CUMULATIVE INDEX

Volumes 16–20

NUCLEAR SCIENCE ABSTRACTS

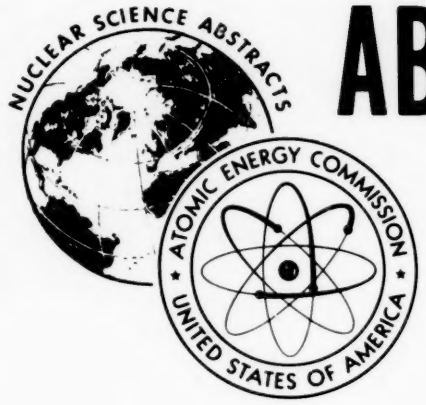

Volumes 16 through 20

1962 – 1966

SUBJECTS (N)

UNITED STATES ATOMIC ENERGY COMMISSION
Division of Technical Information

USAEC DEPOSITORY LIBRARIES

Collections of USAEC reports are maintained in the libraries of the organizations listed below for reference use by the general public. Facilities for making photocopies are available. The USAEC also makes available through these libraries atomic energy reports of countries other than the U. S. that are abstracted in *Nuclear Science Abstracts*.

ALABAMA
Auburn, Auburn University
ALASKA
College, University of Alaska
ARIZONA
Tucson, University of Arizona
ARKANSAS
Fayetteville, University of Arkansas
CALIFORNIA
Berkeley, University of California
Davis, University of California
Los Angeles, University of California
San Diego, Public Library
Stanford, Stanford University
COLORADO
Boulder, University of Colorado
Denver, Public Library
CONNECTICUT
New Haven, Yale University
DELAWARE
Newark, University of Delaware
DISTRICT OF COLUMBIA
Washington, Library of Congress
FLORIDA
Coral Gables, University of Miami
Gainesville, University of Florida
Tallahassee, The Florida State University
GEORGIA
Atlanta, Georgia Institute of Technology
HAWAII
Honolulu, University of Hawaii
IDAHO
Pocatello, Idaho State University
ILLINOIS
Chicago, John Crerar Library
Chicago, University of Chicago
Evanston, Northwestern University
Urbana, University of Illinois
INDIANA
Bloomington, Indiana University
Lafayette, Purdue University
IOWA
Ames, Iowa State University
KANSAS
Manhattan, Kansas State University
KENTUCKY
Lexington, University of Kentucky
Louisville, University of Louisville
LOUISIANA
Baton Rouge, Louisiana State University
New Orleans, Tulane University
MARYLAND
Baltimore, Johns Hopkins University
College Park, University of Maryland
MASSACHUSETTS
Cambridge, Harvard University
Cambridge, Massachusetts Institute of Technology
MICHIGAN
Ann Arbor, University of Michigan
Detroit, Public Library
East Lansing, Michigan State University
MINNESOTA
Minneapolis, University of Minnesota
MISSISSIPPI
State College, Mississippi State University
MISSOURI
Kansas City, Linda Hall Library
Rolla, University of Missouri School of Mines and Metallurgy
St. Louis, Washington University
MONTANA
Bozeman, Montana State College
NEVADA
Las Vegas, Nevada Southern University
Reno, University of Nevada
NEW JERSEY
Princeton, Princeton University
Teaneck, Fairleigh Dickinson University
NEW MEXICO
Albuquerque, University of New Mexico
NEW YORK
Albany, The University of the State of New York
Buffalo, State University of New York at Buffalo
Ithaca, Cornell University
New York, Atomic Industrial Forum, Inc.
New York, Columbia University
New York, New York University
Rochester, University of Rochester
Schenectady, Union College
Syracuse, Syracuse University
Troy, Rensselaer Polytechnic Institute
NORTH CAROLINA
Charlotte, Public Library of Charlotte and Mecklenburg County
Durham, Duke University
Raleigh, North Carolina State College
NORTH DAKOTA
Grand Forks, University of North Dakota
OHIO
Cincinnati, University of Cincinnati
Cleveland, Public Library
Columbus, Ohio State University
Toledo, University of Toledo
Youngstown, Youngstown University
OKLAHOMA
Norman, University of Oklahoma
Stillwater, Oklahoma State University
OREGON
Corvallis, Oregon State University
Portland, Reed College
PENNSYLVANIA
Philadelphia, University of Pennsylvania
Pittsburgh, Carnegie Library
University Park, Pennsylvania State University
PUERTO RICO
Rio Piedras, University of Puerto Rico
RHODE ISLAND
Providence, Brown University
SOUTH CAROLINA
Columbia, University of South Carolina
TENNESSEE
Knoxville, University of Tennessee
Memphis, Public Library
Nashville, Joint University Libraries
Oak Ridge, Oak Ridge Associated Universities
TEXAS
Austin, University of Texas
College Station, Texas A & M University
Dallas, Southern Methodist University
Houston, Rice University
Lubbock, Texas Technological College
San Antonio, Public Library
UTAH
Salt Lake City, University of Utah
VIRGINIA
Blacksburg, Virginia Polytechnic Institute
Charlottesville, University of Virginia
Norfolk, Old Dominion College
WASHINGTON
Pullman, Washington State University
Seattle, University of Washington
WEST VIRGINIA
Morgantown, West Virginia University
WISCONSIN
Madison, University of Wisconsin
Milwaukee, Public Library
WYOMING
Laramie, University of Wyoming

UNITED STATES ATOMIC ENERGY COMMISSION

NUCLEAR SCIENCE ABSTRACTS

Cumulative Index

Volumes 16 through 20
1962 - 1966

SUBJECTS (N)

Division of Technical Information

This eleven-volume set is for sale by the
Superintendent of Documents, U. S. Government Printing Office
Washington, D. C. 20402 Price $36.00

STAFF OF NUCLEAR SCIENCE ABSTRACTS

John W. Norris
Managing Editor

Donald D. Davis
Assistant Managing Editor

David E. Bost
Production Manager

Robert E. Upchurch
Subject Heading Specialist

J. Paul Meredith
Descriptive Cataloging Specialist

Clara L. Fox
Corporate Author Specialist

Mary H. Newman
Reports Evaluator

Brainard L. Patton
Scheduling and Publishing Coordinator

Section Editors

Everett J. Hoffman
Chemistry

Robert C. Kelly
Engineering; Earth Sciences

Lee M. Thompson
General Physics

Charles E. Stuber
High Energy Physics

Hugh E. Voress
Life Sciences

Lawrence T. Whitehead
Nuclear Data

James M. Jacobs
Reactor Technology; Metals and Ceramics

Abstractors

F. S. Armstrong*
Mary M. Brown
Jane G. Buchanan
D. Lamar Cason
Bennie G. Di Bona
Helen G. Donald
James R. Dulaney
Wells L. Green
Bernard O. Griggs
Harry G. Grisham
Mary C. Grissom
Miriam P. Guthrie
Fernando Hamilton
Phyllis C. Hansen
Thomas F. Heagerty
Carolyn D. Houston
Rose V. Jermain
Sidney F. Lanier
Betty L. McDowell
William D. Matheny
John H. Mitchell
Dora H. Moneyhun
Luther Norene
Carol Oen
Jean F. Peckham
Henry D. Raleigh
Mona H. Raridon
Julia S. Redford
Ned W. Rizzardi
Francis L. Sachs
Lila B. Smith
Polly C. Summers
Anne G. Ward
Helen L. Ward
David C. West
Milton O. Whitson
Juanita Wilson

*Atomic Energy of Canada, Ltd.

Acknowledgments

Agreements between the United States Atomic Energy Commission and the following organizations with regard to providing continuing services and specific literature coverage for *Nuclear Science Abstracts* are gratefully acknowledged:

American Institute of Physics; Atomic Energy of Canada Limited; Atomic Energy Research Establishment, United Kingdom; Aktiebolaget Atomenergi, Sweden; European Atomic Energy Community (EURATOM); Gmelin Institute, International Atomic Energy Agency; Japan Atomic Energy Bureau—Japan Atomic Energy Research Institute; Netherlands Patent Office; Reactor Centrum Nederland.

Communication concerning the editorial policy and content of *NSA* should be addressed to the Managing Editor, *Nuclear Science Abstracts*, AEC Division of Technical Information Extension, P. O. Box 62, Oak Ridge, Tennessee 37830.

Use of funds for printing this publication approved by the Director of the Bureau of the Budget, June 28, 1966.

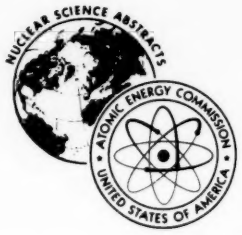

Cumulative Index
Volumes 16-20, Subjects, 1962-1966

NUCLEAR SCIENCE ABSTRACTS

A semimonthly publication of the USAEC Division of Technical Information, Edward J. Brunenkant, Director. Published by the USAEC Division of Technical Information Extension, Robert L. Shannon, Extension Manager.

Nuclear Science Abstracts provides the only comprehensive abstracting and indexing coverage of the international literature on nuclear science and technology. *NSA* covers scientific and technical reports of the U. S. Atomic Energy Commission and its contractors, those of other U. S. Government agencies, and those of other governments, universities, industrial, and research organizations. It also covers patents, books, and journal literature on a worldwide basis. A list of the journals scanned appears in Issues 1 and 13 of each volume. Nearly 400,000 abstracts have appeared in *NSA* through Volume 20. The subject matter covered in *NSA* is described in Issue 1 of each volume and in TID-4552, *Subject Scope of Nuclear Science Abstracts*. The latter is available free from the U. S. Atomic Energy Commission, Division of Technical Information Extension, P. O. Box 62, Oak Ridge, Tennessee 37830.

Abstracts are arranged according to subject categories which are defined in Issue 1 of each volume. If the language of the original item is not English, the language is indicated. Translations are not abstracted if an abstract of the original item has appeared in *NSA*.

AVAILABILITY OF PUBLICATIONS ABSTRACTED

The public availability of all U. S. Atomic Energy Commission reports is indicated in the report number indexes. The availability of other reports, when known, is also indicated. The availability of some unnumbered reports is given in the abstract.

Dissertations abstracted in *Dissertation Abstracts* and included in *NSA* are available from University Microfilms, Inc., 315 N. First Street, Ann Arbor, Michigan 48103.

Information on the availability of the published literature and unpublished conference papers abstracted in *NSA* may be obtained from the Division of Technical Information Extension, P. O. Box 62, Oak Ridge, Tennessee 37830.

HOW TO OBTAIN NUCLEAR SCIENCE ABSTRACTS

NSA is available to the general public on a subscription basis from the Superintendent of Documents, U. S. Government Printing Office, Washington, D. C. 20402, as follows:

For the 24 regular issues, $30.00 domestic, $37.00 foreign. A single issue costs $1.75, plus 25 percent for foreign mailing. Domestic rates apply to the United States, Canada, Mexico, and Central and South American countries except Argentina, Brazil, Guyana, French Guiana, Surinam, and British Honduras. Foreign rates apply to the countries excepted above and to all other countries throughout the world.

For the quarterly, semiannual, and annual indexes, $22.00 domestic, $25.00 foreign.

Multivolume subject and author indexes are available as follows:

Vols. 1-4 (1948-1950). Johnson Reprint Corporation, 111 Fifth Avenue, New York, N. Y. 10003, $30.00.

Vols. 5-10 (1951-1956). Superintendent of Documents, U. S. Government Printing Office, Washington, D. C. 20402, $5.25.

Vols. 11-15, Subjects. Superintendent of Documents, U. S. Government Printing Office, Washington, D. C. 20402, $19.00.

Vols. 11-15, Personal Authors. Superintendent of Documents, U. S. Government Printing Office, Washington, D. C. 20402, $14.25.

Vols. 11-15, Corporate Authors. Superintendent of Documents, U. S. Government Printing Office, Washington, D. C. 20402, $2.50.

Vols. 16-20. (To be issued in 1967.)

Cumulative Report Number Index, Vols. 1—15 Revised, is available from the Superintendent of Documents, U. S. Government Printing Office, Washington, D. C. 20402, $4.00.

Cumulative Report Number Index, Vols. 16—20, is available from the Superintendent of Documents, U. S. Government Printing Office, Washington, D. C. 20402, $4.25.

Annual indexes are available separately from the Superintendent of Documents, U. S. Government Printing Office, Washington, D. C. 20402, as follows:

Vol. 16, Subjects and Authors, $9.75.
Vol. 17, Subjects and Authors, $12.25.
Vol. 18, Subjects and Authors, $12.50.
Vol. 19, Subjects and Authors, $12.50.

Annual indexes for Vol. 20 were not issued since they are a part of the cumulation for Vols. 16–20.

NSA is available on an exchange basis to universities, research institutions, industrial firms, and publishers of scientific information. Inquiries should be directed to the U. S. Atomic Energy Commission, Division of Technical Information Extension, P. O. Box 62, Oak Ridge, Tennessee 37830.

Government agencies may obtain *NSA* free of charge.

INTRODUCTION

Subject entries in this index are generally specific materials, things, and processes. These are followed by modifiers that describe the properties of, and processes applied to, the entries.

The number preceding the colon is the *NSA* volume number, and the number following is the abstract number. The designation (R) following the abstract number indicates that the abstract is of a progress report; (P) indicates a patent; and (T) indicates a translation. Abstracts for reports other than progress reports carry no letter designation. References to report numbers, where appropriate, are included after the abstract number of the citation. Published literature (journal article or book) is identifiable by the absence of a report number.

Special characters are added to modifiers in the field of physics; if the modifier does not establish the experimental or theoretical character of a reference, a symbol (E), (T), or (E/T) is placed immediately after the modifying phrase and before the journal reference number. The value of this identification has been established by the American Institute of Physics.

The user should bear in mind that the ideas presented in the original literature, rather than key words, have been indexed. The indexers have tried to select what seemed the most probable and logical place to look for typical information. Since it is not possible to anticipate where a user would look for information, numerous cross references are included.

Experience in using an index of this type will be the best guide in obtaining the desired information, and a consideration of synonymous or closely related terms as well as recent developments in scientific terminology will prove valuable.

Information must be so indexed as to be of the greatest use to the greatest number of users. This requires that a topic be indexed to headings that most specifically describe it and not ordinarily to the headings that describe its ultimate use, nor to the general class headings that include the specific headings. For example, information on the treatment of thyroid disease with I-131 would be indexed under Thyroid Gland and under Iodine Isotopes I-131, but not necessarily under Radiotherapy. A study of the effects of x radiation on hair would be indexed under both X Radiation and Hair.

The broad, general class headings are used only for general information or for comprehensive reports or articles.

Subject Heading Styles

Generally, the direct form of subject entry is used rather than inverted headings, e.g., Amino Acids rather than Acids, Amino; Helium Isotopes He-4 rather than Helium — isotopes He-4 or Helium — He-4 isotopes. Note, however, that in some cases parenthetic modifying terms or inverted headings of the form Neutrons, Fast are used in preference to a direct entry that would result in the scattering of information. Organic compounds are usually entered in the index in the inverted form so that substituted compounds can be listed near the parent compound; e.g., Benzene, Bromo- rather than Bromobenzene. Subject headings were chosen from TID-5001(5th Rev.) "Subject Headings used by the USAEC Division of Technical Information."

Alphabetization

Subject headings are alphabetized word-by-word. A parenthetic qualifier following a subject heading is disregarded in alphabetizing unless there are two or more headings identical except for the parenthetic qualifier, in which case the qualifier determines the order. Headings involving Greek letters are arranged as if the names of the letters were spelled out.

Examples:

M-Capture
see Electron Capture
Magnesium
Magnesium Alloys
Manganese Fluorides
Manganese(II) Fluorides
Mesons
Mesons (π)
Mesons (ρ)
3-Pentanol, 2,4-Dimethyl-
2-Pentanol, 2-Methyl-
2-Pentanol, 4-Methyl-

Nomenclature of Inorganic Compounds

Inorganic compounds are indexed in the direct form, listing cations in the order of increasing valence in the case of polycationic salts of varying valence and in alphabetic order for polycationic salts in which all cations have the same valence; e.g., Sodium Aluminum Silicates and Potassium Sodium Sulfates.

Multicomponent Alloys and Other Systems

Multicomponent alloys, except well-known trade names, are indexed under a heading in the form "element alloy" for each element in the alloy. The modifier begins with element symbols for each component arranged alphabetically as if the English name for the element were spelled out.

Example: Copper–Gold Alloy is indexed
Copper Alloys
Cu–Au . . .
Gold Alloys
Cu–Au . . .

Well-known alloys such as Zircaloy-2 are indexed directly to the trade name; cross references referring from each component of the alloy to the entry for the trade name are included.

Multicomponent systems of nonmetallic elements are indexed in a manner similar to alloys except the main heading used contains the word "Systems" in place of "Alloys."

Example: Silicon–Tungsten Systems are indexed
Silicon Systems
Si–W...
Tungsten Systems
Si–W...

Multicompound systems and mixtures of compounds are indexed under the main heading for each component compound; the modifiers begin with an alphabetical listing of compound formulas.

Example: Lead Titanate–Lead Zirconate is indexed
Lead Titanates
$PbTiO_3$–$PbZrO_3$...
Lead Zirconates
$PbTiO_3$–$PbZrO_3$...

A mixed system of compounds and elements is indexed using a combined form of the above conventions, e.g., a dispersion of copper and alumina would be indexed

Aluminum Oxides
Al_2O_3–Cu...
Copper Systems
Al_2O_3–Cu...

Physical States and Configurations of Materials

Specification of the physical state, if other than normal, or geometric configuration of the material is included in the modifying phrase, i.e., liquid metals would be indexed to the metal with "liquid" in the modifier, and carbon crucibles would be indexed to Carbon with "crucibles" appropriately placed in the modifier and also to Crucibles if appropriate.

Modifying Phrases

The modifiers appearing under a subject heading are written specifically to describe the relation of the item being indexed to that heading. Effort is exerted to begin the modifier with the word judged to be of greatest use to the greatest number of users: this, however, does not obviate the need to consider all modifiers under the main heading(s) of interest.

Modifiers are usually intended to form a meaningful phrase when combined with the main heading. Some are intended to be read following the main heading, e.g., the entry Hydrogen—sorption by charcoal is read "hydrogen sorption by charcoal"; however, as a result of placing the important word first, many modifiers must be arranged for smooth reading, e.g., Formaldehyde—yields in radiolysis of ethyl ether, effects of deuterium on is read "effects of deuterium on formaldehyde yields in radiolysis of ethyl ether" and Uranium—crystal structure of, effect of cooling rate on allotropic transformations in is read "effect of cooling rate on allotropic transformations in crystal structure of uranium." Prepositions are sometimes omitted if no ambiguity results.

SUBJECTS (N)

N

NAAP
see *Antipyrine, N-Acetyl-4-Amino-*

NAGASAKI
analysis of data on populations for genetic effects of radiation, statistical methods, 17: 7812
atomic explosions in, late effects of, 18: 21854
atomic explosions at, free-field radiation dose from, 20: 16760
autopsy service in, 18: 29172
biological blast effects of atomic explosion at, analytical study of, 19: 13664 (CEX-63.7)
biological effects of atomic explosion on population of, 18: 25722
blood picture in bomb survivors, 16: 20248
blood picture of human populations in, 20: 6810
blood picture of nuclear-explosion survivors in, survey, 20: 20481
blood serum iron content in population of, exposed to atomic bomb radiation, 18: 100
bomb radiation dosimetry in, from roof-tile thermoluminescence, 19: 11536
bomb survivors of, hematological disorders in, 20: 28876
bombing effects on hematology in survivors in, 19: 38378
bombing survivors of, radiation dosage of, 20: 7315(R) (ORNL-3849, pp 151-82)
book: *Effects of Atomic Explosions on Man*, in German, 16: 5124
butanol-extractable iodine in serum of children in, 20: 6832
carcinogenesis and leukemia in, 18: 19581
clinical status of residents of, exposed to atomic bomb radiation in 1945, 19: 31783 (ABCC-61-62)
dental survey on children of, 19: 24228
disease occurrence and mortality patterns of survivors of atomic disaster in, 20: 42697 (ABCC-18-65)
effects of atomic explosions over, review on, 17: 18415
effects of atomic explosion at, on thyroid gland function in children exposed *in utero*, 17: 10371
effects of atomic explosion on population of, 19: 40361(T) (ORNL-tr-437)
eye cataracts in bomb survivors, 16: 20133
fallout monitoring, 1959, 18: 14082
gamma emissions from roof tiles in, thermoluminescent dosimetry of, 20: 16759
genetic effects of radiation on population, 16: 16225
genetic effects of radiation on population, 17: 23211
genetic survey of inbreeding in, 17: 12094
health of population exposed to atomic bomb at, 20: 16271
hematology of bomb survivors, 16: 20249
incidence of diabetes mellitus and glycosuria in, epidemiology of, 19: 15199
leukemia cases in bomb survivors, 16: 20251
leukemia development in humans in, 1946 to 1964, 20: 36645
leukemia in people in, effects on central nervous system, 19: 17502
leukemia incidence in bomb survivors in, 16: 26749
leukemia incidence in bomb survivors in, 1945–1959, 17: 12173
leukemia incidence in population of, exposed to atomic bomb radiation, 19: 31863
leukemia incidence in irradiated population of, 20: 161
leukemia occurrence in bomb survivors in, 17: 14083
leukemia occurrence in bomb survivors in, 18: 25728
medical survey of population of, exposed to 1945 atomic bomb, 1961, 20: 10595(R) (ABCC-60-61)
mortality of atomic bomb survivors in, from malignant neoplasms, 17: 4404
mortality of atomic bomb survivors in, causes and dose relation to, 19: 25998
mortality of bomb survivors, 16: 17511
myopia in children in, effects of environment, inbreeding, and inheritance on, 16: 33325
neutron dose from atomic explosion at, estimation of, 18: 31806
ocular damage to survivors of atomic explosion in, 17: 35466
population exposed to atomic bomb, statistical analysis of, 20: 10663
population of, clinical status of radiation-exposed, 19: 44280(R) (ABCC-63-64)
radiation cataract incidence in bomb survivors, 16: 1548
radiation data for calculation of LD_{50} from, 16: 17435 (A/AC.82/G/L.750)
radiation dose evaluation for populations of, from atomic explosions in 1945, 18: 31783 (CEX-64.3)
radiation dose measurements for population, 16: 15021 (CEX-62.02)
radiation dose to population of, exposed to atomic explosion, 19: 42655 (CEX-62.11)
radiation dosimetry of bomb survivors, Ichiban program for, 20: 39064
radiation effects on survivors of atomic bombing, 17: 1680
radiation effects on human populations in, 17: 4381
radiation effects on tumor incidence in populations, 17: 6333
radiation effects on fertility of population exposed to atomic bomb, 18: 6613 (ABCC-18-62)
radiation effects on hematological system in residents exposed to atomic bomb, long-term, 18: 6640
radiation effects in population of, late, 18: 6612 (ABCC-16-62)
radiation effects on brain from nuclear explosion in, 18: 38850
radiation effects on development of children of, exposed *in utero*, 19: 7166
radiation effects on population of, 19: 21792(R) (ORNL-3650(p.187-219))
radiation effects from atomic bomb on population of, bibliography, 19: 21853 (ABCC-00-62)
radiation effects from atomic explosion on mortality of population of, 19: 33784 (ABCC-15-63)
radiation effects on population of, somatic, 19: 34098
radiation effects from bomb on development and growth of adolescents exposed *in utero*, 19: 45889
radiation effects on population exposed in 1945, summary of 1965 findings on, 20: 20919(R) (ABCC-64-65)
radiation effects on live births among atomic bomb survivors in, 20: 31091
radiation effects on health of population of, 20: 42827(R) (ABCC-58-59)
radiation effects on health of population of, 20: 42828(R) (ABCC-59-60)
radiation effects on population of, exposed to nuclear explosions, 20: 45406
radiation exposure from atomic bomb to shipyard workers in, relation of job absenteeism to, 19: 17543
radiation injuries in adolescents of, 18: 33391
radiation injuries of eyes of residents exposed to atomic explosion, 19: 21873
radiation sickness in residents of, late effects of acute, 18: 37018
radioinduced aging in, hexosamine–collagen ratio for detecting, 20: 12644
radioinduced carcinogenesis in, from atomic bomb explosion, 18: 19580
radioinduced leukemia in, incidence of, 19: 42294
radioinduced thermoluminescence of roof tiles in, 18: 18427
statistical analysis of population for late radiation effects, 17: 6332
survey of conditions, 1963, 18: 18089
survey on incidence of mongolism in offspring of pregnant women exposed to radiation from atomic explosion, 17: 5848
thyroid carcinoma incidence in population of, 17: 21540
thyroid tumors in bomb survivors, 16: 32843
tumor incidence in populations of, 18: 19596
tumor mortality in bomb survivors, 16: 20250

NALORPHINE
radiosensitivity effects on mice, x, 20: 20513

NAPHAZOLINE
effects on inhibition of tissue reaction in irradiated rabbit connective

tissue, 20: 38640
protective effects against lethal whole-body radiation in mice, 16: 14599
radiosensitivity effects on subcutaneous tissue in rabbits, 16: 14600
NAPHTHA
properties as diluent in amine solvent-extraction systems, 18: 37275 (A/CONF.28/P/755)
NAPHTHACENE
bond lengths for, 17: 20580(R) (NP-12207)
conversion into high-purity graphite, 19: 4606(P)
effects on photoconductivity in anthracene crystals, (E), 19: 22381
effects on radioinduced luminescence of bibenzyl, 19: 19963
electric conductivity, effects of pressure, 16: 30942
electron transitions in, oscillator strengths for probability of, (T), 20: 15275
electronic spectra of, tables, 19: 9156 (IS-450)
exchange reactions with deuterium oxide, mechanism of platinum-catalyzed, 16: 16344
graphitization of, mechanism and properties for, 18: 35934 (ML-TDR-64-125(Vol.I))
photolysis of solutions of salts of, in dimethoxyethane and tetrahydrofuran, 17: 28783
properties as free-radical scavenger in radiolysis of halogenated hydrocarbons, 19: 478
pyrolysis and radiolysis of, products from, 18: 3807 (BNL-7413)
radiolysis, 18: 11366 (BNL-7650)
spectra, as impurity in bibenzyl-stilbene crystals, 16: 30985
NAPHTHACENE, 5,6,11,12-TETRAPHENYL-
electroluminescence of, calculations on, 20: 22871(R) (MIT-905-52, (pp 42-73)
fluorescence lifetime, 17: 9054
1-NAPHTHALDEHYDE
reactions with carbonyl reagents, carbon-14 and tritium isotope effects, 16: 23577
NAPHTHALENE
alkyl, phosphor design using, 18: 31642(P)
analysis for sulfur by x-ray absorption methods, 20: 20615
annihilation interactions in mixed and pure, relation of delayed fluorescence and phosphorescence to triplet-triplet, 17: 31112
chemical properties, determination by quantum theory, 16: 15364
complexes with ethenetetracarbonitrile, effects of pressure on properties of, 20: 12534 (COO-1198-216)
complexes with polonium and polonium bromides, chlorides, fluorides, and iodides, preparation of, 20: 1850
crystallization for detecting electromagnetic field activity, 20: 37889
crystallization for detecting electromagnetic field activity, correlation with lunar phases of, 20: 37891
crystallization test for detecting electromagnetic activity, magnetic storm effects on, 20: 37890
deuterium exchange with heavy water, group VIII metal catalysis of, 19: 38597
deuterium isotope effects in hydrogen bonding of imidazole in, 17: 28932
diamino-, mechanism and properties for graphitization of, 18: 35934 (ML-TDR-64-125(Vol.I))
effect on quenching of liquid scintillation solutions, 17: 14981
effects on energy and hydrogen transfer in gamma radiolysis of benzophenone--2-propanol, 18: 27515
effects on hydrogen yields in radiolysis of liquid cyclohexane, 17: 40886
effects on photoreduction of benzophenone, 17: 10680(R) (TID-17584)
effects on radiation resistance of polyethylene, 19: 22322
effects on radioinduced polymerization of butadiene, 17: 4575 (TID-7643(p.109-17))
effects on radioinduced cis-trans isomerization of 2-butene, 17: 39150
effects on radioinduced isomerization of stilbene in benzene, 20: 33334 (NYO-3242-13)
effects on radiolysis of NEDA and NETA petroleum fractions, 19: 481
effects on radiolysis of 2-propanol, 19: 13423 (KFK-243)
effects on radiolytic isomerization of stilbene in benzene solutions, 20: 18735
effects on radiolysis of butyrophenones, 20: 26936
effects on radiolysis of cyclohexane, 18: 12152 (TRECOM-TR-62-90)
effects on yields in gamma radiolysis of cyclohexane, 18: 39302
effects on yields from gamma radiolysis of 2-methyltetrahydrofuran, 19: 28406
effects on yields of biphenyl from gamma radiolysis of benzene, 20: 26988
effects on yields in gamma radiolysis of liquid and vitreous 2-propanol, 20: 41006
electric potentials, 18: 19837(R) (MIT-905-1)
electron capture in, 19: 7539(R) (ORNL-3697(p.131-43))
electron transitions in, oscillator strengths for probability of, (T), 20: 15275
electronic spectra of, tables, 19: 9156 (IS-450)
energy levels of, perturbation technique for, 17: 40833 (ARL-63-27)
energy transfer to 2-α-naphthyl-5-phenyloxazole in solution, 16: 2857(R) (ANL-6398(p.3-4))
exchange reactions with deuterium oxide, mechanism of platinum-catalyzed, 16: 16344
excitation of, pulse-height ratios for, alpha and electron, 18: 20408
excitation transfer in normal-deuterium-labeled crystals of, 16: 16379
fluorescence decay times of, isotope effects of deuterium on, 18: 13805(R) (ANL-6769(p.3-5))
fluorescence of deuterated, in durene, out-of-plane polarization of, 19: 34210
fluorescence quenching in cyclohexane solution of, by oxygen, 17: 4566
fluorescence spectra of solutions of, 16: 22099
fluorescence spectra of single-crystal, 16: 22099
heat of fusion of, 19: 17942 (EUR-2223.d)
hydrogen isotope exchange with hydrobromic acid, 16: 23569
hydrogen isotope exchange with potassium amide in liquid ammonia, 19: 13362
labeling with deuterium, 19: 46307
luminescence of, alpha/beta ratio in, 18: 300
luminescence of, deuterium isotope effects on radiationless transitions in, 19: 2306
luminescence quenching in benzene solution, effects of aromatic halides on, 17: 4563
mass transfer to air-fluidized beds, computer analysis of, 17: 12390 (ANL-SL-SL-2342)
neutron scattering by liquid and solid, cold, 19: 12457 (JINR-P-1903)
octafluoro-, radiolysis of, G values and products of, 19: 15331(R) (BNL-841(p.18-42))
octahydro-, reactions with deuterium in liquid phase on platinum oxide catalysts, 16: 13044
oxidation of, current-voltage measurements for, 19: 36220(R) (MIT-2098-142)
photofluorescence spectra of liquid solutions and single crystals, 16: 22099
photoionization of, energy spectra of electrons from, 18: 281
photoluminescence decay to 250 nsec, 16: 27834
photolysis of, effects of halogenation of decay of triplet states in, 17: 20053(R) (AFCRL-62-626)
preparation and luminescence spectra of pure and anthracene- and durene-containing, 16: 1806(R) (NP-10912)
preparation and properties of carbon-14-labeled-, by nuclear recoil, 17: 33975
preparation of carbon-14-labeled, under neutron irradiation, 17: 30146
preparation of tritium-labeled, by electric discharge, 16: 23548
properties of tritiated, for use as chemical dosimeter, 19: 22289
pyrolysis and radiolysis of, products from, 18: 3807 (BNL-7413)
radiation effects on aerosols of, 17: 3026(R) (TID-17250)
radiation effects on physical properties of, gamma, 17: 29901
radiation effects on reaction of alkyl, with saturated aliphatic hydrocarbon, 17: 8216(P)
radiation effects on scintillation properties of, alpha, beta, and electron, 19: 7994
radiation effects on, recombination of free radicals following, 19: 13465
radiation effects, 19: 22289
radiation effects on, free radical recombination following, 19: 26407
radiation effects on carbon tetrachloride polycrystalline solutions of, spectra of resonance charge transfer in, 20: 18752
radioinduced excitation of singlet and triplet states of, gamma and ultraviolet, 18: 8415
radioinduced fluorescence of organic phosphors in, 20: 3994
radioinduced oxidation on alumina, alumina--silica system, and silica, 18: 1725(R) (ORNL-3488(p.42-54))
radioinduced oxidation of, adsorbed on alumina, aluminosilicate, and silica gel, 19: 4215
radioinduced polarization of fluorescence from, 18: 25594
radioinduced thermoluminescence in, factors affecting, 18: 25472(T) (AEC-tr-6372(p.61-74))
radioinduced thermoluminescence of, in crystalline biphenyl, 19: 40563
radioinduced thermoluminescence of, intensities of fluorescence and phosphorescence in gamma, 20: 33377
radiolysis, 18: 11366 (BNL-7650)
radiolysis effects on hydrogen yield in deaerated petroleum high-boiling fractions, 16: 25416 (PAN-289/ChR)
radiolysis in acetone solutions, triplet state formation in pulse, 19: 36480
radiolysis in boric acid glass, spectra of free radicals in, 18: 10157
radiolysis of, effects on electronic properties, 18: 3863
radiolysis of solid, effects of pi-electron resonances on, 19: 465
radiolysis of solutions of, formation of triplet states in pulse, 20: 23100
radiolysis of, effects of metal ions and temperature on, 20: 29260
radiolysis of, predicted reactions in, 19: 30233(R) (ORNL-3789(p.318-22))
radiolysis of, yield of free radicals of, 18: 20042 (USNRDL-TR-718)
radiolysis of, yields in, 20: 40991
reduction of platinum oxide in heavy water by, catalytic self-activation in, 18: 12092
reduction of platinic oxide by labeled, preparation of platinum oxide

catalysts by, 19: 38596
scintillation response of, alpha, deuteron, and electron, 18: 37242
spectra, deuterium isotopic effects on electron absorption, 16: 29584
spectra in gamma irradiated organic glasses at −196°C, 17: 6148
spectra, modified Urey-Bradley force field for vibrational, 16: 25346
spectra of deuterated and nondeuterated, calculation and interpretation of vibrational, 18: 35556(T)
spectra of deuterated and normal, trapped in solid rare gases, 20: 18016
sublimation and condensation by adiabatic expansion, 16: 4297(T) (NP-tr-827(p.74-6))
thermal accommodation of vaporous, on glass, 19: 32416
thermal decomposition, 20: 40991
use as binder in preparation of dispersions of uranium carbide in uranium, 19: 20512(R) (NCSC-2981-2)
use as binder in preparation of dispersions of uranium carbide in uranium, 19: 20513(R) (NCSC-2981-3)
use as scintillator solvent, 17: 30087
use in preparation of radiation-resistant lubricants, 19: 34214(P)
use in tritium detector, 18: 19887
x-ray scattering by, Raman lines in, (E), 20: 18559 (CALT-221-14)
anthracene–naphthalene, radioinduced thermoluminescence of crystalline, 18: 17879
benzaldehyde-naphthalene, energy transfer by triplets in hydrocarbon glass, 19: 28281(R) (AD-607838)
benzene–benzophenone–naphthalene, radiolysis of, formation of triplet states of solutes in electron, 18: 43655
benzophenone–naphthalene, radiolysis in alcoholic, aqueous, and hydrocarbon solutions, 20: 1920
butyl chloride–naphthalene, radiolysis in alcoholic, aqueous, and hydrocarbon solutions, 20: 1920
CCl_4–naphthalene, radiolysis in alcoholic, aqueous, and hydrocarbon solutions, 20: 1920
cyclohexane–naphthalene, radiolysis of, formation of triplet states of solutes in electron, 18: 43655
dichlorobenzene–naphthalene, radioinduced sulfur-35 production in, 20: 25114
ethanol–naphthalene, radiation effects on hydrogen atom reactions in, 20: 16524
methanol–naphthalene, radiation effects on hydrogen atom reactions in, 20: 16524
methanol–naphthalene, radiolysis yields in, 19: 46324(R) (AGN-8132)
naphthalene–Xe, radiolysis of, spectra of naphthalene triplet state in pulse, 18: 43627
naphthalene–petroleum, radiolysis effects on stability of, 19: 28402
naphthalene–tetrahydrofuran, radiolysis in alcoholic, aqueous, and hydrocarbon solutions, 20: 1920
naphthalene–H_2SO_4, radiolysis in alcoholic, aqueous, and hydrocarbon solutions, 20: 1920
naphthalene–tetramethyl-*p*-benzoquinone, radiolysis in alcoholic, aqueous, and hydrocarbon solutions, 20: 1920
naphthalene–tetrahydrofuran, solvent properties for alkali metals, 19: 40409(R) (MSAR-65-95)
1-chlorobutane–naphthalene, radiolysis in alcoholic, aqueous, and hydrocarbon solutions, 20: 1920
1,4-dioxane-naphthalene, use of bis-(2-alkoxyethyl) ethers as antifreeze in, 16: 5326
2,5-diphenyloxazole–methanol–naphthalene–2,2'-*p*-phenylenebis-5-phenyloxazole, properties of, for scintillation counting of blood glucose, 18: 13659

NAPHTHALENE, BROMO-
luminescence quenching effects on scintillator solutions in benzene and cyclohexane, 17: 4563
radiolysis of, radical captor properties of dinaphthofuranoxyl and DPPH in, 18: 43607

NAPHTHALENE, CHLORO-
radioinduced sulfur-35 production in, 20: 25114

NAPHTHALENE, DECAHYDRO-
dielectric polarization of, temperature dependence, 19: 40468(T) (SC-T-65-721)
perfluoro-, radiation effects on, 19: 38709
radioinduced cracking at high pressure and temperature, beta, 20: 355(R) (NYO-2978-42)
9-chloro-, reduction with tributyltin hydride, 18: 19837(R) (MIT-905-1)

NAPHTHALENE, DIHYDRO-
radiation effects on C_4-cyclodimerization of, 18: 8423

NAPHTHALENE, 1,2-DIMETHYL-
radioinduced excimer emission in liquid, x, 20: 23132

NAPHTHALENE, 1,6-DIMETHYL-
9,10-diphenylanthracene–1,6 dimethylnaphthalene, energy transfer in phosphors of, effect of excimer formation on, 20: 33275

NAPHTHALENE, 2-ETHYL-
radioinduced excimer emission in liquid, x, 20: 23132

NAPHTHALENE, 1-METHYL-
preparation and properties for use in liquid scintillators, 18: 16317
radiation effects on metabolism in rats, x, 20: 20439 (EUR-2628.f)
radioinduced hydrogenation of, beta, 19: 40553(R) (NYO-2978-34)
radiolysis of, yields in, 20: 40991
thermal decomposition, 20: 40991
use of, in liquid scintillation, 18: 16375(P)
uses as solvent in combined liquid and glass particle scintillator, 19: 18324(P)

NAPHTHALENE, 2-METHYL-
radiolysis of, yields in, 20: 40991
thermal decomposition, 20: 40991

NAPHTHALENE, 1,2,3,4-TETRAHYDRO-
decomposition by electron impact, product distribution in liquid-phase, 18: 270 (PAN-432/XVII)
dehydration and dehydrogenation of, on praseodymium oxide, 20: 5567
dehydrogenation and dehydration kinetics using uranium oxide catalyst, 17: 25348
dehydrogenation of, catalytic effects of erbium oxide on, 19: 7533
dehydrogenation of, catalytic effects of praseodymium oxide on, 19: 44023
dehydrogenation on lanthanum oxide, hydrogen formation and kinetics of, 18: 1719
dehydrogenation on erbium oxide, kinetics and products of, 19: 26374
hydrogen abstraction from, by methyl radicals, 19: 21760 (NYO-2728-4)
radioinduced hydrogenation of, beta, 19: 40553(R) (NYO-2978-34)
radiolysis of, appearance potentials and heat of formation for ions from, 18: 294
radiolysis of frozen, kinetics of radical reactions in gamma, 20: 25123 (INR-672/XVII/C)
radiolysis of liquid, mechanism of gamma, 20: 43335
radiolysis of, electron thermalization and electron–ion recombination in, 20: 26981
radiolysis of, excited and superexcited states in, 20: 18783
radiolysis of, in helium, helium–oxygen, and oxygen atmospheres, 19: 13474
radiolysis of, mass-spectrometric studies of ion-molecule reactions in, 20: 12901
6-vinyl-preparation of scintillator polymers of, 19: 13414

1-NAPHTHALENEAZOBENZENE, 2-AMINO-
solubility of, in heavy water, isotope effects on role of hydrogen bonds in, 20: 43287

NAPHTHALENEACETIC ACID
effects with water-d_2 on growth of peppermint, 19: 35920

1,2-NAPHTHALENEDIOL
complexes with flavines, spectra and stability of, 20: 10460 (COO-908-6)

1,4-NAPHTHALENEDIOL
complexes with flavines, spectra and stability of, 20: 10460 (COO-908-6)

2,7-NAPHTHALENEDIOL
deuterium–hydrogen exchange in alkaline solution of, 18: 25453

NAPHTHALENEDIOL, DERIVATIVES
complexes with flavines, electric and magnetic properties of, 20: 10459 (COO-908-5)
complexes with flavines, spectra of, 20: 10461 (COO-908-7)
effects on radiosensitivity of mouse tumors, 19: 26116

1,4-NAPHTHALENEDIOL, 2-METHYL- DIPHOSPHATE, SODIUM SALTS
effects on adenosinetriphosphate content of mouse tumors, 17: 7822
effects on chromosomal DNA in human cells as related to mutagenicity, 19: 33829
effects on phosphorus-32 uptake by irradiated rats, 20: 18379
effects on radiation effects on lipid synthesis in rat brain and liver, 19: 26092
effects on tumor oxygen tension, 18: 17686
preparation and effectiveness as a chemical radiosensitizer of tumors, 17: 105
preparation of tritiated derivatives for tumor therapy, 19: 4191(P)
preparation of tritiated derivatives of, for use as drugs, 20: 18464
protective effects on chromosomal aberrations and mitosis in x irradiated carcinomas and onion root cells, 16: 14555
protective effects of tritium-labeled, on cancer in animals and man, 17: 13897
protective effects against radiation effects on fat synthesis in brain and liver in animals, 17: 13934
protective effects of, against radiation damage to bovine serum albumin, 17: 28757
radiolysis of tritium-labeled, self-, 20: 16535
radiosensitivity effects on tumors, 16: 26752
radiosensitivity effects in cat, dog, and man, 18: 17687
radiosensitivity effects on oral carcinomas, 18: 43355
radiosensitivity effects on phosphorus-32 uptake by rat kidneys and liver, 19: 26011
radiosensitivity effects of, in cancer patients, 20: 5437
radiosensitivity effects on tumors, 20: 18464
radiosensitivity effects on rat tumors, 20: 18533
radiosensitivity effects on mouse ascites tumors, mechanism of, 20: 33082

sensitizing effect of, to action of x radiation, 18: 13537
synthesis of tritiated, 16: 32910
synthesis of tritiated, 18: 5403(P)
therapeutic use of tritium-labeled, for selective irradiation of tumors, 18: 9953
therapeutic use of tritium-labeled, 18: 39032
tritium labeled, effectiveness in palliation of tumors and leukemia, 17: 105
use of tritiated, in radiotherapy of tumors, 19: 46125

2,7-NAPHTHALENEDISULFONIC ACID, 3,6-BIS(*o*-SULFO-*p*-METHYLPHENYLAZO)-4,5-DIHYDROXY-
dianilide of, use of, as extractive photometric reagent in determination of trace amounts of barium and strontium, 20: 33221

2,7-NAPHTHALENEDISULFONIC ACID, 4,5-DIHYDROXY-
analytical uses of azo derivatives of, in complexonometric determination of scandium, 18: 39138
analytical uses of derivatives of, 19: 40426
bisazo derivatives of, analytical uses of, 18: 13700
chelates with uranium(VI), composition and stability, 17: 16073
complex formation with beryllium in aqueous solutions, 19: 38641
complex formation with uranyl ions, 20: 7081
complexes with copper and α,α'-dipyridyl, formation and structure of, 20: 10465 (COO-1020-8)
complexes with thorium and zirconyl, composition and stability constants of, 18: 5260
complexes with uranium, analysis of, potentiometric, 20: 22980
disodium salt of, complexes with copper or iron and triethylenetetraminehexaacetic acid, 20: 10466 (COO-1020-11)
effects on plutonium separation in Purex Process, 20: 7199
nitrobenzeneazo-, reactions with thorium(IV), stability and composition of complexes formed in, 19: 17899
phenylazo-, spectra of thorium complexes with, 17: 33885
sodium salt, composition of uranium complexes with, 19: 28316
uses for spectrophotometric determination of uranium, 20: 14481

NAPHTHALENE-2,7-DISULFONIC ACID, 4,5-DIHYDROXY-3-(6-SULFO-2-NAPHTHYLAZO)-
analytical uses in determination of thorium, 18: 6770

NAPHTHALENE-2,7-DISULFONIC ACID, 4,5-DIHYDROXY-3-(*p*-SULFOPHENYLAZO)-
analytical use for spectrophotometric determination of rare earths, 18: 41341
spectra of thorium complexes with, 17: 33886
uses for spectrometric determination of rare earths, 20: 12806

NAPHTHALENE-6-SULFONIC ACID, 2,3-DIHYDROXY-
analytical use of sodium salt of, for determination of zirconium, 17: 40743
complex formation with uranyl ions, 20: 7081
complexes with uranium, analysis of, potentiometric, 20: 22980
uses for spectrophotometric determination of uranium, 20: 14481

2(1H)-NAPHTHALENONE, OCTAHYDRO-
fragmentation and hydrogen transfer reactions of derivatives of, after electron impact, 17: 23377

NAPHTHALENES
effects on radiolysis of monoimine of phenanthrene-9,10-quinone, 20: 397
effects on rat glucuronide excretion, 18: 38775(R) (ORO-624)
effects on thermal stability of biphenyl at 440°C, 19: 28352
efficiency of scintillators of, for x-ray detection, 20: 16836
electron reactions at 50 to 70 ev, mass spectra from, 17: 35906
energy transfer and annihilation in crystals of, triplet, 18: 717
energy transfer of europium and gadolinium from, to complex with hexafluoro-2,4-pentanedione, 19: 11107
fluorescence decay time in deuterated and natural, device for measuring, 18: 33637
fluorescence of solution scintillators containing, characteristics of, 17: 27451
graphitization of, mechanism and properties for, 18: 35934 (ML-TDR-64-125(Vol.I))
labeling with iodine-131 by uranium fission, 18: 43696
phosphorescence decay time in deuterated and natural, device for measuring, 18: 33637
preparation and properties as scintillators, 19: 17781(R) (ORNL-3750)
radiation effects on catalytic hydrogenation of, 17: 18460(R) (NYO-10186)
radioinduced fluorescence in scintillators of, decay times of beta, 19: 13764
radioinduced inclusions in compounds of 2,3-dimethyl- and 2-methyl-, with thiourea, 16: 3047
radioinduced scintillations in molten, 18: 39295
radioinduced spectra from, x, (E), 20: 7659(R) (ORNL-3849, pp 101-50)
radiolysis effects on organic glasses at −196°C, 16: 11715
radiosensitivity effects on *E. coli* and *S. faecalis*, 18: 38979
radiosensitivity effects on urinary excretion of glucuronic acid by rats, x, 20: 22575 (PRNC-80)
separation by thin-layer electrophoresis, 18: 23156(T) (SC-T-64-612)
spectra in cyclohexane and toluene solutions of, excimer emission, 20: 10854
spectra of deuterium-labeled, isotope effects in mixed crystals on compound-exciton, 17: 23238
spectra of naphthalene, α- and β-tetradeuteronaphthalene, and octadeuteronaphthalene, absorption and vibration, 16: 14743(T)

NAPHTHALENES, IODO-
iodine-131 exchange with potassium iodide, kinetic studies of, 20: 38916
protective effects against radioinduced viscosity increase in lubricating oils, 18: 3874(P)

NAPHTHALENESULFONIC ACID, DINONYL-
alkali salts of, use as liquid cation exchanger for alkali metal ions and ammonium ion in hexane and chloroform, 20: 43447
properties as ion exchanger for separation of rare earths, scandium, and thorium, 20: 20825
solvent properties for alkali metals from nitrate solutions, 18: 1799(R) (ORNL-3496)
solvent properties for various metal ions, 19: 15691
solvent properties for rare earths, 20: 23230
solvent properties for zinc, effects of neutral donors on, 20: 27050
solvent properties for americium and europium trivalent ions, 20: 43447
dinonylnaphthalenesulfonic acid–*n*-heptane, solvent properties for beryllium, 20: 7207

NAPHTHALENESULFONIC ACIDS
analytical use of Beryllon III for spectrophotometric determination of beryllium, 19: 28233
ethanol–naphthalenesulfonic acid–H_2SO_4, radiolysis in aqueous solutions, 20: 1920

NAPHTHAZARIN
complexes with beryllium, cobalt, copper, nickel, and zinc, composition and thermal stabilities, 16: 18893
complexes with hafnium, neodymium, thorium, titanium, and zirconium formation constants and spectra of, 18: 25456
hydro-, complexes of, with beryllium, cobalt, copper, lead, and nickel, 19: 5882
solvent properties for americium and europium, 18: 25622

NAPHTHENIC ACIDS
cobalt salts of, radiation effects on catalytic properties of, 19: 26430
properties for use as liquid ion exchanger, 19: 18063
solvent properties for rare earths from sulfate solutions, 18: 17925 (BM-RI-6396)
solvent properties for uranium from aqueous solutions, 18: 27632(P)
solvent properties for actinides and rare earths, 19: 7263(R) (ORNL-3651)
solvent properties for cerium and yttrium, 20: 4051
solvent properties for uranium, 20: 14642

NAPHTHOFURAN
scintillation properties of, (E), 19: 4198

2-NAPHTHOIC ACID, 1-HYDROXY-
complex with beryllium, stability constant of, 18: 39150 (AAEC/TM-240)
spectra of, fluorescence, 19: 36220(R) (MIT-2098-142)

2-NAPHTHOIC ACID, 3-HYDROXY-
complex with beryllium, stability constant of, 18: 39150 (AAEC/TM-240)
spectra of, fluorescence, 19: 36220(R) (MIT-2098-142)

3-NAPHTHOIC ACID, 2-HYDROXY-
complexes with thorium and zirconium, conductometric and potentiometric studies on, 18: 22100
complexes with uranium, composition and stability of, 19: 32133
complexes with uranyl ions, preparation and properties of, 20: 40898
solvent properties for americium and europium, 18: 25622

NAPHTHOL
analytical use with sodium nitrite for precipitation of uranium from homogeneous solution, 19: 13302
complexes with beryllium, rare earths, thorium, and uranium, preparation and stability of colored, 18: 27366
determination of, method for, 19: 46324(R) (AGN-8132)
effects on polarography of uranyl pyrophosphate complexes, 19: 19816
effects on radioinduced chemiluminescence in organic compounds in presence of oxygen, 19: 46344
effects on radiosensitivity of fruit-spoilage fungi, 20: 13137 (NP-15360)
effects on radiosensitivity of fruit fungi, 20: 33030
hydrogen abstraction from deuterated, effects on styrene polymerization, 16: 14711
molecular properties of alpha and beta, in excited and ground states, 20: 10457 (COO-773-4)
reactions with thorium tetrachloride, mechanisms of, 17: 40806
solvent properties for ruthenium, 18: 39114
solvent properties for ruthenium, effects of ferric ions on, 18: 39115
spectra of aqueous solutions of, pH dependence of fluorescence, 19: 4177(T) (ANL-Trans-112)
yields from radiolysis of naphthalene, effects of metal ions and temperature on, 20: 29260
ethanol–naphthol–H_2SO_4, radiolysis in aqueous solutions, 20: 1920

1-NAPHTHOL, 4-AMINO-
effects on lethal radiation effects on *E. coli*, 18: 125
effects on radiosensitivity of fruit-spoilage fungi, 20: 13137 (NP-

15360)
2-NAPHTHOL, 1-BROMO-
radiosensitivity effects of, use of activation analysis for determining mechanism of, 20: 31172 (SGAE-BL-17/1966)
1-Naphthol, 4-Amino-2-methyl-, hydrochloride
see Vitamin K_5
2-NAPHTHOL, 6-BROMO-
effects on lethal radiation effects on *E. coli*, 18: 125
radiosensitivity effects of, use of activation analysis for determining mechanism of, 20: 31172 (SGAE-BL-17/1966)
1-NAPHTHOL, 2,4-DINITRO-
protective effects against radiation, metabolic factors in, 17: 15794
2-Naphthol-3, 6-Disulfonic Acid, 1-(*o*-Arsonophenylazo)-
see Benzenearsonic Acid, o-2(Hydroxy-3,6-Disulfonaphthylazo)-
1-NAPHTHOL, 2-NITROSO-
analytical use as complexing agent in spectrophotometric determination of ruthenium, 16: 5277
complexes with cobalt, paper chromatographic separation of, 20: 38807
arsenazo I–EDTA–nitrosonaphthol, uses for colorimetric micro-determination of uranium, 20: 29130
2-NAPHTHOL, 1-NITROSO-
analytical use for spectrophotometric determination of ruthenium, 20: 12788
analytical use in precipitation of uranium in rocks in presence of complexone III, 16: 14677
chelate formation effects on cobalt-60 distribution in rat, 16: 12873
complexes with beryllium, rare earths, thorium, and uranium, preparation and stability of colored, 18: 27366
complexes with cobalt, effects of organic solvents on extraction of, 17: 1569
complexes with cobalt, Szilard-Chalmers reactions for enrichment of cobalt-60 in, 18: 22143
solvent properties for cobalt and strontium, 18: 17937 (PAEC(D)CH-638)
solvent properties for americium and europium, 18: 25622
use for gravimetric estimation of molybdenum(VI) ions, 18: 37084
2-NAPHTHOL, 1-(2-PYRIDYLAZO)-
analytical use for determination of uranium, 16: 23600 (CNI-57)
analytical use for complexometric determination of cerium and magnesium in iron and rare earth alloys, 20: 25008
analytical use in solvent extraction and spectrophotometric determination of metals, 16: 139
analytical use in spectrophotometric determination of uranium, 19: 34110 (RL-SA-38)
analytical uses for spectrophotometric determination of uranium, 18: 19900
analytical uses in determination of uranium, 17: 35631 (PG-Report-436)
analytical uses in determination of nickel traces in molybdenum and tungsten, 19: 19799
complexes with inorganic cations, composition of, radiometric and spectrophotometric studies of, 20: 22925
complexes with transition metals, formation constants and distribution equilibria of, 17: 14381
use in spectrophotometric determination of rare earths, 17: 19970
2-NAPHTHOL, 1-(2-THIAZOLYLAZO)-
analytical uses in determination of trace amounts of nickel, 19: 19814
complexes with inorganic cations, composition of, radiometric and spectrophotometric studies of, 20: 22925
1,4-NAPHTHOQUINONE
biochemistry in *Streptococcus faecalis*, 19: 31705(R) (ORNL-3768(p.177-8))
effects on metabolism in Streptococcus in cell membrane, 20: 6723(R) (ORNL-3853, pp 175-6)
preparation and properties of, from *Streptococcus faecalis*, 18: 27012(R) (ORNL-3601(p.207-9))
separation from *Streptococcus faecalis* membrane, 20: 6723(R) (ORNL-3853, pp 175-6)
thioether synthesis from, 19: 31705(R) (ORNL-3768(p.177-8))
1,4-Naphthoquinone, 5,8-Dihydroxy-
see Naphthazarin
1,4-NAPHTHOQUINONE, 2-METHYL-
labeling with tritium in presence of tritiated water, 20: 18711
protective effects against x radiation in mice, 16: 14459(R) (NP-11359 (p.35-75))
proton hyperfine spectra in, 17: 8084
radiosensitivity of, x-ray, 20: 33082
NAPHTHYL SULFIDE
labeling with sulfur-35 by recoil methods, 20: 25114
1-NAPHTHYLAMINE
complexes with beryllium, rare earths, thorium, and uranium, preparation and stability of colored, 18: 27366
deuterium exchange reactions with benzene, 17: 39083
effects on radiosensitivity of fruit-spoilage fungi, 20: 13137 (NP-15360)
reactions with urea, tracer study of, 17: 2709
2-NAPHTHYLAMINE
radioinduced luminescence of, duration of α, β, uv, and x, 18: 8427(T)
spectra of aqueous solutions of, pH dependence of fluorescence, 19: 4177(T) (ANL-Trans-112)
1-NAPHTHYLAMINE, *N*-PHENYL-
deuterium exchange reactions with benzene, 17: 39083
effects on isotope effects in autoxidation of deuterated and normal dibenzyl succinates, 20: 45706
2-NAPHTHYLAMINE, *N*-PHENYL-
effects on radiation effects on intrinsic viscosity in butadiene-styrene polymer, 19: 22342
effects on radiation solubility and swelling in polybutadiene-styrene polymer, 19: 22343
effects on radiation effects on polypropylene, 20: 29290
effects on radioinduced branching in butadiene-styrene polymer, 19: 22344
1,5-NAPHTHYRIDINE
nitrogen-14 hyperfine coupling constant and spin-density in, 17: 8076
spectra of deuterated and normal, PMR, 20: 43282
NAPHTHYRIDINE, NITRO-
spectra of deuterated and normal, PMR, 20: 43282
NARINGIN
deuterium–hydrogen exchange in alkaline solution of, 18: 25453
NASA RESEARCH REACTOR
coolant flow characteristics of, measurement techniques for, 18: 13334 (NASA-TN-D-1725)
coolant leak-rate testing in, 18: 29133
cooling system for, design of emergency and shutdown, 19: 12741
criticality effects of centrally located aluminum, iron, and tungsten rods and tubes, 16: 30019 (NASA-TN-D-1322)
development and testing, 17: 25776(R) (NP-12812)
experimental facilities for radiation testing, in-pile loop, 19: 19414 (CONF-641009-9)
experimental facilities of, maintenance and modification of cryogenic, 20: 32861 (N-66-12348)
hazards analysis for radiation-effects testing at cryogenic temperatures, 16: 28599 (NP-11630)
hazards summary for Plum Brook Mock-Up Reactor, 17: 10130 (NP-12379)
heat transfer analysis during full power operation, 20: 40461 (NASA-TN-D-3552)
hot laboratory facility design for, 16: 644
hot laboratory facility for, 16: 3113
leak-rate testing of containment vessel of, 17: 31754 (NASA-TN-D-1731)
neutron flux distributions and criticality effects in, four-group calculation of, 19: 3778 (NASA-TN-D-2210)
neutron flux mapping, design of instrument for in-core, 16: 15956
operation of, for low-power nuclear tests, 17: 13813 (NASA-TN-D-1560)
structures of, epoxy coating of concrete and steel, 16: 14257
surveillance irradiations in, capsules for, 18: 45096 (TID-7697 (p.1.1.1-22))
testing hydraulic characteristics, 18: 3344 (TID-7663(p.948-1013))
National Aeronautics and Space Administration Reactor
see NASA Research Reactor
NATIONAL REACTOR TESTING STATION
aeroradioactivity survey of area, 19: 13622 (CEX-59.4.10)
analytical branch annual report for 1964, 19: 32059(R) (IDO-14655)
atmosphere monitoring following SL-1 accident, 16: 29248 (TID-7627 (p.581-97))
atmospheric turbulence and diffusion at, effects of MTR-ETR complex on, 19: 39259 (IDO-12041)
design criteria for Lithium-Cooled Reactor Experiment, 17: 15496 (CNLM-4043(Rev.A))
design criteria for test support facility, 17: 15497 (CNLM-4190)
environs monitoring, 16: 4395(R) (IDO-12019)
environs monitoring, 1961, 16: 30693
environs monitoring, 1962, 18: 462
environs monitoring, 1962, 18: 6971(R) (IDO-12033)
environs monitoring, 1963, 19: 637
environs monitoring, 1964, 19: 22562
environs monitoring, 1965, 19: 46642 (IDO-12043)
environs monitoring, 1965, 20: 29434
environs monitoring program, 20: 33578
environs monitoring, 1964, 20: 33586
evaluation of earth materials from localities near, for decontamination of low-level wastes, 18: 13345 (IDO-14624)
filter efficiency improvement program, 16: 29228 (TID-7627(p.215-21))
filter manual, 18: 14107 (IDO-12032)
ground waters in, movement and percent sodium relation to source in, 18: 18037
health and safety activities, 1962, 18: 6971(R) (IDO-12033)
health and safety requirements at, 18: 8547 (IDO-12028)
health physics and safety analysis, 1961, 16: 25652(R) (IDO-12021)
hydrology, 16: 25043 (TID-7628(p.99-114))
hydrology, 19: 46642 (IDO-12043)

hydrology of radioactive waste disposal, 17: 1655
hydrology of subsurface waste disposal at, 19: 40269(R) (IDO-22047-USGS)
iodine-131 uptake by thyroid of native animals at, 18: 8072
iodine-131 release to atmosphere at, 19: 24782
irradiation experiments at, handbook for in-pile, 20: 18135 (IDO-17135)
meteorological research at, 19: 44773 (BNL-914, pp 57-64)
meteorology, 18: 19405 (APEX-445)
meteorology, geology, and population distribution of area, 16: 5368 (APEX-180)
meteorology, Jan. 1961, 16: 29182 (IDO-19310)
monitoring of environs, radiobiological, 17: 33596
monitoring of personnel, 16: 4395(R) (IDO-12019)
monitoring of water supplies for radioactivity, 1961, 16: 30693
nuclear accident of Jan. 3, 1961, meteorological support of radiation measurements, 16: 29182 (IDO-19310)
operation of facilities in Test Reactor Area, preparation of manuals for, 18: 11509 (IDO-16927)
operation of, role of nondestructive testing in, 20: 14197
operational documentary photography manual for facilities at, 18: 9753 (IDO-10037(Rev.1))
personnel dosimetry system at, 19: 44335
radiochemical analysis manual for, 18: 13621 (IDO-14613)
radioisotope migration and retention in lithosphere at, 18: 17349
reactor development and safety at, 20: 2093
respiratory protection program evaluation, 16: 27464 (IDO-12020)
site survey and waste monitoring, 16: 4395(R) (IDO-12019)
siting criteria at, 17: 41101
waste disposal, 16: 25043 (TID-7628(p.99-114))
waste disposal at, hydrology of subsurface, 19: 22529(R) (IDO-22046)
waste disposal at, hydrological aspects of, (E), 19: 35858
waste disposal data, 19: 27834 (IDO-12040)
waste disposal, practices and programs, 16: 25073 (TID-7628(p.536-68))
waste gas injection into lithosphere at, appraisal, 19: 48077 (IDO-12024)
waste management at, 18: 3390 (IDO-16925(p.119-29))
waste processing at, environmental effects of, 20: 45219
waste treatment at, low- and intermediate-level, 20: 26571
wind prediction for, strong southwest, 20: 41129

Natrolite (ion exchanger)
see Cation Exchange Materials

Natural Circulation Reactor
see Submarine Reactors (SSG)

NATURAL GAS
abundance ratios of argon, helium, and neon in, 20: 33522
analysis for carbon isotopes, 16: 22029
analysis of, for argon, helium, and neon, 20: 33522
anomalies of the gamma field over oil and gas fields in Roumania, 18: 5515
composition of, chemical and isotopic, 18: 12366
cost of fuel, comparison with nuclear fuels, 20: 38541
deuterium content in, in petroleum deposits, 20: 7261
economic aspects as energy source, 18: 40216
gamma fields above deposits of, 19: 34375(T)
geophysical testing of reservoirs of, use of radioactive methods for, 19: 28562
neon isotope abundance in helium-bearing, 20: 45898
performance of gas-oil fraction of, as reactor coolant, 20: 25129(T) (AECL-2330, pp 63-70)
production of, Project Gasbuggy studies of underground nuclear explosions in, 19: 46474
production of, Project Gasbuggy for stimulating, 20: 20837
production of, Project Gasbuggy studies of, 20: 25234
production of, use of radioisotopes in exploitation of reservoirs for, 20: 27142
production of, use of underground explosions in, 20: 33443
production of, use of nuclear explosions for increasing, 20: 36973
properties as fuel for MHD generators, 19: 23350
prospecting for, by radiological well logging, 18: 22264(P)
prospecting for, development of equipment for use in radiometric, 18: 39513(T) (AEC-tr-6390(p.290-7))
radiation fields above deposits of, gamma, 20: 35649
radiation stability of gas-oil fraction of, 20: 25128(T) (AECL-2330, pp 33-52)
radioactivity of, comparison of air to, 19: 30456
rare gas content in, variations in, 19: 44239
recovery and storage of, use of underground explosions in, 20: 43463 (UCRL-14756)
storage in underground reservoirs created by nuclear explosions, 20: 39014(R) (TID-23184)
storage underground, economics of nuclear explosives in developing, 20: 39015 (UCRL-14877)
structure control of reservoirs of, use of radiometric methods in, 18: 5513
surveying by aerial radiometric methods, 16: 27453
transportation costs in Canada, 20: 45177
use in magnetohydrodynamic power generation, economics of, 19: 9987
use of liquefied, in magnetohydrodynamic cells, (T), 19: 10000
well productivity, improvement by underground nuclear explosions, 20: 36961 (UCRL-12229)
well stimulation by nuclear explosions, 20: 9093(R) (ORNL-3830, pp 271-4)
xenon content in, from spontaneous fission of uranium-238, 19: 630 (TID-21206)

NATURAL WATERS
(This heading may be modified by location in the form Natural Waters (Wyo.).)
see also Ground Waters
see also Radioactive Waters
see also Surface Waters
age determination of Matsesta, from mesothorium I and radium content in, 19: 655
alpha radioactivity of Polish, 17: 30684
analysis for alkali and alkaline earth metals, flame photometric, 20: 38798 (NIJS-R-465)
analysis for beta radioactivity at JAERI from 1956 to 1960, 16: 11965(R) (JAERI-5003(p.177-81))
analysis for boron traces, spectrophotometric, 18: 11972 (PG-Report-532)
analysis for cesium, flame photometric, 18: 8295
analysis for cesium-137, strontium-89, and strontium-90 by electrodialysis and gamma spectroscopy, 19: 19809
analysis for fallout activities, development of rapid methods for, 19: 32062 (ORO-593)
analysis for fluoride, titrimetric, 18: 1508 (PG-Report-522)
analysis for iodide by radiometric method, 20: 26756
analysis for iodine-131, by ion exchange and beta or gamma counting, 20: 35404
analysis for liquid-solid ratio in, using radiation attenuation gage, 17: 27564(R) (NYO-10219)
analysis for metals, quantitative spectrographic, 16: 17597
analysis for plutonium, 18: 9965 (CEA-2354)
analysis for radioactive contamination, 17: 12516
analysis for radon, design of emanometer for, 17: 134
analysis for radon, bismuth precipitation procedure for, 18: 5241
analysis for strontium-90 and yttrium-90, 16: 28886
analysis for strontium-90 fallout, by solvent extraction and counting, 19: 11017
analysis for thorium, 16: 26934
analysis for thorium using arsenazo III, photometric, 19: 36309
analysis for trace elements by solvent extraction and spectrography, 19: 28253
analysis for trace elements, tracer studies of errors from ion adsorption on glass and plastic in, 19: 30097
analysis for tritium, method for, 18: 3697
analysis for tritium, 18: 41659
analysis for tritium, standardization of, 18: 41660
analysis for tritium, thermal diffusion method for, 20: 41168
analysis for uranium, fluorescence, 17: 28815
analysis for uranium, fluorescence method for chromatographic, 17: 28817
analysis for uranium by paper fluorescence, 17: 40754
analysis for uranium using organic precipitants, photometric, 20: 35446
analysis in South Pacific for tritium, accuracy of, 18: 31370 (INS-R-27)
analysis of oilfield, for beryllium, spectrographic, 18: 1596
beta activity of, methods for determining, 19: 17845
boron content in silt solutions in, 17: 3175
calcium content of Egyptian, 16: 4020
carbon isotope content and distribution in New England, 18: 12352
cerium-144 uptake in, 18: 3448
cesium uptake from, at Cape Thompson, Alaska, 18: 25688 (TID-20638)
cesium-137 content in Japan, 20: 45887 (NP-16290)
cesium-137 content of Italian, 18: 14072 (EUR-481.i)
current velocity of, use of sodium-22 *in situ* diffusion for measurement of, 18: 1906
decontamination by flocculation, 16: 17922
deuterium content variation in hydrologic cycle of North American, 18: 14070
deuterium content of, in regions of global circulation, 19: 22564
distribution and properties of thorium isotopes in, 20: 43535
environs monitoring of, at uranium mill in Colorado, 20: 23409
fission product contamination of, from nuclear plants, 20: 46001
flow of, tracer studies of sewage distribution in, 17: 25534
geochemistry and radioactivity of Lourdes Spa, San Luis Potosi, Mexico, 19: 40835
geochemistry around Umra uranium deposit, India, 17: 16303
geochemistry of, in Umra, Rajasthan, India, 17: 29098
iodine uptake from, at Cape Thompson, Alaska, 18: 25688 (TID-20638)
isotope geochemistry of, 20: 23326
leaching radioactive ores, 16: 5567
lead-210 content in, 17: 30736
lead-210 content in potable, in Illinois, 18: 35738
monitoring for radioactive wastes, 20: 38742

monitoring of, at Juelich Research Center, 19: 48078 (JUL-261-DE)
oxygen-18 content of, in regions of global circulation, 19: 22564
pollution and purification, tracer studies of, 16: 33302
polonium-210 content in potable, in Illinois, 18: 35738
potassium-40 content in, in Vinca, Yugoslavia, 19: 46590(T) (JPRS-31469)
precipitation of uranium from, 16: 6625(T) (CEA-tr-R-1441)
processing for uranium fixation, 20: 25202
radiation monitoring at Ames, Jan.-June 1965, 19: 44302 (TID-22173)
radioactive contamination of, losses in evaporation methods for measurement of, 19: 26577 (INR-568/XIX)
radioactive waste disposal in fresh, 17: 24738
radioactivity and decontamination, 17: 25434
radioactivity control, 16: 33280(T) (CEA-tr-R-1522)
radioactivity control in, methods for, 18: 12393
radioactivity distribution in, from nuclear rocket accidents, 17: 38445 (TID-7653(Pt.I)(p.52-68))
radioactivity effects from, in humans, 16: 20229
radioactivity in Canadian, 18: 18038 (AECL-1874)
radioactivity in French, 18: 14075 (SCPRI(T)-98)
radioactivity in Turkey, 19: 11392(R) (NP-14683)
radioactivity in, protection against, in nuclear energy production, 19: 4410
radioactivity monitoring in Netherlands, 1963, 20: 39118
radioactivity of, in region of Marcoule Center, 17: 42424
radioactivity of Lake of Geneva from fallout, measurement of, 18: 1906
radioactivity of, method for determining, 18: 4892
radioactivity of Polish, 1959, 16: 6626(T) (GAT-Z-5022)
radioactivity of, as indicator of uranium deposits in Hungary and Rumania, 18: 12378
radioactivity of, methods of monitoring for compliance with regulations, 19: 20211
radioactivity of, method for measurement of, 20: 43124
radioactivity, review, 17: 3189
radioelement distribution in, in Florida, 18: 35735
radioisotope collection in, by various materials, 20: 8980(R) (BNWL-36, pp 3.1-122)
radioisotope content in, systematic hydrological surveillance of, 17: 29097
radioisotope content in correlations with fallout, 20: 27161
radium and radon concentrations in Israel, 16: 25624
radium content of, in Azerbaidzhan, 19: 13663
radium in, exposure to, 17: 32314
radium-226 and -228 content in Brazilian, 20: 150(R) (NYO-3086-1 Pt.VI)
radium-226 content of Australian, 18: 16211
radium-226 content in potable, in Illinois, 18: 35738
radon content in, in Belaya Tserkov, Ukraine, 16: 31967
radon content in Sweden, 19: 33746
rare earth contents in Japanese hot springs, activation determination of, 19: 42443
separation of cerium-144, cesium-137, and strontium-90 from, by ion exchange chromatography, 20: 20627
separation of ruthenium-103 and -106, from, by extraction, 18: 9990
separation of thorium and uranium from solids in, 17: 1561(P)
soil content of, effects of neutron meter access tubes on, 18: 16201
strontium and strontium-90 contents of Egyptian, 16: 4020
strontium uptake from Cape Thompson, Alaska, 18: 25688 (TID-20638)
strontium-90 content in Japanese inland, 17: 21947
strontium-90 content in Japanese, 20: 45887 (NP-16290)
strontium-90 removal from, device for, 18: 16249
thorium content in, of Azerbaidzhan, 19: 13663
thorium isotopic composition in, in Kirov District, USSR, 18: 31761
thorium isotopic composition in, in Molodova, Ukraine, 17: 21917
tracer studies, 16: 29292
tracer studies of liquid/solid ratio in, 17: 3657
tracer studies of current speeds in, design of ultrasensitive analyzer for, 17: 3658
tritium activity in, method for measurement of, 20: 31310
tritium content in New Zealand in 1956 to 1963, review of measurements of, 19: 6093 (INS-R-24)
tritium content in, method for determining, 19: 30407
tritium content measurements in eastern Mediterranean area, laboratory program for, 19: 7703(R) (TID-21350)
tritium content of, in Japan, 20: 31398(T) (NSJ-tr-49)
tritium content of, in relation to global circulation, 19: 22564
tritium distribution in Perch Lake, Ontario, 18: 18039 (AECL-1889)
tritium-hydrologic study of, 18: 12372
uranium content of, in Azerbaidzhan, 19: 13663
uranium distribution in, in igneous rocks of humid areas, 18: 39497
uranium isotopic composition in, in Molodova, Ukraine, 17: 21917
uranium isotopic composition in, in Kirov District, USSR, 18: 31761
uranium-234 to uranium-238 occurrence ratio in, in Japan, 19: 6118
uranium-234 to uranium-238 ratio in, 20: 39120
virus particles in, isolation and characterization of, 19: 27897 (ORNL-P-115)
waste disposal in, hazards and movement in, 20: 18157 (BNWL-SA-466)

NATURAL WATERS (HUNGARY)
analysis for radium, radon, and uranium isotopes, 17: 6293

NAVAL REACTORS
see also Carrier Vessel Reactor
see also Maritime Reactors
see also Submarine Advanced Reactor
see also Submarine Fleet Reactor
see also Submarine Reactors (S1C)
see also Submarine Reactors (S5G)
book: *Naval Nuclear Power Installations*, 20: 16116
book: *Naval Nuclear Power Installations*, 20: 18132
conference on nuclear ship propulsion with special reference to nuclear safety, Taormina, Italy, Nov. 14 to 18, 1960, 16: 8386
cooling system for, 18: 43073(P)
design and performance, 18: 11462
design principles of gas-cooled, 17: 29807(T) (TRG-Inf-Ser-314)
development in France, 20: 14176
development, 1962, 17: 5662
economics, 18: 26960
electric switching instrumentation for, on nuclear carriers, (E), 19: 6871 (RTD-TDR-63-3062)
fuel element positioning and withdrawal in, design of equipment for, 17: 17521(P)
fuel elements for, design of thermionic, 18: 24857(R) (GEST-2031)
fuel elements for, fabrication of thermionic, 20: 1437(R) (GEST-2047)
handbook on physics of, 18: 43065 (TID-7050)
physics research program, 18: 43034 (TID-7050(p.1-14))
propulsion of, Joint Committee hearing on nuclear, 20: 30930
water circulation in boiling, effects of ship motion on, 17: 9866

Naval Research Lab. Reactor
see NRL Research Reactor

NAVAL VESSELS
see also Submarines
behavior in waves, 16: 8417
collisions of, effect of angular momentum on, 17: 18242
conference on nuclear ship propulsion with special reference to nuclear safety, Taormina, Italy, Nov. 14 to 18, 1960, 16: 8386
construction rules for nuclear-powered, 18: 7961
contamination by fallout, shielding evaluations for gamma penetration in, 16: 31179 (USNRDL-TR-373)
contamination, gamma penetration into compartments of aircraft carriers, 16: 31180 (USNRDL-TR-412)
contamination of aircraft carriers by penetration of gamma radiation into compartments, 16: 31178 (USNRDL-TR-343)
contamination of surfaces, fall-out simulation, 16: 16611 (USNRDL-TR-549)
decontamination of, 19: 24813
design and nuclear performance of nuclear icebreaker Lenin, 16: 25008
design of radio-controlled nuclear, 20: 42666(P)
development of high performance, 16: 4370 (ONR-9(Vol.3))
fires on, design of alarm system using radioactive material for protection against, 18: 7098
gamma dose distribution in, source distance effect on, 18: 7848 (USNRDL-TR-681)
hull construction of nuclear-powered, collision-resisting, 18: 23090
nuclear-powered, classification standards for, 16: 8397
nuclear-powered, control and instrumentation of organic reactor in, 16: 8404
nuclear-powered, construction of collision resisting ship-sides for, 16: 10137
nuclear-powered, effects of reactor scram on maneuverability, 16: 8413
nuclear-powered, evaluation of collision-resisting sides, 16: 20573
nuclear-powered, evaluation of ports for, 16: 8425
nuclear-powered, legal problems from operation, 16: 8395
nuclear-powered, optimum maneuverability, 16: 8414
nuclear-powered, regulations and rules for, 16: 8399
nuclear-powered, refueling considerations, 16: 8420
nuclear-powered, safety, 16: 8396
nuclear-powered, safety considerations for operation in ports, 16: 8423
nuclear-powered, safety on shore in relation to harbor operation, 16: 8424
nuclear-powered, safety system for dispersal of decay heat after reactor shut-down in, 16: 28514(P)
nuclear-powered, vapor suppression for reactor container in, 16: 8412
nuclear-powered, waste-disposal problems, 16: 8421
nuclear propulsion, evaluation of various reactor types for, 16: 8379
nuclear propulsion, economic studies, 16: 8388
nuclear propulsion, safety aspects, 16: 3302
nuclear propulsion, safety aspects, 16: 8395
nuclear propulsion, safety analysis methods for steam-cooled reactor for, 16: 8402
nuclear propulsion, safety of organic moderated reactors for, 16: 8405
nuclear propulsion, effects of direct-cycle operation of boiling-water reactor on safety, 16: 8406
nuclear propulsion, behavior and testing of boiling-water reactors for,

16: 8407
nuclear propulsion of, review of advantages and disadvantages, 17: 10252
nuclear propulsion of, prospects for, 18: 4837
nuclear propulsion systems for, 18: 35205
nuclear propulsion for, Italian program on, 18: 43071
nuclear propulsion of, status of, 19: 12830
nuclear-powered, experiments on repair of damaged, 19: 22628
nuclear-powered, stopping distances for, 19: 12833
operation during nuclear warfare, 19: 24811
performance of Lenin during first voyage, 16: 25009
power reactors for, effects of ship's motion on kinetics of, 18: 7962
power systems for, development of radioisotope-fueled thermoelectric generator as, 17: 31766(R) (TID-17004)
propulsion of icebreakers, performance of nuclear systems for, 17: 13788
propulsion of, magnetohydrodynamic, 18: 4359
propulsion systems for, nuclear, 19: 40255(P)
protection against radiological effects of nuclear weapons, 19: 24812
radiation control on the USS *Enterprise*, 17: 36043
radiation effects, gamma penetration of aircraft carrier hulls, 16: 6075 (USNRDL-TR-533)
radiation protection in nuclear-powered, 17: 3255
radiation-sensing system for automatically guiding and positioning planes on aircraft carriers, 18: 13991(P)
radioactive aerosols and gases on, monitoring of, 19: 28602
reactor design for, 19: 24159
safety problems on atomic-powered, 18: 37423 (A/CONF.28/P/378)
steam generating plant for, design of, 17: 30656(P)

Navigation, Celestial
see Celestial Navigation

Navigation, Inertial
see Inertial Navigation

NBA
see Benzamidine, N-(p-Nitrophenyl)-

NCR
see Submarine Reactors (S5G)

NEBRASKA
fallout monitoring, 1963, 20: 5649(R) (COO-1340-2, pp 54-83)

NEBULAS
central cavity in rosette, stellar condensation and wind effects on, 20: 27690
collisional cooling of planetary hydrogen, 17: 34682
cosmic-radiation generation in, 17: 11456
dynamics, radiative transfer, and structure in planetary (T), 19: 1139(R) (AFCRL-64-572(A1-20))
electron density in gaseous, monochromators and spectrometers for determination of, 19: 9867
electron excitation cross sections for forbidden spectral lines in gaseous, 18: 32351
element abundances in, 19: 47187 (AD-612182)
formation of central, schematic representation of, 17: 13180(T)
formation of, MGD theory for, 18: 22650(T) (JPRS-24435(p.274-304))
formation of, statistical model for, (T), 20: 2574
gamma absorption in Crab, high-energy, 20: 44084
gamma flux from Crab, 19: 32859
gamma flux from Crab, upper limit for, (E), 19: 44970
gas flow stability in planetary, dilute, (T), 20: 2573
heating by injection of protons, 18: 12826
hydrogen emission spectra in, 18: 10744
hydrogen spectra of Andromeda, measurement and interpretation, 19: 14228
ionization structure of planetary hydrogen, 17: 34681
ionization structure of planetary, 18: 22658
isophotometer tracings of, errors in, 19: 20439(R) (COO-614-31)
kinematics of gaseous, 18: 22657
kinetics of old H II regions in, models for, 20: 25683
magnetic and gravitational fields in planetary particle motion in, (T), 19: 23241
magnetic field in Crab, development of, 18: 8995(T)
mass loss in planetary, 20: 37416
model for H_{II} region formation, 18: 24276
model of Orion, for formation of H_{II} region, 18: 24275
molecular condensation and equilibria in solar, (T), 19: 39352
motion of gravitating gaseous masses in magnetic fields in (T), 19: 1161
optical and radio emission of Crab, calculation of energy distribution of electrons from synchrotron radiation, 19: 2937
origin from fast novae, planetary, (T), 19: 9849
origin of planetary, 16: 16914
photon emission from quasars, limits of, 20: 44947
photon production in Compton-synchrotron process in Crab, high-energy, (T), 19: 44911
photon scattering during escape from, resonance-line, 18: 36141
properties of planetary, in globular cluster, 18: 36133
radiation from Crab, elliptical polarization of continuous, (E), 19: 32868
radiation pressure effects on dynamics of, 18: 18552(T)
radio emission from, polarization of, 18: 10745
radio emission from Crab, coherent plasma mechanism for, 20: 29880
radio sources in Crab, properties of 3C 386, 20: 7699(T)
radio wave emission from, (E), 19: 16329
spectra of gaseous, helium and hydrogen, 20: 25684
spectra of helium in, 16: 16895
spectra of helium and hydrogen in gaseous, recombination, (T), 19: 41238
spectra of, information obtained from, 17: 21209
spectra of, recombination, 18: 16631
spectra of, recombination, 18: 16632
spectra of, recombination, 18: 16633
synchrotron radiation spectra from Crab, 20: 37381(T)
synchrotron spectra of Crab, Compton, (T), 20: 35992
x-ray emission by Crab, 18: 26200
x-ray emission from, small-angle scattering by grains in, 18: 36124 (MIT-2098-60)
x-ray emission from Crab, neutron stars as sources of, 18: 42257
x-ray emission from Crab, lunar occultation of, (E), 19: 4819
x-ray emission from Crab, spectra below 90 kev, (E), 20: 34044
x-ray sources in Crab, neutron-star hypothesis for, 18: 32344
x-ray sources in Crab, 19: 32858
x-ray sources in Crab, neutron-star hypothesis for, 19: 29013 (MIT-2098-123)
x-ray spectra of Crab, (E), 20: 9644
x-ray spectrum of Crab, above 15 kev, (E), 19: 16353

NECK
cancer radiotherapy, 16: 17530
carcinoma of vocal cords, surgical and radiation treatment of, 18: 29493
carcinomas of, presurgical radiotherapy for, 18: 1469
effects of surgery on wound healing in, 20: 14303
granulomas induced by thorium dioxide in, treatment, 17: 35543
granulomas induced in, by thorium dioxide, treatment of, 17: 35543
iodine-131 uptake in trachea of rats, 18: 29203
radiation dose to thorax in diagnostic radiology, 19: 13125
radiation dose to, from mouth radiography, 19: 22064
radiation dose to, from mouth radiography, 19: 22065
radiation effects on carotid arteries following tumor surgery in, 18: 11724
radiation effects on, Thorotrast, 18: 38913
radiation effects on blood vessels in rabbit, protective effects of pyridoxine against, 19: 15221
radiation effects on healing of surgical lesions of, 19: 27962
radiation effects on wound healing in, x, 20: 14303
radiation effects on blood vessels in rabbit, x, 20: 45373
radioinduced tumors in human, Thorotrast, 19: 24319
radiotherapy of, air cooling of skin field during electron beam, 17: 13890
radiotherapy of benign lesions in, incidence of thyroid cancer from, 19: 31971
radiotherapy of carcinomas of, use of high-energy electron beams for, 19: 15251
radiotherapy of carcinomas of, effects of methotrexate on, 19: 24393
radiotherapy of cancers of, 19: 42385
radiotherapy of cancers of, electron, gamma and x, 20: 22818
radiotherapy of carcinomas of, use of electron beams for, 20: 36685
radiotherapy of, effects on ear, 17: 5896
radiotherapy of, effects of, incidence of cancer of larynx in man, 17: 21488
radiotherapy of larynx, oral cavity, and pharynx, protective effects of Tanderil against burns and sickness from, 19: 13110
radiotherapy of lesions of, effects of regional oxygenation on effectiveness of, 18: 41280
radiotherapy of malignancies of, review of electron, 20: 45557
radiotherapy of malignancies of, results with use of betatron, 20: 45559
radiotherapy of non-malignant diseases of, cancer induction in, 16: 25201
radiotherapy of supraglottic carcinomas using telecobalt, 19: 46057
radiotherapy of tumors of, effects of, on ears, 17: 7813
radiotherapy of tumors of, injuries to elastic arteries from, 17: 17797
radiotherapy of tumors of, use of hydrogen peroxide perfusion in, 19: 4035
radiotherapy of tumors of, pathological effects on thyroid gland, 19: 31955
radiotherapy of tumors of, effects on thyroid function, 19: 34071
radiotherapy of tumors of, effects on thyroid function, 19: 43890
radiotherapy of tumors, 19: 46129
radiotherapy of tumors of, 20: 5441
radiotherapy of tumors of, using tantalum-182 wires, 20: 8756
radiotherapy of tumors of, dosimetry for x, 20: 41210
radiotherapy of tumors in region of, use of fast electrons for, 20: 45554
radiotherapy of tumors of, performance of γ and x, 20: 45556
radiotherapy of, cancer induction by, 18: 31202
surgery of, procedures for, 19: 27962
thorium dioxide uptake by lymph nodes and trachea in rat, 18: 31103

Negative Protons
see Antiprotons

Negatrons
see Electrons

NEMATODES
see also Schistosoma
culture of parasitic, in sheep, 18: 43231 (TID-21203)
effects on central nervous system of ground squirrels, 20: 42835(R) (ANL-7136, pp 63-80)
immune response of sheep to irradiated, 18: 43231 (TID-21203)
preparation of irradiated vaccines against parasitic, 19: 7175
radiation effects on immunogenicity of *Trichinella spiralis*, 16: 20137
radiation effects on infectivity and reproductive capacity of *Trichinella spiralis*, 16: 20135
radiation effects on fertilized eggs of, effects of 5-bromodeoxyuridine on, 18: 11717
radiation effects on development of, in Anopheles, gamma, 18: 13527
radiation effects on larvae of lungworm, use for vaccines, 18: 17392
radiation effects on, gamma, 18: 25125
radiation effects on soil, gamma, 18: 38899
radiation effects on, 18: 43231 (TID-21203)
radiation effects on *Syngamus trachea*, x, 20: 70
radiation effects on infectivity of *Nippostrongylus brasiliensis*, in rats, gamma, 20: 3786
radiation effects on propagation of root-knot, in sweet potatoes, 20: 28942
radiation effects on development of *Heterakis gallinarum* embryos, x, 20: 40667
radiation effects on development of *Ascaridia galli* in chickens, x, 20: 42968
radiosterilization of larvae, effects of, on rat eosinophilic response, 18: 17516
Nembutal
see Pentobarbital Sodium
NEOCUPFERRON
solvent properties for americium and europium, 18: 25622
solvent properties for neptunium-239, effects of butylamine on, 19: 13252
solvent properties for neptunium, protactinium, thorium, and uranium, 19: 32297
solvent properties for protactinium and thorium, 19: 42608
solvent properties for protactinium, thorium, and uranium in hydrochloric acid solutions, 20: 1775
NEODYMIUM
see also Rare Earths
abundance determination in stellar atmospheres, 20: 46279
abundance in meteorites and terrestrial matter, 18: 10753
abundance in meteoritic, terrestrial, and solar matter, review on, 19: 13620
abundance in sun, (E), 20: 17237
allotropes at high pressure, 18: 18398
alloying characteristics with transition metals, 18: 41924(R) (IITRI-578P19-13)
alloying effects on oxidation of chromium at 2300°F, 16: 18079(P)
alloying effects on hcp-bcc phase transition in zirconium, 16: 33499
alloying effects on magnesium, 17: 29349
alloying effects on mechanical properties of magnesium–manganese–thorium alloys, 17: 32595
alloying effects on chromium steel, 17: 39580
alpha activity and half life of natural, 19: 31305
alpha reactions (α,xny) at 27 to 52 Mev, gamma spectra from, (E), 20: 6348
analysis for praseodymium, activation, 17: 14151(T) (AEC-tr-5637)
analysis of, colorimetric, 18: 3672(R) (BNL-799(p.64-73))
analysis of, for traces of praseodymium by activation methods, 20: 29082 (SGAE-CH-27/1966)
analysis of, x-ray spectrographic, 19: 5794
anion-exchange behavior in ethanol-containing dilute sulfuric acid, 16: 4148
arc spectra of, analysis of I and II d-c, 17: 35253(R) (IA-775)
atomic mass, (E/T), 20: 11494
atomic structure of, calculation of Hartree-Fock parameters for, 20: 41631
binding by sodium amalgam, 16: 14756
cohesive energy and ionization of, relation between, (T), 19: 47062
conductivity of, electric and thermal, (E), 19: 18510
content and relative abundances in terrestrial materials, 18: 20202
content in African pitchblende, estimation of induced fission vs spontaneous fission from, 20: 37994
content in eclogites from Nowa Wies in Snieznik Klodzki, Poland, 20: 18900
content in igneous rocks, meteorites, and sediments, variation in, 17: 25435
content in sea water and sediment, 17: 30719
content in standard diabase W-1 and standard granite G-1, 19: 26529
content of, in marine organisms, 17: 15604
corrosion by atmosphere at high temperatures, 16: 5315 (WADD-TR-61-123)
crystal field effects in, 19: 13397
crystallization and precipitation of, separation factors in fractional, 17: 8064
density of liquid, at 1035 to 1231°C, 19: 42842 (CONF-650804-6)
density of liquid, at 1035 to 1231°C, 19: 42849 (MLM-1262)
density of liquid, at 1035 to 1231°C, 20: 23697
determination as extracted nitrate complex, spectrophotometric, 19: 9070
determination at controlled potential, coulometric method development, 16: 11523(R) (TID-15106)
determination by copper spark excitation, 16: 22001 (HW-71517)
determination by carrier distillation, spectrographic, 18: 9985
determination by flame spectrophotometry, 18: 6411(R) (ANL-6706)
determination by mass spectrometry, 17: 4460(R) (GEAP-4082)
determination by precipitation as diliturate, gravimetric, 18: 31447
determination by radioactivation on chromatographic paper, 18: 39120
determination by spectrophotometry, effects of complexing reagents on, 19: 11026
determination by spectrochemical methods, voltage-fluctuation patterns in, 19: 40416
determination by titration using sodium tungstate, 18: 21964
determination by thermal-neutron activation methods, sensitivity for, 19: 9071
determination by titration, suitability of tetraethylenepentaminehepta-acetic acid for, 19: 19813
determination in aluminum as trace impurity, activation, 17: 10546
determination in aluminum–neodymium oxide systems, improvement of method for, 19: 7274(R) (IDO-14636)
determination in americium by emission spectrography, 20: 8835 (RFP-414)
determination in cast steels, spectrophotometric, 16: 17602
determination in cerium oxide, spectrophotometric, 16: 12981
determination in cerium solutions, 19: 337
determination in cerium, erbium, and lutetium, mass spectrographic, 19: 2232
determination in concentrates, spectrophotometric, 19: 11025
determination in cerium oxide, spectrographic, 19: 15339 (AEET/Spec./7)
determination in diabase and granite by spark source mass spectrography, 19: 11406
determination in EDTA complexes, spectrophotometric, 17: 6010
determination in fluorite monocrystals, spectrophotometric, 20: 38829
determination in glass, emission spectrographic, 20: 12810
determination in high-purity compounds, spectrographic, 18: 25288
determination in high-purity cerium oxides, spectroscopic, 19: 30109
determination in hydrochloric acid or methanol–nitric acid media, spectrophotometric, 20: 3888 (TID-22402)
determination in hydrochloric acid solutions, spectrographic carrier-distillation, 20: 36729
determination in iron–yttrium garnet powders, spectrographic, 17: 34431
determination in lanthanum oxide, spectrographic, 19: 15338 (AEET/Spec./6)
determination in magnesium–neodymium alloys, x-ray fluorescence, 16: 5283
determination in minerals and rocks, spectrographic, 17: 6008
determination in mixture with praseodymium oxide, x-ray fluorescence, 18: 39135
determination in minerals by neutron activation, 19: 30424
determination in minerals and rocks, activation, 20: 22950
determination in magnesium alloys by successive potentiometric titration, 20: 38830
determination in magnesium alloys, quantometric, 20: 43112
determination in nuclear fuels by isotope dilution, 18: 21970
determination in nitrate solutions by conductometric titration using sodium tungstate, 20: 18608
determination in praseodymium by d-c arc excitation, 16: 22001 (HW-71517)
determination in presence of other rare earths, spectrophotometric, 17: 32002
determination in promethium-147, 18: 35450 (ORNL-TM-922)
determination in praseodymium and samarium mixtures by absorption spectra of their dichlorooxinates, 19: 11027
determination in presence of praseodymium, spectrophotometric, 20: 20568
determination in pure cerium oxide, spectrographic, 20: 29095
determination in rare earth mixtures, activation, 20: 20562 (LYCEN-6538)
determination in rare earth mixtures, polarographic, 20: 26792
determination in rocks, chemical spectrographic method for, 20: 29083(R) (UCRL-14767)
determination in solutions of fission products, development of radio-electrochromatographic method for, 16: 3347(T) (AEC-tr-4497(p.382-8))
determination in silicate rocks, combined cation exchange-spectrochemical, 16: 25287
determination in steel, spectrophotometric, 17: 25142
determination in sodium rare earth sulfates, spectrochemical, 18: 1527
determination in standard igneous rocks G-1, W-1, and G-B by x-ray fluorescence, 20: 29101

determination in silicon carbide by neutron activation, 20: 33167(T) (AEC-tr-6639, pp 42-5)
determination in steel, procedure for, 20: 41415
determination in thorium dioxide, isotope dilution, 18: 1547
determination in thorium and uranium, spectrographic, 20: 26746 (ISO-SA-13)
determination in TBP extracts, spectrophotometric, 20: 29125
determination in uranium thermal neutron fission products by ion exchange, 16: 12965
determination in uranium dioxide for burnup calculations, 16: 23626 (TID-7629(p.152-65))
determination in uranium compounds, spectrographic, 20: 29129
determination, micro-coulometric, 16: 25285
determination of, by radiometric titration using 8-hydroxyquinoline halogen derivatives, 17: 15925
determination of, by radiometric titration using cupferron, 17: 37164
determination of, fluorescence x-ray spectrographic, 18: 1549
determination of, in lanthanum oxide, spectrographic, 17: 15932
determination of, in residues by iron flux method, spectrographic, 17: 19942 (PG-Report-157)
determination of micro amounts of, in rare earth oxides by x-ray fluorescence, 19: 40440
determination of, review on x-ray spectrographic, 17: 23252 (IS-550)
determination of trace amounts of, by reactor neutron activation methods, 20: 26760
determination of, effects of tiron on spectrophotometric, 19: 7325
determination of, spectrophotometric, 19: 11004
determination of, in rare-earth mixtures, photometric, 20: 252
determination of, effects of metal ions on spectrophotometric, 20: 43100
determination of, by titration with chromate ions, 20: 45585
determination using xylenol orange, spectrophotometric, 17: 12199
determination using xylenol orange, spectrophotometric, 17: 25126
determination using hexamethylenetetramine and vanadic acid, indirect, 18: 1558
determination using 4-(2-pyridylazo)resorcinol, spectrophotometric, 18: 19895
determination using 4-(2-pyridylazo)resorcinol, spectrophotometric, 18: 35461
determination using 2-(*p*-sulfophenylazo)-1,8-dihydroxynaphthalene-3,6-disulfonic acid, spectrophotometric, 18: 41341
determination using xylenol orange, spectrophotometric, 18: 43394
determination using *p*-(2-azo-pyridine)-resorcinol, spectrophotometric, 19: 2236
determination using Chromotrope 2B, photometric, 20: 1772
determination using thenoyltrifluoroacetone, photometric, 20: 8859
determination with thorium in monazites, thorium phosphates, and xenotimes, 18: 19885
deuteron reactions (d,*α*) at 15 Mev, cross sections and energy distributions for, 16: 11020
diffusion in germanium, (E), 19: 11755(T)
diffusion in lead and silver crystals, 17: 19997
diffusion in magnesium, 16: 22619
dissolution and ion exchange in ammonium and potassium carbonate solutions, 17: 12240
dissolution and ion exchange behavior in ammonium and potassium carbonate solutions, 17: 39035
distribution between Dowex I-X8 and solutions of potassium acid carbonate and potassium carbonate, 18: 13751
distribution between phases in molten boron oxide–sodium chloride–sodium oxide at 830°C, 20: 7201
distribution in aqueous chloride and nitrate systems with TBP, 20: 7004 (IS-T-42)
effects on carbide stabilization in cast iron, 19: 23024(T) (JPRS-28849 (p.342-50))
effects on crystal structure of cobalt, iron, and nickel intermetallic compounds, 20: 37243
effects on dielectric constant and electric conductivity of cerium aluminate, 19: 15535(T)
effects on dog and rabbit membranes of contact with, 20: 25(R) (TID-22294)
effects on ductility of iodide chromium, 18: 32189
effects on extraction of calcium and strontium, 18: 1811
effects on hydrogen distribution in Zircaloy, 20: 11221
effects on mechanical properties of magnesium-manganese-thorium alloys, 18: 32156(T) (JPRS-25069(p.1-31))
effects on phase transformation temperature of thorium, 20: 37242
effects on properties of electrorefined vanadium, 19: 2795 (BM-RI-6553)
effects on rabbit skin, effects of various solvents on toxic, 20: 25(R) (TID-22294)
effects on secondary electron emission properties of activated aluminum–magnesium alloys, 17: 37545(T)
effects on solubility of hydrogen in iron, 17: 32597
effects on spectrophotometric determination of praseodymium, 20: 22922
electric and galvanomagnetic properties of, effects of temperature on, 20: 7620
electric conductivity in molten iodide, 17: 28888
electric conductivity of, pressure and temperature dependence of, 18: 7238
electric conductivity and Hall coefficient, effects of magnetic ordering and temperature on, 18: 27993
electric conductivity and lattice parameters, 19: 14018
electrochemical characteristics of, in phosphoric acid, 17: 25165 (TID-18697)
electrochemical properties in phosphoric acid, 17: 32034 (CONF-20-22)
electron energies and wave functions of f^3 configuration in intermediate coupling in, 17: 14949 (TID-18035)
electron interactions in, *s-f*, 18: 1667
energy levels of, intermediate coupling effects on low-lying, 17: 25932
energy levels of, ionization energies from, (T), 20: 37439
evaporation during uranic reduction to uranium carbide, 20: 10272(R) (NAA-SR-9339)
evaporation from irradiated fuel, 19: 32282 (NAA-SR-10738)
excited state lifetime in calcium tungstate, measurement of, 17: 10651
fluorescence conversion efficiency of glasses of, 19: 40090
fluorescence in doped aluminum oxide crystals, 18: 27583
fluorescence in niobium-compensated calcium and strontium molybdates, 19: 36393
friction and wear properties of, in vacuum, effects of crystal structure on, 20: 21365
friction characteristics in vacuum, 19: 6255 (NASA-TN-D-2513)
gamma resonant scattering by, 17: 29879(R) (IA-822)
Hall effect in, at 2.4 to 350°K, (E), 20: 24624(T)
hardness at 77 to 293°K, 20: 9510
heat of solution in liquid tin at 750°K, 18: 24183
heat of solution in liquid tin, 19: 41044
heat of solution in liquid tin at 828°K, 20: 11304
heat of sublimation and surface energy of, calculation of, 18: 626
heat of vaporization and vapor pressure of, 17: 22156 (ARL-63-15)
helium and hydrogen ion attenuation at 0.1 to 500 Mev, tables for, 20: 41619 (CEA-R-3042)
hydridation of, kinetic studies of, 16: 31366
ion exchange and solubility in potassium carbonate solutions, 18: 31453
ion exchange on resins at 25°C, 18: 10102
ionization and oxidation on rhenium and tungsten in oxygen atmosphere, 20: 757
ionization on rhenium and tungsten surfaces, effects of adsorbed oxygen on, 20: 31225
liquid, solubility of tantalum and tungsten in, at high temperatures, 20: 41412(R) (IS-1500(Sect. M))
luminescence in barium, calcium, and strontium fluorides at 4.2, 77, and 300°K, 19: 34185(T)
luminescence in monocrystalline lead molybdate at 4.2 to 300°K, infrared, 19: 15513(T)
luminescence of trivalent, in calcium tungstate at 4.2, 77, and 300°K, 19: 17928(T)
magnetic moment of ions of, in crystalline state and in solution, 18: 25350
magnetic properties, antiferromagnetic theory, 16: 4552(T) (AEC-tr-4866)
magnetic properties and neutron diffraction analysis, 16: 18448
magnetic properties at 4.2–300°K, 17: 37710
magnetic properties of, effects of crystalline field and structure on 18: 24186
magnetic properties, 20: 11340
magnetic properties at 2 to 300°K, 20: 43939
magnetic structure of, 18: 10525 (CONF-342-10)
magnetic susceptibility of solid, at 300 to 1250°K, 17: 31011
magnetization up to 110 kgauss, temperature effects, 16: 15457
mass of, spectrometric determination of, 20: 15853
melt technology and non-cutting shaping of, 19: 13969
metabolism in feces, tissues, and urine, 20: 25(R) (TID-22294)
metabolism in rats, effects on liver lipids, 19: 25840(R) (ORINS-49 (p.63-71))
neutron absorption cross section in pitchblende, thermal, 20: 37994
neutron capture cross sections at 0.3 to 10 Mev, 16: 1032(T) (AEC-tr-4685)
neutron capture gamma spectra, 16: 19745(R) (ARF-1193-9)
neutron capture gamma spectrum, 16: 28024(R) (ARF-1193-12)
neutron capture, gamma spectra following, 16: 29750 (ANL-6589)
neutron cross sections at 3.3 to 5.5 Mev, total, 18: 28586
neutron intermediate resonances and total cross sections at 3 to 650 kev, (E), 19: 35462
neutron reactions (n,*γ*) at thermal energies, soft gamma spectra from, 18: 1053
neutron resonance parameters for, 18: 11195(R) (EANDC(E)-49(L))
neutron resonance absorption integrals for, reactivity measurements for, 19: 29338
neutron scattering at 3 to 650 kev, cross sections, phase shifts, and strength functions for, (E), 19: 10319
neutron total cross sections of, (E), 19: 41723
nuclear magnetic moments, spin-orbit coupling, and hyperfine fields,

16: 16831
oxidation at 600 to 1300°C, rate of, 18: 35961
oxidation in air and dry oxygen, 18: 32096
oxidation in dry and moist air at 100 to 800°C, rate of, 20: 21265 (RPI-2714-8)
oxidation kinetics of, effects of moisture and temperature on, 20: 35854
oxidation of, heats of reaction for, (E), 20: 757
oxidation of, kinetics of, 18: 35952 (AWRE-O-45/64)
oxidation of, kinetics of high-temperature, 20: 5859
paramagnetism of polycrystalline, 16: 1686
partition coefficients and reciprocal ionic radii, 17: 27562 (INSJ-54)
performance of cathodes of, in diode ion pumps, 20: 10976 (IS-T-46)
phase transformation temperature, 16: 5315 (WADD-TR-61-123)
phase transformations at 6 to 65 kbar, solid-liquid and solid-solid, 19: 40095
photoelectric effect in, relativistic, 18: 34847
photoelectron distribution from, cesium-137 gamma, 17: 6833
photoelectron emission at $h\nu = 662$ kev, 16: 12296
photonuclear reactions, production of short-lived isomers, 16: 12530
polarographic behavior in tetraethylammonium bromide at dropping mercury electrode, 18: 23463
polarographic behavior in dimethylformamide and dimethylsulfoxide, 19: 40681
polarography at dropping mercury electrode, irreversible and reversible processes in, 18: 17821
polarography in acetonitrile, 18: 41354
polarography of, in acetone solution, 17: 14253
precipitation by benzenephosphinic and benzenephosphonic acids, 18: 27308
preparation and purification, 19: 40948 (IS-1195)
preparation of thin films of, by electrodeposition, 20: 7538 (ORINS-48)
properties as single crystal impurity in proton polarization, 17: 4100
properties, physical and thermodynamic, 19: 40948 (IS-1195)
proton inelastic scattering at 25 to 1700 kev, x-ray yields from, (E), 19: 39881
proton reactions (p,ypxn) at 660 Mev, production of neutron-deficient radioactive rare earths in, 18: 24691
proton reactions (p,n) at 20.5 Mev, Coulomb displacement energies from, (E), 19: 23755
proton reactions at 25 to 100 kev, x-ray production in, 18: 28259
proton scattering by, L- and M-shell ionization yields from, (E), 19: 8067 (UCRL-12136)
proton spallation of, yields from, 18: 4579 (NP-13165(Vol.2)(p.121-32))
purification, 19: 22999(T) (JPRS-28849(p.31-46))
purification techniques, 19: 30338
radiation effects on EPR of calcium fluoride crystals containing, 19: 40602(T)
radioinduced production of helium and hydrogen in, neutron, 19: 26901
reactions with ammonium, potassium, and sodium salts, precipitation, 17: 10621
reactions with hexamethylenediaminetetraacetic acid, 16: 17622(T) (AEC-tr-4456(p.153-65))
reactions with hydrogen, 19: 15466(T) (LA-tr-65-2)
reactions with oxygen in deoxidation of steel, 19: 22166(T) (JPRS-28849 (p.272-8))
reduction and deposition potentials, 19: 7362(T) (UCRL-Trans-1153(L))
relaxation processes in, resonance coupling in, 18: 22056
separation by anion exchange in acetic acid–nitric acid medium, 18: 16131
separation by anion exchange in EDTA, effects of temperature on, 18: 20110
separation by complexing in ethylenediaminetetraacetic and nitrilotriacetic acid, 16: 195
separation by continuous countercurrent ion method, 18: 31679
separation by electrophoresis on zirconium phosphate paper, 17: 4467
separation by extraction using alkali metal amalgams, 17: 40939
separation by paper chromatography, effects of ester composition in alcohol and ketone mixtures on, 17: 40947
separation by partition chromatography with reversed phases, 17: 29025 (AERE-R-4358)
separation by partition chromatography using di-(2-ethylhexyl)-orthophosphoric acid as column material, 18: 3889
separation by precipitation in cadmium and sodium chloride solutions, 17: 12373
separation by reversed-phase partition chromatography using organophosphorus compounds, 18: 25614
separation by solvent extraction using TBP, effects of trilon B, 16: 275
separation by solvent extraction using thenoyltrifluoroacetone, 19: 13257
separation by solvent extraction using TBP, computer program for cascade calculations for, 19: 22092 (IS-T-6)
separation by solvent extraction using dibutylphenyl phosphate, diphenylbutyl phosphate, and TBP, 19: 28454
separation by solvent extraction using bis(2-ethylhexyl) phosphate–Amsco in acid solutions, 20: 7208
separation by trialkylphosphates, 16: 276
separation factor for, in chloride and nitrate systems containing TBP, 20: 40904
separation from americium and samarium by ion exchange, 18: 21707(R) (MLM-1177)
separation from aqueous solutions by solvent extraction using butyl phosphates, synergistic effects of thenoyltrifluoroacetone in, 17: 37306
separation from aqueous solution by solvent extraction as salicylate pyridine complex, 19: 20079
separation from aqueous solutions by solvent extraction using bis(dihexylphosphinyl)-methane, 19: 24619
separation from aqueous solutions by solvent extraction using monomerized and dimerized bis(2-ethylhexyl) phosphate, 20: 27051
separation from cerium, lanthanum, praseodymium, and samarium by ion exchange, 17: 1567
separation from cerium and promethium by reversed-phase chromatography, 17: 33765(R) (GEAP-4278)
separation from cerium and yttrium by solubility of carbonates in water, 20: 7019(T) (LA-tr-65-24)
separation from chloroform–water by solvent extraction using selenoylacetone and selenoyltrifluoroacetone, 20: 26813
separation from erbium by zone crystallization in nitrate medium and by precipitation using ammonium sulfate, 18: 16137
separation from fission products, isotopic distribution in, 19: 22823 (ORNL-TM-1047(p.106-8))
separation from fission products by pH-gradient methods, 19: 36217(R) (IDO-14656)
separation from fission products by solvent extraction and ion exchange, 20: 7203
separation from hydrochloric acid solutions by solvent extraction using dialkyl alkylphosphonates, 20: 36941
separation from irradiated fuel by ion exchange and solvent extraction, 17: 12716(R) (GEAP-4137)
separation from irradiated uranium dioxide by ion exchange, 17: 19928(R) (GEAP-4201)
separation from irradiated uranium dioxide fuels, 18: 15487(R) (GEAP-4361)
separation from irradiated clad uranium dioxide fuels, 18: 24856(R) (GEAP-4430)
separation from irradiated fuel, anion-exchange, 19: 10510(R) (GEAP-4716)
separation from lanthanum using anion exchanger EDE-10, 16: 3086
separation from lanthanum and yttrium, effects of solvent mixture on chromatographic, 17: 6009
separation from lanthanum, 17: 16149(T) (CEA-tr-A-1230)
separation from magnesium–thorium alloy by transfer to liquid scrub alloy in fused salt, 19: 20066
separation from methanol-nitric acid systems using anion exchange resins, 16: 25280 (TID-15598)
separation from metal ions by ion exchange in isopropyl alcohol, 18: 20104
separation from molten fluoride salts, 20: 32804(R) (ORNL-3936, pp 122-71)
separation from nitric acid by solvent extraction with di(2-ethylhexyl) phosphoric acid, 17: 4460(R) (GEAP-4082)
separation from nitric acid solutions by solvent extraction using TBP, 17: 14393
separation from nitric acid solutions by solvent extraction using TBP, effects of ammonium nitrate on, 18: 31665
separation from nitrate solutions by solvent extraction using long-chain tertiary amines, 20: 27063
separation from other rare earths, plutonium, and uranium by molten salt extraction, 17: 1359(R) (ANL-6569)
separation from other rare earths by ion exchange, 17: 4460(R) (GEAP-4082)
separation from other rare earths by paper chromatography, 19: 15675
separation from other rare earths by ion exchange, 19: 18057
separation from other light lanthanides by partition chromatography following production by proton bombardment of erbium, 19: 20078
separation from other rare earths by paper electromigration and focusing chromatography, 19: 30327
separation from other rare earths by thin-layer chromatography, 20: 7202
separation from other rare earths by paper precipitation chromatography using 8-quinolinol, 20: 20814
separation from other rare earths by paper chromatography, 20: 27049
separation from other rare earths by cation exchange in ammonium lactate solutions, 20: 26800
separation from perchlorate solutions by solvent extraction using TBP, 19: 24626
separation from perchloric acid solutions by ion exchange materials, 20: 20823
separation from promethium by solvent extraction using di(2-ethyl-hexyl) orthophosphoric acid, 16: 23788 (ORNL-TM-184)
separation from promethium, chromatographic, 16: 31567
separation from praseodymium and samarium by displacement

chromatography, band distribution in, 17: 6004
separation from praseodymium by high temperature distillation of oxides, 17: 6070
separation from promethium, electrochemical, 17: 14376 (LADC-5634)
separation from praseodymium by ion exchange, 17: 32202
separation from promethium by solvent extraction using D2EHPA, 17: 35864 (AERI-C/R-3)
separation from praseodymium by electrolysis on mercury cathode, 17: 37163
separation from praseodymium by solvent extraction using D2EHPA or TBP, 18: 1834(R) (IS-700(Sect.E))
separation from praseodymium by ion exchange using aluminum, cadmium, cobalt, and zinc, 18: 10200
separation from praseodymium by solvent extraction using D2EHPA or TBP, 19: 9281(R) (IS-900(Sect.E))
separation from praseodymium and samarium by ion exchange, 19: 22411
separation from praseodymium, 19: 26305
separation from praseodymium by solvent extraction using *bis*(2-ethylhexyl) ester of phosphoric acid, 19: 32290
separation from promethium by ion exchange, 19: 38772
separation from praseodymium using phthalate buffer, 19: 46437
separation from praseodymium by solvent extraction using organic phosphorus compounds, 20: 18850
separation from promethium in fission product solutions, eluting agents for ion-exchange, 20: 43411 (BNWL-SA-677)
separation from rare earths using di-(2-ethylhexyl) orthophosphoric acid, chromatographic, 16: 14660
separation from rare earths, 17: 6019
separation from rare earth mixtures by chromatography using di-(2-ethylhexyl)phosphoric acid on Kel-F, 17: 34060
separation from rare earths by ion exchange, 18: 349
separation from rare earths by ion exchange centrifuge chromatography, 18: 17940
separation from rare earths by reverse-phase paper chromatography, 19: 7298
separation from rare earths by cation exchange using ammonium α-hydroxyisobutyrate and lactate, 19: 24432
separation from rare earths by reversed phase partition chromatography using 2-ethylhexyl phenylphosphonate, 19: 24431
separation from rare earths, thorium, and uranium by reversed-phase chromatography using methylenebis(di-*n*-hexylphosphine oxide), 20: 18599
separation from rare earths by solvent extraction using diisoamyl ester of methylphosphonic acid, 20: 27065
separation from rare earths by thin-layer chromatography, 20: 45597
separation from samarium, electrolytic, 18: 13773
separation from samarium, 18: 21708(R) (MLM-1178)
separation from samarium by solvent extraction using bis(2-ethylhexyl) phosphate, 20: 27052
separation from scandium by solvent extraction of diantipyrinylmethane complex, 19: 20080
separation from sulfuric acid by diisobutylphosphoric acid, 18: 1829
separation from thorium by solvent extraction using 2,4-pentanedione, 18: 20106
separation from thiocyanate solutions by solvent extraction using TBP, 19: 24627
separation from transplutonium elements by ion exchange using EDTA, 20: 35596
separation from uranium by anion exchange using carbonate solutions, 18: 361
separation from uranium by complex formation with phthalocyanine, 19: 34279
separation from uranium by partition chromatography on silica-gel column, 20: 9073
separation from uranium by combined ion exchange-solvent extraction using nitric acid–tetrahydrofuran solutions, 20: 20811
separation from yttrium by ion exchange, 18: 1817
separation from yttrium by solvent extraction, 19: 11268
soaps of, preparation and properties of, 20: 35931
solubility and ion-exchange properties in potassium carbonate solutions, 19: 13536
solubility in bismuth at 300 to 700°C, 16: 24216
solubility in cadmium and zinc, 17: 15385(R) (ANL-6683)
solubility in cadmium and zinc, 17: 40421(R) (ANL-6766)
solubility in gold, solid, 20: 17016 (IS-1175)
solubility in liquid cadmium at 325 to 550°C, 16: 32059
solubility in liquid zinc, 18: 1483(R) (ANL-6687(p.27-85))
solubility in liquid zinc, 20: 22966 (ANL-7083)
solvent distribution in diisoamyl methylphosphonate–nitric acid, 20: 45819
solvent extraction from nitric acid solutions by TBP, calculated cascade equilibria for, 18: 25624
solvent extraction by bidentate organophosphorus compounds, 19: 277 (IS-827)
solvent partition between lithium nitrate–potassium nitrate and tributyl phosphate, 16: 10111
solvent properties for tantalum, 20: 13180(R) (IS-RD-4)
solvent properties for magnesium, solid, 20: 17016 (IS-1175)
sorption by cation exchanger, kinetics of, 18: 31516
sorption by ion exchange materials, isotherms for, 18: 31522
sorption by ion-exchange resins, effects of temperature and type of resin on, 19: 9276
sorption by *n*-butanol–nitric acid mixture, 16: 14738
sorption from nitric acid by ion exchange paper, 19: 24435
sorption on ammonium and sodium resins, kinetics of, 18: 10103
specific heats at 300 to 1100°K, 16: 16746
spectra, 19: 5842 (IA-927)
spectra, flame, 16: 30400
spectra in labeled perchloric acid and nitrate solutions, near-infrared and visible, 17: 2932
spectra in lanthanum bromide, absorption, 17: 8045
spectra in lanthanum-magnesium nitrate, spin-lattice relaxation, 18: 27473
spectra in lithium nitrate–potassium nitrate system at 0.35 to 2.6 microns, absorption, 16: 17598
spectra in minerals, visible region absorption, 19: 28558
spectra in thorium oxide at 100°K, nephelauxetic effects on reflection, 18: 25423
spectra in yttrium-aluminum and yttrium-gallium garnets, paramagnetic resonance, 16: 517 (AFCRL-775)
spectra of atomic, ionization potential from, 18: 3773
spectra of, effect of transitions in 4f shell on absorption, 17: 6099
spectra of, emission and x-ray fluorescence, 18: 183
spectra of, isotope shift, line classification, and Zeeman effect of, 18: 7430
spectra of solutions of, infrared, 17: 2983
spectra of trivalent, in lanthanum chloride at 77°K, ultraviolet, 16: 27009
spectra of, analytical applications of flame, 18: 11982
spectra of, assignments of furnace absorption, 19: 22160 (IA-964)
spectra of, atomic absorption, 18: 31513
spectra of, in solution, effects of intra-f^n electronic transitions on absorption, 19: 26314
spectra of, isotopic shifts in, 18: 17819
spectra of, isotope-displacement effect on arc, (E/T), 20: 13418
spectra of, specific mass effects on isotopic displacements in, 20: 1826
spectra of, use of fuel-rich premixed oxyacetylene flame for, emission, 18: 25278
spectra of, x-ray fluorescence, 18: 12022
spectra using d-c arc as excitation source, differentiation of atom and ion, 17: 39796
spectral properties in rare earth oxide matrices, 18: 13869
standards, preparation of primary, 19: 10510(R) (GEAP-4716)
stimulated emission in glass, time behavior of, 17: 41610(T)
substitution in calcium tungstates, theory of coupled, 18: 10089
surface tension of liquid, at 1030 to 1186°C, 17: 551
thermal capacity at 0.4 to 4.0°K, 18: 6114
thermal capacity at 0.4 to 4°K, 19: 13391
thermal capacity at low temperature, magnetic contribution to, (T), 19: 39296
thermal expansion coefficient at low temperature, 17: 18829
thermal expansion at 1.5 to 12°K, 18: 37716
toxic effects on adenosine triphosphate metabolism in mitochondria, 17: 13928
toxicity in laboratory animals, 20: 30970 (COO-1170-5)
use to improve properties of iron, nickel, and cobalt, 19: 23021(T) (JPRS-28849(p.303-9))
uses in deoxidation of steel, 20: 7529
vapor pressure at 1638 to 1791°K, 16: 32062
vapor pressure at 1638 to 1791°K, 16: 2193(R) (NP-11023)
x-ray spectra from mu-mesic atoms of, (E), 20: 38058
x-ray spectra of μ-mesic atoms of, isotope shifts in, (E), 20: 23888
x-ray-diffraction patterns of, effects of cold working on, 20: 39421

NEODYMIUM ACETATES

complexes with thiourea, solubility in water, 20: 1869
crystal structure and thermal stability, 17: 35809
preparation, 20: 25076
preparation, 20: 26853
preparation by oxide solubility in alcohols containing ammonia, 20: 20686
spectra of, infrared absorption, 18: 41446
thermal decomposition of, study of products from, 20: 45658

NEODYMIUM ALLOYS

formation and structure of $R(Me,X)_2$ type compounds in, 19: 30767
Al–Gd–Nd, gadolinium and neodymium antiparallel magnetic moments in, 17: 37775
Al–Gd–Nd, phase studies, Laves, 16: 25798
Al–Nd, crystal structure, 19: 7950
Al–Nd, crystal structure of intermetallic compound NdAl in, 19: 14020
Al–Nd, crystal structure of Laves phases in, 19: 47052
Al–Nd, crystal structure of intermetallic compound $NdAl_3$ in, 20: 11305

Al–Nd, crystal structure and stability of intermetallic compounds in, 20: 21415
Al–Nd, Curie temperature and magnetic moments for, 17: 37775
Al–Nd, magnetic properties of intermetallic compounds of, 20: 39433
Al–Nd, magnetic susceptibilities at 2 to 300°K, 20: 27494(R) (NYO-3454-6)
Al–Nd, phase diagrams and properties, 17: 39581
Al–Nd, phase diagram, 20: 4427
Al–Nd, properties of intermetallic compounds in, tabulation of, 20: 43972
Al–Nd–Tb, neodymium and terbium antiparallel magnetic moments in, 17: 37775
Al–Nd–Tb, phase studies, Laves, 16: 25798
Au–Nd, crystal structure, 17: 16658 (TID-18197)
Au–Nd, oxidation of, kinetics of high-temperature, 20: 5859
Au–Nd, phase studies of solid solutions in, 19: 41062
Be–Nd, crystal structure of, 18: 18399(T)
Be–Nd, structure of $NdBe_{13}$, 19: 23009(T) (JPRS-28849(p.195-6))
Bi–Nd, magnetic properties at 4 to 300°K, 19: 30743(R) (NYO-3454-1)
Bi–Nd, magnetic properties of LnBi type compound in, 19: 42867
Bi–Nd, structure of NdBi in, 18: 7248(T)
Cd–Nd, crystal structure of intermetallic compound $NdCd_a$, 19: 16162
Cd–Nd, electronic configuration and valence of neodymium in $NdCd_{11}$, 17: 18809
Cd–Nd, energy of formation of intermetallic, 19: 17177(R) (ANL-6965 (p.42-83))
Cd–Nd, eutectic temperature in NdCd–Nd region, 19: 32279(R) (ANL-7020(p.3-99))
Cd–Nd, formation of $NdCd_{11}$ compound, free energy of, 18: 35060(R) (ANL-6904)
Cd–Nd, magnetic properties of $NdCd_{11}$, 17: 40421(R) (ANL-6766)
Cd–Nd, phase studies, 18: 17769(R) (ANL-6725(p.99-111))
Cd–Nd, phase studies, 18: 36751 (ANL-6912)
Cd–Nd, phase studies, 20: 27546
Cd–Nd, thermodynamic properties of $NdCd_{11}$ at 400°C, 19: 32279(R) (ANL-7020(p.3-99))
Cd–Nd, thermodynamic properties of liquid, 20: 5594(R) (ANL-6925, pp 21-106)
Co–Mg–Nd, corrosion, 19: 6271(T) (JPRS-27451)
Co–Nd, cobalt ion EPR in intermetallic compounds of, 20: 15963
Co–Nd, cobalt-59 nuclear resonance in cobalt-rich, (E), 19: 4694
Co–Nd, crystal structure of Laves phases in, 19: 47052
Co–Nd, crystal structure of intermetallic compounds in, 20: 37243
Co–Nd, crystal structure of intermetallic compound, 20: 43920
Co–Nd, ferrimagnetism of intermetallic compounds of, (E), 20: 24656
Co–Nd, magnetic properties of, antiferromagnetic effects on, 16: 22624
Co–Nd, magnetic properties of cubic Laves phase in, 19: 13399
Co–Nd, magnetic properties, 19: 38049
Co–Nd, magnetic properties of intermetallic compounds in, 20: 9511
Co–Nd, magnetic properties of intermetallic compound of, (E), 20: 34823
Co–Nd, magnetic properties of intermetallic compound $NdCo_5$ in, 20: 39424
Co–Nd, magnetic structure, 19: 38057
Co–Nd, magnetization of, 18: 5804
Co–Nd, magneto-optic properties of intermetallic compound $NdCo_5$ in, 19: 41084
Co–Nd, preparation of oriented single-crystal spheres of $NdCo_5$, 19: 15989 (AFML-TR-64-362)
Co–Nd, preparation of intermetallic compound $NdCo_5$ by zone melting, 19: 16168
Co–Nd, thermomagnetic properties of, down to liquid helium temperatures, 16: 16742
Cu–Nd, analysis for AlB_2 and $CeCu_2$ type intermetallic compounds, 17: 29335
Cu–Nd, magnetic properties and crystal structure of intermetallic compounds in, 19: 9695
Dy–Nd, electric conductivity and lattice parameters, 19: 14018
Dy–Nd, electric conductivity at 4.2, 77, and 296°K, 20: 22312(R) (AD-622796)
Dy–Nd, electric conductivity of, conduction-electron impurity-scattering effects on, (E), 20: 24644
Dy–Nd, magnetic susceptibility of solid solutions of, 17: 31011
Fe–Nd, crystal structure of intermetallic phases in, 17: 37541(T)
Fe–Nd, crystal structure of $NdFe_7$, 20: 21400
Fe–Nd, crystal structure of intermetallic compounds in, 20: 37243
Fe–Nd, crystal structure of intermetallic compound, 20: 39409
Fe–Nd, magnetic properties at 300 to 1300°K, 20: 7592
Fe–Nd, neutron diffraction study of magnetic behavior and structure of, 18: 24184
Fe–Nd, phase diagram, 20: 11295
Fe–Nd, preparation and thermomagnetic analysis of $NdFe_7$ crystals, 17: 33949
Ga–Mg–Nd, corrosion, 19: 6271(T) (JPRS-27451)
Ga–Nd, crystal structure studies, 19: 44678(R) (ANL-7000, pp 186-200)
Gd–Nd, ferromagnetic spin coupling in, 20: 22314(R) (AD-626865)
Gd–Nd, phase studies, 18: 14457 (DRI-2141)
Gd–Nd, phase transformations and magnetic ordering in, pressure-induced, 20: 40326
Gd–Nd–Ni, magnetic coupling in Haucke and Laves phases in, 20: 27494(R) (NYO-3454-6)
Ge–Nb, crystal structure of intermetallic compounds in, 19: 11762
Ge–Nd, crystal structure, 20: 7591
Ge–Nd, crystal structure of, at or near equiatomic proportions, 20: 19225
Ge–Nd, crystal structure of intermetallic compound NdGe in, 20: 33886 (UCRL-14152)
Ge–Nd, crystal structure of intermetallic compound Nd_5Ge_4 in, 20: 33910
Ge–Nd, crystal structure and magnetic properties, 20: 38369
Ge–Nd, preparation and crystal of NdGe, 20: 19224
Ge–Nd, structure of germanide, 19: 23006(T) (JPRS-28849(p.184-7))
Ho–Nd, phase studies, 18: 14457 (DRI-2141)
Ho–Nd–Ni, magnetic coupling in Haucke and Laves phases in, 20: 27494(R) (NYO-3454-6)
La–Nd, electric conductivity, magnetic susceptibility, and superconductivity at low temperatures, 20: 21873 (NP-15936)
La–Nd, electric conductivity, magnetic susceptibility, and superconducting transition temperatures of, 20: 29753
Lu–Nd, phase studies of samarium-type intermediate phases in, 19: 44672 (AD-619201)
Mg–Mn–Nd, effects of plastic deformation on properties and structure of, 18: 16495
Mg–Mn–Nd, phase studies, 17: 18848
Mg–Mn–Nd–Ni, effects of plastic deformation on properties and structure of, 18: 16495
Mg–Nd, alloying effects on composition and mechanical properties of, 18: 28000
Mg–Nd, analysis of, for neodymium, x-ray fluorescence, 16: 5283
Mg–Nd, corrosion of, effects of cobalt and gallium on, 18: 20482
Mg–Nd, crystal structure of $NdMg_{12}$, 17: 37539(T)
Mg–Nd, crystal structure of magnesium-rich phases in, 18: 39961(T)
Mg–Nd, crystal structure, 20: 2399
Mg–Nd, decomposition of supersaturated neodymium-rich solid solution in, 17: 32594
Mg–Nd, effects of plastic deformation on properties and structure of, 18: 16495
Mg–Nd, effects of plastic deformation on properties and structure of, 18: 34148
Mg–Nd, electric conductivity anomalies below 273°K in dilute, 16: 10734
Mg–Nd, electric conductivity of, 17: 4951
Mg–Nd, electric conductivity of dilute, 18: 7245
Mg–Nd, electric conductivity at low temperatures in magnetic fields, 20: 9530
Mg–Nd, heat resistance, mechanical properties, and recrystallization of, 18: 16496
Mg–Nd, mechanical properties of, effects of alloying elements on, 19: 44709 (JPRS-24761, pp 17–28)
Mg–Nd, microstructure of, effects of heat treatments on, 20: 7615
Mg–Nd, phase studies, 16: 20372(T) (AEC-tr-4457(p.197-204))
Mg–Nd, phase studies and properties, 17: 39581
Mg–Nd, phase studies on, 18: 14506
Mg–Nd, phase studies, 19: 9721
Mg–Nd, phase studies, 19: 41011 (IS-T-15)
Mg–Nd, phase studies, 20: 9531
Mg–Nd, properties and structure of, 20: 17110
Mg–Nd, structure of intermetallic compounds in, 19: 23008(T) (JPRS-28849(p.191-4))
Mg–Nd, thermal stability at 150 to 300°C, 17: 34461
Mg–Nd, thermodynamics of formation of intermetallic compounds, 20: 41412(R) (IS-1500(Sect. M))
Mn–Nd, crystal structure of intermetallic compound Nd_6Mn_{23} in, size-factor limitation in, 19: 23079
Mn–Nd, existence of Nd_6Mn_{23} compound in, 19: 14074
Mn–Nd, magnetic moments of intermetallic compound Nd_6Mn_{23} in, 19: 23109
Mn–Nd, preparation and structure, 20: 15110
Nb–Zr, metallurgical properties and phase studies on, 20: 5891(R) (NYO-2159-1)
Nd–Ag, electric conductivity at low temperatures in magnetic fields, 20: 9530
Nd–Ag, electric conductivity, 20: 25583
Nd–Ag, magnetic properties of intermetallic compound with CsCl structure in, 19: 2814
Nd–Ni, crystal structure of equiatomic intermetallic compound in, 19: 24994
Nd–Ni, crystal structure of intermetallic compounds in, 20: 37243
Nd–Ni, magnetic and structural characteristics of intermetallic compound of type LnNi in, 18: 37697
Nd–Ni, magnetic properties of, antiferromagnetic effects on, 16: 22624
Nd–Ni, magnetic properties of $NdNi_5$ at 4–300°K, 17: 37713
Nd–Ni, magnetic properties of cubic Laves phase in, 19: 13399
Nd–Ni, magnetic properties, 19: 38049

Nd–Ni, magnetic properties of intermetallic compounds in, 20: 9511
Nd–Ni, magnetic susceptibility of $NdNi_5$ at 4 to 300°K, 19: 30743(R) (NYO-3454-1)
Nd–Pd, phase studies, 19: 47051
Nd–Pd, preparation and properties, 19: 16068 (EUR-1894.i)
Nd–Po, preparation and properties of, 20: 35909
Nd–Pr, density and phase studies, 16: 2193(R) (NP-11023)
Nd–Pr, electric conductivity and thermal emf, 19: 28829
Nd–Pr, heat of solution in liquid tin, 19: 41044
Nd–Pr, phase diagram and thermodynamic properties of, 17: 22156 (ARL-63-15)
Nd–Pr, phase equilibria in, 19: 13394
Nd–Pr, phase studies, 16: 19363(R) (NP-11689)
Nd–Pr, phase studies and properties, 17: 39581
Nd–Pr, phase studies and structure, 18: 2282
Nd–Pr, thermodynamic activities and solution ideality, 19: 16087
Nd–Pt, crystal structure of equiatomic intermetallic compound in, 19: 24994
Nd–Pt, magnetic properties, 19: 38049
Nd–Pu, phase studies, 17: 28565(R) (LAMS-2915)
Nd–Pu, phase studies, 18: 7125(R) (LAMS-3021)
Nd–Pu–Y, phase studies, 19: 42849 (MLM-1262)
Nd–Re, magnetic properties, 19: 38049
Nd–Rh, crystal structure of equiatomic intermetallic compound in, 19: 24994
Nd–Sc, phase diagram, 18: 20520 (IS-841)
Nd–Sn, magnetic properties of $NdSn_3$ at 2 to 300°K, 19: 30743(R) (NYO-3454-1)
Nd–Sn, magnetic properties of, at 2 to 300°K, 20: 4423
Nd–Sn, temperature dependence of tin Knight shift and magnetic susceptibility in, 20: 861
Nd–Sn, tin Knight shift and magnetic susceptibility of $NdSn_3$, 20: 12324
Nd–Th, metallurgical properties and phase studies on, 20: 5891(R) (NYO-2159-1)
Nd–Th, phase studies, 18: 2174(R) (USBM-U-1082)
Nd–Th, phase studies, 18: 37623(R) (USBM-RC-1122)
Nd–Th, phase studies of, 20: 37242
Nd–Tl, phase diagram, 16: 29409
Nd–Tm, magnetic properties, 17: 25824
Nd–Tm, magnetic properties and phase transformations in, 20: 21414
Nd–Tm, magnetic susceptibility of delta-phase, temperature dependence of, 18: 20519 (IS-551)
Nd–Tm, phase transformations and magnetic ordering in, pressure-induced, 20: 40326
Nd–Y, electric conductivity at low temperatures, 17: 34443
Nd–Y, electric conductivity at low temperatures, 20: 5888 (NP-15592)
Nd–Y, electric conductivity of dilute, at low temperatures, (E), 20: 15098
Nd–Y, magnetic properties, 17: 25824
Nd–Y, magnetic properties and phase transformations in, 20: 21414
Nd–Y, magnetic susceptibility at 1.5 to 20°K, 17: 34444
Nd–Y, magnetic susceptibility of delta-phase, temperature dependence of, 18: 20519 (IS-551)
Nd–Y, phase diagram, 18: 20520 (IS-841)
Nd–Y, phase studies and atmospheric corrosion, 16: 5315 (WADD-TR-61-123)
Nd–Y, phase studies, 17: 11186 (DRI-2080)
Nd–Y, phase studies, 18: 1489(R) (IS-700(Sect. C))
Nd–Y, phase studies, 16: 32057
Nd–Y, phase transformations and magnetic ordering in, pressure-induced, 20: 40326
Nd–Zn, crystal structure, 18: 5791
Nd–Zn, crystal structure of intermetallic compounds in, 20: 9515
Nd–Zn, crystal structure of intermetallic compound Nd_2Zn_{17} in, 20: 39417
Nd–Zn, lattice parameters of intermetallic compounds in, 19: 24989(R) (TID-21673)
Nd–Zn, melting point of $NdZn_2$, 20: 31743
Nd–Zn, phase studies, 17: 36860(R) (ANL-6648)
Nd–Zn, phase studies, 17: 40421(R) (ANL-6766)
Nd–Zn, structure of NdZn, 17: 36304 (TID-19337)
Nd–Zr, fracture at 78, 197, and 373°K, mechanisms of, 20: 37231
Nd–Zr, preparation and properties, 16: 2128
Nd–Zr, surface tension of liquid, 17: 4943
Pb–Nd–Zn, component distribution in recrystallized, 20: 39435
Sb–Nd, electric properties, 17: 34469
Sb–Nd, electric properties and uses of, 18: 34158
Sb–Nd, magnetic properties of, (E), 19: 20597
Sb–Nd, preparation, semiconducting properties, and structure of, 19: 22965 (AL-TDR-64-239)
Sb–Nd, structure of NdSb in, 18: 7248(T)

NEODYMIUM ALUMINATES
crystal structure, 19: 22170
dielectric constant, 19: 15534(T)
preparation and properties, 20: 8915
preparation of monocrystals of, with perovskite structure, 20: 40920
$MgAl_2O_4$–$NdAlO_3$, constitution diagram and thermal properties, 17: 20016
$MgAl_2O_4$–$NdAlO_3$, phase diagram, 17: 27335

NEODYMIUM ARSENIDES
electric properties and uses of, 18: 34158
preparation, semiconducting properties, and structure of, 19: 22965 (AL-TDR-64-239)
thermoelectric properties, 17: 11296 (AD-278352)

NEODYMIUM AZIDES
preparation, 20: 29166
preparation and spectra of, 19: 13389
thermal decomposition of, differential thermal analysis of, 18: 25446

NEODYMIUM BORATES
polymorphism, x-ray analysis, 16: 162
preparation and properties, 19: 7498
structural properties, 17: 14210 (NBS-MON-25(Sect. 1))
$LaBO_3$–$NdBO_3$, structural polymorphism of, 17: 32124
$NdBO_3$–$SmBO_3$, structural polymorphism of, 17: 32124

NEODYMIUM BORIDES
electric resistance, 19: 6356
electron structure and physical properties of crystals of, 17: 27875
nuclear magnetic resonance of boron-11 in hexavalent, 17: 676
nuclear magnetic resonance of boron-11 in hexa-, Knight shifts in, 17: 32083
physical properties of hexa-, 16: 12154
preparation of hexavalent, conditions for, 19: 2733
preparation, properties, and uses, 17: 2959(T) (AEC-tr-5264)
spectra of, valence state determination from x-ray absorption, 19: 30194
thermal conductivity, 17: 28843
thermodynamic properties of hexavalent, 18: 19928 (CONF-405-6)

NEODYMIUM BROMATES
thermal decomposition of, search for perbromate in, 19: 36402

NEODYMIUM BROMIDES
electric conductivity around melting point, 18: 2231(R) (ORNL-3488 (p. 96-101))
heat capacity and entropy and heat of fusion of, 18: 1643
molecular structure of gaseous, electron diffraction studies of, 20: 31222(T) (ANL-Trans-310)
refractive index of, in aqueous solutions, 19: 46254
spectra of gaseous, energies and intensities of oscillation absorption bands in, 20: 35499
thermal decomposition of hydrates of, mechanisms of, 19: 46271
thermodynamic properties around melting point, 18: 2231(R) (ORNL-3488(p. 96-101))
vapor pressure, 17: 8086
$NdBr_3$–KBr, complex formation in, refractometric studies of, 19: 46254
$NdBr_3$–NaBr, complex formation in, refractometric studies of, 19: 46254
Nd–$NdBr_3$, electric conductivity at 730°C, 18: 2231(R) (ORNL-3488 (p. 96-101))
Nd–$NdBr_3$, electric conductivity at 730°C, 18: 5282

NEODYMIUM CARBIDES
crystal and magnetic structures of, 20: 34839
crystal structure, 17: 6692(T) (AEC-tr-5486)
eutectic temperature between carbon and dicarbide, 19: 41014 (LA-DC-6819)
hydrolysis of, gaseous products from, 20: 29220
lattice parameters and phase transformation temperatures in, 19: 41014 (LA-DC-6819)
microhardness, 19: 41014 (LA-DC-6819)
preparation and hydrolysis in mineral acids and water, 18: 39221
properties at 20 to 1300°C, 20: 36811
properties of, chemical and physical, 20: 17048
reactions with water, formation of gaseous products in, 20: 17048

NEODYMIUM CARBONATES
complexes of, composition in solution of, 20: 10824
preparation by heating aqueous solution of rare earth chlorides and ammonium trichloroacetate, 19: 36399
preparation by precipitation, 17: 15951 (LADC-5579)
preparation from acetates and propionates, 20: 26911
preparation, analysis, and thermal decomposition of, 20: 25065
solubility of, in water charged with carbon dioxide, 20: 45636
spectra of complex, absorption, 16: 5338
thermal decomposition of, compound formations in, 17: 15951 (LADC-5579)
thermal decomposition at 25 to 1400°C, thermogravimetric analysis of, 18: 25354
thermal decomposition, 20: 45693

NEODYMIUM CHLORIDES
chlorine-35 and -37 quadrupole frequency in, 20: 24591(R) (TID-22848)
complexes with phenanthroline, preparation and properties, 19: 40514
complexes with pyrocatechol and pyrogallol, formation and structure of, 18: 31521
complexes with 1,10-phenanthroline, structure and thermal stability of, 18: 25387
crystal field parameters for, 19: 15545

effects of intradermal injections of, on skin of guinea pigs, 18: 1360
electric conductivity and magnetic susceptibilities of, 18: 4281
entropy of formation and vapor hydrolysis, 16: 18911
fluorescence of aqueous solutions of, effects of heavy water on, 20: 25102
formation and stability, 17: 35834
formation of complexes of, in aqueous acid solutions, 18: 31434(R) (UCRL-11317(p.32-51))
heat of formation of, 20: 1806 (BM-RI-6697)
heat of fusion, 17: 28870
heat of vaporization and vapor pressure of, above melting point, 17: 37185
magnetic phases, (T), 20: 20143
magnetic properties from NMR and NQR studies, 20: 42522(R) (COO-1533-2)
magnetic susceptibility at 77 to 550°K, 18: 29626
magnetic transitions in, low-temperature, 18: 39230
magnetic transitions at 0.2 to 4.2°K, 19: 15522
molecular structure of gaseous, electron diffraction studies of, 20: 31222(T) (ANL-Trans-310)
paramagnetic spin-lattice relaxation of hydrated, at 1.1 to 4.2°K, 17: 10652
preparation and thermodynamic properties, 18: 6832
properties of aqueous solutions of, thermodynamic and transport, 20: 22968 (IS-1344)
properties of, magnetic and thermal, 20: 43176 (NP-16302)
reactions with α-alanine in solutions, 17: 1487
reactions with gaseous alkali and alkaline earth metals and hydrogen, thermodynamics of, 20: 43222
reactions with glycine in aqueous solutions, 17: 1486
reactions with isopropylamine, thermogravimetric study of, 20: 36853
reactions with potassium and sodium chlorides, analysis of, 16: 14753
reactions with sodium salicylate in aqueous solutions, preparation of neodymium salicylate by, 20: 26895
refractive index of, in aqueous solutions, 19: 46254
solubility in ordinary alcohols, 17: 28916
solubility of gypsum in aqueous solutions of, 18: 23536
specific gravity and apparent molal volume of aqueous solutions of, at 25°C, 20: 38905
spectra, absorption maxima for calibrating spectrophotometers, 16: 31534
spectra in alcohol at low temperatures, absorption, 16: 28967(T)
spectra in alcohol and aqueous solutions, absorption, 18: 22074
spectra in molten chloride eutectic, near-infrared, 19: 17870
spectra of hydrated, absorption, 16: 31609 (UCRL-6564-T)
spectra of neodymium ions in, line widths of emission, 16: 21205
spectra of single crystals of, exchange coupling in high-resolution absorption, (E), 20: 20140
spectra of, diffuse reflectance, 18: 13689
spectra of, effects of organic solvents on oscillation absorption bands in, 19: 22192
stability of complex, potentiometric determination of, 19: 17904
structural properties of trichloride, 17: 14210 (NBS-MON-25(Sect.1))
temperature-volume relations in aqueous solutions of, 19: 40523
thermal capacity of aqueous solutions of, at 25°C, 20: 12818 (IS-T-52)
thermal capacity of aqueous solutions of, at 25°C, 20: 29144 (IS-1355)
thermal capacity of aqueous solutions of, at 25°C, 20: 38906
thermodynamic properties, 18: 10108
toxic effects on cats, rabbits, and rats, 19: 3883
toxicity, 18: 35266(R) (UCLA-12-529(p.41-7))
vapor pressure, 17: 8086
vapor pressure, 17: 32118
vapor pressure of trivalent, 16: 30429
vapor pressure over molten, 16: 13077
viscosity of aqueous solutions of, at 25°C, 20: 38904
volume-temperature relationships of aqueous solutions of, at 20 to 80°C, 19: 7355 (IS-992)
alkyl aluminum–$NdCl_3$, catalytic effects of, on directional polymerization of 1,3-butadiene in nitrogen, 19: 2318
CsCl–$NdCl_3$, complex formation in, refractometric studies of, 19: 46254
CsCl–$NdCl_3$, phase studies, 20: 38919
dimethylamine–$NdCl_3$, compound formation in ethanol solutions of, 20: 8936
ethanol–$NdCl_3$, solvent properties for lanthanum, 18: 25620
HCl–$NdCl_3$–$PrCl_3$–TBP–H_2O, separation factors for neodymium and praseodymium in, 20: 40904
HCl–$NdCl_3$–$PrCl_3$–TBP–H_2O, solvent distribution of neodymium and praseodymium in, 20: 7004 (IS-T-42)
HCl–$NdCl_3$–$SmCl_3$–TBP–H_2O, solvent distribution of neodymium and samarium in, 20: 7004 (IS-T-42)
$NdCl_3$–KCl, complex formation in, refractometric studies of, 19: 46254
$NdCl_3$–KCl, composition and thermodynamic functions of vapor phase, 17: 5284
$NdCl_3$–KCl, entropy of formation and vapor hydrolysis, 16: 18911
$NdCl_3$–KCl, formation and stability, 18: 17844
$NdCl_3$–KCl, hydrolysis of, thermodynamics of vapor, 16: 31633
$NdCl_3$–KCl, vapor pressure at 900 to 1200°C, 16: 30430
$NdCl_3$–KCl, vapor pressure over molten, 16: 13077
$NdCl_3$–NaCl, complex formation in, refractometric studies of, 19: 46254
$NdCl_3$–Nd_2O_3, thermodynamic properties, 20: 33319
Nd–$NdCl_3$, free energy of solutions of, 19: 11103
Nd–$NdCl_3$, phase studies and vapor pressure, 17: 35818
Nd–$NdCl_3$, phase studies and properties of, 18: 6832
Nd–$NdCl_3$, vapor pressure at high temperatures, 17: 35843

NEODYMIUM CHROMATES
magnetic ordering in orthorhombic, (E), 20: 24646
preparation and properties, 17: 32104

NEODYMIUM CHROMITES
phase studies, 20: 36812
spectra of, infrared, 20: 36807

NEODYMIUM CITRATES
preparation and composition of, 20: 26897
solubility in perchloric acid solutions, 19: 22244

NEODYMIUM COBALTATES
thermal conductivity, 18: 42070

NEODYMIUM COMPLEXES
bromide, composition and stability of, 20: 29225
hexanitrocobaltate, preparation and composition of, effects of temperature on, 20: 29209
pathological effects of, on liver in rats, 18: 13390(R) (ORINS-43)
properties of, as laser material, 17: 25843(R) (AD-282296)
spectra of organophosphorus-trifluorothenoylacetone, infrared, 17: 6050 (TID-15323)
spectra of, band shifts from nephelauxetic effect in, 20: 45699
spectra of, solvent effects of methanol or light or heavy water on, 20: 14560
stability of cationic nitrate, 17: 14393
stability of, effects of ionic size on, 18: 25389
thiocyanate, stability, 19: 32154
with [(2-hydroxyethyl)imino]diacetic acid, dissociation constant of, 19: 38671
with acetic acid chelates, preparation of mixed, 17: 14259
with acetonitrile, pyridinium salts, and triphenylphosphonium, preparation and properties of, 20: 43231
with acetyl-, benzoyl-, and propionylacetonates, stability of, 18: 25389
with acetylacetone, preparation, properties, and solvates, 16: 10016
with acetylacetone and ethylenediaminetetraacetic acid, magnetic properties at low temperatures, 16: 3016
with α-alanine, formation and structure of, 17: 1487
with α-hydroxyglycolate, isobutyrate, and lactate, formation constants, 16: 11635
with α-picolinic acid and α-picolinic acid *N*-oxide, stability constants, 19: 13307
with aminopolycarboxylates, absorption spectra of, 20: 33279
with amygdalin, separation by solvent extraction using butanol, 20: 1796
with antipyrine-salicylates, benzene solvent extraction studies on, 20: 43256
with ascorbic acid, absorption spectra of, 18: 31527
with beta-diketones, preparation, 19: 5866
with β-hydronaphthazarin and naphthazarin, formation constants and spectra of, 18: 25456
with bicarbonate and carbonate, ion exchange studies, 18: 25438
with bis(acetylacetonylidene)ethylenediamine, absorption spectra, 16: 5347
with butyl phosphates, formation and stability of, 20: 26883
with cadmium, cobalt, or zinc and complexone(III), solubility in water and thermal stability, 19: 22239
with carbonates and fluorides, spectrophotometric analysis, 18: 22075
with chloride ion, preparation and properties of, 18: 41461
with citric acid in alkaline solutions, formation and structure, 19: 405
with citric acid, thermal dissociation of, 17: 1485
with citric acid, preparation and properties of, 18: 41460
with citric and tartaric acids, formation, 16: 193
with cupferron, thermal dissociation, 19: 7366
with dibenzoylmethide, preparation and thermal stability of, 18: 12088
with dibutyl phosphate, solubility in dialkyl phosphoric acids in benzene at 25°, 17: 32148
with dibutyl phosphate, solubility in dibutyl phosphoric acid with various diluents, 17: 32149
with dibutylphosphoric acid, properties, 16: 17686
with diethylenetriaminepentaacetic acid, formation and stability constants of, 17: 16001
with diethylenetriaminepentaacetic acid, composition and properties, 18: 5305
with diglycolic acid, stability constant for, 18: 8338
with diglycolic and dipicolinic acids, thermodynamic properties of, 18: 13733
with dilactic, mandelic, and quinic acids, formation and stability constants of, 20: 12817 (IS-1311)
with dimethyl formamide, preparation and properties of, 20: 35491

with dimethyl formamide, preparation and properties of, 20: 35510
with dimethyl sulfoxide, preparation and composition of, 20: 25051
with dipyridyl, reflection spectra, 19: 15498
with DTPA, EDTA, and nitrilotriacetic acid, chemical structure of, 19: 30189
with DTPA, EDTA, and NTA, spectra of, band splitting in absorption, 20: 8935
with EDTA, heat of formation, 18: 1681
with EDTA, formation and stability of, in aqueous solutions, 20: 8946
with EDTA, preparation, composition, and stability of, 20: 29222
with EDTA, stereochemistry of, 18: 23518
with EDTA, thermal properties of, 20: 18679
with Eriochrome Violet B, dropping mercury electrode and polarographic behavior, 16: 14707
with gluconic acid in aqueous solution, 16: 9993
with gluconic acid, stability constants for, 16: 27012
with gluconic acid, stability of, 18: 1697
with gluconic acids, stability constants, 19: 40508
with glucosaminic acid, composition and stability of, 20: 23036
with glycine, formation and structure of, 17: 1486
with glycine, stability constants, 17: 23326
with glycine, stability constants for, 19: 22227
with glycolic acid, binding energy of, infrared spectrophotometric study of, 19: 44004
with glycolic and lactic acids, thermodynamic properties of, 20: 43215
with glyoxylic acid, formation constant of, 18: 22101
with HEDTA, stability constants of, 16: 32054 (IS-304)
with hexamethylenediaminetetraacetic acid in aqueous solution, formation and stability, 18: 5306
with hydroxycitrate, structure, 18: 43525
with isobutyrate and α-hydroxy- and α,β,β′-trihydroxyisobutyrate ligands, stability constants of, 18: 10124
with mandelic acid and α-methylmandelic acid, stability of, 20: 40902
with methoxyacetic, propionic, and thioglycolic acids, formation constants of, 18: 17859
with methylethyl and methylpropyl glycolates, stability of, 18: 22095
with *N*-(hydroxyethyl)ethylenediaminetriacetic acid, electrophoresis of hydrolysis products of, 17: 14264
with *N,N′*-dimethyl-*N,N′*-dinitrosoterephthalamide, mechanism of formation of, 19: 38600
with nicotinic acid and hexathiocyanatochromium in aqueous solutions, formation and stability of, 17: 18080
with nicotinic acid, formation and stability, 17: 35832
with nitric acid, formation and stability, 16: 31627
with nitrilotriacetic acid, enthalpy and entropy of formation, 16: 11601
with nitrilotriacetic acid, ion exchange chromotography of, 16: 30412
with nitrilotriacetic acid, properties and structure of hydrated, 18: 17838
with octyl phosphate, solubility in dialkyl phosphoric acids in benzene at 25°, 17: 32148
with organic reagents, preparation and stability of colored, 18: 27366
with organophosphorus compounds and thenoyltrifluoroacetone, spectra of, 17: 18203
with *p*-hydroxybenzoic acid, preparation and stability of, 18: 13825
with phenanthroline in aqueous solutions, absorption spectra of, 17: 1484
with phenanthroline, infrared spectra of, 20: 16437
with potassium bicarbonate and carbonate, formation constants of, 18: 13751
with potassium carbonate, distribution coefficient and structure, 16: 22055 (TID-16027)
with pyrocatechol and pyrogallol in alkali solutions, formation and structure of, 18: 31521
with pyrogallosulfonic acid, formation of, potentiometric and spectrophotometric studies of, 20: 36837
with S-ethylthioglycolate and mercaptopropionate ions, stability constants of, 17: 25102
with salicylic acid, preparation and stability of, 18: 13825
with selenoylacetone and selenoyltrifluoroacetone, stability of, 20: 26813
with serine, stability and composition, 19: 19874
with serine, stability of, 20: 29208
with sodium triphosphate, preparation, 19: 17880
with sulfosalicyclic acid, spectra of, effects of other rare earths on absorption, 20: 40926
with tartaric acid and trihydroxyglutaric acid, stability constants for, 20: 36838
with terpyridine, composition and spectra of, 19: 30193
with thenoyltrifluoroacetone, magnetic susceptibilities of, 20: 16416(R) (NYO-906-68)
with triethylenetetraminehexaacetic acid, spectra of, absorption, 20: 25106
with triphenylphosphine oxide, properties and spectra of, 19: 42466
with trisbenzoylacetonate and trisbenzoylmethide chelates, luminescence, 16: 14739
with 1,10-phenanthroline, formation and solubility of, 18: 1685
with 1-hydroxycyclopentanecarboxylic acid, stability of, 20: 26910
with 1-hydroxycyclopentanecarboxylic acid, preparation, properties, and structure of, 20: 26837
with 1,10-phenanthroline, magnetic properties and structure of acetate and nitrate, 19: 36405
with 1,10-phenanthroline–thenoyltrifluoroacetone, preparation and composition of, 20: 29221
with 1,2-dihydroxybenzene-3,5-disulfonic acid, absorption spectra of, 18: 13827
with 2,2′-bipyridyl, infrared spectra of, 20: 16437
with 2,2,6,6-tetramethyl-3,5-heptanedione, preparation and volatility of, 20: 7074
with 2,4-hexanedione, formation of, 18: 35546
with 2,4-pentanedione, preparation, 20: 16434
with 2,4-pentanedione and bipyridine or 1,10-phenanthroline, spectra and structure of, 20: 26887
with 2,4-pentanedione, solubilities of, in solvents, 17: 23446
with 8-quinolinol, composition and thermal stability of, 18: 17784

NEODYMIUM COMPOUNDS
see also Phlogodym
analysis for trace elements, spectrographic, 16: 28869 (JEN-107-DQ/I-33)
deposition on silicon, 18: 34034(R) (BMI-1672(Del.))
deposition on silicon wafers, 19: 2716(R) (BMI-1681(Del.))
preparation and properties of argentocyanide, 16: 8747
solubility constants of phthalic and sebacic acid salts, 16: 11563
solubility in water and thermolysis of diliturate, 18: 31447
spectra of 4f transitions in tricyclopentadienide, in 2-methyltetrahydrofuran, 19: 22186
stability of picolinates, 19: 7367
synthesis of organic, using organic acids, 19: 7523
with fatty acids, preparation and properties of, 20: 25076
with potassium suboxide, formation and properties of, 20: 25045

NEODYMIUM ETHYL SULFATES
cerium isotope nuclear alignment in, 16: 8170 (UCRL-9872)
cerium nucleus alignment in, 16: 31097
cerium-137m hyperfine structure constants in, 19: 1624
cerium-139 and -141 gamma spectra in, plane polarization of, 18: 21274
crystal field cleavage in, 17: 8087
crystal field parameters for, 19: 15545
electron spin below 1°K, relations of, with entropy and temperature, 20: 22859(R) (UCRL-16580, pp 149-205)
electron spin resonance of crystals of, 20: 36855
energy-level populations of neodymium ions in, 16: 33631
energy levels at low temperatures, effects on specific heat of, 19: 11046(R) (AROD-2099:22)
gamma distribution from cerium-141 in, 16: 26242
magnetic temperature scale, 19: 47883 (UCRL-16279)
paramagnetic relaxation time of, method of determining, 19: 11046(R) (AROD-2099:22)
paramagnetic resonance in, magneto-optical Faraday effect in, 17: 10617
promethium isotope alignment in, coupling constants and magnetic moments determined by, 17: 19351
quadrupole hyperfine structure of europium isotopes in, 17: 11647 (UCRL-10202)
rare earth ion orientation in, quadrupole coupling constants from, (E), 20: 20146
rare earth ion quadrupole coupling in lattices of, 19: 47883 (UCRL-16279)
rare-earth quadrupole crystal-field shielding in, systematic variation of, (E), 20: 17996
spectra of, analysis of polarized absorption, 17: 35748
spectra of crystalline, electronic, 19: 11046(R) (AROD-2099:22)
spectra of, determination of energy levels and thermal capacity from, 17: 39049
spin lattice relaxation in, 18: 1651
spin level saturation in, magneto-optical Faraday effect measurement of, 17: 10617
temperature scale for, below 1°K, 20: 17614
thermal decomposition, effects of atmosphere, particle size, and upheat rate on, 16: 13048

NEODYMIUM FERRATES
structure of yttrium substituted, 16: 5320

NEODYMIUM FERRATES(III)
crystal structure, 19: 46256

NEODYMIUM FERRICYANIDES
electrochemical properties in aqueous solutions, 18: 6829

NEODYMIUM FLUORIDES
deposition of films of, vapor, 19: 7352 (BMI-1706)
deposition on silicon wafers, 19: 13871(R) (BMI-1691(Del.))
dielectric properties of thin films of, 20: 22324
effects on freezing point depression in sodium fluoride, 18: 5284
energy levels in, coupling of negative hydrogen- and deuterium-ion localized modes to, (E), 20: 32709
fluorine-19 NMR in, (E), 20: 10263(T)

molecular structure of gaseous, electron diffraction studies of, 20: 31222(T) (ANL-Trans-310)
preparation and magnetic moments, 20: 7089
preparation of laser-quality single crystals of, 20: 26362
solubility in beryllium nitrate solutions, 19: 40670
$LiF-NdF_3$, phase studies, 19: 30149(R) (ORNL-3789(p.3-35))
NdF_3-NaF, phase diagrams at 300 to 1300°C, 20: 33278
NdF_3-NaF, phase studies, 19: 30149(R) (ORNL-3789(p.3-35))
NH_4F-NdF_3, chemical properties and crystal structure, 18: 16013

NEODYMIUM FORMATES
decomposition thermograms, 16: 22067(T) (AEC-tr-4460(p.157-62))
preparation and properties, 19: 30163
preparation of, microscopical identification of spherulites in, 18: 10055
structure, 16: 33001

NEODYMIUM GALLATES
structural properties of $Nd_3Ga_5(GaO_4)_3$, 17: 14210 (NBS-MON-25(Sect.1))

NEODYMIUM GERMANATES
crystal structure of, ir spectral studies on, 20: 43218

NEODYMIUM GERMANIUM SULFIDES
preparation and structure of, 20: 23680

NEODYMIUM HAFNATES
preparation and properties, 17: 33889
preparation by reaction of hafnium and neodymium hydroxides, 19: 22191

NEODYMIUM HALIDES
magnetic properties, 19: 9046(R) (IS-900(Sect.C))

NEODYMIUM HYDRIDES
crystal structure, 16: 7567
formation and properties, 17: 1464
magnetic moments, 16: 24173(R) (TID-15819)
magnetic properties at 4.2–300°K, 17: 37710
preparation and properties of, 19: 15466(T) (LA-tr-65-2)
properties and structure, 20: 16453
properties as radiation targets at high temperatures, 18: 18518
spectra of, effects of organic solvents on oscillation absorption bands in, 19: 22192
spectra of, effects of deuterium on infrared, 20: 14568

NEODYMIUM HYDROXIDES
preparation and properties of, 19: 34153(T) (ORNL-tr-661)
preparation and structure of, 19: 42865
reactions with hafnium hydroxides at 100 to 1000°C, 19: 22191
reactions with hydrogen peroxide, 16: 6410
thermal decomposition of, thermographic and x-ray studies on, 20: 25061
$HfO_2-Nd_2O_3$, crystallization of, from reactions of hafnium and neodymium hydroxides, 19: 22191

NEODYMIUM IODATES
solubility of, in water, 20: 45656

NEODYMIUM IODIDES
electric conductivity and magnetic susceptibilities of, 18: 4281
heats of fusion and transition, 17: 28870
magnetic susceptibility at 77 to 550°K, 18: 29626
molecular structure of gaseous, electron diffraction studies of, 20: 31222(T) (ANL-Trans-310)
preparation and structure of tri-, 18: 29602 (LADC-6087)
preparation of hydrates of, 18: 39227
spectra of gaseous, liquid, and solid, energies and intensities of oscillation absorption bands in, 20: 35499
vapor pressure, 17: 8086
$Nd-NdI_3$, electric conductivity and magnetic susceptibilities of, 18: 4281

NEODYMIUM IONS
crystal field potential in calcium fluorides, 18: 27435
crystalline electric field for, origin of, (T), 19: 15545
distribution between phases in boron oxide–sodium chloride–sodium oxide system at 830°C, 18: 33534 (USNRDL-TR-760)
effects on fluorescence of praseodymium-doped lanthanum fluorides, 19: 28309
effects on fluorescence decay of samarium ions in lanthanum chloride crystals, 20: 30782
effects on ground-state splitting in calcium fluoride and strontium fluoride, (T), 19: 9898(T) (JPRS-27372(p.32-5))
effects on lithium niobates, doping, 20: 43242
effects on spectrophotometric determination of erbium, holmium, and neodymium, 20: 43100
electron energy levels and Stark splitting of, in calcium fluoride crystals, 19: 4142
electron paramagnetic resonance of trivalent, in strontium titanate, 18: 2466
electron paramagnetic resonance spectra of trivalent, in strontium titanates, 18: 2467
electron paramagnetic resonance in calcium fluorides, spin-lattice relaxation in, 18: 23527
electron paramagnetic resonance of trivalent, in calcium fluoride, 19: 7512
electron paramagnetic resonance in calcium fluorides, spectral study of, 19: 23980
electron paramagnetic resonance of tetravalent, in calcium fluorides, (E), 19: 41999(T)
electron paramagnetic resonance spectra in lanthanum compounds, 20: 40312
electron spin relaxation time of trivalent, temperature dependence from spin echo studies of, 17: 37787
electron spin resonance of trivalent in hexa-antipyrene iodides, 16: 13074
electron spin resonance of trivalent, hyperfine structure constants from, 17: 37785
electron spin resonance of trivalent, in cadmium sulfide single crystals at 1.4°K and X-band, 18: 5857
electron spin resonance of, 20: 2520(R) (IA-920)
electron spin resonance spectra in lanthanum chlorides and lanthanum bromides, (E), 20: 28653
elution from resin using ammonia-EDTA solutions, 16: 86 (IS-218)
energy exchange to ytterbium ions in calibo glass, (E), 19: 29463
energy level lifetime of trivalent, in calcium fluoride and calcium fluoride and calcium tungstate, (E), 19: 32174
energy-level populations in, in rare-earth ethyl sulfates, 16: 33631
energy levels and crystal-field splittings in yttrium oxides, 20: 30744
energy levels of trivalent, configuration-interaction effects on, 19: 32145
energy transfer from chromium ions to, in lanthanum aluminates, (E), 19: 4150
energy transfer from 4,4′-dimethoxybenzophenone to, effects of terbium ions on two-step, 19: 7387
energy transfer to, from uranyl ions in barium crown glass, radiationless resonance, 18: 24223
energy transfer to ytterbium ions in barium glass, 19: 14241
energy transfer to ytterbium ions in lithium magnesium aluminosilicate glass, (E), 19: 14241
energy transfer to ytterbium ions in silicate glass, luminescence in, 19: 25172(T)
Faraday rotation in calcium fluoride crystals, 18: 5936
fluorescence in lanthanum aluminates, energy transfer from chromium in, 18: 31621
fluorescence in lanthanum chlorides and fluorides, mechanism of concentration quenching of, (E/T), 20: 12297
fluorescence in praseodymium chloride crystals, infrared, 18: 795
fluorescence in praseodymium chloride crystals, 18: 37241
fluorescence of trivalent, in lanthanum trichloride, 20: 26344 (N-65-34948)
fluorescence of, under electron bombardment, 18: 27508
fluorescent properties of trivalent, in crystals, 17: 37177
fluorescent properties in gadolinium oxides, 18: 14598
hydrolysis in aqueous solutions of sodium perchlorate at 25°C, constants for, 20: 43221
hyperfine interactions in tetravalent, constants for, 17: 37686
interactions in lanthanum ethyl sulfate, nondipolar, 19: 2389
interactions in lanthanum chloride, EPR determination of sign of, 20: 45027
laser action and absorption and luminescence spectra of trivalent, in strontium fluoride crystals, 17: 20028(T)
laser emission by cerium fluoride crystals containing, 18: 26119
laser oscillations in barium crown glass containing ytterbium and uranyl ions, 20: 8291
light emission in barium crown glass containing uranyl ion, stimulated, (E), 19: 14239
magnetic moment of trivalent, (E), 19: 7431
magnetic moments with respect to gadolinium ions in aluminium–gadolinium–neodymium alloys, antiparallel, 17: 37775
magnetic moments with respect to terbium ions in aluminium–neodymium–terbium alloys, antiparallel, 17: 37775
magnetic resonance effects in yttrium iron garnets, 16: 9996
magnetic resonance in lutetium aluminate and gallate, 16: 15261 (AFCRL-987)
Maser oscillations of, in calcium tungstate at 0.9 and 1.35 μ, 17: 34605
nuclear magnetic properties of, in lanthanum trichlorides, 16: 33894
optical maser properties in calcium fluorides at 77°K, 16: 12250
optical maser properties in strontium molybdates at 77°K, 16: 12251
paramagnetic resonance spectra of, in calcium fluoride crystal field, 17: 2935 (AD-274000)
paramagnetic resonance in calcium tungstate crystals, lattice sites from, 17: 35712
paramagnetic resonance linewidth of trivalent, in lanthanum magnesium nitrate, (E), 19: 5891
preparation of cerium oxide single crystals containing, (E), 20: 43818
preparation of tetravalent, 16: 1675
production of beams of, in magnetron gas discharges, 18: 7417
radioinduced reduction of trivalent, in strontium fluorides in presence of dysprosium, erbium, gadolinium, holmium, or thulium, gamma, 20: 26982(T)
reactions of trivalent, with chromate ions, quantitative precipitation in, 20: 45585
reactions with cadmium sulfide crystals at 200 kev, replacement collision doping by, (E), 19: 44939

reactions with external magnetic field, calculation of matrix elements in, 18: 4408(T)
reduction mechanisms of alcoholic lithium chloride solutions of trivalent, polarographic studies of, 17: 4507
sorption by powdered silver iodide, effects of acidity on, 19: 13331
spectra and coupling energy levels of trivalent, in lanthanum fluoride, 19: 22209
spectra in alcohol–water solutions, 16: 30397
spectra in barium, calcium, and strontium fluorides, absorption and luminescence, 19: 19854
spectra in calcium fluoride crystals, 17: 29414
spectra in calcium fluorides, stimulated emission of infrared, 18: 22067
spectra in crystalline salts, line widths of emission, 16: 21205
spectra in glass, concentration dependence of fluoresence, 19: 47887(T) (N64-21857, pp 7-12)
spectra in lanthanum fluoride single crystals, optical absorption, 17: 31177
spectra in lanthanum bromide, comparison with lanthanum chloride, 19: 11046(R) (AROD-2099:22)
spectra in lanthanum trifluoride, absorption, 19: 11046(R) (AROD-2099:22)
spectra in praseodymium chloride crystals, infrared-optical double resonance, (E), 19: 26356
spectra in praseodymium–neodymium-doped lanthanum fluoride, optical linewidth and line-shape studies of energy transfer mechanisms in, (E), 20: 2627
spectra in silicate glass, fluorescence, 19: 47886(T) (N64-21857, pp 1-6)
spectra in yttrium chloride, magnetic properties in paramagnetic resonance, 18: 39212
spectra of, in lanthanum bromide and chloride crystals, covalency effects on shifts in, 17: 27311 (AROD-2099.12)
spectra of, in lanthanum bromides and chlorides, 17: 37247
spectra of trivalent, in lanthanum chlorides, 18: 772
spectra of trivalent, in yttrium oxide at 77°K, 18: 5854
spectra of trivalent, level schemes in, 20: 25101
spectra of, calculation of nephelauxetic parameters in, 20: 33291
spectra of, effects of nitrate ions on, 20: 10848
spectra of, effects of chemical bonding and transitions on, 20: 36845
spectra, time-resolved, 16: 20430
spectrum in lanthanum chloride, absorption, 19: 11046(R) (AROD-2099:22)
spectrum in silicate glass, emission, 16: 15126(R) (NP-11584)
spectrum of, in lanthanum chloride crystals, 18: 27401
spin-lattice relaxation rates at 1.4 to 5°K for, in double nitrates and lanthanum ethyl sulfates, 16: 27813
spin-lattice relaxation of trivalent, in lanthanum magnesium nitrate, 16: 27814
spin-lattice relaxation rate of trivalent, in lanthanum double nitrate and ethyl sulfate at 1.4 to 5°K, 18: 2484
spin-lattice relaxation of trivalent, in lanthanum double nitrate at $T \leq 1.5$°K, direct phonon bottleneck process in, 18: 2485
spin lattice relaxation in rare earth salts at 1.2 to 5°K, (E), 20: 28644
spin-lattice relaxation in salts, magnetic field dependence of (E), 19: 2335
spin-lattice relaxation in magnesium neodymium nitrates, magnetic field dependence of, 19: 5921
spin-lattice relaxation rate in garnets, 19: 14121 (AD-608278)
spin-lattice relaxation rates in single crystals of anhydrous lanthanum trichloride, (E), 20: 6542
spin-lattice relaxation of trivalent, in lanthanum chlorides, (E), 20: 12292
spin-lattice relaxation in yttrium ethyl sulfates, (E), 20: 12300
spin-lattice relaxation time in lanthanum trichloride, angular and temperature effects on, 20: 40350
spin-lattice relaxation of, in lanthanum fluorides, 20: 42540
spin-spin coupling in lanthanum ethyl sulfates, free induction signal from, (T), 20: 30778

NEODYMIUM ISOPROPOXIDES
preparation and properties of, 20: 25075

NEODYMIUM ISOTOPES
abundance in irradiated uranium-235, 19: 36217(R) (IDO-14656)
alpha decay systematics for, 17: 7199
carbon-12 reactions with, 17: 41871 (UCRL-10541)
content in Arkansas rain water in Oct. 1964, 20: 16685
diffusion in zirconium at 1000°C, 18: 32136(R) (BMI-X-10093)
energy levels, interactions, nuclear moments, and transitions in, 17: 24381 (AD-403411)
excited states in even, first, 16: 12518
gamma reactions on, cross sections for, 19: 12496
ion reactions with, neutron and photon emission in heavy, 17: 36666 (UCRL-10099(Rev.))
mass differences of, (E), 20: 22153
nuclear gyromagnetic ratios and quadrupole moments, 16: 21446
photon reactions (γ,n), cross sections for, (E), 19: 21287
preparation of self-supporting foils of, 20: 31696
production in fission of uranium-233 and -235, poisoning from, 18: 15473 (ORNL-TM-781)
production in plutonium-239 fission, 18: 38085(T) (AEC-tr-6398(p.288-95))
production in thermal-neutron fission of uranium-235, (E), 19: 45260(R) (IDO-14660)
spectra of, shifts in x-ray, 18: 17064(T)
use of stable, in fuel burnup determination, 19: 28222 (IDO-14642)
yields from thermal-neutron fission of thorium-229, 20: 28303
yields from uranium-235 fission, 18: 34006(R) (ORNL-TM-889)
yields in fission of plutonium-239, uranium-233, and uranium-235, 19: 10510(R) (GEAP-4716)
yields in thorium-232 helium-ion fission, 17: 22567 (UCRL-10673)
yields in uranium-233 thermal fission, (E), 20: 3010(R) (IDO-14663)
yields of, in proton spallation of tantalum at 660 Mev, 18: 4576 (NP-13165(Vol.2)(p.87-100))

NEODYMIUM ISOTOPES Nd-137
beta decay schemes and existence of, (E), 19: 10244 (JINR-P-1857)
decay scheme and half life, (E), 20: 10004

NEODYMIUM ISOTOPES Nd-138
beta decay, (E), 20: 42197
beta decay of, half life for, (E), 20: 22002 (JINR-P-2570)
decay of, conversion electron and gamma spectra of, (E), 19: 12613

NEODYMIUM ISOTOPES Nd-139
beta decay schemes, (E), 19: 10244 (JINR-P-1857)
conversion electron spectra, 18: 7713
decay of isomeric, (E), 19: 12613
gamma spectra, 18: 7713
isomeric state with energy of 232.5 kev, 18: 7725

NEODYMIUM ISOTOPES Nd-140
auger K-electron spectra, 16: 15655
book: *Isobaric Nuclei with Mass Number A = 140*, 18: 2961
decay, auger electron spectra from, 16: 15625 (JINR-P-483(Pt.III))
decay of isomeric, (E), 19: 5261
decay scheme, 18: 4572 (NP-13165(Vol.2)(p.42-9))
decay scheme and energy level, 16: 31125
energy levels of, spin values for three-particle isomeric, 18: 28614
energy levels of, properties of collective, (E), 19: 6671
gamma spectra and half life of isomeric, 19: 29258 (NP-15050)
isomers, existence of new short-period metastable, 16: 17147

NEODYMIUM ISOTOPES Nd-141
decay of, praseodymium-141 levels from, (E), 20: 30416
decay scheme, 18: 9339
decay scheme for, (E), 20: 26084 (JINR-P-2618)
decay scheme for, electron-capture and positron, 17: 31460
determination of metastable, by gamma spectra, 19: 11585
determination of, by neutron activation of stable elements, 20: 33207
gamma spectra, (E), 19: 16840(R) (IDO-17050)
gamma transitions in, effects of radial matrix elements on probabilities of M4, 18: 2861
hyperfine structure, magnetic moment, and spin, 16: 7021 (UCRL-9850)
isomeric transitions, 17: 17147
nuclear spin, 16: 20305(R) (UCRL-10023)
nuclear spin, 17: 4065 (UCRL-9774)
production from neutron reactions (n,2n) with neodymium 142 at 14.7 Mev, 20: 13864
production of isomeric states in yttrium-89 (n,n′γ) reactions at 14 Mev, cross sections for, (E), 19: 41781

NEODYMIUM ISOTOPES Nd-142
atomic mass, (E), 20: 15769
boron-10 and -11 reactions with, terbium-149 isomeric excitation functions from, 17: 26573
carbon-12 reactions with, angular momentum effects on neutron emission in, 17: 26470 (UCRL-10767)
decay of, quasi-particle, 18: 32745(R) (UCRL-11213(p.1-48))
determination in fuels spiked with neodymium-150, equations for, 18: 15487(R) (GEAP-4361)
deuteron reactions (d,d′γ) at 12 Mev, 0+ states from, 19: 41747
deuteron reactions (d,p) at 10 to 12 Mev, energy levels from, (E), 20: 30517
deuteron reactions (d,p), 20: 46580(R) (BMwF-FBK-66-05)
effects on proton polarization in lanthanum magnesium nitrates, 18: 23444 (JINR-P-1626)
effects on proton polarization in magnesium lanthanum nitrate in magnetic field, (E), 19: 9884 (JINR-P-1868)
effects on spectrum of neodymium, mass, 20: 1826
energy levels, 19: 14598
energy levels from (p,p′γ) and (d,d′γ) reactions at 12 Mev, 0+, (E), 19: 41747
gamma scattering by, resonance, 18: 11175 (ANL-6797(p.275-87))
gamma transitions, coefficients of internal pair formation, 16: 12532
helium-4 reactions (He-4,4n), angular momentum effects on excitation functions for, (E), 20: 17784
meson (μ^-) capture by, x-ray spectra from, (E), 20: 29525 (CONF-660209-9)
neutron activation cross sections, 17: 10139
neutron cross sections at 0.414 ev to 10 Mev, 16: 9427 (GA-2451

(Vol.III))
neutron reactions (n,2n), isomeric yields, 16: 6253 (ARGMA-TN-2H1N-30)
neutron reactions (n,2n) with, cross sections for positron production in, 18: 13061
neutron reactions (n,2n) at 14 Mev, shell effects in, (T), 19: 12536
neutron reactions (n,2n) at 14 Mev, cross sections for neodymium-141 isomeric states from, (E), 19: 41781
neutron reactions (n,2n) at 14.7 Mev, neodymium-141 production from, (E), 20: 13864
neutron reactions (n,α) and (n,2n) at 14.7 Mev, cross sections for, (E), 20: 13864
oxygen-16 reactions (O^{16},xn) and (O^{18},pxn) with, excitation functions for, 17: 34954
oxygen-16 scattering at 31 to 45 Mev, B(E2) values for transitions from, (E), 20: 17734
photon reactions (γ,n), cross sections for, (E), 19: 21287
production of isomeric, (E), 19: 10318
proton inelastic scattering by, isobaric analog states in, 20: 46580(R) (BMwF-FBK-66-05)
proton reactions (p,p′γ) at 12 Mev, 0+ states from, (E), 19: 41747
proton reactions (p,3n) with, energy levels from, 20: 40131
proton reactions (p,γ) in stars, 16: 12308
reactions with carbon-12, equilibrium charge distribution in, 17: 24750(R) (UCRL-10624)
x-ray spectra of μ-mesic atoms of, (E), 20: 23888
yields in plutonium-241 thermal fission, (E), 19: 8495

NEODYMIUM ISOTOPES Nd-143
atomic mass, (E), 20: 15769
bremsstrahlung reactions (γ,n) at 22 Mev, isomeric states in, (E), 19: 10318
burnup calculations for, in reactor fuels, 20: 16061(R) (BAW-296)
core isomerism in, (T), 19: 17051
determination in irradiated uranium rod, mass spectrometric, 17: 33833
determination in uranium-233 and -235 fission products, (E), 20: 11960(R) (IDO-14667)
energy level lifetime, 0.74-Mev, 18: 9335
energy levels from neodymium-142 (d,p) reactions, (E), 20: 30517
energy levels of, (T), 20: 30350 (JINR-P-2682)
hyperfine spin lattice relaxation in neodymium-doped magnesium lanthanum nitrate, (E), 20: 28644
hyperfine structure and nuclear moments of, 17: 21068
magnetic properties of, in lanthanum trichlorides, 16: 33894
neutron capture at thermal energies, alpha spectra and branching ratios from, 16: 28124
neutron capture by, gamma spectra from thermal, (E), 20: 3131
neutron capture by, neutron separation energy determination from, (E), 20: 30366
neutron cross sections at 0.414 ev to 10 Mev, 16: 9427 (GA-2451 (Vol.III))
neutron reactions (n,γ), 16: 28055
neutron reactions with, resonances in, 18: 17035
neutron reactions with, radiation widths for resonance, 18: 17036
neutron reactions (n,α), cross section and Qα for, 19: 35615(R) (NP-15037)
neutron reactions (n,α) with, cross sections for thermal, (E), 19: 41809(T)
neutron reactions with, resonances in, (E), 19: 45296
nuclear magnetic moments, 16: 1054
nuclear magnetic moments, 16: 16831
nuclear magnetic moment, (E), 20: 17997
nuclear moments of, E2 and M1, (E), 20: 10077
oxygen-16 scattering at 31 to 45 Mev, B(E2) values for transitions from, (E), 20: 17734
proton elastic scattering by, 20: 46580(R) (BMwF-FBK-66-05)
spin, 16: 17128
yields from uranium-235 fission by thermal neutrons, 16: 23079
yields from uranium-235 thermal fission, 19: 29313
yields from uranium-235 thermal fission, 20: 28749(R) (GEAP-5060)
yields in neutron fission of plutonium-239, uranium-233, and uranium-235, 20: 15133(R) (GEAP-4893)
yields in plutonium-241 thermal fission, (E), 19: 8495
yields in thermal neutron fission of uranium-233 and -235, 20: 43067(R) (IDO-14679, pp 6-46)

NEODYMIUM ISOTOPES Nd-144
alpha activity and half life of, 19: 31305
alpha decay of, data review on, 18: 13071
alpha decay of, energies and rates for, 18: 26640
atomic mass, (E), 20: 15769
carbon nucleus reactions with, measurements of various parameters of, 17: 11645 (UCRL-10099)
carbon-12 reactions with, angular momentum effects on neutron emission from, 17: 26470 (UCRL-10767)
carbon-12 reactions (C-12,7n) at 108 Mev, recoil ranges in, 18: 24734
carbon-12 reactions (C-12,xn) with, neutron and photon emission in (E), 19: 3339
decay of, gamma-gamma angular correlation and intensity from, 17: 31423
determination in uranium-233 and -235 fission products, (E), 20: 11960(R) (IDO-14667)
effects on spectrum of neodymium, mass, 20: 1826
electric dipole transitions in, nuclear structure effects on internal pair formation for, 18: 26581
energy level at 2.18 Mev, lifetime of, 18: 6248
energy level de-excitation characters for, experimental 1^-, 17: 17201
energy levels, 17: 40040
energy levels, 18: 6248
energy levels and gamma spectra of, 18: 17013
energy levels from thermal neutron capture by neodymium-143, (E), 20: 3131
energy levels of, wave functions for ground-state, 17: 857
energy levels of, E1 transition from and lifetime of octupole, (T), 20: 19979
energy levels, polarized gamma-gamma angular correlations, 17: 19256
energy transitions in, from promethium-144 beta decay, (E), 20: 12081
gamma resonant elastic scattering by, cross section for excitation of 2.18-Mev level in, 18: 6248
gamma spectra, 16: 1032(T) (AEC-tr-4685)
half life, 16: 23033
mass difference of samarium-144 and, 18: 32825
meson (μ^-) capture by, x-ray spectra from, (E), 20: 29525 (CONF-660209-9)
neutron cross sections at 0.414 ev to 10 Mev, 16: 9427 (GA-2451 (Vol.III))
oxygen-16 scattering at 31 to 45 Mev, B(E2) values for transitions from, (E), 20: 17734
production from neutron capture by neodymium-143, neutron separation energy determination from, (E), 20: 30366
production in neutron capture by neodymium-143, spin and parity from, 16: 28124
proton inelastic scattering by, 20: 46580(R) (BMwF-FBK-66-05)
proton reactions (p,n) with, 19: 6645
separation from other nuclides, ion-exchange methods for, 17: 211
sorption by humic acids and peat, 16: 11591
x-ray spectra of μ-mesic atoms of, (E), 20: 23888
yields from uranium-235 fission by thermal neutrons, 16: 23079
yields from uranium-235 thermal fission, 19: 29313
yields from uranium-235 thermal fission, 20: 28749(R) (GEAP-5060)
yields in neutron fission of plutonium-239, uranium-233, and uranium-235, 20: 15133(R) (GEAP-4893)
yields in plutonium-241 thermal fission, (E), 19: 8495
yields in thermal neutron fission of uranium-233 and -235, 20: 43067(R) (IDO-14679, pp 6-46)
Zeeman splitting, g values, 16: 5824

NEODYMIUM ISOTOPES Nd-145
alpha decay energy, 18: 13071
atomic mass, (E), 20: 15769
Coulomb excitation at levels to 1.8 Mev, 18: 9335
determination in uranium-233 and -235 fission products, (E), 20: 11960(R) (IDO-14667)
half life, 19: 31305
hyperfine structure and nuclear moments of, 17: 21068
magnetic properties of, in lanthanum trichlorides, 16: 33894
neutron capture at thermal energies, alpha spectra and branching ratios from, 16: 28124
neutron cross sections at 0.414 ev to 10 Mev, 16: 9427 (GA-2451 (Vol.III))
neutron reactions (n,γ), 16: 28055
neutron reactions with, resonances in, 18: 17035
neutron reactions with, radiation widths for resonance, 18: 17036
neutron reactions with, resonances in, (E), 19: 45296
nuclear magnetic moment, (E), 20: 17997
nuclear moments of, E2 and M1, (E), 20: 10077
oxygen-16 scattering at 31 to 45 Mev, B(E2) values for transitions from, (E), 20: 17734
photon reactions (γ,n), threshold energy for, (E), 19: 21287
spin, 16: 17128
yields from uranium-235 fission by thermal neutrons, 16: 23079
yields from uranium-235 thermal fission, 19: 29313
yields from uranium-235 thermal fission, 20: 28749(R) (GEAP-5060)
yields in neutron fission of plutonium-239, uranium-233, and uranium-235, 20: 15133(R) (GEAP-4893)
yields in plutonium-241 thermal fission, (E), 19: 8495
yields in thermal neutron fission of uranium-233 and -235, 20: 43067(R) (IDO-14679, pp 6-46)

NEODYMIUM ISOTOPES Nd-146
abundance in meteorites and terrestrial matter, 18: 10753
alpha decay energy, 18: 13071
alpha inelastic scattering by, nuclear alignment effects in, 16: 32420
atomic mass, (E), 20: 15769

boron-10 and 11 reactions with, angular momentum effects on neutron emission in, 17: 26470 (UCRL-10767)
boron-10 reactions with, terbium-149 isomeric excitation functions from, 17: 26573
boron-11 reactions (B-11,8n) with, anisotropy of terbium-149 production in, 18: 32747(R) (UCRL-11213(p.64-86))
carbon nucleus reactions with, measurements of various parameters of, 17: 11645 (UCRL-10099)
determination in uranium-233 and -235 fission products, (E), 20: 11960(R) (IDO-14667)
effects on spectrum of neodymium, mass, 20: 1826
energy level transitions in, from promethium-146 decay, (E), 20: 12081
energy levels, 17: 40040
energy levels of, (E), 19: 8448
energy levels of, E1 transition from and lifetime of octupole, (T), 20: 19979
gamma reactions (γ,p) with, 19: 6644
meson (μ⁻) capture by, x-ray spectra from, (E), 20: 29525 (CONF-660209-9)
neutron binding energies in, anomalies in, (T), 19: 14523 (JINR-E-1924)
neutron cross sections at 0.414 ev to 10 Mev, 16: 9427 (GA-2451 (Vol.III))
neutron reactions (n,γ) with, production of carrier-free promethium-147 by, 18: 20071
oxygen-16 scattering at 31 to 45 Mev, B(E2) values for transitions from, (E), 20: 17734
rotation states of deformed axial symmetry in, 17: 19282
separation from other nuclides, ion-exchange methods for, 17: 211
x-ray spectra of μ-mesic atoms of, (E), 20: 23888
yields from uranium-235 fission by thermal neutrons, 16: 23079
yields from uranium-235 thermal fission, 19: 29313
yields from uranium-235 thermal fission, 20: 28749(R) (GEAP-5060)
yields in neutron fission of plutonium-239, uranium-233, and uranium-235, 20: 15133(R) (GEAP-4893)
yields in plutonium-241 thermal fission, (E), 19: 8495
yields in thermal neutron fission of uranium-233 and -235, 20: 43067(R) (IDO-14679, pp 6-46)

NEODYMIUM ISOTOPES Nd-147

beta decay, (E), 20: 15810
beta decay of, promethium-147 excited states from, 18: 6232
beta decay of, promethium-147 91-kev level lifetime from, (E), 20: 9985
beta decay spectrum, 19: 12494(T) (AEC-tr-6227/3(p.157-66))
beta spectra, 16: 15689
beta spectra, 17: 7113 (NP-12330(p.166-71))
beta transitions in, polarization from, (E), 20: 4880
beta transitions in, first-forbidden, (E), 20: 12139
chemical behavior in trace quantities, 17: 2960(T) (UCRL-Trans-599(L))
content in atmosphere from underground nuclear explosion, effects of filtering on, 20: 45833 (UCRL-14778)
content in fallout particles, 20: 2053
content in rain water, Fayetteville, Arkansas, Oct. 1964, 20: 16663 (TID-21470)
content in rainwater at Milan following Chinese nuclear explosions, 19: 42643
decay, (E), 19: 16913
decay of, gamma branching in (E), 19: 3240 (ORNL-P-169)
decay of, gamma branching ratios for, (E), 20: 22091
decay, (E), 19: 5156
determination in air by beta measurement, efficiency of counter for, 19: 20169
determination in dust samples, spectrometric, 16: 27461
determination of, gamma spectrometric, 19: 32545 (CEA-R-2461)
diffusion in irradiated artificial graphite, 18: 632
distribution and volatility in air-burst debris, 20: 9184 (USNRDL-TR-933)
distribution from nuclear excavation in basalt, 20: 613
energy levels of, spins and parities of, 18: 21208 (NP-13841)
gamma dose constants for, 20: 46617
half life, 17: 38111
neutron binding energies in, anomalies in, (T), 19: 14523 (JINR-E-1924)
production in neon-22 and oxygen-18 reactions with thorium-232, 18: 24690
release from pyrolytic carbon-coated fuel particles, 19: 39228 (BMI-1734)
separation from erbium-169 and lutetium-177 in lactic acid, electrophoretic, 16: 14793
separation from irradiated neodymium oxides, chromatographic, 17: 8212
separation from yttrium-90 in food by solvent extraction using di-(2-ethylhexyl) phosphoric acid, 19: 15386
uptake by eggs and tissues of chickens following intramuscular and oral administration, 18: 38775(R) (ORO-624)
yields from neutron fission of thorium-232, 18: 9311 (IS-558)
yields from uranium-235 fission by thermal neutrons, 16: 23079
yields from uranium-238 fission, 18: 15240
yields in neutron-induced and spontaneous fission of uranium-238, 18: 1079
yields in proton fission of uranium-238 at 7.1, 9.4, and 12.0 Mev, 20: 37995
yields in thermal neutron fission of plutonium-239, 19: 16873

NEODYMIUM ISOTOPES Nd-148

atomic mass, (E), 20: 15769
determination in fuels spiked with neodymium-150, equations for, 18: 15487(R) (GEAP-4361)
determination in irradiated uranium dioxide as measurement of burnup, 19: 2259
determination in uranium-233 and -235 fission products, (E), 20: 11960(R) (IDO-14667)
deuteron reactions (d,p) with, deformed and spherical nuclei from, (E), 19: 45359
deuteron reactions (d,p) at 10 to 12 Mev, energy levels from, (E), 20: 30517
effects on spectrum of neodymium, mass, 20: 1826
energy levels, 17: 40040
energy levels of, E1 transition from and lifetime of octupole, (T), 20: 19979
gamma reactions (γ,p) with, 19: 6644
neutron activation cross section for, 18: 29000(R) (GEAP-4503)
neutron binding energies in, anomalies in, (T), 19: 14523 (JINR-E-1924)
neutron cross sections at 0.414 ev to 10 Mev, 16: 9427 (GA-2451 (Vol.III))
neutron cross section and resonance integral of (E), 19: 1853(R) (GEAP-4621)
neutron cross sections and resonance capture integral of, thermal (E), 19: 3386
neutron cross section and resonance integral, 19: 10510(R) (GEAP-4716)
neutron reactions (n,2n) at 14 Mev, shell effects in, (T), 19: 12536
neutron resonance integrals for dilute solutions of, (E), 19: 29260 (TID-21744)
oxygen-16 scattering at 31 to 45 Mev, B(E2) values for transitions from, (E), 20: 17734
performance as uranium fuel burnup indicator, 19: 29517
proton reactions (p,t) at 40 Mev, spectra from, (E), 20: 36176(R) (TID-22971, pp 41-140)
proton reactions (p,γ) in stars, 16: 12308
uses in calculations of reactor-fuel burnup, (E), 19: 21667(R) (GEAP-4776)
yields from uranium-235 fission by thermal neutrons, 16: 23079
yields from uranium-235 thermal fission, 19: 29313
yields from uranium-235 thermal fission, 20: 28749(R) (GEAP-5060)
yields in plutonium-241 thermal fission, (E), 19: 8495
yields in thermal neutron fission of uranium-233 and -235, 20: 43067(R) (IDO-14679, pp 6-46)

NEODYMIUM ISOTOPES Nd-149

alpha decay energy; 18: 13071
beta decay of, coincidence measurements of, 18: 19096
beta decay of, gamma energies and intensities in, (E), 19: 43306
beta decay of, γ-γ directional correlations from, (E), 20: 12080
beta decay of, promethium-149 levels from, (E), 20: 17787
beta decay of, promethium-149 energy levels from, (E), 20: 46660
beta decay of, promethium-149 energy-level spins and transitions from, (E), 20: 46745
decay, 20: 14059(R) (IDO-17104)
decay of, gamma intensities and half life from, (E), 19: 41836
decay of, gamma spectra from (E), 19: 3300
decay scheme, 19: 10510(R) (GEAP-4716)
decay scheme, (E), 19: 31217 (IDO-17042(p.11-47))
decay scheme and half life of, (E), 19: 1853(R) (GEAP-4621)
decay scheme, (E), 19: 6658
electron structure and nuclear properties of, 16: 28037 (UCRL-10245)
energy levels from neodymium-148 (d,p) and neodymium-150 (d,t) reactions, (E), 20: 30517
gamma dose constants for, 20: 46617
gamma spectra, (E), 19: 16840(R) (IDO-17050)
half life, (E), 20: 15779
half life, (E), 20: 17787
neutron binding energies in, anomalies in, (T), 19: 14523 (JINR-E-1924)
nuclear spin, 18: 36662
production from deuteron reactions (d,p) with neodymium-148 and (d,t) with neodymium-150, deformed and spherical shapes from, (E), 19: 45359
production in neon-22 and oxygen-18 reactions with thorium-232, 18: 24690

NEODYMIUM ISOTOPES Nd-150

alpha reactions (α,2n) at 18 to 20.5 Mev, samarium-152 energy-level transitions from, (E), 20: 44735
atomic mass, (E), 20: 15769
beta decay of, double, (E), 20: 4828 (COO-818-60)
beta decay of, double, (E), 20: 42263
determination in uranium-233 and -235 fission products, (E), 20: 11960(R) (IDO-14667)
deuteron reactions (d,t) with, deformed and spherical nuclei from, (E),

19: 45359
deuteron reactions (d,p) and (d,t) at 10 to 12 Mev, energy levels from, (E), 20: 30517
effects on spectrum of neodymium, mass, 20: 1826
energy level of, excitation energy and transition probability for first rotational, 17: 31449
energy levels, 17: 40040
energy levels of, properties of octupole, 18: 21172 (JINR-E-1561)
energy levels of, gamma vibrational, (T), 19: 14597
energy levels of, high-spin rotational, (E/T), 20: 19953
gamma reactions (γ,p) with, 19: 6644
mass difference of samarium-150 and, 18: 32825
neutron binding energies in, anomalies in, (T), 19: 14523 (JINR-E-1924)
neutron cross sections at 0.414 ev to 10 Mev, 16: 9427 (GA-2451 (Vol.III))
neutron reactions (n,2n) at 14 Mev, shell effects in, (T), 19: 12536
oxygen-16 inelastic scattering at 43.5 Mev, vibrational-state excitation in, (E), 19: 45321
oxygen-16 scattering at 38 to 48 Mev, level excitation in, 18: 24729
oxygen-16 scattering at 31 to 45 Mev, B(E2) values for transitions from, (E), 20: 17734
photon reactions (γ,n), cross sections for, (E), 19: 21287
proton reactions (p,5n3p) and (p,6n2p) with, cross sections, 18: 30732(R) (NYO-2545-1)
proton reactions (p,t) at 40 Mev, spectra from, (E), 20: 36176(R) (TID-22971, pp 41-140)
proton reactions (p,γ) in stars, 16: 12308
proton spallation of, cross section for, cerium-143 and praseodymium-143 production in, 17: 19229(R) (TID-18444)
yields from uranium-235 fission by thermal neutrons, 16: 23079
yields from uranium-235 thermal fission, 19: 29313
yields from uranium-235 thermal fission, 20: 28749(R) (GEAP-5060)
yields in neutron fission of plutonium-239, uranium-233, and uranium-235, 20: 15133(R) (GEAP-4893)
yields in plutonium-241 thermal fission, (E), 19: 8495
yields in thermal neutron fission of uranium-233 and -235, 20: 43067(R) (IDO-14679, pp 6-46)

NEODYMIUM ISOTOPES Nd-151
beta decay of, promethium-151 gamma spectrum from, 18: 32878
decay of, beta and gamma spectra in, (E), 19: 17054
decay of, gamma intensities and half life from, (E), 19: 41836
energy levels from neodymium-150 (d,p) reactions, (E), 20: 30517
gamma dose constants for, 20: 46617
gamma spectra, 18: 1050
preparation and properties of, for use as neutron sources, 18: 16379

NEODYMIUM LACTATES
preparation and solubility, 20: 22998

NEODYMIUM LAURATES
preparation, 20: 26853

Neodymium Magnesium Nitrates
see Magnesium Neodymium Nitrates

NEODYMIUM MOLYBDATES
preparation and crystal structure of, 20: 31740
$NdMoO_4$–$NaMoO_4$, preparation and properties of monocrystalline, as laser material, 20: 7064

NEODYMIUM NIOBATES
crystal structure of, 17: 35711
distribution in strontium molybdate single crystals, coefficients of, 20: 29746
preparation and structure of, 18: 12673
preparation and structure of perovskite type, 20: 844
transition temperature of, relation of ionic radii to, 18: 12113
$CaMoO_4$–$NdNbO_4$, preparation and spectra of, 18: 26017
$CaWO_4$–$NdNbO_4$, preparation, luminescent properties, and structure of, 18: 26017

NEODYMIUM NITRATES
see also Magnesium Neodymium Nitrates
analysis of, for gadolinium, 17: 21661
complex formation with dipyridine, 18: 1686
complexes with tartaric acid, 18: 41452
complexes with TBP in aqueous solutions, spectra of, 18: 25393
density and viscosity of aqueous solutions of, 20: 14648
determination in potassium nitrate, potentiometric, 19: 26917(R) (IA-984)
effects on blood coagulation, 18: 19535
molar absorbance in dioxane and ethanol-lithium nitrate solutions, 18: 9752 (IA-900)
nitrogen-14 NMR in, (E), 20: 12325
preparation and properties, 18: 9752 (IA-900)
preparation and properties of crystalline hexahydrate, 19: 7375
properties of aqueous solutions of, thermodynamic and transport, 20: 22968 (IS-1344)
radiosensitivity effects and toxic effects in rats, 16: 18763(R) (NP-11660(p.59-66))
separation by fractional crystallization, 16: 27148
separation by solvent extraction using TBP, calculation of cascade stagewise conditions for, 18: 20098 (IS-780)
separation from aqueous solutions by solvent extraction using TBP-nitric acid system, 17: 37307
separation from praseodymium nitrate by solvent extraction using bis(2-ethylhexyl) phosphate–TBP, 20: 3875 (IS-T-37)
solubility in di- and tributyl phosphate, 16: 5342
solubility polytherms of systems with other ceric earths, 18: 20108
solvent extraction behavior in nitric acid–TBP–water systems, 16: 87 (IS-335)
solvent extraction from nitric acid solutions by mixtures of bis(2-ethylhexyl)phosphate and tributyl phosphate, 19: 36536 (IS-T-32)
sorption by phospho-organic resins, 19: 40668
specific gravity and apparent molal volume of aqueous solutions of, at 25°C, 20: 38905
spectra in far infrared at temperature of liquid helium, absorption, 17: 8966
spectra in solutions, absorption, 17: 29879(R) (IA-822)
spectra in solution, absorption, 17: 35684 (IA-809)
spectra of, in aqueous solutions, absorption, 20: 10848
surface stress of aqueous solutions, 19: 22232
thermal decomposition at 25 to 1500°C, 17: 145 (BM-RI-6060)
thermal decomposition at 25 to 1400°C, thermogravimetric analysis of, 18: 25354
thermal decomposition, 19: 19928
thermal decomposition, 20: 29224
toxicity in mice and rats, 18: 17458
$Al(NO_3)_3$–$Nd(NO_3)_3$, density and viscosity of solutions of, 20: 14648
$LiClO_4$–$NdNO_3$–KNO_3–$NaNO_3$, density at 230 to 400°C, 19: 4134
$Nd(NO_3)_3$–HNO_3–H_2O, phase studies at 25°C, 18: 17794
$Nd(NO_3)_3$–HNO_3–H_2O, phase studies at 25°C, 19: 26305
$Nd(NO_3)_3$–HNO_3–$Pr(NO_3)_3$–TBP–H_2O, separation factors for neodymium and praseodymium in, 20: 40904
$Nd(NO_3)_3$–HNO_3–$RbNO_3$–H_2O, solubility isotherm at 25°C, 17: 35842
$Nd(NO_3)_3$–HNO_3–$Pr(NO_3)_3$–TBP–H_2O, solvent distribution of neodymium and praseodymium in, 20: 7004 (IS-T-42)
$NdNO_3$–KNO_3–$NaNO_3$, density at 230 to 400°C, 19: 4134
$Nd(NO_3)_3$–TBP–H_2O, complex formation in, 18: 25393

NEODYMIUM NITRIDES
electric conductivity near Curie point, electron critical diffusion theory of, 19: 41973
magnetic properties, 19: 38067
magnetic properties at 2 to 300°K, 20: 43939
preparation and properties, 17: 21678
preparation by reactive arc melting, 20: 21244
preparation, semiconducting properties, and structure of, 19: 22965 (AL-TDR-64-239)
properties of, electric and magnetic, 17: 32081
thermal capacity at 1.2 to 45°K, 19: 13366

NEODYMIUM OXALATES
carbon-14 exchange between, and alkali metal oxalates, 20: 45634
crystal structure of monoclinic decahydrate of, 20: 36835
dynamic decomposition of, effects of air, carbon dioxide, and nitrogen on, 18: 23507
preparation and crystal structure determination, 19: 15495
reactions of hydrated, with hydrochloric acid, 20: 16447
solubility in EDTA at 25 and 40°C, 19: 9149
solubility in *N,N'*-dimethyl-*N,N'*-dinitrosoterephthalamide at 25°C, 19: 38601
spectra of hydrate of, infrared, 20: 8898
thermal decomposition at 340 to 440°C, 16: 11633
thermal decomposition at 25 to 1500°C, 17: 145 (BM-RI-6060)
thermal decomposition of hydrated, 18: 8376
thermal decomposition at 25 to 1400°C, thermogravimetric analysis of, 18: 25354
thermal decomposition in air and carbon dioxide at 30 to 1100°C, 20: 12862
thermal decomposition of, changes in surface areas of products from, 20: 18680
thermal decomposition of hydrates of, differential thermal analysis of products of, 20: 40900
thermal dissociation of hydrates of, 20: 35509

NEODYMIUM OXIDES
adhesion to aluminum and silicon, 19: 7352 (BMI-1706)
analysis for impurities, spectrographic method for, 16: 20327
analysis for impurities, chemico-spectrographic, 19: 5795
analysis for oxygen, 18: 19907
atomic charge and permittivity of, (E/T), 19: 47901(T)
bonding to silicon, 19: 13871(R) (BMI-1691(Del.))
catalytic effects on dehydrogenation of cyclohexane, 16: 110
catalytic effects on deuterium exchange in cyclohexane, 18: 23573
catalytic effects on dehydrogenation of methylcyclohexene and methylcyclopentene at 330 to 530°C, 19: 30220
catalytic effects on ketone yield from organic acids, 19: 30221
catalytic effects on dehydrogenation of cyclohexane at 515 to 590°C, 19: 30222

catalytic properties, 17: 2991
catalytic properties for parahydrogen conversion and hydrogen-deuterium equilibration at 77 to 642°K, 17: 12290
catalytic properties in hydrogen peroxide decomposition, effects of metal ions on, 19: 5902
compatibility and encapsulation with alloys and metals, 20: 11267 (BNWL-SA-488)
contamination by boron oxide in x-ray-diffractometer furnace, 18: 41400
content in mckelveyite uranium mineral, 19: 40799
crystal lattice transformations at high temperature, (E), 20: 13979
crystal structure of, effects of pressure on polymorphism in, 19: 17885
crystal structure of sesqui-, modifications and phase transformations, 19: 30727 (BM-RI-6616)
crystal structure and petrography of, 20: 24590 (ORNL-P-1158)
crystal structure of A-form of Nd_2O_3, 20: 26889
crystalline parameters and transformations of, stable above 2000°C, 20: 23679
crystallographic modifications and phase transformations of, 20: 16489
deposition of films of, vapor, 19: 7352 (BMI-1706)
deposition on aluminum, electrolytic, 18: 23537
determination in thorium oxide by emission spectroscopy, 20: 16393
diffusion of oxygen in, tracer studies of, 20: 38865(R) (COO-1109-22, Paper 4)
effects of irradiated, on catalytic decomposition of hydrogen peroxide, 20: 25175
effects of, on magnetic properties of manganese ferrites, 17: 14880
effects on catalytic properties of aluminum oxide–chromium oxide systems, 20: 40943
effects on conversion reactions of butane, catalytic, 19: 26373
effects on hydrogen oxidation, catalytic, 19: 26343
effects on optical properties of silicate glasses, 19: 44030
electronegativity and ion radii of, prediction of phases in binary systems with other oxides from, 19: 23061
entropy and heat content at high temperatures, 16: 30356 (BM-RI-6033)
fabrication and properties, 18: 35932(R) (HW-81600(p.2.1-23))
hardness and melting point, 20: 5845
heat of formation on hot metal surfaces, 20: 31225
inhalation of aerosol of, effects of particle size and concentration in guinea pigs and mice, 20: 1593 (COO-1170-4)
magnetic susceptibility at 4.2 to 300°K, 18: 23513
magnetic susceptibility at 4 to 300°K, 20: 3318
magnetic susceptibility, 20: 8912
neutron cross sections at 1.44 ev (E), 19: 3288
nitration, 18: 9752 (IA-900)
oxygen isotopic exchange on, at 300 to 500°C, 20: 8921
oxygen-18 exchange between molecular oxygen and, 19: 46266
pathogenetic effects of inhaled aerosol of, on guinea pigs and mice, 18: 25078
phase studies at 400 to 2200°C, 20: 25048
phase transformation rates in, 18: 32096
phase transformations in, at 1800 to 2400°C, 19: 44731
phase transformations in, at 50 to 1500°C, 20: 5536
phase transformations in, at high pressure and 550 to 1450°C, 20: 26833
physical properties at 600 to 1325°C, 16: 13003(R) (NP-11299)
polymorphism, 16: 3014
preparation by decomposition of nitrate, oxalate, and sulfate, 19: 19928
preparation by thermal decomposition of carbonates, nitrates, oxalates, and sulfates, 17: 145 (BM-RI-6060)
preparation of microspheres of, sol-gel method for, 20: 45791(R) (ORNL-3945, pp 107-28)
preparation of pure, by fractional crystallization, 18: 8449
preparation of pure, by fractional crystallization, 18: 8450
preparation, semiconducting properties, and structure of, 19: 22965 (AL-TDR-64-239)
processing irradiated, for neodymium-147 and promethium-149 separation, 17: 8212
production by thermal decomposition of neodymium oxalate, conditions for optimum surface areas in, 20: 18680
properties of, chemical and physical, 19: 11120
proton reactions at 590 Mev and 18 Bev, yields of iodine isotopes from, (E), 20: 22045
reactions with alkali metal salts(liquid), 16: 18917
reactions with aluminum oxide and oxides of Group II elements at 1400 to 1500°C, 20: 16482
reactions with barium carbonates, ternary oxide formation in, 19: 46242(R) (TID-22207, Paper B)
reactions with boron oxides at high temperatures, 20: 16489
reactions with calcium fluoride, 16: 32050
reactions with hydrogen and oxygen, effects of non-stoichiometry on, 19: 36398
reactions with melted fluorides, 17: 32111
reactions with oxides of tri- and tetravalent elements in solid state, 20: 36840
reactions with oxygen, isotopic-exchange, 19: 2290
reactions with rhodium oxides, 17: 39044
reactions with silicon oxides, 16: 6405
reactions with sodium metaphosphate, spectra of compound formed in, 19: 38668
reactions with water vapor, 19: 374
reactions with water, infrared spectra of products of, 20: 14568
refraction of, calculation of molar and specific, 19: 13395
separation from europium, polarographic, 17: 10572
solubility in ethyl, isopropyl, methyl, and propyl alcohols in presence of ammonia, 20: 20686
spectra in low frequency region, infrared, 18: 23549
spectra of hydrates of, effects of deuterium on infrared, 20: 14568
spectra of, infrared absorption, 17: 27840
spectra of, absorption and fluorescence, 19: 47887(T) (N64-21857, pp 7-12)
spectra of, x-ray absorption, 19: 30194
spectral properties of rare earth-activated, 18: 13868
stabilization of, using metal oxides, 17: 6664 (MND-M-2346)
thermal expansion, 17: 2951 (TID-17339)
thermal expansion of polycrystalline, at temperatures up to 1050°C, 18: 27957 (KAPL-2000-21(p.III.1-6))
thermodynamic properties, 16: 96 (TID-14101)
thermodynamic properties, 16: 25386
thermodynamic properties at 5 to 350°K, 17: 12268
toxicity in mice and rats, 18: 17458
actinide oxides–Nd_2O_3, preparation of sols of, 20: 39341(P)
$Al(NO_3)_3$–Nd_2O_3, compound formation in, at 1200°C, 20: 14539
Al_2O_3–Cr_2O_3–Nd_2O_3, properties for use in dehydrogenation of butane, 20: 40943
Al_2O_3–Nd_2O_3, compound formation in, at 1600 to 1650°C, 20: 14539
Al_2O_3–Nd_2O_3, phase studies, 16: 6433
Al_2O_3–Nd_2O_3–SiO_2, phase studies, 16: 6433
B_2O_3–Nd_2O_3, liquid immiscibility in, 20: 40910
B_2O_3–Nd_2O_3–Na_2O, phase studies at 690 to 1100°C, 20: 26846
CeO_2–Nd_2O_3, equilibrium phase studies on, 18: 23509
Ce_2O_3–Nd_2O_3, phase transformations in, x-ray study of, 16: 10566
$CeTiO_3$–Fe–Nd_2O_3–$SrTiO_3$–TiO_2, thermoelectric properties, 17: 29854(R) (MND-2584-4)
Fe_2O_3–Nd_2O_3, crystal structure and magnetic properties, 20: 4411
IrO_2–Nd_2O_3, phase studies in air, 19: 32751
$NdCl_3$–Nd_2O_3, thermodynamic properties, 20: 33319
Nd_2O_3–Nb_2O_5, crystal structure, preparation, and properties, 19: 32749
Nd_2O_3–Nb_2O_5, properties and structure of compounds formed in, 18: 34199
$NdO_{1.5}$–$PaO_{2.5}$, fluorite phase in, 19: 24511
Nd_2O_3–PrO_2, preparation and phase studies of, 20: 26908
Nd_2O_3–Pr_6O_{11}, x-ray fluorescence analysis for neodymium, 18: 39135
Nd_2O_3–ReO_2, analysis for platinum and rhodium using electron microprobe, 20: 26340(R) (AD-631987)
Nd_2O_3–ReO_2, crystal structure of Nd_2ReO_5 in, 20: 26340(R) (AD-631987)
Nd_2O_3–ReO_2, magnetic properties and structure of compounds formed in, 20: 36784(R) (AD-636054)
Nd_2O_3–ReO_2, phase studies at 1130 and 1300°C, 20: 17007(R) (AD-627468)
Nd_2O_3–ReO_2, preparation and ferromagnetic properties of phases in, 20: 13260(R) (NP-15852)
Nd_2O_3–SiO_2, phase studies, 19: 9694
Nd_2O_3–Sm_2O_3, phase transformations in, x-ray study of, 16: 10566
Nd_2O_3–SrO, phase studies, 20: 302
Nd_2O_3–Ta_2O_5, crystal structure, preparation, and properties, 19: 32749
Nd_2O_3–Ta_2O_5, properties and structure of compounds formed in, 18: 34199
Nd_2O_3–UO_2, compositions and structures of, 17: 12659 (ANL-6631)
Nd_2O_3–UO_2, crystal structure of air- and hydrogen-sintered, 17: 41333(R) (ANL-6677)
Nd_2O_3–UO_2, phase studies, 16: 27643(T) (FTD-TT-62-505)
Nd_2O_3–UO_2, phase studies, 16: 30717(R) (ANL-6516)
Nd_2O_3–UO_2, phase studies, 17: 14740 (TID-11295(2nd Ed.))
Nd_2O_3–WO_3, phase diagrams, 20: 37240
Nd_2O_3–WO_3, preparation and properties, 20: 14534
Nd_2O_3–ZrO_2, crystal structure, differential thermal analysis, and thermal expansion of, 18: 23503
Nd_2O_3–ZrO_2, phase studies, 16: 27642(T) (FTD-TT-62-505)
Nd_2O_3–ZrO_2, phase studies, 19: 41037
Nd_2O_3–ZrO_2, phase studies, 19: 42464
Nd_2O_3–ZrO_2, phase studies, 20: 13283
Nd_2O_3–ZrO_2, phase transformations in, fluorite, 19: 358(T) (ORNL-tr-201)

NEODYMIUM OXYBROMIDES
preparation and crystal structure, 20: 1834

NEODYMIUM OXYCHLORIDES
heat of formation and stability of, 20: 33319

NEODYMIUM OXYFLUORIDES
preparation and properties, 18: 17839

NEODYMIUM OXYSULFATES
preparation and properties, 19: 19928

NEODYMIUM OXYSULFIDES
preparation and structure of divalent, 19: 24498

properties of crystals of, chemical and physical, 17: 8080
NEODYMIUM OXYTELLURIDES
preparation and properties, 17: 2975
preparation and properties, and crystalline structure, 17: 6068
spectra of, nephalauxetic effect in reflection, 19: 36390
NEODYMIUM PALMITATES
preparation, 20: 26853
NEODYMIUM PERCHLORATES
crystal structure of hydrated, 17: 19995
reactions of, with *N,N*-dimethylacetamide, adduct formation in, 19: 36397
spectra of, effects of organic solvents on oscillation absorption bands in, 19: 22192
stability constants of, thermal, 19: 40509
structure, 18: 10079
thermal decomposition of, differential thermal analysis and thermogravimetric studies on, 18: 25396
NEODYMIUM PERRHENATES
preparation and properties of, 20: 43217
NEODYMIUM PHOSPHATES
preparation and single crystal growth of ortho-, 18: 25356
structure, 19: 42458 (NP-15162)
NEODYMIUM PHOSPHIDES
preparation and physicochemical properties of, 20: 45686
preparation, semiconducting properties, and structure of, 19: 22965 (AL-TDR-64-239)
NEODYMIUM PHTHALOCYANINES
preparation and spectra of, 20: 5560
NEODYMIUM PYROPHOSPHATES
preparation and properties, 18: 41454
NEODYMIUM RUTHENATES
magnetic susceptibility at 2 to 1300°K, 16: 16837
NEODYMIUM SALICYLATES
preparation and properties of, 20: 26895
NEODYMIUM SELENIDES
crystal structure, 17: 32125
crystal structure, 18: 1628
crystal structure of, reflection spectra for zonal, (E), 20: 40339
electric conductivity and properties of, 18: 42068
electric properties of, 18: 37718(T)
electric properties, 20: 868
electron structure of mono-, electric conductivity and magnetic susceptibility from, 17: 32082
preparation and properties of Nd_2Se_4, 20: 45689
preparation and structure, 18: 41450
preparation of high-purity, 20: 26843
preparation of, by selenite reduction, 19: 36426
preparation, semiconducting properties, and structure of, 19: 22965 (AL-TDR-64-239)
thermoelectric properties, 17: 11296 (AD-278352)
CaSe–Nd_2Se_3, phase studies, 20: 10857
NdSe–SmSe, electric conductivity and properties of, 18: 42068
NdSe–YbSe, electric conductivity and properties of, 18: 42068
NdSe–YbSe, thermoelectric properties, 17: 11296 (AD-278352)
NEODYMIUM SILICATES
reactions with strontium silicates, products from, 17: 1471
synthesis of complex, 18: 10070
Ca_2SiO_4–$Nd_4(SiO_4)_3$, phase studies, 18: 13787
Ca_2SiO_4–$Nd_4(SiO_4)_3$, phase studies, 19: 36373
NEODYMIUM SILICIDES
crystal structure, 19: 11125
crystal structure, 19: 32755
crystal structure, 19: 40477
crystal structure and microhardness, 19: 42862
crystal structure, 20: 33910
preparation and crystal structure of, 20: 19224
preparation and properties, 19: 357(T) (JPRS-26877(p.25-47))
preparation using arc smelting, 20: 46168
properties of, physicochemical, 20: 17047
NEODYMIUM STEARATES
preparation, 20: 26853
NEODYMIUM SULFATES
see also Ammonium Neodymium Sulfates
crystal structure and bond types of octahydrates, 19: 19915(T)
crystal structure of, infrared spectral studies on, 20: 43219
crystal structure, cation electric field, and magnetic anisotropy in octahydrated, 20: 16435
heat of dehydration, 16: 1783
paramagnetic resonance of trivalent gadolinium ions in octohydrate, zero-field, 16: 16384
reduction of anhydrous, by carbon monoxide, 18: 25427
thermal decomposition, 16: 26993
thermal decomposition at 25 to 1500°C, 17: 145 (BM-RI-6060)
thermal decomposition at 25 to 1400°C, thermogravimetric analysis of, 18: 25354
thermal decomposition, 19: 19928
$Nd_2(SO_4)_3$–Na_2SO_4, thermal stability, 19: 40511
NEODYMIUM SULFIDES
conductivity of, electric and thermal, 18: 39194
crystal growth in barium-activated, 19: 47876 (AD-614435)
crystal structure and thermal properties, 17: 30527
crystal structure, 17: 32125
crystal structure, 18: 1628
electric properties of, 18: 37718(T)
electron structure of mono-, electric conductivity and magnetic susceptibility from, 17: 32082
homogeneity regions in, 20: 3938
physical properties, 18: 1677
preparation, 17: 12293
preparation of high-purity, 20: 26843
preparation of mono-, 17: 14290
preparation of mono-, 19: 18472(T) (JPRS-28739)
properties of crystals of, chemical and physical, 17: 8080
properties of, electric and magnetic, 17: 32081
spectra of, nephalauxetic effect in reflection, 19: 36390
thermal expansion coefficients at 20 to 400°C, 18: 39958(T)
thermoelectric properties, 18: 13800
EuS–Nd_2S_3, compound formation in, 20: 16431
Nd_2S_3–Ag_2S, crystal structure, 20: 26829
Nd_2S_3–SmS, compound formation in, 20: 16431
Nd_2S_3–YbS, compound formation in, 20: 16431
NEODYMIUM SYSTEMS
Al–C–Nd, phase studies of, atomic size effects in, 19: 23111
B–C–Nd, phase studies, 18: 25319 (COO-1140-103)
C–Nd–O, preparation and properties of $Nd_2O_2C_2$ in, 20: 43214
Nd–$NdBr_3$, electric conductivity at 730°C, 18: 2231(R) (ORNL-3488 (p.96-101))
Nd–$NdBr_3$, electric conductivity at 730°C, 18: 5282
Nd–$NdCl_3$, free energy of solutions of, 19: 11103
Nd–$NdCl_3$, phase studies and vapor pressure, 17: 35818
Nd–$NdCl_3$, phase studies and properties of, 18: 6832
Nd–$NdCl_3$, vapor pressure at high temperatures, 17: 35843
Nd–NdI_3, electric conductivity and magnetic susceptibilities of, 18: 4281
Nd–O, mechanical properties, 16: 5315 (WADD-TR-61-123)
Nd–O, phase studies and atmospheric corrosion, 16: 5315 (WADD-TR-61-123)
Nd–O–Ti, reactions in gases, properties of compounds formed by, 20: 45640
Nd–Se, preparation, phase studies, and properties of compounds in, 19: 5862
Nd–Te, crystal chemistry and phase studies of, 18: 23506
Nd–Te, crystal structure and phase equilibria in, 19: 30166
Nd–Te, phase diagrams, evidence for neodymium tellurides in, 20: 9513
Nd–Te, phase studies of compounds in, 18: 37115 (ANL-6856)
Nd–Te, preparation, phase studies, and properties of compounds in, 19: 5862
NEODYMIUM TANTALATES
crystal structure of, 17: 35711
preparation and structure of, 18: 12673
preparation and structure of perovskite type, 20: 844
$NdTaO_4$–$KTaO_3$, crystal structure, 20: 16438
NEODYMIUM TELLURIDES
composition and crystalline parameters of, 17: 20008
crystal structure, 17: 32125
crystal structure, 18: 1628
crystal structure and electric conductivity of, 20: 8905
electric conductivity and properties of, 18: 42068
electric properties, 17: 34469
electric properties and uses of, 18: 34158
electric properties of, 18: 37718(T)
phase studies, 19: 34165
phase studies and electric properties, 16: 15260(R) (AD-262215)
preparation and crystallographic parameters of, 17: 18023
preparation and thermoelectric properties of, 19: 13398
preparation of high-purity, 20: 26843
preparation, properties, and stability of, 20: 26844
preparation, semiconducting properties, and structure of, 19: 22965 (AL-TDR-64-239)
production in neodymium–tellurium systems, 20: 9513
properties, 16: 32068
thermoelectric properties, 17: 11296 (AD-278352)
NEODYMIUM TITANATES
preparation and crystal structure of, 20: 29212
preparation and properties, 19: 2319
NEODYMIUM, TRISCYCLOPENTADIENYL-
preparation by reaction of neodymium fluoride with magnesium cyclopentadienide, 20: 35493
NEODYMIUM TUNGSTATES
formation by high-temperature reactions of neodymium oxides and tungsten oxides, 20: 37240
preparation and crystal structure of, 20: 31740

$Nd_2(WO_4)_3$–Na_2WO_4, phase diagrams, 20: 37241

NEODYMIUM VANADATES
crystallographic and optical properties of hydrated, 19: 44032(T)
preparation and properties, 19: 22245
structure of, x ray diffraction analysis of, 17: 10663

NEODYMIUM YTTRIUM FERRATES
crystalline and magnetic properties of, (E), 19: 7431
magnetic structure of, neutron diffraction for, 17: 28898(T)

NEODYMIUM ZIRCONATES
preparation and properties, 18: 43464
preparation and properties of, 19: 19925

Neohydrin
see Urea, [3-(Chloromercuri)-2-Methoxypropyl]-

NEOMYCIN
determination in cotton clothing, radiometric method for, 20: 40823

NEON
see also Rare Gases
absorption at electron-cyclotron resonance in slightly ionized, 16: 5812
absorption coefficient from 3.6 to 10×10^3 Å, (T), 19: 20833
abundance in primary cosmic radiation, 17: 22403 (AD-282243)
abundance in 3 Centauri A, 16: 4659
acoustic-wave production in low-pressure, r-f breakdown for, 18: 28846
additive effects on molecular spectra, 17: 178
alkali and hydrogen atom trapping in solid, g-factor shifts in, 18: 9016
alkali-metal negative-ion dissociation in, cross sections for, (T), 20: 29947
alpha energy loss and ionization in, 16: 6931
alpha reactions with liquid and solid, emission spectra from, (E), 19: 12101
alpha reactions, beryllium-7 production in, 17: 21098
alpha scattering at 28 Mev, distorted-wave and optical model analysis of, (T), 19: 29294
alpha scattering at 21 to 24 Mev, angular distributions for, (E), 20: 28263 (AECD/EP-10)
analysis for hydrogen, mass spectrographic, 18: 9752 (IA-900)
analysis of, mass spectrometric, 17: 25668
argon ion reactions with, cross sections for, (E), 20: 25747
argon ion reactions at 60 to 500 kev, excitation in, 18: 32448
atom interaction energy in solid, repulsive, 18: 34413
atomic potential functions for, 18: 42313
atomic self-consistent-field functions for neutral, 16: 33634
atomic structure of, x-ray-diffraction studies of electron distributions in, 20: 35475 (IS-T-93)
atomic wave functions for, with five parameters, 17: 32796
atomic weight, 19: 46588 (ORNL-3857)
Auger spectrum of, KLL, (E), 19: 4849
bond lengths and polarities and electronegativity of, 19: 24512
bremsstrahlung emission from plasma of, in thermodynamic non-equilibrium, 17: 42111
bremsstrahlung reactions at 30.5 Mev, proton production in, 17: 31540
bremsstrahlung spectra, 19: 9445 (LA-3130)
bubble release and swelling in solids, model for, 18: 26080
cesium beam scattering by, effects of apparatus resolution on cross sections for, 20: 34114
cesium optical pumping in, spin relaxation time in, 18: 33566
charge exchange in, atom-ion resonance, (T), 19: 19931
charge exchange reactions with krypton, cross sections for, 16: 19554
charge transfer with protons, cross sections for Lyman alpha emission from, 18: 26235
charged-particle stopping power and straggling in, excitation energy for, (T), 19: 41268
chemistry of, predicted, 17: 33894
collisions of atoms of, with alkali metal atoms, ionization produced in, (E), 20: 2639
collisions of atoms of, with singly charged krypton ions, profound stripping and scattering in, (E), 20: 2644
collisions of hydrogenic molecules and metastable, inelastic, (E), 19: 16378
composition of atmospheric, isotopic, 20: 17158(R) (ORNL-3900, pp 82-149)
concentration of, in stone meteorites and its radiogenic and cosmogenic age, 17: 14518
content and isotopic composition in Sikhote-Alin iron meteorite, 16: 22412(T) (AEC-tr-5119)
content and isotopic composition in stone meteorites, radiogenic, spallogenic, and primordial, 18: 26197
content and nature of, in thermal springs in California and Wyoming, 19: 26252
content in amphoteric meteorites, (E), 19: 41225
content in atmosphere and meteorites, 17: 25466
content in iron meteorites, 18: 20205
content in lunar atmosphere, effects of solar wind on, 18: 18546
content in Pantar chondrite, 16: 29587
content in planetary nebula, 18: 36133
content in Sikhote-Alin meteorite, 16: 29627
content in upper atmosphere, from rocket soundings, 18: 37794(T) (NASA-TT-F-141(p.1-21))
contents in 22 iron meteorites, 18: 8973 (NP-13494)
critical and inversion temperatures, 17: 30460
crystal stability of, three-body interactions in, 18: 34706
crystal structure of, isotopic effects on unit-cell volumes, 17: 32106
cyclotron emission from plasma of, in thermodynamic non-equilibrium, 17: 42111
cyclotron harmonic radiation from plasma of, in magnetic field, (E/T), 20: 32637
density in lunar atmosphere, equilibrium, 16: 18285
determination by charged-particle reactions at 2 Mev, 20: 43097
determination in natural gases, volumetric, 20: 33522
determination in pure helium, chromatograph for, 19: 28220 (BNWL-12)
determination in purified helium, use of chromatography and radioactive ionization detector for, 18: 31397
determination in sea water, mass spectrometric, 19: 2247
determination of trace amounts of, by reactor neutron activation methods, 20: 26760
determination of, factors affecting continuous on line, 20: 1734 (EG-Report-36)
deuterium and hydrogen 1s-2p transition in solid, 18: 40453
deuterium hydride ion reactions at 2 to 25 ev, isotope effects in, 20: 33282
deuteron reactions, meson (μ^-) transfer in, 16: 5882
deuteron reactions at 12.9 to 21.0 Mev, electron capture in, 20: 974
deuteron reactions at 0.5 to 25 kev, Lyman alpha emission cross sections for, 18: 32446
deuteron scattering at 11.6 Mev, angular distributions for, (E), 19: 31281
diagnostics of moderate-pressure plasma of, method of detector characteristics for, (E/T), 20: 28533
diagnostics of plasma of, probe characteristics for, (E), 20: 4969
diagnostics of plasma of, using two-probe method of detector characteristics, (E/T), 20: 28534
diamagnetic properties of plasma of, 16: 14152
diffusion and spin relaxation of cesium in, (E), 19: 41278
diffusion in gases, coefficients of, 16: 33613
diffusion in tissue-simulating plastics, 18: 13716(R) (ANL-6769(p.21-9))
diffusion of charge carriers in rarefied ionized, study by diffusion-wave method, 17: 9775
distribution of atomic, in gas discharge in heavy ion source, (E), 19: 27603 (JINR-P-2043)
dysprosium ion stopping in, (E/T), 19: 2984
effects as buffer on spin relaxation of optically pumped cesium, 18: 30403 (NP-14066)
effects of electronegative gas additions on coronal discharges in, 16: 2372
effects on density shifts of sodium-23 hyperfine frequency, 19: 30951
effects on growth rates in Neurospora, 20: 20378
effects on ionization and power loss in theta-pinch plasma, 18: 17167
effects on lifetime of metastable helium atoms, 18: 26238
effects on performance of low-temperature cesium thermionic diode, 18: 12856 (AFCRL-63-607)
effects on radioinduced isotopic exchange in nitrogen, 19: 36482
effects on radiolysis of acetylene, 19: 17991
effects on radiolysis of ethylene, 20: 5582
electric breakdown potential of, measurement of a-c, 20: 3160 (AD-618503)
electric conductivity of positive-column discharge plasma of, (E), 19: 40041
electric conductivity of cesium-seeded, at 2000 to 4000°K, 16: 2328
electric conductivity decay measurements in plasma, 16: 24881 (AFCRL-1119)
electric conductivity of cesium-seeded plasma of, near thermal equilibrium, 17: 33216
electric conductivity in Brayton cycle MHD power generation, (T), 20: 41706
electric conductivity of cesium-seeded plasma of, 18: 11318
electric discharge in, spectroscopic studies of h-f, (E), 19: 1070(T)
electric discharges in, layered structure from high-frequency, 19: 1733
electric discharge in, electron distribution functions in positive column (E/T), 19: 6809
electric discharges in, plasmoid production by h-f, 19: 23853
electric discharge in spark chamber gases of, mechanisms of, (E/T), 19: 13739(T) (UCRL-1171)
electric discharge in, traveling density variations in glow, (E/T), 19: 14141 (RLE-TR-424)
electric discharge in, hollow cathode, (E), 19: 37957
electric discharge in, light image magnification from, 19: 42925 (JINR-P-2256)
electric discharge in, radiation temperature in, 16: 19578
electric discharge in, effects of current on striation motion in glow-type, 16: 19602
electric discharge in, emission luminosity in cold low-pressure arc,

16: 19636
electric discharge in, instability in magnetic field, 16: 31166
electric discharge in, negative radiation temperature of, 17: 5461
electric discharge in, electron distribution from, 16: 15346
electric discharge in, krypton-85 cleanup, 16: 9309
electric discharge in, effects of current on stratification in, 16: 13731
electric discharge in, behavior of, in area of sub-normal low pressure, 17: 16802
electric discharge in, positive column instability in, 17: 33161 (UCRL-10698)
electric discharge in, conductivity of positive-column, 17: 36800
electric discharge in, energy exchange between electrons in, 17: 42125
electric discharge in, ionization effects on, 17: 20656
electric discharge in spark chambers, displacement of, (E/T), 20: 2131 (JINR-P-2344)
electric discharges in, effects of magnetic fields on breakdown time lag of, 20: 2835
electric discharges in, stable plasmoids from h-f, (E), 20: 10188
electric discharges in, electron distribution function for, (E), 20: 21795
electric discharge in, boundary conditions of plasma from, (E), 20: 24535
electric discharge in alkali metal-seeded, (E), 20: 39715
electric discharges in, high-pressure electrodeless, (E), 20: 42509
electric discharges in, anode fall in low-pressure, (E), 20: 46429
electric discharges in, charge-carrier effusion from low-pressure, 20: 46430
electric discharges in, production of stationary consecutive layers and layer waves in low-pressure, 19: 1728
electric discharger in, laser action from, 18: 18624
electric discharge in, moving striations in, 18: 21451
electric discharge in, cathode performance in, 18: 21456
electric discharge in, ionization coefficients for, 18: 21477
electric discharge propagation in rarefied, 18: 21511
electric discharge in, microwave resonance emission spectra of, 18: 24772
electric discharge in, stability of, 18: 24784
electric field effects on cylindrical plasma of, secondary resonances from dipolar, 18: 4660
electric glow discharge in, ion mobilities in, 17: 3641
electric glow discharge positive columns instability in magnetic field in, 16: 14176
electric glow discharges in, changes of normal cathode falls of, 19: 1745
electric glow discharges in, ion energy at cathode of, 17: 25942
electric probe saturation current in plasma of, magnetic field effects on, (E), 19: 14695
electrical discharge in, microwave radiation from, 17: 4194
electromagnetic waves in afterglow plasma of, pulsed, (E), 19: 27630
electron affinities and ionization potentials for, 17: 20741
electron and ion transverse diffusion in plasma of, Hall coefficients and velocities for, 18: 6367
electron beam interaction with plasmas of, 17: 4207
electron beam interactions with gas of, level inversion during excitation by monoenergetic, (E), 20: 31941
electron binding energy of, K-shell, (E), 20: 19405
electron capture by, excitation by, 18: 16709
electron collisions with, lifetimes, excitation functions, densities, total cross sections, and polarization ratios of metastable state, 17: 5046 (UCRL-10477)
electron configuration for, analytical solutions of, 16: 10724
electron correlation energy in helium-like atoms of, 18: 5926
electron densities and energies in, calculations using self-consistent-field approximation, 19: 12067
electron density and temperature of excited, in discharge positive columns, 19: 4622(T) (CEA-tr-R-1412)
electron density and temperature of plasma of, 18: 4647
electron density distribution in plasma column of, radial, (E), 19: 17125
electron diffusion coefficients in, light-chamber technique for thermal, (E), 20: 7727
electron diffusion in, coefficient for thermal, 18: 10790
electron distribution in, solution of Thomas-Fermi-Dirac equation for, 20: 19366
electron drag by traveling magnetic wave in plasma of, (E/T), 19: 27680
electron drift velocity in, at 77 to 443°K, 16: 27742 (NP-11983)
electron elastic scattering by, resonances in differential cross sections for, 17: 34625
electron elastic scattering lengths, 17: 20736
electron elastic scattering by, spin polarization from, (T), 20: 5998
electron elastic scattering by atomic, cross sections for, 18: 11290
electron elastic scattering by, cross sections for, 18: 32381
electron elastic scattering at 15 to 17 ev, resonances in, 18: 32395
electron elastic scattering by, resonances in, 18: 44447
electron energy levels of, autoionizing, 17: 29465
electron energy levels of, optically forbidden transitions in, 18: 10785
electron energy loss, penetration, and range at 5 to 100 Mev, 19: 9445 (LA-3130)
electron excitation of, yield measurements for slow, 16: 4621(T) (AEC-tr-4883)
electron free-free transitions in, method for calculating, 20: 41626
electron inelastic scattering by crystals of, interband excitation in fast, (T), 19: 40083
electron inelastic scattering cross sections, 18: 22669 (AROD-3331:5)
electron inelastic scattering at 500 to 1000 ev, oscillator strengths for, 18: 32401
electron ionization cross sections for, 16: 15569
electron mobility in, 17: 40153(R) (AD-290727)
electron multiple scattering at 40 to 130 kev, linear displacement distributions in, 18: 21316
electron pair production in screened nuclear field in, (T), 19: 43280
electron properties and recombination in, 18: 10767 (RTD-TDR-63-3076)
electron reactions with, excitation cross sections for, 19: 20804(R) (ANL-6938(p.36-45))
electron reactions with, excitation functions for metastable state formation in, 19: 19992
electron reactions with, ionization cross sections in, (E/T), 19: 23261
electron reactions with, excitation of long-lived states in, (E), 19: 23320
electron reactions with, ionization probabilities in, 19: 23273
electron reactions at 0.1 to 20 kev, ionization cross sections for, (E), 19: 43016
electron reactions with, ionization cross sections for, (E/T), 20: 5989
electron reactions with, excitation total cross sections for, (T), 20: 9661
electron reactions with atomic, metastable excitation in, (E), 20: 11455 (UCRL-14450)
electron reactions at 0.001 to 20 ev, cross sections for elastic, 20: 25723 (RT-FI-(65)-60)
electron reactions at 0.5 to 16 kev, mechanisms for multivalent ion production from, (E), 20: 27752
electron reactions at 25 to 150 ev, photon emission in, 18: 24700
electron reactions at 0.36 to 1.9 ev, threshold laws for ionization in, 18: 32427
electron reactions at 2 to 3 kev, ionization cross sections for, 18: 32429
electron reactions in discharge afterglow, 18: 32431
electron reactions with, excitation and ionization in, 18: 36167
electron scattering at 100 kev, Lenz theory for small-angle, (E/T), 19: 8106
electron scattering by, Lenz and Thomas-Fermi-Dirac models for small-angle, (T), 19: 8107
electron scattering by, elastic resonances in, (E), 19: 18702
electron scattering by, screening angles for multiple, (T), 19: 23293
electron scattering at 60 to 400 ev, excitation of optically forbidden states in, (E), 19: 34880
electron scattering by, cross sections extrapolated to zero energy for, 17: 18963
electron scattering by, at 25 kev, 19: 22274 (NP-12721)
electron scattering by Coulomb field of, phase shift approximation for, 17: 31417
electron scattering by atomic, cross sections for, (T), 20: 17286
electron scattering at low energy, resonant, (E), 20: 25743
electron scattering by, corrections to incoherent, 19: 39379
electron scattering at 25 kev, cross sections for and optical transitions in, 18: 20764
electron scattering by, excitation cross sections for, 18: 34430
electron scattering at 50 kev, luminescence from, 18: 44428
electron spectra of, KLL and KL-LLL Auger, (E), 20: 19405
electron temperature and recombination in decaying plasma of, 19: 25594
electron temperatures in afterglow plasma of, using microwave noise, 18: 9551
electron thermal diffusivity in afterglow plasma of, (E), 20: 10149 (SRRC-RR-65-96)
electron thermalization in, calculation of, (T), 20: 28042 (RT-FI-(65)-61)
electron transfer collisions near adiabatic conditions with helium ions, and hydrogen atoms and ions, 16: 16868
electron transmission through gases of, at sub-excitation energies, 18: 32396
electron vacancies in, readjustment to inner, 18: 20729 (CONF-481-6)
electron velocity distribution in positive column of discharge plasma of, radial dependence of, (E), 20: 22294
electron velocity distributions in mixtures of mercury and, 18: 28815
electron-atom and -ion collisions in plasma of, 18: 30888 (NP-14067)
electron-ion recombination in afterglow plasma of, temperature dependence of, 20: 34744
energy level transition probabilities of, data compilation on, 20: 31942
energy levels and transition probabilities for, (T), 19: 18677 (ANL-6959)
energy levels of excited, autoionization, 19: 44934(R) (COO-1277-13)
energy levels of solid, Hartree calculation of ground-state, 17: 642
energy levels of, Hartree-Fock diagrams for ground-state, (E/T), 19: 8080
energy levels of, lifetimes of, (E), 19: 16417
energy levels of, r-f resonance of metastable, (E), 19: 23301
energy levels of, autoionization of, (T), 19: 43006
energy of crystalline, temperature dependence of anharmonic free,

18: 6113
energy transfer to, in iodine fluorescence, 19: 2382
Faraday effect in glow discharge of, 18: 28856
free momentum transfer on metals at 25 to 550°C, 16: 13692 (HE-150-182)
gamma reactions (γ,p) at electron energies to 36 Mev, angular distributions and cross sections, 16: 5921 (HEPL-246)
gamma reactions at 170 Mev, absolute yields from, 16: 18529
glow discharges at 1 to 25 torr, between planar anode and hollow cathode, 20: 30173
glow discharges between plane parallel electrodes in, properties of, (E), 20: 36090
glow discharges in, performance of probes for space potential determination in, 20: 6164
glow discharges in, current density in hollow-cathode, (E), 20: 36091
Hartree-Fock potential of neutral atoms of, analytical expressions for, 18: 16656
heat of fusion and heat of vaporization of, calculation from rigid-sphere equation of state, 18: 224
heat transfer by boiling, in narrow annuli, 19: 9343
heat transfer in boiling, 20: 16610
helium and hydrogen ion attenuation at 0.1 to 500 Mev, tables for, 20: 41619 (CEA-R-3042)
helium atom reactions at 0.04 to 1 kev, ionization cross sections for, 18: 32450
helium ion charge exchange in, cross sections for, 18: 14738
helium ion elastic scattering by, cross section for, 19: 32048(R) (NP-15073)
helium ion elastic scattering by, molecular state crossing for perturbation induced in, (E), 20: 5996
helium ion electron capture in, intensity of u-v radiation from, 18: 18496
helium ion interactions at 0.133 to 1 Mev, free electron and ion production in, 17: 32731 (TID-19137)
helium ion ionization of, cross sections for, 16: 15631 (ORO-539)
helium ion reactions with, charge transfer and ionization cross sections for, 16: 33795(R) (TID-16852)
helium ion reactions at 0.15-Mev, charge transfer and ionization cross sections for, 17: 25865(R) (TID-18705)
helium ion reactions at very low energy, optical radiation from, (E), 20: 7730
helium ion reactions at 0.3 to 3 keV, electron spectra from, 16: 33635
helium ion reactions with, excitation cross sections from, 17: 19340
helium ion reactions at 0.133 to 1.0 Mev, ionization cross sections for, 18: 42317
helium ion reactions at 0.133 to 1.0 Mev, ionization cross sections for, 18: 42318
helium metastable atom scattering by, angular dependence of cross sections, 18: 26237
helium metastable atom scattering by, angular dependence of, 18: 28250
helium reactions at 30 to 1000 ev, ionization cross sections for, 18: 36162
helium scattering on, velocity dependence of total cross sections for, (E), 20: 2614
helium-ion elastic scattering at 10 to 600 ev, cross sections for, (E), 20: 19392
hydrogen ion (H_2 and H_3) dissociation in, (E), 19: 4859
hydrogen ion dissociation in, excited hydrogen atoms in, (E), 19: 29006
hydrogen ion reactions at 10 to 50 kev, equilibrium fractions in, (E), 19: 14243
hydrogen ion reactions at 20 to 120 kev, ionization cross sections for, 20: 31909
hydrogen ion reactions with, excitation cross sections from, 17: 19340
hydrogen line emission in pulsed plasma of, 18: 40667
hydrogen molecule scattering by metastable atoms of, effective cross section of, 19: 25171(T)
hydrogen negative-ion dissociation in, cross sections for, (T), 20: 29947
hydrogen reactions with metastable, de-excitation in, 18: 10799
interaction potentials for atoms of, at high temperature, repulsive, (E), 20: 26302
interactions of gas with plasma at 5 to 200 μ of mercury, 16: 23215
interactions with metastable helium atoms, de-excitation cross sections for, 16: 30972
interactions with graphite, constants for (6-exp) potential in, 17: 29442
ion and light emission from plasma of, time dependence of, (E), 20: 19995(R) (AD-630123)
ion beam reactions with gaseous, charge exchange in, (E), 19: 29008
ion diffusion and drift in, positive, 18: 34449
ion excitation energies and densities in plasma of, (E), 20: 17508 (ARL-65-246)
ion mobilities and recombination coefficients in plasma of, positive, 18: 28827
ion mobilities in, ambipolar diffusion determination of, 18: 785
ion mobilities in, average momentum-transfer cross section for, 18: 36154 (NASA-TN-D-2408)
ion mobility and recombination in plasma of, 20: 22169(R) (AD-622684)
ion reactions at 1 to 30 kev, charge exchange cross sections for alkali metal, (E), 20: 34112
ion reactions at 100 to 450 kev, electron stripping in, 18: 32452
ion reactions at 5 to 35 kev, excitation in, 18: 32447
ion reactions in, charge transfer and ionization cross sections for 60- to 450-kev rare-gas, 17: 28054
ion reactions with plasma of, two-stream instabilities in, (E), 19: 14716
ion resonance in weakly ionized plasma of, 20: 44889
ion scattering by, use for production of neutral beams, 19: 2983
ion stopping by, at 50 kev, 18: 32288
ionization by alpha particles, impurity and temperature effects on energy of, 18: 18467
ionization by electrons at 0.6 to 20 kev, (E/T), 19: 20850
ionization by electrons, cross sections and efficiency curve for, 16: 1764
ionization by electron and proton impact at high energies, cross sections for, (T), 19: 47246
ionization by electron impact at energies up to 100 ev, cross sections for, 17: 31126
ionization by electrons, cross sections for, 18: 20768
ionization by fission fragments in nuclear thermionic cells, 17: 27985
ionization by fission fragments, plasma production in, (E/T), 20: 13939
ionization by fission products, 18: 16740(R) (AD-425231)
ionization by fission fragments, 18: 30487 (TID-7687(p.45-50))
ionization by helium ions, cross sections for, 17: 36451 (TID-19296)
ionization by hydrogen atoms and protons at 10 to 180 kev, cross sections for, 16: 18277
ionization by in-pile fission fragments, (E/T), 19: 16366(R) (AD-609177 (Sect.A))
ionization by light, multi-photon, (T), 19: 16398
ionization by protons at 0.15 to 1.1 Mev, cross sections for, 16: 19559
ionization by protons, cross sections for, 17: 32790
ionization by protons in spark chambers, measurement of, (E), 20: 2128 (JINR-E-2324)
ionization cross section for, electron-impact, 19: 38630
ionization cross sections of, calculation of, 18: 16661
ionization equilibria in sun, (T), 20: 19338
ionization in mass spectrometer, formation of multiply charged ions in, 20: 14584(R) (TID-22444)
ionization in pulse discharge, 16: 878
ionization in spark chambers by charged particles, 18: 24473
ionization near tungsten surface, energy distribution of field ions in, (E), 19: 2971
ionization of deuterated and normal butane and ethylene by energy transfer from, isotope effects in, 16: 28966
ionization of excited, by hydrogen molecular and proton bombardment, 19: 6440(R) (COO-1277-7)
ionization of, measurement of coefficient for first Townsend, 18: 2540
ionization of, by electrons at 0.6 to 20 kev, cross sections for, (E/T), 20: 31906
ionization of, cross sections for ruby-laser-multiphonon, (T), 20: 15276
ionization potential (+6), 18: 16680
ionization potentials of multiply charged, 18: 22117(R) (RRL-133)
ionization striation production in hollow-cathode plasma of, (E), 20: 20085
ionization, Lewis number for, 16: 18930
isotopic composition of atmospheric, 19: 30136
isotopic composition of atmospheric, 19: 46588 (ORNL-3857)
isotopic content of neon-22-enriched, method for determining, 20: 27395
kinetic properties at 2,000 to 10,000°K, (T), 20: 26302
krypton ion reactions with, charge-transfer cross sections for, 16: 27836
light absorption by fully ionized plasma of, (T), 19: 10390 (IPP-6/27)
lithium reactions at 80 kev, energy losses in, (E), 19: 6443
lithium scattering by, interaction potentials from cross sections for, 17: 25933
lithium-7 scattering at 7 to 60 kev, angular distributions from, 18: 21318
magnetic interaction experiments with shock-ionized, 20: 46805 (AD-628323)
magnetic properties of, Hartree-Fock-Slater wavefunction calculations of, 19: 27086
melting temperature of, equations for calculating, 18: 25990
mesic (μ^-) molecule formation rates in, 17: 9586
meson (μ^-) capture by, probability for, 18: 38130
meson (μ) nuclear capture in mesic atoms of, probability for, 17: 24493
meson (μ^-) capture by, measurement of disappearance rate in, 18: 2645
microwave absorption by plasma electrons in, effects of cyclotron resonance on, 17: 31627
microwave discharge afterglow in, electron density in, 17: 11384
microwave emission from plasma of, (E/T), 19: 1792
microwave energy absorption in magnetoplasma of, (E), 19: 37905 (AD-426186)
microwave interaction in afterglow plasma of, 18: 35015
microwave penetration through plasma of, polarization modifications in, (E), 20: 1292
microwave propagation in plasma of, cyclotron resonance echoes from,

(E), 19: 33474
microwave propagation in plasma-filled waveguides containing, 16: 31155
microwave radiation from plasma of, in magnetic field, 17: 22718 (IPPJ-6)
microwave radiation in, negative radiation temperature in cyclotron-resonance, 18: 28874
molecule scattering by, inelastic cross sections for, 19: 14265
neon ion collisions with atoms of, inelastic energy loss in, (E), 19: 41277
neon ion collisions with, resonant electron capture and stripping in, 17: 6863
neon ion inelastic reactions at 20 to 60 ev, electron capture in, 18: 32463
neon ion reactions at 1.0 to 2.5 kev, charge transfer efficiency in, (T), 19: 12066
neon ion reactions with, inelastic energy losses in, 19: 37465
neon ion reactions with, cross sections for, 20: 25747
neon ion reactions with atoms of, at 150 to 400 kev, average inelastic energy loss in, (E/T), 20: 34102
neon ion reactions at 0.3 to 3 kev, electron spectra from, 16: 33635
neon ion scattering at 200 ev to 4 kev, resonant electron capture in, (E), 20: 29944
neon ion scattering on atomic, effects of π and Σ molecular states in, 20: 39601
neon reactions with, resonant electron capture in, 18: 32470
neon-ion reactions at 100 to 400 kev, excitation in, (E), 19: 20862
neutron absorption and scattering at (3 to 25) $\times 10^{-3}$ to 10^{-2} ev, cross sections for, 17: 29588
neutron absorption and scattering cross sections for natural, thermal, 17: 11620 (EANDC(3)-10.U)
neutron moderating properties at 20 to 150°K, 16: 29716
neutron reactions (n,p) at 14.1 Mev, (E), 20: 12118
neutron scattering by liquid, co-operative modes of motion from cold, (E), 20: 2837
neutron total cross sections at 10^{-3} to 10^{-2} ev, 16: 18433
nitrogen ion reactions with, cross sections for, (E), 20: 25747
nitrogen metastable molecule reactions in discharges and afterglows, 18: 32494
noise resonance in afterglow plasma of, narrow-band, 18: 28872
oxygen ion reactions at 15 to 50 kev in, equilibrium fractions for, (E), 19: 18687
performance as filler gas for 14-ft bubble chamber, (E), 19: 36803 (BNL-9146)
performance as spark-detector gas, 18: 18197
performance as working gas in nuclear-thermionic plasma diodes, (E/T), 19: 16440(R) (AD-609177)
performance for uptake of fission gas in passage through boiling-water reactors, 19: 31516(P)
performance in hodoscope tubes, 19: 11583
performance in spark chambers, admixture effects on, 18: 14210 (JINR-P-1498)
performance of alkali-seeded, as carrier gas in MHD generator, (T), 19: 34999 (NASA-TN-D-2873)
performance of lamp with, as light source for photomultiplier gain stabilization, 19: 34478 (ORNL-TM-985)
photo-ionization of, abundances of ionic species from, (E), 19: 37456(R) (ORNL-3778(p.9-12))
photoelectric effect at 852 ev to 40 kev in, cross sections for, (E), 20: 21523
photoemission spectra of plasma of, transition probabilities for, (T), 19: 33486
photoionization by cosmic x rays, cross sections for interstellar K-shell, 20: 37485
photoionization cross sections, (T), 19: 18705
photoionization cross sections for, 17: 647
photoionization cross section at 80 to 600 Å, 18: 14740
photoionization cross sections for 80 to 600 Å, 18: 20728 (AD-412421)
photoionization cross sections at 80 to 600 A, 18: 26239
photoionization in the K-shell of, electron shake-off resulting from, (E), 20: 2622
photoionization of, dielectric breakdown from, (E), 19: 20847
photon reactions with Coulomb field of, pair production total cross sections for high-energy, (T), 20: 17754
photonuclear reactions, 16: 1060
physical properties of liquid, to 50,000 lb/in.^{2}, 18: 15044 (LADC-5956)
plasma of, in positive column at 1 torr, Hall effect and electron drift velocities of, 18: 4678
plasma of, double-probe technique for electron velocity distributions in, 18: 19193
plasma of, image converter measurements on moving striations in positive-column, 18: 22960
plasma of, low-frequency waves in column of, (E), 19: 19309
plasma of, microwave diagnostics, (E), 19: 5351
plasma of, phase shift between electron concentration and light intensity in moving layers of, 19: 1755
plasma of, stability of a-c positive column of, 18: 21412
plasma of, striations in, 17: 20662
polarizabilities of metastable, measurement of, 18: 22696
polarizability of liquid, corrections for zero-field many-body, 17: 4526
polarization of excited, tensor measurements of, 19: 32048(R) (NP-15073)
positron annihilation in liquid, angular distribution of photons from, (E), 20: 32345
positron elastic scattering by, cross sections for epithermal, 17: 29472
positron lifetime spectra in, (E), 19: 18872
positron mean life in, 18: 707
positronium quenching in, ortho-, 16: 5912
potassium atomic beam scattering by, 18: 17121(R) (TID-20362)
potassium beam attenuation in, cross section for, 17: 13628(R) (TID-17888)
potassium beam scattering by, at three temperatures, 17: 36376 (CONF-186-1)
potassium ion scattering by, total cross sections for, (E), 19: 2980
potassium scattering at thermal energies, total cross sections for, 18: 34407 (UCRL-11071)
potential energy integrals at 0°K of solid, (T), 20: 42123
preparation of single crystals of, 16: 2301(R) (TID-14228)
pressure wave propagation in plasma of, 18: 32904
pressure-volume characteristics at low temperatures, 17: 14936 (IS-623)
production and acceleration of plasma of, in betatrons, (E), 19: 12008
properties as counter tube gas, 16: 31870
properties as reactor coolant, 16: 23830 (BNL-5377)
properties as working fluid in Brayton power cycle, 20: 41398
properties as working medium in closed-cycle turbine, 20: 42654
properties at 0°K, theory of, 18: 22839
properties in scintillation detectors, 17: 29209
properties of discharge plasma of, 17: 36796
properties of h-f discharge plasma of, magnetic-field effects on, (E), 20: 20087
properties of high-power low-density induction plasma of, 18: 11319
properties of, thermodynamic and transport, 18: 1112 (ARL-63-151 (p.294-321))
properties of, bibliography on physical and physicochemical, 20: 22969 (JuL-Bibl.-10)
properties, separation, and uses in industry, 19: 13384
proton attenuation by, 17: 18909 (TID-18436)
proton ionization of, cross sections for ion production in, 17: 22264(R) (ANL-6679)
proton ionization cross sections for, 16: 15631 (ORO-539)
proton ionization cross sections for, 16: 15569
proton reactions at 1 to 23 kev, metastable 2S hydrogen atom production in, (E), 20: 982
proton reactions at 10 to 40 kev, excitation cross sections for hydrogen-atom formation in, (E), 20: 25748
proton reactions at 5 to 115 kev, cross sections for electron capture by, (E), 20: 27746
proton reactions at 50 to 200 kev, secondary electron emission in, (E), 20: 29951
proton reactions at 1 to 25 kev, Lyman alpha emission cross sections for, 18: 32446
proton reactions at 0.8 to 3.75 Mev, partial ionization cross sections for, 18: 37849
proton reactions with, meson (μ^-) transfer in, 16: 5882
proton reactions with, ionization cross sections for, 17: 16886
proton reactions with, cross sections for Lyman alpha production in, 17: 25953
proton reactions with neutral ground state of, formation of excited hydrogen atoms in, (T), 20: 41634
proton reactions with, cross sections for double electron capture by 2- to 50-kev, (E), 20: 44140
proton reactions with, electron production cross sections for, 18: 14724(R) (TID-20298)
proton scattering at 4.43 to 4.49 Mev, polarization in, (E), 19: 19155
proton scattering near 100 kev, ionization cross sections for, 16: 21218
radiation effects on fluorescence spectra of, 19: 30264
radiation peaks in pulse-discharge plasma of, mechanism for secondary, (T), 20: 10164
radiation temperature in positive-column plasma at $\lambda = 4$ and 8 mm, 16: 19594
radio wave emission from plasma of, negative-absorption effects on anomalous bremsstrahlung and cyclotron, (E), 20: 17921
radioinduced ionization in thermionic cells, fission-fragment, 18: 20860
radioinduced ionization of, electron dosimetry by, 18: 29764
reaction of atomic, with hydrocarbon molecules, ionization in, 19: 9943
reactions between gases and plasma of, ionization in, 18: 36747
reactions of atomic, rotational transitions in, 18: 32492
reactions with acetylene, deuterium, ethylene, and nitrous oxide, cross sections for, 19: 13324
reactions with carbon black surfaces, 17: 20050
reactions with carbon monoxide, charge-exchange cross sections for, (E), 20: 29948

reactions with cesium, potassium, and sodium in atomic beams, cross sections for, (E/T), 19: 9942
reactions with cesium, excitation transfer in, (E), 20: 15253
reactions with deuterated and undeuterated propane, dissociative charge-exchange, 18: 3743
reactions with deuterium hydride ions, intermolecular isotope effects in, 18: 37134
reactions with gases, dissociative ionization in inelastic, 18: 32487
reactions with graphitized carbon black, gas-surface, 17: 4534
reactions with hydrogen negative ions at 0.2 to 7 kev, electron detachment in, (E), 20: 7735
reactions with hydrogen ion in mass spectrometer, energy-transfer reactions in, 18: 3742
reactions with inert-gas atoms, van der Waals forces for, 18: 34345
reactions with iodine, energy transfer in, 19: 25157
reactions with mercury, cross sections for line broadening from, (E), 20: 2637
reactions with mercury-199 and -201, hyperfine-level excitation in, (E), 20: 4544
reactions with molybdenum, electron spectra from, 18: 24318
reactions with neon ions (divalent), total-charge-transfer cross sections for, 16: 22800
reactions with platinum at 500 to 2500 ev, energy transfer in atomic, 18: 10773
reactions with polyatomic ions, mass spectrometry of dissociation in, 18: 220
reactions with protons and tritons at 0.8 to 3.75 Mev, mass spectra of, 19: 13496
reactions with tungsten surface at 1710 to 2500°K, energy exchange in, 17: 10609 (UCRL-10504)
reactions with tungsten, electron ejection from, (E), 20: 37450
recovery from spark chamber, liquid-nitrogen-cooled adsorption system for, 19: 28633 (MIT-2098-51)
resonances in afterglow plasma of, acoustic, 18: 15357
rubidium-vapor spin relaxation in, (E), 19: 39400
rubidium-87 hyperfine relaxation in, 18: 44825
scandium fluoride absorption spectra in, at 4°K, 20: 45665
scattering atomic beam of, by polycrystalline nickel, 18: 22676
scattering by argon, helium and neon atoms, repulsive potential in elastic, (T), 20: 7723
scattering by copper at 30 kev, (E), 19: 47262
scattering by surfaces, normal momentum transfer in, 18: 40156
scattering of atomic beams of, by argon at thermal energies, cross sections for, 16: 18264
scattering of metastable, in rare gases, errors in measuring cross sections for, 19: 23280
scattering of molecular beams of, by silver single crystals, (E), 20: 44121
scattering on beryllium–copper alloys and nickel at 5 to 25 kev, secondary electrons from, 20: 41620 (NIJS-R-471)
separation from xenon, thermal diffusion factors for, 20: 39321(R) (MLM-1312)
shock waves in, microwave attenuation by, 20: 4934 (AD-619093)
sodium spin-relaxation time in buffer gas of, effect of spin-exchange collisions on optically oriented vapor of, 17: 39771
solubility and thermodynamic properties in molten fluoride systems, 16: 18877
sorption at liquid nitrogen temperature, reversible, 17: 24099
sorption by graphitized carbon black, isotherms for, 16: 31536
sorption by molybdenum, platinum, and tungsten in ion bombardment, 16: 31731
sorption by quartz walls in high-density discharges, (E/T), 19: 46576
sound propagation in afterglow plasma of, Tonks-Dattner resonance determination of, (E), 20: 20044
sound velocity in plasma of, 18: 13138(R) (ORNL-3564(p.44-62))
spectra in glow discharges, (E), 19: 36777
spectra of deuterium and hydrogen in liquid, at 27.2°K, induced infrared, 19: 26320
spectra of excited by electron bombardment, 18: 761
spectra of highly ionized, in high-temperature plasma, 16: 33925 (ARL-62-399)
spectra of highly ionized, in plasma, 18: 40706
spectra of hydrobromic, hydrochloric, and hydriodic acids in, deuterium effects on, 20: 12857
spectra of ionized, operation of theta-pinch discharge as light source for, 20: 25631
spectra of mercury and sulfur isolated in, at high temperatures, 20: 1818 (UCRL-11976)
spectra of, effects of added carbon monoxide on emission, 17: 40855(R) (TID-19512)
spectra of, isotopic shift in, 19: 34124(T)
spectra of, isotope shift in, 17: 29622
spectra of, wavelengths of Lyman lines in, 20: 25731
spectra, electron collision study of excitation functions, 16: 22145
spectra, excited by alpha and electron impacts in pure, 16: 21147
sputtering of potassium chloride crystals at 400 ev, angular distributions from, 16: 19565
sputtering rates on glow-discharge cathodes, 16: 19563
stability of inhomogeneous plasma of, (E), 20: 10191(T)
stability of plasma of, density distribution effect on helical, (E), 20: 38270
stability plasma of, pressure effects on magnetic-field, 18: 6368
stopping in hydrogen, 16: 21628
striations in plasma of, wavelength of moving, (E/T), 19: 14691
structure of single crystal, isotope effects in isothermal compressibility, lattice constant, and thermal expansion in, 20: 6685 (COO-1198-296)
superheat in nucleate boiling of, 18: 26461
thermal accomodation during adsorption of potassium and cesium on tungsten, 17: 16027
thermal capacity of liquid, at boiling point, 18: 19929 (CONF-417-20)
thermal conductivity and viscosity of liquid, at critical point, 17: 25849 (LADC-5791)
thermal conductivity of liquid, 20: 19614 (N-65-17283)
thermal diffusion factor, 19: 36887 (AEET-204)
thermal diffusion of, at 136 to 310°K, isotopic factors for, 17: 20045
thermal diffusion shape factors of columns of, temperature dependent, 18: 5291
thermal transpiration in ultrahigh vacuum, 19: 36619
thermodynamic and transport properties of liquid, 16: 18932
thermodynamic critical point exponents of, quantum theory of corresponding states for, (E/T), 19: 32806
thermodynamic properties of, 17: 21137(R) (NBS-7677)
transition probabilities in luminous plasma, (E), 19: 14713
transition probabilities in shock tubes, 18: 28168
transport coefficients at high temperatures, 16: 25880 (ARL-62-328)
transport properties, 16: 3553
transport properties in pure gaseous and liquid, 16: 18933
transport properties for, during thermal diffusion flow, 20: 39321(R) (MLM-1312)
use in high-field electromagnet cooling, 20: 46543
use in low temperature spark chamber, 20: 41329
use in thermionic-cell conversion devices, 16: 19624
use of liquid, as coolant for cryogenic 200-kgauss magnet, 16: 15408
uses in proportional counters for detection of thermal neutrons, 18: 41798
vapor pressure of liquid and solid, 16: 25968
vapor pressure of liquid, up to critical point, 18: 3722 (UCRL-7167)
vapor pressure ratio of neon-20 and neon-22, anharmonic contribution to, 18: 43475
vapor pressure up to critical point, 18: 41374 (UCRL-7167(Rev.I))
viscosity of, excess transport property determination from, 19: 17365
viscosity of, saturated-liquid, (T), 20: 39940
wave functions for, first-order solutions of Hartree-Fock, 18: 2148
x-ray reactions with, ionization readjustment processes in K-shell, 18: 5929
x-ray attenuation by, coefficients for soft, 17: 22433 (NP-12661)
x-ray reactions at 167 to 913 ev, double Auger electron emission in, (E), 19: 20844
x-ray scattering by atomic, factors for, 17: 39772
x-ray scattering by, corrections for incoherent, 19: 39379
x-ray-absorption coefficients, 17: 39731
xenon ion ionization cross sections, 16: 6880
xenon ion reactions with, charge-exchange cross sections for, (E/T), 19: 34877

NEON FLUORIDES
wave functions of NeF and NeF_2, 20: 14541

NEON HYDRIDES
ions of, charge density contours, Hartree-Fock-Roothaan wavefunctions, and potential curves for, 19: 34167

NEON IONS
aluminum foil bombardment with, defect cluster formation in, 17: 31030
beam production at 17.5-Mev, 18: 2403(R) (PR-P-58)
beams of, analysis of duoplasmatron, 19: 47267
bombardment effects on diffusion of zinc in copper-zinc crystals, 16: 2282
capture of solar, using aluminum foils, 20: 44697
charge exchange with gas targets at 20 to 40 kev, neutral-particle production in, 16: 12248
charge exchange with atoms, cross sections for, 17: 8979
charge transfer cross section of bivalent, in argon, 18: 28246
collisions with argon and neon atoms, inelastic energy loss in, (E), 19: 41277
collisions with neutral neon, resonant electron capture and stripping in, 17: 6863
crystal sputtering to 800 ev, atom emission and spatial distributions from, 16: 22758
cyclotron frequency of divalent and monovalent, (E), 19: 16491
detection of 10 to 100 kev, nuclear track plates for, 17: 3337
detection using photographic emulsions, 18: 37521
diffusion and drift of positive, in neon, 18: 34449

distribution in gas discharge in heavy ion source, (E), 19: 27603 (JINR-P-2043)
dosimetry using nuclear emulsions, photomicrography of ion tracks in, 20: 9263
effects on aluminum and SAP at 9 kev, 19: 47080 (EUR-2478.e)
effects on bacteriophages, 19: 5694
effects on gain of electron multiplier tubes, (E), 20: 43659
effects on germanium films, depth of damage from, (E), 20: 38363
effects on glass surfaces up to 30 kev, 20: 45017
effects on gold films at 15 to 250 ev, 17: 20708
effects on yeast cells, genetic, 16: 9764(R) (UCRL-9897(p.147-50))
effects on yeast, lethal and mutagenic, 20: 6859
electron affinities of, relativistic and nonrelativistic, 17: 27996
electron ionization cross section, 17: 34633
electron reactions in discharge afterglow, 18: 32431
electron reactions with, excitation cross sections for, (T), 20: 31929
electron secondary emission from bombardment of beryllium–copper alloys, energy distribution, 16: 7972
electron transition probabilities of, 2s-2p°, (E), 19: 25173
electron transitions in, collision cross sections for dipolar, 20: 2598
electron-capture cross sections at 0.4 to 3.6 kev, 18: 26229
emission of glass-surface sorbed, rare-gas ion bombardment for, 18: 29862
energy in Zeta pinch discharge in deuterium plasma, 17: 42089
energy levels, 18: 37845
energy levels and wave functions for, (T), 19: 16370 (UCRL-7943-T)
energy levels of, (T), 20: 11450 (UCRL-7842-T)
energy levels of, 20-parameter eigenfunctions and energies of 2^2S states of, 17: 11751
energy loss in gases and solids, 16: 12295
energy loss in hydrogen gas, 16: 12441(R) (TID-14957)
excitation and ionization in Stellarator discharges, 20: 38250
formation by K-shell photoionization of neon, electron shake-off in, (E), 20: 2622
Hartree-Fock wave functions and oscillator strengths for configurations of, 18: 7412
interactions with a tungsten surface, photon emission by, 17: 34593
ionization by electrons, cross sections for, 17: 41653
ionization cross sections of, calculation of, 18: 16661
ionization of carbon monoxide by, cross section for, 17: 35884
ionization of nitrogen by, cross sections for dissociative, 18: 40128
mobilities in parent gas, ambipolar diffusion determination of, 18: 785
mobility of atomic, in afterglow, 19: 33115(R) (AFCRL-64-892)
oscillations in cathode region of glow discharge, plasma, 19: 1762
polarizability and shielding factor for, dipole, (T), 20: 37440
production and acceleration of beams of, 20: 13804
production by hot cathode oscillator discharge for heavy-ion cyclotrons, 19: 37360
production of molecular, reaction rates for, 18: 16722
range-energy relations in matter, (E), 19: 9893 (NAS-NRC-PUB-1133 (p.173-86))
ranges in solids at 50 to 500 kev, 16: 18247
reactions in nuclear emulsions, 17: 3325
reactions in rare gases at 60–450 kev, charge transfer and ionization cross sections for, 17: 28054
reactions of monatomic singly charged, with nitrogen at 10 to 65 kev, rotational and vibrational excitation of singly charged molecular nitrogen ions in, (E), 20: 2618
reactions of, with molecules, atom and charge transfer in, 20: 31224
reactions on helium and neon at 0.3 to 3 kev, electron spectra from, 16: 33635
reactions on metals, secondary electrons from, 17: 16836
reactions with aluminum and copper, emission spectra from bombardment, 18: 28104
reactions with argon, 17: 37646 (KN-62-133(R))
reactions with argon and nitrogen, method for studying interchanges in, 18: 20021
reactions with argon and nitrogen, charge transfer in, 18: 41391
reactions with argon and neon, inelastic energy losses in, 19: 37465
reactions with argon atoms, characteristic energy losses from, (E), 20: 9660(T)
reactions with argon, krypton, neon, and xenon, cross sections for, (E), 20: 25747
reactions with atoms and ions at 0.4 to 2 kev, radiation emission from, 18: 36145
reactions with beryllium–copper alloys at 3 to 90 kev, secondary electron emission from, (E), 20: 21538
reactions with carbon monoxide, charge-exchange cross sections for, (E), 20: 29948
reactions with copper, gold, and graphite at 100 to 30,000 ev, yields of secondary ions from, 17: 7268
reactions with copper and gold at 60, 80, and 90 kev, electron energy spectra from, (E), 20: 15261
reactions with crystal surfaces at 4 to 100 ev, Auger electron yield in, 18: 20780
reactions with crystals, range-energy relations for, (T), 19: 30967
reactions with ethylene molecules at 200 and 400 kev, mass spectra of fragments from, 18: 34433
reactions with gases and solids below 1 Mev, range determinations, 16: 10954 (EFINS-61-68)
reactions with gases, spectra from, 18: 2523 (AFCRL-816)
reactions with gases at 100 to 450 kev, electron stripping in, 18: 32452
reactions with gases, charge exchange in, (E), 19: 29008
reactions with hydrogen molecules at 5 to 35 kev, excitation of Balmer spectral lines in, 18: 26214(T)
reactions with hydrogen, deuterium isotope effects on, 19: 19887
reactions with iron, molybdenum, niobium, silicon carbide, tantalum, titanium oxide, and vanadium, atom ejection patterns in, 16: 2203(R) (TID-14257)
reactions with methane at 2 to 200 ev, 19: 22319
reactions with metal single crystals at 1 to 10 kev, secondary-electron emission in, (E), 19: 39404
reactions with metal surfaces, secondary emission factors for, 20: 31926
reactions with molybdenum at bombarding energies of 10 to 40 kev, 16: 595(T) (NP-tr-792)
reactions with molybdenum, electron spectra from, 18: 24318
reactions with molecular nitrogen ions at 10 to 65 kev, rotational and vibrational excitation in, (E), 19: 41279
reactions with neon, total-charge-transfer cross sections for divalent, 16: 22800
reactions with neon, resonant electron capture in, 18: 32470
reactions with neon gas at 20 to 60 ev, electron capture in, 18: 32463
reactions with neon gas at 1.0 to 2.5 kev, charge transfer efficiency in, (T), 19: 12066
reactions with neon at 100 to 400 kev, excitation in, (E), 19: 20862
reactions with neon, charge-exchange, 20: 4556
reactions with neon atoms at 150 to 400 kev, average inelastic energy loss in, (E/T), 20: 34102
reactions with nickel, product radioactivities from, 18: 1017 (JINR-P-1388)
reactions with nickel, proton-emitting nuclei in, 18: 28567 (JINR-D-1570)
reactions with nitrogen at 0.4 to 2 kev, charge exchange and excitation in, 18: 32449
reactions with nuclear emulsions, effects of energy and mass on grain darkening in, 18: 23916
reactions with organic compounds, fragmentation and ionization in, 19: 17874
reactions with pentaborane-9, mass spectrometric studies of, 19: 13315
reactions with platinum at 500 to 2500 ev, energy transfer in, 18: 10773
reactions with scandium, scandium-44 isomer ratio in, 18: 18872 (JINR-P-1521)
reactions with single crystals of copper, electron emission in, (E), 19: 43009
reactions with thin films at 1 to 30 kev, penetration depth in, 18: 44476
reactions with titanium, nuclear temperature from, (E), 20: 13885
reactions with tungsten at 10–140 kev, secondary electron emission from, 17: 29473
reactions with uranium, production of fissioning isotope with $Z \leq 97$ in, 17: 21082
reactions with xenon atoms, ionization cross sections for, 16: 6880
recombination coefficient of molecular, 18: 786
recombination of diatomic positive, with electrons, 18: 34259 (AD-434907)
reflection by copper crystals at 50 kev, 18: 4341
scattering by copper crystals, structure effects on spectra in, (E), 20: 10261(T)
scattering by neon at 200 ev to 4 kev, resonant electron capture in, (E), 20: 29944
scattering by nickel at 4 to 100 ev, Auger electron emission in, (E), 19: 8096
scattering by rare gases at 80 kev, energy losses from, 18: 34416
scattering by tungsten, electron angular distribution from, 17: 18987
scattering on neon, effects of π and Σ molecular states in, 20: 39601
Slater-Condon parameters of, determined from spectral data, 17: 31118
sorption by tungsten at 40 ev to 5 kev, thermal desorption energies for, 18: 14604
spectra from beams of, extreme ultraviolet, (E), 19: 4853
spectra in strongly ionized plasma, emission, 17: 9764(T)
spectra of multi-ionized, in plasma at high temperatures, 16: 8007
spectra of tetra-, penta-, and hexa-valent, 17: 20753
spectra of VII and VIII, wavelengths in vacuum ultraviolet, 18: 34384
spectral line broadening in, Stark nonhydrogen, 18: 28877
spectral line intensities of lithium-like, 18: 17185
sputtering copper at 30 kev, effects of ion incidence angle on, 17: 688
sputtering of aluminum and gold at 0 to 1 kev, 16: 9280 (ERR-AN-072)
sputtering of aluminum and copper by, energy distributions from, 18: 7404(R) (NP-13430)
sputtering of bcc metal single crystals by, at up to 800 ev, atom ejection in, 17: 37467
sputtering of copper and gold crystals by, high-energy, 16: 19562

sputtering of copper by, at 5 to 15 kev, metastable-atom and photon yields from, 16: 19567
sputtering of copper single crystals by, angular dependence of, 17: 37468
sputtering of copper at 20 kev by, effects of target temperature and angle, 18: 28112
sputtering of germanium at 100 to 800 ev by, target-temperature dependence at 0 to 350°C, 18: 2526
sputtering of gold at 20 to 100 ev, 16: 22757
sputtering of metals by, at 0.1 to 2 kev, 16: 19566
sputtering of metals by, yields in, 16: 22748
sputtering of silicon carbides by, at 10 to 600 ev yields from, 16: 19564
sputtering of silver at 3 to 7 kev by, tracer study of, 18: 751
sputtering on copper, focusing model for, 18: 16672
sputtering on copper at 20 kev, temperature dependence of, 18: 16673
sputtering on copper at 10 to 40 kev, temperature dependence of, 18: 20784
sputtering on copper at 80 to 1200 ev, energy distributions from, 18: 22674
sputtering on copper at 20 kev, angular dependence of, 18: 28262
sputtering on copper at 75 to 1 Mev, yield from, (E), 20: 25744
sputtering on copper at 100 kev to 1 Mev, 20: 37468
sputtering on germanium (100) and (110) surfaces, temperature dependence of yields from, 20: 31915
sputtering on gold at 40 to 100 ev, yields from, (E/T), 20: 13420
sputtering on metals at 20 to 1000 ev, mass dependence of, 18: 20786
sputtering on metals at 45 kev, thermal spikes in, (E), 19: 20838
sputtering on meteorites at 20 kev, erosion rates for, 18: 22655
sputtering on silver at 3 to 7 kev, 18: 37853
sputtering on tungsten, from arc ion source, 19: 34884
sputtering ratio for silver, 16: 9115
sputtering ratio for polycrystalline copper, 16: 9114
sputtering reactions on oriented gold foils at 50 kev, (E), 20: 19372
stripping processes at 100 to 450 kev, cross sections for, 18: 16712
tracks in Ilford emulsions from, grain densities for, 17: 39417 (USNRDL-TR-657)
van der Waals radii of, relation of hydration energy to, 18: 16016
wave functions for $1s^2 2s 2p^6$ configuration of, self-consistent, 18: 20759

NEON ISOTOPES
abundance in Achilles, LaLande, and Peace River chondrites, 20: 16672
abundance in iron meteorites, 16: 4652
abundance in Kapoeta and Staroe Pesjanoe meteorites, 16: 27445
abundance in stone meteorites, relative, 20: 31876
abundance of, in helium-bearing natural gases, 20: 45898
abundance ratios in meteorites, 19: 37450
abundance ratios in atmosphere, (E), 20: 21509
abundances in chondrite pantar, 16: 19167
abundances in ionic species in plasma, (E), 19: 19230 (AD-609186)
abundances in stone meteorites, diffusion losses of, 18: 8975 (NP-13496)
abundances in 47 stone meteorites, 18: 8974 (NP-13495)
content and distribution in pyroxene and feldspar of Khor Temiki meteorite, 20: 25695
content in iron meteorites, (E), 20: 5977
content in meteorites, 18: 18033
content in meteorites, 20: 15193 (NP-15654)
content in Renazzo chondrite, 18: 34390
content in stony meteorites, 17: 30688
contents in mineral fractions of Indarch meteorite, 18: 35714 (BNL-7329)
distribution of atmospheric, 19: 17781(R) (ORNL-3750)
fractionation in gaseous absorption, 17: 4511
helium-3 elastic scattering by, topical model for, 17: 5364
lattice constant of, determination of, for naturally occurring mixture at 4 to 24°K, 17: 34430
neutron reactions (n,p) at 14 Mev, distributions from, (E), 20: 9960(R) (AEET-228)
neutron reactions (n,p) at 14.1 Mev, analysis of, (E), 20: 24429
proton decay, 18: 18876 (KFK-185)
separation by fractionation in film columns, 20: 39322
separation by thermal diffusion, 17: 10240(R) (NP-12208)
separation by thermal diffusion, 18: 21708(R) (MLM-1178)
separation by thermal diffusion, 18: 21709(R) (MLM-1179)
separation by thermal diffusion, 18: 24050(R) (ORNL-3607)
separation by thermal diffusion, 18: 29146(R) (MLM-1192)
separation by thermal diffusion, 18: 35246(R) (MLM-1196)
separation by thermal diffusion, 18: 45173(R) (MLM-1203)
separation by thermal diffusion, effect of alternating current on, 18: 45174(R) (MLM-1204)
separation by thermal diffusion, 18: 45175(R) (MLM-1209)
separation by thermal diffusion, 19: 22846 (ORNL-TM-1047(p.32-9))
separation by thermal diffusion, 19: 24611(R) (MLM-1227)
separation by thermal diffusion, 19: 30632(R) (ORNL-3815)
separation by thermal diffusion, 19: 34607(R) (MLM-1239)
separation by thermal diffusion, factor measurements for, 19: 36887 (AEET-204)
separation by thermal diffusion, column performance for, 19: 36888 (AEET-205)
separation by thermal diffusion, 20: 14444(R) (MLM-1268)
separation in thermal diffusion columns, 17: 12579
separation in thermal diffusion columns, optimum operating conditions for, 19: 13201(R) (MLM-1217)
separation of neon-20 and -22 from, using tube bundle as function of pressure, 20: 39320(R) (MLM-1311)
separation of, review of methods for, 19: 11642
separation of, thermodynamic effects in, (E/T), 19: 9568 (NP-14359)
separation using hot-wire thermal diffusion columns, 20: 39323
spectrum of solar, 18: 24326
thermal diffusion factor for, temperature dependence in, 20: 39326

NEON ISOTOPES Ne-16
production and decay in neon-20 reactions with nickel, possible, 18: 34765 (JINR-P-1679)

NEON ISOTOPES Ne-17
beta decay of, delayed proton emission in, 18: 40523
beta decay of, delayed proton emission in, 18: 42625(R) (ANL-6879 (p.65-8))
beta decay of, log ft values for superallowed transitions in, (E), 20: 24407
beta decay of, proton emission following, 18: 34899
decay, 18: 32813
decay of, delayed proton emission in, (E), 19: 47613
decay of, log ft values for, (T), 19: 21379
decay scheme, 18: 6189
energy levels of, low-lying negative parity, (T), 20: 32398
mass of, isobaric formula for, 19: 1623

NEON ISOTOPES Ne-18
beta decay, 18: 32776
beta decay energies, 16: 7061
beta decay of, branching ratios and half life of, 18: 2911
beta decay of, branching ratios, energies, and half lives, 19: 47603
beta decay of, wave function calculations for transition rate of, 20: 26150
energy levels, 17: 881
energy levels from oxygen-16 (He-3,n) reactions at 11 Mev, (E), 20: 46638
nucleon charge-independent pairing in nondegenerate $2s_{1/2}$ and $1d_{5/2}$ shells of, 20: 24453

NEON ISOTOPES Ne-19
beta decay asymmetry parameter and nuclear magnetic moment of, 17: 26601
beta decay asymmetry parameter for, 18: 22876 (UCRL-11169)
beta spectrum and half life, (E), 19: 5259
decay, positron polarization in, 16: 1018(R) (AFOSR-1396)
energy levels, 17: 881
energy levels, 17: 28298
energy levels, 18: 21352
energy levels, (E), 19: 39827
energy levels, (E), 19: 31241(R) (UCRL-12473(p.1-30))
energy levels, from helium nucleus reactions on oxygen-16, 16: 3743
energy levels of, 17: 2291
half life, 16: 26244
nuclear magnetic moment, 18: 22876 (UCRL-11169)
positron helicity, 16: 24820

NEON ISOTOPES Ne-20
abundance in giant stars, (T), 20: 25698
alpha decay of excited, levels and spins from angular correlations from, (E), 20: 19913
alpha elastic scattering at 28.5 Mev, optical potentials in, (E/T), 20: 4859
alpha fission at 19.5 Mev, angular distributions, 16: 19808
alpha fission of, carbon-12 distributions from, 17: 5368
alpha fission of, distributions and yields from, 16: 33875
alpha inelastic scattering at 50.9 Mev by rotational bands in, (E/T), 19: 21267(R) (UCRL-11828(p.113-16))
alpha inelastic scattering at 50.9 Mev, differential cross sections for, (E), 19: 35405 (UCRL-11681)
alpha particle reactions (α,γ) at 1.2 to 3.2 Mev, resonances from, (E), 19: 43358
alpha reactions (α,d) with, $(d_{3/2})^{\dagger}$ and $(f_{7/2})^{\dagger}$ levels from, 18: 16933 (ANL-6848(p.182-7))
alpha reactions (α,C-12) with, cross section fluctuations in, 18: 24625 (WASH-1046)
alpha reactions (α,d) at 45 to 50 Mev, highly populated levels in, 18: 34779 (UCRL-11341)
alpha reactions (α,γ) at 1.6 to 3.2 Mev, angular correlations and distributions from (E), 19: 1677
alpha reactions (α,γ) with, distributions from, (E), 19: 14517 (CONF-640301(p.109-42))
alpha reactions (α,d) at 42 to 53 Mev, deuteron energy spectra from, (E), 20: 12061
alpha reactions (α,d) at 42 to 53 Mev, energy spectra from, (E), 20: 24358(R) (UCRL-16580, pp 1-93)
alpha reactions ($\alpha,\alpha'\gamma$) with, energy levels from, 17: 858

alpha reactions (α,C^{13}), angular distribution in cluster model analysis of, 17: 17195
alpha reactions ($\alpha,\alpha'\gamma$), particle-gamma coincidence studies, 17: 17290
alpha reactions (α,C^{13}) at 12 to 20 Mev, angular distribution and excitation curve for, 17: 31440
alpha reactions, rates for thermonuclear, 16: 23016
alpha scattering at 42 Mev, 18: 16951(R) (TID-20311)
alpha scattering at 22.8 Mev, excitation of 4.97-Mev (2^-) level by, 18: 19076
alpha scattering at 28.5 Mev by, cross sections for elastic and inelastic, (E), 19: 23642
alpha scattering at 28.5 Mev, (E), 19: 31262
alpha scattering at 18 Mev, cross sections for, (T), 20: 22134
astrophysical application of the 7.20 (4+) Mev state of, 17: 16916
boron-11 reactions (B-11,B-10) and (B-11,Be-10) at 115 Mev, fractional parentage of boron-11 ground state from, (E), 20: 36214
bremsstrahlung reactions (γ,p) at 24 Mev, cross sections for, 17: 17155
bremsstrahlung reactions at 170 Mev with, distributions from, 18: 38084(T) (AEC-tr-6398(p.164-88))
content in atmospheric neon, 19: 30136
content in atmospheric neon, 19: 46588 (ORNL-3857)
content in bronzite chondrites, ratio to helium-4 and neon-22, (E), 20: 5975
content in carbonaceous chondrite and earth, 16: 17892
content in helium-burning stars, 18: 42261
content in meteorites, 18: 20726
content in meteorite Khor Temiki, (E), 19: 44906
content in minerals from Indarch meteorite, (E), 19: 9863
content in Sikhote-Alin meteorite, 16: 29627
content in stone meteorites, 20: 956
content in thucholites, 19: 15745
Coulomb excitation by, 17: 4093
detection, scintillation efficiency of sodium iodide crystals for, 16: 3847(R) (ORNL-3193(p.74-8))
deuteron reactions (d,n) at 2.4 to 6.1 Mev, sodium-21 energy levels from, 16: 7097
deuteron reactions (d,α) and (d,p), measurement of Q_0 values for, 16: 11039
deuteron reactions (d,n), cross sections, 16: 12211(R) (CU(PNPL)-208)
deuteron reactions (d,n), absolute differential cross section and energy spectrum, 16: 12458
deuteron reactions (d,α) at 14.7 Mev, angular distributions from, 16: 28065
deuteron reactions (d,n), distorted-wave Born approximation calculations on, 17: 7170
deuteron reactions (d,nγ), angular correlation measurements, 17: 19254
deuteron reactions (d,p) at 2.4 Mev, angular distributions and cross sections for, 18: 1044
deuteron reactions (d,α) with, isotopic-spin selection-rule violation in, 18: 42741
deuteron reactions (d,nγ) at 1.84 to 2.87 Mev, spin-orbit effects in, (E), 19: 5174
deuteron reactions (d,pγ), neon-21 energy levels from, (E), 19: 8452
deuteron reactions (d,α) at 15 Mev with, cross sections for, (E), 19: 23643
deuteron reactions (d,n) at 1.3 to 2.3 Mev, absolute cross sections for, (E), 19: 23716
deuteron reactions (d,p) at 1.8 and 2.2 Mev, neon-21 energy levels from, (E), 19: 47632
deuteron reactions (d,pγ) at 2.05 Mev, neon-21 levels from, (E), 20: 32476
diffusion in fused quartz cylinders, 16: 1769
diffusion in neon-22, thermal, 17: 31221
effects on yeasts, effects of storage in dark on recovery from, 20: 8724 (UCRL-16545)
electron energy levels of, ^{2}P, (T), 19: 12083
electron magnetic elastic scattering at 41.5 Mev, 17: 7222
electron scattering by, study of nuclear magnetic transitions by inelastic, 17: 19078
electronic charge distribution at high energy, 17: 11388
energy in isobaric multiplets (T), 19: 3368
energy level de-excitation branching in, 18: 34842
energy level distributions, (T), 19: 45313
energy level from fluorine-19 (p,γ) reactions at 669 and 1092 kev, 4.97 Mev, 16: 7113
energy-level lifetimes, 16: 21441
energy level lifetime in, 7.02-Mev, 17: 9573
energy level transitions in, 20: 21984 (BNL-948, pp 751-6)
energy level transitions in, weak cross-over, (E), 20: 34684
energy levels, 16: 28129
energy levels, 17: 881
energy levels, 17: 32723(R) (PR-P-57(p.5-20))
energy levels, 17: 40033
energy levels, 18: 2511
energy levels, 18: 26664
energy levels, 18: 32329
energy levels, 18: 34869
energy levels, 18: 34958
energy levels, 18: 34829
energy levels, 18: 38117
energy levels, (E/T), 19: 25479
energy levels, (E), 19: 37858
energy levels, (T), 20: 1227
energy levels, (E), 20: 12150
energy levels, (T), 20: 19984
energy levels, (E), 20: 40164
energy levels, 18: 14592(R) (PR-P-60)
energy levels, 18: 32277(R) (PR-P-61)
energy levels above 9 Mev, 19: 1053(R) (PR-P-62)
energy levels and gamma spectra, 16: 31088
energy levels and dipole gamma spectra, 16: 21452
energy levels and wave functions, 16: 21501
energy levels and transitions in, 18: 8917(R) (PR-P-59(p.4-20))
energy levels at ground to 6.75 Mev, production and properties of, 18: 21241
energy levels at 5.63 and 5.80 Mev, spin and parity, 16: 14026
energy levels at 8.79 Mev, spin-parity of, 18: 2403(R) (PR-P-58)
energy levels at 8.46 and 8.79 Mev, parity and spin of, 18: 15229
energy levels, de-excitation branching and radiative widths of 5.63 and 5.80 Mev states, 16: 21633
energy levels from fluorine-19 (p,γ) reactions, 16: 11008
energy levels from carbon-12 (C^{13},α) reactions, 18: 15230
energy levels from (C-12,α) reactions with carbon-12, (E/T), 19: 16912
energy levels from alpha reactions (α,γ) with oxygen-16 at 1.1 to 2.55 Mev, (E), 19: 43331
energy levels from fluorine-19 (He-3, d) reactions at 9.5 and 10 Mev, (E/T), 20: 4908
energy levels from oxygen-18 (He-3, n) reactions at 1.3 to 5.8 Mev, 20: 4925
energy levels from carbon-12 (C-12,α) reactions, 8^+, (E), 20: 19913
energy levels from deuteron reactions (d,nγ) with fluorine-19 at 1 Mev, parity and spin of, (E), 20: 22082
energy levels from fluorine-19 proton capture, giant resonance, (E), 20: 28301
energy levels from carbon-12 (C-12,α) reactions, 8^+, (E), 20: 34676
energy levels from carbon-12 (C-12,α) reactions, parities and spins of, (T), 20: 38179
energy levels from carbon-12 (C-12,$\alpha\gamma$) reactions at 15.55 Mev, 20: 38008(R) (AECL-2595)
energy levels in SU(3) shell model, (T), 20: 40163
energy levels in SU(3) classification scheme, odd-parity, (T), 20: 44792
energy levels in, particle-hole matrix-elements for, (T), 20: 10051
energy levels of first-rotational-band states of, 17: 7156
energy levels of, from carbon-12 (C^{13},α) reactions, 17: 42005
energy levels of, from intrinsic deformed-potential wave functions, 18: 2918
energy levels of, intermediate coupling analysis of, 17: 40129
energy levels of, parity and spin of 13.332 and 13.440-Mev, 17: 24476
energy levels of, spin assignments for, 17: 33012
energy levels of, structure of giant dipole resonance for ground and first-excited, 18: 19050
energy levels of, parity and spin of, 18: 26574
energy levels of, lifetime measurements on, 18: 32778
energy levels of, anomalous ordering of, 18: 36651
energy levels of, shell-model calculations for even-parity, 18: 36666
energy levels of, in shell model, 18: 38111
energy levels of, separation method for low-lying, 18: 38120
energy levels of, Hartree-Fock theory for, 18: 42737
energy levels of, Hartree-Fock theory for odd-parity, 18: 42738
energy levels of, detection of T = 2, (E), 19: 5196
energy levels of, collective models for, (T), 19: 14514 (CONF-640301(p.22-38))
energy levels of, shell models for low-lying, (T), 19: 14519 (CONF-640301(p.165-81))
energy levels of, lifetimes of low-lying, (E), 19: 14547
energy levels of, interference effect of short range forces on, (T), 19: 31246(T) (JPRS-29270(p.87-103))
energy levels of, structure of coherent, (T), 19: 33355
energy levels of, search for 4.97-Mev doublet, (E), 19: 39809
energy levels of, projected Hartree-Fock spectra for, (T), 20: 6419
energy levels of, even parity rotational, (T), 20: 24403
energy levels of, electromagnetic properties of giant dipole resonaces in s-d, 20: 26165
energy levels of, T = 2, 20: 42227
energy levels, high-spin, 19: 9771(R) (PR-P-63)
energy-range relations at 0.4 to 6 Mev, 16: 8003
energy spectrum of, SU3 shell-model classification for, 17: 19347
enrichment, methods development for, 18: 27813(R) (ORNL-TM-428)
enrichment, operation of thermal diffusion column for, 18: 27811(R) (ORNL-TM-198)

formation in carbon-12 reaction with carbon-12, 16: 21603
gamma decay, 19: 1053(R) (PR-P-62)
gamma emission by, nuclear property determinations from, 18: 18929
gamma reactions, rates for thermonuclear, 16: 23016
gamma reactions (γ,p) with, cross sections, (E/T), 19: 14528 (LAL-1120)
gamma reactions at 170 Mev, absolute yields from, 16: 18529
gamma reactions (γ,p) at 23.5 Mev, proton spectrum of, 17: 5345
gamma reactions on, giant resonance in, 17: 17160
gamma spectra from, 19: 26922(R) (PR-P-64)
gamma transition in, enhanced E3, 18: 38151
helium-3 reactions (He^3,n) at 3.4 and 4.5 Mev, magnesium-22 energy levels from, 16: 7097
helium-3 reactions (He^3,n) with, differential cross section for, 17: 41873 (WASH-1044)
helium-3 scattering at 28.5 Mev, cross sections for, 17: 24408
helium-3 (He-3,t) reactions, sodium-20 mass and energy levels from, (E), 19: 12557
helium-3 reactions (He-3,n) at 25 Mev, spectra of, 18: 24650
helium-3 reactions (He-3,t) with, Q value for, (E), 19: 19205
helium-3 reactions (He-3,t), sodium-20 energy levels and mass from, (E/T), 20: 24358(R) (UCRL-16580, pp 1-93)
helium-3 reactions (He-3,pγ) at 5.35 Mev, sodium-22 levels from, (E), 20: 30400
interactions with alpha particles (α,γ), dependence upon resonance levels, 17: 16916
ionization for cyclotrons, pulsed sources for, 19: 23224
lattice constant of, determination of, at 4 to 24°K, 17: 34430
matrices for 2s-1d shell of, model-interaction, 19: 41730
meson (μ^-) capture by protons in, rate of, 20: 38166
neutron coupling to rotational core of, model for low-lying positive-parity states in, 17: 41950
neutron elastic and inelastic scattering at 0.5 to 3 Mev, 18: 30835
neutron reactions (n,α) at 6.2 to 10.7 Mev, 16: 17099
neutron reactions (n,d) at 14 Mev, cross sections for, 17: 2242 (TID-16949)
neutron reactions (n,α) with, angular distributions for, 18: 11195(R) (EANDC(E)-49(L))
neutron reactions (n,α) at 14 Mev, angular distributions and Q values for, (E), 19: 35378(R) (EANDC(E)-57(U))
neutron reactions (n,α) at 14.2 Mev, angular and energy distributions from, (E), 20: 17743
neutron reactions (n,α) at 14.1 Mev, angular distributions for, (E), 20: 42216
neutron reactions (n,α) at 14.5 Mev, alpha angular distributions from, (E), 20: 46616
nuclear charge distribution, mean-square radius, 16: 18529
nuclear deformation in, stability of axially asymmetric, 17: 40113
nuclear properties of low-lying excited states, 16: 4620(R) (PR-P-50)
nuclear spin of excited level of, 17: 33125
nuclear structure of, α-particle model of, 17: 5374
nuclear structure of, geometrical position of alpha clusters in, 18: 18943
nucleon binding energies, 16: 11007
nucleon charge-independent pairing in nondegenerate $2s_{1/2}$ and $1d_{5/2}$ shells of, 20: 24453
nucleon inelastic scattering by, collective effects of SU_3 classification in, (T), 19: 19216
particle reactions with, selection rules for alpha-knockout, (T), 20: 3117
photospallation cross sections and mechanisms, 16: 22932
production and separation of, method for, 20: 11191 (JEN-150-DQ/I-51)
production from proton irradiation of aluminum, copper, iron, magnesium, nickel, and silver, 17: 19255
production in alpha reactions (α,t) with fluorine-19 at 28.6 Mev, level population in, (E), 20: 19876
production in carbon-12 (C^{12},αγγ) reactions, nuclear properties from angular correlations of, 18: 1091
production in oxygen-16 reactions at 10 Mev, differential cross sections for, 16: 10999
production in supernova explosion, 17: 16916
production in thermonuclear helium-4 reactions during massive-star evolution, 19: 47202
production of tetravalent ions of, for cyclotrons, 18: 5892
proton elastic and inelastic scattering at low energy, direct interaction mechanism for, 17: 13523
proton inelastic scattering at 14.2 Mev, differential cross sections for excitation of first excited state in, 17: 38277
proton inelastic scattering on, excitation of collective states in, 18: 2898
proton inelastic scattering at 8.5 Mev, angular correlation function for second excited state in, (T), 20: 24457
proton reactions (p,t) with, $T = T_z + 2$ states from, 18: 16923 (ANL-6848(p.125-9))
proton reactions (p,γ) at 1.1 to 2.2 Mev, resonance levels in, 18: 19108
proton reactions (p,γ) at 4.3 to 10.5 Mev, angular distributions and resonances in, 19: 19095 (WASH-1053)
proton reactions (p,γ) at 1.28 to 1.86 Mev, gamma energies and yield, (E), 19: 41838
proton reactions (p,γ) at 1.17 Mev, sodium-21 energy levels from, (E), 19: 41838
proton reactions (p,p′γ) at 8.5 Mev, angular correlations from, (E), 20: 22059
proton reactions (p,p′γ), assignment of 4.97 Mev level from, 16: 21632
proton reactions (p,p′ γ), parity of 4.97 Mev level determined by, 17: 19307
proton reactions (p,γ) at 0.25–1.52 Mev, nuclear density distributions from, 17: 31473
proton reactions with, research on, 17: 29392(R) (NP-12951)
proton scattering at 17 Mev by, cross sections for, 16: 33902
proton scattering by, angular correlations for, 17: 34880 (NP-13018)
proton scattering at 3.35 to 5.15 Mev, excitation functions for, 18: 11283
proton scattering cross sections for, DWBA and SCA calculations of, 18: 28636
proton scattering at high-energies, spin-flip, 18: 38125
proton scattering at 1.5 to 2.8 Mev, angular distributions and excitation curves from, (E), 20: 11995
reactions (Ne-20, Na-24) with gold-197 and uranium-238, angular distributions in, 18: 34763 (JINR-P-1675)
reactions (Ne-20, Na-24) with gold-197 and uranium-238 at 130 Mev, (T), 19: 12539
reactions (Ne-20, ×) with uranium-238, spontaneously fissionable materials from, 18: 30720 (JINR-P-1651)
reactions (Ne-20,xn) with erbium isotopes, (E), 19: 21248(R) (UCRL-11828(p.21-5))
reactions (Ne-20,xn) with erbium isotopes, alpha-active platinum isotopes from, (E), 20: 32458
reactions (Ne-20,xn) with molybdenum-92, cross sections for production of tellurium isotopes in, (E), 20: 46774
reactions (Ne-20,6n) and (Ne-20,7n) with samarium-133, alpha activities from, (E), 19: 16982
reactions (Ne^{20},2pn) with aluminum-27, scandium-44 isomer pair production in, 17: 34877 (JINR-P-1277)
reactions on nuclei at 200 Mev, effects of temporary nuclear structure, 16: 5965
reactions on nuclei, α particles and protons from, 16: 5966
reactions on nuclei at 190 Mev, neutrons from, 17: 9593
reactions with aluminum, carbon, copper, and tantalum nuclei, nitrogen-17 production, 16: 17153
reactions with aluminum, copper, and tantalum, nitrogen-17 production in, 16: 27381
reactions with barium-138, equilibrium charge distribution in, 17: 24750(R) (UCRL-10624)
reactions with barium isotopes, 17: 41871 (UCRL-10541)
reactions with bromine and silver nuclei, models for, 18: 17010
reactions with bromine and silver at 200 Mev, mechanisms of, 18: 24732
reactions with complex nuclei, recoil-range evidence for compound-nucleus formation in, 17: 4088
reactions with emulsion nuclei at 10.4 Mev/nucleon, range-momentum relation for heavy recoil ions in, (E), 19: 39883
reactions with emulsion nuclei at 200 Mev, (E), 20: 40083
reactions with gold-197, holmium-165, and uranium-238 at 10.4 Mev/nucleon, fragment three-dimensional angular correlation for, 17: 25868 (UCRL-10748)
reactions with gold-197 at 127 Mev, angular distributions from one-nucleon-transfer, 19: 1553 (JINR-P-1743)
reactions with gold-197 at 127 Mev, angular distributions from one-nucleon transfer, (T), 19: 41805(T)
reactions with gold-197, angular distributions of exchange products from, (T), 20: 4836 (JINR-P-2298)
reactions with heavy nuclei, angular momentum effects on neutron emission in, 17: 26470 (UCRL-10767)
reactions with holmium-165 and tantalum-181, 17: 4086
reactions with molybdenum-92 and -94 at 100 Mev, delayed proton emission in, (E), 20: 11964 (JINR-E-2464)
reactions with molybdenum-92 and -94, delayed proton emitters from, (E), 20: 17687 (JINR-P-2514)
reactions with nickel at 130 Mev, 17: 7082 (JINR-P-1072)
reactions with nickel at 130 Mev, production of proton emitters in, 18: 24737
reactions with nickel at 150 Mev, possible production and detection of neon-16 in, 18: 34765 (JINR-P-1679)
reactions with nuclei, collision effects in, 17: 28258 (UCRL-10775)
reactions with nuclei, cross sections for nucleon transfer in, 17: 38292
reactions with nuclei, pick-up and stripping, 18: 15195 (JINR-P-1486)
reactions with rare earths, effective charge distribution from, 18: 24624 (UCRL-10806)
reactions with rhodium, interference effects in nuclear transfer, (E/T), 19: 5256
reactions with tantalum at 160 Mev, multinucleon stripping in, 18: 24717
reactions with uranium-238 to 10.4 Mev/nucleon, 17: 833
reactions with uranium-238, spontaneous fission of unknown isotope pro-

duced in, 17: 4052 (JINR-P-1070)
reactions with uranium-238, production of fissionable nuclide in, 17: 21082
reactions with uranium-238, momentum transfer in, 17: 24750(R) (UCRL-10624)
reactions with uranium-238, half life of spontaneously fissionable isomer from, 17: 28241 (JINR-P-1258)
reactions with uranium-238, high angular momentum effects on yields in, 17: 38282
reactions with uranium-238 at 10.4 Mev/nucleon, direct interaction mechanisms in fission, 17: 38286
reactions with uranium-238 at 90 to 150 Mev, production of spontaneously fissioning isomer in, 18: 24725
reactions with uranium-238, spontaneously fissionable materials from, 18: 30720 (JINR-P-1651)
scattering by cadmium-114, differential cross section for inelastic, 17: 20990 (TID-18506)
scattering by carbon, electronic stopping cross sections in, 17: 37670
scattering by gold-197, optical model calculation of differential cross section for elastic, 17: 22550 (BNL-6931)
scattering by gold-197 at 200 Mev, matrix elements for inelastic, (T), 20: 4839 (JINR-P-2333)
scattering by iron-56, excitation cross sections in, 17: 34982
scattering by lead-206, -207, and -208, elastic, 16: 29843
scattering by nuclei, strong absorption model for elastic, 18: 26563
separation by thermal diffusion, 16: 3374
separation from neon-22, effects of helium-4 on, 17: 2689
separation from neon-22 by permeation through vycor membrane, 19: 15977
separation from neon-22 by thermal diffusion, 19: 24611(R) (MLM-1227)
separation from neon-22 by thermal diffusion, transport coefficients in, 19: 30630(R) (MLM-1245)
separation from neon-22 by thermal diffusion, transport coefficients for, 19: 30629(R) (MLM-1238)
separation from neon-21 by thermal diffusion, 19: 36889(R) (MLM-1250)
separation from neon-22 by thermal diffusion, 19: 36889(R) (MLM-1250)
separation from neon-22 by thermal diffusion, 20: 3879(R) (MLM-1266)
separation from neon-22 by thermal diffusion, transport coefficients for, 20: 35828(R) (MLM-1300)
separation from neon isotopes using tube bundle as function of pressure, 20: 39320(R) (MLM-1311)
separation from neon-22 by thermal diffusion, transport properties for, 20: 39320(R) (MLM-1311)
separation from neon isotopes, performance of extraction column for, 20: 39321(R) (MLM-1312)
separation of neon-21 from, by thermal diffusion, 20: 25468 (MLM-1293)
separation studies in thermal diffusion columns, 18: 27810(R) (MLM-1183)
separation studies in thermal diffusion columns, 19: 30629(R) (MLM-1238)
superfluidity effects in, 18: 2951
thermal diffusion in neon-22, 16: 3561
transport coefficients for thermal diffusion at 800°C, 20: 20806(R) (MLM-1274)
triton reactions (t,p) with, level excitation cross sections for, 17: 38619(R) (NP-13150(p.1-3))
vapor pressure ratio to neon-22, anharmonic contribution to, 18: 43475
viscosity coefficients at −195 to +25°C, isotope effects on, (E), 20: 11461
wave functions and one-nucleon transfer reactions for, 20: 34588
He–Ne^{20}–Ne^{22}, thermal diffusion coefficients, 17: 31221
H_2–Ne^{20}–Ne^{22}, thermal diffusion coefficients in, 17: 31221
methane–Ne-20, thermal diffusion in, (E/T), 19: 28292

NEON ISOTOPES Ne-21

abundance of, in helium-bearing natural gases, 20: 45898
abundances in 22 iron meteorites, 18: 8973 (NP-13494)
alpha reactions (α,n), neutron production in, 18: 17055
alpha reactions (α,n) at 1.7 to 2.9 Mev (E), 19: 1612
concentration in gaseous neon, equipment for, 20: 20807(R) (MLM-1287)
content in atmospheric neon, 19: 30136
content in atmospheric neon, 19: 46588 (ORNL-3857)
content in chondrites, 19: 25141
content in iron meteorites, 16: 9016
content in iron meteorites, 18: 20205
content in iron meteorites, (E), 19: 20760
content in meteorites, 18: 20726
content in meteorites, radiometric determination of, 18: 22656
content in meteorite Khor Temiki, (E), 19: 44906
content in meteoritic feldspar and pyroxene, 20: 41162
content in minerals from Indarch meteorite, (E), 19: 9863
content in oceanic red clays, (E), 19: 4358
content in Sikhote-Alin meteorite, 16: 29627
content in stone meteorites, 20: 956
content in thucholites, 19: 15745
Coulomb excitation of, gamma angular distribution in, (E), 19: 16896
determination in iron meteorites, 18: 44342 (COO-382-48)
diffusion in iron and stone meteorites, 18: 5486
electron energy levels of, ^2P, (T), 19: 12083
energy level at 350.2 kev, (E), 20: 3043
energy level transitions in, 17: 11660
energy levels, 17: 881
energy levels, (E), 19: 26917(R) (IA-984)
energy levels, 20: 2520(R) (IA-920)
energy levels and gamma spectra, 16: 31088
energy levels and gamma spectra of, 17: 19317
energy levels and gamma cascades, (E), 19: 47632
energy levels from deuteron beam reactions with light nuclei, 16: 11040
energy levels from neon-21 (p,p′γ) reactions at 1.28 to 1.86 Mev, (E), 19: 41838
energy levels from sodium-23 (d,α) reactions at 4.9 to 5.5 Mev, (E), 19: 47633
energy levels from oxygen-18 (α,n) reactions, triplet, (E), 20: 19909
energy levels from oxygen-18 (α,nγ) reactions at 4.43 and 5.5 Mev, (E), 20: 32427
energy levels from deuteron reactions (d,pγ) with neon-20 at 2.05 Mev, (E), 20: 32476
energy levels from alpha reactions (α,nγ) with oxygen-18 at 4.75 Mev, (E), 20: 32476
energy levels from alpha reactions (α,nγ) with oxygen-18 at 4.7 to 6.0 Mev, (E), 20: 32474
energy levels of, core-particle coupling model for low-lying positive-parity, 17: 41950
energy levels of, lifetimes of low-lying, 17: 33098
energy levels of, properties of positive-parity, 18: 2403(R) (PR-P-58)
energy levels of, SU_3 calculation of, 18: 8919(R) (PR-P-59(p.65-78))
energy levels of, parameters for, 18: 34849
energy levels of, gamma de-excitation analysis of neon-20 (d,pγ) reaction for, (E), 19: 8452
energy levels of, models for collective, (T), 19: 14518 (CONF-640301 (p.143-64))
energy levels of, shell model analysis of, (T), 19: 14560
energy levels of, spin of, (E/T), 19: 23754
energy levels of, SU_3 calculations of, 19: 26922(R) (PR-P-64)
energy levels of, collective representation of low-lying, (T), 19: 41757
energy levels of, mixing ratios, parities, and spins of, (E), 19: 45277 (NP-15363)
energy levels of, low-lying $J = \frac{1}{2}$, (T), 20: 44754
energy levels, nuclear model calculations, 19: 9771(R) (PR-P-63)
energy-level spins and transitions, (E), 20: 40156
enrichment, methods development for, 18: 27812(R) (ORNL-TM-415)
enrichment, methods development for, 18: 27813(R) (ORNL-TM-428)
enrichment, operation of thermal diffusion column for, 18: 27811(R) (ORNL-TM-198)
gamma de-excitation angular correlations and branching ratios, (E/T), 20: 34642
level spins and parities, (E/T), 19: 36220(R) (MIT-2098-142)
neutron capture cross sections at 10, 15, and 60 kev, 17: 9158
neutron reactions (n,α), cross sections and energies, 16: 4871
neutron scattering by, cross sections for thermal, (E), 20: 40129
nuclear structure of, rotation-vibration model for, 20: 6441
occurrence in deep ocean sediments, search for, 19: 13621 (BNL-7881)
production and separation of, method for, 20: 11191 (JEN-150-DQ/I-51)
production by cosmic-ray reactions with iron, magnesium, silicon, and sulfur in stony meteorites, 18: 20204
production from proton irradiation of aluminum, copper, iron, magnesium, nickel, and silver, 17: 19255
production in alpha reactions (α,d) with fluorine-21 at 28.6 Mev, level population in, (E), 20: 19876
production rates by cosmic rays in stone meteorites, 18: 8976 (NP-13497)
proton capture and inelastic scattering at 700 to 1300 kev, 18: 38097
proton reactions (p,γ), sodium-22 energy levels from, 18: 17055
proton reactions (p,γ) at 0.3 to 1.0 Mev (E), 19: 1612
proton reactions (p,p′γ) at 1.28 to 1.86 Mev, neon-21 energy levels from, (E), 19: 41838
proton reactions (p,γ) at 600 to 1400 kev, resonance energies for, 17: 21005
reactions with rubidium, electron spin exchange in, (T), 19: 12082
separation by thermal diffusion, 16: 3374
separation by thermal diffusion, relations with mass difference and pressure, 18: 2128(R) (ORNL-TM-658)
separation by thermal diffusion, development of systems for, 18: 10438(R) (ORNL-TM-736)
separation by thermal diffusion, 18: 34005(R) (ORNL-TM-879)
separation by thermal diffusion, 19: 14911(R) (MLM-1216)
separation by, thermal diffusion, 19: 28717(R) (MLM-1221)
separation from neon by thermal diffusion, 19: 24611(R) (MLM-1227)
separation from neon-20 by thermal diffusion, 19: 36889(R) (MLM-1250)
separation from neon-20 and -22 by thermal diffusion, 20: 25468 (MLM-1293)
separation from neon isotopes, performance of extraction column for, 20: 39321(R) (MLM-1312)

separation from thermal diffusion cascades, system for, 19: 46157(R) (MLM-1254)
separation of, from other neon isotopes by thermal diffusion, 20: 35827(R) (MLM-1299, pp 22-33)
separation studies in thermal diffusion columns, 18: 27810(R) (MLM-1183)
superfluidity effects in, 18: 2951

NEON ISOTOPES Ne-22

content in atmospheric neon, 19: 30136
content in atmospheric neon, 19: 46588 (ORNL-3857)
content in bronzite chondrites, ratio to neon-20, (E), 20: 5975
content in enriched neon, method for determining, 20: 27395
content in meteorites, 18: 20726
content in meteorite Khor Temiki, (E), 19: 44906
content in minerals from Indarch meteorite, (E), 19: 9863
content in Sikhote-Alin meteorite, 16: 29627
content in stone meteorites, 20: 956
content in thucholites, 19: 15745
deuteron reactions (d,p), measurement of Q_0 values for, 16: 11039
deuteron reactions (d,n), absolute differential cross section and energy spectrum, 16: 12458
deuteron reactions (d,n), distorted-wave Born approximation calculations on, 17: 7170
deuteron reactions (d,p) at 2.4 Mev, angular distributions and cross sections for, 18: 1044
deuteron reactions (d,n) at 2.75 Mev, neutron emission in, 18: 34832
deuteron reactions (d,p) with, lifetime of neon-23 1.02-Mev level from, (E), 20: 12060
deuteron reactions (d,d) and (d,t) at 12.14 Mev, cross sections for, (E), 20: 24357(R) (UCRL-14538)
deuteron reactions (d,p) with, neon-23 levels from, (E/T), 20: 34642
diffusion in fused quartz cylinders, 16: 1769
diffusion in neon-20, thermal, 17: 31221
effects on structure of single crystal, isothermal compressibility, lattice constant, and thermal expansion in neon, 20: 6685 (COO-1198-296)
electron energy levels of, 2^3P, (T), 19: 12083
electron pair formation in, following positron decay of sodium-22, (E), 20: 40134
energy level lifetime from alpha reactions (α,pγ) with fluorine-19 at 5.2 Mev, (E), 20: 36211
energy levels, 16: 4815
energy levels, 16: 31108
energy levels, 17: 881
energy levels, 17: 6779(R) (ANL-6603(p.47-52))
energy levels, 18: 8917(R) (PR-P-59(p.4-20))
energy levels, (E), 20: 12150
energy levels, 18: 14592(R) (PR-P-60)
energy levels and gamma spectra, 16: 31088
energy levels at 1.28, 3.35, and 4.47 Mev, branching ratios, multipole mixing ratios, and spins of, 18: 21246
energy levels at 3.34 and 4.47 Mev, spins of, 18: 2403(R) (PR-P-58)
energy levels from oxygen-18 (α,p) reactions at 7.76 to 9.95 Mev, (E), 19: 10280
energy levels from fluorine-19 (α,p) reactions, parity, spin, and widths of, (E), 20: 19938
energy levels in, from neon-20 (t,p) reactions, 17: 38619(R) (NP-13150 (p.1-3))
energy levels in, parity of 1.278-Mev resonance, (E), 19: 41837
energy levels of parameters for, 17: 26432(R) (ORNL-3425(p.16-17))
energy levels of, spin assignments for, 17: 33012
energy levels of, parameters for excited, 18: 26645
energy levels of, branching ratios and lifetimes for, 18: 28592
energy levels of, anomalous ordering of, 18: 36651
energy levels of, wave functions in shell model for, 20: 28371
energy levels of, rotational, 20: 46580(R) (BMwF-FBK-66-05)
enrichment, operation of thermal diffusion column for, 18: 27811(R) (ORNL-TM-198)
internal conversion of 1.277-Mev transition in, 17: 17170
lattice constant of, determination of, at 4 to 24°K, 17: 34430
neutron reactions (n,p) at 14.8 Mev, fluorine-22 production in, (E), 19: 47671
neutron scattering by, cross sections for thermal, (E), 20: 40129
neutron total cross sections at 0.2 to 2.1 Mev, (E), 20: 9981 (WASH-1064)
nuclear deformation in, stability of axially asymmetric, 17: 40113
nucleon binding energies, 16: 11007
production and separation of, method for, 20: 11191 (JEN-150-DQ/I-51)
production from proton irradiation of aluminum, copper, iron, magnesium, nickel, and silver, 17: 19255
proton elastic and inelastic scattering by, excitation functions for, 18: 18984
proton elastic scattering by, differential cross sections for, 19: 11525
proton reactions (p,He-3) and (p,t) with, T = 2 states from, (E), 19: 5196
proton reactions (p,γ) at 1.278 Mev, sodium-23 gamma decay modes from, (E), 19: 41837
proton reactions (p,γ) at 1.28 to 1.86 Mev, sodium-23 energy levels from, (E), 19: 41838
proton reactions (p,γ) with, gamma spectra from, (E), 20: 26113
proton reactions (p,γ) at 200 to 460 kev, resonances in, 16: 15632 (SUI-61-7)
proton reactions (p,$\gamma\hat{\gamma}$), resonances in, 16: 21498
proton reactions (p,γ) at 400 to 1030 kev, sodium-23 energy levels from, 16: 23063
proton reactions (p,γ) at 600 to 1400 kev, resonance energies for, 17: 21005
range in aluminum at 1 to 3 Mev, 17: 7231
reactions (Ne-22, F-18) and (Ne-22, Na-24) with gold-197 at 90 to 140 Mev, (E/T), 19: 12525
reactions (Ne-22, Ne-23) with americium-241 and americium-243, production of isomeric americium-240 and americium-242 by, (E), 20: 46586 (JINR-P-2769)
reactions (Ne-22,f) with uranium-238, gold-199 anomalous cross section for, (E), 20: 28450
reactions (Ne-22,xn) with uranium-238, cross sections for, (E), 20: 13889
reactions (Ne-22,6n) with uranium-238 at 112 to 135 Mev, nobelium-254 production in, (E), 20: 11969 (JINR-P-2471)
reactions (neon-22, 4n) with thorium-232, cross sections for, 16: 24781 (JINR-P-896)
reactions (Ne^{22},αn + 2p3n) with aluminum-27, scandium-44 isomer pair production in, 17: 34877 (JINR-P-1277)
reactions (Ne^{22},4n) on thorium-232, cross sections, 16: 29866
reactions on uranium-238, mendelevium-256 from, 17: 9552
reactions on uranium-238, mendelevium-256 from, 17: 9553
reactions with aluminum, copper, and tantalum, nitrogen-17 production in, 16: 27381
reactions with barium-138, equilibrium charge distribution in, 17: 24750(R) (UCRL-10624)
reactions with bismuth-209, production of neptunium-227 and -228 in, (E), 20: 8071 (JINR-P-2435)
reactions with bismuth-209, production of spontaneously fissioning neptunium isotope in, (E), 20: 42292
reactions with copper at 74–145 Mev, gamma energy spectrum from, 17: 13486 (JINR-P-1119)
reactions with copper, tantalum, tungsten, and uranium at 74 to 145 Mev, gamma energy spectra from, 17: 22509
reactions with gold, interference effects in nucleon transfer, (E/T), 19: 5256
reactions with heavy nuclei, fission excitation functions for, 18: 32839
reactions with medium nuclei, neutron spectra from (E), 19: 3236 (JINR-P-1765)
reactions with nuclei, production of nitrogen-17 in, 16: 7130
reactions with nuclei, cross sections for nucleon transfer in, 17: 38292
reactions with nuclei at 5 to 12 Mev, neutron spectra from, (E), 19: 41810(T)
reactions with plutonium-242, element-104 production in (E), 19: 3233 (JINR-D-1818)
reactions with plutonium-242, production of element-104 in, (E/T), 19: 8410
reactions with plutonium, production of spontaneously fissile isotope in, (E), 19: 37881(T)
reactions with plutonium-242, element-104 production from, 20: 40143
reactions with rare earths, effective charge distribution from, 18: 24624 (UCRL-10806)
reactions with scandium-45 at 60 to 160 Mev, production of scandium-44 isomer pairs in, 18: 34948
reactions with thorium-232 and uranium-238, production of actinium-225 and -226 from, 16: 25411 (JINR-P-978)
reactions with thorium-232, production of thorium-227, actinium-226, actinium-225, and actinium-224, 17: 21081
reactions with thorium-232 at 150 Mev, high angular momentum effects on particle distributions in, 17: 38282
reactions with thorium-232 and uranium-238, yields from, 18: 24689
reactions with thorium-232, yields from, 18: 24690
reactions with thorium-232 at 157 Mev, fission fragment distributions and yields in, 18: 24735
reactions with uranium-238 at 135 Mev, 16: 12432 (JINR-P-899)
reactions with uranium-238, spontaneous fission of unknown isotope produced in, 16: 13951 (JINR-P-898)
reactions with uranium-238, production of mendelevium-256 in, 16: 13947 (JINR-P-866)
reactions with uranium-238, spontaneous fission of unknown isotope produced in, 17: 4052 (JINR-P-1070)
reactions with uranium-238, charge distribution curve and fission product yields for, 17: 17114 (JINR-P-1148)
reactions with uranium-238, production of fissionable nuclide in, 17: 21082
reactions with uranium-238, half life of spontaneously fissionable isomer from, 17: 28241 (JINR-P-1258)
reactions with uranium-238, high angular momentum effects on yields in,

17: 38282
reactions with uranium-238, production of nobelium-256 in, 18: 2839 (JINR-P-1383)
reactions with uranium-238, production of nobelium-256 in, 18: 21183 (JINR-P-1580)
reactions with uranium-238 at 90 to 150 Mev, production of spontaneously fissioning isomer in, 18: 24725
reactions with uranium-238 at 147 Mev, fission fragment distributions and yields in, 18: 24735
reactions with uranium-238, fission yields from, 19: 1648
reactions with uranium-238, spontaneous-fission isomer from, (E), 19: 5129 (JINR-P-1801)
reactions with uranium-238, neutron evaporation from, 19: 37791 (JINR-P-2114)
reactions with uranium, production of spontaneously fissile isotope in, (E), 19: 37881(T)
reactions with uranium-238, fermium-256 production from, 20: 40142
separation by thermal diffusion, 16: 3374
separation by, thermal diffusion, 19: 28717(R) (MLM-1221)
separation from argon-36 and -38 by thermal diffusion, design of hot-wire column for, 18: 14339
separation from natural neon by chemical exchange, 20: 35828(R) (MLM-1300)
separation from neon-20, effects of helium-4 on, 17: 2689
separation from neon-20 by permeation through vycor membrane, 19: 15977
separation from neon-20 by thermal diffusion, 19: 24611(R) (MLM-1227)
separation from neon-20 by thermal diffusion, transport coefficients for, 19: 30629(R) (MLM-1238)
separation from neon-20 by thermal diffusion, transport coefficients in, 19: 30630(R) (MLM-1245)
separation from neon-20 by thermal diffusion, 19: 36889(R) (MLM-1250)
separation from neon-20 by thermal diffusion, 20: 3879(R) (MLM-1266)
separation from neon-20 by thermal diffusion, transport coefficients for, 20: 35828(R) (MLM-1300)
separation from neon isotopes using tube bundle as function of pressure, 20: 39320(R) (MLM-1311)
separation from neon-20 by thermal diffusion, transport properties for, 20: 39320(R) (MLM-1311)
separation from neon isotopes, performance of extraction column for, 20: 39321(R) (MLM-1312)
separation of neon-21 from, by thermal diffusion, 20: 25468 (MLM-1293)
separation studies in thermal diffusion columns, 18: 27810(R) (MLM-1183)
separation studies in thermal diffusion columns, 19: 30629(R) (MLM-1238)
superfluidity effects in, 18: 2951
thermal diffusion in neon-20, 16: 3561
transfer reactions of, with thorium, 17: 11473 (JINR-P-1071)
transport coefficients for thermal diffusion at 800°C, 20: 20806(R) (MLM-1274)
vapor pressure ratio to neon-20, anharmonic contribution to, 18: 43475
viscosity coefficients at −195 to +25°C, isotope effects on, (E), 20: 11461
He–Ne^{20}–Ne^{22}, thermal diffusion coefficients, 17: 31221
H_2–Ne^{20}–Ne^{22}, thermal diffusion coefficients in, 17: 31221
methane–Ne-22, thermal diffusion in, (E/T), 19: 28292

NEON ISOTOPES Ne-23
beta decay, charge and recoil spectra of sodium ions from, 16: 22996(R) (ORNL-3268(p.62-5))
beta decay of, electron-neutrino angular correlations in, 16: 33811
beta decay of, electron shake-off following, 17: 26569
beta decay of, electron-neutrino angular correlation from sodium ion recoil energy spectrum in, 18: 2919
beta decay of, recoil energy spectrum at 100 to 500 ev of sodium-23 ions from, 18: 2919
beta decay of, beta interaction in, (E), 19: 37885
beta decay of, direct-interaction ionization probability for, (T), 20: 19934
beta decay scheme, (E), 19: 27530
energy levels, 17: 881
energy levels from deuteron beam reactions with light nuclei, 16: 11040
energy levels from neon-22 (d,p) reactions, (E/T), 20: 34642
energy levels in, lifetime of 1.02 Mev, (E), 20: 12060
energy levels of, lifetime of 1.02 Mev, (E), 20: 9981 (WASH-1064)
energy levels of, parity and spin of, (E/T), 20: 13773 (IKF-13)
gamma dose constants for, 20: 46617
gamma emission by, 18: 8313
gamma spectra, 17: 9549
gamma spectra, 17: 34966
generation and transfer to recoil spectrometer, gas flow and purification system for, 18: 8681
level spins and parities, (E/T), 19: 36220(R) (MIT-2098-142)

NEON ISOTOPES Ne-24
energy levels, 17: 881
yields from high-energy proton reactions, 20: 18556(R) (BNL-929, pp 66-82)

NEON ISOTOPES Ne-25
reactions (Ne-22, Ne-21) with americium-241, production of isomeric americium-242 by, (E), 20: 46586 (JINR-P-2769)

NEON OXIDES
wave functions of NeO, 20: 14541

NEON SYSTEMS
diffusion of krypton-58 in multicomponent, 19: 2343
Ar^{36}–Ar^{40}–Ne, thermal diffusion coefficients in, 17: 31221
Ar–ethyl acetate–Ne, properties as filler gas for G-M tubes, 18: 31921
Ar–He–Ne, striation production in hollow-cathode plasma at, (E), 20: 20085
Ar–Ne, atomic reactions in plasmas of, (E/T), 19: 16250(R) (AD-609177(Sect.D))
Ar–Ne, chemical reaction kinetics of fission-fragment-ionized, (T), 19: 16249(R) (AD-609177(Sec.B))
Ar–Ne, corona discharge in, effects of additions of electronegative gases on, 16: 2372
Ar–Ne, electric breakdown potentials in, pressure dependence of, (E), 19: 23178
Ar–Ne, electric discharge characteristics in, 16: 11098
Ar–Ne, electric impedance in, in glow discharge tubes, pressure effects on, 16: 19598
Ar–Ne, electron temperatures in plasma of, 18: 9551
Ar–Ne, ignition and operating voltage, 17: 14429
Ar–Ne, interaction potentials for atoms of, at high temperature, repulsive, (E), 20: 26302
Ar–Ne, ionization by in-pile fission fragments, (E/T), 19: 16366(R) (AD-609177(Sect.A))
Ar–Ne, microwave discharges in, formative processes in pulsed, 17: 24133
Ar–Ne, microwave gyro-interactions in magnetoplasma of, 18: 28839
Ar–Ne, molecular ions of, in plasmas, (E), 19: 19230 (AD-609186)
Ar–Ne, noise resonance in afterglow plasma of, 18: 28872
Ar–Ne, performance in spark chambers, 19: 13787
Ar–Ne, performance as working gas in nuclear-thermionic plasma diodes, (E/T), 19: 16440(R) (AD-609177)
Ar–Ne, performance in spark chambers, 19: 22750
Ar–Ne, plasma production by fission-fragment ionization of, (E/T), 20: 13939
Ar–Ne, radioinduced ionization in thermionic cells, fission-fragment, 18: 20860
Ar–Ne, reaction kinetics in Penning mixtures of ionized, (E/T), 19: 16441(R) (AD-609177(Sect.C))
Cs–Ne, performance as working gas in Brayton-cycle MHD cells, (T), 19: 16447 (NASA-TN-D-2651)
D–Ne, crystal structure of solid, (E), 20: 40308
D–Ne, phase separation in liquid, 17: 9029
D–Ne, phase studies, 18: 36105
D–Ne, thermodynamic properties at 24.56°K, 18: 4498
ethane–Ne, kinetic energy effects on carbon-11 reactions with, 19: 40617
ethanol–He–Ne, electron drift velocity variations in, 19: 47116 (BNL-9443)
ethanol–Ne, performance in spark chambers, 19: 22750
ethylene–Ne, kinetic energy effects on carbon-11 reactions with, 19: 40617
He^3–He^4–Ne, thermal diffusion coefficients in, 17: 31221
^{4}He–methane–Ne, performance in proportional counters for thermal neutrons, 18: 30058
He–Ne, electric discharge in, electron density and energy in, 18: 19153
He–Ne, electric discharge in spark chambers, displacement of, (E/T), 20: 2131 (JINR-P-2344)
He–Ne, electric discharge in lasers of, current-voltage characteristics of h-f, (E), 20: 21808
He–Ne, electron energy distribution in discharge plasma of, (E), 20: 34760
He–Ne, emission spectra of, (E), 19: 4833
^{3}He–Ne, emission spectra of, (E), 19: 4833
He–Ne, frequency variations in optical masers of, 18: 30328
He–Ne, gas discharges in lasers of, 18: 28175
He–Ne, heating in shock tubes, 18: 42827
He–Ne, interaction potentials for atoms of, at high temperature, repulsive, (E), 20: 26302
He–Ne, laser oscillation in, satellite, 19: 27065 (ORNL-P-116)
He–Ne, optical maser collision processes in, 18: 32484
He–Ne, performance of lasers of, for plasma density measurements, (E/T), 19: 6783
He–Ne, plasma electron density measurements with lasers of, 17: 28367
He–Ne, repulsive interaction potentials for, 18: 9013
He–Ne, spectra of, evidence for compound in, 19: 34173
He–Ne, use in infrared laser, 18: 4325 (CONF-76-7)
hexafluoroethane–Ne, energy transfer in gamma radiolysis of, 20: 10884

He-3–methane–Ne, performance as filling in thermal neutron detectors, 19: 44373(R) (ANL-6877, pp 15-20)
Hg–Ne, electron density and temperature in plasma of, 17: 11883
H–Ne, crystal structure of solid, (E), 20: 40308
H–Ne, electric breakdown potentials in, pressure dependence of, (E), 19: 23178
H–Ne, electric discharges in, layer phenomena of low-pressure, 19: 1747
H–Ne, electron ionization coefficients, 18: 26220
H–Ne, electron transfer collisions near adiabatic conditions in, 16: 16868
H–Ne, ion mobilities and recombination coefficients in, 18: 28827
H–Ne, liquid-vapor phase equilibria in, 20: 32242
H–Ne, nuclear spin lattice relaxation in, 19: 39378
H–Ne, performance in bubble chambers, 19: 40869 (CONF-650510-14)
H–Ne, performance in bubble chambers, 19: 44375 (BNL-9425)
H–Ne, use in bubble chambers, 19: 39026
H–Ne, use of Platt electrostatic model for calculation of properties of diatomic ions of, 18: 12074
Kr–Ne, molecular ions of, in plasmas, (E), 19: 19230 (AD-609186)
Kr–Ne, thermal diffusion at low temperatures, 17: 2691
methane–Ne, cosmic mesons (μ) energy loss rate in, 17: 29489
methane–Ne, performance in spark chambers, 19: 22750
methane–Ne, thermal diffusion in deuterated, (E/T), 19: 28292
Ne–H_2O, performance in spark chambers, 19: 22750
Ne–K, excitation transfer in first excited state of potassium, cross sections for collision-induced, (E), 20: 11499
Ne–Na, excitation transfer in first excited states of sodium, cross sections for collision-induced, (E), 20: 11499
Ne–O, electric discharge in, cathode performance in, 18: 21456
Ne–O, optical maser collision processes in, 18: 32484
Ne–O, radiolysis of, ozone formation in, 18: 20095
Ne–Rb, optical pumping of rubidium-87 in, 20: 2596 (UCRL-16241)
Ne–Rn, thermal diffusion, 16: 3561
Ne–Xe, diffusion of xenon-133 in, 19: 13295
Ne–Xe, spectra of xenon in, detection of laser lines in (E), 19: 1173
NH_3–Ar–Ne, properties as filler gas for G-M tubes, 18: 31921

Neopentane
see Propane, 2,2-Dimethyl-

Neopentyl Alcohol
see 1-Propanol, 2,2-Dimethyl-

Neoplasms
see Tumors

NEPA Reactors
see Aircraft Reactors

Nepheline Syenites
see Syenites

NEPHELOMETERS
see also Sedimentation Apparatus
design and development for radioactive wastes, 19: 42690(R) (ORNL-3782, pp 91-101)
design of radiometric, 19: 24836(P)

NEPHELOMETRY
X-agent effects on protein, 17: 38670

NEPHROSIS
induced by injected mercuric chloride in rats, 20: 3666
occurrence of acute, from x-ray therapy of lymphosarcomas, 17: 27203
pathology of, induced by injected uranium nitrate in rats, 20: 3666
radioinduced in dogs, pathology of, 20: 1686
radioinduced in man, 18: 38791

NEPTUNATES
preparation attempts by pyrolysis of neptunyl nitrate and metal nitrate mixtures, 18: 20012

NEPTUNIUM
see also Actinides
analysis, 17: 6025
analysis for impurities, by ion exchange and spectrography, 17: 15896
analysis of irradiated, for curium-242, 17: 40692 (DP-603)
analysis of, use of anion exchange in spectrographic, 18: 41558 (ANL-6811)
bibliography on, 19: 17390 (AERE-R-4792)
book: *Kinetics of Reduction-Oxidation Reactions of Uranium, Neptunium, and Plutonium in Aqueous Solutions*, in Russian, 20: 25098
chemistry and properties of, survey on, 19: 4161
chemistry, compounds, handling, and radiation hazards of, review of, 18: 16051
clearance of inhaled, from lungs, 17: 2796 (HW-SA-2700)
compressibility and phase diagram of, 20: 39423
crystal structure of, valence electrons and interatomic bonds in, 20: 40296
deposition from ammonium formate–perchloric acid solutions by electrolysis, 20: 25081
deposition of, in bone of rats, effects of diethylenetriaminepentaacetic acid on, 17: 35311(R) (HW-76000(p.143-8))
deposition of, on aluminum, plutonium, and stainless steel, from aqueous media and alcohols, method for quantitative electrolytic, 20: 45675
deposition on aluminum, platinum, and stainless steel, target preparation by electrolytic, 20: 43396
deposition on stainless steel, parameters for quantitative electrolytic, 20: 21287 (AE-217)
determination by controlled potential coulometry, 16: 30326 (HW-SA-2635)
determination by complexonometric titration, 20: 22944
determination, coulometric, 16: 18810 (DP-673)
determination in aluminum as trace impurity, activation, 17: 10546
determination in mixtures of actinides and fission products by paper chromatography, 20: 5509
determination in neptunium–plutonium alloys, spectrophotometric, 19: 38546(R) (RFP-552)
determination in plutonium and uranium solutions by arsenazo photometry, 17: 14189
determination of, automatic colorimetric method for, 17: 38918 (DP-840)
determination of, design of controlled-potential coulometer for, 17: 18000
determination of, electrochemical methods for, 18: 5239
determination of, spectrophotometric, 17: 10533 (HW-SA-2657)
determination of, spectrophotometric, 17: 23265
determination of, evaluation of organic reagents for spectrophotometric, 20: 7035
determination of, using Arsenazo III, photometric, 20: 36778
determination of, review of methods for, 20: 38821
determination using ethanol-aqueous solution and quercetin, 16: 31573
determination using thoron, 16: 31574
determination using arsenazo III, method for, 18: 10005
determination using xylenol orange, photometric, 20: 16408
determinations in the presence of plutonium, calorimetric, 19: 28717(R) (MLM-1221)
diffusion from irradiated uranium, effects of burnup and irradiation level on, 16: 25841 (HW-72321)
diffusion in aqueous solutions, tracer techniques for measurement of self-, 19: 398
diffusion in sintered uranium dioxide at 1250 to 1600°C, 20: 11312
distribution and effects in ecological systems, 17: 33609
distribution between magnesium chloride and magnesium–zinc alloy at 800°C, 18: 1483(R) (ANL-6687(p.27-85))
distribution between phosphate solution and cation exchange resin, 18: 27446
distribution between γ-alumina and molten chlorides, 20: 3959
distribution of inhaled, in tissues, 17: 2796 (HW-SA-2700)
distribution of, between molten magnesium chloride and liquid zinc–magnesium alloy, 19: 36553
electric conductivity at 300°K, reduced Ziman, 18: 34164
electric conductivity at low temperature, radioactive self-damage effects on, (E), 19: 20649
electric conductivity of alpha, at 5 to 300°K, 19: 44675(R) (ANL-7000, pp 155-75)
electric conductivity of, effects of temperature on, 20: 7604
electrodeposition from acid solutions, effects of pH, 16: 3349(T) (AEC-tr-4497(p.400-10))
electrodeposition of, carrier technique for quantitative, 18: 8339
electrodeposition on stainless steel plates, 19: 32059(R) (IDO-14655)
electron energy levels, properties of low-lying, 16: 9326
elution from anion resin, 16: 16394
fission and production in plutonium and uranium irradiations, 16: 29789 (WAPD-TM-331)
Hall coefficient of alpha, at 5 to 420°K, 19: 44675(R) (ANL-7000, pp 155-75)
handling, 16: 19175 (ANL-6540)
ion exchange in concentrated hydrochloric and perchloric acids, distribution coefficients for, 18: 17759
neutron capture cross sections at high energies, 16: 11501(R) (ANL-6413)
neutron capture cross sections at 20 kev, 19: 38786 (LA-DC-7111)
neutron flux and spectrum measurements on foils of, 20: 21427(R) (NASA-CR-54904)
neutron total cross section of, fast, 17: 20982 (HW-SA-2875)
neutron transmission at 35 to 105 ev, 16: 18460
oxidation by chromium(VI) in perchlorate solutions, 19: 22194
oxidation of, spot tests on, 18: 5234
oxidation state in aqueous media, determination of, 18: 19896
oxidation-reduction reactions of, bibliography on kinetics of, 20: 31215 (LA-3507)
precipitation of, with thorium and uranium peroxides, 17: 16079
precipitation with lanthanum trifluoride, oxidation states in, 20: 20561 (JAERI-1099)
preparation and properties of, review of, 19: 18686
preparation of soils of, by electrolysis, 20: 25518 (AERE-R-5097, Paper 15)
preparation of targets by electrodeposition, 17: 12598

preparation of thick and thin sources of, by electroplating and electrophoresis, 20: 18562(R) (EUR-2640.e)
preparation on 50-gram scale, 18: 22432
production, 20: 16543
production of, review of methods for, 20: 20796
properties for complexing, 20: 1848
properties for laser applications, 19: 22205
properties of, electric and thermoelectric, 18: 7242
properties of, pressure-temperature-resistance, 17: 3495 (UCRL-9808)
properties of, review on, 18: 7235
properties of, at low temperatures, 20: 39448 (AERE-X-PR-2596-9)
purification facilities at Purex Plant, 18: 10180 (HW-SA-3282)
purification of, radiochemical method for, 20: 8838 (UCRL-14258)
radiation effects on low-temperature electric conductivity of, self, 20: 39448 (AERE-X-PR-2596-9)
reactions of, compensatory effect in kinetics of, 18: 35563
reactions with sodium bromate in molten lithium nitrate–sodium nitrate, 20: 7073
recovery of, in the Purex and Redox processes, 16: 30493 (HW-SA-1963)
reduction by vanadium in perchloric acid, kinetics and thermodynamics of, 18: 23485
reduction of pentavalent, by iodide ion, kinetics of, 17: 16003
separation by cation exchange on KU-1 and KU-2 resins, 16: 26933
separation by solvent extraction using tri-n-butyl phosphate, 16: 11794
separation by solvent extraction using thenoyltrifluoroacetone and triisooctylamine, 16: 12966
separation from acid solutions by solvent extraction using *N*-benzoyl-phenylhydroxylamine, 20: 45812
separation from aluminum alloyed fuels during chemical processing, flowsheets for, 20: 12926 (IDO-14669)
separation from americium, plutonium, and uranium by reversed-phase partition chromatography, 16: 4224 (KR-11)
separation from americium and uranium by solvent extraction using triisooctylamine, 20: 27003
separation from americium-241 by solvent extraction, 20: 43072(R) (IDO-14679, pp 193-229)
separation from aqueous solutions by solvent extraction using butyl phosphates, synergistic effects of thenoyltrifluoroacetone in, 17: 37306
separation from aqueous media by solvent extraction using lanthanum fluoride and TTA, 18: 19896
separation from aqueous and alcohol-containing hydrochloric acid solutions by ion exchange, 20: 29358
separation from berkelium by solvent extraction, 19: 22112
separation from fission products by solvent extraction using N,N-disubstituted amides, 18: 343 (DP-541)
separation from fission products by precipitation with barium sulfate, 20: 16343
separation from fission products using focusing chromatography, 20: 18601
separation from fission product solutions by ion exchange, 20: 29357
separation from fission products in acid-deficient nitrate system by solvent extraction using 4-methyl-2-pentanone, 20: 31319 (ISO-SA-10)
separation from hydrochloric acid solutions by solvent extraction using 2-ethylhexanol, 19: 36252
separation from irradiated uranium by ion exchange, 18: 23726
separation from irradiated reactor fuels by solvent extraction, 19: 11292
separation from irradiated uranium, chromatographic, 19: 18053 (PAN-575/IXA-V)
separation from irradiated fuel elements, 19: 40675
separation from irradiated uranium by reversed-phase partition chromatography, 20: 10954
separation from irradiated fuels, 20: 16582
separation from irradiated uranium dioxide in chlorine trifluoride by volatilization, 20: 29330(R) (EURAEC-1601)
separation from irradiated uranium dioxide and uranium hydride using phthalocyanine, 20: 43153
separation from irradiated fuels, review of methods for, 20: 46134
separation from neutron-irradiated biological materials by ion exchange, 20: 36762
separation from nitrate solutions with plutonium and uranium by solvent extraction using tertiary amine, 16: 27119(P)
separation from nitric acid solutions by anion exchange resins, 17: 40924 (DP-531)
separation from niobium and zirconium by ion exchange, 18: 25294
separation from nitrate solutions by anion exchange, prevention of gas formation in resin beds used in, 19: 9249 (DP-923)
separation from nitric acid solutions by solvent extraction using dialkyl phosphoric acid, 19: 20075
separation from nitrate solutions by solvent extraction using organo-phosphorus compounds, 19: 20077
separation from nuclear materials by solvent extraction, reagents for, 20: 20561 (JAERI-1099)
separation from other elements with atomic numbers 89 to 95 by paper chromatography, 16: 20340
separation from other transuranic elements by solvent extraction using alkylphosphoric acids, 17: 30625
separation from other actinides by liquid ion exchange, 19: 15358
separation from perchloric acid solutions by solvent extraction using bis(di-*n*-phosphinyl)alkanes, 20: 45786(R) (COO-119-234, pp 277-96)
separation from plutonium and uranium by cation exchange, 16: 26936
separation from plutonium by anion exchange, 17: 40925 (DP-689)
separation from plutonium, uranium, and other elements by ion exchange, 18: 25295
separation from plutonium, solvent-extraction, (E), 19: 15665 (CEA-R-2607)
separation from plutonium by solvent extraction, acidity effects on, 19: 24611(R) (MLM-1227)
separation from protactinium by ion exchange, 18: 23409 (RT/CHI(63)-31)
separation from protactinium by solvent extraction, 20: 43383
separation from Purex Process wastes by solvent extraction, 17: 4625 (HW-SA-2767)
separation from Purex waste by anion exchange, 17: 40923 (DP-453)
separation from rare earth compounds by extraction, 16: 291
separation from rare earths and yttrium by solvent extraction, 18: 352
separation from solutions by solvent extraction using hydroxylamine derivatives, 19: 32297
separation from thorium by ion exchange followed by solvent extraction using trioctylphosphine oxide, 20: 242
separation from transuranium elements by solvent extraction using trioctylphosphine oxide, 19: 28717(R) (MLM-1221)
separation from uranium, 16: 22983 (AWRE-O-46/58)
separation from urine by solvent extraction using mono-2-ethylhexyl phosphoric acid, 17: 37297
separation from uranium and fission products in Purex and Redox processes, 18: 13913 (HW-SA-3283)
separation from uranium by complex formation with phthalocyanine, 19: 34279
separation from uranium and its fission products by ion exchange using 8-quinolinol, 20: 36754
separation from waste solutions, 20: 42689
separation in Purex process, facility for continuous, 18: 13912 (HW-SA-2928)
separation of, from hydrochloric acid by solvent extraction using tri-octylamine, 17: 16156
separation of, from nitric acid solutions, by solvent extraction using trilaurylamine, 17: 18194
separation of plutonium-238 from irradiated, pilot plant facility for, 17: 35936 (CONF-187-1)
separation of, from zinc, in hydrochloric acid solutions by ion-exchange chromatography, 20: 45809
separation of, from irradiated reactor fuels, solvent extraction process for, 20: 45815
solvent extraction by tributyl phosphate and di-2-amyl 2-butylphosphonate in short-residence contactors, 19: 40645 (CONF-650918-1)
solvent partition between lithium nitrate–potassium nitrate and tributyl phosphate, 16: 10111
spectra in labeled perchloric acid and nitrate solutions, near-infrared and visible, 17: 2932
spectra of, theoretical band-head, 17: 24750(R) (UCRL-10624)
spectra of, electron-transfer, 20: 23033
structure, 17: 16559
superconductivity in, search for, 18: 26473
thermal capacity of impure, at 8 to 320°K, 19: 34714
thermoelectric powers at 20°K to room temperature, 16: 15290
thermoelectric power at 20 to 300°K, 18: 36510
transfer from plasma to milk in sheep, tracer study, 17: 10326
vapor pressure at 1700 to 1950°K, 18: 33570
vaporization of, thermodynamics of, 20: 38876 (UJV-1598)
x-ray fluorescence yield for L shell of, 19: 3276

NEPTUNIUM ALLOYS

Al–Np, metallographic examination in clean laboratories, (E), 19: 22969 (DPSPU-65-30-18)
Al–Np, phase studies on, 18: 41984
Np–Pu, crystal structure and phase studies, 18: 25892(R) (ANL-6868 (p.234-66))
Np–Pu, electrical properties from 1 to 300°K, (E), 19: 37115
Np–Pu, phase diagram, 16: 4473
Np–Pu, phase studies and properties of, bibliographic study of, 16: 32115 (KFK-105)
Np–Pu, preparation and properties, 18: 25892(R) (ANL-6868(p.234-66))
Np–Pu, preparation and properties of crystalline, 18: 39806(R) (ANL-6757)
Np–Pu, spectrophotometric analysis for plutonium, 19: 38546(R) (RFP-552)
Np–Pu, structure of single crystal of, 18: 34171

NEPTUNIUM BROMIDES
heat of formation, 20: 29229
NEPTUNIUM CARBIDES
crystal structure and phase studies, 18: 25970(R) (ANL-6868(p.303-25))
production and properties of, 18: 7262
thermionic emission constants of, 17: 16783 (LADC-5128)
NpC–ThC, crystal structure and phase studies, 18: 25970(R) (ANL-6868 (p.303-25))
NEPTUNIUM CHLORIDES
complexes with cyclopentadiene, preparation and properties of, 20: 43230
complexes with dimethylacetamide, preparation and properties of, 20: 31235
heat of formation, 20: 29229
reactions with aluminum chlorides, complex formation in, 17: 10586 (HW-SA-2597)
reactions with dinitrogen pentoxide, 20: 33295
NEPTUNIUM COMPLEXES
composition and stability of pentavalent, 18: 27362(T) (KFK-tr-150)
formation in aqueous solutions, 16: 7575
formation in aqueous solutions, 16: 14702(T) (FTD-TT-61-246)
formation in aqueous solutions by ion exchange, 17: 27350
nitrato- and oxynitrato-, preparation of, 20: 33295
oxychloride, preparation and properties of, 20: 31235
preparation and properties of tetravalent, 17: 16075
separation of pentavalent chelates by extraction, 17: 27350
spectra and stability of, in methanol and water, 19: 7414
stability, 20: 1848
with bromide and chloride, electron transfer in, 18: 3709 (HW-SA-2965)
with bromide and chloride in solutions, spectrophotometric and ion exchange studies, 18: 33526 (IA-924)
with bromine and chlorine, stability of, 20: 2520(R) (IA-920)
with chloride, anion exchange and nonaqueous studies, 17: 10585 (HW-SA-2596)
with chromium, equilibria and kinetics in perchlorate solutions, 18: 13750
with citric and tartaric acids, 16: 5335
with citric and tartaric acids, 16: 5335
with dimethylacetamide, preparation of, 20: 33295
with EDTA, mandelic, oxalic, and phenylarsonic acids, solvent extraction studies on formation of, 20: 20561 (JAERI-1099)
with fluorides and sulfates, properties and stability of, 20: 29148
with glycolic and lactic acids, preparation and properties of, 20: 14556
with hydroxyquinoline and thenoyltrifluoroacetone, effects of organic solvents on extraction of, 17: 1569
with organic acids, formation and stability of, 17: 23236
with oxalate ions, equilibrium solubility in perchloric and oxalic acids, 18: 25392
with phenolphthalein, mole ratio and variation methods for determining sorptive properties of, 20: 5530 (SC-RR-65-625)
with phosphoric acids, preparation by ion-exchange reaction, 18: 27446
with 8-quinolinol and its derivatives, properties of, 19: 28287 (KFK-281)
with 8-quinolinol, preparation and properties, 19: 46288
NEPTUNIUM COMPOUNDS
preparation and properties of, by reaction of neptunium dioxide with alkaline earth oxides, 17: 23359
properties of, review of, 18: 16051
stability, 20: 1855
NEPTUNIUM FLUORIDES
chemistry, 16: 6435
chemistry of, 20: 31315(R) (ANL-7175, pp 42-103)
heat of formation, 20: 29229
molecular structure of, mean amplitudes of vibration at 0 and 298°K in, 20: 38897
properties and reactions of, 20: 5595(R) (ANL-6925, pp 107-64)
separation from uranium hexafluoride, 19: 13553(P)
NEPTUNIUM(III) FLUORIDES
NpF_3–NaF, phase studies, 19: 30149(R) (ORNL-3789(p.3-35))
NEPTUNIUM(IV) FLUORIDES
reactions with calcium, preparation of neptunium by, 18: 22432
thermodynamic properties at 50 to 1600°K for ideal gaseous state at one atmosphere pressure, 16: 26979
NEPTUNIUM(VI) FLUORIDES
crystal structure, 19: 15663(R) (ANL-6900(p.143-202))
magnetic susceptibility at 4 to 337°K, effects of uranium hexafluoride, 16: 30944
molecular force constants of, calculation of, 17: 25174
molecular force constants of, 20: 26865
molecular structure of, mean-square amplitudes of interatomic distances in, 18: 1639
spectra of gaseous, absorption, 20: 20803(R) (ANL-7055, pp 99-162)
spectra of gaseous, absorption, 20: 31248
NEPTUNIUM GERMANATES
preparation and properties, 17: 25216
NEPTUNIUM HYDRIDES
phase studies, 19: 26339
thermodynamic properties, 19: 26339
NEPTUNIUM IODIDES
heat of formation, 20: 29229
NEPTUNIUM IONS
see also Neptunyl Ions
activity coefficients and potentials of (V-VI) couples, effects of hydrogen ion concentration, 16: 22124
atomic radial wavefunctions for trivalent and tetravalent, Slater modified Hartree-Fock, 17: 18066
behavior with Dowex-1 anion exchange resin in nitric acid system, 17: 2992
chemistry of pentavalent, 17: 27350
crystal field shielding in, Slater Modified Hartree-Fock calculations of, 18: 3792
determination of mixtures of tetravalent and pentavalent, in nitric acid solutions, spectrophotometric, 18: 13616 (DP-543)
determination of pentavalent, using Chlorophosphonazo III, photometric, 17: 19981
diffusion coefficients of tetravalent, in Dowex 1-X4 and Permutit SK anion exchange resins, 16: 25309 (DP-727)
distribution coefficients of tetravalent, in potassium sulfate solutions, 16: 27146
effects on methanol exchange in dilute solutions, NMR spectra of, 20: 26838
electron energy levels of trivalent, 18: 27398
heat of solution in hydrochloric acid, 16: 3013
optical properties of tetravalent, in lead molybdate single crystals, 19: 22205
oxidation of pentavalent, by vanadium(V), kinetics of, 17: 40766 (DP-434)
oxidation of (V) to (VI) by ammonium nitrate, 16: 166
reactions in pure and mixed solvents and in presence of inert salts, exchange, 20: 3964
reduction of different valence states of, by uranium(IV) in chloride and perchlorate solutions, 19: 38584 (SC-RR-65-219)
reduction of hexavalent, to pentavalent, by platinum in chloride media, 16: 11638
reduction of pentavalent, by vanadium(III) in perchlorate solutions, kinetics of, 16: 13055
reduction of pentavalent, mechanism of, 17: 10596 (TID-15793)
reduction of pentavalent, to neptunium(IV) by hydrazine nitrate and iron(II) sulfate, 17: 14189
reduction of pentavalent, by uranium(IV) in aqueous perchlorate and chloride solutions, 20: 7082
separation of (IV), (V), and (VI) by solvent extraction, behavior in dodecylbenzenesulfonic acid, 16: 3075
solvent extraction of tetravalent, from nitric acid by TTA and TBP or TBPO in cyclohexane, synergic effects in, 16: 10108
solvent extraction of pentavalent, from nitric acid by TBP and TTA in cyclohexane, synergic effects in, 16: 10107
solvent extraction of pentavalent, from isobutyl alcohol by TTA, 16: 31681
spectra in lithium halide solutions, absorption, 18: 9752 (IA-900)
spectra of complex, in methanol and water, 19: 7414
spectra of trivalent, in heavy water–lithium chloride solutions, absorption, 17: 29879(R) (IA-822)
spectra of trivalent, in lanthanum trichloride single crystals, 17: 37191
spectra of, effects of chemical bonding and transitions on, 20: 36845
NEPTUNIUM ISOTOPES
alpha emission energies, 16: 9455
contents in irradiated BR-2 fuel elements, 19: 10501 (BLG-231)
energy levels of odd-even, hindrance factors for ground-state, (T), 20: 46756
fission barriers and half lives of, spontaneous, (T), 20: 28357
gamma reactions on, cross sections for, 19: 12496
neutron cross sections, 19: 33243 (JAERI-4032)
neutron cross sections of, tabulation, (E), 19: 45250 (BNL-325(2nd Ed.) (Suppl. 2)(Vol.III))
neutron fission of, average number of fission neutrons in, 17: 33016
nuclear properties of, pairing force effects on, (T), 19: 39927
production of spontaneously fissioning, in neon-22 reactions with bismuth-209, 20: 42292
NEPTUNIUM ISOTOPES Np-227
fission of, half life for spontaneous, (E), 20: 8071 (JINR-P-2435)
production in neon-22 reactions with bismuth-209, (E), 20: 8071 (JINR-P-2435)
NEPTUNIUM ISOTOPES Np-228
fission of, half life for spontaneous, (E), 20: 8071 (JINR-P-2435)
production in neon-22 reactions with bismuth-209, (E), 20: 8071 (JINR-P-2435)

NEPTUNIUM ISOTOPES Np-234
beta decay of, transition rates for, (T), 20: 17742
photoproton emission and angular distributions, 16: 7079
positron decay scheme, 17: 4066
NEPTUNIUM ISOTOPES Np-235
beta decay of, nuclear finite size effects on absolute reduced half lives of first forbidden transitions in, (T), 20: 28355
NEPTUNIUM ISOTOPES Np-236
neutron-proton residual interactions in, coupling rules for, (T), 19: 6641
production of isomeric, in deuteron reactions with uranium-238, (E), 20: 40092
NEPTUNIUM ISOTOPES Np-237
activity measurements by foil counting, 16: 1317(R) (LAMS-2627 (p.145-9))
alpha angular distributions from oriented, 16: 7092
alpha decay and thermal neutron fission, nuclear orientation effects, 16: 16061
alpha emission from, use of p-n semiconductor detector for measuring, 20: 29552
alpha fission, 16: 11704(R) (TID-15148)
alpha fission at 22.7 to 45.7 Mev, fragment mass and yields from, (E), 20: 28337
alpha reactions (α,cm), (α,n), (α,2n), and (α,3n) at 5 to 25 Mev, cross sections for, (E), 20: 28337
analysis for protactinium-233, 20: 43383
analysis of foils of, method for, 20: 22870 (LA-DC-7625)
bibliography on chemical, nuclear, and physical properties and separation processes, 16: 3306 (MND-P-2581-I)
bibliography on properties and separation processes, 16: 5080 (MND-P-2581-III(Pt. I))
calibration as neutron-threshold detector, effects of boron-10 shields, 16: 3181 (NDL-TR-9)
charge state and energy loss of, from americium-241 surface deposits, (E), 20: 426
content in spent power reactor fuels, evaluation of, 20: 14435 (BNWL-SA-503)
conversion electron spectra of, sensitivity of beta counters for, 17: 29191 (AWRE-O-29/63)
conversion electron spectra of, sensitivity of beta counters for, 17: 29191 (AWRE-O-29/63)
costs and uses, review of future and present, 17: 31681(R) (HW-76559)
decay scheme, 16: 12540
detection and measurement of, using scintillation ion exchange resin, 19: 32098
determination in human urine, evaluation of methods for, 16: 23375 (TID-7616(p.51-9))
determination in human lungs, whole-body counting, 17: 5704 (TID-12790)
determination in presence of plutonium and fission products using trioctylamine extraction, 17: 40694 (DP-762)
determination in presence of uranium-235, extraction-radiometric, 20: 43072(R) (IDO-14679, pp 193-229)
determination in radioactive waste solutions, 17: 40693 (DP-748)
determination in the presence of plutonium-239, coincidence methods for, 20: 43158
determination in urine, radiochemical, 17: 1176(R) (HW-70050(p.78-142))
determination in urine, radiochemical, 17: 14138 (HW-67067)
determination in urine, radiochemical, 18: 31371 (KY-429)
determination of inhaled, in man by whole-body gamma spectrometry, 17: 24853
determination using proportional detectors, 19: 34470 (CEA-R-2765)
deuteron fission at 21 Mev, cross sections and fragment angular distributions from, 17: 28314
deuteron fission of, fragment anisotropy in compound-nucleus, (E), 19: 12586
deuteron fission of, angular anisotropies from fast, (E/T), 19: 14527 (LA-DC-6673)
deuteron fission of, angular anisotropies from fast, (E/T), 19: 14527 (LA-DC-6673)
deuteron reactions with, products of, · 20: 4928
distribution and retention in rat adrenals, 18: 23221
distribution in tissues and toxic effects of inhaled dusts, 16: 7383 (HW-70949)
distribution of, in liver and kidney in rats, 17: 35293(R) (HW-76000 (p.36-8))
ecological effects, 17: 33609
effect on rat kidneys and liver, 20: 8566
effects of, in skin, pathological, 17: 35312(R) (HW-76000(p.149-55))
effects of injected, on fat accumulation in rat liver, 20: 10522(R) (BNWL-122, pp 79-80)
effects of injected, in liver of sheep, 19: 40350 (HW-SA-3723)
effects on acetate metabolism in rat liver lipids, 18: 41031(R) (HW-80500(p.76-8))
electrodeposition on nickel, 18: 34005(R) (ORNL-TM-879)
energy level transitions in, effect of pairing correlations on E1 (T), 19: 3321
energy level transitions in, conversion electron intensities from, (E), 20: 11956 (EUR-2632.d)
energy levels, 17: 2316
energy levels, 17: 28297
energy levels, 18: 7698 (UCRL-11028)
energy levels, 18: 42690
energy levels, (E), 19: 39946
energy levels, (E), 20: 12158
energy levels, (E), 20: 34561
energy levels, (E), 20: 34562
energy levels, (E), 19: 35378(R) (EANDC(E)-57(U))
energy levels, (T), 19: 21251(R) (UCRL-11828(p.31-4))
energy levels and spins, 16: 31092
energy levels and spins of, 17: 9596
energy levels from americium-241 alpha decay, (E), 20: 26132
energy levels from americium-241 decay, (E), 20: 32375 (ITEF-351)
energy levels from alpha decay of americium-241, (E), 20: 46792
energy levels of, parameters for, 18: 11282
energy levels of, half life of 60-kev, 18: 34813
energy levels of, lifetime of 103-kev, (E), 19: 23676
extrusion of wires of, 19: 16043
fission anisotropies and cross sections at 12 kev to 1.5 Mev, 16: 29734
fission fragment measurements in strong backgrounds using nuclear emulsions, 16: 25558 (JINR-P-979)
fission fragment measurement in high backgrounds, photographic emulsions for, 17: 30880
fission product decay curves for, calculation of, 19: 36831
fission, use in neutron spectrometry, 19: 31245 (ZfK-RN-27)
gamma decay, 18: 34802
gamma magnetic transitions in, orbit-flip effects on, 17: 5350
gamma spectra of, sensitivity of beta counters to, 17: 29191 (AWRE-O-29/63)
helium-ion fission of, cross sections, and charge and mass distributions of, 16: 33809
helium ion fission at 42.8 Mev, deformation of transition-state nucleus in, (E), 20: 12077
helium ion fission at 20 to 40.5 Mev, charge and mass distributions, cross sections, and nuclear radii, 16: 12449 (TID-15147)
helium ion reactions at 20.0 to 40.5 Mev, charge and mass distributions in fission, (E), 20: 11954 (COO-347-18)
helium-3 reactions with, products of, · 20: 4928
internal conversion, nuclear penetration effects on E1, 16: 23102
internal conversion fluorescence yields from, (E), 19: 16853 (NP-14687)
internal conversion in, nuclear structure effects on L-shell, (T), 19: 27486
magnetic octupole moments, 16: 8226
metabolism and toxic effects of, in rats, 17: 35291(R) (HW-76000 (p.22-30))
metabolism in adrenal gland of rats, 18: 41029(R) (HW-80500(p.70-2))
metabolism of, 20: 28885
metabolism of inhaled and ingested, 16: 25120(R) (HW-72500(p.41-3))
Mossbauer effect in neptunium oxides, 18: 34920
Mössbauer effect in neptunium dioxide, after alpha decay, (T), 19: 18699
Mössbauer effect in, review of applications of, 19: 27416 (CONF-650425-1)
neutron absorption cross sections as function of neutron spectra and temperature, 18: 28918(R) (HW-79280(p.3.1-21))
neutron activation rates, calculation of neutron spectral distributions from, 16: 5500 (WAPD-T-1380)
neutron activation cross sections at 0.46 to 1.3 Mev, 17: 40421(R) (ANL-6766)
neutron capture cross sections, 16: 20302(R) (ANL-6477(p.217-23))
neutron cross sections, 17: 4037
neutron cross sections of, effective, 17: 33325(R) (ORNL-3445(p.251-97))
neutron cross sections at 1 kev to 10 Mev, 18: 28718
neutron cross sections, 18: 36567 (CONF-446-10)
neutron cross sections and resonance parameters for, thermal, (T), 20: 24334 (BNL-10083)
neutron cross sections and resonance integrals, 20: 34622
neutron cross sections and resonance integrals, 20: 44602 (BNL-982)
neutron fission at 0.5 to 9.0 Mev, angular momentum effects in (E), 19: 1679
neutron fission cross sections at 10^3 to 10^7 ev, 16: 26525
neutron fission cross section, 16: 26505 (TID-13546)
neutron fission cross sections at 5 to 37 Mev, · 17: 24416
neutron fission cross sections for, thermal and epithermal, 18: 38073(T) (AEC-tr-6398(p.59-63))
neutron fission cross sections of, energy dependence of fast, 19: 15861 (NDL-TR-46)
neutron fission cross sections at 24 kev, (E), 19: 35416

neutron fission cross sections at 1.0 to 4.5 Mev, (E), 20: 9981 (WASH-1064)
neutron fission cross sections at 40 to 500 kev, (E), 20: 17852
neutron fission cross sections at 1.0 to 5.0 Mev, ratio to uranium-235, (E), 20: 24346 (LA-DC-7617)
neutron fission cross sections at 1 to 6 Mev, (E), 20: 46588 (LA-DC-7853)
neutron fission lifetime, 16: 32394 (LADC-5367)
neutron fission lifetime, 17: 17299
neutron fission of, fragment angular distributions from, 17: 22661
neutron fission of, fragment anisotropy in compound-nucleus, (E), 19: 12586
neutron fission of, fragment anisotropy in, (E), 19: 12586
neutron fission of, fragment mass distributions from, (E), 20: 17861
neutron fission of, mass yield curves for thermal, 20: 26190
neutron fission of, angular anisotropies from fast, (E/T), 19: 14527 (LA-DC-6673)
neutron fission rates in FRO critical assemblies, (E/T), 19: 45522 (AE-195)
neutron fission ratios relative to uranium-235, (E), 19: 42077 (ANL-7014)
neutron fission rates of, fast, (E), 20: 14202
neutron reaction cross sections, 16: 14041
neutron reactions on, neptunium-238 production by, 17: 819
neutron reactions with, fast neutron in-pile detection by threshold, 18: 2020 (EUR-289.e)
neutron reactions (n,f), cross sections for, 18: 16947 (NP-13661)
neutron reactions (n,2n) at 14 Mev, shell effects in, (T), 19: 12536
neutron reactions (n,F), thermal, 19: 22801
neutron reactions (n,f) at 0.4 to 4.15 Mev, energy dependence of cross sections for, (E), 19: 45258 (IAE-833)
neutron reactions with, plutonium-238 production in, 20: 19134 (DUN-SA-5)
neutron reactions (n,f) at 0.75 Mev, cross section and threshold energy for, 20: 21427(R) (NASA-CR-54904)
neutron sensitivity of foil-glass dosimeters of, 20: 5713 (AD-623384)
nuclear magnetic moments in neptunium oxide, 18: 26522(R) (ANL-6868 (p.326-30))
nuclear orientation of, in neptunium dioxides, 17: 5056
photofission cross sections at 7.0 Mev, 16: 23082
preparation and properties, 17: 193 (LAMS-2756)
preparation by electrodeposition from solutions, 20: 25081
preparation on multigram scale, 18: 39163 (LA-DC-6402)
processing calutron-separated, methods for, 19: 22848 (ORNL-TM-1047 (p.53-7))
production and uses of, review of, 20: 46134
production by neutron reactions with uranium-235 in thermal power reactors, 18: 41896
production by resonance neutron activation of depleted uranium, 17: 1176(R) (HW-70050(p.78-142))
production in commercial power reactors, process for, 20: 2210
production in fast power reactors, economics of, 18: 26927 (TID-20647)
production in power reactors, fuel cycle for, 20: 32837
production in power reactors, calculated rates and values of, 20: 35002 (BNWL-223)
production in reactors, fuel cycle costs relation to, 19: 29599
production in tracer quantities, 17: 29960
production in U. S. power reactors, estimates for future, 20: 14946 (DP-1015)
production of alpha sources of, electrospraying method for, 20: 16553
production of, process control in, 18: 41330
proton fission at 4 to 12 Mev, cross sections for, 18: 15257
proton fission of, 18: 24625 (WASH-1026)
radiation effects on, self, 20: 39448 (AERE-X-PR-2596-9)
reactions with acids at room temperature, 17: 193 (LAMS-2756)
recovery from radioactive wastes by solvent extraction, 20: 27036(R) (IDO-14661, pp 1-44)
separation and purification from irradiated neptunium targets, 18: 41570
separation and purification from irradiated enriched and natural uranium, 18: 41570
separation from fission products by solvent extraction with thenoyltrifluoroacetone and triisooctylamine, 16: 12966
separation from irradiated neptunium dioxide, facility and equipment for, 17: 40926 (DP-719)
separation from irradiated neptunium dioxide by anion exchange, performance of equipment and process for, 17: 40927 (DP-729)
separation from plutonium-238 by ion exchange, 17: 40922 (DP-417)
separation from plutonium-238, ion exchange process for, 18: 41572
separation from power reactor fuels, economics of, 19: 20036 (BNWL-25)
separation from Purex process plant streams, 18: 13910 (HW-56675(Del.))
separation from radioactive wastes, design of ion exchange column for, 18: 41571
separation from unconverted neptunium-237 and plutonium-238 from, ion exchange process for, 18: 41572
separation from waste solutions, method for, 20: 20561 (JAERI-1099)
stopping times of recoil, in neptunium dioxide, 20: 22037
toxic effects and tissue distribution in rats, 16: 30196 (HW-SA-2614)
toxic effects of, in sheep, 17: 35292(R) (HW-76000(p.31-5))
toxicity, in inhaled dust, 16: 25124(R) (HW-72500(p.56-60))
transfer from plasma to milk, 16: 25121(R) (HW-72500(p.44-9))
use as fast-neutron threshold detector, 17: 34268
use in neutron dosimeters based on fission fragment damage principle, 20: 35740 (BNWL-SA-516)
use in solid-state fission counters, 17: 18646

NEPTUNIUM ISOTOPES Np-238

beta decay and energy levels, 18: 9343
beta decay, energy levels from, 16: 12483
decay, 20: 20561 (JAERI-1099)
energy level shifts in, model of neutron-proton residual interaction for, 20: 8115
energy levels and quasiparticle assignments for, from americium-242m decay, 18: 36581 (UCRL-11379)
fission of compound-nucleus states of, anisotropies in, (E/T), 19: 14527 (LA-DC-6673)
neutron fission lifetime of compound nuclei of, 17: 17299
neutron reactions (n,F), thermal, 19: 22801
neutron-proton residual interactions in, coupling rules for, (T), 19: 6641
preparation by neutron irradiation of neptunium-237, 20: 20561 (JAERI-1099)
production in neutron reactions on neptunium-237, 17: 819

NEPTUNIUM ISOTOPES Np-239

analysis for cerium-143, extraction-radiometric, 20: 43072(R) (IDO-14679, pp 193-229)
content in air from Chinese detonations in 1964, 20: 8980(R) (BNWL-36, pp 3.1-122)
content in atmosphere after Chinese atmospheric tests, 20: 23344 (AEET-240)
content in Columbia River and water supplies in Hanford, Washington area, Jan. to June 1965, 20: 7297 (BNWL-165)
content in fallout particles, 20: 2053
content in fallout from Chinese nuclear test of May 14, 1965, 20: 33530
content in Hanford reactor effluent, 19: 685(R) (HW-81746(p.3.33-6))
content in reactor effluent water, effects of sodium silicate addition on, 18: 36752 (HW-75782)
content in reactor effluent, effect of SiO_2 on, 20: 45215 (BNWL-282)
content in Savannah River water, July through Dec. 1965, 20: 27195(R) (DPST-66-30-1)
detection in gastrointestinal tract from drinking water, continuous monitoring system for, 20: 27191 (BNWL-SA-212)
determination by precipitation with barium sulfate and gamma spectroscopy, 20: 16343
determination in heavy-water moderator by sequential analysis, 18: 27287 (DP-886)
determination in irradiated uranium dioxide, 18: 3891
determination in instrumental activation analysis of pitchblende, 18: 43409
determination in reactor effluents, methods for, 17: 35627(R) (AFSWC-TDR-62-146)
determination in reactor effluent water, monitor for, 18: 13619 (HW-66689)
determination of, gamma spectrometric, 19: 32545 (CEA-R-2461)
distribution and volatility in air-burst debris, 20: 9184 (USNRDL-TR-933)
dosimetry of, equation for internal, 20: 18955
ecological effects, 17: 33609
electrodeposition on stainless steel, method for rapid, 19: 36361
electrophoretic properties, 20: 29351
energy level lifetimes, 74.6-kev, 17: 19272
energy level transitions in, effect of pairing correlations on E1 (T), 19: 3321
energy levels, 18: 7698 (UCRL-11028)
energy levels, 18: 34850
energy levels, 18: 42690
energy levels, (E), 20: 34561
energy levels of, parameters for, 18: 11282
energy levels of, half life of 73.6-kev, (E), 19: 32547 (EUR-2274.e)
gamma coincidence counting in fuels, 17: 2096
gamma decay, 16: 3692
gamma dose constants for, 20: 46617
gamma emission, magnetic quadrupole, 16: 5987
gamma spectra, 17: 34966
gamma spectra of, (E), 19: 23701
half life of millimicrosecond isomer, 17: 7655(R) (ANL-6600)
metabolism in rats, effects of plutonium-239 on, 18: 41030(R) (HW-80500(p.73-5))

preparation, 17: 16551
preparation of, by separation from americium-243 or irradiated uranium, 20: 27003
production in tracer quantities, 17: 29960
removal from rats, effects of DTPA on, 18: 41030(R) (HW-80500(p.73-5))
separation by solvent extraction using hydroxylamine derivatives, 19: 13252
separation from animal tissues using complexing agents, 19: 12945
separation from fission products, chromatographic, 19: 23998(R) (TID-21733)
separation from irradiated uranium, determination of epicadmium-to-subcadmium neutron capture ratio from, 18: 26249
separation from mixed fission products, 19: 15364
separation from neutron-irradiated uranium using focusing chromatography, 20: 29351
separation from radionuclide mixtures by liquid ion exchange, 20: 35427
separation from reactor fuels, technique for, 17: 29572 (KR-44)
separation from uranium and fission products by solvent extraction from nitric acid, 17: 27446
separation from uranium dioxide by solvent extraction, 18: 3891
separation from uranium and fission products, chromatographic, 18: 29557 (KR-83)
separation from water by adsorption on minerals, 16: 25035 (HW-69225)
separation of ionic, at submicromolar concentrations by paper electrophoresis, 16: 17710
sorption by Columbia River particulate material, 18: 35761 (HW-79279)
sorption from reactor effluent by particles in Columbia River, 19: 215(R) (HW-81746(p.3.81))

NEPTUNIUM ISOTOPES Np-240
beta decay and energy levels, 18: 9343
energy level shifts in, model of neutron-proton residual interaction for, 20: 8115
fission probabilities of, spontaneous, 18: 28613
gamma dose constants for, 20: 46617
half life of isomeric, (E), 20: 32460
neutron-proton residual interactions in, coupling rules for, (T), 19: 6641

NEPTUNIUM ISOTOPES Np-241
decay of isomeric, (E), 20: 42202

NEPTUNIUM NITRATES
preparation of hydrated, from aqueous solutions, 20: 33295
preparation of solvated, from nonaqueous solutions, 20: 33295
separation from aqueous nitric acid solutions by solvent extraction using dibutyl carbitol and TBP, 19: 22415
separation from nitric acid solutions by complex formation with organic phosphorus compounds, 19: 20077
spectra of hexa- and tetravalent in nitric acid and tri-n-octylamine-xylene solutions, absorption, 16: 2947

NEPTUNIUM NITRIDES
decomposition of, at 2210 to 2830°C, 20: 43233
decomposition pressure, 18: 37115 (ANL-6856)
decomposition pressure, 19: 40958

NEPTUNIUM OXALATE COMPLEXES
equilibrium solubility in perchloric and oxalic acids, 18: 25392
formation, 16: 2995(T) (CEA-tr-R-1375)

NEPTUNIUM OXIDES
chemistry of, literature survey of solid-state, 19: 15412 (KFK-225)
crystal structure powder diffraction patterns, 19: 17795
crystal symmetry and properties of pentavalent, 18: 41413
evaporation and thermodynamic properties of, 20: 23015
evaporation *in vacuo* at 1850 to 2475°K, thermodynamics of, 20: 10840
fabrication of targets of, for neutron irradiation, 18: 41984
Mössbauer effect of neptunium-237 in, after alpha decay, (T), 19: 18699
neptunium-237 nuclear orientation in, 17: 5056
neptunium-237 Mossbauer effect in, 18: 34920
neptunium-237 recoil stopping time in, 20: 22037
preparation from molten salts, 17: 32073
preparation of hexavalent and pentavalent, 17: 35703 (TID-17786)
preparation of hydrates of trivalent, by ozone oxidation of aqueous hydroxide, 18: 41412
preparation of sols of, with yttrium oxides, 20: 39341(P)
preparation of thin-film radiation targets of, using evaporation-condensation, 20: 11183 (ORNL-P-1900)
processing of irradiated, for plutonium-238 recovery, 17: 40927 (DP-729)
properties of pentavalent, comparison to americium, plutonium, and uranium, 17: 27350
reactions with alkaline earth oxides, 17: 23359
reactions with dinitrogen pentoxide, 20: 33295
reactions with germanium dioxide and silicon dioxide, 17: 25216
separation of neptunium-237 and plutonium-238 from irradiated, facility and equipment for, 17: 40926 (DP-719)
$Al–NpO_2$, compacting by powder metallurgy, 18: 41984
$EuO_2–NpO_2$, phase studies by x-ray diffraction, 20: 2379
$HfO_2–NpO_2$, preparation of sols of, 20: 39442(P)
$Li_2O–NpO_2$, crystal structure, preparation, and properties, 19: 32746
$Li_2O–NpO_2$, crystal structure, preparation, and properties, 19: 32747
$Li_xO–NpO_2–O$, crystal structure and thermal stability of phases in, 18: 27358 (KFK-196)
$Li_xO–NpO_2–O$, lattice constants and thermal stability, 18: 36036
$NpO_2–Na_2O$, crystal structure, preparation, and properties, 19: 32746
$NpO_2–Na_2O$, crystal structure, preparation, and properties, 19: 32747
$NpO_2–Nb_2O_5$, crystal structure, preparation, and properties, 19: 32748
$NpO_x–O–Na_2O$, crystal structure and thermal stability of phases in, 18: 27358 (KFK-196)
$NpO_x–O–Na_2O$, lattice constants and thermal stability, 18: 36036
$Np_2O_3–P_2O_5$, preparation, lattice constants, and properties, 19: 32750
NpO_2–rare earth oxides, preparation of sols of, 20: 39341(P)
$NpO_2–Ta_2O_5$, crystal structure, preparation, and properties, 19: 32748
$NpO_2–ZrO_2$, preparation of sols of, 20: 39442(P)

NEPTUNIUM OXYCHLORIDES
complexes with arsonium compounds and cesium, preparation and properties of, 20: 31235
preparation by dehydration of solution of neptunium and chloride ions, 18: 43536(P)

NEPTUNIUM PEROXIDES
precipitation from nitric acid solutions, 18: 344 (DP-594)
preparation and solubility in hydrogen peroxide–nitric acid solutions, 17: 12227 (TID-16192)
solubility in hydrogen peroxide–nitric acid systems, 18: 344 (DP-594)

NEPTUNIUM SILICATES
preparation and properties, 17: 25216

NEPTUNIUM(IV) SULFATE COMPLEXES
properties of, polarographic studies of, 17: 29003

NEPTUNIUM SYSTEMS
C–Np–U, phase studies, 18: 25970(R) (ANL-6868(p.303-25))
Np–O, evaporation and thermodynamic properties of, 20: 23015

NEPTUNYL IONS
electronic structure and magnetic properties, 19: 32163
oxygen exchange between water and ionic, rates of, 18: 5281
spectra of, electronic configuration model for interpretation of solution absorption, 20: 26870
temperature effects on, in nitric acid, 17: 20116

NEPTUNYL NITRATES
preparation of hydrated, from aqueous solutions, 20: 33295
preparation of solvated, from nonaqueous solutions, 20: 33295
separation by solvent extraction using organophosphoric compounds, 16: 1860(T) (AEC-tr-4671)

NERVA Project
see Rocket Reactors (Kiwi)

NERVE CELLS
activity of, models for, 18: 2404(R) (TID-19651)
development in postnatal rats, tracer study, 20: 20391(R) (TID-22825)
development in rat embryos, 19: 33834
effects of radiation sickness on DNA, phosphatase, and RNA in cerebral, in rats, 20: 31010
effects of radiation sickness on nuclei in adrenal, hypothalamus, and thyroid gland, in rats, 20: 35313
electric impulses from brain, pulse analyzers for, 18: 29188
firing patterns in auditory cortex of cats, observation of joint probabilities of, 16: 4610(R) (TID-14435)
formal threshold type, realizability of Boolean functions by, 16: 4610(R) (TID-14435)
glucose metabolism in gliol, effects on appetite inhibition, 20: 10541
nucleic acid metabolism in, effects of behavioral activation on, 20: 20391(R) (TID-22825)
permeability of squid axon membranes to ions, 18: 29
properties of large nets of, 19: 18383(R) (TID-21595)
radiation effects on neuron substructure in rats, 16: 16278
radiation effects on nucleoproteins and electrical response, 16: 17440(T) (JPRS-12921(p.12-33))
radiation effects in brain of rats, 16: 23474
radiation effects in embryonic neural tube, 16: 23476
radiation effects, survey, 16: 23480
radiation effects, high-dose gamma, 16: 23484
radiation effects of alpha particles from cyclotron, 16: 23492
radiation effects on spinal cord neurons, 16: 23502
radiation effects on ribonucleic acid content of gasserian ganglion cells in rats, 16: 32759
radiation effects on desoxyribonucleic acid content of gasserian ganglion cells in rats, 16: 32760
radiation effects on electrophoretic mobility and protein fraction of, 16: 32811
radiation effects on, in supraoptic cytoplasm and nucleus in rats, 17: 7868
radiation effects on, in rats, 17: 10461
radiation effects on, in rats, 17: 10466
radiation effects on glycogen content of, in frogs, 17: 37069(T)

(JPRS-21170(Del.))
radiation effects on, galactic, 17: 41712 (RM-3043-PR)
radiation effects on, in mice, 17: 40545 (BNL-7284)
radiation effects on, in brain, deuteron, 17: 40606
radiation effects on, in rabbit brain, 18: 1381(T) (OTS-62-11069 (No.3)(p.768-80))
radiation effects on nucleic acid metabolism in, of rabbit brain, 18: 1382(T) (OTS-62-11069(No.3)(p.781-96))
radiation effects on glycogen content of, in brain of rabbits, 18: 1383(T) (OTS-62-11069(No.3)(p.797-808))
radiation effects on secretory function of rat hypothalamus, x, 18: 3529
radiation effects on rat, gamma, 18: 5115
radiation effects on, 18: 11824
radiation effects on dog, polonium-210 and strontium-90, 18: 13463(T) (JPRS-23559(Del.)(p.36-42))
radiation effects on Nissl granules in rat spinal cord, 18: 33349
radiation effects on degeneration of pelvic ganglia in man, cyclotron, 19: 13043
radiation effects on rat dorsal ganglion, protective effects of AET against x, 19: 15224
radiation effects on tritiated-thymidine uptake by neuroblasts in grasshoppers, 19: 15073
radiation effects on neuroblasts, in salamander embryos, 19: 28026
radiation effects on, review of, 19: 31824
radiation effects on fine structure in frog, x, 19: 42285
radiation effects on rat olfactory, x, 20: 8708
radiation effects on rat olfactory bulb, effects of gases in nasal cavities on x, 20: 16215 (AD-628443)
radiation effects on electrical activity of olfactory, x, 20: 20431 (AD-630323)
radiation effects on tigroid substances in, radio wave, 20: 22592
radiation effects on ribonucleoproteins of, gamma and x, 20: 42866
radiation effects on myelinization of, in rats, 20: 45322(R) (UCLA-12-595, pp 6-28)
radiation injuries, relation to proteolytic enzymes in cytoplasm, 16: 23494
radiation injuries of, in rats, 18: 38781
radiation injuries of, in rats, 18: 38919
radiation injuries of, in rats, 18: 38920
radiation injuries of rat, pathology of, 20: 68
radioinduced cytochemical changes in rat, x, 17: 33638
radiosensitivity, 18: 48 (USNRDL-TR-670)
radiosensitivity of, fluorescence emission effects on uv, 18: 11776
radiosensitivity of rabbit, 19: 5637
radiosensitivity of, in rat brains, effects of age on, 19: 8874
radiosensitivity of embryonic grasshopper, effects of tonicity on, 19: 13119
radiosensitivity of neutrons of rabbit cortex, 19: 40355(T) (FTD-TT-65-48, pp 111-12)
radiosensitivity of developing, γ and x, 20: 22620(R) (TID-22823)
removal of cervical sympathetic, effects of, on radioinduced cataract development in rabbits, 17: 21490

NERVES
activity, biochemical basis of, 16: 1405
effects of section of sciatic, on bone blood flow, 20: 16192
electric activity of optic, measurement of, in frogs, 18: 27027
electrical activity, effects of alpha particles, 16: 16197
grafts of, in man, rats, and dogs, effect of radiation processing of graft on take, 18: 9869
grafts, radiosterilization, 16: 26810
inactivation of, effects of, on calcium metabolism in skeleton, 17: 15755
magnetic field effects on vagal inhibition in frogs, 19: 21776 (UCRL-12389)
physiology of, 18: 43165
radiation and age effects on function of rat motor, x, 17: 35518
radiation and surgery effects on canine sciatic, 19: 29954
radiation damage, effective mechanism at low doses, 16: 6319
radiation effects on isolated, 16: 16255
radiation effects on electrical characteristics, comparison of ionizing and ultraviolet, 16: 16256
radiation effects on response in frog's muscle to electric stimuli, 16: 16257
radiation effects on presynaptic failure of neuromuscular transmissions, 16: 16258
radiation effects of alpha particles on fibers from frog skin, 16: 20134
radiation effects on frog sciatic, deuteron and alpha, 16: 23486 (UCRL-9799)
radiation effects on bioelectric activity, 16: 23503
radiation effects of beta particles on compound action potentials, 16: 23504
radiation effects on response of cholinergic and enteric, to drugs in guinea pig, 16: 28752 (UCLA-461)
radiation effects on, in red bone marrow, 16: 32742(T) (JPRS-15018 (p.64-72))
radiation effects on sciatic, at various intervals post-exposure, 17: 1252
radiation effects on nervus ischiadicus of frogs, method of measuring effects of dose rate on, 17: 7816
radiation effects on electrical excitation of isolated, 17: 10417
radiation effects on degeneration and regeneration of peripheral, in rabbits, 17: 12160
radiation effects on electrical activity of α- and β-fibers of sciatic, in frogs, 17: 21483
radiation effects on action potential of frog sciatic, alpha, 17: 23101
radiation effects on electric properties of, in rats, 17: 24961
radiation effects on action current curve of frog ischiadicus, 17: 25000
radiation effects on endings of, beta, 17: 30361
radiation effects on Annelid, x, 17: 33626
radiation effects on electrical activity and permeability of membranes of isolated, 18: 47(R) (TID-19617)
radiation effects on functional state of excitable systems in, of frogs, 18: 3500 (UCRL-11005)
radiation effects on regeneration after traumatic injury of, in dogs, 18: 23250(T) (JPRS-24704(p.12-17))
radiation effects on action-potential of, effects of sodium azide on, 18: 23277
radiation effects on functioning of vestibular, in presence of vibrations, 18: 31213
radiation effects on vestibular, gamma and proton, 18: 31214
radiation effects on functional state of vagus, in cats, dogs, and rabbits, 18: 41176
radiation effects on electric activity of, in rabbits, 19: 3914(T)
radiation effects on electric activity of cat and rabbit, 19: 3915(T)
radiation effects on growth in chicken embryos, 19: 10802
radiation effects on physiological response of fish, gamma, 19: 17536
radiation effects on activity of rat, prenatal, 19: 17619
radiation effects on gastrointestinal tract, in rabbits, 19: 21910
radiation effects on sensitivity of animal, gamma, 19: 26086
radiation effects on sodium-22 efflux in isolated rat, 19: 26087
radiation effects on activity of afferent, in cats and rats, 19: 26107
radiation effects on regeneration process in rat sciatic, 19: 33909
radiation effects on human optic, following hypophyseal therapy, necrotic gamma, 19: 36070
radiation effects on, in developing insect larvae, morphological, 19: 43849
radiation effects on, deuterons, 19: 45874
radiation effects on regenerative capacity of, 20: 1635
radiation effects on excised diaphragm-nerve preparations, 20: 18293 (NP-14898)
radiation effects on action potentials of, in cold-blooded animals, x, 20: 29021
radiation effects on function and ultrastructure of isolated rat sympathetic ganglion, x, 20: 31055
radiation effects on rat peripheral, regeneration following local and whole-body x, 20: 35263
radiation effects on excitability of ganglions of solar plexus, x, 20: 38687
radiation effects on leg, gamma, 20: 40783
radiation effects on membrane properties and action potential of, x, 20: 40606 (BMwF-FBK-66-02)
radiation effects on excitation threshold of frog, mechanisms for x, 20: 42868
radiation effects on, of brain meninges in dogs, 20: 42881
radiation exposure of isolated ganglion of, β, 20: 14332
radiation injuries, histology, 16: 28831
radiation processing of peripheral homografts of, 18: 9869
radiation sickness effects on, in dogs, 16: 30292
radiation sickness effects on morphology of, in rats, 17: 30409
radiation sickness effects on regeneration of sciatic, in dogs, 19: 7061(T)
radioinduced excitability changes in vagus, effects of histamine and serotonin on x, 18: 37023
radioinduced microscopic effects on, in frog interauricular septum, 17: 30368
radiosensitivity in worms, 16: 30283
radiosensitivity of tissues, review, 16: 7415 (BNL-675(p.176-99))
radiosensitivity of sensory, 19: 13074
radiosensitivity of rat, 20: 22698
regeneration in dogs with radiation sickness, 20: 36614
response inhibition of auditory, effects of acoustic intensity on, 19: 39270(R) (TID-21894)
role of olfactory system in x ray arousal of rats, 19: 15140
sensitivity to ultraviolet light, 17: 10310(R) (TID-17789)
signals, operation of instrumentation for processing, 16: 4610(R) (TID-14435)
structure of isolated endings, 18: 43151 (ISS-63/50)
suturing during simultaneous treatment of thermal burns and radiation

sickness, 17: 19861
thorium(IV) oxide effects on vasomotor changes of Shwartzman reaction in rabbits, 17: 17717
ultraviolet absorption by cuttlefish, 16: 21925(T)

NERVOUS SYSTEM

see also Brain
see also Nerve Cells
see also Spinal Cord
amino acid metabolisms in visual system of rats after unilateral enucleation, tracer study, 18: 31092
analysis for copper, activation method for, 18: 41331
audiogenic convulsive seizures and low-level irradiation, 16: 23499
book: *Effects of Ionizing Radiation on the Central Nervous System*, 19: 15203
book: *Ionizing Radiation: Neural Function and Behavior*, 20: 10689
book: *Irradiation and the Nervous System*, 17: 27194
book: *Problems of Ionizing Radiation Effects on the Nervous System*, 17: 27193
book: *Radiotherapy of Diseases of the Nervous System*, 19: 265
book: *Yearbook of Nuclear Medicine*, Vol. I, 1966, 20: 36690
cell migration in maturing, radiosensitivity and labeling studies, 16: 7419 (BNL-675(p.246-61))
conference on effects of radiation, Vienna, June 5 to 9, 1961, 16: 16253
defects in human, leukemogenic effects of, 20: 14346
development in postnatal rats, tracer study, 20: 20391(R) (TID-22825)
dosimetry of beta particles from internally deposited phosphorus-32 in, central, 20: 38651
effects of bromide on conditioned reflexes in dogs, 18: 33319
effects of cesium-137 on, in man after single exposure, 18: 6687
effects of curare alkaloids on, tracer studies in mice, 19: 31777
effects of dietary iodine on, in rats, 20: 45307
effects of ethanol on conditioned reflexes of dog, 20: 29009
effects of leukemia on central, in Hiroshima and Nagasaki patients, 19: 17502
effects of melanins on, in mammals, 18: 21700 (BNL-7855)
effects of pyridine drugs on, tracer studies, 19: 32271
effects of radiation and brain trauma on regulation of peripheral blood system by, in rats, 18: 27188
effects of strontium-90 on mouse central, effects of chloral and strychnine on, 19: 17578
effects of surgical ablation of rat olfactory, on conditioned stimulation by x rays, 20: 45412
effects of toxins on central, in rats, 17: 7902(T)
effects on development of radiation lesions of bone marrow in albino rats, 16: 1532
function in effects of beta radiation, heat, and xylene on inflammatory edema in rabbit ears, 20: 35342
irradiation of central, dynamic effects on nerve cells of, 19: 31824
irradiation of mouse, treatment of leukemia using, 18: 41283
metabolic influence during radiation sickness, 16: 20192
metabolism, effects of physical activity, 16: 34
metabolism of nuclei acids and proteins in, 16: 9811(R) (TID-14972)
morphology of subcutaneous, in radiodermatitis, 19: 19591
motor end plate fine-structure changes after myasthenia gravis and denervation, 16: 11376(R) (AD-259234(p.18-30))
nucleic acid antimetabolite effects on cat, 16: 23478
permeability of perilemma, study using carbon-14-labeled sugars, 16: 16117
phospholipid exchange rate in, during radiation sickness, 16: 14588
photosensitization of crayfish ventral nerve cord with methylene blue dye, 17: 35260(R) (TID-19135)
radiation and diphtheria toxin effects on activity of central, in rats, 17: 7899(T)
radiation and staphylococcal toxin effects on active and trace conditioned reflexes in rats, 17: 7898(T)
radiation chemotherapy and protection, 16: 2919
radiation effect on mammalian, following prenatal exposure, 20: 22756
radiation effects in rabbits, 16: 63
radiation effects on cerebral cortex, 16: 64
radiation effects on pattern and threshold of electroshock seizures, 16: 75
radiation effects on rat, effects of partial shielding, 16: 1477(T) (JPRS-10170(p.128-34))
radiation effects on learning and conditioned reflexes, 16: 2892 (TID-14294)
radiation effects, 16: 6303(T) (JPRS-11322(p.227-47))
radiation effects, head exposure, 16: 6304(T) (JPRS-11322(p.248-73))
radiation effects on neuromotor ability, 16: 7347(R) (TID-14692)
radiation effects of x rays, delayed, 16: 7416 (BNL-675(p.200-3))
radiation effects, 16: 8629
radiation effects on, 16: 9900
radiation effects of external doses not exceeding 1000 r, 16: 11488(T) (JPRS-12480)
radiation effects on protoporphyrin III affinity in central, 16: 14539
radiation effects on nucleic acids of liver, 16: 2895
radiation effects on pancreas, 16: 2896
radiation effects, 16: 16243
radiation effects, aerobic and anaerobic metabolic studies, 16: 16274
radiation effects, 16: 16277
radiation effects on vegetative, 16: 16280
radiation effects in rats, 16: 16282
radiation effects, comparison of response variability and degree of higher activity, 16: 16283
radiation effects at low levels, 16: 16286
radiation effects, hypotheses on action mechanisms, 16: 16288
radiation effects on degeneration and restoration of interneuron synapses, 16: 17437(T) (FTD-TT-62-362)
radiation effects in hamsters on central, brain exposure, 16: 17506
radiation effects on adrenergic transmission in cats, 16: 20143
radiation effects, review, 16: 24558
radiation effects on synapses, whole-body exposure, 16: 23442
radiation effects, conference, 16: 23471
radiation effects, 16: 23472
radiation effects, survey of gamma, beta, and x-radiation, 16: 23480
radiation effects of repeated low dose and single high dose, 16: 23482
radiation effects, demyelination, malacic myelopathy, and myodegeneration in monkeys and rats, 16: 23483
radiation effects, electron microscope study, 16: 23485
radiation effects, morphologic and pathophysiologic, survey of Russian work, 16: 23487
radiation effects of protons at 185 Mev, 16: 23489
radiation effects, functional changes, 16: 23497
radiation effects, review, 16: 23506
radiation effects on performance, head exposure in monkeys, 16: 23512
radiation effects in rats, 16: 23420 (USNRDL-TR-561)
radiation effects on central, 16: 25235
radiation effects on higher, in prenatally exposed progenies, 16: 25236
radiation effects on, of animals irradiated during embryonic development, 16: 25237
radiation effects on, in rats irradiated during embryo genesis, 16: 25238
radiation effects on, of white rats exposed during embryonic period, 16: 25239
radiation effects on, of rat progenies exposed during late antenatal period, 16: 25240
radiation effects on, of rats chronically exposed prenatally, 16: 25241
radiation effects on, of rabbits exposed prenatally, 16: 25243
radiation effects on, of rats exposed prenatally, 16: 25245
radiation effects on, of rats exposed prenatally, 16: 25246
radiation effects in, conference on, 16: 26741(T) (FTD-TT-62-657)
radiation effects on developing, 16: 28830
radiation effects on ganglia in guinea pigs, 16: 30304
radiation effects on ribonucleoproteins in, 16: 30303
radiation effects, 17: 27069(T) (JPRS-19284)
radiation effects in monkeys, 17: 13984(R) (TID-18003)
radiation effects on, 17: 17887
radiation effects on, 17: 33504
radiation effects on activity of central, in dogs, 17: 30363
radiation effects on central, in offspring in rats, 17: 7881
radiation effects on central, in mice injected with stimulants, 17: 10263
radiation effects on central, in monkeys, 17: 12176
radiation effects on central, in dogs, 17: 12177
radiation effects on central, in dogs, 17: 13993
radiation effects on central, in rats, 17: 14045
radiation effects on changes in different types of, in rats, 17: 7895(T)
radiation effects on chicken and pigeon, localization of, 17: 19917
radiation effects on conditioned and unconditioned respiratory reflexes in rabbits, 17: 7891(T)
radiation effects on conditioned secretory-motor alimentary reflexes in dogs, gamma, 17: 7893(T)
radiation effects on control of metabolic activity, 17: 14031
radiation effects on cytochromoxidase and succinic dehydrogenase activity in rabbit, fractionated gamma and x-ray, 17: 31979
radiation effects on developing, in embryos, 17: 7852
radiation effects on developing, in embryos, 17: 7857
radiation effects on developing, in embryos, 17: 7883
radiation effects on developing, 17: 13989(T) (JPRS-17819(p.1-14))
radiation effects on developing, 17: 13997
radiation effects on developing, 17: 15638 (TID-18139)
radiation effects on electrical activity of central, x, 17: 33627
radiation effects on function, 17: 5888
radiation effects on function, effects of acute, chronic, and fractionated exposure, 17: 17778(T) (JPRS-18395(p.311-20))
radiation effects on genetics in guiena pig, gamma, 17: 30343
radiation effects on glycogen content of, in frogs, 17: 37069(T) (JPRS-21170(Del.))
radiation effects on higher parts of central, 17: 7888(T)

radiation effects on higher, 17: 7889(T)
radiation effects on higher, in dogs, 17: 7892(T)
radiation effects on higher, in rats, 17: 7897(T)
radiation effects on higher, in rats exposed *in utero*, 17: 7900(T)
radiation effects on histopathology of central, in rats following brain exposure, 17: 7904(T)
radiation effects on histopathology of, 17: 17829
radiation effects on higher, in dogs, 17: 17834
radiation effects on higher nervous activity of dogs irradiated as embryos, 17: 30401
radiation effects on, in offspring of irradiated rats, 17: 14029
radiation effects on, in rats exposed *in utero*, 17: 21508
radiation effects on, in man and animals, 17: 30441
radiation effects on motor alimentary conditioned reflexes in rat, gamma, 17: 7890(T)
radiation effects on morphology of, in rats, 17: 7901(T)
radiation effects on motor defense reflexes elaborated with visual stimuli in rabbits, gamma and x, 17: 7894(T)
radiation effects on mobility of nervous processes of dogs irradiated as embryos, 17: 30454
radiation effects on mouse, gamma, 17: 40615
radiation effects on myotactic reflex in rabbits, 17: 2869
radiation effects on neurological disturbances in tortoises, 17: 30382
radiation effects on nucleic acid metabolism in, in rats, 17: 40602
radiation effects on, of eyes and skin in man, 17: 5851
radiation effects on protein metabolism in, 17: 15781
radiation effects on rabbit and rat, effects of rate on, 17: 21551
radiation effects on reactions of, 17: 31908
radiation effects on, review, 17: 38841
radiation effects on ribonucleic acid metabolism, 17: 10356 (BNL-6546)
radiation effects on ribonucleic acid metabolism in rat, 17: 37060 (BNL-6600)
radiation effects on stomach, in rats, 17: 30432
radiation effects on sympathetic, 17: 21592
radiation effects on trace conditioned reflex system in rats, 17: 7896(T)
radiation effects, pathological, 17: 23126
radiation effects, recovery, 17: 23136
radiation effects, whole-body critical exposure, 17: 31816(R) (ORO-605)
radiation effects on, deuteron-beam focal exposure, 17: 13963 (BNL-6186)
radiation effects on, effects of hypothermia on internal-source, 17: 5889
radiation effects on rats, three-generation parental-exposure, 17: 19862
radiation effects on central, 18: 47(R) (TID-19617)
radiation effects on response of, to analgesics and other drugs, 18: 47(R) (TID-19617)
radiation effects on, in prenatally irradiated rats, x, 18: 69
radiation effects on food-deprived rat, x, 18: 80
radiation effects on central, 18: 122(T)
radiation effects on liver cell glycogen content after exposure of, 18: 3512
radiation effects on developing, in rat fetuses, 18: 3497(R) (TID-19749)
radiation effects in mice, rabbits, and rats on central, protective effects of drugs against, 18: 5014
radiation effects on rabbit, gamma, 18: 5131(T)
radiation effects on, in frogs, 18: 6669
radiation effects on response to stimuli of, in rabbits, chronic gamma, 18: 6671
radiation effects on, in monkeys, 18: 8102 (BNL-7620)
radiation effects on sympathetic and parasympathetic control of peripheral blood vessels in dogs, 18: 9838
radiation effects on electroshock seizures in rat central, 18: 9885
radiation effects on central, protective and therapeutic effects of drugs against, 18: 9921
radiation effects on animal, influence of drugs on x, 18: 11882
radiation effects on, in frogs, x, 18: 13474
radiation effects on rat, x, 18: 15836(T)
radiation effects after spinal cord irradiation on rat, x, 18: 17528
radiation effects on, of rabbit stomach, 18: 17586
radiation effects on, effects of phenothiazine in, x, 18: 17711
radiation effects on monkey and rat, x, 18: 19586
radiation effects on, in antenatally irradiated dogs, 18: 19608(T)
radiation effects on rat, x, 18: 19729
radiation effects on, in rabbit ears, 18: 21832(T) (JPRS-24301(Del.) (p.17-22))
radiation effects on peripheral, in liver of dogs and rabbits, 18: 23309
radiation effects on dogs and rabbits, 18: 23377
radiation effects on rabbit, exposed *in utero*, 18: 25121
radiation effects on audiogenic seizure in mice and rats, gamma, 18: 25206
radiation effects on neurosecretion in pituitary gland, protection against, by 5-hydroxytryptamine, 18: 27224
radiation effects on cat, proton, 18: 27111
radiation effects on catabolism and anabolism in, x, 18: 29380
radiation effects on dog and monkey central, gamma-, neutron-, and x-, 18: 29382
radiation effects on sympathetic nerves controlling blood circulation, 18: 29517
radiation effects on rat, as affected by prenatal irradiation, gamma, 18: 29290
radiation effects on, electroencephalographic study, 18: 29302
radiation effects on dog, after head irradiation, x, 18: 31142
radiation effects from deposited phosphorus-32 on, in rat, 18: 33278 (STI/DOC/10/28(p.39-66))
radiation effects on conditioned reflexes in normal and bromide-treated dogs, 18: 33319
radiation effects on sensitivity of rabbit, x, 18: 35380
radiation effects on central, in rabbits, 18: 35304(R) (AD-439300)
radiation effects on response of, to conditioned reflexes, 18: 37016
radiation effects on, book, 18: 37019
radiation effects on calcium metabolism by bones and teeth as affected by, x, 18: 37003
radiation effects on developing, in animals and man, 18: 38845
radiation effects on, gamma, 18: 38895
radiation effects on response to conditioned reflex of dogs, 18: 38779 (TID-21084)
radiation effects on response of, to drug-induced convulsions in rats, 18: 41175
radiation effects on autonomic, in cats, dogs, and rabbits, 18: 41176
radiation effects on development of, in rabbits, 18: 41105(T)
radiation effects on autonomic, in cats, 18: 41174
radiation effects on dog and guinea pig central, microdose x, 19: 3947
radiation effects on rabbit, 19: 5637
radiation effects on amino acid content of guinea pig, prenatal, 19: 5673
radiation effects on, electroencephalographic study of occupational, 19: 8859
radiation effects on mammalian central, 19: 8950
radiation effects on rat, protective effects of ACTH and phenobarbital against, 19: 8972
radiation effects on control center of autonomic, in rabbits, 19: 19509(T) (JPRS-29250(p.9-13))
radiation effects on dog, antenatal, 19: 19536
radiation effects on, 19: 19572
radiation effects on, in rabbits, 19: 21910
radiation effects on thalamic area of brain, in rabbits, 19: 21891
radiation effects on electrical activity of, in man, 19: 24293
radiation effects on, conference on, 19: 26078
radiation effects on rat embryo central, *in utero*, 19: 26083
radiation effects on histochemical and histological changes in rat central, 19: 26090
radiation effects on cable properties and functional changes in rat central, 19: 26095
radiation effects on electrophysiology of dog central, low-level, 19: 26098
radiation effects on conditional reflexes in dogs, repeated low dose, 19: 26101
radiation effects on rabbit, protective effects of aminazine against head exposure, 19: 26138
radiation effects on dorsal root ganglia of newborn rats *in vitro*, 19: 26084
radiation effects on responses in prenatally irradiated animals, ionizing, 19: 28109
radiation effects in rabbit, pathological, 19: 31818
radiation effects on central, review, 19: 31824
radiation effects on catecholamine content in rat, (E), 19: 31829
radiation effects on reactions of central, in rats, 19: 31839
radiation effects on, of rats, 19: 31841
radiation effects on, of developing embryos, 19: 33938
radiation effects on, in rat embryos, 19: 33834
radiation effects on reactions of rat, to burns, 19: 33921
radiation effects on intestinal motor function of dog, x, 19: 35956
radiation effects on ganglionic cells in chicken embryo, 19: 36071
radiation effects on function of, synergistic effects of acceleration and vibration during space flight, 19: 38358 (AD-612660)
radiation effects in human, 19: 40349 (BNL-9345)
radiation effects on, innervating mammary gland, 19: 40353(T) (FTD-TT-65-48, pp 16–17)
radiation effects on, in rabbits, 19: 40355(T) (FTD-TT-65-48, pp 111–12)
radiation effects on activity of, in dogs, 19: 40356(T) (FTD-TT-65-48, pp 469–70)
radiation effects on, synergistic effects of stress induced by vibration on, 19: 40354(T) (FTD-TT-65-48, pp 38-9)
radiation effects on morphology of dog, proton, 19: 42321
radiation effects on burro central, following cranial irradiation, gamma, 19: 42299
radiation effects at ultra-high frequency energy on, climate effects on,

19: 43774
radiation effects on rabbit and rat, pathological, 19: 45812(R) (ORO-631, pp 1-35)
radiation effects on human, from radiotherapy of nasal cavity, 19: 45983
radiation effects on development of, in rat embryos, 20: 60(R) (NYO-901-37, pp 33-68)
radiation effects on developing, in dog fetus, 20: 1627(T)
radiation effects on performance of learned response by rats, effects of nembutal on x, 20: 3772
radiation effects on adaptive responses of rat, x, 20: 5319
radiation effects on central, γ, 20: 5329
radiation effects on conditioned reflex in goats, γ, 20: 5369
radiation effects on physiology of rat, γ, 20: 5292(R) (COO-205-55, Paper 1)
radiation effects on physiology of frog, γ, 20: 5293(R) (COO-205-55, Paper 2)
radiation effects on physiology of frog, γ, 20: 5292(R) (COO-205-55, Paper 1)
radiation effects on conditioned reflex activity of dogs, γ, 20: 6872
radiation effects on dog, effects of oxidation-inhibiting compounds on x, 20: 6817
radiation effects on development of, in fetuses, 20: 8619 (CONF-631008, pp 2-36)
radiation effects on development of, in fetuses, γ and x, 20: 8620 (CONF-631008, pp 33-47)
radiation effects on development of, in chick embryos, γ and x, 20: 8260 (CONF-631008, pp 33-47)
radiation effects on developing, in fetuses, x, 20: 8621 (CONF-631008, pp 48-81)
radiation effects on developing, in fetuses, x, 20: 8622 (CONF-631008, pp 82-91)
radiation effects on activity of alanine–2-oxoglutarate and aspartate–2-oxoglutarate-aminotransferase in rat, x, 20: 10593
radiation effects on vestibular apparatus in dogs and rabbits, gamma, proton, and x-ray, 20: 10610(T) (NASA-TT-F-353, pp 157-84)
radiation effects on human respiratory center, x, 20: 12702
radiation effects on rat, after neonatal spinal cord exposure, proton, 20: 14299
radiation effects on rabbit, x, 20: 14350
radiation effects on dog, α, 20: 16268
radiation effects combined with labyrinthectomy on rabbit, γ, 20: 18338
radiation effects on mouse and rat, γ, 20: 18376
radiation effects on cat and rat central, x, 20: 18292(R) (N-65-17068)
radiation effects on, controlling metabolic activity in rats, x, 20: 20433 (AD-630390)
radiation effects on central, review, 20: 20449
radiation effects on, in burros and sheep, neutron, 20: 20489
radiation effects on conditions reflexes in rats exposed *in utero*, x, 20: 20492
radiation effects on rat, effects of parabiosis on x, 20: 22720
radiation effects on, review on Soviet research in, 20: 22687
radiation effects on human following Thorotrast angiography, 20: 22759
radiation effects on, gamma, 20: 24871(R) (AD-625949)
radiation effects on neuromuscular competence and response to stimuli in monkeys, massive pulsed-dose reactor, 20: 24872 (AFRRI-SR-66-2)
radiation effects on synaptic mechanisms in cats, whole-body x-ray, 20: 26657(R) (SRIA-115PS3-1)
radiation effects on dog, x, 20: 26686
radiation effects on conditioned reflexes in dogs, effects of orally administered powdered Chinese magnolia on, 20: 26670
radiation effects on rat central, whole-body x, 20: 26671
radiation effects on compensatory mechanisms in labyrinthectomized rabbit, x, 20: 26643
radiation effects on conditioned reflexes in dogs, β, 20: 29009
radiation effects on central and reflex, controlling vomiting, 20: 33014
radiation effects on animal, clinical and experimental studies on low-dose x, 20: 33037
radiation effects on physiology of rabbit, x, 20: 33056
radiation effects on response of rabbit, x, 20: 33057
radiation effects on aminotransferase activities in rat, neutron, 20: 36601
radiation effects on function of basis processes in human, uv, 20: 36626
radiation effects on stimulation of solar plexus, x, 20: 38687
radiation effects on, in animals, 20: 38653
radiation effects on regulatory function of rabbit, x, 20: 38654
radiation effects on conditioned reflex in fish and rabbits, 20: 38655
radiation effects on central, following therapy, 20: 40659
radiation effects on fetal rat, 20: 40654
radiation effects on cytology and cytochemistry of ribonucleoproteins of, gamma and x, 20: 42866
radiation effects on acetylcholine metabolism in rabbit, γ, 20: 42875
radiation effects on rat, protective effects of barbamyl and serotonin on γ, 20: 43008
radiation effects on cells of goldfish, γ, 20: 45428
radiation effects on animal, prenatal, 20: 45468
radiation effects on central, in rats, 17: 7902(T)
radiation injuries, review of Soviet work, 16: 23496
radiation injuries, acute syndrome in burros, 16: 23498
radiation injuries and repair, 16: 32741(T) (JPRS-15018(p.47-63))
radiation injuries after exposure of head, 17: 5887
radiation injuries to, review on, 18: 21881
radiation injuries of mitochondria in cells of, in mammals, 18: 38952
radiation injuries of, in mice, 19: 13058
radiation injury, effects of electric radiation, 16: 28811
radiation sickness effects on central, in animals, 18: 9884
radiation sickness effects on rabbit autonomic, 18: 13514
radiation sickness effects on central, in dogs, 18: 23310
radiation sickness effects on, pathology of, 19: 38433(T)
radiobiology of nervous receptors, 16: 16254
radiodiagnosis of spinal cord resulting in injuries of, Thorotrast, 18: 19659
radiodiagnosis of tumors of, using technetium-99m, 19: 26184
radiodiagnosis of diseases of, 19: 36207
radioinduced autonomic dystonias in human, 20: 6791(T) (JPRS-33039, pp 1-8)
radioinduced cerebellar defects in mouse, x, 18: 11740
radioinduced changes in, following radiotherapy, 16: 11477
radioinduced changes under effects of interoceptive stimulation, 16: 17444(T) (JPRS-13342(p.4-11))
radioinduced changes in, of rabbits exposed prenatally, 16: 25242
radioinduced changes in, of rabbits exposed prenatally, 16: 25244
radioinduced changes in cerebral cortex in second generation progenies, 16: 28816
radioinduced effects on activity of rat, x, 17: 30362
radioinduced necroses of central, delayed post-therapeutic, 18: 33290
radioinduced stimulation of, in rats, 18: 6622 (USNRDL-TR-682)
radioinduced stimulation, 18: 48 (USNRDL-TR-670)
radioprotective effects of thiamine combined with narcotics, 16: 18775
radiosensitivity, 16: 17440(T) (JPRS-12921(p.12-33))
radiosensitivity and reactivity of, in dogs, 18: 1403
radiosensitivity effects of thiamine combined with narcotics on, 16: 26742(T) (FTD-TT-62-831)
radiosensitivity effects when under influence of radioprotective agents, 18: 17663
radiosensitivity effects of drug stimulation of, in mice, 20: 12685
radiosensitivity effects of drug depression or stimulation of mouse, 20: 18459
radiosensitivity effects on radiation injuries, muscle tissue in rabbits, 20: 36602
radiosensitivity, in mice, 16: 32793
radiosensitivity in rats, 17: 19809 (USNRDL-TR-624)
radiosensitivity of central, during ontogenesis, 16: 1517
radiosensitivity of blood vessel control, 16: 23438
radiosensitivity of central, effects of narcotics on, 16: 28813
radiosensitivity of vascomotor reflexes, 16: 28850
radiosensitivity of, relation to course of radiation sickness, 16: 32865
radiosensitivity of central, 17: 4393
radiosensitivity of central, in rats, 17: 15744
radiosensitivity of embryonic rat, 17: 15745
radiosensitivity of developing, 17: 27169
radiosensitivity of developing, 17: 38896
radiosensitivity of, effects of thiamine in frogs and lobsters on, 18: 11559(R) (TID-19977)
radiosensitivity of, in cats and rats, 18: 33278 (STI/DOC/10/28(p.39-66))
radiosensitivity of, effects of arsenic compounds on, 18: 36971
radiosensitivity of, in fish, 19: 2100
radiosensitivity of, in rats, 19: 2061 (BNL-8451)
radiosensitivity of rabbit, 19: 3914(T)
radiosensitivity of cat and rabbit, 19: 3915(T)
radiosensitivity of rat, 19: 8827
radiosensitivity of mammalian, 19: 10786(R) (TID-21440)
radiosensitivity of, 19: 12970
radiosensitivity of, in developing fetuses, 19: 15213
radiosensitivity of animal, review on, 19: 17515
radiosensitivity of, in man, 19: 31953
radiosensitivity of, in rats, 19: 33879
radiosensitivity of, 19: 33822
radiosensitivity of, effects of biological stress in mice on, 19: 42334
radiosensitivity of, in mammals, 19: 45981
radiosensitivity of human, 19: 45892
radiosensitivity of, in rat fetuses, 19: 45894
radiosensitivity of, biochemical exponents of, 20: 115
radiosensitivity of, γ, 20: 38773
radiosensitivity of, in man and monkeys, 20: 42934
radiosensitivity, reaction mechanisms in sympathetic, 16: 17462(T)
radiosterilized homografts for surgery of, 18: 31176

radiosurgery of, strontium-90 needle for, 18: 33436
radiotherapy effects on, late, 16: 16207
radiotherapy effects on, protective effects of Voyal against, 19: 13117
radiotherapy effects on human gliomas, 19: 22035
radiotherapy of carcinomas, effects on, supervoltage x, 18: 29541
radiotherapy of diseases of, humoral effects, 18: 11787
radiotherapy of diseases of, 19: 10975
radiotherapy of diseases of, prevention and reduction of generalized local reactions in, 19: 13109
radiotherapy of diseases of, use of low doses for, 20: 36707
radiotherapy of tumor of, effects of triethylenemelamine on, 19: 13146
reactions to irradiation of retina of eye, 16: 32810
response to radiation and trauma, 17: 5886
response to radioinduced lesions, effects of pharmacological inhibition on, 18: 6658
role in changes of metabolic reactivity of irradiated organisms, 16: 16284
role in changes of metabolic reactivity of irradiated organisms, 16: 23422(T) (AEC-tr-5190)
role in radiation sickness, 16: 6301(T) (JPRS-11322(p.180-213))
role in radiation injuries, 16: 6302(T) (JPRS-11322(p.214-26))
role of autonomic, in radiation effects on avoidance conditioning in rats, 19: 26103
splanchnic, effects on radiation avoidance by rats, 16: 26747
strontium-90 effects on, in dogs, 16: 5191
surgical techniques for, anterolateral cordotomy, 18: 15734(R) (ACRH-20(p.37-46))
toxic effects of inhaled radon on autonomic, 18: 31119
transfer of radiation effects by, in mice, 20: 5421
zinc-65 uptake and distribution in, of sheep, 16: 28712 (HW-SA-2338)

NETHERLANDS
cesium-137 content in milk, 1959–60, 16: 9837
cesium-137 content in milk, 16: 10321
environs monitoring at Reactor Centrum Nederland Research Establishment, Petten, 18: 37439 (CONF-337-7)
facilities of Institute for Atomic Sciences in Agriculture, Wageningen, 18: 38774(R) (EUR-1881.e)
fallout monitoring, 1959, 17: 3201 (AD-275905)
fallout monitoring, 1961 and 1962, 18: 29910
fallout monitoring, 1958 through 1963, 19: 618 (EUR-1820.d,f,i,n)
fallout monitoring, 1962, 19: 18143 (EUR-1838.d.f.i.n)
fallout monitoring, 1964, 20: 4155 (EUR-2516.d,f,i,n)
fallout monitoring, 1964, 20: 33575
food irradiation research in, 19: 11624
legal control of radioisotopes in, 19: 32487
nuclear energy organization, legislation, and training in, 20: 18183
nuclear industry in, development of, 20: 12557
nuclear power development in, 19: 47923
nuclear power development in, role of Euratom in, 20: 10395
nuclear research facility in, siting of, 17: 41099
nuclear research in, review of, 20: 12556
nuclear science research program at Central Lab. TNO, Delft, 20: 8499
potassium-40 content in milk, 16: 10321
radiation measurements in Amsterdam, low-level environmental, 16: 438
radiation processing of food in, review of, 20: 31628
radioactive contamination of foods, 1961 and 1962, 18: 29910
radioactivity monitoring in biosphere, 1963, 20: 39118
radioactivity of food in, 1964, 20: 23411
radioisotope uses in, economics of industrial, 20: 27377
radionuclide content in food in Amsterdam, 1960 to 1963, 20: 20949
reactor development in, 18: 44933(R) (NP-14367)
strontium-90 content in milk, 1959 and 1960, 16: 9837

NETR
see Air Force Engineering Test Reactor

Network Analyzers
see Computers

NETWORK THEORY
analysis using digital computers, 17: 35260(R) (TID-19135)
developments in, 16: 5776(R) (NP-11141)
output of R-C network charged by random pulse train (E/T), 19: 1963 (SC-DC-64-491)
research on, 17: 24561(R) (PIBMRI-1112-63)
research on, at Illinois University, 17: 36440(R) (NP-13061)
research programs on, 19: 26915(R) (AD-609133)
research progress on, 18: 15711(R) (TID-20256)
research progress on, 19: 23164(R) (SU-SEL-64-103)

NEUFLEX PROCESS
(Preparation of solvent extraction feed from unirradiated zirconium-base fuels)
preparation of solvent extraction feeds from zirconium-base fuels, 18: 17932 (ORNL-3465)

NEUROLOGY
development, M.I.T. summary for Sept. to Nov. 1961, 16: 13183(R) (TID-15140)
developments in, 16: 7634(R) (TID-13000)
pulse analyzers for, transistorized multichannel, 18: 29188
radiation effects on, of neonatal rats, x, 17: 35521
radiodiagnosis in, review on, 19: 17723
research on, 17: 21401(R) (TID-18585)
research programs at M.I.T. electronics lab, 16: 19476(R) (TID-15642)
research programs on, 16: 30172(R) (TID-16489)
research programs on, 17: 6801(R) (TID-17303)
research programs on communication aspects of, 17: 13879(R) (TID-17943)
research programs on, 19: 39270(R) (TID-21894)
research programs at M.I.T. electronics lab., 20: 4478(R) (TID-22179)
research progress on, 18: 2404(R) (TID-19651)
research progress on, 18: 15711(R) (TID-20256)
research progress, 18: 42162(R) (TID-20963)
research progress on, 19: 25071(R) (TID-21667)
systems, computer simulation of, 16: 4610(R) (TID-14435)
tracer techniques in, 17: 7724
use of accelerated ion beams in, 16: 23488

Neurons
see Nerve Cells

NEUROSPORA
aminoacyl-sRNA synthetase enzyme in, characterization of, 19: 31704(R) (ORNL-3768(p.157-63))
colony counter for, 19: 42687(R) (ORNL-3782, pp 31-4)
counter design for, 20: 38546
desoxyribonucleic acid occurrence and properties in mitochondria of, 18: 43209
effects of diethyl- and dimethylnitrosamine on, mutagenic, 20: 40632(R) (ORNL-3922, pp 175-91)
effects of methanesulfonate on, mutagenic, 20: 40632(R) (ORNL-3922, pp 175-91)
effects of storage time, temperature, and atmosphere on, 19: 2068(R) (ORNL-3700(p.34-57))
enzyme locational specificity in, genetic factors in, 20: 31012
gene action, mutations, and recombination in, mechanisms of, 17: 35453(R) (TID-19287)
genetic analysis of, 19: 2078 (ORNL-P-652)
genetic factors in, 18: 8053
genetic factors in, 18: 8054
genetic studies of, 19: 21772(R) (TID-21709)
genetics of, complementation and recombination, 18: 13394
growth rates in, effects of rare gases on, 20: 20378
leucine biosynthesis in, genetic regulation of enzymes for, 20: 18196
metabolism of methionine and *S*-adenosylmethionine by, 17: 33463(R) (ANL-6723(p.149-52))
metabolism of tryptophan by, indolepyruvic acid formation in, 20: 10540 (HW-SA-3728)
mutagen specificity in, 18: 27003(R) (ORNL-3601(p.27-46))
mutagenic and toxic effects of chemisterilants on, 18: 15868
mutagenic effect of certain polycyclic hydrocarbon carcinogens in, 18: 27008(R) (ORNL-3601(p.146-51))
mutagenic effects of 3,4-benzpyrene in, 19: 2068(R) (ORNL-3700(p.34-57))
mutagenic effects of acridines on, in absence of light, 20: 40510(R) (TID-23137)
mutants in, effects of carbon dioxide on leaky and nonleaky, 20: 40624(R) (ORNL-3922, pp 52-8)
mutation induction in, spectra of allelic complementation and leakiness in chemical, spontaneous, and radiation, 19: 8862
mutations, genetic analysis, 17: 7692
mutations, genetic factors, 17: 19764
mutations in, nitrous acid-induced ad-3B, 20: 16159(R) (ORNL-3900, pp 150-81)
mutations in, utilization of chemically induced, 20: 18347
mutations of, enzymatic and antigenic properties of proteins in, 19: 2002(R) (ORNL-3700(p.63-8))
mutations of, mechanisms for, 18: 35262(R) (TID-20914)
radiation effects on conidia germination in, protective effects of calcium gluconate against x, 17: 40612
radiation effects on tryptophan synthetase in, uv, 19: 108
radiation effects on cell nuclei of, protective effects of anoxia against x, 19: 31788(R) (ORNL-3768(p.33-57))
radiation effects on, gamma, 19: 43648(R) (UCLA-12-565, pp 87-96)
radiation effects on mutations and survival in, protective effects of anoxia against x, 19: 42363
radiation effects on mutations and survival in, protective effects of anoxia against x, 19: 42364
radiation effects on oxygen concentrations in conidia of, x, 19: 42365
radiation effects on conidia of, protective effects of endogenous anoxia and MEA against x, 19: 42365
radiation effects on conidia of, γ and x, 20: 3780
radiation effects on, mechanisms of repair of uv, 20: 10716
radiation injuries of, photoreactivation of uv-induced, 20: 6777(R)

(ORNL-3853, pp 54-61)
radioinduced inactivation of, mechanism for photoreactivation of uv, 20: 40629(R) (ORNL-3922, pp 94-8)
radioinduced mutants in, physiological and structure relations within TD locus in, 19: 17517
radioinduced mutant reversion in, for glutamic dehydrogenase production, uv, 20: 20462
radioinduced mutants of, γ, 20: 45248(R) (NYO-2043-129)
radioinduced mutations, 16: 31491
radioinduced mutations of, genetic analysis of, 18: 29292
radioinduced mutations of, genetic analysis of, 18: 29292
radioinduced mutations of, genetic damage in, 19: 2068(R) (ORNL-3700 (p.34-57))
radioinduced mutations of, 19: 2078 (ORNL-P-652)
radioinduced mutations in, x, 19: 2111
radioinduced mutations in AD-3 region of, kinetics of, 19: 15153
radioinduced mutations in, allelic complementation from uv and x, 19: 15081
radioinduced mutations in, biochemistry and genetics of uv and x, 19: 15082
radioinduced mutations in, complementation and reversion of uv, 19: 31788(R) (ORNL-3768(p.33-57))
radioinduced mutations in Neurospora, uv, 18: 19621
radioinduced mutations in, stability of uv, 20: 6708
radioinduced mutations of, 20: 6777(R) (ORNL-3853, pp 54-61)
radioinduced mutation rates in ad-3 regions of, x, 20: 16159(R) (ORNL-3900, pp 150-81)
radioinduced mutations in, utilization of, 20: 18347
radioinduced mutations in, uv, 20: 18196
radioinduced mutations of, uv and x, 20: 31012
radioinduced mutations in, photoreactivation of uv, 20: 40624(R) (ORNL-3922, pp 52-8)
radioinduced mutations in, x, 20: 42926
radioinduced nonallelic mutations in, x, 20: 40624(R) (ORNL-3922, pp 52-8)
radioinduced revertants in mutants of, complementation studies of uv, 20: 6829
radioinduced revertants in mutants of, enzyme studies of uv, 20: 6829
radiosensitivity, 19: 21893
radiosensitivity of conidia of, relation of karyokinetic stage to, 19: 7066
radiosensitivity of, effects of acriflavine on, 20: 10716
radiosensitivity of, photoprotection against x, 20: 14358
radiosensitivity of, effects of developmental stage on, 20: 18297(R) (UCLA-12-576, pp 81-8)
ribonuclease activity in, 20: 6720(R) (ORNL-3853, pp 143-50)
ribonucleic acid synthesis in, 19: 2007(R) (ORNL-3700(p.150-4))
RNA in, characterization of, 20: 40535(R) (ORNL-3922, pp 128-35)
simulated space flight tests for biocompatibility, 20: 40508(R) (ORNL-3922, pp 196-9)
sulfate metabolism in, tracer study of, 18: 29199(R) (TID-20768)
synthesis of nucleic acids, 16: 30
tryptophan synthetase activity in, 19: 31674(R) (ORNL-3768(p.64-9))
x-ray-induced inactivation of conidia, 16: 4105

NEUTRAL RED

distribution in tissues of mice and rats, effects of radioprotective drugs on, 18: 17660
effects of X agent on precipitation or crystallization of, 18: 33671
effects of X agent on precipitation or crystallization of, 18: 33672
effects of X agent on precipitation or crystallization of, 18: 33673
effects of X agent on sedimentation of, effects of aluminum-foil shielding on, 19: 11231
effects of X agent on sedimentation of, 19: 11232
effects of X agent on sedimentation of, effects of color on, 19: 11230
radiation effects on excretion of, in dogs operated by Pavlov or Heidenhain methods, x, 20: 45402
uptake by frog sartorius muscle, effects of heavy water on, 20: 5317
X-agent effects on sedimentation of, effects of environment on, 19: 26448
X-agent effects on solutions of, 19: 26449

NEUTRINO BEAMS

production of monochromatic, using 200-Bev proton synchrotron, (T), 20: 11398 (UCID-1008)
production of, description of CERN layout for, 20: 39746 (CERN-66-24)

NEUTRINO PAIRS

emission from stellar plasma, (T), 20: 7692
equilibrium with electron pairs at high temperature, (T), 19: 16347
production in electron–positron interactions, (T), 19: 37605(T)
production in electron dipole transitions, (T), 19: 5004
production in nuclear Coulomb field, 18: 868
production in photon annihilation, 18: 36292
production in photon interactions, (T), 19: 45027 (NP-15199)
production in photon interactions, cross sections for, (T), 20: 7829
production in photon transition, 16: 7003
production in stars, processes for, 17: 41708
production in stars, (T), 20: 2587
production in stellar evolution, (T), 19: 44927(T)

NEUTRINOS

see also Antineutrinos
see also Cosmic Neutrinos
absorption and emission rates, relation to cosmology, 16: 27865 (UCRL-9855)
absorption by dense matter, mechanisms for, 18: 9175
absorption by nuclei, collective vibrations from, (T), 19: 12567
absorption in Coulomb field of nuclei, cross sections for high-energy, 17: 20999
abundance of electron- and meson (μ)-associated, in universe, 18: 8984
angular correlation in neutron decay, 16: 4698
angular correlation with electrons, problems in measurements by cloud chamber method, 16: 12338
angular correlations with electrons in beta decay of helium-6 and neon-23, 16: 33811
angular correlations in antimony-122, beta decay, (E/T), 19: 33341
angular correlation with beta particles in first forbidden nonunique beta decay, (E), 20: 15857
astronomy and, 17: 20803(T) (JPRS-18605)
bibliography, 20: 17352 (NEIC-RR-21)
bibliography, 20: 19445 (NEIC-RR-20)
book: *Neutrino*, 19: 14401
book: *Neutrino Astrophysics*, 20: 11436
capture by chlorine-37, rate of, (T), 20: 37366
capture by nuclei, response of solar-neutrino detector using, (T), 20: 23848
charge acquisition in minimal interactions of, (T), 19: 39513
charge and electromagnetic moments, survey of experimental determinations of, 18: 28327 (TID-20711)
collection along channels of magnetic quadrupole lenses from decay of mesons (π), 16: 4690 (NP-10773)
collection in open cavities, 17: 2161 (JINR-P-1014)
conference on, 20: 21594 (CERN-65-32)
conference on high-energy experiments with, 18: 12889 (CERN-63-37)
conservation laws for two-component fields of (T), 19: 1448
coupling to intermediate bosons, (T), 19: 29097
currents of, classification of, 17: 11479 (LNF-62/98)
decay and relativistic properties, (T), 20: 41806
degeneracy in cosmology, universal, 17: 695
degeneracy in universe, limits on, (E/T), 19: 4812
density in universe, (T), 20: 27809
density of, in universe, experimental and theoretical data on, 17: 16910
detection and identification of intermediate, design of experiment for, 17: 4126 (BNL-6512(p.32-6))
detection and measurement, 16: 4358
detection and measurement in cosmic rays, 16: 33666
detection and measurement of solar, using the beryllium-9 reaction, 17: 40062
detection and measurement of solar, 20: 20365
detection apparatus for solar, 18: 14908
detection, bubble chamber devices for, 17: 15142
detection, design of spark chamber for, 16: 31923
detection equipment for, 18: 26166 (BNL-837(p.170-89))
detection of cosmic ray-produced, experiment for, 20: 4561 (COO-818-64)
detection of cosmic, equipment for, 20: 20365
detection of, design of liquid scintillation system for, 16: 31925
detection of high-energy, 17: 23678
detection of solar, review, 18: 24295
detection of solar, by capture in chlorine-37, 18: 40568
detection of solar, possible method for, 18: 44341 (BNL-8217)
detection of solar, method for, 19: 16595
detection of solar, experiment for, 20: 18556(R) (BNL-929, pp 66-82)
detection of solar, performance of nuclei for, 20: 37793
detection of, spark chamber for, 17: 23664
detection of, cadmium-loaded scintillator for, 20: 4847 (UCRL-12085(Pt.1))
detection of, chamber performance and photographs for, 18: 12452 (CERN-63-37(p.215-17))
detection of, development of 12-ft bubble chamber for, 20: 21032 (CERN-65-32, pp 259-62)
detection of, for determination of terrestrial abundances of radioactive potassium, thorium, and uranium, (T), 20: 14750
detection of, method for, (T), 20: 10073
detection of, method for, 20: 21030 (CERN-65-32, pp 223-4)
detection of, review of equipment for, 18: 16326
detection of, review of methods for, 20: 7798 (NEIC-RR-18)
detection underground, experiments on, 19: 34982
detection underground, laboratory for, 20: 21612 (CERN-65-32, pp 225-30)
detection using gallium-71 (ν,e$^-$) reactions, (T), 20: 11537
discovery, 18: 4446

distributions in nuclear reactions with targets, momentum and space, (T), 19: 25489
doublets of, prediction by quaternion formulation of wave functions, 17: 24191
effects on biological processes, 20: 29402
effects on decay constant of bound mesons(μ), 18: 40533
effects on meson (π) decay branching ratio, 18: 37943
electric charge, charge radius, and magnetic moment of, 17: 41797
electrodynamics of, effects on cosmological models, 17: 7005
electromagnetic form factors for ν_e and ν_μ, 18: 4460
electromagnetic form factor for, with vector boson-mediated weak interactions, 18: 14868
electromagnetic form factors of, (T), 19: 6552
electromagnetic properties of, 19: 16661
electromagnetic properties of, survey on, 19: 37666
electromagnetic wave absorption by, 18: 6043
elementary particle models with two, 17: 9273
elementary particle models with two, unified, 17: 39935
emission and interactions in stars, (T), 20: 4534
emission by copper-63 following neutron capture, 20: 6050
emission by degenerate electron plasma of stars, 18: 44849 (AFCRL-64-528)
emission by excited nuclei, pair, 18: 34932
emission by massive stars in late stages of evolution, (T), 19: 37447
emission by neutron stars, rate of, (T), 19: 18671
emission by red giant stars, energy loss by, 17: 15046
emission by stars, evolutionary time scales for late carbon-burning phases with, 17: 24201
emission by stars, theory for, 18: 14703 (NP-13704)
emission by sun, models for flux of, 18: 42259
emission by sun, spectroscopy of, (T), 19: 8058
emission by supernova, 16: 5837
emission from collapsing stars, methods for observing, 20: 37379
emission from excited states in sodium-23, 19: 43366
emission from exploding supernovas, energy transfer in, (T), 20: 25680
emission from fission fragments, detection of, (T), 20: 4847 (UCRL-12085(Pt.1))
emission from high-temperature stars, surface intensity and stellar energy loss from, (T), 20: 41612
emission from massive stellar centers, energy loss by, 18: 7379
emission from neutron stars, cooling rates from, (T), 20: 4532
emission from neutron stars, cooling-time effects of, (T), 20: 15201
emission from neutron stars, (T), 20: 34075
emission from partially degenerate helium cores in stars cooling from, (T), 19: 41237
emission from point mass, effects on gravitation of, (T), 19: 44910
emission from stars, 16: 4732
emission from stars under gravitational collapse, 18: 37834
emission from stars, mass loss from, 18: 44343
emission from star-like sources, evaluation of, 19: 12055
emission from stars, neutral current effects in, (T), 19: 20772(T)
emission from stars, (T), 20: 7706
emission from stellar plasma, (T), 19: 4790
emission from stellar plasmas, mechanism of, 20: 13519
emission from sun, temperature of solar interior from, (T), 20: 23848
emission from sun, solar interior temperature determination from, 20: 37380
emission from Tau A, 20: 27693
emission in beta decay, book, 17: 9618
emission in beta decay, direction of, 19: 23163(R) (ORNL-3650(p.111-86))
emission in electron-positron annihilation in stars, 16: 22826
emission in evolution of supernovas, 18: 7377
emission in fission fragment beta decay, detection of, 20: 4848 (UCRL-12085(Pt.2))
emission in gravitational collapse of fluid sphere, (T), 19: 16711
emission in intermediate boson or heavy lepton decay, detection of, 17: 21111 (SLAC-5(p.29-31))
emission in late stages of stellar evolution, effects of, 17: 32850
emission in meson (μ^-) capture by copper, 17: 5377
emission in meson (μ) capture by boron-10, correlations for, 18: 28735
emission in meson ($\pi^\pm$) decay, spatial distributions of, 19: 35045
emission in photon interactions with photons, cross section for, 17: 20940
emission in stars, theory, 16: 24659
emission in stellar evolution, review, 17: 17650
emission in stellar evolution, 18: 18551(T)
emission in stellar evolution, luminosity of, (T), 19: 44927(T)
emission in stellar processes, (T), 20: 4533
emission in supernova processes, electron and meson (μ) associated, 17: 32880
emission of pairs of, by stellar plasma, 17: 11446
emission processes in carbon-burning stars, effects of energy-loss, (T), 20: 15194
energy and mass, theoretical concepts, 16: 9376
energy density in universe, 17: 2145 (JINR-E-1032)
energy density in universe, 18: 37838
energy density of high-energy, in the universe, 17: 9439
energy spectra, (E), 19: 46643(R) (LAL-1136)
energy spectra and flux of, from magnetic-finger focused meson (K^+) and (π^+) beams, (T), 19: 30877 (BNL-9062)
energy spectra in atmosphere, (T), 20: 34239
equation of motion for zero-mass, Lorentz invariance of, (T), 19: 18776
exchange forces with electron in nuclei, 17: 24484
existence in celestial atmospheres, 18: 42253 (JINR-E-1752)
existence of two, 18: 38182
existence of two kinds of, evidence for, 17: 37942
existence of two, postulation for, 17: 11478 (LNF-62/97)
existence of two, proof of, 17: 28152 (NEVIS-113)
existence of two, relation to lepton conservation laws, 17: 22468
existence of two types of, survey of experimental and theoretical data for, 17: 24301
existence of two types of, 17: 34758
existence of two varieties of, experimental proof for, 17: 15153
existence of two, approximate symmetries in, 16: 31038
existence of, review of evidence for, 20: 19517
existence with mass and partial conservation of muon charge, 18: 9194
experiment at CERN on, preliminary results, 19: 1391
experiment at CERN on, conclusions from (E/T), 19: 1393
experimental facility for, at Argonne synchrotron, 16: 31922
experimental physics of, 18: 42367 (JINR-E-1803)
experiments at CERN on, analysis of data from, 18: 40375
experiments at CERN on, 19: 37662
experiments at CERN on, bubble and spark chamber, 19: 39612
experiments on, 18: 20900 (CERN-64-6(p.99-123))
experiments with, at Stanford linear accelerator, 17: 21118 (SLAC-5 (p.193-221))
experiments with high-energy, interpretation of, 17: 11471 (JINR-E-1120)
experiments with high-energy, lectures on, 19: 16660
experiments with high-energy, review on, 19: 25358
facilities for studying, 19: 43175
field equations for, vectorial optics for, 19: 31091
field equations for, dimensionality of real world from strength of, 20: 6218
field of negative or positive 1-spinors for, for singular-electromagnetic-field tensor, (T), 19: 41348
field theory for, geometrodynamic, 20: 4619
field theory for, quantum, 20: 39853 (JEN-157-DF/I-48)
field theory of, 19: 39639
fields for two, formulation of, 18: 32557
flux calculation of, method for, 20: 21608 (CERN-65-32, pp 169-74)
flux calculations of, methods for, 19: 31010 (NPA/Int.63/11)
flux in CERN experiment, calculations of, 18: 12893 (CERN-63-37 (p.79-109))
flux in CERN experiment, calculations of, 19: 1134
flux in CERN experiment, focusing system for increasing, 19: 37244 (CERN-65-17)
flux in universe, (T), 20: 9646
flux of solar, (T), 20: 37377
flux of, method for calculating, 20: 21608 (CERN-65-32, pp 169-74)
flux of, methods for calculating, 20: 21600 (CERN-65-32, pp 97-108)
fluxes through an aperture, 17: 3977
form factors of, calculation of electromagnetic, 18: 2591 (TID-19682)
formalism of neutrino theory of light, 19: 18936
gas of, theory for, 17: 31654 (PAN-384/VII)
generation and behavior in space, 16: 6938
geometric theory of, 19: 39503
helicity and mass, 18: 28327 (TID-20711)
helicity of, method for experimental observation of, 20: 34167(T)
intensity of solar, using capture in chlorine-37, (E), 19: 30968 (BNL-9093)
interaction amplitudes of, unitary spin analysis of, 20: 37751
interaction of, proton background in CERN experiments on, (E), 20: 11571
interaction with nucleons, (T), 20: 21598 (CERN-65-32, pp 79-82)
interactions and properties, 16: 33666
interactions and properties of, survey, 16: 33726
interactions and properties of standing, 17: 7016
interactions and production of, cross sections for, 17: 28151 (NEVIS-111)
interactions and properties of, electromagnetic, 18: 5841(R) (AROD-2800.12)
interactions and properties of muon, review, 18: 10893
interactions and properties of, review on, 19: 23474
interactions and production in stars, review on, 19: 25139
interactions and properties of, (E/T), 20: 999
interactions at high energy, 16: 10812 (CERN-61-30)

interactions at high energy, techniques for experiments on, 17: 23626
interactions at high energy, cross sections for, (T), 19: 25384
interactions at high energies, semileptonic, (T), 20: 19527
interactions at high energies, weak, (T), 20: 21614 (CERN-65-32, pp 275-84)
interactions at high energies in spark chambers, 20: 34146 (CU-1932-256)
interactions in bubble and spark chambers at high energies, lower limit for intermediate boson mass from, (E/T), 20: 21596 (CERN-65-32, pp 11-24)
interactions in bubble chambers at high energies, intermediate boson mass from, 20: 21597 (CERN-65-32, pp 25-30)
interactions in CERN spark chamber experiment, 19: 1392
interactions in Coulomb field, vector boson and meson (μ) production in, 19: 23475
interactions in earth, heat production by, 18: 42525
interactions in emulsions, location and analysis of, (E), 20: 6052
interactions in Freon bubble chamber, 18: 26265 (BNL-837(p.114-36))
interactions in heavy-liquid bubble and spark chambers, 18: 26266 (BNL-837(p.160-9))
interactions in nuclear Coulomb fields, cross sections for meson (K), meson (μ), and meson (π) production, 17: 5288
interactions in nuclear emulsions, method for determining, 20: 21609 (CERN-65-32, pp 175-80)
interactions in nuclear field, direct production of lepton pairs from, (T), 20: 25858
interactions of, 17: 7037
interactions of, cross sections for elastic and inelastic, 17: 11478 (LNF-62/97)
interactions of, electromagnetic, 17: 17018
interactions of, experimental program at CERN for detecting, 16: 31924
interactions of, experiments to study weak, 17: 20580 (UCRL-10022 (p.144-50))
interactions of high-energy, structure of cross sections for, (T), 19: 10102
interactions of high-energy, in heavy-liquid bubble chamber, 19: 29042 (CERN-65-12)
interactions of high-energy, review on, 19: 39611
interactions of high-energy, review of experiments on, 20: 11580
interactions of, meson (π) production in, 17: 13350 (JINR-P-1152)
interactions of meson (μ), upper limits for, 18: 26321
interactions of solar, with electrons, methods for detecting, 20: 37792
interactions of, theory of weak, 17: 20567 (UCRL-10022(p.42-5))
interactions of, astrophysics in, 18: 26187 (BNL-837(p.193-233))
interactions of, astrophysics in, (T), 19: 8064
interactions of, CERN experiment on, 19: 35180
interactions of, damping theory in weak (T), 19: 3039
interactions of, description of large-area liquid scintillation detector for studying, 20: 33689
interactions of, electrodynamics of weak, 18: 28740
interactions of, effects on weak interaction theory (T), 19: 1298
interactions of, effects of weak magnetism in, (T), 19: 8492
interactions of, experiments on, 20: 21606 (CERN-65-32, pp 157-60)
interactions of, form factors in weak, (T), 19: 12316
interactions of, intermediate vector boson production in, (T), 20: 13464
interactions of, lectures on, 19: 29039 (ANL-6989)
interactions of, measurement of meson (μ) polarization from, 20: 30003
interactions of, photon production in, 18: 36382
interactions of, production amplitudes for, (T), 19: 27223
interactions of, review, (T), 20: 6036 (CERN-64-13(Vol.4), pp 51-95)
interactions of, review of experimentation in, 20: 9781
interactions of, review, (E), 20: 19439 (ANL-7130, pp 273-84)
interactions of, research on, 20: 37735(R) (COO-818-96)
interactions of, strong, 18: 40280
interactions of, selection rules for two-body, (T), 19: 8243
interactions of, SU(6) symmetry for N* production in, (T), 19: 18832
interactions of, shadow universe model for, (T), 19: 35127
interactions of, supercharged particle production in high-energy, (T), 19: 41483(T)
interactions of, shadow universe concept for, (T), 20: 6045(T)
interactions of, summary on detection and properties of, 20: 21613 (CERN-65-32, pp 269-74)
interactions, theoretical implications of experiments on, 16: 31920
interactions, theoretical investigations of, 16: 31921
interactions, two-neutrino hypothesis, 16: 24694 (NP-11731)
interactions underground, experimental possibilities for studying, 17: 34764
interactions with nuclear Coulomb field, muon pair production in, 16: 1086
interactions with mesons ($K_{\pi 2}$), 16: 4728
interactions with nucleons, pion production cross sections, 16: 12558
interactions with nucleons, weak processes during, 16: 12563
interactions with electrons, cross sections for, 16: 13880
interactions with neutrons, cross sections for, 16: 13880
interactions with protons, intermediate-boson-production cross sections, 16: 4719
interactions with electrons, field-theoretical analysis, 16: 22901
interactions with nucleons, 16: 22949
interactions with nucleons at high energies, boson nonproduction in, 16: 26130
interactions with hyperons and nucleons, vector current structure for, 16: 26184
interactions with nucleons, meson (π) production in, 16: 26074 (JINR-P-905)
interactions with nucleons at 0 to 5 Bev, cross sections for inelastic, 16: 27973
interactions with nucleons at high energies, search for anomalous, 16: 27990
interactions with nucleons, meson (π) production in, 16: 28001
interactions with nucleons, meson (π) production in, 16: 28002
interactions with nucleons, meson (π) production in, 17: 743
interactions with nucleons, cross sections, 17: 2145 (JINR-E-1032)
interactions with electrons, elastic, 17: 2199
interactions with particles, effects of lepton-current local action on, 17: 3997
interactions with nucleons, meson (π) production amplitudes for, 17: 7023
interactions with protons, cross sections for meson (K^+) production in, 17: 6953 (LNF-62/89)
interactions with nucleons, cross section for, 17: 9439
interactions with nucleons, cross sections for, 17: 11563
interactions with neutrons and protons, relations between cross sections for meson (π) production in, 17: 13348 (JINR-P-1141)
interactions with electrons, charge renormalization in elastic, 17: 16958 (UCRL-10336)
interactions with neutrons and protons, rates of $e^{\pm}$ producing, 17: 19149
interactions with protons, meson (π) production cross sections for, 17: 20919
interactions with neutrons, electron-meson (μ) production ratio in, 17: 20933
interactions with protons, cross section and form factors for meson (K) production in, 17: 22464
interactions with photons in external gravitational field, pair production and scattering in, 17: 25996
interactions with nucleonic Coulomb fields, polarization of bosons produced in, 17: 31317
interactions with neutrons, applicability of weak interaction theory to, 17: 31324
interactions with neutrons, cross sections for, assuming Regge-particle mediators, 17: 36588
interactions with nucleons, meson production in, 17: 37970
interactions with nucleons, Regge pole domination of, 17: 39887
interactions with nuclear fields, charged vector meson production in, 17: 41741 (LNF-63/44)
interactions with nucleons, unitary symmetry of weak current structure in, 17: 41781
interactions with neutrons at 1 Bev, hyperon (Σ^+) polarization from, 18: 882
interactions with protons at 200 Mev, cross section for, 18: 896
interactions with nuclear and proton Coulomb fields, effects on intermediate boson production in, 18: 2653
interactions with protons, six-fermion couplings in, 18: 6023
interactions with matter, review of experimental and theoretical studies of, 18: 7542
interactions with nucleons at high energies, one-neutrino hypothesis for, 18: 7555
interactions with nucleons, production of polarized baryons and leptons in weak, 18: 9125
interactions with nucleons, cross sections for production of heavy vector mesons in, 18: 9202
interactions with neutrons, hyperon production in, 18: 10940
interactions with electrons, mesons (μ), and neutrons, theory of, 18: 12890 (CERN-63-37(p.1-20))
interactions with electrons, nonlocality and dissymmetry in Ke, mode in, 18: 12930
interactions with nucleons, spark chamber performance for, 18: 12448 (CERN-63-37(p.43-75))
interactions with neutrons, analysis of, 18: 12892 (CERN-63-37(p.33-41))
interactions with protons at 2 to 10 Bev, rates and total cross sections for, 18: 12895 (CERN-63-37(p.163-77))
interactions with polarized electrons, 18: 12902 (JINR-P-1487)
interactions with neutrons in nuclei, analysis of elastic, 18: 13040 (CERN-63-37(p.203-13))
interactions with nucleons, unitary universal model for, 18: 14904
interactions with electrons and mesons (μ), unitary symmetry in weak, 18: 14940
interactions with neutrons and protons, use of 1000-Bev accelerator to

study, 18: 16750 (BNL-7534(p.88-106))
interactions with neutrons, theory for elastic, 18: 16759 (CERN-64-13 (Vol.III)(p.81-110))
interactions with electrons, cross sections for elastic, 18: 16760 (LAMS-3013)
interactions with leptons, parity nonconservation in, 18: 22774
interactions with cosmic rays in universe, theory of, 18: 24348
interactions with nucleons, $W^{\pm}$ production and form factors in, 18: 26268 (BNL-837(p.249-56))
interactions with nucleons at high energies, meson production in, 18: 28413
interactions with nucleons, conserved vector current hypothesis testing by, 18: 34561
interactions with electrons, spin correlations in, 18: 34614
interactions with nucleons, meson (μ) pair production in, 18: 36344
interactions with nucleons, J = ⅝ isobar production in, 18: 37909
interactions with nucleons, electron production in, 18: 40280
interactions with nuclear coulomb field, lepton-pair production in universal four-fermion theory of, 18: 40500 (AD-603251)
interactions with leptons (T), 19: 3071
interactions with nucleons (E/T), 19: 2941
interactions with neutrons, polarization of mesons (μ^-) from, (E/T), 19: 5201
interactions with matter, effects of existence of hadrons having nonzero mean hypercharge on, (T), 19: 4939
interactions with nucleons in liquids, (E), 19: 4947
interactions with nucleons, N* production in, (T), 19: 4981
interactions with leptons, angular and spin correlations in, (T), 19: 5007
interactions with nucleons, unitary symmetry for SU(3) relations in, (T), 19: 8165
interactions with gravitational field, 4-component spinorial equation in, (T), 19: 8271
interactions with nucleons, intermediate bosons in, (E), 19: 8149
interactions with protons, resonances in, 19: 9767(R) (IS-900(Sect.P))
interactions with protons, N^*_{33} production in, (T), 19: 10055
interactions with nucleons, PC violation in meson (π) production in, (T), 19: 10073
interactions with nucleons, lepton emission in, (T), 19: 12253
interactions with deuterons, cross sections for inelastic, (T), 19: 12255
interactions with electrons and mesons (μ), polarization in, (T), 19: 14343
interactions with leptons, weak, 19: 14401
interactions with antineutrinos and photons, effects of neutrino mass on, (T), 19: 16472 (JINR-P-1933)
interactions with nucleons in SU_3 model, hyperon production in, (T), 19: 16594
interactions with leptons, photon structure from elastic, (T), 19: 18769
interactions with nucleons, meson (K) and (π) peripheral production in, (T), 19: 18815
interactions with electrons, recoil polarization in, (T), 19: 18905
interactions with elementary particles, production amplitudes in, (T), 19: 20925 (ICTP-64/3)
interactions with nucleons, neutral weak currents in, (T), 19: 20988
interactions with neutrons, SU(6) for N* production in, (T), 19: 20996
interactions with nucleons, single meson (K) and (π) production in, (T), 19: 23477
interactions with nucleons, N* production in, (T), 19: 25292
interactions with nucleons, meson production in, (T), 19: 25315
interactions with electrons, spin correlations in cross sections for, (T), 19: 27186
interactions with protons, asymptotic relations for meson (π)-production cross sections in, (T), 19: 29065 (JINR-P-2062)
interactions with protons, U_{12} predictions for N* production in, (T), 19: 31065
interactions with neutrons, transverse proton polarization in, (T), 19: 31075
interactions with nucleons, form factors and polarization effects in, (T), 19: 35081
interactions with nucleons, cross sections and form factors for, (T), 19: 35128
interactions with protons, asymptotic relations between meson (π) production cross sections in, (T), 19: 35134
interactions with electrons, recoil electron energy spectra in, (T), 19: 37620
interactions with nucleons, meson (π) production in, (T), 19: 37631
interactions with nucleons, resonance production in, (T), 19: 39517
interactions with electrons, weak boson production in, (T), 19: 39567
interactions with electrons, polarization effects in, (T), 19: 39587
interactions with nuclear nucleons, meson (π) production in, (T), 19: 41754
interactions with neutrons, analysis of, (T), 19: 47301 (CERN-65-30)
interactions with nucleons, charge ratio of mesons (π) produced in, (T), 19: 47377
interactions with nucleons, SU(6) for N* and Y^*_1 production in, 20: 1020
interactions with antineutrinos, bootstrap method for W boson exchange in, 20: 2721
interactions with protons at high energy, cross sections for meson (π^+) production in, (T), 20: 2733
interactions with baryons at high energy, De Santis model for, 20: 2784
interactions with electrons, experiment for detecting, 20: 4848 (UCRL-12085(Pt.2))
interactions with antineutrinos, pure gravitational tensor field from, (T), 20: 4763
interactions with protons, production of (3,3) resonance by, (T), 20: 4476(R) (IS-1200(Sect.P))
interactions with neutrons, radiative meson (μ) production from, (T), 20: 4611
interactions with nucleons, baryon resonance production in, (T), 20: 6065
interactions with nucleons at high energies, conservation hypotheses for, (T), 20: 9784
interactions with nucleons, nonpolarized lepton state from, (T), 20: 11577
interactions with neutrons, mass of intermediate bosons from, (T), 20: 13504
interactions with neutrons, charge-retention currents for elastic, (T), 20: 15327
interactions with nucleons, lepton production in, (T), 20: 15387
interactions with leptons at high energies, local-current commutation relations for, 20: 17387
interactions with neutrons, meson (π) production cross sections for, (E), 20: 19438 (ANL-7130, pp 257-71)
interactions with electrons and positrons, two- and four-component theories in, 20: 19463
interactions with electrons, polarization in, (T), 20: 19464
interactions with nucleons, asymmetries in meson (π) production in, 20: 19478
interactions with nucleons, asymmetries in meson (π) production from, (T), 20: 21638
interactions with neutrons, flux determination from, (E), 20: 21603 (CERN-65-32, pp 115-20)
interactions with neutrons, meson (μ^-) angular and energy distributions from, (T), 20: 23950
interactions with baryons and leptons, properties of, (T), 20: 24010 (CERN-65-24(Vol.3), pp 65-86)
interactions with leptons and nucleons, (E/T), 20: 24260
interactions with antineutrinos, cross section for photon production in annihilation, (T), 20: 27809
interactions with neutrons, models for proton polarization from, 20: 27815
interactions with mesons (K^0), coherent regeneration and meson (K^0_2) decay in, (T), 20: 27885
interactions with bound electrons, cross section for, (T), 20: 32005
interactions with neutrons and protons at very-high energies, cross sections for, (T), 20: 32036
interactions with nucleons, baryon resonance production in, 20: 32080
interactions with nucleons at high energies, inelastic, 20: 34146 (CU-1932-256)
interactions with nucleons, W meson production in, (T), 20: 34157 (UJV-1576)
interactions with nucleons, polarized N* production from, (T), 20: 44276
interactions with nucleons, differential cross sections for lepton polarization and N* production in, (T), 20: 46334 (IS-T-96)
interactions with baryons in SU(3), inelastic, 20: 46382
interactions with nucleons, collinear meson production in SU(6) from, (T), 20: 46383
interactions with electrons, two-body approximation of elastic, 16: 24688 (JINR-P-947)
interactions without strangeness change, (E), 19: 16681
isospinor field for, 18: 34527
magnetic charge of, (T), 19: 35042(T)
magnetic charge of, testing of, (T), 19: 35044
mass, (T), 19: 41482(T)
mass and magnetic moment of, (T), 19: 29124
mass in meson (μ) decay, (T), 19: 31066
mass of, meson (μ) decay rate effects of non-zero rest, 17: 31291
mass of, from spinor connection in Riemannian space, 19: 27207
mass of, method for high-accuracy measurement of, 19: 1276
mass of, upper limits for, 18: 37943
masses of electronic and muonic, 17: 16991
model for elementary particles, unified, 17: 4022
model for elementary particles, 19: 43165
model for properties of, 19: 16645
models for, description of electromagnetic, (T), 19: 41377
momentum distribution in nuclear reactions with targets, (T), 19: 25488
motion in superdense matter, (T), 20: 951 (NP-15517)
motion in superdence matter, partial external trajectories of, (T),

20: 19446 (NP-15932)
occurrence and properties of, 17: 34811
pair production in Coulomb field by, cross-section for, 18: 28742
photon composition from, 18: 36253 (UCRL-7425)
photoproduction in nuclear coulomb field, 17: 9407
photoproduction in nuclear coulomb field, 17: 9473
photoproduction on protons in superdense stars, cross sections for, 17: 39834
photoproduction on protons, pseudoscalar term in, 18: 44526
physics of, experiments on, 18: 10842 (BNL-787)
possible existence of two, approximate symmetries in, 16: 31038
process involving high-energy, 16: 970
production and acceleration in plasma, (T), 19: 21500
production and losses in massive stars and supernovae, (T), 19: 14201
production at CERN, 18: 26165 (BNL-837(p.91-113)
production by gravitational field of astrophysical objects, (T), 19: 4821
production by meson beam focused by plasma lens, 19: 20915 (BNL-8967)
production by 200-Bev proton synchrotron, (T), 19: 20738 (UCRL-11983)
production facilities for, summary of, 20: 21605 (CERN-65-32, pp 153-6)
production from cosmic ray reactions with dense matter, differential energy spectra for, (T), 20: 37712
production in accelerators, effects of focusing on (T), 19: 2925 (MURA-698)
production in CERN proton synchrotron, (E/T), 19: 12003
production in cosmic ray interactions with atmospheric nuclei, 17: 41716
production in electron pair annihilation in stars, spectra of, 18: 30393
production in electron reactions with helium-4 and tritium in stellar collapse, (T), 19: 43520(T)
production in helium-3 ($p,e^+\nu$) reactions in solar interiors, (T), 19: 32869
production in high-energy proton bombardment of accelerator targets, estimate of flux from, 18: 32320 (UCRL-10948)
production in massive helium stars, 18: 36150
production in meson (π^-) and (π^+) decay, amplitudes, 16: 15604
production in meson (π) decay, properties, 16: 26147
production in meson (π^+) decay, 17: 9252
production in meson (K^0) decay, 17: 9245
production in meson(π) decay, 17: 11471 (JINR-E-1120)
production in meson (μ^-) capture by oxygen-16, (E), 20: 6273 (AD-617398)
production in meson (μ^-) reactions with helium-3, probability for, (T), 20: 22152
production in nuclear targets, momentum distribution for, (T), 19: 19131
production in particle inelastic reactions at 1 to 10 Bev, 16: 5861 (JINR-P-772)
production in proton interactions in cosmic radio sources, 18: 32346
production in relativistic mesons (π) and (K) decay, spectra of, 18: 12894 (CERN-63-37(p.111-29))
production in solar reactions, 18: 28703
production in space and properties, 16: 33727
production in stars, 19: 34835 (N64-22572)
production in stars, energy balance in universe from, (T), 20: 2587
production in sun, (T), 20: 34068(T)
production in target irradiation at high energy, (T), 19: 19132
production in thermonuclear reactions, (T), 20: 2587
production of beams of, in CERN synchrotron, 17: 23637
production of beams of, using high-intensity proton linac, (E), 19: 9808 (TID-21282)
production of CERN experiment on, 20: 21602 (CERN-65-32, pp 111-14)
production of, design of 750-Mev linear proton accelerator for, 17: 15325(R) (TID-17766)
production of high-intensity beams of, 16: 31926
production of high-energy beams from a 300-Bev synchrotron, 17: 20589 (UCRL-10022(p.222-30))
production of solar, mechanism and rate of, 17: 15047
production of solar, in carbon-nitrogen and proton-proton cycles in sun, 18: 37835
production of, astrophysics of, 19: 9872
production of, isotopic sources for, 20: 6050
production of, review of methods for, 20: 7798 (NEIC-RR-18)
properties and use in cosmogonical analysis, review of, 19: 23465
properties in beta decay, theory of, 17: 4111
properties in beta decay and in space, review, 17: 34795
properties in space, 17: 16917
properties in 4-spinor field, theoretical, 16: 10927
properties of, 20: 24010 (CERN-65-24(Vol.3), pp 65-86)
properties of single four-component, with two physical states, 16: 27966
properties of, lectures on, 20: 21616 (JINR-P-2429)
properties of, quantum laws for, (T), 19: 39661
properties of, research at CERN on, 18: 20967
properties of, review of theories and experimental data on, 18: 10907
properties of, review of, 18: 20919
properties of, review of, 20: 17406
properties of, tensorial description of, 19: 35052
properties, review, 17: 34729 (JINR-P-1269)
quantum numbers in theories having two, 17: 15096
quantum theory for, 19: 47409
radiation from fields of, structure of, 20: 8000
radius of, electromagnetic, (T), 19: 25290
reactions (ν,e^-) with chlorine-37, (T), 19: 16342
reactions (ν,e^-) with deuterium, (T), 20: 10073
reactions (ν,e^-) of solar, with chlorine-37, of, at Earth, (T), 20: 23847
reactions (ν,e^-) of solar, with chlorine-37 at earth, rate of, 20: 23847
reactions (ν,μ^-) with nuclei, test for time reversal violation in, (T), 20: 13835
reactions in matter at ~500 Mev, 17: 9468
reactions in nuclear Coulomb fields, polarization effects in intermediate boson production in, 18: 7533
reactions in type II supernova explosions, (T), 19: 14200 (UCRL-12191)
reactions (ν,e^-) on nuclei, cross sections, 16: 18517
reactions of solar, with terrestrial chlorine-37, probabilities of, 18: 14907
reactions of, experiments on, 20: 30002
reactions of, test of Cabibbo's theory of CP-violation in, 19: 31082
reactions on nuclei and nucleons at 1 Bev, particle production cross sections, 16: 27965
reactions on nuclei, multiple meson production from, 17: 19176
reactions with aluminum-27 and copper-63 at 1.5 to 4 Bev, cross sections for intermediate boson production in, 18: 10955
reactions with aluminum and copper at 2 to 10 Bev, rates and total cross sections for, 18: 12895 (CERN-63-37(p.163-77))
reactions with beryllium-9, 17: 40062
reactions with chlorine-37, cross sections for, (T), 20: 6393
reactions with chlorine-37, cross section for, (T), 20: 38111
reactions with iron, intermediate-boson-production cross sections, 16: 4719
reactions with iron and lead, diffraction mechanism for mesons (μ) and (π) production in, 17: 21091
reactions with lead, meson (π) pair production in, (T), 19: 16530
reactions with matter, 16: 33727
reactions with matter, intermediate vector bosons from, (T), 20: 2759 (UR-875-102)
reactions with matter, lepton production in, (T), 20: 4866
reactions with nuclei at intermediate energy, 16: 21425
reactions with nuclei at high energies, boson nonproduction in, 16: 26130
reactions with nuclei, 17: 17018
reactions with nuclei, intermediate boson production in, 17: 29546
reactions with nuclei in earth's crust, meson (μ) production in, 17: 41716
reactions with nuclei, cross section asymptotic behavior for production of mesons (π^+) in inelastic, 17: 41826
reactions with nuclei, asymptotic cross sections for, 18: 11256
reactions with nuclear Coulomb fields, vector boson production in, 18: 12896 (CERN-63-37(p.179-201))
reactions with nuclei, W production in, 18: 26269 (BNL-837(p.257-65))
reactions with nuclei, structure effects in, 18: 36656
reactions with nuclei at 60 Bev, meson (π) pair production in, 18: 40642
reactions with nuclear Coulomb field, lepton pair production in, 18: 44552
reactions with nuclei, polarization of mesons (μ^-) from, (E/T), 19: 5201
reactions with nuclei, induced transformations in, 19: 34984
reactions with nuclei, cross sections for, (T), 19: 39943
reactions with nuclear nucleons, meson (π) production in, (T), 19: 41754
reactions with nuclei, nuclear structure effects in, (T), 20: 12100
reactions with Z = 13 to 35 nuclei, lepton-pair production cross sections for, 18: 40500 (AD-603251)
representation of ν_e and ν_μ in separate SU(3) fields, 19: 16676
research at CERN, 20: 25780 (CERN-66-13)
research at CERN on, 18: 30508 (CERN-64-26)
research on solar, using isotopic composition of extraterrestrial and terrestrial material, 20: 37369
research programs on, effects on CERN scheduling, 17: 4128 (BNL-6512 (p.40-2))
research programs on, data affecting, 17: 4129 (BNL-6512(p.43-5))
review of physics of, 18: 18652
role in cosmology, 18: 40111
scattering by nuclei near 1 Bev, lepton pair production cross sections, 16: 29705
scattering by nuclear Coulomb field, vector boson production in, 18: 12891 (CERN-63-37(p.21-32))
scattering by nuclei, bremsstrahlung from, (T), 19: 8482
scattering by nuclei, transverse muon polarization from quasielastic, 20: 32468
scattering by nuclei, quasi-elastic, (T), 20: 44740
shielding of, in CERN experiments, 17: 4127 (BNL-6512(p.37-9))
solar flux and elastic scattering, limits on, 18: 20713
solar flux and elastic scattering, upper limit on, 19: 37452

spectra from meson (μ) and (π) decay and meson (μ^-) capture, 16: 15562
spectra from neutron production in compression of nuclear matter, (T), 20: 8097
spectra of solar, use for solar structure parameter determination, 20: 37378
spinor field of, gravitational field equations in the presence of, 17: 13372
statistics for gases of, (T), 19: 35101
theories having two 2-component or one 4-component, 17: 15141
theory, 18: 2593 (TID-19707)
theory for, 18: 837 (JINR-D-1345)
theory for photons using, (T), 19: 41387
theory for stars of, 18: 28208
theory for two kinds of, 18: 16782
theory having three, 17: 19109
theory of electron- and meson (μ)-associated, 18: 34598
theory of, four component, 17: 13421
theory of four-component Dirac, 17: 24190
theory of, four-component, 17: 39932
theory of four types of, in unitary symmetry group, 18: 32596
theory of gases of, statistical, 17: 34745
theory of light, gauge invariance of electromagnetic field in, 17: 24331
theory of two, selection rules for, 18: 2583 (CEA-2259)
theory of two-, in weak interactions, 19: 10101
theory of two, in composite elementary-particle model, 18: 14918
theory of, C, P, T transformations on a space-time curve in, 18: 10905
theory of, equivalence of Majorana and two-component, 19: 16512
theory of, in geometrodynamics, 20: 15561
theory of, two-component, 18: 32628
theory, experimental verification of two-component, 16: 10930
transformation for, analogy in, 18: 28335
transport in stellar gravitational collapse, relativistic theory for, 20: 32296
two-neutrino hypothesis, 17: 24189
wave equations for, 18: 18707
wave equations for free fields of, (T), 19: 21110

NEUTRINOS (ν_e)

angular distributions and energy spectra in atmosphere, (T), 20: 23948
charge moment of, method for determining, 18: 12916 (TID-20112)
detection of solar, apparatus for, 20: 4523 (COO-818-63)
existence of, approximate symmetries for, 16: 31038
flux at sea level, 19: 34985
flux of, upper limits on, (E), 19: 12216
form factor of, intermediate vector-boson theory for electromagnetic, 20: 21669
interactions in meson (μ^2) decay, weak-current, (T), 20: 11578
interactions with neutrons at high energies, analysis of, (E), 19: 10069
interactions with protons, baryon conservation in, (E), 19: 12216
interactions with protons, positron spectra from, (E), 20: 992 (COO-818-65)
interactions with protons, cross sections for, 20: 993 (COO-818-70)
interactions with protons, positron spectra from, (E), 20: 2680 (COO-818-58)
interactions with electrons, neutral lepton currents in, (T), 20: 7809
interactions with electrons, S-operator theory for, 20: 15481
interactions with protons, liquid scintillator for measuring cross sections for, 20: 21027 (CERN-65-32, pp 41-4)
interactions with nucleons at high energies, intermediate boson production in, (E), 20: 21595 (CERN-65-32, pp 1-10)
photoproduction, 16: 4732
production in electron-positron beam interactions, (T), 19: 12261
production in electron capture processes in stars, energy losses from, (T), 19: 16348
properties, 19: 35179
properties of, comparison with ν_μ, (T), 20: 9722(T)
reactions with deuterium, cross sections for, 20: 993 (COO-818-70)

NEUTRINOS ($\bar{\nu}_e$)

angular distributions and energy spectra in atmosphere, (T), 20: 23948
interactions of cosmic, with electrons, mesons (μ^-) from, (T), 20: 23949

NEUTRINOS (ν_μ)

angular distributions and energy spectra in atmosphere, (T), 20: 23948
charge, 16: 26115
emission from stars, 18: 2517
emission in meson (μ) decay, experimental consequences of the Majorova theory for, 17: 13435
existence of, approximate symmetries for, 16: 31038
flux at sea level, 19: 34985
form factor of, intermediate vector-boson theory for electromagnetic, 20: 21669
interactions above 10^{12} ev, model for, (T), 20: 11558 (JINR-E-2496)
interactions in meson (μ^2) decay, weak-current, (T), 20: 11578
interactions with neutrons at high energies, analysis of, (E), 19: 10069
interactions with protons at high energies, intermediate boson production in, (E), 19: 10070
interactions with neutrons, radiative charged lepton production in, (T), 19: 16546
interactions with electrons, Feinberg-Pais field theory of, 19: 33075
interactions with polarized protons, CP violation in, (T), 19: 35111
interactions with nucleons, cross section for pion production in, (T), 19: 43158
interactions with neutrons, polarization of mesons (μ^-) from, (T), 19: 45050
interactions with protons, cross sections for elastic, (T), 20: 7819
interactions with protons, effects of W meson on lepton pair production in, (T), 20: 15347
interactions with protons, effects of vector mesons on lepton production by, (T), 20: 17504
interactions with mesons (μ) at very high energies, (T), 20: 17366(T)
interactions with nucleons at high energies, intermediate boson production in, (E), 20: 21595 (CERN-65-32, pp 1-10)
interactions with neutrons, cross sections for N* production in, (T), 20: 21599 (CERN-65-32, pp 89-96)
mass, 18: 22776
mass, 17: 19125
mass, (E), 20: 13461 (UCRL-16365)
mass of, from radiative corrections to ($\pi \rightarrow \gamma\mu\nu$) decay, (T), 20: 7811
mass of, method for determining, (T), 19: 25329
mass of, sensitivity of vector coupling constant to T-invariance and, (T), 19: 27215
mass of, upper limit for, 18: 10845 (JINR-P-1454)
mass of, upper limit for, 17: 39896
production in electron-positron beam interactions, (T), 19: 12261
properties, 19: 35179
properties of, comparison with ν_e, (T), 20: 9722(T)
reactions with nuclei, intermediate boson production in, (E/T), 19: 33049

NEUTRINOS ($\bar{\nu}_\mu$)

angular distributions and energy spectra in atmosphere, (T), 20: 23948
interactions with protons, polarization of mesons (μ^+) from, (T), 19: 45050

NEUTRON-ABSORPTION ANALYSIS

development for helium-3–helium-4 mixtures, 19: 24611(R) (MLM-1227)
effects of probe arrangement on, 18: 29929 (NP-13993)
equipment and methods for hydrogenous material, 20: 3913(P)
equipment and methods of, for use in materials analysis, 20: 22917
equipment for determining water in soils, 18: 35808 (HW-82009)
equipment for monitoring boron in chemical process tanks, 19: 22404 (HW-65531)
instrument for, 18: 33470(T) (AEC-tr-6399(p.83-91))
instrument for measuring moisture in friable materials, 18: 33466(T) (AEC-tr-6399(p.43-50))
isotope abundance effects on, 17: 38958
method for pyrotechnic cartridges, 20: 39334
method of, for mineral beneficiation products, 20: 33183(T) (AEC-tr-6639, pp 114-17)
moisture measurements by, method for finding sensitivity and precision of, 19: 7766 (IFA-MR-21)
neutron source preparation and arrangement for, 19: 36299
of rocks in boreholes, 20: 37018
reliability of, in moisture content measurements, 20: 8848
research program, 16: 2967(R) (TID-14310)
use for analysis of coal, 17: 27240(R) (TID-18883)
use for density measurement in two-phase hydrogen, 19: 36752 (NASA-TN-D-2787)
use for determination of moisture in soil and building materials, 18: 19905
use for determination of plutonium-239 in reactor fuels, 20: 233 (SGAE-PH-28/1965)
use for moisture content of building materials, 18: 31384
use for moisture determinations, review, 17: 4465
use for moisture determinations in coal and soil, 18: 39565 (COO-712-73)
use for nondestructive determination of burnup in nuclear fuels, 20: 11004
use for void-fraction measurements in boiling water, (E), 19: 18109 (CONF-654-53)
use in determination of carbon-hydrogen ratio of hydrocarbons, 18: 19904
use in determining mixing in concrete, 19: 2221(R) (SRO-79)
use of isotopic neutron sources in, 18: 43387 (ORNL-P-479)
uses of, 19: 26728

Neutron Activation Analysis
see Activation Analysis

NEUTRON ACTIVATION CROSS SECTIONS

calculation for structural materials, methods for, (T), 19: 45461 (N64-25922)
calculation of, 20: 44609 (CONF-660303, pp 315-27)
calculation of, for corrosion products in Yankee, 20: 45126 (WCAP-6072)
computer library collection of, 20: 44608 (CONF-660303, pp 309-14)

determination of epithermal and fast, 17: 7306
determination of, in swimming pool reactor irradiations, 17: 7100 (NP-12330(p.95-6))
measurement for nuclei with $68 \leq A \leq 208$ at 24 kev, (E), 20: 12135
measurement in Project Gnome, 16: 17072 (PNE-113P)
measurement of, on nickel, using a magnetic spectrograph with nuclear emulsions, 17: 31545
measurement of, resonance self-shielding in, 17: 4030
measurement of, for various nuclei at 14.7 Mev, 18: 24613 (NP-13930 (p.139))
of nuclear reactions induced by 20-Mev deuterons, 17: 31548
tables, 16: 23008 (XDC-60-8-81)
tables, 18: 18879 (NP-13722)
tables of, for metastable isomers, 20: 16336(R) (NYO-10175)

NEUTRON BEAMS

albedo for limestone concrete of fast, 20: 44988 (NASA-TM-X-1287)
amplification of, method for, 17: 36632
attenuation by borated boiling water, void fraction determination by, 19: 3577
attenuation, mathematical analysis, 16: 3657 (NARF-61-33T)
characteristics of, for use in radiotherapy, 19: 22056
collimating tube design for AARR, 20: 30787(R) (ANL-7190, pp 11-142)
collimation, apparatus for testing, 16: 14922 (TID-15378)
collimation effects on energy spectrum of 2.7-Mev, 16: 8160
collimation of, effects of total reflections on, 17: 13477
collimation of narrow, equipment for, 16: 6597
collimation of, absorbing material for, 19: 17375
collimators for, performance of reflecting multi-channel, 17: 32982
control by graphite-lined cavity, spatial distribution of neutron flux in, 17: 13470 (NYO-9657)
depolarization by targets, calculation of, (T), 20: 4476(R) (IS-1200 (Sect.P))
depolarization in passage through magnetized iron, 18: 24568 (NP-13930 (p.78-9))
description of, from Dutch research reactors, 17: 15508
development for cancer radiotherapy, 18: 35437
diffraction of slow, crystal studies by, 19: 23971
divergence in spectrometers, equations for maximum, 17: 23749
dosimetry, 17: 20237 (CEA-2250)
dosimetry and irradiations with fast, for therapeutic uses, 17: 12083
dosimetry in tissue, isodose charts for, 19: 46121
dosimetry of, 20: 8712
dosimetry of, 19: 775 (MITNE-47)
dosimetry of, use of threshold detectors for, 19: 42726
effects on blood coagulation, 20: 28985
effects on boron compound and chromium and nickel oxide catalysts for para- to orthohydrogen conversion at 77°K, 20: 23790
effects on copper and zinc metabolism in horses and swine, 20: 32907(R) (ORO-648, pp 62-70)
effects on dyeing and tensile properties of cotton, review of, 20: 35821
effects on erythrocyte chimerism and immunologic tolerance in cattle twins, 20: 32908(R) (ORO-648, pp 71-90)
effects on leukemic and tumor cells, 19: 42274
effects on orchard grass chromosomes, 20: 24886
effects on phase transformations in minerals, 20: 35946
effects on solids, elastic explosions from, (T), 20: 30740
effects on young chickens, 20: 32909(R) (ORO-648, pp 91-102)
emission from Ispra-I reactor, effects of gamma heating on, (E), 19: 10641 (EUR-2178.e)
energy and flux calculations for, in double-rotor chopper, 17: 30818
energy and spatial distributions in straight cylindrical channel through water, (E), 19: 45465
energy determinations in, by scattering analysis, 17: 41291
energy loss of, at 10 to 1000 Mev, in biological tissue, calculation of, 16: 30931 (ORNL-3260)
energy spectra in time-variable, method for determining exact, (T), 20: 11937
energy spectra of, from HIFAR reactor, 18: 3348
extraction from reactors, systems for, 18: 21566 (KR-64(Sect.XXIX))
filtering and shielding techniques for, 18: 21130 (KR-64(Sect.XXX))
filters for cold and thermal, crystalline, 18: 42579 (BLG-260)
filters for diffraction analysis, 18: 37145
flux distribution measurements in, from drift-tube neutron generators, (E), 20: 6263 (NP-15635)
focusing and polarization of, electromagnetic, 19: 741
focusing by multiple scattering, 18: 32272 (NP-14112)
intensity determination using helium-3, 18: 11185 (ANL-6797(p.384-7))
intensity of collimated thermal, measurements of, (T), 20: 24314
intensity of swimming pool reactor, core modifications to enhance, 19: 29797
intensity of thermal, at reactor beam ports, 19: 25768
magnetic resonance in, effect of target on para-, (T), 19: 29343
measurement of energy and line width of monochromatic, at 6.8 to 18 Mev, 16: 25589
measurement of, from HT-1 beam hole of MTR, (E), 19: 31217 (IDO-17042(p.11-47))
modulation of (d,t)-produced, with 5 Mc/sec repetition rate, 18: 16614
monitoring of, design of counter for, 16: 31818 (EIR-25)
monitoring 2.5-Mev, indirect method for, (E), 20: 5777
optical devices for, use at beam-hole experiments, 17: 32981
polarization and flipping efficiency in diffractometry, (T), 19: 10991
polarization by transmission through polarized proton target, 20: 34664
polarization from deuteron–deuteron interactions, (E), 20: 46785
polarization in field of Stern-Gerlach-type magnet, 19: 35357
polarization measurements on fast, using scattering asymmetry, 17: 32939
polarization of, development of method for measuring, 17: 2210
polarization of equipment for, 18: 14182
polarization of, guide for changing plane of design of system of, 17: 9149(P)
polarization of thermal, magnetized-mirror, 17: 18537 (KR-37)
polarization of thermal, 18: 9300
polarization of thermal, measurement by magnetized mirrors, 18: 11140 (ANL-6797(p.35-44))
polarization of thermal, 18: 42584 (IAE-597)
polarization of, apparatus for magnetized-mirror, 18: 11141 (ANL-6797(p.45-55))
preparation of monoenergetic, use of recoil proton spectrometers for, 16: 33715
production, 17: 32978
production above 30 Mev at proton synchrotron facilities using deuterium targets (E), 19: 1108 (NASA-CR-56934(p.152-9))
production and analysis of 2.4-Mev, (E), 20: 13088
production and use of polarized, survey of experiments on, 17: 2241 (NIRL/R/16(p.61-7))
production and uses of polarized, in mev to 10-kev range, (E), 20: 6259 (CONF-650217, pp 111-23)
production by electron linear accelerators, parameters for, 17: 33135
production by proton bombardment of beryllium at 9 Bev, (E), 20: 7673 (JINR-P-2424)
production in crystal monochromators, 16: 18454
production in heavy water reactors, 19: 42066(P)
production in proton-accelerator generator, 18: 44317 (AECL-2059)
production in swimming pool reactors, effects of fuel elements on, 20: 26533(R) (BNL-954, pp 16-49)
production in UCLA Spiral-Ridge Cyclotron, 17: 38329 (CERN-63-19 (p.144-8))
production of cold, for elastic scattering studies, 16: 33703(T) (AEC-tr-5232)
production of, design of 750-Mev linear proton accelerator for, 17: 15325(R) (TID-17766)
production of fast, for radiotherapy, 19: 42400
production of high flux, reactor design for, 18: 38577 (A/CONF.28/P/49)
production of high-flux 2.5- and 14-Mev, 18: 42617
production of high-intensity, 19: 1529
production of high-intensity, using cyclotron with separated orbits, 19: 41174
production of intense monoenergetic, (E/T), 19: 44882
production of low-energy, monochromatic, polarized, 17: 41281
production of moderated, from pulsed accelerators, 17: 32978
production of monochromatic, by total deflection, 17: 2214
production of monochromatic, polarized, slow, 17: 41850
production of monoenergetic, method for, (E), 19: 23355(R) (BNL-867(p.1-117))
production of monochromatic, from 50 to 150 Mev, 20: 19789
production of monochromatic cold, intensity and wavelength resolution for, 20: 21949
production of monoenergetic pulsed, apparatus for, 20: 46576(P)
production of narrow medium-energy, for small-angle scattering measurements, (E), 19: 44862 (IAE-867)
production of polarized, by (p,n) reactions on aluminum, 16: 4781
production of polarized, at 18 to 120 Mev, 16: 19734
production of polarized thermal, 16: 26198 (NP-11859)
production of polarized cold, resonance and thermal, 16: 26205
production of polarized, by reflection from magnetized cobalt mirror, 17: 38019(T) (AEC-tr-5734(p.94))
production of polarized, crystal collimators for, 18: 2837(R) (EANDC(OR)-22L)
production of polarized, 18: 20368
production of polarized monochromatic thermal, 18: 32712 (CEA-R-2329)
production of polarized, by scattering on polarized protons, 19: 1538
production of polarized, 19: 31207
production of pulsating, (E/T), 19: 18634 (NP-14614)
production of pulsed polarized, at 10 to 700 kev, (E), 19: 37247(R) (ORNL-3778(p.83-4))
production of pulsed, design of generator for, 20: 13745(P)

production of pulsed, design and operation of rotating mechanical chopper for, (E), 20: 29555
production of pure, fast, 17: 33447(R) (ANL-6723(p.28-32))
production of regular flat-spectrum, device for, 20: 15687(P)
production of, shielding requirements in, 17: 5057
production of sinusoidally modulated, (E), 20: 13704(R) (MIT-2344-4, pp 101-5)
production of subthermal, by total internal reflection, 18: 21120 (AMRA-TR-63-25)
production of thermal, using split reactor cores, 17: 12030
production of thermal, reactor core modification for enhanced, 20: 10432
production of 14-Mev polarized, generator for, 18: 16902
production using high-intensity proton linac, (E), 19: 9808 (TID-21282)
production using liquid-nitrogen-cooled targets, for measuring small angle scattering cross sections, 20: 46572
profile measurements on, automatic scanner for, 17: 39399
properties for use in radiotherapy, biological, clinical, and physical, 19: 7222
properties of cyclotron, 17: 11627 (TID-15088)
properties of, coherence, (T), 20: 15328
radial distribution of thermal, from horizontal channel of VVRS reactor, method of analyzing, 18: 30697
radiation hazards of synchrocyclotron, 19: 41171(T) (N64-33402)
reactions with nuclei, technique for angular distribution measurements from, 20: 9786
reflection of thermal, from collimator walls, 18: 21126 (KR-64(Sect.XXIV))
research program using, 18: 34799
scattering by crystals, effects of diffraction and secondary extinction, 16: 18455
scattering by cylindrical volume, computer program for analysis of, 17: 31634 (NAA-SR-Memo-8516)
scattering by deuterium, polarization of recoil deuterons from, (T), 20: 997 (ORNL-P-1607)
scattering by matter, angular and spatial distributions of multiple, (T), 19: 41650(T)
scattering by mosaic single crystals, reflectivity of, (E/T), 19: 14477
scattering by nuclei at 14 Mev, nuclear temperature after excitation in, 18: 15235
scattering from cylindrical targets, computer program for analyzing, 17: 28223 (NAA-SR-Memo-8427)
selection in cyclotrons for time-of-flight studies, 16: 14117
separation of cold component from, using Soller collimators, 18: 33148 (IFA-FN-23)
shapes of, from electron beam reactions with uranium, 18: 8955 (SAL-1)
shielding studies for, 18: 32948(R) (EUR-534.d(Pt.I))
shielding studies for, ESTAKOS equipment for, 18: 32949(R) (EUR-534.d(Pt.II))
signal-to-noise ratio of thermal, test facility for, 19: 37202(R) (BNL-900(p.1-28))
spectra in, from split-core swimming-pool reactors, 18: 4848 (EANDC(OR)-26U)
spectra in UA-RR-1 thermal column, 20: 18147
spectroscopy with proton recoil telescope, 17: 8649
spin flipping by r-f magnetic resonance, 17: 13878(R) (KR-36)
temperature distribution in graphite stacks, measurement of, 17: 26395 (PAN-101/IX)
time-of-flight measurements on, data processing system for, (E), 20: 46552 (AERE-R-5237)
timing pulsed, 18: 3354
transmission of polarized, in ferromagnets, magnetic saturation effects on, 18: 15162
transmission of polarized, through magnetized soft iron, 19: 35357
transmission through thick targets, depolarization of, 20: 28245
transport equation for, 17: 2182
transport of polarized thermal, 18: 21125 (KR-64(Sect.XXIII))
use in detecting hidden explosives in luggage, 18: 38716(P)
use in industry, 19: 9348(T) (FTD-MT-63-261)
use in radiotherapy of cancers, 19: 32000
use in radiotherapy of cancers, 19: 32001
use in two-phase hydrogen density measurements, 19: 29185
use of pulsed, for neutron spectra in moderators and multiplying media, 19: 31191 (INR-564/IX-A)
use of thermal, in therapy, 17: 35274 (BNL-6824)
use of, surgical, 19: 43905
uses in determination of moisture content of soils, 20: 19118
uses of thermal, for radiography, 18: 33995

NEUTRON CAPTURE CROSS SECTIONS

see also Capture-to-Fission Ratios

calculation for nuclei with $20 \leq A \leq 240$ from 0.1 to 25 Mev using nonlocal optical model, (T), 20: 46583 (IKF-17)
calculation for rare-earth nuclei from 1 to 10 kev, 20: 17653 (LA-3463)
calculation for transuranic elements, 20: 34622
calculation of, at 10^3 to 10^5 ev, 16: 26518
calculation of average thermal, for media containing zirconium hydride, (T), 20: 37991
calculation of Doppler functions in, 18: 2833 (AEEW-R-266)
calculation of Doppler-broadened, 18: 2965
calculation of fast neutron removal cross sections, 18: 34888
calculation of, multilevel effects on, 18: 2969
calculation of multigroup, effect of resonance overlap on, (T), 20: 44582 (NAA-SR-11963)
computer analysis of, for tissue-equivalent cylindrical phantom, 19: 3821 (ORNL-P-655)
Doppler broadening of resonance, in fast power reactors, (T), 20: 10385(T) (EURFNR-10F)
effects of nucleon parity number on radiative, 17: 24417
energy dependence of radiative, to 50 kev (E/T), 19: 3391
for monodirectional fission source, effective fast, 16: 24797 (WADC-TR-58-266)
measurement, 20: 26095 (SGAE-PH-34/1965)
measurement and calculation for 31 elements and 48 compounds, 19: 31434
measurement at 0.2 to 2.5 Mev for praseodymium-141, (E), 20: 21969(R) (ANL-7055, pp 230-3)
measurement at 1 to 10 kev for various elements, 16: 29883(R) (TID-16309)
measurement at 30 kev, detector design for, 17: 26521
measurement at 30 to 170 kev, method of, 20: 42293
measurement by pile oscillator method, 17: 29576 (PAN-410/IX)
measurement by pile-oscillator method in EWA reactor, 18: 38665
measurement, detector design for, 16: 14084
measurement experience at Brookhaven, 17: 42226
measurement for erbium-170 and gadolinium-158 at 4 kev to 2 Mev, (E), 20: 6280(R) (ANL-6925(p.249-51))
measurement for fast neutrons using indium resonance detector in water, 20: 37990
measurement for lanthanum-139, praseodymium-141, and ytterbium-176, 20: 46963(R) (ANL-7132)
measurement for manganese in fast reactors, 20: 34950
measurement in DR-3 Reactor, in-pile components for gamma spectrometer for, 19: 22737
measurement in fast reactors, method for, 19: 47944 (ANL-7034)
measurement in nuclear explosions, 19: 38786 (LA-DC-7111)
measurement methods, 17: 2341(R) (TID-17186)
measurement of effective, by oscillation of fissionable sample in critical assemblies, 17: 42006
measurement of fast, methods for, 17: 34860
measurement of fast, methods for, 19: 14529 (MMPP-FRPC-64-2)
measurement of infinitely dilute resonance integrals, method for, 20: 40146
measurement of, pile oscillator for, 17: 36967 (AERI-P/R-6)
measurement of resonance, method for, 20: 9943 (ORNL-P-1885)
measurement of, air scattering effects in, (T), 19: 35359
measurement of, calibration methods for, 18: 18875 (JINR-P-1547)
measurement of, design of remotely operated laboratory for, 18: 12294
measurement of, detector systems for, 19: 46566(R) (TID-22141, pp 67-79)
measurement of, for reactor materials, (E), 20: 32370(R) (ANL-7175, pp 212-16)
measurement of, high-efficiency detector for, 19: 4517
measurement techniques and resonance parameters from, 20: 19812 (GA-6919)
measurement using gamma scintillation detector, 18: 8659
measurement using Moxon-Rae detectors, 30 kev, 19: 32787(R) (NIRS-3(1-17))
measurements at intermediate energies, 16: 26509
measurements, development of equipment for, 16: 2566(R) (TID-14187)
measurements of, self-shielding in, 18: 7696(R) (ORNL-TM-761)
measurements, spectroscopy applications to, 16: 14055
measurements using large liquid scintillation detectors, 16: 14059
Monte Carlo program for, 16: 20933 (WAPD-TM-273)
multilevel effects in, 18: 7702 (WAPD-T-1630)
nucleon number parity effect on, (T), 19: 33284
relations with source energy and spectrum hardening factors, 17: 19207 (WAPD-T-1524)
research programs at ORNL, 18: 24620(R) (ORNL-TM-874)
resonance effects in Doppler calculations, (T), 20: 2972
systematics of thermal, 18: 44735 (NRL-6124)
tables, 16: 26194 (JAERI-6010)
tables, 17: 32709 (IFA/SN/17)
tables, 18: 15562
tables of, for fission products, 17: 24406 (WAPD-TM-333)
theory of radiative, statistical, 16: 17070 (NDA-2093-7)

Neutron Choppers

see Neutron Spectrometers

NEUTRON CROSS SECTIONS

(Cross sections for particular neutron-induced reactions are included at the target nuclide heading and at the neutron heading, e.g., Cadmium Isotopes Cd-114 and Neutrons, Thermal)
see also Neutron Activation Cross Section
see also Neutron Capture Cross Sections
see also Neutron Fission Cross Sections
see also Neutron Resonance Cross Sections
see also Neutron Scattering Cross Sections
see also Neutron Total Cross Sections
accuracy, 17: 26042
accuracy from 0.1 to 100 kev, for calculations on fast reactors, 20: 45092
accuracy of, sensitivity of multiplication factor calculations to, 20: 46964(R) (BNWL-284)
analysis and evaluation of, multilevel-multichannel formalism for, 17: 3814
analysis of inelastic, optical model, 17: 39966 (BNL-818)
averaging group, computer program for, 18: 15145 (NAA-SR-Memo-9276)
bibliography for inelastic scattering and (n,2n) processes, 16: 17074 (VDIT-50)
bibliography on, 19: 31216 (AWRE-O-13/65)
bibliography on, 19: 39778 (BNL-9355)
bibliography on Russian work, 17: 11613 (BNL-768)
bibliography on self-shielding, 16: 13940 (CNLM-1802-10)
bibliography on, of threshold reactions, 18: 34753(R) (EANDC(E)-50(L))
calculated values of, for comparison of calculated and measured activation rates, 17: 12722 (TID-17839)
calculation, 16: 9653 (KAPL-2000-16)
calculation above 1 kev, 16: 26517 (TID-13526)
calculation, computer program for, 16: 32358 (GEAP-3644)
calculation for fast reactor analysis, computer program for, 20: 5055 (BNWL-146)
calculation for fast neutrons, computer program for, 20: 44586 (NAA-SR-Memo-12019)
calculation for homogeneous reactors, computer programs for, 19: 24002
calculation for materials with grain structure, method for, 19: 42041 (GA-6286)
calculation for natural non-fissile elements, computer program for, 19: 39776 (AEEW-M-517)
calculation for nuclei with $6 \leq A \leq 27$ at 0 to 16 Mev using local optical potential with average parameters, (T), 20: 46555 (LA-3538(Vol.1))
calculation for reactor cells, methods for, 19: 40152 (GA-6462)
calculation for reactions (n,2n) on medium and heavy nuclei, method of, (T), 20: 1187
calculation for tantalum-181 and tungsten from 1 kev to 14 Mev, (T), 20: 2961
calculation for use in reactor diffusion and transport codes, computer program for, 16: 33783 (IDO-16758)
calculation from Breit-Wigner resonance parameters, computer program for, 20: 11958 (GAMD-6562)
calculation from charged particle nuclear reactions, (T), 20: 26097 (UCRL-14568)
calculation from resonance parameters, computer program for, 20: 13786 (ORNL-TM-1396)
calculation from spectral measurements in bulk media, adequacy of, 20: 34905 (GA-7059)
calculation in fast reactors, 16: 26519
calculation methods, evaluation for use in reactivity calculations, 16: 3608 (CEND-145)
calculation of, computer program for, 18: 1018 (KAPL-M-NCF-4)
calculation of Doppler-broadened, Breit-Wigner formalism for, (T), 19: 29327
calculation of "effective," in thermal reactors, 16: 12403 (EANDC (E) 14)
calculation of effective, 17: 42199(T) (EURAEC-777)
calculation of effective removal cross sections for fast neutrons, 16: 19884 (XDC-60-1-215)
calculation of fast, computer program for, 20: 28272 (JAERI-1104)
calculation of group-averaged, computer programs for, 20: 15665 (AWRE-O-103/65)
calculation of inelastic, for thirty even-even nuclei at 0.8 to 3.3 Mev, 16: 2493 (TID-14206)
calculation of multigroup, computer program for, 18: 9291 (GA-4132)
calculation of multigroup, computer program for, 18: 13031 (GA-4436)
calculation of multigroup, for fast reactors, 18: 38249 (A/CONF.28/P/510)
calculation of multigroup, computer program for, 20: 20201(R) (ANL-7110, pp 311-401)
calculation of optical-model, computer program for, 18: 40507 (KAPL-3020)
calculation of point, from resonance parameters, computer program for, 20: 42141 (NAA-SR-11980(Vol.6))
calculation of spectrum-averaged, 16: 9653 (KAPL-2000-16)
calculation of thermal, SWAK program for, 17: 28243 (KAPL-M-RPC-6)
calculation of thermal, computer program for, 18: 38051 (KAPL-M-6145)
calculation of thermal, computer programs for, 20: 19844 (WANL-TME-1228)
calculation of, computer program for, 18: 40809 (HW-75521)
calculation of, computer program for, 19: 35379 (IDO-17087)
calculation of, computer programs for, 19: 37784 (CONF-650524-2)
calculation of, computer program for, 20: 13751 (AEEW-M-606)
calculation of, computer program for, 20: 13774 (JAERI-1096)
calculation of, computer programs for, 20: 17698 (WANL-TME-1132)
calculation of, computer program development for, 20: 30791(R) (ANL-7204, pp 32-64)
calculation of, FORM code for, 18: 13050 (NAA-SR-Memo-9174)
calculation of, impossible Legendre coefficients in, 20: 30355 (ORNL-P-2084)
calculation of, methods for, 19: 23996(R) (ORNL-3650(p.1-110))
calculation of, multilevel formalism for, (T), 19: 29325
calculation of, optical model for, 20: 20183
calculation of, SWAK 36-group computer program for, 18: 44706 (KAPL-M-6175)
calculation using optical model with diffuse complex potential, 17: 2268
calculation using optical model, 18: 38055 (TID-20943)
calculation using compound nucleus model, parameters for, 20: 15863
calculational methods for, 18: 42649 (TID-7050(p.24-89))
calculations, computer program for, 16: 31058 (UCRL-6912)
calculations for nuclei with $28 \leq A \leq 240$ at 0 to 16 Mev, using local optical potential with average parameters, 20: 46556 (LA-3538(Vol.2))
calculations for shielding data, computer programs for, 16: 21691 (DC-60-7-9)
calculations for thermal reactors, resonance effects in multigroup, 20: 22384
calculations for water moderated reactors reactivity sensitivity, 20: 24707 (CONF-660303-6)
calculations of Doppler broadened, computer program for, 19: 39777 (AEEW-M-518)
compilation and evaluation of, 20: 46966(R) (NAA-SR-12010)
compilation for reactions on nuclei with Z = 13 to 28, with charged-particle emission, 20: 44671(T) (INDSWG-101, pp 164-223)
compilation on punch cards, 19: 31461(R) (ANL-7010(p.235-87))
compilations of, status of, 20: 20177(R) (BNL-929, pp 83-105)
computation of effective fast removal, 16: 19884 (XDC-60-1-215)
computer code library for 40-group calculations, 16: 12422 (BAW-158)
computer processing of, conversion of MUFT/KATE to DRAM format for, 18: 38068 (KAPL-M-6157)
computer program for calculating multigroup averaged, 18: 18849 (AAEC/E-114)
computer program for calculating Doppler-broadened, 18: 27844 (LAMS-3075)
computer program for plotting differential, 20: 1149 (GAMD-6507)
computer program for averaging of, 20: 9941 (GAMD-6692)
computer programs for, (T), 19: 19063 (AWRE-O-97/64)
computer programs for calculation of, 19: 27735(R) (NAA-SR-10850)
conference, 20: 44603 (CONF-660303)
correction of fast, by integral experiments, (T), 20: 9976 (RT/FI(65)30)
correlation with radioactivity of products, equations for, 17: 31441
data compilation at BNL, review, 20: 44606 (CONF-660303, pp 226-34)
data evaluation by computer, 20: 44607 (CONF-660303, pp 270-86)
data evaluation using computers, 20: 42145
data from recent calculations and experiments, 16: 24776 (BNL-732)
data on, collection and dissemination of, 17: 4040
data on, computer program for maintenance of, 17: 39946 (NAA-SR-Memo-8823)
data plotting of, computer program for, 20: 17699 (WANL-TME-1317)
data preparation for reactor calculations, 20: 44583 (NAA-SR-11980 (Vol.1))
data reduction and analysis, computer programs for, 16: 12012 (MND-C-2501)
data requests at U.K. Nuclear Data Library, 20: 6254 (AEEW-M-503)
data requests for, compilation of EANDC, 19: 35377 (EANDC-43(U))
data requests for, compilation of, 20: 1161 (WASH-1057)
data requests from Euratom countries, compilation, 19: 31188 (EANDC(E)-58(U))
data required for fast and intermediate reactors, 16: 3666 (EANDC(E)-21)
data requirements for nuclear power development, 20: 32839
data retrieval of, computer program for, 20: 3009 (GA-6685)
data review, October 1961, 16: 2481 (BNL-694)
data storage and retrieval program for Nuclear Data Library, 18: 25879 (AWRE-O-4/64)
date on 14-Mev, for stable isotopes, (E/T), 20: 38838
derivation of SUPERNOVA multigroup, for beryllium oxide- and

graphite-moderated systems, 18: 36786 (UCRL-7827)
description of information storage and retrieval system for Sigma Center at Brookhaven, 19: 3804 (BNL-883)
design and research at Rensselaer Polytechnic Inst., 18: 9802
determination by activation and mass spectrometric methods, 20: 3864 (AERE-L-166)
determination by pile oscillator method, theory, 18: 38059
determination by reactivity measurements, 20: 44621 (CONF-660303, pp 773-81)
determination by using integral measurement data, 20: 44577 (CONF-660303, pp 304-8)
determination for threshold detectors, method for, 20: 24363(T) (CEA-tr-A-1845)
determination of, flux effects on, 17: 2242 (TID-16949)
determination of fast, computer system for, 20: 13806
determination of group, by computers, for multigroup calculations, 17: 399 (AWRE-0-1/61)
determination of monoenergetic, 17: 1359(R) (ANL-6569)
determination of, source of discrepancies in, 20: 44611 (CONF-660303, pp 486-501)
development of four-group, for SNAP core calculations, 17: 17422 (NAA-SR-Memo-7789)
display of Atomics International, graphical, 17: 41866 (NAA-SR-Memo-8904)
Doppler broadening, 17: 24383 (AEEW-R-226)
Doppler broadening of, differential equations for, 18: 28530 (WAPD-BT-30(p.41-6))
Doppler broadening integral for, derivation of, (T), 20: 3375 (IDO-17120)
effect of uncertainties in, on fast reactor calculations, 20: 45069 (CONF-660303, pp 809-20)
effects of uncertainties in, on reactor safety, 20: 45068 (CONF-660303, pp 430-53)
energy dependence of nuclear, (T), 20: 6404
errors in, reactor sensitivity to, 20: 26422 (BNL-10058)
Euratom requests for, 17: 22553 (EANDC(E)-43L)
fluctuations for 2- to 5-Mev neutrons, on nuclei with A near 30, 16: 24845
for (n,2n) reactions, analysis for nuclei A > 30, 19: 37202(R) (BNL-900 (p.1-28))
for fast-reactor reflectors, (T), 19: 29200
for fission-product nuclides, 19: 29263 (WAPD-TM-333(Add.1))
for nuclei of Z = 1 to 20, 18: 44726 (BNL-325(2nd Ed.)(Suppl.2)(Vol.I))
for nuclei of Z ≥ 93, experimental data on, 19: 33243 (JAERI-4032)
for nuclei 1 ≤ Z ≤ 20, 19: 37202(R) (BNL-900(p.1-28))
for phosphorus and sulfur isotopes, fast, (E), 20: 37166
Hanford library for isotopes Z = 196 through 240, 17: 41862 (HW-75716 (Vol.3))
Hanford library for Z = 97 to 200, revised, 17: 41861 (HW-75716(Vol.2))
Hanford library for Z = 1 to 96, revised, 17: 41860 (HW-75716(Vol.1))
Hanford library revisions, 18: 29144 (HW-75715)
inelastic, relation between energy moments and Placzek moments in, 17: 19204 (TID-18429)
interpretation for fissile nuclide, (T), 20: 44624 (CONF-660303, pp 873-94)
libraries for multigroup, computer programs for preparation of, 20: 46966(R) (NAA-SR-12010)
libraries of multigroup, computer program for preparation of, 20: 13706 (NAA-SR-Memo-10884 and Add.)
library for carbon-12 from 0.01 to 15 Mev, 20: 42160 (KAPL-3099)
library for fast reactor analysis, 19: 40286(R) (NAA-SR-11200)
library for Monte Carlo codes FMC-N, 18-0, and 18-1, 20: 4830 (GEMP-384)
library for nuclei 1 ≤ A ≤ 91, 20: 17673 (BNWL-CC-325(Vol.1))
library for nuclei 90 ≤ A ≤ 161, 20: 17674 (BNWL-CC-325(Vol.2))
library for nuclei 159 ≤ A ≤ 239, 20: 17675 (BNWL-CC-325(Vol.3))
library for tungsten isotopes from 0 to 10 Mev, 20: 44589 (WANL-TME-1472)
library of multigroup, for reactor materials, 19: 40286(R) (NAA-SR-11200)
library of multithermal, for reactor materials, 20: 19844 (WANL-TME-1228)
library of 16-group, for SNAP shield analysis, 20: 34782 (NAA-SR-Memo-11718)
library of 23-group, 17: 39945 (NAA-SR-Memo-8742)
library of 26-group, for fast reactor analysis, 19: 24043
library of, description, 18: 37597 (A/CONF.28/P/168)
library of, for reactor and shielding transport calculations, 20: 30723 (NAA-SR-11831)
library of, UKAEA, 19: 45249 (AWRE-O-55/65)
library of, Winfrith, 18: 21156 (AEEW-R-351)
library preparation for reactor and shielding calculations, 20: 26333 (CONF-660303-2)
measurement, 17: 4271
measurement and analysis for fissile nuclides, (E/T), 20: 44623 (CONF-660303, pp 840-72)
measurement and uses of microscopic, 18: 28541
measurement at ORNL, 18: 7696(R) (ORNL-TM-761)
measurement at 100 ev to 100 kev, review of, 20: 26093 (ORNL-P-2106)
measurement at 14.7 Mev, utilization of alpha particle associated with neutron in reaction T(d,n)α, 16: 13751
measurement at 14 Mev, for nuclei having Z < 31, 19: 10254 (ORNL-3672)
measurement by sample-oscillation method for reactor materials (E/T), 19: 3512 (CEA-R-2487)
measurement, correlation to integral experiments, 16: 26532 (BNL-5604; BNL-5892)
measurement, design of instrument for, 16: 21333 (CRRP-1078)
measurement during high-altitude nuclear explosions, time-of-flight, 18: 34751 (CONF-481-71)
measurement for fast neutrons and resonance neutrons, 20: 46559 (ORNL-P-2493)
measurement for neutron attenuation studies, 19: 3454 (TID-21294)
measurement for nonfissile nuclei, 20: 28282 (ORNL-P-2091)
measurement for nuclei near A = 55, 18: 42650 (TID-21144)
measurement for nuclei with Z ≥ 94, 19: 29326
measurement for reactions (n,αγ), (n,2n), and (n,pγ), 17: 34861
measurement for reactor reflectors, leakage effects on, (T), 20: 34512 (ANL-7170)
measurement for thorium from 0.015 to 1.00 kev, (E), 20: 6377
measurement in kev region, methods and theory for, 17: 34859
measurement, modified pile oscillator for, 16: 2783
measurement of differential and total, for slow neutrons, 18: 24606 (NP-13930(p.73-4))
measurement of nonelastic collision, sphere method for, 17: 34855
measurement of nonelastic, for iron, (E), 19: 33221
measurement of, principles and limitations of time-of-flight, 17: 2269
measurement of shape elastic, by self-screening method, 17: 38004(T) (AEC-tr-5734(p.27-8))
measurement of thermal and epithermal, 16: 18435
measurement of thermal, using pulsed-source method, 18: 26828
measurement of total, at 1.44 ev, 19: 3288
measurement of total, on radioactive samples, 20: 44604 (CONF-660303, pp 67-74)
measurement of, with fast choppers, 17: 4037
measurement of, development and improvement of methods for, 18: 33011 (A/CONF.28/P/259)
measurement of, developments in, 20: 38103
measurement of, estimating neutron spectra from 14-Mev source for, 19: 16823
measurement of, fabrication of samples of radioactive material for, 19: 34663
measurement of, instrumentation development for, 20: 4246(R) (RPI-328-40, pp 49-55)
measurement of, instrumentation development for, 20: 15731(R) (RPI-328-49)
measurement of, parallel-plate fission chamber for, 20: 39256
measurement program at the MTR, 17: 4036
measurement program, 20: 46599(R) (RPI-328-68, pp 1-62)
measurement techniques, description and evaluation of, 20: 44610 (CONF-660303, pp 381-403)
measurement using solid state detectors, 17: 38061 (AE-115)
measurement using Karlsruhe Van de Graaff generator, program for, 18: 24246 (NP-13930(p.137-8))
measurement using underground explosions, 19: 18093 (LA-DC-6897)
measurement using pulsed sources, 19: 29174 (ORNL-P-1116)
measurement using neutrons from nuclear detonation, (E), 19: 39889
measurement using atomic explosions as pulsed sources, 20: 24304 (LA-DC-7799)
measurement using electron linacs, 20: 24355 (RPI-328-50)
measurement using electron linacs, 20: 24356 (RPI-328-51)
measurement using boron monitors, errors in, (E), 20: 30352 (NASA-TR-R-240)
measurements, 18: 24625 (WASH-1046)
measurements in fast reactors, 16: 26506
measurements of, methods and problems in, 17: 7128 (NP-12330(p.369-77))
measurements of, program for, 18: 8912(R) (HW-78388(p.10.1-25))
measurements of thermal, for fissile isotopes, 19: 29328
measurements of, compilation of requests for, 19: 45255 (EANDC-45(U))
measurements of, effective factors for, (T), 19: 47577 (IDO-17107)
measurements of, summary for HAPO 1956–1964, 19: 22870(R) (HW-83601)
model of low-energy, optical, 17: 37998(T) (AEC-tr-5734(p.1-2))
MUFT library compilation, 17: 24373 (WCAP-3709)
multilevel effects in, 18: 7702 (WAPD-T-1630)
multiple-scattering corrections to, computer program for, 18: 26530 (BNL-8028)
of reactor materials, magnetic tapes for fine-energy-detail, 16: 10946

(APEX-704)
parameters in, for fissile materials, 17: 4035
preparation for calculations on fast reactors, 20: 20229(R) (ANL-7110, pp 99-229)
preparation of group-averaged spectrum-weighted, computer program for, 20: 44584 (NAA-SR-11980(Vol.3))
preparation of, computer program for, 20: 28266 (AWRE-O-27/66)
production for reactor calculations, (T), 19: 35720
program for automatic data storage and analysis, 19: 25465
program of fast, 19: 33237(R) (ANL-7020(p.226-30))
properties of, echoes, giant resonances, and size resonances in, (T), 19: 33315
punched card library of, 16: 26520
radiative capture, near 30 and 65 kev, 17: 17222
reducing many-group to few group, computer code for, 17: 786 (LAMS-2747)
reduction of many-group to few-group, computer program for, 17: 12581 (LAMS-2801)
requests for, Euratom, 17: 39971 (EANDC(E)-47(L))
requests for, compilation of, 20: 36158 (EANDC-55(U))
requirements for reactor design calculations, 20: 45070 (CONF-660303, pp 823-39)
research on, (E/T), 20: 30360 (WASH-1068)
research on fast, review of, (E/T), 20: 30349 (JAERI-1102)
resonance phenomena in, review of, 17: 41996
resonances in, numerical techniques for analysis of, 20: 21994 (BNL-10094)
review for neutron spectrum and dose measurements by foil activation, 19: 31316
review of evaluations of, 18: 4538 (EANDC(UK)-26U)
review of evaluations of, 18: 26559 (WASH-1047)
review of evaluations of, by AEC Nuclear Cross Sections Advisory Group, 18: 32751 (WASH-1048)
six- and sixteen-group for fast and intermediate critical assemblies, 16: 4680 (LAMS-2543)
spectrum hardening for non-1/v thermal, 17: 20961
statistics of, optical-model studies of, 18: 13233 (BNL-823(p.1-19))
survey of future requirements for the nuclear power industry, 20: 45107 (CONF-660303, pp 1025-34)
tables, 18: 17255
tables, 18: 17287 (NP-13666)
tables, 16: 26194 (JAERI-6010)
tables for alloys, compounds, and elements, for reactor studies, 16: 29824
tables for aluminum, beryllium, deuterium, iron, nitrogen, oxygen, and silicon from 0.037 ev to 18 Mev, 20: 44661 (UNC-5139)
tables for reactions (n,α) (n,d), (n,He^3), (n,nα), (n,2n), (n,np), (n,p), and (n,t) at 14–15 Mev, 17: 26422 (EUR-122.e)
tables for reactor materials, 16: 12420 (APEX-515)
tables of, for fast reactor materials, 17: 28245 (KFK-120)
tables of, for reactor materials, 17: 39975 (LAMS-2941)
tables of, for threshold reactions, 17: 26421 (EUR-10.e)
tables of nine and sixteen group, for reactor analysis, 17: 22789 (GEMP-173)
tables of nine-group, 18: 21170 (GEMP-279)
tables of reaction, for nuclei to 230, 18: 9307 (CEA-2380)
tables of, for reactor fuel cycle analysis, 19: 45546 (HW-79951(Pt.3))
tabulation, 20: 26533(R) (BNL-954, pp 16-49)
tabulation for beryllium, 16: 21334 (DC-60-12-98)
tabulation for data tape for slowing-down code GAM-1, 16: 22984 (GA-2451(Vol.I))
tabulation for fission products, 20: 28278 (JUL-354-RG)
tabulation for GAM-I data tape, 16: 9427 (GA-2451(Vol.III))
tabulation for plutonium isotopes at 0.001 to 15 Mev, 20: 13770 (GA-6576)
tabulation for transuranium elements, 20: 24334 (BNL-10083)
tabulation for uranium-235, 20: 24361 (WANL-TME-1384)
tabulation for 14-Mev neutrons, 20: 32380 (SC-RR-66-229)
tabulation of 16 groups, for Sandia Pulsed Reactor II, 19: 48063 (SC-RR-65-344)
tabulation of 19-group, for fast reactor analysis, 19: 45244 (AEEW-M-472)
tabulation of 20-group fast, for reactor analysis (E/T), 19: 3476 (IA-980)
tabulation of 9- and 16-group, for reactor analysis, 20: 4829 (GEMP-173(Suppl.1))
tabulation of, CINDA, 20: 26088 (NYO-72-73)
tabulation of, effective factors for, 20: 24341 (IDO-17107(Suppl.1))
tabulation of, for CINDA, (E), 19: 8406 (UNC-5090)
tabulation of, for nuclei of $88 \leq Z \leq 98$, (E), 19: 45250 (BNL-325 (2nd Ed.)(Suppl.2)(Vol.III))
tabulations, (E), 20: 3018 (NYO-72-27)
tabulations for MOSEL reactor materials, 20: 14062 (JUL-214-RG)
tabulations for tantalum-181 and tungsten from 1 kev to 14 Mev, 20: 8064 (GEMP-388)
tabulations for thorium fuel cycle development, 20: 21967 (AEET-234)
tabulations for uranium-235 from 1.86 ev to 10 Mev, 20: 17697 (WANL-TME-1028)
tabulations of, CINDA Supplement No. 1, 20: 8077 (NYO-72-52(Suppl. 1))
tabulations of, for europium, gadolinium, hafnium, and samarium at 0.025 ev to 10 Mev, 20: 8074 (KFK-352)
theory, 18: 4600
theory of fluctuations of, 19: 37202(R) (BNL-900(p.1-28))
total, for 44 elements, 17: 20982 (HW-SA-2875)
variations in, from statistical fluctuation of compound nucleus level density, 17: 40046
Westcott parameters of americium, curium, plutonium, and uranium isotopes, (T), 20: 11959 (HW-77389)

NEUTRON DECAY
chemical effects, survey, 16: 22247
heat transfer calculations for, 16: 26231 (TRG-Report-322)
radiative corrections in, 17: 11469 (JINR-E-1100)
use in spectral measurements, 18: 2082

NEUTRON-DIFFRACTION ANALYSIS
attenuation factor for, 19: 25036
book: *Applications of Neutron Diffraction in Chemistry*, 18: 13607
book: *Magnetic Neutronography*, 20: 36370
book: *Single Crystal Diffractometry*, 20: 46962
collimator design for neutron powder diffractometry, (E), 19: 40492
comparison with x-ray-diffraction analysis, 16: 27697(T) (AEC-tr-5170)
conference on, 16: 26890 (AERE-R-3818)
conference on, 18: 37138
correction for extinction in crystals, 16: 2310
correction for secondary extinction effects on, 17: 784 (AERE-R-3692)
corrections for secondary extinction in single crystals, 16: 18455
cryostats for, design of, 19: 40852
crystal adjustment for single specimens, 16: 5546
crystal lattice parameters for, fundamental and modulated reciprocal, 20: 34802 (ANL-7147)
crystal structure and magnetic properties from, conference on, 17: 37790
crystal structure from time-of-flight, integrated intensity formula for determination of, 18: 780
crystal structure from time-of-flight, 18: 37674 (A/CONF.28/P/488)
crystal structure factors from, computer program for, 19: 43466 (AEET-203)
data collection in, procedures and problems in, 18: 37146
data recording and computer control for, 19: 4523
data recording in, method for fast, 18: 29657
determination of interatomic force constants from, 17: 37804
development for studying crystals, 18: 1491(R) (ORNL-3488(p.102-22))
developments in, for use in inorganic chemistry, 20: 38882
effects of extinction on diffuse measurements, 17: 8518 (BNL-6052)
effects of particle size on scattering extinction in, 20: 5016(T)
effects of sample motion on patterns from, 18: 12775
electronic equipment for automatic facility for, 16: 27290
equipment and methods development for, 17: 6809(T) (AEC-tr-5567)
equipment and techniques for, review of, 17: 37795
equipment and techniques for, 18: 25971(R) (ANL-6868(p.331-7))
equipment and techniques for crystal- and magnetic-structure, (E), 19: 4449 (ANL-6920)
equipment for, 18: 16352
equipment for, at Dutch research reactors, 17: 15508
equipment for crystal-structure studies by, design manual for, 17: 30796 (AERE-R-4305)
equipment for crystallographic and magnetic, 19: 34431
equipment for high-pressure, 20: 43473(T)
equipment for, use of silicon diode detector, 20: 43730
extinction and interference effects for crystalline, 20: 12309
feasibility of high-pressure, 17: 12750 (ARF-1183-4)
filters for, development of, 18: 37145
furnace design for use in, 17: 12545
furnace design for high-temperature, (E), 19: 18099 (LA-DC-6382)
furnace for, design of high-vacuum, 20: 29106
goniostat design for use in, 17: 12571
impurity effects in, 18: 16434
instruments and methods for, review, 17: 7070
intensity in powder, frequency dependence of, 20: 45013
intensity measurements in, physical factors affecting total, 16: 26892 (AERE-R-3818(p.5-18))
intensity measurements in, goniostat for three-dimensional, 19: 24827
interplanar spacing conversion tables for diffraction angles (E/T), 19: 1048 (JAERI-6015)
lectures on magnetic materials, 20: 30784
limitations and possibilities in determining magnetic structures, 16: 3508
method for single crystal- and powder-, time-of-flight, 20: 32701
method for structural determinations of powders in fast pulse reactor, 18: 32174
method of, for solid oxygen, 17: 40821
methods, 17: 38027(T) (AEC-tr-5734(p.140-52))
methods and theory for, review of, 17: 5059

methods for hydrogen-bonded crystals, 18: 16055
methods of, in crystal lattice dynamics, 18: 10656
modified Polaroid film holder for, 18: 5591
neutron beam polarization and flipping efficiency in, (T), 19: 10991
neutron sources for, pulsed and steady-state sources, (T), 20: 5726 (CONF-650217, pp 102-7)
neutron sources for, use of pulsed thermal, 20: 6258 (CONF-650217, pp 82-101)
nuclear null-matrix use in, 20: 36355 (ANL-7182)
null matrix applications in, 16: 7516
of ferroelectrics, 17: 6647 (BNL-5747)
of liquid-like binaries, radial density functions for, 17: 37524
of magnetic bonding in ordered salts (E/T), 19: 2269 (BNL-8514)
of ordering in manganese–nickel alloys, 20: 39407(T) (ANL-Trans-344)
of samples under high pressure, equipment and methods for, 20: 34816 (IDO-17170)
of single crystals, accurate intensity measurements in, 18: 41380
of structure and dynamical behavior of solids and liquids, 19: 36817 (RT/FI(64)-20)
photographic detectors for, 16: 29165 (ANL-FGF-328)
photography of patterns, sensitivity and spatial resolution of screen-film combinations, 16: 8961
recording time formula for, 19: 29228(R) (AEET/NP/10)
research in, 17: 38044(T) (AEC-tr-5734(p.255-66))
research program at Puerto Rico Nuclear Center, 18: 35495 (BNL-7290)
research programs on, at MIT in 1963, 18: 16894(R) (MIT-3031-1)
sample drying for, 20: 3914 (AERE-M-1654)
single-crystal, effects of simultaneous reflections on, 18: 32157
spark detector for, 16: 6538 (IFA-FN-21)
spectrometer for, performance of three-axis, (E), 19: 44531
studies of magnetic exchange interactions in transition metal compounds, 19: 27710 (KR-93)
techniques and uses, 16: 31571 (RCN-8)
theory of double Bragg scattering by single crystals, 16: 26211
theory of thermal neutron scattering by crystals and solids, 18: 11152
use for determining atomic magnetic moments in iron–nickel alloys, 18: 27990
use for determining moisture content in highway construction materials, 19: 9446 (NP-14604)
use for determining moisture content in soils and construction materials, 19: 9447 (NP-14610)
use for determining structures of biological molecules, 20: 40632(R) (ORNL-3922, pp 175-91)
use in crystal structure study of copper-nickel-zinc alloy, 19: 32762
use in determination of preferred orientation in steels, 18: 36033
use in determination of interplanar spacings in polymers, 20: 3308
use in determining crystal structure of potassium oxalate, 19: 29228(R) (AEET/NP/10)
use in determining magnetic properties of solid, 20: 17158(R) (ORNL-3900, pp 82-149)
use in magnetic moment distributions for impurities in iron, (T), 20: 40330
use in materials testing, conference on, 20: 4116
use in structure determination of tungsten oxide, 20: 33890
use in studies of metals and alloys, 19: 25029
use of high-flux reactors for, 18: 33154
use of isotopic neutron sources in, 18: 43387 (ORNL-P-479)
use of Polaroid film in, 16: 8962
use of time-of-flight method in, for crystal structure studies, 17: 25163 (PAN-404/II)
use to study preferred orientations, 16: 33615
uses for phase evaluation for structure determination, 20: 29720
uses in crystal structure and magnetization studies of compounds similar to perovskite, 18: 27389
uses in determining magnetic moments of iron oxides, 18: 27390

NEUTRON DIFFRACTOMETERS

book: *Applications of Neutron Diffraction in Chemistry*, 18: 13607
book: *Single Crystal Diffractometry*, 20: 46962
collimator design for powder, (E), 19: 40492
collimators for, 20: 6268
collimators for, calculation of optimum, 17: 8599 (UCRL-6825)
comparison with x-ray diffractometers, 16: 27697(T) (AEC-tr-5170)
control and data handling of Argonne automatic, system for, 20: 26542
control of, computer program for, 20: 35735 (AERE-R-5213)
control system for relative-positioning, 19: 42686(R) (ORNL-3782, pp 29-30)
crystal design for, 20: 19769
data collection from automatic counting and recording system for, 18: 27786 (CEA-2335)
description for McMaster University pool reactor, 16: 8951
description of automatic single-crystal, 17: 18576
description of DIDO, 17: 6417
description of remote-control, 17: 37417(T)
design, 16: 25085 (JAERI-7022)
design, 16: 32980
design, 17: 16469
design, 18: 14173
design and fabrication of double, 20: 7345
design and operation at Rossendorf, 16: 14952
design and operation of automatic measurement system, 16: 14953
design and operation of, 17: 32368
design and operation, 18: 33881 (NP-14131)
design and operation of two-coordinate, 19: 46835(T)
design and performance of automatic multi-purpose, 17: 37802
design and performance of single crystal, with automatic programming-control system, 17: 37803
design and performance of small automatic, 20: 16882
design and performance of time-of-flight, 20: 34816 (IDO-17170)
design of automatic single-crystal, 16: 11857 (NRL-5744)
design of automatic, for single crystal structure studies, 18: 6992 (KR-57)
design of automatic double-crystal, for crystal- and magnetic-structure analysis, (E), 19: 4449 (ANL-6920)
design of automatic double-crystal, 19: 34431
design of automatic double-crystal, engineering drawings for, 20: 675
design of computer-controlled, 19: 280(R) (ORNL-3679(p.94-116))
design of crystal, 16: 20678
design of dual, for CP-5 reactor, 17: 8517 (ANL-6537)
design of, engineering drawings for, 17: 27674
design of high intensity, 17: 20318
design of multiple, for PLUTO, 18: 37506 (AERE-R-4643)
design of programed multichannel, 18: 2000
design of semi-automatic, for crystal and magnetic structure studies, 18: 29948
design of time-of-flight, for studying solids under high pressures, 19: 45476 (IDO-17106)
detectors for, description of slow, 20: 24791 (IKF-16)
development, 16: 6802(R) (KR-12)
development, 20: 40796(R) (IS-1500(Sect.C))
instrumentation of manually programmed, 20: 27303
monochromator for, evaluation of mosaic crystals as, 17: 41854
operation and performance of double-axis, for powder investigations, 20: 16799
operation of, summary of, 18: 2403(R) (PR-P-58)
performance of automatic three-circle, 18: 37527
performance of, using time-of-flight spectrometers, (E), 19: 9481 (JINR-P-1909)
shielding design and fabrication for, 20: 42681(R) (IS-1500(Sect. R))
specifications for, 17: 16467
survey, 17: 18571
theory of gravity, for the absolute determination of coherent scattering cross sections, 17: 14640
use in study of uranium crystal structure, 16: 31379

Neutron Fission

see Fission

NEUTRON FISSION CROSS SECTIONS

see also Capture-to-Fission Ratios

calculation by multilevel formalism, simple approach to, 16: 24386
calculation for transuranic elements, 20: 34622
calculation of, computer program for, 19: 45282 (ORNL-TM-1180)
calculation of, multi-level model for, (T), 20: 3374 (IA-1053)
data evaluation, 20: 1160 (WAPD-T-1847)
effects of inelastic scattering on, in fast reactors, 20: 34949
measurement and interpretation of low-energy, (T), 20: 17850
measurement experience at Brookhaven, 17: 42226
measurement for uranium-235 from 20 ev to 2 Mev, (E), 20: 24347 (LA-DC-7618)
measurement for uranium-235 in fast reactors, 20: 34950
measurement in fast reactors, method for, 19: 47944 (ANL-7034)
measurement of effective, by oscillation of fissionable sample in critical assemblies, 17: 42006
measurement of fast, methods for, 19: 14529 (MMPP-FRPC-64-2)
measurement of, fast electronics for, 18: 24015
measurement of, method for analyzing foils for, 20: 22870 (LA-DC-7625)

NEUTRON MONOCHROMATORS

beam intensity measurements for chopper and crystal, thermal, (T), 20: 24314
beam spectra from crystal-type, 16: 18454
calibration and performance, (E/T), 19: 29170 (IEA-78)
control systems for three-rotor choppers, (E), 20: 13713
description of crystal, 18: 2837(R) (EANDC(OR)-22L)
description of, for production of polarized slow beams, 17: 41850
description of helical-slot velocity selector, (E), 19: 26659 (JAERI-1069)
design, 17: 2214
design and construction, 16: 15635(R) (TID-15384)

design and evaluation for operation at 0.001 to 2 ev, 16: 1003(T) (AEC-tr-4687)
design and operation of crystal, 16: 10192 (TID-14863)
design and performance of cold, 16: 31873
design and performance, 18: 32712 (CEA-R-2329)
design and performance of, for long-wavelength neutrons, 20: 21007
design and performance of rotating-crystal, for time-of-flight spectroscopy, 20: 27344
design for slow neutrons, (E), 19: 22694 (IEA-76)
design of beryllium-crystal, 16: 18467
design of crystal, for producing polarized beams, 17: 41281
design of curved-crystal Cauchois-type, 16: 18465
design of L-shaped converter without accelerator, 19: 3228(P)
design of mechanical, 16: 6578
design of rotating disc, 16: 11879
design of rotating-disk, 17: 10937
design of slow, 20: 31477 (CEA-R-2981)
design with surface coatings for neutron reflection suppression, 20: 32368(P)
development of cold, 20: 21949
development of curved and flat crystalline, for use in neutron spectrometers, 17: 4775(T) (NP-tr-923)
development of, for production of pure, fast neutron beam, 17: 33447(R) (ANL-6723(p.28-32))
development of, summary, 17: 18549(R) (TID-18408)
effective cutoff energies for, for spherical, cylindrical, and slab geometries, 17: 3787
efficiency of, from multiple Bragg reflection in large mosaic crystals, (T), 19: 47562
evaluation of mosaic crystals as, 17: 41854
neutron parasitic reflections in crystalline, 17: 38044(T) (AEC-tr-5734 (p.255-66))
neutron reflection from, by oriented single crystals, (E/T), 20: 13709 (PAEC-IPA(D)PH-652)
neutron reflectivity of mosaic single crystal, collimated, (E/T), 19: 14477
neutron transmission functions for choppers, 16: 3868(R) (ORNL-3193 (p.204-15))
nonmonochromatic higher order contamination in crystal, determination of, 18: 26499 (RISO-73)
performance of aluminum, 20: 7445(T)
performance of oriented-single-crystal, for removal of second-order reflections, (E), 20: 8055
phase synchronization of multiple-chopper, 20: 21111
properties of single-crystal, 18: 5636 (PAN-270)
pulse forms and transmission functions for two-rotor, 17: 10938
resolution function, 16: 7153
scattering in, inelastic, 19: 14260
structure of crystals for, 17: 6058(T) (AEC-tr-5566)
use for determining molecular structure in biological materials, 20: 40632(R) (ORNL-3922, pp 175-91)
use of crystal, in epithermal-neutron radiography, 19: 46563
velocity selector for, mechanical, 17: 39378 (IDO-16878)

NEUTRON PHOTOGRAPHY

backing materials for, evaluation of, 16: 20665
book: *Magnetic Neutronography*, 20: 36370
book: *Neutron Radiography*, 20: 4115
characteristics of beam facility at Argonne, 18: 41933 (TID-11295(3rd Ed.))
collimators and foil-film combinations for, 20: 16619
comparison with other radiographic methods, 17: 10814 (ANL-FGF-335)
development, 17: 4687 (ANL-FGF-378)
development and use, 16: 12421 (ARF-1164-15)
development of, for large masses, 17: 10189 (AD-275297(p. 112-15))
equipment design for, 17: 16484(P)
equipment development, characteristics of activation foils, multiwire spark chambers, phosphors, semiconductors, and scintillators, 16: 9252(R) (ARF-1164-21)
equipment for, design of portable, 20: 7243
equipment for, using thermal neutron beam from Juggernaut Reactor, 18: 33995
equipment, methods, and uses of, review, 19: 15728
fading in, gamma-induced, 18: 16359
feasibility for nondestructive testing of materials, 16: 11930 (WAL-TR-142/67)
film blackening in, methods for enhancing, 20: 667
film holder for, modification of Polaroid, 18: 1491(R) (ORNL-3488 (p.102-22))
fundamentals of, for nondestructive testing, 17: 30147
image brightness intensifiers for thermal, 20: 25269
image converter materials and methods, comparisons of, 16: 23965 (ANL-6515(p.28-52))
image display for, performance of lithium fluoride thermoluminescent sheets for, 20: 46074
image formation in, efficiency of thermal neutrons for, 17: 10880 (ARF-1164-27)
image in, effects of detector characteristics and scattering on, 16: 23966 (ANL-6515(p.53-80))
image intensifier for, possible development of, 19: 11470 (ANL-6917)
image intensifier for thermal, 19: 26642
image quality from neutron beams, effects of scattering and image detector resolution, 16: 4739(R) (ARF-1164-18)
image storage, using lithium fluoride thermoluminescence, 20: 22853(R) (ANL-7060)
image-intensification system testing, 20: 42579(R) (ANL-7245, pp 29-47)
imaging equipment and methods in, 18: 25675(R) (ANL-6868(p.219-28))
imaging qualities and gamma and thermal neutron sensitivity of detectors for, 16: 22321(R) (ARF-1164-24)
methods, 18: 41625 (ANL-6846)
methods and uses of, evaluation of, 16: 20810
methods and uses of, as inspection technique, 17: 8380 (ANL-FGF-386)
methods and uses, review, 16: 19148(R) (ANL-6279)
methods for, using Japanese TTR-1 beam, 19: 26516
methods of, for metallographic studies of cadmium–tin alloys, 19: 34709
methods of, using crystal monochromator, 19: 46563
program at Los Alamos, 18: 39466 (LA-DC-6289)
review, 20: 29627
review and development of techniques for field use, 17: 30677
sensitivity and spatial resolution of screen-film combinations (Li^6–ZnS and Li^6F–ZnS), 16: 8961
sensitivity for lead and uranium, 19: 15729
shield enclosure for encapsulated irradiated fuel for, 18: 26068 (ANL-6799)
techniques for radiographic testing, 16: 30650
testing of polaroid camera for, 17: 10999 (ANL-FGF-340)
use for irradiated fuel elements and building materials, 19: 20129
use for radiographic inspection of irradiated fuel elements, 17: 25426
use for radiographic testing of irradiated fuel elements, 19: 11377
use in inspection of heavy metals and hydrogenous materials, 18: 4240 (CONF-356-1)
use in inspection work, 19: 13603
use in irradiated fuel radiography, 18: 20591
use in nondestructive examination of irradiated fuel capsules, 18: 43774 (TID-7697(p.2.22.1-11))
use in nondestructive testing of brazed joints, 19: 13935 (ANL-6924)
use of gadolinium foil-photographic film combinations in, 20: 621 (LA-DC-6978)
use of Polaroid film in, 16: 8962
use to determine cadmium burnup in reactor control rods, 18: 15458

Neutron Radiography
see Neutron Photography

Neutron Removal Cross Sections
see Neutron Capture Cross Sections

NEUTRON RESONANCE CROSS SECTIONS

calculation formulas for, (T), 19: 17233
calculation of Doppler-broadened, methods for, 18: 7666
calculation of multigroup, effect of resonance overlap on, (T), 20: 44582 (NAA-SR-11963)
calculation of, uncertainties in, 17: 36652 (EIR-55)
calculation of, development of methods for epithermal energies, 20: 42579(R) (ANL-7245, pp 29-47)
calculation of, methods development for, 20: 20201(R) (ANL-7110, pp 311-401)
calculation of, multigroup data preparation for, (T), 20: 38451
calculation using statistical methods, (T), 20: 34504
computer program for, 18: 30088 (AEEW-R-323)
determination, 18: 21164 (CONF-481-36)
determination for elements near A = 100 by boron-10 absorption, 16: 28036 (TID-16059)
dispersion relations for low-energy, 17: 26045
Doppler broadening, 16: 24393
Doppler broadening, 16: 26214 (AERE-M-1035)
Doppler broadening, calculation, 17: 28307
Doppler broadening of isolated, approximate formulas for, (T), 19: 43275 (LA-3315)
Doppler broadening of capture, in fast power reactors, (T), 20: 10385(T) (EURFNR-10F)
Doppler effect on, 20: 34500
integrals in, contribution of negative energy levels to, 17: 26047
line shapes in, calculation of, 17: 26043
measurement by component subtraction method, 16: 730
measurement of, equipment and methods for, 17: 39968 (BNL-7234)
measurement of, method for, 20: 9943 (ORNL-P-1885)
measurement of, neutron-source requirements for, 20: 46559 (ORNL-P-2493)
parameters for low-energy, 17: 26044
parameters in, analysis of, 17: 26046

review, (E/T), 19: 29324
statistics of, 18: 2956
tables of, for fission products, 17: 24406 (WAPD-TM-333)
NEUTRON SCATTERING CROSS SECTIONS
behavior with respect to incident energy and target mass number, 17: 36861(R) (ANL-6764)
bibliography on inelastic, 17: 11587 (AE-88)
calculation for fast neutrons, computer program for, 20: 44645 (NAA-SR-11706)
calculation of anisotropic elastic, 18: 28919(R) (NAA-SR-9090)
calculation of cold, in homonuclear diatomic liquids, 20: 32353
calculation of cold, in homonuclear diatomic liquids, 20: 32354
calculation of differential, for thermal neutrons, 17: 15167 (BNL-719 (Vol.I)(p.144-71))
calculation of differential, for thermal neutrons, evaluation of techniques for, 17: 15168 (BNL-719(Vol.I)(p.172-202))
calculation of differential slow, for gases, 17: 26539
calculation of differential, for gas molecules, (T), 20: 3135
calculation of, DSDE computer program for, 17: 19200 (NAA-SR-Memo-7940)
calculation of fast, Legendre polynomial coefficients for, 17: 34852
calculation of inelastic, incoherent approximation, 17: 4050 (ANL-6551)
calculation of inelastic, computer program for, 20: 8059
calculation of, multilevel effects on, 18: 2969
calculation of thermal, using Boltzmann equation, 18: 42599 (TID-7050 (p.289-330))
calculation of thermal, (T), 19: 29192
calculation of, using nuclear model, 20: 26092 (ORNL-P-2072)
calculations for moderators with semi-rigid molecules, 16: 28102 (IDO-16749)
calculations for polar liquids, 17: 15171 (BNL-719(Vol.I)(p.289-301))
classical limits in general system, 16: 15614 (TID-15383)
computer program for calculating, 18: 44703 (IDO-16984)
corrections for absorption and double scattering in measurements of fast, computer program for calculating, 18: 11143 (CEA-2374)
data retrieval from tables using computer program, 18: 39794 (NAA-SR-Memo-9721)
derivation of equation for, by simple systems, 17: 15170 (BNL-719 (Vol.I)(p.276-88))
determination for fissile elements, expressions for, 18: 18865 (ANL-6792(p.695-709))
Fermi approximation for thermal, 18: 11149
intermediate resonance structure in, 18: 34768 (MIT-2098-61)
libraries of, computer program for editing, 20: 36135 (AAEC-TM-310)
limits, theoretical studies, 16: 15635(R) (TID-15384)
measurement at thermal energies, experimental arrangement for, 18: 11138 (ANL-6797(p.21-6))
measurement by time-of-flight technique, computer programs for analysis of, 20: 32379 (ORNL-TM-1208)
measurement for Z = 3 to 92 nuclei at 1.0 to 14.8 Mev, 18: 30736(R) (TID-20658)
measurement of differential, techniques for, 17: 34851
measurement of differential, thick target method for, 19: 21298
measurement of differential, for reactor moderators, 20: 8035 (GA-5798)
measurement of fast, methods for, 19: 14529 (MMPP-FRPC-64-2)
measurement of inelastic differential, method for, 19: 42154 (KFK-261)
measurement of inelastic, liquid scintillation detectors for, 19: 46766(R) (TID-22141, pp 67-79)
measurement of low-energy inelastic, apparatus for, 19: 19095 (WASH-1053)
measurement, time-of-flight methods in, 16: 14044
measurements, 18: 3038(R) (ANL-6801)
measurements for intermediate and light nuclei at 0.4 to 1.2 Mev, 18: 9331
measurements of energy versus target-mass, (E), 19: 31215(R) (ANL-7010(p.1-19))
measurements of, computer program for correcting, 18: 44776
models for, 18: 22862
multiple scatter corrections by Monte Carlo, 16: 9454
of a system of atoms in liquids, use in determining liquid structure, 16: 15262 (ANL-6523)
of free molecules, determination of, 16: 33684 (NP-12134)
optical model calculations of, 18: 32726 (AERE-R-4649)
resonance structure in continuum shell model, theory of, 18: 26531 (LADC-6007)
table of 1-Mev, elastic, 17: 21040
tables, 16: 26194 (JAERI-6010)
tables for nuclei with Z = 3 to 92, 20: 44668(T) (INDSWG-101, pp 73-108)
theory of, using irreversible statistical mechanics of moderately dense fluids, 18: 20633 (TID-20512)
NEUTRON SHIELDING
albedo dependence on hydrogen content of, 18: 19257 (BRL-1224)
albedo distributions for fast, (E/T), 20: 2932 (ORNL-3822(Vol.1))
albedo distributions for fast, (E/T), 20: 2933 (ORNL-3822(Vol.2))
albedo distributions for fast, (E/T), 20: 2934 (ORNL-3822(Vol.3))
albedo distributions for fast, (E/T), 20: 2935 (ORNL-3822(Vol.4))
albedo distributions for fast, (E/T), 20: 2936 (ORNL-3822(Vol.5))
albedo distributions for fast, (E/T), 20: 2937 (ORNL-3822(Vol.6))
analysis of deep penetrations of, Monte Carlo methods for, 18: 28914
analysis of fast, two-component method for, 20: 26334 (DC-60-4-87)
analysis of, Monte Carlo code geometry for, 17: 26393 (LAMS-2856)
analysis of, two-component method for, 17: 3810
analysis using Monte Carlo code, (T), 19: 19331 (RRA-T44)
analysis using S_n method, 20: 10224 (ORNL-TM-1196)
attenuation kernel in hydrogen, computer analysis of, (T), 19: 35352 (TIM-792)
bibliography on materials for, 19: 25615 (AED-C-01-08)
bibliography on, for nuclear weapons radiation, 18: 15422 (NBS-MON-69)
book: *Neutron Attenuation in Optically Thick Shields*, 19: 14742
book: *Problems in Dosimetry and Shielding*, 18: 17246
by metals during thermal neutron activation, sample-size dependence, 18: 6184(T) (SC-T-523)
calculation methods for accelerators, 16: 17161
calculation of retardation density and thermal flux in scattering medium with fast neutron source, 17: 32984
calculations for accelerators and space vehicles, 17: 2416 (UCRL-10439)
calculations for window designs for hot cells, 16: 684
calculations for, by two-group and three-group programs, 17: 24648
capture and scattering in, (T), 20: 20103
characteristics for reactor uses, computer analysis of, (T), 19: 10453 (EUR-2152.e)
composition of, containing boric acid esters of monoaliphatic alcohols, 17: 9815(P)
computer program for, 17: 7496 (AEEW-M-261)
computer program for problems in, generalized Monte Carlo, 17: 22535 (MND-MC-2856)
design analysis of, for power reactors, 18: 4804(T) (AEC-tr-6155)
design and analysis of, transport code for (T), 19: 3463
design and construction of, for neutron generator, 18: 3030
design calculations for cyclotrons, 16: 7188
design calculations for cyclotrons, 16: 23166(T) (UCRL-Trans-842)
design for diffraction experiments, 17: 38043(T) (AEC-tr-5734(p.251-4))
design for hardened structures, (T), 20: 3276
design for meson (π) production facility using proton linear accelerator, 20: 2559
design for neutron sources, 20: 1323(P)
design for use with beams, 18: 21130 (KR-64(Sect.XXX))
design for Van de Graaff generator, 20: 46937
design of fast, Monte Carlo computer program for, (T), 19: 12725 (WAPD-TM-481)
design of honeycomb structure, 16: 30776(P)
design of laminated, 18: 38236 (A/CONF.28/P/684)
design of 4-in. portable, for a radiochemistry enclosure, 17: 3694
design of 4-inch portable, for radiochemistry enclosure, 17: 2747
design using liquids, 17: 40225(P)
development in West Germany, (E), 19: 14750
development of boron-filled polyvinyl chloride plastisols, 17: 15375 (LAMS-2800)
development of high-temperature cadmium oxide covers, 19: 24841 (FZK-208)
development of high-density concrete for, (E), 19: 29450
development of light-weight boron materials for, 16: 21690(R) (AD-267561L)
development of low-activation, for reactor environmental chembers, (E), 19: 29454
development of plastic-lined, 18: 24809(P)
development of rare-earth paints as, 18: 13184(P)
dose and flux calculations for, computer programs for, 17: 40220(T) (AEC-tr-6063)
dose and spectrum calculations for finite configurations, methods for, 17: 41116
dose distributions in iron and water, 19: 31435
dose rate behind concrete, method for calculating (T), 19: 3458
dosimetry in ducts in, 18: 21546 (NP-13805)
energy distributions in, method of counting efficiencies for studying, 19: 31440
evaluation of combinations of materials for, 18: 40740
fabrication of boron carbide, 16: 28647(R) (ORNL-2340(Pts.1-5))
fabrication of densified lithium fluoride as, 18: 19264
fabrication of high-density borated graphite, 20: 15027(P)
fabrication on site, 16: 27615(P)
flux distributions in laminated, 18: 42874
gamma dose rates behind, (E/T), 20: 6625 (UNC-5118)
gamma production in, effects on irradiation targets enclosed in, 16: 33532
gamma secondary radiation in light-weight, 18: 3032
heat generation in concrete, from capture and thermalization (T),

19: 3462
material for, casting large Boral, 17: 12640
material for, method for production of Boral, 17: 12639
materials and theory for, 17: 22766 (PA-TR-3009)
materials, bituminous composition as, 16: 3515(P)
materials, development of hydrided rare earth-titanium alloy, 16: 12100(R) (LAR-4)
materials development for, 17: 2415 (RIA-62-654)
materials, evaluation of organic, 16: 17221 (DC-52-5-41)
materials evaluation for, for neutron detectors, (E), 19: 13723 (HW-84329)
materials evaluation for, (E/T), 19: 14753
materials evaluation for, (E/T), 19: 14759
materials, fabrication of bricks, 16: 4522(P)
materials for, 17: 16731(P)
materials for, description of polymer-dispersion, 17: 41375(P)
materials for, development of polyethylene particles in an organic binder as, 17: 31638(P)
neutron albedos around concrete, (E), 19: 29456
neutron angular distribution and capture radiation in slabs of borated polyethylene, lead, and steel, 17: 11900 (NARF-62-16T)
neutron diffusion in, computer program for calculating, 17: 28220 (EUR-106.f)
neutron distributions in and behind, calculations of, 18: 40744
neutron flux calculations in cylindrical, using Lie series, 18: 32720
neutron flux density and dose rates outside, 18: 30689 (JUL-158-ST)
neutron fluxes in, thermal, 17: 40217(T) (AEC-tr-6044)
neutron migration, Monte Carlo schemes for calculating, 16: 2469 (UCRL-5918-T)
neutron transmission through rectangular ducts in, 17: 3802
neutron transmission through ducts in heavy-water–iron, (T), 19: 12723 (AE-166)
neutron transport in, analysis of fast, (E), 19: 21199 (CEX-65.02)
neutron transport in homogeneous, Monte Carlo code for, (T), 19: 33193 (MND-C-2933)
neutron transport in, removal-diffusion theory for, 19: 39751 (AE-185)
penetration by fast neutrons, distributions from, 18: 28911
performance, (E/T), 19: 14757
performance of air and concretes as, against point fission sources, (T), 19: 25616 (ORNL-TM-973)
performance of borated-graphite and -iron oxides, 20: 14180 (COO-1430-1)
performance of concretes as, 19: 29455
performance of concrete, removal cross section uses in calculations of, 19: 31434
performance of concretes for, 20: 10229
performance of graphite–iron laminar, (T), 19: 14749
performance of high-density concretes as, (E), 19: 19329 (ORNL-3704)
performance of ilmenite-loaded concrete, 18: 13174 (CEAL-1007)
performance of laminated iron–heavy systems as, 18: 28908
performance of laminar, (E), 19: 14752
performance of lithium hydride as, (T), 19: 21614 (NAA-SR-Memo-10559)
performance of lithium hydrides as, (E), 19: 35723
performance of water as, nomograms for calculation of, 17: 42157
performance of Westinghouse Test Reactor, 18: 4851 (ORNL-TM-332)
performance of, few- and multigroup P3 analyses of, (T), 20: 2939 (WAPD-T-1710)
performance of, methods for calculating, 19: 14763
preparation of glass, 20: 12273(P)
production of, method for, 18: 24079(P)
properties and uses of materials for, 16: 30844
properties of concrete structures, 18: 6404(R) (ORNL-3499(Vol.I)(p.131-6))
properties of glasses as, 19: 11805
properties of iron-ore, 18: 40738
properties of iron–aqueous, 18: 40739
properties of iron–serpentine concretes for, 20: 32677
properties of multilayer, 18: 15594 (NARF-58-29R)
properties of multilayer, 18: 15595 (NARF-58-40R)
quantum mechanics of, 18: 22986
radiation attenuation in, multigroup code for, (T), 19: 35568(T) (ORNL-tr-610)
reflection and transmission by walls for, calculation of fast, 17: 40218(T) (AEC-tr-6051)
requirements for irradiated mixed-oxide fuel elements, (E), 19: 14729 (HW-84451)
research program at HAPO on, review of, 17: 28408 (HW-SA-3032)
slowing-down spectra in heavy-water–iron laminar, (E), 19: 29457
streaming through ducts in concrete, (E/T), 19: 23939 (NP-14882)
testing, (E), 19: 14728 (APEX-581)
testing facility for, 18: 21546 (NP-13805)
testing of, facility for, 19: 19333
transmission through slabs of, analysis of fast, 17: 39948 (NARF-63-5T)
use of densified wood laminates as, 20: 33777
use of polyethylene as, 17: 26222
void effects in, 17: 26399 (RAS-33)

Neutron Source Reactor
see Brookhaven Neutron Source Reactor

NEUTRON SOURCES
see also Reactor Thermal Columns
see also Sigma Piles
accelerator tubes for, use of epoxy compounds for cementing isolation rings in, 20: 44059
alpha pulse height analysis of beryllium–polonium, 18: 19465(R) (MLM-1160)
beam amplification, 17: 36632
beam intensity measurements of, for determination of density of two-phase hydrogen, 19: 36752 (NASA-TN-D-2787)
beam pulsing in Cockcroft-Walton, design of trigger for, 20: 35975
beam sorter design for drift-tube, (E), 20: 6262 (NP-15633)
behavior of beryllium–polonium, 17: 8490 (BMI-1606)
bibliography on calibration and standards, 16: 4237 (CEA-BIB-11)
book: *Isotopic neutron sources*, 18: 15164
book: *Neutron Activation as an Analytical Method*, 19: 13260
book: *Neutron Irradiation and Activation Analysis*, 19: 11040
book: *Portable Neutron Generators in Nuclear Geophysics*, 19: 29221
calibration, 16: 1318(R) (LAMS-2627(p.150-60))
calibration, 20: 2520(R) (IA-920)
calibration, 18: 19468(R) (MLM-1176)
calibration and construction of standard photo-, of activity 3.11×10^6 nps, 18: 2784
calibration and design of spontaneous-fission, 17: 41133
calibration by manganese sulfate-bath method, absolute, 19: 23609
calibration by manganous-sulfate-bath method, corrections for, (E), 20: 8054
calibration for intrinsic-trace process control, 16: 24570
calibration for measurement of moisture content in soil, 17: 35400
calibration of americium–beryllium and radium–beryllium, (E), 19: 16822
calibration of Be–Pu, (E), 19: 36889(R) (MLM-1250)
calibration of beryllium-polonium, in manganese sulfate bath, 18: 22853
calibration of beryllium–radium, for use in standard pile, 18: 30968
calibration of beryllium–plutonium, 19: 25462
calibration of beryllium-polonium, 20: 13107
calibration of Canadian radium–beryllium, absolute and relative, 20: 6265
calibration of fast, intermediate, and thermal, 17: 9493
calibration of fission, method for, 17: 41132
calibration of flux from radium–beryllium, 19: 22799
calibration of NBS standard thermal, 16: 21339
calibration of NBS-I, in manganese sulfate bath of heavy water, 17: 41849
calibration of radium–beryllium, absolute, 17: 36635
calibration of radioactive, use of manganese sulfate bath for absolute, 19: 33188 (AAEC/TM-288)
calibration of radium–beryllium, using manganese sulfate bath, 19: 35358
calibration of, technique improvements in manganese bath for, 18: 9298
calibration of thermal, 17: 28232
calibration of, by manganese sulfate bath method, 18: 21124 (IA-800)
calibration of, determination of error caused by finite geometry in, 18: 19466(R) (MLM-1170)
calibration of, determination of absolute emission in, 19: 15877
calibration of, determination of manganese sulfate content in baths for, (E/T), 19: 47552
calibration of, effect of neutron scattering on, 19: 22797
calibration of, facility for, 18: 10308(R) (UCRL-7571)
calibration of, manganese sulfate method for, 20: 36144 (ZFK-RN-33)
calibration of, with different spectral composition, 20: 2947
calibration using concentrated manganese sulfate baths and water, determination of capture with charged-particle emission for, (E), 19: 45232
calibration using manganese-56, 20: 3321(R) (ANL-7082, pp 29-53)
calibration using manganese sulfate bath method, 20: 24310
characteristics and performance of pulsed reactors and electron linacs, 16: 18459
collimation of, for use in well logging, 19: 24740(P)
collimator for 14-Mev, development of steel, 18: 19821
collimators for, development of, 20: 13701 (JUL-294-NP)
comparison of accelerators and reactors as, 19: 31461(R) (ANL-7010 (p.235-87))
conference on accelerator targets as, 19: 28944 (EUR-1815.e(Rev.))
conference on Intense Neutron Generator, 19: 39752 (AECL-2177)
construction and application of generators, 18: 7668
construction of NG 200/1, 20: 11942
container for beryllium–radium, 17: 23592
containment of $\alpha + {}^{9}Be$, using pyrex and quartz, 18: 18857
control of, equipment for, 17: 32344(T) (AEC-tr-5901)

cooling system for deuterium and tritium (d,n), 18: 7645
counting rates for, effects of temperature on measured, 18: 21709(R) (MLM-1179)
description and performance of 14-Mev, 20: 44596
description for activation analysis, 16: 9964
description of, for activation analysis, 17: 32009
description of polarized 14-Mev, using D-T reaction, 18: 16902
description of polarized, for mev to 10-kev energies, (E), 20: 6259 (CONF-650217, pp 111-23)
description of positive-ion accelerator for activation analysis, 17: 32330
description of pulsed-thermal, using accelerators and research reactors, 16: 18458
description of pulsed, for in-pile uses, 18: 21605
description of pulsed deuteron-tritium, 19: 27392 (INR-573/IXA)
description of pulsed, using deuteron–tritium reactions, 20: 32358
description of standard, using beryllium–radium in water bath, 19: 12458 (JUL-179-RX)
description of tube for 14-Mev neutrons, 16: 19517
description of, using reactions of LAMPF proton beam with moderated targets, (E), 20: 5935 (CONF-650217, pp 73-6)
design, 17: 22546
design, 17: 21401(R) (TID-18585)
design, 18: 4075(P)
design, 18: 15564
design, 19: 25467(P)
design, 20: 13743(P)
design, 20: 26079(P)
design, 20: 34689(P)
design, 18: 15540 (TID-20284)
design and construction for pulsed and continuous operation, 16: 28021
design and construction of accelerator as 14-Mev, 19: 23614
design and development of sealed-tube 14-Mev, using D-T and T-T reactions, 17: 7069
design and operation of 14-Mev pulsed, 16: 3861(R) (ORNL-3193 (p.173-4))
design and operation of cold, 18: 30690(T) (ANL-Trans-42)
design and operation of proton-accelerator, 18: 44317 (AECL-2059)
design and performance of spark ion source, 16: 6992
design and performance of 300-kev electrostatic, 16: 21657
design and performance of DIDO liquid hydrogen cold, 16: 32380
design and performance in geophysical prospecting, 17: 20224
design and performance of PANACEA americium-beryllium, 17: 34195(R) (JLI-2748-0-7)
design and performance of mobile, for activation analysis, 18: 36565
design and performance of pulsed, for diffusion studies, 19: 14479
design and performance of pulsed-reactor, (E), 19: 31607 (LA-DC-6786)
design and performance of pulsed, with spark ion source, 19: 31204
design and performance of portable, 19: 31209
design and performance of pulsed, with modulated flux, (E), 20: 13720
design and performance of, with variable pulse frequency and width, 20: 13721
design and performance of cold, 20: 32351
design and preparation of antimony-beryllium, for JRR-2, 17: 30126
design and theory of 14-Mev, 20: 35455
design and uses of low-voltage, review, 16: 6991
design and uses of pulsed, 19: 21216
design for activation analyses, 20: 8832 (NP-15780)
design for continuous and pulsed operation, 16: 16483
design for cross section measurements, developments in, 20: 38103
design for efficient irradiation, 20: 23251(P)
design for fast reactors, 17: 36982
design for laboratory production of short-lived radioisotopes, 16: 8765
design for Operation HENRE, 20: 11930 (CEX-65.03)
design for production of monoenergetic pulsed neutron beams, 20: 46576(P)
design for pulsed fast reactors, 20: 28697
design for pulsed neutron-neutron logging in gas and oil wells, 20: 37017
design for simulating thermonuclear explosions, 18: 21546 (NP-13805)
design for thermal neutron flux standardization, 18: 40486
design for uranium exposure in controlled and measured vacuum, 20: 9575 (LA-3413)
design for use as moisture probe, volume of influence of, 19: 36678
design for use in equipment for activation analysis, 18: 29595
design for use in petroleum searches, 18: 39755(T) (AEC-tr-6390 (p.378-86))
design for well logging, 16: 419
design for well logging, 17: 3200(P)
design for well logging, 17: 16415(P)
design for well logging, 20: 9160(P)
design of alpha-beryllium, 18: 6152(P)
design of antimony–beryllium easily regenerable, 18: 40484
design of Argonne Thermal Source Reactor, 16: 21714 (ANL-6440)
design of beryllium-antimony, for reactor minimum power levels, 16: 13195(P)
design of beryllium–plutonium, 17: 9497(P)
design of beryllium plus alpha-emitter, 18: 4524(P)
design of beryllium and lithium target, for use with high energy ion beams, 20: 1143(P)
design of compact, 18: 5542(P)
design of compact, using duoplasmatron ion source, 18: 24247 (NP-13930(p.140))
design of controlled gas-filled tube for use as, 18: 31863(P)
design of Convergatron amplifier, 17: 1735(P)
design of Convergatron neutron amplifier, 17: 1601(P)
design of discharge-tube, for well logging, 20: 29444(P)
design of fast, 17: 8314(P)
design of fast pulsed-source assembly SORA, 19: 3793
design of fission-spectrum, using BSR neutrons, (E), 19: 8377 (ORNL-TM-987)
design of, for well logging, 17: 18585(P)
design of generator for constant neutron output, 18: 40497(P)
design of high-energy erbium–tritium, 20: 7315(R) (ORNL-3849, pp 151-82)
design of high-output sealed-off, for activation analysis, 20: 38839
design of howitzer, for neutron absorption studies, 20: 40057
design of Japanese generator, 16: 22294
design of L-shaped converter without accelerator, 19: 3228(P)
design of linear accelerator for well logging, 19: 2934(P)
design of liquid-shielded, 17: 40225(P)
design of low cost plutonium-beryllium, 19: 3198
design of monoenergetic, 16: 18281(P)
design of neutron amplifier, 16: 28617(P)
design of parallel-electrode, 20: 17669(P)
design of plasma device as, 16: 2619(P)
design of plasma-pinch, 18: 11159(P)
design of polarized, 18: 40094
design of portable, for use in activation analysis, 18: 29590
design of portable pulsed, 18: 34749(P)
design of portable, 19: 23622(P)
design of portable, 19: 39770
design of portable, for activation analysis, 19: 43261
design of portable water-cooled water-reflected critical assembly, 20: 19782 (LA-3374)
design of probe, for soil moisture measurements, 16: 5291
design of pulse generator for well logging, 18: 5508
design of pulsed, 19: 4498
design of pulsed, 19: 23621(P)
design of pulsed, 19: 25466(P)
design of pulsed, 19: 29223(P)
design of pulsed, 20: 24320(P)
design of pulsed, 19: 23991(R) (ANL-7003)
design of pulsed fast reactor, 20: 14096
design of pulsed reactor, 17: 9915(P)
design of pulsed, using fissile material, 18: 7669(P)
design of pulsed-beam, 20: 13745(P)
design of pulsed, for reactivity measurements, 19: 33222
design of pulsed, using an accelerator tube, 19: 34395(P)
design of radioisotope, 18: 28158
design of radium–beryllium, 18: 40491
design of regular flat-spectrum, using heavy water diffuser, 20: 15687(P)
design of sealed-bulb, 20: 28260
design of sealed, for activation analysis, 19: 34121
design of self-contained, 18: 1934(P)
design of shuttered accelerator-type, 18: 8639(P)
design of standard thermal, 20: 17654 (RT/PROT-(65)31)
design of strong pulsed, 18: 24570 (NP-13930(p.141-3))
design of T(d,n), 20: 24321(P)
design of thermal, for linear accelerator, 18: 23896
design of thermal, for calibration of radiometers, 20: 37073 (NP-16201)
design of thermonuclear, 16: 19877(P)
design of tritium gas target for production of fast neutrons, 18: 10618 (AE-127)
design of, utilizing nuclear reaction of deuterium and tritium, 17: 9056
design of zirconium hydride–uranium reactor with fission-source plate for shielding evaluations, 16: 32519 (NAA-SR-7432)
design of 14-Mev tritium-deuterium, with alpha-particle detector, 17: 14432
design of 14-Mev tritium–deuterium-saturated, with titanium absorber, 18: 9304(P)
design of 14-Mev, for use in medical research, 19: 2(R) (HW-81746(p.2.32-5))
design of, for planetary surface analysis, 20: 27170 (UCRL-14654-T)
design of, for pulsed irradiation, 19: 24188
design of, for use in activation analysis of petroleum products for chlorine, 20: 29116

design of, having sinusoidally modulated intensity, (E), 20: 13704(R) (MIT-2344-4, pp 101-5)
design of, using deuteron and triton reactions with titanium, 18: 15170(P)
design of, using ion collisions, 19: 16834(P)
design of, with automatic target temperature control, 20: 13744(P)
design relations for, 18: 15446 (CEA-2378)
design using alkali metal hydrides or hydroxides as targets, 20: 9958(P)
design using deuteron reactions (d,n) with tritium, with low-voltage accelerators, 20: 42136 (AD-637457)
design using deuteron beams, with improved voltage control, 20: 44600(P)
design using ion-beam deflection magnets for stabilization of output, 18: 39581
development, 17: 11936(R) (ANL-6672)
development, 17: 15858(R) (ORNL-3397(p.71-112))
development, 17: 21315(R) (GEAP-4162)
development and evaluation of thermal, 18: 4515
development and performance of 50-c, for production of radioisotopes, 16: 29279(R) (BMI-X-10009)
development and performance of 300-kv generator, 19: 43254
development and properties of actinium–beryllium, for industrial geophysics studies, 18: 25873
development and standardization of, 17: 4271
development and uses of 14-Mev, 19: 17781(R) (ORNL-3750)
development at Karlsruhe Nuclear Research Centre, 19: 17442
development for industrial radiography, 17: 10880 (ARF-1164-27)
development for use in well logging, 19: 18189(P)
development for use in activation analysis, 19: 42448
development of antimony–beryllium regenerable, 18: 36563
development of antimony–beryllium, with heavy water moderator, 20: 16830(R) (UCRL-14534, pp 8-12)
development of beryllium–polonium, for production of radioisotopes, 16: 29278(R) (BMI-X-199)
development of Cockcroft Walton type, 18: 22858
development of cold, 16: 18449
development of cold, status of European, 17: 5296 (EANDC-22L)
development of cold, 17: 32980
development of cold, using ice-d_2, 20: 36148
development of constant output T(d,n), 19: 19069
development of electrostatic generator, 19: 11870
development of fast, 17: 34860
development of fast, for radiotherapy, 19: 22054
development of, for in-process radiotracer production, 17: 6511(R) (BMI-1583(Del.))
development of, for short-time pulses, 17: 28329
development of gaseous targets for use in, 18: 22636
development of high-flux, using excitation of heavy nuclei, 19: 33198
development of high-intensity compact, pulsed, 19: 43251 (KFK-304)
development of high-output tubes for activation analysis, 20: 3005
development of high-intensity pulsed, conference on, 20: 6256 (CONF-650217)
development of ING, engineering problems in, 19: 31183 (AECL-2212)
development of Intense Neutron Generator, engineering problems in, 19: 39760 (AECL-2177, Paper 7))
development of Intense Neutron Generator, 20: 34467 (AECL-2557)
development of intense, 20: 36538(R) (AECL-2407)
development of intense, using proton accelerators, 20: 39542
development of limited-energy, produced by decay of excited nuclei, (E), 20: 4802 (IDO-17115)
development of monoenergetic from reactor-produced nitrogen-17, 19: 29889(R) (ANL-6971(p.90-116))
development of monoenergetic, using lithium 7(p,n) reactions and accelerators, 19: 29889(R) (ANL-6971(p.90-116))
development of plutonium oxide–beryllium oxide standard, 16: 1289(R) (MLM-1114)
development of plutonium glass, 18: 32172
development of polarized fast, review of, 19: 19078
development of portable 14-Mev, 17: 38998
development of pulsed, for subcritical assemblies, 16: 6915 (TID-7619 (p.161-82))
development of pulsed-reactor-type, 16: 18457
development of pulsed, for use in reactor startup, 17: 7541(R) (GEAP-4047)
development of pulsed high-intensity fission, 19: 45874 (GA-6168)
development of pulsed, bibliography for, 20: 5200 (TID-3571 (Suppl.1))
development of pulsed, for power reactor startup, 20: 8386(R) (GEAP-4841)
development of pulsed, for power reactor startup, 20: 22414(R) (GEAP-4961)
development of pulsed, for power reactor startup, 20: 28233 (GEAP-5079)
development of pulsed, for power reactor startup, 20: 42628(R) (GEAP-5145)
development of sealed ion-accelerator type, 16: 31760
development of sealed-tube, 19: 13250
development of separated-orbit cyclotron as, 19: 39755 (AECL-2177, Paper 2))
development of simple, compact, for radiotherapy, 17: 21532
development of tritium-target, 20: 696(R) (ORNL-3829)
development of, using alpha emitters and an oxygenous target, 17: 37892(P)
development of vanadium-51 (p,n), 19: 19137
development of 14-Mev, for operation HENRE, 19: 8666(R) (ORNL-3697(p.165-9))
development of 150-kv ion accelerator for use as, 17: 21122
development using electron linacs and research reactors, 16: 18456
development using Orbitron ion sources, 19: 21208
development using electron linear accelerators, 20: 46592(R) (ORNL-3973(Vol.1), pp 1-13)
dose and energy distributions from americium–beryllium, americium–boron, plutonium–beryllium, and polonium–beryllium, 19: 39766 (ORNL-TM-1171)
dose conversion factors for plutonium-beryllium and polonium-beryllium, 19: 31208
dose conversion factors for, in soft tissue, 20: 32355
dose conversion factors for americium–boron and americium–beryllium, 20: 32356
dose distribution in water-filled Lucite sphere from beryllium-polonium, 18: 6715(R) (ORNL-3499(Vol.II)(p.85-9))
dose distribution in air from point, estimates of, (E), 19: 25460
dose rates from point fission, through concretes, (T), 19: 29449
dose rates from shielded and unshielded isotopic, 18: 18621 (ORNL-3576)
dose yield as function of gamma yield in polonium–beryllium, 17: 15224
dosimetry for deuteron–deuteron, in water, 18: 15152
dosimetry of alpha particles in beryllium–polonium, design of spark detector for, 18: 4124
dosimetry of fast neutrons from plutonium-beryllium, 16: 10960 (TID-14865)
dosimetry of fast neutrons from beryllium–polonium, graphs for, 16: 33334
dosimetry of fast neutron, for chronic exposure of mice, 20: 40504(R) (ORNL-3922, pp 146-60)
dosimetry of neutrons near, 17: 34281
dosimetry, flux measurements, and spectrometry of, multisphere technique for, 19: 46757 (CEA-R-2772)
economics for Intense Neutron Generator, 19: 39753 (AECL-2177, Introduction)
effectiveness of americium–beryllium and plutonium–beryllium, in prompt-gamma activation analysis, 17: 3676
effects on reactor stable periods, 17: 42213
efficiency measurements by gold foil activation, 18: 26505
efficiency of beryllium–plutonium, effects of composition on, 20: 20553(R) (MLM-1142)
efficiency of D-T, effects of target "reloading" on, 18: 24579
emission from, 17: 34195(R) (JLI-2748-0-7)
emission from, method for determining simultaneous, 20: 11947(P)
emission of beryllium–plutonium, 18: 45174(R) (MLM-1204)
emission of K x-rays from continuous, (E/T), 20: 24351(R) (MIT-905-52, pp 1-41)
emission rates from, 17: 9495
emission rates of beryllium–plutonium-239, 19: 28717(R) (MLM-1221)
emission rates of, determination by Gauss' quadrature formula, 18: 45173(R) (MLM-1203)
emission strength analyses for, 18: 16376(R) (MLM-1157)
energy distribution analysis by DAEDALUS code, 16: 1010
energy distributions from beryllium-polonium and beryllium-radium, 17: 13356
energy spectra of beryllium–polonium, measurement method for, 17: 41134
energy spectra of americium-241–beryllium, 20: 40069(R) (EANDC(E)-66(U))
energy spectrum of americium-241–beryllium, 18: 26510
engineering problems of pulsed, 20: 40455 (BNL-10454)
equipment for FRJ-2 cold beam, 20: 12503(T) (AERE-Trans-1042)
evaluation for biological application, 20: 45379
evaluation of (γ,n), in Molten Salt Reactor Experiment shutdown, 18: 43082 (ORNL-TM-935)
evaluation of actinium–beryllium, 19: 23612
evaluation of, for small laboratories, 18: 21139
experimental facilities of Intense Neutron Generator, 19: 39757 (AECL-2177, Paper 4)
experiments using pulsed, laboratory, 16: 14255
fabrication, 20: 16914(R) (ORNL-3900, pp 182-93)
fabrication and postirradiation handling of antimony-beryllium, difficulties encountered in, 20: 9377 (CONF-650620, pp 85-104)
fabrication and testing of plutonium-enriched, 18: 27810(R) (MLM-1183)

fabrication of americium–beryllium (E), 19: 3224
fabrication of americium–beryllium, in glove box, 19: 6283
fabrication of beryllium–plutonium, 16: 22529 (AERE-R-3670)
fabrication of, for JANUS reactor, 16: 30717(R) (ANL-6516)
facility for using, 20: 12954(P)
feasibility of heterogeneous isotopic, 20: 24298 (AD-625406)
feasibility of isotopic, with variable intensity, 20: 24299(R) (AD-625415)
feasibility of use of upgraded PHERMEX linac as photo-, (E), 20: 5936 (CONF-650217, pp 77-81)
feasibility of 14-Mev, for Operation HENRE, 20: 26063 (CEX-65.01)
flux and spectrum variations with distance from, 17: 34297
flux angular distribution of T(d,n), 16: 21370
flux calculations for antimony-beryllium thermal neutron sources, 19: 31199 (TPI-104)
flux calibration by foil activation, 16: 13934
flux distribution from pulsed, 18: 13026 (AE-129)
flux distribution from, activation methods for determining, (E), 19: 28627 (EUR-1815.e(Rev.)(p.235-40))
flux distributions from point, in water system with internal spherical cavity, 18: 34731 (NASA-CR-54110)
flux distributions from drift-tube, (E), 20: 6263 (NP-15635)
flux evaluation in 14.2-Mev, 18: 22854
flux from antimony-124–beryllium, 20: 24307
flux from 150 kev Cockcroft-Walton, 17: 22536 (SAM-TDR-63-18)
flux intensification, 19: 39754 (AECL-2177, Paper 1))
flux measurements for plutonium–beryllium, 16: 10366(R) (BMI-X-189)
flux pattern for 14-Mev generator, determination of, 19: 3459
flux patterns for 14-mev, 20: 21946
fluxes at ground level from vertically collimated upward-pointing 14-Mev, 18: 40478 (RM-4120-AEC)
fluxes in paraffin, 18: 16892 (JUL-140-RX)
gamma emission from, comparison of americium–beryllium and plutonium–beryllium in prompt-gamma activation analysis, 17: 7953 (CUA-NE-24)
gamma emission from low-level, use in ore analysis, 19: 28275
gamma spectra from beryllium–plutonium, 16: 18467
gamma spectra from beryllium–polonium, 17: 7102 (NP-12330(p.104-8))
gamma spectra of beryllium–polonium, 18: 15237
handling of, design of laboratory and equipment for remote, 18: 12294
health physics problems of, in well logging, 20: 41216
health problems of, 20: 41215
hydrogen dispenser for, design of, 19: 4447(P)
image intensifier television system for, 20: 39174
inspection and recanning of beryllium–plutonium, 18: 30114 (MLM-1188)
intensity in subcritical cores, relative, (E), 20: 22392
intensity of beryllium–radium, method for absolute measurement of, 17: 15222
intensity of Harwell plutonium-240 standard, 20: 44594
intensity of pulsed, measurement of, (E), 19: 8376(R) (GA-5176)
intensity of, design of detector for measuring, 19: 13809(P)
intensity of, methods of increasing, 18: 16957(T) (AEC-tr-6371)
ion source design for fast, high-yield r-f, 17: 26397 (PAN-246)
ion source for, design of high-frequency, 18: 14170
ion sources for, 18: 16904
ion sources for pulsed, performance of r-f, 20: 36147
ion sources for, deuterium–tritium mixture for, 19: 29222(P)
magnetic field confinement to ion source area in, development of shielding for, 18: 4073(P)
measurement of, detector calibration for, 19: 32570
measurements using pulsed, theory of, 17: 26065
moderator for, 17: 37154 (HW-73913)
modification of Tex generator pulsing system for lower neutron background, 17: 33126
modification to pulsing technique, 19: 6625
monitoring of deuterium (d,n), using deuterium (d,p) reaction, 20: 13715
multiplication factor for localized, 16: 24405
multiplier development for, for use in activation analysis, 18: 39517(T) (AEC-tr-6390(p.365-71))
neutron absorption in cavity surrounding, 18: 18856
neutron activation and spectra in concrete walls around accelerator, 20: 3264
neutron angular and flux distributions from, 16: 5816
neutron angular distribution-energy relationship for, calculation of, 20: 21934 (AD-621473)
neutron angular flux from different, relations among, 17: 3748
neutron background in laboratory containing, room-scattered, (E/T), 20: 13714
neutron collimation from deuterium (d,n), 19: 35496
neutron diffusion from, stochastic analysis of anisotropic, 16: 31061
neutron distribution and yield from (d,d), measurements of, 16: 27320
neutron distributions from with different spectra, similarity of spatial, 20: 28239
neutron distribution around hemispherical, thermal, 16: 4616(R) (NP-11098(p.35-7))
neutron distributions from pulsed, in slowing-down media, 18: 4009
neutron dose conversion factors for beryllium-plutonium and beryllium-polonium, 19: 7205(R) (ORNL-3697(p.159-64))
neutron doses from beryllium–polonium, calculation method for, 17: 41111
neutron emission by, absolute determination of number in, by associated particle method, 18: 26503
neutron emission by, measurement by manganese activation method, 18: 26504
neutron emission from pulsed, quantitative measurement at high energies, 16: 19725 (SCR-467)
neutron emission from, determination of number of simultaneous, 18: 25857(P)
neutron emission measurement, 17: 10849(R) (HW-73337(p.29-76))
neutron emission rates of beryllium–plutonium (E), 19: 3380
neutron energy and flux from beryllium–plutonium, (E), 19: 8384
neutron energy distributions from polonium-beryllium, 17: 29570
neutron energy from beryllium–plutonium-238 of air, 19: 28576(R) (UCRL-12167)
neutron energy spectra from polonium-beryllium, performance of scintillation spectrometer in measuring, 18: 41789
neutron flux at large distance from point, air-ground interface effects on, 18: 26511
neutron flux from eccentric point, in spherical reactors, 18: 26869
neutron flux in heterogeneous multiplying media using pulsed, (T), 19: 33230
neutron flux in SM-1 reactor with plutonium–beryllium, 19: 48040
neutron growth rate of plutonium-beryllium, 18: 21707(R) (MLM-1177)
neutron intensity from antimony-beryllium, 17: 30126
neutron production of americium-beryllium, absolute, 17: 22665 (ORNL-TM-550)
neutron production by D-D, indirect monitoring of, (E), 20: 5777
neutron spectra and yields from (α,n) reactions in heterogeneous isotopic, (E), 20: 2949
neutron spectra from beryllium–lead-210, 18: 36564
neutron spectra from radium–beryllium, up to 12 Mev, (E), 19: 5119
neutron spectra from polonium-beryllium, from photographic emulsions, 19: 31203
neutron spectra from americium–beryllium and radium–beryllium, (E), 20: 6269
neutron spectra from americium–lithium, 20: 20201(R) (ANL-7110, pp 311-401)
neutron transport equation for point, solution of, 18: 11154
neutron wave excitation by modulated and pulsed, (E/T), 20: 13722
neutron yield from beryllium–plutonium, variation in, 20: 9166(R) (BNWL-36, pp 2.1-58)
neutron yields from (radium + mesothorium)–beryllium, time dependence of, 20: 32352
operation and uses of high intensity, in industry, 16: 32355 (AERE-R-3920)
operation of neutron generator, 16: 2967(R) (TID-14310)
operation of pulsed, using Cockcroft-Walton deuteron accelerator, 19: 14194
performance of accelerator-pulsed, 20: 2956
performance of accelerator-bombarded exponential piles as pulsed, (E), 20: 6257 (CONF-650217, pp 11-24)
performance of accelerators as pulsed, for nuclear engineering studies, 20: 32360
performance of accelerator, for tumor therapy, 20: 33141
performance of accelerator based, comparison of, 20: 34478
performance of americium–beryllium and americium–boron, 20: 7315(R) (ORNL-3849, pp 151-82)
performance of beryllium–plutonium, 20: 18568(R) (NBL-230)
performance of cylindrical and spherical assemblies as, 20: 26394(R) (ANL-7193)
performance of fast-burst reactors as pulsed, (E), 20: 6671 (CONF-650217, pp 1-10)
performance of gas-filled tube, with Penning-type ion source, 19: 35367
performance of low-background deuteron-deuteron, for nuclear analyses, 20: 28236 (NP-16039)
performance of lucite, scattering shape effects on, 20: 34470 (EUR-2953.e)
performance of mechanically pulsed fast-burst reactors as, 20: 6672 (CONF-650217, pp 25-35)
performance of neutron source reactors, 20: 26533(R) (BNL-954, pp 16-49)
performance of nitrogen-17, 20: 4802 (IDO-17115)
performance of nuclear explosions as, 20: 27077 (LA-DC-7272)
performance of oscillating, 19: 41641(R) (MIT-2344-3, pp 137-54)
performance of oxygen-18 (p,n) gas target, 20: 4927
performance of pulsed, for kinetics measurements on small plutonium assemblies, (E), 19: 12750 (HW-SA-3565)

performance of pulsed, in low energy neutron spectroscopy, 19: 29174 (ORNL-P-1116)
performance of pulsed, for reactor studies, (T), 19: 40151 (EIR-79)
performance of pulsed and steady, for diffraction and scattering analysis, (T), 20: 5726 (CONF-650217, pp 102-7)
performance of pulse-modulated, for reactor criticality measurement, 20: 10425 (EUR-2523.f)
performance of pulsed research reactors as, 20: 12495 (EUR-2538.e)
performance of Sioux Falls, 18: 19344 (ACNP-64006)
performance of tritium (d,n), 19: 37292
performance of underground nuclear explosions as, 19: 44157 (LA-DC-7304)
performance of, using reaction H(t,n), 17: 33035
performance of 14-Mev, 18: 13636(R) (ORNL-3537(p.71-105))
performance of, for soil moisture measurements, 18: 27774
performance of, using alpha, beta, and gamma emitters, 18: 27828
performance of, using portable particle accelerators, (E), 19: 10218 (CEA-Note-461)
photo-, uses in startup of research reactors, 18: 11490
power production in Intense Neutron Generator, nuclear, 19: 39758 (AECL-2177, Paper 5))
power supply for, design of, 18: 40481
power supply system for Intense Neutron Generator, r-f, 19: 39759 (AECL-2177, Paper 6))
preparation and performance of titanium–tritium targets for, 19: 9049(T) (NP-tr-1198)
preparation of americium-beryllium-curium, 19: 3219
preparation of deuterium-zirconium targets for pulsed, 18: 18860
preparation of polonium-208–beryllium, 18: 13049 (MLM-914)
preparation, properties, and uses of americium-241, 16: 29281 (ORNL-3335)
pressure control in deuterium, 19: 10239
procurement of plutonium–beryllium, problems involved, 16: 2967(R) (TID-14310)
production and industrial uses of, conference on, 20: 19128
production of beryllia pellets for, 19: 28780
production of pseudo-random square-wave, using shift register with binary feedback (T), 19: 3507 (CEA-R-2230)
production of pulsating, (E/T), 19: 18634 (NP-14614)
properties and spectra of, 19: 39772
properties and uses, 16: 29710
properties of, 19: 5125
properties of accelerator targets for, 19: 28945 (EUR-1815.e(Rev.) (p.182-5))
properties of beryllium, 19: 36302
properties of helium-3 cyclotron for use as, 20: 20565 (ORNL-P-1216)
properties of linear accelerator, 16: 14074
properties of nitrogen-17 or oxygen-18 (α,n), 17: 41124
properties of positive ion accelerators for, 17: 29568
properties of pulsed, 16: 14078
properties of pulsed, dynamic and static, (T), 20: 34907 (ORNL-TM-1213)
properties of radium, 18: 28533
properties of radioisotopic, 19: 851
properties of synchrocyclotron, 16: 14073
properties 150-kv positive-ion accelerator as, 17: 24369(R) (GA-3542)
pulse techniques using thermal, survey on, 19: 33219
pulse transformer design for generator for well logging, 18: 39604(P)
pulsed, fast reactor design for use as, 19: 21745(P)
pulsed, fast reactor design for use as, 19: 21746(P)
pulsing of, theory of techniques for, 18: 2811
radiation characteristics of pulsed Kukla reactor, 18: 10374 (D2-9878-4)
radiation dosimetry of plutonium–beryllium, 16: 10223
radiation hazards from, 18: 1462
radiation hazards from, 19: 38480
radioactivity induced in irradiated Ra-Be, 16: 3720
radioisotope production in the Intense Neutron Generator, 19: 39762 (AECL-2177, Paper 9))
reactivity effects of fast, on subcritical reactors, 18: 30992(R) (ORNL-3619(p.3-11))
reactivity effects from pulsed, in reactors, 19: 27752 (ORNL-TM-1113)
reactivity effects on swimming pool reactors, (T), 19: 27823
reactivity effects on multi-region reactors, (T), 19: 10488 (ORNL-TM-993)
reactivity transients from pulsed, in reactors, 18: 24851 (ORNL-TM-570)
reactor criticality effects of external, 16: 14251
recoil atom distribution from applications of, theory of, (T), 19: 6399
requirements of, for EGCR startup, 17: 15471 (TID-18107)
research programs on, at Japanese universities, 1964, 19: 37211
research programs on, at Siemens-Schuckertwerke laboratories, Erlangen, Germany, 19: 42228
research programs on, at AECL, 19: 45694(R) (AECL-2251)
research with pulsed, conference on, 20: 13710 (STI/PUB/104(Vol.1))
research with pulsed, conference on, 20: 13711 (STI/PUB/104(Vol.2))
research with pulsed, review of, 20: 13725
review of reactor-associated, 17: 4278
safety hazards in operation of pulsed, in AGN-201 reactor, (E), 19: 12842 (NP-14591)
sensitivity of low-level, 18: 31386
shield design and construction for neutron generator, 18: 3030
shielding design for, 20: 1323(P)
shielding for, 20: 10439(R) (ORNL-3830, pp 285-98)
shielding measurements for fast, (E), 20: 9265
shielding of Intense Neutron Generator, 19: 39761 (AECL-2177, Paper 8))
shielding of, nomograms for calculation of aqueous, 17: 42157
shielding of Van de Graaff, 20: 46937
shielding of, performance of metal-water, 18: 19262
spectra analysis for beryllium-polonium and plutonium-240, computer program for, 20: 16875
spectra from americium-241–beryllium–curium-242, gamma and neutron, 19: 26718 (ORNL-3802)
spectra from antimony-beryllium, 17: 26054
spectra from antimony–beryllium, 17: 34831 (CONF-39-68)
spectra from beryllium-polonium, 16: 12406
spectra from beryllium–polonium and beryllium–radium, 16: 17060
spectra from beryllium–polonium, 18: 7054(R) (ORNL-3499(Vol.II) (p.120-4))
spectra from boron-9(d,n) reactions, 20: 31786(R) (ORO-2891-5)
spectra from boron–polonium, gamma and neutron, 16: 7040
spectra from D-T, estimation of, 18: 28559
spectra from moderated plutonium-beryllium, 18: 10308(R) (UCRL-7571)
spectra from polonium–beryllium, in paraffin moderator, (E), 20: 15683
spectra from tritium (d,n), at 400 kev, 16: 14063
spectra from 14-Mev, method for estimating, 19: 16823
spectra from, angular variations of, (E), 19: 25455 (ORNL-TM-1087)
spectra of americium–lithium, 19: 29468(R) (ANL-7017)
spectra of beryllium–polonium, 16: 24762 (TID-15743)
spectra of beryllium-polonium, 17: 23757
spectra of beryllium–plutonium, 17: 26402
spectra of beryllium-polonium and beryllium-plutonium, 18: 13032 (IA-856)
spectra of, determination of fast, 18: 7072
spectra of, measurements of, 17: 9494
spectra of plutonium-, polonium-, and radium-beryllium, 16: 13942 (DC-58-1-90)
spectra of plutonium-, polonium-, and radium-beryllium, 17: 1175(R) (HW-70050(p.31-77))
spectra of plutonium–beryllium, 17: 18932
spectra of, analysis of errors in measurement of, 18: 13357(R) (MLM-1148)
spectrometer design for use with D-D, (E), 20: 13088
spectroscopy of pulsed, using time-of-flight methods, 18: 18224
spectroscopy using white, 17: 41873 (WASH-1044)
spectrum of americium–beryllium, (E), 20: 44592
spectrum of beryllium–plutonium, measurement, 16: 7045
spectrum of beryllium–polonium, 17: 41120
spectrum of beryllium–polonium, 18: 7061 (UCRL-10732)
stabilization of output for deuterium–tritium, 16: 18282(P)
stabilizers for, development of ion beam position, 18: 991
standard, comparisons of flux density of, 17: 9069
standardization, 17: 41077
standardization of, developments in, 17: 9106
standardization of radium–beryllium, by gold-foil activation techniques, 17: 36424 (NP-13020(p.289))
survey, 17: 32978
survey of pulsed, 20: 46565
survey of reactions for use as, 17: 15249 (BNL-6765)
survey on thermal, 20: 19796
target assembly for tritium (d,n), TV-monitored, 19: 28950 (EUR-1815.e(Rev.)(p.241-5))
target design for high-yield, 19: 1529
target design for accelerator, 19: 4782(P)
target design for, lithium tritide–aluminum, 19: 33233(P)
targets for D-D, performance of self-regenerating, (E/T), 20: 6334
targets for, use of rare earths and yttrium in, 19: 10376(P)
theory and uses of, 17: 17102
thermal flux-density standards, slowing-down spectrum and neutron temperature in, (E), 20: 46566
tritium hazards in, method for reducing, 20: 7302 (NP-15632)
tritium target for (d,n), 20: 21948
use for producing radiotracers in process streams, 19: 2687
use for production of intrinsic radiotracers for process control, 16: 10366(R) (BMI-X-189)
use for reactivity measurements on subcritical assemblies, 17: 31697
use for reactivity measurements on subcritical assemblies, pulsed, 18: 21607
use for remote activation analysis, 19: 10983(R) (TEES-2671-3)

use for well logging, 19: 46624(P)
use in activation analysis, 18: 21953 (AERE-R-4576)
use in activation analysis, 19: 36322
use in activation analysis, 19: 38565
use in age estimation by potassium–argon method, 20: 29413
use in analysis of remote surfaces, 20: 31211
use in cadmium probe for moisture measurements, 16: 22504
use in calibration of radiometers, 20: 37074 (NP-16202)
use in calibration of radiometers, 20: 37075 (NP-16204)
use in control of flooding of oil deposits, 18: 5520
use in control of soil irrigation, 20: 633
use in critical assembly experiments, computer program for data analysis from, 20: 12355 (GAMD-6781)
use in determining moisture content of soils, 18: 425
use in geophysics, research program in Soviet Union on, 20: 37001
use in humidity measurements on loose materials, 20: 46022
use in industrial automation and control, 20: 23543(T) (AEC-tr-6466/1, pp 82-99)
use in instrumentation, 19: 26728
use in measurement of density of steam–water mixtures, 16: 13273 (AERE-EL/M-97)
use in measurement of speed of ships, 20: 25368(P)
use in measuring moisture content of soil, 19: 7720
use in measuring soil moisture, 20: 632
use in measuring space-dependent source transfer function in sub-critical reactor cores, 20: 45082
use in moisture gage, 20: 5819
use in moisture measurement in raw materials for pig iron, 18: 4140
use in neutron–gamma well-logging of earth formations for hydrogen, 20: 25314(P)
use in nondestructive testing of materials, 20: 41115(P)
use in prospecting for minerals, 20: 33169(T) (AEC-tr-6639, pp 50-4)
use in reactor startups, review of safety aspects of, 17: 23576
use in snow property measurement, 17: 34139
use in soil moisture meters, 20: 14771
use in soil moisture measurements, 20: 39131
use in startup and operation of Molten Salt Reactor Experiment, 18: 43082 (ORNL-TM-935)
use in steam void determination in loops, 19: 20294
use in studies on soil moisture on lysimeters and small watersheds, 17: 35403
use in teaching, 16: 6912 (TID-7619(p.109-22))
use in well logging for chlorine in subsurface formations, 20: 29446(P)
use in well logging, 20: 43163(P)
use of (α,n), for detector calibration, 20: 35756 (LA-DC-7702)
use of actinium–beryllium, in well logging, 18: 5498
use of antimony–beryllium, for radiography, 20: 7243
use of atomic explosions as pulsed, in measurement of cross sections, 20: 24304 (LA-DC-7799)
use of beryllium and polonium, in activation analysis of alloys for indium, 18: 17747
use of beryllium–lead-210, in moisture gages, 17: 29887
use of collimated beam, for shielding studies, 16: 19885
use of curium–americium–beryllium, design of facility for, 20: 9017
use of deuterium (d,n) reactions in associated-particle method, (E), 20: 44813
use of electrostatically focused ion source in d-c, 17: 14431
use of, for humidity measurements at building sites, 17: 15903
use of, for well logging, 17: 8678(P)
use of, for well logging, 17: 8679(P)
use of gamma emitters as, preparation and survey of, 18: 16379
use of h-f sine-wave modulated, for subcritical reactivity measurements, (T), 19: 14785 (AEEW-R-398)
use of, health physics problems in, 17: 29149
use of, in well logging, 17: 8677(P)
use of isotopic, in chemical analysis, 18: 43387 (ORNL-P-479)
use of isotopic, in irradiation facilities, 20: 2997
use of lithium-6 deuteride as, 16: 33789 (BNL-5366)
use of modulated and pulsed, in thermal neutron wave experiments, 20: 34486
use of nuclear explosions as pulsed, for cross section measurements, 18: 36557 (TID-7695(p.25-30))
use of polonium-beryllium for activation of liquid biological materials, 20: 9016
use of proton accelerators as pulsed, 20: 44581 (CONF-660303, pp 1055-63)
use of pulsed, 16: 6914 (TID-7619(p.138-60))
use of pulsed accelerators as, 17: 32979
use of pulsed, for measuring reactivity of critical assemblies, 17: 32894 (CONF-39-47)
use of pulsed in critical mass determinations in plutonium production processes, 16: 586(R) (HW-70716)
use of pulsed, in large reactor neutronics analysis, 18: 3226
use of pulsed, in measurement of diffusion parameters, 16: 28013 (NP-11733)
use of pulsed, in start-up of power reactors, 17: 29790(R) (GEAP-4083)
use of pulsed, in startup of power reactors, 18: 1240(R) (GEAP-4305)
use of pulsed, in subcritical reactivity measurements, 18: 3124
use of pulsed, in well logging, 18: 5509
use of pulsed, for power reactor startup procedures, (E), 19: 12778(R) (GEAP-4644)
use of pulsed, for measurements in heavy water systems, (E), 20: 14076
use of pulsed, for experiments in intermediate and fast critical assemblies, 20: 14083
use of pulsed, for SAPHIR reactivity measurements, (E), 20: 14199
use of pulsed, for subcritical reactivity measurements in IRR-1, (E), 20: 14200
use of pulsed, for measuring spectra in moderators and reactor lattices, (E/T), 20: 13735
use of pulsed, for determining neutron diffusion parameters in fluids and rocks, 20: 14772
use of pulsed, for aerospace research, 20: 32365
use of pulsed, for ANNA critical assembly parameter measurements, 20: 47077
use of pulsed, in subcritical reactivity measurements, 18: 15471 (GA-4838)
use of pulsed, in startup of power reactors, 18: 17297(R) (GEAP-4388)
use of pulsed, in reactivity measurements, 18: 42940 (TID-7050 (p.1319-57))
use of pulsed, in developing methods of measuring subcritical reactivity, 19: 6125 (HW-80913)
use of pulsed, in well logging, 19: 38871(P)
use of vanadium-51 (p,n) reaction as absolute, 18: 1080
use of 14-Mev, for radiotherapy, 18: 3649
use of 250-kv Cockcroft-Walton accelerator with frozen water-d_2 target, 16: 21654
use of, in neutron–gamma well-logging apparatus, 20: 25315(P)
use of, measurement methods for, 20: 29593
use to measure soil bulk density, 17: 30729
uses for analysis and prospecting of boron deposits, 19: 13261
uses for material analysis evaluation, 16: 23964 (ANL-6515(p.9-27))
uses in activation analysis, 19: 24460
uses in activation analysis, 20: 35420
uses in determination of moisture content of soils, 18: 27821
uses in determining direction of ground-water flow, 20: 31430
uses in equipment for moisture measurements, 20: 31627
uses in geological explorations and prospecting, 16: 33299
uses in geology, 17: 305
uses in liquid level measurements, review, 19: 18357
uses in soil density and moisture determinations, 18: 27824
uses in soil moisture determinations, 20: 14756
uses in USSR, 16: 33354
uses in well logging, 16: 8986 (CEA-NOTE-352)
uses of beryllium–radium, in industrial moisture gages, 17: 29886
uses of fast, for soil humidity determination, 16: 13411 (NP-11381)
uses of fast, in Operation HENRE transport studies, (E), 19: 21199 (CEX-65.02)
uses of, in soil amelioration studies, 17: 12484
uses of in-pile cryogenic, for basic radiation-damage studies, (E), 20: 5569 (CONF-650217, pp 108-10)
uses of portable, 19: 30547
uses of pseudo-random-pulsed, for reactor reactivity measurements, (T), 19: 31541(R) (GEAP-4767)
uses of pulsed, in well logging, 17: 1640
uses of pulsed thermal, for inelastic-scattering analysis of matter, (T), 20: 6258 (CONF-650217, pp 82-101)
uses of pulsed, for analyzing heavy-water subcritical assemblies, (E), 19: 27817 (EIR-73)
uses of pulsed, for kinetics analyses in heavy water lattices, 20: 14066(R) (MIT-2344-4, pp 63-9)
uses of pulsed, in reactor physics studies, 18: 15482
uses of 100- to 400-kv, in activation analysis, 20: 29118
yield and angular distribution from Zr–tritium target, 16: 21371
yield of electron-linear-accelerator uranium-target, 19: 44860 (IAE-614)
yield of tritium (d,n), using mixed deuterium ion beams, (E), 19: 28949 (EUR-1815.e(Rev.)(p.229-34))
yield of, experimental space-integration method for, 18: 30949 (NYO-9077)
yields from, 16: 29709
yields from beryllium–plutonium, measurement of, 19: 30629(R) (MLM-1238)
yields from photo-, for activation analysis, 20: 16332 (GA-6691)
yields from polonium-, plutonium-, and radium-beryllium, 16: 24388
yields from pulsed, activation methods for measuring, 19: 14480
yields from tritium (d,n), measurement of, 19: 23615
yields from tritium (d,n), measurement by associated particle method,

19: 23613
yields of beryllium–polonium, comparison of calculated and measured, 18: 45173(R) (MLM-1203)
yields of d-d neutrons from different targets, 17: 32768
yields of 14-Mev, lead activation technique for measuring, 19: 29186
beryllium–plutonium, variation in yield determination of, 20: 9166(R) (BNWL-36, pp 2.1-58)

NEUTRON SPECTRA

agreement of one-dimensional transport theory calculations with experiment, 17: 26392(R) (GA-3853)
analysis of, computer program for, 18: 7054(R) (ORNL-3499(Vol.II) (p.120-4))
analysis of thermal-neutron-induced fast, in natural uranium, 16: 21338
analysis of time-of-flight, computer program for, 20: 16877
analysis of, least square matrix method for, 19: 2645
analysis using orthonormal expansions, (T), 19: 1535
analysis using resonance detector foils, 18: 40783 (KR-87)
angular dependence of thermal, in lattices, 17: 9477 (BNL-5924)
asymptotic and transient, for different moderators and sources, 17: 24369(R) (GA-3542)
calculation and measurement, 18: 22862
calculation for clean critical assembly with high enrichment, 18: 42938 (TID-7050(p.1245-75))
calculation for fast neutrons, computer program for, 20: 44586 (NAA-SR-Memo-12019)
calculation for graphite irradiation capsules, 18: 1297 (HW-SA-3185)
calculation for heterogeneous reactors, thermal and epithermal, 18: 36790
calculation for organic-cooled heavy-water-moderated power reactors, 17: 4306 (TID-17231)
calculation for pulsed systems, 17: 15210 (BNL-719(Vol.IV)(p.1331-59))
calculation for radiation damage experiments, 16: 22817
calculation for research reactors, 18: 38630
calculation in homogeneous reactors, computer program for, 20: 12357 (KR-75)
calculation in reactors, computer program for, 19: 40176 (AGN-TM-407)
calculation of above-thermal, 16: 24370
calculation of asymptotic thermal, in graphite, 17: 15186 (BNL-719 (Vol.II)(p.656-65))
calculation of asymptotic thermal, in infinite beryllium medium with constant plane source, 18: 7667
calculation of, by up-scattering equation, 17: 15182 (BNL-719(Vol.II) (p.570-91))
calculation of differential fast, from threshold detector data, 20: 4256
calculation of epithermal, in reactors, 18: 28536
calculation of epithermal and thermal, computer program for, 20: 4804 (KAPL-3098)
calculation of expected, for mechanical selector, 17: 24378
calculation of fast, induced in americium-243, iron-54, and nickel-58, 18: 2332
calculation of fast, in reactor pressure vessels using multigroup removal source method, 19: 3451 (AEEW-R-377)
calculation of fast, computer program for, 20: 28272 (JAERI-1104)
calculation of fast-reactor, shape function for, 20: 34933
calculation of few-group spatially dependent epithermal, variational method for, 18: 32714 (CONF-446-7)
calculation of heterogeneous water-moderated reactor, transport equation for, 18: 23030
calculation of, in infinite homogeneous media, 17: 15179 (BNL-719 (Vol.II)(p.439-63))
calculation of in-pile, for over a few hundred ev, 18: 30943 (CEA-R-2403)
calculation of infinite-medium, computer program for, 16: 29711 (HW-71953)
calculation of leakage, for highly enriched uranium solutions, 16: 3612
calculation of reactor lattice, 19: 27754 (TRG-Report-754)
calculation of region-dependent fast, computer program for, 20: 46966(R) (NAA-SR-12010)
calculation of spatial variation of, in media of varying composition or temperature, 17: 15181 (BNL-719(Vol.II)(p.565-9))
calculation of spatial variation of thermal, in lattices, 17: 15183 (BNL-719(Vol.II)(p.592-609))
calculation of spatially-dependent, 17: 26020
calculation of space-dependent neutron kinetic equations using digital computer, 18: 15439
calculation of thermal, 16: 9653 (KAPL-2000-16)
calculation of thermal, GATHER-II code for, 16: 24440
calculation of thermal, in subcritical homogeneous and inhomogeneous media, 17: 15212 (BNL-719(Vol.IV)(p.1375-90))
calculation of thermal, in polyethylene, 17: 15164 (BNL-719(Vol.I) (p.100-16))
calculation of thermal, from scattering law data, 17: 15166 (BNL-719(Vol.I)(p.121-43))
calculation of thermal, in heterogeneous media, review of theoretical methods, 17: 15178 (BNL-719(Vol.II)(p.RD1-34))
calculation of thermal, in a medium with two different temperatures, 17: 15187 (BNL-719(Vol.II)(p.666-84))
calculation of thermal, in homogeneous and heterogeneous media, 17: 15189 (BNL-719(Vol.II)(p.706-97))
calculation of thermal, and of bump in spectrum where the Maxwellian meets the 1/E tail, 17: 15184 (BNL-719(Vol.II)(p.610-13))
calculation of thermal, in reactor lattice, 17: 22820
calculation of thermal, computer program for, 17: 26391 (EUR-105.e)
calculation of thermal, SWAK program for, 17: 28243 (KAPL-M-RPC-6)
calculation of thermal, in lattice cells, SPECTROX method for, 17: 42209
calculation of thermal ,in multi-region systems , 18: 1208 (JAERI-1050)
calculation of thermal, review of, 18: 2749
calculation of thermal, methods for, 18: 2780 (CONF-39-104)
calculation of thermal, in homogeneous media, comparison of codes for, 18: 21122 (EUR-1605.e)
calculation of thermal, using scattering kernels, 18: 42600 (TID-7050 (p.330-49))
calculation of thermal, in bomb debris, 20: 5609 (LA-3403)
calculation of thermal, in reactor lattices, computer program for, 20: 8343 (ANL-7023)
calculation of thermal, for water-moderated assemblies, (T), 20: 34971
calculation of thermal, in plutonium–uranium fueled water reactors, (T), 20: 12370
calculation of, using multigroup reactor physics techniques, 17: 12722 (TID-17839)
calculation of, computer program for, 20: 4805 (ORNL-TM-1245)
calculation of, emission emerging from graphite column of thermal reactor, 18: 18853 (ZFK-TPH-8)
calculation using the modified heavy gas model and two-group theory, 16: 27727(R) (HW-73116(p.4-16))
calculation using the generalized-heavy-free-gas approximation, 17: 15185 (BNL-719(Vol.II)(p.614-55))
calculations for reactor shields, 16: 19728 (XDCL-59-2-7)
computer calculation of, based on foil data, 19: 775 (MITNE-47)
computer program for solving multigroup, 16: 24763 (TRG-Report-229)
data handling and reduction from time-of-flight facility, computer program for, 18: 44701 (GAMD-2887)
deformation in enriched heterogeneous lattices, 18: 38317 (A/CONF.28/P/675)
derivation from differential scattering cross section data and transport theory, 16: 14740
description of, in orthonormal series, 18: 26824(R) (ANL-6885)
determination by activation rate reduction, 17: 26041
determination by activation measurements for epithermal and fast neutrons, 18: 40780 (EUR-1643.e(p.205-27))
determination from D-T sources, approximate, 18: 28559
determination in Argentine Reactor RA-1, use of aluminum and manganese detectors for, 16: 7252
determination in absorber-moderator systems, tabulation, (E/T), 19: 16814 (AERE-R-4776)
determination in heavy water assemblies, activation techniques for epithermal, 20: 36524 (AE-230)
determination in liquid hydrogen, (E/T), 20: 34471(R) (GA-7064)
determination in pool reactors by activation methods, 17: 10139
determination of fast, review of activation methods for, 19: 46763 (RCN-37)
determination of, in thermal reactors, 16: 34111 (AAEC/TM-132)
determination of intermediate, review of activation methods for, 20: 13070 (RCN-40)
determination of multigroup, computer program for, 18: 34730 (KR-77)
determination of thermal, in moderated fuel elements, 17: 26802
determination of thermal, using cadmium filters, 19: 14478
determination outside shields of pulsed accelerators, 20: 2553
determination using proportional counters, orthonormal expansion methods for, 20: 43692
determination using boron trifluoride proportional counter, 20: 43694
discrepancy between calculated and measured, for one-dimensional water slabs, 17: 26392(R) (GA-3853)
distribution in core and reflector of swimming-pool reactor, 17: 17600(T) (CEA-tr-A-1194)
effects on ductility of irradiated steel, 20: 43997(R) (NRL-Memo-1663)
effects on radiation damage interpretation, 18: 2357
enhancement in beryllium-moderated reactor systems, computer program for calculating, 16: 33970 (AAEC/E-91)
equations for thermal, in reactors, 17: 17095
equations for thermal, near interface between two media, 20: 8058
errors in time-of-flight, computer program for correcting, 20: 30344 (EUR-2779.e)
evaluation of, analytic methods for, 17: 34178

expansion with foil-activation measurements, orthonormal, 18: 15426(R) (ANL-6810)
expansion with foil-activation measurements, orthonormal, 18: 19456(R) (ANL-6840)
expansion with foil-activation measurements, orthonormal, 19: 31460(R) (ANL-7010(p.179-233))
experimental and theoretical agreement of, 17: 24369(R) (GA-3542)
extraction hole effects on thermal, 16: 26199 (NP-11932)
formulation of, semi-empirical, 18: 32716
from fission, measurement by in-pile cavity method, 17: 3785
hardening of thermal, in boric acid–water solution, 19: 45226 (KFK-294)
in beryllium oxide, borated heavy water, and borated normal water, (E), 19: 8376(R) (GA-5176)
in ETR water loop, 17: 37003(R) (HW-78118)
in fast assemblies, parametric representation of, 17: 38503
in heavy water lattices, calculation of, 18: 6451
in heterogeneous assembly of heavy moderators with variable temperature, 16: 15804
in heterogeneous assemblies, 17: 9848 (KFK-108)
in heterogeneous media, theoretical analysis of, (T), 19: 8376(R) (GA-5176)
in heterogeneous reactors, theory of space-dependent, 17: 26803
in heterogeneous reactors, effects of energy dependence of diffusion coefficients on, 19: 3525
in heterogeneous thermal reactors, 17: 36896
in infinite gas, 16: 7955(R) (PR-P-51)
in moderator with temperature discontinuity, 18: 21145
in multiplying and nonmultiplying media, 17: 3736
in multiplying media, determination of asymptotic, 18: 28552
in pulsed assemblies, time-dependent, 17: 34560(R) (TID-19195)
in r-z reactor cores, computer program for, 19: 5432 (KAPL-M-6185)
in shielding materials, 17: 38416 (HW-78274)
in thermal reactors, hardening by selective absorption in fuel rods, 20: 10324 (RFR-174)
in two-region system, theory of thermal, 17: 19213
in uranium dioxide CANDU-type fuel with heavy and light water mixtures as coolants, 16: 12424 (CRRP-985C)
in uranium dioxide lattices moderated by light water-heavy water mixtures, 19: 3806(R) (KR-79)
in uranium–heavy water lattice cells, 18: 3092 (AE-123)
in uranium-water lattices, computation of, 17: 18996
in VVR-S reactor, epithermal, 18: 43033 (PAN-505/1X-A)
measurement, 17: 9488
measurement, 17: 16438
measurement above 0.5 Mev, using emulsions, 16: 28614
measurement at various Hanford plant areas, (E), 19: 20201 (HW-SA-3525)
measurement at 0.5 to 14 Mev using threshold reactions, 16: 27308
measurement at 0.6 to 16 Mev, development of activation detectors for, 17: 26394 (LAMS-2883)
measurement at 2.34 to 10.4 kev using a chopper, 16: 25586
measurement at 2.5 to 30 Mev using threshold detectors, 18: 7061 (UCRL-10732)
measurement at 2.5 to 30 Mev, technique for, 19: 9538
measurement by foil techniques, threshold parameters for, 18: 16367
measurement by modulation of target potential, 20: 19890
measurement by proton recoil telescope and nuclear emulsions, 17: 8648
measurement by resonance detector foils, 16: 4336
measurement by sandwich foils, 17: 32418
measurement by scanning proton recoil in emulsion, 18: 13028 (AWRE-NR-5/63)
measurement by time-of-flight, 17: 10240(R) (NP-12208)
measurement by time-of-flight and foil techniques, in water and boric acid solutions, 17: 15173 (BNL-719(Vol.II)(p.318-36))
measurement by time-of-flight techniques, 18: 15482
measurement, foil technique for, 16: 14946
measurement from reactors during steady state on pulsed operation, 16: 30570 (BNL-4795)
measurement in Aquilon reactor, (E/T), 20: 3582 (CEA-R-2482)
measurement in blocks of depleted uranium, 20: 34962
measurement in bulk media, 20: 44580 (CONF-660303, pp 782-95)
measurement in depleted uranium using pulsed sources, (E/T), 20: 14202
measurement in fast reactors using resonance absorbers, 16: 7694
measurement in fast reactors using recoil-proton methods, 17: 34285
measurement in fast reactors, subcritical facility for, 19: 38128 (KFK-302)
measurement in fast reactors, performance of foil detectors for, (T), 20: 8346 (EUR-2532.e)
measurement in heavy-water lattices, 17: 15193 (BNL-719(Vol.III)(p.879-99))
measurement in heavy water-moderated aluminum-plutonium-fueled reactor, 20: 46964(R) (BNWL-284)
measurement in HERALD thermal column, (E), 20: 5191 (AWRE-R-4/65)
measurement in heterogeneous lattices, 17: 15177 (BNL-719(Vol.II)(p.411-36))
measurement in heterogeneous media, integral and differential, 20: 3600
measurement in heterogeneous assemblies, methods for, (E/T), 20: 4801(R) (GA-6634)
measurement in heterogeneous assemblies, techniques for, 20: 19778(R) (GA-6824)
measurement in hydrogenous moderators using pulsed sources, (E/T), 20: 13737
measurement in JUGGERNAUT and ZPR-VI, (E), 19: 17177(R) (ANL-6965(p.42-83))
measurement in laminated iron–water, performance of threshold detectors for, 20: 1304 (AE-196)
measurement in moderators and reactor lattices, use of pulsed sources for, (E/T), 20: 13735
measurement in NRL Research Reactor, 20: 16335(R) (NBS-TN-276)
measurement in paraffin, 20: 2931 (AD-616518)
measurement in poisoned heavy water and water, (E), 19: 5114(R) (GA-5486)
measurement in poisoned heavy water and water, (E), 19: 41646
measurement in PRTR fuel clusters, 19: 25759(R) (HW-84369(p.39-43))
measurement in reactors, significance of, 17: 3541 (TID-17211)
measurement in reactors, 17: 11594 (SCTM-205-62(53))
measurement in reactors by use of activation foils, 17: 31669 (AAEC/TM-191)
measurement in reactors, 18: 35066 (STI/DOC/10/28(p.73-7))
measurement in reactor channels and cores using resonance detectors, 19: 25693
measurement in reactors using threshold detectors, 20: 1414
measurement in reactors, methods for, 20: 22382 (RT-FI(65)57)
measurement in reactors, review of methods for, 20: 40378
measurement in thermal reactor during moderation, effects of absorption and leakage on, 18: 4521
measurement in uranium-heavy water lattices of thermal, 17: 15172 (BNL-719(Vol.II)(p.305-17))
measurement in VERA using fast pulsed sources, (E/T), 20: 14086
measurement in water for determining temperature of neutron gas, 18: 4516
measurement in water-moderated bare homogeneous assemblies using fission chambers, 18: 26885
measurement in ZEEP by reaction rates with selected nuclides, 16: 17233 (CRRP-985-D)
measurement near a cadmium disk using foil activation, 17: 15176 (BNL-719(Vol.II)(p.401-10))
measurement, nuclear emulsion technique, 16: 22327 (NARF-61-36T)
measurement of, and its influence on primary knock-on atom spectra in finite test specimens, 17: 34292
measurement of asymptotic and steady-state, in multiplying media (E), 19: 3191(R) (RPI-328-16)
measurement of, at 0.5 to 15 Mev, 17: 14933 (EANDC(OR)-19(L))
measurement of, by time-of-flight, 17: 15218 (PAN-353/I-A)
measurement of, by reduction of thermal activation rates, 17: 33245 (WAPD-T-1582)
measurement of deviation from 1/E distribution in epicadmium, 18: 34735
measurement of differential and integral, in heavy water-moderated reactors, 20: 45090
measurement of, effects of linear accelerator intensity, neutron source, precollimator, and scatterer on, 17: 24369(R) (GA-3542)
measurement of effective temperature of thermal, 18: 30694
measurement of epithermal, in reactors, 17: 31694
measurement of fast, using threshold-detector activation, 16: 26530
measurement of fast, in civilian power reactors, 17: 34296
measurement of fast, using threshold detectors, 18: 2020 (EUR-289.e)
measurement of fast, by method of counting efficiencies, 18: 7072
measurement of fast, using lithium-6 semiconductor counter telescope, 18: 23986
measurement of fast, from bremsstrahlung interactions in lead, (E), 19: 25455 (ORNL-TM-1087)
measurement of fast, using (n,α) and (n,p) reactions in silicon diodes, 19: 28661
measurement of fast, for determination of given radioisotope in mixture of radioisotopes, 19: 30131
measurement of fast, by magnetic analysis of neutron-induced charged particles, (E/T), 19: 31460(R) (ANL-7010(p.179-233))
measurement of fast, from photon reactions with lead and uranium-238, (E), 20: 29529(R) (RPI-328-56, pp 94-112)
measurement of fast, calibration of large proton-recoil detector for, 20: 43669 (CONF-661001-4)
measurement of fast, using threshold foil activation, 20: 46575
measurement of, from pulsed sources and reactors, 17: 9494
measurement of indices in reactor of, by oscillation method, 18: 33021 (LFEN-N1.12)

measurement of leakage, near critical assemblies, 17: 34275
measurement of leakage, from uranium-235 spheres, 20: 21939(R) (GA-6930)
measurement of low-energy, in-core, 18: 42941 (TID-7050(p.1357-96))
measurement of pulsed-chopped, 16: 29883(R) (TID-16309)
measurement of reactor, using threshold detectors, 18: 31912 (NP-14089)
measurement of, status of technique development for, 16: 31052 (GA-3176)
measurement of stationary, mean emission time correction for pulsed-source (T), 19: 3514 (GAMD-4131)
measurement of temperature distribution in core of VVR-S reactor, 18: 38638
measurement of thermal and resonance fluxes at irradiation locations in FRM, 16: 15998 (FRM-26)
measurement of thermal, in graphite-moderated reactor, 17: 15175 (BNL-719(Vol.II)(p.359-400))
measurement of thermal, in homogeneous medium with two different temperatures, 17: 26755 (EUR-23.e)
measurement of thermal, in graphite assemblies, 18: 33028
measurement of thermal, across discontinuity in properties and temperature, 20: 8057
measurement of thermal, by neutron activation, 20: 20200(R) (ANL-7110, pp 29-98)
measurement of thermal, in beryllium oxide, 20: 21939 (GA-6930)
measurement of, using decay spectrometers, 18: 2082
measurement of, using multiple-threshold detectors, 18: 2083
measurement of, activation detector development for, 20: 33628(R) (NAA-SR-Memo-11816)
measurement of, effects of gamma radiation on, 19: 40122(R) (GEAP-4862)
measurement of, from americium–lithium sources, 20: 20201(R) (ANL-7110, pp 311-401)
measurement of, using pulse analyzers, 19: 26922(R) (PR-P-64)
measurement program for fast neutron, 20: 46561(R) (RPI-328-68, pp 63-83)
measurement using threshold detectors, in-pile, 17: 34286
measurement using foils, accuracy improvement in, 18: 11512(R) (NARF-63-9p)
measurement using foil activation in heavy- and light-water reactors and shields (E/T), 19: 3771 (AE-155)
measurement using resonance activation, 20: 2971
measurement using Fermi chopper, 20: 2994
measurement using nuclear emulsions, 20: 5196(R) (IS-1200(Sect.E))
measurement using europium-activated lithium iodide phosphors, 20: 11116
measurement using Bonner sphere and nuclear emulsions, performance for, 20: 29522 (CONF-651109, pp 286-305)
measurement using nuclear emulsions, techniques for fast, 20: 29848 (CONF-651109, pp 199-212)
measurement using time-of-flight technique, 20: 46574
measurement with MIT fast chopper, 16: 24369
measurements, development of equipment for, 16: 2566(R) (TID-14187)
measurements, factors influencing, 16: 15612 (GA-2544)
measurements in heterogeneous media, 17: 15174 (BNL-719(Vol.II) (p.337-58))
measurements in reactors using emulsions, plate scanning microscope for, 19: 34440
measurements of, asymptotic, 17: 2341(R) (TID-17186)
measurements of asymptotic, in multiplying media, 17: 32971 (CONF-11-6)
measurements of fast, analysis of reliability of matrix models and methods for, 18: 26120
measurements of fast and intermediate, in bulk media, adequacy of, 20: 34905 (GA-7059)
measurements of very hard thermal, deviations from Maxwell shape in, 19: 31201 (ZfK-RN-25)
measurements of, using semiconductor detectors, 18: 23884 (NP-13930(p.159-77))
measurements using bubble chambers, 16: 20683
modification of thermal flux in research reactors, 18: 38631
neutron conservation in experimental, 17: 26392(R) (GA-3853)
neutron energy in, method for determining maximum, 19: 34505
neutron temperature measurement in RFR by activation probe method, 18: 38640
normalization for radiation damage in silicon, 19: 34747 (NAA-SR-10612)
of mixtures of two noninteracting gases heated to various temperatures, 16: 19730
perturbations of thermal, near absorbers, 18: 15460
prediction of spatially dependent, at energies above thermal, 16: 28413 (TID-16220)
pulsed, effects of reflectors on, (E), 19: 8376(R) (GA-5176)
radiation damage dependence on, 16: 24636
radiation damage dependence on, 16: 24638
research on time-dependent, 17: 22666(R) (TID-18561)
sensitivity of transient, to different scattering kernels, 17: 3737
shape analysis of time-of-flight, computer program for, 20: 19833 (RT/FI-(65)48)
size effects on, 17: 26392(R) (GA-3853)
spatial dependence across absorption and temperature discontinuities, 17: 24369(R) (GA-3542)
spatial dependence of thermal, across temperature and absorption discontinuity, 17: 26029
thermalization in reactor moderators, 17: 4029
time dependence of, in D_2O (E/T), 19: 3191(R) (RPI-328-16)
time dependent fast, space independent thermalization, 16: 18413
use of thermal, for reactor design, 20: 22376 (GA-6901)
variation of fast, with distance from source, 17: 34297
variation with burnup in Russian VVR-S reactor, 18: 38641
without high-energy component, system for obtaining, 17: 24369(R) (GA-3542)

Neutron Spectrographic Analysis
see Neutron Spectroscopy

NEUTRON SPECTROMETERS

accessories for, 16: 30717(R) (ANL-6516)
analyzers and polarizers for, preparation of single-crystal, 17: 30804
background determination for time-of-flight, method of, 19: 813
beam divergence in, equations for maximum, 17: 23749
beam intensity measurements for chopper, thermal, (T), 20: 24314
Bonner spheres with, data from, 17: 18377 (TID-7652(p.523-94))
book: *Scintillation Spectrometry of Gamma Emissions and Fast Neutrons*, 18: 39690
boron-10 absorbers for, fabrication of compact, 20: 41272(R) (ORNL-3875, pp 53-74)
burst shape measurement and prediction for multi-rotor choppers, 18: 20339 (TID-20504)
burst shape measurement and prediction for, 19: 7817
calibration and development of 4π-recoil, 19: 31460(R) (ANL-7010 (p.179-233))
calibration and performance of triple-table, 18: 5636 (PAN-270)
calibration and testing of Perlow, 16: 22326 (HW-69471)
calibration by nuclear emulsions, 18: 16358
calibration of in-pile, 19: 35368
calibration of Perlow, 17: 1175(R) (HW-70050(p.31-77))
calibration of slow choppers, 16: 14066
calibration of time-of-flight, for fast neutrons, (E), 19: 26674
characteristics and construction of curved slit neutron shutter for thermal and cold neutron range, 16: 10203
characteristics of epithermal, using semiconductors, 16: 13315
characteristics of time-of-flight, nomographs of, 16: 22363
characteristics of r-f polarized, 18: 20368
characteristics of curved-crystal, using various crystals as monochromators, 19: 6184 (IDO-17022)
chopper arrangements and characteristics at NRU reactor, 16: 3208
chopper calculations for divergent beam geometries in, 18: 20385
chopper design and operation for, rotating mechanical, 20: 29555
chopper rotor burst shapes, use of P-gram construction in calculation of, 17: 18547 (TID-18396)
chopper rotor deformation above 19,000 rpm, 16: 14070
chopper techniques and uses, 16: 14065
choppers for crystal, engineering drawings for, 18: 43992
choppers for slow neutrons, design and performance of, 19: 18300
choppers for, calculational method for multirotor, 18: 30040
choppers for, design of three-rotor, 18: 20388
choppers for, for wavelength range 7 to 15 Å, 20: 21007
circuit design and operation for fast, 16: 5519
circuit design for time-of-flight, walk-correction, 20: 5796
circuit for improving resolution in time-of-flight many-layer, 18: 20338 (PAN-469/I)
circuits for fast time-of-flight, problems with, 20: 46082
coincidence system for time-of-flight, design of fast-slow, 18: 5650
construction and calibration of long, 16: 23849 (TID-15746)
construction of fast chopper for resonance neutrons, 20: 23500
construction of lead slowing-down-time, 19: 15926
control circuits for automatic operation of crystal, 19: 36801 (AEET/NP/12)
control of synchronous motors in chopper, 20: 11177 (UJV-1388/65)
control of systems of, computer, 18: 33876 (BNL-8180)
control of, using IBM-1620 computer, 18: 24009
control system for triple axis, programmed automatic, 20: 31543
control systems for, description of automatic preprogrammed, 17: 32433
controller and digital read-out system for, tape-programmed, 19: 18255 (ELI-89)
converter for, time-to-pulse height, 19: 26695
converters for time-of-flight, time-to-pulse height, 18: 30014
counting rates in, sample orientation effects on, 17: 18605 (TID-18405)
cross section measurements with fast choppers, 17: 4037

data acquisition and processing system for time-of-flight, performance of computer, 20: 4245 (ORNL-P-1723)
data analysis and control system using digital computer, 20: 21982 (BNL-948, pp 718-40)
data control and processing system for, automatic, 18: 2024 (RT/EL(63)9)
data corrections for helium-3, computer program for, 20: 19047 (UCRL-16595)
data processing for, design of devices for, 16: 33168(T) (AEC-tr-5411)
data processing system for time-of-flight, computerized, 18: 33958
data processing, design of tape-to-card converter for, 16: 8826 (AERE-R-3346)
data readout system for time-of-flight, design of, 20: 29566
data recording system design for multichannel, 16: 22377
data recording system for, design of automatic, 18: 18215
data unfolding techniques for contoured semiconductor, 20: 33627(R) (N-66-10648)
description of, at CNEN, 17: 15241
description of chopper, (E), 19: 18098 (KAPL-3074)
description of combined crystal-chopper unit, 19: 3806(R) (KR-79)
description of crystal and time-of-flight types, 16: 18463
description of crystal, 17: 7070
description of crystal, long-wavelength, and powder, 17: 37801
description of crystal, at installations in India, 20: 5715 (AEET-227)
description of fast, (E), 19: 22695 (IEA-83)
description of phased-rotor, for neutron scattering experiments, 17: 22308
description of pulse-shape discriminator and unscrambling code for proton-recoil scintillation, 19: 30527 (ORNL-P-1110)
description of thermal-neutron time-of-flight, (E), 19: 9480 (JINR-P-1899)
description of time-of-flight, for 0.005 to 100 ev, 16: 1184 (AERE-R-3829)
description of time-of-flight, for D-D neutrons, 18: 16323
description of time-of-flight fast, 20: 7429
description of, using protons from neutron beta decay, 18: 14285
design, 16: 33171
design, 17: 15213(R) (GA-3409)
design, 17: 31259 (CONF-16-2)
design, 18: 11269
design, 19: 1940
design, 19: 8670
design, 20: 39255
design, 19: 26917(R) (IA-984)
design, 18: 21708(R) (MLM-1178)
design, 20: 7315(R) (ORNL-3849, pp 151-82)
design, 18: 15612 (UCRL-7611)
design and calibration of associated-particle time-of-flight, for nanosecond operation, 17: 26624
design and calibration of spherical, 19: 26709
design and characteristics of new type, for fast neutrons, 17: 18625
design and construction of single crystal, 16: 24650
design and construction of double-crystal, 16: 33198
design and construction for fast neutrons, 20: 38159
design and construction of broad range magnetic, 20: 39194 (AD-638137)
design and development, 17: 4807 (MITNE-8)
design and development of third axis for crystal-type, at Chalk River Plant, 17: 18595 (CRGP-956)
design and evaluation for time-of-flight measurements, 16: 8906 (ORO-462)
design and operation of fast-slow coincidence scintillator, 16: 30592 (UCRL-5975)
design and operation of, 18: 16352
design and operation of Universal Spectrometer I for use at Brookhaven, 18: 27749 (BNL-851)
design and operation of solid-state, (E), 19: 17177(R) (ANL-6965 (p.42-83))
design and operation of, using two window filters, 19: 15931
design and operation of semiconductor, for in-core measurements, 19: 44450(R) (IBK-120a)
design and operation of rotating crystal, for FRJ-2, 20: 28836 (JUL-338-NP)
design and operation of cold-neutron time-of-flight, 20: 31567
design and operation of Karlsruhe crystal, 20: 35787
design and performance of fast, 16: 6584
design and performance of two-crystal, using neutron recoil with neutron scattering in coincidence, 16: 10204
design and performance of proton-recoil, using liquid hydrogen radiator, 16: 10238
design and performance of rotating-crystal in time-of-flight measurements, 16: 14071
design and performance of fast choppers, 16: 18459
design and performance of ORNL fast-chopper time-of-flight, 16: 18460
design and performance of silicon surface-barrier-type, for fast neutrons, 16: 20745
design and performance of gaseous scintillation, using helium-3, 16: 20710
design and performance of scintillation, 16: 25549 (ASD-TDR-62-52)
design and performance of the JAERI crystal-type, 16: 25557 (JAERI-1030)
design and performance of fast, using silicon surface-barrier semiconductor detector, 16: 27263 (TID-16326)
design and performance of gaseous scintillation, using helium-3, 16: 31836(T) (AEC-tr-5367)
design and performance of chopper, 16: 31850
design and performance of organic crystal, 16: 31856
design and performance of time-to-pulse height converter for, 16: 33231
design and performance of proton-recoil, using a hydrogeneous radiator and a semiconductor detector, 17: 3308 (NP-12226)
design and performance of proton-recoil proportional, with gamma discrimination, 17: 6462
design and performance of single-crystal, 17: 22016
design and performance of gamma-insensitive, 17: 23757
design and performance of time-of-flight, 17: 38039(T) (AEC-tr-5734 (p.227-31))
design and performance of helium-3, 17: 39415 (UCRL-6911(Pt.I))
design and performance of chopper, 18: 6990 (BLG-189)
design and performance for WWR-type reactors, 18: 8686
design and performance of neutron-decay-type, 18: 12478
design and performance of multiple-threshold, 18: 12479
design and performance of crystal, 18: 14232
design and performance of time-of-flight, 18: 33944
design and performance of time-of-flight, for measurement of total neutron cross sections, 19: 5147
design and performance of single-crystal, 19: 9540
design and performance for Swedish reactors, 19: 11603
design and performance, 19: 13695
design and performance, 19: 22785
design and performance of scintillation time-of-flight, 19: 28642
design and performance of crystal, 19: 34559
design and performance of lightweight fission, for energies from thermal to Mev, 19: 34563
design and performance of DIDO triple-axis, 19: 46753 (AERE-R-4895)
design and performance of time-of-flight, 19: 46829
design and performance of hybrid system, 20: 7445(T)
design and performance of solid-state, for 15- to 35-Mev neutrons, 20: 11139
design and performance of gamma-block stilbene, 20: 13063 (JAERI-1092)
design and performance for polarization analysis, 20: 14856 (KFK-345)
design and performance of helium-3, 20: 19047 (UCRL-16595)
design and performance of lithium-6-semiconductor, for fast neutrons, 20: 21034 (EUR-2712.e)
design and performance for neutron small-angle scattering experiments, 20: 28255
design and performance of fast chopper with adjustable slit, 20: 28257
design and performance of time-of-flight, with rotating-crystal chopper, 20: 27344
design and performance of fast chopper with adjustable slit, 20: 28848
design and performance of time-of-flight, 20: 31566
design and performance of multi-arm, 20: 33617 (BNL-940, pp 179-82)
design and performance of FR-2 rotating-crystal, 20: 35160
design and use of fast chopper for epithermal region, 16: 25586
design and uses of time-of-flight, for pulsed Triga reactor, 18: 15607 (GA-3075)
design, calibration, and use of fast delayed coincidence, 17: 11627 (TID-15088)
design for analysis of proton-nuclei interactions at 50 to 700 Mev, 17: 12796(R) (ORNL-3360(p.286-95))
design for Bulk Shielding Facility, 20: 5181(R) (ORNL-3029)
design for elastic, inelastic, and quasi-elastic scattering measurements, three-rotor chopper, 17: 15233
design for energies below 15 Mev, 19: 15872(R) (ORNL-3714(Vol.I) (p.78-86))
design for energies between thermal and 10 kev, 19: 15872(R) (ORNL-3714(Vol.I)(p.78-86))
design for fast and slow neutron, 20: 21140(P)
design for fast neutrons using silicon surface barrier detectors, 18: 18177 (TID-20418)
design for fast neutrons, 18: 39707(P)
design for High Temperature Lattice Test Reactor, 18: 22335(R) (HW-80020(p.14-22))
design for high-intensity time-dependent fast neutron environment, 18: 24008
design for measurement in strong background, 18: 5632(R) (ORNL-3499 (Vol.I)(p.181-7))
design for neutron decay spectrometry, 18: 22363
design for pulsed fast reactor SORA, 18: 6519 (EUR-490.e)

design for slow neutrons, 20: 13065 (JUL-295-NP)
design for slow neutrons, 20: 42681(R) (IS-1500(Sect. R))
design for use in DIDO Reactor, 16: 18442
design for use in gamma scattering experiments, 18: 43114(R) (NP-14236)
design of address scaler and temporary memory for a transistorized time-of-flight analyzer, 16: 20763
design of associated-particle time-of-flight, (E), 20: 13088
design of, at MIT reactor, 17: 10141
design of automatic low-temperature, 19: 778(R) (ORNL-3676(p.47-8))
design of boron trifluoride, 19: 24874(P)
design of crystal, 16: 3960
design of crystal-type, 16: 18464
design of crystal, for measurement of neutron widths scattering, 17: 15287
design of crystal, engineering drawings for, 17: 18647
design of crystal, 17: 38040(T) (AEC-tr-5734(p.232-4))
design of crystal, for producing polarized beams, 17: 41281
design of crystal, for measuring small changes in effective neutron temperature in TRIGA-Mark (II), 19: 29786
design of curved-crystal Cauchois-type, 16: 18465
design of curved-slit, 16: 27273
design of curved-slit chopper, 17: 38042(T) (AEC-tr-5734(p.244-6))
design of devices for processing data from, 16: 20771
design of diffractometer for crystalline samples, 16: 25593
design of double, 20: 4476(R) (IS-1200(Sect.P))
design of double slow, 17: 15235
design of fast and slow, 20: 39261
design of fast chopper, 17: 8587 (AWRE-NR/P-4/62)
design of fast time-of-flight, for tandem accelerator, 17: 6465
design of fast, using surface-barrier diodes, 18: 2098
design of fast, using two semiconductor detectors spaced by lithium fluoride, 18: 18243(P)
design of fast, using semiconductor detectors, 18: 43942 (TID-21202)
design of fast, using stilbene crystal and photomultiplier, 19: 30574
design of flexible pulsed-beam rotating-crystal, for scattering studies, 19: 28632 (KFK-263)
design of, for fast neutron time-of-flight measurements, 16: 33153 (PAN-324/I-A)
design of, for production of short monoenergetic neutron bursts, 16: 30573 (GAMD-1961)
design of helium-3-filled ionization-chamber, 17: 2291
design of helium-3 fast, 17: 8584(AD-286928)
design of isochronous flight path, for fast neutrons, 17: 30797 (CONF-22-12)
design of liquid helium-3, 19: 40928(P)
design of liquid-helium time-of-flight coincidence, 20: 8165
design of lithium-6 sandwich semiconductor, for epithermal range, (E), 20: 5714 (AD-623722)
design of magnetic, for neutrons from 1 to 15 Mev, 19: 28671
design of mechanical chopper, with synchronous rotating collimator, 17: 41267
design of multi-rotor fast chopper, 16: 18461
design of multi-rotor choppers, 17: 38041(T) (AEC-tr-5734(p.240-3))
design of nanosecond-range time-of-flight, for fast neutrons, 16: 11882
design of nanosecond time coder with large analysis range for time-of-flight, 18: 24018
design of nanosecond time coder with large analysis range for, 18: 24019
design of neutron guide at FRM Reactor, 16: 19117
design of neutron guide at FRM reactor, 16: 27272(T) (SCL-T-421)
design of nonpulsed time-of-flight, 20: 44592
design of polarization, for HFBRR, engineering drawings for, 20: 672
design of precision crystal, 18: 23881 (NP-13930(p.128-9))
design of proton recoil telescope as, 17: 8649
design of proton-recoil, using solid-state detectors, 18: 41795
design of proton-recoil and semiconductor, (E), 19: 17156(R) (EUR-2197.d)
design of proton-recoil, using semiconductor detectors, 19: 22730
design of proton-recoil, for fast neutrons, 19: 26693
design of proton-recoil, for fast, 19: 28691
design of proton-recoil, for fast neutrons, 19: 34490
design of proton-recoil, for fast neutrons, 20: 11096 (EUR-2491.e)
design of proton-recoil, using semiconductor detectors, 20: 19018(R) (ANL-7110, pp 231-310)
design of proton-recoil, 20: 46049(R) (ORNL-3973(Vol.2), pp 96-103)
design of recoil, for fast neutrons, 18: 20365
design of remotely operated low-energy, 20: 41272(R) (ORNL-3875, pp 53-74)
design of resonance neutron chopper, 18: 12463 (PAN-442/I,I-A)
design of resonance, 18: 12464 (PAN-443/I,IA)
design of rotating-crystal, with mechanical energy preselector, 17: 37424
design of rotating-cyrstal, 18: 23879 (NP-13930(p.126))
design of scintillation time-of-flight, 19: 20355
design of semiconductor, 17: 41238 (AD-289566)
design of shielded-diode, 19: 23996(R) (ORNL-3650(p.1-110))
design of silicon-gold surface barrier, for fast neutrons, 16: 3854(R) (ORNL-3193(p.119-23))
design of silicon-gold surface barrier, for fast neutrons, 16: 3853(R) (ORNL-3193(p.116-19))
design of silicon diode, for flux measurement in swimming pool reactors, 20: 27352
design of silicon-junction fast, 18: 18206
design of slow chopper at Ispra I reactor, 16: 14068
design of slow-chopper time-of-flight, 18: 494 (RT/FI(63)-26)
design of slow-neutron chopper for, 16: 8896 (AERE-R-3779)
design of slowing-down-time lead, for nondestructive assay of plutonium-239 and uranium-235 in fuels, 20: 7014 (NP-15688)
design of solid-state, 19: 23991(R) (ANL-7003)
design of spark, 16: 14978(P)
design of telescope-type, 18: 6411(R) (ANL-6706)
design of time-of-flight, using semi-monochromatizing chopper, 16: 14069
design of time-of-flight, for fast neutrons, 16: 22355
design of time-of-flight, for slow neutron cross section measurements, 16: 33199
design of time-of-flight, for cyclotrons, 17: 361 (NYO-9360)
design of time-of-flight, for neutrons from proton reactions, 17: 18377 (TID-7652(p.523-94))
design of time-of-flight, engineering drawings for, 17: 36174
design of time-of-flight, engineering drawings for, 18: 5678
design of time-of-flight, 18: 11482 (HW-79054(p.47-53))
design of time-of-flight, for cyclotrons, 18: 14215 (NP-13641)
design of time-of-flight, for linear accelerator, 18: 14216 (NP-13702)
design of time-of-flight, 18: 14230
design of time-of-flight, with variable-bandwidth encoder, 18: 20363
design of time-of-flight, for fission neutrons, 18: 20384
design of time-of-flight, for fast neutrons, 18: 23882 (NP-13930(p.144-6))
design of time-of-flight digital system for, 18: 24022
design of time-of-flight, for thermal velocities, 18: 25863
design of time-of-flight, 18: 30024
design of time-of-flight, for thermal neutrons, 18: 30025
design of time-of-flight scintillation, 18: 34752(R) (CU(PNPL)-234)
design of time-of-flight, for use with pulse-height analyzers, 18: 39606 (AAEC/TM-259)
design of time-of-flight, for angular distribution measurements, 18: 39669
design of time-of-flight, 18: 41830
design of time-of-flight, 18: 41831
design of time-of-flight, with gamma-neutron discrimination, 18: 41832
design of time-of-flight, using recoil alpha particles, 19: 4489
design of time-of-flight, with nanosecond resolution, 19: 13749
design of time-of-flight, 19: 13786
design of time-of-flight, for fast neutrons, 19: 18273
design of time-of-flight transistorized, (E), 19: 22686 (CEA-R-2405)
design of time-of-flight, for continuous fast-neutron beams, 19: 43392
design of time-of-flight, using avalanche transistors, 20: 21110
design of time-of-flight encoder for, 20: 37067 (AECL-2578)
design of time-of-flight, 20: 46574
design of time-selector for choppers, for two-dimensional analysis, 20: 13075 (UJV-1450/65)
design of transistorized 1024-channel time-of-flight, 16: 14087
design of transistorized 1024-channel time-of-flight analyzer, 16: 20762
design of twin-rotor type for solid-state research, 16: 7152
design of two-dimensional selector, 16: 20765
design of, using semiconductor triodes, 16: 33211
design of vertical-arm, engineering drawings for, 17: 32454
design of 1024-channel magnetic drum time analyzer for, 16: 20779
design of 2-rotor, 17: 19559(T) (UCRL-Trans-899(L))
design of 20-MHz transistorized timer for, 16: 20766
design of 200-m time-of-flight, 18: 14275
design of 256-channel time-of-flight, with magnetic memory, 18: 14262
design of 3-nsec time-of-flight, 16: 11907
design of, using back-scattering of protons from polyethylene films, 18: 23883 (NP-13930(p.147-57))
design of, with two scintillators, 20: 21143(P)
design parameters for choppers, 16: 3180 (ANL-6449)
design using photographic film detector, 18: 12444 (AD-415810)
design using two semiconductor detectors, 18: 23884 (NP-13930(p.159-77))
design with four choppers for study of thermal neutron scattering, 16: 7151
design with lithium-6 target and silicon diodes, 16: 13754
development, 16: 1944(R) (ORNL-3189(p.172-9))
development, 17: 2051(R) (CU(PNPL)-219)
development, 17: 14933 (EANDC(OR)-19(L))
development, 18: 42622(R) (ANL-6879(p.2-20))
development, 18: 11195(R) (EANDC(E)-49(L))
development, 18: 14590(R) (NIRL/R/60)

development, 18: 27753(R) (ORNL-3578(p.6-36))
development, 20: 5737(R) (ORNL-3858(Vol.I), pp 59-64)
development and performance, 19: 7205(R) (ORNL-3697(p.159-64))
development and performance of rotating-crystal, 19: 35378(R) (EANDC(E)-57(U))
development and performance of, 20: 12545(R) (PAEC(A)AR651)
development and testing, 17: 36347(R) (NARF-62-18P)
development and use of, in cross section measurements, 17: 17623(R) (IDO-16827)
development and use of, 17: 41873 (WASH-1044)
development for epithermal neutrons, 20: 46048(R) (ORNL-3973(Vol.1), pp 60-4)
development for fast and intermediate neutrons, 19: 11532
development for integral neutron thermalization measurements, 16: 15612 (GA-2544)
development for low thermal energies, 17: 35253(R) (IA-775)
development for measurement of double-differential scattering cross sections, 18: 8912(R) (HW-78388(p.10.1-25))
development for use with Nevis synchrocyclotron, 17: 31077(R) (CU(PNPL)-228)
development of, 20: 23808(R) (NIRS-4, pp 3-12)
development of activation detectors for, for 0.6 to 16 Mev, 17: 26394 (LAMS-2883)
development of charged-particle-collimated lithium-6-fluoride, 20: 46043 (MLM-1339)
development of epithermal, 20: 5737(R) (ORNL-3858(Vol.I), pp 59-64)
development of fast, 16: 16520 (CEA-2002)
development of fast, for in-pile measurements, 17: 42236
development of fast, using lithium-6 sandwich, 19: 3785
development of fast, for reactor shielding measurements, 19: 2642
development of fast, using 4π recoil proportional counting, 19: 2643
development of fast, for measuring recoil proton track lengths, 19: 7538(R) (ORNL-3697(p.113-30))
development of helium-3, 17: 15251(R) (CU(PNPL)-220)
development of helium-3-filled proportional counter as, 18: 12453 (CONF-340-15)
development of helium-3, 19: 2646
development of lithium-6-loaded glass scintillation, 16: 27382
development of lithium-6 fluoride-sandwiched silicon, 20: 43718
development of multisphere, 19: 46757 (CEA-R-2772)
development of proton-recoil, for 10 to 450 Mev, 18: 7051(R) (ORNL-3499(Vol.II)(p.109-11))
development of proton-recoil scintillation, 19: 2647
development of proton-recoil scintillation, 19: 15872(R) (ORNL-3714 (Vol.I)(p.78-86))
development of punched-card readout system for, 17: 356 (CREL-1073)
development of rotating-crystal, 18: 10376(R) (HW-79054(p.82-9))
development of scintillation time-of-flight, 19: 18296
development of semiconductor proton recoil telescope, 19: 11533
development of slowing-down-time lead, for nondestructive assay of plutonium-239 and uranium-235 in fuels, 19: 30082 (NP-14969)
development of stilbene-crystal, 17: 20564(R) (TID-18442)
development of thin radiator telescope, 19: 18303
development of time-of-flight, summary, 17: 18549(R) (TID-18408)
development of time-of-flight, 18: 27793
development of time-of-flight, for photoneutrons, 19: 18298
development of time-of-flight with large memory capacity, 19: 47115(R) (ANL-6983)
development of time-of-flight, using computers, 19: 47336
development of, using helium-3(n,p) reaction, 18: 8614(R) (PR-P-59(p. 46-64))
development of velocity-type, 16: 12211(R) (CU(PNPL)-208)
development of velocity-type, 16: 13689(R) (CU(PNPL)-211)
development of velocity-type, 16: 13690(R) (CU(PNPL)-212)
development of 30,000-rpm chopper, 17: 22666(R) (TID-18561)
development using lithium-6 (n,t) reactions, 19: 11534
developments in technique for Nevis, 17: 41996
diagnostic use for deuterium plasma thermonuclear reactions, 19: 19251 (NP-14689)
dimensions, calculating optimum, 16: 5502(T) (CEA-tr-X-404)
discriminators for time-of-flight, design of fast, 17: 30805
drive units for time-of-flight, improved hydrostatic bearings for, 17: 18588 (AERE-R-4214)
efficiency and resolution of proton-recoil, computer program for, 18: 7053(R) (ORNL-3499(Vol.II)(p.115-19))
efficiency and resolution of Rubbine proton-recoil, 19: 7781 (AERE-R-4686)
efficiency for intermediate energy neutrons, 16: 33217
efficiency of neon-21 filled, 16: 6596
efficiency of semiconductor-sandwich, (E), 20: 4238 (EUR-2487.e)
efficiency of stilbene crystal fast, matrix treatment for, 19: 44492
electronic equipment for automatic facility for, 16: 27290
energy and flux calculations for double-rotor chopper, 17: 30818
energy spectrum from double-reflection, 17: 36108 (AERI-P/R-4)
experience with Yugoslav three-crystal, 19: 4486(T) (AEC-tr-6227/2 (p.113-29))
fabrication and testing of gamma insensitive, 19: 34540
facilities for low-energy neutron cross section measurements, summary of U. S., 18: 29976 (EANDC(US)-46U)
filter, performance of beryllium crystal for removal of high orders in thermal region of crystal type, 16: 8956
firing control system utilizing thyratrons, 16: 13689(R) (CU(PNPL)-211)
firing control systems using thyratrons, 16: 13690(R) (CU(PNPL)-212)
focusing effects in triple-axis, 18: 4100
focusing of triple-axis, graphical method for, (T), 19: 26668 (RCN-34)
helium-3, design and range extension of, 16: 31831 (UCRL-6911(Pt.II))
helium-filled proportional counter, design of, 20: 9166(R) (BNWL-36, pp 2.1-58)
instability of elliptical chopper rotors at high speeds, 16: 18462
instrumentation for analyzing data from time-of-flight, 18: 27846(R) (ORNL-3578(p.60-6))
inversion matrix for, using the helium-3(n,p)T reaction, 17: 34239 (UCRL-10770)
line-shape errors from differentiation method with single-crystal scintillation, (T), 19: 44493
luminosity and resolution of crystal diffraction, theory, 16: 22356
luminosity and resolution of triple-axis crystal, 19: 11566
luminosity and resolution of crystal, (T), 20: 16874
measurement units for, 19: 33704
neutron beam production for, reactor core modification for enhanced thermal, 20: 10432
neutron beams for, reactor core modifications to enhance, 19: 29797
neutron transmission measurements with pulsed accelerator, 17: 4038
operation and control of system of, computer for, 20: 16869
operation at ORR, 20: 17158(R) (ORNL-3900, pp 82-149)
operation of fast chopper, 20: 30325(R) (RPI-328-56, pp 113-34)
operation of Nevis synchrotron velocity, 17: 602(R) (CU(PNPL)-218)
operation of rotating-crystal, use of preselector for suppression of reflection of higher orders in, 18: 23880 (NP-13930(p.127))
operation of scintillator, amplitude-time discrimination of gamma background in, 17: 39433
operation of time-of-flight, with deflection-bunching system at Karlsruhe cyclotron, 20: 39546
operations of diffraction, summary of, 18: 2403(R) (PR-P-58)
optical properties of crystal, secondary extinction effects on, 20: 23491
performance, 17: 16353
performance at 10 to 17 Mev, 19: 35378(R) (EANDC(E)-57(U))
performance evaluation of time-of-flight, 16: 3179 (ANL-6448)
performance evaluations of nine types, 17: 3314 (UCRL-10275)
performance evaluations of fast, 17: 34863
performance for angular and energy distributions, effects of finite geometry on, 19: 32583
performance for cross section measurements, 19: 29174 (ORNL-P-1116)
performance for fast neutrons using nuclear emulsions, 17: 34293
performance for GLEEP fast neutron spectra determination, 19: 40256 (AERE-M-1590)
performance for neutron dosimetry, 18: 38732
performance for resonance measurement in copper and zinc, 20: 7430
performance of at Nevis synchrocyclotron, 17: 15251(R) (CU(PNPL)-220)
performance of Bonner sphere and nuclear emulsion, 20: 29522 (CONF-651109, pp 286-305)
performance of bubble chambers as, 16: 20683
performance of chopper and rotating-crystal, 19: 42154 (KFK-261)
performance of double time-of-flight, 19: 45252 (CEA-R-2734)
performance of emulsion, helium-3, and liquid scintillator 4π, 20: 4249 (UCRL-16311)
performance of europium-activated lithium iodide, for fast neutrons, 17: 34291
performance of fast, determination of characteristics for, 17: 41265
performance of fast, with lithium iodide scintillator, 17: 41266
performance of fast chopper, as source for measuring neutron diffusion, 19: 29176 (PAN-539/IX)
performance of fast, using lithium-drifted surface-barrier detectors, (E), 19: 28659
performance of foil-activation, for in-pile uses, 17: 31694
performance of helium-3, 17: 41873 (WASH-1044)
performance of helium-3, for attenuation measurements, 19: 22745
performance of helium-3, extended range, 20: 22010(R) (NYO-72-28)
performance of helium-3, for cyclotron environs monitoring, 20: 29846 (CONF-651109, pp 154-60)
performance of high-pressure helium-3 ionization, 20: 31573
performance of liquid-hydrogen bubble chambers as, 16: 13351
performance of lithium-6 semiconductor, 18: 23986
performance of lithium fluoride-silicon sandwich surface-barrier, 19: 11531

performance of lithium iodide, scintillators in, 19: 18272
performance of lithium-6 semiconductor, 19: 23163(R) (ORNL-3650(p.111-86))
performance of lithium-6 semiconductor, 19: 44457 (NP-15475)
performance of MIT fast chopper, 16: 24369
performance of neutron-decay, 20: 43745
performance of phased-rotor, 16: 14064
performance of proton-recoil, (E), 20: 4997(R) (EUR-2494.d)
performance of proton-recoil and lithium-6 semiconductor, for fast neutrons, 20: 33715
performance of rotating-crystal, 19: 19095 (WASH-1053)
performance of scintillation-type, for fast neutrons, 18: 41772 (KFKI-1491/A)
performance of scintillation, 19: 13731 (NP-14722)
performance of semiconductor-type, 17: 34290
performance of semiconductor, 19: 44478 (ZFK-PHA-12, pp 132-9)
performance of semiconductor, (E), 20: 4997(R) (EUR-2494.d)
performance of semiconductor sandwich, 20: 33620 (EUR-2793.e)
performance of single-crystal, (T), 19: 8379 (UCRL-7611(Rev.I))
performance of spherical helium-3 chamber, 19: 34539
performance of synchrocyclotron velocity, for neutron total cross section measurement, 19: 19095 (WASH-1053)
performance of three-axis, for neutron scattering by hydrogen and vanadium, 19: 44527
performance of three-axis, for use in diffraction analyses, (E), 19: 44531
performance of time-of-flight coincidence, 17: 34864
performance of time-of-flight, for diffractometry, (E), 19: 9481 (JINR-P-1909)
performance of time-of-flight, with semiconductor time-to-amplitude converter, 20: 19071
performance of time-of-flight, error analysis for determining, 20: 33618 (CONF-660303-35)
performance of, using (n,t) reactions on lithium-6, 17: 30803
performance of, using stilbene crystals, 17: 36143 (AERE-R-4269)
performance of, without preamplifiers, 16: 27320
performance of, for neutron flux measurements, 18: 26590
performance of, for radiation detection in activation analysis, 20: 35767
performance of, using proton recoils, 20: 14444(R) (MLM-1268)
performance using semiconductor detectors, 16: 20752
performance with pulsed and steady-state sources, for diffraction and scattering studies, (T), 20: 5726 (CONF-650217, pp 102-7)
phasing two-chopper systems of, with motor-generator drive, 17: 4838
positioning of triple-axis, graphical method for, 18: 23870 (AERE-R-4380)
properties of organic-scintillator, 17: 41120
properties of semiconductor, 18: 20334 (KR-64(Sect.XXXI))
properties of time-of-flight, for slow neutrons, 20: 13061 (IDO-17134)
properties of twin-rotor, in monochromatization, 17: 15237
proportional counter applications as, 18: 29991
pulse analyzers for, time-to-pulse height, 20: 7394
pulse discriminator for time-of-flight, zero cross-over, 18: 25803 (NAS-NRC-Pub-1184(p.146-9))
pulse-height distributions from scintillation, unfolding of, (T), 19: 28732 (ORNL-3743)
pulse-time coder for time-of-flight, 18: 23996
resolution function of two-rotor velocity selector, 19: 738
resolution function of neutron chopper, for total cross section measurements, (T), 19: 20331
resolution of lithium-sensitized solid-state, analysis by iterative methods, 18: 44931(R) (ANL-6936(p.39-72))
resolution of time-of-flight, 17: 11779 (BNL-767(p.278-87))
resolution of time-of-flight, 18: 41839
resolution of time-of-flight, geometric, 20: 6297(R) (ORNL-3858(Vol.2), pp 82-90)
resolution using phased-rotor velocity selectors, 16: 14067
resolution width of crystalline, with plane crystals, 18: 2095
resonance effects (S-wave) in time-of-flight transmission experiments, 16: 13927 (CEA-1998)
response of proton-recoil, 17: 36145 (ASD-TDR-62-838)
rotors for, evaluation of, 20: 7396
simulation of mechanical chopper, 16: 29133
spectra unfolding in proton-recoil, computer program for, 20: 16875
spectral line shape from single-crystal scintillation, reconstruction of, (T), 20: 14869
spectral range of helium-3, extension of, 18: 20359
steering and data registration for, design of mechanism for, 17: 16454
survey, 17: 30888
survey, 20: 19794
survey on crystal, 20: 19795
synchronization system for rotating crystal, design of phase locked frequency multiplier for, 20: 39201 (EUR-2999.e)
thermostat design for, for −200 to −100°C, 19: 9489 (RT/EL(64)-11)
time analyzer design and performance, 16: 349(T) (AEC-tr-4694)
time analyzer design and performance, 16: 350(T) (AEC-tr-4700)
time coder for time-of-flight, nsec, 18: 12457 (EUR-491.e)
time focusing of, 19: 1956(R) (IDO-16994)
time-of-flight, for use with cyclotrons, 16: 27379
time-amplitude converter for time-of-flight, 18: 41819
time-of-flight analysis of Bragg beams from crystal, 19: 7765 (IDO-17029)
transmission data for, computer program for, 17: 37995 (KAPL-M-EC-32)
transmission functions of 3-axis, for calculation of phonon line widths, 17: 23360
transmission functions for choppers with straight slits, 18: 7063
use for analysis of condensed systems, 20: 7038
use for differentiating fresh water and petroleum, 19: 4082
use for neutron radiography, 16: 23965 (ANL-6515(p.28-52))
use for reactor shielding studies, 19: 780 (ORNL-P-548)
use in fast neutron polarization experiments, method for simultaneous asymmetry measurements for, 20: 7372
use of CDC 160-A computer for multiparameter-multichannel analysis for, 18: 23859
use of fast chopper for diffusion measurements in organic glass, 19: 45222 (INR-624/IX-A/R)
use of fast-chopper, for analysis of thorium-232 S-wave resonances, 19: 19095 (WASH-1053)
use of helium-3 sandwich-type solid-state, 18: 37510 (BRL-Memo-1545)
use of lithium-6(n,t)helium-4 reaction in, 17: 8661
use of lithium-6 semiconductor, for measuring fast neutron spectra in reactors, 20: 34911
use of organic phosphors in, (E/T), 19: 34516
use of proton recoil telescope and nuclear emulsions as, 17: 8648
use of semiconductor detectors as fast, 17: 23766
use of silicon surface-barrier detectors in, for fast neutrons, 20: 5181(R) (ORNL-3029)
use of single-crystal, for thermal spectrum measurement, 19: 15887
use of time-of-flight, with pulsed electron linac for pulsed photoneutron studies, 17: 33032
use of 1.7-nsec resolution time-of-flight, 18: 42628 (CEA-R-2382)
uses of time-of-flight for neutron-scattering analyses, 18: 36080(R) (RPI-328-8)
velocity selector for, mechanical, 17: 39378 (IDO-16878)

NEUTRON SPECTROSCOPY

activation methods for, in pool reactors, 17: 10139
bibliography on, 19: 36817 (RT/FI(64)-20)
calibration of organic scintillators for fast, 19: 13735 (ORNL-P-993)
chamber design for fast reactors, 16: 18443
collimators for, design of rubber Soller slit, 17: 3340
control systems for, development of automatic, 20: 35759 (RT-EL-(66)2)
corrections to transmission method for thermal, 17: 41851
counting efficiency method of, 17: 8646
data acquisition and processing system for time-of-flight, performance of computer, 20: 4245 (ORNL-P-1723)
data analysis, theoretical methods, 16: 14095
data collection system for, time-shared computer, 18: 4154 (BNL-7396)
data recording systems for time-of-flight, design of magnetic-tape, 20: 7355 (AERE-NP/GEN/26)
data reduction, 16: 15612 (GA-2544)
description of threshold-detector method for 2.5- to 30-Mev, (E), 19: 14469 (UCRL-11760)
design of instruments for recoil proton collimation in, 17: 10889 (AD-252467)
design of multichannel recording system for digital storage of three parameter, 16: 13341
design of "window" filters for, 18: 18225
detector for, lithium-6 semiconductor, 17: 41238 (AD-289566)
detectors for, performance and uses of threshold, 20: 15175 (UCRL-16312)
development for pulsed and steady neutron sources, (T), 20: 5726 (CONF-650217, pp 102-7)
development for use in nuclear research in U.S.S.R., 20: 34665
development of threshold foil, 19: 2644
development using stars in nuclear emulsions, 20: 41276 (UCRL-16769)
developments in, for neutron resonance phenomena in various elements, 17: 41996
energy resolution and statistics in high-energy, sampling effects on, 16: 23934
equipment and methods for, 19: 31207
equipment for, at Dutch research reactors, 17: 15508
equipment for, design of 30-Mev linear electron accelerator as, 17: 2342
equipment for fast high-intensity time-dependent, 20: 25437(P)
facilities for, at IBR reactor, 17: 38007(T) (AEC-tr-5734(p.42-7))
formulation of, in reactors, 17: 34274
improvements in, 17: 11638(R) (TID-17720(p.38-61))
instrumentation for analyzing data from time-of-flight, 18: 27846(R)

(ORNL-3578(p.60-6))
intensity increase in time-of-flight, by sweeping the beam over the target, 17: 4810(T) (AEC-tr-5540)
interpretation of activation measurements, 17: 34277
limitations of time-of-flight, 17: 2269
linear accelerators in time-of-flight, 17: 38001(T) (AEC-tr-5734(p.11-19))
method for fast, scintillation, 20: 19790
methods for asymptotic, in multiplying media, (E), 19: 25457 (RPI-328-28)
methods for, at 0.5 to 15 Mev, 17: 8626
methods for epithermal and thermal, 17: 34280
methods for fast, in reactors, 17: 34279
methods for fast, in biological exposure chambers, 17: 34283
methods for, in fast reactors, 17: 34267
methods for intermediate-energy, using activation detectors, 20: 14860 (RT/FI(65)-33)
methods for second-order reflection removal using oriented single crystals, (E), 20: 8055
methods for time-of-flight, with pulsed sources, 18: 18224
methods for, review of differential and integral, (E), 20: 6260 (CONF-651101-43)
methods of millimicrosecond, in polarization analysis, 16: 4793
methods of, review and use in dosimetry, 17: 8645
methods of, time-of-flight, 17: 38000(T) (AEC-tr-5734(p.7-10))
multisphere technique for, 20: 41280(T) (NP-tr-1410)
neutron resonances in, method of correcting for missed, (T), 19: 15900
nuclear emulsion applications in, 18: 30747
performance of emulsions and junction detectors for fast, 18: 23960
performance of method using orthonormal expansions of activation measurements (T), 19: 1535
performance of (n,t) reaction with lithium-6 for fast, 17: 34284
resolution of chopped crystal beams and mechanical monochromators for, 16: 7153
resolution technique in, 17: 41997
response function in time-of-flight, 20: 46049(R) (ORNL-3973(Vol.2), pp 96-103)
source for, 14-Mev, 17: 15218 (PAN-353/I-A)
technique for time-of-flight, using(γ,n) reactions to study energy levels of heavy nuclei, 20: 44631 (CONF-660303, pp 1064-72)
threshold detection for in-pile, 18: 2020 (EUR-289.e)
time-of-flight analyzer criteria, 16: 14093
time-of-flight applications to capture-cross-section measurements, 16: 14045
time-of-flight applications to isotope resonances, 16: 14046
time-of-flight applications to fissile-isotope studies, 16: 14051
time-of-flight applications to reactor spectra, 16: 14061
time-of-flight applications to total cross sections, 16: 14047
time-of-flight applications to resonance parameters, 16: 14048
time-of-flight data recording and sorting systems, 16: 14089
time-of-flight data analysis using computers, 16: 14100
time-of-flight, delay system for use in, 17: 11036
time-of-flight measurements in nuclear physics, 16: 14041
time-of-flight measurements in reactor studies, 16: 14042
time-of-flight measurements in liquid and solid state physics, 16: 14043
time-of-flight measurements in scattering cross sections, 16: 14044
time-of-flight measurements in graphite-uranium lattices, 16: 14062
time-of-flight measurements at 0.2 to 15 Mev using linear accelerators, 16: 14075
time-of-flight measurements below 100 kev, 16: 14077
time-of-flight measurements, detector comparisons for, 16: 14079
time-of-flight measurements at low energies using extended counter banks, 16: 14086
time-of-flight measurement trends, 16: 14092
time-of-flight measurements of reaction cross sections of radioisotopes, 16: 14055
time-of-flight technique limitations between 100 ev and 100 kev, 20: 44610 (CONF-660303, pp 381-403)
units, nomograph for conversion between, 16: 29717
use for molecules, 20: 11377
use for nuclear structure determinations, 18: 13112
use in analysis of interatomic forces, 17: 36427 (NP-13020(p.318-39))
use in fission analysis, 17: 13598
use in kinetics and structure determinations in liquids and solids, 20: 20164
use in plasma diagnostics, 18: 15405
use in study of atomic vibrations in crystal lattices, 19: 41996(T)
use of Bonner spheres and threshold detectors in, 17: 12797(R) (ORNL-3360(p.296-305))
use of cloud chambers for homogeneous reactors, 16: 18440
use of computers in, 20: 21982 (BNL-948, pp 718-40)
use of in-core, for determining configuration of ZPR-VI assemblies, 19: 6828(R) (ANL-6944(p.53-76))
use of ionization chambers for spectral analysis, 16: 18468
use of neutron reactions with silicon-28 in fast, 20: 27290
use of nuclear emulsions in homogeneous reactors, 16: 18441
use of nuclear emulsion stars for, from 20 to 300 Mev, (E/T), 19: 46769 (UCRL-16325)
use of organic scintillators in proton-recoil, 20: 43672 (ORNL-P-2471)
use of slow, for measuring structure factors of liquids, 20: 34343
use of threshold detectors for fast, 17: 34268
use of time-of-flight, for crystal structure analysis, 20: 34817 (INR-702/II/PS)
uses for studies of rotational behavior of ammonium ions in several salts, 20: 31241

NEUTRON TOTAL CROSS SECTIONS
analysis and measurement, 18: 40612
calculation for scattering resonances, (T), 19: 17177(R) (ANL-6965 (p.42-83))
calculation of, multi-level model for, (T), 20: 3374 (IA-1053)
determination at 0.3 to 1.5 Mev, automated facility for, 19: 19095 (WASH-1053)
determination for fissile elements, expressions for, 18: 18865 (ANL-6792(p.695-709))
determination in Bev range, 17: 38306
fluctuations at high energies, 20: 38173
mathematical deductions from high-energy, 17: 13501
measurement, 17: 38010(T) (AEC-tr-5734(p.57-61))
measurement at Harvard University, 19: 35371(R) (AD-612914)
measurement at high energies, 19: 47550(R) (TID-22141, pp 81-93)
measurement at low temperatures, apparatus for, 17: 14441
measurement for carbon and iron at 14.6 Mev, (E), 20: 2962
measurement in FRG-1, design of crystal spectrometer for, 18: 14232
measurement of fast, techniques for, 17: 34850
measurement of fast, methods for, 19: 14529 (MMPP-FRPC-64-2)
measurement of, for highly radioactive materials, 17: 26050
measurement of thermal, mathematical statistics of, 17: 24431
measurement of, using directional detectors, 17: 7095 (NP-12330 (p.61-5))
measurement of, calculations on transmission, 18: 11196(R) (HW-79054(p.64-81))
measurement of, development of automated facility for, 18: 44931(R) (ANL-6936(p.39-72))
measurement of, equipment for, 18: 11269
measurement of, neutron chopper for, 19: 20331
measurement of, research on, 20: 4846(R) (RPI-328-40, pp 43-8)
measurement techniques for fast, (E), 19: 41723
measurement, time-of-flight methods in, 16: 14045
measurement using a continuous spectrum, 16: 27731(R) (HW-73116 (p.37-50))
measurement using silicon detectors, 20: 13101
measurements of fast, 20: 19805(R) (ANL-7110, pp 1-28)
measurements of 3 to 15 Mev, systematic, 17: 15254 (HW-SA-2901)
resonance structure of, at 0.3 to 2.7 Mev, 18: 13066
temperature effects of magnetic order on, 18: 36034
use in determination of resonance absorption cross sections, 20: 9943 (ORNL-P-1885)
values of 12.5 to 21.0-Mev, 17: 40049

Neutron Transport Theory
see Neutrons

NEUTRONS
(When identified by mode of production or energy see headings such as Neutrons, Fission or Neutrons, Thermal)
see also Antineutrons
see also Cosmic Neutrons
see also Dineutrons
see also Neutron Beams
see also Neutron Sources
see also Tetraneutrons
absorption and attenuation in glass shielding windows, 16: 3153
absorption and attenuation by plastics, 19: 16093
absorption and diffusion in AGOT graphite, 20: 10272(R) (NAA-SR-9339)
absorption and production in reactors, contributions to oscillation measurements by, 19: 3524
absorption and reflection by polyethylene, calculations of, 18: 4685
absorption and resonance disadvantage factor in reactors, 17: 40303
absorption and scattering at 1 Mev, 16: 3662
absorption and scattering in air, calculations, 16: 14203 (NARF-62-1T)
absorption and scattering, interference potential in resonance, 17: 17468
absorption and transmission by palladium, 17: 29596
absorption and transmission by nuclei, optical model calculations of, 18: 24595 (NP-13930(p.6-13))
absorption and transmission probabilities in reactor lattices, use of Argonaut Reactor in studying, 17: 29732
absorption and transport of, research on, 20: 26533(R) (BNL-954, pp 16-49)
absorption, ARES code for computing, 16: 24391

absorption at low energies, resonance, (T), 19: 33208
absorption by adjacent cadmium and indium foils, 19: 825
absorption by annular and rod-grid elements in uranyl nitrate critical assemblies, (E), 20: 14091
absorption by block surrounded with moderator, effective integrals for resonance, 16: 2470(T) (AEC-tr-4668)
absorption by boron carbide–copper tubular control elements, 19: 917
absorption by boron-10 and lithium-6 at 10.7 to 247.0 kev, cross sections for, (E), 20: 9981 (WASH-1064)
absorption by burnable poison lumps in reactors, 18: 28975
absorption by cadmium and indium tantalates, 18: 38276 (A/CONF.28/P/476)
absorption by cadmium-113, gold, and tungsten-186, Doppler effect in resonance, 20: 35841(R) (NAA-SR-11900)
absorption by coarse-grained materials, resonance, 17: 31479
absorption by combinations of lead oxide and other oxides, 19: 11682
absorption by concrete, thermal stresses from, 19: 29478
absorption by control rods, calculation method for resonance, 20: 1356
absorption by crystals, crystal binding effects on resonant, 16: 28022 (UAC-6187)
absorption by dysprosium and hafnium isotopes, resonance integrals for, 18: 40753 (IDO-16977(p.1-20))
absorption by elements, coefficients for, 16: 23966 (ANL-6515(p.53-80))
absorption by even-odd nuclei, closed-shell effects on, 19: 37808(R) (ORNL-3778(p.69-75))
absorption by excited nuclei, 16: 32445
absorption by fissile materials, 19: 3226
absorption by fission products, effects on fast-reactor reactivity, (T), 19: 10489 (RT/FI(64)-19)
absorption by fuel-moderator lattices, narrow resonance approximation for reciprocal effects in, 18: 1211
absorption by fuel rods after long irradiation, equation for, 16: 19733
absorption by fuel-rod clusters, resonance integrals for, 17: 820
absorption by fuel spheres, Dancoff correction for resonance, 18: 15502
absorption by gold and indium, resonance, 18: 2970
absorption by gold foils, measurement and calculation of resonance, 18: 32719
absorption by gold wires, self-shielding effects in, 18: 28720
absorption by gold-197, Doppler effect and resonance integral for, (E), 19: 29334
absorption by gold, indium-115, iridium-191, lutetium-176, plutonium-239, and uranium-235, effective cutoff energies for, (T), 20: 9949
absorption by gold, method for measuring resonance, 20: 15731(R) (RPI-328-49)
absorption by gold and tungsten isotopes, Doppler coefficients and resonance integrals for, (E/T), 20: 28265(R) (AI-66-85)
absorption by graphite in gas-cooled reactors, calorimeter for determining, 19: 48031
absorption by hafnium-177, resonance integrals for, 19: 25486
absorption by heavy water-moderated lattices, calculation of, 18: 40750 (CONF-446-36)
absorption by holmium-165, resonance parameters for, (E), 20: 22004 (JINR-P-2593)
absorption by isotopic mixtures, resonance integrals for, 17: 28219 (ANL-6709)
absorption by lead oxide-rare earth systems, 18: 8825
absorption by liquid hydrogen, cross sections for, 20: 8163
absorption by lithium aluminate as burnable reactor poison, 20: 30865(P)
absorption by lumped absorbers, escape probability approximations in, 18: 36553 (NAA-SR-9744)
absorption by manganese-55, resonance integrals for, 19: 23657
absorption by materials, modification of Hurwitz spectra by leakage, 16: 586(R) (HW-70716)
absorption by materials with grain structure, 16: 24394
absorption by materials, DIRAC optical distribution function for, 18: 21151
absorption by materials, data reduction program for, 19: 14886 (KAPL-M-6430)
absorption by materials, resonance integrals for, (E), 20: 14008(R) (ANL-7122, pp 42-69)
absorption by matter, shell transmission theory for, 18: 4536 (EANDC-33U(p.161-3))
absorption by mercury, in reactor safety device, 18: 11391(P)
absorption by mixed absorbers, effects of interfering resonances in, 18: 2971
absorption by mixtures of thorium-232 and uranium-238, resonance integral measurements for, 19: 37779
absorption by mixtures, computer program for resonance, 19: 40112(R) (ANL-7046(p.36-66))
absorption by moderator-containing control rods, calculation of effectiveness of, 18: 26832
absorption by moisture in building materials, 20: 5819
absorption by molecules, cross sections for resonance, (T), 20: 6266
absorption by multilayer control rods, calculation of effectiveness of, 18: 26831
absorption by non-saturating fission products, (E), 19: 10480 (CRRP-1185)
absorption by nucleus with smoothly changing cross section, effects of resonance absorber, 16: 13970
absorption by nuclei at low energies, cross sections for fringe-area, 16: 26212
absorption by nuclei at 0.021 to 10.1 kev, 18: 36080(R) (RPI-328-8)
absorption by nuclei, optical model calculations of cross sections for, 18: 26663
absorption by nuclei in fast reactors, Doppler effects in, 18: 38252 (A/CONF.28/P/644)
absorption by nuclei, cross sections for Doppler effect calculations, (T), 19: 31508 (UNC-5064)
absorption by nuclei in large fast reactors, Doppler effects in, (E/T), 19: 31242 (UNC-5112)
absorption by nuclei in homogeneous media with heavy moderators, resonance, (T), 20: 11941
absorption by nuclei, resonance integrals for, (E), 20: 15691 (CEA-R-2840)
absorption by nuclei, resonance parameters of, 20: 19812 (GA-6919)
absorption by nuclei, Doppler-broadened resonance, 20: 21951
absorption by nuclei, Doppler broadening in resonance, 20: 34551
absorption by planar lattice of rods, effective boundary conditions for, 18: 15477
absorption by plane slabs, blackness coefficients for, 17: 28437 (KAPL-2000-20)
absorption by plates in water-moderated lattices, 17: 18993
absorption by plates, effects of mutual screening on resonance, 17: 24379
absorption by plutonium-239 and uranium-238 in fast reactors, 18: 6446 (EANDC(E)-46L)
absorption by plutonium-239 at 7 to 550 ev, cross sections and resonance parameters for, (E), 19: 23650
absorption by plutonium-239 and -240 at 0.532 to 1.44 ev, mutual shielding between resonances in, 19: 29335
absorption by plutonium-240, resonance, (E/T), 19: 37782 (BNWL-97)
absorption by plutonium-240, calculations for resonance, (E/T), 20: 6577(R) (BNWL-149, pp 22-35)
absorption by plutonium-240, resonance integrals for, (E/T), 20: 10350(R) (BNWL-152)
absorption by plutonium-240 at 1.05 ev in homogeneous systems, temperature dependence of resonance, (T), 20: 12001
absorption by plutonium-240, Doppler effects on resonance, 18: 28714
absorption by poisoning materials, burnup effects on, (E), 19: 40163
absorption by promethium-149, cross sections for, (E), 20: 6589
absorption by rare earths, reactivity measurements for resonance integrals for, 19: 29338
absorption by rhenium and thulium, resonance integrals for, (E/T), 19: 16843 (IITRI-578P24-12)
absorption by rhodium-103, resonance integral for, (E), 19: 31217 (IDO-17042(p.11-47))
absorption by slugs surrounded by moderator, resonance, 16: 29730
absorption by sodium, resonance, 20: 30358(R) (RPI-328-56, pp 1-48)
absorption by soft tissues, 17: 2860
absorption by solids for study of atomic vibrations, 17: 36433 (NP-13020(p.392-400))
absorption by spheres distributed randomly, computer analysis of, 17: 12583 (WAPD-TM-352)
absorption by spheres, flux distributions from, (T), 19: 33189 (AP-Note-426)
absorption by target materials, radioisotope production in, 20: 45784(P)
absorption by thin foils, activation measurements of resonance integrals for, 17: 26423 (GA-3125)
absorption by thorium in graphite–thorium compacts, resonance self-shielding factors from, 16: 32518 (AEEW-R-163)
absorption by thorium-232 and uranium-238 in mixed dioxides, 18: 28717
absorption by thoria and thorium rods at nonuniform temperatures, 18: 38373(R) (BAW-3125-1)
absorption by thoria and thorium rods at nonuniform temperatures, 19: 10500(R) (BAW-3125-2)
absorption by thoria and thorium rods, resonance, 18: 38373(R) (BAW-3125-1)
absorption by thorium-232–uranium-238 mixtures, resonances in, (E/T), 19: 5198
absorption by thoria and thorium rods, resonance, 19: 10500(R) (BAW-3125-2)
absorption by thorium and thorium oxides, resonance integrals for, (E), 19: 16838(R) (BAW-3125-3)
absorption by thorium dioxide rods at 20 to 1548°C, Doppler coefficient for resonance, 19: 29332
absorption by thorium-232–uranium-238 mixtures, resonance, (E),

19: 31217 (IDO-17042(p.11-47))
absorption by thorium, Doppler coefficient for, 20: 35841(R) (NAA-SR-11900)
absorption by thorium-232, integrals for resonance, (E/T), 19: 19075
absorption by tungsten, resonance integrals and Doppler coefficients for, 20: 6279(R) (AI-65-225)
absorption by tungsten, resonance integrals for, (E/T), 20: 18045(R) (AI-66-16)
absorption by tungsten isotopes, resonance parameters from, 20: 30358(R) (RPI-328-56, pp 1-48)
absorption by tungsten nuclei at 4 to 27 ev, 18: 26539(R) (ORNL-3582 (p.58-60))
absorption by tungsten, Doppler effect in, 18: 30715 (BNL-860)
absorption by uranium and uranium oxide, resonance, 16: 24759 (AE-77)
absorption by uranium-235, at 0.8 to 62 ev, 18: 7926(R) (GA-3307)
absorption by uranium-238, cadmium ratios for, 17: 34987
absorption by uranium-238 in natural uranium, 18: 28716
absorption by uranium-238 metal and dioxide rods, effective resonance, 16: 33788 (BAW-1244)
absorption by uranium-238, at 0 to 2 kev, 17: 19318
absorption by uranium-238, epi- and sub-cadmium, 17: 26062
absorption by uranium, transport theory calculations of thermal utilization in, 18: 16955 (ZFK-TPH-1)
absorption by uranium-238 in critical and subcritical assemblies, (E/T), 19: 8607
absorption by uranium oxides, resonance integrals for, (T), 19: 10301
absorption by uranium-238 in homogeneous media with heavy moderators, resonance, (T), 20: 11941
absorption by uranium-235 at 0.1 to 2.3 ev, spin dependence of cross sections for, (E), 20: 30360 (WASH-1068)
absorption by uranium-238 in 1/E spectrum, effective temperature for resonance, (T), 20: 35034
absorption by uranium-238 in lattices and rods, resonance, 16: 24764 (WAPD-T-1497)
absorption by uranium-238, effects of temperature on resonance, 16: 28010 (AEEW-R-102)
absorption by uranium-235, shielding effects of uranium-238 on resonance, 17: 9525
absorption by xenon-135 in reactors, optimum power decrease for minimizing, (T), 20: 8358
absorption, calculation of Doppler broadened resonance, 16: 3721
absorption calculations for, approximation to Doppler broadening function for resonance, 18: 9297
absorption cross sections in heterogeneous systems, resonance, 17: 17470
absorption cross sections and transmission coefficients for, 18: 42762
absorption cross sections at 24 kev, (E), 19: 45230
absorption cross sections of nuclei with $20 \leq A \leq 240$ from 0.1 to 25 Mev, calculations using nonlocal optical model, (T), 20: 46583 (IKF-17)
absorption cutoff energies in cadmium, gadolinium, and samarium 1/v detector filters, effective, 16: 18219
absorption density in reactor fuels, equations for, 18: 19336
absorption in annular-ring geometries, resonance, (T), 20: 34972
absorption in black cylinders, linear extrapolation distance for, 18: 2799
absorption in block in moderator, spatial distribution of, 17: 24375
absorption in cavity-source system, 18: 18856
absorption in cements, measurements for $E_0 \leq 30$ Mev, 20: 24575 (LNF-66/7)
absorption in ceramic-fueled fast reactors, Doppler coefficient of resonance, 16: 33973 (ANL-6601)
absorption in clustered pin superheater lattices, resonance, 17: 38481 (TID-7674(p.54-5))
absorption in composite cylinders, 16: 24760 (CRT-1079)
absorption in concrete, 18: 40768
absorption in control rods, efficiency of, 18: 28961
absorption in dilute fast reactors at 1 kev, effect of resonance overlapping on Doppler change in, 18: 11408
absorption in doubly heterogeneous media, resonance, (T), 20: 36429 (GA-7077)
absorption in fast and thermal reactors, 18: 38302 (A/CONF.28/P/172)
absorption in fast ceramic reactors, Doppler coefficients of, (T), 19: 10483 (GEAP-4630)
absorption in fast power reactors, Doppler calculations for resonance, 20: 8388 (IA-1057)
absorption in fast breeder reactors, effect of randomness on group cross sections for resonance, 20: 22391
absorption in fast reactors, Doppler effects on resonance, 18: 4790 (CONF.334-4)
absorption in fuel rods, assembly for measuring cross sections for, 20: 1384(P)
absorption in fuel rods, effective resonance integral for, (E), 20: 36435
absorption in gold, manganese, and tantalum, 19: 32058(R) (GA-5978)
absorption in gold, thorium, and uranium foils, resonance, 17: 19408
absorption in hafnium, cross sections for resonance, 18: 34883
absorption in heavy water–uranium systems, pulsed-neutron measurement of, 18: 42950
absorption in heterogeneous systems, Doppler broadened resonance, 16: 24439
absorption in heterogeneous reactors, resonance, 17: 13697
absorption in heterogeneous fuel cells, pulsed source determination of, 18: 3125
absorption in heterogeneous structures, approximation formulas for resonance, 18: 32718
absorption in heterogeneous reactors, theory of resonance, 18: 44977
absorption in heterogeneous reactors, surface resonance, (T), 19: 25635
absorption in heterogeneous media including moderator scattering, intermediate resonance, (T), 19: 47953 (BNL-9393)
absorption in heterogeneous systems, resonance integral for, (T), 20: 2973
absorption in heterogeneous media with moderator scattering, resonance integrals for, (T), 20: 2974
absorption in heterogeneous assemblies, resonance, (T), 20: 6579(R) (BNWL-149, pp 48-56)
absorption in heterogeneous media, intermediate resonance, 20: 28247
absorption in heterogeneous media, resonance, (T), 20: 28249
absorption in heterogeneous systems, equivalence theorem for resonance, 16: 1208
absorption in heterogeneous systems containing several resonance materials, 16: 33994 (WAPD-BT-26(p.1-8))
absorption in homogeneous media, resonance, 16: 10943
absorption in homogeneous media, mathematical analysis of resonance, 17: 17467
absorption in homogeneous critical assemblies, resonance, 19: 45521 (AAEC/TM-118)
absorption in infinite lattices, calculation of resonance, (T), 19: 14765(R) (ANL-6977)
absorption in infinite homogeneous mixtures, calculation method for resonance, 20: 26070
absorption in infinite homogeneous mixtures, resonance, 20: 28251
absorption in intermediate resonances of heterogeneous systems, (T), 20: 34505
absorption in large ceramic-fueled fast reactors, Doppler effect on, 16: 33992 (TID-16805)
absorption in low-energy resonances (T), 19: 3215
absorption in lumps with nonuniform temperature distribution, resonance, 17: 5310
absorption in materials having grain structures, resonance, 17: 11604
absorption in materials with grain structure, resonance, 20: 2993
absorption in matter, mechanisms of, 19: 47152
absorption in media, Doppler-broadened contour functions for resonance, 18: 40464 (AAEC/E-117)
absorption in moderators, spectral distribution of resonance, 18: 30700
absorption in nonhomogeneous systems, resonance, 18: 44718
absorption in nuclear reactors, calculations of, 17: 35091 (EUR-360.i)
absorption in nuclei in crystals to determine replacement probabilities, (T), 19: 35495
absorption in particles, resonance (E/T), 19: 3214
absorption in probes of optional geometry, method for determining, 19: 12461
absorption in reactors, spatial distribution of resonance, 16: 24392
absorption in reactor control rods, rod effectiveness determinations, 16: 30040
absorption in reactors, developments in resonance, 18: 32724 (A/CONF.28/P-262)
absorption in reactor materials, self-shielding in, 18: 42606 (TID-7050 (p.552-95))
absorption in reactors, Doppler effects on, (E/T), 19: 17243
absorption in reactors, resonance, (T), 19: 31509
absorption in reactors, design of self-adjusting element for, 19: 38098(P)
absorption in reactor lattices, resonance integral calculation for, 20: 5077
absorption in reactors, resonance, (T), 20: 8352
absorption in reactors, computer program for calculating, 20: 11932 (GA-6637)
absorption in reactor materials, self-shielding factors for, 20: 36431 (KFK-384)
absorption in reactors, multigroup cross sections for resonance, (T), 20: 38451
absorption in reactors, annotated bibliography of poisons for, 20: 45080
absorption in rod clusters, Dancoff factor for resonance, (T), 20: 10326 (RFR-265)
absorption in semihomogeneous fuel elements, parameters for, 18: 23064 (TID-7662(p.299-316))
absorption in separated tungsten isotopes, resonance integrals for, (E), 19: 29333

absorption in slab lattices, epithermal, 16: 749
absorption in slab lattices, resonance integrals for, 19: 29337
absorption in square lattices, Monte Carlo code for, 16: 21715 (BAW-154)
absorption in thorium-232 and uranium-238 mixtures, resonance, (E/T), 19: 47575 (IDO-16986)
absorption in thorium metals and thorium dioxides, computer program for calculating resonance, 20: 11932 (GA-6637)
absorption in two-nuclide system, computer program for resonance, 18: 44700 (AAEC/E-126)
absorption in two-region cells, computer program for calculating resonance, 20: 12351 (ANL-7033)
absorption in unresolved resonance region, statistical treatment of, 20: 30420
absorption in uranium-238 lattices, resonance integrals for, 17: 31478
absorption in uranium-fueled, heavy water-moderated, organic-cooled lattices, resonance, (T), 20: 32785
absorption in uranium-235–uranium-238 mixtures, Doppler coefficient for resonance, (E), 20: 34627
absorption integrals for cobalt, gold, indium, silver, and uranium-238, infinite-dilution, 20: 6558(R) (ANL-7115, pp 42-67)
absorption integral for indium, experimental measurement of, 18: 30949 (NYO-9077)
absorption integral representations, resonance, 16: 8159 (IDO-16718)
absorption integrals for epithermal, pile oscillator measurement of, (E/T), 19: 1547 (CEA-R-2486)
absorption integrals for small particles, 18: 40805 (AAEC/E-120)
absorption, intermediate-width-resonance theory for resonance, 16: 23105
absorption materials for, 16: 32120 (TID-16597)
absorption of, by boron trifluoride, reactor safety uses of, 16: 31822 (NAA-SR-6542)
absorption of, Doppler broadened cross sections for resonance, 17: 24383 (AEEW-R-226)
absorption of epithermal, cadmium-cutoff energies for, 18: 2796
absorption of low-energy, surface, 17: 7212
absorption of, mathematical analysis of resonance, 17: 17471
absorption of pile, effects on neutron activation analysis, 17: 15877 (MMPP-226-1)
absorption of, resonant, 17: 22534 (MMPP-NPC-1-2)
absorption of, specifications of type-3 sections for, 16: 31250 (APAE-Memo-312)
absorption of, temperature dependence of effective resonance integrals for, 17: 41848
absorption of underground explosion, activation of terrestrial environment in, 20: 16160 (UCRL-14739(Pt.2))
absorption of, computer program for resonance, 19: 27393 (KAPL-M-6143)
absorption of, Euratom's Bureau of Nuclear Standards for measurements on, 20: 26591
absorption of, geometrical effects on resonance, (T), 20: 40062
absorption of, interference effects in resonant, 18: 15190 (CONF-187-76)
absorption of, intermediate resonance, (T), 20: 11928 (BNL-9790)
absorption of, method for measuring resonance, 20: 28237(R) (TID-22844, pp 1-35)
absorption of, Monte Carlo methods for calculation of resonance, 20: 18046 (BNL-9644)
absorption of, parameters for least squares analysis of, 19: 37758 (BNL-9243)
absorption of, pulsed technique for measuring resonance, 20: 15731(R) (RPI-328-49)
absorption of, shell-model effects on optical-model, 18: 38155
absorption of, statistical resonances for unresolved region of, 20: 21940 (GAMD-6908)
absorption of, theory of resonance, 18: 16895 (NP-13662)
absorption rate calculation using Monte Carlo method, 17: 4882
absorption resonances and escape probability in thorium oxide–uranium oxide rods, 18: 40487
absorption resonance integrals in flat source approximation, 18: 40545
absorption resonance integral dependence on moderator properties, (T), 19: 6622
absorption resonance integral calculations for, equivalence principle for, (T), 20: 2977
absorption resonance integrals for, computer program for calculating, 20: 6291 (NAA-SR-Memo-11538)
absorption resonance cross sections and integrals, Doppler effect on, 20: 34500
absorption resonance integrals for, calculation using statistical methods, (T), 20: 34504
absorption resonance integral for thorium-232, calculation using Monte Carlo method, (T), 20: 34626
absorption resonances in plutonium–uranium carbide-fueled fast breeder power reactor mockup, Doppler broadening of, (E), 20: 26487
absorption resonance integral for rhenium, (E), 20: 42333
absorption resonance escape probability in plutonium-240, measurement using iridium foils, 20: 42137 (AEEW-M-661)
absorption resonance in cylindrical rings of fuel and moderator, Dancoff corrections to, 17: 26805
absorption theorem for, maximum, 20: 21953
absorption, theory of resonance, 16: 24390
absorption-fission ratio in uranium-235, (T), 19: 17233
absorption, calculation of resonance, 16: 18410
absorption, computer program for integral calculation in resonance, 16: 5644 (GA-2525)
absorption, effects of nonuniform temperature distributions on resonance, 16: 21340
absorption, effect of nonuniform temperature distribution on temperature dependence of resonance, 16: 2710
absorption, method of calculating resonance, 16: 731
absorption, numerical analysis of resonance, 16: 5931 (ORNL-3205)
absorptions in slabs, spatial distribution calculation of resonance, 16: 18416
acceleration by gravity, 18: 7696(R) (ORNL-TM-761)
acceleration by gravity, (E), 19: 37688
acceleration of, gravitational, 18: 11139 (ANL-6797(p.30-4))
activation of foils by, calculation of, 18: 38643
activation of nickel-64 by 14-Mev, 20: 14461(R) (ORNL-3889, pp 48-70)
age and moments of slowing-down density distribution in hydrocarbons, 16: 13928 (NAA-SR-Memo-6866)
age and slowing-down flux at indium resonance from line fission source in heavy water, 16: 12415
age and slowing-down time in beryllium, (T), 20: 30333
age, attenuation, and diffusion length in biphenyl and monoisopropyl-biphenyl, 16: 29733
age calculation from activation data, computer program for, 20: 36142 (NASA-TM-X-1260)
age from plutonium–beryllium source, determination in graphite, 16: 22969 (TID-15614)
age in aluminum-biphenyl, biphenyl-iron, and monoisopropylbiphenyl, (E), 19: 8381
age in Dowtherm-A, 18: 21138
age in finite systems, solutions of equation for, 18: 9294 (ORNL-TM-765)
age in graphite and water, 18: 9296
age in heterogeneous lattices, 18: 6414
age in isopropylbiphenyl and water, from uranium-235 fission, 16: 13969
age in moderators, moments calculations, 16: 733
age in nonmultiplying media, method for calculating, 18: 15132 (GA/Phys/63-7)
age in Th–HOH and Th–HOH–Al lattices, 16: 1007
age in thorium oxide–heavy water–water lattices, 16: 734
age in water, 16: 3611 (NASA-TN-D-1102)
age in water, Monte Carlo calculation of, 18: 42592 (TID-7050(p.125-37))
age measurements in infinite homogeneous media, use of foil detectors in, 16: 1008
age measurements in biphenyl and mineral oil, 16: 735
age measurements in diphenyl, graphite, water, and water-metal mixtures, 18: 24996(R) (NAA-SR-8888(Sect.VI))
age measurements in graphite, water, and water–zirconium mixtures, 19: 10675(R) (NAA-SR-9999)
age of fission, in water, 16: 15264(R) (HW-71747)
age of fission, in graphite, 17: 3783
age of monoenergetic and fission-source, Fermi continuous slowing-down model for, 18: 30692
age theory for criticality calculations, eigenvalue problem in, 20: 37993
age theory for, generalization of Fermi, 18: 38049 (A/CONF.28/P/827)
age to absorption in water, calculation of average, 20: 30340
age to indium resonance in lead–water and thorium–water lattices, 20: 34985
age-to-indium resonance in water, RBU Monte Carlo calculations of, 18: 38054 (NAA-SR-Memo-9500)
age, cross sections, diffusion length, scattering, and thermalization, experiments and calculations on, 19: 35719
ages in concrete at 1.44 ev to 2.5 Mev, 18: 26515
ages in hydrogen at 0.1 kev to 18 Mev, (T), 19: 29260 (TID-21744)
ages in moderator materials, fission and non-fission, 17: 22566 (TID-18590)
ages in moderators and moderator–metal systems, moments calculations of, 16: 22977
ages in water–zirconium systems, 20: 10272(R) (NAA-SR-9339)
albedo, exact solution of transient-state problem, 16: 7039
albedo flux from atmosphere, (E), 19: 41606
albedo for slab walls, 18: 30702
albedo on Moon's surface from cosmic radiation, 17: 34715
albedo on shielding, hydrogen content dependence of, 18: 19257 (BRL-1224)
albedo on slabs, transport solution for, 18: 21134 (TID-20540)
analysis by time-of-flight, 19: 14533(R) (NYO-1082-1)

analytical uses of production by (α,n) reactions, 20: 24985
angular correlations with gamma rays in deuteron reactions (d,n) with boron-11 at 0.62 and 0.94 Mev, 17: 26570
angular correlations with gamma rays in deuteron reactions (d,nγ) with boron-11 at 1.0 and 0.7 Mev, 18: 26680
angular correlations in chlorine-37 (p,nγ) reactions at 5.5 Mev, (E), 19: 17042
angular correlations with gamma rays in deuteron reactions (d,nγ) with boron-11 and carbon-13, 19: 25539
angular correlations in meson (π⁻) capture by carbon-12, (T), 19: 27476
angular distributions from alpha reactions (α,n) with boron-11, 16: 17119
angular distributions and energy spectra from deuteron-proton interactions, 16: 21475
angular distributions from alpha reactions with lithium-7 at 13.5 to 13.9 Mev, 16: 21602
angular distributions and energies from alpha reactions (α,n) with beryllium-9 at 4.3 to 5.6 Mev, 16: 24852
angular distribution asymmetry in meson (μ⁻) capture by calcium, 16: 5864(T) (UCRL-Trans-759)
angular distributions from deuteron reactions (d,n) with carbon-12 at 13 Mev, 17: 797 (NP-12129)
angular distributions from point source in air, functions for describing, 17: 5294 (BRL-Memo-1432)
angular distributions from deuteron reactions (d,n) in fluorine-19, 17: 11636(R) (TID-17720(p.8-14))
angular distributions at the surface of cadmium rods at the center of a reactor, 17: 11303(R) (HW-75228)
angular distributions from (α,n) reactions with beryllium-9 and carbon-12, 17: 17154
angular distributions and energy spectra from deuteron reactions (d,n) with nitrogen-14, 18: 6198
angular distribution from reactions (He³–t) at 460 to 1087 kev, 18: 6206
angular distributions from meson (π⁻)–proton inelastic interactions, 18: 30580
angular distributions for 20- to 55-Mev bremsstrahlung, forward asymmetry in, 18: 19038
angular distributions from alpha reactions with tantalum at 40 and 80 Mev, 18: 40517 (UCRL-11375)
angular distribution measurements on, using emulsion plates, 19: 836
angular distributions from nitrogen-14 (d,n) reactions (E), 19: 3277
angular distributions from reactions (p,n) with beryllium-9 at 2.300 to 2.560 Mev (E/T), 19: 3229 (AE-158)
angular distribution and energy of cascade, from proton-copper reactions at 1 Bev, (E/T), 19: 17159(R) (ORNL-3714(Vol.II)(p.97-118))
angular distributions from beryllium-9 (d,n) reactions at 2 to 3 Mev, (E/T), 19: 17034
angular distribution of, high-efficiency detector for, 19: 20333
angular distribution from tritium (d,n) reactions, 19: 23666
angular distributions and energy spectra from (d,n) reactions at 11.7 Mev, (E), 19: 33365
angular distributions from manganese-55 (α,n) reactions at 14 and 17 Mev, (E), 19: 33240 (IFA-CRD-30)
angular distributions from meson (π⁻)-proton interactions at 200 to 300 Mev, (E), 19: 33062
angular distribution and energy spectra from helium-4 (He-3,n) reactions at 29.8 Mev, (E), 19: 41659 (IAE-835)
angular distributions from boron-11 (d,n) reactions at 1 to 11 Mev, (E/T), 19: 41732
angular distribution from d-d reactions at 20 to 300 kev, 19: 41832
angular distributions from meson (μ⁻) capture by spin 0 nuclei, asymmetry of, (E), 19: 45274 (NEVIS-136)
angular distributions from beryllium-9 (d,n) reactions at 2.6 to 7 Mev, (E), 20: 8060 (ANL-7095)
angular distributions from carbon-13 (d,n) reactions at 1.68 to 3.23 Mev, (E/T), 20: 8062(R) (COO-720-058)
angular distributions from alpha reactions (α,n) with manganese-55 at 14 and 17 Mev, (E), 20: 10000
angular distributions from tritium (d,n) reactions at 500 kev, (T), 20: 9987
angular distribution and energy of, from boron-11 (d,n) reaction, (E), 20: 15858
angular distributions from meson (μ⁻) capture by sulfur, asymmetry in, (E), 20: 15720 (JINR-E-2516)
angular distributions from meson (μ⁻) capture by calcium, (E), 20: 15721 (JINR-E-2517)
angular distributions from alpha reactions (α,n) with carbon-12 at 14 Mev, (E), 20: 17803
angular distributions and energy from deuteron reactions with deuterium and tritium, (T), 20: 21934 (AD-621473)
angular distribution from (μ⁻,n) reactions with nuclei of different spins, anisotropy in, (E), 20: 24375
angular distributions from deuteron reactions (d,n) with lithium-7 at 0.8 and 1 Mev, (E), 20: 30402
angular distributions from capture of polarized mesons (μ⁻) by copper, iron, and lead, (E), 20: 40096
angular momenta and energies in heavy-ion reactions, 17: 41871 (UCRL-10541)
attenuation and energy deposition in liquid hydrogen (E/T), 19: 1925 (FZK-182)
attenuation and energy deposition in hydrogen, Monte Carlo program for calculating, 19: 31194 (NP-15046)
attenuation and heat deposition in liquid hydrogen, 17: 38442 (TID-7653(Pt.I)(p.17-28))
attenuation and heat deposition in liquid hydrogen, 17: 38443 (TID-7653(Pt.I)(p.29-34))
attenuation by anhydrous shielding, calculations of, 19: 31425
attenuation by beryllium, pulse decay constant for, (T), 20: 4815
attenuation by bound moderators, 16: 24376
attenuation by carbon and carbon–iron layers, 18: 40480
attenuation by concretes, 16: 24224
attenuation by heavy and light boron-poisoned water, 16: 24366
attenuation by heavy gases, 16: 24378
attenuation by heavy water lattices, 17: 35086 (DP-832)
attenuation by high-density concrete aggregates having hydrous iron ore, 16: 32113 (HW-56489)
attenuation by hydrogen slabs at 8.1 Mev, Monte Carlo calculations, 17: 28411
attenuation by ilmenite-loaded concrete, 18: 13174 (CEAL-1007)
attenuation by iron-water shields, 16: 26192 (AEEW-R-125)
attenuation by Japanese residences, 19: 42655 (CEX-62.11)
attenuation by lithium hydride shields, 18: 40736 (NAA-SR-9364)
attenuation by lithium hydrides, 20: 5181(R) (ORNL-3029)
attenuation by matter, few- and multigroup P3 analyses of, (T), 20: 2939 (WAPD-T-1710)
attenuation by optically thick shields, calculation of, (E/T), 19: 31461(R) (ANL-7010(p.235-87))
attenuation by paraffin at 5 Mev, solid-state spectrometric study of, 18: 37510 (BRL-Memo-1545)
attenuation by reactor shielding, (E), 19: 17156(R) (EUR-2197.d)
attenuation by reactor and shield materials, 16: 3880(R) (ORNL-3193)
attenuation by shielding materials, solutions of transport equation from, 16: 32520 (XDC-60-2-28)
attenuation by slabs of lead, borated polyethylene, and steel, 17: 11900 (NARF-62-16T)
attenuation by thick shields, Monte Carlo code geometry for, 17: 26393 (LAMS-2856)
attenuation by thin layers of hydrogenous materials, 19: 35572
attenuation by underground concrete structures, (T), 19: 3474
attenuation data analysis, improvements in, 16: 14096
attenuation data analysis using computers, 16: 14097
attenuation in annular space in concrete, 17: 38054(T) (AEC-tr-6009)
attenuation in annular and ordinary ducts, geometrical streaming, (T), 19: 12726
attenuation in as-cured barite concrete, 17: 36833 (HW-71113)
attenuation in bulk shielding, computer code for calculation, 16: 19236 (HW-73381)
attenuation in bulk media, 17: 3805
attenuation in castable polyethylenes, 17: 26399 (RAS-33)
attenuation in concrete, effects of concrete composition, 16: 24908
attenuation in concrete, 17: 2416 (UCRL-10439)
attenuation in concrete-shielded bunkers and tunnel, 18: 9556 (ORNL-3464)
attenuation in concretes, mechanisms for, 19: 29455
attenuation in concretes, mechanisms of, 19: 40061 (BNWL-SA-79)
attenuation in concrete-iron and iron-water systems, 20: 42517
attenuation in heterogeneous slab lattices, 16: 17237 (NASA-TN-D-1184)
attenuation in hydrogen, two-phase density measurements using, (E), 19: 29185
attenuation in iron serpentine concrete, effects of high temperatures, 16: 18592 (HW-73255)
attenuation in iron production raw materials, moisture content determination from, 17: 34205
attenuation in iron, approximation theory of, 18: 4686
attenuation in laminated shielding, 18: 38236 (A/CONF.28/P/684)
attenuation in laminated shields of concrete and lead (E/T), 19: 3450 (AE-157)
attenuation in limonite and serpentine concretes, 19: 19332
attenuation in lithium hydride, measurement of, (E), 20: 26065 (NDA-42)
attenuation in lithium hydride-uranium shields, 20: 32672 (NAA-SR-Memo-11786)
attenuation in magnetite and ordinary concretes, accuracy of shield calculations for, 19: 43464
attenuation in materials and soils, 16: 4943 (NP-11129)
attenuation in paraffin and polyethylene, temperature dependence,

16: 13930 (TID-14821)
attenuation in plastic man phantom, 16: 1315(R) (LAMS-2627(p.127-36))
attenuation in polyethylene, 17: 39956
attenuation in reactor materials, 17: 36347(R) (NARF-62-18P)
attenuation in shielding, P-3 multigroup calculations of, 17: 26218
attenuation in shield configurations, 17: 38416 (HW-78274)
attenuation in shielding materials, measurement of, 18: 15425 (UNC-5072)
attenuation in shielding materials, 19: 30895
attenuation in slabs of borated polyethylene, (E/T), 20: 34793
attenuation in thermal shielding for power reactors, calculation of, 18: 21636 (HW-72844)
attenuation in thin iron and polyethylene layers, (E), 19: 35571
attenuation in uranium–stainless steel–water mockups, 17: 42155(T) (AEC-tr-6056)
attenuation of, by concrete and iron, 16: 32604 (EIR-27)
attenuation of, by shielding materials, review of, 17: 4279
attenuation of, generalized Monte Carlo computer program for problems in, 17: 22535 (MND-MC-2856)
attenuation of reactor, in serpentine sand, (E), 20: 6524
attenuation of, analysis, (E/T), 19: 14758
attenuation of, analysis, (E/T), 19: 14757
attenuation of, analysis of two-component materials weight efficiency for, 19: 31426
attenuation of, comparisons of various calculations of, (T), 19: 29190
attenuation of, measurement of soil moisture by, 20: 43558
attenuation of, spatially decoupled simultaneous differential equations for, 18: 15159
attenuation resonances at low energies, computer analysis, 16: 14098
beta decay, 18: 34799
beta decay, (T), 19: 10045
beta decay of, electromagnetic corrections to weak interactions from, 17: 19141
beta decay of, method for testing time-invariance by, 17: 28414
beta decay of moving longitudinally polarized free, angular distributions from, (T), 19: 41496
beta decay of polarized, in magnetic field, (T), 19: 14346
beta decay of, radiative corrections to, 17: 2180
beta decay of, vector coupling constant renormalization in, 17: 22511
beta decay of, electron polarization in, (T), 19: 18765
beta decay of, half life for, 18: 21129 (KR-64(Sect.XXVII))
beta decay of, parameters for, 18: 21128 (KR-64(Sect.XXVI))
beta decay, theory of, 17: 4111
beta spectrum, (T), 19: 5136
bibliography on photoproduction, 17: 39982 (NP-13139)
bibliography on space research on, 20: 35985 (NASA-SP-7026)
binding and pairing energies in nuclei with A = 143 to 177, (E), 19: 29367
binding energies in heavy nuclei, 16: 18474
binding energies in nuclei with A = 81 to 209, 18: 30813
binding energies in nuclei, measurement of, 18: 32881
binding energies in A = 91 to 209 nuclei, determination from (d,p) and (d,t) reactions, 18: 34966
binding energies in nuclei from A = 91 to 209, (E), 19: 29362
binding energies in nuclei with A = 69 to 100, 19: 29365
binding energies in nuclides with A = 92 to 132, 19: 29366
binding energies in $86 \leq N \leq 92$ nuclei, 20: 3098
binding energies of pairs of, in nuclei, 19: 29354
binding energy in beryllium-10, carbon-13, and nitrogen-15, 18: 11166 (ANL-6797(p.179-82))
binding energy in nuclei, 19: 21275
binding energy in two-cluster nuclear molecule, (T), 19: 37852
binding energy of pairs of, in nuclei, variation with neutron numbers, 20: 17729
binding in nuclei, neutron-proton exchange energy for, (T), 19: 23651
biological effectiveness of, survey of experiments on relative, 17: 1665
biological effects, 17: 24892(R) (NYO-10451)
biological effects, 18: 25095(T) (FTD-TT-63-1046)
biological effects of, units of measurement for, 18: 31184
biological effects of, conference on, 18: 38926
biological effects of, survey, 18: 38927
biological effects of, conference on, 18: 41218
biophysical considerations of, 18: 41234
book: *An Introduction to Transport Theory*, 17: 15227
book: *An Introduction to Neutron Transport Theory*, 18: 24581
book: *Biological Effects of Neutron Radiation*, 19: 38437
book: *Effects of Nuclear Radiation on Solids*, 19: 30841
book: *Group Constants for Nuclear Reactor Calculations*, 19: 12472(T)
book: *Interaction of Radiation with Matter*, 18: 10978
book: *Introduction to Neutron Distribution Theory*, 19: 12471
book: *Investigations of Neutron Physics*, 18: 40492
book: *Magnetic Neutronography*, 20: 36370
book: *Natural Neutron Background of the Atmosphere and Earth Crust*, 20: 43547
book: *Neitronnaya Fizika* (Neutron Physics), in Russian, 16: 29722
book: *Neutron Irradiation and Activation Analysis*, 19: 11040
book: *Neutron Physics* (E/T), 19: 3227(T)
book: *Neutron Radiography*, 20: 4115
book: *Neutrons*, 16: 1016
book: *Nuclear Technology in Construction*, 19: 38828
book: *Numerical Methods of Reactor Analysis*, (E/T), 19: 6849
book: *Physics of Low-Energy Neutrons*, 20: 34506
book: *Physics of Nuclear Kinetics*, 19: 23616
book: *Radiation Physics. II. Neutron and Gamma Ray Dosimetry*, 19: 22772
book: *Slowing Down and Thermalization of Neutrons*, 20: 32361
book: *Soviet Progress in Neutron Physics*, 19: 12470(T)
book: *The Biological Action of Neutron Radiation*, 19: 45822(T) (JPRS-31822)
book: *The Two-Nucleon Interaction*, 18: 909
book: *Theory of Neutron Slowing Down in Nuclear Reactors*, 20: 36434
book: *Theory of the Fission Chain Reaction*, 18: 995
bound states in nuclei, calculation using a nonlocal single-particle model, 17: 41943
bound states of, search for three-body, (E), 20: 44650 (ORNL-P-2412)
bound states of, three-body, (T), 20: 19501
buckling and diffusion in uranium dioxide rod clusters, void effects on, (E/T), 20: 8465 (RFX-316)
buckling and extrapolation length in heavy water–plutonium lattices, 20: 34946
buckling and flux distributions in lattices of slightly enriched uranium and heavy water, (E), 19: 42049(R) (MIT-2344-3, pp 155-64)
buckling and integral spectrum in uranium-235–beryllium oxide subcritical assemblies, 18: 44968 (AAEC/E-123)
buckling by slab, extrapolation distance for (T), 19: 3191(R) (RPI-328-16)
buckling by unirradiated metal or oxide lattices with heavy-water moderator, computer program for two-group, 18: 36776 (CRRP-1198)
buckling in ECO lattices, computer program for calculating, 20: 8457 (EUR-2551.e)
buckling in enriched uranium carbide-graphite assemblies, material, 18: 40784 (NAA-SR-9772)
buckling in enriched uranium dioxide–heavy-light-water lattices, progressive substitution measurement of, 19: 3521 (TID-21238)
buckling in enriched uranium heavy-water lattices, 20: 45084
buckling in graphite-plutonium/uranium clean lattices at 400°C (E), 19: 1834 (AEEW-R-318)
buckling in graphite moderated plutonia-urania assemblies, 20: 20197 (AEEW-R-438)
buckling in graphite lattices fueled with plutonium and uranium dioxides, (E), 20: 20198 (AEEW-R-464)
buckling in graphite lattices fueled with plutonium and uranium dioxides, (T), 20: 20199 (AEEW-R-466)
buckling in Halden Boiling Reactor second fuel charge (E/T), 19: 3631 (HPR-34)
buckling in heavy water–uranium dioxide lattices, 18: 36777 (DP-873)
buckling in heavy water–uranium carbide lattices, 18: 38326 (A/CONF.28/P/743)
buckling in heavy water-uranium partially enriched lattices, material, 18: 42923(R) (MITNE-46)
buckling in heavy water-moderated uranium carbide lattices, 20: 34921
buckling in heavy water-moderated natural uranium lattices, pulsed and static, 20: 34939
buckling in heavy water-moderated natural uranium lattices, 20: 34924
buckling in heavy-water organic-cooled assembly, 18: 40828 (EUR-1830.e(Pt.III))
buckling in irregularly shaped bodies, geometric, 19: 29210
buckling in light-water-uranium lattices, 20: 2520(R) (IA-920)
buckling in reflected reactors, radial, (T), 19: 29557
buckling in reflected reactors, radial, (T), 20: 10339
buckling in reflected reactors, radial, (T), 20: 45085
buckling in subcritical assemblies, theory of material, 18: 33029
buckling in thorium–uranium fueled beryllium oxide moderated exponential piles, 20: 32820
buckling in two-region assemblies, progressive substitution technique with variation of diffusion coefficients for, 18: 33035
buckling in uranium–heavy water lattices, 18: 44972 (MIT-2344-1)
buckling in uranium-235 fueled subcritical assemblies moderated by beryllium oxide–fertile material mixtures, (E/T), 20: 36418 (AAEC-E-146)
buckling in uranium-fueled heavy and light water-moderated experimental cores, (E/T), 20: 36422 (AEEW-R-467)
buckling in water-moderated slightly enriched uranium lattices, 18: 35113 (TID-8540(p.529-609))
buckling in water-moderated and -reflected uranium dioxide lattices, effect of transverse buckling on, 19: 29558
buckling in water-moderated uranium dioxide assemblies, (T),

20: 10382(R) (WCAP-3269-13)
buckling measurements for critical assemblies, analysis of progressive substitution methods for material, 18: 33040
capture, 17: 41873 (WASH-1044)
capture and scattering by tungsten isotopes at 0 to 70 ev, (E), 20: 46599(R) (RPI-328-68, pp 1-62)
capture and thermalization in cadmium–water systems, 18: 15133 (JEN-127-DF/1-39)
capture and transmission by iron, lead, and sulfur, 18: 24620(R) (ORNL-TM-874)
capture by aluminum-27 at 14 Mev, gamma spectra from, 17: 17207
capture by aluminum, copper, and tungsten, secondary gamma emission from, (E), 20: 12267
capture by aluminum at 0 to 1 Mev, cross sections for, (E), 20: 46599(R) (RPI-328-68, pp 1-62)
capture by antimony-121, rhenium-187, and strontium-84, isomeric cross section ratios for, (E), 20: 22052
capture by barium-135 at 18 to 1500 ev, gamma transitions from, (E), 19: 47701
capture by barium-135 at 18 to 1500 ev, gamma transitions in resonance, (E), 19: 27423 (JINR-P-1972)
capture by benzene-chromium-tricarbonyl, new molecule formation in, 17: 28998
capture by bismuth, tin, and yttrium, gamma spectra from, (E), 19: 25475(R) (ORNL-TM-1044)
capture by bismuth, iron, lead, and nickel at 7.4 Mev, gamma spectra from, (E), 20: 10060
capture by boron in PWR-2, 16: 792
capture by boron in PWR-2 fuel assembly, 17: 11995 (WAPD-T-1371(Rev.))
capture by boron-10, applications in therapy of brain tumors, 16: 16215
capture by boron-10, use in radiotherapy of brain tumors, 18: 33431 (TID-20856)
capture by boron-10 in cell mixtures, local effects of, 20: 20360(R) (PRNC-73)
capture by boron-10 and lithium-6 at 10.7 to 247.0 Bev, cross sections for, (E), 20: 30360 (WASH-1068)
capture by bromine, resonances in, 17: 22556 (JINR-P-1218)
capture by bromine isotopes in irradiation of bromoethane, 19: 4205
capture by cadmium-113, effects of polarization on gamma distributions from, (E), 19: 14331(T) (CEA-tr-R-1814)
capture by calcium-44, gamma spectrum from, 17: 22264(R) (ANL-6679)
capture by cerium-144, resonance integral and thermal cross sections for, 16: 26294
capture by chlorine, cobalt, manganese, and vanadium, gamma spectra from, (E), 19: 19095 (WASH-1053)
capture by chlorine-35 and scandium-45, cross sections for, (E), 19: 41806(T)
capture by chromium-51, L/K ratio in, 18: 26665
capture by chromium-50, chromium-51 energy-level spins and transitions from, (E), 20: 44693
capture by cobalt-59, parameters of 132-ev energy level from, 17: 39967 (BNL-6780)
capture by copper-63 and lead-206 and 207 at 30 kev, gamma spectra from direct, 17: 38210
capture by copper and molybdenum, radiative, (E/T), 19: 10263
capture by copper, gold, indium, and manganese, cadmium ratios for, 19: 29468(R) (ANL-7017)
capture by deuterium, calculations with elastic unitarity and nonsymmetric three-body wave functions, (T), 20: 44748
capture by deuterons and protons at 14.4 Mev, cross sections, 16: 6963
capture by dysprosium isotopes at 0.023 to 1 ev, cross sections for radiative, 18: 18897
capture by elements, gamma spectra from, 19: 25468(R) (ARF-1193-17)
capture by elements in rat tissues by, 19: 19601
capture by erbium-166, gamma spectra and erbium-167 level scheme from, (E), 20: 3127
capture by fluorine-20, nuclear magnetic resonance from beta-decay anisotropy in polarized, 17: 41948
capture by fluorine-19, gamma spectra from, (E), 19: 25475(R) (ORNL-TM-1044)
capture by gadolinium, 18: 21164 (CONF-481-36)
capture by gadolinium-155 and -157, gadolinium-156 and -158 Mössbauer effect following, (E), 19: 39863
capture by gadolinium-156, cross sections for, (E), 20: 19835 (SGAE-PH-35/1965)
capture by germanium-73, excited levels from, (E), 20: 28474
capture by gold and tantalum, graphic representation of double, 19: 10352
capture by gold at 30 kev, cross sections, 18: 4533 (EANDC-33U(p.87-101))
capture by gold at 30 to 1500 kev, cross sections for, (E), 20: 30360 (WASH-1068)
capture by gold-197, gamma spectra from resonance, 18: 6256
capture by gold, potential and resonance, 18: 11201 (JINR-P-1456)
capture by graphite, pile oscillation determination of cross section for, 17: 39978 (NP-13134)
capture by graphite, cross section for, (E), 19: 5123
capture by hafnium and tungsten isotopes at 30 to 1200 ev, 18: 24571(R) (RPI-328-6)
capture by hafnium and tungsten isotopes (E), 19: 3191(R) (RPI-328-16)
capture by hafnium isotopes at 30 to 400 ev, (E), 19: 23630(R) (RPI-328-20(p.42-6))
capture by hafnium-177, gamma spectra of, 18: 40626
capture by hafnium-178, interference in cross section for radiative, 17: 38014(T) (AEC-tr-5734(p.72-3))
capture by heavy nuclei, statistical analysis of energy levels for, 17: 28282
capture by holmium-165 at 0 to 55 ev, resonance spins from, (E), 20: 15681
capture by hydrogen in water, 2.2-Mev gamma ray from, 18: 29146(R) (MLM-1192)
capture by hydrogen in man, estimation of total hydrogen content by, 20: 30993
capture by hydrogen, gamma ray energy from, 20: 45046(R) (IDO-17192)
capture by impurities in crystals, use in vibration studies, (T), 19: 10227
capture by impurity atoms in crystals, 19: 16407(T)
capture by indium-115, conversion-electron from thermal, (E), 19: 41808(T)
capture by iron and manganese, gamma spectra from resonance, (E), 20: 15731(R) (RPI-328-49)
capture by iron and manganese, gamma spectra from, (E), 20: 28287(R) (TID-22844, pp 36-53)
capture by iron at 0 to 200 kev, cross sections for, (E), 20: 46599(R) (RPI-328-68, pp 1-62)
capture by iron-54, energy levels from, (T), 19: 21277
capture by iron-56 at 14 Mev, gamma spectrometer for measuring spectra from, 20: 43708
capture by iron-58, mercury-202, and zinc-64 and -68, resonance, 18: 1038
capture by iron, thorium, and uranium-238 at 1 to 30 kev, cross sections for, 18: 18863 (ANL-6792(p.11-27))
capture by lumped boron, spiked-poison technique for measuring, 18: 2798
capture by magnesium-24, spectra of resonance and thermal, 19: 35399 (ORNL-P-1307)
capture by magnesium-24 and sulfur-33, resonances from, (E), 19: 45356
capture by manganese-55 at 200 to 525 ev, multiple scattering corrections for radiative, (T), 20: 11967 (JINR-P-2455)
capture by medium-weight nuclei, transition partial-width fluctuations in, 16: 14056
capture by mercury-198 and -199, gamma spectra from resonance, 18: 6256
capture by mercury-199, gamma spectra from, 20: 46599(R) (RPI-328-68, pp 1-62)
capture by molybdenum-95, *p*-wave resonant, 16: 33886
capture by molybdenum, rubidium, samarium, tin and zirconium isotopes, cross sections for radiative, (T), 19: 19106
capture by nickel at 0 to 200 kev, cross sections for, (E), 20: 46599(R) (RPI-328-68, pp 1-62)
capture by niobium-93 at 30 to 4000 ev, cross sections, resonance parameters, and strength functions for, (E), 19: 33287
capture by nuclei, gamma spectra from, 16: 14054
capture by nuclei, measurement of, 16: 27367
capture by nuclei, analysis with time-of-flight multi-dimensional selector, 16: 28055
capture by nuclei, gamma production in, 17: 5058
capture by nuclei, mono-energetic gamma production in, 17: 13560
capture by nuclei in stars, 17: 24197
capture by nuclei, generalized Doppler functions for resonance, 18: 2833 (AEEW-R-266)
capture by nuclei at 0.01 to 1 Mev, cross sections for, 18: 18864 (ANL-6792(p.29-50))
capture by nuclei at 30 and 65 kev, cross sections for radiative, 18: 34274(R) (NIRS-2(p.3-15))
capture by nuclei at binding energies, levels from, 18: 42650 (TID-21144)
capture by nuclei in various spectra, rates for resonance, 19: 29339
capture by nuclei in resonance region, data analysis method for, (T), 19: 35434
capture by nuclei at 5 to 100 kev, cross sections for, 19: 37825 (ORNL-P-1226)
capture by nuclei, resonance integrals for, 18: 44707 (NAA-SR-Memo-9886)
capture by nuclei, gamma spectra from, 19: 23163(R) (ORNL-3650(p.111-86))
capture by nuclei $23 \leq Z \leq 27$ at 14 Mev, gamma spectra from, (E), 20: 19829 (NIJS-R-455)

capture by nuclei at 1 to 5 ev, gamma spectra from, (E), 20: 30385
capture by nuclei with 23 ≤ A ≤ 209 at 14.7 Mev, cross sections for, (E), 20: 46614
capture by nuclei, nuclear resonance fluorescence from, 18: 13063
capture by nuclei, electron distributions from, 18: 20332 (KR-64 (Sect. XII))
capture by nuclei, use of lead spectrometer for studying, 18: 24608 (NP-13930(p.110-11))
capture by nuclei, analysis of gamma spectra from, 18: 24620(R) (ORNL-TM-874)
capture by nuclei, fluctuations in multiple, 18: 30759
capture by nuclei, resonance self-shielding corrections for, 18: 30766
capture by nuclei, structure studies by gamma emission following, 18: 32876
capture by nuclei, probability of large cross sections for (T), 19: 3373
capture by nuclei, gamma spectroscopy from, 19: 4505
capture by nuclei, effects of resonance interference in, (T), 19: 21335
capture by nuclei, circular polarization of gamma rays from, (E), 19: 23633 (UJV-1211/64)
capture by nuclei, precise absolute intensity determination of gamma rays from, (T), 19: 27505
capture by nuclei, spin assignments from, 19: 31207
capture by nuclei, gamma emission, 19: 31267
capture by nuclei, radiation spectroscopy for, 19: 31310
capture by nuclei, measurement techniques for radiative, 19: 45375
capture by nuclei, helicity representation for, 19: 47610
capture by nuclei, gamma spectra from, 20: 1252
capture by nuclei, multiple scattering corrections for radiative, (T), 20: 11967 (JINR-P-2455)
capture by nuclei, resonance scattering of gammas from, (E), 20: 13771 (IA-1050)
capture by nuclei, method for analysis of γ-γ cascades from, (E), 20: 13062 (IEA-96)
capture by nuclei, resonance widths in, (E), 20: 17676 (CEA-R-2810)
capture by nuclei, computer program for resonance parameters from, 20: 24340 (GA-5816)
capture by nuclei, cross sections for nucleosynthesis in, 20: 24350 (LA-DC-7774)
capture by nuclei, neutron separation energy determination from, (E), 20: 30366
capture by nuclei, average level widths of compound nucleus from, (E), 20: 32424
capture by nuclei, use as gamma source for nuclear photo-excitation studies, 20: 34682
capture by nuclei, collective model for direct radiative, 20: 34670
capture by palladium up to 150 ev, resonances in, (E), 19: 33308
capture by palladium, spectra from resonance, 19: 35378(R) (EANDC(E)-57(U))
capture by platinum-195, resonance gamma rays from, 16: 33885
capture by platinum-195, gamma spectra from resonance, 18: 6256
capture by platinum-195, gamma spectra from resonance, 17: 7655(R) (ANL-6600)
capture by plutonium-239 resonance levels, gamma spectra from, (E), 19: 29245 (JINR-P-2014)
capture by plutonium-240, resonance, (T), 20: 9989
capture by praseodymium-141, gamma energies from, 17: 38156
capture by praseodymium-141, gamma spectra for, 17: 22557 (JINR-P-1223)
capture by protactinium-233, resonance integral for, (E), 20: 34619
capture by protons, 18: 40356
capture by rare earth nuclei at 1 to 10 kev, cross sections for, (T), 20: 17653 (LA-3463)
capture by resonance nuclides in water-moderated assemblies, energy and spatial interference in (E/T), 19: 3570
capture by rhenium-186 and -188, measurement of gamma rays from, 17: 21078
capture by rhenium-185 and -187, cross sections and resonance parameters for, (E), 20: 30360 (WASH-1068)
capture by rhenium, rhenium-185, rhenium-187, and tungsten, resonance integrals for, (E), 20: 34621
capture by rhenium isotopes, tantalum isotopes, and tungsten isotopes at 30 to 170 kev, cross sections for, (E), 20: 42293
capture by rhodium-103, resonance integral of, (E), 19: 19095 (WASH-1053)
capture by rhodium-103, conversion electron spectrum from, (E), 20: 17810
capture by samarium-150, spectra from, 17: 7273
capture by samarium and tin isotopes at 30 kev, cross sections for radiative, 18: 34274(R) (NIRS-2(p.3-15))
capture by samarium isotope at 30 kev, 19: 23163(R) (ORNL-3650 (p.111-86))
capture by sodium at 10 to 135 kev, cross sections for, (E), 20: 17718
capture by sodium at 0 to 700 kev, cross sections for, (E), 20: 46599(R) (RPI-328-68, pp 1-62)
capture by soils, radioactivity induced in, 20: 12582
capture by structural materials at 0 to 50 kev, cross sections for, 17: 41883
capture by tellurium-130, cross sections for production of tellurium-131 isomer pairs in, 20: 26191
capture by terbium-159 at 0.05 to 11.14 ev, level spins from, 18: 28708
capture by thallium-203 and -205 at 10 ev to 50 kev, cross sections for radiative, (E), 19: 5249
capture by thorium, 18: 13233(R) (BNL-823(p.1-19))
capture by thorium-232 and uranium-238 at 5 to 200 kev, cross sections for radiative, 18: 9330
capture by thorium and uranium dioxides, resonance, 18: 11192 (BAW-1286)
capture by thorium, measurement of resonance integrals for, 18: 26621
capture by thorium and thorium dioxide, Doppler effect in resonance, (E), 19: 37780 (BAW-3125-4)
capture by thorium at 20 to 222 ev, resonance parameters for, (E), 19: 43353
capture by tin isotopes, gamma spectra from resonance and thermal, (E), 19: 35402 (ORNL-P-1353)
capture by tin-124 at 62 ev, angular distribution from radiative, (E), 19: 45379
capture by tin-124 in tin compounds, antimony-125 distribution from, (E), 20: 45718
capture by tungsten, Doppler effects in, 19: 24064(R) (ANL-6997)
capture by tungsten-182 and -183, gamma spectra from resonance, 18: 6256
capture by tungsten-186, resonance integral for, (E), 20: 34620
capture by tungsten isotopes at 0.01 to 10 ev, cross sections for, (E), 20: 44605 (CONF-660303, pp 182-203)
capture by tungsten-182 at 4.1 to 114 ev, gamma spectra from, (E), 20: 46599(R) (RPI-328-68, pp 1-62)
capture by tungsten-183 at 7.6 to 41 ev, gamma spectra from, (E), 20: 46599(R) (RPI-328-68, pp 1-62)
capture by uranium carbide breeding blanket in fast reactor, effects of reflector on, 18: 4746
capture by uranium-238, cross section integrals for, 18: 28713
capture by uranium-238 in fast reactor region, resonance, 18: 15480
capture by uranium-238, Doppler shifts at 300 to 500°K, 18: 28712
capture by uranium-238 lattice, slowing-down calculations for, 18: 42593 (TID-7050(p.137-54))
capture by uranium-238, resonance integrals for, 18: 28713
capture by uranium-238 in enriched uranium-dioxide fuels, 18: 28989
capture by uranium-238 in critical assembly rod lattice, 18: 42939 (TID-7050(p.1275-1319))
capture by uranium-238, spontaneous fission of isotopes produced in, (E), 19: 21403
capture by uranium-238 in heavy water lattices, anti-trap factor for resonance, 19: 29502 (CEA-R-2475)
capture by uranium-238, ratio to uranium-235 fission, 19: 35605(R) (ANL-7045(p.24-48))
capture by uranium-238 at 1.0 to 1.2 kev, cross sections for, (E), 20: 9981 (WASH-1064)
capture, computer analysis of gamma spectra from, 16: 14099
capture cross sections at Stellar temperatures, 19: 12604
capture gamma spectroscopy, use of lithium-drifted germanium diodes in, 20: 37072 (KFK-429)
capture in annular traps, resonance, 17: 17469
capture in arsenic trichloride, chemical reactions of recoil arsenic-76 from, 19: 30311
capture in boron and uranium-235, measurements by calibration of resulting gamma radiation, 16: 15629 (KAPL-M-DAG-2(Rev.1))
capture in boron-bearing slab cores, (E/T), 20: 14063 (KAPL-M-6528)
capture in cadmium–water systems, 18: 38043 (A/CONF.28/P/678)
capture in charged-particle stripping reactions with nuclei, Coulomb distortions in, 18: 26646
capture in copper, manganese, and nickel, (E), 19: 16972
capture in enriched lattices, foil measurements of, 18: 40782 (KR-84)
capture in fuel and poison, measurement, 16: 2496 (TID-14261)
capture in heterogeneous media, variational principle for, 18: 3121
capture in heterogeneous reactor fuel elements, variational principle for resonance, 18: 26870
capture in iron, width of resonances for, 17: 40108
capture in liquid organic halides, mechanisms for reactions following radiative, 17: 16076
capture in mercury, gamma spectrum from, 17: 38018(T) (AEC-tr-5734 (p.88-90))
capture in natural uranium rod clusters, resonance integrals for, (E), 20: 34546
capture in niobium-93, total radiation widths for p- and s-wave resonance, 18: 2936
capture in reactors, resonance, 18: 3178 (GAMD-3712(Rev.))

capture in rod arrays, Dancoff correction factor for resonance, 16: 12680
capture in rod arrays with resonance absorption and interference, computer program for epithermal, 18: 40785 (WAPD-TM-427)
capture in soil, gamma dose rates and integrated doses from, 19: 24750 (UCRL-12339(Vol.I))
capture in soils, gamma dose rates and integrated doses from, 19: 24751 (UCRL-12339(Vol.II))
capture in stars, effects on stellar element abundances, 20: 13410
capture in stars, integrated flux distributions for, 20: 29887
capture in stellar nuclei, mechanisms for, (T), 19: 41235
capture in structural materials, (T), 19: 45461 (N64-25922)
capture in thorium and thorium dioxide rods, Doppler coefficients for, (E), 20: 45088
capture in uranium-238, cadmium ratio for, 17: 5373
capture in uranium isotope mixtures, approximate solutions for resonance, 19: 31461(R) (ANL-7010(p.235-87))
capture in water-moderated 1% enriched uranium lattices, 18: 13233(R) (BNL-823(p.1-19))
capture of, angular correlation of gamma rays from, 17: 38013(T) (AEC-tr-5734(p.71))
capture of, approximation methods for resonance, 18: 7673 (CONF-187-26)
capture of, computer program for calculating resonance integrals for, 17: 28238 (AEEW-M-304)
capture of, effects on velocity distributions, 18: 28544
capture of, evaluation of approximations of resonance, 18: 2804
capture of, evidence for element synthesis by stellar, 17: 32883
capture of, gamma spectra from, 18: 7696(R) (ORNL-TM-761)
capture of, magnetic spectrometers for analyzing spectra from, 17: 36153 (LADC-5954)
capture of polarized, beta decay of polarized nuclei from, 18: 21201 (KR-64(Sect.XXVIII))
capture of s and p, nuclear levels in, (E/T), 19: 12553
capture of slow, interference between direct and resonance, 16: 4746
capture of 30 to 65 kev, cross sections for radiative, 17: 17222
capture of, gamma spectra and giant resonances in, 18: 26611
capture of, two-dimensional gamma spectrometer for analyzing, 20: 13075 (UJV-1450/65)
capture probabilities for plane lattices, 18: 3102 (UCRL-7023)
capture processes in stars, 17: 9158
capture processes in element formation, role of neutron numbers 98, 108, and 116, 17: 17157
capture processes for element (Z > 20) synthesis, 17: 41706(T)
capture rates in boron and uranium-235 in Plastic Mockup Assembly, 16: 9429 (KAPL-M-PJT-9)
capture rates in slabs, computer program for epithermal, 18: 15149 (WAPD-TM-407)
capture resonance parameters, measurement of, 17: 39968 (BNL-7234)
capture resonance integrals for, computer program with Doppler broadening for, 18: 38052 (KAPL-M-6158)
capture resonance integrals for, method for measuring infinitely dilute, 20: 40146
capture resonance integrals in uranium-233, Monte Carlo studies of, 17: 3774
capture resonance integrals in uranium-238, 17: 3775
capture resonance integral in plutonium-240 in aluminum–plutonium rods, reactivity determination of, 17: 3776
capture resonance integrals in gold, indium-115, and rhenium-185, 17: 3777
capture resonance integral in samarium-150, 17: 3778
capture resonance integral in indium foils, 17: 3779
capture resonance integrals in dysprosium and tungsten, 17: 3780
capture resonance integrals in infinite homogeneous media, 17: 3782
capture resonance integrals of, calculation of effective, 17: 7054 (AEEW-R-118)
capture resonance integrals in uranium metal and oxide, 17: 11667
capture resonance integrals in uranium metal and oxide, 17: 11668
capture resonance integrals for uranium-238 in hydrogen mixtures, effects of temperature, 17: 28308
capture resonance integrals of lattice, interaction correction to, 17: 36887
capture resonance integral calculations for homogeneous reactors, 17: 40280 (UCRL-6901)
capture resonance integrals in tight lattices, 18: 15442
capture resonance integrals of, approximation for, 18: 34741
capture resonance integral calculations for lattices, effective surface in calculation of, 18: 34744
capture resonance integrals for, computer program for calculating, 18: 36775 (CRRP-1197)
capture resonance integral measurements for fuel elements, 18: 44973 (PAN-102/IX)
capture resonance integrals for, 18: 44707 (NAA-SR-Memo-9886)
capture resonance integrals for, computer program for infinite dilution, 19: 29182 (WAPD-TM-494)
capture resonance parameters, analysis by time-of-flight methods, 16: 5993
capture resonance energies in tungsten isotopes, (E), 19: 31233(R) (RPI-328-35(p.112-16))
capture resonances in fission products, self-shielding of, 17: 3772
capture resonances in zirconium, tin, lanthanum, and praseodymium, 18: 24620(R) (ORNL-TM-874)
capture resonances of "s," numerical analysis of time-of-flight experiments, 17: 17096
capture, scattering, and transmission by rhodium-103, resonances in, 18: 1008 (JINR-P-1313)
capture therapy, shielding of skin during, 16: 26841 (BNL-5197)
capture-to-fission alpha ratio measurement, multiple coincidence technique for, 17: 9514 (TID-17675)
capture-to-fission ratio measurement, 18: 6173(R) (ORNL-3499(Vol.I) (p.15-17))
capture to fission ratio for uranium-235, 18: 30707 (AECL-1965)
capture to 50 kev, 18: 40630
capture-to-fission ratio for uranium-235 at 0.01 to 1 Mev, 18: 18864 (ANL-6792(p.29-50))
capture-to-fission ratio for uranium-235 in epithermal region, 18: 28564 (CONF-446-5)
capture-to-fission ratios at 3.25 ev to 1.8 kev, 18: 42646 (ORNL-TM-954)
capture-to-fission ratios for low-enrichment uranium-heavy water lattices, 18: 42923(R) (MITNE-46)
capture-to-fission ratio for plutonium-239, 19: 14828(R) (GEAP-4723)
capture-to-fission ratios in plutonium and uranium, measurement preparations for, 19: 16836(R) (ANL-6900(p.330-4))
capture-to-fission ratio for uranium-235, epicadmium, (E), 19: 21334
capture-to-fission ratios for plutonium-239 and -241 at epicadmium energies, 20: 3321(R) (ANL-7082, pp 29-53)
capture-to-fission ratio measurement in low-flux assemblies, method for direct, 20: 3430
capture-to-fission ratio measurements, design of time-of-flight system with on-line computer for, 20: 41232(R) (ORNL-3875, pp 75-90)
capture-to-fission ratios in low-power reactors, measurement of, 20: 45071 (CONF-660303, pp 1092-7)
capture, scattering, and transmission by rhodium-103, parameters for resonance, 18: 11276
cavitation induced by, ultrasonic, 18: 32266 (CERN-64-30(p.315-24))
chain reactions of, statistical theory of, 17: 7059
chain reactions of, statistical theory of, 17: 7060
chain reactions of, statistical theory of, 17: 7061
chain reactions of, statistical theory, 18: 38039 (A/CONF.28/P/652)
charge form factor, 16: 25877(R) (ANL-6534)
charge form factors of, 16: 33770
charge form factor for, 17: 24328
charge form factor for, relativistic calculation of (T), 19: 1365
chemical effects on quartz, 16: 28979 (TID-12303)
chemical effects on ammonium sulfate, 17: 25307
chemical effects on silica gels, 17: 33979
chemical effects on telluric acid, 18: 3808 (CEA-2286)
chemical effects on crystalline urea and acetamide hydrochloride, radiocarbon-labeled compounds produced by, 18: 5380
chemical effects on biphenyl and terphenyls, 18: 6849 (TID-19677)
chemical effects on nitrogenous compounds, 18: 12151 (TID-20192)
chemical effects on catalytic activity of aluminum oxides and phosphates in dehydration of alcohols, 18: 12160
chemical effects on graphite–gas systems, 18: 13835 (HW-78948)
chemical effects on potassium halides, 18: 13842(R) (TID-20296)
chemical effects on hydrocarbons, 18: 16079(T) (CEA-tr-A-1411)
chemical effects on nickel oxide, 18: 17882
chemical effects on diketone complexes, 18: 17717(R) (TID-20438)
chemical effects on carbon tetrachloride–white phosphorus reactions, 18: 20091
chemical effects on amides and amidines, 18: 20092
chemical effects on aromatic petroleum fractions, 18: 19836 (EUR-496.f)
chemical effects on polyallyl nitriles, 18: 22122(T) (JPRS-24289(Del.) (p.41-3))
chemical effects on phosphatides, 18: 29778
chemical effects on crude oils in presence of sedimentary rocks and water, 18: 37174 (A/CONF.28/P/830)
chemical effects on rates of reactions between magnesium powder and oxygen, 18: 41530
chemical effects on recoil phenomena in hexamminecobalt(III) chlorides, 18: 43668
chemical effects on sodium chloroiridates and chloroiridites, 18: 43632
Cherenkov radiation at small angles from, 16: 29703
classification in eightfold way symmetry scheme, 18: 14958
collimation of, computer analysis of efficiency of collimators, (T), 19: 21612 (NAA-SR-Memo-10557(Pt.I))
collimation of, computer analysis of efficiency of collimators, (T),

19: 21613 (NAA-SR-Memo-10557(Pt.II))
collimation of, from deuterium (d,n) reactions, (E), 19: 16832
collision density at epithermal energies, calculation, 17: 26406
collision density in reactor moderators, asymptotic form of, 18: 1195
collision density and resonance integral in homogeneous absorber-moderator mixtures, (T), 19: 23607
collision density in fast reactors, effects on Doppler-effect calculations, 20: 38422 (ANL-7120, pp 449-61)
collision probabilities in spheres with arbitrary radial source distribution, 17: 3750
collision probabilities of, in spheres with arbitrary radial source distribution, 17: 7056 (HW-SA-2696)
collision probabilities for heterogeneous lattice cells of n-media, first-, 17: 24653
collision probabilities of, in regular rod lattices, 17: 24377
collision probabilities in cylindrical-fueled infinite lattices, 17: 31693
collision probabilities in rod lattices, Dancoff correction tables for, 18: 9299
collision probability codes for cylindrical lattices for IBM-704, 18: 24844 (ANL-6836)
collision probability in infinite rectangular cylinder, first-, (T), 19: 6626
collision probabilities in cluster-type fuel elements, method of calculating, (T), 20: 1138
collision, diffusion, and slowing down in reactors, theory of, 18: 11375
collisions in shielding materials, critical removal angles for, (E), 19: 38020
color centers in lithium and sodium fluorides induced by, zero-phonon lines of, (E), 20: 45035
computer system for control of laboratory for, digital, 20: 13806
conference on detection and dosimetry of, 17: 41106
conference on inelastic scattering in liquids and solids, 16: 7145 (STI/PUB/35)
conference on neutron physics, Karlsruhe, Germany, Oct. 8 to 10, 1963, 18: 24567 (NP-13930)
conference on thermalization of, Brookhaven National Laboratory, April 30 to May 2, 1962, 17: 15160 (BNL-719(Vols.I,II,III, and IV))
conservation in close coupled critical assemblies, 16: 3613
conservation in close coupled critical assemblies, 16: 3614
containment of, liquid helium bottle for, 20: 26078
correlation in reactors, Boltzmann equation for, 19: 42042 (JINR-P-2216)
correlation with protons in heavy nuclei, role in beta decay, 19: 12507
correlations in nuclei, (T), 19: 45279 (NP-15415)
coupling in transfer reactions, levels with different total angular momentum from, 17: 7155
coupling to neon-20 rotational core, model for low-lying positive-parity states in, 17: 41950
coupling to protons in beta decay, vector constant for, 18: 9361
coupling to protons in thulium-170 and yttrium-90, 19: 14644
cross sections, 18: 17287 (NP-13666)
cross sections for, 18: 17255
cross sections in fast reactors, program for group collapsing of, 19: 35609 (BNWL-84)
currents in thin regions of asymmetric configuration, 17: 11596 (TID-15752)
data on, at Aldermaston Library, 17: 36638 (AWRE-O-70/63)
decay constant in beryllium, 20: 40376
decay constant of pulse of, time-dependent, (T), 20: 36151
decay constants and spectra in water-moderated multiplying assembly, 16: 719
decay constants and spectra in multiplying assemblies, 16: 15523 (GA-2656)
decay constants and extrapolation length in graphite, pulsed, (E), 19: 41647
decay constants for pulsed, in homogeneous non-multiplying media, (T), 20: 9938 (BNL-9770)
decay constants for plutonium fueled uranium-water lattices, (E), 20: 12397(R) (EURAEC-1506)
decay constants in beryllium systems, 20: 42601
decay constants of pulsed, spectral correction analysis of (T), 19: 3205
decay, electron-neutrino angular correlation in, 16: 4698
decay in inner Van Allen belt, 17: 5195
decay in space following bomb explosion, electron distribution from, 17: 34669
decay in space, electron spectra from, (T), 19: 4864(T) (FTD-TT-64-1077(p.200-6))
decay in Van Allen belts, buildup of intensity, 17: 5067
decay of free, beta, 19: 31207
decay of geomagnetically trapped, spatial distribution of protons from, 20: 32266
decay of, half life and interaction probabilities in, 16: 19729
decay of ionospheric nuclear-explosion-produced, vlf disturbances caused by, 18: 13002
decay of, model for weak leptonic interactions in, 18: 2621
decay of non-oriented, polarization in, 19: 39582
decay of nuclear explosion, product production contours for, 17: 23497 (D1-82-0241)
decay of orbiting reactor leakage, trapped electron flux from, (T), 20: 7988
decay of polarized, CP-parity non-conservation in, (T), 19: 47312 (NP-15460)
decay of polarized, CP violation in, 20: 6087
decay of pulsed, in diphenyl, 20: 46966(R) (NAA-SR-12010)
decay of, radiative corrections to, 16: 33710
decay of solar, proton flux from, 20: 21495
decay of, symmetry violations in leptonic, 18: 7551
decay of, unitary symmetry of weak current structure in, 17: 41781
decay of, angular, energy, and polarization correlations for leptonic, (T), 20: 6088
decay of, axial vector current in leptonic, 18: 40318
decay of, branching ratios for leptonic, (T), 19: 21019
decay of, conserved-vector current theory for, 18: 36262
decay of, coupling constants in, (T), 19: 18816
decay of, coupling constants in, (T), 19: 35388 (KFK-307)
decay of, effects of external magnetic field on, (T), 20: 44274
decay of, electron energy spectra from V–A interaction in, 18: 36267
decay of, equal-time axial-vector current commutators in sum rules for, (T), 20: 19511
decay of, G_2 symmetry for, 20: 21719
decay of, high energy fragments from baryon nonconserving, 20: 37734 (COO-818-87)
decay of, intermediate vector boson for electromagnetic corrections to, (T), 20: 7832
decay of, model for, (T), 19: 16624
decay of, model for leptonic, 20: 15360
decay of, modified vector-boson propagator for leptonic, (T), 20: 11588
decay of, phase-space integrals for, (T), 20: 17732
decay of, radiative corrections for, 18: 37951
decay of, radiative corrections to, (T), 19: 8234
decay of, renormalization axial-vector coupling constants for, (T), 20: 19808 (ANL-7130, pp 409-20)
decay of, spectrometer design for study of, 18: 22363
decay of, SU(3) symmetry for leptonic, 20: 32176
decay of, U(12) symmetry for weak interactions in, (T), 19: 21028
decay of, vector and axial coupling of broken SU(6) for, 19: 32984
density and flux distributions in ANNA critical assembly, (E/T), 19: 31502 (INR-470/IX-A)
density distributions in multizone reactors, 16: 12671
density distributions in heavy water-moderated lattices, 18: 35143(R) (DP-915)
density distribution in two-zone heterogeneous graphite exponential pile, buckling, (E), 19: 45524 (AEEW-R-428)
density distributions in reactors, kinetic equations for, (T), 19: 47963
density distributions in multilayer unit cells, 20: 42680 (INR-698/IX-A/RP)
density fluctuation determinations by statistical correlation methods, 16: 12678
density fluctuations in zero-power reactors, equations for, 18: 35080 (TID-7679(p.347-55))
density fluctuations in reactors, subcriticality measurements by analysis of, 19: 25694
density fluctuations in reactors, cross correlation of, 20: 8364
density fluctuations in reactors, hydraulic noise effects on, (T), 20: 12360 (ORNL-TM-1332)
density fluctuations in homogeneous multiplying media, angular correlations in, (T), 20: 30863
density in paraffin, effects of sample shape on, 18: 28983
density in reactors, theory of multiplet, 18: 10825
density in reflected reactors, pulsed two-region calculations, 20: 38453
density in slabs and half spaces, spatial-distribution functions for calculating, 18: 34745
density in thermal reactors, computer program for time behavior of, 17: 31683 (JEN-115-DF/I-34)
density in time-dependent media, 20: 19788
density of albedo, above atmosphere, (E), 19: 27339
detection and discrimination from gamma rays, 18: 34752(R) (CU(PNPL)-234)
detection and flux measurement for, design of boron-12 beta decay detector for, 20: 33725(P)
detection and measurement in pulsed toroidal discharge, 16: 1122(T) (NP-tr-788(p.16-22))
detection and measurement in reactors, 17: 34279
detection and measurement of, design of mechanical chopper for, 18: 12463 (PAN-442/I,I-A)
detection and measurement of, design of mechanical chopper for, 18: 12464 (PAN-443/I,IA)

detection and measurement, performance of spectrometer at 0.005 to 100 ev, 16: 1184 (AERE-R-3829)
detection and measurement using foils, elimination of flux perturbation, 16: 2346
detection and measurement, development of silicon-gold surface barrier dosimeter for, 16: 1943(R) (ORNL-3189(p.166-71))
detection and measurement at 10 to 600 kev, use of inelastic scattering, threshold reactions for, 16: 1938 (DOFL-TM-60-42)
detection and measurement, effects of boron-10 shields on calibration of threshold detectors, 16: 3181 (NDL-TR-9)
detection and measurement, solid-state detectors for, 16: 3186 (UCRL-6505)
detection and measurement, use of silicon-gold diodes in, 16: 3845(R) (ORNL-3193(p.58-62))
detection and measurement, 16: 4358
detection and measurement, 16: 4009(R) (UCSF-21)
detection and measurement, thermocouple device for, 16: 4360(P)
detection and measurement in shutdown and startup channels of MERLIN reactor, 16: 6103 (JUL-10-RE)
detection and measurement, use of semiconductor detectors for, 16: 5492 (JÜL-20-RE)
detection and measurement in gamma background, description of scintillation counter for, 16: 5531
detection and measurement, development of activation threshold detector for, 16: 6539 (NDL-TR-15)
detection and measurement, bibliography, 16: 1947 (REIC-Memo-23)
detection and measurement using multiple-wire spark counters, 16: 7709
detection and measurement, calibration of area monitor for, 16: 11971(R) (JAERI-5003(p.209-14))
detection and measurement, dosimeter development for military tactical conditions, 16: 11844 (AD-259711)
detection and measurement at 1 to 100 kev, design of apparatus, 16: 13758
detection and measurement by induced activities in gold foils, 16: 13934
detection and measurement, design of short dead-time corona streamer spark detector for, 16: 13340
detection and measurement of spatial distribution, apparatus, 16: 14977(P)
detection and measurement practices, analyses, 16: 15028(R) (UCRL-6658(Rev.))
detection and measurement in reactors, fundamentals of activation probes, 16: 15797
detection and measurement, design of traveling flux monitor for, 16: 5488 (DP-659)
detection and measurement in bremsstrahlung beam of 22-Mev betatron, 16: 17158 (SCR-481)
detection and measurement, summary of methods for, 16: 17058 (NYO-7877(Rev.1))
detection and measurement with boron tribluoride counters during emission from plutonium billets, 16: 16809 (PG-Report-314)
detection and measurement of delayed fission, in reactor cooling circuits, 16: 16523 (CEA-2101)
detection and measurement in ANP Reactors (SCW), 16: 18654 (FXM-429)
detection and measurement in presence of gamma flux, detector, 16: 17878(P)
detection and measurement from high-energy pulsed source, evaluation of scintillation detectors for, 16: 19725 (SCR-467)
detection and measurement in radiation effects environments, 16: 19074 (NARF-62-4T)
detection and measurement, terphenyl–boron liquid scintillator for, 16: 19079 (TID-15701)
detection and measurement at 4 to 76 Mev, efficiency of a plastic scintillator for, 16: 19125
detection and measurement, semiconductor counter for, 16: 20755
detection and measurement, gamma-insensitive scintillation counter for, 16: 20787
detection and measurement, liquid scintillation counters for, 16: 20709
detection and measurement, interaction of two adjacent detectors in, 16: 22368
detection and measurement, development of spark counter for, 16: 22325 (DP-523)
detection and measurement, semiconductor detectors for, 16: 20754
detection and measurement, cerium-activated vitreous scintillators for, 16: 20716
detection and measurement, design of fission chamber and preamplifier assembly for, 16: 24552
detection and measurement, design and performance of solid-state fission counters for, 16: 24553
detection and measurement, separation from gamma pulses, 16: 24579
detection and measurement in shelters during Upshot-Knothole tests 1 and 8, 16: 24016 (WT-789)
detection and measurement with scintillators, 16: 24327
detection and measurement, characteristics of scintillation systems for, 16: 23848 (SCTM-326-61(14))
detection and measurement, construction of long counter for, 16: 23849 (TID-15746)
detection and measurement by semiconductor detectors, 16: 23870
detection and measurement by aluminum and copper activation tapes, 16: 24904 (DC-61-2-98)
detection and measurement, development of scintillation crystals for, 16: 25570 (TID-16107)
detection and measurement, frequency response of current ion chamber for, 16: 25587
detection and measurement methods for biological and physical applications, 16: 25594
detection and measurement, design of scintillation counter for, 16: 27156 (AD-269792)
detection and measurement in reactors, feasibility of regenerating detectors for in-core, 16: 27254 (HW-73335)
detection and measurement, efficiency of long counters for, 16: 27303
detection and measurement in reactors, improvement of technique for, 16: 28459(P)
detection and measurement using semiconductor detectors, 16: 27358
detection and measurement using lithium-6-loaded glass scintillators, 16: 27382
detection and measurement, design of helium-3 scintillation counter for, 16: 27402(R)
detection and measurement, design of high level monitor for, 16: 28360 (DP-693)
detection and measurement using the boron-10 (n,α) lithium-7 reaction, 16: 28063
detection and measurement, liquid scintillation counters for, 16: 30603(T) (AEC-tr-5368)
detection and measurement, gamma-insensitive scintillation counter for, 16: 31834(T) (AEC-tr-5364)
detection and measurements of slow resonance, 16: 31851
detection and measurement, development of scintillation counters for, 16: 31874
detection and measurements using organic crystal detectors for, 16: 31856
detection and measurement of, development semiconductor diodes for, 16: 33162(R) (WCAP-2053)
detection and measurement using cerium-activated vitreous scintillators, 16: 33169(T) (AEC-tr-5415)
detection and measurements of intermediate energy, 16: 33217
detection and measurement in deuterium reactions (H^3,n), silicon p-n junction use for, 15: 5539
detection and measurement, design of moderated foil dosimeter for, 16: 8903 (HW-71710)
detection and measurements using triode semiconductor monitor, 16: 13320
detection and measurement at high temperatures, development of silicon carbide junctions for, 17: 358(R) (EURAEC-51)
detection and measurement with silicon junction detectors, 17: 1757
detection and measurement, dosimeter development, 17: 3207 (HW-SA-2785)
detection and measurement, effects of orientation of detector to neutron source, 17: 3237 (Y-1405)
detection and measurement, design of single and multispheres of polyethylene, bare or cadmium-covered, placed over lithium iodide detectors, 17: 3306 (LADC-5427)
detection and measurement at 5 to 35 Mev, efficiency of bubble chamber for, 17: 3307 (LAMS-2764)
detection and measurement of epithermal, design of helium-3 scintillation detector for, 17: 3313 (UCRL-7068)
detection and measurement by a long counter, directional resolution and shielding properties, 17: 3320
detection and measurement of, 17: 4271
detection and measurement in calibration of Cockcroft-Walton Accelerator, 17: 5412 (NDL-TM-6)
detection and measurement of, description of instruments for, 17: 6447
detection and measurement, use of lutetium foils in, 17: 7549(R) (HW-74761(p.5.1-35))
detection and measurement, screening for accidental exposure using sodium-24 detector, 17: 5775 (TID-14529)
detection and measurement using thallium-activated sodium iodide, 17: 6474
detection and measurement using a proportional counter, energy dependence of, 17: 6477
detection and measurement of intermediate-energy, detector for, 17: 6478
detection and measurement of, mixed with neutrons using a dual ionization chamber system, 17: 6479
detection and measurement around nuclear installations, survey of methods for, 17: 6482
detection and measurement using a thermopile, 17: 6485

detection and measurement of, energy variation of sensitivity of a polyethylene-moderated boron trifluoride proportional counter for, 17: 8585 (AE-91)
detection and measurement of, design of detectors for use in power reactors, 17: 10986
detection and measurement of, design of fission chamber for operation at very high temperatures, 17: 10987
detection and measurement using a proton-recoil proportional counter, 17: 11002 (CNEN-158)
detection and measurement of, performance of gas scintillation counter for, 17: 11005 (IKF-5)
detection and measurement by damage effects in solids, 17: 12554 (CEA-2206)
detection and measurement of, design of recoil-proton telescopes for, 17: 12795(R) (ORNL-3360(p.281-5))
detection and measurement, design of counter-telescope for, 17: 14651 (TID-18055)
detection and measurement, development of silicon carbide junction for, 17: 14653 (WCAP-2175)
detection and measurement of, scintillation pulse discrimination in, 17: 18643
detection and measurement using solid-state fission counters, 17: 18646
detection and measurement of, using enriched-uranium foil in Hurst Threshold Detector, 17: 23747 (TID-18647)
detection and measurement in reactors, jacketed-gage for, 17: 23802(P)
detection and measurement, design of fission and ionization chambers for, 17: 25602 (PAN-411/IX)
detection and measurement at very low flux levels, apparatus for application of Szilard-Chalmers effect to, 17: 25613
detection and measurement at low dose levels, chemical, 17: 26211
detection and measurement using activation foils, evaluation of factors affecting, 17: 26236
detection and measurement using wire activation methods, 17: 29722 (PAN-409/IX)
detection and measurement in tissue, 17: 28676(R) (NYO-10050)
detection and measurement of, from atomic explosion in shelters and homes, 17: 29883 (WT-1174)
detection and measurement of, in reactors using wire-type detectors, 17: 31705(P)
detection and measurement in pit with earth and concrete walls, effects of boron liner on background reduction for, 17: 31636 (UCRL-4047)
detection and measurement of, development of miniature silicon carbide detectors for, 17: 30859 (WCAP-2128)
detection and measurement of, compensated ionization chamber for, 17: 30862
detection and measurement of, survey of, 17: 30888
detection and measurement of, development of semiconductor detectors for, 17: 32404(R) (WCAP-2274)
detection and measurement of, efficiency of lithium-glass scintillator for, 17: 32405 (ZFK-RN-19)
detection and measurement of, by scintillation discs, efficiency of, 17: 32406
detection and measurement of pulsed, electron linac-neutron spectrometer system for, 17: 33032
detection and measurement in presence of high gamma flux, use of proportional detectors in, 17: 34235 (EUR-300.f)
detection and measurement of, methods for, 17: 34267
detection and measurement in reactors, unified formulations for, 17: 34274
detection and measurement of, using gold-foil detectors, 17: 34276
detection and measurement by activation methods, 17: 34277
detection and measurement in high-power reactors, 17: 34282
detection and measurement of, in radiation-damage studies, techniques for, 17: 34295
detection and measurement using silicon carbide detectors, 17: 34300
detection and measurement using thermocouple-type detectors, 17: 34301
detection and measurement of, design of high-temperature fission chamber for, 17: 34302
detection and measurement of, pulse-shape discrimination method for, 17: 34869
detection and measurement of, use of semiconductor detectors for, 17: 36145 (ASD-TDR-62-838)
detection and measurement of, development of semiconductor detectors for, 17: 36155(R) (WCAP-2346)
detection and measurement in nuclear accidents, dosimetry aspects of, 17: 37370
detection and measurement of, coating silicon carbide detectors with uranium-235 film for, 17: 37420(R) (WCAP-2382)
detection and measurement using cadmium-covered cobalt wires, 17: 37426
detection and measurement of, multifilament detector with non-overloading preamplifier for, 17: 37434
detection and measurement of, design of instrument for, 17: 39430
detection and measurement of, engineering drawings of dosimeter for, 17: 39443
detection and measurements of, engineering drawings of monitor for, 17: 39445
detection and measurement in stationary reactors, impulse correlations between two counters for, 17: 42214
detection and measurement of, design and performance of survey meter for, 18: 486(R) (AD-297107)
detection and measurement of, performance of boron trifluoride proportional counters for, 18: 503
detection and measurement of, proportional detector for, 18: 2837(R) (EANDC(OR)-22L)
detection and measurement of, semiconductor detectors for, 18: 2035(R) (WCAP-2403)
detection and measurement of, design of counter for, 18: 2403(R) (PR-P-58)
detection and measurement using activation wires, design of wire scanner with automatic decay correction system for, 18: 4111
detection and measurement of, use of boron phosphides for, 18: 4136(P)
detection and measurement in presence of gamma radiation by scintillation detector, 18: 6411(R) (ANL-6706)
detection and measurement, miniature ionization chamber for, 18: 5680(P)
detection and measurement, thermionic counter for, 18: 5684(P)
detection and measurement of, by associated-particle method, 18: 6163 (NP-13349)
detection and measurement of slow, preparation and properties of boron-containing scintillator for, 18: 7064
detection and measurement of, in mixed fields, 18: 8646(R) (NYO-2740-1(p.54-74))
detection and measurement by foil activation, student experiment for, 18: 11156
detection and measurement of, design and performance of spectrum index detectors for, 18: 10384(T) (EURAEC-877)
detection and measurement in presence of gamma radiation, 18: 10406
detection and measurement of, design of self-powered coaxial detector for in-pile, 18: 10408
detection and measurement of, efficiency of long counter for, 18: 12462 (PAN-437/IA)
detection and measurement of, flat-response detector for, 18: 14223 (UCRL-11170)
detection and measurement, design of 4π paraffin-moderated boron trifluoride detector for, 18: 14237
detection and measurement of, development of thermoelectric detector for, 18: 14272
detection and measurement using liquid scintillator, 18: 13636(R) (ORNL-3537(p.71-105))
detection and measurement by ionization chambers for moisture measurements, 18: 13671
detection and measurement using Hurst proportional detector, multisphere instrument, and single-sphere instrument, 18: 16299 (LAMS-2977)
detection and measurement by luminescent dosimeters, 18: 16305 (NP-13748)
detection and measurement of, using lithium-6 salicylate scintillator, 18: 16308 (TID-7689(p.103-5))
detection and measurement of, development of semiconductor detectors for, 18: 18179(R) (WCAP-2562)
detection and measurement of, portable transistorized radiometer with corona counters for, 18: 18189
detection and measurement by scintillation bubble chambers, 18: 18204
detection and measurement using organic phosphors, 18: 18208
detection and measurement of, device for 2π-directional, 18: 19285
detection and measurement using organic scintillators, gamma-neutron discrimination in, 18: 20350
detection and measurement of, semiconductor counters for, 18: 20334 (KR-64(Sect.XXXI))
detection and measurement of, helium-filled scintillation detector for, 18: 20398
detection and measurement in reactor, feasibility of in-core ion chambers for, 18: 21563(R) (GEAP-4483)
detection and measurement of, using semiconductor detectors, 18: 22347(T,R) (EURAEC-1008)
detection and measurement of, using high-temperature xenon-filled fission counter, 18: 22372(P)
detection and measurement of, from uranium fluoride deposits in process equipment, 18: 23875 (K-1586)
detection and measurement of, development of transistorized monitor for, 18: 23966
detection and measurement using d-c fission chamber filled with helium, 18: 25777 (AEEW-M-395)
detection and measurement of, fission chambers for in-pile, 18: 25780(R) (GEAP-4604)
detection and measurement in-pile, detector development for, 18: 27750(R)

(HW-79280(p.7.1-22))
detection and measurement of, design of instruments for, 18: 27791(R) (WCAP-2596)
detection and measurement using ionization chambers, 18: 27803
detection and measurement using mica containing fissionable materials, 18: 29048(R) (HW-80284(p.6.1-10))
detection and measurement from plutonium-uranium alloy, method for, 18: 29568(T) (EURAEC-1014)
detection and measurement of, survey of reactions for absolute, 18: 30695
detection and measurement of, by determination of atoms formed in neutron reactions with target, 18: 30745
detection and measurement, uses of nuclear emulsions for, 18: 30747
detection and measurement using rhodium-103 threshold detector, 18: 30748
detection and measurement, 18: 32301
detection and measurement using proportional counters, effect of location in paraffin block, 18: 31926
detection and measurement of, equipment for, 18: 31937
detection and measurement of, charged-fragment detectors for, 18: 35807(R) (GEMP-83)
detection and measurement of, corona counters for, 18: 35860
detection and measurement of, plastic scintillation detector efficiency for, 18: 35873
detection and measurement in power reactors, 18: 38400 (A/CONF.28/P/80)
detection and measurement of reactor, 18: 38337
detection and measurement of epithermal, using resonance activation analysis, 18: 40780 (EUR-1643.e(p.205-27))
detection and measurement of, testing of silicon carbide barrier counter for, 18: 39614(R) (EURAEC-1027)
detection and measurement of, development of film badge for, 18: 39651
detection and measurement using activation detectors, 18: 41762 (CEA-R-2491)
detection and measurement in nuclear excursion, Hanford Criticality Dosimeter for, 18: 41765 (HW-71710(Rev.))
detection and measurement in presence of gamma radiation, efficiency of scintillation counter for, 18: 41794
detection and measurement of, photographic, 18: 41625 (ANL-6846)
detection and measurement of photo-, from light and medium elements, 18: 43932 (IFA-M-34)
detection and measurement using modular counters, 18: 43972
detection and measurement using modular counters, 18: 43973
detection and measurement of, performance of semiconductor detector for, 18: 43991
detection and measurement by foil detectors, effects of flux anisotropies on, 19: 826
detection and measurement in high-temperature environment, pulse instrumentation for (E/T), 19: 753 (AEEW-R-383)
detection and measurement at 7 kev to 16 Mev, rem counter calibration for, 19: 755 (AERE-R-4524)
detection and measurement in-pile, ion chamber system for, 19: 761 (GEAP-4643)
detection and measurement of, in-pile fission chamber assembly for, 19: 779 (ORNL-3699)
detection and measurement in plutonium extraction plant, instrumentation for, 19: 2437 (NP-14343(p.Ib1-10))
detection and measurement of, using activation detectors, 19: 4453 (HW-81338)
detection and measurement of, design of spark chamber for, 19: 5569(R) (MIT-2098-64)
detection and measurement of, sensitivity of instruments for, 19: 4499
detection and measurement using aluminum and gold foils, comparison with fission counter results, (E), 19: 8376(R) (GA-5176)
detection and measurement using boron trifluoride detectors, 19: 8376(R) (GA-5176)
detection and measurement, calibration of threshold foil system for, 19: 7786 (NDL-TM-16)
detection and measurement of, design of warning dosimeter for, 19: 7802
detection and measurement of fluxes of, using rhodium activation, 19: 9497(T) (CEA-tr-A-1715)
detection and measurement, efficiency of gas scintillation detector for, 19: 9771(R) (PR-P-63)
detection and measurement of, comparison of proportional detectors for, 19: 11423(R) (UCRL-12004)
detection and measurement of, development of continuous monitors for, 19: 12865(R) (NAA-SR-10501)
detection and measurement and energy determination, 19: 11590
detection and measurement, ionization chamber for, 19: 11600
detection and measurement in reactors, survey of methods for, 19: 12732
detection and measurement of, development of instruments for, 19: 13702(R) (HW-81984(p.7.1-26))
detection and measurement of, efficiency of organic phosphors for, 19: 15873(R) (ORNL-3714(Vol.II)(p.134-46))
detection and measurement in reactors, design of Campbell system for, 19: 15857(R) (GEAP-4747)
detection and measurement of, near uranium converter in Triga reactor, 19: 17371
detection and measurement of reactor-produced, instruments for, (E), 19: 15874 (PAN-561/IX-A)
detection and measurement of, corona counters for, 19: 18280
detection and measurement using silicon carbide counter, (E), 19: 18256(R) (EURAEC-1215)
detection and measurement at various Hanford plant areas, (E), 19: 20201 (HW-SA-3525)
detection and measurement using semiconductor and scintillation detectors, 19: 20330(T) (AEC-tr-6547)
detection and measurement of, use of LiI(Eu) scintillation counter for, 19: 20375
detection and measurement of, development of nuclear emulsion dosimeter for, 19: 20161 (NP-14869)
detection and measurement using lithium-6 salicylate scintillators, 19: 22818(R) (ORNL-3650(p.221-38))
detection and measurement in reactors, development of stable instruments for, 19: 24016(R) (GEMP-87)
detection and measurement in reactors, instruments for, (E), 19: 22688 (CONF-640607(Vol.I)(Paper C-4))
detection and measurement in reactors, (E), 19: 22689 (CONF-640607(Vol.I)(Paper A-6))
detection and measurement of, ionization chambers for, 19: 22716
detection and measurement, design of calorimeter for, 19: 22767
detection and measurement of, design of fission chamber for, 19: 22807(P)
detection and measurement in reactors, instruments for, (E), 19: 24011 (CONF-640607(Vol.I)(Paper A-11))
detection and measurement in Garigliano reactor, instruments for, (E), 19: 24069 (CONF-640607(Vol.I)(Paper B-4))
detection and measurement in reactors, ionization chambers for, (E), 19: 24165 (CONF-640607(Vol.I)(Paper A-12))
detection and measurement of, transistorized system for, 19: 24855
detection and measurement of, using corona counters, 19: 26691
detection and measurement of, performance of dosimeter for, 19: 28576(R) (UCRL-12167)
detection and measurement, fabrication of 4π counter for, 19: 29228(R) (AEET/NP/10)
detection and measurement, development of miniature detectors for, 19: 30535(R) (WCAP-2644)
detection and measurement, development of miniature detectors for, 19: 30536(R) (WCAP-2666)
detection and measurement of, 19: 30547
detection and measurement of pulsed, boron trifluoride counter gating system for, 19: 32556
detection and measurement by particle tracks in crystals, 19: 32563
detection and measurement, 19: 32601(P)
detection and measurement of, methods for, 19: 34425(R) (HW-84384 (p.7.1-27))
detection and measurement using multi-layer detectors, time-of-flight error in, 19: 34509
detection and measurement in reactors, instruments for, 19: 35623
detection and measurement, for reactor control and monitoring, 19: 38091 (GEMP-90)
detection and measurement of, instruments for, 19: 36749(R) (HW-84609 (p.7.1-17))
detection and measurement of, monitor for, 19: 40286(R) (NAA-SR-11200)
detection and measurement using bubble chamber, 19: 38993 (NP-15143)
detection and measurement using bubble chamber, 19: 38994(R) (NP-15145)
detection and measurement of, electronic circuit and equivalent proportional counters for, 19: 39001
detection and measurement using boron-11 activation detector, (E), 19: 40867 (BNWL-64)
detection and measurement of, engineering drawings of ionization chamber for, 19: 40923
detection and measurement in reactors, count-rate meter for, 19: 42714(R) (ORNL-3782, pp 11-19)
detection and measurement of, development of personal monitors for, 19: 42716(R) (ORNL-3782, pp 52-64)
detection and measurement from pulsed sources, Bonner sphere method for, 19: 43415 (MATT-347)
detection and measurement of, gamma-insensitive dosimeter for, 19: 44544(P)
detection and measurement of, instrumentation for, 19: 44369 (AERE-R-4552)
detection and measurement in reactor cores, methods for, 19: 44450(R) (IBK-120a)
detection and measurement of, geometrical efficiencies of detectors for,

(T), 19: 44505
detection and measurement of, calibration of survey probe for, 19: 46752 (AERE-M-1564)
detection and measurement of, multisphere technique for, 19: 46757 (CEA-R-2772)
detection and measurement of, performance of polyethylene for, 19: 46759 (EGG-1183-1017)
detection and measurement of, energy dependence of alanine dosimeter for, 20: 394
detection and measurement of, development of solid-state rate meter for, 20: 646 (AD-614432)
detection and measurement near reactors, monitor for, 20: 1362
detection and measurement in reactors, using boron-10-coated ionization chambers, (E), 20: 5717 (AEEW-M-508)
detection and measurement of in-pile, detectors for, (E), 20: 5728 (IBM-65-825-1487)
detection and measurement of, semiconductor detectors for, 20: 7459(P)
detection and measurement of, cadmium cut-off energies for fission and 1/v detectors for, (T), 20: 11131
detection and measurement in high gamma backgrounds, 20: 11154
detection and measurement of, semiconductor detectors for, 20: 13116(P)
detection and measurement using lithium-6 glass detectors, (E), 20: 13090
detection and measurement of, background gamma discrimination in, 20: 13111
detection and measurement by track imaging in insulating materials, 20: 14854 (CONF-660304-3)
detection and measurement in reactors, using activation detectors, 20: 14860 (RT/FI(65)-33)
detection and measurement at low-counting rates, performance of boron fluoride counter for, 20: 14863
detection and measurement at 0.025 ev to 100 Mev, detector for, 20: 16819 (LA-3435)
detection and measurement using corrugated-plate spark chambers, 20: 16894
detection and measurement using boron trifluoride proportional detectors, 20: 16895
detection and measurement in reactors, instruments for, 20: 16903
detection and measurement of, performance of ionization chambers and proportional counters for, 20: 19047 (UCRL-16595)
detection and measurement using semiconductor detectors, 20: 21026 (BNL-948, pp 704-17)
detection and measurement of, performance of dielectric track detectors for, 20: 21091
detection and measurement of, engineering drawings of instrument for, 20: 23508
detection and measurement of, in simultaneous emission, instrument for, 20: 23511(P)
detection and measurement of, instrumentation development for, 20: 27267(R) (TID-22844, pp 62-75)
detection and measurement near Argonne ZGS, film for, 20: 29523 (CONF-651109, pp 639-46)
detection and measurement of, design of stilbene scintillation counter for, 20: 31532
detection and measurement in reactors, instrument development for, 20: 31596
detection and measurement of, frequency response of ionization chambers for, 20: 31597
detection and measurement of, review of methods for, 20: 33625 (MLM-1326)
detection and measurement in well logging, scintillation counter for, 20: 33723(P)
detection and measurement of, silver counter for, 20: 35755 (LA-3498)
detection and measurement of, evaluation of instruments for, 20: 35767
detection and measurement of, construction of gas scintillators for, 20: 37127
detection and measurement of, design of Rem responding rate meter for, 20: 37068 (BNL-10321)
detection and measurement of, development of portable monitor for, 20: 37071 (DP-993)
detection and measurement techniques, 20: 46599(R) (RPI-328-68, pp 1-62)
detection and measurement using uranium-235-coated silicon carbide diodes, 20: 46073
detection and production from cosmic nucleons, multiplicity monitor, 19: 43027
detection and spectroscopy using semiconductor detectors, 17: 41238 (AD-289566)
detection at high temperatures, silicon carbide detector for, 18: 33918
detection by dielectric liquid ionization chambers, 20: 13107
detection by lithium-7 gamma de-excitation, 17: 41125
detection in boreholes using a scintillation counter, 17: 4863(P)
detection in concrete-walled laboratory, room-scattered background for, 20: 13714
detection in drill holes, probe design for, 17: 10836
detection in electron-deuteron interactions, 16: 10916
detection in emulsion, analysis of recoil-proton tracks for, (T), 19: 22699 (UCRL-11296)
detection in mixed gamma-neutron fields, device for, 17: 14684
detection in pulsed-source diffusion experiments, instrumentation for, (E), 20: 7409
detection in reactors, cross-correlation of counts in separate time intervals (T), 19: 3555
detection in reactors, design and performance of gamma-compensated ionization chamber for, 20: 41360(P)
detection of Bev-range, performance of scintillation counters for, 20: 11106 (NP-15786)
detection of, design of scintillation counter for, 17: 4839
detection of, design of visual sensing device for radiography, 17: 16484(P)
detection of, development of foil-type materials for, 17: 36347(R) (NARF-62-18P)
detection of, device for, 17: 4868(P)
detection of divergent, performance of multiple-wire spark counters for, 20: 41317
detection of, helium-3 proportional counter for, 18: 5686(P)
detection of high-energy, methods for, 17: 24364
detection of, in-core sensors for rocket reactors for, 16: 28540 (NP-11862)
detection of, reactions for resonance and threshold, 17: 28237 (AE-102)
detection of, research on, 17: 41109
detection of, scintillators for, 17: 29229(P)
detection of simultaneously emitted, method and device for, 18: 25857(P)
detection of, survey instrument for, 17: 27685 (LA-2860)
detection of 0.1- to 20-Mev, response functions of organic NE-213 for, 20: 43672 (ORNL-P-2471)
detection of 2.6- and 14.4-Mev, efficiency of NE-213 organic phosphors for, 20: 46047 (ORNL-3893)
detection of, audio-visual warning system for, 20: 5733 (LA-DC-6790)
detection of, bibliography on instrumentarion for, 20: 34761 (STI-PUB-21-18)
detection of, Bonner single-sphere instrument for, 19: 44454 (LA-DC-7323)
detection of, calorimeter performance for, 20: 14170 (EGG-1183-2019)
detection of, circuit for fast cancellation of gamma background in, 18: 41867
detection of, computer program for calculating self-shielding and filter cutoff energy for activation foil, 20: 36137 (AEEW-M-621)
detection of, counter performance for, 20: 13367 (UCRL-16445(Rev.))
detection of, design and fabrication of activation detectors for, 20: 27357(P)
detection of, design and performance of diamond scintillation detector for, 20: 41290
detection of, design and performance of two-impulse scintillation detector for, 20: 41337
detection of, design of metal-foil activation detector for, 20: 41358(P)
detection of, design of spherical boron trifluoride proportional counter for, 20: 41271(R) (ORNL-3875, pp 44-52)
detection of, design and performance of ionization chamber for, 20: 43716
detection of, design of scintillation counter for, 20: 43750
detection of, efficiency of long shielded counters for, 19: 39034
detection of, equipment for, 20: 23906 (N-65-10044)
detection of, fabrication of high pressure helium-3 gas scintillation detector for, 20: 43733
detection of, fast circuits for, 20: 29536
detection of, frequency response of ionization chambers for, 20: 46076
detection of, ionization chamber for, 20: 7391
detection of, ionization chamber for, 20: 23512(P)
detection of, liquid scintillators for, 19: 18297
detection of, lithium borate crystals for, 20: 21049
detection of, miniature fission chambers for, 20: 680(P)
detection of, performance of lithium iodide in, 18: 14269
detection of, performance of NM-64 monitor for, 19: 7792
detection of, performance of time-of-flight scintillation counter for, 19: 11542
detection of, performance of scintillation counters for, 19: 18262 (NP-14686)
detection of, performance of Eastman Type A film for, 20: 5742(R) (UCRL-14351)
detection of, performance of boron fluorides and lithium glass for, 20: 8035 (GA-5798)
detection of, radiometer for, 19: 22778
detection of, rem dosimeter performance for, 20: 31514(R) (UCRL-14881)
detection of, response of organic scintillators for, 19: 15902

detection of, review on, 18: 25850
detection of, scintillation detectors for, 19: 18327
detection of, scintillation counter for, 19: 42748
detection of, semiconductor sensitivity for, 20: 21059
detection of, sensitivity of glass-base dosimeter with radioinduced optical density changes for, 20: 43679
detection of, silicon detectors for, 20: 13101
detection of, stilbene scintillation detector for, 20: 14900
detection of, techniques for, 20: 31606
detection of, use of regenerating fission chambers for, 18: 35837 (HW-81986)
detection of, 4π-recoil proportional counter response for, 19: 15853 (ANL-6897)
detection of, 4π spectrometers for, 20: 4249 (UCRL-16311)
detection probabilities in reactors, use in reactor parameter measurement, 20: 8363
detection, silicon carbide junction barrier counter development, 16: 17816(R) (EURAEC-107)
detection up to 80 kev, lithium-6-loaded glass phosphors for, 16: 5541
detection, use of zinc sulfide crystal as low-level sensor, 16: 7679 (DC-60-7-733)
detection using coated silicon-carbide diodes, in-pile, (E), 19: 28690
detection using corrugated-plate spark chambers, 20: 11120
detection using glass phosphors, 19: 15927
detection using ionization chambers, 18: 10373 (CONF-187-57)
detection using lithium-6-loaded glass scintillation detectors, 16: 14082
detection using paraffin-moderated boron trifluoride counters, (E), 19: 40890
detection using scintillation spectrometers, pulse-height spectra in, 18: 33925
detection with absolute fission counters, 17: 41129
detector development for in-pile monitoring, 18: 27751(R) (HW-80284 (p.7.1-18))
detector for, standardization of Radsan, 17: 6443 (USNRDL-TR-598)
detector for 40 to 120 Mev, directional, 18: 10381 (SC-DC-64-268)
detector for, performance of long, 18: 14198 (AWRE-NR/A-1/59)
detectors for, calibration of, 17: 14648 (IKF-6)
detectors for, comparison, 16: 14079
detectors for, effective cadmium cutoff energies for cylindrical, 18: 8644 (JAERI-1052)
detectors for, properties of threshold, 17: 21401(R) (TID-18585)
detectors for, pulse transformers for pulse counting channels for, 18: 10364 (AEEW-R-306)
development of detectors for, 20: 39221
diffraction, 17: 35190
diffraction by aluminum, magnesium, and vanadium at high pressures, 20: 14059(R) (IDO-17104)
diffraction by barium cobalt iron(II) ferrate(III) powders, effects of particle size on, 20: 5016(T)
diffraction by cadmium-lead alloys and lead, attenuation in, (E/T), 19: 25036
diffraction by crystals, magnetic structure determination by, 19: 11745
diffraction by crystals, for crystal-structure studies, 19: 16414
diffraction by ideal crystals, 18: 16510
diffraction by magnetic compounds of iron with silicon, germanium, and tin, 20: 10231
diffraction by manganese vanadite, 19: 38061
diffraction by manganese oxides, long-range magnetic order from, (E), 20: 13993
diffraction by MnSb–CrSb and CrTe–CrSb systems, 19: 38060
diffraction by ordered platinum–manganese alloys at 26 and 250°C, 20: 5912
diffraction by potassium cyanide crystals, 19: 13287
diffraction by praseodymium, 18: 24172
diffraction by rolled steels, structural analysis by, 18: 2115
diffraction by uranium dioxide, magnetic structure determination by, (E), 19: 40091
diffraction by vortex lines in superconducting niobium, 19: 38058
diffraction by zinc, scattering length for, (E), 20: 17667
diffraction from antiferromagnetic and ferromagnetic salts, covalency effects on, 19: 47895
diffraction in crystalline solids, 17: 7068
diffraction in manganese–nickel alloys, ferromagnetic moment per atom from polarized, 17: 37527
diffraction in near-stoichiometric iron sulfides, magnetic and structural properties from, 17: 37783
diffraction of, doubly curved guide for suppression of higher orders in, 20: 19787
diffraction patterns from crystal spectrometers, 16: 20678
diffraction phenomena in ferromagnetic transition metals, models for band theoretical interpretation of, 17: 34586
diffusion, (T), 19: 43258
diffusion, acceleration of group diffusion calculations in EQUIPOISE-3 program, 17: 26403
diffusion adjoint formulation, multi-energy, 16: 10936 (DC-58-9-198)
diffusion and depletion in reactors, few-group cross sections in multi-region calculations for (T), 19: 3564
diffusion and extrapolation lengths in P_1 scattering approximation, calculation using variational methods, 20: 34491
diffusion and flux distribution in reflected cylindrical reactor, 16: 28446
diffusion and multiplication in beryllium oxide–natural uranium lattices, (E/T), 20: 14080
diffusion and production in reactors, application to reactivity concept and kinetic measurements, 17: 26816
diffusion and slowing down, effects of cross section resonant structure, 16: 2473(T) (AEC-tr-4711)
diffusion and slowing down in moderators, expression formulation, 16: 2474(T) (AEC-tr-4719)
diffusion and slowing down in moderators, equations for, 17: 2514
diffusion and slow down in heterogeneous moderators containing holes, (T), 19: 47563
diffusion and thermalization in ice at –196°C and water at 0.5 to 286°C, 16: 7166
diffusion and thermalization in ice at –196°C and water at 0.5 to 286°C, 16: 24765(T) (AEC-tr-5143)
diffusion and thermalization in finite moderating media, 16: 26206
diffusion and thermalization in hydrided Zircaloy-2, 16: 26207
diffusion and thermalization, experimental aspects, 17: 15190 (BNL-719(Vol.III)(p.RE1-62))
diffusion and thermalization in non-isothermal media, 17: 37996 (TID-17646)
diffusion and thermalization in materials, 18: 34752(R) (CU(PNPL)-234)
diffusion and transport in cylinders, effects of voids, 16: 21330 (AD-267646)
diffusion and transport in reactor control rods, 16: 33981 (GEAP-3937)
diffusion and transport analyses of, 18: 36080(R) (RPI-328-8)
diffusion and transmission through matter, methods of calculating, 19: 25464
diffusion and transport of, spatial averaging of, (T), 19: 31185 (AP-Note-422)
diffusion and transport calculations in NPR tube-in-tube fuel geometry, 19: 42128(R) (BNWL-95, pp 18-23)
diffusion anisotropy in periodic lattices, 17: 5311
diffusion, approximation analysis of macroscopic, 16: 22970(T) (AEC-tr-5168)
diffusion approximation for, grey-slab inclusion in finite-difference, 17: 24366 (AAEC/TM-186)
diffusion approximation in homogeneous media, 20: 34477
diffusion areas in uranium dioxide-fueled critical assemblies, 17: 35119
diffusion, BOUND computer programs for one energy P_3 approximation, 16: 8318 (WAPD-TM-303)
diffusion boundary conditions, study in exponential piles, 17: 42233
diffusion calculations, computer code for, 16: 701
diffusion calculations by multichannel flux synthesis, 16: 12413
diffusion, calculation by single-velocity kinetic equations, 16: 14243(T) (FTD-TT-61-124(p.2-35))
diffusion calculations in two and three dimensions, EQUIPOISE program for few-group, 16: 18412
diffusion calculations, EQUIPOISE 3A two-group code, 16: 20930 (ORNL-3199(Add.))
diffusion calculations, QUICKIE and ULCER programs for IBM-7090, 16: 24436
diffusion calculations for, computer program for, 16: 29712 (K-1520)
diffusion calculations for, convergence of EQUIPOISE methods for, 17: 26414
diffusion calculations in control elements, linear extrapolation distance for, 17: 28235
diffusion calculations in three dimensions, computer program for one-group, 17: 36627 (CRRP-1159)
diffusion calculations for, absorber representation in finite-difference, 18: 11136 (AEEW-R-311)
diffusion calculations for, synthesis technique for time-dependent problems in, 18: 15154
diffusion calculations for, computer code for one-dimensional, 18: 15144 (NAA-SR-Memo-9204)
diffusion calculations for, computer time problem in input-output for two-dimension, 18: 36559 (WAPD-T-1681)
diffusion calculations for, computer programs for, 18: 42942 (TID-7050(p.1461-1511))
diffusion calculations, computer program for one-dimensional, 20: 20201(R) (ANL-7110, pp 311-401)
diffusion coefficient calculations for heterogeneous lattices, 16: 12417
diffusion coefficients, group averaging of, 16: 18415
diffusion coefficients in heavy water at 20 to 220°C, 16: 24374
diffusion coefficients for whole-reactor analysis, computer program for cell-averaged, 18: 32710 (AEEW-R-370)

diffusion coefficients for, method of averaging (T), 19: 3218
diffusion coefficients in reactors, few-group calculations of, (E/T), 19: 10219 (CONF-654-24)
diffusion coefficient of, relations with source distribution, (T), 19: 12456(R) (GEAP-4731)
diffusion coefficients for, derivation from transport theory, 19: 14474
diffusion coefficients for, energy-group averaging of, (T), 19: 31186 (AP-Note-440)
diffusion coefficients in reactors with empty channels, 20: 40377
diffusion, computer program for solving equations for, 16: 10393 (ORNL-3199)
diffusion, computer program for transfer functions, 17: 7530 (AEEW-R-189)
diffusion constants for, computer program for calculating, 17: 28220 (EUR-106.f)
diffusion constant measurements in hydrogenous materials, 18: 37113 (A/CONF.28/P/763)
diffusion constants in phenyls, water, water-d_2, and zirconium hydride, 18: 40475 (JÜL-160-NP)
diffusion constants for blackness regions in overlapping energy group models, (T), 19: 14470 (WAPD-BT-31(p.27-35))
diffusion cooling in small assemblies, 16: 3870(R) (ORNL-3193(p.223-8))
diffusion cooling coefficient for, summation of, 18: 42614
diffusion cooling coefficient and asymptotic spectrum temperature in moderators (E/T), 19: 3206
diffusion, decay constant of fully thermalized fluxes, 16: 28013 (NP-11733)
diffusion, developments in programming IBM-701 computers for multigroup calculations, 16: 12404 (NP-11332)
diffusion equations in two dimensions, computer program for solution of few-group, 16: 10394 (ORNL-3200)
diffusion equations, computer program for solution, 16: 18621 (UCRL-6076(Suppl.1))
diffusion equations, methods of multidimensional group computations of, 17: 7057 (TID-14262)
diffusion equation for, with variable coefficients, solution by a power series method, 17: 11590 (NP-12368)
diffusion equations for, mathematical aspects of PDQ-5 program for solving two-dimensional, 17: 19209 (WAPD-TM-364)
diffusion equations for, computer program for solving, 17: 28228 (WAPD-T-1589)
diffusion equations for, flux linear relation to adjoint functions in two-group, 17: 28233
diffusion equation for, computer program for three-dimensional time-dependent, 18: 9290 (AEEW-R-223)
diffusion equations for, computer program for solving, 18: 9295 (WAPD-TM-369)
diffusion equations for, group rebalancing in solving, 18: 13033 (ORNL-TM-788)
diffusion equations for, development of multigroup, 18: 15475
diffusion equations for, approximate solution of three-dimensional group, 18: 15148 (WAPD-TM-377)
diffusion equation for, computer program for solving multigroup, 18: 18851 (IA-862)
diffusion equations for, computer program for solving two-group space-time, 18: 24572 (WAPD-TM-416)
diffusion equation for, computer program for solving one-dimensional, 18: 27842 (AEEW-R-369)
diffusion equations for, structure and solutions of, 18: 32959 (A/CONF.28/P/263)
diffusion equation for, generalized endpoint method for solving, 18: 35056
diffusion equations in XY geometry for, development of two-group, 18: 38034 (A/CONF.28/P/410)
diffusion equations for, iteration procedures in solution of, 18: 42607 (TID-7050(p.1414-41))
diffusion equations for reactor transient analysis, computer program for (T), 19: 1836 (AEEW-R-389)
diffusion equations for, interface conditions and numerical techniques for multigroup (T), 19: 3208
diffusion equations for, computer programs for variational solution of multigroup, 19: 3225
diffusion equations for, simulation of, (T), 19: 5440
diffusion equations for, computer solutions of multigroup, (T), 19: 12749 (EUR-2173.i)
diffusion equations for, finite difference approximation to, (T), 19: 14471 (WAPD-BT-31(p.51-8))
diffusion equation for heterogeneous reactors, energy-dependent one-dimensional, (T), 19: 24035
diffusion equation for slab geometry, (T), 19: 25463
diffusion equation for, buckling matrix solution of multigroup, (T), 19: 27391(R) (GEAP-4846)
diffusion equations for, mesh calculations for, 19: 27751 (KAPL-M-6198)
diffusion equations for reactors, boundary perturbation effects in multigroup, (T), 19: 29195
diffusion equation for, program system for multigroup, 19: 41649
diffusion equation for one-dimensional slab geometry, (T), 19: 43255
diffusion equations for reactors, computer program for solving, 20: 3382 (WAPD-TM-532)
diffusion equations for heterogeneous reactors, computer program for solving, 20: 5057 (GA-6540)
diffusion equations in slab geometry, computer program for solving two-group time-dependent, 20: 9942 (IDO-17125)
diffusion equations for, technique for solving, (T), 20: 17652 (CEA-R-2867)
diffusion equations for, numerical solution by Kantorovich method, (T), 20: 17656
diffusion equations for reactors, computer program for solving, 20: 20207 (ORNL-TM-1302)
diffusion equation for, computer program for solution of one-dimensional multigroup, 20: 19777 (CEA-R-2923)
diffusion equations for, iterative methods for solution of, 20: 22400
diffusion equation for, formalisms of method of weighted residuals for, 20: 21957
diffusion equation for, solution by variational methods using discontinuous trial functions, 20: 33772
diffusion equation for, variational principle for, 20: 34954
diffusion equation for, solution by variational techniques, 20: 34490
diffusion equation for, method for numerical solution of multigroup time-dependent, 20: 34498
diffusion equation for, efficiency of Σ_0/Σ_t estimator in Monte Carlo programs for solution of, 20: 34955
diffusion equations for, solution using method of weighted residuals, (T), 20: 24302 (GA-6273)
diffusion equations for, stabilized march technique for, 20: 28246
diffusion equation for, variational principle using discontinuous trial functions for, 20: 36143 (WAPD-T-1885)
diffusion equations for, computer program for solving time-dependent multigroup, 20: 36138 (AWRE-O-3/66)
diffusion equations for, computer program for solution of time-dependent two-dimensional multigroup, 20: 42143 (WANL-TNR-133(Rev.))
diffusion equations for, method for solving three-dimensional, 20: 46967
diffusion, FICS program for calculating, 16: 26196 (KAPL-M-RPC-3)
diffusion formulas for homogeneous, axially symmetric, anisotropic media, Monte Carlo, 16: 2466 (AAEC/E-66)
diffusion from aluminum-clad uranium fuel, use of interposed chromium and nickel coatings for reduction of, 19: 18443(P)
diffusion from point source in exponential atmosphere, (T), 19: 43252 (LA-3349)
diffusion hardened spectra and lengths, direct calculation of, 16: 19736
diffusion hardening in water, re-analysis of data on, 18: 44709 (WAPD-T-1634)
diffusion hexagonal and tetragonal cells, equations for, (T), 19: 37771
diffusion in a cylindrical reactor, computer program for, 17: 12580 (DP-804)
diffusion in a cylindrical reactor, generalized potential theory, 20: 38448
diffusion in a finite cylindrical reactor, boundary conditions for, by P_L approximation of the transport equation, 17: 26417
diffusion in Advanced Reactivity Measurement Facility, 18: 40753 (IDO-16977(p.1-20))
diffusion in air-gap geometry, Dancoff correction for, 17: 5309
diffusion in air-filled aluminum-tube lattices in heavy water, (E/T), 20: 13705(R) (MIT-2344-4, pp 135-44)
diffusion in anisotropic media with no strong distributed absorption or fission, (E/T), 20: 13705(R) (MIT-2344-4, pp 135-44)
diffusion in ANNA critical assembly, two-group spectral parameters for, (E), 19: 31503 (INR-572/IX-A)
diffusion in atmosphere from atomic explosions at 500,000 ft, 16: 12208 (AFSWC-TDR-62-17)
diffusion in benzene, cross sections and decay constants for, 19: 21217
diffusion in benzene, parameters for, (T), 20: 15676
diffusion in beryllium oxide- and graphite-moderated systems, cross sections for, 18: 36786 (UCRL-7827)
diffusion in beryllium, spatial distributions of 3- and 15-Mev, 19: 16821
diffusion in beryllium oxide, parameters for, (E), 19: 33229
diffusion in beryllium oxides and graphite, pulsed, (E), 20: 13727
diffusion in biphenyl, heavy water, water and zirconium hydride, thermal parameters of, (E), 19: 35378(R) (EANDC(E)-57(U))
diffusion in biphenyl at 24 to 105°C, parameters of pulsed, (E), 20: 35990
diffusion in CANDU type lattice, analysis of spectra in, (T), 19: 29632 (EUR-1849.e)
diffusion in coaxial regions, 17: 4027
diffusion in coupled reactors, multigroup equations for, 19: 35705 (EUR-2416.e)
diffusion in critical assembly, probability calculation of, 17: 26413

diffusion in cubes and slabs, asymptotic decay constants in, 19: 29212
diffusion in cylindrical voids, 16: 22978
diffusion in cylindrical geometries, computer program for, 17: 19201 (RISO-55)
diffusion in cylindrical flux trap assembly, solution of group equations for, 17: 28031
diffusion in cylindrical geometry, mesh spacing for finite-difference one-dimensional, 18: 42588 (ORNL-TM-957)
diffusion in cylindrical reactors, boundary conditions for, 19: 24033
diffusion in cylindrical and slab geometries, equations for space-dependent spectra of, 19: 35362
diffusion in cylinders, methods of calculating, 19: 40286(R) (NAA-SR-11200)
diffusion in Dowtherm-A, 18: 984 (RT/F1(63)-22)
diffusion in EL-4 lattice mockup, (E), 19: 14824 (DP-919)
diffusion in epoxy resin and organic glass, method for measuring, 20: 46570
diffusion in fast-breeder reactors, evaluation of reflectors to prevent leakage in, 18: 4700
diffusion in fast pulsed reactors, two-space-point model for, (T), 19: 24028 (EUR-2273.e)
diffusion in fast reactors, multigroup calculations for, 19: 40161 (ZfK-TPh-11)
diffusion in finite multiplicative media, multigroup, 18: 2785
diffusion in finite slab lattices, (T), 19: 25692
diffusion in fluid fuel reactors, computer program for, 18: 23062 (ORNL-TM-847)
diffusion in fully reflected reactors, 17: 5312
diffusion in generalized geometry, potential-theory method for multigroup, 18: 38050 (A/CONF.28/P/842)
diffusion in graphite, measurement of, 17: 5293 (BNL-5987)
diffusion in graphite at 20°C, parameters for, 18: 990
diffusion in graphite, anisotropy and parameters for, 18: 976 (CEA-2210)
diffusion in graphite, approach-to-equilibrium during, 18: 28550
diffusion in graphite–paraffin lattices, 18: 38060
diffusion in graphite lattices, multigroup calculations of, 19: 8601 (NAA-SR-Memo-7891)
diffusion in graphite, 19: 10675(R) (NAA-SR-9999)
diffusion in graphite, measurement of, 19: 12865(R) (NAA-SR-10501)
diffusion in graphite, 19: 27735(R) (NAA-SR-10850)
diffusion in graphite, equilibrium and pulsed measurement of, 20: 10272(R) (NAA-SR-9339)
diffusion in graphite, parameters for pulsed and static, (E/T), 20: 17661
diffusion in grey control rods, extrapolation length for, (T), 19: 21649
diffusion in heavy water, measurements by pulsed source method, 16: 739
diffusion in heavy water–water systems, 17: 3792
diffusion in heavy water, parameters for, 17: 26067
diffusion in heavy water at 10 to 50°C, parameters for, 18: 993
diffusion in heavy water-moderated systems, calculational methods for, 18: 35112 (RISO-81)
diffusion in heavy-water organic-cooled reactors, computer programs for, 18: 38325 (A/CONF.28/P/742)
diffusion in heavy-water-filled ducts, (E/T), 19: 14755
diffusion in heavy water, time-dependent spectra for, 19: 23605
diffusion in heavy water, pulsed-source technique for measuring, (E), 20: 14076
diffusion in heterogeneous medium, computer code for two-group, 18: 30094 (EUR-1839.e)
diffusion in heterogeneous reactors, homogenization methods for, 18: 42926 (TID-7050(p.620-56))
diffusion in heterogeneous materials, self-shielding in, 18: 42925 (TID-7050(p.595-620))
diffusion in heterogeneous media, homogenization method for calculating, 19: 29171 (JPL-TR-32-686)
diffusion in hexagonal geometry, numerical solution of, 18: 2806
diffusion in hexagonal and tetragonal cells, equations for, (T), 19: 37771
diffusion in hollow slowing-down control rods, calculation of boundary conditions for, 17: 28491
diffusion in hollow cylinders, equations for, 19: 22497
diffusion in homogeneous systems, four-group, 18: 13027 (AHSB(S)R-60)
diffusion in homogeneous lattices, computer program for multigroup, 18: 34730 (KR-77)
diffusion in homogeneous slabs, variational principles with boundary conditions for, (T), 19: 27407
diffusion in homogeneous slabs, variational principles with boundary conditions for, (T), 19: 27408
diffusion in homogeneous slabs, variational principles with boundary conditions for, (T), 19: 27409
diffusion in ice, 17: 12774(R) (ORNL-3360(p.63-7))
diffusion in ice and water, 17: 38052(T) (AEC-tr-5734(p.286-7))
diffusion in ice and water at 0 and 20°C, 17: 38053(T) (AEC-tr-5734 (p.288-92))
diffusion in ice, parameters for, 18: 6139(R) (ORNL-3499(Vol.I)(p.33-9))
diffusion in ice, parameters for, (E/T), 19: 16855(R) (ORNL-3714 (Vol.I)(p.1-30))
diffusion in ice, temperature dependence of, (E), 19: 31195 (ORNL-P-1167)
diffusion in infinite media, 17: 789
diffusion in infinite homogeneous medium, anisotropic scattering effects on, 18: 980 (LADC-5903)
diffusion in infinite homogeneous medium, solution of monoenergetic Boltzmann equation for, 18: 2789
diffusion in iron-water shields, 16: 24597
diffusion in iron, spectra of, 19: 35356
diffusion in laminated shields, Monte Carlo computer program for, 18: 42866 (ML-TDR-64-52)
diffusion in large heterogeneous media, method for describing, 18: 3225
diffusion in lattice containing cavities, coefficients for, (T), 19: 16815 (CEA-R-2278)
diffusion in lattices, computer analysis of, 19: 19359 (RPI-328-19)
diffusion in lead, heavy monoatomic gas model for, 20: 2943
diffusion in light water, capture effects on, (T), 19: 27399
diffusion in limited reactor regions, boundary-control method for, 17: 11598 (WAPD-T-1457)
diffusion in matrices, mathematical models for, 16: 12702
diffusion in matter, iterative analysis of, (T), 19: 12459 (TID-21110)
diffusion in matter, variational flux-synthesis analysis of, (T), 19: 21638 (CONF-650501-4)
diffusion in media, Monte Carlo code for, 20: 8044 (UCRL-7630(Suppl.1))
diffusion in mobile media, 17: 24376
diffusion in moderators, two-group boundary conditions in square lattices, 16: 24772
diffusion in moderating materials, effects of kernels of die-away parameters on, 17: 34560(R) (TID-19195)
diffusion in moderating media, one-group treatment for demonstration of neutron wave technique in, 17: 39962
diffusion in moderators, fast chopper as source for measuring, 19: 29176 (PAN-539/IX)
diffusion in moderators and multiplying media, research on pulsed-beam methods for, 19: 31191 (INR-564/IX-A)
diffusion in monatomic hydrogen, time-dependent moments equations solutions for, 20: 15675
diffusion in multi-region symmetric reactors, two-group analysis, 16: 1188 (CRNE-1023)
diffusion in multi-layer slab systems, 17: 4031
diffusion in multilayer graphite-steel shields, multigroup calculations of, 18: 42869 (UJV-1032/64)
diffusion in multiplying medium, asymptotic and steady-state spectra of, 19: 29561
diffusion in nonabsorbing medium of nonuniform temperature, 16: 12408
diffusion in nonisothermal media, (T), 20: 30322 (BNL-947)
diffusion in nonmultiplying media, interpretation of pulsed, (T), 20: 13731
diffusion in nonseparable reactor geometries, modified Ritz method for, 20: 22385
diffusion in one and two dimensions, computer program for, 19: 14466 (ORNL-TM-842)
diffusion in organic liquids, effects of non–1/v capture on pulsed, (E), 20: 13730
diffusion in organic glass, parameters, (E), 20: 28234 (INR-690/IX-A/R)
diffusion in ortho- and parahydrogen, parameters for, (E), 19: 35365
diffusion in parallel-plate lattices, 20: 22398
diffusion in parallel-slab subcritical assemblies, 20: 20195 (AAEC/TM-302)
diffusion in periodic heterogeneous lattices, method of calculating, 17: 13473
diffusion in plane heterogeneous systems, time-dependent equations for, 20: 40059
diffusion in Plexiglas, 16: 8289 (DC-59-9-124)
diffusion in Plexiglas with empty channels, pulsed measurements of, 18: 33036
diffusion in polyethylene, extrapolation lengths at different energies for, 18: 21132 (RPI-328-4)
diffusion in polyethylene cells, spectra in, (E/T), 19: 29218
diffusion in polythene, extrapolation lengths for, 18: 28556
diffusion in pulsed moderating systems, calculation of multigroup extrapolation distances, 16: 750
diffusion in pulsed assemblies, wave model for, 18: 40472 (EUR-1643.e (p.137-41))
diffusion in P_1 approximation, equations for multigroup, 17: 2215
diffusion in r-θ geometry, iterative methods for solution of, 18: 9292 (KAPL-M-DBM-3)
diffusion in r-θ geometry, iterative methods for solution of, 18: 42609 (TID-20165)
diffusion in radial geometry, computer program for, 19: 14461

(AEEW-M-469)
diffusion in reactor core, computer program for calculating, 16: 3379 (AEEW-M-160)
diffusion in reactor matrices, computer program for solving equations for, 16: 19237 (KAPL-M-FDF-1)
diffusion in reactors, DDB computer code for calculating, 16: 28361 (GAMD-2797(Vol.I))
diffusion in reactors, DDB computer code for calculating, 16: 28362 (GAMD-2797(Vol.II))
diffusion in reactors, calculation using Schroedinger equation, 16: 14249
diffusion in reactors, kinetic equations of two-group theory for, 17: 2499
diffusion in reactors, solution of the kinetic equation in periodic reactivity changes, 17: 26817
diffusion in reactors, autocorrelation functions and fluctuations of, 17: 24773
diffusion in reactors, five-group analysis of, 17: 31672 (AEEW-R-249)
diffusion in reactors, symmetry properties of eigenfunctions occurring in, 17: 40306
diffusion in reactors, calculation using active and passive surface technique, 17: 42228
diffusion in reactors, radial-streaming, 18: 7889 (AEEW-R-272)
diffusion in reactors, program for few-group two-dimensional, 18: 17280 (WCAP-6059)
diffusion in reactors, solution of spatio-temporal equations for, 18: 16890 (EUR-596.e)
diffusion in reactor lattices, computer programs for, 18: 44971 (KAPL-M-6186)
diffusion in reactor lattices, computer solution for (T), 19: 3518 (NP-14429)
diffusion in reactors, integration techniques and invariant imbedding in equations for (T), 19: 3549
diffusion in reactors, equations for space- and time-dependent, (T), 19: 10485 (HW-72740)
diffusion in reactors, computer programs for, 19: 14790 (KAPL-2165-2)
diffusion in reactors, analysis using KARE program, (E), 19: 14807 (KAPL-M-6186(Rev.I))
diffusion in reactor control plates, models for, (T), 19: 17197
diffusion in reactors with complex geometry, method for solving equations for, 19: 17234
diffusion in reactors with complex geometry, (T), 19: 17235
diffusion in reactor fuel rods, use of Laplace transformation in solution of equations for, 19: 18128
diffusion in reactors, space-time behavior of, (T), 19: 27755
diffusion in reactor lattices, Monte Carlo method for, (T), 19: 35713
diffusion in reactors, calculations for, 19: 35506
diffusion in reactors, computer program for, 19: 40176 (AGN-TM-407)
diffusion in reactors, use of poison in direct solution of equation for, 19: 42052
diffusion in reactors, lectures on, 19: 45531 (N64-29786)
diffusion in reactors, computer calculations of, (T), 19: 47912 (ANL-7050, pp 347-68)
diffusion in reactors, variational calculations of, (T), 19: 47945 (ANL-7050, pp 159-77)
diffusion in reactors, use for fuel-cycle and power-distribution calculations, (T), 19: 47946 (ANL-7050, pp 231-49)
diffusion in reactors, two-dimensional codes for, (T), 20: 5056 (CONF-654-22)
diffusion in reactors, mesh size corrections for computer codes for, 20: 5069
diffusion in reactors, variational multichannel synthesis for, (T), 20: 8038 (KAPL-3095)
diffusion in reactors, accuracy of variational method for, (T), 20: 12369
diffusion in reactors, computer program for, 20: 14056 (AWRE-O-99/65)
diffusion in reactor reflectors, few-group constants for, 20: 34934
diffusion in rectangular cells, 17: 26007
diffusion in S_4 cylindrical geometry cell, computer code for, 19: 33195 (NAA-SR-Memo-9202)
diffusion in shielding materials, Monte Carlo schemes for calculating, 16: 2469 (UCRL-5918-T)
diffusion in slab geometry, computer program for calculation of, 16: 33984 (INTERNUC-67)
diffusion in slab geometry, P-2 approximation for disadvantage factors in, 17: 34560(R) (TID-19195)
diffusion in slab geometry, orthogonal polynomial angular expansion of the Boltzmann equation for, 17: 39961
diffusion in slabs, random-walk treatment of, (T), 20: 46551 (AD-640260)
diffusion in solids, solution of equations for, 16: 23763
diffusion in solids, lattice structure effects on, 18: 24577
diffusion in spherical geometry, P_3 boundary conditions for, 18: 2795
diffusion in spherical geometry, multigroup adjoint computer program for (T), 19: 1522 (IA-936)
diffusion in stacked cylindrical disks, computer program modification for calculation, 16: 31224 (UCRL-5682(Suppl.1))
diffusion in swimming pool reactor, (E/T), 19: 25769
diffusion in thermal reactors, modified two-group theory model for, 17: 28231
diffusion in thick slabs, 18: 15169
diffusion in thin slabs, discrete ordinate quadratures for, 17: 5313
diffusion in three-dimensional lattices, computer program for few-group, 18: 42587 (NP-14349)
diffusion in triangular mesh, computer program for multigroup, 18: 42578 (BLG-230)
diffusion in two-dimensional space with XY geometry, computer program for, 19: 21198 (CEA-R-2759)
diffusion in two-group reactor model, one-velocity, 18: 38322 (A/CONF. 28/P/706)
diffusion in two-region assemblies of enriched uranium and heavy water, 19: 42048 (MIT-2344-3, pp 125-36)
diffusion in unmatched foils, data thickness corrections for, 16: 33991 (TID-16733)
diffusion in uranium rods, laplacians for, 18: 7891 (CEA-Note-209)
diffusion in uranium, asymptotic spectra in, 19: 19067
diffusion in variable-mesh hexagonal geometry, solution of equation for, 18: 11148 (WAPD-T-1610)
diffusion in water at ~0° and ice at −80°C, 17: 2211
diffusion in water, parameters for, 17: 15220 (TID-18007)
diffusion in water, parameters for, 17: 26066
diffusion in water in cube, slab, and sphere geometry, 17: 34560(R) (TID-19195)
diffusion in water-moderated plutonium lattices, 18: 36782(R) (HW-81659(p.33-44))
diffusion in water, pulse technique for measuring, 18: 38043 (A/CONF. 28/P/678)
diffusion in water, design of pulse generator for measuring, 19: 14479
diffusion in water, measurement using pulsed source, (E), 19: 27392 (INR-573/IXA)
diffusion in water, P_3 calculations of pulsed, (T), 19: 37767 (WAPD-T-1788)
diffusion in water in spherical containers, parameters for, (T), 20: 15686
diffusion in zirconium hydrides, decay-time constants and spectra for, (E), 20: 11943
diffusion in 60° geometry, seven-point difference equations for, (T), 19: 29193
diffusion in 60° geometry, seven-point difference equations with arbitrary mesh spacing for, 20: 44590 (WAPD-T-1802)
diffusion length and mean free path, calculation from Markov chain statistics, 16: 12411
diffusion length and pulse parameters for water, 18: 26516
diffusion length calculations for, 16: 24373
diffusion length in liquids, design of apparatus for measuring, 16: 10942
diffusion length in heavy water, 16: 28018
diffusion length in water, 17: 5308
diffusion length in water and aqueous solutions of poisons, 17: 14740 (TID-11295(2nd Ed.))
diffusion length in infinite media, effect of several approximations on, 17: 26024
diffusion length in semi-infinite beryllium block, effect of cold and trapped neutrons on, (T), 19: 43257
diffusion length in water, from time-decaying fields, (E), 19: 47560
diffusion length in two-region slab lattice, (T), 20: 34482
diffusion length measurements in water, 16: 737
diffusion length measurements in AGOT graphite, Bragg-induced cold neutron effects in, 20: 44585 (NAA-SR-Memo-11866)
diffusion length of, exact equations for, 18: 34742
diffusion lengths in paraffin and polyethylene, effects of temperature, 16: 736
diffusion lengths in crystals, calculation, 16: 8161
diffusion lengths in bismuth-graphite systems and graphite, 16: 24375
diffusion lengths in slab lattices, calculations of anisotropic, (T), 19: 19355 (BNL-8950)
diffusion lengths and energy spectra in semi-infinite beryllium block, (T), 19: 33206
diffusion lengths in graphite, 20: 22520(R) (NAA-SR-11805)
diffusion lengths and temperatures in boron-poisoned heavy and light water, 20: 34469 (DP-MS-66-30)
diffusion lengths in graphite, 20: 35841(R) (NAA-SR-11900)
diffusion lengths in poison-bearing water, calculations using diffusion theory and transport theory, 20: 40053
diffusion lengths in graphite, 20: 46966(R) (NAA-SR-12010)
diffusion, model study in Kansas State standard pile, 16: 24761 (TID-15667)
diffusion, multiplication, and stopping of, use of impulse method in studying, 17: 34847
diffusion, non-iterative solution, 16: 12345
diffusion, numerical solution by digital computers, 16: 21341
diffusion of, computer program for, 17: 22532 (KAPL-2165-1)

diffusion of, computer code for solution in few-group approximation, 17: 26396 (PAN-107/IX)
diffusion of, convergence of codes for, 18: 2803
diffusion of, development of Nordheim equation from, 17: 29564 (CNAM-7)
diffusion of, effects of cavities on, 17: 20966
diffusion of, FICS program for analysis of, 17: 19197 (KAPL-M-RPC-3(Rev.1))
diffusion of, Fortran program for solution of two-dimensional, 17: 19208 (WAPD-TM-363)
diffusion of, in hexagonal lattices of circular rods, calculation of, 16: 33677 (AAEC/TM-123)
diffusion of, in light water, calculation models for, 16: 31204 (GEAP-3943)
diffusion of monoenergetic, Boltzmann time-independent equation in spherical geometry for, 20: 24316
diffusion of, new asymptotic theory for, 18: 2788
diffusion of, numerical solution of multigroup equations for, 17: 26014
diffusion of, numerical solution of multigroup equation for, 18: 2802
diffusion of, one- and two-dimensional multigroup, 17: 26013
diffusion of pulsed, extrapolation distances for, 16: 26208
diffusion of pulsed, in water assemblies, 17: 22538 (TID-18565)
diffusion of pulsed, in moderator materials, 17: 38058
diffusion of pulsed, in moderators, 18: 38048 (A/CONF.28/P/762)
diffusion of pulsed, in shutdown reactor cores, (T), 20: 36437
diffusion of, reactor transfer functions for, 17: 7531 (AEEW-R-197)
diffusion of reactor, streaming effect in, 19: 12757
diffusion of, solutions for two-energy-group, 17: 26008
diffusion of, solution of Boltzmann transport equation for, 17: 26400
diffusion of, three-group approximation of, 17: 15432
diffusion of, TRAM code for calculating, 17: 28222 (KAPL-M-RPC-1(Rev.1))
diffusion of, variational method for space and time synthesis in, 17: 3820
diffusion of, variational procedure for calculating fast few-group constants for, 17: 5298 (KAPL-2220)
diffusion of, alternating-direction iteration theory for, 19: 29167 (CONF-650505-2)
diffusion of, analysis using transport theory with boundary conditions, 19: 31190(R) (GEAP-4782)
diffusion of, asymptotic resolution of kinetic equations for, (T), 19: 31206
diffusion of, calculation of thermal utilization factor in energy-dependent, (T), 19: 47558
diffusion of, code for multi-group time-dependent, 19: 27397 (WANL-TNR-133)
diffusion of, computer program for one-dimensional few-group, 18: 13190 (WCAP-6058)
diffusion of, computer program for, 18: 15432 (NAA-SR-Memo-9423)
diffusion of, computer program for N-group, 18: 22857
diffusion of, computer simulation of reactor, 18: 24847 (HW-79446)
diffusion of, computer program for (T), 19: 1525 (KAPL-2165-3)
diffusion of, computer analysis using perturbation theory, 19: 4578 (AI-Memo-64-102)
diffusion of, complex bucklings in three-group theory for solution of equations for, 19: 5118
diffusion of, computer analysis of, (T), 19: 19065 (WAPD-TM-395)
diffusion of, computer programs for, 19: 29181 (WAPD-TM-477)
diffusion of, computer codes for multigroup, 19: 29505 (FZK-211)
diffusion of, energy averaging of coefficients for, 18: 26517
diffusion of, KARE program for, (E), 19: 37760 (KAPL-M-6186(Rev.II))
diffusion of, monoenergetic Boltzmann equation for, 18: 30701
diffusion of, multidimensional, multigroup, multiregion code for, 18: 15131 (EUR-532.e)
diffusion of, multigroup equations for, 18: 21155
diffusion of, nonlinear iteration method for, (T), 19: 29166 (CONF-650501-3)
diffusion of, polarization effects in, (T), 19: 37775
diffusion of, program for few-group constants in, 18: 16893 (KAPL-M-6119)
diffusion of, Ritz difference equations on a triangulation for one-group, 19: 29180 (WAPD-T-1756)
diffusion of, synthesis of multigroup equations for, 19: 31461(R) (ANL-7010(p.235-87))
diffusion of, transport theory for extension of coefficient of, 20: 21944
diffusion of, use in study of molecular structure, 18: 13714 (AD-415804)
diffusion of, variational calculations of spatial and temporal, 18: 28539
diffusion of, wave theory for, 18: 38060
diffusion, one-dimensional multigroup calculation of annular void coefficients, 16: 18417
diffusion, one-dimensional few-group code for, 16: 26195 (KAPL-M-CT-1)
diffusion parameters in water at 26.7°C, 16: 12407
diffusion parameters in biphenyl, monoisopropylbiphenyl, and Dowtherm, measurement, 16: 19731
diffusion parameters in water-d_2, 17: 2219
diffusion parameters for water, measurement by pulsed and poisoning methods, 17: 15197 (BNL-719(Vol.III)(p.946-65))
diffusion parameters in water, 17: 26398 (PAN-403/IX)
diffusion parameters in carbon black, 19: 5113 (CONF-446-79)
diffusion parameters for pulsed, spectral correction analysis of, (T), 19: 33216
diffusion parameters in heavy water from 25 to 250°C, (E), 19: 33224
diffusion parameters in heavy-water–water mixtures at 21°C, (E), 19: 35351 (TID-21851)
diffusion parameters in ice, temperature dependences of, 19: 43253 (ORNL-TM-1204)
diffusion parameters for cylinders of water–heavy water, 20: 2951
diffusion parameters in water, sample geometry effects on, (E), 20: 2952
diffusion parameters in diphenyl at 85 and 105°C, (E), 20: 2953
diffusion parameters organic liquids and water, pulsed, (E), 20: 13729
diffusion parameters for uniform reactor matrices, (T), 20: 30851
diffusion parameters in organic glass, resins, and water, 20: 34508
diffusion parameters in water, measurement and calculation of, (E/T), 20: 40055
diffusion problems for anisotropic scattering medium, solution by singular integral method, 16: 9420
diffusion programs for, characteristics of two-dimensional, 18: 28540
diffusion, solution to non-linear diffusion equations for semi-infinite media, 16: 13932 (UCRL-6721)
diffusion, stochastic analysis of anisotropic, 16: 31061
diffusion theory, approximations by monatomic heavy-gas model, 16: 29725
diffusion theory calculations for self-shielded regions, 16: 5918 (WAPD-T-1384)
diffusion theory calculations, computer program for, 16: 9132 (HW-71545)
diffusion theory for, transport effects in, 18: 28970
diffusion theory for, multigroup, 18: 42594 (TID-7050(p.154-75))
diffusion theory for, scattering-kernel effects on fuel and poison depletion rates for, 18: 44705 (KAPL-M-6151)
diffusion theory for, mathematical methods in (T), 19: 1090
diffusion theory for, boundary conditions for asymptotic, 19: 5124
diffusion theory for, two-dimensional multigroup, 19: 12455 (EUR-2174.i)
diffusion theory for, bilinear averaging process in, (T), 19: 29027
diffusion theory for, use in analysis of control rods, 19: 31496 (AP-Note-399)
diffusion theory for, boundary terms in time-dependent synthesis techniques for, (T), 19: 33207
diffusion theory for, transport-equivalent, 19: 45221(R) (GEAP-4913)
diffusion theory for wave-type experiments on, 20: 32363
diffusion theory, generalized multigroup, 16: 28020
diffusion theory, multi-group, 17: 5581 (NYO-10206)
diffusion theory of, associated with reactor criticality studies, 17: 2515
diffusion theory of, direct solution of difference equations for, 17: 19212
diffusion theory, orthogonality relations for adjoint functions in, 17: 25680
diffusion theory of, asymptotic, 18: 994
diffusion theory of epithermal neutron logging in borehole geometry, problems in one-energy-group, 18: 5494
diffusion theory of, reduction of transport theory to multigroup, 18: 15165
diffusion theory of, comparison with energy-dependent transport theory solutions, 18: 21153
diffusion theory of, transport-equivalent, 18: 42583(R) (GEAP-4547)
diffusion theory of, transport effects in, 19: 6624
diffusion theory of, development of transport equivalent, (T), 19: 12456(R) (GEAP-4731)
diffusion theory of, variational principles in, 20: 1136
diffusion theory parameter calculation, variational procedure, 16: 9653 (KAPL-2000-16)
diffusion theory parameters using bilinear averaging, multigroup, 20: 1140
diffusion theory representation of fuel clusters containing control rods, 20: 3428
diffusion theory representation for control rods of thermal reactors, (T), 20: 16090 (WAPD-T-1841)
diffusion through hollow cylinders, computer analysis, 16: 22968 (SPM-423)
diffusion through gold and indium foils and palladium, 19: 5147
diffusion, transport corrections to, 16: 24371
diffusion with upscatter, computer program for multigroup, 19: 3190 (NAA-SR-Memo-9891)
diffusion-depletion calculations, representation of few-group cross sections in, 19: 19362 (WAPD-T-1721)
diffusion, effects of cross-section resonance structure on, 18: 38009 (A/CONF.28/P/357)
disadvantage factor calculations for slab geometry, 17: 26405
disadvantage factor of two-region slab lattice, (T), 19: 19366
disadvantage factor in cylindrical geometry, 19: 42063

disadvantage factor in uranium-water lattices, (E/T), 20: 30855
discovery, 18: 4446
dispersion in homogeneous systems, analysis of wave experiments for, 20: 34511
dispersion law for reactor, (T), 19: 17231
dispersion law of moderators, (T), 20: 2991
distribution and thermalization in reactors, computer program for, 19: 23998(R) (TID-21733)
distribution at two-medium interfaces, angular and energy, (E), 19: 8382
distribution fluctuations in reactor with cellular structure, method for calculating, 17: 19211
distribution fluctuations in reactors, effects on power spectra, 18: 28979
distribution fluctuations in power reactors, theory of, 18: 29067
distribution fluctuations in small plutonium-fueled assemblies, 18: 28302
distribution from atomic explosions, 16: 8452
distribution from atomic explosions, 16: 11367(T) (JPRS-11873)
distribution from TRIGA Reactor, 16: 25016 (DOFL-TM-60-27)
distribution from pulsed plane source, 16: 24758 (AE-71)
distribution from pulsed source in hydrogen, P_1-approximation for, 18: 13026 (AE-129)
distribution from alpha reactions with tantalum, 19: 33281
distribution functions for, multiple collision densities for Monte Carlo calculation of, 17: 26028
distribution functions for, Monte Carlo calculation of, 17: 39949 (NP-13117)
distribution functions in cylindrical geometry, 19: 3189 (CRRP-1201)
distribution functions in infinite media in steady state, (T), 19: 8378 (TID-21429)
distribution functions for, analytic expressions for Monte Carlo calculation of, 19: 10240
distribution in absorbing rod, P_n approximation for, 20: 6267
distribution in Army Reactors (PM-3), from antimony–beryllium sources, (E/T), 19: 29188
distribution in burro irradiated at HPRR, 20: 7315(R) (ORNL-3849, pp 151-82)
distribution in concrete shelter entranceways, 16: 708
distribution in critical system, Monte Carlo calculations of, 17: 11462 (UCRL-6707)
distribution in finite-layer reactor, two-group theory for, 17: 24654
distribution in FRJ-1 Merlin Reactor, 17: 7634 (JUL-75-RE)
distribution in homogeneous spherical fast reactors, 16: 28427(T) (CEA-tr-R-1596)
distribution in homogeneous moderator, space-energy, 18: 40479
distribution in hydrogenous moderators, second spatial moment of, 18: 34736
distribution in hydrogenous moderators containing voids, second spatial moment of, 19: 3193
distribution in infinite medium, steady-state, (T), 20: 40052
distribution in large closed-cycle reactor primary shields, 19: 45601(R) (WCAP-3750)
distribution in monoenergetic criticality problems, calculation of, 19: 14284
distribution in multiplying assemblies, 17: 17091 (LADC-5383)
distribution in pulsed-neutron-irradiated semi-infinite media, (T), 19: 8389
distribution in radial shield of Experimental Boiling Water Reactor at 100-Mw operation, calculation, 19: 10547 (IEA-74)
distribution in reactors, fluctuation frequency spectrum of, 18: 6448 (NP-13443)
distribution in reactors, correlation theory calculations of, 20: 45053
distribution in shielding, emergent gamma flux from, 16: 31177 (NARF-62-6T)
distribution in shield without hydrogen, (T), 19: 5392
distribution in soils following nuclear detonations, 16: 12814 (WT-1117)
distribution in spherical bodies, point source transport solutions for position- and velocity-dependent, 17: 9492
distribution of air-burst-induced, in soil, effects of moisture, 16: 2817 (USNRDL-TR-530)
distribution of centerline uncollided at the end of finite cylinders, empirical determination, 16: 14204 (TID-14973)
distribution of counts by a detector in reactor, probability method for, 17: 40287
distribution of fission-induced, in cylindrical phantoms, 20: 7315(R) (ORNL-3849, pp 151-82)
distribution of, numerical method for computing, 17: 3817
distribution oscillations in subcritical assemblies, 18: 28978
distributions and collision probabilities of, in superlattices, 17: 40300
distributions around reactors (T), 19: 3486
distributions around reactors, (E/T), 19: 14772
distributions around TRIGA Mark F reactor, (E), 19: 24173 (NDL-TR-56)
distributions at air-ground interfaces, from small atomic explosions, 17: 19198 (LA-2390(Suppl.))
distributions from inelastic meson (π^-)-proton interactions at 374, 417, and 454 Mev, differential, 17: 9205 (UCRL-10564)
distributions from reactions, theory of, 17: 34984
distributions from sources with different spectra, similarity of spatial, 20: 28239
distributions from deuteron disintegration scattering on light nuclei, angular and energy, (T), 19: 27481
distributions from deuteron disintegration scattering on light nuclei, (T), 19: 27481
distributions in ANNA critical assembly, (E), 19: 17364 (PAN-563/IX-A)
distributions in bulk shielding, comparison of calculations and experimental data, 16: 714
distributions in boiling-water reactors (T), 19: 1845
distributions in beryllium oxide-moderated critical assemblies, (E/T), 19: 45537
distributions in cube-shaped room with source in center, 18: 21137
distributions in cylindrical lattices, 18: 28545
distributions in cylindrical lattices, resonance effects on, 18: 28545
distributions in fuel elements in heterogeneous reactors, effects of many-layer probes on, 18: 6449
distributions in fast and thermal reactors, 18: 38302 (A/CONF.28/P/172)
distributions in Geesthacht Research Reactor, methods of measurement of, 17: 38504
distributions in graphite lattices, measurements of fine structures in, (E), 19: 5429 (CEA-R-2479)
distributions in heavy water subcritical assemblies, 18: 28984
distributions in heavy-water-moderated steam-generating, 18: 38424 (A/CONF.28/P/174)
distributions in heterogeneous reactors, method for calculating, 19: 42060
distributions in irradiation positions of German FRM, 17: 31756
distributions in JEEP, 18: 28921(R) (TID-20649)
distributions in light-water-moderated reactors, effects of energy on, 18: 21608
distributions in monoisopropyl diphenyl–uranium and uranium–water lattices, 17: 13472
distributions in multiplying media, theory of prompt-decay constants and spectra for, 18: 21149
distributions in multiplying media, prompt-decaying eigenstates for thermal and slowing-down range in, 18: 21150
distributions in mixed-fuel heavy water-moderated reactors, 18: 28973
distributions in multiplying medium, space-time correlations in, 19: 33200
distributions in multi-component unbounded media, angular and energy, 16: 2472(T) (AEC-tr-4707)
distributions in Milne problem with sources of the form X^n, angular and flux, 16: 5816
distributions in poisoned slabs, variational calculations of, 18: 28537
distributions in reactor lattices, nonuniform spatial, 16: 728
distributions in reactors, methods of calculating and measuring, 17: 28492
distributions in reactors, solution of multigroup equations for, 17: 38506
distributions in reactors, effects of fuel inhomogeneities on, 18: 4741 (EUR-401.e)
distributions in reactors, instruments for measuring, 18: 8606(R) (HW-78388(p.7.1-10))
distributions in reactors, optimization of, 18: 28968
distributions in reactors, cylindrical-cell approximations to, 18: 30961
distributions in reactors, boundary-value solutions for, 18: 44976
distributions in reactors, analog-computer simulation of, 19: 3515 (HW-82397)
distributions in reactors containing pulsed neutron sources, (T), 19: 10488 (ORNL-TM-993)
distributions in reactors, noise and power-spectral-density effects on, (T), 19: 14793 (ORNL-3757)
distributions in reactors, calculation using centers and limit cycles, (T), 19: 21634 (BNL-9010)
distributions in reactors, calculations of, (T), 19: 21640 (IDO-16983)
distributions in reactors, computer generation of contour maps of, (E), 19: 30641 (IDO-17042(p.64-71))
distributions in reactors, variational calculations of, 20: 15666 (CONF-660204-4)
distributions in shielding, development of hand calculations for, 16: 26432 (APEX-652)
distributions in shutdown reactor with photoneutron source, 17: 26797
distributions in subcritical assemblies, 17: 42207
distributions in semi-infinite media, albedo problem, 18: 28971
distributions in subcritical reactors, effects of extraneous sources on, 18: 30992(R) (ORNL-3619(p.3-11))
distributions in shield materials, computer program for, 18: 38237 (KAPL-M-6159)

distributions in shield materials, computer program for, 18: 38238 (KAPL-M-6160)
distributions in small assemblies of slabs (T), 19: 1847
distributions in thermal plutonium-fueled reactors, 18: 38299 (A/CONF. 28/P/165)
distributions in three space dimensions in steady-state reactors, 18: 38301 (A/CONF.28/P/169)
distributions in Triso reactor, flux-mapping system for, (E), 19: 24070 (CONF-640607(Vol.I)(Paper C-1))
distributions in unreflected subcritical reactor core, 16: 3655 (AD-257584)
distributions in uranium carbide, space-energy, 18: 42611
distributions of, correlations and fluctuations in, 17: 26010
distributions of, in EGCR, calculation of, 17: 17566 (TID-18245)
distributions of, in plane homogeneous reactor at power level, 17: 19591
distributions of, time moments of energy-time, 17: 22541
distributions of, theorems on fluctuations and fluctuation spectra in, 19: 41653
Doppler coefficients of fertile and refractory materials, 20: 2958
dosage calculation for highly enriched uranium solutions, 16: 3612
dosage determinations, use of film badges for, 16: 4039(T) (NP-tr-824)
dosage determinations in persons exposed to critical assemblies, 16: 8653
dosage determinations in tissue of, from plutonium–beryllium source, 16: 10223
dosage determination, units and measurements, 16: 15042
dosage determination during zero-power reactor incident, 16: 16618
dosage determinations for personnel exposed to nuclear excursion, computer program for, 16: 20877 (Y-1386)
dosage determinations by an attenuation technique, 17: 8450
dosage determination, improvement by use of polyurethane attenuators, 17: 16332(R) (UCRL-7143)
dosage determinations in plutonium processing plant, 17: 34146 (CONF-67-18)
dosage measurements, pile oscillator technique for, 16: 19951
dosage measurement by external counting, 17: 18323 (HW-73891(Rev.))
dosage measurements, from (α,n) and (γ,n) sources in tissue-equivalent phantom, 17: 28684 (UCRL-10267)
dosage to man in supersonic flight in upper atmosphere from solar flare radiation, 18: 30399
dose albedo on concrete, formula for differential (T), 19: 3471
dose and radiative capture rates in concrete, lithium hydride, and water, (T), 19: 14743
dose calculation in man from exposure to criticality accident, 18: 38731
dose distribution and linear energy transfer of, computer calculation of, 17: 33617(R) (ORNL-TM-640)
dose distribution in air-over-ground geometry, spatial, 19: 20217
dose distribution in air from point sources, evaluation of, (E), 19: 25460
dose distributions in water-filled Lucite sphere, 18: 6715(R) (ORNL-3499(Vol.II)(p.85-9))
dose distributions from sources in air, (T), 20: 46928(R) (ORNL-3973(Vol.1), pp 26-47))
dose equivalent rates of, orthonormal expansion method for, (T), 20: 43693
dose equivalent rates of, orthonormal expansion method for, 20: 43694
dose estimation for, from criticality accidents in solutions of fissile material, 18: 27723 (NP-13724)
dose estimation for, computer code for, 19: 31930 (NYO-3267-2)
dose from critical excursion in Alecto, 17: 40411(T) (AEC-tr-6067)
dose from NERVA Reactor Experiment A2, (E), 19: 38235 (LA-3296)
dose from Wood River Junction criticality accident, 20: 5666 (TID-21995)
dose measurement in mixed gamma fields, instruments for, 20: 31505(R) (BNWL-235-4, pp 30-4)
dose measurements, 17: 24892(R) (NYO-10451)
dose measurements in tissue, conversion factors for, 19: 17491 (ORNL-P-802)
dose measurements in tissue of 60 to 400 Mev, 19: 25910 (ORNL-TM-1038)
dose rate at ground from source in air, angular distributions of, 18: 15166
dose rate determination of intermediate energy, instrument for, 16: 29106 (LA-2717)
dose rate in duct entranceways, Monte Carlo calculations of, 19: 38017 (NP-15094)
dose rate in water, statistical estimation of, (T), 19: 17157(R) (ORNL-3714(Vol.I)(p.43-67))
dose rate measurement over broad energy range, 19: 4465 (NP-14358)
dose rates and fluxes from 30-Mev proton reactions in aluminum and beryllium, 17: 22698
dose rates and flux density outside shielding, measurement of, 18: 30689 (JUL-158-ST)
dose rates behind porous plugs, from Ground Test Reactor, 18: 15593 (NARF-58-28R)
dose rates from radioisotope and fission-product sources, 18: 22984 (NYO-10721)
dose rates in air, effects of air-ground interface on, 18: 42363 (CEX-62.14)
dose rates in cylindrical volume source, source function coefficient evaluation, 16: 11118 (DC-57-11-103)
dose rates in shelters, effects of compartmentalization on, 18: 25712 (USNRDL-TR-722)
dose rates of reactor, calorimetric measurement of, absorbed, 19: 45467
dose-rate equivalent of intermediate, difference procedure for calculating, 19: 28584
dose-rate meter for, design of portable, 20: 31600
dose-rates in critical assembly environment, air-scattered, 20: 22386
doses and flux in Bulgarian IRT-1000 research reactor, (E), 19: 19420
doses in tissue at 60 to 400 Mev, calculation methods for, 19: 17159(R) (ORNL-3714(Vol.II)(p.97-118))
doses in tissue from 100- to 400-Mev, 18: 6714(R) (ORNL-3499 (Vol.II)(p.56-60))
doses of, permissible flux for tissue at 60- to 400-Mev, 20: 7659(R) (ORNL-3649, pp 101-50)
dosimeter design for, 19: 44543(P)
dosimetry, 17: 41118
dosimetry, 18: 35260(R) (AERE-PR/HPM-5)
dosimetry, 19: 14463(R) (EUR-2179.e)
dosimetry and flux measurements of, methods for, 19: 19415 (CRC-1210)
dosimetry around pulsed sources, systems for, 19: 44370 (AERE-R-4883)
dosimetry at Harwell, developments, 17: 18621
dosimetry at high temperatures, development of compounds for, 19: 24841 (FZK-208)
dosimetry at Triga reactor facility, techniques for, 20: 36523 (AD-635819)
dosimetry at 0.5 to 1 Mev, 17: 8485
dosimetry by activation techniques, 18: 16355
dosimetry by indium-foil activity, 16: 15026 (TID-15398)
dosimetry by measurement of body sodium-24 activity, 16: 33196
dosimetry by nuclear emulsions, sources of error in, 17: 16434
dosimetry by tritium production in lithium fluorides, 19: 6229
dosimetry by variations in resistivity of metals subjected to irradiation, 18: 30247
dosimetry calculations from foil-activation data, computer program for, 18: 32017 (HW-81367)
dosimetry, design of readout system for, 16: 13924(R) (AD-261974)
dosimetry from beryllium–radium source using optical glass, 17: 23786
dosimetry from critical assemblies, technique for, 20: 7354 (AERE-M-1641)
dosimetry from plutonium(IV) fluoride processing equipment, 16: 22967 (LAMS-2692)
dosimetry in accelerator environment, methods for, 20: 41543 (RPP-R-2)
dosimetry in accidents at Argonne, planning for, 19: 30477
dosimetry in accidental and normal conditions, methods for, 19: 44332
dosimetry in and behind beryllium slabs, tabulations for, 20: 22307 (DC-61-3-69)
dosimetry in chest, use of phantoms for, 20: 46030(R) (AERE-PR-HPM-9, pp 6-17)
dosimetry in criticality accidents, 19: 36729
dosimetry in different energy ranges, review, 17: 3333
dosimetry in event of accident at Savannah River Plant, equipment and methods for, 20: 11029 (DP-1006)
dosimetry in gamma mixtures, 17: 41121
dosimetry in gamma background, tissue-equivalent ionization chamber for, 17: 41113
dosimetry in human body using activation foils, 20: 24946
dosimetry in irradiation experiments in DIDO reactors, 18: 45137 (TID-7697(p.5.6.1-9))
dosimetry in IRT-2000 reactor using ferrosulfates, 19: 22775
dosimetry in living organisms, 18: 38730
dosimetry in medical facility of MIT research reactor, 17: 34269
dosimetry in mixed radiation fields, use of multisphere detector for, 20: 43673 (PPAD-596-E)
dosimetry in neutron background, calorimeter for, 20: 27362(P)
dosimetry in presence of gamma rays, detectors for, 19: 36036
dosimetry in radiation damage studies, units for, 18: 29044(R) (HW-79280(p.6.1-16))
dosimetry in radiation damage studies, 19: 18259 (HW-SA-3541)
dosimetry in reactors, 16: 12188
dosimetry in reactor facilities, 16: 23335 (SC-4680(M))
dosimetry in reactors using activation detectors, review of, 17: 34270
dosimetry in reactors, review of methods for, 17: 34271
dosimetry in reactors, calorimetric, 18: 3043 (TID-19678)
dosimetry in reactors, review of methods for, 18: 33879 (HW-SA-3585)
dosimetry in reactors for radiation effects studies, 18: 41933 (TID-11295

(3rd Ed.))
dosimetry in reactors, activation monitor for, 19: 7797
dosimetry in reactors, using liquid phosphors, 19: 15888
dosimetry in reactors, using colored polyvinyl alcohol films, 20: 2135
dosimetry in reactors, pneumatic system for, 20: 13069 (NASA-CR-54468)
dosimetry in sheep, 18: 38728
dosimetry, in the presence of gamma radiation, 17: 5774 (TID-13984)
dosimetry in tissues, 18: 33431 (TID-20856)
dosimetry in tissues, activation method for, 18: 38729
dosimetry in tissues of 60- to 400-Mev, 19: 40372
dosimetry in tissues, performance of low-temperature calorimeters for, 20: 43668(R) (ANL-7136, pp 1-16)
dosimetry in tissue at large distances from source, 17: 23093 (UCRL-10559)
dosimetry in 10-Bev synchrophasotron, 19: 39315 (JINR-P-2177)
dosimetry methods, 18: 12477
dosimetry near bare pulsed reactor, phantom-nuclear emulsion technique for, 18: 31917 (UCRL-10907)
dosimetry near particle accelerators, 17: 14660
dosimetry of, 19: 40800(R) (AERE-PR/HPM-7)
dosimetry of, 19: 6126(R) (HW-83605)
dosimetry of, 19: 24748(R) (PG-Report-647)
dosimetry of, at right-angle bends in concrete shelter entrances, 17: 3798
dosimetry of atomic explosion, at Hiroshima and Nagasaki, 18: 31806
dosimetry of beryllium–polonium, measurement method for, 17: 41111
dosimetry of, by activation methods, 17: 20344 (CEA-2251)
dosimetry of, conference on, 17: 31052
dosimetry of, conference on, 17: 34266
dosimetry of criticality accident, 19: 36699 (BNWL-SA-5)
dosimetry of, design of isodose detector system for, 17: 11034
dosimetry of, development and evaluation of instruments and methods for, 17: 6437 (JUL-69-ST)
dosimetry of fast and slow, semiconductor apparatus for, 17: 20386(P)
dosimetry of first- and multiple-collision, multisphere technique for, 20: 41280(T) (NP-tr-1410)
dosimetry of fission spectrum, air and *in vivo*, 19: 8951
dosimetry of, from accelerators, 17: 41115
dosimetry of, glass detector for, 17: 16474(P)
dosimetry of high-energy, methods for, (T), 20: 4505 (ORNL-P-1738)
dosimetry of, in IRT-1000 reactor, 17: 41112
dosimetry of, in radiation damage analysis, 17: 3884
dosimetry of in-pile, conference on, 20: 11110 (STI/DOC/10/46)
dosimetry of in-pile, review of, 20: 11144
dosimetry of in-pile, status in Canada, 20: 11145
dosimetry of in-pile, status in France, 20: 11146
dosimetry of in-pile, status in Germany, 20: 11147
dosimetry of in-pile, status in Hungary, 20: 11148
dosimetry of in-pile, status in Netherlands, 20: 11149
dosimetry of in-pile, methods for, 20: 11150
dosimetry of in-pile, status in United Kingdom, 20: 11151
dosimetry of in-pile, status in Yugoslavia, 20: 11152
dosimetry of intermediate-energy, 17: 14661
dosimetry of mixed gamma radiation and, design of apparatus for, 18: 511
dosimetry of nuclear explosion, (T), 19: 40938
dosimetry of pulsed and steady-state, 17: 5780 (USNRDL-TR-583)
dosimetry of pulsed, 18: 10374 (D2-9878-4)
dosimetry of reactor, activation method for integral, 20: 9273
dosimetry of secondary, from low-energy solar-flare protons, 19: 17159(R) (ORNL-3714(Vol.II)(p.97-118))
dosimetry of, theory of, 17: 8647
dosimetry of thermal to 10 Mev, detector for absorbed, 17: 41110
dosimetry of, use of ionization chambers for, 17: 8650
dosimetry of, using treated glass, 17: 3347(P)
dosimetry of, using proposed universal unit, 18: 4947(T) (AEC-tr-6189)
dosimetry of 0.5 ev to 0.5 Mev, 17: 41122
dosimetry of, after criticality accident, 19: 33986 (BNWL-SA-6)
dosimetry of, book on, 19: 5125
dosimetry of, calculational methods in, 19: 38897
dosimetry of, calibration of silicon surface-barrier detector for, 19: 26669 (TID-21844)
dosimetry of, calibration of photographic film detectors for, 20: 4237 (BNL-9665)
dosimetry of, Canadian service for, 20: 7309 (NP-15642, pp 13-19)
dosimetry of, combined chemical and computer method, for thermal to 15 Mev, 19: 29889(R) (ANL-6971(p.90-116))
dosimetry of, depth variation in, 19: 36035
dosimetry of, design of rem counter for, 18: 14195 (AE-132)
dosimetry of, design of ionization chamber for, 19: 31787(R) (NYO-2740-2)
dosimetry of, design on boron polyethylene-moderated counters for, 20: 39214(T) (NP-tr-1394)
dosimetry of, design of ionization chamber for, 20: 41268(R) (NYO-2740-3, pp 5-165)
dosimetry of, detector for, 19: 32603(P)
dosimetry of, development of thermoluminescent detectors for, 20: 4236 (BNL-9605)
dosimetry of, development of instrument for personal and general-area, 19: 767(R) (HW-81746(p.5.46-53))
dosimetry of, development of boron trifluoride rem counter for, 19: 2624
dosimetry of, development of metal-foil detector for, 19: 20340
dosimetry of, development of calorimeter for, 19: 29889(R) (ANL-6971 (p.90-116))
dosimetry of, equipment and methods for, 18: 31315
dosimetry of, equipment and techniques for, 19: 7538(R) (ORNL-3697 (p.113-30))
dosimetry of, equipment and techniques of, 19: 22780
dosimetry of, equipment for, 19: 46847
dosimetry of, equipment and techniques for, 20: 35758 (PG-Report-711)
dosimetry of, evaluation methods for, 18: 31314
dosimetry of, film badge system for, 19: 11462
dosimetry of, from Phoebus 1A-321 rocket reactor, 20: 35120 (LA-3393)
dosimetry of, in-pile, 20: 33709
dosimetry of, maximum permissible exposure dose for, 18: 31829
dosimetry of, methods for personnel, 19: 36728
dosimetry of, methods for, 20: 43671 (ORNL-P-2467)
dosimetry of, passive analytic techniques in, 18: 35831 (AFSWC-TDR-62-107)
dosimetry of, performance of chemical and luminescent detectors for, 18: 38728
dosimetry of, performance of photographic film detectors for, 18: 39679
dosimetry of, performance of semiconductor detectors for, 19: 34066
dosimetry of, performance of photographic film detector for, 19: 42731
dosimetry of, performance of film and silicon diodes for, 20: 29518 (BNWL-SA-27)
dosimetry of, performance of proportional detectors for, 20: 41268(R) (NYO-2740-3, pp 5-165)
dosimetry of, performance of cadmium-covered film detectors with sulfur pellets for, 20: 46030(R) (AERE-PR-HPM-9, pp 6-17)
dosimetry of, photographic, 19: 46853
dosimetry of, physical problems in, 20: 25386 (ORNL-P-2105)
dosimetry of, portable microcalorimeter for, 20: 21024 (AD-630693)
dosimetry of, review of methods for, 19: 28589
dosimetry of, review of research at Harwell, 20: 23487
dosimetry of, scintillation detector for, (E), 19: 22697 (JUL-213-ST)
dosimetry of, system for, 20: 14915(P)
dosimetry of, tissue-equivalent proportional counters for, 20: 13060 (CEA-R-2891)
dosimetry of, use of silver-activated metaphosphate glass for, 19: 42722(T) (CEA-tr-A-1750)
dosimetry of, use of probe method in, 20: 37081
dosimetry of, using induced activity, 18: 14196 (AEEW-M-335)
dosimetry of, using tissue-equivalent ionization chambers, 19: 27949 (TID-21889)
dosimetry of, using radiochemical nitrate yields, 19: 39042
dosimetry outside reactor shielding, 18: 9934
dosimetry procedures for NMPO experiments in ETR, 18: 32220 (CONF-589-1)
dosimetry using boron-loaded nuclear track plates in spherical water moderator, 20: 35778
dosimetry using double-moderator detector, 18: 33951
dosimetry using film badges, 19: 4417
dosimetry using packs of Eastman Type A (NTA) film, 16: 30599 (UCRL-9513)
dosimetry using silver-activated phosphate glass, 16: 9051
dosimetry using thermoluminescent phosphor, (E), 19: 4455 (HW-84398)
dosimetry using thermoluminescent phosphors, 19: 40868 (BNWL-SA-23)
dosimetry using ultrasonic waves, 17: 8665(P)
dosimetry with proportional detectors, 17: 18644
dosimetry with solid state track detectors, medical uses, 20: 41262 (BNWL-SA-619)
dosimetry, role of momentum in, 20: 605
dosimetry, using photographic film and scintillators, 19: 28676
dynamics in reactors, space-time, 18: 33016 (A/CONF.28/P/271)
economy in regenerative reactor employing thorium–uranium-233 cycle, 17: 24774
effect on integrated MOS circuits, 20: 46097(R) (AD-630344)
effect on internal friction in pure iron, 18: 28054
effect on nuvistors and miniature electron tubes, 20: 46101
effect on pyrolysis of terphenyls, 19: 40630
effective temperature, definitions of, 18: 38642
effects combined with gamma rays on survival of burros, 20: 32965(R) (ORO-648, pp 1-25)
effects in barley seed, genetic, 20: 97
effects in hydrogen plasma in strong uniform magnetic field, 16: 3776
effects in plants, genetic, 19: 21861(R) (NP-14937(p.116-25))

effects in silkworms, genetic, 19: 21915
effects in silkworms, genetic, 19: 21916
effects in Tradescantia and Vicia, genetic, 19: 36014
effects in Tradescantia, biological, 19: 40800(R) (AERE-PR/HPM-7)
effects mixed with gamma radiation on neuro-endocrine changes in dogs, 19: 26018
effects of acute and chronic exposure to, review, 18: 17568
effects of atomic bomb, on Hiroshima victims, correlation of dose and acute symptoms in, 19: 8853
effects of bilateral and unilateral exposure to, on swine, 20: 32965(R) (ORO-648, pp 1-25)
effects of bipolar gain of transistors, Q-factor technique for, 19: 32613(R) (AD-608960)
effects of, combined with gamma radiation on electronic parts, effects of neutron-gamma ratio on transient, 18: 647 (D2-9878-3(Sect.E))
effects of, combined with gamma radiation on electric properties of silicone dielectric fluids, 18: 656 (NARF-63-7T)
effects of exposure of cotton seeds to, on plant growth and fiber texture, 19: 8860
effects of high-intensity pulses of, on magnetic ferrites, 18: 5818 (USAELRDL-TR-2286)
effects of high-altitude explosion-produced, on ionosphere, 18: 29823 (RM-3932-PR)
effects of high-level, on ecology of bird populations, 20: 17
effects of in-pile, on nickel alloys and steels, 18: 28075
effects of in-pile, on alloys and metals, 18: 27952(R) (EURAEC-926)
effects of in-pile, on thermocouples, (T), 19: 22657 (CONF-640607 (Vol.II)(Paper D-5))
effects of in-pile, on thermocouples, (E), 19: 24014 (CONF-640607 (Vol.II)(Paper D-4))
effects of in-pile, on thermocouples, (E), 19: 24015 (CONF-640607 (Vol.II)(Paper G-2))
effects of in-pile, on SNAP 10A fuels, (E), 20: 6678 (NAA-SR-Memo-11374)
effects of iron–nitrogen solid solution at >1 Mev, nitrogen-loss-enhancement, 19: 1004(R) (ORNL-3676(p.125-56))
effects of magnetic fields on, (T), 20: 30734(R) (TID-22970, pp 1-63)
effects of mechanical properties of zinc crystals, 18: 44262
effects of mixed gamma radiation and, on forest litter production, 19: 13082
effects of mixed gamma radiation and, on sheep and goats, 18: 8109 (RTD-TDR-63-3077)
effects of, on monkey response to repetitious work, 17: 19852
effects of, on mortality of mice, fission spectrum, 17: 19811 (USNRDL-TR-627)
effects of pulsed, combined with gamma radiation on the turn-off characteristics of silicon-controlled rectifiers, 18: 648 (D2-9878-3 (Sect.F))
effects of pulsed, on cables, resistors, and ferrite cores, 18: 14544 (USAELRDL-TR-2306)
effects of pulsed, on radioisotope release from NERVA fuels, (E), (USNRDL-TR-811)
effects of reactor, on radiation stability of strongly basic anion exchange resins, 19: 44055 (IAE-788)
effects of repeated exposures of, on graphite, 19: 34739 (BNL-8223)
effects of resonance, on reactivity in WWR-S reactor, 20: 38536
effects of, review, 18: 4600
effects of whole-body exposure, hematological, 16: 11430(R) (ANL-6464 (p.12))
effects of 14-Mev, on *Escherichia coli*, relative biological efficiency in, 20: 31107
effects of, alone and mixed with high-level gamma radiation, in burros, swine, and sheep, 18: 11645(R) (ORO-614)
effects of, combined with gamma radiation on monkeys, 18: 6616 (SAM-TDR-63-55)
effects of, compared with gamma and x radiation, 18: 41233
effects of, measurement and shielding, 18: 17375
effects of, on cataract induction, comparison of RBE of x rays with, 20: 40618(R) (NYO-2740-3, pp 166-215)
effects of, on iron–nickel alloys, 20: 33949
effects of, on photosensitivity of molybdenum trioxide single crystals, 20: 46235
effects of, problems in monitoring, 17: 18851 (ASD-TDR-62-530)
effects of, with gamma radiation on size of litters produced by male mice, 20: 20453
effects on absorption spectra of zinc sulfide crystals, 19: 32209
effects on activation of dust samples, inhalation hazards from, 19: 26589
effects on adrenal, spleen, and testes weights in mice, 20: 33068
effects on age hardening of beryllium–copper alloys, 19: 44760
effects on aging of aluminum–lithium alloys, 18: 18434
effects on Al–UAl, dispersion fuel plates, 18: 8716 (CONF-339-5)
effects on algae, biological, 20: 1681
effects on alkali halide single crystals, annealing of, (E), 19: 17974
effects on alkali metal and alkaline earth bromates, 20: 36899
effects on alkali halide crystals, 20: 43303
effects on alkyl bromide, 19: 22325
effects on alkyl bromides, Finkelstein reaction for measuring partial organic retention in, 20: 29292
effects on alloys and stainless steels at cryogenic temperatures, 20: 2459
effects on alpha iron, model of, 19: 11669(R) (GEMP-41A)
effects on α iron, interstitial cluster and vacancy production from, (T), 20: 38361
effects on alpha uranium, relation burnup and swelling in, 18: 5829
effects on α-uranium, dislocation loops induced in, 19: 6367
effects on alpha-uranium, orientation and Burgers vectors of dislocation loops from, 20: 5848
effects on alumina-coated uranium dioxide fuel particles, 19: 39227 (BMI-1729)
effects on aluminum and gold, effects of quenched-in vacancies on stage I recovery from, 18: 4321
effects on aluminum–plutonium alloy, 18: 5811 (ANL-6651)
effects on aluminum-base fuels, 18: 5812 (ANL-6665)
effects on aluminum-containing reactor fuels, annealing of, 18: 28076
effects on aluminum oxide, ESR spectra of, 18: 28078
effects on aluminum-lithium alloys, molybdenum-uranium alloys, and uranium, 18: 37733 (A/CONF.28/P/62)
effects on aluminum-clad uranium dioxide fuel, 19: 7978 (GEAP-3694)
effects on aluminum oxides, ESR in, 19: 18513
effects on aluminum-matrix dispersion fuel plates, 19: 32679(R) (IDO-17037)
effects on aluminum–copper single crystals, effects of aluminum content on strength-annealing of, 19: 44739(R) (ANL-7000, pp 233-77)
effects on aluminum, copper, gold, and platinum, low-temperature recovery of residual resistivity from, (E), 19: 47097
effects on aluminum–silicon alloys, recovery from, 20: 905
effects on aluminum oxides, (E), 20: 3446(R) (GEST-2045)
effects on aluminum alloys, 20: 18020(R) (ORNL-3900, pp 2-81)
effects on aluminum oxides, EPR studies of, 20: 18740
effects on aluminum–copper alloys, molybdenum, and nickel, 20: 27569(R) (BNWL-207, pp 3.7-13)
effects on aluminum, correlation with Frenkel defects, 20: 45037
effects on aminotransferase activities in central nervous system and skeletal muscle in rats, 20: 36601
effects on ammonium and potassium dichromates, effects of radiation, thermal, and uv annealing on, 18: 16114
effects on ammonium and potassium sulfates, effects of ultrasonics on, 19: 4220
effects on ammonium and potassium sulfates, ultrasonic reversal of, 19: 13471
effects on animal cells in tissue culture, 18: 38931
effects on anion-exchange resins, 19: 38697 (ZFK-RN-17(p.139-64))
effects on antifriction and strength properties of structural materials, 20: 41498
effects on antimony compounds, thermal annealing of, 19: 2403
effects on antimony oxides and potassium antimony hydroxides, annealing of, 20: 9021
effects on aqueous suspensions of plutonium dioxide, 20: 41009 (AERE-R-3268)
effects on *Arabidopsis thaliana*, biological, 19: 21914
effects on argon clathrates, 19: 45679(R) (NYO-1859-11)
effects on argon diffusion in single crystals of potassium chloride, 19: 42918
effects on atmospheric contamination by activation of airborne dusts, 18: 41702
effects on austenitic stainless steel, 20: 21383
effects on austenitic stainless steel and nickel alloys, mechanisms for embrittlement, 20: 25623
effects on A302B steel, effects of stresses on, 18: 24190(R) (GA-5037)
effects on A302B steel, annealing effects on, 20: 2455
effects on A302B steel at 450 to 480°F, 20: 37289
effects on barley seed, 16: 9885
effects on barley, oat, and wheat seed and shoots, 20: 28960
effects on barley, genetic, 18: 27003(R) (ORNL-3601(p.27-46))
effects on barley, mutagenic, 16: 17469
effects on base current component of transistors, 18: 32233 (SC-R-64-195)
effects on base current in silicon transistors, 19: 40936 (SC-R-65-912)
effects on bcc alpha-iron, computer study of, 20: 2473
effects on bcc metals, 19: 23355(R) (BNL-867(p.1-117))
effects on bcc metals, annealing of, 20: 19267
effects on bcc metals, 20: 20183
effects on behavior of monkeys, 19: 45898
effects on bend properties of molybdenum and niobium alloys, 18: 32226 (ORNL-TM-880)
effects on benzene–bromoethane mixtures, reactions of recoil bromine-82 in, 20: 25174
effects on beryllium, effects of microstructure on, 18: 7320

effects on beryllium oxide, 18: 8893
effects on beryllium oxide bricks, 18: 12755
effects on beryllium oxide compacts and crystals, 18: 14374(R) (ORNL-3523(p.227-75))
effects on beryllium oxide at 900°C, 18: 20605
effects on beryllium oxide, 18: 30233 (GA-5123)
effects on beryllia, 18: 41933 (TID-11295(3rd Ed.))
effects on beryllia, influence of neutron energy on, 18: 44235 (AAEC/TM-266)
effects on beryllium oxide, 19: 3620(R) (GA-3561)
effects on beryllium oxide crystals, 19: 12865(R) (NAA-SR-10501)
effects on beryllium oxides, (T), 19: 14104
effects on beryllium oxide crystals and powders, (E), 19: 26357
effects on beryllium oxidation by carbon dioxide at 600 to 1000°C, 20: 2442
effects on beryllia-moderated-reactor materials, 20: 5115(R) (GA-4967)
effects on beryllium oxides, 20: 5181(R) (ORNL-3029)
effects on beryllium at 750°C, 20: 14059(R) (IDO-17104)
effects on beryllia, 20: 33938 (CEA-R-2943)
effects on beryllia flakes, 20: 37281
effects on beryllia microstructure, 20: 39450 (CEA-R-2963)
effects on beryllia, model of, 20: 43985 (AAEC-TM-318)
effects on bis-salicylaldehyde triethylenetetramine cobalt chloride, 20: 25173
effects on bleaching of alkali halide crystals, 19: 11227(T)
effects on blood picture and constituents in dogs, 18: 35317 (RTD-TDR-63-3012)
effects on boron-doped graphite, interstitial loops from, 20: 23782
effects on box elder, genetic, 16: 14522
effects on brain in neutron capture therapy, 16: 23495
effects on brazed and welded Inconel and stainless steel joints, 20: 44027
effects on brittleness of iron, iron alloys, and steels at low temperature, 18: 30229 (BNL-8015)
effects on brittleness of steels in reactor pressure vessels, 18: 30253
effects on brittleness of reactor pressure vessels, 18: 30258
effects on brittleness of ferrite-pearlite steels, 18: 37745 (A/CONF.28/P/339)
effects on brittleness of alloys and metals, review of, 19: 11809
effects on bromine in liquid hexane, 20: 45762
effects on bromobenzene, 19: 11220
effects on bromobenzene temperature effect on, 20: 376
effects on bromobenzene, 20: 10890
effects on bulk compressibility and electric conductivity of polyepoxides, 20: 21418 (AD-627049)
effects on burros, pathological, 20: 18188(R) (ORO-635)
effects on bursting pressure and fatigue life of stainless steel pressure tubes, 20: 2435 (WAPD-T-1720)
effects on cables and resistors, 20: 2187 (ECOM-2545)
effects on cables and transducers, transient, 20: 9301 (IDO-17103)
effects on cadmium sulfide, 18: 30245(T) (ORNL-tr-179)
effects on calcium fluoride crystals, damage from, 20: 17804
effects on can-fuel bond in fuel elements, 19: 41089 (HW-56028)
effects on capacitor dielectrics, 20: 23764(R) (AD-626474)
effects on capacitive liquid level indicators, 20: 35807 (LA-DC-7654)
effects on carbide thermionic emitters, in-pile, 18: 35929(R) (GA-4769 (Pt.I))
effects on carbohydrate and protein metabolism in brains, 20: 115
effects on carbon precipitation in alpha iron, 19: 990 (BNL-8418)
effects on carbon dioxide-graphite reactions, (E), 19: 19953 (AERE-R-4201)
effects on carbon dioxide-graphite reactions, effects of hydrogen and water vapor on chemical, 19: 19954 (AERE-R-4839)
effects on carbon graphitization in reactors, (E), 19: 34633
effects on carbon steel, 20: 11227
effects on carbon steel ASTM A-212B, 20: 36492(R) (ORNL-3951, pp 217-24)
effects on carbon steel and iron, annealing effects on, 20: 44006
effects on carbon-molybdenum systems, 19: 30648(R) (HW-84573(p.3.1-74))
effects on carbon-coated fuel particles, 19: 39129(R) (ORNL-TM-1116)
effects on carbon-coated uranium dioxide particles, 20: 35834(R) (BMI-1767)
effects on carrier lifetime and detectivity of antimony–indium semiconductors, 20: 37295
effects on catalytic oxidation of graphite by ferric hydroxide, 18: 44254
effects on catalytic properties of neodymium oxide for use in decomposition of hydrogen peroxide, 20: 25175
effects on catalytic activity of silicon dioxide–silver sulfate–vanadium oxide in oxidation of sulfur dioxide, 20: 29291
effects on cattle, burros, sheep, and swine, pathological, 19: 3891(R) (ORO-625(p.1-27))
effects on cattle, pathological, 20: 18188(R) (ORO-635)
effects on cavitation threshold of degassed water, 19: 28383
effects on cellulose, comparison with gamma rays, 19: 9203
effects on ceramic fuels, 18: 29040(R) (GEAP-4480)
effects on ceramic fuel elements and uranium dioxide, 18: 30116(R) (ORNL-3619(p.123-46))
effects on ceramic and plastic dielectric materials, 18: 40010 (USAELRDL-TR-2323)
effects on ceramic-coated fuel particles, 18: 40023
effects on ceramics and metallic-ceramic bonds, 19: 26883 (LA-3285)
effects on ceramic fuel materials, 20: 7513
effects on ceramic insulators, 20: 27614
effects on cesium-diode converter performance, 20: 9300 (IAE-949)
effects on chemical reactions in benzene-water solutions, 16: 8758 (NP-11262)
effects on chlorine and phosphorus diffusion in silicon, (E), 20: 28612
effects on chromates deposited on magnesium oxide, 19: 13452
effects on chromium–nickel steel, 18: 7322
effects on chromium-51 recoil processes in potassium chromate systems with oxides, 19: 13499
effects on chromium-51 recoil distribution in potassium chromate, annealing reactions in, 19: 13503
effects on chromium compounds, 20: 31297
effects on chromosome aberrations in bean root tips at 14 Mev, oxygen effects on, 19: 132
effects on chromosomes in Tradescantia, genetic, 19: 36016
effects on chromosome break induction in barley, interaction in, 19: 38399
effects on chromosome aberrations in barley and *Vicia faba* seeds, effects of Myleran on, 20: 31136
effects on chromosomes in barley seed, effects of diethyl pyrocarbonate on, 20: 36589
effects on chromosomes, repair mechanisms for, 20: 40609 (CONF-660418-1)
effects on chromosomes in bone marrow and leukocytes of man, whole-body mixed with γ, 20: 45405
effects on chromosomes, RBE for aberrant, 18: 41228
effects on chromosome aberrations in human leukocytes, 19: 2073(R) (ORNL-3700(p.95-7))
effects on circuits, measurement in Pulstar reactor, 20: 6679 (NP-15645)
effects on *Cl. perfringens*, alpha toxin, 19: 38446
effects on clad boron carbide poison plates, 18: 7310 (WAPD-261)
effects on clad boron–iron systems, 19: 11681
effects on clad plutonium carbide–uranium carbide, 18: 7985(R) (BMI-1650(Del.))
effects on clad uranium carbide fuel elements, 19: 42905 (NAA-SR-11134)
effects on cloud chamber performance, 18: 39637
effects on clustering in aluminum–copper alloys at −195°C, 20: 23780
effects on coal tar pitch, 19: 30257
effects on coaxial cables, 18: 37518 (USAELRDL-TR-2334)
effects on cobalt complexes, effects of gamma pre-irradiation on recoil phenomena in, 18: 16113
effects on cobalt chelates, oxygen effects in annealing of recoil damage in, 18: 37225
effects on cobalt complexes, recoil mechanism in, 20: 9022
effects on cobalt acetylacetonate, annealing of, 20: 10888
effects on cobalt halopentammine complexes, annealing of, 20: 10889
effects on cobalt complexes, 20: 12897
effects on cobalt complexes on ion exchanger, 20: 18764
effects on cobalt complexes, reactions of recoil cobalt-60 in, 20: 25172
effects on cobalt complexes, thermal annealing of recoil damage from, 20: 29259
effects on cobalt complexes, annealing of, 20: 38965
effects on cobalt complexes, annealing of, 20: 43366
effects on cobalt-nitroammine complexes, mechanism of thermal annealing in, 19: 13502
effects on cod muscle enzymes, time-temperature factors affecting, 18: 41888
effects on coke-type graphite at 425 to 1200°C, 20: 29812
effects on color center formation in sodium chloride crystals, 19: 34239
effects on color center formation in ionic crystals, 19: 34241
effects on color changes and fall of leaves, 20: 36609
effects on color centers, crystal structure, and optical properties of potassium chloride crystals, 20: 43306
effects on complexes of cobalt with 3,3-diacetyl-2,4-pentanedione, annealing of chemical recoil damage in, 20: 12896
effects on components of R.P.I. Linac, (E), 19: 30886 (RPI-328-27)
effects on compounds, molecular transformations in, 19: 7585
effects on concentration of interstitials and vacancies in niobium, calculation of, 19: 41106
effects on conductivity of n-type silicon, 19: 40935 (SC-DC-65-1247)
effects on contact melting of metals, 18: 16538
effects on copper, annealing of dislocation loops in, 18: 4320

effects on copper single crystals, 18: 14560
effects on copper single crystals, annealing of, 18: 42136
effects on copper single crystals, defects produced in, 19: 6369
effects on copper single crystals, (E), 19: 23128(T) (ANL-Trans-174)
effects on copper phthalocyanine after treatment with electrons, gamma rays, or heat, annealing of, 19: 30277
effects on copper single crystals, strengthening in, 19: 34760
effects on copper crystals, microstrain from, (E), 19: 47107
effects on copper phthalocyanines, hot and thermal processes in hot zone from copper-64 recoil in, 20: 9004
effects on copper strength, 20: 20365
effects on copper alloys, deformation, 20: 35942
effects on copper–nickel alloys, 19: 1004(R) (ORNL-3676(p.125-56))
effects on copper–nickel alloys, 19: 11682
effects on copper, relation between prismatic dislocations and change in volume during annealing, 18: 20599
effects on copper, annealing and recrystallization in, 19: 37192
effects on copper, electron microscopy of defects from, 20: 906
effects on copper, electric conductivity changes and stored energy release in, 20: 29824
effects on copper, electron microscopy of defects from, 20: 46955
effects on corneal epithelium in mice, 17: 30359
effects on corneal epithelium, mitotic, 18: 38948
effects on corrosion behavior and mechanical properties of Inconel, 16: 9260 (KAPL-M-EEB-17)
effects on corrosion of aluminum by water, 18: 2300
effects on corrosion and mechanical properties of ZrNb3Sn1 alloy and Zircaloy, 18: 18418(T,R) (EURAEC-971)
effects on corrosion of mild steel in HWCTR, 18: 28073
effects on corrosion of Zircaloy-2 by steam–water sprays, 18: 28932(R) (EURAEC-1013)
effects on corrosion and mechanical properties of niobium–tin–zirconium alloy and Zircaloy-2, 18: 32235(T,R) (EURAEC-1068)
effects on corrosion and mechanical properties of niobium–tin–zirconium alloys, 18: 37612 (A/CONF.28/P/477)
effects on corrosion and properties of Zircaloy-2, 18: 41933 (TID-11295 (3rd Ed.))
effects on corrosion behavior of aluminum and copper, 19: 26907
effects on corrosion and mechanical properties of aluminum and aluminum–magnesium alloys, 19: 44752 (CEA-tr-A-1818)
effects on corrosion and mechanical properties of zirconium–niobium–tin alloy and Zircaloy-2, 20: 11354
effects on corrosion resistance of boron-modified austenitic stainless steels, 20: 17118(R) (EURAEC-1564)
effects on corrosion of zirconium alloys, 20: 27425(R) (BNWL-207, pp 5.1-12)
effects on creep in graphite at 40°C, 19: 32783
effects on creep in type 304 stainless steel, 20: 889(R) (BNWL-120, pp 4.1-59)
effects on creep of metals, 18: 22481(R) (EURAEC-964)
effects on creep of cold-worked Zircaloy-2, 18: 32222 (HW-SA-3477)
effects on creep of graphite, 18: 44257
effects on creep of graphite at 40°C, 19: 42909 (RD/B/N-327)
effects on creep of metals at high temperature, extrapolation method for, 20: 41495(R) (EURAEC-1621)
effects on creep rupture and fatigue strength of aluminum, 20: 33969
effects on creep-rupture properties of tungsten and rhenium–tungsten alloys, 19: 11682
effects on creep-rupture properties of INOR-8, 19: 37165(R) (GEMP-47A, pp 85-99)
effects on creep-rupture of tungsten, energy dependence of, 20: 27409(R) (GEMP-58A)
effects on critical shear stress of nickel, annealing of, 20: 45038
effects on crosslinking and polymerization of, 19: 13431
effects on cryogenic temperature sensors, (E), 19: 4538 (LA-DC-6649)
effects on crystalline deoxyribonucleic acid, 17: 33980
effects on crystal structure and mechanical properties of beryllium oxide and magnesium oxide, 18: 30261
effects on crystal lattice equilibrium, 18: 37734 (A/CONF.28/P/92)
effects on crystal structure of apatite, 19: 7547
effects on crystal structure of beryllium oxide, 19: 11680
effects on crystal structure of solids, reactor irradiation facilities for studies of, 19: 12853
effects on crystal structure of beryllium oxide, 19: 25064
effects on crystal structure of beryllium oxide, x-ray diffraction studies of, 19: 25067
effects on crystals, Frenkel pair recombination in, 19: 34763
effects on crystal structure and electric properties of lead zirconium titanate–niobium oxide systems, 19: 47096
effects on crystal structure of zinc oxide, 20: 11359
effects on crystal structure of graphite, x-ray studies of, 20: 17130
effects on crystal structure of aluminum and aluminum alloys at −196°C, 20: 19260
effects on crystal orientation in metals, use of stereo electron metallography for studying, 20: 23777 (TRG-Report-1161)
effects on crystal structure of lithium fluoride and quartz, 20: 23185
effects on crystal structure defects in gold, 20: 31788
effects on crystals, 20: 33952
effects on crystal lattice of carbon steel, 20: 41497
effects on crystal structure of doped iron, (E), 20: 45039
effects on crystal structure of metals, recovery from, (E/T), 20: 45040
effects on cultured hamster cells, biological, 20: 42841(R) (ANL-7136, pp 266-89)
effects on cupferrate, 19: 11222
effects on current capacity of niobium stannide, (E), 20: 40301
effects on cysteic acid, cysteine, and cystine, chemical, 20: 16540
effects on cytoplasm of wasp Habrobracon eggs, 16: 28751(R) (TID-16471)
effects on decomposition of nickel oxalate, 19: 42559
effects on defect energy levels in germanium crystals, 18: 5817 (PAN-438/II)
effects on defect structure in crystals, 19: 1013
effects on defect distributions in copper, gold, and silver, 19: 9749
effects on defects in uranium dioxide single crystals, 18: 5824
effects on defects in graphite, 19: 14100
effects on defects in iron, 20: 33951
effects on deformation properties of A302B steel, 20: 2436 (WERL-8844-4)
effects on deformation mechanisms in iron, 20: 5851
effects on deformation structure of aluminum–copper alloys and copper, 20: 44003
effects on densification and homogenization of uranium dioxide–zirconium dioxide fuels, 20: 21432 (WAPD-301)
effects on density of uranium carbides, 19: 25056 (TRG-Report-862)
effects on density of uranium monocarbide at 750°C, 20: 29804(R) (EURAEC-1637)
effects on developing mouse fetuses, effects of dose on, 20: 12683
effects on development of Ascaris eggs in swine, 20: 33026
effects on diamond crystals, small-angle x-ray scattering from defects in, 19: 39230 (BNL-9332)
effects on dielectric properties of alumina, 18: 36228(R) (GEST-2033)
effects on dielectric and mechanical properties of dielectrics, combined effects of low-temperature, vacuum, and, 20: 21152 (N-65-22353)
effects on diethylmercury and diphenylmercury, 19: 15587
effects on diffusion in metals, 18: 30287
effects on diffusion in aluminum–copper alloys, 19: 1004(R) (ORNL-3676(p.125-56))
effects on diffusion of krypton in rubidium chloride, 20: 8999
effects on dimensions and stored energy of reactor graphite at 30 to 306°C, 18: 670
effects on dimensions of graphite, effects of temperature, 18: 4302 (HW-SA-2274(Rev.))
effects on dimensions of graphite, effects of chemical additives on, 18: 7305 (HW-SA-3020)
effects on dimensions of uranium–molybdenum alloys, 18: 8870 (NAA-SR-6262)
effects on dimensions of Zircaloy-4-clad uranium dioxide tubes irradiated in boiling reactor, 18: 14534 (DP-837)
effects on dimensional stability of steel, 18: 20584 (SC-R-64-120)
effects on dimensional stability of extruded boron carbide–graphite, 18: 32221 (GA-4557)
effects on dimensions of graphite bars, 18: 34231
effects on dimensions of graphite, effects of fabrication variables on, 18: 36049(R) (TID-20931)
effects on dimensions of uranium and uranium alloys, 18: 37736 (A/CONF.28/P/145)
effects on dimensions of low-permeability graphite, 19: 14085 (HW-SA-3664)
effects on dimensions of CSF and TSX graphite in NPR, (E), 19: 37161 (BNWL-56)
effects on dimensions of clad uranium alloy fuel tubes in pressurized heavy-water reactor, 19: 37163 (CONF-650904-3)
effects on dimensions of dilute uranium alloys, cavitational swelling, 19: 37164 (CONF-650904-4)
effects on dimensional stability of U_3Si_2, 19: 42805 (NAA-SR-10621)
effects on dimensional changes in thorium–uranium alloys, 19: 44737(R) (ANL-7000, pp 111-18)
effects on dimensions of EGCR graphite, effects of tensile stresses on, 19: 44744 (HW-SA-3592)
effects on dimensional stability of boronated graphite, 20: 9564 (BNWL-161)
effects on dimensions and thermal expansion of pyrolytic graphite, effects of annealing on, 20: 11225
effects on dimensional changes in raw-coke graphites, 20: 13322 (BNWL-178)
effects on dimensions of aluminum–uranium compound-dispersion fuels,

20: 19178(R) (IDO-17154)
effects on dimensional stability of reactor fuel plates, 20: 27609
effects on dimensional stability of graphite at 450 to 1200°C, 20: 31782 (BNWL-SA-67)
effects on dimensions of graphite, effects of chemical additions on, 20: 31667
effects on dimensions of sodium-saturated graphite, 20: 31667
effects on diode and transistor gain, Q-factor technique for, 19: 36865 (FZK-224)
effects on diodes and transistors, 20: 16909 (N-65-18250)
effects on diodes, transistors, and microelectronic circuits, 20: 16908 (N-65-17526)
effects on diphenylpicrylhydrazyl, EPR studies of, 20: 29289
effects on dislocation arrangements in zirconium, 18: 12718 (AE-130)
effects on dislocation mobility in iron, 19: 37159 (BNL-9289)
effects on dislocation channeling in deformed rhenium, 20: 745(R) (BNWL-120, pp 3.1-22)
effects on dislocation densities in crystals of lithium fluoride and potassium chloride, 20: 43305
effects on disordered regions in n-type, 18: 7316
effects on displacement efficiency in iron, computer experiments on, 19: 6376
effects on dissociation of hydrogen and other diatomic molecules, 18: 988
effects on distribution of arsenic-76 and -77 in arsenic and labeled germanium chlorides in benzene, 18: 43674
effects on distribution of radioactive selenium between red and gray allotropic modifications, 20: 38961
effects on DNAase activity in rat urine, 20: 18262
effects on domestic animals, delayed pathological, 19: 45812(R) (ORO-631, pp 1-35)
effects on ductile-brittle transition of steel, correlation of, 18: 644 (CONF-39-99)
effects on ductile-brittle transition of pressure vessel steels, 18: 7307 (NRL-5984)
effects on ductile-brittle transition in steel, 18: 8863(R) (EURAEC-817)
effects on ductile-brittle transition in pressure-vessel steels, 18: 28040(R) (EURAEC-1022)
effects on ductile-brittle transitions in iron alloys, 18: 36045(R) (EURAEC-1100)
effects on ductile-brittle transition temperature of steel, correlation of, 19: 16222 (WAPD-TM-471)
effects on ductility of pressure vessel steels, 18: 41933 (TID-11295 (3rd Ed.))
effects on ductility of steels, research on, 19: 9735(R) (NRL-Memo-1424)
effects on ductility of Armco iron, effects of nitrogen on, 19: 28871 (EURAEC-1347)
effects on ductility of chromium–nickel steel, 19: 34755
effects on ductility of type-304 stainless steel, 20: 7644
effects on ductility of austenitic stainless steels and nickel alloys, 20: 31801
effects on ductility of steel, 20: 43993(R) (EURAEC-1691)
effects on ductility of type 316 stainless steels, 20: 44015
effects on EBR-I Core IV prototype fuel rods, 18: 4297 (ANL-6670)
effects on EBWR fuel rods, 19: 39125(R) (BNWL-91)
effects on EGCR prototype fuel elements, 20: 891 (GEAP-3893)
effects on Einkorn wheat, mutagenic, 19: 2152
effects on elastic moduli of graphite monocrystals, 18: 30254
effects on elastic properties of copper, ultrasonic study of, 19: 1002(R) (ORNL-3676(p.66-73))
effects on elastic properties of glasses, 19: 7984
effects on elasticity of graphite polycrystals, 19: 20640
effects on elastic modulus of graphite, ultrasonic testing of, 19: 28878
effects on elastic properties of polycrystalline graphite, (E/T), 20: 2446
effects on elastic constants of copper and graphite, pulse method for determining, (E), 20: 35945
effects on electric and optical properties of gallium arsenide, 18: 2312
effects on electric conductivity of zinc at 77°K, 18: 4322
effects on electric conductivity of iron–nickel alloy, 18: 5821
effects on electric conductivity of uranium at 20 and 77°K, 18: 5826
effects on electric conductivity of uranium dioxide crystals, 18: 8719(R) (EURAEC-746)
effects on electric switchgear for space nuclear electric systems, 18: 10346(R) (X64-11113)
effects on electric conductivity of uranium dioxide, 18: 14362(R) (EURAEC-850)
effects on electric conductivity of thin germanium films, 18: 16532
effects on electric properties of silicon planar transistors, 18: 22535 (SC-TM-64-69)
effects on electric and magnetic properties of gold–manganese alloys, 18: 24210
effects on electric conductivity of polyvinyl chloride, 18: 29776
effects on electric conductivity of aluminum oxide at high temperatures, 18: 30175 (TID-7687(p.51-7))
effects on electric properties of germanium and silicon diodes, 18: 32254
effects on electric conductivity of aluminum, annealing of, 18: 34222
effects on electric conductivity, Hall constant, and thermoelectric power of aluminum–copper alloys, 18: 37782
effects on electric properties of semiconductors, 18: 39995 (GA-3087)
effects on electric properties of zone-refined silicon, 18: 40005 (ONR-16(Vol.1)(p.246-62))
effects on electric conductivity and Hall coefficient of graphite, effects of annealing on, 18: 42131
effects on electric conductivity of uranium dioxide crystals, 19: 4586 (EURAEC-1190)
effects on electric conductivity of aluminum–tin alloy, (E), 19: 4731
effects on electric conductivity of glass, 19: 19976
effects on electric conductivity of polyethylene, 19: 20017
effects on electric conductivity of doped and pure iron, 19: 25058
effects on electrical components and subassemblies, 19: 25750 (NP-15022(Vol.III))
effects on electrically insulating materials, 19: 24584
effects on electric and mechanical properties of epoxide polymers, 19: 28408
effects on electric cables and transducers, transient, (E), 19: 30483 (IDO-17042(p.48-63))
effects on electric conductivity of oriented pyrocarbon, recovery of, 19: 32784
effects on electric cables, 19: 39056 (N64-29558)
effects on electric properties of glassy carbon, 19: 42913
effects on electric conductivity of beryllium, thoria, and zirconia, 20: 2460
effects on electric cables, signal transients from, 20: 2186 (ECOM-2415)
effects on electric properties of magnesium germanium silicides, 20: 2502
effects on electric conductivity and polarization of polymers, 20: 4030
effects on electric and physical properties of polymeric materials, 20: 11344 (N65-35361)
effects on electric properties of aluminum, mechanism for recovery from, 20: 11362
effects on electric conductivity of aluminum, dose dependence of stage II annealing of, 20: 13340
effects on electric properties of indium–antimony alloys, 20: 17150(T)
effects on electric properties of germanium and silicon, 20: 21150 (HMI-B-45)
effects on electric insulation materials, 20: 23521 (NASA-CR-54387)
effects on electric connectors and dielectrics at low pressure and high temperature, 20: 23524
effects on electric resistivity of tungsten, recovery from, 20: 27595
effects on electric conductivity of cadmium oxide and nickel hydroxide, 20: 29821
effects on electric equipment, review of, 20: 46098
effects on electronic devices and materials, 18: 658 (REIC-32)
effects on electrochemical behavior of iron and steel, 18: 25553
effects on electronic components, 18: 30240 (WANL-TME-109)
effects on electrodes in nickel–cadmium batteries, 18: 34213(R) (AI-64-11)
effects on electronic components, transient, 18: 36054
effects on electronic equipment, 18: 35805(R) (BSR-847)
effects on electronic equipment and components, 19: 9547
effects on electron tubes, hardening against, 19: 20399(R) (NP-14946)
effects on electronic equipment, transient, 20: 2190
effects on electronic equipment in SNAP environment, 20: 4262 (NP-15610)
effects on electronic equipment, transient, 20: 13130 (SC-DC-65-1892)
effects on electronic components in space, review of, 20: 16911
effects on electronic components, 20: 19098(R) (N-65-17953)
effects on electronic components, research program on, 20: 19107(R) (N-65-21263)
effects on electron mobility and Hall effect in n-germanium, 20: 26374(T)
effects on electronic equipment, 20: 25448
effects on electronic components, 20: 33732(R) (N-66-16985)
effects on electronic components, 20: 33733(R) (N-66-17104)
effects on electron spin resonance of graphite, (E), 20: 44008
effects on embrittlement of stainless steel at high temperature, effects of heat treatment on, 18: 28061
effects on embrittlement of pressure-vessel steels, 18: 37749 (A/CONF.28/P/420)
effects on embrittlement of stainless steel and Nimonic alloy at 25 to 800°C, 19: 34756
effects on embrittlement of stainless steel, 20: 4460(R) (ORNL-3870, pp 140-5)
effects on embrittlement of steel, method for comparing, 20: 27611
effects on embrittlement of reactor structural steels, 20: 29825

effects on embrittlement of stainless steel at 700 to 900°C, 20: 33946 (ORNL-TM-1516)
effects on embryos of mice, RBE of x radiation, 20: 40618(R) (NYO-2740-3, pp 166-215)
effects on endosperm-embryo relations in Triticum seeds, 18: 43218(R) (EUR-1882.e(p.7-26))
effects on energy storage in graphite, 18: 671
effects on engineering materials in vacuum and/or at cryotemperatures, 18: 20581(R) (FZK-172)
effects on enhanced diffusion in alpha brass, flux dependence of, 18: 44244
effects on enriched calcium oxide–uranium dioxide–zirconium dioxide and cerium dioxide–uranium dioxide fuels at high burnup, 20: 35834(R) (BMI-1767)
effects on erythrocyte enzymes in horses, 17: 38751
effects on *Escherichia coli*, genetic, 19: 43751(T)
effects on ethyl bromide, isotopic and phase effects in, 20: 20751
effects on exchange capacity of resins, 19: 42921
effects on exciton spectra of cuprous oxide, 18: 2328
effects on exciton spectrum of copper oxide, 20: 2505
effects on expansion and microstructure of beryllium oxide, 19: 25061
effects on expansion and cracking of beryllium oxide lattices, 19: 25065
effects on explosives and propellants, bibliography on, 20: 4461 (REIC-Memo-28)
effects on extruded uranium dioxide fuel elements, 19: 992 (CRFD-1192)
effects on eyes of accelerator personnel, 18: 21882
effects on eyes, pathological, 19: 45843
effects on eyes of mice, cataract induction in, 18: 8105(R) (NYO-2740-1 (p.81-154))
effects on eyes of rabbits, threshold dose for cataract induction in, 19: 8886
effects on F centers in alkali metal halide crystals at 14 Mev, 20: 30739
effects on fast diode switching times, 20: 21157
effects on fast-reactor components and materials, evaluation of, (E/T), 19: 35634
effects on fatigue properties of A302-B steel, 18: 40003 (NRL-6127)
effects on fatigue properties of A302-B steel plate, 19: 34748 (NRL-Memo-1596)
effects on fatigue properties of Magnox AL80, 20: 9580
effects on fatigue of A212 and A302B steels, 20: 39406 (WAPD-T-1864)
effects on faults in aluminum as function of concentration, 19: 44755
effects on ferrites with high permeability, (E), 19: 4736
effects on ferritic steel, spectral effects on, 18: 10581 (WAPD-T-1622 (Rev.))
effects on ferromagnetic materials, point-fault, 18: 32255
effects on Ferrovac E iron, defects produced in, 19: 37160 (BNL-9290)
effects on Ferrovac E, 20: 20177(R) (BNL-929, pp 83-105)
effects on fertilized eggs of *Pleurodeles waltlii*, 16: 28776
effects on field-effect transistors, 18: 36055
effects on field-effect and bipolar transistors, 19: 2666 (SC-R-64-1333)
effects on films for measuring nuclear explosion gamma radiation, 16: 5493 (NDL-TR-13)
effects on fine structure of optical absorption bands in, magnesium oxide, 19: 40632
effects on first-order displacive transitions in quartz and cristobalite, 19: 7987
effects on fission-gas release in uranium dioxide, 19: 28893
effects on fission-product distributions in urania pellets, 20: 11365
effects on fluorocarbons, chemical, 19: 11171 (TID-21576)
effects on forests, 19: 33956
effects on forests, ecological, 20: 2080 (BNL-917, pp 20-36)
effects on forests, ecological, 20: 2081 (BNL-917, pp 39-60)
effects on formation of carbon-14-labeled polymers in ammonia–ethylene mixtures, 20: 1922
effects on formation of radiophosphorus oxidation states in aqueous inorganic sulfate solutions, 20: 33341
effects on fracture toughness of hafnium, 19: 7979 (KAPL-3076)
effects on fracture toughness of Zircaloy-2, 20: 27576(R) (BNWL-207, pp 4.44-55)
effects on frequency of chlorophyll mutations in wheat seeds, 17: 38689
effects on fruit flies, 19: 31696
effects on fuel and poison elements, in-pile measurements of, 20: 16089(R) (WAPD-MRP-114)
effects on fuel element cladding, 19: 23996(R) (ORNL-3650(p.1-110))
effects on fuel elements under superheat conditions, 19: 42903 (GEAP-4775)
effects on fueled graphite, 19: 39129(R) (ORNL-TM-1116)
effects on fueled graphite spheres, 19: 44749 (ORNL-P-1507)
effects on fused chloride and fluoride salts, 18: 34050(R) (ORNL-3626 (p.59-164))
effects on gain degradation in silicon semiconductors, 20: 21169
effects on gain of transistors, 19: 30594(R) (AD-608961)
effects on gain of 2N1051 transistors, 19: 32618 (SC-RR-65-224)
effects on gas-cooled-reactor fuel elements, 18: 29019
effects on gaseous phosphine and phosphine–silane mixtures, yields of disilane and silane in, 20: 43315
effects on gastrointestinal tract in conventional and germfree mice, 20: 45359 (ORNL-P-2407)
effects on genetic response of Drosophila spermatozoa, 18: 19647
effects on germanium n-type crystals, etchings for, 18: 2333
effects on germanium alloy p-n-p transistors, 18: 7308 (USAELRDL-TR-2310)
effects on germanium and silicon semiconductor devices, 18: 22527(R) (NASA-CR-40)
effects on germanium and silicon at 0.2 to 14.1 Mev, 19: 1003(R) (ORNL-3676(p.112-21))
effects on germanium bicrystals, 19: 4544
effects on germanium tunnel diodes, 19: 4542
effects on germanium, 19: 11786
effects on germanium and silicon transistors, (E/T), 19: 22816
effects on germination of tobacco seeds, 18: 38897
effects on gladiolus hybrids, seeds, and tubers, 20: 35290
effects on glass fiber–polytetrafluoroethylene systems, 18: 28067
effects on glassy carbon and reactor graphite, 19: 23154
effects on grain boundary cavitation and cracking in uranium, 20: 29807 (TRG-Report-325)
effects on graphite, 18: 653 (GA-4282)
effects on graphite, review of, 18: 2372
effects on graphite at 78°K, 18: 2374
effects on graphite, 18: 2377
effects on graphite, 18: 4298 (BNL-6835)
effects on graphite, energy release in recovery from, 18: 4319
effects on graphite, effects of flux level on, 18: 7318
effects on graphite oxidation kinetics in acid solutions, 18: 24202(T) (GA-tr-5174)
effects on graphite, contraction, 18: 29048(R) (HW-80284(p.6.1-10))
effects on graphite, 18: 30953(R) (ORNL-3619(p.147-200))
effects on graphite lattice, dimensional changes in, 18: 32240
effects on graphite, 18: 37740 (A/CONF.28/P/163)
effects on graphite, prediction for in-reactor conditions, 18: 39996 (HW-79793)
effects on graphite at 900 to 1200°C, defects from, 18: 44252
effects on graphite, 18: 44054(R) (ORNL-3670(p.174-200))
effects on graphite dimensional changes, 19: 9741
effects on graphite moderator, 19: 20614 (HW-81250A)
effects on graphite cylinders, 19: 25052(R) (ORNL-3731(p.154-206))
effects on graphite, theory for predicting, 19: 26904
effects on graphite thermal conductivity, 19: 29612 (AHSB(S)R-82)
effects on graphite, alternate exposure and annealing, 19: 34738 (BNL-8222)
effects on graphite, annealing of, 19: 34757
effects on graphite at 350 to 500°C, 19: 36949(R) (BNL-900(p.121-97))
effects on graphite, 19: 37166 (HW-84609(p.6.1-5))
effects on graphite mechanical properties, 19: 39237
effects on graphite, use of bromine adsorption in determining, 19: 41109(P)
effects on graphite, 19: 42922
effects on graphite, defect nucleation in, 20: 2447
effects on graphitized carbon black, temperature dependence of ESR from, (E), 20: 20144
effects on graphitized carbon black, EPR determination of anneal effects from, 20: 21435
effects on graphite–uranium carbide fuel spheres, 20: 34993 (ORNL-TM-1512)
effects on graphite, annealing of, 20: 35939
effects on graphite energy storage, relations with annealing, 20: 37283
effects on graphite dimensions, two-phase model for, (T), 20: 44007
effects on grasshopper embryos, 17: 24896 (TID-18723)
effects on grasshopper embryos, lethal, 16: 23413 (TID-15962)
effects on growth of Euglena cells, 18: 17501
effects on growth of *Euglena* cells, 18: 17501
effects on growth of pine trees, 18: 36976
effects on growth of ascaris eggs in pigs, 19: 7128
effects on growth of uranium at 77°K, 19: 25059
effects on growth of mice, 19: 31833
effects on hair cells of *Tradescantia occidentalis*, RBE of, 18: 1409
effects on Hall coefficient and input resistance of indium antimonides and arsenides, 19: 4545
effects on hard and soft magnetic materials, 19: 37179
effects on hardening in mild steels, dose and temperature effects on, 19: 37186
effects on hardening and embrittlement in body-centered-cubic transition metals, 20: 2472
effects on hardness of graphite, 18: 669
effects on hardness of copper single crystals, annealing of, (E), 19: 4728

effects on hardness of beryllia, 19: 41087 (AAEC/E-135)
effects on hardness of molybdenum and tungsten, 20: 2457
effects on hardness and impact properties of beryllium, 20: 39436
effects on hardness of crystals of potassium chloride and lithium fluoride, 20: 43304
effects on Hastelloy X, 18: 40835 (IDO-28616)
effects on Hastelloy X, Incoloy 825, and Inconel 625, 20: 33962
effects on heavy water, isotope effects in, 20: 8981 (CEA-R-2794)
effects on helium distributions in urania fuels, 18: 28068
effects on helium formation in beryllium oxide, 19: 14098
effects on helium diffusion from beryllium oxide, kinetics of, 20: 21428 (NP-15942)
effects on helium bubble formation in metals, 20: 25623
effects on hematopoiesis, effects of fractionated exposure on, 20: 28984
effects on hexamminocobalt nitrate, annealing of, 19: 46391
effects on high-purity uranium, 18: 39998 (HW-SA-3673)
effects on high-purity uranium, 19: 2856 (HW-79559)
effects on high-temperature creep of alloys and metals, 18: 28039(R) (EURAEC-1020)
effects on high-temperature thermocouples, 19: 20401 (ORNL-P-1065)
effects on high-temperature reactor materials, 19: 25053(R) (ORNL-3731 (p.207-28))
effects on holes in silicon, 18: 32231 (SC-R-64-193)
effects on hollow uranium dioxide pellets in collapsible Zircaloy-2 sheaths, 20: 2415 (AECL-2276)
effects on human blood *in vitro*, 18: 27066(R) (ORNL-3601(p.105-9))
effects on human chromosomes, 18: 19582
effects on human marrow, cytological, 18: 19602
effects on human somatic cells, genetic, 18: 43227 (ORNL-P-419)
effects on hydridation and oxidation of zirconium alloys, for use as fuel element cladding, 20: 7519 (RCN-41)
effects on hydrocarbons and crude oils in presence of sedimentary rocks and water, 19: 22335
effects on hydrogen adsorption by aluminum oxide, 18: 25468 (BNL-845)
effects on hydrolysis of uranium monocarbide, yields in, 18: 13853
effects on hydrolysis of uranium carbides and plutonium carbide–uranium carbide systems, 19: 40586
effects on hysteresis loops in monocrystalline barium titanates, 19: 38705
effects on IFA-3 aluminum alloy, 18: 37637 (A/CONF.28/P/591)
effects on ignition characteristics of uranium, 19: 32447(R) (ANL-7020 (p.175-97))
effects on image orthicon and vidicon camera heads, 16: 25836 (AD-270724)
effects on image restoration in photographs, 20: 43344
effects on impact properties of carbon steel, 18: 2358
effects on impact properties of nickel steel, 20: 31669
effects on in-pile thermionic materials, 18: 26259
effects on in-pile thermocouples, 19: 37197
effects on incidence of chromosomal aberrations in mice, 17: 31958
effects on Inconel and Hastelloy-X, 19: 37167(R) (HW-84609(p.8.1-7))
effects on indium antimonide, 18: 44241(T) (AI-Trans-58)
effects on induced activity in polyethylene, 20: 17822
effects on infrared transmission of indium arsenide crystals, 18: 8898(T)
effects on infrared photoconductors, 19: 13820
effects on infrared absorption spectrum of silicon, (E), 20: 40340
effects on inheritance of mice to susceptibility to pentobarbital, 20: 45374
effects on Initial Engine Test components, 18: 24937 (APEX-917)
effects on insulated-gate transistors, 20: 23522 (UCRL-11936)
effects on integrated silicon circuits, damage from, 20: 35811
effects on interaction of induced chromosome breaks in barley seed, 19: 42343
effects on internal friction of graphite, 18: 8730 (WADC-TR-58-360 (Pt.V))
effects on internal friction and elastic modulus of metals, 18: 44240(T) (AEC-tr-6475)
effects on internal friction of cold-worked zirconium, 19: 2827
effects on internal friction spectra of iron, 19: 7983
effects on internal friction of iron, torsion pendulum for recording, 19: 9751
effects on internal friction in copper, 19: 9754
effects on interstitial loops in molybdenum, 18: 16536
effects on interstitial dislocation loops in beryllium oxide at high temperatures, 20: 38377
effects on iodine reactions with Zircaloy-2, 20: 23585(R) (GEAP-3771-18)
effects on iodine-131 production in tellurium dioxide, oxidation states in, 20: 23200
effects on iron, 19: 11682
effects on iron, 19: 16216(R) (HW-84281(p.4.19-24))
effects on iron and steel, 20: 2474
effects on iron and ferritic steel, 20: 27596
effects on iron at 0°K, computer study of primary damage state from, 18: 28057
effects on iron at 77°K, magnetic coaxing studies of, 20: 37288
effects on iron, defect annealing of, 18: 8891
effects on iron–nickel alloys, annealing of, 18: 2327
effects on iron slabs, calculation of heating, 18: 17243 (GAMD-3690)
effects on iron–nickel alloy single crystal magnetic properties, (E), 20: 24649
effects on iron, damage distribution within displacement spike in, 19: 6377
effects on iron, interstitials from, 20: 31789
effects on iron, precipitation of impurities in, 18: 18411 (AE-138)
effects on isotope exchange between carbon oxides, 17: 29011
effects on kidney tissues and renal clearance of mice, 20: 36608
effects on labeled organic retentions in halohydrocarbon mixtures with bromine, 19: 40624
effects on lactation in dairy cattle, 19: 43801
effects on lactation by dairy cows, whole-body, 19: 45760(R) (ORO-631, pp 83-121)
effects on lattice streaking of beryllium oxide, annealing of, 19: 14105
effects on lattice parameters in lithium fluoride, 19: 15635
effects on lattice perturbations in semiconductors, 20: 908
effects on lattice parameter of copper–boron systems, 20: 2441
effects on lattice parameters of uranium monocarbide, annealing of, 20: 17140
effects on lattice parameters in graphite, 20: 23784
effects on lattice parameters of metals, 20: 31669
effects on lead iodide and potassium chloride crystals, correlated atomic collisions in, 20: 9582
effects on length of Zircaloy-clad uranium dioxide fuel elements, 19: 18533 (CRFD-1174)
effects on lethality in mice, pulsed, 18: 8178
effects on lethality in dogs, dose and exposure effects on, 19: 43832
effects on leukocyte chromosomes, 19: 45813(R) (ORO-631, pp 36-44)
effects on life span of first and second generation offspring after male mice exposure, 16: 31472 (LADC-5323)
effects on life span of guinea pigs, 20: 12628 (AD-626997)
effects on liquid cerium–cobalt–plutonium alloy in contact with sodium, 19: 16219 (LA-DC-6753)
effects on liquid sodium dilation of graphite, 19: 39235 (NAA-SR-11309)
effects on lithium fluoride at low temperatures, 18: 2329
effects on lithium fluoride crystals, 18: 5858
effects on lithium fluoride crystals, 18: 30270
effects on lithium fluorides, x-ray study of damage in, 18: 39324
effects on lithium fluorides, EPR studies of, 19: 11794
effects on lithium carbonate, preparation of carrier-free fluorine-18 by, 19: 13510
effects on lithium-drifted silicon p-i-n diodes, (E), 19: 28702
effects on lithium sulfate monohydrate and monodeuterate, 19: 42526 (TID-22035)
effects on lithium fluoride thermal conductivity and lattice faults, (E), 20: 411
effects on lithium fluoride, NMR studies of, 20: 14602
effects on lithium fluoride single crystals at 77 and 80°K, optical absorption measurements of, 20: 28668
effects on lithium fluoride crystals, R_N band from, 20: 34841
effects on living tissues, review, 18: 17525
effects on long-term mechanical properties of metals and alloys, research program on, 19: 11777(R) (EURAEC-1243)
effects on long-term mechanical properties of metals and alloys at high temperatures, research program on, 19: 11778(R) (EURAEC-1268)
effects on low-melting organic coolants, 18: 33617 (AECI-1915)
effects on lower yield point of alpha-iron and ferritic steels, computer calculation of, 20: 27584(R) (GEMP-400A, pp 169-84)
effects on luminescence of thallium-activated alkali halides, 19: 19966
effects on macroscopic growth of magnesium oxide crystals, 18: 20597
effects on magnesia–plutonia fuels, 18: 12725 (HW-SA-3127)
effects on magnesium oxide crystals, growth in, 19: 34759
effects on magnesium oxide single crystals, zero-phonon transition spectra from, (E), 20: 9585
effects on magnesium oxide crystals, symmetry of color center from, (E), 20: 32717
effects on magnesium oxide, exchange-coupled F-center pairs in, 20: 34821
effects on magnetic properties of ferrites, 18: 663
effects on magnetic properties of iron, 18: 2326
effects on magnetic properties of iron–nickel alloys, 18: 5822
effects on magnetic properties of ferrites, 18: 7330
effects on magnetic properties of Permalloy thin films, 18: 7333
effects on magnetic properties of iron–silicon systems, 18: 8892
effects on magnetic materials, 18: 10346(R) (X64-11113)
effects on magnetic properties of single-crystal iron–nickel alloys, 18: 12743
effects on magnetic properties of nickel, 18: 14548

effects on magnetic Barkhausen effect in iron and nickel, 18: 18414 (NP-13771)
effects on magnetic materials, 18: 30290
effects on magnetic properties of iron–nickel alloys, 18: 36056
effects on magnetic moments in aluminum-iron alloys, 18: 37774
effects on magnetic materials and logic circuit, 19: 13868
effects on magnetic properties of defects in nickel, 19: 20647
effects on magnetic properties of defects in iron, 19: 20648
effects on magnetism of cobalt, iron, and nickel, 19: 20652
effects on maize seed development, 18: 38942
effects on maize under different physiological conditions, genetic, 17: 10380
effects on maize, mutagenic, 19: 43712 (BNL-9383)
effects on maize, mutagenic, 20: 22661
effects on maize, genetic, 20: 40618(R) (NYO-2740-3, pp 166-215)
effects on mammary tumor incidence in rats, 16: 31387(R) (ANL-6535 (p.22-5))
effects on man, biological, 20: 8711
effects on man, biological, 20: 10698
effects on man, biological, 20: 28970
effects on man, bone marrow transplants effects against, 18: 17667
effects on man, protective effects of bone marrow grafts against, 20: 5420
effects on martensite content of 304 and 348 stainless steels, annealing and cold work relations in, 20: 46225 (BNWL-238)
effects on mass transfer of uranium, 19: 14099
effects on materials, correlations of exposure units for, 18: 28074
effects on materials of Astron thermonuclear reactor, 18: 30897 (UCRL-6804)
effects on materials, exo-electron emission in annealing of recoil damage in, 18: 37775
effects on materials, additivity of gamma effects and, 19: 2405
effects on materials, instrumentation for analyzing, (E), 19: 11471 (HW-75132)
effects on materials and electronic devices, thresholds, 19: 16242
effects on materials at cryogenic temperatures, measurement in reactors, (E), 20: 5569 (CONF-650217, pp 108-10)
effects on materials, design of calorimeter for measuring heating, 16: 26502
effects on matter, theory, 17: 16883
effects on mechanical properties of alloys in nuclear superheated steam environments, 18: 4161 (GEAP-4351)
effects on mechanical properties of fuel element cladding materials, 18: 8868 (HW-SA-3268)
effects on mechanical properties of metals, dose estimations from, 18: 10585
effects on mechanical properties of uranium, 18: 12735 (TRG-Report-611(p.9-10))
effects on mechanical resistance and volume of fused silicate ceramics, 18: 12738
effects on mechanical properties of Zircaloy-4, 18: 14533 (CONF-187-98)
effects on mechanical properties of steels and zirconium alloys, 18: 16525 (NP-13657)
effects on mechanical properties of austenitic stainless steels, 18: 24192 (HW-SA-3221)
effects on mechanical properties of pressure vessels, 18: 30111(R) (GEMP-35A)
effects on mechanical properties of niobium-stabilized stainless steel, 18: 34218 (ORNL-TM-881)
effects on mechanical properties of reactor pressure vessels, 18: 36048(R) (SWRI-1243-14)
effects on mechanical properties of austenitic and ferritic steels, 18: 37739 (A/CONF.28/P/162)
effects on mechanical properties of fcc crystals, 18: 37754 (A/CONF.28/P/471)
effects on mechanical properties of Magnox Al 80, 18: 37617 (A/CONF.28/P/857)
effects on mechanical properties of metals, extrapolation of, 18: 37752 (A/CONF.28/P/460)
effects on mechanical properties of structural materials, 18: 40019
effects on mechanical properties of zirconium alloys, 18: 42108 (AECL-1986)
effects on mechanical properties of stainless steel, 18: 44050(R) (ORNL-3670(p.116-21))
effects on mechanical properties of INOR-8, 18: 44055(R) (ORNL-3670 (p.216-24))
effects on mechanical properties of metals and alloys, data tabulations on, 19: 4714 (HW-81334(Pt.2))
effects on mechanical properties of stressed A-302B steel, 19: 7977(R) (GA-5636)
effects on mechanical properties of A-302B steel subjected to multiaxial stresses, 19: 9731 (GA-5273)
effects on mechanical properties of steel, 19: 16226
effects on mechanical properties of cadmium-indium-silver alloys, effects of tin on, 19: 18402 (WCAP-3269-29)
effects on mechanical properties of reactor graphite, 19: 20637
effects on mechanical properties of austenitic stainless steel as function of temperature, 19: 23119 (BNWL-1)
effects on mechanical properties of zinc crystals in presence of surface-active mercury, 19: 23131
effects on mechanical and physical properties of thorium, 19: 26879 (BNWL-24)
effects on mechanical properties of iron, 19: 36949(R) (BNL-900(p.121-97))
effects on mechanical properties of Zircaloy-2, 19: 37162 (BNWL-SA-236)
effects on mechanical properties of aluminum–chromium–iron–yttrium alloys, 19: 36952(R) (GEMP-47A, pp 13-26)
effects on mechanical properties of cladding materials for SNAP hydride reactors, 19: 39166 (NAA-SR-Memo-11149)
effects on mechanical properties of chrome nickel stainless steels, 19: 41093(T) (FTD-TT-65-125)
effects on mechanical properties of metals, displacement spike density model for, 19: 44599(R) (GEMP-50A)
effects on mechanical properties of stainless steel at high temperatures, 20: 2430 (ORNL-P-1713)
effects on mechanical properties of Incoloy 800, 20: 2458
effects on mechanical properties of INOR-8, 20: 4308(R) (ORNL-3870, pp 243-60)
effects on mechanical properties of stainless steels under stress, thermodynamic method for evaluating, 20: 5913(R) (EURAEC-1488)
effects on mechanical properties and structures of isotactic polystyrene, 20: 7168
effects on mechanical properties and microstructure of type-304 stainless steel at 21 and 315°C, 20: 7643
effects on mechanical properties of beryllium, 20: 13323 (CONF-170, pp 138-59)
effects on mechanical properties of Inconel 600 and X-750, 20: 13333
effects on mechanical properties of austenitic stainless steels, 20: 13333
effects on mechanical properties of low-alloy manganese–molybdenum–nickel–niobium steel, 20: 19258 (UJV-1470/65)
effects on mechanical properties and point defects in niobium, 20: 21320(R) (AD-625475)
effects on mechanical properties of austenitic stainless steels, 20: 27573(R) (BNWL-207, pp 4.8-31)
effects on mechanical properties of Zircaloy-2, 20: 27574(R) (BNWL-207, pp 4.32-4)
effects on mechanical properties of reactor materials, nondestructive methods for measuring, 20: 27580(R) (GA-6996)
effects on mechanical properties of molybdenum, 20: 29820
effects on mechanical properties of hafnium control rods, 20: 31668
effects on mechanical properties of pressure vessel steels and structural steels, 20: 37286
effects on mechanical properties of cold-worked iron, 20: 37304
effects on mechanical properties of vanadium-base alloys, 20: 41506
effects on mechanical properties of iron, role of interstitial impurities in, 20: 44001
effects on mechanical properties of Inconel X, 20: 44013
effects on mechanical properties of A302B pressure vessel steels, comparison of U. S. and Japanese, 20: 46236
effects on mechanical properties of ASTM A302B steel, 20: 46237
effects on medical x-ray film, 20: 12545(R) (PAEC(A)AR651)
effects on meiotic irregularities in plants, 16: 1585
effects on Meissner effect in niobium, 20: 34423
effects on melting point and vaporization of uranium dioxide, 18: 8864 (HW-69234)
effects on melting point of uranium dioxide, 19: 16223 (WCAP-6065)
effects on melting tungsten–uranium dioxide and uranium dioxide fuel elements, 20: 2416 (AECL-2289)
effects on mercury-coated zinc single crystals, 18: 12740
effects on metabolism in dairy cattle, 19: 43801
effects on metal oxides, effects of crystal structure on, 20: 17148
effects on metal-oxide transistors, (E), 19: 28701
effects on metallic reactor materials, 19: 25046(R) (HW-83615)
effects on metallurgical reactions in aluminum–copper, copper–nickel, and iron–nitrogen alloys, 19: 37173 (ORNL-P-1448)
effects on metals and alloys, 18: 14537(R) (HW-79766(p.4.1-76))
effects on metals at low temperatures, saturation phenomena in defect production in, 18: 16531(T) (AI-Trans-38)
effects on metals, 20: 29819
effects on metals, mechanisms of damaging, 19: 24916(R) (GEMP-334A)
effects on mice, 16: 4060
effects on mice, 19: 2072(R) (ORNL-3700(p.83-8))
effects on mice, fractionation and low-dose-rate, 18: 3494 (TID-18386)
effects on mice, comparison with x rays, 17: 2886
effects on mice, genetic, 16: 32010

effects on mice, genetic, 18: 27007(R) (ORNL-3601(p.83-91))
effects on mice, lethal, 20: 42934
effects on mice, RBE for, 18: 31148
effects on microcircuit digital gates, 20: 19100 (N-65-18004)
effects on microelectronic circuits, 20: 25446(R) (AD-631705)
effects on microhardness of alloys, 18: 14569
effects on microörganisms, 17: 24937
effects on microstructure of molybdenum, 18: 14366(R) (HW-79766(p.3.1-64))
effects on microstrain yield stress in copper single crystals, 18: 36058
effects on microstructure of uranium dioxide, 19: 13985 (GEAP-4535)
effects on microstructure of bcc metals, theoretical studies of, 20: 9378(R) (GEMP-54A)
effects on microstructure of iron and molybdenum, mechanisms of, 20: 9566(R) (BNWL-166, pp 3.15-23)
effects on microstructure of uranium at 4.5°K, 20: 11224
effects on microstructure of molybdenum, 20: 11227
effects on microstructure of beryllium oxide, 20: 13331
effects on microstructure of uranium carbides, 20: 13332
effects on microstructure of uranium nitride–20 plutonium nitride fuels, 20: 27405(R) (BNWL-198, pp 3.1-21)
effects on microstructure of plutonia–urania fuels, effects of preparation procedures on, 20: 29805(R) (NUMEC-3432-21)
effects on mineral content of plasma of burros, 20: 45290(R) (UCLA-12-595, pp 29-32)
effects on mobile interstitials in alloys and metals, 18: 39993 (EUR-1643.e(p.246-53))
effects on mobility of dislocations in lithium fluoride crystals, 19: 22310
effects on molecular motions and structure of crystalline stereoregular polymers, 20: 20753
effects on molybdenum, 18: 2294 (HW-SA-2953)
effects on molybdenum, 18: 7298(R) (HW-78962(p.3.1-14))
effects on molybdenum and niobium, annealing of, 18: 20596
effects on molybdenum, recovery from, 18: 34221
effects on molybdenum-uranium alloys and uranium, 18: 37757 (A/CONF.28/P/735)
effects on molybdenum, steel, and tungsten, 19: 4719(T) (AEC-tr-6227/2 (p.63-72))
effects on molybdenum–uranium alloy fuel, 19: 14087 (NAA-SR-8955)
effects on molybdenum–uranium alloy fuel, 19: 14088 (NAA-SR-8956)
effects on molybdenum, 19: 16209(R) (HW-84281(p.3.1-16))
effects on molybdenum, annealing of, 19: 20634
effects on molybdenum–uranium alloy fuel elements at 260 to 600°C, 19: 26900
effects on molybdenum, 19: 30648(R) (HW-84573(p.3.1-74))
effects on molybdenum, dislocation loop interactions in annealing of, (E), 19: 37182
effects on molybdenum–uranium alloy fuel, 19: 41090 (NAA-SR-11121)
effects on molybdenum, annealing of, 20: 2476
effects on molybdenum crystal structure, 20: 15136 (RL-REA-2595, pp 51-62)
effects on monkey testicles, 16: 1463 (AF-SAM-61-72)
effects on monkey social behavior, 18: 13502
effects on monkey testes, 18: 23330
effects on monkeys, behavioral, 20: 14286 (AD-625837)
effects on monkeys, leukemic, 19: 28074
effects on monkeys after whole-body exposure, leukomogenic, 19: 28074
effects on MOS transistor characteristics, mechanisms for, 20: 13133
effects on mosaic structure of aluminum single crystals, 18: 5831
effects on mouse skin, comparison with effects of electrons and x rays, 20: 45426
effects on mouse testes, 18: 41230
effects on multiplication values in silicon p-n junctions, 19: 9549
effects on mutations in X_1 and X_2 *Vicia faba* L, 17: 28648
effects on mutations in mammals, 20: 16159(R) (ORNL-3900, pp 150-81)
effects on mutations in *Pisum sativum*, 20: 35269
effects on n- and p-type lead telluride, 18: 37115 (ANL-6856)
effects on n-p-n silicon transistors, 20: 2184(R) (AD-614618)
effects on n-p-n silicon transistors, 20: 2185(R) (AD-618194)
effects on *n*-propyl bromide, bromobenzene, 4-bromo-*o*-xylene, and benzyl bromide, thermal annealing of, 19: 40576
effects on n-type antimony–indium alloy at 78°K, 20: 2500
effects on n-type silicon at 293°K, 20: 40303
effects on NERVA electronic components, 18: 30237 (NP-14069)
effects on NERVA engine components under dynamic operation conditions, 19: 14867 (FZK-170-2)
effects on NERVA resistance-temperature transducers, 20: 13127 (CONF-651101-61)
effects on nervous system in rabbits and rats, pathological, 19: 45812(R) (ORO-631, pp 1-35)
effects on neutron sensors, 18: 23888 (PWAC-424)
effects on nickel single crystals, 18: 14559
effects on nickel, 19: 16225
effects on nickel crystals, recovery above room temperature, 19: 39251
effects on nickel-base alloys as function of preirradiation treatment, 20: 27575(R) (BNWL-207, pp 4.35-43)
effects on nickel, interstitial and vacancy clusters from, (E), 20: 38367
effects on nil ductility temperature of A212B stainless steel, 19: 18259 (HW-SA-3541)
effects on niobium–uranium alloys, 18: 37618 (A/CONF.28/P/864)
effects on niobium and stainless steel-clad plutonium uranium carbide fuel elements, 20: 27593(R) (UNC-5134(Vol.2))
effects on niobium-stabilized stainless steel, 20: 37284
effects on nitride precipitation in iron, 19: 1005 (ORNL-P-556)
effects on nitrogenous bases in DNA in bean seeds, 19: 42322
effects on noise in diodes, 20: 9307
effects on nonfissionable alloys and metals, bibliography on, 16: 24269 (STI/PUB/21/6)
effects on notch ductility of structural steels, 19: 11781(R) (NRL-Memo-1556)
effects on notch ductility of pressure vessel of Yankee Power Reactor, 19: 11781(R) (NRL-Memo-1556)
effects on notch ductility of steels, neutron spectral and annealing effects in, 20: 43997(R) (NRL-Memo-1663)
effects on nuclear magnetic resonance in polyethylene, 18: 17864 (JINR-P-1518)
effects on nuclear thermionic cells, 18: 20882
effects on nucleation in graphite, 18: 37776
effects on nucleic acids in testis of rats, 18: 38939
effects on oats and wheat, 18: 13494
effects on oats, genetic, 20: 18417
effects on operating characteristics of transducers and strain gages, 19: 2668
effects on optical absorption and photoconductivity of rutile, 18: 7280 (BNL-7501)
effects on optical rotation of quartz, 19: 1018
effects on optical absorption spectra of thermally bleached lithium fluoride crystals, (E), 20: 24615
effects on optical absorption spectra of sodium chloride crystals, (E), 20: 34834
effects on optical absorption of alkali borate glass containing arsenic or manganese, 20: 36887
effects on order-disorder transition in iron–nickel alloy, 20: 44025
effects on organic tissues, relation of tissue composition to, 18: 5109
effects on organic liquid coolants, 18: 38264 (A/CONF.28/P/15)
effects on organic compounds in reactor irradiation tests, 19: 28367
effects on organic fluorine compounds, 20: 7134
effects on oxidation of zirconium, 16: 31369
effects on oxidation of graphite at 350 to 500°C, 18: 20580 (BNL-7964)
effects on oxidation rates of graphite, amelioration of, 18: 27597
effects on oxidation of graphite, 19: 11793
effects on oxidation of zirconium alloys by low-oxygen water, 19: 16016(R) (HW-84281(p.5.1-5))
effects on oxidation of graphite by carbon dioxide, 20: 9578
effects on oxidation-reduction potential of electrolytes, 20: 17118(R) (EURAEC-1564)
effects on oxidation of pyrolytic carbon by steam at 1000 to 1400°C, 20: 23600 (GA-7005)
effects on oxidation of Zircaloy-2 process tubes in PRTR, 20: 27427(R) (BNWL-207, pp 5.16-18)
effects on oxides and sodium chloride, use of color center technique for studies of, 18: 42141
effects on oxygen-defect complex formation in silicon, infrared absorption spectra of, (E), 20: 13998
effects on oxygen-doped germanium, oxygen-defect complexes for determining recovery from, (E), 20: 30742
effects on p-type germanium, annealing of, 20: 23781
effects on paramagnetic center formation in ammonium selenates, 20: 38398
effects on parameters of silicon diodes, 19: 13817
effects on pea seeds, genetic, 20: 81
effects on pearl color, 19: 2863
effects on peas, genetic, 19: 43734
effects on performance of high-temperature thermocouples, 19: 18344 (ORNL-P-1066)
effects on performance of stainless steel-clad Alumel–Chromel thermocouples, in-pile, 20: 4263 (ORNL-TM-1320)
effects on periodically annealed graphite, 18: 662
effects on Permalloy magnetic films, 19: 14113
effects on phase transformations in tin, 16: 7939 (SCTM-199-61(11))
effects on phase transformations in zirconia, 18: 8885
effects on phase transformations in calcium orthosilicate, cristobalite, lead oxide, quartz, and silicon oxide, 20: 4462
effects on phase transformation points in polymorphic solids, thermodynamic calculation of, 20: 45034
effects on phases in niobium–zirconium-base alloys, 18: 39999 (KAPL-

2251)
effects on phenolic resin-bonded laminates at –423°F, 20: 46540
effects on phonon infrared absorption spectra in magnesium oxide, 19: 41108
effects on phosphorus trichloride, diphosphorus tetrachloride yields from, 20: 26987
effects on photo- and thermal annealing of phosphorus-32 in potassium chloride, 19: 13487
effects on photoelectric properties of silicon p-n junctions, (E), 19: 26715
effects on photomultiplier tubes, transient, 19: 26629 (ECOM-2519)
effects on phthalocyanines, 20: 36886
effects on physical properties of sand and sandy loam soil, 17: 12099
effects on physical properties of graphite in repeated irradiations and annealings, 18: 2378
effects on physical properties of lithium hydrides, 18: 24188 (APEX-329)
effects on physical properties of 212B steel, 18: 28072
effects on physical properties of graphite, 18: 32238
effects on physical properties of nuclear graphite, 19: 6361 (HW-82152)
effects on physical properties of graphite, 20: 756
effects on physical properties of graphite and Hastelloy N, 20: 31683(R) (ORNL-3936, pp 95-121)
effects on pipes under internal pressure, 18: 4316
effects on plants, mutagenic, 20: 8656
effects on plants, genetic, 20: 18420
effects on plants, genetic, 20: 18188(R) (ORO-635)
effects on plants, genetic, 18: 1373 (BNL-7360)
effects on plants, genetic, 18: 38774(R) (EUR-1881.e)
effects on plants, genetic, 18: 38935
effects on plasticity of graphite, 18: 668
effects on plastic deformation of nickel, 19: 11682
effects on plastic, glass-laminate, and ceramoplastic materials, 19: 39232 (FZK-227)
effects on plastic deformation of alpha-uranium monocrystals, 20: 5916
effects on platinum, damage from, 19: 23144
effects on plutonium carbide and plutonium carbide–uranium carbide, 18: 5813 (ANL-6678)
effects on plutonium fuels, 18: 18439
effects on plutonium-uranium carbide fuel elements, 18: 18280 (ANL-6792(p.297-313))
effects on plutonium dioxide–uranium dioxide pellets, 19: 2857 (HW-SA-3129)
effects on plutonium and uranium isotopic composition of enriched thoria–urania fuel, 19: 12492 (ORNL-TM-1024(Rev.1))
effects on plutonium-uranium dioxide fuel elements, 19: 14828(R) (GEAP-4723)
effects on plutonium dioxide–uranium dioxide fuel rods in EBWR, 19: 16218 (HW-SA-3626)
effects on plutonium carbide–uranium carbide, 19: 24923(R) (UNC-5081)
effects on plutonium nitride–uranium nitride fuels, 19: 39125(R) (BNWL-91)
effects on plutonia–urania fuels, 19: 39125(R) (BNWL-91)
effects on plutonia and urania ceramics and cermets, (E), 20: 5192 (BNWL-SA-251)
effects on plutonium dioxide–uranium dioxide fuel elements, 20: 46226 (BNWL-SA-791)
effects on polarization of fluorine nuclei and protons in polymers, 20: 4037
effects on polycrystalline graphite, ESR studies of, 20: 23785
effects on polycrystalline ammonium selenate, ESR spectral studies on, 20: 26925 (NP-16037)
effects on polycrystalline graphite, 20: 35938
effects on polyethylene and teflon, positron lifetimes in, 19: 14089 (NRS-26)
effects on polyethylene crystals, infrared spectra of, 19: 15600
effects on polymerization of monomers in wood, 20: 5818
effects on polymerization induction, 18: 5389
effects on polypropylene mechanical relaxation and molecular mobility, 18: 12158
effects on polysaccharide content of rat testes, 19: 8930
effects on potassium chloride, chemical states of phosphorus-32 produced in, 18: 25567
effects on potassium and sodium chlorides, chemistry of sulfur-35 production in, 19: 13504
effects on potassium trioxalatoferrates, annealing of, 20: 12903
effects on potassium chromate, production of chromium-51 in, 20: 23197
effects on potassium chloride crystals, optical properties of F centers from, 20: 34836(T)
effects on potassium chloroiridates, 20: 35546
effects on praseodymium complexes with β-diketones, 20: 16416(R) (NYO-906-68)
effects on pre-precipitation rate of aluminum–zinc alloys, 18: 24206
effects on preamplifier components, 18: 24822 (PWAC-427)
effects on precipitation kinetics of aluminum-copper alloy, 19: 28876
effects on precipitation behavior and tensile properties of chromium–nickel–niobium steel, 20: 33950
effects on pressure transducers, 18: 659 (UCRL-13092)
effects on pressure vessel steel, 18: 26925 (GEAP-4423)
effects on pressure-vessel steels, 18: 40004 (NRL-Memo-1502)
effects on pressure vessel steel, 18: 40829 (EURAEC-1175)
effects on pressure transducers, pulsed in-pile, 18: 39567 (IDO-16977 (p.44-54))
effects on pressure-vessel steels, 19: 2859 (NRL-6160)
effects on pressure-vessel steels, research program on, 19: 4716(R) (NRL-Memo-1534)
effects on pressure vessel steel, 19: 4715 (NRL-6151)
effects on pressure transducer components, transient and permanent, 19: 39055 (GA-6266)
effects on pressure transducers, 20: 14170 (EGG-1183-2019)
effects on pressure vessel steel embrittlement, 20: 27610
effects on pressure vessel steels, 20: 41494(R) (EURAEC-1617)
effects on pressure vessel steel, criteria for evaluating, 20: 46228 (NRL-6415)
effects on production in coffee plants, 17: 34201
effects on properties of niobium–tin–zirconium alloy, 18: 14545(T,R) (EURAEC-863)
effects on properties of EGCR graphite, 19: 11779 (HW-71500B)
effects on properties of reactor-grade graphite, 19: 40959
effects on properties of molybdenum, combined impurity and, 20: 5851
effects on properties of uranium carbides, 20: 9592
effects on proteins of cotton seeds, 18: 37205(T) (AEC-tr-6398(p.403-7))
effects on protein loss into gastrointestinal tract in mice, dose effects on, 20: 32933
effects on pulse fission chambers, (E), 20: 5807 (AEEW-M-493)
effects on pure and doped iron, point defects produced by, 19: 47094(T) (ORNL-tr-668)
effects on pyrolytic graphite at high temperatures, 18: 34232
effects on pyrolytic carbon, 18: 37676 (A/CONF.28/P/573)
effects on pyrolytic carbon, 19: 13878(R) (GA-5606(Pt.1))
effects on pyrolytic-carbon-coated uranium carbide particles, 19: 20463 (ORNL-TM-431)
effects on pyrolytic carbon-coated uranium carbide and dioxide fuel particles, 19: 44740 (BMI-1737)
effects on pyrolytic carbon-coated fuel particles, 19: 44748 (ORNL-P-1505)
effects on pyrolytic carbon coatings of reactor fuel pellets, 20: 18076 (ORNL-TM-1385)
effects on pyrolytic-carbon-coated urania particles, 20: 23582(R) (BMI-1765)
effects on quartz and fused silica crystals, 18: 8874 (NYO-2937-1)
effects on quenched-and-annealed uranium, 19: 18451 (DP-328)
effects on radiation-resistant electronic equipment, 18: 33869
effects on radioinduced defects in graphite, 18: 14554
effects on rare gas trapping in calcium fluorides, 18: 27972(T,R) (EURAEC-1043)
effects on rat bone growth, 19: 2143
effects on rat stress accommodation, 18: 25100
effects on rat teeth, whole-body, 19: 26003
effects on rate-controlling mechanism for slip in body-centered-cubic metals, 20: 43998 (ORNL-3993)
effects on reactions between carbon dioxide and graphite, 19: 11159 (AERE-R-4332)
effects on reactions between carbon dioxide and graphite, 19: 11160 (AERE-R-4659)
effects on reactions between carbon dioxide and graphite in presence of methane, 19: 11161 (AERE-R-4817)
effects on reactions between carbon dioxide and graphite, 19: 11162 (AERE-R-4819)
effects on reactions of carbon with carbon dioxide, 19: 11163 (AERE-R-4828)
effects on reactions between bromine and cyclohexane, organic retentions of bromine-80m and -82 in, 19: 38713
effects on reactions between stainless steel and U_3Si_2 in presence of sodium, 19: 42805 (NAA-SR-10621)
effects on reactor structural materials at high temperatures, 18: 24193 (HW-SA-3436)
effects on reactor pressure vessels, measurement of, 18: 23780(R) (SWRI-1243-11)
effects on reactor materials tensile properties, 18: 26096
effects on reactor fuel elements, swelling, 18: 28044(R) (HW-80284 (p.8.1-4))
effects on reactor pressure vessels, 18: 28945
effects on reactor fuels and construction materials, 19: 14096
effects on reactor fuel processing materials, 19: 15571(R) (TID-21385)
effects on reactor-fuel composition and reactivity, (T), 19: 19350

(AD-605022)
effects on reactor materials, exposure unit for, (T), 19: 18548
effects on reactor fuels and structural materials, (E), 19: 30829 (TID-7697(Add.))
effects on reactor materials, (E), 19: 35622
effects on reactor materials, method for studying, 19: 38822 (BNWL-SA-2)
effects on reactor materials, summary of ETR tests of, 20: 27572(R) (BNWL-207, pp 4.4-7)
effects on reactor materials, heating, (E), 19: 26628 (CEA-R-2581)
effects on recoil bromination of aromatic compounds, 20: 31296
effects on recrystallization of pure aluminum, 19: 4721
effects on recrystallization of high-purity aluminum, 19: 16241
effects on refractory carbides, 20: 23774(R) (ORNL-3913, pp 75-109)
effects on refractory concretes, 20: 44005
effects on regenerating in-core neutron chambers, 19: 26649 (BNWL-14)
effects on reproduction in domestic animals, 19: 45813(R) (ORO-631, pp 36-44)
effects on resistance of thin-film resistors, method for measuring, 20: 694
effects on resistance strain gages, in-pile, 20: 29578 (EUR-2649.e)
effects on resistivity in tungsten, isothermal recovery from, 19: 37165(R) (GEMP-47A, pp 85-99)
effects on rhenium, 19: 47106
effects on rhombic sulfur, 18: 30250
effects on rice, genetic, 18: 1388
effects on rice, genetic, 18: 38934
effects on rice, mutagenic, 18: 21867
effects on rocket reactor thermal control materials, 18: 20603
effects on rupture properties of niobium-stabilized stainless steel under constant stress rate conditions, 19: 44750 (ORNL-TM-1216)
effects on SAP-clad uranium carbide fuel elements, 20: 46220 (AECL-2571)
effects on saturated fluorocarbons, chemical, 19: 46404
effects on secondary breakdown in transistors, 18: 25756
effects on seeds of deciduous trees, RBE gamma, 20: 38594(R) (ORO-2066-10)
effects on selected transducers at 150 to 220°F for NERVA program, 18: 22525 (FZK-159-1)
effects on semiconductors in reactors, 19: 11790
effects on semiconductors, 19: 34766
effects on semiconductors and transistors, 20: 14920 (TID-22664)
effects on semiconductor diode characteristics, transient, 20: 35809
effects on semiconductor detectors, 20: 46099
effects on serum proteins, 17: 38752
effects on sheep, pathological, 20: 18188(R) (ORO-635)
effects on silicon p-i-n junction, 18: 2321
effects on silicon field-effect transistors, 18: 4304 (NP-13342)
effects on silicon carbide luminescence, 18: 16122
effects on silicon crystals, Hall effect measurements of, 18: 16534
effects on silicon, annealing of, 18: 22541
effects on silicon rectifiers, 18: 32228 (SC-R-64-182)
effects on silicon transistors, energy dependence of, 18: 32234 (SC-R-64-196)
effects on silicon avalanche diodes, single collision, 18: 34248
effects on silicon carbide p-n junctions, 18: 42082(T)
effects on silicon transistors, annealing of, 19: 4551
effects on silicon transistors, 19: 13813 (WL-TDR-64-97)
effects on silicon field-effect transistors, 19: 13819
effects on silicon planar transistors, (E), 19: 22817
effects on silicon transistors, 19: 28696 (AD-607561)
effects on silicon carbide diodes, 19: 30536(R) (WCAP-2666)
effects on silicon transistors and Mylar capacitors, transient, 19: 30595 (GA-6008)
effects on silicon semiconductors, comparison of gamma and, 19: 32615 (NAA-SR-10856)
effects on silicon, spectrum normalization for, 19: 34747 (NAA-SR-10612)
effects on silicon carbide detectors, 19: 34592(R) (EURAEC-1384)
effects on silicon defect centers from, 19: 39252
effects on silicon diodes, 20: 4299(R) (ORNL-2711)
effects on silicon diodes, displacement clusters from, 20: 7460
effects on silicon integrated circuits and transistors, 20: 7464
effects on silicon carbide transistors, 20: 12276 (NYO-3405-4)
effects on silicon semiconductors, transient annealing in, 20: 31613 (SC-DC-66-1443)
effects on silicon, transient annealing of, 20: 37129 (SC-DC-66-1820)
effects on silkworm eggs, lethal, 20: 72
effects on single crystals of graphite, (E), 19: 23142
effects on sintered beryllium oxides, 18: 2380
effects on sintered uranium carbide pellets, 18: 24072(T,R) (EURAEC-934)
effects on sintered uranium dioxide, 18: 30157(T,R) (EURAEC-933)
effects on size of litters produced by male mice, 20: 20453
effects on skin, 16: 26841 (BNL-5197)
effects on slip in copper single crystals, 20: 7646
effects on slurries of uranium-235 dioxide in liquid ammonia, 19: 37176 (ORNL-TM-1150)
effects on SNAP electronic components, 19: 24883 (NAA-SR-10284)
effects on social distractibility behavior of female monkeys, 20: 36639
effects on sodium phosphates, 20: 12902
effects on sodium selenate crystals, ESR of paramagnetic centers from, (E), 20: 15972
effects on solid xenon compounds, 20: 43373
effects on solid-solid phase transformations, (E), 20: 40306
effects on solids, theory of, 19: 11236
effects on sorption rate of hydrogen by manganese dioxide, 20: 8985
effects on space flight control systems, 19: 849(R) (FDL-TDR-64-30)
effects on spermatogenesis in man, design of irradiation facility for study of, 18: 29245 (TID-20783)
effects on spin-lattice relaxation time of praseodymium ions in lanthanum chloride, 20: 40350
effects on stability of carbon tetrafluoride, in-pile, 18: 30995(R) (ORNL-3619(p.278-335))
effects on stability of metallic reactor fuels, 19: 11792
effects on stability of carbon-14-labeled heterocyclics, 20: 20783
effects on stacking fault annihilation in gold films, 19: 44739(R) (ANL-7000, pp 233-77)
effects on stainless steels at low temperatures, 18: 28048 (NP-13980)
effects on stainless-to-Zircaloy joints, 18: 45022(R) (GNEC-327)
effects on stainless steel-clad uranium dioxide fuel rods (E), 19: 3727 (ORNL-TM-921)
effects on stainless steel, 19: 2871
effects on stainless steel-UO_2 plates, (E), 19: 4717 (ORNL-3709)
effects on stainless steels, (E), 19: 4670
effects on stainless steel- and Zircaloy-clad uranium dioxide fuel elements, 19: 8616(R) (GEAP-4725)
effects on stainless steel (type-304) embrittlement at high temperatures, 19: 28885
effects on stainless steel dispersion fuel elements for Army PM reactors, (E), 19: 31545 (MND-Z706-13)
effects on stainless steel and Zircaloy-2, 19: 40286(R) (NAA-SR-11200)
effects on stainless steel, 19: 42801(R) (BMI-1721(Del.))
effects on stainless steel-clad uranium mononitride, 20: 888 (BMI-1731)
effects on stainless steels, 20: 46148
effects on stainless steels, 20: 46149
effects on standing wave impedance probe components, 18: 12412 (AFCRL-63-753)
effects on steel subjected to multiaxial stress distributions, 18: 5815(R) (GA-4742)
effects on steel, method for measuring, 19: 7992
effects on steels, 18: 40020
effects on steels, method for comparison of, 20: 41504
effects on steels, equipment for measuring, 20: 41113
effects on stored energy and dimensions of graphite, 19: 28879
effects on stored energy release of beryllia, effects of dosage on, 20: 15142
effects on stored-energy distributions in graphite, 19: 28884
effects on strain fatigue of austenitic stainless steels and nickel alloys, 20: 21426 (N-65-24714)
effects on strains and stresses of annular fuel elements, (T), 19: 17259
effects on strength of copper crystals, prestressing effects on, 18: 8879
effects on strength of beryllium oxide, 18: 18436
effects on strength of copper alloy single crystals, annealing of, (E), 19: 4729
effects on strength of copper and aluminum–copper alloy, 19: 11682
effects on strength of copper alloys, effects of aluminum and gallium on, 19: 44739(R) (ANL-7000, pp 233-77)
effects on strength of copper single crystals, mechanism of, 20: 45030
effects on strength of copper single crystals, mechanism of, 20: 45031
effects on strength of copper single crystals, mechanism of, 20: 45032
effects on stress relaxation in materials, 18: 42120(T) (AEC-tr-6474)
effects on stress-strain curves of copper single crystals, 18: 16530(T) (AEC-tr-6373)
effects on stress-strain curves of copper crystals, 18: 18417(T) (ANL-Trans-3)
effects on stress-strain curves of copper, strengthening theory on, 18: 24200(T) (ANL-Trans-19)
effects on stress-rupture properties of niobium-stabilized chromium–nickel stainless steel, 18: 44054(R) (ORNL-3670(p.174-200))
effects on stress-rupture properties of A-286 stainless steel, 19: 11682
effects on stress-strain properties of type 304 stainless steel, 19: 40961
effects on stress-rupture properties of Inconel and 304 stainless steel, 20: 5181(R) (ORNL-3029)
effects on stress-rupture of Inconel at high temperatures, 20: 4299(R) (ORNL-2711)
effects on stress-rupture properties of chromium–nickel–niobium alloys,

20: 5917
effects on stress-rupture properties of A-286 alloy and René 41, 20: 11358
effects on stress-rupture of chromium–nickel–niobium steel, 20: 13328 (ORNL-TM-1359)
effects on stressed tubes of A302B steel, 18: 36046(R) (GA-5495)
effects on structural properties of steels, 18: 16527(R) (NRL-Memo-1393)
effects on structure of metals, 19: 997(R) (NYO-2994-1)
effects on structure of chlorophyll-less mutant of *Euglena* cells, 19: 8805
effects on structure of metals, 19: 23132
effects on structure of carbon steel and iron, 19: 23133
effects on structure of molybdenum, 19: 37195
effects on structure of polybutadiene, 19: 40561
effects on structure of molybdenum, combined effect of carbon impurity atoms on, 20: 895
effects on structure of alpha-quartz, 20: 17149(T)
effects on structure of sintered beryllium oxide, x-ray diffraction studies on, 20: 21433(T) (UCRL-Trans-10012)
effects on structure of graphite, energy release at high temperatures from, 20: 31802
effects on structure of germanium, 20: 36357 (INR-684/II/PH)
effects on sulfur oils, 20: 45735
effects on sulfur-35 recoils in alkali metal chlorides, chemical, 19: 9166 (COO-32-106)
effects on superconducting properties of lead, 18: 15068
effects on superconductors, 18: 34683(R) (NP-14136)
effects on superconductivity of niobium stannide (E), 19: 1506
effects on superconducting properties of indium and tin foils, 20: 30301
effects on superconducting niobium–tin alloys, 20: 34459
effects on superheat reactor fuel cladding materials, 20: 28750(R) (GEAP-5061)
effects on survival and tumorigenesis in mice, 18: 23230(R) (ANL-6823(p.15-19))
effects on survival of burros, 18: 38775(R) (ORO-624)
effects on survival of burros, 20: 32965(R) (ORO-648, pp 1-25)
effects on Swedish charcoal iron, annealing of, 19: 11789
effects on swelling in molybdenum–uranium alloys with finely dispersed phases, 19: 14097
effects on swelling of alpha uranium, 19: 14101
effects on swelling of uranium, 19: 14102
effects on swine, 19: 5635
effects on swine, pathological, 20: 18188(R) (ORO-635)
effects on tandem-extruded stainless steel–Zircaloy-2 joints, 18: 7284 (DP-859)
effects on tantalum, effect of oxygen concentration on annealing of, 20: 19268
effects on tantalum alloy capsules containing liquid plutonium–cobalt–cerium alloy fuel, 20: 43814 (LA-DC-7581)
effects on tellurium compounds, chemical state of iodine-131 formed in, 18: 33661
effects on tellurium oxide, chemistry of iodine-131 produced by, 19: 13505
effects on tensile properties of Zircaloy-2, 18: 24191 (HW-SA-3194)
effects on tensile properties of niobium with 0.6% zirconium, 18: 24196 (PWAC-278)
effects on tensile properties of carbon steel, 18: 37748 (A/CONF.28/P/412)
effects on tensile properties of chromium–nickel–niobium steel at 650 800°C, 18: 42128
effects on tensile properties of niobium- and titanium-stabilized chromium–nickel steels at room temperature to 850°C, 18: 42129
effects on tensile properties of fuel cladding materials in superheat environments, 19: 2880
effects on tensile creep ductility of alpha uranium, under strain and stress, 19: 23141
effects on tensile fracture strain of graphite, at 25, 550, and 600°C, 19: 39238
effects on tensile properties of Zircaloy-2 and -4, 19: 40961
effects on tensile properties of Hastelloy X-280, effects of cold working and aging on, 20: 889(R) (BNWL-120, pp 4.1-59)
effects on tensile properties of Zircaloy-2, effects of hydrogen content on, 20: 5851
effects on tensile properties of magnesium and magnesium alloys, 20: 7639
effects on tensile properties of copper–niobium–zirconium alloys, 20: 9590
effects on tensile-strain limits of graphite, 20: 11225
effects on tensile properties of Hastelloy X-280, pre-exposure effects on, 20: 23769 (BNWL-202)
effects on tensile properties of refractory metal alloys, 20: 27571(R) (BNWL-207, pp 4.1-3)
effects on tensile fracture strain of graphite, 20: 27578 (BNWL-SA-56)
effects on tensile properties of molybdenum, niobium, and tungsten, effects of annealing on, 20: 27582(R) (GEMP-400A, pp 63-98)
effects on tensile-strain fracture in EGCR-type graphite, 20: 29811
effects on tensile properties of Incoloy 800, Inconel 600, and Zircaloy-2, 20: 33964
effects on tensile properties of aluminum alloy 6061, (E), 20: 35941
effects on ternary plutonium–uranium alloys and plutonium carbide–uranium carbide fuels, in-pile, (E), 20: 14007(R) (ANL-7122, pp 1-41)
effects on terphenyl decomposition at 200 to 450°C, 19: 2410
effects on testis in rats, histochemical studies of, 18: 38940
effects on textiles, 19: 24556
effects on thermal conductivity of graphite at 200 to 600°C, 18: 672
effects on thermal conductivity of graphite, measurement by a rapid thermal-pulse method, 18: 655 (HW-SA-2874)
effects on thermal conductivity of beryllium oxide at 0 to 85°C, 18: 5827
effects on thermal conductivity of nuclear-grade graphite, 18: 7319
effects on thermal expansion coefficients of uranium, 18: 12733 (TRG-Report-611(p.6-7))
effects on thermal conductivity of uranium, 18: 12734 (TRG-Report-611 (p.8))
effects on thermal conductivity of pyrolytic carbon and graphite, 18: 20450(R) (BMI-1661(Del.))
effects on thermal conductivity of uranium dioxide pellets, 18: 28071
effects on thermal conductivity of uranium dioxide, 18: 32219 (CEA-R-2372)
effects on thermal conductivity of pyrolytic graphite, 18: 34033(R) (BMI-1669(Del.))
effects on thermal annealing of cobalt complexes, 18: 35609
effects on thermal conductivity of uranium dioxide at 150 to 1600°C, 19: 11776 (AERE-R-4690)
effects on thermal properties of alkali-halide crystals and solid solutions, 19: 19986
effects on thermal capacity of graphite at 1.7 to 16°K, 19: 23152
effects on thermally stimulated conductivity of p-type silicon, (E), 19: 41985
effects on thermal conductivity of polyethylene at 0 to 170°C, 19: 40603
effects on thermal ratcheting in aluminum-clad urania fuel elements, 19: 44737(R) (ANL-7000, pp 111-18)
effects on thermal insulation in reactors, 19: 44088
effects on thermal conductivity of uranium, 19: 47101
effects on thermal conductivity and electric properties of uranium dioxide, 20: 2452
effects on thermal conductivity of germanium and silicon, 20: 7648
effects on thermal cracking of petroleum gas-oil fractions, 20: 18785(T)
effects on thermionic cell performance, 18: 20881
effects on thermistors and transistors, 20: 5808 (N65-35081)
effects on thermo-electric fuel elements, 19: 28872(R) (GEST-2039)
effects on thermocouples, design of apparatus for studying, 18: 23840 (RT/ING(64)-2)
effects on thermocouples, 18: 41723 (UJV-987/64)
effects on thermoelements in reactors, 18: 32237
effects on thermophysical properties of isopropylbiphenyl, 20: 1923
effects on thin magnetic films, coating effects on, (E), 19: 28881
effects on thiourea, yields of compounds labeled with phosphorus-32 and sulfur-35 from, 19: 46365
effects on thorium and uranium, effects of postirradiation annealing on, 18: 14366(R) (HW-79766(p.3.1-64))
effects on thorium–uranium alloys and compounds, review, 19: 37175 (ORNL-TM-1142)
effects on time of flowering of rear, 16: 1593
effects on time-to-rupture of metals and alloys, 19: 47081(R) (EURAEC-1432)
effects on tin compounds, yields of antimony-125 from, 19: 46388
effects on tin-119 Mössbauer effect in magnesium–tin oxide crystals, damage, 20: 3065
effects on tissues, 20: 8712
effects on tissues, 20: 18548
effects on tobacco resistance to blue mold disease, mutagenic, 20: 40613 (N-66-18147)
effects on toxin formation by *Cl. perfringens*, 19: 38448
effects on transducers and electric cables, transient, 18: 8608 (IDO-16914)
effects on transformations in uranium oxysulfide–uranium sulfide, 19: 44737(R) (ANL-7000, pp 111-18)
effects on transistors, 18: 43903
effects on transistor current gain, mechanism, 19: 15936 (SC-R-64-1373)
effects on transistorized circuits, methods for analyzing, 19: 42771 (SC-R-65-941)
effects on transistors, 19: 44548 (NP-15422)
effects on transistors, physical parameters for predicting, 20: 2184(R) (AD-614618)
effects on transistors, method for predicting, 20: 2185(R) (AD-618194)
effects on transistor gain degradation, (E/T), 20: 9302 (RLDP-65-13)

effects on transition joints between Inconel 600 and Zircaloy-2, 20: 27574(R) (BNWL-207, pp 4.32-4)
effects on traveling-wave tubes, transient, 19: 13818
effects on tree growth, 18: 33282 (TID-20876)
effects on trimethylsilane, 19: 45679(R) (NYO-1859-11)
effects on trioxalatochromium ions on anion-exchange resin, 20: 45777
effects on triphenylphosphine and triphenylphosphine oxide, 20: 9003
effects on tris-(ethylenediamine)-cobalt(III) complexes, 19: 42533
effects on tritium formation in irradiation of amines and hydrocarbons in quartz ampoules, 19: 26440
effects on tritium gas bubble formation in aluminum–lithium alloys, (E), 20: 19265
effects on tungsten, 20: 2475
effects on tungsten, 20: 25474(R) (BNL-954, pp 122-67)
effects on tungsten tensile properties, annealing of, 20: 33965
effects on tungsten single crystals, 20: 35944
effects on twinning in niobium–vanadium alloys, 20: 39462
effects on type 304 stainless steel, 19: 7847 (APED-4542)
effects on type 304 stainless steel, methods of reducing, 20: 43999 (ORNL-TM-1544)
effects on type 347 stainless steel, 20: 37168(R) (BMI-1771)
effects on type 347 stainless steel, 20: 37169(R) (BMI-1774)
effects on UHTREX fuel, 19: 9734 (LA-DC-6713)
effects on uniform silicon avalanche diodes, 18: 16528 (SC-DC-64-346)
effects on unpaired electron concentrations in lithium fluoride single crystals, 19: 42544
effects on urania, 19: 36953(R) (HW-84609(p.5.1-5))
effects on urania, 19: 39125(R) (BNWL-91)
effects on uranium dioxide pellets sintered at low temperatures, 18: 5819 (UNC-5061)
effects on uranium and uranium dioxide, in-pile, 18: 11432(R) (DP-875)
effects on uranium carbide, 18: 12754
effects on uranium dioxides, autoradiography of, 18: 18438
effects on uranium carbides, in-pile, 18: 24860(R) (UNC-5071)
effects on uranium dioxides, temperature distribution in, 18: 37730 (A/CONF.28/P/17)
effects on uranium alloy fuel elements, 18: 37735 (A/CONF.28/P/97)
effects on uranium dioxide films, 18: 37742 (A/CONF.28/P/338)
effects on uranium dioxide single crystals, 18: 37611 (A/CONF.28/P/444)
effects on uranium carbide, 18: 39828(R) (UNC-5080)
effects on uranium dioxide, formation and distribution of uranium metal in, 18: 39997 (HW-82263)
effects on uranium dioxide melting point (E), 19: 2867
effects on uranium, 19: 26898
effects on uranium rods, induced expansion in, 19: 30830
effects on uranium expansion, 20: 4470
effects on uranium dioxide–lithium fluoride mixtures, 20: 12898
effects on uranium dioxide–zirconium dioxide mixtures, 20: 13330
effects on uranium and uranium alloys, 20: 21436
effects on uranium dioxide oxidation in carbon dioxide atmosphere, 20: 23171
effects on uranium recrystallization, 20: 27598
effects on urinary excretion of amino acids, 18: 19638
effects on vacancy repeated yielding characteristics of copper–tin alloys, 19: 20635
effects on vacancy agglomerate induction in copper, interpretation of contrast phenomena in, 20: 11353(T) (ANL-Trans-259)
effects on vapor-grown single crystals of uranium dioxide, 19: 20603
effects on vegetation at GNL reactor site, Georgia, 19: 36038
effects on volume variations in iron, 20: 27594(T) (ORNL-tr-1236)
effects on vulcanization of rubbers, 19: 11200
effects on water at 14.6 Mev, reaction rates and yields from, (T), 20: 16509 (TID-22666)
effects on water in presence of inert salts, 19: 26397
effects on water, effects of salts on, 20: 8981 (CEA-R-2794)
effects on wear resistance of carbon steel, 20: 11227
effects on welding of teflon and other polymeric materials, 18: 325
effects on wheat seedlings in relation to polyploidy, 16: 1613
effects on wheat seed, effects of oxygen tension and storage temperature on, 18: 31221
effects on wheat seeds, genetic, 20: 3762
effects on wheat, biological, 19: 21913
effects on work hardening of copper, 18: 20600
effects on work hardening of copper single crystals, 18: 24211
effects on work performance of monkeys, chronic-exposure, 20: 32962 (AD-627686, pp 423-33)
effects on work-hardening parameters of copper single crystals, 18: 28077
effects on x-ray line broadening of beryllium oxide, 18: 20608
effects on x-ray scattering by beryllium oxide, 18: 20607
effects on xenon diffusion in uranium dioxide, 18: 18386
effects on xenon tetrafluoride, Szilard-Chalmers, 18: 31580
effects on yellow-anthered dallisgrass, genetic, 18: 8193
effects on yield of early maturing cotton, 20: 42899
effects on yield strength and grain size relation in iron and iron–carbon alloys, 18: 7328
effects on Young's modulus of reactor graphite, 19: 14048
effects on zeolites, 18: 35234(R) (HW-81862)
effects on zinc oxide smokes, 20: 37281
effects on zinc uptake by plants, 20: 6711(R) (ORNL-3849, pp 43-100)
effects on Zircaloy-2 corrosion by water, 18: 14407(R) (HW-79766(p.5.1-16))
effects on Zircaloys, in-pile, 18: 28023
effects on Zircaloy-2 corrosion by fog, 18: 37324 (A/CONF.28/P/16)
effects on Zircaloy-2 and zirconium–niobium–tin alloy, 19: 16208(R) (EURAEC-1249)
effects on Zircaloy-clad uranium dioxide, 19: 18542
effects on Zircaloy-clad urania, 19: 24093(R) (WAPD-MRP-111)
effects on Zircaloy-2 pressure tubes, 19: 30821 (BNWL-42)
effects on Zircaloy-2, 19: 37167(R) (HW-84609(p.8.1-7))
effects on zirconium, 19: 11814
effects on zirconium alloys corrosion by water, 19: 32693 (AECL-2257)
effects on 347 stainless steel, 19: 39091(R) (BMI-1723(Del.))
effects on 5-Mc magnetic tunnel-semiconductor logic circuits, 19: 40939
effects with recurrent intercrossing on genetic variability in Phaseolus, 20: 5406
eigenfunctions and energy levels of, in nonhomogeneous nuclei, 17: 33010
eigenvalue problem from Boltzmann equation for thermal equilibrium approach, 17: 24369(R) (GA-3542)
electric charge of, upper limits for, 17: 17012
electric dipole moment of, low pass filter for determination of, 19: 41338 (ORNL-TM-1149)
electric dipole moment of, as test of CPT invariance, (T), 20: 9801
electric dipole moment of, (E), 20: 39470(R) (ORNL-3924)
electric form factor, sign, 16: 9423
electric structure factor from thermal neutron scattering by rare gases, (E), 20: 40129
electromagnetic form factors of, 16: 33758
electromagnetic form factors for, 17: 9344
electromagnetic form factor for, from electron-deuteron scattering, 18: 37879 (NP-14173)
electromagnetic radiation from, in magnetic field, (T), 19: 29104
electromagnetic structure, 16: 9399
electron emission and polarization, 16: 10843
embrittlement of ferritic steels by, and recovery, 20: 44019
embrittlement of stainless steel by, effects of grain size on, 20: 13335
embrittlement of Soudotenax and T-1 pressure vessel steels by, 20: 17117 (EURAEC-1558)
emission and polarization from proton reactions (p,n) with lithium-7 at 4 to 6 Mev, (E), 20: 9983
emission at 0° in proton reactions with nuclei at 143 Mev, 16: 15676
emission by californium-252 spontaneous-fission products, (E/T), 19: 8396 (ISS-64/35)
emission by compound nuclei, 17: 9593
emission by compound nuclei, computer analysis of, (T), 19: 21245 (ORNL-TM-196)
emission by confined plasma, 18: 2985(R) (UCRL-10852)
emission by dysprosium and terbium compound nuclei (E), 19: 3339
emission by energy levels of nitrogen-14, (E/T), 19: 17012
emission by excited fission nuclei, (T), 20: 6313
emission by fusing deuteron plasma in high-intensity pulsed discharges, 16: 29899 (CLM-R-20)
emission by nuclei, Q-values for, 18: 32727 (BNL-846)
emission by Picket Fence and Scylla plasma, 18: 6302(R) (LAMS-3004)
emission by plasma, 17: 36810
emission by plutonium-239, uranium-233 and -235 fission fragments, 19: 33384
emission by radium sources, 18: 28533
emission by Scylla III, 17: 29655 (LADC-5531)
emission by sources, measurement of absolute, 19: 15877
emission by sun, upper bounds of flux of, 20: 21495
emission by terbium and dysprosium compound nuclei, 17: 36666 (UCRL-10099(Rev.))
emission by uranium-235 in region of symmetrical fission, 16: 31123
emission by uranium-235 fission fragments, 18: 24701
emission from beryllium–lead-210 source, spectra of, 18: 36564
emission from beryllium–plutonium sources, rates of (E), 19: 3380
emission from compound nuclei, angular momentum effects in evaporation, 18: 28628
emission from excited fission fragments, 17: 13354
emission from KIWI-TNT destruct, dose measurements of, 19: 42135 (LA-3304)
emission from meson (μ^-) reactions with hydrogen (liquid), 16: 15583
emission from meson (π^-) absorption in copper, lead, and tin, spectra, 18: 32733 (ISS-64/10)

emission from nonmultiplying assemblies, mean time calculation method, 16: 2467 (GA-2189)
emission from plasma, 19: 21483(R) (ORNL-3760(p.30-56))
emission from plutonium-239 and uranium-233 and -235 fission fragments, (E/T), 19: 41681 (ANL-Trans-205)
emission from proton reactions with carbon-13 and nitrogen-15, 18: 38072 (UCRL-7676)
emission from source, absolute determination of number in, by associated particle method, 18: 26503
emission from sun, (T), 20: 9634 (D1-82-0484)
emission from sun, evidence of high-energy, 20: 23857
emission from triton reactions with deuterium plasma yields for, (E), 19: 5292(T) (AEC-tr-6518(p.180-4))
emission from, of heavy ion reactions with nuclei, spectra of, (E) 19: 41810(T)
emission in alpha reactions (α,n) with carbon-13 in stars, 16: 23016
emission in alpha reactions (α,n) with beryllium-9 at 10–14 Mev, angular distributions for, 17: 38297
emission in alpha reactions (α,n) with beryllium-9 and carbon-13 at 14–23 Mev, angular distributions for, 17: 38298
emission in alpha reactions (α,n) with nuclei at 42 Mev, angular and energy distributions in, 17: 38208
emission in bremsstrahlung reactions (γ,n) with heavy elements, (E), 20: 15724 (MIT-2098-224)
emission in charged-particle reactions, threshold energies from, 17: 34862
emission in compound-nucleus reactions forming polonium-210, 18: 26647
emission in cosmic proton reactions in lead, 18: 14767
emission in cosmic meson reactions in lead, 18: 14768
emission in decay of compound nuclei, effect of spin on, (T), 20: 12048
emission in deuteron reactions (d,n) with nitrogen-14, yield curves for, 17: 24496
emission in deuteron reactions (d,n) with lithium-7 at 0.68–2.0 Mev, angular distributions and polarizations for, 17: 38253
emission in deuteron interactions at 275 to 450 kev, polarization in, 18: 9122
emission in deuteron reactions (d,n) with fluorine-19 and lithium-7 at 1.98 Mev, spectra of, 18: 13108
emission in deuteron reactions (d,nγ) with beryllium-9 at 0.94 Mev, time-of-flight spectra for, 18: 14230
emission in deuteron reactions (d,n) with tritium at 1 and 3 Mev, angular distributions for, 18: 28655
emission in deuterium theta pinch, 18: 32921
emission in deuterium plasma thermonuclear reactions, diagnostics from, 19: 19251 (NP-14689)
emission in deuteron photodisintegration, vertex functions for, (T), 19: 25317
emission in deuteron stripping reactions, computer program for cross section calculations for, 19: 41677 (ORNL-TM-1151)
emission in dysprosium-150 and 151 and terbium-149 production in heavy ion reactions, angular momentum effects on, 17: 26470 (UCRL-10767)
emission in fission and (α,n) reactions, counter design for simultaneous measurement of, 20: 16905(P)
emission in heavy ion reactions with uranium-238, evaporation in, 19: 37791 (JINR-P-2114)
emission in heavy-ion reactions with nuclei, angular distributions, (T), 20: 8089(T) (BNL-tr-30)
emission in helium reactions (He-3,n) with nuclei at 25 Mev, spectra of, 18: 24650
emission in helium-4 (d,np) reactions at 14.6 and 20.2 Mev, 18: 30837
emission in helium hypernuclei nonmesic decay, (E), 20: 11977 (TID-22536)
emission in meson (μ^-) capture by heavy nuclei, 16: 7100
emission in meson (μ) capture in lead and silver, 16: 18474
emission in meson (μ) capture by heavy nuclei, 16: 18486
emission in meson (π^-) capture by complex nuclei, 16: 25902 (LNF-62/37(p.138-42))
emission in meson(μ^-) reactions with helium-4, spectra of, 17: 24320
emission in meson (π^-) capture by emulsion nuclei, energy spectra of, 17: 26543
emission in meson (π^-) capture by nuclei, spectra of, 18: 7769
emission in meson (μ^-) capture by oxygen-16, mechanism for, 18: 15196 (JINR-P-1530)
emission in meson (π^-) capture by nuclei, spectra of, 18: 19084
emission in meson (π^-) capture by complex nuclei at 150 Mev/c, spectra of, (E), 19: 8437
emission in meson (μ^-) capture by deuterons and helium-3, (E), 19: 29254 (NEVIS-128 and Add.)
emission in meson (π^-) reactions with xenon at 9 Bev/c, high four-momentum transfer in, (E), 19: 47698
emission in meson(μ^-) capture by several elements, multiplicity distributions in, 18: 40516 (UCRL-11243)
emission in minerals, rocks, and uranium, 18: 16209
emission in neutron reactions (n,p) with deuterium at 14.7 Mev, energy spectra of, 18: 6010
emission in nuclear weapons detonation, dosimetry of, 18: 44918 (ORNL-P-311)
emission in oxygen ion reactions with gold, 18: 9323 (UCRL-11088)
emission in oxygen-16 reactions with metals at 167 Mev, 19: 10336
emission in photon reactions with medium nuclei up to 80 Mev, 18: 38152
emission in photon reactions with bismuth and lead (E/T), 19: 3249
emission in plutonium-240 and uranium-234 symmetric fission, 17: 19280
emission in plutonium-239 and uranium-235 (n,f) reactions at 24 kev, secondary, (E), 19: 45297
emission in polarized meson (μ^-) capture by helium-4, asymmetry parameter of, 17: 19338
emission in powerful pulse discharges, (T), 19: 5311
emission in proton reactions (p,n), thresholds, 16: 7068
emission in proton reactions (p,n) with vanadium-51 at 1.67 to 2.05 Mev, 16: 8177
emission in proton reactions (p,n) at 6–12 Mev, spectra of, 17: 24444
emission in proton reactions (p,n) with boron-10 at 4.8–10.6 Mev, excitation function for, 17: 24456
emission in proton reactions (p,n) with nuclei at 18.5 Mev, angular distributions for, 18: 40587
emission in proton quasi-elastic scattering by light nuclei, fragmentation theory for, 18: 40536
emission in proton reactions (p,n) with nuclei, equipment for measuring angular distributions of, 18: 39669
emission in proton reactions (p,n) with lithium-7 at 3 to 4 Mev, polarization from, (E), 19: 31274)
emission in proton reactions with lithium-6, (E), 20: 3140
emission in proton reactions (p,n) with lithium-7 near threshold, (E), 20: 30525
emission in reactions between complex nuclei, excitation functions for, 17: 22634
emission in rupture of uranium nucleus, 18: 16957(T) (AEC-tr-6371)
emission in spontaneous fission of californium-252, (E), 19: 43397
emission in underground nuclear explosions, engineering drawings of diagnostic pinhole assemblies for determining, 19: 18337
emission lifetimes from compound nuclei, 16: 32394 (LADC-5367)
emission of secondary, in meson (π^-)-proton interactions, (E), 20: 13525
emission of, determination of simultaneous, 20: 11947(P)
energy and flux distributions in Kansas University Reactor, 16: 25025 (TID-15977)
energy and flux in reactors, relation between core composition and cadmium ratio for, (E/T), 19: 29560
energy and flux measurements on, methods of, 20: 14883
energy and flux of skyshine, around synchrotron, (E), 19: 20741
energy and intensity spectra of solar, above 1 Mev, (T), 19: 44902
energy and intensity spectra of solar, near earth, (E/T), 19: 44903
energy and population of knock-ons in neutron-irradiated polyatomic materials, 16: 1804 (GEMP-101)
energy and spatial distributions in finite cylindrical rods of fissile material, 16: 8158 (DC-60-11-51)
energy and spatial distributions in straight cylindrical channel through water, (E), 19: 45465
energy dependence of, 17: 37999(T) (AEC-tr-5734(p.3-6))
energy deposition and transfer in liquid hydrogen, 16: 29641 (NASA-TN-D-1115)
energy distribution, multigroup theory for calculation, 16: 1013
energy distribution, method for determination, 16: 7006(T) (AEC-tr-4963)
energy distributions from plutonium fluorides, 16: 22967 (LAMS-2692)
energy distribution in homogeneous media, 17: 788
energy distribution of fast, from lead, 17: 873
energy distributions from proton reactions (p,n) with vanadium-51, 17: 4063 (UCRL-6530)
energy distributions from beryllium-polonium and beryllium-radium sources, 17: 13356
energy distributions of scattered, in water, 17: 26401
energy distributions from polonium–beryllium source, 17: 29570
energy distributions at graphite-water boundary, 17: 34895
energy distributions in reactors, effects of core division by moderator material on, 18: 24849 (NP-13930(p.130))
energy distribution in hydrogenous moderator of long counter, (T), 19: 21202
energy-exchange kernels and spectra in water, 18: 2814
energy from americium-241–Be reactions, 19: 23163(R) (ORNL-3650 (p.111-86))
energy from, deposited at depth in simulated tissue, 18: 38726
energy in nuclei ($A \gtrsim 200$), Fermi, 18: 19118
energy level positions in nuclei, 18: 9360
energy levels, 16: 3598 (AD-257272)
energy loss in polyethylene–ethylene spherical-cavity dosimeters, (T), 20: 11135

energy measurements by attenuation techniques, 16: 31057 (UCRL-6264)
energy measurement by transmission, technique for, 20: 38028
energy of, determination from recoil proton tracks in emulsion, 17: 36126
energy of incident, in neutron-capture therapy, 20: 35367
energy of system of interacting, ground-state, (T), 20: 30523
energy of, boron trifluoride detector for measuring, 19: 24874(P)
energy release in organic liquids, 17: 8197
energy response in boron-10 shielded uranium-235 fission chamber, 17: 1768
energy spectra and flux measurements in reactors, methods for, 16: 23377 (TID-7616(p.69-77))
energy spectra and flux in exponential experiments, transients in, (T), 19: 29504 (EUR-1910.e)
energy spectra and flux measurements of accelerator, methods for, 20: 31786(R) (ORO-2891-5)
energy spectra behind water shielding, method of counting efficiencies for studying, 19: 31440
energy spectra changes in heterogeneous reactor, use of lutetium in measurements, 16: 718
energy spectra distributions, threshold detector technique for calculation and measurement, 16: 717
energy spectra, effects of reflection from homogeneous, slowing-down half space, 16: 24773
energy spectra from proton reactions (p,n) with gold, nickel, rhodium, and tantalum, 17: 17293
energy spectra from point source in heavy monatomic gas, 18: 4522
energy spectra from fast reactor at 100 ev to 50 kev, (E), 19: 10494
energy spectra from beryllium-9 (α,n) reactions at 7.3 and 10.1 Mev, (E), 19: 30527 (ORNL-P-1110)
energy spectra from proton reactions (p,n) with deuterium at 30 and 50 Mev, 19: 33298
energy spectra from (p,n) reactions on lanthanum, praseodymium, and tin at 6 to 14 Mev, (E/T), 20: 1239
energy spectra from lithium-7 (p,n) reactions near threshold, (T), 20: 6356
energy spectra from (p,n) reactions at 30 and 50 Mev, (E/T), 20: 6361
energy spectra in reflector of Melusine, (E), 19: 21729 (CEA-R-2442)
energy spectra in finite graphite blocks, equilibrium, (T), 19: 21205
energy spectra in poisoned media, comparison with scattering model, (E/T), 19: 27388 (GA-6291)
energy spectra in bulk media by time-of-flight method, (E/T), 19: 27390 (GA-6313)
energy spectra in multiplying medium, asymptotic and steady-state, (E), 19: 39768 (RPI-328-21)
energy spectra in heterogeneous thermal reactors, diffusion approximation for space-dependent, (T), 19: 42056
energy spectra in heterogeneous nonabsorbing media, (T), 20: 2942
energy spectra in nonstationary beams, method for determining exact, 20: 11937
energy spectra in graphite after fast-pulse injection, time-dependent, (E/T), 20: 11940
energy spectra in TRIGA Mark II, 20: 22502
energy spectra in fast reactors, methods for calculating, 20: 34905 (GA-7059)
energy spectra in BR-1, analysis using ionographic emulsions, 20: 35790
energy spectra in emulsions, computer program for, 20: 46028 (AD-639048)
energy spectra of, analysis by interactions with varying magnetic field, 17: 5285
energy spectra of stray, from Bevatron, (E), 19: 4778
energy spectra of HPRR and Ichiban critical assemblies, 20: 7315(R) (ORNL-3849, pp 151-82)
energy spectra of, computer program for measuring, 20: 36137 (AEEW-M-621)
energy spectral distributions in power reactors, calculated and measured using threshold detector technique, 16: 5500 (WAPD-T-1380)
energy states in local and nonlocal potentials, 20: 32566
energy states in lead-208, 20: 32566
energy states in nuclei, correlation of positions of, 19: 47583 (NP-15467)
energy transfer in tissue-equivalent cylindrical phantoms, 18: 38725
equivalent ionization chambers for, 20: 46059
escape from atmosphere, flux of cosmic-ray produced, 17: 41714
escape from heterogeneous cluster-type fuel rods, Dancoff factor and equivalence theorem for resonance, (T), 19: 42055
escape from infinite cylindrical absorbers, probability for, 18: 2801
escape from reactor shield voids, calculation of, 20: 8045(T) (AI-Trans-203)
escape from slab lattices, superposition principle in Monte Carlo calculations for resonance, (T), 19: 3551
escape in regular arrays of fuel rods, resonance, (T), 19: 21648
escape integrals in heterogeneous reactors, resonance, (T), 19: 25695
escape of, Doppler-broadened cross sections for resonance, 18: 4586 (WAPD-T-1626)
escape probabilities and fluxes outside self-absorbing cylindrical sources, 16: 4702
escape probabilities from fuel rods and rod lattices, 17: 31698
escape probabilities for hollow cylinders, tables of, 18: 1219
escape probabilities for slabs, (T), 19: 29196
escape probabilities from manganese sulfate baths, calibration of neutron sources from, 20: 24310
escape probabilities for 19-rod bundles of fuel rods, computer program for calculation of resonance, 16: 23258 (CVNA-130)
escape probabilities of resonance, calculation by Gurevich-Pomeranchuk theory, 17: 2207 (ZFK-TPH-3)
escape probabilities in thermal reactors, computer program for resonance, 19: 40153 (IA-1001)
escape probabilities in lattices, Monte Carlo analysis of resonance, (T), 19: 14472 (WAPD-T-1718)
escape probability calculation, 16: 12405
escape probability for, resonance, 18: 38049 (A/CONF.28/P/827)
escape probability formulation for intensive reactor quantities (T), 19: 3548
escape probability in lumps, improved estimate of, (T), 19: 17177(R) (ANL-6965(p.42-83))
escape probability in lumped absorbers, (T), 19: 27405
escape probability in homogeneous thorium reactors, resonance, 19: 47969
escape probability in homogeneous thorium reactor, resonance, 19: 47970
escape probability in homogeneous thorium reactor, resonance, 17: 3781
escape probability for, level separation corrections to resonance, (T), 19: 27538
evaporation from excited nuclei, distributions, 17: 17162
evaporation, correlation by Simpson pile, 18: 14774
exchange between coupled reactor cores (T), 19: 3719 (LA-DC-6530)
exchange in nitrogen-14 reactions (N^{14},N^{15}) with nitrogen-14 at 18 Mev, mechanisms of, 17: 38228
exchange in nitrogen-14(N^{14},N^{15}) reactions at 9.0 to 18.0 Mev, cross sections for, 18: 7770
exchange in proton reactions (p,t) with nuclei, Regge pole theory for, 17: 38226
exchange in proton interactions with protons in Bev range, (T), 20: 17394
exchange of, in high-energy ion-ion reactions, 17: 11492 (TID-16044)
existence in stellar mass, 18: 22664
existence of tetra-, (T), 19: 39547
experimental studies using a tandem accelerator, 18: 6156 (CONF-354-1)
experiments using, review of Argonne 4.5-Mev Van de Graaff, 20: 9945
extrapolation length in slab geometry, (T), 20: 2988
extrapolation length in water, (T), 20: 46562(R) (RPI-328-68, pp 84-144)
extrapolation length measurements in graphite and water, 20: 46966(R) (NAA-SR-12010)
Fermi age and thermalization in beryllium oxide, 16: 6212(R) (GA-1532)
Fermi age from uranium-233 fission, 16: 3867(R) (ORNL-3193(p.203))
filtering of, performance of bismuth and quartz crystals for, 18: 34752(R) (CU(PNPL)-234)
fission asymmetry contribution, 18: 13041 (CNAEM-12)
flux amplifiers of, design of transistorized, 18: 14242
flux and leakage through heavy water–iron laminates, (E/T), 20: 4800 (AE-198)
flux and multiplication in fast reactors, heterogeneity effects on, (T), 20: 18063
flux and population fluctuations in zero-power reactors, 16: 30035
flux and slowing-down density in reactors, 18: 6445 (AAEC/E-111)
flux and spectra calculations from activation data, coefficients for, 18: 18879 (NP-13722)
flux and spectra measurements, in German FR-2 research reactor, 16: 8912(T) (CEA-tr-A-1024)
flux and spectra measurements in void tank irradiation chamber, 16: 17311 (SCR-480)
flux and spectra of, semiconductor proton recoil telescope for measuring, 19: 11533
flux and spectrum of, cancer therapy using 70 Mev synchrotron, 19: 38517
flux and thermal utilization in reactor lattices, 19: 33572
flux and thermal utilization in square cell reactor lattices, effects of multipoles on, (T), 20: 5063
flux at aircraft altitudes, anomalous increases in, (E), 19: 41579
flux at large distance from point source of, air-ground interface effects on, 18: 26511
flux attenuation in KS-150 reactor shielding, 20: 20269 (UJV-1454/65)
flux attenuation to desired level for detector, method for, 19: 32601(P)
flux beneath shield of meson production facility, (T), 20: 3262
flux beneath shield of meson production facility, (T), 20: 20100 (ORNL-TM-1423)
flux calculation in reactor cells, methods for improving the cylindrical reflecting boundary condition in, 17: 3749

flux calculation technique for classroom use, 18: 6151
flux calculations, 16: 2718
flux calculations for subcritical reactor with extraneous sources, 16: 15787 (ORNL-TM-182)
flux calculations, refinements in two-group, 16: 24401
flux calculations, computer program for two-group current-equivalent parameters in, 16: 24930 (AE-75)
flux calculations, 17: 435
flux calculations at reactor core-reflector boundaries, 17: 9813
flux calculations for an exponential pile, two-group, 17: 11303(R) (HW-75228)
flux calculations for, two-group, 17: 17462
flux calculations at a point, Monte Carlo methods for, 17: 26412
flux calculations in two-dimensional multiregion reactor theory, analytic method for, 17: 35110
flux calculations for reactor on central rod drop, method for, 17: 42190 (IA-820)
flux calculations for, correction functions for, 18: 22849(R) (HW-80020(p.23-30))
flux calculations from activation data, computer program for differential, 19: 16833
flux calculations in three dimensions, computer program for one-group, (T), 19: 45218 (DP-938)
flux calculations in Sandia Pulsed Reactor II, tabulations of, 19: 48063 (SC-RR-65-344)
flux changes in reactors, Pontryagin's maximum principle for, 18: 23025 (TID-7662(p.265-77))
flux control in high-temperature BBC/KRUPP, 18: 26968
flux control in radiation effects testing, 18: 2363
flux data, code for processing threshold-detector, 16: 12013 (NDL-TR-21)
flux decay constant in graphite crystalline assemblies, asymptotic, 19: 47554
flux decay constants for finite non-multiplying media, (T), 20: 6580 (CEA-R-2702)
flux decay constants in beryllium and graphite, pulsed, (T), 20: 17662
flux decay constants of pulsed, limit of discrete time eigenvalues for, (T), 20: 24309
flux decay in a subcritical assembly, 17: 5305
flux decay in liquid uranium, neutron- and pile-physics theories for, 20: 24319
flux decay in reactor moderators, computer program for spectral analysis of, 20: 6585 (NAA-SR-Memo-10941)
flux deformation in boiling water reactors without control rods, (T), 19: 19358 (EURAEC-1303)
flux densities in lattice cells, boundary conditions for gap geometry, 18: 17256
flux densities in heterogeneous reactors, calculation of fast fission factor for, 20: 30859
flux density calculations by nonlinear variational principle, 16: 14254
flux density calculation from accelerator shielding, skyshine, (E/T), 20: 25651 (DESY-66/3)
flux density fluctuations in Halden BWR-I, experiments for, 18: 35157 (TID-7679(p.449-68))
flux density in heavy water-moderated uranium carbide lattices, 20: 34922
flux density in reactors with limited coolant heatup, 18: 38305 (A/CONF.28/P/374)
flux density in reactors, methods for determining integral, 19: 17236
flux density in reactors during exchange of fuel elements, method for local reduction of, 19: 24045(P)
flux density in reactors, instruments for measurement of, 20: 1359
flux density measurements using lithium-7 formation in boron-10 monitor, 18: 42621 (AERE-R-4663)
flux density measurements of, absorption alignment chart for, 19: 33704
flux density near planar boundary between vacuum and water, experimental measurement of linear extrapolation distance for, 18: 30949 (NYO-9077)
flux density of, activation detectors for measuring differential, 20: 33636
flux density of, construction and testing of precision long counter for measuring, 20: 37069 (BNWL-260)
flux depression by metal foils, Monte Carlo calculation of, 16: 24362
flux depression in infinite homogeneous media at energies below the resonance, 17: 3782
flux depression in pulsed heterogeneous assemblies, decay rate-dependence of (T), 19: 3520 (RPI-328-9)
flux depressions in reactors, from absorber rods, (T), 19: 27758
flux determination in irradiation experiments in General Electric Test Reactor, 18: 45138 (TID-7697(p.5.7.1-5))
flux determination for, metal-foil threshold detector for, 20: 25440(P)
flux distortions in heterogeneous reactors, method for calculating, 17: 40296
flux distortions in reactor rod configurations, eigenfunctions for calculating, 18: 23029
flux distribution measurement by induced radioactivity, device for, 16: 1969
flux distribution simulation by electric analogy, 16: 14256
flux distribution in multi-region reactor, space-dependent kinetics of, 16: 18628
flux distribution of water-moderated, 16: 19724 (AFCRL-573)
flux distribution synthesis, 16: 19735
flux distribution in branched thermal column, 16: 19930
flux distribution in reactor, shape of, 16: 25004(T) (AERE-Trans-888)
flux distribution gage for, 16: 25562 (NP-11705)
flux distribution in natural uranium, equilibrium, 16: 26529
flux distribution in reactor, correlation of statistical fluctuations in, 16: 34009
flux distribution in, heterogeneous reactors with moderating fuel elements, 17: 3751
flux distribution in slabs, 17: 3806
flux distribution of, activation method for measuring, 17: 4286(P)
flux distribution scanning in reactors, apparatus for, 17: 8683(P)
flux distribution of, measurement by foil activation, 17: 11608
flux distribution measurements near discontinuities, 17: 15194 (BNL-719(Vol.III)(p.900-31))
flux distribution in reactor cores, relations with power output, 17: 17410 (GEAP-3914)
flux distribution measurements with gold foil absorbers in water, corrections for, 17: 18600 (ORNL-3407)
flux distribution in power reactors, kinetic equations for, 17: 21317 (KAPL-2217)
flux distribution in sandwich reactor lattices, relation to Bloch's theorem, 17: 24606 (AEEW-R-136)
flux distribution in multi-legged entranceways, 17: 26220
flux distribution measurements using fission of thorium-232 and uranium-238 by fast neutrons, 17: 29606
flux distribution calculation for bare homogeneous thermal reactor during fuel burnup, 17: 29729
flux distribution in reactor fuel regions composed of thin cells, 17: 35107 (WAPD-T-1571)
flux distribution of, computer program for calculating, 17: 34836 (EUR-350-i)
flux distribution in low source reactor startups, kinetics of, 17: 38507
flux distribution in reactor channels, automatic device for measuring, 17: 37437
flux distribution in thermal reactor absorber and moderator, equations for, 18: 3129
flux distribution in semi-infinite medium with anisotropic scattering and absorption, Milne problem for, 18: 16900(T)
flux distribution in German FRM pool research reactor, 18: 23108
flux distribution determination from activity of medium flowing in reactor, 18: 26865(T) (AEC-tr-6227/1(p.47-9))
flux distribution measurements in high-temperature BBC/KRUPP Reactor, 18: 26967
flux distribution in gas-cooled reactors, measurement of, 18: 28930(P)
flux distribution measurements for intermediate, uses of resonant detectors for, 18: 29990
flux distribution in cylindrical cell, calculation of, 18: 32277(R) (PR-P-61)
flux distribution in power reactors, development of equipment for monitoring, 18: 35247(R) (NAA-SR-9700)
flux distribution of, small fission chambers for, 18: 37531
flux distribution in reactors, measurement by activation of coolant in irradiation element, 18: 42952(P)
flux distribution in heterogeneous lattices, computer program for, 18: 42586 (KEA-114)
flux distribution at perturbations in light-water-moderated uranium dioxide lattice, (E), 19: 8600 (KEA-205)
flux distribution in Kahl power reactor, relaxation method for calculating, 19: 21655
flux distribution in reactors, apparatus for determining, 19: 24871(P)
flux distribution in bent air duct through water, 19: 27701 (EIR-78)
flux distribution in shield voids, 19: 27745
flux distribution in polyethylene and water, asymptotic spectra of, (E), 19: 29177 (RPI-328-29)
flux distribution of, activation methods for determining, (E), 19: 28627 (EUR-1815.e(Rev.)(p.235-40))
flux distribution in cylindrical duct, method for calculating, (T), 19: 31211
flux distribution and collision probability in multizone lattices, (T), 19: 35715
flux distribution and leakage through perforated iron plates in heavy water, 19: 37774
flux distribution measurements in reactors, optimization of regenerating detectors for, 19: 38138

flux distribution in subcritical sphere with central point source, (T), 19: 40162
flux distribution in EBWR during power operation, (E), 19: 42076 (ANL-6751)
flux distribution in reactors, method for determining, 19: 45560 (ANL-7011)
flux distribution in WWR-S, (T), 19: 48072
flux distribution in light-water-moderated reactors, 20: 3500
flux distribution in Shippingport Pressurized Water Reactor, 20: 3519
flux distribution of, transport equation for, 20: 2940
flux distribution in reactors, xenon oscillation effects on, (T), 20: 6590
flux distribution in cylindrical cells, energy-dependent, (T), 20: 5928(R) (PR-P-66)
flux distribution in cylindrical geometry, singular integral equations for, 20: 9947
flux distribution around 10-Bev synchrophasotron, spatial, (E), 20: 11390 (JINR-P-2446)
flux distribution in homogeneous suspension reactors, (E), 20: 14072
flux distribution in Dowtherm A and water, extrapolation distances from pulsed, (E), 20: 13726
flux distribution in matter, dependence on parameters of scattering nuclei, (T), 20: 13734
flux distribution in exponential assemblies, (E/T), 20: 20214
flux distribution in multilayer unit cells, method for measuring, (E), 20: 20204 (INR-656/IX-A/R)
flux distribution in reactors, computer program for, 20: 22488 (AD-621121)
flux distribution in uniform isotropic media, time-dependent Green function for, 20: 21959
flux distribution in concrete, fast and thermal, 20: 23808(R) (NIRS-4, pp 3-12)
flux distribution in reactors, gamma scanning technique for measuring, 20: 28741 (EURAEC-1613)
flux distribution in Wigner-Seitz cell, transport codes for, 20: 30854
flux distribution in reactor matrices, disadvantage factor for, (T), 20: 36423 (APED-4335)
flux distribution in reactors, analog analysis of transient, 20: 36432 (WCAP-2828)
flux distribution in reactors, disadvantage factors for, 20: 36426 (CONF-660606-11)
flux distribution in fast reactors, analysis of transient, 20: 38431 (ANL-7120, pp 625-31)
flux distribution in high-power slab reactors, 20: 38452
flux distribution in reactors, measurement techniques for, 20: 40379
flux distribution Shippingport core 2 seed 1, wire measurements of, 20: 45125 (WAPD-PWR-TE-203)
flux distribution in BORAX-V, 20: 45202 (ANL-6964)
flux distribution in heavy water-moderated aluminum-plutonium-fueled reactor, 20: 46964(R) (BNWL-284)
flux distributions in asymmetric core, three-dimensional code and two flux synthesis techniques for calculation, 16: 743
flux distributions in boiling water reactor, perturbation theory calculation, 16: 7253
flux distributions in iron-water regions external to core, diffusion-theory method for calculating, 16: 8290 (GNEC-187)
flux distributions in cylinders, 17: 7062
flux distributions of, in reactors with large cavities, 17: 24658
flux distributions in shielding, multigroup approximation calculation of, 17: 29566 (WAPD-T-1563)
flux distributions in reactors near the source of an exponential column, radial, 17: 40307
flux distributions of, use of cadmium-covered depleted uranium in monitoring, 18: 7661(R) (HW-77954(p.4.78-84))
flux distributions in reactors, design of 4-π beta and 4-π gamma ionization chambers for mapping, 18: 8677
flux distributions in reactor operating under continuous fuel cycle at equilibrium, 18: 11402
flux distributions in activation analysis, geometry-related, 18: 12024
flux distributions in concentric fuel annuli, one-group collision-probability calculations for, 18: 17252
flux distributions within certain energy spectra, theory for defining, 18: 16903
flux distributions in graphite–plutonium–uranium systems, 18: 11146(R) (ANL-6797(p.143-7))
flux distributions in reactors, activation method for determining, 18: 24840(P)
flux distributions for graphite systems, modified gas equation for, 18: 28088(R) (HW-80284(p.10.1-28))
flux distributions in reactor equipment for measuring, 18: 30962
flux distributions in shielding arrangements, methods of calculating, 18: 32949(R) (EUR-534.d(Pt.II))
flux distributions in water system with internal cavity, 18: 34731 (NASA-CR-54110)
flux distributions in cylindrical lattice cells, computer program for epithermal, 18: 36775 (CRRP-1197)
flux distributions of, effects of axial motion of fuel on, 18: 36794 (NP-14204)
flux distributions in swimming pool reactor, 18: 38618 (A/CONF.28/P/718)
flux distributions in heavy water, organic-cooled reactors, 18: 38502 (A/CONF.28/P/711)
flux distributions in critical assemblies, 18: 38306 (A/CONF.28/P/499)
flux distributions in heterogeneous lattices, 18: 38320 (A/CONF.28/P/690)
flux distributions of, statistical variations in, 18: 40470 (EUR-1643.e (p.125-30))
flux distributions in uranium rod–heavy water lattices, 18: 42923(R) (MITNE-46)
flux distributions in reactor cores, single-channel synthesis of three-dimensional, 18: 42927 (TID-7050(p.657-78))
flux distributions in reactor cores, multichannel synthesis of three-dimensional, 18: 42928 (TID-7050(p.678-710))
flux distributions in reactor cores, variational synthesis of three-dimensional, 18: 42929 (TID-7050(p.710-28))
flux distributions in iron-water-d_2 laminates, 18: 42874
flux distributions in heavy water reactor, spatial dependence of zero-power, 18: 44974 (TID-21190)
flux distributions in critical assemblies, computer program for adjoint, 19: 1521 (IA-911)
flux distributions in single- and multi-cell cores, computer programs for (T), 19: 1835 (AEEW-R-354)
flux distributions in TREAT, energy release rate from, 19: 1840 (NAA-SR-Memo-5397)
flux distributions in reflected reactors, effects of foreign element or rig on, 19: 1844
flux distributions and intensities from water-moderated reactors (E), 19: 3774 (CEA-R-2536)
flux distributions in water-moderated assembly, four-group calculation of, 19: 3778 (NASA-TN-D-2210)
flux distributions in boiling-water reactor, steam void effects on (E/T), 19: 3630 (HPR-20)
flux distributions in water, expectation values for (T), 19: 3222
flux distributions in reactors, iodine and xenon instabilities of, (T), 19: 5431 (IDO-16985)
flux distributions in stars, (T), 19: 6433
flux distributions in JEN reactor, automatic sample changer for activation measurements of, 19: 10655
flux distributions in cylindrical reactors, computer analysis of, (T), 19: 12748 (EUR-2162.e)
flux distributions of, design of detector for determining, 19: 13809(P)
flux distributions in iron–water shielding, 19: 17163
flux distributions in critical assemblies, (E), 19: 17221 (PAN-560/IX-A)
flux distributions in slightly enriched BWR, computer program for, 19: 19357 (EURAEC-1302)
flux distributions in gas-cooled graphite-moderated reactor using plutonium recycled fuel, 19: 19364
flux distributions in reactors, computer programs for, 19: 21644 (WAPD-TM-478)
flux distributions and disadvantage factors in two-region cells, (T), 19: 21212
flux distributions in homogeneous reactors, computer programs for, 19: 24002
flux distributions in homogeneous, source-free medium, Case's method for solution of half-space problems in, 19: 29184
flux distributions in multi-layered plane reactor shielding, solution of differential equations for, 19: 31512
flux distributions in reactors, energy and spatial variations of, (E/T), 19: 31184 (AP-Note-371)
flux distributions in reactors, solid-state instrument for mapping, 19: 30592(P)
flux distributions in tissue-equivalent material and water phantoms, 19: 32787(R) (NIRS-3(1-17))
flux distributions in reactors, development of microwave techniques for measuring, 19: 35703(R) (BNWL-38)
flux distributions in power reactors, xenon nonconvergence calculations of, 19: 35709 (WAPD-T-1673)
flux distributions in cylindrical reactor cells, computer program for, 19: 35704 (EUR-2181.e)
flux distributions in reactor cells, space-energy, (T), 19: 40152 (GA-6462)
flux distributions in research reactor VVR-S, (E), 19: 42183
flux distributions in thermionic fuel elements, 19: 47978 (CEA-R-2782)
flux distributions in Grosswelzheim Superheat Reactor, (E/T), 19: 47992 (KEA-311)
flux distributions of, device for measuring, 20: 684(P)

flux distributions in reflector and primary shield of New Production Reactor, 20: 3544
flux distributions in reactors, meter design for measuring, 20: 5061 (ZFK-RN-22)
flux distributions in reactors, statistical fluctuations in, (T), 20: 5066
flux distributions in air near ground-air interface, (T), 20: 6528
flux distributions in arbitrarily shaped reactors, (T), 20: 8353
flux distributions in multiple-pin fuel elements, computer program for, 20: 12384 (AGN-TM-411)
flux distributions in natural uranium–water matrices, 20: 16028
flux distributions in reactors, Courant-Wallace expressions for, (T), 20: 22372 (AFRRI-TN-65-1)
flux distributions in 19-element natural uranium-fueled assemblies, 20: 24706 (AECL-2423)
flux distributions in time-dependent media, 20: 32357
flux distributions in sodium-cooled reactors, 20: 35841(R) (NAA-SR-11900)
flux distributions in cylindrical fuel solutions, effects of voids, 20: 38532 (NASA-TN-D-3555)
flux distributions and spectra in iron–water shielding, (E/T), 20: 40287
flux distributions in swimming-pool reactors, correlation with two-group diffusion theory, 20: 42600
flux distributions in reactors, statistical fluctuations in, 20: 46976
flux dosimetry using cobalt alloys, 18: 44050(R) (ORNL-3670(p.116-21))
flux effects on cross section determinations, 17: 2242 (TID-16949)
flux fine structure in uranium dioxide clusters, 18: 21612 (CEA-2387)
flux flattening in thermal reactors, 17: 4258
flux flattening in heterogeneous reactors, calculation of, (T), 20: 12364 (UJV-1365/65)
flux fluctuations in chain reactions, statistical theory, 18: 38039 (A/CONF.28/P/652)
flux fluctuations in multi-point reactor, (T), 19: 17226
flux fluctuations in reactors, (T), 19: 19073
flux from eccentric point source in spherical reactors, buckling in, 18: 26869
flux from foil activation data, computer program for determining, 20: 37076 (SC-DC-66-1512)
flux from monoenergetic point sources in air, 16: 9414 (KN-60-57(R))
flux from shock region of collapsing plasma, 17: 9754
flux in atmosphere, albedo, 18: 11080
flux in atmosphere, latitude effect on albedo, (E), 19: 27126
flux in atmosphere, determination using indium activation, 20: 28106(T)
flux in beryllium blocks, decay of, (T), 19: 43256
flux in close-packed lattices, disadvantage factor for, 20: 34927
flux in critical slabs, multiple collision formulation of, 18: 7660 (EUR-479.e)
flux in cylindrical-rod lattices, P-3 calculations for (T), 19: 3527
flux in cylindrical absorbing regions, computer program for, (T), 20: 9939 (EUR-2536.e)
flux in fast reactor Doppler-effect calculations, resonance correction to group, (T), 19: 42057
flux in fast reactor Doppler-effect calculations, resonance correction to group, (T), 19: 42058
flux in fast reactor cores, Monte Carlo calculations of heterogeneity of, 20: 22397
flux in fields of, statistical fluctuation theory for, 20: 24315
flux in finite multiplying media, calculation of, 19: 29468(R) (ANL-7017)
flux in FR-2 research reactor with boric acid poisoning, (E), 19: 24179
flux in heavy water reactors, methods for calculating, 18: 38495 (A/CONF.28/P/683)
flux in heavy water–iron laminates, (E/T), 19: 21210
flux in heterogeneous media, energy and space dependence of scalar, (T), 19: 29194
flux in heterogeneous multiplying media, with pulsed neutron source, (T), 19: 33230
flux in heterogeneous reactors, kinetic equations for, 19: 35716
flux in infinite moderator, grey rod extrapolation distance for, (T), 20: 13712
flux in JRR-1, analysis of variations in, 19: 21737
flux in light water assemblies, ($k\beta/l$) pulsed-source technique for, (E), 20: 14162
flux in LITR and ORR reactors, measurements of, 20: 46102(R) (ORNL-4013)
flux in loosely coupled cores, space-time behavior of, 20: 8467
flux in Magnox reactors, three-dimensional, 18: 38473 (A/CONF.28/P/552)
flux in meson production-facility shielding, calculation of, 19: 17159(R) (ORNL-3714(Vol.II)(p.97-118))
flux in natural-uranium, light-water exponential piles, resonance, 20: 28722
flux in nonmultiplying medium, recursion formula in Lie-series method for, 20: 2941
flux in nonseparable reactor geometries, modified Kantorowitsch method for calculating, 20: 24717
flux in ORR, spectra of, 19: 30651(R) (ORNL-3789(p.239-47))
flux in plate laminations, (T), 19: 31430
flux in power reactors after shutdown, detector for, 19: 43566
flux in power reactors, design of fast counting channel for, 19: 48033
flux in pressurized-water reactors, detector for, 20: 25438(P)
flux in pulsed assemblies, variational calculation of, 18: 7659 (CONF-187-27)
flux in reactor, calculations by individual source-sink method, 16: 26500
flux in reactor core, coolant nitrogen-16 activity monitoring for control of, 20: 10430
flux in reactor deuterium-containing probe for measuring, 20: 13119(P)
flux in reactor fission plates, transient-temperature method for measuring, 17: 38572
flux in reactor fuel pin clusters, method for determining, 19: 45525 (EUR-2470.e)
flux in reactor regions of no source terms, equations for energy-dependent, 17: 20955
flux in reactor thermal column, (E/T), 19: 33197 (NIJS-R-437)
flux in reactors, statistical variations of, 17: 1069
flux in reactors, digital period meter for measuring, 18: 30956
flux in reactors, use as design tool (T), 19: 3679
flux in reactors, matrix operator method for calculating, (T), 19: 17225
flux in reactors, silicon carbide detectors for measuring, 19: 36824 (WCAP-5482)
flux in reactors, detectors for monitoring, 19: 36806 (BNWL-SA-163)
flux in reactors, computer programs for calculating, 19: 40157 (ORNL-TM-1175)
flux in reactors, regenerating chambers for monitoring, 19: 43525
flux in reactors, wire activation system for determining, 19: 43565
flux in reactors, calibration of graphite damage, (E), 19: 48070
flux in reactors, instrumentation for measuring, 20: 2107
flux in reactors, survey of conventions for reporting, 20: 7631 (HNWL-SA-332)
flux in reactors, correlation theory for, 20: 8348 (JINR-P-2391)
flux in reactors, performance of synthesis method for calculating, (E/T), 20: 12368 (WAPD-T-1737)
flux in reactors, group-theory method for eigenvalue problems in, (T), 20: 12373
flux in reactors, detectors for monitoring, 20: 18023
flux in reactors, few-time-step depletion calculations of, 20: 18052 (WAPD-T-1836)
flux in reactors, variation principles for critical, 20: 22399
flux in reactors, sequential delay sampling time analyzer for measurement of, 20: 23489
flux in reactors, absolute power measurement from fluctuations in, (E), 20: 26436
flux in reactors, foil thermal disadvantage factors for measuring, 20: 34904 (CONF-660606-3)
flux in reactors, computer programs for graphic display of, 20: 46140 (WAPD-TM-611)
flux in recombines of L54 reactor, from delayed-neutron precursors, 18: 45038
flux in shielding of ULYSSE reactor, 17: 38494(T) (AEC-tr-6010)
flux in slab reactor with natural uranium, production of flat, (T), 20: 18058
flux in small cylinders, slabs, and spheres, time dependence of, 18: 2813
flux in small reactor cells, disadvantage factors for, 18: 30965
flux in thorium–uranium-233 breeding blankets, disadvantage factors for, 20: 34943
flux in three-region, heavy-water-moderated, cylindrical cells, 18: 42948
flux in two-group point reactor model, 20: 34919
flux in Univ. of Florida Training Reactor, calculations of, 20: 30862
flux in upper atmosphere during 1964 solar minimum, (E), 20: 37908
flux in Vostok satellites, 18: 1962(T) (FTD-TT-63-968(p.321-5))
flux in ZPR-III fast assembly, calculations of (E/T), 19: 3540
flux lifetime distribution in physical systems, analysis of correlation method for measuring, (T), 20: 21035 (FEI-21)
flux mapping in reactor cores, 16: 33267(P)
flux mapping in reactors, 20: 39252(P)
flux mapping in subcritical reactor with indium activation foils, 16: 3811 (AD-257585)
flux maps in Sandia Engineering Reactor, 19: 12845 (SC-RR-64-1757)
flux measurement, 17: 9488
flux measurement at reactor sites, intercalibration program for, 17: 37003(R) (HW-78118)
flux measurement by irradiation of ribbon-shaped copper probes, 16: 4335
flux measurement by self-shielding method, 19: 33201
flux measurement, equipment for, 17: 8612
flux measurement for tissue dose, errors of fission threshold detectors, 16: 1316(R) (LAMS-2627(p.137-44))
flux measurement in reactors, use of dysprosium foils for, 16: 31844

flux measurement in reactors, apparatus for integrated, 17: 1782(P)
flux measurement in reactor, logarithmic instrument for, 17: 22018
flux measurement in reactors, device for, 17: 29221(P)
flux measurement in Hanford reactors, foil technique for, 18: 8688
flux measurement in reactors, device for continuous, 18: 14290(P)
flux measurement in reactors, design of ionization chamber, 18: 24039(P)
flux measurement in reactors, multiple threshold detectors for, 18: 37552
flux measurement in reactors, use of ceramic foils for, 19: 18439
flux measurement in-core, methods for, 19: 22660(R) (HW-83298(p.7.1-30))
flux measurement in gamma fields, design of ionization chamber for, 19: 32611(P)
flux measurement in reactors, device for, 19: 34588(P)
flux measurement in reactors, computer program for, 19: 47866 (KAPL-M-6460)
flux measurement in reactors, method and device for, 20: 18043(P)
flux measurement in reactors, method for direct, 20: 20213
flux measurement in swimming pool reactors, design of silicon diode spectrometers for, 20: 27352
flux measurement of, 17: 4864(P)
flux measurement of, equipment for, 17: 10006(P)
flux measurement of, method and design of apparatus for, 17: 16477(P)
flux measurement of, ionization chamber arrangement for, 18: 22371(P)
flux measurement of, performance of zirconium scatterer technique for, 20: 4806(R) (RPI-328-40, pp 1-42)
flux measurement system for reactors, using single fixed-position detector, 20: 34885
flux measurement techniques in space, 16: 21228
flux measurement using $Li^6(n,\alpha)H^3$ reaction, absolute, 16: 33797
flux measurement using dysprosium, cadmium ratio for, 17: 4338 (TID-17268)
flux measurement using foils, review, 17: 8625
flux measurement using neutron probe equipped with pulse fission chamber and ferrite transformer, 17: 8622
flux measurement using foils, equipment for use in, 17: 14633
flux measurement using foils, corrections for perturbations in, 17: 28234
flux measurement using proton-recoil solid-state detectors, solid angles for, 17: 36140 (AE-116)
flux measurement using foils, computer program for, 18: 23871 (ANL-6822)
flux measurement using activation analysis, 18: 35840 (R64SD-10)
flux measurement using argon-41 activation for continuous monitoring, 19: 10675(R) (NAA-SR-9999)
flux measurement using glass scintillators, Monte Carlo corrections for, 20: 26062 (CEA-R-2971)
flux measurement using silver activation foils, corrections for, 20: 29539
flux measurement, detector for operation at high fluxes, 18: 27807(P)
flux measurements, development of aluminum-gold alloy for, 16: 11893
flux measurements, thermopile for, 16: 327 (AD-255794)
flux measurements using nickel, effects of thermal neutron cross sections of cobalt-58 isomers, 16: 722
flux measurements in irradiation capsules by argon activation, 16: 8941
flux measurements by automatic activated-wire mapping system, 16: 8942
flux measurements by foil-activation methods, 17: 30871
flux measurements with semiconductor detectors, 16: 8943
flux measurements, description of ion chamber system for, 16: 8944
flux measurements for local power density using neutron telescope, 16: 8945
flux measurements, sensing device design for, 16: 14975(P)
flux measurements in Sandia Pulsed Reactor Facility, 16: 15788 (SCR-463)
flux measurements by fission counters, 16: 19114
flux measurements, development of miniature silicon carbide detectors, 16: 22333(R) (WCAP-1874)
flux measurements, development of miniature silicon carbide detectors, 16: 22334(R) (WCAP-1929)
flux measurements with metal foils, effects of self-shielding and thickness on, 16: 24364
flux measurements, effects of detectors on, 16: 24365
flux measurements in tissue-equivalent phantoms, 16: 23460 (AERE-R-3696)
flux measurements, 16: 28434
flux measurements using gold and manganese foils, 16: 14927(T) (CEA-tr-A-1090)
flux measurements of, technique for measuring angular distribution of, 17: 3789
flux measurements in ducts in water, 17: 3799
flux measurements using gold and manganese foils, comparison with aluminum–cobalt wires, 17: 4333(R) (IDO-16805(p.7-35))
flux measurements in WWS-reactor, 17: 5582
flux measurements in zero-energy reactors, instruments for, 17: 6483
flux measurements in reactors, device for, 17: 9966(P)
flux measurements using fission chambers, 17: 8670(P)
flux measurements by gold foil activation, self-shielding coefficients for, 17: 11609
flux measurements at cavity walls, 17: 13470 (NYO-9657)
flux measurements at 35-Mev betatron installation, 17: 14545
flux measurements, materials for threshold, 17: 22782 (AEET/CD/10)
flux measurements in concentric-annuli fuel elements, 17: 26756 (EUR-24.e)
flux measurements in reactors using self-powered detectors, 18: 3077
flux measurements by fission-product formation in thorium wire, 18: 12496(P)
flux measurements in reactors, design of apparatus using a neutron-activatable fluid for, 18: 13204(P)
flux measurements in water at 23 to 300°C, temperature dependence of, 18: 15155
flux measurements of, methods for analyzing threshold-detector, 18: 18175 (EUR-588.e)
flux measurements in reactors, development of microwave spectroscopy method for, 18: 18861(P)
flux measurements in reactors using pellet-type activation detectors, 18: 24829(P)
flux measurements at TRIGA F reactor, 18: 24957 (NDL-TR-59)
flux measurements of, from T(d,n) reaction, 18: 26590
flux measurements in reactors by silicon diode detectors, 18: 29996
flux measurements on, threshold detectors for, 18: 30037
flux measurements in standard piles, 18: 30967
flux measurements on reactor, using threshold detectors, 18: 31912 (NP-14089)
flux measurements using out-of-pile detectors and gas circulating loop, 18: 33009(P)
flux measurements using gas flow, 18: 31943
flux measurements of, bibliography on, 18: 37516 (SRB-63-7)
flux measurements using current fluctuations from ionization chamber with logarithmic amplifier (E/T), 19: 752 (AEEW-R-375)
flux measurements using ionization chambers, errors in, 19: 6199
flux measurements, 19: 14463(R) (EUR-2179.e)
flux measurements in reactors, wire scanner for, 19: 28646
flux measurements in reactors, system for, 19: 35693(P)
flux measurements in reactors, device for, 19: 42064(P)
flux measurements using resonance activation, 20: 2971
flux measurements in Pulstar reactor, techniques for, (E), 20: 8462 (NP-15644)
flux measurements in reactors, using fission chambers and proportional detectors, 20: 16896
flux measurements in reactors, ionization chambers for, 20: 16897
flux measurements in reactors using thermopiles, 20: 16899
flux measurements in NRL Research Reactor, 20: 16335(R) (NBS-TN-276)
flux measurements using argon activation, analog system for solving equations for, 20: 27263 (NAA-SR-11355)
flux measurements in reactor cores, method for absolute, 20: 32776
flux measurements of, multisphere technique for, 20: 41280(T) (NP-tr-1410)
flux measurements in PWR Core 2, system description for, 20: 42647 (WAPD-PWR-2226)
flux measurements in ATRC, 20: 45046(R) (IDO-17192)
flux measurements at air-earth interface, 16: 12817 (WT-1419)
flux measurements in concentric annular fuel elements, analysis of fine, 17: 25880
flux measurements in critical assemblies, techniques for, 17: 28439 (KAPL-M-JNB-1)
flux measurements, properties of semiconductor detectors for in-core, 18: 38345 (A/CONF.28/P/858)
flux measurements, standard detectors for, 19: 3226
flux measurements, standardization of, 20: 14461(R) (ORNL-3889, pp 48-70)
flux measurements, design of fission chamber and preamplifier assembly for, 16: 24552
flux measuring apparatus for, in reactors, 17: 10019(P)
flux moderation in paraffin, 20: 20524 (RT-PROT-(65)32)
flux moments in gap geometry, boundary condition for, 20: 22390
flux monitor development for, 20: 3982(R) (AGN-8156)
flux monitor for, development of, 19: 27735(R) (NAA-SR-10850)
flux monitoring by argon activation, argon mass flowrate computer for, 18: 39617 (NAA-SR-9745)
flux monitoring, development of techniques for continuous in-core, 16: 798
flux monitoring during startup of boiling-water reactors, in-pile system for, 20: 22438
flux monitoring in JEN-1 Reactor, preparation of materials for, 19: 7285
flux monitoring in reactors using argon activation, (E/T), 19: 28689
flux monitoring in reactors, device for, 20: 2173
flux monitoring in pressurized-water reactors, self-powered detectors for, 20: 2174

flux monitoring in reactors, development of regenerating detectors for, 20: 6567 (HW-SA-3600)
flux monitoring in power reactors, instrumentation for in-core, 20: 10400
flux monitoring in reactors, solid-state instrumentation for, 20: 18034
flux monitoring in reactors, instrumentation for, 20: 18035
flux monitoring in reactors using argon, 20: 20206 (NAA-SR-11356)
flux monitoring of, for activation analysis accuracy, 18: 39084
flux monitoring of, equipment for continuous, 20: 8316(R) (NAA-SR-11450, Sect.7)
flux-monitoring system using argon activation, 16: 17850
flux monitoring system development, 20: 42579(R) (ANL-7245, pp 29-47)
flux monitoring for activation determination of oxygen, 17: 38926
flux monitoring using sensitive fluid in-core, development of method of, 18: 35839 (NAA-SR-9748)
flux monitoring using detector current fluctuations, (T), 19: 28686
flux monitors in reactors, technique for optimizing composition of regenerating, 19: 2634
flux noise in aqueous uranium dioxide suspensions, 16: 12708
flux of albedo, at 45° latitude, (E), 19: 25194
flux of, and experimental measurement theory, 17: 7063
flux of, instrumentation for reactor in-core measurement of, 16: 31269 (NP-11754(Vol.I)(Sect.IV))
flux of, KARE input for calculating, 18: 1209 (KAPL-M-JA-6(Rev.VI))
flux of, nomographs for monitoring by activation methods, 18: 34012
flux of, P_N calculations for, 18: 40485
flux of, use of cobalt and aluminum–cobalt wires for measuring, 20: 14867
flux over soil and water, cause of difference in, 19: 7705
flux pattern from 14-Mev generator, determination of, 19: 3459
flux peaking at fuel gaps in Heavy Water Components Test Reactor fuel assemblies, 19: 8633(R) (DP-935)
flux peaking at sharp corners, diffusion theory for, 17: 17092 (TID-16485)
flux peaking in highly enriched clean critical assembly, 18: 42938 (TID-7050(p.1245-75))
flux perturbation by gold foils, 16: 24359
flux perturbation in activation analysis, 17: 33778 (CONF-17-6)
flux perturbations by absorbing foils, comparison of experiments and theories, 17: 26410
flux perturbations due to infinite plane absorbers, (T), 19: 21220
flux perturbations of, effects of infinite plane absorbers on exponential, (T), 20: 17655
flux recording on tape and wire, development of equipment for, 18: 31942
flux scanning in reactors, 17: 6489(P)
flux shapes in reactors, variational techniques for calculation of three-dimensional, 20: 34953
flux spectra determination by foil activation, (E/T), 20: 44579 (CONF-660303, pp 532-53)
flux spectra in ORNL Research Reactor, 18: 23099(R) (ORNL-3591 (p.156-9))
flux spectra in reactors, semi-empirical method for determining, 18: 44934 (TID-7696(p.5.4.1-21))
flux stability in gas-graphite power reactors, spatial (T), 19: 3615 (CEA-R-2480)
flux stability in reactors, kinetic equations for, 19: 14800
flux stability in reactors containing xenon-135, computer program for, 20: 14061 (IDO-17127)
flux synthesis and depletion in three-dimensional, computer program for, 19: 5436 (WAPD-TM-468)
flux synthesis approximations in the time direction, 16: 24543
flux, synthesis of three-dimensional, 16: 745
flux traverses for, diffusion theory fitting of, 17: 39944 (HW-69871)
flux trends in spherical reactors, statistical theory, 16: 12015 (RM-2869-PR)
flux variation analysis, method for, 17: 7638
flux variation in reactors, calculation of removal cross sections for two-thermal group model, 16: 32552 (AEEW-R-133)
flux variations and multiplication in aqueous uranium dioxide suspensions, 16: 12707
flux variations in reactors, system for measuring, 18: 23016 (TID-7662(p.46-52))
flux variations in reactors, minimization of, 18: 23020 (TID-7662 (p.179-88))
flux variations in square lattices, method for calculating, (T), 20: 12366 (UJV-1439/65)
flux variations in multiplying medium, (T), 20: 21954
flux variations in steady-state operating reactors, 20: 38445 (RT-FI-(66)1)
flux-shape eigenfunctions for two-zone slabs, tables of, 20: 16024 (RFR-231)
flux-shape eigenfunctions for two-zone cylinders, tables of, 20: 16025 (RFR-232)
fluxes and lifetimes in plutonium(IV) oxide–polystyrene arrays, 18: 11398(R) (HW-79054(p.54-63))
fluxes at ground level from vertically collimated upward-pointing 14-Mev neutron source, 18: 40478 (RM-4120-AEC)
fluxes in graphite reactor shields, two-group calculations of, 17: 39954(T) (AEC-tr-6062)
fluxes in MERLIN, measurement of, 17: 35183
fluxes in metal-hydrogen shielding in N.S. *Savannah*, 16: 8411
fluxes in paraffin containing beryllium–carbon–radium source, 18: 16892 (JUL-140-RX)
fluxes in reactor core, computer program for calculation, 16: 10379 (APEX-702)
fluxes in reactors, semiconductor measurement of, 17: 8627
fluxes in reactors, activation measurement of, 19: 45542(R) (BAW-272)
fluxes in Rossendorf Reactor, 18: 19431 (ZFK-RN-21)
fluxes in shields for marine reactors, theoretical prediction of penetration, 16: 8410
fluxes in unpoisoned assemblies, measurement of, 20: 20183
fluxes of, method for solving Boltzmann equation for, 19: 21222
fluxes of, stochastic process method for calculating, 18: 11142 (ASD-TDR-63-89)
fluxes on axes of fissile cylinders, computer program for calculating, 18: 9606 (TRG-Report-648)
form-factor determination in electron scattering, 16: 10915
form factor determination from electron inelastic scattering, (T), 19: 4903
form factor determination from meson (π) electroproduction on protons, (T), 19: 45065
form factor for deuteron-electron elastic scattering, (T), 20: 7839
form factor of, charge, 18: 37960
form factor of, deuteron-electron interactions to determine electromagnetic, (T), 19: 16652
form factor of, electromagnetic, 18: 22728(R) (NP-13870)
form factor relation to separate-singlet vector-meson coupling in U(6), $\omega\phi$ mass difference for electric, 20: 19572
form factors, 16: 18379
form factors (E), 19: 1385
form factors and structure of, from deuteron-electron scattering, 17: 34968
form factors for, 18: 10881 (SLAC-25(Pt.I)(p.134-48))
form-factors for, from electron-neutron coincidences, 17: 9253
form factors for, measurement by electron elastic scattering, 17: 9266
form factors for nickel(II) salts, 17: 37773
form factors for, review, 17: 9464
form factors from deuteron-electron interactions, electromagnetic, (T), 20: 11666
form factors from inelastic electron interactions with deuterons, (E), 20: 30027
form factors from electron scattering by deuterium, electromagnetic, (E), 20: 39795
form factors from deuteron-electron interactions, electromagnetic, (T), 20: 41883
form factors in SU(6) symmetry, charge, (T), 19: 8181
form factors of, charge, 18: 9128
form factors of, determination of charge, 18: 2937
form factors of, electron-deuteron scattering for charge, Pauli, and ratio to proton, 17: 24317
form factors of electromagnetic, (E), 19: 41326 (HUX-2752-9)
form factors of, from deuteron-electron elastic scattering, 17: 11505
form factors of, from deuteron-electron inelastic interactions, 17: 34827
form factors of, determination from deuteron-electron interactions, (T), 19: 39541
form factors of, determination using electron-deuteron interactions, (T), 20: 27898
form factors of, electromagnetic, 18: 10934
form factors of, effect of polarizability on slope of electric, 18: 36277
form factors of, electromagnetic, 18: 40326
form factors of, electromagnetic, (T), 19: 10063
form factors of, electromagnetic, (T), 19: 16607
form factors of, electromagnetic, (T), 19: 35120
form factors of, electromagnetic, (E), 19: 35154
form factors of, electromagnetic, (E), 20: 17349 (LAL-1155)
form factors of, electromagnetic, 20: 24008 (CERN-65-24(Vol.2), pp 67-87)
form factors of, from meson (π) electroproduction, 18: 26312
form factors of, from deuteron-electron inelastic interactions, 18: 32601
form factors of, from meson (π) electroproduction (T), 19: 1372
form factors of, from triton wave function, (T), 20: 11623
form factors of, from deuteron-electron inelastic interactions, (E), 20: 11626
form factors of, from electron-deuteron elastic interactions, (E), 20: 11644
form factors of, from deuteron–electron interactions, (E), 20: 19509
form factors of, magnetic, 18: 22552(R) (LAL-1090)
form factors, theory, 16: 16941 (NP-11592(Vol.I)(p.121-37))
form factors, (E), 19: 4975

gamma dipole absorption by neutron-proton pairs in helium-4, 16: 32426
generation time in reactors, determination by pulsed neutron method, 17: 1024 (IDO-16791(p.151-56))
group constants for reactor simulation, computing reduced delayed, 18: 27843 (HW-81076)
half life, 18: 2837(R) (EANDC(OR)-22L)
half life measurement, 20: 18174(R) (NP-15771)
hazards from, 18: 18088
hazards from 0.1 to 1.0 Mev, 19: 681(R) (HW-81746(p.2.29-31))
hazards from, quantities and units for protection against, 19: 36130
heating effects in NERVA, calculations, (T), 19: 29772
impulse response of exponential piles, method for, 18: 33032
in atmosphere, earth crust, and rocks, 20: 43547
intensity distributions in Stern-Gerlach experiment, 16: 22973
intensity of pulses of, integrating detector for measuring, 20: 7436
interaction cross sections, 16: 13880
interaction strengths of, (T), 20: 30001
interaction with protons, in shell model, 18: 38115
interactions at 20 kev to 2 Mev, crossed-beam studies of, 19: 1259
interactions in detectors, 17: 4820
interactions in fissile assemblies, 16: 12701
interactions in nuclear explosives, foil activation wheel method for measurement of, 18: 36556 (TID-7695(p.21-4))
interactions in stars, 16: 9333(T) (FTD-TT-61-314)
interactions in thermal reactors, method of calculation of high energy events, 16: 1189 (DP-609)
interactions of bound, with antiprotons at 3 Bev/c, 18: 18900
interactions of $d_{3/2}$, with $g_{9/2}$ protons in niobium-92, 18: 22893
interactions of, length for, 18: 28684
interactions of, mass distribution in resonance, 18: 20975
interactions of, scattering-length correction to, (T), 19: 39499
interactions, phase-shift determination by pair-production analysis, 16: 19689
interactions with antiprotons, meson (π) production and multiplicities, 16: 3711
interactions with alpha particles at 2 to 3 Mev, phase-shift analysis, 16: 8130
interactions with antineutrinos and neutrinos, rates of $e^{\pm}$ producing, 17: 19149
interactions with antiprotons, cross sections for large-absorption, 17: 20944
interactions with alpha particles at 2–24 Mev, polarization asymmetry in elastic, 17: 32932
interactions with antiprotons, production of intermediate-state vector mesons in annihilation, 18: 2619
interactions with antineutrinos and neutrinos, production of polarized baryons and leptons in weak, 18: 9125
interactions with alpha particles at 14.1 Mev, angular distributions for elastic, 18: 9134
interactions with accelerator beams using neutron-gas targets, 18: 16600 (BNL-7534(p.406-13))
interactions with antiprotons, SU_3 invariance in annihilation, 18: 36313
interactions with antiprotons, production of ω and ϕ in annihilation, 18: 40227 (BNL-8235)
interactions with antiprotons at 1.96 Bev/c, anti-isobar ($\frac{3}{2},\frac{3}{2}$) production in, 18: 44510 (BNL-8268)
interactions with antiprotons, mesons(K), and protons at 6 to 22 Bev/c, total cross sections for, 18: 44515 (BNL-8323)
interactions with antiprotons, SU(3) and SU(4) relations in annihilation, (T), 19: 4970
interactions with antiprotons, intermediate boson production in annihilation, (T), 19: 10074
interactions with antihyperons and antinucleons at high energies, annihilation in, (T), 19: 12260
interactions with antihyperons ($\bar{\Sigma}^-$), selection rules for annihilation, (T), 19: 16633
interactions with alpha particles at 22.15 Mev, cuspology and effective range theory for, 19: 27168 (UCRL-12030-T)
interactions with antiprotons, annihilation in, (E), 19: 31035
interactions with antiprotons at 1.96 Bev/c, $\bar{N}^*$ production in, (E), 19: 41438
interactions with antiprotons, intermediate vector boson production in, (T), 19: 41484(T)
interactions with antiprotons, broken $\bar{U}(12)$ analysis of annihilation, (T), 19: 45008 (JINR-E-2246)
interactions with alpha particles, phase equivalent potentials for elastic, (T), 20: 13482
interactions with antiprotons in emulsions at 3 Bev/c, inelastic, (E), 20: 17359
interactions with antiprotons, $\rho\rho$ resonance in, (E/T), 20: 24042
interactions with antiprotons, cross sections in broken $\bar{U}(12)$ for annihilation, 20: 25855
interactions with alpha particles at 6 to 30 Mev, differential cross sections for, (E), 20: 30390
interactions with antiprotons at 5 to 20 Bev/c, meson-exchange model for forward elastic, 20: 30039
interactions with antiprotons at rest in deuterium, annihilation, (E), 20: 32015
interactions with antiprotons, SU_{6W} predictions for, 20: 32056
interactions with antiprotons and protons, Regge-pole theory for charge-exchange, 20: 32069
interactions with antiprotons at 2 to 6 Bev/c, Regge-pole model for cross sections for, (E/T), 20: 39801
interactions with bound electrons, cross sections for, (E), 19: 41274
interactions with biological materials, 20: 10698
interactions with concretes, albedos from, (E), 19: 29456
interactions with cosmic neutrinos, meson (μ^-) angular and energy distributions from, (T), 20: 23950
interactions with deuterons, polarization effects in elastic, 16: 4791
interactions with deuterons below 8 Mev, phases, 16: 8135
interactions with deuterons at 14.1 Mev, 16: 2521
interactions with deuterons at 14.4 Mev, determination of neutron-neutron scattering length from, 16: 21472
interactions with deuterons, angular distributions from, 16: 33718
interactions with deuterons and neutrons at 14.1 Mev, 16: 33732
interactions with deuterons, spins in, 16: 33786
interactions with deuterons at 0.5 to 1.0 Mev, polarization effects, 16: 26101
interactions with deuterons below 2 Mev, polarization effects, 16: 26102
interactions with deuterons at 0.5 to 1.95 Mev, differential cross sections and polarization in, 17: 737
interactions with deuterons, scattering lengths for, 17: 7089 (NP-12330 (p.15-16))
interactions with deuterons, amplitudes and polarization in elastic, 17: 9189 (JINR-P-1087)
interactions with deuterons and protons at 200 Mev, cross sections for, 17: 9309
interactions with deuterons at low energy, s-phases for, 17: 22424 (JINR-P-1213)
interactions with deuterons and protons, vertex function restrictions in, 17: 26285 (NP-12882)
interactions with deuterons, doublet scattering lengths for, 17: 28210
interactions with deuterons, three-body formalism in, 17: 31330
interactions with deuterons, threshold effects on, due to existence of the di-neutron, 17: 31345
interactions with deuterons at 1.0 Mev, polarization in elastic, 17: 32935
interactions with deuterons, matrix elements of the Hamiltonian in, 17: 32937
interactions with deuterons, bound state between two product neutrons in, 17: 39871
interactions with deuterons, upper bounds on scattering lengths in, 17: 13466
interactions with deuterons at low energies, 18: 18658
interactions with deuterons, 18: 18907
interactions with deuterons, upper bound on doublet length for, 18: 22763
interactions with deuterons at 2.8 to 3.6 Mev, dineutron threshold effects in, 18: 24444
interactions with deuterons, proton spectrum from, 18: 24398 (NP-13961)
interactions with deuterons, final-state (n-n) interaction effects in charge-exchange, 18: 28340
interactions with deuterons, deuteron wave function distortion effects in elastic, 18: 30562
interactions with deuterons, distortion of deuteron wave function in, 18: 32625
interactions with deuterons at 32 and 40 Mev, impulse approximation for elastic, 18: 34537
interactions with deuterons, amplitude for doublet, 18: 37898
interactions with deuterons and protons at 2 and 3 Bev, cross sections for, 18: 40221 (BNL-7973)
interactions with deuterons (T), 19: 3372
interactions with deuterons at low energies, phase shifts and scattering lengths in, (T), 19: 10081
interactions with deuterons, Mott-Massey theory for, 19: 12179
interactions with deuterons at low energy, (T), 19: 12319
interactions with deuterons and helium-3, bibliography, (E/T), 19: 21238 (LA-3205)
interactions with deuterons at low energies, elastic, (T), 19: 27202
interactions with deuterons, doublet scattering length in, (T), 19: 33052
interactions with deuterons, ^2S scattering length for, (T), 19: 35087
interactions with deuterons, singularities of amplitudes for elastic, (T), 19: 41504
interactions with deuterons, elastic, (T), 19: 43178
interactions with deuterons at high energy, equation for partial amplitudes of, 20: 2740
interactions with deuterons, binding energies and cross sections for, (T), 20: 4614

interactions with deuterons, breakup, (T), 20: 11607
interactions with deuterons, review of, 20: 19982
interactions with deuterons, Padé approximant for S-matrix for inelastic, 20: 15363
interactions with deuterons, doublet and quartet scattering lengths for, (T), 20: 27820
interactions with deuterons at 14 Mev, differential cross sections for elastic, (T), 20: 30050
interactions with deuterons at 14 Mev, neutron spectra from disintegration, (T), 20: 42291
interactions with deuterons at 14.4 Mev, (T), 20: 46400
interactions with electrons, spin-independent, 18: 9164
interactions with electrons at low energies, measurement of, 18: 10839 (ANL- 6797(p.15-20))
interactions with electrons, 18: 10681(R) (CEAL-1009)
interactions with electrons, polarizability effects on form factors from, 18: 36277
interactions with electrons, theory for, 19: 1309
interactions with electrons, review of form factors for, 19: 18763
interactions with electrons, effective potential for, (E), 19: 45098
interactions with electrons, nucleon electromagnetic form factors for, (T), 20: 32033
interactions with electrons from thermal neutron scattering by rare gases, (E), 20: 40129
interactions with electrons, 17: 2171(T) (AEC-tr-5465)
interactions with gamma radiation ($\gamma + n \rightarrow p + \pi^-$) at 715 Mev, polarization of protons from, 17: 13430
interactions with gamma rays, meson (π) production in, 18: 7514
interactions with gamma radiation at 275 Mev, meson (π^-) production in, 18: 40310
interactions with gamma radiation at medium energies, effects of inelastic channel on, (T), 20: 15394
interactions with hyperons (Σ^-), bound states, 16: 10921
interactions with hyperons (Λ) and protons at low energies, boson production and properties, 16: 12374
interactions with hyperons (Λ) and (V) and protons, heavy bosons from, 18: 7517
interactions with hyperons (Λ) and protons, unitary symmetry in strong, 18: 14940
interactions with hyperons (Ξ^-), unitary symmetry for S-wave, 18: 36310
interactions with hyperons (Λ), cross sections for elastic, 19: 1256
interactions with hyperons (Ξ^-), unitary symmetry in, (T), 19: 8151
interactions with hyperons (Λ), resonance, (E), 19: 35449
interactions with hyperons (Σ^-) from meson (π^-) interactions with deuterons, final-state, (T), 20: 21681
interactions with mesons (π^-) at 2.8 Bev, cross sections at 10 to 180°, 16: 4724
interactions with mesons (K^+), threshold effects in, 16: 8055 (NP-11232 (p.252-7))
interactions with mesons (K), charge independence in, 16: 8062 (NP-11232(p.321-6))
interactions with mesons (π^0), multiple meson (π^0) production, 16: 12548
interactions with mesons (K^-) at 630 to 1100 Mev/c, cross sections, 16: 13895
interactions with mesons (K^-), Λ-π resonance in, 16: 21482
interactions with mesons (π^-), meson (π^-) production in, 16: 32353
interactions with mesons (π^-) at 2.8 Bev/c, 17: 9317
interactions with mesons (π^-) at large angles, elastic, 17: 9428
interactions with mesons (π^-), "glancing" collisions in, 17: 9434
interactions with mesons(π^-) at 1.89 to 2.36 Mev/c, spin 2 ($\Sigma\pi$) resonant states in, 17: 24335
interactions with mesons (π), multiplet structure in strong, 17: 26373
interactions with mesons (K), meson (π) production in, 18: 4469
interactions with mesons (π^-) at 7 Bev, peripheral, 18: 6005
interactions with mesons (K^+), theory using Feynman diagrams for, 18: 9205
interactions with mesons (π^-) at 4.5 Bev, total cross sections for, 18: 10933
interactions with mesons (K^+) at 47.7 to 364 Mev, cross sections and phase shifts for elastic, 18: 12959
interactions with mesons (π^-) at 0.3 to 1 Bev, resonance-like effects in, 18: 14959
interactions with mesons (π^+) at 1230 Mev/c, meson (η^0) and (ω^0) production in, 18: 14955
interactions with mesons (K^-) at 765 Mev/c, meson (η) production in, 18: 16783
interactions with mesons (π), meson (π) phases from dispersion relations for, 18: 28422
interactions with mesons (π) and photons, vector meson production in, 18: 34620
interactions with mesons (K^-) at 1.15 Bev/c, resonance ($\Sigma\pi$) production in, 18: 36339
interactions with neutrons, N^{*--} production in, 18: 40253 (UCRL-11543(Rev.))
interactions with mesons (π^-) at 9 Bev/c, 18: 40290
interactions with mesons (π^+) at 1.23 Bev/c, multipion resonances in, 18: 42376 (TID-20762)
interactions with mesons (π^+), distributions from, 18: 42418
interactions with mesons(K^-) at 1.15 Bev/c, ($\Sigma\pi$) resonances in, 18: 44523 (UCRL-11568)
interactions with mesons (π^-) at 10 Bev, inelastic, (E), 19: 4905
interactions with mesons (π^+) at 6 Bev/c, charge-exchange cross sections, (E), 19: 4946
interactions with mesons (K^+) at 900 Mev/c, one meson (π) production in, (E), 19: 10064
interactions with mesons (K^-), resonant states in, (T), 19: 18801
interactions with mesons (K^-) at 1.15 Bev/c, Y_1^* production in, (T), 19: 18803
interactions with mesons (K) at high energies, Regge trajectories in, (T), 19: 23417
interactions with mesons (K-) at 916 Mev/c, Y_1^* resonance from, (E), 19: 25265(R) (UCRL-11776)
interactions with mesons (π), design of experiments on, 19: 27159 (LA-3126)
interactions with mesons (K^+) at 2.3 Bev/c, absorption effects in, (T), 19: 27246
interactions with mesons (π^-) at 9 Bev/c, quasielastic, (E), 19: 37608(T)
interactions with mesons (π^+) at 1.7 Bev/c, meson (ρ) and (ω) production in, (E), 19: 41528
interactions with mesons (K-), final-state interactions in ($\Lambda\pi$-), (T), 19: 41405
interactions with mesons (K-) at rest, hyperon (Σ^-) production in, (E), 19: 41494
interactions with mesons (π^-) at 1.2 to 4.5 Bev/c, cross sections for backward elastic, (E), 19: 47310 (NP-15376)
interactions with mesons (K^+) at 2.3 Bev/c, charge-exchange, (E), 20: 1009
interactions with mesons (K^+) at 2.3 Bev/c, K^* production in, (E), 20: 1010
interactions with mesons (π^-) at 1.38 to 4.05 Bev/c, backward elastic, (E), 20: 2713
interactions with mesons (π^-) and neutrons in neutron stars, neutrino cooling from, (T), 20: 4532
interactions with mesons (K^-) at 828 to 1112 Mev/c, Y_1^*(1765) resonance in, (E), 20: 11656
interactions with mesons (K^-) at 600 to 850 Mev/c, hyperon (Λ)-meson (π) resonances in, (E), 20: 13522
interactions with mesons (π^+) at 1.7 Bev/c, meson (ω) and (ρ^0) production and decay in, (E), 20: 15403
interactions with mesons (K^-) and (K^+) at high energies, real amplitudes for, (T), 20: 17378
interactions with mesons (π) at 1.7 Bev/c, products from, (E/T), 20: 19273(R) (BNL-929, pp 3-43)
interactions with mesons (π^+), Regge-pole analysis of meson (ω) production in, (T), 20: 19510
interactions with mesons (π^-), peripheral mechanism in, (T), 20: 30081
interactions with mesons ($K^\pm$) at 5 to 20 Bev/c, meson-exchange model for forward elastic, 20: 30039
interactions with mesons (K^-) at 0.920 to 1.120 Bev/c, Σ-η resonances from, (E), 20: 32103
interactions with mesons (π^-) and neutrons in stars, rates of, (T), 20: 34075
interactions with mesons (K^-) at 2.24 Bev/c, η^* (960) production in, (E), 20: 39786
interactions with mesons ($K^\pm$) at 2 to 6 Bev/c, Regge-pole model for cross sections for, (E/T), 20: 39801
interactions with mesons (π^-) at 3.5 Bev/c, (E), 20: 39842
interactions with mesons (K^-) at 0.8 to 1.1 Bev/c, Y_1^* resonant amplitudes from, (E), 20: 41886
interactions with neutrons, scattering length in, 16: 6962
interactions with nucleons at 100 to 650 Mev, scattering amplitudes, 16: 10913
interactions with neutrons, scattering length for, 16: 21472
interactions with neutrons, measurement of polarization in, 16: 28015(T) (AEC-tr-5305)
interactions with nucleons, cross sections for, 17: 5057
interactions with nucleons in nuclei, resonance widths in, 17: 13487 (JINR-P-1130)
interactions with neutrons, energies of, 17: 13516
interactions with neutrinos, meson (π) production in, 17: 13348 (JINR-P-1141)
interactions with neutrino, electron-meson (μ) production ratio in, 17: 20933
interactions with nucleons, scattering amplitude uniqueness and vector meson exchange in, 17: 24336
interactions with neutrons at 8.3 Bev, total cross sections for,

17: 26382
interactions with neutrinos, applicability of weak interaction theory to, 17: 31324
interactions with neutrinos, cross sections for, assuming Regge-particle mediators, 17: 36588
interactions with nucleons in the nuclear surface region, mechanisms for, 17: 38178
interactions with neutrons in reaction n + d → 2n + p, 17: 39871
interactions with nucleons in Fermi distribution, low energy optical potentials for, 17: 13468
interactions with neutrinos at 1 Bev, hyperon (Σ^+) polarization from, 18: 882
interactions with neutrons at thermal energies, experimental measurement of cross sections for, 18: 11138 (ANL-6797(p.21-6))
interactions with neutrinos, hyperon production in, 18: 10940
interactions with neutrinos, theory of, 18: 12890 (CERN-63-37(p.1-20))
interactions with neutrinos, analysis of, 18: 12892 (CERN-63-37 (p.33-41))
interactions with neutrinos in nuclei, analysis of elastic, 18: 13040 (CERN-63-37(p.203-13))
interactions with nucleons, mass-difference effects in kinematics of, 18: 14822
interactions with neutrinos, use of 1000-Bev accelerator to study, 18: 16750 (BNL-7534(p.88-106))
interactions with neutrinos, theory for elastic, 18: 16759 (CERN-64-13(Vol.III)(p.81-110))
interactions with neutrons in final state of triton three-particle photodisintegration, 18: 24632
interactions with neutrons at low energies, scattering length and effective range for, 18: 24451
interactions with neutrons, neutron-neutron singlet S-state scattering length in, 18: 24462
interactions with neutrons, S-state, 18: 24398 (NP-13961)
interactions with neutrinos, form factors in, 18: 26268 (BNL-837 (p.249-56))
interactions with neutrons in final state, comparison with p-p final-state interactions, 18: 28340
interactions with neutrinos at high energies, meson production in, 18: 28413
interactions with neutrons at 1.9 Bev/c, experimental study of charge symmetry in, 18: 37888 (UCRL-11550)
interactions with neutrons, 18: 40649
interactions with neutrons, ^1S scattering length for, 18: 44782
interactions with neutrons and protons at 2.6 to 8.3 Bev, total cross sections for, 19: 1551 (JINR-P-1725)
interactions with neutrons, charge symmetry in (T), 19: 3099
interactions with neutrinos, polarization of mesons (μ^-) from, (E/T), 19: 5201
interactions with neutrons at 3.69 Bev/c, 19: 9775(R) (UCRL-11466)
interactions with neutrinos (ν_e) and (ν_μ) at high energies, analysis of, (E), 19: 10069
interactions with nucleons at low energies, charge-independent, (T), 19: 12217
interactions with neutrinos (ν_μ), radiative charged lepton production in, (T), 19: 16546
interactions with neutrinos in SU_3 model, hyperon production in, (T), 19: 16594
interactions with neutrinos, SU(6) for N* production in, (T), 19: 20996
interactions with neutrons at 1.8 Bev/c, (E), 19: 25265(R) (UCRL-11776)
interactions with neutrinos at high energy, in heavy-liquid bubble chamber, 19: 29042 (CERN-65-12)
interactions with neutrinos, transverse proton polarization in, (T), 19: 31075
interactions with nucleons, elastic scattering matrix for, (T), 19: 31014 (UCRL-7942)
interactions with neutrons and protons at 2.6 to 8.3 Bev, total cross sections for, (E), 19: 37610(T)
interactions with neutrons in neutron stars, antineutrino production in, (T), 19: 37448
interactions with nucleons in nuclei, (T), 19: 45279 (NP-15415)
interactions with neutrons in s-state, reactor in space for measuring cross section of, (T), 19: 45036 (NP-15476)
interactions with neutrinos (ν_μ), polarization of mesons (μ^-) from, (T), 19: 45050
interactions with neutrinos, analysis of, (T), 19: 47301 (CERN-65-30)
interactions with neutrinos, charge ratio of mesons (π) produced in, (T), 19: 47377
interactions with neutrons at 1.4 to 4.0 Bev/c, backward elastic, (E), 20: 2700(T)
interactions with neutrinos, radiative meson (μ) production from, (T), 20: 4611
interactions with neutrons, N*- production in, (E/T), 20: 6042 (UCRL-16189)
interactions with neutrons, theory for partially inelastic, (T), 20: 7785 (GA-6712)
interactions with nucleons, Dashen-Frautschi method for singlet scattering lengths in, (T), 20: 7840
interactions with neutrons, cross section for, (T), 20: 7870
interactions with neutrons, scattering length for, (E), 20: 9768
interactions with neutrons, N*- production from, (E), 20: 11624
interactions with neutrons, charge independence and lengths for, (T), 20: 11649
interactions with neutrinos, mass of intermediate bosons from, (T), 20: 13504
interactions with neutrons in triton-triton reactions, (T), 20: 15733 (UCRL-7769)
interactions with neutrinos, charge-retention currents for elastic, (T), 20: 15327
interactions with neutrons and protons, charge independence in scattering lengths for, 20: 15356
interactions with nucleons, scattering lengths for, (T), 20: 17350 (N-65-19395)
interactions with neutrinos, meson (π) production cross sections for, (E), 20: 19438 (ANL-7130, pp 257-71)
interactions with neutrons, Coulomb-modified S-wave dispersion relation for, 20: 21680
interactions with neutrinos (ν_μ), cross sections for N* production in, (T), 20: 21599 (CERN-65-32, pp 89-96)
interactions with neutrinos, flux determination from, (E), 20: 21603 (CERN-65-32, pp 115-20)
interactions with neutrons, direct measurement of, 20: 24054
interactions with neutrinos, models for proton polarization from, 20: 27815
interactions with neutrinos at very-high energies, cross sections for, (T), 20: 32036
interactions with neutrons, total cross sections for, (E), 20: 34584
interactions with nucleons, analysis of, 20: 34179
interactions with protons at 12 Bev/c, angular distributions for, (E), 20: 37747
interactions with neutrons in stars, properties of, 20: 44074
interactions with protons at 210 to 217 Mev, polarization effects on, 16: 3638
interactions with protons at 8.3 Bev, total cross section, 16: 5922 (JINR-D-788)
interactions with protons in deuterium electrodisintegration, 16: 6956
interactions with protons at 14 Mev, 16: 6929
interactions with protons at 16 and 24 Mev, polarization in, 16: 6982
interactions with protons at 16 and 24 Mev, polarization in, 16: 6983
interactions with protons at 9 Bev, meson (π^-) production, 16: 4723
interactions with protons, precision measurement of scattering amplitude using hydrocarbon mirrors, 16: 8104 (UCRL-6320)
interactions with protons, static potential shapes, 16: 8145
interactions with protons, excitation effects on cross sections, 16: 9400
interactions with protons at 1 to 10 Bev, 16: 10912
interactions with protons, tensor force approximations, 16: 10837
interactions with protons at 140 Mev, scattering parameters, 16: 10873
interactions with protons at 212 Mev, depolarization in quasi-elastic, 16: 10876
interactions with protons at 140 Mev, polarization in, 16: 12371
interactions with protons at 0.5 Mev, cross sections, 16: 12211(R) (CU(PNPL)-208)
interactions with protons at 0.5 Mev, cross sections, 16: 13689(R) (CU(PNPL)-211)
interactions with protons at 16 to 23 Mev, angular distributions, 16: 13690(R) (CU(PNPL)-212)
interactions with protons, isotopic spin dependence of cross sections at 600 to 1000 Mev, 16: 2431
interactions with protons in the pair correlation model, excitation of even-even nuclei by, 16: 17150
interactions with protons and tritons at 14.6 Mev, elastic scattering, 16: 16520 (CEA-2002)
interactions with protons, coherent amplitudes, 16: 18420
interactions with protons, theory, 16: 18099 (NP-11463(Pt.1)(p.179-85))
interactions with protons at 27 Bev, cross sections for inelastic, 16: 21286
interactions with protons at 100 to 300 Mev, model, 16: 22906
interactions with protons, meson spectra from, 16: 22921
interactions with protons at 200 Mev, 16: 24684 (JINR-P-920)
interactions with protons at 310 Mev, phase shift analysis, 16: 24687 (JINR-P-944)
interactions with protons, scattering phase shift analysis, 16: 24692 (JINR-P-970)
interactions with protons at 0.5 and 3.2 Mev, total cross sections, 16: 24706
interactions with protons, angular distributions of mesons (π^0) produced

in, 16: 26082 (JINR-P-981)
interactions with protons, phase shift analysis of, 16: 32350
interactions with protons in odd-odd nuclei, 16: 32446
interactions with protons at 200 Mev, cross sections, 16: 29700
interactions with protons, potential for elastic, 16: 29672
interactions with protons at 350 Mev, meson (π)-nucleon coupling constant from, 16: 26105
interactions with protons at 128 Mev, triple-scattering parameters, 16: 26140
interactions with protons near 30 Bev, inelastic cross sections, 16: 26252
interactions with protons of bound nuclear at 5.1 Bev, cross sections for, 16: 27931
interactions with protons at 13.7 to 350 Mev, phase parameter representation for, 17: 740
interactions with protons at 0.4926 and 3.205 Mev, precision measurements of the total cross section of, 17: 6976
interactions with protons in the deuteron, 17: 9224
interactions with protons, deuteron binding energy from, 17: 9240
interactions with protons at Bev, elastic charge-exchange cross sections for, 17: 9263
interactions with protons at 25 Bev, charge exchange cross sections for, 17: 9423
interactions with protons, quantum mechanical relations for, 17: 11932
interactions with protons, strange particle production in, 17: 13386
interactions with protons, axial-vector form factors in, 17: 15115
interactions with protons at 23.1 Mev, polarization in, 17: 17024
interactions with protons, meson (π^+) exchange and backward peaking in high-energy, 17: 19117
interactions with protons, differential cross sections for, 17: 19517
interactions with protons, effects of polarization on, 17: 19058
interactions with protons at 22.5 and 110 Mev, angular distributions from, 17: 19076
interactions with protons at 630 Mev, cross section and meson (π)–nucleon coupling constant for elastic, 17: 20847 (JINR-P-1207)
interactions with protons at 660 Mev, phase-shift analysis of, 17: 22426 (JINR-P-1221)
interactions with protons at 9 Bev, meson (π) production in, 17: 22443
interactions with protons below 20 Mev, effective range analysis of, 17: 22487
interactions with protons, total cross section for, 17: 22564 (ORNL-3383)
interactions with protons at 10 Mev, meson(π) contributions to dispersion relations for, 17: 24349
interactions with protons in chlorine-38 and potassium-40, shell model for, 17: 24507
interactions with protons at 142 Mev, phase shifts for, 17: 24308
interactions with protons, inelastic deuteron form factor similarity to amplitudes in, 17: 29533
interactions with protons, distorted wave approximation for phase-shifts in, 17: 31295
interactions with protons at 140 Mev, quasifree, 17: 31342
interactions with protons at 5 Bev, Regge pole contributions to cross section of, 17: 34816
interactions with protons at 0–40 Mev, analysis of differential and total cross sections for, 17: 34868
interactions with protons, polarization in, 17: 36669 (WASH-1042)
interactions with protons, cross section for, 17: 37661(R) (TID-19415)
interactions with protons at 9 Bev, meson (π) production in, 17: 37442
interactions with protons in nuclei, doublet splittings from, 17: 40031
interactions with protons, theory of nonlocal potential in, 17: 22501
interactions with protons at high energies, inelastic cross sections for, 18: 1092
interactions with protons at 630 Mev, phase-shift analysis of, 18: 847 (JINR-P-1375)
interactions with protons at 5.5 Bev, cross sections for, 18: 2626
interactions with protons at 2.04 and 2.85 Bev, meson (ρ) effects in charge-exchange, 18: 2662
interactions with protons at 2.04 and 2.85 Bev, backward peak in, 18: 2663
interactions with protons in nuclei ($50 \leq A \leq 58$), effective, 18: 6231
interactions with protons in triplet state, domination by deuteron Regge pole, 18: 9116
interactions with protons, angular distributions from, 18: 9159
interactions with photons, meson (π) interaction effects in (γ,3π), 18: 9196
interactions with protons, Traiman-Yang criterion for, 18: 10847 (JINR-P-1461)
interactions with protons at 5.5 Bev, total cross section for, 18: 10969
interactions with protons at 600 Mev, meson (π^-) and (π^+) emission in, 18: 10970
interactions with protons at 991 Mev, meson (π) anomalies in, 18: 18697
interactions with photons, amplitudes for meson production in, 18: 18699
interactions with protons at 0.1 and 0.548 Mev, cross sections and final polarization in radiative, 18: 18891
interactions with protons at 0.1 and 0.548 Mev, effects of parity nonconserving internucleon potentials on radiative capture in, 18: 18892
interactions with protons at 600 Mev, meson ($\pi^\pm$) production in, 18: 842 (JINR-P-1334)
interactions with protons at 128 Mev, triple-scattering parameter for, 18: 20933
interactions with protons at 126 Mev, polarization in, 18: 20934
interactions with protons, Regge trajectories for, 18: 20936
interactions with protons at 23.1 Mev, phase shift analysis of, 18: 20904 (JINR-P-1553)
interactions with protons, proton recoil spectrum for elastic, 18: 22720 (ISS-64/1)
interactions with protons in heavy nuclei and high isomeric states, 18: 22926
interactions with protons at 23 Mev, 18: 24625 (WASH-1046)
interactions with protons at 23.1 Mev, depolarization parameter for, 18: 24393 (LADC-6357)
interactions with protons, 18: 24400 (NYO-1807-9)
interactions with protons near 140 Mev, phase-shift analysis of, 18: 24403 (UCRL-7563-T)
interactions with protons at 128 Mev, meson (π)-nucleon coupling constants from, 18: 24423
interactions with protons, potentials for, 18: 26285
interactions with protons at 1.6 Bev/c in bubble chamber, pion production by, 18: 26376
interactions with protons at 0 to 350 Mev, phase parameters for, 18: 30516 (NYO-1807-12)
interactions with protons at 25 Bev, charge-exchange cross sections for, 18: 30539
interactions with protons at 10 Mev, resonance effects in, 18: 30604
interactions with protons in niobium-92, 18: 30788
interactions with protons, sonic spark chamber analysis of charge-exchange, 18: 31889 (CERN-64-30(p.191-202))
interactions with protons, charge-independent pairing in, 18: 34600
interactions with protons, meson effects in nuclear, 18: 34915
interactions with protons near 50 Mev, phase-shift analysis of, 18: 37902
interactions with protons, absorptive damping in, 18: 40301
interactions with protons in emulsions at 600 Mev, cross sections for, 18: 39673
interactions with protons at 290 to 970 Mev, cross sections for, 18: 42403
interactions with protons, representation of residual, 18: 44545
interactions with protons, effects on deuteron form factors, 19: 1255
interactions with polarized protons below 10 kev, polarization from, 19: 1538
interactions with protons and deuterons at 15 to 120 Mev, total cross sections for (E), 19: 3293
interactions with protons in odd-odd deformed nuclei, residual, (T), 19: 6641
interactions with protons, quasi-spin operators for LS coupling, (T), 19: 8471
interactions with protons, partial-wave summation for high-energy potential, (T), 19: 10042
interactions with protons at 2 to 150 Mev, soft-core model for, (T), 19: 10046
interactions with protons, cross sections for elastic, 19: 10107
interactions with protons, amplitudes for, (T), 19: 12183
interactions with protons, potentials for high-energy, (T), 19: 14325 (UCRL-1011)
interactions with protons at 1.5 Bev, isospin analysis of, (T), 19: 14342
interactions with protons at low energy, virtual level description of, (T), 19: 14369
interactions with protons in nuclei, (T), 19: 14622
interactions with protons at 40 and 160 Mev, differential cross sections for, (T), 19: 16856 (ORNL-P-788)
interactions with protons, pseudoscalar coupling in, (T), 19: 16484
interactions with polarized protons, 19: 16656
interactions with protons, single-particle exchange models for, (T), 19: 16579
interactions with protons in nuclei, Bogolyubov transformation for pairing, (T), 19: 19160
interactions with protons, multimeson resonances in, (T), 19: 18864
interactions with protons, Treiman-Yang criterion for, (T), 19: 21046
interactions with protons in nuclei, isobaric states in, (T), 19: 21304
interactions with protons, pairing correlations in, (T), 19: 21381
interactions with protons at 30 and 60 Mev, amplitudes for, (T), 19: 23450
interactions with protons in nuclei, (T), 19: 23678
interactions with protons in nuclei, collective excitations in, (T), 19: 23771
interactions with protons, charge exchange in, 19: 25268

interactions with protons at 161 Mev, cross sections for, (E), 19: 25347
interactions with protons at 310 to 700 Mev, polarization in elastic, (E), 19: 25265(R) (UCRL-11776)
interactions with protons in odd-odd nuclei, (T), 19: 27489
interactions with protons to 15 Mev, cross sections for, (T), 19: 27187
interactions with protons, meson (π^-) production near threshold, (E), 19: 27236
interactions with phonons near degeneracy point, (T), 19: 29467
interactions with protons in helium-3(d,He-3) reactions, final-state, (E), 19: 33314
interactions with protons in helium-4(d,α) reactions, final-state, (E), 19: 33314
interactions with protons at 20 to 28 Mev, total cross sections for, (E), 19: 32998
interactions with protons at 1.40 to 3.55 Bev/c, charge-exchange, (E), 19: 33048
interactions with protons, determination of high-energy secondary particles in, 19: 33051
interactions with protons at 95 to 310 Mev, phase-shift analysis of, (T), 19: 35147
interactions with protons at 25 and 50 Mev, phase-shift analysis of, (T), 19: 35148
interactions with protons, 19: 35371(R) (AD-612914)
interactions with protons in odd nuclei, effective, (T), 19: 35431
interactions with protons in closed-shell nuclei, (T), 19: 35470
interactions with protons at high energies, cross sections for, (E), 19: 35181
interactions with protons at 6.2 Bev, charge exchange in, (E), 19: 37558
interactions with protons, gamma asymmetry and circular polarization in, (T), 19: 39538
interactions with protons at 3 to 10 Bev, cross sections for elastic, (E), 19: 41347
interactions with protons in nuclei, R(5) and R(8) groups in quasi-spin formalism for pairing, 19: 41839
interactions with protons in nuclei, (T), 19: 43383
interactions with protons at 50 Mev, phase shift analysis for, (T), 19: 43046 (NIRL/R/98)
interactions with protons, design of high pressure diffusion cloud chamber for studying elastic, 19: 44494
interactions with protons at 23 to 630 Mev, angular dependence of phase shift analysis of, 19: 45015 (JINR-P-2241)
interactions with protons in tritium-Λ hypernucleus, tensor, (T), 19: 47657
interactions with protons at 630 Mev, phase shifts in, 20: 994 (JINR-P-2332)
interactions with protons at 23 Mev, correlation function for, (E), 20: 2685 (LA-DC-7250)
interactions with protons at 20 to 120 Mev, polarization in, (E), 20: 2701
interactions with protons at 19.3 Bev/c, amplitude for, (E/T), 20: 2712
interactions with protons at 300 to 700 Mev, polarization parameters of, (E), 20: 4590 (UCRL-11926)
interactions with protons, Schroedinger equation with tensor forces for, (T), 20: 4597
interactions with protons at 2 to 10 Bev, real amplitude for elastic, (E), 20: 7787 (JINR-E-2413)
interactions with protons at 0.17 to 310 Mev, phase shifts in, (T), 20: 7788 (JINR-E-2440)
interactions with protons at 23 Mev, correlation coefficients for, (E), 20: 9981 (WASH-1064)
interactions with photons, hyperon and meson production in, 20: 9774
interactions with protons, technique for angular distribution measurements from, 20: 9786
interactions with protons at 600 Mev, meson (π) production in, (E), 20: 11564 (JINR-P-2462)
interactions with protons at medium energies, polarization in, (T), 20: 11617
interactions with protons, elastic-scattering matrix from phase-shift analyses of, (E/T), 20: 11622
interactions with protons, charge independence and lengths for, (T), 20: 11649
interactions with protons at 8 Bev/c, differential cross sections for elastic charge-exchange, (E), 20: 11606
interactions with protons at 600 Mev, meson ($\pi^\pm$) production in, (E), 20: 13453 (JINR-P-2511)
interactions with protons, soft-core potential for phase-shift energy dependence in elastic, (T), 20: 13489
interactions with protons, real part of forward amplitude of, (T), 20: 13493
interactions with protons at 129 and 150 Mev, cross sections for, (E), 20: 13500
interactions with protons, effective ranges in $^1S_0$ states of, (T) 20: 13512
interactions with protons at 585 Mev, meson (π^+) and (π^-) production cross sections for, (E), 20: 15310 (JINR-P-2508)
interactions with protons at 2 to 10 Bev, amplitude for, (E), 20: 17363(T)
interactions with protons, deuteron and gamma production in, 20: 17413
interactions with protons, charge exchange model for, 20: 19273(R) (BNL-929, pp 3-43)
interactions with protons at 205 Mev, polarization parameters of, (E), 20: 19453 (UR-875-126, Paper 5)
interactions with protons at 605 Mev, elastic, (E), 20: 19441 (JINR-E-2560)
interactions with protons at 23.1 Mev, phase shift analysis for, (E), 20: 19442 (JINR-E-2609)
interactions with protons, amplitude for elastic, (T), 20: 19504
interactions with protons, 2^+ meson exchange in, (T), 20: 19512
interactions with protons, deuteron compositeness from effective-range formula for, 20: 21689
interactions with protons in nuclei, quasi-particle random-phase approximation in, 20: 22147
interactions with protons, exchange processes and $^1S_0$ scattering length for, (T), 20: 24017 (UCRL-11985)
interactions with protons at 14.1 Mev, angular distributions from, (E), 20: 24020
interactions with protons at 630 Mev, phase shifts for, (E), 20: 24018(T) (AERE-Trans-1047)
interactions with protons, generalized Bogoliubov transformation for pairing, 20: 24426
interactions with protons, relativistic reconstruction of scattering matrix for, 20: 25786 (JINR-P-2630)
interactions with protons at 585 Mev, meson ($\pi^\pm$) production in, (E), 20: 25809(T)
interactions with protons at 630 Mev, discrimination between sets of phase shifts in, 20: 25860
interactions with polarized protons at 23 Mev, spin correlation coefficients for, (E), 20: 30360 (WASH-1068)
interactions with protons at 20 to 28 Mev, total cross sections for, (E), 20: 30004
interactions with protons, total cross sections for, (E/T), 20: 30028
interactions with protons at 5 to 20 Bev/c, meson-exchange model for forward elastic, 20: 30039
interactions with protons in nuclear emulsions, meson (π^+) and (π^-) charge asymmetry from, (E), 20: 30082
interactions with protons, cross sections for deuteron formation in, (T), 20: 32004
interactions with protons, direct and charge-exchange, (T), 20: 32048
interactions with proton at 1.0 to 6.3 Bev, elastic, (E), 20: 34228
interactions with protons at 590 Mev, time-reversal invariance in, (T), 20: 34233
interactions with protons, Regge-pole model for charge-exchange, 20: 34192
interactions with protons in nuclei, short-range, (T), 20: 38056
interactions with protons at 600 Mev, cross section for meson (π^-) production in, (E), 20: 38186
interactions with protons at 630 Mev, phase shift analysis and triple scattering parameters of, (E), 20: 37739 (JINR-E-2726)
interactions with protons, amplitudes for Regge pole exchange model of, 20: 37862
interactions with protons at 2 to 6 Bev/c, Regge-pole model for cross sections for, (E/T), 20: 39801
interactions with protons at 600 Mev, meson (π) production in, (E), 20: 39826
interactions with protons at 600 Mev, cross sections for meson ($\pi^\pm$) production in, (E/T), 20: 39834
interactions with protons at 400 and 630 Mev, optimal experiments for measuring parameters of, 20: 39752 (JINR-E-2765)
interactions with protons at 19.8 Bev/c, angular and energy distributions of secondary particles from inelastic, (E), 20: 39761 (JINR-P-2809)
interactions with protons at 23.1 Mev, spin correlation parameter for, (E), 20: 41877
interactions with protons below 1 Bev, review of polarization in, (E), 20: 41916
interactions with protons at 15 to 30 Mev, recoil technique for differential cross section measurements on, 20: 44632 (CONF-660303, pp 1084-91)
interactions with protons at 1.0 to 6.3 BeV, differential cross sections for elastic, (E), 20: 46341 (SLAC-66)
interactions with protons at 203 Mev, (E), 20: 46723
interactions with protons at low energies, effective range approximation based on Regge poles for, 20: 46379
interactions with protons at 605 Mev, polarization and triple scattering parameter for elastic, (E), 20: 46381
interactions with photons, meson (π) production in, (T), 19: 33387
interactions with tissue, mathematical analysis, 17: 2787(R) (ORNL-3347(p.73-100))

interactions with tritons at 14 Mev, cross section for inelastic, 18: 15258
interactions with tritons, breakup and scattering cross sections of, 19: 14533(R) (NYO-1082-1)
isotope transparency to, energy level power function determination by, 17: 38003(T) (AEC-tr-5734(p.25-6))
kinetic behavior in reactors, 18: 42932 (TID-7050(p.855-77))
kinetics and reactions of, research using reactors, 20: 23238
kinetics in aluminum-reflected tungsten-based fast critical assemblies (E), 19: 3539
kinetics in BBRR, 19: 48056 (BNL-9510)
kinetics in coupled KIWI cores, models for, 19: 40240 (LA-3263)
kinetics in critical, nonmultiplying, and subcritical media, space-time, 20: 32784
kinetics in fast plutonium-fueled reactors, computer program for calculating, 19: 45530 (JAERI-1082)
kinetics in graphite–uranium rocket reactors, (T), 19: 21715 (AD-605574)
kinetics in heavy water-moderated natural uranium lattices, 20: 34923
kinetics in intermediate and fast critical assemblies, pulsed, 20: 14083
kinetics in multiplying systems, unification of theory for, 20: 32779
kinetics in pressure tube and pressure vessel type heavy water reactors, 19: 45626
kinetics in reactors, variational method for, 18: 15468 (EUR-217.d(Pt. I and II))
kinetics in reactors, calculation of, 19: 1849
kinetics in reactors, time-dependent perturbation theory for, 19: 3546
kinetics in reactors, collision probabilities in (T), 19: 3553
kinetics in reactors, computer programs for, 19: 14787 (HW-80968)
kinetics in reactors, computer programs for, 19: 14786 (CRRP-1184(App. 1))
kinetics in reactor lattices, boundary conditions for calculating, (T), 19: 17220 (ORNL-TM-1022)
kinetics in reactors, analysis of, (T), 19: 29741 (LA-3257)
kinetics in reactors, computer program for calculation of, 19: 40148 (BNWL-111)
kinetics in reactors, energy- and space-dependent solutions for, (T), 19: 43522
kinetics in reactors, cylindrical functions for, 19: 42956
kinetics in reactors, spatial and spectral coupling in, (T), 20: 1411 (CONF-650413-13)
kinetics in reactors, hole and void effects, (T), 20: 5064
kinetics in reactors, theory for experiments on noise from, (T), 20: 5076
kinetics in reactors, computer program for, 20: 8347 (GA-6612)
kinetics in reactors, computer program for, 20: 12354 (GAMD-6644 (Add.))
kinetics in reactors, computer program for solution of equations for, 20: 11946
kinetics in reactors, computer program for, 20: 14060 (IDO-17114)
kinetics in reactors, computer program for, 20: 14064 (LA-3427)
kinetics in reactors, computer program for, 20: 20202 (AWRE-O-4/66)
kinetics in reactors, statistical analysis for determining, 20: 22381 (RT-FI(65)49)
kinetics in reactors, iterative variational method for elliptical problems in, 20: 22387
kinetics in reactors, statistical theory for, 20: 22418
kinetics in reactors, statistical theory of, 20: 30844
kinetics in reactors, research on, 20: 36388(R) (AEET-248)
kinetics in reactors, computer program for, 20: 36427 (CRRP-1235)
kinetics in reactors, space and energy dependence of, 20: 45081
kinetics in reflected critical assemblies, decay constants for, 19: 42040(R) (BNWL-95, pp 40-54)
kinetics in Rover reactors, method for calculating, 20: 24780 (LA-DC-6751)
kinetics in sodium-cooled fast breeder reactors, determination of, 20: 24708 (KFK-382)
kinetics in system with xenon feedback, computer program for, 18: 40781 (KAPL-3061)
kinetics in thorium–uranium-233 fast-thermal coupled system (T), 19: 3542
kinetics in thorium-fueled heavy water reactors, calculation of, 20: 32774
kinetics in thorium–uranium-233 breeding blankets, 20: 34942
kinetics in water moderated reactors, analysis of, 20: 36424 (CEA-R-2883)
kinetics in water-moderated plutonia–urania lattices, 20: 34925
kinetics in ZPR-VI, parameters for (E), 19: 3538
kinetics of, statistical analysis of, 19: 35368
leakage from close-packed natural uranium-heavy water lattices in ZEEP, 18: 33018 (CRRP-627)
leakage from reactor cores, fuel burnup calculation effects of, 18: 3144
leakage from reactor core, spectra of, 18: 19439
leakage from reactor cores, calculation by HERESY I, 18: 42884(R) (NYO-3194-1)
leakage through reactor shield voids, calculation of, 18: 1192(T) (AEC-tr-6108)
lifetime and worth calculations, development of computer program for, 16: 31196 (ANL-6555)
lifetime in critical assemblies, pulse techniques for determining, 18: 38312 (A/CONF.28/P/648)
lifetime in crystals and liquids, upper bounds for time-decay constants of, (T), 19: 47553
lifetime in multiplying assemblies, 17: 24369(R) (GA-3542)
lifetime in reactors, (T), 19: 8605
lifetime in reactors, analysis of Rossi-α experiment on, (T), 20: 5070
lifetime in reactors, space-dependent formula for Rossi-α measurements of, (T), 20: 12375
lifetime in subcritical reactors, proof of formula for Rossi-α method for measuring, 20: 45083
lifetime measurements in thermal reactor, 16: 3659
lifetime measurement of, in subcritical reactors, 18: 15481
lifetime of, lower limits on, (E), 19: 12216
lifetime of, lower limit for mean, (E), 20: 21636
lifetimes in beryllium oxide, tungsten carbide, and uranium reflectors, 17: 5299 (LA-2743)
lifetimes in beryllium-oxide-moderated slightly enriched uranium oxide cores, 17: 7535 (CEA-2201)
lifetimes in glass scintillation detectors, Monte Carlo calculations, 16: 21125(R) (ANL-6517)
lifetimes in heavy water thermal system, measurement of, 18: 44715
lifetimes in lead slabs, (E), 19: 33221
lifetimes in subcritical reactors, 18: 28921(R) (TID-20649)
lifetimes in thermal reactors, measurement by Rossi-alpha-method, 17: 29733
magnetic diffusion of, in disordered iron–nickel alloys, 17: 20494
magnetic fields around stars of, 19: 18670
magnetic form factors, 16: 7139
magnetic moment, (T), 19: 8167
magnetic moment, (T), 20: 6074
magnetic moment from sum rules and SU(6) symmetry, (T), 19: 47306 (JINR-E-2343)
magnetic moment in covariant version of Wigner's supermultiplet theory, 19: 23444
magnetic moment of, meson contribution to, 17: 24288
magnetic moment of, dispersion theory for anomalous, 19: 45108
magnetic moment of, dispersion-theoretical calculation of, 20: 17390
magnetic moment of, relative to protons, (T), 20: 34235
magnetic moment of, relative to N*(1238), (T), 20: 34235
magnetic moment ratio to protons in Wigner SU(4) supermultiplet theory, 19: 29043 (IC/65/16)
magnetic moment with respect to protons in SU_4 symmetry, 19: 23403
magnetic moments of, Vigier rotator model for anomalous, 17: 34802
magnetic moments of, in SU(6), 19: 35060(T)
magnetic moments of, self-consistent calculation of isovector part of, 20: 2704
mass determinations for, accuracy of, 19: 29350
mass difference (n-p) in quantum field theory, 19: 1424 (NP-14404(p.271-99))
mass difference between protons and, 17: 13381
mass difference between protons and, electromagnetic, 17: 15140
mass difference between protons and, 18: 5996
mass difference between protons and, dispersion calculations of, 18: 26374
mass difference between protons and, from tritium (p,n) reactions, 18: 26616
mass difference with protons, 16: 8054 (NP-11232(p.243-51))
mass difference with protons, 16: 11035
mass difference with protons, meson (π) cloud effects on, 16: 21285
mass relative to protons, (T), 19: 41511
mass relative to protons, small-mass charged particles from, 19: 45119
mass relative to protons, S-matrix theory for, 20: 13511
mass relative to protons, (T), 20: 19508
mass relative to protons, (T), 20: 21673
mass relative to protons from spontaneous symmetry breakdown, 20: 21678
mass relative to protons, dispersion-theoretical perturbation series in particle models for, 20: 21683
mass relative to protons, bound-state model for, 20: 30042
mass relative to protons, model for electromagnetic, 20: 32057
mass relative to protons, field-theoretical sum rules for calculating, 20: 41824
mass with respect to protons, s-matrix calculations for difference in, 18: 36315
mean free path in moderators at 14 Mev, (T), 19: 23608
measurement of atomic explosion-induced, use of fission threshold detectors for, 16: 29111 (ORNL-1671)
measurement of in-pile, characteristics of ionization chambers for,

18: 31938
measurement of multiplicity in photonuclear reactions, statistical method, 17: 14679
measurement of natural, in boreholes, 20: 35655
measurement of, near the core-face of subcritical fast reactors, 16: 32603 (ANL-6595)
measurement of, properties of 4π counters for, 18: 31939
measurement of, use of activation detectors in, 18: 31944
measurement, time-of-flight methods in, 16: 14047
measurements by activation, sensitivity of method for, 17: 9490
metallurgical annealing effects on metals at 4.5°K, 18: 14562
meter access tubes, effects on soil temperature and water, 18: 16201
migration areas in heterogeneous reactors with periodic structure, 18: 32717
moderation and multiplication in reactors, properties of media for, 20: 32776
moderation at very low temperature, 16: 26193 (CEA-2012)
moderation by beryllia and beryllium, 18: 38032 (A/CONF.28/P/362a)
moderation by cold media, 18: 13233(R) (BNL-823(p.1-19))
moderation by reactor coolant, two-thermal-group diffusion model of, 17: 5306
moderation in aluminum–water systems, Monte Carlo code for slowing-down moments, (T), 20: 8040 (NAA-SR-Memo-11239)
moderation in beryllium and beryllium oxides, (E), 19: 19066
moderation in fluids, flow measurement using, 20: 11080(P)
moderation in graphite-moderated water-cooled reactors, 18: 24888 (HW-SA-3507)
moderation in graphite, iron, and lead, pulsed-source measurements of, (E), 20: 13741
moderation in heterogeneous graphite–water mixtures, measurement of, (E), 19: 25461
moderation in hydrogenous media, eigenfunction analysis of, (T), 19: 8374 (AE-164)
moderation in non-multiplying infinite homogeneous media, 16: 13926 (ANL-6498)
moderation in non-homogeneous media, 18: 28531
moderation in pure material, solving equation for conjugate moments, 16: 29726
moderation in water and water-d_2, 18: 38044 (A/CONF.28/P/680)
moderation in yttrium hydrides, 18: 28558
moderation in zirconium hydride lattices, 18: 38311 (A/CONF.28/P/645)
moderation of, parameters for, 17: 11605
moderation of simulated fission spectrum, 17: 9495
moderation of, accuracy of diffusion theory for, (T), 19: 10222 (UCRL-12128)
moderation of, in soils for determination of moisture content, 20: 43094
moderation of, materials for low-temperature, 19: 19095 (WASH-1053)
moderation of, use of pulsed sources for measuring, (E/T), 20: 13735
momentum distributions in nuclei, 19: 45279 (NP-15415)
momentum distribution from (π^-, 2N) reactions, (T), 20: 13874
monitor for, analysis of, 16: 30574 (HW-71142)
monitoring deuteron-triton reaction-induced, 19: 14533(R) (NYO-1082-1)
monitoring, development of remote system for, 17: 16332(R) (UCRL-7143)
monitoring, epithermal use of silver-109 in, 16: 19066 (CRDC-1083)
monitoring in activation analysis, use of gold wire for, 18: 11985
monitoring in industrial buildings, 19: 38884
monochromatization of, higher order contamination in, 18: 26499 (RISO-73)
motion in annular voids in cylindrical reactors, reactivity effects of, (T) 19: 29523
multiplication and fluctuations in reactors, (T), 19: 21641 (JINR-P-1996)
multiplication at surface of transport containers, adjoint-problem calculation of, 18: 34726 (AWRE-O-21/64)
multiplication, design of water-moderated assembly for, 16: 9345(R) (GA-2471)
multiplication factor in natural-uranium–graphite reactors, optimization of, 20: 20217
multiplication in pulsed neutron injected cores, 16: 6122
multiplication in reactors, branching limit theorem, 16: 15794
multiplication in small bare homogeneous sphere, isotropic constant-cross-section calculations, 16: 9417 (UCRL-6660)
multiplication in HFIR, effects of voids in island region, 16: 9579 (ORNL-TM-114)
multiplication in reactors, branching mechanisms, 16: 15793
multiplication in 3%-enriched uranium(VI) oxide, Monte Carlo calculations, 16: 18157(R) (HW-72586(p.35-43))
multiplication in heterogeneous media, coupling of two systems for, 17: 24660
multiplication in systems of aluminum, 90%-enriched uranium, and water, 17: 40294
multiplication in fuel element, theory of, 18: 7897
multiplication in single fuel element, theory of, 18: 11151
multiplication in paraffin–uranium fluoride systems, 18: 16891(R) (GA-4881)
multiplication in pulsed media, C(R) analysis of, 18: 34495 (GA-5404)
multiplication in reactors, stochastic models for, 18: 35070 (TID-7679 (p.29-59))
multiplication in homogeneous medium, temperature dependence of, (T), 19: 8604
multiplication in uranium–water lattices, factor for infinite, (E/T), 19: 10495
multiplication in reflected media, global method for calculating, 19: 12462
multiplication in fission, principle of invariant imbedding in one-dimensional, (T), 19: 16857 (P-996(RAND))
multiplication in natural uranium-light water exponential pile, calculations from material buckling, 19: 21645
multiplication in arrays of fissile units, 19: 44977 (IDO-17095)
multiplication in reflected reactors, correlation of, 20: 5058 (JINR-P-2335)
multiplication in fissionable media, computer programs for calculating, 20: 6581 (CEA-R-2872)
multiplication in aluminum- and Zircaloy-clad uranium dioxide, effective, (T), 20: 18065
multiplication in fissionable materials, theory of first-passage distributions for, 20: 20101
multiplication in uranium trioxide water-moderated systems, 20: 46997
multiplication measurements *in situ*, 16: 2621 (RFP-245)
multiplication measurements on uranium systems containing boron, 16: 2622 (RFP-246)
multiplication of, in Experimental Gas Cooled Reactor fuel assemblies, 17: 9853 (ORNL-TM-433)
multiplication of, use of two-dimensional and two-group diffusion program for calculating, 17: 24646
multiplicity measurements on photo-, method for, 18: 42616
nuclear deformation variation with number of, 17: 15308
nuclear generation time in reactors, variation with reactivity, 20: 3386
optical potential of, symmetry term in, 17: 17204
pairing correlations with protons, linear Bogoliubov transformation for, (T), 20: 10058
pairing correlations with protons in spherical even nuclei, 20: 38177
pairing forces in deformed nuclei, 18: 34939
pairing with protons following proton-bombardment cascade in nuclei, perturbation theory for, 18: 24664
parameters for critical assemblies, progressive substitution method for, 18: 33041
penetrabilities and reaction cross sections for nuclei to mass 230, 18: 9307 (CEA-2380)
penetration and slowing-down in reactor shielding, method for predicting, (T), 20: 15935
performance for activation analysis, second-order effects on, 18: 23428
photoemission from oxygen-16 at threshold to 60 Mev, cross sections and resonances in, 18: 16943 (IS-676)
photoemission from oil and water in oil prospecting using photon beams at 2.25 to 15 Mev, 19: 22572
photoemission from beryllium-9, polarization in, 16: 21410
photoemission spectrum of cobalt, 16: 6017
photoproduction, 16: 29858
photoproduction cross sections for medium–weight nuclei, 18: 43932 (IFA-M-34)
photoproduction cross sections and spectra on carbon-12 and oxygen-16 to 33 Mev, (E), 19: 45330
photoproduction cross sections for, 16: 24778 (CEA-2148)
photoproduction from light nuclei at 0 to 80 Mev, 17: 40095
photoproduction from phosphorus, silicon, and sulfur, cross sections for, 18: 2921
photoproduction from carbon-12, spectra of, (E), 19: 16855(R) (ORNL-3714(Vol.I)(p.1-30))
photoproduction from aluminum-27, spectra of, (E), 19: 16855(R) (ORNL-3714(Vol.I)(p.1-30))
photoproduction from lead-206, spectra of, (E), 19: 16855(R) (ORNL-3714(Vol.I)(p.1-30))
photoproduction from lead-208, spectra of, (E), 19: 16855(R) (ORNL-3714(Vol.I)(p.1-30))
photoproduction from bismuth-209, spectra of, (E), 19: 16855(R) (ORNL-3714(Vol.I)(p.1-30))
photoproduction from oxygen-16, spectra of, (E), 19: 16855(R) (ORNL-3714(Vol.I)(p.1-30))
photoproduction from copper and water targets, yields from, (E), 19: 16867
photoproduction from lead, yields of, (E), 19: 41833
photoproduction from beryllium and water, review, 16: 29823
photoproduction from beryllium-9 and carbon-13 in region of 3 Mev, 16: 9653 (KAPL-2000-16)
photoproduction in bremsstrahlung reactions at 24 Mev, direct photoeffect and evaporation contributions in, 17: 38209
photoproduction in elements found in uranium ores, 17: 41885

photoproduction in silicon at 15 to 38 Mev, displacement effects in, 18: 7329
photoproduction in PRTR, flux measurements of, 18: 40834 (HW-80253)
photoproduction in nuclei at 5.4–10.8 Mev, cross sections for, (E), 19: 8490
photoproduction in shielding materials, (E), 19: 14728 (APEX-581)
photoproduction in heavy water, 19: 19806
photoproduction in infinite medium of heavy water by delayed gammas following uranium-235 irradiation, 16: 24495
photoproduction in reactions with oxygen-16, spectra from, 16: 15695
photoproduction in electron-photon cascades in thick targets, 20: 3261
photoproduction in oxygen-16, dipole effects in, (T), 20: 8123
photoproduction in accelerator shielding, (T), 20: 25657 (SLAC-PUB-179)
photoproduction in heavy water, yields for, (E), 20: 26096 (TID-22889)
photoproduction in beryllium-moderated reactors, calculational method for delayed, (T), 20: 32767 (UCRL-14720)
photoproduction in shielding materials by bremsstrahlung-induced electromagnetic cascades, (E), 20: 36347 (DESY-66/13)
photoproduction of, analysis of reactions for, 17: 28246 (NDA-Memo-2123-1)
photoproduction of, apparatus for study of energy spectra and polarization in, 19: 45303
photoproduction of, angular distributions in bremsstrahlung reactions at 55 Mev, 16: 13988
photoproduction of, angular distributions from bismuth-209, 16: 17089
photoproduction of polarized, in gamma reactions on deuterium at 2.75 Mev, 19: 3636
photoproduction on nitrogen-14 and oxygen-18 at 30.5 Mev, 17: 11756
photoproduction on nuclei, distributions from, 17: 33074
photoproduction on oxygen-16, cross sections for, 17: 34988
photoproduction on carbon-12 and oxygen-16 at 15–33 Mev, cross sections and energy spectra for, 17: 38269
photoproduction on calcium-40 and sulfur-32 at 32 Mev, energy spectra for, 17: 38270
photoproduction on sulfur-32 at 30 Mev, direct interactions in, 17: 38272
photoproduction on nuclei, polarization in, 17: 38242
photoproduction on lead-208, nuclear level parameters from, 17: 40080
photoproduction on calcium at 15–30 Mev, cross sections for, 17: 40103
photoproduction on protons in superdense stars, cross sections for, 17: 39834
photoproduction on bismuth-209 at 85 Mev, angular distributions for, 17: 41979
photoproduction on lead-208, time-of-flight spectra of, 17: 40432(R) (NYO-10063(p.63-70))
photoproduction on aluminum at 16 to 26.5 Mev, energy spectra of, 18: 2874
photoproduction on carbon-13 at low energies, E1-M1 interference term in, 18: 7744
photoproduction on oxygen-18 at 20 Mev, angular and energy distributions from, 18: 9396
photoproduction on uranium-235, cross sections for, 18: 9397
photoproduction on aluminum, phosphorus, and sulfur, 18: 11195(R) (EANDC(E)-49(L))
photoproduction on copper isotopes, cross sections for, 18: 13103
photoproduction on thick targets, measurement of, 18: 21308
photoproduction on beryllium-8 at 2.75 Mev, polarization in, 18: 28687
photoproduction on lead, cross sections for, 18: 28728
photoproduction on oxygen-16 at 16.1 to 23 Mev, analysis of yield curves for, 18: 30769
photoproduction on calcium-40 at 15 to 30 Mev, cross sections for, 18: 30773
photoproduction on nuclei, cross sections for, 18: 32843
photoproduction on helium-3 at 5 to 120 Mev, cross sections for, 18: 36678
photoproduction on helium-3 at 5 to 120 Mev, cross sections for, 18: 36643
photoproduction on bismuth and lead isotopes, cross sections for, 18: 40588
photoproduction on niobium-93 at 15 to 30 Mev, yields from, 18: 42633 (IFA-M-30)
photoproduction on oxygen-16, analysis of groups from, 18: 42751
photoproduction on oxygen-16 at 17.6 Mev, cross sections for, 18: 42743
photoproduction on oxygen-16 at 31 Mev, threshold for, 18: 44772
photoproduction on carbon-12 and oxygen-16, particle-hole model for, 18: 44842
photoproduction on deuterons at 2.5 to 150 Mev, covariant theory for, 18: 44553
photoproduction on magic nuclei, threshold level effects in, (E/T), 19: 5253
photoproduction on carbon and magnesium to 30 Mev, cross sections for, (E), 19: 10332
photoproduction on nuclei, cross sections for, (E), 19: 10356
photoproduction on uranium, spectra of, 19: 13695
photoproduction on nuclei, measurement of cross sections for, 19: 16961
photoproduction on sulfur-32 at threshold to 22.1 Mev, cross sections for, (E), 19: 19170
photoproduction on holmium, anisotropy in giant-resonance region of, (E), 19: 19197
photoproduction on nuclei at 10 to 28 Mev, cross sections for, (E), 19: 19217
photoproduction on carbon-13, time-of-flight spectrometry of, 19: 18298
photoproduction on nuclei at 10 to 28 Mev, cross sections for, (E), 19: 21305
photoproduction on bismuth-209 and tantalum-181, angular distributions from, (E), 19: 21288
photoproduction on lithium-6, (E), 19: 23704
photoproduction on nuclei, polarization in, (T), 19: 25500
photoproduction on helium-4 at 1 Bev, (E), 19: 25506
photoproduction on heavy nuclei, damping of giant resonances in, (T), 19: 25532
photoproduction on light nuclei, cross sections for, (E), 19: 25542
photoproduction on nuclei, field model for, 19: 27467
photoproduction on zirconium-90, cross sections for, (T), 19: 27479
photoproduction on calcium-40, cross sections for dipole, (T), 19: 27482
photoproduction on nuclei at 6 to 30 Mev, cross sections for, (E), 19: 27523
photoproduction on oxygen at 300 Mev, (E), 19: 31269
photoproduction on iodine-127 at 0.3 to 1 Bev, cross sections and yields for, (E), 19: 31291
photoproduction on uranium, spectra from, 19: 31304
photoproduction on deuterium at 2.75 Mev, polarization of, (E), 19: 33330
photoproduction on arsenic-75, dipole-quadrupole interaction in, (E/T), 19: 33346
photoproduction on aluminum, spectra of, (E), 19: 35378(R) (EANDC(E)-57(U))
photoproduction on light nuclei, cross sections for, 19: 37831(R) (TID-21940)
photoproduction on carbon and magnesium to 30 Mev, total cross sections for, (E), 19: 37833(R) (TID-21940(Paper II))
photoproduction on nuclei $51 \leq Z \leq 83$, energy spectra from, (E), 19: 36220(R) (MIT-2098-142)
photoproduction on deuterium, laboratory observation of, 19: 41712
photoproduction on deuterium at 11.0 to 22.9 Mev, polarization in, 16: 16924 (NP-11509)
photoproduction on carbon-12 to 52 Mev, cross sections for, (E), 20: 2296
photoproduction on lithium-6 at 5.7 to 32 Mev, cross sections for, (E), 20: 1217
photoproduction on beryllium-9, polarization from, (T), 20: 8111
photoproduction on lithium-7 at 25 Mev max, energy spectra of, (E), 20: 8117
photoproduction on oxygen-18 at 20 Mev, angular distributions and energy from, 20: 10102
photoproduction on nuclei at 8 to 16 Mev, spectra from, (E), 20: 15723 (MIT-2098-162)
photoproduction on beryllium and deuterium by fission gamma rays, (E/T), 20: 17830
photoproduction on aluminum, carbon, and sulfur at threshold to 200 Mev, cross sections for, (E), 20: 22094
photoproduction on deuterons in water shielding for reactors, flux distribution from, (T), 20: 24801
photoproduction on beryllium-9 at 6 and 80 Mev, cross sections for, (E), 20: 24430
photoproduction on beryllium-9 to 85 Mev, energy spectra and polarization from, (E), 20: 24432
photoproduction on lithium-6 at 5 to 97 Mev, cross sections for, (E), 20: 24437
photoproduction on lithium-6 at 30 Mev, energy spectra from, (E), 20: 26140
photoproduction on nuclei, use for determining bremsstrahlung pulse barycenter, 20: 25427
photoproduction on protons, research program on, (E), 20: 27921
photoproduction on nuclei, 20: 34671
photoproduction on nuclei, yields from, (E), 20: 26200
photoproduction on nuclei, energy spectra from, (E), 20: 42165(R) (MIT-2098-251, pp 16-20)
photoproduction on helium-3 at 12 to 170 Mev, angular distributions and energies from, (E), 20: 44711(T)
photoproduction on protons at 0.3 to 5.8 BeV, (E), 20: 46348(T) (SLAC-Trans-44)
photoproduction resonances in deformed nuclei, 16: 2553
photoproduction yields from erbium and holmium, 16: 17083
photoproduction yields from bremsstrahlung reactions with carbon and oxygen at 31 Mev, 16: 24864
physics in large fast reactors, review of, 18: 40489
physics of, conference on, 17: 4034
physics of pulsed, (E/T), 20: 46564
physics of, research on, 18: 7662(R) (ORNL-3499(Vol.II))

physics research in Project Gnome, 18: 10215
physics, reactions, and scattering of, 18: 11195(R) (EANDC(E)-49(L))
plutonium-239 and uranium-235 partial cross sections for, 17: 31414(T) (AEC-tr-5917)
polarimeter for, time-of-flight, 20: 16876
polarizability coefficients for, determination of electric, (E), 20: 24362(T) (ANL-Trans-294)
polarizability of meson (π) contribution to, (T), 19: 20949
polarizability of, electric and magnetic, 18: 34526
polarizability of, from photon scattering by helium, 18: 34538
polarizability of, electric, (E), 19: 12576
polarization, 17: 34817
polarization and strength functions of, comparison in various models for, 17: 17101
polarization angular dependence from nitrogen-14 (d,n) reactions at 3.7 Mev, (E), 19: 33366
polarization asymmetries from proton reactions (p,n) with lithium-7 at 0.1 to 2.4 Mev, 16: 17091
polarization by reflection from cobalt–iron mirrors, facility for, 19: 39265(R) (IA-1021)
polarization by scattering on nuclei at 2.09 Mev, optical model analysis, 16: 21539
polarization by scattering on zirconium at 3.4 Mev, 18: 42613
polarization by scattering, (E/T), 20: 20365
polarization direction change in rotating magnetic field, adiabatic, 18: 11150
polarization, from d-d interactions at 300 to 500 kev, 16: 4778
polarization, from d-d and d-t interactions, 16: 4779
polarization, from light nuclei, 16: 3668 (NYO-7864)
polarization, from (d,n) reactions on deuterium, 16: 5920
polarization from (d,n) reactions with lithium-7, 17: 17087
polarization from deuterium photodisintegration, 17: 19136
polarization from deuterium (d,n) reaction at 20 to 160 kev, 18: 19071
polarization from proton reactions (p,n) with carbon-13 and nitrogen-15 at 6.9 to 12.3 Mev, (E/T), 19: 10338
polarization from deuterium (d,n) reactions, 19: 17035
polarization from carbon-12 (d,n) reactions at 4 to 7.5 Mev, (E), 19: 35435
polarization from deuteron reactions (d,n) with deuterium at 1.5 and 1.9 Mev, (E), 20: 16876
polarization from deuteron reactions (d,n) with carbon-12 at 6 Mev, (E), 20: 28467
polarization from antineutron-proton interactions, models for, 20: 27815
polarization from deuteron reactions (d,n) with tritium at 6.6 Mev, (E), 20: 30442
polarization in (d,n) reactions, 18: 18950
polarization in carbon-12 (d,n) reactions, 18: 16908 (ANL-6848(p.16-23))
polarization in carbon-12 (d,n) reactions, (E), 19: 14643
polarization in deuteron reactions (d,n) with tritium at 5 Mev, 16: 27355
polarization in deuteron reactions (d,n) with tritium at 16 and 24 Mev, 17: 17083
polarization in deuterium (d,n) helium-3 reactions, 18: 34963
polarization in deuteron reactions (d,n) with deuterium at 3 Mev, 18: 36680
polarization in deuteron reactions (d,n) with tritium at 9 to 19 Mev, 18: 40636
polarization in deuterium (d,n) reactions at 4.7 and 5.6 Mev, (E), 19: 5247
polarization in deuteron reactions (d,n) with carbon at 2.8 Mev, 19: 39950
polarization in decay of collective states excited by meson (μ) capture, (T), 19: 41769
polarization in deuterium (d,n) reactions at 1.9 to 3.7 Mev, angular distributions of, (E), 20: 4895
polarization in deuterium-deuteron reactions, 20: 8078(R) (NYO-1082-2)
polarization in deuteron reactions (d,n) with nitrogen-15 at 1.6 to 3.0 Mev, (E), 20: 30427
polarization in elastic and inelastic scattering on nuclei at 0.3 to 3 Mev, 18: 24694
polarization in electric and magnetic fields, 20: 41902
polarization in hyperon (Σ^+) decay, (E), 20: 39748 (COO-881-76)
polarization in lithium-7 (p,n) reactions, 18: 7682 (NP-13418)
polarization in photodisintegration of deuterium, 17: 34560(R) (TID-19195)
polarization in photodisintegration of beryllium-9 and deuterium, 18: 6197
polarization in proton reactions (p,n) with lithium-7 at 4 to 10 Mev, 16: 2411 (TID-14213)
polarization in proton reactions (p,n) with tritium at 2.9 to 12 Mev, 16: 13885
polarization in proton reactions (p,n) with lithium-7 at 4.5 Mev, angular distributions for, 17: 26564
polarization in proton reactions (p,n) with nuclei, 19: 5149
polarization in proton reactions (p,n) with carbon-13 and nitrogen-15 at 6.9 to 12.3 Mev, 19: 47710
polarization, in scattering from nuclei, 16: 4793
polarization in the carbon-12(d,n) nitrogen-13 reaction, 17: 17264
polarization in tritium (p,n) reactions at 1.9 to 3.5 Mev, 18: 17052
polarization in two-nucleon systems at 310 to 700 Mev, (E/T), 20: 39844
polarization measurements with liquid helium scintillation detector, 16: 13337
polarization measurement at low and medium energies, methods for, 16: 15543
polarization measurement by meson (μ^-) capture, 16: 25922 (NP-11977 (p.49-52))
polarization measurements in Mev region, apparatus for, 18: 43939 (RFX-97)
polarization methods for cold, resonance, and thermal, 16: 26205
polarization of, by scattering, compound nuclear and direct contributions to, 17: 11752
polarization of deuteron-deuteron, measurement by solenoid, 17: 9294
polarization of, from interaction of polarized deuterons with tritons at 170 kev, 17: 729
polarization of, from (d,n) reactions in nitrogen-14 at 1.32 Mev, 17: 17127 (TID-18256)
polarization of, from (γ,n) reactions on deuterons, 17: 11551
polarization of, in reactions d(γ,n), 17: 11805(R) (TID-17728)
polarization of, in deuteron and proton reactions with deuterium and tritium at 1.9–23.7 Mev, 17: 34919
polarization of instrument for measurement of, 20: 38163
polarization of photo-, from carbon, deuterium, and oxygen, 18: 36080(R) (RPI-328-8)
polarization of photo-, from oxygen-16, (E), 19: 23631(R) (RPI-328-20(p.53-4))
polarization of photo-, from oxygen-16, (E), 19: 36220(R) (MIT-2098-142)
polarization of, theory for, 17: 18537 (KR-37)
polarization of 2.8-Mev, in elastic scattering by nuclei, 17: 17294
polarization of, apparatus for measuring, 20: 8165
polarization of, analyzer for measurement of, 20: 14856 (KFK-345)
polarization of, determination by scattering on helium, (T), 19: 45217 (COO-7-0363)
polarization of, in photoproduction on bismuth, 18: 30799
polarization of, in interactions with polarized proton targets, 19: 1524 (JINR-P-1797)
polarization of, preparation of single-crystals of cobalt-iron alloy for, 19: 42886(T)
polarization precession in lithium-7 (p,n) reactions at 2.9 to 5 Mev, (E), 19: 37242 (AE-189)
polarization studies, 20: 4822(R) (ANL-7081, pp 22-35)
polymerization induction by, 18: 5389
potentials in medium-density gases, 16: 3663
power functions and radiative capture of, optical model calculations on, 17: 37998(T) (AEC-tr-5734(p.1-2))
production and economy of, in reactors, review of, 20: 36145
production and escape in reactors, computer code for, 16: 26466 (GEMP-123)
production and polarization in meson (π^-)–proton interactions at 310 Mev, 18: 34512 (UCRL-11140)
production and properties survey, 16: 28170
production by (α,n) reactions in heterogeneous isotopic neutron sources, (E), 20: 2949
production by (α,n) and (γ,n) reactions with nuclei, (E), 20: 4802 (IDO-17115)
production by accelerators, targets for, 18: 28236 (EUR-1815.d,f,e)
production by cosmic mesons (μ), 17: 13087
production by cosmic-proton reactions on space vehicles, 17: 16876
production by cosmic radiation at high altitudes, 18: 15168
production by cosmic-ray reactions in atmosphere at ground level, 20: 37483
production by d-t reactions in Cockcroft-Walton accelerators, 16: 28234
production by fission, 17: 7655(R) (ANL-6600)
production by (γ,tn) reactions, excitation functions of, 17: 5347
production by helium-3 reactions with elements $Z \leq 22$, (E), 19: 19095 (WASH-1053)
production by ion collisions, apparatus for, 19: 16834(P)
production by proton reactions with nuclei at 6 Bev, 18: 21698(R) (ANL-6860)
production by reaction of high-energy protons with aluminum, heavy water, lead, and uranium, (E), 19: 31215(R) (ANL-7010(p.1-19))
production by tritium–deuteron reactions at 8 to 200 kev, yield, 16: 21358 (SERL-TR-M-61)
production by Van de Graaff generator, 20: 36146
production cross sections in boron-11 (p,n) reactions at 4 to 11.5 Mev, (E), 19: 14509
production for activation analysis, 18: 11998
production in accelerators, 20: 35454
production in alpha reactions with nuclei, 16: 33803
production in alpha reactions with air, nitrogen, oxygen, and water,

17: 9527
production in antiproton-proton interactions at 5 to 9 BeV/c, differential and total cross sections for, (E), 20: 46362
production in Brookhaven Alternating Gradient Synchrotron proton beam at 30° and 30 Bev, 16: 21650 (NP-11624)
production in cascades by heavy-particle reactions in matter, 16: 13944 (DESY-A2.85)
production in compression of nuclear matter, neutrino spectra from, (T), 20: 8097
production in cosmic radiation interactions with atmospheric particles, 17: 41714
production in cosmic-ray interactions, theory of albedo, 18: 2743
production in cosmic proton reactions with aluminum shielding, 18: 15421 (NASA-TN-D-2122)
production in cosmic showers, transverse momentum of, 18: 14770
production in d-t and d-p interactions, 17: 7241
production in D-T plasma, 17: 9753
production in dense plasma foci, (T), 19: 12637(R) (LA-3202-MS)
production in deuteron reactions (d,n) with deuterons, preparation of target materials for, 16: 19676 (TID-15688)
production in deuterium plasma without reversed trapped field, 17: 9766
production in deuterium plasma, 17: 11866
production in deuteron reactions (d,n) with calcium-40, carbon-12, and oxygen-16, energy distributions in, 17: 38170
production in deuteron reactions (d,n) with tritium, 19: 23614
production in deuteron reactions with tritium, coincidence measurement of, 19: 22696 (IKF-D-32)
production in deuterium by fast linear pinch, 19: 33445
production in deuterium (d,n) reactions, collimation in, (E), 19: 35496
production in fast magnetic plasma compression devices, 18: 6390
production in gamma reactions (γ,n) with carbon-12 and oxygen-16 at 30.5 Mev, 17: 11755
production in graphite and nickel by 660-Mev protons, (E), 19: 38018
production in heated and confined plasma, 18: 6403(P)
production in heavy elements, Monte Carlo calculation of, 19: 26922(R) (PR-P-64)
production in heavy water reactors, methods for high-flux, 20: 20183
production in helium-3 reactions with tritium at 3.23 Mev, 16: 21573
production in high-energy cyclic electron accelerators, 16: 33920
production in hyperon (Σ^-) reactions with helium-4 at rest, (E), 19: 5226
production in IGY neutron monitor, counting rate and multiplicity spectrum of, 20: 21551
production in K^--proton interactions at 293 to 513 Mev/c, 16: 27914 (UCRL-10175)
production in ${}_{\Lambda}He^4$ decay, 16: 12360
production in lead by cosmic protons, 17: 12976
production in lithium bombardment of light nuclei, (E), 20: 10088
production in Martian atmosphere, biological implications of, 17: 32881
production in massive shields, effect on gamma background, 17: 25591(R) (ANL-6646(p.50-65))
production in meson (μ^-) capture in hydrogen (liquid), spectrum, 16: 9395
production in meson π-proton interactions, 17: 5252
production in meson (π^-)–proton interactions at 10 Bev/c, 18: 30517 (PAN-492/VI)
production in meson (π^-)–proton interactions at 313 and 371 Mev, cross sections for, 18: 34516 (UCRL-11435)
production in meson (π)-proton interactions at 450 Mev, (E), 20: 13524
production in meson (π^-)-proton interactions at 350 to 800 Mev, (E), 20: 13527
production in multiregion cylinder of finite height, computer program for calculation, 16: 2774(R) (IDO-16710)
production in neutron fission of uranium-235, angular distributions, 16: 23141
production in neutron monitor by cosmic radiation, 17: 12977
production in nuclear reactions, multiple, 17: 41901
production in nuclear reactions on light nuclei, 18: 11232
production in oxygen-16 reactions with gold, 17: 28251 (UCRL-10689)
production in (p,n) reactions on nuclei, theory for, 17: 2279
production in photon reactions (γ,n) with sulfur-32 at 22 Mev, cross sections for, 17: 28286
production in photon reactions (γ,n) with beryllium-9, magnetic dipole transitions and neutron polarization in, 17: 29610
production in photodisintegration (γ,np) of heavy nuclei to 200 Mev, (T), 19: 10295
production in proton reactions with nuclei (Z = 4 to 50) at 32 Mev, 16: 21479
production in proton reactions, cross sections for multiple, 16: 23096
production in proton reactions with nuclei at 9 to 25 Bev, 16: 33837
production in proton reactions with rhodium at 5 to 12 Mev, 17: 11631 (TID-16049)
production in proton bombardment of lithium-7, cross sections for, 17: 17220
production in proton nuclear reactions at 450 Mev, 18: 18933
production in proton-antiproton collisions, unitary symmetry model for, 18: 20953
production in proton shielding, 18: 24805 (UNC-5049)
production in proton reactions with heavy nuclei at 0.3 to 1.0 Bev, 18: 34961
production in proton reactions (p,n) with aluminum-27, carbon-13, and nitrogen-14, thresholds for, 19: 23683
production in proton–vanadium-51 reactions at 1.5 to 2.3 Mev, (E), 19: 41676 (ORNL-P-1468)
production in proton-proton interactions at 2.0 Bev, (E/T), 19: 41503
production in proton reactions (p,n) with nuclei at 14.8 Mev, 16: 26326 (UCRL-6733)
production in reactions (μ^-, nν) on sulfur nuclei with polarized muons, angular asymmetries, 16: 21426
production in reactions (α,n) on beryllium-9, angular distributions, 16: 24804
production in reactors, review of, 19: 12732
production in shielding of meson production facilities, flux calculation for, (T), 20: 10223 (ORNL-P-1787)
production in single fission events in pulsed reactor, statistical fluctuations in, 18: 19433
production in slab and spherical reactors, relation of critical size to, 17: 17425 (RM-3256-PR)
production in solar flares, 18: 44416
production in solar flares, (T), 19: 44902
production in SORA reactor, 19: 10652
production in stars, 18: 17055
production in steady-state plasma, 20: 10219(P)
production in subcritical cores, relative source strengths of, (E), 20: 22392
production in supernova, 18: 4661(T)
production in thallium (γ,xn) reactions to 107 Mev, (E), 19: 14608
production in theta pinch plasma without reversed magnetic field, 18: 6298 (63-RL-3226E)
production in triton reactions (t,n) in deuterium plasma, density determination from spectra of, 17: 42128
production in tritium bombardment by deuterons, 19: 18189(P)
production in triton reactions with boron at 0.54 to 2.40 Mev, (E), 19: 37891
production of, by deuteron bombardment of boron-11 at 1.6 to 2.7 Mev, 17: 13605
production of cascade and evaporation, from proton–carbon reactions, 17: 36347(R) (NARF-62-18P)
production of high-density gases of, from nuclei, 16: 18535
production of, in deuterium plasmas, 17: 948 (62-RL-2936E)
production of, in fission, 17: 19393
production of intense bursts of, apparatus for, 17: 9496(P)
production of polarized, in tritium (d,n) reactions at 0.1 to 7.7 Mev, 16: 11012
production of polarized, summary of reactions for, 17: 17125 (TID-18137)
production of polarized, in neutrino interactions with nucleons, 18: 9125
production of polarized, in (d,n) reaction on deuterium, 18: 16992
production of polarized, in proton reactions (p,n) at 50 Mev, (E), 19: 28962(R) (NIRL/R/81)
production of pulses in explosions and reactors, 16: 14077
production of pulsed, in accelerators, 19: 23163(R) (ORNL-3650 (p.111-86))
production of secondary, in proton reactions with nuclei at 160 Mev, (E/T), 19: 21244 (ORNL-P-844)
production of 14-Mev, by deuteron–triton reactions, 16: 29882 (PAN-277/I-A)
production of 14-Mev, in deuteron–tritium reactions, evaluation of target materials for, 17: 34833 (DOFL-TR-1148)
production of 14-Mev, in tritium (d,n) reactions at 250 kev, 19: 37292
production of 14-Mev, design of accelerator for, 19: 47176
production of 14-Mev, by deuteron reactions with tritium, 20: 22976
production of 28-Mev beam, 17: 15272
production of, computer analysis of angular distributions from, 20: 8041 (ORNL-TM-1241)
production of, tritium gas target for, 20: 21948
production on nuclei, cross sections for, 17: 11672
production source in Mark II Baked Picket Fence, 16: 15719(R) (LAMS-2682)
production using accelerators, targets for, 20: 19296 (EUR-2641.d,f,e)
propagation from high-altitude nuclear explosions, shadow-cone geometry for, 18: 40431
propagation in cavities, Monte Carlo calculations for, (T), 19: 27385 (CEA-R-2774)
propagation in graphite thermal columns, 17: 26070
propagation in media, measurement, 16: 23814(P)
propagation of Bragg-reflected, in bounded mosaic crystals, (T),

20: 28622
propagation of waves of, P_1 space-energy dependent theory of, 19: 29211
propagation through multiregion media, 17: 26071
properties for use in activation analysis, 20: 38838
properties in biological materials, absorption, effectiveness, and energy distribution, 19: 36727
properties in unitary symmetry model, electromagnetic, 18: 24388 (JINR-P-1616)
properties of gases of, at zero temperature, 18: 37905
properties of superdense stars of, at absolute zero, (T), 19: 16351
properties of, book on, 18: 17097
properties of, for use in radiotherapy, 19: 28200
properties of, theory of, 18: 11137 (ANL-6797(p.2-14))
protection against, effects of AET-Thiogel A on mice subjected to lethal doses of, 16: 31386(R) (ANL-6535(p.19-20))
proton radiative capture at 50 Mev, 16: 5911
pulse amplitudes from pulsed fast reactor, statistical distribution of, (T), 19: 27750 (JINR-P-2076)
pulse effects in nonmultiplying assemblies, time behavior of, 20: 8050
pulse propagation in graphite, (E/T), 19: 19072
pulsed techniques for reactivity measurements, 18: 35076 (TID-7679 (p.219-28))
pulsed techniques for impulse-response of reactors, cross-correlation techniques with random excitation for, 18: 35075 (TID-7679(p.203-18))
pulsed, problems of experiments with, 18: 38058
pulsing of reactor, for activation analysis, 19: 17831
pulsing techniques, time effects in, 18: 30949 (NYO-9077)
pulsing techniques for critical and subcritical assemblies, 18: 33030
quality factor at energies to 680 Mev, recombination method for determining, 19: 31212
range in water for polonium–beryllium, 16: 3658 (NP-11106)
range-dose calculations for, in tissues at 60 to 400 Mev, 18: 43320 (ORNL-P-322)
RBE for human body, 20: 42865
reaction (n,α) with tellurium isotopes, cross-section systematics near shell closure, (T), 20: 46658
reaction (n,γ) with silicon-31, cross sections for, (E), 20: 34557
reaction (n,γ) and (n,2n) with nuclei of bromobenzene and ethyl bromide in benzene, chemical effects from, 20: 43334
reaction cross sections and scattering experiments at FRM, 20: 20331
reaction rates in reactor lattices, calculation of, 19: 27754 (TRG-Report-754)
reaction rates in thorium–uranium breeding blankets, 20: 34944
reaction with natural uranium, number of fissions in, 19: 40640
reaction with tellurium-130 in telluric acid to produce iodine-131, 20: 43404
reaction with uranium-235 at 0.1 to 50 ev, probability of ternary fission in, (E), 19: 25471 (JINR-P-2025)
reactions (n,α), (n,2n), and (n,p), neutron spectrum measurement using, 18: 7061 (UCRL-10732)
reactions (n,α) on chlorine-35 in potassium chloride, 18: 6871
reactions (n,α) with silicon-29 at 2.2 to 3.8 Mev, cross sections for, 18: 7731
reactions (n,γ) with bromine and chlorine, products from, 18: 6851(T) (CEA-tr-R-1534)
reactions (n,γ) with chromium-53, 18: 7783
reactions (n,p) with nuclei, angular distribution calculations using distorted-wave Born approximation, 18: 7750
reactions (n,p) with nickel-58 at 2.2 to 3.8 Mev, cross sections for, 18: 7731
reactions (n,α) with silicon-29, nuclear properties from, 18: 16995
reactions (n,α) at 14 Mev, statistical analysis of excitation functions and energy spectra, 18: 17057
reactions (n,α) at 14 Mev, statistical model cross sections for, 18: 17058
reactions (n,α) with carbon-12 at 14 Mev, angular distributions for, 18: 19040
reactions (n,α), (n,d), (n,p) with cesium-133 and iodine-127, 18: 18952
reactions (n,α) and (n,2n) with phosphorus-31 at 14.8 Mev, cross sections for, 18: 19032
reactions (n,α), (n,p), and (n,2n) with aluminum, copper, holmium, iron, palladium, and tellurium at 14.7 Mev, cross sections for, 18: 19037
reactions (n,α) and (n,p) with gallium-71 and zinc-68 at 14 Mev, copper-68 decay studies from, 18: 19057
reactions (n,α) and (n,γ) with rhodium-103 at 0.023 ev, 24 and 116 kev, and 2.49 and 14.67 Mev, cross sections for, 18: 18928
reactions (n,α) with nuclei at 14 Mev, nuclear shell effects in cross sections for, 18: 18977
reactions (n,α) with uranium-238, instrument for detection of alpha particles from, 18: 20403
reactions (n,α) with boron-10 gases, pressure wave generation in, 18: 21268
reactions (n,α) with boron-10 in kev range, yield ratio for ground and excited states of lithium-7 from, 18: 24620(R) (ORNL-TM-874)
reactions (n,αn) with gallium, cross sections for, 18: 25300
reactions (n,α) with lanthanum-139, alpha energy spectrum for, 18: 26606
reactions (n,α) with nuclei at 14 Mev, angular and energy distributions for, 18: 28640
reactions (n,α) and (n,p), optical model for cross sections of, 18: 28666
reactions (n,α) with lithium-7 at 14 Mev, hydrogen-4 production cross section for, 18: 28672
reactions (n,α) with cobalt-59 up to 20.3 Mev, 18: 28588
reactions (n,α) and (n,p) with argon, measurement of cross sections for, 18: 30736(R) (TID-20658)
reactions (n,α) and (n,p) with potassium-39 at 4 to 13.7 Mev, cross sections for, 18: 32784
reactions (n,α) with boron-10, gamma emission by excited lithium-7 produced in, 18: 31385
reactions (n,α) of, angular distribution for, 18: 34876
reactions (n,α) with nuclei at 14 Mev, total cross sections for, 18: 34887
reactions (n,α) with nuclei, direct interaction model for knockout and pickup, 18: 34769 (NP-14085)
reactions (n,α) of, statistical model analysis of, 18: 34810
reactions (n,α) with calcium-40 at 14 Mev, differential cross sections for, 18: 34841
reactions (n,α) with molybdenum isotopes at 15 Mev, energy spectra of, 18: 36597
reactions (n,α) at 14 Mev, statistical model anomalies for, 18: 38156
reactions (n,α) with silicon-28 at 14.55 Mev, cross sections for, 18: 38069 (NP-14111)
reactions (n,α) and (n,p), cross section energy dependence in, 18: 40631
reactions (n,α) with fluorine-19, distributions from, 18: 42620(R) (AEET/NP/8)
reactions (n,α) with boron-10, cross sections for, 18: 42621 (AERE-R-4663)
reactions (n,α) and (n,p) with nuclei, cross sections for, 18: 42659
reactions (n,α) with nuclei $6 \leq Z \leq 30$ at 14.5 Mev, 18: 44779
reactions (n,α) and (n,p) with aluminum-27, recoil ranges of magnesium-27 and sodium-24 in, 18: 44765
reactions (n,α), (n,d), (n,p), and (n,t) with nuclei at 14 Mev, measurement of cross sections for, 18: 44768
reactions (n,α), (n,d), and (n,p) at 14.7 Mev, cross sections for (E), 19: 3319
reactions (n,α) with lanthanum-139 at 14 Mev, nuclear surface structure analysis from (E/T), 19: 3241 (PAN-515/I)
reactions (n,α) with copper-63 at 12.5 to 16.5 Mev, cross sections for, 19: 6666
reactions (n,α), (n,2n), and (n,p) with nuclei at 12.6 to 19.6 Mev, excitation functions for, (E), 19: 6669
reactions (n,α) with lithium-6, tritium production in, 19: 6229
reactions (n,α) with lithium-6 at 1 to 600 kev, cross sections for, (E/T), 19: 10281
reactions (n,α), (n,2n), and (n,p) with fluorine-19 and sodium-23, cross sections for, (E/T), 19: 10287
reactions (n,α) with aluminum-27, sodium-24 production in, 19: 11649
reactions (n,α) with nuclei at 14.8 Mev, cross sections for, (E), 19: 12592
reactions (n,α) and (n,p) with silicon isotopes at 5.2 to 9.0 Mev, cross sections for, (E), 19: 12511
reactions (n,α) with silicon-29 at 14.37 to 14.57 Mev, (E), 19: 14559
reactions (n,α) with niobium-93, alpha spectrum from, 19: 14533(R) (NYO-1082-1)
reactions (n,α) with oxygen-16 at 14 Mev, (E), 19: 14592
reactions (n,α) with aluminum-27 at 13.4 to 14.2 Mev, cross section variation for, (E), 19: 14612
reactions (n,α) with manganese-55 at 14.8 Mev, cross section for, (E), 19: 14615
reactions (n,α) with nuclei, alpha substructures in, (T), 19: 16946
reactions (n,α) and (n,2n) with nuclei at 14 Mev, excitation cross sections for, (E), 19: 16951
reactions (n,α) with fluorine-19 at 4.7 and 14.1 Mev, (E), 19: 17038
reactions (n,α) with aluminum-27 at 14.1 Mev, (E), 19: 17038
reactions (n,α) with carbon-12 at 14.5 Mev, angular distributions from, (E/T), 19: 17039
reactions (n,α) and (n,p) with nuclei at 14 Mev, shell effects in, (T), 19: 17040
reactions (n,α) with boron-10 for boron detection, 19: 17807
reactions (n,α) with cobalt-59 at 12.6 to 19.6 Mev, (E), 19: 21290
reactions (n,α) with silicon-28 at 14.8 Mev, angular distributions from, (E), 19: 21318
reactions (n,α) with germanium-73 at 14 Mev, cross sections for, (E), 19: 21325
reactions (n,α) with aluminum-27 at 14.1 Mev, angular and energy distributions from, (E), 19: 23720
reactions (n,α), (n,αn), and (n,nα) with nickel-58 at 14.1 Mev, angular and

energy distributions from, (E), 19: 23720
reactions (n,α) with silicon-28 at 14 Mev, (E), 19: 23782
reactions (n,α) with lithium-6, 19: 24410
reactions (n,α), (n,p), and (n,t) with nuclei at 14.8 Mev, cross sections for, (E), 19: 27516
reactions (n,α) with carbon-12 at 14 Mev, angular distributions from, 19: 29228(R) (AEET/NP/10)
reactions (n,α), (n,np), and (n,p) with silicon at 14 Mev, ionization of reaction products from, 19: 29236 (GA-6136)
reactions (n,α) with silver at 14 Mev, angular and energy distributions from, (E), 19: 29279
reactions (n,α) and (n,p) with bromine, potassium, and rubidium, (E), 19: 33394
reactions (n,α) and (n,αγ) with boron-10, ratio of, 19: 35398 (ORNL-P-1304)
reactions (n,α) with potassium-41 at 4.4 to 8.4 Mev, cross sections for, (E), 19: 35378(R) (EANDC(E)-57(U))
reactions (n,α) with calcium-44 at 6.7 to 15.4 Mev, cross sections for, (E), 19: 35378(R) (EANDC(E)-57(U))
reactions (n,α) (n,n′) (n,p) with calcium-40 at 3.7 to 7.5 Mev, cross sections for, (E), 19: 35378(R) (EANDC(E)-57(U))
reactions (n,α_0) with silicon-28 at 5.2 to 7.2 Mev cross sections for, (E), 19: 35378(R) (EANDC(E)-57(U))
reactions (n,α_0) with silicon-29 at 5.2 to 7.2 Mev, cross sections for, (E), 19: 35378(R) (EANDC(E)-57(U))
reactions (n,α) with cobalt-59 at 14.1 Mev, cross section for, (E), 19: 35378(R) (EANDC(E)-57(U))
reactions (n,α) with manganese-55 at 12.5 to 19.6 Mev, cross sections for, (E), 19: 35378(R) (EANDC(E)-57(U))
reactions (n,α) with samarium-149 at 0.004 to 0.1 ev, spectra from, (E), 19: 35378(R) (EANDC(E)-57(U))
reactions (n,α) with aluminum-27, cross section for, (E), 19: 35378(R) (EANDC(E)-57(U))
reactions (n,α) with neon-20 at 14 Mev, angular distribution and Q values from, (E), 19: 35378(R) (EANDC(E)-57(U))
reactions (n,α) with cobalt-59 at 12.6 to 19.6 Mev, cross sections for, (E), 19: 35378(R) (EANDC(E)-57(U))
reactions (n,α) with copper-63 at 12.6 to 16.6 Mev, cross sections for, (E), 19: 35378(R) (EANDC(E)-57(U))
reactions (n,α) with lithium-6 at 10 to 600 kev, cross sections for, (E), 19: 35378(R) (EANDC(E)-57(U))
reactions (n,γ) in activation analysis, data compilation for, 18: 11961 (AEET/Anal./28)
reactions (n,γ) and (n,2n) with nuclei at 0.024 to 14.7 Mev, cross sections for ground- and isomeric-state production in, 18: 13070
reactions (n,γ) with cesium-133, ratio for production of cesium-134 ground and 137-kev state in, 18: 13072
reactions (n,F) with uranium-235 (E/T), 19: 3235 (JINR-P-1761)
reactions (n,f) with uranium-233, prompt gamma spectra from, 19: 6631 (IDO-17025)
reactions (n,f) with uranium-235 at 2 to 70 ev, cross sections for, (E), 19: 45299
reactions (n,γ) with fluorine-19, spectra from, 18: 26541(R) (ORNL-3582(p.68-71))
reactions (n,γ) with nuclei, gamma spectra from, 17: 26442(R) (ORNL-3425(p.57-60))
reactions (n,γ) with nuclei, gamma spectra for, 17: 26443(R) (ORNL-3425(p.60-3))
reactions (n,γ) with nuclei having A = 23 to 32, spectra from, 18: 26542(R) (ORNL-3582(p.71-5))
reactions (n,γ) with tin nuclei, spectra from, 18: 26540(R) (ORNL-3582 (p.62-7))
reactions (n,γ) with uranium-238 at 0.001 to 5.6 ev, cross sections for, 18: 15171 (AEEW-M-414)
reactions (n,γ) with nuclei, dose distributions from, 18: 16962
reactions (n,γ) with nuclei at 1 to 50 kev, cross sections for, 18: 19116
reactions (n,γ) with indium and indium-115, spectra from, 18: 11164 (HW-79054(p.4-11))
reactions (n,γ) with nuclei, gamma spectra from, 18: 20333 (KR-64 (Sect.XX))
reactions (n,γ) with samarium at 10 to 20 ev, spectra from, 18: 20388
reactions (n,γ) with neodymium-146, production of carrier-free praseodymium-147 by, 18: 20071
reactions (n,γ) with cerium-142, production of carrier-free praseodymium-143 by, 18: 20071
reactions (n,γ) with molybdenum-98, production of carrier-free technetium-99m by, 18: 20071
reactions (n,γ) of polarized, polarization of photons from, 18: 21200 (KR-64(Sect.XXII))
reactions (n,γ) with rhenium, gamma spectra from, 18: 21205 (NP-13807)
reactions (n,γ) with nickel-60, angular correlation of 7.54–0.284 Mev cascade in, 18: 21240
reactions (n,γ) with nuclei, analysis of gamma spectra from, 18: 21202 (KR-64(Sect.XXXII))
reactions (n,γ) with copper, gamma spectra for, 18: 22867 (CONF-481-44)
reactions (n,γ) with gold-197 at 20 to 200 kev, cross sections for, 18: 24591(R) (LMSC-4-50-62-1)
reactions (n,γ) with nickel-64 at 100 to 2000 kev, cross sections for, 18: 24591(R) (LMSC-4-50-62-1)
reactions (n,γ) with nuclei, studies of nuclear structure and compound nucleus decay in, 18: 24607 (NP-13930(p.104-8))
reactions (n,γ) with silver-109, gamma spectra from, 18: 28600
reactions (n,γ) with aluminum-27 at 14 Mev, spectra from, 18: 30724 (NIJS-R-420)
reactions (n,γ) with promethium-147, macroscopic cross section for, 18: 34006(R) (ORNL-TM-889)
reactions (n,γ) with nuclei, relation between cross section and scattering length for, 18: 34762 (JINR-P-1671)
reactions (n,γ) with cobalt-59, 18: 34827
reactions (n,γ) with nuclei, direct and semi-direct, 18: 36618
reactions (n,γ) of, radioisotope production by, 18: 37592
reactions (n,γ) on bromine-79, energy distribution function for production of bromine-80 by, 18: 37230
reactions (n,γ) with chlorine, gold, iron, and silver at epithermal to 30 kev, energy dependence of, 18: 38075(T) (AEC-tr-6398(p.70-80))
reactions (n,γ) with oxygen-18 at 0.2 to 1.0 Mev, cross sections for, 18: 40628
reactions (n,γ) and (n,n′) with indium isotopes, cross sections for, 18: 40627
reactions (n,γ) with deuterons, parity nonconservation studies for, 18: 40504 (EUR-1643.e(p.196-203))
reactions (n,γ) and (n,p) with cesium-133 and iodine-127 at 2.6 Mev, cross sections for, 18: 42639 (KFKI-1467/f)
reactions (n,γ) on cobalt-59 in cobalt(II) complexes, recoil effects from, 18: 43671
reactions (n,γ) with chlorine-35 in meteorites, 18: 44358
reactions (n,γ) on triphenylgallium, formation of recoil products in, 18: 43673
reactions (n,α) with aluminum-27 at 14.8 Mev, energy spectra from, 18: 11295
reactions (n,α) with aluminum-27 at 12.8 to 14.3 Mev, excitation function for, (E), 19: 37838 (USNRDL-TR-846)
reactions (n,α) with terbium-159 at 14.2 Mev, alpha energy spectrum of, (E), 19: 39780 (INR-596/PL)
reactions (n,α) with osmium-192 at 14 Mev, production of tungsten-189 in, (E), 19: 39801
reactions (n,α) and (n,p) with rubidium at 13 to 17 Mev, cross sections for, (E), 19: 39823
reactions (n,α) with bromine at 13 to 17 Mev, cross sections for, (E), 19: 39823
reactions (n,α_0) with sulfur-32 at 3.6 Mev, angular distribution for, (E/T), 19: 43304
reactions (n,α) with rubidium-85 at 14 Mev, chemical state of bromine-82 formed by, 19: 42565
reactions (n,α) with sulfur-32, cross sections and Q values for, 19: 45679(R) (NYO-1859-11)
reactions (n,α) with boron-10, spectra from, 19: 44450(R) (IBK-120a)
reactions (n,α) with lithium-6, spectra from, 19: 44450(R) (IBK-120a)
reactions (n,α) with silicon-29 at 13.6 to 15.6 Mev, excitation function for, 19: 45290 (ZFK-PHA-12, pp 110-12)
reactions (n,αγ), (n,dγ), (n,n′γ), (n,pγ), and (n,n′αγ) with carbon-12, nitrogen-14, and oxygen-16 at 14.8 Mev, gamma angular distributions from, (E/T), 19: 47593(R) (TID-22012, pp 156-75)
reactions (n,α), (n,2n), and (n,p) with iron-54 at 2.2 to 16.8 Mev, cross sections for, (E/T), 19: 47668
reactions (n,α) with nuclei at 14.6 Mev, angular and energy distributions from, (E/T), 19: 47637
reactions (n,α) and (n,p) with silicon-28 at 13.5 to 14.4 Mev, cross section for, (E), 20: 1163
reactions (n,α) and (n,p) with chlorine-35 and -36 and sulfur-32 and -33, phosphorus-32 and -33 production in, (E), 20: 3020 (ORNL-TM-1065)
reactions (n,α) with scandium-45, cross sections for, 20: 1947
reactions (n,α) and (n,2n) with beryllium, multigroup cross sections for, 20: 2960
reactions (n,α) with lithium-6 at 1.2 to 8.0 Mev, cross sections for, 20: 4299(R) (ORNL-2711)
reactions (n,α) with lithium-6, alpha and triton energy distributions from, 20: 5181(R) (ORNL-3029)
reactions (n,α), (n,γ), and (n,2n) with ruthenium-104 at 14.7 Mev, cross sections for, (E), 20: 6338
reactions (n,α) with argon-40 at 13.0 to 20.2 Mev, cross sections for, (E/T), 20: 6357
reactions (n,α), (n,d), and (n,t) with nitrogen-14 and -15, angular distributions from, (E/T), 20: 8078(R) (NYO-1082-2)

reactions (n,α) with silver-107, total cross sections for, 20: 8078(R) (NYO-1082-2)
reactions (n,α) and (n,n′) with boron-10 at 1.0 to 4.75 Mev, differential and integrated cross sections for gamma rays from, (E), 20: 9981 (WASH-1064)
reactions (n,α) with calcium-40, phosphorus-31, and sulfur-32 at 14 Mev, spectra from, (E/T), 20: 10010
reactions (n,α), (n,αn), and (n,nα) with argon-40 at 13.0 to 20.2 Mev, cross sections for, (E/T), 20: 10093
reactions (n,α) with aluminum-27 at 12.6 to 19.6 Mev, cross sections for, (E), 20: 9990
reactions (n,α_0) with sulfur-32 at 3.2 Mev, angular and energy distributions from, (E), 20: 11993
reactions (n,α) at 14.8 Mev, direct interaction models for, (T), 20: 12002
reactions (n,α) with phosphorus-31 at 14.8 Mev, cross section for, (E), 20: 12134
reactions (n,α) with silicon-28 at 14.8 Mev, angular distributions from, (E/T), 20: 12030
reactions (n,α) with calcium-40 at 4.7 Mev, alpha angular distributions in, (E), 20: 12119
reactions (n,α) with oxygen-16 at 14 Mev, angular distribution for, (E/T), 20: 12120
reactions (n,α) with boron-10 and lithium-6, excitation functions for, (E), 20: 13741
reactions (n,α) and (n,p) with potassium-39 and sodium-23 at 4 to 14 Mev, cross sections for, (E/T), 20: 13773 (IKF-13)
reactions (n,α) and (n,p) with silicon-28 at 13.95 Mev, recoil ionization defects from, (E), 20: 13989
reactions (n,α) with silicon-29 at 13.4 to 15.0 Mev, excitation function for, (E), 20: 15800
reactions (n,α) with germanium-72 at 14.6 Mev, isomeric cross section ratio for, (E/T), 20: 15773
reactions (n,α) with boron-10 at 23 ev to 0.5 Mev, excited-to-ground state branching ratio for, (E), 20: 17719
reactions (n,α) with calcium-44, cross sections for, (E), 20: 17804
reactions (n,α) with barium-138 and calcium-44, cross sections for, (E/T), 20: 17809
reactions (n,α) with neon-20 at 14.2 Mev, angular and energy distributions from, (E), 20: 17743
reactions (n,α) at 3.0 and 4.7 Mev, total cross sections for, (E), 20: 17767
reactions (n,α), (n,2n), and (n,p) with nuclei at 0 to 20 Mev, cross sections for, 20: 19810 (EUR-119.e(Vol.2))
reactions (n,α) with lithium-6, tritium production in, 20: 18763
reactions (n,α) with argon-40 at 14.1 Mev, alpha angular and energy distributions from, (E), 20: 19853
reactions (n,αn′) with heavy nuclei, direct, (T), 20: 22018
reactions (n,αn′) with uranium-238 at 14.7 Mev, cross sections for, (E), 20: 22017
reactions (n,α) with oxygen-16 at 14 Mev, mechanisms for, (E), 20: 15738
reactions (n,α) with bromine and silver in nuclear emulsions at 18.3 Mev, angular distributions and energy spectra from, (E), 20: 26209
reactions (n,α) with sulfur-32 at 2.5 to 3.2 Mev, angular distributions from, (E), 20: 28308
reactions (n,α) and (n,p) with bromine-79 and-81 at 14.8 Mev, cross sections for, (E), 20: 28447
reactions (n,α) with boron-11 at 14.2 Mev, lithium-8 production in, (E), 20: 30363
reactions (n,α) with aluminum-27 at 13.5 to 14.8 Mev, cross sections for, (E), 20: 32528
reactions (n,α), (n,αn′), and (n,n′α) with sodium-23 at 12.6 to 18.7 Mev, cross sections for, (E), 20: 32540
reactions (n,α) and (n,p) with silicon-28 at 13.95 and 14.6 Mev, angular and energy distributions from, (E), 20: 32431
reactions (n,α) with fluorine-19 at 4.7 Mev, angular and energy distributions from, (E), 20: 32434
reactions (n,α) in alumina and magnesia, calculation of gas volume from, 20: 31799
reactions (n,α) with oxygen-18 at 14.7 Mev, cross section for, (E), 20: 33228
reactions (n,α) with boron-10 at 10 to 500 kev, absorption and total cross sections for, 20: 34513(R) (ANL-7179)
reactions (n,α) with boron-10 and lithium-6 at 10.7 to 247 kev, cross sections for, (T), 20: 34526 (NP-16125)
reactions (n,α) and (n,p) with nuclei at 14.8 Mev, cross sections for, (E), 20: 36212
reactions (n,α), (n,γ), (n,2n), and (n,p) with cadmium isotopes at 0.0005 to 15.0 Mev, cross sections for, 20: 36159 (GA-6997)
reactions (n,α), (n,γ), (n,2n), and (n,p) at 0.0005 to 15.0 Mev, cross sections for, 20: 36159 (GA-6997)
reactions (n,α) with bismuth-209, gold-197, iridium, silicon-28, silicon-29, and silver-107 at 12 to 23 Mev, (E), 20: 38036
reactions (n,α), (n,p), and (n,2n) with iron-54 and selenium isotopes at 14.4 Mev, cross sections for, (E), 20: 40079 (ORO-3346-2)
reactions (n,α) and (n,p) with nuclei, cross sections for, (E), 20: 40069(R) (EANDC(E)-66(U))
reactions (n,α) with nuclei, resonance activation integral cross sections for, (E), 20: 40069(R) (EANDC(E)-66(U))
reactions (n,α) with sodium-23 at 12.6 to 18.7 Mev, cross sections for, (E), 20: 40069(R) (EANDC(E)-66(U))
reactions (n,α) and (n,p) with nuclei, cross sections for, (E), 20: 40069(R) (EANDC(E)-66(U))
reactions (n,α) with germanium-73 at 14 Mev, cross sections for, (E), 20: 40098
reactions (n,α) with calcium-40 and fluorine-19 at 6 Mev, cross sections for, (E), 20: 40100
reactions (n,α_0) with carbon-12 at 16 and 17 Mev, total cross sections for, 20: 42367
reactions (n,α) with oxygen-16 at 14.9 Mev, alpha angular distribution from, (E), 20: 42370
reactions (n,α_0) with sulfur-32 from 2.5 to 3.2 Mev, differential cross sections for, (E), 20: 42375
reactions (n,α) with oxygen-16 and silicon-28, DWBA analysis of, (T), 20: 42391
reactions (n,α) with neon-20 and oxygen-16 at 14.1 Mev, angular distributions for, (E), 20: 42216
reactions (n,α) with nuclei, cross sections for, (T), 20: 44609 (CONF-660303, pp 315-27)
reactions (n,α) with boron-10 and lithium-6, cross sections by shell transmission method, 20: 44617 (CONF-660303, pp 701-12)
reactions (n,α) with lithium-6 at 25, 67, and 100 kev, cross sections for, (E), 20: 44620 (CONF-660303, pp 763-5)
reactions (n,α) and (n,p) with germanium-72, cross sections for, (E), 20: 46759
reactions (n,α) with lithium-7 and rhodium-103 at 14.7 Mev, cross sections for, (E), 20: 46614
reactions (n,α) with nuclei with $27 \leq A \leq 181$, ratio of forward to backward yields of recoil nuclei, (E), 20: 46614
reactions (n,α) with neon-20 at 14.5 Mev, alpha angular distribution from, (E), 20: 46616
reactions (n,α) and (n,p) with nickel-64 at 14.7 Mev, radioisotope production in, (E), 20: 46626
reactions (n,α), (n,2n), (n,p), and (n,pn) at 14.6 Mev, mechanisms and shell effects, 16: 12487
reactions (n,d) and (n,t) with nuclei, polarization in direct, 18: 36624
reactions (n,d) and (n,p) with helium-3 at 0.3 to 4 Mev, cross sections for, 18: 44725 (AWRE-O-78/64)
reactions (n,d) and (n,p) with nuclei, scintillation telescopes for, 19: 15891
reactions (n,d) and (n,p) with boron-10 at 14.4 Mev, differential cross sections for, (E), 19: 39798
reactions (n,d) with oxygen-16 at 14 Mev, distorted-wave approximation for, 18: 34774 (ORNL-P-144)
reactions (n,d) with sulfur-32 at 14 Mev, 18: 34818
reactions (n,d) with fluorine-19, phosphorus-31, and sulfur-32 and -34 at 14.1 Mev, cross sections for, 18: 38083(T) (AEC-tr-6398(p.157-63))
reactions (n,d) with oxygen-16 at 15 Mev, angular distributions for, 18: 44762
reactions (n,d) with nuclei, variational treatment of, (T), 19: 12528
reactions (n,d) with iodine-127, energy levels of tellurium-126 from, 19: 14533(R) (NYO-1082-1)
reactions (n,d) with sulfur-34, cross section for, 19: 14533(R) (NYO-1082-1)
reactions (n,d) with sulfur-32, energy levels of phosphorus-31 from, 19: 14533(R) (NYO-1082-1)
reactions (n,d) with nitrogen-15, effects of compound nucleus processes on, 19: 14533(R) (NYO-1082-1)
reactions (n,d) with tritium at 14.4 Mev, neutron-neutron scattering length from, (E), 19: 21404
reactions (n,d) with oxygen-16, local energy approximation for finite-range effects in, (T), 19: 23736
reactions (n,d) with silicon-28 at 14 Mev, (E), 19: 23782
reactions (n,d) with nuclei at 14.4 Mev, differential cross sections for, (E), 19: 35487
reactions (n,d) with fluorine-19, phosphorus-31, and sodium-23 at 14 Mev, (E/T), 19: 47644
reactions (n,d) with copper-63, nickel-58, and zinc-64 at 14 Mev, energy levels from, (E), 20: 4896
reactions (n,d) with ruthenium-100 and -102, cross sections for, (E), 20: 6338
reactions (n,d) with oxygen-16, exchange amplitudes for, (T), 20: 12126
reactions (n,d) with carbon-12, helium-4, lithium-6, and -7 at 152 Mev, energy spectra from, (E), 20: 28403
reactions (n,d) with nitrogen-14, nitrogen-15, sulfur-32, and sulfur-34 at 14 Mev, (E), 20: 38150
reactions (n,d) with copper isotopes at 14.08 Mev, angular distributions

from, (E), 20: 40069(R) (EANDC(E)-66(U))
reactions (n,d) with zinc-64, angular distributions from, (E), 20: 40069(R) (EANDC(E)-66(U))
reactions (n,d), (n,np), and (n,2n) with helium-4 near 20 Mev, 18: 28698
reactions (n,f) with uranium-235 at 0.025 ev to 8 Mev, energy dependence of average neutron number from, 18: 15253
reactions (n,f) with plutonium-239, plutonium-241, uranium-233, and uranium-235, resonance integrals for, 18: 21166 (CRRP-1183)
reactions (n,f) with uranium-235 and uranium-238 at 2.5 and 14 Mev, probability of ternary, 18: 21219
reactions (n,f) with uranium-235, beta decay and delayed gammas following, 18: 21297
reactions (n,f) with plutonium-241 at 2 to 100 ev, cross sections for, 18: 24586 (IDO-16976)
reactions (n,f) with plutonium-239 and uranium-233, -235, and -238, energy dependence of neutron yield from, 18: 24640
reactions (n,f) with uranium-235, alpha values for epithermal, 18: 28715
reactions (n,f) with uranium-235, alpha values for epithermal, 18: 28557
reactions (n,f) with uranium-232 at 4 to 400 ev, cross sections for, 18: 36611
reactions (n,f) with plutonium-241 at 0.2 to 100 ev, cross sections for, 18: 40505 (IDO-16995)
reactions (n,f) with plutonium-239 and protactinium-231 at 1.5 to 1500 kev, cross sections for, 18: 40526
reactions (n,f) with uranium-235 at 6 Mev, mass-energy relations for, 18: 44931(R) (ANL-6936(p.39-72))
reactions (n,f) with natural thorium at 14.7 Mev, yields in, 18: 44836
reactions (n,f) with natural uranium at 14.7 Mev, yields in, 18: 44835
reactions (n,f) with uranium-235, coupling effects in, (T), 19: 37839(T) (ANL-Trans-195)
reactions (n,f) with bismuth at 14.8 Mev, cross sections for, 19: 37872
reactions (n,f) with thorium-232 and uranium-238 at 14.5 Mev, yields from, 19: 43368
reactions (n,f) with plutonium-239 and uranium-235 at 24 kev, secondary-neutron yield from, (E), 19: 45279
reactions (n,f) with uranium-238 at 14.7 Mev, delayed neutron emission in, (E), 20: 28296
reactions (n,f) with uranium-235 at 14 Mev, statistical analysis of, (T), 20: 34568
reactions (n,f) with plutonium-239, uranium-233, and uranium-235, energy dependence of fission-fragment angular distribution in, (E), 20: 42171(T) (LA-tr-66-41)
reactions (n,f) with uranium isotopes, energy dependence of delayed-neutron yield in, (E), 20: 44670(T) (INDSWG-101, pp 158-63)
reactions (n,f) with plutonium-241 at 20 to 200 ev, cross sections for, (E), 20: 44625 (CONF-660303, pp 910-18)
reactions (n,f) with plutonium-241 at 0.01 to 0.5 ev, cross section for, (E), 20: 44635 (IN-1012)
reactions (n,f) with uranium-238 at 14.5 Mev, fission-fragment energies from, (E), 20: 46750
reactions (n,f) with thorium-232, delayed-neutron yield at threshold, (E), 20: 46787
reactions (n,f) with thorium-232 at 14.8 Mev, yields from, (E), 20: 46625
reactions (n,γ) with mercury-199, 19: 1053(R) (PR-P-62)
reactions (n,γ) with chlorine-37, chemical effects on recoil chlorine-38 from, 19: 459
reactions (n,γ) with aluminum-27, backscattering range from, 19: 3346
reactions (n,γ) with nuclei, bibliography on, 19: 5262
reactions (n,γ) with nuclei, spectra from, (E), 19: 8670
reactions (n,γ) with thorium-232 and uranium-238, cross sections for, (T), 19: 8409
reactions (n,γ) in butyl and propyl bromides, chemical effects of, 19: 13488
reactions (n,γ) with indium-115 at 1.4 to 9.1 ev, isomeric states in, 19: 16938
reactions (n,γ) with iron, molybdenum, and silver, cross sections for, (E), 19: 16958
reactions (n,γ) in potassium rhenium bromide–potassium tin chloride type mixed crystals, chemical effects of, 19: 15644
reactions (n,γ) with scandium-45, cascade transitions in, (E), 19: 16897
reactions (n,γ) with nuclei at 24 kev, cross sections for, (E), 19: 16935
reactions (n,γ) with iron-56 at 1.5 to 4.0 Mev, gamma spectra from, (E), 19: 19095 (WASH-1053)
reactions (n,γ) at 20 to 500 ev, cross sections for, (E), 19: 19095 (WASH-1053)
reactions (n,γ) with yttrium-89 at 225 to 925 kev, cross section for, (E), 19: 19095 (WASH-1053)
reactions (n,γ) with fluorine-19 spectra from resonance, (E), 19: 19185
reactions (n,γ) with gold and tantalum at 1 to 4 Mev, spectra from, (E/T), 19: 21317
reactions (n,γ) with niobium-93, spectra from, (E), 19: 21330
reactions (n,γ) with bromine-79 at 0.024 to 3.1 Mev, isomeric cross section ratio for, (E), 19: 21331
reactions (n,γ) with deuterons, elastic unitarity effects in, (T), 19: 21371
reactions (n,γ) and (n,2n) in metal phenyl compounds, recoil products from, 19: 22361
reactions (n,γ) with nuclei, polarization from, (E), 19: 23726
reactions (n,γ) with gold-197 at 13 to 683 kev, cross sections for, (E), 19: 27507
reactions (n,γ) with nuclei, gamma energies and half-lives in, 19: 29227 (AEET/ANAL/32)
reactions (n,γ) with uranium-235, strength functions for, (T), 19: 29249 (JINR-P-2068)
reactions (n,γ) with nuclei, spin cut-off coefficient for, (T), 19: 29341
reactions (n,γ) with uranium-235 at 0.002 to 30 kev, 19: 29247 (JINR-P-2024)
reactions (n,γ) with thallium-203, 19: 30126
reactions (n,γ) with calcium-42 and vanadium-51, energy levels from, (E), 19: 31241(R) (UCRL-12473(p.1-30))
reactions (n,γ) with triphenylarsine and tetraphenylgermane, 19: 30312
reactions (n,γ) with cadmium-113, gamma angular asymmetry from, (E/T), 19: 33371
reactions (n,γ) with argon-40, activation cross section for, (E), 19: 35378(R) (EANDC(E)-57(U))
reactions (n,γ), with silver-109, activation cross section for, (E), 19: 35378(R) (EANDC(E)-57(U))
reactions (n,γ) with iron-58 at 2200 m/sec, cross section for, (E), 19: 35378(U) (EANDC(E)-57(U))
reactions (n,γ) with manganese-55, spectra from, (E), 19: 35378(R) (EANDC(E)-57(U))
reactions (n,γ) with iron-56, spectra from, (E), 19: 35378(R) (EANDC(E)-57(U))
reactions (n,γ) with cobalt-59 at 10 to 400 Mev, spectra from, (E), 19: 35378(R) (EANDC(E)-57(U))
reactions (n,γ) with mercury-199 at 0.1 to 8 Mev, spectra from, (E), 19: 35378(R) (EANDC(E)-57(U))
reactions (n,γ) with nuclei in Mev range, level density from compound-nucleus, (T), 19: 35448
reactions (n,γγ') with chlorine-35, angular correlations in, (E), 19: 35426
reactions (n,γ) with nuclei, rotational-vibrational effects on spectra from, 18: 11162 (ANL-6797(p.89-110))
reactions (n,γ) with dysprosium-164, spectra from, 18: 11163 (ANL-6797(p.133-42))
reactions (n,γ) with samarium-150, conversion-electron spectrum from, 18: 11165 (ANL-6797(p.148-55))
reactions (n,γ) with nuclei, partial widths for E1 gamma rays and relation to giant resonance, 18: 11168 (ANL-6797(p.211-19))
reactions (n,γ) with heavy nuclei, gamma-ray M1 transitions from, 18: 11169 (ANL-6797(p.220-9))
reactions (n,γ) with tin isotopes, gamma spectra from resonance, 18: 11170 (ANL-6797(p.230-5))
reactions (n,γ) with calcium-48, gamma spectrum from, 18: 11171 (ANL-6797(p.243-6))
reactions (n,γ) with deuterium, cross section and gamma yield using polarized neutrons, 18: 11172 (ANL-6797(p.247-58))
reactions (n,γ) with nuclei, variation of the energy of, 18: 11174 (ANL-6797(p.271-4))
reactions (n,γ) with niobium-93, total radiation widths for s- and p-wave, 18: 11177 (ANL-6797(p.294-300))
reactions (n,γ) with nuclei, partial radiation widths of, 18: 11179 (ANL-6797(p.322-3))
reactions (n,γ) with tungsten-184, coincidence gamma spectra from resonance, 18: 11180 (ANL-6797(p.324-32))
reactions (n,γ) with uranium-239, fluctuations in partial widths for, 18: 11181 (ANL-6797(p.333-41))
reactions (n,γ) with nitrogen-15, resonance, 18: 11182 (ANL-6797 (p.342-57))
reactions (n,γ) with rhodium-105, cross section for, 18: 11186 (ANL-6797(p.388))
reactions (n,γ) of polarized, nuclear polarization from, 18: 11188 (ANL-6797(p.397-403))
reactions (n,γ) with dysprosium-163 and lutetium-176, spectra from, 18: 10366 (ANL-6797(p.111-32))
reactions (n,γ) with nuclei, measurement of gamma spectra from, 18: 10367 (ANL-6797(p.156-78))
reactions (n,γ) with gadolinium-155, transition intensities for, 18: 11284
reactions (n,γ) with nuclei, collective-model relation to gamma spectra from, 18: 11167 (ANL-6797(p.194-210))
reactions (n,γ) with tin-118, -120, and -124, p-wave resonances of, 19: 39784 (ORNL-P-1352)
reactions (n,γ) with rhenium-185 and -187 at 4 kev to 6 Mev, cross sections for, (E), 19: 40112(R) (ANL-7046(p.36-66))
reactions (n,γ) with nuclei, gamma spectra of resonances of, (E), 19: 39781 (JAERI-1073)
reactions (n,γ) with iodine-127 at 0.025 ev and 24 kev, cross sections, (E), 19: 39816

reactions (n,γ) with mercury isotopes at 20 to 210 ev, spectra from (E), 19: 40896
reactions (n,γ) with vanadium, vanadium-52 energy levels from, (E), 19: 41725
reactions (n,γ) with chromium isotopes, gamma spectra from, (E), 19: 41807(T)
reactions (n,γ) with mercury-199, mercury-200 parity assignments from, 19: 41846
reactions (n,γ) with rhenium-185 in mixed crystals, chemical transformations from, 19: 40585
reactions (n,γ) with xenon-126, cross sections for, (E), 19: 43313
reactions (n,γ) with tellurium-128 and -130 in telluric acid, chemical and nuclear transformations in, 19: 42566
reactions (n,γ) with boron-11 at 20 kev, cross sections for, (E), 19: 45246(R) (ANL-6877,pp 5-14)
reactions (n,γ) with uranium-235 at 0.002 to 30 kev, cross sections for, (E), 19: 45292 (BNL-tr-16)
reactions (n,γ) with tungsten-187, cross section for, 19: 44599(R) (GEMP-50A)
reactions (n,γ) with yttrium-89 at 0.145 to 1.225 Mev, cross sections and isomer ratios for, (E), 19: 45376
reactions (n,γ) in chromium oxides, reactions of recoils from, 19: 46398
reactions (n,γ) with manganese-55 to 10 kev, cross sections for, (E/T), 19: 47634
reactions (n,γ) with arsenic-75, gamma spectra from, (E), 20: 3011 (IPA-NR-22)
reactions (n,γ) with nuclei at 1 ev to 50 kev, cross sections for, (E), 20: 3032
reactions (n,γ) with nuclei, level studies from, 20: 4821(R) (ANL-7081, pp 2-21)
reactions (n,γ) with hydrogen, gamma spectra from, (E), 20: 4856
reactions (n,γ) with cesium-133, rhenium-187, and scandium-45, isomeric cross section ratios for, (E/T), 20: 6301 (TID-22165)
reactions (n,γ) with americium-241, separation of daughters from, (E), 20: 5823(T) (ORNL-tr-892)
reactions (n,γ) with lutetium-175 and molybdenum-98 at 0.4 to 3 Mev, cross sections for, (E), 20: 6556(R) (ANL-7105, pp 36-58)
reactions (n,γ) with gold-197, gold-198 resonance parameters and spins from, (E), 20: 6392
reactions (n,γ) with nuclei, gamma spectra from, (T), 20: 6427
reactions (n,γ) of polarized, with nuclei, automation of experiments on, 20: 7388
reactions (n,γ) with nuclei at 0.1 to 15 Mev, cross section tabulations for, 20: 8084 (UCRL-14007(Rev. 1))
reactions (n,γ) with osmium-184 and -190, cross sections for, (E), 20: 8175
reactions (n,γ) with nickel-64 at 0.176 to 1.958 Mev, cross sections for, (E), 20: 9981 (WASH-1064)
reactions (n,γ), with yttrium-89 at 0.14 to 1.22 and 14.5 Mev, cross sections for, (E), 20: 9981 (WASH-1064)
reactions (n,γ) with oxygen-18 at 205.2 to 979.8 kev, cross sections for, (E), 20: 9981 (WASH-1064)
reactions (n,γ) with gold-197 at 0.14 to 1.22 Mev, cross sections for, (E), 20: 9981 (WASH-1064)
reactions (n,γ) with cadmium-113 at 18 kev, gamma spectra from, (E), 20: 9244(R) (ANL-7029, pp 4-8)
reactions (n,γ) with phosphorus-31 in triphenylphosphine and triphenylphosphine oxide, 20: 9003
reactions (n,γ) with bromine-81 in carbon tetrachloride and n-hexane, ground-state and isomeric bromine-82 production from, 20: 10938
reactions (n,γ) with cobalt-59 in cobalt complexes, chemical effects of, 20: 14584(R) (TID-22444)
reactions (n,γ) and (n,p) with sulfur in cysteic acid, cysteine, and cystine, recoil chemistry of, 20: 14584(R) (TID-22444)
reactions (n,γ) with ytterbium isotopes, resonances in, (E), 20: 15839
reactions (n,γ) with palladium-110 and tellurium-130, isomeric cross-section ratios in, (E), 20: 15777
reactions (n,γ) with uranium-238 at 0.01 to 3 Mev, cross sections for, (T), 20: 17720
reactions (n,γ) with copper-64 and gold-197, threshold cross sections and energies for, 20: 16335(R) (NBS-TN-276)
reactions (n,γ) with silicon-28, silicon-29 levels from, (E), 20: 19846
reactions (n,γ) and (n,n′) with gold-197 and rhodium-103, resonances in, (E), 20: 19866
reactions (n,γ) with rhenium-185 at 4 kev to 2.6 Mev, cross sections for, (E), 20: 21969(R) (ANL-7055, pp 230-3)
reactions (n,γ) with rhenium-187 at 4 kev to 7.6 Mev, cross sections for, (E), 20: 21969(R) (ANL-7055, pp 230-3)
reactions (n,γ) with rhodium-103, gamma spectra from, (E), 20: 15754
reactions (n,γ) with gold-197 at 24.8 kev, cross sections for, (E), 20: 24378
reactions (n,γ) with krypton-78, production of krypton-79 by, 20: 26089 (ORNL-3839)
reactions (n,γ) with iodine-127 and -129, production of isomeric xenon-129 and -131 by, 20: 26089 (ORNL-3839)
reactions (n,γ) with nuclei, cross sections for, 20: 26095 (SGAE-PH-34/1965)
reactions (n,γ) with mercury near 5 Mev, gamma spectra from, (E), 20: 30358(R) (RPI-328-56, pp 1-48)
reactions (n,γ) with gold-197 and yttrium-89, cross sections for, (E), 20: 30360 (WASH-1068)
reactions (n,γ) with indium-113 and -115, cross sections for, (E), 20: 30360 (WASH-1068)
reactions (n,γ) with cobalt-59, gamma spectra from, (E), 20: 30360 (WASH-1068)
reactions (n,γ), with vanadium-51, manganese-55, copper-63, copper-65, and iodine-127 at 0.1 to 14 Mev, cross sections for, (T), 20: 30378
reactions (n,γ) with hydrogen, deuteron binding energy from, (E), 20: 32488
reactions (n,γ) with nuclei, method for calculating cross sections for, 20: 32374(R) (IITRI-578P25-15)
reactions (n,γ) with protactinium-231, uranium-232 yields from, 20: 34550
reactions (n,γ) with lanthanum-140, cross section for, (E), 20: 34614
reactions (n,γ) with samarium-149, conversion electron spectra from, (E), 20: 34637
reactions (n,γ) with cobalt-59, production of cobalt-60 in, 20: 35576
reactions (n,γ) with nuclei, spectroscopy of, 20: 36191
reactions (n,γ) and (n,n) with uranium-238 at 5 to 1000 ev, cross sections and resonance parameters for, (E), 20: 36202
reactions (n,γ) with chlorine-35, M1 transitions in, (T), 20: 36208
reactions (n,γ) with tungsten isotopes, energy levels from, (E), 20: 39470(R) (ORNL-3924)
reactions (n,γ) with tin isotopes, gamma spectra of, (E), 20: 39470(R) (ORNL-3924)
reactions (n,γ) with nickel-64, nickel-65 production in, 20: 40081 (PAEC(D)IS-653)
reactions (n,γ) with hafnium-178, hafnium-179 decay scheme from, (E), 20: 42285
reactions (n,γ) with palladium-108 and silver-109, preparation of carrier-free silver-111 by, 20: 41023
reactions (n,γ) with nuclei, cross sections for, (T), 20: 44609 (CONF-660303, pp 315-27)
reactions (n,γ) with hafnium-178 and ytterbium-176, energy-level transitions in isomeric hafnium-179 and ytterbium-177 from, (E), 20: 44709
reactions (n,γ) with germanium and selenium, effects of energy on isomeric cross section ratios in, 20: 44816
reactions (n,γ) with molybdenum-100, 20: 44817
reactions (n,γ), cross section calculation, 16: 19766
reactions (n,He-3) with arsenic-75, cobalt-59, manganese-55, and rhodium-103 at 14.8 Mev, (E), 19: 14615
reactions (n,He-3) with cesium-133 at 14.7 Mev, cross sections for, (E), 19: 25496
reactions (n,He-3) with nuclei at 14.8 Mev, effective cross sections for, (E), 20: 15739
reactions (n,n′) and (n,2n) with lead-208, neutron source yield measurements by, 19: 29186
reactions (n,nˢ) and (n,p) with excited nuclei, cross sections for direct, (T), 20: 17714
reactions (n,nˆ) with carbon-12 at 15 to 80 Mev, 18: 24642
reactions (n,n′) with indium-115, cross section for, (E), 19: 35378(R) (EANDC(E)-57(U))
reactions (n,nˆ) with carbon-12 at 13 to 18 Mev, 3α decay mode cross section for, (E), 20: 4878
reactions (n,n′)3α with carbon-12 at 15.55 Mev, (E), 19: 10299
reactions (n,n′ γ) with Z = 3 to 92 nuclei at 1.0, 4.0, and 14.8 Mev, cross sections and spectra for, 18: 30736(R) (TID-20658)
reactions (n,n′γ) with copper at 0.7 to 1.4 Mev, cross sections for, 18: 42619 (AE-150)
reactions (n,n′γ) with nuclei at 0.3 to 2.6 Mev, excitation cross sections for, (E/T), 19: 31284
reactions (n,n′γ) with nuclei at 0 to 14 Mev, energy absorption in, 19: 39769 (SC-DC-65-1544)
reactions (n,n′γ) with bismuth-209, gold-197, and lead-206, gamma spectra from, (E), 19: 41669 (LA-DC-7096)
reactions (n,n′γ) with yttrium-89 at 14 Mev, cross sections for, 19: 41781
reactions (n,n′γ) with nuclei for $60 \geq A \geq 100$, cross sections for, 19: 45263 (JAERI-1078)
reactions (n,n′γ) with aluminum-27 at 3.5 to 4.5 Mev, gamma angular distributions from, (E/T), 19: 47588(R) (TID-22012, pp 22-52)
reactions (n,n′γ) with magnesium and silicon at 3.0 to 4.35 Mev, gamma angular distributions from, (E/T), 19: 47589(R) (TID-22012, pp 53-66)
reactions (n,n′γ) with argon-40 at 3.0 to 4.5 Mev, gamma angular distributions from, (E/T), 19: 47590(R) (TID-22012, pp 67-98)
reactions (n,n′γ) with iron-56 at .97 to 4.76 Mev, gamma angular distributions and cross sections from, (E/T), 19: 47591(R) (TID-22012, pp 99-128)

reactions (n,n'γ) with lead-206, -207, and -208 at 1.0 to 4.6 Mev, gamma angular distributions from, (E/T), 19: 47592(R) (TID-22012, pp 129-55)
reactions (n,n'γ) with boron-10 and -11, calcium-40, cerium, cobalt, and uranium at 3.0 to 14.8 Mev, gamma angular distributions and cross sections from, (E/T), 19: 47594(R) (TID-22012, pp 176-205)
reactions (n,n'γ) with cerium-140 at 3.25 Mev, gamma angular distributions from, (E), 20: 9981 (WASH-1064)
reactions (n,n'γ) with argon-40 at 3.0 to 4.5 Mev, (E/T), 20: 10093
reactions (n,n'γ) with iron-56 at 0.95 to 4 Mev, cross sections and gamma angular distributions from, (E), 20: 12108
reactions (n,n'γ) with iron-56 at 0.95 to 4.0 Mev, angular distributions and level parities and spins from, (E), 20: 17736
reactions (n,n'γ) with aluminum, carbon, iron, lead, and oxygen at 14 Mev, cross sections for, 20: 30498
reactions (n,n'γ) with nuclei, elemental analysis by, 20: 27170 (UCRL-14654-T)
reactions (n,n'γ) with boron-10 and iron at 2 to 15 Mev, gamma spectra from, (E), 20: 30358(R) (RPI-328-56, pp 1-48)
reactions (n,n'γ) with nuclei near 4 Mev, gamma production cross sections for, (E/T), 20: 34515 (CONF-660303-34)
reactions (n,n) and (n,p) with helium-3, measurement of cross sections for, 18: 30736(R) (TID-20658)
reactions (n,n) and (n,γ) with lithium-7, cross sections for, (T), 19: 39820
reactions (n,n') with rhodium-103, evaluation of activation for use as threshold detector, 18: 30748
reactions (n,n) with nuclei, field model for, 19: 27467
reactions (n,n) with helium-3 to 1.5 Mev, phase-shift analysis of, 20: 3060
reactions (n,pn) with zirconium-90 at 14 Mev, production of yttrium-89 isomers in, (E), 19: 47566 (AERE-R-5009)
reactions ($n,p_{0,1}$) with silicon-28 at 5.2 to 7.2 Mev, cross sections for, (E), 19: 35378(R) (EANDC(E)-57(U))
reactions (n,p) and (n,γ) with tritium at 14.4 Mev, (E), 19: 21405
reactions (n,p) and (n,α) with elements, helium and hydrogen production in alloys from, 19: 26901
reactions (n,p) and (n,2n) with silicon at 14 Mev, ionization energy of reaction products from, 19: 29236 (GA-6136)
reactions (n,p) at 14 Mev, theory for, 18: 14592(R) (PR-P-60)
reactions (n,p) at 14 Mev, shell effects in, 18: 44789
reactions (n,p) of, emulsion plate camera for measuring, 18: 25866
reactions (n,p) on helium-3, energy distribution function for production of tritium by, 18: 37230
reactions (n,p) on tetraphenylgermanium, formation of recoil products in, 18: 43673
reactions (n,p) on cobalt-59 and zinc-64, production of carrier-free copper-64 and iron-59 by, 19: 30267
reactions (n,p) with magnesium-24, use for production of carrier-free sodium-24, 18: 12523 (SGAE-1963/3B)
reactions (n,p) with titanium-47 at 2.0 to 3.6 Mev, cross section of, 18: 15296
reactions (n,p) with nickel-58 at 2 to 6 Mev, ratio for ground- and isomeric-state production in, 18: 19060
reactions (n,p) with titanium-46, -48, and -50 at 14.7 Mev, cross sections for, 18: 18924
reactions (n,p) with silicon-28 at 14.1 Mev, exchange effects and finite range in, 18: 18998
reactions (n,p) with nuclei, optical model analysis of, 18: 21165 (CONF-490-1)
reactions (n,p) with nuclei at 14 Mev, cross section fluctuations in, 18: 28682
reactions (n,p) with deuterium at 13.6 Mev, spectra of, 18: 28684
reactions (n,p) with deuterium, phenomenological analysis of, 18: 28697
reactions (n,p) with iron-56 up to 20.3 Mev, 18: 28588
reactions (n,p) with nuclear emulsions, 18: 30747
reactions (n,p) with sulfur-32 for preparation of carrier-free phosphorus-32, 18: 32002
reactions (n,p) with tin-112 and -124 at 14.1 Mev, 18: 32865
reactions (n,p) with iron-54, cross section of, 18: 34885
reactions (n,p) with sulfur-32, absolute measurement of yields from, 18: 36751 (ANL-6912)
reactions (n,p) with nuclei at 50 to 150 Mev, 18: 42695
reactions (n,p) with magnesium-24, 19: 1053(R) (PR-P-62)
reactions (n,p) with iron-54 and zirconium at 3.55 to 6.02 Mev, cross sections for (E), 19: 3383
reactions (n,p) with iron-54 at 2.3 to 3.5 Mev, cross sections for (E), 19: 3230 (AE-160)
reactions (n,p) with oxygen-18 at 19 Mev, nitrogen-18 production in, (E), 19: 5225
reactions (n,p) with nickel-60 and titanium-46 at 12.5 to 16.5 Mev, cross sections for, (E), 19: 6666
reactions (n,p) with chlorine-35 to prepare sulfur-35, 19: 9572
reactions (n,p) with silicon-28, angular distributions from, (E), 19: 11526
reactions (n,p) with nuclei, Green's functions for, (T), 19: 12606
reactions (n,p) with deuterium, angular distributions from, (E), 19: 12612
reactions (n,p) with nuclei, use for neutron spectral analysis, 19: 11532
reactions (n,p) with oxygen-16 in water, nitrogen-16 specific activity from, (T), 19: 14847 (WAPD-BT-31(p.37-42))
reactions (n,p) with iron-56 at 13.4 to 14.2 Mev, cross section variation for, (E), 19: 14612
reactions (n,p) with chlorine-35, fast neutron detection with, 19: 14619
reactions (n,p) with ethyl and methyl chlorides and methane, sulfur-35-labeled products in, 19: 13495
reactions (n,p) with iron-54 at 2.2 to 6.2 Mev, cross sections for, (E), 19: 19095 (WASH-1053)
reactions (n,p) with nickel-58, cobalt-58 production in, 19: 17984
reactions (n,p) with iron-56 at 12.6 to 19.6 Mev, (E), 19: 21290
reactions (n,p) with chlorine-35 in various chlorides, protective effects against oxidation of sulfur produced in, 19: 20004
reactions (n,p) with cobalt-59 at 14.8 Mev, cross sections for, (E), 19: 23725
reactions (n,p) with silicon-28 at 14 Mev, (E), 19: 23782
reactions (n,p) with deuterium at 14.4 Mev, phenomenological model analysis of, (T), 19: 23811
reactions (n,p) with helium-3, resonances in, (T), 19: 25537
reactions (n,p) with oxygen-16, flux determination using, 19: 28627 (EUR-1815.e(Rev.)(p.235-40))
reactions (n,p) with nickel-58 at 8.4 to 22 Mev, angular and energy distributions from, (E), 19: 29286
reactions (n,p) with nickel-58 at 22 Mev, angular and energy distributions from, (E), 19: 29286
reactions (n,p) with nuclei, cross sections for, (T), 19: 29323
reactions (n,p) with nickel-58 at 1.04 to 2.67 Mev, cross sections and isomer ratios for, (E), 19: 31215(R) (ANL-7010(p.1-19))
reactions (n,p) with polarized helium-3 at 0.117 ev, 19: 35374 (BNL-9195)
reactions (n,p) with potassium-41 at 3.2 to 8.4 Mev, cross sections for, (E), 19: 35378(R) (EANDC(E)-57(U))
reactions (n,p) with calcium-42 at 3.0 to 8.5 Mev, cross sections for, (E), 19: 35378(R) (EANDC(E)-57(U))
reactions (n,p) with calcium-44 at 5.6 to 8.5 Mev, cross sections for, (E), 19: 35378(R) (EANDC(E)-57(U))
reactions (n,p) with nickel-58 at 14.1 Mev, cross section for, (E), 19: 35378(R) (EANDC(E)-57(U))
reactions (n,p) with fluorine-19 at 12.5 to 19.6 Mev, cross sections for, (E), 19: 35378(R) (EANDC(E)-57(U))
reactions (n,p) with titanium-46 at 12.5 to 19.6 Mev, cross sections for, (E), 19: 35378(R) (EANDC(E)-57(U))
reactions (n,p) with titanium-48 at 12.5 to 19.6 Mev, cross sections for, (E), 19: 35378(R) (EANDC(E)-57(U))
reactions (n,p) with iron-56, cross section for, (E), 19: 35378(R) (EANDC(E)-57(U))
reactions (n,p) with iron-56 at 12.6 to 19.6 Mev, cross sections for, (E), 19: 35378(R) (EANDC(E)-57(U))
reactions (n,p) with nickel-60 at 12.6 to 16.6 Mev, cross sections for, (E), 19: 35378(R) (EANDC(E)-57(U))
reactions (n,p) with titanium-46 at 12.6 to 16.6 Mev, cross sections for, (E), 19: 35378(R) (EANDC(E)-57(U))
reactions (n,p) with closed-shell nuclei, effective two-body interaction in, (T), 19: 35470
reactions (n,p) with nitrogen-14 in air, ionization yields of, (E), 19: 35420
reactions (n,p) with helium-3 at 4 to 300 kev, cross sections for, (E), 19: 37828 (ORNL-P-1375)
reactions (n,p) with iron-54 at 3.55 to 17.4 Mev, cross sections for, (E), 19: 37846
reactions (n,p) with neon-22 at 14.8 Mev, fluorine-22 production in, (E), 19: 47671
reactions (n,p) with iron-56 at 14 Mev, cross sections for, (E), 19: 47673
reactions (n,p) with copper-65 at 14 Mev, cross sections for, 19: 47673
reactions (n,p) with calcium-42 and calcium-43, cross sections for, 20: 1947
reactions (n,p) with nickel isotopes at 14 Mev, angular and energy distributions from direct, (E), 20: 6440
reactions (n,p) with ruthenium-99 and -101 at 14.7 Mev, cross sections for, (E), 20: 6338
reactions (n,p) with ruthenium-102 and -104 at 14.7 Mev, cross sections for, (E), 20: 6338
reactions (n,p) with chlorine-37 at 13.0 to 20.2 Mev, cross sections for, (E/T), 20: 6357
reactions (n,p) with sulfur-33, phosphorus-33 production in, (E), 20: 8178(P)
reactions (n,p) with oxygen-18 at 14.7 to 18.6 Mev, cross sections for, (E), 20: 9981 (WASH-1064)
reactions (n,p) with iron-54 at 2.3 to 3.8 Mev, cross sections for, 20: 10006
reactions (n,p) with magnesium-24 at 12.6 to 19.6 Mev, cross sections for, (E), 20: 9990

reactions (n,p) with light nuclei at 14.8 Mev, cross sections for, (E), 20: 12133
reactions (n,p) with neon at 14.1 Mev, (E), 20: 12118
reactions (n,p) with helium-3 and nitrogen-14, excitation functions for, (E), 20: 13741
reactions (n,p) with sulfur-33, cross sections for, (E), 20: 14461(R) (ORNL-3889, pp 48-70)
reactions (n,p) with cesium-133 and gallium-69 at 14.6 Mev, isomeric cross section ratio for, (E/T), 20: 15773
reactions (n,p) with cesium-133 and gallium-69 at 14.6 Mev, isomeric cross section ratio for, (E/T), 20: 15773
reactions (n,p) with magnesium-24 and nickel-58, threshold cross sections and energies for, 20: 16335(R) (NBS-TN-276)
reactions (n,p) with potassium-41, cross sections for, (E/T), 20: 17809
reactions (n,p) with silicon-28 at 9.1 to 21 Mev, angular distributions from, (E/T), 20: 19813 (IKF-14)
reactions (n,p) with tin isotopes at 14 Mev, cross sections for production of isomeric indium isotopes from, (E), 20: 19939
reactions (n,p) with helium-3 gas, pressure wave generation in, (T), 20: 21803
reactions (n,p) with deuterium at 8.4, 14.1, and 22 Mev, proton spectra from, (E), 20: 24415
reactions (n,p) with nickel-58, recoil-ion ranges from, (E), 20: 24423
reactions (n,p) with nuclei at 14.8 Mev, cross sections for, (E), 20: 30394
reactions (n,p) with sulfur-33, effective cross sections for, (E), 20: 24424
reactions (n,p) with neon at 14.1 Mev, analysis of, (E), 20: 24429
reactions (n,p) with nickel at 14 Mev, proton spectra from, (E), 20: 26226
reactions (n,p) with iron and nickel at 0.82 to 3.7 Mev, cross sections for, 20: 28746(R) (GEAP-4795)
reactions (n,p) with deuterium at 152 Mev, cross sections and peak widths from, (E), 20: 28404
reactions (n,p) with zinc-64 at 14.8 Mev, cross sections for, (E), 20: 28447
reactions (n,p) with zirconium isotopes, cross sections for, (E), 20: 30418
reactions (n,p) with iron-56 at 13.5 to 14.8 Mev, cross sections for, (E), 20: 32528
reactions (n,p) with phosphorus-32, cross section for, (E), 20: 34557
reactions (n,p) with nickel-58, production of cobalt-58 in, 20: 35576
reactions (n,p) with aluminum-27, calculations using finite-range distorted-wave Born approximation, (T), 20: 38112
reactions (n,p) with nuclei, cross sections for, (T), 20: 44609 (CONF-660303, pp 315-27)
reactions (n,p) with tritium at 20.8 Mev, search for three-body neutron bound state in, (E), 20: 44650 (ORNL-P-2412)
reactions (n,p) with helium-3, spin dependence of, (E), 20: 44804
reactions (n,p) with tritium at 20.8 Mev, trineutrons from, (E), 20: 44809
reactions (n,p) with nuclei with $14 \leq A \leq 190$ at 14.7 Mev, cross sections for, (E), 20: 46614
reactions (n,p), with nuclei, cross sections for, 19: 29228(R) (AEET/NP/10)
reactions (n,t) with boron-10 at 14.4 Mev, triton angular distributions in, 18: 34830
reactions (n,t) with lithium-7 at 14.4 Mev, triton spectrum from, 18: 44808
reactions (n,t) with lithium-6, use for neutron spectral analysis, 19: 11532
reactions (n,t) with lithium-6, use for neutron spectral analysis, 19: 11534
reactions (n,t) with nitrogen-14, energy levels of carbon-12 from, 19: 14533(R) (NYO-1082-1)
reactions (n,t) with lithium-6 at 60 to 100 kev, angular distributions from, (E), 19: 27515
reactions (n,t) with lithium-6, cross sections for, (T), 20: 1180
reactions (n,t) with nitrogen-14 at 14 Mev, (E), 20: 38150
reactions (n,xγ) with $Z = 3$ to 92 nuclei at 14.8 Mev, cross sections and gamma spectra for, 18: 30736(R) (TID-20658)
reactions (n,xn) with polonium-210, production of polonium-208 and -209 in, 18: 19465(R) (MLM-1160)
reactions (n,xn) with tritium at 14.1 Mev, charged-particle spectra in, (E), 19: 39939
reactions (n,2nf) with uranium-235 at 9 to 18 Mev, fragment mass yields in, (E), 19: 12587
reactions (n,2np) with deuterium, models for, (T), 19: 6630 (AD-601793)
reactions (n,2n2p) with aluminum-27, threshold cross section and energy for, 20: 16335(R) (NBS-TN-276)
reactions (n,2n) and (n,p) with nuclei, cross sections for positron production in, 18: 13061
reactions (n,2n) with erbium-170, europium-151, thallium-205, and ytterbium-176 at 14.8 Mev, cross sections for, 18: 19036
reactions (n,2n) with nuclei at 14 Mev, isomeric cross-section ratios for, 18: 18966
reactions (n,2n) with nuclei, neutron angular correlations for, 18: 18963
reactions (N,2N) with nuclei, calculations of energy-level densities from, 18: 24596 (NP-13930(p.14))
reactions (n,2n) with nuclei at 14 Mev, cross section fluctuations in, 18: 28682
reactions (n,2n) with tin-112 and -124 at 14.1 Mev, 18: 32865
reactions (n,2n) and (n,np) with nuclei above 100 Mev, cross sections for, 18: 40514 (NYO-10693)
reactions (n,2n) and (n,p) with nuclei, cross sections for, (E), 19: 5230
reactions (n,2n) with sodium-23 at 12.5 to 16.5 Mev, cross sections for, (E), 19: 6666
reactions (n,2n) with nuclei at 14.8 Mev, cross sections for, (E), 19: 12592
reactions (n,2n) with beryllium-9 at 14 Mev, excited states in, (E), 19: 12502
reactions (n,2n) with nuclei at 14 Mev, shell effects in, (T), 19: 12536
reactions (n,2n) with nuclei, statistical model analysis of cross sections for, (T), 19: 14503 (BNL-897)
reactions (n,2n) and (n,3n) with uranium-233 at 4 to 15 Mev, cross sections for, (E/T), 19: 14501 (AWRE-O-100/64)
reactions (n,2n) with copper-65 at 13.4 to 14.2 Mev, cross section variation for, (E), 19: 14612
reactions (n,2n) with erbium-170, europium-151, thallium-205, and ytterbium-176, (E), 19: 14614
reactions (n,2n) with beryllium-9, effects on reactivity of beryllium-containing reactors, (T), 19: 17223
reactions (n,2n) with copper-63 at 14.1 Mev, cross section for, (E), 19: 19117
reactions (n,2n) with copper-63 at 12.6 to 19.6 Mev, (E), 19: 21290
reactions (n,2n) with beryllium, 19: 25020
reactions (n,2n) with nuclei at 14.8 Mev, isomeric cross section ratios in, (E), 19: 27517
reactions (n,2n) with potassium-39 at 13.1 to 23.5 Mev, cross sections for, (E), 19: 35378(R) (EANDC(E)-57(U))
reactions (n,2n) with nickel-58 at 14.1 Mev, cross section for, (E), 19: 35378(R) (EANDC(E)-57(U))
reactions (n,2n) with cobalt-59 at 14.1 Mev, cross section for, (E), 19: 35378(R) (EANDC(E)-57(U))
reactions (n,2n) with fluorine at 12.5 to 19.6 Mev, cross sections for, (E), 19: 35378(R) (EANDC(E)-57(U))
reactions (n,2n) with potassium-39 at 12.5 to 19.6 Mev, cross sections for, (E), 19: 35378(R) (EANDC(E)-57(U))
reactions (n,2n) with titanium-46 at 12.5 to 19.6 Mev, cross sections for, (E), 19: 35378(R) (EANDC-(E)-57(U))
reactions (n,2n) with gallium-69 at 12.5 to 19.6 Mev, cross sections for, (E), 19: 35378(R) (EANDC(E)-57(U))
reactions (n,2n) with niobium-93, cross section for, (E), 19: 35378(R) (EANDC(E)-57(U))
reactions (n,2n) with copper-63 at 12.6 to 19.6 Mev, cross sections for, (E), 19: 35378(R) (EANDC(E)-57(U))
reactions (n,2n) with nickel-58 at 12.6 to 19.6 Mev, cross sections for, (E), 19: 35378(R) (EANDC(E)-57(U))
reactions (n,2n) with copper-65 at 12.6 to 19.6 Mev, cross sections for, (E), 19: 35378(R) (EANDC(E)-57(U))
reactions (n,2n) with zinc-64 at 12.6 to 19.6 Mev, cross sections for, (E), 19: 35378(R) (EANDC(E)-57(U))
reactions (n,2n) with sodium-23 at 12.6 to 16.6 Mev, cross sections for, (E), 19: 35378(R) (EANDC(E)-57(U))
reactions (n,2n) with cobalt-59 at 12.6 to 16.6 Mev, cross sections for, (E), 19: 35378(R) (EANDC(E)-57(U))
reactions (n,2n) with copper-65, nickel-58, and zinc-64 at 12.6 to 19.6 Mev, (E), 19: 35441
reactions (n,2n) with deuterium, theoretical description of, 19: 37901
reactions (n,2n) with molybdenum-92 at 14.8 Mev, isomer production in, (E), 19: 39790
reactions (n,2n) with fluorine-19 and nitrogen-14 at 14.6 Mev, total cross sections for, (E), 19: 39797
reactions (n,2n) with iodine-127, search for 2.6-hr iodine-126m in, 19: 41716
reactions (n,2n) with neodymium-142, samarium-144, terbium-159, and erbium-168 at 14 Mev, production of isomeric states in, (E), 19: 41781
reactions (n,2n) with scandium-45 at 14 Mev, (E), 19: 47596(R) (TID-22141, pp 94-7)
reactions (n,2n) with nuclei ($Z \sim 28$) at 12.6 to 19.6 Mev, excitation functions for, (E/T), 19: 47571 (EUR-2456.e)
reactions (n,2n) with medium and heavy nuclei, cross sections for, (T), 20: 1187
reactions (n,2n) with copper-63 at 16.59 to 17.71 Mev, excitation curve for, (E), 20: 6319
reactions (n,2n) with beryllium-9 at 14 Mev, excitation and decay mechanisms of, (E), 20: 6320
reactions (n,2n) with beryllium-9, effects on slowing-down in beryllia and beryllium, (T), 20: 8042 (TID-22446)

reactions (n,2n) with manganese-55 at 12.6 to 19.6 Mev, cross sections for, (E), 20: 9990
reactions (n,2n) with cobalt-59 at 12.6 to 19.6 Mev, cross sections for, (E), 20: 9990
reactions (n,2n) with organic halides, chemical effects of, 20: 9007
reactions (n,2n) with phosphorus-31 at 14.8 Mev, cross section for, (E), 20: 12134
reactions (n,2n) with nuclei, cross sections for, (E/T), 20: 12040
reactions (n,2n) with neodymium-142 at 14.7 Mev, neodymium-141 production from, (E), 20: 13864
reactions (n,2n) with nuclei at 12 to 18 Mev, cross sections for, (E), 20: 15863
reactions (n,2n) with rubidium-85, cross section for, (E), 20: 14461(R) (ORNL-3889, pp 48-70)
reactions (n,2n) with osmium-192 at 14.6 Mev, isomeric cross section ratio for, (E/T), 20: 15773
reactions (n,2n) with scandium-45 at 14 Mev, scandium-44 isomeric yield ratio from, (E), 20: 17777
reactions (n,2n) with calcium-48, effective cross sections for, 20: 19943
reactions (n,2n) with beryllium-9 above 2.7 Mev, integral cross section for, (E), 20: 24419
reactions (n,2n) and (n,p) with nickel-58 at 13.2 to 15.5 Mev, cross sections for, (E), 20: 34518 (INR-680/1/PH)
reactions (n,2n) with nuclei, cross section for, (T), 20: 34623
reactions (n,2n) with vanadium-51, cross section for, (E), 20: 34624
reactions (n,2n) with nuclei at 14.5 Mev, cross section predictions from adjacent nuclei (α,2n) and (p,2n) reactions, (T), 20: 36178 (UCRL-14575)
reactions (n,2n) with cobalt-59 at 13.2 to 15.7 Mev, isomeric pair production cross sections for, (E/T), 20: 36164 (INR-668/1/PH)
reactions (n,2n) with beryllium-9, neutron-neutron bound state in, (E), 20: 40091
reactions (n,2n) with nuclei at 14.8 Mev, activation cross sections for, (E), 20: 42207
reactions (n,2n) with nuclei, cross sections for, (T), 20: 44609 (CONF-660303, pp 315-27)
reactions (n,2n) with niobium-93, discrepancy between measured and predicted cross sections for, 20: 44616 (CONF-660303, pp 682-9)
reactions (n,2n) with tungsten-182 and tungsten-186 at 14.8 Mev, (E), 20: 46784
reactions (n,2n) with nuclei with $14 \leq A \leq 92$ at 14.6 Mev, cross sections for, (E), 20: 46614
reactions (n,2n) with nuclei with $45 \leq A \leq 144$, cross sections for, (E), 20: 46614
reactions (n,2n) with nuclei with $14 \leq A \leq 181$ at 13.56 to 14.7 Mev, excitation functions for, (E), 20: 46614
reactions (n,2n), and (n,p) with ruthenium-96 at 14.7 Mev, cross sections for, (E), 20: 6338
reactions (n,2n), (n,p), and (n,nα) with copper-65 at threshold to 20.2 Mev, cross sections for, (E), 20: 28306
reactions (n,2n)2α with beryllium-9 at 15 Mev, mechanism of, (E), 20: 42362
reactions (n,2p), (n,He-3), and (n,2p) with rhodium-103 at 14.7 Mev, cross sections for, (E), 20: 6338
reactions (n,3n) with lead-206 at 17.1 to 29 Mev, cross sections for, 19: 1640
reactions (n,3n) with tritium at 14 Mev, cross section for, (E), 20: 4849(R) (UCRL-14360, pp 1-50)
reactions and scattering of, 17: 36669 (WASH-1042)
reactions and scattering on nuclei, computer program for cross sections of, 18: 1018 (KAPL-M-NCF-4)
reactions and scattering, 18: 24625 (WASH-1046)
reactions and thermalization in critical assemblies, 18: 36781(R) (HW-81659(p.26-32))
reactions and transport in thermonuclear reactor blankets, 20: 6454 (AD-619671)
reactions at 14 Mev with nuclei with Z = 3 to 30, gamma spectra from, 19: 23163(R) (ORNL-3650(p.111-86))
reactions at 14 Mev, counter telescope for charged-particle production in, 19: 46821
reactions in beryllium–uranium critical assemblies, 18: 26248
reactions in bromine salts, recoil distributions from, 19: 28395
reactions in collapsing stars, adiabatic exponent for equilibrium in, (T), 20: 2588
reactions in critical systems, variational principle for ratios of, (T), 20: 18059
reactions in fast reactors, multigroup calculations of, 18: 38249 (A/CONF.28/P/510)
reactions in food, radioactivity from, 20: 29599
reactions in gas-cooled graphite-moderated reactors, steady-state, 18: 1270
reactions in graphite–thorium systems, Doppler measurements for, 16: 729
reactions in inert gas-filled thermionic diodes, space-charge neutralization in, 18: 20861
reactions in iridium, cluster formation from, (E), 20: 38382
reactions in lithium hydride and water, gamma spectra from, 19: 25749 (NP-15022(Vol.I))
reactions in matter, temperature determination from, 17: 34218(P)
reactions in nuclear emulsions at 20 to 300 Mev, gray prong per star analysis of, (E), 20: 41276 (UCRL-16769)
reactions in plutonium–uranium fueled water reactors, cross sections for, (T), 20: 12370
reactions in plutonium-239–thorium-232 systems, resonance interference effects on cross sections for, (T), 20: 21970 (ANL-7144)
reactions in reactors, computer analysis of, (T), 19: 12490 (ORNL-3689)
reactions in spherical materials, self-shielding effects in activation, 18: 6764
reactions in stars, nucleosynthesis from, 20: 34674
reactions in subcritical lattices, measurement, (E), 20: 14185(R) (MIT-2344-4, pp 70-9)
reactions in systems of cylinders, 17: 24370 (HW-77279)
reactions in tissue of, effects of neutron energy on, 20: 3708 (CEA-R-2833)
reactions in tissue phantom at high energies, 20: 14330
reactions (n,α) and (n,p) with nuclei, cross sections and Q-values, 16: 1017 (AE-58)
reactions (n,α) with boron-10 at 0.2 to 8.2 Mev, boron-10 decay, 16: 3713
reactions (n,α) with fluorine-19 at 0.2 to 8.2 Mev, 16: 3713
reactions (n,α), (n,2n), and (n,p), with nuclei at 14 Mev, isomer-pair production cross sections, 16: 7054
reactions (n,α) with arsenic-75 at 14 Mev, angular distributions and energies from, 16: 12484
reactions (n,α) with neon-20 at 6.2 to 10.7 Mev, 16: 17099
reactions (n,α) and (n,p) in cesium iodide at 12.1 to 21.5 Mev, energy spectra and cross sections from, 16: 21552
reactions (n,α), (n,2n), and (n,p) with nuclei around Z = 40, cross sections, 16: 21586
reactions (n,α) with carbon-12 at 14.1 Mev, angular distributions and cross sections in, 17: 4060 (NYO-9765)
reactions (n,α) and (n,p) with silicon-28 at 14 Mev, emission from, 17: 9567
reactions (n,α) in lithium-6, electron microscopic observation of, 17: 11615 (BNL-6082)
reactions (n,α) and (n,p) with nuclei at 14.5 Mev, cross-section calculations by statistical theory for, 17: 11754
reactions (n,α) with nickel-58, cross sections for, 17: 17139
reactions (n,α) with nuclei, statistical model calculations of cross sections for, 17: 17206
reactions (n,α) with carbon-12 at 14 Mev, mechanisms of, 17: 17288
reactions (n,α) and (n,γ) on rhodium-103, cross sections, 17: 19297
reactions (n,α) with carbon, nitrogen, and oxygen, angular distribution of alpha particles from, 17: 19306
reactions (n,α) with aluminum-27, forward-backward asymmetry of sodium-24 recoil nuclei from, 17: 19336
reactions (n,α) and (n,p) with aluminum-27 and sodium-23, ratio of cross sections for, 17: 21034
reactions (n,α), (n,d), and (n,p) with cesium iodide at 14.6 Mev, cross sections for, 17: 21035
reactions (n,α), (n,2n), and (n,p), cross sections and product half lives for, 17: 25857(R) (PR-P-56(p.4-18))
reactions (n,α) with aluminum-27 at threshold, cross sections for, 17: 26421 (EUR-10.e)
reactions (n,α), (n,2n), and (n,p) with calcium at 14.9 Mev, cross sections for, 17: 26549
reactions (n,α) with aluminum-27 and cobalt-59 at 14 Mev, angular and energy distributions from, 17: 26550
reactions (n,α) with aluminum-27 at 15 Mev, differential cross sections and energy spectra for, 17: 26605
reactions (n,α) and (n,nα) at 14.8 Mev, differential cross sections, energy spectra, and level density parameters for, 17: 26606
reactions (n,α) with silicon-28, intensity fluctuations of excitation function for, 17: 28295
reactions (n,α) on arsenic-75, distributions from, 17: 29951
reactions (n,α) with aluminum-27 at 14 Mev, angular and energy distributions from, 17: 31477
reactions (n,α) and (n,2n) with beryllium, helium production in, 17: 31017 (AAEC/E-108)
reactions (n,α) with gold-197, holmium-165, and lutetium-175 at 14.7 Mev, alpha energy spectra and differential cross sections for, 17: 34917
reactions (n,α) with nuclei at 14 Mev, cross section trends in, 17: 36409 (NP-13020(p.166-8))
reactions (n,α) with fluorine-19, counter telescope study of, 17: 36417 (NP-13020(p.255-9))
reactions (n,α) with nuclei ($165 \leq A \leq 197$) at 14 Mev, energy spectra

for, 17: 38296
reactions (n,α) and (n,p) with silicon-28 and -29 at 1.0–5.5 Mev, cross sections and energy spectra for, 17: 38302
reactions (n,α) with lithium-6 at 255 kev, triton polarization angular distributions from, 17: 38250
reactions (n,α) with silicon-28 at 12.15–18.4 Mev, cross section fluctuations in, 17: 38221
reactions (n,α) with aluminum-27 and copper-63, effective threshold energy for, 17: 38116
reactions (n,α) and (n,p) with ($23 \leq A \leq 77$) at 5–25 Mev, statistical model analysis of cross sections for, 17: 38212
reactions (n,α), (n,2n), and (n,p) with nuclei $60 > A > 24$, absolute cross sections for, 17: 40049
reactions (n,α) with even-even nuclei, calculation using a direct interaction process, 17: 39994
reactions (n,α) with aluminum-27, range of recoil sodium-24 from, 17: 41910
reactions (n,α) with nitrogen-14 and oxygen-16, 18: 2840 (NYO-9766)
reactions (n,α) with aluminum-27 and cesium iodide, 18: 2845(R) (TID-19657)
reactions (n,α) and (n,p) with aluminum-27 at 14.8 Mev, nuclear recoil ranges in, 18: 2859
reactions (n,α) with nuclei at 14 Mev, nuclear shell effects on cross sections for $3 \leq A \leq 235$, 18: 4632
reactions (n,α) on lithium-6, cross sections, 18: 4089 (EANDC-33U (p.136-49))
reactions (n,α) with phosphorus-31 at 2.5 to 5.0 Mev, excitation function for, 18: 6227
reactions (n,α) with silicon-28 and -29, spectra from, 18: 6163 (NP-13349)
reactions (n,αγ) and (n,pγ) with potassium-39, coincidence study of, 17: 17196
reactions (n,αn′) with copper-65 at 14.5 Mev, cross sections, 16: 8219
reactions [(n,αn) + (n,nα)] with nuclei, separation energies for, 17: 2242 (TID-16949)
reactions (n,α_0) with calcium-40, energy spectra and differential cross section of, 17: 34928
reactions (n,d) with vanadium-51, angular distributions from, 16: 21554
reactions (n,d) with $f_{7/2}$ proton shell nuclei at 14 Mev, cross sections for ground-state transitions in, 17: 34920
reactions (n,d) with lithium-7 at 14.8 Mev, cross section for, 17: 38115
reactions (n,dn) and (n,tn) with lithium-6 and -7 respectively, cross sections for 5 to 14 Mev, 16: 23120
reactions (n,f) with uranium-235, fragment kinetic energy and prompt neutron distributions in, 18: 2935
reactions (n,γ), spectral analysis, 16: 18437
reactions (n,γ) on nuclei, gamma resonance effects, 16: 21454
reactions (n,γ) on odd-Z nuclei below 40 kev, cross sections, 16: 23138
reactions (n,γ) with nuclei, isotopic effect of secondary reactions of recoil atoms in, 16: 24861
reactions (n,γ) with sulfur-34, 16: 28982 (UCRL-10360)
reactions (n,γ), spectral analysis, 16: 29791(T) (AEC-tr-5221)
reactions (n,γ) with chlorine, gamma spectra from, 17: 806 (TID-16985)
reactions (n,γ) with gadolinium-155 and 157, gamma and electron conversion spectra from, 17: 7175
reactions (n,γ) with molybdenum-95, gamma spectra from resonances in, 17: 6776(R) (ANL-6603(p.1-8))
reactions (n,γ) with chlorine-35 and molybdenum-95, spin and parity of levels in cascades from, 17: 13519
reactions (n,γ) and (n,p) in aluminum-27, cross sections for, 17: 13521
reactions (n,γ) with europium-155, gamma energy from, 17: 19304
reactions (n,γ) on iridium-191, cross sections, 17: 19316
reactions (n,γ) with bismuth-209, figure of merit for, 17: 24509
reactions (n,γ) with nuclei, gamma spectra for, 17: 26419(R) (ARF-1193-23)
reactions (n,γ) with gold-197, gold-198 activity for varied fluxes in, 17: 26510
reactions (n,γ), charge of recoil atoms from, 17: 28969
reactions (n,γ) on tellurium-130, yields from in-pile, 17: 29941
reactions (n,γ), scintillation detector for cross sections of, 17: 30876
reactions (n,γ), 17: 35190
reactions (n,γ) with molybdenum-95, niobium-93, and zirconium-91, gamma spectra of p- and s-wave resonances in, 17: 34951
reactions (n,γ) with helium-3 at 2.45–4.6 Mev, differential and total cross sections for, 17: 34983
reactions (n,γ) in VVR-S reactor, background from, 17: 40409 (NP-13135)
reactions (n,γ) with gold-197, cross section for, 18: 1080
reactions (n,γ) with scandium-45 at 0.15 to 14.65 Mev, cross sections for, 18: 1037
reactions (n,γ) with uranium-238, gamma spectra for, 18: 1006 (IKF-8)
reactions (n,γ) with cesium-133, europium-151, and silver-109, lifetimes of excited states produced by, 18: 6259
reactions (n,γ) with nuclei, angular correlations from, 18: 2403(R) (PR-P-58)
reactions (n,He^3) with nuclei at 14.5 Mev, cross-section upper limits, 16: 8219
reactions (n,n′α) with lithium-7, cross section determination for, 16: 19748 (LA-1697)
reactions (n,n′γ) on lithium-7, cross sections for, 17: 5357
reactions (n,n′γ) with nuclei, fast-slow coincidence system for measuring angular correlations in, 17: 29207
reactions (n,n′γ) with strontium-88, angular distribution for, 18: 2846(R) (TID-19709)
reactions (n,n′γ) with iron-56 at 2.06 ± 0.10 Mev, angular correlations in products from, 18: 6199
reactions (n,n′) with indium-115, effective threshold energy for, 17: 38116
reactions (n,nα) with vanadium-51, cross section for, 17: 31797(R) (BNL-782(p.51-9))
reactions (n,nγ) with magnesium-24, 1.37-Mev gamma ray angular distribution from, 17: 20564(R) (TID-18442)
reactions (n,nγ) with iron-56, 0.85-Mev gamma ray angular distribution from, 17: 20564(R) (TID-18442)
reactions (n,np) and (n,p) with sulfur-32 at 14.4 Mev, nuclear temperature calculations, 16: 8205
reactions (n,p) in molybdenum, cross sections for, 17: 9592
reactions (n,p) on beryllium-9, cross sections for, 17: 7198
reactions (n,p) on chlorine-35, yields from in-pile, 17: 29942
reactions (n,p) on nuclei at 14.5 Mev, pairing-energy effects on, 16: 23103
reactions (n,p) on nickel-58 and zinc-64 at 1.8 to 4.8 Mev, 16: 31082
reactions (n,p) on sulfur-32, yields from in-pile, 17: 29940
reactions (n,p) with nuclei at 14 Mev, direct and evaporation mechanisms, 16: 4850
reactions (n,p) with nuclei at 14 Mev, cross section ratios for, 16: 6019
reactions (n,p) with nuclei at 14 Mev, angular distributions and spectra from, 16: 11028
reactions (n,p) with nuclei at 14 Mev, cross sections for, 16: 12477
reactions (n,p) with odd-odd deformed nuclei, 16: 29781 (JINR-P-999)
reactions (n,p) with oxygen-16 at 12.6 to 16.3 Mev, cross sections for, 17: 2223 (KAPL-2214)
reactions (n,p) with silicon-28, proton angular distribution from, 17: 9566
reactions (n,p) with benzene and its irradiation products at 0.03 to 0.3 ev, cross sections for, 17: 20058
reactions (n,p) with silicon-28 at 14 Mev, distorted-wave Born approximation with exchange interaction, 17: 24497
reactions (n,p) with deuterium at 14.4 Mev, proton spectra from, 17: 26306
reactions (n,p) with nuclei $24 \leq A \leq 58$, cross sections for threshold, 17: 26421 (EUR-10.e)
reactions (n,p) with sulfur-32 at 14.6 Mev, proton angular distributions and energy for, 17: 29602
reactions (n,p) with sulfur-32, measurement of neutron fluxes with, 17: 29202 (NIRL/R/31)
reactions (n,p) with aluminum-27 and cobalt-59 at 14.8 Mev, angular and energy distributions from, 17: 31470
reactions (n,p) with cobalt-59 at 14.8 Mev, 17: 36407 (NP-13020 (p.155-9))
reactions (n,p) with low-Z nuclei at 14 Mev, cross sections for, 17: 36410 (NP-13020(p.169-73))
reactions (n,p) with lithium-6 at 3.5 to 14.8 Mev, cross sections for, 17: 38115
reactions (n,p) with nickel-58, phosphorus-31, sulfur-32, and titanium-46, effective threshold energy for, 17: 38116
reactions (n,p) with beryllium-9 at 15.5 Mev, cross section for, 17: 38125
reactions (n,p) with cesium-133, iodine-127, and potassium-39 at 12 to 22 Mev, proton spectra from, 17: 41968
reactions (n,p) with gold-197 and indium-115 at 14.8 Mev, proton energy spectra from, 18: 1046
reactions (n,p) with aluminum-27 at 14 Mev, angular distributions from, 18: 1054
reactions (n,p) with nuclei, exchange effects in, 18: 2860
reactions (n,p) with silicon-30 at 14 Mev, cross section for, 18: 4607
reactions (n,p) with deuterium at 14.7 Mev, neutron spectra from, 18: 6010
reactions (n,p) with silicon-28 at 14 Mev, analysis of direct, 18: 9358
reactions (n,p) with nuclei, theory of compound-nucleus and direct, 18: 9440
reactions (n,pn) with carbon-12 at 120 to 150 Mev, gamma spectra of residual nuclei, 16: 21466
reactions (n,t) with medium-heavy nuclei, cross sections for, 17: 9619
reactions (n,2n) and (n,p) with cobalt-59 and zinc-64 at 13.8 to 14.8 Mev, 16: 21385
reactions (n,2n) and (n,p) with rhenium isotopes at 14.1 Mev, cross sections for, 17: 24380 (AD-402668)

reactions (n,2n), bibliography on, 17: 11587 (AE-88)
reactions (n,2n) in deuterium, kinetics of, 17: 13488 (NDL-TR-40)
reactions (n,2n) with nuclei, cross-section calculations, 16: 7072
reactions (n,2n) with fluorine-19 in fluoroorganic compounds, 16: 28974 (IA-738)
reactions (n,2n) with beryllium at 3.2 to 4.5 Mev, cross sections, 16: 29742
reactions (n,2n) with lithium-6 and -7 at 10.2 and 14.1 Mev, cross sections for, 17: 11722
reactions (n,2n) with silver-107 and silver-109 at 14 Mev, cross sections for, 17: 26547
reactions (n,2n) with nuclei at 14 Mev, cross sections for, 17: 26551
reactions (n,2n) with antimony-121, iron-54, phosphorus-31, and silver-107, measurement of cross sections for, 17: 34903
reactions (n,2n) with bismuth and lead, angular correlations and cross sections for, 17: 34912
reactions (n,2n) with nuclei at 12–20 Mev, cross sections for, 17: 38213
reactions (n,2n) with beryllium-9, bismuth-209, and deuterium at 14 Mev, 17: 40053
reactions (n,3n) with beryllium at 14 Mev, cross section measurements in shell symmetry for, 18: 9354
reactions (n,3n) with thorium at 14 Mev, cross section measurements in shell symmetry for, 18: 9354
reactions of reflected, with unit spherical target, (T), 20: 13742
reactions of, resonance statistics effects in, 18: 2956
reactions of, with shielding materials, determination of heat from, 17: 4283
reactions of 350-kev polarized, with oriented holmium-165, nuclear deformation and spin-spin interaction effects in, 18: 24620(R) (ORNL-TM-874)
reactions of, cross sections for, 18: 16947 (NP-13661)
reactions of, equipment for high-energy experiments on, 20: 7315(R) (ORNL-3849, pp 151-82)
reactions of, optical models of, 19: 31215(R) (ANL-7010(p.1-19))
reactions of, statistical errors in flux level parameters in resonance, 16: 24771
reactions on calcium, titanium, and vanadium nuclei at 14.5 Mev, 16: 31090
reactions on crystalline solids at high energies, theory for damage, 16: 24256
reactions on magnetic oxides, total cross sections for, 18: 34752(R) (CU(PNPL)-234)
reactions on matter, equipment for studying, 17: 15508
reactions on near-magic nuclei, widths of resonances in, 17: 13557
reactions on NRX fuel rods, cross sections for, 17: 31758
reactions on nuclei, cross sections for epithermal, 17: 7306
reactions on nuclei, strength functions and widths for, 17: 19222 (TID-16603)
reactions on uranium dioxide pellets, fission-gas release from, 18: 28042 (EURAEC-1048)
reactions other than (n,γ), activation analysis with, 17: 27230 (IA-839)
reactions with absorbing materials, activation measurements of resonance integrals by component subtraction method, 16: 730
reactions with actinium-227, neptunium-237, and protactinium-231, fission fragment mass distributions from, (E), 20: 17861
reactions with air, hydrogen, and sulfur fluoride, ionization, 18: 10346(R) (X64-11113)
reactions with aligned nuclei, resonances in, 18: 4540 (JINR-P-1369)
reactions with alpha-iron, defect clusters from, 19: 28888
reactions with α-iron, damage from, 19: 47105
reactions with aluminum, carbon, copper, lead, and tin at 8.3 Bev, inelastic and total cross sections, 16: 15622 (JINR-D-880)
reactions with aluminum–lithium alloys, tritium production by, 17: 33110(P)
reactions with aluminum-27 and sodium-23 at 14.6 Mev, cross sections for, 17: 40027
reactions with aluminum-27, cascade and evaporation, 18: 7689(R) (ORNL-3499(Vol.II)(p.31-53))
reactions with aluminum, carbon, fluorine, and hydrogen at 2.77 Mev, total cross sections for, 18: 21159 (CEA-2399)
reactions with aluminum-27, sodium-24 yields in, 18: 24592 (NP-13913)
reactions with aluminum, bismuth, carbon, copper, and water, energy deposition from, 18: 44751
reactions with aluminum and oxygen at 15 Mev to 0.0001 ev, library data for, 19: 1543 (AEEW-M-445)
reactions with aluminum-27 and magnesium-24, sodium-24 preparation by, 19: 15610
reactions with aluminum at 0.001 ev to 15 Mev, cross sections for, 19: 16839 (GA-5884)
reactions with aluminum, carbon, nitrogen, and oxygen at 90 to 150 Mev, total cross sections for, (E), 19: 23808
reactions with aluminum, magnesium, and sulfur at 14 Mev, gamma emission in, (E), 19: 37890
reactions with aluminum and silicon isotopes, Q values for, 19: 44450(R) (IBK-120a)
reactions with aluminum halides to produce krypton and xenon isotopes, 20: 18731
reactions with aluminum, copper, iron, and magnesium at 12 to 16 Mev, total cross sections for, (E), 20: 28396
reactions with aluminum and nickel, cross sections for, (T), 20: 34512 (ANL-7170)
reactions with aluminum at 4.6°K, defect annealing in, (E), 20: 38380
reactions with aluminum, carbon, cerium, chromium, curium, lead, oxygen, tungsten, and uranium at 25 to 400 Mev, 20: 46932(R) (ORNL-3973(Vol.2), pp 71-84)
reactions with americium-241, americium-242 from, (E), 19: 31217 (IDO-17042(p.11-47))
reactions with americium-241 and -243, curium-242, and -244 and plutonium-238 production in, (E), 20: 12394 (BNWL-SA-472)
reactions with americium-241, plutonium-238, and thorium-230 at 0.1 to 1.2 Mev, fission fragment angular distributions from, (E/T), 20: 17848
reactions with americium-241 at 4 and 5 Mev, fission fragment angular distributions from, (E/T), 20: 17848
reactions with antimony, arsenic, selenium, and tellurium at 0.003 to 0.008 ev, total cross sections, 16: 24811
reactions with antimony, arsenic, selenium, and tellurium at 0.003 to 0.008 ev, total cross sections for, 16: 28032 (NP-11631)
reactions with arsenic and bromine at 0.1 to 10 kev, total cross sections for, 18: 40591
reactions with arsenic-75, total cross sections at 0.05 to 40 ev, (E), 19: 6712
reactions with atoms in solids, energy exchange cross sections for, 17: 19205 (TID-18432)
reactions with atoms, molecules, and nuclei, cross section tabulations for, (E), 20: 3018 (NYO-72-27)
reactions with benzene and biphenyl at 0.001 to 0.1 ev, total cross sections for, 19: 1641
reactions with benzene, decomposition G values in, 19: 7576
reactions with benzene, sodium acetate, and toluene at 0.03 to 0.5 ev, total cross sections for, (E), 19: 25483
reactions with beryllium oxide at 11.6 Mev, diffusion parameters, 16: 10951 (DC-59-12-221)
reactions with beryllium, cross sections for, 19: 29235 (GA-5905)
reactions with biological materials and matter, processes in, 19: 5125
reactions with bismuth, lead, and thallium at 14.2 Mev, total cross sections for, 18: 32872
reactions with bismuth, indium, iodine, and vanadium at 3.2 to 5.2 Mev, (E), 19: 14576
reactions with bismuth, polonium-210 production in, 19: 20008
reactions with bismuth, production of polonium-210 in, 20: 20585
reactions with borated steel, stainless steel, and tungsten, production of secondary gammas in, 16: 716
reactions with boron-10, branching ratios of, 17: 352 (AE-84)
reactions with boron, gold, and helium-3, cross sections for, 18: 6181 (RISÖ-61)
reactions with boron-10, chemical effects on methanol of recoils from, 19: 4224
reactions with boron-10 in gases, pressure wave generation in fission, (E), 19: 39836
reactions with boron-10, boron-11, carbon, and oxygen at 10 to 500 kev, cross sections for, (E), 20: 28353
reactions with bromine at 0.1 to 2 kev, spin dependence of strength functions from total cross sections for, (E), 19: 16953
reactions with bromoethane, pressure and temperature effects on bromine-80 recoil reactions in, 19: 40626
reactions with calcium, potassium, and sodium at 8.58 to 11.59 Mev, total cross sections for, 18: 24591(R) (LMSC-4-50-62-1)
reactions with calcium, carbon, and iron at 8 to 14 Mev, total cross sections for, 18: 42703
reactions with calcium, cerium, and cobalt at 3.0 to 4.5 Mev, gamma spectra from, (E), 19: 19095 (WASH-1053)
reactions with calcium, chromium, and nickel isotopes, resonances in, 19: 21454
reactions with calcium oxide crystals, M-like centers in, 19: 22366
reactions with calcium at 3.5 to 5.0 Mev, gamma production in, (E), 20: 6408
reactions with calcium and potassium at 2.37 to 15.98 Mev, total cross sections for, (E), 20: 9981 (WASH-1064)
reactions with calcium at 2.2 to 5.3 Mev, total cross section for, (E), 20: 38183
reactions with calcium-41 at 1 to 2 Mev, total cross sections for, (E), 20: 40087
reactions with carbon at 0.025 ev to 15 Mev, cross sections, 17: 793 (AWRE-O-71/60)
reactions with carbon at 31 to 33 Mev, cross sections for, 17: 38329 (CERN-63-19(p.144-8))

reactions with carbon and oxygen at 14 Mev, gamma spectra from, 18: 16329
reactions with carbon dioxide, catalysis of decomposition, 19: 2400
reactions with carbon-12, oxygen-16, and silicon-28 at 14 Mev, cross sections for scattering, (E/T), 19: 21441
reactions with carbon-12 at 2.5 to 5 Mev, total cross section for, 19: 40115 (CONF-650602-33)
reactions with carbon at 0.7 to 45 Mev, cross sections for, (E), 20: 24356 (RPI-328-51)
reactions with carbon-12(n,n')3α at 15.5 Mev, (E), 20: 44849
reactions with cesium and niobium at 14 Mev, total cross sections for, (E), 20: 17702
reactions with chlorate and perchlorate ions for labeling with chlorine-38, 19: 17982
reactions with chlorine, lead, potassium, sodium, and sulfur at 14.7 Mev, gamma emission in, (E), 20: 42146 (AD-638014)
reactions with chromates for chromium-51 production, 19: 18070
reactions with chromic oxide, production of chromium-51 in, 19: 22295
reactions with chromium in ammonium chromate, chromium acetylacetonate, and potassium chromate, preparation of pure chromium-51 using, 20: 43401
reactions with cobalt and rare earth isotopes, 18: 17035
reactions with cobalt-59 below 30 kev, resonance parameters in (E), 19: 1616
reactions with cobalt-59 at 0.1 to 30 kev, resonance parameters for, (E), 19: 5172
reactions with cobalt in acetylacetonates, recoil effects from, 19: 30313
reactions with complex nuclei at 25 to 400 Mev, data from inelastic, (E), 20: 44720
reactions with copper, platinum, and silver at 385 Mev, spallation phenomena in, 18: 2853
reactions with copper, dislocation breakaway stress from, 19: 7986
reactions with copper crystals, deformation in, 19: 23145
reactions with copper, iron, and steel, induced activity in, 19: 37178
reactions with copper-63, gold-197, indium-115, manganese-55, and phosphorus-31, rates for, (E/T), 19: 45522 (AE-195)
reactions with copper, silver, and platinum foils at 400 Mev, beryllium-8 production from, (E), 20: 24374
reactions with copper above 10 ev, chemical binding effects on total cross sections for, 20: 32392
reactions with copper phthalocyanine, crystal-structure effects on recoil atoms after, 20: 40309
reactions with curium-244 at 0.01 to 900 ev, total cross sections for, 18: 26650
reactions with curium-244 and plutonium-238 at 1 kev to 14 Mev, cross sections for, (T), 20: 30346 (GEMP-411)
reactions with deuterons and tritons at 14.4 Mev, charge dependence of nuclear forces in breakup, 18: 9416
reactions with diatomic molecules, theory of dissociation in, 20: 27039(T) (AED-tr-5152)
reactions with dysprosium isotopes, cross sections for, 18: 28719
reactions with elemental constituents of lunar surface, 16: 11339 (UCRL-5916)
reactions with elements in tissues of human body, 19: 7051
reactions with emulsion, nuclei, star production in, (E), 20: 8069 (JINR-P-2383)
reactions with erbium, cross sections, energy levels, and resonances for, 18: 4591
reactions with erbium-162 at 0.005 to 0.1 ev, total cross sections for, (E), 20: 28453
reactions with even-even isotopes near threshold, channel analysis of fission, (E/T), 19: 31230 (ORNL-P-1082)
reactions with even-even tin isotopes, total cross sections for, (E), 20: 30490
reactions with even intermediate elements, level spacings from total cross sections for, (E/T), 20: 32389
reactions with fission products, cross-section calculations for SIZZLE code, 20: 6659 (NAA-SR-Memo-11473)
reactions with fissionable isotopes, comparison of multilevel and single-level effects on cross sections for, (T), 20: 44630 (CONF-660303, pp 997-1003)
reactions with fissile nuclei, model for Doppler coefficients for, 20: 46567
reactions with fuels in fast ceramic reactors, cross sections for, 18: 35146(R) (GEAP-4601)
reactions with gadolinium-158 at 14 Mev, activities produced in, 16: 4620(R) (PR-P-50)
reactions with gadolinium, effects on reactivity worths of, (E), 19: 29320
reactions with gases and liquids, effects of close-range order on total cross sections for, 18: 40634
reactions with germanium-76, arsenic-77 production by, 18: 39782(T) (AEC-tr-6390(p.533-9))
reactions with germanium crystals, recoil atom energy losses in, (E), 19: 37191
reactions with germanium at 0.4 to 18.6 Mev, germanium recoil atom ionization spectrum from, (E), 20: 17265
reactions with gold and uranium-238, 18: 35247(R) (NAA-SR-9700)
reactions with gold and stainless steel, 19: 12865(R) (NAA-SR-10501)
reactions with gold foil, absolute measurement of efficiency of neutron sources by, 18: 26505
reactions with gold, incident flux angular distribution for activating, (E), 19: 31460(R) (ANL-7010(p.179-233))
reactions with gold and iodine at 24 Mev, Monte Carlo capture cross sections for, (T), 20: 32378 (NASA-TR-R-239)
reactions with graphite, vacancy production in, 17: 34507
reactions with graphite, structural changes in, 19: 23156
reactions with graphite components, induced stresses in, 19: 28886
reactions with graphite, magnesium, and polyethylene in channels of FRJ-2 reactor, heating from, 20: 5202
reactions with hafnium and tungsten isotopes, resonance parameters for, (E), 20: 9981 (WASH-1064)
reactions with heavy emulsion nuclei, cascade from, 17: 22564 (ORNL-3383)
reactions with heavy nuclei at low energies, cross sections for resonance, 18: 6295
reactions with heavy nuclei, yields of heavier nuclei from, 18: 6154 (ANL-6756)
reactions with heavy nuclei, fission cross sections and yields for, 18: 18863 (ANL-6792(p.11-27))
reactions with heavy nuclei, fission fragment anisotropy in, (E), 19: 12586
reactions with heavy isotopes to produce other heavy isotopes, 19: 27504
reactions with heavy and medium nuclei, rates for, (T), 20: 11989
reactions with heavy even-even nuclei, model of, 20: 22520(R) (NAA-SR-11805)
reactions with helium at 147 Mev, total cross sections for, 18: 38123
reactions with helium-4, spin coupling to deuteron-tritium reaction channels, (T), 20: 11978 (UCRL-7961-T)
reactions with helium, plasma production in, ionization, (T), 19: 10442
reactions with holmium-165, spins of resonances in, (E), 19: 16988
reactions with holmium-165 at 0 to 55 ev, resonance spins from, (E), 19: 41665 (JINR-P-2209)
reactions with holmium-165 at 14 Mev, total cross sections for, (E), 20: 12089
reactions with holmium-165 at 7.85 Mev, spin-spin interaction in total cross sections for, 20: 34608
reactions with holmium-165, spins of resonances in, 20: 34664
reactions with holmium-165 at 14 Mev, effect of nuclear alignment on total cross section for, (E), 20: 46746
reactions with hydrogen atoms, energy exchange study, 16: 3656(R) (GA-2503)
reactions with hydrogen, proton recoil energy loss distribution from, 16: 24791 (ORNL-3089)
reactions with hydrogen at 0.0001 ev to 20 Mev, cross sections for, 19: 45248 (AWRE-O-23/65)
reactions with hydrogen, interaction effect in capture, (T), 20: 3059
reactions with hydrogen and deuterium at 90 to 150 Mev, total cross sections for, (E), 20: 34584
reactions with hydrogenous compounds at 0.025 to 0.4 ev, total cross sections for, (E), 20: 40069(R) (EANDC(E)-66(U))
reactions with indium at 14 Mev, alpha spectra from, 17: 7207
reactions with indium-115, isomeric splitting ratio of first three resonances in, 18: 24610 (NP-13930(p.114-15))
reactions with indium-115 and samarium-149 at 0.4 to 14 ev, cross sections for, 18: 36585
reactions with indium-115, ratios of isomers from, (E), 19: 35378(R) (EANDC(E)-57(U))
reactions with iodine-129, production of iodine-130 isomer in, (E), 20: 15772
reactions with iodine in cyclohexane, isomeric transition reactions of iodine-130 following, 20: 35556
reactions with iron, yield of gamma rays from, 16: 33799
reactions with iron to prepare manganese-54, 19: 22312
reactions with iron, manganese, and vanadium at 18 to 260 kev, total cross sections for, (E), 20: 40069(R) (EANDC(E)-66(U))
reactions with isotopes, tables on resonance integrals, (E/T), 19: 29260 (TID-21744)
reactions with krypton at 6.4 to 12 Mev, disintegration, 16: 17099
reactions with lanthanum-138 at 0.2 to 2000 ev strength functions from, (E), 19: 35403 (ORNL-P-1354)
reactions with lanthanum-138 at 0.2 ev to 2 kev, resonance parameters from, (E), 20: 39470(R) (ORNL-3924)
reactions with lead-208 and oxygen-16, phenomenological potentials for, 16: 22988(R) (ORNL-3268(p.8-10))
reactions with lead-204 at 6 to 50 kev, resonances in, (E), 19: 25475(R)

(ORNL-TM-1044)
reactions with lead and uranium-238 at 7.5 to 30 kev, effective cross sections for, (E), 20: 40069(R) (EANDC(E)-66(U))
reactions with lead at 1.7 and 2.1 Mev, total inelastic cross sections for, (E), 20: 44618 (CONF-660303, pp 726-34)
reactions with light elements at 14 Mev, total effective cross section for (E), 19: 1654
reactions with light nuclei at 14 Mev (E/T), 19: 1557 (NP-14297)
reactions with lithium-6, theory of, 16: 28031 (LA-2714)
reactions with lithium-6 and lithium-7 at 14.1 Mev, total cross sections, 16: 29736
reactions with lithium-7 at 13.98 Mev, cross sections for tritium production in, 17: 1524 (AWRE-NR/A-2/62)
reactions with lithium-6 and lithium-7 at 14 Mev, energy and yield of neutrons from, 17: 2206 (LA-1589)
reactions with lithium-6 and -7 at 1.5 to 7.5 Mev, 18: 1040
reactions with lithium for activation analysis, 18: 23427
reactions with lithium-6, fission recoil products from, 19: 7565
reactions with lithium atoms, ionization in, (T), 19: 23288
reactions with lithium fluorides, tritium production and diffusion from, (E), 19: 23146
reactions with lithium-6, energy from, 19: 31461(R) (ANL-7010(p.235-87))
reactions with lithium-6 and -7, cross sections for, (E), 20: 30360 (WASH-1068)
reactions with lithium at 4.2 to 6.1 Mev, total cross sections for, (E), 20: 40069(R) (EANDC(E)-66(U))
reactions with lutetium, 16: 33580(R) (HW-74190)
reactions with magnesium and silicon, production of short-lived radioisotopes in, 17: 26633
reactions with magnesium-24, cross section for, (E), 19: 35378(R) (EANDC(E)-57(U))
reactions with manganese, absolute measurement of efficiency of neutron sources by, 18: 26504
reactions with matter, measurements of absorbed dose in, 16: 3227
reactions with matter as related to image formation, 16: 12421 (ARF-1164-15)
reactions with materials in accelerators, tables of radioisotopes produced in, 17: 794 (CERN-62-22)
reactions with matter, measurement of induced activity from, 17: 34905
reactions with materials, equations for activation in, 17: 38120
reactions with matter, resonance effects in, 19: 47542 (ANL-7050, pp 457-70)
reactions with materials, conventions for reporting damage in, 20: 7631 (BNWL-SA-332)
reactions with methane at 0 to 0.306 ev, Krieger-Nelkin method for calculating differential scattering cross sections, 16: 2482 (IDO-16692)
reactions with meteorites, 17: 15008
reactions with metals at high energies, residual radioactivity from, 20: 31831
reactions with MHD cell gases, ionization in, 19: 29031 (AE-173)
reactions with mixed oxide fuels, Doppler delay in (T), 19: 3554
reactions with molybdenum at 10 to 1000 ev, total cross sections, 16: 25877(R) (ANL-6534)
reactions with molybdenum and tungsten at 0.05 to 1.00 Mev, capture cross sections, 16: 29744
reactions with molybdenum, interstitial loops in, 19: 20636
reactions with natural zirconium at 0.1 ev to 100 Mev, cross section tabulations for, 18: 6153 (AHSB(S)-R-62)
reactions with neon-22 at 0.2 to 2.1 Mev, total cross sections for, (E), 20: 9981 (WASH-1064)
reactions with neptunium-237 and thorium-230 at 12 kev to 1.5 Mev, fission anisotropies and cross sections, 16: 29734
reactions with neptunium-237, cross sections for, 18: 36567 (CONF-446-10)
reactions with neptunium-237, thorium-229, and -230, cross sections for fission, 18: 38073(T) (AEC-tr-6398(p.59-63))
reactions with neptunium, plutonium, and uranium isotopes at 24 kev, fission cross sections for, (E), 19: 35416
reactions with neptunium-237 at 1.0 to 4.5 Mev, fission cross sections for, (E), 20: 9981 (WASH-1064)
reactions with neptunium, plutonium, and uranium isotopes at 40 to 500 kev, fission cross sections for, (E), 20: 17852
reactions with neptunium-237 and uranium-235 and -238 at 1.0 to 5.0 Mev, fission cross section ratios for, (E), 20: 24346 (LA-DC-7617)
reactions with nickel-58 at 14 Mev, cross sections for, 16: 4620(R) (PR-P-50)
reactions with nickel-58 at 1.04 to 2.67 Mev, cobalt-58 cross section and isomer ratio in, 17: 22638
reactions with nickel at 15 Mev, cross section and energy spectrum of, 17: 38132
reactions with nickel-uranium alloys, secondary electron yields from fission fragments in, (E), 19: 12508
reactions with niobium and rubidium to 1.3 kev, resonance parameters and radiation widths from, (E), 19: 41727
reactions with niobium, resonance parameters for, (E), 20: 30360 (WASH-1068)
reactions with nitrogen-14 in atmosphere, 18: 20817
reactions with nitrogen-15 at 0.45 to 2.20 Mev, total cross sections for, 18: 36674
reactions with nitrogen–oxygen systems, nitrogen fixation in, 19: 2395
reactions with nitrogen-14 at 4.5 to 14.5 Mev, total cross sections for, (T), 19: 35396 (NP-15095)
reactions with non-fissile materials, production of thermal energy in, 17: 11619 (CEA-2172)
reactions with nuclei, energy distributions immediately following the event, 16: 6469
reactions with nuclei at 3.7 Mev, cross-section measurements, 16: 8224
reactions with nuclei at 0.1 to 100 Mev, total cross sections for, 16: 11021
reactions with nuclei, detection and spectroscopy of charged particles emitted from, 16: 12801(R) (IA-685)
reactions with nuclei, cross sections and excitation function, 16: 21352 (NP-11667)
reactions with nuclei at 30 kev, 16: 22991(R) (ORNL-3268(p.43-7))
reactions with nuclei below 5 Mev, resonance theory, 16: 23145
reactions with nuclei, solution of Schroedinger equation for calculation of cross sections, 16: 29745
reactions with nuclei, generalized nuclear model for, 16: 33843
reactions with nuclei at 28.4 Mev, total cross sections for A 6 to 240, 16: 5969
reactions with nuclei (n,γ), isomeric cross section ratios for, 17: 832
reactions with nuclei at 14.8 Mev, cross sections, product half lives, and Q values for, 17: 2242 (TID-16949)
reactions with nuclei, mechanisms of, 17: 11708
reactions with nuclei at low energies, theory of, 17: 11740
reactions with nuclei at 25 to 400 Mev, 17: 12783(R) (ORNL-3360 (p.182-98))
reactions with nuclei, data table for, 17: 21033
reactions with nuclei, Doppler broadened cross sections for, 17: 24383 (AEEW-R-226)
reactions with nuclei at 12 to 19 Mev, energy dependence of cross sections for, 17: 26618
reactions with nuclei, studies of P-wave strength functions to determine spin-orbit coupling in, 17: 26637
reactions with nuclei at 2–10 kev, inelastic scattering and radiative capture cross sections for, 17: 29631
reactions with nuclei, review of, 17: 29149
reactions with nuclei for industrial purposes, 17: 28946(T) (CEA-tr-A-1308)
reactions with nuclei, calculation of low-energy intranuclear cascades in, 17: 31526
reactions with nuclei at intermediate energies, theory of, 17: 32990
reactions with nuclei, mass-flow function in, 17: 33027
reactions with nuclei, optical model for radiative capture and inelastic, 17: 33048
reactions with nuclei, nomograph for determining activities from, 17: 34029
reactions with nuclei, cross sections for threshold, 17: 36653 (EUR-119.e)
reactions with nuclei at 14.7 Mev, rare, 17: 36707
reactions with nuclei at 14 Mev, reaction mechanisms in, 17: 41993
reactions with nuclei at 14.8 Mev, cross sections for rare, 18: 1077
reactions with nuclei, total inelastic cross sections for, 18: 2963
reactions with nuclei, cross section tabulations for, 18: 4538 (EANDC(UK)-26U)
reactions with nuclei, effects of crystalline fields on resonant, 18: 6164 (NP-13354)
reactions with nuclei at 14 Mev, 18: 13636(R) (ORNL-3537(p.71-105))
reactions with nuclei, gamma production cross sections for, 18: 21169 (GEMP-278)
reactions with nuclei, neutron distributions from fission, 18: 21197 (KR-64(Sect.XVIII))
reactions with nuclei, optical model studies of, 18: 24594 (NP-13930 (p.1-5))
reactions with nuclei at 12.5 to 19.6 Mev, cross sections for, 18: 24602 (NP-13930(p.43-9))
reactions with nuclei at 14 Mev, cross sections and gamma spectra for, 18: 24604 (NP-13930(p.54-5))
reactions with nuclei, promulgation of cross sections for, 18: 28541
reactions with nuclei at 14 Mev, gamma spectra of radioisotopes from, 18: 30734 (SAR-G-63-38)
reactions with nuclei, gamma radiation from, 18: 30735(R) (TID-20657)
reactions with nuclei, nomographs for induced radioactivity in, 18: 34012
reactions with nuclei, tunneling in Coulomb field in, 18: 34894

reactions with nuclei, bibliography on cross sections for, 18: 34753(R) (EANDC(E)-50(L))
reactions with nuclei in activation analysis, parameters for, 18: 33492
reactions with nuclei at 4 to 5 Mev, compound-nucleus level widths from, 18: 36645
reactions with nuclei, radiation widths for, 18: 17033
reactions with nuclei, radiation widths for, 18: 17036
reactions with nuclei, total cross sections for, 18: 26543(R) (ORNL-3582(p.75-82))
reactions with nuclei, threshold cross sections for, 18: 37552
reactions with nuclei in reactors for radioisotope production, 18: 39781(T) (AEC-tr-6390(p.488-92))
reactions with nuclei, calculations of cross sections for, 18: 42673
reactions with nuclei, angular momentum effects in fission (E), 19: 1679
reactions with nuclei, Doppler-broadened cross sections for (T), 19: 1537
reactions with nuclei, 19: 1987
reactions with nuclei, twenty-six-group cross sections for fission (E/T), 19: 3374
reactions with nuclei, computer program for cross sections for, 19: 3375
reactions with nuclei, computer analysis of cross section data for, 19: 8390 (AEEW-M-347)
reactions with nuclei, cross section tables, (E), 19: 8406 (UNC-5090)
reactions with nuclei at 11 to 101 kev, optical-model study of cross sections for, 19: 8457
reactions with nuclei, multigroup flux-weighted cross sections for, (T), 19: 10220 (GEMP-329)
reactions with nuclei, cross sections, (E/T), 19: 10643 (EURAEC-1198)
reactions with nuclei to 16 Mev, cross sections for two-particle emission in, (T), 19: 10283
reactions with nuclei, computer analysis of yields from, (T), 19: 12489 (ORNL-3673)
reactions with nuclei, (T), 19: 11590
reactions with nuclei at 35 ev to 8 kev, total cross sections for, (E), 19: 12572
reactions with nuclei, fission fragment anisotropy in, (T), 19: 12584
reactions with nuclei, thresholds for, (E), 19: 14539 (TID-21627)
reactions with nuclei, analytical uses of single-nucleon-transfer, (T), 19: 14494 (ANL-6878(p.249-75))
reactions with nuclei, computer analysis of cross sections and resonances of, (E), 19: 14506 (BNL-8710)
reactions with nuclei, measurement of total cross sections for, (E), 19: 18098 (KAPL-3074)
reactions with nuclei, group cross sections for, (T), 19: 19063 (AWRE-O-97/64)
reactions with nuclei, cross sections for, (T), 19: 21228 (ANL-6970)
reactions with nuclei, availability of cross section data for, (E), 19: 21225 (AECL-2168)
reactions with nuclei, chain element activity in intermittent, (T), 19: 21226 (AEET/HP/Th-19)
reactions with nuclei at high energies, secondary nucleon yields from, (E/T), 19: 21242 (NP-14837)
reactions with nuclei, computer analysis of cross sections for, (T), 19: 25472 (KAPL-M-6424)
reactions with nuclei, effects on reactor design criteria, (E/T), 19: 29321
reactions with nuclei, beam paramagnetic resonance in, (T), 19: 29343
reactions with nuclei, computer analysis of cross sections, (E/T), 19: 31200 (WAPD-TM-501)
reactions with nuclei, cross sections for, (E), 19: 31244 (ZfK-RN-23)
reactions with nuclei, infinitely dilute resonance integrals in, (T), 19: 33234 (AAEC/TM-270)
reactions with nuclei, echoes, giant resonances, and size resonances in cross sections for, (T), 19: 33315
reactions with nuclei at 2 to 60 kev, strength functions of, (E), 19: 35404 (ORNL-P-1371)
reactions with nuclei, cross section of, 19: 35506
reactions with nuclei in Mev region, optical model parameters for inelastic, 19: 37793 (MIT-2098-152)
reactions with nuclei, cross sections for gamma production in, (T), 19: 4326 (GEMP-360)
reactions with nuclei to 80 kev, statistical properties of resonance parameters in, (E), 19: 45296
reactions with nuclei of $88 \leq Z \leq 98$, cross sections, (E), 19: 45250 (BNL-325(2nd Ed.)(Suppl.2)(Vol.III))
reactions with nuclei, fission systematics for, (T), 19: 47614
reactions with nuclei, Doppler broadening of cross sections for, (T), 20: 3375 (IDO-17120)
reactions with nuclei, cross sections and polarization studies from, 20: 4822(R) (ANL-7081, pp 22-35)
reactions with nuclei at 0.1 to 15 Mev, gamma production cross sections for, 20: 4849(R) (UCRL-14360, pp 1-50)
reactions with nuclei, code for multigroup transfer matrices in, (T), 20: 8043 (TID-22447)
reactions with nuclei, width fluctuation factor for, (T), 20: 13824
reactions with nuclei, computer programs for charged particle cross sections from, 20: 17671 (AEEW-M-611)
reactions with nuclei, sensitivities of, for activation analysis, 20: 16332 (GA-6691)
reactions with nuclei at 14 Mev, design and performance of counter telescope for, 20: 21054
reactions with nuclei up to 100 Mev, cross-section energy-dependence model for, 20: 24360(R) (UCRL-16580, pp 107-48)
reactions with nuclei, giant resonances in, (T), 20: 24383
reactions with nuclei, semiconductor performance for charged particle detection from, 20: 25376 (AECD/EP-9)
reactions with nuclei at 14 Mev, millisecond isomer production in, (E), 20: 28431
reactions with nuclei at 14 Mev, cross sections, Q-values, and sensitivities for, 20: 32380 (SC-RR-66-229)
reactions with nuclei at 80 to 150 Mev, total cross sections for, (E), 20: 34583
reactions with nuclei, conference on structure analysis by, 20: 34656
reactions with nuclei, mechanisms for, 20: 34658
reactions with nuclei, channel theory of fission, 20: 34661
reactions with nuclei, determination of resonance parameters for, 20: 34662
reactions with nuclei, strength functions for, 20: 34663
reactions with nuclei, resonances and strength functions from, 20: 34665
reactions with nuclei, theory of doorway states in, 20: 34666
reactions with nuclei, resonance parameters from, (T), 20: 36160 (GA-7060)
reactions with nuclei, collision integral for anisotropic chain-type, 20: 36213
reactions with nuclei at 7.8 to 64 kev, activation cross sections for, (E), 20: 40069(R) (EANDC(E)-66(U))
reactions with nuclei with $Z = 13$ to 28, with charged-particle emission, 20: 44671(T) (INDSWG-101, pp 164-223)
reactions with *o*- and *p*-hydrogen, cross section codes for, (T), 19: 16367 (GA-5652)
reactions with oil and water for measurements of Lid Tank Facility dose-rate measurements, 16: 17064 (CNLM-3244)
reactions with organic mercury, phosphorus, and sulfur compounds, products from, 20: 33336(R) (PRNC-86)
reactions with orientated holmium-165 at 350 kev, 18: 32820
reactions with oxygen-16 at 0 to 15 Mev, cross sections for, 18: 9353
reactions with oxygen-18 at 0.14 to 2.47 Mev, total cross sections for, (E), 19: 12526
reactions with oxygen-18 at 2.45 to 19.0 Mev, total cross sections for, (E), 19: 12527
reactions with oxygen-16 below 15 Mev, elastic cross sections and Legendre moments for, 19: 37792 (KAPL-M-6452)
reactions with oxygen isotopes, reactor power level monitoring with nitrogen-17 from, 20: 30938
reactions with *p*-azoxyanisole, molecular motion from total cross sections for, 18: 43453
reactions with palladium-110 and titanium-50 at 14–15 Mev, rhodium-110 and scandium-50 isomeric state production in, 17: 40079
reactions with palladium at 1.2 to 10 ev, cross sections and transmission measurements for, 18: 24609 (NP-13930(p.112-13))
reactions with phosphorus pentoxide, phosphorus-32 production in, 18: 24051(T) (JPRS-24590)
reactions with phosphates, phosphorus-32 preparation in, 19: 15582
reactions with plutonium-241 at 0.02 to 2 kev, Doppler broadening of cross sections, 16: 1020 (IDO-16679)
reactions with plutonium-241 and protactinium-233, cross sections, 16: 2774(R) (IDO-16710)
reactions with plutonium-239, uranium-233, and uranium-235, calculation of excitation functions in, 17: 2265
reactions with plutonium-239 at 0.061 to 6.5 kev, capture-to-fission ratios in, 17: 11936(R) (ANL-6672)
reactions with plutonium-238 at 0.4 to 1.4 Mev, cross section for, 17: 31398 (CONF-46-37)
reactions with plutonium-239 at 0.06 to 0.3 ev, cross sections for fission, 18: 17002
reactions with plutonium-239–uranium-238 systems, Doppler coefficients for, 18: 19322 (ANL-6792(p.777-89))
reactions with plutonium-239 and uranium-238, Doppler coefficients for, 18: 19360 (ANL-6792(p.765-75))
reactions with plutonium-239, Doppler coefficients from cross sections for fission, 18: 19361 (ANL-6792(p.791-802))
reactions with plutonium-239 and uranium-238, Doppler coefficients for, 18: 19362 (ANL-6792(p.823-52))
reactions with plutonium-239–uranium-238 systems, Doppler coefficients for, 18: 19363 (ANL-6792(p.853-72))
reactions with plutonium and uranium isotopes, cross sections for fission, 18: 23064 (TID-7662(p.299-316))

reactions with plutonium and uranium isotopes, delayed and prompt neutron yields in, 18: 23026 (TID-7662(p.334-47))
reactions with plutonium-241 at 0.025 to 0.75 ev and 13.8 to 1000 ev, total cross sections for, 18: 36568 (CRRP-1186)
reactions with plutonium-239 in BR-5 Reactor, capture to fission ratio for, 18: 36582
reactions with plutonium-239 and uranium-233, resonance width distributions of, 18: 40519
reactions with plutonium-239 and uranium-233, capture and fission cross sections for (E), 19: 3384
reactions with plutonium-240 at 60 to 500 kev, cross section for fission, (E), 19: 5158
reactions with plutonium-239, and uranium-233 and -235, fragment distributions from, (E), 19: 8670
reactions with plutonium-241 at 0.025 to 1000 ev, total cross sections for, (E), 19: 8416
reactions with plutonium-239, cross sections for fission, (E), 19: 9485 (NP-14488)
reactions with plutonium-239 and uranium-233, -235, and -238, capture-to-fission ratios for, (E), 19: 10300
reactions with plutonium-239, fragment mass distributions in fission, 17: 26447(R) (ORNL-3425(p.79-82))
reactions with plutonium isotopes at 0.65 to 8.25 Mev, fission fragment anisotropy in, (E), 19: 12585
reactions with plutonium-240, effects of transition states on, (T), 19: 14526 (LA-DC-6670)
reactions with plutonium-241 at 1 kev to 15 Mev, cross sections for, 19: 14502 (AWRE-O-101/64)
reactions with plutonium-241, cross section for fission, (E/T), 19: 14572
reactions with plutonium and uranium isotopes, fractional yields from fission, (T), 19: 16845 (LA-3169)
reactions with plutonium-239 and uranium-233 and -235, absorption and fission cross sections for, 19: 17348 (NP-14795)
reactions with plutonium-239 and uranium-235, cross sections for fission, (E), 19: 15926
reactions with plutonium and uranium isotopes, fission cross sections for, 19: 19057
reactions with plutonium and uranium isotopes, fission ratios for, (E), 19: 21227 (ANL-6941)
reactions with plutonium-239 at 200 to 600 ev, symmetries in fission, (E), 19: 21241 (LA-DC-6639)
reactions with plutonium-239, uranium-233 and -235, cross sections for, 19: 29229 (BNL-918)
reactions with plutonium-239 and uranium-235, fission integrals for, (E), 19: 29224 (AE-181)
reactions with plutonium-239 and uranium-235 at 40 kev, fission neutron spectra from, (E), 19: 29269
reactions with plutonium, analysis using fast integral experiments, (T), 19: 31507 (TRG-Report-439(Rev.))
reactions with plutonium and uranium, fission fragment energy and mass from, (E), 19: 31215(R) (ANL-7010(p.1-19))
reactions with plutonium and uranium isotopes, cross sections for fission, (E), 19: 39889
reactions with plutonium-239 at 20 to 120 ev, fission cross sections for, (E), 19: 44157 (LA-DC-7304)
reactions with plutonium-239, Doppler shifts at 300 to 600°K, 20: 6556(R) (ANL-7105, pp 36-58)
reactions with plutonium-239, Doppler contributions to cross sections for, 20: 6558(R) (ANL-7115, pp 42-67)
reactions with plutonium-242, resonance parameters and total cross sections for, (E), 20: 9981 (WASH-1064)
reactions with plutonium-239, fission and total cross sections for, 20: 9981 (WASH-1064)
reactions with plutonium-239 and uranium-233 and -235, energy dependence of fragment yields from, (E), 20: 9981 (WASH-1064)
reactions with plutonium-239 and uranium-233 and -235 at 0.025 and 0.057 ev, fission neutron yields from, (E), 20: 9981 (WASH-1064)
reactions with plutonium-241 at 30 to 89 ev, fission cross sections for, (E), 20: 9981 (WASH-1064)
reactions with plutonium-239 and uranium-238, cross sections for resonance self-shielding in, (T), 20: 12374
reactions with plutonium-239 and uranium-235, fission neutron spectra from, (E), 20: 17825
reactions with plutonium-239 and uranium-235, alpha particle and fission fragment energies and yields from fission, (E), 20: 17839
reactions with plutonium-239 at 0.16 ev to 5 kev, fission cross sections for, (E/T), 20: 17851
reactions with plutonium-239 and uranium-235 at 0.0322 to 0.275 ev, fission cross sections for, (E), 20: 17854
reactions with plutonium-240 at 0.03 to 2.0 Mev, fission cross sections for, (E), 20: 17855
reactions with plutonium-239 at 200 to 600 ev, symmetry of fission, (E), 20: 17858
reactions with plutonium-239 and uranium-233 and -235, fission fragment distributions from, (E), 20: 17863
reactions with plutonium-239 to 200 ev, resonance parameters in, (E), 20: 19856
reactions with plutonium-239 at 15 to 82 ev, cadmium-115 yields from symmetric resonance fission, (E), 20: 22135
reactions with plutonium-239 at 20 ev to 2 Mev, fission cross sections for, (E), 20: 24348 (LA-DC-7620)
reactions with plutonium-240 at 0.1 and 1.6 Mev, prompt neutron yields from, (E), 20: 24377
reactions with plutonium-239, total kinetic energies of symmetric fission fragments from, (E), 20: 26213
reactions with plutonium-240 at 20 ev to 2 Mev, capture and fission cross sections for, (E), 20: 26086 (LA-DC-7623)
reactions with plutonium-238, angular distributions and cross sections for fission, (E), 20: 28459
reactions with plutonium-239 at 30 kev to 14.7 Mev, ratio of asymmetric to symmetric fission in, (E), 20: 30404
reactions with plutonium-242 at 0.02 to 400 ev, total cross sections for, (E), 20: 30465
reactions with plutonium-242, resonances and total cross sections for, (E), 20: 30360 (WASH-1068)
reactions with plutonium-241 at 20 to 74 ev, fission and resonance widths and cross sections for, (E), 20: 30360 (WASH-1068)
reactions with plutonium-240, resonances in, (E), 20: 30360 (WASH-1068)
reactions with plutonium and uranium isotopes, total energy release from, 20: 35003 (BNWL-232)
reactions with plutonium-239 and uranium-233 and -235 in subcritical assemblies, fission rates for, (E/T), 20: 36418 (AAEC-E-146)
reactions with plutonium-239 up to 200 ev, capture and fission cross sections for, 20: 36168 (JINR-P-2713)
reactions with plutonium-239 at 13.1 to 15.4 Mev, cross sections for fission, 20: 36165 (INR-688/1/PH)
reactions with plutonium-240 at 0.01 to 10 ev, total cross sections for, (E), 20: 46579 (AERE-NP-GEN-9)
reactions with polarized nuclei, resonance effects in, 18: 21127 (KR-64(Sect.XXV))
reactions with polarized nuclei, precession in, (T), 19: 5254
reactions with polyethylene, gamma activity from, 19: 30243
reactions with polyethylene, total cross section for, (E), 19: 43259
reactions with potassium-39 at 4.0 to 8.0 Mev, cross sections for charged particle production in, (E), 19: 35378(R) (EANDC(E)-57(U))
reactions with protactinium-231, uranium-232 production in, 17: 39200(R) (ORNL-3452(p.239))
reactions with protactinium-233 at 0.01 to 1.0 ev, total cross sections for, 18: 40543
reactions with promethium-147 and -148, total cross sections for, (E/T), 20: 32376 (KAPL-3090)
reactions with protactinium-233 at 0.01 ev to 10 kev, total cross sections for, (E), 20: 42151 (IN-1014)
reactions with quartz crystals, induced optical absorption in, 19: 34232
reactions with rare earths at 0.015 to 0.3 ev, total cross sections, (E), 19: 16841 (IEA-75)
reactions with rare earths at 0.0005 to 1 ev, total cross sections for, 19: 39779 (IEA-86)
reactions with rare earths at 0.025 ev to 10 Mev, cross sections for, 20: 8074 (KFK-352)
reactions with reactor matrices composed of coaxial cylindrical regions, calculation of fast fission effect for, 18: 21609
reactions with reactor materials, distributions from, 18: 37741 (A/CONF.28/P/167)
reactions with reactor materials, cross section libraries for, 18: 37597 (A/CONF.28/P/168)
reactions with reactor coolant gases, plasma production from, 18: 40680
reactions with samarium-149 at 0.1 to 0.9 ev, 18: 17037
reactions with scintillators, pulse-height distributions from, 18: 35859
reactions with shielding, gamma dose effects, 16: 23245 (NDL-TR-19)
reactions with silicon-28, magnesium-25 energy levels from, 17: 9556
reactions with silicon in semiconductor-detector diodes, 17: 37256
reactions with silica, volume changes in, 18: 5834
reactions with silicon, induced doping in, 18: 18156
reactions with silicon in semiconductor detectors, 18: 24599 (NP-13930 (p.26-38))
reactions with silicon at 5 to 9 Mev, semiconductor detector studies of cross sections for, 18: 24600 (NP-13930(p.39-40))
reactions with silicon, ionization produced by recoil atoms in, 19: 26911
reactions with silver isotopes, cadmium buildup in, (T), 19: 33246 (KAPL-M-6455)
reactions with silicon-28, use in fast neutron spectroscopy, 20: 27290
reactions with sodium-23 at 0.01 to 14 Mev, data compilation for, 18: 13039 (AEEW-R-254)
reactions with sodium at 1 to 4 Mev, optical model analysis of cross sections for, (T), 19: 14504 (BNL-904)

reactions with sodium, cross sections for, 19: 14828(R) (GEAP-4723)
reactions with sodium at 1 ev to 40 kev, cross sections for, (T), 20: 13753 (BNL-961)
reactions with sodium at 1 ev to 40 kev, cross sections for, (T), 20: 24335 (BNL-10085)
reactions with soils, calculation of gamma dose from, 16: 7769 (NDL-TR-18)
reactions with solids, structure of displacement cascades produced by, 17: 31053
reactions with spherical nuclei below 1 Mev, optical model for, 17: 40042
reactions with spin-½ nuclei, scattering widths for, 18: 17034
reactions with stilbene phosphor at 1 to 15 Mev, light pulse distributions from, 16: 3669 (TID-13075)
reactions with subcritical systems, albedo method for studying, 16: 33675
reactions with sulfur, phosphorus-32 production in, 19: 13847
reactions with sulfur, production of phosphorus-32 in, 20: 35568 (IEA-103)
reactions with tantalum-182 below 3.0 ev, total cross sections for, 18: 24584 (IDO-16956)
reactions with technetium-99 at 14 Mev, 19: 46160(R) (ORNL-3832, pp 29-32)
reactions with technetium-99, cross sections for, 20: 10940
reactions with technetium at 14 Mev, activation cross sections for, (E), 20: 14461(R) (ORNL-3889, pp 48-70)
reactions with technetium-99 at 14.8 Mev, activation cross sections for, 20: 22039
reactions with tellurium and tin isotopes at 14.2 Mev, antimony and indium ground state and isomer production cross sections for, 17: 26465 (PAN-400/I)
reactions with tellurium-130 in telluric acid, iodine-131 preparation by, 19: 15577
reactions with tellurium, iodine-131 production in, 19: 15611
reactions with telluric acid, preparation of carrier-free iodine-131 by, 19: 17981
reactions with tellurium and tin isotopes at 14.9 Mev, isomeric cross sections for, (E), 19: 33241 (INR-461/I)
reactions with tellurium to produce iodine-131, 20: 36917
reactions with tellurium, production of iodine-131 in, 20: 41399 (IEA-110)
reactions with thorium-232 and uranium-238 at 4.7 to 18.1 Mev, fission fragment mass yields in, (E), 19: 12587
reactions with terphenyls, decomposition in, 18: 38266 (A/CONF.28/P/53)
reactions with thallium for production of gamma source, 18: 32008
reactions with thorium-232 and uranium-235 at 2 to 8 Mev, total cross sections, 16: 29737
reactions with thorium-231 and 233 and uranium-235 at 0.4–3.8 Mev, K-band sequence from cross sections and fragment angular distributions in fission, 17: 26445(R) (ORNL-3425(p.72-5))
reactions with thorium, Doppler coefficient for, 18: 23064 (TID-7662(p.299-316))
reactions with thorium-232 and uranium-238, resonance cross sections for, 18: 24673
reactions with thorium-232 and uranium-238, collision probability in (T), 19: 3390
reactions with thorium and uranium isotopes, fission fragment angular distributions from, (E/T), 19: 8485
reactions with thorium-232 at 3 to 14 Mev, delayed-neutron yields in fission, 19: 21443
reactions with thorium-232 and uranium isotopes, mass yields from fission, 19: 29252 (LA-DC-6674)
reactions with thorium-232 and uranium-235, flux recovery assumptions for fission and resonance capture in, 19: 29336
reactions with thorium-232 at 0.56 Mev, differential cross section for, 19: 40115 (CONF-650602-33)
reactions with thorium-232 and uranium-238 at 14 Mev, delayed neutron precursors from, (E/T), 20: 17831
reactions with thorium-232, fission fragment yields from, (E), 20: 17860
reactions with thorium-230, resonance parameters for, (E), 20: 30360 (WASH-1068)
reactions with tin isotopes, strong p-wave resonances from, (E), 20: 39470(R) (ORNL-3924)
reactions with transneptunium elements, transcurium elements from, (T), 19: 13845 (ANL-6932)
reactions with tritium at 0.025 ev to 20 Mev, cross sections, (E), 19: 31223 (LA-3270)
reactions with tungsten isotopes at 0.001 ev to 15 Mev, cross sections, (E), 19: 19083 (GA-5885)
reactions with tungsten-182, -183, -184, and -186 at .01 to 10 ev, capture cross sections for, (E), 20: 11957 (GA-6832)
reactions with tungsten-184, resonance parameters for, (E), 20: 24421
reactions with tungsten-180 at 0.1 to 400 ev, resonance parameters from, (E), 20: 39470(R) (ORNL-3924)
reactions with tungsten isotopes, resonance parameters from, (E), 20: 39470(R) (ORNL-3924)
reactions with uranium, measurement of conversion ratio and resonance escape probability, 16: 724
reactions with uranium dioxide in CANDU type fuel elements, effects of coolant and fuel temperature changes, 16: 4677 (CRRP-985-B)
reactions with uranium-235 at 0.02 to 10 ev, channel effects in fission, (E), 19: 29369
reactions with uranium-235, effects of neutron energy on energy of fission products from, 16: 24809
reactions with uranium-235, fission fragment anisotropy in, 17: 26448(R) (ORNL-3425(p.82-9))
reactions with uranium-235, uranium-238, and plutonium-239, multiplication in, 16: 26241
reactions with uranium-238 at 14 Mev, fission-product energies from, 16: 26355
reactions with uranium-238 at 14 Mev, energy and mass distributions from, 17: 4075
reactions with uranium-235, effects of energy on energy of fission products from, 17: 9526
reactions with uranium-235 at individual resonances, fission symmetry of, 17: 26572
reactions with uranium, antimony-127 and 129 fission yields in, 17: 28278
reactions with uranium, palladium-111 and 111m cumulative yields in fission, 17: 28280
reactions with uranium-238, blocking effects of resonance of cross sections in, 17: 33021
reactions with uranium-235 and plutonium-239, fission, 17: 38005(T) (AEC-tr-5734(p.29-36))
reactions with uranium-235, cross sections for, 18: 6155 (AWRE-O-82/63)
reactions with uranium-235 at 12 to 690 kev, cross sections for, 18: 6172(R) (ORNL-3499(Vol.I)(p.11-15))
reactions with uranium-233 and -235, kinetic energy of fragments from fission, 18: 16946 (NP-13654)
reactions with uranium-238, Doppler coefficients from cross sections for radiative capture, 18: 19361 (ANL-6792(p.791-802))
reactions with uranium-235 at 0.06 to 10 ev, probability of triple fission in, 18: 18896
reactions with uranium-235, fission fragment energy distributions from, 18: 22874 (PAN-476/II)
reactions with uranium-233, multilevel analysis of, 18: 28721
reactions with uranium-235, capture-to-fission ratio for, 18: 27790(R) (ORNL-3578(p.46-59))
reactions with uranium-235 at 0.1 to 1.0 Mev, cross sections for fission (E), 19: 3374
reactions with uranium-235 at 3.25 ev to 1.8 kev, capture to fission ratios for (E), 19: 3385
reactions with uranium-238, Doppler broadening of resonances by sample motion in (T), 19: 3389
reactions with uranium-235, statistical model for fission, 19: 5207
reactions with uranium-233 at 8 to 17 ev, fission cross sections for, (E), 19: 8423
reactions with uranium-235 and -238 at 14 Mev, krypton and xenon isotope yields, 19: 12597
reactions with uranium-235 at 4 Mev, fission fragment kinetic-energy distributions from, (E), 19: 12569
reactions with uranium-235 at 0.003 to 0.3 ev, ratio of binary to ternary fission in, (E), 19: 12570
reactions with uranium-233, capture-fission ratios for, (E), 19: 14484 (AECL-2148)
reactions with uranium-233 at 4 to 15 Mev, fission cross sections for, (E/T), 19: 14501 (AWRE-O-100/64)
reactions with uranium-235, statistical model for fission, 19: 14550
reactions with uranium-236, energy balance and prompt neutron emission in fission, (T), 19: 16848 (MIT-905-30)
reactions with uranium-238 at 14.7 Mev, yields of zirconium isotopes from fission in, 19: 19135
reactions with uranium at 4.5°K, point defects in, 19: 20642
reactions with uranium-235, fission-product charge distributions in, (E/T), 19: 25534
reactions with uranium-235 at 1 to 15 Mev, cross section tabulations for, (E/T), 19: 27417 (GA-5944)
reactions with uranium-235, cross sections for fission, (E), 19: 26655 (IAE-697)
reactions with uranium-235 at 0.002 to 30 kev, fission, (E), 19: 29247 (JINR-P-2024)
reactions with uranium-235, strength functions for fission, (T), 19: 29249 (JINR-P-2068)
reactions with uranium-235 at 1.5 Mev, fission neutron spectra from, (E), 19: 29269
reactions with uranium-235 up to 20 kev, statistical properties of

levels in fission, (E/T), 19: 29277
reactions with uranium-235, ternary fission in, (E), 19: 29278
reactions with uranium-235 and -238, ratio of gamma activity per unit fission in, (E), 19: 29330
reactions with uranium-235 at 3 Mev, alpha-particle emission in fission, (E), 19: 29376
reactions with uranium-235, saddle-point rotational states from resonance fission, (E/T), 19: 31229 (ORNL-P-1067)
reactions with uranium-235 at 0.04 to 14 Mev, cross section for fission, (E), 19: 33283
reactions with uranium-235, capture/fission ratio in, (E), 19: 35723
reactions with uranium-235 and -238 and plutonium-239 at 2.086 and 4.908 Mev, neutron spectra from, (E), 19: 35440
reactions with uranium-238 from 0.001 ev to 15.0 Mev, cross sections for, 19: 39764 (GA-6087(Rev.))
reactions with uranium-235 at 3.25 ev to 1.8 kev, capture-to-fission ratio for, (E), 19: 41749
reactions with uranium-235 at 14.9 Mev, yttrium-90, niobium-96, and lanthanum-140 yields from fission, (E), 19: 41779
reactions with uranium-235, fission neutron spectra from, (T), 19: 43270 (IA-1007)
reactions with uranium-235 at 0.002 to 30 kev, fission cross sections for, (E), 19: 45292 (BNL-tr-16)
reactions with uranium dioxides, Doppler coefficients for, 19: 45532 (ORNL-TM-1219)
reactions with uranium dioxide surfaces, uranium atom ejection during fission, (T), 19: 47580 (LA-3352)
reactions with uranium-233 and -235 at 0.1 to 0.2 Mev, fission cross section structure from, (E), 20: 3089
reactions with uranium-238, effective temperature for Doppler broadening of resonances in, 20: 5135 (WCAP-3269-40)
reactions with uranium-235 in SGR lattices, epicadmium/subcadmium fission ratios for, (E), 20: 6586 (NAA-SR-Memo-11313)
reactions with uranium-233 and -235, fission fragment kinetic energy from, (T), 20: 6421
reactions with uranium-235, delayed gamma emission in fission, (E), 20: 6316
reactions with uranium-235 at 0.1 to 50 ev, binary- and ternary-fission, (E), 20: 8143
reactions with uranium-235 and -238 at 1.5 to 4.5 Mev, fission cross section ratios for, (E), 20: 9981 (WASH-1064)
reactions with uranium-235 at 300 to 800°K, resonance integrals for, 20: 10272(R) (NAA-SR-9339)
reactions with uranium-237, -238, and -239 at 14 Mev, fission fragment mass distributions from, (T), 20: 9986
reactions with uranium-235 at 0.2 ev to 10 kev, capture to fission ratio for, (E), 20: 9981 (WASH-1064)
reactions with uranium dioxide pellets, effective resonance temperature correlation for, 20: 12372
reactions with uranium-235, fission fragment energy and mass distributions in, (E/T), 20: 12117
reactions with uranium isotopes in heavy-water lattices, 20: 14103(R) (MIT-2344-4, pp 48-62)
reactions with uranium-235, cross sections for, 20: 13749 (AEEW-M-502)
reactions with uranium-235 at 150 to 335 kev, fission cross section for, (E), 20: 15818
reactions with uranium-235 and -238, twenty-group cross sections for, 20: 18057
reactions with uranium-235 at 1.86 ev to 10 Mev, cross sections for, 20: 17697 (WANL-TME-1028)
reactions with uranium-235, nucleon pairing effects on threshold fission, (T), 20: 17847
reactions with uranium-235 at 2 ev to 30 kev, fission, radiative capture, and total cross sections for, (E), 20: 17856
reactions with uranium-235, fission fragment kinetic energy from, (E/T), 20: 17867
reactions with uranium-233 at 1.7 to 30 ev, least-squares analysis of fission cross sections for, (T), 20: 17853
reactions with uranium-233, resonance fission integral for, (E), 20: 17722
reactions with uranium-235 at 0.1 to 2 Mev, cross sections for elastic, (E/T), 20: 15032(R) (ANL-7152, pp 50-72)
reactions with uranium-235 at 380 to 620 kev, fission cross sections for, (E), 20: 30425
reactions with uranium-238, capture cross sections for, (E), 20: 24345 (LA-DC-7613)
reactions with uranium-233 at 20 ev to 2 Mev, cross sections for fission, (E), 20: 24349 (LA-DC-7622)
reactions with uranium-233 at .0001 ev to 10 Mev, cross sections for, 20: 26080 (BAW-393-5)
reactions with uranium-235, prompt neutron angular spectra from ternary fission, (E), 20: 26211
reactions with uranium-235 and -238, electron emission from fission fragments from, (E), 20: 26212
reactions with uranium-235 at 0.04 to 1.0 Mev, prompt neutron yields from fission, (E), 20: 30360 (WASH-1068)
reactions with uranium-235 at 0.01 to 40 ev, fission cross sections for, (E), 20: 30360 (WASH-1068)
reactions with uranium-235 at 1 to 20 ev, capture-to-fission ratios for, (E), 20: 30360 (WASH-1068)
reactions with uranium-233, capture and fission cross sections for, (E), 20: 30358(R) (RPI-328-56, pp 1-48)
reactions with uranium-238, computer program for calculating cross sections for, 20: 30356 (ORNL-TM-1448)
reactions with uranium-235 at 0.03 to 200 ev, cross sections for, (E/T), 20: 30342 (AERE-M-1670)
reactions with uranium-238, capture-to-fission ratios for, 20: 32391
reactions with uranium at 1 to 10 Mev, cross sections for, 20: 35841(R) (NAA-SR-11900)
reactions with uranium-238 at 14 Mev, krypton and xenon isotope yields from fission, (E), 20: 36171 (NP-16155)
reactions with uranium-235 at 14 Mev, fragment activity and gamma spectra from, (T), 20: 36181 (USNRDL-TR-1009)
reactions with uranium-235, spins of resonances in, (E), 20: 44619 (CONF-660303, pp 755-62)
reactions with uranium-235 at 8- to 40-ev, symmetry from fission, 17: 19220 (PNE-114F)
reactions with uranium isotopes, distributions of fragments from, fission, 17: 31029
reactions with vanadium-50 at 3 to 60 kev, resonance parameters and total cross sections for, (E), 20: 30360 (WASH-1068)
reactions with vanadium at 21.65 to 152.6 kev, resonance parameters for, (E), 20: 40069(R) (EANDC(E)-66(U))
reactions with X-211 turbomachinery materials, activation response of, 20: 28591 (DC-59-3-90)
reactions with xenon-124, electron-capture production of iodine-125 in, 18: 18263
reactions with yttrium-89 at 15 kev, level parameters from, (E), 19: 5172
reactions with ytterbium isotopes, spectra of resonance, 19: 41661 (JINR-P-2158)
reactions with yttrium-89 at 4 kev to 3 Mev, capture cross sections for, (E), 20: 26394(R) (ANL-7193)
reactions with zinc-70 at 14 to 15 Mev, nickel-67 production in, (E), 19: 27564
reactions with zirconium isotopes, strength functions for, (E), 19: 35401 (ORNL-P-1346)
reactivity effects in compressible fissile media, 18: 42345
reactivity effects in SNAP reactors, 19: 10619 (NAA-SR-Memo-10421)
reactor criticality effects of photoneutrons in beryllium-moderated reactors, 16: 7301(XDC-58-4-58)
reflection and transport by soil at Nevada Test Site, 17: 24599 (BRL-
reflection and transmission by aluminum slabs, Monte Carlo results on, 18: 24564 (BRL-1238)
reflection and transmission by strongly absorbing slab, (T), 19: 27414
reflection and transmission by strongly absorbing slab, (T), 19: 33205
reflection and transmission of, multiple collision calculation of, 17: 34839 (EUR-367.e)
reflection by cobalt mirrors, analysis of total, (E), 19: 21201(T) (KFK-tr-164)
reflection by concrete, (E), 20: 46928(R) (ORNL-3973(Vol.1), pp 26-47)
reflection by oriented single crystals in neutron monochromators, (E/T), 20: 13709 (PAEC-IPA(D)PH-652)
reflection by powders, 17: 38049(T) (AEC-tr-5734(p.280-2))
reflection from cobalt mirrors, total, 18: 11157
reflection from metallic mirrors, total, 17: 4033
reflection from semi-infinite slab, angular distribution and reflection coefficient for, 17: 28437 (KAPL-2000-20)
reflection from slabs of concrete, angular distributions for, (E/T), 20: 34797
reflection from strongly absorbing media, 16: 4745
reflection in elliptic systems, 19: 41645
reflection in large mosaic crystals, monochromator efficiency and multiple Bragg, (T), 19: 47562
reflection of, design of refractometer for, 18: 23838 (NP-13930(p.122-4)) 1190)
reflection of, image source method for calculating, 20: 1061
relaxation length in air in BREN Operation, 18: 429 (CEX-62.03)
relaxation of pulse of, in heavy medium (T), 19: 3192
research in U.S.A., review of, 18: 43147
research with pulsed, 17: 17419(R) (MITNE-26)
resonance absorption measurement by pulsed source, feasibility of, 20: 4806(R) (RPI-328-40, pp 1-42)
resonance absorption integrals of, effects of resonance overlap on, 20: 30421
resonance calculations for, methodology for, 20: 11945
resonance escape integrals in heterogeneous systems, (T), 20: 8356
resonance escape probability from cylinders, computer program for

calculating, 20: 1133 (IDO-17075)
resonance escape probability in reactors, methods for determining, (T), 20: 28723
resonance escape probability in reactors, moderator void dependence of, (E/T), 20: 28724
resonance escape probability in arrayed cladded fuel lattice, Dancoff factor for, 20: 30842
resonance escape probability in water-moderated thorium lattices, (E), 20: 34973
resonance escape probability in thorium–water lattices, (E), 20: 34985
resonance escape probability and thermal utilization in water-moderated natural uranium exponential assemblies, (E), 20: 34974
resonance integrals for uranium-238, methods for calculating, (T), 20: 1158 (ORNL-TM-1296)
resonance integrals for thorium dioxide and uranium carbide and dioxide, temperature-dependent, (T), 20: 1148 (CRRP-1222)
resonance integral for gold-197, 20: 8316(R) (NAA-SR-11450, Sect.7)
resonance integrals for uranium-235, capture and fission, (E/T), 20: 10274(R) (NAA-SR-11605, Sect. 1)
resonance integral for gold-197, (E/T), 20: 10275(R) (NAA-SR-11650, Sect. 5)
resonance integrals for plutonium-240 and uranium-238, (T), 20: 9950
resonance integrals for, cadmium cutoff energies for, (T), 20: 9951
resonance integrals for heterogeneous media containing gold particles, (E/T), 20: 9952
resonance integrals in MITR, measurement of effective, (E), 20: 14186(R) (MIT-2344-4, pp 145-8)
resonance integrals for, second order approximations for effective, 20: 17650 (AAEC/E-144)
resonance integrals for, sample preparation methods for, 20: 45046(R) (IDO-17192)
resonance parameter measurements in reactor materials, 20: 46966(R) (NAA-SR-12010)
role in lithium-6 three-body model, 16: 17079
role in lithium-6 three-body model, 16: 17079
role in nuclear reactions, review, 18: 4600
role in nuclear reactions, review, 18: 4600
scattering and transport in fusion reactor blanket assemblies, 20: 6451 (AD-619668)
scattering angular distributions of, computer program for correcting, 20: 44597
scattering at air-ground interface, Monte Carlo calculation of, 16: 26200 (ORNL-3287)
scattering at interfaces, equations for (T), 19: 3467
scattering at low energies, complex potential model for, 16: 5865
scattering at low energies, quasi-elastic magnetic, 17: 32985
scattering at low energies, temperature dependence in elastic and inelastic (T), 19: 3191(R) (RPI-328-16)
scattering at 0.05 to 1.5 ev, 17: 34560(R) (TID-19195)
scattering at 0.10, 0.15, and 0.25 ev by water at 22°C, quasi-elastic, 17: 5297 (HW-75147)
scattering at 24 Mev, polarization in, 17: 4096
scattering at 4 and 14.8 Mev, gamma production cross sections for, 18: 28579 (TID-20689)
scattering by A = 208 nuclei at 8 Mev, excitation of 3^- collective state in inelastic, (E/T), 20: 13870
scattering by air, computer program for determining energy and angular distribution, 16: 19881 (DC-60-7-119)
scattering by alkali and alkaline earth hydroxide lattices, spectra from inelastic, 18: 39154 (EUR-1643.e(p.174-80))
scattering by alkali halides, anharmonic effects in, 19: 26922(R) (PR-P-64)
scattering by alloys and disordered systems, diagnostic uses of diffuse elastic, (E), 19: 43485
scattering by alpha particles at 2 to 23 Mev, 16: 8103 (TID-14475)
scattering by alpha particles at 16 to 26 Mev, angular distributions for, 18: 28698
scattering by alpha particles, phase shifts for, (T), 19: 45217 (COO-7-0363)
scattering by aluminum and sodium, 18: 21698(R) (ANL-6860)
scattering by aluminum at 2.76 Mev, energy spectra and total cross section for, 17: 13514
scattering by aluminum, beryllium, carbon, iron, and polyethylene, dose measurements in small-volume, 18: 26532 (NAA-SR-9418)
scattering by aluminum, argon, and sodium, inelastic, (E), 19: 31217 (IDO-17042(p.11-47))
scattering by aluminum-27 at 1 to 5 Mev, cross sections for elastic and inelastic, (T), 19: 37781 (BNL-927)
scattering by aluminum-27 and silicon-28 at 14.2 Mev, core excitation model for inelastic, (E/T), 19: 37854
scattering by aluminum and chromium single crystals, time-of-flight method for, (E), 19: 47894
scattering by aluminum, magnesium, and silicon at 3 to 4.5 Mev, gamma angular distributions from inelastic, (E/T), 19: 47638
scattering by aluminum-27 at 14.2 Mev, differential cross sections for inelastic, (E), 20: 4891
scattering by aluminum, copper, iron, and magnesium at 12 to 14 Mev, total cross sections for, (E), 20: 11949 (AD-625747)
scattering by aluminum, iron, and teflon at 130 to 160 kev, cross sections for, (E), 20: 13716
scattering by aluminum-27 at 4.5 and 7.5 Mev, gamma production in, (E), 20: 24344 (LA-DC-7612)
scattering by aluminum-27 and fluorine-19 at 14.2 Mev, cross sections for, (E), 20: 40069(R) (EANDC(E)-66(U))
scattering by aluminum, iron, and uranium, inelastic, 20: 44613 (CONF-660303, pp 577-98)
scattering by aluminum at 2.52 Bev, nonelastic, (E), 20: 44828
scattering by ammonium salts, energy distributions and lattice dynamics from inelastic, 16: 32371
scattering by ammonium halides, energy distribution for, 17: 20975
scattering by ammonium iodide solid solutions, measurement of ion motion by, 19: 23255 (PAN-S69/II)
scattering by ammonium salts, inelastic, 19: 29228(R) (AEET/NP/10)
scattering by ammonium perchlorates and perchloric acid, inelastic, (E), 19: 32168
scattering by anharmonic crystals, 17: 31387
scattering by anharmonic crystals, phonon frequencies and lifetimes from inelastic, 18: 2830
scattering by anharmonic crystals, energy distributions in, 18: 15163
scattering by anharmonic crystals, damping theory for, 18: 30688 (N64-14946)
scattering by anharmonic crystals, scattering function for inelastic, 18: 34460
scattering by anharmonic crystals, functions for inelastic, 18: 34748
scattering by anharmonic crystals, damping theory for, 19: 35363
scattering by anharmonic crystals at low temperatures, inelastic, (T), 19: 40093
scattering by anharmonic crystals, one-phonon resonances in inelastic, (T), 19: 43491
scattering by antiferromagnetic crystals, effects of phonon and spin interactions on, 16: 29720
scattering by antimony, molybdenum, tungsten, and uranium, elastic, (E), 19: 17017
scattering by antimony, cadmium, copper, and tin at 1 Mev, cross sections for inelastic, (E), 20: 30383
scattering by argon-40 at 3 to 4.5 Mev, gamma angular distributions from inelastic, (E/T), 19: 47639
scattering by atactic and isotactic propylene, spectra of, 18: 13819
scattering by atomic systems, four-correlation function for resonance, 16: 22859
scattering by atoms and molecules, distributions from, 18: 36080(R) (RPI-328-8)
scattering by atoms and molecules, elastic and inelastic, 18: 40474 (IDO-16977(p.23-43))
scattering by atoms of crystal lattice, effects of magnetic moment and spin on, 19: 12466
scattering by barium, molybdenum, potassium, sodium, and strontium at 2.5 Mev, inelastic cross sections, 16: 29741
scattering by barium titanates, 17: 23862(R) (AD-286036)
scattering by barium-138, cerium-140, copper-63, iron-56, and zirconium-90, inelastic, (E), 19: 16973
scattering by barium, cerium, copper, iron, and zirconium at 0 to 200 kev, inelastic, (E/T), 20: 34652
scattering by benzene, biphenyl, and terphenyl, cross sections for low-energy, 20: 6272
scattering by beryllium and beryllium oxide crystal phonons at 0.015 to 0.132 ev, 16: 32383
scattering by beryllium, 17: 17623(R) (IDO-16827)
scattering by beryllium powder, 17: 22967(R) (IDO-16857)
scattering by beryllium-9 at 0.2 to 2.0 Mev, differential cross sections and polarization for, 17: 41536(R) (ANL-6767)
scattering by beryllium, cross sections and kernels for, 18: 4513 (GA-4638)
scattering by beryllium-9 at 0.2 to 2.0 Mev, 18: 7675 (CONF-327-8)
scattering by beryllium, inelastic, 19: 1956(R) (IDO-16994)
scattering by beryllium, coherent effects in, (T), 19: 8376(R) (GA-5176)
scattering by beryl containing one percent adsorbed water, determining water molecule motions from, (E), 19: 12069
scattering by beryllium, scattering law for, (E), 19: 33192(R) (GA-6096)
scattering by beryllium-9 at 14 Mev, differential cross sections for elastic, (E/T), 19: 35410
scattering by beryllium-9 at 14 Mev, (E), 19: 47609
scattering by beryllium, beryllium oxide, and graphite at 22°C, (E), 19: 1544 (AERE-R-4732)
scattering by beryllium oxide, microstructure and temperature effects in, 20: 5180 (NAA-SR-Memo-11604)

scattering by beryllium-9 at 2.60 to 2.77 Mev, polarization from elastic, (E), 20: 30414
scattering by beryllium oxides, phonon spectra from, 20: 36140(R) (GA-7091)
scattering by beryllium, measurement of dispersion relation by, 20: 42541
scattering by beta brass, cross sections for, 17: 6705
scattering by beta brass, critical, (E), 19: 47904
scattering by bismuth-209 and carbon-12, distributions from, 17: 5359
scattering by bismuth, tantalum, thorium, and uranium at 15.2 Mev, 17: 26638
scattering by bismuth, lead, and sulfur at 14 Mev, excitation cross sections from inelastic, 17: 26440(R) (ORNL-3425(p.46-9))
scattering by bismuth, tantalum, thorium, and uranium at 15.2 Mev, angular distributions in elastic, 18: 21340
scattering by bismuth, carbon, lead, silicon, and zirconium, elastic, (E), 19: 5238
scattering by bismuth at 2.5 Mev, cross sections for, (T), 20: 36392(R) (ANL-7219, pp 28-54)
scattering by boron, anisotropy of elastic, 18: 15136 (NAA-SR-Memo-9019)
scattering by boron, nitrogen, and oxygen, amplitudes for coherent, (T), 19: 27555
scattering by boron-10, resonances in cross sections for, (T), 19: 27555
scattering by boron-11 in orthoboric acid, 20: 12836
scattering by boron, calcium, carbon, and potassium at 14.0 Mev, cross sections for elastic, (E), 20: 22119
scattering by boron-10 and -11 in boron oxides, amplitudes for coherent, 20: 30335
scattering by boron, calcium, carbon, and potassium, elastic, (E/T), 20: 46574
scattering by bromine, energy and frequency distributions in, 16: 31051 (AECL-1578)
scattering by cadmium at 0.45 Mev, differential cross section, and polarization in, 17: 16770(R) (ANL-6666)
scattering by cadmium, indium, and silver at 0.3 to 1.5 Mev, differential cross sections for, (E), 20: 13829
scattering by calcium, carbon, and oxygen at 14 Mev, gamma spectra from, 17: 24511
scattering by calcium-40 at 14.1 Mev, differential cross sections for, 18: 38127
scattering by calcium and carbon, cross sections for, (E), 19: 19095 (WASH-1053)
scattering by calcium at 1 to 14 Mev, differential cross sections for elastic, (E/T), 20: 9981 (WASH-1064)
scattering by calcium-40 at 3.15 Mev, cross sections for compound elastic, (E/T), 20: 15865
scattering by calcium at 2.15 to 6.53 Mev, differential elastic cross sections for, 20: 38183
scattering by calcium-41 at 1 to 2 Mev, cross sections for elastic, (E), 20: 40087
scattering by carbon, deuterium, and oxygen at 1 Mev, polarization in, 17: 19045 (TID-16659)
scattering by carbon-12, mechanism for resonances in elastic, 17: 26608
scattering by carbon-12 at 14 Mev, differential and excitation cross sections for, 17: 28301
scattering by carbon-12 and oxygen-16, effects of Wood-Saxton potential on elastic, 17: 40013
scattering by carbon at low energies, phase-shift calculation of cross sections for, 18: 1036
scattering by carbon-12 at 14.1 Mev, elastic and inelastic, 18: 26600
scattering by carbon-12 at 17.2 to 21 Mev, resonances in cross sections for elastic, 18: 28572 (ORNL-3615)
scattering by carbon-12 at 14 Mev, angular distributions from, 18: 42629 (CEA-R-2407)
scattering by carbon-12 and magnesium-24 at 14 Mev, gamma emission in inelastic, 18: 44794
scattering by carbon-12 at 1 to 2 Mev, polarization in, 18: 44844
scattering by carbon-12 in organic scintillators, recoil detection in, 19: 15902
scattering by carbon-12 at 17 to 21 Mev, resonances in, (E), 19: 21310
scattering by carbon at 4.4 to 8.5 Mev, polarization from, (E), 19: 23722
scattering by carbon, strong-coupling calculations for, (T), 19: 27526
scattering by carbon-12, lithium-6, and lithium-7 at 14 Mev, inelastic, (E), 19: 47609
scattering by carbon, iron, and lithium-7 at 14.6 Mev, angular distributions, cross sections, and energy levels in inelastic, 20: 1144 (AD-614451)
scattering by carbon, iron, and lithium-7 at 14.6 Mev, inelastic, (E/T), 20: 2962
scattering by carbon-12 at 2.48 and 3.77 Mev, cross sections for, (T), 20: 8100
scattering by carbon-12 at 0.1 to 4.5 Mev, Feshbach theory for, 20: 8104
scattering by carbon-12 and oxygen-16 at 3.0 to 4.7 Mev, carbon-13 and oxygen-17 level parameters from elastic, (E), 20: 17767
scattering by carbon-12 and oxygen-16 at 14.1 Mev, gamma emission in, (E), 20: 19817 (INR-661/1A/PL)
scattering by carbon-12 and oxygen-16, resonance parameters for elastic, (T), 20: 22010(R) (NYO-72-28)
scattering by carbon-12 below 4.5 Mev, unified reaction theory for elastic, 20: 28333
scattering by carbon-12, polarization in elastic, (E/T), 20: 32359
scattering by carbon-12 at 14.1 Mev, level excitation from, (E), 20: 32408
scattering by carbon-12 at 16 to 20 Mev, optical-model analysis of elastic, (E/T), 20: 40088
scattering by carbon-12 at 14 Mev, calculations by dispersion method for inelastic, (T), 20: 40104(T)
scattering by carbon-12 at 1 to 10 Mev, differential elastic, (E), 20: 41556
scattering by carbon-12 at low energy, channel coupling in, (T), 20: 44653 (PUC-937-219)
scattering by carbon-12 at 7.5 Mev, gamma spectra from inelastic, (E), 20: 46588 (LA-DC-7853)
scattering by carbon at 1 to 10 Mev, (E), 20: 46599(R) (RPI-328-68, pp 1-62)
scattering by carbon-12 at 6.0, 7.0, and 7.5 Mev, gamma, angular distribution from inelastic, (E), 20: 46588 (LA-DC-7853)
scattering by cesium, amplitude for coherent, 20: 15736
scattering by chemically bound atoms, impulse approximation for resonance, 18: 6049
scattering by chlorine-35 and -37 at 4 and 6 Mev, level parities and spins from inelastic, (E), 20: 32550
scattering by chlorine at 14.2 Mev, elastic and inelastic, (E), 20: 44746
scattering by chromium, determination of atomic magnetic moment by, 16: 23000(R) (ORNL-3268(p.76-9))
scattering by chromium oxide, ferric oxide, and franklinite, inelastic, 16: 32369
scattering by chromium, magnetic, (E), 19: 18520
scattering by chromium, iron, and nickel, cross sections for inelastic, 19: 35605(R) (ANL-7045(p.24-48))
scattering by closed-shell nuclei, intermediate resonances in, 18: 34768 (MIT-2098-61)
scattering by closed-shell $f_{7/2}$ nuclei at 14.1 Mev, evaporation mechanism in inelastic, (E), 19: 37788 (INR-591/1A/PL)
scattering by coal, 19: 5777(R) (TID-20080)
scattering by cobalt–iron alloys, magnon spectrum in, 19: 38062
scattering by cobalt-59 at 5.2 Mev, differential cross sections for inelastic, (E), 20: 8062(R) (COO-720-058)
scattering by cobalt indium, gold, silver, and tantalum at 3.5 to 8.5 Mev, level density parameters from, (E), 20: 13827
scattering by cobalt, temperature dependence of amplitudes for magnetic, 20: 20335
scattering by cobalt-59, level spin assignments from, (E), 20: 30360 (WASH-1068)
scattering by compound nuclei at 3.1 Mev, cross sections, 16: 29743
scattering by complex nuclei, optical model analysis of elastic, 18: 15221
scattering by complex nuclei below 50 Mev, data survey for elastic polarized, 20: 3014 (LA-DC-7386)
scattering by concrete at 0.1 to 14 Mev, differential dose albedo for, 18: 40734 (AD-600684)
scattering by concrete, graphite, and water, angular distributions for, (E), 20: 28597
scattering by conduction electrons and impurities in metals, polarization effects on, 20: 26377(T)
scattering by copper, iron, and nickel at 700 to 1300 kev, cross sections for elastic, 18: 4511 (CONF-250-13)
scattering by copper at 0.5 to 10 Mev, optical model calculation of cross sections for (E/T), 19: 1567 (RFR-223)
scattering by copper at 0.8 to 1.75 Mev, cross sections and energy levels for (T), 19: 3243 (RFR-239)
scattering by copper crystal dislocations, (E), 19: 6411
scattering by copper crystals, phonon spectra from inelastic, 19: 35588
scattering by copper, dispersion relations for lattice vibrations from, (E), 19: 41996(T)
scattering by copper-65 and zinc-67, resonant, 20: 7430
scattering by copper, potentials from second-order multiple scattering theory elastic, 20: 19933
scattering by crystal imperfections, diffusion effects, 16: 960
scattering by crystals, effects of crystal anharmonicities calculated by Feynman ordered operator calculus, 16: 7150
scattering by crystals, computer program for cross section evaluation, 16: 10390 (GA-2492)
scattering by crystals, slow inelastic, 16: 22982
scattering by crystals, elastic resonance, 16: 26203(T) (AEC-tr-5145)

scattering by crystals, incoherent approximation, 16: 29727
scattering by crystals, determination of polarization vectors from inelastic, 16: 32170 (AECL-1572)
scattering by crystals, effects of four-phonon interactions on energy distributions in, 17: 11510
scattering by crystals with impurity nuclei, reconstruction of vibrational spectrum of, 17: 22547
scattering by crystals, method for calculating, 17: 28226 (UCRL-7267)
scattering by crystals, research programs on, 18: 16894(R) (MIT-3031-1)
scattering by crystal lattices, one-phonon, 18: 26130
scattering by crystals and fluids, 18: 26509
scattering by crystals, phonon spectra from incoherent, 18: 26520(T)
scattering by crystals, 18: 34455
scattering by crystals, conference on, 18: 37138
scattering by crystals, (T), 19: 8388
scattering by crystals, elastic, 19: 12466
scattering by crystals, properties of cross sections for inelastic, (T), 19: 14633
scattering by crystals at small angles, lattice defects from, 19: 18717
scattering by crystalline polyethylene at 0.027 ev, 19: 23617
scattering by crystals, phonon correlation function and coherent inelastic, 19: 23976(T)
scattering by crystalline perchloric acid monohydrate, barrier to rotation height of hydronium group by, 19: 30158
scattering by crystals, incoherent, (T), 19: 39176
scattering by crystal defects, data tabulations of sin x/x for, 19: 43467 (AERE-R-4934)
scattering by crystals, effects of anharmonicity and impurities on, (T), 19: 43266
scattering by crystals, theory for inelastic, 19: 43267
scattering by crystals of polyethylene at 0.17 to 0.50 ev, (E/T), 20: 2964
scattering by crystals, two-level impurity effects on one-quantum inelastic, (T), 20: 8306(T)
scattering by crystals, phase determination from, 20: 17041
scattering by crystals and liquids, research on slow inelastic, 20: 22316 (JINR-P-2081)
scattering by crystals, automatic data analysis of, 20: 32681 (BNL-10238)
scattering by crystals, design of pressure vessel for measurement of pressure-induced phonon energy shifts from inelastic, 20: 36358 (SGAE-PH-43/1966)
scattering by cylinders, Monte Carlo calculation of, 18: 2824
scattering by cylinders, Monte Carlo calculations on, 18: 6147(R) (ORNL-3499(Vol.I)(p.159-61))
scattering by defects in neutron-irradiated graphite, elastic, 18: 24207
scattering by deformed nuclei at high energies, 16: 8228
scattering by deformed nuclei, inelastic, 19: 10361
scattering by deuterons, Lee model field theory analysis of, 16: 4613(R) (NP-11098(p.14-22))
scattering by deuterium at 0.5 to 1.95 Mev, differential cross section and polarization of, 17: 6777(R) (ANL-6603(p.9-19))
scattering by deuterium and hydrogen, solution of transport equations for, anisotropic, 17: 20958 (LAMS-2873)
scattering by deuterium, anisotropy of elastic, 18: 15134 (NAA-SR-Memo-9017)
scattering by deuterium and hydrogen below 1 ev, kernels for, 18: 28546
scattering by deuterium and hydrogen molecules at 0.007 to 3 ev, cross sections for, 18: 30818
scattering by deuterium at 3.8 and 4.6 Mev, polarization in elastic, (E), 20: 19870
scattering by deuterons at 1 to 5 Mev, angular distributions for elastic, (E), 20: 42359
scattering by deuterium at 8 Mev, differential cross section for elastic, (E), 20: 46588 (LA-DC-7853)
scattering by diamond and silicon, Debye-Waller factor for, 20: 24791 (IKF-16)
scattering by disordered crystals, (T), 19: 8386
scattering by doped crystals, electron-phonon interaction effects in inelastic, (T), 19: 20671
scattering by elements, transfer matrices for, (T), 19: 19087 (NAA-SR-Memo-9055)
scattering by elements at 14 Mev, collective-state excitation by inelastic, (E/T), 19: 23697
scattering by elements, optical model calculations for elastic, (T), 19: 41827
scattering by ethane at 0.020 to 0.064 ev, inelastic, 20: 4810
scattering by ethylene polymers at 0.089 to 1.0 ev cross sections for, 18: 16891(R) (GA-4881)
scattering by ethylene at 22 to 72 Mev, inelastic, (E), 19: 12478
scattering by ethylene polymers at 0.167 to 0.499 ev, inelastic, (E), 19: 47572 (GA-6547)
scattering by even-even nuclei at 2.5 Mev, shell model calculations for, 20: 24338 (CONF-660411-1)
scattering by excitons in crystals, cross sections for, (T), 20: 18006
scattering by fcc manganese–palladium alloys, magnetic, (E/T), 19: 37118
scattering by ferromagnets, magnetic field effects on, 18: 4520
scattering by ferromagnets, property studies by, 18: 7658 (BNL-7550)
scattering by ferromagnets, magnetic inelastic, (T), 19: 16415
scattering by ferromagnet at Curie temperature, Landau approximation for, (T), 19: 19023
scattering by ferromagnetic materials, Landau approximation for inelastic magnetic, 19: 23603
scattering by ferroelectric salts, uses for analysis of low-frequency vibrations, 19: 45241
scattering by ferromagnetic materials near phase-transition point, polarized, (T), 20: 17987(T)
scattering by ferromagnetic terbium, magnon spin-wave dispersion relations for inelastic, (E), 20: 24609
scattering by ferromagnetic alloys, cross sections for elastic, (E/T), 20: 26346 (NP-16010, pp 1-41)
scattering by ferromagnetic materials, critical, (T), 20: 28672
scattering by ferromagnets in region of ferroacoustic resonance, cross sections for inelastic, (T), 20: 32722(T)
scattering by ferromagnetic materials, critical magnetic, 20: 40316
scattering by fluid composed of nonspherical molecules, (T), 19: 16382
scattering by fluorine-19, resonances from, 17: 19223 (TID-16621)
scattering by fluorine-19, differential cross sections for, (E), 20: 30360 (WASH-1068)
scattering by free molecules at low energy, (T), 19: 33212
scattering by fused quartz at 0.00065 to 2.0 ev, cross sections for, (E), 20: 22010(R) (NYO-72-28)
scattering by gadolinium at 0.01 to 0.4 ev, cross sections for, (E), 20: 22010(R) (NYO-72-28)
scattering by gallium, amplitudes for coherent, 18: 13113(T)
scattering by gas and solid targets, nuclear plate camera for measuring, 20: 27317
scattering by gaseous moderators, SOPHIST I code for, 16: 9583 (UCRL-5956)
scattering by gaseous ammonia molecules at 0.005 ev, cross section for, 18: 18854
scattering by gaseous and solid deuterated methane, (E), 20: 30360 (WASH-1068)
scattering by gaseous deuterated methane at 0 to 156 Mev, intramolecular coherent, (E), 20: 38000
scattering by gaseous methane at 0.025 ev, calculation of, (T), 20: 38004
scattering by gases and liquid in effective-width model, (T), 20: 44595
scattering by Gaussian and harmonic well potentials, 18: 18666
scattering by germanium, inelastic, 19: 26922(R) (PR-P-64)
scattering by gold, mercury, and thallium at 300 to 1500 kev, 18: 21698(R) (ANL-6860)
scattering by gold-197 and tantalum-181 at 5.5 and 7.5 Mev, gamma spectra from, (E), 19: 6677
scattering by gold-197 at 400 to 700 kev, cross sections for inelastic, (T), 19: 17037
scattering by gold-197, cross sections for inelastic, 19: 16883
scattering by gold, mercury, and thallium at 0.3 to 1.5 Mev, cross sections for, (E), 19: 19095 (WASH-1053)
scattering by gold, mercury, and thallium at 0.3 to 1.5 Mev, cross sections for, (E), 19: 19224
scattering by graphite, heavy water, and water, 16: 21331 (AERE-R-4019)
scattering by graphite at 0.03 to 0.15 ev, 16: 33910
scattering by graphite, 17: 3731
scattering by graphite, kernel for (E/T), 19: 3379
scattering by graphite, phonon spectra of, (E), 19: 19095 (WASH-1053)
scattering by graphite at 0.17 to 0.30 ev, excited levels from inelastic, (E), 20: 34812 (BNL-940, pp 94-5)
scattering by graphite, equipment for, 20: 41075 (AERE-R-5217)
scattering by hafnium, cross sections for slow, 18: 38088
scattering by hard-sphere nuclei, total elastic cross sections, 16: 18419
scattering by heavy ice at 4 and 77°K, cross sections for, 17: 41853
scattering by heavy water at 22 and 150°C, law for, 18: 28528 (AERE-R-4582)
scattering by heavy nuclei, analysis of inelastic, 18: 34910
scattering by heavy and medium nuclei, inelastic, 18: 38146
scattering by heavy elements, inelastic, 18: 44931(R) (ANL-6936(p.39-72))
scattering by heavy and medium nuclei, inelastic, 18: 44777
scattering by heavy nuclei, cross sections for, 18: 44760
scattering by heavy water, molecular conglomerates in, 19: 21221
scattering by heavy media, synthetic kernels for, (T), 20: 9955
scattering by heavy gases, correlation function for multiple elastic, (T), 20: 26073
scattering by helium (liquid), spectra of density fluctuations by

excitation in, 16: 17061 (AROD-431:45)
scattering by helium II, anomalous fluctuations in cross sections for, 17: 25924
scattering by helium, asymmetry of double, 18: 11277
scattering by helium, polarization in, 18: 38121
scattering by helium at 1.12 to 2.57°K, energy transfer in, 19: 26922(R) (PR-P-64)
scattering by helium-4 at 25 to 34 Mev, angular distributions and polarization in, (E), 19: 45259 (IAE-834)
scattering by helium-4 at 22 to 29 Mev, helium-5 energy levels from elastic, (E), 20: 6335
scattering by helium-4 at 262 kev, polarization in, (E), 20: 13717
scattering by helium-4 at 8 to 31 Mev, cross sections for elastic, (E/T), 20: 34654
scattering by hematites, magnetic, (E/T), 19: 11766
scattering by hematites at 0.0053 ev, spin wave spectra from inelastic, (E), 20: 38355 (ITEF-355)
scattering by hexagonal lattices, computer code for coherent elastic, 19: 31189 (GA-6026)
scattering by hexagonal cobalt, spin-wave-dispersion relations from polarized inelastic, (E), 20: 24648
scattering by holmium nitrides, studies of atomic magnetic moments by, 16: 23001(R) (ORNL-3268(p.80-1))
scattering by holmium-165 at 350 kev, nuclear deformation effects in, 19: 35397 (ORNL-P-1302)
scattering by hydrogen-charged nickel–palladium alloys, magnetic, 17: 2217
scattering by hydrogen (liquid ortho and para), 17: 15213(R) (GA-3409)
scattering by hydrogenous compounds, 17: 32986
scattering by hydrogen in zirconium hydrides at 0.01 to 0.55 ev, analysis of elastic, 18: 13043 (GA-4490(Rev.))
scattering by hydrogen, analytical applications of, 18: 13670
scattering by hydrogen multigroup equations for, 18: 15476
scattering by hydrogenous moderators, inelastic, 18: 40544
scattering by hydrogen-bonded ferroelectrics, inelastic, 18: 39155 (EUR-1643.e(p.181-7))
scattering by hydrogen layers in alkali and alkaline earth hydroxides, spectra of inelastic, (E), 19: 45482
scattering by hydrogenous reactor moderators, reaction rate curves for, (E/T), 20: 19776 (AE-223)
scattering by hydrogenous compounds, cross sections for, 20: 22010(R) (NYO-72-28)
scattering by hydrogen in palladium, diffusion constants from inelastic, 20: 34856
scattering by ice and water, total effective cross section for, 16: 28019
scattering by impurity centers in crystals, theory of inelastic, 16: 13938
scattering by impurity centers of crystals, theory of magnetic, 17: 11511
scattering by impurity atoms in crystals, (T), 19: 43493
scattering by indium-115, determination of d-wave strength function from inelastic, 18: 2905
scattering by indium-115 at 1 to 14.6 Mev, isomeric production cross section for, 18: 28709
scattering by indium-115, isomeric states from inelastic, (E), 19: 21237 (KFK-265)
scattering by indium-115, cross sections for inelastic, 20: 12160
scattering by indium-113 and -115, cross sections for inelastic, (E), 20: 30360 (WASH-1068)
scattering by intermediate and heavy nuclei at 0.5 to 0.8 Mev, cross sections for elastic, 18: 26568
scattering by ionic single crystals, effects of charged defects on, 16: 22919
scattering by iridium, rhenium, and samarium isotopes, spin determinations from, (E), 19: 35378(R) (EANDC(E)-57(U))
scattering by iridium-191, cross sections and spin assignments for resonant, (E), 20: 13796
scattering by iron, cross sections for gamma production in inelastic, 16: 12489
scattering by iron and water, dieaway curves for, 17: 2341(R) (TID-17186)
scattering by iron, tungsten, and uranium, elastic, 17: 4225(R) (ANL-6635(p.28-50))
scattering by iron at 0.80 to 4 Mev, inelastic, 17: 17473
scattering by iron and nickel at Curie point, 17: 20979
scattering by iron, amplitude for magnetic, 17: 37815
scattering by iron–manganese–zinc, alloy, 17: 38031(T) (AEC-tr-5734 (p.188-92))
scattering by iron near Curie temperature, relation to spin-density fluctuations, 18: 11158
scattering by iron, nickel, and niobium at 0.6 to 2.4 Mev, 18: 16958(T) (NP-tr-1114)
scattering by iron-56 and magnesium-24, gamma angular distributions in inelastic, 18: 19015
scattering by iron at 2 to 5 Mev, inelastic, 18: 34740
scattering by iron-56 at 1 to 4 Mev, cross sections for elastic and inelastic, (E/T), 19: 10296
scattering by iron at 0.9 to 4 Mev, gamma angular distributions from, (E/T), 19: 14538 (TID-20387)
scattering by iron at 0.45 to 2.3 Mev, differential cross sections for, (E), 19: 35378(R) (EANDC(E)-57(U))
scattering by iron and lead at 7 and 14.5 Mev, shell model for elastic, 20: 6434
scattering by iron-54 and iron-56 at 1.20 to 2.61 Mev, gamma angular distributions for, (E), 20: 8152
scattering by iron at 0.45 to 2.28 Mev, cross sections for elastic and inelastic, (E), 20: 30417
scattering by iron and yttrium-89 at 5 Mev, cross sections for inelastic, (E), 20: 39470(R) (ORNL-3924)
scattering by isopropylbiphenyl, cross sections for, (E), 20: 26098(T) (AECL-2330, pp 255-83)
scattering by lanthanum-139 and praseodymium-141 at 1 to 2 Mev, energy levels from inelastic, (E), 19: 33364
scattering by lattice defects in ferromagnetic crystals, 17: 11610
scattering by lattice defects in cold-formed metals and irradiated materials, 18: 24194 (NP-13930(p.116-17))
scattering by lattice vibrations in doped crystals, (T), 19: 12476
scattering by lead, excitation cross sections in inelastic, 16: 21545
scattering by lead isotopes, energy level excitations in inelastic, 17: 7099 (NP-12330(p.86-94))
scattering by lead-208, cross sections for level excitations in inelastic, 17: 31447
scattering by lead-208 at 0.715–1.342 Mev, parity and spin for resonances in, 17: 26441(R) (ORNL-3425(p.49-55))
scattering by lead-206 at 2.5 Mev, zero-spin states from inelastic, 18: 1074
scattering by lead and molybdenum at 3.3 and 3.7 Mev, angular distributions and polarization of elastic, 18: 15222
scattering by lead-204 at 2.2 to 19 Mev, cross sections for inelastic, 19: 1640
scattering by lead-rich iron-lead alloys, magnetic moment distribution from, 19: 38040
scattering by lead-208 and oxygen-16 at 0.5 to 4 Mev, phase shift analysis of, (E), 19: 39785 (ORNL-P-1356)
scattering by lead, tantalum, thallium, and tungsten at 14 Mev, cross sections for inelastic, (E), 19: 41718
scattering by lead, tantalum, thallium, and tungsten at 14 Mev, cross sections for inelastic, 20: 6437
scattering by lead-206 and -208 at 3.15 Mev, cross sections for elastic, (E), 20: 10105
scattering by lead and silicon, cross sections for free and coherent, 20: 15682
scattering by lead at 350°C, inelastic, 20: 26396(R) (IDO-17140)
scattering by lead-208 at 0.715 to 1.761 Mev, resonances in, (E), 20: 32519
scattering by lead at low energy, neutron polarization in, (E), 20: 42140 (JINR-P-2764)
scattering by light nuclei at 14 Mev, optical model for elastic, 18: 1048
scattering by light and intermediate nuclei at 0.5 to 0.8 Mev, cross sections for, 18: 26571
scattering by light nuclei, optical model calculations for, 18: 30729 (NP-14056)
scattering by light elements, calculation method for, (T), 19: 26917(R) (IA-984)
scattering by light and medium-weight nuclei at 14-Mev, (E), 19: 43373
scattering by light nuclei, computer program for calculations using evaporation model, 20: 46560 (ORNL-TM-1552)
scattering by liquids, 16: 24271 (AERE-R-4043)
scattering by liquid ortho-para- and para- hydrogen, inelastic, 16: 31053 (GA-3371)
scattering by liquid sodium, 17: 4976
scattering by liquids, inelastic, 17: 11414
scattering by liquids and solids, conference on, 17: 15228
scattering by liquids, study of thermal motions in, 17: 15238
scattering by liquid sodium, 17: 22967(R) (IDO-16857)
scattering by liquid-like binary, description of, 17: 28137 (BNL-6364)
scattering by liquid scintillator, computer program for calculating, 17: 34848
scattering by liquids, radial distribution curve determination by, 17: 37225
scattering by liquid methane and parahydrogen at 0.009 to 0.17 ev, inelastic, 18: 4512 (GA-4292)
scattering by liquid helium at high momentum, (E), 19: 12474
scattering by liquid helium at small momentum transfers, inelastic, (E), 19: 19053
scattering by liquid methane, model of, 19: 29228(R) (AEET/NP/10)
scattering by liquid and solid argon at 0.02 to 0.1 ev, (E), 19: 37786

(IDO-17089)
scattering by liquids, determination of thermal motion from, (T), 19: 44817
scattering by liquids, dynamics of, (E), 19: 45235
scattering by liquids, review on, (E), 20: 19799
scattering by liquids and solids, elastic and inelastic nuclear and magnetic, 20: 20164
scattering by liquids, kinetics studies using, 20: 19620
scattering by liquid metals, spectra for, (T), 20: 26348 (NP-16010, pp 102-39)
scattering by liquid argon, energy distribution in inelastic, 20: 25975
scattering by liquid aluminum, bismuth, lead, thallium, tin, and zinc, structure factors from inelastic, 20: 27535
scattering by liquid lead, (E), 20: 30360 (WASH-1068)
scattering by liquid lead, analysis of inelastic, (T), 20: 30347(R) (IDO-17147, pp 13-28)
scattering by liquid and solid cyclohexane, diffusive motion determination from, (E), 20: 33253 (BNL-940, pp 138-41)
scattering by liquid methane, Langevin equation of Brownian motion for analyzing, 20: 33255 (BNL-940, pp 149-54)
scattering by liquids, theory for, 20: 26349 (NP-16010, pp 140-77)
scattering by liquids, hindered-translator model for, (T), 20: 38006
scattering by liquids, dynamic processes in slow inelastic, 20: 40338
scattering by lithium, effects of tantalum-backing on, 17: 5348
scattering by lithium-6 and -7 at 1.5 to 7.5 Mev, cross sections for, 17: 13536
scattering by lithium isotopes, neutron spectra from, 18: 7671 (AWRE-NR-6/63)
scattering by lithium and its isotopes, anisotropy of elastic, 18: 15135 (NAA-SE-Memo-9018)
scattering by lithium-6 and -7 at 14 Mev, angular and energy distributions from, 18: 21263
scattering by lithium-6 and -7, inelastic, (T), 19: 29440 (NAA-SR-Memo-10881)
scattering by lithium-6, level excitation in inelastic, 19: 33274
scattering by lithium-7 at 4 to 9 Mev, inelastic, (E), 19: 35378(R) (EANDC(E)-57(U))
scattering by lithium-6 and -7 at 4.4 Mev, polarization from, (E/T), 19: 47570 (COO-7-0361)
scattering by lithium-7 at 2.45 Mev, angular distributions from inelastic, (E), 20: 12106
scattering by lithium-6 and -7 at 4.4 Mev, polarization in elastic, 20: 32433
scattering by lithium-7 at 14 Mev, excitation of 5.7 Mev level by inelastic, (E), 20: 42364
scattering by lithium at 1 to 10 Mev, (E), 20: 46599(R) (RPI-328-pp 1-62)
scattering by macroscopic systems, applications of Wigner representation to theory of, 18: 13037
scattering by macroscopic systems, quasiclassical theory for, 19: 10238
scattering by magnetic crystals, inelastic, 16: 18451
scattering by magnetites, measurements of acoustical and optical spin waves from, 16: 31582 (AECL-1575)
scattering by magnetite, magnetic, 17: 37829
scattering by magnetic materials, 17: 37814
scattering by magnetite, polarization dependence of spin wave, 17: 39065
scattering by magnesium-24 at 14 Mev, first excited state excitation by inelastic, 18: 6264
scattering by magnetized ferromagnetic slab, calculation of in-pile anisotropy from, 18: 19276
scattering by magnesium-24 to 14.1 Mev, 18: 26600
scattering by magnetic structures, 18: 44419 (BNL-7311)
scattering by magnetic materials at and near Curie point, (T), 19: 12467
scattering by magnesium-24 at 14 Mev, angular distributions for inelastic, 20: 1219
scattering by magnetic materials, survey on, 20: 19797
scattering by magnesium-24 and iron-56 at 3.3 and 3.5 Mev, angular correlations for inelastic, (E), 20: 26131
scattering by magnetized crystals, wave mechanical calculation for, 20: 26075
scattering by magnetite, temperature effects on magnon spectra from, (E), 20: 30765
scattering by magnesium, frequency of normal lattice modes from, 20: 38397
scattering by manganese zinc ferrates, 17: 37832
scattering by manganese-55, multilevel effects in, 18: 7702 (WAPD-T-1630)
scattering by manganese fluorides, inelastic, 18: 10091
scattering by manganese fluoride single crystals, spin-wave dispersion at 4.2°K from, 18: 11135
scattering by manganese, differential cross sections for, (E), 19: 8469
scattering by manganese at 700 to 1200 kev, cross sections for, (E), 20: 30360 (WASH-1068)
scattering by manganese fluorides and manganese aluminates, magnetic inelastic, 20: 32706
scattering by materials, 19: 16817(R) (GA-5554)
scattering by matter, effects of atomic weights on, (T), 19: 33192(R) (GA-6096)
scattering by matter, s-wave resonances in, (E/T), 19: 45215 (CEA-R-2780)
scattering by medium nuclei at 3.3 Mev, polarization in elastic, 18: 2846(R) (TID-19709)
scattering by media, angular distributions from, 18: 28535
scattering by metals and oxides, law for metal atom in, 16: 32375
scattering by metal crystals, effects of conduction electron-phonon interactions on, 17: 2216
scattering by metals, electric properties from, 18: 36028
scattering by metals, Fermi surface determination from, (T), 20: 34835
scattering by methane (liquid), 16: 32236
scattering by methane (solid), energy distribution from, 17: 20977
scattering by methane gas, excitation in, 18: 40574
scattering by methane, spin correlation effects on (T), 19: 3377
scattering by methane, spin correlation effects on cross sections for, (T), 19: 23737
scattering by methylene at 2 to 14 Mev, total cross sections for (E), 20: 8062(R) (COO-720-058)
scattering by methane, effects of molecular rotation on differential cross sections for, 20: 25740
scattering by moisture in soils, 19: 11405
scattering by moisture in soils, use of cadmium for calibration of probes for measuring, 19: 38869
scattering by molecules, 16: 10981
scattering by molecules, cross sections, 17: 19379
scattering by molecular crystals, 17: 36429 (NP-13020(p.346-53))
scattering by molecules at chemical bond energies, 17: 38036(T) (AEC-tr-5734(p.213-17))
scattering by molecules at low energies, cross sections for, 18: 32715 (KFKI-64-3)
scattering by molecular crystals, (E), 19: 13401
scattering by molecules of liquid and solid methane at 1.5 to 4.5 Mev, inelastic, (E), 19: 32189
scattering by molecular crystals, (T), 19: 45492
scattering by molecules, cross sections for resonance, (T), 20: 6266
scattering by molecules, (T), 20: 19800
scattering by molecules, review on, (E), 20: 19801
scattering by molecular crystals, elastic and inelastic magnetic, 20: 20165
scattering by molecules, cross sections for elastic and quasielastic, (T), 20: 26076
scattering by molecules, nuclear spin correlation effects on, (T), 20: 34814 (BNL-940, pp 169-72)
scattering by molecules, effects of nuclear spin correlations on, (T), 20: 38004
scattering by molecules, effect of nuclear spin correlations on, 20: 42144
scattering by molybdenum, 17: 5393
scattering by molybdenum, anisotropy of elastic, 18: 15139 (NAA-SR-Memo-9023)
scattering by monatomic gases, computer program for calculation of cross sections, 16: 22965 (GAMD-680)
scattering by monatomic gases, computer program for calculation of cross sections, 16: 22966 (GAMD-2408)
scattering by monatomic gas, angular moments of kernel for, 18: 40465 (AE-148)
scattering by monatomic gases, differential cross sections for, (T), 20: 30337
scattering by mosaic single crystals, 18: 37142
scattering by nickel and vanadium, inelastic, 16: 32387
scattering by nickel, critical, 17: 37831
scattering by nickel at 14 Mev, differential cross sections for elastic, 18: 2888
scattering by nickel, anisotropy of elastic, 18: 15138 (NAA-SR-Memo-9021)
scattering by nickel phase transitions in small-angle polarized, (E/T), 20: 17986(T)
scattering by nickel, properties of magnetic, (T), 20: 24585 (AD-627302)
scattering by nickel and zirconium at 14 Mev, cross sections for elastic and inelastic, (E), 20: 34687
scattering by niobium crystals, lattice dynamics from inelastic, 18: 715
scattering by niobium and natural zirconium at 0.3 to 1.5 Mev, cross sections for, 18: 6221
scattering by niobium superconductors, 18: 22832
scattering by niobium hydride, thorium hydride, and zirconium hydride, spectra from inelastic, (E), 19: 23600(R) (RPI-328-20(p.35-9))
scattering by niobium at 0.9 to 1.25 Mev, gamma spectra from inelastic,

(E), 19: 31215(R) (ANL-7010(p.1-19))
scattering by niobium-93, energy levels from inelastic, (E), 20: 6280(R) (ANL-6925, pp 249-51)
scattering by niobium at 0.275 to 0.85 Mev, differential cross sections for elastic, (E/T), 20: 9981 (WASH-1064)
scattering by niobium-93, excited states from inelastic, (E), 20: 21969(R) (ANL-7055, pp 230-3)
scattering by niobium-93 at 14 Mev, differential elastic cross sections for, (E), 20: 44615 (CONF-660303, pp 675-81)
scattering by nitrogen-15 at 1.9 to 3.5 Mev, cross sections for elastic, 16: 21394
scattering by nitrogen and oxygen at 14 Mev, cross sections for, 17: 33006 (UCRL-7192)
scattering by nitrogen-15 up to 10 Mev with formation of compound particle-hole states, resonances in elastic, 18: 18890
scattering by nitrogen-15 at 440 to 1960 kev, angular distributions for elastic, 18: 28643
scattering by nitrogen-14 at 4.5 to 11.6 Mev, optical model analysis of elastic, (T), 19: 5132 (NP-14480)
scattering by nitrogen-14 at 4.5 to 14.5 Mev, cross sections for elastic, (T), 19: 35396 (NP-15095)
scattering by nitrogen at 1.595 to 3.207 Mev, differential cross sections for elastic, (E), 20: 24354 (ORNL-P-2026)
scattering by nitrogen-14 at 1.595 to 3.25 Mev, differential cross sections for elastic, 20: 34681
scattering by nitrogen-14 at 1.78 to 3.21 Mev, differential cross sections for, (E), 20: 39470(R) (ORNL-3924)
scattering by nonspherical nuclei, elastic, 17: 17246
scattering by nonspherical nuclei, inelastic, 17: 17248
scattering by nonspherical nuclei, optical model analysis of, (T), 19: 43276 (NAA-SR-Memo-11456)
scattering by normal liquids, energy and momentum transfers in, 16: 7155
scattering by nuclei, optical model potential, 16: 3872(R) (ORNL-3193 (p.237-50))
scattering by nuclei, polarization effects, 16: 4792
scattering by nuclei at 2.9 Mev, gamma production cross sections for, 16: 7095
scattering by nuclei at 2.8 Mev, polarizations in elastic, 16: 11026
scattering by nuclei (light) at 0.1 to 2.4 Mev, polarization asymmetries in, 16: 17091
scattering by nuclei, wave distortion in inelastic, 16: 21591
scattering by nuclei, non-local potential model for, 16: 21390
scattering by nuclei at 14 Mev, optical-model analysis, 16: 23089
scattering by nuclei, resonance elastic, 16: 23109
scattering by nuclei at A = 34 to 242, S- and P-wave strength functions, 16: 26334
scattering by nuclei at 14 Mev, cross sections for elastic small-angles, 16: 28044
scattering by nuclei, polarization of elastic, 16: 29714
scattering by nuclei at 3.5 Mev, polarization in, 16: 32438
scattering by nuclei, angular distribution, excitation, and polarization measurements following, 17: 2243(R) (TID-17083)
scattering by nuclei, search for selectively excited spin-zero states in even-even nuclei by, 17: 7075 (AROD-2577:2)
scattering by nuclei, inelastic, 17: 11708
scattering by nuclei, neutron, prong, and proton distributions and spectra for, 17: 22564 (ORNL-3383)
scattering by nuclei at 0.4 to 1.2 Mev, cross sections for, 17: 26476
scattering by nuclei below 10 ev, spins of resonant states from, 17: 26604
scattering by nuclei, threshold effects in elastic, 17: 31514
scattering by nuclei, effects of polarization on, 17: 34894
scattering by nuclei, optical model for, 17: 40042
scattering by nuclei, spectra and angular distributions of inelastic, 17: 41991
scattering by nuclei, review of data on inelastic, 17: 41992
scattering by nuclei at 6 Mev, energy spectra for inelastic, 18: 998 (AD-299005)
scattering by nuclei at 6 Mev, inelastic, 18: 999 (AD-299028)
scattering by nuclei at high energies, inelastic cross sections for, 18: 1092
scattering by nuclei, intermediate state lifetime from K-shell ionization probability in elastic, 18: 2897
scattering by nuclear many-body systems, self-diffusion in incoherent inelastic, 18: 6149
scattering by nuclei with A near 100, optical model analysis of, 18: 7676 (CONF-340-3)
scattering by nuclei with A near 20, 18: 7677 (CONF-340-6)
scattering by nuclei ($24 \leq A \leq 68$), angular correlations for inelastic, 18: 7780
scattering by nuclei at 3 Mev, angular correlation functions for compound inelastic, 18: 9402
scattering by nuclei, spin of low-energy resonances from, 18: 11183 (ANL-6797(p.363-8))
scattering by nuclei, cross sections for, 18: 15476
scattering by nuclei at 0.3 Mev, angular distributions for elastic, 18: 17090
scattering by nuclei at 3.25 Mev, polarization in, 18: 19103
scattering by nuclei with two extra nucleons, inelastic, 18: 18906
scattering by nuclei at 0.1 to 16 Mev, cross sections for, 18: 18864 (ANL-6792(p.29-50))
scattering by nuclei at 1 to 4 Mev, cross sections for energy level excitation in, 18: 21217
scattering by nuclei, instrumentation for inelastic, 18: 24620(R) (ORNL-TM-874)
scattering by nuclei at small angles, cross section increase in, 18: 26519
scattering by nuclei at 2 to 6 Mev, resonance structures in continuum-shell-model, 18: 26531 (LADC-6007)
scattering by nuclei, optical model calculations of cross sections for, 18: 26663
scattering by nuclei around A = 75, strength function and spin for inelastic, 18: 28675
scattering by nuclei, angular distributions from, computer standardization of, 18: 30086 (AEEW-M-444)
scattering by nuclei with rotational and vibrational spectra at 0.5 to 3 Mev, 18: 30835
scattering by nuclei, optical model calculations of cross sections for, 18: 32726 (AERE-R-4649)
scattering by nuclei at 1 Mev, optical model analysis of elastic, 18: 34828
scattering by nuclei, diffraction mechanism for elastic, 18: 34848
scattering by nuclei near A = 20 at 0.2 to 2.2 Mev, 18: 38116
scattering by nuclei at small angles near s-wave resonance, polarization in, 18: 40586
scattering by nuclei, computer program for angular distributions from, 18: 44737 (ORNL-TM-930)
scattering by nuclei at 14 Mev, measurement of cross sections for elastic, 18: 44768
scattering by nuclei at 14 Mev, differential cross sections for inelastic (E), 19: 3382
scattering by nuclei, analysis of (T), 19: 3246
scattering by nuclei (T), 19: 3280
scattering by nuclei at 6 Mev, angular distributions for, (E), 19: 5171
scattering by nuclei, polarization from, (T), 19: 6699
scattering by nuclei, effects on paramagnetic resonances, (E/T), 19: 8398 (JINR-P-1840)
scattering by nuclei at 3 to 650 kev, cross sections, phase shifts, and strength functions for, (E), 19: 10319
scattering by nuclei, Green's functions for inelastic, (T), 19: 12606
scattering by nuclei ($1 \leq Z \leq 92$) at 0.1 to 14 Mev, angular distribution coefficients for elastic, 19: 14540 (TID-21629)
scattering by nuclei at 3.5 to 4.8 Mev, differential cross sections for elastic, (E/T), 19: 14564
scattering by nuclei, average compound-nucleus cross sections for, (E/T), 19: 17011
scattering by nuclei, unified theory for elastic, 19: 17036
scattering by nuclei at 0.2 to 2.0 Mev, compound elastic, (T), 19: 19190
scattering by nuclei at 85 to 700 kev, differential cross sections for elastic, (E), 19: 21298
scattering by nuclei at 14 to 24 Mev, optical model analysis of, (T), 19: 23700
scattering by nuclei, asymptotic approximation for elastic, (T), 19: 27540
scattering by nuclei, non-spherical optical model for, (T), 19: 33238 (CONF-650524-1)
scattering by nuclei at low energies, methods for measurement of inelastic, 19: 33235 (AERE-R-4263)
scattering by nuclei at 3 to 650 kev, intermediate resonances and total sections for, (E), 19: 35462
scattering by nuclei at 14.1 Mev, gamma yields from inelastic, 19: 35417
scattering by nuclei at 0.8 Mev, angular distributions of elastic, (T), 19: 37884
scattering by nuclei with energy level splitting, resonant transition in, (T), 19: 37224(T)
scattering by nuclei, electrodynamic effects in Coulomb, (T), 19: 41334 (JINR-P-2229)
scattering by nuclei, computer program for matrices of inelastic, (T), 19: 47544 (KAPL-M-6467)
scattering by nuclei, Coulomb field and magnetic moment interactions in, 19: 47115(R) (ANL-6983)
scattering by nuclei at high energies, direct-interaction inelastic, (T), 20: 3256
scattering by nuclear Coulomb field, polarization determination from, (T), 20: 4832 (IAE-901)
scattering by nuclei, p-wave phase shifts in small-angle, (T), 20: 4909
scattering by nuclei, errors in optical model analysis of, 20: 6296(R)

(ORNL-3858(Vol.1), pp 1-12)
scattering by nuclei, determination of nuclear equation of state by inelastic, (T), 20: 6379
scattering by nuclei with A = 12 to 209 at 14 Mev, inelastic, (E), 20: 8153
scattering by nuclei at 1 Mev, differential cross sections for, (E/T), 20: 9981 (WASH-1064)
scattering by nuclei, computer program for angular data from, 20: 9972 (NAA-SR-11231)
scattering by nuclei at 14 Mev, differential cross sections for inelastic, (E), 20: 10007
scattering by nuclei, angular distributions from inelastic, 20: 10083
scattering by nuclei in matter, (T), 20: 13734
scattering by nuclei at 0.8 Mev, cross sections for elastic, (T), 20: 15770
scattering by nuclei at 84 to 350 Mev, differential cross sections and polarization from second-order multiple scattering theory elastic, 20: 19933
scattering by nuclei at low energies, intermediate structure, (T), 20: 21988 (BNL-948, pp 876-904)
scattering by nuclei at 0.8 to 4.1 Mev, nuclear shell effects on inelastic, (E), 20: 22023
scattering by nuclei at 0.3 to 0.8 Mev, angular distributions from elastic, (E), 20: 22023
scattering by nuclei, polarization from, (E), 20: 24362(T) (ANL-Trans-294)
scattering by nuclei, time-of-flight analysis of inelastic, (E), 20: 24481
scattering by nuclei at low energies, compound nucleus properties from resonance, (T), 20: 24468
scattering by nuclei, resonance effects on spectra from, (T), 20: 24313
scattering by nuclei at 14.1 Mev, spectra for inelastic, (E), 20: 28268 (FEI-30)
scattering by nuclei, gamma differential cross sections from inelastic, (T), 20: 28343
scattering by nuclei, levels and spins from inelastic, (T), 20: 28343
scattering by nuclei, method for low-background inelastic, (E), 20: 28236 (NP-16039)
scattering by nuclei, technique for measuring resonance, 20: 30358(R) (RPI-328-56, pp 1-48)
scattering by nuclei, analysis of inelastic, 20: 34659
scattering by nuclei, optical model analysis of, 20: 34673
scattering by nuclei, slowing down parameters and Legendre polynomial coefficients for, 20: 37988 (WAPD-TM-572)
scattering by nuclei, computer analysis of data on differential elastic, 20: 44578 (CONF-660303, pp 335-53)
scattering by nuclei, computer program for solving T matrices for, 20: 44663 (WAPD-TM-571)
scattering by nuclei with Z = 13 to 92, cross sections for elastic, 20: 44669(T) (INDSWG-101, pp 109-57)
scattering by nuclei, spin-orbit effects in, (T), 20: 44780
scattering by nuclei with Z = 4 to 92 at 5 Mev, angular distributions from elastic, (E), 20: 46794
scattering by nuclei with Z = 13 to 83 at 3.2 Mev, elastic, (E/T), 20: 46644
scattering by oriented holmium-165 at 350 kev, polarization in, (E), 19: 33326
scattering by oriented polyethylene, frequencies in, 20: 35504
scattering by oxygen-16, cross sections for, 17: 7174
scattering by oxygen, cross sections and Legendre coefficients of angular distribution for, 17: 13488 (NDL-TR-40)
scattering by oxygen-16 at 0 to 15 Mev, Legendre coefficients for angular distributions from, 18: 9353
scattering by oxygen-16 at 2 to 4 Mev, resonances in elastic, 18: 24620(R) (ORNL-TM-874)
scattering by oxygen-18 at 405 to 2702 kev, angular distributions for elastic, 18: 28642
scattering by oxygen at 0.347 to 14.0 Mev, angular distributions from elastic, 19: 14732(R) (TO-B-63-83)
scattering by oxygen-16 at 3.0 to 4.7 Mev, cross sections for elastic, (E), 19: 19095 (WASH-1053)
scattering by oxygen-16 at 3.2 to 4.2 Mev, cross sections for, (E), 19: 19095 (WASH-1053)
scattering by oxygen-16 at 3 to 4 Mev, (E), 20: 44651 (ORNL-P-2434)
scattering by oxygen at 1 to 10 Mev, (E), 20: 46599(R) (RPI-328-68, pp 1-62)
scattering by palladium at 15, 77, and 298°K, paramagnetic, (E), 20: 6544
scattering by paramagnetic crystals, effects of spin-phonon interactions on, 16: 29719
scattering by paramagnetic manganese oxides, energy spectra in, 19: 38063
scattering by paramagnetic materials, (E), 19: 43486
scattering by phonons and magnons in single crystals, line broadening studies, 16: 7148
scattering by phonons, anharmonic and impurity effects on, (T), 20: 34806 (BNL-940, pp 23-8)
scattering by phosphorus-31 at 14.2 Mev, differential cross sections for, (E), 19: 23718
scattering by plane slab crystal, effects of resolution of collimators on, 19: 14473
scattering by plates containing poison spheres, self-shielding, 18: 42924 (TID-7050(p.537-52))
scattering by plutonium-239 at 7.8 to 44.5 ev, resonance spins, 16: 13992
scattering by plutonium-239 and uranium-235 at 0.6 to 1.6 Mev, cross sections, 16: 29740
scattering by plutonium-239, anisotropy of elastic, 18: 15142 (NAA-SR-Memo-9026)
scattering by plutonium-239, resonance, (E), 20: 4849(R) (UCRL-14360, pp 1-50)
scattering by plutonium-239, spin values, average fission width, and total spin correlation from resonance, (E), 20: 6414
scattering by plutonium-239 and uranium-233 and -235, amplitudes for coherent, (T), 20: 19845
scattering by polar liquids, theory of hindered rotations in, 17: 15171 (BNL-719(Vol.I)(p.289-301))
scattering by polarized deformed nuclei at 1 Mev, optical-model cross sections for, 18: 19017
scattering by polarized nuclei at 0.3 to 14 Mev, spin-spin interactions in, 18: 24645
scattering by polarized nuclei, in electric or magnetic fields, (T), 19: 27426 (JINR-P-2026)
scattering by polarized nuclei in external magnetic field, (T), 20: 3120
scattering by polyethylene and water, inelastic, 16: 32364 (TID-16691)
scattering by polyethylene, 17: 15213(R) (GA-3409)
scattering by polycrystalline diamond, inelastic, 17: 20968
scattering by polyethylene and vanadium, 17: 34560(R) (TID-19195)
scattering by polyethylene at 0.215 and 0.625 ev, 18: 733(R) (TID-19610)
scattering by polycrystalline pile-irradiated copper, small-angle, 18: 14558
scattering by polyphenyls, molecular dynamics in, 18: 40473 (EUR-1643.e(p.143-54))
scattering by polycrystals, 18: 44420 (GAMD-3631)
scattering by polyethylene and water at low energy, chopper study of, (E), 19: 3191(R) (RPI-328-16)
scattering by polyethylene, frequency spectrum and scattering kernel for, (T), 19: 8376(R) (GA-5176)
scattering by polyethylene, kernel for, (T), 19: 10235
scattering by polyethylene and water, differential cross sections for, (E), 19: 23599(R) (RPI-328-20(p.24-34))
scattering by polyethylene at 0.158 to 0.650 ev, cross sections of inelastic, (E/T), 19: 31197(R) (RPI-328-35(p.125-35))
scattering by polythene and heavy water at 0.04 to 0.4 ev, coherent, (E), 19: 33192(R) (GA-6096)
scattering by polyethylene at 0.0154 to 0.317 mev, (E), 20: 21943
scattering by polyphenyls, method for calculating, 20: 28258
scattering by polyethylene and water at 0.83 to 1.8 ev, differential cross sections for inelastic, (E), 20: 30334
scattering by polyethylene and zirconium hydrides, differential cross sections for inelastic, (E), 20: 46563(R) (RPI-328-68, pp 145-60)
scattering by potassium and sodium, anisotropy of elastic, 18: 15137 (NAA-SR-Memo-9020)
scattering by potassium-39 at 1.49 to 3 Mev, cross sections for, (E), 19: 41737
scattering by potassium manganese fluorides, diffuse, (E/T), 20: 19273(R) (BNL-929, pp 3-43)
scattering by potassium iodides, dispersion relation for normal-mode vibrations from inelastic, (E), 20: 32710
scattering by potassium at 14 Mev, optical-model analysis of elastic, (T), 20: 38171
scattering by potassium-39 at 14 Mev, cross sections for elastic, (E/T), 20: 42393
scattering by precipitations in aluminum–copper alloys at long wavelength, 20: 3285
scattering by proton interactions, statistical correlation of water content with, 17: 34204
scattering by quantized magnetic flux lines in superconductors, (T), 19: 12450
scattering by rare earth oxides, 17: 37830
scattering by rare earth metals and compounds, magnetic, 17: 37819
scattering by reactor moderators, cross sections for, (E/T), 20: 19778(R) (GA-6824)
scattering by reinforced concretes, albedo intermediate-energy calculations of, 19: 43462 (ORNL-TM-1205)
scattering by rhodium-103, scintillation detector for resonance, 17: 30877
scattering by semi-infinite halfspace, albedo in, (T), 19: 10234
scattering by silicon single crystals, phonon dispersion relations for,

16: 7173
scattering by silicon at 200 to 700 kev, differential cross sections and polarization in, 16: 23117
scattering by silicon-28 at 14.1 Mev, 18: 26600
scattering by silicon-28 and sulfur-32 at 14 Mev, differential cross sections for (E/T), 19: 3298
scattering by silicon and sulfur at 2.45 to 5.80 Mev, energy spectra of, (E), 19: 19095 (WASH-1053)
scattering by silicon and sulfur at 2.45 to 5.80 Mev, (E/T), 19: 23620
scattering by silicon and sulfur at 2.45 to 5.80 Mev, elastic and inelastic, (E), 20: 10103
scattering by silicon-28 and sulfur-32 at 2.45 to 5.80 Mev, cross sections for elastic and inelastic, (E), 20: 15811
scattering by silicon at 0.57 to 2.28 Mev, cross sections for elastic, (E/T), 20: 30345 (EUR-2798.e)
scattering by silicon at 0.57 to 2.28 Mev, differential cross sections for, (E), 20: 40069(R) (EANDC(E)-66(U))
scattering by silicon-28 at 7.5 Mev, gamma spectra from inelastic, (E), 20: 46588 (LA-DC-7853)
scattering by silicon-28 at 4.0, 7.0, and 7.5 Mev, gamma angular distribution from inelastic, (E), 20: 46588 (LA-DC-7853)
scattering by silicon at 7.5 Mev, time spectrum at 135°, (E), 20: 46588 (LA-DC-7853)
scattering by silicon at 7.5 Mev, angular distribution for elastic, (E), 20: 46588 (LA-DC-7853)
scattering by silicon-28 at 7.5 Mev, differential cross sections for inelastic, (E), 20: 46588 (LA-DC-7853)
scattering by simple metal-transition metal alloys, cross sections for magnetic, 16: 24333
scattering by single crystals, anharmonic effects in coherent inelastic, 16: 19741
scattering by single crystals, angular distributions of double Bragg, 16: 26211
scattering by single crystal chromium, magnetic, 17: 37821
scattering by single crystals, coherent extinction and second-order, 20: 15671
scattering by small cylinders, Monte Carlo analysis of, 18: 982 (NAA-SR-Memo-9060)
scattering by sodium-23 at 0.5 to 4 Mev, cross sections for, 16: 23064
scattering by sodium-23 at 0 to 4 Mev, nuclear model calculations of, 18: 24597 (NP-13930(p.15))
scattering by sodium-23 up to 4 Mev, excitation cross section for, 18: 32805
scattering by sodium and water, Monte Carlo solutions for multiple, 20: 26062 (CEA-R-2971)
scattering by solids, crystal structure effects on, 17: 38045(T) (AEC-tr-5734(p.267-9))
scattering by solid hexane, low-frequency molecular vibrations in inelastic, 19: 2314
scattering by solid methane, diagnostic uses of, (E/T), 19: 45239
scattering by solids, measurement of molecular motions by, 20: 18674
scattering by solids under pressure, apparatus for measurement of, 20: 31756
scattering by solids, spectroscopy for, 20: 32687
scattering by solids, magnetic and thermal property studies from, 20: 34804 (BNL-940, pp 1-7)
scattering by solid and liquid cyclohexane, inelastic, 20: 38005
scattering by solid methane, effects on molecular rotation from, (T), 20: 40323
scattering by spherical nuclei at low energy, polarization in elastic, 18: 42702
scattering by spin waves in hexagonal cobalt, inelastic, 16: 13820
scattering by spin waves in magnetic crystals, 16: 15326
scattering by spin waves, measurement of form factors for, 17: 22530 (AERE-R-4299)
scattering by spin waves in ferromagnetic materials, inelastic, 18: 9302
scattering by spin fluctuation in pyrrhotite, temperature dependence of inelastic, 18: 26498 (PAN-280)
scattering by spinless targets, computer program for, 20: 15670 (WAPD-TM-524)
scattering by spin-zero nuclei, generalized optical model for resonances in, (T), 20: 24469
scattering by spin waves in terbium, exchange parameters from inelastic, (E), 20: 34813 (BNL-940, pp 159-62)
scattering by spin-waves in iron–nickel alloys, angular distributions from, (T), 20: 36354 (AERE-R-4535)
scattering by statistical media, time-dependent motions of nuclei in, 17: 21216
scattering by stretch-oriented polyethylene, frequency limit of stretch-bead acoustic mode from, 20: 10865
scattering by strontium titanate single crystal, 17: 5141
scattering by sulfur-32 at 14.1 Mev, 18: 26600
scattering by sulfur-32 at 14.6 Mev, differential cross sections for (E), 19: 3320
scattering by systems with local degrees of freedom, elastic, 18: 36682
scattering by tantalum at 2 to 300 kev, 16: 25877(R) (ANL-6534)
scattering by thallium bromide at 105 and 296°K, dispersion relations in, 19: 26922(R) (PR-P-64)
scattering by the Coulomb field of nuclei, theory of, 17: 7074
scattering by thin plates, Monte Carlo calculations for, 16: 29715
scattering by thorium-232, anisotropy of elastic, 18: 15140 (NAA-SR-Memo-9024)
scattering by thorium-232 and uranium-238, excitation functions in, (T), 19: 8409
scattering by transition metals, relation to Pauling's theories on magnetic properties, 19: 6313
scattering by tritium at 1.0 to 6.0 Mev, phase-shift analysis for elastic, (T), 20: 17769
scattering by tritium at 14 Mev, differential cross sections for elastic, (E), 20: 42373
scattering by tungsten, anisotropy of elastic, 18: 15143 (NAA-SR-Memo-9027)
scattering by tungsten-182, tungsten-184, and tungsten-186 at 0.3 to 1.5 Mev, optical-model analysis of, (T), 20: 44646 (NAA-SR-11973)
scattering by uranium dioxide at 0.007 to 0.09 ev, inelastic, 16: 31050 (AECL-1577)
scattering by uranium-238 at 14.7 Mev, 17: 21027
scattering by uranium, anisotropy of elastic, 18: 15141 (NAA-SR-Memo-9025)
scattering by uranium-238 at 0.001 to 5.6 ev, cross sections for, 18: 15171 (AEEW-M-414)
scattering by uranium-238 at 550 to 1305 kev, angular and energy distributions from, 18: 18863 (ANL-6792(p.11-27))
scattering by uranium-238 at 95 kev, cross sections for inelastic, (E), 19: 29257 (NP-15012)
scattering by uranium nitrides, magnetic structure from, (E), 20: 10255
scattering by uranium-238 at 95 kev, cross section for inelastic, (E), 20: 9996
scattering by uranium-238, (n,an') reaction effects on anomaly in small-angle elastic, (E), 20: 22017
scattering by uranium-238 at small angles, anomalous elastic, (E), 20: 44764
scattering by uranium at 4 Mev, neutron polarization measurement by elastic, (E), 20: 46785
scattering by vanadium at 0.15 ev, 16: 31054 (HW-SA-2541)
scattering by vanadium, time-of-flight-spectrum for inelastic, 17: 20973
scattering by vanadium at low energies, 18: 733(R) (TID-19610)
scattering by vanadium-51 at 0.6 to 25 kev, 18: 2943
scattering by vanadium and vanadium hydride, spectra from inelastic, 18: 24605 (NP-13930(p.59-71))
scattering by vanadium and water, angular distributions in, (E), 19: 8376(R) (GA-5176)
scattering by vanadium at 20 Mev, frequency distribution of, (E), 19: 35378(R) (EANDC(E)-57(U))
scattering by vanadium, spectra from elastic, (E), 20: 7445(T)
scattering by water, constants for approximation functions, 16: 21342
scattering by water at 0.15 to 0.40 ev, 16: 31054 (HW-SA-2541)
scattering by water at 0.10 to 0.25 ev, quasi-elastic, 16: 31055 (HW-SA-2542)
scattering by water and water-d_2, 16: 32382
scattering by water, comparison with theoretical calculations, 17: 13678(R) (HW-75914)
scattering by water, cross sections for, 17: 22537 (TID-18481)
scattering by water, models for, 17: 18996
scattering by water, law for, 17: 31079(R) (HW-77311(p.4-11))
scattering by water at low energies, small-energy rotational transitions in, 17: 36634
scattering by water, law for, 18: 11147(R) (HW-79054(p.12-20))
scattering by water at 22 and 150°C, 18: 15129 (AERE-R-4484)
scattering by water, water-d_2, and hydrofluoric acid aqueous solutions, spectra of, 18: 27440
scattering by water, kernel for, 18: 34739
scattering by water molecules, angular- and position-dependent spectrum of (E), 19: 3201
scattering by water vapor at low energy, (T), 19: 33212
scattering by water, van Hove function for, (E), 19: 45236
scattering by water, cross sections for inelastic, (E), 20: 4807(R) (RPI-328-40, pp 56-66)
scattering by water at 3.3 and 8.0 Mev, energy and dose-rate distributions in, 20: 28598
scattering by water at 0.304 ev, width of 0.200-ev vibration level from, (E), 20: 34480
scattering by yttrium manganites, magnetic, 18: 3772
scattering by yttrium, anisotropy of elastic, 18: 15199 (NAA-SR-Memo-9022)
scattering by yttrium-89 at 0.00064 to 8.0 ev, cross sections for,

(E/T), 20: 22010(R) (NYO-72-28)
scattering by Z = 13 to 83 nuclei at 2.8 Mev, angular distributions from elastic, 18: 38080(T) (AEC-tr-6398(p.120-5))
scattering by Z = 30 to 50 nuclei at 400 kev, cross sections for elastic, 18: 38074(T) (AEC-tr-6398(p.64-9))
scattering by Z = 12 to 83 nuclei at 14 Mev, cross sections for inelastic, (E), 19: 25475(R) (ORNL-TM-1044)
scattering by zirconium-90, metastable state production cross section, 17: 22628
scattering by zirconium hydride at 0.018, 0.032, and 0.064 Mev, frequency distribution in, (E), 19: 35378(R) (EANDC(E)-57(U))
scattering by zirconium hydrides and heavy water at 0.06 to 10 ev, differential cross sections for, (E), 20: 2963
scattering by zirconium hydrides, (E), 20: 27344
scattering by zirconium-90, zirconium-91 neutron single-particle levels from, (T), 20: 32552
scattering by 302°K water at 0.15 to 1.8 ev, differential cross sections for, (E/T), 20: 32350 (KAPL-M-6536)
scattering by 36 elements, 2 polymers, and stainless steel, angular distributions from, 16: 12419 (ANL-5567(Rev.))
scattering by $50 < A < 90$ nuclides, potential, 18: 2849
scattering, calculation using approximation which allows for chemical binding, 17: 15185 (BNL-719(Vol.II)(p.614-55))
scattering calculations using Monte Carlo method, direction- and track-selection schemes for, 20: 44588 (ORNL-TM-1484)
scattering cross sections for straight cylindrical ducts, 16: 3657 (NARF-61-33T)
scattering cross section and spatial distribution of slowing down, relation between energy dependence of, 18: 2787
scattering cross sections for, resonance structure in, 18: 16941 (ANL-6848(p.241-8))
scattering cross sections in moderators, computer code for inelastic, 20: 8059
scattering cross sections for, optical model analysis of, 20: 41796(R) (MIT-2098-251, pp 74-103)
scattering data in ROC nuclear data library, computer program for conversion of form of elastic, 20: 37989 (WAPD-TM-573)
scattering effects on reactivity measurements in Advanced Reactivity Measurement Facility, (E/T), 19: 29551
scattering equation for, extension of, 20: 40056
scattering from beryllium, cross sections for inelastic, (T), 19: 35455
scattering from bismuth-209 and lead-206 at 7 Mev, large-angle elastic, (E), 19: 33334
scattering from concrete slab, Monte Carlo method for determining, 20: 13742
scattering from polycrystalline materials, one-phonon coherent peaks in, (T), 19: 35364
scattering from SNAP-type radiators, computer code for, 19: 31198 (TIM-799)
scattering from uranium at 1240 kev, spectra of, 18: 27793
scattering from uranium-238 at 550 kev, spectra of, 18: 27793
scattering in a Fermi liquid at low energies, 16: 965
scattering in air, angular distribution, 16: 19732
scattering in aluminum and bismuth, excitation cross sections for, (E), 19: 41274
scattering in anisotropic medium, generalized first-flight collision probability for, (T), 20: 9954
scattering in antiferromagnets with weak ferromagnetism, (T), 19: 47899(T)
scattering in attenuating media, Monte Carlo estimators for calculation of (T), 19: 1527 (ORNL-TM-974)
scattering in biological systems, use of slow inelastic, 20: 45268 (AD-638991)
scattering in biphenyl, spectra of inelastic, 18: 34302
scattering in chromium, magnetic, 19: 38039
scattering in copper-zinc alloys, short-range order diffuse, 17: 22193
scattering in copper and vanadium, multiple, (T), 19: 12577
scattering in crystals with electron impurity centers, single-phonon Green's function for, (T), 19: 20710
scattering in crystals, single-phonon coherent, (T), 19: 45475 (IAE-750)
scattering in fast reactors, matrices for inelastic, 18: 21598 (IA-899)
scattering in ferromagnetic crystals containing impurities, inelastic, (T), 20: 20158
scattering in hexagonal geometries, computer program for determining, 20: 26424 (CEA-R-2977)
scattering in homogeneous medium, free-gas collision operator for, 20: 4811
scattering in infinite plane slab, 18: 37942
scattering in iron sulfide, equations for solution of inelastic, 19: 14260
scattering in iron–nickel alloys, paramagnetic, (E), 20: 8303
scattering in liquids and solids, inelastic, 17: 20967 (STI/PUB/62 (Vol.II))
scattering in liquids and solids, structural research by, 17: 38026(T) (AEC-tr-5734(p.119-39))
scattering in liquids, Van Hove functions from spectra of, 18: 29666
scattering in magnetic crystals, critical, 18: 37149
scattering in manganese fluoride single crystals, critical magnetic, 19: 38038
scattering in many-particle systems, method for differential cross sections of inelastic, 19: 42154 (KFK-261)
scattering in Maxwellian gases, average cosine for, (T), 20: 1135 (RT/FI(65)12)
scattering in methane, contribution of molecular rotation to inelastic, 19: 1540
scattering in moderators near resonances, (T), 19: 6627
scattering in moderators, decay constant for pulsed, 20: 4816
scattering in multibend ducts, Monte Carlo program for, 17: 21201 (NARF-62-13T)
scattering in nonmagnetic medium, index of refraction for, (T), 19: 29183
scattering in nuclei, optical potentials for distorted wave analyses of elastic, 17: 38184
scattering in paramagnetic materials, effect of spin-spin interaction on, 17: 7072(T)
scattering in plane geometry, Jacobi polynomials for Boltzmann equation for, 20: 8047
scattering in regular crystals, inelastic channels in resonance, (T), 20: 12313
scattering in shielding experiments, ANNEX-2 program for analysis of, 17: 40216 (NAA-SR-Memo-8516(Rev.))
scattering in single crystals, measurement of one-phonon, 19: 46753 (AERE-R-4895)
scattering in slabs, initial value problem for anisotropic, 19: 39765 (INR-611/IX-A/R)
scattering in solids, spectra from, (E), 20: 4476(R) (IS-1200(Sect. P))
scattering in the static approximation, multiple, 17: 4032
scattering in thin plates, probabilities for double, single, and triple, 16: 21125(R) (ANL-6517)
scattering in thin plates, Monte Carlo calculations of elastic energy-dependent multiple, 17: 11595 (TID-15571)
scattering in titanium–zirconium alloy, inelastic, 17: 38060(T)
scattering in water, comparison of Nelkin's kernel with experiment, 17: 11303(R) (HW-75228)
scattering kernels (T), 19: 1519 (BNL-8433)
scattering law for, procedure for calculating, 18: 22848(R) (GA-4659)
scattering law for, 18: 24625 (WASH-1046)
scattering law for water, 18: 28088(R) (HW-80284(p.10.1-28))
scattering laws, data recording and sorting systems for, 16: 14089
scattering laws for graphite moderators of thermal reactors, 18: 17266
scattering laws for, integral parameters for (T), 19: 1518 (AE-154)
scattering length in magnesium, coherent, 17: 34841
scattering length from deuteron-meson (π^-) interactions, neutron-neutron, (E), 19: 20995
scattering length from meson (π^-) capture by helium-3, (T), 19: 45354
scattering length from deuteron-meson (π^-) interactions, (E), 20: 15511
scattering matrices for, method for evaluating multigroup, 20: 34499
scattering, Milne problem with first order anisotropic, 16: 15617
scattering model for, effects on calculated reactor parameters, 20: 45065 (CONF-660303, pp 146-50)
scattering models for, formalism and properties of, 20: 44587 (NP-16291)
scattering of, analysis of inelastic, into interference and self terms, 16: 32374
scattering of, by water, calculated kernels for, 16: 32359 (GEAP-3944)
scattering of, calculation of energy deposition in, by a Monte Carlo method, 17: 26160
scattering of, computer code for Hauser Feshbach calculations on, 17: 11591 (NP-12370)
scattering of, computer program for treatment of anisotropic elastic, 17: 15215 (NAA-SR-Memo-7776)
scattering of, computer program for, 17: 31384 (HW-78288)
scattering of, determination of J-values of s-type resonances from, 17: 5300 (NRL-5851)
scattering of, detection of noncollinear spin densities in ferromagnets by magnetic, 17: 31215
scattering of, DSN calculation of anisotropic, 17: 3815
scattering of, exact solution of velocity-dependent Milne problem in, 17: 26033
scattering of, for control and regulation of moisture content in bulk materials, 17: 1694
scattering of, in acoustic fields, analysis of, 17: 9195 (NP-12399)
scattering of, integration of the Egelstaff S-function for, 17: 24037(R) (HW-76128)
scattering of, lattice and spin waves in inelastic, 17: 22271 (MMPP-NPC-1-4)
scattering of long-wavelength, by irradiated beryllium oxide, 17: 20962
scattering of long-wave, by solids, density fluctuations from, 20: 28255
scattering of low-energy, validity of laws for, 17: 24369(R) (GA-3542)

scattering of, many-particle evaporation spectra for inelastic, 17: 31393 (CONF-46-6)
scattering of polarized, by lithium-6 and -7, 16: 4790
scattering of polarized, by antiferromagnetic and ferromagnetic materials, 16: 7141
scattering of polarized, by spin-waves in exchange-coupled lattices, 16: 18452
scattering of polarized, in helical magnetic structures, 16: 26188
scattering of polarized, at 0.1 to 25 Mev, 17: 17094 (TID-18277)
scattering of polarized, by nuclei, 17: 36414 (NP-13020(p.214-26))
scattering of polarized, by spin waves in magnetic material, 18: 7853(R) (KR-58)
scattering of polarized, elastic, 18: 40511 (NP-14205)
scattering of polarized, on polarized nuclei, 19: 35373 (BNL-903)
scattering of polarized, by carbon-12, (E), 20: 9983
scattering of polarized, by helium-4 at 12.0 Mev, elastic, (E), 20: 44732
scattering of, quasi-classical approximation in, 17: 11606
scattering of, sample orientation effects on spectrometer counting rate on, 17: 18605 (TID-18405)
scattering of slow, by molecular hydrogen and deuterium, cross sections for, (T), 19: 33194 (N64-18279)
scattering of slow, asymptotic formula for law of, 19: 45231
scattering of, study of long range nuclear potential by small-angle, 17: 24477
scattering of, theory of paramagnetic, 16: 33782 (CEA-1996)
scattering of, threshold effects and Wigner cusp phenomenon, 18: 997
scattering of, transport equation solutions for anisotropic, 17: 29569
scattering of, use of synthetic method for slab geometry problems in, 17: 5303 (TID-15405)
scattering of 14-Mev, performance of time-of-flight spectrometer for angular distribution measurement from, 20: 19071
scattering of 3.3-Mev polarized, asymmetry in elastic, (E/T), 19: 10343
scattering of, computer program for angular distributions and cross sections for compound-nuclear-state, 18: 26556 (ORNL-TM-875)
scattering of, computer program for, 19: 15981(R) (ORNL-3714(Vol.I) (p.70-7))
scattering of, computer program for Legendre coefficients for elastic, 20: 13699 (GA-6690)
scattering of, computer program for angular distributions from elastic, 20: 13697 (AEEW-M-605)
scattering of, computer program for evaluation of angular distributions for, 20: 40063
scattering of, conference on inelastic, 19: 43262
scattering of, conference on inelastic, 19: 45234
scattering of, conference on inelastic, 19: 45243
scattering of, conference on inelastic, 20: 34803 (BNL-940)
scattering of, energy transfer matrices for anisotropic elastic, 18: 16897 (UCRL-7624)
scattering of, facility for low energy inelastic, 20: 15731(R) (RPI-328-49)
scattering of, gas targets for experiments on, 19: 42964(R) (ORNL-3782, pp 144-52)
scattering of, HFBR experimental facilities for measuring inelastic, 19: 19413 (BNL-8802)
scattering of, input functions for anisotropic, (T), 19: 27406
scattering of, instrumentation for angular distribution in elastic and inelastic, 19: 25475(R) (ORNL-TM-1044)
scattering of, laboratory experiments at Dutch high-flux reactor on, 18: 26965
scattering of, lectures on inelastic and magnetic, 20: 30784
scattering of, measurement of biological film thickness on percolating filters by, 18: 27770
scattering of, measurement of binder content in asphalt by, 18: 41885
scattering of, measurement of moisture content in asbestos and plywood by, 19: 5791
scattering of, metallographic studies using, 19: 4599
scattering of, Monte Carlo solutions for multiple, 20: 26062 (CEA-R-2971)
scattering of, numerical analysis of critical magnetic, 20: 19785 (RISO-118)
scattering of, optical model analysis of elastic, 18: 36698
scattering of, optical model calculations of, 19: 37202(R) (BNL-900 (p.1-28))
scattering of, research with inelastic, 18: 38570 (A/CONF.28/P/12)
scattering of, research on inelastic, 20: 20183
scattering of, research on low-energy inelastic, 20: 28288(R) (TID-22844, pp 54-61)
scattering of, S_n analysis of anisotropic (T), 19: 1536
scattering of, theory of, 18: 34624
scattering of, theory of inverse, 20: 26396(R) (IDO-17140)
scattering of, two-dimensional multigroup analysis of, (T), 19: 21197 (CEA-R-2747 and Add.)
scattering of, uses for analyzing magnetic systems, (T), 19: 43484
scattering of, use in research on underground water supplies, 20: 37135
scattering of, use of, in analysis of soil for water content, 20: 39141
scattering on aluminum-27 at 14 Mev, excitation of 4.5-Mev state by inelastic, (E), 20: 12031
scattering on ammonium halide crystals, lattice dynamics from, 17: 37805
scattering on bare slabs, Green's function for anisotropic, 17: 38059
scattering on beryllium-9 at 0.2 to 2.0 Mev, parity and spin of beryllium-10 energy levels from, 18: 7771
scattering on carbon-12, helium-4, and oxygen-16 at low energies, phase-shifts and polarization in elastic, 17: 26542
scattering on carbon-12 at 14 Mev, gamma angular correlations in inelastic, 17: 38267
scattering on carbon-12 at 30 Mev, wave function localization in optical model for, 17: 38183
scattering on carbon-12 and oxygen-16, optical model for bound states in, 18: 6211
scattering on copper at 14.5 Mev, isospin term of optical potential from, 17: 40071
scattering on crystals, interatomic force constants from inelastic, 17: 37804
scattering on dilute nickel alloys, magnetic moment distributions from, 17: 37694
scattering on drift rings, theory of, small-angle, 17: 36591
scattering on fluorine-19 at 1 to 300 kev, fluorine-20 nuclear levels from resonances in, 18: 7766
scattering on heavy and light water, models for, 20: 44587 (NP-16291)
scattering on helium-4 at 1.79 Mev, angular distributions for, 17: 31430
scattering on helium, elastic, 19: 45303
scattering on holmium-165 and manganese-55 at 2, 5, and 14 Mev, deformation magnitude and sign from cross section asymmetries for elastic, 17: 31471
scattering on iron-56 and magnesium-24 at 2.0 and 3.5 Mev, gamma angular correlations in inelastic, 17: 38275
scattering on iron–palladium alloys, atomic magnetic moments from, 17: 37693
scattering on iron-56 and lead-208 at 4.1–24.0 Mev, nonlocal optical potentials for elastic, 17: 38185
scattering on iron, spin wave absorption in polarized, (E), 19: 14634
scattering on iron, spin correlations from diffuse magnetic, (E), 20: 13994
scattering on lithium-6 at 90 Mev, exact distorted-wave calculations for inelastic, 17: 38194
scattering on magnetic materials, 17: 38027(T) (AEC-tr-5734(p.140-52))
scattering on magnetic alloys, disorder effects from, 17: 37799
scattering on nuclei at 1 to 5 Mev, inelastic, 16: 9413 (CEA-2083)
scattering on nuclei ($12 \leq A \leq 209$) at 6 Mev, compound-nucleus and direct reactions in, 17: 38207
scattering on nuclei at 14 Mev, cross sections for inelastic, 17: 41958
scattering on nuclei ($A \sim 100$) at 0.275 to 0.85 Mev, nonlocal optical model analysis of elastic, 18: 6241
scattering on nuclei at 0.65 Mev, angular distributions for elastic, 18: 17089
scattering on nuclei, polarization effects on distribution of, (T), 19: 19108
scattering on nuclei to 50 Mev, bibliography on polarization and elastic, 19: 35390 (LA-3281)
scattering on nuclei, potential model for elastic, (E/T), 19: 47581 (LA-DC-6730)
scattering on resonant nuclei, complex scattering amplitudes for coherent Bragg, 17: 37798
scattering on sulfur, distorted waves approximation in elastic and inelastic, 17: 38182
scattering on water at 25 and 75°C, energy distributions for inelastic, 17: 37806
scattering on zinc crystals, lattice dynamics from inelastic, 17: 39601
scattering resonances, 20: 20201(R) (ANL-7110, pp 311-401)
scattering return to reactor matrices, detector for measuring, 18: 19285
scattering spectra for, Monte Carlo analysis of time-of-flight, 17: 41868 (TID-18080)
scattering studies, integration of Egelstaff S-functions for, 17: 31681(R) (HW-76559)
scattering with first-order anisotropy, elementary theory of time-dependent elastic, 20: 34479
self-shielding effects in slab absorbers, 16: 4945 (UCRL-6526)
self-shielding factor of cobalt-60 foil for, 18: 34737
self-shielding factors for multiple concentric cylinders, Monte Carlo calculations of, 18: 42882 (NASA-TN-D-1587)
self-shielding in activation analysis, 17: 19939 (IA-756)
separation energies in even A ($84 \leq N \geq 98$) nuclei, 18: 24681
separation energies for, 18: 26576
separation energies for nuclei, (E), 19: 39862
shielding against plutonium-238-in-plutonium dioxide, comparison of computation methods for, 20: 46936 (ORNL-TM-1632)

shielding against, facility for testing, 19: 19333
shielding against, performance of lead-filled plastics for, 20: 1319
shielding against, multi-layer material for, 20: 28601(P)
shielding against, properties of concretes for, 20: 32679
shielding against, material properties for, 20: 36352
shielding by concrete, 20: 3253
shielding calculations for power reactors, 19: 14744
shielding calculations for reactors, Monte Carlo method for, 19: 45469
shielding, evaluation of elastomeric materials for, 16: 8291 (RIA-61-1344)
shielding in closely packed slab lattices, self-, (E), 19: 21636 (CONF-654-32)
shielding in heterogeneously distributed pure absorber, self-, (T), 20: 4808 (UCRL-14432-T)
shielding in meson production facilities, flux calculation beneath, (T), 20: 10223 (ORNL-P-1787)
shielding in uranium slab lattices, self- (E), 19: 3533
shielding measurements in heavy concrete, 20: 41534 (DESY-66/18)
shielding of, fabrication of organic materials for, 20: 30732(P)
shielding of, from electron accelerators with 30-Mev maximum energy, (T), 19: 34828
shielding of, in high-energy electron accelerators, 19: 17170
shielding scattered, in space power plants (T), 19: 3716 (FZK-154)
shielding space vehicles from secondary, produced in spherical proton shielding, (T), 20: 3242 (NASA-SP-71, pp 225-8)
shielding studies, 20: 6520(R) (ORNL-3858(Vol.1), pp 42-6)
single-particle states of, energies of, 17: 17231
slowdown and thermalization in heavy water, (E), 20: 26068
slowdown in liquid argon, analysis of, (T), 20: 30166 (NYO-3326-13)
slowdown in water at 1.46 ev, time distribution and spatial dependence of, (E), 20: 26067
slowing-down age in paraffin, 20: 4813
slowing-down and fast group constants from pulsed, 19: 41654
slowing down and migration time, review of, (E/T), 19: 27387 (GA-6290)
slowing down and thermalization of, computer program for, 18: 22852 (NAA-SR-9233)
slowing-down and thermalization in water, time behavior of, (E), 19: 35353
slowing-down and thermalization of, computer program for, 20: 4804 (KAPL-3098)
slowing-down and thermalization in graphite, time constants for pulsed, (E), 20: 13728
slowing down approximations in transport theory of, 17: 11592 (NP-12480)
slowing-down by homogeneous isotropic moderator, random functional approach to (T), 19: 1530
slowing down by multiple elastic scattering, evaluation of average energy in, 18: 22861
slowing-down by sintered beryllium oxide, 16: 1034 (AEC-tr-4689)
slowing-down calculations, computer program for, 16: 3611 (NASA-TN-D-1102)
slowing down, calculation method for shielding, 17: 12776(R) (ORNL-3360(p.96-7))
slowing down calculations using Monte Carlo method, effects of epithermal neutron interactions with bound protons on, (T), 20: 34485
slowing down density distribution in homogeneous media, computer program for analysis of, 16: 26197 (NAA-SR-7357)
slowing-down density from beryllium-radium sources in graphite prism, 17: 15223
slowing-down density in heavy media, calculation methods for, 17: 39951(T) (AEC-tr-6055)
slowing-down distributions in infinite media, from point sources, 16: 22974
slowing down distribution in infinite media, computer code for calculating moments of, 18: 40477 (NAA-SR-Memo-9802)
slowing down distributions in water, salt water, and silicon dioxide, 19: 35370(T)
slowing-down equation for, constant solution of, 18: 34747
slowing-down fraction, CAGE program for computed lethargy levels, 16: 8157 (DC-58-6-221)
slowing down in a bare multiplying medium, time-dependent, 17: 3735
slowing down in a reactor thermal column, calculation of, 17: 5307
slowing down in a spherical nonfissionable medium, point-source solution to transport equations for, 17: 38055
slowing down in absorbing media, equations for, 19: 37769
slowing down in beryllium, 18: 26248
slowing-down in beryllia and beryllium, age and fast-effect calculations for, 20: 8042 (TID-22446)
slowing down in concretes, measurement of, 19: 14754
slowing down in Dowtherm A at 10 to 260°C, 16: 24774
slowing-down in graphite and iron from 14 to 4.9 Mev, 16: 4744
slowing down in graphite, 18: 44969 (CEA-R-2478)
slowing down in graphite, age to indium resonance of, (E), 20: 26069
slowing down in heavy water, Greuling-Goertzel approximation, 16: 19726 (TID-15645)
slowing down in heterogeneous media, calculation by Wilkins' theory, 17: 790
slowing down in heavy water, toluene, and water, 17: 34829 (CONF-39-63)
slowing-down in heavy medium, theory for, 18: 6145(R) (ORNL-3499 (Vol.I)(p.118-27))
slowing down in heavy media, 18: 40494
slowing down in heavy water, time dependence of, (E/T), 20: 21936 (AE-216)
slowing down in hydrogenous mixtures, (T), 19: 10229
slowing down in hydrogenous mixtures, heavy nuclei effects on, (T), 19: 23606
slowing down in hydrogen, solution of space-energy-angle dependent equations for, (T), 19: 27404
slowing down in hydrogenous mixtures, equation for, 20: 28248
slowing down in ice at 90 and 273°K, 17: 32989
slowing down in infinite homogeneous moderator, stochastic calculation of, 16: 18411
slowing-down in infinite homogeneous medium, exact theory, 16: 4743
slowing-down in infinite homogeneous beryllium moderator, effects of reactions (n,2n) and (n,α) on, 16: 15615
slowing down in infinite homogeneous media, Boltzmann equation for, 18: 26500
slowing down in infinite homogeneous media, Boltzmann equation for, 18: 26501
slowing down in infinite media, chemical binding and thermal motion effects on, 18: 26513
slowing down in infinite media, calculation methods for, 19: 6828(R) (ANL-6944(p.53-76))
slowing down in infinite medium, calculation using variational techniques, 20: 34494
slowing down in liquid hydrogen, parameters for, (T), 19: 6628
slowing down in matrices, exact solution to equation for, 17: 3819
slowing down in matter, stochastic analysis of, 17: 13476
slowing down in mixture of elements, energy distribution in, (T), 19: 16829
slowing down in moderator, asymptotic law in theory of, 17: 2208(T) (FTD-TT-62-1045)
slowing down in moderators, effective resonance integrals for, 17: 5314
slowing down in multilayered media of, distribution equations for, 19: 35369(T)
slowing down in nonabsorbing moderator, 18: 15151
slowing down in pure water, below 2.1 Mev, (E/T), 19: 29201
slowing down in reactors, theory of, 17: 22548
slowing down in reactor systems, 18: 42590 (TID-7050(p.15-24))
slowing down in resonance-capture media, model for, 18: 42593 (TID-7050(p.137-54))
slowing down in reactor shields, method for prediction of, 19: 40156 (NP-15161)
slowing down in reactors, transfer matrices for, (T), 20: 19784 (NAA-SR-11530)
slowing down in thin plates of hydrogenous material, Monte Carlo method for studying, 19: 45216 (CEA-R-2804)
slowing down in uniform media, analytic approximations in, 18: 42591 (TID-7050(p.89-125))
slowing down in uniform media, Monte Carlo calculations for, 18: 42592 (TID-7050(p.125-37))
slowing-down in water, measurement, 17: 15198 (BNL-719(Vol.III) (p.966-76))
slowing down in water, pulsed measurements of, 18: 42589 (PAN-503/IX-A)
slowing down in water and tungsten–water media, (E/T), 19: 29203
slowing down in water–Zircaloy systems, (T), 19: 31192 (KAPL-3080)
slowing down in water, space- and time-dependent density for, (E), 20: 11927 (AE-208)
slowing-down kernels for, measurement of, 18: 28551
slowing-down lengths in beryllium oxide at 0.3 and 1.4 ev, 16: 33806
slowing down length in moderator mixtures, calculation of, 17: 34842
slowing down, mathematical formalisms for, 16: 26209 (BNL-5821)
slowing down, model study in Kansas State standard pile, 16: 24761 (TID-15667)
slowing-down, Monte Carlo programs for, 16: 8305 (DC-58-8-64)
slowing down of, analytic approximation techniques for integral equations for, 18: 7119
slowing down of (d,d), to 1.44 ev in paraffin wax, 16: 26210
slowing down of, definition of a suitable "mean" collision number in, 17: 22543
slowing down of, pulsed-source measurements of, 17: 34829 (CONF-39-63)
slowing-down of, renewal theory for, 17: 11603
slowing down of, analysis limitations for, (T), 20: 32363

slowing down of, computer program for, 20: 13698 (DTMB-1820)
slowing down of, effects of hydrogenous media on, 18: 38008 (A/CONF.28/P/356)
slowing down of, near resonances, 18: 28544
slowing down of, transfer matrices for multigroup, (T), 20: 19784 (NAA-SR-11530)
slowing-down parameters in liquid hydrogen, 18: 28554
slowing down process of, in heavy water, effect of chemical bonding on, 17: 15226
slowing-down spectra in light and heavy water, 16: 9411 (AAEC/E-78)
slowing-down spectra in slab, Greuling-Goertzel method with angular dependence for, 18: 28527 (AE-140)
slowing-down spectra in natural uranium-heavy water lattices, (E/T), 19: 19070
slowing-down spectrum, computer program for calculation, 16: 24945 (MND-C-2500-5)
slowing-down spectrum in CANDU-type reactor cell, 17: 26881
slowing-down spectrum in water, 17: 28437 (KAPL-2000-20)
slowing-down spectra of, in discontinuous media, 17: 36633
slowing-down theory, review of, 17: 34835 (EUR-342.i)
slowing down theory for, anisotropic scattering in, 18: 21135 (UCRL-7006-T)
slowing down time in water, calculation of, 19: 37202(R) (BNL-900 (p.1-28))
slowing-down time in water, spatial dependence of, (E/T), 20: 34487
slowing-down time in water, spatial dependence of, (E), 20: 34488
slowing-down with resonance absorption, solution to Boltzmann equation for, 16: 704
slowing-down with anisotropic scattering, analysis by Laplace transforms, 16: 12412
solar, search during solar minimum for, 20: 44452
spatial distribution in water at indium resonances from 1.4-Mev source, 16: 1009
spatial distribution in water, foil activation analysis of, 16: 1010
spatial distribution of, from fission source in water, 17: 3784
spatial variations and spectra of, in uranium–water lattices, 17: 11940 (CRRP-895)
spectra and buildup factors in infinite conical configurations of water, computer program for calculation, 16: 31218 (NASA-TN-D-1434)
spectra and thermalization analyses in thermal reactors, 18: 38006 (A/CONF.28/P/73)
spectra and yield from helium-3 reactions (He-3,n) with nuclei at 19 to 25 Mev, 20: 22132
spectra and yields in deuteron reactions on thick targets, (E), 19: 35428
spectra at 50 to 160 Mev, comparison of experimental and calculated, (E/T), 19: 17160(R) (ORNL-3714(Vol.II)(p.119-33))
spectra from Accelerator Pulsed Fast Assembly, leakage, 20: 36140(R) (GA-7091)
spectra from alpha reactions (α,n) with beryllium-9 and polonium-beryllium source, 19: 31203
spectra from alpha reactions (α,n) with aluminum-27 at 17 Mev, level density parameters from evaporation, (E), 20: 38115
spectra from alpha reactions (α,n) with manganese-55 at 17 Mev, level density parameters from evaporation, (E), 20: 38115
spectra from alpha reactions (α,n) with iron-56 at 17 Mev, level density parameters from evaporation, (E), 20: 38115
spectra from alpha reactions (α,n) with silver at 17 Mev, level density parameters from evaporation, (E), 20: 38115
spectra from bismuth-209 (γ,n) reactions at 12 to 16 Mev, (E), 19: 41834
spectra from deuteron-triton interactions at 5 to 12 Mev, 17: 11526
spectra from deuteron reactions with tritium, energy, 18: 2404(R) (TID-19651)
spectra from deuteron three-body-breakup reactions with helium-3, 20: 24388
spectra from deuteron three-body-breakup reactions with tritium, 20: 24388
spectra from gamma reactions (γ,n) with beryllium-9 at 3 to 17 Mev, energy levels from, (E), 20: 6390
spectra from meson (μ) capture by helium-3, (T), 19: 41783
spectra from moderators at 20 to 80°K, (E), 20: 11944
spectra from SPERT capsule driver core, analysis of, 19: 32680(R) (IDO-17052)
spectra from uranium-235 spheres, leakage, 20: 21939(R) (GA-6930)
spectra in ALRR, nuclear emulsion analysis, 20: 42681(R) (IS-1500 (Sect. R))
spectra in aluminum–plutonium–water systems, 18: 11436(R) (HW-79054(p.31-42))
spectra in beryllium, (E/T), 20: 2968
spectra in borated light water, infinite-medium, (T), 19: 33192(R) (GA-6096)
spectra in borated water, (E), 20: 15731(R) (RPI-328-49)
spectra in Doppler region, calculation of, (T), 19: 47539 (ANL-7050, pp 51-76)
spectra in fast assembly, accelerator-pulsed time-of-flight measurements of, 20: 36430 (GA-7091(App.C))
spectra in fast reactors, modal representation of, (T), 19: 29538
spectra in fast reactors, subcritical facility for measurement, 19: 38128 (KFK-302)
spectra in graphite, following fast neutron pulse, (T), 19: 16824
spectra in heavy and light water, (E/T), 20: 24312
spectra in heavy water, 19: 23209(R) (RPI-328-20)
spectra in heavy water, analysis of time-dependent, 19: 37766 (RPI-328-23)
spectra in heavy water, pulsed-source measurement of time-dependent, (E/T), 20: 13736
spectra in heavy water and polyethylene, time-dependent, (E), 20: 30324(R) (RPI-328-56, pp 52-93)
spectra in heavy-water natural uranium lattice, angular, (E), 20: 30846
spectra in homogeneous multiplying media, (E), 19: 18734 (CEA-R-2455)
spectra in homogeneous infinite media, 20: 8051
spectra in hydrogenous media, eigenfunction analysis of, 20: 2999
spectra in infinite homogeneous media, computer analysis of, (T), 19: 14468 (RPI-328-18)
spectra in iron, nickel, and stainless steel, measurements of, (E), 19: 37770
spectra in lattices, 17: 4046
spectra in light water-moderated reactors, computer analysis of, 18: 35128(R) (GEAP-4642)
spectra in light-water-moderated reactors, computer code for calculating, 19: 24032
spectra in light-water lattices, cell theory calculation of, 19: 47968
spectra in liquid hydrogen, determination of, (E/T), 20: 34471(R) (GA-7064)
spectra in media, analysis of asymptotic, 18: 36080(R) (RPI-328-8)
spectra in multiplying hydrogen-moderated uranium-235 assemblies, asymptotic, 18: 15474 (TID-20302)
spectra in multiplying media, measurement of asymptotic, (E), 19: 25457 (RPI-328-28)
spectra in multiplying media, measurement of asymptotic, 20: 6591
spectra in multiplying and non-multiplying media, (T), 20: 46562(R) (RPI-328-68, pp 84-144)
spectra in natural uranium, measurement of exponential, (E), 19: 39763 (EUR-2413.e)
spectra in nonmultiplying media, asymptotic, 18: 15147 (TID-20170)
spectra in ORR, measurement of fluctuation, 20: 26535 (ORNL-TM-1401)
spectra in paraffin-moderated uranium-235 assemblies, (E), 19: 23596(R) (RPI-328-20(p.1-8))
spectra in paraffin–zirconium oxide media, 20: 4806(R) (RPI-328-40, pp 1-42)
spectra in polyethylene, measurements of spatially dependent asymptotic, (E), 19: 23597(R) (RPI-328-20(p.9-15))
spectra in polyethylene and water, spatially dependent asymptotic, (E), 19: 33215
spectra in reactor matrices, 17: 28437 (KAPL-2000-20)
spectra in reactors, harmonic analysis of instantaneous counting of random pulse flow for, 18: 38336
spectra in reactors, use for reactivity analysis, (E), 19: 25688 (ORNL-TM-1066)
spectra in reactors, methods for calculating, 19: 27412
spectra in reactor cores, effects of temperature on, 19: 40122(R) (GEAP-4862)
spectra in reflected cores and reflector regions, 20: 22396
spectra in samarium-poisoned graphite, 18: 11145 (GA-4812)
spectra in thermal reactors, calculation of, 19: 12729(R) (EACRP-U-17)
spectra in thermal reactors, flux synthesis method for determining, 20: 47003
spectra in uranium–water systems, measured and theoretical, 19: 33192(R) (GA-6096)
spectra in uranium dioxide tubes at 50 to 750°C, (E/T), 20: 45089
spectra in water containing erbium and gadolinium, temperature-dependent, (E/T), 20: 2966
spectra in water-moderated uranium-235-fueled subcritical assemblies, 19: 35723
spectra in ZR-2 assembly measurement of, 18: 38335
spectra measuring methods for, 20: 20183
spectra of, for cadmium curtain between source and probe, 17: 26392(R) (GA-3853)
spectra of, from phosphorus-31, 17: 13528
spectra of secondary, from proton reactions with nuclei between beryllium and bismuth at 450 Mev, (E), 19: 17160(R) (ORNL-3714(Vol.II)(p.119-33))
spectra of space-dependent fluxes of, calculation of, 20: 22520(R) (NAA-SR-11805)
spectra of 14.8-Mev, 17: 36347(R) (NARF-62-18P)

spectra of, from heavy-ion bombardment of gold, 19: 10370
spectra of, from lithium-7 reactions on lithium-6, 18: 17009
spectra of, from proton reactions at 4 to 14 Mev, 18: 26601
spectral density of fluctuations of, negative reactivity measurements from, 18: 35074 (TID-7679(p.171-81))
spectrometry in multisection fission chamber, time-of-flight, 19: 26655 (IAE-697)
spectrometry in uranium fluoride–paraffin critical lattices, 18: 28982
spectroscopy below 10 ev, differential and integral methods for, (E), 20: 6260 (CONF-651101-43)
spectroscopy of, method for, (T), 19: 15900
spectroscopy of, using single-crystal devices, (T), 19: 8379 (UCRL-7611(Rev.I))
spectroscopy of, using iterative unfolding method, (T), 19: 20316 (ANL-6984)
spectrum from ZENITH plutonium core-7 (E/T), 19: 1863 (AEEW-R-374)
standard for, use of californium-252 as primary, 17: 9627
statistical behavior in multiplying media, 16: 24775
statistics in multiplying systems, 18: 42935 (TID-7050(p.1010-1130))
statistics in reactors, importance-function, (T), 19: 8598 (EUR-1897.e)
stimulation of nonmesonic hyperon (Λ) decay, 17: 13407
stopping in peat and water, 17: 10559
streaming from EGCR core, current estimates of, 17: 17548 (TID-18096)
streaming in beam tubes, 16: 706
streaming in concrete ducts, dose measurements for, 18: 21546 (NP-13805)
streaming in heavy water pipes, 17: 3803
streaming in straight cylindrical shield ducts, 17: 3801
streaming in water-d_2-filled pipes, 17: 11588 (AE-98)
streaming through straight aluminum ducts, 17: 39947 (NARF-63-3T)
streaming through bent ducts, (E/T), 19: 23948
strength function calculation from transmission data, computer program for, 19: 10217 (BNL-8711)
strength function for nuclei $220 \leq A \leq 248$, peak in s-wave, 19: 47115(R) (ANL-6983)
strength functions in optical model, 16: 1015
strength functions, s- and p-wave, 16: 6949
strength functions and widths for lead and tin isotopes, 17: 28261
strength functions for ellipsoidal nuclei, s-wave, 17: 29599
strength functions in optical models, collective vibration effects on p and s-wave, 17: 38197
strength functions of optical model for, 18: 7678 (CONF-346-5)
strength functions for, inelastic scattering determination in, 18: 8919(R) (PR-P-59(p.65-78))
strength functions for, P- and S-wave, 18: 18988
strength functions in rare earth region, target spin dependence of, 19: 41656 (BNL-9245)
strength functions of, level spin dependence of, (E/T), 20: 19273(R) (BNL-929, pp 3-43)
strengths of single, in nuclei, 17: 33049
structure of, from form factors and scattering amplitudes, (E/T), 19: 47565 (AD-614270)
structure of, general survey of, 19: 45125
structure of, review on, 18: 44524
structure of, review of, 19: 18763
tables of resonance integral functions, 19: 45214 (ANL-7024)
temperature distribution in hot mixtures of water–water-d_2, 17: 26814
temperature distributions in core, boron-filter measurement of, 18: 33037
temperature distribution across water-boron-poisoned water interface, (E/T), 19: 21207
temperature in reactor fuel elements, calculation of, 17: 1055
temperature measurement of, using gadolinium filter, 16: 33189
temperature measurement using gadolinium filter, 17: 18617
temperature measurements in TRIGA-Mark (II), 19: 29786
temperature of, use of lutetium in measurement of, 17: 11586 (AAEC/TM-164)
temperatures in CANDU-type reactor lattice cell, 17: 26880
temperatures in fuel elements, determination by lutetium activation, 17: 40295
temperatures in graphites sleeves, 18: 7858 (AEEW-R-144)
temperatures of, relation between activation and kinetic, 17: 39960
theory of thermalization, utilization, and resonance absorption, 17: 11975
thermal utilization in plate lattices, 16: 14250
thermal utilization coefficient of, in heavy-water-moderated reactors, external blocking effect in, 17: 22807
thermal utilization factor for, determination from fuel-element extrapolation lengths, 17: 28230
thermal utilization in heterogeneous reactors, formulation of polyenergetic, 18: 3115
thermal utilization in heterogeneous lattices, simple formulation of polyenergetic, 18: 15445
thermal utilization, 18: 32277(R) (PR-P-61)
thermal utilization in square lattice cells, 18: 42947
thermal utilization in heterogeneous reactors, resonance interference effects on, (T), 19: 25695
thermal utilization in reactor lattice cells during fuel irradiation, 19: 29512
thermal utilization in ceramic-fueled, water-moderated reactors, models for, (T), 19: 38229 (WCAP-5492)
thermal utilization in SGR uranium carbide lattices, (E), 20: 6586 (NAA-SR-Memo-11313)
thermal utilization factors for, correlation of calculated and measured, 20: 21938(R) (BNWL-193, pp 16-20)
thermal utilization in reactors, determination of, (E/T), 20: 28725
thermal utilization in reactors, determination of, (E/T), 20: 28726
thermalization, 17: 22666(R) (TID-18561)
thermalization, 18: 38056(T) (AEC-tr-6398(p.126-38))
thermalization, 18: 40493
thermalization, (E/T), 20: 9944 (RPI-328-44)
thermalization, 18: 42598 (TID-7050(p.285-9))
thermalization, (E/T), 19: 47548(R) (TID-22141, pp 3-33)
thermalization and transport in lattices, analytical expressions for, 17: 2505
thermalization and transport in reactor cores, 17: 9878
thermalization and scattering by benzene and polyphenyls, 17: 15163 (BNL-719(Vol.I)(p.69-99))
thermalization and transport, 18: 11376
thermalization at large bucklings in beryllium, effects of coherent scattering on, 19: 25458 (RPI-328-33)
thermalization by liquid hydrogen, 16: 7167
thermalization by isopropylbiphenyl and water, 18: 24566 (NP-13921)
thermalization by water-d_2, time-dependent spectral studies of, (E/T), 19: 31196(R) (RPI-328-35(p.1-34))
thermalization calculations, Monte Carlo sampling technique for multi-phonon processes, 16: 9353 (AE-62)
thermalization, developments in program for measurement of integral,
thermalization, diffusion effect in, 16: 29732
thermalization experiments, review, 17: 12011
thermalization for Mass-1 and Nelkin scattering kernels, non-1/v, 18: 44719
thermalization in heterogeneous reactors, 16: 2688(T) (AEC-tr-4677)
thermalization in plane lattices, 16: 2708
thermalization in heavy gases with energy-dependent absorption, 16: 3660
thermalization in heavy-gas moderators, Boltzmann equation solutions, 16: 7011
thermalization in heterogeneous and quasi-homogeneous media, generalization of Wilkins theory for homogeneous media, 16: 19739
thermalization in graphite, 16: 30066 (GA-2307)
thermalization in heterogeneous reactors, 16: 29725
thermalization in heavy crystalline moderators, theory, 16: 29728
thermalization in heterogeneous systems, Monte Carlo calculation of, 17: 779
thermalization in heavy gas moderators, equations for, 17: 2514
thermalization in moderators, pulsed-source measurements of, 17: 4044
thermalization in reactor lattice, methods of calculation of, 17: 13475
thermalization in a free gas and a crystalline medium, solution of spatial- and time-dependent eigenvalue problem for, 17: 15209 (BNL-719(Vol.IV)(p.1299-1330))
thermalization in heavy crystals, theory, 17: 15169 (BNL-719(Vol.I)(p.203-37))
thermalization in infinite homogeneous media, 17: 15179 (BNL-719(Vol.II)(p.439-63))
thermalization in a cylindrical fuel cell, diffusion theory for, 17: 15188 (BNL-719(Vol.II)(p.684-705))
thermalization in graphite, 17: 15192 (BNL-719(Vol.III)(p.805-37))
thermalization in heavy water, 17: 15193 (BNL-719(Vol.III)(p.879-99))
thermalization in reactor cell, computer calculation, 17: 13878(R) (KR-36)
thermalization in solids, 17: 19205 (TID-18432)
thermalization in solids, approximate models for, 17: 20957 (LA-2834)
thermalization in a reactor lattice, analysis of, 17: 22822
thermalization in zirconium hydride, 17: 26030
thermalization in bare homogeneous multiplying medium, analysis of time-dependent, 17: 26408
thermalization in moderators, calculation of generalized heavy free gas operator for, 17: 29562 (AEEW-M-350)
thermalization in zirconium hydride, 17: 32974 (GA-4328)
thermalization in beryllium, effects of coherent scattering on, 17: 34560(R) (TID-19195)
thermalization in infinite homogeneous media, equation for, 17: 34891
thermalization in homogeneous media, models for, 17: 42200(T) (EURAEC-778)
thermalization in beryllium, effects of coherent scattering on, 18: 2820
thermalization in beryllium, coherent scattering effects on, 18: 11153
thermalization in rocks, temperature effects on, 18: 10292

thermalization in zirconium hydride, measurement of, 18: 26514
thermalization in water, parameters for, 18: 26871
thermalization in graphite, analysis by WKB method, 18: 28542
thermalization in poisoned media, eigenfunction analysis of, 18: 30698
thermalization in moderators, experimental age measurements for, 18: 30949 (NYO-9077)
thermalization in thermal reactors, calculations of, 18: 33010 (A/CONF.28/P/258)
thermalization in infinite homogeneous media, theory of, 18: 34727 (CEA-R-2368)
thermalization in beryllium, coherent-scattering effects in, 18: 36080(R) (RPI-328-8)
thermalization in plutonium and uranium solutions, models for, 18: 36780(R) (HW-81659(p.20-5))
thermalization in cylindrical symmetrical two-zone reactor cell with natural uranium and heavy water, 18: 36789
thermalization in heterogeneous reactors, method for calculating, 18: 38616 (A/CONF.28/P/705)
thermalization in hydrogenous media, 18: 38011 (A/CONF.28/P/366)
thermalization in cylindrically symmetric cells, 18: 38037 (A/CONF.28/P/643)
thermalization in gases, time eigenvalues and degenerate kernels in, 18: 40467 (BNL-7842)
thermalization in graphite, WKB calculations of, 18: 42580 (BNL-7812)
thermalization in graphite, pulse-equilibrium calculations of, 19: 3505 (BNL-7823)
thermalization in beryllium, effects of coherent scattering on (T), 19: 3191(R) (RPI-328-16)
thermalization in graphite with poison and temperature discontinuity (E), 19: 3203
thermalization in graphite, wave reflection in (E/T), 19: 3204
thermalization in Marius, spectral indices for, (E/T), 19: 10643 (EURAEC-1198)
thermalization in thermal columns in heavy-water reactors, (E), 19: 17358 (ANL-6915)
thermalization in graphite, (T), 19: 16828
thermalization in water, chemical binding effects in, (T), 19: 19071
thermalization in weakly absorbing medium, (T), 19: 21204
thermalization in graphite, (E), 19: 21211
thermalization in beryllium, effects of coherent scattering on, (E), 19: 23598(R) (RPI-328-20(p.16-23))
thermalization in cluster fuel elements, model for, (T), 19: 24056
thermalization in infinite media, analysis by method of moments, 19: 25459
thermalization in moderating assemblies, analysis of pulsed, 19: 29178 (RPI-328-31)
thermalization in beryllium, effects of coherent scattering on, 19: 29217
thermalization in ice, water, and heavy water, (E), 19: 33226
thermalization in light and heavy water, time-dependent, (T), 19: 33227
thermalization in system of moderators at different temperatures, (T), 19: 33209
thermalization in cylindrically symmetric two-zone reactor cell, (T), 19: 35714
thermalization in beryllium, scattering effects on, (E), 19: 37765 (RPI-328-22)
thermalization in gases, liquids, and solids, Van Hove theory for relaxation times in, 19: 39773
thermalization in heavy water, interference scattering effects on, (T), 19: 47559
thermalization in moderating assemblies, time-, energy-, and space-dependent theory of, 20: 3003
thermalization in graphite, (T), 20: 4818
thermalization in beryllium, beryllium oxides, heavy water, polyethylene, water, and zirconium hydrides, (E/T), 20: 8035 (GA-5798)
thermalization in heterogeneous reactors, computer program for, 20: 10323 (KR-101)
thermalization in heterogeneous and homogeneous reactors, computer program for calculating, 20: 10329 (RT/FI(65)24)
thermalization in crystalline media, variational methods for, (T), 20: 9957
thermalization in moderators, (T), 20: 12275 (GA-6861)
thermalization in heterogeneous systems, Monte Carlo calculations of, (T), 20: 11935 (RFR-154)
thermalization in graphite, wave excitation in, (E/T), 20: 13722
thermalization in paraffin, pulse transfer function for, (E/T), 20: 13724
thermalization in beryllium and graphite, pulsed-source measurements of, (E), 20: 13738
thermalization in water and zirconium hydrides, pulsed-source measurements of, (E), 20: 13739
thermalization in graphite-water systems at large temperature gradients, (E), 20: 13740
thermalization in reactor moderators, review of integral, 20: 19779 (GA-8904)
thermalization in reactors, computer program for, 20: 22374(R) (BNWL-193, pp 5-15)
thermalization in zirconium hydrides, models for, 20: 22377 (GA-6930, App. B)
thermalization in heavy water, time dependence of, (E/T), 20: 21936 (AE-216)
thermalization in beryllium and graphite, (E), 20: 21942(T) (KFK-tr-188)
thermalization in beryllium, application of C(λ) method to, (T), 20: 24308
thermalization in nonisothermal media, (T), 20: 30322 (BNL-947)
thermalization in reactors, space-dependent, (T), 20: 30861
thermalization in heterogeneous systems, approximate treatment of, 20: 30864
thermalization in graphite and graphite-moderated enriched uranium systems, time-dependent, (E/T), 20: 30327
thermalization in heavy water lattices, phenomenological model application, 20: 38455
thermalization in multiplying media containing plutonium, 20: 40384(R) (EURAEC-1660)
thermalization in infinite medium, (T), 20: 40052
thermalization in heavy water, (T), 20: 46562(R) (RPI-328-68, pp 84-144)
thermalization in a heterogeneous medium, model for, 20: 47006(R) (EURAEC-1666)
thermalization in reactors, numerical methods for determining, 20: 46999
thermalization in reactor metals, 17: 2468 (CRRP-985-E)
thermalization in graphite and water, 17: 7055 (HW-SA-2415)
thermalization in heavy water coolants, 17: 11962 (TID-17574)
thermalization in moderators, chemical binding effect in, 18: 38031 (A/CONF.28/P/360)
thermalization, measurements using electron linear accelerator, 16: 28011 (GA-2510)
thermalization model for, 20: 26533(R) (BNL-954, pp 16-49)
thermalization near equilibrium, 18: 22862
thermalization of, study by matrix eigenvalue techniques of, 16: 29883(R) (TID-16309)
thermalization of, variational methods in, 17: 4043
thermalization of, Boltzmann equation solutions by phase integral method, 17: 15201 (BNL-719(Vol.IV)(p.1075-1102))
thermalization of, time decay constants in solution of Boltzmann equation for, 17: 15202 (BNL-719(Vol.IV)(p.1103-30))
thermalization of, solution of time-dependent Boltzmann equation for, 17: 15206 (BNL-719(Vol.IV)(p.1232-54))
thermalization of, solution of time-, energy-, and space-dependent Boltzmann equation for, 17: 15210 (BNL-719(Vol.IV)(p.1331-59))
thermalization of, mechanisms of, 17: 15213(R) (GA-3409)
thermalization of, IBM-7090 programs for calculating, 17: 15217 (ORNL-TM-461)
thermalization of, representation of eigenvalues in, 17: 15221 (TID-18008)
thermalization of, equations for calculating, in multiregion or multitemperature geometries, 17: 15181 (BNL-719(Vol.II)(p.565-9))
thermalization of, calculation by up-scattering equation, 17: 15182 (BNL-719(Vol.II)(p.570-91))
thermalization of, Tempest II code in Fortran for IBM 709 and 7090 calculations of, 17: 19202 (TID-18284)
thermalization of, solution of energy- and time-dependent, 17: 24368 (GA-3469)
thermalization of, pressure vessel for measuring, 17: 24369(R) (GA-3542)
thermalization of, discrete energy representation of, 17: 26031
thermalization of, velocity polynomials in, 17: 26032
thermalization of, space and time dependent eigenvalue problem in, 17: 26390 (EUR-22.e)
thermalization of, eigenvalues of Wilkin's equation for solving problems of, 17: 31386
thermalization of, energy-dependent Milne problem solution for, 17: 32969 (BNL-6949)
thermalization of, velocity polynomial calculation of, 17: 32973 (CONF-39-46)
thermalization of, research on, 17: 31794(R) (BNL-782(p.1-17))
thermalization of, effective mass kernels in, 17: 34560(R) (TID-19195)
thermalization of, research progress on, 17: 37993(R) (GA-4426)
thermalization of, research progress on, 17: 39943(R) (GA-4176)
thermalization of, eigenvalue problems in, 18: 6148
thermalization of pulsed, theory of time-dependent, 19: 37202(R) (BNL-900(p.1-28))
thermalization of, transient phenomena in theory of, 18: 21142
thermalization of, transient phenomena in theory of, 18: 21143
thermalization of, time eigenvalues and degenerate kernels for, 18: 28553
thermalization of, pulse-source measurement of, 18: 38036 (A/CONF.28/P/509)
thermalization of, correlation-function method for, 18: 40471 (EUR-1643.e(p.131-6))
thermalization of, Monte Carlo calculations for, 18: 42602 (TID-7050 (p.379-409))

thermalization of, chemical binding effects on spectra in, 18: 42615
thermalization of, scattering-law parameters for, 19: 1518 (AE-154)
thermalization of, time eigenvalues and degenerate kernels in (T), 19: 1519 (BNL-8433)
thermalization of, heavy monatomic gas model for (T), 19: 1539
thermalization of, theory for, 19: 1542
thermalization of, energy-transfer moments in (T), 19: 3509 (CEA-R-2472)
thermalization of, models for (T), 19: 3510 (CEA-R-2473)
thermalization of, spatially independent problems in theory of, 19: 8385
thermalization of, time-dependent, (T), 19: 16830
thermalization of, spatial transients in, 19: 23604
thermalization of, approximation for energy increases in, (T), 19: 37761 (KAPL-M-6471)
thermalization of, transient phenomena in, (T), 19: 37773
thermalization of, integral, 19: 41640(R) (GA-6323)
thermalization of, temperature-dependent, (T), 19: 41652
thermalization of, error estimates for integral-equation eigenvalue problems in, 20: 3411
thermalization of, research on, 20: 4806(R) (RPI-328-40, pp 1-42)
thermalization of, integral, (E/T), 20: 19778(R) (GA-6824)
thermalization of, research on, 20: 28237(R) (TID-22844, pp 1-35)
thermalization of, research on, 20: 30324(R) (RPI-328-56, pp 52-93)
thermalization of, mean number of collisions in, (T), 20: 37992
thermalization of, lectures on, (T), 20: 44587 (NP-16291)
thermalization parameters for, (T), 19: 33223
thermalization problem of two different media, 17: 2213
thermalization, relation of real and imaginary parts of Van Hove correlation function for describing, 16: 7149
thermalization, relation of real and imaginary parts of Van Hove correlation function for describing, 16: 24766(T) (AEC-tr-5146)
thermalization representation for effective cross section calculations, 17: 42199(T) (EURAEC-777)
thermalization spectra for, routing delay for normalization of, 18: 14218 (TID-20244)
thermalization studies, 16: 2566(R) (TID-14187)
thermalization studies at Kurchatov Atomic Energy Institute, review, 18: 38012 (A/CONF.28/P/367)
thermalization, theory development, 16: 32357 (GA-3122)
thermalization theory of, applications to hot-atom chemical reactions, 18: 31587
thermalization theory for, using simple scattering kernel, 19: 14467 (PAN-545/IXA)
thermalization time in water, measurement of, 18: 7656 (AE-125)
thermalization, variational methods for calculating, 16: 29713 (TID-12780)
thermalization with isotropic kernels, (T), 19: 33225
time-of-flight analysis, development of magnetic-tape recording system for, 16: 1937 (CREL-1036)
time-of-flight methods, conference on, 16: 14040
time-of-flight measurements from (γ,n) reactions, 18: 10689 (LNF-63/47 (p.160-9))
transfer functions for, use of power spectra in reactor-system analysis of, 18: 35071 (TID-7679(p.107-33))
transfer in (N-14,N-13) reactions on nitrogen-14, (E), 19: 43390
transfer in calcium-40 (p,d) reactions at 30 Mev, 18: 18981
transfer in lead-207 (N^{14},N^{13}) reactions, 17: 36649 (CONF-62-12)
transfer in nuclear reactions having arbitrary Q, 16: 29870
transfer in nuclear reactions, 17: 36650 (CONF-62-13)
transfer in reactions, reduced widths from, 18: 16929 (ANL-6848(p.160-7))
transfer of two, in nitrogen-15 reactions with zirconium isotopes, 17: 38080 (JINR-P-1273)
transfers in aluminum, copper, gold, nickel, and tantalum bombardment with nitrogen-14 and -15, 16: 26221 (JINR-P-973)
transmission by filters for separation of thermal and intermediate energies, 18: 30693
transmission by finite water slabs, 20: 4999(R) (ORNL-2599)
transmission by hydrogenless shielding materials, 19: 47870
transmission by lead and tungsten, resonance parameters from, 18: 24620(R) (ORNL-TM-874)
transmission by plutonium-241-enriched plutonium dioxide, cross sections for, 18: 11184 (ANL-6797(p.369-75))
transmission by polarized holmium-165 at 8.3-Mev, 20: 6275(R) (AD-619534)
transmission by shielding, angular distributions in, 20: 5181(R) (ORNL-3029)
transmission by slow chopper, 18: 494 (RT/FI(63)-26)
transmission by tin isotopes, nuclear radii from, 18: 24620(R) (ORNL-TM-874)
transmission by very thick layers, Monte Carlo analysis of, 18: 28914
transmission coefficients for, s-wave, 18: 34866
transmission in concrete, iron, polyethylene, soil, and water at 0.5 to 14 Mev, 17: 9478 (BRL-1174)
transmission in indium and silver, (E), 19: 15926
transmission in iron-56 at 0.1 to 50 kev, 1148-ev resonance in, (E), 19: 5121
transmission in kev region using single-level Breit-Wigner formula for resonances, 18: 6150
transmission in palladium at 1.2 to 100 ev, resonances in, (E), 19: 45233
transmission in perfect crystals, anomalous, (T), 20: 38387
transmission in protactinium-233, tantalum-182, and uranium-233, (E), 20: 44604 (CONF-660303, pp 67-74)
transmission in shielding, 17: 36835
transmission in shielding materials, (E), 19: 14728 (APEX-581)
transmission in silver-109 at 30 ev to 20 kev, resonance parameters for, (E), 20: 12072
transmission in slab geometries, Monte Carlo codes for, 19: 14731 (TO-B-63-82)
transmission in slabs, Monte Carlo calculations of, 19: 14732(R) (TO-B-63-83)
transmission in thorium-232, p-wave resonance, 18: 11247
transmission in titanium hydride, 18: 37142
transmission measurements on, data handling and resonance analysis in, 16: 27368
transmission of, computer program for data on, 17: 37995 (KAPL-M-EC-32)
transmission of, in air, computer program for, 16: 33365 (UNC-5031)
transmission of, optical model coefficients for, 17: 32968(BNL-765)
transmission of polarized, through holmium-165, 16: 23107
transmission of polarized, effects of polarized nuclei on, 17: 36669 (WASH-1042)
transmission of polarized, by polarized targets, 18: 36696
transmission of polarized, through a superconductor in the mixed state, (T), 20: 2998
transmission probabilities through purely absorbing tubes, tables, 16: 28009 (AECL-1504(Pts.I&II))
transmission resonances of s-wave, analytical program for, 17: 5295 (CEA-2156)
transmission resonances of, computer analysis of, 18: 2779 (CEA-2346)
transmission resonances in time-of-flight experiments, IBM 7094 computer calculations for, 19: 37777
transmission through slab of liquid hydrogen calculation by Monte Carlo method, 16: 24605
transmission through rectangular ducts, 17: 3802
transmission through cadmium, 17: 26034
transmission through nickel-coated copper tubes, 18: 34752(R) (CU(PNPL)-234)
transmission through polarized nuclei in europium and europium sulfides, field measurements from, 18: 35560
transmission through bent aluminum ducts (E/T), 19: 3473
transmission through lithium hydride (E/T), 19: 3220
transmission through lithium hydride slabs, (T), 19: 29173 (NAA-SR-Memo-10853)
transmission through beryllium-Hevimet slabs, 19: 29438 (APEX-502)
transmission through thick slabs, computer program for, 19: 29440 (NAA-SR-Memo-10881)
transmission through heterogeneous multiplying and nonmultiplying media, 19: 41643 (ORNL-TM-1184)
transmission through lithium hydride slabs, Monte Carlo analysis of, 19: 41642 (NAA-SR-10853)
transmission through boral, 20: 4999(R) (ORNL-2599)
transmission through heterogeneous shields, 20: 4999(R) (ORNL-2599)
transmission through orientated holmium-165 at 8 and 15 Mev, total cross sections for, (E/T), 20: 10066
transmission through slabs, transfer-matrix method for, (T), 20: 15934
transmission through iron-water mixtures, 20: 34784
transmission through heavy concrete at high energy, (E), 20: 34787
transmission through magnetized cobalt and nickel, Stern-Gerlach experiment for measuring polarized, 20: 34819
transmission through cobalt, effect of Bloch domains on polarized, 20: 34820
transmissions in chlorine-containing crystals, 405-ev resonance for chlorine-35 from, (E), 19: 43271 (JINR-P-2198)
transmutation doping of semiconductors, 18: 37662 (BNL-874(p.10-11))
transport, 18: 13175 (ESD-TDR-63-231)
transport, albedo logic for double-S_n analysis, 16: 15264(R) (HW-71747)
transport analysis of pulses of, 18: 2812
transport and energy deposition in cryogenic propellant tanks of nuclear rockets, Monte Carlo method for (T), 19: 3717 (FZK-156)
transport approximation of energy-dependent Boltzmann equation, for anisotropic scattering with energy degradation, 17: 26404
transport at large distances from source, lattice model concept of, 20: 9956
transport at 400 to 50 Mev, computer program for, 18: 36578 (ORNL-3610)
transport by shields, Monte Carlo calculation of deep, 18: 15424 (NP-13719)

transport calculations for, iteration procedure for, 18: 2781 (LADC-5904)
transport calculations for, alternation between diffusion and S_n cycles in, 18: 2792
transport calculations for strong absorbers, equivalent radii for P_1, 18: 7663 (TID-19819)
transport calculations in fast reactors, 18: 29131
transport calculations for, Monte Carlo computer program for, 18: 42585 (KAPL-3013)
transport calculations for, Monte Carlo techniques in, 18: 42608 (TID-7050(p.1441-61))
transport calculations for, adjoint solutions in (T), 19: 3504 (AWRE-O-52/64)
transport calculations for source-detector problems, adjoint, (T), 19: 29172 (LADC-6488)
transport calculations using Monte Carlo method, energy-independent biasing functions for, 20: 2985
transport calculations using P_1 and P_3 scattering moments, one-dimensional, 20: 34932
transport calculations for, computer programs for, 20: 46558 (ORNL-3856)
transport calculations using Monte Carlo method, 20: 46930(R) (ORNL-3973(Vol.1), pp 52-9)
transport, computer program for solution of equations for, 16: 13931 (UCRL-6604)
transport, computer codes for Monte Carlo calculations, 16: 16633 (DC-59-12-83)
transport cross sections for, optical model of, 17: 17472
transport effects in neutron wave experiment, (T), 20: 15685
transport equation, solutions for spherical geometry, 16: 2468 (ORNL-3216)
transport equation, Yvon's approximation method for solving, 16: 6120
transport equation diffusion approximation, 16: 7008
transport equation solution for infinite homogeneous media, 16: 10935 (AE-63)
transport equations, development of SNG-TAC and DSN-TAC codes for, 16: 12801(R) (IA-685)
transport equation, discrete S_n method for solution, 16: 15613 (LA-2595)
transport equations, albedo logic for S_n analysis, 16: 18414
transport equation solution by residue iteration method, 16: 19727 (TID-15664)
transport equation for, Green functions for synthetic kernel, 16: 26201 (PAN-284/IX)
transport equation solutions for parallel plane radiation obliquely incident on parallel plane dispersion, 16: 32270 (DASA-1257)
transport equations for, computer program for solution of, 16: 32361 (IA-761)
transport equation solutions for, computer program for P-3 approximation, 16: 32365 (WAPD-TM-207)
transport equations for, computer program for solving time-dependent radiation hydrodynamics, 17: 785 (LAMS-2713)
transport equation for, iterative solution of, 17: 3816
transport equation in slab geometry, computer program for solution of, 17: 4024 (KAPL-M-EJB-1)
transport equation for, synthetic method solution of, 17: 5302 (TID-15404)
transport, equations for linear extrapolation length and disadvantage factor for cylinders, 17: 9486
transport equations for, modification of Greuling-Goertzel method, 17: 9487
transport equation for, solution of, 17: 13469 (AE-89)
transport equation solution in plane geometry for heavy gas, infinite medium, and constant total cross section, 17: 15211 (BNL-719 (Vol.IV)(p.1360-74))
transport equations for, integral forms, 17: 15180 (BNL-719(Vol.II) (p.464-84))
transport equations for, elementary solutions method for, 17: 22533 (MMPP-NPC-1-1)
transport equations for, truncation errors in solutions of slab geometry, 17: 22529 (AD-282968)
transport equations for, existence and uniqueness theorems for, 17: 28225 (TID-18885)
transport equation in finite slab, method for solving one-dimensional, 17: 28227 (WAPD-T-1392)
transport equation solution for, computer program for, 17: 37994 (IA-761(App.))
transport equation for monoenergetic, elementary solutions for, 18: 996
transport equation for, solution of one-dimensional multigroup, 18: 975 (AWRE-O-12/63)
transport equation for, solution methods for, 18: 985(T) (AEC-tr-6107)
transport equation for, approximate solution of time-dependent, 18: 733(R) (TID-19610)
transport equations for, computer program for solving multi-energy, 18: 2782 (WAPD-TM-272)
transport equation solution for cylinders, computer program for, 18: 2783 (WAPD-TM-396)
transport equation for, Case-Wigner method of solving, 18: 4517
transport equations for, time-dependent, 18: 4523
transport equation for, DSN method for solving, 18: 7657 (AEEW-R-161)
transport equation in slabs, numerical solution of double P_3, 18: 7655 (AAEC/TM-224)
transport equation for point source, space-velocity distributions from solution of, 18: 11154
transport equation for one-velocity group, application of Case's solution for, 18: 11155
transport equations for, solutions for nonlinear, 18: 13241
transport equation with anisotropic scattering, degenerate solutions for, 18: 15161
transport equation for, solution of uniform, 18: 18855
transport equations for, computer program for, 18: 21123 (GA-4972)
transport equations for adjacent half spaces, solution of one-speed, 18: 21133 (TID-20503)
transport equation for, numerical techniques for, 18: 22851 (LA-2996)
transport equation for, anisotropic scattering effects in, 18: 24565 (LA-3051)
transport equations for monoenergetic, variational boundary conditions for spherical harmonics approximation to, 18: 24573
transport equation computer code, two-dimensional multigroup, 18: 26497 (AWRE-O-66/63)
transport equation in plane geometry for, transformation of, 18: 34743
transport equations for, iterative solutions of, 18: 38309 (A/CONF.28/P/632)
transport equation for, Galerkin method for numerical solution of, 18: 40488
transport equations in cylindrical geometry, Gaussian-quadrature solutions of, 18: 44714
transport equations for, solution of integral, 18: 44022 (RM-3942-PR)
transport equation for, iterative method for solving energy-dependent, (T), 19: 5115
transport equation for heterogeneous media, Green function solution of, (T), 19: 6623
transport equation for, analytical solution of energy-dependent, (T), 19: 37772
transport equation for, approximate solution of nonlinear, (T), 19: 41651
transport equation for, approximation to multi-dimensional, (T), 19: 33204
transport equation for convex homogeneous body, eigenvalue spectrum of, (T), 19: 33218
transport equation for, P_1 approximation to time-dependent, (T), 19: 23610
transport equation for, relation to non-equilibrium thermodynamics, 19: 47551 (UJV-1354/65)
transport equation for slab geometry, eigen-values of, (T), 19: 27413
transport equation for slab geometry, time- and velocity-dependent, (T), 19: 45227 (NIJS-R-449)
transport equation in one-velocity and isotropic-scattering approximation, 19: 45220 (EUR-2411.i)
transport equation, modified spherical harmonic approximations for, 19: 35350 (TID-21038)
transport equation with anisotropic scattering, iterative method for solving, (T), 19: 21223
transport equation with anisotropic scattering, solution of one-dimensional, (T), 19: 35361
transport equations for, generalized variational method for, (T), 19: 8383
transport equations for, generalized P-N approximation method for solving, 19: 12463
transport equations for, method of moments for solving, (T), 19: 14464 (LA-3060)
transport equations for, discrete ordinates angular quadrature of, (T), 19: 14465 (LA-3186)
transport equations for, in slab geometry, numerical integration of, 19: 17168
transport equations for, lower bounds for eigenvalues for, 19: 16831
transport equations for pulse calculations, P_3 approximation to, (T), 19: 29197
transport equations for, angular moments in integral, 19: 29214
transport equations for, methods for solving, 19: 31202
transport equations for, eigenvalues of Boltzmann, (T), 19: 33217
transport equations for, for criticality determination in two-region cells, 19: 42035 (ANL-6590)
transport equations for, time eigenvalue (T), 19: 1519 (BNL-8433)
transport equations in cylindrical and plane geometry, computer program for, 19: 45219 (EUR-2410.i)
transport equation for, normal-mode solution of, 20: 1141
transport equation for critical slab, solution by perturbation theory, 20: 3423
transport equation for, variational vacuum boundary conditions for P_N approximation to, 20: 2978
transport equation for, approximation by moments equations, 20: 2981
transport equation for, numerical method for solving linear, 20: 2983

transport equation for, method for solving, 20: 2984
transport equations for, computer program for solving, 20: 2990
transport equation for one-speed, solutions in plane geometry, 20: 3000
transport equation for, approximation by discrete ordinates equations, 20: 2982
transport equation for, solution by S_n approximation, 20: 10224 (ORNL-TM-1196)
transport equation for multi-region cylindrical geometry, computer program for solution in P_5 approximation, 20: 9940 (EUR-2584.e)
transport equation for slab geometry, solutions for, 20: 11933 (INR-630/IX-A/PR(Pt.2))
transport equations for, adjoint, 20: 14094
transport equation in plane multiregion geometries, first-order solutions of, 20: 15674
transport equation for, computer program for solution of one-dimensional multigroup, 20: 19783 (NAA-SR-10951)
transport equations for, computer program for solving, 20: 21937 (AEET-210)
transport equation for, P_3-approximation for, 20: 26074
transport equation for, space-time flux synthesis methods for solving Boltzmann, 20: 28235 (NAA-SR-11821)
transport equation for, structure of solution for, 20: 34474
transport equation with anisotropic scattering in slab geometry, (T), 20: 34483
transport equation for, variational formulations of, 20: 34492
transport equation for, continuity conditions for P_N approximations to, 20: 34493
transport equation for, approximation method for solving, 20: 34495
transport equations for two-dimensional geometry, accuracy of S_2, (T), 20: 34481
transport from point time-dependent source in atmosphere, 16: 18404 (UNC-5006)
transport from point source at altitude 10^5 feet, flux density calculations for, (T), 20: 21935 (AD-624041)
transport, generalized variational method for calculating, 16: 24372
transport in a slab, invariant imbedding approach to, 17: 17103
transport in absorber-moderator systems, tabulation, (E/T), 19: 16814 (AERE-R-4776)
transport in absorbing media, equations for, 19: 37769
transport in adjacent half-spaces, Case's method in one-speed, 18: 21140
transport in adjacent semi-infinite media, time-dependent, (T), 20: 2987
transport in adjacent semi-infinite media, time-dependent monoenergetic, (T), 20: 30339
transport in air from atomic bombs, shielding against, 19: 38892
transport in air of 3 and 14 Mev, comparison of geometries, 17: 9483
transport in aluminum, carbon, and polyethylene slabs, data tabulations for, (T), 19: 47868 (RRA-T52)
transport in anisotropic scattering media, computer program for, 19: 1526 (ORNL-3715)
transport in arbitrary geometry with anisotropic scattering, equation solutions for (T), 19: 3209
transport in bare slabs, finite Fourier transforms for energy-independent, (T), 20: 26072
transport in beryllia- and graphite-moderated subcritical assemblies, (E), 19: 19360 (UCRL-12200)
transport in complex geometry, analysis by three-dimensional Monte Carlo calculations, (E/T), 20: 3348
transport in complex reactor geometries, computer programs for, 20: 32768 (UNC-5148)
transport in compressible fissile media, dynamic reactivity effects in, 18: 23027 (TID-7662(p.447-90))
transport in concrete, 17: 24367 (BRL-1189)
transport in cylindrical geometry, spherical harmonic approximation of, 16: 19738
transport in cylindrical and spherical geometry, S_n solutions for, 17: 17463
transport in cylindrical lattices, 17: 26005
transport in cylindrical geometry, calculation of, 18: 3112
transport in cylindrical rods, equations for, 18: 18858
transport in cylindrical and slab geometries, discrete-ordinates method for, 18: 26512
transport in cylindrical lattices, collision probabilities for, 18: 26872
transport in cylindrical geometry, FORTRAN II program for IBM 7090, 18: 34729 (IDO-16968)
transport in cylindrical geometry, collision probabilities for, 18: 38045 (A/CONF.28/P/681)
transport in cylindrical heterogeneous reactor cell, computer program for one-group, 18: 42922 (KR-71)
transport in cylindrical geometry, even-order spherical-harmonics method for, 18: 44717
transport in cylindrical or slab cell, multigroup one-dimensional spherical harmonic calculation of, 18: 44704 (IDO-16998)
transport in cylindrical geometries, disadvantage factor in (T), 19: 3213
transport in cylindrical geometry, unsymmetrical spherical-harmonics method in, (T), 19: 10231
transport in cylinders and slabs, one-group collision-probability code for, 20: 15668 (EUR-2624.e)
transport in cylindrical rods in square reactor lattices, monoenergetic equation for, 20: 26437
transport in cylindrical, planar, and spherical cells, computer program for, 20: 26061 (CEA-R-2896)
transport in differentially heated media, (T), 20: 8052
transport in diffusing, multiplying and slowing-down media, multi-group theory for, 18: 15150(T) (AEC-tr-6332)
transport in dissipative media, first-order diffusion and telegraphist's equations for, 18: 44712
transport in enriched uranium-water assembly with resonance absorbers, flux measurements from study of, 19: 3777 (IDO-17009)
transport in fast reactors, validity of approximation in, 17: 26023
transport in fast reactors, equation for, 18: 17288
transport in fast reactors, 22-group constants for, 18: 26824(R) (ANL-6885)
transport in fast ceramic reactors, theory, 18: 35146(R) (GEAP-4601)
transport in fast reactors, resonance self-shielding in, (T), 20: 8355
transport in fertile zone of JRR-1, (E), 19: 17367(T) (CEA-tr-X-552)
transport in finite moderators, time-dependent solutions for, 17: 11597 (TID-16085)
transport in finite nonabsorbing slab, with isotropic elastic scattering, 18: 34746
transport in finite black sphere, spherical harmonic method for Milne analog in, 19: 19068
transport in finite slab geometries, source functions for, (T), 20: 2930 (AD-614636)
transport in fixed three-dimensional body, equations for, 19: 21203
transport in fuel elements, monoenergetic treatment, 16: 21344
transport in gap geometry, boundary conditions for monoenergetic, 18: 2791
transport in gaseous core reactors, computer program for, 20: 22370 (AD-621021)
transport in general geometry, spherical-harmonics approximation for, (T), 19: 25456 (RPI-328-7)
transport in graphite and water, decay constants in pulsed, (T), 19: 10230
transport in graphite-moderated gaseous-core rocket reactors, (T), 19: 14875 (GNE/Phys/64-16)
transport in graphite moderated lattices, multigroup calculation methods for, (T), 19: 17279 (NAA-SR-10531)
transport in graphite, temperature-dependent variation of mean free path of, (E), 20: 21955
transport in hafnium–uranium-235-water systems, resonance interference in, (E/T), 19: 21643 (WAPD-T-1728)
transport in heavy media, theory for, 17: 41846(T) (AEC-tr-6094)
transport in heavy-water-moderated lattices, space-dependent spectra in, 19: 29568
transport in heavy-water moderated lattices, (T), 20: 45066 (CONF-660303, pp 151-70)
transport in heavy water matrices, spatial dependence of, 18: 13242
transport in heterogeneous materials, cross sections and self-shielding factors for, 17: 5301 (TID-13710)
transport in heterogeneous media, Green functions for, 18: 2793
transport in heterogeneous reactors, collision probabilities for, 18: 38310 (A/CONF.28/P/640)
transport in heterogeneous systems, factorization method for multigroup integral equations for (T), 19: 1523 (JAERI-1058)
transport in heterogeneous anisotropically scattering shields, energy-dependent, (T), 20: 2989
transport in homogenized-fuel regions, 17: 26004
transport in homogeneous reactors, computer programs for, 19: 24002
transport in homogeneous plane slabs, (T), 19: 39771
transport in homogeneous multiplying systems, (T), 20: 16030
transport in homogeneous media, asymptotic equation for, 20: 26077
transport in homogeneous media, calculations of using P-3 approximation, 20: 40064
transport in infinite slabs, operator equations for, 17: 9485
transport in infinite media, generalization of Fick's law for, 18: 26518
transport in infinite slab reactors, equations for, 18: 26867
transport in infinite slab of finite thickness, variational approach to calculation of, 18: 32721
transport in infinite homogeneous media, (T), 19: 31499 (BNWL-3)
transport in infinite homogeneous medium, (T), 19: 12464
transport in inhomogeneous and finite media, 18: 38234 (A/CONF.28/P/363)
transport in inhomogeneous moderators, graphic method for solving, (T), 20: 13732
transport in iron, 17: 29563 (BRL-1199)
transport in iron and iron-water mixtures, (E/T), 20: 4998 (JINR-P-2359)

transport in isotropic media and slab geometries, generalization of Fick's law for, (T), 19: 10237
transport in laminated iron–heavy water systems, 18: 28908
transport in large lethargy interval, number of collisions in, (T), 19: 6621
transport in lattices, EQUIPOISE method for calculating, 19: 47541 (ANL-7050, pp 179-89)
transport in lattices, disadvantage factor calculations for, (T), 20: 18049 (RT/FI(65)-42)
transport in linear and spherical geometries, equations for, 18: 43114(R) (NP-14236)
transport in matter, model for, 17: 8705
transport in matter, computer analysis of, (T), 19: 19063 (AWRE-O-97/64)
transport in matter, use of importance sampling for, 19: 45458 (AE-190)
transport in matter, code for multigroup transfer matrices in, (T), 20: 8043 (TID-22447)
transport in matter, computer code for multigroup anisotropic, (T), 20: 8039 (LA-3373)
transport in moderating media, energy-dependent theory for, 17: 19203 (TID-18428)
transport in multiplying and scattering media, 17: 3821
transport in multiplying media, 18: 42581 (CEA-R-2476)
transport in multiplying system, approach to equilibrium of pulsed, (T), 19: 27403
transport in natural uranium, 16: 15611 (CEA-1997)
transport in non-multiplying media, Monte Carlo code for, (T), 19: 33193 (MND-C-2933)
transport in nonmultiplying media, review of pulsed-source measurements on, 19: 37762 (KFK-301)
transport in nonuniform slabs, solution for time-dependent, (T), 20: 8036 (INR-637/IX-A/R)
transport in nuclear rockets, IBM-7090 Monte Carlo program for calculating, 17: 20959 (UNC-5043)
transport in one-dimensional slab geometry, computer program for calculating, 16: 13929 (ORNL-TM-168)
transport in one-dimensional slab and sphere, Green's functions for one-velocity, 18: 44722
transport in one-dimensional rod, invariant imbedding theory for, 19: 33199
transport in one-dimensional rods, invariant-imbedding theory for, 20: 1315
transport in one-dimensional geometries, (T), 20: 36136 (AE-227)
transport in organic moderator, 18: 34734
transport in plane geometry, eigenfunction expansion method for Boltzmann equation for, 18: 38035 (A/CONF.28/P/498)
transport in plane geometry, analytical and numerical methods for, 18: 40735 (EUR-1643.e(p.87-108))
transport in plane slab, energy-dependent isotropic equation for, 18: 40482
transport in plane multi-region geometries, first-order solutions for one-speed, 19: 29215
transport in plane geometry, eigenfunctions and full-range completeness for, (T), 20: 6252 (AD-617880)
transport in plane geometry, half-range completeness and half-space problems for, (T), 20: 6253 (AD-617882)
transport in plane geometry, orthogonality relations for, 20: 15684
transport in plane geometry, solutions of multigroup equations for, (T), 20: 15667 (EIR-72)
transport in plane parallel plate, separation of spatial and angular variables in equation for, 20: 15673
transport in plates, criticality conditions of, 19: 3197
transport in plutonium critical assemblies, foil activation studies of, 20: 6579(R) (BNWL-149, pp 48-56)
transport in pool reactors, 18: 38613 (A/CONF.28/P/670)
transport in pulsed fast liquid-metal-cooled reactors, two-group calculations of, (T), 19: 17216 (EUR-2217.e)
transport in reactors, nine and sixteen group cross sections for analysis of, 17: 22789 (GEMP-173)
transport in reactor coolant ducts, 18: 3133
transport in reactor fuel elements with nonuniform temperature distribution, Doppler effects in, 17: 38510
transport in reactors, equations for, 18: 26866
transport in reactors, variational calculations of, 18: 28966
transport in reactor shielding, (T), 19: 17156(R) (EUR-2197.d)
transport in reactor reflectors, heat transfer model for, 19: 21656
transport in reactor matrices, program for, 19: 33190 (CEA-R-2614)
transport in reactors, matrix factorization in equations for (T), 19: 3550
transport in reactors, depletion calculations for (T), 19: 3562
transport in reactors, statistical dynamics of, (T), 19: 8598 (EUR-1897.e)
transport in reactors, nonlinear Peierls equations for, 19: 25690
transport in reactors, reduced Boltzmann equations for, 19: 35717
transport in reactors, (T), 19: 47921(R) (ANL-7090, pp 30-54)
transport in reactors, collision-probability calculations of, (T), 19: 47540 (ANL-7050, pp 93-112)
transport in reactors, (T), 20: 3375 (IDO-17120)
transport in reactors, S2 and S4 calculations of, (T), 20: 6264 (WAPD-T-1849)
transport in reactors, solutions of energy-dependent Boltzman equation for, 20: 18068
transport in reactors, (T), 20: 18070
transport in reactors, computer programs for, 20: 22380 (ORNL-TM-1246)
transport in reactor systems, 20: 30804
transport in reactors, equations for, 20: 30862
transport in reactors, kinetic equations for, 20: 34910
transport in reflected multiplying slab, 20: 32782
transport in restricted geometry, discrete spectrum of operators for monoenergetic, 20: 24317
transport in rocket reactors, (T), 19: 35841
transport in rocket reactors, (T), 19: 35842
transport in rods having variable cross sections, 16: 18408
transport in shield materials, computer program for, 19: 3463
transport in shielding materials up to 400 Mev, calculations for (E/T), 19: 3461
transport in shielding plate layers, solution of Boltzmann equation for, 19: 3196
transport in shielding, removal-diffusion theory for, 19: 39751 (AE-185)
transport in shielding materials, formulation of, (T), 20: 1303 (AD-614250)
transport in shields, P_3 method for flux calculation from, 20: 32673 (NAA-SR-Memo-11872)
transport in slab geometry, computer program for calculation, 16: 23274 (WAPD-TM-320)
transport in slab geometry, double P_N analysis of, 17: 24365 (AAEC/E-107)
transport in slab geometry, 17: 26003
transport in slab geometry, one-velocity, 17: 26027
transport in slab geometry, solution of time-dependent, 17: 28224(R) (TID-18884)
transport in slab geometry, computer program for, 17: 29565 (IDO-16856)
transport in slab geometries, free-surface boundary condition for, 18: 18859
transport in slab geometry, spatial expansion of, equation for, 18: 28532
transport in slab geometry, modified P_3 approximations to equations for, 18: 34728 (DTMB-1814)
transport in slab geometries, computer programs for, 18: 34732 (WAPD-TM-436)
transport in slab geometry, polynomial spatial expansions of Boltzmann equation for, 18: 40466 (APED-4342)
transport in slab geometry, solution of initial-value problem for (T), 19: 1531
transport in slab geometries, angular distributions in (T), 19: 3211
transport in slab geometry with anisotropic scattering, (T), 20: 2986
transport in slab geometry, solution to one-velocity time-independent Boltzmann equation for, 20: 3004
transport in slab geometry, tables of functions for, 20: 4803 (INR-630/IX-A/PR)
transport in slab geometry, spectral theory for stationary operator for, 20: 17658
transport in slab geometry with anisotropic scattering, initial-value problem for, 20: 28242
transport in slab geometry with isotropic scattering, initial-value problem for, 20: 28243
transport in slab geometry, numerical integration of equations for, 20: 30326
transport in slab geometries, reflection and transmission in, 20: 36134 (AAEC-E-149)
transport in slabs, matrix formalism for P_L approximations to, 18: 979 (KAPL-M-RAR-1)
transport in slabs, calculations of escape probabilities, 18: 28543
transport in slabs, blackness theory approximations to, 18: 42603 (TID-7050(p.409-48))
transport in SNAP shielding, cross section library for, 20: 34782 (NAA-SR-Memo-11718)
transport in source-free systems, perturbation calculations of multigroup, 18: 42577 (AWRE-O-32/64)
transport in source-free multiplying media, Milne problem for, 18: 44702 (GAMD-2906)
transport in source free medium, Boltzmann equation expansion with Jacobi polynomials for, 20: 28259
transport in spherical geometry, one-group, 17: 17458
transport in spherical geometry, spherical harmonics approximation of, 17: 17459
transport in spherical geometry, theoretical method for problems in, 18: 2794
transport in spherical reactors, Boltzmann solutions with vacuum-interface boundary conditions for, 18: 38334 (TID-20933)

transport in spherical geometry, computer program for adjoint, 19: 1521 (IA-911)
transport in spherical reactors, j_N analysis of, 20: 16022 (EUR-2627.e)
transport in spherical configurations, eigenfunctions for Boltzmann equation for, 20: 24301 (CEA-R-2926)
transport in three-dimensional geometry, Monte Carlo computer program for, 18: 42870 (UNC-5093)
transport in three-dimensional rectangular geometry, computer program for, 20: 30726 (TID-22964)
transport in three-dimensional geometry, computer codes for, 20: 40460(R) (IDO-17191)
transport in two-dimensional laminated materials, method for solution of one-dimensional stationary equation for, 20: 21945
transport in two-region slab lattice, calculation of disadvantage factor for, 20: 17668
transport in uranium-heavy water subcritical lattices, pulse measurements of, 18: 44972 (MIT-2344-1)
transport in voids, correction for streaming losses in, (T), 19: 10236
transport in water, Monte Carlo calculation of buildup factors and energy spectra, 16: 2620 (NASA-TN-D-850)
transport in water, eigenfunction analysis of, 18: 36080(R) (RPI-328-8)
transport in water-moderated systems, few-group calculations for, 18: 42596 (TID-7050(p.197-229))
transport in water, analysis of, (E/T), 20: 35001 (BNWL-222)
transport, inequalities in one-velocity theory for anisotropic scattering, 16: 10939 (ORNL-3229)
transport kernel for anisotropic scattering in slab geometry, spectral analysis of, 18: 13036
transport of, computer program for solving stationary, 17: 24371 (IA-806)
transport of, difference equations in, 17: 26026
transport of, discrete ordinate equations for, 17: 26012
transport of epithermal, effects of fuel depletion on, 18: 28974
transport of, in multilayer cylindrical geometry, spherical harmonics approximation of, 17: 17089 (CRT-1088)
transport of, in plane and spherical geometry, 17: 17456
transport of, integral equation of energy-dependent, 17: 11601
transport of, MOCA-2 code for calculating, 17: 26017
transport of, modified P_3 approximations to, 17: 26022
transport of monoenergetic, in non-moderating assemblies, 17: 11598 (TID-16304)
transport of monoenergetic, nonstationary kinetic theory of, 18: 36560
transport of monoenergetic, computer analysis of, (T), 19: 6845 (WAPD-TM-482)
transport of monoenergetic, computer program for, 19: 27394 (KAPL-M-6420)
transport of multi-energy, computer analysis of, 19: 25696(R) (HW-84369(p.11-19))
transport of, non-iterative and stable solution of discrete ordinates equations for, 17: 29567 (WAPD-T-1577)
transport of pulsed, in reactors, (T), 19: 21637 (CONF-650406-2)
transport of, spherical harmonics approximation for, 17: 17457
transport of, theory of estimating, 18: 2822
transport of, thin-region parameters in slab geometry for, 17: 34560(R) (TID-19195)
transport of, two-dimensional calculations of, 17: 26015
transport of, within spherical medium, distribution function and neutron source term in, 17: 20960
transport of, analytic tests of multigroup descriptions of, 18: 28534
transport of, analytic methods in energy-dependent, 18: 38033 (A/CONF. 28/P/401)
transport of, anisotropic scattering in half-space, 18: 13034
transport of, anisotropic scattering effects in, (T), 19: 16826
transport of, approximate solutions to monoenergetic Milne problems in, 20: 34496
transport of, Boltzmann equation in spherical harmonics for, (T), 19: 35355
transport of, boundary conditions in age theory of, 20: 34476
transport of, computer program for, 19: 15981(R) (ORNL-3714(Vol.I) (p.70-7))
transport of, computer program for preparing data for Monte Carlo calculations for, 19: 21196 (AWRE-O-81/64)
transport of, computer program for application of spherical harmonics to, 19: 31187 (CRT-1218)
transport of, computer program for calculating energy spectra from, 20: 4805 (ORNL-TM-1245)
transport of, computer analysis of angular distributions from, 20: 8041 (ORNL-TM-1241)
transport of, computer programs for determining source convergence for, 20: 11934 (ORNL-TM-1325)
transport of, computer program for, 20: 22304 (AD-612031)
transport of, computer program for P_n multigroup scattering matrices in, 20: 30323 (ORNL-TM-1537)
transport of, errors associated with spatial harmonics in, (T), 19: 29205
transport of, error estimates for integral equation eigenvalue problems in, 20: 36149
transport of, few-group constants for systems having rapid spectral variation with position in, 19: 29219
transport of, for computer program, Monte Carlo calculations, 19: 47546 (KFK-298)
transport of, from proton-induced nuclear evaporation, 18: 28538
transport of, Green's function for monoenergetic, (T), 19: 21215
transport of, group constants for, 18: 40798
transport of, invariant imbedding in, (T), 19: 29175 (P-1495(RAND))
transport of, irreversible processes in, 18: 22856
transport of, kernel method in equation for, 20: 18069
transport of, modified spherical harmonic approximations in equations for (T), 19: 3210
transport of, moments and discrete ordinates equations for, (T), 19: 47547 (LA-DC-7320)
transport of, monoenergetic critical equation for, (T), 19: 21214
transport of, Monte Carlo calculations for, 18: 40468 (EUR-1643.e (p.115-18))
transport of, Monte Carlo computer program for, 18: 42610 (UCRL-7630 (Rev.1))
transport of, Monte Carlo technique for selecting scattering angles from anisotropic distributions in, (T), 19: 10232
transport of, Monte Carlo technique for selecting scattering angles from anisotropic distributions in, (T), 19: 10233
transport of, Monte Carlo code for, 19: 16818 (ORNL-3622)
transport of, Monte Carlo code for, 19: 43463 (TIM-941)
transport of, Monte Carlo calculations of, 19: 47545 (KFK-297)
transport of, multi-group constants for, 18: 38041 (A/CONF.28/P/668)
transport of, multiple collision (random walk) analysis of, 18: 40469 (EUR-1643.e(p.119-23))
transport of, multigroup diffusion theory for, 19: 10224
transport of, multiple collision method for solving problems in, (T), 19: 31210
transport of, orthogonality of eigenfunctions in one-speed, (T), 19: 8380
transport of, polarization effects in, (T), 20: 4814
transport of, preparation of cross section data for computer analysis of, (E/T), 19: 31200 (WAPD-TM-501)
transport of, radiative transfer equation solutions for, (T), 20: 15572
transport of, research on anisotropic, 20: 26533(R) (BNL-954, pp 16-49)
transport of, standardization of computer programs for, 20: 30721 (EUR-2778.e)
transport of, stochastic theory of, 19: 19074
transport of, systematic approximations for first-collision probabilities in, 19: 14475
transport of, wave parameters in monoenergetic, (T), 19: 29213
transport of, wave concept of, 20: 28250
transport operator for homogeneous medium, real eigenvalues of monoenergetic, (T), 20: 40054
transport problems of, computer program for solution of, 17: 17093 (TID-18117)
transport problems, review, 18: 38057
transport processes in zero-power point reactors, detectors for random, (T), 20: 24716
transport properties in elementary materials at 0.3 to 2.7 Mev, 17: 787(T) (AEC-tr-5413)
transport solutions to monoenergetic critical problems, 18: 6136 (ANL-6787)
transport studies, 16: 2566(R) (TID-14187)
transport theory, 16: 31062
transport theory, 17: 17455
transport theory, 20: 46928(R) (ORNL-3973(Vol.1))
transport theory, analytical solution for energy-dependent problem, 16: 4742
transport theory, analytical solution for energy-dependent problem in, 16: 24769(T) (AEC-tr-5204)
transport theory, application to reactor reactivity measurements, 17: 2470 (EIR-28)
transport theory at high energies, velocity dependent, 17: 5315
transport theory calculations in heterogeneous reactors, 18: 38344 (A/CONF.28/P/845)
transport theory, diffusion cooling phenomenon in nonstationary, 16: 22981
transport theory equations for, numerical solution of, 17: 41852
transport theory, for one-dimensional criticality studies, 16: 8156 (ANL-6459)
transport theory, FORTRAN program MO150 for, 16: 20934 (WAPD-TM-315)
transport theory for, using a semidirect variational method, 16: 22975
transport theory for, in critical slab systems, 16: 34011
transport theory for, energy-dependent, 17: 28229
transport theory for, integral-difference equations in, 17: 34832 (CONF-39-71)

transport theory for infinite media, 17: 39952(T) (AEC-tr-6057)
transport theory for, reduction to multigroup diffusion theory, 18: 2790
transport theory for spatially dependent distribution in heterogeneous media, 18: 9303
transport theory for one-dimensional rod, 18: 22855
transport theory for, correlation functions in invariant imbedding, 18: 26508
transport theory for, numerical, 18: 30704
transport theory for, developments in, 18: 32709 (A/CONF.28/P/261)
transport theory for, numerical solution of equations in, 18: 32722
transport theory for, multigroup, 18: 42595 (TID-7050(p.175-97))
transport theory for, relations to multigroup diffusion theory, 18: 44713
transport theory for, review, (T), 19: 9768 (LAMS-3079)
transport theory for, vacuum boundary conditions for spherical harmonics method of calculating, 19: 12460
transport theory for, invariant imbedding techniques in, 19: 15985
transport theory for, applications of, 19: 19064 (MMPP-FRPC-64-1)
transport theory for slab geometry, spherical harmonics method in, 19: 29198
transport theory for, approximation for scattering anisotropy in, 19: 33202
transport theory for, computer program for multigroup constants for, 19: 37759 (BNWL-35)
transport theory for wave parameters of, monoenergetic, 19: 43268
transport theory for, dynamic programming and inverse problem in, (T), 19: 47537 (AD-612468)
transport theory for reactors, invariant-imbedding techniques in, 20: 1415
transport theory for, variational principles in, 20: 2979
transport theory for, variational principles in, 20: 2980
transport theory for, spherical harmonics approximation in, 20: 4820
transport theory for, boundary value problems in, 20: 8048
transport theory for, spherical harmonics method in, 20: 8056
transport theory for, Boltzmann equation for anisotropic scattering in, 20: 11936
transport theory for, Bessel and Bickley functions for, (T), 20: 13707 (ORNL-TM-1415)
transport theory for, special functions in, (T), 20: 13708 (ORNL-TM-1417)
transport theory for, exponential transform for, 20: 20099 (ORNL-RSIC-14)
transport theory for, generalized invariant imbedding of, 20: 21947
transport theory for, bibliography on, 20: 26064 (IFA-FR-48)
transport theory for, vacuum boundary conditions for spherical harmonic method in, 20: 30332
transport theory for, dispersion law of linear Boltzmann equation in, 20: 30338
transport theory for reactor, 20: 32366
transport theory for, 20: 34472 (UCRL-14921-T)
transport theory for, radiative transfer for, (T), 20: 33977
transport theory for, Jacobi polynomial solution of one-dimensional and monoenergetic Boltzmann equation in, 20: 34473
transport theory for, solution of Milne problem for two half-spaces with different media, 20: 38003
transport theory for, inscattering approximations in, 20: 40060
transport theory for random walk of, in moderator containing holes, 20: 46573
transport theory, isoperimetric and other inequalities in one-velocity, 16: 5919
transport theory in semi-infinite media using invariant-imbedding methods, 16: 18406
transport theory in homogeneous systems, 18: 13233(R) (BNL-823 (p.1-19))
transport theory in pulsed multiplying assemblies, 20: 3001
transport theory, matrix symmetrization in multigroup, 16: 18407
transport theory, multi-group, 16: 26538
transport theory, one-velocity Boltzmann equation solution, 16: 2475
transport theory of collision probabilities in cylindrical geometry, 16: 19740
transport theory of, review of, 17: 4272
transport theory of, three soluble problems in linear, 17: 9480 (NP-12458)
transport theory of, P_N calculation method for classroom use in, 17: 26233
transport theory of, computer program for solving Carlson discrete S_n approximation to Boltzmann equation in, 17: 36626 (AEEW-R-273)
transport theory of, spherical-harmonics method for solution of problems in, 18: 15156
transport theory of, reduction to multigroup diffusion theory, 18: 15165
transport theory of, derivation of some invariant imbedding equations in, 18: 16898
transport theory of, correction to invariant imbedding equations obtained by particle counting in, 18: 16899
transport theory of, solutions to the source-free energy-dependent Boltzmann equation for, 18: 21153
transport theory of, abstract approach to unique solution of, 18: 21154
transport theory of, stochastic analysis of, 19: 29189
transport theory of, Chandrasekhar equations for, 20: 8049
transport theory of, use of Poincare-Bertrand formula in, 20: 4812
transport theory of, integral, 20: 9953
transport theory of, use of generalized functions and Poincare-Bertrand formula in, 20: 21956
transport theory of, properties of P_L and double P_L relaxation lengths in, 20: 21958
transport theory of, kinetic equations in, 20: 26071
transport theory of, use in critical assembly analysis, 20: 35171
transport theory of, eigenfunction expansion method for solving problems in, 20: 46569
transport theory, solution by angular segmentation method for shield configurations, 16: 10938 (NARF-61-43T)
transport theory, solution of Vick's problem and corresponding partial probabilities for, 16: 29723
transport theory, second fundamental theorem in one-velocity, 17: 4025 (ORNL-3330)
transport theory, velocity-dependent Milne's problem in, 16: 22976
transport theory, validity in critical size and reactivity calculations, 16: 26539
transport theory with anisotropic scattering, diffusion length in, 20: 1137
transport theory, Yvon approximation method, 16: 21336
transport through atmosphere from burst at 70,000 ft, 16: 5916 (AFSWC-TR-61-85)
transport through single-bend aluminum ducts in water shields, (E), 19: 47863 (AD-613480)
transport with anisotropic scattering, geometrical effects on, (T), 20: 16021 (CEA-R-2890)
transport with linearly anisotropic scattering, half-space (T), 19: 3212
transport with linearly anisotropic scattering, equations for half-space, 20: 11939
transport, Yvon approximation method in, 16: 24770
transport-theoretical calculations of disadvantage factors in lattices, 18: 28969
tunneling transfer in reactions of identical nuclei, 20: 6387
ultrasonic cavitation induced by, 17: 23646
uranium-238 resonance integral measurements in ECEL critical assembly, 18: 28960 (NAA-SR-9390)
use as probe for moisture control in mixtures for agglomeration, 20: 13156
use for analysis of coal deposit drillings, 19: 28560
use for determination of moisture in crude and fertilizer lime, 19: 26247
use for determining moisture content in materials, 20: 25355
use for measurement of moisture content of sintering materials, 18: 18299
use for moisture determination in concrete, numerical analysis method for, 20: 25355
use for radiography of boron in reactor alloys, (E), 20: 3471(R) (GEAP-4861)
use for soil density and moisture content determinations, for efficiency of probes, 20: 29506
use for soil density and moisture-content determinations, efficiency of air-gap and direct-transmission methods for, 20: 29505
use for study of rotational and vibrational freedom of hydrogen atoms in molecules, 17: 21607
use for temperature measurement by thermalization, 17: 12550(P)
use for therapy, 20: 10728
use in activation analysis, limits and techniques in, 16: 5265 (CF-60-11-42(Rev.))
use in cancer therapy, review, 18: 29461
use in determination of moisture in solids by reflection, 18: 6758
use in determining hydrogen content of materials, 18: 8319(P)
use in humidity measurements on loose materials, 20: 46022
use in level measurement in steel vessels, 18: 8619
use in Lunar and planetary composition studies, 20: 46106
use in measurement of phonon frequencies in polyethylene, 20: 3315
use in moisture gages, 20: 16924
use in moisture measurements, effects of density on, 18: 13672
use in nuclear physics, conference on, 18: 10621 (ANL-6797)
use in paving-mixture and soil density and moisture determinations, conference on, 20: 29504
use in production of short-lived nuclides, 20: 43022
use in radiography, 18: 13596
use in radiography, comparison with x rays, 18: 39471
use in radiography of biological materials, 19: 24392
use in semiconductor fabrication, 18: 2116
use in soil density and moisture measurements, 18: 39719 (RT/GEO(64)-10)
use in soil moisture determination, 18: 5505
use in soil-water determinations in well logging, 18: 5524
use in study of self diffusion in liquids, 16: 6870
use in therapy, evaluation of, 18: 41299
use in tumor radiotherapy, 18: 29471

use in tumor therapy, model for, 18: 19816
use in vulcanization of elastomers, resins, and rubber, economics of, 19: 1016
use in well logging, theory of, 18: 5501
use in well logging, 18: 5523
use in well logging, 18: 12373(P)
use in well logging in oil prospecting, 18: 12374(P)
use in well logging, calibration of apparatus for, 18: 12375(P)
use in well logging, boundary effects in, 19: 13654
use in well logging, method for, 19: 15772
use in well logging for chlorine, apparatus and method for, 20: 27179(P)
use of polarized, as research tool in nuclear physics, 18: 12929
use of pulsed, for reactivity measurements (T), 19: 3558
use of pulsed, in power reactor physics measurements during startup, 18: 29041(R) (GEAP-4606)
use of pulsed, in neutron and reactor physics, review on developments in, 19: 1528
use of pulsed, in power reactor reactivity measurements, 19: 12779(R) (GEAP-4732)
use of 14.5-Mev, in activation analysis of geological samples, 19: 36243(R) (X64-17610)
use of 14-Mev, for activation analysis, precision in, 19: 38569
use to produce high concentrations of vacancies in crystalline solids, 16: 24309
uses for strengthening metals and alloys, 20: 11366
uses in humidity measurements, 19: 30616
uses of pulses of, for criticality measurements on lattices, 18: 28981
uses of reactor, for commercial radiation chemistry, (E/T), 19: 40559
velocity distribution in infinite homogeneous media, space-independent Boltzmann equation for, (T), 20: 9948
velocity measurements from meson (π^-) interactions with protons, 16: 18322 (UCRL-9951)
velocity selector for, on the JRR-3 reactor, 20: 47066
wave functions for, P-wave strength in, 17: 724
wave propagation in subcritical assembly, 16: 6915 (TID-7619(p.161-82))
wave propagation in time-dependent P_1 approximation, (T), 19: 33203
wave propagation in multigroup transport approximations, (T), 20: 34484
yield in (d,n) reactions with deuterium and tritium, total, 17: 28254 (UCRL-10752(Suppl.))
yield in deuteron reactions (d,n) with tritium, 19: 23613
yield in deuteron reactions (d,n) with tritium, 19: 23615
yield in proton reactions (p,n) with $90 \lesssim A \leq 209$ nuclei at 5.5 and 9.5 Mev, cross sections and strength functions from, (E/T), 20: 26181
yield in z-pinch plasma compression, 17: 9738
yield in 15-Mev electron linear accelerator, 17: 30125
yields from alpha reactions (α,n) with carbon-14 at 2.5 to 5.1 Mev, (E), 20: 22110
yields from beams, beam energies and target thickness effects, 16: 23964 (ANL-6515(p.9-27))
yields from beryllium-9 (α,n) reactions at 2 to 12 Mev, 19: 29272
yields from beryllium–plutonium sources, effects of elemental ratios on, 20: 20553(R) (MLM-1142)
yields from deuterium (d,n) and tritium (d,n) reactions, 18: 34815
yields from deuteron reactions with deuterided erbium and titanium, (E), 19: 21301
yields from gamma reactions (γ,n) with nuclei in oil and water at 5 to 10 Mev, (E), 19: 34392(T)
yields from gamma reactions (γ,n) with nuclei in oil and water at 2.25 to 15 Mev, (T), 19: 34393(T)
yields from lithium-7 (p,n) reactions near threshold, (E/T), 20: 6355
yields from meson (π^-) capture by nuclei, (E/T), 20: 6292 (NP-15601)
yields from nitrogen-14 (d,n) reactions at 1.4 to 3.8 Mev, 18: 26673
yields from proton reactions (p,n) with vanadium-51 at 1.6 to 2.2 Mev, 18: 24591(R) (LMSC-4-50-62-1)
yields from pulsed sources, activation methods for measuring, 19: 14480
yields in (α,n) reactions at 2 to 5.4 Mev, 19: 45301
yields in fission, measurement of, (E), 20: 46553 (EANDC(UK)-3)
yields in helium ion fission of rhenium and thorium-232 at energies up to 40 Mev, 18: 26670
yields in nuclear reactions, (T), 19: 43377
yields in proton reactions with beryllium, lead, tin, and depleted uranium at 0.5 to 2.0 Bev, (E), 20: 34675
yields in uranium-235 thermal neutron fission, average, 18: 11194 (CONF-346-7)
yields of, from proton reactions in copper, 17: 22695
yields of secondary, in nucleon reactions with nuclei at high energies, (E/T), 19: 21242 (NP-14837)

NEUTRONS, COLD

diffraction by vortex lines in superconductors, 20: 28256
energy distribution in molecular motions in polyethylene at low frequency, 17: 37760
flux measurements in BEPO, DIDO, and EL-3 reactors, 16: 32380
interactions with bound protons at low temperatures, total cross sections for, 18: 17081
interferometer design for, 16: 22388
lifetimes in 1-m^3 cubic cavity with beryllium walls, 16: 29721
performance for radiography, (E), 19: 40722
production and gravitational properties of ultradense gas of, 19: 23619
production by inelastic scattering in hydrogen-containing substances, 16: 7169
production by total reflection, 18: 24569 (NP-13930(p.119-20))
production in Russian IRT reactor, 18: 30690(T) (ANL-Trans-42)
production of beams of, monochromators for, 20: 21949
production of, equipment for, 17: 12032
production of, gamma and fast neutron heating in moderators for, 20: 36152
production of, moderator materials for, (E), 20: 11944
reactions (n,p) in cyclohexane, temperature dependence of cross sections for, (E), 20: 11938
reactions with liquid and solid polyphenyls, total cross sections for, (E), 20: 28254
reactions with rhenium-185 and -187, total cross sections for, (E), 20: 3030
reactions with rotating molecules in condensed matter, (E/T), 19: 23355(R) (BNL-867(p.1-117))
reactions with thorium dioxide, uranium dioxide, and uranium at 0.0045 to 0.028 ev, total cross sections for, (E/T), 20: 21966 (AE-222)
reflection by cobalt films, total, (E), 19: 5122
scattering and slowing-down by hydrogenous compounds, 17: 11602
scattering by benzene, biphenyl, and biphenyl–phenyl ether system at
scattering by acoustic spin waves in magnetites, polarized, 16: 32366
scattering by aluminum, temperature dependence of phonons in, 16: 7176
scattering by ammonia, hydrogen, and methane, inelastic, 16: 32379
scattering by amyl, ethyl, and methyl alcohols, inelastic, 16: 32381
0.019 to 0.08 ev, 19: 27411
scattering by beryllium oxide at 100 to 400°K, cross sections for, 17: 29446
scattering by beryllium oxides, cross sections for, 17: 11671
scattering by beryllium oxide crystals, 18: 20574
scattering by biphenyl, spectrum for inelastic, 17: 38032(T) (AEC-tr-5734(p.194-5))
scattering by bromine (liquid), quasi-elastic, 17: 15241
scattering by copper-zinc alloy, small-angle, 17: 38034(T) (AEC-tr-5734(p.199-202))
scattering by copper monocrystals, inelastic, 17: 38035(T) (AEC-tr-5734 (p.210-12))
scattering by crystals, detection of structural defects by, 17: 18794
scattering by defects in solids, radiation damage studies by, 19: 12469
scattering by crystals, relation between cross sections and oscillation frequencies, 16: 7171
scattering by crystals, relation between cross sections and oscillation frequencies, 16: 24767(T) (AEC-tr-5156)
scattering by defects in solids, cross section calculation for, 19: 25620 (AERE-R-4853)
scattering by deuterated liquid methane, (E), 20: 46571
scattering by ethyl ether near critical point, inelastic, (E), 20: 8971
scattering by gaseous methane and ammonia, (T), 20: 44599
scattering by glycerol and water, 17: 15245
scattering by heavy and light water, (E), 19: 19077
scattering by heavy ice, temperature dependence of small-angle, (E),
scattering by ethylene and hydrogen, angular distributions of, 16: 32372
scattering by glycerol, water, and water-d_2, atomic and vibratory motions from, 16: 32373
19: 21218
scattering by hydrogenous materials, 17: 22540
scattering by hydrogen-bonded liquids, quasi-elastic, 17: 9489
scattering by hydrogenous compounds at low temperatures, total cross sections for, 18: 17081
scattering by hydrogen (liquid), cross sections for (T), 19: 3378
scattering by hydrogen in liquid argon, cross sections for, (T), 20: 7967
scattering by hydrides, determination of localized modes of hydrogen excess in, (E), 20: 20107 (EUR-2734.e)
scattering by hydrogen, methanol, and vanadium, 16: 31873
scattering by hydrous substances, inelastic, 16: 32385
scattering by ice at 2.5×10^{-4} to 3×10^{-3} ev, 16: 1014
scattering by iron(II) chloride, spectroscopy of iron(II) ion by, 16: 16824
scattering by lead (liquid), 17: 41873 (WASH-1044)
scattering by light and heavy water, spectral studies of water structural dynamics from, 16: 7163
scattering by liquids, 17: 4042
scattering by liquids, inelastic, 18: 7403 (BNL-7414)
scattering by liquids, microdynamic structural study from, 18: 26507
scattering by liquid and solid argon at 4.1 A, inelastic, 18: 28518
scattering by liquid and solid organic compounds, molecular rotation determinations from, 18: 43658
scattering by liquid argon, inelastic, (E), 19: 8345

scattering by liquid and solid argon, inelastic, (E), 19: 12475
scattering by liquid helium II, theory, 19: 14454
scattering by liquid and solid aluminum, inelastic, (E), 19: 14075
scattering by liquid hydrogen, consistent-vibrations model for cross sections of, (T), 19: 29168 (FZK-199)
scattering by liquid methane, use of Langevin equation of Brownian motion for analysis of, 20: 313
scattering by liquids, cooperative modes of motion from, (E), 20: 2837
scattering by liquids, law of corresponding states for, (T), 20: 28241
scattering by liquid nitrogen, quasi-phonon dispersion in, (E), 20: 44598
scattering by liquid helium, localized excitation in, 16: 7154
scattering by liquid methane, energy distribution, 16: 19743
scattering by liquids, 16: 22980
scattering by lucite, geometrical optimization for, 20: 34470 (EUR-2953.e)
scattering by magnetic materials, use in magnetism studies, 18: 32713 (CEA-R-2412)
scattering by magnesia, spectra of, 19: 29228(R) (AEET/NP/10)
scattering by magnetic materials at Curie temperature, angular resolution for, 20: 22325
scattering by magnetic materials, critical, 20: 28256
scattering by materials, energy spectra from, (E), 20: 31567
scattering by methane, distributions from, (E), 19: 45237
scattering by moderator materials, inelastic, 18: 13030(R) (GA-4434)
scattering by molecular hydrogen, cross sections and spectra for, (T), 20: 17664
scattering by organic materials and water, 19: 12457 (JINR-P-1903)
scattering by nickel-palladium alloys, vibration defect modes in, 16: 15693
scattering by ortho-hydrogen at 12 to 21°K, distributions from, 19: 4146
scattering by phonons in nickel, 18: 11195(R) (EANDC(E)-49(L))
scattering by phonons in nickel, 18: 37711
scattering by phosphonium iodides, low-frequency molecular motions and barrier to rotation in, 20: 12859
scattering by polycrystalline beryllium oxide, inelastic, 17: 7130 (NP-12330(p.384-91))
scattering by polycrystalline metals, cross sections for inelastic, 17: 15247 (AERE-R-4101)
scattering by polyethylene and water at 0.15 to 1.81 ev, cross sections for, (E), 19: 19095 (WASH-1053)
scattering by polyethylene at 100°K, phonon frequency spectrum in, 19: 27401
scattering by polyethylene, phonon spectra from, 19: 32151
scattering by polyphenyls, 19: 45238
scattering by polycrystals, differential inelastic, 16: 19737
scattering by possible moderating materials using spinning sample method, 16: 7158
scattering by potassium dihydrogen phosphates, 17: 20976
scattering by radioinduced defects in single crystals of potassium bromide and sodium chloride, 20: 26365(T)
scattering by sodium chloride-type crystals, structure factors for, 17: 27392(T)
scattering by sodium at 80 to 198°C, inelastic, 16: 32378
scattering by solid and liquid lead, inelastic, 17: 26418
scattering by tin (liquid and solid), comparative studies of, 17: 15239
scattering by tin at 210 to 240°C, 16: 32377
scattering by titanium hydride, inelastic, 16: 32376
scattering by vanadium, elastic and inelastic, 17: 12032
scattering by vanadium, time-of-flight spectrum for inelastic, 17: 20972
scattering by vanadium, spectrum for inelastic, 17: 38033(T) (AEC-tr-5734(p.196-8))
scattering by vanadium and water, 17: 38039(T) (AEC-tr-5734(p.227-31))
scattering by vanadium and vanadium hydride, (E), 19: 12076
scattering by vanadium, phonon frequency distribution in, 16: 7175
scattering by vanadium, inelastic, 16: 32384
scattering by water, quasi-elastic, 17: 15246
scattering by water, quasi-elastic, 17: 36630 (TID-17871)
scattering by water, 18: 15128 (AE-133)
scattering by xylene, proton frequency spectra from, 18: 37151
scattering by zinc crystals, phonon dispersion relations from inelastic, 16: 27674
scattering by zirconium hydrides, distributions from inelastic, (E), 19: 45240
scattering from water, inelastic and quasi-elastic, 16: 7165
scattering in liquids, theory of quasi-elastic, 17: 39700(T)
scattering, monochromator for measuring, 16: 31873
scattering of, by liquids, relations of, with frequency spectra, 16: 32367 (TID-16830)
scattering of, installation for studying, 17: 15234
scattering of, review of inelastic, 18: 21121 (BNL-7958)
scattering on graphite at 950°C, high energy modes in frequency distribution of, 18: 5292
scattering on heavy water, temperature dependence of inelastic, 18: 38042 (A/CONF.28/P/673)
separation from horizontal beam of VVR-S reactor, 18: 38600 (A/CONF.28/P/480)
separation from neutron beams of VVR-S Russian reactor, 18: 33148 (IFA-FN-23)
source development, 17: 32980
source of, design and performance of, 20: 32351
source of, leakage flux from ice-d_2, (E), 20: 36148
sources of, 16: 29716
sources of, status of European, 17: 5296 (EANDC-22L)
sources, properties of various moderators as, 16: 7170
spectra in WWR-M reactor column, 19: 38281
transmission by polycrystals, 18: 42579 (BLG-260)
transport in matter, pulsed, (T), 20: 13733
use in steel radiography, 20: 16616
use in structural analysis, methods of, 17: 38916
use in study of condensed states of substances, 18: 30690(T) (ANL-Trans-42)

NEUTRONS, DELAYED

abundance and period of, from neutron fission of plutonium isotopes, 20: 35003 (BNWL-232)
analytical uses, 17: 10534 (IA-784)
control and economy of, in liquid-metal-fueled reactors, 17: 9856 (TID-14537)
decay constant for, best-mean, 18: 40797
detection and measurement of effective fraction of, in multiplication configurations or reactors, 18: 30959
detection and measurement of, equipment and method for, 20: 9290
detection in irradiated fuel elements for determination of plutonium-239 and uranium-235, 19: 28223(R) (NP-14973)
detection of, as indication of uranium in minerals and rocks, 20: 27181
determination of effective fraction, inhour equation for, 16: 19907 (CENRD-163)
distributions of, in beryllium reactor after shutdown, 17: 42212
distributions of, from fission fragments, 18: 21196 (KR-64(Sect.XVII))
effectiveness in Fireball Reactor, 16: 15897 (FXM-411)
effects on behavior of fast reactor after reactivity excursions, 18: 4748
effects on energy-release calculations in reactor meltdown, 17: 19553 (APDA-150)
effects on pulsed-neutron measurements, correction for, 18: 44720
effects on reactivity, laboratory experiments on, 19: 29563
effects on reactivity transients in reactors, 20: 34977
effects on reactor stability, (T), 20: 30850
effects on reactor kinetics, computer program for calculation, 16: 16632 (ANL-6511)
effects on shape of distribution curve of reactor, 17: 11949 (IFK-2)
effects on stability of power reactors, (T), 20: 22443
effects on steady fission chain, 19: 38135
emission after fission, distributions of, (T), 19: 27436 (NP-14833)
emission, angular momentum effects in, 16: 11697(R) (TID-15020 (p.49-56))
emission by antimony-135, (E), 19: 36220(R) (MIT-2098-142)
emission by antimony and arsenic isotopes, 20: 18838
emission by bromine-87, bromine-88, and bromine-89, (E), 20: 46762
emission by fission products, 20: 42681(R) (IS-1500(Sect. R))
emission by 54-sec bromine-86, 17: 22610
emission following fission, review, 16: 29823
emission from antimony and arsenic fission products, (E), 20: 17833
emission from plutonium and uranium isotopes, systematics of, 18: 18864 (ANL-6792(p.29-50))
emission in fission, 19: 21443
emission in neutron fission of uranium-238 at 14.7 Mev, (E), 20: 28296
emission in photonuclear reactions, (T), 19: 5145
emission in thorium-232 fission at 1.6 to 2.6 Mev, (E), 20: 17680 (FEI-26)
emission of, contribution to Nordheim equation, 17: 29564 (CNAM-7)
emission of, experimental measurement of half-period for, 18: 30949 (NYO-9077)
emission probability by halide nuclei from uranium-235 fission, 18: 32755
energy spectra and yields of, (E/T), 20: 17830
flux in Plutonium Recycle Critical Facility, 18: 11435(R) (HW-79054 (p.21-30))
fraction in critical assemblies, pulse techniques for determination of effective, 18: 38312 (A/CONF.28/P/648)
fraction in fast reactors, calculation of effective, 18: 36785 (TRG-Report-83)
fraction measurement in BSR-I by boron-substitution method, effective, 16: 18632
group numbers reduction by least squares, 18: 36552 (LA-3082)
half lives of groups of, 20: 9290
kinetics in highly enriched heavy water reactors, (E), 20: 20209 (TID-22730)
measurement of, statistical method for, 19: 31460(R) (ANL-7010

(p.179-233))
model of, for reactor transfer functions, 20: 1356
monitoring of, in determination of uranium by activation, 16: 31546 (ORNL-3342)
production by antimony and arsenic fission, research on, 19: 35378(R) (EANDC(E)-57(U))
production in decay of plutonium-239, 17: 41886
production in decay of 2-second antimony-135, (E/T), 20: 24351(R) (MIT-905-52, pp 1-41)
production in photofission of uranium-238, 17: 41887
production of, contribution of bromine and iodine isotopes to, 18: 21221
reactivity effects of, in VVR-M, (E), 19: 17380
reactor criticality effects, 18: 43083
spectra in lithium-9 decay, (E), 20: 3130
use in determining oil-water interface in rocks, 20: 43553
use in uranium determination in boreholes, 20: 41157
yield at neutron fission threshold of thorium-232, (E), 20: 46787
yields from fission fragments, (E/T), 20: 17831
yields from gamma reactions (γ,p) with oxygen-18, 19: 27578
yields from uranium-238 fast fission, (E), 20: 17832
yields in bare and reflected critical assemblies, 18: 23026 (TID-7662(p.334-47))
yields in electron bombardment of uranium at 8 to 13 Mev, 18: 24574
yields in fast reactors (E/T), 19: 3674
yields in fission of plutonium-239 and thorium-232, 16: 8173
yields in Molten Salt Reactor Experiment, effective, 17: 4337 (ORNL-TM-380)
yields in natural-uranium-fueled gas-cooled graphite-moderated reactors, 18: 1271
yields in neutron fission of uranium isotopes, energy dependence of, (E), 20: 44670(T) (INDSWG-101, pp 158-63)
yields in neutron fission of thorium-232 at threshold, (E), 20: 44672(T) (LA-tr-66-34)
yields in photofission of heavy nuclei, (E), 20: 28300
yields in thorium-232 and uranium-238 photofission, 16: 23115
yields in uranium-238 photofission, (E), 20: 6315
yields of, two-dimensional S_N perturbation theory for effective, 19: 29567

NEUTRONS, EPITHERMAL
absorption and fission processes in reactors, 19: 1843
absorption and flux spectra in cylindrical lattice cells, computer program for, 19: 46917(R) (DP-975)
absorption in slabs of 1/v absorbers, (T), 20: 2946
capture by indium foils, effects of flux anisotropy on cadmium correction factors for, (E), 20: 34510
capture by thorium-232, resonance integrals for, (E), 19: 21336
capture by tungsten isotopes at 35 ev to 10 kev, 19: 37806(R) (ORNL-3778(p.53-64))
capture in rectangular or parallelogram geometry, computer program for, 19: 6844 (WAPD-TM-437)
capture-to-fission rate for uranium-233 and -235 (E/T), 19: 3387
capture-to-fission ratio for uranium-235, 19: 37785 (CONF-650602-26)
detection and measurement of, radiometer calibration techniques for, 19: 15871 (NP-14732)
detection and spectroscopy of, using lithium-6 semiconductor detector, (E), 20: 5714 (AD-623722)
detectors for, in well logging, 20: 39138(P)
distribution in homogeneous media, energy and space, (T), 20: 14774
distributions in reactors, diffusion theory for, 19: 29525
dosimeter for, development of activation, 20: 14862
dosimetry in personnel using silver-activated phosphate glass, 20: 628
dosimetry in phantoms, 20: 18185(R) (BNL-929, pp 126-47)
dosimetry of, cobalt-silver activity ratio method for, 20: 21025 (AERE-R-5122)
dosimetry of, detector for, 20: 41362(P)
dosimetry of, using tissue-equivalent chamber, 20: 14421
effects on neutron filter cutoff energies, (T), 20: 17663
energy spectra of, methods for analyzing, 19: 11532
energy spectrum in absorbing medium with temperature gradient, (T), 19: 33228
flux determination using gold activation detectors, (T), 20: 21053
flux in reactor thermal column, (E/T), 19: 33197 (NIJS-R-437)
flux index monitors for, 19: 42707 (AERE-R-4866)
flux of, indium foils for measuring, 19: 34481
interactions with bound protons, effects on slowing-down calculations using Monte Carlo method, (T), 20: 34485
kinetics in critical assemblies, determination of, 20: 34906 (NAA-SR-Memo-11799)
production, properties, and use for therapy, 20: 1714
properties for production of transuranic elements, 20: 26533(R) (BNL-954, pp 16-49)
reaction rates in reactor matrices, computer program for calculating, 20: 2992
reactions (n,γ) with nuclei in thermal reactors, gamma spectra from, (E), 19: 35849 (RT/FI(64)-16)
reactions in enriched-uranium heavy water lattices, (E), 19: 42044(R) (MIT-2344-3, pp 37-54)
reactions in thermal reactors, computer analysis of fission, (T), 19: 10507 (DP-928)
reactions with hafnium isotopes, s-wave strength functions from, (E), 19: 37804(R) (ORNL-3778(p.38-44))
reactions with matter, production of recoil protons in, 18: 31639
reactions with plutonium-239 and uranium-235, fission resonance integral for, (E), 20: 17751
reactions with plutonium-239, yields of zinc-72 from fission, 20: 28448
reactions with tantalum-182 at 5 to 100 ev, cross sections, (E), 19: 31217 (IDO-17042(p.11-47))
reactions with uranium-233 and -235, capture-to-fission ratios for, (E), 19: 14510 (CONF-654-27)
reactions with uranium-233, resonance integrals for fission, (E), 19: 21336
reactions with uranium-235 at 3 ev to 2 kev, capture/fission ratio for, (E), 19: 23629 (ORNL-3738)
reactions with uranium-235 at 0.025 to 1 ev, ternary fission yield in, (E), 19: 29237 (IDO-17073)
reactions with uranium-235 at 0.02 to 80 ev, fission cross sections for, (E), 20: 22012 (UCRL-14606)
reactions with uranium-235, resonance parameters from, 20: 24361 (WANL-TME-1384)
reactions with uranium-235, capture-to-fission ratio for, (E), 20: 34617
reactions with uranium-233 and uranium-235, capture-to-fission ratios for, (E), 20: 34618
scattering by electrons in metals, cross sections for, (T), 20: 44135
scattering by hydrogenous materials at 0.018 to 0.080 ev, (E), 19: 21200 (KFK-264)
scattering by hydrogenated iron, magnetic, 19: 40075 (IEA-84)
scattering by polyethylene and water, inelastic, (E/T), 19: 47549(R) (TID-22141, pp 34-49)
scattering by polyethylene, differential inelastic cross sections for, (E), 20: 44576 (CONF-660303, pp 122-33)
slowing down in concretes, albedo and capture-gamma dose rates for, 20: 6519(R) (ORNL-3858(Vol.1), pp 20-41)
slowing down in heterogeneous media, numerical program for, 20: 34475
spectra in complex media, similitude theory for, 20: 14776
spectra in uranium, measuring method for, 19: 38136
spectra measurement in heavy water assemblies, activation techniques for, 20: 36524 (AE-230)
transport in cylindrical lattice cells, (T), 19: 29191
use in well logging, analytical theory for, 20: 18932

NEUTRONS, FAST
absorption and total cross sections for 24 kev, on metals, 18: 4531 (EANDC-33U(p.41-3))
absorption by even zirconium isotopes, structure in resonant, (E), 19: 37809(R) (ORNL-3778(p.76-81))
absorption by polymers, 19: 15578
absorption by reactor fuels, Doppler coefficients for resonance, (T), 20: 22378 (KFK-367)
absorption by thorium-232 and uranium-235 and -238, 18: 44984
absorption cross section for, measurement using indium resonance detector in water, 20: 37990
absorption dose of, in bone marrow, 18: 25048
absorption from flat, infinite, and uniform source by foils, calculation of probability for, 16: 33784
absorption in boron slab lattices, epithermal, 17: 19206 (WAPD-T-1377)
absorption in shielding materials, measurement of 3- and 15-Mev, (E), 20: 9265
absorption in thorium at 190 kev, Doppler broadening of resonance, 18: 1049
age-diffusion equation for, 18: 21603
age-to-resonance of, experimental measurement of, 18: 30949 (NYO-9077)
ages in cylindrical bore holes, 17: 10833
analytical use in determination of water content of living trees, 16: 26905(T) (CEA-tr-A-1127)
angular distribution of, measurement of, 17: 3808
angular distributions from alpha bombardments, carbon-12 detectors for, 18: 16951(R) (TID-20311)
angular distribution for photo-, calculation of, 18: 34935
angular distribution and spectra in paraffin, measurement of, 20: 2931 (AD-616518)
angular distributions behind iron shielding, 20: 40286
angular distribution from scattering on light nuclei, 16: 15644
attenuation and moderation in hematite concrete, (E), 20: 12263 (JINR-P-2479)
attenuation and thermalization in water, (E/T), 19: 29202
attenuation and thermalization in water, (E/T), 20: 30340
attenuation, bibliographic survey of, 16: 32356 (CEA-Note-345)

attenuation by borated polyethylene and water, 18: 2826
attenuation by cadmium foil covers, 19: 31460(R) (ANL-7010(p.179-233))
attenuation by concrete, 17: 22695
attenuation by concrete, 17: 22700
attenuation by concrete shields, 17: 13608 (AWRE-NR-1/63)
attenuation by concretes, 18: 35092(T) (JPRS-25467(p.1-8))
attenuation by ethylene polymer slabs, 17: 3808
attenuation by high-density concretes, 16: 24227
attenuation by hydrogen, 16: 13936
attenuation by iron–water mixtures, 18: 40739
attenuation by lithium hydrides, 18: 2825
attenuation by lithium hydride, 18: 6144(R) (ORNL-3499(Vol.I)(p.116-18))
attenuation by lithium hydride shields, 18: 40736 (NAA-SR-9364)
attenuation by lithium hydride, (E/T), 19: 17157(R) (ORNL-3714(Vol.I)(p.43-67))
attenuation by lithium hydrides and lithium-6 hydrides in water, 19: 27705 (XDC-59-10-69)
attenuation by magnetite concrete, 17: 2743
attenuation by moderating media, 16: 14076
attenuation by polyethylene, flux profiles of, 17: 9481 (TID-15547)
attenuation by reactor shields, effects of voids on, 17: 26399 (RAS-33)
attenuation by sodium, 18: 42612
attenuation by water, 17: 28221 (EUR-107.f)
attenuation by water, flux profiles for, 18: 16891(R) (GA-4881)
attenuation by yttrium and zirconium, effects of hydrogen content, 16: 6074 (DC-57-7-51)
attenuation by zirconium hydrides, 18: 42618
attenuation functions, modified coefficients for, 16: 21335 (XDC-60-2-76)
attenuation in air-filled annular ducts, method for prediction of, (T), 20: 1139
attenuation in concrete shielding, 16: 3800
attenuation in graphite and water, 18: 986(T) (AEC-tr-6113)
attenuation in graphite, iron, and lead, 18: 19261
attenuation in hydrogenous materials, 16: 6076 (XDC-57-1-32)
attenuation in iron, 18: 32951
attenuation in iron surrounding cylindrical ducts, (E/T), 20: 20092 (AE-220)
attenuation in lithium hydrides, 17: 26219
attenuation in lithium hydrides, 18: 28913
attenuation in lithium hydride SNAP-10A shield (T), 19: 3722 (NAA-SR-9647)
attenuation in polyethylene slab, calculation of probabilities for, 17: 26222
attenuation in polyethylene slabs, 17: 32988
attenuation in reactor beams, single crystal filters for, (E), 19: 6161
attenuation in zirconium hydrides at 0.5 to 12 Mev, 18: 28912
attenuation of reactor, in serpentine sand, (E), 20: 6524
background count in underground low-level gamma-counting laboratory, 19: 20093(R) (ANL-6938(p.194-205))
biological effectiveness, relative, 17: 25038
biological effects, effects of dose on recovery rate, 17: 5909 (TID-14019)
biological effects, 17: 19844
book: *Fast Neutron Physics. Part II. Experiments and Theory*, 17: 34849
buckling in laminated lattices of 10 to 30% enrichment, 18: 42943 (UJV-971/63)
capture and inelastic scattering on indium-113 and -115, cross sections for, 18: 34962
capture by cesium, iodine, silver, and tin, gamma spectra from, 17: 13513
capture by copper and nickel, gamma spectra from, 17: 21010
capture by even zirconium isotopes, s-wave strength functions from, 18: 26544(R) (ORNL-3582(p.82-4))
capture by gold and silver, cross sections for, 18: 4534 (EANDC-33U(p.114-35))
capture by indium-113, indium-115, and yttrium-89, cross sections for isomer production in, (E), 20: 42326
capture by iron at 1, 1.2, and 1.4 Mev, (E), 19: 8412
capture by light nuclei, 17: 24473
capture by nuclei, effects on nuclide abundances, 17: 32869
capture by nuclei, gamma production data for, 20: 15725 (NP-14855)
capture by nuclei, mechanisms in, 20: 34669
capture by tantalum-181, tungsten-182, tungsten-183, tungsten-184, and tungsten-186, (T), 19: 21464
capture by thorium-232 at 0.19–1.1 Mev, cross sections for, 17: 28279
capture by tungsten isotopes at 1 to 200 kev, cross sections for (E/T), 19: 3376
capture by tungsten isotopes at 35 ev to 10 kev, 19: 37806(R) (ORNL-3778(p.53-64))
capture by uranium-238, gamma spectra from, 17: 21008
capture by uranium-238, Doppler effect in, 19: 3388
capture by uranium-238, Doppler effect in, 20: 35068
capture by yttrium-89, isomer ratios from, (T), 20: 19920
capture cross sections for holmium-165, indium-115, manganese-55, and sodium-23 from 1.0 to 19.5 Mev, radiative, (E), 20: 42332
capture gamma spectra comparison, 17: 17255
capture gamma spectra, 16: 14060
capture in fast reactors, Doppler coefficient of resonance, (T), 19: 10497
capture in gold, mercury, silver, tantalum, tungsten, and uranium at 18 to 300 kev, cross sections for radiative, 17: 21009
capture in manganese sulfate baths and water with charged-particle emission, (E), 19: 45232
capture in thorium-232, partial widths of radiative, 17: 20980 (CEA-2228)
capture in thorium, Doppler coefficients for, 18: 2964
capture in uranium-235 and uranium-238 matrices, Doppler effect in, 20: 38430 (ANL-7120, pp 616-24)
capture of, gamma emission in, 17: 11659
capture, two-group calculation of gamma radiation from, 16: 26202(T) (AEC-tr-5077)
capture-to-fission ratio of uranium-235 at 12 to 690 kev, 18: 34886
carcinogenic effects on kidney and pancreas, 16: 49 (USNRDL-TR-529)
chemical effects on quartz, 16: 27709
conference on physics of, Houston, Texas, Feb. 26, 27, and 28, 1963, 17: 41988
correlations of, assembly for studying angular and energy, 19: 40894
cross section and propagation measurements in fast reactors, review, 18: 38013 (A/CONF.28/P/368)
cross section measurements for, calculations on total, 18: 11196(R) (HW-79054(p.64-81))
cross sections, 18: 17287 (NP-13666)
cross sections for 14-Mev, measurement of total, 17: 7095 (NP-12330)(p.61-5))
cross sections for, total, 18: 24625 (WASH-1046)
cross sections in carbon, fluorine, and vanadium at 2.6 to 2.85 Mev, (E), 19: 27400
cross sections in elements, method of determining, 20: 20183
density distribution in reactors, stability of PROGONKA method for calculating, 19: 29513
detection and measurement of, high-sensitivity semiconductor detector for, 17: 23746(R) (TID-18552)
detection and measurement of, design of spectrometer for, 17: 23757
detection and measurement by ionization chambers, 17: 23772
detection and measurement using a General Dynamics Hurst-type dosimeter, Monte Carlo calculation of energy response in, 17: 26221
detection and measurement of, disposable dosimeter for, 17: 29205
detection and measurement of, using (n,t) reactions on lithium-6, 17: 30803
detection and measurement of, ionization chambers for, 17: 30866
detection and measurement of flux, sensitivity of long counters, 17: 1175(R) (HW-70050(p.31-77))
detection and measurement of, ionization chamber design for, 17: 4846
detection and measurement using helium-3-filled semiconductor counter, 17: 6481
detection and measurement by nuclear emulsions in personnel monitoring, 17: 8606
detection and measurement of, photographic films for, 17: 8614
detection and measurement at 0.5 to 15 Mev, 17: 8626
detection and measurement using scintillation detectors, calculation of pulse-height distributions and counting efficiencies of, 17: 8644
detection and measurement of, design of instrument for, 17: 10889 (AD-252467)
detection and measurement of, design of argon–hydrogen ionization chamber for, 17: 11035
detection and measurement of, design modifications for cost reduction of instrument for, 17: 14610(R) (ORNL-3378(p.28-36))
detection and measurement by organic scintillators, 17: 14350
detection and measurement, sensitivity of boron trifluoride counters for, 17: 18624
detection and measurement of, design of silicon n-p-p junction rectifier for, 17: 32411
detection and measurement, boron trifluoride-paraffin counter for, 17: 32432
detection and measurement of, using proportional counters, 17: 32445
detection and measurement of, using threshold detectors, 17: 34268
detection and measurement in reactors, 17: 34279
detection and measurement in DR-1 reactor, 17: 34280
detection and measurement in biological irradiation chambers, 17: 34283
detection and measurement of, using (n,t) reaction with lithium-6, 17: 34284
detection and measurement using threshold detectors, 17: 34289
detection and measurement using semiconductor detectors, 17: 34290
detection and measurement using europium-activated lithium iodide, 17: 34291
detection and measurement using nuclear emulsions, 17: 34293

detection and measurement using iron-54 and nickel-58 detectors, 17: 34294
detection and measurement using titanium threshold detectors, 17: 34299
detection and measurement of, Monte Carlo calculation of dosimeter energy response for, 17: 34306
detection and measurement of, development of silicon-junction dosimeter for, 17: 36137(R) (AD-289692)
detection and measurement, development of instrumentation for, 17: 36347(R) (NARF-62-18P)
detection and measurement of, engineering drawings of proportional detector for, 17: 39446
detection and measurement of, development of high-sensitivity dosimeter for, 17: 41250(R) (TID-19491)
detection and measurement of, design and performance of scintillation counter for, 18: 493 (PAN-266)
detection and measurement of, efficiency of scintillation detectors for, 18: 501
detection and measurement using boron trifluoride counters in hollow spheres of paraffin, 18: 2054
detection and measurement of, spectrometer for, 18: 2098
detection and measurement of fluxes of, using manganese sulfate baths, 18: 4533 (EANDC-33U(p.87-101))
detection and measurement by associated-particle method, 18: 4535 (EANDC-33U(p.150-8))
detection and measurement below 100 kev, recoil counter for, 18: 4085 (EANDC-33U(p.25-40))
detection and measurement of fluxes of, boron pile for, 18: 4086 (EANDC-33U(p.44-51))
detection and measurement of fluxes of, standards for, 18: 4087 (EANDC-33U(p.52-63))
detection and measurement of fluxes of, using manganese sulfate baths, 18: 4088 (EANDC-33U(p.102-13))
detection and measurement of fluxes of, absolute, 18: 4089 (EANDC-33U (p.136-49))
detection and measurement of fluxes of, conference on, 18: 4084 (EANDC-33U)
detection and measurement of, effects on Hurst detector for, 18: 5635(R) (ORNL-3499(Vol.I)(p.194-6))
detection and measurement of, design of instrument with background discriminator for, 18: 5668
detection and measurement of, by associated-particle method, 18: 6161 (NP-13346)
detection and measurement using cesium and sodium iodides, 18: 12456 (EIR-59)
detection and measurement of, decay spectrometer for, 18: 14285
detection and measurement in gamma background, design of scintillation detector for, 18: 18181
detection and measurement of, efficiency of surface-barrier silicon detectors for, 18: 18183
detection and measurement of, method for, 18: 18186
detection and measurement of, design of silicon-junction spectrometer for, 18: 18206
detection and measurement using boron trifluoride counters, 18: 18207
detection and measurement using semiconductor detectors, 18: 20413
detection and measurement using threshold detectors, 18: 23885 (NP-13930(p.178-80))
detection and measurement using boron trifluoride counter in hollow paraffin sphere, 18: 23900
detection and measurement of 14-Mev, semiconductor counter telescope for, 18: 23985
detection and measurement using lithium-6 semiconductor counter telescope, 18: 23986
detection and measurement in gamma background, transistorized pulse-shape discriminator for, 18: 23994
detection and measurement of photo-, 18: 28629
detection and measurement of, time-of-flight systems for, 18: 27793
detection and measurement outside Shippingport PWR pressure vessel, 18: 29065
detection and measurement using proportional counters, 18: 29991
detection and measurement of, using lithium-6-covered surface barrier junctions, 18: 29992
detection and measurement using scintillation counters, 18: 29993
detection and measurement using threshold detectors, 18: 29994
detection and measurement of, survey of reactions and detector preparation methods for, 18: 29995
detection and measurement of, time-of-flight spectrometer for, 18: 30024
detection and measurement of, direction-sensitive monitor for, 18: 31865 (AE-144)
detection and measurement of, uses of silver-activated phosphate glasses for, 18: 31927
detection and measurement using threshold detectors, 18: 32949(R) (EUR-534.d(Pt.II))
detection and measurement using indium, method for, 18: 33978(P)
detection and measurement of background of cosmic, 18: 36220
detection and measurement using hexane-filled ionization chamber, 18: 37512 (NP-14130)
detection and measurement of, spectrometer for, 18: 39707(P)
detection and measurement using threshold detectors, 18: 40780 (EUR-1643.e(p.205-27))
detection and measurement using threshold detectors, 18: 40517 (UCRL-11375)
detection and measurement of, development of high-sensitivity dosimeter for, 18: 39623(R) (TID-21077)
detection and measurement using scintillation detectors, 18: 41772 (KFKI-1491/A)
detection and measurement at 1 to 20 Mev, efficiency of scintillation detectors for, 18: 41778
detection and measurement from beryllium-polonium source by scintillation spectrometer, 18: 41789
detection and measurement using semiconductor spectrometer, 18: 43942 (TID-21202)
detection and measurement of, spectrometers for, 19: 780 (ORNL-P-548)
detection and measurement in reactors, 19: 9475 (CEA-R-2451)
detection and measurement by induced activity, 19: 11590
detection and measurement of, using organic scintillators, 19: 15872(R) (ORNL-3714(Vol.I)(p.78-86))
detection and measurement of, radiometer calibration techniques for, 19: 15871 (NP-14732)
detection and measurement using surface-barrier junctions and lithium-6, (E), 19: 20334
detection and measurement of, high-sensitivity dosimeter for, 19: 22698(R) (TID-21547)
detection and measurement of, design of hodoscope for, 19: 24064(R) (ANL-6997)
detection and measurement using threshold detectors, 19: 22776
detection and measurements using boron trifluoride counter, 19: 22779
detection and measurement, scintillation counter for, 19: 22798
detection and measurements in IRT reactor, 19: 24185
detection and measurements of, efficiency of scintillators for, 19: 24848
detection and measurement of, gamma rejection in, 19: 31460(R) (ANL-7010(p.179-233))
detection and measurement of, design of Hurst type dosimeter for, 19: 32577
detection and measurement of ultrafast, threshold scintillation counter for, 19: 34576
detection and measurement using organic phosphors, (E/T), 19: 34516
detection and measurement of, performance of dielectric liquid-filled ionization chambers for, 19: 34535
detection and measurement of, foundations of high-efficiency scintillation detectors for, 19: 34571
detection and measurement of, detector with gamma-background cut-off by photomultiplier space charge for, 19: 34572
detection and measurement of, detector with gamma-cut-off by photomultiplier gas amplification for, 19: 34573
detection and measurement in NPR, (E), 19: 38232 (HW-SA-3330)
detection and measurement by sulfur-32 activation, 19: 45679(R) (NYO-1859-11)
detection and measurement using fission foils, 19: 45679(R) (NYO-1859-11)
detection and measurement of, system for, 19: 44452 (K-1642)
detection and measurement of, design of threshold detector for, 20: 681(P)
detection and measurement of dose equivalent and fluence of, device for, 20: 2123 (ANL-7085)
detection and measurement in thermal-neutron flux, 20: 5060(R) (TID-22357)
detection and measurement using silicon surface-barrier detectors, 20: 5181(R) (ORNL-3029)
detection and measurement of, using copper-62 activation in copper-63, (E), 20: 6289 (KN-63-10(R))
detection and measurement of, coincidence counters for, (E), 20: 7408
detection and measurement in polarization experiments, spectrometric method for simultaneous, 20: 7372
detection and measurement of, proton-recoil spectrometer for, 20: 11096 (EUR-2491.e)
detection and measurement of 15- to 35-Mev, design and performance of solid state spectrometer for, 20: 11139
detection and measurement at 1 to 50 Mev, device for, 20: 13081
detection and measurement of, boron trifluoride probe for, 20: 14913(P)
detection and measurement in thermal neutron background, semiconductor detector for, 20: 21034 (EUR-2712.e)
detection and measurement of, counter for, 20: 21140(P)
detection and measurement of, instrumentation development for, 20: 29529(R) (RPI-328-56, pp 94-112)

detection and measurement of, performance of organic scintillators for, 20: 33630 (ORNL-3888)
detection and measurement using proton-recoil and lithium-6 semiconductor spectrometers, 20: 33715
detection and measurement of, design of silver-activated zinc sulfide sandwiched scintillation detectors for, 20: 41335
detection and measurement of fluxes of, performance of activable-cathode G-M counters for, 20: 43729
detection and measurement using liquid organic scintillators, 20: 46048(R) (ORNL-3973(Vol.1), pp 60-4)
detection and measurement, design of silicon-gold surface barrier detector for, 16: 3853(R) (ORNL-3193(p.116-19))
detection and measurement, development of scintillation detector for, 16: 1005(T) (UCRL-Trans-689)
detection and measurement in shielding, first-collision moments method for, 16: 1024 (NARF-61-12T)
detection and measurement, design of high-efficiency detector, 16: 3836(R) (ORNL-3193)
detection and measurement, properties of silicon-gold surface barrier detector, 16: 3854(R) (ORNL-3193(p.119-23))
detection and measurement, design of scintillation detector, 16: 5501(T,P) (CEA-tr-R-1393)
detection and measurements, design of spectrometer for, 16: 6584
detection and measurement of fluxes by threshold-detector activation, 16: 8913(T) (CEA-tr-A-1025)
detection and measurement of flux by threshold detectors, 16: 9703(T) (CEA-tr-A-1026)
detection and measurement in JEN-1, 16: 11323
detection and measurement from plutonium-beryllium source, 16: 10960 (TID-14865)
detection and measurement, design of transistorized survey meter, 16: 11859(R) (ORNL-3191(p.1-18))
detection and measurement in water on top of the P102 dolly during critical experiments, 16: 14316 (PREDC-3079)
detection and measurement, evaluation of detector materials for, 16: 12801(R) (IA-685)
detection and measurement, sensitivity of long counters by Monte-Carlo method, 16: 14934
detection and measurement, semiconductor detectors for, 16: 14964
detection and measurement, recoil-proton ionization chamber for, 16: 17874(P)
detection and measurement at 14 Mev, design of activation detector for, 16: 19106
detection and measurement with europium-activated lithium iodide scintillators, 16: 19116
detection and measurement by semiconductor detectors, 16: 23899 (AERE-R-3874)
detection and measurement using threshold detectors, 16: 26530
detection and measurement at 0.5 to 14 Mev, 16: 27308
detection and measurement, design and performance of transistorized multi-channel monitor, 16: 29114 (TID-15474)
detection and measurement of, use of organic scintillators for, 16: 31989(T) (FTD-TT-62-678)
detection and measurement of 14-Mev pulsed, design of instrument for, 16: 1950 (UCRL-9861)
detection and measurement, design of spectrometer for, 16: 6584
detection and monitoring TREAT fuel meltdown, 19: 31460(R) (ANL-7010(p.179-233))
detection at 0.1 to 14 Mev, performance of scintillation counters for, (T), 19: 9495 (UCRL-12150)
detection by anthracene and terphenyl, angular anisotropy of scintillation response in, (E), 20: 7158
detection by fission-track production in mica, 18: 35861
detection by organic scintillators, (T), 19: 38997 (UCRL-16149)
detection in plastic scintillators, computer program for simulation of, 20: 39196 (AE-236)
detection in reactors using threshold reactions, 18: 2020 (EUR-289.e)
detection methods for reactor, 19: 45684
detection of Bev-range, scintillation detector efficiency for, 20: 13109
detection of, efficiency of filament scintillator for, 17: 7118 (NP-12330) (p.199-201))
detection of, energy response of instruments for, 18: 4119
detection of, by nucleating ultrasonic cavitation in liquids, 19: 18319
detection of, design and performance of portable monitor for, 20: 16848
detection of, double pulse scintillation counters for, 18: 43989
detection of, efficiency of Hornyak button-type scintillator for, 19: 30559
detection of, fission foil detectors for, 19: 15861 (NDL-TR-46)
detection of, methods development for, 20: 19018(R) (ANL-7110, pp 231-310)
detection of, multiple wire-cavity spark counter for, 19: 15892
detection of, organic scintillators for, 20: 27307
detection of, performance of organic scintillation detector for, 19: 46774
detection of, performance of boron trifluoride proportional detectors for, (E), 20: 7405
detection of, performance of dielectric liquid-filled cloud chamber for, 20: 13112
detection of, self-triggering projection discharge chamber for, 19: 30564
detection, proportional detector for, 16: 26204(T) (AEC-tr-5217)
detection using (n,γ) and (n,p) reactions, 19: 14619
detection using lithium-drifted germanium and silicon surface-barrier detectors, (E), 19: 28659
detection using lithium fluoride thermoluminescence, 20: 39219
detection using plastic scintillator, computer program for calculating efficiency of, 18: 23891 (UCRL-11339)
detection using scintillators, efficiency of, 18: 41850
detection using ultrasonic cavitation in liquids, 19: 34498
detector for, design of proton-recoil, 19: 13750
detectors of, activation rates for threshold, 17: 28221 (EUR-107.f)
diffusion and thermalization of, theory of, 18: 40496
diffusion and transport in fast reactors, 18: 38300 (A/CONF.28/P/166)
diffusion in carbon black, parameters for, 18: 28548
diffusion in fast breeder reactors, S_n and few-group calculations of, 19: 10228
diffusion in fast reactors, computer program for calculating, 20: 6583 (JAERI-1091)
diffusion in heavy water, analysis by pulsed-source method, 17: 34870
diffusion in heavy water, time-dependent spectra in, (E), 19: 29208
diffusion in hydrogen at 2, 4, 6, 8, 10, 12, and 14 Mev, 17: 17460
diffusion in iron and lead in water, energy spectra for, (E), 19: 31205
diffusion in laminated iron–water systems, (E/T), 20: 1304 (AE-196)
diffusion in parallel-plate lattice, 17: 19196 (CRRP-1140)
diffusion in parallel-plate lattices, calculation of, 20: 32763 (AECL-2543)
diffusion in spherical reactors, few-group calculations of, 18: 19275
diffusion in water, pulsed-source measurements of, (E), 19: 29207
diffusion length in water, experiment for, 18: 30949 (NYO-9077)
diffusion of, one-group theory for, 17: 3804
diffusion of, with strong forward scattering, 18: 2807
diffusion parameters for, variational calculation of, 16: 24400
distribution and thermalization in reactor graphite, 19: 21646
distribution around reactor fuel rods, method for calculating spatial, 20: 34916
distribution at air-ground interface, 18: 2828
distribution in water shields, (E), 19: 17157(R) (ORNL-3714(Vol.I) (p.43-67))
distributions in and behind shielding, calculations of, 18: 40744
distributions in cube-shaped room with source in center, 18: 21137
distributions in enriched-uranium heavy-water lattices, computer analysis of, 20: 13703(R) (MIT-2344-4, pp 17-47)
distributions in enriched-uranium heavy-water lattices, 20: 45077 (MIT-2344-5)
distributions in liquid hydrogen in nuclear rockets, 18: 28401
distributions in reactor, use of depleted uranium for monitoring, 18: 8866(R) (HW-78388(p.8.1-7))
distributions in WWR-S channels, spatial and spectral, 17: 38570 (UJV-943/63)
distributions in water of swimming-pool reactors, (E), 19: 21735 (ORNL-P-1092)
distributions in water, first- and last-flight expectation values in Monte Carlo calculations of, (T), 19: 27395 (ORNL-RSIC-3)
distributions of, by leakage, from Experimental Gas Cooled Reactor, 17: 17554 (TID-18106)
distributions of, after penetrating shields, 18: 28911
Doppler coefficients of reactor materials, 20: 46966(R) (NAA-SR-12010)
dosage calculations, computer program for, 16: 7225 (APEX-293)
dosage determinations in biological experiments, 17: 6315 (ORNL-1559)
dosage determinations, around human phantoms by nuclear emulsions, 17: 6323 (UCRL-9967)
dosage determinations around and in human phantoms by nuclear emulsions, 17: 10868 (UCRL-9967(Rev.))
dosage determinations for chronic low-level exposure of mice, lethal, 17: 33487(R) (NP-13010(p.66-73))
dosage determinations for mice, lethal, 18: 25165
dosage determinations by sulfur activation, 16: 1305(R) (LAMS-2627 (p.66-71))
dosage determination using films, 16: 5619
dose absorption from, in bone marrow, 18: 38878
dose albedo on concrete, differential (E/T), 19: 3472
dose albedo on concrete, differential, (E/T), 19: 38021
dose depth and oxygen enhancement ratio in therapy using, 19: 28203
dose depth distributions in biological objects in mixed gamma-neutron fields, 19: 22080
dose distribution in human phantom, evaluation using hair, 18: 37029 (A/CONF.28/P/812)
dose estimates of, in SL-1 accident, 17: 16315 (LADC-5359)
dose estimations for, in man, 18: 1487(R) (HW-77609(Sect.3))

dose measurements of, in graphite irradiation in Belgian Reactor-2, 19: 48030
dose rate behind shielding plugs in Battelle shielding facility, 18: 21543 (BMI-1384)
dose rate calculations incorporating energy dependence of detector response, tables, 16: 8166 (DC-60-9-76)
dose rate from point source in air, first-last collision model of air/ground interface effects on, 18: 15167
dose rate in concrete bunkers, 18: 5474(R) (ORNL-3499(Vol.I)(p.153-5))
dose rate measurements within and behind beryllium oxide, 18: 24806 (XDC-61-1-149)
dose rates along center lines of concrete ducts, (E/T), 20: 34799
dose rates and energy distributions in concrete, from plane and point sources, (T), 19: 37764 (ORNL-RSIC-4)
dose rates behind concrete and water slabs, 17: 36628 (ORNL-TM-646)
dose rates in concrete-lined ground holes, from overhead irradiation, 18: 5473(R) (ORNL-3499(Vol.I)(p.147-52))
dose rates in concrete-lined bunkers, 18: 14060 (ORNL-3513)
dose rates in concrete and water from point isotropic fission sources, (T), 19: 45464 (ORNL-TM-1167)
dose rates in ethylene as function of penetration distance in hydrogen, 16: 15757 (DC-59-9-75)
dose rates in shield assemblies, computer program for calculating, 16: 11117 (DC-57-11-101)
dosimeter for isotropic fluxes of, 19: 15872(R) (ORNL-3714(Vol.I)(p.78-86))
dosimeter for, design of multi-element, 19: 28693
dosimeter for, semiconductor, 20: 21095
dosimetry, 18: 2086
dosimetry, 18: 8548(R) (NYO-2740-1(p.31-53))
dosimetry, 20: 29078(R) (AD-633252)
dosimetry and spectrometry of, activation, 17: 41114
dosimetry as LET function, design and performance of instrument for, 18: 31950
dosimetry at AB Atomenergi, Sweden, 17: 41117
dosimetry at surfaces of biological shield of TRIGA Mark II Research Reactor, 16: 17310 (ORNL-TM-178)
dosimetry by aluminum, carbon, or tissue-equivalent material, 17: 23748 (USNRDL-TR-621)
dosimetry by analysis of hair for phosphorus-32, 16: 1339(R) (ORNL-3189(p.234-5))
dosimetry by fission threshold monitors in irradiation capsules, 18: 43940 (TID-7697(p.5.5.1-10))
dosimetry by phosphorus-32 activation in human hair, 17: 41017 (CEA-2302)
dosimetry by phosphorus-32 activation, 18: 23890 (SCPRI(S)-92)
dosimetry by thermoluminescent detector, 18: 10387
dosimetry calibrations for Irradiation Standards and Procedure Committee, 18: 31906 (HW-81871)
dosimetry for radiation damage studies, 18: 34263 (ANL-6826)
dosimetry in animal tissue, method for, 19: 38439
dosimetry in animals and cultured cells using ionization chambers, 20: 39227
dosimetry in ASTRA reactor by calorimetric methods, 17: 38571
dosimetry in biological studies, equipment and methods for, 20: 35349
dosimetry in bone marrow estimated from elemental constitution, 18: 31196
dosimetry in bone marrow, calculations of, 18: 31197
dosimetry in dogs and phantoms, 20: 20432 (AD-630332)
dosimetry in gamma background, performance of boron trifluoride proportional detectors for, 20: 31561
dosimetry in heavy particle fields, performance of tissue-equivalent ionization chamber for, 20: 46030(R) (AERE-PR-HPM-9, pp 6-17)
dosimetry in man, biological method for, 19: 44322
dosimetry in mice, 18: 38732
dosimetry in MIT Reactor using calorimeter and threshold detectors, 20: 20723(R) (MIT-334-33)
dosimetry in mixed fields, properties of glasses for, 20: 31462
dosimetry in mixed fields, tissue-equivalent ionization chamber for in-phantom, 20: 31524
dosimetry in reactors, using threshold detectors, 19: 28644
dosimetry in research reactors, 17: 41108
dosimetry in seeds, 20: 38693
dosimetry in tissues, problems in, 18: 25107
dosimetry in tissues, use of computers for, 20: 43668(R) (ANL-7136, pp 1-16)
dosimetry in tissue-equivalent phantom, 19: 2628
dosimetry in water, 18: 15152
dosimetry in water using threshold detectors, tissue-equivalent depth, 19: 15047
dosimetry methods for, 17: 41107
dosimetry near neutron sources and reactors, 17: 34281
dosimetry of, by thorium fission, 17: 8662
dosimetry of, comparison of methods for, 17: 6480
dosimetry of concrete-reflected, angular dependence of, (E/T), 19: 17157(R) (ORNL-3714(Vol.I)(p.43-67))
dosimetry of, cross section measurements for, 17: 31056
dosimetry of, design of scintillation detectors for, 17: 9491
dosimetry of, first-collision, 17: 34178
dosimetry of, for radiation damage analysis, 17: 12722 (TID-17839)
dosimetry of, from betatrons, 17: 42021
dosimetry of, from beryllium–polonium sources, 16: 33334
dosimetry of, in cryogenic in-pile loops, 17: 1781
dosimetry of, in intense flux fields, 17: 18645
dosimetry of, isotope fission cross sections for long-term, 17: 31057
dosimetry of scattered, at air-ground interface, 18: 2829
dosimetry of therapeutic beams of, 19: 42400
dosimetry of, uses of iron and nickel for, 17: 26787 (TID-7641(p.283-9))
dosimetry of, using threshold detectors, 17: 32294(T) (CEA-tr-A-1221)
dosimetry of, using resistivity variations in neutron-irradiated materials, 17: 41126
dosimetry of, activation method for, 19: 22773
dosimetry of, as function of reactor power, 20: 26924(R) (MIT-334-48)
dosimetry of, based on sulfur-32 (n,p) reactions in human hair, 19: 18195 (LA-DC-6646)
dosimetry of, book on, 20: 7446
dosimetry of, calorimetric, 19: 13741
dosimetry of, design of scintillation ratemeter for, (E), 19: 20312 (AERE-R-4525)
dosimetry of, design of single-sphere instrument for, 20: 7366 (LA-DC-7323A)
dosimetry of, detector for, 20: 41362(P)
dosimetry of, development of instruments for personnel, (E), 19: 20318 (HW-SA-3526)
dosimetry of, development of semiconductor devices for, 19: 38992 (COO-1226-8)
dosimetry of, development of solid-state device for, 20: 11094(R) (COO-1226-10)
dosimetry of, gamma radiation effects on nuclear emulsion, 18: 16357
dosimetry of, graphite and tissue-equivalent ionization chambers for, 19: 22800
dosimetry of, in gamma background, 20: 25378 (AFRRI-SR-66-3)
dosimetry of, in neutron exposure facility, 19: 29890(R) (ANL-6971 (p.117-19))
dosimetry of, in research reactor for biological studies, 18: 41107
dosimetry of, latent image fading in monitoring films used in, 19: 26657 (IDO-12031)
dosimetry of, performance of ferrous sulfate–sulfuric acid detector for, 18: 30056
dosimetry of, performance of silver-activated metaphosphate glass for, 20: 5713 (AD-623384)
dosimetry of, performance on insulators for, 20: 5719 (CEA-R-2846)
dosimetry of, performance of lithium fluoride thermoluminescent detector for, 20: 5572 (USNRDL-TR-909)
dosimetry of, performance of semiconductor for 0 to 50,000 rads, 20: 25374 (AD-631742)
dosimetry of, performance of film and silicon diodes for, 20: 29518 (BNWL-SA-27)
dosimetry of, proton recoil proportional counter for, 19: 38968 (AEET/HP/D-1)
dosimetry of, pulse shape discrimination in scintillator, 20: 29524 (CONF-651109, pp 647-52)
dosimetry of, rate meter for, 19: 18263 (NP-14706)
dosimetry of, review, 19: 29889(R) (ANL-6971(p.90-116))
dosimetry of, review of methods for, 19: 34569
dosimetry of, scintillator-film combination for, 20: 16861
dosimetry of, sources of errors in, in use of nuclear emulsions for, 18: 23961
dosimetry of, use of aluminum stearate gels and aluminum octoate gels for, 18: 31949
dosimetry of, use of carbohydrate solutions for, 19: 22774
dosimetry of, use of proportional detectors for, 19: 39043
dosimetry of, use of threshold detectors for, 19: 42726
dosimetry of, using photographic film detectors, 19: 22781
dosimetry of, using proton-recoil detectors, (T), 20: 654 (NP-15466)
dosimetry of, using semiconductor detectors, (E), 20: 2134 (TID-22335)
dosimetry of, using hair activation, 20: 16758
dosimetry of, using cesium-137 gamma spectrometry following thorium fission, 20: 31530
dosimetry outside shielding of low-power heavy water reactors, 16: 25026
dosimetry, performance of semiconductor detectors, 16: 30581 (HW-SA-2624)
dosimetry using activation detectors, use of iron, magnesium, nickel, titanium, and zinc in, 17: 34288
dosimetry using activation detectors and ionization chambers, 20: 39228
dosimetry using boron trifluoride detectors, method for, 18: 33980(P)

dosimetry using ferrous sulfate–sulfuric acid solution, 18: 10372 (CONF-187-55)
dosimetry using fission foils, method for direct, 18: 33979(P)
dosimetry using glycine aqueous solutions, 19: 18271
dosimetry using lithium fluoride, (E), 19: 4484 (UCRL-11613)
dosimetry, using liquid and plastic phosphors, 16: 5617
dosimetry using nuclear emulsions, methodological errors in, 17: 27692
dosimetry using nuclear emulsions, 18: 16357
dosimetry using scintillation detector, pulse shape discrimination in, 19: 763(R) (HW-81746(p.2.19-23))
dosimetry using sulfur tablets in film badges, 17: 39412 (CRRD-1161)
dosimetry using sulfur disks, reduction of sulfur dose threshold in, 20: 647 (AERE-M-1631)
dosimetry using thorium, 18: 30749
dosimetry, development of sensitive device for, 19: 11498(R) (TID-21446)
effect on anthracene oils, 20: 45717
effect on fast switching diodes, 20: 46100
effect on strain and stress distributions in fuel elements, 18: 24943
effectiveness in mice, relative biological, 19: 21817(R) (BNL-867 (p.119-50))
effectiveness of, relative biological, 17: 34179
effects at 0.43 to 1.80 Mev, biological, 16: 1558
effects in graphite, effects of annealing on, 20: 31803
effects in iron, 19: 34741(R) (BNWL-79(p.3.1-22))
effects in leukemic and tumor cells, biological, 19: 42274
effects in mice, 16: 11466 (USNRDL-TR-550)
effects in mice, 16: 12915
effects in mice, hematological, 19: 27955
effects in moderators for cold neutron production, heating from, 20: 36152
effects in rats, hematological, 19: 27949 (TID-21889)
effects in silkworm gonads, genetic, 19: 43786
effects in Tradescantia, effects of temperature on, 16: 18785
effects of acute and chronic exposure to, 20: 45419
effects of age on whole-body sublethal acute biological effects of, in rats, 18: 3501 (USNRDL-TR-673)
effects of cadmium-transmitted, on ferroelectric properties of barium titanates, 18: 32251
effects of dose levels on relative biological effectiveness and elimination of chromosomal aberrations, 16: 1603
effects of hardness of iron, effects of dose rate on, 20: 25619(R) (ORNL-3949)
effects of, on chick embryos and mouse ascites tumors and testis, relative, 17: 12143
effects of, on *E. coli*, oxygen enhancement ratio for, 17: 12144
effects of, on intestines and skin of rats, relative biological, 17: 12145
effects of, on lattices in quartz crystals, 16: 33517 (NYO-10444)
effects of, on skin of pigs, fractionated and single, 17: 12146
effects of, on skin and tumors, reduced oxygen enhancement effect in, 17: 12147
effects of, on structure of aluminum single crystals, 16: 33521 (PAN-322/I-B)
effects of, on teeth of rats, effects of age on, 17: 23095 (USNRDL-TR-634)
effects of, on tumors in rats, oxygen effect in, 17: 12142
effects of single and repeated exposure on gonads of mice and rats, 18: 17623
effects of small doses of, on *Drosophila melanogaster*, 18: 36946 (A/CONF.28/P/386)
effects of 10^{20} nvt exposure, on molybdenum containing carbon, 19: 42901 (BNWL-SA-151)
effects of 200-kev, on phage induction in *E. coli*, RBE for, 20: 29002
effects of 200-kev, on chromosomes, RBE for, 20: 29002
effects of, combined with x rays on Drosophila chromosome exchange yield, 20: 24914
effects of, compared to x rays and gamma rays on mice, 18: 17559
effects on A-center formation rate in oxygen-containing silicon, (E), 19: 11801(T)
effects on A-286, rhenium–tungsten alloy, and tungsten, 18: 30111(R) (GEMP-35A)
effects on absorption spectra of silicon crystals in near infrared region, 18: 44264
effects on absorption spectra of Yakutian diamonds, 19: 41098
effects on adrenal cortex function in rats, 19: 38443
effects on aging and resistivity of aluminum–magnesium alloys, 18: 34244
effects on aging in Japanese nuclear-explosion survivors, 20: 20480
effects on agricultural plants, 20: 18409
effects on alumina, beryllia, and magnesia, 19: 30828(R) (ORNL-3789(p.230-8))
effects on alumina, beryllia, and magnesia, 20: 23774(R) (ORNL-3913, pp 75-109)
effects on aluminum, recovery mechanisms for, 18: 2334
effects on aluminum and gold at low temperatures, 18: 36051
effects on aluminum, annealing of, 19: 25069
effects on aluminum, 19: 36949(R) (BNL-900(p.121-97))
effects on aluminum–copper alloys, effects of aluminum content on, 19: 44739(R) (ANL-7000, pp 233-77)
effects on aluminum and titanium alloys and metals at cryogenic temperatures, in-pile loops for testing, 20: 11345(R) (NASA-CR-54787)
effects on amino acid synthesis in *Micrococcus glutamicus*, 20: 42914
effects on animal cells in culture, effects of oxygen on biological, 20: 31123
effects on animal cells in tissue culture, 18: 41181
effects on animals and plants, genetic, 20: 1622 (WT-820)
effects on annealing of Frenkel defects in crystals, computer simulation of, 20: 37294
effects on anthracene oil, at 150 to 350°C, (E), 19: 22290
effects on anthracene oil and terphenyl mixture, 20: 356 (SGAE-CH-19/1965)
effects on anthracene oil, decomposition by, 20: 33342
effects on antibiotic production of Actinomycetes, 18: 31223
effects on antimony-doped germanium single crystals at 100°C, 20: 2495
effects on apple tree roots, genetic, 20: 38692
effects on aqueous solutions of phenylalanine and tyrosine, 18: 39357
effects on aqueous corrosion of zirconium alloys, 19: 30650(R) (ORNL-3789(p.126-38))
effects on aqueous solutions in reactors, production of chemicals by, 19: 40548 (BNWL-82)
effects on asparagus, mutagenic, 18: 33323
effects on barley chromosomes, effects of dose on aberrant, 20: 18355
effects on barley and wheat, mutagenic, 20: 22658
effects on barley, 18: 25178
effects on behavior of monkeys, 19: 28029
effects on behavior of monkeys, 19: 33857
effects on behavioral responses of male monkeys, 20: 36638
effects on beryllium at 450 to 650°C, 18: 20579 (AAEC/E-115)
effects on beryllium oxide at 75 and 500 to 700°C, 18: 20610
effects on beryllium oxide compacts, 18: 22529(R) (ORNL-3591 (p.147-55))
effects on beryllium oxides at 0.3 to 4.2×10^{21} nvt, 18: 22531 (ORNL-TM-742)
effects on beryllia components, 18: 30953(R) (ORNL-3619(p.147-200))
effects on beryllium oxide compacts at 583 to 1100°C, 18: 34224
effects on beryllia single crystals, x-ray diffraction studies of, 18: 44048(R) (ORNL-3670(p.56-63))
effects on beryllia compacts, 19: 2860 (ORNL-P-631)
effects on beryllia microstructure at high temperatures, 19: 4710 (AAEC/E-130)
effects on beryllium oxide, 19: 25062
effects on beryllium oxide single crystals, 19: 30834
effects on beryllia, effects of bentonite additives on, 19: 40959
effects on beryllium oxide thermal conductivity due to microcracking, 20: 2443
effects on beryllium oxide crystals, 20: 8316(R) (NAA-SR-11450, Sect.7)
effects on beryllium oxide, 20: 7510
effects on beryllia at 950 to 1050°C, 20: 27585(R) (GEMP-400A, pp 221-62)
effects on beryllium, 20: 39454 (EUR-3055.e)
effects on beryllia at 800 to 980°C, 16: 18083 (GA-2648)
effects on biphenyl, 19: 34218
effects on blood cells in mice, 20: 40502(R) (ORNL-3922, pp 115-27)
effects on blood plasma iron clearance time in sheep, whole-body, 18: 31179
effects on blood picture of rats, effects of dose on, 20: 6902
effects on blood–brain barrier permeability in burros and sheep, 20: 20489
effects on bone marrow of mice, biological, 19: 29889(R) (ANL-6971 (p.90-116))
effects on boronated graphite, 20: 17116 (BNWL-199)
effects on bread wheat, frequency and spectrum of mutagenic, 19: 9853
effects on brittle-to-ductile transition temperature of polycrystalline tungsten, 20: 2422(R) (GEMP-52A, pp 11-21)
effects on buckwheat seeds, 18: 41189
effects on burros, 18: 38889
effects on cadmium sulfide single crystal electrophysical properties 20: 34829
effects on carbon-containing foils of molybdenum, 18: 2314
effects on carbon precipitation in alpha-iron, 20: 11227
effects on cardiac function, 20: 18328
effects on cardiovascular and hematopoietic system of rats, 19: 38441
effects on catalysts for use in electrochemical reactions, 19: 30296(P)
effects on catalytic properties of manganese dioxide, 19: 4225
effects on cataract development in rabbit eyes, threshold dose for, 19: 15142
effects on central nervous system in dogs and monkeys, 18: 29382

effects on ceramic materials, 20: 46224 (BNL-10560)
effects on ceramic materials, 16: 10607 (DC-55-6-101)
effects on Charpy impact and tensile properties of chromium–molybdenum steel, 18: 40018
effects on chemical and physical properties of rat blood, 19: 38440
effects on chemical reactions of iron with oxygen, 20: 5846
effects on chemisorption and surface defects in magnesium oxide, 18: 22140
effects on cherry graft development, 18: 19691
effects on chimeric bract induction in *Euphorbia pulcherrima*, 20: 32969(R) (ORO-648, pp 123-58)
effects on chinchillas, biological, 20: 6900
effects on chlorophyll mutation frequency, meiosis, and mitosis in peas, 20: 36621
effects on chromosome aberrations in *Crepis capillaris* seeds, moisture effects on post-, 19: 19581
effects on chromosome aberration frequency in winter wheat, 19: 31836
effects on chromosomes of bone marrow cells, 20: 22582
effects on chromosomal bridges at anaphase in barley seeds and Tradescantia, 20: 29031
effects on chromosomes, 19: 2062 (BNL-8462)
effects on chromosomes in humans, whole-body, 16: 17493
effects on chrysanthemum, 20: 32969(R) (ORO-648, pp 123-58)
effects on coated thorium and uranium carbide and oxide fuel particles, 20: 4458 (GA-6485)
effects on coated carbide fuel particles, 20: 9596
effects on cobalt oxides, (E), 20: 11355
effects on cobalt complexes, 20: 38962
effects on color of fused silica, 19: 47082 (NASA-CR-304)
effects on coloration induction in fused silica, spectra of thermal annealing effects on, 19: 23125 (NP-14958)
effects on conductivity of silicon diodes, (E), 19: 22811
effects on conifer-hardwood, effects of environmental factors on, 20: 12672
effects on content of steroids in blood of burros, 20: 18296(R) (UCLA-12-576, pp 57-60)
effects on contraction and expansion in graphite, 18: 36043 (BNL-7214)
effects on copper crystals, x-ray diffraction study of, 19: 999(R) (ORNL-3676(p.27-31))
effects on copper–nickel alloys, redistribution kinetics of segregated zones from, 18: 24208
effects on copper, thermal activation of slip in, 18: 20594
effects on copper, iron, and tungsten crystals, anisotropy of atomic displacements in, 19: 16228
effects on corrosion and hydridation of Zircaloy-2, 18: 2343
effects on corrosion resistance of boronated stainless steel, 19: 39110
effects on corrosion and tensile properties of hafnium-to-Zircaloy-2 welded joints, 19: 41092 (WAPD-TM-457)
effects on corrosion of selected metals by Santowax OM at 500 to 700°F, 20: 5846
effects on corrosion of zirconium alloys by water, 20: 23767 (BNWL-88)
effects on corticosterone content in plasma of burros, 20: 22727
effects on cracking in type 347 stainless steel, 20: 29618(R) (GEAP-4982)
effects on creep and dimensional changes in graphite, 20: 37282
effects on creep in graphite, mechanisms of, 19: 32782
effects on creep of Zircaloy-2 at 300°C, 20: 27603
effects on creep-rupture of A-286 alloy, effects of boron content on, 20: 9378(R) (GEMP-54A)
effects on creep-rupture properties of tungsten–25 rhenium alloy, 19: 44598(R) (GEMP-49A)
effects on creep-rupture properties of INOR-8, effects of annealing on, 19: 44599(R) (GEMP-50A)
effects on creep-rupture properties of A-286 alloy and Hastelloy X, 20: 2456
effects on creep-rupture of molybdenum, tungsten, and tungsten–25 rhenium alloy, 20: 5851
effects on creep-rupture of Hastelloy N, effects of irradiation temperature on, 20: 9378(R) (GEMP-54A)
effects on creep-rupture of TZM molybdenum alloy, 20: 9378(R) (GEMP-54A)
effects on creep-rupture properties of tungsten, 20: 17152
effects on creep-rupture properties of TZM alloy, 20: 27582(R) (GEMP-400A, pp 63-98)
effects on creep-rupture of A-286 alloy, effects of boron additions on, 20: 27584(R) (GEMP-400A, pp 169-84)
effects on creep-rupture properties of Inor-8, 20: 33963
effects on critical currents in superconductors, 18: 9265
effects on crystal structure of copper, 18: 14557
effects on crystal structure of carbonates, oxides, and titanates, 18: 34241
effects on crystal lattices, 20: 43987 (BNL-10569)
effects on crystallinity and thermal conductivity of pyrolytic carbons, 20: 44009
effects on culture and morphology of *Bacillus mesentericus*, 19: 38449
effects on current-carrying behavior of superconducting Nb_3Sn, 18: 18424
effects on DBTT of weld heat-affected-zones in A-212B steel, 20: 25619(R) (ORNL-3949)
effects on decomposition of water in reactor, 19: 38698 (ZFK-RN-17 (p.199-207))
effects on decomposition of terphenyls at 350°C, 20: 20722 (EUR-2401.f)
effects on defect induction in beryllium oxide, 20: 23786
effects on defects in diamond-lattice semiconductors, 19: 11811
effects on defects in aluminum, 20: 13338
effects on defects in silicon crystals, (E), 20: 42567(T)
effects on deformation of copper–tin alloys, 19: 44753
effects on deformation of copper–tin alloys, 20: 21434
effects on deformation properties of hydrided Zircaloy-2, 20: 27421
effects on deformed copper single-crystal Bordoni internal friction peak, 19: 1002(R) (ORNL-3676(p.66-73))
effects on degradation of terphenyl in in-pile loop, 20: 26924(R) (MIT-334-48)
effects on density, lattice parameters, and size of beryllium oxide crystals at 75 to 100°C, annealing effects on, 18: 20609
effects on density and dimensions of beryllia, 19: 27778(R) (GA-4124)
effects on density and tensile properties of beryllium, 20: 5849
effects on dental lesions in rats, 17: 19807 (USNRDL-TR-620)
effects on diamonds, stresses in, 19: 20639
effects on dielectric properties of aluminum and silicon oxides, 18: 36059
effects on different type graphites at 800 to 1200°C, 20: 2417 (BNWL-112)
effects on diffusion in α-aluminum–copper alloys, 19: 30840
effects on dimensions of EGCR graphite, 18: 41933 (TID-11295(3rd Ed.))
effects on dimensions of graphite, 19: 30736(R) (GA-5033)
effects on dimensions of molybdenum, effects of carbon on, 20: 745(R) (BNWL-120, pp 3.1-22)
effects on dimensions of aluminum–europium oxide dispersions, 20: 5174(R) (ORNL-3870, pp 214-29)
effects on dimensions of beryllia, effects of alumina and bentonite additions on, 20: 9378(R) (GEMP-54A)
effects on dimensions of graphite combined with effects of sodium, 20: 9570 (CONF-650620, pp 47-84)
effects on dimensions of carbon and graphite irradiated at 150 to 650°C, 20: 11225
effects on dimension of alumina, 20: 13337
effects on dimensions of graphite, effects of carbon black content on, 20: 19252 (BNWL-201)
effects on dimensional stability of carbon and graphite at 900 to 1800°C, 20: 21419 (BNWL-191)
effects on dimensions of graphite, 20: 21420 (BNWL-215)
effects on dimensions and strength of beryllia, effects of silica additions on, 20: 27409(R) (GEMP-58A)
effects on dimensions and electric resistivity of ceramic materials, 20: 27588 (LA-DC-6822)
effects on dimensional changes in furfuryl alcohol-impregnated graphite, 20: 29813
effects on dimensions of graphite and carbon crystals, 20: 44020
effects on dislocations in annealed copper, 19: 39241
effects on dislocation channeling in molybdenum, effects of prestrain on, 20: 745(R) (BNWL-120, pp 3.1-22)
effects on dislocation motion in iron, 20: 9576(R) (ORNL-3878)
effects on displacement cascades in gold films, 19: 44739(R) (ANL-7000, pp 233-77)
effects on DNA synthesis in pea seedlings, 20: 28989
effects on dogs, effects of geometry on, 19: 8783 (BNL-8571)
effects on dogs, sheep, and swine, air and *in vivo* dosimetry of, 19: 8951
effects on dominant lethal mutations in mature sperm and gonad damage in animals, RBE of, 19: 17607
effects on dormant seeds, 20: 32969(R) (ORO-648, pp 123-58)
effects on double Bragg scattering in beryllium oxide, 18: 37772
effects on *Drosophila melanogaster*, anoxia effects on, 18: 11831
effects on Drosophila and silkworms, genetic, 20: 26655(R) (NP-15975)
effects on Drosophila, comparison of RBE of x radiation with, 20: 38645
effects on ductile-to-brittle transition temperature in Zircaloy-2, 19: 34627(R) (BNWL-79(p.6.1-20))
effects on ductility of molybdenum- and niobium-base alloys, 18: 44049(R) (ORNL-3670(p.77-111))
effects on ductility of Ferrovac iron, study of dislocation kinetics in, 19: 37158 (BNL-9264)
effects on ductility of types 304 and 348 stainless steel, 20: 889(R) (BNWL-120, pp 4.1-59)
effects on ductility of Zircaloy-2, 20: 2420(R) (DPST-65-83-8)

effects on ductility of aluminum–chromium–iron–yttrium alloy, 20: 7499(R) (GEMP-53A)
effects on ductility of iron–chromium–aluminum–yttrium alloys, effects of annealing at 350°C on, 20: 27411(R) (GEMP-400A, pp 135-63)
effects on ductility of type 304 stainless steel, effects of carbon content and titanium additions on, 20: 31669
effects on ductility of type 304 stainless steel, 19: 39236 (WCAP-3269-36)
effects on *durum* and bread wheats, first generation, 16: 1599
effects on *E. coli* and *S. cerevisiae* survival, 18: 41231
effects on Ecballium, mutagenic, 20: 8690
effects on Ehrlich ascites tumor cells, 18: 29543
effects on Einkorn wheat, RBE of, 18: 41227
effects on elastic properties of graphite, 20: 44018
effects on electric conductivity of pyrolytic graphite, 18: 12741
effects on electric conductivity and Hall effect of germanium, 18: 32243
effects on electric conductivity of glasses, 19: 18543
effects on electric conductivity and Hall coefficients of germanium, 19: 41104(T)
effects on electric and magnetic properties of copper–iron alloys, 19: 42915
effects on electric resistivity of metals at 4°K, 19: 44739(R) (ANL-7000, pp 233-77)
effects on electric properties of silicon carbides, 20: 2503
effects on electric properties of silicon, annealing during fabrication of p-n junctions of, 20: 2440
effects on electric conductivity of tungsten, effects of annealing on, 20: 7632(R) (GA-6679)
effects on electrical components and structural materials for use in SNAP-8 program, 20: 9563 (BMI-X-10152)
effects on electric properties of ferroelectric materials, 20: 11352 (NP-15707)
effects on electric conductivity of tungsten, 20: 15040(R) (GA-6721)
effects on electric properties of conductivity-modulated silicon p-i-n diodes, 20: 16912
effects on electric conductivity and Hall effect in zinc sulfide single crystals, 20: 36865
effects on electric components for SNAP 8, 20: 45194 (NAA-SR-11924)
effects on electric properties of cadmium sulfide single crystals, 20: 46957(T)
effects on electronic equipment, computer program for data retrieval on, 19: 46870(R) (AD-612191)
effects on electronic components, pulsed and steady-state, 16: 29136
effects on embrittlement of A-286 alloy at high temperature, additive effects of boron on, 18: 28062
effects on embrittlement of type 304 stainless steel, 20: 4460(R) (ORNL-3870, pp 140-5)
effects on embrittlement of types 304 and 304L stainless steels at 650 to 842°C, 20: 4460(R) (ORNL-3870, pp 140-5)
effects on embrittlement of type 304 stainless steel, role of grain boundary carbides in, 20: 4460(R) (ORNL-3870, pp 140-5)
effects on embrittlement of type 304 stainless steel, role of titanium additions in, 20: 4460(R) (ORNL-3870, pp 140-5)
effects on embrittlement of molybdenum steels with dispersed second phase, 20: 5846
effects on embrittlement of iron and iron–titanium alloys, effects of nitrogen on, 20: 23801
effects on engineering properties of structural reactor materials, review on, 18: 32216 (A/CONF.28/P/242)
effects on EPR spectra of diamonds, effects of heat treatment on, 18: 22536
effects on erythrocytes in blood and saline suspensions, 19: 24350
effects on *Escherichia coli*, biological, 19: 15018 (ORNL-P-758)
effects on ESR in zinc sulfide crystals, 19: 32210
effects on ESR spectra of pure zinc sulfide, 18: 23664
effects on ESR spectra of polycrystalline graphite, temperature effects on, 18: 32239
effects on excitation spectra of copper-activated and pure zinc sulfides, 18: 24575
effects on eye color mutations in *Dahlbominus fuscipennis* at 14 Mev, 20: 33023
effects on eye lens of mice, 18: 1375 (BNL-7371)
effects on eyes of mice, pathological, 19: 34098
effects on ferroelectric transition behavior in barium titanates, 20: 10244
effects on fertility in mice, whole-body exposure, 16: 23467
effects on fission-gas-generation and temperature in plutonia–urania, profiles of, 20: 29618(R) (GEAP-4982)
effects on flour beetles, Tribolium, biological, 20: 1613 (HW-SA-3537)
effects on fluorescence spectra of uranyl ion in cesium uranyl nitrate, 18: 25554
effects on formation of labeled xenon compounds in lithium fluoride–uranium dioxide mixture, 19: 36500
effects on gain of n-p-n silicon planar transistors, 19: 24884 (SC-TM-261-63(14))
effects on gas bubble formation in magnesium oxide, 20: 4387(R) (ORNL-3870, pp 38-43)
effects on gas formation and compression fractures in beryllium, 20: 2478
effects on gastrointestinal tract, whole-body exposure, 17: 7815
effects on gastrointestinal tract in guinea pig, relative potency of, 16: 31475 (USNRDL-TR-576)
effects on gelation of triethylene glycol dimethacrylate at 14 Mev, 20: 20720 (AD-630891)
effects on generation-recombination noise in germanium single crystals, 20: 26361
effects on genetics of barley seeds, post-treatment modification of, 18: 11842
effects on genetic variability in *durum* wheat, 19: 42267
effects on germanium and silicon, x-ray-diffraction study of, 18: 39992 (EUR-1643.e(p.231-45))
effects on germanium and silicon, 19: 2864
effects on germanium photoconductivity, (E), 19: 4550(T)
effects on germanium point diodes, surface identification by, (E), 19: 4552
effects on germanium, 19: 11682
effects on germanium, annealing of, 19: 20626
effects on germanium at 80°K, 19: 44754
effects on germanium, annealing of, 20: 2509
effects on germanium, electron-microscope observations of, 20: 4467
effects on germanium p-n junctions, 19: 20627
effects on gladiolus hydrids, seeds, and tubers, 20: 35290
effects on gonads of mice, 17: 31891
effects on grain, effects of post-irradiation soaking and temperature changes on mutagenic, 20: 22779
effects on graphite thermal conductivity, 18: 2335
effects on graphite in liquid nitrogen, 18: 2375
effects on graphite, relation of flux level and spectra to accumulation of damage in, 18: 2376
effects on graphite single crystals, electron microscope studies on, 18: 44259
effects on graphite, 18: 44957(P)
effects on graphite, 19: 11682
effects on graphite, 19: 11711
effects on graphite, 19: 22976(R) (GA-4901)
effects on graphite dimensional changes, comparison with bromination, 19: 30762
effects on graphite basal plane contraction, (T), 19: 41100
effects on graphite joints and graphite-coated particles in carbonized pitch matrix, 20: 17119 (GAMD-6789)
effects on graphite structural properties, 20: 28744(R) (GA-6869)
effects on graphite, interstitial cluster growth from, 20: 44021
effects on green and yellow excited absorption spectra of cuprous oxides, 18: 20077
effects on growth and survival of durum wheat, comparison with effects of mutagenic agents, 17: 10388
effects on growth of *Escherichia coli*, 18: 29247 (TID-20785)
effects on growth of mice compared to x radiation, 18: 31198
effects on growth on bone marrow cells in spleen of mice, biological, 20: 8710
effects on growth and mutations in Triticum, 20: 31080
effects on growth and morphology of *Vicia sativa* and *V. villosa* from seed exposure, 20: 32988
effects on growth in peas treated with vitamin C, 20: 45387
effects on hair regrowth in mice, 18: 41140
effects on hardness and thermoelectromotive force of metals, 18: 28066
effects on hardness of fcc metals, 18: 30285
effects on hardness of aluminum single crystals, 19: 20641
effects on hardness of molybdenum, effects of annealing and temperature on, 19: 37165(R) (GEMP-47A, pp 85-99)
effects on hardness of carbon steels, combined effects of carbon content and irradiation temperature on, 20: 11342 (EURAEC-1502)
effects on hardness of A302B and nickel–chromium–molybdenum steels, effects of irradiation temperature on, 20: 11342 (EURAEC-1502)
effects on hardwood-pine forests, effects of age and dose on recovery from, 20: 12675
effects on hot hardness of tungsten single crystals, 19: 44599(R) (GEMP-50A)
effects on hot hardness of molybdenum, 19: 44598(R) (GEMP-49A)
effects on hot-hardness of tungsten single crystals, dosage effects of, 20: 2422(R) (GEMP-52A, pp 11-21)
effects on hot-hardness of tungsten single crystals, 20: 9378(R) (GEMP-54A)
effects on hot-hardness of tungsten single crystals, 20: 27582(R) (GEMP-400A, pp 63-98)
effects on hot-hardness of molybdenum and molybdenum alloys, effects of test temperature on, 20: 27582(R) (GEMP-400A-pp 63-98)

effects on human blood picture in Nagasaki, 20: 20481
effects on hydrogen and oxygen sorption by zirconium alloys, 20: 27599
effects on hydrogen sorption and mechanical properties of Zircaloy-2, 20: 27601
effects on impact strength of A-302B steel, combined stress and, 20: 11227
effects on impact properties of hydrided Zircaloy-2 and zirconium–2.5 niobium alloy, 20: 27602
effects on impact properties of zirconium–2.5 niobium and Zircaloy-2, effects of hydrogen on, 20: 31669
effects on improving flue-cured tobacco, 18: 31160
effects on in-pile corrosion of nuclear materials by aqueous solutions, 20: 5852(R) (EURAEC-1522)
effects on Incoloy, 19: 38178(R) (GEAP-4790)
effects on Inconel, Hastelloy X, and stainless steel, 19: 30649(R) (HW-84573(p.4.1-31))
effects on Inconel 600–Zircaloy-2 transition joints, 20: 23768 (BNWL-190)
effects on induction of lens opacities in mice, RBE for, 19: 26004
effects on induction of sulfur-35 recoil atoms in ferroelectric tri-glycine sulfate, annealing effects on, 19: 42570
effects on induction of chromosome aberrations of blood cells in rats, 20: 6901
effects on infrared absorption spectra of silicon, 19: 32773 (AD-611145)
effects on injection of A centers in single crystals of silicon, 18: 44263
effects on intact mouse thymus, effects of hypoxia on, 20: 32982
effects on intestinal permeability to polyvinylpyrrolidone in rats, 18: 41080(R) (HW-80500(p.127-8))
effects on intestinal permeability, in rats, 19: 34098
effects on iodine-131-containing calcium iodate, thermal annealing effects on, 18: 27511
effects on iodine-126 and -128 retention in potassium iodate, 19: 13500
effects on iron and steel, additive effects of nitrogen on, 18: 28041(R) (EURAEC-1046)
effects on iron and steel, effects of nitrogen on, 18: 37763(R) (EURAEC-1103)
effects on iron and steel, research program on, 19: 18534(R) (EURAEC-1318)
effects on iron and steel, research program on effects of nitrogen on, 19: 44741 (EURAEC-1383)
effects on iron and steel, research program on effects of nitrogen on, 19: 44742(R) (EURAEC-1430)
effects on iron with nickel impurities at 77°K, 19: 28880
effects on isomeric terphenyl, decomposition, 20: 20739
effects on large animals, facility for studying, 18: 41219
effects on large mammals, effects of geometry on, 19: 8783 (BNL-8571)
effects on lattice atom displacement probabilities in copper, gold, iron, and silver, (T), 19: 47104
effects on lattice defects in quartz, 20: 27621
effects on learning by monkeys, 19: 28030
effects on lethality in flour beetles, dose ratio of x rays to, 19: 10852
effects on life span of mice, chronic exposure, 19: 8790(R) (NP-14448(p.116-31))
effects on life span of mice, 16: 18764(R) (NP-11660(p.67-75))
effects on life span on mice, 17: 13972(R) (NP-12484(p.45-53))
effects on life span and morphology of peripheral blood in white rats, 18: 19677
effects on life span of mice, chronic exposure, 16: 26658(R) (NP-11966 (p.36-42))
effects on lithium fluoride single crystals, 19: 9219(T)
effects on lithium-drifted germanium detectors at 1 to 16 Mev, (E), 20: 7462
effects on longevity of guinea pigs and rats, 20: 36640
effects on low-temperature dielectric relaxation in fused silica, 18: 20616
effects on luminescence of zinc sulfide, 19: 19967
effects on luminescence of thallium-activated alkali metal halide crystals, 19: 34238
effects on luminescence of potassium chloride and thallium-activated potassium chloride, 19: 34240
effects on magnesium oxides, x-ray line broadening in, (E), 20: 2445
effects on magnetic properties of type II superconductors, 18: 9262(R) (NP-13492)
effects on magnetic amplifier control devices for nuclear ramjets, 18: 33825 (AD-435095)
effects on magnetic properties of iron, effects of magnetic field on, 18: 39994 (EURAEC-1157)
effects on magnetic hysteresis of iron, combined nickel impurity and, 20: 17134
effects on magnetic properties of iron–silicon systems, 20: 27566 (AERE-R-5194)
effects on maize, 19: 3964
effects on maize, 18: 1374 (BNL-7367)
effects on maize seeds, genetic, 20: 31092
effects on maize seed, biological RBE of, 20: 42843 (BNL-10358)
effects on mammalian cells, 17: 23171
effects on mammalian species, lethal, 18: 8101 (BNL-7603)
effects on mammals, whole-body relative biological, 18: 17499
effects on mammary tumor incidence in rats, 17: 33448(R) (ANL-6723 (p.33-40))
effects on mechanical properties of stainless steel, 18: 13354(R) (BMI-1657(Del.))
effects on mechanical properties of Type 347 stainless steel, 18: 17351(R) (BMI-1659(Del.))
effects on mechanical properties of type 347 stainless steel pressure tubes, effects of high temperature on, 18: 28052 (WAPD-T-1574)
effects on mechanical properties of Zircaloy sheaths, 18: 30231 (DP-888)
effects on mechanical properties of manganese–molybdenum steel and Zircaloy-2, 18: 30263
effects on mechanical properties of 1100 aluminum, 18: 34032(R) (BMI-1668(Del.))
effects on mechanical properties of 1100 aluminum, 18: 34033(R) (BMI-1669(Del.))
effects on mechanical properties of Teflon and Teflon-based materials in liquid hydrogen, 18: 39361
effects on mechanical properties of type 347 stainless steel, 18: 40028
effects on mechanical properties of beryllia, 18: 44234 (AAEC/E-127)
effects on mechanical properties of iron and steel, 19: 1004(R) (ORNL-3676(p.125-56))
effects on mechanical properties of type 347 stainless steel, 19: 2716(R) (BMI-1681(Del.))
effects on mechanical properties of Zircaloy-2 pressure tubes, 19: 6362 (HW-83164)
effects on mechanical properties of iron, 19: 7976(R) (EURAEC-1238)
effects on mechanical properties of SAP, 19: 7855(R) (RISÖ-90)
effects on mechanical properties of type 347 stainless steel, 19: 22864(R) (BMI-1704(Del.))
effects on mechanical properties of beryllium, 19: 25042 (AAEC/E-133)
effects on mechanical properties of high-temperature structural metals and alloys, 19: 30820 (BNWL-23)
effects on mechanical properties of Inor-8, 19: 34742(R) (BNWL-79(p.4.1-30))
effects on mechanical properties of Hastelloy X-280, 19: 34742(R) (BNWL-79(p.4.1-30))
effects on mechanical properties of Incoloy 800, 19: 34742(R) (BNWL-75(p.4.1-30))
effects on mechanical properties of Inconel 625 as function of exposure temperature, 19: 34742(R) (BNWL-79(p.4.1-30))
effects on mechanical properties of type 304 stainless steel at 550°C and 30,000 psi, 19: 34742(R) (BNWL-79(p.4.1-30))
effects on mechanical properties of boronated stainless steel, 19: 39110
effects on mechanical properties of type 304 stainless steel and Zircaloy-2, 19: 39229(R) (BMI-X-10134)
effects on mechanical properties of hafnium control rods, 19: 41092 (WAPD-TM-457)
effects on mechanical properties of beryllia, 19: 44599(R) (GEMP-50A)
effects on mechanical properties of Hastelloy X-280, Incoloy 800, Inconel 600, and INOR-8, 20: 889(R) (BNWL-120, pp 4.1-59)
effects on mechanical properties of stainless steel at 25 to 850°C, 20: 2477
effects on mechanical properties of aluminum alloy 6061, 20: 4460(R) (ORNL-3870, pp 140-5)
effects on mechanical properties of A302B and AMMO2 manganese–molybdenum steels, 20: 5846
effects on mechanical properties of Inconel 600, Inconel 625, Inconel 718, and Incoloy 800, 20: 5851
effects on mechanical properties of carbon or low-alloy steel, 20: 5921
effects on mechanical properties of type 304 stainless steel and Zircaloy-2, 20: 7628(R) (BMI-X-10146)
effects on mechanical properties of Inconel 625, 20: 7630 (BNWL-153)
effects on mechanical properties of Inconel 600 and 702, 20: 9408 (BNWL-154)
effects on mechanical properties of Hastelloy R-235 and X-280, 20: 9408 (BNWL-154)
effects on mechanical properties of SA212B and SA302B steels, 20: 19178(R) (IDO-17154)
effects on mechanical properties of beryllium, 20: 19178(R) (IDO-17154)
effects on mechanical and thermal properties of beryllium oxides, 20: 29810
effects on mechanical properties of hot-pressed and extruded beryllium, 20: 31794
effects on mechanical properties of low-alloy pressure vessel steel, 20: 31796
effects on mechanical properties of Hastelloy X-280 and Inconel 625, 20: 31669

effects on mechanical properties of type 347 stainless steel, 20: 35834(R) (BMI-1767)
effects on mechanical properties of titanium–vanadium alloys, 20: 36391(R) (ANL-7219, pp 1-27)
effects on mechanical properties of Incoloy-800, Inconel-600, and Zircaloy-2, 20: 39457 (GEAP-5100-9)
effects on mechanical properties of cladding materials, 20: 42579(R) (ANL-7245, pp 29-47)
effects on *meta*- and *ortho*-terphenyl, decomposition in, 19: 30228 (CRC-1219)
effects on meta- and ortho-terphenyl, 20: 1928
effects on metabolism of rats, delayed, 20: 14368
effects on metals at low temperatures, 19: 6364(R) (NP-14443)
effects on metals, 19: 11807
effects on metals at cryogenic temperatures, 19: 14086(R) (N65-13446)
effects on metals at cryogenic temperatures, 19: 25048(R) (NP-14889)
effects on metals at 4.5°K, annealing of, 18: 14561
effects on mice, 18: 41221
effects on mice, 18: 38933
effects on mice, 18: 38732
effects on mice, 17: 5671(R) (LAMS-2780(p.85-129))
effects on mice, 18: 25165
effects on mice of, dose fractionation, biological, 20: 3728
effects on mice, comparison of RBE of γ radiation with, 20: 38647
effects on mice, comparison with effects of x radiation, 18: 21828 (USNRDL-TR-713)
effects on mice, chronic exposure, 18: 11760
effects on mice, comparison with x rays and gamma rays, 18: 17560
effects on mice, effects of previous exposure, 17: 5776 (TID-14698)
effects on mice, effects of LET on early, 17: 10358 (BNL-6575)
effects on mice, effects of dose distribution on, 18: 8104(R) (NYO-2740-1(p.7-30))
effects on mice, leukemogenic, 20: 6901
effects on mice, latent somatic, 20: 45417
effects on mice, low-level exposure, 18: 11632(R) (NP-13555(p.107-17))
effects on mice, lethal, 17: 33449(R) (ANL-6723(p.41-3))
effects on mice, physical factors affecting leukemogenic, 18: 19577
effects on mice, RBE for late somatic, 18: 41232
effects on microcracking in beryllia, development of compositions resistant to, 20: 27585(R) (GEMP-400A, pp 221-62)
effects on microhardness and microstructure of type 304 stainless steel, 19: 33603(R) (GEAP-4816)
effects on microhardness of molybdenum and tungsten, effects of test temperature on, 20: 9378(R) (GEMP-54A)
effects on microorganism development in stored wheat, 20: 7472
effects on microstructure of hot-pressed beryllium oxide, annealing effects on, 18: 34225
effects on microstructure of sintered beryllium oxide, 18: 34226
effects on microstructure of high-purity iron, 20: 745(R) (BNWL-120, pp 3.1-22)
effects on microstructure of molybdenum, isothermal recovery of, 20: 9378(R) (GEMP-54A)
effects on microstructure of nickel, electron microscopy study of, 20: 9565(R) (BNWL-166, pp 3.10-14)
effects on microstructure of sintered beryllia, mechanisms of, 20: 23775 (ORNL-P-1194)
effects on microstructure of beryllia, mechanisms of, 20: 27585(R) (GEMP-400A, pp 221-62)
effects on microstrain in copper single crystals, 20: 31669
effects on microstructure of pressure vessel-grade steel, 18: 26092
effects on mitosis in mammalian cells, 18: 41229
effects on mitosis in Pisum, 20: 24890
effects on modulus-of-rupture of beryllia, 19: 40959
effects on molded graphite, effects of pitchbinder on, 20: 13247(R) (GA-6831)
effects on molten lithium nitrate, chemical, 19: 30230 (MATT-329)
effects on molybdenum creep-rupture properties, 19: 28887
effects on monocrystalline and nuclear graphite, 18: 2373
effects on morphology of liver cells in mice, 19: 28081
effects on morphology of organs in rats, 19: 38444
effects on mortality of rats in different positions, RBE of, 19: 38438
effects on mouse chromosomes, aberrant, 19: 10879
effects on mouse intestine, 18: 41226
effects on mouse life spans, 14 Mev, 19: 31677(R) (ORNL-3768 (p.119-30))
effects on murine leukemia cells *in vitro*, survival curves for, 20: 5361
effects on mutagenic, 18: 43218(R) (EUR-1882e(p.7-26))
effects on mutation induction in *Act. antibioticus*, comparison of chemicals with, 19: 26023
effects on mutations in winter wheat seedlings from seed exposure, 19: 36061
effects on mutation frequency in wheat, 20: 36620
effects on n- and p-type silicon, 20: 40334(T)
effects on *n*-type silicon, defect clusters from, (E), 20: 31792
effects on NERVA engine components, 19: 14868 (FZK-170-4)
effects on NERVA electrical components, 19: 14871 (FZK-170-7)
effects on NERVA engine components, 19: 14872 (FZK-170-8)
effects on NERVA engine components, 19: 13812 (FZK-184-3)
effects on NERVA turbine pump assembly bearings under dynamic operation conditions, 19: 14869 (FZK-170-5)
effects on NERVA turbine pump assembly bearings under dynamic operation conditions, 19: 14870 (FZK-170-6)
effects on nickel oxide structure, 20: 23800
effects on nickel foils, 20: 43990 (BNWL-SA-782)
effects on niobium, 19: 32718 (AD-608398)
effects on nitride precipitation in alpha-iron, 20: 9576(R) (ORNL-3878)
effects on notch ductility of A302-B steel, 19: 11780 (NRL-6179)
effects on occurrence of sex-linked, recessive, lethal mutations in Drosophila, 17: 19914
effects on occurrence frequency of mutations in Drosophila, 17: 31936
effects on operation of pressure transmitter at high temperatures, 19: 20400 (NP-14955)
effects on optical properties of zirconium oxide film, 20: 4304(R) (ORNL-3870, pp 171-83)
effects on optical transmission spectra of zinc sulfide single crystals, 20: 31272
effects on ortho-para conversion in liquid hydrogen, 19: 11168 (NASA-TN-D-2591)
effects on ortho-para conversion in liquid hydrogen, (E), 19: 28403
effects on oxidation of copper and iron, 18: 22118 (TID-20541)
effects on oxide film corrosion on Zircaloy-2 and zirconium, 19: 47099
effects on oxide films on zirconium, effects of vacuum annealing on, 20: 27600
effects on oxygen chemisorption by calcia and magnesia, 20: 18787
effects on oxygen-doped silicon, (E), 20: 40302
effects on p-type silicon, energy levels of defects from, 20: 46950
effects on peas, genetic, 20: 36634
effects on peas, mutagenic, 19: 35962
effects on performance of high-frequency silicon transistors, 19: 15938
effects on performance of psychological tests by monkeys, 20: 35281
effects on perovskite crystals, 18: 22540
effects on phase transformations in barium, calcium, and strontium titanates, 20: 9006
effects on phase transformations in barium titanates, 20: 37301
effects on phenyl metal compounds, chemical effects of energetic recoil atoms created by, 19: 42568
effects on phosphorus-doped silicon, 20: 43986 (AD-637937)
effects on photoconductivity of semiconducting germanium, (E), 19: 11799(T)
effects on physical properties of graphite, 18: 667
effects on physical properties of graphite, 19: 30831
effects on physical properties of Santowax WR at 425 to 800°F, 20: 17122 (MIT-334-34)
effects on pig skin, biological, 19: 32001
effects on pig skin, effects of dose fractionation on, 20: 3735
effects on plant cells, effects of chromosome volume and DNA content on, 18: 29236 (BNL-7697)
effects on plastic deformation properties of niobium single crystals, 20: 9576(R) (ORNL-3878)
effects on plutonium dioxide–uranium dioxide fuel pins for fast reactors, transient, 20: 892 (GEAP-4804)
effects on Poisson's ratio of PGA graphite, 20: 11225
effects on polycrystalline graphite, 20: 39466
effects on polystyrene, comparison with gamma effects, 19: 17988
effects on polystyrene, 19: 30233(R) (ORNL-3789(p.318-22))
effects on polystyrene, 18: 22113(R) (ORNL-3591(p.223-30))
effects on potassium dihydrogen arsenate, compression effects on arsenic-74 and -76 annealing in, 19: 13497
effects on potato seedlings, 19: 3965
effects on potatoes, 18: 31170
effects on potatoes following tuber exposure, 20: 24898
effects on pressure vessel design for pressurized water reactors, 18: 3083
effects on pressure-vessel steels, research program on, 18: 34219 (RCN-26)
effects on pressure vessel steels under fatigue cycling, 18: 40008 (SWRI-1228-30)
effects on properties of iron, 18: 10589
effects on properties and spectra of diamond, annealing effects on, 18: 12739
effects on properties of cobalt–copper alloys, 19: 41095(T) (ORNL-tr-667)
effects on properties of beryllia, effects of composition on, 20: 2424(R) (GEMP-52A, pp 37-42)
effects on properties of fueled graphite spheres, 20: 4306(R) (ORNL-3870, pp 194-213)

effects on properties of type 6061 aluminum alloy, 20: 5846
effects on properties of boronated graphite, 20: 9377 (CONF-650620, pp 85-104)
effects on properties and structure of pyrolytic carbons, 20: 13247(R) (GA-6831)
effects on properties and structure of graphite at 495 to 1035°C, 20: 21421 (GA-6888)
effects on properties of pressure vessel steels, 20: 21228 (AE-221)
effects on proton spin diffusion and relaxation in ethylene polymers, 18: 18445(T)
effects on proton polarization in polyethylenes, (E), 20: 22345
effects on pure and doped iron at 78°K, 18: 14549
effects on pyrimidine mutation induction in *Salmonella typhimurium*, genetic analysis of, 19: 45878
effects on pyrolytic graphite, 20: 39465
effects on quartz, 18: 40013
effects on quartz, ultrasonic study of, 18: 18432
effects on rabbit lenses, 18: 17549
effects on rabbit eyes, 19: 17583
effects on rabbit eyes, effects of chemical radioprotective compounds on, 20: 18476
effects on rabbits, 19: 31832
effects on rabbits, effects of elevated air temperature on, 17: 33621(T) (JPRS-20379)
effects on rat blood picture, lifespan, and neoplasms, 18: 17482(T) (FTD-TT-63-1049)
effects on rat lifespan, effects of irradiation age on, 18: 23292
effects on rat thyroid glands, 18: 43266
effects on rats and dogs, 18: 11654 (USNRDL-TR-693)
effects on rats, protective effects of testosterone against, 17: 1352
effects on reactions between beryllium oxide and graphite at 1500°C, equipment and setup for studying, 20: 2431 (ORNL-TM-1255)
effects on reactor vessel mechanical performance, 18: 8905
effects on reactor pressure vessel steel under stress, 19: 20631
effects on reactor materials, monitoring of, 19: 31461(R) (ANL-7010 (p.235-87))
effects on rectifiers, 18: 39589
effects on reproductive performance of flour beetles (*Tribolium castaneum*), effects of temperature and sex on, 18: 41084(R) (HW-80500(p.147-9))
effects on reproductive capacity of flour beetles, *Tribolium castaneum*, 20: 84
effects on resistance-temperature transducers at low temperatures, 20: 2191
effects on resistivity of tungsten, 19: 44598(R) (GEMP-49A)
effects on resistivity of tungsten, 20: 27582(R) (GEMP-400A, pp 63-98)
effects on response of scintillation gamma spectrometers, 18: 18219
effects on rice, mutagenic, (E), 19: 29930
effects on rice, RBE comparison of gamma radiation and, 20: 36649
effects on rubidium uranyl nitrates, 20: 43365
effects on rupture life of tungsten–25 rhenium sheet, 20: 2422(R) (GEMP-52A, pp 11-21)
effects on rupture life of INOR-8, effects of postirradiation annealing on, 20: 2423(R) (GEMP-52A, pp 27-35)
effects on rupture life of INOR-8, effects of irradiation temperature on, 20: 2423(R) (GEMP-52A, pp 27-35)
effects on rupture life of tungsten, 20: 27409(R) (GEMP-58A)
effects on rupture life of Hastelloy N, effects of irradiation temperature and preirradiation annealing on, 20: 27409(R) (GEMP-58A)
effects on rupture life of tungsten–25 rhenium alloy, 20: 27582(R) (GEMP-400A, pp 63-98)
effects on rupture life of Hastelloy N, effects of welding on, 20: 27584(R) (GEMP-400A, pp 169-84)
effects on rupture strength of type 304 stainless steel, 20: 33961
effects on Santowax WR, 19: 30231(R) (MIT-334-12)
effects on Santowax WR, effects of temperature on, 20: 20723(R) (MIT-334-33)
effects on seedling development in Vicia spp. for fodder, 17: 38691
effects on seeds, 20: 45360 (ORNL-P-2435)
effects on seeds of red clover, Ultuna, genetic, 19: 45882
effects on seeds of tomatoes, genetic, 20: 1638
effects on seeds of wheat, genetic, 20: 1655
effects on seeds of barley, effects of oxygen and moisture on biological, 20: 1667
effects on segregation in nickel–40 copper alloy, 20: 9576(R) (ORNL-3878)
effects on semiconductor detector performance, 19: 11610
effects on semiconductors, radiosensitivity levels for, 20: 16911
effects on semiconducting properties of gallium arsenides, 20: 31617(T),
effects on sexual cells of male mice, 17: 33668
effects on sheep embryos, following prenatal exposure to, 20: 32966(R) (ORO-648, pp 26-35)
effects on sigma phase structure of molybdenum–rhenium alloys, 19: 37051
effects on silica glass, annealing of, (E), 19: 47108
effects on silica gels, x-ray scattering studies on, 20: 19254 (CONF-650629-3)
effects on silicon surface-barrier detectors, 18: 20357
effects on silicon transistor design tradeoffs, 19: 4541
effects on silicon near-infrared absorption bands, 19: 11228(T)
effects on silicon carbide p-n junctions, 19: 16244
effects on silicon-controlled rectifiers, 19: 42774
effects on silicon diodes, 20: 4999(R) (ORNL-2599)
effects on silicon-controlled rectifiers, 20: 9306
effects on silicon near infrared absorption spectra, 20: 34837(T)
effects on single crystals of beryllium oxide, 19: 42919
effects on single crystals of strontium titanate, 20: 29826
effects on sintered beryllia compacts, irradiation temperature effects in, 19: 11782 (ORNL-TM-1011)
effects on sintered aluminum, beryllium, and magnesium oxides at 100 to 1100°C, 20: 27613
effects on slip lines in single-crystal molybdenum, 19: 30822 (BNWL-44)
effects on SNAP electrical devices in high-temperature vacuum, 19: 24880 (BMI-X-10120)
effects on solid lubricant materials, 18: 20585 (WANL-TNR-109)
effects on solid-solid phase transformations under pressure, 20: 33968
effects on solids and liquids, defect formation in, 19: 991 (CEA-R-2510)
effects on sorptive properties of ion exchange materials, 19: 44091
effects on spectra of point defects in silicon, 19: 33513 (AD-611194)
effects on sperm composition in rat testes, 19: 10833
effects on sperm of silkworms, genetic, RBE to gamma, 20: 38626
effects on spleen cells in tissue culture, 17: 31946
effects on spleen colonization by transplanted bone marrow cells in mice, 20: 22707
effects on stability of anthracene oils, 19: 46333 (SGAE-CH-20/1965)
effects on stainless steel types 304 and 347, 19: 2872
effects on stainless steel, 19: 30642(R) (BMI-1707(Del.))
effects on stored energy release in molybdenum, 19: 40961
effects on stored-energy release when annealing molybdenum, 19: 27709(R) (GA-5734)
effects on strength of magnesium oxide crystals, 18: 20595
effects on strength of aluminum–copper and copper single crystals, 18: 26074
effects on strength of EBOR-fueled, beryllia-based fuel elements, 19: 32678(R) (GEMP-48A)
effects on stress corrosion of stainless steels by magnesium chloride, 19: 47079 (AERE-R-5014)
effects on stress rupture of A-286 alloy and Hastelloy X, 20: 5851
effects on stress relaxation in Nimonic 80A, 20: 23791
effects on stress relaxation of Nimonic 80A springs, 20: 31669
effects on stress-rupture properties of A-286 and Rene-41 at 650°C, 18: 32258
effects on stress-rupture properties of INOR-8 at 816°C, 19: 44598(R) (GEMP-49A)
effects on stress-rupture of Zircaloy-2, 20: 746(R) (BNWL-120, pp 6.1-11)
effects on stress-rupture properties of Hastelloy N, 20: 31669
effects on strontium titanate single crystals, 18: 34246
effects on strontium titanates, 19: 11682
effects on structural defects in beryllium oxides, electron microscopy of, 18: 12745
effects on structural materials in OMRE, 18: 35937 (NAA-SR-9796)
effects on structural alloys and metals, review on, 18: 37786
effects on structure of amorphous germanium, 19: 6373
effects on structure of A-286 alloy, electron microscope studies of, 19: 47088 (NMI-4998, pp 95-106)
effects on structure of quenched aluminum, electron microscopic studies on, 20: 9562 (AE-206)
effects on structure of molybdenum, effects of prestrain on, 20: 17132
effects on structure of iron, electron transmission microscopy study of effects of heating on, 20: 23779
effects on structure of plutonia–urania, 20: 29618(R) (GEAP-4982)
effects on structure of pyrolytic carbon, 20: 35862(R) (ORNL-3951, pp 3-83)
effects on superconductivity of niobium stannide (E), 19: 1023
effects on surface homogeneity of graphitized carbon black, 18: 44256
effects on surfaces of silicon planar transistors, effects of annealing on, 20: 27619
effects on survival of 5-bromo-deoxycytidine-treated bone marrow cells, 20: 14333
effects on tantalum hardness, 19: 21690(R) (LA-3244)
effects on temperature of plutonia–urania, effects of diametral gap size on, 20: 29618(R) (GEAP-4982)
effects on tensile properties of reactor casing steels, effects of irradiation temperature on, 18: 8877(T) (EURAEC-816)
effects on tensile properties of tungsten and Zircaloy-2, 18: 18307
effects on tensile properties of type 347 stainless steel pressure tube, effects of annealing on, 18: 20450(R) (BMI-1661(Del.))

effects on tensile properties of aluminum, its alloys, and stainless steels, 18: 28079
effects on tensile properties of alloys, 18: 30238(R) (NP-14102)
effects on tensile properties of type 347 stainless steel, 19: 13871(R) (BMI-1691(Del.))
effects on tensile properties of Zircaloy-2, 19: 14110
effects on tensile properties of Hastelloy N at 500 to 800°C, 19: 26908
effects on tensile properties of aluminum alloy 6061, 19: 28889
effects on tensile properties of Inconel 600–Zircaloy-2 transition joint, 19: 34742(R) (BNWL-79(p.4.1-30))
effects on tensile properties of Incoloy, Inconel, Hastelloy-X, and austenitic stainless steels, 19: 34743 (GEAP-4754)
effects on tensile properties of Nimonic PE16, and chromium–nickel steel, 19: 37185
effects on tensile properties of type 304 stainless steel, 19: 44743 (GEAP-3634)
effects on tensile properties of Incoloy 800, (E), 20: 3471(R) (GEAP-4861)
effects on tensile properties of copper–niobium–zirconium alloy, 20: 2414 (AECL-2272)
effects on tensile properties of hafnium, 20: 5850
effects on tensile properties of SAP 865, 895, and 930, effects of test temperature on, 20: 5838(R) (RISO-110)
effects on tensile properties and tube burst pressure of Zircaloy-2, 20: 9569(R) (BNWL-166, pp 6.1-3)
effects on tensile properties of iron, effects of dose rate on, 20: 9576(R) (ORNL-3878)
effects on tensile properties of type 410 stainless steel, 20: 9576(R) (ORNL-3878)
effects on tensile properties of types 270 and 330 nickel, 20: 9576(R) (ORNL-3878)
effects on tensile properties of aluminum–chromium–iron–yttrium alloys, 20: 9378(R) (GEMP-54A)
effects on tensile properties of iron–chromium–aluminum–yttrium alloys, 20: 13179(R) (GEMP-55A, pp 13-28)
effects on tensile properties of iron and iron–titanium alloys, effects of nitrogen content on, 20: 13324(R) (EURAEC-1529)
effects on tensile properties of aluminum and titanium at cryogenic temperatures, 20: 21427(R) (NASA-CR-54904)
effects on tensile properties of type 347 stainless steel, 20: 23582(R) (BMI-1765)
effects on tensile properties of Incoloy, Inconel, and Zircaloy-2, 20: 23585(R) (GEAP-3771-18)
effects on tensile properties of molybdenum–50 rhenium, effects of annealing temperature on, 20: 27409(R) (GEMP-58A)
effects on tensile properties of structural alloys at 30°R, 20: 27589(R) (NASA-CR-54881)
effects on tensile properties of zirconium–2.5 niobium alloy, 20: 27604
effects on tensile properties of aluminum, titanium, and titanium-base alloy at cryogenic temperatures, 20: 31784(R) (NASA-CR-54976)
effects on tensile properties of type 316L and type 17-4 PH stainless steels, 20: 33960
effects on terphenyls, interpretation of, 20: 1927
effects on terphenyl, 20: 40946 (AECL-2589)
effects on terphenyl coolants, 18: 30988 (NAA-SR-6920)
effects on terphenyls, 18: 33619 (MITNE-48)
effects on testis, effects of dose fractionation, 17: 24967
effects on therapy dosimetry, 18: 37058
effects on thermal conductivity of germanium and silicon, 18: 2319
effects on thermal conductivity of beryllium oxide at 2 to 300°K, 18: 20611
effects on thermal conductivity of germanium single crystals, (E), 19: 13814
effects on thermally activated flow stress in iron, 19: 39242
effects on thermal diffusivity of pyrolytic carbon and graphite, 19: 42900 (BMI-1739)
effects on thermal diffusivity of beryllium oxide–0.5 magnesium oxide, 19: 44599(R) (GEMP-50A)
effects on thermal conductivity of silicon monocrystals at 80 to 300°K, 20: 2487
effects on thermal conductivity of ternary arsenides, 20: 2488
effects on thermal control coatings for spacecraft, 20: 2428 (NASA-SP-55, pp 365-79)
effects on thermal conductivity of germanium, 20: 4466
effects on thermal diffusivity of beryllia, 20: 9378(R) (GEMP-54A)
effects on thermal diffusivity of pyrolytic carbon and pyrolytic graphite, 20: 31667
effects on thermal diffusivity of beryllia, 20: 31667
effects on thermistors at 14 Mev, 19: 26716
effects on thermocouples, 18: 44261
effects on thermoelectric properties of semiconductors, 18: 34237
effects on thermoelectric capacity of germanium at low temperatures, (E), 19: 39240
effects on thymus of mice, tumor induction in, 17: 33450(R) (ANL-6723 (p.44-9))
effects on thyroid function in rats, 19: 38442
effects on tissues, biological, 20: 18548
effects on tissues, mechanism of, 20: 45256
effects on transistors, permanent damage, 16: 9254 (DOFL-TR-975 (Vol.I, Pt.1))
effects on transport properties of germanium, 18: 8884
effects on tree seeds, 17: 33661
effects on *Tribolium castaneum*, genetic, 20: 11184(R) (BNWL-122, pp 137-9)
effects on tumor cell populations, model for, 18: 31242
effects on tumor cell reproductive capacity *in vivo*, dose-response relation in, 16: 17496
effects on tungsten, annealing of, 20: 42551
effects on type 347 stainless steel, 19: 22865(R) (BMI-1711(Del.))
effects on type-II superconductors, 18: 10583
effects on uranium carbides, review on, 18: 12695
effects on variability induction in gibberellin-producing strains of *F. moniliforme*, 20: 32991
effects on variegation in Einkorn wheat, mutagenic, 20: 20497
effects on viability and chromosome aberration in potato seeds, 17: 31938
effects on *Vicia faba*, effects of DNP on recovery from mutagenic, 20: 22670
effects on *Vigna sinensis* seeds, 20: 32969(R) (ORO-648, pp 123-58)
effects on water, LET in, 18: 27497 (WAPD-BT-30(p.53-64))
effects on wear resistance of copper, iron, lead bronze, and steel, 20: 15140
effects on weight of mouse organs, 18: 31199
effects on wheat, seed and seedling exposure, 17: 15748
effects on wheat seeds, mutagenic, 20: 22743
effects on wheat, mutagenic, 17: 39362
effects on wheat, mutagenic, 19: 2161
effects on winter wheat, mutagenic, 18: 33374
effects on x-ray diffraction pattern of beryllia single crystals, 20: 4391(R) (ORNL-3870, pp 75-82)
effects on x-ray diffraction by germanium and silicon, (E), 20: 24612
effects on x-ray low-angle scattering properties of molybdenum, effects of carbon on, 20: 9565(R) (BNWL-166, pp 3.10-14)
effects on yield strength of copper and aluminum-copper, relation to type and density of defects, 18: 18425
effects on yield stress of A-212B steel, effects of postirradiation annealing on, 20: 25619(R) (ORNL-3949)
effects on zinc sulfide, phase transitions induced by, 18: 23665
effects on Zircaloy-2 mechanical properties, 18: 36047 (HW-82102)
effects on Zircaloy-2 pressure tubes in PRTR, 19: 21686 (HW-84540)
effects on Zircaloy-2 PRTR pressure tubes, evaluation of post-, 19: 23120 (BNWL-5)
effects on Zircaloy-2 tubes, 19: 30737(R) (HW-84573(p.6.1-11))
effects on zirconium corrosion by steam, 18: 22152
effects on zirconium alloys, 18: 37668 (A/CONF.28/P/158)
effects on zirconium by hydrofluoric acid, 19: 46957(R) (ORNL-3832, pp 100-6)
effects on 12- to 50-Å precipitated particles in metals, 16: 21106
effects on 347 stainless steel, 19: 46912(R) (BMI-1727(Del.))
effects on 347 stainless steel, 19: 46913(R) (BMI-1733(Del.))
effects with creep on deformation and dimensional changes in graphite, 19: 30837
effects, biological, 16: 17522
embrittlement of type 304 stainless steel, effects of boron additions on, 20: 31669
emission and return fluxes of, in heavy-water reactors, (E), 20: 14070(R) (MIT-2344-4, pp 115-34)
emission from nuclear explosions, dosimetry of, 20: 16760
emission from split-core swimming-pool reactors, 18: 4848 (EANDC(OR)-26U)
emission in deuteron reactions (d,n) with fluorine-19 at 3 Mev, spectra of, 18: 27793
emission in reactions (d,nγ), coincidence methods for, 17: 34864
energies and fluxes around Saclay Proton Synchrotron, scattered, 17: 42009 (CEA-2303)
energy distributions in reactors, 18: 22990
energy of, time-to-pulse-height converter for measuring, 17: 34254
energy of, accuracy of time-of-flight determination of, 18: 41839
energy spectra in ORGEL-type reactors, effects of organic coolant on, 17: 35090 (EUR-305.e)
energy spectra in bare homogeneous reactor with two-component moderator, equations for, (T), 19: 47964
energy spectra of, determination by proton spectra measurements from neutron scattering on polyethylene films, 18: 23883 (NP-13930(p.147-57))
energy spectra of, methods for analyzing, 19: 11532

energy spectra of, performance of lithium-6 semiconductor spectrometer for measuring, 19: 44457 (NP-15475)
energy spectra of, penetrating layers of iron and heavy water, (E/T), 19: 47561
energy spectra of, performance of ionization chambers for determining, 20: 7443
energy spectra of, measurement using europium-activated lithium iodide phosphors, 20: 11116
energy spectrum in Triga Mark II reactor, 18: 1303 (RT/FI(63)-20)
energy spectrum in fast reactors, 500-kev to 3.8-Mev, (E), 20: 34911
energy spectrum measurements, modified standard foil technique for, 16: 14946
fission cross sections and excitation functions for, 17: 34865
flux and heating in SNAP-8DS shielding, calculation of, (T), 20: 12468 (NAA-SR-Memo-9916)
flux calculations with Penelope program, corrections for, 17: 39953(T) (AEC-tr-6061)
flux decay in lead slabs, (E), 20: 2950
flux densities in High Flux Reactor, 19: 45681 (RCN-36)
flux density measurements using activation of P compounds, 20: 39222
flux distribution in atmosphere, 18: 26101
flux distribution in water phantoms, 19: 10861
flux distribution from anisotropic sources, 19: 19095 (WASH-1053)
flux distribution in reactors, activation and threshold detectors for determining, 19: 35711
flux distribution in EBWR shielding, calculations of, 19: 35760 (IEA-85)
flux distribution in in-pile loop (BLO 3), 20: 20722 (EUR-2401.f)
flux distribution in cylindrical rod and slab geometries, computer program for, 20: 28718 (JAERI-1105)
flux distribution measurement, use of semiconductors, 16: 7696
flux distributions of pulsed, in multiplying and non-multiplying uranium systems, 18: 34738
flux distributions in multilayer biological reactor shields, diffusion approximation for, 18: 38283 (A/CONF.28/P/721)
flux distributions in reactors, energy and spatial and spectral, (E/T), 19: 31184 (AP-Note-371)
flux distributions in enriched uranium lattices, (E), 19: 42043(R) (MIT-2344-3, pp 15-36)
flux distributions in light-water moderated reactor, computer program for, 20: 38450
flux evolution in multiplying media (T), 19: 3581
flux evolution in multiplying medium, energy, space, and time dependence of, (T), 20: 21950
flux in annular ducts through laminated iron-heavy water shields, (E/T), 20: 1317
flux in annular uranium fuel elements, 18: 8919(R) (PR-P-59(p.65-78))
flux in atmosphere, detector for measuring, 17: 37911
flux in atmosphere, variations of, 18: 9047 (D1-82-0257)
flux in atmosphere, solar minimum measurements of, 20: 42055
flux in IRT-2000 reactor, measurement of, 19: 22777
flux in LITR and ORR, 19: 22818(R) (ORNL-3650(p.221-38))
flux in LITR and ORR, measurement of, (E), 20: 12501 (ORNL-TM-1163)
flux in moderators, computer program for calculation of Fourier transform of, 20: 46557 (NAA-SR-Memo-11892)
flux measurement at 14 Mev by stilbene scintillator, 19: 28628 (EUR-1815.e(Rev.)(p.246-53))
flux measurement by phosphorus and sulfur activation, 18: 16356
flux measurement by cobalt activation, 16: 8921
flux measurement by aluminum-27(n,α) and magnesium-24(n,p) reactions, 16: 17730
flux measurement in IRT-2000, 20: 28840
flux measurement of, use of sulfur-32 (n,p) reaction for, 17: 9529
flux measurement using indium detector, 19: 42734
flux measurement using metallic foils, 20: 21427(R) (NASA-CR-54904)
flux measurement with large liquid scintillator, method for absolute, 19: 28641
flux measurement with phosphorus–polythene discs, 16: 31845
flux measurement, counter for, 18: 16362
flux measurement, use of nickel and titanium detectors in integral, 19: 26671(T) (CEA-tr-A-1822)
flux measurements in zero-energy reactor by rhodium activation, 17: 29824 (AEEW-R-85)
flux measurements by (n,α) and (n,p) reactions, 17: 30165
flux measurements on, phosphorus–sulfur detectors for absolute, 17: 30872
flux measurements using threshold detectors, 17: 4102
flux measurements, 17: 20237 (CEA-2250)
flux measurements by foil activation, 17: 33325(R) (ORNL-3445(p.251-97))
flux measurements in power reactors, method for integrated, 17: 41119
flux measurements using copper, iron, nickel, and titanium threshold detectors, 18: 30750
flux measurements on, using threshold detectors, 18: 35836 (CRC-1101)
flux measurements in shield of Shippingport Reactor, 18: 43039 (WAPD-PWR-TE-161)
flux measurements for graphite assemblies, 18: 42918 (CEA-R-2548)
flux measurements using sulfur activation, Geiger-Mueller counter calibration for, 19: 24856
flux measurements using iron wires, developments in, 20: 14433(R) (BAW-298)
flux measurements by phosphorus activation, 16: 10219
flux measurements in PM-2 and SM-1 core and vessel mockups, 16: 18646 (APAE-95)
flux monitoring in reactors, method for, 20: 45728
flux monitoring using activation reactions, 18: 19437
flux of, measurement using sulfur threshold detectors, 17: 20349 (NAA-SR-Memo-4365)
flux of monochromatic, thick organic radiators for determining absolute, 20: 39223
flux of, portable instruments for determining average energy of, 17: 20348 (JÜL-90-ST)
flux of solar, at 20 to 160 Mev, (E), 20: 37375
flux of, NMR measurement of, 20: 11169(P)
flux of, quartz and silicon dioxide films for measuring, 20: 16851
flux of, variational procedure for calculating, 17: 38057
flux patterns from a 14-Mev generator, 20: 21946
flux propagation in fast reactors, measurement of long-range, 16: 26531
fluxes and spectra of, threshold detectors for measuring, 19: 34570
fluxes in Engineering Test Reactor, 17: 36969 (IDO-16894)
induction of chromosomal aberrations in *Tradescantia*, effects of dose rate and exposure time on, 16: 1589
interactions at 20 kev to 2 Mev, crossed-beam studies of, 19: 1259
interactions of, effects of energy on, 16: 33574
interactions with alpha particles at 15 Mev, D-wave contribution in, 17: 31326
interactions with deuterons at 14 Mev, cross sections for, 18: 5649
interactions with protons at 630 Mev, total cross sections, (E), 19: 10242 (JINR-P-1824)
interactions with deuterons at 5.635 and 9.035 Mev, cross sections for elastic, (E), 20: 13520
ionization by, in nuclear plasma diodes, 18: 24373
kinetics in subcritical assemblies, pulsed, (T), 20: 14087
leakage from EGCR, analysis of, 17: 17564 (TID-18243)
leakage spectra from lithium hydride slabs, 17: 34830 (CONF-39-65)
lethal radiation dosage determinations for Ehrlich ascites tumor cells, 16: 12906
lithium fluoride thermoluminescent response to, 20: 22853(R) (ANL-7060)
measurement in ETR cycle 27, 17: 15498 (IDO-16728)
measurement of, by reaction with nickel-58, effects of cobalt-58 isomers on, 16: 29753 (IDO-16744)
measurement of, in low intensity regions, 16: 33779 (AEEW-M-269)
measurements of, matrix treatment of spectrometric, 19: 44492
medically used sources of, dose distribution in, 20: 9166(R) (BNWL-36, pp 2.1-58)
moderation of, use of, in moisture determination, 16: 28651(R) (TID-16338)
monitoring at Orsay proton synchrocyclotron, 17: 22704
monitoring in TREAT, hodoscope for, 19: 23991(R) (ANL-7003)
monitoring of, design of transistorized, portable rate meter for, 17: 16468
monitoring of, engineering drawings of device with optional burst detector for, 19: 6211
multiplication factor for, in thermal reactors, 18: 24846 (EUR-1618.e)
multiplication factor in dense reactor grid, (T), 20: 24318
mutagenic effects on Drosophila sperm, 16: 28817
pathological effects in tissues in mice, fractionated and protracted, 16: 26656 (R) (NP-11966(p.1-26))
penetration and scattering of, shielding materials effects on, 20: 18020(R) (ORNL-3900, pp 2-81)
penetration effects in moderators, 16: 21337
penetration in concrete, (E), 20: 38352
penetration in homogeneous medium from disk source, (T), 20: 26335
performance in activation analyses, 20: 3863(R) (IS-1200(Sect. C))
photoproduction on lead and uranium-238, spectra of, (E), 20: 29529(R) (RPI-328-56, pp 94-112)
polarization, 17: 7655(R) (ANL-6600)
polarization by copper and zirconium, measurement as function of scattering angle, 17: 7065
polarization by ice-d_2 and oxygen (liquid), 17: 7064
polarization in precession magnets, 19: 21209
polarization measurements, diffusion cloud chamber for, 17: 32422
polarization measurements on beams of, 17: 32939
polarization of (d,t), using polarized deuterons, 17: 7066
polarization of, energy and geometry corrections in analysis of, 17: 24372 (IFA/A/23)
polarization of, from nuclear reactions, review of, 17: 42000

polarization of, method for measuring, 17: 39958
polarization of, device for measuring, 18: 30039
polarization of, formalism for numerical evaluation of, 20: 19791
polarization of, measurement using parallel-plate avalanche counters, 19: 42765
polarization of, projection discharge chamber for measuring, 19: 30564
polarization of, scintillation counter for determining, 18: 30054
polarization precession, electromagnet for, (E), 19: 37242 (AE-189)
polarization, problems, 16: 2415
production by D-T reaction, 19: 22054
production from cosmic meson (μ) reactions with nuclei at 58 mwe underground, differential energy spectrum from, (E), 20: 37710
production in fission neutron reactions with iron, 18: 40531
production in thermal neutron reactions with lithium deuteride, 17: 41963
production in thermal reactor channels, method for, 19: 21742
production of, design of high yield r-f ion source for, 17: 26397 (PAN-246)
production of, methods for, 17: 34860
production of monoenergetic, in deuteron-tritium reactions, 18: 37817 (NP-14123)
production of polarized, sources for, 19: 19078
production of pure fluxes in IRT Reactor, 16: 24705
production of vacancies in gamma-irradiated sodium chloride by, 17: 11377
production of 14-Mev polarized, generator for, 18: 16902
production of 28-Mev beams of, using D-T reaction, 18: 44711
production of, in 14-Mev generator, 20: 35455
production of, reactor-pulse technique for, 20: 35456
production to 6 Mev, lithium-6 deuteride targets for, 19: 28952 (EUR-1815.e(Rev.)(p.258-62))
propagation of monoenergetic, in oxygen and water, (E), 19: 14462 (EUR-2161.f)
protection against, effects of MEG in mice, 18: 17656
pulsed techniques for subcritical assemblies, 18: 33019 (EUR-593.e)
radiolytic effects on water, separation from gamma effects, 16: 10053
reactions (n,α) with silicon-28 at 13.5 to 14.7 Mev, cross-section oscillations in, 16: 21413
reaction cross sections for reactor materials (E/T), 19: 3476 (IA-980)
reaction cross sections for, MAG program for, (T), 19: 16851 (NAA-SR-Memo-10544)
reaction studies, 17: 4060 (NYO-9765)
reactions (n,α) with silicon at 13.6 to 15 Mev, cross sections for, 18: 16971
reactions (n,α) with nitrogen-14 and oxygen-16, cross sections, 18: 24643
reactions (n,α) with lithium-6 coatings on surface barrier junctions, 18: 29992
reactions (n,α) with copper-63, 18: 30750
reactions (n,α) and (n,p) with argon isotopes, cross sections for, 18: 42670
reactions (n,α) and (n,p), production of radioisotopes of high specific activity by, 19: 2701
reactions (n,α) with beryllium-9, excited states of helium-6 from, (E), 19: 5195
reactions (n,α) with silicon-29, mechanisms for, (E), 19: 14537 (PAN-540/I)
reactions (n,α) with copper-63, cross section for, (E), 19: 16908
reactions (n,α) with lithium-6, absolute measurement of cross sections of, 19: 28641
reactions (n,α) and (n,p) in silicon diodes, neutron spectrum measurements by, 19: 28661
reactions (n,γ) with copper and manganese, gamma spectra from, 18: 24699
reactions (n,γ) with fluorine-19, spectra from resonant, 18: 26541(R) (ORNL-3582(p.68-71))
reactions (n,γ) with nuclei, experimental study of, 18: 38071 (NP-14214)
reactions (n,γ) with nuclei, gamma spectra from, 18: 44807
reactions (n,γ) with uranium-238 at 0.12 to 7.6 Mev, cross sections for, 18: 44763
reactions (n,γ) with gold-197 at 0.12 to 1.8 Mev, cross sections for, 18: 44764
reactions (n,γ) with elements, sensitivity of activation analysis by, 19: 26241
reactions (n,γ) with uranium-238 at 27 to 40 kev, spectrum from, 19: 35400 (ORNL-P-1343)
reactions (n,α) and (n,p) with nuclei, effects on neutron-source calibration by manganous-sulfate-bath method, (E), 20: 8054
reactions (n,α) with calcium-40 at 4.7 Mev, distributions from, (E), 20: 9959(R) (AEET-214)
reactions (n,α), (n,2n), (n,np), (n,p) and (n,t) with nuclei below 20 Mev, excitation functions for, (E/T), 20: 19883
reactions (n,α) with lithium-7 at 14.7 Mev, cross section for hydrogen-4 production in, (E), 20: 34537
reactions (n,α) with chlorine-36, phosphorus-33 production in, (E), 20: 37166
reactions (n,α), (n,2n), (n,p), and (n,t) with nuclei, cross sections for, (E), 20: 40069(R) (EANDC(E)-66(U))
reactions (n,d) and (n,p) with nuclei at 8 to 22 Mev, distributions from, (E), 20: 3012 (IKF-11)
reactions (n,d) with copper-63 and -65, angular distributions from, (E/T), 19: 41755
reactions (n,f) at 0.4 to 4.15 Mev, energy dependence of cross sections for, (E), 19: 45258 (IAE-833)
reactions (n,f) with plutonium-239, thorium-232, uranium-233, uranium-235, and uranium-238, delayed gammas from, 18: 21296
reactions (n,f) with thorium-232 and uranium-235, cross sections for, 18: 40508 (LAMS-774)
reactions (n,f) with thorium-232, uranium-233, -235, -236, and plutonium-239 at 14 Mev, 18: 40509 (LAMS-938)
reactions (n,f) with uranium-235, a statistical properties of, 18: 42720
reactions (n,f) with uranium-235 and -238, delayed neutron yields from, (E), 19: 45300
reactions (n,f) with uranium-235, (E), 20: 19805(R) (ANL-7110, pp 1-28)
reactions (n,f) with uranium at 14 Mev, alpha and fission-fragment angular distributions from, (E), 20: 19861
reactions (n,f) with uranium-235 at 0.36 to 0.65 Mev, cross section for, 20: 19935
reactions (n,f) with uranium-235 at 5, 6, and 7 Mev, mass dependence of total fission-fragment energy in, (E), 20: 42297
reactions (n,γ) with iron-56 at 1148 ev, spectra from, (E), 19: 37807(R) (ORNL-3778(p.64-9))
reactions (n,γ) with rhenium at 20 to 1000 kev, cross sections for, (E), 19: 45298
resctions (n,γ) with uranium-238 at 30 kev, gamma spectra from, (E), 20: 1168
reactions (n,γ) with nickel-64 at 0.2 to 2.0 Mev, cross sections for, (E/T), 20: 4911
reactions (n,γ) with tin-124 at 62 ev, angular distributions from, (E), 20: 6317
reactions (n,γ) with rhenium and tantalum at 30 to 170 kev, cross sections for, (E), 20: 11986
reactions (n,γn') with nuclei, effects on capture and non-elastic spectra, (T), 20: 44614 (CONF-660303, pp 613-22)
reactions (n,γ) with silver-109, Westcott factor for, (E), 20: 46627
reactions (n,n') with rhodium-103 at 14.2 Mev, cross sections for, (E), 20: 34549
reactions (n,nα), (n,2n), and (n,p) with copper-65 at 2 to 20.3 Mev, cross sections for, (E), 20: 40149
reactions (n,n'γ) with nuclei, angular distributions from, 18: 11187 (ANL-6797(p.389-92))
reactions (n,n'γ) and (n,2n) with carbon at 14 Mev, spectrometry of angular distributions from, 18: 24603 (NP-13930(p.51-3))
reactions (n,np) and (n,p) with zinc-64 at 14 Mev, (E), 20: 22048
reactions (n,n'3α) with carbon-12 at 14 Mev, mechanisms for, 18: 40599
reactions (n,p) with aluminum-27 and titanium-46, 18: 13636(R) (ORNL-3537(p.71-105))
reactions (n,p) with nickel-58, burnup corrections in activation, 18: 19438
reactions (n,p) with iron-54, nickel-58, and titanium-46, 18: 30750
reactions (n,p) with copper-65, cross section for and preparation of nickel-65 by, 18: 41897
reactions (n,p) with zinc-67, copper-67 production by, 18: 41532
reactions (n,p) with magnesium, production of carrier-free sodium-24 by, 18: 43675
reactions (n,p) with lead-204, cross sections for, 19: 30126
reactions (n,p) with sulfur-32, cross section for, (E), 19: 35378(R) (EANDC(E)-57(U))
reactions (n,p) with sulfur-33 cross section for, (E), 19: 35378(R) (EANDC(E)-57(U))
reactions (n,p) with titanium-46, cross section for, (E), 19: 35378(R) (EANDC(E)-57(U))
reactions (n,p) with titanium-47, cross section for, (E), 19: 35378(R) (EANDC(E)-57(U))
reactions (n,p) with sulfur-33, cross sections for, (E), 19: 35378(R) (EANDC(E)-57(U))
reactions (n,p) with nickel-58 and titanium-46, flux density determinations, by, 19: 35711
reactions (n,p) with oxygen-16 at 12 to 17 Mev, cross sections, (E), 19: 40163
reactions (n,p) with natural neon at 14 Mev, distributions from, (E), 20: 9960(R) (AEET-228)
reactions (n,p) with titanium-46, -47, and -48, effective cross sections for, (E), 20: 24422
reactions (n,p) with sulfur-33, phosphorus-33 production in, (E), 20: 37166
reactions (n,p) with sulfur-32, neutron dosimetry using, 20: 39228

reactions (n,t) with lithium-6, distributions from, 18: 16965
reactions (n,2n) with antimony-12 and -123, recoil behavior from, 18: 15292
reactions (n,2n) with beryllium-9, cross sections for, 18: 32738 (PWAC-433)
reactions (n,2n) with nickel-58 and ruthenium-96, (E), 19: 27440 (TID-21812)
reactions (n,2n) with nitrogen-14 at 14.1 Mev, cross sections for, (E), 19: 45325
reactions (n,2n) with beryllium-9 at 14.5 Mev, angular correlations and cross sections for, (E), 19: 45252 (CEA-R-2734)
reactions and scattering on thorium-232 and uranium-238 at 1.6 to 7.0 Mev, (E), 19: 14571
reactions at 8.3 Bev, cross sections for, 16: 18537
reactions in emulsions, proton recoil spectra of, 16: 5528
reactions in glass and polymers, density and length distribution of fission tracks from, 18: 37228
reactions in graphite-uranium lattices, Monte Carlo analysis of, 17: 15158 (AEEW-M-286)
reactions in magnesium oxide, F-center production, (E), 20: 37998
reactions in multiplying media, prompt neutron kinetics from modulated and pulsed, (T), 20: 14088
reactions in plexiglass, polyethylene, and water, cross sections and spatial distributions, 16: 17059
reactions in plexiglass, polyethylene, and water, cross sections and spatial distribution for, 16: 22971(T) (JPRS-13609)
reactions in slabs containing uranium-235 and -238, 17: 26795
reactions in water, charged-particle slowing-down spectra from, 20: 1924
reactions (n,α) with carbon-12, spin of 2.4-Mev state and total cross section for 5-Mev excitation in, 17: 22614
reactions (n,α) with carbon-12 at 14.85 Mev, neutron-identification circuit for, 17: 23618
reactions (n,α) and (n,p) with silicon at 6 to 9 Mev, fluctuations in cross sections for, 17: 29613
reactions (n,α), (n,2n), and (n,p) with nuclei, cross sections for, 17: 31056
reactions (n,α) with aluminum-27, angular distribution for, 17: 31493
reactions (n,α) with indium and phosphorus, 17: 7094 (NP-12330(p.46-52))
reactions (n,α) on nuclei, distributions from, 17: 13506
reactions (n,α) and (n,2n) on tellurium isotopes, 17: 19289
reactions (n,α) and (n,p) on silicon, excitation functions, 17: 19295
reactions (n,α) with carbon-12 and oxygen-16 at 5.0 to 8.8 Mev, excitation functions for, 17: 34874 (CONF-13-7)
reactions (n,α) and (n,p) with nuclei ($12 < A < 150$) at 14 to 15 Mev, cross section behavior in, 17: 38162
reactions (n,α) and (n,p) with nuclei, threshold energies for, 18: 2838(R) (EANDC(OR)-23L)
reactions (n,α) and (n,p) with silicon-28 and 29, spectra from, 16: 26306
reactions (n,αγ), (n,2n), and (n,pγ), cross sections for, 17: 34861
reactions (n,γ) with nuclei, review of, 17: 41995
reactions (n,γ) on gold-197, cross sections for, 18: 4537 (EANDC-33U(p.164-7))
reactions (n,n′α) with lithium-7 at 4 to 15 Mev, cross sections for, 17: 34879 (LA-2235)
reactions (n,p) and (n,np) with nickel at 14.1 Mev, cross sections for, 16: 33839
reactions (n,p) on nickel-58, cross sections for, 17: 13502
reactions (n,p) on tin nuclei, cross sections, 17: 19374
reactions (n,p) with molybdenum isotopes, cross sections for, 17: 7101 (NP-12330(p.97-103))
reactions (n,p) with aluminum-27, cross section for, 18: 2845(R) (TID-19657)
reactions (n,t) on lithium-7, cross sections for, 17: 31436
reactions (n,t) on medium nuclei, cross sections for, 17: 31434
reactions (n,2n) and (n,3n) with heavy nuclei, cross sections for, 17: 34971
reactions (n,2n) on nuclei, cross sections, 17: 19344
reactions of, with beryllium nuclei, 16: 33509 (AFSWC-TDR-62-15)
reactions of, kinetic energies of products from fission, 18: 36584
reactions of, research at Hungarian Institute of Nuclear Studies, (E), 19: 33279
reactions on beryllium, cross sections for inelastic, 18: 16966
reactions on bismuth-209, resonances in, 17: 31459
reactions on lead-208, total cross sections for, 16: 33905
reactions on nickel at 175 to 300 kev, total cross sections, 18: 17038
reactions on nuclei, activation cross sections for, 17: 7306
reactions on nuclei at 5 to 20 Mev, excitation functions for, 17: 13497
reactions on nuclei at 14 Mev, alpha distributions from, 17: 13511
reactions on nuclei at 14 Mev, total cross sections for, 17: 36676
reactions on sodium, thorium, and uranium, cross sections for, 18: 16973
reactions on uranium-235 and -238, 18: 4532 (EANDC-33U(p.64-86))
reactions with aluminum, alpha, neutron, and proton spectra from, 17: 7093 (NP-12330(p.39-45))
reactions with aluminum, gamma production in, 18: 13088
reactions with aluminum, iron, and uranium at 1.5 to 5 kev, total cross sections for, (E), 19: 31215(R) (ANL-7010(p.1-19))
reactions with americium-243 at 14 Mev, formation of spontaneously fissioning isomer of americium-242 in, 18: 34759 (JINR-D-1693)
reactions with calcium at 2 to 3 Mev, total cross sections for, (E), 20: 9981 (WASH-1064)
reactions with calcium at 3.5–5.0 Mev, gamma rays from, (E), 20: 10101
reactions with carbon-12 at 630 Mev, total cross section, (E), 19: 10242 (JINR-P-1824)
reactions with carbon-12 at 2.8 to 5 Mev, R-function and optical-potential fitting of cross sections for, 19: 29233 (CONF-650410-1)
reactions with carbon-12 and hydrogen, total cross sections, (E), 19: 37811(R) (ORNL-3778(p.94))
reactions with chlorine, phosphorus, silicon, and sulfur at 3–5 Mev, total cross sections for, 17: 28287
reactions with components in type 347 stainless steel, helium and hydrogen production in, 20: 7490(R) (BMI-1745, Sect.A)
reactions with elements, for activation analysis, 19: 32058(R) (GA-5978)
reactions with elements and compounds at 3 to 15 Mev, removal cross sections, 16: 29739
reactions with fluorine-19 and sodium-23, cross sections, 18: 16969
reactions with fluorine, evidence of direct processes in, 16: 21549
reactions with fused silica, induced crystallinity in, 18: 10599
reactions with gadolinium at 2.4 to 15.7 Mev, total cross sections for, (E), 20: 30419
reactions with germanium crystals, energy levels induced in, 18: 8897(T)
reactions with gold-197, Doppler shifts and resonance integrals in, (E), 20: 4841(NAA-SR-Memo-11511)
reactions with gold and platinum, beta and gamma spectra from, (E), 20: 10107
reactions with gold foils, recoil atoms from, 20: 21441
reactions with graphite, induced dimension changes in, 18: 26095
reactions with granite, seawater, and soils, gamma dose curves from, (T), 19: 46589 (UCRL-14332)
reactions with iron-56 and manganese-55, backscattering from, 19: 3347
reactions with iron and lead in boron carbide at 4 to 14.9 Mev, removal cross sections, 16: 29738
reactions with isotopes for activation analysis, table of data on, 18: 15955 (NP-13761)
reactions with light nuclei, tritium yields from, 19: 47721 (LA-3385)
reactions with lithium-7, triton production in, 17: 34878 (LA-2234(Del.))
reactions with lithium-6 and -7, 18: 15198 (LAMS-2979)
reactions with lithium-drifted silicon detectors, damage effects in, 18: 33913
reactions with matter, mechanism of, 17: 12083
reactions with natural uranium, fission ratios in, (E), 19: 29329
reactions with neptunium-237, cross sections for, 18: 28718
reactions with neptunium, plutonium, and uranium isotopes, fission rates for, (E), 20: 14202
reactions with niobium-93 at 1.7 and 2.1 Mev, differential gamma production cross sections for, (E/T), 20: 30360 (WASH-1068)
reactions with nitrogen-15 at 3.2 to 6.6 Mev, total cross sections for, (E), 20: 9981 (WASH-1064)
reactions with nuclei, angular distributions for, 17: 28240 (BNL-400(Vols.I and II))
reactions with nuclei, optical model theory for, 17: 34852
reactions with nuclei, resonance processes in, 17: 34853
reactions with nuclei, polarization effects in, 17: 34854
reactions with nuclei, statistical-model theory for, 17: 34857
reactions with nuclei, counter techniques in, 17: 41994
reactions with nuclei at 10 to 100 kev, total cross sections of, 18: 4525 (BNL-7349)
reactions with nuclei at 12.5 to 21 Mev, cross sections for, 18: 16970
reactions with nuclei at 14 Mev, systematics of cross sections for, 18: 24601 (NP-13930(p.41-2))
reactions with nuclei, total cross sections for, 18: 26543(R) (ORNL-3582(p.75-82))
reactions with nuclei near 400 Mev, evaporation effects in, 18: 30751
reactions with nuclei, removal cross sections for, 18: 34888
reactions with nuclei at 28 Mev, total cross sections, 18: 44711
reactions with nuclei, resonances in capture and total cross sections for, 19: 1636
reactions with nuclei having $Z < 31$ at 14 Mev, distributions from, (E), 19: 10254 (ORNL-3672)
reactions with nuclei, angular anisotropies from fission, (E/T), 19: 14527 (LA-DC-6673)
reactions with nuclei, measurement of cross sections for, 19: 14529 (MMPP-FRPC-64-2)
reactions with nuclei, scintillation spectrometer for charged-particle emission in, 19: 15894
reactions with nuclei, delayed neutrons from fission, (T), 19: 27436

(NP-14833)
reactions with nuclei, combined R-function and optical-potential fitting formula for cross sections of, 19: 29233 (CONF-650410-1)
reactions with nuclei to 20 Mev, graphs of excitation functions for, 19: 31226 (NP-15018)
reactions with nuclei at 2 to 15 Mev, substructure in giant resonances in total cross sections of, (E), 19: 33239 (HW-SA-3588)
reactions with nuclei, total cross section measurements for, (E), 19: 41723
reactions with nuclei at 50 to 1400 kev, distributions from, (E/T), 20: 8088(T) (ANL-Trans-242)
reactions with nuclei, survey on, 20: 9973 (NP-15816)
reactions with nuclei, cross section corrections for, (T), 20: 9976 (RT/FI(65)30)
reactions with nuclei at 8 to 21 Mev, cross sections for nonelastic, (E), 20: 11985
reactions with nuclei, use in nuclear structure analysis, 20: 12132
reactions with nuclei, cross sections for gamma production in, (E), 20: 24344 (LA-DC-7612)
reactions with nuclei, review of cross section research on, (E/T), 20: 30349 (JAERI-1102)
reactions with nuclei, survey of, 20: 32535
reactions with nuclei for activation analysis, 20: 38838
reactions with nuclei with Z = 11 to 16, total cross sections for, 20: 44743
reactions with organic scintillators, response functions for, 19: 2648
reactions with osmium, production of tungsten-189 in, 20: 10108
reactions with osmium-190 and osmium-192, 20: 10108
reactions with oxygen-16 at 14 Mev, deuteron and proton spectra from, 18: 22890
reactions with oxygen, nitrogen isotope production in, 19: 7607
reactions with oxygen-16 at 1 Mev, R-function and optical-potential fitting of cross sections for, 19: 29233 (CONF-650410-1)
reactions with plutonium-239, cross sections for fission, 18: 4530 (EANDC-33U(p.14-23))
reactions with plutonium-239 and uranium-235 at 0.08 to 1.25 Mev, fission, 18: 36583
reactions with plutonium-239 at 1 kev to 15 Mev, cross section tabulations, (E), 19: 12480 (AWRE-O-79/64)
reactions with plutonium-240 at 1 kev to 15 Mev, cross section tabulations, (E), 19: 12481 (AWRE-O-91/64)
reactions with plutonium-239 at 1 Mev, fission product yields from, (T), 20: 9970 (LA-3383)
reactions with plutonium-241, prompt neutron yields from fission, (E), 20: 17826
reactions with plutonium-239 and uranium-235 and -238 at 1.09, 1.7, and 2.1 Mev, gamma spectra from, (E), 20: 30360 (WASH-1068)
reactions with plutonium-238 and -239, neutron production cross sections for, (E), 20: 36436
reactions with plutonium and uranium isotopes, evaluation of published data on fission cross sections for, 20: 44622 (CONF-660303, pp 796-808)
reactions with praseodymium at 14-Mev, total cross section for, 18: 26577
reactions with reactor fissile, fertile, and structural materials, 16: 26505 (TID-13546)
reactions with rhodium-103, strength functions from, 18: 17032
reactions with selenium at 0.1 to 5 kev, resonances in, 19: 1637
reactions with shielding materials at 350 Mev, evaporation and cascade nucleons from, 18: 3033
reactions with silicon-28 and -29 at 4.6 to 8.5 Mev, 17: 34884 (TID-19047)
reactions with sodium in phantom, 17: 5736
reactions with sulfur, effects of impurities on, 17: 30580 (AERE-M-1244)
reactions with technetium-99 at 14.1 Mev, cross sections for, (E), 19: 45325
reactions with terphenyl, yields in, 20: 7130 (SGAE-CH-23/1965)
reactions with thallium-activated cesium iodide crystals, alpha emission in, 17: 34873 (CONF-13-5)
reactions with thorium-232 at 2.95 and 14.8 Mev, yield of fission fragments $89 \leq A \leq 140$ from, 17: 26467 (TID-18776)
reactions with thorium and uranium, prompt neutrons from, 18: 2838(R) (EANDC(OR)-23L)
reactions with thorium-232 and uranium-235 and -238, Doppler effects in, 18: 18867 (ANL-6792(p.897-912))
reactions with thorium-232, nuclear emulsion for analysis of fission, 18: 23959
reactions with thorium-232 at 2.95 and 14.8 Mev, fission, 18: 38194
reactions with thorium-232, mass yields from fission, 19: 10351
reactions with thorium-230, fission cross sections and fragment angular anisotropies in, (E), 19: 25475(R) (ORNL-TM-1044)
reactions with thorium-232 and uranium-238, fission fragment mass distributions from, (T), 19: 27443(T) (ANL-Trans-149)
reactions with thorium-232 at 1.42 to 14.9 Mev, prompt neutron yields fission, (E), 19: 29266
reactions with thorium-232 at 1.6 to 2.6 Mev, delayed neutrons from fission, (E), 20: 17680 (FEI-26)
reactions with thorium-232, fission fragment angular anisotropy and mass asymmetry from, (E), 20: 17869
reactions with uranium-238 at 13.7 to 14.8 Mev, cross section for fission, 17: 24478
reactions with uranium-238, alpha emission in fission, 17: 7097 (NP-12330(p.71-8))
reactions with uranium-238, neutrons-per-fission from, 17: 36677
reactions with uranium-238, Doppler coefficients for, 18: 18866 (ANL-6792(p.885-95))
reactions with uranium-235, delayed neutron reduced groups for fission, 18: 36552 (LA-3082)
reactions with uranium-238, prompt-neutrons-per-fission from (E), 19: 1617
reactions with uranium-235, Doppler effect in fission, 19: 3388
reactions with uranium-238 at 2 to 5 Mev, cross sections and angular distributions from fission, (E), 19: 10284
reactions with uranium-235 at 4 Mev, anisotropy and asymmetry in fission, (E), 19: 17041
reactions with uranium-235 at 4 Mev, fragment distributions from fission, (E), 19: 16835 (AEET/NP/9)
reactions with uranium-235 at 3 ev to 2 kev, capture/fission ratio for, (E), 19: 23629 (ORNL-3738)
reactions with uranium-235 at 7.5 and 14.8 Mev, prompt neutron yields from fission, (E), 19: 29267
reactions with uranium-233, mass yields from, (E), 19: 35413
reactions with uranium-235 and -238, fission rates for, 19: 41672(R) (MIT-2344-3, pp 5-14)
reactions with uranium-235 in reactor fuels, measurement of fission, (T), 19: 45229 (UJV-1324/65)
reactions with uranium-235 and -238, fission ratios of, (E), 20: 1147 (CRRP-1220)
reactions with uranium-235 at 720 kev, fragment kinetic-energy distributions from, (E), 20: 3110
reactions with uranium-235 and -238, chain, (T), 20: 8037 (JINR-P-2415)
reactions with uranium-238 in sodium-graphite reactors, fast fission factors for, 20: 10272(R) (NAA-SR-9339)
reactions with uranium-235 at 3 Mev, alpha distributions from ternary fission, (E), 20: 9959(R) (AEET-214)
reactions with uranium-238, fine structure in mass distribution of fission fragments from, (E), 20: 12121
reactions with uranium-235 at 100 kev to 2.6 Mev, fission neutron yields from, (E), 20: 17823
reactions with uranium-238 at 1.5 to 15 Mev, delayed neutron yields from fission, (E), 20: 17832
reactions with uranium-235, mass dependence of fission fragment energies from, (E/T), 20: 17868
reactions with uranium-234, cross sections for fission, 17: 7204
reactions with uranium-238, prompt yield in, fission, 18: 32730 (EANDC(OR)-31(L))
reactions with uranium-235 at 3.9 to 6.4 Mev, prompt neutron yields from fission, (E), 19: 31215(R) (ANL-7010(p.1-19))
reactions with uranium-235, fragment angular anisotropy and mass symmetry in fission, 19: 29228(R) (AEET/NP/10)
reactions with uranium-234, angular distribution and cross sections, 16: 29785 (ORNL-3306)
reactions with uranium-235, kinetic energies of fission fragments from, 16: 33802
reactions with various atomic nuclei, gamma spectra from, 16: 2502(T) (AEC-tr-4718)
reactions with yttrium and zirconium, yttrium-90 isomer production in, 16: 3705
reactions with chromium, effects of energy on capture cross sections, 16: 24810
reactivity effects of, spatial dependence of, 18: 40796
reflection and transmission by walls, calculation of, 17: 40218(T) (AEC-tr-6051)
reflection and transmission in carbon, copper, and iron, (E), 19: 23601
reflection by concretes, dose albedo distributions for, (E/T), 20: 2932 (ORNL-3822(Vol.1))
reflection by concretes, dose albedo distributions for, (E/T), 20: 2933 (ORNL-3822(Vol.2))
reflection by concretes, dose albedo distributions for, (E/T), 20: 2934 (ORNL-3822(Vol.3))
reflection by concretes, dose albedo distributions for, (E/T), 20: 2935 (ORNL-3822(Vol.4))
reflection by concretes, dose albedo distributions for, (E/T), 20: 2936 (ORNL-3822(Vol.5))
reflection by concretes, dose albedo distributions for, (E/T), 20: 2937 (ORNL-3822(Vol.6))

reflection by hydrogenous materials, albedo for, 18: 15146 (RRA-M31)
reflection of, angular-dependent albedo for, 18: 2827
relaxation length in hydrogenous material, point kernel analysis, 16: 10937 (DC-60-2-79)
research program in the United Kingdom, 16: 26504
response of organic phosphors to, 16: 3557
scattering at 15.2 Mev, angular distributions from, 17: 852
scattering at 8.1, 11.9, and 14.1 Mev, cross sections for nonelastic, 17: 22609
scattering by air, angular distribution of, 18: 2829
scattering by, aluminum-27 at 1 to 4 Mev, 17: 13509
scattering by aluminum-27 at 2.76 Mev, angular distributions for, 17: 26518
scattering by aluminum, iron, lead, and zirconium at 2 to 14 Mev, elastic cross sections for, 19: 5148
scattering by aluminum, concrete, graphite, lithium hydride, and steel cylinders, (E/T), 19: 17157(R) (ORNL-3714(Vol.I)(p.43-67))
scattering by aluminum and sodium at 0.3 to 1.5 Mev, cross sections for elastic, 19: 31462(R) (ANL-7028)
scattering by aluminum, concrete, graphite, lithium hydride, and steel cylinders, (E/T), 20: 3265
scattering by aluminum-27, beryllium-9, and sodium-23 at 0.3 to 1.5 Mev, cross sections for, 20: 34644
scattering by aluminum, graphite, and steel cylinders, spectra from, (E/T), 20: 38007
scattering by beryllium, methods for calculating, 18: 13051 (NAA-SR-Memo-9214)
scattering by bismuth and carbon, time-of-flight measurement of differential cross sections for, 17: 9295
scattering by bismuth-209 at 2.82 Mev, angular distribution and evaluation of statistical and optical models in, 18: 13123
scattering by bismuth monocrystals, inelastic, (E), 19: 14524 (JINR-P-1847)
scattering by cadmium, indium, and silver at 0.2 to 1.5 Mev, cross sections for elastic, 19: 31462(R) (ANL-7028)
scattering by cadmium-111 at 14.07 to 14.78 Mev, activation cross sections for, (E), 20: 30360 (WASH-1068)
scattering by calcium, elastic, 17: 11593 (PAN-354/I-A)
scattering by calcium, angular distributions, 16: 2418
scattering by carbon-12, polarization in elastic, 17: 11741
scattering by carbon-12 of 14 Mev, angular distributions for elastic and inelastic, 17: 13483 (CEA-2216)
scattering by carbon nuclei, correlations from inelastic, 17: 19372
scattering by carbon-12, excitation of 7.65-Mev level by, 18: 16967
scattering by carbon-12, excited states from inelastic, 18: 16968
scattering by carbon-12, cross sections for elastic, 18: 26547(R) (ORNL-3582(p.93-4))
scattering by carbon-12 at 14 Mev, inelastic, 18: 41830
scattering by carbon-12 and silicon at 14 Mev, 18: 41831
scattering by carbon-12 at 14 Mev, energy levels in, 18: 42628 (CEA-R-2382)
scattering by carbon at 2.8 to 4.7 Mev, asymmetries from, (E), 19: 8456
scattering by closed-shell nuclei at 14 Mev, level density and nuclear temperature from inelastic, 17: 31492
scattering by coal, use in determining constituents, 18: 29579
scattering by coal, inelastic, 20: 39025 (ORO-2980-12)
scattering by cobalt, copper, and zinc at 0.3 to 1.5 Mev, optical model analysis of, 18: 28695
scattering by cobalt and copper, gamma spectra from inelastic, (E), 20: 7414
scattering by copper and zirconium, polarization effects in, 17: 31432
scattering by Coulomb field of nucleus, 18: 15213
scattering by cylinders, intensities of, 18: 2823
scattering by cylinders, dose rates from, 18: 6146(R) (ORNL-3499 (Vol.I)(p.155-9))
scattering by deuterium of, cross sections and Legendre coefficients of angular distribution for, 17: 13488 (NDL-TR-40)
scattering by deuterium, elastic, 18: 16964
scattering by elements, elastic and inelastic, (E/T), 20: 19805(R) (ANL-7110, pp1-28)
scattering by ferromagnetics, spiral, effects of magnetic field on elastic, 19: 5116
scattering by gold, mercury, and thallium at 300 to 1500 kev, cross sections for, (E), 19: 31215(R) (ANL-7010(p.1-19))
scattering by graphite and lithium fluoride, 17: 38038(T) (AEC-tr-5734 (p.222-6))
scattering by heavy weight nuclei at 4.0 to 6.5 Mev, 18: 26671
scattering by helium at 23 Mev, polarization effects in, 18: 44798
scattering by helium-4 at 10 to 700 Mev, polarization from, (E), 20: 1134 (ORNL-P-1604)
scattering by helium-3 at 3.33 to 7.90 Mev, polarization from elastic, (E), 20: 32452
scattering by hydrogen at 22.5 Mev, differential cross sections for, 17: 851
scattering by in-pile fission sources, displacement cross sections, 16: 22964 (CEA-2142)
scattering by iodine-127 at 800 kev, inelastic, 18: 17039
scattering by iron-56 at 0.8 to 4.0 Mev, energy-level excitation in, 17: 13492
scattering by iron, angular distribution for inelastic, 18: 17048
scattering by iron, tantalum, uranium, and zirconium, elastic, (E), 19: 14765(R) (ANL-6977)
scattering by iron, effects of resonance cross section structure on, (E), 19: 25484
scattering by iron at 0.45 to 2.28 Mev, cross sections for elastic and inelastic, (E), 20: 30417
scattering by iron-54 and iron-56 at 2.5 Mev, gamma angular distribution from inelastic, (E), 20: 44813
scattering by lead at 1.5 to 4.2 Mev, elastic differential cross sections for, 17: 26626
scattering by lead-206, -207, and -208 at 3.5 Mev, spectra of, 18: 13112
scattering by lead-208 at 0.7 to 1.9 Mev, 18: 26545(R) (ORNL-3582 (p.86-90))
scattering by lead-208, resonances in, (E), 19: 37763(R) (ORNL-3778 (p.89-92))
scattering by light nuclei at 14 Mev, 18: 11226
scattering by light nuclei in fast reactors, resonance, 16: 26521
scattering by lithium isotopes, cross sections for, (E), 19: 6703
scattering by lithium-6 and -7 at 3.35 and 4.83 Mev, cross sections for, (E), 20: 24343 (LA-DC-7603)
scattering by magnesium at 14 Mev, cross sections for elastic and inelastic, 17: 28275
scattering by magnesium at 2.0 to 5.0 Mev, angular distributions from, 16: 15686
scattering by manganese to 14 Mev, energy spectra of inelastic, (E), 20: 31566
scattering by medium weight nuclei at 4.0 to 6.5 Mev, 18: 26668
scattering by nickel, oxygen, and silicon at 90 kev, angular distributions and cross sections for, 16: 33800
scattering by niobium and zirconium at 0.3 to 1.5 Mev, cross sections for elastic, (E), 19: 31215(R) (ANL-7010(p.1-19))
scattering by niobium-93, gamma rays from inelastic, 20: 27316
scattering by nitrogen-15 at 1 to 12 Mev, cross sections for, (T), 20: 6426
scattering by nuclei at 14 Mev, cross sections for, 17: 15286
scattering by nuclei, measurement of angular distributions of, 17: 41998
scattering by nuclei, excitation functions for inelastic, 17: 34856
scattering by nuclei, gamma detection techniques for inelastic, 17: 34858
scattering by nuclei, techniques for angular distribution measurements from, 17: 34851
scattering by nuclei at 2.5 Mev, cross sections for inelastic, 18: 14851
scattering by nuclei at 13.8 to 14.7 Mev, energy dependence of backward elastic, 18: 38136
scattering by nuclei at 0.3 to 1.5 Mev, differential cross sections for elastic (E), 19: 3381
scattering by nuclei, cross sections, (E/T), 19: 29322
scattering by nuclei, angular distributions from, (E/T), 19: 31252
scattering by nuclei, gamma yields from inelastic, (E), 19: 35406(T) (ANL-Trans-177)
scattering by nuclei, computer program for multiple, 19: 37778
scattering by nuclei at 0.8 to 4.5 Mev, compound-nucleus analysis of, (T), 20: 3021 (ORNL-TM-1238)
scattering by nuclei at 2.8 Mev, gamma spectra from, (E), 20: 8085 (USNRDL-TR-916)
scattering by nuclei, gamma production data for, 20: 15725 (NP-14855)
scattering by nuclei at 3.4 Mev, charge and mass dependence of polarization for elastic, (T), 20: 26207
scattering by nuclei at 4.0 Mev, polarization angular distributions from, (E), 20: 30360 (WASH-1068)
scattering by nuclei at 24 Mev, angular distributions in elastic, 16: 8214
scattering by nuclei at 3.4 to 4.6 Mev, angular distributions, 16: 26507
scattering by oxygen, polarization effects in, 17: 31433
scattering by oxygen-16, cross sections for, 18: 26546(R) (ORNL-3582 (p.90-2))
scattering by oxygen-18 at 2.9 to 4.1 Mev, cross sections (E), 19: 3259
scattering by oxygen-16 at 2 to 4 Mev, resonances in, (E), 19: 37810(R) (ORNL-3778(p.85-8))
scattering by plane and spherical reflectors, back-, 18: 16896 (NP-13720)
scattering by polyethylene and zirconium hydride at 0.238 to 0.570 ev, cross sections for inelastic, (E), 20: 30325(R) (RPI-328-56, pp 113-34)
scattering by sodium-23, direct processes in inelastic, (T), 19: 43310
scattering by square-mound-potential gas, 17: 11607
scattering by sulfur-32 at 4.6 Mev, angular distribution in elastic and inelastic, 17: 5327
scattering by sulfur-32, distributions from inelastic, 18: 16972

scattering by tantalum-181 and tungsten-184, cross sections for inelastic, 17: 11936(R) (ANL-6672)
scattering by tantalum-181 at 0.3 to 1.5 Mev, angular distributions and energy-level excitations in, 17: 32991 (ANL-6727)
scattering by tantalum-181 at 0.3 to 1.5 Mev, spectra from, (E), 19: 31215(R) (ANL-7010(p.1-19))
scattering by thorium and uranium at 3.5 to 13.5 Mev, angular distributions and cross sections, 16: 33801
scattering by tungsten-184, 17: 19720 (ANL-6698)
scattering by tungsten-184, level excitation in, 17: 36669 (WASH-1042)
scattering by tungsten-184 at 0.3 to 1.5 Mev, cross sections for, 17: 38147
scattering by tungsten-184 at 0.3 to 1.5 Mev, differential cross sections for, (E), 19: 31215(R) (ANL-7010(p.1-19))
scattering by uranium-235 and uranium-238, elastic, 17: 3764
scattering by uranium, cross sections for elastic, 17: 17159
scattering by uranium at 0.3 to 1.5 Mev, cross sections for elastic and inelastic, 18: 2876
scattering by uranium-235 at 0.3 to 1.5 Mev, differential cross section for elastic, 18: 11240
scattering by uranium-238 at 0.05 to 15 Mev, rotational-optical model analysis of, 18: 38133
scattering by uranium at 0.57 Mev, electric polarizability from elastic, (E), 19: 12576
scattering by uranium and uranium-235 at 0.3 to 1.5 Mev, elastic and inelastic, (E), 19: 31215(R) (ANL-7010(p.1-19))
scattering by uranium at 0.83 Mev, cross sections and polarization from, (E), 20: 13868
scattering by uranium-235 at 0.4 to 0.6 Mev, cross sections for elastic, (E), 20: 19935
scattering by uranium-238 at 75 to 1620 kev, excitation functions and differential cross sections for, (E), 20: 22056
scattering by vanadium, phonon frequency distribution from, 19: 20553 (KFK-262)
scattering from aluminum, graphite, and steel cylinders, Monte Carlo calculations for, (E), 19: 35349 (ORNL-TM-1156)
scattering in boron-10 glass phosphors at 1 to 500 kev, Monte Carlo methods for studying multiple, (E), 20: 43700
scattering in fast reactors, evaporation formula for inelastic, 18: 38307 (A/CONF.28/P/511)
scattering in rectangular concrete ducts, (E/T), 20: 6519(R) (ORNL-3858(Vol.1), pp 20-41)
scattering in underground concrete structures, methods for calculating, (E/T), 20: 1307 (RRA-M45)
scattering in underground concrete structures, calculations for, (E/T), 20: 1308 (RRA-T41)
scattering in underground concrete and iron structures, methods for calculating, (E/T), 20: 1310 (RRA-T51)
scattering of, by tungsten, 16: 33974(R) (ANL-6610)
scattering of, collective nuclear energy levels from inelastic, 17: 848
scattering of, equipment for measuring, 17: 10240(R) (NP-12208)
scattering of, for moisture content determination in building materials, 17: 34206
scattering of, inelastic, 17: 38138
scattering of polarized, at 1.95 Mev, 18: 30816
scattering of, resonance phenomena in, review on, 17: 41999
scattering of 14-Mev, cross sections for nonelastic, 17: 7096 (NP-12330 (p.66-70))
scattering of 84-Mev, semiclassical optical model for, 17: 7266
scattering of, measurement of moisture content of crude ores by elastic, 18: 35910
scattering of, studies of condensed state of matter by, 18: 15312
scattering of, use for differentiating fresh water and petroleum, 19: 4082
scattering on tungsten, lead, bismuth, thorium, and uranium, angular distribution of elastic, 17: 17097
scattering probabilities for multigroup reactor analysis, calculation of inelastic, 19: 37768 (WCAP-3269-34)
scattering rate in beryllium oxide–thorium–uranium oxide, elastic, 17: 41481 (AAEC/TM-213)
scattering resonances in fast reactors, computer program for, 18: 24811 (ANL-6805)
scattering theory, 17: 35079(R) (ANL-6749)
shielding design for, Monte Carlo computer program for, (T), 19: 12725 (WAPD-TM-481)
shielding for, in diffraction experiments, 17: 38043(T) (AEC-tr-5734 (p.251-4))
shielding of, development of materials for, 20: 35570(R) (MLM-1299, pp 17-21)
shielding of, energy-dependent removal cross sections in, (T), 19: 35347 (AE-184)
shielding point sources of, by air and concrete, (T), 19: 25616 (ORNL-TM-973)
shielding relativistic, 16: 7188
shielding relativistic, 16: 23166(T) (UCRL-Trans-842)
slowdown of, elastic, 18: 40495
slowing down by hydrogen, moisture determination in wood by, 19: 17846
slowing down density at 1.44 ev, 16: 2471(T) (AEC-tr-4691)
slowing down in graphite and water without polarization loss, (T), 20: 1134 (ORNL-P-1604)
slowing down in homogeneous water assemblies, numerical analysis of, (E), 19: 19095 (WASH-1053)
slowing-down in hydrogenous moderators, 17: 26068
slowing down in water and water-steel combinations, experiment for, 18: 30949 (NYO-9077)
slowing down of, solutions for equations for, 17: 32983
slowing down times for 14-Mev, (E), 19: 19095 (WASH-1053)
slowing-down of radium–beryllium, in water, 18: 44710
slowing-down time in water to cadmium edge, 18: 21148
sources for chronic exposure of mice, dosimetry, 20: 40504(R) (ORNL-3922, pp 146-60)
sources of, for radiotherapy, 17: 35381
spatial distribution in iron, 16: 2623
spectra and fast-fission effect in thermal uranium–water reactors, 20: 22506
spectra and multigroup constant calculations for, computer program for, 17: 41844 (GA-4265)
spectra at exit of channel B of Yugoslavian RA reactor at 2 Mw, 19: 24181
spectra behind laminated heavy-water–iron shielding, (E), 19: 29457
spectra from radium–beryllium sources, (E), 19: 5119
spectra in AFRRI TRIGA, 20: 40454 (AD-636542)
spectra in depleted uranium, pulsed-source measurements of, (E/T), 20: 14202
spectra in homogeneous hydrogen-containing medium, methods for determining, 16: 22972
spectra in lead sphere with graphite shell, (E/T), 19: 29546
spectra in liquid hydrogen, (E), 20: 2967
spectra in liquid hydrogen, 20: 24303(R) (GA-6897)
spectra in MERLIN, measurement of, 17: 35183
spectra in paraffin, (E/T), 20: 3257
spectra in polyethylene, 17: 39957
spectra in reactors, computer analysis of, (T), 19: 12762 (WCAP-3269-26)
spectra in reactors, methods for calculating, 19: 27412
spectra in reactor shields of concrete and water, (E/T), 20: 1318
spectra in reactors, computer program for interpretation of activation measurements of, 20: 35745 (EUR-2985.e)
spectra in Russian BR-5, 16: 26204(T) (AEC-tr-5217)
spectra in sodium and uranium, (E), 19: 33232
spectra in Triga Mark-II, (T), 20: 12505
spectra in tungsten, Doppler effects on, 20: 34905 (GA-7059)
spectra in VERA core, proportional detector for measuring, 18: 37507 (AWRE-NR-2/64)
spectra in water, 19: 23996(R) (ORNL-3650(p.1-110))
spectra in water, pulsed-neutron measurement of, 18: 22848(R) (GA-4659)
spectra in ZPR-VI assembly 4Z, 19: 40113(R) (ANL-7071)
spectra inside human phantoms, 19: 18269 (UCRL-11599(Rev.))
spectra measurements in IRR-1 core, 17: 35253(R) (IA-775)
spectra measurements, nuclear emulsion technique, 16: 22327 (NARF-61-36T)
spectra of, counting efficiency method for studying, 17: 8646
spectra of fission-produced, near 14 Mev, 18: 2838(R) (EANDC(OR)-23L)
spectra of from lithium hydride-water slabs, 19: 23996(R) (ORNL-3650(p.1-110))
spectra of, from Tower Shielding Reactor II, 18: 6526(R) (ORNL-3499 (Vol.I)(p.105-8))
spectra of, in Bulk Shielding Reactor core and shielding, 18: 6525(R) (ORNL-3499(Vol.I)(p.98-105))
spectra of in-core uncollimated, 18: 44926(R) (ANL-6923(p.46-78))
spectra of in-core, (E), 19: 31460(R) (ANL-7010(p.179-233))
spectra of, measurement, 17: 4225(R) (ANL-6635(p.28-50))
spectra of, measurement using the lithium-6(n,t)helium-4 reaction, 17: 8661
spectra of, method of threshold-foil measurement for, 17: 26038
spectra of, method for measuring, 17: 16438
spectra of, methods of measuring, 17: 8645
spectra of region-dependent, computer program for, 20: 46966(R) (NAA-SR-12010)
spectra of thermal-neutron-induced, in natural uranium, 16: 21338
spectra of, activation methods for determining, 19: 46763 (RCN-37)
spectra of, calculation of differential, 20: 4256
spectra of, ionization chamber for measuring, 18: 31951
spectra of, measurement using time-of-flight spectrometer, 18: 14275
spectra of, measuring using threshold detectors, (E), 19: 39007
spectra of, measurement program for, (E), 20: 46561(R) (RPI-328-68,

pp 63-83)
spectra of, nuclear emulsions for measuring, 19: 20374
spectra of, recoil spectrometers for analyzing, 18: 20365
spectrometer design for, time-of-flight, 16: 22355
spectrometer for, design of isochronous flight-path, 17: 30797 (CONF-22-12)
spectrometer for, organic scintillator, 17: 41120
spectrometer for, time-of-flight, 19: 18273
spectroscopy by threshold-detector method at 2.5 to 30 Mev, (E), 19: 14469 (UCRL-11760)
spectroscopy of, activation methods for, 17: 10139
spectroscopy of, apparatus for high-energy time-dependent, 20: 25437(P)
spectroscopy of, emulsion and junction detectors for, 18: 23960
spectroscopy of, instruments for, (E), 19: 22686 (CEA-R-2405)
spectroscopy of, produced by bremsstrahlung in lead, (E), 19: 25455 (ORNL-TM-1087)
spectroscopy of, performance of nuclear emulsions for, 20: 29848 (CONF-651109, pp 199-212)
spectroscopy of, scintillation spectrometer efficiency for, 19: 13731 (NP-14722)
spectroscopy of, scintillation method for, 20: 19790
spectroscopy using emulsion, recoil, and threshold detectors, (E), 19: 22695 (IEA-83)
spectrum calculation from threshold detector measurements, methods for, 19: 12754
spectrum determination from activation measurement, least-square matrix method for, 19: 23618
spectrum in depleted and 93%-enriched uranium, 20: 34905 (GA-7059)
spectrum measurements in swimming pool reactors using activation detectors, 18: 43971
thermalization by water in concretes and soils, uses for water determinations, 18: 41600
thermalization in paraffin, from 15.9 Mev, 18: 24578
thermalization in moderating nonmultiplying media, theory, 16: 9422
thermalization of pulsed, variational techniques for, 19: 29206
thermalization, time dependent behavior for space independent, 16: 18413
time-of-flight measurement for, design of spectrometer for, 16: 33153 (PAN-324/I-A)
transmission by concrete bricks, paraffin, and wood at 4.5 and 14.5 Mev, 19: 1812(R) (HW-81746(p.2.36-8))
transmission by polythene and steel, 18: 28547
transmission of, along air-filled ducts in water, 16: 33971 (AEEW-R-69)
transmission through lithium hydride, 17: 12779(R) (ORNL-3360(p.105-11))
transmission through lithium hydride, angular distribution of, 17: 12780(R) (ORNL-3360(p.111-21))
transmission through shielding slabs, analysis of, 17: 39948 (NARF-63-5T)
transmission through borated polyethylene and lead slabs, 18: 13177 (NARF-62-16T)
transmission through lithium hydride slabs, 19: 12724 (NAA-SR-Memo-10584)
transmission through ducts in heavy-water–iron shielding, (T), 19: 12723 (AE-166)
transmission through ducts in concretes, (E/T), 19: 23939 (NP-14882)
transmission through aluminum, paraffin, and water, energy spectra from, (E), 20: 12268
transmission through lithium hydride shields, (E), 20: 46928(R) (ORNL-3973(Vol.1), pp 26-47)
transport calculations for beryllium-reflected cermet reactor cores, 18: 28088(R) (HW-80284(p.10.1-28))
transport equation for, asymptotic solution of one-velocity, 18: 11144 (CONF-187-50)
transport equation for, solution of, 19: 29179 (RT/FIMA(64)-2)
transport equation in multidimensional geometries, angle-space synthesis method for, 20: 40360 (WAPD-T-1890)
transport in air, ground, and shielding, studies in HENRE Operation, (E), 19: 21199 (CEX-65.02)
transport in air, Sn-method for calculating, 20: 6261 (LA-3415)
transport in aluminum, carbon, and polyethylene, Monte-Carlo study of, 19: 27396 (RRA-T47)
transport in graphite and water, (E), 20: 8035 (GA-5798)
transport in hydrogenous slabs, Monte Carlo calculations of, 17: 34843
transport in liquid hydrogen and water at 0.5 to 15 Mev, spectra of, (E), 19: 27386 (GA-5750)
transport in multiplying media, modulated and pulsed experiments on, (T), 20: 13723
transport in nonmoderating media, P_n analysis of, 18: 7664 (TID-19909)
transport in nonmultiplying media, pulsed, (E/T), 20: 13719
transport in steel and uranium blocks, 18: 26521
transport in water slabs, leakage spectra for, 18: 6143(R) (ORNL-3499(Vol.I)(p.108-15))
transport in water, 18: 40735 (EUR-1643.e(p.87-108))
transport in water (E/T), 19: 3223
transport theory for, few-group constants for, 18: 42597 (TID-7050 (p.229-76))
transport through iron slabs, 16: 5917 (BRL-Memo-1374)
tumor induction in mice by, combined with γ rays, 20: 45417
use for radiotherapy, cellular biology and physics of, 19: 9007
use in activation analysis of meteorites for oxygen and silicon, 19: 43927 (CONF-650405-16)
use in activation determination of light elements, 20: 35390 (CEA-R-2965)
use in activation analysis, parameters for, 17: 6026
use in chlorine well logging, 20: 25316(P)
use in determination of oxygen in meteorites, 19: 30125
use in determining liquid level in containers, 18: 5597(P)
use in determining moisture content of solids, 18: 8303
use in diagnostic radiography, 19: 7228
use in exponential experiments, theory for, 18: 26877
use in nondestructive testing of steel for oxide inclusions, 19: 11379(P)
use in radiography of large masses, 17: 10189 (AD-275297(p.112-15))
use in radiography, advantages of, 20: 667
use in radiotherapy, 20: 10736
use in therapy, 19: 4033
use in therapy, 19: 42400
use in therapy, 18: 11934
use in therapy, effect of dose fractionation on, 18: 9944
use in therapy, evaluation of, 18: 41299
use in therapy, evaluation of, 18: 41226
use of reactor-produced, in activation analysis, 18: 43371(R) (GA-5073)
use of reactor-produced, in activation analysis, 19: 32058(R) (GA-5978)
uses for determining nuclear radii of tin isotopes, 18: 26538(R) (ORNL-3582(p.56-7))
uses in activation analysis of lunar surfaces, 17: 16894
uses in defectoscopy and for thickness measurements on heavy metals, 20: 25454
uses in well logging, 19: 7722(P)

NEUTRONS, FISSION

absorption by mice, phantom study, 20: 5286 (CONF-650616-16)
absorption by mice, phantom studies of depth-dose relations in, 20: 5286 (CONF-650616-16)
age and distribution moments in graphite, 18: 981 (NAA-SR-Memo-8684)
age in aluminum–water mixtures, 20: 9379(R) (NAA-SR-11650, Sect.4)
age in water, effects of spin polarization on, 20: 30329
age measurements for aluminum- and iron-water systems, 20: 8316(R) (NAA-SR-11450, Sect.7)
age to indium resonance in water, 18: 2800
age-to-indium resonance in water, 18: 4514 (NAA-SR-8621)
age to indium resonance in graphite, point source technique for, 18: 28529 (NAA-SR-8683)
age to indium resonance in water (E), 19: 1532
age to indium resonance in water, computer analysis, (E), 19: 6620 (NAA-SR-Memo-8662)
age to indium resonance in arbitrary nuclide mixtures, (T), 19: 10221 (GNE/PHYS/64-7)
age to indium resonance in iron-water mixtures, calculation of, 19: 12865(R) (NAA-SR-10501)
age to indium resonance in aluminum–water systems, (E), 20: 2970
age to indium resonance energy in iron-water mixtures, (E), 20: 17659
age to indium resonance in water-moderated thorium lattices, (E), 20: 34973
age to resonance in concrete, (E), 20: 3255
age-to-indium resonance in water–zirconium mixtures, 18: 40476 (NAA-SR-9503)
age-to-indium resonance in zirconium–water mixtures, 18: 44708 (NAA-SR-Memo-9965)
age-to-indium resonance energy in iron–water systems (E), 19: 3532
ages in moderators, tables on, (E/T), 19: 29260 (TID-21744)
ages to indium resonance in water–zirconium systems, 18: 28555
attenuation by iron–water mixtures, 18: 40739
attenuation by lithium hydride shields, 18: 40736 (NAA-SR-9364)
attenuation kernel in hydrogen, computer analysis of, (T), 19: 35352 (TIM-792)
capture by tungsten-184, (E), 20: 46784
capture in media near underground explosions, radioactivity from, (T), 19: 679 (HNS-1229-54)
decay of high-altitude explosion, artificial radiation belts from, 20: 24226
detection and measurement of, spectrometer for, 18: 20384
detection and measurement from californium-252 and curium-244, design of boron trifluoride proportional counter for, 20: 46039 (DP-1035)
detection of, system for, 20: 46553 (EANDC(UK)-3)
distribution along straight cylindrical ducts in water, (E), 20: 38351
distribution in cylindrical tissue-equivalent phantom, 19: 3821 (ORNL-P-655)

distributions from thermal neutron fission of uranium-235, 18: 24697
distributions in iron and water, 19: 31435
distributions of, computer program for, energy, spatial, and velocity, 19: 39767 (ORNL-TM-1192)
dosage determinations for mice, lethal, 17: 37138 (LADC-5747)
dosimetry in mouse phantoms, 20: 41268(R) (NYO-2740-3, pp 5-165)
effects in mouse oöcytes, genetic, 19: 43789
effects in mouse spermatogonia, genetic, 19: 43789
effects in silkworm gonads, genetic, 19: 43786
effects on austenitic and nickel-base steels, 19: 7996
effects on batteries, hardening against, 20: 21162
effects on blood picture in man, 17: 23175
effects on copper and zinc content and enzyme activity in blood of mammals, 20: 16222 (AFWL-TR-65-112)
effects on dogs and sheep, 18: 41222
effects on dogs, induction of intrapulmonary hemorrhage in, 18: 41223
effects on ductility of stainless steel, 20: 17141
effects on elongation, stress, and work hardening in low-alloy and mild steels, 19: 4726
effects on goats, pathological, 20: 38629
effects on growth and mutations in Triticum, 20: 31080
effects on hematopoietic system in sheep, 20: 38637
effects on *Hibiscus esculentus* and *Vigna sinensis* seeds, effects of environment on, 20: 32969(R) (ORO-648, pp 123-58)
effects on intestines in rats, use of polyvinylpyrrolidone leakage for measurement of, 19: 10891
effects on mice, 17: 37138 (LADC-5747)
effects on mice, biological, 20: 33055
effects on mice, pathological, 20: 42833(R) (ANL-7136, pp 16-46)
effects on mice, pathological, 18: 41224
effects on microstructure of silicon transistors, energy dependence of, 20: 29579 (NAA-SR-11887)
effects on mouse lethality compared with gamma rays, 18: 19576
effects on mouse oocytes, effects of time on mutagenic, 19: 31791(R) (ORNL-3768(p.89-93))
effects on mouse offspring, effects of time between irradiation and conception on frequency of mutagenic, 20: 18368
effects on photoconductivity of germanium at 4.2°K, (E), 19: 23129
effects on rat reproduction, 20: 10601(R) (BNWL-122, pp 135-6)
effects on rats, co-carcinogenic with 2,7-diacetylaminofluorene, 20: 42840(R) (ANL-7136, pp 164-90)
effects on rice, wheat, and other plants, genetic, 20: 26655(R) (NP-15975)
effects on seeds, species differences in, 19: 45817(R) (ORO-631, pp 145-71)
effects on silkworm gonial cells, mutagenic, 19: 45883
effects on structure and properties of copper and iron, 18: 18307
effects on thermal conductivity of germanium, 19: 1014
emission in thermal fission of plutonium-239, uranium-233 and 235, energy spectra of, 17: 26394 (LAMS-2883)
emission of di- and tetra-, 17: 31073(R) (ANL-6719)
emission of, rate and yields for, (T), 20: 6313
emission probabilities, energy spectra, and number distribution widths for, in fast reactions, 17: 34865
energy spectra of californium-252, plutonium-239, and uranium-235, (E), 19: 29269
energy spectra of uranium-235 and -238 and plutonium-239, (E), 19: 35440
energy spectra of uranium-235, method for calculating, (T), 19: 43270 (IA-1007)
flux distributions from point source in water, transfusion-method computer calculation of thermal, 18: 36555 (ORNL-3487)
flux measurements on, using threshold detectors, 18: 35836 (CRC-1101)
fluxes in graphite, diffusion theory calculations of, 17: 41847(T) (AEC-tr-6095)
lifetime to 1.46-ev indium resonance energy in aluminum–water mixtures, (E), 20: 46568
measurement of effective delayed neutron fraction-prompt neutron lifetime ratio, (E/T), 20: 28238
multiplication factor in beryllium oxide, 18: 13035
multiplication in beryllium in spherical geometry, 18: 13240
number of, calculation from fission-fragment mass distribution, 16: 32360 (IA-757)
production of high-intensity pulsed beams of, conference on, 20: 6256 (CONF-650217)
production of in fission of nuclei, formula for average number from, 17: 33016
production of, design of source for, (E), 19: 8377 (ORNL-TM-987)
reactions (n,γ) and (n,2n) with tungsten-186, (E), 20: 46784
reactions (n,p) with praseodymium-141, cerium-141 production by, 20: 34614
reactions (n,2n) with nuclei, cross sections, 19: 29319
reactions (n,p) with cobalt-59, cross sections for, 17: 28292
reactions with iron, threshold detector determination of fast neutron spectra from, 18: 40531
reactions with plutonium-239, fragment activity and gamma spectra from, (T), 20: 36181 (USNRDL-TR-1009)
reactions with uranium-233, mass yields from fission, 19: 436 (USNRDL-TR-769)
reactions with uranium-235, fragment activity and gamma spectra from, (T), 20: 36181 (USNRDL-TR-1009)
reactions with uranium-233, fragment activity and gamma spectra from, 20: 36181 (USNRDL-TR-1009)
reactions with uranium-238, fragment activity and gamma spectra from, (T), 20: 36181 (USNRDL-TR-1009)
reactivity worth in fast reactors, 16: 24398
reflection by hydrogenous materials, albedo for, 18: 15146 (RRA-M31)
shielding point sources of, by air and concrete, (T), 19: 25616 (ORNL-TM-973)
slowing down in carbon, collision density with elastic and inelastic scattering, 18: 4518
slowing-down in graphite and sodium, 17: 41845(T) (AEC-tr-6092)
slowing down in metals and moderators, measurement of, 19: 27735(R) (NAA-SR-10850)
slowing down in water, comparisons of calculations and measurements, 18: 15153
slowing down in water, spin polarization effects on, (T), 20: 2969
slowing down of, moments for, 17: 39950(T) (AEC-tr-6040)
slowing-down density distribution in iron-water mixtures at indium resonance energy, Monte Carlo code for, 20: 17660
slowing-down in iron–water systems, to indium resonance, (E/T), 19: 31193 (NAA-SR-Memo-10918)
slowing-down spectra in beryllium and beryllium oxide, 18: 24576
spectra in rectangular cells, Monte Carlo computer program for, 18: 42576 (AERE-R-4553)
spectra of low-energy, measurement of, 20: 19018(R) (ANL-7110, pp 231-310)
spectra of uranium-235, in concrete, (E/T), 20: 34794
spectra of, angular and energy, (T), 19: 33356
spectrometric calibration of, by nuclear emulsions, 18: 16358
spectroscopy using semiconductor sandwich detectors, (E), 20: 4238 (EUR-2487.e)
transmission by liquid hydrogen slab, computer programs for, 18: 13029 (D2-4643-2)
transport in semi-infinite media, P_1 approximation treatment of, 17: 39955(T) (AEC-tr-6070)
yield from fissionable materials, determination of mean number of, 17: 35253(R) (IA-775)
yields from californium, plutonium, and uranium isotopes, (E), 20: 17823
yields from californium, plutonium, and uranium isotopes, use of boron pile for measuring, 20: 46554 (EANDC(UK)-52-S)
yields from plutonium-239, uranium-233 and -235 fission fragments, (E), 20: 9998
yields from plutonium-239, uranium-233, and uranium-235, (E), 20: 15718 (IDO-17083)
yields in radium-226 proton fission, fragment mass dependence of, (E), 20: 28430
yields per fission from nuclei ($238 \leq A \leq 252$), 18: 18863 (ANL-6792(p.11-27))
yields per fission of nuclei ($232 \leq A \leq 239$), 18: 18864 (ANL-6792 (p.29-50))

NEUTRONS, FUSION

capture in media near underground explosions, radioactivity from, (T), 19: 679 (HNS-1229-54)
moderation in fused-salt–graphite systems, (E/T), 19: 29428
production in dense plasma, (E), 19: 33407(R) (LA-3320(p.19-23))
reactions with uranium-238, fragment activity and gamma spectra from, (T), 20: 36181 (USNRDL-TR-1009)

NEUTRONS, PROMPT

angular correlations between fission fragments and, methods for, 20: 3025
angular distributions and velocities from californium-252 fission, 16: 26320 (UCRL-9713(Rev.))
attenuation by concrete, 16: 25415 (ORNL-3309)
attenuation by concrete, 16: 29212 (ORNL-TM-346)
attenuation in zero-power reactor Anna, (E), 19: 33671
decay constant for, in aqueous uranyl nitrate, 18: 6140(R) (ORNL-3499(Vol.I)(p.57-8))
decay constant for, in multiplying media, 18: 15147 (TID-20170)
decay constant in hydrogen-moderated enriched uranium, 18: 5967(R) (ORNL-3499(Vol.I)(p.49-50))
decay constant in ZPR-VI, 19: 3538
decay constant in uranium cylinders with stainless steel reflectors, (E), 20: 36440
decay constant of, 17: 4339 (TID-17270)
decay constants for, method for measurement of, 20: 30848
decay constants in uranium critical assemblies, 17: 15069 (ORNL-TM-

470)
decay constants in reactor assemblies, method of measuring, 18: 15482
decay constants in solid-moderated, enriched uranium subcritical assemblies (E), 19: 3560
decay constants in plutonium critical assemblies, (E), 19: 33220
decay constants in solid-moderated, enriched uranium subcritical assemblies, 19: 42051 (UCRL-12013)
decay constants of, in far-subcritical assemblies, 17: 4045
decay constants of, prediction by point-model kinetic theory, 20: 30862
decay in bare reactors, effects of floor-reflected neutrons on Rossi-α measurement of, (E), 19: 33565 (ORNL-P-140)
decay in enriched uranium cylinders with gaps, 18: 5971(R) (ORNL-3499 (Vol.I)(p.64-7))
decay in fully-enriched assemblies, 17: 26069
decay in heavy-water subcritical assemblies, 17: 31692
decay in plutonium-water assembly, probability method for, 19: 3508 (CEA-R-2454)
decay in reactors, Monte Carlo method for analysis of, 19: 42039 (BNWL-95, pp 36-9)
decay in slightly enriched lattices, pulsed-source technique for measuring, (E), 20: 14076
decay in VERA, pulsed-source measurements of, (E), 20: 14089
decay rates in reflected reactors, spatial dependence of, (E), 19: 29530
detection of, measurement of power reactivity from probabilities for, 18: 9705
detection probability of, Rossi-α experiment for, (T), 20: 1419
diffusion theory of, nonlinear kinetics in multigroup, 18: 2831
distributions from neutron-induced and spontaneous fission, 18: 21197 (KR-64(Sect.XVIII))
effects on energy-release calculations in reactor meltdown, 17: 19553 (APDA-150)
effects on sheep, 18: 31228
emission by fission fragments, 18: 19837(R) (MIT-905-1)
emission by fission fragments, intensity of, 19: 23665
emission by uranium-233 fission fragments, 17: 33089
emission from uranium-235 fission fragments, (E), 20: 17824
emission in californium-252 spontaneous fission, statistics of, 18: 24651
emission in fast fission of uranium-238, yields of (E), 19: 1617
emission in fission of heavy nuclei, (T), 19: 19129
emission in fission of uranium-235, (E), 19: 31248
emission in neutron fission, (E), 19: 16926
emission in neutron-induced fission, review on, 19: 29253 (LA-DC-6675)
emission in spontaneous fission of californium-252, (E), 20: 39470(R) (ORNL-3924)
emission in thermal fission of uranium-235, energy distributions of, 17: 26585
emission in thorium-232 photofission, angular distribution and energy spectra for, (E), 19: 8458
emission in uranium-235 fission at 0.4–11.3 Mev, angular and energy distributions for, 17: 33042
emission in uranium-233 and -235 fission, 18: 16946 (NP-13654)
emission in uranium-236 fission, Monte Carlo calculations of, (T), 19: 16848 (MIT-905-30)
emission of, research on, 20: 42325
emission of, time-of-flight method for measuring, 20: 17864
emission, role of closed shells on, 16: 12573
energy distributions of, from uranium-233 neutron fission, 18: 2935
energy spectra of, from fission of uranium-235 by slow neutrons, 17: 21387(R) (KR-42)
flux of, fission-induced, calculation of, (E/T), 19: 5569(R) (MIT-2098-64)
half lives in metallic uranium critical assemblies, 17: 12770(R) (ORNL-3360(p.39-40))
interactions of, with fission fragments, 16: 32363 (ORNL-3338)
kinetics in fast core of fast-thermal reactor, variational method for, 20: 30852
kinetics in fast neutron multiplying media, modulated and pulsed experiments for, (T), 20: 14088
life spans of, in HIFAR, 16: 34110 (AAEC/TM-128)
lifetime calculation of, using the statistical theory of neutron chain reactions, 17: 7061
lifetime calculations, computer program for, 16: 16632 (ANL-6511)
lifetime in ALRR, 20: 42681(R) (IS-1500(Sect. R))
lifetime in Bulgarian IRT reactor, (E), 19: 19422
lifetime in fast assemblies, 17: 26064
lifetime in hydrogen-moderated, enriched-uranium assemblies, 17: 3791
lifetime in MARYLA reactor, noise-technique measurement of, 19: 29783 (PAN-565/IX,XI)
lifetime in mixed spectrum critical assembly, 20: 3402
lifetime in reactors, method for measuring, 20: 9225 (RT/FI(65)34)
lifetime in Russian VVR-S reactor, 18: 38659
lifetime in spherical assemblies, 20: 22383(T) (AEC-tr-6693)
lifetime in subcritical cylinders of enriched uranium, 20: 34941
lifetime in Swedish reactor FRO, 20: 14178 (AE-207)
lifetime in TRIGA Mark II reactor, (E), 19: 5549
lifetime in ZPR-IX reflected assembly (E/T), 19: 3559
lifetime, inhour equation for calculations, 16: 19907 (CENRD-163)
lifetime measurements on, simplification of time analyzers for, 19: 23602
lifetime measurements using pulsed-neutron techniques, 20: 34508
lifetime of, low flux measurement of ratio of, to delayed fraction, 17: 42236
lifetime of, relations with multiplication factor in diffusion theory, 19: 31495(R) (ANL-7010(p.21-76))
lifetime of, short time-variance method for measuring, 19: 27830
lifetime of, two-dimensional S_N perturbation theory for, 19: 29567
lifetimes, 18: 30963
lifetimes in critical assemblies of enriched uranium, 18: 34496
lifetimes in enriched-uranium cylinders, 18: 28303
lifetimes in enriched uranium assemblies, 19: 23996(R) (ORNL-3650(p.1-110))
lifetimes in fast critical systems, 18: 4738 (ANL-6681)
lifetimes in fast assembly SORA (E/T), 19: 3794
lifetimes in Portuguese Research Reactor (RPI), 18: 31035 (LFEN-16)
lifetimes in reflected uranium–heavy water systems, 18: 35116
lifetimes in subcritical assemblies, pulsed measurement of, 18: 44972 (MIT-2344-1)
production, effects of change of nuclear potential, 16: 18509
production in fission of plutonium-240, 16: 9444(T) (AEC-tr-4710)
production in uranium-235 fission, distributions of, 18: 21198 (KR-64(Sect.XIX))
production time in SPERT IV reactor, 17: 42396 (IDO-16903)
reactions in reactor assemblies, Rossi-α theory of kinetics of, 19: 24036
spectra from californium-252 spontaneous fission, (T), 19: 45302
use in period measurements for subcritical systems, 18: 30949 (NYO-9077)
use in reactor period determination, 18: 4694
yield from fast fission of uranium-238, 18: 32730 (EANDC(OR)-31(L))
yields from fast fission of uranium-235, 19: 31462(R) (ANL-7028)
yields from fission of uranium-235 at 3.9 to 6.4 Mev, (E), 19: 31215(R) (ANL-7010(p.1-19))
yields from fragments in uranium-233 and -235 thermal fission, (E), 19: 19079 (AECL-2163)
yields from neutron-induced fission of plutonium-240, measurement of, (E), 20: 24377
yields from nuclear fission, 18: 6213
yields from thorium-232 fast fission, (E), 19: 29266
yields from uranium-235 thermal fission, (E), 19: 29267
yields from uranium 235 neutron fission, (E), 20: 30360 (WASH-1068)
yields in bare and reflected critical assemblies, 18: 23026 (TID-7662(p.334-47))
yields in neutron fission of thorium-232 and uranium-235, (E), 19: 29372
yields in photofission of uranium-238 at 7 Mev, (E), 19: 29268
yields in photofission of uranium-238 at 7 Mev, (E), 19: 29372

NEUTRONS, THERMAL
absorption and diffusion in beryllium oxide, 17: 36625 (AAEC/TM-203)
absorption and diffusion in graphite, source measurements of, 18: 36554 (NAA-SR-9803)
absorption by antimony-indium crystals during diffraction, anomalous, 17: 38020(T) (AEC-tr-5734(p.98-101))
absorption by asphalts containing 1 to 25 wt% boron, 19: 2356(P)
absorption by bismuth, 18: 38727
absorption by boral, 17: 34845
absorption by Boral, 18: 36561
absorption by dysprosium isotopes, cross sections and infinitely dilute resonance integrals for, (T), 20: 24420
absorption by elements in soil, 17: 30091
absorption by gadolinium-156, cross section for, (E), 20: 11987
absorption by hydrogen, cross section for, (E), 19: 21219
absorption by hydrogen, sensitivity of hydrogen determination by, 19: 36260
absorption by nuclei, Monte Carlo analysis of, (T), 19: 10223 (WAPD-T-1734)
absorption by plutonium-240 in plutonium oxide grains dispersed in beryllium oxide, effective cross sections for, (T), 20: 24311
absorption by polymers, 19: 15578
absorption by silver, cross sections for, 19: 33350
absorption by thorium-232, cross sections for, 19: 16910
absorption by uranium-238, cadmium ratios for, 17: 34987
absorption by uranium-235, level spacing in uranium-236 from, 18: 7752
absorption cross section for AGOT graphite, 18: 38053 (NAA-SR-Memo-9427)
absorption cross sections for, regularities in, 18: 44735 (NRL-6124)
absorption cross sections for boron (E/T), 19: 1520 (CRRP-1203)
absorption density distributions in heavy water reactors, calculation of, (T), 20: 12365 (UJV-1438/65)

absorption in gold, effective cross section for, 17: 38023(T) (AEC-tr-5734(p.107-8))
absorption in natural boron standard, cross sections for, (E), 20: 13807
absorption in pile activation analysis, 19: 28271
absorption in presence of strong gamma component, utilization of bismuth, 16: 15616
absorption integrals and cross sections for fission products, tabulation of, 20: 28278 (JUL-354-RG)
absorption of, cross sections for activation in, 17: 26466 (PAN-407/IX)
absorption of, use of correlated sampling in Monte Carlo calculations of changes in (T), 19: 3217
absorption rates and fluxes of, Monte Carlo calculations of, 18: 42602 (TID-7050(p.379-409))
adjunct flux, determination by perturbation methods, 16: 10941
albedos for concretes, 19: 1815 (RRA-M44)
albedos for, experimental measurement of, 18: 30949 (NYO-9077)
angular albedos for concrete, differential, (T), 20: 3266
angular distribution measurements at the surface of a cadmium rod, 17: 3788
angular distribution of, measurement of, 18: 2797
attenuation, bibliographic survey of, 16: 32356 (CEA-Note-345)
attenuation by absorbing disc, 16: 9415 (MS-91(2nd. Ed.))
attenuation by Boral, 16: 5738
attenuation by concretes, 18: 35092(T) (JPRS-25467(p.1-8))
attenuation by cylindrical air ducts in water, 18: 38046 (A/CONF.28/P/688)
attenuation by gadolinium oxide–titanium system, 17: 42322(P)
attenuation by gold and indium foils, 16: 3855(R) (ORNL-3193(p.123-8))
attenuation by hydrogen atoms in soil water, 16: 9424
attenuation by iron–water mixtures, 18: 40739
attenuation by lithium hydride shields, 18: 40736 (NAA-SR-9364)
attenuation by lithium hydrides and lithium-6 hydrides in water, 19: 27705 (XDC-59-10-69)
attenuation by phonons in single crystals, (T), 20: 38371
attenuation by tissue-equivalent phantom of head, 17: 35274 (BNL-6824)
attenuation by water beyond 30 cm, 17: 3817
attenuation in air-filled annular ducts, method for prediction of, (T), 20: 1139
attenuation in air-field cylindrical ducts in water shields, (T), 20: 10221 (NP-15692)
attenuation in concretes, 17: 1042 (JUL-54-RE)
attenuation in iron-water and water shields from point fission source, 18: 32950 (WAPD-TM-448)
attenuation in polyethylenes, hydrogen content determination from, 17: 26399 (RAS-33)
attenuation of reactor, in serpentine sand, (E), 20: 6524
book: *Slow Neutrons*, 17: 39964
book: *Slow Neutrons*, 19: 33214(T)
book: *Thermal Neutron Scattering*, 20: 19792
buckling in plutonium-graphite assemblies, 18: 24852
capture by aluminum, copper, iron, and magnesium, pile oscillator method for measuring cross sections of (E), 19: 1546 (CEA-R-2485)
capture by americium-241, spontaneously fissioning americium-242 isomer from, (E), 20: 1191
capture by americium-241, spontaneously fissionable americium-242 isomer production from, (E), 20: 26210
capture by ammonium and potassium fluophosphates, radiative, 17: 29000
capture by arsenic-75 and phosphorus-31, chemical effects from, 19: 30282
capture by arsenic-75, gamma energy and intensity in, 20: 4849(R) (UCRL-14360, pp 1-50)
capture by arsenic-75 in benzenearsonic acid, arsenic-76 enrichment by, 20: 25187
capture by bismuth, gamma spectra from, (E), 19: 19095 (WASH-1053)
capture by boron-11 and silver-109, polarization of product nuclei in, (E), 20: 12098
capture by boron, cross sections for, (E), 19: 5170
capture by cadmium-108, cross section for, 18: 7782
capture by cadmium-113 in cadmium sulfides, recoil defects from, 20: 4000
capture by calcium-43, calcium-44 energy-level transitions from, (E), 20: 42335
capture by cerium-140, cross section for, 18: 44818
capture by chlorine-35, electron pair production in, (E), 20: 13762 (CONF-233(Vol.4), pp 700-9)
capture by chromium in dichromate solutions, chemistry of, 17: 4595
capture by chromium-52 and chromium-53, gamma correlations in, (E), 19: 33267
capture by cobalt complexes, rate-determining step in recombination following, 19: 32218
capture by cobalt 59, cross sections for, (E), 20: 10025
capture by cobalt-59, iron-56, manganese-55, and mercury-199, (E), 19: 14561
capture by cobalt-59, cobalt-60 energy-level structure from, (E), 20: 46736
capture by cobalt-59, spin dependence of cross sections for, 17: 22626
capture by concretes, 19: 1815 (RRA-M44)
capture by deuterium, wave functions for, 18: 42739
capture by deuterium, (E/T), 19: 5257
capture by deuterons, helium-3 and hydrogen-3 structures from, 18: 22906
capture by dysprosium-164, conversion-electron spectrum from, 20: 17822
capture by erbium-166 and erbium-167, emission of internal conversion electrons during, 17: 22587
capture by erbium-167, gamma spectra from, (E), 20: 15757
capture by foils, calculation of corrections for, 18: 38644
capture by foils, calculations for, 18: 38643
capture by gold-197, interference effects in radiative, 17: 38016(T) (AEC-tr-5734(p.83-5))
capture by gold-197, interference between potential and resonance, (E), 19: 10252 (NP-14583)
capture by gold-197, gamma spectra from, (E), 20: 15756
capture by gold-197, internal conversion coefficients of transitions from, (E), 20: 24465
capture by gold-197, production of high-specific-activity gold-198 in, 20: 29610
capture by heavy nuclei, gamma spectra from, 17: 13590
capture by holmium-166, lutetium-176, and thulium-170, 17: 17181
capture by holmium-165, gamma spectra from, (E), 20: 15758
capture by holmium-165, conversion-electron spectrum from, 20: 17822
capture by indium-115, indium-116 isomers from, 20: 17822
capture by iodine-125, cross sections and resonance integrals for, 18: 44754
capture by iodine-127, iodine-128 low-lying levels from, (E), 20: 15831
capture by iron-54 and -56, strengths for, 18: 32846
capture by iron-56, gamma spectra from, (E), 20: 46599(R) (RPI-328-68, pp 1-62)
capture by lanthanum-139 and praseodymium-141, lanthanum-140 and praseodymium-142 energy-level structure from, (E), 20: 46651
capture by light and medium nuclei, energy dependence of radiative (E/T), 19: 3391
capture by light nuclei, measurement of cross sections for, 18: 6159 (LADC-5990)
capture by lutetium-176, lutetium-177 levels from, 20: 17822
capture by lutetium-176, multipolarities of lower transitions from, (E), 20: 24466
capture by mercury isotopes, cross sections for, 18: 9336
capture by mercury-199, γ-γ cascades in, (E), 19: 21292
capture by neodymium-143, gamma spectra from, (E), 20: 3131
capture by nickel isotopes, gamma transitions from, (E), 20: 26208
capture by nitrogen-containing cobalt complexes, chemical effects of, 19: 46386
capture by nuclei, recoil energies from, 17: 5001
capture by nuclei, gamma spectra from, 17: 19329
capture by nuclei, method for soft-gamma coincidence detection in, 17: 38015(T) (AEC-tr-5734(p.74-82))
capture by nuclei ($15 \leq A \leq 100$), cross sections for M1 transition in, 17: 38196
capture by nuclei, gamma spectra from, 18: 4627
capture by nuclei, 18: 42622(R) (ANL-6879(p.2-20))
capture by nuclei, beta emission asymmetries from polarized, 16: 23086
capture by nuclei, circular polarization of gamma quanta from, 16: 29806
capture by nuclei, gamma spectra from, 18: 21193 (KR-64(Sect.XIV))
capture by nuclei, resonance scattering and absorption of gamma rays from, 18: 24620(R) (ORNL-TM-874)
capture by nuclei, research program using FRM on, 18: 24961 (NP-13930(p.80-103))
capture by nuclei, gamma spectra from, 18: 26666
capture by nuclei, measurement of gamma spectra from, 18: 28569 (MITNE-37)
capture by nuclei, gamma elastic scattering from, 18: 32792
capture by nuclei, photoneutron reactions from gamma emission in, 18: 32843
capture by nuclei, gamma spectra from, (E), 19: 6695
capture by nuclei, gamma spectra from, (E), 19: 35439
capture by nuclei, gamma radiation from, (E), 19: 37805(R) (ORNL-3778 (p.44-53))
capture by nuclei, gamma spectra from, (E), 20: 15787
capture by nuclei, analysis of gamma spectra from, 20: 34660
capture by nuclei, data analysis of scintillation detection of gammas from, 20: 46038 (CEA-R-3034)
capture by palladium, gamma spectra from, (E), 20: 15755
capture by potassium-39, potassium-40 energy levels from, (E), 20: 46652
capture by rhodium-105, cross section for, 18: 44817
capture by rhodium-103, production of isomeric rhodium-104 in, (E), 20: 44689

capture by rhodium-103, rhodium-104 energy-level transitions from, (E), 20: 44690
capture by samarium-149, conversion electron and gamma spectra for, 17: 28305
capture by samarium-149, gamma spectrum from, (E), 19: 23784
capture by samarium-149, samarium-150 energy-level spins and transitions from, (E), 20: 46744
capture by scandium-45, scandium-46 levels from, (E), 20: 28373
capture by selected elements, gamma spectra, 16: 13941 (DC-58-1-30)
capture by sintered mixtures of lead oxide or silicate with rare earth oxides, 19: 23941
capture by stainless steel, gamma spectra from, (E), 19: 5545 (ORNL-3609)
capture by strontium-88, radiation widths of gamma emission from, 19: 47115(R) (ANL-6983)
capture by tellurium, gamma spectra from, (E), 20: 17681 (IAE-966)
capture by tellurium isotopes, gamma spectra from, (E), 20: 42286
capture by titanium-48, nuclear-force time-reversal invariance determination from cascade from polarized, (E), 20: 19906
capture by uranium-238, gamma spectra from, (E), 19: 19095 (WASH-1053)
capture by xenon-126 and xenon-136, cross sections for, (E), 19: 35412
capture by zirconium isotopes, gamma spectra from, 18: 6179(R) (ORNL-3499(Vol.I)(p.42-6))
capture cross sections for, 17: 38138
capture cross sections for media containing zirconium hydride, averaging of, (T), 20: 37991
capture cross sections for soil, 20: 45885 (AD-639446)
capture gamma spectra comparison, 17: 17255
capture gamma spectra for, 17: 38063(R) (IITRI-1193-26)
capture, gamma spectra from resonance, 16: 14057
capture gamma spectra, 16: 14060
capture in atmosphere, from high-altitude point sources, (T), 20: 24300 (AD-626147)
capture in chlorine-35, electron pair production in, 17: 38017(T) (AEC-tr-5734(p.87))
capture in copper, manganese, and nickel, (E), 19: 16972
capture in dysprosium, praseodymium and terbium, gamma spectra for (E), 19: 3256
capture in gadolinium, gamma spectra from, 17: 7182
capture in gaseous and liquid phosphines, 18: 1753
capture in hafnium, 16: 21395
capture in rhodium-103, level excitation by, 18: 15211(T) (AEC-tr-6340)
capture in ruthenium-106, (E), 19: 6678
capture in semiconductors, transmutation doping and defect formation by, 18: 30278
capture of, by trimethylphosphine, effects on bonds of, 16: 25454 (BNL-4850)
capture of, excited state production by, 17: 31073(R) (ANL-6719)
capture of, high resolution gamma rays from, 17: 26332
capture of, measurement of gamma spectra from, 17: 36659 (LADC-5952)
capture of, radiation damage by Mossbauer effect in, 17: 5036(R) (ORNL-3364(p.1-26))
capture of, resonance scattering detection by gammas from, 18: 9310 (IA-863)
capture of, gamma spectra from, (E), 20: 24329(R) (ANL-7108, pp 1-4)
capture of, gamma-gamma cascades from, 19: 14563
capture of, isomer ratios in, 18: 44786
capture probabilities for, computer program for, 18: 42585 (KAPL-3013)
capture resonance scattering detection by gamma radiation from, (E/T), 20: 2520(R) (IA-920)
capture resonance levels, Doppler broadening of, 16: 26214 (AERE-M-1035)
capture, two-group calculation of gamma radiation from, 16: 26202(T) (AEC-tr-5077)
chopper for, design and performance of, 18: 6990
conference, 17: 37997(T) (AEC-tr-5734)
cross sections and diffusion parameters for, computer program for, 18: 38051 (KAPL-M-6145)
cross sections for, total, 17: 41527(R) (ANL-6720(p.2-15))
cross sections of materials for, effective, 17: 40219(T) (AEC-tr-6058)
cytological and genetic effects on rice seeds, 16: 32763
decay constant in small crystalline moderator assemblies, asymptotic, 17: 15203 (BNL-719(Vol.IV)(p.1158-74))
decay constant measurement in ice and beryllium at −125 to −100°C, 17: 15199 (BNL-719(Vol.III)(p.981-96))
decay constant of, in graphite, variation of pulsed source method for measurement of, 17: 22542
decay constants in heavy water, effects of temperature on, 20: 8337
decay of, electron-proton plasma from, 18: 32920
density and flux depression by absorbing foils, 16: 3907
density and temperature distributions in reactor, theoretical studies of, 18: 16903
density disadvantage factors in water-moderated enriched lattices, temperature dependence of, (T), 19: 3528
density distribution in reflected reactor, Fermi age theory calculation of, 17: 9888
density distribution in reactors, stability of PROGONKA method for calculating, 19: 29513
density distributions in indium, shift effect in, 16: 740
density measurements by activation using liquid scintillators, 18: 22339 (PAN-440/IX)
detection and image storage using lithium fluoride thermoluminescent sheets, 20: 46074
detection and measurement of, adaptation of gamma dosimetric films for, 17: 23740 (IA-802)
detection and measurement of, using borazole derivatives, 17: 23741 (NP-12675)
detection and measurement using tourmaline dosimeter, 17: 24761
detection and measurement of, efficiency of boron- and lithium-loaded scintillators for, 17: 29197 (EUR-133.i)
detection and measurement of, disposable dosimeter for, 17: 29205
detection and measurement of, characteristics of imaging detectors for, 17: 3677
detection and measurement of, ionization chamber design for, 17: 4846
detection and measurement using flat slow scintillation detector, 17: 8640
detection and measurement of design and efficiency of proportional counter for, 17: 34237 (RISÖ-60)
detection and measurement of high-intensity, at high temperatures, 17: 34272
detection and measurement in DR-1 reactor, 17: 34280
detection and measurement, counters for, 17: 36868(R) (GEMP-78)
detection and measurement of fluxes of, using manganese sulfate baths, 18: 4088 (EANDC-33U(p.102-13))
detection and measurement of, design of silicon surface barrier detector for, 18: 5654
detection and measurement of, pulse amplitude distributions in boron fluoride detectors for, 18: 5660
detection and measurement of, development of ionization chamber for, 18: 8673
detection and measurement of, sensitivity of boron trifluoride proportional detectors for, 18: 14245
detection and measurement of, use of scintillation counters for, 18: 14246
detection and measurement from reactor, apparatus for, 18: 16371(P)
detection and measurement of, efficiency of surface-barrier silicon detectors for, 18: 18183
detection and measurement using conversion electrons from cadmium and gadolinium, 18: 21564(R) (GEMP-81)
detection and measurement in reactors, digital techniques for, 18: 24004
detection and measurement of, time-of-flight spectrometer for, 18: 30025
detection and measurement of effective temperature of, in Melusine Reactor, 18: 30694
detection and measurement of, uses of silver-activated phosphate glasses for, 18: 31927
detection and measurement of, glass proportional detector for, 18: 37529
detection and measurement of, efficiency of cylindrical counters for, 18: 37530
detection and measurement of, use of helium-3–methane–neon mixtures in proportional counters for, 18: 41798
detection and measurement of, efficiency of silicon surface-barrier detectors for, 18: 43954
detection and measurement using cobalt wire activation monitors, 19: 754 (AERE-R-4111)
detection and measurement of, using beta activation device, 19: 4450 (CEA-R-2560)
detection and measurement of, properties of borazarenes and borazoles for scintillation, 19: 7548
detection and measurement in reactors, 19: 9475 (CEA-R-2451)
detection and measurement by induced activity, 19: 11590
detection and measurement using thermoluminescent detectors, 19: 13752
detection and measurement of, radiometer calibration techniques for, 19: 15871 (NP-14732)
detection and measurement using N,N′,N″-trimethylborazine scintillators, 19: 17781(R) (ORNL-3750)
detection and measurement of, survey meter for, 19: 18336
detection and measurement of, development of fluoroglass dosimeters for, 19: 22723
detection and measurement using europium-activated lithium iodide crystals, 19: 30513 (AEET/TP/4)
detection and measurement, development of instrumentation for, 19: 38090(R) (GEMP-88)
detection and measurement using dysprosium oxide, 20: 4260(P)
detection and measurement of, boron trifluoride probe for, 20: 14913(P)

detection and measurement using borax-impregnated K-2 emulsion plates, 20: 16891
detection and measurement of, counter for, 20: 21140(P)
detection and measurement of, activation detector for, 20: 27275
detection and measurement, evaluation of boron-zinc sulfide scintillation detector for, 16: 351(T) (AEC-tr-4702)
detection and measurement, lithium-loaded scintillator for, 16: 2370
detection and measurement, calibration of boron trifluoride detector for, 16: 3851(R) (ORNL-3193(p.102-9))
detection and measurement by gold foils in water, 16: 3843(R) (ORNL-3193(p.52-5))
detection and measurement, development of scintillator for, 16: 8918(T) (FTD-TT-61-261)
detection and measurement by foils in water, 16: 3848(R) (ORNL-3193 (p.78-94))
detection and measurement using thermoluminescence of lithium fluoride, 16: 21171
detection and measurement, calibration of converted Pee Wee survey instrument for, 16: 20640 (LAMS-2697)
detection and measurement using plastic scintillators, 16: 20717
detection and measurement, gamma-insensitive scintillation detector for, 16: 20718
detection and measurement in presence of gamma radiation and fast neutrons using glass dosimeter, 16: 22324 (DOFL-TR-1050)
detection and measurement of, patent application for bending-body device for, 16: 27470(T,P) (AEC-tr-5163)
detection and measurement of, design of fission detector for, 16: 29131
detection and measurement by activation of gold foils, 16: 31056 (LADC-5381)
detection and measurement, gamma-insensitive scintillation detector for, 16: 31837(T) (AEC-tr-5370)
detection and measurement using plastic scintillators, 16: 33164(T) (AEC-tr-5401)
detection and measurement using a scintillation detector with resolving time of 10^{-8} sec, 16: 33249
detection by activated lithium iodide crystals, energy discrimination and scintillation pulse height for, 18: 8665(T)
detection by argon-filled boron-coated proportional counter in corona zone, 16: 13331
detection by boron-trifluoride-gas-filled ionization chamber, design and patent for, 17: 16481(P)
detection by converter-and-photographic film detectors, 17: 3332
detection by fission-track production in mica, 18: 35861
detection in presence of intense gamma background, semiconductor detector for, 19: 44480 (ZFK-PHA-12, pp 144-6)
detection of, efficiency and properties of silicon surface barrier detectors for, 17: 25599 (PAN-377/I-B,IX)
detection of, resolution study of photographic image method for, 17: 37430
detection of, scintillation detector for, 17: 30879
detection of, corona discharge detectors for, 18: 16328
detection of, design of liquid scintillation detector for, 19: 32585
detection of, design and performance of ionization chamber with silver electrodes for, 20: 43680
detection of, design of boron-containing plastic scintillator for, 20: 46093
detection of, development of survey meters for, 20: 41272(R) (ORNL-3875, pp 53-74)
detection of, discriminating semiconductor device for, 20: 5802(P)
detection of, equipment for, 19: 1940
detection of, liquid scintillator system for, 18: 33953
detection of, performance of silicon p-n junctions for, 19: 7803
detection of, performance of scintillation detectors for, 19: 13791
detection of, performance of helium-3, methane, and neon mixtures for, 19: 44373(R) (ANL-6877, pp 15-20)
detection of, performance of semiconductor detectors with uranium salts for, 19: 44479 (ZFK-PHA-12, pp 140-3)
detection of, performance of liquid scintillators for, 20: 5746 (ZFK-RN-18)
detection of, proportional detector gases for, 18: 30058
detection of, scintillation detectors for, 19: 13790
detection of, scintillation detectors for, 19: 18296
detection of, scintillation counters for, 19: 34551
detection of, scintillation counter efficiency for, 19: 42749
detection of, sensitivities of activation elements for, 20: 25379 (ANL-6953)
detection of, survey of instruments for, 20: 19796
detection, photographic, 16: 8922
detection using boron trifluoride proportional counters, 19: 46822
detection using coaxial-symmetrical flow spark counter, 18: 20348
detection using europium-activated lithium iodide crystals, system for, 19: 34513
detection using helium-3 proportional counter, 20: 25441(P)
detection using silver-activated zinc sulfide, pulse-shape discriminator for, 19: 44368 (AERE-M-833)
detectors for, reaction rates in, 18: 7026 (AEEW-R-217)
detectors for, bibliography on, 20: 11088 (AED-C-28-01)
detectors for, evaluation of threshold, 19: 22801
diffraction by aluminum, bismuth, and quartz, extinction effect in, (E), 20: 12309
diffraction by bismuth and potassium nitrate at high pressures, 19: 32680(R) (IDO-17052)
diffraction by nickel oxides, magnetic moment distribution from, 20: 8046
diffraction of, review, 17: 5059
diffraction scattering by solids, measurement of, 17: 7070
diffusion, analysis of the one-thermal-group model for, 16: 7005 (WAPD-T-1234)
diffusion and distribution in hydrogen and heavy gases, (T), 20: 15677
diffusion and scattering in cold polyethylene, 17: 28437 (KAPL-2000-20)
diffusion approximation and variational expression for distribution in space-energy, 16: 18409
diffusion coefficients in water-d_2 at 20 to 220°C, 17: 26415
diffusion coefficient measurements in water-d_2, corrections for, 17: 26416
diffusion coefficient measurements in heavy water, 17: 15193 (BNL-719(Vol.III)(p.879-99))
diffusion coefficient in beryllium at 60 to 400°K, (T), 19: 21206
diffusion coefficient for Maxwellian proton gas, (T), 19: 33210
diffusion coefficient in heavy water containing voids, (E), 20: 2957
diffusion coefficients in petroleum and silicate, determination of, using pulsed source, 20: 14772
diffusion coefficients in fluids and rocks, determination of, using pulsed source, 20: 14772
diffusion coefficients for lattices with voids, (E), 20: 24713
diffusion constants in organic glass, measurement using neutron chopper, 19: 45222 (INR-624/IX-A/R)
diffusion cooling and heating in water, (E), 19: 12465
diffusion, effects of velocity distribution on, 16: 1004(T) (UCRL-Trans-687)
diffusion equations with two overlapping groups, solution of, (T), 19: 33211
diffusion equations for, derivation of Nordheim equation from, (T), 19: 41644
diffusion equilibrium in crystalline media, 17: 7129 (NP-12330(p.378-83))
diffusion from hemispherical source, 16: 4616(R) (NP-11098(p.35-7))
diffusion in beryllium, effect of Bragg cutoff on, 17: 5316
diffusion in beryllium absorption cross sections and transfer and diffusion lengths for, 18: 26502
diffusion in biphenyl and monoisopropylbiphenyl, parameters for, 18: 989
diffusion in concrete, pulsed-source method for parameters of, 18: 7849
diffusion in finite media, analysis of, 18: 6137 (NP-13447)
diffusion in finite solid media, effects of Bragg cutoff on, 16: 1011
diffusion in graphite, energy modes in, 18: 2809
diffusion in heavy water at 20 to 220°C, 17: 7058 (TID-15165)
diffusion in heavy water, parameters for, 18: 4519
diffusion in heavy- and light-water (E/T), 19: 1520 (CRRP-1203)
diffusion in heavy water, decay constants of, (E), 19: 42045(R) (MIT-2344-3, pp 55-108)
diffusion in heavy water, (E/T), 20: 11931 (CONF-651101-53)
diffusion in heavy water, 16: 9641(R) (DP-685)
diffusion in heptane, parameters for, 18: 987
diffusion in heterogeneous and homogeneous media, computer program for, 19: 16816 (EUR-2187.e)
diffusion in heterogeneous media, anisotropy in, 16: 9418(T) (AEC-tr-4716)
diffusion in highly trapping media, 16: 31059
diffusion in hollow-tube-fueled thermal reactors (E/T), 19: 1841
diffusion in infinite homogeneous source-free medium, parameters for, 18: 992
diffusion in light water, 16: 9419
diffusion in light water, 16: 12416
diffusion in moderators, parameters for, 17: 11605
diffusion in moderating media, neutron-wave technique for, 18: 13038
diffusion in moderators, photon diffusion analogy with, 18: 18852 (MATT-231)
diffusion in moderators, fast chopper as source for measuring, 19: 29176 (PAN-539/IX)
diffusion in non-absorbing media, effect of temperature differences on, 17: 15207 (BNL-719(Vol.IV)(p.1255-71))
diffusion in organic moderators, 17: 13471 (RT/FI(62)-57)
diffusion in organic reactor coolants, temperature dependence of, 20: 26066(T) (AECL-2330, pp 251-4)
diffusion in parallel-plate lattice, 17: 19196 (CRRP-1140)
diffusion in parallel-plate lattices, calculation of, 20: 32763 (AECL-2543)

diffusion in plexiglas system with empty channels, 18: 21141
diffusion in plutonium-fueled aluminum-water lattices, (E), 20: 12396(R) (EURAEC-1505)
diffusion in polythene, 17: 36631
diffusion in polythene, extrapolation lengths for, 18: 24571(R) (RPI-328-6)
diffusion in reactor moderators, 18: 15482
diffusion in reactor moderators, effects of empty channels on, 18: 21602
diffusion in reactor graphite, length of, (E), 19: 21646
diffusion in Santowax-R at 200 to 400°C, length of, 18: 38040 (A/CONF. 28/P/653)
diffusion in semi-infinite beryllium slab, effects of Bragg cutoff on, 16: 1012
diffusion in semi-infinite graphite slabs, effect of Bragg cutoff on, (T), 19: 43260
diffusion in sintered beryllium oxide, 17: 24374
diffusion in two-layer medium, 18: 26506
diffusion in uranium–heavy water lattices, 18: 44972 (MIT-2344-1)
diffusion in uranium-water lattices, activation ratios for spectra in, 19: 29569
diffusion in uranium, (E), 20: 3031
diffusion in water-d_1 at 20 to 220°C, coefficients, 17: 2212
diffusion in water as function of temperature formulas for, 17: 32976
diffusion in water around a point source of uranium-235, ratio of flux to source strength for, 17: 39959
diffusion in water for various scattering laws, 17: 32972 (CONF-11-7)
diffusion in water slabs, extrapolation lengths for (E), 19: 1533
diffusion in water-d_2, parameters of (E), 19: 3207
diffusion in water-moderated lattices, two-dimensional, (T), 19: 21654
diffusion in water, parameters for, (E), 20: 36141 (IEA-107)
diffusion in water–water-d_2 mixtures, parameters for, (E), 20: 40061
diffusion in well with timbered layer, attenuation decrement and mean lifetime for nonstationary, (E), 20: 27175
diffusion length and transport mean-free path in graphite at 100 to 300°K, (T), 19: 47556
diffusion length and temperature in boron-bearing water and heavy water, (E), 20: 34503
diffusion length in water, 17: 2209
diffusion length in light water, experimental measurement, 17: 15191 (BNL-719(Vol.III)(p.799-804))
diffusion length in water at 20 to 50°C, 17: 19210
diffusion length in water at 24 to 82°C, 18: 30691
diffusion length in graphite, experiment for, 18: 30949 (NYO-9077)
diffusion length in water, experiment for, 18: 30949 (NYO-9077)
diffusion length in concrete, (E), 20: 3255
diffusion length in water at 18 to 255°C, (E), 20: 15679
diffusion length in paraffin, temperature dependence, 16: 9653 (KAPL-2000-16)
diffusion length in graphite, 16: 34070 (NAA-SR-Memo-7415)
diffusion length in water at 16 to 89°C and in Dowtherm A at 185°C, 16: 9421
diffusion length in absorbing aqueous solutions, 16: 738
diffusion lengths in polyethylene and water, 17: 28437 (KAPL-2000-20)
diffusion lengths in water, 17: 20956 (GEAP-4018)
diffusion lengths in matter, iterative calculations of (T), 19: 1534
diffusion lengths in Santowax-R at 200 to 400°C, 20: 15680
diffusion lengths in Santowax R poisoned with boron, (E), 20: 13718
diffusion measurements in biphenyl and graphite, pulsed, (E/T), 20: 9379(R) (NAA-SR-11650, Sect. 4)
diffusion near boundaries of absorbing rods immersed in a moderator, study by elementary diffusion theory, 18: 15441
diffusion of, effect of temperature gradients on, 17: 7071
diffusion of, in reactor lattice, theory of, 17: 4229 (CRRP-1116)
diffusion of initial burst of, in moderating media (T), 19: 3216
diffusion of, measurement of water content in building materials by, 17: 15902
diffusion of, one-group theory for, 17: 3804
diffusion of, SWAK program for calculating, 17: 28243 (KAPL-M-RPC-6)
diffusion of, computer code listing for, 18: 15130 (EUR-358.i(Suppl.))
diffusion parameters in water and ice, 17: 4028
diffusion parameters in graphite and bismuth, 17: 15200 (BNL-719 (Vol.III)(p.1034-73))
diffusion parameters in light and heavy water and graphite, calculation of, 17: 15204 (BNL-719(Vol.IV)(p.1186-1210))
diffusion parameters of, calculation for pulsed systems, 17: 15210 (BNL-719(p.Vol.IV)(p.1331-59))
diffusion parameters, measurement, 17: 15190 (BNL-719(Vol.III) (p.RE1-62))
diffusion parameters of, in water poisoned with boron or cadmium, 17: 32975
diffusion parameters in water, measurement by pulsed neutron method, 18: 9301
diffusion parameters for water, 18: 26828
diffusion parameters of, review of, 18: 40490
diffusion parameters of, computer analysis, (T), 19: 6843 (WAPD-TM-373)
diffusion parameters in water, measurement using pulsed neutron techniques, 20: 2954
diffusion parameters in ice and water, temperature dependence of, (E), 20: 28240
diffusion parameters in solid biphenyl, 16: 18405
diffusion theory calculation of leakage flux from semi-infinite media, 18: 38047 (A/CONF.28/P/708)
diffusion theory parameters for depletion calculation, variational procedure for, 18: 42605 (TID-7050(p.494-519))
disadvantage factors in thermal reactors, 18: 38255(R) (KR-72)
disadvantage factors in reactors, computer program for, 19: 23998(R) (TID-21733)
disadvantage factors in reactors, calculation methods for, (T), 19: 29784(R) (TID-21794)
disadvantage factors for, in water-urania lattices, 19: 31462(R) (ANL-7028)
disadvantage factor for square cell of uranium dioxide-water lattices, (E), 20: 10333
disadvantage factors for slab geometries, 16: 12681
distribution analysis for, activation-autoradiographic method of, 18: 30697
distribution at cadmium rod surfaces, measurement of angular, 18: 3097 (HW-SA-2934)
distribution in channels of heavy water reactor model, 17: 4264
distribution in cylindrical fuel cells, diffusion theory for, 17: 15188 (BNL-719(Vol.II)(p.684-705))
distribution in graphite blocks, 20: 45060
distribution in heavy gaseous moderators, 17: 34834 (EUR-292.i)
distribution in heterogeneous reactor, space-energy, (T), 19: 5438
distribution in heavy-water-moderated thoria-urania lattices with flux traps, 19: 31495(R) (ANL-7010(p.21-76))
distribution in homogeneous media, energy and space, (T), 20: 14774
distribution in infinite plates, 16: 7007
distribution in non-absorbing gaseous media, Milne's problem for, 17: 15205 (BNL-719(Vol.IV)(p.1211-31))
distribution in nonabsorbing media, Milne's problem for, 16: 1006
distribution in Philippine Research Reactor core, equation for, 19: 8669
distribution in reactor matrices, computer program for, 17: 36871 (KR-47)
distribution in slowing-down media, 18: 4009
distribution in sphere of natural uranium, foil activation measurements of Maxwellian, 18: 40483
distribution in uranium-heavy water lattices, 17: 15172 (BNL-719 (Vol.II)(p.305-17))
distribution in water-moderated plutonia–urania lattices, calculation of, 19: 25684(R) (HW-84369(p.5-9))
distribution in water, from anisotropic fast source, (E/T), 20: 30340
distribution near material boundaries, theory for calculating, 17: 31385 (JEN-114-DF/I-33)
distribution of drill holes, effect of transport on, 17: 1640
distributions around single heavy-water-moderated fuel rods, (T), 20: 14067(R) (MIT-2344-4, pp 80-8)
distributions in cube-shaped room with source in center, 18: 21137
distributions in cells, computer analysis of, 18: 28921(R) (TID-20649)
distributions in cylindrical reactor cells, (T), 19: 12751 (PAN-534/IX-A)
distributions in enriched-uranium heavy-water lattices, 20: 14065(R) (MIT-2344-4, pp 4-16)
distributions in hydrogen-moderated, fuel-bearing assemblies, 17: 28437 (KAPL-2000-20)
distributions in heterogeneous reactor cell, three-group method of calculating energy and spatial, 17: 13474
distributions in heavy-water-moderated, organic-cooled fuel elements, 18: 11415
distributions in heavy water–uranium lattices, 18: 28967
distributions in low-enrichment superheater cells, 17: 7595(R) (ACNP-62018)
distributions in light water moderated matrices, energy and spatial, 17: 38493 (WAPD-T-1594)
distributions in moderators, effects of absorbers on, 18: 15460
distributions in reactors, 17: 31794(R) (BNL-782(p.1-17))
distributions in reactor, equations for, 17: 38505
distributions in reactors, pulsed-source analysis of, 18: 28551
distributions in reactor lattices, calculation of space-energy, 18: 40473 (EUR-1643.e(p.143-54))
distributions in reactors, multigroup calculations of, 19: 1851
distributions of slowing-down density of, in graphite prism, 17: 15223
distributions of, P_n approximation for (T), 19: 1846
dose measurements of, in graphite irradiation in Belgian Reactor-2, 19: 48030
dose rate behind shielding plugs in Battelle shielding facility, 18: 21543 (BMI-1384)
dosimeter for, deformable-glass, 20: 11168(P)

dosimeter for, design of multi-element, 19: 28693
dosimeter for, development of activation, 20: 14862
dosimetry, adaptation of photographic films for, 17: 35253(R) (IA-775)
dosimetry at surfaces of biological shield of TRIGA Mark II Research Reactor, 16: 17310 (ORNL-TM-178)
dosimetry by cobalt activation, 16: 8914(T) (CEA-tr-A-1027)
dosimetry by phosphorus-32 activation, 18: 23890 (SCPRI(S)-92)
dosimetry by source-depletion method, 17: 34278
dosimetry in accidental and normal conditions, methods for, 19: 44332
dosimetry in biological cavity of NRX Reactor, 18: 38727
dosimetry in criticality accidents using multisphere technique, 19: 44323
dosimetry in gamma background using film badges, 20: 16807 (CLOR/IBJ-42/D)
dosimetry in man, biological method for, 19: 44322
dosimetry in mixed fields, properties of glasses for, 20: 31462
dosimetry in mixed fields, tissue-equivalent ionization chamber for in-phantom, 20: 31524
dosimetry in personnel using silver-activated phosphate glass, 20: 628
dosimetry in research reactors, 17: 41108
dosimetry in tissues, 20: 37025(R) (PG-Report-705)
dosimetry in tissue-equivalent phantoms using activated gold wires, 20: 38745(R) (NYO-3267-3)
dosimetry methods for, 17: 41107
dosimetry of, 20: 8712
dosimetry of, cobalt-60 standards for, 17: 41242 (EUR-422.e)
dosimetry of, in cryogenic in-pile loops, 17: 1781
dosimetry of, design of single-sphere instrument for, 20: 7366 (LA-DC-7323A)
dosimetry of, design and performance of luminescent dosimeters for, 20: 9291
dosimetry of, detector for, 20: 41362(P)
dosimetry of, in research reactor for biological studies, 18: 41107
dosimetry of, performance of insulators for measurement of, 19: 44385 (CERN-65-4(Vol.II), I12-19)
dosimetry of, performance of silver-activated metaphosphate glass for, 20: 5713 (AD-623384)
dosimetry of, performance of insulators for, 20: 5719 (CEA-R-2846)
dosimetry of, performance of lithium fluoride thermoluminescent detector for, 20: 5572 (USNRDL-TR-909)
dosimetry of, performance of foils in pocket ion chambers for, 20: 11119
dosimetry of, rate meter for, 19: 18263 (NP-14706)
dosimetry of, use of silver-activated metaphosphate glass for, 19: 42722(T) (CEA-tr-A-1750)
dosimetry of, using radioluminescent phosphate glass, (E), 19: 44509
dosimetry using capture gamma, 18: 41779
dosimetry using capture gammas and film badges, effects of cadmium ratio on, 19: 36833
dosimetry, using film and silver-activated phosphate glass, 16: 31060
dosimetry using lithium fluoride, (E), 19: 4484 (UCRL-11613)
dosimetry using lithium fluoride, 20: 2178
dosimetry, standardization of sources and instruments for, 19: 4463 (NP-14356)
effects combined with chemicals on growth and mutation frequency of rice seeds, 19: 8854
effects in impurity-doped crystals, effects of lattice defects on annealing processes for, 18: 3857
effects in oat seeds, genetic, 20: 1665
effects in plant cells, chemical protection, 17: 23149
effects of cadmium-transmitted, on ferroelectric properties of barium titanates, 18: 32251
effects of dose levels on relative biological effectiveness and elimination of chromosomal aberrations, 16: 1603
effects of dose of, to seeds, on growth of carrot, flax, radish, and tomato plants, 20: 45453
effects of exposure of seed, on seedling growth, 16: 1525
effects of fast reactor fuels, calculation of, 20: 27405(R) (BNWL-198, pp 3.1-21)
effects of microstructure of uranis single crystals, 20: 11224
effects of recurrent selections and, in oat breeding, 19: 21988
effects on absorption bands of lithium fluoride at 77°K, 18: 32241
effects on absorption spectra of Yakutian diamonds, 19: 41098
effects on aging, helium agglomeration, and recrystallization in aluminum–lithium alloys, 19: 23126 (PAN-546/XIV)
effects on albumin and serum, chemical protection against, 18: 11869
effects on alkali metal bromates, yields of bromate decomposition and bromide ion in, 18: 43639
effects on alkali-halide color centers and dislocations, (E), 19: 41976
effects on α-phase uranium, 19: 26881(R) (EURAEC-1333)
effects on ammonium dihydrogen phosphate, 18: 6872
effects on austenitic and nickel-base steels, 19: 7996
effects on azides and nitrates, 20: 45754
effects on bacterial resistance of prunus seedlings grown from exposed seeds, 19: 33887
effects on barley, rice, and wheat, 17: 30055
effects on beryllia–thoria–urania dispersions, 18: 44233 (AAEC/E-125)
effects on beryllia impregnated with urania–thoria–yttria, 20: 27586(R) (GEMP-400A, pp 269-77)
effects on blood serum, protective effects of chemical agents against, 18: 11850
effects on borated graphite, damage from, 20: 46234
effects on boronated graphite, 20: 17116 (BNWL-199)
effects on brain tumors and rabbit ears, 17: 10475
effects on bread wheat, frequency and spectrum of mutagenic, 18: 9853
effects on breakdown potentials of air gaps in electronic equipment, (E), 20: 33738
effects on bromopentamminerhodium nitrate and chloropentammineiridium chloride, 20: 43340
effects on cadmium, isochronal annealing of, 19: 998(R) (ORNL-3676 (p.12-23))
effects on cadmium, isochronal annealing of, 19: 1001(R) (ORNL-3676 (p.61-5))
effects on cadmium sulfides and tellurides, damage, 19: 1003(R) (ORNL-3676(p.112-21))
effects on cadmium sulfide and telluride, 19: 16221 (ORNL-3767)
effects on cadmium sulfide electric conductivity, (E), 20: 38405
effects on "Cappelli" durum wheat, mutagenic, 17: 10390
effects on catalytic properties of magnesium oxide for decomposition of nitrous oxide, 19: 44680(R) (ANL-7000, pp 227-32)
effects on chromium compounds, 20: 33328 (BNL-9376)
effects on chromosomes of *Sorghum vulgare* seeds, 19: 13085
effects on coated uranium(IV) oxide particles, 18: 2348
effects on coated uranium carbide particles, 18: 37747 (A/CONF.28/P/398)
effects on cobalt complexes, 20: 38962
effects on cobalt–dysprosia dispersed in soda-potash glass, effects of boron carbide additions on, 20: 31668
effects on conductivity of helium-3 plasma, (E), 20: 39683
effects on corrosion resistance of boronated stainless steel, 19: 39110
effects on creep properties of A-286 alloy, 20: 5846
effects on creep-rupture properties of A-286 alloy and Hastelloy X, 20: 2456
effects on current induction in commercial capacitors, 20: 21151 (IBM-66-825-1944)
effects on cytology and morphology of tomatoes, 17: 10452
effects on decomposition of potassium bromate, thermal annealing of, 20: 45753
effects on defects in diamond-lattice semiconductors, 19: 11811
effects on dielectric and tensile properties of crystalline vitreous materials, 20: 23802
effects on dimensions of aluminum–europium oxide dispersions, 20: 5174(R) (ORNL-3870, pp 214-29)
effects on dimensions and electric resistivity of ceramic materials, 20: 27588 (LA-DC-6822)
effects on diploid and hexaploid species of *Avena*, 17: 10457
effects on distribution of antimony recoil atoms in potassium antimonates, 19: 42552
effects on ductility of stainless steel, 20: 17141
effects on ductility of type 304 stainless steel, effects of carbon content and titanium additions on, 20: 31669
effects on durum and bread wheats, first generation, 16: 1599
effects on electric and thermal conductivity and optical absorption of alkali halides, 19: 26388
effects on embrittlement of A-286 alloy at high temperature, additive effects of boron on, 18: 28062
effects on embrittlement of type 304 stainless steel, effects of boron on, 20: 898
effects on embrittlement of type 304 stainless steel, 20: 4460(R) (ORNL-3870, pp 140-5)
effects on embrittlement of types 304 and 304L stainless steels at 650 to 842°C, 20: 4460(R) (ORNL-3870, pp 140-5)
effects on embrittlement of type 304 stainless steel, role of grain boundary carbides in, 20: 4460(R) (ORNL-3870, pp 140-5)
effects on embrittlement of type 304 stainless steel, role of titanium additions in, 20: 4460(R) (ORNL-3870, pp 140-5)
effects on embryo-endosperm ratios in seeds, 17: 10386
effects on *Escherichia coli*, biological, 19: 15018 (ORNL-P-758)
effects on fibrous fissiochemical fuels, 19: 46324(R) (AGN-8132)
effects on fission gas release and microstructure in uranium dioxide, 20: 27590 (ORNL-3930)
effects on fission-gas-generation and temperature in plutonia–urania, profiles of, 20: 29618(R) (GEAP-4982)
effects on gaseous methane–phosphine mixture, formation of phosphorus-32-labeled products in, 19: 5962
effects on germanium, introduction of interstitial arsenic donors in, 18: 22544

effects on germanium monocrystals, 16: 6504
effects on germanium monocrystals, 16: 24245(T) (AEC-tr-5147)
effects on glasses, ESR studies of, 20: 5019
effects on grass seeds, genetic, 18: 25177
effects on green and yellow excited absorption spectra of cuprous oxides, 18: 20077
effects on growth and survival of durum wheat, comparison with effects of mutagenic agents, 17: 10388
effects on growth and viability of sweet clover after seed exposure, compared with x radiation, 16: 1600
effects on high resistivity n and p type silicon, donor production from, 20: 35806 (CEA-R-2918)
effects on high-temperature ductility of niobium-stabilized austenitic stainless steel, 19: 32774 (AE-186)
effects on improving flue-cured tobacco, 18: 31160
effects on in-pile corrosion of nuclear materials by aqueous solutions, 20: 5852(R) (EURAEC-1522)
effects on intergranular void and crack formation in austenitic steel at 650 to 850°C, 20: 44016
effects on iodine-126 and -128 retention in potassium iodate, 19: 13500
effects on krypton trapping by uranium carbide surfaces, 20: 19255 (EUR-2749.e)
effects on lithium fluoride single crystals, formation of colloidal lithium particles after annealing in, 18: 5859
effects on lithium bromide and fluoride single crystals, 20: 14603
effects on lithium fluoride crystals, point defects from, 20: 18007
effects on luminescence of thallium-activated alkali metal halide crystals, 19: 34238
effects on luminescence of potassium chloride and thallium-activated potassium chloride, 19: 34240
effects on magnetic susceptibility of lithium fluoride, 18: 32217 (BLG-190)
effects on magnetic susceptibility of lithium fluoride single crystals, 19: 7568
effects on mechanical properties of iron and steel, 19: 1004(R) (ORNL-3676(p.125-56))
effects on mechanical and physical properties of boral, 19: 9737 (UJV-1145/64)
effects on mechanical properties of boronated stainless steel, 19: 39110
effects on mechanical properties of stainless steel at 25 to 850°C, 20: 2477
effects on mechanical properties of aluminum alloy 6061, 20: 4460(R) (ORNL-3870, pp 140-5)
effects on mechanical properties of silver–15 indium–5 cadmium alloy, 20: 31668
effects on mitosis in *Pisum sativum* root tip cells, 20: 36644
effects on mouse tumor growth and transplantability, 18: 41225
effects on mutation frequency in dormant rice seed, 19: 8855
effects on mutation induction in potato plants, 19: 42318
effects on mutation induction in cotton species *Gossypium barbadense*, 20: 36623
effects on mutations in rice, 16: 32764
effects on n-type cadmium sulfides and cadmium tellurides, 20: 41271(R) (ORNL-3875, pp 44-52)
effects on *Nicotiana tabacum*, mutagenic, 18: 9852
effects on non-fissile materials, in-pile, heating, 17: 42198(T) (AEC-tr-6091)
effects on nonfissile materials, calculation of in-pile heating, 19: 989 (AERE-M-760)
effects on oat seeds, genetic, 19: 26053
effects on oats and wheat, 18: 13494
effects on oats, effects of ploidy on frequency of mutagenic, 19: 38419
effects on oats, genetic, 18: 3579
effects on optical properties of tourmaline, 19: 13501
effects on optical absorption in F centers of potassium chloride crystals, 19: 18017(T)
effects on optical absorption spectra of lithium fluoride, 20: 17143
effects on organic retentions of bromine-80 and -82 in alkyl halides and hydrocarbons, 19: 38715
effects on organic halogen compounds, 20: 43367
effects on p-type silicon, nuclear compensation in, 20: 27257 (AWRE-O-24/66)
effects on photoconductive properties of cadmium sulfides and selenides, 20: 32736
effects on physical properties and structure of uranium mononitride, 19: 2861
effects on physical properties of boronated graphite, 19: 32776 (BNWL-96)
effects on physical properties of cadmium sulfides, 20: 4027
effects on plants, genetic, 20: 26644
effects on plated cadmium–indium–silver alloys, 19: 44736 (ANL-6883)
effects on plutonia–urania fuels, 20: 15135(R) (NUMEC-3432-18)
effects on polymerization of vinyl compounds, role of LET in, 18: 31638
effects on polystyrene, positronium lifetimes in, (E), 20: 32704
effects on potassium dihydrogen arsenate, compression effects on arsenic-74 and -76 annealing in, 19: 13497
effects on potassium bromide, formation of F centers in, 19: 13501
effects on potential of mercury oxide electrode, 20: 1932
effects on properties of heat-resistant pyroceramics, 19: 42911
effects on properties of type 6061 aluminum alloy, 20: 5846
effects on properties of boronated graphite, 20: 9377 (CONF-650620, pp 85-104)
effects on purines and pyrimidines, 19: 40557
effects on pyrolytic carbon-coated thorium and/or uranium fuel elements, 20: 27568 (BMI-1772)
effects on regenerating liver cells of mice, 18: 3479 (BNL-7353)
effects on rice seed, chlorophyll mutations from, 20: 40641
effects on rice seeds, 16: 1608
effects on rice, effects of diethyl sulfate on, 18: 38936
effects on rice, mutagenic, 20: 8652
effects on rubidium uranyl nitrates, 20: 43365
effects on scintillation properties of lithium iodide crystals, 19: 24882 (LA-DC-7108)
effects on seeds of red clover, Ultuna, genetic, 19: 45882
effects on seeds of *Trifolium subterraneum*, genetic, 20: 8704
effects on seeds of *Vigna sinensis*, biological, 20: 14341
effects on semiconductors, 20: 2516
effects on small animals, chambers for studying, 19: 25988
effects on somatic mutation induction in sand oats, dose rate effects on, 19: 15172
effects on soybeans, 18: 38848
effects on soybeans, mutagenic, 20: 45358(R) (NP-16208)
effects on soybean seeds, genetic, 20: 45388
effects on spring wheat, comparison with gamma and x rays, 17: 12155
effects on stainless steel-clad urania fuel elements, 20: 29806 (ORNL-TM-1511)
effects on stress rupture of A-286 alloy and Hastelloy X, 20: 5851
effects on stress-rupture properties of A-286 and Rene-41 at 650°C, 18: 32258
effects on structure of beryllium and quartz, 19: 6368
effects on structure of A-286 alloy, electron microscope studies of, 19: 47088 (NMI-4998, pp 95-106)
effects on sulfur-35 production and valence state in ammonium chloride, 20: 35545
effects on summer wheat seeds, mutagenic, 20: 35317
effects on superconducting current density in uranium-vanadium silicide systems, (E), 19: 14435(R) (NP-14676)
effects on superconducting properties of aluminum–niobium alloys and vanadium silicides, (E), 20: 30260
effects on surface homogeneity of graphitized carbon black, 18: 44256
effects on survival of cells in tissue cultures, 18: 8100 (BNL-7542)
effects on sweet cherry trees, genetic, 20: 16244
effects on swelling of uranium, effects of pre- and postirradiation heat treatments on, 19: 44739(R) (ANL-7000, pp 233-77)
effects on tensile properties of Hastelloy N at 500 to 800°C, 19: 26908
effects on tensile properties of aluminum alloy 6061, 19: 28889
effects on tensile properties of type 304 stainless steel, 19: 44743 (GEAP-3634)
effects on tensile properties of Nimonic PE16, 20: 31669
effects on thermal conductivity of sintered uranium dioxide, 18: 36514
effects on thermocouples, 19: 18390(R) (GEMP-43A)
effects on tissues, biological, 20: 8712
effects on transmutations in crystalline solids, 19: 11682
effects on transmutation doping of semiconductors, 19: 13439
effects on urania fuel plates, effects of fuel density, operating temperature, fissioning rate, and metal additions on, 20: 23778 (WAPD-TM-455)
effects on uranium single crystals, 18: 42123
effects on uranium single crystal growth, 19: 44739(R) (ANL-7000, pp 233-77)
effects on variegation in Einkorn wheat, 20: 20497
effects on wheat seeds, mutagenic, 20: 22743
effects on wheat, genetic, 20: 45392
effects on wheat, effects of boron on, aberrant and mutagenic, 19: 2153
effects on wheat, mutagenic, 17: 39362
effects on wheat, mutagenic, 19: 2161
effects on yeast, mutagenic, 19: 2091
effects on yield of solvated electrons in organic borate glasses at −196°C, 19: 7581
effects on zinc sulfide crystals, 19: 34230
eigenvalue spectra, 17: 34560(R) (TID-19195)
embrittlement of Inconel alloys and austenitic stainless steels, 20: 15141
emission from accelerating sources, kinetics of, (T), 20: 12371
emission from split-core swimming-pool reactors, 18: 4848 (EANDC(OR)-26U)

energy and spatial distribution of, in heavy water-uranium lattices, 16: 32362 (MITNE-17)
energy distribution in paraffin, 18: 32723
energy distribution in plane geometry of light water, effects of diffusion cooling on, 19: 3194
energy distribution in beryllium oxide finite and semi-infinite blocks, (T), 19: 47555
energy distribution of, synthetic scattering model for calculating, 19: 47557
energy distribution in infinite homogeneous medium for 1/v absorption, computer program for, 16: 4441 (GAMD-1581)
energy grouping in reactor analysis, upscattering fraction definition for, (T), 19: 24031(R) (RPI-328-20(p.47-9))
energy spectra in horizontal beamhole of Soviet VVR-S reactor, 17: 35176
energy spectra in subcritical test assembly for Beloyarsk Power Reactor, 18: 13304
energy spectra in Cekmece TR-1, 19: 35853
energy spectra of, determination by activation techniques, (T), 19: 16825
extrapolation length in graphite, 18: 2808
extrapolation length in water, 18: 2810
filter design for removing, from reactor spectrum, 16: 24641
fission fragment damage in glasses, minerals, and plastics, plutonium particle size analysis by, 20: 27189 (BNWL-SA-26)
flux amplification in water-moderated reactors, thermal columns for, 16: 24955
flux and multiplication in Saxton reactor, subcritical, 20: 12418(R) (WCAP-3739)
flux at free boundary, spatial transients in, 19: 23604
flux average energy of, boron-lined counter for determining, 20: 21074
flux axial distribution at various moderator levels in NRX reactor, 16: 17232 (CRC-1058)
flux behavior in exponential and pulsed experiments, Boltzmann transient, 18: 21142
flux behavior in exponential and pulsed experiments, Boltzmann transient, 18: 21143
flux buckling in subcritical assemblies, measurement of, 18: 42916 (CEA-R-2490)
flux buckling measurements in water–natural uranium exponential pile, 18: 26880
flux buckling measurements in exponential piles, experiment for, 18: 30949 (NYO-9077)
flux calculation for reactor supercell, 17: 26804
flux calculation for irradiation capsules in heterogeneous reactors, 18: 45135 (TID-7697(p.5.3.1-8))
flux calculations for, improvement of cylindrical reflecting boundary condition in, 17: 2466 (BNL-6309)
flux calculations with Penelope program, corrections for, 17: 39953(T) (AEC-tr-6061)
flux calculations for fuel element, 18: 26899 (HW-50086)
flux calculations for antimony-beryllium sources, 19: 31199 (TPI-104)
flux calculations using Monte Carlo method, computer programs for, 20: 19786 (WAPD-T-1835(Rev.))
flux calibration of, from WWR-C reactor, 17: 19684
flux contours in reactor, on-line printer for automatic plotting of, 20: 8359
flux densities in High Flux Reactor, 19: 45681 (RCN-36)
flux density in graphite cylinders, 18: 36562
flux determination in reactors, using coincidence measurements on gold foils, 19: 24037
flux determination using gold activation detectors, 20: 21053
flux disadvantage factors for, measurement using foil activation, 20: 34951
flux distribution in superheater core, 17: 26037
flux distribution in fuel element and moderator, calculational method for Wigner-Seitz cell approximation for, 18: 1212
flux distribution in subcritical trap assembly with spontaneous fission source, 18: 7896
flux distribution in reactor fuel element and associated moderator, constant source assumption for, 18: 15440
flux distribution measurements within and behind beryllium oxide, 18: 24806 (XDC-61-1-149)
flux distribution in reactor shielding, removal age-diffusion calculation of, 18: 28915 (AEEW-R-361)
flux distribution in reactors, comparison of various methods of measuring, 18: 30960
flux distribution spectral indices in reactors, oscillation method of measuring, 18: 33021 (LFEN-N1.12)
flux distribution in rectangular lattice of cylindrical elements, 18: 38327 (A/CONF.28/P/826)
flux distribution in experimental assemblies, analog method for estimating, 18: 45134 (TID-7697(p.5.2.1-8))
flux distribution in TRIGA Mark II reactor in pulsed and steady operation, (E), 19: 5548
flux distribution in VVR-S reactor fuel element, (T), 19: 5553
flux distribution in complex lattices, program for calculating, 19: 12865(R) (NAA-SR-10501)
flux distribution in water phantoms, 19: 10861
flux distribution in clusters of uranium oxide rods, semi-empirical formula for, (E/T), 19: 17258
flux distribution in axial direction of reactor, 19: 24044(P)
flux distribution in EBWR shielding, calculations of, 19: 35760 (IEA-85)
flux distribution in source-free absorbing medium, temperature effect on, (T), 19: 41652
flux distribution in soil in Operation Bren, 19: 47569 (CEX-62-50)
flux distribution in heavy water moderated, organic-cooled reactors, hyperfine structure of, 20: 18055
flux distribution in hexagonal lattices, determination of, (T), 20: 22371 (AD-621026)
flux distribution in monoisopropylbiphenyl-uranium lattices, 20: 26429(T) (AECL-2330, pp 284-94)
flux distribution in horizontal reactor channels, beryllium reflector effects on, 20: 32765 (IAE-957)
flux distribution in pitchblende, 20: 37994
flux distribution around point source of fast neutrons in infinite hydrogenous medium, (T), 20: 40058
flux distribution in Physical Constants Testing Reactor and external thermal column, 16: 18156(R) (HW-72586(p.28-34))
flux distributions in simple-geometry natural uranium-heavy water-organic lattices, 17: 26759 (EUR-206.e)
flux distributions in reflected reactors, computer program for calculating, 17: 29716 (MITNE-34)
flux distributions in reactors, apparatus for measuring, 17: 29194 (CEA-2271)
flux distributions in spherical water-filled containers, 17: 3331
flux distributions in and near steel rods in graphite moderator, 17: 4026 (TID-14073)
flux distributions in plutonium-fueled lattices, P-3 calculations of, 17: 37003(R) (HW-78118)
flux distributions in infinite beryllium medium with constant plane source, 18: 7667
flux distributions in concrete-walled ducts, calculations of, 18: 9557 (ORNL-3507)
flux distributions inside stacks of foils, 18: 16901
flux distributions in water system with internal cavity, 18: 34731 (NASA-CR-54110)
flux distributions in exponential piles, time-dependent, 18: 35225
flux distributions from point isotropic fission source in water, transfusion-method computer calculation of, 18: 36555 (ORNL-3487)
flux distributions near plane interface between monatomic gases, calculation of, 18: 36558 (TID-20935)
flux distributions in uranium rod–heavy water lattices, 18: 42923(R) (MITNE-46)
flux distributions in enriched swimming pool reactor core (E), 19: 1936 (PAEC(D)RE-648)
flux distributions in organic–heavy-water lattices (E), 19: 1909
flux distributions in ANNA critical assembly (T), 19: 3519 (PAN-533/IX-A)
flux distributions in iron-water and water shields (T), 19: 3221
flux distributions in heavy-water lattices of enriched uranium metal rods, (E/T), 19: 5433 (MITNE-33)
flux distributions in heavy water lattices with single uranium rod, (E/T), 19: 42047 (MIT-2344-3, pp 115-24)
flux distributions from pulsed source in heterogenous rock-fluid system, 19: 42649
flux distributions in reactor moderators and reflectors, temperature effects on, (T), 19: 47956 (IAE-723)
flux distributions in Tower Shielding Reactor II, 20: 5181(R) (ORNL-3029)
flux distributions in paraffin, (E), 20: 15683
flux distributions of, activation autoradiographic method for determining, 20: 27284
flux distributions in light-water moderated reactor, computer program for, 20: 38450
flux from radium–beryllium sources, calibration of, 19: 22799
flux importance function in heterogeneous lattices, (T), 20: 34969
flux importance function for, use in calculations for reactor cells, 20: 34970
flux in activation analysis, sensitivity of, 19: 28272
flux in annular ducts through laminated iron-heavy water shields, (E/T), 20: 1317
flux in critical assemblies, one-group parameters for, (T), 20: 14073
flux in empty cylindrical channels surrounded by hydrogenous media, 18: 17249 (EIR-60)
flux in heterogeneous media, method for calculating, 17: 34838 (EUR-358.i)

flux in homogeneous slab reactor, fuel distribution for flat, (T), 19: 35708 (UJV-1310/65)
flux in indium foils, effects of flux anisotropies on perturbations in, (E), 19: 21213
flux in IRT-2000 reactor, measurement of, 19: 22777
flux in LITR and ORR, measurement of, (E), 20: 12501 (ORNL-TM-1163)
flux in reactor shielding, DTK calculation of, 18: 19279 (NAA-SR-Memo-9458)
flux in reactor thermal column, (E/T), 19: 33197 (NIJS-R-437)
flux in reactors, detector foil perturbation of, 17: 34840 (NP-12662)
flux in reactors, equipment for measuring, 17: 42240(P)
flux in scattering medium, theory of, 17: 32984
flux in slab, computer program for angular, 18: 977 (GAMD-3033)
flux in swimming-pool reactor, beam port void effects on scalar, (E/T), 19: 17376
flux in water and uranyl fluoride–water solutions, perturbation by aluminum–dysprosium foils, 20: 15669 (NASA-TN-D-3237)
flux in water in Lid Tank Facility, (E/T), 20: 4299(R) (ORNL-2711)
flux in water medium in Lid Tank Facility, 20: 46935 (ORNL-TM-1603)
flux in 19-pin oxide fuel elements, 17: 26040
flux mapping of, using semiconductor detectors and tunnel diodes, 18: 24827
flux measurement by nonperturbing foils, 17: 26411
flux measurement by fission tracks in solids, 19: 26707
flux measurement by manganese activation, absolute, 16: 27334
flux measurement in graphite, optimum foil thickness of dysprosium for, 18: 43949
flux measurement in high-power reactors, fission chamber for, 16: 19091
flux measurement of, design of monitor using encased thermocouple, 18: 14288(P)
flux measurement, development of boronated glass for, (E), 19: 19095 (WASH-1053)
flux measurements using sodium powders, 17: 4825
flux measurements, use of lithium-coated solid-state surface barrier detector for, 17: 35253(R) (IA-775)
flux measurements in power reactors, method for integrated, 17: 41119
flux measurements using gold foil activation, 18: 23876 (KFK-180)
flux measurements using indium and silver nitrates and rhodium sulfate, 18: 23896
flux measurements by activation methods, in-time integration of, 18: 30696
flux measurements by transmutation phenomenon, in-time integrated, 18: 30745
flux measurements using vanadium foils, 19: 24034
flux measurements using gold activation, Geiger-Mueller counter calibration for, 19: 24856
flux measurements using foil detectors, 19: 32567
flux measurements in water using gold activation, corrections to, 20: 5181(R) (ORNL-3029)
flux measurements using gold activation, corrections to, 20: 4299(R) (ORNL-2711)
flux measurements using aluminum–cobalt wires, developments in, 20: 14433(R) (BAW-298)
flux measurements in water-cooled fuel-plate test rig for DIDO reactors, 20: 47062 (AERE-M-1758)
flux measurements in criticality accidents using multi-sphere technique, 19: 44323
flux measurements in Argentina Reactor (RA-1), 16: 3956 (NP-11107)
flux measurements, development of aluminum-gold alloy for, 16: 11893
flux measurements with gold foils, corrections for, 16: 24361
flux measurements by metal foil activation, 16: 24363
flux measurements at 5 ev using thick gold detectors, 16: 23841 (CEA-2162)
flux measurements by foil activation, effects of inter-foil interactions on, 16: 30939
flux of, calibration of National Bureau of Standards, 17: 28232
flux of, measurement by activation and scintillation counting, 17: 25601 (PAN-408/IX)
flux of pulsed, in water, (E), 19: 29209
flux of, boron thermistors for measuring, 20: 13126(P)
flux of, distribution of eigenvalue curves in analysis of, (T), 20: 3002
flux optimization in AARR core, 19: 31495(R) (ANL-7010(p.21-76))
flux perturbation by indium foils in water, 17: 26409
flux perturbation in diffusing media by the introduction of detectors, 17: 6484
flux perturbation in water by re-entrant holes, 20: 34501
flux perturbation by probes, 16: 24360
flux perturbations by absorbing probe, review, 17: 26407
flux perturbations of, effects of flux anisotropy on, 18: 21152
flux ratios in multi-region reactors, method for determining, (T), 19: 17224
flux space energy distribution, diffusivity in, 16: 29732
flux space-energy distribution of, use of perturbation theory in multigroup method of calculating, 16: 29731
flux spectrum in medium with temperature discontinuity, 16: 2476
flux stability in reflected slab reactor with xenon and temperature reactivity feedback, 17: 26809
flux standardization of, assembly for absolute, 17: 26237
flux standardization of, equipment for, 18: 40486
flux trapping by water-d_2, 16: 33785
fluxes in Bulk Shielding Facility, (E/T), 20: 4299(R) (ORNL-2711)
fluxes in concrete and water, from point isotropic fission sources, (T), 19: 45464 (ORNL-TM-1167)
fluxes in concrete branched rectangular ducts, (E/T), 20: 46928(R) (ORNL-3973(Vol.1), pp 26-47))
fluxes in Engineering Test Reactor, 17: 36969 (IDO-16894)
fluxes in graphite, diffusion theory calculations of, 17: 41847(T) (AEC-tr-6095)
fluxes in multilegged concrete ducts, 18: 6405(R) (ORNL-3499(Vol.I) (p.137-46))
fluxes in oil, at Lid Tank Facility, 20: 4999(R) (ORNL-2599)
fluxes in paraffin, 16: 23964 (ANL-6515(p.9-27))
fluxes in reactor shielding, 17: 40217(T) (AEC-tr-6044)
fluxes in vertical irradiation facilities of CP-5, 19: 45668 (ANL-7026)
gamma rays from capture of, nondestructive technique to defect burnable poisons in fuel materials, 20: 41112 (IITRI-578P11-54)
genetic effects in lespedeza seeds, 16: 31488
genetic effects on dormant flax seed, 16: 21934
image intensifier for, 20: 39174
intensity distribution from Soller-type collimator, 20: 13702 (LA-DC-7594)
interaction with matter, resonance, 18: 40496
interactions of polarized, with protons in magnetic-fields, (T), 20: 36053
interactions of, spin-orbit, 17: 20963
interactions of, with Fermi liquids, theory for, 17: 15114
interactions with protons, Fermi approximation to cross sections for, 18: 11149
interactions with bound and free protons at 0.005 to 0.05 ev, cross sections for, 16: 29729
leakage in a hexagonal lattice, 17: 26752 (CRRP-1147)
leakage kernels and slowing down parameters of, errors in spatial harmonics for, (T), 20: 1142
lifetime calculations for slab and spherical geometry, (T), 20: 34489
lifetime in borehole model, (E/T), 19: 18184
lifetime in cadmium–graphite lattice, 18: 42582 (CEA-R-2515)
lifetime in infinite medium, determination of, using pulsed source, 20: 14772
lifetime in thorium oxide–water–heavy water lattices, 16: 6096 (BAW-1234)
lifetime in well-logging experiments, computer program for calculating, 20: 14775
lifetime measurement in water moderator, 17: 15195 (BNL-719 (Vol.III)(p.932-4))
lifetime measurements of pulsed, in graphite, 17: 15196 (BNL-719 (Vol.III)(p.935-45))
lifetime of, method for measuring, 19: 35360
measurement in ETRC core, 19: 32680(R) (IDO-17052)
measurement in soil–water systems, scintillation detector for, 20: 19092
monitor design, 16: 10255
monitoring of, engineering drawings of device with optional burst detector for, 19: 6211
monochromatization of, properties of twin-rotor pulsing device for, 17: 15237
monochromatization of, velocity selector for, (E), 19: 22694 (IEA-76)
motion of pulses of, in graphite, 18: 40800
multiplication factor in reactor, effects of fast fission in two-region fuel element, 16: 19911 (HW-SA-2586)
multiplication in graphite–uranium lattices (E), 19: 3569
nuclear reactions, energy distribution of capture gamma radiation, 16: 6469
performance in activation analyses, 20: 3863(R) (IS-1200(Sect. C))
polarization, 16: 26198 (NP-11859)
polarization of, after passage through soft iron, 17: 9479 (NP-12447)
polarization of beams of, 18: 9300
polarization of, by reflection from magnetized cobalt mirror, 17: 32977
polarization of, apparatus for magnetized-mirror, 18: 11141 (ANL-6797(p.45-55))
polarization of, calculation of, 18: 30703
polarization of, measurement by magnetized mirrors, 18: 11140 (ANL-6797(p.35-44))
production by accelerators and reactors, comparison of, 19: 31461(R) (ANL-7010(p.235-87))
production in thermal columns in heavy water reactors, (E), 19: 17358 (ANL-6915)
production in 70-Mev electron linear accelerator shielding, 19: 20749
production of beams of, reactor core modifications to enhance, 19: 29797

production of, design of high-flux component in Bulk Shielding Reactor for, 17: 3576 (ORNL-TM-399)
production of monochromatic, polarized beams of, 17: 41850
production of pulsed beams of, using accelerator-bombarded exponential piles, (E), 20: 6257 (CONF-650217, pp 11-24)
production of 10^{14}/cm²/sec fluxes of, in modified Brookhaven Graphite Research Reactor, (E/T), 19: 33664 (BNL-9086)
production of, using reactions of LAMPF proton beam with moderated targets, (E), 20: 5935 (CONF-650217, pp 73-6)
propagation in base multiplying media, exceptional frequencies in, (T), 19: 17232
propagation in graphite, thermalization effects in one-group analysis for pulse, (T), 20: 15678
propagation in moderating media away from a sinusoidally modulated point source, neutron-wave technique for, 17: 3747
propagation in steel–uranium and uranium slabs, (E), 19: 12454 (EUR-1637.f)
propagation in thermal columns of pulsed reactors, 17: 35215
propagation of burst of, through extended multiplying system, 18: 35247(R) (NAA-SR-9700)
propagation of pulses of, in multi-region media, 17: 34871
propagation of pulsed, Moore's method for analysis of, 19: 29204
propagation of pulsed, in infinite water geometry, 20: 2944
propagation of pulsed, in absorbing media, (E/T), 20: 32362
properties of slow-neutron dispersion, counting and optical, (T), 19: 34551
properties of, use of impulse method for investigating, 17: 34846
pulse propagation in graphite, from reactors, 20: 2955
pulse propagation in graphite, measurement using modulated and pulsed sources, 20: 34486
pulse propagation in homogeneous systems, general linear model for dispersion in, 20: 36150
radioinduced mutations in rice, 20: 40640
radioisotope production by, materials activation by, 19: 33704
reaction (n,γ) with dysprosium at 900 to 6000 Mev, spectra of, 18: 42734
reaction of, with plutonium-239 and plutonium-241, 18: 1487(R) (HW-77609(Sect.3))
reactions (n,γ) with cobalt-58 and sodium-22, cross sections for, 18: 7777
reactions (n,γ) with silver-107 and 109, 88-kev transition in, 18: 7782
reactions (n,α) with boron-10 and lithium-6 in chromates and cobalt complexes, effects on recoil atom retention, 19: 13489
reactions (n,α) with boron-10, cross section for, (E), 19: 20088
reactions (n,α) with uranium-235, cross sections for, (E), 19: 26917(R) (IA-984)
reactions (n,α) with boron-10, reactions of recoils from, 19: 36514
reactions (n,γ) with indium-115, gamma spectra from, 18: 15215
reactions (n,γ) with nuclei, cross sections for production of short-lived isomers in, 18: 15219
reactions (n,γ) with cobalt-58, burnup in, 18: 19438
reactions (n,γ) with nuclei, gamma-gamma correlations from, 18: 21199 (KR-64(Sect.XXI))
reactions (n,γ) with chlorine-35, angular distributions of electron-positron pairs from, 18: 21236
reactions (n,γ) with selenium-77, sum-coincidence studies of gamma cascades from, 18: 21329
reactions (n,γ) with copper and manganese, gamma spectra from, 18: 24699
reactions (n,γ) with tin nuclei, spectra from, 18: 26540(R) (ORNL-3582 (p.62-7))
reactions (n,γ) with cadmium-113, conversion electron spectra from, 18: 27795
reactions (n,γ) with nuclei, use for photonuclear resonant scattering, 18: 30765
reactions (n,γ) with silicon semiconductors, phosphorus-31 production in, 18: 33920
reactions (n,γ) with iron-56, spectra of, 18: 36627
reactions (n,γ) and (n,2n) with germanium compounds, germanium isotope effects on recoil products in, 18: 39347
reactions (n,γ) with gadolinium and samarium, spectra from, 18: 40529
reactions (n,γ) with gold-198, absorption cross section for, 18: 39119
reactions (n,γ) with bismuth-209 and uranium-238, spectra from, 18: 42646 (ORNL-TM-954)
reactions (n,α) with neodymium-143, samarium-147, and samarium-149, cross sections for, 19: 35615(R) (NP-15037)
reactions (n,α) with heavy nuclei, cross sections for, (E), 19: 41809(T)
reactions (n,α) with calcium-40 and -43 and oxygen-17, Q-values for, (E), 20: 11983
reactions (n,α) with potassium-39, sulfur-32, and -33, cross sections and Q-values for, (E), 20: 11983
reactions (n,α) with boron-10, branching ratio for, (E), 20: 22071
reactions (n,α) with samarium-149 at 0.004 to 0.1 ev, spins of resonances from, (E), 20: 28370
reactions (n,f) and (n,γ) with nucleic, cross sections for, (E), 20: 3031
reactions (n,f) with nuclei, 18: 11189 (ANL-6797(p.424-37))
reactions (n,f) with plutonium-239 and -241, fragment mass distributions from, 18: 15260
reactions (n,f) with uranium-235, prompt neutron distributions from, 18: 21198 (KR-64(Sect.XIX))
reactions (n,f) with uranium-235, mass distribution for binary and ternary, 18: 21280
reactions (n,f) with uranium-235, yields for, 18: 24677
reactions (n,f) with uranium-235, neutron emission by fission fragments in, 18: 24701
reactions (n,f) with plutonium-239 and uranium-235, interference effects in fission cross sections for, 18: 26569
reactions (n,f) with uranium-235, fragment range from, 18: 28580 (WAPD-BT-30(p.47-52))
reactions (n,f) with uranium-235, gamma angular distribution from, 18: 42637 (KFKI-16/1963)
reactions (n,f) with uranium-235, statistical properties of, 18: 42720
reactions (n,f) with uranium-235, use of cerium-144 and lanthanum-140 production as monitor for, 19: 1586
reactions (n,f) with uranium-235, fragment distributions from, (E), 19: 5126 (CEA-R-2408)
reactions (n,f) with uranium-233, prompt gamma spectra from, 19: 6631 (IDO-17025)
reactions (n,f) with uranium-235, ternary, (E), 19: 23640
reactions (n,f) with uranium-235, gamma angular distribution in, (E), 19: 41722
reactions (n,f) with plutonium-239 and plutonium-241, yields from, 19: 22870(R) (HW-83601)
reactions (n,f) with uranium-235, ionization energy losses of fragments from, (E), 20: 3029
reactions (n,f) with uranium-235, fragment charge distribution in, (E), 20: 11980 (USNRDL-TR-935)
reactions (n,f) with uranium-235, statistical analyses of, (T), 20: 34568
reactions (n,f) with plutonium-239 and plutonium-241, fission-fragment energy and mass distributions in, (E), 20: 42261
reactions (n,f) with uranium-235, mass dependence of fission-fragment energy, (E), 20: 42297
reactions (n,f) with uranium-235, search for three- and four-body neutron bound states in, (E), 20: 42298
reactions (n,f) with uranium-235, cesium-132, -134, and -136 and rubidium-86 yields in, 20: 42178
reactions (n,f) with uranium-233 and -235, cesium-137 yields in, 20: 42176
reactions (n,f) with isomeric americium-242, cross sections for, (E), 20: 44708
reactions (n,f) with uranium-236, fission-fragment energy and yields in, (E), 20: 46749
reactions (n,f) with plutonium-239, fission-product range distribution in aluminum, (E), 20: 46761
reactions (n,f) with uranium-233 and uranium-235, yields of bromine isotopes from, (E), 20: 46762
reactions (n,f) with uranium-235, palladium-115 yield from, (E), 20: 46624
reactions (n,γ) with cesium-133, cesium-134 isomer cross-section ratio for, (E), 19: 5131 (KFKI-18/1963)
reactions (n,γ) with silicon, phosphorus production in, 19: 11205
reactions (n,γ) with argon-40, cross sections for, (E), 19: 12535
reactions (n,γ) with holmium-165, conversion electron spectra from, (E), 19: 16942
reactions (n,γ) in aluminum-27, and lead-208, spectra from, (E), 19: 25485
reactions (n,γ), with scandium-45, levels populated in, (E), 19: 25526
reactions (n,γ) with lutetium-176, isomer production in, (E), 19: 31283
reactions (n,γ) on argon-41, cross section for, 19: 31303
reactions (n,γ) with mercury-199, energy levels from, (E), 19: 31309
reactions (n,γ) with nuclei in thermal reactors, gamma spectra from, (E), 19: 35849 (RT/FI(64)-16)
reactions (n,γ) with gold-197, gamma spectrum from, (E), 19: 37797 (IAE-772)
reactions (n,γf) with transuranic nuclei, (T), 19: 39864
reactions (n,γ) with holmium, gamma spectra from, 19: 41670 (LA-DC-7097)
reactions (n,γ) with nuclei, spectra from, 19: 40896
reactions (n,γ) in ammonium and sodium chloroiridates, products from, 19: 42572
reactions (n,γ) with phosphorus-31 and sulfur-32, gamma spectra from, (E), 19: 43288
reactions (n,γ) with tungsten, osmium and rhenium production from, 19: 44599(R) (GEMP-50A)
reactions (n,ν) with iron-54, gamma spectra from, (E), 19: 45322
reactions (n,γ) with iodine-127, spectra from, (E/T), 20: 1151 (IFA-RN-20)

reactions (n,γ) with mercury-199, gamma angular distributions from, (E), 20: 1152 (IFA-RN-21)
reactions (n,γ) with americium-241, americium-242 isomer production in, 20: 1155 (JINR-P-2347)
reactions (n,γ) with iron-54, gamma spectra from, 20: 3109
reactions (n,γ) with hydrogen, cross section for, (E), 20: 3058
reactions (n,γ) with thallium-203, thallium-204 energy levels from, (E), 20: 6411
reactions (n,γ) with scandium-45, gamma spectra from, (E), 20: 9981 (WASH-1064)
reactions (n,γ) with chlorine-35, angular correlations in, (E), 20: 10009
reactions (n,γ) with nickel, gamma spectra from, (E), 20: 9966 (IAE-885)
reactions (n,γ) with holmium-165, gamma spectra from, (E), 20: 11982(T) (LA-tr-65-34)
reactions (n,γ) with thulium-169, thulium-170 levels from, (E), 20: 17782
reactions (n,γ) with nuclei, research at RC-1 reactor, 20: 20334
reactions (n,γ) with vanadium-51, vanadium-52 level scheme from, (E), 20: 19899
reactions (n,γ) with manganese-55, gamma spectra from, 20: 22064
reactions (n,γ) with cadmium-113, internal conversion spectra from, (E), 20: 22066
reactions (n,γ) with sulfur-32, sulfur-33 level spins from, (E), 20: 22077
reactions (n,γ) with erbium-167, erbium-168 gamma spectra and level scheme from, (E), 20: 24484
reactions (n,γ) with arsenic-75, levels from, (E), 20: 24455
reactions (n,γ) with mercury near 5 Mev, gamma spectra from, (E), 20: 30358(R) (RPI-328-56, pp 1-48)
reactions (n,γ) with tungsten isotopes, gamma spectra from, (E), 20: 30360 (WASH-1068)
reactions (n,γ) with beryllium-10, cross sections for, (E), 20: 30347(R) (IDO-17147, pp 13-28)
reactions (n,γ) with gold-197, gold-198 levels from, (E), 20: 30409
reactions (n,γ) with hafnium isotopes, gamma spectra and energy levels from, (E), 20: 30466
reactions (n,γ) with cesium-133 and iodine-127, gamma spectra from, (E), 20: 32422
reactions (n,γ) with scandium-45, (E), 20: 34574
reactions (n,γ) with iron-54, iron-55 levels from, (E), 20: 34677
reactions (n,γ) with titanium-48, time invariance of nuclear forces from, 20: 30505
reactions (n,γ) with samarium-149, samarium-150 levels from, 20: 36215
reactions (n,γ) with strontium-87, strontium-88 neutron binding energy levels from, (E), 20: 38141
reactions (n,γ) with scandium-45, gamma spectra from, (E), 20: 42382
reactions (n,γf) with plutonium-239, and uranium-233 and -235, probability of, (T), 19: 5182
reactions (n,p) with copper-65, cross section for and preparation of nickel-65 by, 18: 41897
reactions (n,p) with chlorine-35 in sodium chloride, yields of sulfur-35 from, 20: 25134
reactions in clays and soils, gamma spectra from, 20: 43607
reactions in meat, phosphorus-32 production by, 19: 42671
reactions in silicon semiconductor devices, activation in, 19: 32600(P)
reactions in solids, review of chemical consequences of, 19: 13498
reactions (n,α) with chromium-53, chromium-54 energy levels and spins from, 17: 28320
reactions (n,α) and (n,γα) with beryllium-7, parity conservation in, 17: 29609
reactions (n,α) with tellurium-120 and -123, 17: 29879(R) (IA-822)
reactions (n,α) with aluminum-27 near 14 Mev, cross section fluctuations for, 17: 40089
reactions (n,α) with uranium-235, 17: 41930
reactions (n,α) with boron-10, branching ratio for lithium-7 ground and first excited state production in, 18: 2940
reactions (n,α) and (n,γ), heat transfer calculations for, 16: 26231 (TRG-Report-322)
reactions (n,α) on samarium-149, cross sections, 16: 33881
reactions (n,d) with oxygen-16, deuteron angular distribution for, 17: 40096
reactions (n,γ) with nuclei, gamma spectra for, 17: 26443(R) (ORNL-3425(p.60-3))
reactions (n,γ) with samarium-150, 17: 26494
reactions (n,γ) with cadmium-114, europium-154, and holmium-166, gamma spectra from, 17: 28332
reactions (n,γ) with plutonium-239, cross section for, 17: 32723(R) (PR-P-57(p.5-20))
reactions (n,γ) with erbium-164, cross sections for, 17: 34981
reactions (n,γ) with cadmium, gadolinium, and samarium, low-energy gamma rays from, 17: 36408 (NP-13020(p.160-5))
reactions (n,γ) with nuclei, gamma intensities from, 17: 40045
reactions (n,γ) with phosphorus-31 in phosphorus trichloride, chemical reactions following, 17: 40852 (NP-13229)
reactions (n,γ) with gold, anomalous, 17: 41942
reactions (n,γ) with nuclei, spectrometer performance for, 18: 2058
reactions (n,γ) with cadmium-113 in cadmium sulfide, cadmium-114 recoil effect on luminescence and photoconductivity, 18: 4324
reactions (n,γ) with fluorine-19, energy spectra from, 18: 6214
reactions (n,γ) with mercury-200, energy levels from, 18: 9388
reactions (n,p) with nitrogen-14, cross section for, 17: 22561 (NP-12658)
reactions of, product yields in fission, 17: 39985 (USNRDL-TR-633)
reactions of, with nuclear isomers, cross sections and uses of, 16: 29790(T) (AEC-tr-5187)
reactions with absorber materials, effects of burn-up on absorption cross sections for, 17: 15214 (GEAP-4017)
reactions with absorbing materials, cross sections, 16: 2774(R) (IDO-16710)
reactions with americium-241 at 0.032 to 80 ev, cross sections for fission, (E), 19: 10335
reactions with americium-241, fission fragment mass yield curves for, (E), 19: 43326
reactions with americium-241, yields of americium-242, curium-242, and plutonium-242 from, 20: 14631
reactions with americium-242, americium-243 yields from, 20: 14631
reactions with argon, gold, and sodium, cross sections for, 18: 15302
reactions with aromatic phosphorus compounds, phosphorus-32 formation in, 19: 38700
reactions with beryllium and beryllium oxide, fast fission factors for, (E), 20: 28277 (JUL-337-RG)
reactions with boron-10, 18: 8099 (BNL-5741)
reactions with boron-10, 18: 8100 (BNL-7542)
reactions with boron and uranium-235, cross sections, 18: 24578
reactions with boron-10 in boron–copper system, production of helium-4 and lithium-7 by, 20: 2444
reactions with boron glass, helium production by, 20: 44011
reactions with cadmium-108, activation cross sections for, 18: 21220
reactions with californium-252 and uranium-235, prompt gamma rays from, 20: 6314
reactions with cesium-133 and praseodymium-141 at 0.01 to 10 ev, total cross sections for, 19: 29232 (CONF-758-2)
reactions with chlorine-35 in organic chlorine compounds, production of sulfur-35 in, 20: 25114
reactions with deuterium and lithium for production of 14-Mev neutrons, 17: 41963
reactions with dysprosium-163, hafnium-177, and thulium-169 at 1 to 4 ev, spins of resonances in, (E), 19: 5180
reactions with elements, for activation analysis, 19: 32058(R) (GA-5978)
reactions with fissionable nuclei, analysis and interpretation of cross sections for, 18: 42752
reactions with gadolinium, spins of resonances in, (T), 19: 27559
reactions with gaseous and liquid nitrogen and oxygen, coherent effects in, (E), 19: 35354
reactions with gold at 0.001 to 0.1 ev, total cross sections for, (E), 19: 18300
reactions with gold, activity from, (T), 20: 19834 (SGAE-CH-24/1965)
reactions with gold, gold-198 yields from, (E), 20: 19878
reactions with heated tellurium dioxide to produce iodine-131, 20: 12922(P)
reactions with helium-3, electric conductivity of plasma produced in, (E), 20: 24488 (AE-218)
reactions with hydrogen gas, energy exchange in, 18: 30699
reactions with iron, cross sections for manganese-53 production in, 19: 12605
reactions with liquid and solid polyphenyls, total cross sections for, (E), 20: 28254
reactions with lithium carbonate, formation of fluorine-18 in, 18: 43633
reactions with lithium-6 deuterides, production of 14-Mev neutron flux in, 16: 33789 (BNL-5366)
reactions with manganese-54, activation cross section for, 18: 40474 (IDO-16977(p.23-43))
reactions with matter as probe of molecular motions, 19: 40455 (BNL-9297)
reactions with metals, neutron shielding effects in, 18: 6184(T) (SC-T-523)
reactions with minerals and ores, gamma spectra from, 20: 33161(T) (AEC-tr-6639, pp 13-17)
reactions with neodymium-148, cross sections and resonance capture integral for (E), 19: 3386
reactions with nitrogen, gamma production in, 17: 4210 (DASA-1318)
reactions with nitrogen-14 in hydrazine sulfate, yields of carbon-14-labeled compounds in, 18: 43636
reactions with nuclei, cross sections for, 18: 2837(R) (EANDC(OR)-22L)
reactions with nuclei, capture-to-fission ratios in, 18: 2403(R) (PR-P-58)
reactions with nuclei, charge and mass distributions from fission, 18: 21195 (KR-64(Sect.XVI))

reactions with nuclei, nuclear structure studies using, 18: 32780
reactions with nuclei, energy release in fission, (E/T), 19: 21224 (AECL-2160)
reactions with nuclei, activation-rate reduction to a differential spectrum in, (T), 19: 43327
reactions with nuclei, shell effects on cross sections for, (E), 19: 47618
reactions with nuclei, with charged-particle emission, 20: 44666(T) (INDSWG-101, pp 1-22)
reactions with nuclei, cross-section multilevel analysis, 16: 14101
reactions with oriented uranium-235, distributions from fission, 18: 26554(R) (ORNL-3582(p.121-6))
reactions with plutonium-239 and uranium-233 and 235, fragment velocities in fission, 17: 24422
reactions with plutonium-239, uranium-233 and 235, neutron energy spectra from fission, 17: 26394 (LAMS-2883)
reactions with plutonium-239, fragment mass distributions in fission, 17: 26447(R) (ORNL-3425(p.79-82))
reactions with plutonium-239, capture-to-fission ratio for, 17: 28277
reactions with plutonium-239 and uranium-235, phase analysis of, 17: 31413(T) (AEC-tr-5916)
reactions with plutonium-239 and uranium-233, neutrons emitted in, 17: 19280
reactions with plutonium-239 and uranium-235, triple-fission, 17: 38006(T) (AEC-tr-5734(p.37-41))
reactions with plutonium-239, capture to fission ratio for, 18: 1001 (AERE-R-4173(Add.))
reactions with plutonium-241 at 0.1 to 11 ev, fission cross sections for, 18: 7768
reactions with plutonium-239 and uranium-233 and 235, directional correlation of fission fragments and prompt gammas from, 18: 9400
reactions with plutonium-241, cross section for fission, 18: 34914
reactions with plutonium and uranium, cross sections for, 18: 38064 (A/CONF.28/P/717)
reactions with plutonium-239 and uranium-233 at 0.057 ev, eta values for, 18: 40474 (IDO-16977(p.23-43))
reactions with plutonium-241, heavy fragment yields in, (E), 19: 8495
reactions with plutonium-239 and uranium-233, krypton and xenon isotope yields from, (E), 19: 12597
reactions with plutonium-239 and uranium-233 and -235, gamma angular distributions from fission, (E), 19: 12623
reactions with plutonium-239 at 0.16 ev to 5 kev, cross sections for fission, (E), 19: 12501
reactions with plutonium-239 and uranium-233 and -234, fragment energy distribution from fission, (E), 19: 14570
reactions with plutonium-239 at 100 to 220 ev, cross sections for, (E), 19: 16855(R) (ORNL-3714(Vol.I)(p.1-30))
reactions with plutonium-239, fragment mass distribution in fission, 19: 16873
reactions with plutonium and uranium isotopes, cross sections for, (T), 19: 21678 (ANL-6972)
reactions with plutonium and uranium isotopes, xenon-135 yields in, 19: 29314
reactions with plutonium-239, fission product ranges in, (E), 19: 29373
reactions with plutonium-239 and uranium-235, yields of krypton-85 in fission, (E), 19: 39800
reactions with plutonium-239 and uranium-235, fission cross sections for, 19: 47567 (CEA-R-2775)
reactions with plutonium-239 and -241 and uranium-233 and -235, xenon-135 yields from fission, (E), 20: 11990
reactions with plutonium-241, capture-to-fission ratio for, (E), 20: 15774
reactions with plutonium and uranium isotopes, fission neutron yields from, 20: 17823
reactions with plutonium-241, prompt neutron yields from fission, (E), 20: 17826
reactions with plutonium-141 at 20 to 200 ev, fission cross sections for, (E), 20: 26082 (IDO-17174)
reactions with plutonium-239 and uranium-235, x-ray yields from fission, (E), 20: 26182
reactions with plutonium-239, fission fragment ranges in aluminum from, (E), 20: 28476
reactions with plutonium-239, yields of zinc-72 from fission, 20: 28448
reactions with plutonium isotopes, abundance and period of delayed neutrons from, 20: 35003 (BNWL-232)
reactions with plutonium-239, ranges of products from fission, (E), 20: 34525 (KFK-401)
reactions with plutonium-239 and uranium-235, fission resonance integral for, (E), 20: 17751
reactions with plutonium-239, total kinetic energies of symmetric fission fragments from, (E), 20: 26213
reactions with plutonium isotopes, fission fragment energy correlations for thermal, 20: 39470(R) (ORNL-3924)
reactions with protactinium-233, total cross sections for, 18: 40474 (IDO-16977(p.23-43))
reactions with quartz crystals, induced color centers in, 19: 18016
reactions with rare gases at (3 to 25) $\times 10^{-3}$ ev, absorption and scattering cross sections for, 17: 29588
reactions with rhenium-187, activation cross section for, 18: 40578
reactions with rhenium-185 and -187, total cross sections for, (E), 20: 3030
reactions with semiconductor impurities, 19: 7769(R) (NYO-3124-1)
reactions with semiconductors, recoil and transmutation in, 16: 6817(R) (ORNL-3213(p.57-80))
reactions with thermocouples, composition changes from, 17: 30826
reactions with thorium dioxide, uranium dioxide, and uranium at 0.0045 to 0.028 ev, total cross sections for, (E/T), 20: 21966 (AE-222)
reactions with thorium-229, fission yields from, 20: 28303
reactions with thorium-229, product mass distribution from fission, 20: 30373
reactions with transuranium elements at 0.4 to 200 ev, cross sections for, (T), 20: 24334 (BNL-10083)
reactions with tungsten and gold at low temperatures, Doppler effect in resonance, 17: 9532
reactions with tungsten isotopes, cross sections for, (E), 20: 9981 (WASH-1064)
reactions with uranium-water lattices, effective cross sections for, 17: 22599
reactions with uranium-235, kinetics and mass distribution of binary and ternary fission in, 17: 26446(R) (ORNL-3425(p.76-9))
reactions with uranium-235, prompt neutron emission in fission, 17: 26585
reactions with uranium-235, mass-yield distribution variation with neutron energy for fission, 17: 31391 (CONF-12-2)
reactions with uranium-235, fragment distributions and mechanisms in fission, 17: 7098 (NP-12330(p.79-85))
reactions with uranium-235, ternary fission product parameters for, 17: 9583
reactions with uranium-235 at 6.68 ev, resonance, 17: 11655
reactions with uranium-235 at 0.4–11.3 Mev, prompt neutron angular and energy distributions from fission, 17: 33042
reactions with uranium-235, with distributions from ternary fission, 17: 34958
reactions with uranium-235, prompt gamma emission in, 18: 1000 (AEET/NP/7)
reactions with uranium-235, long-range particles from fission, 18: 4587(T) (AEC-tr-6183)
reactions with uranium-233 and -235, mass yields in fission, 18: 7700 (USNRDL-TR-679)
reactions with uranium-235, neutron emission in, 18: 9325(T) (AEC-tr-6285)
reactions with uranium-235, average neutron yield in fission, 18: 11194 (CONF-346-7)
reactions with uranium-235, energy balance for ternary fission, 18: 17003
reactions with uranium-235, fragment mass distributions from, 18: 16338
reactions with uranium-235, mass distributions from fission, 18: 20358
reactions with uranium-235, angular distributions and energy spectra of neutrons emitted in, 18: 24697
reactions with uranium-235, long-range alpha particles from fission, 18: 40606
reactions with uranium-235, alpha distributions from ternary fission, 18: 42652(T) (ANL-Trans-68)
reactions with uranium-235, mean beta energy from fission (E), 19: 1653
reactions with uranium-232, capture cross sections and resonance integrals for, (E), 19: 10302
reactions with uranium-235, fission fragment energy spectra from, (E), 19: 11516
reactions with uranium-235, fission gas release from, 19: 15394
reactions with uranium-233 and -235 and plutonium-239, gamma angular distributions from, (E), 19: 16869
reactions with uranium-233 and -235, prompt neutron yields from fission fragments in, (E), 19: 19079 (AECL-2163)
reactions with uranium-235, fission fragment angular and energy distributions from, (E), 19: 19085 (JEN-131-DF/I-42)
reactions with uranium-233 and uranium-235, mass yields from, 19: 19133
reactions with uranium-235, cross sections for, (E), 19: 21230 (CEA-R-2552)
reactions with uranium-235, fragment energy spectrum in fission, (E), 19: 21296
reactions with uranium-235, tellurium-131 and -133 isomer pair yields from fission, (E), 19: 21390
reactions with uranium-235, prompt neutrons emitted by fragments in, 19: 23665
reactions with uranium-235, duration of gamma emission from fission, (E), 19: 25480
reactions with uranium-233 and -235 and plutonium-239, fission fragment mass distributions from, (T), 19: 27443(T) (ANL-Trans-149)

reactions with uranium-235, fission fragment ranges from, (E), 19: 27527
reactions with uranium dioxide, mass spectra of krypton and xenon from, 19: 26912
reactions with uranium-235 at 0.025 to 1 ev, ternary fission yield in, (E), 19: 29237 (IDO-17073)
reactions with uranium-235, tritium yields from, 19: 29518
reactions with uranium-235, prompt neutron yields from fission, (E), 19: 29267
reactions with uranium-235, fission fragment yields from, 19: 29313
reactions with uranium-235, independent radiochemical yields from fission, (T), 19: 33329
reactions with uranium-235, neutron spectra from fission, (T), 19: 33356
reactions with uranium-235, energy dependence of gamma angular anisotropy from fission, (E), 19: 33370
reactions with uranium at 4.5°K, electric conductivity changes in, 19: 34762
reactions with uranium-233 and uranium-235, fission yields in, 19: 35442
reactions with uranium-235, fission fragment energy distributions from, (E), 19: 37819(R) (ORNL-3778(p.129-39))
reactions with uranium-235, fission products from, 19: 36217(R) (IDO-14656)
reactions with uranium-235 at 2200 m/sec, cross sections for fission, (E), 19: 41691
reactions with uranium-235, positron emission of fission products from, (E), 19: 41799(T)
reactions with uranium-235, yields of isotopes from fission, (E), 19: 45260(R) (IDO-14660)
reactions with uranium-235, K x ray emission during, (E), 19: 45294
reactions with uranium-235, yields of antimony-124 and -126 and empirical Z_p function in fission, (E), 19: 47611
reactions with uranium-235, fragment kinetic-energy distributions from, (E), 20: 3110
reactions with uranium-235, fission yields from, (E), 20: 6288 (KAPL-3113)
reactions with uranium-235, BCS model calculations of mean primary charge distribution from fission, (T), 20: 10054
reactions with uranium-235, fission fragment kinetic energy and mass distributions from, (E), 20: 9997
reactions with uranium-233 and -235, capture-to-fission ratios for, (E), 20: 11960(R) (IDO-14667)
reactions with uranium-233 and -235, fission yields from, (E), 20: 11960(R) (IDO-14667)
reactions with uranium-235, palladium-115 yields from fission, (E), 20: 11981 (USNRDL-TR-943)
reactions with uranium-235, fission-fragment mass-energy correlations from, (E), 20: 12076
reactions with uranium-233 and -235, zirconium-95 yields from, (E), 20: 13783 (ORNL-TM-1333)
reactions with uranium-235, yields of argon isotopes and cobalt-56 in ternary fission, (E), 20: 13862
reactions with uranium-235, prompt neutron yields from fission, (E), 20: 17824
reactions with uranium-235, gamma energies and yields from fission, (E), 20: 17828
reactions with uranium-235, gamma angular distributions from fission, (E), 20: 17829
reactions with uranium-235 at 0.005 to 0.2 ev, ratio of binary-to-ternary fission in, (E), 20: 17840
reactions with uranium-235, fission fragment mass distributions after prompt neutron emission, (E/T), 20: 17866
reactions with uranium-235, mass dependence of fission fragment energies from, (E/T), 20: 17868
reactions with uranium-236, fission fragment yields from, (T), 20: 28262 (AD-632242)
reactions with uranium-235 and -238, promethium-148 yields from fission, 20: 28271 (JAERI-1103)
reactions with uranium-235 at 0.003 to 0.3 ev, fission, (E), 20: 30513
reactions with uranium-233 and -235, yields of xenon-133 and -135 from fission, 20: 30533
reactions with uranium-235, fragment activity and gamma spectra from, (T), 20: 36181 (USNRDL-TR-1009)
reactions with uranium-236, neutron yields from fission, 17: 5351
reactions with uranium-235, gamma spectra from, fission, 17: 9521
reactions with uranium-235, kinetic energies of fission fragments from, 16: 33802
reactions with water, use in neutron moisture probe, 16: 698
reactions (n,α) with beryllium-7, alpha properties from, 16: 21401
reciprocity theorems for, 17: 5304
reflection by beryllium, lithium fluoride, and sodium chloride single crystals, 16: 20637 (JAERI-1030(Suppl.))
reflection by concretes, Monte Carlo calculations of, 18: 28910
reflection by slabs of aluminum, concrete, iron, lead, and polyethylene, differential, 20: 42142 (NP-16234)
reflection from collimator slits, total, 17: 13477
reflection from collimator walls, multiple, 18: 21126 (KR-64(Sect.XXIV))
reflection from slabs of iron, (E/T), 20: 34796
research with, survey of, 17: 36658 (LADC-5951)
resonance escape factors for homogeneous mixture of uranium with graphite and uniform water moderator, 16: 12023
scattering and slowing-down by hydrogenous compounds, 17: 11602
scattering and transmission of, experiments on, in German FRM reactor, 18: 23114
scattering by alkali metals, uses for calculating phonon dispersion relations, (E), 19: 43264
scattering by aluminum, beryllium, and bismuth, cross sections for, 18: 26662
scattering by aluminum and beryllium crystals, interference effects in inelastic, (E), 19: 12477
scattering by aluminum powder, distributions from inelastic, (E), 19: 20551 (IDO-17063)
scattering by ammonia (gaseous and liquid), cross sections for, 17: 9510 (PAN-214)
scattering by ammonium perchlorate and hexamethylbenzene, cross section measurements of rotational motions in, 18: 44439
scattering by ammonia and hydrogen sulfide at 0.025, 0.07, and 0.1 ev, 19: 14476
scattering by ammonia and hydrogen sulfide, differential cross sections for, 19: 32680(R) (IDO-17052)
scattering by ammonium compounds, distribution from incoherent, 19: 45242
scattering by anharmonic crystal, 17: 5317
scattering by anharmonic crystals, damping theory for, 18: 28560
scattering by anharmonic crystals, spectral line shape of inelastic, (T), 19: 43499
scattering by antiferromagnetic and ferromagnetic crystals, polarization effects in elastic, 17: 22544
scattering by antiferromagnets, cross section of inelastic magnetic, (T), 20: 4809
scattering by argon, krypton, and xenon, electron-neutron interaction potential from, (E), 19: 45098
scattering by argon-36, anomalous, 16: 8213
scattering by asymmetrically deformed square well potential, S-wave strength function in, 18: 16956 (ZFK-TPH-7)
scattering by atoms in condensed systems, 17: 4041
scattering by atomic aggregates, Fermi approximation to cross sections for, 18: 11149
scattering by benzene, total cross sections for, 17: 15243
scattering by benzene and polyphenyls, 17: 15163 (BNL-719(Vol.I) (p.69-99))
scattering by benzene, biphenyl, *m*-, *o*-, and *p*-terphenyl, angular distributions and diffusion constants from, (E), 20: 4817
scattering by beryllium, kernel for, 18: 2819
scattering by beryllium, kernel for, 18: 30784
scattering by beryllium powder at 0.04 to 0.10 ev, inelastic (E), 19: 3200
scattering by beryllium oxides, differential cross sections for, (T), 20: 4801(R) (GA-6634)
scattering by beryllium, vanadium, and water at 0.07 ev; cross sections for inelastic, 16: 14064
scattering by beryllium oxide, effects of microstructure and temperature on cross sections for, 16: 33528
scattering by binary rare earth alloys, magnetic, 18: 25980(R) (ORNL-3582(p.9-10))
scattering by bromine (liquid) at 0.037 and 0.0088 ev, angular and frequency distributions from, 17: 15240
scattering by butane, ethane, and methane, calculation methods for, (E), 19: 47576(R) (IDO-17081, pp 49-76)
scattering by calcium hydroxide and magnesium hydroxide, 17: 29445
scattering by carbon tetrachloride, diffraction spectra from, (E), 20: 9960(R) (AEET-228)
scattering by chemically bound systems, computer program for calculation, 17: 4023 (KAPL-2225)
scattering by chromium–iron–nickel and iron–manganese alloys at high temperatures, 18: 16506
scattering by chromium–palladium alloys, magnetic, 18: 25978(R) (ORNL-3582(p.5-6))
scattering by chromium–manganese alloys, magnetic, 18: 25979(R) (ORNL-3582(p.7-8))
scattering by chromium, 19: 23611(T)
scattering by chromium, phonon spectra from, (E), 19: 43265
scattering by cobalt crystals at high temperature, coherent magnetic, 17: 21061
scattering by cobalt, magnetic, 18: 37710
scattering by cobalt, manganese, and nickel carbonates, cross sections and polarization of elastic and inelastic, 18: 42320(T)
scattering by cobalt-59, spin dependence of cross sections for, 17: 22626

scattering by complex magnetic crystalline structures, elastic, 17: 28236(T)
scattering by complex molecules, 18: 2805
scattering by complex spherical potentials, cross sections for, 16: 28039
scattering by concretes, accuracy of Monte Carlo method for calculating albedo from, 20: 6519(R) (ORNL-3858(Vol.1), pp 20-41)
scattering by copper, total cross sections for, 20: 36140(R) (GA-7091)
scattering by coupled atoms, differential cross sections for, (T), 20: 9946
scattering by crystals, perturbation theory of anharmonicity effects in inelastic, 17: 15230
scattering by crystals, incoherent cross sections, 17: 19381
scattering by crystal impurity nuclei, inelastic, 17: 38030(T) (AEC-tr-5734(p.186-7))
scattering by crystals and liquids, review of dynamics of, 17: 38056
scattering by crystals and solids, theoretical study of, 18: 11152
scattering by crystals, anomalous dispersion in, 18: 37148
scattering by crystals with point defects,cross sections for, 18: 44721
scattering by crystals, vibration interaction effects on inelastic, (T), 19: 11769
scattering by crystals, phonon interactions in, 19: 23983
scattering by crystals at 30 to 1000 ev, cross section for, (E), 19: 45489
scattering by crystals, engineering drawings of diffractometer for studying, 20: 675
scattering by crystals, structure analysis using inelastic, 20: 20170
scattering by crystals, structure determination from inelastic, 20: 28603 (BNL-10134)
scattering by crystals, dynamic structure property determination from, (T), 20: 34835
scattering by crystals, phonon dispersion relations from inelastic, 16: 32370
scattering by crystals, effects of electron-phonon and phonon-phonon interactions on inelastic, 16: 32386
scattering by Debye solids and diffusive media, examples of scattering law, 16: 9412 (AERE-R-3847)
scattering by defects in solids, inclusion of relaxed atoms in calculation of cross sections for, 18: 42314
scattering by deuterated methane (T), 19: 1639
scattering by diatomic liquid elements, coherent inelastic (E/T), 19: 3199
scattering by diatomic molecules, formulas for, 16: 33791 (KR-26)
scattering by diphenyl and Dowtherm "A," angular and energy distributions from inelastic, 17: 15244
scattering by dislocations in nickel, magnetic, 19: 29220
scattering by doped semiconductors, coherent, (E), 19: 14079
scattering by ethane, propane, and water, model for, 19: 32680(R) (IDO-17052)
scattering by ethane, cross sections for inelastic, (E), 20: 9981 (WASH-1064)
scattering by ethylene and propylene, angular distribution for, 17: 38028(T) (AEC-tr-5734(p.164-6))
scattering by ferromagnetic crystal, inelastic, (T), 19: 33347
scattering by ferromagnetic materials at small angles, inelastic, (T), 19: 33213
scattering by free molecules, classical selfcorrelation for cross section of, 17: 19236
scattering by gallium, cross sections for coherent, 18: 19112(T)
scattering by gases, computational techniques for cross-section determinations in, 17: 15167 (BNL-719(Vol.I)(p.144-71))
scattering by gases, evaluation of computational techniques for determination, 17: 15168 (BNL-719(Vol.I)(p.172-202))
scattering by gaseous, liquid, and solid methane, inelastic, 19: 8076
scattering by gaseous and liquid methanethiol and methanol, cross sections for, 20: 325
scattering by gaseous and liquid ethane at 0.020 to 0.046 ev, molecular motion determination from inelastic, (E), 20: 33254 (BNL-940, pp 142-8)
scattering by gaseous methane, effect of interference scattering on, 16: 29718
scattering by germanium–iron phases, uses for crystal-structure analyses, (E), 20: 9960(R) (AEET-228)
scattering by graphite, theory, 17: 15165 (BNL-719(Vol.I)(p.117-20))
scattering by graphite, effects of temperature, 16: 1035(T) (AEC-tr-4690)
scattering by graphite, phonon frequency distributions in, 16: 7174
scattering by graphite, water, and water-d_2, 16: 13925 (AERE-R-3931)
scattering by halogen acids, distributions from slow inelastic, (E), 19: 44038
scattering by harmonically bound protons, cross section for, 17: 19228 (TID-18424)
scattering by heavy and medium nuclei at 1.509 Mev, polarization in elastic, 17: 31410 (TID-19051)
scattering by heavy water containing poison, spectra of (E), 19: 3202
scattering by heavy water, water, and zirconium hydride, cross sections for, (E), 20: 21939(R) (GA-6930)
scattering by heavy water, model for incoherent, 16: 24379
scattering by helium near λ curve, cross sections for, (T), 19: 29342
scattering by helium II (liquid), Green functions for, 16: 10977
scattering by hexamethylbenzene, studies of hindered rotational motions and phase transitions by, 20: 18717
scattering by holmium-165, spin dependence of (E), 19: 3338
scattering by hot gases, use for temperature measurement, 18: 26157
scattering by hydrogen sulfide (liquid), total cross sections for, 17: 9509 (PAN-213)
scattering by hydrogenous materials, 17: 14933 (EANDC(OR)-19(L))
scattering by hydrogenous compounds, 18: 24625 (WASH-1046)
scattering by hydrogen in water molecule, cross sections for, 18: 36551 (GA-5373)
scattering by hydrogenous compounds, (E), 19: 19095 (WASH-1053)
scattering by hydrogen in tissue, 19: 22018 (BNL-8165)
scattering by hydrides, theory, 19: 25454 (NAA-SR-10899)
scattering by hydrogenous moderators, differential cross sections for, (E/T), 19: 27389 (GA-6295)
scattering by hydrogenated nickel-palladium alloy, magnetic, 19: 40075 (IEA-84)
scattering by hydrogen and vanadium, performance of three-axis spectrometer for, 19: 44527
scattering by hydrogen molecules, Fadeev equations for, (T), 20: 13417
scattering by hydrogen, computer program for, 20: 17684 (JAERI-1085)
scattering by hydrogenous moderators, cross sections for, (T), 20: 36139 (GA-7055)
scattering by ice, water, and water vapor at 0.18×10^{-3} to 2.8×10^{-3} ev, 16: 7162
scattering by ideal gases in acoustical fields, total cross sections for, (T), 20: 30256
scattering by iron and nickel at 0°K, polarization effects in, 17: 9520
scattering by iron(II) chloride near Neel temperature, cross section for small-angle, 17: 16006
scattering by iron–silicon systems, magnetic structure studies in, 17: 34465
scattering by iron–uranium alloys, magnetic, 17: 37824
scattering by iron, distributions from magnetic, 18: 2837(R) (EANDC(OR)-22L)
scattering by iron–palladium–rare earth alloys, magnetic, 18: 25977(R) (ORNL-3582(p.2-4))
scattering by light and heavy water, 17: 15161 (BNL-719(Vol.I) (p.26-53))
scattering by light and heavy water at 0.03, 0.06, and 0.12 ev, space-time correlation functions for, 16: 7161
scattering by light and heavy water, angular and energy distributions, 16: 7164
scattering by linear molecules, (T), 20: 38002
scattering by liquid methane, cluster model for, 17: 22967(R) (IDO-16857)
scattering by liquid hydrogen disulfide, at 5.8 to 187 Mev, 17: 31388
scattering by liquids and solids, studies of atomic motion by, 17: 9513 (TID-17489)
scattering by liquid methane, comparison with theoretical results, 17: 15216 (NP-12502)
scattering by liquids, space-time correlation function representation of cross sections for, 17: 15219 (PAN-355/I-B)
scattering by liquids and solids, spectrometer for studying inelastic, 17: 15235
scattering by liquids and solids, incoherent inelastic, 18: 18932
scattering by liquid sodium, cross sections for inelastic, 18: 22860
scattering by liquids, specimen container for, 18: 29653
scattering by liquids, coherent (T), 19: 1638
scattering by liquid argon, inelastic, (E), 19: 8345
scattering by liquid sodium, coherent, (T), 19: 12473
scattering by liquids, models for, 19: 23738
scattering by liquid methane, use of Langevin equation of Brownian motion for analysis of, 20: 313
scattering by liquid argon, coherent, (T), 20: 4819
scattering by liquid and solid lead, distributions from multiple, (E/T), 20: 6255 (AERE-R-5016)
scattering by liquid and solid argon, differential cross sections for inelastic, (E), 20: 9981 (WASH-1064)
scattering by liquids and solids, 20: 8046
scattering by liquid and solid argon, inelastic, 20: 14059(R) (IDO-17104)
scattering by liquids, 20: 19798
scattering by liquids, review on, (E), 20: 19799
scattering by liquid and solid argon, inelastic, 20: 26396(R) (IDO-17140)
scattering by liquids and polyethylene, theory of, 20: 26396(R) (IDO-17140)
scattering by liquid argon, statistical evaluation of elastic, 20: 34329 (BNL-940, pp 183-90)

scattering by liquids, hindered-translator model for one-particle motions in, 20: 37999
scattering by liquids, smeared potential model, 16: 7156
scattering by liquids, incoherent approximation for cross section, 16: 7157
scattering by liquids, 16: 22979
scattering by liquids, incoherent approximation for cross sections, 16: 24768(T) (AEC-tr-5158)
scattering by liquid methylamine, total cross sections for, 16: 28016
scattering by lithium deuteride and hydride, (E), 19: 44732
scattering by low-impurity metal crystals, oscillation frequency and resonance location determination from, (E), 20: 22320
scattering by lucite, paraffin, and water, 16: 7169
scattering by macroscopic systems, applications of Wigner representation to theory of, 18: 13037
scattering by macroscopic systems, quasiclassical theory for, 19: 10238
scattering by magnetic structures with large superlattice repeat distance, 19: 23611(T)
scattering by magnetic materials, spin-wave excitation by inelastic, 19: 41987
scattering by magnetic materials, survey on, 20: 19797
scattering by magnetic materials at Curie temperature, angular resolution for, 20: 22325
scattering by magnetic ions in crystals, orbital electron contribution to, (T), 20: 28673
scattering by magnesium, frequencies of normal modes from inelastic, (E), 20: 34810 (BNL-940, pp 78-82)
scattering by manganese oxide and manganese zinc ferrite, measurement of magnetic inelastic, (E), 19: 8375 (BNL-7645)
scattering by many-body systems, nonequilibrium properties form, 20: 24305
scattering by many-body systems, nonequilibrium properties from, 20: 24305
scattering by matter, single-particle effects on inelastic, 17: 15095
scattering by matter, cross sections for inelastic, 19: 47543 (ANL-7050, pp 471-85)
scattering by matter, analytic uses of pulsed-beam inelastic, (T), 20: 6258 (CONF-650217, pp 82-101)
scattering by mercury, neutron gravity refractometer for measurement of, 19: 14481
scattering by metals, analysis of, 19: 43263
scattering by methane, 17: 4330(R) (IDO-16781)
scattering by methane (liquid), 17: 4333(R) (IDO-16805(p.7-35))
scattering by methane at −148°C, 17: 17623(R) (IDO-16827)
scattering by methane, inelastic, 16: 3661
scattering by methane gas at 0.015 and 0.0252 ev, rotational level effects, 16: 7087
scattering by methane, 16: 33787
scattering by moderating molecules, cross sections for, 18: 33010 (A/CONF.28/P/258)
scattering by moderators, cross sections and kernels for, (T), 19: 29169 (GA-6281)
scattering by moderators, 16: 12409
scattering by moderators, data analysis scheme, 16: 21332 (AERE-R-4041)
scattering by molecules with rotational freedom, cross sections for, 17: 22545
scattering by molecules, 17: 17623(R) (IDO-16827)
scattering by molecules, 17: 36629 (PAN-255)
scattering by molecular benzene, angular distribution and cross section for, 18: 13764
scattering by molecules, distributions from, 18: 40474 (IDO-16977 (p.23-43))
scattering by molecules, modification of Krieger-Nelkin approximation for, (T), 19: 5120
scattering by molecules, computer programs for cross sections for, 19: 35379 (IDO-17087)
scattering by molecules, kinetic equations for, (T), 19: 35366
scattering by molecular hydrogen, cross sections and spectra for, (T), 20: 17664
scattering by molecules, (T), 20: 19800
scattering by molecules, review on, (E), 20: 19801
scattering by molecules, mass-tensor approximation for, 20: 28253
scattering by nickel, polarization effects in spin-orbit, 18: 11261
scattering by non-axially symmetric deformed potential, s-wave intensity function in, 18: 34787
scattering by nonabsorbing media, effects of chemical binding on Milne-problem extrapolation distance in, 18: 21147
scattering by nuclei in crystals, theory for, 17: 31074 (ANL-6744)
scattering by nuclei, resonance widths for, 17: 15287
scattering by nuclei, boundary diffusion effects on cross sections for, (T), 19: 21424
scattering by nuclei at 5.8 and 7.5 Mev, gamma spectra from inelastic, (E), 20: 22069
scattering by nuclei, intensity measurements for inelastic, (T), 20: 24314
scattering by nuclei, calculation using complex potential, 16: 13935
scattering by organic compounds, determination of carbon-hydrogen ratios by, 17: 5949 (BNL-5814)
scattering by organic molecules, dynamics of, 18: 37150
scattering by organic moderators, cross sections for inelastic, 19: 8387
scattering by ortho- and para-hydrogen, cross sections for, 17: 15242
scattering by ortho- and parahydrogen, (T), 20: 44591
scattering by p-azoxyanisole, effects of magnetic field causing polarization of sample, 16: 7159
scattering by paraffin at 80°C, spectra and yield in, 17: 9493
scattering by paramagnetic manganese fluoride, 17: 20978
scattering by plane-parallel crystal plate, 16: 13937
scattering by plasma, temperature measurements from, 17: 31621
scattering by polar liquids, 17: 22539 (TID-18587)
scattering by polarized nuclei in ferromagnetic materials, 18: 24580
scattering by polyethylene, 17: 15164 (BNL-719(Vol.I)(p.100-16))
scattering by polythene, distributions from, 18: 24571(R) (RPI-328-6)
scattering by polyethylene, inelastic, (E), 19: 14482
scattering by polyethylene, phonon spectra from, 19: 32151
scattering by polyethylene, inelastic, 20: 26396(R) (IDO-17140)
scattering by polycrystalline aluminum, one-phonon coherent, (T), 20: 30745
scattering by polycrystalline vanadium, phonon frequency distribution from inelastic, 20: 34507
scattering by propane at 0.01 to 0.10 ev, cross sections, 16: 10944
scattering by pyrrhotite crystal, magnetic inelastic, 18: 21131 (PAN-279)
scattering by rare gases, electron-neutron interaction from, (E), 20: 40129
scattering by rare earths, paramagnetic, 16: 13933
scattering by reactor moderators, development of computer programs for calculating, 20: 8035 (GA-5798)
scattering by reactor moderators, computer program for, 20: 19780 (JAERI-1094)
scattering by reactor moderators, methods for calculating, (T), 20: 19781 (JAERI-1095)
scattering by reactor moderators, sensitivity of reactor parameters on, 20: 28714 (BNWL-SA-616)
scattering by rotating states in molecules, 18: 24299 (NP-13930 (p.56-7))
scattering by semi-infinite nonabsorbing gas, energy-dependent Milne problem for, 18: 21144
scattering by shielding materials, albedo measurements on, 19: 40065 (NP-15152)
scattering by silicon polymers, 17: 36669 (WASH-1042)
scattering by single crystals of beta brass, coherent, (E), 19: 11767
scattering by sintered beryllium oxide at 290 to 1500°K, cross sections for, 16: 1033(T) (AEC-tr-4688)
scattering by sodium at 0.026 to 0.10 ev, 17: 4330(R) (IDO-16781)
scattering by sodium (liquid) at 0.025 to 0.1 ev and 23 to 200°C, 17: 4333(R) (IDO-16805(p.7-35))
scattering by sodium (liquid), energy transfer in, 17: 17183
scattering by solids, 17: 38044(T) (AEC-tr-5734(p.255-66))
scattering by solids, 18: 22862
scattering by solids, inelastic, 19: 12468
scattering by solid solutions, one-phonon peak in, (T), 19: 41991(T)
scattering by solid and liquid terphenyls, 16: 18418
scattering by spinel-type solid solutions, theory of, 17: 2218(T)
scattering by spin system of paramagnetic materials, 17: 7073(T)
scattering by spin waves in yttrium iron garnets, polarization dependence of inelastic, (E), 20: 24647
scattering by tantalum, effects of lattice dynamics on, 18: 44207
scattering by thermodynamic systems, Van Hove's function for, (T), 19: 27398
scattering by thermodynamic systems, Van Hove function for, (T), 19: 30853
scattering by thorium, titanium, and zirconium hydrides, inelastic, (E/T), 19: 47549(R) (TID-22141, pp 34-49)
scattering by titanium and zirconium hydrides, inelastic, (E/T), 19: 31234(R) (RPI-328-35(p.120-4))
scattering by transition metal hydrides, hydrogen vibration effects in, (E/T), 19: 5887
scattering by uniaxial antiferromagnetic materials, distributions from, 17: 5318(T)
scattering by unordered solids, inelastic, (T), 19: 10226
scattering by uranium dioxide, crystal properties from, (E), 19: 42894
scattering by vanadium and water at 0.001 to 1 ev, differential cross sections for, (E), 19: 33192(R) (GA-6096)
scattering by water, comparison of Nelkin and Radkowsky kernels for, 17: 9482 (WAPD-T-1481)
scattering by water, 17: 11589 (HW-75526)
scattering by water-d_2, intramolecular, 17: 20964

scattering by water-d_2, intermolecular, 17: 20965
scattering by water molecules, 18: 2815
scattering by water at 95°C, law for, 18: 8912(R) (HW-78388(p.10.1-25))
scattering by water at fixed angles, time-dependent pair correlation function for inelastic, (T), 19: 10225
scattering by water, differential cross sections for, (E/T), 19: 29216
scattering by water and zirconium hydrides, differential cross sections for, (E/T), 20: 4801(R) (GA-6634)
scattering by water, angular distributions and diffusion constants from thermal, (E), 20: 6270
scattering by water-d_2 and zirconium hydride, angular distributions and diffusion constants from, (E), 20: 6271
scattering by water, elastic, (T), 20: 28252
scattering by water, model for, (E/T), 20: 30330
scattering by water-d_2, model for calculating, (T), 20: 42139 (IN-1020)
scattering by water, calculation of angular distribution, 16: 21343
scattering by white tin, inelastic, (T), 19: 11770
scattering by white tin, uses for crystal-lattice analyses, (E), 19: 42889
scattering by ytterbium-176, isomeric states from, (E), 19: 45357
scattering by yttrium, amplitude of, 17: 26615(T)
scattering by yttrium, 19: 47888
scattering by zirconium hydrides at 296 and 750°K, cross sections for, 20: 36140(R) (GA-7091)
scattering cross sections for, DSDE computer program for calculating, 17: 19200 (NAA-SR-Memo-7940)
scattering cross section for, spectrometer for measuring inelastic, 18: 10376(R) (HW-79054(p.82-9))
scattering cross sections for, Boltzmann calculations of inelastic, 18: 42599 (TID-7050(p.289-330))
scattering cross sections in crystalline and liquid substances, (T), 19: 45228 (NP-15469)
scattering cross sections of, fluid kinetic models for, 20: 34509
scattering, design of four-rotor neutron spectrometer for studying, 16: 7151
scattering, development of instrument for velocity distribution measurements in, 16: 21333 (CRRP-1078)
scattering, Doppler approximations and models for, 16: 26209 (BNL-5821)
scattering from magnetized cobalt mirrors, spin reversal in, 19: 21300
scattering from oxyhydrogen flame, temperature measurement by, 20: 37310
scattering function for n-body scatterer, method for evaluating, (T), 19: 5117
scattering in complex magnetic structures, inelastic, 17: 39702(T)
scattering in dilute systems, density expansion of self-correlation function for, 20: 34468 (BNL-940, pp 175-8)
scattering in doped ferromagnets, theory of inelastic magnetic, 17: 13478(T)
scattering in f.c.c. cobalt, spin-wave, 20: 8305
scattering in ferrites, effects of spin-spin interaction in, 17: 37634(T)
scattering in ferrites, effects of spin-photon interaction on one-quantum, 17: 37635(T)
scattering in liquid metals, Kohn anomaly in coherent, (T), 20: 2948
scattering in liquids and solids, (T), 20: 19793
scattering in magnetic crystals, theory, 17: 32987
scattering in materials, 18: 34752(R) (CU(PNPL)-234)
scattering in moderators, elastic and inelastic, (T), 19: 29192
scattering in pentane, angular distributions from inelastic, (E), 20: 38001
scattering in reactors, analysis of inelastic, (E/T), 20: 13700 (JAERI-1086)
scattering in real gases, cluster expansion for inelastic, (T), 20: 15672
scattering in rectangular concrete ducts, (E/T), 20: 6519(R) (ORNL-3858(Vol.1), pp 20-41)
scattering in silicon single crystals, oscillatory signal interference effects on, 19: 19076
scattering in uranium dioxide, reactivity effects of inelastic, 17: 3763
scattering in water, double differential cross sections for, 20: 36140(R) (GA-7091)
scattering, inelastic in inorganic and organic compounds, Egelstaff scattering law curves, 16: 1021 (IDO-16699)
scattering kernel generation for, computer programs for, 18: 978 (KAPL-M-FDF-5)
scattering kernel for polyethylene and water, calculated moments of, 17: 38418 (KAPL-M-FDF-3)
scattering kernels for graphite, spectra of crystalline, 19: 23595(R) 19: 23595(R) (GA-5305)
scattering kernels and laws for, method for calculating, 20: 3412
scattering kernels for water at 423 and 550°K, (T), 20: 42138 (IN-1019)
scattering law determinations from experimental data, 17: 15162 (BNL-719(Vol.I)(p.54-65))
scattering law evaluation, 16: 12410
scattering law for graphite, spectra measurements for, 18: 33028
scattering law for atomic systems, 18: 32711 (AERE-NP/GEN-29)
scattering lengths of, comparison of coherent, 18: 23878 (NP-13930 (p.76-7))
scattering of, by gaseous hydrogen sulfide, 16: 33685 (NP-12135)
scattering of, determining pair correlation function from, 17: 19204 (TID-18429)
scattering of, in heavy water and water, 16: 33577(R) (AE-79)
scattering of, intermediate function in, 17: 22475
scattering of polarized, spin density matrix formalism for, 18: 14813 (KR-65)
scattering of 0.05 to 1.5 ev, inelastic, 17: 22666(R) (TID-18561)
scattering of, analysis of inelastic, (T), 19: 5160
scattering of, analysis of approximations used in, 19: 43250 (COO-917-15)
scattering of, boundary effects on cross section measurements for, (T), 19: 14156
scattering of, computer program for calculating Legendre moments from, 19: 45223 (JAERI-1084)
scattering of, convolution approximation of Van Hove function for, 20: 17665
scattering of, crystal-diffraction techniques for inelastic, (E/T), 20: 19795
scattering of, mechanical and time-of-flight techniques for inelastic, 20: 19794
scattering of, quasiclassical approximation in theory of, 20: 17666
scattering of, solid-state studies by, 19: 47889
scattering of, studies of condensed state of matter by, 18: 15312
scattering of, time-dependent correlation functions for, (T), 20: 30336
scattering on atomic nuclei, van Hove equation for, 20: 44593
scattering on bonded atoms, differential cross section calculation for, 17: 38037(T) (AEC-tr-5734(p.219-21))
scattering on bound atoms, asymptotic formulas for, (T), 19: 19107
scattering on manganese(II) fluorides, covalent spin distributions from polarized, 17: 37692
scattering on molecular gases, mass tensor approximation for, 17: 39963
scattering, properties of space-time correlation function for, 16: 7147
scattering, theory of law for, 16: 7146
scattering, total cross sections for inelastic, 16: 32368
selector for, mechanical, 17: 18559(T) (UCRL-Trans-899(L))
separation from reactor flux, design of structure for, 20: 40368(P)
shielding against, properties of boron–glycerin–litharge cement for, 19: 18441
slowing down in fissionable materials and moderators, 20: 20183
slowing down of, mathematical theory of, 18: 32723
space-energy separability of, in pulsed systems, 17: 15210 (BNL-719 (Vol.IV)(p.1331-59))
space-energy separability assumption validity for water moderators, 16: 10940 (WAPD-T-1065)
spectra as function of lattice position, computer program for calculation, 16: 26459 (BNL-5826)
spectra, calculation from scattering law data, 17: 15166 (BNL-719 (Vol.I)(p.121-43))
spectra, calculation of spatial variation in lattices, 17: 15183 (BNL-719(Vol.II)(p.592-609))
spectra, calculation of asymptotic, in graphite, 17: 15186 (BNL-719 (Vol.II)(p.656-65))
spectra, calculation in a medium with two different temperatures, 17: 15187 (BNL-719(Vol.II)(p.666-84))
spectra calculations of, review of methods for, 18: 38010 (A/CONF.28/P/365)
spectra, comparison of self-adjoint variational and 36-group calculations of, 16: 24368
spectra, computer program for, 16: 24367
spectra, effects of resonance absorbing cylinders on, 16: 15264(R) (HW-71747)
spectra, extraction hole effects on, 16: 26199 (NP-11932)
spectra from deuteron reactions (d,n) with tritium at 400 kev, 16: 14063
spectra from VVR-C, 18: 9736
spectra in beryllium and graphite, (E/T), 20: 18127(R) (GA-6753(Pt.1))
spectra in beryllium oxide, 20: 21939(R) (GA-6930)
spectra in beryllium oxides, temperature effects on, 20: 36140(R) (GA-7091)
spectra in biphenyl, effects of methyl borate concentration on, 20: 36140(R) (GA-7091)
spectra in boric acid solutions, 17: 9528
spectra in boric acid–water solutions, hardening of, 19: 45226 (KFK-294)
spectra in boric acid–water systems, determination using integral activation techniques, (E), 20: 2965
spectra in cluster fuel elements, model for, (T), 19: 24056
spectra in complex media, similitude theory for, 20: 14776
spectra in composite fuel elements, method of predicting, 18: 15506
spectra in cooled moderators, (E), 20: 2945
spectra in diphenyl, methyl borate concentration effects on, 20: 36140(R) (GA-7091)

spectra in enriched heterogeneous lattices, deformation of, 18: 38317 (A/CONF.28/P/675)
spectra in finite mass media, properties of, · 20: 21933 (AD-621119)
spectra in graphite-moderated reactor, measurement of, 17: 15175 (BNL-719(Vol.II)(p.359-400))
spectra in graphite, measurement, 17: 15192 (BNL-719(Vol.III) (p.805-37))
spectra in graphite systems, 18: 21146
spectra in graphite-moderated lattices, (E/T), 19: 8601 (NAA-SR-Memo-7891)
spectra in graphite, use of random sampling and multiparameter analysis for, 19: 37776
spectra in graphite–uranium-235 systems, effects of chemical binding, 16: 720
spectra in heavy crystalline media, 16: 24377
spectra in heavy-gas moderators, theoretical calculations, 17: 15208 (BNL-719(Vol.IV)(p.1289-98))
spectra in heavy water lattices, method for calculating, 18: 6451
spectra in heavy water-moderated natural uranium lattices, (E/T), 20: 45090
spectra in heavy water–20% enriched uranyl sulfate systems, 16: 30999 (JAERI-1034)
spectra in heavy-water-moderated natural uranium elements, 20: 39452 (EUR-2981.f)
spectra in heterogeneous media, 17: 3733
spectra in heterogeneous media, methods of calculating, 17: 15178 (BNL-719(Vol.II)(p.RD1-34))
spectra in heterogeneous systems, transport calculation of, 19: 1523 (JAERI-1058)
spectra in heterogeneous cylindrical lattice, program for energy, 19: 33191 (EUR-2294.e)
spectra in heterogeneous lattice cells, computer program for, 19: 41648
spectra in homogeneous poisoned, effect of the Gaussian approximation and various scattering laws on, 17: 3732
spectra in homogeneous media, calculation of, 18: 21122 (EUR-1605.e)
spectra in homogeneous Frankfurt research reactor, (E), 19: 33672
spectra in homogeneous hydrogen-moderated mixture, program for Wigner-Wilkins, 19: 45224 (JEN-133-DF/I-43)
spectra in homogeneous mixtures, computer program for, 19: 45225 (JEN-135-DF/I-44)
spectra in lattices, free-gas-theory calculations of, (T), 19: 47538 (ANL-7050, pp 33-40)
spectra in light and heavy water, time-dependent, (T), 20: 28232 (AE-226)
spectra in liquid hydrogen, 20: 24303(R) (GA-6897)
spectra in moderator with temperature discontinuity, 18: 21145
spectra in multi-region systems, computer program for, 18: 1208 (JAERI-1050)
spectra in organic-cooled heavy-water-moderated power reactors, 17: 3734
spectra in paraffin and in paraffin-moderated subcritical assemblies, space-dependent, 20: 34968
spectra in plutonium–uranium fueled water reactors, (T), 20: 12370
spectra in plutonium dioxide–uranium dioxide lattices, measurement by neutron activation, 20: 20200(R) (ANL-7110, pp 29-98)
spectra in poison-bearing beryllium at high temperature, (E/T), 20: 34502
spectra in reactor lattices, calculation of bump where the Maxwellian meets the 1/E tail, 17: 15184 (BNL-719(Vol.II)(p.610-13))
spectra in reactors, computer analysis of, 19: 6840 (KAPL-M-6413)
spectra in reactors, space dependent, (T), 19: 8599 (EUR-2108.i)
spectra in reactors, computer analysis of, (T), 19: 12762 (WCAP-3269-26)
spectra in reactor moderators, 19: 42037 (BNWL-95, pp 4-17)
spectra in reactor lattices, computer program for calculating, 20: 8343 (ANL-7023)
spectra in reactor cells, lutetium–dysprosium foil activation method for determining, 20: 10338
spectra in reactors, computer program for, 20: 20205 (JAERI-1097)
spectra in reactors, effective temperatures, 16: 12658 (RISÖ-33)
spectra in subcritical homogeneous and inhomogeneous media far from a planar source, 17: 15212 (BNL-719(Vol.IV)(p.1375-90))
spectra in two-temperature lattice, theoretical calculations, 16: 23283
spectra in uranium–water lattices, measuring method for, 19: 38136
spectra in uranium light-water lattices, (T), 20: 9954
spectra in water, · 20: 36140(R) (GA-7091)
spectra in water and heavy water, (E/T), 19: 33231
spectra in water for slab geometry, 18: 15158
spectra in water near temperature discontinuity, (E/T), 20: 30331
spectra in water with absorbers, 18: 34733
spectra in water-moderated uranium dioxide cores, 19: 6848
spectra in water-moderated assemblies, (T), 20: 34971
spectra in Yugoslav heavy water reactor, 20: 30939
spectra in zirconium hydrides, transient properties of, (E/T), · 20: 21941 (IAE-977)
spectra measurements in borated water, (E), 20: 28237(R) (TID-22844, pp 1-35)
spectra near graphite–paraffin interface, 20: 8057
spectra near graphite–paraffin interface, 20: 8058
spectra of, calculation of, 18: 2749
spectra of, computational methods for, 18: 2780 (CONF-39-104)
spectra of, computer program for calculating, 17: 26391 (EUR-105.e)
spectra of, computer program for calculating, 18: 9291 (GA-4132)
spectra of, computer program for spatially dependent, 18: 9293 (KAPL-M-RPC-10)
spectra of, determination by activation rate reduction, 17: 26041
spectra of, determination by transmission methods, 17: 41851
spectra of, in borated water, 18: 2818
spectra of, in homogeneous and heterogeneous media, theoretical calculations of, 17: 15189 (BNL-719(Vol.II)(p.706-97))
spectra of, in media with absorption and temperature discontinuity, 17: 26029
spectra of, in multiplying media, 18: 2821
spectra of, in pressure-tube reactors, 18: 7888 (AEEW-R-186)
spectra of, in samarium-poisoned graphite, 18: 2817
spectra of, in split reactor cores, 17: 12030
spectra of, near absorbers in moderators, 18: 2816
spectra of, relation to scattering law, 17: 17088 (BNL-770)
spectra of, deduction from activation rates of foils, (E/T), 20: 16857
spectra of, eigenfunction analysis of, 18: 15205(R) (TID-20132)
spectra of, emerging from graphite column of thermal reactor, 18: 18853 (ZFK-TPH-8)
spectra of, method for measuring, 19: 15887
spectra of, near absorbing foils in moderators, (E), 19: 27402
spectra temperature distribution in heterogeneous systems, 16: 1002 (PAN-233/IX)
spectra, theoretical calculations, 16: 24938 (HW-71649)
spectral calculations using scattering kernels, 18: 42600 (TID-7050 (p.330-49))
spectral measurements in-core, 18: 42941 (TID-7050(p.1357-96))
spectroscopy of, activation methods for, 17: 10139
spectroscopy of, design of "window" filters for, 18: 18225
spectroscopy of, design of chopper for, (E), 19: 18098 (KAPL-3074)
spectroscopy of, in Triga Mark II thermal column, (E), 19: 42184
spectroscopy of, review of problems and methods of, 19: 31207
spectroscopy of, time-of-flight spectrometer for, (E), 19: 9480 (JINR-P-1899)
spectrum, description of spatially dependent using variational principles, 16: 28416 (WAPD-BT-25(p.1-24))
spectrum effects in fuel and moderator for graphite lattice calculations (E/T), 19: 1839 (NAA-SR-7892)
spectrum in VVR-5 reactor, 18: 7684 (NP-13420)
spin reversal of polarized, with depolarization, 16: 19742
temperatures of, from spherical source in water, 18: 4516
therapeutic effects on tumors, 16: 30207 (BNL-4905)
thermalization in homogeneous systems, 17: 17465
transmission by bismuth single crystals, 17: 15236
transmission by graphite, measurement by pulse method, 18: 28549
transmission by light and heavy water, determination of hydrogen content in heavy water by, 20: 36740
transmission by plane cadmium covers, 18: 44716
transmission by single crystals, 18: 42579 (BLG-260)
transmission by water, flux and reflection in, 17: 34828 (BRL-1204)
transmission in helium-3–helium-4 mixture, determination of composition from, 20: 28210
transmission in hydrocarbons, hydrogen determination by, 19: 28258
transmission of, along air-filled ducts in water, 16: 33780 (AEEW-R-70)
transmission through cadmium covers, measurement of, 17: 19199 (NAA-SR-7770)
transmission through ducts in heavy-water–iron shielding, (T), 19: 12723 (AE-166)
transmission through cadmium, effects of radiation exposure on, 19: 32680(R) (IDO-17052)
transmission through single crystals, interference phenomena in, 20: 36360 (ZFK-RN-32)
transmission through magnetized nickel–palladium alloy sheet containing absorbed hydrogen, 16: 14001
transmission through aluminum and beryllium, 16: 33199
transport calculation methods for, in reactor lattices, 18: 38007 (A/CONF.28/P/74)
transport calculations for, multigroup, 18: 42601 (TID-7050(p.349-78))
transport equation for, asymptotic solutions of, 17: 17090 (GA-3298)
transport equation for slab geometry, computer program for solving, 18: 18850 (EUR-533.i)
transport equation in finite bodies, spectrum of, (T), 20: 17657
transport equation for, computer program for Boltzmann, 20: 13698 (DTMB-1820)

transport equation for, P_1 analytical solution of energy- and space-dependent, 20: 30328
transport equation for, regular eigenfunctions of time-dependent, 20: 32364
transport in enriched heavy-water lattices, (E/T), 19: 5433 (MITNE-33)
transport in graphite, calculations using P-3 approximation, (T), 20: 40064
transport in heavy water–light water moderated assemblies, 18: 28921(R) (TID-20649)
transport in heavy gas moderators, 16: 7010
transport in homogeneous media, computer program for, 19: 3225
transport in hydrogen in bound water of concrete, cross section for, 18: 7849
transport in infinite slabs, asymptotic angular dependent leakage spectra in, (T), 19: 33196 (NIJS-R-435)
transport in one-dimensional slab geometry, 19: 6839 (KAPL-M-6123)
transport in organic liquids, 18: 38038 (A/CONF.28/P/651)
transport in pulsed water systems, measurement of extrapolation lengths for, 17: 11600 (WAPD-T-1490)
transport mean free path in graphite, poison method for, 18: 15160
transport of polarized beams of, 18: 21125 (KR-64(Sect.XXIII))
transport of, few-group approximation to multigroup, 18: 42604 (TID-7050(p.448-94))
transport of, solution of energy- and space-dependent, 19: 27410
transport theory for spatially dependent distribution in heterogeneous media, 18: 9303
use as magnetic probes, 20: 25717 (BNL-946)
use for asphalt-content determination in paving mixture, bombardment-counting-technique for, 20: 29509
use for brain tumor therapy, 19: 10928 (BNL-8664)
use for brain tumor therapy, 19: 32044
use for nondestructive materials testing, method and apparatus for, 20: 25272(P)
use for soil humidity measurements, 16: 16620
use in activation analysis, parameters for, 17: 6026
use in activation studies, self-shielding effects of metals in, 18: 33488
use in biological radiography, 19: 22018 (BNL-8165)
use in concrete moisture-content determination, 20: 18610
use in heterogeneous reactors, equations for, 18: 19320
use in neutron capture therapy, 20: 18507 (BNL-10009)
use in neutron capture therapy, 20: 18508 (BNL-10038)
use in nuclear physics, advanced course on, 18: 21185 (KR-64)
use in production of glass with internal stresses, 19: 4611(P)
use in radiographic, image analysis in, 20: 20866
use in radiography, 17: 3678
use in radiography of irradiated materials, television system for, 19: 28621
use in reproduction of printed matter, 18: 3928(P)
use in weld radiography, 20: 11005(P)
use in well logging, 18: 5522
use of, in hydrogenous plasma temperature measurement, 16: 27249 (AROD-2504:2)
use to determine atomic motions in liquid argon, (E), 19: 16416
uses for determining nuclear radii of tin isotopes, 18: 26538(R) (ORNL-3582(p.56-7))
utilization factors for, in lattice cells, 18: 21597 (EUR-1606.e)
utilization factor for square cell of uranium dioxide–water lattices, (E), 20: 10333
utilization factor in water-moderated natural uranium exponential assemblies, 20: 34974
utilization factor calculations for reactors, 16: 9679(T) (AEC-tr-4678)
utilization in reactor lattices, inhomogeneous perturbation theory for calculating (T), 19: 3526
utilization in reactor matrix, effects of spatially varying source on, (T), 19: 10493
velocity selection of, using helical-slot monochromator, (E), 19: 26659 (JAERI-1069)
wave propagation from pulses of, experimentation with, 18: 2809
wave propagation in time-dependent P_1 approximation, (T), 19: 33203

NEVADA

(See also headings of the form Nevada (Nye Co.))

cattle radioactivity in 1959, 16: 1329(R) (LAMS-2627(p.226-33))
cesium-137 uptake by animals and plants in, coefficients of variance for, 19: 1997
climatological observations at Tonopah Test Range, 18: 13371 (SC-TM-354-63(72))
crustal structure of, from underground-explosion seismic wave propagation, 17: 41001
crustal structure of, from underground-explosion seismic wave propagation, 17: 41004
crustal structure of, from underground and underwater-explosion seismic wave propagation, 17: 41007
crustal structure of earth in vicinity of Las Vegas, gravity and seismic studies on, 18: 18036
earthquake shocks in, analysis of depth data on, 19: 24733 (VESIAC-8580VU)
fallout monitoring, 1961 and 1962, 17: 34156 (TID-18892)
fallout monitoring, 1962, 17: 34182
fallout monitoring, 1962, 17: 38705 (CONF-244-1)
fallout monitoring, October to December 1961, 18: 6951 (UCLA-518)
fallout monitoring, 1961 to 1963, 18: 29193 (CONF-548-1)
fallout monitoring, 1959 through 1961, 19: 9378
fallout monitoring, 1959, 1960, and 1961, 19: 30409
fallout monitoring after underground Pike Event, 1964, 19: 30403 (TID-21764)
geologic map of Frenchman Flat Quadrangle, 18: 31052 (TEI-848)
geologic map of Topopah Spring SW Quadrangle, 18: 26986 (TEI-846)
geology of Buckboard Mesa, 19: 610 (PNE-5001P)
radiological monitoring of air above Las Vegas area, 17: 41018
rock radioactivity in Nevada Test Site and vicinity, 19: 18146 (TEI-858)
strontium-90 uptake by animals and plants in, coefficients of variance for, 19: 1997

NEVADA (CHURCHILL CO.)

geologic and hydrologic studies of Shoal site, 19: 26528 (VUF-1001)
geologic investigations, 17: 3167 (TID-17224)
geologic maps, photographs, and logs, 17: 3168 (TID-17224(Suppl.))
geology, hydrology, and seismicity evaluations for Project Shoal, 16: 19159 (TEI-796)

NEVADA (CLARK CO.)

occurrence and properties of allanite pegmatites, 16: 17889

NEVADA (LINCOLN CO.)

geologic map of Paiute Ridge Quadrangle, 18: 26984 (TEI-826)

NEVADA (NYE CO.)

geologic map of Ammonia Tanks Quadrangle, 17: 4732
geologic map of Buckboard Mesa Quadrangle, 17: 4730
geologic map of Buckboard Mesa Quadrangle, 18: 39477 (TEI-852)
geologic map of Cane Spring Quadrangle, 17: 4720
geologic map of Camp Desert Rock Quadrangle, 17: 4721
geologic map of Frenchman Flat Quadrangle, 17: 4719
geologic map of Jackass Flats Quadrangle, 17: 4729
geologic map of Jangle Ridge Quadrangle, 17: 4734
geologic map of Lathrop Wells Quadrangle, 17: 4726
geologic map of Mercury Quadrangle, 17: 4728
geologic map of Mine Mountain quadrangle, 17: 4722
geologic map of northwest Specter Range Quadrangle, 17: 4725
geologic map of northwest Topopah Spring Quadrangle, 17: 4741
geologic map of Oak Spring Quadrangle, 17: 4739
geologic map of Paiute Ridge Quadrangle, 17: 4735
geologic map of Paiute Ridge Quadrangle, 18: 26984 (TEI-826)
geologic map of Plutonium Valley Quadrangle, 17: 4736
geologic map of Quartet Dome Quadrangle, 19: 20151 (TEI-860)
geologic map of Rainier Mesa Quadrangle, 17: 4740
geologic map of Scrugham Peak Quadrangle, 17: 4724
geologic map of Scrugham Peak Quadrangle, 18: 35704 (TEI-849)
geologic map of Silent Butte Quadrangle in, 18: 41639 (TEI-850)
geologic map of Skull Mountain Quadrangle, 17: 4731
geologic map of Skull Mountain Quadrangle, Nevada Test Site, 18: 26985 (TEI-845)
geologic map of Striped Hills Quadrangle, 17: 4723
geologic map of Thirsty Canyon SE Quadrangle, 19: 20150 (TEI-859)
geologic map of Tippipah Spring Quadrangle, 17: 4737
geologic map of Timber Mountain Quadrangle, 17: 4738
geologic map of Yucca Flat Quadrangle, 17: 4727
geologic map of Yucca Lake Quadrangle, 17: 4733
geology, 16: 7747 (TEI-789)
geology and radioactivity of U12b tunnels in, 16: 29186 (TEI-797)
geology of ground water test well C, Nevada Test Site, 16: 22409 (TEI-818)
geology of U12e.04 tunnel site, 16: 29184 (TEI-776)
geology survey of U12e tunnel system, summary, 16: 15000 (TEI-773)
geophysics of granite stock in Climax area, 17: 1638
ground-water test well B at Nevada Test Site, lithologic data, tests, and construction, 16: 19160 (TEI-808)
ground water tritium-age at Nevada Test Site, 16: 5585
seismic refraction survey of Porpoise site area south of Climax Granitic Stock in, 19: 6586 (NP-14518)

NEVADA PROVING GROUNDS AREA

algal distribution, 19: 33801
animal depositories and ecological peculiarities of, for underground explosion effects, 17: 33505
atmospheric radiation scattering and transmission properties under cloudy conditions, 16: 5563
cratering data in desert alluvium at, 16: 19164
ecological distribution of rodents, 16: 5149 (TID-14374)
ecological study of mites on kangaroo rats in, 18: 13

ecology, effects of fall-out, 16: 28670(R) (UCLA-507)
ecology, effects of underground nuclear explosion, 17: 19750 (PNE-226(P))
ecology, effects on vegetative retention of fallout, 17: 33546
ecology of animals, effects of nuclear detonations, 17: 33580
ecology of, effects of underground nuclear explosions on, 17: 35342(R) (UCLA-515(p.81-98))
ecology of, effects of fallout on, 18: 4961
fallout monitoring, 1961 and 1962, 17: 34156 (TID-18892)
gamma detection and measurement at, 16: 1943(R) (ORNL-3189(p.166-71))
geology, 16: 11946
geology and hydrology, 16: 29185 (TEI-787)
geology and physical properties of alluvium in test site, 17: 36010 (PNE-234P)
geology of ground water test well C, 16: 22409 (TEI-818)
geology of Oak Spring group, 17: 1650
geology of U12b.08 tunnel in, 16: 22408 (TEI-814)
geology of U12e.04 tunnel site, 16: 29184 (TEI-776)
ground water test well, 16: 10278 (TEI-803)
ground water tritium-age, 16: 5585
ground waters in, chemistry and movements of, 18: 33194 (TEI-838)
hydrology, interbasin movement of ground water, 17: 1653
hydrology, potential aquifers in carbonate rocks, 17: 1654
logs for wells and test holes drilled in test site prior to 1960, 16: 8992 (TEI-804)
mining operations in, effects of Sedan event on, 17: 19729 (PNE-204F)
monitoring for beta activities in rabbits and rodents after reactor test (Kiwi-A), 17: 27054 (TID-18864)
monitoring for fall-out, 1951 through 1958, 16: 22434 (TID-7632(p.4-24))
monitoring for radioactivity from rocket reactor test, 1959, 16: 32693 (TID-16835)
monitoring of environs, 1962, 16: 20907
monitoring of environs, 1962, 17: 18455
plant ecology, effects of atomic explosions, 17: 5655 (HW-SA-2546)
radiobiological monitoring of environs, 17: 33543
rock radioactivity, 19: 18146 (TEI-858)
seismic refraction survey of Porpoise site area, 19: 6586 (NP-14518)
stratigraphy and structure of Rainier and USGS tunnel areas on, effects of underground explosions on, 18: 1908
survey for waste disposal prospects, 17: 4370 (TEI-829)
wind measurements in mesodecline over Tonopah test range, 17: 8405

NEVADA TEST SITE

alluvium porosity at, measurement of, using density logs, 17: 25432 (TID-18690)
archeological status of, 20: 35640 (LA-3520)
atomic explosion-produced gamma radioactivity at, 17: 3156 (TEI-832)
balloon tracking in vicinity of, long-range, 19: 21769 (TID-21661)
characteristics and taxonomy of soil fungi from, 19: 35880
climatology of Tonopah Test Range, 1963, 18: 29154 (SC-TM-64-576)
decontamination of materials at, evaluation of, 18: 10307 (TID-19108)
description of cryogenic facilities at Jackass Flats for Rover Program, 18: 22847
drilling of large holes for underground explosions, 18: 43102 (CONF-645-1)
ecological studies at, 18: 9817
ecological studies on plants and mammals, 1963, 18: 11569(R) (UCLA-520(p.81-108))
ecological studies on animals and plants, 1964, 19: 21811(R) (UCLA-12-541(p.101-30))
ecology, 16: 45(R) (TID-14147)
ecology of animals of, effects of nuclear explosions on, 20: 45265
ecology of arthropods at, 19: 6901 (TID-21394)
ecology of mammals of, 19: 33702 (TID-21941)
ecology of Orthoptera of, 19: 3831
ecology of plants of, 19: 12904 (HW-SA-3402)
ecology of plants of, 19: 25817 (UCLA-12-553)
ecology of reptiles of, 18: 8065
effects of large underground Sedan explosion on lizard population, 18: 23181 (UCLA-12-522)
environs monitoring for radioactivity, October to December, 1961, 18: 6951 (UCLA-518)
environs monitoring, 1957 to 1962, 18: 35770 (TID-19416)
environs monitoring, 1962 to 1964, 18: 37383
environs monitoring, 19: 7728 (NVO-162-15)
environs monitoring, 16: 9030 (TID-14776)
environs monitoring of, maintenance and performance of alpha survey meters for, 16: 10325
environs monitoring by measurement of strontium-90 levels in native animals, 1958 to 1961, 16: 10309 (UCLA-500)
fallout hazard from, 17: 37386
fallout monitoring station for, description of remote, 18: 31910 (NBS-5471)
fallout monitoring, 1963, 19: 6104
fallout radioactivity of air, precipitation, and vegetation at, 1963, 18: 11569(R) (UCLA-520(p.81-108))
gamma radioactivity at, natural, 17: 3156 (TEI-832)
gamma spectra of soil samples from, 17: 37014(R) (NYO-9505(p.95-111))
geologic map of Skull Mountain Quadrangle, 18: 26985 (TEI-845)
geologic studies of Pre-Schooner sites in basalt in Buckboard Mesa, preshot, 20: 511 (PNE-505P)
geology and radioactivity of U12b tunnels at, 16: 29186 (TEI-797)
geology of area of U12e tunnel system at, 16: 11936 (TEI-806)
geology of Jackass Flats Quadrangle, 18: 8005 (TEI-843)
geology of site of SULKY nuclear cratering experiment, preshot, 19: 32331 (PNE-719P)
geology of U12e tunnel at, 16: 15000 (TEI-773)
geology of U12i and U12i.01 tunnels and lithology of U12i.01 drill hole, 18: 8004 (TEI-842)
geology of Yucca Flats, 17: 1649
geology of 410 Area, 16: 7747 (TEI-789)
ground shock from small-scale cratering detonations in basalt at, seismic measurements on, 20: 25231 (PNE-504F)
ground water discharge, movement, and occurrence in tuffaceous rocks of, 20: 5643 (TEI-862)
ground-water test well B, lithologic data and construction of, 16: 19160 (TEI-808)
inventory of plants and small mammals, 20: 45264(R) (UCLA-12-595, pp 72-89)
iodine-131 from, hazards to children of, 18: 4044
lizard population at Sedan test site, 17: 21397 (PNE-224F)
meteorological program, 19: 44774 (BNL-914, pp 65-8)
mining on, equipment and excavations for, 20: 14754 (NVO-38-1)
monitoring for radioactive iodine isotopes at, after underground explosion during Operation Niclick, 18: 445 (NVO-162-1)
monitoring system for postshot drilling at, 19: 40834(R) (UCRL-14151)
neutron activation of soils of, gamma dose curves from, (T), 19: 46589 (UCRL-14332)
neutron transport and reflection by soil at, 17: 24599 (BRL-1190)
nuclear rocket reactor tests at, safety aspects, 19: 46707
nuclear rocket tests at, safety aspects of, 20: 37034
nuclear-explosion seismic-wave amplitudes and travel times between Ordway, Colorado and, 17: 41006
plant ecology of target area at, 17: 23145
plant ecology on target areas at, 17: 33576
Pluto site at, geology of, 18: 22260 (TEI-841)
radiation effects on vegetation at, 20: 8661
radiation effects on growth and morphology of plants at, 20: 18386
radiation effects on animal and plant ecology at, 20: 18211(R) (UCLA-12-576, pp 89-111)
radiation hazards to children from testing at, 18: 4043
radiation monitoring at, 18: 35772(R) (UCLA-12-529(p.69-84))
radiation monitoring at, system for remote, 19: 40878 (NVO-162-5(Rev.))
radioecology, 20: 45264(R) (UCLA-12-595, pp 72-89)
radioinduced chromosome aberrations in mouse, 19: 27948(R) (TID-21862)
radiological telemetering system used at, 18: 22338 (NVO-162-5)
radiosensitivity of algae and fungi in soils of, 19: 35991
research programs at, ecological and radiation effects, 19: 43662(R) (UCLA-12-565, pp 97-128)
rock stresses in Rainier Mesa of, 18: 39511 (WT-1869)
seismic data from HAYMAKER Event, 17: 3152 (NP-12276)
seismic data from YORK Event, 17: 3153 (NP-12277)
seismic data from WICHITA Event, 17: 3154 (NP-12278)
seismic data from BOBAC Event, 17: 3151 (NP-12275)
shrubs from, rooting of stem cuttings of, 20: 45264(R) (UCLA-12-595, pp 72-89)
tick distributions, populations, and seasonal occurrences at, 17: 40539
tunnel U12e, properties of tuff specimens from, 16: 23987 (TEI-811)
tunnels at, geology of U12k and U12k.01, 16: 23988 (TEI-817)
vegetation at, growth of, following nuclear explosions, 16: 5113
water supply wells for, behavior of, 17: 1633 (TEI-788)
wind measurements in mesodecline at, 17: 4701

NEW ENGLAND REGION

aerial gamma monitoring of, correlation with areal geology, 18: 43798 (CEX-59.4.14)
ages of granites and volcanic rocks in, 18: 3989(R) (NYO-10517 (p.65-84))
carbon isotope distribution in lakes of, 18: 12352
geologic dating of Ammonoosuc volcanics and Monson gneiss in, rubidium–strontium method for, 20: 16711(R) (MIT-1381-13)
mortality of dentists in comparison with general population and physicians, 20: 45502 (PHS-999-RH-18)
radiation exposure levels of population in northern, 18: 35751
radioinduced leukemia in, background, 18: 20214

NEW HAMPSHIRE

aerial gamma monitoring of, correlation with areal geology, 18: 43798

(CEX-59.4.14)
distribution of thorium and uranium in Conway granite in, 18: 35729
geology of Binary and Conway granites in, 18: 11523(R) (TID-19927)
geology of Conway granites in, 17: 29091(R) (TID-18953)
geology of Conway granites in, 18: 11522(R) (TID-19926)
radiation effects on congenital malformations in infants in, natural background, 19: 33853
radiation exposure in, background, 18: 43838
radiation monitoring of lakes in, 20: 7265
radioactivity from natural sources, 17: 27629
radioactivity in ground waters, 1959 and 1960, 16: 22403 (NP-11638)
radioactivity in ground water in, 20: 37006
thorium and uranium occurrence in White Mountain batholith, 16: 5576
thorium and uranium occurrence in older plutonic rocks in, 16: 5577
thorium content in Conway granite in, lognormality of, 17: 34126
thorium content of granites on White Mountains, 16: 27422 (TID-16370)
thorium content of Conway granite in, 17: 6297
thorium prospecting in Conway granite of White Mountains in, 17: 299(R) (TID-16781)
thorium reserves in Conway Granite, 16: 5555(R) (TID-14471)

NEW JERSEY
aerial surveying for environmental levels of gamma radiation, 1961, 18: 1946 (CEX-61.6.3)
age estimation and paleography of sediments in Triassic Basin in, 20: 18924(R) (NYO-1669-11)
fallout in precipitation at Westwood in 1963 and 1964, 19: 7701 (NYO-2415-12)
fallout monitoring in precipitation in Westwood, 1961 and 1962, 17: 20242 (NYO-9534)
fallout monitoring, following Soviet 1961 tests, 17: 33535
radiation-producing machines in use, 1961, 16: 27510
strontium-90 content of primary teeth of children in, 20: 16763
tritium-hydrologic research in, 18: 12372
water supply for New York City area of, desalting evaluation for, 20: 42658 (NP-16250)

NEW MEXICO
see also Albuquerque Area (N. Mex.)
aeroradioactivity survey and geology of Gnome test site area, 19: 13623 (CEX-59.4.24)
bird survey in, 19: 17410 (HW-SA-3359)
cesium-137 content in residents from 1956 to 1961, 16: 1328(R) (LAMS-2627(p.223-5))
cosmic-ray energy spectra at high altitude over, in 1962, 20: 4569
fallout monitoring, 1962 and 1963, 18: 16224(R) (LAMS-3034(p.180-3))
fallout monitoring to determine cesium-137 body burden, 1963 and 1964, 18: 43833(R) (LA-3132-MS(p.153-69))
geology and formation of galenas in West-Central, 16: 13376
ground crust structure in eastern, interpreted from Gnome explosion, 17: 21911
pollution survey of Animas River in, 18: 35763 (NP-14161)
uranium occurrence in carbonate rocks in northwestern, 16: 5574
vegetation survey of Trinity crater 20-years post-explosion, 19: 24236 (COO-1296-1)

NEW MEXICO (EDDY CO.)
geology and hydrology, 16: 31959(R) (PNE-130F)
uranium-bearing asphaltite nodules in dolomites, Carlsbad, 16: 5593

NEW ORLEANS
strontium-90 content of teeth of children born in, 20: 32913

New Production Reactor
see Hanford Production Reactors (N)

NEW YORK
(See also headings of the form New York (Westchester Co.))
aerial gamma monitoring of, correlation with areal geology, 18: 43798 (CEX-59.4.14)
contamination of water supply of New York City, during radiological warfare, model study of, 17: 39293(R) (NP-13151)
control of radium luminous dial watches in New York City, 19: 30469
effects of 20-megaton thermonuclear explosion on New York City area, 17: 2733
fall-out monitoring, 1954 to 1962, 16: 22450 (TID-7632(p.271-8))
fall-out monitoring in New York City, 1961, 17: 1677
fallout monitoring in New York City, 1962, 17: 40494(R) (TID-18790 (App.II))
fallout monitoring of diet in, 19: 42677
fallout monitoring in, New York Operations Office program for, 20: 521(R) (HASL-164)
geologic studies on intrusion and metamorphism in rocks in, 20: 18924(R) (NYO-1669-11)
geology and hydrology of Nuclear Service Center site in western, 18: 35755
health physics program in New York City, 20: 18966
nuclear port survey, 17: 6312 (NP-12238)
radiation control regulations, 17: 27597 (NP-12924)
radiation control in New York City, 4-yr survey of, 17: 39322
radiation dose from diagnostic radiography of population of, 19: 28580
radiation monitoring program in, 18: 22304
radiation protection code for industry, 17: 8434
radiation protection program of, 19: 38887
radiation safety program for industries in, 19: 18213
radioactive contamination of waters of Hudson-East River complex, model study, 17: 3211 (NYO-8102)
radioactivity of ground and surface waters in Suffolk Co., 19: 18169
radioisotopes for industry in, 18: 18255
radium-228 monitoring in foods at, 20: 148(R) (NYO-3086-1 Pt.IV)
strontium-90 accumulation in bones from contaminated diet, 20: 43619
strontium-90 content of diet and bones of residents of, effects of calcium content on, 19: 9376
strontium-90 fallout in, 18: 39505
strontium-90 monitoring of soil in city of, 18: 10280
thyroid cancer incidence in, 1941 to 1962, 18: 36981
uranium content of diets in, 20: 8740 (CONF-727, pp 136-41)
water supply for New York City area of, desalting evaluation for, 20: 42658 (NP-16250)

NEW YORK (WESTCHESTER CO.)
geochronology of Manhattan Prong in, 19: 22567(R) (NYO-1669-10)
geology of Manhattan Prong in, 18: 14067(R) (NYO-7243)

NEW ZEALAND
age estimations of biotites from Alpine Fault in, effects of argon and strontium diffusion on isotopic-ratio, 16: 13379
carbon-14 content of volcanic ash in, 20: 20893
carbon-14 content of atmosphere at Markara, 20: 31410
distribution of deuterium in hydrothermal areas of, 17: 8929 (NP-12335)
environmental radioactivity measurements, 20: 40521(R) (NP-16270)
fall-out monitoring, 1960 to 1961, 16: 394 (AERE-R-3766)
fall-out monitoring in rain water, 1956 to 1959, 16: 396 (NS-R-12)
fall-out monitoring, 1961, 16: 6645(R) (HASL-117)
fall-out monitoring, 1954 to 1961, 16: 7768 (DXRL-1)
fall-out monitoring, 16: 9008
fall-out monitoring, Jan. to April 1962, 16: 29181 (DXRL-F4)
fallout deposition in rain water, 17: 29106
fallout determination in rainwater in, from 1956 to 1959, 20: 43530
fallout monitoring, 16: 23408(R) (DXRL-F3)
fallout monitoring, 17: 4690(R) (DXRL-F5)
fallout monitoring in, 17: 5750(R) (DXRL-F6)
fallout monitoring, 1963, 17: 32285(R) (DXRL-F8)
fallout monitoring, 1963, 18: 14073(R) (NP-13473)
fallout monitoring, 1963, 18: 20234(R) (NP-13859)
fallout monitoring, 1964, 18: 31756(R) (NP-14098)
fallout monitoring 1956 to 1962, 19: 28420(R) (NP-14825)
fallout monitoring in, 1964, 19: 35892 (NP-15082)
fallout monitoring in, National Radiation Laboratory program for, 20: 521(R) (HASL-164)
fallout monitoring, 1965, 20: 14734(R) (NP-15844)
fallout monitoring, 1965, 20: 20882(R) (HASL-171)
fallout monitoring in, 1962 to 1965, 20: 35653
fallout monitoring, 1965, 20: 43581(R) (NP-16245)
fallout, radioisotope levels in, 17: 5751(R) (HASL-132)
fallout, July to Sept. 1964, 19: 9371(R) (NP-14618)
geochronology of metamorphic and plutonic rocks in, by rubidium-strontium method, 20: 20888
isotope distribution in thermal areas of, 20: 45924
isotopic ratios in thermal area, 16: 16581
isotopic ratios in thermal area, 16: 16582
leukemia incidence in, survey of, 19: 31997
monitoring for fallout radioactivity, 1962 and 1963, 18: 6944(R) (HASL-142)
monitoring for fallout in, program for, 19: 13682
monitoring strontium-90 content from fallout in, milk in, 19: 13682
radiation monitoring of rain water in, 17: 5758
radiation monitoring in, 1965, 20: 31446(R) (NP-16015)
radiation protection, organization, 16: 1346
radiation protection program, 20: 43581(R) (NP-16245)
radioisotope content in rain water, Lower Hutt, 1959 to 1961, 16: 22410 (TID-15817)
radioisotope distribution in geothermal areas of, 19: 28420(R) (NP-14825)
sulfur isotope content in volcanic materials from, 20: 18909
sulfur isotope content in volcanic minerals of, 20: 45921
sulfur isotopic ratios in geothermal and volcanic waters in, 18: 43800 (INS-R-25)
sulfur isotopic ratios in geothermal and volcanic environment of Wairakei region of, 20: 45925
technological applications of radiation, 1960, 16: 9078
tritium content in waters in 1956 to 1960, 16: 16078
tritium content in geothermal bore water, correlation with chloride-enthalpy relations, 18: 43788 (INS-R-29)
tritium content in rain water in, 20: 20893

tritium content in waters in, 1956 to 1963, review of, 20: 45926
tritium measurements in natural waters in 1956 to 1963, review, 19: 6093 (INS-R-24)

NI-O-NEL
corrosion by air at 1750°F after 10,000 hours, 17: 41379
corrosion by ammonium fluoride–formic acid–nitric acid solutions anodic protection against, 18: 35959
corrosion by nitric acid, 17: 6192(T,R) (EURAEC-382)
corrosion by Sulfex solutions and Zirflex solutions, 17: 2461(R) (BNL-731(p.18-46))
corrosion by superheated steam, 17: 38465 (TID-7674(p.11-16))
corrosion by superheated steam at 1050 and 1150°F, 18: 1241(R) (GEAP-4332)
corrosion by superheated steam containing chloride, 18: 30129 (GEAP-4450)
corrosion by VBWR coolant water, 18: 45020(R) (GEAP-4619)
corrosion in Eurochemic head-end equipment, 18: 39843 (NP-9807)
corrosion in solvent extraction processes, 18: 8761
corrosion in waste fixation in glass, 19: 33676 (ORNL-3640)
corrosion of, by nitric vapors at 375°C, 16: 33071(T,R) (EURAEC-337)
corrosion of, by Sulfex and Zirflex process solutions, 16: 33064 (BNL-752)
corrosion of low-carbon, by solutions produced in head-end processes for fuel, 19: 20481 (ORNL-3787)
corrosion of welded, by fixed wastes at 200 to 500°C, 18: 19448(R) (ORNL-TM-757)
performance as cladding for superheater fuel elements, 18: 28025
performance in nuclear superheated steam environments, 18: 4161 (GEAP-4351)
performance in nuclear-superheater environment, 19: 10541(R) (GEAP-4703)
properties as fuel element cladding material, 17: 36928(R) (GEAP-4126)
properties as fuel element cladding materials, 17: 36929(R) (GEAP-4243)
properties as superheat fuel cladding, 19: 4597 (SAN-8003(p.13-89))
radiation effects on, in nuclear superheater environments, 18: 45020(R) (GEAP-4619)
reactions with iodine at 350°C, 19: 8615(R) (GEAP-3771-14)
stress-corrosion cracking in water, 17: 41380

Niagara Mohawk Power Reactor
see Nine-Mile Point Power Reactor

Nibufin
see Phosphinic Acid, Dibutyl-, p-Nitrophenyl Ester

Niccolates
see Nickelates

NICHROME
bonding to iron–nickel–tungsten alloy, roll, 17: 14827(R) (LAR-17)
calcination of nitrated, phase transformations in, 17: 15524 (IDO-14601)
chlorination of, corrosion and reaction rates in processing by, 18: 39386
compatibility with plutonium dioxide at 900°C, 18: 35932(R) (HW-81600(p.2.1-23))
composition and fabrication of dispersion-strengthened, 17: 23959(R) (NP-12793)
corrosion by air and nitrogen–oxygen atmospheres at 1750 and 1850°F, 17: 25723 (IDO-28605)
corrosion by boiling hydrofluoric acid–nitric acid solutions, 20: 37169(R) (BMI-1774)
corrosion by FTW-65 Purex waste, 19: 31617(R) (ORNL-TM-1081)
corrosion by fuel storage-basin water, electrochemical, 20: 28853(R) (IDO-14661, pp 45-82)
corrosion by liquid potassium, sodium, and potassium–sodium alloy, 19: 34643
corrosion by steam at 750°C of type V, 19: 44616(R) (ANL-7000, pp 122-37)
corrosion by superheated steam, 18: 44931(R) (ANL-6936(p.39-72))
corrosion of type V, by superheated steam at 550°C, 18: 32139(R) (HW-81269(p.5.1-23))
development of zirconia-coated, for use as high-temperature extrusion billet liner, 18: 39859 (IITRI-B244-18)
dissolution in nitric acid using electrolytic dissolver, 18: 5416 (IDO-14604)
dissolution of, effects of changes of anode basket material on electrolytic, 18: 5415(R) (IDO-14599)
emissivity of coated, in vacuum, 18: 24138(R) (PWA-2206(Vol.I))
emissivity of coated, in vacuum, 18: 24139(R) (PWA-2206(Vol.II))
emissivity of coated, in vacuum, 18: 24140(R) (PWA-2206(Vol.III))
evaporation at 2050°F, effects of oxide film on, 20: 9410(R) (BNWL-166, pp 5.1-3)
heat flux on submerged, during boiling of organic coolants, 20: 12965
joining to aluminum in heater for boiling detection, 19: 37001 (ORNL-TM-1165)
krypton-85 release from stressed wire of, 18: 33450(R) (NYO-2757-4)
kryptonation of wire of, 18: 33450(R) (NYO-2757-4)
meltdown during transient nucleate boiling with natural circulation of water, 18: 3967
oxidation at 1020 and 1120°C in oxygen at 0.14 to 85 torr, 20: 27426(R) (BNWL-207, pp 5.13-15)
oxidation of types V and V-Cb, by air and nitrogen–oxygen at 1750 and 1850°F, 17: 28528(R) (IDO-28607)
oxidation of, use of krypton-85 for studying effects of creep on, 20: 18570(R) (NYO-2757-5)
phase transformation studies during calcination of nitrates of, 17: 30582(R) (IDO-14611)
preparation of kryptonated, by diffusion, 20: 18570(R) (NYO-2757-5)
properties of cladding of, high-temperature, 17: 7571 (TID-17402)
radioinduced relaxation of stresses in, 18: 42120(T) (AEC-tr-6474)
reactions with plutonia at 1200°C, 19: 36953(R) (HW-84609(p.5.1-5))
reactions with plutonia at 1093°C, 20: 19178(R) (IDO-17154)
separation from uranium by solvent extraction, pilot plant processes for, 17: 228 (IDO-14569)
separation of uranium from enriched fuel of, continuous electrolytic process for, 20: 7191 (IDO-14643)
tensile properties of, effects of thoria on, 17: 34410(R) (NP-13057)
tensile properties of, effects of thoria additions on, 18: 592(R) (AD-421756)
thermal decomposition of simulated, 17: 4492 (IDO-14597)
vaporization from probe surface in electric arcs, (E), 20: 32593
vibration of wires of, effects of length on, 18: 16376(R) (MLM-1157)
Nichrome–PuO_2, properties at high temperatures, 19: 39125(R) (BNWL-91)

NICKEL
see also Transition Metals
abrasion of, friction, wear, and work-hardening during, 18: 18363
abundance in solar atmosphere, (T), 20: 19332
abundance in solar corona, (T), 20: 31865
abundance in 3 Centauri A, 16: 4659
abundance in 3 Centauri A, 17: 32851
alloying characteristics with rare earths, 18: 41924(R) (IITRI-578P19-13)
alloying effects on beryllium binary systems, 16: 13593(T) (CEA-tr-X-259)
alloying effects on energy storage in copper, 16: 10480(R) (GA-2691)
alloying effects on zirconium corrosion in hydrochloric acid at 150 to 250°C, 16: 13533
alloying effects on delta-prime phase of plutonium, 17: 3535
alloying effects on beryllium–zirconium intermetallic compounds, 17: 14725(R) (BBC-114)
alloying effects on titanium, 17: 16580(P)
alloying effects on mechanical properties of vanadium, 17: 25771 (ASD-TDR-62-667)
alloying effects on magnesium, 17: 29349
alloying effects on mechanical properties of magnesium–manganese–thorium alloys, 17: 32595
alloying effects on beryllium–zirconium alloys to 2500°F, 17: 34397(R) (BBC-119)
alloying effects on ignition temperature of plutonium in air and oxygen, 17: 36860(R) (ANL-6648)
alloying effects on titanium corrosion by mercury at 538°C, 17: 36861(R) (ANL-6764)
alloying effects on hardness of chromium, 17: 37548
alloying effects on corrosion of zirconium and its alloys in steam and water, 17: 37495(T) (TRG-Inf-Ser-100)
alloying effects on ductility and electric conductivity of hardened steel, 17: 39545(T,R) (EURAEC-599)
alloying effects on uranium, 17: 39623
alloying effects on uranium, effects of quenching temperature on, 17: 39627
alloying effects on corrosion and mechanical properties of zirconium alloys, 18: 545(R) (GEAP-4368)
alloying effects on magnetic properties of irradiated iron, 18: 2326
alloying effects on corrosion of beryllium by steam and water, 18: 4192 (AERE-R-4422)
alloying effects on corrosion resistance of zirconium in carbon dioxide, 18: 12576 (GEAP-4089(Vol.I)(Paper 3))
alloying effects on corrosion and mechanical properties of zirconium alloys, 18: 12542(R) (GEAP-4484)
alloying effects on titanium corrosion by mercury at 320 to 454°C, 18: 15663(R) (ANL-6808)
alloying effects on composition and mechanical properties of magnesium–neodymium alloys, 18: 28000
alpha attenuation in foils of, differential energy loss measurements of, 18: 699
alpha elastic scattering at 24.7 Mev, relative cross sections for, 18: 34902
alpha elastic scattering at 24.7 Mev, optical-model analysis of, (E/T), 20: 30413
alpha elastic scattering at 25 to 85 Mev, analysis of cross sections for, (T), 20: 36204

alpha particle energy loss and straggling in foils of, 20: 44144
alpha reactions (α,Li^6) with, 18: 16951(R) (TID-20311)
alpha reactions (α,Li-6) at 42 Mev (E/T), 19: 3337
alpha reactions (α,p), proton spectra from, 16: 2538
alpha reactions (α,n) at 11 to 20 Mev, spectra from, 16: 23100
alpha reactions with, secondary electron emission from, 18: 33911
alpha scattering at 43 Mev, excitation of collective levels by inelastic, 16: 21514
alpha scattering at 25 Mev by, differential cross sections for elastic (E), 19: 1234 (PAN-347)
alpha scattering at 28 Mev, distorted-wave and optical model analysis of, 19: 29294
ammonia, hydrogen sulfide, oxygen, and water vapor on rate of, 17: 2942 (K-1533)
analysis and determination, 20: 14500
analysis for antimony, arsenic, bismuth, and zinc, activation, 19: 2237
analysis for carbon dioxide, carbon monoxide, hydrogen, and nitrogen by hot-vacuum extraction, 17: 14147 (PG-Report-412)
analysis for cerium and manganese, photometric, 19: 36297
analysis for cobalt by neutron activation, 17: 12210
analysis for cobalt, use of Compton compensated spectrometry in activation, 18: 13710
analysis for cobalt, nondestructive activation, 19: 5828
analysis for copper and iron by x-ray fluorescent spectroscopy, 17: 2913
analysis for impurities, methods of spectrochemical, 16: 22038
analysis for impurities by activation methods, 19: 19796
analysis for nitrogen, isotope-dilution method for, 19: 40444
analysis for oxygen by sulfur monochloride method, 16: 14631(T) (UCRL-Trans-801(L))
analysis for oxygen, activation, 18: 19886
analysis for rhenium by anion exchange, 19: 13220
analysis for scandium after solvent extraction using diantipyrilmethane, 18: 13702
analysis for surface oxygen by neutron activation methods, 19: 24410
analysis for trace impurities, mass spectrometric, 19: 26226 (CEA-R-2721)
analysis for zinc, 16: 3334(T) (AEC-tr-4497(p.243-50))
analysis of, for electronic structure of impurities in, neutron magnetic diffusion, 17: 20494
annealing of cold-rolled, effects on structures, 17: 14848(R) (TID-17893)
annealing of neutron radiation effects on electric conductivity of, 16: 27700(T) (AEC-tr-5263)
anodic overvoltages of electrodes of, in molten fluorides, 20: 284 (EUR-804.e)
argon-ion reactions on, secondary from, 17: 16836
argon ion reactions with surface of, 18: 747(T) (NP-tr-1068)
argon reactions with films of, at 100 ev, dislocation dipoles and loops from, 17: 27920
atomic beam scattering on polycrystalline, angular distributions in, 18: 22676
atomic displacements in crystals of, from electron bombardment at 0.5 to 1.3 Mev, 16: 13651
atomic Slater-Condon parameters for, 17: 2426
behavior in fused lithium chloride–potassium chloride eutectic, chromatographic and electrophoretic, 18: 43479
beta absorption by, 18: 14609
beta reactions with thin foils of, bremsstrahlung energy spectra from, (E), 19: 23950
bonding of coatings of, to aluminum and uranium, 17: 6606
bonding of, electron microscopy of vacuum-hot-pressure, 17: 23864(R) (BMI-1619(Del.))
bonding to aluminum, chromium, magnesium, molybdenum, or tungsten, method of measuring quality of, 20: 8503(P)
bonding to aluminum by extrusion, 18: 27937
bonding to lead shielding, effects on mechanical properties, 17: 34383
bonding to magnesia, 17: 34365 (LADC-5598)
bonding to molybdenum–titanium alloy and tungsten by vacuum hot-pressing, 20: 5866
bonding to uranium by catalyst and solid state diffusion, 17: 25786 (UCRL-13075)
book: *Nickel and Its Alloys (Vol. I)*, 18: 10462(T) (OTS-63-11098 (Vol.I))
brazing to molybdenum, 17: 42401(R) (AD-296862)
brazing to tungsten, 16: 25737 (WAL-TR-460.54/1-2)
bremsstrahlung production by strontium-90–yttrium-90 beta particles in, (E), 19: 45284 (TID-22169)
bremsstrahlung reactions (y,p) at 24 Mev, direct photoeffect and evaporation contributions in, 17: 38209
bremsstrahlung reactions (y,α) at 32.5 Mev, spectra from, 18: 42680
bremsstrahlung reactions (y,n) at 10 to 28 Mev, cross sections for, (E), 19: 21305
bremsstrahlung reactions (y,n) with, neutron yields from, 20: 26200
bremsstrahlung yields from, with incorporated strontium-90–yttrium-90, 20: 5000 (ORNL-IIC-5, pp 91-8)
bromine ion slowing down in, at 10 to 100 MeV, (E), 19: 37457(R) (ORNL-3778(p.123-5))
carbon ion reactions at 2 to 10 Mev/amu, equilibrium charge-state populations in, (E), 19: 43007
carbon-12 elastic scattering at 124.5 Mev (E/T), 19: 3364
carcinogenic effects of, bibliography on, 20: 45286 (ORO-3461-8b)
carcinogenicity of injected, 16: 8502
catalytic deuteration of alkyl benzenes on, mechanisms of π-complexes in, 18: 16040
catalytic effects on exchange of deuterium with hydrogen of alkylbenzenes, 17: 12288
catalytic effects on deuterium exchange between benzene and heavy water, 17: 27384
catalytic effects on isotope exchange between ammonia and deuterium, 17: 27386
catalytic effects on isotope exchange between anisole or xylene and deuterium oxide, 17: 27387
catalytic effects on isotope exchange between deuterium and toluene, 17: 27389
catalytic effects on isotope exchange between deuterium oxide and propene, 17: 27390
catalytic effects on labeling of hydrocarbons by tritium, 17: 28936
catalytic effects on hydrogen exchange between ammonia and deuterium, 18: 13760
catalytic effects on fluorine reactions with xenon, 19: 4144
catalytic effects on decomposition of tritium-labeled compounds, 19: 7491
catalytic effects on carbon dioxide–graphite reactions, 19: 13901(R) (TID-21415)
catalytic effects on hydrogen exchange of alkylaromatic hydrocarbons and toluic acid derivatives with deuterium oxide, 19: 38688
catalytic properties in deuterium exchange reactions, 19: 38597
catalytic properties of films of, for deuterium exchange in polymethylcyclopentanes, 16: 31601
cavitation by liquid sodium, 18: 34075 (NASA-CR-54071)
cavitation damage in water, 20: 16974 (NP-15889)
cesium ion reactions on, negative-ion yields from, 17: 5087
charged particle elastic scattering by, 17: 41529(R) (ANL-6720(p.29-42))
charged particle reactions with, cross sections for, 17: 34886 (UCRL-10783)
charged particle reactions with, tabulations of cross sections for, (E), 19: 14534 (ORNL-CPX-2)
charged particle reactions with, (E), 19: 25475(R) (ORNL-TM-1044)
chlorination of, corrosion and reaction rates in processing by, 18: 39386
chlorination of, kinetics of, 20: 7086
chlorine ion energy losses in, at 2 to 40 MeV, (E), 19: 6461
coating of tubes using, for use as diffusion barriers, 16: 15098(P)
coating on 6061 aluminum, corrosion resistance of electroless, 20: 45046(R) (IDO-17192)
coating with borides, kinetics and mechanism, 16: 15205(T) (FTD-TT-62-233)
coating with radioactive rare earth for use as radiation source, 18: 24056
coating with thorium by electrolysis, 16: 20963
color centers and recombination luminescence of sodium chloride doped with, 19: 27715
comminution of, effects of impact strength, microhardness, shear modulus, and thermal expansion on, 18: 44220(T)
compatibility of coatings of, with plutonium, thorium, and uranium, 17: 8843
compatibility of thoria-dispersed, with cesium at 1800°F, 18: 22444(R) (MSAR-63-126)
compatibility with lead telluride, 16: 24161 (NAA-SR-Memo-7172)
compatibility with bismuth germanium telluride at 500 to 700°C, 17: 23971 (WCAP-1868)
compatibility with plutonium dioxide–uranium dioxide pellets at 1000°C, 17: 41358(R) (NUMEC-P-105)
compatibility with uranium nitrides at 900°C, 18: 30108(R) (BMI-X-10083)
compatibility with uranium nitrides at 600 to 1200°C, 18: 32037(R) (BMI-X-10092)
compatibility with arc-melted europium oxide and molybdate at 1150°C, 18: 44053(R) (ORNL-3670(p.166-72))
compatibility with uranium nitride, 19: 2717(R) (BMI-X-10100)
compatibility with graphite–nitrogen environment at 1000 and 1200°C, 19: 40966 (BNWL-92)
compatibility with boron carbide and uranium dioxide at 1200°C, 19: 40966 (BNWL-92)
compatibility with hypostoichiometric plutonium mononitride at 820°C, 20: 7493(R) (BMI-1748(Del.))
compatibility with Zircaloy-2 at 600 to 750°C, 20: 23613
compatibility with cadmium and indium tantalates, (E), 19: 17202
compressibility at high pressures, 17: 3494 (UCRL-6696-T)

compression textures in, 18: 44145(R) (ORNL-3670(p.11-16))
conductivity in magnetic fields at low temperatures, electric and thermal, 17: 20475
consolidation by high energy-rate pneumatic impaction, process development for, 20: 27440(R) (BNWL-198, pp 2.1-20)
content in ablation products of iron meteorites, 19: 30910 (EUR-1819.e(p.59-61))
content in blood and skin in rabbits with radiodermatitis, 19: 33910
content in blood and skin of man and rabbits suffering from radiodermatitis, 20: 45309
content in distilled beryllium, calculation and determination of, 19: 22104 (UCRL-12253)
content in high-purity depleted uranium metal, 19: 24481 (GAT-T-1141)
content in $M_{23}C_6$ type carbides in austenitic steels, 16: 19378(T) (AEC-tr-5059)
content in organs and tissues of humans outside continental U. S., 19: 21831
content in ORR pressurized-water corrosion loop, 19: 30150(R) (ORNL-3789(p.113-21))
content in Pacific sector of Antarctic Ocean, 19: 42634(R) (YALE-2912-10)
content in red giant stars, theory for, 18: 16634
content in red-colored Paleozoic deposits in Northern Tien Shan, 20: 14780(T) (AEC-tr-6579)
content in river waters, 17: 30687
content in rocks, effects of clay content on, 20: 29417
content in skin and blood, effects of radiodermatitis on, 18: 33285(T) (JPRS-25502)
content in Van Arkel-refined zirconium, comparison with Knoll-refined, 17: 33819
contents in meteorites, 18: 34398
corrosion, 18: 22451
corrosion by acid cadmium chloride solutions, 16: 5675
corrosion by acids and chloride salts in chemical plants, 16: 20983
corrosion by aluminum–silicon and water of coatings of, on uranium, 19: 40949 (ISC-640)
corrosion by anisole–boron trifluoride, evaluation of, 20: 19135(R) (K-C-718)
corrosion by aqueous solutions, galvanic, 18: 41959 (WCAP-1844)
corrosion by atmosphere at high temperatures, 16: 5315 (WADD-TR-61-123)
corrosion by boiling niobium pentafluoride, 17: 26944(R) (BMI-1630 (Del.))
corrosion by boiling cesium, 19: 13913(R) (AFML-TR-64-327)
corrosion by boric acid–potassium hydroxide solutions, 18: 30133 (WCAP-3737)
corrosion by cesium, contamination effects in ion propulsion systems, 17: 21835
corrosion by cesium at 750°C, 18: 20873
corrosion by cesium at 1000°C, 18: 42348 (GEST-2035)
corrosion by cesium at 400°C, 20: 4337
corrosion by cesium at 400°C, 20: 11227
corrosion by flowing water at pH 5 and 1000°C, dynamic, 20: 43833 (ORNL-TM-1030)
corrosion by fluorine and fluoride melt in fluorinator, 16: 10455 (ORNL-3253)
corrosion by fluoride salt melts at 500 to 650°C, 17: 35251(R) (BMI-1632(Del.))
corrosion by fluorine at 600°C, 18: 1484(R) (ANL-6687(p.86-152))
corrosion by fluorine-gas mixtures at 450 to 500°C, 18: 26824(R) (ANL-6885)
corrosion by fluoride-volatility process fused salts, 19: 2716(R) (BMI-1681(Del.))
corrosion by fluorine, 19: 15663(R) (ANL-6900(p.143-202))
corrosion by fluorine–oxygen mixtures, 19: 15663(R) (ANL-6900(p.143-202))
corrosion by fluorine–molten salt in fluoride volatility pilot plant during fuel processing, 19: 18051 (ORNL-3623)
corrosion by fluorine at 30 to 200°C, 19: 30642(R) (BMI-1707(Del.))
corrosion by fluoride volatility process atmospheres, 20: 7192(R) (K-1649)
corrosion by fluorine and molybdenum and tellurium fluorides at 500°C, (E), 20: 14008(R) (ANL-7122, pp 42-69)
corrosion by fluorine, 20: 35846 (CEA-R-2932)
corrosion by halide volatility separation process gases and liquids, 20: 33413(R) (K-1669)
corrosion by hydrofluoric acid–nitrogen oxide systems, 17: 2461(R) (BNL-731(p.18-46))
corrosion by hydrofluoric acid, 17: 25720 (BMI-X-234)
corrosion by hydrofluoric acid–nitrogen dioxide solutions and nitrosyl chlorides, 18: 3671(R) (BNL-799(p.26-54))
corrosion by hydrofluoric acid–nitrogen dioxide systems, 18: 11958(R) (BNL-823(p.20-47))
corrosion by hydrofluoric acid–nitrogen oxide solutions, 19: 15331(R) (BNL-841(p.18-42))
corrosion by hydrochloric acid–fluorine solutions, 19: 15663(R) (ANL-6900(p.143-202))
corrosion by hydrogen fluoride–oxygen, 19: 31462(R) (ANL-7028)
corrosion by hydrofluoric acid–nitrogen oxide, 19: 36216(R) (BNL-900(p.29-72))
corrosion by hydrofluoric acid–nitrogen oxide solutions, 20: 20177(R) (BNL-929, pp 83-105)
corrosion by hydrofluoric acid–oxygen systems at high temperatures, 20: 23602(R) (ORNL-3913, pp 53-73)
corrosion by liquid aluminum fluoride–potassium fluoride–zirconium fluoride under fluorination conditions at 600°C, 19: 6267 (BMI-X-316)
corrosion by liquid potassium, sodium, and potassium–sodium alloy, 19: 34643
corrosion by lithium fluoride–sodium fluoride–zirconium fluoride systems, 16: 4450(R) (BMI-1546)
corrosion by molten fluorides at 500°C, 17: 29279 (BMI-X-227)
corrosion by molten chlorides, 18: 3298(R) (ORNL-2221(Pts.1-5)(Del.))
corrosion by nitric acid, 17: 6192(T,R) (EURAEC-382)
corrosion by process environments in fluid-bed fluoride volatility process, tests, 19: 26764 (ANL-6979)
corrosion by reagents in fluoride volatility process, 18: 43706(R) (ANL-6800(p.197-296))
corrosion by sodium hydroxides, 17: 7606(R) (ORNL-1515)
corrosion by sodium chloride, determination of rate of, by tracers, 20: 12545(R) (PAEC(A)AR651)
corrosion by steam and water, 17: 37001(R) (ANL-6780)
corrosion by superheated steam, 19: 16010 (ACNP-62024)
corrosion by uranium hexafluoride up to 1000°C, 18: 20469 (CEA-2385)
corrosion by water and vapor at 450°F, 16: 5668 (MND-E-2655)
corrosion by water in pressurized water reactors, 16: 7855
corrosion by water, 16: 13532 (MND-E-2727)
corrosion by water of, plates of plutonium–aluminum fuel elements, 20: 11227
corrosion by zirconium fluoride at 350 to 830°C, 16: 33438
corrosion in molten-salt fluoride-volatility process for spent aluminum-base fuels, 18: 43717 (ORNL-P-391)
corrosion mass transfer in lithium (liquid), 16: 10450 (AD-259882)
corrosion of A, effects of oxidation-dissolution cycles in graphite fuels on, 17: 35618(R) (ORNL-TM-545)
corrosion of A, in simulated chloride volatility process waste solutions at 25 and 50°C, 17: 35618(R) (ORNL-TM-545)
corrosion of, by carbon tetrachloride–chlorine system following exposure to oxygen, 17: 10246(R) (ORNL-TM-403)
corrosion of, by liquid lithium fluoride–sodium fluoride–zirconium tetrafluoride, 17: 6571 (ORNL-TM-411)
corrosion of, by niobium pentafluoride, 17: 22111 (BMI-X-229)
corrosion of, in fluorinator, 17: 14763 (BMI-X-218)
corrosion of "L", under fluorination conditions at 500°C, 16: 4501 (TID-13688)
corrosion of plated coatings of, on aluminum by water and hydroxide solutions at 330°C, 19: 46945 (BNWL-98)
corrosion of pure and thoria-dispersed, by oxygenated steam at 650°C and water at 360°C, 18: 25919(R) (ANL-6868(p.190-200))
corrosion of tubes of, in liquid-liquid heat exchangers, 16: 9153 (MND-E-2681)
corrosion of unwelded and welded 200 plate by fluoride volatility process environments at 450 to 500°C, 19: 32280(R) (ANL-7020(p.100-49))
corrosion of welded, by nitrogen environments containing fluorine, hydrochloric acid, and oxygen at 450 and 500°C, 18: 15426(R) (ANL-6810)
corrosion of welded, by fixed wastes at 200 to 500°C, 18: 19448(R) (ORNL-TM-757)
corrosion of welds of, by gases, 18: 24813(R) (ANL-6880(p.49-67))
corrosion of 200, by fluoride volatility environments, 20: 5595(R) (ANL-6925, pp 107-64)
corrosion of, electrochemical, 18: 14404(R) (EURAEC-95)
corrosion of, measurement of, by beta backscattering and x-ray induction, 20: 19196
corrosion of, review, 19: 7868
corrosion resistance of plating of, on aluminum in aqueous systems at 300 and 330°C, 18: 24083 (HW-81196)
corrosion resistance of coatings of, on uranium, 19: 4143
corrosion resistance to mercury at 900°F, 20: 2264
corrosion testing, 17: 34355
cosmic-ray spallation reactions with, in iron meteorites, chromium isotopes from, (E), 20: 7747 (NP-15591)
crack propagation, rates in air and in vacuum at 1200°F, 16: 5723 (NRL-5702)
crack propagation and strength, 16: 19335 (ASD-TR-61-207)
creep and self-diffusion in, 17: 30985(R) (TID-19070)
creep at high temperature and low stress, 16: 4543 (NRL-5704)

creep in, equations for analysis of first-stage, 20: 7499(R) (GEMP-53A)
creep of, effects of stress and temperature on, 18: 24136 (NP-13909)
creep properties, effects of substructure, 16: 10505 (ASD-TR-61-440)
creep properties of, effects of nitrogen on, 17: 14838 (NRL-5880)
crystal lattice dynamics of, 18: 9317(R) (PR-P-59(p.37-45))
crystal structure of, effects of deformation and recrystallization on, 17: 8863
crystal structure of plastically deformed, 17: 32576 (UCRL-10778)
crystal structure, 17: 41873 (WASH-1044)
crystal structure of, geometry of configurations of interstitial atoms in fcc, 18: 6571(T) (AI-Trans-12)
crystal structure and magnetic properties of plating of, on aluminum, 18: 24083 (HW-81196)
crystal structure changes in thermal expansion, Bradburn Fürth equation of state for calculating, 18: 30206
crystal structure of, Krebs model for kinetic, (E), 20: 34811 (BNL-940, pp 83-7)
crystal vibrations, 18: 32277(R) (PR-P-61)
crystallization after cold rolling and heat treatments, effects of tantalum on, 19: 37016
crystallization kinetics in strongly deformed monocrystals, 20: 33934
crystallization of, effects of tantalum on, 19: 16164
crystallization temperature, effects of transition element binary solid solutions, 16: 25822
de Haas-van Alphen effect in whisker crystals of, high-field, 18: 44137 (IS-985)
decomposition voltage potential in fluorides at 500°C, 19: 17781(R) (ORNL-3750)
decontamination of, using acid oxalate–peroxide solutions, 19: 4046(R) (ORNL-3627(p.247-8))
defect frequency in palladium crystals, (T), 19: 31449 (SGAE-PH-14/1964)
deformation rate, temperature effects on, 16: 2227
deformation, stored energy increase and release after, 16: 25821
deposition by electroless plating, 19: 7855(R) (RISO-90)
deposition by electroplating, 18: 44029(R) (AD-600126)
deposition from sulfamate bath, properties of deposits, 19: 36948 (BDX-613-66)
deposition of coatings of, on uranium by decomposition of carbonyl vapor, evaluation of, 16: 13521
deposition of coatings of, on uranium dioxide particles, 17: 1857
deposition of coatings of, by Electroless process, review of, 17: 14734 (IGO-TM/CA.010)
deposition of coatings of, on nickel tubes for use as diffusion barriers, 16: 15098(P)
deposition of coatings of, on plutonium oxide spheres, 16: 4985(R) (NUMEC-P-80)
deposition of coatings of, on surfaces from nickel carbonyl, effects of ammonia, hydrogen sulfide, oxygen, and water vapor on rate of, 17: 2942 (K-1533)
deposition of electroless, on aluminum, 18: 23140 (RFP-367)
deposition of electroless, on beryllium, 19: 9638 (RFP-478)
deposition of films of, by vacuum evaporation, 18: 8930
deposition of, bath for electrolytic, 18: 8742(P)
deposition of, on solid electrodes by voltammetry, 19: 37010
deposition of, tracer studies of effects of organic addition agents on electrolytic, 18: 10099
deposition on aluminum-clad fuel elements by chemical method, 18: 20453 (HW-72415)
deposition on aluminum and uranium in fuel element fabrication, 19: 18443(P)
deposition on aluminum oxide powder, method of, 19: 11704
deposition on aluminum alloy 6061, 20: 5866
deposition on aluminum, facility for continuously regenerated electroless, 20: 27408 (DUN-800)
deposition on and stripping from uranium, 19: 11711
deposition on beryllium of coatings of electroless, 20: 5849
deposition on beryllium and niobium–1 zirconium, electroless, 20: 5867
deposition on bismuth telluride, electrolytic, 20: 11543(R) (GIC-2605-3)
deposition on cadmium–indium–silver alloy and uranium, electrolytic, 18: 39846
deposition on chromium-plated molybdenum and tungsten for corrosion protection, 19: 32700
deposition on fast-burst reactor components, electrolytic, 20: 5867
deposition on fuel elements, computer analysis of process controller for, 19: 5449 (HW-67979)
deposition on fuel rods for corrosion protection, method for, 20: 39350(P)
deposition on spherical particles of plutonium dioxide and plutonium dioxide–uranium dioxide, 20: 747 (EURAEC-1391)
deposition on substrates, 19: 44344 (K-L-1944)
deposition on tungsten, method for, 18: 44115
deposition on uranium, electrolytic, 18: 41482(P)
deposition on uranium, electrolytic, 18: 41490(P)
deposition on uranium by electrolytic methods, 19: 4143
deposition on uranium by carbonyl decomposition, 19: 13843(R) (SAN-366-1)
deposition on uranium bars, process for electrolytic, 19: 16049(P)
deposition on uranium by diffusion from molten magnesium bath, 19: 40949 (ISC-640)
deposition on uranium dioxide particles, 19: 44596 (EURAEC-1392)
deposition on uranium–10 molybdenum to prevent stress-corrosion cracking in air, electrolytic, 20: 5867
deposition on uranium surfaces, method for electrolytic, 20: 13211 (BNWL-124)
deposition on uranium, electrolytic, 20: 31670
deposition on uranium dioxide spheres using nickel and nickel oxide powders, 20: 33848 (Y-1538)
deposition on urania, method for, 20: 46144(R) (HW-67765)
deposition on uranium, electrolytic, 17: 1819(T,P) (AEC-tr-5496)
deposition on uranium bars, bath for, 19: 46944(P)
deposition on zinc-coated uranium, electrolytic, 19: 40949 (ISC-640)
deposition with niobium, tantalum, titanium, and zirconium from anhydrous solutions, electrolytic, 18: 26057
desorption and diffusion from metals, activation energies for, 16: 19568
desorption energy of silver on, tracer study, 17: 36474
desorption of carbon monoxide from surfaces of, photo-, (E), 19: 22525
detection of inclusions of, in zirconium alloys by x-ray emission in electron microscopy, 20: 20593
determination as corrosion product in fuel solution of Berlin Research Reactor, 20: 1541
determination as impurity in and volatilization from tungsten, semi-quantitative spectrographic, 16: 4131 (BM-RI-5903)
determination as impurity in bismuth, spectrographic, 17: 27309
determination as trace in standard rocks G-1 and W-1, spectrographic, 16: 20831
determination as trace impurity in uranium, 18: 29591
determination as trace impurity in plutonium–thorium–uranium and thorium–uranium alloys, 19: 17798
determination by atomic-absorption spectroscopy, 17: 40716 (TID-7655 (p.379-89))
determination by activation, substoichiometric, 18: 21997
determination by back-titration with EDTA using silver-110m-labeled silver iodate as indicator, 20: 26769
determination by charged-particle reactions at 2 Mev, 20: 43097
determination by potentiometric titration of acid liberated by complex formation, 19: 46205
determination by radiocoulometric titration using solid non-isotopic indicator, 19: 43952
determination by radiometric titration, 20: 16386
determination by spectroscopy using high-frequency plasma flames, 18: 10020
determination by spectrochemical methods, voltage-fluctuation patterns in, 19: 40416
determination by thermal-neutron activation methods, sensitivity for, 19: 9071
determination by titration, suitability of tetraethylenepentaminehepta-acetic acid for, 19: 19813
determination by x-ray fluorescence analysis, 19: 22154
determination in antimony, activation techniques for, 16: 3326(T) (AEC-tr-4497(p.179-88))
determination in alloys, 17: 10539 (TID-16296)
determination in Armco iron, use of radioisotopes for, 17: 33822
determination in aluminum, activation, 18: 43407
determination in aluminum, activation, 19: 28224 (SGAE-CH-13/1964)
determination in aqueous solutions, coulometric, 19: 36889(R) (MLM-1250)
determination in aluminum, activation, 19: 46207
determination in actinide carbides, 20: 8874
determination in aluminum ingots, x-ray fluorescence, 20: 8828 (K-1638)
determination in asbestos using ion exchange, activation, 20: 16336(R) (NYO-10175)
determination in aluminum, activation, 20: 22896
determination in americium and plutonium by spark-source mass spectrography, 20: 40816 (RFP-699)
determination in beryllium–magnesium alloys by spectral analysis, 16: 22037
determination in beryllium and beryllium oxide, 17: 21643
determination in beryllium, activation, 17: 25123
determination in biphenyl, spectrophotometric, 17: 28809
determination in beryllium oxide, spectrophotometric, 18: 3694
determination in boron, x-ray-fluorescence, 18: 29564(R) (NBL-210 (p.41-7))
determination in beryllium oxide, device for quantitative, 19: 11007
determination in biological materials, 19: 33692(R) (NYO-1397-1)
determination in beryllium oxide, spectrographic comparison of standards

on, 20: 6998 (AAEC/TM-294)
determination in blood and hair of man, activation, 20: 36728
determination in boron by x-ray fluorescence, 20: 43091 (UCRL-14879)
determination in clay, acetic acid leachates, sand, and silt, spectrochemical, 16: 4379
determination in cadmium and zinc sulfides, spectrometric, 16: 11569
determination in cerium, erbium, and lutetium, mass spectrographic, 19: 2232
determination in copper, effects of threshold reactions on activation, 19: 4085
determination in copper, activation, 19: 5824
determination in chromium-molybdenum alloy, use of fluorescent x-ray instrument for, 19: 13221
determination in copper by activation, 19: 40422
determination in diabase W-1 and granite G-1, spectrographic, 16: 17895
determination in dioxides of titanium, zirconium, and thorium by x-ray fluorescence, 17: 144
determination in dilute hydrofluoric acid using dimethylglyoxime, gravimetric, 17: 33799 (PG-Report-476)
determination in ethylenediamine tartrate solutions, polarographic, 16: 11511 (CRDC-1059)
determination in europium oxide, spectrographic, 17: 2931
determination in fuel element descaling solutions, spectrophotometric, 19: 7274(R) (IDO-14636)
determination in fused fluorides by voltammetry, 19: 17781(R) (ORNL-3750)
determination in fuel descaling make-up solutions, 19: 32059(R) (IDO-14655)
determination in ferromagnetic films, activation, 20: 14489
determination in high-purity molybdenum, niobium, tantalum, and tungsten, spectrophotometric, 17: 38959
determination in hydrogenated and nonhydrogenated fats, activation, 18: 25282
determination in high-purity tantalum by spectrography using d-c arc method, 20: 20608
determination in indium using α-benzildioxine, spectrophotometric, 16: 1719
determination in iron, activation, 19: 10980 (EURAEC-1273)
determination in iron, spectrophotometric, 20: 3863(R) (IS-1200(Sect. C))
determination in iron by bremsstrahlung activation method, 20: 18613
determination in igneous and metamorphic apatites, spectrographic, 20: 26787
determination in lithium chloride–potassium chloride eutectic by controlled potential stripping, 16: 16310
determination in liquid lithium fluoride–sodium fluoride–potassium fluoride systems, voltammetric, 18: 29585
determination in lanthanum oxide, spectrographic, 20: 22895
determination in lanthanum oxide, spectrographic, 20: 22945
determination in molybdenum in sulfuric acid, 16: 11567
determination in magnesium–manganese alloys, spectrophotometric, 16: 18817 (PG-Report-295)
determination in meteorites, activation, 17: 33851
determination in molybdenum and its compounds, spectrographic, 18: 17766
determination in molybdenum, tungsten, and their alloys, classical methods for, 18: 19921
determination in mass spectrometer at 10^{-6} gram, 18: 39057 (CONF-520-1)
determination in mixed oxides with rare earths, complexonometric, 18: 39139
determination in meteorites, activation, 19: 7349
determination in minerals by neutron activation, 19: 30424
determination in marine plants and animals, spectroscopic, 19: 36314
determination in mixtures by x-ray fluorescence using promethium-147/aluminum and tritium/zirconium sources, 20: 3883 (ORNL-IIC-5, pp 154-81)
determination in MSRE fuel, polarographic, 20: 14454(R) (ORNL-3889, pp 17-24)
determination in mosaic virus and nucleic acids in tobacco plants, activation, 20: 38846
determination in nickel plating solutions by flame spectrophotometry, 16: 12960 (TIM-406)
determination in natural water, quantitative spectrographic, 16: 17597
determination in niobium and zirconium by radioactivation analysis, 16: 23633 (TID-7629(p.239-44))
determination in niobium and its alloys, 16: 25294
determination in nickel steel and electro-etch residues, activation, 17: 5984
determination in neptunium by ion exchange and spectrography, 17: 15896
determination in niobium, chemico-spectrographic method for, 17: 40758
determination in nucleic acids, activation, 18: 19892
determination in niobium or niobium oxide by d-c arc excitation, photometric, 19: 26268
determination in niobium or niobium oxide by fusion and d-c arc excitation, photometric, 19: 26269
determination in nickel ores by neutron activation, 20: 33161(T) (AEC-tr-6639, pp 13-17)
determination in organic reactor coolants, spectrographic, 18: 184
determination in other metals, volumetric, 19: 7274(R) (IDO-14636)
determination in polyphenyls, x-ray spectrographic, 17: 27227 (EUR-28.f)
determination in polyphenyls by activation analysis, 17: 38945
determination in plutonium alloys, spectrophotometric, 17: 41350(R) (MLM-1162)
determination in petroleum and its products, activation, 18: 15968
determination in polyphenyls, x-ray-spectrographic, 18: 19844 (ISPRA-455)
determination in presence of copper by differential spectrophotometry, 18: 35442 (AERE-R-3840)
determination in presence of 71 elements, spectrographic, 18: 43420
determination in pure water by extraction photometry, 19: 15388
determination in pure molybdenum and tungsten, photometric, 19: 19799
determination in presence of manganese by activation methods, 19: 19796
determination in powdered samples by spectrochemical methods, 19: 22120
determination in plutonium using dimethylglyoxime, spectrophotometric, 19: 38546(R) (RFP-552)
determination in plutonium fluorides and peroxides, review on spectrographic, 20: 14464 (RFP-597)
determination in plutonium–uranium–zirconium alloy by anion exchange-partition chromatography and spectrography, 20: 26764
determination in plutonium by carrier distillation methods, spectrographic, 20: 40814 (RFP-664)
determination in powder samples by spectrographic methods, semi-quantitative, 20: 43104
determination in rare earth oxides, spectrographic method for, 16: 20327
determination in reactor-grade uranium dioxide, activation, 19: 5827
determination in reactor coolants, polarographic, 19: 11003
determination in rare earth oxides by atomic absorption spectrophotometry, 20: 33151 (IS-T-88)
determination in stratospheric aerosols, 16: 25609 (AFCRL-62-299)
determination in Santowax OMP by spectrographic methods, 17: 7959 (RT/CHI(62)13)
determination in SAP, x-ray spectrographic, 17: 27226 (EUR-21.f)
determination in steels, polarographic, 17: 28797 (AEET/ANAL/8)
determination in spent dissolver decontamination solutions, 17: 37292(R) (ORNL-TM-586)
determination in solutions of alkali metals, 18: 3298(R) (ORNL-2221 (Pts.1-5)(Del.))
determination in soil, activation, 18: 21994
determination in small solid samples by mass spectroscopy, design of ion source for, 18: 23406 (CONF-512-4)
determination in steel by x-ray fluorescence, 18: 25275
determination in silicon, activation, 18: 33502
determination in solar corona, 18: 40109
determination in sea water, activation, 18: 43790(R) (TID-21137)
determination in silicon, activation, 19: 2240
determination in solids by spark source mass spectrometry, quantitative, 19: 13247
determination in solutions, coulometric, 19: 17781(R) (ORNL-3750)
determination in sea water by neutron activation methods, 19: 22574
determination in sea water by quantitative solvent extraction and spectrography, 19: 28253
determination in sea water and silts, spectroscopic, 19: 36315
determination in stainless steel, electron microprobe, 19: 38536 (ACF-6)
determination in sodium loop transfer samples, methods for, 20: 12766 (GEAP-4178)
determination in silicon dioxide, activation, 20: 20634
determination in silicates, activation, 20: 26782
determination in sintered and zone refined boron-10, spectrographic, 20: 43090(R) (TID-23342)
determination in SAP, methods for, 20: 45574 (EUR-3064.f)
determination in terphenyls, activation, 17: 28813
determination in tantalum by d-c arc method, spectrographic, 18: 19894
determination in thorium at 50 to 500 ppm, spectrophotometric, 18: 23414 (Y-1464)
determination in tantalum by anion exchange in hydrofluoric–nitric acid mixtures, 18: 35455
determination in tungsten and tungsten alloys, spectrophotometric, 19: 15362
determination in tantalum by activation, 19: 24416
determination in uranium leach solutions, 16: 14668
determination in uranium compounds and metal, colorimetric, 16: 22005 (PG-Report-325)
determination in uranium compounds by reversed-phase partition chromatography, 16: 23636 (TID-7629(p.276-84))
determination in uranium base alloys, photometric, 16: 26928

determination in uranium(IV-VI) oxide by carrier distillation excitation, effects of graphite electrode grade on, 17: 10538 (TID-16295)
determination in urine, spectrographic, 17: 17625(R) (MLM-1144)
determination in uranium using dithizone, spectrophotometric, 18: 1533
determination in uranium-233-labeled uranium dioxide, spectrographic, 18: 9980
determination in uranium, methods for, 18: 9991
determination in uranium alloys, photometric, 18: 19845 (JAERI-1053)
determination in uranium alloys, gravimetric, 18: 29558 (LA-3088)
determination in uranium tetrafluoride produced by fluidized-bed process, absorptiometric, 19: 10982 (PG-Report-614)
determination in uranium and its compounds and alloys, methods for, 19: 19823
determination in uranium trioxide, spectrophotometric, 20: 7011 (NLCO-964)
determination in uranium tetrafluoride, spectrographic, 20: 14473
determination in uranium by carrier distillation, spectrographic, 20: 18563 (EUR-2647.f)
determination in uranium–zirconium alloy by anion exchange-partition chromatography and spectrography, 20: 26764
determination in uranium trioxide by emission spectrography, 20: 40802 (HW-65402(Rev.1))
determination in uranium(IV-VI) oxides, effects of graphite electrode grade on carrier-distillation spectroscopic, 20: 40807 (NLCO-976)
determination in uranium by atomic absorption spectrophotometry, 20: 40815 (RFP-698)
determination in urine by atomic absorption spectroscopy, 19: 24611(R) (MLM-1227)
determination in various base materials, spectroscopic techniques for, 20: 7005 (IS-T-51)
determination in water, silver-spark spectrographic, 17: 1381 (IDO-14591)
determination in zirconium alloys, chemical, 18: 12542(R) (GEAP-4484)
determination in zirconium by activation, 19: 24418
determination in zinc sulfate and sulfide, interfering reactions in activation, 20: 36755
determination in zinc sulfate using ion exchange and activation methods, 20: 36756
determination, micro-coulometric, 16: 25285
determination of, in uranium fission products, 17: 15892
determination of, in presence of alkali metals, chemical spectrographic, 17: 15923
determination of, in residues by iron flux method, spectrographic, 17: 19942 (PG-Report-157)
determination of, in uranium concentrates and ores, spectrographic, 17: 23254 (PG-Report-220)
determination of, method for, 17: 28801 (IDO-14316(Suppl.4))
determination of trace amounts in rare earth compounds, spectrographic, 16: 28869 (JEN-107-DQ/I-33)
determination of traces in beryllium, photometric, 17: 19963
determination of traces of, using oxycellulose, 17: 35656
determination of traces of, in tungsten, spectrographic, 18: 13610 (BM-RI-6308)
determination of traces of, in water by atomic absorption spectrometry, 18: 33461 (DP-879)
determination of traces of, in polyphenyls, 19: 302 (RT/CHI(64)-11)
determination of traces of, in uranium carbides, 19: 4061 (PG-Report-516)
determination of traces in cobalt oxide, spectrographic, 19: 15336 (AEET/Spec./3)
determination of traces of, in nickel, spectrophotometric, 19: 17779 (LA-3152)
determination of traces of, in uranium using electron microprobe, 20: 225 (CONF-650810-2)
determination of trace amounts of, in iron, activation, 20: 14471
determination of trace amounts of, in beryllium by spectrography, 20: 16352
determination of trace amounts of, in water, activation, 20: 24990
determination of trace amounts of, by reactor neutron activation methods, 20: 26760
determination of traces of, in crude oils, by nondestructive activation analysis, 20: 33196
determination of trace amounts of, in tungsten and molybdenum by atomic absorption spectrophotometry, 20: 43154
determination of, properties of formaldoxime for spectrophotometric, 18: 39085
determination of, in ferrite computer cores by neutron activation methods, 20: 45584
determination simultaneously with cobalt in aluminum, petroleum, and polyphenyls, activation, 18: 17739
determination simultaneously with lead in uranium by square-wave polarography, 18: 17740
determination using thioglycolic acid, spectrophotometric, 18: 17764
determination using α-mercaptopropionic acid, spectrophotometric, 19: 24426
determination using radiocoulometric methods, 20: 10769
deuteron attenuation by films of, at 1.5 to 4.5 MeV, 16: 15668
deuteron disintegration in nuclear fields, (E), 20: 46786
deuteron elastic scattering at 11.8 Mev, angular distributions, 16: 3637
deuteron elastic scattering at 6.5 Mev, polarization, 17: 17263
deuteron elastic scattering at 11.8 Mev, distorted-wave theory of, 17: 26429(R) (ORNL-3425(p.5-8))
deuteron elastic scattering at 11.8 Mev, optical model analysis of, 17: 38192
deuteron elastic scattering by, nuclear tensor potentials from, 18: 17041
deuteron elastic scattering at 26 Mev, angular distributions from, 18: 28634
deuteron elastic scattering at 15 Mev, strong absorption model analysis of, 18: 42708
deuteron elastic scattering at 26 Mev, optical model analysis of, (E/T), 20: 3053
deuteron inelastic scattering at 15 Mev, 17: 4089
deuteron reactions (d,α) at 15 Mev, cross sections and energy distributions for, 16: 11020
deuteron reactions (d, helium-3) at 21.6 Mev, determination of configurations of states by, 16: 21562
deuteron reactions (d,t) with, spectra from, 17: 7655(R) (ANL-6600)
deuteron reactions at 11.8 Mev, optical model parameters for, 18: 1051
deuteron reactions (d,p) at 10 Mev, dependence of angular distribution on total angular-momentum transfer in, 18: 42742
deuteron reactions at 11 to 12 Mev, total cross sections for, (E), 19: 35429
deuteron reactions (d,np) at 13.6 Mev, (E), 19: 39940
deuteron scattering at 27.6 Mev, elastic and inelastic cross sections, 16: 2488 (NP-10975)
deuteron scattering at 12 Mev, angular distributions, 16: 13953 (JÜL-30-KP)
deuteron scattering at 3 to 30 Mev, optical model analysis of, 17: 11676
deuteron scattering at 21.6 Mev, optical model predictions of polarization in, 17: 38247
deuteron scattering at 21.6 Mev, optical model parameters for, 17: 38190
deuteron scattering at 26.5 Mev, total cross sections for, (E), 19: 5164
deuteron total cross sections at 11 Mev, (E), 19: 43323
development for SEFOR core materials, 20: 38531 (GEAP-5133)
development of coatings of, for niobium–titanium–vanadium alloys, 16: 19334(R) (ARF-2227-5)
development of coatings of, for oxidation protection of vanadium alloys at high temperatures, 17: 35997(R) (IITRE-B6001-5)
development of coatings of, for high-temperature oxidation protection of vanadium alloys, 16: 12083(R) (ARF-2227-4)
diffraction patterns of powdered, neutron, 20: 12545(R) (PAEC(A)AR651)
diffusion and mobility of antimony-124 in, temperature dependence of, 17: 23997(T)
diffusion and solubility of, in beryllium, 17: 23872(R) (TID-18626)
diffusion and solubility of deuterium and hydrogen in single crystals, 19: 37132
diffusion in alpha iron at 700 to 900°C, 17: 29337
diffusion in aluminium, annealing effects on, 17: 14829 (NAA-SR-Memo-7871)
diffusion in aluminum, electronic probe microanalyzer study of, 18: 543 (CEA-2291)
diffusion in aluminum, 18: 5733 (NAA-SR-8387)
diffusion in chromium–nickel alloys, 20: 834(T) (AERE-Trans-1031)
diffusion in cobalt and cobalt–nickel alloys, magnetic effect on, 17: 27841
diffusion in copper–zinc alloy, 18: 7994(R) (GTR-21)
diffusion in copper, formation of porosity during, 18: 10544 (UCRL-10383)
diffusion in gamma uranium, 17: 41333(R) (ANL-6677)
diffusion in gamma uranium, 18: 25969(R) (ANL-6868(p.287-302))
diffusion in gamma uranium, 18: 44208
diffusion in gamma-cerium, measurements on electro-, 19: 22978 (HW-SA-3481)
diffusion in gamma cerium, electro-, 19: 34722
diffusion in gamma-phase uranium, 20: 19175 (ANL-6568)
diffusion in gamma-cerium, gamma-uranium, and epsilon-plutonium, electro-, 20: 23734
diffusion in graphite, 18: 2275
diffusion in graphite, 18: 39911 (UCRL-7324)
diffusion in graphite, 19: 26832
diffusion in lead sulfide crystals at 600 to 700°C, 17: 29351
diffusion in nickel at 930 to 1300°C, mechanism of self-, 19: 44708(T) (JPRS-24761, pp 1–11)
diffusion in niobium at 950 to 1100°C, 19: 26857
diffusion in pyrolytic graphite, 20: 5846
diffusion in silver at 600 to 850°C, 17: 19998
diffusion in single-crystal magnesia, 20: 31719(R) (UCRL-16658, pp 155-69)

diffusion in titanium at 800 to 1200°C, 16: 12156
diffusion in titanium, 16: 15207
diffusion in titanium at 900 to 1650°C, 17: 34454
diffusion in uranium, 18: 5733 (NAA-SR-8387)
diffusion of bismuth (liquid) into boundaries of oriented crystals of, 17: 11241
diffusion of cesium through membranes of, surface ionization following, (E), 19: 6449
diffusion of cobalt-60 in, effects of argon and hydrogen environment on, 17: 18791
diffusion of cobalt-57 in, Mossbauer spectra determination of, 18: 4246(R) (ORNL-3470(p.16-19))
diffusion of copper in, at 800 to 1050°C, 20: 4363 (AEET/CD/31)
diffusion of hydrogen in solid, 16: 5727(T) (AEC-tr-4948)
diffusion of hydrogen in, at high temperatures, 18: 36231 (USAELRDL-TR-2431)
diffusion of, in liquid lead, 16: 28647(R) (ORNL-2340(Pts.1-5))
diffusion of, in silver at 600 to 850°C, 17: 20457 (NYO-9438)
diffusion of molybdenum in, as function of temperature, 20: 2357(T) (AERE-Trans-1032)
diffusion of nickel-63 in, measurements of grain-boundary, 18: 30204
diffusion of sulfur in, 19: 2812
diffusion of titanium in, gamma attenuation analysis of, 19: 988
diffusion on surfaces of crystalline, self-, 19: 6302 (NYO-2994-3)
diffusion on surfaces of single crystals of, self-, 19: 6303 (NYO-2994-3 (App.B))
diffusion through sodium to molybdenum surface, 18: 27893 (NASA-SP-41 (p.73-4))
diffusion-barrier properties of coatings of, for aluminum–uranium interfaces, 17: 4926 (EUR-17.f)
dislocation dissociation in crystals of, 18: 2238
dislocation structure of, deformed at 23°C, 18: 4249(R) (ORNL-3470 (p.33-9))
dissociation energy of gaseous and heat of vaporization of solid, correlation of, 17: 6095
dissolution and ion exchange behavior in ammonium carbonate solutions, 17: 39035
dissolution by Purex waste solutions, 20: 24809(R) (BNWL-213)
dissolution in aqua regia, 16: 4221 (IDO-14565)
dissolution rate in liquid aluminum, 17: 10577 (ANL-FGF-292)
distribution coefficient in hydrochloric acid and ion exchange resins, 16: 7503
distribution in deep-sea silts and sea water, 20: 18892 (NYO-3450-1, pp 41-89)
distribution in shallow marine environments, 20: 18895 (NYO-3450-1, pp 217-76)
distribution in Zircaloy-2 and zirconium oxide, use of electron microprobe for determination of, 17: 27746(R) (DPST-63-71-1)
distributions in hot-pressed tantalum carbide, 17: 37558
distributions in sea water, geographical and vertical, 19: 22574
ductility of, at −269°C, 20: 21416
ductility of, effects of liquid cesium on, 18: 14354(R) (ARF-B215-12)
effect on properties of low-alloy steels for reactor pressure vessels, 20: 39444(P)
effect on slip anisotropy in zone-refined beryllium, 19: 34686(R) (NMI-1266)
effects as catalyst on hydrogenation of ethylene, deuterium–hydrogen exchange in, 20: 40942
effects as coating on light and refractory metals and their alloys, 19: 4605
effects in x-ray spectrochemical analysis of steel, correction for inter-element, 20: 22957
effects of additions of, on oxidation of zirconium borides, 18: 32200
effects of alloying additions of, on oxidation rates of niobium, tantalum, and tungsten, 20: 11227
effects of binder of, on cryogenic properties of titanium and tungsten carbides, 20: 11293
effects of foils of, on charge states of oxygen-16 ions, 20: 15854
effects of, on potentiometric-acidimetric determination of zirconium, 17: 23288
effects of sintering aids of, on thermal conductivity of uranium and plutonium uranium carbides, 20: 31666
effects of small concentrations of, on conductivity of iron irradiated by fast neutrons at 78°K, 17: 22231
effects on aluminum alloy dissolution by hydrofluoric acid, 17: 1564(R) (IDO-14593)
effects on beryllium crystals, 18: 24066(R) (NMI-2126)
effects on beryllium crystals, 18: 24067(R) (NMI-2127)
effects on copper oxidation, 20: 4320(R) (ORNL-3870, pp 70-4)
effects on copper or silver infiltrants in graphite, 20: 29764
effects on corrosion of aluminum, 17: 18707
effects on corrosion resistance of Zircaloy-2 to water at high temperatures, 18: 37644
effects on corrosion resistance of zirconium, 18: 41972(P)
effects on corrosion of steels by liquid sodium at 450, 600, and 750°C, 19: 4629
effects on corrosion resistance of chromium–cobalt–tungsten alloys, 19: 18415
effects on corrosion of zirconium by superheated steam, 19: 22899
effects on corrosion of graphite by water vapor, 20: 31667
effects on critical cylinder diameters of hydrogen moderated uranium compounds, 19: 18736 (K-1629)
effects on deformation of zone-refined beryllium, 19: 18460(R) (NMI-1265)
effects on determination of iridium in ores by neutron activation analysis, 20: 36751
effects on dissolution of aluminum by nitric acid, 17: 23431 (IDO-14606)
effects on ductility of iodide chromium, 18: 32189
effects on ductility of molybdenum, 19: 37041(R) (NP-15174)
effects on electric conductivity and mechanical properties of niobium–titanium alloys, 19: 26872
effects on eutectic temperature of iron–plutonium alloys, 19: 40958
effects on exchange of deuterium between aniline and deuterium oxide, 20: 43275
effects on fabrication and mechanical properties of sintered tungsten powder compacts, 20: 27495(RFP-706)
effects on fluorescence of salicylate, 17: 33879
effects on fluorescence of uranium in sodium carbonate–sodium fluoride melts, 18: 33506
effects on hardness of niobium, 19: 26859
effects on hardness of molybdenum, 20: 31741
effects on heterometric determination of vanadium, 19: 36289
effects on heterometric determination of vanadium using 5,7-diiodo-8-hydroxyquinoline, 20: 257
effects on homomolecular isotopic exchange of carbon monoxide, catalytic, 19: 26328
effects on hot hardness of zirconium oxides, 20: 5846
effects on hydrogen para-ortho conversion and isotopic exchange, effects of oxygen on catalytic, 19: 26345
effects on intergranular corrosion of 20Cb stainless steel, 20: 29643
effects on internal friction in magnesium, 19: 11727 (NYO-2471-4)
effects on internal friction of molybdenum and tungsten, 20: 27508
effects on iron irradiated at 77°K by fast neutrons, 19: 28880
effects on isotopic exchange between cyclobutane and deuterium, 20: 304
effects on magnetic hysteresis of iron, combined fast-neutron radiation and, 20: 17134
effects on mechanical properties of magnesium-manganese-thorium alloys, 18: 32156(T) (JPRS-25069(p.1-31))
effects on mechanical properties of aluminum–copper–iron–tin–titanium–vanadium alloys, 19: 46985 (AD-613651)
effects on microstructure and phase composition of sintered carbides of uranium and plutonium–uranium, 20: 9461
effects on oxidation of copper, 18: 14412(T,R) (EURAEC-961)
effects on oxidation of copper, 19: 7864(R) (EURAEC-1225(Pt.1))
effects on oxidation of graphite, 19: 22911
effects on oxidation resistance of beryllium–niobium and beryllium–zirconium alloys, 20: 5844
effects on phase transformations in steel, 18: 24152(T,R) (EURAEC-1001)
effects on phase transformations in gallium–plutonium alloys and plutonium, 19: 13889(R) (MLM-1208)
effects on phase transformation in plutonium, 19: 40958
effects on phase transformations in gallium–plutonium alloy and plutonium, differential thermal analysis of, 20: 41452 (MLM-1172)
effects on photometric determination of cerium in cast iron and steels, 20: 43143
effects on plasticity of zirconia, 18: 27882 (GEAP-4473)
effects on point defects in iron, 19: 47094(T) (ORNL-tr-668)
effects on preparation of uranium carbide by carbothermic reduction of oxide, 20: 33841 (NAA-SR-10624)
effects on properties of uranium carbide dispersions in chromium or iron, 18: 42106(P)
effects on properties of beryllium–Zircaloy-2 braze alloys, 19: 26819 (NMI-4787)
effects on properties of zirconium alloys, 19: 36990(P)
effects on properties of boron steel, 20: 39426
effects on properties of plutonium carbide–uranium carbide systems, 17: 29330(R) (UNC-5056)
effects on radiation damage in silicon crystals, 18: 34228
effects on sintered density of uranium monocarbide and uranium plutonium carbide pellets, 20: 27416(R) (UNC-5134(Vol.1))
effects on sintering of uranium carbide, 17: 1898(R) (ORO-579)
effects on sintering of plutonium and uranium carbides, 18: 14432 (TID-7676(p.70-4))
effects on sintering rates of tungsten, 18: 34098
effects on sintering of zirconium boride, 19: 26794

effects on sintering properties of carbides of uranium and plutonium–uranium, 20: 9461
effects on sintering of zirconium diboride, 20: 31668
effects on sintering of high density tungsten–uranium oxide systems, 16: 27601 (LAMS-2716)
effects on sintering of plutonium carbide–uranium carbide systems, 17: 29298(R) (UNC-5055)
effects on spectrophotometric determination of aluminum, 19: 13226
effects on spectrophotometric determination of zinc using 1-(2-thiazolylazo)-2-naphthol, 19: 19814
effects on spectrophotometric determination of thorium, 19: 24408
effects on strength of zone-refined beryllium, 19: 11680
effects on thermoelectric properties of thorium arsenide, 19: 16091
effects on titanium corrosion by mercury, 19: 44616(R) (ANL-7000, pp 122-37)
effects on tritium exchange between tritiated ethyl malonate and hydrocarbons, catalytic, 20: 16492
effects on uranium carbide–zirconium carbide solid solutions, 18: 12567
effects on vacuum sintering properties of plutonium carbide–uranium carbide, 20: 9462
effects on zirconium corrosion by steam and water, 18: 37632 (A/CONF.28/P/341)
effects on zirconium alloys for use in reactors, 20: 9560(P)
effects on zirconium alloys for use in nuclear reactors, 20: 9561(P)
electric breakdown and electron emission in vacuum, mechanisms of, 18: 20139
electric conductivity, effects of neutron irradiation on, 16: 578(T) (SCL-T-371)
electric conductivity, effects of magnetic fields up to 400 kgauss, 16: 15451
electric conductivity, 16: 23662 (AE-76)
electric conductivity of thin vacuum-deposited films of, thickness and temperature dependence of, 19: 2799 (COO-623-101)
electric conductivity of thin films of, 19: 44344 (K-L-1944)
electric discharge in, self-absorption and total intensity values of spectra from, 17: 13136(T)
electric mobility in bismuth (liquid) at 500°C, 17: 4946
electrochemical behavior in acids, effects of internal hydrogen, 16: 5312(R) (TID-14370)
electrochemical machining of, effects of friction, surface finish, and tool erosion on, 17: 34386
electrochemical proton discharge on, isotope effects of deuterium, hydrogen, and tritium on, 18: 37118
electrochemical reactions of, isotope separation factors in hydrogen evolution by desorption in, 18: 29646
electrochemical reactions of, isotope separation in hydrogen evolution in, 18: 29647
electron backscattering by (111) face, kinematic theory calculations of, 19: 20868
electron backscattering coefficients for, empirical equations of, 19: 37794 (NASA-TN-D-2909)
electron band structure of, effects of electron configurations on, (T), 20: 6534 (SC-DC-65-1843)
electron bombardment of, ion desorption spectrum from, (E), 19: 9941
electron emission from cesiated and vacuum surfaces of, (E), 19: 41284
electron inelastic scattering, energy distribution, 17: 13595(T)
electron interaction effects in films of, superimposed on superconducting lead films, (E), 20: 11918
electron penetration at 1 to 10 kev, 16: 18368
electron polarization in, determination by annihilation of polarized positrons, (E), 19: 37898
electron propagation through vacuum boundary with, relative transition radiation yields from, (E), 20: 13352
electron reactions at 0.3–1.6 Mev with, secondary emission from relativistic, 17: 25926
electron reactions at 70 Mev with thin foils of, secondary emission from, 19: 37463
electron reactions at 6 to 60 kev, transient radiation from, (E), 20: 15268
electron reactions at 6 to 23 kev, optical transition radiation from, 20: 21518
electron scattering by, energy loss mechanisms in relativistic, 18: 34258(R) (AD-417250)
electron scattering by, effects of angle of incidence and energy on inelastic, 19: 16406(T)
electron scattering at 0.6 to 1.8 Mev, backscatter and secondary emission in, (E), 19: 29441 (NASA-TN-D-2782)
electron scattering by films of, differential cross sections for multiple, (E), 20: 4485
electron secondary emission in argon ion bombardment, 16: 6845
electron secondary emission coefficient, 16: 12276
electron secondary emission from thin foils of, (E), 20: 13103
electron spin density in, doubly and triply degenerate, 18: 792
electron transition radiation intensity from, 16: 27916(T) (AEC-tr-5234)
electronic work function of cesium-coated, 18: 16742(R) (GA-4804)
embrittlement of, by sulfur, 16: 28646(R) (ORNL-2247(Pts.1-5))
emission behavior, current-field characteristics of, 17: 21989
emission properties of oxide-coated electrodes of, effects of recrystallization on, 17: 31125
emissivity, 17: 31009
emissivity of coated, in vacuum, 18: 24138(R) (PWA-2206(Vol.I))
emissivity of coated, in vacuum, 18: 24139(R) (PWA-2206(Vol.II))
emissivity of coated, in vacuum, 18: 24140(R) (PWA-2206(Vol.III))
emissivity of lithiated and oxidized nickel "C" coatings at 200 to 1450°F, 16: 30802(R) (PWA-1966)
energy bands, 16: 12219(R) (NP-11304)
energy level transitions in, Coster-Kronig, (T), 20: 15238 (CONF-233 (Vol.3), pp 398-418)
energy level widths for, K, (T), 20: 15239 (CONF-233(Vol.3), pp 419-39)
energy levels, 17: 41873 (WASH-1044)
energy levels in, g-factors of low, (E/T), 20: 11479
energy release by cold-worked or neutron-irradiated, stages III and IV of, 19: 16225
erosion by water at 70°F, effects of annealing on cavitation, 20: 29640 (NP-16048)
erosion of 201, by liquid sodium, 20: 5861
evaporation from porous tungsten ionizers, 20: 21570 (N-65-29785)
evaporative lifetime on tungsten and oxygenated tungsten from 1250 to 1750°K, (E), 20: 40307
explosibility of powders of, 19: 36698 (BM-RI-6516)
fabrication and properties of drawn wires of, 18: 35933(R) (ML-TDR-64-56)
failure of combustion reactor in fuel processing, mechanism of, 19: 10667 (BMI-X-322)
fatigue behavior of, in cyclic loading, 17: 22204
fatigue of cold-rolled, α-ray-diffraction studies of, 20: 29623(R) (TID-22970, pp 121-256)
fatigue properties at 1500°F, effects of environment, 16: 526 (NRL-5666)
Fermi surface properties of de Haas-van Alphen effect in, 19: 9767(R) (IS-900(Sect.P))
ferromagnetic behavior of crystals of, at low temperatures, 16: 25547 (AROD-2302.8)
ferromagnetic properties, 17: 16699
fission fragment ranges in, 20: 3982(R) (AGN-8156)
fission product deposition on, in turbulent air streams, 18: 3067
fission product plateout on, from helium system, 16: 29369 (GA-1934)
fluidization of fine particles of, effects of interparticle forces on gaseous, 20: 7047 (ANL-7086)
fluorescence yields in proportional and scintillation detectors, 18: 3796
fluoride films on foils of, ultra-microtome studies of, 19: 6250 (GAT-T-1219(Rev.1))
fracture under impulsive loading, 16: 25759 (NP-11890)
friction of sliding against nickel in sodium at 340 to 650°C, 17: 40423(R) (BMI-1639(Del.))
gamma attenuation, (E), 19: 19333
gamma backscattering at 662 kev, (E), 19: 13789
gamma heating in, calculations for, (E/T), 20: 6517 (CONF-651101-41)
gamma reactions (γ,n) with, neutron angular distribution from, 18: 34935
gamma reactions (γ,n) at 10 to 28 Mev, cross sections for, (E), 19: 19217
gamma reactions (γ,α) at 31 Mev, alpha spectra from, (E), 20: 38037
gamma reactions at 6.13 Mev, electron pair production cross sections for, (E), 19: 39787 (SGAE-PH-19/1965)
gamma reactions at 6.13 Mev, pair-production cross sections for, (E), 20: 37746
gamma reactions (γ,n) and gamma scattering cross sections, 16: 5935
gamma reactions (γ,d) and (γ,p) at 30 to 90 Mev, 16: 24835
gamma reactions (γ,p), cross sections for, 17: 21030
gamma reactions (γ,α) at 21 and 30 Mev with, spectra and relative yields for, 17: 24481
gamma reactions on, effects of E1 resonances on, 16: 33906
gamma reactions with magnetized, polarized electrons from, (E), 19: 27556
gamma resonant scattering by, 17: 29879(R) (IA-822)
gamma resonant scattering in, (E), 19: 6683
gamma resonant scattering by, (E), 19: 12543
gamma scattering spectra for, 17: 35253(R) (IA-775)
gamma spectra from 14-Mev neutron activation, determination by, 19: 26241
gamma spectrum for, thermal neutron capture, 17: 38063(R) (IITRI-1193-26)
gold film adhesion to substrates of, vapor-deposited, 20: 27516
gold-197 Mössbauer spectra in host lattices of, isomer shifts in, 17: 13254
gold-197 nuclear Zeeman effect in, 18: 9405
gold-197 Mössbauer isomer shift and residual electric conductivity in, (E), 19: 10346

gold-197 Mössbauer effect in, relation between chemical shift and electronegativity in, 20: 7055 (UCRL-16436)
grain boundary and intergranular cracking under stress, effects of purity, 16: 5716 (NP-10972)
grain boundary diffusions, 16: 19426
grain boundary migration in zone-refined, review on, 20: 3626 (ORNL-P-1722)
graphite recrystallization from melts of, 19: 30736(R) (GA-5033)
hardness of heat-treated, electroless coatings of, at 175 to 1000°F, 17: 22164 (K-1460)
Hartree-Fock potential of neutral atoms of, analytical expressions for, 18: 16656
heat of sublimation and vaporization of solid, 17: 6093
heat of vaporization, 17: 10240(R) (NP-12208)
heat transfer and pressure drop in eccentric tubes, 16: 25526 (NYO-9649)
heat transfer from, to boiling water, 17: 35995
heat transfer from spheres of, to water at 30 to 94°C, 20: 31440(R) (ANL-7175, pp 159-83)
heat transfer to water by, 20: 20925(R) (ANL-7055, pp 177-212)
heat transfer to water by spheres of, 20: 42580(R) (ANL-7245, pp 60-73)
helium and hydrogen ion attenuation at 0.1 to 500 Mev, tables for, 20: 41619 (CEA-R-3042)
helium ion range-energy relations in, (E), 19: 9888 (NAS-NRC-PUB-1133(p.17-37))
helium-4 energy-range relations to 2 Mev, 16: 8003
helium-4 reactions (He^4,Be^7) at 33 to 41 Mev, 17: 31516
helium-3 elastic scattering at 20 Mev, differential cross sections for, 18: 21359
helium-3 elastic scattering at 20 Mev, differential cross sections, 18: 26681
helium-3 reactions (He^3,n) at 20 Mev, final-state differential cross section for, 18: 15256
helium-3 reactions (He-3,n) at 19 to 25 Mev, angular distributions and cross sections for, (E), 20: 22132
hydrogen atom and ion reactions at 10 to 40 kev, secondary electron emission from, (E), 20: 31533
hydrogen atom recombination on, energy transfer during, 18: 40157
hydrogen ion range-energy relations in, (E), 19: 9888 (NAS-NRC-PUB-1133(p.17-37))
hydrogen ion reactions, sputtering yields, 16: 2203(R) (TID-14257)
hydrogen ion reactions at 1 to 30 kev, electron emission in, 17: 24173
hydrogen ion reactions at high energies, light and uv emission in, 16: 4639
hydrogen sorption on films of, isotope effect in, 18: 3858
hyperfine field at iron-57 nuclei in lattice of, temperature dependence of, 20: 30750
hysteresis in magnetic rotation in cold-rolled and recrystallized, 16: 10561
impregnation of carbon by liquid, 18: 25957(P)
inflammability of powdered, at 180 to 1100°C, 18: 44211
interfacial capacities and transient potentials of electrodes of, 16: 5312(R) (TID-14370)
internal friction in cold-worked, 16: 29397
iodine ion slowing-down in, at 10 to 100 Mev, (E), 19: 37457(R) (ORNL-3778(p.123-5))
iodine reactions at 20 to 120 Mev, stopping cross sections for, 18: 14207 (CONF-354-4)
iodine-127 attenuation in, at 25 to 115 Mev, cross sections for, 18: 716
ion bombardment of (100) face of, Auger electron emission in, (E), 19: 8096
ion elastic scattering by, nuclear radius and surface-thickness analysis from, (E/T), 19: 33251 (UCRL-11781)
ion emission from cesiated and vacuum surfaces of, (E), 19: 41284
ion energy loss rates in, 18: 8917(R) (PR-P-59(p.4-20))
ion exchange behavior in organic solvents containing organic acids, 18: 25305
ion exchange behavior in hydrochloric acid–organic solvent media, 18: 39124
ion exchange in concentrated hydrochloric and perchloric acids, distribution coefficients for, 18: 17759
ion exchange paper chromatography, 18: 17785
ion penetration in films of, method for determination of low-energy krypton and radon, 16: 11762
ion range in, from nickel-58 (n,p) reactions, (E), 20: 24423
ion range-energy relations in, (E), 19: 9893 (NAS-NRC-PUB-1133(p.173-86))
ion ranges at 10 to 100 Mev, bromine and iodine, 20: 41647
ion ranges in, determination from collection experiments, 17: 6820
ion reactions at 36 to 115.5 Mev, dissociation in, 18: 24723
ion reactions at 4 to 100 ev, Auger electron yield in, 18: 20780
ion reactions with, proton-emitting nuclei in, 18: 28567 (JINR-D-1570)
ion reactions with foils of, sticking factors of rare gas, 19: 34610
ion reactions with surfaces of, isotopic effect in secondary electron emission in, (E), 19: 41249
ion scattering at 12 to 25 kev, secondary electrons from, 20: 41620 (NIJS-R-471)
ion scattering on, energy loss in boron and nitrogen, (E/T), 20: 9668
iridium-193 Mössbauer effect in, (E), 19: 21255(R) (UCRL-11828 (p.57-8))
iron-57 internal field in, at 77°K to Curie point, 20: 12298
joining to refractory metals, methods for, 18: 7956(R) (GA-3992(Pt.I))
krypton ion adsorption and retention, in electric discharge, 16: 29516
laser beam reactions with, uv spectra from plasma produced from, (E), 20: 38300
lattice vibrations in single crystals of, dispersion relations for, 19: 2828
lead distribution in, effects of cerium additions on, 19: 23019(T) (JPRS-28849(p.292-6))
lithium-6 reactions at 36 and 63 Mev, dissociation in, 18: 15277
magnetic field effects on thermocouple wires of, 17: 30828
magnetic fields at nuclei in, 17: 13245
magnetic fields at nuclei in, (E), 19: 20578
magnetic fields in low-temperature, De Haas-Van Alphen effect from, 20: 42523(R) (IS-1500(Sect.P))
magnetic moment distribution in, 17: 37822
magnetic moment distribution of, polarized neutron-beam technique for, 20: 40325
magnetic moments of, neutron-diffraction analysis of effects of copper, molybdenum, and silicon on, 18: 27990
magnetic properties, effects of hydrogen, 16: 21010(R) (AD-264878)
magnetic properties of, electron correlations for, 18: 2266
magnetic properties of, temperature variation of anisotropy of, 19: 38076
magnetic properties near Curie point, (E), 19: 41972
magnetic properties of thin films of, near Curie point, (E), 20: 24658
magnetic susceptibilities, 16: 25882 (ASD-TR-61-630)
magnetization of, distribution of internal, (T), 20: 30734(R) (TID-22970, pp 1-63)
magnetocrystalline anisotropy of single crystals of, 16: 25882 (ASD-TR-61-630)
magnetoresistance of crystals of, at 31 and 160 k gauss, longitudinal and transverse, 17: 37714
magnetostriction and residual stresses after plastic elongation, 16: 9214(R) (TID-14810)
manganese-54 hyperfine field in, 17: 40087
mechanical properties, effects of various gases at high temperatures, 16: 22644
mechanical properties of, effects of electrons at 0.2 to 1.8 Mev on, 17: 3577(R) (TID-17067)
mechanical properties at high temperatures, effects of hydrogen on, 18: 27966 (ORNL-3600)
mechanical properties of crystalline, effects of heat treatments on, 18: 32042(R) (HW-81269(p.3.1-38))
mechanical properties at −196 to 2800°C, temperature effects on, 18: 42065
mechanical properties at room temperature to 300°C, 19: 22863(R) (AD-606809)
mechanical properties of composites of, with glass, 20: 39405 (UCRL-16844)
mechanical properties at cryogenic temperature, 17: 6542
melting temperature of, equations for calculating, 18: 25990
mesic atom (μ^-) decay in, anomaly in, 17: 6888
mesic atoms of, meson (μ^-) decay in, 16: 24278 (JINR-P-971)
mesic (μ^-), effect of atomic binding on decay rate of mesons (μ^-) in, 17: 774
meson (μ^-) capture by, x rays from, 18: 19044
meson (μ^-) capture by, probability for, (T), 20: 28456
meson (π^-) reactions (π^-,nγ) with, energy spectra from, (E), 19: 21315
meson (μ) capture, Fermi interactions in, 16: 15590
meson (μ) cascades in, x-ray emission from, 16: 15692
meson (μ) scattering, x-ray emission in, 16: 19705
meson (μ^-) capture rate and lifetime in, 17: 775
meson (μ^-) capture by, x-ray spectra from, 17: 26578
metabolism by Habrobracon, 19: 10741 (TID-21559)
mixing with copper in fluidized-packed beds, particulate movement in, 18: 25658
molecular beam scattering from plates of, decrease of frictional resistance in, 18: 40155
motion of particulate, on graphite surfaces, 18: 27872
motion of particulate, in fluidized beds, 19: 15663(R) (ANL-6900 (p.143-202))
negative ion emission, after positive ion bombardment, 18: 28121
neon-20 reactions with, at 130 Mev, 17: 7082 (JINR-P-1072)
neon-20 reactions with, product radioactivities in, 18: 1017 (JINR-P-1388)
neon-20 range-energy relations at 0.4 to 6 MeV, 16: 8003
neon-20 reactions at 130 Mev, production of proton emitters in,

18: 24737
neutron absorption and inelastic scattering by, gamma spectra from, 20: 13966 (UNC-5140)
neutron absorption cross section in pitchblende, thermal, 20: 37994
neutron attenuation in, (E), 19: 19333
neutron capture by, at 0 to 50 kev, cross sections for, 17: 41883
neutron capture by, 18: 40630
neutron capture by, average level widths of compound nucleus from, (E), 20: 32424
neutron capture cross sections, 16: 26509
neutron capture cross sections at 4 to 220 kev, total, 18: 42650 (TID-21144)
neutron capture cross section of, energy dependence of radiative (E/T), 19: 3391
neutron capture cross sections at 0 to 200 kev, (E), 20: 46599(R) (RPI-328-68, pp 1-62)
neutron capture gamma spectra, fast and thermal, 16: 14060
neutron capture gamma spectrum, 16: 28024(R) (ARF-1193-12)
neutron capture gamma spectra, 17: 17255
neutron capture gamma spectra, 18: 24625 (WASH-1046)
neutron capture gamma spectra, high-energy, 19: 25468(R) (ARF-1193-17)
neutron capture in, resonance and thermal, (E), 19: 16972
neutron critical scattering in, 17: 11222
neutron cross sections, thermal, 16: 2783
neutron cross sections, library of 40-group BPG and spectral "B" codes, 16: 12422 (BAW-158)
neutron cross sections for, nine and sixteen group, 17: 22789 (GEMP-173)
neutron cross sections for, fast, 17: 28245 (KFK-120)
neutron cross sections and nuclear data for, 18: 7680 (KFK-120(Pt.III))
neutron cross sections, 18: 28043(R) (HW-79280(p.8.1-6))
neutron cross sections at 1.44 ev (E), 19: 3288
neutron cross sections for, from 0.414 ev to 5.5 Mev, 19: 45244 (AEEW-M-472)
neutron cross sections for, 9- and 16-group, 20: 4829 (GEMP-173(Suppl.1))
neutron cross sections for, 20: 4830 (GEMP-384)
neutron cross sections for, 20: 14062 (JUL-214-RG)
neutron cross sections and shielding coefficients for, 20: 22383(T) (AEC-tr-6693)
neutron cross sections for, (T), 20: 34512 (ANL-7170)
neutron differential elastic cross section at 13.9 Mev, (E), 19: 35378(R) (EANDC(E)-57(U))
neutron diffraction patterns of crystals of, 17: 37802
neutron diffraction by powders of, thermal, 17: 7070
neutron diffusion pattern of crystals of, 17: 20318
neutron double Bragg scattering by single crystals of, angular distributions in, 16: 26211
neutron elastic scattering at $\theta = 0°$, 16: 4741(R) (TID-14157)
neutron elastic scattering at 2.8 Mev, polarizations in, 16: 11026
neutron elastic scattering and polarization by, at 2.8 Mev, 17: 17294
neutron elastic scattering by, angular distribution for fast, 17: 36669 (WASH-1042)
neutron elastic scattering at 14 Mev, differential cross sections for, 18: 2888
neutron elastic scattering at 700 to 1300 kev, cross sections for, 18: 4511 (CONF-250-13)
neutron elastic scattering anisotropy in, 18: 15138 (NAA-SR-Memo-9021)
neutron elastic scattering at 0.65 Mev, angular distributions for, 18: 17089
neutron elastic scattering at 0.3 Mev, angular distributions for, 18: 17090
neutron elastic scattering at 3.25 Mev, polarization in, 18: 19103
neutron elastic scattering at 0.3 to 1.5 Mev, differential cross sections for (E), 19: 3381
neutron elastic scattering at 0.3 to 1.5 Mev, angular distributions from, (E), 19: 19095 (WASH-1053)
neutron elastic scattering at 0.2 to 2.0 Mev, compound, (T), 19: 19190
neutron elastic scattering at 85 to 700 kev, differential cross sections for, (E), 19: 21298
neutron elastic scattering at 0.8 Mev, angular distributions of, (T), 19: 37884
neutron elastic scattering at 1 Mev, differential cross sections for, (E/T), 20: 9981 (WASH-1064)
neutron elastic scattering at 0.8 Mev, cross sections for, (T), 20: 15770
neutron elastic scattering at 3.2 Mev, (E/T), 20: 46644
neutron flux and spectrum measurements on foils of, 20: 21427(R) (NASA-CR-54904)
neutron flux measurements using, effects of cobalt-58 on, 16: 722
neutron form factors and spin density distributions for, comparison with Hartree-Fock calculations, 17: 6646 (BNL-5674)
neutron inelastic scattering at 14 Mev, 16: 3686
neutron inelastic collision cross sections, 16: 10984
neutron inelastic scattering, vibration defect modes in cold, 16: 15693
neutron inelastic collision cross sections, 16: 29793(T) (FTD-TT-62-953)
neutron inelastic scattering in, phonon scattering spectra from, 16: 32387
neutron inelastic scattering cross sections, 17: 15385(R) (ANL-6683)
neutron inelastic scattering by, cross sections for, 18: 16958(T) (NP-tr-1114)
neutron inelastic scattering at 14 Mev, collective-state excitation by, (E/T), 19: 23697
neutron inelastic scattering by, gamma yields from, (E), 19: 35406(T) (ANL-Trans-177)
neutron inelastic scattering at 0.9 to 10 Mev, cross sections for, 19: 35605(R) (ANL-7045(p.24-48))
neutron inelastic scattering by crystals of, at 0°K, polarization effects in, 17: 9520
neutron inelastic scattering at 14 Mev, differential cross sections for, (E), 20: 10007
neutron inelastic scattering at 5.8 and 7.5 Mev, gamma spectra from thermal, (E), 20: 22069
neutron magnetic scattering by dislocations in, 19: 29220
neutron magnetic scattering by, properties of, (T), 20: 24585 (AD-627302)
neutron microscopic cross sections for, 17: 41866 (NAA-SR-Memo-8904)
neutron radiative capture cross sections at 30 and 65 kev, 18: 34274(R) (NIRS-2(p.3-15))
neutron radiative capture at 7.4 Mev, gamma spectra from, (E), 20: 10060
neutron reactions (n,t), cross section, 16: 7048
neutron reactions at 3.7 Mev, cross-section measurements, 16: 8224
neutron reactions at 0.1 to 100 Mev, total cross sections for, 16: 11021
neutron reactions (n,p) at 14 Mev, angular distributions and spectra from, 16: 11028
neutron reactions at thermal energies, cross sections, 16: 10961 (TID-14868)
neutron reactions at 3 to 15 Mev, removal cross sections, 16: 29739
neutron reactions, solution of Schroedinger equation for cross-section calculation, 16: 29745
neutron reactions (n,p) and (n,np) at 14.1 Mev, cross sections for, 16: 33839
neutron reactions (n,t), cross sections for, 17: 2242 (TID-16949)
neutron reactions (n,t) with, cross sections for, 17: 9619
neutron reactions with, uses for neutron dosimetry, 17: 26787 (TID-7641 (p.283-9))
neutron reactions (n,t) on, cross sections for, 17: 31434
neutron reactions (n,p) with, cross section and energy spectrum for, 17: 31545
neutron reactions (n,p) at 15 Mev, cross section and energy spectrum of, 17: 38132
neutron reactions (n,γ) with, spectrometer performance for thermal, 18: 2058
neutron reactions (n,γ) with, dose distributions from, 18: 16962
neutron reactions with, gamma production in, 18: 21169 (GEMP-278)
neutron reactions with, for fast-neutron spectrometry, 18: 29995
neutron reactions with, gamma radiation from, 18: 30735(R) (TID-20657)
neutron reactions at 4 to 5 Mev, compound-nucleus level widths from, 18: 36645
neutron reactions (n,γ) at epithermal to 30 kev, energy dependence in, 18: 38075(T) (AEC-tr-6398(p.70-80))
neutron reactions (n,γ) with, gamma spectra from fast, 18: 44807
neutron reactions (n,n'γ) at 0.3 to 2.6 Mev, excitation cross sections for, (E/T), 19: 31284
neutron reactions (n,γ) at 0.025 ev, spectra from, 19: 40896
neutron reactions (n,n'γ) with, cross section for, 19: 45263 (JAERI-1078)
neutron reactions (n,p) at 14 Mev, proton spectra from, (E), 20: 26226
neutron reactions (n,p) at 0.82 to 3.7 Mev, cross sections for, 20: 28746(R) (GEAP-4795)
neutron removal cross sections for, effective fast, 16: 24797 (WADC-TR-58-266)
neutron resonance cross sections, 17: 7595(R) (ACNP-62018)
neutron resonance absorption integrals for, (E), 20: 15691 (CEA-R-2840)
neutron scattering angular distribution, 16: 12419 (ANL-5567(Rev.))
neutron scattering at 0 to 500°C, 16: 18444
neutron scattering at 90 kev, angular distributions and cross sections for, 16: 33800
neutron scattering by, at Curie point, 17: 20979
neutron scattering by, critical, 17: 37831
neutron scattering by, cross sections for, 17: 41873 (WASH-1044)
neutron scattering by phonons in, cold, 18: 11195(R) (EANDC(E)-49(L))
neutron scattering by, cross sections for, 18: 15476
neutron scattering at 2.5 Mev, cross sections for inelastic, 18: 14851
neutron scattering cross sections at 0.5 to 0.8 Mev, 18: 26571
neutron scattering by, gamma production cross section for, 18: 28579 (TID-20689)
neutron scattering by phonons in, cold, 18: 37711

neutron scattering by, at and near Curie point, (E/T), 19: 12467
neutron scattering by, angular distributions of, 19: 31252
neutron scattering by powders of, near 1 Å, 16: 22356
neutron scattering by, phase transitions in small-angle polarized, (E/T), 20: 17986(T)
neutron scattering at 14 Mev, cross sections for elastic and inelastic, (E), 20: 34687
neutron spectra in, measurement of, (E), 19: 37770
neutron spin-orbit scattering by, polarization effects in thermal, 18: 11261
neutron total cross section of, fast, 17: 20982 (HW-SA-2875)
neutron total cross section at 200 ev to 1 Mev, 17: 36669 (WASH-1042)
neutron total cross section of, effective, 18: 11195(R) (EANDC(E)-49(L))
neutron total cross sections at 0.3 to 2.7 Mev, resonance structure in, 18: 13066
neutron total cross sections at 175 to 300 kev, 18: 17038
neutron transmission through magnetized, Stern-Gerlach measurement of polarized, 20: 34819
neutron transport properties at 0.3 to 2.7 Mev, 17: 787(T) (AEC-tr-5413)
nickel-61 Mössbauer spectra in, parity effects on, 17: 13238
nickel-61 NMR in single-domain powder of, 20: 45000
nickel-61 nuclear magnetic resonance in, 19: 39418
nitrogen ion ranges at 0.4 and 2.5 Mev, (E), 19: 41269
nitrogen ion sputtering reactions at 0 to 8 kev, 16: 587 (NASA-TR-R-105)
nitrogen-14 reactions, neutron transfer in, 16: 26221 (JINR-P-973)
nitrogen-14 energy-range relations at 0.4 to 6 Mev, 16: 8003
nuclear magnetic resonance of nickel-61 in, line shapes, saturation behavior, and temperature studies in, 17: 34603
nuclear magnetic resonance relaxation in, effects of Bloch wall position fluctuations on, 18: 6195
nuclear magnetic relaxation rates in, theory of, 18: 32273 (NP-14118)
nucleon reactions at high energies, secondary nucleon yields from, (E/T), 19: 21242 (NP-14837)
nucleon scattering at 2.8 and 6.8 Mev, angular distributions from, 18: 38080(T) (AEC-tr-6398(p.120-5))
oxidation by carbon dioxide–carbon monoxide mixtures, 20: 21383
oxidation by oxygen at 500 to 1200°C, 19: 6249(R) (EURAEC-1111(Pt.1))
oxidation mechanisms, 19: 26765(R) (EURAEC-1295)
oxidation of, growth of oxide crystals in, 17: 39492(T,R) (EURAEC-726)
oxidation of, growth of nickel oxide crystals in, 17: 39483(R) (EURAEC-660)
oxidation of high-purity, at 1200°C, 20: 33812 (BM-RI-6800)
oxidation of, nucleation-germination phenomena in, 17: 16596(T,R) (EURAEC-559)
oxidation of thoria-dispersion-hardened, 17: 27730(R) (HW-77052)
oxidation of thoria dispersion-hardened, kinetics of, 17: 37003(R) (HW-78118)
oxidation of, beta backscattering for evaluation of, 19: 2751
oxidation tests of flame-sprayed coatings of, on vanadium alloys, 16: 6706(R) (ARF-2227-3)
oxidation, tracer studies, 17: 39017 (ANL-6684)
oxidation, tracer studies of mechanism of, 19: 9098 (UCRL-7631-T)
oxygen ion energy losses in, at 2 to 40 Mev, (E), 19: 6461
oxygen sorption on, high-energy electron diffraction studies of, 19: 39178
oxygen-16 reactions at 167 Mev, charged-particle yields in, 17: 28252 (UCRL-10693)
oxygen-ion transmission through thin foils of, charge-state distribution after, (E), 19: 47179
oxygen-16 reactions at 167 Mev, charged-particle emission in, 18: 34780 (UCRL-11349)
oxygen-16 reactions at 167 Mev, particle spectra from, (E/T), 19: 10336
oxygen-16 scattering at 164 Mev, distributions from multiple, 18: 42319
performance as catalyst for hydrogen reactions, 19: 2345
performance as collector electrode for thermionic cells, 20: 11540(R) (AD-626444)
performance as electrodes in barium-filled thermionic cells, 18: 44498(R) (MND-2812-3)
performance as electrodes in barium-filled thermionic cells, 18: 44497(R) (MND-2812-2)
performance as electrode in molten salts at 850°C, 18: 39156 (EUR-1643.e(p.327-45))
performance as electrode in neon glow discharge, effect of active gas additives on, 18: 21456
performance as electrode, tracer study of diffusion and evaporation, 18: 37476(T) (AEC-tr-6398(p.232-45))
performance as emitter electrode in cesium plasma diode, 18: 32890 (LAMS-3086)
performance as liquid-phase sintering promoter for uranium monocarbide, 20: 21296 (Y-1510)
performance as melting-point temperature sensors up to 6000°F, (E), 19: 30489 (SC-DC-65-1237)
performance as reflector in fast rocket reactors, 19: 29769
performance in accelerating electrodes in cesium-contact ion thrustors, 20: 31383
performance in thermionic cells, 18: 26933
performance of coatings of, on cadmium–indium–silver control rods, 16: 25796
performance of coatings of, on Pebble Bed Reactor fuel, 16: 9663 (NYO-9064)
performance of electrodes of, in thermionic converters, 19: 20906
performance of electrodes of, in contact ion engines, 19: 13613
permeability of, to helium and hydrogen, bibliography on, 17: 37492(R) (SCL-B-107)
phase transformations, effect of pressure and irradiation on solid-solid, (E), 20: 40306
phonon spectra, 18: 24959 (NP-13910)
photodesorption of carbon monoxide from, efficiency and mechanism of, 19: 7408
photoelectric emission from, by ultraviolet radiation at 10 to 50 ev, 18: 706
photoelectric properties, 17: 6801(R) (TID-17303)
photoelectrons from magnetized crystals of, polarization of, (E), 20: 37475
photoinduced carbon monoxide desorption from, 19: 5974
photon reactions (γ,n) and (γ,p) with, shell structure effects on cross sections for, (T), 20: 24428
photon reactions (γ,d) and (γ,p) at 24 Mev, yield ratios for, 17: 28289
photon reactions, release of adsorbed carbon monoxide by, 16: 31722 (NYO-9805)
photon reactions up to 80 Mev, neutron emission in, 18: 38152
photon reactions with, proton angular distributions and yields at >8 Mev, 17: 28265
photoproton angular distributions from, 16: 2533
plastic deformation of sintered, 16: 21081
plastic deformation of, electron-positron annihilation in, 18: 37694
plasticity of, effects of added cerium, magnesium, and zirconium on, 20: 46213
platinum-195 Mössbauer effect in, g-factor and internal fields from, (E), 20: 32487
point defects in crystals of, induced by quenching and radiation, 17: 37589
point defects in irradiated, 16: 33553
polarization of silver nuclei in, 18: 31361(R) (UCRL-11213(p.87-138))
polarographic behavior in lithium chloride–potassium chloride eutectic, 18: 8381
polishing with corundum grains, tracer studies of surface processes in, 18: 27935
porosity of coatings of, electrodeposited on uranium, 17: 34353
porosity of coating of, on uranium surfaces, x-ray fluorescence determination of, 20: 13211 (BNWL-124)
positron annihilation in, effects of electronic structure on, 18: 42443
positron annihilation in ferromagnetic, angular correlations from polarized, (E), 20: 32703
positron lifetime in, 16: 3626
potential–pH diagram for metallic, in water, 18: 8324 (KAPL-M-MSB-1)
potentials of electrodes of, in alcohols, salt solutions, and water, 16: 25322 (TID-16292)
potentials of electrodes of, effects of internal hydrogen on, 17: 28830 (TID-18985)
powder metallurgy of, 19: 2774
powders of, arrangement in lines-of-force pattern by electric fields, 18: 5848 (SC-TM-40-59(51))
precipitation from nitric acid solution using sodium borohydride, 18: 13358(R) (MLM-1151)
precipitation using dimethylbenzenearsonic acid, 19: 9136
precipitation using trichlorobenzenearsonic acid, 19: 9137
preparation and properties of tungsten-fiber reinforced, 20: 43848(R) (BNWL-269, pp 5.1-36)
preparation and structure of films of, evaporated on rock salt crystals, 17: 29333(T) (NP-tr-1032)
preparation for electron microscopy, 18: 7298(R) (HW-78962(p.3.1-14))
preparation of crystals of, by zone melting at 2320 to 3800°K, 17: 32590
preparation of films of, by electroplating on copper, 17: 35353(R) (IA-775)
preparation of foamed, for aerospace uses, 19: 37141
preparation of highly dispersed, by irradiation of oxalate, 16: 32161
preparation of kryptonated, by ion bombardment, 20: 18570(R) (NYO-2757-5)
preparation of porous sintered, 19: 11715(P)
preparation of single crystals of, 16: 3398 (PAN-245/I-B)
pressure spalling of, properties of, (T), 20: 12539 (LA-DC-7692)
production in supernova interiors, rapid nuclear processes for, 17: 39835
production of porous membranes of, for diffusion barriers, 17: 25718(P)
production of very pure powders of, electrolytic method for,

16: 5659(T)(P) (CEA-tr-X-421)
properties and reactions at elevated temperatures, 16: 4527 (DMIC-160)
properties and structure of shock-hardened, 17: 35264(R) (UCRL-10706(p.111-203))
properties and structure of, deposited by carbonyl process, 20: 7551 (BDX-613-77)
properties as cladding for corrosion protection of uranium, 20: 7522
properties as coatings on copper neutron-transmission tubes, 18: 34752(R) (CU(PNPL)-234)
properties as neutron shield, 17: 38043(T) (AEC-tr-5734(p.251-4))
properties as neutron reflector in fast-breeder reactors, 18: 4700
properties as reactor reflector, 16: 24421
properties as reactor reflector, 17: 42224
properties as reflector in fast reactor, 18: 4746
properties as thermionic cathode, 17: 12747(R) (AFCRL-62-373)
properties as thermocouple material, fabrication methods effects on, 17: 30824
properties as threshold neutron detectors for radiation damage investigations, 17: 41118
properties as threshold detector, 18: 17278 (KAPL-M-6101)
properties at −400 to 100°F, 18: 42020 (PB-171809(Rev.))
properties for use as reactor material, 16: 4994
properties for use in cermet filters for purification of sodium (liquid), 17: 18682(T) (FTD-TT-62-1473(p.31-7))
properties for use as oxidation-resistant coating for uranium, 19: 13925
properties for use in packed column for boron isotope separations using anisole–boron trifluoride, 20: 25467 (K-1653)
properties for use as thermal shielding at high temperatures in vacuum, 20: 41440(R) (ALO-3632-4)
properties in neutron flux measurement, 18: 8688
properties of coatings of, on vanadium base alloys at high temperatures, 17: 12610(R) (ARF-B-6001-2)
properties of, dispersion velocity dependence on mechanical and thermal, 17: 27873
properties of, effects of uranium on, 17: 418 (NP-12164)
properties of electron beam melted, 16: 19280
properties of, electrical and thermal, 17: 25381 (ASD-TDR-62-118)
properties of, for use as cathode in electrolytic separation of deuterium, 17: 22074
properties, theory of infrared and optical, 16: 25758 (NP-11675)
properties, effects of rare earths on, 19: 23021(T) (JPRS-28849(p.303-9))
protective effects against nucleic acid decomposition by nuclease, 18: 25085 (SGAE-BL-5/1964)
protective effects of coatings of, against corrosion of thorium and uranium during long-term storage, 16: 25713 (BMI-1563)
protective effects of coatings of, against oxidation of niobium–vanadium alloys at 2000 to 2400°F, 16: 27587 (ARF-2227-6)
proton attenuation at 1 to 1000 Mev, 17: 18909 (TID-18436)
proton attenuation at 28.7 Mev in, 17: 37861
proton attenuation at 23 Mev, 19: 22818(R) (ORNL-3650(p.221-38))
proton attenuation by films of, at 1.5 to 4.5 Mev, 16: 15668
proton elastic and inelastic scattering at 6.8 Mev, 17: 24414
proton elastic scattering at 6.8 Mev, 16: 7120
proton elastic scattering at 57 Mev, angular distributions and polarizations, 16: 23056
proton elastic scattering at 9–22 Mev, optical-model analysis of, 17: 28316
proton inelastic scattering by, effects of E1 resonances on, 16: 33906
proton inelastic scattering at 14.5 Mev, statistical model prediction for yields in, 17: 38206
proton nonelastic scattering cross sections at 10 Mev, 17: 13581
proton reaction cross sections at 28 Mev, shell closure effect on total, 18: 22903
proton reactions (p,n) at 18.5 Mev, angular distributions of quasielastic, 18: 40587
proton reactions (p,p') at 10.5 Mev, cross sections for, (E), 20: 13897
proton reactions (p,xN) at 660 Mev, angular distributions from, (E/T), 20: 28270 (FEI-28)
proton reactions at high energies, 16: 4882(R) (ANL-6427)
proton reactions at 540 Mev, cross section for production of rare gases from, 17: 19255
proton reactions at 130 to 400 Mev, production cross sections for isotopes in, 17: 28943(R) (TID-18961)
proton reactions at 130 to 400 Mev, isotope formation cross sections for, 18: 22881
proton reactions at 0.5 to 3 Mev, formation cross sections for nuclides from, 18: 43601(R) (TID-21007)
proton reactions at 660 Mev, secondary neutron production in, (E), 19: 38018
proton reactions at 590 Mev and 18.3 Bev, potassium isotopes yields in, in, (E), 20: 17717
proton reactions at 0.05 to 2.9 Bev, induced activity data and cross sections for spallation, (E/T), 20: 32549
proton reactions (p,n) at 14.8 Mev, neutron spectra from, 16: 26326 (UCRL-6733)
proton reactions (p,n) at 5 to 12 Mev, neutron spectra from, 17: 17293
proton reactions (p,γ) at 1424 kev, gamma-ray resonance yield curves from thick targets, 18: 9432
proton reactions with, radioisotope production in, 18: 1021 (ORNL-TM-663)
proton reactions with, rare gas and tritium production cross sections for, 18: 15189 (CERN-64-12)
proton reactions with flat shields of, nucleon angular distributions and yields from, (E), 19: 43461 (NP-15385)
proton reactions with slabs of, secondary nucleon emission in, 20: 28596
proton scattering, angular distributions, 16: 29881(R) (ORNL-1383)
proton scattering by, optical models for, 17: 19342
proton scattering by, neutron, prong, and proton spectra and distributions for, 17: 22564 (ORNL-3383)
proton scattering at 40 Mev, proton polarization resulting from, 17: 36701
proton scattering by, polarization from, 18: 40597
proton shielding performance of, for space vehicles, (T), 20: 3242 (NASA-SP-71, pp 225-8)
proton total cross sections at 8.5 to 11 Mev, (E), 19: 43323
proton total cross sections at 16.4 Mev, (E), 20: 1208
proton total cross section at 17 Mev, (E), 20: 44662 (USC-136-111)
proton total reaction cross section at 16.6 Mev, measurement of, 18: 1086
proton total reaction cross sections, 18: 18987
radiation annealing effects at 4.5°K, 18: 14562
radiation annealing of Frenkel defects in, statistical model for, 18: 32252
radiation damage, 16: 29460
radiation damage, cross section for atomic displacement by electrons at 0.5 to 3 Mev, 16: 564 (61-GC-166)
radiation damage in, production and recovery of electron-induced, 16: 27719
radiation damage in, electron microscopy study of fast-neutron, 20: 9565(R) (BNWL-166, pp 3.10-14)
radiation damage to crystals of, basic mechanism study of, 16: 13643 (TID-14667)
radiation effects of neutrons on relaxation of elastic stresses in bent plates, 16: 22704
radiation effects of neutrons on electric conductivity, annealing, 16: 22706
radiation effects on relaxation of elastic stresses in bent plates of, neutron, 16: 22704
radiation effects on electric conductivity of, annealing, neutron, 16: 22706
radiation effects and isochronal annealing data at 4°K, 16: 6810(R) (ORNL-3213(p.15-23))
radiation effects on relaxation of elastic stresses in, kinetics, 16: 27699(T) (AEC-tr-5257)
radiation effects on electric conductivity of, neutron, 16: 31267 (NP-11754(Vol.I)(Sect.II))
radiation effects of fission fragment bombardment, 16: 33407
radiation effects on, gamma, 18: 26067(R) (AI-8971)
radiation effects on mechanical properties, 17: 591
radiation effects on pure, reactor-neutron, 17: 5001
radiation effects on electric resistance of, 17: 6732 (62-GC-207)
radiation effects on, comparison with quenching, 17: 8711(R) (TID-17556)
radiation effects on electric conductivity of, neutron, 17: 10138
radiation effects, 17: 8877 (AFCRL-62-316)
radiation effects, 17: 11129
radiation effects on, thermal annealing of neutron, 17: 14903
radiation effects on properties of electrolytic, 17: 18885
radiation effects on corrosion, mechanical, physical and thermal properties of, 17: 32679
radiation effects on content of, in yeast nucleic acids, 17: 35540
radiation effects on tensile properties of, neutron, 17: 37572 (HW-78178)
radiation effects on, mechanisms for annealing and producing, 18: 2322
radiation effects on, preparation of samples for studying, 18: 7290(R) (HW-77954(p.3.1-20))
radiation effects on magnetic properties of, neutron, 18: 14548
radiation effects on plastic deformation and magnetic susceptibility of single crystals of, neutron, 18: 14559
radiation effects on, at low temperatures, saturation phenomena in defect production by neutron, 18: 16531(T) (AI-Trans-38)
radiation effects on magnetic Barkhausen effect of, electron and neutron, 18: 18414 (NP-13771)
radiation effects on mechanical properties of, 18: 18430
radiation effects on hardness and thermoelectromotive force of, neutron, 18: 28066
radiation effects on ferromagnetism of, 18: 30289
radiation effects on, neutron, 18: 32255
radiation effects on structure of, neutron, 19: 997(R) (NYO-2994-1)

radiation effects on catalytic reactions of, in formic acid decomposition, 19: 4196(R) (ORNL-3627(p.220-3))
radiation effects on plastic deformation, 19: 11682
radiation effects on, 19: 15991(R) (BNL-841(p.63-101))
radiation effects on, release of stored energy in recovery from neutron, 19: 16225
radiation effects on content of, in blood, liver, and spleen in dogs, 19: 17537
radiation effects on reactions with dimethylglyoxime, gamma, 19: 17781(R) (ORNL-3750)
radiation effects on content in dog tissues, 19: 19540
radiation effects on magnetic properties of defects in, neutron, 19: 20647
radiation effects on magnetism of, at 28°K, neutron, 19: 20652
radiation effects on tensile properties of, 19: 23996(R) (ORNL-3650 (p.1-110))
radiation effects on reactions with dimethylglyoxime, gamma, 19: 23163(R) (ORNL-3650(p.111-86))
radiation effects on electric resistivity in, electron, 19: 25070
radiation effects on catalytic activity in conversion of cyclohexane, 19: 26417
radiation effects on function of electrodes of porous, proton, 19: 28908
radiation effects on, gamma, 19: 36451(R) (BNL-900(p.73-104))
radiation effects on magnetic properties of, electron, (E), 19: 39239
radiation effects on, recovery from neutron, 19: 39251
radiation effects on electric resistivity at 4°K, fast neutron, 19: 44739(R) (ANL-7000, pp 233-77)
radiation effects on capacity of, gamma, 19: 7995
radiation effects on crystals of, neutron, 16: 33552
radiation effects on crystals of, at 3 Mev, Kossel patterns in electron, 16: 16786
radiation effects on magnetic susceptibility of crystals of, neutron, 17: 22260
radiation effects on crystals of, 17: 23872(R) (TID-18626)
radiation effects on thin films of, neutron, 16: 22680
radiation effects on ferromagnetic resonance of thin films of, helium-3, 20: 12318
radiation effects on battery electrodes of, gamma, 20: 17124(R) (N-65-17608)
radiation effects on battery electrodes of, gamma, 20: 21425(R) (N-65-24491)
radiation effects on electric conductivity of, stage IV recovery from electron, (E), 20: 31800
radiation effects on phase transformations in, under high pressure, 20: 33968
radiation effects on electric conductivity and magnetism of, electron, 20: 37297
radiation effects on diffusion in copper at 200 to 520°C, alpha, 20: 37300
radiation effects on, as control rod coating, 20: 39461 (WCAP-6074)
radiation effects on foils of, neutron, 20: 43990 (BNWL-SA-782)
radiation effects on critical shear stress, annealing of neutron, 20: 45038
radiation effects on, in nickel–cadmium batteries, 18: 34213(R) (AI-64-11)
radiation heating deposition rates in, cross sections for, 17: 36347(R) (NARF-62-18P)
radiation, deformation, and quenching effects on susceptibility relaxation and recovery, 18: 14571
radiochemistry, 16: 10046 (NAS-NS-3051)
radioinduced defects in, effects of Frenkel pair recombination on, 20: 7651
radioinduced defects in annealed, Frenkel pair recombination volume from alpha, 20: 21447
radioinduced defects in, neutron, 20: 27569(R) (BNWL-207, pp 3.7-13)
radioinduced heating of, gamma, 18: 10346(R) (X64-11113)
radioinduced interstitial point defects in, produced by argon ions at 100 ev, 18: 5828
radioinduced interstitial and vacancy clusters in, neutron, (E), 20: 38367
radioinduced lattice defects in, electron microscopic observations of, 19: 11812
radioinduced production of helium and hydrogen in, neutron, 19: 26901
radioinduced relaxation of elastic stresses in, 17: 455
radioinduced relaxation of stresses in, 18: 42120(T) (AEC-tr-6474)
radioluminescence and optical flash in sodium chloride phosphor doped with, x, (E), 19: 27719
rare-gas ion reactions at 1 to 10 kev, secondary-electron emission in, (E), 19: 39404
reactions with aluminum oxides, effects of sulfur and magnesium on, 20: 35834(R) (BMI-1767)
reactions with benzenearsonic acid and its derivatives in acid media, precipitation, 17: 12198
reactions with beryllium, copper, stainless steel, and niobium alloys to 760°C *in vacuo*, 19: 44606 (PWAC-483)
reactions with beryllium to 500°C in carbon dioxide and *in vacuo*, 19: 22997 (TRG-Report-842)
reactions with bromine at 300 to 1600°K and 10^{-7} to 10^{-4} mm mercury, mass spectrometry of products from, 18: 4900 (CONF-117-32)
reactions with carbon dioxide, 16: 2993 (NP-10967)
reactions with chlorine, transfer of translational energy in surface, 16: 13061
reactions with crucibles of refractory compounds with boron, carbon, and nitrogen at 400 to 1500°C, 19: 37112
reactions with fast neutrons, helium and hydrogen production in type 347 stainless steel in, 20: 7490(R) (BMI-1745, Sect.A)
reactions with fluorine, mechanism of, 17: 15998
reactions with fluorine, kinetics and mechanism, 17: 39017 (ANL-6684)
reactions with hydrogen sulfide, 19: 30067(R) (ORNL-3789(p.56-98))
reactions with liquid sodium at high temperatures, 20: 38499 (ANL-7120, pp 839-47)
reactions with magnesium to 450°C, 19: 22997 (TRG-Report-842)
reactions with Magnox to 500°C in argon and *in vacuo*, 19: 22997 (TRG-Report-842)
reactions with metals to 1000°C in different atmospheres, 19: 22997 (TRG-Report-842)
reactions with organic matrix materials in ice-water system, 18: 15722 (TID-20332)
reactions with plutonium oxide during sintering, 17: 14209 (LA-2828)
reactions with plutonium–thorium–uranium alloys at 650°C, 19: 44674(R) (ANL-7000, pp 69-83)
reactions with radioinduced Frenkel defects in silicon crystals, 17: 37610
reactions with silver nitrate in nonaqueous solvents, 16: 5311(R) (TID-14361)
reactions with sodium at high temperatures, 19: 39090(R) (ANL-7046 (p.78-82))
reactions with sodium, high-temperature, 20: 15033(R) (ANL-7152, pp 87-96)
reactions with sodium at high temperatures, 20: 20925(R) (ANL-7055, pp 177-212)
reactions with sulfur-bearing alumina at high temperatures, 20: 37168(R) (BMI-1771)
reactions with sulfur-bearing alumina at high temperatures, 20: 37169(R) (BMI-1774)
reactions with titanium nitride, 20: 7097
reactions with tritium atoms at 50 to 100 kev, research on, 20: 22857(R) (ORNL-3913, pp 111-32)
reactions with uranium di- and monocarbides and nitride at 1000°C, 16: 30829
reactions with uranium carbides during fritting, 18: 12663
reactions with uranium nitride, 19: 26756 (CEA-R-2762)
reactions with uranium to 700°C *in vacuo*, 19: 22997 (TRG-Report-842)
reactions with uranium nitride at 600 to 1200°C, 20: 19187 (BMI-1760)
reactivity effects as reflector on beryllium-oxide-moderated uranium-235-fueled subcritical systems, 16: 18622 (UCRL-6729)
reactivity effects in beryllia-moderated subcritical assemblies, (E), 19: 10490 (UCRL-7686)
reactivity worths, 19: 38178(R) (GEAP-4790)
reactor reflector critical thickness, 16: 24410
recovery and recrystallization after cold deformation, 16: 21082
recovery in stressed, electrical, magnetic, and mechanical studies of, 16: 27676
refractive index of gaseous, (E/T), 20: 5879 (D-910092-6)
reinforcing by tungsten fibers in pneumatically compacted plates, 19: 39093 (BNWL-SA-141)
review of status and future potential of, for defense, 18: 8718 (DMIC-Memo-183)
rupture moduli in glass system, 18: 4262 (UCRL-11011)
ruthenium magnetic hyperfine field in, (E), 19: 37857
self-diffusion, 17: 8711(R) (TID-17556)
self-diffusion in, effects of tensile straining on, 17: 1954 (UCRL-10457)
separation as ferrocyanide on filter paper by precipitation chromatography, 17: 40932
separation by anion exchange in acetic acid–nitric acid medium, 18: 16131
separation by anion exchange in acid-organic solvent media, 18: 23707(R) (TID-20609)
separation by anion exchange in mixed aqueous and non-aqueous systems, 19: 2243
separation by electrophoresis on zirconium phosphate paper, 17: 4467
separation by reversed-phase column chromatography, 17: 1401
separation by reversed-phase chromatography, use of tri-caprylyl-monoethyl ammonium chloride and trioctylamine in, 18: 43395
separation by solvent extraction of diethyldithiocarbamate, radiochemical, 17: 19964
separation by solvent extraction using dibenzoylmethane as chelating agent, 17: 19974

separation by solvent extraction of the dibenzoylmethane complex, 17: 21790
separation by solvent extraction using bis-salicylaldehyde–ethylenediamine, 18: 22181
separation from acid leach slurries by liquid ion exchange, 19: 24630
separation from aluminum and iron by column and electrochromatography in molten sulfates, 20: 35430
separation from aqueous solutions by mixer-settlers, review, 16: 23793
separation from aqueous solutions by mixer-settlers, review, 16: 30498(T) (AEC-tr-5327)
separation from aqueous solutions by solvent extraction using diphenylarsinic acid, 17: 21787
separation from aqueous sulfate solutions, electrolytic, 18: 3917(P)
separation from aqueous sulfuric acid solutions by solvent extraction using *N*-octylanilinobenzylphosphonate, 18: 27330
separation from berkelium by solvent extraction, 19: 22112
separation from beryllium by ion-exchange chromatography, 17: 3075(T) (AWRE/Trans/33)
separation from cerium and chromium, 16: 23658
separation from cerium and lanthanum nitrate solutions by chromatographic extraction, 19: 22431
separation from cerium by ion exchange chromatography, 19: 26480
separation from cerium and manganese by solvent extraction using TBP, 19: 36297
separation from chromium, manganese, rare earths, and silver by ion exchange chromatography, 20: 20634
separation from cobalt and iron using tri-*n*-octylamine-cellulose anion exchanger, 16: 4231
separation from cobalt and zinc by carrier precipitation, 17: 2242 (TID-16949)
separation from cobalt and copper by ion exchange, 17: 6180 (IA-769)
separation from cobalt, methods for, 17: 27401
separation from cobalt in thiocyanate solutions using hexone, 19: 15571(R) (TID-21385)
separation from cobalt by multistage solvent extraction, 19: 17984
separation from cobalt by ion exchange, 19: 30334
separation from cobalt and copper by extraction chromatography, 20: 433 (INP-412/C)
separation from cobalt and copper by extraction chromatography using trioctylamine, 20: 27055
separation from HRT fuel by uranyl peroxide precipitation, testing of equipment for, 16: 18988 (ORNL-TM-223)
separation from hydrochloric acid solutions by solvent extraction using 2-ethylhexanol, 19: 36252
separation from iron by thin-layer chromatography, 19: 9266
separation from iron by extraction-chromatography using tetrabutyl hypophosphate–tetrabutyl pyrophosphate mixture, 19: 42439
separation from lithium chloride by solvent extraction, pulse column operation for, 16: 33070(R) (ORNL-TM-297)
separation from lithium chloride solutions by oxine precipitation-carbon adsorption method, 20: 43092 (Y-1553)
separation from manganese and zinc by cation exchange, 19: 13535
separation from metal ionic mixtures, electrochromatographic, 17: 10753
separation from metal mixtures by thin layer chromatography, 20: 36753
separation from molybdenum or uranium by thin-layer chromatography, 19: 9266
separation from nitric or sulfuric acid solutions, ion exchange selectivity scales for, 19: 9257
separation from other metals by ion exchange chromatography in tartrate medium, tracer studies of, 19: 7627
separation from other metals by ion exchange, 19: 15692
separation from other metals by reversed-phase chromatography, 19: 30331
separation from other metals by partition chromatography of chloride solutions, tracer studies of, 19: 32288
separation from other inorganic ions by paper chromatography, 20: 12939
separation from other metals by extraction chromatography using TOPO, tracer studies of, 20: 27054
separation from palladium by solvent extraction using tri-*n*-octylphosphine oxide, 19: 19753 (IS-T-3)
separation from pitchblende residues, leaching processes for, 20: 43420 (MCW-1508)
separation from plutonium by anion exchange, 17: 4629
separation from plutonium by ion exchange, 20: 35585 (EURAEC-1639)
separation from rare earths by ion exchange in isopropyl alcohol, 18: 20104
separation from rare earths by ion exchange chromatography, 20: 18827
separation from rhenium by anion exchange chromatography, 19: 24433
separation from ruthenium by cation exchange, 16: 22270
separation from salts by solvent extraction using Schiff bases in chloroform, 20: 10759 (INP-427/C)
separation from scandium by precipitation using cinnamic acid, 18: 43426
separation from scandium by ion exchange chromatography, 20: 16574
separation from scandium by ion exchange chromatography, 20: 20821
separation from silver by partition chromatography, 20: 4054
separation from solution by ion exchange using polyamidoximes, 18: 35653(P)
separation from solutions by liquid ion exchange, 19: 15676
separation from solutions by extraction using liquid ion exchangers, 19: 18063
separation from solutions by solvent extraction, review of methods for, 19: 13543
separation from stainless steel waste solutions by electrolysis over mercury cathode, 16: 12794 (IDO-14570)
separation from sulfate solution by ion exchange, relative effectiveness of mineral cation exchangers, 16: 30389
separation from thorium, titanium, and zirconium using ammonium cinnamate, 16: 28900
separation from thorium salt solutions, electrolytic, 18: 3904
separation from thorium by ion exchange in nitric acid solution, 20: 20624
separation from thorium and uranium by paper chromatography, 18: 33505
separation from titanium by cation exchange chromatography, 17: 32054
separation from titanium using benzoylphenylhydroxylamine, direct weight gravimetric, 17: 38940
separation from trivalent rare earths by cation exchange, 17: 10734 (IS-508)
separation from uranium-233, solvent-extraction, 17: 40387
separation from uranium by cation exchange chromatography, 19: 13245
separation from uranium by ion exchange, 19: 44119
separation from uranium by ion exchange and elution with ascorbic acid, 18: 25611(T) (AEC-tr-6227/1(p.1-8))
separation from uranium by partition chromatography on silica-gel column, 20: 9073
separation from uranium by combined ion exchange–solvent extraction using nitric acid–tetrahydrofuran solutions, 20: 20811
separation from waste solutions, development of methods for, 16: 1855(R) (IDO-14560)
separation from zirconium by ion exchange chromatography, 16: 31577
separation from zirconium by zone melting, 18: 8456
separation from zirconium by ion exchange on pyrocatechol-*O,O*-diacetic acid, 18: 33508
separation of cobalt-58 from neutron-irradiated target of, by reversed-phase partition chromatography, 20: 25196 (INR-677/V/XIII/C)
separation of, from indium and gallium using cinnamic acid, 17: 15924
separation of, from boron, method for, 17: 17999
separation of, from chromium, cobalt, and iron by ion exchange, 17: 23258 (SC-4784(RR))
separation of magnesium from, by complex formation and solvent extraction, 19: 19833 (CEA-R-2628)
separation of rare earths from, by precipitation using ammonium cinnamate, 20: 45611
separation of scandium from, by ion exchange chromatography, 19: 533
separation of scandium from, by precipitation using ammonium cinnamate, 20: 25012
separation of, from thallium by ion-exchange chromatography, 20: 36935
separation using aromatic Schiff bases, 20: 45802
shock wave interactions with, thermodynamic parameters from mirror-image approximation for particle velocity and pressure in, 17: 37676
silver hyperfine structure constants in, 18: 16954 (UCRL-11143)
silver-104 and -110 polarization in, (E), 19: 16995
sintering effects on uranium carbide, 16: 5690(R) (ORO-477)
sintering of powdered, topological study of, 18: 32060(R) (TID-20826)
sintering with cobalt and tungsten carbide, carburizing process in, 19: 30708
Slater-Condon parameters of, determined from spectral data, 17: 31118
sliding friction measurements for ball and flat, specimens in sodium environs at room temperature to 650°C, 17: 35251(R) (BMI-1632(Del.))
soaps of, preparation and properties of, 20: 35931
solubility in beryllium, 17: 20474
solubility in bismuth (liquid) at 482 to 1010°C, 16: 6716 (NEPA-1221)
solubility in bismuth, lead, lithium, mercury, and sodium at 600°C, 18: 14401 (BNL-7553)
solubility in liquid cadmium, 17: 1985
solubility in liquid sodium, effects of free energy gradient on, 18: 22488 (NAA-SR-8381)
solubility in liquid metals at 600°C, 18: 27886 (NASA-SP-41(p.21-6))
solubility in liquid zinc, 20: 22966 (ANL-7083)
solubility in lithium (liquid) at 482 to 1010°C, 16: 6718 (NEPA-1465)
solubility in lithium at high temperature, 16: 16689 (TID-7626(Pt.I) (p.143-5))
solubility in lithium at 1200 to 1700°F, 19: 36980 (PWAC-355)
solubility in mercury, 17: 28906
solubility in molten potassium, 20: 2237
solubility in potassium, 20: 11227
solubility in rubidium at 1000 to 2000°F, 17: 16634 (AGN-8063)

solubility in silicon, determination by neutron activation, 17: 8828
solubility in silicon, determination of solid, 17: 30151
solubility in tungsten, effects of iron on, 20: 865
solubility in uranium nitride at 800 to 1000°C, 19: 26756 (CEA-R-2762)
solubility in $ZrBe_{13}$ and Zr_2Be_{17} at 70 to 2500°F, 17: 29313(R) (BBC-118)
solubility in $ZrBe_{13}$ and Zr_2Be_{17} at 70 to 2500°F, 18: 27946(R) (BBC-1201
solvent extraction using mono-octyl ester of α-aniline benzylphosphonic acid, 16: 13157
solvent partition in aqueous bromide–TBP systems, 18: 25382
solvent partition in tributyl phosphate–hydrochloric acid or –nitric acid systems, 18: 33685
solvent properties for cerium, 18: 39969
sorption by ammonium molybdo-, tin, titanium, and zirconium phosphates, comparison of, 20: 45795(R) (ORNL-3945, pp 176-88)
sorption by cellulose ion exchangers from acetone and ethanol mixtures with hydrochloric acid, 18: 16140
sorption by gamma-alumina and inorganic ion exchange materials from fused salts, 19: 38771
sorption from nitric acid by ion exchange paper, 19: 24435
sorption from perchloric acid solutions by ion exchange materials, 20: 20823
sorption of americium-241 and protactinium-233 by, from water–ethanol solutions, 18: 23724
sorption of hydrogen by evaporated films of, electric conductivity measurements in, 17: 21672(T) (SCL-T-480)
sorptive properties for hydrogen and hydroxyl ions, 17: 25853 (PAN-372/V)
sorptive properties for hydrogen and hydroxyl ions, 18: 23448 (PAN-466/V)
sorptive properties for hydrogen, 19: 7484
sorptive properties for nitrogen activated by electron impact, 19: 7507
sorptive properties of films of, for hydrogen and deuterium, 16: 26877
sorptive properties of films of, for carbon monoxide, effects of heterogeneity of surface on, 16: 31600
sorptive properties of films of, for krypton and xenon, relation of surface area to, 17: 39589
sorptive properties of annealed and oxidized single crystals of, for undecanoic and nonadecanoic acids, 20: 1570 (TID-22150)
sorptive properties of evaporated films of, for krypton and xenon, 20: 21387
sorptive properties of evaporated films of, for carbon monoxide at 0°C, 20: 21388
sorptive properties of evaporated films of, for carbon dioxide at room temperature, 20: 21389
sorptive properties for bromine-82, 20: 39337
spalling of, stress effects on time-dependent, 18: 30182
spark patterns produced by grinding of, 18: 19493(T) (SC-T-64-47)
spectra in lithium chloride–potassium chloride, crystal field, 16: 30371 (TID-16693)
spectra in reaction zone of acetylene air flame, excitation of atomic, 17: 27371(T)
spectra of, correlation of dissociation energies and excitation potentials in flame, 17: 14234
spectra of, in aluminum–iron alloys and iron–silicon systems, 17: 30516 (TID-19080)
spectra of, K x-ray, 17: 30484
spectra of normal vibrational modes in, frequency, 18: 18452 (AERE-R-4562)
spectra of, in zeta pinch, 19: 25564
spectra of, measurement of K x-ray, 18: 44429
spectra of, muonic K and L x-ray, 18: 42626(R) (ANL-6879(p.69-87))
spectral characteristics, 16: 26953 (ARL-62-336)
spin wave dispersion in, s-d interaction and Fermi surface for, 20: 30775
sputtering at 50 to 600 ev by rare gas ions, 17: 8931(R) (NP-12389)
sputtering by argon and neon ions, in glow discharges, 16: 19563
sputtering by argon, angular dependence of ion-electron emission in, (E), 19: 6475
sputtering by argon ions at 30 to 170 kev, (E), 19: 44937(R) (TID-22140)
sputtering by argon ions, electron diffraction analysis of damage from, (E/T), 20: 13981
sputtering by argon ions at threshold to 600 ev, yields from, (E), 20: 34116
sputtering by cesium at 2–5 kv, 17: 21830
sputtering by cesium ions, 18: 40168
sputtering by helium ions at 600 ev, yield curves for, 17: 25870(R) (X62-11400)
sputtering by hydrogen ions, yields from, 18: 8926
sputtering by krypton ions at 1200 ev, energy distributions for ejected atoms from, 18: 7404(R) (NP-13430)
sputtering by krypton and mercury at 10 to 2000 ev, energy spectra and yields from, 18: 20787
sputtering by mercury ions at 10 ev, energy distribution from, 18: 9004
sputtering by mercury ions, 18: 20666
sputtering by mercury ions, adsorption effects on ejection patterns in, (E), 19: 23270
sputtering by noble-gas ions at 0.1 to 1 kev, yields, 16: 19566
sputtering by noble-gas ions at 100 to 600 ev, yields from, 16: 22753
sputtering by potassium ions, positive surface ionization in, (E), 19: 16412
sputtering by rare gas ions at 20 to 1000 ev, mass dependence of, 18: 20786
sputtering of crystals of, by argon and neon ions, angular distribution from, 17: 688
sputtering of crystals of, by cations to 800 ev, atom spatial distributions from, 16: 22758
stability of, effects of thermal cycling on, 18: 16492
stacking-fault energy, 18: 20550
strength, effects of high-temperature thermomechanical treatment, 16: 30819
stress-strain curve for crystals of, magnetic measurement of, 17: 11234
stripping and replating of coatings of, on uranium, 18: 14375 (RFP-342)
structural properties of, effects of thermal cycling on, 18: 22510
structure of, neutron radiography of internal, 17: 1984
superconductivity of coated wires of, 19: 28962(R) (NIRL/R/81)
superconductivity in film laminates with lead, gapless, (E), 20: 34442
surface friction in sliding on nickel, effects of surface films, 16: 23803 (R60GL185)
surface properties for molten chloride and fluoride salts, 18: 34050(R) (ORNL-3626(p.59-164))
surface tension at melting point, 17: 39612
surface tension of, measurement by electron bombardment heating, 17: 37538
surface tension of, measurement by pendant drop method, 19: 47065
surface treatments for, coating and mechanical, 20: 29706 (NASA-TM-X-53448)
tensile properties of, effects of purity and neutrons on, 17: 37572 (HW-78178)
tensile properties of, testing, (E), 19: 20554 (LA-3161)
tensile properties of 201, effects of intergranular changes on, 20: 37169(R) (BMI-1774)
thermal capacity, 18: 30209
thermal capacity and conductivity of, nonlinear estimation method for transient determination of, (T), 20: 27522
thermal capacity of, effects of magnetic order on, 20: 4320(R) (ORNL-3870, pp 70-4)
thermal conductivity, 17: 21389(R) (MLM-1145)
thermal conductivity, 17: 27789(R) (MLM-1156)
thermal conductivity of radiator fins of, 17: 6673 (ORNL-2065)
thermal conductivity of, in layers with aluminum and oxide films, 18: 42101(P)
thermal conductivity of powdered, 18: 44922(R) (ANL-6800(p.326-402))
thermal cycling effects on coating of, 19: 29468(R) (ANL-7017)
thermal diffusion of deuterium and hydrogen in alpha, at 400 to 600°C, 20: 2397
thermal expansion at 480 to 530°C, 18: 42037
thermal expansion coefficient of, x-ray determination of, 19: 47023(T) (LA-tr-65-20)
thermal properties, 16: 22597 (WADD-TR-60-924)
thermal properties, 18: 26896(R) (ANL-6868(p.133-74))
thermal radiation properties of, 17: 542 (WADD-TR-60-370(Pt.II))
thermal radiation spectral emittance, temperature effects, 17: 41563 (WADD-TR-60-370(Pt.III))
thermal radiative properties, 17: 6650 (DMIC-177(Vol.I))
thermal resistance of coatings of, electrodeposited on molybdenum, 16: 30841
thermionic emission from crystalline, in cesium, potassium, and rubidium vapors, 18: 12794
thermionic emission of electrodes of, in gases, 17: 11435
thermodynamic properties at high pressures and temperatures, 19: 40459 (NP-15324)
thermodynamic properties of oxygen in liquid, 20: 4454
thermodynamics in lithium and potassium chloride systems (liquid), oxygen equilibrium potential diagram for, 16: 20426
thermoelectric emission and work function of, in cesium vapor, (E), 19: 6447
thermoelectric potentials at 25 to 900°C, 19: 4656 (ORNL-3605(Vol.1) (p.116-38))
thermoelectric properties, 18: 30493 (TID-7687(p.247-93))
thermoluminescence effects on sapphire and sodium borate glass, 16: 13060
thickness measurement by alpha energy degradation, 20: 3982(R) (AGN-8156)
thickness of coatings of, measurement, 19: 34428
thickness of coatings of, on uranium fuel cores, Hall-effect devices for measuring, 20: 25271
thickness uniformity of commercial films of, 17: 11104 (TID-16252)

toxic effects in Habrobracon, 19: 10741 (TID-21559)
tracer applications survey, 16: 1359
transition probabilities of forbidden lines of, calculation of, 18: 14736
tritium sorption on films of, isotope effects in mercury displacement of, 18: 3858
triton energy losses in, 16: 2491 (TID-14145)
triton ranges and stopping cross sections in, 17: 17212
triton scattering and slowing-down by, at 2.7 Mev, 16: 27782
twinning in, effects of loading and shock on, 18: 612
use as catalyst in sintered actinide carbon preparation, 19: 32687(P)
use as diffusion barrier between aluminum clad and uranium fuel, 18: 13264
use as interfacial coating in diffusion bonding of niobium to niobium, 18: 30154 (USBM-U-1107)
use as liner in tritium detection cell, 19: 32612(P)
use in determination of lead-210 and polonium-210, 20: 12785
use in fast-neutron activation dosimetry, 17: 34288
use in magnetostrictive delay line for wire spark chamber, 19: 787 (UCRL-11620)
use in neutron detection, 18: 41762 (CEA-R-2491)
use in separation of uranium isotopes by vaporization, 16: 9095(T,P) (AEC-tr-4993)
use in tungsten to tungsten diffusion bonding, 20: 25553(P)
use of plating by, in metallographic mounting, 20: 43906 (ORNL-P-2361)
use of powdered, to promote phase separation in liquid-liquid extraction process, 19: 36571(P)
uses as filter for deuterium and tritium separation, 19: 2702
uses as interlayer in cladding uranium with magnesium, 19: 4143
uses in fuel elements as layer between sheath and fuel, 19: 5461(P)
vapor pressure, 20: 331
vapor pressure and evaporation coefficient at 1190 to 1355°C, 16: 30981
vaporization from probe surface in electric arcs, (E), 20: 32593
vibrational frequency distribution of, neutron inelastic scattering studies of, 17: 39713 (BNL-7240)
viscosity of liquid, based on atomic parameters, 20: 20656 (UCRL-11930)
wear characteristics of plated coatings of, for use in rotary switches, 19: 42216 (SC-DR-65-269)
welding by friction, 17: 1908
welding effects on beryllium, fusion, 16: 5692 (WADD-TR-60-917)
welding of pipes and plates of, Hanford procedures for, 19: 20524 (TID-20625(Vol.IV)(Rev.I))
welding of, argon-arc and electron-beam methods of, 20: 21310
welding of, characteristics of electron beam, 18: 34112
welding of, Hanford guide to procedures, specifications, and qualification test records for, 18: 24104 (TID-20625(Vol.III))
welding procedures for, 20: 33413(R) (K-1669)
welding to INOR-8, strength testing of joints in, 18: 4174(R) (ORNL-3470(p.157-72))
welding to Kovar and nickel, quality of, 19: 23347(R) (NYO-3429-2)
welding to type 6061-T6 aluminum alloy, cold-pressure, 20: 11214(R) (NASA-CR-54717)
welding, ultrasonic, 16: 4515 (NP-11054)
wetting by liquid sodium, effects of additions of barium and calcium to sodium and of oxide films, 16: 25782
wetting by molten chlorides and fluorides, sessile drop observations, 18: 23437 (CONF-322-12)
wetting niobium–titanium carbide and niobium–vanadium carbide systems by, using resting drop method, 18: 7241
wetting of niobium carbide–titanium carbide and niobium carbide–vanadium carbide systems by, 19: 18522(T)
wetting properties for metallic carbides, 20: 1837
work function in cesium, (E), 19: 16182
work function in cesium–hydrogen atmosphere, (E), 19: 37097
work function of cesium-covered, (E), 19: 37098
work function of, in hydrogen, effects of copper surface layers on, 16: 19608
work function of, reduction of, 17: 27972
x-ray absorption at room temperature and −180°C, 17: 39798
x-ray emission lines of, widths of K, 17: 18925
x-ray spectrum from mesic (μ), 17: 22264(R) (ANL-6679)
x-ray mass absorption at 1.49 to 16.61 kev, (E), 19: 25146(R) (TID-21542)
x-ray scattering by surfaces of, anomalous, (E), 19: 18591
x-ray spectra from μ-mesic atoms of, nuclear charge distribution from, 19: 27518
x-ray spectra of, performance of spectroanalyzer with promethium-147 beta source for K, 20: 11133
x-ray total cross sections at 15 to 30 Mev, (E), 19: 12573
xenon-133 ranges and retention at 1–150 kev, energy and flux dependence of, 17: 28002
xenon-131 ranges in, at 5 to 30 kev, 18: 20672
yield stress of, effects of molybdenum on temperature dependence of, 18: 44145(R) (ORNL-3670(p.11-16))
Young's modulus of, as function of temperature, 18: 39970

NICKEL ACETATES
magnetic susceptibility of tetrahydrate of, at liquid helium temperatures, 18: 12062

NICKEL ALLOY COUPLES
Alumel/Chromel, performance to 2200°F, 19: 44348 (PWAC-473)
Alumel/Chromel, thermocouple tables, smoothed, 19: 20265 (ORNL-3649(Vol.2)(Sect.2.3))
Alumel/Chromel, thermocouple tables for cryogenic, smoothed, 19: 20274 (ORNL-3649(Vol.2)(Sect.2.12))
Alumel/Chromel, aging and thermoelectric power of thermocouples, 20: 4398 (TRG-Report-1021)
Alumel/Chromel, development for in-pile measurements, 19: 46722 (PWAC-462)
Alumel/Chromel, fabrication and properties as thermocouple at high temperature, 19: 22927 (TIM-888)
Alumel/Chromel, performance as thermocouples up to 6000°F, (E), 19: 30489 (SC-DC-65-1237)
Alumel/Chromel, performance of thermocouples of, for PWR-1 seed 4 analysis, 20: 1477 (WAPR-PWR-TE-166)
Alumel/Chromel, performance to 2200°F, 19: 44348 (PWAC-473)
Alumel/Chromel, radiation effects on thermoelectric properties of, (E), 19: 24014 (CONF-640607(Vol.II)(Paper D-4))
Alumel/Chromel, radiation effects on stainless steel-clad, 20: 4263 (ORNL-TM-1320)
Alumel/Chromel, testing of thermocouples of, 20: 4299(R) (ORNL-2711)
Alumel/Chromel, thermocouple tables, smoothed, 19: 20265 (ORNL-3649 (Vol.2)(Sect.2.3))
Alumel/Chromel, thermocouple tables, smoothed, 19: 42688(R) (ORNL-3782, pp 74-83)
Chromel/constantan, thermocouple tables, smoothed, 19: 20268 (ORNL-3649(Vol.2)(Sect.2.6))
Chromel/canstantan, thermocouple tables, smoothed, 19: 42688(R) (ORNL-3782, pp 74-83)
Constantan/Fe, radiation effects on thermoelectric properties of, (E), 19: 24014 (CONF-640607(Vol.II)(Paper D-4))
Constantan/Cr, radiation effects on thermoelectric properties of, (E), 19: 24014 (CONF-640607(Vol.II)(Paper D-4))
constantan/Cu, thermocouple tables, smoothed, 19: 20267 (ORNL-3649(Vol.2)(Sect.2.5))
constantan/Fe, thermocouple tables, smoothed, 19: 20266 (ORNL-3649(Vol.2)(Sect.2.4))
constantan/Fe, thermocouple tables for cryogenic JN/JP, smoothed, 19: 20275 (ORNL-3649(Vol.2)(Sect.2.13))
constantan/Fe, thermocouple tables for cryogenic YN/YP, smoothed, 19: 20276 (ORNL-3649(Vol.2)(Sect.2.14))
constantan/Cu, thermocouple tables for cryogenic, smoothed, 19: 20273 (ORNL-3649(Vol.2)(Sect.2.11))
Cr/Cu–Mn–Ni, neutron radiation effects on, 18: 44261
Cu/Cu–Ni, radiation effects on, at cryogenic temperatures, (E), 19: 4538 (LA-DC-6649)
Cu–Mn–Ni/Fe, neutron radiation effects on, 18: 44261
Cu/Nimonic-75, diffusion characteristics of, 19: 917
Invar/Ni, tensile properties of, testing, (E), 19: 20554 (LA-3161)
Mo–Ni/Ti, solid state bonding of, 18: 24112
Mo/Ni/Ti, solid state bonding of, 18: 24112
Ni–Ru/Re–W, thermoelectric potential at 200 to 1800°C, 19: 37031(R) (GEMP-47A, pp 101-6)

NICKEL ALLOYS
see also A-286 Alloy
see also Durimet 20
see also Hastelloy C
see also Hastelloy D
see also Hastelloy F
see also Hastelloy R235
see also Hastelloy X
see also Haynes Stellite No. 31
see also Haynes 25 Alloy
see also Hevimet
see also Inconel
see also Inconel X
see also INOR-8
see also Monel
see also Ni-O-Nel
see also Nichrome
see also Nimonic 75
see also Nimonic-80
see also Nimonic-90
see also Nimonic DS
see also René-41
see also René-62
see also Waspaloy
analysis for boron, spectrographic, 20: 33158 (Y-1543)
analysis for elements, spark-source mass spectrographic, 19: 34114

(WAPD-T-1662)
analysis for hafnium or zirconium using catechol violet, colorimetric, 19: 19780
analysis for niobium and tantalum, photometric method for, 19: 40442
analysis for samarium, 19: 40445
analysis for titanium using diantipyrinylmethane, photometric, 16: 18841
analysis for zirconium traces by x-ray fluorescence, 17: 21644
analysis for zirconium, 18: 31409
analysis of, for trace impurities by deuteron activation methods, 20: 40812 (ORO-2980-14)
analysis, spectrographic, 16: 11539
bibliography, 16: 19248 (NP-11628)
bibliography on, Defense Metals Information Center selected accessions, January 1963, 17: 14739 (NP-12525)
bibliography on, DMIC selected accessions, Sept. 1962, 17: 419 (NP-12170)
bibliography on, DMIC accessions, May 1963, 17: 29246 (AD-407822)
bibliography on high-strength, 17: 6521 (NP-12417)
bibliography on performance above 1000°F, 19: 2728 (PDL-50140)
bonding with beryllium and beryllium-transport alloys, diffusion, 16: 6704
book: *Nickel and Its Alloys (Vol. I)*, 18: 10462(T) (OTS-63-11098 (Vol.I))
brazing, 17: 3459(P)
brazing alloys for René 62, properties of, 19: 40989
brazing and welding properties, review, 16: 10424 (ASD-TR-61-322 (p.661-76))
brazing of, criteria for, 17: 11163 (DMIC-181)
brazing properties, review, 16: 10424 (ASD-TR-61-322(p.661-76))
casting, 17: 4910(R) (MAB-139-M(C7))
compatibility of EPE7, with plutonium carbide–uranium carbide, 20: 31675
compatibility with uranium carbide fuels in sodium, 18: 35957 (NAA-SR-7502)
corrosion, 18: 22451
corrosion by acids, carbon dioxide, and liquid metals, alloying effects of molybdenum on, 17: 34352
corrosion by air, carbon oxides, hydrogen sulfide, and sulfur dioxide to 1200°C, 18: 39844
corrosion by aqueous solutions, review, 18: 32081 (A/CONF.28/P/243)
corrosion by cesium at 400°C, 20: 4337
corrosion by fluorine in ADP Process equipment, 16: 4215 (ANL-6342)
corrosion by fluoride mixture under hydrofluorination conditions at 650°C, 17: 40423(R) (BMI-1639(Del.))
corrosion by fluorine–molten salt in fluoride volatility pilot plant during fuel processing, 19: 18051 (ORNL-3623)
corrosion by fluorine and molybdenum and tellurium fluorides at 500°C, (E), 20: 14008(R) (ANL-7122, pp 42-69)
corrosion by fluorine, 20: 35846 (CEA-R-2932)
corrosion by fused-salt fuels, 17: 7565(R) (PWAC-161)
corrosion by liquid lead, 17: 31763(R) (MND-P-3003)
corrosion by liquid potassium, sodium, and potassium–sodium alloy, 19: 34643
corrosion by lithium and lithium hydride, 16: 25718 (NP-11952)
corrosion by lithium at 1500 to 1900°F, 17: 6570 (ORNL-2674)
corrosion by steam at high temperatures, 16: 26467(R) (HW-73100)
corrosion by steam at 3000 psi and 550°C, 18: 7143(R) (HW-77954 (p.5.20-3))
corrosion by steam at 3000 psi and 550°C, 18: 8752(R) (HW-78388 (p.9.1-4))
corrosion by steam, effects of oxygen and pressure on, 19: 13883(R) (HW-81984(p.9.1-6))
corrosion by superheated steam, 17: 21230 (TID-7658(p.27-47))
corrosion by superheated steam at 550°C, 18: 32139(R) (HW-81269 (p.5.1-23))
corrosion by superheated steam, effects of surface preparation on, 18: 41962
corrosion by water, electrochemical, 16: 12055
corrosion by water or water vapor in radiation environment, 19: 7870
corrosion during Zircaloy-2 dissolution in molten fluoride mixture, 17: 40424(R) (BMI-1642(Del.))
corrosion of, alloying effects of aluminum, chromium, molybdenum, and titanium on, 17: 20412 (HW-76952)
corrosion of, by fused salts, 16: 28646(R) (ORNL-2247(Pts.1-5))
corrosion of, by liquid lithium fluoride–sodium fluoride–zirconium tetrafluoride, 17: 6571 (ORNL-TM-411)
corrosion of Duranickel and Nicloy-9 in solvent extraction processes, 18: 8761
corrosion of, in fluorinator, 17: 14763 (BMI-X-218)
corrosion of, in high-temperature water cooled reactors, 17: 6567 (HW-SA-2745)
corrosion of INCO-61 by molten fluoride mixture in hydrofluorinator at 500°C, 17: 36222 (BMI-X-253)
corrosion of Incoloy-804 in solvent extraction processes, 18: 8761
corrosion of Inconel 600 and Monel 400, by boiling water reactor coolants, effects of ammonia on suppression of, 20: 26920 (AECL-2562)
corrosion of Monel-400, by hydrofluoric acid dissolver solutions, 20: 33411 (IDO-14674)
corrosion of TD nickel by lithium fluoride, 19: 12150
corrosion of tubes of, in liquid-liquid heat exchangers, 16: 9153 (MND-E-2681)
corrosion of type L, by fluoride-volatility process solutions at 500°C, 17: 23864(R) (BMI-1619(Del.))
corrosion of type L, by aluminum fluoride–potassium fluoride–uranium fluoride system at 600°C, 19: 13871(R) (BMI-1691(Del.))
corrosion of type-304, in superheated steam, 19: 4197 (SAN-8003 (p.90-133))
corrosion of types A and TD, by steam at 650°C, 17: 26750(R) (ANL-6717)
corrosion of, review, 19: 7868
corrosion resistance and hardening mechanism of, review of, 18: 18322
corrosion resistance to mercury at 900°F, 20: 2264
corrosion studies of, technical progress review, 17: 11129
corrosion studies, 18: 14396
corrosion studies on, technical progress review on, 18: 18307
creep at high temperature and low stress, 16: 4543 (NRL-5704)
creep buckling data, 17: 7565(R) (PWAC-161)
crystal structure of, effects of deformation and recrystallization on, 17: 8863
crystal structure and phase studies, 18: 25970(R) (ANL-6868(p.303-25))
development and properties of superalloys, 16: 10402 (ASD-TR-61-322 (p.25-39))
development of, for brazing uses, 17: 14786 (KR-33)
developments in high-temperature, 16: 27641(T) (FTD-TT-62-503)
diffusion of hydrogen in Nichrome at high temperatures, 16: 8713 (NEPA-1841)
dissolution of Corronel 230 and Hastelloy G by Purex waste solutions, 20: 24809(R) (BNWL-213)
dissolution of Nichrome in nitrate systems, electrolytic, 16: 7613 (IDO-14575)
dissolution of Nichrome fuel element materials in nitric acid, electrolytic, 16: 20534(R) (IDO-14574)
drilling, 17: 6615
ductility of Hastelloy W, effects of aging and temperature on, 19: 30737(R) (HW-84573(p.6.1-11))
effects of beryllium additions on, 20: 37275
effects of decontaminating and descaling solution on metal loss on Hy-80, 20: 21238 (NP-15928)
electric conductivity of Copel XM as function of temperature, 19: 11475 (NAA-SR-Memo-10366)
electronic structure, 17: 16700
emissivity of coatings of, to 2000°F, 16: 30801(R) (PWA-1878)
emissivity of oxidized coatings of, at 200 to 1450°F, 16: 30802(R) (PWA-1966)
end milling of U-500, 17: 6614
extrusion by hydrostatic methods, 19: 44651
fabrication of fuel-cladding, 18: 32033 (A/CONF.28/P/225)
formation and structure of $R(Me,X)_2$ type compounds in, 19: 30767
friction testing to 2000°F, 16: 3475 (WADC-TR-59-603(Pt.II))
frictional properties, 17: 8818 (UCRL-13052)
helium penetration through the walls of tubes of, 17: 39226
joining by brazing, soldering, or welding, 20: 29666 (RSIC-484)
joining by mechanical fastening, 20: 29667 (RSIC-509)
lead distribution in E1765, effects of cerium additions on, 19: 23019(T) (JPRS-28849(p.292-6))
lubrication of, by ceramic-bonded calcium fluoride coatings, 19: 18395 (NASA-TN-D-2688)
machining properties, 16: 4528 (DMIC-Memo-134)
machining properties of, 20: 29665 (RSIC-482)
magnetic properties, research program on correlation of microstructure with, 19: 30742(R) (NYO-3087-4)
mechanical properties of IN-100, 16: 15153(R) (ASD-TR-7-886(IV))
mechanical properties at cryogenic temperatures, 16: 27622(R) (AD-271176)
mechanical properties and thermal cycling of, 16: 28647(R) (ORNL-2340 (Pts.1-5))
mechanical properties, effects of combined alternating and static stress, 17: 4965
mechanical properties of nickel-200 and -270 at high temperatures, effects of hydrogen on, 18: 27966 (ORNL-3600)
mechanical properties of Inco 713c sheet at 1700 to 1900°F, 18: 30168 (ASD-TDR-62-869(Pt.II))
mechanical properties of Hastelloy W weld metal, effects of aging on, 20: 43888 (BNWL-290(Pt.1))
microconstituent identification, 17: 1928 (DMIC-Memo-160)
oxidation by air and oxygen at 1120°C of Hastelloy X-280, 20: 762(R) (BNWL-120, pp 5.1-18)

performance as substrate for niobium stannide films (E), 19: 984
performance of Incoloy 804 in nuclear superheater environment, 18: 24886(R) (GEAP-4565)
performance of Rene-62, in nuclear-superheater environment, 19: 10541(R) (GEAP-4703)
permeability of, to helium and hydrogen, bibliography on, 17: 37492(R) (SCL-B-107)
phase studies, 17: 11204(T,R) (EURAEC-444)
phase studies and structure, 16: 5742
physical properties of warm-rolled nichrome fuel sheet, 16: 7884 (DC-60-7-64)
powder metallurgy, status of, 16: 24110(R) (MAB-139-M(C4))
properties and structures of intermetallic compounds with lanthanides, 16: 1687
properties as bearing material for steam and water, 17: 3427(R) (NP-12233)
properties as cladding and structural materials in reactors, 18: 32072
properties as cladding and structural material in reactors, 18: 41947
properties as cladding for corrosion protection of uranium, 20: 7522
properties as fuel element cladding in steam and water environments, 18: 34076 (TID-8540(p.213-330))
properties as fuel cladding, 18: 32033 (A/CONF.28/P/225)
properties at low temperatures, 18: 22493(R) (PB-171809-6)
properties for aerospace uses, 19: 47068
properties for cryogenic applications, 19: 23070
properties for structural use in gas-cooled reactors, 16: 19993 (NYO-9793)
properties for use as canning materials for fuel elements, 18: 39981
properties of, as cladding for reactor fuel elements, 17: 8820 (XDCL-60-8-40)
properties of Hastelloy as fuel elementsleeve, 19: 24078(R) (GA-4710)
properties of heat-resistant, effects of molybdenum and tungsten on, 18: 44222
properties of, handbook on, 18: 10535 (N63-18835)
properties of, review of, 19: 6352
properties of, review of methods of improving, 19: 18523
radiation damage in Hastelloy X-280, effects of cold working and aging on neutron, 20: 889(R) (BNWL-120, pp 4.1-59)
radiation effects on mechanical properties, fast neutron, 16: 572 (REIC-20)
radiation effects on relaxation of elastic stresses in bent Nichrome plates, neutron, 16: 22704
radiation effects on relaxation of elastic stresses in, neutron, 16: 27699(T) (AEC-tr-5257)
radiation effects on properties, review, 16: 33546
radiation effects on corrosion by water, 17: 2018
radiation effects on mechanical properties of, 17: 21230 (TID-7658 (p.27-47))
radiation effects on mechanical properties of, 17: 27730(R) (HW-77052)
radiation effects on tensile properties of type 330, 17: 34557(R) (ORNL-3480(p.117-42))
radiation effects on mechanical properties of, critical factors in interpretation of, 17: 41515
radiation effects on mechanical properties of, 18: 7294(R) (HW-77954 (p.4.19-77))
radiation effects on mechanical properties and microstructure of, at 50 to 650°C, 18: 24193 (HW-SA-3436)
radiation effects on stress-rupture strength of, reactor, 18: 37746 (A/CONF.28/P/339a)
radiation effects on embrittlement of Nimonic, neutron, 19: 34756
radiation effects on, evaluation for fast-reactor uses, (E/T), 19: 35634
radiation effects on tensile properties of Nimonic PE16, neutron, 19: 37185
radiation effects on mechanical properties of Hastelloy X-280, fast neutron, 20: 889(R) (BNWL-120, pp 4.1-59)
radiation effects on tensile properties of types 270 and 330, fast-neutron, 20: 9576(R) (ORNL-3878)
radiation effects on strain fatigue of, neutron, 20: 21426 (N-65-24714)
radiation effects at cryotemperatures on tensile and shear properties of, 20: 46539
radioinduced embrittlement of, neutron, 20: 25623
radioinduced strain relaxation in, 17: 454
reactions with chlorine-36-labeled trichloroethylene, hydrochloric acid formation in, 18: 35637
reactions with refractory oxide crucibles at high temperatures in vacuum, 16: 6756
reactor criticality effects of Hastelloy, 19: 24078(R) (GA-4710)
refining by electron beam melting, 18: 27875
reinforcement with aluminum oxide fibers, 16: 10499 (AD-267891)
strengthening of solid solutions, 16: 6734
surface treatments for, coating and mechanical, 20: 29706 (NASA-TM-X-53448)
tensile properties, 16: 22586 (DMIC-Memo-150)
tensile properties of René 62, 19: 39156(R) (CEND-532)
testing for advanced BONUS core, 18: 29043 (GNEC-345)
thermal conductivity, 17: 6673 (ORNL-2065)
thermal cycling tests, 17: 7565(R) (PWAC-161)
thermal expansion at 480 to 530°C, 18: 42037
thermal properties of, data compilation, 17: 8801 (DMIC-177(Vol.2))
thermal radiative properties, 17: 6650 (DMIC-177(Vol.I))
thermal stability study of dispersion-strengthened SLIS, 19: 41021(R) (NMI-8002.1)
thermal stress properties of Nimonic-PE-16, 19: 24076(R) (GA-4966)
use in gas turbines for aerospace applications, survey, 16: 13512 (DMIC-Memo-145)
vacuum-brazing, 16: 2175(R) (GEMP-3A)
wear and corrosion testing as journal bearing material, 20: 43823 (AECL-2566)
weldability of IN-102 and A-625-M, 18: 44054(R) (ORNL-3670(p.174-200))
welding of, criteria for fusion and resistance, 17: 11163 (DMIC-181)
welding of, Hanford guide to procedures, specifications, and qualification test records for, 18: 24104 (TID-20625(Vol.III))
welding properties, 16: 10486 (TID-14971)
welding properties, review, 16: 10424 (ASD-TR-61-322(p.661-76))
welding to niobium alloys, use of palladium insert in fusion, 18: 32128(P)
Al–Be–Ni, phase studies, 16: 29417
Al–Co–Cu–Fe–Ni, corrosion of Alnico V by water, 19: 28756 (ORNL-TM-1029)
Al–Co–Cu–Fe–Ni, internal magnetic fields at iron sites in, Mössbauer measurement of, 20: 24617
Al–Co–Cu–Fe–Ni, strength coefficient, 16: 10560
Al–Cr–Co–Fe–Mo–Ni–Ti, joining of Udimet 500 and 700, by mechanical fastening, 20: 29667 (RSIC-509)
Al–Cr–Co–Fe–Mo–Ni–Ti, mechanical properties at high temperatures, 17: 14811 (ASD-TDR-61-529)
Al–Cr–Co–Fe–Mo–Ni–Ti, mechanical properties of, at 70 to 2000°F, 17: 18758 (NAA-SR-Memo-8052)
Al–Cr–Co–Fe–Mo–Ni–Ti, mechanical properties at 1500°F, 17: 22852(R) (GA-2696)
Al–Cr–Co–Fe–Ni–Ti, radiation effects on, 18: 7292(R) (HW-77954 (p.4.1-12))
Al–Cr–Co–Fe–Mo–Ni–Ti, stress-rupture properties of Udimet 700, at high temperatures and strain rates, 20: 11265 (AD-626375)
Al–Cr–Co–Fe–Mo–Ni–Ti, surface treatments for Udimet 500 and 700, coating and mechanical, 20: 29706 (NASA-TM-X-53448)
Al–Cr–Co–Mo–Ni–Ti, corrosion of Udimet 500 by lithium fluoride in cyclic high-temperature environment, 20: 4326 (TRW-ER-6561)
Al–Cr–Co–Mo–Ni–Ti, fabrication and properties of atomized, extruded, and sintered Udimet 700, 18: 10449(R) (IITRI-B247-12)
Al–Cr–Co–Mo–Ni–Ti, fabrication of Udimet 700, by extrusion, 18: 18329(R) (ASD-TDR-7-945(IV))
Al–Cr–Co–Mo–Ni–Ti, joining of M-252, by mechanical fastening, 20: 29667 (RSIC-509)
Al–Cr–Co–Mo–Ni–Ti, properties of Udimet 700, as extrusion liner for use at 1900 to 3600°F, 18: 18329(R) (ASD-TDR-7-945(IV))
Al–Cr–Co–Mo–Ni–Ti, strength, effects of severe stress and thermal histories, 16: 21023 (ASD-TR-61-194)
Al–Cr–Co–Mo–Ni–Ti, surface treatments for Astroloy, coating and mechanical, 20: 29706 (NASA-TM-X-53448)
Al–Cr–Co–Mo–Ni–Ti–V–Zr, surface treatments for IN-100, coating and mechanical, 20: 29706 (NASA-TM-X-53448)
Al–Cr–Co–Mo–Ni–Ti, tensile properties, statistical evaluation, 16: 3448 (ASD-TR-61-516)
Al–Cr–Co–Mo–Ni–Ti, thermal radiation properties of, 17: 542 (WADD-TR-60-370(Pt.II))
Al–Cr–Co–Ni–Nb–Ti–W, surface treatments for Mar-M 200, coating and mechanical, 20: 29706 (NASA-TM-X-53448)
Al–Cr–Cu–Ni, electric conductivity in magnetic fields at 4.2°K, 18: 32700
Al–Cr–Cu–Ni, electric conductivity of, temperature dependence of, 18: 32701
Al–Cr–Fe –Mo–Ni–Nb–Ti, corrosion and mechanical properties of Inconel 713C as gas turbine material, 16: 32114 (IDO-28591)
Al–Cr–Fe–Mo–Ni–Nb–Ti–W, corrosion by carbon dioxide, helium, nitrogen, and steam of PRDL-102, 20: 9408 (BNWL-154)
Al–Cr–Fe–Mo–Ni–Nb, fabrication and properties of atomized, extruded, and sintered Inco 713C, 18: 10449(R) (IITRI-B247-12)
Al–Cr–Fe–Mo–Ni, fabrication and properties of atomized, extruded, and sintered PH15–7Mo, 18: 10449(R) (IITRI-B247-12)
Al–Cr–Fe–Mo–Ni–Ti, heat treatment effects on welded, 16: 7842 (DC-59-10-174)
Al–Cr–Fe–Mo–Ni–Ti–W, joining of D-979, by mechanical fastening, 20: 29667 (RSIC-509)
Al–Cr–Fe–Mo–Ni, mechanical properties at high temperatures, 17: 14811 (ASD-TDR-61-529)
Al–Cr–Fe–Mo–Ni–Ti, mechanical properties at 1100 to 1200°F,

17: 22852(R) (GA-2696)
Al–Cr–Fe–Mo–Ni–Nb–Ti, mechanical properties of René-62, 19: 24081(R) (GNEC-361)
Al–Cr–Fe–Mo–Ni–Ti, mechanical properties and microstructure of, effects of heat treatments and molybdenum content on, 20: 23721
Al–Cr–Fe–Mo–Ni–Nb–Ti, oxidation of Inconel 718 by water vapor in helium at 1700°F, 19: 30820 (BNWL-23)
Al–Cr–Fe–Mo–Ni–Ti, properties of, for use at 1600 to 2100°F, 16: 13575 (DC-60-1-55)
Al–Cr–Fe–Mo–Ni–Ti, radiation effects on, 18: 7292(R) (HW-77954 (p.4.1-12))
Al–Cr–Fe–Mo–Ni–Nb–Ti, radiation effects on Inconel 718, 18: 7292(R) (HW-77954(p.4.1-12))
Al–Cr–Fe–Mo–Ni–Nb–Ti, radiation effects on mechanical properties of Inconel 718, neutron, 19: 30820 (BNWL-23)
Al–Cr–Fe–Mo–Ni–Ti, radiation effects on tensile properties of Nimonic PE16, thermal-neutron, 20: 31669
Al–Cr–Fe–Mo–Ni, tensile properties, 17: 16640 (DMIC-Memo-164)
Al–Cr–Fe–Mo–Ni–Nb–Ti, thermal response and microstructure of Inconel 718 at 1200 and 1400°F, 19: 39158 (GEAP-4751)
Al–Cr–Fe–Ni–Ti, precipitation processes in, 17: 16718
Al–Cr–Fe–Ni, tensile properties, 17: 16640 (DMIC-Memo-164)
Al–Cr–Mo–Ni–Ti, development of Udimet 700, for use in extrusion billet liners, 18: 39859 (IITRI-B244-18)
Al–Cr–Mo–Ni, fabrication of vertical-rib sandwich panels of, by roll-welding, 20: 25509(R) (AD-632831)
Al–Cr–Mo–Ni–Nb–Ti–W, phase diagrams, 20: 9533
Al–Cr–Ni, corrosion resistance and hardening mechanism of, 18: 18322
Al–Cr–Ni, crack propagation rates in air and in vacuum at 1300°F, 16: 5723 (NRL-5702)
Al–Cr–Ni, properties at high temperatures, effects of γ′ particle size on, 16: 21008 (AD-263483)
Al–Cr–Ni–Ti, corrosion resistance and hardening mechanism of, 18: 18322
Al–Cr–Ni–Ti, corrosion of Inconel 702 by superheated steam, 18: 21668(R) (GEMP-274)
Al–Cr–Ni–Ti, corrosion by trichloroethylene, tracer studies of, 20: 29655
Al–Cr–Ni–Ti–W, heat resistance of, effects of composition and time on, 16: 2217(T) (NP-tr-809)
Al–Cr–Ni–Ti, oxidation of Inconel 702 by water vapor in helium at 1700°F, 19: 30820 (BNWL-23)
Al–Cr–Ni–Ti–W, properties for use at 1600 to 2100°F, 16: 13575 (DC-60-1-55)
Al–Cr–Ni–Ti, radiation effects on decomposition of, 17: 14911
Al–Cr–Ni–Ti, radiation effects on mechanical properties of Inconel 702, neutron, 18: 8868 (HW-SA-3268)
Al–Cr–Ni–Ti, radiation effects on tensile properties of Inconel 702, neutron, 19: 30820 (BNWL-23)
Al–Cr–Ni–Ti, thermal conductivity of Inconel 702 at 50 to 930°C, 19: 2798 (CONF-764-10)
Al–Cr–Ni–W, phase studies and properties, 16: 12170
Al–Cu–Fe–Ni, corrosion by water, 16: 13532 (MND-E-2727)
Al–Cu–Ni, crystal structure of compounds in, 17: 14883(T)
Al–Cu–Ni, embrittlement of hydrogenated, solute-induced, 20: 5846
Al–Dy–Ni, phase studies, Laves, 16: 25798
Al–Fe–Ni, corrosion by water at 260 to 350°C, effects of silicon on, 16: 30739 (ANL-FGF-298)
Al–Fe–Ni, corrosion by water at high temperatures, 16: 22550
Al–Fe–Ni, corrosion by water at high temperatures, resistance optimization studies on, 16: 3454 (HW-68253)
Al–Fe–Ni, corrosion by water at 360°C, 17: 1878
Al–Fe–Ni, corrosion of, by water above 315°C, 17: 7552(R) (HW-74761 (p.8.1-15))
Al–Fe–Ni, corrosion by water at 300°C, 17: 13678(R) (HW-75914)
Al–Fe–Ni, corrosion by dry steam, 17: 22119
Al–Fe–Ni, corrosion by water at 330°C, 17: 27730(R) (HW-77052)
Al–Fe–Ni, corrosion by ultra-pure water at 25, 50, and 100°C, 18: 32093
Al–Fe–Ni, corrosion by sintered compacts of, by water and steam, 19: 4607(P)
Al–Fe–Ni, mechanical properties of X8001, 18: 12653 (ORNL-3557)
Al–Fe–Ni, thermal properties, strength, and structure, 16: 12167
Al–Fe–Ni–Pu–Ti, corrosion by water at 350°C, 20: 46143(R) (HW-66081)
Al–Fe–Ni–U, reactions with steam at 1200 to 1600°C, 19: 17174(R) (ANL-6900(p.232-303))
Al–Gd–Ni, magnetic properties and structure of $GdAl_2$–$GdNi_2$ phase in, 20: 27494(R) (NYO-3454-6)
Al–Hg–Ni, corrosive effects on titanium of mercury-based, 19: 44616(R) (ANL-7000, pp 122-37)
Al–Mn–Ni, composition of X phase in, 17: 11249
Al–Mn–Ni–Ti, corrosion by halide volatility separation process gases and liquids, 20: 33413(R) (K-1669)
Al–Nb, oxidation of, at 760°C, effects of additives on, 16: 27590(R) (DRI-2043)
Al–Nb, oxidation of, by air, effects of metallic additives on, 16: 24174 (TID-16032)
Al–Nb, oxidation rates of, effects of silicon, tin, titanium, and vanadium on, 16: 10456(R) (TID-14956)
Al–Nb, phase studies, 16: 549
Al–Nb, phase studies, 16: 10544(R) (TID-14954)
Al–Nb, phase studies, 16: 22616
Al–Nb, reaction of Ni_3Nb with Ni_3Al, 16: 19390
Al–Ni, alloying effects on beryllium–zirconium intermetallic compounds, 17: 14725(R) (BBC-114)
Al–Ni, alloying effects on mechanical and oxidation properties of zirconium beryllides at high temperatures, 18: 27946(R) (BBC-120)
Al–Ni, corrosion by water at 260 to 315°C of X-8001, 16: 3405 (ANL-6204)
Al–Ni, corrosion by water at 50 to 80°C, 16: 12061
Al–Ni, corrosion by water at 230 and 265°C, effects of silicon additions on, 16: 22544 (KR-19)
Al–Ni, corrosion by water, effects of silicon on, 17: 21387(R) (KR-42)
Al–Ni, corrosion by molten fluoride mixture at 650°C, 17: 34345 (BMI-X-247)
Al–Ni, corrosion by molten fluoride mixture in hydrofluorinator at 500°C, 17: 36222 (BMI-X-253)
Al–Ni, corrosion in hydrofluorination processing of reactor fuels, 17: 39179(R) (ORNL-3452(p.26-50))
Al–Ni, corrosion by liquid fluoride salts, 18: 2178 (BMI-X-260)
Al–Ni, corrosion by potassium fluoride–zirconium fluoride under hydrofluorination conditions at 600°C, 18: 7985(R) (BMI-1650(Del.))
Al–Ni, corrosion by water, effects of heat flux on, 18: 14408 (ORNL-3541)
Al–Ni, corrosion resistance and hardening mechanism of, 18: 18322
Al–Ni, corrosion by heavy water, 18: 37637 (A/CONF.28/P/591)
Al–Ni, crystal structure of nitrogen-containing, 16: 2259
Al–Ni, deformation and second-phase particles in, 16: 25693 (ARL-62-357)
Al–Ni, dislocation densities of, deformed at 23°C, 18: 4249(R) (ORNL-3470(p.33-9))
Al–Ni, dislocations in, electron microscope study of, 19: 24980(R) (COO-987-4)
Al–Ni, dissolution in nitric acid, effects of mercuric nitrate catalyst on, 18: 31658(R) (IDO-14635)
Al–Ni, effects on oxidation of beryllides, 17: 20450(R) (BBC-116)
Al–Ni, explosibility of powders of, 19: 36698 (BM-RI-6516)
Al–Ni, heat resistance and tensile properties, 16: 12130
Al–Ni, isolation of Ni_3Al in multicomponent alloys, 16: 15210
Al–Ni, magnetic susceptibility, 16: 18039 (TID-14769)
Al–Ni, nuclear magnetic resonance of aluminum-27 in, 17: 31202
Al–Ni, nuclear magnetic resonance shifts of aluminum-27 in NiAl and Ni_3Al, 18: 7670 (AD-423292)
Al–Ni, oxide film formation on surface of, morphology of, 16: 4573
Al–Ni, phase diagrams for, determination of, by solid-state diffusion, 16: 3496
Al–Ni, phase diagrams for, determination of, by solid state diffusion, 16: 22603(T) (HW-tr-37)
Al–Ni, phase studies, 16: 22641
Al–Ni, phase studies and surface tension at 1640°C, 17: 12702
Al–Ni, phase studies of, atomic size effects in, 19: 23111
Al–Ni, preparation and heat treating, 16: 2175(R) (GEMP-3A)
Al–Ni, radiation effects, 16: 15178(R) (GEMP-9A)
Al–Ni, reaction of Ni_3Al with Ni_3Nb, 16: 19390
Al–Ni, specific heats at 1.5 to 4°K, of beta-phase, 19: 30743(R) (NYO-3454-1)
Al–Ni, stoichiometry and temperature effects on pest degradation in NiAl in, 18: 42055
Al–Ni, superconducting transition in, (E), 20: 9915
Al–Ni, thermal capacity of beta-phase, at low temperatures, 20: 27494(R) (NYO-3454-6)
Al–Ni, thermal properties and strength, 16: 12167
Al–Ni, use as multi-threshold detector in neutron spectrum measurements, 18: 12479
Al–Ni, use as multiple threshold detector for neutrons, 18: 37552
Al–Ni–Nb, crystal structure of intermetallic compounds, 17: 27828
Al–Ni–Nb, crystal structure of M-phase, (E/T), 20: 30734(R) (TID-22970, pp 1-63)
Al–Ni–Nb, mechanical properties at 800 and 900°C, 17: 39557
Al–Ni–Nb, oxidation rate of Ni_3Al–Ni_3Nb, 18: 20478
Al–Ni–Nb, oxidation of, phase distributions in layers from studies of, 20: 14990
Al–Ni–Nb, phase diagram, 20: 46512
Al–Ni–Nb, phase studies at 1140°C, 20: 15121
Al–Ni–Nb, properties, 18: 8828
Al–Ni–Nb, reactions between Ni_3Al and Ni_3Nb in, 17: 27827
Al–Ni–Nb, superconductivity, 20: 46512

Al–Ni–Pu, casting of aluminum-base, for fuel elements, 20: 46144(R) (HW-67765)
Al–Ni–Pu, composition for use as reactor fuel, 17: 18693(P)
Al–Ni–Pu, corrosion by water at 350°C, 20: 46143(R) (HW-66081)
Al–Ni–Pu, development for fuel elements, 18: 40818(P)
Al–Ni–Pu, fabrication by pneumatic injection casting, 17: 27758 (HW-69204)
Al–Ni–Pu, fabrication activities, summary, 17: 31681(R) (HW-76559)
Al–Ni–Pu, phase studies and properties of, bibliographic study of, 16: 32115 (KFK-105)
Al–Ni–Pu, preparation of corrosion-resistant, 17: 36219(P)
Al–Ni–Pu preparation and corrosion resistance, 18: 41493(P)
Al–Ni–Pu, preparation and properties as reactor fuel, 19: 37150(P)
Al–Ni–Pu, radiation effects on injection-cast capsules, proposal for, 16: 568 (HW-68434)
Al–Ni–Pu, radiation stability, neutron, 16: 24640
Al–Ni–Pu, radiation effects on Zircaloy-clad, 17: 13678(R) (HW-75914)
Al–Ni–Pu, radiation effects on injection-cast Zircaloy-clad, 17: 26181
Al–Ni–Pu, radiation effects on Zircaloy-2-clad, 18: 8721(R) (HW-78388 (p.5.1-22))
Al–Ni–Pu, radiation effects on injection-cast Zircaloy-clad, 18: 8867 (HW-SA-2909)
Al–Ni–Pu, welding to aluminum, stainless steel, and zirconium alloys, 18: 44120
Al–Ni–Pu–Ti, phase studies and properties of, bibliographic study of, 16: 32115 (KFK-105)
Al–Ni–Sc, crystal structure of intermetallic compound ScNiAl in, 19: 30701
Al–Ni–Sn–Zr, corrosion by steam at 400°C, 19: 32696(R) (EURAEC-783)
Al–Ni–Sn–Zr, fabrication and properties, 19: 36965(T,R) (EURAEC-618)
Al–Ni–Ta, crystal structure of intermetallic phase TaNiAl in, 19: 6338
Al–Ni–Ta, crystal structure of ordered intermediate phases, 19: 28817
Al–Ni–Ti, corrosion resistance and hardening mechanism of, 18: 18322
Al–Ni–Ti, corrosion by water at 350°C, 20: 46143(R) (HW-66081)
Al–Ni–Ti–Zr, corrosion by steam at 400°C, 19: 32696(R) (EURAEC-783)
Al–Ni–Ti–Zr, fabrication and properties, 19: 36965(T,R) (EURAEC-618)
Al–Ni–U, bonding of, diffusion of aluminum in, 19: 11748
Al–Ni–U, corrosion by steam, 20: 30794(R) (IDO-17147, pp 1-12)
Al–Ni–U, radiation effects on, at high temperatures, 17: 5023
Al–Ni–U, reactions with water during TREAT transients, 18: 1486(R) (ANL-6687(p.167-87))
Al–Ni–U, reactions with steam, reactor safety studies of, 18: 33678(R) (ANL-6875)
Al–Ni–U, reactions with flowing steam, 19: 11679
Al–Ni–U, reactions with steam at 800 to 1300°C, 19: 11682
Al–Ni–U, reactions with water during Kiwi-TNT transients, 20: 20925(R) (ANL-7055, pp 177-212)
Al–Ni–Zr, corrosion by steam at 400°C, 19: 32696(R) (EURAEC-783)
Al–Ni–Zr, fabrication and properties, 19: 36965(T,R) (EURAEC-618)
Al–Ni–Zr, oxidation and mechanical properties, 17: 32621
Al–Ni–Zr, thermal expansion of, to 1100°C, 19: 24982(R) (EURAEC-1270)
Au–Mn, nuclear magnetic moments and hyperfine structure of gamma transitions of gold-197 in, 16: 22999(R) (ORNL-3268(p.70-4))
Au–Mo–Ni, performance for bonding graphite to metals, 20: 31683(R) (ORNL-3936, pp 95-121)
Au–Mo–Ni, properties as brazing alloy, 17: 12653(P)
Au–Ni, brazing on INOR-8 heat exchanger for Molten Salt Reactor Experiment, 18: 10512
Au–Ni, correlation of Mössbauer isomer shift and residual electric resistivity in, 18: 44291 (ORNL-P-400)
Au–Ni, corrosion by boric acid–potassium hydroxide solutions, 18: 30133 (WCAP-3737)
Au–Ni, creep testing of brazed joints at high temperatures in shear, 18: 4174(R) (ORNL-3470(p.157-72))
Au–Ni, elastic constants of single-crystal, effects of pressure on, 20: 29623(R) (TID-22970, pp 121-256)
Au–Ni, electric conductivity and Mossbauer shifts of gold in, 18: 26534(R) (ORNL-3582(p.16-17))
Au–Ni, electron transfer in dilute, 17: 37189
Au–Ni, heat of formation and phase studies, 16: 10502 (AROD-2287.15)
Au–Ni, magnetic field at gold nuclei in dilute, 16: 12547
Au–Ni, magnetic fields at gold nuclei in, 17: 13245
Au–Ni, magnetic fields and isomer shifts in, (E), 19: 37042(R) (ORNL-3778(p.4-6))
Au–Ni, magnetic properties of Au in, 18: 36511
Au–Ni, Mössbauer isomer shift correlation with residual electrical resistance of, 17: 26453(R) (ORNL-3425(p.103-11))
Au–Ni, optical properties of films, 17: 16696
Au–Ni, performance for high-temperature brazing, 18: 2212
Au–Ni, performance as metal-to-ceramic seals, 18: 29928(R) (NP-13979)
Au–Ni, use as brazing alloys for refractory metals, 18: 7956(R) (GA-3992(Pt.I))
Au–Ni, use as brazing alloy in Inconel joints, 18: 27915 (KAPL-2000-21(p.V.1-20))
Au–Ni, use for brazing Inconel in reactor environments, 17: 36272
Au–Ni–Sn, solute interactions in dilute, (E/T), 20: 2349 (UCRL-16320)
Au–Ni–Ta, properties of, as brazing alloy for graphite, 16: 9249(P)
Ba–Ni, performance of thermionic cell with cathode of, 17: 27981
Ba–Ni, phase studies, 20: 4442
Be–Co–Fe–Ni, phase studies, 16: 2180 (NMI-1252)
Be–Co–Ni, phase studies, 16: 2180 (NMI-1252)
Be–Co–Ni, phase studies of, containing traces of manganese, 16: 2180 (NMI-1252)
Be–Cr–Fe–Ni, tensile properties at room temperature, 19: 30667(R) (COO-1319-24)
Be–Fe–Ni, phase studies, 16: 2180 (NMI-1252)
Be–Ni, analysis for impurities in, development of electron microprobe for, 20: 29083(R) (UCRL-14767)
Be–Ni, corrosion by water at 343°C, 17: 6568(R) (NMI-1905)
Be–Ni, crystal structure at early aging stage after annealing at 425 and 500°C, 16: 7912
Be–Ni, diffusion of beryllium into, electronic probe microanalyzer study of, 18: 543 (CEA-2291)
Be–Ni, diffusion of beryllium in, enthalpy of, 20: 11326
Be–Ni, electric conductivity in, localized impurity-state determination from, (E), 20: 24659
Be–Ni, electron multiplication in, (E), 19: 18528
Be–Ni, field emission microscopy of, 20: 25596(T)
Be–Ni, fracture studies, 19: 20462(R) (NRL-6258)
Be–Ni, phase diagram, 17: 14740 (TID-11295(2nd Ed.))
Be–Ni, phase studies, 16: 25810
Be–Ni, phase studies and surface tension at 1500°C, 17: 12702
Be–Ni, phase studies, 18: 26005
Be–Ni, preparation by coal reduction of beryllium oxide, 17: 35821
Be–Ni, preparation of single crystals of, 18: 14372(R) (NMI-2124)
Be–Ni, preparation by zone melting, 19: 44694(R) (NP-15432)
Be–Ni, preparation by splatcooling and hot-pressing, 20: 4381(R) (NMI-8001.4)
Be–Ni, properties, 17: 34339
Be–Ni, properties of localized impurity states in, 20: 21390
Be–Ni, properties of, effects of alloying additions on, 20: 46208
Be–Ni, radiation effects on precipitation reactions of, 16: 33567
Be–Ni, radiation effects on properties of precipitation-hardening, 17: 31054
Be–Ni, structure, effects of ultra-rapid quenching on, 17: 14812(R) (ASD-TDR-62-181)
Be–Ni, x-ray scattering studies on aging in, 18: 39959(T)
Bi–Ni, density at 800°C, 18: 12700
Cd–Ni, crystal structure of nitrogen-containing, 16: 2259
Ce–Co–Cu–Fe–Ni–Pu, phase studies, 20: 5848
Ce–Co–Cu–Ni–Pu, phase studies, 19: 24986(R) (MLM-1220)
Ce–Ni, crystal structure of equiatomic intermetallic compound in, 19: 24994
Ce–Ni, crystal structure of intermetallic compounds in, 20: 37243
Ce–Ni, density and expansion coefficients at 25 to 800°C, 19: 37032 (LA-DC-6580)
Ce–Ni, effect of annealing on coercive force of deformed, 17: 16716
Ce–Ni, magnetic and structural characteristics of intermetallic compound of type LaNi in, 18: 37697
Ce–Ni, magnetic properties of $CeNi_4$ at 4–300°K, 17: 37713
Ce–Ni, magnetic properties, 19: 38049
Ce–Ni, magnetic properties of intermetallic compounds in, 20: 9511
Ce–Ni, magnetic properties of intermetallic compounds of, 20: 32699
Ce–Ni, magnetic susceptibility of $CeNi_5$ at 4 to 300°K, 19: 30743(R) (NYO-3454-1)
Ce–Ni, mechanical properties, 18: 22517
Ce–Ni, phase studies, 17: 40342(R) (LAMS-2973)
Ce–Ni, phase studies, 18: 24815(R) (MLM-1184)
Ce–Ni, phase studies, 18: 30975(R) (LAMS-3096)
Ce–Ni, phase studies, 18: 41927(R) (MLM-1199)
Ce–Ni, phase studies, 19: 40961
Ce–Ni, properties and structure of, 18: 39969
Ce–Ni–Pu, phase studies and properties of, bibliographic study of, 16: 32115 (KFK-105)
Ce–Ni–Pu, phase studies, 18: 4166(R) (MLM-1171)
Ce–Ni–Pu, phase studies, 18: 24815(R) (MLM-1184)
Ce–Ni–Pu, phase studies, 18: 41927(R) (MLM-1199)
Ce–Ni–Pu, phase studies, 18: 41933 (TID-11295(3rd Ed.))
Ce–Ni–Pu, phase studies, 19: 13889(R) (MLM-1208)
Ce–Ni–Pu, phase studies, 19: 24986(R) (MLM-1220)
Ce–Ni–Pu, phase studies, 19: 39163(R) (MLM-1244)
Ce–Ni–Pu, phase studies, 20: 21342(R) (MLM-1301)
Ce–Ni–Pu, properties of, 17: 27789(R) (MLM-1156)

Co–Cu–Mn–Ni, corrosion by liquid sodium at 700 and 1200°F, 20: 9422 (NAA-SR-11326)
Co–Fe–Mn–Ni, mechanical properties at 70 to 2000°F, 17: 18758 (NAA-SR-Memo-8052)
Co–Fe–Mo–Ni, properties of Maraging Steel for use in space electric power systems, 20: 4379 (NASA-CR-54091)
Co–Fe–Ni, development of hardened martensitic, as high-temperature magnetic materials, 20: 43815(R) (NASA-CR-54356)
Co–Fe–Ni, diffusion of deuterium and hydrogen in Nilo K at 40 to 400°C, 18: 5771 (AWRE-O-49/63)
Co–Fe–Ni, diffusion of helium in Kovar, 19: 908 (TID-21249)
Co–Fe–Ni, ductility of Kovar, effects of liquid cesium on, 18: 14354(R) (ARF-B215-12)
Co–Fe–Ni, welding to Kovar and nickel, quality of, 19: 23347(R) (NYO-3429-2)
Co–Mo–Ni, mechanical properties of welded plates of, 19: 11718 (AD-604052)
Co–Mo–Ni, strength of laminated, 17: 23970(R) (WAL-TR-766.2/3-3)
Co–Mo–Ni–Ti, fabrication of vertical-rib sandwich panels of, by roll-welding, 20: 25509(R) (AD-632831)
Co–Ni, antiferromagnetism of, 17: 37828
Co–Ni, atomic magnetic properties, 16: 16839
Co–Ni, cobalt-59 and nickel-61 NMR absorption in, effects of temperature and pressure on, 19: 23812
Co–Ni, corrosion by boiling hydrochloric and phosphoric acids, calculated, 18: 32089 (TID-20777(p.25-32))
Co–Ni, diffusion in, magnetic effect on, 17: 27841
Co–Ni, electrodeposition from sulfamate bath, effects of variables on deposit properties, 19: 36948 (BDX-613-66)
Co–Ni, magnetic fields at cobalt nuclei in, 17: 13245
Co–Ni, magnetic moment distribution in, 17: 37822
Co–Ni, magnetic moments in, distribution of, 19: 23058
Co–Ni, nuclear polarization of cobalt-60 in, (E), 19: 10249 (NP-14477)
Co–Ni, phase diagrams, 20: 33939 (DP-1051)
Co–Ni, plastic behavior of, 17: 581
Co–Ni, plastic deformation of single crystals of, 17: 6695(T) (AEC-tr-5568)
Co–Ni, self-diffusion of cobalt-60 and nickel-63 in, 16: 33501
Co–Ni, self-diffusivities in, 16: 24169 (NYO-9430)
Co–Ni, self-diffusion in, tracer studies of volume, 19: 9708
Co–Ni, stacking fault tetrahedra stability in, 16: 19381(T) (UCRL-Trans-824)
Co–Ni, thermodynamic properties of oxygen in liquid, 20: 4454
Co–Ni, vacancies in, quenched-in, 16: 12158
Co–Ni–Nb, mechanical properties and structure of, 17: 20478
Co–Ni–Sc, crystal structure of Laves phases in, 20: 41412(R) (IS-1500 (Sect. M))
Co–Ni–Sc, scandium-45 NMR in cubic Laves-phase intermetallic compounds of, Knight shift and linewidth in, (E), 20: 24654
Co–Ni–Ti, creep testing of Nivco, 20: 43815(R) (NASA-CR-54356)
Co–Ni–Ti–Zr, mechanical and thermophysical properties of Nivco, at 80 to 1600°F, 18: 41928(R) (NASA-CR-54089)
Co–Ni–Ti–Zr, properties of Nivco in space electric power systems, 20: 4379 (NASA-CR-54091)
Co–Ni–U, phase studies on, eutectic temperature and composition from, 16: 17297(R) (LAMS-2681)
Co–Ni–W, oxidation in air at 2000°F, 17: 14724(R) (ARF-2158-15)
Co–Ni–W, properties at high temperatures, 17: 14827(R) (LAR-17)
Cr–Co–Cu–Mo–Ni–W, corrosion resistance to strong acids, 19: 18415
Cr–Co–Fe–Mo–Ni, corrosion and mechanical properties of Multimet Alloy N-155 as gas turbine material, 16: 32114 (IDO-28591)
Cr–Co–Fe–Mn–Ni, corrosion by mercury at high temperatures, 18: 7152
Cr–Co–Fe–Mn–Ni–W, corrosion by mercury at high temperatures, 18: 7152
Cr–Co–Fe–Mo–Ni, corrosion by superheated steam at 1050 to 1150°F, 19: 2853
Cr–Co–Fe–Mn–Mo–Ni–W, corrosion of Rsonel, by coal gasification products at high temperatures, 19: 42127(R) (TID-22009)
Cr–Co–Fe–Mn–Mo–Ni, corrosion of Vitallium, by boiling hydrofluoric acid–nitric acid solutions, 20: 37169(R) (BMI-1774)
Cr–Co–Fe–Mn–Mo–Ni–Ti, corrosion of Hanford 22, by boiling hydrofluoric acid–nitric acid solutions, 20: 37169(R) (BMI-1774)
Cr–Co–Fe–Mo–Ni, corrosion of Haynes 21, by boiling hydrofluoric acid–nitric acid solutions, 20: 37169(R) (BMI-1774)
Cr–Co–Fe–Mn–Mo–Ni–Ti, corrosion of Hanford 23 and 24, by boiling hydrofluoric acid–nitric acid solutions, 20: 37169(R) (BMI-1774)
Cr–Co–Fe–Mn–Mo–Ni–W, mechanical properties at high temperatures, 17: 14811 (ASD-TDR-61-529)
Cr–Co–Fe–Mo–Ni–W, mechanical properties of, at 70 to 2000°F, 17: 18758 (NAA-SR-Memo-8052)
Cr–Co–Fe–Mn–Ni–W, tensile properties of L-605, effects of cold deformation on, 20: 39399 (NASA-TN-D-3528)
Cr–Co–Fe–Mo–Ni, welding characteristics, 16: 4510 (DMIC-Memo-140)
Cr–Co–Fe–Ni, corrosion by superheated steam at 1050 and 1150°F, 19: 2853
Cr–Co–Fe–Ni, machining properties, 16: 4528 (DMIC-Memo-134)
Cr–Co–Fe–Ni, properties of Elgiloy at –400 to 100°F, 18: 42020 (PB-171809(Rev.))
Cr–Co–Mo–Ni, drilling of hardened Astroloy, 17: 6617
Cr–Co–Mo–Ni–W, erosion by mercury vapor at 640°F of Stellite 6B, 20: 11214(R) (NASA-CR-54717)
Cr–Co–Mo–Ni, fabrication and properties of thoria-dispersion-strengthened, 18: 18277(R) (AD-432420)
Cr–Co–Mo–Ni–Ti, machining, 16: 3417(R) (ASD-TR-7-532a(IV))
Cr–Co–Mo–Ni, mechanical properties of, effect of rhenium admixture on, 16: 24200
Cr–Co–Mo–Ni, mechanical properties of S-1, to 1800°F, 17: 29070(R) (NP-12934)
Cr–Co–Mo–Ni–W, oxidation by air at 1600°F of Stellite 6B, 20: 11215(R) (NASA-CR-54718)
Cr–Co–Mo–Ni, tensile properties of Udimet 500, effects of thoria additions on, 18: 592(R) (AD-421756)
Cr–Co–Mo–Ni–W, testing for bearing parts in liquid sodium, 20: 22520(R) (NAA-SR-11805)
Cr–Co–Ni, corrosion of Udimet 500, by lithium fluoride, 19: 12150
Cr–Co–Ni, deposition of, on molybdenum for oxidation protection, 16: 30840
Cr–Co–Ni, neutron reactions with, activation response of, 20: 28591 (DC-59-3-90)
Cr–Co–Ni, stress-rupture behavior of, effects of molybdenum, niobium, and tungsten on, 18: 44165
Cr–Co–Ni, thermal resistance of layers of, electrodeposited on molybdenum, 16: 30841
Cr–Co–Ni–W, corrosion of, by decontaminating solution, 16: 24496 (TID-7626(Pt.I)(p.87-91))
Cr–Co–Ni–W, corrosion of, by water in pressurized water reactors, 16: 7855
Cr–Co–Ni–W, corrosion by mercury at high temperatures, 16: 32079 (NAA-SR-6306)
Cr–Co–Ni–W, machining characteristics of HS-25, 17: 6609
Cr–Co–Ni–W, machining of HS-25, 17: 6611
Cr–Co–Ni–W, metallurgy of, for heat transfer loops, 17: 22092(R) (GE63FPD66)
Cr–Co–Ni–W, use of, in fabrication of mercury corrosion loop, 16: 11810(R) (AGC-0584-04-1)
Cr–Cu–Fe–Mo–Ni, corrosion and metallurgical changes in, caused by steam at 1200 to 1500°F, 16: 24126
Cr–Cu–Fe–Mo–Ni–Ti, corrosion of, by reactor fuel dissolver solutions, 17: 6566 (HW-SA-2307)
Cr–Cu–Fe–Mo–Ni, corrosion by copper chloride at high temperatures, 18: 4796(R) (GEAP-4153)
Cr–Cu–Fe–Mo–Ni, corrosion by boiling magnesium chloride, 18: 4796(R) (GEAP-4153)
Cr–Cu–Fe–Mo–Ni–Ti, corrosion and fabrication properties for use as nuclear fuel reprocessing plant dissolver, 18: 25996
Cr–Cu–Fe–Mn–Ni–Ti, corrosion of Corronel-230, by FTW-65 Purex wastes, 19: 31617(R) (ORNL-TM-1081)
Cr–Cu–Fe–Mn–Mo–Ni–Ti, corrosion of Hanford 21, by boiling hydrofluoric acid–nitric acid solutions, 20: 37169(R) (BMI-1774)
Cr–Cu–Fe–Mn–Mo–Ni, corrosion of Illium R, by boiling hydrofluoric acid–nitric acid solutions, 20: 37169(R) (BMI-1774)
Cr–Cu–Fe–Mo–Ni, descaling by sodium carbonate–sodium hydroxide solutions, 18: 22441 (HW-79048)
Cr–Cu–Fe–Mn–Ni, effects of ammonium fluoride–formic acid–nitric acid anodic solutions against corrosion of, 18: 35959
Cr–Cu–Fe–Mo–Ni, effects of ammonium fluoride–formic acid–nitric acid anodic solutions against corrosion of, 18: 35959
Cr–Cu–Fe–Mo–Ni, performance of Ni–O–Nel 825 in nuclear superheater environment, 18: 24886(R) (GEAP-4565)
Cr–Cu–Fe–Ni, corrosion of, by water in pressurized water reactors, 16: 7855
Cr–Cu–Fe–Ni, corrosion of, effect of Teflon on, 17: 24639(WAPD-BT-28(p.53-9))
Cr–Cu–Fe–Ni, radiation effects on magnetic properties of, 17: 32692
Cr–Cu–Ge–Ni–Pd, use as brazing alloy in Inconel joints, 18: 27915 (KAPL-2000-21(p.V.1-20))
Cr–Fe–Ni, oxidation of Nicral D at 900 to 1100°C, 16: 24124(T) (AEC-tr-5235)
Cr–Fe–Ni, reactions of, with carbon dioxide, 16: 2993 (NP-10967)
Cr–Eu–Ni, fabrication of reactor control rods of, 19: 28803(P)
Cr–Fe–Mn–Mo–Ni–W, corrosion and metallurgical changes in, caused by steam at 1200 to 1500°F, 16: 24126
Cr–Fe–Mn–Mo–Ni–Ti, corrosion of Hanford 20, by boiling hydrofluoric acid–nitric acid solutions, 20: 37169(R) (BMI-1774)
Cr–Fe–Mn–Mo–Ni–Ti, corrosion of Hanford 17, by boiling hydrofluoric acid–nitric acid solutions, 20: 37169(R) (BMI-1774)

Cr–Fe–Mn–Mo–Ni, specification for type 355 plate, sheet, and strip for irradiation testing, 17: 41347 (HW-75208)
Cr–Fe–Mn–Ni, corrosion of, by water in pressurized water reactors, 16: 7855
Cr–Fe–Mn–Ni, corrosion of, effects of carbon, nitrogen, niobium, and titanium on, 16: 13536
Cr–Fe–Mn–Ni, corrosion by superheated steam, cycle tests of, 17: 21229 (TID-7658(p.20-6))
Cr–Fe–Mn–Ni, corrosion of Incoloy, by superheated steam, 17: 38465 (TID-7674(p.11-16))
Cr–Fe–Mn–Ni, corrosion of Incoloy by oxygenated steam at 500°C and 3000 psi, 17: 38466 (TID-7674(p.16))
Cr–Fe–Mn–Ni, corrosion of Incoloy-800 by ferric chloride and superheated steam, 18: 1241(R) (GEAP-4332)
Cr–Fe–Mn–Ni, corrosion by boiling magnesium chloride, 18: 4796(R) (GEAP-4153)
Cr–Fe–Mn–Ni, corrosion by copper chloride at high temperatures, 18: 4796(R) (GEAP-4153)
Cr–Fe–Mn–Ni, corrosion by superheated steam at 1020°F, 18: 7957(R) (GEMP-257)
Cr–Fe–Mn–Ni, corrosion of aluminum-modified Incoloy 800, by steam at 650°C, 18: 19456(R) (ANL-6840)
Cr–Fe–Mn–Ni, corrosion of Incoloy 800 by superheated steam, 18: 27909
Cr–Fe–Mn–Ni, corrosion by mercury at 600 to 1000°F, 18: 27913
Cr–Fe–Mn–Ni, corrosion of Incoloy, by superheated steam at 550°C, 18: 32139(R) (HW-81269(p.5.1-23))
Cr–Fe–Mn–Ni, corrosion of Corronel 230, by boiling hydrofluoric acid–nitric acid solutions, 20: 37168(R) (BMI-1771)
Cr–Fe–Mn–Ni, corrosion of Corronel 230, by boiling hydrofluoric acid–nitric acid solutions, 20: 37169(R) (BMI-1774)
Cr–Fe–Mn–Ni, descaling by sodium carbonate–sodium hydroxide solutions, 18: 22441 (HW-79048)
Cr–Fe–Mn–Ni, fabrication and property specifications for fuel element tubes of Incoloy-800, 18: 1241(R) (GEAP-4332)
Cr–Fe–Mn–Ni, mechanical properties at high temperatures, 17: 14811 (ASD-TDR-61-529)
Cr–Fe–Mn–Ni, mechanical properties of, effects of steam at 1050°F on, 18: 4795(R) (GEAP-3924)
Cr–Fe–Mn–Ni, mechanical properties at high temperatures, 18: 4796(R) (GEAP-4153)
Cr–Fe–Mn–Ni, oxidation of Incoloy-800 by helium–steam at 1700°F, 18: 32043(R) (HW-81269(p.4.1-64))
Cr–Fe–Mn–Ni, phase diagrams of, effects of additive on, 16: 30822
Cr–Fe–Mn–Ni, properties as fuel element cladding material, 17: 36928(R) (GEAP-4126)
Cr–Fe–Mn–Ni, properties as fuel element cladding material, 17: 36929(R) (GEAP-4243)
Cr–Fe–Mn–Ni, radiation effects on, in superheated steam, 17: 21235 (TID-7658(p.59-77))
Cr–Fe–Mn–Ni, thermal-stress-fatigue properties of Incoloy, 18: 596(R) (ATL-A-139)
Cr–Fe–Mn–Ni, thermal stress fatigue tests of Incoloy 800, 19: 13980(R) (ATL-A-144)
Cr–Fe–Mo–Ni, compatibility with niobium beryllide at 2000°F, 17: 532 (GEMP-105)
Cr–Fe–Mo–Ni, corrosion of, by acid, 16: 12057
Cr–Fe–Mo–Ni, corrosion of, by fluorides (liquid), 16: 630
Cr–Fe–Mo–Ni, corrosion of, by hydrofluoric acid in volatility pilot plant, 16: 20538 (ORNL-TM-186)
Cr–Fe–Mo–Ni, corrosion of, by water in pressurized water reactors, 16: 7855
Cr–Fe–Mo–Ni–Ti, corrosion and mechanical properties of Inconel 901 as gas turbine material, 16: 32114 (IDO-28591)
Cr–Fe–Mo–Ni, corrosion by aqueous chlorides at 500 to 550°F, 17: 500(R) (KAPL-2000-19(p.IV.1-IV.11))
Cr–Fe–Mo–Ni, corrosion by molten fluorides at 500°C, 17: 29279 (BMI-X-227)
Cr–Fe–Mo–Ni, corrosion of Hastelloy X-280, by helium–water system at 1700, 1900, and 2100°F, 20: 5846
Cr–Fe–Mo–Ni, corrosion by carbon dioxide, helium, nitrogen, and steam of Hastelloy X-280, 20: 9408 (BNWL-154)
Cr–Fe–Mo–Ni, corrosion by water vapor at 815, 930, and 1038°C of Hastelloy X-280, 20: 9409 (BNWL-155)
Cr–Fe–Mo–Ni, corrosion of Hymu-80 by potassium chloride–uranium trichloride eutectic at 900°C, 20: 21261 (LA-3470)
Cr–Fe–Mo–Ni, corrosion by molten fluoride salts, 16: 32080 (ORNL-TM-328)
Cr–Fe–Mo–Ni, creep and stress-rupture properties in air, liquid metal, and salt at 1350 to 1650°F, 16: 13588 (TIM-287)
Cr–Fe–Mo–Ni, creep of irradiated, at 1600°, 16: 28642(R) (BMI-1581 (Del.))
Cr–Fe–Mo–Ni–Nb–W, descaling by sodium carbonate–sodium hydroxide solutions, 18: 22441 (HW-79048)
Cr–Fe–Mo–Ni, effects of ammonium fluoride–formic acid–nitric acid anodic solutions against corrosion of, 18: 35959
Cr–Fe–Mo–Ni, evaporation at 2050°F of Hastelloy X-280, effects of oxide film on, 20: 9410(R) (BNWL-166, pp 5.1-3)
Cr–Fe–Mo–Ni, mechanical properties of Inconel 713C, 16: 15153(R) (ASD-TR-7-886(IV))
Cr–Fe–Mo–Ni, mechanical properties at high temperatures, 17: 14811 (ASD-TDR-61-529)
Cr–Fe–Mo–Ni–Ti, oxidation of V-57, induced by cyclic strain at high temperatures, 18: 18311 (62RL3190M)
Cr–Fe–Mo–Ni–Ti–W, oxidation of M-308, induced by cyclic strain at high temperatures, 18: 18311 (62RL3190M)
Cr–Fe–Mo–Ni, oxidation of Hastelloy X-280 by helium–steam at 1700°F, 18: 32043(R) (HW-81269(p.4.1-64))
Cr–Fe–Mo–Ni–Nb, oxidation of Inconel 625 by water vapor in helium at 1700°F, 19: 30820 (BNWL-23)
Cr–Fe–Mo–Ni, oxidation at 2050°F of Hastelloy X-280, 20: 5851
Cr–Fe–Mo–Ni–W, properties of, mechanical and physical, 20: 33861 (BAW-237)
Cr–Fe–Mo–Ni, radiation effects on mechanical properties of, fast neutron, 16: 572 (REIC-20)
Cr–Fe–Mo–Ni, radiation effects on mechanical properties, 17: 18852 (BNL-6249)
Cr–Fe–Mo–Ni–Nb, radiation effects on Inconel 625, 18: 7292(R) (HW-77954(p.4.1-12))
Cr–Fe–Mo–Ni–Ti, radiation effects on Nimonic, in-pile, 18: 28075
Cr–Fe–Mo–Ni, radiation effects on mechanical properties of Hastelloy X-280 at 280°C, 18: 32043(R) (HW-81269(p.4.1-64))
Cr–Fe–Mo–Ni–Nb, radiation effects on mechanical properties of Inconel 625, neutron, 19: 30820 (BNWL-23)
Cr–Fe–Mo–Ni, radiation effects on mechanical properties of Hastelloy X-280, fast-neutron, 20: 9408 (BNWL-154)
Cr–Fe–Mo–Ni, radiation effects on tensile properties of Hastelloy X-280, neutron, 20: 23769 (BNWL-202)
Cr–Fe–Mo–Ni–W, radiation effects on mechanical properties of Hastelloy X-280, fast-neutron, 20: 31669
Cr–Fe–Mo–Ni, stress-corrosion cracking by boiler water at 500°F and sea water at 550°F, 17: 27749 (KAPL-M-CC-3)
Cr–Fe–Mo–Ni–Ti, tensile and crack-propagation properties of, at 75 to 1500°F, 16: 12081(R) (AD-260547)
Cr–Fe–Mo–Ni, tensile properties of, for use as forging die at 2400°F, 16: 27623(R) (ARF-2220-15)
Cr–Fe–Mo–Ni, tensile properties, 17: 16640 (DMIC-Memo-164)
Cr–Fe–Mo–Ni, tensile properties at room temperature, 19: 30667(R) (COO-1319-24)
Cr–Fe–Mo–Ni–Nb–W, tensile properties of IN-102, 19: 39156(R) (CEND-532)
Cr–Fe–Mo–Ni–Nb, thermal response and microstructure of Inconel 625 at 1200 and 1400°F, 19: 39158 (GEAP-4751)
Cr–Fe–Mo–Ni–Nb–W, welding properties of Inco IN-102, 20: 4306(R) (ORNL-3870, pp 194-213)
Cr–Fe–Ni, carburization of, by flowing carbon dioxide, 16: 30167 (ORNL-3313(p.19-64))
Cr–Fe–Ni, carburization in carbon dioxide at 593 to 815°C, effects of chromium content on, 18: 4254(R) (ORNL-3470(p.89-93))
Cr–Fe–Ni, carburization in carbon dioxide at 600 to 800°C, effects of varying chromium content on, 19: 26772
Cr–Fe–Ni, compatibility with niobium beryllide at 2000°F, 17: 532 (GEMP-105)
Cr–Fe–Ni, corrosion and metallurgical changes in, caused by steam at 1200 to 1500°F, 16: 24126
Cr–Fe–Ni, corrosion of, by boiling potassium, 16: 30167 (ORNL-3313 (p.19-64))
Cr–Fe–Ni, corrosion of, by decontaminating solution, 16: 24496
Cr–Fe–Ni, corrosion of, by liquid metals, 16: 32087
Cr–Fe–Ni, corrosion of, by liquid metals and salts, 16: 28646(R) (ORNL-2274(Pts.1-5))
Cr–Fe–Ni, corrosion by fused fluorides, 17: 7606(R) (ORNL-1515)
Cr–Fe–Ni, corrosion by carbon dioxide, 17: 6560 (AAEC/E-98)
Cr–Fe–Ni, corrosion of, by steam at 1050°F, 17: 16587 (GEAP-4165)
Cr–Fe–Ni, corrosion of G-157, by air and nitrogen–oxygen atmospheres at 1750 and 1850°F, 17: 25723 (IDO-28605)
Cr–Fe–Ni, corrosion by air at 1750°F after 10,000 hours, 17: 41379
Cr–Fe–Ni, corrosion by liquid sodium, 18: 3298(R) (ORNL-2221(Pts.1-5) (Del.))
Cr–Fe–Ni, corrosion products of alloy 600, solubility in ammoniated and lithiated water, 18: 18313 (KAPL-3017)
Cr–Fe–Ni, corrosion resistance and hardening mechanism of, 18: 18322
Cr–Fe–Ni, corrosion cracking of, stacking fault energy and dislocation structure in stress, 18: 22448 (UCRL-10890)
Cr–Fe–Ni, corrosion of Incoloy 800 by steam, 18: 26824(R) (ANL-6885)
Cr–Fe–Ni, corrosion by carbon dioxide at 750 to 1050°C, effects on mechanical properties, 18: 35960

Cr–Fe–Ni, corrosion of Incoloy by superheated steam, 18: 44931(R) (ANL-6936(p.39-72))
Cr–Fe–Ni, corrosion of Incoloy 800 by VBWR coolant water, 18: 45020(R) (GEAP-4619)
Cr–Fe–Ni, corrosion and mechanical properties of Incoloy 800, 18: 45022(R) (GNEC-327)
Cr–Fe–Ni, corrosion of Incoloy 800 by helium–steam at high temperatures, 18: 44036(R) (HW-82651(p.4.1-49))
Cr–Fe–Ni, corrosion by supercritical water, (E), 19: 14851(R) (WCAP-2703)
Cr–Fe–Ni, corrosion of austenitic, review of aqueous, 19: 16013 (CEA-R-2600)
Cr–Fe–Ni, corrosion cracking by sodium chloride atmosphere at 600°F, stress-, 19: 30667(R) (COO-1319-24)
Cr–Fe–Ni, corrosion films on, structure of oxide, 19: 40967(R) (COO-1319-27)
Cr–Fe–Ni, corrosion cracking in, mechanisms of stress-, 20: 16968 (COO-1319-33)
Cr–Fe–Ni, corrosion cracking by magnesium chloride, effects of surface preparation on stress-, 20: 23598(R) (COO-1319-34)
Cr–Fe–Ni, corrosion by boiling magnesium chloride, effects of composition and microstructure on, 20: 23599 (COO-1319-36)
Cr–Fe–Ni, corrosion by boiling magnesium chloride solutions and by water, cracking in stress-, 20: 31676(R) (COO-1319-39)
Cr–Fe–Ni, corrosion cracking of, circulating autoclave for studies of stress, 20: 33814 (COO-1319-40)
Cr–Fe–Ni, development and properties of superalloys of, 16: 10402 (ASD-TR-61-322(p.25-39))
Cr–Fe–Ni, development of, for use in ANP program, 16: 28647(R) (ORNL-2340(Pts.1-5))
Cr–Fe–Ni, diffusion of fission products in, at 800, 1000, and 1150°C, 18: 22477(R) (BMI-X-10081)
Cr–Fe–Ni, diffusion of fission products in, 19: 7891 (BMI-1696)
Cr–Fe–Ni, diffusion of fission products in, 19: 28850
Cr–Fe–Ni, diffusion of fission products in, effects of concentrations on, 20: 11212(R) (BMI-X-10143)
Cr–Fe–Ni, effects of short-range order on dislocations and stacking fault energy in, 18: 8815
Cr–Fe–Ni, effects of ammonium fluoride–formic acid–nitric acid anodic solutions against corrosion of, 18: 35959
Cr–Fe–Ni, electron-beam welding to tubesheet joints, 20: 2283 (KAPL-3110)
Cr–Fe–Ni, electron-microprobe analysis for components, 18: 25269(R) (NLCO-905)
Cr–Fe–Ni, fabrication, properties, and applications of, to large power generating equipment, 16: 629
Cr–Fe–Ni, fabrication, 18: 10454(R) (TID-20081)
Cr–Fe–Ni, fabrication and properties of wires of, 19: 9596(R) (COO-1319-18)
Cr–Fe–Ni, fabrication into omega seals by high-energy-rate process, (E), 19: 22450 (KAPL-3094)
Cr–Fe–Ni, fabrication of ingots and single crystals of, 19: 24932(R) (COO-1319-12)
Cr–Fe–Ni, fatigue tests on pressure vessel cladding of, 20: 13255 (KAPL-3108)
Cr–Fe–Ni, fission product diffusion in irradiated, at 600 to 1200°C, 20: 21232 (BMI-1763)
Cr–Fe–Ni, hard surfacing of age-hardenable, 17: 37512 (KAPL-M-JJI-1)
Cr–Fe–Ni, joining by brazing, 19: 11711
Cr–Fe–Ni, joining of Alloy 600 to Zircaloy-4, development of processes for, 19: 13941 (KAPL-3073)
Cr–Fe–Ni, mechanical properties at 70 to 2000°F, 17: 18758 (NAA-SR-Memo-8052)
Cr–Fe–Ni, mechanical properties, 18: 45022(R) (GNEC-327)
Cr–Fe–Ni, mechanism of stress corrosion cracking of, in sodium chloride, 20: 11233(R) (COO-1319-32)
Cr–Fe–Ni, optical properties of, at high temperatures, emittance and reflectance, 16: 12236 (WADD-TR-60-370)
Cr–Fe–Ni, performance of Incoloy, Incoloy 800, Incoloy 801, and Ni–O–Nel in nuclear superheater environment, 18: 24886(R) (GEAP-4565)
Cr–Fe–Ni, performance of Incoloy, Incoloy 800, Ni–O–Nel, and RA 330 in nuclear superheater environment, 18: 24884(R) (GEAP-4419)
Cr–Fe–Ni, performance of Incoloy B as cladding for superheater fuel elements, 18: 28025
Cr–Fe–Ni, phase studies, 17: 12664 (GEAP-4060)
Cr–Fe–Ni, phase studies, 18: 10454(R) (TID-20081)
Cr–Fe–Ni, properties of Ni-SPAN C at –400 to 100°F, 18: 42020 (PB-171809(Rev.))
Cr–Fe–Ni, properties and performance as fuel cladding for Marviken superheater elements, 19: 28770
Cr–Fe–Ni, properties as cladding material for water-cooled reactors, 19: 32756
Cr–Fe–Ni, properties for fuel cladding for steam-cooled reactors, 20: 35840 (KR-89, pp 131-52)
Cr–Fe–Ni, radiation effects on corrosion of, by fluoride eutectics, 16: 32175(R) (ORNL-1531)
Cr–Fe–Ni, radiation effects on corrosion of, by various gases, 16: 33430(R) (EURAEC-318)
Cr–Fe–Ni, radiation effects on mechanical properties of, 16: 33519 (ORNL-TM-337)
Cr–Fe–Ni, radiation effects on mechanical properties of, fast neutron, 16: 572 (REIC-20)
Cr–Fe–Ni, radiation effects on Incoloy, 18: 45020(R) (GEAP-4619)
Cr–Fe–Ni, reactions of Nimonic PE16 with plutonium carbide–uranium carbide, 20: 9438
Cr–Fe–Ni, specification for age-hardenable, for irradiation testing, 17: 41345 (HW-74960)
Cr–Fe–Ni, specification for plate, sheet, and strip for irradiation testing, 17: 41346 (HW-74961)
Cr–Fe–Ni, stress-corrosion cracking by boiler water at 500°F and sea water at 550°F, 17: 27749 (KAPL-M-CC-3)
Cr–Fe–Ni, stress-corrosion cracking, 18: 4920(R) (TID-19731)
Cr–Fe–Ni, stress corrosion cracking in, 19: 24933(R) (COO-1319-15)
Cr–Fe–Ni, stress corrosion cracking in, 19: 24934(R) (COO-1319-21)
Cr–Fe–Ni, stress corrosion cracking of Alloy 600 by wetted thermal insulation, 19: 46949 (CONF-650905-2)
Cr–Fe–Ni, stress release in, at 600 to 750°C, effects of additives and ratios of components on, 16: 30842
Cr–Fe–Ni, stress-corrosion cracking of, design of testing equipment for, 18: 10454(R) (TID-20081)
Cr–Fe–Ni, stress-corrosion cracking in, effects of fourth-component additions on, 19: 40967(R) (COO-1319-27)
Cr–Fe–Ni, stress-corrosion by chlorides, oxygen, and water, 19: 40967(R) (COO-1319-27)
Cr–Fe–Ni, tensile properties, 17: 16640 (DMIC-Memo-164)
Cr–Fe–Ni, tensile properties at room temperature, 19: 30667(R) (COO-1319-24)
Cr–Fe–Ni, tensile properties to 1200°F, effects of composition on, 19: 40967(R) (COO-1319-27)
Cr–Fe–Ni, tensile properties at 25 to 625°C, effects of composition on, 20: 23598(R) (COO-1319-34)
Cr–Fe–Ni, thermal cycling of tubular, effects of fused salts on, 16: 28647(R) (ORNL-2340(Pts.1-5))
Cr–Fe–Ni, thermal neutron magnetic scattering at high temperatures, 18: 16506
Cr–Fe–Ni, thermal properties of, in carbon monoxide and hydrogen, 17: 18839
Cr–Fe–Ni, use of, in fabrication of level indicators for molten salt reactor fuels, 16: 31823 (ORNL-TM-331)
Cr–Fe–Ni–Mn, mechanical properties at high temperatures, 18: 4796(R) (GEAP-4153)
Cr–Fe–Ni–Nb, corrosion of Inconel 600 in air at 1150°C, 18: 28044(R) (HW-80284(p.8.1-4))
Cr–Fe–Ni–Nb–Ti, corrosion of R-27, by superheated steam at 550°C, 18: 32139(R) (HW-81269(p.5.1-23))
Cr–Fe–Ni–Nb–Ti, descaling by sodium carbonate–sodium hydroxide solutions, 18: 22441 (HW-79048)
Cr–Fe–Ni–Nb–Ti, radiation effects on, 18: 7292(R) (HW-77954(p.4.1-12))
Cr–Fe–Ni–Nb–Ti, radiation effects on hardness of R-27, at 50 and 280°C, 18: 32043(R) (HW-81269(p.4.1-64))
Cr–Fe–Ni–Ru–W, properties at 1400 to 2000°F, 17: 14808(R) (ARF-2158-24)
Cr–Fe–Ni–Sn–Zr, properties for use as fuel element cladding, 19: 20497(P)
Cr–Fe–Ni–Ti, corrosion of, by water in pressurized water reactors, 16: 7855
Cr–Fe–Ni–Ti, corrosion by air at 1750°F after 10,000 hours, 17: 41379
Cr–Fe–Ni–Ti, ductility of Ni-span C, effects of liquid cesium on, 18: 14354(R) (ARF-B215-12)
Cr–Fe–Ni–Ti–W, oxidation resistance at 1200°C, 19: 36992(P)
Cr–Fe–Ni–W, mechanical properties at room temperature, 17: 14724(R) (ARF-2158-15)
Cr–Ga–Fe–Ni, phase diagram, 16: 32060
Cr–Gd–Fe–Ni, corrosion of, by water, 16: 17967(R) (USBM-U-887)
Cr–Gd–Fe–Ni, fabrication and structure, 16: 3474(R) (USBM-U-863)
Cr–Gd–Ni, fabrication of reactor control rods of, 19: 28803(P)
Cr–Mn–Mo–Ni, properties for use in liquid-hydrogen bubble chamber, 19: 42808
Cr–Mn–Ni, properties for use in liquid-hydrogen bubble chamber, 19: 42808
Cr–Mo–Ni, compatibility with plutonium and uranium carbides, 20: 30790(R) (ANL-7204, pp 1-31)
Cr–Mo–Ni, corrosion of, by acid, 16: 12057
Cr–Mo–Ni, corrosion of Incoloy and Timken 16-25-6, by sodium at 1200°F, 18: 20472 (NAA-SR-Memo-9340)

Cr–Mo–Ni, corrosion by acids at 800 to 2375°F, effects of heat treatments and microstructure on, 20: 21277
Cr–Mo–Ni, crystal structure of, neutron diffraction studies of atom ordering in, 19: 9676
Cr–Mo–Ni, effect of ferrite content on strength of, 17: 23924 (TID-7620(Pt.I)(p.243-50))
Cr–Mo–Ni, intercrystalline corrosion by hydrochloric acid, 17: 34356
Cr–Mo–Ni, oxidation of, causes of catastrophic, 16: 4500 (ORNL-TM-51)
Cr–Mo–Ni, phase studies, 16: 19412
Cr–Mo–Ni, phase studies at 500 to 1200°C, 20: 27556
Cr–Mo–Ni, thermal properties of, at high temperatures, 16: 4551 (WADD-TR-60-904)
Cr–Mo–Ni–Nb, corrosion and oxidation resistance in fused salts, 18: 41968(P)
Cr–Mo–Ni–Nb–W, creep-rupture properties, 17: 39531(R) (EURAEC-689)
Cr–Mo–Ni–Nb–Ti–W, melting temperatures in, effects of chromium and nickel content on, 16: 19411
Cr–Mo–Ni–Nb–Ti–W, melting temperatures in, effects of chromium and nickel content on, 16: 32127(T) (JPRS-14484)
Cr–Mo–Ni–Ta, corrosion and oxidation resistance in fused salts, 18: 41968(P)
Cr–Mo–Ni–V, corrosion and oxidation resistance in fused salts, 18: 41968(P)
Cr–Mo–Ni–W, corrosion and oxidation resistance in fused salts, 18: 41968(P)
Cr–Ni, aging and thermoelectric power of Alumel–Chromel thermocouples, 20: 4398 (TRG-Report-1021)
Cr–Ni, air and helium effects on voltage drifts in thermocouples of, 17: 30829
Cr–Ni, analysis for yttrium, spectrophotometric in, 18: 8300
Cr–Ni, analysis for yttrium using Arsenazo-III, spectrophotometric, 20: 10773
Cr–Ni base thermocouples, performance in helium, 17: 348
Cr–Ni, behavior of Chromel-P thermocouple wire in carbon dioxide–carbon monoxide, 19: 22664 (ORNL-P-1070)
Cr–Ni, casting and properties of, addition effects of molybdenum, niobium, and tungsten on, 16: 15216
Cr–Ni, combustion behavior, 16: 10508 (DC-55-5-17)
Cr–Ni, compatibility with plutonia at 1093°C, 20: 9407 (BNWL-18)
Cr–Ni, corrosion of Corronel 230, by boiling flowing hydrofluoric acid–hydrogen peroxide solutions, 17: 35618(R) (ORNL-TM-545)
Cr–Ni, corrosion of Corronel 230, effects of oxidation-dissolution cycles in graphite fuels on, 17: 35618(R) (ORNL-TM-545)
Cr–Ni, corrosion by air at 1750°F after 10,000 hours, 17: 41379
Cr–Ni, corrosion of niobium-modified and unmodified, by superheated steam at 1020 and 1350°F, 18: 7957(R) (GEMP-257)
Cr–Ni, corrosion resistance and hardening mechanism of, 18: 18322
Cr–Ni, corrosion by dilute sulfuric acid solution at 25°, 18: 32089 (TID-20777(p.25-32))
Cr–Ni, corrosion by steam, 18: 41933 (TID-11295(3rd Ed.))
Cr–Ni, corrosion by waste melts, 19: 22405(R) (HW-83298(p.4.1-25))
Cr–Ni, corrosion by Purex waste–colemanite melt at 900°C, 19: 25775(R) (HW-84603(p.8-31))
Cr–Ni, corrosion by steam at high temperature, 19: 45572(R) (GEAP-4755)
Cr–Ni, corrosion by trichloroethylene, tracer studies of, 20: 29655
Cr–Ni, corrosion of Blaw Nox NA 55 and NA 64 by boiling hydrofluoric acid–nitric acid solutions, 20: 37169(R) (BMI-1774)
Cr–Ni, corrosion of, in fluidized-bed fluoride volatility process, 20: 45789(R) (ORNL-3945, pp 48-71)
Cr–Ni, creep and oxidation testing, 16: 10515 (DC-60-2-210)
Cr–Ni, creep and oxidation testing, 16: 34068(R) (GEMP-144)
Cr–Ni, creep and corrosion tests on fuel sheets of, 18: 24939(R) (GEMP-285)
Cr–Ni, creep properties, 18: 21668(R) (GEMP-274)
Cr–Ni, creep-rupture properties at 1300 to 1740°F, 17: 33312(R) (GEMP-215)
Cr–Ni, creep-rupture properties at 1300 to 1750°F, 18: 7957(R) (GEMP-257)
Cr–Ni, creep-properties of fuel sheets of, at 1300 to 1750°F, 18: 40925(R) (GEMP-304)
Cr–Ni, creep-rupture properties at 1300 to 1750°F, 18: 33127(R) (GEMP-295)
Cr–Ni, crystal structure and phase studies of, at 1245 to 1300°C, 16: 22573(R) (AD-266459)
Cr–Ni, crystal structure and phase studies, 17: 30985(R) (TID-19070)
Cr–Ni, deformation rate of, temperature effects on, 16: 2227
Cr–Ni, deposition of coatings of, on molybdenum, niobium, and tantalum, 17: 22147
Cr–Ni, deposition of, on molybdenum for oxidation protection at 1100°C, 16: 9149 (ARDE(MX)-89/60)
Cr–Ni, deposition of, on molybdenum for oxidation protection, 16: 30840
Cr–Ni, descaling by sodium carbonate–sodium hydroxide solutions, 18: 22441 (HW-79048)
Cr–Ni, development and testing as coating for uranium(IV) oxide fuel spheres, 18: 37613 (A/CONF.28/P/554)
Cr–Ni, diffusion of chromium-51 and nickel-63 in, 18: 36023
Cr–Ni, diffusion in, activation energy and frequency factor for self-, 19: 40961
Cr–Ni, diffusion of chromium and nickel in, 20: 834(T) (AERE-Trans-1031)
Cr–Ni, effects on stress-relieving on ductility and corrosion resistance of, 17: 23924 (TID-7620(Pt.I)(p.243-50))
Cr–Ni, electric conductivity of Chromel P as function of temperature, 19: 11475 (NAA-SR-Memo-10366)
Cr–Ni, electric properties, 16: 12160
Cr–Ni, electrotransport of components of, effects of chromium concentration on, 16: 3487
Cr–Ni, evaluation of, for high-temperature protection of vanadium alloys, 16: 2168(R) (ARF-2227-2)
Cr–Ni, fabrication and testing of uranium-dioxide-fueled, 17: 3447 (PREDC-759)
Cr–Ni, fabrication and properties of thoria-dispersion-strengthened, 18: 18277(R) (AD-432420)
Cr–Ni, fission product plateout on, from helium system, 16: 29369 (GA-1934)
Cr–Ni, gold film adhesion to substrates of, vapor-deposited, 20: 27516
Cr–Ni, irradiation testing at 815°C of fueled, summary of long-term, 17: 25688(R) (GEMP-177A)
Cr–Ni, lubrication by fused fluoride coatings in air, hydrogen, liquid sodium, and vacuum, 18: 33695 (NASA-TN-D-2348)
Cr–Ni, magnetic field effects on thermocouple wires of, 17: 30828
Cr–Ni, magnetic moment distributions in dilute, 17: 37694
Cr–Ni, mechanical properties of, effects of creep exposure at 1000 to 1800°F on, 16: 5709 (ASD-TR-61-339)
Cr–Ni, metallurgical properties of austenitic, (E), 20: 3471(R) (GEAP-4861)
Cr–Ni, neutron elastic scattering by, cross sections for, (E/T), 20: 26346 (NP-16010, pp 1-41)
Cr–Ni, neutron-induced composition changes in, 17: 30826
Cr–Ni, neutron radiation effects on stress-rupture strength of A-286, 17: 4992
Cr–Ni, neutron radiation effects on physical properties of, 17: 31023
Cr–Ni, oxidation of burner rig stages of, effects of dynamic head and niobium on, 16: 13574 (DC-59-2-36)
Cr–Ni, oxidation by air and steam, 18: 21668(R) (GEMP-274)
Cr–Ni, oxidation of, kinetics, mechanism, and microstructure of internal, 20: 23619
Cr–Ni, performance in nuclear-superheater environment, 19: 10541(R) (GEAP-4703)
Cr–Ni, performance of, on Pebble Bed Reactor fuel, 16: 9663 (NYO-9064)
Cr–Ni, phase studies, 18: 2163(R) (IS-700(Sect.M))
Cr–Ni, phase studies, 19: 9604(R) (IS-900(Sect.M))
Cr–Ni, properties of, evaluation summary of, for ANP uses, 16: 10513 (DC-59-11-162)
Cr–Ni, properties as fuel element material, 17: 38544 (GEMP-239)
Cr–Ni, properties as fuel cladding and sheet materials, 18: 13315(R) (GEMP-231)
Cr–Ni, properties of K-state, 19: 9604(R) (IS-900(Sect.M))
Cr–Ni, properties of, effects of additions and impurities on, 20: 46194(T) (AD-634697)
Cr–Ni, protective effects of, against oxidation of niobium–vanadium alloys at 2000 to 2400°F, 16: 27587 (ARF-2227-6)
Cr–Ni, protective properties of coatings of, for tungsten alloys, 17: 14808(R) (ARF-2158-24)
Cr–Ni, radiation effects on, of long-term neutron exposures, 16: 32034(R) (GEMP-15A)
Cr–Ni, radiation effects on electric conductivity of, 17: 39688
Cr–Ni, radiation effects on thermoelectric properties, 18: 32237
Cr–Ni, radiation effects on, in use as fuel matrix, 19: 11679
Cr–Ni, reactions with beryllium to 600°C in carbon dioxide and *in vacuo*,
Cr–Ni, reactions with Magnox alloy to 550°C in argon and carbon dioxide, 19: 22997 (TRG-Report-842)
Cr–Ni, reactions with plutonia and urania in air and hydrogen at high temperatures, 19: 22867(R) (HW-81603(p.2.1-23))
19: 22997 (TRG-Report-842)
Cr–Ni, reactions with plutonia at high temperatures, 19: 39125(R) (BNWL-91)
Cr–Ni, reactions with plutonium–thorium–uranium alloys at 650°C, 19: 44674(R) (ANL-7000, pp 69-83)
Cr–Ni, strength and creep of, effects of rare earths on, 16: 3502
Cr–Ni, stress-corrosion cracking in water, 17: 41380
Cr–Ni, structure of chromium phase of, at 1300°C, 16: 5707(R) (AD-261335)
Cr–Ni, structure of, short-range order in atomic, 19: 28815(T) (ORNL-tr-632)

Cr–Ni, tensile properties of, at 60 to 2000°F, effects of niobium on, 16: 19341 (DC-59-2-83)
Cr–Ni, tensile properties of, effects of molybdenum on, 20: 25587
Cr–Ni, thermal properties of, in carbon monoxide and hydrogen, 17: 18839
Cr–Ni, thermal resistance of, electrodeposited on molybdenum, 16: 30841
Cr–Ni, thermodynamic properties, 20: 834(T) (AERE-Trans-1031)
Cr–Ni, use as catalyst in preparation of radioactive diamonds, 19: 32277(P)
Cr–Ni, use of, in thermocouples, 16: 20633 (DC-59-10-202)
Cr–Ni, use of Incoloy 800 in magnetic force welding, 18: 29001(R) (HW-79280(p.5.1-25))
Cr–Ni, welding of, magnetic-force, 18: 12547(R) (HW-76303(p.3.1-37))
Cr–Ni–Nb, aging and thermal conductivity of, 20: 25588
Cr–Ni–Nb, phase diagram, 17: 4978
Cr–Ni–Nb, phase diagram, 17: 27825
Cr–Ni–Nb, phase studies, 16: 10551
Cr–Ni–Nb, phase studies, 18: 18307
Cr–Ni–Nb, phase studies on intermetallic compounds in, 20: 17075
Cr–Ni–Nb, radiation effects on stress-rupture properties of, neutron, 20: 5917
Cr–Ni–Nb, stress-rupture testing, summary of in-pile, 18: 4764(R) (ORNL-3470(p.129-56))
Cr–Ni–Nb, structural transformations in, 18: 615
Cr–Ni–Nb, tensile properties of, at 60 to 2000°F, 16: 19341 (DC-59-2-83)
Cr–Ni–Nb–Ta–Ti, properties of Inco 82 as filler material in weldments, 18: 4174(R) (ORNL-3470(p.157-72))
Cr–Ni–Sm, fabrication of reactor control rods of, 19: 28803(P)
Cr–Ni–stainless steel 304, corrosion in Saxton steam generator, 20: 30884(R) (WCAP-3269-16)
Cr–Ni–stainless steel, strain fatigue limits of, biaxial, 20: 12418(R) (WCAP-3739)
Cr–Ni–Ti, corrosion resistance and hardening mechanism of, 18: 18322
Cr–Ni–Ti, use as brazing alloy, 19: 30690(R) (ML-TDR-64-270)
Cr–Ni–U, fabrication of, edge sealing by fusion welding in, 16: 9161 (DC-59-2-86)
Cr–Ni–U, fabrication of clad ribbon of, 16: 9191 (DC-58-11-103)
Cr–Ni–U, melting point, 16: 6104(R) (LAMS-2647)
Cr–Ni–U, radiation effects on enriched, 17: 41333(R) (ANL-6677)
Cr–Ni–W, mechanical properties at room temperature and oxidation at 2000°F, 17: 14724(R) (ARF-2158-15)
Cr–Ni–W, properties, 17: 14825(R) (LAR-12)
Cr–Ni–W, properties, 17: 14826(R) (LAR-14)
Cr–Ni–W, properties, 17: 14827(R) (LAR-17)
Cr–Ni–Zr, corrosion of, oxygen gradients in, 17: 6579
Cr–Ni–Zr, corrosion by water at 400°C, 17: 39656
Cr–Ni–Zr, corrosion by steam, 18: 41933 (TID-11295(3rd Ed.))
Cr–Ni–Zr, oxidation by superheated steam at 540°C, 18: 15663(R) (ANL-6808)
Cs–Ni–Pu, phase studies and properties of, bibliographic study of, 16: 32115 (KFK-105)
Cu–Au–Ni, gold-197 hyperfine structure coupling in, (E), 20: 39470(R) (ORNL-3924)
Cu–Au–Ni, Mössbauer isomer shift correlation with residual electrical resistance of, 17: 26453(R) (ORNL-3425(p.103-11))
Cu–Au–Ni, properties as brazing alloy for copper-to-stainless steel joints, 18: 2199 (NAA-SR-Memo-9088)
Cu–Fe–Ni, neutron scattering by, cross sections for magnetic, 18: 27990
Cu–Fe–Ni, radiation effects on, uniaxial anisotropy from low-temperature magnetic anneal of electron, (E), 20: 23789
Cu–Fe–Ni, separation of ruthenium from, by cation exchange, 16: 22270
Cu–Fe–Ni, yield stresses of, internal strain effects on, 20: 33889 (UCRL-16846)
Cu–Mn–Ni, corrosion by nitric acid, 17: 6192(T,R) (EURAEC-382)
Cu–Mn–Ni, corrosion by liquid sodium at 700 and 1200°F, 20: 9422 (NAA-SR-11326)
Cu–Mn–Ni, electric conductivity of constantan as function of temperature, 19: 11475 (NAA-SR-Memo-10366)
Cu–Ni, analysis for zinc by x-ray fluorescence methods, 19: 15373
Cu–Ni, analysis of cast, for impurities, 18: 2157(R) (BMI-1644(Del.))
Cu–Ni, atom segregation in, 17: 34557(R) (ORNL-3480(p.117-42))
Cu–Ni, brazing alloy for metallized alumina-to-niobium alloy seals, 19: 40980 (LA-3302)
Cu–Ni, catalytic properties for ethylene hydrogenation, effects of argon-ion bombardment and annealing, 17: 12186
Cu–Ni, catalytic properties for benzene hydrogenation, 19: 17417(R) (NYO-3217-1)
Cu–Ni, corrosion of, by acids and chloride salts in chemical plants, 16: 20983
Cu–Ni, corrosion by simulated N-reactor secondary water, 17: 37480 (HW-76358)
Cu–Ni, corrosion by sodium chloride solutions at 80°C, calculated, 18: 32089 (TID-20777(p.25-32))
Cu–Ni, crystal structure and phase studies, 17: 30985(R) (TID-19070)
Cu–Ni, deposition on carbon steel tubes in feedwater heaters, 17: 32509
Cu–Ni, diffusion of copper-64 and nickel-63 in, 18: 36024
Cu–Ni, diffusion in, activation energy and frequency factor for self-, 19: 40961
Cu–Ni, effects of decontaminating and descaling solution on metal loss on, 20: 21238 (NP-15928)
Cu–Ni, elastic constants of, relation to cohesion and stability of intermetallic phases, 18: 44228
Cu–Ni, electric conductivity and Hall constant of paramagnetic, 18: 14481(T) (AEC-tr-6344)
Cu–Ni, electric conductivity in magnetic fields at 4.2°K, 18: 32700
Cu–Ni, electron thermoemission at 500 to 1100°K, 17: 3583
Cu–Ni, equipment and techniques for TIG welding of reactor tubes of, 18: 14438
Cu–Ni, erosion by water at 70°F, effects of annealing on cavitation, 20: 29640 (NP-16048)
Cu–Ni, heat capacity of constantan at 0.15 to 4.2°K, 17: 35263(R) (UCRL-10706(p.1-110))
Cu–Ni, heat of mixing at 1200°C, 17: 35694 (NYO-4691)
Cu–Ni, oxidation of, selective, 17: 11135(T,R) (EURAEC-483)
Cu–Ni, oxidation of, growth of nickel oxide crystals in, 17: 39492(T,R) (EURAEC-726)
Cu–Ni, oxidation of crystalline, 18: 41366(R) (EURAEC-1129)
Cu–Ni, oxidation, electron microscopic studies of selective, 19: 7864(R) (EURAEC-1225(Pt.1))
Cu–Ni, parameters for tungsten arc welding of 2-inch pipes of, 19: 22928 (WERL-8844-7)
Cu–Ni, performance as catalyst for hydrogen reactions, 19: 2345
Cu–Ni, phase separation and vacancies in, 18: 14482(T) (AEC-tr-6347)
Cu–Ni, radiation effects on segregation in, neutron, 16: 33568
Cu–Ni, radiation effects on thermoelectric properties, 18: 32237
Cu–Ni, radiation effects on engineering properties of, 18: 32216 (A/CONF.28/P/242)
Cu–Ni, radiation effects on deformed quenched, isochronal annealing of neutron, 19: 1004(R) (ORNL-3676(p.125-56))
Cu–Ni, radiation effects on, 19: 11682
Cu–Ni, radiation effects on segregation in, 19: 37173 (ORNL-P-1448)
Cu–Ni, radiation effects on segregation in, fast-neutron, 20: 9576(R) (ORNL-3878)
Cu–Ni, radioinduced segregation in, rehomogenization kinetics of fast-neutron, 18: 24208
Cu–Ni, reactions of, with carbon dioxide, 16: 2993 (NP-10967)
Cu–Ni, stress corrosion cracking of Alloy 400 by wetted thermal insulation, 19: 46949 (CONF-650905-2)
Cu–Ni, tensile properties of, containing tungsten fibers, at high temperatures, 20: 25570 (N-65-35957)
Cu–Ni, tensile properties of composites of tungsten fibers and, 20: 31770
Cu–Ni, thermal capacity of, effects of magnetic order on, 20: 4320(R) (ORNL-3870, pp 70-4)
Cu–Ni, uses of lead–tin-coated Constantan as superconducting level gages, 18: 40442
Cu–Ni, vacancies in, quenched-in, 16: 12158
Cu–Ni, welded joints of, effects of multiple repairs and 400°F interpass temperature on, 19: 34655 (NP-15134)
Cu–Ni–Nb, fabrication and properties of impregnated, 18: 4270
Cu–Ni–Nb, phase studies on, 20: 29764
Cu–Ni–Ta, crystal structure, 19: 44718
Cu–Ni–Ta, fabrication and properties of impregnated, 18: 4270
Cu–Ni–Ta, phase studies, 19: 42874
Cu–Ni–Ta, phase studies, 20: 23725
Cu–Ni–Ta, phase studies on, 20: 29764
Cu–Ni–W, ductility and tensile properties of tungsten-base, 20: 43822
Cu–Ni–W, fabrication by sintering, 18: 30145(R) (AD-401528)
Cu–Ni–W, gamma attenuation in, from point sources, 16: 11122 (DC-59-12-229)
Cu–Ni–W, gamma reactions in, buildup factor studies of, 16: 10668 (DC-60-2-215)
Cu–Ni–W, gamma reactions in, point source data from, 16: 11123 (DC-60-4-108)
Cu–Ni–W, mechanical properties of liquid-phase sintered, 19: 37140
Cu–Ni–W, mechanical properties and microstructure of, 19: 44691 (NASA-TN-D-3015)
Cu–Ni–W, mechanical properties of sintered composites of tungsten-base, 20: 11291
Cu–Ni–W, properties of composite-type, 20: 29624(R) (TID-22970, pp 257-329)
Cu–Ni–W, sintering of tungsten-base, in presence of liquid phase, 20: 7544
Cu–Ni–Zn, analysis of, for cobalt by isotope dilution, 16: 5276
Cu–Ni–Zn, crystal structure of, neutron diffraction study of, 19: 32762

Cu–Ni–Zn, neutron diffraction study of long-range order in single-crystal, 19: 25026
Cu–Ni–W, sintering of, rearrangement shrinkage in liquid-phase, 20: 27465
Dy–Gd–Ni, magnetic coupling in Haucke and Laves phases in, 20: 27494(R) (NYO-3454-6)
Dy–Ni, crystal structure of equiatomic intermetallic compound in, 19: 24994
Dy–Ni, crystal structure of intermetallic compounds in, 20: 37243
Dy–Ni, dysprosium-161 Mössbauer effect in, (E), 20: 13992
Dy–Ni, dysprosium-161 isomer shift in, 20: 13992
Dy–Ni, dysprosium hyperfine magnetic field in intermetallic compounds of, (E), 20: 22330
Dy–Ni, hyperfine fields in intermetallic compounds of, temperature dependence of, 19: 42877
Dy–Ni, magnetic and structural characteristics of intermetallic compound of type LnNi in, 18: 37697
Dy–Ni, magnetic properties of, antiferromagnetic effects on, 16: 22624
Dy–Ni, magnetic properties, 19: 38049
Dy–Ni, magnetic properties of cubic Laves phase in, 19: 13399
Dy–Ni, magnetic properties of intermetallic compounds in, 20: 9511
Dy–Ni, oxidation by air at 500°C and water at 93 and 177°C, 17: 34330(R) (USBM-U-1057)
Dy–Ni, phase studies, 16: 17967(R) (USBM-U-887)
Dy–Ni, physical properties, (E), 19: 16188
Er–Ni, crystal structure of equiatomic intermetallic compound in, 19: 24994
Er–Ni, crystal structure of intermetallic compounds in, 20: 37243
Er–Ni, magnetic and structural characteristics of intermetallic compound of type LnNi in, 18: 37697
Er–Ni, magnetic properties of, antiferromagnetic effects on, 16: 22624
Er–Ni, magnetic properties of $ErNi_5$ at 4–300°K, 17: 37713
Er–Ni, magnetic properties of cubic Laves phase in, 19: 13399
Er–Ni, magnetic properties, 19: 38049
Er–Ni, magnetic properties of intermetallic compounds in, 20: 9511
Er–Ni, magnetic structure and transitions in, 17: 39714 (BNL-7325)
Er–Ni, oxidation by air at 400°C and water at 93 and 177°C, 17: 34330(R) (USBM-U-1057)
Er–Ni, phase studies, 16: 17967(R) (USBM-U-887)
Er–Ni, physical properties, (E), 19: 16188
Er–Ni, preparation for solid solubility studies, 19: 41021(R) (NMI-8002.1)
Eu–Ni, crystal structure of intermetallic compounds in, 20: 39415
Eu–Ni, fabrication of control rods of, 19: 28802(P)
Eu–Ni, magnetic properties, 20: 2369
Eu–Ni, preparation, hardness, and microstructure, 20: 2369
Fe–Mn–Ni, martensitic reaction nucleation rate in, 20: 29623(R) (TID-22970, pp 121-256)
Fe–Mn–Ni, phase studies of, martensitic transformation characteristics in, 16: 6750
Fe–Mn–Ni, preparation and tensile properties, 19: 17443(P)
Fe–Mn–Ni, structure of antiferromagnetic, 17: 22186
Fe–Mo–Ni, brazing to molybdenum, 17: 42401(R) (AD-296862)
Fe–Mo–Ni, corrosion of, by chloride solutions, 16: 23528(R) (ORNL-3290)
Fe–Mo–Ni, corrosion of, by molten fluoride salts, 16: 20974 (BMI-X-198)
Fe–Mo–Ni, corrosion of, under hydrofluorination conditions during dissolution of Zircaloy-2, 16: 5665 (BMI-X-184)
Fe–Mo–Ni, corrosion by fluorine and hydrofluoric acid, 17: 8740 (BMI-X-213)
Fe–Mo–Ni, corrosion by hydrofluoric acid, 17: 25720 (BMI-X-234)
Fe–Mo–Ni, corrosion by molten fluorides at 500°C, 17: 29279 (BMI-X-227)
Fe–Mo–Ni, corrosion by molten fluoride mixture at 650°C, 17: 34345 (BMI-X-247)
Fe–Mo–Ni, corrosion by molten fluoride mixture in hydrofluorinator at 500°C, 17: 36222 (BMI-X-253)
Fe–Mo–Ni, corrosion by Hy–Mu-80, by fluoride salt melts at 500 to 650°C, 17: 35251(R) (BMI-1632(Del.))
Fe–Mo–Ni, corrosion of Alloy 79-4, by dissolution-fluorination cycles during volatility single vessel studies, 17: 37292(R) (ORNL-TM-586)
Fe–Mo–Ni, corrosion in hydrofluorination processing of reactor fuels, 17: 39179(R) (ORNL-3452(p.26-50))
Fe–Mo–Ni, corrosion by liquid fluoride salts, 18: 2178 (BMI-X-260)
Fe–Mo–Ni, corrosion by potassium fluoride–zirconium fluoride under hydrofluorination conditions at 600°C, 18: 7985(R) (BMI-1650(Del.))
Fe–Mo–Ni, corrosion by fluorides in Fluoride Volatility Process, 18: 17351(R) (BMI-1659(Del.))
Fe–Mo–Ni, corrosion by fused salt fluoride volatility media, 18: 35641(R) (ORNL-TM-785)
Fe–Mo–Ni, corrosion by fluoride volatility process fused salts, 19: 2716(R) (BMI-1681(Del.))
Fe–Mo–Ni, corrosion of HyMu-80, by aluminum fluoride–potassium fluoride–uranium fluoride–zirconium fluoride system at 600°C, 19: 13871(R) (BMI-1691(Del.))
Fe–Mo–Ni, corrosion by metallic fluorides, effects of hydrogen fluoride on, 19: 18421(R) (BMI-1697(Del.))
Fe–Mo–Ni, diffusion of hydrogen in, effects of glass and oxide coatings on, 16: 2179 (NAA-SR-6109)
Fe–Mo–Ni, effects of ammonium fluoride–formic acid–nitric acid anodic solutions against corrosion of, 18: 35959
Fe–Mo–Ni, magnetic properties of thin film of, uniaxial anisotropic behavior, in, 16: 26644(R) (NP-11755)
Fe–Mo–Ni, magnetization directions in cold-worked, effects of mechanical and thermal history on, 18: 12678
Fe–Mo–Ni, neutron scattering by, cross sections for magnetic, 18: 27990
Fe–Mo–Ni, preparation and magnetic properties of films of, 18: 12676
Fe–Mo–Ni, magnetic properties of cube-textured sheets of, 18: 12677
Fe–Mo–Ni, radiation effects on corrosion of, by aqueous chlorides, 16: 14772 (ORNL-3265)
Fe–Mo–Ni, radiation effects on magnetic properties of, 17: 32692
Fe–Mo–Ni, radiation effects on magnetic properties of, proton, 17: 37701
Fe–Mo–Ni, radiation effects on magnetic properties of polycrystalline, electron, 18: 12744
Fe–Mo–Ni, radiation effects on domain orientation and magnetism of molybdenum Permalloy, 19: 23158
Fe–Mo–Ni, radiation effects on, uniaxial anisotropy from low-temperature magnetic anneal of electron, (E), 20: 23789
Fe–Mo–Ni, radioinduced magnetic annealing effects in, 19: 4722
Fe–Mo–Ni–Ru–W, properties at 1400 to 2000°F, 17: 14808(R) (ARF-2158-24)
Fe–Mo–Ni–Ti–W, joining to alumina ceramics by soldering, 19: 11699 (IPP-4/15)
Fe–Mo–Ni–V, effects of ammonium fluoride–formic acid–nitric acid anodic solutions against corrosion of, 18: 35959
Fe–Mo–Ni–W, coatings for, 17: 6563 (DC-61-7-6)
Fe–Ni, allotropic transformation in, 17: 10240(R) (NP-12208)
Fe–Ni, analysis of films of, for iron and nickel, 20: 14489
Fe–Ni, analysis of, for nickel by activation methods, 20: 45584
Fe–Ni, analysis of, for iron by activation methods, 20: 45584
Fe–Ni, anisotropic energy of electron-irradiated, 17: 11274
Fe–Ni, atomic magnetic moments and ordering in, 17: 37818
Fe–Ni, bonding of, to stainless steel and Zircaloy-2, 16: 30744 (CVNA-44)
Fe–Ni, bonding of, to Zircaloy-2 tubing, 16: 5021 (GNEC-176(Del.))
Fe–Ni, composition dependence of spin wave energies in, 18: 34187
Fe–Ni, corrosion by fluoride-volatility process solutions at 500°C, 17: 23864(R) (BMI-1619(Del.))
Fe–Ni, corrosion by hydrofluoric acid, 17: 25720 (BMI-X-234)
Fe–Ni, corrosion by molten fluorides at 500°C, 17: 29279 (BMI-X-227)
Fe–Ni, corrosion by molten fluoride mixture at 650°C, 17: 34345 (BMI-X-247)
Fe–Ni, corrosion by molten fluoride mixture in hydrofluorinator at 500°C, 17: 36222 (BMI-X-253)
Fe–Ni, corrosion in hydrofluorination processing of reactor fuels, 17: 39179(R) (ORNL-3452(p.26-50))
Fe–Ni, corrosion by liquid fluoride salts, 18: 2178 (BMI-X-260)
Fe–Ni, corrosion by potassium fluoride–zirconium fluoride under hydrofluorination conditions at 600°C, 18: 7985(R) (BMI-1650(Del.))
Fe–Ni, corrosion by cesium at 750°C, 18: 20873
Fe–Ni, corrosion of, book, 18: 22451
Fe–Ni, corrosion of, review, 19: 7868
Fe–Ni, density-of-states effects on magnetic stiffness of, (E/T), 19: 23969
Fe–Ni, deposition on graphite structures as reinforcement, 19: 32715(P)
Fe–Ni, diffusion of fission products in, effects of concentrations on, 20: 11212(R) (BMI-X-10143)
Fe–Ni, effects of alloying on strength of, 18: 24161
Fe–Ni, elastic wave generation from electromagnetic wave absorption and electron reactions on, 17: 37732
Fe–Ni, electric and thermal conductivity of, in magnetic fields at low temperatures, 17: 20475
Fe–Ni, electric conductivity of, effect of composition on, 19: 34675(R) (EURAEC-1394)
Fe–Ni, electrodeposition of Permalloy on wire, 19: 11657(R) (NYO-1480-2)
Fe–Ni, electron-positron annihilation in plastically deformed, 18: 37694
Fe–Ni, electronic specific heat, 17: 16698
Fe–Ni, fission product diffusion in irradiated, at 600 to 1200°C, 20: 21232 (BMI-1763)
Fe–Ni, flow stress at room temperature, relations with strain, 18: 18413(R) (EURAEC-975)
Fe–Ni, formation and structure of surface layers during corrosion of, 17: 22125
Fe–Ni, hyperfine structure of iron-57 spectra in, 17: 13236

Fe–Ni, iron-57 gamma absorption in, s-electron density from isomer shifts in spectra of, 17: 37777
Fe–Ni, magnetic and structural properties of sputtered films of, 18: 42040
Fe–Ni, magnetic diffusion of neutrons in disordered, 17: 20494
Fe–Ni, magnetic fields at iron nuclei in, 17: 13245
Fe–Ni, magnetic fields at iron-57 nuclei in, (E), 19: 20578
Fe–Ni, magnetic moment distribution in, measurement by neutron diffraction, 17: 20491
Fe–Ni, magnetic moment distributions in dilute, 17: 37694
Fe–Ni, magnetic moment distributions in, 17: 37822
Fe–Ni, magnetic moments of, neutron diffraction analysis of effects of copper, molybdenum, and silicon on, 18: 27990
Fe–Ni, magnetic properties of Ni_3Fe, use of alloying additives to modify, 17: 39526 (AERE-M-1282)
Fe–Ni, magnetic properties of neutron-bombardment-ordered single-crystal, 18: 12743
Fe–Ni, magnetic properties of electrodeposited Permalloy, 18: 27944 (AERE-R-4229)
Fe–Ni, magnetic properties of grain-oriented, 19: 23164(R) (SU-SEL-64-103)
Fe–Ni, magnetic studies of radiation effects on, 17: 456
Fe–Ni, martensite burst transformation in crystals of, 17: 3496 (UCRL-10415)
Fe–Ni, martensite formation in, 19: 40283 (COO-1198-237)
Fe–Ni, mechanical properties at 70 to 2000°F, 17: 18758 (NAA-SR-Memo-8052)
Fe–Ni, mechanical properties of, 19: 34675(R) (EURAEC-1394)
Fe–Ni, Mossbauer effect in, 17: 29627
Fe–Ni, Mössbauer effect studies of ordering in, 17: 36478
Fe–Ni, Mössbauer study of internal magnetic fields of, 18: 39940
Fe–Ni, Mössbauer effect in, 19: 38042
Fe–Ni, mutually induced x-ray fluorescence in, 18: 9038
Fe–Ni, neutron elastic scattering by, cross sections for, (E/T), 20: 26346 (NP-16010, pp 1-41)
Fe–Ni, neutron radiation effects on, 18: 32255
Fe–Ni, neutron scattering on magnetic, disorder effects from, 17: 37799
Fe–Ni, neutron scattering in, paramagnetic, (E), 20: 8303
Fe–Ni, neutron scattering by spin-waves in, angular distributions from, (T), 20: 36354 (AERE-R-4535)
Fe–Ni, order-disorder transitions in, 17: 37825
Fe–Ni, ordering in irradiated, (E), 19: 14055
Fe–Ni, overdriving effects on polymorphism dynamics in, 19: 20555 (LA-3215)
Fe–Ni, phase transformations in, hydrostatic pressure effects on, 16: 4550 (WADD-TR-60-893)
Fe–Ni, physical properties of, effects of molybdenum admixtures on, 18: 24159
Fe–Ni, preparation of single crystals of, 16: 3398 (PAN-245/I-B)
Fe–Ni, properties of, for application to 1200°F, 16: 10403 (ASD-TR-61-322(p.40-54))
Fe–Ni, properties of Invar at –400 to 100°F, 18: 42020 (PB-171809(Rev.))
Fe–Ni, properties for coating metals, 20: 43880
Fe–Ni, radiation effects on, 16: 33565
Fe–Ni, radiation effects on, magnetic measurements of, 16: 4588 (NP-10802)
Fe–Ni, radiation effects on, magnetic measurements of, 16: 13650
Fe–Ni, radiation effects on magnetic properties of, 16: 6824(R) (ORNL-3213(p.137-9))
Fe–Ni, radiation effects on structure of, neutron, 16: 16782
Fe–Ni, radiation effects on anisotropy and magnetism of, 16: 31380
Fe–Ni, radiation effects on electric resistance, 17: 597
Fe–Ni, radiation effects on magnetic properties of, 17: 32692
Fe–Ni, radiation effects on magnetic properties of, 17: 37621
Fe–Ni, radiation effects on, annealing of neutron, 18: 2327
Fe–Ni, radiation effects on electric conductivity of, neutron, 18: 5821
Fe–Ni, radiation effects on magnetic properties of, neutron, 18: 5822
Fe–Ni, radiation effects on magnetic properties of thin films of Permalloy, helium-3 and neutron, 18: 7333
Fe–Ni, radiation effects on magnetic properties of, neutron, 18: 36056
Fe–Ni, radiation damage in Permalloy magnetic films, 19: 14113
Fe–Ni, radiation effects on output pulses from, fast-neutron, 19: 13868
Fe–Ni, radiation effects on domain orientation and magnetism, 19: 23158
Fe–Ni, radiation effects on ferromagnetic properties of, 19: 22863(R) (AD-606809)
Fe–Ni, radiation effects on ferromagnetic resonance of thin films of, helium-3, 20: 12318
Fe–Ni, radiation effects on magnetic properties of single crystals of, neutron, (E), 20: 24649
Fe–Ni, radiation effects on diffusion stages and magnetic properties of, electron and neutron, 20: 33949
Fe–Ni, radioinduced order-disorder transitions, 17: 16701
Fe–Ni, radioinduced uniaxial anisotropy energy of films of, composition dependence of helium-3, (E), 20: 24668
Fe–Ni, radioinduced order-disorder transition in, neutron, 20: 44025
Fe–Ni, radioinduced defects in, retained by tempering, 20: 46945
Fe–Ni, reactions with Magnox alloy to 450°C, 19: 22997 (TRG-Report-842)
Fe–Ni, short-range ordering in, (E), 19: 43506
Fe–Ni, structures in shock-loaded, deformation and transformation, 20: 817 (CONF-710)
Fe–Ni, tensile properties at room temperature, 19: 30667(R) (COO-1319-24)
Fe–Ni, thermal diffusion of hydrogen in gamma-, at 400 to 600°C, 20: 2397
Fe–Ni, thermodynamic properties of oxygen in liquid, 20: 4454
Fe–Ni, use for brazing graphite to graphite, 17: 1913(P)
Fe–Ni, use of, in coolant-flow rotameters for water-cooled reactors, 16: 27393(P)
Fe–Ni, xenon-133 release from, at 400 to 1400°C, 17: 23946(R) (BMI-X-10039)
Fe–Ni–Pd–Ru–W, properties at 1400 to 2000°F, 17: 14808(R) (ARF-2158-24)
Fe–Ni–Pd–W, mechanical properties at room temperatures, 17: 14724(R) (ARF-2158-15)
Fe–Ni–Pt–Ru–W, effects of annealing on room-temperature properties of, 17: 14807(R) (ARF-2158-21)
Fe–Ni–Pt–Ru–W, properties at 1400 to 2000°F, 17: 14808(R) (ARF-2158-24)
Fe–Ni–Ru–Ta–W, properties at 1400 to 2000°F, 17: 14808(R) (ARF-2158-24)
Fe–Ni–Ru–W, mechanical properties at room temperature, 17: 14724(R) (ARF-2158-15)
Fe–Ni–Ru–W, properties at high temperatures, 17: 14806(R) (ARF-2158-18)
Fe–Ni–Ru–W, tensile properties, 17: 14805(R) (ARF-2158-12)
Fe–Ni–Sc, crystal structure of Laves phases in, 20: 41412(R) (IS-1500 (Sect. M))
Fe–Ni–Ti, performance as brazing alloy for graphite, 18: 37649 (A/CONF.28/P/432)
Fe–Ni–Ti, radiation effects on electric resistance, 17: 597
Fe–Ni–U, analysis for iron and uranium by controlled-potential coulometry, 20: 3879(R) (MLM-1266)
Fe–Ni–U, eutectic temperature and composition of, 16: 17297(R) (LAMS-2681)
Fe–Ni–W, deformation properties of dispersed and sintered composites of, elastic and plastic, 20: 29686
Fe–Ni–W, development for high-temperature uses, 17: 14805(R) (ARF-2158-18)
Fe–Ni–W, diffusion in sintered, 20: 865
Fe–Ni–W, ductility and tensile properties of tungsten-base, 20: 43822
Fe–Ni–W, ductility and strength of sintered composite, effects of tungsten content on, 20: 43885 (ASRL-TR-132-2)
Fe–Ni–W, fabrication of tungsten sheet bars by zone refining of, 19: 7884
Fe–Ni–W, mechanical properties of liquid-phase sintered, 19: 37140
Fe–Ni–W, mechanical properties of compacts of, 17: 1919 (ASRL-TR-94-4)
Fe–Ni–W, mechanical properties of, effects of strain rate on, 20: 11284 (UCRL-14599)
Fe–Ni–W, mechanical properties of sintered composites of tungsten-base, 20: 11291
Fe–Ni–W, oxidation at high temperatures, 17: 14806(R) (ARF-2158-18)
Fe–Ni–W, oxidation in air at 2000°F, effects of aluminum, ruthenium, and titanium additions, 17: 14724(R) (ARF-2158-15)
Fe–Ni–W, preparation of highly densified and machinable, 20: 25554(P)
Fe–Ni–W, properties at high temperatures, 17: 14807(R) (ARF-2158-21)
Fe–Ni–W, properties at high temperatures, 17: 14825(R) (LAR-12)
Fe–Ni–W, properties at high temperatures, 17: 14826(R) (LAR-14)
Fe–Ni–W, properties at high temperatures, 17: 14827(R) (LAR-17)
Fe–Ni–W, properties of sintered, 19: 7915
Fe–Ni–W, properties of composite-type, 20: 29624(R) (TID-22970, pp 257-329)
Fe–Ni–W, zone refining of cemented, production of tungsten sheet bars by, 20: 29688
Fe–Ni–W–Zr, oxidation in air at 2000°F, 17: 14724(R) (ARF-2158-15)
Fe–Ni–Zr, corrosion of, by deoxygenated steam, 17: 19720 (ANL-6698)
Fe–Ni–Zr, corrosion by steam at 540°C, 17: 35079(R) (ANL-6749)
Fe–Ni–Zr, corrosion by superheated steam, 17: 41333(R) (ANL-6677)
Fe–Ni–Zr, corrosion by oxygenated sodium at 540 and 650°C, 18: 19456(R) (ANL-6840)
Fe–Ni–Zr, corrosion by steam, 18: 41933 (TID-11295(3rd Ed.))
Fe–Ni–Zr, corrosion by superheated steam, 19: 14765(R) (ANL-6977)
Fe–Ni–Zr, corrosion by liquid metals, measurement of, 19: 17177(R) (ANL-6965(p.42-83))
Fe–Ni–Zr, corrosion by steam at 540°C, effects of alloy microstructure on, 19: 44616(R) (ANL-7000, pp 122-37)

Fe–Ni–Zr, corrosion by steam at 540°C, effects of pressure on, 19: 44616(R) (ANL-7000, pp 122-37)
Fe–Ni–Zr, oxidation by superheated steam at 540°C, 18: 15663(R) (ANL-6808)
Ga–Lu–Ni, crystal structure studies, 19: 44678(R) (ANL-7000, pp 186-200)
Ga–Ni, phase studies of nitrogen-containing, 16: 16768
Gd–Ho–Ni, magnetic coupling in Haucke and Laves phases in, 20: 27494(R) (NYO-3454-6)
Gd–Nd–Ni, magnetic coupling in Haucke and Laves phases in, 20: 27494(R) (NYO-3454-6)
Gd–Ni, crystal structure of equiatomic intermetallic compound in, 19: 24994
Gd–Ni, crystal structure of intermetallic compound $GdNi_3$ in, 20: 11308
Gd–Ni, crystal structure of intermetallic compounds in, 20: 37243
Gd–Ni, effect of annealing on coercive force of deformed, 17: 16716
Gd–Ni, fabrication and phase studies on, (E), 19: 16189
Gd–Ni, fabrication of control rods of, 19: 28802(P)
Gd–Ni, magnetic and structural characteristics of intermetallic compound of type LaNi in, 18: 37697
Gd–Ni, magnetic properties of, antiferromagnetic effects on, 16: 22624
Gd–Ni, magnetic properties of $GdNi_5$ at 4–300°K, 17: 37713
Gd–Ni, magnetic properties of cubic Laves phase in, 19: 13399
Gd–Ni, magnetic properties, 19: 38049
Gd–Ni, magnetic properties of intermetallic compounds in, 20: 9511
Gd–Ni, magnetic susceptibility of $GdNi_5$ at 4 to 300°K, 19: 30743(R) (NYO-3454-1)
Gd–Ni, oxidation by air at 450°C and water at 93 and 177°C, 17: 34330(R) (USBM-U-1057)
Gd–Ni, phase diagram, 17: 14740 (TID-11295(2nd Ed.))
Gd–Ni, phase diagram, 19: 6293
Gd–Ni, phase diagram, 16: 32060
Gd–Ni, phase studies, 16: 17967(R) (USBM-U-887)
Gd–Ni, physical properties, (E), 19: 16188
Gd–Ni, preparation for solid solubility studies, 19: 41021(R) (NMI-8002.1)
Ge–Hf–Ni, crystal structure of intermetallic compounds in, 20: 23726
Ge–Ni, phase studies, 16: 22595 (TID-15971)
Ge–Ni, phase studies of nitrogen-containing, 16: 16768
Ge–Ni–Sc, crystal structure, G phases in, 17: 14876
Ge–Ni–Ta, crystal structure of intermetallic compounds in, 20: 23726
Ge–Ni–Th, crystal structure of intermetallic compound $ThNi_2Ge_2$ in, 19: 23037
Hf–Ni, crystal structure of intermetallic compound $Ni_{16}Hf_7$ in, 16: 30787 (IS-257)
Hf–Ni, crystal structure of intermetallic compounds NiHf and $NiHf_3$ in, 16: 12122
Hf–Ni, crystal structure of intermetallic compounds, 20: 41412(R) (IS-1500(Sect. M))
Hf–Ni, magnetic properties of intermetallic compounds of, 20: 32699
Hf–Ni, magnetic susceptibility of $HfNi_5$ at 4 to 300°K, 19: 30743(R) (NYO-3454-1)
Hf–Ni, phase diagram, 16: 25819
Hf–Ni, phase diagram, 16: 10578
Hf–Ni, properties of, high-temperature, 18: 32214(P)
Hg–Ni, phase studies, 19: 36949(R) (BNL-900(p.121-97))
Hg–Ni, vapor pressures of intermetallic compounds in, 19: 23091
Hg–Ni–Zr, corrosive effects on titanium of mercury-based, 19: 44616(R) (ANL-7000, pp 122-37)
Ho–Nd–Ni, magnetic coupling in Haucke and Laves phases in, 20: 27494(R) (NYO-3454)
Ho–Ni, crystal structure of equiatomic intermetallic compound in, 19: 24994
Ho–Ni, crystal structure of intermetallic compounds in, 20: 37243
Ho–Ni, magnetic and structural characteristics of intermetallic compound of type LaNi in, 18: 37697
Ho–Ni, magnetic properties of, antiferromagnetic effects on, 16: 22624
Ho–Ni, magnetic properties of $HoNi_5$ at 4–300°K, 17: 37713
Ho–Ni, magnetic properties of cubic Laves phase in, 19: 13399
Ho–Ni, magnetic properties, 19: 38049
Ho–Ni, magnetic properties of intermetallic compounds in, 20: 9511
Ho–Ni, magnetic susceptibility of $HoNi_5$ at 4 to 300°K, 19: 30743(R) (NYO-3454-1)
In–Mg–Ni, crystal structure of $MgNi_2In$ in, 17: 20468
In–Ni, indium hyperfine magnetic field in, (E), 20: 17992
In–Ni, magnetic fields at indium nuclei in, hyperfine, 20: 22859(R) (UCRL-16580, pp 149-205)
In–Ni, phase studies of nitrogen-containing, 16: 16768
In–Ni–Ti, crystal structure of $TiNi_2In$ in, 17: 20468
Ir–Ni–U, crystal structure studies, 19: 44678(R) (ANL-7000, pp 186-200)
La–Ni, crystal structure of equiatomic intermetallic compound in, 19: 24994
La–Ni, magnetic properties of, antiferromagnetic effects on, 16: 22624
La–Ni, magnetic properties of intermetallic compounds of, 20: 32699
La–Ni, preparation for solid solubility studies, 19: 41021(R) (NMI-8002.1)
Li–Ni, oxidation of, effect of lithium on, 19: 30684
Li–Ni, phase studies, 20: 4442
Lu–Ni, crystal structure of equiatomic intermetallic compound in, 19: 24994
Lu–Ni, crystal structure of intermetallic compounds in, 20: 39415
Lu–Ni, magnetic properties of $LuNi_5$ at 4–300°K, 17: 37713
Lu–Ni, magnetic properties of $LuNi_5$, 20: 37279
Lu–Ni, preparation and structure of, 20: 2385(T)
Mg–Hg–Ni, corrosive effects on titanium of mercury-based, 19: 44616(R) (ANL-7000, pp 122-37)
Mg–Mn–Nd–Ni, effects of plastic deformation on properties and structure of, 18: 16495
Mg–Ni, analysis for magnesium, electrographic, 20: 267
Mg–Ni, crystal structure of nitrogen-containing, 16: 2259
Mg–Ni, distribution of praseodymium between magnesium chloride–potassium chloride–sodium chloride and, at 600°C, 19: 32279(R) (ANL-7020(p.3-99))
Mg–Ni, elastic constants of, relation to cohesion and stability of intermetallic phases, 18: 44228
Mg–Ni, heat resistance, mechanical properties, and recrystallization of, 18: 16496
Mg–Ni, production of splatcooled, 19: 41021(R) (NMI-8002.1)
Mg–Ni, solvent properties for rare earth elements in molten chloride salts, 20: 3865 (ANL-7064)
Mg–Ni, thermodynamics of compound formation in, from vapor pressure measurements, 16: 19353 (IS-440)
Mn–Ni, conduction electron momentum in, electron–positron annihilation studies, 17: 11275
Mn–Ni, crystal structure of, neutron diffraction studies on, 20: 39407(T) (ANL-Trans-344)
Mn–Ni, electron-positron annihilation contribution to electric conductivity of, 17: 29368
Mn–Ni, electronic specific heat, 17: 16698
Mn–Ni, fabrication of sintered foils of, for neutron dosimetry, 18: 41980 (PAN-496/XIV)
Mn–Ni, magnetic moment distributions in dilute, 17: 37694
Mn–Ni, magnetic structure from polarized neutron diffraction, 18: 37710
Mn–Ni, magnetic structure of, from polarized neutron scattering, 20: 20335
Mn–Ni, neutron elastic scattering by, cross sections for, (E/T), 20: 26346 (NP-16010, pp 1-41)
Mn–Ni, order-disorder transformations in, 17: 18824
Mn–Ni, phase studies, 20: 39407(T) (ANL-Trans-344)
Mn–Ni, phase transformations in, 17: 25783 (UCRL-7210)
Mn–Ni, polarized neutron diffraction for ferromagnetic moment per atom of $MnNi_5$, 17: 37527
Mn–Ni, radiation effects on atomic mobility and electric conductivity of, gamma, 18: 42138
Mn–Ni–Pd, use for braze bonding stainless steel cans to stainless steel–uranium dioxide cermets, 19: 4635
Mn–Ni–Sc, crystal structure of Laves phases in, 20: 41412(R) (IS-1500 (Sect. M))
Mn–Ni–U, eutectic temperature and composition of, 16: 17297(R) (LAMS-2681)
Mo–Ni, analysis of, for oxygen by sulfur monochloride method, 16: 14631(T) (UCRL-Trans-801(L))
Mo–Ni, atomic radii and interatomic distances in intermetallic compounds in, 18: 28029
Mo–Ni, atomic structure of, short-range order and size-effect coefficients for, (E), 20: 4421
Mo–Ni, brazing and welding, 18: 3298(R) (ORNL-2221(Pts.1-5)(Del.))
Mo–Ni, corrosion of, by acid, 16: 12057
Mo–Ni, corrosion by molten fluorides, 18: 3298(R) (ORNL-2221(Pts.1-5)(Del.))
Mo–Ni, corrosion in solvent extraction processes, 18: 8761
Mo–Ni, corrosion resistance and hardening mechanism of, 18: 18322
Mo–Ni, corrosion and oxidation resistance in fused salts, 18: 41968(P)
Mo–Ni, creep-rupture properties, 18: 3298(R) (ORNL-2221(Pts.1-5)(Del.))
Mo–Ni, crystal structure of, x-ray studies of short-range order of, 19: 25041
Mo–Ni, crystal structure stacking faults in, effects of rolling textures on, 19: 44723
Mo–Ni, phase studies at 500 to 1200°C, 20: 27556
Mo–Ni, development of, for ANP program, 16: 28646(R) (ORNL-2274 (Pts.1-5))
Mo–Ni, development of, for ANL program, 16: 28647(R) (ORNL-2340 (Pts.1-5))
Mo–Ni, development, 18: 3298(R) (ORNL-2221(Pts.1-5)(Del.))
Mo–Ni, diffusion in, effects of crystal deformation on, 16: 25831
Mo–Ni, electric conductivity of, effects of crystal structure on,

20: 41457(R) (ORO-3291-3)
Mo–Ni, fabrication by sintering, 18: 30145(R) (AD-401528)
Mo–Ni, intercrystalline corrosion by hydrochloric acid, 17: 34356
Mo–Ni, phase diagram, 18: 44194
Mo–Ni, short-range order in, x-ray diffuse-scattering determination of, (E), 20: 11325
Mo–Ni, specific heats of, methods of measuring, 20: 41457(R) (ORO-3291-3)
Mo–Ni, structure of, short-range order in atomic, 19: 28815(T) (ORNL-tr-632)
Mo–Ni, thermal capacity data and order-disorder reactions in, 20: 37278
Mo–Ni, thermal properties of, at high temperatures, 16: 4551 (WADD-TR-60-904)
Mo–Ni–Nb–Ta–Ti, corrosion resistance and ductility, 19: 34735(P)
Mo–Ni–Pt–Ru–W, properties at 1400 to 2000°F, 17: 14808(R) (ARF-2158-24)
Mo–Ni–Ru–W, properties at high temperatures, 17: 14807(R) (ARF-2158-21)
Mo–Ni–Ti–W, joining to alumina ceramics by soldering, 19: 11699 (IPP-4/15)
Mo–Ni–W, mechanical properties, effects of aging temperature and molybdenum and tungsten content on, 20: 5851
Mo–Ni–Zr, corrosion by pressurized water and workability of, 18: 20461
Mo–Ni–Zr, heat treatment effects on mechanical properties and workability of, 18: 20461
Mo–Ni–Zr, oxidation and mechanical properties, 17: 32621
Nd–Ni, crystal structure of equiatomic intermetallic compound in, 19: 24994
Nd–Ni, crystal structure of intermetallic compounds in, 20: 37243
Nd–Ni, magnetic and structural characteristics of intermetallic compound of type LnNi in, 18: 37697
Nd–Ni, magnetic properties of, antiferromagnetic effects on, 16: 22624
Nd–Ni, magnetic properties of $NdNi_5$ at 4–300°K, 17: 37713
Nd–Ni, magnetic properties of cubic Laves phase in, 19: 13399
Nd–Ni, magnetic properties, 19: 38049
Nd–Ni, magnetic properties of intermetallic compounds in, 20: 9511
Nd–Ni, magnetic susceptibility of $NdNi_5$ at 4 to 300°K, 19: 30743(R) (NYO-3454-1)
Ni–Ag, deposition on beryllium, 19: 13914 (CONF-729-4)
Ni–Ag, production of, by sintering at 470 to 1150°C, 17: 32497
Ni–Nb, corrosion of, by steam and water, 16: 29346
Ni–Nb, crystal structure of intermetallic compound $NbNi_3$ in, 19: 9699
Ni–Nb, diffusion in solid solutions of Ni_3Nb, tracer studies of, 19: 7916
Ni–Nb, mechanical properties at 1000°C, 19: 26859
Ni–Nb, mechanical properties and oxidation rate, 19: 32754
Ni–Nb, oxidation kinetics of, at 500 to 900°C, 19: 13929
Ni–Nb, oxidation kinetics at 500 to 900°C, 19: 20494
Ni–Nb, paramagnetic susceptibility and lattice parameters of solid solutions of, 18: 8848
Ni–Nb, phase diagrams, 20: 15115
Ni–Nb, phase studies, 19: 11682
Ni–Nb, phase studies, 19: 26859
Ni–Nb, properties, 19: 26848
Ni–Nb, structure of intermetallic compound NbNi in, 17: 1981(T)
Ni–Nb, vacuum-pressure braze cladding of, 18: 7177
Ni–Nb–Ru, crystal structure studies, 19: 44678(R) (ANL-7000, pp 186-200)
Ni–Nb–Ta, diffusion of nickel in, effects of annealing temperature and composition on, 20: 17089
Ni–Nb–Ta–Sn–Ti, corrosion resistance and ductility of, 19: 34735(P)
Ni–Nb–Ta–Ti, corrosion resistance and ductility of, 19: 34735(P)
Ni–Nb–Ta–Ti–W, corrosion resistance and ductility, 19: 34735(P)
Ni–Nb–Ta–Ti–V, corrosion resistance and ductility, 19: 34735(P)
Ni–Nb–Ti, phase diagrams of, ternary chemical compounds in, 20: 43971
Ni–Nb–V, corrosion of, by steam and water, 16: 29346
Ni–Nb–V, oxidation, 17: 6562(R) (ARF-B-6001-1)
Ni–Nb–W, solid-state bonding of, 18: 24112
Ni–Nb–Zr, hydrogen embrittlement of, review of, 20: 37187
Ni–Pd, activity coefficient of nickel in, 19: 13280(R) (TID-21569)
Ni–Pd, corrosion by cesium at 750°C, 18: 20873
Ni–Pd, corrosion in waste fixation in glass, 19: 33676 (ORNL-3640)
Ni–Pd, hydrogen additive effects on neutron magnetic scattering by, 17: 2217
Ni–Pd, magnetic properties at 90 to 1100°K, 20: 7585(T) (ANL-Trans-251)
Ni–Pd, neutron inelastic scattering, vibration defect modes in cold, 16: 15693
Ni–Pd, neutron magnetic scattering in hydrogenated, 19: 40075 (IEA-84)
Ni–Pd, neutron scattering cross sections, 16: 30781 (BNL-6263)
Ni–Pd, neutron transmission through magnetized, effects of absorbed hydrogen on, 16: 14001
Ni–Pd, phase studies at 800 to 1400°C, 20: 338
Ni–Pd, polarization of protons in, 17: 6945 (BNL-5648)
Ni–Pd, spectrum of, vibrational frequency, 16: 30781 (BNL-6263)
Ni–Pd–U, crystal structure studies, 19: 44678(R) (ANL-7000, pp 186-200)
Ni–Pd–W, mechanical properties at room temperatures and oxidation at 2000°F, 17: 14724(R) (ARF-2158-15)
Ni–Pr, crystal structure of equiatomic intermetallic compound in, 19: 24994
Ni–Pr, crystal structure of intermetallic compounds in, 20: 37243
Ni–Pr, effect of annealing on coercive force of deformed, 17: 16716
Ni–Pr, magnetic and structural characteristics of intermetallic compound of type LnNi in, 18: 37697
Ni–Pr, magnetic properties of, antiferromagnetic effects on, 16: 22624
Ni–Pr, magnetic properties of $PrNi_5$ at 4–300°K, 17: 37713
Ni–Pr, magnetic properties of cubic Laves phase in, 19: 13399
Ni–Pr, magnetic properties, 19: 38049
Ni–Pr, magnetic properties of intermetallic compounds in, 20: 9511
Ni–Pr, magnetic properties of intermetallic compounds of, 20: 32699
Ni–Pr, magnetic susceptibility of $PrNi_5$ at 4 to 300°K, 19: 30743(R) (NYO-3454-1)
Ni–Pr, magnetic susceptibility of $PrNi_2$ at 4 to 300°K, 19: 30743(R) (NYO-3454-1)
Ni–Pt, activity coefficient of nickel in, 19: 13280(R) (TID-21569)
Ni–Pt, phase studies at 800 to 1400°C, 20: 338
Ni–Pt–U, crystal structure studies, 19: 44678(R) (ANL-7000, pp 186-200)
Ni–Pu, phase diagram, 17: 4984
Ni–Pu, phase diagram, 17: 16567
Ni–Pu, phase studies and properties of, bibliographic study of, 16: 32115 (KFK-105)
Ni–Pu, phase studies, 19: 39163(R) (MLM-1244)
Ni–Pu, structural characteristics, 16: 7913
Ni–Pu, structure of intermetallic compounds in, 17: 3536
Ni–rare earth, crystal structure of intermetallic compounds in, 20: 37243
Ni–rare earth, magnetic and structural properties of intermetallic compounds of, 18: 8861
Ni–rare earth, magnetic properties and structure, 20: 4448
Ni–rare earths, magnetic properties of $LnNi_2$ series, 20: 37279
Ni–rare earth, magnetic susceptibility at 4 to 300°K of intermetallic, 19: 30743(R) (NYO-3454-1)
Ni–Re, electric and thermal properties at 293.3 to 1123.3°K, 18: 39967
Ni–Re, fabrication of sheets of high-purity, 19: 24955(R) (USBM-RC-1157)
Ni–Re, gold film adhesion to substrates of, vapor-deposited, 20: 27516
Ni–Re, nickel retention by molten, under high pressure, 19: 24955(R) (USBM-RC-1157)
Ni–Re, tensile properties of high-purity, 19: 24955(R) (USBM-RC-1157)
Ni–Re, use in tungsten to tungsten diffusion bonding, 20: 25553(P)
Ni–Rh–Ti, superconductivity, 18: 21112
Ni–Rh–U, crystal structure studies, 19: 44678(R) (ANL-7000, pp 186-200)
Ni–Ru, phase studies, 16: 12162
Ni–Ru–W, properties, 17: 14826(R) (LAR-14)
Ni–Ru–W, properties, 17: 14827(R) (LAR-17)
Ni–Sc, crystal structure, 17: 41333(R) (ANL-6677)
Ni–Sc, structure of intermetallic compounds ScNi and Sc_2Ni in, 17: 1988
Ni–Sc, structure of intermetallic compounds in, 19: 23011(T) (JPRS-28849(p.199-200))
Ni–Sm, crystal structure of equiatomic intermetallic compound in, 19: 24994
Ni–Sm, crystal structure of intermetallic compounds in, 20: 37243
Ni–Sm, fabrication of control rods of, 19: 28802(P)
Ni–Sm, magnetic and structural characteristics of intermetallic compound of type LnNi in, 18: 37697
Ni–Sm, magnetic properties of, antiferromagnetic effects on, 16: 22624
Ni–Sm, magnetic properties of $SmNi_5$ at 4–300°K, 17: 37713
Ni–Sm, magnetic properties of cubic Laves phase in, 19: 13399
Ni–Sm, magnetic properties, 19: 38049
Ni–Sm, magnetic properties of intermetallic compounds in, 20: 9511
Ni–Sm, oxidation by air at 500°C, 17: 34330(R) (USBM-U-1057)
Ni–Sm, physical properties, (E), 19: 16188
Ni–Sn, magnetic fields at tin nuclei in, 17: 13245
Ni–Sn, phase studies, 16: 22595 (TID-15971)
Ni–Sn, preparation of Ni_3Sn_4, 18: 2163(R) (IS-700(Sect.M))
Ni–Sn–Ti–Zr, corrosion by steam at 400°C, 19: 32696(R) (EURAEC-783)
Ni–Sn–Ti–Zr, fabrication by extrusion, 18: 22428(T,R) (EURAEC-838)
Ni–Sn–Ti–Zr, fabrication and properties, 19: 36965(T,R) (EURAEC-618)
Ni–Sn–Zr, corrosion by steam at 400°C, 18: 22428(T,R) (EURAEC-838)
Ni–Sn–Zr, corrosion by steam at 400°C, 19: 32696(R) (EURAEC-783)
Ni–Sn–Zr, fabrication and properties, 19: 36965(T,R) (EURAEC-618)
Ni–Sn–Zr, properties as cladding for fuel elements, 20: 25614(P)
Ni–Sn–Zr, thermal expansion of, to 1100°C, 19: 24982(R) (EURAEC-

1270)
Ni–Sr, phase studies, 20: 4442
Ni–Ta, atomic structure of, short-range order and size-effect coefficients for, (E), 20: 4421
Ni–Ta, crystal structure of intermetallic compound Ta_3Ni in, 16: 18078
Ni–Ta, crystal structure and electric and magnetic properties, 18: 32181
Ni–Ta, crystal structure of intermetallic compound $TaNi_3$ in, 19: 9699
Ni–Ta, crystal structure of intermetallic compound $TaNi_2$, 19: 16150
Ni–Ta, crystal structure of ordered intermediate phases, 19: 28817
Ni–Ta, crystal structure of $TaNi_2$, 19: 30787
Ni–Ta, crystal structure, 19: 44718
Ni–Ta, crystallization of, effects of fine precipitates on, 19: 16164
Ni–Ta, crystallization after cold rolling and heat treatments, 19: 37016
Ni–Ta, crystallization, 20: 11227
Ni–Ta, diffusion in solid solutions of Ni,Ta, tracer studies of, 19: 7916
Ni–Ta, effects of additives on high-temperature properties of eutectic, 20: 17108
Ni–Ta, electric conductivity of, anomalies in, 20: 31775
Ni–Ta, mechanical properties and microstructure of, effects of small additions of selected elements on, 20: 27550
Ni–Ta, phase diagram, 16: 18072
Ni–Ta, separation of Ni_2Ta compound from, 17: 34334(T) (UCRL-Trans-969)
Ni–Ta, structure of intermetallic compound TaNi in, 17: 1981(T)
Ni–Tb, crystal structure of intermetallic compounds in, 20: 37243
Ni–Tb, magnetic and structural characteristics of intermetallic compound of type LnNi in, 18: 37697
Ni–Tb, magnetic properties of, antiferromagnetic effects on, 16: 22624
Ni–Tb, magnetic properties of $TbNi_5$ at 4–300°K, 17: 37713
Ni–Tb, magnetic properties of cubic Laves phase in, 19: 13399
Ni–Tb, magnetic properties, 19: 38049
Ni–Tb, magnetic properties of intermetallic compounds in, 20: 9511
Ni–Tc, phase studies at 1050°C, 17: 41460
Ni–Th, corrosion by water at 120 to 260°C, 19: 22889 (ANL-7006)
Ni–Th, phase studies, 16: 30877
Ni–Th, phase studies, 19: 14044
Ni–Th, preparation by electrolysis of oxides in fluoride melts, 20: 27402 (BM-RI-6789)
Ni–Ti, alloying effects of, on physical metallurgy of cobalt alloys, 16: 29312 (DMIC-171)
Ni–Ti, corrosion resistance and hardening mechanism of, 18: 18322
Ni–Ti, crystal structure of Ti_2Ni, 17: 29362
Ni–Ti, crystal structure of Ti_3Ni, 17: 41333(R) (ANL-6677)
Ni–Ti, crystal structure of equi-atomic, model of, 20: 41412(R) (IS-1500(Sect. M))
Ni–Ti, deposition of coatings of, by plasma jet spraying, 17: 517 (NOTS-TP-2616)
Ni–Ti, diffusion of, in B–Ni system, 17: 6591 (ASD-TDR-62-734)
Ni–Ti, diffusion of, in C–Ni system, 17: 6591 (ASD-TDR-62-734)
Ni–Ti, effects of aluminum, cobalt, iron, silicon, and tungsten on properties of Nitinol, 20: 2310 (AD-618681)
Ni–Ti, electric conductivity of, at 1.1 to 35°K, maxima in, 16: 27818
Ni–Ti, magnetic resistivity of, at 1.1 to 4.2°K, negative-value non-existence in, 16: 27818
Ni–Ti, mechanical properties of intermetallic compounds in, effects of composition and structure on, 17: 541 (WADD-TR-60-184(Pt.III))
Ni–Ti, performance as metal-to-ceramic seals, 18: 29928(R) (NP-13979)
Ni–Ti, properties as brazing alloy for aluminum oxides, 18: 22548(R) (AD-414164)
Ni–Ti, sorptive properties for zirconium, tracer studies of, 20: 35912
Ni–Ti, welding by solid-state methods, 19: 22937
Ni–Ti–W, joining to alumina ceramics by soldering, 19: 11699 (IPP-4/15)
Ni–Ti–Zr, fabrication and properties, 19: 36965(T,R) (EURAEC-618)
Ni–Ti–Zr, tensile properties at room temperature, 18: 18380
Ni–Ti–Zr, thermal expansion of, to 1100°C, 19: 24982(R) (EURAEC-1270)
Ni–Tm, crystal structure of equiatomic intermetallic compound in, 19: 24994
Ni–Tm, crystal structure of intermetallic compounds in, 20: 39415
Ni–Tm, magnetic and structural characteristics of intermetallic compound of type LnNi in, 18: 37697
Ni–Tm, magnetic properties of $TmNi_5$ at 4–300°K, 17: 37713
Ni–Tm, magnetic properties of cubic Laves phase in, 19: 13399
Ni–Tm, magnetic properties of intermetallic compounds in, 20: 9511
Ni–Tm, magnetic susceptibility of $TmNi_5$ at 4 to 300°K, 19: 30743(R) (NYO-3454-1)
Ni–Tm, preparation and structure of $MgCu_2$-type, 20: 2385(T)
Ni–U, analysis for nickel, gravimetric, 18: 29558 (LA-3088)
Ni–U, atomic radii and interatomic distances in intermetallic compounds in, 18: 28029
Ni–U, diffusion in, effects of pressure on, 16: 27685 (CEA-1664)
Ni–U, diffusion in, activation energy for inter-, 20: 2328 (INR-625/XIV/R)
Ni–U, effects on preparation of uranium carbide by carbothermic reduction of oxide, 20: 33841 (NAA-SR-10624)
Ni–U, eutectic temperature in, 16: 17297(R) (LAMS-2681)
Ni–U, metallographic tests on arc melted, 20: 29775
Ni–U, neutron reactions with, secondary electron yields from fission fragments in, (E), 19: 12508
Ni–U, phase diagrams of, determination of, by solid-state diffusion, 16: 3496
Ni–U, phase diagrams of, determination of, by solid-state diffusion, 16: 22603(T) (HW-tr-37)
Ni–U, phase diagram, 17: 25786 (UCRL-13075)
Ni–U, phase studies, 17: 29255 (ZFK-WF-13)
Ni–U, phase studies, 17: 39620
Ni–U, phase studies, 17: 40153(R) (AD-290727)
Ni–U, phase transformation (β–α'), 17: 39626
Ni–U, production of splatcooled, 19: 41021(R) (NMI-8002.1)
Ni–U, secondary electron emission by fission fragments in, (E), 19: 17253(R) (AD-609177(Sect.F))
Ni–V, crystal structure of intermetallic compounds in, 19: 987
Ni–V, crystal structure of intermetallic compound VNi_3 in, 19: 9699
Ni–V, crystallographic parameters, 17: 18822
Ni–V, electronic specific heat, 17: 16698
Ni–V, hardness and oxidation properties, 17: 35997(R) (IITRE-B6001-5)
Ni–V, magnetic moment distributions in dilute, 17: 37694
Ni–V, neutron elastic scattering by, cross sections for, (E/T), 20: 26346 (NP-16010, pp 1-41)
Ni–W, analysis of, for oxygen by sulfur monochloride method, 16: 14631(T) (UCRL-Trans-801(L))
Ni–W, atomic structure of, short-range order and size-effect coefficients for, (E), 20: 4421
Ni–W, creep at 750 to 1200°C, effects of composition on, 19: 6342
Ni–W, creep properties at 750 to 1200°C, effects of tungsten content on, 20: 5851
Ni–W, creep properties at high temperatures, 20: 31669
Ni–W, crystal structure of, short-range order in, 20: 27557
Ni–W, diffusion of nickel-63 and tungsten-185 in, 18: 36025
Ni–W, diffusion in, activation energy and frequency factor for self-, 19: 40961
Ni–W, ductility at low temperatures, 18: 28028
Ni–W, effects of additives on high-temperature properties of eutectic, 20: 17108
Ni–W, fabrication by sintering, 18: 30145(R) (AD-401528)
Ni–W, mechanical properties of liquid-phase sintered, 19: 37140
Ni–W, mechanical properties and microstructure of, effects of small additions of selected elements on, 20: 27550
Ni–W, oxidation kinetics at 500 to 900°C, 20: 5854(T) (JPRS-32341, pp 8-16)
Ni–W, solid-state bonding of, 18: 24112
Ni–W, structure of, short-range order in atomic, 19: 28815(T) (ORNL-tr-632)
Ni–W, thermal capacity of, at 293 to 1100°K, 16: 12166
Ni–Y, crystal structure, 19: 9604(R) (IS-900(Sect.M))
Ni–Y, crystal structure of YNi, 19: 9677
Ni–Y, crystal structure of equiatomic intermetallic compound in, 19: 24994
Ni–Y, crystal structure, 20: 4297(R) (IS-1200(Sect.M))
Ni–Y, crystal structure of intermetallic compound YNi_3 in, 20: 7586
Ni–Y, crystal structure of intermetallic compound YNi_3 in, 20: 11308
Ni–Y, crystal structure of intermetallic compounds in, 20: 37243
Ni–Y, evaluation of, as coating for vanadium alloys, 16: 2168(R) (ARF-2227-2)
Ni–Y, gadolinium EPR in, 18: 33587
Ni–Y, magnetic and structural characteristics of intermetallic compound of type LnNi in, 18: 37697
Ni–Y, magnetic properties of, antiferromagnetic effects on, 16: 22624
Ni–Y, magnetic properties of YNi_5 at 4–300°K, 17: 37713
Ni–Y, magnetic properties of intermetallic compounds in, 20: 9511
Ni–Y, oxidation by air at 500 to 1400°C, 19: 2750
Ni–Y, oxidation of nickel-rich, effects of yttrium content on high-temperature, 20: 33812 (BM-RI-6800)
Ni–Y, phase diagram, 16: 2248
Ni–Y, phase studies and atmospheric corrosion, 16: 5315 (WADD-TR-61-123)
Ni–Y, production of splatcooled, 19: 41021(R) (NMI-8002.1)
Ni–Yb, atomic radii and interatomic distances in intermetallic compounds in, 18: 28029
Ni–Yb, magnetic properties of, antiferromagnetic effects on, 16: 22624
Ni–Zn, critical temperature of superconducting, transition metal impurity effects on depression of, (E), 20: 37955
Ni–Zn, crystal structure of nitrogen-containing, 16: 2259
Ni–Zn, diffusion of copper in, 18: 7994(R) (GTR-21)

Ni–Zn, phase studies of nitrogen-containing, 16: 16768
Ni–Zr, analysis for zirconium, electrographic, 20: 267
Ni–Zr, brittleness and fracture of, effects of hydrogen on, 19: 44716
Ni–Zr, corrosion by steam at 540°C, 17: 35079(R) (ANL-6749)
Ni–Zr, corrosion by steam at 400°C, 18: 24150(T,R) (EURAEC-538)
Ni–Zr, corrosion by steam at 400°C, hydrogen sorption during, 18: 34060(T,R) (EURAEC-1062)
Ni–Zr, corrosion films on, microprobe studies of, 19: 9621 (DP-906)
Ni–Zr, corrosion by superheated steam at 540 and 650°C, 19: 22899
Ni–Zr, corrosion by steam of, 19: 24982(R) (EURAEC-1270)
Ni–Zr, corrosion by steam, effects of aluminum, tin, or titanium on, 19: 24982(R) (EURAEC-1270)
Ni–Zr, corrosion by steam at 540°C, 19: 44616(R) (ANL-7000, pp 122-37)
Ni–Zr, crystal growth and structure of, 19: 22863(R) (AD-606809)
Ni–Zr, crystal structure, 16: 10570
Ni–Zr, crystal structure of intermetallic compound $Ni_{10}Zr_7$ in, 16: 30787 (IS-257)
Ni–Zr, crystal structures of intermetallic compounds NiZr and $NiZr_2$ in, 16: 12122
Ni–Zr, crystal structure of Brillouin zones in, effects of electron-atom ratios on, 19: 26836
Ni–Zr, crystal structure of intermetallic compounds, 20: 41412(R) (IS-1500(Sect. M))
Ni–Zr, effects of additives on high-temperature properties of eutectic, 20: 17108
Ni–Zr, electrochemical potential and hydrogen overvoltage, 17: 34403 (GEAP-4192)
Ni–Zr, embrittlement effects of hydrogen on, 18: 34169
Ni–Zr, extrusion of, effects on structure, 17: 6654(R) (EURAEC-394)
Ni–Zr, hardening of, by formation of intermetallic compounds, 19: 24982(R) (EURAEC-1270)
Ni–Zr, hardening of, by addition of aluminum, tin, or titanium, 19: 24982(R) (EURAEC-1270)
Ni–Zr, hydrogen overvoltage measurements in, 17: 27728(R) (GEAP-4076)
Ni–Zr, hydrogen overvoltage at Zr_2Ni in sulfuric acid, 18: 12642 (GEAP-4089(Vol.II)(Paper 22))
Ni–Zr, impact testing of, high-velocity, 20: 33490 (CONF-651026, pp 737-68)
Ni–Zr, magnetic susceptibility of $ZrNi_5$, at 4 to 300°K, 19: 30743(R) (NYO-3454-1)
Ni–Zr, mechanical properties of, 19: 24982(R) (EURAEC-1270)
Ni–Zr, mechanical properties and microstructure of, effects of small additions of selected elements on, 20: 27550
Ni–Zr, oxidation by oxygen at 700°C, 17: 41333(R) (ANL-6677)
Ni–Zr, oxidation kinetics at 500 to 900°C, 20: 5854(T) (JPRS-32341, pp 8-16)
Ni–Zr, oxidation kinetics and oxide film breakaway at 600 to 850°C, 20: 25497
Ni–Zr, phase diagram, 16: 10578
Ni–Zr, phase diagram, 16: 25819
Ni–Zr, phase studies, 17: 11204(T,R) (EURAEC-444)
Ni–Zr, phase studies, 17: 40153(R) (AD-290727)
Ni–Zr, phase studies and properties of extruded, effects of annealing, quenching, and tempering on, 18: 24150(T,R) (EURAEC-538)
Ni–Zr, reactions with hydrogen and structure of intermetallic compounds in, 16: 19356 (NAA-SR-7132)
Ni–Zr, reactions with hydrogen, thermochemical and structural aspects of, 20: 27436
Ni–Zr, resistance to scaling at elevated temperatures, 19: 32770(P)
Ni–Zr, sorptive properties for hydrogen, 19: 24982(R) (EURAEC-1270)
Ni–Zr, tensile properties, 19: 36965(T,R) (EURAEC-618)
Pb–Ni, molal volume of, at 800°C, 16: 12135
Pb–Ni, radiation effects on magnetization of, neutron, 20: 25628
Sb–Mn–Ni, antimony-121 and -123 NMR in ferromagnetic, (E/T), 19: 23663
Sb–Ni, structure of NiSb, effects of magnetic structure on, 18: 37115 (ANL-6856)

NICKEL ARSENIC SULFIDES
structural properties, 17: 14210 (NBS-MON-25(Sect.1))

NICKEL ARSENIDES
effects on separation of uranium from ore concentrates by solvent extraction using TBP, 17: 16144 (NLCO-867)
structure, effects of magnetic moments on, 18: 37115 (ANL-6856)
use of powdered, to promote phase separation in liquid-liquid extraction process, 19: 36571(P)

NICKEL BORIDES
crystal structure and composition of ternary, 19: 7447
preparation and magnetic properties, 16: 13567 (ARL-66)
stability and structure of, 17: 8083
structural characteristics, 16: 7913
surface tension of molten, 19: 47021(T) (JPRS-31225)
Ni–Ni_3B, development of fiber-reinforced composites of, 20: 2219 (AMRA-CR-64-05/4)

NICKEL BROMATES
thermal decomposition of, search for perbromate in, 19: 36402

NICKEL BROMIDES
additive effects on electric conductivity and density of fused alkali metal nitrate systems, 18: 8334 (TID-19997)
bromine-81 quadrupole bonding and resonance in solid layer type, 16: 7538
electron energy losses in, and mechanisms of, 17: 13165
fission fragment tracks in, water vapor etching of, 18: 18437
solution spectra extinction coefficients and peak positions for tetrahedral complexes in organic-salt melts, 18: 3713(R) (ORNL-3470 (p.11-15))
vaporization of, 17: 2956 (UCRL-9840)
CsBr–$NiBr_2$, spectra of nickel(II) in melts of, absorption, 20: 3921(R) (ORNL-3870, pp 56-60)
LiBr–$NiBr_2$, spectra of nickel(II) in melts of, absorption, 20: 3921(R) (ORNL-3870, pp 56-60)
$NiBr_2$–KBr, spectra of nickel(II) in melts of, absorption, 20: 3921(R) (ORNL-3870, pp 56-60)

NICKEL CARBIDES
reactions and properties of low-temperature produced, 16: 13019(T) (AEC-tr-5021)
BC–NiC, corrosion by water at high temperatures, 16: 24107 (GEAP-3831)
BC–NiC, radiation effects on properties of, 16: 24107 (GEAP-3831)
NiC–TiC, emissivity of, measurements of, 17: 16787(R) (PWA-2163)

NICKEL CARBONATES
neutron elastic and inelastic scattering by, cross sections and polarization of, 18: 42320(T)
structural properties, 17: 14210 (NBS-MON-25(Sect.1))

NICKEL CARBONYLS
carbon and oxygen isotope exchange in, 16: 29295(R) (NYO-8771)
complexes with cyclic phosphite esters, 20: 1561 (IS-T-31)
decomposition in ion source of mass spectrometer, mechanism of, 20: 14584(R) (TID-22444)
determination in carbon dioxide and carbon monoxide, 17: 30473 (PG-Report-483)
effects on radiolysis of benzene and benzene–cyclohexane mixtures, 19: 32226
exchange reactions with carbon monoxide, 17: 8052
metabolism in rats, tracer study, 20: 40536(R) (ORO-3461-1)
poisoning in man, use of dithiocarb for therapy of, 20: 40536(R) (ORO-3461-1)
radiation effects on reactions of, with cyclohexane, 18: 13893
radiolysis, 17: 39145
radiolysis of gases from, magnetic susceptibility measurements of, 17: 36347(R) (NARF-62-18P)
spectra of, appearance potentials and fragmentation of ions in, 20: 8882 (IS-983)
toxicity in rats, 20: 40536(R) (ORO-3461-1)
toxicology of, bibliography on, 20: 45285 (ORO-3461-8a)
use of, in preparation of nickel deposits, 20: 7551 (BDX-613-77)
cyclohexane–nickel carbonyl, radiation effects on, gamma, 18: 39353

NICKEL CATALYSTS
activity in isotope exchange reaction of *p*-xylene with deuterium oxide, 16: 22080
deuterium exchange with water on, in alkaline solution, 18: 227
effects of Raney, on isomerization of deuterated ethylbenzene and toluene, 19: 28348
effects on deuterium exchange between heavy water and propene, 18: 27369
exchange between deuterium and hydrogen on clean surfaces, 16: 11649
preparation of Raney, 20: 3974 (ORNL-TM-1314)
properties for recombination of radiolytic hydrogen and oxygen in steam at 560 to 860°F, 18: 35497(R) (GNEC-354)
properties in tritium exchange between hydrogen and steam, 18: 10081
radiation effects on activity, beta, 16: 13109
radiation effects on hydrogenation of propene by, 17: 16084
radiation effects on activity and sorptive properties of, gamma and neutron, 17: 27483
radiation effects on activity of, beta and x, 19: 36521(P)
role in reaction of ethylene with hydrogen, 17: 30154
sorptive properties for cyclohexene, hydrogen sulfide, and methyl sulfide, 16: 31597
uses in hydrogenation, tracer studies of product contamination by, 20: 1889

NICKEL CHLORIDES
corrosive effects on stainless steels under stress, mechanism of, 16: 30733 (ARF-2181-12)
corrosive effects on austenitic stainless steel, 19: 22893 (DP-957)
decomposition of, tracer study of thermal, 19: 26917(R) (IA-984)
effects on copper corrosion by mineral acids, 16: 484(R) (AD-256309)

effects on electric conductivity and density of fused alkali metal nitrate systems, 18: 8334 (TID-19997)
effects on radioinduced graft polymerization of rayon to styrene, 18: 285
effects on radiolysis of ethanol and methanol, 20: 7150
effects on sintering of tungsten, 20: 21291 (NP-15944)
electron energy losses in, and mechanisms of, 17: 13165
fission fragment tracks in, water vapor etching of, 18: 18437
free energy of formation at 400 and 450°C, 19: 38575 (BNL-9343)
hexammine, recoil chemistry of cobalt-57 in annealed, 19: 11208
hydrogen ion tunneling in nickel chloride hexammines, 18: 35558
metabolism in rats, tracer study, 20: 40536(R) (ORO-3461-1)
positron annihilation in, origin of second lifetime component from, (E), 20: 19486
potentials of nickel electrodes in, 16: 25322 (TID-16292)
radioinduced damage to lattices of, fission-fragment, 18: 32253
reactions with isopropylamine, thermogravimetric study of, 20: 36853
separation by reversed-phase partition chromatography using organophosphorus compounds, 18: 25614
separation from salt mixtures by extraction chromatography using organic phosphorus compounds, 20: 10759 (INP-427/C)
solution spectra extinction coefficients and peak positions for tetrahedral complexes in organic-salt melts, 18: 3713(R) (ORNL-3470 (p.11-15))
spectra of nickel(II) in mixtures of tri-n-butyl-benzylphosphonium chloride and, absorption, 20: 3921(R) (ORNL-3870, pp 56-60)
spectra of 3d orbital transitions in tetrahedral $NiCl_4^{-2}$ in molten salts, spin-allowed, 18: 3713(R) (ORNL-3470(p.11-15))
thermal decomposition mechanisms, 19: 39265(R) (IA-1021)
vaporization of, 17: 2956 (UCRL-9840)
benzyltributylphosphonium chloride–$NiCl_2$, density equations for molten, 20: 3921(R) (ORNL-3870, pp 56-60)
CsCl–$NiCl_2$, density equations for molten, 20: 3921(R) (ORNL-3870, pp 56-60)
CsCl–$NiCl_2$, phase diagram, 16: 7561
CsCl–$NiCl_2$, spectra of nickel(II) in melts of, absorption, 20: 3921(R) (ORNL-3870, pp 56-60)
LiCl–$NiCl_2$, spectra of nickel(II) in melts of, absorption, 20: 3921(R) (ORNL-3870, pp 56-60)
$MgCl_2$–$NiCl_2$, spectra of nickel(II) in melts of, absorption, 20: 3921(R) (ORNL-3870, pp 56-60)
$NiCl_2$–KCl, spectra of nickel(II) in melts of, absorption, 20: 3921(R) (ORNL-3870, pp 56-60)
$NiCl_2$–NaCl, spectra of nickel(II) in melts of, absorption, 20: 3921(R) (ORNL-3870, pp 56-60)
$NiCl_2$–RbCl, spectra of nickel(II) in melts of, absorption, 20: 3921(R) (ORNL-3870, pp 56-60)
Ni–$NiCl_2$, free energy of solutions of, 19: 11103

NICKEL COMPLEXES

bis(maleonitriledithiolato), molecular structure of, 19: 23355(R) (BNL-867(p.1-117))
formation of, optimum conditions for, 19: 13374
formation of, thermodynamics and kinetics of, 18: 17717(R) (TID-20438)
magnetic interactions in, 20: 3863(R) (IS-1200(Sect. C))
separation of porphyrin, from oil solutions, 18: 5405(P)
tetracyano, gamma reactions (γ,n) and (γ,p) with nickel-58 in, chemical species from, 20: 45748
with adenosine triphosphate, infrared spectra of, in heavy water, 19: 5936
with adenosine triphosphate, stability constants of, 16: 7556
with adenosinephosphoric acids, stability constants of, 16: 28948
with α,β,γ,δ-tetraphenylporphine, Szilard-Chalmers recoil reactions in, 19: 15647
with α, β, γ, δ-tetraphenylporphines, retentions in Szilard-Chalmers (n,γ) recoil reactions in, 19: 40612
with aminoacetone-*N*,*N*-diacetic acid, dissociation and stability constants of, 18: 19946
with ammonia, chloride, sulfate, and thiocyanate, nuclear magnetic resonance studies of ligand exchange rates in, 19: 352 (UCRL-11584)
with ammonia, radiolysis of, 18: 10169
with cupferron, thermal dissociation, 19: 7366
with diacetamide, properties and spectra of, 20: 8494 (TID-22449)
with dialkyl phosphoric acids, preparation and properties, 18: 25429
with dimethylglyoxime, infrared spectra of, 20: 40796(R) (IS-1500 (Sect.C))
with EDTA, bonding and structure of, 17: 33896
with EDTA, destruction by oxidation, 19: 32047 (KFK-287)
with EDTA, radiation effects on stability, 19: 30250
with ethylenediaminetetraacetic acid, radioprotective effects of, in mice, 18: 13567
with glycolic acid, binding energy of, infrared spectrophotometric study of, 19: 44004
with hydronaphthazarin, preparation, composition, and thermal stability, 19: 5882
with mercaptohydroquinone and 4-mercaptoresorcinol, stability of, 19: 26237
with mercaptosuccinic acid and 2,3-dimercaptosuccinic acid, formation and properties of, 18: 8394 (TID-20013)
with phosphoorganic compounds in TTA and 2,4-pentanediones, synergism in, 20: 261
with substituted 2-(pyridyl)- and 2-(quinolyl)-1,3-indanediones, acid dissociation and formation constants of, 18: 25457
with tetraphenylporphine in dioxane, gamma radiolysis of, 20: 36889
with thenoylacetone and TTA, formation constants of, 19: 30215
with triethylenetetraaminehexaacetic acid, formation constants of, 18: 8396 (TID-20015)
with urea, spectral analysis, 16: 13012(R) (TID-15227)
with 1,3-bis(2'-pyridyl)-1,2-diazaprop-2-ene, spectra, 17: 33816
with 1-substituted tetrazoles, 19: 15417 (TID-19078)
with 2-methyl-4,6-heptanedione, stability constants of, 19: 11056(T) (AEC-tr-6227/3(p.183-92))
with 7-anilinobenzyl-8-quinolinol, solubility constants, 16: 5344
with 8-quinolinols, luminescence yields of, 20: 10456 (COO-773-3)

NICKEL(II) COMPLEXES

hydrogen ion tunneling in nickel chloride hexammines, 18: 35558
isotropic shifts of ionic, evidence for ion pairing in, 19: 2298
monoacetylacetonato, kinetics of formation of, 19: 19445(R) (TID-21660)
oxidation of 4-carboxy-1,2-cyclohexanedionedioxime, in alkaline media, 17: 4506
spectra of, assignment of ligand-field, 17: 6115 (NYO-9868)
spectrum of tetrahedral $NiCl_4^{=}$ in molten salts, 17: 18044
with acetylacetone, solvent effects on formation of, 19: 19445(R) (TID-21660)
with carbamic acid, synthesis, 16: 6425
with diethylenetriaminepentaacetic acid, preparation, properties, and structure, 16: 11610
with ethylenimine, properties, 16: 17708(R) (TID-14812)
with halide ions in fused alkali metal nitrate systems, formation of, 18: 8335 (TID-19998)
with hexamethylphosphoramide, NMR contact shifts in, 20: 12828 (TID-21587)
with methanol, isotopic dilution studies on, 17: 2948(R) (TID-17216)
with *N*-(2-pyridylmethyl)iminodiacetic acid, stability of, 17: 15993
with naphthazarin, composition and thermal stability, 16: 18893
with oximes, solubility and stability of, 17: 6114 (IS-434)
with salicylaldehyde and its derivatives, magnetic moments of, 20: 36823
with tetraethylenepentamine and triethylenetetramine, dissociation and formation of, 17: 32067
with tetraethylenepentamine and triethylenetetramine, exchange reactions with nickel-63 ions, 17: 32067
with thiocyanate, spectrophotometric analysis of, 19: 15571(R) (TID-21385)
with triethylenetetramine, kinetics of exchange reactions with ethylenediaminetetraacetic acid–cuprate(II), 16: 32978
with 1-(2-pyridylazo)-2-naphthol, formation constants and distribution equilibria of, 17: 14381
with 2,4-pentanedione, stability constants in mixed solvents, 19: 26295 (TID-21811)
with 2,4-pentanedione, kinetics of formation of, 19: 36343(R) (TID-21847)
with 2,4-pentanedione, solvent effects on formation of, 19: 36343(R) (TID-21847)

NICKEL COMPOUNDS

crystallography of, with perovskite-like structure, 19: 25014
cyclopentadienyl, decomposition in ion source of mass spectrometer, 20: 14584(R) (TID-22444)
preparation and properties of bis-(β-diketone) polymers, 17: 12188
radiation chemistry of aqueous ammoniate, 16: 11712
thermal decomposition of, application of activated complex theory to, 18: 36900 (UCRL-10791)

NICKEL COUPLES

Invar/Ni, tensile properties of, testing, (E), 19: 20554 (La-3161)
Al/Ni, corrosion by water at 50°C, 20: 43824 (ANL-6236)
Al/Ni, diffusion of xenon in, 16: 29368 (BNL-5113)
Al/Ni/U, diffusion kinetics, 18: 5733 (NAA-SR-8387)
Al/Ni/U, diffusion in, metallographic study of, 16: 9175
Au/Ni/Rh, use for electric contacts in rotary switches, 19: 35871 (SC-DC-64-2086)
Cu/Ni, hot pressing effects on, at 2 to 12 ksi and 1000°F, 16: 4450(R) (BMI-1546(Del.))
Mo/Ni/Nb/stainless steel, diffusion in bimetallic tubing of, with molybdenum and nickel diffusion barriers, inter-, 20: 11215(R) (NASA-CR-54718)
Mo/Ni/Nb–Zr/stainless steel, diffusion in bimetallic tubing of, with molybdenum and nickel diffusion barriers, inter-, 20: 11215(R) (NASA-CR-54718)

Mo/Ni/stainless steel/Ta, diffusion in bimetallic tubing of, with molybdenum and nickel diffusion barriers, inter-, 20: 11215(R) (NASA-CR-54718)
Ni/U, diffusion in, effects of pressure on, 16: 27685 (CEA-1664)
Pb/Ni, superconductivity of film, ferromagnetic effects on, (T), 19: 45197

NICKEL CYANIDE COMPLEXES
chemical properties of, 16: 30930(R) (NYO-2669)
formation and stability in molten salts, 19: 32122(R) (NYO-2747-3)

NICKEL CYANIDES
properties for precipitation of cesium from sea water, 17: 30726

NICKEL DEUTERIDES
phase studies, 20: 45635

NICKEL FERRATES (III)
demagnetization under shock compression and heating, (E), 19: 30848(R) (UCRL-12473(p.31-63))
magnetic fields in, Mössbauer study of effective, 19: 38026 (INP-407/PL)
magnetic properties of, shock effects on, 20: 4708(R) (UCRL-14360, pp 50-73)
paramagnetism of, Mössbauer observation of, (E), 19: 28339
preparation and magnetic properties, 16: 13567 (ARL-66)

NICKEL FERROCYANIDES
ion exchange properties for cesium, 18: 27331

NICKEL FLUOANTIMONATES
preparation, 19: 26917(R) (IA-984)

NICKEL FLUOBORATES
complexes with pyridine, preparation and properties of, 20: 14225 (TID-21577)

NICKEL FLUORIDES
see also Potassium Nickel Fluorides
additive effects on electric conductivity and density of fused alkali metal nitrate systems, 18: 8334 (TID-19997)
effects on freezing point depressions in sodium fluoride, 17: 37213
enthalpy of formation of, 20: 31213(R) (ANL-7175, pp 119-58)
free energy of formation, 19: 36216(R) (BNL-900(p.29-72))
heat of sublimation and vapor pressure of, 20: 26874
preparation and thermodynamic properties, 18: 3671(R) (BNL-799(p.26-54))
reduction by hydrogen in molten fluoride systems, 18: 3298(R) (ORNL-2221(Pts.1-5)(Del.))
solution spectra measurements in alkali metal fluoride salt melts, 18: 3713(R) (ORNL-3470(p.11-15))
spectrum in molten lithium fluoride–potassium fluoride–sodium fluoride eutectic, 19: 9096 (ORNL-P-403)
thermodynamic properties of, emf measurements of, 20: 29215
vapor pressure at 1077 to 1283°C, 19: 36384
vaporization of, 17: 2956 (UCRL-9840)
NiF_2–KF, anodic overvoltages of nickel electrodes in molten eutectic, 20: 284 (EUR-804.e)

NICKEL FLUOSILICATES
nuclear magnetic resonance of fluorine and protons in, at 0.15 to 4.2°K, 18: 34275 (NP-14114)

NICKEL HYDRIDES
disintegration at high pressures, 17: 8831
enthalpy of formation of normal and deuterated, 20: 26826
formation of face centered cubic, 16: 1796
properties and structure, 17: 28830 (TID-18985)
spectra of deuterated and normal, rotational analysis of violet bands of, 19: 28294
spectra of normal and deuterated, bands in the violet region of, 18: 1655

NICKEL HYDROXIDES
dehydration, emanation during, 16: 31661
radiation effects on electric conductivity of, neutron, 20: 29821
tritium exchange with water, 16: 31367

NICKEL IODIDES
iodine-127 quadrupole bonding and resonance in solid layer type, 16: 7538
solution spectra extinction coefficients and peak positions for tetrahedral complexes in organic-salt melts, 18: 3713(R) (ORNL-3470 (p.11-15))
vaporization of, 17: 2956 (UCRL-9840)

NICKEL IONS
chromatography on acetylated filter paper, 16: 6379
complexing of divalent, in molten dimethylsulfone, 18: 3713(R) (ORNL-3470(p.11-15))
coordination in lithium fluoride–potassium fluoride–sodium fluoride melt, 18: 12077
effects of monovalent, in irradiated lithium and sodium fluorides, 19: 457
effects on cobalt determination in steel, 20: 43145
effects on copper determination, 20: 36726
effects on crystalline electric fields, method for calculating, 20: 5006(R) (ORNL-3870, pp 50-5)
effects on hydrolysis of α-D-glucose 1-phosphate, 20: 16421
effects on hydrolysis of polyphosphates, 20: 29152
effects on nuclear resonance in potassium compounds, 16: 31538
effects on oxidation of carbon, catalytic, 19: 28302
effects on radiolysis of methanol, 19: 9216
effects on spectrophotometric determination of erbium, holmium, and neodymium, 20: 43100
electrogeneration and application to coulometric titrations, 18: 8315
electron paramagnetic resonance spectra of, in strontium titanate, 18: 2467
electron paramagnetic resonance spectrum of divalent, in calcium oxide single crystals, 18: 2468
electron spin resonance spectra in calcium oxide crystals, 18: 9752 (IA-900)
electrotransport in chromium–nickel alloys, effects chromium concentration on, 16: 3487
energies in high-speed plasma beams in vacuum arcs, 18: 40708
exchange reactions with water in aqueous complexes, oxygen-17 nuclear magnetic resonance studies of, 18: 31431(R) (UCRL-11317(p.1-14))
magnetic form factor for divalent, in nickelous oxide, 16: 32980
magnetic properties of divalent, in nickel fluosilicate, 16: 15443
methanol exchange between solvent and solvated, 19: 11105
paramagnetic resonance in double-nitrate crystals, 16: 20412
photopolarographic reduction, uv, 20: 12798
polarography in nitrate melt, oscillographic, 19: 2271 (EUR-1908.e)
production of beams of, in magnetron gas discharges, 18: 7417
radioinduced reduction of, in irradiated aqueous sulfate glasses at 77°K, 20: 33378
radiolysis of aqueous solutions of, pulse, 19: 38728
radioprotective effects in mice, 18: 13567
reactions of divalent, with methanol, isotopic dilution studies on, 17: 2948(R) (TID-17216)
reactions with acetylacetone, kinetics, 19: 19445(R) (TID-21660)
reactions with permanganate ions during pulse-radiolysis of solutions, 20: 10914
reactions with potassium niobates, 18: 1664
reactions with 2,4-pentanedione in 2-propanol–water, thermodynamics of, 20: 16416(R) (NYO-906-68)
recoil ranges of, in alpha reactions with nickel-58, 18: 22869 (CONF-481-48)
reduction at boron carbide electrodes in voltammetry, 19: 24409
reduction in liquid fluorides, electrochemical, 18: 43445 (ORNL-P-324)
reflectance effects on zirconium oxide, 18: 14722(R) (TID-20233)
separation by thin-layer ionophoresis, 18: 10185
separation from titanium using vanillin, 19: 333
Slater-Condon parameters of, determined from spectral data, 17: 31118
solvent extraction from molten nitrate by liquid silicone–TBP at 150°C, 19: 19833 (CEA-R-2628)
sorption by aminodiacetate resin Dowex A-1, 20: 16358
sorption from perchloric acid solutions by cellulose and acid resin sulfonic acid exchangers, 18: 35473
spectra of divalent, in alkali halide melts, absorption, 20: 3921(R) (ORNL-3870, pp 56-60)
spectra of zero-field splitting in, 17: 37754
spectra of, in nickel glass after reduction, 20: 13260(R) (NP-15852)
stability constants and structure, effects of ligand fields, 17: 28911
toxicity of, in mouse, determination by LD_{50} on thirtieth day of, 17: 17719

Nickel Iron Nitrides
see Iron Nickel Nitrides

NICKEL ISOTOPES
alpha inelastic scattering at 44 Mev, 18: 36700
alpha inelastic scattering by even-even, 18: 40608
alpha inelastic scattering at 25 to 100 Mev, phase shift in, (T), 19: 43312
alpha reactions (α,p) at 42 Mev, (E), 19: 8487
approximation model for, quasiparticle, 18: 19073
binding energies of even-even, calculations using shell model with reaction matrix, (T), 20: 38066
carbon-12 reactions with, neutrons from, 17: 9593
charged particle reactions with, tabulations of cross sections for, (E), 19: 14534 (ORNL-CPX-2)
collective motions in, effects of spin-dependent forces on, 16: 23093
deuteron elastic scattering and reactions, cross sections for, 17: 29575 (PAN-242)
deuteron reactions (d,n) on, distributions from, 17: 28335
deuteron reactions (d,p) with, angular distribution from, 18: 24625 (WASH-1046)
deuteron reactions (d,p) with, spins of states from, (E), 19: 14495 (ANL-6878(p.279-301))
deuteron reactions (d,t) at 15 Mev, (E/T), 19: 37863
deuteron reactions (d,p) and (d,t) with, nuclear structure studies using, 20: 6435
electron inelastic scattering by, form factors for magnetic dipole, 18: 24625 (WASH-1046)

energy level calculations for, with pairing interaction, 18: 34927
energy levels, (E/T), 19: 37863
energy levels in even, calculations of vibrational, 20: 15851
energy levels, interactions, nuclear moments, and transitions in, 17: 24381 (AD-403411)
energy levels of, theory of low-lying vibrational, 17: 5365
energy levels of, spins of, 18: 42624(R) (ANL-6879(p.35-63))
energy levels of, shell model calculations of, 20: 6385
energy levels of, one- and two-phonon, (T), 20: 12123
energy levels of, surface delta interaction for, 20: 26169
gamma emission and decay of, from 30-Mev proton reactions on zinc, 18: 42655
gamma reactions on, cross sections for, 19: 12496
gamma scattering by, resonance, 18: 11175 (ANL-6797(p.275-87))
helium-3 elastic scattering by, optical model for, 17: 5364
helium-3 reactions (He-3,t) at 18 Mev, (E), 20: 42334
model of, neutron orbits in shell, 19: 19095 (WASH-1053)
neon-20 reactions at 150 Mev, possible production and detection of neon-16 in, 18: 34765 (JINR-P-1679)
neon-20 reactions on, neutrons from, 17: 9593
neutron cross sections, 16: 7012 (DC-59-7-171)
neutron cross sections, data tape for reactor analysis, 16: 8322 (XDC-59-11-72)
neutron reactions with, 18: 11195(R) (EANDC(E)-49(L))
neutron reactions with, resonances in, 19: 21454
nuclear model for, testing by proton inelastic scattering, 20: 44658 (UCRL-16984)
nuclear potentials, evidence for distortion, 16: 21565
nuclear structure of even, (T), 20: 21976
preparation of foil targets of, 20: 19297 (IAE-973)
preparation of foils of, by rolling, 20: 25519 (AERE-R-5097, Paper 21)
production in helium ion and proton reactions with niobium at 240 to 880 Mev, cross sections for, 18: 42745
proton elastic scattering at 14.5 Mev, cross sections for, 19: 47705
proton elastic scattering at 6.9 Mev, differential cross sections and polarization from, (T), 20: 30495
proton elastic scattering at 14.5 Mev, cross sections for, (E/T), 20: 34638
proton inelastic scattering by even, microscopic description of, (T), 20: 22118
proton reactions (p,t) with, analytical uses of, (T), 19: 14498 (ANL-6878(p.425-48))
proton reactions at 14.5 Mev, total cross sections for, (E), 20: 42162 (LA-DC-8075)
proton reactions on, cobalt-57 yields from, 17: 8153
proton reactions (p,n) at 17 Mev on even, effects of excited isobaric states, 16: 26333 (UCRL-6830)
proton reactions (p,α) at 20.5 Mev on, cross sections, 17: 33070
proton reactions, cross sections for production of cobalt-57, 18: 27832(R) (ORNL-TM-530(Rev.))
separation in calutrons, 18: 34007(R) (ORNL-TM-890)
separation of stable, in calutrons, 18: 34005(R) (ORNL-TM-879)

NICKEL ISOTOPES Ni-56

binding energies and spectra of, from residual two-body interaction theory, 18: 4605
decay of, conversion electron and gamma spectra in, (E), 19: 16944
decay of, gamma spectra from, (E), 20: 13815
decay scheme, 18: 1083
decay scheme of, energy levels in, 17: 22632
energy levels and mass of, determination of, 18: 21357
energy levels from nickel-58 (p,t) at 28 Mev, 19: 47706
energy levels from proton reactions (p,t) with nickel-58 at 28 Mev, (E), 20: 3041
energy levels of, half lives of, 18: 1083
energy levels of, detection using (p,t) reactions with nickel-58, (E), 19: 39819
internal conversion coefficients, 18: 36623
mass, 19: 47706
neutron total cross section, 17: 41873 (WASH-1044)
production in helium-3 reactions with iron-56, (E), 19: 16974
production in iron-56 (α,4n) reactions at 20 to 68 Mev, excitation functions for, 19: 27500
production in lithium-6 reactions with iron-54 at 21 to 63 Mev, excitation functions for, 18: 9398
production in lithium-6 reactions with iron-54 at 21 to 63 Mev, statistical analysis of, 18: 9399
proton reactions (p,d) and (p,t) at 28 Mev, (E), 19: 47706
recoil ranges of residual, in helium-3 reactions with iron-56, 20: 10090
yield in alpha and proton reactions with copper, 20: 30531

NICKEL ISOTOPES Ni-57

beta decay half life (E), 19: 3295
core isomerism in, (T), 19: 17051
decay of, gamma spectra from, (E), 20: 13815
decay of, K/L ratio for electron-capture, (E), 20: 11984
decay scheme, 17: 5378
energy levels from (p,d) reactions, spins of, 18: 21299
energy levels from nickel-58 (p,d) at 28 Mev, 19: 47706
energy levels from nickel-58 (He-3, α) reactions at 15 and 18 Mev, (E/T), 20: 4912
energy levels from nickel-58 (He-3,α) reactions, spins of, (E), 20: 15860
energy levels of, from helium-3 reactions (He-3,α) with nickel-58, (E), 20: 4892
gamma dose constants for, 20: 46617
gamma spectra, 18: 24585(R) (IDO-16969)
gamma spectra, (E), 19: 27440 (TID-21812)
half life, (E), 19: 35441
nuclear state alignment of, 17: 11703
nucleon interactions in, properties from effective, (T), 20: 17735
production at ORNL, 19: 26718 (ORNL-3802)
production in (n,2n) reactions with nickel-58, (E), 19: 27440 (TID-21812)
production in alpha and proton reactions with copper at 320 to 700 Mev, cross sections for, 18: 32849
production in helium-3 reactions with iron-56, (E), 19: 16974
production in iron-56 (α,3n) reactions at 20 to 68 Mev, excitation functions for, 19: 27500
production in lithium-6 reactions with iron-54 at 21 to 63 Mev, excitation functions for, 18: 9398
production in lithium-6 reactions with iron-54 at 21 to 63 Mev, statistical analysis of, 18: 9399
production of carrier-free, by nickel-58 (n,2n) reactions, 16: 13114
recoil ranges of residual, in helium-3 reactions with iron-56, 20: 10090

NICKEL ISOTOPES Ni-58

alpha elastic and inelastic scattering at 43 Mev, 16: 21421
alpha elastic and inelastic scattering at 43 Mev, distorted waves approximation in, 17: 38182
alpha elastic and inelastic scattering at 43 Mev, cross sections for, (E/T), 19: 12521
alpha elastic and inelastic scattering by, angular distributions for, (E), 19: 27446
alpha elastic and inelastic scattering at 22.2 Mev, angular distributions from, (E), 19: 45312
alpha elastic scattering at 7 to 12 Mev, angular distributions from, 18: 21292
alpha inelastic scattering, excitation by, 16: 24777 (CEA-2146)
alpha inelastic scattering by, excitation of two-phonon states, 16: 29839
alpha inelastic scattering at 43 Mev, collective excitations by, 17: 22627
alpha inelastic scattering at 43 Mev, excitation of collective modes in, 17: 38257
alpha inelastic scattering at 43 Mev, collective states excited in, 17: 38266
alpha inelastic scattering at 40 Mev, plane wave Born approximation for, 17: 38204
alpha inelastic scattering by, distorted wave analysis of, 17: 41873 (WASH-1044)
alpha inelastic scattering at 44 Mev, 18: 16925 (ANL-6848(p.137-42))
alpha inelastic scattering by, levels from, (T), 19: 14489 (ANL-6878 (p.143-73))
alpha inelastic scattering by, form factors from, (T), 19: 19172
alpha inelastic scattering at 43 Mev, distorted-wave calculation of, 19: 41692
alpha inelastic scattering at 25 to 100 Mev, cross sections for, (E/T), 19: 43294
alpha inelastic scattering at 25 to 100 Mev, phase shift in, (T), 19: 43312
alpha inelastic scattering by, (T), 20: 21973 (BNL-948, pp 175-221)
alpha inelastic scattering at 64.3 Mev, strong absorption model for, 20: 22086
alpha inelastic scattering at 43 and 64.3 Mev, multiple excitation of collective levels from, (T), 20: 26130
alpha reactions, 18: 7696(R) (ORNL-TM-761)
alpha reactions (α,p) at 42 Mev, angular distributions of protons from, 18: 16951(R) (TID-20311)
alpha reactions (α,αn), (α,α2n), (α,αp), and (α,αpn) at 46 to 68 Mev, recoil ranges of product ions from, 18: 21294
alpha reactions (α,p) at 18 Mev, total angular momentum transfer in, (E/T), 19: 19210
alpha reactions (α,α') at 44.4 Mev, differential cross sections, 16: 11013
alpha reactions (α,αpn), cross sections for, 16: 33814
alpha reactions (α,p) at 42 Mev, angular distribution anisotropies and emission spectra from, 17: 38206
alpha reactions (α,γ) and (α,p) at 4.9 to 6.1 Mev and 4.9 to 11 Mev, cross sections for, 18: 9411
alpha reactions at 3 to 10 Mev, gamma yields from, 16: 23065
alpha reactions at 27 to 42 Mev, proton evaporation from, 16: 23113
alpha reactions at 42 Mev, proton emission in, (E), 20: 12062
alpha reactions to 48 Mev, shell effects in, 18: 26599

alpha reactions with, ion recoil ranges in, 18: 22869 (CONF-481-48)
alpha scattering at 43 Mev, optical potential ambiguities in, 17: 34944
alpha scattering at 64.3 Mev, differential cross sections for, 18: 15275
alpha scattering at 28.5 Mev, nuclear states from, 18: 17046
alpha scattering at 43 Mev, interference effects in, 18: 24713
alpha scattering at 64.3 Mev, 18: 32747(R) (UCRL-11213(p.64-86))
alpha scattering at 34.4 Mev, angular distributions for, (E), 19: 47623
alpha scattering at 21 Mev, angular distributions from, (E/T), 20: 30353(R) (ORNL-3940, pp 1-61)
alpha scattering by, 17: 40436(R) (NYO-10063(p.105-15))
bremsstrahlung reactions (γ,n), (γ,2n), and (γ,p) at 24 Mev, direct photoeffect and evaporation, 17: 38209
bremsstrahlung reactions (γ,p) at 22 Mev, energy spectra from, (E), 19: 14566
bremsstrahlung reactions (γ,n) with, cross sections for, 20: 26200
decay in alpha reactions (α,xnyp) with iron-54, shell structure effects in, (T), 19: 41741
deuteron elastic scattering at 13.6 Mev, angular distributions, 16: 18523
deuteron elastic scattering cross section, 16: 29817
deuteron elastic scattering cross sections at 12.8 Mev, 17: 11688
deuteron elastic scattering at 7 to 12 Mev, angular distributions from, 18: 21292
deuteron elastic scattering at 6.5 Mev, angular distributions from, (E), 19: 5251
deuteron elastic scattering at 27.5 Mev, angular distribution for, (E/T), 20: 3057
deuteron elastic scattering at 13.6 Mev, differential cross sections for, (E), 20: 38128
deuteron elastic scattering at 13.6 Mev, optical model analysis of, (T), 20: 42294
deuteron elastic scattering by, angular distributions from, 20: 46580(R) (BMwF-FBK-66-05)
deuteron inelastic scattering at 13.6 Mev, angular distributions, 16: 18522
deuteron inelastic scattering cross sections, 16: 29817
deuteron inelastic scattering at 15 Mev, angular distributions from, 17: 38271
deuteron inelastic scattering at 13.6 Mev, differential cross sections for, 17: 38259
deuteron reactions (d,p) at 9 Mev, proton angular distributions, 16: 3715
deuteron reactions (d,p), angular distributions, 16: 15700
deuteron reactions (d,p), differential cross section and reduced width, 16: 15701
deuteron reactions (d,p), angular distributions and cross sections, 16: 18511
deuteron reactions at 21.6 Mev, angular distributions and cross sections, 16: 21557
deuteron reactions (d,t) at 21.6 Mev, angular distributions and cross sections for, 16: 28134
deuteron reactions (d,p) at 27.5 Mev, cross section, 16: 29817
deuteron reactions (d,t) of, at 21.6 Mev, 16: 32287 (TID-16662)
deuteron reactions (d,p) at 13.6 Mev, proton angular distributions from, 17: 2315
deuteron reactions (d,helium-3) at 15 Mev, 17: 4090
deuteron reactions (d,p) at 13.8 Mev, proton polarization from, 17: 7286
deuteron reactions (d,t) at 21.6 Mev, 17: 6780(R) (ANL-6603(p.52-5))
deuteron reactions at 20 Mev, cross sections for, 17: 17216
deuteron reactions (d,p) at 13.6 Mev, angular distributions from, 17: 24414
deuteron reactions (d,α), (d,αn), (d,αp), (d,2np), and (d,2pn) at 0–24 Mev, excitation functions and inverse cross sections for, 17: 28317
deuteron reactions (d,p) at 9 and 15 Mev, spectroscopic factors for, 17: 38172
deuteron reactions (d,d) and (d,p) at 8.9 and 11.8 Mev, distorted waves approximation in, 17: 38182
deuteron reactions (d,p) with, compound nucleus formation effects in, 17: 38222
deuteron reactions at 12.8 Mev, 18: 6180 (PAN-257)
deuteron reactions with, cross sections for, 18: 6229
deuteron reactions (d,p) with, single-particle states of final nuclei in, 18: 9417
deuteron reactions (d,p) at 10 Mev, spin dependence of angular distributions from, 18: 9424
deuteron reactions (d,n) at 7 Mev, 18: 16917 (ANL-6848(p.98-103))
deuteron reactions (d,α) and (d,p) at 3 to 4.3 Mev, energy levels from, 18: 19046
deuteron reactions (d,d), (d,d′), (d,p) at 27.5 Mev, 18: 19003
deuteron reactions (d,n) at 11.7 Mev, neutron spectra from, (E), 19: 33365
deuteron reactions (d,t) at 15 Mev, (E/T), 19: 37863
deuteron reactions (d,p), proton polarization from, (E), 20: 6422
deuteron reactions (d,p) at 7 Mev, cross sections and nickel-59 levels from, (E), 20: 13858
deuteron reactions (d,n), at 7.0 Mev, (E), 20: 19805(R) (ANL-7110, pp 1-28)
deuteron reactions (d,n) at 11.7 Mev, neutron spectra and angular distributions from, (E), 20: 22109
deuteron reactions (d,p) with, proton yields from, (E), 20: 26208
deuteron reactions at 0 to 22 Mev, excitation functions for, (E), 20: 34529(R) (UR-3591-2)
deuteron scattering at 12.8 Mev, elastic, 18: 6180 (PAN-257)
deuteron scattering at 22 Mev, angular distribution of polarized, (E), 19: 33303
deuteron splitting in, perturbation theory of, 16: 33718
deuteron stripping reactions (d,p) with, 16: 30930(R) (NYO-2669)
deuteron total cross sections at 11 Mev, (E), 19: 43323
effects on nickel oxide crystal lattice constants, (E), 19: 4158
electron energy levels of, g-factors and hyperfine-interaction constants for, (E), 20: 9962(R) (ANL-7029, pp 9-12)
electron inelastic scattering by, partial-wave analysis of, 17: 11710
electron inelastic scattering by, effects of surface oscillations on form factors for, (T), 19: 6716
electron inelastic scattering by, shell model analysis of excitation in, (T), 19: 6718
electron inelastic scattering by, level excitation in, (E), 20: 30360 (WASH-1068)
electron inelastic scattering from first excited state of, form factors from, (E), 20: 34605
electron scattering shape parameters, 16: 11007
energy level calculations for, using s-state forces, 18: 38163
energy level transitions in, E2, (T), 19: 16940
energy levels, 16: 2488 (NP-10975)
energy levels, 16: 28071
energy levels, 18: 34906
energy levels, 18: 40608
energy levels, (E), 19: 31257
energy levels, 20: 4849(R) (UCRL-14360, pp 1-50)
energy levels and E3 and E4 gamma spectra, 16: 21450
energy levels from nickel-60 (p,t) at 28 Mev, 19: 47706
energy levels from scattering, vibrational, (E/T), 20: 44795
energy levels from beta decay of copper-58, (E), 20: 46242(R) (TID-23239)
energy levels from proton inelastic scattering at 9.10 to 9.55 Mev, (E), 20: 46734
energy levels of, 16: 33854
energy levels of, determination of, from 43-Mev alpha scattering reactions, 16: 32400 (TID-16665)
energy levels of, microscopic models for vibrational, (T), 20: 3083
energy levels of, effective interactions and seniorities in, (T), 20: 28400
energy levels of, energy calculations using shell model with reaction matrix, (T), 20: 38066
fabrication as radiation target, 18: 27813(R) (ORNL-TM-428)
gamma emission, analysis of collective E3 and E4, 16: 26271
gamma reactions (γ,p) with, cross sections, (E/T), 19: 14528 (LAL-1120)
gamma reactions (γ,n) and (γ,p) with, in potassium tetracyanonickelate, chemical species from, 20: 45748
gamma reactions (γ,n), cobalt-57 yields from, 17: 26611
helium-3 elastic scattering at 12 Mev, 18: 38144
helium-3 elastic scattering at 33 Mev, cross sections for, (E/T), 19: 43339
helium-3 inelastic scattering by, DWBA analysis of, (T), 19: 39885
helium-3 reactions (He-3,d) with, 18: 21204 (LADC-6302)
helium-3 reactions at 22 Mev, deuteron angular distributions in, 18: 24590 (LADC-6370)
helium-3 reactions (He-3,d) with, isobaric analog states from, (E), 19: 25514
helium-3 reactions (He-3,n) with, Q-value for, (E), 19: 31320
helium-3 reactions (He-3,α) at 24.5 Mev, energy levels from, (E), 20: 4892
helium-3 reactions (He-3, α) at 15 and 18 Mev, nickel-57 levels from, (E/T), 20: 4912
helium-3 reactions (He-3,α) at 15 and 18 Mev, (E), 20: 15860
helium-3 reactions (He-3,t) at 22 Mev, Coulomb displacement-energy from, (E), 20: 22095
helium-3 reactions (He-3,t) at 18 Mev, (E), 20: 42334
helium-3 reactions (He-3,d) at 16.5 Mev, copper-59 energy levels from, (E), 20: 44837
helium-3 scattering at 33 Mev, (E/T), 20: 24330(R) (ANL-7108, pp 31-6)
helium-4 reactions at 46 to 68 Mev, angular momentum and nuclear shell effects in, (E/T), 19: 10340
helium-4 reactions at 70 to 100 Mev, excitation functions for, (E), 20: 34529(R) (UR-3591-2)
ion inelastic scattering by, collective-level excitation in, (T), 19: 35383 (JINR-P-2142)
ion inelastic scattering by, collective level excitation in complex, (T), 20: 13890

ion reactions with, angular momentum effects in, 17: 36657 (JINR-P-1347)
lithium-6 reactions at 66 Mev, gallium-63 from, 19: 12556
meson (μ^-) capture by, (E), 19: 37897
neutron activation cross sections at 14 Mev, 16: 4620(R) (PR-P-50)
neutron activation rates for threshold detectors, 17: 3541 (TID-17211)
neutron activation cross sections for threshold detectors, 17: 3541 (TID-17211)
neutron activation cross sections, 17: 10139
neutron activation rates for, fast, 17: 28221 (EUR-107.f)
neutron activation of foils of, fast, 17: 36347(R) (NARF-62-18P)
neutron capture at 15 to 300 kev in, cross sections and gamma spectra for fast, 17: 21010
neutron capture by, gamma polarization following thermal, 16: 29806
neutron capture by, gamma spectra from thermal, (E), 20: 9966 (IAE-885)
neutron capture by, gamma transitions from thermal, (E), 20: 26208
neutron capture in, gamma angular correlations in thermal, 17: 41527(R) (ANL-6720(p.2-15))
neutron cross sections of, at 13 to 15 Mev, 16: 32176(R) (PR-P-53)
neutron cross sections at 1.44 ev (E), 19: 3288
neutron inelastic scattering by, gamma yields from, (E), 19: 35406(T) (ANL-Trans-177)
neutron inelastic scattering at 14.1 Mev, evaporation mechanism of, (E), 19: 37788 (INR-591/IA/PL)
neutron reaction yields from, 16: 13114
neutron reactions (n,p), (n,np), and (n,2n) at 13.86 to 14.88 Mev, 16: 2480 (ANU/P-236)
neutron reactions(n,p), cross section of fission, 16: 2772 (AAEC/E-59 (Suppl.1))
neutron reactions (n,p) at 14 Mev, direct and evaporation mechanisms, 16: 4850
neutron reactions (n,2n) at 14.8 Mev, cross sections for, 16: 7072
neutron reactions (n,p) at 2 to 5 Mev, cross sections, 16: 18499
neutron reactions (n,p), calculation of cross sections for, 16: 23133
neutron reactions (n,p) in, use of, in measuring fast fluxes, 16: 29753 (IDO-16744)
neutron reactions (n,p) at 1.8 to 4.8 Mev, excitation functions, 16: 31082
neutron reactions (n,p) at 2 to 5 Mev, comparison of experimental and theoretical cross sections for, 16: 32396 (NP-11745)
neutron reactions (n,d), (n,np), (n,py), and (n,pn) at 14 Mev, cross sections for, 17: 2242 (TID-16949)
neutron reactions (n,p), separation energies for, 17: 2242 (TID-16949)
neutron reactions [(n,d) + (n,np) + (n,pn)] at 14.8 Mev, cross sections, product half life, and Q value for, 17: 2242 (TID-16949)
neutron reactions (n,2n) at 14.8 Mev, cross sections for, 17: 2242 (TID-16949)
neutron reactions (n,n′) and (n,p) at 14 Mev, cross sections for, 17: 2242 (TID-16949)
neutron reactions (n,$\alpha\gamma$), (n,αn), and (n,2p) at 14.8 Mev, cross sections for, 17: 2242 (TID-16949)
neutron reactions (n,p) on, yields from epithermal and fast, 17: 7306
neutron reactions (n,p), cross sections for fast, 17: 12722 (TID-17839)
neutron reactions (n,p) at 1.6 to 14.8 Mev, cross sections for, 17: 13502
neutron reactions (n,α), cross section for ground state transition, 17: 17139
neutron reactions at 1.04 to 2.67 Mev, cobalt-58 cross section and isomer ratio in, 17: 22638
neutron reactions (n,p), preparation of cobalt-58 by, in reactor, 17: 24508
neutron reactions (n,p) at threshold, cross sections for, 17: 26421 (EUR-10.e)
neutron reactions (n,p) with, properties as neutron threshold detectors, 17: 28237 (AE-102)
neutron reactions (n,p) with, cross sections for fast, 17: 31056
neutron reactions (n,p) with, cross sections for threahold, 17: 31057
neutron reactions (n,p), production of cobalt-58 by, 17: 30165
neutron reactions (n,p), use in neutron flux measurements, 17: 30165
neutron reactions (n,p) on, neutron dosimetry by, 17: 32294(T) (CEA-tr-A-1221)
neutron reactions (n,p) with, use for integration of fast-neutrons flux, 17: 34294
neutron reactions (n,d) at 14 Mev, cross sections for ground-state transitions in, 17: 34920
neutron reactions (n,np) at 14.7 Mev, cross sections for, 17: 36707
neutron reactions (n,p) at 2.2 to 3.8 Mev, cross sections for, 17: 38061 (AE-115)
neutron reactions (n,p) with, effective threshold energy for, 17: 38116
neutron reactions (n,p) at 12.5 to 21.0 Mev with, cross sections for, 17: 40049
neutron reactions (n,2n) at 12.5 to 21.0 Mev with, cross sections for, 17: 40049
neutron reactions (n,np) at 14.8 Mev, cross section of, 18: 1077
neutron reactions with, fast neutron in-pile detection by threshold, 18: 2020 (EUR-289.e)
neutron reactions (n,p) at 2.2 to 3.8 Mev, cross sections for, 18: 7731
neutron reactions (n,p) with, cross sections for positron production in, 18: 13061
neutron reactions at 12.5 to 21 Mev, cross sections for, 18: 16970
neutron reactions (n,p) with burnup corrections for, 18: 19438
neutron reactions (n,p) at 2 to 6 Mev, ratio for ground- and isomeric-state production in, 18: 19060
neutron reactions (n,p) as flux monitor, fast, 18: 19437
neutron reactions (n,p) with, optical model analysis of, 18: 21165 (CONF-490-1)
neutron reactions (n,p) with, for neutron flux measurements, 18: 23885 (NP-13930(p.178-80))
neutron reactions (n,p), measurement of fast neutron fluxes by, 18: 30750
neutron reactions (n,γ) with, angular correlations in, 18: 32277(R) (PR-P-61)
neutron reactions (n,p), production of cobalt-58 by, 19: 2701
neutron reactions (n,2n) and (n,p) with, cross sections for, (E), 19: 5230
neutron reactions (n,2n) at 14 Mev, shell effects in, (T), 19: 12536
neutron reactions (n,p) with, cobalt-58 production by, 19: 17984
neutron reactions (n,p), thermal, 19: 22801
neutron reactions (n,α), (n,αn), and (n,$n\alpha$) at 14.1 Mev, angular and energy distributions from, (E), 19: 23720
neutron reactions (n,2n) with, (E), 19: 27440 (TID-21812)
neutron reactions (n,p) with, use to measure neutron integral flux, 19: 26671(T) (CEA-tr-A-1822)
neutron reactions (n,p) at 8.4 to 22 Mev, angular and energy distributions from, (E), 19: 29286
neutron reactions (n,d) at 22 Mev, angular and energy distributions from, (E), 19: 29286
neutron reactions (n,2n) with, fission-averaged cross sections, 19: 29319
neutron reactions (n,p) with, cross sections for, (T), 19: 29323
neutron reactions (n,p) at 1.04 to 2.67 Mev, cross sections and isomer ratios for, (E), 19: 31215(R) (ANL-7010(p.1-19))
neutron reactions (n,p) with, flux density determinations using, 19: 35711
neutron reactions (n,p) at 14.1 Mev, cross section for, (E), 19: 35378(R) (EANDC(E)-57(U))
neutron reactions (n,2n) at 14.1 Mev, cross section for, (E), 19: 35378(R) (EANDC(E)-57(U))
neutron reactions (n,2n) at 12.6 to 19.6 Mev, cross sections for, (E), 19: 35378(R) (EANDC(E)-57(U))
neutron reactions (n,2n) at 12.6 to 19.6 Mev, excitation functions of, (E), 19: 35441
neutron reactions (n,2n) at 12.6 to 19.6 Mev, excitation function for, (E/T), 19: 47571 (EUR-2456.e)
neutron reactions to 16 Mev, cross sections for two-particle emission in, (T), 19: 10283
neutron reactions (n,d) and (n,p) at 8 to 22 Mev, distributions from, (E), 20: 3012 (IKF-11)
neutron reactions (n,d) at 14 Mev, energy levels from, (E), 20: 4896
neutron reactions (n,p) at 14 Mev, angular and energy distributions from direct, (E), 20: 6440
neutron reactions (n,p) threshold cross section and energy for, 20: 16335(R) (NBS-TN-276)
neutron reactions (n,2n) at 10 to 20 Mev, cross sections for, 20: 19810 (EUR-119.e(Vol.2))
neutron reactions (n,p) at 0 to 20 Mev, cross sections for, 20: 19810 (EUR-119.e(Vol.2))
neutron reactions (n,p) at 5.0 Mev, cross section and threshold energy for, 20: 21427(R) (NASA-CR-54904)
neutron reactions (n,p) with, recoil-ion range in nickel from, (E), 20: 24423
neutron reactions (n,2n) and (n,p) at 13.2 to 15.5 Mev, cross sections for, (E), 20: 34518 (INR-680/I/PH)
neutron reactions (n,p) with, cobalt-58 production in, 20: 35576
neutron reactions (n,2n) at 3 Mev above threshold, cross section for, (E), 20: 46614
neutron reactions (n,2n) at 13.56 to 14.7 Mev, excitation functions for, (E), 20: 46614
neutron reactions (n,2n) at 14.6 Mev, cross section for, (E), 20: 46614
neutron scattering at 1 to 4 Mev, cross sections for energy level excitation in, 18: 21217
neutron threshold reactions with, cross sections for, 17: 36653 (EUR-119.e)
neutron total cross section, 17: 41873 (WASH-1044)
neutron total cross sections for, level spacings from, (E/T), 20: 32389
nuclear moment of inertia, determination of, 17: 38206
nucleon interactions in, potentials for, 18: 26638
nucleon interactions in, properties from effective, (T), 20: 17735
oxygen reactions (O-16,4n) with, production of proton emitters in, 18: 40598
photon reactions (γ,n) and (γ,p) with, properties of, (T), 20: 42220

preparation as radiation target material, 18: 27811(R) (ORNL-TM-198)
properties as neutron threshold detector, 17: 35260(R) (TID-19135)
properties for use as threshold detector in shielding studies, 18: 32949(R) (EUR-534.d(Pt.II))
proton angular distributions to excited 2+ and 3– states, parity change determinations from, 16: 21556
proton compound-elastic scattering at 5.45 Mev, differential cross section for, 18: 11289
proton cross sections at 8.8 Mev, (E), 19: 29276
proton differential elastic scattering cross sections at 30.3 Mev, 18: 36631
proton elastic and inelastic scattering at 6.8 Mev, 17: 24414
proton elastic scattering at 22.2 Mev, angular distributions and cross sections, 16: 9462
proton elastic scattering at 14.5 Mev, polarization angular dependence in, 16: 18518
proton elastic scattering at 7 to 12 Mev, cross sections for, 17: 16770(R) (ANL-6666)
proton elastic scattering, isotopic, isotonic, and shell closure effects on polarized, 17: 19360
proton elastic scattering at 4.2 Mev, angular distribution of, 17: 22656
proton elastic scattering at 10.9 and 11.7 Mev, differential cross sections for, 18: 7762
proton elastic scattering at 9.4 Mev, cross sections and polarization for, 18: 18964
proton elastic scattering at 7 to 12 Mev, angular distributions from, 18: 21292
proton elastic scattering at 30 Mev, polarization in, 18: 36633
proton elastic scattering at 6.9 Mev, (E), 19: 5237
proton elastic scattering at 14.5 to 21 Mev, effects of structure on polarization in, (E), 19: 8441
proton elastic scattering at 6.9 Mev, isotope effects on polarization in, (E), 19: 14630
proton elastic scattering at 50 Mev, differential cross sections for, (E), 19: 28962(R) (NIRL/R/81)
proton elastic scattering at 3.00 to 3.56 Mev, angular distribution for, (E), 19: 37879(T)
proton elastic scattering at 39 Mev, polarization in, 19: 45378
proton elastic scattering by, optical model parameters for distributions polarizations from, (E/T), 20: 1157 (ORNL-P-1616)
proton elastic scattering at 160 Mev, differential cross sections for, (E/T), 20: 4906
proton elastic scattering at 160 Mev, differential cross sections for, (E/T), 20: 9979 (TID-22478)
proton elastic scattering by, intermediate resonance structure in, (E/T), 20: 10038
proton elastic scattering at 25 to 50 Mev, polarization from, (E), 20: 15728(R) (RHEL/R-112, pp 23-36)
proton elastic scattering at 45 Mev, differential cross sections for, (T), 20: 21963 (AD-626656)
proton elastic scattering at 40 Mev, cross sections for, (E/T), 20: 30353(R) (ORNL-3940, pp 1-61)
proton elastic scattering at 40 Mev, differential cross sections and polarization for, (E), 20: 32510
proton elastic scattering at 39 Mev, polarization in, (E), 20: 36176(R) (TID-22971, pp 41-140)
proton elastic scattering at 49 Mev, angular distribution of polarization in, (E), 20: 38049
proton elastic scattering at 30 Mev, optical-model analysis of, (T), 20: 42255
proton elastic scattering at 6.14 and 6.53 Mev, angular distribution of polarization in, (E), 20: 46783
proton inelastic scattering at low energies, reaction mechanisms for, 16: 21393
proton inelastic scattering at 7 to 8 Mev, proton polarization from, 16: 26290
proton inelastic scattering at 14.65 Mev, 16: 28071
proton inelastic scattering, angular correlations from, 16: 32427
proton inelastic scattering at 6.6 Mev, 17: 7178
proton inelastic scattering at 5.73 Mev, compound nucleus and direct interaction contributions from gamma angular correlations in, 17: 38276
proton inelastic scattering at 10 Mev, differential cross sections for, 18: 7763
proton inelastic scattering by, angular correlations for, 18: 7780
proton inelastic scattering at 10.3 Mev, 18: 21252
proton inelastic scattering at 40 Mev, 18: 30808
proton elastic scattering at 17.8 Mev, polarization in, (E/T), 19: 14599
proton inelastic scattering at 30 Mev, differential cross sections for, (E), 19: 28962(R) (NIRL/R/81)
proton inelastic scattering at 7 Mev, energy levels and cross sections for, (E), 20: 13858
proton inelastic scattering at 8.0 Mev, levels from, (E), 20: 28342
proton inelastic scattering at 40 Mev, cross sections for, (E/T), 20: 30353(R) (ORNL-3940, pp 1-61)
proton inelastic scattering at 9.10 to 9.55 Mev, spins of levels from, (E), 20: 38181
proton inelastic scattering at 17.6 Mev, testing nuclear model by, (E/T), 20: 44658 (UCRL-16984)
proton inelastic scattering at 9.2 and 10.5 Mev, proton spin flip in, (E), 20: 46597 (RLO-1388-14)
proton quasi-elastic scattering at 30 to 150 Mev, (E), 19: 5569(R) (MIT-2098-64)
proton quasi-elastic scattering at 160 Mev, (E/T), 20: 46725
proton reactions (p,γ) with, resonances in, 18: 13055 (NRL-5897)
proton reactions (p,α) at 50 Mev, 18: 14590(R) (NIRL/R/60)
proton reactions (p,d) at 17 to 18.5 Mev, neutron shell configuration studies from, 18: 21291
proton reactions (p,d) at 28 Mev, angular dependence on final state spin in, 18: 21299
proton reactions (p,α) at 11 to 12.5 Mev, 18: 34855
proton reactions (p,d) with, isobaric analog states from, (T), 19: 14492 (ANL-6878(p.207-13))
proton reactions (p,n) at 5 to 10 Mev, thresholds for, (E), 19: 14607
proton reactions (p,p′) at 8 to 11 Mev, spectra from, (E), 19: 19095 (WASH-1053)
proton reactions (p,t) at 28 Mev, energy levels from, (E), 19: 39819
proton reactions (p,d) and (p,t) at 28 Mev, (E), 19: 47706
proton reactions (p,t) at 28 Mev, nickel-56 energy levels from, (E), 20: 3041
proton reactions (p,pn) at 450 Mev, differential recoil from, (T), 20: 4893
proton reactions (p,pn) at 370 Mev, nuclear structure effects on cross section for, (E), 20: 8120
proton reactions (p,xpyn) at 370 Mev, cross sections for, (E), 20: 8120
proton reactions (p,d) at 18.5 to 27.5 Mev, differential cross sections for, (E/T), 20: 9975 (PUC-937-174)
proton reactions (p,d) with, form-factor calculations for, (T), 20: 10056
proton reactions (p,n) at 14.2 Mev, angular distributions, Q values, and spectra from, 20: 13345(R) (NP-15772)
proton reactions (p,d) at 57 Mev, energy spectra from, (E), 20: 17725
proton reactions (p,n) with, 202-kev level from, (E), 20: 19914
proton reactions (p,n) with, accelerator beam calibration from threshold energy for, 20: 28401
proton reactions (p,n) at 14.2 Mev, Q-values and differential cross sections for, (E/T), 20: 34520 (INSJ-97)
proton reactions (p,n) with, thresholds for, (E), 20: 38053
proton reactions (p,n) with, threshold energy for, (E), 20: 38054
proton reactions at 57 Mev on, proton distributions from, 17: 7197
proton reactions at 8 to 13 Mev, gamma and neutron yields in, 18: 44775
proton reactions at 30 Mev, optical-model analysis of total cross sections for, (T), 20: 42255
proton reactions (p,α) and (p,p′) at 17.5 Mev, alpha spectra from, 16: 7112
proton reactions (p,α) at 18 Mev, seniority wave function effects on angular distributions and cross sections, 16: 21578
proton reactions (p,d), distributions from, 16: 26258
proton reactions (p,α), (p,d), (p,p), and (p,t) at 57 Mev, 16: 29774 (JAERI-1020(p.194-200))
proton reactions (p,pn) at 370 Mev, cross sections for, 17: 796 (NEVIS-109)
proton reactions (p,p′γ), angular correlation symmetries in, 17: 11684
proton reactions (p,pn) and (p,2p), 17: 11703
proton reactions (p,γ), resonance-curve shapes and resonance energies for, 17: 19349
proton reactions (p,γ), resonance yield curves and energies for, 17: 19357
proton reactions (p,γ) with, resonance yield curves for, 17: 32998 (CONF-52-3)
proton reactions (p,n) with, threshold energy for, 17: 36669 (WASH-1042)
proton reactions (p,t) at 40 Mev, angular distributions and energy spectra for, 17: 38232
proton reactions (p,d) at 57 Mev, neutron binding energies in, 17: 38229
proton reactions (p,α) at 12.6 to 14.25 Mev, angular distributions in, 17: 41906
proton reactions (p,γ) at 1424 kev, yield curves for, 18: 2843 (TID-19193)
proton reactions (p,t) with, 18: 9319(R) (TID-19940(p.22-76))
proton reactions with, angular distributions for, 17: 39974 (INSJ-59)
proton reactions with, distributions from, (E), 19: 10257(R) (TID-21335 (p.33-107))
proton reactions with, reduced widths and strength functions for, (E/T), 19: 17009
proton scattering at 2 to 5 Mev, resonances in, 16: 21543
proton scattering by, polarization in inelastic, 16: 26226 (NYO-10131)
proton scattering at 8 Mev by, angular distribution of elastic, 16: 29471(R) (ANL-6574)
proton scattering cross sections of, fluctuations of, 17: 21048
proton scattering by, excitation function for elastic, 17: 22264(R)

(ANL-6679)
proton scattering at 9.4–22.2 Mev, local optical potentials for, 17: 38185
proton scattering at 29 Mev, 18: 14590(R) (NIRL/R/60)
proton scattering at 40 Mev, analysis of, 18: 16924 (ANL-6848(p.130-6))
proton scattering by, energy levels from, 18: 30867
proton scattering by, polarization from, 18: 40597
proton scattering at 30 Mev, optical-model analysis of (E/T), 19: 3315
proton scattering by, intermediate structures and statistical fluctuations in cross sections for, (T), 19: 8440
proton scattering at 40.5 Mev, polarization effects in, (E), 19: 37823(R) (ORNL-3800(p.1-49))
proton scattering at 35 to 160 Mev, spectra from, (E), 19: 36220(R) (MIT-2098-142)
proton scattering at 40 Mev, (T), 19: 37862
proton scattering at 18.6 and 19.1 Mev, (E/T), 20: 4849(R) (UCRL-14360, pp 1-50)
proton scattering at 19 Mev, excited 2^+ and 3^- levels from, (E/T), 20: 12065
proton scattering at 45 Mev, cross sections for elastic, (E), 20: 40162
proton total cross sections at 8.5 to 11 Mev, (E), 19: 43323
proton total cross sections at 30 and 50 Mev, (E), 20: 15729(R) (RHEL/R-112, pp 37-66)
proton total scattering cross sections at 30 Mev, 18: 36632
reactions with oxygen-16, compound nucleus formation cross sections for, 17: 17118 (JINR-P-1162)
spectra of radiation damage in, calculation of fast-neutron, 18: 2332
use as fast-neutron threshold detector, 17: 34268

NICKEL ISOTOPES Ni-59

abundance in stone meteorites, 19: 8052 (NYO-8924)
activity measurements in iron meteorites, 17: 28943(R) (TID-18961)
activity measurements in stone meteorites, 17: 28943(R) (TID-18961)
content in Bondoc meteorite, cosmogenic, 19: 32884
decay in helium-3 reactions (He-3,xnyp) with iron-56, shell structure effects in, (T), 19: 41741
decay of, inner bremsstrahlung transitions and interference of K-capture gamma transitions in, 17: 28322
determination in stone meteorites, 18: 43601(R) (TID-21007)
deuteron elastic scattering, absorptive effects in, 16: 26342
deuteron reactions (d,p), neutron level shifts, 16: 11034
deuteron reactions (d,p) with, compound nucleus formation effects in, 17: 38222
electron capture decay of, virtual, 17: 11709
energy level transitions from neutron capture by nickel-58, (E), 20: 26208
energy levels, 17: 2315
energy levels, 17: 9534
energy levels, 18: 38163
energy levels at 0.470 and 0.880 Mev, parity and spin of, 18: 11173 (ANL-6797(p.270))
energy levels from (p,d) reactions, spins of, 18: 21299
energy levels from nickel-60 (p,d) at 28 Mev, 19: 47706
energy levels from thermal-neutron capture in nickel, (E), 20: 9966 (IAE-885)
energy levels from deuteron reactions (d,p) with nickel-58 at 7 Mev, (E), 20: 13858
energy levels from proton reactions (p,d) with calcium-40 at 55 Mev, neutron-hole, (E), 20: 19877
energy levels from helium-3 reactions (He-3,α) with nickel-60 at 15 Mev, (E), 20: 22127
energy levels, modified shell model for, 16: 18511
energy levels of, 16: 33854
energy levels of, spins and transition correlations of, 17: 32725(R) (PR-P-57(p.37-43))
energy levels of, spin of, 17: 33090
energy levels of, spins of, 18: 28693
energy levels of, spin of, 18: 42622(R) (ANL-6879(p.2-20))
energy levels of, reduced widths and strength functions of, (E), 19: 17009
energy levels of, from helium-3 reactions (He-3,α) with nickel-60, (E), 20: 4892
energy levels of, strength functions for single-particle, 20: 6345
energy levels of, effective interactions and seniorities in, (T), 20: 28400
energy levels of, energy calculations using shell model with reaction matrix, (T), 20: 38066
excited states of, spins of, 17: 25859(R) (PR-P-56(p.35-42))
gamma spectra, 17: 11709
neutron capture by, gamma energy and intensity from, 16: 33819
neutron energy level positions in, 18: 9360
nuclear spin and parity, ground-state, 16: 15700
production in reactions of cosmic rays with meteorites, 16: 1808(R) (TID-12849)
production of carrier-free, by nickel-58 (n,γ) reaction, 16: 13114
proton reactions (p,α) at 18 Mev, seniority wave function effects on angular distributions and cross sections, 16: 21578
single-particle states of, from (d,p) reactions with nickel-58, 18: 9417

NICKEL ISOTOPES Ni-60

alpha elastic and inelastic scattering at 43 Mev, 16: 21421
alpha elastic scattering at 7 to 12 Mev, angular distributions from, 18: 21292
alpha inelastic scattering, excitation by, 16: 24777 (CEA-2146)
alpha inelastic scattering at 43 Mev, collective excitations by, 17: 22627
alpha inelastic scattering at 43 Mev, collective states excited in, 17: 38266
alpha inelastic scattering at 43 Mev, excitation of two-phonon levels in, 18: 11267
alpha inelastic scattering at 44 Mev, 18: 16925 (ANL-6848(p.137-42))
alpha inelastic scattering by, form factors from, (T), 19: 19172
alpha inelastic scattering at 34.4 Mev, excitation of two-phonon states in, (E), 19: 33316
alpha inelastic scattering at 44 Mev, cross section angular dependence in, 19: 47608
alpha particle scattering and vibrational states, 16: 32410
alpha reactions (α,p) at 42 Mev, angular distributions of protons from, 18: 16951(R) (TID-20311)
alpha reactions (α,p) at 18 Mev, total angular momentum transfer in, (E/T), 19: 19210
alpha reactions at 3 to 10 Mev, gamma yields from, 16: 23065
alpha reactions at 27 to 42 Mev, proton evaporation from, 16: 23113
alpha reactions at 42 Mev, proton emission in, (E), 20: 12062
alpha scattering at 43 Mev, angular distributions to excited states, 16: 21560
alpha scattering at 28.5 Mev, nuclear states from, 18: 17046
alpha scattering at 44 Mev, angular distributions from, (E/T), 19: 19169
alpha scattering at 34.4 Mev, angular distributions for, (E), 19: 47623
alpha scattering by, 17: 40436(R) (NYO-10063(p.105-15))
bremsstrahlung reactions (γ,p) at 24 Mev, direct photoeffect and evaporation contributions in, 17: 38209
decay in alpha reactions (α,xnyp) with iron-56, shell structure effects in, (T), 19: 41741
deuteron differential elastic scattering cross sections at 14.7 to 18.1 Mev, 16: 12426 (INSJ-44)
deuteron elastic and inelastic scattering at 5 to 13.5 Mev, 18: 6177(R) (ORNL-3499(Vol.I)(p.29-31))
deuteron elastic scattering at 13.6 Mev, angular distributions, 16: 18523
deuteron elastic scattering cross sections at 12.8 Mev, 17: 11688
deuteron elastic scattering by, 18: 21161 (CONF-417-26)
deuteron elastic scattering at 7 to 12 Mev, angular distributions from, 18: 21292
deuteron elastic scattering at 6.5 Mev, angular distributions from, (E), 19: 5251
deuteron elastic scattering at 5 to 15 Mev, polarizability effects on optical model potentials in, (E/T), 19: 27551
deuteron elastic scattering at 34.4 Mev, angular distributions from, (E/T), 20: 30353(R) (ORNL-3940, pp 1-61)
deuteron elastic scattering at 13.6 Mev, cross section for, (E), 20: 30497
deuteron elastic scattering at 13.6 Mev, differential cross sections for, (E), 20: 38128
deuteron elastic scattering at 13.6 Mev, optical model analysis of, (T), 20: 42294
deuteron elastic scattering by, angular distributions from, 20: 46580(R) (BMwF-FBK-66-05)
deuteron inelastic scattering at 13.6 Mev, angular distributions, 16: 18522
deuteron inelastic scattering at 15 Mev, angular distributions from, 17: 38271
deuteron inelastic scattering at 13.6 Mev, differential cross sections for, 17: 38259
deuteron inelastic scattering by, effect of data normalization on optical model parameters for, (T), 19: 27550
deuteron inelastic scattering at 15 Mev, single excitations in, (E), 19: 35486
deuteron inelastic scattering at 15 Mev, excitation of two-phonon states by, (E), 19: 45346
deuteron inelastic scattering at 9.9 to 13.6 Mev, differential cross sections for, (E/T), 19: 47635
deuteron reactions (d,p) at 9 Mev, proton angular distributions, 16: 3715
deuteron reactions (d,p), angular distributions, 16: 15700
deuteron reactions (d,p), differential cross section and reduced width, 16: 15701
deuteron reactions (d,p), angular distributions and cross sections, 16: 18511
deuteron reactions at 21.6 Mev, angular distributions and cross sections, 16: 21557
deuteron reactions (d,t) at 21.6 Mev, angular distributions and cross sections for, 16: 28134
deuteron reactions (d,p) at 13.6 Mev, proton angular distributions from, 17: 2315

deuteron reactions (d,p) at 13.8 Mev, proton polarization from, 17: 7286
deuteron reactions (d,He³) with, angular distributions from, 17: 7655(R) (ANL-6600)
deuteron reactions (d,p) at 13.6 Mev, angular distributions from, 17: 24414
deuteron reactions (d,2α) at 0–24 Mev, excitation functions and inverse cross sections for, 17: 28317
deuteron reactions at 12.8 Mev, 18: 6180 (PAN-257)
deuteron reactions with, cross sections for, 18: 6229
deuteron reactions (d,p) with, single-particle states of final nuclei in, 18: 9417
deuteron reactions (d,p) at 10 Mev, spin dependence of angular distributions from, 18: 9424
deuteron reactions (d,t) at 14.7 Mev, spin dependence of angular distributions from, 18: 21301
deuteron reactions (d,n) at 11.7 Mev, neutron spectra from, (E), 19: 33365
deuteron reactions (d,t) at 15 Mev, (E/T), 19: 37863
deuteron reactions (d,p), proton polarization from, (E), 20: 6422
deuteron reactions (d,n) at 11.7 Mev, neutron spectra and angular and angular distributions from, (E), 20: 22109
deuteron reactions (d,p) with, proton yields from, (E), 20: 26208
deuteron scattering at 5 to 13.5 Mev, 17: 41873 (WASH-1044)
deuteron scattering at 12.8 Mev, elastic, 18: 6180 (PAN-257)
deuteron scattering at 5 to 13.5 Mev, differential cross sections for, 18: 28577 (ORNL-3637)
deuteron total cross sections at 11 Mev, (E), 19: 43323
electron energy levels of, g-factors and hyperfine-interaction constants for, (E), 20: 9962(R) (ANL-7029, pp 9-12)
electron inelastic scattering by, partial-wave analysis of, 17: 11710
electron inelastic scattering by, shell model analysis of excitation in, (T), 19: 6718
electron inelastic scattering by, level excitation in, (E), 20: 30360 (WASH-1068)
electron inelastic scattering from first excited state of, form factors from, (E), 20: 34605
electron-pair annihilation in, internal pair production coefficients from, (E), 19: 43330
energy gap in, 18: 36649
energy gap in, effective hamiltonian for, 17: 21074
energy level densities at excitation energies of 20 Mev, (T), 19: 27561
energy level lifetime in, 4+, 17: 17219
energy level transitions in, E2, (T), 19: 16940
energy level transitions in, M1-M2 mixing ratios as test of purity of vibrational, (T), 19: 25503
energy levels, 16: 12503
energy levels, 16: 17081
energy levels, 16: 23073
energy levels, 16: 28071
energy levels, 17: 2051(R) (CU(PNPL)-219)
energy levels, 18: 40608
energy levels, 20: 4849(R) (UCRL-14360, pp 1-50)
energy levels and E3 and E4 gamma spectra, 16: 21450
energy levels from scattering, vibrational, (E/T), 20: 44795
energy levels of, determination of, from 43-Mev alpha scattering reactions, 16: 32400 (TID-16665)
energy levels of, lifetime of second excited, 17: 41956
energy levels of, parameters for, 18: 19046
energy levels of, lifetime of second excited, 18: 34752(R) (CU(PNPL)-234)
energy levels of, identification of 3⁺ 3-phonon, (E), 19: 5192
energy levels of, microscopic models for vibrational, (T), 20: 3083
energy levels of, parity and spin of, 20: 8083 (PUC-937-171A)
energy levels of, effective interactions and seniorities in, (T), 20: 28400
energy levels of, energy calculations using shell model with reaction matrix, (T), 20: 38066
energy-level transition probabilities of, E2, (T), 20: 3115
energy-level transitions, (E), 20: 42254
fabrication as radiation target, 18: 27813(R) (ORNL-TM-428)
gamma emission, analysis of collective E3 and E4, 16: 26271
gamma reactions (γ,π⁻) with, cross sections for, (T), 19: 19146
gamma transition energies in, determination of, (E), 19: 6664
gamma transitions, coefficients of internal pair formation, 16: 12532
helium-3 elastic scattering at 33 Mev, cross sections for, (E/T), 19: 43339
helium-3 reactions at 22 Mev, deuteron angular distributions in, 18: 24590 (LADC-6370)
helium-3 reactions (He-3,d) with, isobaric analog states from, (E), 19: 25514
helium-3 reactions (He-3,α) at 24.5 Mev, energy levels from, (E), 20: 4892
helium-3 reactions (He-3,t) at 22 Mev, Coulomb displacement-energy from, (E), 20: 22095
helium-3 reactions (He-3, α) at 15 Mev, angular distributions from, (E), 20: 22127
helium-3 reactions (He-3,α) at 17.5 Mev, angular-momentum effects in, (E), 20: 32508
helium-3 reactions (He-3,t) at 18 Mev, (E), 20: 42334
helium-3 reactions (He-3,d) at 16.5 Mev, copper-61 energy levels from, (E), 20: 44837
helium-3 scattering at 33 Mev, (E/T), 20: 24330(R) (ANL-7108, pp 31-6)
helium-4 reactions with, zinc-64 compound nucleus production in, (E), 19: 19090 (UCRL-11862)
helium-4 reactions with, formation and decay of zinc-64 in, 20: 38152
lithium-6 reactions at 66 Mev, gallium-63 from, 19: 12556
meson (μ⁻) capture by, (E), 19: 37897
neutron capture at 15 to 300 kev in, cross sections and gamma spectra for fast, 17: 21010
neutron capture by, gamma spectra from thermal, (E), 20: 9966 (IAE-885)
neutron capture by, gamma transitions from thermal, (E), 20: 26208
neutron capture in, gamma angular correlations in thermal, 17: 41527(R) (ANL-6720(p.2-15))
neutron cross sections of, at 13 to 15 Mev, 16: 32176(R) (PR-P-53)
neutron inelastic scattering by, gamma yields from, (E), 19: 35406(T) (ANL-Trans-177)
neutron reactions (n,p) at 14 Mev, direct and evaporation mechanisms, 16: 4850
neutron reactions (n,p), production of carrier-free cobalt-60 by, 16: 13114
neutron reactions (n,np), (n,pγ), and (n,pn) at 14 Mev, cross sections for, 17: 2242 (TID-16949)
neutron reactions (n,p) with, cross sections for fast, 17: 31056
neutron reactions (n,d) at 14 Mev, cross sections for ground-state transitions in, 17: 34920
neutron reactions (n,γ) with, angular correlations from, 18: 2403(R) (PR-P-58)
neutron reactions (n,γ) with, 18: 14592(R) (PR-P-60)
neutron reactions (n,γ) with, angular correlation of 7.54–0.284 Mev cascade in, 18: 21240
neutron reactions (n,p) at 12.5 to 16.5 Mev, cross sections for, (E), 19: 6666
neutron reactions to 16 Mev, cross sections for two-particle emission in, (T), 19: 10283
neutron reactions (n,p) at 12.6 to 16.6 Mev, cross sections for, (E), 19: 35378(R) (EANDC(E)-57(U))
neutron reactions (n,p) at 14 Mev, angular and energy distributions from direct, (E), 20: 6440
neutron reactions (n,p) at 0 to 20 Mev, cross sections for, 20: 19810 (EUR-119.e(Vol.2))
neutron scattering at 1 to 4 Mev, cross sections for energy level excitation in, 18: 21217
neutron total cross section, 17: 41873 (WASH-1044)
neutron total cross sections for, level spacings from, (E/T), 20: 32389
nuclear surface oscillations in, calculation of, 17: 40019
nucleon capture at 10 to 40 Mev, cross sections and mechanism for direct, (T), 20: 17737
parity and spin of, from deuteron scattering data, 20: 15850
preparation as radiation target material, 18: 27811(R) (ORNL-TM-198)
proton angular distributions to excited 2+ and 3– states, parity change determinations from, 16: 21556
proton capture by, use for testing cosmological theory, (T), 19: 4808
proton capture cross sections at 10 to 20 Mev, (E/T), 19: 21442
proton compound-elastic scattering at 5.45 Mev, differential cross section for, 18: 11289
proton cross sections at 8.8 Mev, (E), 19: 29276
proton differential elastic scattering cross sections at 30.3 Mev, 18: 36631
proton elastic and inelastic scattering at 6.8 Mev, 17: 24414
proton elastic scattering at 7 to 12 Mev, cross sections for, 17: 16770(R) (ANL-6666)
proton elastic scattering, isotopic, isotonic, and shell closure effects on polarized, 17: 19360
proton elastic scattering by, excitation functions for, 17: 22264(R) (ANL-6679)
proton elastic scattering at 4.2 Mev, angular distribution of, 17: 22656
proton elastic scattering at 9.4 Mev, cross sections and polarization for, 18: 18964
proton elastic scattering at 7 to 12 Mev, angular distributions from, 18: 21292
proton elastic scattering at 30 Mev, polarization in, 18: 36633
proton elastic scattering at 6.9 Mev, (E), 19: 5237
proton elastic scattering at 6.9 Mev, isotope effects on polarization in, (E), 19: 14630
proton elastic scattering at 3.00 to 3.56 Mev, angular distribution for, (E), 19: 37879(T)
proton elastic scattering at 39 Mev, polarization in, 19: 45378
proton elastic scattering at 25 to 50 Mev, polarization from, (E),

20: 15728(R) (RHEL/R-112, pp 23-36)
proton elastic scattering at 45 Mev, differential cross sections for, (T), 20: 21963 (AD-626656)
proton elastic scattering at 40 Mev, cross sections for, (E/T), 20: 30353(R) (ORNL-3940, pp 1-61)
proton elastic scattering at 39 Mev, polarization in, (E), 20: 36176(R) (TID-22971, pp 41-140)
proton elastic scattering at 49 Mev, angular distribution of polarization in, (E), 20: 38049
proton elastic scattering at 30 Mev, optical-model analysis of, (T), 20: 42255
proton elastic scattering at 6.53 Mev, angular distribution of polarization in, (E), 20: 46783
proton inelastic scattering at low energies, reaction mechanisms for, 16: 21393
proton inelastic scattering at 14.65 Mev, 16: 28071
proton inelastic scattering at 6.6 Mev, 17: 7178
proton inelastic scattering, gamma angular distribution from, 17: 17205
proton inelastic scattering by, angular distributions for, 17: 39974 (INSJ-59)
proton inelastic scattering by, angular correlations for, 18: 7780
proton inelastic scattering at 3 to 4.3 Mev, energy levels from, 18: 19046
proton inelastic scattering at 40 Mev, 18: 30808
proton elastic scattering at 17.8 Mev, polarization in, (E/T), 19: 14599
proton inelastic scattering at 30 Mev, differential cross sections for, (E), 19: 28962(R) (NIRL/R/81)
proton inelastic scattering at 40 Mev, polarization asymmetry in, (E), 20: 24440
proton inelastic scattering at 40 Mev, cross sections for, (E/T), 20: 30353(R) (ORNL-3940, pp 1-61)
proton inelastic scattering at 17.8 Mev, cross sections for, (T), 20: 30437
proton inelastic scattering at 10.5 and 14.0 Mev, spin flip in, (E), 20: 32557
proton inelastic scattering at 17.8 Mev, testing nuclear model by, (E/T), 20: 44658 (UCRL-16984)
proton inelastic scattering at 10.5 and 14.0 Mev, proton spin flip in, (E), 20: 46597 (RLO-1388-14)
proton reactions (p,d) at 17 to 18.5 Mev, neutron shell configuration studies from, 18: 21291
proton reactions (p,d) at 28 Mev, angular dependence on final state spin in, 18: 21299
proton reactions (p,d) at 55 Mev, cross sections for, 18: 36570 (INSJ-73)
proton reactions (p,p′γ) with, angular distributions and energy spectra from (E/T), 19: 1568(R) (TID-21113)
proton reactions (p,γγ), triple correlations in, (E/T), 19: 10342
proton reactions (p,d) with, isobaric analog states from, (T), 19: 14492 (ANL-6878(p.207-13))
proton reactions (p,d) at 55 Mev, deuteron spectra from, (E), 19: 16852(R), (NP-14647)
proton reactions (p,γγ) with, triple correlations in, (E), 19: 23628 (NRL-6186)
proton reactions (p,pγ) at 5 to 7 Mev, level structure from, (E), 19: 35480
proton reactions (p,p′γ) at 3.4 to 5 Mev, cross sections for, (E), 20: 12159
proton reactions (p,d) at 55 Mev, angular distributions and spectroscopic factors from, (E), 20: 19877
proton reactions (p,n) with, accelerator beam calibration from threshold energy for, 20: 28401
proton reactions (p,p′γ) at 13 Mev, energy levels from, (E), 20: 32490
proton reactions (p,n) with, thresholds for, (E), 20: 38053
proton reactions (p,n) with, threshold energy for, (E), 20: 38054
proton reactions at 30 Mev, optical-model analysis of total cross sections for, (T), 20: 42255
proton reactions (p,α) and (p,p′) at 17.5 Mev, alpha spectra from, 16: 7112
proton reactions (p,n) at 6–12 Mev, neutron spectra from, 17: 24444
proton reactions (p,n) with, threshold energy for, 17: 36669 (WASH-1042)
proton reactions (p,α) at 10.02 to 14.43 Mev, angular distributions in, 17: 41906
proton reactions with, distributions from (E), 19: 10257(R) (TID-21335 (p.33-107))
proton scattering at 31 Mev, cross sections for inelastic, 16: 21576
proton scattering at 30.8 Mev, angular distributions, 16: 26282
proton scattering at 8 Mev by, angular distribution of elastic, 16: 29471(R) (ANL-6574)
proton scattering cross sections of, fluctuations of, 17: 21048
proton scattering at 29 Mev, 18: 14590(R) (NIRL/R/60)
proton scattering at 40 Mev, analysis of, 18: 16924 (ANL-6848(p.130-6))
proton scattering at 55 Mev by, differential cross sections for, 18: 36571 (INSJ-74)
proton scattering by, polarization from, 18: 40597
proton scattering at 30 Mev, optical-model analysis of (E/T), 19: 3315
proton scattering at 40 Mev, (T), 19: 37862
proton scattering at 18.6 and 19.1 Mev, (E/T), 20: 4849(R) (UCRL-14360, pp 1-50)
proton scattering at 19 Mev, excited 2^+ and 3^+ levels from, (E/T), 20: 12065
proton scattering at 45 Mev, cross sections for elastic, (E), 20: 40162
proton total cross sections at 8.5 to 11 Mev, (E), 19: 43323
proton total cross sections at 30 and 50 Mev, (E), 20: 15729(R) (RHEL/R-112, pp 37-66)
proton total scattering cross sections at 30 Mev, 18: 36632
transition mixing ratios (E2/M1) for, measurement of $2^{+\prime} \rightarrow 2^+$, 17: 17205

NICKEL ISOTOPES Ni-61

alpha scattering by, 17: 40436(R) (NYO-10063(p.105-15))
Coulomb excitation by nitrogen ions, (E), 19: 16895
deuteron reactions at 21.6 Mev, angular distributions and cross sections, 16: 21557
deuteron reactions (d,t) at 21.6 Mev, angular distributions and cross sections for, 16: 28134
deuteron reactions (d,t) at 15 Mev, (E/T), 19: 37863
deuteron reactions (d,p), proton polarization from, (E), 20: 6422
deuteron reactions at 10 to 20 Mev, excitation functions for, (E), 20: 38148
electron-nuclear double resonance and hyperfine structure variation of, in aluminum oxide crystals, 18: 718
energy level at 0.282 Mev, parity and spin of, 18: 11173 (ANL-6797 (p.270))
energy level at 0.284 Mev, spin of, 18: 28693
energy level at 284 kev, spin of, 18: 21240
energy level transitions from neutron capture by nickel-60, (E), 20: 26208
energy levels, 17: 2315
energy levels and nuclear potential, 18: 32881
energy levels from Coulomb excitation by neon-20, 17: 4093
energy levels from (p,d) reactions, spins of, 18: 21299
energy levels from thermal-neutron capture in nickel, (E), 20: 9966 (IAE-885)
energy levels, modified shell model for, 16: 18511
energy levels of, spin of, 18: 42622(R) (ANL-6879(p.2-20))
energy levels of, reduced widths and strength functions of, (E), 19: 17009
energy levels of, structure from isomeric transition in, (T), 20: 19970
energy levels of, energy calculations using shell model with reaction matrix, (T), 20: 38066
gamma spectra of, parity effects on Mössbauer, 17: 13238
helium-3 reactions with, zinc-64 compound nucleus production in, (E), 19: 19090 (UCRL-11862)
helium-3 reactions with, formation and decay of zinc-64 in, 20: 38152
helium-3 reactions (He-3,t) at 18 Mev, (E), 20: 42334
magnetic fields acting on, in ferromagnetic materials, 19: 20578
magnetic moment, 16: 26322
Mössbauer effect in, bibliography on, 18: 14650
Mössbauer effect in, from Coulomb excitation, (E), 19: 33337
Mössbauer effect in, measurement using Coulomb excitation, 20: 26196
Mössbauer effects in, following Coulomb excitation, 20: 3920(R) (ORNL-3870, pp 27-37)
neutron capture by, gamma energy and intensity from, 16: 33819
neutron capture cross sections, 18: 24620(R) (ORNL-TM-874)
neutron cross sections of, at 13 to 15 Mev, 16: 32176(R) (PR-P-53)
neutron energy level positions in, 18: 9360
neutron reactions (n,p), production of carrier-free cobalt-61 by, 16: 13114
neutron reactions (n,np) at 14.8 Mev, cross sections for, 17: 2242 (TID-16949)
neutron strength functions of, s-wave, (E), 19: 35404 (ORNL-P-1371)
nuclear magnetic moments, 16: 1054
nuclear magnetic moments of ground state, Mössbauer-parity experiment for measuring sign, 16: 22998(R) (ORNL-3268(p.67-9))
nuclear magnetic moment, 17: 19358
nuclear magnetic moment, 17: 41938
nuclear magnetic moment, 18: 36640
nuclear magnetic resonance in pure nickel powders, line shapes, saturation behavior, and temperature studies in, 17: 34603
nuclear magnetic resonance absorption in 0.5% cobalt–nickel alloy, effects of temperature and pressure on, 19: 23812
nuclear magnetic resonance in metallic nickel, 19: 39418
nuclear magnetic resonance of, in single-domain nickel powders, 20: 45000
nuclear moments, 17: 22222 (MMPP-NPC-1-3)
nuclear properties, study by Mössbauer effect, 16: 21447
nuclear radius, 17: 36679
nuclear spin and parity, ground-state, 16: 15700
oxygen ion reactions at 25 Mev, Mössbauer spectra from, (E), 20: 19832 (ORNL-P-1966)
proton reactions (p,n) with, thresholds for, (E), 19: 6704
proton scattering at 7 Mev, (E), 19: 5569(R) (MIT-2098-64)

single-particle states of, from (d,p) reactions with nickel-60, 18: 9417

NICKEL ISOTOPES Ni-62

alpha elastic scattering at 7 to 12 Mev, angular distributions from, 18: 21292
alpha elastic scattering at 25 to 85 Mev, (T), 19: 19206
alpha inelastic scattering, excitation by, 16: 24777 (CEA-2146)
alpha inelastic scattering at 43 Mev, collective excitations by, 17: 22627
alpha inelastic scattering at 43 Mev, collective states excited in, 17: 38266
alpha inelastic scattering by, nuclear-structure effects on, 18: 7751
alpha inelastic scattering at 44 Mev, 18: 16925 (ANL-6848(p.137-42))
alpha inelastic scattering by, levels from, (T), 19: 14489 (ANL-6878 (p.143-73))
alpha inelastic scattering by, form factors from, (T), 19: 19172
alpha inelastic scattering at 25 to 100 Mev, cross sections for, (E/T), 19: 43294
alpha inelastic scattering at 25 to 100 Mev, phase shift in, (T), 19: 43312
alpha inelastic scattering at 44 Mev, collective states in, 19: 47608
alpha reactions (α,p) at 42 Mev, angular distributions of protons from, 18: 16951(R) (TID-20311)
alpha reactions (α,n), cross sections for, 16: 33814
alpha reactions at 3 to 10 Mev, gamma yields from, 16: 23065
alpha reactions at 27 to 52 Mev, proton evaporation from, 16: 23113
alpha reactions at 42 Mev, proton emission in, (E), 20: 12062
alpha scattering at 44 Mev, angular distributions from, (E/T), 19: 19169
alpha scattering at 25 to 100 Mev, angular distributions, (E/T), 19: 21269(R) (UCRL-11828(p.132-3))
alpha scattering by, 17: 40436(R) (NYO-10063(p.105-15))
alpha scattering by, phase rule energy variation in, 18: 38142
bremsstrahlung reactions (γ,p) at 24 Mev, direct photoeffect and evaporation contributions in, 17: 38209
deuteron elastic scattering at 13.6 Mev, angular distributions, 16: 18523
deuteron elastic scattering at 7 to 12 Mev, angular distributions from, 18: 21292
deuteron elastic scattering at 6.5 Mev, angular distributions from, (E), 19: 5251
deuteron elastic scattering at 13.6 Mev, differential cross sections for, (E), 20: 38128
deuteron elastic scattering at 13.6 Mev, optical model analysis of, (T), 20: 42294
deuteron inelastic scattering at 13.6 Mev, angular distributions, 16: 18522
deuteron inelastic scattering at 15 Mev, angular distributions from, 17: 38271
deuteron inelastic scattering at 13.6 Mev, differential cross sections for, 17: 38259
deuteron reactions (d,p), angular distributions, 16: 15700
deuteron reactions (d,p), differential cross section and reduced width, 16: 15701
deuteron reactions (d,p) at 13.6 Mev, proton angular distributions from, 17: 2315
deuteron reactions (d,p) at 13.6 Mev, angular distributions from, 17: 24414
deuteron reactions (d,p) at 10 Mev, spin dependence of angular distributions from, 18: 9424
deuteron reactions (d,n) at 11.7 Mev, neutron spectra from, (E), 19: 33365
deuteron reactions (d,p) at 15 Mev, (E/T), 19: 37863
deuteron reactions (d,p), proton polarization from, (E), 20: 6422
deuteron reactions (d,n) at 11.7 Mev, neutron spectra and angular distributions from, (E), 20: 22109
deuteron reactions (d,p) with, proton yields from, (E), 20: 26208
electron inelastic scattering from first excited state of, form factors from, (E), 20: 34605
energy level lifetimes from Doppler shift attenuation measurements, (E), 19: 16950
energy level of, lifetime of 1.172-Mev, 18: 11249
energy level transitions in, E2, (T), 19: 16940
energy levels, 16: 23073
energy levels, 18: 2841(R) (ORNL-3488(p.1-17))
energy levels, 18: 40608
energy levels, (E), 19: 23767
energy levels, 20: 4849(R) (UCRL-14360, pp 1-50)
energy levels and shell-model properties, (E), 19: 37823(R) (ORNL-3800(p.1-49))
energy levels at 1.17 to 2.89 Mev, model for, 16: 33872
energy levels excited by alpha scattering, 18: 32747(R) (UCRL-11213 (p.64-86))
energy levels from scattering, vibrational, (E/T), 20: 44795
energy levels from copper-63 (d,He-3) reactions, (E), 20: 46242(R) (TID-23239)
energy levels of, alpha inelastic scattering excitation of, 17: 40094
energy levels of, anharmonicity in vibrational motion of, 18: 7754
energy levels of, Coulomb excitation of, 17: 32723(R) (PR-P-57(p.5-20))
energy levels of, determination of, from 43-Mev alpha scattering reactions, 16: 32400 (TID-16665)
energy levels of, excited by (d,p) reactions, 17: 34948
energy levels of, lifetimes of first-excited, 18: 2403(R) (PR-P-58)
energy levels of, lifetimes of, 18: 8917(R) (PR-P-59(p.4-20))
energy levels of, power functions for, 17: 38003(T) (AEC-tr-5734(p.25-6))
energy levels of, three-phonon, 17: 9576
energy levels of, shell model analysis of, (T), 19: 37824(R) (ORNL-3800(p.50-7))
energy levels of, microscopic models for vibrational, (T), 20: 3083
energy levels of, from neutron reactions with copper-63 at 14 Mev, (E), 20: 4896
energy levels of, parity and spin of, 20: 8083 (PUC-937-171A)
energy levels of, energy calculations using shell model with reaction matrix, (T), 20: 38066
energy-level transitions from proton inelastic scattering at 17.5 Mev, (E), 20: 46741
helium reactions (He-3,d) at 22 Mev, angular and energy distributions for, 18: 19082
helium-3 elastic scattering at 33 Mev, cross sections for, (E/T), 19: 43339
helium-3 reactions (He-3,d) with, distorted-wave analysis of, 18: 21204 (LADC-6302)
helium-3 reactions (He-3, d) with, quasi-boson plus quasi-proton scheme for, 19: 25517
helium-3 reactions (He-3,d) at 22 Mev, (E), 20: 1216
helium-3 reactions (He-3,d), core excitation in, (T), 20: 13816
helium-3 reactions (He-3,d) at 22 Mev, angular distributions from, (T), 20: 17692 (ORNL-TM-1414)
helium-3 reactions (He-3,t) at 22 Mev, Coulomb displacement-energy from, (E), 20: 22095
helium-3 reactions (He-3,t) at 18 Mev, (E), 20: 42334
helium-3 scattering at 33 Mev, (E/T), 20: 24330(R) (ANL-7108, pp 31-6)
meson (μ^-) capture by, (E), 19: 37897
neutron capture by, gamma spectra from thermal, (E), 20: 9966 (IAE-885)
neutron capture by, gamma transitions from thermal, (E), 20: 26208
neutron capture cross sections, 18: 24620(R) (ORNL-TM-874)
neutron capture in, gamma angular correlations in thermal, 17: 41527(R) (ANL-6720(p.2-15))
neutron elastic scattering at 4 Mev, polarized, 18: 40511 (NP-14205)
neutron inelastic scattering in, phonon scattering spectra from, 16: 32387
neutron reactions, carrier-free yields from, 16: 13114
neutron reactions (n,np) at 14.8 Mev, cross sections for, 17: 2242 (TID-16949)
neutron reactions with, determination of mass-flow function from, 17: 33027
neutron scattering by, excitation function fluctuation in, 17: 41873 (WASH-1044)
neutron scattering at 4.0 Mev, polarization angular distributions from, (E), 20: 30360 (WASH-1068)
neutron total cross section, 17: 41873 (WASH-1044)
neutron total cross sections for, level spacings from, (E/T), 20: 32389
nuclear properties of, (E/T), 19: 41755
nuclear radius, 17: 36679
nucleon coupling to anharmonic surface vibrations of, (T), 20: 26125
preparation as radiation target material, 18: 27811(R) (ORNL-TM-198)
proton elastic and inelastic scattering at 6.8 Mev, 17: 24414
proton elastic scattering, isotopic, isotonic, and shell closure effects on polarized, 17: 19360
proton elastic scattering at 4.2 Mev, angular distribution of, 17: 22656
proton elastic scattering at 3.4 to 4.2 Mev, angular distributions for, 18: 11274
proton elastic scattering at 7 to 12 Mev, angular distributions from, 18: 21292
proton elastic scattering of 6.9 Mev, (E), 19: 5237
proton elastic scattering at 6.9 Mev, isotope effects on polarization in, (E), 19: 14630
proton elastic scattering at 3.00 to 3.56 Mev, angular distribution for, (E), 19: 37879(T)
proton elastic scattering at 6.53 Mev, angular distribution of polarization in, (E), 20: 46783
proton inelastic scattering at 11 Mev, excitation of two-phonon levels in, 17: 40068
proton inelastic scattering at 11 Mev, angular distributions for, 18: 6175(R) (ORNL-3499(Vol.I)(p.24-6))
proton reactions (p,d) at 28 Mev, angular dependence on final state spin in, 18: 21299
proton reactions (p,d) with, isobaric analog states from, (T), 19: 14492 (ANL-6878(p.207-13))
proton reactions (p,p'γ) at 3.4 to 5 Mev, cross sections for, (E), 20: 12159

proton reactions (p,p'γ) at 13 Mev, energy levels from, (E), 20: 32490
proton reactions (p,n) at 5.5 to 14.3 Mev, excitation functions for, (E), 20: 36157(R) (CU-1019-51)
proton reactions (p,n) with, thresholds for, (E), 20: 38053
proton reactions at 20 to 50 Mev with, cross sections and excitation functions for, 17: 26426 (NYO-10387)
proton reactions at 20 to 50 Mev, copper-63 compound nucleus formation in, (E), 20: 38147
proton reactions (p,p') at 11 Mev, 17: 19335
proton reactions (p,n) with, thresholds for, 17: 22568 (WASH-1041)
proton scattering at 4.71 Mev, spin of 2.05-Mev level from, 17: 26589
proton scattering by, excitation functions for, 18: 4529 (CONF-327-4)
proton scattering by, excitation function fluctuations in, 18: 7696(R) (ORNL-TM-761)
proton scattering by, at 17.5 Mev, 18: 26536(R) (ORNL-3582(p.54))
proton scattering by, polarization from, 18: 40597
proton scattering at 12 Mev, cross sections for, 19: 47585 (ORNL-3851)
proton scattering at 18.6 and 19.1 Mev, (E/T), 20: 4849(R) (UCRL-14360, pp 1-50)
proton scattering at 19 Mev, excited 2⁺ and 3⁻ levels from, (E/T), 20: 12065
proton scattering by, isobaric analog states from, (E), 20: 44761
transition probabilities in, E2, 18: 32778

NICKEL ISOTOPES Ni-63

alpha inelastic scattering by, levels from, (T), 19: 14489 (ANL-6878 (p.143-73))
beta activity of, use of 4π proportional counters for measuring, 20: 31548
beta decay of, corrections for foil absorption in 4π counting of, (E), 19: 26654 (EUR-2248.e)
beta decay of, neutrino degeneracy and post Fermi end-point energy in, (E), 20: 24399
beta self-absorption in solutions of, effects of teflon on, 18: 12175
beta transitions in, angular momentum retardation of, 18: 40557
counting techniques for, international comparison of proportional, 18: 31866 (AWRE-O-26/64)
deposition, computer program for evaluating radiochemical data on, 19: 40636 (WAPD-TM-516)
detection and measurement of, using scintillation ion exchange resin, 19: 32098
determination in sea water by liquid scintillation counting, 20: 12779 (USNRDL-TR-924)
diffusion in alpha-irradiated copper, 19: 47032
diffusion in alpha-irradiated copper, 20: 37300
diffusion in chromium-nickel alloys, relation of high-temperature creep to, 18: 36023
diffusion in cobalt–nickel alloys, self-, 16: 33501
diffusion in cobalt–nickel alloys, 19: 9708
diffusion in copper-nickel alloys, relation of high-temperature creep to, 18: 36024
diffusion in copper at 250 to 520°C, 20: 21367
diffusion in gamma-iron and nickel, measurements of grain-boundary, 18: 30204
diffusion in nickel–tungsten alloys, relation of high-temperature creep to, 18: 36025
diffusion in sodium chloride crystals, coefficients for, 18: 39224
effects of ingested, on reproduction of Habrobracon, 19: 10741 (TID-21559)
electrodeposition of, development of methods for, 17: 35670 (AERE-M-1257)
energy level transitions from neutron capture by nickel-62, (E), 20: 26208
energy levels, 17: 2315
energy levels, 17: 41873 (WASH-1044)
energy levels at 0.158 and 0.528 Mev, parity and spin of, 18: 11173 (ANL-6797(p.270))
energy levels from thermal-neutron capture in nickel, (E), 20: 9966 (IAE-885)
energy levels of, excited by (d,p) reactions, 17: 34948
energy levels of, spins of, 18: 28693
energy levels of, sign of, 18: 42622(R) (ANL-6879(p.2-20))
energy levels of, from copper-63 (d,He-3) reactions, 19: 21358
energy levels of, quasi-particle method for, (T), 19: 25501
energy levels of, energy calculations using shell model with reaction matrix, (T), 20: 38066
exchange reactions with tetraethylenepentamine- and triethylene-tetramine-nickel (II) complexes, 17: 32067
formation and transport in Inconel reactor cooling systems, 16: 1182 (AECL-1265(Paper 4))
half life, 16: 14021
neutron capture by, gamma energy and intensity from, 16: 33819
nuclear spin and parity, ground-state, 16: 15700
production at PRR, methods for, 20: 12545(R) (PAEC(A)AR651)
production of carrier-free, by nickel-62 (n,γ) reactions, 16: 13114
radioinduced diffusion in copper, model of alpha, 20: 39451 (EUR-2968.e)
radiometric assay by liquid scintillation counting, 16: 5382
separation from cobalt-58, 16: 215
use as tracer to study extraction of metal ions, 20: 45802
use in diffusion measurements of thermal energy of extreme environments from aborted aerospace launchings, 19: 11310(R) (SC-DC-64-1433)
use in luminous paints in watchmaking, 19: 28706
use in triggering Penning discharge, 20: 45877
use on filters to measure dusts, 16: 26652
uses in thickness gage for measuring soot in furnace, 18: 30081

NICKEL ISOTOPES Ni-64

activation using 14-Mev neutrons, 20: 14461(R) (ORNL-3889, pp 48-70)
alpha elastic scattering at 7 to 12 Mev, angular distributions from, 18: 21292
alpha inelastic scattering, excitation by, 16: 24777 (CEA-2146)
alpha inelastic scattering by, nuclear-structure effects on, 18: 7751
alpha inelastic scattering at 44 Mev, 18: 16925 (ANL-6848(p.137-42))
alpha inelastic scattering by, levels from, (T), 19: 14489 (ANL-6878 (p.143-73))
alpha inelastic scattering by, form factors from, (T), 19: 19172
bremsstrahlung reactions (γ,p) at 24 Mev, direct photoeffect and evaporation contributions in, 17: 38209
deuteron elastic scattering at 13.6 Mev, angular distributions, 16: 18523
deuteron elastic scattering at 7 to 12 Mev, angular distributions from, 18: 21292
deuteron elastic scattering at 6.5 Mev, angular distributions from, (E), 19: 5251
deuteron elastic scattering at 13.6 Mev, differential cross sections for, (E), 20: 38128
deuteron elastic scattering at 13.6 Mev, optical model analysis of, (T), 20: 42294
deuteron inelastic scattering at 13.6 Mev, angular distributions, 16: 18522
deuteron inelastic scattering at 13.6 Mev, differential cross sections for, 17: 38259
deuteron reactions (d,p), angular distributions, 16: 15700
deuteron reactions (d,p) at 13.6 Mev, proton angular distributions from, 17: 2315
deuteron reactions (d,p) at 13.6 Mev, angular distributions from, 17: 24414
deuteron reactions (d,t) at 14.7 Mev, spin dependence of angular distributions from, 18: 21301
deuteron reactions (d,n) at 11.7 Mev, neutron spectra from, 19: 33365
deuteron reactions (d,p) at 15 Mev, (E/T), 19: 37863
deuteron reactions (d,p), proton polarization from, (E), 20: 6422
deuteron reactions (d,n) at 11.7 Mev, neutron spectra and angular distributions from, (E), 20: 22109
deuteron stripping reactions (d,p) with, 16: 30930(R) (NYO-2669)
effects on nickel oxide crystal lattice constants, (E), 19: 4158
energy level structure of, 17: 22568 (WASH-1041)
energy level transitions in, E2, (T), 19: 16940
energy levels, 18: 40608
energy levels and shell-model properties, (E), 19: 37823(R) (ORNL-3800 (p.1-49))
energy levels from scattering, vibrational, (E/T), 20: 44795
energy levels of, alpha inelastic scattering excitation of, 17: 40094
energy levels of, microscopic models for vibrational, (T), 20: 3083
energy levels of, effective interactions and seniorities in, (T), 20: 28400
energy levels of, energy calculations using shell model with reaction matrix, (T), 20: 38066
energy-level transitions from proton inelastic scattering at 17.5 Mev, (E), 20: 46741
helium-3 elastic scattering at 33 Mev, cross sections for, (E/T), 19: 43339
helium-3 reactions (He-3,d) at 22 Mev, (E), 20: 1216
helium-3 reactions (He-3,t) at 22 Mev, Coulomb displacement-energy from, (E), 20: 22095
helium-3 reactions (He-3,t) at 18 Mev, (E), 20: 42334
helium-3 scattering at 33 Mev, (E/T), 20: 24330(R) (ANL-7108, pp 31-6)
neutron capture cross sections, 18: 24620(R) (ORNL-TM-874)
neutron capture cross section at 0.12 to 1.96 Mev, 18: 24625 (WASH-1046)
neutron compound inelastic scattering at 3 Mev, angular correlation functions for, 18: 9402
neutron radiative capture cross sections at 100 to 2000 kev, 18: 24591(R) (LMSC-4-50-62-1)
neutron reactions (n,np) at 14.8 Mev, cross sections for, 17: 2242 (TID-16949)
neutron reactions (n,γ) at 0.2 to 2.0 Mev, cross sections for, (E/T), 20: 4911
neutron reactions (n,γ) at 0.176 to 1.958 Mev, cross sections for, (E), 20: 9981 (WASH-1064)
neutron reactions (n,γ) with, nickel-65 production in, 20: 40081

(PAEC(D)IS-653)
neutron reactions (n,α) and (n,p) at 14.7 Mev, radioisotope production in, (E), 20: 46626
neutron total cross section, 17: 41873 (WASH-1044)
neutron total cross sections for, level spacings from, (E/T), 20: 32389
nuclear properties of, (E/T), 19: 41755
proton elastic and inelastic scattering at 6.8 Mev, 17: 24414
proton elastic scattering at 9.5 to 22.2 Mev, angular distributions and cross sections, 16: 9462
proton elastic scattering at 4.2 Mev, angular distribution of, 17: 22656
proton elastic scattering at 3.4 to 4.2 Mev, angular distributions for, 18: 11274
proton elastic scattering at 7 to 12 Mev, angular distributions from, 18: 21292
proton elastic scattering at 6.9 Mev, (E), 19: 5237
proton elastic scattering at 6.9 Mev, isotope effects on polarization in, (E), 19: 14630
proton elastic scattering at 50 Mev, differential cross sections for, (E), 19: 28962(R) (NIRL/R/81)
proton elastic scattering at 3.00 to 3.56 Mev, angular distribution for, (E), 19: 37879(T)
proton inelastic scattering at 11 Mev, excitation of two-phonon levels in, 17: 40068
proton inelastic scattering at 11 Mev, energy level structure from, 17: 41954
proton inelastic scattering at 11 Mev, angular distributions for, 18: 6175(R) (ORNL-3499(Vol.I)(p.24-6))
proton inelastic scattering at 10 Mev, differential cross sections for, 18: 7763
proton inelastic scattering at 11-Mev, angular distribution of, (E), 19: 16855(R) (ORNL-3714(Vol.I)(p.1-30))
proton inelastic scattering at 9.3, 10.5, and 14 Mev, proton spin flip in, (E), 20: 46597 (RLO-1388-14)
proton reactions (p,n) at 3 to 5 Mev, isobaric-analog states in copper-65 from, 18: 19079
proton reactions (p,n) at 100 to 400 Mev, excitation functions for, 20: 30464
proton reactions (p,nγ), energy levels from, 16: 4813
proton reactions (p,n) with, excitation function and recoil behavior for, 17: 28247(R) (TID-18788)
proton scattering at 9.6 and 11.7 Mev by, differential cross sections for, 17: 11643 (UCRL-6930)
proton scattering at 9.6 and 11.7 Mev, excitation levels determined by, 17: 17239
proton scattering at 9.4–22.2 Mev, local optical potentials for, 17: 38185
proton scattering at 7 Mev, (E), 19: 5569(R) (MIT-2098-64)
proton scattering by, isobaric analog states from, (E), 20: 44761

NICKEL ISOTOPES Ni-65
beta and gamma spectra and energy levels, 16: 17148
beta decay of, energy levels and half life from, 17: 26586
beta decay of, gamma spectra for, 18: 19048
beta decay of, gamma spectra from, (E), 19: 45320
beta transitions in, angular momentum retardation of, 18: 40557
content in Hanford reactor coolant, estimation of aluminum component corrosion from, 19: 925(R) (HW-81746(p.3.44-9))
content in Hanford reactor effluent, 19: 685(R) (HW-81746(p.3.33-6))
decay of, activity measurements for gamma, 20: 9196
decay of, beta and gamma spectra from, 18: 24639
energy level analogy to copper-65, 18: 19079
energy levels, 17: 2315
energy levels from nickel-64 (n,γ) reactions at 0.2 to 2.0 Mev, radiation widths of, (E/T), 20: 4911
energy levels of, excited by (d,p) reactions, 17: 34948
energy levels of, energy calculations using shell model with reaction matrix, (T), 20: 38066
gamma dose constants for, 20: 46617
gamma emission from liquid and solid, resonance scattering of 1.114-Mev, 17: 41981
gamma spectra, 17: 34966
gamma spectra, 20: 44634(R) (IDO-17188)
neutron reactions (n,α) at 14 Mev, nuclear shell effects in cross sections for, 18: 18977
nuclear spin and parity, ground-state, 16: 15700
preparation of carrier-free, by neutron reactions (n,p) on copper-65, 18: 41897
preparation of high-specific-activity, using Szilard-Chalmers effects of 8-hydroxyquinolates, 16: 27043(T) (CEA-tr-X-444)
production at PRR, methods for, 20: 12545(R) (PAEC(A)AR651)
production by neutron reactions (n,γ), 18: 37592
production by neutron reactions (n,γ) with nickel-64, 20: 40081 (PAEC(D) IS-653)
production in alpha and proton reactions with copper at 320 to 700 Mev, cross sections for, 18: 32849
production of carrier-free, by nickel-64 (n,γ) reactions, 16: 13114
yields in proton spallation of copper at 24 Bev, 16: 24859

NICKEL ISOTOPES Ni-66
alpha inelastic scattering by, form factors from, (T), 19: 19172
production in 80-Mev proton fission of terbium-159, absolute cross section for, 17: 16052(R) (TID-18261(p.44-8))
yield from neutron fission of uranium-235, 16: 21347 (AWRE-0-58/61)
yield in multiple fission of uranium-235, 16: 28068

NICKEL ISOTOPES Ni-67
beta decay, (E), 19: 27564
production in neutron reactions with zinc-70 at 14 to 15 Mev, (E), 19: 27564

NICKEL MOLYBDATES
preparation and structure of, 19: 43991 (N64-26433)
preparation, crystal structure, and magnetic susceptibility of, 20: 26864

NICKEL NIOBATES
crystal structure, 16: 11650
crystallographic and magnetic structure, 16: 7532

NICKEL NITRATES
additive effects on electric conductivity and density of fused alkali metal nitrate systems, 18: 8334 (TID-19997)
analytical use for ion exchange separation of americium, curium, and rare earths, 20: 18562(R) (EUR-2640.e)
complexes with pyridine, preparation and properties of, 20: 14225 (TID-21577)
complexes with uranyl nitrate, formation in solution, 19: 28317
purification by zone melting, 18: 544 (CEA-2310)
salting-out properties in uranyl nitrate extraction from aqueous solutions, 17: 10770
separation by reversed-phase partition chromatography using organophosphorus compounds, 18: 25614
spectra in tributyl phosphate, infrared, 16: 31610 (AERE-R-3031)
thermal decomposition of hexahydrate of, 17: 4492 (IDO-14597)
$Ni(NO_3)_2$–$Th(NO_3)_4$, crystal structure of octahydrates, 19: 19852

NICKEL ORES
analysis for nickel by neutron activation, 20: 33161(T) (AEC-tr-6639, pp 13-17)
neutron capture gamma spectrometry in boreholes in, 18: 5522
Cu–Ni, sulfur-34 content in sulfides from Soviet Union deposits of, 18: 33767

NICKEL OXALATES
decomposition of surface of, comparison of radiation and thermal, 18: 335
decomposition of, kinetics of, 19: 42559
decomposition to nickel oxide, 19: 24978 (AROD-2884.3)
irradiation, preparation of metal and oxide by, 16: 32161
radiation effects on thermal decomposition of, 18: 20061
radiation effects on thermal decomposition of, 18: 44246
radiation effects on rate of decomposition of, beta and gamma, 20: 38955
radioinduced decomposition of, neutron, 19: 42559
sorptive properties for labile factor activity in chicken plasma, 17: 1201
spectra in iron oxalate–nickel oxalate mixtures, x-ray, 16: 13567 (ARL-66)
thermal decomposition kinetics, 18: 40971 (BNL-7683)

NICKEL OXIDES
see also Nickel Uranium Oxides
analysis for cobalt, tracer technique for, 20: 16335(R) (NBS-TN-276)
analysis for cobalt, copper, iron, and manganese by paper chromatography and precipitation using phosphorus-32-labeled phosphate, 20: 35409
analysis for impurities by activation methods, 19: 19796
analysis for iron by radioisotope dilution, 20: 16335(R) (NBS-TN-276)
analysis for nickel, use of fluorescent x-ray instrument for, 19: 13221
catalytic activity for decomposing nitrous oxide, 17: 41333(R) (ANL-6677)
catalytic effects on hydrocracking of polyphenyls, 17: 28434 (IDO-16858)
catalytic effects on radioinduced polymerization of isobutene, 18: 12220
catalytic effects on decomposition of tritium-labeled compounds, 19: 7491
catalytic properties of, isotopic exchange studies of, 18: 13739
cobalt-57 Mössbauer effect in, time independence of charge states determination from, (E), 20: 32713
crystal lattice constants of, isotope effects on, 19: 4158
crystal structure of, electron microscopic fringes from antiferromagnetic domain walls in, 19: 18514
crystal structure of lithium-doped, 20: 41458(R) (TID-23268)
diffusion into magnesium oxide single crystals, 19: 43997(R) (UCRL-11889)
distribution in sulfur trioxide–uranium trioxide–water systems, 16: 18896
effects of injected, carcinogenic, 16: 8503
effects on density and volume changes of graphite, 17: 36202(R) (SCC-13)

effects on fritting of beryllium oxide, 18: 22500(T) (UCRL-Trans-1042(L))
effects on hardness of zirconia at room temperature, 17: 32484(R) (GEAP-4284)
effects on homomolecular isotopic exchange of carbon monoxide, catalytic, 19: 26328
effects on mechanical properties of aluminum, 17: 37551
effects on neutron-irradiation effects on graphite, 17: 36349(R) (SCC-18)
effects on physical properties and radiation stability of graphite, 18: 7305 (HW-SA-3020)
effects on preparation of uranium carbide by carbothermic reduction of oxide, 20: 33841 (NAA-SR-10624)
effects on radioinduced reactions of isobutane and propylene on silica gel, 16: 13085(R) (TID-15251)
effects on radioinduced polymerization of acrylonitrile, 18: 12171
effects on radioinduced copolymerization, 19: 18000
effects on radioinduced polymerization of styrene, 20: 43338
effects on radioinduced reactions of isobutane and olefins, 18: 13836(R) (NYO-10025)
effects on sedimentation in aqueous thoria slurries, 19: 13278(R) (NYO-10295)
effects on structure and electric conductivity of calcium oxide–zirconium oxide, 19: 32736(T) (NP-tr-1236(p.66-73))
electron distribution and magnetic form factor of crystals of, 17: 37816
electron energy losses in, and mechanisms of, 17: 13165
emissivity of, measurements of, 17: 16787(R) (PWA-2163)
emittance at high temperatures, total hemispherical, 17: 6731
energy bands, 16: 12219(R) (NP-11304)
fabrication and mechanical properties of fine-grained polycrystalline, 19: 24978 (AROD-2884.3)
fabrication and properties of pure high-density fine-grained ceramics of, 19: 24979 (AROD-2884.4)
formation of thin films of, studies of the initial stages of, 19: 26765(R) (EURAEC-1295)
free energy of formation at 1100°F, 17: 32571(R) (MSAR-63-105)
free energy of formation, (E), 19: 17202
growth of crystals of, on copper–nickel alloys and nickel, 17: 39492(T,R) (EURAEC-726)
growth of crystals of, 17: 39483(R) (EURAEC-660)
growth of crystals of, on nickel, 17: 39483(R) (EURAEC-660)
hardness of crystals of, 16: 10728
incorporation into uranium dioxide lattice, 17: 27487
ion reactions at 40 kev, lattice disorders from krypton and xenon, (E), 20: 27597
magnetic form factor for nickel ions in, 16: 32980
mechanical properties, effects of grain parameters on, 19: 32048(R) (NP-15073)
melting temperature, evaluation for space technology, 18: 16521
neutron diffraction by, magnetic moment distribution from thermal, 20: 8046
neutron reactions at thermal energies, cross sections, 16: 10961 (TID-14868)
performance of cesium-coated, as collector for thermionic cells, 18: 20870
polarography in lithium and lithium sodium metaphosphates at 750 and 730°C, 18: 1516
preparation of crystals of, by zone melting at 2320 to 3800°K, 17: 32590
preparation of crystals of, by flame fusion, 17: 1941(R) (NP-12214)
preparation of double oxide with uranium trioxide, 18: 22014(R) (ORNL-3591(p.84-101))
preparation of highly dispersed, by irradiation of oxalate, 16: 32161
preparation of thin targets of, by oxidization of foils, 17: 35253(R) (IA-775)
preparation of thin films of, for use as isotopic oxygen targets, 17: 5945
preparation, properties, and aerospace applications, 19: 37142
production using tracer techniques for control of fractionation of impurities, 20: 23532(T) (AEC-tr-6466/1, pp 293-6)
properties, absorption, radiative, and thermionic emission, 16: 26953 (ARL-62-336)
proton diffusion in films of, effects of aluminum, molybdenum, tungsten, and zinc on, 18: 27457
proton reactions at 660 Mev, 17: 41884
radiation effect on sorption of carbon monoxide and oxygen on, gamma, 19: 40578
radiation effects on lithium-doped catalysts, in carbon monoxide oxidation, 16: 4600
radiation effects on chemisorption of hydrogen and oxygen by, fast neutron, 17: 3558
radiation effects on magnetic properties, 17: 12737
radiation effects on oxygen sorption, 17: 22249
radiation effects on catalytic activity of, 18: 17902
radiation effects on adsorptive and catalytic properties of, for heterogeneous oxidation of carbon monoxide, 19: 17952 (CEA-R-2604)
radiation effects on reduction by hydrogen, 19: 19975
radiation effects on reduction at 275°C, 19: 23140
radiation effects on catalytic activity in conversion of cyclohexane, 19: 26417
radiation effects on catalytic oxidation of carbon monoxide on, at 25°C, 19: 40577
radiation effects on catalytic activity in hydrogen *para-ortho* conversion, neutron, 19: 32775 (AFAPL-TR-65-9)
radiation effects on films of, on glass, 16: 21108
radiation effects on films of, on glass, 17: 5020
radiation effects on catalytic effects of, on para- to orthohydrogen conversion at 77°K, 20: 23790
radiation effects on structure of, fast-neutron, 20: 23800
radiation effects on reduction of, by hydrogen, 20: 31285
radiation effects on catalytic activity, surface excess oxygen, and electric conductivity of, gamma, 20: 36885
radiation effects on catalytic activity of, in decomposition of hydrogen peroxide, 20: 43364
radioinduced blistering of polycrystalline, helium ion, (E), 20: 29816
radioinduced catalytic activity of, 20: 362
radioinduced decomposition of, neutron, 18: 17882
radioinduced sorptive properties for gases, 17: 18152
radioinduced transition radiation from, fast electron, 18: 12747
radioinduced tritium release from lithium-doped, neutron, 16: 18955
radiolysis of azoethane adsorbed on, 18: 39316
radiolysis of azoethane adsorbed on, energy transfer in gamma, 20: 23116
reactions with oxides of europium and dysprosium, 18: 26896(R) (ANL-6868(p.133-74))
reactions with uranium oxides at high pressure and 900 to 1200°C, 16: 25302 (BMI-1585)
reactor reflector critical thickness, 16: 24410
separation from urania in organic slurries, centrifugal, 20: 36933
sintering of, mechanism of first stage in, 18: 4217(T) (AEC-tr-6159)
sintering of powders of, 20: 755(T) (IS-Trans-20)
solubility in borax at 760 to 900°C, 20: 3951
solubility in uranium(VI) oxide–water systems at 300°C, 16: 11636
solubility in vanadium oxide at 685°C, enthalpy for, 20: 7072
sorptive properties of hydrous, for cesium and strontium, 18: 45155(R) (TID-20980)
spectra in low frequency region, infrared, 18: 23549
spectra of, in 300 to 1000 mμ region, reflectance, 17: 15970
spectral characteristics, 16: 26953 (ARL-62-336)
stability of, galvanic cell studies of, 19: 43997(R) (UCRL-11889)
strength of polycrystalline, effects of compressive surface layers on, 20: 33860 (AD-634361)
strength of sintered, effects of grain size on, 19: 22952
uses in coating uranium dioxide spheres with nickel, 20: 33848 (Y-1538)
Al_2O_3–NiO_3, catalytic effects on hydrocracking of high boilers in reactor coolant, 17: 28435 (IDO-16877)
Al_2O_3–NiO, formation of delta-phase spinel, 19: 4664(T) (UCRL-Trans-1130)
Al_2O_3–NiO, use as multi-threshold detector for neutron spectrum measurements, 18: 12479
$Cr_2FeNi_2O_8$, crystal structure at 4.2 and 290°K, 17: 39400
Cr_2O_3–NiO, analysis by x-ray fluorescence, 18: 25275
Cr_2O_3–NiO–O, phase studies on, 20: 13260(R) (NP-15852)
Cr_2O_3–NiO–SiO_2, endurance of aluminum phosphate-bonded coating of, 17: 6675(R) (PWA-2128)
CuO–NiO–SO_3–UO_3–D_2O, critical phenomena and liquid-liquid immiscibility at 260 to 410°C, 17: 33922
CuO–NiO–SO_3–UO_3–water-d_2, liquid-liquid immiscibility and phase studies of, 17: 25067(R) (ORNL-3417(p.77-98))
CuO–NiO–SO_3–UO_3–H_2O, phase studies, 19: 23163(R) (ORNL-3650 (p.111-86))
Fe_2O_3–La_2O_3–NiO, phase diagrams at 800 to 1400°C, 19: 972
Fe_2O_3–La_2O_3–NiO, phase studies, 20: 5851
Fe_2O_3–NiO, analysis by x-ray fluorescence, 18: 25275
Fe_2O_3–NiO, phase diagrams to 1500°C, 19: 972
Fe_2O_3–NiO–ZnO, neutron radiation effects on magnetic properties of, 17: 2042
La_2O_3–NiO, phase diagrams to 1500°C, 19: 972
La_2O_3–NiO, phase studies, 20: 5851
Li_2O–Ni_2O, effects on radioinduced polymerization of acrylonitrile, 18: 12171
MgO–NiO, ordering in solid solutions of, effects of heat on, 16: 2924 (ASD-TR-61-92)
MgO–NiO, phase studies at 800 to 1400°C, 20: 338
MgO–NiO, preparation and plastic properties of single crystals of, 17: 41425 (HR-63-274)
MnO–NiO, phase studies at 800 to 1400°C, 20: 338

MoO_3–NiO, radiation effects of catalytic activity in hydrodesulfurization of hydrocarbons, 17: 16117(P)
Ni–NiO_x, durability as cathode in ion thruster, 19: 13615
NiO–Nb_2O_5, phase diagram, 19: 44711
NiO–Nb_2O_5, phase studies, 19: 26846
NiO–N_2O_5–UO_3–H_2O, formation of NiO·3UO_3 at 300°C in, 18: 12084
NiO–rare earth oxides, preparation and magnetic properties, 19: 42463
NiO–Sc_2O_3, phase studies, 20: 29168
NiO–SiO_2, sorptive properties for cesium, 17: 36995(R) (TID-19187)
NiO–SO_3–UO_3–D_2O, critical phenomena and liquid-liquid immiscibility at 260 to 410°C, 17: 33922
NiO–SO_3–UO_3–H_2O, formation of NiO · 3UO_3 at 300°C in, 18: 12084
NiO–SO_3–UO_3–water-d_2, liquid-liquid immiscibility and phase studies of, 17: 25067(R) (ORNL-3417(p.77-98))
NiO–WO_3, radiation effects on catalytic activity in hydrodesulfurization of hydrocarbons, 17: 16117(P)
NiO–ZrO_2, characterization of hot-pressed, 17: 27728(R) (GEAP-4076)
PbO–NiO, analysis by beta backscattering, 18: 41350

NICKEL PERCHLORATES

complexes with pyridine, preparation and properties of, 20: 14225 (TID-21577)
separation by reversed-phase partition chromatography using organophosphorus compounds, 18: 25614

NICKEL PHOSPHIDES

electron structure and physical properties of crystals of, 17: 27875

Nickel Potassium Fluorides

see Potassium Nickel Fluorides

NICKEL SALTS

boiling of aqueous solutions, hydrodynamic model for nucleate pool, 16: 20605
neutron form factor for divalent, 17: 37773
specific heat at 0.1 and 1.5°K, 18: 36509

NICKEL SELENIDES

entropies of transition metal, 16: 11600
magnetic properties, (E), 20: 4849(R) (UCRL-14360, pp 1-50)

NICKEL STEEL

analysis for molybdenum and tin using 8-quinolinol, spectrophotometric, 16: 16314
analysis for samarium, 19: 40445
analysis of, activation, 17: 5984
cavitation by bismuth, lead, and mercury, 16: 13537
cavitation by bismuth, lead, and mercury, 16: 33434(T) (AEC-tr-5382)
cobalt distribution in, optimization for PWR fuel elements, 17: 24613 (BAW-115)
corrosion by carbon dioxide at 450 to 825°C, 18: 16444
corrosion by steam and water at 100 to 600°C, 17: 23894
creep-rupture properties of maraging Almar 15 at 900°F, 18: 41928(R) (NASA-CR-54089)
diffusion and permeation of hydrogen isotopes in maraging, 20: 25559 (AWRE-O-19/66)
ductility of, effects of hydrogen on, 18: 24153(T,R) (EURAEC-1002)
fatigue of, at low strain cycles, 17: 1944 (TID-16455)
fission product plateout on, from helium system, 16: 29369 (GA-1934)
fracture toughness of maraging, effects of microstructure on, 20: 31670
mechanical properties, 17: 11099(R) (NP-12475)
performance in very thick pressure vessels, 18: 40772
properties at −400 to 100°F, 18: 42020 (PB-171809(Rev.))
properties of, review of methods of improving, 19: 18523
radiation effects at 60 to 400°C, 17: 24014(T,R) (EURAEC-530)
radiation effects on tensile properties of ASTM A353B, irradiated at 30°R, fast-neutron, 20: 27589(R) (NASA-CR-54881)
radiation effects on impact properties of, neutron, 20: 31669
weldability of, 18: 39411(R) (APCI-541103)
welding of, causes and effects of micro-flaws in, 17: 519 (WAL-TR-642.4/1)
welding parameters for maraging, electron-beam, 20: 5867
B–C–Cr–Mn–Mo–Ni–Nb–V, precipitation of niobium carbide in, 18: 37726
B–Cr–Mo–Ni, fabrication and properties, 18: 15565
B–Cr–Ni, corrosion resistance and tensile properties, 19: 28761
C–Co–Ni, tensile properties of strain-aged, 20: 31716(R) (UCRL-16658, pp 121-32)
C–Cr–Co–Mn–Mo–Ni, mechanical properties of welded, 19: 22863(R) (AD-606809)
C–Cr–Mn–Mo–Ni, mechanical properties of welded, 19: 22863(R) (AD-606809)
C–Cr–Mn–Mo–Ni–Si, strength and toughness of dynamically strain-aged, 20: 7584 (UCRL-16363)
C–Cr–Mn–Mo–Ni–Si–V, strength and toughness of dynamically strain-aged, 20: 7584 (UCRL-16363)
C–Cr–Mo–Ni–V, mechanical properties, effects of composition variations on, 19: 9645 (AD-604867)
C–Cr–Mo–Ni–Nb, mechanical properties, effects of low-temperature tempering on, 19: 9647 (AD-604876)
C–Cr–Mo–Ni, mechanical properties, effects of low-temperature tempering on, 19: 9647 (AD-604876)
C–Cr–Mo–Ni–V, mechanical properties, effects of low-temperature tempering on, 19: 9647 (AD-604876)
C–Cr–Ni–Nb, precipitation of niobium carbide in, 18: 37726
Co–Mo–Ni, mechanical properties of, effects of strain rate on, 20: 11284 (UCRL-14599)
Co–Mo–Ni, properties of Mar-aging, 16: 24153 (DMIC-Memo-156)
Co–Mo–Ni, tensile properties of strain-aged, 20: 31716(R) (UCRL-16658, pp 121-32)
Co–Ni, fracture toughness properties of, effects of carbon content on, 20: 11273(R) (NRL-6364)
Cr–Mn–Mo–Ni, development of high-strength weldable low-alloy, 20: 27481(R) (EURAEC-1419 and App.)
Cr–Mn–Mo–Ni, ductility of low-alloy, effects of alloying additions on, 20: 27481(R) (EURAEC-1419 and App.)
Cr–Mn–Mo–Ni, welding of very thick plates of, process development for, 20: 23621(R) (EURAEC-1548)
Cr–Mn–Ni, mechanical properties of austenitic cast, at 2.5 to 4.5°K, 20: 19232
Cr–Mo–Ni, corrosion by mercury and sodium amalgam at 200 to 500°C, 18: 18312(T) (CEA-tr-A-1455)
Cr–Mo–Ni, extrusion of type 4340, Dynapak, 19: 30686(R) (AD-608945)
Cr–Mo–Ni, fabrication and properties of reactor pressure vessel of, 18: 27926
Cr–Mo–Ni, fatigue of type 4130, energy criterion for, (T), 20: 27521
Cr–Mo–Ni, formation of Fe_2Mo in, 20: 35899(T) (AI-Trans-208)
Cr–Mo–Ni, fracture toughness properties of 12% maraging, 20: 11273(R) (NRL-6364)
Cr–Mo–Ni, hardness of welded type 4340, effects of heat treatments on, 20: 11215(R) (NASA-CR-54718)
Cr–Mo–Ni, oxidation of, causes of catastrophic, 16: 4500 (ORNL-TM-51)
Cr–Mo–Ni, performance in very thick pressure vessels, 18: 40772
Cr–Mo–Ni, phase transformations in martensitic, 18: 39917(T,R) (EURAEC-1120)
Cr–Mo–Ni, properties of Super-Elso, 19: 41008 (EURAEC-1407)
Cr–Mo–Ni, properties of Super-Elso, effects of heat treatments on, 20: 41447(R) (EURAEC-1669)
Cr–Mo–Ni, protection and rupture potentials in sodium bicarbonate–sodium chloride solutions at 40 and 80°C, 17: 25728(T) (EURAEC-677)
Cr–Mo–Ni, radiation effects on, surveillance tests on, 17: 31062
Cr–Mo–Ni, radiation effects on, neutron, 18: 40829 (EURAEC-1175)
Cr–Mo–Ni, radiation effects on ductility of, neutron, 19: 9735(R) (NRL-Memo-1424)
Cr–Mo–Ni, radiation effects on notch ductility of, neutron, 19: 11781(R) (NRL-Memo-1556)
Cr–Mo–Ni, radiation hardening in low-alloy, effects of irradiation temperature on fast-neutron, 20: 11342 (EURAEC-1502)
Cr–Mo–Ni, radioinduced embrittlement of, neutron, 20: 27610
Cr–Mo–Ni, tempering behavior of pressure-vessel, 19: 26817 (KAPL-3092)
Cr–Mo–Ni, transformation temperatures in Super Elso, effects of heating rate on, 20: 21331(R) (EURAEC-1569)
Cr–Mo–Ni, weld embrittlement in joints in, effects of time at high temperatures on, 20: 21393
Cr–Mo–Ni, welding techniques for HY-80, 20: 11261
Cr–Mo–Ni–Nb–V, development as HY-180/210 steel, 20: 5851
Cr–Mo–Ni–V, development, 19: 20462(R) (NRL-6258)
Cr–Mo–Ni–V, fatigue crack propagation in, effects of air or salt water environment on, 20: 11273(R) (NRL-6364)
Cr–Mo–Ni–V, mechanical properties, effects of carbon on, 19: 9646 (AD-604872)
Cr–Mo–Ni–V, mechanical properties of, effects of processing on, 20: 33858(R) (AD-634094)
Cr–Ni, additive effects of boron on properties of, for use as reactor heat shields, 17: 33261
Cr–Ni, analysis of, for molybdenum and tin using 8-quinolinol, spectrophotometric, 16: 16314
Cr–Ni, brittle fracture of super ELSO, 19: 20549(R) (EURAEC-1282)
Cr–Ni, compatibility with boron carbide, 17: 18759 (NAA-SR-Memo-8055)
Cr–Ni, corrosion cracking of, effects of carbon on, 16: 5677
Cr–Ni, corrosion of, by acids at high temperature, 16: 24129
Cr–Ni, corrosion of, by water at 70°C, 16: 10460
Cr–Ni, corrosion of, effects of vanadium pentoxides on, 16: 12059
Cr–Ni, corrosion by sodium bicarbonate solution, effects of chlorine and oxidants on, 17: 12616
Cr–Ni, corrosion by nitric acid containing chromium ions, effects of silicon on, 17: 14774(T) (AEC-tr-5646)
Cr–Ni, corrosion by sodium bicarbonate–sodium chloride solution, 17: 25726(T) (EURAEC-675)
Cr–Ni, corrosion by sodium acid carbonate–sodium chloride solutions and sulfates at 20°C, 17: 25727(T) (EURAEC-676)

Cr–Ni, corrosion by sodium at 1000°C, 17: 27756
Cr–Ni, corrosion by liquid lithium at 1000 and 1200°C, 18: 10480(T) (JPRS-22697(p.97-105))
Cr–Ni, corrosion by mercury and sodium amalgam at 200 to 500°C, 18: 18312(T) (CEA-tr-A-1455)
Cr–Ni, corrosion by nitric acid of boron alloyed, 18: 27983
Cr–Ni, corrosion by water and steam at high temperatures, effects of surface treatment on, 19: 34644
Cr–Ni, corrosion by aqueous dichromate-nitric acid, 20: 41418(R) (GEAP-5150)
Cr–Ni, corrosion by aqueous iron chloride, effects of carbon, manganese, and silicon traces on, 20: 41418(R) (GEAP-5150)
Cr–Ni, ductility of, alloying effects of molybdenum and uranium on temper embrittlement, 16: 7887 (NP-11168)
Cr–Ni, effects of niobium and zirconium on, 17: 11210
Cr–Ni, effects of cerium on properties of, 17: 39607
Cr–Ni, fission product plateout on, from helium system, 16: 29369 (GA-1934)
Cr–Ni, fracture of, dislocation in niobium carbide in area of, 20: 23757
Cr–Ni, hardness of heat-affected zones of welded joints in Super Elso, 19: 44686(R) (EURAEC-1362)
Cr–Ni, heat strength of, relation of, to kinetic oxidation coefficient, 16: 18077
Cr–Ni, loop corrosion tests at supercritical pressure and temperature on, 20: 2262 (WCAP-2056(Pt.6))
Cr–Ni, oxidation in air and in nitrogen with 0.1% oxygen at high temperatures, 17: 34351
Cr–Ni, passivation characteristics of, effect of temperature on, 16: 10461
Cr–Ni, potentiokinetic studies on corrosion by copper sulfate, nitric acid, and sulfuric acid, 17: 25729(T) (EURAEC-678)
Cr–Ni, preparation of, containing controlled-impurity carbon, manganese, and silicon, 20: 41418(R) (GEAP-5150)
Cr–Ni, properties of cast austenite, effects of rare earths on, 19: 22879(T) (JPRS-28849(p.319-25))
Cr–Ni, protection and rupture potentials in sodium bicarbonate–sodium chloride solutions at 40 and 80°C, 17: 25728(T) (EURAEC-677)
Cr–Ni, radiation effects on stress-rupture properties of tubular, 17: 33323(R) (ORNL-3445(p.199-217))
Cr–Ni, radiation effects on plastic deformation of, 17: 32684
Cr–Ni, radiation effects on tensile properties at 590 to 750°C, 17: 39689
Cr–Ni, radiation effects on mechanical and structural properties of, neutron, 18: 7322
Cr–Ni, radiation effects on austenitic, in-pile, 18: 28075
Cr–Ni, radiation effects on embrittlement of, 18: 37749 (A/CONF.28/P/420)
Cr–Ni, radiation effects on ductility of, 19: 34755
Cr–Ni, radiation effects on tensile properties of, 19: 37185
Cr–Ni, review on radiation effects on crystal lattice of, 18: 14565
Cr–Ni, specifications for castings for corrosive service, 17: 12611 (TID-17861)
Cr–Ni, stress-corrosion cracking in water, 17: 41380
Cr–Ni, thermal stresses in fuel element cladding of, 19: 34693
Cr–Ni–Nb, effects of aging at 600 to 800°C on microstructure of, 20: 21355 (TRG-Report-1168)
Cr–Ni–Nb, oxidation resistance of, effects of yttrium on, in carbon dioxide at high temperature, 20: 35914
Cr–Ni–Nb, radiation effects on tensile properties of, at 650 to 800°C, 18: 42128
Cr–Ni–Nb, radiation effects on tensile properties of, at room temperature to 850°C, 18: 42129
Cr–Ni–Nb, radiation effects on, neutron, 19: 7996
Cr–Ni–Nb, radiation effects on stress-rupture of, 20: 13328 (ORNL-TM-1359)
Cr–Ni–Nb, radiation effects on precipitation behavior and tensile properties of, neutron, 20: 33950
Cr–Ni–Nb, radioinduced embrittlement at high temperatures, 18: 5830
Cr–Ni–Ti, ageing of corrosion-resistant, structural changes in, 19: 47026(T) (ORNL-tr-795)
Cr–Ni–Ti, embrittlement failure in superheater pipes, causes of, 17: 37521(T) (TRG-Inf-Ser-191)
Cr–Ni–Ti, radiation effects on tensile properties of, at room temperature to 850°C, 18: 42129
Cr–Ni–Ti, radiation effects on, neutron, 19: 7996
Cr–Ni–Ti–W, analysis of carbide phase isolated from, activation, 18: 25289
Mn–Mo–Ni, stress rupture properties at 500 and 600°C of stainless-clad, 18: 10567
Mn–Mo–Ni–Nb, radiation effects on mechanical properties of low-alloy, neutron, 20: 19258 (UJV-1470/65)
Mn–Mo–Ni–V, welding procedures for, electro-slag, 20: 2281(R) (EURAEC-1408)
Mn–Ni, grain size and transformation of austenized Wel-Monix, 20: 33866 (EURAEC-1649)
Mo–Ni–V, fracture toughness, 18: 44138 (KAPL-3031)
Mo–Ni–V, fracture toughness, 19: 24984 (KAPL-3088)
Mo–Ni–V, fracture toughness tests on specimens of, of different sizes, 20: 27479 (CONF-660406-1)
Ni–Nb–Ti, properties of Mar-aging, 16: 24153 (DMIC-Memo-156)

NICKEL STRONTIUM LANTHANUM OXIDES
crystal structure, 20: 12865

NICKEL SULFATES
additive effects on gamma-induced polymerization of acrylonitrile in aqueous solution, 18: 29716(T,R) (AEC-tr-6231(p.175-85))
effects on ammonia yield in radiolysis of ethylenediamine aqueous solutions, 18: 5381
magnetic and crystal structure, 16: 18445
magnetic properties of crystalline, 19: 9046(R) (IS-900(Sect.C))
magnetic structure, 16: 13785
magnetic susceptibility and reflectance spectra of, 20: 26864
polymerization effects on acrylonitrile in aqueous solution, 16: 30455
potentials of nickel electrode in, 16: 25322 (TID-16292)
production using tracer techniques for control of fractionation of impurities, 20: 23532(T) (AEC-tr-6466/2, pp 293-6)
radiation effects on electric conductivity of solutions of, gamma, 20: 36912
radioinduced phosphorus in, oxidation states of, 20: 33341
radiolysis of aqueous solutions containing, 19: 503
radiolysis of hydrated, yields in, 19: 40610
radiolysis of hydrated, gamma, 20: 36903
separation from iron and uranium by solvent extraction using alkyl phosphoric acids, 18: 13936

NICKEL SULFIDES
see also Nickel Arsenic Sulfides
carcinogenicity of injected, 16: 8503
crystal structure at 85 to 770°K, neutron diffraction studies of, 17: 1952 (UCRL-7028)
crystal structure from neutron diffraction, 18: 37147
explosibility of powders of ores of, 19: 36698 (BM-RI-6516)
magnetic properties, (E), 20: 4849(R) (UCRL-14360, pp 1-50)
structural properties, 17: 14210 (NBS-MON-25(Sect.1))
sulfur-35 exchange with thiophene, 20: 3976
surface area measurements by isotopic exchange method, 16: 13056
thermal conductivity, 17: 8010(R) (TID-17767)

NICKEL SYSTEMS
Al–B–C–Cr–Mo–Ni–Ta–W–Zr, corrosion and properties of TAZ-8A, 20: 46166 (NASA-TN-D-3597)
Al–B–Ni, phase studies, 16: 19403
Al–B–Ni, phase studies of spherulite in, 16: 22641
Al–C–Cr–Co–Mo–Ni–Ti, extrusion of Udimet 700 into T-sections, 19: 7874(R) (ASD-TDR-7-911(V))
Al–C–Cr–Co–Mo–Ni–Ti, gas contents of atomized powder compacts of Inco-713C and Udimet 700, 19: 7874(R) (ASD-TDR-7-911(V))
Al–C–Cr–Mo–Ni–Ti–W, sorptive properties for zirconium, tracer studies of, 20: 35912
Al–C–Mo–Ni–Si–U–Zr, preparation and fabrication as refractory fuel material, 18: 34071(P)
Al–C–Ni, phase studies of, atomic size effects in, 19: 23111
Al–C–Ni–Nb, phase studies, 20: 15103
Al–C–Ni–Ta, phase studies, 20: 15103
Al–Cr–Dy_2O_3–Ni–Ti, properties as reactor control material, 18: 42889
Al–Cr–Er_2O_3–Ni–Ti, properties as reactor control material, 18: 42889
Al–Cr–Eu_2O_3–Ni–Ti, properties as reactor control material, 18: 42889
Al–Cr–Fe–Mn–Mo–Ni–Si, machining characteristics, 17: 14778(R) (ASD-TR-7-532a(IX))
Al–Cr–Gd_2O_3–Ni–Ti, properties as reactor control material, 18: 42889
Al–Cr–Ni–Si, fabrication methods effects on thermoelectric properties of, 17: 30824
Al–Cr–Ni–Sm_2O_3–Ti, properties as reactor control material, 18: 42889
Al–Cu–Fe–Mn–Ni–Si–Ti, corrosion by molten fluoride mixture at 650°C, 17: 34345 (BMI-X-247)
Al–Fe–Mg–Ni–Si–Ti–Zr, coating with aluminum–nickel layers by chemical deposition, 19: 39143(P)
Al–Fe–Mg–Ni–Si, corrosion by water and steam, 20: 763 (BNWL-125)
Al–Fe–Mg–Ni–Si, performance as fuel element cladding, 20: 8439(R) (KR-97)
Al–Fe–Ni–Si, corrosion by water and steam, 20: 763 (BNWL-125)
Al–Fe–Ni–Si, fabrication methods effects on thermoelectric properties of, 17: 30824
Al–Mg–Ni–Si, fatigue properties of IFA-3 aluminum-base, 20: 7566 (KR-99)
Al–Mg–Ni–Si, fatigue properties at 250 to 350°C, low-cycle, 20: 13308
Al–Mg–Ni–Si, properties for use as fuel element canning material, 17: 14735 (KR-31)
Al–Mn–Ni–Si, air and helium effects on voltage drifts in thermocouples of, 17: 30829
Al–Mn–Ni–Si, behavior of Alumel thermocouple wire in carbon dioxide–

carbon monoxide, 19: 22664 (ORNL-P-1070)
Al–Mn–Ni–Si, magnetic field effects on thermocouple wires of, 17: 30828
Al–Mn–Ni–Si, neutron-induced composition changes in, 17: 30826
Al–Mn–Ni–Si, radiation effects on thermoelectric properties, 18: 32237
Al–Mn–Ni–Si, reactions with beryllium to 600°C in carbon dioxide and *in vacuo*, 19: 22997 (TRG-Report-842)
Al–Mn–Ni–Si, reactions with Magnox alloy to 550°C in argon and carbon dioxide, 19: 22997 (TRG-Report-842)
Al–Ni–Pu–Si, radiation effects on Zircaloy-clad, 20: 46143(R) (HW-66081)
Al–Ni–Si, corrosion by water at 315°C, alloying effects of magnesium and zinc on, 17: 37005(R) (KR-49)
Al–Ni–Si, corrosion behavior and mechanical properties in high-temperature water, 18: 25931
Al–Ni–Si, corrosion by ultra-pure water at 25, 50, and 100°C, 18: 32093
Al–Ni–Si, corrosion resistance of sintered, 19: 11682
Al_2O_3–Ni, catalytic effects on isotope exchange between anisole or xylene and deuterium oxide, 17: 27387
Al_2O_3–Ni, catalytic effects on deuterium oxide exchange reaction with *p*-xylene, 18: 13822
Al_2O_3–Ni, compaction of powdered, methods for, 20: 33842 (NASA-TN-D-3511)
Al_2O_3–Ni, development of arc-sprayed, for high-temperature extrusion billet liners, 18: 39859 (IITRI-B244-18)
Al_2O_3–Ni, mechanical properties of alumina-whisker reinforced, 20: 43848(R) (BNWL-269, pp 5.1-36)
Al_2O_3–Ni, oxidation and properties of, effects of high temperatures on composites of, 20: 43845(R) (AD-637573)
Al_2O_3–Ni, oxidation and properties of, effects of high temperatures on cermet, 20: 43845(R) (AD-637573)
Al_2O_3–Ni, testing shim seals for thermionic cells, 18: 42348 (GEST-2035)
Al_2O_3–Ni, wear properties of plasma-arc-deposited coatings of, 20: 21319 (AD-621064)
B–Cd–Ni, crystal structure, 20: 14532
B–C–Fe–Ni–Si, corrosion of, by water in pressurized water reactors, 16: 7855
B–Co–Ni–Si, corrosion by liquid sodium at 700 and 1200°F, 20: 9422 (NAA-SR-11326)
B–Cr–Fe–Ni, properties, 16: 3516(P)
B–Cr–Fe–Ni–Si, galling tests of Colmonoy 5 and 6 for HTGR valve seats, 19: 11304 (GAMD-3058)
B–Cr–Fe–Ni, joining plates of, containing boron-10 by resistance foil-seam welding process, 16: 3423 (KAPL-M-SAT-7)
B–Cr–Fe–Ni, neutron attenuation by, 16: 15612 (GA-2544)
B–Cr–Fe–Ni, nuclear properties, 16: 21839(R) (IDO-16760)
B–Cr–Fe–Ni, properties of, as reactor control material, 16: 32120 (TID-16597)
B–Cr–Fe–Ni, radiation effects, 16: 810
B–Cr–Fe–Ni, radiation effects on burnable poison of, 16: 32156 (WAPD-262)
B–Cr–Ni, corrosion by cesium at 750°C, 18: 20873
B–Cr–Ni, corrosion by molten lead, 19: 32656(R) (MND-P-3006)
B–Cr–Ni, phase composition of, effects of aluminum and titanium on, 16: 27652
B–Cr–Ni, phase studies, 16: 532(T) (NP-tr-787)
B–Cr–Ni, protective effects as coating on molybdenum and molybdenum–titanium alloy, 19: 47061
B–Cr–Ni–Si, corrosion by liquid sodium at 700 and 1200°F, 20: 9422 (NAA-SR-11326)
Be–B–Ni, crystal structure of compounds in, 20: 29795
B–Fe–Ni–Si, corrosion by liquid sodium at 700 and 1200°F, 20: 9422 (NAA-SR-11326)
B–Hf–Ni, crystal structure, 20: 20685
B–Mo–Ni, crystal structure and phase diagrams, 18: 22502
B–Mo–Ni, phase composition and properties of, 20: 43973
B–Ni, diffusion of, in Ni–Ti alloys, 17: 6591 (ASD-TDR-62-734)
B–Ni, gamma and neutron attenuation in, 19: 19333
B–Ni–Ag, crystal structure, 20: 14532
B–Ni–Si, brazing alloy for tungsten carbide–cobalt cermet to TZM molybdenum alloy, 20: 4307(R) (ORNL-3870, pp 238-42)
B–Ni–Si, corrosion by liquid sodium at 700 and 1200°F, 20: 9422 (NAA-SR-11326)
B–Ni–Sn, phase studies on nickel corner of, 17: 8857
B–Ni–Ti, crystal structure, 20: 20685
B–Ni–U, crystal structure, 20: 14532
B–Ni–U, crystal structure, 20: 20685
B–Ni–V, crystal structure, 20: 20685
B–Ni–Y, crystal structure, 20: 14532
B–Ni–Zr, crystal structure, 20: 20685
B–Ni–Zr, crystal structure of stoichiometric, 20: 39416
B–Ni–Zr, phase studies, 16: 33496
B–Pb–Ni, crystal structure, 20: 14532
B_4C–Ni, corrosion in boiling reactor environment, 18: 10573 (GEAP-4296)
B_4C–Ni, radiation effects on, 18: 10573 (GEAP-4296)
C–Cr–Co–Fe–Mn–Mo–Ni–W, corrosion by mercury at high temperatures, 18: 7152
C–Cr–Co–Fe–Ni–W, corrosion of Star J, by potassium at 1600°F, 20: 27432(R) (NASA-CR-54892)
C–Cr–Co–Fe–Ni–W, friction and wear measurements on Stellite 6 in pressurized water environment, 19: 22462 (WAPD-288)
C–Cr–Co–Ni–Ti, production of, by sintering at 470 to 1150°C, 17: 32497
C–Cr–Fe–Mn–Ni, performance of Incoloy in nuclear superheated steam environments, 18: 4161 (GEAP-4351)
C–Cr–Fe–Mo–Ni–Nb–Ta–W–V, production of corrosion and oxidation resistant, 18: 12618(P)
C–Cr–Fe–Mo–Ni, reinforcement of graphite by, 19: 39114(P)
C–Cr–Mn–Ni, corrosion by steam, 18: 30143
C–Cr–Ni, production of, by sintering at 470 to 1150°C, 17: 32497
C–Cr–Ni–P, use for braze bonding stainless steel cans to stainless steel–uranium dioxide cermets, 19: 4635
C–Cu–Fe–Mn–Ni, magnetic field effects on thermocouple wires of, 17: 30828
C–Cu–Fe–Mn–Ni, neutron-induced composition changes in, 17: 30826
C–Fe–Mn–Ni, preparation and tensile properties, 19: 17443(P)
C–Fe–Mn–Ni, tensile properties of Invar sheet at cryogenic temperatures, 19: 13989 (LA-3192)
C–Fe–Mo–Ni, corrosion of HyMu 80 by potassium fluoride–zirconium fluoride under hydrofluorination conditions at 600°C, 18: 7985(R) (BMI-1650(Del.))
C–Fe–Mo–Ni, corrosion of HyMu 80 by liquid fluoride salt at 500°C in presence of fluorine and hydrofluoric acid, 18: 10468 (BMI-X-269)
C–Fe–Mo–Ni, corrosion of HyMu-80 by fluoride melt at 650°C during hydrofluorination of stainless steel and Zircaloy-2, 18: 30128 (BMI-X-288)
C–Fe–Mo–Ni, corrosion of HyMu-80 in fluoride volatility process, 18: 34034(R) (BMI-1672(Del.))
C–Fe–Mo–Ni, corrosion of HyMu 80 in molten-salt fluoride-volatility process for spent aluminum-base fuels, 18: 43717 (ORNL-P-391)
C–Fe–Mo–Ni, corrosion of HyMu 80 by molten salt under fluorination and hydrofluorination conditions, 19: 2744 (BMI-X-315)
C–Fe–Mo–Ni, corrosion of HyMu 80 by liquid aluminum fluoride–potassium fluoride–zirconium fluoride under fluorination conditions at 600°C, 19: 6267 (BMI-X-316)
C–Fe–Ni, internal friction and martensite structure in, 16: 19368 (TID-15643)
C–Fe–Ni, martensite formation in, 19: 40283 (COO-1198-237)
C–Hf–Ni, phase studies of nickel-rich, 20: 826 (NP-15535)
C–Mg–Ni, phase studies of, atomic size effects in, 19: 23111
C–Mn–Ni–Si, use for braze bonding stainless steel cans to stainless steel–uranium dioxide cermets, 19: 4635
C–Ni, concentration and temperature effects on density of, 19: 20567(T) (LA-tr-65-5)
C–Ni, diffusion of, in Ni–Ti alloys, 17: 6591 (ASD-TDR-62-734)
C–Ni, sorptive properties for zirconium, tracer studies of, 20: 35912
C–Ni, surface graphitization in, 16: 6738
C–Ni–Nb, structure of filled Ti_2Ni type compounds in, 19: 37107
C–Ni–Nb–Ti–Zr, creep properties in ultra-high vacuum of AS-30, long-time, 19: 37039(R) (NASA-CR-54393)
C–Ni–Pu, properties for use as liquid fuel in homogeneous reactor, 18: 32212(P)
C–Ni–Th, phase studies, 20: 5848
C–Ni–Th, solid state equilibria in, 19: 6315
C–Ni–U, phase diagrams, 16: 4569
C–Ni–U, phase studies, 17: 32637
C–Ni–U, phase studies, 20: 4368 (CEA-R-2845)
C–Ni–U, phase studies, 20: 9553
C–Ni–U, solid state equilibria in, 19: 6315
C–Ni–UO_2, radiation effects on fibrous fuels of, 20: 23071(R) (AGN-8169)
C–Ni–Zn, phase studies of, atomic size effects in, 19: 23111
Ce–Ni–Si, formation of compounds with AlB_2 type structure in, 19: 30767
C–Ni–Zr, phase studies of nickel-rich, 20: 826 (NP-15535)
Co–Ni–ThO_2, oxidation and properties of composite, effects of high temperatures on, 20: 43845(R) (AD-637573)
Cr–Co–Fe–Mn–Ni–Si–W, bonding of, controlling factors in diffusion, 19: 24964
Cr–Co–Ni–NbC–TaC–TiC, oxidation tests of Kennametal K 162B and 183A at 1400 and 1500°C, 19: 9624 (SCNC-270)
Cr–Cr_3C_2–Ni, self-welding to ceramics, graphite, and metals in SNAP reactor environment at 700 to 1300°F, 20: 7570 (NAA-SR-9643)
Cr–Cu–Fe–Mn–Ni–Si, corrosion of Incoloy 800 by superheated steam, 18: 21668(R) (GEMP-274)

Cr–Cu–Fe–Mn–Ni–Si, corrosion of Incoloy 800 by superheated steam containing chloride, 18: 30129 (GEAP-4450)
Cr–Cu–Fe–Mn–Ni–Si, corrosion of Incoloy 800 by superheated steam, 18: 30130 (GEAP-4495)
Cr–Cu–Fe–Mn–Ni–Si, fabrication of Incoloy 800 tubes for use as fuel cladding, 18: 32101 (GEAP-4557)
Cr–Cu–Fe–Mn–Ni–Si, performance of Incoloy 800 as fuel cladding for supercritical-water reactors, 18: 35691(R) (WCAP-3374-1)
Cr–Cu–Fe–Mn–Ni–Si, properties of Incoloy 800 as fuel sheaths in nuclear superheat reactors, 18: 44033 (GEAP-4633)
Cr–Cu–Fe–Mn–Ni–Si, strain cycle tests of Incoloy 800 tubes, 18: 39813 (GEAP-4462)
Cr–Fe–Mn–Mo–Ni–Si, corrosion and metallurgical changes in, caused by steam at 1200 to 1500°F, 16: 24126
Cr–Fe–Ni–P, corrosion cracking in, mechanisms of stress-, 20: 16968 (COO-1319-33)
Cr–Fe–Ni–Si, corrosion cracking in, mechanisms of stress-, 20: 16968 (COO-1319-33)
Cr–Fe–Ni–Si, fabrication methods effects on thermoelectric properties of, 17: 30824
Cr–Mn–Ni–Si, mechanical properties of, effects of steam at 1050°F on, 18: 4795(R) (GEAP-3924)
Cr–Ni–P, corrosion of Nicrobraz-50 by boric acid–potassium hydroxide solutions, 18: 30133 (WCAP-3737)
Cr–Ni–P, radiation effects on AWS BNi-7 braze, in-reactor, 20: 44027
Cr–Ni–P, use in joining metals, 19: 10714(P)
Cr–Ni–PuO_2, preparation by pneumatic impaction, 19: 9603(R) (HW-81601(p.2.1-35))
Cr–Ni–PuO_2, properties of cermets of, 20: 9407 (BNWL-18)
Cr–Ni–Si, corrosion by liquid sodium at 700 and 1200°F, 20: 9422 (NAA-SR-11326)
Cr–Ni–Si, fabrication methods effects on thermoelectric properties of, 17: 30824
Cr–Ni–Si, use for brazing Inconel in reactor environments, 17: 36272
Cr–Ni–ThO_2, oxidation and properties of composite effects of high temperatures on, 20: 43845(R) (AD-637573)
Cr–Ni–UO_2, fabrication procedure for, 16: 9159 (DC-54-4-71)
Cr–Ni–UO_2, oxidation of, effects of stress, temperature, and time on, 16: 21028 (DC-60-1-108)
Cr–Ni–UO_2, properties of cermets of, 20: 9407 (BNWL-18)
Cr–Ni–UO_2, radiation effects on molybdenum-clad, 16: 9253 (DC-59-6-195)
Cr–Ni–UO_2, radiation stability, 19: 11792
CrO–Ni, catalytic effects on isotope exchange between hydrogen and water, 17: 33869 (IFA/IS/20)
CrO_3–Ni, properties for use as catalyst for hydrogen–deuterium exchange, 20: 5534
Cu–Ni–Si, corrosion of, by acid, 16: 12057
Cu–Ni–Si, use for braze bonding stainless steel cans to stainless steel–uranium dioxide cermets, 19: 4635
Dy_2O_3–Ni, use of alloy clad, for high-temperature uncooled articulating control rods, 20: 35859 (CONF-660606-9)
Dy_2O_3–Ni, use of cermet of, in high-temperature reactor control rods, 20: 33781
Eu_2O_3–Ni, development of, for use in HTRE-3 control rod poison tips, 16: 11213 (DC-60-6-53)
Eu_2O_3–Ni, thermal-cycling-induced growth in, 16: 825
Fe–Mo–Ni–Si, corrosion of, by lithium fluoride–sodium fluoride–zirconium fluoride systems at 500°C, 16: 4502 (TID-13691)
Fe–Ni–Ru–Si–W, properties at 1400 to 2000°F, 17: 14808(R) (ARF-2158-24)
Fe–Ni–Si, fabrication methods effects on thermoelectric properties of, 17: 30824
Fe–Ni–Si, neutron scattering by, cross sections for magnetic, 18: 27990
Fe–Ni–WC, internal friction of, effects of composition on, 19: 39170(T) (FTD-TT-64-1001)
Ge–Ni–O, magnetic structure, 19: 38057
glass–Ni, internal stresses in, 17: 39522 (AD-291849)
graphite–Ni, graphite crystal growth in, 19: 23074(T)
graphite–Ni, graphite recrystallization from melts of, 19: 22976(R) (GA-4901)
H–Ni–Zr, crystal structure of compound $NiZrH_3$ in, 16: 10570
Mg–Ni–Si, corrosion by steam and water at high temperatures, 19: 30669(R) (HW-84573(p.5.1-22))
Mo–Ni–NbC–TiC, friction coefficients with alumina and solar glass of K-162B Kentanium, *in vacuo*, 20: 7571 (NAA-SR-9644)
Mo–Ni–NbC–TiC, friction coefficients with alumina with molybdenum disulfide coating of K-162B Kentanium, *in vacuo*, 20: 7571 (NAA-SR-9644)
Mo–Ni–NbC–TiC, self-welding to ceramics, graphite, and metals in SNAP reactor environment at 700 to 1300°F, 20: 7570 (NAA-SR-9643)
Mo–Ni–NbC–TaC–TiC, thermal expansion at 68 to 1800°F, 18: 20513 (CNLM-4234)
Mo–Ni–ThO_2, compaction of powdered, methods for, 20: 33842 (NASA-TN-D-3511)
Mo–Ni–ThO_2, development and properties of dispersion-strengthened, 20: 31669
Mo–Ni–ThO_2, oxidation and properties of composite, effects of high temperatures on, 20: 43845(R) (AD-637573)
Mo–Ni–ThO_2, preparation and tensile properties, 19: 26854
Mo–Ni–TiC, oxidation of, by air at 600 to 1300°C, effects of molybdenum content on, 20: 29653
Mo–Ni–TiC, phase studies and sintering of, 19: 9685
Ni–H_2O, gamma heating in, calculations for, (E/T), 20: 6517 (CONF-651101-41)
Ni–H_2O, neutron angular and energy distributions at interface of, (E), 19: 8382
Ni–H_2O, oxidation potential-pH diagrams for, 17: 501(R) (KAPL-2000-19(p.V.1-V.31))
Ni–NaCl, thermostimulated electron emission from crystallophosphor of, 19: 25170(T)
Ni–NbC–TaC–TiC, oxidation tests of Kennametal K 150A at 1400 and 1500°C, 19: 9624 (SCNC-270)
Ni–NbC–TaC–TiC, thermal expansion at 68 to 1800°F, 18: 20513 (CNLM-4234)
Ni–Nb–N, structure of filled Ti_2Ni type compounds in, 19: 37107
Ni–Nb–O, structure of filled Ti_2Ni type compounds in, 19: 37107
Ni–Ni_3B, development of fiber-reinforced composites of, 20: 2219 (AMRA-CR-64-05/4)
Ni–$NiCl_2$, free energy of solutions of, 19: 11103
Ni–NiO_4, durability as cathode in ion thruster, 19: 13615
Ni–O–Ti, crystal structure of Ti_4Ni_2O in, 17: 29362
Ni–O–Ti, crystal structure of Ti_4Ni_2O, 17: 41333(R) (ANL-6677)
Ni–O–Zr, phase studies, 16: 547
Ni–P, deposition on steel, 17: 12613
Ni–P, deposition on beryllium, 20: 27454
Ni–P, properties as plating for fuel-element spacer rings, 19: 22933
Ni–Pd–Si, metastable amorphous ferromagnetic phases in, 19: 33687 (CALT-221-10)
Ni–PuC–UC, properties, 19: 24923(R) (UNC-5081)
Ni–PuC–UC, thermal diffusivities of, 19: 39163(R) (MLM-1244)
Ni–rare earth–Si, crystal structure of $R_3Ni_6Si_2$ compounds in, 20: 31253
Ni–Re–Si, phase studies and crystal structure, 18: 22077
Ni–Sc–Si, crystal structure, G phases in, 17: 14876
Ni–Si, corrosion by steam and water at high temperatures, 19: 30669(R) (HW-84573(p.5.1-22))
Ni–Si, fabrication methods effects on thermoelectric properties of, 17: 30824
Ni–Si, phase studies, 16: 22595 (TID-15971)
Ni–SiO_2, catalytic effects on isotope exchange between anisole or xylene and deuterium oxide, 17: 27387
Ni–Si–Th, crystal structure of compound in, 19: 20568
Ni–Si–Ti, phase studies, 18: 549(R) (NP-13241)
Ni–Si–U, melting point, 16: 6104(R) (LAMS-2647)
Ni–Te, structure and superconductivity in, 17: 27816(T) (UCRL-Trans-921)
Ni–ThO_2, annealing, 17: 3457
Ni–ThO_2, bonding of TD-Nickel, method for diffusion, 20: 5867
Ni–ThO_2—bonding to refractory metals, process for TD Nickel diffusion, 20: 31670
Ni–ThO_2, compaction of powdered, methods for, 20: 33848 (NASA-TN-D-3511)
Ni–ThO_2, compatibility of TD nickel with graphite nitrogen environment at 1000 and 1200°C, 19: 40966 (BNWL-92)
Ni–ThO_2, corrosion, oxidation, and strength of, 17: 32501
Ni–ThO_2, corrosion testing, 17: 34355
Ni–ThO_2, corrosion by fluorine at 600°C, 18: 1484(R) (ANL-6687 (p.86-152))
Ni–ThO_2, corrosion resistance in water at 360°C and oxygenated steam at 650°C, 19: 11682
Ni–ThO_2, corrosion by boiling cesium, 19: 13913(R) (AFML-TR-64-327)
Ni–ThO_2, corrosion by lithium fluoride in cyclic high-temperature environment, 20: 4326 (TRW-ER-6561)
Ni–ThO_2, corrosion in oxidizing atmospheres at high temperatures, 20: 43842
Ni–ThO_2, corrosion of TD nickel by lithium fluoride, 19: 12150
Ni–ThO_2, creep fracture at 18,000 psi and 900 to 1100°C, 19: 16169
Ni–ThO_2, creep of TD Nickel at 325 to 1100°C, 20: 23753
Ni–ThO_2, development and properties of dispersion-strengthened, 20: 31669
Ni–ThO_2, diffusion of chromium in, for corrosion protection, 20: 29748
Ni–ThO_2, drawing, 17: 3457
Ni–ThO_2, electric conductivity of wires of, at 80 to 1600°F, 18: 41928(R) (NASA-CR-54089)
Ni–ThO_2, evaluation for aerospace applications, 18: 12554 (NASA-TN-D-1944)

Ni–ThO_2, joining by brazing, soldering, or welding TD nickel, 20: 29666 (RSIC-484)
Ni–ThO_2, oxidation in oxygen at 700 to 1000°C, 18: 7139(R) (HW-77954(p.5.5-11))
Ni–ThO_2, oxidation rates, 18: 8752(R) (HW-78388(p.9.1-4))
Ni–ThO_2, oxidation at 900 to 1400°C, 18: 10488
Ni–ThO_2, oxidation at 600 to 1000°C, kinetics of, 18: 12035 (HW-79350)
Ni–ThO_2, oxidation at 900 to 1400°C, 19: 11682
Ni–ThO_2, oxidation and properties of composite, effects of high temperatures on, 20: 43845(R) (AD-637573)
Ni–ThO_2, preparation, 17: 3526
Ni–ThO_2, preparation and tensile properties, 19: 26854
Ni–ThO_2, properties, 17: 3526
Ni–ThO_2, properties of dispersion-strengthened, 17: 4967
Ni–ThO_2, properties of extruded, 19: 2831
Ni–ThO_2, properties of TD nickel as cladding material for SNAP hydride reactors, 19: 39166 (NAA-SR-Memo-11149)
Ni–ThO_2, properties at high temperatures, 20: 4418
Ni–ThO_2, radiation effects on, 18: 7292(R) (HW-77954(p.4.1-12))
Ni–ThO_2, radiation effects on mechanical properties of, neutron, 18: 14537(R) (HW-79766(p.4.1-76))
Ni–ThO_2, recrystallization behavior of cold-rolled, 18: 42029
Ni–ThO_2, recrystallization properties, 20: 5851
Ni–ThO_2, rupture strength of, effects of microstructure on, 20: 39398 (NASA-TN-D-3527)
Ni–ThO_2, stability of thoria phase in, 18: 8853
Ni–ThO_2, substructure of TD nickel, electron transmission microscopic studies, 20: 43882(R) (AD-636487)
Ni–ThO_2, surface treatments for TD nickel, coating and mechanical, 20: 29706 (NASA-TM-X-53448)
Ni–ThO_2, texture of, effects of annealing and cold rolling on, 20: 46169
Ni–ThO_2, welding of dispersion-hardened, magnetic force, 20: 7532(R) (BNWL-150, pp 5.1-33)
Ni–ThO_2–U, agglomeration and segregation of thoria in, at 800°C, 20: 43902 (NMI-7018)
Ni–ThO_2–W, oxidation and properties of composite, effects of high temperatures on, 20: 43845(R) (AD-637573)
Ni–TiB_2, preparation, 17: 6591 (ASD-TDR-62-734)
Ni–TiC, corrosion of, by molten sodium, 16: 28646(R) (ORNL-2247 (Pts.1-5))
Ni–TiC, preparation, 17: 6591 (ASD-TDR-62-734)
Ni–UC, phase studies, 17: 1843
Ni–UC, thermal diffusivities of, calculations of, 19: 39163(R) (MLM-1244)
Ni–UC, x-ray diffraction analysis, 17: 29330(R) (UNC-5056)
Ni–UN, phase studies, 17: 32637
Ni–UO_2, preparation of fibrous, for fissiochemical reactions, 20: 3982(R) (AGN-8156)
Ni–UO_2, radiation effects on fibrous fissiochemical fuels of, 19: 46324(R) (AGN-8132)
Ni–UO_2, thermodynamic stability of fibrous fuels of, 20: 23071(R) (AGN-8169)
Ni–WC, internal friction of, effects of composition on, 19: 39170(T) (FTD-TT-64-1001)
Ni–ZrB_2, oxidation kinetics at 500 to 1000°C, 20: 5845
Sb–B–Ni, crystal structure, 20: 14532

NICKEL TELLURIDES
structure, effects of magnetic moments on, 18: 37115 (ANL-6856)

NICKEL TITANATES
crystal structure of, 16: 30717(R) (ANL-6516)

NICKEL TUNGSTATES
magnetic susceptibility and reflectance spectra of, 20: 26864
reduction by carbon monoxide, isotherms for, 16: 22072(T) (AEC-tr-5125)

NICKEL URANATES
crystal structure and density of, 20: 2400

NICKEL URANIUM OXIDES
formation of $NiO{\cdot}3UO_3$ in aqueous systems of nickel oxide–sulfur trioxide–uranium(VI) oxide and nickel oxide–nitrogen pentoxide–uranium(VI) oxide at 300°C, 18: 12084

NICKEL ZINC FERRITES
magnetic properties, 18: 26058
radiation effects on magnetic diffusion in, gamma, 20: 16532

NICKEL ZIRCONIUM HYDRIDES
crystal structure from neutron diffraction, 18: 37140

NICKELATES
see also Lithium Nickelates
electron yields from cathodes of, 19: 41124(R) (NP-15108)

NICOTINAMIDES
see also Phenatine
effects on chromosome aberration induction in carcinoma and sarcoma cells by nitrogen mustard and triethylamine, 20: 40550
effects on desoxyribonucleic acid synthesis in irradiated rat tumors, 19: 8980
effects on development of irradiated bone marrow cells in tissue culture, 19: 31784 (EUR-2415.e)
effects on growth of Ehrlich ascites tumors in mice, 17: 33476(R) (ANL-6723(p.215))
effects on radiosensitivity of tumors, 16: 21966
effects on radiosensitivity of Ehrlich ascite cells, 16: 21967
effects on radiosensitivity of thymocytes, 17: 7823
effects on radiosensitivity of mouse tumors, 19: 26116
effects on respiration in rat thymocytes in culture, 20: 5340
effects on synthesis of desoxyribonucleic acid by irradiated tumor cells, 16: 5180
*N*¹-methyl-, radiation effects on intestinal absorption and elimination of, in rats, 17: 40661 (TID-18205)
preparation of labeled, 19: 32271
protective effects of, against radiation damage to bovine serum albumin, 17: 28757
protective effects against radiation injury to Ehrlich carcinoma, 19: 211
protective effects against radiation damage in rat thymocytes, 19: 7187
protective effects against radiation effects on DNA synthesis in ascites tumor cells, 19: 28041
radiation effects on, x, 18: 6852
radiation effects on leak of, in ascites tumor cells, 19: 15051
radiation protection of, against decline in DNA synthesis, 17: 33639
radiosensitivity effects on normal and tumor cells, 16: 6335
radiosensitivity effects on Ehrlich tumors, 17: 35478
radiosensitivity effects on cell membrane permeability, gamma, 18: 13508
radiosensitivity effects on rat thymocyte nuclei, 20: 18455
sorption by rats, intestinal, 17: 13986(R) (UCLA-510)
6-amino-, effects on radiosensitivity of human and tumor cells, 18: 8210

NICOTINE
see also Tobacco
content in tobacco plants, effects of irradiation of seed on, 18: 17591
effects on calcium uptake and release by frog ventricular muscle, 18: 1347
effects on ileum of irradiated guinea pigs, protective effects of cysteamine against, 19: 22002
labeling with carbon-14, 19: 32267
metabolism in bacteria and liver extracts, tracer study, 19: 31766
radiation effects on toxicity of, in mice, 17: 15678
radiation effects on content in nicotiana plants, 18: 19690
synthesis in *Nicotiana glutinosa* from carbon-14 dioxide, labeling in pyrrolidine, 18: 36936
benzopyrene–nicotine, effects on Tunicata eggs, 20: 8599

NICOTINIC ACID
analysis for selenium, activation, 16: 22021
complexes of, with rare earths and hexathiocyanatochromium, stability constants of, 17: 18080
complexes with cobalt, effects on bone fracture healing in irradiated rabbits, 17: 2855
complexes with rare earths, stability, 17: 35832
degradation of carbon-14-labeled, carbon-by-carbon, 18: 37167
effects on cholesterol and specific radioactivity in rabbit liver, 20: 28895
effects on nicotine synthesis in tobacco plants, 18: 17591
labeling with carbon-14, method for, 19: 28430
preparation of tritium-labeled, 17: 30567
protective effects against radiation effects on amino acid content in wheat sprouts, 18: 33398
radiation effects, in foods, 16: 17948(T) (AERE-Trans-882)
radiation effects on metabolism of, in rats, 17: 14050
radiation effects on content of, in eggs and wheat, 19: 17575
radiation effects on content of, in guinea pigs, 19: 17581
radiation effects on content in oysters, gamma, 20: 45347
radiosensitivity effects on Ehrlich tumors, 17: 35479
radiosensitivity effects on rats, 18: 5139(T) (JPRS-22123)
radiosensitivity effects on mouse sarcomas, 19: 13113
radiosensitivity effects on rabbit eyes, 20: 18476
radiosterilization effects on content of, in strawberries, gamma, 20: 13142(R) (UCD-34P80-3, pp 52-4)

NIGERIA
cesium content in alkali granites in Northern, 17: 34125
fall-out monitoring, 1960 to 1961, 16: 394 (AERE-R-3766)
fallout monitoring in, to 1961, 19: 18219
granite potassium–rubidium ratios, 16: 13381

NIMONIC-75
diffusion into copper at 900°C, 20: 5850
joining by brazing, soldering, or welding, 20: 29666 (RSIC-484)
machining properties of, 20: 29665 (RSIC-482)
reactions with aluminum to 500°C *in vacuo*, 19: 22997 (TRG-Report-842)
reactions with beryllium to 600°C in carbon dioxide and *in vacuo*, 19: 22997 (TRG-Report-842)

reactions with carbon dioxide to 700°C, 19: 22997 (TRG-Report-842)
reactions with Magnox alloy to 550°C *in vacuo*, 19: 22997 (TRG-Report-842)
reactions with uranium to 500°C *in vacuo*, 19: 22997 (TRG-Report-842)
Cu/Nimonic-75, diffusion characteristics of, 19: 917

NIMONIC-80
brazing and welding of, criteria for, 17: 11163 (DMIC-181)
compatibility of 80A, with plutonium carbide–uranium carbide, 20: 31675
compatibility with fissionable materials, 17: 29255 (ZFK-WF-13)
corrosion by sodium at 650°C, 18: 25937
corrosion resistance and hardening mechanism of, review of, 18: 18322
crystal structure of, effects of deformation and recrystallization on, 17: 8863
extrusion by hydrostatic methods, 19: 18436
joining by brazing, soldering, or welding, 20: 29666 (RSIC-484)
machining properties of, 20: 29665 (RSIC-482)
radiation effects on stress relaxation in, fast-neutron, 20: 23791
radiation effects on stress relaxation of springs of, fast-neutron, 20: 31669
reactions with beryllium to 600°C in carbon dioxide and *in vacuo*, 19: 22997 (TRG-Report-842)
reactions with Magnox alloy to 550°C, 19: 22997 (TRG-Report-842)
reactions with plutonium carbide–uranium carbide, 20: 9438
Eu_2O_3–nimonic, radiation effects on mechanical properties of, neutron, 17: 41496 (NP-13106)

NIMONIC-90
brazing and welding of, criteria for, 17: 11163 (DMIC-181)
compatibility with tantalum at 760 to 900°C, 20: 31675
corrosion by air, carbon oxides, hydrogen sulfide, and sulfur dioxide to 1200°C, 18: 39844
corrosion resistance and hardening mechanism of, review of, 18: 18322
crack-propagation resistance, 18: 5769 (AD-290278)
creep-rupture properties, 17: 39531(R) (EURAEC-689)
crystal structure of, effects of deformation and recrystallization on, 17: 8863
joining by brazing, soldering, or welding, 20: 29666 (RSIC-484)
machining properties of, 20: 29665 (RSIC-482)
reactions with Magnox alloy to 500°C in carbon dioxide–carbon monoxide, 19: 22997 (TRG-Report-842)

NIMONIC DS
reactions with carbon dioxide to 600°C, 19: 22997 (TRG-Report-842)
reactions with Magnox alloy to 550°C *in vacuo*, 19: 22997 (TRG-Report-842)

NIMROD Synchrotron
see Harwell Synchrotron

NINE MILE POINT POWER REACTOR
design, 19: 24139
design and safety analysis of, 20: 12408 (NP-15660(Vol.1))
economic aspects, 19: 31569
economic comparison with CANDU Reactor, 18: 35172
economics of, under Canadian conditions, 18: 40919
hazards analysis, 20: 12408 (NP-15660(Vol.1))
hazards analysis, 20: 12410 (NP-15660(Suppl.1))
hazards analysis of, 20: 10380 (TID-22438)
operation and safeguards of, regulatory actions relative to, 19: 12795
radioisotope production in, economic and technical feasibility of, 19: 28723
safety analysis, 19: 25636
site evaluation analysis, 20: 12409 (NP-15660(Vol.2))

NINGYONITES
processing of, for uranium extraction, 19: 9395

NIOBATES
see also Aluminum Niobates
see also Barium Niobates
see also Cadmium Niobates
see also Calcium Niobates
see also Cerium Niobates
see also Cobalt Niobates
see also Dysprosium Niobates
see also Erbium Niobates
see also Europium Niobates
see also Fluoniobates
see also Gadolinium Niobates
see also Holmium Niobates
see also Iron Niobates
see also Lanthanum Niobates
see also Lead Niobates
see also Lithium Niobates
see also Lithium Zinc Niobates
see also Lutetium Niobates
see also Magnesium Niobates
see also Manganese Niobates
see also Neodymium Niobates
see also Nickel Niobates
see also Potassium Chloroniobates
see also Potassium Niobates
see also Praseodymium Niobates
see also Rare Earth Niobates
see also Samarium Niobates
see also Scandium Niobates
see also Sodium Niobates
see also Terbium Niobates
see also Thulium Niobates
see also Ytterbium Niobates
see also Yttrium Niobates
see also Zinc Niobates
crystallographic and magnetic structure of bivalent transition metal, 16: 7532
formation of complex, from transition metals, 18: 17790
halo, properties of, 19: 9604(R) (IS-900(Sect.M))
ionic charge and polymerization of anions of, in aqueous solution, 19: 13379
piezoelectric properties, review, 17: 3527
preparation and crystal structure, 17: 32100
structure, 16: 6426
surface tension and thermal expansion of, 17: 8091

NIOBIC ACIDS
complexes with amines, infrared spectra and thermal studies on, 18: 17804
spectra and thermal studies on aging of, infrared, 18: 17804

NIOBIUM
abundance in giant stars, 17: 3913
abundance in solar atmosphere, 16: 29599 (AFOSR-3024)
aging, 17: 3466 (ASD-TR-61-351)
alloying characteristics with rare earths, 18: 41924(R) (IITRI-578P19-13)
alloying effects on stainless steel corrosion, 16: 13536
alloying effects on tantalum and tungsten alloys, 16: 13562(R) (AD-259116)
alloying effects on air-casting and properties of chromium–nickel alloys, 16: 15216
alloying effects on oxidation of chromium-nickel fuel ribbon, 16: 13574 (DC-59-2-36)
alloying effects on mechanical properties of aluminum-chromium-iron alloy, 16: 17276(P)
alloying effects on mechanical properties of steel, 16: 16737
alloying effects on tensile properties of chromium–nickel alloys, 16: 19341 (DC-59-2-83)
alloying effects on corrosion resistance of zirconium alloys to steam and water, 16: 29337(R) (ARF-2198-26)
alloying effects on corrosion of chromium–molybdenum steel by carbon dioxide, 16: 29344(T) (AEC-tr-5303)
alloying effects on physical metallurgy of cobalt alloys, 16: 29312 (DMIC-171)
alloying effects on grain size of uranium, 16: 33380
alloying effects on chromium–nickel steel, 17: 11210
alloying effects on corrosion and mechanical properties of zirconium, 17: 32484(R) (GEAP-4284)
alloying effects on hardness of chromium, 17: 37548
alloying effects on corrosion of zirconium alloys in steam and water, 17: 37495(T) (TRG-Inf-Ser-100)
alloying effects on uranium, 17: 39623
alloying effects on uranium, effects of quenching temperature on, 17: 39627
alloying effects on austenitic steel, 17: 41437(T,R) (EURAEC-598)
alloying effects on copper–zirconium alloys, 17: 11225
alloying effects on titanium, 17: 16580(P)
alloying effects on iron self-diffusion, 17: 22177
alloying effects on corrosion and mechanical properties of zirconium, 17: 23865(R) (GEAP-4139)
alloying effects on corrosion of zirconium by steam and water, 17: 23889(R) (ARF-B198-39)
alloying effects on mechanical properties of vanadium, 17: 25771 (ASD-TDR-62-667)
alloying effects on corrosion and mechanical properties of zirconium alloys, 18: 545(R) (GEAP-4368)
alloying effects on heat of transport of hydrogen in zirconium, 18: 5800
alloying effects on corrosion resistance of zirconium in carbon dioxide, 18: 12576 (GEAP-4089(Vol.I)(Paper 3))
alloying effects on corrosion and mechanical properties of zirconium alloys, 18: 12542(R) (GEAP-4484)
alloying effects on fission–plutonium–uranium alloys, 18: 15563
alloying effects on grain size of uranium, 18: 16509
alloying effects on iron–nickel alloys, 18: 24161
alpha reactions (α,n) and (α,p) at 42 Mev, angular distributions of neutrons and protons from, 18: 16951(R) (TID-20311)

alpha reactions (α,n) at 12 to 18 Mev (E/T), 19: 3362
alpha reactions (α,p) at 42 Mev, (E), 19: 8487
alpha reactions (α,xn), counting of technetium isomers produced in, 16: 11691(R) (TID-15020(p.15-22))
alpha reactions (α,n) at 42 Mev, 17: 26639
alpha reactions (α,n) at 42 Mev, angular and energy distributions in, 17: 38208
alpha reactions at 42 Mev, proton emission in, (E), 20: 12062
analysis, 16: 25294
analysis, 17: 6022
analysis for carbides, nitrides, and oxides by anodic staining, 19: 46929 (NMI-4998, pp 57-64)
analysis for carbon, hydrogen, nitrogen, and oxygen, review of methods for, 16: 12995
analysis for carbon dioxide, carbon monoxide, hydrogen, and nitrogen by hot-vacuum extraction, 17: 14147 (PG-Report-412)
analysis for carbon, gasometric, 17: 23255 (PG-Report-239)
analysis for carbon, hydrogen, iron, nitrogen, and oxygen, review of methods for, 18: 33516
analysis for common impurities by d-c arc excitation, photometric, 19: 26268
analysis for common impurities by fusion and d-c arc excitation, photometric, 19: 26269
analysis for copper by absorption spectroscopy, effects of ions on, 20: 36726
analysis for hafnium or zirconium using catechol violet, colorimetric, 19: 19780
analysis for hydrogen, nitrogen, and oxygen, 18: 10022
analysis for hydrogen, nitrogen, and oxygen, vacuum fusion, 18: 33491
analysis for hydrogen, gravimetric, 18: 33538
analysis for impurities and alloying elements, methods survey, 16: 5267 (MAB-178-M)
analysis for impurities using thioacetamide, 16: 14676
analysis for impurities, chemico-spectrographic method for, 17: 40758
analysis for impurities, review of methods for, 18: 13656
analysis for impurities, review of methods for, 18: 33515
analysis for impurities by activation, 19: 24416
analysis for impurities by anodic staining, 19: 34107 (ORNL-3821)
analysis for iron, lead, silicon, and tantalum, spectrographic, 16: 1721
analysis for iron using 4,7-diphenyl-1,10-phenanthroline, spectrophotometric, 16: 2974
analysis for iron traces, spectrophotometric, 17: 7984
analysis for nickel in high-purity, spectrophotometric, 17: 38959
analysis for niobium-94 and -95, gamma-spectrometric, (E), 19: 22684 (AE-174)
analysis for nitrogen, design of modified Kjeldahl apparatus for, 16: 8682 (TID-11411)
analysis for nitrogen, 18: 10023
analysis for nitrogen and oxygen by d-c carbon-arc, gas chromatographic technique, 19: 9069
analysis for nitrogen and oxygen, using inert gas fusion-chromatographic method, 19: 15404
analysis for nitrogen, isotope-dilution method for, 19: 40444
analysis for oxygen by heat extraction, 16: 7515
analysis for oxygen, fast-neutron activation, 16: 26914
analysis for oxygen, comparison of inert gas-fusion and vacuum extraction methods for, 16: 28872 (TID-11794)
analysis for oxygen, vacuum-fusion, 16: 30332 (WAL-TR-823/5)
analysis for oxygen, 17: 27257
analysis for oxygen, comparison of activation and vacuum fusion methods, 18: 19922
analysis for oxygen, comparison of fast neutron activation and vacuum fusion methods for, 18: 43419
analysis for oxygen, method for, 19: 24419
analysis for rhenium by anion exchange, 19: 13220
analysis for sulfur, luminescent method for, 18: 33513
analysis for tantalum, spectrophotometric, 16: 16313
analysis for tantalum, activation, 16: 18014 (AD-263880)
analysis for tantalum, buffer effects in spectrochemical, 17: 15899
analysis for tantalum, use of radioisotopes for, 17: 33822
analysis for tantalum traces, x-ray spectrographic, 18: 33458 (BM-RI-6483)
analysis for tantalum by ion exchange in hydrofluoric–nitric acid mixtures, 18: 35455
analysis for tantalum, activation, 19: 4096
analysis for tantalum and tungsten, activation, 19: 5833
analysis for tantalum by neutron activation methods, 19: 32069
analysis for tantalum by activation, 19: 36295
analysis for tantalum by electron excitation, x-ray spectrographic, 20: 246
analysis for zirconium, 16: 30343
analysis for zirconium, photometric, 18: 37102
analysis, neutron activation, 16: 23633 (TID-7629(p.239-44))
analysis of high-purity, for copper, spectrophotometric, 17: 25140
analysis of high-purity, for impurities, spectrochemical, 18: 17720 (BM-RI-6414)
analysis of oxygen, method for, 20: 29108
analysis of pure, for trace impurities, activation, 19: 17785 (SGAE-CH-11/1964)
analysis of, survey of methods for, 18: 3703
analysis of, for iron by atomic absorption spectrophotometry, 20: 43162
analysis of, review of methods for, 19: 36304
analysis of, use of activation methods for, 18: 29577
analysis, review, 16: 8688
anelastic behavior, 18: 5770 (ASD-TDR-62-323)
annealing and melting of, reactions with nitrogen, oxygen, and water vapor in, 19: 40490
annealing of cold-worked, analysis of isochronal, 20: 33919
annealing properties of single-crystal, containing deformation in twins, 20: 5846
annealing twins and stacking faults in, 16: 536
annealing twins and twin-boundary intersections in, 20: 23665
anodic oxide film capacitance on, effects of proton space charge on, 19: 13365
arc-cast and powder metallurgy of, 16: 28646(R) (ORNL-2247(Pts.1-5))
argon ion reactions, atom ejection patterns in, 16: 2203(R) (TID-14257)
behavior in albitization process of granitoids in Ognitsk complex in Eastern Sayany, 19: 657
behavior in surface waters, fission product, 16: 399(T) (CEA-tr-A-1012)
bibliography on, 17: 6521 (NP-12417)
bibliography on, 18: 32076
bibliography on analytical chemistry of, 18: 33482
bibliography on, Defense Metals Information Center selected accessions, January 1963, 17: 14739 (NP-12525)
bibliography on, DMIC selected accessions, Sept. 1962, 17: 419 (NP-12170)
bibliography on, DMIC accessions, May 1963, 17: 29246 (AD-407822)
bibliography on metallurgical properties, 16: 15164 (AGARDograph-50)
bibliography on preparation, fabrication, and uses of, 18: 34151
bonding, additive effects of interfacial materials on diffusion, 17: 34330(R) (USBM-U-1057)
bonding by ceramic adhesives, 17: 25750
bonding by gas-pressure at high temperature, 16: 13555
bonding methods for, 16: 22564 (DMIC-Memo-153)
bonding of, to molybdenum–uranium alloys, for use as diffusion barrier material, 17: 18716 (NAA-SR-7973)
bonding of, to Inconel 600 and stainless steels, process development for explosive, 20: 21295(R) (WANL-PR-(EE)-002)
bonding to alumina, 17: 34365 (LADC-5598)
bonding to alumina, process development for, 20: 27487(R) (GEMP-400A, pp 263-8)
bonding to aluminum oxides, 18: 41928(R) (NASA-CR-54089)
bonding to aluminum oxide, process development for, 19: 37031(R) (GEMP-47A, pp 101-6)
bonding to beryllium oxide, process development for, 19: 37031(R) (GEMP-47A, pp 101-6)
bonding to beryllium oxide, method for, 20: 4354(P)
bonding to beryllium and stainless steel by extrusion, 18: 27937
bonding to Inconel 600 and types 321 and 347 stainless steels, explosive, 20: 11243(R) (WANL-PR(EE)-001)
bonding to itself and other refractory metals by solid-state diffusion methods, 19: 16050(P)
bonding to molybdenum–titanium alloy and tungsten by vacuum hot-pressing, 20: 5866
bonding to niobium by diffusion using interfacial coatings, 18: 30154 (USBM-U-1107)
bonding to refractory metals, temperature requirements for solid-state diffusion, 17: 25688(R) (GEMP-177A)
bonding to tungsten-coated alumina–yttria system, 17: 34365 (LADC-5598)
bonding to type 316 stainless steel, 17: 36200(R) (NP-13033)
bonding to uranium carbide and iron–uranium carbide cermets, 20: 9468
book: *Analytical Chemistry of Niobium and Tantalum*, 18: 39142
book: *Behavior and Properties of Refractory Metals, 19: 14066*
book: *Columbium and Tantalum*, 18: 4187
book: *Critical Review of the Analytical Methods of the Titanium, Vanadium, and Chromium Transition Element Groups*, 18: 3702
book: *Niobium and Its Alloys*, 16: 32047
book: *Niobium and Tantalum*, 17: 36331
book: *Production Technology of Niobium and Niobium Alloys*, 20: 43984
book: *Rare Metal Extraction by Chemical Engineering Techniques*, 18: 13952
book: *Vanadium, Niobium, Tantalum. The Metallurgy of the Pure Metals and Their Alloys*, in German, 18: 25906
brazing, 16: 27584(P)

brazing, 17: 22140
brazing, exothermic, 17: 27760(R) (NP-12901)
brazing methods for, 16: 22564 (DMIC-Memo-153)
brazing of, 17: 6558
brazing of, development of alloys for, 18: 5758
brazing of, evaluation of alloys for, 17: 1897(R) (NP-12144)
brazing of sandwich structures of, alloys for, 17: 36257
brazing of, development of alloy for, 20: 25552(P)
brazing properties, review, 16: 10424 (ASD-TR-61-322(p.661-76))
brazing to alumina–molybdenum mixtures using vanadium braze, 18: 44496(R) (MND-2812)
brazing to aluminum oxides in thermionic diodes, 18: 24368 (JPL-TR-32-548)
bremsstrahlung production by strontium-90–yttrium-90 beta particles in, (E), 19: 45284 (TID-22169)
bremsstrahlung reactions (γ,p) at 24 Mev, direct photoeffect and evaporation contributions in, 17: 38209
bremsstrahlung reactions (γ,α) at 32.5 Mev, spectra from, 18: 42680
bremsstrahlung reactions with, isomer production in, (E), 20: 46733
bremsstrahlung yields from, with incorporated strontium-90–yttrium-90, 20: 5000 (ORNL-IIC-5, pp 91-8)
brittle-ductile transition, 16: 21068
brittle fracture and twinning in crystals of, relation of, 17: 25772 (ASD-TDR-63-360)
brittle fracture of, relationship to twinning, 18: 32131 (ASD-TDR-63-360 (Pt.II))
casting, 17: 4910(R) (MAB-139-M(C7))
casting, melting, and properties of, 17: 16532
catalytic effects on decomposition of acetylene, 18: 29689
cesium surface ionization, 17: 21830
charged particle reactions with, cross sections for, 17: 34886 (UCRL-10783)
chlorination of, corrosion and reaction rates in processing by, 18: 39386
chlorination of, kinetics, 19: 42454 (BM-RI-6649)
cladding tubes of, with beryllium, 19: 30691 (N64-28460)
coating by aluminum-base alloys, method for, 20: 43962
coating by anodic treatment and vapor deposition, 16: 25701 (WADD-TR-61-64)
coating by iridium, protective effects of, 20: 15004(R) (N65-20790)
coating development for oxidation protection at high temperatures, 16: 6543 (ONR-9(Vol.I)(p.104-27))
coating developments for, 18: 541(R) (AD-419549)
coating of, effects of, on compression and high-temperature damage and oxidation, 17: 32526
coating of, for oxidation protection at high temperatures, 18: 8743(P)
coating of sheet, development of protective, 16: 27603 (MAB-181-M)
coating of wires of, by Nb_3Sn, 18: 4291
coating of wires, with superconducting niobium-tin alloy, 16: 15463
coating of, effects of additives on, 20: 43827 (GTR-19)
coating of, for corrosion protection, 20: 43905 (ORNL-3212)
coating of, for oxidation protection at 2300°F, 19: 20483 (SCNC-318)
coating of, for oxidation protection at 0 to 2000°F, 20: 43827 (GTR-19)
coating of, review of techniques for protective, 19: 4605
coating techniques for, review of, 18: 7270
coating testing for, 17: 36283 (AD-295530)
coating with aluminum, aluminum alloys, beryllium, and beryllium alloys, 16: 527 (SCNC-326)
coating with alumina by plasma spraying, 17: 36983(R) (AD-290068)
coating with aluminum–tin-base alloys for protection against oxidation, 17: 39465 (SCNC-328(Del.))
coating with alumina and molybdenum by plasma spraying, 17: 42401(R) (AD-296862)
coating with aluminum–tin alloy method for, 20: 4355(P)
coating with aluminum alloy, use of titanium as middle layer for, 20: 4356(P)
coating with aluminum–tin alloys, 20: 4357(P)
coating with aluminum–tin for oxidation protection at 2000°F, 20: 43836 (TID-17070)
coating with boron, properties of boride layers formed by, 18: 6824
coating with calcium titanates, endurance properties of, 16: 25761(R) (PWA-2088)
coating with chromium–silicon–titanium systems by vapor deposition, 16: 15125 (NP-11483)
coating with chromium-nickel, stainless steel and zirconium at 1200°C, 17: 22147
coating with disilicides, 18: 34209
coating with niobium disilicide, growth kinetics and diffusion reactions of, 20: 37190
coating with zinc, 16: 499 (NRL-5643)
coatings, development of oxidation-resistant, 16: 2173 (DMIC-Memo-137)
coatings for, 16: 24148(R) (ASD-TR-61-676)
coatings for, for high-temperature uses, 16: 27687
coatings for, properties of ceramic, 18: 7273
coatings for, development of oxidation-protection, 20: 7514 (DC-60-4-179)
coatings for, development of corrosion-protection, 20: 9426 (TID-12809)
coatings for, evaluation of protective, 20: 29651
combustion in fluorine, 18: 1485(R) (ANL-6687(p.153-66))
combustion of, in fluorine, calorimetry of, 16: 28641(R) (ANL-6543)
compaction by gas pressures, method for isostatic, 19: 941
compatibility of coatings of, with plutonium, thorium, and uranium, 17: 8843
compatibility of coating of, with uranium carbide–zirconium carbide thermionic diode at 1800 to 2500°C, 20: 29820
compatibility with lead telluride at 600 to 700°C, 17: 23927 (WCAP-1703)
compatibility with lead telluride at 500 to 700°C, 17: 23971 (WCAP-1868)
compatibility with fissium–plutonium–uranium alloys at 550 to 650°C, 17: 35078(R) (ANL-6739)
compatibility with sodium at 650°C, 17: 41333(R) (ANL-6677)
compatibility with plutonium nitride at 1430°C, 17: 40423(R) (BMI-1639(Del.))
compatibility with uranium carbide and uranium carbide–uranium sulfide at 1150°C, 17: 40422(R) (ANL-6784)
compatibility with thorium uranium beryllides, borides, and carbides at 1090°C, 17: 40423(R) (BMI-1639(Del.))
compatibility with plutonium nitride and thorium–uranium carbide, 18: 7985(R) (BMI-1650(Del.))
compatibility with plutonium carbide–uranium carbide, 18: 8729 (UNC-5074)
compatibility with plutonium nitrides, 18: 13354(R) (BMI-1657(Del.))
compatibility with plutonium carbide–uranium carbide systems at 1500°F, 18: 16426(R) (UNC-5068)
compatibility with fissium–plutonium–uranium alloys at 650°C, 18: 19456(R) (ANL-6840)
compatibility with thorium and uranium borides and carbides, 18: 20450(R) (BMI-1661(Del.))
compatibility with fissium–plutonium–uranium and plutonium–uranium alloys at 550 to 650°C, 18: 26893(R) (ANL-6868(p.11-108))
compatibility with beryllium–thorium–uranium alloy at 1500°F, 18: 34032(R) (BMI-1668(Del.))
compatibility with beryllium–thorium–uranium alloy, 18: 34034(R) (BMI-1672(Del.))
compatibility with ceramic insulation materials at high temperatures, 19: 7851 (CNLM-5942)
compatibility with plutonium carbide–uranium carbide, 19: 24923(R) (UNC-5081)
compatibility with uranium dioxide, 20: 5181(R) (ORNL-3029)
compatibility with uranium carbide–zirconium carbide system at 2000°C, 20: 4335
compatibility with plutonium-uranium carbides, 20: 6600(R) (ANL-7105, pp 1-35)
compatibility with uranium carbide and uranium carbide–10 uranium sulfide at 1150°C, 20: 9556
compatibility with plutonium–uranium carbides at 590 and 820°C, 20: 9437
compatibility with cesium at 550°C, 20: 13203
compatibility with uranium phosphides at high temperatures, 20: 23540(R) (ANL-7176, pp 45-72)
compatibility with solid solution uranium carbide–zirconium carbide at high temperatures, 20: 27490 (LA-DC-6901)
compatibility with plutonium carbides at 1200 to 1400°C, 20: 29820
compatibility with hydrogen in presence of thermal gradient, 20: 43832 (NASA-TN-D-3546)
conductivity at 273 to 1273°K, electric and thermal, 18: 27988(T)
conference on refractory metals, Oslo, Norway, June 23 to 26, 1963, 18: 34068
conference on, University of Sheffield, Sept. 1960, 16: 25708
consolidation by powder-metallurgy and melting processes, 18: 4224
contact potential difference between polycrystalline foils of tungsten and, 18: 8827
contamination by residual gases in vacuum systems, 18: 14355 (CONF-373-7)
contamination by residual gases in high vacuum, 18: 39826 (ORNL-3674)
contamination by rolling in argon atmosphere, 19: 9592(R) (ASD-8-170(IV))
contamination in high vacua at 578 to 1202°C, analysis of, 18: 4255(R) (ORNL-3470(p.98-125))
content in alkali igneous rocks, 16: 31970
content in animals of, 19: 33724
content in arid and humid clays in Russia, geochemistry of, 18: 1893
content in ascidian *Styela plicata*, 19: 21840
content in distilled beryllium, calculation and determination of, 19: 22104 (UCRL-12253)
content in food of, 19: 33724
content in man of, 19: 33724

content in schlieren granite segregations, 19: 24699
contrast effect in, absorption, 17: 23954 (LADC-5478)
corrosion by acids and chloride salts in chemical plants, 16: 20983
corrosion by air, carbon dioxide, nitrogen, and oxygen, 17: 3435
corrosion by alkali metals, 18: 37634 (A/CONF.28/P/343)
corrosion by alkaline media at 21 and 98°C, 19: 22900
corrosion by aluminum, tin, and zinc at 800 to 1100°C, 19: 40961
corrosion by atmosphere at high temperatures, 16: 5315 (WADD-TR-61-123)
corrosion by biphenyl, 20: 25491(T) (AECL-2330, pp 179-95)
corrosion by bismuth at 750°C, 19: 36949(R) (BNL-900(p.121-97))
corrosion by bismuth and tin, 20: 2275
corrosion by bismuth–lead alloys at 450 to 750°C, 20: 25474(R) (BNL-954, pp 122-67)
corrosion by boiling mercury, 19: 15991(R) (BNL-841(p.63-101))
corrosion by carbon dioxide, nitrogen, and oxygen, effects of temperature on, 17: 29289
corrosion by cesium at 1600 to 2500°F, 16: 16684 (TID-7626(Pt.I) (p.109-10))
corrosion by cesium at high temperatures, design of capsules for testing, 17: 3426(R) (NP-12189)
corrosion by cesium at 1000°C, 18: 42348 (GEST-2035)
corrosion by cesium at 1600, 1800, and 2500°F, 20: 5846
corrosion by chloride solutions, 16: 23528(R) (ORNL-3290)
corrosion by fused-salt fuels, 17: 7565(R) (PWAC-161)
corrosion by gas–oil, hydrogenated terphenyl, and monoisopropylbiphenyl at 330 to 400°C, 20: 25492(T) (AECL-2330, pp 196-217)
corrosion by high-temperature gases, protection against, 16: 29347
corrosion by impurities in liquid metal coolant in Dounreay Fast Reactor, 16: 26475 (TID-7622(p.35-56))
corrosion by impure Santowax, 17: 23891 (NAA-SR-7755)
corrosion by lead (liquid) at high temperatures, 17: 7606(R) (ORNL-1515)
corrosion by liquid lithium, effects of additives on, 18: 14409 (ORNL-3551)
corrosion by liquid cesium, role of oxygen in, 18: 16447
corrosion by liquid metals and their alloys with thorium and uranium, 19: 4617 (IS-888)
corrosion by liquid thorium and uranium alloys, 19: 9281(R) (IS-900 (Sect.E))
corrosion by liquid chromium-uranium, 19: 9281(R) (IS-900(Sect.E))
corrosion by liquid potassium, sodium, and potassium–sodium alloy, 19: 34643
corrosion by liquid lithium, 20: 4999(R) (ORNL-2599)
corrosion by liquid chromium–uranium, 20: 4077(R) (IS-1200(Sect. E))
corrosion by lithium, effects of oxygen, 16: 22552
corrosion by lithium at 1500 to 1900°F, 17: 6570 (ORNL-2674)
corrosion by lithium at 400 and 1000°C, effects of grain size on, 18: 4255(R) (ORNL-3470(p.98-125))
corrosion by lithium at 2000 to 3000°F, 18: 14420
corrosion by lithium, effects of carbon, nitrogen, or oxygen on, 18: 27914
corrosion by lithium at 1500 to 2000°F, 19: 36980 (PWAC-355)
corrosion by lithium at 800°C, effects of oxygen on, 19: 40961
corrosion by lithium, time dependence of, 20: 5181(R) (ORNL-3029)
corrosion by lithium, alloying effects on, 20: 4299(R) (ORNL-2711)
corrosion by mercury at high temperatures, 18: 7152
corrosion by mercury at 350 to 1350°F, 19: 32657(R) (MND-P-3007)
corrosion by molten chromium-uranium eutectic, 18: 1834(R) (IS-700(Sect.E))
corrosion by molten chromium–uranium eutectic at 900, 950, and 1000°C, 19: 26773
corrosion by oxygenated sodium at 650°C, 18: 19456(R) (ANL-6840)
corrosion by oxygen-contaminated lithium, effects of zirconium on, 19: 40961
corrosion by polyphenyls at 330 to 400°C, 16: 22547 (p.42-62))
corrosion by potassium at 1450 to 2000°F, 16: 16678 (TID-7626(Pt.I)
corrosion by potassium at 1500 to 1800°F, 18: 5728 (ASD-TDR-63-270(Pt.II))
corrosion by potassium vapor at 1500 to 1800°F, 18: 18282 (BNL-844)
corrosion by potassium, effects of oxygen on, 18: 27914
corrosion by potassium at 2000 to 3000°F, centrifuge for determining, 19: 28762
corrosion by potassium at 200, 600, and 815°C, effect of oxygen on, 19: 34642 (ORNL-3751)
corrosion by potassium–sodium alloys, 20: 5181(R) (ORNL-3029)
corrosion by potassium at 200, 600, and 815°C, effects of oxygen on, 20: 4321(R) (ORNL-3870, pp 136-9)
corrosion by reactor coolant, 16: 491(T) (CEA-tr-A-979)
corrosion by sodium at 760 to 1315°C, 18: 4160(R) (BNL-799(p.74-100))
corrosion by sodium at 650°C, 18: 15663(R) (ANL-6808)
corrosion by sodium at 650°C, 18: 26893(R) (ANL-6868(p.11-108))
corrosion by sodium at 1260°C, 19: 28764
corrosion by steam at 1000°F, 17: 23890(R) (BMI-X-10040)
corrosion by steam at 540°C, effects of additives on, 17: 36221 (BMI-1636)
corrosion by steam at 1000°F, 18: 2184
corrosion by steam and water, 18: 37635 (A/CONF.28/P/445)
corrosion by sulfuric acid, impedance measurements of anodic films formed in, 18: 10484
corrosion by terphenyls, 16: 22551
corrosion by terphenyls at 400 to 450°C, 17: 37478 (EUR-379.e)
corrosion by Tramex Process solutions, 17: 12183(R) (ORNL-3375)
corrosion by various alkaline media at 25 and 98°C, 20: 31669
corrosion, effects of surface saturation with silicon, 16: 25721(T) (FTD-TT-61-31(p.60-9))
corrosion in reactors, 19: 20488
corrosion of, at high temperatures, electron microscopic determination of, 17: 16583(R) (EURAEC-545)
corrosion of, by liquid tin at 630 and 800°C, 17: 18704
corrosion of, in oxygen, steam, and sulfate solutions at 300 to 650°C, 17: 20426
corrosion of, beta backscattering for evaluation of, 19: 2751
corrosion of, book, 18: 22451
corrosion of, measurement of, by beta backscattering and x-ray induction, 20: 19196
corrosion of, review, 19: 7868
corrosion protection coatings for, bibliography on properties of, 20: 21257 (AD-621546)
corrosion resistance, 16: 10464
corrosion resistance and electrochemical properties, 18: 4206
corrosion resistance of, effects of alloying and coating on, 18: 34084
corrosion resistance to mercury at 900°F, 20: 2264
corrosion studies of, technical progress review, 17: 11129
corrosion studies, 18: 14396
corrosion studies on, technical progress review on, 18: 18307
creep and rupture of, numerical methods for analysis of, 20: 15041 (GEMP-397)
creep in, cyclic stress induced, 19: 44700(R) (TID-22117)
creep of pure, at 800 to 1200°C, 17: 22178
creep of, effects of oxygen on, 18: 41933 (TID-11295(3rd Ed.))
creep properties, effects of rolling conditions, 16: 10505 (ASD-TR-61-440)
creep tests at low temperatures, 18: 34119 (ATN-64(9236)-9)
creep-rupture and tensile properties of, effects of nitrogen on, 20: 37218
creep-rupture properties at 1900 to 2600°F, effects of oxygen on, 18: 42017 (NRL-6095)
critical current behavior in superconducting, 18: 16883
critical current density and superconductivity of poly- and single crystals of, 18: 4288
critical current density in superconducting, structural effects on, (E), 19: 16767
critical surface temperature relations with cesium ion current, 16: 24280 (NASA-TN-D-1307)
crystal lattice dynamics of, 17: 32725(R) (PR-P-57(p-37-43))
crystal lattice dynamics of, measured by neutron inelastic scattering, 18: 715
crystal lattice dynamics of, model of dislocation motion for, 19: 13984(R) (GA-5520)
crystal lattice vibrations in, inelastic neutron scattering measurements of, 20: 42573
crystal structure, 16: 3479 (WADD-TR-61-181)
crystal structure of, 16: 30169(R) (ORNL-3313(p.133-78))
crystal structure, 17: 32565 (ASD-TR-61-181(Pt.III))
crystal structure, 18: 2403(R) (PR-P-58)
crystal structure of annealed, stacking faults in, 18: 14462(R) (EURAEC-851)
crystal structure, 18: 32138(R) (DRI-2166)
crystal structure, 18: 35933(R) (ML-TDR-64-56)
crystal structure deformation at 4.2 to 373°K, flow and yield stress measurements of, 18: 44213
crystal structure deformation in, mechanism of thermally activated flow in, 18: 44214
crystal structure of, electron microscopic fringes from coherent domain walls in, 19: 18514
crystal structure of, 19: 43480
crystal structure of, effects of high-temperature contamination by atmosphere and nitrogen on, 20: 4401(T) (ANL-Trans-218)
crystal structure preferred orientation, 20: 4389(R) (ORNL-3870, pp 61-4)
crystal structure at 110 to 400°K, 20: 7614
crystal structure of, determination by phonon dispersion, 20: 37273
crystallite nucleation by electron-beam heating in films of, 17: 32489
crystallization and mechanical properties of electron-beam-melted, 19: 37133
crystallization and recovery of cold worked, 19: 44698 (PWAC-465)
crystallization behavior, 17: 16653(R) (NP-12634)

crystallization kinetics in strongly deformed monocrystals, 20: 33934
crystallization of electron-beam-melted, 17: 41465
crystallization of, during soldering and welding, 20: 13267(T) (AD-624909)
crystallization rate after uniaxial compression and annealing, 19: 20604
crystallographic dislocations in, dynamics of, 18: 34122(R) (GA-4900)
current density in contact points of oxidized wires of superconducting, (E), 20: 30277
current fluctuations in superconducting, 18: 26484
current losses in type II superconducting, 20: 28187
defects in crystals of, stacking-fault, (E/T), 20: 13971 (AD-625834)
deformation, 17: 3466 (ASD-TR-61-351)
deformation at high temperatures, 18: 12606(T) (JPRS-23121(p.6-12))
deformation at low and moderate temperatures, 17: 11223
deformation at low temperatures, 19: 20605
deformation behavior at low and moderate temperatures, 16: 29420
deformation behavior of, effects of interstitial atom-dislocation interactions on, 17: 25827
deformation behavior of, in transition temperature range, 20: 13253 (IS-T-65)
deformation by filing at room temperature, x-ray-diffraction study of, 17: 25768 (AD-403526)
deformation by twinning at −196°C, 19: 18490
deformation flow stress in, temperature dependence of, 17: 20462
deformation of crystalline, effects of annealing on, 19: 952(R) (GA-5620)
deformation of flash-annealed and recrystallized, mechanism of, 18: 12691
deformation of flash- and vacuum-annealed, mechanisms of, 18: 20543
deformation of polycrystalline, at room temperature, 18: 44193
deformation of single crystals of, at 1400 to 2300°C, 18: 44191
deformation of, at 77 and 78°K by twinning, slip, and catastrophic flow, 20: 33892
deformation properties, 18: 2163(R) (IS-700(Sect.M))
deformation properties of, electron microscopic study of plastic, 20: 29761
deformation texture of rolled, effects of impurities and processing on, 17: 27880
deformation, thermally activated, 17: 27879
deformation twins in single crystals of, annealing of, 18: 44149(R) (ORNL-3670(p.36-43))
deformation twins in single crystals of, annealing of, 20: 27551
degasification in vacuum heating, 18: 30214
degassing reactions at 1600 to 2300°C, 18: 39977
density, 18: 42042
density, 20: 17053
density of compacts of, effects of pressure and lattice polygonization on, 19: 22939
density of compacts of, 17: 27829
deposition by electrolytic methods, 20: 35870
deposition from fused salts, mechanism for electrolytic, 20: 9449
deposition from fused salt mixtures, electro-, 20: 11260
deposition from molten salt solutions at high temperature, electrolytic, 16: 5358(T)
deposition from molten fluorides, electrolytic, 19: 16034
deposition from potassium fluoniobate, electrolytic, 16: 5361(T)
deposition of coatings of, development of methods for, 19: 20456 (EUR-2111.d)
deposition of coatings of, on microminiaturized uranium dioxide particles, techniques for vapor, 16: 18005
deposition of coatings of, on uranium dioxide fuels, 16: 32084(T,R) (EURAEC-227)
deposition of coatings of, on uraniferous ceramic particles, 17: 11112(T,R) (EURAEC-409)
deposition of coatings of, on uranium oxide particles, 17: 12595(T,R) (EURAEC-309)
deposition of coating of, electrolytic, 18: 14439
deposition of superconducting films of, vacuum, 18: 2751
deposition of superconducting high-purity films by a-c sputtering, 18: 2752
deposition of superconducting films, 18: 13014
deposition on aluminum and uranium, chemical vapor, 20: 11260
deposition on ceramic particles, 17: 11116(T) (EURAEC-487)
deposition on finely dispersed particles, method for, 20: 4314(P)
deposition on magnesium oxide, epitaxial growth of, 19: 7860
deposition on other metals by electroplating methods, 19: 42827
deposition on uranium carbide, 20: 2300(P)
deposition on vanadium-base alloys for oxidation protection, 19: 20459(R) (IITRI-B6019-6)
deposition with nickel, tantalum, titanium, and zirconium, electrolytic, 18: 26057
determination, 17: 6022
determination and separation of, review of, 18: 3691
determination as impurity in and volatilization from tungsten, semi-quantitative spectrographic, 16: 4131 (BM-RI-5903)
determination by atomic absorption spectroscopy using induction-coupled plasmas, 20: 40796(R) (IS-1500(Sect.C))
determination by infrared spectroscopy of the oxinate, 17: 19969
determination by quinol method, standard solution for photometric, 19: 32079
determination by solvent extraction using cyclohexanone, gravimetric, 17: 30497
determination by spectrochemical methods, voltage-fluctuation patterns in, 19: 40416
determination by thermal-neutron activation methods, sensitivity for, 19: 9071
determination by x-ray fluorescence, 17: 31999
determination by x-ray fluorescence spectroscopy, 19: 38549
determination, colorimetric, 18: 348
determination in alloys, ores, and slags, fluorescence spectrometric, 17: 32007
determination in aqueous solutions, polarographic, 18: 31379
determination in alloys using vacuum cup electrode, spectrographic, 19: 22103 (TIM-904)
determination in alloys, minerals, and rocks by neutron activation, 19: 24420
determination in alloys and metals, photometric, 19: 40442
determination in aqueous solutions, design of oxyacetylene burner for measuring sensitivity of spectrophotometric, 20: 29083(R) (UCRL-14767)
determination in borides, carbides, and nitrides, methods for, 19: 24403 (NP-14952)
determination in complex alloys, 16: 7503
determination in concentrates, minerals, and ores by ion exchange, 16: 16312
determination in carbonatites, spectrophotometric, 16: 31575
determination in carbonatites, spectrographic, 17: 27228 (EUR-32.f)
determination in columbite ores and in tantalum, 18: 3703
determination in columbite–tantalite ores, x-ray fluorescence spectrometric, 19: 19754 (JEN-134-DQ/I-39)
determination in columbites and samarskites, 20: 43131
determination in diabase W-1 and granite G-1, spectrographic, 16: 17895
determination in diabase and granite by spark source mass spectrography, 19: 11406
determination in erbium, mass spectrographic, 19: 2232
determination in fluorine, combustion, 17: 1359(R) (ANL-6569)
determination in fissium, spectrophotometric, 17: 33812
determination in fluorite and zircons, radiospectroscopic, 18: 6756
determination in ferro-niobium by precipitation and spectrophotometry, 19: 28242
determination in graphite, rocks, and stainless steel simultaneously with tantalum, activation, 18: 1519
determination in granite, spectrochemical, 18: 17755
determination in hydrogen peroxide using Methylthymol Blue, selective, 16: 12983
determination in hydrochloric acid solution, spectrophotometric, 16: 14672
determination in heat-resisting alloys by x-ray fluorescence, 16: 28877
determination in high-alloy steels, rapid method for, 19: 17844
determination in hafnium carbide–niobium carbide, method for, 19: 46941 (NP-15514(Vol.3))
determination in high-purity tantalum by spectrography using d-c arc method, 20: 20608
determination in iron and nickel base alloys, spectrographic, 16: 11539
determination in iron alloys, x-ray spectrochemical, 17: 5997
determination in irradiated fuel effluents, methods for, 20: 22862 (CEA-R-2553)
determination in minerals and ores, x-ray fluorescence, 16: 152
determination in molybdenum, tungsten, and uranium alloys, photometric, 17: 30496
determination in minerals by precipitation from homogeneous solution, 19: 7321
determination in minerals and silicate rocks, radiometric-spectrophotometric, 19: 43943
determination in minerals and rocks using paper chromatography, 20: 35389 (CEA-R-2791)
determination in niobium oxide–tantalum oxide mixtures, spectrographic, 17: 15857(R) (ORNL-3397(p.57-70))
determination in niobium carbide–zirconium carbide systems, oxidimetric, 17: 25150
determination in niobium-tin coated metal ribbon, intensity ratio technique for x ray spectrometric, 18: 15972
determination in niobium–zirconium alloys, spectrophotometric, 18: 35465
determination in niobium–tin alloys, chemical and x-ray (E), 19: 335
determination in niobium carbide–zirconium carbide, method for,

19: 46941 (NP-15514(Vol.3))
determination in niobium–tungsten alloys, gravimetric, 20: 10794
determination in ores by x-ray fluorescence, 16: 9967
determination in ores, spectrographic, 16: 30348
determination in ores from Araxá area, Minas Gerais, Brazil, 17: 1382 (IEA-53)
determination in ores by neutron activation of short-lived radionuclides, 17: 4481
determination in ores in the presence of tantalum, spectrophotometric, 17: 14170
determination in ores, spectrometric-scintillation counting, 17: 32025
determination in ores, activation, 18: 13626(R) (NYO-10174)
determination in ores, photometric, 18: 13694
determination in ores, spectrographic, 19: 36225 (AEET/Spec./8)
determination in presence of tantalum, volumetric, 16: 7504
determination in presence of ethylenediaminetetraacetic acid, effects of pH on polarographic, 16: 12982
determination in presence of tantalum, polarographic, 16: 25290
determination in pyrophosphoric acid solutions, polarographic, 17: 2924
determination in presence of molybdenum, gravimetric, 17: 30500
determination in presence of yttrium and zirconium by x-ray spectrum method, 18: 5226
determination in presence of tantalum, spectrophotometric, 18: 5238
determination in presence of 71 elements, spectrographic, 18: 43420
determination in protactinium, spectrographic, 19: 284 (AERE-R-4615)
determination in presence of fluoride ions, molybdenum, and tantalum using 4-phenyldaphnetin, gravimetric, 19: 2233
determination in presence of other elements, calorimetric, 19: 13207(T) (FTD-TT-64-592)
determination in presence of tantalum by precipitation using *N*-benzoyl-*N*-*o*-tolylhydroxylamine, 19: 24437
determination in process feed solutions by extraction chromatography, 20: 16333 (KR-81)
determination in rocks, spectrochemical, 16: 28901
determination in steel, chromatographic, 16: 12801(R) (IA-685)
determination in steel as molybdoniobic acid, spectrophotometric, 16: 16315
determination in steel, spectrophotometric, 18: 35479
determination in solids by spark source mass spectrometry, quantitative, 19: 13247
determination in steel by neutron activation, 19: 43942
determination in silicates, activation, 20: 26782
determination in titanium alloys, gravimetric, 16: 25269 (NP-11834)
determination in tantalum by proton activation, 16: 31570
determination in tantalum, buffer effects in spectrochemical, 17: 15899
determination in tantalum oxide, spectrographic, 17: 28796 (AEET/ANAL/7)
determination in tantalum by d-c arc method, spectrographic, 18: 19894
determination in tantalum and tantalum oxides of, spectrophotometric, 18: 25284
determination in tantalum by anion exchange in hydrofluoric–nitric acid mixtures, 18: 35455
determination in titanium and zirconium alloys, gravimetric, 18: 35478
determination in thorium oxide, spectrochemical, 19: 46226
determination in the presence of fluoride, spectrophotometric, 20: 14455(R) (ORNL-3889, pp 25-32)
determination in uranium compounds by reversed-phase partition chromatography, 16: 23636 (TID-7629(p.276-84))
determination in uranium base alloys, photometric, 16: 26928
determination in uranium alloys using xylenol orange, spectrophotometric, 18: 1543
determination in uranium alloys, photometric, 18: 19845 (JAERI-1053)
determination in uranium and its compounds and alloys, methods for, 19: 19823
determination in uranium tetrafluoride, spectrographic, 20: 14473
determination in uranium dioxide, x-ray spectrographic, 20: 18558 (AECL-2526)
determination in uranium compounds after separation by solvent extraction using *N*-benzoylphenylhydroxylamine, spectrographic, 20: 24976 (GAT-524)
determination in water, silver-spark spectrographic, 17: 1381 (IDO-14591)
determination in zirconium alloys, chemical, 18: 12542(R) (GEAP-4484)
determination in zirconium, oscillographic, 19: 32092
determination methods for, 16: 28884
determination of, design of quantometer for x-ray, 17: 40751
determination of, effects of phosphomolybdate on spectrographic, 17: 15930
determination of, in presence of tantalum and zirconium, using lumogallion, photometric, 17: 15929
determination of, in alloys, ores, and slags, x-ray spectrum, 17: 15900
determination of, in presence of alkali metals, chemical spectrographic, 17: 15923
determination of, in presence of tantalum, titanium, and zirconium, spectrophotometric, 17: 21657
determination of, in titanium and zirconium alloys, photometric, 17: 21658
determination of, in presence of tantalum and titanium as complex using 1-butanol, 17: 21659
determination of, luminescent, 17: 15928
determination of radioactive, in foods and water, 18: 41357
determination of, survey of methods for, 18: 3703
determination of traces of, in tungsten, using anion exchange column, 19: 28217(R) (AD-608074)
determination of trace amounts of, in uranium and uranium alloys, 20: 3897
determination of trace amounts of, by reactor neutron activation methods, 20: 26760
determination of, using 7,8-dihydroxy-4-methylcoumarin, 17: 4464
determination of, using 8-quinolinol, titrimetric, 17: 21650
determination of, x-ray spectrometric, 18: 1589
determination of, x-ray spectrometric, 18: 1590
determination of, spectrophotometric, 18: 10013
determination of, spectrophotometric, 18: 10014
determination of, photometric, 18: 31411
determination of, tracer techniques for, 18: 33483
determination of, development of photometric and titrimetric methods for, 19: 17841
determination of, review on methods for, 19: 22108
determination of, review of methods for, 19: 36304
determination of, polarographic method for, 19: 40443
determination of, hydrogen peroxide method for spectrophotometric, 20: 3904
determination of, using Arsenazo III, photometric, 20: 36778
determination, pyrogallol complexometric, 16: 16327
determination, reagents for absorptiometric, 17: 7983
determination simultaneously with tantalum in minerals and ores, activation, 20: 16336(R) (NYO-10175)
determination using thiocyanic acid, spectrophotometric, 16: 23659
determination using 4-(2-pyridylazo)resorcinol, spectrophotometric, 17: 1408
determination using xylenol orange, photometric, 17: 12215
determination using lumogallion reagent, fluorescence, 17: 14193
determination using 4-(2-pyridylazo)-resorcinol, absorptiometric, 17: 38960
determination using 2,3,7-trihydroxy-6-fluorone, photometric, 18: 5222
determination using carbon tetrachloride and diethyl ether, 18: 9988
determination using diazo and monoazo compounds, photometric, 18: 19913
determination using thiocyanate, conditions for spectrometric, 18: 31392
determination using *N*-benzoylphenylhydroxylamine, spectrophotometric, 20: 18586
deuteron elastic scattering at 11.8 Mev, angular distributions, 16: 3637
deuteron elastic scattering at 11.8 Mev, optical model analysis of, 17: 38192
deuteron elastic scattering at 15 Mev, strong absorption model analysis of, 18: 42708
deuteron reactions (d,α) at 15 Mev, cross sections and energy distributions for, 16: 11020
deuteron reactions (d,n) with, cross sections and mechanism of, (E), 20: 38159
deuteron scattering at 11.8 Mev, 17: 31539
development of coatings of, for thermal protection, 17: 410 (DMIC-175)
dialysis in solutions, 16: 32984
diffusion and position energies of interstitial impurities in, (T), 20: 28679
diffusion and reactions of silicon and titanium in, 17: 34460
diffusion at 1100°C, effects of plating metals on, 17: 23876(R) (USBM-U-1031)
diffusion barriers between hafnium–20 tantalum cladding on tantalum–10 tungsten, performance of, 20: 16943(R) (IITRI-B237-45)
diffusion coefficient measurements in, for niobium-95 at 2000 to 2400°C, 18: 4172(R) (ORNL-3470(p.67-74))
diffusion from sodium at high temperatures, factors affecting, 20: 40357 (NAA-SR-11766)
diffusion in barrier materials at 1700 and 1800°C, 17: 1918 (ASD-TDR-62-432)
diffusion in beta titanium, 18: 39906 (NRL-6141)
diffusion in beta-zirconium, temperature dependence of, 18: 41933 (TID-11295(3rd Ed.))
diffusion in chromium, inter-, 20: 5846
diffusion in gamma uranium, 17: 41333(R) (ANL-6677)
diffusion in gamma uranium, 18: 25969(R) (ANL-6868(p.287-302))
diffusion in gamma uranium, 18: 44208
diffusion in gamma-phase uranium, 20: 19175 (ANL-6568)
diffusion in molybdenum at 1850 to 2350°C, tracer studies of, 19: 16200

diffusion in molybdenum, coefficient for, 20: 11227
diffusion in monocrystalline and molten samples, tracer studies of, 19: 7917
diffusion in niobium and niobium carbides, 16: 12128
diffusion in niobium carbides at 1800°C, 17: 29350
diffusion in niobium–zirconium alloys, tracer studies of, 17: 30988(T) (FTD-TT-63-258)
diffusion in niobium and niobium carbides, activation energies for, 18: 624
diffusion in niobium–titanium alloys at 1000 to 2000°C, 19: 18461 (NRL-6221)
diffusion in niobium carbides at 1700 to 2300°C, 20: 43954
diffusion in pyrolytic carbon, 18: 37676 (A/CONF.28/P/573)
diffusion in tantalum at 900 to 2500°C, 20: 4320(R) (ORNL-3870, pp 70-4)
diffusion in thorium and uranium dioxides, 19: 47070
diffusion in titanium base alloys, 16: 15207
diffusion in titanium at 900 to 1650°C, 17: 34454
diffusion in type 316 stainless steel, 17: 36200(R) (NP-13033)
diffusion in uranium carbide at 820°C, 16: 6686(R) (NDA-2162-5)
diffusion in uranium dioxide single crystals, 19: 5904
diffusion in vanadium, concentration gradients of, 18: 20512 (ASD-TDR-62-7(Pt.II))
diffusion in, effects of annealing temperature and porosity on self-, 20: 17090
diffusion in, self-, 20: 5846
diffusion in, tracer studies of self-, 19: 41064
diffusion of atoms in bcc, activation energy for interstitial, (T), 19: 40086
diffusion of boron and carbon in, conditions for, 18: 20540
diffusion of boron and carbon in, 18: 36001
diffusion of boron in surface of, 20: 11228
diffusion of carbon and niobium in, activation energies for, 18: 624
diffusion of hydrogen in, at 95 to 1065°C, 16: 10027
diffusion of hydrogen in, relaxation effect in, 20: 23730
diffusion of interstitials in, alloying effects of zirconium on, 16: 33500
diffusion of iridium, molybdenum, osmium, rhenium, tantalum, tungsten, and zirconium in, 16: 2194(R) (NP-11060)
diffusion of nickel in, at 950 to 1100°C, 19: 26857
diffusion of niobium-95 and tantalum-182 in, temperature dependence, 18: 27967 (ORNL-3617)
diffusion of niobium-95 and tantalum-182 in, 18: 44151(R) (ORNL-3670 (p.129-31))
diffusion of niobium-95 and tantalum-182 in, 18: 44153 (ORNL-P-425)
diffusion of niobium-95 and tantalum-182 in, at 874 to 2400°C, 19: 41064
diffusion of niobium-95 and tantalum-182 in, 20: 4385(R) (ORNL-3870, pp 15-19)
diffusion of oxygen in, at 600 and 815°C, 19: 42810
diffusion of oxygen in, at 600 and 815°C, 20: 4321(R) (ORNL-3870, pp 136-9)
diffusion of silicon coating into, phase and structure studies, 16: 533(T) (NP-tr-789)
diffusion of tantalum in liquid, coefficient for, 20: 14969
diffusion of tin in, containing zirconium or titanium, 20: 17632
diffusion of tungsten in, 19: 11682
diffusion of uranium in, temperature dependence of, 20: 11290
diffusion of xenon in, 16: 5711 (CNLM-2154)
diffusion penetration by plutonium-uranium alloys, 16: 28555 (TID-7623 (p.105-21))
diffusion, tracer study, 16: 18049
dislocation configuration in deformed foils of, 20: 4386(R) (ORNL-3870, pp 20-6)
dislocation damping interactions in, effects of nitrogen on interstitial, 16: 33491
dislocation damping in superconducting, 20: 20113(R) (NYO-3001-1)
dislocation distribution in deformed, effects of tungsten on, 18: 44146(R) (ORNL-3670(p.17-20))
dislocation dynamics from internal friction, 17: 37508(R) (GA-4495)
dislocation etch pits in, 20: 9576(R) (ORNL-3878)
dislocation in cold-worked crystals of, 17: 23947(R) (GA-3585)
dislocation on {110} planes in bcc, dissociation of, 20: 33918
dislocation parameters for, 20: 17033
dislocation relaxation spectra in cold-worked, 16: 22587 (GA-3076)
dislocation-relaxation spectra of cold-worked, 16: 25807 (GA-1745)
dislocation relaxation structure of, 19: 22977(R) (GA-6163)
dislocation structures in annealed polycrystalline, etch pit studies on, 18: 22506
dislocation velocity in single crystals of, stress dependence of, 18: 44149(R) (ORNL-3670(p.36-43))
dislocations in annealed and deformed crystals of, 17: 29336
dislocations in, calculations of stress field effects of, 17: 13620(R) (NBS-7644)
dislocations in primary slip systems of crystals of, dynamical behavior of, 17: 37526
dissociation energy of gaseous and heat of vaporization of solid, correlation of, 17: 6095
dissolution, development of head-end processes for, 16: 8717 (ORNL-3241)
dissolution in fused lead chloride, 16: 1854(R) (IDO-14553)
dissolution in fused halides, formation of niobium chlorides by, 18: 16032
dissolution of, in chloride and chloride–fluoride melts, anodic processes in, 17: 18835
distribution between nitric acid and 10% trilaurylamine solutions, 17: 12364 (NP-12394)
distribution coefficient in hydrochloric acid and ion exchange resins, 16: 7503
distribution in irradiated uranium(IV) oxides, (E), 19: 30835
distribution in zirconium oxide, use of electron microprobe for determination of, 17: 27746(R) (DPST-63-71-1)
domain structure of foils of, from electron transmission microscopy, 18: 5784
ductility at liquid helium temperatures, 17: 30996
ductility, effects of hydrogen and oxygen, 17: 8834
ductility of, at −269°C, 20: 21416
ductility of, effects of liquid cesium on, 18: 14354(R) (ARF-B215-12)
ductility of, effects of solid-solution hardening at grain boundaries on, 19: 23078
effect on properties of low-alloy steels for reactor pressure vessels, 20: 39444(P)
effects of additions of, on extrusion and forging of tungsten alloys, 17: 6589 (ASD-TDR-62-670)
effects of alloying additions of, on thermal stability of $TiAl_3$, 20: 11335
effects of content of, on stress-corrosion of chromium–iron–nickel-base alloys by boiling magnesium chloride, 20: 23599 (COO-1319-36)
effects of fuel cladding of, on performance of fast power breeder reactors, 20: 35070
effects of, on aluminum-iron alloys, 16: 30820
effects of, on chromium-iron-manganese-nickel alloys, 16: 30822
effects of, on stress release of chromium–iron–nickel alloys, 16: 30842
effects of, on thoria compacts, 16: 30777 (ANL-6529)
effects on austenitic grain size and ductility of low-alloy steel, 20: 27481(R) (EURAEC-1419 and App.)
effects on colorimetric determination of vanadium in uranium compounds, 20: 12802
effects on corrosion of chromium–molybdenum steel by carbon dioxide, 16: 22556
effects on corrosion of antimony–zirconium alloys by water at 680°F, 17: 6561(R) (ARF-2198-34)
effects on corrosion of iron–zirconium alloys by steam at 750°F, 17: 6561(R) (ARF-2198-34)
effects on corrosion of steels by liquid sodium, 18: 14417
effects on corrosion resistance of molybdenum–nickel alloys, 18: 41968(P)
effects on corrosion resistance of zirconium, 18: 41972(P)
effects on corrosion of steels by liquid sodium at 450, 600, and 750°C, 19: 4629
effects on corrosion and mechanical properties of zirconium, 19: 7867 (GEAP-4504)
effects on crystal structure of alpha-iron, 20: 13317
effects on crystal structure and properties of thoria-tungsten cermets, 20: 37185
effects on determination of plutonium using Arsenazo III and its analogs, 20: 45614
effects on ductility of steel, 17: 14862(T) (EURAEC-515)
effects on ductility of iodide chromium, 18: 32189
effects on fabricability of titanium–vanadium alloys, 19: 44587(R) (ANL-7000, pp 3-63)
effects on ferroelectric and physical properties of hot-pressed lead titanate–lead zirconate, 18: 613
effects on ferroelectric properties of lead stannate–titanate–zirconate mixtures, 18: 29151(R) (SC-DC-64-890)
effects on fluorescence and laser properties of rare earth-activated calcium molybdate and strontium molybdate crystals, 19: 36393
effects on fracture mechanisms in beryllium single crystals, 20: 23714
effects on grain size of uranium, 19: 23047
effects on grain size and transformations in alpha-uranium and uranium alloys at 720 to 800°C, 20: 31666
effects on grain size of tungsten, 20: 39400 (NASA-TN-D-3531)
effects on hot-cracking susceptibility of Monel, 19: 30751 (WERL-8844-8)
effects on hydrogen embrittlement of steel, 18: 24153(T,R) (EURAEC-1002)
effects on internal friction of cold-worked zirconium, 19: 2827
effects on kidney function in rats, 18: 23203 (UR-646)
effects on mechanical properties of thorium–uranium alloys, 18: 18304
effects on mechanical properties of tungsten of alloying additions of,

20: 5851
effects on metastable phases in uranium, 19: 16055 (AEET/Met.-2)
effects on microstructure of uranium, 19: 14024
effects on microstructure of tungsten–thoria dispersion-hardened alloys, 20: 31781
effects on oxidation of zirconium, 16: 7528(T) (CEA-tr-X-428)
effects on oxidation resistance of graphite, 18: 24087 (WADD-TR-61-72(Vol.XXX))
effects on oxidation resistance and strength of chromium–magnesia composites, 19: 41022(R) (NP-15292)
effects on phase transformations in steel, 18: 24152(T,R) (EURAEC-1001)
effects on precipitation in carbon–iron systems, 16: 33424
effects on properties of beryllium–calcium alloys at high temperatures, 18: 35951(P)
effects on properties of tantalum, 19: 41067
effects on properties of boron steel, 20: 39426
effects on radiation growth and swelling of uranium, 18: 37736 (A/CONF.28/P/145)
effects on sintering of zirconium boride, 19: 26794
effects on strength of thorium at high temperatures, 19: 20560 (ORNL-3777)
effects on stress-rupture behavior of chromium–cobalt–nickel alloys, 18: 44165
effects on superconducting transition temperature of vanadium silicide, 19: 39196
effects on tensile properties of carbon steel, 16: 7891 (NP-11196(p.43-61))
effects on thermal properties of thoria–urania systems, 16: 7924 (ANL-6397)
effects on thermal expansion of tungsten carbide cermets, 16: 19371 (TIM-410)
effects on thermoelectric properties of tantalum, 19: 30812
effects on zirconium corrosion by steam and water, 18: 37632 (A/CONF.28/P/341)
elastic properties, 19: 20579
elastic properties at 4.2 to 300°K, (E), 20: 4422
elastic properties of, sonic frequency resonance method for determining, 20: 7596
elastic-wave attenuation in superconducting, at 5 to 30 Mc, 17: 11400
elasticity and texture of, 17: 23872(R) (TID-18626)
elasticity constants of polycrystalline, 19: 28828
electric characteristics of anodized compacts of, 16: 2233
electric characteristics of anodized films of, 16: 2233
electric conductivity at 4°K, 16: 24888(R) (NBS-7244)
electric conductivity at 20 to 1755°C, 18: 18354(R) (TID-20412)
electric conductivity of superconducting, surface, (E), 19: 11941
electric conductivity of, effects of plastic deformation on, 19: 14005
electric conductivity, 19: 16053(R) (AD-424622)
electric conductivity of, containing hydrogen, (E), 19: 23060
electric conductivity of, effects of nitrogen content and temperature on, 19: 30811
electric conductivity at 80 to 400°K, 20: 23749
electric conductivity of, effects of impurities and strain on, 20: 31742
electric conductivity of superconducting, from helicon-like resonances, (E/T), 20: 40031
electric conductivity enhancement of superconducting, through hydrogen treatment, 20: 46510 (NASA-TN-D-3638)
electric current-carrying capacity of superconducting, 17: 24152
electric current losses and magnetic properties of superconducting, 18: 9262(R) (NP-13492)
electric current strengths in two-component diffusion layers on, in magnetic fields, 18: 30217
electric currents in superconducting wires of, 50-c critical, 17: 34595
electric-field emission current from normal and superconducting, 16: 10720
electric properties of contacts with normal metals below transition temperature, 17: 36453 (TID-19310)
electric properties of superconducting, at 50 cps, 18: 44677
electric properties of, compilation of, 19: 32718 (AD-608398)
electrochemical behavior in lithium chloride–potassium chloride eutectic, 17: 30555
electrochemical machining of, effects of friction, surface finish, and tool erosion on, 17: 34386
electrochemical properties in potassium sulfate solutions, 18: 10470(R) (EURAEC-812)
electrode potentials, effects of anode polarization on, 17: 25741
electron binding energies of, measurements for, 17: 18924
electron emission in MHD generators from electrodes of, (E), 20: 39736
electron energy levels, 18: 40123
electron energy losses at 150 to 250 ev, (E), 19: 19335
electron field emission patterns of, 18: 29662
electron states in superconducting, 18: 34708
electron tunneling in superconducting, 17: 643
electron tunneling in superconducting, in mixed state, (T), 19: 12430 (NP-14644)
electron tunneling in superconducting point contacts of, infrared frequency response of, (E), 20: 44548
electronegativity, 18: 13797
electronic specific heats and magnetic susceptibility of, variation with temperature, 18: 8837
electronic structure, physical properties, and alloying properties, 18: 34202
electronic structure of, at superconducting critical temperatures, 20: 31747
electrorefining in potassium fluoride–sodium fluoride electrolyte, 18: 35926 (BM-RI-6506)
emissivities of surface at 500 to 1100°C, 16: 18051
emissivities with and without nitrogen at 810 to 2132°C, 16: 21077
emissivity, 18: 12669
emissivity from 1200 to 2000°K, surface roughness effects on, (E), 19: 32798(T)
emissivity of coated, in vacuum, 18: 24138(R) (PWA-2206(Vol.I))
emissivity of coated, in vacuum, 18: 24139(R) (PWA-2206(Vol.II))
emissivity of coated, in vacuum, 18: 24140(R) (PWA-2206(Vol.III))
emissivity of, at 1200 to 2300°C, 20: 11314
emittance properties of disilicide oxidation-protective coatings on, 19: 13869(R) (ASD-TDR-63-269)
energy level transitions in, Coster-Kronig, (T), 20: 15238 (CONF-233 (Vol.3), pp 398-418)
energy level widths for, K, (T), 20: 15239 (CONF-233(Vol.3), pp 419-39)
enthalpy, 20: 5851
enthalpy and heat capacity at 273 to 2740°K, (E/T), 19: 39217
enthalpy at 298 to 1415°K, 19: 4681
enthalpy of solid, measurements of, to 2400°C by drop technique, 20: 7114
etching dislocations on oriented single-crystal faces of, 20: 866
etching using ferric chloride and free hydrofluoric acid, 18: 14508
evaporation and condensation of, design of electron beam device for, 18: 43753
extrusion as clad in uranium carbide fuel elements, 19: 24952 (NMI-2523)
extrusion by hydrostatic methods, 19: 18436
extrusion by hydrostatic methods, 19: 44651
extrusion of alloy-clad billets of, 20: 4299(R) (ORNL-2711)
extrusion of arc-melted, 20: 4999(R) (ORNL-2599)
extrusion of, effects of surface contamination on, 18: 7179
extrusion of, factors affecting, 18: 14443
fabrication and properties, 16: 19396
fabrication and properties as refractory material, 16: 19404
fabrication and properties review, 16: 29328
fabrication and properties of, review of, 17: 29253 (NRC-7129)
fabrication and properties for process equipment in aerospace, cryogenics, and nuclear engineering, 17: 39556
fabrication and properties for use as superconductors, 18: 34179
fabrication and properties of drawn and swaged wires of, 18: 35933(R) (ML-TDR-64-56)
fabrication and properties of, handbook on, 20: 5874 (AGARDograph-94)
fabrication by electroforming, 19: 42827
fabrication by explosive forming, 16: 20994(R) (NP-11621)
fabrication by hot isostatic pressing, 20: 11260
fabrication characteristics and methods, 18: 4225
fabrication for use in reactors, 19: 37008
fabrication into superconducting delay lines, (E), 20: 3612 (CONF-651001-6)
fabrication of bars and tubes of, 19: 32712(P)
fabrication of, effects of carbon and nitrogen on, 17: 32612
fabrication of irradiation specimens of, 17: 6558
fabrication of powdered, method for, 18: 34117(P)
fabrication of reactor components of, by electron beam and TIG welding, 18: 14447
fabrication of rods or tubes of, method for, 19: 22954(P)
fabrication of thin-wall tubes of, methods for, 18: 14423 (CONF-373-9)
fabrication of tubing of, by spinning, 16: 12068 (CNLM-3342)
fabrication of tubes of, by rotary swaging, 18: 41993(P)
fabrication of, mechanical tests to evaluate, 18: 34101
fabrication of, review of primary working operations for, 18: 34104
fabrication, properties, uses, and welding, 16: 19398
fabrication, ultrasonic tube drawing, 16: 7868 (NYO-10008)
fabrication, ore processing, properties, and uses of, 18: 35949
fabrication, oxidation, and properties of, 18: 35986 (ERR-FW-049A)
fabrication, properties, and uses of, review on, 18: 34178
Faraday unipolar induction in type II superconductors of, 20: 40016
fatigue of, effect of crystal structure on, 20: 4443
Fermi surface of, 18: 13133(R) (NBS-8212)
film formation on, tracer study of composition of anodic, 17: 34335
fluorination, 18: 3038(R) (ANL-6801)

forming of, electrolytic, 19: 11711
forming of, electrolytic, 18: 14439
fragilization in hydrogen at room temperature, effect of oxygen in solid solution and of deformation velocity, 17: 29343
fringe patterns in electron microscopy of foils of, 18: 32039(R) (EURAEC-974)
gamma reactions on, effects of E1 resonances on, 16: 33906
geochemistry and mineralogy of, in Cherry Mountains (Urals), USSR, book, 19: 20190
geology of deposits, 16: 22417
Ginzburg-Landau parameters of superconducting, (E/T), 20: 2906
Ginzburg-Landau parameters for superconducting, temperature variation of, (E/T), 20: 26036
gliding in tension of single crystals of, at 1400 to 2300°C, 18: 2245
grain boundaries, structure and properties, 16: 19429
grain refinement by recrystallization, 18: 3298(R) (ORNL-2221(Pts.1-5) (Del.))
growth of stabilized crystals of, using induction plasma torch, 16: 5661
hardening of, dispersion methods of, 19: 28843
hardness, 17: 11093(R) (NMI-2112)
hardness anisotropy in crystals of, 16: 25818
hardness, microstructure, and cold working properties of high-purity, effects of carbon, 16: 16747
hardness of cast and powdered, at 20 to 2120°C, 18: 39985
hardness of, as function of oxygen concentration, 19: 34642 (ORNL-3751)
hardness of, effects of nickel on, 19: 26859
hardness testing, sticking to diamonds in, 16: 12163
heat capacity of high-purity, at 0.35 to 25°K, 20: 32684(R) (UCRL-16658, pp 21-38)
helium ion reactions at 320 to 880 Mev, cross sections for isotope production in, 18: 42745
helium nucleus reactions at 240 to 880 Mev, 17: 7149 (UCRL-10461)
hydrogen evolution on electrodes of, in hydrochloric and solutions, 19: 34179
hydrogen overvoltage on, 18: 1671
hydrolysis, effects of sulfuric acid on, 17: 30461
impurities in, ordering of interstitial, 20: 18003
impurity atom relaxation strength in, anisotropy of Snoek, (E), 20: 13980
inflammability of powdered, at 180 to 1100°C, 18: 44211
interactions in interstitial sites in bcc lattice of crystals of, 17: 20460 (UCRL-7184)
internal friction in, 17: 27783(R) (GA-4227)
internal friction in, interstitial-dislocation interactions in, 17: 35770
internal friction in, activation energies and attempt frequencies for deformation-induced, 17: 36321
internal friction in plastically deformed bcc, 18: 34039(R) (GA-5340)
internal friction peaks in cold-worked (E), 19: 2824
internal friction of, effects of nitrogen and oxygen on, 19: 14053
internal friction of, effects of nitrogen and oxygen on, 19: 23035
internal friction measurements in deformed high-purity, 19: 27709(R) (GA-5734)
internal friction of, effects of nitrogen and oxygen on, 20: 11227
internal friction peak in, dislocation-relaxation, 20: 15122
internal friction of cold-worked, effects of restraining on, 20: 21378
internal friction of cold-worked, effects of nitrogen and oxygen on, 20: 33893
interstitial atom-dislocation effects in, 17: 3466 (ASD-TR-61-351)
ion exchange in concentrated hydrochloric and perchloric acids, distribution coefficients for, 18: 17759
ion exchange properties, 17: 28896
iron-57 Mössbauer effect in, localized magnetic moments from, 19: 18511
joining of, review of, 17: 34360 (CONF-94-5)
joining of, to tantalum, impurity effects on, 16: 29319(R) (USBM-U-952)
joining to refractory metals, methods for, 18: 7956(R) (GA-3992(Pt.I))
joining to tantalum, methods for, 17: 36268
joining to uranium carbide and zirconium carbide, 16: 19323(P)
lattice defect observations in crystals of, use of electron microscopy for, 18: 4251(R) (ORNL-3470(p.49-52))
Luders band velocity in, effects of stress on, 18: 44199
machining, 16: 3417(R) (ASD-TR-7-532a(IV))
machining of, optimum conditions for turning, 19: 30696 (RDB(C)TM-278)
machining properties, 16: 4528 (DMIC-Memo-134)
magnetic behavior of superconducting, 18: 18841
magnetic field distribution in annealed and plastically deformed type-II-superconducting, (E), 20: 13672
magnetic field effects on complex permeability and conductivity of, 19: 22998 (UCRL-11251)
magnetic field penetration depth in superconducting, temperature dependence of, (E), 19: 14435(R) (NP-14676)
magnetic field penetration in superconducting, radial velocity of, (E), 19: 39702
magnetic field penetration depth in superconducting, (E/T), 19: 39726
magnetic field structure in superconducting, 18: 22832
magnetic field transitions in superconducting, surface effects on a-c, (E), 20: 21918
magnetic flux distribution in superconductors of, measurement of, 20: 8003(R) (MIT-3226-8)
magnetic flux jumps in superconducting, speed of, (E/T), 19: 45199
magnetic flux jumps in superconducting, (E/T), 19: 37750
magnetic flux movement through superconducting, energy losses from, (E), 19: 6618
magnetic flux penetration in superconducting, ultrasonic attenuation for determination of, (E), 20: 13684
magnetic flux pinning in superconducting, quantized, (E), 20: 21909
magnetic flux pinning in superconducting thin films of, (E), 20: 30278
magnetic flux retention in hysteretic superconducting, 20: 44521
magnetic flux trapping in superconducting crystal spheres of, 19: 14445
magnetic fluxoid transitions and loss in multiply connected superconductors of, (E/T), 20: 6246
magnetic hysteresis losses from surface of superconducting, mechanism for, 18: 956
magnetic hysteresis loops in superconducting, intrinsic properties of, (E), 20: 19741
magnetic hysteresis in superconducting, effects of surface properties on, 20: 28195
magnetic hysteresis of superconducting, surface contamination effects on, (T), 20: 28196
magnetic moments of superconducting spheres of, residual, (E), 19: 45195
magnetic properties, 17: 4171(R) (NBS-7280)
magnetic properties of cold-draw wires of, 17: 21137(R) (NBS-7677)
magnetic properties at low temperatures, 18: 34712
magnetic properties of, compilation of, 19: 32718 (AD-608398)
magnetic properties of superconducting, effects of lattice defects on, 20: 30253 (CEA-R-2808)
magnetic quantized flux pinning in superconducting, 18: 32698
magnetic resonances in superconducting, low-frequency mixed-state, (E), 20: 21894
magnetic susceptibility, 17: 14941(R) (NBS-7608)
magnetic susceptibility, 17: 41333(R) (ANL-6677)
magnetic susceptibilities of, temperature dependence of, 20: 17069
magnetization curves of impure superconductivity, 17: 13147
magnetization curve of type II superconducting, (E), 19: 45200
magnetization of impure superconducting, (T), 20: 40036
magnetization of nonideal type-II superconducting wires of, Procopiu-effect analog in longitudinal, (E), 20: 24277
magnetization of superconducting, irreversible, (E/T), 19: 16777
magnetization of superconducting, peak effect in, 20: 44528
magnetization of type-II superconducting, adiabatic, (E), 20: 24278
magnetocalorie effects in superconducting, reversible, (E), 19: 39703
magnetostriction in pure monocrystalline, 19: 39199
magnetothermal effects in superconductors of, (E), 19: 14433 (CONF-651-44)
mechanical properties, effects of interstitial impurity levels, 16: 2170 (BM-RI-5872)
mechanical properties, 16: 3479 (WADD-TR-61-181)
mechanical properties, effects of titanium, vanadium, and zirconium, 16: 3443 (ASD-TR-61-3)
mechanical properties, effects of impurities, 16: 18015 (AD-263881)
mechanical properties, effects of additives, 16: 22644
mechanical properties, effects of hydrogen pickup, 16: 25402
mechanical properties, effects of oxygen on, 16: 29372 (IS-503)
mechanical properties of extruded, at high temperatures, 16: 29375(R) (NMI-2106)
mechanical properties of, effects of oxygen on, 17: 4447 (IS-500(Sect. M))
mechanical properties at 1600 and 1800°F, 17: 7606(R) (ORNL-1515)
mechanical properties of, effects of impurities on, 17: 16652(R) (NP-12633)
mechanical properties of, effects of hydrogen on, 17: 16728
mechanical properties, radiation effects on, 17: 18868
mechanical properties of, effects of surface gas contamination on, 17: 20479
mechanical properties of, at low temperatures, effects of hydrogen and oxygen on, 17: 20501
mechanical properties, 17: 32565 (ASD-TR-61-181(Pt.III))
mechanical properties of, effects of carbon and nitrogen on, 17: 32612
mechanical properties and strength of, additive effects of oxygen on, 17: 39527 (AROD-2530:2)
mechanical properties of deformed, effects of annealing temperature and vacuum pressure on, 17: 41396
mechanical properties of electroclad and electroformed, 18: 14439
mechanical properties of argon arc and electron beam welded, 18: 27927
mechanical properties of, effects of trace elements on, 18: 34206

mechanical properties at −196 to 2800°C, temperature effects on, 18: 42065
mechanical properties of, effects of heat treatment on, 19: 7959
mechanical properties at low temperatures, 19: 9604(R) (IS-900(Sect.M))
mechanical properties and internal friction of, effects of strain-aging on, 19: 14028
mechanical properties of single crystal, effects of high vacuum purification on, 20: 838
mechanical properties of arc-cast, heat treatment effects on, 20: 4999(R) (ORNL-2599)
mechanical properties of, additive effects on, 20: 5181(R) (ORNL-3029)
mechanical properties of, effects of hot plastic deformation on, 20: 4403(T) (JPRS-32317)
mechanical properties of, effects of impurities on, 20: 4425
mechanical properties, 20: 4299(R) (ORNL-2711)
mechanical properties and structure of, effects of hot rolling in air, argon, and vacuum on, 20: 11249
mechanical properties of, effects of alloying additions on, 20: 11288(T) (AD-622477)
mechanical properties of, effects of alloy additions on, 20: 11302
mechanical properties of single-crystal, as function of orientation, 20: 29762
mechanical properties of single-crystal and polycrystalline, 20: 33892
mechanical twinning in, effects of interstitials on, 18: 8818
melting and welding of, purification using cerium-niobium electrode in, 18: 29617
melting of, composition of gases evolved during electron beam, 20: 872
melting of, effects of additives, arc current, and electrode density on vacuum-arc, 18: 24070 (RTD-TDR-63-4089)
melting of, performance of plasma electron beam source for, 18: 41952
melting of, performance of induction furnace for cold-mold, 20: 2352(R) (USBM-RC-1205, pp 9-10)
melting point determinations, 17: 29330(R) (UNC-5056)
melting point of zone-refined, 20: 31721(T) (AD-630971)
melting point of, effects of gas impurities on, 20: 17094
mercury ion reactions, atom ejection patterns in, 16: 2203(R) (TID-14257)
meson (μ^-) capture by, probability for, (T), 20: 28456
metabolism by dogs and rats, effects of particle properties and size on, 19: 3852
metallographic techniques for studying corrosion of, 19: 7863 (BNL-7642)
metallography, 17: 36269
metallurgical effects on tensile properties of carbon steel, 16: 25792
metallurgical effects on properties of aluminum–titanium-zirconium alloys, 16: 25813
metallurgical effects on stacking fault energy in chromium–iron–nickel alloys, 18: 22448 (UCRL-10890)
metallurgical properties, 16: 15164 (AGARDograph-50)
metallurgical properties, 16: 22616
metallurgy, 16: 29326
metallurgy of, bibliography on, 17: 36203 (TID-3572)
metallurgy of, book on, 20: 46147(T) (NASA-TT-F-359)
metallurgy of, in steels and superalloys, 19: 985
metallurgy of, research on, 20: 5851
microstructure of, 16: 30170(R) (ORNL-3313(p.179-208))
microstructure of, effects of carbon, nitrogen, and oxygen on, 17: 36269
microstructure of single-crystal, Berg-Barrett x-ray microscopy of, 19: 26835
microstructure of, effects of heat treatment at 1625°C on, 20: 23716
microstructures, 19: 44610 (TIM-943)
microwave surface in superconducting, (E), 20: 21916
movement in ground water at Savannah River Plant, 17: 4700
neon ion reactions, atom ejection patterns in sputtering by, 16: 2203(R) (TID-14257)
neutron absorption cross sections, 16: 18429
neutron absorption cross sections at 24 kev, (E), 19: 45230
neutron average total cross sections at 11 to 101 kev, (E/T), 19: 8457
neutron capture by, 18: 40630
neutron capture cross sections, 16: 26509
neutron capture cross sections, 17: 2222 (JINR-P-1010)
neutron capture cross section of, energy dependence of, 17: 37999(T) (AEC-tr-5734(p.3-6))
neutron capture cross sections, energy dependence of, 18: 15562
neutron capture cross sections at 0.01 to 1 Mev, 18: 18864 (ANL-6792(p.29-50))
neutron capture cross section of, energy dependence of radiative (E/T), 19: 3391
neutron capture gamma spectrum, 16: 28024(R) (ARF-1193-12)
neutron capture gamma spectra from, thermal, (E), 19: 25475(R) (ORNL-TM-1044)
neutron capture resonance integrals, (E), 20: 40146
neutron cross sections, thermal, 16: 2783
neutron cross sections, 16: 33579 (GA-2911)
neutron cross sections for, nine and sixteen group, 17: 22789 (GEMP-173)
neutron cross sections for, 9- and 16-group, 20: 4829 (GEMP-173 (Suppl.1))
neutron cross sections for, 20: 4830 (GEMP-384)
neutron diffraction by vortex lines in superconducting, 19: 38058
neutron Doppler coefficients for, fast, (E/T), 19: 29199
neutron elastic scattering at 0.3 to 1.5 Mev, differential cross sections for, 18: 6221
neutron elastic scattering at 0.275 to 0.85 Mev, nonlocal optical model analysis of, 18: 6241
neutron elastic scattering at 5.0 Mev, angular distribution, 18: 26668
neutron elastic scattering at 400 kev, cross section for, 18: 38074(T) (AEC-tr-6398(p.64-9))
neutron elastic scattering at 0.3 to 1.5 Mev, differential cross sections for (E), 19: 3381
neutron elastic scattering at 0.3 to 1.5 Mev, angular distributions from, (E), 19: 19095 (WASH-1053)
neutron elastic scattering at 0.3 to 1.5 Mev, cross sections for fast, (E), 19: 31215(R) (ANL-7010(p.1-19))
neutron elastic scattering at 1 Mev, differential cross sections for, (E/T), 20: 9981 (WASH-1064)
neutron elastic scattering at 0.275 to 0.85 Mev, differential cross sections for, (E/T), 20: 9981 (WASH-1064)
neutron elastic scattering at 0.68 to 1.25 Mev, (E/T), 20: 19805(R) (ANL-7110, pp 1-28)
neutron elastic scattering at 5 Mev, angular distributions from, (E), 20: 46794
neutron inelastic collision cross sections, 16: 10984
neutron inelastic collision cross sections, 16: 29793(T) (FTD-TT-62-953)
neutron inelastic scattering cross sections, 17: 15385(R) (ANL-6683)
neutron inelastic scattering by, cross sections for, 18: 16958(T) (NP-tr-1114)
neutron inelastic scattering at 4.0 to 6.5 Mev, energy spectra, 18: 26668
neutron inelastic scattering by, gamma yields from, (E), 19: 35406(T) (ANL-Trans-177)
neutron inelastic scattering by, cold, (E/T), 20: 28670
neutron interaction threshold values for fission spectrum, 16: 7036
neutron intermediate resonances and total cross sections at 3 to 650 kev, (E), 19: 35462
neutron reactions at 3.7 Mev, cross-section measurements, 16: 8224
neutron reactions (n,γ) below 40 kev, cross sections, 16: 23138
neutron reactions in, yields of helium and hydrogen produced by fast, 19: 44746 (NAA-SR-Memo-10626)
neutron resonance integral, 16: 9653 (KAPL-2000-16)
neutron resonance absorption integrals for, 16: 26511
neutron resonance integrals, 17: 5320 (AE-81)
neutron resonance parameters for, 18: 11195(R) (EANDC(E)-49(L))
neutron resonance parameters and radiation widths for (E/T), 19: 3238 (JINR-P-1771)
neutron resonance level widths and spacings at 30 to 4000 ev, 19: 35378(R) (EANDC(E)-57(U))
neutron resonance parameters, (E), 20: 9981 (WASH-1064)
neutron resonance parameters, (E), 20: 30360 (WASH-1068)
neutron scattering angular distribution, 16: 12419 (ANL-5567(Rev.))
neutron scattering, fast, 16: 26505 (TID-13546)
neutron scattering at 0.4 to 1.2 Mev, cross sections for, 17: 26476
neutron scattering cross sections at 0.3 to 1.5 Mev, 17: 35079(R) (ANL-6749)
neutron scattering at 1 Mev, nonlocal model analysis of, 17: 41873 (WASH-1044)
neutron scattering by, cross sections for, 17: 41873 (WASH-1044)
neutron scattering at 0.275 and 0.85 Mev, optical model analysis of, 18: 7676 (CONF-340-3)
neutron scattering cross sections at 0.1 to 1.6 Mev, 18: 18864 (ANL-6792(p.29-50))
neutron scattering by, optical model analysis of, 18: 24625 (WASH-1046)
neutron scattering at 0.275 to 0.850 Mev, 18: 42623(R) (ANL-6879 (p.21-34))
neutron scattering by, average compound-nucleus cross sections for, (E/T), 19: 17011
neutron scattering by, angular distribution in, 19: 31252
neutron total cross section of, fast, 17: 20982 (HW-SA-2875)
neutron total cross section at 200 ev to 10 kev, 17: 36669 (WASH-1042)
neutron total cross sections at 10 to 100 kev, 18: 4525 (BNL-7349)
neutron total cross sections at 0.3 to 2.7 Mev, resonance structure in, 18: 13066
neutron total cross sections at 35 ev to 8 kev, (E), 19: 12572
neutron total cross sections of, measurement using neutron velocity spectrometer, (E), 19: 19095 (WASH-1053)
neutron total cross sections at high energies, fluctuations in, 20: 38173
neutron transport properties at 0.3 to 2.7 Mev, 17: 787(T) (AEC-tr-5413)

niobium-93 relaxation rates in metallic, (E), 19: 27577
nitridation at high temperatures, 19: 30675(R) (SRIA-132)
nitridation at high temperatures in ultrahigh vacuum, 17: 12230(R) (TID-17638)
nitridation at very low pressures and high temperatures, 17: 25781(R) (TID-18738)
notch sensitivity, 17: 3467 (ASD-TR-61-474)
nuclear levels in, spacing distributions and correlations for, 18: 2955
nuclear magnetic resonance of crystals of, 17: 1926 (DI-82-0194)
nuclear magnetic resonance in superconducting, 20: 33607
nuclear quadrupole resonance, 17: 10592 (IS-520)
nuclear spin-lattice relaxation in, 16: 27662
optical properties at high temperatures, emittance and reflectance, 16: 12236 (WADD-TR-60-370)
optical properties in polycrystalline, 18: 10062
optical properties of, determination of integral semispherical and monochromatic degrees of blackness at 1200 to 2500°K, 18: 39930(T)
oxidation, 16: 13568 (ARL-239(Pt.II))
oxidation, 17: 7606(R) (ORNL-1515)
oxidation, 18: 2163(R) (IS-700(Sect.M))
oxidation at high temperatures, 17: 12612
oxidation at high temperatures, 17: 14773(R) (TID-18063)
oxidation at high temperatures, 19: 30675(R) (SRIA-132)
oxidation at high temperatures in ultrahigh vacuums, 17: 12230(R) (TID-17638)
oxidation at low pressure at 1200 to 1700°C, 19: 13924
oxidation at low pressures and high temperatures, 20: 5181(R) (ORNL-3029)
oxidation at low pressures at 870 to 3500°F, 20: 4324 (PWAC-460)
oxidation at very low pressures and high temperature, 17: 25781(R) (TID-18738)
oxidation at 1060 to 1650°C and 5×10^{-4} to 2×10^{-3} torr, 18: 8763
oxidation at 150 to 1000°C, 16: 32088
oxidation at 150 to 1000°C and 760 to 10^{-3} mm Hg, 16: 1745
oxidation at 1900 to 2300°F, effects of aluminum–zinc and zinc coatings, 16: 21031 (DC-60-8-25)
oxidation at 300 to 1200°C and oxygen pressures of 0.1 mm Hg to 1 atm, 16: 4496 (NP-11056(p.16-31))
oxidation at 300 to 600°C, thermal, 18: 8758
oxidation at 400 to 1325°C, 16: 27568
oxidation at 400 to 1100°C, structure of oxide films formed in, 18: 10478(T) (JPRS-22697(p.64-78))
oxidation at 400 to 700°C, 19: 9604(R) (IS-900(Sect.M))
oxidation at 450 to 1050°C, effects of pressure on, 17: 28863
oxidation at 500 and 1000°, alloying effects of metals on, 18: 14413(T) (FTD-TT-63-1020)
oxidation at 800, 900, and 1000°C at low oxygen pressures, 19: 34639(R) (BNWL-79(p.5.1-11))
oxidation at 850°C in oxygen at low pressures, mechanism of, 18: 566 (NP-13284)
oxidation by air and gas mixtures, kinetics of, 18: 34083
oxidation by air at 800°C, effects of phosphiding treatment on, 19: 6268 (IS-854)
oxidation by air at 800°C, effects of phosphide coatings on, 20: 5851
oxidation by air at 500 to 900°C, effects of alloying additions on, 20: 11227
oxidation by dry air at 20 to 300°C, 18: 37639(R) (EURAEC-1130)
oxidation by oxygen and water vapor, mechanism and rate of, 17: 1441
oxidation by oxygen at 1200 to 1700°C, effects of pressure on, 20: 11227
oxidation by steam at 1050 to 1500°C, 20: 31669
oxidation characteristics, review, 16: 12997 (CNLM-1724)
oxidation, development of coatings and techniques for protection against, 16: 10406 (ASD-TR-61-322(p.101-18))
oxidation, electron diffraction study, 17: 14270
oxidation in air at 1000 to 1200°C, effects of molybdenum on, 19: 11693
oxidation in hydrochloric, nitric, phosphoric, and sulfuric acids and sodium hydroxide, anodic, 18: 25929
oxidation in the solid-solution range, mechanisms of, 18: 39838(R) (EURAEC-1041)
oxidation kinetics and thermochemistry, 16: 4495 (NP-11056(p.3-15))
oxidation kinetics, 16: 32974
oxidation kinetics, 19: 28757(T) (FTD-TT-64-1154)
oxidation kinetics, 20: 29644
oxidation mechanism, 16: 22156
oxidation mechanism of, studies of dislocations and precipitates in, 17: 39484(R) (EURAEC-688)
oxidation mechanism, 17: 39486(R) (EURAEC-747)
oxidation of platinum-clad, at 1200 and 1400°C, 18: 12652(R) (NP-13593)
oxidation of, at 336 to 475°C, characteristics of, 17: 34354
oxidation of films of, conductance during anodic, 19: 6325
oxidation of foils of, kinetics of, 19: 40974
oxidation of, in hydrochloric, nitric, phosphoric, and sulfuric acid solutions, 17: 25246
oxidation of, kinetics of, effects of silicon and titanium on, 17: 8746
oxidation of, kinetics of anodic, 17: 16675
oxidation of, kinetics and mechanism of, 18: 7155
oxidation of refined, at 350 to 1200°C, kinetics of, 18: 10479(T) (JPRS-22697(p.79-96))
oxidation of, structure of anodic films formed during, 17: 29285
oxidation of, surface temperature during, 17: 30943
oxidation of, beta spectroscopic and tracer studies of oxygen and metal transport in, 19: 34645
oxidation of, effects of alloying on, 18: 25936
oxidation of, effects of coatings on, 20: 33825
oxidation of, effects of fluoride coating on, 20: 39348
oxidation of, effects of specimen shape and stress on, 20: 41412(R) (IS-1500(Sect. M))
oxidation of, kinetics and rate of, 18: 32094
oxidation of, solid-state anodic, 20: 9431
oxidation of, stress generation in surface layers during, 20: 4320(R) (ORNL-3870, pp 70-4)
oxidation of, subscale layers in, 18: 37627
oxidation of, temperature dependence of, 20: 16982
oxidation of, to form metal–metal oxide electrode, 19: 22936
oxidation of, tracer studies of anodic film formation in, 19: 16021
oxidation properties of, for use in sodium coolant system, 19: 22981 (LA-DC-7050)
oxidation protection of, by ceramic coatings, 20: 7528
oxidation rate of, at 1100°C, effects of alloying materials on, 20: 23614
oxidation resistance of, at high temperatures, 17: 16653(R) (NP-12634)
oxidation resistance of, development of coatings for improving, 18: 10491
oxide films on surface of electrodes of, valency changes in, 17: 25203
oxygen addition to, techniques for controlled, 19: 15538
oxygen ion reactions with surface of, secondary oxide ion from, (E), 20: 15976(T)
oxygen ordering in, Curie temperature of, (T), 20: 28680
oxygen removal from, by contact with gas mixture, 19: 36972(P)
paramagnetism in superconducting wires of, (E), 19: 25447
passivation by oxide film, electrochemical studies of, 18: 10485
performance as collector in thermionic generators, (E), 19: 18739(R) (NP-14830)
performance as collector in thermionic generators, 19: 43028(R) (AD-609966)
performance as electrodes in barium-filled thermionic cells, 18: 44498(R) (MND-2812-3)
performance as electrodes in barium-filled thermionic cells, 18: 44499(R) (MND-2812-4)
performance as electrodes in barium-filled thermionic cells, 18: 44497(R) (MND-2812-2)
performance as emitter in cesium-vapor solar-thermionic cells, 17: 9117
performance as fuel cladding in fast reactors, 18: 24952(R) (ANL-6880(p.6-48))
performance as fuel cladding for liquid-metal-cooled breeder reactors, (E), 19: 35800
performance as superconductor, for inverter applications, 19: 40845(R) (N64-33676)
performance in superconducting storage systems for memory devices, 18: 26490
performance of coatings of, on Pebble Bed Reactor fuel, 16: 9663 (NYO-9064)
performance of pelletized, for control of radiant heat transfer in nuclear rockets, (E), 19: 24148 (NASA-CR-210)
performance of superconducting, for large-volume solenoids, (E), 19: 10189 (RLE-TR-427)
performance of superconducting, for linac resonant cavities, 19: 27012 (MURA-714(p.540-4))
permeability of, electromagnetic induction equipment and techniques for measuring, 18: 32149(R) (UCRL-11317(p.131-49))
phase studies on, 20: 32312(R) (UCRL-16658, pp 133-43)
phase transformations in thin foils of, containing interstitials, 18: 25992
phase transition in alloyed and unalloyed, effects of interstitials on ductile-to-brittle, 16: 25751 (DMIC-Memo-155)
photoeffects in anodized electrodes of, 19: 35585 (TID-21972)
photoeffects in anodized electrodes of, open- and short-circuit, 19: 41080
photoelectric properties of anodized, 18: 14722(R) (TID-20233)
photoelectric properties of electrodes of, 16: 13705(R) (TID-14943)
photoemission from crystalline, effects of argon ion bombardment at 500 ev on work function for, 18: 4356
photogalvanic effects of anodized, 18: 569
photon reactions with, proton angular distributions and yields at >8 Mev, 17: 28265
photonuclear reactions, 16: 1060
photovoltaic effects in anodized electrodes of, 16: 10457(R) (TID-14977)
physical properties, 16: 15209
physical properties of, additive effects of oxygen on, 17: 37554

physical properties of, effects of alloying additions and chemical reactions on, 18: 34205
physical properties, 19: 32718 (AD-608398)
physicochemical properties, 16: 3436
plastic deformation, effects of temperature, 16: 3464 (PWAC-359)
plastic deformation of, dislocation patterns from, 18: 30225
plastic deformation of, mechanism of, 19: 40961
plastic deformation in single crystals of, 20: 9576(R) (ORNL-3878)
plastic deformation mechanisms in single-crystal, 20: 25619(R) (ORNL-3949)
plastic strain in, use of stress relaxation technique for studying, 19: 2810
polarization in aluminum chloride–diethyl ether solution for plating, 19: 25010
polarization in aqueous sulfate solutions, electrochemistry of passivating oxide film formed in, 18: 34063
polishing, electrolytic, 16: 18014 (AD-263880)
powder metallurgy, status of, 16: 24110(R) (MAB-139-M(C4))
powder metallurgy of, in the USSR, 17: 1823(T) (JPRS-15978)
powder metallurgy of, 19: 2774
precipitate structure in, 17: 39486(R) (EURAEC-747)
precipitation by iron hydroxides, 16: 27509
preparation and examination of films of, by electron microscope, 16: 10525(R) (EURAEC-21)
preparation and properties of thin films of, as hard superconductor, 18: 15055
preparation and properties of thin-film hard superconducting, 18: 28501
preparation and properties of single crystals of, 19: 39138
preparation and properties of single crystals of, 20: 41481
preparation and purification, 18: 2163(R) (IS-700(Sect.M))
preparation and purification of crystals of, 16: 18015 (AD-263881)
preparation by arc reduction processes, 19: 9146
preparation by calciothermic reduction of niobium pentoxide, 19: 15540
preparation by reduction of pentoxide by carbon, 16: 1647 (IS-339)
preparation by reduction of oxides by carbon, equilibria in, 16: 2209(T) (AEC-tr-4867)
preparation by reduction of pentachloride in hydrogen plasma jet, 20: 4314(P)
preparation by reduction of pentoxide of, using aluminum, 20: 41412(R) (IS-1500(Sect. M))
preparation by zinc reduction of niobium halides, 20: 9405(P)
preparation from electrolytic powders, 17: 3392(T) (JPRS-16063)
preparation from mixture of niobium carbide and oxide, 16: 9146
preparation from mixture of carbide and oxide by vacuum reduction process, 19: 9145
preparation from vapor phase, 18: 32121
preparation of bicrystals of, 19: 22863(R) (AD-606809)
preparation of, by oxide reduction, thermodynamics of, 17: 14269
preparation of, by carbothermic reduction of pentoxide, 17: 16530(T) (JPRS-18277)
preparation of crystals of, by electron beam melting, 18: 27871(T)
preparation of crystals of, by horizontal zone melting by electron bombardment, 16: 19281
preparation of, design of apparatus and method for, 17: 20408(P)
preparation of, design of apparatus and method for, 17: 20409(P)
preparation of films of, by sputtering and superconductivity, 16: 22755
preparation of films of, by vacuum-arc process, 16: 31769
preparation of high-purity, 17: 4447 (IS-500(Sect.M))
preparation of high-purity, 20: 4297(R) (IS-1200(Sect.M))
preparation of kryptonated, by diffusion, 20: 18570(R) (NYO-2757-5)
preparation of large single crystals of, by strain-anneal method, 19: 16042
preparation of porous, by volatilization of titanium from niobium–titanium alloys, 19: 16035
preparation of pure, by electrolysis, 17: 29275(P)
preparation of, separation of metal from reaction products in, 17: 20410(P)
preparation of single crystals of, by arc-zone melting, 18: 18339
preparation of single crystals of, by electron-beam zone melting, 18: 22463(T) (JPRS-22336(p.6-9))
preparation of single crystal, 19: 9604(R) (IS-900(Sect.M))
preparation of standard solutions, 19: 32079
preparation of superconducting films of, method for, 19: 1501
preparation of thin superconducting films of, getter sputtering technique for, 18: 13015
preparation of thin films of, by jet-polishing and electro-polishing, 20: 27464
preparation of, use of vacuum techniques in, 17: 23885
preparation of, by reduction of niobium pentachloride using hydrogen, 18: 20009
preparation of, electric arc reduction process for, 19: 39133
preparation of, vacuum techniques for, 19: 11686
preparation, properties, and uses of, review on, 18: 34189
preparation, properties and uses of, chemical process monograph on, 19: 18407
pressing and sintering of powdered, 19: 22939
pressing and sintering of powders of, removal of impurities during, 16: 3436
production by arc reduction of niobium carbide and oxide mixture, 18: 34067
production by carbide-oxide reaction in vacuum, 17: 21600
production by carbide-oxide reaction in arc furnace, 17: 21601
production by electrolysis, 16: 12040
production by fusion electrolysis, 17: 4901(P)
production by reduction of pentachloride using hydrogen, 17: 16548
production by vacuum reduction, 18: 35948
production from tin slags, 20: 14956
production of, electrolytic, 17: 16547
production of high-quality sheet, panel summary on, 20: 39357 (MAB-212A-M)
production of reactor-grade, from pyrochlore minerals, 19: 16006
production of superconducting films of, 16: 10493
production with defect-free surfaces by electropolishing, 19: 37013
production, economics, and uses of, 1964, 20: 9384
properties, 16: 3460 (NP-11108)
properties and reactions at elevated temperatures, 16: 4527 (DMIC-160)
properties and separation processes for, review on, 17: 32508
properties and structure, 19: 4701
properties and structure of polycrystals of, plastic deformation and yield stress, 17: 29339
properties and uses of, mechanical and physical, 17: 16715
properties and uses of, review of, 19: 36966
properties and uses of, review on, 20: 2307 (AD-613023)
properties as cladding for corrosion protection of uranium, 20: 7522
properties as collector in thermionic cells, 20: 4570(R) (AD-614592)
properties as control rods, 19: 21690(R) (LA-3244)
properties as emitter in thermionic converters, 17: 20607
properties as fuel element cladding, 18: 15563
properties as high-temperature coating, 20: 29650
properties as nuclear space power plant radiator, 17: 35222 (PWA-2240)
properties as reactor material, 16: 18050
properties at high temperatures, 17: 34409(R) (NMI-1253)
properties at high temperatures for use as heating element, 19: 4699
properties at high temperatures, compilation to 1957, 20: 43908 (PWAC-237)
properties for aerospace uses, 19: 47068
properties for exothermic brazing, 17: 16608(R) (NP-12615)
properties for high-temperature use, alloying effects of vanadium on, 18: 14454 (BM-RI-6390)
properties for structural use in gas-cooled reactors, 16: 19993 (NYO-9793)
properties for use as reactor material, 16: 4994
properties for use at high temperatures, 18: 34201
properties for use as fuel cladding material, 19: 11679
properties for use as reactor material, 19: 13907
properties for use as oxidation-resistant coating for uranium, 19: 13925
properties for use as fuel-element cladding, 19: 22884
properties for use as fuel cladding material in reactors, 19: 39206
properties in hydrochloric acid solutions, 16: 17634(T) (AEC-tr-4459 (p.77-82))
properties of bimetal tubes for type 316 stainless steel and, 20: 11214(R) (NASA-CR-54717)
properties of coated, at high temperatures, 16: 9189 (ASD-TR-61-66 (Pt.II))
properties of, effects of annealing on, 17: 36324
properties of electron beam melted, 16: 19280
properties of electrodes of, as electrolytic dissolver material, 16: 1854(R) (IDO-14553)
properties of, for use in thermionic reactors, 17: 5577 (GA-3523)
properties of, for formation of transition metal pseudosilicides, 17: 18668(R) (AFOSR-2647)
properties of, for use in silicate technology, 18: 7250
properties of, mechanical and structural, 17: 3499 (WADD-TR-61-181 (Pt.II))
properties of pentavalent, in aqueous solution, 20: 1875
properties of, review on, 17: 36332
properties of single crystals of, work-hardening, 18: 2263
properties of single crystals of superconducting, magnetic and thermal, 17: 14867
properties of superconductive r-f cavities of pure, 17: 9021
properties of superconducting mixed-state, magnetic and ultrasonic attenuation, 20: 17608
properties of thorium oxide- and yttrium oxide-coated electrodes of, 17: 25810
properties of welded sheaths, sheets, and tubes of, corrosion, mechanical, and physical, 18: 7172

properties of, at 2000°C, for use in thermionic converters, 20: 29729
properties of, dependence of technological uses on, 19: 42880
properties of, effects of alloying elements on, 20: 43905 (ORNL-3212)
properties of, effects of sodium coolant on, 20: 46995
properties of, effects of other metals on mechanical and physical, 19: 11734
properties of, physicochemical, mechanical, and radiation stability, 19: 26818 (NAA-SR-8617(Vol.III))
properties of, review on, 18: 34180
properties, review, 16: 33495
properties, review, 17: 12596
properties, structure, and uses of, review on, 18: 27984
properties, tables of, mechanical and thermal, 16: 10509 (DC-56-3-115)
protection at high temperatures, coatings for, 19: 2762
proton elastic scattering at 9–22 Mev, optical-model analysis of, 17: 28316
proton nonelastic scattering cross sections at 10 Mev, 17: 13581
proton reactions at 240 to 880 Mev, 17: 7149 (UCRL-10461)
proton reactions at 100 Mev, isomeric state from, 17: 17141
proton reactions at 240 to 720 Mev, cross sections for isotope production in, 18: 42745
proton reactions at 40 Mev to 25 Bev, lithium isotopes from, (E), 20: 31205
proton reactions (p,n) at 9 Mev with, neutron spectrum from, 17: 20994 (UCRL-7233)
proton reactions with, lithium-6 and -7 fragments from, 18: 16977
proton scattering, angular distributions, 16: 29881(R) (ORNL-1383)
pulse transmission by coaxial cables of superconducting, (E), 19: 39740
purification, 19: 9604(R) (IS-900(Sect.M))
purification by electron-bombardment melting on a cooled hearth, 16: 32046
purification by electron-beam melting, 17: 34330(R) (USBM-U-1057)
purification by electric-arc zone melting, tracer studies of, 18: 22464(T) (JPRS-22336(p.23-34))
purification by zinc–niobium compounds, 16: 499 (NRL-5643)
purification by zone refining, 16: 27658
purification by zone refining, distribution of additions after, 18: 10461(T) (JPRS-22697(p.46-63))
purification of, methods for, 17: 35950
purification of, by electron-beam floating zone refining, 20: 27414 (ORNL-P-2108)
purification of, radiochemical method for, 20: 8838 (UCRL-14258)
radiation damage, point defects in neutron, 16: 24258
radiation damage to tensile properties of, effects of annealing and of zirconium on, 18: 24196 (PWAC-278)
radiation effects on mechanical properties, fast neutron, 16: 572 (REIC-20)
radiation effects of neutrons on embrittlement of, 16: 33557
radiation effects on mechanical properties, 17: 18868
radiation effects on electric conductivity of, isochronal recovery curves for, 17: 22248
radiation effects on self-diffusion-controlled reactions in, 17: 31055
radiation effects on magnetic properties and critical temperature of superconducting, fast-neutron, 18: 10583
radiation effects on mechanical properties of, review, 18: 20456 (ORNL-3593)
radiation effects on, stage III recovery from neutron, 18: 20596
radiation effects on hardness and thermoelectromotive force of, neutron, 18: 28066
radiation effects on, in-pile, 18: 27952(R) (EURAEC-926)
radiation effects on oxidation of, by dry argon–nitrogen–oxygen, argon–oxygen, and oxygen systems at 20°C, 18: 37639(R) (EURAEC-1130)
radiation effects on tensile properties of, neutron, 19: 25046(R) (HW-83615)
radiation effects on mechanical properties of, neutron, 19: 30820 (BNWL-23)
radiation effects on, fast-neutron, 19: 32718 (AD-608398)
radiation effects on concentration of interstitials and vacancies in, calculation of, 19: 41106
radiation effects on yielding and flow in bcc, 20: 2472
radiation effects on in-pile corrosion of, by aqueous solutions, 20: 5852(R) (EURAEC-1522)
radiation effects on plastic deformation properties of single-crystal, fast-neutron, 20: 9576(R) (ORNL-3878)
radiation effects on, annealing of neutron, 20: 19267
radiation effects on mechanical properties and point defects in, neutron, 20: 21320(R) (AD-625475)
radiation effects on tensile properties of, effects of annealing on neutron, 20: 27582(R) (GEMP-400A, pp 63-98)
radiation effects on carbide fuel cladding of, neutron, 20: 27593(R) (UNC-5134(Vol.2))
radiation effects on, for use as sensor material, 20: 29486(R) (NASA-CR-54964)
radiation effects on Meissner effect in, neutron, 20: 34423
radiation heating deposition rates in, cross sections for, 17: 36347(R) (NARF-62-18P)
radioinduced production of helium and hydrogen in, neutron, 19: 26901
rare gas release, 16: 4167
reaction with nitrogen, oxygen, and water vapor, embrittling effects of, 19: 46296
reactions of, with uranium ceramics at 1200 to 2000°C, 16: 33468 (GA-3124)
reactions of, with niobium bromides at 400 to 450°C, products in, 17: 23297 (IS-544)
reactions with aluminum oxides at high temperatures, 19: 44979(R) (NP-15419)
reactions with alumina, 20: 16978
reactions with aluminum oxide and yttrium oxide, 20: 27531
reactions with aluminum oxides at 1800 to 2200°K, kinetics of, 20: 29174
reactions with benzenearsonic acid and its derivatives in acid media, precipitation, 17: 12198
reactions with beryllium, magnesium, and zirconium oxides at 1600 to 2100°C, 16: 4555(T) (FTD-TT-61-74)
reactions with beryllium to 500°C in carbon dioxide and *in vacuo*, 19: 22997 (TRG-Report-842)
reactions with borides, carbides, and nitrides at 900 to 2200°C, 20: 25578(T) (N-65-35787)
reactions with carbon dioxide to 600°C, 19: 22997 (TRG-Report-842)
reactions with carbon and nitrogen at 1150 to 2370°C, 20: 12845
reactions with carbon monoxide at 1300 to 1700°C, 20: 21270
reactions with diazo and monoazo compounds, color, 18: 19913
reactions with eutectic chromium–uranium alloy at 900 to 1000°C, 17: 14740 (TID-11295(2nd Ed.))
reactions with fast neutrons, helium and hydrogen production in type 347 stainless steel in, 20: 7490(R) (BMI-1745, Sect.A)
reactions with fissium–plutonium–uranium alloys at 750°C, 19: 44587(R) (ANL-7000, pp 3-63)
reactions with flowing steam at 1050 to 1500°C, oxidation in, 19: 24940
reactions with graphite at 1700 to 2300°C, kinetics of, 20: 43954
reactions with hydrogen, nitrogen, and oxygen, kinetics of, 18: 4207
reactions with hydrogen in ATR gas loop, study of possible, 19: 30644 (BNWL-48)
reactions with hydrogen sulfide at 1000 to 1400°C, 20: 14554
reactions with lead chloride, effects of chlorine, 16: 17761 (IDO-14579)
reactions with liquid sodium at high temperatures, 20: 38499 (ANL-7120, pp 839-47)
reactions with magnesium to 650°C, 19: 22997 (TRG-Report-842)
reactions with metal oxides at high temperatures, 19: 44685 (CONF-650908-5)
reactions with metals to 700°C in different atmospheres, 19: 22997 (TRG-Report-842)
reactions with methane at low pressures and high temperatures, 20: 5181(R) (ORNL-3029)
reactions with niobium oxides, 20: 16483
reactions with nitrogen and oxygen at high temperatures, 20: 4299(R) (ORNL-2711)
reactions with oxygen, 19: 40463(R) (SRIA-425-5)
reactions with plutonium nitride, 18: 34032(R) (BMI-1668(Del.))
reactions with plutonium carbide–uranium carbide at 1000°C, 19: 24992(R) (UNC-5094)
reactions with plutonia at high temperatures, 19: 39125(R) (BNWL-91)
reactions with plutonium uranium carbide and uranium monocarbide at 820°C, 20: 27416(R) (UNC-5134(Vol.1))
reactions with refractory metal borides, carbides, nitrides, and oxides, 20: 14989
reactions with silica, interfacial, 16: 31595
reactions with sodium at 2100 to 2400°C, 19: 39090(R) (ANL-7046(p.78-82))
reactions with sodium, high-temperature, 20: 15033(R) (ANL-7152, pp 87-96)
reactions with sodium at high temperatures, 20: 20925(R) (ANL-7055, pp 177-212)
reactions with steam at high temperatures, kinetics of, 19: 32447(R) (ANL-7020(p.175-97))
reactions with steam at 1050 to 1500°C, 20: 6552(R) (ANL-6925, pp 187-233)
reactions with sulfur dioxide, 20: 33270
reactions with uranium di- and monocarbides and nitride at 1000°C, 16: 30829
reactions with uranium-bearing reactor fuels, 17: 27961
reactions with uranium carbide-zirconium carbide systems, 18: 30486 (TID-7687(p 27-44))
reactions with uranium to 600°C *in vacuo*, 19: 22997 (TRG-Report-842)
reactions with uranium carbide–zirconium carbide solid solutions at high

temperatures, compatibility in, 20: 2332 (LA-3307)
reactions with uranium carbide–zirconium carbide, 20: 9400
reactions with uranium carbides, thermodynamic calculation of, 20: 9432
reactions with xylenol orange, 16: 9992
reactions with zinc vapors deposited on, kinetics of, 18: 7271
reactor criticality effects, 18: 15562
reactor criticality effects, 18: 30963
reactor criticality effects, 19: 24079(R) (GA-5487)
reactor criticality effects per atom, (E), 19: 42077 (ANL-7014)
recrystallization temperature, effects of heating rate on, 16: 6737
recrystallization behavior, 16: 22581 (AROD-2530:1)
recrystallization center growth rate, temperature dependence, 16: 29428
recrystallization of, effects of carbon and nitrogen on, 17: 32612
recrystallization behavior of electron-beam-melted, 17: 37555
recrystallization temperature and strength of, effects of molybdenum and titanium additions on, 20: 7618
reduction by aluminum, cadmium, and zinc, 17: 25150
reduction by hydrofluoric acid for titration, 18: 5245
reduction of concentrates and slags of, effects of carbon, iron, and silicon on, 17: 32492
reduction of lead and silver chlorides in fused halides by, 18: 16032
refining by electron beam melting, 18: 27875
refining, development and testing of apparatus for, 16: 18015 (AD-263881)
refining in electron-beam melting furnace, 20: 29634
refining of, use of iodide for, 17: 10635
relaxation effect in, effects of treatments and hydrogen content on, 19: 16053(R) (AD-424622)
relaxation peaks at 100 to 300°K, 16: 33505
relaxation spectra of dislocations in well-annealed, 17: 14730(R) (GA-3845)
review of engineering properties of, 18: 8790 (DMIC-188)
review of status and future potential of, for defense, 18: 8718 (DMIC-Memo-183)
rolling, 17: 36266
rolling, effects of media and temperature on friction in, 17: 30953
rolling in air and vacuum at 300 to 1300°C, 20: 19200
rolling of, effects of degree of deformation on cold, 19: 22944
scavenging effects on carbon, nitrogen, and oxygen in chromium, 18: 12692
separation by electrolysis of cryolitic solutions of pentoxide, 16: 10106
separation by solvent extraction using dodecylbenzenesulfonic acid, 16: 3075
separation by solvent extraction using amines, 17: 14375 (BM-RI-6205)
separation by solvent extraction using butyl phosphates, 18: 16157(P)
separation by solvent extraction using TBP-Amsco, effects of oximes on, 19: 13532(R) (ORNL-TM-1020)
separation by solvent extraction using TBP-Amsco, effects of keto-oximes and nitrates on, 19: 13532(R) (ORNL-TM-1020)
separation from acid solution by solvent extraction with tri-*n*-octyl phosphine oxide-cyclohexane systems, 16: 22275
separation from acid solutions using ammonium pyrrolidinedithiocarbaminate, 17: 28807
separation from alkaline solutions by solvent extraction using quaternary ammonium compounds, 17: 39185(R) (ORNL-3452(p.168-88))
separation from alkaline solutions by hydrated titanium oxide, 19: 5985 (AERE-R-4516)
separation from aqueous solutions containing iron and other impurities by anion exchange, 16: 17775(P)
separation from aqueous solutions by solvent extraction using Amsco-TBP, suppression of, by oximinoketones and oxalic acid, 17: 3070(R) (ORNL-TM-265)
separation from berkelium by solvent extraction, 19: 22112
separation from cesium by ion exchange on zinc ferrocyanide, 20: 7198
separation from chloride solutions by solvent extraction using amines, 18: 1799(R) (ORNL-3496)
separation from citric, hydrochloric, oxalic, and tartaric acid solutions using ammonium pyrrolidinedithiocarbaminate, 17: 33838
separation from fission products by solvent extraction using TBP and TOPO, 17: 243
separation from fission products by solvent extraction using D2EHPA, 18: 16147
separation from fission products in air samples by paper chromatography, 19: 317
separation from fission product solutions by ion exchange, 20: 29357
separation from fuel reprocessing solutions, 17: 10519(T,R) (EURAEC-460)
separation from hafnium and tantalum by paper chromatography, 19: 44124
separation from hydrochloric, nitric, and sulfuric acid solutions by solvent extraction using *N*-benzoylphenylhydroxylamine, 17: 27305
separation from hydrofluoric and sulfuric acid solutions by solvent extraction using tributyl phosphate, 18: 362
separation from hydrochloric acid solutions by solvent extraction using 2-ethylhexanol, 19: 36252
separation from hydrochloric acid solutions by solvent extraction using tetrabutyl pyrophosphate and tetrabutyl hypophosphate, tracer studies of, 19: 46451
separation from hydrochloric acid solutions by solvent extraction using quaternary ammonium chlorides, 20: 20816
separation from hydrofluoric acid solutions by solvent extraction using dialkyl alkylphosphonates, 20: 36941
separation from irradiated molybdenum using diisobutyl ketone, 17: 10714
separation from iron, manganese, tin, and titanium in fluoride solutions using pyrogallol, 18: 10189
separation from iron, tantalum, tin, and titanium by solvent extraction, 18: 39395
separation from irradiated fuels, 19: 20084(P)
separation from irradiated uranium dioxide in chlorine trifluoride by volatilization, 20: 29330(R) (EURAEC-1601)
separation from low-grade ores by chlorination, 19: 28437 (BM-RI-6635)
separation from low grade ores, reductive chlorination process for, 20: 4072(P)
separation from metal solutions by anion exchange in ammonium and hydrogen chlorides and fluorides, 18: 17941
separation from mercury, 19: 15332(R) (BNL-841(p.52-62))
separation from molybdenum and yttrium by carrier precipitation, 17: 2242 (TID-16949)
separation from molybdenum and tantalum using 4-phenyldaphnetin, 19: 2233
separation from molybdenum, method for carrier-free, 20: 262
separation from molybdenum by solvent extraction using tetra-*n*-butyl-ammonium bromide, 20: 12933
separation from molybdenum, tantalum, and tungsten by solvent extraction using methyl isobutyl ketone, 20: 40796(R) (IS-1500(Sect.C))
separation from neptunium and zirconium by ion exchange, 18: 25294
separation from neptunium by solvent extraction using 4-methyl-2-pentanone, 20: 31319 (ISO-SA-10)
separation from nitric acid solution by solvent extraction using amines, 17: 23433(R) (MITNE-31)
separation from nitric or sulfuric acid solutions, ion exchange selectivity scales for, 19: 9257
separation from organophosphorus solvents using acid solutions, 19: 13532(R) (ORNL-TM-1020)
separation from other fission products by sorption on silica gel, 18: 16144
separation from other fission products by solvent extraction, 19: 18075
separation from other metal ions by ion exchange, 19: 40658
separation from other fission products by solvent extraction using benzene–oxine solutions, 19: 46440
separation from other elements by precipitation with bismuth phosphate carrier, 20: 7204
separation from other fission products and uranium by chromatography on ion-exchange paper, 20: 35440
separation from other fission products by ion exchange, 20: 35587 (IEA-101)
separation from other elements by ion exchange using triisoöctylamine, 20: 43439
separation from oxalic acid solutions by ion exchange and solvent extraction, 17: 40747
separation from oxalic acid solution by solvent extraction using triiso-octylamine, effects of uranium on, 19: 22409
separation from protactinium, chromotographic, 16: 16396
separation from proton-irradiated zirconium, 17: 18149
separation from protactinium by solvent extraction using *N*-benzoyl-phenylhydroxylamine, 18: 13707
separation from protactinium and zirconium by solvent extraction using benzoylphenylhydroxylamine, 18: 23728
separation from protactinium by solvent extraction using diisobutyl-carbinol, 19: 7632
separation from protactinium by solvent extraction, 19: 30337
separation from protactinium by solvent extraction using quaternary ammonium chlorides, 20: 20816
separation from protactinium by solvent extraction using isoamyl alcohol, 20: 36940
separation from Purex solution by solvent extraction using D2EHPA, 17: 39186(R) (ORNL-3452(p.189-94))
separation from Purex 1WW by solvent extraction using organophosphorus reagents, 19: 13532(R) (ORNL-TM-1020)
separation from solutions by solvent extraction using hydroxamic acid, 17: 39185(R) (ORNL-3452(p.168-88))
separation from soil, radiochemical methods for, 18: 22185
separation from solutions by solvent extraction, review of methods for, 19: 13543
separation from steel, radiochemical evaluation of extraction process for, 17: 236

separation from strontium by ion exchange, 19: 22443(P)
separation from strontium by rapid solvent extraction using bis(2-ethylhexyl) phosphate, 20: 33191
separation from sulfuric acid solutions by solvent extraction using *N*-benzoyl-*N*-phenylhydroxylaminates, 18: 5237
separation from tantalum by solvent extraction, 16: 7609 (BM-RI-5918)
separation from tantalum and purification by distillation of pentachlorides, 16: 22062(T) (AEC-tr-4460(p.14-32))
separation from tantalum by solvent extraction with hydrofluoric acid–sulfuric acid–methyl isobutyl ketone, 16: 25492
separation from tantalum, process for, 16: 31689(P)
separation from tantalum and zirconium by solvent extraction, 17: 6022
separation from tantalum by solvent extraction of fluorotantalate using chloroform, 17: 12216
separation from tantalum and titanium, methods for, 17: 27401
separation from tantalum using reaction of pentoxides with hexachloropropene, 17: 30553
separation from tantalum by chlorination at 540 to 600°C, 17: 35946
separation from tantalum, processes for, 17: 35949
separation from tantalum by double fluoride salts, 17: 39029(T) (AEC-tr-6069)
separation from tantalum and titanium by solvent extraction of thiocyanate complexes, 18: 348
separation from tantalum using *N*-benzoyl-*N*-phenylhydroxylamine, 18: 1809
separation from tantalum and titanium, chromatographic, 18: 1580
separation from tantalum and zirconium by thin-layer chromatography, 18: 17949
separation from tantalum and titanium by solvent extraction using ammonium pyrrolidinedithiocarbaminate, 18: 27342
separation from tantalum by solvent extraction using hydrofluoric acid–TBP, 18: 33688
separation from tantalum by solvent extraction using TBP, effects of hydrofluoric and sulfuric acids on, 18: 39396
separation from tantalum by precipitation from homogeneous solution, 19: 7640
separation from tantalum by ion exchange, 19: 20054
separation from tantalum by reversed-phase paper chromatography, 20: 9072
separation from tantalum by ion exchange, 20: 35442
separation from tantalum by column extraction using TBP in kerosene, tracer studies of, 20: 43131
separation from tantalum by solvent extraction using TBP, 20: 43437
separation from tantalum by paper chromatography using amines, 20: 43446
separation from thorium using liquid-metal extraction, 17: 28465 (TID-7650(p.436-53))
separation from thorium nitrate solutions, 17: 40389
separation from titanium by cation exchange chromatography, 17: 32054
separation from titanium and zirconium using phenylacetylhydroxamic acid, gravimetric, 17: 38933
separation from tributyl phosphate, 17: 40953(P)
separation from uranium concentrates, 16: 4208(R) (NLCO-800)
separation from uranium by oxidation-reduction in fused salts, 16: 10100 (IS-286)
separation from uranium and zirconium by solvent extraction, 16: 17766
separation from uranium by cation exchange chromatography, 19: 13245
separation from waste water, methods for, 19: 40276
separation from waste solutions by flotation methods, 20: 10447
separation from water by foaming, 20: 36934
separation from waste solutions by solvent extraction using bis(2-ethylhexyl) phosphate, 20: 45796(R) (ORNL-3945, pp 195-8)
separation from zirconium fuel solutions using TBP, 16: 1649(R) (ORNL-TM-1)
separation from zirconium by solvent extraction using acetylacetone, 16: 29042
separation from zirconium by solvent extraction using *N*-benzoylphenylhydroxylamine, 16: 12989
separation from zirconium by TTA in benzene, chromatographic, 17: 20113
separation from zirconium by paper chromatography, 17: 37157
separation from zirconium using salicylhydroxamic acid, radiochemical, 19: 2224
separation from zirconium by solvent extraction, 19: 26265
separation from zirconium by solvent extraction using benzoyltrifluoroacetone or trifluoroacetylacetone, 20: 18833
separation from zirconium by solvent extraction using *N*-benzoylphenylhydroxylamine, 20: 18586
separation from zirconium by solvent extraction using 8-hydroxyquinaldoxime and caproic acid, 20: 18849
separation from zirconium by ion exchange, 20: 27044
separation from zirconium by solvent extraction using dioctyl ester of methylenediphosphonic acid, 20: 33421
separation of fission product, radiochemical, 16: 24564
separation of, from tantalum by solvent extraction with 8-quinolinol, 17: 18213
separation of, from boron, method for, 17: 17999
separation of, from samarskite by solvent extraction, 17: 20110
separation of, from sulfuric acid solutions by solvent extraction, 17: 30629
separation of nitrogen and oxygen from, degasification processes for, 20: 29633
separation of protactinium from, by peroxide precipitation, 17: 40940
separation of protactinium from, 19: 36538 (MLM-1233J)
separation of protactinium from, 19: 36539 (MLM-1234J)
separation of protactinium from, using *N*-phenylbenzohydroxamic acid, 20: 27062
separation of protactinium from, by selective precipitation from oxalic-hydrochloric acid mixtures, 20: 41043
separation of protactinium from, by hydrolysis in oxalic and hydrochloric acid, 20: 41044
separation of rare earths from, by solvent extraction using butyric acid, 20: 45612
separation of, from other fission products by fractional electrolytic dissolution, 20: 35589 (NP-16170)
separation of, from tantalum by reaction of the mixed pentachlorides with calcium fluoride and calcium oxide, 20: 43170 (IS-T-107)
separation with titanium from aqueous solutions by sorption ion exchangers, 17: 241
sintering behavior of electrolytic powders of, at 1000 to 2300°C, 16: 30761
sintering of powders of, 16: 13557
sintering of powders of, kinetics of hot-press, 17: 8770
solubility in alpha-iron at 600 to 900°C, 20: 13317
solubility in bismuth (liquid) at 482 to 1010°C, 16: 6716 (NEPA-1221)
solubility in bismuth, 17: 2464(R) (BNL-731(p.59-94))
solubility in cesium, 19: 11682
solubility in cobalt–tungsten carbide systems, chemical determination of, 20: 39427
solubility in liquid and solid magnesium, 18: 28002
solubility in liquid plutonium at 700 to 1000°C, 20: 15043 (LA-3436)
solubility in liquid cerium–cobalt–plutonium alloy at 500 to 900°C, 20: 15043 (LA-3436)
solubility in liquid zinc, 20: 22966 (ANL-7083)
solubility in liquid plutonium at 700 to 950°C, 20: 33779
solubility in lithium (liquid) at 482 to 1010°C, 16: 6718 (NEPA-1465)
solubility in lithium at 760 to 1540°C, 19: 26282 (CONF-650411-4)
solubility in lithium at 1200 to 1700°F, 19: 36980 (PWAC-355)
solubility in lithium and potassium, effects of carbon, nitrogen, and oxygen on, 20: 7579 (TIM-850)
solubility in lithium at 760 to 1540°C, 20: 33863 (CNLM-6335)
solubility in magnesium–zinc alloys, 20: 31314(R) (ANL-7175, pp 1-41)
solubility in mercury, 17: 31798(R) (BNL-782(p.60-91))
solubility in molten potassium, 20: 2237
solubility in potassium, effects of oxygen on, 19: 26282 (CONF-650411-4)
solubility in potassium, 20: 11227
solubility in potassium at 760 to 1205°C, 20: 33863 (CNLM-6335)
solubility in pure potassium at 1000°C, 19: 40946(R) (AI-65-93)
solubility in rubidium at 1000 to 2000°F, 17: 16634 (AGN-8063)
solubility in sodium at 1470 to 2507°F, equilibrium, 16: 30365(R) (NRL-5844)
solubility in zinc (liquid), 16: 544
solubility of oxygen in, at 500 to 1900°C, 18: 5805
solvent extraction using triisooctylamine, 16: 13148
solvent extraction using acetylacetone, 16: 29042
solvent extraction of, as salt of *N*-phenylbenzohydroxamic acid, 16: 30503
solvent extraction from strong hydrochloric acid, 16: 31687
solvent extraction by tributyl phosphate and di-2-amyl 2-butylphosphonate in short-residence contactors, 19: 40645 (CONF-650918-1)
solvent extraction by Alamine 336–dibutyl cellosolve in contactor, 19: 44108 (AERE-R-4440(Pt.3))
solvent extraction from nitric acid solutions, effects of solvent degradation on, 19: 46430 (ORNL-P-1601)
solvent properties for oxygen at 1000°C, 16: 13611
solvent properties for oxygen, 17: 39527 (AROD-2530:2)
solvent properties for nitrogen and oxygen, 18: 34177
solvent properties for nitrogen at 450 to 1000°C, 20: 13303
solvent properties for hydrogen, pressure and temperature dependence of, 20: 27506
solvent properties for nitrogen, 20: 31250
sorption by platinum, gold, silver, stainless steel, glass, and polyvinyl chloride, tracer study of, 17: 35693 (NP-12983)
sorption from aqueous solutions by pyroclastic rocks, 17: 35940 (UJV-951/63)

sorption from nitric acid by ion exchange paper, 19: 24435
sorptive properties for hydrogen in potassium–sodium alloy at 350°C, 16: 25402
sorptive properties for nitrogen and oxygen in vacuum, research program, 17: 10602(R) (TID-16820)
sorptive properties for nitrogen at high temperatures and low pressures, 18: 12041(R) (TID-19489)
sorptive properties and work function of, 18: 20564
sorptive properties for nitrogen in ultrahigh vacuum and constant pressure, 18: 22002 (CONF-209-26)
sorptive properties for nitrogen and oxygen in ultrahigh vacuum, 18: 35958(R) (SRIA-126)
sorptive properties for nitrogen, 18: 41933 (TID-11295(3rd Ed.))
sorptive properties for nitrogen and oxygen in ultrahigh vacuum to 1800°C, 19: 906(R) (TID-21114)
sorptive properties for nitrogen, oxygen, and nitrogen–oxygen mixtures, 19: 30675(R) (SRIA-132)
sorptive properties for nitrogen at 25 to 1800°C and 6×10^{-9} to 6×10^{-5} torr, 19: 47031
sorptive properties for nitrogen and oxygen at very low pressures, 20: 775(R) (SRIA-425-6, pp 10-33)
sorptive properties for oxygen, 20: 916(R) (SRIA-415-6)
sorptive properties for nitrogen, oxygen, and nitrogen–oxygen mixtures, 20: 5851
sorptive properties for nitrogen and oxygen, 20: 8887(R) (SRIA-425-7)
sorptive properties for nitrogen and oxygen, kinetics of, 20: 21351(R) (SRIA-425-8)
sorptive properties of evaporated films of, for carbon monoxide at 0°C, 20: 21388
sorptive properties of evaporated films of, for carbon dioxide at room temperature, 20: 21389
sorptive properties for nitrogen at 10^{-5} to 10^{-8} torr and 1400 to 1900°K, 20: 29178
spalling of aluminum coatings on, at high temperatures, 18: 20474 (TID-12794)
spark patterns produced by grinding of, 18: 19493(T) (SC-T-64-47)
specific heat in magnetic field, 18: 2773
specific heat of superconducting, measurement of anomalous lattice, 18: 9287
specific heat of superconducting crystals of, 17: 36442(R) (NP-13084)
specific heat of superconducting, in magnetic fields, (E), 20: 2906
specific heat of unannealed wires of, at low temperature in magnetic fields, 20: 19751
specific heat of unannealed wires of, at low temperature in magnetic fields, 20: 46524
specifications for sheet rolled, 16: 24160 (MAB-184-M)
spectra in compounds and metal, L-series of fluorescent x-ray, 16: 4165(T) (NP-tr-822)
spectra of, absorption, 18: 1489(R) (IS-700(Sect.C))
spectra of, atomic absorption, 17: 10549
spectra of, flame, 17: 19990 (IS-517)
spectra of L_{β_5} emission bands of, 17: 8082
spectra of, L_{II} and L_{III} x ray absorption edges of, 17: 22201(T)
spectra of, effects of impurities on M-emission band of, 18: 39197
spectra of, effects of electronic structure on x-ray emission, 20: 12846
spectra of, Ohlin structure near limit of continuous x-ray, (E), 19: 44940
spectra of, use of fuel-rich premixed oxyacetylene flame for emission, 18: 25278
spectra, L-series, 19: 6355
sputtering at 50 to 600 ev by rare gas ions, 17: 8931(R) (NP-12389)
sputtering by cesium ions, 18: 40168
sputtering by helium ions at 600 ev, yield curves for, 17: 25870(R) (X62-11400)
sputtering by mercury ions at 10 ev, energy distribution from, 18: 9004
sputtering by noble-gas ions at 100 to 600 ev, yields from, 16: 22753
sputtering of crystals of, by argon, mercury, neon, and xenon ions at low energies, atom ejection in, 17: 37467
strain aging and London yielding of single crystals of, impurity effects on, 20: 29790
strain-aging, effects of titanium, vanadium, and zirconium additions, 16: 21063
strain aging, effect of stress on, 20: 43965
strain-aging process in, yield-point return and internal friction studies of, 20: 2376
straining in polycrystalline, effects of aging, grain size, and pre-strain on micro-, 18: 18379
strength at high temperatures, effects of alloying on, 20: 43969
stress relaxation and thermal activation, 19: 30757
stress relaxation prior to yield point in, 20: 5851
structure of annealed and/or explosively shocked, 18: 18403
structure of rolled, deformation effects on, 17: 14798
structure of, effects of ionic bombardment on lattice, 19: 27063 (INR-555/XIV)
structure, radiation and thermal effects, 16: 18026(R) (EURAEC-78)
superconducting behavior of deformed and undeformed, orientation dependence of, (E), 19: 6604
superconducting critical fields and temperatures for, 17: 41592
superconducting critical field of, resistivity and temperature dependence of, 18: 2772
superconducting critical alternating currents in, density dependence on frequency of, 18: 13018
superconducting critical fields of films of, 18: 21114
superconducting critical current oscillations in, field dependence of, 18: 28512
superconducting critical fields in, 18: 34704
superconducting critical currents in, 18: 36434
superconducting critical alternating currents in, (E/T), 19: 33169
superconducting critical characteristic curves for, 19: 41630
superconducting critical currents and fields in flux-pump fed coils of, (E), 20: 21924
superconducting critical current in, effects of lattice defects on, 20: 31759
superconducting critical temperature of, effect of interstitial gases on, (E), 20: 40025
superconducting current density and resistive transition characteristics of, 18: 22837
superconducting energy gap in monocrystalline, anisotropy of, 18: 15107
superconducting energy gaps in, 18: 36501
superconducting energy gap in, ultrasonic determination of, 18: 36506
superconducting films of, preparation by "protected sputtering", 18: 36536
superconducting, joule heating at contacts with normal copper, 17: 12830
superconducting magnetic flux pump of, 18: 36521
superconducting penetration depth in, temperature variation of, (E), 20: 1131
superconducting point contacts of, macroscopic quantum interference effects in, (E/T), 20: 11911
superconducting properties of films of, 18: 2751
superconducting properties of evaporated and sputtered films of, 18: 34157
superconducting properties of, (E), 19: 16764 (AROD-3473:2)
superconducting properties of, effects of oxygen on, 19: 25031
superconducting properties of high-purity, at 1.1 to 9.25°K, (E), 20: 4774 (IS-T-22)
superconducting properties of fine wires of, in copper matrix, 20: 13673
superconducting properties of thin films of, 20: 19723 (N-65-17508)
superconducting properties of, effects of λ transition on, 20: 21875
superconducting properties of cold-worked, heat-treatment effects on, (E), 20: 26029
superconducting properties of high-purity, (E), 20: 30315
superconducting properties of high-purity, (E), 20: 42117
superconducting single crystals of, ultrasonic attenuation measurements on, 18: 36503
superconducting surface losses in, temperature dependence of, (E), 19: 14435(R) (NP-14676)
superconducting transitions of gallium–vanadium and niobium–tin coated wires of, mechanical constraint effects on, 17: 28098
superconducting transition temperature of films of, effects of impurities on, 18: 2752
superconducting transition temperature of, pressure dependence of, (E), 20: 19762
superconducting transition temperature of, uniaxial stress effects on, (E), 20: 28228
superconducting transition temperature at high pressures, (E), 20: 28227
superconducting vortex motion in, guided, (E/T), 19: 8341
superconducting wire of, intermediate-state resistance of, 18: 6134
superconducting wire of, preparation and uses of, 19: 22947
superconductive properties of, technical applications of, 17: 16705
superconductivity of, negative surface free-energy effects in, 17: 9034
superconductivity in, mechanisms of high-field, 17: 9042
superconductivity energy gap of, ultrasonic attenuation measurements of, 17: 25826
superconductivity and uses of, 17: 34451
superconductivity of, effects of dissolved gases on, 17: 37848
superconductivity, 17: 41604
superconductivity of, upper critical field for, 18: 2776
superconductivity of wires of, coated with Nb_3Sn, 18: 4284
superconductivity of, ultrasonic measurement of, 18: 13022
superconductivity of, magnetic field effects on, 18: 15069
superconductivity of, 18: 15084
superconductivity of thin films of, 18: 15117
superconductivity of annealed wires of, 18: 30673(R) (SSD-TDR-63-311)
superconductivity of, upper critical field for, 18: 34713
superconductivity energy gaps in, electron tunnelling measurements of, 18: 36495
superconductivity of, effects of long-range order on, 18: 42564

superconductivity of, effects of crystal dislocations on, 18: 44688
superconductivity of monocrystalline, magnetic field effects on, 19: 1490
superconductivity of, additive effects of oxygen on, (E), 19: 6609
superconductivity in, effects of fiber structure on, (E), 19: 8366
superconductivity of, Hall effect in, (E), 19: 27383
superconductivity of coated wires of, 19: 28962(R) (NIRL/R/81)
superconductivity of crystalline, effects of oxygen on, 19: 32048(R) (NP-15073)
superconductivity in films of, (E), 19: 37867
superconductivity of powders of, critical persistent currents in, 17: 6875
superconductivity at 1 to 9.25°K, (E), 20: 4476(R) (IS-1200(Sect.P))
superconductivity of, effects of crystal imperfections on, 20: 4297(R) (IS-1200(Sect.M))
superconductivity of, temperature dependence of Ginzburg-Landau parameter for, 20: 17585 (AD-627910)
superconductivity in, nuclear spin-lattice relaxation time for, (E), 20: 37941
superconductivity of, 20: 40047
surface energy of solid, 16: 4566
surface ionization of, determination of heat of sublimation from, 19: 24506
surface tension at melting point, 17: 39612
surface tension of, measurement by pendant drop method, 19: 47065
technology and uses of, review, 20: 43817(T) (JPRS-36718)
temperature in superconducting, magnetic field effects on, (E), 19: 5105
tensile properties, effects of temperature, 16: 3464 (PWAC-359)
tensile properties at +20, −78, and −190°C, 16: 19382
tensile properties of zone refined, at 4.2 to 373°K, 16: 22593 (NP-11795)
tensile properties of zone-refined rod and sheet, 16: 27661
tensile properties at 0 to 2200°C, 17: 1863
tensile properties of electron-beam zone-melted, 18: 30161
tensile properties of wrought, effects of oxygen on, 18: 34196
tensile properties of, effects of interstitial and substitutional solutes on, 18: 34203
tensile properties of, effects of interaction of interstitial solute and substructure on, 18: 34204
tensile properties of, method of testing, 18: 34210
tensile properties at room temperature at 77°K, 19: 11682
tensile properties of, effects of hydrogen on, 19: 26866
tensile properties of crystals of, 17: 539 (UCRL-10356)
tensile properties of, effects of lithium and oxygen on, 20: 5181(R) (ORNL-3029)
tensile properties of, effects of exposure to cesium at 1200°C on, 20: 11227
tensile properties of single-crystal, effects of strain rate and temperature on, 20: 11227
tensile properties of, effects of mechanical twinning on, 20: 15049(R) (N65-16256)
tensile properties of, effects of temperature and strain rate on, 20: 31669
tensile properties at 1100 to 1300°C, effects of vacuum on, 20: 46198
tensile strength of single crystals of, effects of temperature on, 17: 16652(R) (NP-12633)
tensile-yield stresses, effects of strain rates, 16: 27669
testing for use as cladding of fissium–plutonium–uranium alloy fuel, 18: 10572 (CONF-373-2)
testing for use in thermionic collector electrodes, 20: 23992(R) (AD-626593)
thermal absorbance, emittance, and reflectance, 16: 9193 (DMIC-Memo-141)
thermal capacities, in normal and superconducting states, 16: 33627
thermal capacity at 0.4 to 4.2°K, 18: 22840
thermal capacity and total emittance at 1250 to 2350°K, 19: 23049
thermal capacity at superconducting lower critical field of, λ-transition in, (E), 19: 33165
thermal capacity at 0.35 to 25°K, measurements of, (E), 19: 33180
thermal capacity below 3.3°K, 20: 13692
thermal capacity of, from 1471 to 2260°K, 17: 23976
thermal capacity of normal and superconducting, at 1.2 to 12°K, 18: 22841
thermal capacity of superconducting, in magnetic fields, 18: 40457
thermal capacity of superconducting, in mixed state, (E), 19: 5094
thermal capacity of superconducting, at 0.25 to 25°K, (E), 19: 19019 (UCRL-11901)
thermal capacity of normal and superconducting, 19: 43997(R) (UCRL-11889)
thermal capacity of superconducting, (T), 20: 2905
thermal capacity of superconducting, in magnetic fields, 20: 4786
thermal capacity of superconducting, (E), 20: 21907
thermal conductivity at 0.2 to 1.2°K, 16: 16874
thermal conductivity, 17: 18818
thermal conductivity at 1.6 to 15°K, 17: 39600
thermal conductivity and emissivity at 1000 to 2000°C, 18: 27959 (ML-TDR-64-59)
thermal conductivity of superconducting thermal switches of, at 0.3 to 2°K, (E), 19: 23584
thermal conductivity of, 19: 32718 (AD-608398)
thermal conductivity, 20: 4299(R) (ORNL-2711)
thermal conductivity of superconducting, (E), 20: 21914
thermal conductivity of dirty and pure type II superconductors of, (E), 20: 34465
thermal conductivity and blackness at high temperatures, 20: 43976
thermal diffusion of oxygen in, 20: 29769
thermal expansion properties at low temperatures, 17: 1967
thermal expansion of, alloying effects on, 18: 22516
thermal expansion at 800 to 2000°C, 18: 32198
thermal expansion to 2000°C, 18: 34190
thermal expansion to 2000°C, 19: 4678(T)
thermal expansion of, effects of impurities on, 19: 23088
thermal expansion to 2500°C, 19: 41009 (GEMP-375)
thermal expansion coefficient of, x-ray determination of, 19: 47023(T) (LA-tr-65-20)
thermal expansion of, at 25 to 2500°C, 20: 27552
thermal properties of, data compilation, 17: 8801 (DMIC-177(Vol.2))
thermal radiation properties of uncoated, 16: 32039(R) (PWA-1863)
thermal radiation properties of surface-oxidized, 16: 32039(R) (PWA-1863)
thermal radiative properties, 17: 6650 (DMIC-177(Vol.I))
thermionic emission properties, 17: 20622
thermionic emission properties, 17: 20624
thermionic emission from crystalline, in cesium, potassium, and rubidium vapors, 18: 12794
thermionic emission characteristics for use in cesium thermionic converter, 18: 14792
thermodynamic properties at zero pressure and 293 to 3000°K, 16: 19354 (LAMS-2640)
thermodynamic properties of, bibliography on, 17: 27793 (NP-12938)
thermodynamic properties of mixed state of superconducting, determination from magnetocaloric effects, 20: 1122
thermodynamic properties at 0 to 2740°K, 20: 7117
thermodynamic properties, 20: 10816(T) (NASA-TT-F-285)
thermodynamic properties at 0 to 2740°K, 20: 17100
thermoelectric emission and work function of, in cesium vapor, (E), 19: 6447
thermoelectric properties, 18: 30493 (TID-7687(p.247-93))
thermoelectric properties at 300 to 1200°K, 19: 26833
thermoelectric properties of, 19: 32718 (AD-608398)
thermophysical properties, 18: 34207
thermophysical properties at 1300 to 3000°K, (E), 20: 41762
toxic properties of, review of, 18: 13423
tracer, survey, 16: 1359
twin boundaries in, annealing effects on, 18: 4246(R) (ORNL-3470 (p.16-19))
twinning in crystals of, 16: 13632
twinning in, effects of carbon, hydrogen, nitrogen, and oxygen on, 17: 39611
twinning of flash-annealed, at 77°K, 17: 39590
ultrasonic attenuation in superconducting, magnetic field effects on, (E), 19: 10192
ultrasonic attenuation in mixed state of superconducting, (E), 20: 26045
ultrasonic attenuation in mixed state of, (E), 20: 34431
ultrasonic transverse-wave attenuation in superconducting, temperature dependence of, 18: 2760
ultrasonic wave attenuation in superconducting, 20: 44529
uptake by Sargassum, 18: 37382
use as cathode in electrolytic reduction of uranyl and plutonium(IV) ions, 19: 42474
use as diffusion barrier between aluminum clad and uranium fuel, 18: 13264
use for bremsstrahlung production with strontium-90-yttrium-90 sources, 19: 2672
use for electroless and electrolytic coating of bearings and dies, review of, 19: 4604
use for superconducting transformers, 18: 26466
use in oxygen gettering in liquid sodium, 18: 1245 (LADC-5936)
use in superconducting transformer and charging circuit for magnet, 18: 37310 (AERE-M-1397)
use of, in nuclear rockets, 17: 8710 (TID-16315(Del.))
use of survey of, 18: 4188
use with rare earth oxides in photon radiation sources, 19: 16048(P)
uses in nuclear technology, 17: 12679
uses of granular or powdered, in fuel element end cap cavity to reduce pressure, 18: 42988(P)
vacancies in, entropy and heat of formation of, 20: 22972 (TID-22851)
vacancies in, method of mixtures measurement of concentration and en-

ergy of formation of, 20: 32726(T)
vacancy annihilation and precipitation in, clustered, 18: 7244
vacancy formation in, energy of, 17: 37547(T)
vapor pressure, 20: 331
vapor pressure at 2250 to 2570°K, 17: 8553
vaporization by electron bombardment, 19: 34660
welding, 17: 6631
welding, 17: 8760(T) (FTD-TT-62-1244)
welding, 17: 22140
welding, 20: 4299(R) (ORNL-2711)
welding and properties of welded, 16: 4516 (NP-11126)
welding at 100 to 150 kv, electron beam equipment and techniques for, 16: 19272
welding by T1G method, detrimental effects of nitrogen and oxygen on, 17: 34330(R) (USBM-U-1057)
welding electron beam and vacuum refined, butt, 18: 27927
welding of, effects of, on properties, 17: 11242
welding of, effects of carbon, nitrogen, and oxygen on, 17: 23876(R) (USBM-U-1031)
welding of, equipment and properties for electron-beam, 17: 34378
welding of, evaluation of electron-beam, 16: 31763
welding of fuel ribbon, development of edge sealing techniques, 16: 7862 (DCL-58-2-39)
welding of, review of, 17: 29301
welding of tube of, 17: 23915 (TID-7620(Pt.I)(p.144-54))
welding of, argon-arc and electron-beam methods of, 20: 21310
welding of, cerium–niobium consumable electrode for, 18: 29617
welding of, effects of melting methods on argon-arc and electron-beam, 18: 22465
welding of, electron-beam and vacuum arc, 18: 24108
welding of, electron-beam and tungsten-arc, 18: 34058(R) (WANL-PR(P)-003)
welding of, embrittlement in, 18: 34108
welding of, feasibility of vacuum-diffusion, 19: 22946(T)
welding of, flash, 19: 34662
welding of, properties of electron-beam and TIG, 18: 10510
welding properties, 16: 10486 (TID-14971)
welding properties, review, 16: 10424 (ASD-TR-61-322(p.661-76))
welding sheaths, sheets, and tubes of, techniques for, 18: 7172
welding techniques for, 20: 4999(R) (ORNL-2599)
welding to alumina, electron-beam, 17: 25691(R) (RBESO-3404-2)
welding to carbides by vacuum diffusion, 19: 22931(T) (JPRS-29550)
welding to stainless steel, 20: 21309
welding to tantalum, effects of carbon, nitrogen, and oxygen on embrittlement, 16: 3474(R) (USBM-U-863)
welding to tantalum and alloys by diffusion and pressure bonding, 16: 19374(R) (USBM-U-921)
welding to vanadium sheet, tongue effect in, 16: 2155
welding, method for spot, 20: 789 (AD-619333)
work function, 18: 8827
work hardening in, mechanisms of, 17: 29363
work hardening mechanism, 18: 12622 (ASD-TDR-62-354(Pt.II))
work hardening of crystals of, at −196 to 100°C, 17: 1942 (PWAC-375)
workability of sheet, determination of, 19: 16109
x-ray emission by, yield of L-shell, 18: 7732
x-ray emission spectra of, L and K, (E), 20: 41350
x-ray spectra of, emission bands in, 20: 27730
x-ray yields from, L-shell, 18: 40573
yield behavior of polycrystalline, 18: 4261 (TID-19788)
yield strength, effects of nitrogen on, 16: 13612
yield strength of single crystals of, 19: 11728 (TID-21599)
yield stress in, effects of grain size on, 17: 41458
yield stress of, correlation of thermal component of, 17: 18793
yield stress of crystals of, effects of temperature on, 17: 39551
yield stress of flash-annealed, effects of strain rate on room-temperature, 18: 584
Young's modulus for, effects of temperature on, 19: 14006

NIOBIUM ALLOY COUPLES

Fe/Nb–Zr/stainless steel/V, diffusion in bimetallic tubing of, with iron and vanadium diffusion barriers, inter-, 20: 11215(R) (NASA-CR-54718)
Fe/Nb–Zr/stainless steel, diffusion in bimetallic tubing of, with iron diffusion barrier, inter-, 20: 11215(R) (NASA-CR-54718)
Mo–Nb/Re–W, thermoelectric potential at 200 to 1800°C, 19: 37031(R) (GEMP-47A, pp 101-6)
Mo–Nb/Re–W, thermoelectric potential to 1800°C, 19: 44598(R) (GEMP-49A)
Mo/Ni/Nb–Zr/stainless steel, diffusion in bimetallic tubing of, with molybdenum and nickel diffusion barriers, inter-, 20: 11215(R) (NASA-CR-54718)
Nb/Nb–Ti, diffusion at 1300 to 2000°C, inter-, 20: 11227
Nb–Zr/stainless steel, diffusion in, 17: 34413 (TID-19109)
Nb–Zr/stainless steel, diffusion in bimetallic tubing of, inter-, 20: 11215(R) (NASA-CR-54718)

NIOBIUM ALLOYS

see also Hastelloy F
analysis, 16: 25294
analysis for beryllium, colorimetric, 16: 30346
analysis for carbon, hydrogen, molybdenum, oxygen, titanium, tungsten, and zirconium, evaluation of methods for, 18: 1520
analysis for cerium, photometric, 17: 32021
analysis for hafnium, titanium, and zirconium by ion exchange, 20: 7039
analysis for impurities by anodic staining, 19: 34107 (ORNL-3821)
analysis for molybdenum, polarographic, 19: 19781
analysis for nitrogen, 18: 10023
analysis for oxygen, comparison of fast neutron activation and vacuum fusion methods for, 18: 43419
availability, fabrication, and properties of refractory sheet, 19: 9617
bending sheet of, methods and problems of, 18: 34107
bibliography on, 18: 32076
bibliography on corrosion-resistant, 18: 20475 (VDDIT-87)
bonding to copper and stainless steel, 17: 1897(R) (NP-12144)
bonding to themselves or other refractory metal alloys, 19: 16050(P)
book: *Niobium and Its Alloys*, 16: 32047
book: *Production Technology of Niobium and Niobium Alloys*, 20: 43984
book: *Vanadium, Niobium, Tantalum. The Metallurgy of the Pure Metals and Their Alloys*, in German, 18: 25906
book, *Niobium Alloys*, 19: 4701
brazing and welding properties, review, 16: 10424 (ASD-TR-61-322 (p.661-76))
brazing honeycomb structures of, remelt temperature techniques for, 20: 39365
brazing of, development of filler materials for, 17: 3389(R) (USBM-U-978)
brazing properties, review, 16: 10424 (ASD-TR-61-322(p.661-76))
cavitation damage resistance in lithium to 2000°F, design of rotating disk test unit for determining, 17: 39552
coating by chromium–silicon–titanium for oxidation protection, 18: 30127 (ASD-TDR-62-934(Pt.II))
coating development and evaluation, 16: 2120 (ASD-TR-61-66(Pt.I))
coating developments for, 18: 541(R) (AD-419549)
coating development for oxidation protection, 18: 25896(R) (PF-63-3)
coating for, mechanical properties and oxidation resistance of, 18: 7272
coating of, for oxidation protection at high temperatures, 18: 8743(P)
coating of, protective effects of disilicides at 2800 to 3200°F, 17: 12585 (AD-277775)
coating of, for oxidation protection at 0 to 2000°F, 20: 43827 (GTR-19)
coating of, review of techniques for protective, 19: 4605
coating of, with oxidation-resistant silicides, fluidized-bed process for, 20: 43881
coating techniques for, review of, 18: 7270
coating with aluminum–chromium–titanium and chromium–silicon–titanium systems, 18: 7274
coating with aluminum alloy, use of titanium as middle layer for, 20: 4356(P)
coating with aluminum–tin alloys, 20: 4357(P)
coating with aluminum–tin for oxidation protection at 2000°F, 20: 43836 (TID-17070)
coatings for, 17: 6510 (ASD-TDR-62-934)
coatings for, development of oxidation-protection, 20: 7514 (DC-60-4-179)
coatings for, problems of protective, 20: 43877
coatings on, lifetime and performance of niobium silicide, 20: 5910
compatibility with uranium carbides, 16: 11153 (ORO-501)
compatibility with hydrogen in presence of thermal gradient, 20: 43832 (NASA-TN-D-3546)
composition, corrosion resistance, and mechanical properties of, review on, 17: 32508
conference on refractory metals, Oslo, Norway, June 23 to 26, 1963, 18: 34068
consolidation by powder-metallurgy and melting processes, 18: 4224
corrosion by acids at high temperature, 16: 24129
corrosion by acids, 18: 4206
corrosion by alkali metals at high temperatures for space reactor uses, 18: 14419
corrosion by aqueous solutions, review, 18: 32081 (A/CONF.28/P/243)
corrosion by atmosphere at high temperatures, 16: 5315 (WADD-TR-61-123)
corrosion by flowing sodium at 650°C, 18: 3038(R) (ANL-6801)
corrosion by liquid potassium at high temperatures, 20: 39028
corrosion by steam at 1000 to 1300°, additive optimization, 16: 25695(R) (BMI-X-188)
corrosion by steam and water at 315 to 400°C, 17: 25735
corrosion by steam at 540 and 650°C, 18: 24080 (BMI-X-286)
corrosion of, by steam at 1000 to 1300°F, 17: 14764(R) (BMI-X-10030)
corrosion of, in air at 1000°C, effects of rare earth additions on, 16: 33432 (WADD-TR-61-123(Pt.II))
corrosion of, in pressurized water reactors, 17: 16598

corrosion studies, 18: 14396
corrosion studies on, technical progress review on, 18: 18307
corrosion, stability, and strength of, 20: 43905 (ORNL-3212)
crack-propagation properties of FS-82, 17: 3462(R) (AD-275938)
crack-propagation resistance of D-14 and FS82, 18: 5769 (AD-290278)
creep in, rate-controlling mechanisms in, 19: 985
creep properties of, review of, 18: 7204 (DMIC-Memo-170)
creep properties of, comparison of, 20: 27545
crystal growth by recrystallization, methods for, 18: 4223
degradation and training in superconducting, metallurgy of, 19: 2816
development and evaluation of, for use in nuclear superheater, 17: 14764(R) (BMI-X-10030)
development and properties of heat-resistant, 19: 26848
development for brazing tantalum alloys, 18: 549(R) (NP-13241)
development for high-temperature reactor applications, 18: 2226(R) (NMI-1258)
development for high-temperature applications, review, 18: 34069
development for high-temperature uses, 16: 27691(P)
development for service in steam at 1000 to 1300°F, 16: 27558(R) (BMI-X-195)
development for use at high temperatures, 19: 985
development of clad, for high temperatures, 20: 46206
development of coated FS-85, 17: 36279(R) (AD-287509)
development of corrosion-resistant, 19: 931 (TID-21221(p.87-109))
development of F-48 type, 17: 13876(R) (BMI-1603(Del.))
development of high-temperature-resisting, 16: 30167 (ORNL-3313(p.19-64))
development of infiltrated, 18: 44066(T) (LA-tr-64-27)
development of oxidation-resistant coatings for, 16: 2173 (DMIC-Memo-137)
development of steam-corrosion-resistant, for nuclear superheaters, 17: 1816(R) (BMI-X-10016)
development, properties, and uses as engineering materials in aerospace vehicles, 16: 10409 (ASD-TR-61-322(p.307-36))
effects on lead–nickel alloy magnetization, 20: 25628
electric conductivity, hardness, and structure of, 18: 25999
engineering properties of, review of, 18: 8790 (DMIC-188)
extrusion by Dynapak process, effects of die geometry and lubrication on, 18: 7180
extrusion of, effects of surface contamination on, 18: 7179
extrusion of, factors affecting, 18: 14443
extrusion parameters for Cb-132M billets, 20: 43831(R) (NASA-CR-72057)
fabrication and properties as refractory material, 16: 19404
fabrication and properties of, review of, 17: 29253 (NRC-7129)
fabrication and properties for process equipment in aerospace, cryogenics, and nuclear engineering, 17: 39556
fabrication and properties of, 18: 7264
fabrication and properties for use as superconductors, 18: 34179
fabrication and properties of, handbook on, 20: 5874 (AGARDograph-94)
fabrication characteristics and methods, 18: 4225
fabrication for high temperature uses, development of techniques for, 16: 10427 (ASD-TR-61-322(p.817-32))
fabrication of bars and tubes of, 19: 32712(P)
fabrication of F-48, 17: 3379(R) (BMI-1596(Del.))
fabrication of high-strength tubing from, 18: 2205(R) (WANL-PR-(N)-003)
fabrication of rods of, 20: 7546(P)
fabrication of sheets of, 19: 34651(R) (AD-612490)
fabrication of sheet, 17: 6593(R) (ASD-TR-7-784(VII))
fabrication of small ingots of, by skull arc casting in vacuum, 17: 25759
fabrication of tube shells by flow turning, process development for, 20: 4301(R) (ORNL-3870, pp 102-35)
fabrication of, mechanical tests to evaluate, 18: 34101
fabrication of, with high stress-rupture strength up to 2200°F, 19: 46976(P)
fabrication, properties, uses, and welding, 16: 19398
fabrication, oxidation, and properties of, 18: 35986 (ERR-FW-049A)
gamma emission by, radiative widths for, (E), 19: 23626 (JINR-P-1995)
heat treatment of chromium–silicon–titanium-coated nut and bolt of F-48, 18: 35978 (AD-431856)
joining of, review of, 17: 34360 (CONF-94-5)
machining characteristics, 17: 34358(R) (ASD-TDR-63-581)
machining characteristics of, 19: 4637
machining of, effects of mechanical and physical properties on, 18: 12609
machining studies, 16: 20990(R) (ASD-TR-7-532a(VI))
mechanical properties, effects of alloying additions, 16: 7897 (WADC-TR-57-344(Pt.V))
mechanical properties, 17: 6517 (MAB-188-M)
mechanical properties at high temperatures, 17: 34409(R) (NMI-1253)
mechanical properties of, review, 18: 20456 (ORNL-3593)
mechanical properties of, effects of heat treatment on, 19: 7959
mechanical properties of, prepared by electron-beam melting, 19: 30768
mechanical properties and oxidation rate, 19: 32754
melting and welding of, purification using cerium-niobium electrode in, 18: 29617
metallurgical properties, 16: 15164 (AGARDograph-50)
notch sensitivity of F-48, 17: 3467 (ASD-TR-61-474)
oxidation, 17: 6564(R) (DRI-2056)
oxidation and contamination rates, 18: 4207
oxidation at high temperatures, 17: 12612
oxidation at low pressures and high temperatures, 20: 5181(R) (ORNL-3029)
oxidation characteristics, review, 16: 12997 (CNLM-1724)
oxidation mechanism, 16: 22156
oxidation of binary, alloying effects of boron, silicon, and metals on, 17: 22122
oxidation of silicon and titanium coated, kinetics, 16: 32085
oxidation protection of, development of coatings for, 18: 30190
phase diagrams of binary and ternary, 17: 27778 (DMIC-183)
phase studies of binary, 18: 4283
powder metallurgy of, in the USSR, 17: 1823(T) (JPRS-15978)
preparation by carbothermal reduction of oxides, 18: 41948
preparation of oxidation-resistant, 19: 24929(P)
preparation of thin films of, by jet-polishing and electro-polishing, 20: 27464
processing and properties of Cb-74, 18: 7269
production and evaluation of sheet-rolled, 17: 14723 (AD-278821)
properties, 16: 3460 (NP-11108)
properties and uses of, review of, 19: 36966
properties and uses of, review on, 20: 2307 (AD-613023)
properties as cladding and structural materials in reactors, 18: 41948
properties as cladding for corrosion protection of uranium, 20: 7522
properties as fuel cladding material for reactors, 18: 8840
properties as fuel element cladding in steam and water environments, 18: 34076 (TID-8540(p.213-330))
properties at high temperatures, methods for improving, 16: 12152
properties at high temperature, 16: 27622(R) (AD-271176)
properties for aerospace uses, 19: 47068
properties for alkali metal containment, research on, 17: 27535 (BNL-801)
properties for use as jacket material for fast reactor fuels, 18: 21698(R) (ANL-6860)
properties for use as fuel-element cladding, 19: 22884
properties for use as fuel cladding material in reactors, 19: 39206
properties of F-48, at high temperatures, 16: 28642(R) (BMI-1581(Del.))
properties of F-48, 17: 3379(R) (BMI-1596(Del.))
properties of high-temperature, 19: 37149(P)
properties of superconducting, size factor and, 17: 25927
properties of welded sheaths, sheets, and tubes of, 18: 7172
properties of, chemical and mechanical, 17: 12655 (AD-277776)
properties of, review, 17: 1826
properties of, review, 17: 1963(T) (FTD-TT-62-1256)
properties of, review on, 17: 36332
properties of, review on, 18: 34180
properties of, research on fundamental, 19: 23163(R) (ORNL-3650(p.111-86))
radiation effects on mechanical properties and microstructure of, at 50°C, 18: 24193 (HW-SA-3436)
rolling sheet, 17: 6517 (MAB-188-M)
rolling to foil, review, 18: 35962 (AD-434397)
specifications for sheet rolled, 16: 24160 (MAB-184-M)
strain-aging, effects of titanium, vanadium, and zirconium additions, 16: 21063
strength and uses of, review on, 18: 27984
strengthening of, studies of local-order mechanism of, solid-solution, 19: 13979 (ASD-TDR-63-567(Pt.II))
technology and uses of, review, 20: 43817(T) (JPRS-36718)
tensile properties, 16: 22586 (DMIC-Memo-150)
tensile properties of FS-82, 17: 3462(R) (AD-275938)
tensile properties of F48, directional variation of, 17: 36282 (AD-295529)
tensile properties of, effects of beryllium and zirconium on, 20: 37245
thermal diffusivity at 1800 to 2600°K, 18: 36029
thermal expansion at 80 to 400°K, 20: 23749
thermal properties of, data compilation, 17: 8801 (DMIC-177(Vol.2))
thermal radiative properties, 17: 6650 (DMIC-177(Vol.I))
use for electroless and electrolytic coating of bearings and dies, review of, 19: 4604
use of survey of, 18: 4188
weld ductility of, comparison of, with weld ductility of tantalum-base alloys, 20: 13264(R) (WANL-PR(P)-008)
welding, 18: 8783(T) (JPRS-22597)
welding by solid-state methods, 19: 22937
welding characteristics of types D31 and FS82, 16: 4510 (DMIC-Memo-140)
welding metallurgy, 16: 13556
welding of commercial, effects of, on properties, 17: 11243

welding of, cerium–niobium consumable electrode for, 18: 29617
welding of, embrittlement in, 18: 34108
welding of, survey of methods for, 19: 11711
welding properties, review, 16: 10424 (ASD-TR-61-322 (p.661-76))
welding sheaths, sheets, and tubes of, techniques for, 18: 7172
welding studies, 18: 5752(R) (WANL-PR(P)-001)
welding to nickel alloys, use of palladium insert in fusion, 18: 32128(P)
welding, ultrasonic, 16: 19295 (ASD-TR-7-888(1))
Al–Cr–Co–Ni–Nb–Ti–W, surface treatments for Mar-M 200, coating and mechanical, 20: 29706 (NASA-TM-X-53448)
Al–Cr–Fe–Mo–Nb–Ti, brazing of René 62 T-joints, 18: 44103(R) (ORNL-3670(p.259-61))
Al–Cr–Fe–Mo–Ni–Nb–Ti, corrosion and mechanical properties of Inconel 713C as gas turbine material, 16: 32114 (IDO-28591)
Al–Cr–Fe–Mo–Ni–Nb–Ti–W, corrosion by carbon dioxide, helium, nitrogen, and steam of PRDL-102, 20: 9408 (BNWL-154)
Al–Cr–Fe–Mo–Ni–Nb, fabrication and properties of atomized, extruded, and sintered Inco 713C, 18: 10449(R) (IITRI-B247-12)
Al–Cr–Fe–Mo–Nb–Zr, machining characteristics, 17: 14778(R) (ASD-TR-7-532a(IX))
Al–Cr–Fe–Mo–Nb–Ti, mechanical properties at 1100 to 1500°F, 17: 22852(R) (GA-2696)
Al–Cr–Fe–Mo–Ni–Nb–Ti, mechanical properties of René-62, 19: 24081(R) (GNEC-361)
Al–Cr–Fe–Mo–Ni–Nb–Ti, oxidation of Inconel 718 by water vapor in helium at 1700°F, 19: 30820 (BNWL-23)
Al–Cr–Fe–Mo–Ni–Nb–Ti, radiation effects on Inconel 718, 18: 7292(R) (HW-77954(p.4.1-12))
Al–Cr–Fe–Mo–Ni–Nb–Ti, radiation effects on mechanical properties of Inconel 718, neutron, 19: 30820 (BNWL-23)
Al–Cr–Fe–Mo–Ni–Nb–Ti, thermal response and microstructure of Inconel 718 at 1200 and 1400°F, 19: 39158 (GEAP-4751)
Al–Cr–Fe–Nb–Zr, properties, 17: 1997(P)
Al–Cr–Mo–Ni–Nb–Ti–W, phase diagrams, 20: 9533
Al–Cr–Nb, oxidation at 1100°C, effects of composition on, 20: 11338
Al–Cr–Nb, phase studies, 20: 11338
Al–Cr–Nb–Ti, oxidation above 1200°C, 16: 2175(R) (GEMP-3A)
Al–Cr–Nb–Ti, oxidation behavior at high temperatures, 17: 36224 (GEMP-218)
Al–Cr–Nb–Ti–V, properties for brazing niobium, 20: 25552(P)
Al–Cr–Nb–W, oxidation resistance at 590 to 1370°C, 16: 9196(R) (GEMP-103A)
Al–Cu–Nb, crystal structure, 19: 44718
Al–Cu–Nb, phase studies, 19: 42874
Al–Cu–Nb, phase studies, 20: 23725
Al–Cu–Nb, phase studies on, 20: 29764
Al–Cu–Nb–Zr, creep properties of, 17: 586(P)
Al–Ge–Nb–Sn, phase studies, 20: 13275
Al–Hf–Nb–Ti, fabrication and mechanical properties at 70 to 1650°F, 18: 12538(R) (ARF-B201-27)
Al–Hf–Nb–Ti–Zr, fabrication and tensile properties at 70 and 1600°F, 18: 12538(P) (ARF-B201-27)
Al–Hf–Nb–Ti, oxidation by air at 1000°F, 18: 12538(R) (ARF-B201-27)
Al–Mo–Nb–U, preparation and properties as reactor fuel, 19: 26873(P)
Al–Nb, alloying effects on oxidation resistance of $ZrBe_{13}$ at 1300 to 1600°F, 17: 29313(R) (BBC-118)
Al–Nb, alloying effects on oxidation properties of zirconium beryllides at high temperatures, 18: 27946(R) (BBC-120)
Al–Nb, crystal structure and phase studies of superconducting, 18: 32149(R) (UCRL-11317(p.131-49))
Al–Nb, crystallization of intermetallic compounds in, effects of casting temperature on, 20: 27554
Al–Nb, elastic properties, 20: 25580
Al–Nb, electric conductivity above superconducting transition temperature, 20: 8028
Al–Nb, fabrication and production of stoichiometric, 19: 42831
Al–Nb, fabrication of sintered bodies of, 20: 15026(P)
Al–Nb, intermetallic compounds in, properties of, for use in aerospace technology, 20: 29770
Al–Nb, magnetic field penetration in Nb_3Al superconductors, (E), 20: 8030
Al–Nb, magnetic field penetration into superconducting intermetallic compounds of, (E), 20: 21908
Al–Nb, magnetic properties of superconducting, 18: 9262(R) (NP-13492)
Al–Nb, magnetic susceptibility and specific heat of superconducting binary complex phases of, 18: 37715
Al–Nb, negative surface energy model of superconductivity of, 17: 9040
Al–Nb, oxidation resistance, effect of metallic additions on, 17: 4902(R) (DRI-2061)
Al–Nb, oxidation kinetics of, at 500 to 900°C, 19: 13929
Al–Nb, oxidation kinetics at 500 to 900°C, 19: 20494
Al–Nb, oxidation, 20: 5896 (TID-22388)
Al–Nb, phase diagram of, 17: 22161 (DRI-2096)
Al–Nb, phase diagram, 20: 31769
Al–Nb, phase equilibria of, 17: 4902(R) (DRI-2061)
Al–Nb, phase studies, 18: 18307
Al–Nb, phase studies of, 20: 5896 (TID-22388)
Al–Nb, phase studies, 20: 11338
Al–Nb, phase studies, 20: 13275
Al–Nb, preparation and heat treating, argon–arc melting method for, 17: 18743 (EUR-132.f)
Al–Nb, preparation and superconductivity properties of intermetallic compounds of, 18: 4287
Al–Nb, preparation and properties of $NbAl_3$ for possible use as reactor material, 19: 20464 (SCNC-316)
Al–Nb, preparation of superconducting films of, 19: 33187(R)
Al–Nb, properties as coating for refractory metals, 20: 4418
Al–Nb, properties of intermetallic compound, 20: 37260
Al–Nb, radiation effects on superconducting properties of, fast-neutron, 18: 10583
Al–Nb, radiation effects on superconductivity of, neutron, 18: 34683(R) (NP-14136)
Al–Nb, radiation effects on superconducting properties of boron- and uranium-doped, thermal neutron, (E), 20: 30260
Al–Nb, spalling at high temperatures, 18: 20474 (TID-12794)
Al–Nb, superconductivity of, 17: 1989
Al–Nb, superconductivity, 17: 41604
Al–Nb, superconducting transition of Nb_3Al, effects of vanadium on, 18: 34283 (UCRL-11390)
Al–Nb, superconductivity of fused, 20: 15123
Al–Nb, use in superconducting magnets, 17: 20438
Al–Nb–Sn, crystal structure and alloying properties, 17: 16727
Al–Nb–Sn, phase study of Cr_3O-type structures in, 19: 44702 (TID-22200)
Al–Nb–Sn, superconducting properties of Nb_3SnAl, 17: 27861
Al–Nb–Sn–Ti, fabrication and mechanical properties at 70 to 1650°F, 18: 12538(R) (ARF-B201-27)
Al–Nb–Sn–Ti, oxidation by air at 760 to 1360°C, 17: 27780(R) (DRI-2104)
Al–Nb–Sn–Ti, oxidation by air at 760 to 1360°C, 17: 29249(R) (DRI-2090)
Al–Nb–Sn–Ti, oxidation by air at 1000°F, 18: 12538(R) (ARF-B201-27)
Al–Nb–Ta–Ti, corrosion by mercury, 18: 10492
Al–Nb–Ta–Ti–Zr, corrosion by mercury, 18: 10492
Al–Nb–Ta–Ti, corrosion cracking in titanium-base, stress-, 20: 16967 (AD-628277)
Al–Nb–Ta–Ti, corrosion by sodium chloride, effects of stress on, 20: 33858(R) (AD-634094)
Al–Nb–Ta–Ti, fatigue crack propagation in, study of low-cycle, 19: 20462(R) (NRL-6258)
Al–Nb–Ta–Ti, fracture toughness of plasmarc welds in titanium-base, 20: 11273(R) (NRL-6364)
Al–Nb–Ta–Ti, mechanical properties of, effects of processing on, 19: 20462(R) (NRL-6258)
Al–Nb–Ta–Ti, mechanical properties of titanium-base, 20: 33858(R) (AD-634094)
Al–Nb–Ta–Ti, properties at −400 to 100°F, 19: 26803(R) (AD-611165)
Al–Nb–Ta–Ti, welding characteristics, 16: 4510 (DMIC-Memo-140)
Al–Nb–Ti, development of high-temperature, effects of hafnium, tin, and zirconium additions on, 16: 15167 (ARF-2201-15)
Al–Nb–Ti, fabrication and tensile properties at 70 and 1600°F, 18: 12538(R) (ARF-B201-27)
Al–Nb–Ti, fission-product permeability at 2200 to 3200°F, 17: 6645 (BMI-1604)
Al–Nb–Ti, mechanical and metallurgical properties, 16: 4547 (WADC-TR-59-595(Pt.II))
Al–Nb–Ti, oxidation above 1200°C, 16: 2175(R) (GEMP-3A)
Al–Nb–Ti, oxidation at 1370°C, 16: 15179 (GEMP-106A)
Al–Nb–Ti, oxidation resistance at 590 to 1370°C, 16: 9196(R) (GEMP-103A)
Al–Nb–Ti, oxidation resistance, effect of metallic additions on, 17: 4903(R) (DRI-2075)
Al–Nb–Ti, oxidation behavior at high temperatures, 17: 36224 (GEMP-218)
Al–Nb–Ti, oxidation resistance of $(Nb–Ti)Al_3$, effects of chromium, silicon, and tin on, 18: 8749(R) (DRI-2134)
Al–Nb–Ti, oxidation by air at 1000°F, 18: 12538(R) (ARF-B201-27)
Al–Nb–Ti, oxidation, 20: 5896 (TID-22388)
Al–Nb–Ti, oxidation protection by aluminum–tin coatings with chromium and titanium additions, 20: 7580 (TIM-945)
Al–Nb–Ti, phase studies, 16: 15228
Al–Nb–Ti, phase studies on, 20: 5896 (TID-22388)
Al–Nb–Ti, properties as corrosion-protection coating for niobium, 20: 9426 (TID-12809)
Al–Nb–Ti, properties of, mechanical and physical, 20: 13271

Al–Nb–Ti, properties at high temperatures, 20: 43963
Al–Nb–Ti–W–V–Zr, properties for use to 1200°F, 20: 4393 (PWAC-472)
Al–Nb–Ti–Zr, fabrication and mechanical properties at 70 to 1650°F, 18: 12538(R) (ARF-B201-27)
Al–Nb–Ti–Zr, oxidation resistance at 1000°C, alloying effects, 16: 9248(P)
Al–Nb–Ti–Zr, oxidation by air at 1000°F, 18: 12538(R) (ARF-B201-27)
Al–Nb–U, preparation of, 19: 32771(P)
Al–Nb–V, corrosion by steam and water, 16: 29346
Al–Nb–V, crystal structure and phase studies of superconducting, 18: 32149(R) (UCRL-11317(p.131-49))
Al–Nb–Zr, corrosion by steam and water, 16: 29346
Al–Nb–Zr, hardness, 17: 27779(R) (DRI-2102)
Al–Nb–Zr, oxidation resistance at 1000°C, 16: 9248(P)
Al–Nb–Zr, phase isotherms at 1100 and 1300°C, 17: 39529(R) (DRI-2117)
Al–Nb–Zr, phase studies, 17: 6729
Al–Nb–Zr, preparation, 17: 6652(R) (DRI-2057)
Al–Ni–Nb, crystal structure of intermetallic compounds in, 17: 27828
Al–Ni–Nb, crystal structure of M-phase, (E/T), 20: 30734(R) (TID-22970, pp 1-63)
Al–Ni–Nb, oxidation rate of Ni_3Al–Ni_3Nb, 18: 20478
Al–Ni–Nb, oxidation of, phase distributions in layers from studies of, 20: 14990
Al–Ni–Nb, phase diagram, 20: 46512
Al–Ni–Nb, phase studies at 1140°C, 20: 15121
Al–Ni–Nb, properties, 18: 8828
Al–Ni–Nb, reactions between Ni_3Al and Ni_3Nb in, 17: 27827
Al–Ni–Nb, superconductivity, 20: 46512
Au–Nb–Rh, crystal structure and superconductivity, 18: 25970(R) (ANL-6868(p.303-25))
Au–Nb–Rh, superconductivity in, (E), 19: 16774
Au–Nb–V, phase structure and superconductivity of, 18: 11117
Be–Ca–Nb, development of corrosion-resistant, 17: 37473(P)
Be–Cr–Nb, tensile properties of, 20: 37245
Be–Cu–Nb, crystal structure of intermetallic compounds in, 20: 23726
Be–Nb, coating developments for, 17: 532 (GEMP-105)
Be–Nb, compatibility with chromium, Hastelloy X, Inconel X, and molybdenum at 2000 and 2500°F, 17: 532 (GEMP-105)
Be–Nb, corrosion by lithium at high temperatures, 20: 4299(R) (ORNL-2711)
Be–Nb, crystal structure of intermetallic compound $NbBe_{12}$ in, 16: 16717 (DC-58-11-114)
Be–Nb, crystal structure and mechanical properties, 18: 37713
Be–Nb, crystallization in, 18: 39948
Be–Nb, development of, for high-temperature uses, 17: 16637(R) (BBC-115)
Be–Nb, development of high-temperature, 17: 20451(R) (BBC-117)
Be–Nb, elastic properties of intermetallic compound $NbBe_{12}$ in, at high temperatures, 16: 7921
Be–Nb, evaporation rates of $NbBe_{12}$ and Nb_2Be_{17}, 17: 36293(R) (DRI-2079)
Be–Nb, high-temperature oxidation resistance of intermetallic compounds in, 18: 27912
Be–Nb, intermetallic compounds in, properties of, for use in aerospace technology, 20: 29770
Be–Nb, machining of, applicability of electric-discharge in, 16: 33446 (DC-60-3-173)
Be–Nb, mechanical and physical properties of intermetallic compounds in, 19: 7942
Be–Nb, oxidation kinetics of, at 700 to 1500°C, 16: 12051 (NAA-SR-6493)
Be–Nb, oxidation mechanisms, 16: 9156(R) (TID-14955)
Be–Nb, oxidation of intermetallic compounds $NbBe_{12}$ and Nb_2Be_{17} in, at 1200 to 2000°F, 16: 24123 (TID-16030)
Be–Nb, oxidation of stoichiometric, at 1200 to 1800°F, kinetic studies, 16: 27562(R) (TID-16019)
Be–Nb, oxidation of, at 1200 to 1800°F, 17: 530(R) (DRI-2042)
Be–Nb, oxidation, 17: 6653(R) (DRI-2071)
Be–Nb, oxidation, 17: 6643(R) (BBC-112)
Be–Nb, oxidation of intermetallic compounds in, at high temperatures, effects of aluminum additives on, 17: 14725(R) (BBC-114)
Be–Nb, oxidation of intermetallic compounds $NbBe_{12}$ and Nb_2Be_{17} in, at 1200 to 1800°F, 17: 15947(R) (DRI-2088)
Be–Nb, oxidation resistance of, at 1100 to 1700°F, 17: 20450(R) (BBC-116)
Be–Nb, oxidation of aluminum-containing $NbBe_{12}$ and Nb_2Be_{17} at 650 to 1000°C, 17: 27781(R) (DRI-2105)
Be–Nb, oxidation resistance of $NbBe_{12}$ and Nb_2Be_{17} at 1600 to 1900°F, alloying effects of aluminum on, 17: 29313(R) (BBC-118)
Be–Nb, oxidation of $NbBe_{12}$ and Nb_2Be_{17} at 550 to 1100°C, effects of aluminum additions on, 18: 7136(R) (DRI-2128)
Be–Nb, oxidation by dry and moist air at 1600 to 1900°F, effects of aluminum additions on, 18: 27946(R) (BBC-120)
Be–Nb, oxidation resistance of intermetallic compounds in, at 1000 to 2000°F, 19: 7943
Be–Nb, oxidation of intermetallic compounds $NbBe_{12}$ and Nb_2Be_{17} in, 19: 11680
Be–Nb, oxidation resistance of, effects of aluminum, nickel, silicon, and tantalum additions on, 20: 5844
Be–Nb, oxidation rate of, at 1100°C, 20: 23614
Be–Nb, oxidation in air at 800 to 2200°F, 20: 43886(R) (BBC-111)
Be–Nb, performance as thermionic emitters, 18: 30479(R) (DRI-2137)
Be–Nb, phase studies and recrystallization properties of, 18: 44203
Be–Nb, properties of, below 1000°C, 16: 2235
Be–Nb, properties of intermetallic compounds in, 16: 10517 (DC-60-4-80)
Be–Nb, properties of intermetallic compounds $NbBe_{12}$, Nb_2Be_{17}, and Nb_2Be_{19} in, effects of fabrication and processing on, 16: 25748 (ASD-TDR-62-476)
Be–Nb, properties to 2750°F, 17: 532 (GEMP-105)
Be–Nb, properties, 17: 14740 (TID-11295(2nd Ed.))
Be–Nb, properties of intermetallic compounds in, 17: 25790
Be–Nb, thermal conductivities at 300 to 1000°C, 16: 19393
Be–Nb, thermal expansion coefficients, 17: 20450(R) (BBC-116)
Be–Nb–W, tensile properties of, 20: 37245
Be–Nb–Zr, properties to 2750°F, 17: 532 (GEMP-105)
Be–Nb–Zr, properties for brazing niobium, 18: 5758
Be–Ni, development of NiBe fiber-reinforced composites of, 20: 2219 (AMRA-CR-64-05/4)
Bi–Nb, phase studies, 19: 37072
Bi–Nb, pressure-temperature phase diagrams, (E), 19: 5092
Bi–Nb, superconducting transition in, (E), 19: 5092
Ca–Nb–Zr, corrosion by superheated steam, 19: 40977(P)
Ca–Nb–Zr, preparation of corrosion-resistant, 19: 4612(P)
Ce–Nb, corrosion by lithium at high temperatures, 20: 4299(R) (ORNL-2711)
Ce–Nb–Zr, preparation for use in nuclear reactors, 20: 9560(P)
Co–Mo–Nb, yield strength and ductility at high temperatures, 20: 25611(P)
Co–Nb, crystal structure of beta phase of, 18: 34145
Co–Nb, crystal structure of μ phases in, 20: 27555
Co–Nb, decomposition and structure of supersaturated, 20: 43938
Co–Nb, mechanical properties and oxidation rate, 19: 32754
Co–Nb, phase diagram, 18: 42078
Co–Nb, phase studies, 17: 28565(R) (LAMS-2915)
Co–Nb, phase studies, 19: 23096
Co–Nb, phase studies, 20: 23752
Co–Nb, properties, 19: 26848
Co–Nb, solvent properties for silicon in beta phase of, 18: 34145
Co–Nb, thermodynamic properties, 19: 18526
Co–Nb–Rh, crystal structure and superconductivity, 18: 25970(R) (ANL-6868(p.303-25))
Co–Nb–Rh, superconductivity in, (E), 19: 16774
Co–Nb–Ta, phase studies, 18: 25970(R) (ANL-6868(p.303-25))
Co–Nb–V, oxidation properties at 2000°F in air, 17: 35997(R) (ITRE-B6001-5)
Co–Ni–Nb, mechanical properties and structure of, 17: 20478
Cr–Co–Nb, corrosion resistance to strong acids, 19: 18415
Cr–Co–Nb, phase studies on intermetallic compounds in, 20: 17075
Cr–Cu–Fe–Nb–Zr, fabrication for steam-service, 17: 18713 (GEAP-4115)
Cr–Cu–Nb–Zr, corrosion by high-pressure flowing steam at 300, 400, and 500°C, 17: 34346(R) (GEAP-4211)
Cr–Cu–Nb–Zr, properties for steam-service fuel element cladding, optimization studies, 17: 14731(R) (GEAP-3979)
Cr–Fe–Mo–Ni–Nb, corrosion by boiling magnesium chloride, 18: 4796(R) (GEAP-4153)
Cr–Fe–Mo–Ni–Nb–W, descaling by sodium carbonate–sodium hydroxide solutions, 18: 22441 (HW-79048)
Cr–Fe–Mo–Ni–Nb, oxidation of Inconel 625 by water vapor in helium at 1700°F, 19: 30820 (BNWL-23)
Cr–Fe–Mo–Ni–Nb, radiation effects on Inconel 625, 18: 7292(R) (HW-77954(p.4.1-12))
Cr–Fe–Mo–Ni–Nb, radiation effects on mechanical properties of Inconel 625, neutron, 19: 30820 (BNWL-23)
Cr–Fe–Mo–Ni–Nb–W, tensile properties of IN-102, 19: 39156(R) (CEND-532)
Cr–Fe–Mo–Ni–Nb, thermal response and microstructure of Inconel 625 at 1200 and 1400°F, 19: 39158 (GEAP-4751)
Cr–Fe–Mo–Ni–Nb–W, welding properties of Inco IN-102, 20: 4306(R) (ORNL-3870, pp 194-213)
Cr–Fe–Nb–Zr, corrosion by air, carbon dioxide, and water, 17: 504
Cr–Fe–Ni–Nb, corrosion of Inconel 600 in air at 1150°C, 18: 28044(R) (HW-80284(p.8.1-4))
Cr–Fe–Ni–Nb–Ti, corrosion of R-27, by superheated steam at 550°C, 18: 32139(R) (HW-81269(p.5.1-23))

Cr–Fe–Ni–Nb–Ti, descaling by sodium carbonate–sodium hydroxide solutions, 18: 22441 (HW-79048)
Cr–Fe–Ni–Nb–Ti, radiation effects on, 18: 7292(R) (HW-77954(p.4.1-12))
Cr–Fe–Ni–Nb–Ti, radiation effects on hardness of R-27, at 50 and 280°C, 18: 32043(R) (HW-81269(p.4.1-64))
Cr–Ga–Nb, phase studies on intermetallic compounds in, 20: 17075
Cr–Ge–Nb, phase studies on intermetallic compounds in, 20: 17075
Cr–Mo–Nb, corrosion by steam at 1000°F, 17: 493(R) (BMI-X-10003)
Cr–Mo–Nb, mechanical properties and oxidation rate, 19: 32754
Cr–Mo–Nb, oxidation at 800 to 1200°C, 18: 34080
Cr–Mo–Nb, phase diagrams at 1000 to 1550°C, 20: 33936
Cr–Mo–Nb, phase studies, 16: 3493
Cr–Mo–Nb, phase studies, 16: 12157
Cr–Mo–Nb, phase studies, 18: 30187
Cr–Mo–Nb, phase studies at 1000 to 2000°C, 18: 44180
Cr–Mo–Nb, properties and structure at high temperatures, 18: 26012
Cr–Mo–Nb, properties, 19: 26848
Cr–Mo–Nb–Ta, composition having superior high-temperature strength, 18: 25917(P)
Cr–Mo–Nb–Ti, corrosion by steam at 1000°F, 17: 23890(R) (BMI-X-10040)
Cr–Mo–Nb–Ti–V, corrosion by steam at 1000°F, 17: 23890(R) (BMI-X-10040)
Cr–Mo–Nb–Ti–V, corrosion by steam at 540 and 650°C, 18: 8747(R) (BMI-X-10071)
Cr–Mo–Nb–Ti–V, corrosion by steam at 540 and 650°C, 18: 22415(R) (BMI-X-10082)
Cr–Mo–Nb–Ti–Zr, mechanical and oxidation properties of, at high temperatures, 16: 27691(P)
Cr–Mo–Nb–U, preparation and properties as reactor fuel, 19: 26873(P)
Cr–Mo–Ni–Nb, corrosion and oxidation resistance in fused salts, 18: 41968(P)
Cr–Mo–Ni–Nb–Ti–W, melting temperatures in, effects of chromium and nickel content on, 16: 19411
Cr–Mo–Ni–Nb–Ti–W, melting temperatures in, effects of chromium and nickel content on, 16: 32127(T) (JPRS-14484)
Cr–Nb, cellular precipitation of intermetallic compound $NbCr_2$ in, 18: 26022
Cr–Nb, compatibility with sodium at 650°C, 17: 41333(R) (ANL-6677)
Cr–Nb, corrosion by liquid sodium, 17: 11935(R) (ANL-6658)
Cr–Nb, corrosion by steam at 1000°F, 17: 23890(R) (BMI-X-10040)
Cr–Nb, corrosion by flowing sodium at 650°C, 17: 37001(R) (ANL-6780)
Cr–Nb, corrosion by potassium at 1500 to 1800°F, 18: 5728 (ASD-TDR-63-270(Pt.II))
Cr–Nb, corrosion by potassium vapor at 1500 to 1800°F, 18: 18282 (BNL-844)
Cr–Nb, corrosion by sodium at 650°C, 18: 26893(R) (ANL-6868(p.11-108))
Cr–Nb, corrosion by steam at 750 to 900°F, 18: 27861 (KAPL-2000-21 (p.VII.1-5))
Cr–Nb, creep and tensile properties, 17: 32568 (CONF-53-5)
Cr–Nb, decomposition of, x-ray diffraction studies of, 17: 14871
Cr–Nb, development and properties for reactor cladding, 18: 7266
Cr–Nb, elastic properties, 19: 20579
Cr–Nb, electric and mechanical properties, 18: 24158
Cr–Nb, free energies of formation of Laves phases in, 16: 13636
Cr–Nb, mass transport by sodium, 18: 15563
Cr–Nb, mechanical properties, 18: 27861 (KAPL-2000-21(p.VII.1-5))
Cr–Nb, mechanical properties at 1100 and 1300°C, 19: 11734
Cr–Nb, mechanical properties of, effects of composition on, 20: 11288(T) (AD-622477)
Cr–Nb, oxidation rate of, at 1100°C, 20: 23614
Cr–Nb, oxidation of, kinetics, mechanism, and microstructure of internal, 20: 23619
Cr–Nb, oxidation of, effects of chromium content on, 20: 46157
Cr–Nb, phase diagram, 17: 27825
Cr–Nb, phase studies, 18: 18307
Cr–Nb, phase studies of intermetallic compound, 20: 37239
Cr–Nb, phase transformations in, 20: 17046
Cr–Nb, physical properties of, 17: 4225(R) (ANL-6635(p.28-50))
Cr–Nb, precipitation of $NbCr_2$ in, cellular, 20: 5846
Cr–Nb, properties of, at high temperatures, 16: 30779 (BMI-1277)
Cr–Nb, thermal expansion, 18: 27861 (KAPL-2000-21(p.VII.1-5))
Cr–Nb–Sn–U–Zr, corrosion, 17: 39640
Cr–Nb–Ti, compatibility with sodium at 650°C, 17: 41333(R) (ANL-6677)
Cr–Nb–Ti, corrosion of, by steam and water, 16: 29346
Cr–Nb–Ti, corrosion by steam at 1000°F, 17: 23890(R) (BMI-X-10040)
Cr–Nb–Ti, mechanical properties for high-temperature applications, 19: 39192
Cr–Nb–Ti, phase diagrams, 19: 26862
Cr–Nb–Ti, phase diagrams, 20: 15078
Cr–Nb–Ti, phase studies at 600, 800, and 1000°C, 17: 11212
Cr–Nb–Ti, phase studies, 17: 16543
Cr–Nb–Ti, phase studies, 17: 27826
Cr–Nb–Ti, phase studies of $NbCr_2$–$TiCr_2$, 17: 29346
Cr–Nb–Ti, phase studies, 17: 39558
Cr–Nb–Ti, phase studies, 18: 18307
Cr–Nb–Ti, phase studies at 1280 to 1540°C, 19: 26858
Cr–Nb–Ti, phase studies, 20: 17091
Cr–Nb–Ti, tensile properties of, effects of composition on, 20: 17112
Cr–Nb–Ti–V, corrosion by steam at 1000°F, 17: 23890(R) (BMI-X-10040)
Cr–Nb–Ti–V, corrosion by steam at 1000°F, 18: 2184
Cr–Nb–Ti–V, corrosion by steam at 540 and 650°C, 18: 8747(R) (BMI-X-10071)
Cr–Nb–Ti–V, corrosion by steam at 540 and 650°C, 18: 22415(R) (BMI-X-10082)
Cr–Nb–Ti–V, corrosion by steam at 540, 565, 650, and 750°C, 18: 32036(R) (BMI-X-10091)
Cr–Nb–Ti–V, corrosion by steam at 540°C, 18: 41933 (TID-11295 (3rd Ed.))
Cr–Nb–Ti–V, corrosion by steam at high temperatures, 19: 2758
Cr–Nb–Ti–V, corrosion by air and superheated steam, 19: 9620 (BMI-1700)
Cr–Nb–Ti–V, fabrication by extrusion and rolling, 18: 22415(R) (BMI-X-10082)
Cr–Nb–Ti–V, mechanical properties of corrosion-resistant, 19: 9620 (BMI-1700)
Cr–Nb–Ti–V, performance in nuclear-superheater environment, 19: 10541(R) (GEAP-4703)
Cr–Nb–Ti–V, properties for use as cladding materials in nuclear superheat applications, 18: 24080 (BMI-X-286)
Cr–Nb–Ti–V, properties as cladding materials, 20: 5846
Cr–Nb–Ti–V, tensile properties at 540, 675, and 815°C, 18: 32036(R) (BMI-X-10091)
Cr–Nb–Ti–Zr, corrosion by steam at 540°C, 17: 36221 (BMI-1636)
Cr–Nb–U, phase studies, 18: 8835
Cr–Nb–U, phase studies, 19: 11679
Cr–Nb–U, preparation and properties as reactor fuel, 19: 26874(P)
Cr–Nb–V, corrosion of, by steam and water, 16: 29346
Cr–Nb–V, corrosion by steam at 1000°F, 17: 23890(R) (BMI-X-10040)
Cr–Nb–V, corrosion by steam at 540°C, 18: 8747(R) (BMI-X-10071)
Cr–Nb–V, corrosion by steam at 540°C, 18: 22415(R) (BMI-X-10082)
Cr–Nb–V, fabrication and mechanical properties of sheet of, 19: 20552(R) (IITRI-B6021-6)
Cr–Nb–V–Zr, development and properties for reactor cladding, 18: 7266
Cr–Nb–Zr, corrosion of, by steam and water, 16: 29346
Cr–Nb–Zr, corrosion by steam at 1000°F, 17: 493(R) (BMI-X-10003)
Cr–Nb–Zr, corrosion by high-pressure flowing steam at 300, 400, and 500°C, 17: 34346(R) (GEAP-4211)
Cr–Nb–Zr, corrosion by potassium at 1500 to 1800°F, 18: 5728 (ASD-TDR-63-270(Pt.II))
Cr–Nb–Zr, corrosion films on, composition of, 18: 12580 (GEAP-4089 (Vol.II)(Paper 19))
Cr–Nb–Zr, corrosion by potassium vapor at 1500 to 1800°F, 18: 18282 (BNL-844)
Cr–Nb–Zr, corrosion mechanisms of, 18: 39840 (GEAP-4521)
Cr–Nb–Zr, corrosion by water at 360°C and steam at 400°C, mechanism of, 19: 30681
Cr–Nb–Zr, corrosion by steam at 400 and 450°C, 19: 30668(R) (EURAEC-1274)
Cr–Nb–Zr, oxidation by steam at 750 and 900°F, 18: 2162(R) (IITRI-B198-46)
Cr–Nb–Zr, phase diagram, intermetallic compounds in, 20: 23684
Cr–Nb–Zr, phase studies, 17: 11108(T,R) (EURAEC-307)
Cr–Nb–Zr, phase studies, 17: 14749(T,R) (EURAEC-408)
Cr–Nb–Zr, phase studies, 18: 28036
Cr–Nb–Zr, phase studies, 16: 32084(T,R) (EURAEC-227)
Cr–Nb–Zr, tensile properties of, effects of composition and heat treatment on, 16: 29380 (TID-6155)
Cr–Ni–Nb, aging and thermal conductivity of, 20: 25588
Cr–Ni–Nb, phase diagram, 17: 4978
Cr–Ni–Nb, phase diagram, 17: 27825
Cr–Ni–Nb, phase studies, 16: 10551
Cr–Ni–Nb, phase studies, 18: 18307
Cr–Ni–Nb, phase studies on intermetallic compounds in, 20: 17075
Cr–Ni–Nb, radiation effects on stress-rupture properties of, neutron, 20: 5917
Cr–Ni–Nb, stress-rupture testing, summary of in-pile, 18: 4764(R) (ORNL-3470(p.129-56))
Cr–Ni–Nb, structural transformations in, 18: 615
Cr–Ni–Nb, tensile properties of, at 60 to 2000°F, 16: 19341 (DC-59-2-83)
Cr–Ni–Nb–Ta–Ti, properties of Inco 82 as filler material in weldments, 18: 4174(R) (ORNL-3470(p.157-72))
Cu–Nb, fabrication and properties of impregnated, 18: 4270
Cu–Nb, oxidation at 500 to 900°C, 19: 40976
Cu–Nb, phase studies and properties, 16: 6759

Cu–Nb, preparation and properties of impregnated, 17: 32495
Cu–Nb–Sn–Zr, corrosion by steam at 400 and 450°C, 19: 30668(R) (EURAEC-1274)
Cu–Nb–Zr, abrasion between cylinders and flats of, in water at 550°F, 20: 7490(R) (BMI-1745, Sect.A)
Cu–Nb–Zr, alloy element distribution in bulk metal and oxide film on, 20: 5851
Cu–Nb–Zr, corrosion by air, carbon dioxide, and water, 17: 504
Cu–Nb–Zr, corrosion by high-pressure flowing steam at 300, 400, and 500°C, 17: 34346(R) (GEAP-4211)
Cu–Nb–Zr, corrosion by superheated steam at 500°C, hydrogen uptake from, 17: 41368(T,R) (EURAEC-784)
Cu–Nb–Zr, corrosion by superheated steam at 500°C, hydrogen uptake from, 18: 14386(T,R) (EURAEC-822)
Cu–Nb–Zr, corrosion and hydridation by steam and water, 18: 30134(T,R) (EURAEC-955)
Cu–Nb–Zr, corrosion and hydridation by steam and water, effects on tensile properties, 19: 4616(R) (EURAEC-1161)
Cu–Nb–Zr, corrosion films on, microprobe studies of, 19: 9621 (DP-906)
Cu–Nb–Zr, corrosion by steam at 400 and 450°C, 19: 30668(R) (EURAEC-1274)
Cu–Nb–Zr, corrosion and hydrogen absorption characteristics of, effects of heat treatment on, 20: 25488 (WAPD-TM-500)
Cu–Nb–Zr, effects of hydrogen content on delayed failure of, 17: 14810(R) (ARF-B6005-2)
Cu–Nb–Zr, failure of, factors affecting delayed, 17: 38551(R) (SRO-93)
Cu–Nb–Zr, fatigue of hydrided, effects of heat treatment on, 17: 34404(R) (IITRI-B6005-8)
Cu–Nb–Zr, hot hardness tests on plasticity of oxide film formation on, 19: 25009
Cu–Nb–Zr, hydride precipitates in, effects of heat treatment on strain-induced orientation of, 18: 18341 (AECL-1888)
Cu–Nb–Zr, hydrogen distribution in oxidized, tritium autoradiographic studies of, 19: 13910 (AECL-2085)
Cu–Nb–Zr, hydrogen embrittlement, 18: 5776(R) (IITRI-B6005-11)
Cu–Nb–Zr, hydrogenation of, delayed failure from, 17: 28533(R) (SRO-83)
Cu–Nb–Zr, hydrogenation of, delayed failure from, 17: 42352(R) (SRO-94)
Cu–Nb–Zr, hydrogenation of, delayed failure from, 18: 3190(R) (SRO-95)
Cu–Nb–Zr, mechanical properties of hydrided, effects of fabrication, specimen geometry, and temperature, 17: 22155(R) (ARF-B6005-5)
Cu–Nb–Zr, mechanical properties of, effects of hydrogen content on, 18: 14386(T,R) (EURAEC-822)
Cu–Nb–Zr, radiation effects on tensile properties of, fast-neutron, 20: 2414 (AECL-2272)
Cu–Nb–Zr, radiation effects on tensile properties of, neutron, 20: 9590
Cu–Nb–Zr, stress-rupture of, effects of hydrogen embrittlement on, 17: 31733(R) (SRO-84)
Cu–Nb–Zr, testing for power reactor pressure tubes, 18: 37666 (A/CONF.28/P/22)
Cu–Ni–Nb, fabrication and properties of impregnated, 18: 4270
Cu–Ni–Nb, phase studies on, 20: 29764
Er–Nb, phase studies and atmospheric corrosion of, 16: 5315 (WADD-TR-61-123)
Fe–Mn–Nb–Ta–Ti, analysis of, methods for, 19: 28242
Fe–Mo–Nb, electric conductivity at 1.5 to 77°K, 18: 34183
Fe–Mo–Nb, magnetization, magnetoresistance, and resistivity of, 19: 7955
Fe–Nb, analysis for trace metals, polarographic, 20: 14455(R) (ORNL-3889, pp 25-32)
Fe–Nb, analysis of, for niobium and tantalum by ion exchange, 16: 16312
Fe–Nb, corrosion of, by steam and water, 16: 29346
Fe–Nb, crystal structure of cold-worked and heat-treated, 18: 13354(R) (BMI-1657(Del.))
Fe–Nb, crystal structure of μ phases in, 20: 27555
Fe–Nb, diffusion into liquid iron at 1923°K, 18: 26010
Fe–Nb, elastic properties, 19: 20579
Fe–Nb, electric conductivity of, at low temperatures, 17: 20489
Fe–Nb, fabrication into diaphragms, 18: 7985(R) (BMI-1650(Del.))
Fe–Nb, fabrication, 18: 15664(R) (BMI-1655(Del.))
Fe–Nb, fabrication by cold rolling, 18: 17351(R) (BMI-1659(Del.))
Fe–Nb, interactions of, with impurities during diffusion, electron probe microanalysis of, 16: 5281
Fe–Nb, isomer shift of iron-57 in $NbFe_2$ at 300 and 800°K, 19: 44678(R) (ANL-7000, pp 186-200)
Fe–Nb, mechanical properties and oxidation rate, 19: 32754
Fe–Nb, phase diagram, 16: 30332 (WAL-TR-823/5)
Fe–Nb, phase studies of precipitation of Laves phases from, 16: 25827
Fe–Nb, properties, 19: 26848
Fe–Nb, solubility of nitrogen in, 19: 41065
Fe–Nb, superconductivity of, 18: 15082
Fe–Nb–Sn–Zr, corrosion by steam at 400 and 450°C, 19: 30668(R) (EURAEC-1274)
Fe–Nb–Zr, corrosion of, by steam and water, 16: 29346
Fe–Nb–Zr, corrosion by steam at 400 and 450°C, 19: 30668(R) (EURAEC-1274)
Fe–Nb–Zr, oxidation by steam at 750°F, 18: 2162(R) (IITRI-B198-46)
Ga–Nb, crystal structure of intermetallic phase Nb_3Ga_2 in, 19: 6340
Ga–Nb, crystal structure of intermetallic compounds in, 20: 871
Ga–Nb, crystallographic parameters, 17: 18822
Ga–Nb, electric conductivity above superconducting transition temperature, 20: 8028
Ga–Nb, fabrication, properties, testing, and uses of superconducting, 19: 16110
Ga–Nb, phase studies and structure, 19: 6349
Ga–Nb, preparation of superconducting, vapor deposition technique for, 17: 18892 (ASD-TDR-62-1111)
Ga–Nb, preparation and superconductivity properties of intermetallic compounds of, 18: 4287
Ga–Nb, preparation of superconducting, empiricism for, 18: 14518
Ga–Nb, preparation of superconducting films of, 19: 33187(P)
Ga–Nb, properties of superconducting, 18: 6127
Ga–Nb, superconductivity of fused, 20: 15123
Ga–Nb, superconducting properties, (E), 20: 21897
Ga–Nb–Zr, phase studies, 17: 6729
Ge–Nb, composition range, decomposition pressure, and thermodynamic stability of Nb_3Ge, 17: 37518 (UCRL-7157)
Ge–Nb, composition range, decomposition pressure, and thermodynamic stability of Nb_3Ge phase in, 17: 40813
Ge–Nb, decomposition pressure and thermodynamic properties of $NbGe_2$ and Nb_5Ge_3, 17: 37494 (UCRL-7158)
Ge–Nb, decomposition pressures and thermodynamic stability of $NbGe_2$ and α- and β-Nb_5Ge_3, 17: 40814
Ge–Nb, effects of Nb_3Sn on crystal structure of $GeNb_3$ in, 18: 12705
Ge–Nb, phase studies, 20: 13275
Ge–Nb, preparation and properties of superconducting, 17: 18892 (ASD-TDR-62-1111)
Ge–Nb, preparation and superconductivity properties of intermetallic compounds of, 18: 4287
Ge–Nb, superconductivity of Nb_3Ge, (E), 19: 39625
Ge–Nb–Sn, superconducting properties of Nb_3SnGe, 17: 27861
Hf–Mo–Nb–W, mechanical properties, 19: 23039
Hf–Nb, critical current density of superconducting, in transverse field of 30 kgauss, 18: 6128
Hf–Nb, crystal structure and phase studies, 18: 12623 (ASD-TDR-63-204)
Hf–Nb, fabrication and properties of high-temperature, 20: 27472 (BM-RI-6777)
Hf–Nb, magnetization of high-field superconducting type-II, mixed state paramagnetism in, (E), 20: 8018
Hf–Nb, oxidation resistance to air at 2500°F, effects of aluminum and chromium on, 19: 36978(R) (IITRI-B6040-2)
Hf–Nb, phase diagrams, 18: 25985 (WADD-TR-60-132(Pt.III))
Hf–Nb, phase strengthening, 17: 6555
Hf–Nb, phase studies, 16: 27627(R) (NMI-9243)
Hf–Nb, phase studies, 17: 6668(R) (NMI-9246)
Hf–Nb, phase studies, 17: 12583(R) (NMI-9249)
Hf–Nb, phase studies, 18: 30228
Hf–Nb, phase studies on, 18: 34163
Hf–Nb, phase studies, 18: 42087
Hf–Nb, phase studies, 19: 40960
Hf–Nb, properties at high temperature, 17: 3469 (BM-RI-6101)
Hf–Nb, properties of welded, 17: 11242
Hf–Nb, superconducting transitions in high magnetic fields, 17: 25938
Hf–Nb, work function for, 20: 40297
Hf–Nb–Ta, fabrication and properties, 16: 514(R) (AD-255012)
Hf–Nb–Ta–V, mechanical properties, 17: 14809(R) (ARF-B231-8)
Hf–Nb–Ta–V, oxidation of siliconized, at 2200°F, 17: 23942(R) (ARF-B6001-3)
Hf–Nb–Ta–V, oxidation life at 2200°F of siliconized, static, 17: 35997(R) (IITRE-B6001-5)
Hf–Nb–Ta–W, fabrication and properties of high-temperature, 20: 27472 (BM-RI-6777)
Hf–Nb–Ti, coating of C-103 with silicides for oxidation protection, evaluation, 19: 7876(R) (ML-TDR-64-71)
Hf–Nb–Ti, creep properties at 2200°F, 18: 37621(R) (IITRI-B6021-3)
Hf–Nb–Ti, fabricability, strength, and weldability of, 20: 29763
Hf–Nb–Ti–W, fabrication and properties of high-temperature, 20: 27472 (BM-RI-6777)
Hf–Nb–Ti–W, properties for elevated-temperature service, 19: 6241 (BM-RI-6558)
Hf–Nb–Ti–W–Zr, properties for elevated-temperature service, 19: 6241 (BM-RI-6558)
Hf–Nb–V, fabrication and tensile properties of, effects of nitrogen and oxygen on, 16: 16712(R) (ARF-2231-3)
Hf–Nb–V, fabrication and properties of high-temperature, 20: 27472

(BM-RI-6777)
Hf–Nb–V, oxidation of siliconized, at 2200°F, 17: 23942(R) (ARF-B6001-3)
Hf–Nb–V, oxidation life at 2200°F of siliconized, static, 17: 35997(R) (IITRE-B6001-5)
Hf–Nb–V, preparation and properties, 16: 22577(R) (ARF-2231-4)
Hf–Nb–V, strength at high temperatures, 20: 2407(P)
Hf–Nb–W, corrosion by refluxing potassium at 1800 to 2400°F, 20: 25485 (NASA-TN-D-3429)
Hf–Nb–W, crystal structure and phase studies at 1100, 1300, and 1600°C, 18: 18342(R) (DRI-2153)
Hf–Nb–W, crystal structure and phase studies, 18: 32138(R) (DRI-2166)
Hf–Nb–W, effect of carbon on phase equilibria of, 19: 32729(R) (DRI-1092-211)
Hf–Nb–W, effects of carbon on phase equilibria in, 19: 22973(R) (DRI-1092-203)
Hf–Nb–W, effects of carbon and oxygen on phase equilibria in, 20: 7558(R) (DRI-1092-221)
Hf–Nb–W, effects of carbon and oxygen additions on phase equilibria in, 20: 7559(R) (DRI-1092-225)
Hf–Nb–W, effects of carbon and oxygen on phase equilibria in niobium-rich region of, 20: 21329(R) (DRI-1092-229)
Hf–Nb–W, erosion by water of rotating disks of, 19: 44625 (TIM-894)
Hf–Nb–W, fabrication and properties of C-129 foil, 19: 24945 (ASD-TDR-63-829(Pt.I))
Hf–Nb–W, fabrication and properties of high-temperature, 20: 27472 (BM-RI-6777)
Hf–Nb–W, mechanical properties of C-129, 19: 13978 (AMRA-TR-64-16)
Hf–Nb–W, phase equilibria of niobium-rich regions, 17: 16641(R) (DRI-2091)
Hf–Nb–W, phase equilibria in, effects of carbon and oxygen on, 20: 35885(R) (DRI-1092-232)
Hf–Nb–W, phase studies, 17: 39529(R) (DRI-2117)
Hf–Nb–W, phase studies, 18: 8792(R) (DRI-2131)
Hf–Nb–W, preparation and properties of, 17: 27779(R) (DRI-2102)
Hf–Nb–W, properties for elevated-temperature service, 19: 6241 (BM-RI-6558)
Hf–Nb–W, weldability of C-129, 17: 39498 (DMIC-Memo-169)
Hf–Nb–W–V, oxidation of siliconized, at 2200°F, 17: 23942(R) (ARF-B6001-3)
Hf–Nb–W–V, oxidation life at 2200°F of siliconized, static, 17: 35997(R) (IITRE-B6001-5)
Hf–Nb–W–Y, development and evaluation of C-129Y, 19: 11667 (D2-20282-1)
Hf–Nb–W–Y, development and evaluation of C-129Y, 20: 11227
Hf–Nb–W–Y, evaporation tests of C-129Y in high vacuum, 18: 44049(R) (ORNL-3670(p.77-111))
Hf–Nb–W–Y, evaporation losses of C-129Y, at 1200 to 1500°C in high vacuum, 19: 37043 (ORNL-P-1394)
Hf–Nb–W–Y, evaporation losses in high vacuum of C-129Y, 20: 4301(R) (ORNL-3870, pp 102-35)
Hf–Nb–W–Y, fabricability, strength, and weldability of, 20: 29763
Hf–Nb–W–Y, properties of welds in C-129Y, 19: 40989
Hf–Nb–W–Y, properties for use in aerospace vehicles, 20: 15119
Hf–Nb–W–Y, properties for high-temperature service, 20: 39445(P)
Hf–Nb–W–Y, tensile properties of C-129Y, effects of welds on, 20: 29712(R) (WANL-PR-(P)-009)
Hf–Nb–W–Y, weld bend tests of C-129Y, 19: 13955(R) (WANL-PR-(P)-005)
Hf–Nb–W–Y, weldability evaluation of C-129Y, 18: 41979 (ORNL-TM-929)
Hf–Nb–W–Y, weldability of C-129Y sheets, 18: 44049(R) (ORNL-3670 (p.77-111))
Hf–Nb–W–Y, weldability study of C-129Y, 19: 24957(R) (WANL-PR(P)-006)
Hf–Nb–W–Y, weldability studies of C-129Y, 19: 46966(R) (WANL-PR(P)-007)
Hf–Nb–W–Y, weldability evaluation of, 20: 39366
Hf–Nb–W–Y, welding of C-129Y, electron-beam and tungsten-arc, 18: 22426(R) (WANL-PR(P)-002)
Hf–Nb–W–Y, welding of C-129Y, tungsten-arc, 18: 34058(R) (WANL-PR(P)-003)
Hf–Nb–W–Y, welding parameters for C-129Y, electron-beam, 20: 5867
Hf–Nb–W–Zr, properties for elevated-temperature service, 19: 6241 (BM-RI-6558)
Hg–Nb, phase studies, 19: 36949(R) (BNL-900(p.121-97))
In–Nb, preparation of β-tungsten-structure superconducting, 16: 25803
In–Nb, preparation and superconductivity properties of intermetallic compounds of, 18: 4287
In–Nb, preparation of superconducting, empiricism for, 18: 14518
In–Nb, pressure-temperature phase diagrams, (E), 19: 5092
Ir–Nb, crystal structure and phase studies of Nb_3Ir_1, 19: 6308
Ir–Nb, crystal structure and atomic volumes, 19: 16154
Ir–Nb, electric and mechanical properties, 18: 24158
Ir–Nb, magnetic susceptibility and specific heat of superconducting binary complex phases of, 18: 37715
Ir–Nb, mechanical properties at 1100 and 1300°C, 19: 11734
Ir–Nb, mechanical properties of, effects of composition on, 20: 11288(T) (AD-622477)
Ir–Nb, oxidation rate of, at 1100°C, 20: 23614
Ir–Nb, phase diagrams, 18: 25985 (WADD-TR-60-132(Pt.III))
Ir–Nb, phase diagram, 19: 16155
Ir–Nb, phase studies, 17: 6668(R) (NMI-9246)
Ir–Nb, phase studies, 18: 25988
Ir–Nb, phase studies, 20: 11227
Ir–Nb, superconductivity of, 18: 15084
Ir–Nb, superconductivity in close-packed intermediate phases of, 20: 17624
Ir–Nb–Rh, crystal structure and superconductivity, 18: 25970(R) (ANL-6868(p.303-25))
Ir–Nb–Rh, superconductivity in, (E), 19: 16774
La–Nb, electric and mechanical properties, 18: 24158
La–Nb, mechanical properties at 1100 and 1300°C, 19: 11734
La–Nb, mechanical properties of, effects of composition on, 20: 11288(T) (AD-622477)
La–Nb, oxidation rate of, at 1100°C, 20: 23614
Li–Nb, interactions at grain boundary, 20: 9498(R) (NYO-3228-6)
Mg–Nb, phase diagrams, 18: 28002
Mo–Nb, analysis for niobium, 17: 30500
Mo–Nb, coating development of, for high-temperature applications in air, 16: 10415 (ASD-TR-61-322(p.482-502))
Mo–Nb, compatibility with sodium at 650°C, 17: 41333(R) (ANL-6677)
Mo–Nb, corrosion of, by steam and water, 16: 29346
Mo–Nb, corrosion of, by fluorine-containing fluids, 17: 8750(P)
Mo–Nb, corrosion by steam at 1000°F, 17: 23890(R) (BMI-X-10040)
Mo–Nb, corrosion by sodium at 650°C, 17: 36861(R) (ANL-6764)
Mo–Nb, corrosion by flowing sodium at 650°C, 17: 37001(R) (ANL-6780)
Mo–Nb, corrosion by potassium at 1500 to 1800°F, 18: 5728 (ASD-TDR-63-270(Pt.II))
Mo–Nb, corrosion by sodium at 650°C, 18: 15663(R) (ANL-6808)
Mo–Nb, corrosion by potassium vapor at 1500 to 1800°F, 18: 18282 (BNL-844)
Mo–Nb, corrosion by sodium at 650°C, 18: 26893(R) (ANL-6868(p.11-108))
Mo–Nb, corrosion by hydrochloric, phosphoric, and sulfuric acids, effects of alloy composition on, 20: 14997
Mo–Nb, creep strength of, effects of composition on, 20: 11302
Mo–Nb, crystal lattice vibrations in, inelastic neutron scattering measurements of, 20: 42573
Mo–Nb, crystal structure of, phonons in disordered, (E), 20: 5911
Mo–Nb, crystal structure and electric conductivity of, 20: 29766
Mo–Nb, crystal structure of, determination by phonon dispersion, 20: 37273
Mo–Nb, diffusion in bcc, 19: 23112
Mo–Nb, electric and mechanical properties, 18: 24158
Mo–Nb, electric conductivity at 300°K, effects of 1% iron solute on, 18: 12688
Mo–Nb, electric conductivity at 1.5 to 77°K, 18: 34183
Mo–Nb, electronic specific heat and magnetic susceptibility of, variation with temperature, 18: 8837
Mo–Nb, electronic structure of, at superconducting critical temperatures, 20: 31747
Mo–Nb, extrusion, 19: 20500 (AFML-TR-64-387)
Mo–Nb, fabrication and properties of extruded and rolled, 18: 5727(R) (AD-294579)
Mo–Nb, fabrication and properties, 18: 26893(R) (ANL-6868(p.11-108))
Mo–Nb, forging characteristics, 16: 9162 (DMIC-Memo-143)
Mo–Nb, hardness, 20: 15073
Mo–Nb, hardness of, at 20 to 2000°C, effects of molybdenum content on, 16: 30839
Mo–Nb, hydrogen affinity of, 18: 24165
Mo–Nb, iron magnetic moment in, discontinuous, (E), 19: 38031
Mo–Nb, Knight shift of niobium-93 in, 17: 16709
Mo–Nb, magnetic susceptibility and hydrogen affinity, 17: 3523
Mo–Nb, mass transport by sodium, 18: 15563
Mo–Nb, mechanical properties of, effects of composition on, 17: 24001
Mo–Nb, mechanical properties at 1100 and 1300°C, 19: 11734
Mo–Nb, mechanical properties of, effects of composition on, 20: 11288(T) (AD-622477)
Mo–Nb, mechanical and thermal properties of niobium-base, 20: 43940
Mo–Nb, metallurgy of, bibliography on, 17: 36203 (TID-3572)
Mo–Nb, microstructures, 19: 44610 (TIM-943)
Mo–Nb, neutron inelastic scattering by, Kohn effect from, (E), 20: 34805 (BNL-940, pp 8-15)
Mo–Nb, niobium-93 nuclear magnetic relaxation in, (E), 19: 41989
Mo–Nb, oxidation kinetics and mechanism of, 18: 34078
Mo–Nb, oxidation at 1000 to 1200°C, 18: 34079

Mo–Nb, oxidation, 18: 37627
Mo–Nb, oxidation at 400 to 1200°C, 18: 41960
Mo–Nb, oxidation in air at 1000 to 1200°C, 19: 11693
Mo–Nb, oxidation of coated, by air at high temperatures, 19: 27768(R) (SCNC-308)
Mo–Nb, oxidation by oxygen at 40 to 1200°C, 20: 5851
Mo–Nb, oxidation by air at 1000 to 1200°C, effects of composition on, 20: 11227
Mo–Nb, oxidation rate of, at 1100°C, 20: 23614
Mo–Nb, paramagnetic susceptibility, 16: 10576
Mo–Nb, preparation of vacuum-arc-cast, 16: 18016(R) (AD-265129)
Mo–Nb, preparation and properties of single crystals of, 20: 41481
Mo–Nb, preparation by electron-bombardment zone-melting methods, 16: 32046
Mo–Nb, properties of wrought, 17: 6672 (NP-12383)
Mo–Nb, properties of welded, 17: 11242
Mo–Nb, recrystallization temperature and strength of, effects of molybdenum content on, 20: 7618
Mo–Nb, self-diffusion of niobium in, 20: 35907
Mo–Nb, solid-state bonding of, 18: 24112
Mo–Nb, solvent properties of, for oxygen at 1000°C, 16: 13611
Mo–Nb, strength of, effects of carbon additions on, 17: 6672 (NP-12383)
Mo–Nb, superconductivity of, below 1°K, 16: 615
Mo–Nb, superconductivity below 20 millidegrees in, 17: 31217
Mo–Nb, superconductivity of, 18: 15084
Mo–Nb, superconductivity of, 18: 15085
Mo–Nb, superconductivity of, measurement of heat capacity to test theory of, 18: 36486
Mo–Nb, superconductivity of, 18: 36487
Mo–Nb, superconductivity, 20: 40047
Mo–Nb, superconducting transition temperature of 75Nb–25Mo, pressure effects on, 20: 44568
Mo–Nb, thermal capacity of solid solutions of, at low temperatures, 19: 4703
Mo–Nb, thermal expansion coefficient determination by x-ray method, 19: 47023(T) (LA-tr-65-20)
Mo–Nb, thermal expansion of, 20: 43964
Mo–Nb, thermodynamic properties, 16: 13636
Mo–Nb, yield strength of, effects of oxygen on, 17: 18811
Mo–Nb–Pt–U, corrosion resistance in water, 19: 20497(P)
Mo–Nb–Pt–U, properties for use as reactor fuel, 19: 20497(P)
Mo–Nb–Ru–Ti–V, oxidation of siliconized, at 2200°F, 17: 23942(R) (ARF-B6001-3)
Mo–Nb–Ru–Ti–V, oxidation life at 2200°F of siliconized, static, 17: 35997(R) (IITRE-B6001-5)
Mo–Nb–Ta, corrosion of, by fluorine-containing fluids, 17: 8750(P)
Mo–Nb–Ta, fabrication and properties, 16: 514(R) (AD-255012)
Mo–Nb–Ta, mechanical properties of, effects of composition on, 17: 24001
Mo–Nb–Ta, mechanical properties at high temperatures, 19: 34734
Mo–Nb–Ta, properties of wrought, 17: 6672 (NP-12383)
Mo–Nb–Ta, tensile properties at 3000°F, 18: 12562(R) (X63-12299)
Mo–Nb–Ta–W, cavitation damage of Cb-132M in liquid sodium to 1500°F, 20: 46154 (NASA-CR-72035)
Mo–Nb–Ta–W, corrosion of, by fluorine-containing fluids, 17: 8750(P)
Mo–Nb–Ta–W, creep slip of solution-hardened, at 980 to 1370°C, 19: 47049
Mo–Nb–Ta–W–Zr, creep tests on NB132M at 3200°F, 20: 5885(R) (NAS-CR-54773)
Mo–Nb–Ta–W, deformation mechanisms in solution-hardened niobium-base, 20: 17082
Mo–Nb–Ta–W, electric conductivity of Cb-132, at 80 to 400°K, 20: 23749
Mo–Nb–Ta–W, mechanical properties of, effects of composition on, 17: 24001
Mo–Nb–Ta–W, mechanical properties, 18: 18307
Mo–Nb–Ta–W, mechanical properties of solution-hardened, strain-aging studies of, 19: 7935
Mo–Nb–Ta–W, mechanical properties at 77 to 423°K, 19: 34724
Mo–Nb–Ta–W, properties as hollow turbine vanes, 20: 16963
Mo–Nb–Ta–W, strain aging of solution-hardened, 20: 5851
Mo–Nb–Ta–W, tensile properties, 17: 27812(R) (WADD-TR-61-134(Pt.II))
Mo–Nb–Ta–W, tensile properties at 3000°F, 18: 12562(R) (X63-12299)
Mo–Nb–Ta–W, tensile properties at 3000°F, 19: 16156
Mo–Nb–Ta–W, thermal expansion of Cb-132, at 80 to 400°K, 20: 23749
Mo–Nb–Ta–W, vacuum arc furnace design for melting of, 18: 44071
Mo–Nb–Ti, coating evaluation for D-31, 19: 9607 (ML-TDR-64-70)
Mo–Nb–Ti, coating of D-31 with silicides for oxidation protection, evaluation, 19: 7876(R) (ML-TDR-64-71)
Mo–Nb–Ti, coating of, for oxidation protection at 2300°F, 19: 20483 (SCNC-318)
Mo–Nb–Ti, coating with aluminum–tin-base alloys for protection against oxidation, 17: 39465 (SCNC-328(Del.))
Mo–Nb–Ti, coatings for, for high-temperature uses, 16: 27687
Mo–Nb–Ti, corrosion resistance, 16: 10464
Mo–Nb–Ti, corrosion by steam at 1000°F, 17: 493(R) (BMI-X-10003)
Mo–Nb–Ti, corrosion by steam at 1000°F, 17: 23890(R) (BMI-X-10040)
Mo–Nb–Ti, corrosion by potassium at 1500 to 1800°F, 18: 5728 (ASD-TDR-63-270(Pt.II))
Mo–Nb–Ti, corrosion by sodium at 650°C, 18: 15663(R) (ANL-6808)
Mo–Nb–Ti, corrosion by potassium vapor at 1500 to 1800°F, 18: 18282 (BNL-844)
Mo–Nb–Ti, corrosion by sodium at 650°C, 18: 26893(R) (ANL-6868 (p.11-108))
Mo–Nb–Ti, elastic properties and shear modulus of annealed and quenched, 18: 35999
Mo–Nb–Ti, evaluation of protective coatings for, 20: 29651
Mo–Nb–Ti, extrusion properties, 16: 12065(R) (AMC-TR-7-775(V))
Mo–Nb–Ti, fabrication and structure, 16: 10470 (ASD-TR-7-784(VI))
Mo–Nb–Ti, fabrication of rolled sheet, 17: 6597(R) (DMIC-176)
Mo–Nb–Ti, fabrication by vacuum rolling, 17: 36270
Mo–Nb–Ti, fabrication and properties, 18: 26893(R) (ANL-6868(p.11-108))
Mo–Nb– Ti, fabrication, oxidation, and properties of, 18: 35986 (ERR-FW-049A)
Mo–Nb–Ti, forging characteristics, 16: 9162 (DMIC-Memo-143)
Mo–Nb–Ti, machining, 16: 3417(R) (ASD-TR-7-532a(IV))
Mo–Nb–Ti, machining studies on pressed, sintered, and arc-cast, 16: 30742(R) (ASD-TR-7-532a(VII))
Mo–Nb–Ti, mechanical and thermal properties of niobium-base, 20: 43940
Mo–Nb–Ti, oxidation at 1000 to 1200°C, 18: 34079
Mo–Nb–Ti, oxidation of coated, by air at high temperatures, 19: 27768(R) (SCNC-308)
Mo–Nb–Ti, oxidation at 500 to 1200°C, 19: 36981
Mo–Nb–Ti, oxidation protection by aluminum–tin coatings with chromium and titanium additions, 20: 7580 (TIM-945)
Mo–Nb–Ti, properties of coated, at high temperatures, 16: 9189 (ASD-TR-61-66(Pt.II))
Mo–Nb–Ti, properties of arc-melted, 19: 27768(R) (SCNC-308)
Mo–Nb–Ti, specifications for machining, 18: 12609
Mo–Nb–Ti, thermal absorbance, emittance, and reflectance of, 16: 9193 (DMIC-Memo-141)
Mo–Nb–Ti, welding, 16: 30741 (ASD-TDR-62-292)
Mo–Nb–Ti, welding of D-31, ultrasonic, 17: 36240(R) (AD-290604)
Mo–Nb–Ti, welding of, ultrasonic, 19: 16025 (AD-425218)
Mo–Nb–Ti, x-ray diffraction of nonmetallic phases chemically extracted from, 19: 7973
Mo–Nb–Ti–U–Zr, ductility of uranium-base, effects of aging, forging, and rolling on, 20: 43883 (AD-637777)
Mo–Nb–Ti–U–Zr, mechanical properties for possible structural use, 19: 9651 (AMRA-TR-64-28)
Mo–Nb–Ti–U–Zr, mechanical properties of high-strength uranium-base, 20: 39440(P)
Mo–Nb–Ti–U–Zr, transformation diagram and kinetics of, 17: 25769(R) (AMRA-CR-63-02/1(F))
Mo–Nb–Ti–V, coating for oxidation protection, 19: 20459(R) (IITRI-B6019-6)
Mo–Nb–Ti–V, corrosion by steam at 1000°F, 17: 23890(R) (BMI-X-10040)
Mo–Nb–Ti–V, elastic properties and shear modulus of annealed and quenched, 18: 35999
Mo–Nb–Ti–V, mechanical properties of low-ruthenium content, at 2000°F, 16: 33444(R) (ARF-2231-6)
Mo–Nb–Ti–V, mechanical properties of, at high temperatures, effects of molybdenum, tantalum, and tungsten additions on, 16: 33444(R) (ARF-2231-6)
Mo–Nb–Ti–V, phase studies, 19: 7967
Mo–Nb–Ti–V, preparation and properties, 16: 22577(R) (ARF-2231-4)
Mo–Nb–Ti–W, forging characteristics, 16: 9162 (DMIC-Memo-143)
Mo–Nb–Ti–W–Zr, forging characteristics, 16: 9162 (DMIC-Memo-143)
Mo–Nb–Ti–Zr, analysis using vacuum cup electrode, 19: 22103 (TIM-904)
Mo–Nb–Ti–Zr, coating with aluminum–tin-base alloys for protection against oxidation, 17: 39465 (SCNC-328(Del.))
Mo–Nb–Ti–Zr, corrosion by lithium at 1600°F, 19: 36980 (PWAC-355)
Mo–Nb–Ti–Zr, creep properties of niobium-modified TZM, 20: 29705(R) (NAS-CR-54973)
Mo–Nb–Ti–Zr, fabrication and properties of cast and extruded, 18: 12536(R) (AD-412904)
Mo–Nb–Ti–Zr, fabrication and properties of extruded and rolled, 18: 22412(R) (AD-422106)
Mo–Nb–U, corrosion by water at 650°F, alloying effects of platinum on, 18: 16449(P)
Mo–Nb–U, isothermal transformations of gamma-phase, 19: 40958
Mo–Nb–U, microstructure and phases of heat-treated, 18: 42051
Mo–Nb–U, nonmetallic inclusions in, 16: 30874
Mo–Nb–U, phase boundaries at 675, 700, and 720°C, 18: 5801

Mo–Nb–U, phase diagrams, 16: 30868
Mo–Nb–U, phase studies and properties of, at 450 and 500°C, 16: 30871
Mo–Nb–U, phase studies and properties of, at 500°C, 16: 30867
Mo–Nb–U, phase studies and properties of, at 500 to 560°C, 16: 30869
Mo–Nb–U, phase studies of, at 575 to 1200°C, 16: 30870
Mo–Nb–U, phase studies, 18: 18387
Mo–Nb–U, phase studies, 17: 39631
Mo–Nb–U, production of fine-grained, 19: 30663(P)
Mo–Nb–U, transformation of gamma phase of, isothermal, 19: 7910 (UCRL-7824)
Mo–Nb–U–Zr, alloying effects of chromium and vanadium on aging and stability of, 17: 39644
Mo–Nb–U–Zr, mechanical properties, 17: 39643
Mo–Nb–U–Zr, mechanical properties of gamma-phase uranium-base, 20: 15060 (UCRL-7771)
Mo–Nb–U–Zr, nonmetallic inclusions in, 16: 30874
Mo–Nb–U–Zr, phase structure of, at 800 and 1000°C, 16: 30872
Mo–Nb–U–Zr, phase studies below 800°C, 17: 39633
Mo–Nb–U–Zr, phase transformation in, at 430 to 550°C, 16: 30873
Mo–Nb–V, corrosion of, by steam and water, 16: 29346
Mo–Nb–V, corrosion by steam at 1000°F, 17: 493(R) (BMI-X-10003)
Mo–Nb–V, ductility, strength, and weldability of, 18: 14448
Mo–Nb–V, fabricability, strength, and weldability of, 20: 29763
Mo–Nb–V, mechanical properties of, effects of composition on, 17: 24001
Mo–Nb–V, preparation and properties, 16: 22577(R) (ARF-2231-4)
Mo–Nb–V, properties, 17: 34419(R) (WADC-TR-57-344(Pt.VII))
Mo–Nb–V–Zr, bend ductility of B-66, effects of argon atmosphere contamination on, 19: 9592(R) (ASD-8-170(IV))
Mo–Nb–V–Zr, bonding of B-66, method for diffusion, 20: 5867
Mo–Nb–V–Zr, casting and testing of B-66 ingots, 18: 571(R) (AD-297246)
Mo–Nb–V–Zr, coating evaluation for B-66, oxidation-resistant, 19: 36945 (AD-610867)
Mo–Nb–V–Zr, coating of B-66, with chromium–silicon–titanium systems and silicides, 18: 14373(R) (NP-13498)
Mo–Nb–V–Zr, coatings for B-66 foils, development of high-temperature oxidation-resistant, 18: 30118(R) (RTD-TDR-63-4006(Pt.I))
Mo–Nb–V–Zr, coatings on B-66, properties of oxidation-resistant, 19: 26801(R) (AD-607530)
Mo–Nb–V–Zr, compatibility of rocket nozzles of, with hydrogen, 20: 19228
Mo–Nb–V–Zr, composition, crystal structure, and phases of precipitates in, 16: 22582 (ASD-TDR-62-7)
Mo–Nb–V–Zr, contamination of B-66 by rolling in argon atmosphere, 19: 9592(R) (ASD-8-170(IV))
Mo–Nb–V–Zr, corrosion protection by silicide coatings, 19: 11682
Mo–Nb–V–Zr, corrosion by cesium and lithium above 2500°C, 19: 28766
Mo–Nb–V–Zr, corrosion of B-66, by lithium, effects of oxygen on, 20: 4301(R) (ORNL-3870, pp 102-35)
Mo–Nb–V–Zr, corrosion by cesium vapor and liquid lithium at 2500 to 3400°F of B-66, 20: 5851
Mo–Nb–V–Zr, corrosion by refluxing potassium at 1800 to 2400°F, 20: 25485 (NASA-TN-D-3429)
Mo–Nb–V–Zr, creep-rupture properties of B-66, temperature dependence, 18: 44049(R) (ORNL-3670(p.77-111))
Mo–Nb–V–Zr, creep-rupture properties of, 20: 2336 (ORNL-P-1634)
Mo–Nb–V–Zr, ductility transition temperature of B-66, effects of protective coatings and welding on, 20: 27466
Mo–Nb–V–Zr, ductility, strength, and weldability of, 18: 14448
Mo–Nb–V–Zr, evaporation tests of B-66 in high vacuum, 18: 44049(R) (ORNL-3670(p.77-111))
Mo–Nb–V–Zr, evaporation losses of B-66, at 1200 to 1500°C in high vacuum, 19: 37043 (ORNL-P-1394)
Mo–Nb–V–Zr, evaporation losses in high vacuum of B-66, 20: 4301(R) (ORNL-3870, pp 102-35)
Mo–Nb–V–Zr, extrusion, 17: 3445(R) (NP-12225)
Mo–Nb–V–Zr, extrusion of tubing from, optimization studies, 17: 11140(R) (AMC-TR-7-775(VII))
Mo–Nb–V–Zr, extrusion of tubes of, 17: 23895(R) (AD-403514)
Mo–Nb–V–Zr, extrusion of, program outline for, 17: 25749(R) (WANL-PR-(N)-001)
Mo–Nb–V–Zr, extrusion by Dynapak process of B-66, 19: 30686(R) (AD-608945)
Mo–Nb–V–Zr, fabrication of rolled sheets of B-66, 18: 12591(R) (AD-409960)
Mo–Nb–V–Zr, fabrication of B-66, by rolling, 18: 12593(R) (AD-411155)
Mo–Nb–V–Zr, fabrication and mechanical properties of B-66, 18: 18292(R) (N63-20341)
Mo–Nb–V–Zr, fabrication of B-66, by extrusion and forging, 18: 20484(R) (AD-418992)
Mo–Nb–V–Zr, fabrication of B-66, by extrusion, 18: 20487(R) (WANL-PR-(N)-002)
Mo–Nb–V–Zr, fabrication and properties of coated B-66, 18: 24068(R) (NP-13955)
Mo–Nb–V–Zr, fabrication of extruded B-66, 18: 24093(R) (AD-424593)
Mo–Nb–V–Zr, fabrication and properties of B-66 tubing, 18: 27924(R) (WANL-PR-(N)-004)
Mo–Nb–V–Zr, fabrication of B-66, by rolling, 18: 30106(R) (AD-430773)
Mo–Nb–V–Zr, fabrication B-66 into sheets, 18: 30146(R) (AD-414497)
Mo–Nb–V–Zr, fabrication of B-66 tubing, 18: 41933 (TID-11295(3rd Ed.))
Mo–Nb–V–Zr, fabrication by forging and by extrusion, 19: 11711
Mo–Nb–V–Zr, fabrication and properties of B-66 sheet, 19: 20499(R) (AD-606291)
Mo–Nb–V–Zr, fabrication and properties of B-66 foil, 19: 24945 (ASD-TDR-63-829(Pt.I))
Mo–Nb–V–Zr, fabrication and properties of B-66 strip and foil, 19: 24946 (ASD-TDR-63-829(Pt.II))
Mo–Nb–V–Zr, fabrication of tubing of B-66, 20: 16998
Mo–Nb–V–Zr, joining of foils of B-66, for honeycomb panel fabrication, 18: 37661 (ASD-TDR-63-799(Pt.I))
Mo–Nb–V–Zr, mechanical properties of Pfaudler silicide and TRW chromium–silicon–titanium-coated B-66, in air at 70 to 2600°F, 18: 20523(R) (NP-13811)
Mo–Nb–V–Zr, mechanical properties of B-66, 19: 13978 (AMRA-TR-64-16)
Mo–Nb–V–Zr, oxidation and mechanical properties of coated B-66, 17: 39525(R) (AD-416459)
Mo–Nb–V–Zr, oxidation protection of B-66 by chromium–silicon–titanium coatings at 2000 to 2700°C, 18: 30127 (ASD-TDR-62-934(Pt.II))
Mo–Nb–V–Zr, properties of B66 sheet, 18: 573(R) (AD-422116)
Mo–Nb–V–Zr, properties as space reactor fuel cladding, 18: 9713 (CONF-375-3)
Mo–Nb–V–Zr, properties of coated B-66, to 2600°F, 18: 14373(R) (NP-13498)
Mo–Nb–V–Zr, properties of B-66, to 2600°F, 18: 14353(R) (AD-408310)
Mo–Nb–V–Zr, properties of B-66 foils at high temperatures, effects of coatings on mechanical and thermophysical, 18: 34128 (RTD-TDR-63-4068)
Mo–Nb–V–Zr, properties of welds in B-66, 19: 40989
Mo–Nb–V–Zr, reactions with cesium at 3400°F, metallographic specimen preparation of B-66, 19: 46954 (NMI-5025(Pt.I), pp 39-58)
Mo–Nb–V–Zr, reactions with uranium carbide, nitride, and dioxide, metallographic specimen preparation of B-66, 19: 46954 (NMI-5025 (Pt.I), pp 39-58)
Mo–Nb–V–Zr, rolling of foils of B-66, 19: 7871(R) (AD-422001)
Mo–Nb–V–Zr, stress-rupture properties of B-66, 19: 40961
Mo–Nb–V–Zr, tensile properties of welded plates of B-66, 20: 4301(R) (ORNL-3870, pp 102-35)
Mo–Nb–V–Zr, tensile properties of B-66, effects of welds on, 20: 29712(R) (WANL-PR-(P)-009)
Mo–Nb–V–Zr, tensile strength of B-66, at 1100 to 1400°C, 17: 30950(R) (NMI-2117)
Mo–Nb–V–Zr, tests of B-66 tubing, nondestructive, 19: 13950 (ORNL-TM-990)
Mo–Nb–V–Zr, thermal properties, 18: 7201 (ASD-TDR-63-597)
Mo–Nb–V–Zr, thermal properties to melting point, 20: 878
Mo–Nb–V–Zr, weld bend tests of B-66, 19: 13955(R) (WANL-PR-(P)-005)
Mo–Nb–V–Zr, weld stability in B-66, 20: 5866
Mo–Nb–V–Zr, weld structural stability in, 18: 22459(R) (NP-13816)
Mo–Nb–V–Zr, weldability of B-66, 17: 39498 (DMIC-Memo-169)
Mo–Nb–V–Zr, weldability of B-66 sheet, 18: 44049(R) (ORNL-3670 (p.77-111))
Mo–Nb–V–Zr, weldability study of B-66, 19: 24957(R) (WANL-PR(P)-006)
Mo–Nb–V–Zr, weldability studies of B-66, 19: 46966(R) (WANL-PR(P)-007)
Mo–Nb–V–Zr, weldability evaluation of, 20: 39366
Mo–Nb–V–Zr, welding of B66, effects of parameters on T1G welds in, 18: 573(R) (AD-422116)
Mo–Nb–V–Zr, welding of B-66, power force programmed ultrasonic, 18: 12594 (AD-427997)
Mo–Nb–V–Zr, welding of B-66, tungsten-arc, 18: 34058(R) (WANL-PR(P)-003)
Mo–Nb–V–Zr, welding of B-66, equipment and procedures for, 19: 9629(R) (AD-608818)
Mo–Nb–V–Zr, welding parameters for B-66, electron-beam, 20: 5867
Mo–Nb–V–Zr, welding properties of B-66, 20: 27466
Mo–Nb–V–Zr, welds in B-66, thermal stability of, 20: 27468
Mo–Nb–W, consolidation from elemental powders by hot pressing and annealing, 18: 41982
Mo–Nb–W, corrosion of, by fluorine-containing fluids, 17: 8750(P)
Mo–Nb–W, creep strength of, effects of composition on, 20: 11302
Mo–Nb–W, extrusion, 17: 6592 (ASD-TDR-62-781)
Mo–Nb–W, extrusion and properties of, 19: 18419(R) (AD-424207)
Mo–Nb–W, extrusion, 19: 20500 (AFML-TR-64-387)
Mo–Nb–W, fabrication and tensile properties at high temperatures,

18: 12562(R) (X63-12299)
Mo–Nb–W, fabrication of, effects on mechanical properties, 18: 20485 (ASD-TDR-62-670(Pt.II))
Mo–Nb–W, factors affecting vacuum-arc melting of, 18: 24070 (RTD-TDR-63-4089)
Mo–Nb–W, mechanical properties of, effects of composition on, 17: 24001
Mo–Nb–W, melting, 17: 6592 (ASD-TDR-62-781)
Mo–Nb–W, phase studies and properties of, 16: 22618
Mo–Nb–W, workability, 17: 6592 (ASD-TDR-62-781)
Mo–Nb–W–V, mechanical properties of, effects of composition on, 17: 24001
Mo–Nb–W–Zr, composition, crystal structure, and phases of precipitates in, 16: 22582 (ASD-TDR-62-7)
Mo–Nb–W–Zr, creep testing of F-48, at 2200°F, 17: 35251(R) (BMI-1632(Del.))
Mo–Nb–W–Zr, fabrication and structure, 16: 10470 (ASD-TR-7-784(VI))
Mo–Nb–W–Zr, fabrication and properties of rolled sheet, 17: 6597(R) (DMIC-176)
Mo–Nb–W–Zr, fabrication by vacuum rolling, 17: 36270
Mo–Nb–W–Zr, forging characteristics, 16: 9162 (DMIC-Memo-143)
Mo–Nb–W–Zr, friction and wear of, at high temperatures and in vacuum, 16: 5708 (ASD-TR-61-301)
Mo–Nb–W–Zr, hardness of niobium-base, effects of composition on hot-, 20: 31669
Mo–Nb–W–Zr, homogenization kinetics of sintered, 18: 26047
Mo–Nb–W–Zr, mechanical properties, 17: 14727(R) (BMI-1600(Del.))
Mo–Nb–W–Zr, mechanical properties of warm-extruded and rolled, 17: 32567 (BMI-X-249)
Mo–Nb–W–Zr, mechanical and oxidation properties of F-48, 17: 34415 (UCRL-6187(Rev.))
Mo–Nb–W–Zr, mechanical properties, 18: 18307
Mo–Nb–W–Zr, mechanical properties at 1000 to 1600°C, 19: 23043
Mo–Nb–W–Zr, mechanical properties, 19: 28833
Mo–Nb–W–Zr, mechanical properties of niobium-base, effects of composition on, 20: 7599
Mo–Nb–W–Zr, phase studies, 19: 7968
Mo–Nb–W–Zr, properties of coated, at high temperatures, 16: 9189 (ASD-TR-61-66(Pt.II))
Mo–Nb–W–Zr, properties of F-48, as journal bearing material, 17: 25382 (ASD-TR-61-705)
Mo–Nb–W–Zr, shear strength of F-48 fasteners at room temperature and 1600°F, 17: 36281 (AD-295526)
Mo–Nb–W–Zr, tensile properties, 17: 3378(R) (BMI-1583(Del.))
Mo–Nb–W–Zr, tensile properties, 17: 27878
Mo–Nb–W–Zr, tensile strength of F-48, at 1100 to 1500°C, 17: 30950(R) (NMI-2117)
Mo–Nb–W–Zr, welding, 16: 30741 (ASD-TDR-62-292)
Mo–Nb–Zr, corrosion of, by steam and water, 16: 29346
Mo–Nb–Zr, corrosion resistance and mechanical properties, 17: 37535
Mo–Nb–Zr, oxidation by steam at 900°F, 18: 2162(R) (IITRI-B198-46)
Mo–Nb–Zr, oxidation in air, composition of scale formed during, 18: 10477(T) (JPRS-22697(p.27-38))
Mo–Nb–Zr, phase diagram, 18: 8809(T) (JPRS-22593)
Mo–Nb–Zr, phase studies, 18: 625
Mo–Nb–Zr, phase studies on, 18: 16494
Mo–Nb–Zr, phase studies and properties, 18: 26056
Mo–Nb–Zr, phase studies of, isothermal sections at 1200°C in, 20: 41464
Mo–Nb–Zr, phase transformation kinetics, 16: 15166 (ARF-2198-21)
Mo–Ni–Nb–Ta–Ti, corrosion resistance and ductility, 19: 34735(P)
Nb–Ag, fabrication and properties of impregnated, 18: 4270
Nb–Ag, preparation and properties of impregnated, 17: 32495
Nb–Os, crystal structure and phase studies of Nb_3Os_5, 19: 6308
Nb–Os, electronic structure of, at superconducting critical temperatures, 20: 31747
Nb–Os, magnetic susceptibility and specific heat of superconducting binary complex phases of, 18: 37715
Nb–Os, superconductivity of, 18: 15082
Nb–Os, superconductivity of, 18: 15084
Nb–Os–Rh, superconductivity in, (E), 19: 16774
Nb–Pd, crystal structure of intermetallic compounds in, 19: 987
Nb–Pd, crystal structure of intermetallic compound NbPd, in, 19: 9699
Nb–Pd, crystal structure and electric conductivity of, 20: 29766
Nb–Pd, crystallographic parameters, 17: 18822
Nb–Pd, electric and mechanical properties, 18: 24158
Nb–Pd, electric conductivity and Hall constant of, 17: 580
Nb–Pd, magnetic properties at 90 to 1100°K, 20: 7585(T) (ANL-Trans-251)
Nb–Pd, magnetic susceptibility and specific heat of superconducting binary complex phases of, 18: 37715
Nb–Pd, mechanical properties at 1100 and 1300°C, 19: 11734
Nb–Pd, mechanical properties of, effects of composition on, 20: 11288(T) (AD-622477)
Nb–Pd, phase studies and structure, 16: 12169
Nb–Pd, phase studies, 18: 25988
Nb–Pd, properties as brazing materials, 19: 24916(R) (GEMP-334A)
Nb–Pd, superconductivity of, 18: 15084
Nb–Pd–Rh, crystal structure and superconductivity, 18: 25970(R) (ANL-6868(p.303-25))
Nb–Pd–Rh, superconductivity in, (E), 19: 16774
Nb–Pt, crystal structure of intermetallic compounds in, 19: 987
Nb–Pt, crystal structure of intermetallic compound $NbPt_3$ in, 19: 9699
Nb–Pt, crystal structure of equiatomic intermetallic compound in, 19: 24994
Nb–Pt, lattice parameters and solubility of intermetallic compounds $PtNb_2$ and $PtNb_3$ in, 17: 32638
Nb–Pt, magnetic susceptibility and specific heat of superconducting binary complex phases of, 18: 37715
Nb–Pt, phase studies, 18: 25988
Nb–Pt, superconductivity of, 18: 15084
Nb–Pt, superconductivity in close-packed intermediate phases of, 20: 17624
Nb–Pt–Rh, crystal structure and superconductivity, 18: 25970(R) (ANL-6868(p.303-25))
Nb–Pt–Rh, superconductivity in, (E), 19: 16774
Nb–Pu, phase studies and properties of, bibliographic study of, 16: 32115 (KFK-105)
Nb–Pu–U, fabrication, 17: 35251(R) (BMI-1632(Del.))
Nb–Pu–U, hardness, 17: 23864(R) (BMI-1619(Del.))
Nb–Pu–U, hardness and phase studies, 16: 4450(R) (BMI-1546(Del.))
Nb–Pu–U, phase studies, 16: 17966(R) (BMI-1514(Del.))
Nb–Pu–U, phase studies, 17: 25685(R) (BMI-1624(Del.))
Nb–Pu–U, preparation and properties, 18: 37601 (A/CONF.28/P/58)
Nb–Pu–U, properties as reactor fuel, 17: 8763
Nb–Pu–U, properties for reactor use, 17: 41422 (CEA-2300)
Nb–Pu–U, properties, 19: 4647 (CEA-R-2531)
Nb–Pu–U–Zr, hardness and phase studies, 16: 4450(R) (BMI-1546(Del.))
Nb–Pu–U–Zr, phase studies, 16: 17966(R) (BMI-1541(Del.))
Nb–rare earth, preparation, 17: 8795(P)
Nb–Re, crystal structure and phase studies of $Nb_{13.5}Re_{10.5}$, 19: 6308
Nb–Re, deformation in, x-ray studies of, 18: 39881 (AD-603473)
Nb–Re, deformation of, x-ray-diffraction studies of, 20: 35929
Nb–Re, electric and mechanical properties, 18: 24158
Nb–Re, electronic structure of, at superconducting critical temperatures, 20: 31747
Nb–Re, extrusion, 17: 11093(R) (NMI-2112)
Nb–Re, fabrication by hot rolling, 17: 25689(R) (NMI-2115)
Nb–Re, fabrication by rolling, 17: 30912(R) (NMI-2118)
Nb–Re, faulting in, x-ray diffraction study of, 19: 9649 (AD-608738)
Nb–Re, hardness, 16: 20955(R) (NMI-2105)
Nb–Re, hardness, 17: 11093(R) (NMI-2112)
Nb–Re, hydrogen affinity of, 18: 24165
Nb–Re, hydrogen absorption in, 20: 43832 (NASA-TN-D-3546)
Nb–Re, magnetic susceptibility and hydrogen affinity, 17: 3523
Nb–Re, magnetic susceptibility and specific heat of superconducting binary complex phases of, 18: 37715
Nb–Re, mechanical properties at 1100 and 1300°C, 19: 11734
Nb–Re, mechanical properties of, effects of composition on, 20: 11288(T) (AD-622477)
Nb–Re, oxidation rate of, at 1100°C, 20: 23614
Nb–Re, phase diagram, 16: 2250
Nb–Re, phase diagram, 17: 8727
Nb–Re, phase studies, 16: 546
Nb–Re, preparation, 16: 10534(R) (NMI-2102)
Nb–Re, properties at high temperatures, 17: 34409(R) (NMI-1253)
Nb–Re, properties at high temperatures, 18: 2226(R) (NMI-1258)
Nb–Re, rolling of, 17: 27733(R) (NMI-2116)
Nb–Re, solvent properties of, for oxygen at 1000°C, 16: 13611
Nb–Re, structure of chi phase in, 18: 8812
Nb–Re, superconductivity of, 18: 15084
Nb–Re, tensile properties at RT to 1400°C, effects of fabrication methods on, 17: 30950(R) (NMI-2117)
Nb–Re–W, factors affecting vacuum-arc melting of, 18: 24070 (RTD-TDR-63-4089)
Nb–Re–Zr, oxidation by oxygen at 1000°C, kinetics and microstructures of, 20: 37193
Nb–Rh, crystal structure and superconductivity, 18: 25970(R) (ANL-6868 (p.303-25))
Nb–Rh, crystal structure of intermetallic compounds in, 19: 16154
Nb–Rh, magnetic susceptibility and specific heat of superconducting binary complex phases of, 18: 37715
Nb–Rh, phase diagrams, 18: 25985 (WADD-TR-60-132(Pt.III))
Nb–Rh, phase diagram, 19: 16153
Nb–Rh, phase studies, 16: 27627(R) (NMI-9243)
Nb–Rh, phase studies, 17: 6668(R) (NMI-9246)
Nb–Rh, phase studies, 17: 12588(R) (NMI-9249)

Nb–Rh, phase studies, 18: 25988
Nb–Rh, phase studies, 20: 11227
Nb–Rh, superconductivity of, 18: 15084
Nb–Rh, superconductivity in close-packed intermediate phases of, 20: 17624
Nb–Rh–Ru, crystal structure and superconductivity, 18: 25970(R) (ANL-6868(p.303-25))
Nb–Rh–Ru, superconductivity in, (E), 19: 16774
Nb–Rh–Ti, superconductivity, 18: 21112
Nb–Rh–Zr, superconducting transition temperature, 19: 44678(R) (ANL-7000, pp 186-200)
Nb–Ru, electronic structure of, at superconducting critical temperatures, 20: 31747
Nb–Ru, phase diagrams, 18: 25985 (WADD-TR-60-132(Pt.III))
Nb–Ru, phase studies, 16: 27627(R) (NMI-9243)
Nb–Ru, phase studies, 17: 6668(R) (NMI-9246)
Nb–Ru, phase studies, 17: 12588(R) (NMI-9249)
Nb–Ru, phase studies, 17: 25821
Nb–Ru, phase studies, 18: 18307
Nb–Ru, phase studies above 1100°C, 18: 44197
Nb–Ru, phase studies, 20: 5851
Nb–Ru, preparation, 16: 16724(R) (NMI-9238)
Nb–Ru, solvent properties of, for oxygen at 1000°C, 16: 13611
Nb–Ru, superconductivity of, 18: 15082
Nb–Ru, superconductivity of, 18: 15084
Nb–Ru, superconductivity and electronic specific heat of, 18: 36488
Nb–Ru, thermodynamic properties, paramagnetic susceptibility, and superconducting transition temperature, 18: 20557
Nb–Sc, critical current density of superconducting, in transverse field of 30 kgauss, 18: 6128
Nb–Sc, crystal structure and phase studies, 18: 12623 (ASD-TDR-63-204)
Nb–Sc, phase studies of solid solution formation in, 19: 41050
Nb–Sn, a-c losses in, 18: 9262(R) (NP-13492)
Nb–Sn, analysis for niobium and tin, chemical and x-ray (E), 19: 335
Nb–Sn, anomalous specific heat of Nb_3Sn in liquid helium region, 20: 46521
Nb–Sn, chemical deposition of superconducting films of, 18: 15040 (IDA/HQ-63-1412(Vol.I)(p.80-4))
Nb–Sn, composition and structure of superconducting, 18: 38025
Nb–Sn, constitution diagram and superconductivity, 17: 30993
Nb–Sn, critical currents for superconductors of, 17: 14938 (LADC-5472)
Nb–Sn, critical currents in, intermetallic compound Nb_3Sn in, 17: 16805
Nb–Sn, critical current-field characteristics of short wire samples in superconducting solenoids, 17: 37730
Nb–Sn, critical currents in Nb_3Sn, angular and field dependence of, 17: 39764
Nb–Sn, critical currents in Nb_3Sn, field and angular dependence of, 18: 4504
Nb–Sn, critical currents of superconducting, 18: 26464
Nb–Sn, critical currents and fields in magnetic fields of 200 kgauss, (E), 19: 23541
Nb–Sn, critical field limits at superconducting temperatures, 17: 3635
Nb–Sn, crystal lattice stiffness parameter of intermetallic Nb_3Sn at 4.2 to 300°K, (E), 20: 28633
Nb–Sn, crystal structure, equilibrium solubilities, and constitutional diagram for, 17: 16727
Nb–Sn, crystal structure, equilibrium solubilities, and phase diagram for, 17: 16727
Nb–Sn, crystal structure of $NbSn_2$, 18: 18391
Nb–Sn, crystal structure, 19: 9604(R) (IS-900(Sect.M))
Nb–Sn, crystal structure of intermetallic compound Nb_6Sn_5 in, 19: 24996
Nb–Sn, crystal structure of intermetallic compounds in, 20: 4297(R) (IS-1200(Sect.M))
Nb–Sn, crystal structure of intermetallic compound Nb_3Sn in, 20: 7612
Nb–Sn, crystallization of chemical-vapor-deposited crystals of Nb_3Sn, 20: 15113
Nb–Sn, crystallography and phase equilibrium in, 18: 34165
Nb–Sn, current capacity, neutron irradiation effects on, 20: 40301
Nb–Sn, current intensity of superconducting Nb_3Sn in magnetic field, 17: 34647
Nb–Sn, deposition on niobium wires, 18: 4291
Nb–Sn, development, properties, and uses of superconducting, 18: 13010
Nb–Sn, development of 112 kgauss superconducting magnets of, 19: 19058
Nb–Sn, effects of cold working and heat treatment on properties of, 17: 41636
Nb–Sn, effects of microstructure on critical current density and superconductivity of, 18: 4290
Nb–Sn, effects of processing variables on critical current density and superconductivity of Nb_3Sn, 18: 4289
Nb–Sn, effects of Nb_3Sn in, on crystal structure of $GeMo_3$, $GeNb_3$, and Mo_3Si, 18: 12705
Nb–Sn, electric conductivity of, magnetic effects on, 16: 24888(R) (NBS-7244)
Nb–Sn, electric conductivity of Nb_3Sn in high magnetic field, 17: 20439
Nb–Sn, electric conductivity at 18 to 850°K, 18: 39953
Nb–Sn, electric conductivity above superconducting transition temperature, 20: 8028
Nb–Sn, fabrication of niobium-zirconium clad wires of, 17: 41333(R) (ANL-6677)
Nb–Sn, fabrication of Nb_3Sn into superconductive solenoids, 18: 14445
Nb–Sn, fabrication into superconducting element, 18: 15127(P)
Nb–Sn, fabrication, properties, testing, and uses of superconducting, 19: 16110
Nb–Sn, fabrication of stranded superconducting wires and solenoids of, 20: 9897
Nb–Sn, fabrication of superconducting solenoids from stranded wires of, 20: 17593 (CONF-650922, pp 597-603)
Nb–Sn, fast neutron effects on critical current in, 18: 9265
Nb–Sn, gamma emission by tin-119 in, isomer energy shifts in, 16: 12545
Nb–Sn, gamma resonance absorption by tin-119 in, 16: 7129
Nb–Sn, growth of Nb_3Sn crystals in, 17: 34317 (AD-413113)
Nb–Sn, growth of Nb_3Sn single crystals, 18: 4171(R) (ORNL-3470(p.3-5))
Nb–Sn, impurity effects on superconducting properties of, 18: 44679
Nb–Sn, intensity ratio technique for x-ray spectrometric analysis, 18: 15972
Nb–Sn, intermediate-resistance state in, presence of, between normal and superconducting states, 16: 15461
Nb–Sn, intermediate phases in, 17: 6703
Nb–Sn, Knight shift in relation to transition temperature in intermetallic phases in, 19: 30707
Nb–Sn, lattice parameter measurements for Nb_3Sn at 20 to 975°C, 18: 3714(R) (ORNL-3470(p.41-4))
Nb–Sn, magnetic field effects on superconductivity of, 17: 37887
Nb–Sn, magnetic field production by solenoids of superconducting Nb_3Sn, 101-kgauss, 18: 958
Nb–Sn, magnetic flux compression in superconducting, 18: 28509
Nb–Sn, magnetic field penetration in superconducting Nb_3Sn, 18: 36530
Nb–Sn, magnetic flux jumping in superconducting tubes of, 18: 42560
Nb–Sn, magnetic field generation in hollow cylinder at 14°K by wires of Nb_3Sn, 18: 44682
Nb–Sn, magnetic flux jump in hollow cylinders of, 19: 33159
Nb–Sn, magnetic flux jumping in superconducting, (T), 19: 35326
Nb–Sn, magnetic flux jumps in superconducting Nb_3Sn in pulsed magnetic fields, (E), 20: 2921
Nb–Sn, magnetic flux jumps and trapping in superconducting, (E), 20: 4793
Nb–Sn, magnetic field penetration in Nb_3Sn supercoductors, (E), 20: 8030
Nb–Sn, magnetic flux jumps in superconducting intermetallic compounds of, sample geometry effects on, (E), 20: 9916
Nb–Sn, magnetic flux trapping and compression in superconducting, (E), 19: 6605
Nb–Sn, magnetic field penetration into superconducting intermetallic compounds of, (E), 20: 21908
Nb–Sn, magnetic flux trapping threshold in superconducting Nb_3Sn, (E), 20: 21926
Nb–Sn, magnetic flux jumping in hollow cylinders of superconducting, (E), 20: 24272
Nb–Sn, magnetic field trapping by superconducting hollow cylinders of intermetallic compounds of, temperature dependence of, (E), 20: 32316
Nb–Sn, magnetic flux jumping in high-field high-current superconducting, stability against, (T), 20: 32320
Nb–Sn, magnetic flux penetration in superconducting, (E), 20: 42132
Nb–Sn, magnetic hysteresis in superconducting, (E), 19: 35334
Nb–Sn, magnetic moment at superconducting transition in, (T), 19: 33181
Nb–Sn, magnetic properties of superconducting, 18: 4495
Nb–Sn, magnetic properties of Nb_3Sn, 18: 30687
Nb–Sn, magnetic shielding by superconducting plates of, 20: 26035
Nb–Sn, magnetic shielding properties of superconducting, for accelerator extraction systems, 20: 39523
Nb–Sn, magnetization discontinuities in superconducting, (E), 19: 37740
Nb–Sn, maximum critical field of superconductors of, 17: 8959
Nb–Sn, mechanical constraint effects on superconducting transitions of niobium wires coated with, 17: 28098
Nb–Sn, microstructure and mechanical properties, 17: 4886(R) (AD-275610)
Nb–Sn, microwave surface resistance in superconducting, (E), 20: 21916
Nb–Sn, negative surface energy model of superconductivity of, 17: 9040
Nb–Sn, performance as superconducting magnet, 18: 42554
Nb–Sn, performance of superconducting magnets using Nb_3Sn ribbon (E), 19: 571
Nb–Sn, performance of superconducting, for linac resonant cavities, 19: 27012 (MURA-714(p.540-4))
Nb–Sn, performance of superconducting solenoids of, in superfluid

helium, (E), 20: 24268
Nb–Sn, phase and superconductivity studies on (E), 19: 1505
Nb–Sn, phase diagrams, structure, and properties, 16: 29392(T) (AEC-tr-5323)
Nb–Sn, phase diagram, 18: 27982
Nb–Sn, phase diagram, 18: 28003
Nb–Sn, phase diagram, 19: 16157
Nb–Sn, phase diagram and peritectic decomposition of intermetallic compound Nb_3Sn, 19: 16167
Nb–Sn, phase diagram, 19: 25030
Nb–Sn, phase studies, 18: 2163(R) (IS-700(Sect.M))
Nb–Sn, phase studies, 18: 14396
Nb–Sn, phase studies, 19: 40961
Nb–Sn, phase studies, 20: 13275
Nb–Sn, physical properties of gas-phase-deposited Nb_3Sn, 17: 32647
Nb–Sn, preparation and properties of intermetallic compounds of, 17: 406 (ASD-TDR-62-269)
Nb–Sn, preparation and superconducting properties of, 17: 8853
Nb–Sn, preparation of Nb_3Sn, 17: 17965(P)
Nb–Sn, preparation of superconductors with extremely high critical field strengths, 17: 18684
Nb–Sn, preparation of superconducting, with extremely high critical field strengths, 17: 18684
Nb–Sn, preparation of single crystals of, 18: 954 (NP-13274(p-40-6))
Nb–Sn, preparation and superconductivity properties of intermetallic compounds of, 18: 4287
Nb–Sn, preparation of superconducting, empiricism for, 18: 14518
Nb–Sn, preparation and properties of thin-film hard superconducting, 18: 28501
Nb–Sn, preparation and quenching characteristics of surface-coated wires of, 18: 36528
Nb–Sn, preparation and properties of films of Nb_3Sn (E), 19: 984
Nb–Sn, preparation of thin films of, by codeposition, (E/T), 19: 4601
Nb–Sn, preparation and properties of intermetallic compound Nb_3Sn on ceramic substrates, 19: 16040
Nb–Sn, preparation of superconducting films of, 19: 33187(P)
Nb–Sn, preparation and sintering of Nb_3Sn, 19: 44592 (CLM-R-43)
Nb–Sn, preparation of superconducting Nb_3Sn using diffusion layers, 20: 17649
Nb–Sn, preparation of thin films of Nb_3Sn, 20: 19723 (N-65-17508)
Nb–Sn, preparation of multilayer continuous intermediate phase wires of, 20: 29781
Nb–Sn, pressure effects on superconductivity of, 18: 15078
Nb–Sn, production of single crystal, 17: 36440(R) (NP-13061)
Nb–Sn, properties for superconducting coils, 17: 29386 (CEA-2239)
Nb–Sn, properties as superconducting magnet, 17: 32712 (LNF-63/26)
Nb–Sn, properties of superconducting, 18: 6127
Nb–Sn, properties for use as superconductive wires, 18: 34200
Nb–Sn, properties of sintered Nb_3Sn, as superconducting magnetic coil, 19: 44592 (CLM-R-43)
Nb–Sn, radiation effects on superconducting properties of, fast-neutron, 18: 10583
Nb–Sn, radiation effects on current-carrying behavior of superconducting Nb_3Sn, fast neutron, 18: 18424
Nb–Sn, radiation effects on superconductivity of, neutron, 18: 34683(R) (NP-14136)
Nb–Sn, radiation effects of fast neutrons on superconductivity of Nb_3Sn (E), 19: 1023
Nb–Sn, radiation effects of neutrons on superconductivity of (E), 19: 1506
Nb–Sn, radiation effects on superconducting, neutron, 20: 34459
Nb–Sn, resistive states in superconducting, 18: 15065
Nb–Sn, solvent properties for Ti_3Sn and Mo_3Al, 18: 4271
Nb–Sn, specific heat anomaly at superconducting transition, (E), 19: 35345
Nb–Sn, structure analysis of superconducting wire, 17: 18724
Nb–Sn, structure of gamma phase in, 19: 30730 (CALT-221-8)
Nb–Sn, superconducting, critical current in, at 0.1 to 60 kgauss, 16: 15406
Nb–Sn, superconducting, critical field in, at 4.2°K, 16: 15462
Nb–Sn, superconducting, critical fields in bulk and wire form of, 16: 15427
Nb–Sn, superconducting, effects of temperature on critical field in, 16: 15467
Nb–Sn, superconducting, magnetic properties of, 16: 15426
Nb–Sn, superconducting, magnetic quenching characteristics of, 16: 15396
Nb–Sn, superconducting, phase studies of, 16: 25791
Nb–Sn, superconducting, preparation and properties of, 16: 22600(T) (AEC-tr-5123)
Nb–Sn, superconducting, preparation and properties of, 16: 29405
Nb–Sn, superconducting, preparation of, 16: 12047
Nb–Sn, superconducting, preparation of, as layers on niobium wires, 16: 15463
Nb–Sn, superconducting, use of, as iron-core-magnet coils, 16: 15430
Nb–Sn, superconducting, use of, as magnet coils for fields over 100 kgauss, 16: 15460
Nb–Sn, superconducting, use of, to produce a 28.5-kgauss magnet, 16: 15429
Nb–Sn, superconducting solenoids of, design and testing of, 16: 4610(R) (TID-14435)
Nb–Sn, superconducting wires of, magnetic and physical properties of, 16: 15464
Nb–Sn, superconductivity of, 16: 16830
Nb–Sn, superconductivity of, 17: 406 (ASD-TDR-62-269)
Nb–Sn, superconductivity, 17: 4886(R) (AD-275610)
Nb–Sn, superconductivity in, 17: 5084
Nb–Sn, superconductivity in, 17: 6807 (UCRL-9819)
Nb–Sn, superconductivity of, critical persistent currents in, 17: 6875
Nb–Sn, superconducting properties in strong magnetic fields, 17: 619
Nb–Sn, superconductive properties and technical applications of, 17: 16705
Nb–Sn, superconduction with extremely high critical field strength, 17: 18798
Nb–Sn, superconductivity transition temperature of Nb_3Sn, effects of pressure on, 17: 18843
Nb–Sn, superconducting critical currents in niobium wire cored with, 17: 24062 (UCRL-10402)
Nb–Sn, superconductivity properties of Nb_3Sn in, 17: 32615
Nb–Sn, superconducting critical fields of Nb_3Sn in, 17: 32224
Nb–Sn, superconductivity of sintered Nb_3Sn, 17: 34447
Nb–Sn, superconductivity and uses of Nb_3Sn, 17: 34451
Nb–Sn, superconductivity of, isotope effects on, 17: 34617
Nb–Sn, superconducting properties of Nb–Nb_2Sn, sintered compacts, 17: 36470
Nb–Sn, superconductivity, 17: 41604
Nb–Sn, superconductivity of Nb_3Sn-coated niobium wire, 18: 4284
Nb–Sn, superconducting transition temperatures in, pressure effects on, 18: 6120
Nb–Sn, superconducting wire of, intermediate-state resistance of, 18: 6134
Nb–Sn, superconducting properties of Nb_3Sn, and Nb_3Sn_2, 18: 6135
Nb–Sn, superconducting critical alternating currents in, 18: 13018
Nb–Sn, superconducting magnets of Nb_3Sn, stabilization of, 18: 15045
Nb–Sn, superconducting critical currents in magnetic fields, 18: 15076
Nb–Sn, superconducting band gap for, 18: 15099
Nb–Sn, superconductivity of, effects of substitution of other elements for part of tin on, 18: 21110
Nb–Sn, superconducting magnets of, 18: 24547
Nb–Sn, superconductivity of intermetallic compounds in, 18: 28003
Nb–Sn, superconducting magnets of, 18: 34715
Nb–Sn, superconducting transition temperature of, pressure effects on, 18: 36429
Nb–Sn, superconducting critical currents in, 18: 36434
Nb–Sn, superconducting magnetic flux pump of Nb_3Sn, 18: 36521
Nb–Sn, superconducting cylinders of Nb_3Sn, hysteresis losses in, 18: 36527
Nb–Sn, superconducting properties of vapor-deposited, effects of composition on, 18: 36529
Nb–Sn, superconductivity of solid solutions based on Nb_3Sn, 18: 36531
Nb–Sn, superconducting tunneling in Nb_3Sn, 18: 36498
Nb–Sn, superconducting critical currents in transverse fields, 18: 44698
Nb–Sn, superconducting penetration depth of Nb_3Sn (E/T), 19: 1507
Nb–Sn, superconducting energy gap in Nb_3Sn (E/T), 19: 1508
Nb–Sn, superconductivity of Nb_3Sn, magnetic-field effects on (E/T), 19: 1509
Nb–Sn, superconducting transitions in Nb_3Sn (E), 19: 1510
Nb–Sn, superconductivity of Nb_3Sn, microwave studies of (E), 19: 1511
Nb–Sn, superconducting transitions of Nb_3Sn in pulsed fields (E), 19: 1512
Nb–Sn, superconductivity degradation in Nb_3Sn ribbons (E), 19: 1515
Nb–Sn, superconducting properties of, containing Nb_3Sn filament bundles (E), 19: 1517
Nb–Sn, superconducting transitions in Nb_3Sn films, models for (E), 19: 1513
Nb–Sn, superconducting transitions in Nb_3Sn disks, (E), 19: 1514
Nb–Sn, superconducting transition temperature in, effect of pressure on, (T), 19: 12438
Nb–Sn, superconducting properties of, 19: 12453
Nb–Sn, superconductivity and kinetics of formation of intermetallic compound Nb_3Sn, 19: 16157
Nb–Sn, superconductivity of intermetallic compound Nb_3Sn, effects of vacancy distribution on, 19: 16166
Nb–Sn, superconducting transitions in fast-pulsed magnetic fields, (E), 19: 16779
Nb–Sn, superconducting properties of, current and magnetic field effects

on, (E), 19: 19060
Nb–Sn, superconducting, preparation and magnetization of, 19: 26791
Nb–Sn, superconductivity of hollow sintered cylinders of, (E), 19: 41609
Nb–Sn, superconductivity critical currents in intermetallic compound Nb_3Sn, 19: 45213
Nb–Sn, superconductivity of intermetallic compounds of, above 4.2°K, (E), 19: 47508
Nb–Sn, superconducting electromagnet of, 19: 47526
Nb–Sn, superconductivity of Nb_3Sn, (T), 20: 1264 (NBS-8843)
Nb–Sn, superconducting transitions in sintered, (E), 20: 8029
Nb–Sn, superconducting properties of, effects of tensile stress on, 20: 8007
Nb–Sn, superconductivity of Nb_3Sn, 20: 13666 (IPP-4/22)
Nb–Sn, superconductivity of fused, 20: 15123
Nb–Sn, superconductivity of diffusion layers of Nb_3Sn, (E), 20: 17632
Nb–Sn, superconducting critical currents in intermetallic compounds of, (E), 20: 21921
Nb–Sn, superconducting critical currents and fields in flux-pump fed coils of, (E), 20: 21924
Nb–Sn, superconducting critical currents in intermetallic compounds of, in high fields, (E), 20: 21922
Nb–Sn, superconductivity of Nb_3Sn in, 20: 23745
Nb–Sn, superconductivity of multilayer continuous intermediate phase wires of, effects of heat treatments on, 20: 29781
Nb–Sn, superconducting transition temperatures of $NbSn_2$ and Nb_6Sn_5, 20: 30279
Nb–Sn, superconductivity of, effect of annealing temperature on, 20: 34424
Nb–Sn, superconducting properties of, at elevated temperatures, 20: 34417(R) (N-65-34464)
Nb–Sn, surface impedance in superconducting, 18: 26489
Nb–Sn, theory for superconductivity of Nb_3Sn in, 17: 18830
Nb–Sn, thermal conductivity at 2.6 to 28°K, 18: 974
Nb–Sn, thermal expansion coefficient change at superconductivity transition temperature of Nb_3Sn, 17: 18845
Nb–Sn, thermal expansion of Nb_3Sn at 80 to 1290°K, 18: 39972
Nb–Sn, use for exciting electrical machines, 18: 42555
Nb–Sn, use in accelerators and storage rings as superconductors, 18: 16602 (BNL-7534(p.417-47))
Nb–Sn, use in magnetic shielding for energetic protons, 17: 11899 (N62-10900(Pt.IV))
Nb–Sn, use of Nb_3Sn in superconducting magnets, 17: 20438
Nb–Sn, valence bonding in Nb_3Sn intermetallic compound in, 18: 32208
Nb–Sn, vapor deposition of Nb_3Sn, and properties, 18: 4226
Nb–Sn, wire cross sections of, for microscopy, preparation of, 16: 29333
Nb–Sn–Ti, superconductivity of fused, 20: 15123
Nb–Sn–V, superconductivity of fused, 20: 15123
Nb–Sn–V–Zr, corrosion by steam at 400 and 450°C, 19: 30668(R) (EURAEC-1274)
Nb–Sn–Zr, chemical and mechanical properties of, program for studying radiation effects on, 17: 22229(T-R) (EURAEC-560)
Nb–Sn–Zr, corrosion of, by steam to 550°C, 16: 32084(T,R) (EURAEC-227)
Nb–Sn–Zr, corrosion by steam and water, 17: 6581
Nb–Sn–Zr, corrosion by steam and water, 17: 6535(T) (EURAEC-352)
Nb–Sn–Zr, corrosion by water, 17: 22094 (HW-71023)
Nb–Sn–Zr, corrosion and mechanical properties of, 17: 39472(T,R) (EURAEC-668)
Nb–Sn–Zr, corrosion by steam and water, 17: 39659
Nb–Sn–Zr, corrosion by superheated steam at 400°C, 18: 8735(T,R) (EURAEC-782)
Nb–Sn–Zr, corrosion by steam and water, effects of heat treatment on, 18: 12574 (APED-4364)
Nb–Sn–Zr, corrosion films on, composition of, 18: 12580 (GEAP-4089 (Vol.II)(Paper 19))
Nb–Sn–Zr, corrosion by steam at 400°C, hydrogen pickup in, 18: 14545(T,R) (EURAEC-863)
Nb–Sn–Zr, corrosion by steam and water, 18: 14358(R) (EURAEC-135)
Nb–Sn–Zr, corrosion of $ZrNb_3Sn$ by steam and water, 18: 14360(R) (EURAEC-199)
Nb–Sn–Zr, corrosion by water and steam, 18: 30110 (EUR-86.d)
Nb–Sn–Zr, corrosion and hydrogen pickup in steam and water, effects of heat treatment on, 18: 30138
Nb–Sn–Zr, corrosion mechanisms of, 18: 39840 (GEAP-4521)
Nb–Sn–Zr, corrosion by steam at 400 and 450°C, effects of metal additions on, 18: 41938(T,R) (EURAEC-1058)
Nb–Sn–Zr, corrosion and hydrogen pickup in water and steam at 600 to 900°F, 18: 41957 (KAPL-3018)
Nb–Sn–Zr, corrosion resistance of, effects of various additives on, 18: 41972(P)
Nb–Sn–Zr, corrosion by terphenyls, 19: 2759
Nb–Sn–Zr, corrosion by water at 360°C and steam at 400°C, mechanism of, 19: 30681
Nb–Sn–Zr, corrosion by steam at 400 and 450°C, 19: 30668(R) (EURAEC-1274)
Nb–Sn–Zr, corrosion by water in ETR G-7 loop, 19: 30669(R) (HW-84573(p.5.1-22))
Nb–Sn–Zr, corrosion resistance of, effects of additives and cold working on, 19: 36990(P)
Nb–Sn–Zr, corrosion by steam, effects of antimony, chromium, iron, and vanadium additions on, 20: 2255(R) (EURAEC-1323)
Nb–Sn–Zr, corrosion in reactor, ETR test of, 20: 27425(R) (BNWL-207, pp 5.1-12)
Nb–Sn–Zr, corrosion by steam, composition of oxide film formed by, 20: 31669
Nb–Sn–Zr, creep and fatigue properties of $ZrNb_3Sn$, 18: 14359(R) (EURAEC-136)
Nb–Sn–Zr, crystal structure of, effects of hydrogen on, 16: 33487(T,R) (EURAEC-243)
Nb–Sn–Zr, dispersion and solution strengthening effects on, 18: 5794
Nb–Sn–Zr, effects of metal additions on corrosion of Nb_3SnZr by steam, 18: 18319(T,R) (EURAEC-953)
Nb–Sn–Zr, effects of physical parameters and radiation on fuel element cladding of, (E), 20: 7519 (RCN-41)
Nb–Sn–Zr, elongation of, due to thermal cycling, 16: 10526(R) (EURAEC-136)
Nb–Sn–Zr, fabrication of tubing of, 17: 6600(T) (EURAEC-354)
Nb–Sn–Zr, fabrication and mechanical testing, 18: 37612 (A/CONF.28/P/477)
Nb–Sn–Zr, fabrication and properties of, effects of metal additions on, 18: 41938(T,R) (EURAEC-1058)
Nb–Sn–Zr, fatigue properties of $ZrNb_3Sn$, 18: 14360(R) (EURAEC-199)
Nb–Sn–Zr, hardness of zirconium-base, effects of tempering at 400 to 700°C on, 20: 31669
Nb–Sn–Zr, heat treatment and tensile properties of, 17: 22094 (HW-71023)
Nb–Sn–Zr, hydrogen pickup in steam and water, effects of heat treatment on, 18: 12574 (APED-4364)
Nb–Sn–Zr, length variations induced by thermal cycling in $ZrNb_3Sn$ tubes, 18: 14359(R) (EURAEC-136)
Nb–Sn–Zr, mechanical properties, 16: 33487(T,R) (EURAEC-243)
Nb–Sn–Zr, mechanical properties of, at 25 to 850°C, effects of oxygen, 17: 1947 (TID-17174)
Nb–Sn–Zr, mechanical properties of, hydrogen effects on, 17: 6696(T) (EURAEC-353)
Nb–Sn–Zr, mechanical properties and phases of, effects of hydrogen on, 17: 12693
Nb–Sn–Zr, mechanical properties, 18: 8735(T,R) (EURAEC-782)
Nb–Sn–Zr, phase diagrams, 18: 12633 (GEAP-4089(Vol.I)(Paper 4))
Nb–Sn–Zr, phase studies, 17: 6697(T) (EURAEC-358)
Nb–Sn–Zr, phase studies, 18: 14358(R) (EURAEC-135)
Nb–Sn–Zr, phase studies, 18: 14360(R) (EURAEC-199)
Nb–Sn–Zr, preparation, 16: 20980(T,R) (EURAEC-26)
Nb–Sn–Zr, preparation of, 17: 8890(T,R) (EURAEC-494)
Nb–Sn–Zr, properties for reactor applications, 18: 12633 (GEAP-4089 (Vol.I)(Paper 4))
Nb–Sn–Zr, properties of $ZrNb_3Sn$, 18: 14358(R) (EURAEC-135)
Nb–Sn–Zr, properties for use as cladding materials in water, 18: 30110 (EUR-86.d)
Nb–Sn–Zr, radiation effects on, neutron, 17: 8890(T,R) (EURAEC-494)
Nb–Sn–Zr, radiation effects on, 17: 39472(T,R) (EURAEC-668)
Nb–Sn–Zr, radiation effects on properties of $ZrNb_3Sn_x$, neutron, 18: 14545(T,R) (EURAEC-863)
Nb–Sn–Zr, radiation effects on corrosion and mechanical properties of, neutron, 18: 18418(T,R) (EURAEC-971)
Nb–Sn–Zr, radiation effects on corrosion and mechanical properties of, neutron, 18: 32235(T,R) (EURAEC-1068)
Nb–Sn–Zr, radiation effects on corrosion and mechanical properties of, neutron, 18: 37612 (A/CONF.28/P/477)
Nb–Sn–Zr, radiation effects on oxidation by low-oxygen water, neutron, 19: 16016(R) (HW-84281(p.5.1-5))
Nb–Sn–Zr, radiation effects on corrosion and mechanical properties of, neutron, 19: 16208(R) (EURAEC-1249)
Nb–Sn–Zr, radiation effects on corrosion and mechanical properties of, neutron, 20: 11354
Nb–Sn–Zr, radiation effects on corrosion of, by water, effects of fabrication history on fast-neutron, 20: 23767 (BNWL-88)
Nb–Sn–Zr, stability of martensite structure at 400 to 700°C at times to 2000 hr, 19: 14041
Nb–Sn–Zr, stability of martensite structure in zirconium-base, 20: 11227
Nb–Sn–Zr, superconductivity of fused, 20: 15123
Nb–Sn–Zr, tensile properties of, effects of oxygen on, 16: 15184 (KAPL-2000-17)
Nb–Sn–Zr, tensile properties of, effects of composition and heat treatment on, 16: 29380 (TID-6155)

Nb–Sn–Zr, thermal cycling of, changes in length by, 16: 19380(T,R) (EURAEC-201)
Nb–Sn–Zr, treatment for improved corrosion resistance, 17: 36216(P)
Nb–Sn–Zr, welding, 17: 6535(T) (EURAEC-352)
Nb–stainless steel–Zr, compatibility studies, 20: 8447 (PWAC-491)
Nb–stainless steel, creep and oxidation properties of, 17: 30927
Nb–Ta, atomic structure of solid solutions of, x-ray-scattering study of, (E), 20: 43975(T)
Nb–Ta, corrosion by hydrochloric, phosphoric, and sulfuric acids, effects of alloy composition on, 20: 14997
Nb–Ta, critical currents in superconducting, 18: 22833
Nb–Ta, current distribution in type II superconductors of, 20: 40029
Nb–Ta, current flow patterns in superconducting, in longitudinal fields, (E/T), 20: 17617
Nb–Ta, deformation in tantalum-base, mechanisms of thermally activated, 20: 29724
Nb–Ta, degassing, fusion, and sintering of, vacuum techniques for, 16: 12046
Nb–Ta, electric and mechanical properties, 18: 24158
Nb–Ta, electric current capacity in superconducting, 17: 24085
Nb–Ta, electric conductivity in the mixed state of superconducting, r-f, (E/T), 20: 24286
Nb–Ta, electron beam melting, 17: 3375(R) (ASD-TR-7-826(II))
Nb–Ta, electron tunneling in superconducting point contacts of, infrared frequency response of, (E), 20: 44548
Nb–Ta, fabrication and properties of high-temperature, 20: 27472 (BMI-1777)
Nb–Ta, Ginzburg-Landau parameters of superconducting, (E/T), 20: 2906
Nb–Ta, Hall effect in superconducting sheets of, (E), 19: 19039
Nb–Ta, Hall effect in superconducting, (E), 19: 39710
Nb–Ta, hardness, 20: 15073
Nb–Ta, magnetic flux motion in, 18: 40446
Nb–Ta, magnetic flux line motion in superconducting, (E/T), 19: 8355
Nb–Ta, magnetic flux motion in superconducting, (E/T), 20: 21910
Nb–Ta, magnetic induction measurements for superconducting, 17: 37717
Nb–Ta, magnetic properties of superconducting, 20: 36359(R) (TID-22992)
Nb–Ta, magnetization of nonideal type-II superconducting wires of, Procopiu-effect analog in longitudinal, (E), 20: 24277
Nb–Ta, mechanical properties of, effects of composition on, 17: 24001
Nb–Ta, mechanical properties, 17: 31010
Nb–Ta, mechanical properties at 1100 and 1300°C, 19: 11734
Nb–Ta, mechanical properties of, effects of composition on, 20: 11288(T) (AD-622477)
Nb–Ta, oxidation rate of, at 1100°C, 20: 23614
Nb–Ta, paramagnetic susceptibility, 16: 10576
Nb–Ta, paramagnetic helical current flow in superconducting, (E), 19: 23576
Nb–Ta, phase studies based on thermochemical data, 18: 33603
Nb–Ta, powder metallurgy, 17: 3375(R) (ASD-TR-7-826(II))
Nb–Ta, production of, by electrolysis, 16: 12040
Nb–Ta, properties at high temperatures, effects of carbon, molybdenum, oxygen, titanium, tungsten, and zirconium on, 19: 37151(P)
Nb–Ta, properties at high temperatures, effects of carbon, oxygen, titanium, and zirconium on, 19: 37152(P)
Nb–Ta, radiation effects on superconducting properties of, 18: 10583
Nb–Ta, resistive states in superconducting, 18: 15065
Nb–Ta, segregation of tantalum by controlled solidification of, effects of titanium additions on, 20: 14969
Nb–Ta, shear properties of single crystal, effects of composition on, 20: 37215
Nb–Ta, specific heat of superconducting, in magnetic fields, (E), 20: 2906
Nb–Ta, spectrographic analysis for hafnium, thorium, titanium, and zirconium simultaneously, 18: 19912
Nb–Ta, structure of intermediate state of superconducting, (E), 19: 10191
Nb–Ta, superconducting resistive transitions in, 18: 11124
Nb–Ta, superconducting critical currents in, effect of surface conditions on, 20: 28185
Nb–Ta, superconducting current distribution in sheets of, 20: 30273
Nb–Ta, superconductivity of, time effects in, 18: 16881
Nb–Ta, surface barrier to magnetic flux penetration of, 18: 9262(R) (NP-13492)
Nb–Ta, surface barrier in superconducting, 18: 22842
Nb–Ta, surface current in mixed state of superconducting wires of, (E/T), 20: 26048
Nb–Ta, temperature dependence of mixed-state upper critical field in, 17: 29456
Nb–Ta, tensile properties at 3000°F, 18: 12562(R) (X63-12299)
Nb–Ta, thermal capacity of superconducting, in magnetic fields, 18: 40457
Nb–Ta, thermal capacity of superconducting, in magnetic fields, 20: 4786
Nb–Ta, thermal conductivity of single crystals of, 18: 36494
Nb–Ta, thermal conductivity of superconducting, (E/T), 20: 34428
Nb–Ta, work function of, 19: 7958
Nb–Ta, work hardening in tantalum-base, mechanisms of, 20: 4384(R) (ORNL-3870, pp 7-14)
Nb–Ta, yield strength of, effects of oxygen on, 17: 18811
Nb–Ta–Sn, superconductivity of, 17: 406 (ASD-TDR-62-269)
Nb–Ta–Sn, superconductivity of fused, 20: 15123
Nb–Ta–Sn–V, superconductivity of, 17: 406 (ASD-TDR-62-269)
Nb–Ta–Sn–V, superconducting properties of $(Nb,Ta,V)_3Sn$ (E), 19: 1504
Nb–Ta–Ti, coating of, for oxidation protection at 2300°F, 19: 20483 (SCNC-318)
Nb–Ta–Ti, properties of arc-melted, 19: 27768(R) (SCNC-308)
Nb–Ta–Ti–V, coating by pack siliconization, 18: 37621(R) (IITRI-B6021-3)
Nb–Ta–Ti–V, coating for oxidation protection, 19: 20459(R) (IITRI-B6019-6)
Nb–Ta–Ti–V, creep properties and fabrication, 19: 13885(R) (IITRI-B6021-4)
Nb–Ta–Ti–V, effects of boron, carbon, hafnium, and silicon on fabrication and tensile properties on, 19: 32719(R) (AD-609727)
Nb–Ta–Ti–V, fabrication and properties, 17: 4924(R) (ARF-B231-7)
Nb–Ta–Ti–V, fabrication and properties at high temperatures, 18: 37621(R) (IITRI-B6021-3)
Nb–Ta–Ti–V, fabrication and mechanical properties of sheet of, 19: 20552 (IITRI-B6021-6)
Nb–Ta–Ti–V, mechanical properties of, at 2000°F, 16: 33444(R) (ARF-2231-6)
Nb–Ta–Ti–V, oxidation of siliconized, at 2200°F, 17: 23942(R) (ARF-B6001-3)
Nb–Ta–Ti–V, oxidation life at 2200°F of siliconized, static, 17: 35997(R) (IITRE-B6001-5)
Nb–Ta–Ti–V, preparation and properties, 16: 22577(R) (ARF-2231-4)
Nb–Ta–Ti–W, brazing, method for, 20: 25556(P)
Nb–Ta–V, arc melting, 17: 3375(R) (ASD-TR-7-826(II))
Nb–Ta–V, availability, properties, and uses of, 20: 29760
Nb–Ta–V, brazing techniques for, 19: 30690(R) (ML-TDR-64-270)
Nb–Ta–V, coating of, with aluminum–silicon in tin, 16: 24163(R) (NP-11711)
Nb–Ta–V, coating of, with ceramics and metals, 16: 24148(R) (ASD-TR-61-676)
Nb–Ta–V, coating with silicides and silicon for protection against oxidation to 4000°F, 18: 30105(R) (AD-429028)
Nb–Ta–V, coatings for, development of aluminum–tin and silicide, 16: 29341 (NP-11990)
Nb–Ta–V, coatings for, for high-temperature uses, 16: 27687
Nb–Ta–V, development as brazing alloy for refractory metals, 20: 4301(R) (ORNL-3870, pp 102-35)
Nb–Ta–V, development and properties of, 20: 31709(R) (IITRI-B6042-5)
Nb–Ta–V, fabrication of rolled sheet, 17: 6597(R) (DMIC-176)
Nb–Ta–V, fabrication and properties of dispersion-strengthened, 18: 5732(R) (IITRI-B6007-5)
Nb–Ta–V, fabrication and properties of sheet bar of, 18: 10508
Nb–Ta–V, fabrication and mechanical properties of sheet of, 19: 20552(R) (IITRI-B6021-6)
Nb–Ta–V, forging characteristics, 16: 9162 (DMIC-Memo-143)
Nb–Ta–V, mechanical properties and quality of, effects of processing variables on, 16: 19336 (ASD-TR-61-684)
Nb–Ta–V, mechanical properties of, effects of composition on, 17: 24001
Nb–Ta–V, mechanical properties, 17: 31010
Nb–Ta–V, mechanical properties and stability of dispersion-strengthened, 17: 30971(R) (IITRI-B6007-3)
Nb–Ta–V, oxidation of, protective effects of aluminum-tin, beryllide, and silicon-titanium coatings against, 17: 22109(R) (ASD-TDR-63-160)
Nb–Ta–V, phase diagram, 19: 41036
Nb–Ta–V, preparation and properties, 16: 22577(R) (ARF-2231-4)
Nb–Ta–V, properties of, at cryogenic and ultrahigh temperatures, 16: 545
Nb–Ta–V, properties as brazing alloy material, 17: 29320(R) (GEMP-23A)
Nb–Ta–V, properties of, data tabulations of mechanical, metallurgical, and physical, 18: 5774 (DMIC-189)
Nb–Ta–V, tensile properties of vanadium-base, effects of carbon and silicon additions on, 20: 21333(R) (IITRI-B6042-4)
Nb–Ta–V, thermal properties, 18: 7201 (ASD-TDR-63-597)
Nb–Ta–V, thermal properties to melting point, 20: 878
Nb–Ta–V–Zr, strength at high temperatures, 20: 2407(P)
Nb–Ta–W, bend tests of electron-beam welds in SCb-291, 19: 13954(R) (WANL-PR(P)-004)
Nb–Ta–W, corrosion of, by fluorine-containing fluids, 17: 8750(P)

Nb–Ta–W, corrosion by boiling sodium, 19: 22890 (BNL-9018)
Nb–Ta–W, corrosion by sodium at 1260°C, 19: 28764
Nb–Ta–W, corrosion by sodium at 1266°C, 19: 36949(R) (BNL-900 (p.121-97))
Nb–Ta–W, corrosion by refluxing potassium at 1800 to 2400°F, 20: 25485 (NASA-TN-D-3429)
Nb–Ta–W, creep strength of, effects of composition on, 20: 11302
Nb–Ta–W, development, 16: 12045
Nb–Ta–W, fabrication and tensile properties at high temperatures, 18: 12562(R) (X63-12299)
Nb–Ta–W, fabrication and properties of SCb-291 foil, 19: 24945 (ASD-TDR-63-829(Pt.I))
Nb–Ta–W, mechanical properties at 2600°F of coated, evaluation of, 17: 16633(R) (AD-296341)
Nb–Ta–W, mechanical properties of, effects of composition on, 17: 24001
Nb–Ta–W, properties of, for use as high-temperature structural materials, 16: 3443 (ASD-TR-61-3)
Nb–Ta–W, tensile and creep properties at 2800 to 3400°F, 17: 37506 (BLR-62-26)
Nb–Ta–W, tensile properties of SCb-291, effects of welds on, 20: 29712(R) (WANL-PR-(P)-009)
Nb–Ta–W, tensile strength at 1100 to 1900°C, 17: 30950(R) (NMI-2117)
Nb–Ta–W, weld bend tests of SCb-291, 19: 13955(R) (WANL-PR-(P)-005)
Nb–Ta–W, weldability study of SCb-291, 19: 24957(R) (WANL-PR(P)-006)
Nb–Ta–W, weldability studies of SCb-291, 19: 46966(R) (WANL-PR(P)-007)
Nb–Ta–W, welding of SCb-291, electron-beam and tungsten-arc, 18: 22426(R) (WANL-PR(P)-002)
Nb–Ta–W, welding of SCb-291, tungsten-arc, 18: 34058(R) (WANL-PR(P)-003)
Nb–Ta–W–Zr, analysis for alloying elements and impurities, comparison of results from 25 laboratories on FS-85, 20: 18567 (MAB-217-M)
Nb–Ta–W–Zr, analysis using vacuum cup electrode, 19: 22103 (TIM-904)
Nb–Ta–W–Zr, bonding of FS-85, to Inconel 600 and stainless steels, process development for explosive, 20: 21295(R) (WANL-PR-(EE)-002)
Nb–Ta–W–Zr, bonding to Hastelloy N, Inconel 600, and types 321 and 347 stainless steels of FS-85, explosive, 20: 11243(R) (WANL-PR(EE)-001)
Nb–Ta–W–Zr, coating of FS-85, with chromium–molybdenum–silicon and chromium–silicon–titanium systems, 18: 14353(R) (AD-408310)
Nb–Ta–W–Zr, coating of FS-85, with platinum and platinum–rhodium alloy, 18: 20445(R) (AD-434441)
Nb–Ta–W–Zr, coating of FS-85, with palladium–platinum alloy and platinum, 18: 34029(R) (AD-601740)
Nb–Ta–W–Zr, coating of FS-85 for oxidation protection at high temperatures, 19: 7845(R) (AD-608135)
Nb–Ta–W–Zr, coating of FS-85 for oxidation protection, development of diffusion barriers for ductile, 19: 36957(R) (NP-15113)
Nb–Ta–W–Zr, coatings on FS-85, properties of oxidation-resistant, 19: 26801(R) (AD-607530)
Nb–Ta–W–Zr, contamination of FS-85, by residual gases in high vacuum, 18: 39826 (ORNL-3674)
Nb–Ta–W–Zr, corrosion of platinum- and platinum–rhodium-clad FS-85, by air at 2200 and 2550°F, 18: 20445(R) (AD-434441)
Nb–Ta–W–Zr, corrosion of FS-85 by boiling cesium, 19: 13913(R) (AFML-TR-64-327)
Nb–Ta–W–Zr, corrosion of FS-85, by lithium, effects of oxygen on, 20: 4301(R) (ORNL-3870, pp 102-35)
Nb–Ta–W–Zr, corrosion by lithium in niobium–1-zirconium alloy forced-convection loop, 20: 5853 (TIM-898)
Nb–Ta–W–Zr, creep behavior in ultrahigh vacuum at 2000 and 2200°F, 20: 13256 (NASA-TN-D-3222)
Nb–Ta–W–Zr, creep of FS-85, at 2000°F and 4000 psi stress under vacuum conditions, 18: 44142(R) (NASA-CR-54123)
Nb–Ta–W–Zr, creep of FS-85, at 2000 to 2200°F in ultrahigh vacuum, 20: 21344 (N-65-26653)
Nb–Ta–W–Zr, creep properties of FS-85, 20: 4301(R) (ORNL-3870, pp 102-35)
Nb–Ta–W–Zr, creep properties of FS-85, 20: 31669
Nb–Ta–W–Zr, creep test data of FS-85 at 2000°F and 7000 psi, 19: 9662(R) (NASA-CR-54228)
Nb–Ta–W–Zr, creep-rupture of FS-85 at 982 to 1204°C, effects of annealing on, 20: 35895 (ORNL-TM-1456)
Nb–Ta–W–Zr, ductility of FS-85, effects of aging on bend, 20: 4301(R) (ORNL-3870, pp 102-35)
Nb–Ta–W–Zr, ductility transition temperature of FS-85, effects of protective coatings and welding on, 20: 27466
Nb–Ta–W–Zr, evaporation tests of FS-85 in high vacuum, 18: 44049(R) (ORNL-3670(p.77-111))
Nb–Ta–W–Zr, evaporation losses of FS-85, at 1200 to 1500°C in high vacuum, 19: 37043 (ORNL-P-1394)
Nb–Ta–W–Zr, evaporation losses in high vacuum of FS-85, 20: 4301(R) (ORNL-3870, pp 102-35)
Nb–Ta–W–Zr, fabricability, strength, and weldability of, 20: 29763
Nb–Ta–W–Zr, fabrication and properties, 18: 7265
Nb–Ta–W–Zr, fabrication of FS-85, by rolling, 18: 12593(R) (AD-411155)
Nb–Ta–W–Zr, fabrication and mechanical properties of FS-85, 18: 18292(R) (N63-20341)
Nb–Ta–W–Zr, fabrication of FS-85, by forging, 18: 20484(R) (AD-418992)
Nb–Ta–W–Zr, fabrication and properties of forged and rolled FS-85, 18: 24093(R) (AD-424593)
Nb–Ta–W–Zr, fabrication and properties of FS-85 sheet, 18: 30106(R) (AD-430773)
Nb–Ta–W–Zr, fabrication FS-85 into sheets, 18: 30146(R) (AD-414497)
Nb–Ta–W–Zr, fabrication by forging and cold rolling, 19: 11711
Nb–Ta–W–Zr, fabrication and properties of FS-85 sheet, 19: 20499(R) (AD-606291)
Nb–Ta–W–Zr, mechanical properties, 17: 14802(R) (AD-278727)
Nb–Ta–W–Zr, mechanical properties of coated and uncoated FS-85, in air to 2600°F, 17: 36188(R) (AD-289857)
Nb–Ta–W–Zr, mechanical properties of FS-85, 19: 13978 (AMRA-TR-64-16)
Nb–Ta–W–Zr, preparation and specifications for corrosion loop testing, 20: 4380 (NASA-CR-54761)
Nb–Ta–W–Zr, properties as space reactor fuel cladding, 18: 9713 (CONF-375-3)
Nb–Ta–W–Zr, properties of coated FS-85, to 2600°F, 18: 14353(R) (AD-408310)
Nb–Ta–W–Zr, properties of welds in FS-85, 19: 40989
Nb–Ta–W–Zr, properties as hollow turbine vanes, 20: 16963
Nb–Ta–W–Zr, tensile properties of FS-85 at room temperature to 2600°F, 17: 36279(R) (AD-287509)
Nb–Ta–W–Zr, tensile properties of FS-85, effects of welds on, 20: 29712(R) (WANL-PR-(P)-009)
Nb–Ta–W–Zr, thermal properties, 18: 7201 (ASD-TDR-63-597)
Nb–Ta–W–Zr, thermal properties to melting point, 20: 878
Nb–Ta–W–Zr, weld bend tests of FS-85, 19: 13955(R) (WANL-PR-(P)-005)
Nb–Ta–W–Zr, weldability of FS-85, 17: 39498 (DMIC-Memo-169)
Nb–Ta–W–Zr, weldability of FS-85 sheet, 18: 44049(R) (ORNL-3670 (p.77-111))
Nb–Ta–W–Zr, weldability study of FS-85, 19: 24957(R) (WANL-PR(P)-006)
Nb–Ta–W–Zr, weldability studies of FS-85, 19: 46966(R) (WANL-PR(P)-007)
Nb–Ta–W–Zr, weldability of FS-85, effects of oxygen contamination on, 20: 13264(R) (WANL-PR(P)-008)
Nb–Ta–W–Zr, weldability of FS-85, effects of oxygen contamination on, 20: 29712(R) (WANL-PR-(P)-009)
Nb–Ta–W–Zr, weldability evaluation of, 20: 39366
Nb–Ta–W–Zr, welding of FS-85, electron-beam and tungsten-arc, 18: 34058(R) (WANL-PR(P)-003)
Nb–Ta–W–Zr, welding properties of FS-85, 20: 27466
Nb–Ta–Y–Zr, grain size and hardness of, effects of yttrium additions on, 19: 40953 (PWAC-441)
Nb–Ta–Zr, coating evaluation for FS-82, 19: 9607 (ML-TDR-64-70)
Nb–Ta–Zr, corrosion by lithium at 2000 to 3000°F, 18: 14420
Nb–Ta–Zr, forging characteristics, 16: 9162 (DMIC-Memo-143)
Nb–Ta–Zr, nitrogen and oxygen contents of, effects of yttrium additions on, 19: 40953 (PWAC-441)
Nb–Ta–Zr, properties for use in thermal protective systems in space vehicles, 18: 32199
Nb–Ta–Zr, radiation effects on fuel rod jackets of, 19: 26876 (ANL-6750)
Nb–Ta–Zr, reactions with uranium monocarbide at 1000 to 2400°C, 18: 8795 (HW-72031)
Nb–Ta–Zr, superconducting critical currents at 4.2°K, 17: 554
Nb–Ta–Zr, superconductivity, 17: 4886(R) (AD-275610)
Nb–Ta–Zr, superconducting critical current density in, effect of microheterogeneity on, 20: 40020
Nb–Ta–Zr, welding, 16: 30741 (ASD-TDR-62-292)
Nb–Tc, magnetic susceptibility and NMR measurements in, 18: 8837
Nb–Tc, phase studies on, 17: 11220
Nb–Th, corrosion by water at 120 to 260°C, 19: 22889 (ANL-7006)
Nb–Th, phase studies, 16: 30877
Nb–Th, superconducting properties of eutectic, 17: 32650
Nb–Th–U, mechanical properties and phase studies at high temperatures, 17: 12660 (ATL-A-128)
Nb–Th–Zr, corrosion by water at 300 to 500°C, 17: 39651
Nb–Th–Zr, phase studies and structure at 550 to 1100°C, 17: 39650
Nb–Ti, analysis of, for titanium, titrimetric, 16: 1722
Nb–Ti, analysis of, x-ray fluorescence, 16: 22008 (TIM-576)
Nb–Ti, bulk superconductivity in, 18: 24553
Nb–Ti, calculation of upper critical field of, 17: 20452 (BSD-TDR-

63-62)
Nb–Ti, coating of, for oxidation protection at 2300°F, 19: 20483 (SCNC-318)
Nb–Ti, coating with aluminum–tin-base alloys for protection against oxidation, 17: 39465 (SCNC-328(Del.))
Nb–Ti, coating with aluminum alloy for oxidation protection, 20: 4315(P)
Nb–Ti, corrosion of, by steam and water, 16: 29346
Nb–Ti, corrosion by steam at 1000°F, 17: 493(R) (BMI-X-10003)
Nb–Ti, corrosion by steam at 1000°F, 17: 23890(R) (BMI-X-10040)
Nb–Ti, corrosion by liquid sodium, 18: 21698(R) (ANL-6860)
Nb–Ti, corrosion by lithium at 2000°F, 19: 36980 (PWAC-355)
Nb–Ti, corrosion by hydrochloric, phosphoric, and sulfuric acids, effects of alloy composition on, 20: 14997
Nb–Ti, critical currents in superconducting coils and wire of, 17: 24062 (UCRL-10402)
Nb–Ti, critical current density of superconducting, in transverse field of 30 kgauss, 18: 6128
Nb–Ti, critical currents in cold-rolled, anisotropy of, 18: 36524
Nb–Ti, critical current training in superconducting, (E), 19: 10215
Nb–Ti, critical currents of superconducting, effect of magnetic-field rise time on, (E), 19: 43238
Nb–Ti, current density and magnetic field in cold-worked superconductors of, (E), 19: 41637
Nb–Ti, development of superconducting magnets of, (E/T), 19: 6607
Nb–Ti, development and properties of, as brazes for joining aluminum oxide and niobium–zirconium alloy, 20: 27445 (LA-DC-7159)
Nb–Ti, diffusion of iron and niobium in, 16: 15207
Nb–Ti, diffusion in, 17: 34454
Nb–Ti, diffusion of niobium in, at 1000 to 2000°C, 19: 18461 (NRL-6221)
Nb–Ti, diffusion in bcc, 19: 23112
Nb–Ti, electric and mechanical properties, 18: 24158
Nb–Ti, electric conductivity of, at 1.1 to 3.5°K, maxima in, 16: 27818
Nb–Ti, electric conductivity and mechanical properties of, effects of platinum metals on, 19: 26872
Nb–Ti, evaporation of titanium from, vapor pressure determinations by, 19: 25012
Nb–Ti, fabrication by rolling, 18: 15663(R) (ANL-6808)
Nb–Ti, fabrication and properties, 18: 26893(R) (ANL-6868(p.11-108))
Nb–Ti, fabrication, properties, testing, and uses of superconducting, 19: 16110
Nb–Ti, filament structure of superconducting, 18: 18846
Nb–Ti, flux jumping and training in superconducting solenoids of, 18: 26470
Nb–Ti, forging characteristics, 16: 9162 (DMIC-Memo-143)
Nb–Ti, formation and aging characteristics of α-martensitic phase in quenched, 18: 16508
Nb–Ti, friction and wear of, at high temperatures and in vacuum, 16: 5708 (ASD-TR-61-301)
Nb–Ti, hardness, 20: 15073
Nb–Ti, internal friction of, effects of nitrogen and oxygen on, 19: 23035
Nb–Ti, local order in, x-ray diffuse scattering studies of, 17: 36289 (ASD-TDR-63-567(Pt.I))
Nb–Ti, local order and solution strengthening in, 19: 6312
Nb–Ti, magnetic flux penetration in superconducting, (E), 20: 42132
Nb–Ti, magnetic induction measurements for superconducting, 17: 37717
Nb–Ti, magnetic resistivity of, at 1.1 to 4.2°K, negative-value non-existance in, 16: 27818
Nb–Ti, maximum critical field of superconductors of, 17: 8959
Nb–Ti, mechanical and metallurgical properties, 16: 4547 (WADC-TR-59-595(Pt.II))
Nb–Ti, mechanical properties at high temperatures, 16: 10509 (DC-56-3-115)
Nb–Ti, mechanical properties at 1100 and 1300°C, 19: 11734
Nb–Ti, mechanical properties of, effects of composition on, 20: 11288(T) (AD-622477)
Nb–Ti, oxidation at 500 to 1200°C, 17: 37486
Nb–Ti, oxidation at 1000 to 1200°C, 18: 34079
Nb–Ti, oxidation, 18: 37627
Nb–Ti, oxidation of coated, by air at high temperatures, 19: 27768(R) (SCNC-308)
Nb–Ti, oxidation, 20: 5896 (TID-22388)
Nb–Ti, oxidation protection by aluminum–tin coatings with chromium and titanium additions, 20: 7580 (TIM-945)
Nb–Ti, oxidation rate of, at 1100°C, 20: 23614
Nb–Ti, performance in 100-kOe superconducting electromagnets, 18: 30227
Nb–Ti, phase studies on, 20: 5896 (TID-22388)
Nb–Ti, preparation and properties of thin-film hard superconducting, 18: 28501
Nb–Ti, properties, 16: 3492
Nb–Ti, properties of welded, 17: 11242
Nb–Ti, properties for high-temperature use, additive effects of borides, carbides, and oxides on, 18: 14454 (BM-RI-6390)
Nb–Ti, properties of arc-melted, 19: 27768(R) (SCNC-308)
Nb–Ti, properties and structure of, 20: 46205
Nb–Ti, reactions with metals at 540 to 760°C *in vacuo*, 19: 44606 (PWAC-483)
Nb–Ti, recrystallization temperature and strength of, effects of titanium content on, 20: 7618
Nb–Ti, solvent properties of, for oxygen at 1000°C, 16: 13611
Nb–Ti, superconducting, effects of temperature on critical field in, 16: 15467
Nb–Ti, superconductivity, 16: 16830
Nb–Ti, superconductivity of thin wires of, 17: 8858
Nb–Ti, superconductivity of, pulsed-magnetic-field studies of, 17: 18907 (TID-17310)
Nb–Ti, superconducting critical currents at 4.2°K, 17: 28101
Nb–Ti, superconductivity, 17: 34438
Nb–Ti, superconductivity, 17: 37560
Nb–Ti, superconductivity of, upper critical fields for, 18: 2776
Nb–Ti, superconductivity of, mechanism for high-field, 18: 4499
Nb–Ti, superconducting critical alternating currents in, 18: 13018
Nb–Ti, superconducting properties of, 18: 28524
Nb–Ti, superconductivity of, surface effects on, 18: 34683(R) (NP-14136)
Nb–Ti, superconducting transition temperature, effects of phase transformation on, 18: 42025(T) (AI-Trans-49)
Nb–Ti, superconducting properties, 18: 44681
Nb–Ti, superconductivity of, (E), 19: 6613
Nb–Ti, superconductivity and phase transformations, 19: 7965
Nb–Ti, superconducting critical current and magnetization of, (E), 19: 8338
Nb–Ti, superconducting transition anomalies in, (E), 19: 10214
Nb–Ti, superconducting properties of, 19: 12453
Nb–Ti, superconducting critical currents in solenoids passing through lambda point, s-c, (E), 19: 14438
Nb–Ti, superconducting critical currents in, effect of circulating currents on, 19: 23551
Nb–Ti, superconductivity of, effects of heat treatment on, 19: 23108
Nb–Ti, superconducting-normal transitions in variable fields, mechanisms of, (E), 20: 2902
Nb–Ti, superconducting critical fields in, Pauli paramagnetism effects on upper, (E), 20: 6236
Nb–Ti, superconductivity of, 20: 13666 (IPP-4/22)
Nb–Ti, superconducting critical field of, spin-orbit effects on upper, (E), 20: 32330
Nb–Ti, superconducting critical current of, effect of precipitates on, 20: 32322
Nb–Ti, superconducting properties of, at elevated temperatures, 20: 34417(R) (N-65-34464)
Nb–Ti, temperature dependence of mixed-state upper critical field in, 17: 29456
Nb–Ti, tensile properties, 18: 37695
Nb–Ti, transformation characteristics during continuous cooling, 18: 20545
Nb–Ti, upper critical fields of superconducting, 18: 11109
Nb–Ti, volatilization of titanium from, for preparation of electrolytic capacitor anodes, 19: 16035
Nb–Ti, x-ray diffraction of nonmetallic phases chemically extracted from, 19: 7973
Nb–Ti–U, phase studies at 600, 650, and 1000°C, 17: 39630
Nb–Ti–V, aging characteristics and phase studies, 16: 6746
Nb–Ti–V, annealing, 17: 35078(R) (ANL-6739)
Nb–Ti–V, coating development for, 16: 2168(R) (ARF-2227-2)
Nb–Ti–V, coating for oxidation protection at high temperatures, 19: 15996(R) (IITRI-B6019-4)
Nb–Ti–V, coating for oxidation protection at 1800 to 2500°F, 19: 20459(R) (IITRI-B6019-6)
Nb–Ti–V, coating of, with nickel by flame spraying, oxidation tests of, 16: 6706(R) (ARF-2227-3)
Nb–Ti–V, coating with silicide, 17: 12610(R) (ARF-B6001-2)
Nb–Ti–V, coating with silicides for high-temperature oxidation protection, 17: 30938(R) (NP-12971)
Nb–Ti–V, coatings of pack-siliconized, effects of processing time at 2000 to 2200°F on thickness of, 17: 35997(R) (IITRE-B6001-5)
Nb–Ti–V, compatibility with sodium at 650°C, 17: 41333(R) (ANL-6677)
Nb–Ti–V, compatibility with sodium at 650°C, 18: 26893(R) (ANL-6868 (p.11-108))
Nb–Ti–V, corrosion of, by steam and water, 16: 29346
Nb–Ti–V, corrosion by steam at 1000°F, 17: 493(R) (BMI-X-10003)
Nb–Ti–V, corrosion by steam at 1000°F, 17: 23890(R) (BMI-X-10040)
Nb–Ti–V, corrosion by sodium at 650°C, 17: 35078(R) (ANL-6739)
Nb–Ti–V, corrosion by sodium at 650°C, 17: 36861(R) (ANL-6764)
Nb–Ti–V, corrosion by flowing sodium at 650°C, 17: 37001(R) (ANL-6780)

Nb–Ti–V, corrosion by sodium at 650°C, 18: 15663(R) (ANL-6808)
Nb–Ti–V, corrosion by sodium at 650°C, 19: 31462(R) (ANL-7028)
Nb–Ti–V, corrosion by sodium at 650°C, effects of oxygen on, 19: 35604(R) (ANL-7045(p.1-23))
Nb–Ti–V, corrosion by acids and bases of vanadium-base, 20: 11230 (BM-RI-6715)
Nb–Ti–V, creep and tensile properties of, at 1800°F, 16: 6747
Nb–Ti–V, creep-rupture testing at 870°C, 18: 4255(R) (ORNL-3470(p.98-125))
Nb–Ti–V, development of, for high-temperature uses, 16: 5680 (ARF-2210-6)
Nb–Ti–V, development and properties of, as brazes for joining aluminum oxide and niobium–zirconium alloy, 20: 27445 (LA-DC-7159)
Nb–Ti–V, development and properties of, 20: 31709(R) (IITRI-B6042-5)
Nb–Ti–V, effect of silicide coatings on ductile-to-brittle transition of, 19: 32692(R) (AD-426040)
Nb–Ti–V, elastic properties and shear modulus of annealed and quenched, 18: 35999
Nb–Ti–V, elastic properties, 20: 6556(R) (ANL-7105, pp 36-58)
Nb–Ti–V, evaluation of properties of, 19: 15995 (IITRI-B231-11)
Nb–Ti–V, evaporation tests of Armour alloy in high vacuum, 18: 44049(R) (ORNL-3670(p.77-111))
Nb–Ti–V, fabrication and high-temperature properties of, effects of nitrogen and oxygen on, 16: 12084(R) (ARF-2231-2)
Nb–Ti–V, fabrication and high-temperature strength, 16: 6707 (ARF-2231-1)
Nb–Ti–V, fabrication and tensile properties of, effects of nitrogen and oxygen on, 16: 16712(R) (ARF-2231-3)
Nb–Ti–V, fabrication of, evaluation of methods and additives for, 16: 29348 (ARF-2231-5)
Nb–Ti–V, fabrication by rolling, 18: 15663(R) (ANL-6808)
Nb–Ti–V, fabrication and properties at high temperatures, effects of molybdenum, tantalum, and tungsten additions on, 18: 22418(R) (IITRI-B6021-1)
Nb–Ti–V, fabrication and properties, 18: 26893(R) (ANL-6868(p.11-108))
Nb–Ti–V, fabrication for fuel-coating tests, 19: 14765(R) (ANL-6977)
Nb–Ti–V, fabrication and mechanical properties of sheet of, 19: 20552(R) (IITRI-B6021-6)
Nb–Ti–V, forgeability and tensile strength, 17: 25771 (ASD-TDR-62-667)
Nb–Ti–V, hardening by carbide and oxide dispersions, 17: 41428(R) (IITRI-B6007-4)
Nb–Ti–V, hardness of sodium-treated, 17: 35079(R) (ANL-6749)
Nb–Ti–V, mechanical properties of, at 2000°F, effects of interstitials on, 16: 2167(R) (ARF-2210-5)
Nb–Ti–V, mechanical and oxidation properties, 17: 41427(R) (IITRI-B231-9)
Nb–Ti–V, mechanical properties of, effects of pack silicide coatings on, 18: 39819(R) (IITRI-B6019-5)
Nb–Ti–V, melting points, 18: 44497(R) (MND-2812-2)
Nb–Ti–V, microstructure of, effects of annealing temperature on, 19: 44587(R) (ANL-7000, pp 3-63)
Nb–Ti–V, oxidation of aluminum coated, 17: 12656 (AD-277779)
Nb–Ti–V, oxidation of siliconized, at 2200°F, 17: 23942(R) (ARF-B6001-3)
Nb–Ti–V, oxidation life at 2150 to 2200°F of siliconized, effects of preparation method on static, 17: 35997(R) (IITRE-B6001-5)
Nb–Ti–V, oxidation protection by aluminum–tin coatings with chromium and titanium additions, 20: 7580 (TIM-945)
Nb–Ti–V, oxidation by air at 900 to 1200°C, kinetics and mechanisms of, 20: 37191
Nb–Ti–V, preparation and properties, 16: 22577(R) (ARF-2231-4)
Nb–Ti–V, properties as cladding for reactor fuel elements, 18: 6412(R) (GEAP-3888)
Nb–Ti–V, properties as fuel cladding, 19: 24064(R) (ANL-6997)
Nb–Ti–V, protective coatings for, 17: 6562(R) (ARF-B-6001-1)
Nb–Ti–V, radiation effects on mechanical properties up to 750°C, neutron, 20: 41506
Nb–Ti–V, tensile properties of vanadium-base, effects of carbon and silicon additions on, 20: 21333(R) (IITRI-B6042-4)
Nb–Ti–V, use as brazing alloy for fabrication of refractory metals, 18: 44049(R) (ORNL-3670(p.77-111))
Nb–Ti–V–Zr, oxidation of siliconized, at 2200°F, 17: 23942(R) (ARF-B6001-3)
Nb–Ti–V–Zr, oxidation life at 2200°F of siliconized, static, 17: 35997(R) (IITRE-B6001-5)
Nb–Ti–V–Zr, phase studies, 18: 549(R) (NP-13241)
Nb–Ti–V–Zr, properties, 19: 26848
Nb–Ti–V–Zr, properties, effects of composition on, 20: 2340 (ORNL-TM-1131)
Nb–Ti–W, composition and preparation of oxidation-resistant, 17: 36218(P)
Nb–Ti–W, creep strength of, effects of composition on, 20: 11302
Nb–Ti–W, properties of, mechanical and physical, 19: 11740
Nb–Ti–W, shear strength of fasteners of, at room temperature and 1600°F, 17: 36281 (AD-295526)
Nb–Ti–W–V, coating for oxidation protection, 19: 20459(R) (IITRI-B6019-6)
Nb–Ti–W–V, oxidation of siliconized, at 2200°F, 17: 23942(R) (ARF-B6001-3)
Nb–Ti–W–V, oxidation life at 2200°F of siliconized, static, 17: 35997(R) (IITRE-B6001-5)
Nb–Ti–W–V, preparation and properties, 16: 22577(R) (ARF-2231-4)
Nb–Ti–W–V, properties for elevated-temperature service, 19: 6241 (BM-RI-6558)
Nb–Ti–W–V–Zr, properties for elevated-temperature service, 19: 6241 (BM-RI-6558)
Nb–Ti–Zr, annealing, 17: 35078(R) (ANL-6739)
Nb–Ti–Zr, bend tests of coated D-36, 19: 7844(R) (AD-602500)
Nb–Ti–Zr, bonding of D-36, method for diffusion, 20: 5867
Nb–Ti–Zr, brazing of honeycomb structures of, 18: 39874
Nb–Ti–Zr, brazing, equipment and methods for, 18: 27938
Nb–Ti–Zr, coatings for D-36 foils, development of high-temperature oxidation-resistant, 18: 30118(R) (RTD-TDR-63-4006(Pt.I))
Nb–Ti–Zr, corrosion of, by steam and water, 16: 29346
Nb–Ti–Zr, corrosion by steam at 1000°F, 17: 493(R) (BMI-X-10003)
Nb–Ti–Zr, corrosion by potassium at 1500 to 1800°F, 18: 5728 (ASD-TDR-63-270(Pt.II))
Nb–Ti–Zr, corrosion by sodium at 650°C, 18: 15663(R) (ANL-6808)
Nb–Ti–Zr, corrosion by potassium vapor at 1500 to 1800°F, 18: 18282 (BNL-844)
Nb–Ti–Zr, corrosion by sodium at 650°C, 18: 26893(R) (ANL-6868(p.11-108))
Nb–Ti–Zr, ductility transition temperature of D-36, effects of protective coatings and welding on, 20: 27466
Nb–Ti–Zr, fabrication of high-quality tubing of, 17: 16603 (ANL-FGF-409)
Nb–Ti–Zr, fabrication and testing of brazed honeycomb sandwich panels of D-36, 18: 10494 (AD-427700(p.245-80))
Nb–Ti–Zr, fabrication and properties, 18: 26893(R) (ANL-6868(p.11-108))
Nb–Ti–Zr, fabrication and properties of D-36 foil, 19: 24945 (ASD-TDR-63-829(Pt.I))
Nb–Ti–Zr, fabrication and properties of D-36 strip and foil, 19: 24946 (ASD-TDR-63-829(Pt.II))
Nb–Ti–Zr, fabrication of honeycombed-sandwich panels from D-36, 20: 7541
Nb–Ti–Zr, joining of foils of D-36, for honeycomb panel fabrication, 18: 37661 (ASD-TDR-63-799(Pt.I))
Nb–Ti–Zr, microstructure of, effects of annealing temperature on, 19: 44587(R) (ANL-7000, pp 3-63)
Nb–Ti–Zr, oxidation of, at 1000°C, 16: 9248(P)
Nb–Ti–Zr, oxidation of, by air above 700°C, 16: 3408 (NP-11119)
Nb–Ti–Zr, oxidation, 18: 7157
Nb–Ti–Zr, oxidation-resistant coatings on D-36, performance of commercial, 20: 16973 (NASA-TN-D-3275)
Nb–Ti–Zr, phase diagram, 16: 5743
Nb–Ti–Zr, phase studies on, at 570 to 1100°C, 20: 29785
Nb–Ti–Zr, properties, 18: 2163(R) (IS-700(Sect.M))
Nb–Ti–Zr, properties of D-36 foils at high temperatures, effects of coatings on mechanical and thermophysical, 18: 34128 (RTD-TDR-63-4068)
Nb–Ti–Zr, shear strength of fasteners of, at room temperature and 1600°F, 17: 36281 (AD-295526)
Nb–Ti–Zr, superconductivity of, effects of composition on, 20: 29784
Nb–Ti–Zr, superconductivity of, effects of cold working and heat treatments on, 20: 29787
Nb–Ti–Zr, superconductivity of, effects of microstructure on, 20: 29788
Nb–Ti–Zr, thermal properties, 18: 7201 (ASD-TDR-63-597)
Nb–Ti–Zr, thermal properties to melting point, 20: 878
Nb–Ti–Zr, welding of brazed joints of, electron-beam, 18: 32123
Nb–Ti–Zr, welding properties of D-36, 20: 27466
Nb–transition metal, critical temperature of superconducting, 20: 1129
Nb–U, analysis for impurities, visual, 17: 6528 (TID-7625(p.45-51))
Nb–U, analysis of, for iron, absorptiometric, 16: 12957 (PG-Report-272)
Nb–U, analysis of, for uranium by controlled-potential coulometry, 17: 23269
Nb–U, casting of, testing of products from, 20: 29803
Nb–U, combustion kinetics of, 20: 43612
Nb–U, corrosion of, by sodium at 1600 and 1800°C, 16: 17966(R) (BMI-1541(Del.))
Nb–U, corrosion mechanisms of, stress, 16: 12056
Nb–U, corrosion by water at 650°F, alloying effects of platinum on, 18: 16449(P)
Nb–U, decomposition of gamma solid solution in, mechanism of, 16: 30831
Nb–U, detection of metastable phases in, 18: 18385
Nb–U, development of high-temperature plutonium-spiked, 16: 14375(R) (BMI-1557(Del.))

Nb–U, diffusion of uranium in, mechanism of, 16: 2223
Nb–U, diffusion in, 17: 39608
Nb–U, fabrication, 18: 3298(R) (ORNL-2221(Pts.1-5)(Del.))
Nb–U, fabrication and properties of impregnated, 18: 4270
Nb–U, formation of oriented oxide films on gamma-phase, 17: 16536
Nb–U, grain size of end-quenched, 19: 23047
Nb–U, isothermal transformations of gamma-phase, 19: 40958
Nb–U, mechanical properties, 17: 14740 (TID-11295(2nd Ed.))
Nb–U, mechanical properties of, 17: 39636
Nb–U, mechanical properties and phase studies, 17: 39637
Nb–U, mechanical properties and phase studies, 17: 39625
Nb–U, mechanical properties, 17: 39635
Nb–U, mechanical properties of gamma-phase uranium-base, 20: 15060 (UCRL-7771)
Nb–U, mechanical properties, 20: 29803
Nb–U, metallography of irradiated, 19: 13572
Nb–U, metallographic tests on arc melted, 20: 29775
Nb–U, microstructure of uranium-rich, effects of heat treatments on, 20: 21372
Nb–U, neutron activation of uranium-238 in thin plates of, 17: 2097
Nb–U, phase diagram and structure, 16: 30857
Nb–U, phase diagram, 16: 30858
Nb–U, phase diagram of, determination of, by solid-state diffusion, 16: 3496
Nb–U, phase diagram of, determination of, by solid-state diffusion, 16: 22603(T) (HW-tr-37)
Nb–U, phase diagrams of, metastable phases in, 20: 23717
Nb–U, phase studies, 16: 22616
Nb–U, phase studies, 16: 30858
Nb–U, phase studies and properties of, at 450 and 500°C, 16: 30871
Nb–U, phase studies, 17: 29255 (ZFK-WF-13)
Nb–U, phase studies, 17: 39624
Nb–U, phase studies, 17: 39632
Nb–U, phase studies and radiation effects on, 18: 37618 (A/CONF.28/P/864)
Nb–U, phase studies, 19: 11679
Nb–U, phase studies, 19: 20587
Nb–U, phase studies, 20: 11224
Nb–U, phase studies, 20: 17035
Nb–U, phase studies on uranium-rich, 20: 21372
Nb–U, phase transformation, effects of cooling rate on onset temperature for $\gamma \rightarrow \beta$, 17: 16672
Nb–U, phase transformations, 18: 14477 (UCRL-7595)
Nb–U, phase transformations in, 18: 24124 (CEA-2341)
Nb–U, phase transformation kinetics, 18: 37677 (A/CONF.28/P/701)
Nb–U, phase transitions in, effects of heat treatment on, 19: 7939
Nb–U, phase transformations and microstructure of, effects of heat treatment on, 19: 14024
Nb–U, phase transformation kinetics in, 20: 17036
Nb–U, preparation and use as reactor fuel in foamy state, 17: 41478(P)
Nb–U, preparation, 18: 2163(R) (IS-700(Sect.M))
Nb–U, preparation by carbon reduction of mixed oxides, 19: 9604(R) (IS-900(Sect.M))
Nb–U, processing by volatilization, 18: 37280 (A/CONF.28/P/771)
Nb–U, production of niobium-base, method for, 20: 41412(R) (IS-1500 (Sect. M))
Nb–U, properties of, as fuel alloy at high temperatures, 16: 24633
Nb–U, properties for use as fuel element in gas-graphite reactors, 18: 4818
Nb–U, properties as reactor fuel, 18: 34130 (TID-8540(p.331-410))
Nb–U, properties as reactor fuel, 18: 42024 (UJV-926/63)
Nb–U, properties as fuel, material, 20: 25614(P)
Nb–U, radiation effects on, at 1600 and 1800°F, 16: 4450(R) (BMI-1546(Del.))
Nb–U, radiation effects on dimensional stability of, 16: 28642(R) (BMI-1581(Del.))
Nb–U, radiation effects on, 17: 3882
Nb–U, radiation effects on stability, 17: 3378(R) (BMI-1583(Del.))
Nb–U, radiation and fission fragment effects on, 19: 11810
Nb–U, reactions of, with hydrogen at 264 and 571°C, 16: 17665
Nb–U, reactions of, with hydrogen at 264 and 571°C, 16: 17665
Nb–U, segregation in arc-melted, mechanism and methods for eliminating, 18: 22454 (BMI-1218)
Nb–U, self-diffusion coefficients of gamma-phase uranium in, 16: 29416
Nb–U, self-diffusion in, 17: 23872(R) (TID-18626)
Nb–U, spectrographic analysis for aluminum, 18: 35451 (PG-Report-390)
Nb–U, structure of, effects of cooling rate from gamma phase on, 18: 34127 (RT/MET(64)-2)
Nb–U, structures, tempered from the γ region, 17: 14870
Nb–U, superconducting transitions in high magnetic fields, 17: 25938
Nb–U, thermal cycling effects on dimensional stability of, 16: 9657(R) (NAA-SR-1109)
Nb–U, transformation of retained β phase in, by tempering from $\beta + \gamma$, range, kinetics of, 17: 27824
Nb–U, transformation of gamma phase of, isothermal, 19: 7910 (UCRL-7824)
Nb–U, uranium recovery from scrap, 16: 11774(R) (NLCO-685)
Nb–U–Zr, corrosion of, by sodium at 1600 and 1800°C, 16: 17966(R) (BMI-1541(Del.))
Nb–U–Zr, corrosion mechanisms of, stress, 16: 12056
Nb–U–Zr, corrosion, 17: 39640
Nb–U–Zr, corrosion resistance and dimensional stability of, methods of preparation for, 18: 44093(P)
Nb–U–Zr, fabrication of corrosion-resistant dimensionally-stable, 17: 22148(P)
Nb–U–Zr, fission product release from, in TREAT meltdown, 19: 17174(R) (ANL-6900(p.232-303))
Nb–U–Zr, mechanical properties and phase studies, 17: 39642
Nb–U–Zr, mechanical properties, 17: 41333(R) (ANL-6677)
Nb–U–Zr, mechanical properties of gamma-phase uranium-base, 20: 15060 (UCRL-7771)
Nb–U–Zr, mechanical properties of gamma-phase, effects of dynamic loading on, 20: 27496 (UCRL-14805)
Nb–U–Zr, phase studies and structure, 16: 30862
Nb–U–Zr, phase studies and polythermal diagrams, 16: 30863
Nb–U–Zr, phase studies and structure, 16: 30864
Nb–U–Zr, phase studies, 17: 39632
Nb–U–Zr, phase studies and properties of, 18: 39912 (UCRL-7869)
Nb–U–Zr, properties of metastable γ-phase, 20: 5843
Nb–U–Zr, properties of, at 150 to 350°C, mechanical and physical, 20: 21356 (UCRL-14724)
Nb–U–Zr, radiation effects on, reactor-excursion, 19: 31462(R) (ANL-7028)
Nb–U–Zr, reactions of molybdenum with uranium in, 18: 34174
Nb–U–Zr, reactions with water during Kiwi-TNT transients, 20: 20925(R) (ANL-7055, pp 177-212)
Nb–U–Zr, thermal cycling effects on crystal structure and dimensional stability, 17: 39639
Nb–U–Zr, transformation of gamma phase of, isothermal, 19: 7910 (UCRL-7824)
Nb–V, coating development for oxidation protection of, at high temperatures, 16: 19334(R) (ARF-2227-5)
Nb–V, coating for oxidation protection, 19: 20459(R) (IITRI-B6019-6)
Nb–V, compatibility with sodium at 650°C, 17: 41333(R) (ANL-6677)
Nb–V, composition and mechanical and physical properties of, 18: 7267
Nb–V, corrosion of, by steam and water, 16: 29346
Nb–V, corrosion resistance, 16: 10464
Nb–V, corrosion by superheated steam, 17: 20417
Nb–V, corrosion by steam at 1000°F, 17: 23890(R) (BMI-X-10040)
Nb–V, corrosion by steam at 1000°F, 18: 2184
Nb–V, corrosion by potassium at 1500 to 1800°F, 18: 5728 (ASD-TDR-63-270(Pt.II))
Nb–V, corrosion by steam at 540 and 650°C, 18: 8747(R) (BMI-X-10071)
Nb–V, corrosion by potassium vapor at 1500 to 1800°F, 18: 18282 (BNL-844)
Nb–V, corrosion by liquid sodium, 18: 21698(R) (ANL-6860)
Nb–V, corrosion by steam at 540 and 650°C, 18: 22415(R) (BMI-X-10082)
Nb–V, corrosion by lithium at 815°C, effects of oxygen on, 20: 2340 (ORNL-TM-1131)
Nb–V, corrosion by acids and bases of vanadium-base, 20: 11230 (BM-RI-6715)
Nb–V, corrosion by hydrochloric, phosphoric, and sulfuric acids, effects of alloy composition on, 20: 14997
Nb–V, corrosion by refluxing potassium at 1800 to 2400°F, 20: 25485 (NASA-TN-D-3429)
Nb–V, creep and tensile properties of, at 1800°F, 16: 6747
Nb–V, creep and tensile properties, 17: 32568 (CONF-53-5)
Nb–V, creep strength and ductility of, effects of mechanical twinning on, 20: 15049(R) (N65-16256)
Nb–V, creep testing of, summary of slow-bend, 18: 4255(R) (ORNL-3470(p.98-125))
Nb–V, deformation twinning in, 18: 42019 (ORNL-3678)
Nb–V, development of, for high-temperature uses, 16: 5680 (ARF-2210-6)
Nb–V, development and properties of, as brazes for joining aluminum oxide and niobium–zirconium alloy, 20: 27445 (LA-DC-7159)
Nb–V, diffusion penetration of, by plutonium–uranium alloys, 16: 28555 (TID-7623(p.105-21))
Nb–V, diffusion in bcc, 19: 23112
Nb–V, diffusion kinetics, 19: 42837 (AD-610234)
Nb–V, dislocation and mechanical twinning in, effects of impurities on, 17: 23961 (ORNL-TM-542)
Nb–V, ductile-to-brittle transitions in, enhancement of, 20: 43893 (KAPL-3119)
Nb–V, ductile-to-brittle transitions in, grain boundary effects on, 20: 43894 (KAPL-3146)
Nb–V, ductility, strength, and weldability of, 18: 14448

Nb–V, effects of additives on dispersion strength of, 17: 23943(R)
Nb–V, evaluation for use in lithium-cooled reactors, 18: 44049(R) (ORNL-3670(p.77-111))
Nb–V, fabrication of, evaluation of methods and additives for, 16: 29348 (ARF-2231-5)
Nb–V, fabrication and properties, 17: 4924(R) (ARF-B231-7)
Nb–V, fabrication, oxidation, and properties for use above 2000°F, 17: 39562
Nb–V, fabrication and properties of dispersion-strengthened, 18: 5732(R) (IITRI-B6007-5)
Nb–V, fabrication and properties, 18: 26893(R) (ANL-6868(p.11-108))
Nb–V, fabrication and properties of, effects of metals and carbon on, 18: 27858(R) (IITRI-B6007-6)
Nb–V, fabrication, properties, testing, and uses of superconducting, 19: 16110
Nb–V, fabrication and mechanical properties of sheet of, 19: 20552(R) (IITRI-B6021-6)
Nb–V, hardness, 20: 15073
Nb–V, hydrogen embrittlement, 16: 2256
Nb–V, interdiffusion in, 19: 47058
Nb–V, lattice defect observations in crystals of, use of electron microscopy for, 18: 4251(R) (ORNL-3470(p.49-52))
Nb–V, machinability, properties, weldability, and workability of, 17: 32581
Nb–V, mechanical properties of, at high temperatures, 16: 19339 (BM-RI-5987)
Nb–V, mechanical properties of, effects of composition on, 17: 24001
Nb–V, mechanical properties and stability of dispersion-strengthened, 17: 30971(R) (IITRI-B6007-3)
Nb–V, melting points, 18: 44497(R) (MND-2812-2)
Nb–V, oxidation protection of, at 2000 to 2400°F, coatings for, 16: 27587 (ARF-2227-6)
Nb–V, oxidation of aluminum coated, 17: 12656 (AD-277779)
Nb–V, oxidation kinetics of, 18: 7156
Nb–V, oxidation of, temperature dependence of, 20: 16982
Nb–V, oxidation rate of, at 1100°C, 20: 23614
Nb–V, performance as cladding for plutonium–uranium fuel alloys, (E), 20: 14007(R) (ANL-7122, pp 1-41)
Nb–V, properties of welded, 17: 11242
Nb–V, properties as high-temperature brazing alloys, 17: 25688(R) (GEMP-177A)
Nb–V, properties as brazing alloy material, 17: 29320(R) (GEMP-23A)
Nb–V, properties as fuel element cladding, 18: 15563
Nb–V, properties for high-temperature brazing, 19: 11669(R) (GEMP-41A)
Nb–V, radiation effects on fuel rod jackets of, 19: 26876 (ANL-6750)
Nb–V, radioinduced twinning in, neutron, 20: 39462
Nb–V, structural properties of solid solutions of, 19: 13979 (ASD-TDR-63-567(Pt.II))
Nb–V, tensile and creep properties at 2800 to 3400°F, 17: 37506 (BLR-62-26)
Nb–V, tensile strength of B-33, at 1100 to 1400°C, 17: 30950(R) (NMI-2117)
Nb–V, thermal expansion of, 20: 43964
Nb–V, thermodynamic properties, 16: 13636
Nb–V, twinning in, relation of dislocation substructure to, 20: 4389(R) (ORNL-3870, pp 61-4)
Nb–V, twinning transition temperature, effects of oxygen and vanadium content on, 19: 30809
Nb–V, twinning transition temperature, effects of cold-rolling reduction and annealing temperature on, 19: 30809
Nb–V–Zircaloy-2, radiation effects on phases in, neutron, 18: 39999 (KAPL-2251)
Nb–V–Zr, corrosion of, by steam and water, 16: 29346
Nb–V–Zr, creep properties of, at 982 and 1204°C, 20: 27545
Nb–V–Zr, creep testing of, summary of slow-bend, 18: 4255(R) (ORNL-3470(p.98-125))
Nb–V–Zr, development and properties of niobium-base Cb-753, 20: 19214 (N-65-22097)
Nb–V–Zr, melting points, 18: 44497(R) (MND-2812-2)
Nb–V–Zr, phase studies, 17: 11108(T,R) (EURAEC-307)
Nb–V–Zr, phase studies, 17: 14749(T,R) (EURAEC-408)
Nb–V–Zr, phase studies, 18: 28036
Nb–V–Zr, preparation and properties, 16: 22577(R) (ARF-2231-4)
Nb–V–Zr, properties of Cb-753, 20: 21411
Nb–V–Zr, radiation effects on phases in, neutron, 18: 39999 (KAPL-2251)
Nb–W, analysis for niobium and tungsten, gravimetric, 20: 10794
Nb–W, arc melting behavior, effects of oxygen, titanium, and zirconium additions on, 17: 22127(R) (ASD-TDR-63-296)
Nb–W, corrosion of, by steam and water, 16: 29346
Nb–W, corrosion of, by fluorine-containing fluids, 17: 8750(P)
Nb–W, corrosion by cesium and lithium above 2500°F, 19: 28766
Nb–W, corrosion by lithium at high temperatures, 20: 2269
Nb–W, corrosion by liquid lithium and cesium vapor at 2500 to 3400°F, 20: 5851
Nb–W, corrosion by cerium–cobalt–plutonium alloy fuels, effects of carbon on, 20: 31679(R) (LA-3524)
Nb–W, corrosion by molten plutonium alloys, carbon effects on, 20: 43829(R) (LA-3582)
Nb–W, creep strength of, effects of composition on, 20: 11302
Nb–W, diffusion coefficients for, at 1700 to 2300°C, 20: 35926
Nb–W, electric and mechanical properties, 18: 24158
Nb–W, electronic structure of, at superconducting critical temperatures, 20: 31747
Nb–W, extrusion of, comparison of high-velocity and conventional, 17: 1889 (ASD-TDR-62-506)
Nb–W, extrusion and properties of, 19: 18419(R) (AD-424207)
Nb–W, extrusion and swaging, 20: 15101
Nb–W, fabrication and tensile properties of, effects of carbides on, 17: 27812(R) (WADD-TR-61-134(Pt.II))
Nb–W, fabrication and properties, 18: 5727(R) (AD-294579)
Nb–W, fabrication of, effects on mechanical properties, 18: 20485 (ASD-TDR-62-670(Pt.II))
Nb–W, fabrication and properties of high-temperature, 20: 27472 (BM-RI-6777)
Nb–W, factors affecting vacuum-arc melting of, 18: 24070 (RTD-TDR-63-4089)
Nb–W, hardness, 20: 15073
Nb–W, kinetics of hot-press sintering of powdered, 17: 8770
Nb–W, magnetic induction measurements for superconducting, 17: 37717
Nb–W, mechanical properties of, effects of composition on, 17: 24001
Nb–W, mechanical properties at 1100 and 1300°C, 19: 11734
Nb–W, mechanical properties of, effects of composition on, 20: 11288(T) (AD-622477)
Nb–W, mechanical properties of, 20: 33875 (N-66-16551)
Nb–W, oxidation kinetics at 900 to 1300°C, 19: 34648
Nb–W, oxidation kinetics at 500 to 900°C, 20: 5854(T) (JPRS-32341, pp 8-16)
Nb–W, oxidation by air at 900 to 1300°C, effects of niobium content on, 20: 5851
Nb–W, oxidation at 900 to 1300°C, 20: 46201
Nb–W, preparation of vacuum-arc-cast, 16: 18016(R) (AD-265129)
Nb–W, preparation of thin films of, for transmission electron microscopy, 20: 27464
Nb–W, preparation and properties of single crystals of, 20: 41481
Nb–W, production by arc-melting, 17: 22127(R) (ASD-TDR-63-296)
Nb–W, properties of, evaluation of, for alkali metal containment, 16: 21037(R) (NP-11614)
Nb–W, properties of welded, 17: 11242
Nb–W, properties for high-temperature uses, 20: 15101
Nb–W, reactions with cesium at 3400°F, metallographic specimen preparation of, 19: 46954 (NMI-5025(Pt.I), pp 39-58)
Nb–W, reactions with uranium carbide, nitride, and dioxide, metallographic specimen preparation of, 19: 46954 (NMI-5025(Pt.I), pp 39-58)
Nb–W, solid-state bonding of, 18: 24112
Nb–W, tensile properties of, effects of thermal-mechanical processing variables on short-time, 18: 2215 (ASD-TDR-63-782)
Nb–W, tensile properties at 3000°F, 18: 12562(R) (X63-12299)
Nb–W, tensile properties of, effects of carbon, vanadium, and zirconium on, 18: 34197
Nb–W, tensile properties of, 20: 37245
Nb–W–V, mechanical properties of, effects of composition on, 17: 24001
Nb–W–V, oxidation of siliconized, at 2200°F, 17: 23942(R) (ARF-B6001-3)
Nb–W–V, oxidation life at 2200°F of siliconized, static, 17: 35997(R) (IITRE-B6001-5)
Nb–W–V, phase diagram, properties, and structure of vanadium-rich corner of, 19: 9681
Nb–W–V, preparation and properties, 16: 22577(R) (ARF-2231-4)
Nb–W–V, properties for elevated-temperature service, 19: 6241 (BM-RI-6558)
Nb–W–V–Zr, ductility, strength, and weldability of, 18: 14448
Nb–W–V–Zr, mechanical properties of, effects of carbon on, 17: 34419(R) (WADC-TR-57-344(Pt.VII))
Nb–W–V–Zr, properties for elevated-temperature service, 19: 6241 (BM-RI-6558)
Nb–W–Y–Zr, corrosion by refluxing potassium at 1800 to 2400°F, 20: 25485 (NASA-TN-D-3429)
Nb–W–Zr, aging characteristics of Cb-752 and D-43, 18: 44049(R) (ORNL-3670(p.77-111))
Nb–W–Zr, alloying effects of carbon on creep properties, 17: 1998(P)
Nb–W–Zr, bend tests of coated Cb-752 and D-43, 19: 7844(R) (AD-602500)
Nb–W–Zr, bend tests of electron-beam welds in Cb-752, 19: 13954(R) (WANL-PR(P)-004)
Nb–W–Zr, bonding of, controlling factors in diffusion, 19: 24964

Nb–W–Zr, brazing, equipment and methods for, 18: 27938
Nb–W–Zr, casting and testing of Cb-752 and D-43 ingots, 18: 571(R) (AD-297246)
Nb–W–Zr, coating of D-43, with chromium–silicon–titanium systems and silicides, 18: 14373(R) (NP-13498)
Nb–W–Zr, coating of, with oxidation-resistant silicides, fluidized-bed process for, 20: 43881
Nb–W–Zr, coatings on Cb-752, properties of oxidation-resistant, 19: 26801(R) (AD-607530)
Nb–W–Zr, coatings on D-43, performance of Disil, 19: 37034 (N64-27085)
Nb–W–Zr, contamination of Cb-752, by residual gases in high vacuum, 18: 39826 (ORNL-3674)
Nb–W–Zr, corrosion by sodium at 650°C, 18: 15663(R) (ANL-6808)
Nb–W–Zr, corrosion by sodium at 650°C, 18: 26893(R) (ANL-6868 (p.11-108))
Nb–W–Zr, corrosion protection by silicide coatings, 19: 11682
Nb–W–Zr, corrosion by boiling sodium, 19: 22890 (BNL-9018)
Nb–W–Zr, corrosion by sodium at 1260°C, 19: 28764
Nb–W–Zr, corrosion by sodium at 1266°C, 19: 36949(R) (BNL-900 (p.121-97))
Nb–W–Zr, corrosion by flowing lithium, 20: 2238
Nb–W–Zr, corrosion by bismuth and tin, 20: 2275
Nb–W–Zr, corrosion of Cb-752, by lithium, effects of oxygen on, 20: 4301(R) (ORNL-3870, pp 102-35)
Nb–W–Zr, corrosion by refluxing potassium at 1800 to 2400°F, 20: 25485 (NASA-TN-D-3429)
Nb–W–Zr, creep behavior in ultrahigh vacuum at 2000 and 2200°F, 20: 13256 (NASA-TN-D-3222)
Nb–W–Zr, creep of AS-30 at 2000°F, long-time, 19: 18459(R) (NASA-CR-54287)
Nb–W–Zr, creep properties of Cb-752, 20: 4301(R) (ORNL-3870, pp 102-35)
Nb–W–Zr, creep tests on AS-30 at 3200°F, 20: 5885(R) (NAS-CR-54773)
Nb–W–Zr, creep-rupture properties of D-43, temperature dependence, 18: 44049(R) (ORNL-3670(p.77-111))
Nb–W–Zr, creep-rupture properties of, 20: 2336 (ORNL-P-1634)
Nb–W–Zr, ductility and tensile properties of arc-welded D-43, 19: 37034 (N64-27085)
Nb–W–Zr, ductility transition temperature of Cb-752 effects of protective coatings and welding on, 20: 27466
Nb–W–Zr, effect of carbon on phase equilibria of, 19: 32729(R) (DRI-1092-211)
Nb–W–Zr, effects of carbon on phase equilibria in, 19: 22973(R) (DRI-1092-203)
Nb–W–Zr, effects of carbon and oxygen on phase equilibria in, 20: 7558 (DRI-1092-221)
Nb–W–Zr, effects of carbon and oxygen additions on phase equilibria in, 20: 7559(R) (DRI-1092-225)
Nb–W–Zr, effects of carbon and oxygen on phase equilibria in niobium-rich region of, 20: 21329(R) (DRI-1092-229)
Nb–W–Zr, erosion by mercury vapor of Cb-752, 20: 11214(R) (NASA-CR-54717)
Nb–W–Zr, evaporation tests of D-43 in high vacuum, 18: 44049(R) (ORNL-3670(p.77-111))
Nb–W–Zr, evaporation losses of D-43, at 1200 to 1500°C in high vacuum, 19: 37043 (ORNL-P-1394)
Nb–W–Zr, extrusion, 17: 3445(R) (NP-12225)
Nb–W–Zr, fabricability, strength, and weldability of, 20: 29763
Nb–W–Zr, fabrication of sheets, 17: 8757(R) (NP-12446)
Nb–W–Zr, fabrication into H sections, 18: 7163(R) (NP-13410)
Nb–W–Zr, fabrication of rolled sheets of D-43 and Cb-752, 18: 12591(R) (AD-409960)
Nb–W–Zr, fabrication of H sections of Cb-752 and D-43, by drawing and extrusion, 18: 12595(R) (AD-429144)
Nb–W–Zr, fabrication and properties of extruded and rolled D-43, 18: 22411(R) (AD-417692)
Nb–W–Zr, fabrication and properties of coated D-43, 18: 24068(R) (NP-13955)
Nb–W–Zr, fabrication and properties of Cb-752 sheet, 18: 34025(R) (AD-428036)
Nb–W–Zr, fabrication and properties of rolled sheets of Cb-752, 19: 882(R) (AD-600403)
Nb–W–Zr, fabrication and properties of forged Cb-752, 19: 6240(R) (ASD-8-170(V))
Nb–W–Zr, fabrication and properties of rolled Cb-752, 19: 6239(R) (ASD-8-108(VI))
Nb–W–Zr, fabrication and properties of Cb-752 foil, 19: 24945 (ASD-TDR-63-829(Pt.I))
Nb–W–Zr, fabrication and properties of Cb-752 strip and foil, 19: 24946 (ASD-TDR-63-829(Pt.II))
Nb–W–Zr, fasteners for use to 3000°F, 19: 32702(R) (AD-609653)
Nb–W–Zr, forging characteristics, 16: 9162 (DMIC-Memo-143)
Nb–W–Zr, forging of, method optimization for closed-die, 16: 15152(R) (ASD-TR-7-782(VIII))
Nb–W–Zr, grain size and microhardness of D-43, effects of annealing temperature on, 19: 37034 (N64-27085)
Nb–W–Zr, hardness of annealed and as-cast, 18: 32138(R) (DRI-2166)
Nb–W–Zr, machining, properties, welding, and working of, 18: 14486
Nb–W–Zr, mechanical properties of Pfaudler silicide and TRW chromium–silicon–titanium-coated D-43, in air at 70 to 2600°F, 18: 20523(R) (NP-13811)
Nb–W–Zr, mechanical properties of Cb-752 and D-43, 19: 13978 (AMRA-TR-64-16)
Nb–W–Zr, phase diagram, 17: 3531
Nb–W–Zr, phase diagram, 18: 8809(T) (JPRS-22593)
Nb–W–Zr, phase equilibria of niobium-rich regions, 17: 16641(R) (DRI-2091)
Nb–W–Zr, phase equilibria in, effects of carbon and oxygen on, 20: 35885(R) (DRI-1092-232)
Nb–W–Zr, phase studies, 17: 39529(R) (DRI-2117)
Nb–W–Zr, phase studies, 18: 8792(R) (DRI-2131)
Nb–W–Zr, phase studies on, 18: 16494
Nb–W–Zr, phase studies, 18: 32138(R) (DRI-2166)
Nb–W–Zr, preparation and properties of, 17: 27779(R) (DRI-2102)
Nb–W–Zr, properties of, for alkali metal containment, 16: 24165(R) (NP-11824)
Nb–W–Zr, properties of Cb-752 as structural material for re-entry vehicles, 18: 7203 (D2-35105)
Nb–W–Zr, properties of coated D-43, to 2600°F, 18: 14373(R) (NP-13498)
Nb–W–Zr, properties of X-110, to 2600°F, 18: 14353(R) (AD-408310)
Nb–W–Zr, properties as hollow turbine vanes, 20: 16963
Nb–W–Zr, radiation effects on mechanical properties of Nb-752, neutron, 18: 14537(R) (HW-79766(p.4.1-76))
Nb–W–Zr, radiation effects on hardness of Cb-752, at 50°C, 18: 32043(R) (HW-81269(p.4.1-64))
Nb–W–Zr, radiation effects on ductility of D-43, fast-neutron, 18: 44049(R) (ORNL-3670(p.77-111))
Nb–W–Zr, radiation effects on mechanical properties of Cb-752, neutron, 19: 30820 (BNWL-23)
Nb–W–Zr, radiation effects on tensile properties of Cb-752, neutron, 20: 27571(R) (BNWL-207, pp 4.1-3)
Nb–W–Zr, rolling of foils of Nb-752, 19: 7871(R) (AD-422001)
Nb–W–Zr, stress effects in corrosion of D-43, by potassium, 20: 2270
Nb–W–Zr, stress-corrosion of D-43, in potassium at 2000 to 2200°F, 19: 9622(R) (NASA-CR-54200)
Nb–W–Zr, tensile and creep properties at 2800 to 3400°F, 17: 37506 (BRL-62-26)
Nb–W–Zr, tensile properties of D-43, to 3000°F, 19: 37034 (N64-27085)
Nb–W–Zr, tensile properties of, effects of disilicide coatings on, 20: 27549
Nb–W–Zr, tensile properties of Cb-752, effects of welds on, 20: 29712(R) (WANL-PR-(P)-009)
Nb–W–Zr, tensile properties of, 20: 37245
Nb–W–Zr, thermal properties, 18: 7201 (ASD-TDR-63-597)
Nb–W–Zr, thermal properties to melting point, 20: 878
Nb–W–Zr, thermophysical properties of D-43, 18: 44049(R) (ORNL-3670(p.77-111))
Nb–W–Zr, weld bend tests of Cb-752, 19: 13955(R) (WANL-PR-(P)-005)
Nb–W–Zr, weld structural stability in, 18: 22459(R) (NP-13816)
Nb–W–Zr, weldability of D-43 sheets, 18: 44049(R) (ORNL-3670 (p.77-111))
Nb–W–Zr, weldability study of Cb-752, 19: 24957(R) (WANL-PR(P)-006)
Nb–W–Zr, weldability studies of Cb-752, 19: 46966(R) (WANL-PR(P)-007)
Nb–W–Zr, weldability evaluation of, 20: 39366
Nb–W–Zr, welding of Nb-752 and D-43, electron-beam and tungsten-arc, 18: 22426(R) (WANL-PR(P)-002)
Nb–W–Zr, welding of Cb-752 and D-43, tungsten-arc, 18: 34058(R) (WANL-PR(P)-003)
Nb–W–Zr, welding properties of Cb-752, 20: 27466
Nb–Y, corrosion by lithium at high temperatures, 20: 4299(R) (ORNL-2711)
Nb–Y, crystal structure and phase studies, 18: 12623 (ASD-TDR-63-204)
Nb–Y, phase diagram, 19: 23005(T) (JPRS-28849(p.158-65))
Nb–Y, phase studies, 16: 19394
Nb–Y, phase studies and atmospheric corrosion, 16: 5315 (WADD-TR-61-123)
Nb–Y, phase studies of solid solution formation in, 19: 41050
Nb–Y–Zr, corrosion by steam at 400-500°C, 20: 2276(P)
Nb–Y–Zr, grain size and hardness of, effects of yttrium additions on, 19: 40953 (PWAC-441)
Nb–Y–Zr, preparation for use in nuclear reactors, 20: 9561(P)
Nb–Zircaloy-4–Zr, fabrication of tubular, methods for, 19: 47998(R) (SRO-118)

Nb–Zircaloy-2, radiation effects on phases in, neutron, 18: 39999 (KAPL-2251)
Nb–Zn, crystal structure of intermetallic compounds in, 20: 11328
Nb–Zn, oxidation resistance of intermetallic compounds, 18: 7271
Nb–Zn, phase diagram, 16: 499 (NRL-5643)
Nb–Zn, phase diagram, 16: 6543 (ONR-9(Vol.I)(p.104-27))
Nb–Zn, phase diagram, 20: 31669
Nb–Zn, phase studies, 19: 23077
Nb–Zn, properties of, as protective coating for niobium, 16: 6543 (ONR-9(Vol.I)(p.104-27))
Nb–Zn, properties as high-temperature coating, 20: 29650
Nb–Zn, structure of intermetallic compound $NbZn_3$ in, 16: 5731
Nb–Zn, superconductivity of, critical persistent currents in, 17: 6875
Nb–Zn, vapor pressures of compounds in, 16: 499 (NRL-5643)
Nb–Zn–Zr, mechanical properties, 18: 7292(R) (HW-77954(p.4.1-12))
Nb–Zr, a-c conductivity of superconducting, 17: 41541 (BSD-TDR-63-147)
Nb–Zr, a-c losses in superconducting wires of, 17: 28099
Nb–Zr, a-c resistance of, 17: 20538 (BSD-TDR-63-60)
Nb–Zr, a-c power losses in superconducting, 18: 36426
Nb–Zr, aging characteristics, 16: 15192 (ORNL-3245)
Nb–Zr, aging of, 16: 30167 (ORNL-3313(p.19-64))
Nb–Zr, aging studies of, 20: 5181(R) (ORNL-3029)
Nb–Zr, aging studies on welds of, 20: 5181(R) (ORNL-3029)
Nb–Zr, analysis for niobium, spectrophotometric, 18: 35465
Nb–Zr, analysis for zirconium by spectrography of solutions, 20: 14446 (N64-25607)
Nb–Zr, analysis of electron-beam welds of, 19: 22984(R) (NASA-CR-54167)
Nb–Zr, analysis of, gamma spectra measurements in activation, 19: 38566
Nb–Zr, annealing effects on superconductivity in, 16: 12131
Nb–Zr, annealing, 17: 35078(R) (ANL-6739)
Nb–Zr, annealing specifications for, 20: 35110 (CNLM-5584(Vol.3))
Nb–Zr, anodization measurements of compositional segregation in, 18: 4250(R) (ORNL-3470(p.45-8))
Nb–Zr, anomalous critical currents in superconducting noninductive coils of, (E), 20: 13674
Nb–Zr, attenuation of 5- to 30-Mc elastic waves in superconducting, 17: 11400
Nb–Zr, beta phase stabilization in, 17: 11213
Nb–Zr, bonding of, to Inconel 600 and stainless steels, process development for explosive, 20: 21295(R) (WANL-PR-(EE)-002)
Nb–Zr, bonding to aluminum and beryllium oxides, 18: 41928(R) (NASA-CR-54089)
Nb–Zr, bonding to beryllium, 19: 11711
Nb–Zr, bonding to metallized alumina, brazing alloy for, 19: 40980 (LA-3302)
Nb–Zr, bonding to alumina–yttria, brazing alloy for, 19: 40980 (LA-3302)
Nb–Zr, bonding to types 321 and 347 stainless steels, explosive, 20: 11243(R) (WANL-PR(EE)-001)
Nb–Zr, bonding to aluminum oxide, development and properties of brazes for, 20: 27445 (LA-DC-7159)
Nb–Zr, brazing and welding of, 20: 5181(R) (ORNL-3029)
Nb–Zr, brazing techniques for bonding to graphite, 20: 2294
Nb–Zr, brazing to beryllium using silver, 19: 44606 (PWAC-483)
Nb–Zr, brazing to beryllium using silver alloys, effects of carbon and silicon coatings on, 19: 44606 (PWAC-483)
Nb–Zr, brittle fracture in liquid-metal coolant loop tubing of, 19: 22984(R) (NASA-CR-54167)
Nb–Zr, brittle fracture of hydrided and nonhydrided cold-worked, 20: 27477(R) (BNWL-207, pp 6.7-12)
Nb–Zr, brittleness of, effects of hydrogen on, 19: 18498
Nb–Zr, brittleness and fracture of, effects of hydrogen on, 19: 44716
Nb–Zr, brittleness at −23 to 265°C, 20: 746(R) (BNWL-120, pp 6.1-11)
Nb–Zr, brittleness of, effects of hydrogen on, 20: 11227
Nb–Zr, burst testing of tubular, 19: 24089(R) (SRO-114)
Nb–Zr, calculation of upper critical field of, 17: 20452 (BSD-TDR-63-62)
Nb–Zr, carburization by uranium carbide, 18: 10537 (NAA-SR-Memo-9015)
Nb–Zr, carburization of, for prevention of galling, 19: 44609 (TIM-927)
Nb–Zr, casting methods improvement for preparation of macrohomogeneous ingots of, 18: 4250(R) (ORNL-3470(p.45-8))
Nb–Zr, cavitation damage in mercury and water, 18: 3955 (NP-13319)
Nb–Zr, cavitation damage in mercury and water, 19: 9623 (NP-14632)
Nb–Zr, cavitation damage in bismuth–lead alloy at 500°F, 19: 24938 (NP-15024)
Nb–Zr, cavitation in bismuth–lead alloy at 500 and 1500°F, ultrasonic-induced, 19: 39116 (NP-15263)
Nb–Zr, cavitation damage in bismuth–lead alloy at 500 and 1500°F, 20: 771 (NP-15558)
Nb–Zr, cavitation damage in mercury and water, 20: 16974 (NP-15889)
Nb–Zr, cavitation damage in liquid, at high temperatures, 20: 33835
Nb–Zr, characteristics of superconducting solenoid of, 17: 12539
Nb–Zr, chromatographic analysis for hydrogen, 17: 2909(T,R) (EURAEC-383)
Nb–Zr, coating development for oxidation protection, 18: 25896(R) (PF-63-3)
Nb–Zr, coating of, evaluation of properties before and after, 17: 1887(R) (AD-273746)
Nb–Zr, coating of D-14, with chromium and titanium from fused salt baths, 18: 18294(R) (NP-13758)
Nb–Zr, coating of D-14 for oxidation protection, 18: 34052 (RTD-TDR-63-4063)
Nb–Zr, coating testing for, 17: 36283 (AD-295530)
Nb–Zr, coating with enamel frits, 16: 13570 (CNLM-2989)
Nb–Zr, coating with aluminum–tin-base alloys for protection against oxidation, 17: 39465 (SCNC-328(Del.))
Nb–Zr, coating with chromium or titanium by deposition from fused-salt baths, 18: 29675
Nb–Zr, coating with silicides for oxidation protection, evaluation, 19: 7876(R) (ML-TDR-64-71)
Nb–Zr, coating with nickel, electroless, 20: 5867
Nb–Zr, coating with silicon by fluidized-bed process, 20: 29630
Nb–Zr, coatings for, development of oxidation-protection, 20: 7517 (PWAC-499)
Nb–Zr, compatibility with fissium–plutonium–uranium alloys at 550 to 650°C, 17: 35079(R) (ANL-6749)
Nb–Zr, compatibility with sodium at 650°C, 17: 41333(R) (ANL-6677)
Nb–Zr, compatibility with plutonium carbide–uranium carbide, 18: 8729 (UNC-5074)
Nb–Zr, compatibility with plutonium carbide–uranium carbide systems at 1500°F, 18: 16426(R) (UNC-5068)
Nb–Zr, compatibility with cesium at 1800 and 2500°F, 18: 22444(R) (MSAR-63-126)
Nb–Zr, compatibility with fissium–plutonium–uranium alloys at 550 to 650°C, 18: 26893(R) (ANL-6868(p.11-108))
Nb–Zr, compatibility with uranium carbide fuels in sodium, 18: 35957 (NAA-SR-7502)
Nb–Zr, compatibility with ceramic insulation materials at high temperatures, 19: 7851 (CNLM-5942)
Nb–Zr, compatibility with plutonium carbide–uranium carbide, 19: 24923(R) (UNC-5081)
Nb–Zr, compatibility with alkali metals at high temperatures, 20: 2236
Nb–Zr, compatibility with TZM alloy in flowing lithium, 20: 2238
Nb–Zr, compatibility with uranium dioxide, 20: 5181(R) (ORNL-3029)
Nb–Zr, compatibility with type 316 stainless steel in 650°C, 20: 7518 (PWAC-501)
Nb–Zr, compatibility with lithium, 20: 8447 (PWAC-491)
Nb–Zr, compatibility with plutonium–uranium carbides at 590 and 820°C, 20: 9437
Nb–Zr, compatibility with TZM molybdenum alloy in refluxing potassium at 2000°F, 20: 13192(R) (NASA-CR-54843)
Nb–Zr, contamination in high vacua at 578 to 1202°C, analysis of, 18: 4255(R) (ORNL-3470(p.98-125))
Nb–Zr, contamination by residual gases in vacuum systems, 18: 14355 (CONF-373-7)
Nb–Zr, contamination by residual gases in high vacuum, 18: 39826 (ORNL-3674)
Nb–Zr, content test and phase studies, 16: 10526(R) (EURAEC-86)
Nb–Zr, corrosion and hydridation of, by gases, steam, and water, 16: 22541 (AECL-1513)
Nb–Zr, corrosion and properties study, 16: 12653(R) (EURAEC-130)
Nb–Zr, corrosion of, by cesium at 1600 to 2500°F, 16: 16684 (TID-7626(Pt.I)(p.109-10))
Nb–Zr, corrosion of, by potassium at high temperatures, 16: 16680 (TID-7626(Pt.I)(p.69-86))
Nb–Zr, corrosion of, by liquid rubidium at 1800°F, 16: 14834 (AGN-8034)
Nb–Zr, corrosion of, by potassium at 1450 to 2000°F, 16: 16678 (TID-7626(Pt.I)(p.42-62))
Nb–Zr, corrosion of, by sodium at 1500 to 2400°F, 16: 16677 (TID-7626 (Pt.I)(p.23-34))
Nb–Zr, corrosion of, by sodium at 2200°F, 16: 20042(R) (BNL-696)
Nb–Zr, corrosion of, by steam and water, 16: 29346
Nb–Zr, corrosion of, by steam and water at 750 to 900 and 680°F, 16: 29337(R) (ARF-2198-26)
Nb–Zr, corrosion of, by steam at 400°C and 200 atm, rates of, 16: 20981(T,R) (EURAEC-27)
Nb–Zr, corrosion of, by steam or water at 360, 400, and 480°C, effects of heat treatment on rates of, 16: 20982(T,R) (EURAEC-85)
Nb–Zr, corrosion of, by steam to 550°C, 16: 32084(T,R) (EURAEC-227)
Nb–Zr, corrosion of, by water, 16: 32086
Nb–Zr, corrosion of, by water at 300 and 350°C, 16: 12735(R) (EURAEC-80)
Nb–Zr, corrosion of, by water at high temperatures and pressures, effects of anions on, 16: 22557

Nb–Zr, corrosion of, effects of heat treatment on, 16: 10526(R) (EURAEC-86)
Nb–Zr, corrosion of, effects of heat treatment on, 16: 3406 (GEAP-3729)
Nb–Zr, corrosion, fabrication, and phase studies, 16: 18613(R) (EURAEC-22)
Nb–Zr, corrosion resistance, 16: 10464
Nb–Zr, corrosion resistance of, effects of heat treatment on, 16: 20980(T,R) (EURAEC-26)
Nb–Zr, corrosion by air, carbon dioxide, and water, 17: 504
Nb–Zr, corrosion by cesium at high temperatures, design of capsules for testing, 17: 3426(R) (NP-12189)
Nb–Zr, corrosion by potassium, 17: 4905(R) (NP-12334)
Nb–Zr, corrosion by steam and water, 17: 6581
Nb–Zr, corrosion of, by steam at 500°C and 1 atm. pressure, 17: 8715(T,R) (EURAEC-451)
Nb–Zr, corrosion by liquid sodium, 17: 11935(R) (ANL-6658)
Nb–Zr, corrosion by steam and water at high temperatures, effects of iron additions on, 17: 12618
Nb–Zr, corrosion by steam at 280 to 500°C and 15 to 800 lb/in.², 17: 12619
Nb–Zr, corrosion of, in water at 680°F and steam at 750 and 900°F, 17: 16586 (GEAP-4098)
Nb–Zr, corrosion of, by rubidium at 1000 to 2000°F, 17: 16634 (AGN-8063)
Nb–Zr, corrosion by mercury at high temperatures, 17: 19726 (BNL-759(p.54-77))
Nb–Zr, corrosion by sodium at 1400 to 2400°F, 17: 19726 (BNL-759 (p.54-77))
Nb–Zr, corrosion by uranyl sulfate solution at 280°C, in-pile, 17: 27750 (ORNL-3099)
Nb–Zr, corrosion resistance and tensile properties of welds in, 17: 32496
Nb–Zr, corrosion hydrogen embrittlement of, 17: 32525
Nb–Zr, corrosion by high-pressure flowing steam at 300, 400, and 500°C, 17: 34346(R) (GEAP-4211)
Nb–Zr, corrosion by sodium at 650°C, 17: 36861(R) (ANL-6764)
Nb–Zr, corrosion by flowing sodium at 650°C, 17: 37001(R) (ANL-6780)
Nb–Zr, corrosion by steam at 500°C, 17: 39468(T,R) (EURAEC-520)
Nb–Zr, corrosion by superheated steam at 500°C, hydrogen sorption during, 17: 39470(T,R) (EURAEC-619)
Nb–Zr, corrosion by steam and water, 17: 39659
Nb–Zr, corroaion of, by steam at 500°C and 1 atm. pressure, 17: 8715(T,R) (EURAEC-451)
Nb–Zr, corrosion by superheated steam at 500°C, hydrogen uptake from, 17: 41368(T,R) (EURAEC-784)
Nb–Zr, corrosion by potassium (liquid), 17: 41339 (GE-62FPD365)
Nb–Zr, corrosion by sodium at 760 to 1315°C, effects of barium, magnesium, and oxygen additions on, 18: 4160(R) (BNL-799(p.74-100))
Nb–Zr, corrosion by potassium at 1500 to 1800°F, 18: 5728 (ASD-TDR-63-270(Pt.II))
Nb–Zr, corrosion by mercury at high temperatures, 18: 7152
Nb–Zr, corrosion by superheated steam at 500°C and water at 350°C, hydrogen uptake from, 18: 14386(T,R) (EURAEC-822)
Nb–Zr, corrosion by water at 300°C, 18: 14357(R) (EURAEC-79)
Nb–Zr, corrosion by water vapor at 400°C, 18: 14418
Nb–Zr, corrosion by liquid cesium, role of oxygen in, 18: 16447
Nb–Zr, corrosion by boiling cesium in loop, 18: 18279 (AGN-8041 (Del.))
Nb–Zr, corrosion by potassium vapor at 1500 to 1800°F, 18: 18282 (BNL-844)
Nb–Zr, corrosion by potassium at 2000 to 2200°F, 18: 24091
Nb–Zr, corrosion by sodium at 650°C, 18: 26893(R) (ANL-6868(p.11-108))
Nb–Zr, corrosion by lithium, effects of carbon, nitrogen, or oxygen on, 18: 27914
Nb–Zr, corrosion and hydridation by steam and water, 18: 30134(T,R) (EURAEC-955)
Nb–Zr, corrosion by steam and water, 18: 37612 (A/CONF.28/P/477)
Nb–Zr, corrosion by water, 18: 37633 (A/CONF.28/P/342)
Nb–Zr, corrosion and hydrogen absorption in steam, 18: 39847
Nb–Zr, corrosion by boiling mercury and sodium, 18: 41933 (TID-11295 (3rd Ed.))
Nb–Zr, corrosion by barium vapor, 18: 44499(R) (MND-2812-4)
Nb–Zr, corrosion by steam, effects of antimony, chromium, copper, germanium, iron, tellurium, and vanadium on, 19: 4615(R) (EURAEC-1115)
Nb–Zr, corrosion and hydridation by steam and water, effects on tensile properties, 19: 4616(R) (EURAEC-1161)
Nb–Zr, corrosion cracking by boiling mercury, 19: 7863 (BNL-7642)
Nb–Zr, corrosion mass transfer in potassium to types 316 and 321 stainless steel, 19: 9622(R) (NASA-CR-54200)
Nb–Zr, corrosion by boiling cesium, 19: 13913(R) (AFML-TR-64-327)
Nb–Zr, corrosion by two-phase potassium in loop, 19: 13917 (SY-5463-R)
Nb–Zr, corrosion by Santowax OM coolant at 320 to 400°C, out-of-pile and in-pile, 19: 13911 (AECL-2118)
Nb–Zr, corrosion by boiling mercury, effects of magnesium on, 19: 15991(R) (BNL-841(p.63-101))
Nb–Zr, corrosion of, review of oxidation and hydriding kinetics and radiation effects in, 19: 16011 (AERE-R-4820)
Nb–Zr, corrosion by boiling potassium in loop test, 19: 20476 (ORNL-3503)
Nb–Zr, corrosion by boiling sodium, 19: 22890 (BNL-9018)
Nb–Zr, corrosion by liquid potassium, 19: 23996(R) (ORNL-3650(p.1-110))
Nb–Zr, corrosion stress cracking in mercury, 19: 28763
Nb–Zr, corrosion by sodium at 1260°C, 19: 28764
Nb–Zr, corrosion by ultrasonic-induced cavitation in liquid metals, 19: 28767
Nb–Zr, corrosion by steam at 400 and 450°C, effects of alloy additions on, 19: 30668(R) (EURAEC-1274)
Nb–Zr, corrosion by boiling potassium, 19: 34640 (CNLM-6246)
Nb–Zr, corrosion by potassium–sodium alloy at 1250°F in stainless steel loop, carbon and nitrogen mass transfer in, 19: 34640 (CNLM-6246)
Nb–Zr, corrosion by mercury at high temperatures, 19: 36949(R) (BNL-900(p.121-97))
Nb–Zr, corrosion by sodium at high temperatures, 19: 36949(R) (BNL-900(p.121-97))
Nb–Zr, corrosion by bismuth at 748°C, 19: 36949(R) (BNL-900(p.121-97))
Nb–Zr, corrosion of welds in, effects of heat treatments on lithium, 19: 36980 (PWAC-355)
Nb–Zr, corrosion by lithium, effects on zirconium content on, 19: 36980 (PWAC-355)
Nb–Zr, corrosion by lithium, effects of oxygen contamination on, 19: 36980 (PWAC-355)
Nb–Zr, corrosion by lithium, effects of heat treatment and oxygen on, 19: 44620 (CNLM-6344)
Nb–Zr, corrosion resistance of, effects of production method and aging on, 19: 44629
Nb–Zr, corrosion by potassium–sodium at 1250°F, effects of carbon, nitrogen, and oxygen on, 19: 44626 (TIM-896)
Nb–Zr, corrosion by potassium at 2000°F, 20: 768(R) (NASA-CR-54226)
Nb–Zr, corrosion by boiling and condensing alkali metals, 20: 2268
Nb–Zr, corrosion by potassium at high temperatures, 20: 2271
Nb–Zr, corrosion by bismuth and tin, 20: 2275
Nb–Zr, corrosion by potassium–sodium alloy, 20: 2273
Nb–Zr, corrosion by potassium–sodium alloys, 20: 5181(R) (ORNL-3029)
Nb–Zr, corrosion by lead at 1400°F, 20: 4308(R) (ORNL-3870, pp 243-60)
Nb–Zr, corrosion by potassium–sodium eutectic, 20: 4323(R) (ORNL-3870, pp 308-11)
Nb–Zr, corrosion by lithium at high temperatures, 20: 4299(R) (ORNL-2711)
Nb–Zr, corrosion by potassium, 20: 4301(R) (ORNL-3870, pp 102-35)
Nb–Zr, corrosion by lithium, effects of oxygen on, 20: 4301(R) (ORNL-3870, pp 102-35)
Nb–Zr, corrosion by cesium at 1600, 1800, and 2500°F, 20: 5846
Nb–Zr, corrosion by potassium at 1070°C, 20: 7518 (PWAC-501)
Nb–Zr, corrosion by sodium at 2000°F, 20: 9423(R) (NASA-CR-54735)
Nb–Zr, corrosion by hydrochloric, phosphoric, and sulfuric acids, effects of alloy composition on, 20: 14997
Nb–Zr, corrosion of welded joints of, by water and steam, 20: 19195
Nb–Zr, corrosion by liquid alkali metals, test loops for studying, 20: 21284
Nb–Zr, corrosion by lead at 1400°F, 20: 23603 (ORNL-TM-1437)
Nb–Zr, corrosion by mercury and sodium at high temperatures, 20: 25474(R) (BNL-954, pp 122-67)
Nb–Zr, corrosion by refluxing potassium at 1800 to 2400°F, 20: 25485 (NASA-TN-D-3429)
Nb–Zr, corrosion by mercury at 593 to 703°C, 20: 29646
Nb–Zr, corrosion by cerium–cobalt–plutonium alloy fuels, effects of carbon on, 20: 31679(R) (LA-3524)
Nb–Zr, corrosion by lead at 1400°F, 20: 31683(R) (ORNL-3936, pp 95-121)
Nb–Zr, corrosion by steam at 400°C and 120 atm, effects of heat treatment on, 20: 33824
Nb–Zr, corrosion resistance of, effect of heat treatment on, 20: 33849
Nb–Zr, corrosion by liquid potassium at high temperatures, 20: 41419(R) (GMAD-3643-5)
Nb–Zr, corrosion of zirconium-base, by steam at high temperatures, 20: 41422
Nb–Zr, corrosion by molten plutonium alloys, carbon effects on, 20: 43829(R) (LA-3582)
Nb–Zr, corrosion by lithium at 2000°F, 20: 43837 (TIM-823)
Nb–Zr, crack propagation tests on pressure tubes of, 20: 7501(R) (TID-22426)
Nb–Zr, crack propagation in hydrided zirconium-base, 20: 9490(R) (BNWL-166, pp 6.15-18)

Nb–Zr, creep and tensile properties, 17: 32568 (CONF-53-5)
Nb–Zr, creep and fatigue properties of $ZrNb_2$, 18: 14359(R) (EURAEC-136)
Nb–Zr, creep and rupture properties at 1600 to 2200°F, 19: 37029 (CNLM-4267)
Nb–Zr, creep at 600°C, 19: 31462(R) (ANL-7028)
Nb–Zr, creep properties of, at high temperatures, alloying effects of copper and molybdenum on, 16: 16772(P)
Nb–Zr, creep properties at 2200°F, 18: 37621(R) (IITRI-B6021-3)
Nb–Zr, creep properties, effects of vacuum gases on slow-bend, 18: 44049(R) (ORNL-3670(p.77-111))
Nb–Zr, creep properties, effects of cold working and annealing on, 20: 4301(R) (ORNL-3870, pp 102-35)
Nb–Zr, creep rupture and fatigue evaluation of, 18: 29103(R) (APS-5071-R)
Nb–Zr, creep rupture properties of, effects of annealing on, 19: 7929
Nb–Zr, creep strength of, effects of vacuum on cantilever beam bend tests of, 18: 14456 (CONF-373-10)
Nb–Zr, creep testing of, summary of slow-bend, 18: 4255(R) (ORNL-3470(p.98-125))
Nb–Zr, critical alternating currents in superconducting films of, 18: 9269
Nb–Zr, critical currents in, effects of carbon, oxygen, and size on, 16: 30798 (ORNL-3303)
Nb–Zr, critical currents in external magnetic field and superconducting properties, 17: 545(T) (AEC-tr-5473)
Nb–Zr, critical current in magnets of, 17: 27944 (NP-12908)
Nb–Zr, critical current and magnetization properties of, 17: 34549(R) (ORNL-3480(p.41-5))
Nb–Zr, critical current degradation and flux jumping in solenoids of heat-treated, 17: 36469
Nb–Zr, critical current-field characteristics of short wire samples in superconducting solenoids, 17: 37729
Nb–Zr, critical current-field relation in, 17: 41542 (BSD-TDR-63-148)
Nb–Zr, critical currents in superconducting, effects of heat treatment on, 18: 6127
Nb–Zr, critical current density of superconducting, in transverse field of 30 kgauss, 18: 6128
Nb–Zr, critical current in rolled strip of superconducting, field-dependent anisotropy of, 18: 6130
Nb–Zr, critical current density of superconducting, in a pulsed magnetic field, 18: 18833
Nb–Zr, critical currents in wires and strips of superconducting, anisotropy and proximity effect in, 18: 36525
Nb–Zr, critical currents in ribbons of superconducting, effects of magnetic field direction and annealing on, 18: 36526
Nb–Zr, critical current training in superconducting, (E), 19: 10215
Nb–Zr, critical currents in superconducting, 19: 16797
Nb–Zr, critical current degradation in wide-strip superconductors of, (E), 19: 41639
Nb–Zr, critical currents of superconducting, effect of magnetic-field rise time on, (E), 19: 43238
Nb–Zr, critical currents in, effect of omega transformation on, (E), 19: 47511
Nb–Zr, critical current of disperse superconducting phases in, 20: 9900
Nb–Zr, critical current density in superconducting, magnetic field dependence of, (E), 20: 26031
Nb–Zr, critical currents in, effects of annealing and orientation on, (E), 20: 42569
Nb–Zr, critical-current induced transitions in superconducting, 20: 24273
Nb–Zr, crystal structure of, effects of hydrogen on, 16: 33487(T,R) (EURAEC-243)
Nb–Zr, crystal structure of, preparation of oxide replicas for studies of, 20: 27561
Nb–Zr, crystal structure and electric conductivity of, 20: 29766
Nb–Zr, crystallization and recovery of cold-worked, 19: 44698 (PWAC-465)
Nb–Zr, current-carrying capacity in superconducting solenoids, 17: 6209
Nb–Zr, current density reduction in magnets of, 17: 25873
Nb–Zr, current degradation in superconducting solenoids of, 19: 37735(R) (N64-33921)
Nb–Zr, current density and magnetic field in cold-worked superconductors of, 19: 41637
Nb–Zr, current decay propagation in superconducting, persistent, (E), 19: 47507
Nb–Zr, current degradation in superconducting solenoids of, (E), 20: 21920
Nb–Zr, current degradation in superconductors of, low-frequency alternating, (E), 20: 34449
Nb–Zr, current losses in type II superconducting, 20: 28187
Nb–Zr, current losses and magnetic field aberrations from high-field superconducting wires of, in adiabatic demagnetization apparatus, 20: 37970
Nb–Zr, current-carrying capacity of superconducting, temperature and field dependence of, 18: 34681 (BSD-TDR-64-87)
Nb–Zr, degradation of large superconducting magnets of, (E), 19: 25444
Nb–Zr, degradation phenomena in small superconducting coils of, (E), 20: 17629
Nb–Zr, development, properties, and uses of superconducting, 18: 13010
Nb–Zr, development as reactor material, 19: 914
Nb–Zr, development as fuel jacket material for fast reactors, 20: 38465 (ANL-7120, pp 289-300)
Nb–Zr, diffusion of interstitials in, 16: 33500
Nb–Zr, diffusion of components in, tracer studies of, 17: 30988(T) (FTD-TT-63-258)
Nb–Zr, diffusion in type 316 stainless steel, 17: 36200(R) (NP-13033)
Nb–Zr, diffusion and solubility of hydrogen in, 19: 13349
Nb–Zr, diffusion in bcc, 19: 23112
Nb–Zr, dimensional changes during annealing in, temperature gradient effects on, 18: 26028
Nb–Zr, ductility of zirconium-base, effects of high temperatures on, 20: 41422
Nb–Zr, effects of heat treatment and radiation on mechanical properties, 17: 3550
Nb–Zr, effects of hydrogen on delayed failure of, 17: 14810(R) (ARF-B6005-2)
Nb–Zr, effects of aging temperature on hardness, 17: 22160(R) (DRI-2094)
Nb–Zr, effects of environment, heat treatment, and temperature on corrosion of, 17: 32524
Nb–Zr, effects of cold working and heat treatment on properties of, 17: 41636
Nb–Zr, effects of hydrogenation on delayed failure susceptibility of, 18: 18406
Nb–Zr, effects of surface treatments on emittance of, 19: 22984(R) (NASA-CR-54167)
Nb–Zr, effects of lithium and oxygen on tensile properties of, 20: 5181(R) (ORNL-3029)
Nb–Zr, effects of physical parameters and radiation on fuel element cladding of, (E), 20: 7519 (RCN-41)
Nb–Zr, electric and mechanical properties, 18: 24158
Nb–Zr, electric conductivity in fixed and swept magnetic fields, 17: 41546 (CONF-176-7)
Nb–Zr, electric conductivity of nonideal superconducting, a-c, 18: 18836
Nb–Zr, electric conductivity, 18: 22475 (BATT-4673-T7)
Nb–Zr, thermal conductivity, 18: 22475 (BATT-4673-T7)
Nb–Zr, electric current degradation in superconducting solenoids of, (E), 19: 6608
Nb–Zr, electric conductivity at 4 to 273°K, 19: 13992 (ML-TDR-64-234)
Nb–Zr, electric conductivity at 200 to 1446°C, 19: 47015 (TIM-854)
Nb–Zr, electric conductivity to 1500°C, 20: 5851
Nb–Zr, electric properties of superconducting, 17: 35260(R) (TID-19135)
Nb–Zr, electric properties of contacts to normal metals, 17: 36453 (TID-19310)
Nb–Zr, electric properties near breakdown in superconducting, 18: 9264
Nb–Zr, electric power losses at 50 cps in superconducting, 18: 44677
Nb–Zr, electric properties of normal region in superconducting magnet of, 20: 17610
Nb–Zr, electrochemical potential and hydrogen overvoltage, 17: 34403 (GEAP-4192)
Nb–Zr, electron field emission patterns of, 18: 29662
Nb–Zr, electronic properties, 18: 44150(R) (ORNL-3670(p.44-53))
Nb–Zr, embrittlement effects of hydrogen on, 18: 34169
Nb–Zr, embrittlement by contamination during vacuum treatments, 19: 42809
Nb–Zr, emissivity, 17: 6675(R) (PWA-2128)
Nb–Zr, emissivity measurements at 800 to 5000°K, 18: 20566
Nb–Zr, emissivity of coated, in vacuum, 18: 24138(R) (PWA-2206 (Vol.I))
Nb–Zr, emissivity of coated, in vacuum, 18: 24139(R) (PWA-2206 (Vol.II))
Nb–Zr, emissivity of coated, in vacuum, 18: 24140(R) (PWA-2206 (Vol.III))
Nb–Zr, emissivity, effects of surface treatments on, 20: 4301(R) (ORNL-3870, pp 102-35)
Nb–Zr, emissivity to 1500°C, total hemispherical, 20: 5851
Nb–Zr, emissivity of titanate coatings on, 20: 15057(R) (PWA-2750)
Nb–Zr, emissivity of titanate-coated, at high temperatures, 20: 43816(R) (PWA-2877)
Nb–Zr, emittance at 100 to 1200°C, measurement of total hemispherical, 18: 5809
Nb–Zr, emittance properties of iron titanate coatings on, 19: 18465(R) (PWA-2518)

Nb–Zr, energy gap of high-field superconducting, 18: 26481
Nb–Zr, erosion by water of rotating disks of, 19: 44625 (TIM-894)
Nb–Zr, erosion by mercury, water, and bismuth–lead alloy, cavitation, 20: 29640 (NP-16048)
Nb–Zr, evaporation tests in high vacuum, 18: 44049(R) (ORNL-3670 (p.77-111))
Nb–Zr, evaporation losses of FS-85, at 1200 to 1500°C in high vacuum, 19: 37043 (ORNL-P-1394)
Nb–Zr, evaporation losses in high vacuum, 20: 4301(R) (ORNL-3870, pp 102-35)
Nb–Zr, extrusion at high energy rates, 18: 8769 (LADC-5763)
Nb–Zr, extrusion by hydrostatic methods, 19: 18436
Nb–Zr, extrusion, 19: 20500 (AFML-TR-64-387)
Nb–Zr, extrusion as clad in uranium carbide fuel elements, 19: 24952 (NMI-2523)
Nb–Zr, fabrication, melting, welding, and workability of, 16: 16716 (CNLM-2166)
Nb–Zr, fabrication of arc-melted, for production of 43-kgauss superconducting solenoid, 16: 6564
Nb–Zr, fabrication of beta-quenched, 16: 24137
Nb–Zr, fabrication of tubing of, by spinning, 16: 12068 (CNLM-3342)
Nb–Zr, fabrication of, for mercury corrosion loop, 17: 11131 (AGC-0584-
Nb–Zr, fabrication and properties of cold-rolled, 17: 41333(R) (ANL-6677) 04-5)
Nb–Zr, fabrication and properties, 18: 2158(R) (EURAEC-176)
Nb–Zr, fabrication of tube shells of, by floturning, 18: 4255(R) (ORNL-3470(p.98-125))
Nb–Zr, fabrication and superconductivity properties of, 18: 4285
Nb–Zr, fabrication and properties, 18: 14357(R) (EURAEC-79)
Nb–Zr, fabrication of tubular, as reactor fuel cladding, 18: 19456(R) (ANL-6840)
Nb–Zr, fabrication effects on superconducting current capacities of, 18: 21098
Nb–Zr, fabrication and properties, 18: 26893(R) (ANL-6868(p.11-108))
Nb–Zr, fabrication into tube shells by flow turning, 18: 44049(R) (ORNL-3670(p.77-111))
Nb–Zr, fabrication, properties, testing, and uses of superconducting of, 19: 16110
Nb–Zr, fabrication into tubing, development of methods for, 19: 24954 (TID-21790)
Nb–Zr, fabrication into superconducting delay lines, (E), 20: 3612 (CONF-651001-6)
Nb–Zr, fabrication of superconductors of, 20: 39372(P)
Nb–Zr, fabrication of Zircaloy-4-clad pressure tubing of, 20: 43862 (TID-23312)
Nb–Zr, fabrication of loops of, for liquid potassium and sodium, 20: 43879
Nb–Zr, fast neutron effects on critical current in, 18: 9265
Nb–Zr, fatigue behavior in potassium at 800°F, 17: 12036(R) (SY-5396-R3)
Nb–Zr, fatigue due to hydrogen embrittlement, 17: 526(R) (ARF-2230-12)
Nb–Zr, fatigue in lithium at 1600°F from cantilever bending, 17: 35223(R) (SY-5396-R5)
Nb–Zr, fatigue in lithium at 1600°F and potassium at 800°F from cantilever bending, 18: 6516 (SY-5396-R6)
Nb–Zr, fatigue in lithium at 1600°F and potassium at 800°F, cantilever-bending, 18: 12624(R) (ASD-TDR-63-270(Pt.IV))
Nb–Zr, fatigue of, effects of applied stress and hydrogen sorption on static, 16: 25746(R) (ARF-2230-9)
Nb–Zr, fatigue of hydrided, effects of heat treatment on, 17: 34404(R) (IITRI-B6005-8)
Nb–Zr, fatigue properties of $ZrNb_2$, 18: 14360(R) (EURAEC-199)
Nb–Zr, feasibility of labeled, for spacecraft shield ablation measurements, 20: 36353
Nb–Zr, filament structure of superconducting, 18: 18846
Nb–Zr, flux annihilation in superconducting, (E/T), 19: 43239
Nb–Zr, flux creep and jump in superconducting, effect of Joule heating on, 20: 21884
Nb–Zr, flux jumping and training in superconducting solenoids of, 18: 26470
Nb–Zr, forging characteristics, 16: 9162 (DMIC-Memo-143)
Nb–Zr, formation of niobium carbide surface films on, activation energies for, 20: 14992
Nb–Zr, fracture of, effects of hydrogen content and temperature on, 19: 26839
Nb–Zr, fracture properties of zirconium-base, effects of hydrogen and temperature on, 20: 31669
Nb–Zr, grain growth of, effects of cold working and annealing on, 19: 20473(R) (NASA-CR-54629)
Nb–Zr, grain growth in liquid-metal coolant loop tubing of, 19: 22984(R) (NASA-CR-54167)
Nb–Zr, Hall coefficient in normal and superconducting, 17: 12668 (NRL-5874)
Nb–Zr, Hall effect measurements on superconducting magnets of, 20: 17600(R) (ORNL-3908, pp 114-48)
Nb–Zr, hardness, 20: 15073
Nb–Zr, hardness of, effects of cooling rate on, 18: 44133 (CRRM-1200)
Nb–Zr, hardness of, effects of cooling rate and niobium content on, 19: 40961
Nb–Zr, heat treatment for improved corrosion resistance, 19: 34635(P)
Nb–Zr, heat treatment effects on texture of, 20: 37198
Nb–Zr, heat-treatment effects on critical current and temperature of superconducting, 18: 44690
Nb–Zr, hemispherical emittance values at 100 to 1200°C, total, 18: 4255(R) (ORNL-3470(p.98-125))
Nb–Zr, hydridation of, metallographical studies of, 17: 39470(T,R) (EURAEC-619)
Nb–Zr, hydridation effects on properties of, 19: 40959
Nb–Zr, hydridation of, kinetics, 20: 2222 (EURAEC-1390)
Nb–Zr, hydride nucleation and growth in, 20: 2253 (AECL-2297)
Nb–Zr, hydrogen distribution in oxidized, tritium autoradiographic studies of, 19: 13910 (AECL-2085)
Nb–Zr, hydrogen embrittlement of, 17: 8715(T,R) (EURAEC-451)
Nb–Zr, hydrogen embrittlement, 18: 5776(R) (IITRI-B6005-11)
Nb–Zr, hydrogen embrittlement of, review of, 20: 37187
Nb–Zr, hydrogen overvoltage measurements in, 17: 27728(R) (GEAP-4076)
Nb–Zr, hydrogen overvoltages at, in sulfuric acid, 18: 12642 (GEAP-4089(Vol.II)(Paper 22))
Nb–Zr, hydrogen uptake by, 20: 7520
Nb–Zr, hydrogenation, 18: 551(T,R) (EURAEC-224)
Nb–Zr, in-pile stress rupture tests, 17: 14740 (TID-11295(2nd Ed.))
Nb–Zr, inductance of superconducting solenoids of, 20: 26032
Nb–Zr, internal friction measurements, 18: 4255(R) (ORNL-3470(p.98-125))
Nb–Zr, internal friction peak in, dislocation-relaxation, 20: 15122
Nb–Zr, internal friction and relaxation processes in, 20: 17106
Nb–Zr, joining to alumina bodies in ceramic-to-metal seals for high temperatures, 17: 34366 (LAMS-2917)
Nb–Zr, longitudinal critical currents in cold-drawn superconducting, 17: 14961
Nb–Zr, magnetic behavior of superconducting wires of, 18: 13019
Nb–Zr, magnetic diffusivity in cylinder of type-II superconducting, (E), 20: 24279
Nb–Zr, magnetic field stabilization inside superconducting tubes of, 18: 11111
Nb–Zr, magnetic field effects on superconductivity of, 18: 15077
Nb–Zr, magnetic flux jumps in superconducting, 18: 34724
Nb–Zr, magnetic field effects on temperature in superconducting, (E), 19: 5105
Nb–Zr, magnetic fluxoid annihilation instability in superconducting, (E/T), 19: 12441
Nb–Zr, magnetic flux behavior in wires of superconducting, (E), 19: 16795
Nb–Zr, magnetic flux jumping under adiabatic conditions in superconducting wires of, (E), 19: 33164
Nb–Zr, magnetic field penetration in superconducting, radial velocity of, (E), 19: 39702
Nb–Zr, magnetic flux degradation in superconducting coils of, (E), 19: 47512
Nb–Zr, magnetic field effects on ultrasonic wave propagation in, 20: 863
Nb–Zr, magnetic flux annihilation and instabilities in inhomogeneous superconducting, (E), 20: 1132
Nb–Zr, magnetic flux jumps in superconducting NbZr in pulsed magnetic fields, (E), 20: 2921
Nb–Zr, magnetic fields on surface of superconducting, in external magnetic field, (E), 20: 2924
Nb–Zr, magnetic field penetration of thick slabs of superconducting type-II, velocity of, (T), 20: 8011
Nb–Zr, magnetic flux jumps in superconducting, sample geometry effects on, (E), 20: 9916
Nb–Zr, magnetic flux motion in thin-walled tubes of hard superconducting, spatial variations of, (T), 20: 9917
Nb–Zr, magnetic field strength at surface of superconducting, EPR measurements for, (E), 20: 21898
Nb–Zr, magnetic fluxoid annihilation instability in superconducting, (E/T), 20: 21927
Nb–Zr, magnetic flux penetration in superconducting, (E), 20: 42132
Nb–Zr, magnetic hysteresis losses from surface of superconducting, 18: 956
Nb–Zr, magnetic hysteresis losses of high-field superconducting, (T), 20: 26044
Nb–Zr, magnetic induction measurements for superconducting, 17: 37717
Nb–Zr, magnetic moment, 18: 13008(R) (ORNL-3564(p.100-25))

Nb–Zr, magnetic properties of superconducting, 16: 15426
Nb–Zr, magnetic properties of superconducting, effects of cold-working and heat treatment on, 16: 15465
Nb–Zr, magnetic properties of superconducting, effects of cold-working and heat treatment on, 16: 15466
Nb–Zr, magnetic properties of superconducting, effects of temperature on critical field of, 16: 15467
Nb–Zr, magnetic susceptibility, 20: 17106
Nb–Zr, magnetization and transport current in wire of, 17: 39749
Nb–Zr, magnetization of superconducting, relation to magnetic field of a solenoid constructed of the alloy, 18: 9277
Nb–Zr, magnetization of superconducting, 18: 9279
Nb–Zr, magnetization of superconducting wires of, 18: 42563
Nb–Zr, magnetization of superconducting, (E/T), 19: 27372
Nb–Zr, magnetization discontinuities in superconducting, (E), 19: 37740
Nb–Zr, magnetization of superconducting, effect of external current on, (E/T), 20: 19735
Nb–Zr, magnetization of nonideal type-II superconducting wires of, Procopiu-effect analog in longitudinal, (E), 20: 24277
Nb–Zr, magnetization of high-field superconducting, a-c losses and hysteresis in, (E), 20: 26043
Nb–Zr, magnetization of superconducting, (E), 20: 42133
Nb–Zr, magnetothermal effects in superconductors of, (E), 19: 14433 (CONF-651-44)
Nb–Zr, magnets of superconducting wires of, 18: 6108
Nb–Zr, mass transport by sodium, 18: 15563
Nb–Zr, mass transfer by sodium, 18: 15568
Nb–Zr, mass transfer from type 316 and 321 stainless steel to, in liquid potassium, research program on, 19: 20474(R) (NASA-CR-54281)
Nb–Zr, mass transfer from Type 316 and 321 stainless steels to, in liquid potassium at 1400°F, 19: 40970(R) (NASA-CR-54390)
Nb–Zr, mass transfer of carbon and nitrogen to, from type-316 stainless steel in liquid potassium, 20: 2239
Nb–Zr, maximum critical field of superconductors of, 17: 8959
Nb–Zr, mechanical properties of, to 550°C, 16: 32084(T,R) (EURAEC-227)
Nb–Zr, mechanical properties, 17: 504
Nb–Zr, mechanical properties of, hydrogen effects on, 17: 6696(T) (EURAEC-353)
Nb–Zr, mechanical properties at –300 to 1200°F, 17: 11075(R) (AD-278043)
Nb–Zr, mechanical properties, 17: 11108(T,R) (EURAEC-307)
Nb–Zr, mechanical properties of hydrided, effects of fabrication, specimen geometry, and temperature on, 17: 22155(R) (ARF-B6005-5)
Nb–Zr, mechanical properties of, effects of high-temperature lithium and potassium on, 17: 30939(R) (SY-S396-R4)
Nb–Zr, mechanical properties of LB-2-coated, effects of coating oxidation test on, 17: 36284 (AD-295547)
Nb–Zr, mechanical and superconductivity properties of, 17: 37542(T)
Nb–Zr, mechanical properties of, effects of hydrogen content on, 17: 39468(T,R) (EURAEC-520)
Nb–Zr, mechanical properties of, effects of hydrogen content on, 17: 39470(T,R) (EURAEC-619)
Nb–Zr, mechanical properties of, effects of hydrogen content on, 17: 41368(T,R) (EURAEC-784)
Nb–Zr, mechanical properties, 18: 7292(R) (HW-77954(p.4.1-12))
Nb–Zr, mechanical properties of, effects of heat treatment on, 18: 12637 (GEAP-4089(Vol.I)(Paper 11))
Nb–Zr, mechanical properties of welded, 18: 37680 (A/CONF.28/P/757)
Nb–Zr, mechanical properties at 1100 and 1300°C, 19: 11734
Nb–Zr, mechanical properties and TTT curves, 19: 18517
Nb–Zr, mechanical properties at high temperatures, 19: 44674(R) (ANL-7000, pp 69-83)
Nb–Zr, mechanical properties of, effects of carbon and oxygen on, 19: 44605 (PWAC-464)
Nb–Zr, mechanical properties of, effects of aging, oxygen content, and production method on, 19: 44629
Nb–Zr, mechanical properties of, effects of oxygen on, 20: 4297(R) (IS-1200(Sect.M))
Nb–Zr, mechanical properties of, effects of composition on, 20: 11288(T) (AD-622477)
Nb–Zr, mechanical properties of, effects of beta grain size on, 20: 21368
Nb–Zr, mechanical properties of cold-worked zirconium-base, 20: 31669
Nb–Zr, mechanical properties of, effects of oxygen on, 20: 35887 (IS-T-92)
Nb–Zr, mechanical properties of, effects of composition and heat treatments on, 20: 37236
Nb–Zr, mechanical properties of, effects of oxygen on, 20: 41412(R) (IS-1500(Sect. M))
Nb–Zr, metallographic inspection of test samples of, 16: 32126(T,R) (EURAEC-328)
Nb–Zr, metallography, 16: 20042(R) (BNL-696)
Nb–Zr, metallographic techniques for studying corrosion of, 19: 7863 (BNL-7642)
Nb–Zr, metallographic techniques for preparation of, for microscopy, 20: 16959
Nb–Zr, metallurgical aspects of superconducting, 18: 6129
Nb–Zr, metallurgical bonding to Hastelloy X and stainless steel by extrusion, 18: 27937
Nb–Zr, microstructure and superconductivity of, effects of cold rolling and heat treatment on, 17: 29369
Nb–Zr, microstructure and training of high-field superconductors of, 18: 4286
Nb–Zr, microstructures, 19: 44610 (TIM-943)
Nb–Zr, microstructure of, effects of annealing temperature on, 19: 44587(R) (ANL-7000, pp 3-63)
Nb–Zr, microstructure, effects of tempering on, 20: 13304
Nb–Zr, microstructure of cast, with low oxygen contents, 20: 19245
Nb–Zr, nickel coatings on, thermal cycling effects, 19: 29468(R) (ANL-7017)
Nb–Zr, nitrogen and oxygen content of, effects of yttrium additions on, 19: 40953 (PWAC-441)
Nb–Zr, nondestructive testing of superconducting wires of, methods development for, 18: 4250(R) (ORNL-3470(p.45-8))
Nb–Zr, nuclear spin-lattice relaxation in type II superconductors of, (E), 19: 41611
Nb–Zr, omega transformation in, 17: 12706
Nb–Zr, omega transformation and segregation processes in, 20: 17105
Nb–Zr, oxidation of, at 1000°C, 16: 9248(P)
Nb–Zr, oxidation of, at 400 and 600°C, kinetics of, 16: 4503(R) (TID-14242)
Nb–Zr, oxidation of, at 525 to 1090°C, 16: 2254
Nb–Zr, oxidation of, by air above 700°C, 16: 3408 (NP-11119)
Nb–Zr, oxidation of, causes of second transition point in, 16: 7857
Nb–Zr, oxidation of, during forging, development of coatings to prevent, 16: 13570 (CNLM-2989)
Nb–Zr, oxidation of, in air and steam, effects of additives on, 16: 32078 (AERE-R-4134)
Nb–Zr, oxidation characteristics at 400 to 2200°F, 17: 18705
Nb–Zr, oxidation of, protective effects of aluminum-tin, beryllide, and silicon-titanium coatings against, 17: 22109(R) (ASD-TDR-63-160)
Nb–Zr, oxidation of, effects of zirconium on resistance to, 17: 29291
Nb–Zr, oxidation by water at 360°C, 17: 35078(R) (ANL-6739)
Nb–Zr, oxidation by water containing lithium hydroxide, 18: 2192
Nb–Zr, oxidation in air and steam, 18: 7135 (AERE-R-4459)
Nb–Zr, oxidation in air, composition of scale formed during, 18: 10477(T) (JPRS-22697(p.27-38))
Nb–Zr, oxidation at 500 and 1000°, alloying effects of metals on, 18: 14413(T) (FTD-TT-63-1020)
Nb–Zr, oxidation by carbon dioxide up to 600°C, 18: 30192
Nb–Zr, oxidation at 400 to 600°C and 1 to 760 torr, kinetics and mechanism of, 19: 18409 (COO-1000-1)
Nb–Zr, oxidation at low pressures at 1000 to 1600°F, 19: 24931 (CNLM-5351)
Nb–Zr, oxidation by high-pressure, high-velocity helium at 2050°F, 19: 34639(R) (BNWL-79(p.5.1-11))
Nb–Zr, oxidation protection by aluminum–tin coatings with chromium and titanium additions, 20: 7580 (TIM-945)
Nb–Zr, oxidation by oxygen at 400 to 600°C, kinetics and mechanisms of, 20: 11227
Nb–Zr, oxidation rate of, at 1100°C, 20: 23614
Nb–Zr, oxidation of, mechanism of breakaway, 20: 25496
Nb–Zr, oxidation kinetics and oxide film breakaway at 600 to 850°C, 20: 25497
Nb–Zr, oxidation of, distribution of niobium in oxide film in, 20: 25504
Nb–Zr, oxidation of, kinetics, mechanism, and microstructure of internal, 20: 23619
Nb–Zr, oxidation by oxygen at 1000°C, kinetics and microstructures of, 20: 37193
Nb–Zr, oxygen addition mechanism and solubility in, 19: 2820
Nb–Zr, oxygen content of, 19: 22984(R) (NASA-CR-54167)
Nb–Zr, oxygen content in, 20: 8447 (PWAC-491)
Nb–Zr, paramagnetic susceptibility, 16: 10576
Nb–Zr, paramagnetic helical current flow in superconducting, (E), 19: 23576
Nb–Zr, paramagnetism in cold-worked superconducting wires of, 19: 39749
Nb–Zr, parameters for zirconium self-diffusion in, 20: 2356(T) (AERE-Trans-1030)
Nb-Zr, performance in superconducting solenoids, 17: 4781
Nb–Zr, performance of superconducting magnets of, 18: 11100 (LNF-63/67)
Nb–Zr, performance in superconducting coils for inductive energy storage, 18: 15047

Nb–Zr, performance as cladding for uranium carbide fuels, 18: 23817(R) (ANL-6880(p.72-8))
Nb–Zr, performance as fuel cladding in fast reactors, 18: 24952(R) (ANL-6880(p.6-48))
Nb–Zr, performance as cladding for uranium carbide fuels, 18: 24860(R) (UNC-5071)
Nb–Zr, performance as superconducting magnet, 18: 42554
Nb–Zr, performance as space radiator for thermionic reactor, 19: 3728 (PWA-2319)
Nb–Zr, performance as superconducting solenoids, (E), 19: 10189 (RLE-TR-427)
Nb–Zr, performance of superconducting coils of, in magnetic mirror systems, (E), 19: 10449
Nb–Zr, performance in high-field superconducting magnets, (E), 19: 19018 (ORNL-TM-1083)
Nb–Zr, performance of superconducting, for linac resonant cavities, 19: 27012 (MURA-714(p.540-4))
Nb–Zr, performance of superconducting magnets of, 19: 31335(R) (UCRL-12303)
Nb–Zr, performance as reactor pressure tubes, evaluation, (E), 19: 31551(R) (SRO-115)
Nb–Zr, performance in superconducting magnets, 20: 1120(R) (ORNL-3836, pp 90-110)
Nb–Zr, performance of superconducting solenoids of, 20: 4775 (UCRL-16376)
Nb–Zr, performance as cladding for alloy and carbide fuels, (E), 20: 14007(R) (ANL-7122, pp 1-41)
Nb–Zr, phase diagrams of, effects of oxygen on, 16: 16719 (EURAEC-137)
Nb–Zr, phase diagrams, 17: 556
Nb–Zr, phase diagrams, 18: 12633 (GEAP-4089(Vol.I)(Paper 4))
Nb–Zr, phase diagram, 18: 12635 (GEAP-4089(Vol.I)(Paper 9))
Nb–Zr, phase strengthening in, 17: 6555
Nb–Zr, phase studies, 16: 20981(T,R) (EURAEC-27)
Nb–Zr, phase studies, 16: 20982(T,R) (EURAEC-85)
Nb–Zr, phase studies, 16: 21061
Nb–Zr, phase studies, 16: 22616
Nb–Zr, phase studies, 16: 30783 (EURAEC-283)
Nb–Zr, phase studies and properties, 16: 12735(R) (EURAEC-80)
Nb–Zr, phase studies, 17: 537(R) (TID-17006)
Nb–Zr, phase studies, 18: 14396
Nb–Zr, phase studies of, 18: 18383
Nb–Zr, phase studies, 18: 26003
Nb–Zr, phase studies, 19: 11682
Nb–Zr, phase studies, 20: 35924
Nb–Zr, phase studies of, 20: 41443(R) (COO-588-12)
Nb–Zr, phase transformation kinetics, 16: 15166 (ARF-2198-21)
Nb–Zr, phase transformations in, time-temperature curves for, 18: 12636 (GEAP-4089(Vol.I)(Paper 10))
Nb–Zr, phase transformations in, dilatometric observations of, 19: 14019
Nb–Zr, phase transformations in, omega, 19: 16163
Nb–Zr, phase transformation kinetics, 20: 4390(R) (ORNL-3870, pp 65-9)
Nb–Zr, phase transformations in, effects of niobium content on metastable, 20: 7619
Nb–Zr, phase transformation in, start temperature for martensitic, 20: 19230
Nb–Zr, phase transformation in, kinetics of beta-, 20: 23746
Nb–Zr, phase transformations of, factors affecting, 20: 37234
Nb–Zr, physical properties of, 17: 4225(R) (ANL-6635(p.28-50))
Nb–Zr, pickling conditions for, 18: 12587
Nb–Zr, plastic deformation and tensile properties of, effects of temperature on, 16: 3464 (PWAC-359)
Nb–Zr, plastic flow of, determination by hardness, 20: 37230
Nb–Zr, power losses in superconducting solenoids of, 19: 16448(R) (TID-21380(p.85-111))
Nb–Zr, power losses in superconducting, a-c, (E), 19: 35324
Nb–Zr, preparation of powders of, by igneous electrolysis, 17: 16529(T,R) (EURAEC-509)
Nb–Zr, preparation and properties of heat-treated, 17: 32626
Nb–Zr, preparation and properties of thin-film hard superconducting, 18: 28501
Nb–Zr, preparation of powders of, 20: 2222 (EURAEC-1390)
Nb–Zr, pressure testing of tubular, 19: 47998(R) (SRO-118)
Nb–Zr, procurement and quality evaluation of stock of, for corrosion studies, 19: 40952 (ORNL-TM-1179)
Nb–Zr, production by fused salt electrolysis in sodium chloride–sodium fluoniobate–zirconium tetrafluoride, 18: 16431
Nb–Zr, propagation of normal region in superconducting solenoid of, 20: 42100
Nb–Zr, properties of welded, 17: 11242
Nb–Zr, properties as claddings for uranium carbide fuels, 17: 16650 (NAA-SR-7696)
Nb–Zr, properties of superconducting, at 9,250 Mcps, 17: 16722
Nb–Zr, properties of, effects of annealing temperature and time on critical, 17: 20504
Nb–Zr, properties during superconducting transition, 17: 27942 (NIRL/R/32)
Nb–Zr, properties as superconducting magnet, 17: 32712 (LNF-63/26)
Nb–Zr, properties as cladding for fissium–plutonium–uranium fuel elements, 17: 41333(R) (ANL-6677)
Nb–Zr, properties of superconducting, 17: 41604
Nb–Zr, properties as cladding for reactor fuel elements, 18: 6412(R) (GEAP-3888)
Nb–Zr, properties for use for containment of boiling mercury or sodium, 18: 12627(R) (BNL-823(p.66-93))
Nb–Zr, properties of, 18: 12565
Nb–Zr, properties for superconducting solenoids, 18: 26474
Nb–Zr, properties for use as superconductive wires, 18: 34200
Nb–Zr, properties for use in water-cooled reactors, 18: 37668 (A/CONF.28/P/158)
Nb–Zr, properties for use as fuel cladding for water-cooled power reactors, 18: 37692
Nb–Zr, properties for use as fuel cladding material, 19: 11679
Nb–Zr, properties as pressure tubes in power reactors, 19: 17328
Nb–Zr, properties for liquid metal loops, 19: 40112(R) (ANL-7046 (p.36-66))
Nb–Zr, properties of cold-worked fuel sheathing tubes of, 19: 39150 (AECL-2250(Pt.I))
Nb–Zr, properties for use in water-cooled reactors, 19: 42813
Nb–Zr, properties at low temperatures, 20: 3920(R) (ORNL-3870, pp 27-37)
Nb–Zr, properties of bimetal tubes of type 316 stainless steel and, 20: 11214(R) (NASA-CR-54717)
Nb–Zr, properties for containment of potassium at high temperatures, 20: 18020(R) (ORNL-3900, pp 2-81)
Nb–Zr, properties of TIG-welded, 20: 23731
Nb–Zr, properties of zirconium-base, for fuel cladding for water-cooled reactors, 20: 35849 (KR-89, pp 82-96)
Nb–Zr, properties at high temperatures, compilation to 1957, 20: 43908 (PWAC-237)
Nb–Zr, properties as bore seal material, 20: 46145 (NASA-CR-54093)
Nb–Zr, properties of zirconium-base, for use in water cooled reactors, 20: 46159(P)
Nb–Zr, pulse transmission by coaxial cables of superconducting, (E), 19: 39740
Nb–Zr, purification by electron-beam melting, 20: 5181(R) (ORNL-3029)
Nb–Zr, radiation effects on stress-rupture strength of, tube burst tests of, 16: 6823(R) (ORNL-3213(p.124-33))
Nb–Zr, radiation effects on superconducting, proton, 17: 6756
Nb–Zr, radiation effects on oxidation of, 17: 12621
Nb–Zr, radiation effects, 17: 17447
Nb–Zr, radiation effects on properties of precipitation-hardening, 17: 31054
Nb–Zr, radiation effects on, 17: 18389 (TID-7652(p.808-18))
Nb–Zr, radiation effects on rupture-stress properties of, 17: 31068
Nb–Zr, radiation effects on stress-rupture properties, 17: 34557(R) (ORNL-3480(p.117-42))
Nb–Zr, radiation effects on properties as semiconductor material, 17: 36347(R) (NARF-62-18P)
Nb–Zr, radiation effects on mechanical properties of, neutron, 18: 14537(R) (HW-79766(p.4.1-76))
Nb–Zr, radiation effects on tensile properties of, 18: 26096
Nb–Zr, radiation effects on bend properties of, neutron, 18: 32226 (ORNL-TM-880)
Nb–Zr, radiation effects on hardness of, at 50°C, 18: 32043(R) (HW-81269 (p.4.1-64))
Nb–Zr, radiation effects on mechanical properties of hydrided, 18: 42108 (AECL-1986)
Nb–Zr, radiation effects on ductility of, fast-neutron, 18: 44049(R) (ORNL-3670(p.77-111))
Nb–Zr, radiation effects on creep of, 19: 24089(R) (SRO-114)
Nb–Zr, radiation effects on tensile properties of, neutron, 19: 25046(R) (HW-83615)
Nb–Zr, radiation effects, 19: 27735(R) (NAA-SR-10850)
Nb–Zr, radiation effects on fuel rod jackets of, 19: 26876 (ANL-6750)
Nb–Zr, radiation effects on mechanical properties of, neutron, 19: 30820 (BNWL-23)
Nb–Zr, radiation effects on tensile properties of, neutron, 20: 27571(R) (BNWL-207, pp 4.1-3)
Nb–Zr, radiation effects on impact properties of hydrided, fast-neutron, 20: 27602
Nb–Zr, radiation effects on tensile properties of, fast-neutron, 20: 27604
Nb–Zr, radiation effects on sorptive properties of, for hydrogen and oxygen, fast-neutron and gamma, 20: 27599
Nb–Zr, radiation effects on impact properties of, effects of hydrogen on

fast-neutron, 20: 31669
Nb–Zr, radiation effects on critical current peak vs magnetic field behavior of superconducting, 20: 44505
Nb–Zr, reactions with uranium monocarbide at 1000 to 2400°C, 18: 8795 (HW-72031)
Nb–Zr, reactions with sodium at 2100 to 2400°C, 19: 39090(R) (ANL-7046(p.78-82))
Nb–Zr, reactions with metals at 540 to 760°C *in vacuo*, 19: 44606 (PWAC-483)
Nb–Zr, reactions with fission–plutonium–uranium alloys at 750°C, 19: 44587(R) (ANL-7000, pp 3-63)
Nb–Zr, reactions with oxygen at 2000°F, 19: 47016 (TIM-901)
Nb–Zr, reactions with TZM molybdenum alloy at 2000°F in refluxing potassium, 20: 9423(R) (NASA-CR-54735)
Nb–Zr, reactions with sodium, high-temperature, 20: 15033(R) (ANL-7152, pp 87-96)
Nb–Zr, reactions with sodium at high temperatures, 20: 20925(R) (ANL-7055, pp 177-212)
Nb–Zr, reactions with plutonium uranium carbide at 820°C, 20: 27416(R) (UNC-5134(Vol.1))
Nb–Zr, reactions with oxygen at 1000 to 1600°F, mechanisms of, 20: 31669
Nb–Zr, reactions with liquid sodium at high temperatures, 20: 38499 (ANL-7120, pp 839-47)
Nb–Zr, reactions with uranium mononitride at high temperatures, 20: 37168(R) (BMI-1771)
Nb–Zr, reactions with plutonium nitride and uranium nitride at high temperatures, 20: 37169(R) (BMI-1774)
Nb–Zr, reactor creep tests on heat-treated, 20: 7501(R) (TID-22426)
Nb–Zr, relation between structure anisotropy and superconducting anisotropy in, 17: 20493
Nb–Zr, resistance to sodium corrosion, 17: 31798(R) (BNL-782(p.60-91))
Nb–Zr, resistive states in superconducting, 18: 15065
Nb–Zr, rupture properties of, effects of exposure to potassium at 1400°F on stress-, 20: 13191(R) (NASA-CR-54476)
Nb–Zr, shear strength of fasteners of, at room temperature and 1600°F, 17: 36281 (AD-295526)
Nb–Zr, solubility in sodium (liquid), 17: 14839(R) (NRL-5904)
Nb–Zr, solubility in cesium at 2500°F, 19: 13913(R) (AFML-TR-64-327)
Nb–Zr, solubility in sodium at 800 to 1380°C, 20: 5846
Nb–Zr, solvent properties of, for oxygen at 1000°C, 16: 13611
Nb–Zr, solvent properties for hydrogen, 20: 5849
Nb–Zr, solvent properties for oxygen at 1000 to 1200°C, 20: 16980
Nb–Zr, solvent properties of zirconium-base, for hydrogen to 550°C, 20: 27435
Nb–Zr, sorptive properties for hydrogen from steam at 500°C, 17: 39468(T,R) (EURAEC-520)
Nb–Zr, sorptive properties for oxygen at 1000°C and 10^{-4} to 10^{-7} torr, 18: 27903 (NASA-SP-41(p.307-12))
Nb–Zr, sorptive properties for nitrogen, 18: 44049(R) (ORNL-3670 (p.77-111))
Nb–Zr, sorptive properties for nitrogen, kinetics of, 20: 4301(R) (ORNL-3870, pp 102-35)
Nb–Zr, sound absorption in superconducting, u-h-f, 17: 39767
Nb–Zr, specifications of, for use in corrosion test loop fabrication, 20: 21293 (R-66SD3007)
Nb–Zr, stability of carbon-strengthened, at 2000°F, 20: 4397 (TIM-955)
Nb–Zr, strength of CS1830 series of, effects of fabrication on short-time, 17: 36290 (CNLM-4408)
Nb–Zr, strength properties, 19: 20474(R) (NASA-CR-54281)
Nb–Zr, strengthening by oxygen addition and quenching, 19: 39223(P)
Nb–Zr, stress rupture of tubular, 16: 30167 (ORNL-3313(p.19-64))
Nb–Zr, stress-rupture in-pile testing, 17: 5040(R) (ORNL-3364(p.125-50))
Nb–Zr, stress-rupture of, effects of hydrogen embrittlement on, 17: 31733(R) (SRO-84)
Nb–Zr, stress-rupture properties at 980 to 1200°C, 18: 4255(R) (ORNL-3470(p.98-125))
Nb–Zr, stress rupture at 550 and 600°C, 19: 29468(R) (ANL-7017)
Nb–Zr, structure of, temperature effects on, 16: 12653(R) (EURAEC-130)
Nb–Zr, structure effects on mechanical and superconducting properties of, (E), 19: 28863
Nb–Zr, structure and superconducting properties of, effects of oxygen on, 20: 42535
Nb–Zr, superconducting, phase equilibria in, 16: 27671
Nb–Zr, superconducting, behavior of, 16: 30170(R) (ORNL-3313(p.179-208))
Nb–Zr, superconducting, magnetic quenching characteristics of, 16: 15396
Nb–Zr, superconducting, transition temperatures of, 16: 6825(R) (ORNL-3213(p.139-40))
Nb–Zr, superconductivity, 16: 16830
Nb–Zr, superconducting, use of, as iron-core-magnet coils, 16: 15430
Nb–Zr, superconducting, use of, as magnet coils for fields over 100 kgauss, 16: 15460
Nb–Zr, superconducting, use of, for 55-kgauss magnets, 16: 15427
Nb–Zr, superconducting, use of, in 30-kgauss solenoid, 16: 15431
Nb–Zr, superconducting, use of, to produce 59-kgauss magnet, 16: 15428
Nb–Zr, superconducting critical currents in, 17: 553
Nb–Zr, superconductivity of, effects of magnetic-field orientation on, 17: 5037(R) (ORNL-3364(p.27-56))
Nb–Zr, superconductivity in, 17: 6807 (UCRL-9819)
Nb–Zr, superconductivity of, pulsed-magnetic-field studies of, 17: 18907 (TID-17310)
Nb–Zr, superconductivity of thin wires of, 17: 8858
Nb–Zr, superconductive properties and technical applications of, 17: 16705
Nb–Zr, superconducting properties, 17: 22365
Nb–Zr, superconducting critical currents in coils and wires of, 17: 24062 (UCRL-10402)
Nb–Zr, superconducting transitions in high magnetic fields, 17: 25938
Nb–Zr, superconducting properties for use in high-field magnets, 17: 28074
Nb–Zr, superconducting critical currents at 4.2°K, 17: 28101
Nb–Zr, superconducting critical fields of, 17: 32224
Nb–Zr, superconductivity, 17: 34438
Nb–Zr, superconductivity and uses of Nb$_3$Zr, 17: 34451
Nb–Zr, superconductor transition to normal state in solenoids of, 17: 37742
Nb–Zr, superconducting critical current dependence on dI/dt in, 17: 37523
Nb–Zr, superconducting-normal transitions in, 18: 952 (ANL-SBC-1)
Nb–Zr, superconducting behavior of film of, prepared using exploding wires, 18: 2753
Nb–Zr, superconductivity of, upper critical fields for, 18: 2776
Nb–Zr, superconductivity of, mechanism for high-field, 18: 4499
Nb–Zr, superconducting transition temperatures in, pressure effects on, 18: 6120
Nb–Zr, superconducting critical current of, dependence on applied transverse magnetic field, 18: 6131
Nb–Zr, superconducting critical current of ultrafine wire of, dependence on wire size, 18: 6132
Nb–Zr, superconducting wire of, intermediate-state resistance of, 18: 6134
Nb–Zr, superconducting solenoids of, flux jumping in, 18: 13017
Nb–Zr, superconducting critical alternating currents in, 18: 13018
Nb–Zr, superconducting magnets of, 18: 24547
Nb–Zr, superconducting magnets of, 18: 34715
Nb–Zr, superconducting cylinders of, hysteresis losses in, 18: 36527
Nb–Zr, superconducting behavior of films of, 18: 42574
Nb–Zr, superconducting properties, 18: 44681
Nb–Zr, superconducting properties of, 19: 12453
Nb–Zr, superconducting properties of, (E), 19: 16764 (AROD-3473:2)
Nb–Zr, superconducting transitions in fast-pulsed magnetic fields, (E), 19: 16779
Nb–Zr, superconducting, alternating current characteristics of, 19: 18480
Nb–Zr, superconducting critical fields for, (T), 19: 19025
Nb–Zr, superconducting critical currents of, (E), 19: 19056
Nb–Zr, superconducting properties of, effects of heating to 300°C for 10 hr on, 19: 20609(P)
Nb–Zr, superconductivity, 19: 39695
Nb–Zr, superconducting critical current density in, method for increasing, (E), 20: 1121(T) (AI-Trans-97)
Nb–Zr, superconducting properties of, effects of heat treatments and microstructure on, 20: 2395
Nb–Zr, superconducting-normal transitions in variable fields, mechanisms of, (E), 20: 2902
Nb–Zr, superconducting properties, 20: 4390(R) (ORNL-3870, pp 65-9)
Nb–Zr, superconducting properties, (E), 20: 4792
Nb–Zr, superconducting solenoids of, mechanism of current degradation in, 20: 8004
Nb–Zr, superconducting point contacts of, macroscopic quantum interference effects in, (E/T), 20: 11911
Nb–Zr, superconductivity of, 20: 13666 (IPP-4/22)
Nb–Zr, superconductivity of, effects of omega-transformation on, (E), 20: 19722 (N-65-17099)
Nb–Zr, superconducting critical currents and fields in flux-pump fed coils of, (E), 20: 21924
Nb–Zr, superconductivity disruption in, in magnetic field, 20: 28181
Nb–Zr, superconducting critical currents in wires of, magnetic field dependence of, (E), 20: 28175
Nb–Zr, superconductivity of, effects of cold working and heat treatments on, 20: 29787
Nb–Zr, superconductivity of, effects of microstructure on, 20: 29788
Nb–Zr, superconductivity of, effects of cold working and heat treatments

on, 20: 29789
Nb–Zr, superconducting critical current density of wires of, (E), 20: 30267(T)
Nb–Zr, superconducting critical fields of, angular dependence of upper, (E), 20: 30270
Nb–Zr, superconductivity of, in pulsed magnetic fields, effects of aging on, 20: 32312(R) (UCRL-16658, pp 133-43)
Nb–Zr, superconducting properties of, at elevated temperatures, 20: 34417(R) (N-65-34464)
Nb–Zr, superconducting properties in strong d-c magnetic fields, (E), 20: 37950
Nb–Zr, superconductivity for magnets, 20: 40015(R) (ORNL-TM-1598)
Nb–Zr, superconducting critical current density in, effect of structure on, 20: 40021
Nb–Zr, superconductivity in surface layers of, (E), 20: 40023
Nb–Zr, superconductivity, 20: 40047
Nb–Zr, superconducting properties of copper-enclosed, pressure effects on, 20: 44526
Nb–Zr, superconducting critical field measurements for, resistive effects on surface, 20: 44534
Nb–Zr, surface current effects in superconducting, 20: 30280
Nb–Zr, temperature cycling effects on critical currents in wire of, 18: 42553
Nb–Zr, tensile properties, 16: 20981(T,R) (EURAEC-27)
Nb–Zr, tensile properties at 4.2, 77, and 300°K, 17: 5037(R) (ORNL-3364(p.27-56))
Nb–Zr, tensile properties at 4.2 to 300°K, 17: 41477
Nb–Zr, tensile properties, 18: 3038(R) (ANL-6801)
Nb–Zr, tensile properties at 20 to 950°C, 18: 25966(R) (ANL-6868 (p.120-32))
Nb–Zr, tensile properties of, effects of copper and specimen geometry on, 19: 26805 (AECL-2207)
Nb–Zr, tensile properties of cold-worked, for use as fuel sheathing, 19: 28807 (AECL-2250)
Nb–Zr, tensile properties of, effect of texture on, 19: 30805
Nb–Zr, tensile properties of pressure tubing of, effects of hot working on, 19: 46539(R) (TID-22249)
Nb–Zr, tensile properties of zirconium-base, effects of strain rate and temperature on, 20: 9490(R) (BNWL-166, pp 6.15-18)
Nb–Zr, tensile properties of, effects of precipitation hardening on, 20: 23698
Nb–Zr, testing for power reactor pressure tubes, 18: 37666 (A/CONF.28/P/22)
Nb–Zr, testing for use in liquid-metal turbine blades and nozzles, 20: 2240
Nb–Zr, testing magnets of, 17: 24053(R) (ORNL-3432)
Nb–Zr, testing of, method for maintaining high-purity gas environment for, 19: 18408
Nb–Zr, testing superconducting magnets of, 17: 21388(R) (LNF-63/11)
Nb–Zr, testing tubular, 19: 35778(R) (SRO-116)
Nb–Zr, thermal analysis of ω phase of, 19: 47037
Nb–Zr, thermal conductivity of normal and superconducting, at 1.6–12°K, 17: 39598
Nb–Zr, thermal cycling, effects on crystal structure and dimensional stability, 17: 14729 (CRGM-1106)
Nb–Zr, thermal expansion coefficient at 75 to 1890°F, 19: 16057(R) (AGN-8131)
Nb–Zr, thermal expansion of, effects of hydride phase on, 20: 31745
Nb–Zr, thermal phase transitions in superconducting, 18: 42575
Nb–Zr, thermal properties of, at 500 to 5000°F, 17: 16636 (ASD-TDR-62-765)
Nb–Zr, thermal propagation of normal region in wires of, effect of copper plating on velocity of, 17: 37716
Nb–Zr, thermal propagation of normal boundary in superconducting, (E/T), 19: 16766
Nb–Zr, thermal propagation of normal transitions of superconducting, 20: 24273
Nb–Zr, thermodynamic properties, 16: 13636
Nb–Zr, thermodynamic properties of capsules of, 17: 27792 (NP-12933)
Nb–Zr, thermodynamic properties of nitrogen equilibrium solid solutions in, 20: 13263 (ORNL-TM-1355)
Nb–Zr, thermoelectric power at 9.2 to 330°K, effects of zirconium content on, 20: 17067
Nb–Zr, thermophysical properties, 18: 44049(R) (ORNL-3670(p.77-111))
Nb–Zr, training effect in coil of superconducting, (E), 20: 11895
Nb–Zr, transfer of carbon and nitrogen to, from stainless steels in potassium, 20: 2270
Nb–Zr, transformation kinetics in, 18: 4250(R) (ORNL-3470(p.45-8))
Nb–Zr, transformation kinetics, study of, 18: 44147(R) (ORNL-3670 (p.21-2))
Nb–Zr, transformation kinetics in, 19: 41033
Nb–Zr, transformation temperatures of, effects of cooling rates on, 20: 37233
Nb–Zr, transients in superconducting coil of, 17: 22267 (BSD-TDR-62-116)
Nb–Zr, transport current effects on magnetization of superconducting wires of, 17: 34622
Nb–Zr, transport current effects on magnetic properties of superconducting (E), 19: 3176
Nb–Zr, tube-burst tests on, 20: 5181(R) (ORNL-3029)
Nb–Zr, ultrasonic attenuation in superconducting, in strong magnetic fields, (E), 19: 21188
Nb–Zr, ultrasonic attenuation in superconductors of, temperature dependence of, 19: 25436(R) (RTD-TR-65)
Nb–Zr, ultrasonic attenuation in nonideal superconducting, flux jumping and magnetization effects on, (E), 20: 17606
Nb–Zr, upper critical fields of superconducting, 18: 11109
Nb–Zr, uptake of carbon, nitrogen, and oxygen by, in liquid metal loops, 20: 41419(R) (GMAD-3643-5)
Nb–Zr, use as loop material for forced-convection corrosion of refractory alloys by lithium, 20: 5853 (TIM-898)
Nb–Zr, use as solenoid lens in electron microscope, 19: 15841
Nb–Zr, use for superconducting magnet coils, 20: 5614
Nb–Zr, use in accelerators and storage rings as superconductors, 18: 16602 (BNL-7534(p.417-47))
Nb–Zr, use in condensers for space power plants, 19: 9331 (PWA-2320 (Vol. I))
Nb–Zr, use in heat transfer tube, 20: 14699(P)
Nb–Zr, use in superconducting magnets, 17: 20438
Nb–Zr, use in superconducting solenoids, 17: 23712
Nb–Zr, use in superconducting solenoids, 18: 36520
Nb–Zr, use in superconducting solenoid, 19: 23594(P)
Nb–Zr, use of superconducting, for magnet development, 20: 34418(R) (N-66-16181)
Nb–Zr, welding, 17: 22092(R) (GE63FPD66)
Nb–Zr, welding, aging behavior in, 17: 8769
Nb–Zr, welding of, effects of gases on, 16: 20807 (NP-11694)
Nb–Zr, welding of, in various atmospheres, 17: 509 (CW-R&DL-29)
Nb–Zr, welding of, 17: 6558
Nb–Zr, welding of, nondestructive testing of zones of, 20: 13320
Nb–Zr, welding properties, 18: 4255(R) (ORNL-3470(p.98-125))
Nb–Zr, welding to current contacts, 17: 36267
Nb–Zr, welding to T-111 alloy, 20: 43830(R) (NASA-CR-72029)
Nb–Zr, wetting by sodium, effects of temperature on, 20: 37168(R) (BMI-1771)
Nb–Zr, x-ray diffraction of nonmetallic phases chemically extracted from, 19: 7973
Nb–Zr, 50-c critical currents in superconducting wires of, 17: 34595
Ni–Nb, corrosion of, by steam and water, 16: 29346
Ni–Nb, crystal structure of intermetallic compound $NbNi_3$ in, 19: 9699
Ni–Nb, diffusion in solid solutions of Ni_3Nb, tracer studies of, 19: 7916
Ni–Nb, mechanical properties at 1000°C, 19: 26859
Ni–Nb, mechanical properties and oxidation rate, 19: 32754
Ni–Nb, oxidation kinetics of, at 500 to 900°C, 19: 13929
Ni–Nb, oxidation kinetics at 500 to 900°C, 19: 20494
Ni–Nb, paramagnetic susceptibility and lattice parameters of solid solutions of, 18: 8848
Ni–Nb, phase diagrams, 20: 15115
Ni–Nb, phase studies, 19: 11682
Ni–Nb, phase studies, 19: 26859
Ni–Nb, properties, 19: 26848
Ni–Nb, structure of intermetallic compound NbNi in, 17: 1981(T)
Ni–Nb, vacuum-pressure braze cladding of, 18: 7177
Ni–Nb–Ru, crystal structure studies, 19: 44678(R) (ANL-7000, pp 186-200)
Ni–Nb–Ta, diffusion of nickel in, effects of annealing temperature and composition on, 20: 17089
Ni–Nb–Ta–Sn–Ti, corrosion resistance and ductility of, 19: 34735(P)
Ni–Nb–Ta–Ti, corrosion resistance and ductility of, 19: 34735(P)
Ni–Nb–Ta–Ti–V, corrosion resistance and ductility, 19: 34735(P)
Ni–Nb–Ta–Ti–W, corrosion resistance and ductility, 19: 34735(P)
Ni–Nb–Ti, phase diagrams of, ternary chemical compounds in, 20: 43971
Ni–Nb–V, corrosion of, by steam and water, 16: 29346
Ni–Nb–V, oxidation of coatings of, 17: 6562(R) (ARF-B-6001-1)
Ni–Nb–W, solid state bonding of, 18: 24112
Ni–Nb–Zr, hydrogen embrittlement of, review of, 20: 37187
Ni–Th–Zr, properties and structure of, 18: 37670 (A/CONF.28/P/337)
Pb–Nb, tunneling between superconducting films of, 18: 6125
Sb–Nb, crystal structure of intermetallic compound $NbSb_2$ in, 19: 23028
Sb–Nb, crystal structure of intermetallic compounds in, 19: 39209
Sb–Nb, phase relations and structures in, 18: 37714
Sb–Nb, preparation and superconductivity properties of intermetallic compounds of, 18: 4287
Sb–Nb, preparation of intermetallic compounds in, by chemical transport in temperature gradient, 19: 26333
Sb–Nb–Sn, superconducting properties of Nb_3SnSb, 17: 27861

Sb–Nb–Sn–Zr, corrosion by steam at 400 and 450°C, 19: 30668(R) (EURAEC-1274)
Sb–Nb–Zr, corrosion of, in 680°F water, 17: 16582 (ARF-B198-36)
Sb–Nb–Zr, corrosion by water at 680°F, 17: 30905(R) (ARF-B198-42)
Sb–Nb–Zr, corrosion by steam at 400 and 450°C, 19: 30668(R) (EURAEC-1274)
Sb–Nb–Zr, oxidation by water at 680°F, 18: 2162(R) (IITRI-B198-46)

NIOBIUM ARSENIDES

crystal structure, 17: 18738(R) (AFOSR-2645)
crystal structure, 18: 1622
crystal structure, 19: 7945
preparation by chemical transport in temperature gradient, 19: 26333

NIOBIUM BORIDES

analysis for boron by pyrohydrolysis, 19: 19761 (NP-14876)
analysis for boron, method for, 19: 46941 (NP-15514(Vol.3))
analysis, methods for, 19: 24403 (NP-14952)
bibliography on phase relations of, 17: 30913 (NP-12972)
bibliography on phase relations of, 18: 10518 (AD-410526)
bibliography on preparation and properties of, 17: 10579 (ASD-TDR-62-873)
bonding in nuclear magnetic resonance analysis of, 17: 8081
boron-11 quadrupole resonance in, 17: 3511
chemical bonding and electric conductivity of, 20: 16439
combustion in fluorine, calorimetry of, 18: 43440(R) (ANL-6800(p.305-25))
compact preparation, 17: 6520(R) (NP-12373)
corrosion by hydrogen chloride at 2250°C, 19: 46956 (NP-15514 (Vol.1))
corrosion of, by hydrochloric acid, 17: 20405(R) (NP-12710)
crystal structure and thermal properties, 19: 7467
deformation properties and hardness of, at high temperatures, 20: 33920
electric properties of, effects of non-metallic atoms on, 17: 8854
emissivity and thermal conductivity at 1263 to 2242°K, 18: 35939(R) (NP-14192)
emissivity, measurement of spectral, 17: 16632(R) (AD-274654)
emissivity measurements to 3000°K, equipment for, 18: 20567
enthalpy of formation of, 20: 31213(R) (ANL-7175, pp 119-58)
erosion by gases at 3000°K, 16: 16726(R) (NP-11311)
fabrication and properties of MHD cell electrodes of, 19: 6495
fabrication and properties of, for use at high temperatures, 20: 29772
galvanomagnetic properties, 17: 416(R) (NP-12130)
heat capacity and thermodynamic properties at 5 to 350°K, 18: 1642
heat of formation of di-, 19: 32118(R) (ANL-7020(p.165-74))
lattice parameters and thermal expansion at 25 to 1700°C, 19: 47009 (NP-15514(Vol.2))
melting temperature, evaluation for space technology, 18: 16521
oxidation and thermodynamic properties at high temperatures, 18: 35939(R) (NP-14192)
oxidation by carbon dioxide at 2250°C, 19: 46956 (NP-15514(Vol.1))
oxidation of, in argon–carbon dioxide mixtures at 2250°C, 17: 6520(R) (NP-12373)
oxidation rate of, at 1100°C, 20: 23614
preparation and purification, 19: 46941 (NP-15514(Vol.3))
preparation by carbon reduction of oxide with boric oxide, 20: 19702
preparation by powder metallurgical techniques, 17: 34328(R) (NP-12991)
preparation of polynuclear, 20: 3863(R) (IS-1200(Sect. C))
preparation, properties, and uses of, review on, 16: 27640(T) (FTD-TT-62-430)
preparation, properties, and aerospace applications, 19: 37142
properties for very high temperature applications, 18: 10539 (RTD-TDR-63-4096(Pt.I))
properties, mechanical and physical, 16: 30853
properties, mechanical and physical, 19: 7456
reactions with carbon, 20: 14555
reactions with graphite to 2200°C, 19: 38654
spectra at 1500 to 2500°K, infrared, 18: 22497 (WADD-TR-60-646 (Pt.3, Vol.II))
spectra of niobium in, L, 19: 6355
spectral emissivity at 1540 to 2000° K, 16: 9142(R) (NP-11264)
structural characteristics, 16: 7913
superconducting transition temperatures of, 18: 36493
thermodynamic properties at 300 to 1200°K, 16: 25401
thermodynamic properties of, tables of, 17: 40777(R) (RAD-SR-63-183)
thermodynamic properties, 19: 7448
thermodynamic properties, 20: 10816(T) (NASA-TT-F-285)

NIOBIUM BROMIDES

complexes of, with pyridine, structure of, 17: 23297 (IS-544)
complexes with acetonitrile, butyronitrile, and propionitrile, properties of, 18: 41416
complexes with diethyl and dimethyl sulfides and tetrahydrothiophene, compositions and properties, 16: 11629
complexes with picoline and pyridine, magnetic properties and spectra of, 18: 22053
heat of formation, 16: 20450
heat of formation of oxytrivalent and pentavalent, 16: 30424
reactions of, with niobium at 410 to 450°C, products in, 17: 23297 (IS-544)
reactions with dimethyl- and diphenyl sulfoxides, properties and spectra of products in, 18: 25398
reactions with niobium oxides, phase studies of equilibrium products in, 19: 363
reactions with primary and secondary aliphatic amines, 16: 12945
reactions with pyridine, 17: 10500 (IS-385)
spectra of, electronic, 19: 34160
structure, x-ray analysis of, 18: 5308
thermodynamic properties, 20: 10816(T) (NASA-TT-F-285)

NIOBIUM CARBIDES

analysis for carbon using electron microprobe, 19: 43966
analysis for oxygen by heat extraction, 16: 7515
analysis, methods for, 19: 24403 (NP-14952)
bibliography on phase relations of, 17: 30913 (NP-12972)
bibliography on phase relations of, 18: 10518 (AD-410526)
bibliography on properties, 17: 27809 (UCRL-7284)
bonding and vacancies in, 18: 16483(T) (AEC-tr-6374)
bonding to tantalum, 16: 15151 (APED-3870)
chlorination, 20: 22983
comminution of, effects of impact strength, microhardness, shear modulus, and thermal expansion on, 18: 44220(T)
compact preparation, 17: 6520(R) (NP-12373)
compressibility of, effect of high pressure on, 20: 9520
containment in graphite crucibles at 3800 to 4700°K, 20: 43174 (NASA-CR-608)
corrosion by carbon dioxide and hydrochloric acid at 2250°C, 17: 34328(R) (NP-12991)
corrosion by hydrogen chloride at 2250°C, 19: 46956 (NP-15514 (Vol.1))
corrosion by hydrogen fluoride at 2000 to 3100°K, 20: 2261(R) (UCRI-326)
corrosion by manganese–uranium alloy at 1100°C, 17: 7658(R) (LAMS-2815)
crystal structure, 18: 16507
crystal structure, 18: 25970(R) (ANL-6868(p.303-25))
deformation properties and hardness of, at high temperatures, 20: 33920
densification of pressed and sintered, effects of dispersion on, 18: 18335
deposition of coatings of, on graphite, 16: 4523(P)
deposition of coatings of, on graphite by carburization, 16: 30767(P)
deposition on graphite surfaces, 19: 42835(P)
deposition on graphite surfaces, 19: 42836(P)
determination in niobium and niobium alloys by anodic staining, 19: 34107 (ORNL-3821)
determination in niobium by anodic staining, 19: 46929 (NMI-4998, pp 57-64)
diffusion into zirconium at 1760°C, 19: 40412 (TIM-924)
diffusion of carbon and niobium in, 16: 12128
diffusion of carbon in, at 2940°K, 16: 29408
diffusion of carbon and niobium in, at 1800°C, 17: 29350
diffusion of carbon and niobium in, activation energies for, 18: 624
diffusion of carbon in, at 1800 to 2700°C, layer-growth measurements of, 20: 2398
diffusion of carbon in, at 1700°K, coefficient for, 20: 14992
diffusion of carbon in, at 1100 to 1500°C, 20: 23662(T) (LA-tr-66-21)
diffusion of carbon in, at 1700 to 3000°C, 20: 27530
dislocations in, in area of fracture in chromium–nickel steels, 20: 23757
effects on ferrite grain growth in mild steels, 19: 985
effects on mechanical properties of tungsten, 16: 3478 (WADD-TR-60-37(Pt.II))
effects on properties of graphite, with and without copper and silver infiltration, 20: 29764
effects on radiation resistance and mechanical properties of plutonium or uranium carbides, 18: 44230(P)
effects on stacking faults in austenitic steel, 19: 985
effects on tantalum carbide–titanium carbide–tungsten carbide systems, 16: 27659
elastic properties of polycrystalline, 20: 35908
elastic properties of stoichiometric, 20: 39430
electric conductivities and Hall coefficients, 16: 6749
electric conductivity of, at high temperatures, 17: 8856
electric conductivity at high temperatures, 18: 28012(T)
electric conductivity of, at 1200 to 3500°K, 20: 41729
electric properties of, effects of non-metallic atoms on, 17: 8854
electric properties of, rigid band model for interpreting, 18: 24137 (NP-13944)
electric resistance at 1200 to 3500°K, 20: 41729
emissivity at 800 to 5000°K, relation of structure to, 18: 20566
enthalpy equations, 20: 5846

entropy of formation at 298°K, 18: 19974
erosion by gases at 3000°K, 16: 16725(R) (NP-11311)
evaporation rate and vapor pressure at 1100 to 2000°C, 16: 2208(T) (AEC-tr-4865)
extrusion of, development of techniques for, 20: 796
fabrication and properties of sintered filters of, 18: 18336
fabrication by hot-pressing, 20: 31699
fabrication of large parts from, 19: 40988
Fermi level, 19: 47009 (NP-15514(Vol.2))
figure of merit and atomic characteristics, 19: 2284
formation by carburization of niobium–zirconium alloy, 19: 44609 (TIM-927)
formation by niobium pentachloride dissociation on graphite and niobium surfaces, mechanism of, 20: 21241(T) (LA-tr-66-15)
formation in niobium steel, 17: 11209
formation of, by reduction of niobium pentoxide, 17: 21692
formation on niobium–1 zirconium alloy, activation energies for, 20: 14992
free energy of formation at 1180 to 1370°K, 18: 19970
friction between surfaces of, at high temperatures in vacuum, argon, helium, and nitrogen atmospheres, 19: 28825
hardness of cast, at 20 to 1500°C, 20: 41429(R) (USBM-RC-1249)
hardness of, effects of temperature on, 17: 36316
hardness of sintered, to 1200°C, 20: 23743
heat of formation, 17: 20502
heat of formation of, 20: 43251
hot pressing of high density, apparatus for, 16: 19267
inflammability of powdered, at 180 to 1100°C, 18: 44211
interactions with gas flow in MHD generators, 20: 41738
magnetic susceptibility, 17: 14858(T) (AEC-tr-5651)
melting point, 17: 11201(T) (AEC-tr-5598)
melting temperature, evaluation for space technology, 18: 16521
oxidation by carbon dioxide at 2250°C, 19: 46956 (NP-15514(Vol.1))
oxidation of, at 1000 to 2000°K, kinetics of, 17: 21665(R) (ASD-TDR-62-203(Pt.II))
oxidation of cast, by air at 450 to 800°C, 20: 41429(R) (USBM-RC-1249)
oxidation of, in argon–carbon dioxide mixtures at 2250°C, 17: 6520(R) (NP-12373)
oxidation of, x-ray studies of, 18: 2283
performance as emitter for thermionic converter, effects of surface condition on, 18: 28305 (APL-TDR-64-63)
performance in high-temperature reactors for space propulsion, 16: 28631
performance in high-temperature reactor fuels, 20: 12378
plastic deformation of crystalline, 18: 14497
plastic deformation, 19: 11682
precipitation at grain boundaries in austenitic steel, 16: 33422
precipitation in austenitic steels, effect of heat treatment on, 16: 33423
precipitation in austenitic creep-resisting steels, 18: 37726
precipitation on dislocations in austenite steel, 16: 537
preparation and properties of, 18: 16498
preparation and properties of cast, 20: 41429(R) (USBM-RC-1249)
preparation and properties of 100–1000 A particles of, 20: 43951
preparation and purification, 19: 46941 (NP-15514(Vol.3))
preparation by reduction of oxides by carbon, equilibria in, 16: 2209(T) (AEC-tr-4867)
preparation by reduction of niobium pentoxide, conditions for, 18: 35947(T)
preparation of high-purity, using cobalt or iron-nickel alloy bath, 19: 42828
preparation of high-purity, auxiliary metal bath for, 20: 27452
preparation of thin films of, 18: 16507
preparation, properties, and aerospace applications, 19: 37142
production and properties of, 18: 7262
production by graphite–niobium reactions at 1700 to 2300°C, kinetics of, 20: 43954
properties as magnetohydrodynamic electrodes, 18: 7458 (PWA-2125)
properties as thermionic cathodes to 3000°C, 18: 12426
properties for matrix material in particulate uranium carbide fuels, 20: 39353 (BNwF-FBK-66-07)
properties for thermionic power generation, vaporization, 18: 27980
properties, mechanical and physical, 16: 30853
properties of, dispersion velocity dependence on mechanical and thermal, 17: 27873
properties of, at 2000°C, for use in thermionic converters, 20: 29729
radiation capacity at 1200 to 3500°K, 20: 41729
radiation effects on, neutron, 20: 23774(R) (ORNL-3913, pp 75-109)
reactions with copper and nickel mattes, slags, molten salts, and refractory metals, 20: 14989
reactions with graphite at 1800 to 2200°C, contact, 18: 30208
reactions with magnesium and zirconium oxides at 1800 to 2000°C, 18: 43463
reactions with molybdenum at 1000 to 2100°C, 16: 4555(T) (FTD-TT-61-74)
reactions with molybdenum, niobium, tantalum, and tungsten at 900 to 2200°C, 20: 25578(T) (N-65-35787)
reactions with niobium pentoxide in vacuum, 17: 21600
reactions with niobium pentoxide in arc furnace, 17: 21601
reactions with niobium oxides, kinetics of, 17: 25256
reactions with niobium oxides by vacuum reduction process for preparation of niobium metal, 19: 9145
reactions with niobium oxides to prepare crude niobium metal, 19: 9146
reactions with niobium oxide–tungsten oxide and niobium oxide–tungsten carbide to form niobium–tungsten alloy, 20: 29677
reactions with niobium oxides, properties of intermediate products in, 18: 10069
reactions with nitrogen at 1150 to 2370°C, 20: 12845
reactions with titanium, 20: 13194
review, 18: 39899 (LA-2942)
screening of metal–metal bonds in, effects on overlapping, 18: 17781(T) (AEC-tr-6388)
sintering of, effects of cobalt chloride and iron on, 16: 27611
solubility in low-carbon manganese steel, 17: 20471
spectra of niobium in, L, 19: 6355
spectra, reflection, 17: 6520(R) (NP-12373)
spectral emittance at 800 to 5000°F, 16: 18939
stability in acids, alkalis, and oxidizers, 16: 2952
stability in acids, alkalis, and oxidizers, 16: 11583(T) (AEC-tr-5040)
superconducting critical currents of, (E), 19: 27371
superconducting properties, 19: 20572
superconductivity of, negative results, 17: 11391
superconductivity of, high-field, (E), 19: 25449
superconductivity, 19: 43997(R) (UCRL-11289)
superconductivity of platelets and whiskers of, electric and magnetic transport properties in, (E), 20: 8015
superconductivity, susceptibility, and thermal capacity of, (E), 20: 34443
testing as high-temperature heater for electric resistance furnaces, 20: 15112
thermal capacity at 1289 to 2778°K, 17: 35751
thermal capacity at 7 to 320°K, 19: 42848 (LA-DC-6565)
thermal capacity at 10 to 320°K, 20: 15097
thermal capacity of, at 7.5 to 320°K, 19: 46998 (LA-3331)
thermal decomposition, 17: 32036 (CONF-40-2)
thermal expansion, 17: 6520(R) (NP-12373)
thermal expansion, 17: 20405(R) (NP-12710)
thermal expansion at 25 to 2080°C, 18: 30195
thermal expansion at high temperatures, 18: 32178
thermal expansion at 25 to 2030°C, 19: 47009 (NP-15514(Vol.2))
thermal expansion at 30 to 2843°C, 20: 5846
thermal properties to 5000°F, 16: 18938
thermal properties, 16: 22597 (WADD-TR-60-924)
thermal properties of, at 500 to 5000°F, 17: 16636 (ASD-TDR-62-765)
thermionic emission from crystalline, in cesium, potassium, and rubidium vapors, 18: 12794
thermionic properties, 16: 13626
thermionic properties at 1400 to 2000°K, 17: 25811
thermodynamic functions of, concentration and temperature dependences of, (T), 19: 23041(T)
thermodynamic properties, 17: 3470 (BMI-1601)
thermodynamic properties at 298.15 to 2000°K, 18: 23435 (BM-RI-6446)
thermodynamic properties of, Schottky-Wagner model predictions and observations of, 19: 7453
thermodynamic properties, 20: 10816(T) (NASA-TT-F-285)
thermodynamic stability of, review of data on, 19: 23064
thermoelectric emission of, on metal substrates, 19: 6351
thermoelectric emission in cesium vapor, 20: 29800
thermoelectric properties, temperature dependence, 16: 15230
thermoemission properties of, 17: 39799
use as cathode in thermionic converter, 17: 25845(R) (AD-404255)
use of, in nuclear rockets, 17: 8710 (TID-16315(Del.))
vaporization at 2260 to 2940°K, 16: 29408
welding to high melting metals by vacuum diffusion, 19: 22931(T) (JPRS-29550)
wetting by liquid cobalt, copper, iron, and nickel, 20: 1837
C–NbC–UC, phase equilibria and uranium carbide stability in, 17: 39588
C–NbC–UC, preparation as reactor fuel material, 20: 2305(P)
Co–NbC–TaC–TiC, thermal expansion at 68 to 1800°F, 18: 20513 (CNLM-4234)
Co–NbC–TaC–WC, thermal expansion at 68 to 1800°F, 18: 20514 (CNLM-4479)
Co–NbC–TaC–TiC–WC, thermal expansion at 68 to 1800°F, 18: 20514 (CNLM-4479)
Co–NbC–WC, mechanical properties of, effects of composition on, 20: 13274
Co–NbC–WC, physical properties and structure, 19: 42861
Cr–Co–Ni–NbC–TaC–TiC, oxidation tests of Kennametal K 162B and 183A at 1400 and 1500°C, 19: 9624 (SCNC-270)

GaC–NbC, preparation and crystal structure of H-phase in, 19: 39208
graphite–NbC, fabrication and properties of hot-pressed composites of, 20: 31688 (NASA-CR-507)
graphite–NbC, fabrication and physical properties of, 20: 39367
graphite–NbC, preparation and properties as electrode to 3000°C, 18: 12425
graphite–NbC, thermal expansion of, at 1000 to 2500°C, 20: 35900
HfC–NbC, analysis for hafnium and niobium, method for, 19: 46941 (NP-15514(Vol.3))
HfC–NbC, preparation and physical properties of solid solutions in, 19: 37091
HfC–NbC, preparation and properties, 20: 11330
HfC–NbC, thermoemission properties at 1100 to 2500°C, 19: 23075
HfC–NbC–ZrC, phase studies and structure, 18: 2281
HfN–NbC–NbN, superconducting properties, 20: 17589 (CONF-650922, pp 541-9)
MoC–NbC, use of, in nuclear rockets, 17: 8710 (TID-16315(Del.))
Mo–Ni–NbC–TiC, friction coefficients with alumina and solar glass of K-162B Kentanium, *in vacuo*, 20: 7571 (NAA-SR-9644)
Mo–Ni–NbC–TiC, friction coefficients with alumina with molybdenum disulfide coating of K-162B Kentanium, *in vacuo*, 20: 7571 (NAA-SR-9644)
Mo–Ni–NbC–TiC, self-welding to ceramics, graphite, and metals in SNAP reactor environment at 700 to 1300°F, 20: 7570 (NAA-SR-9643)
Mo–Ni–NbC–TaC–TiC, thermal expansion at 68 to 1800°F, 18: 20513 (CNLM-4234)
NbC–NbN, critical supercurrents in, (E), 19: 39688
NbC–NbN, reflection spectra of, 17: 6520(R) (NP-12373)
NbC–NbN, superconducting critical currents of, (E), 19: 27371
NbC–NbN, superconductivity of platelets and whiskers of, electric and magnetic transport properties in, (E), 20: 8015
NbC–NbN, superconducting properties, 20: 17589 (CONF-650922, pp 541-9)
NbC–NbN, superconductivity of ternary-alloyed interstitial compounds of, 20: 34444
NbC–NbN–VN, superconducting properties, 20: 17589 (CONF-650922, pp 541-9)
NbC–NbN–ZrC, Hall coefficient for solid solutions of, 19: 47009 (NP-15514(Vol.2))
NbC–NbN–ZrN, superconducting properties, 20: 17589 (CONF-650922, pp 541-9)
NbC–Nb_2O_5, reduction of, electric arc method for, 19: 39133
NbC–SiC, oxidation tests at 1400 and 1500°C, 19: 9624 (SCNC-270)
NbC–SiC–TiC, oxidation tests at 1400 and 1500°C, 19: 9624 (SCNC-270)
NbC–SiC–ZrC, oxidation tests at 1400°C, 19: 9624 (SCNC-270)
NbC–TaC, high-field superconductivity of, (E), 19: 25449
NbC–TaC, melting point, 17: 11201(T) (AEC-tr-5598)
NbC–TaC, phase separation in solid solutions of, effects of tungsten carbide on short-range, 20: 27511
NbC–TaC, phase studies, 16: 2210(T) (AEC-tr-4871)
NbC–TaC, preparation and properties, 20: 11330
NbC–TaC, superconductivity of solid solutions of, 18: 22843
NbC–TaC, superconductivity, 18: 32149(R) (UCRL-11317(p.131-49))
NbC–TaC, superconducting properties of solid solutions of, 18: 34684 (UCRL-11368)
NbC–TaC, superconductivity, 19: 43997(R) (UCRL-11889)
NbC–TaC, wetting by liquid copper, 20: 1837
NbC–TaC–ZrC, melting point, 17: 11201(T) (AEC-tr-5598)
NbC–TiC, oxidation tests at 1400°C, 19: 9624 (SCNC-270)
NbC–TiC, phase studies, 16: 2210(T) (AEC-tr-4871)
NbC–TiC, wetting by nickel, 19: 18522(T)
NbC–UC, carbon-stable regions in, 17: 32617
NbC–UC, compatibility with stainless steel, 18: 44053(R) (ORNL-3670 (p.166-72))
NbC–UC, corrosion and oxidation resistance and compatibility with graphite, 18: 30142
NbC–UC, diffusion of xenon-133 from low-dose, low-temperature irradiated fuels of, (E), 20: 4471
NbC–UC, fabrication and testing, 18: 14381 (TID-7676(p.163-9))
NbC–UC, performance as thermionic emitters, 18: 35929(R) (GA-4769(Pt.I))
NbC–UC, preparation and high-temperature stability, 18: 44231(P)
NbC–UC, properties for cathodes in thermionic space power plants, 20: 15046(R) (N65-15820)
NbC–UC, thermodynamic properties, 18: 2222 (LADC-5907)
NbC–UC, thermoelectric properties of temperature dependence of, 16: 15230
NbC–UC, thermoelectric emission, 19: 6351
NbC–UC, vacuum emission of, 20: 19211(R) (N-65-21350)
NbC–UC, vaporization at high temperatures in vacuum, 17: 41338(R) (GA-4391)
NbC–UC–ZrC, preparation and high-temperature stability, 18: 44231(P)
NbC–VC, wetting by nickel, 19: 18522(T)
NbC–W, phase equilibria at 2000 to 3000°C, 18: 39968
NbC–W, phase studies at 2000 to 3000°C, (E), 19: 20583(T)
NbC–W, phase studies, 19: 40961
NbC–W_2C, melting point, 17: 11201(T) (AEC-tr-5598)
NbC–ZrC, analysis for niobium in, oxidimetric, 17: 25150
NbC–ZrC, analysis for niobium and zirconium, method for, 19: 46941 (NP-15514(Vol.3))
NbC–ZrC, corrosion by carbon dioxide and hydrochloric acid at 2250°C, 17: 34328(R) (NP-12991)
NbC–ZrC, electric conductivity, 17: 34328(R) (NP-12991)
NbC–ZrC, Hall effect, 17: 6520(R) (NP-12373)
NbC–ZrC, melting point, 17: 11201(T) (AEC-tr-5598)
NbC–ZrC, oxidation tests at 1400°C, 19: 9624 (SCNC-270)
NbC–ZrC, oxidation by carbon dioxide at 2250°C, 19: 46956 (NP-15514(Vol.1))
NbC–ZrC, phase studies, 16: 2210(T) (AEC-tr-4871)
NbC–ZrC, preparation and properties as electrode to 3000°C, 18: 12425
NbC–ZrC, preparation and properties, 20: 11330
NbC–ZrC, reflection spectra of, 17: 6520(R) (NP-12373)
NbC–ZrC, superconducting critical currents of, (E), 19: 27371
Ni–NbC–TaC–TiC, oxidation tests of Kennametal K 150A at 1400 and 1500°C, 19: 9624 (SCNC-270)
Ni–NbC–TaC–TiC, thermal expansion at 68 to 1800°F, 18: 20513 (CNLM-4234)

NIOBIUM CHLORIDES

analysis for uranium, x-ray fluorescence spectrometric, 19: 5774 (LA-3159)
atom clusters in complex, bonding in, 17: 28826 (NYO-10551)
complex with phosphoryl chloride, structure of, 17: 21674
complexes of, with pyridine, structure of, 17: 23297 (IS-544)
complexes with acetonitrile, butyronitrile, and propionitrile, properties of, 18: 41416
complexes with bipyridyl, phenanthroline, picoline, and pyridine, magnetic properties and spectra of, 18: 22053
complexes with diethyl and dimethyl sulfides and tetrahydrothiophene, compositions and properties, 16: 11629
density and viscosity at melting point to 325°C, 17: 30998
dissociation of niobium pentachloride on surface of, mechanism of niobium carbide formation by, 20: 21241(T) (LA-tr-66-15)
dissociation on graphite and niobium surfaces, mechanism of niobium carbide formation by, 20: 21241(T) (LA-tr-66-15)
electron paramagnetic resonance of tetravalent, 17: 157
enthalpy of formation, 18: 22054
fixation by calcium chloride, 17: 34052(T,R) (EURAEC-634)
formation by niobium dissolution in fused halides, 18: 16032
heat of formation and hydrolysis of oxytrivalent, 16: 30425
pharmacology and toxicology, 16: 2876 (UCLA-491)
phase studies of, with tin chlorides, 18: 8383
preparation of penta-, by chlorination of niobium carbide, 17: 40832(P)
preparation of polynuclear, 20: 3863(R) (IS-1200(Sect. C))
production from oxide using carbon tetrachloride entrained by carbon dioxide at 700°C, 16: 33071(T,R) (EURAEC-337)
production of penta-, 16: 32084(T,R) (EURAEC-227)
radiation effects on complexing reactions of, gamma, 18: 12138 (BM-RI-6382)
reactions of pentavalent, with lithium dialkylamides, 16: 11592
reactions of, with potassium chloride in vapor phase, 17: 18079
reactions with dimethyl- and diphenyl sulfoxides, properties and spectra of products in, 18: 25398
reactions with methanol, methoxide complex formation equilibrium in, 19: 11075
reactions with niobium pentoxide, 17: 25265
reactions with niobium oxides, phase studies of equilibrium products in, 19: 363
reactions with potassium chloride, tracer study of gaseous, 16: 23709 (JINR-P-957)
reactions with primary and secondary aliphatic amines, 16: 12945
reactions with pyridine, 17: 10500 (IS-385)
reactions with thorium chlorides in melts, tensiometric and thermal analyses, 16: 4169
reactions with triphenylarsine oxide and triphenylphosphine oxide, 19: 17907
reactions with water vapor, kinetics of, 18: 5263
reactions with zirconium oxide films, 16: 9141(R) (NMI-2101)
reduction by carbon, hydrogen, or metals, methods for, 17: 35950
reduction of, for deposition of niobium coatings, 19: 20456 (EUR-2111.d)
reduction to metal in hydrogen plasma jet, 20: 4314(P)
reduction to niobium by hydrogen, 18: 20009
reduction to niobium using zinc, 20: 9405(P)
reduction using hydrogen, 17: 16548
separation by reversed-phase partition chromatography using organophosphorus compounds, 18: 25614
separation from tantalum chloride, methods for, 20: 4077(R) (IS-1200

(Sect. E))
separation from tantalum chloride, methods for, 20: 41064(R) (IS-1500 (Sect.E))
spectra of, electronic, 19: 34160
synthesis of anhydrous, 17: 30553
thermodynamic properties, 20: 10816(T) (NASA-TT-F-285)
toxic effects on dogs, mice, rabbits, and rats, 19: 45768
$AlCl_3$–KCl–$NbCl_4$, phase studies, 17: 25252
$AlCl_3$–KCl–$NbCl_5$, phase studies by thermographic methods, 19: 36378
CsCl–$NbCl_4$, phase diagram and structure of, 17: 1490
KCl–NaCl–$NbCl_4$, phase diagram and structure of, 17: 1489
$NbCl_4$–KCl–NaCl, phase studies, 16: 30431
$NbCl_4$–KCl, phase studies, 16: 30431
$NbCl_5$–KCl–$TaCl_5$, phase studies, 17: 25251
$NbCl_5$–KCl–$ZrCl_4$, thermodynamic properties and crystallization, 17: 21713
$NbCl_4$–NaCl, phase studies, 16: 30431
$NbCl_4$–NaCl–$TaCl_4$, phase studies, 17: 25251
$NbCl_5$–Nb_2O_5, phase studies and properties, 17: 25265
$NbCl_5$–$POCl_3$–$TiCl_4$, phase studies, 18: 1630
$NbCl_4$–RbCl, phase diagram and structure of, 17: 1490

NIOBIUM COBALTATES
ion magnetic exchange interactions in, 18: 16048

NIOBIUM COMPLEXES
acetonitrile, crystal structure of, 20: 40796(R) (IS-1500(Sect.C))
formation and properties of, in oxalic acid–sulfuric acid systems, 20: 7039
formation and stability, 16: 17681
nitrato-, preparation of quinquevalent, 20: 33292
pentachloromethoxo-, electron spin resonance of niobium-93 in, 19: 17884
preparation and structure of pentachloroalkoxo-, 17: 25189
preparation of co-ordination-type, 17: 37192
preparation of, by chlorination of carbide, 20: 22983
properties of EDTA, polarographic studies, 16: 22087
with ammonium, cesium, and tetramethylammonium chlorides, crystallographic and spectral properties of, 19: 378
with carbamic acid, synthesis, 16: 6425
with cesium oxychloride, chemistry of, 19: 13328
with citric acid, isotopic exchange in, 17: 14363
with cupferron, separation by solvent extraction, 17: 25137
with EDTA, polarography of, 17: 10544
with EDTA, migration in electrodialysis cell, 19: 20052 (ORNL-TM-1035)
with ethers and organic sulfides, preparation and properties of fluoride, 19: 17895
with gallic acid, absorption spectra of solutions of, 18: 13715 (AFOSR-TN-59-1183)
with molybdenum, formation and reduction, 16: 16315
with nitrilotriacetic acid, titration of, 18: 5230
with phosphoromolybdenum, formation and structure of, 17: 1469
with pyrogallol, structure of, 17: 12292
with salicylic acid and amines, formation and stability, 17: 25250
with thiocyanate, effects of hydrochloric and sulfuric acids on solvent extraction of, 18: 347
with thiocyanate, effects of acetone, carbon tetrachloride, and tin and zinc chlorides on spectra of, 18: 31392
with tiron, formation constants of, 19: 17908
with triphenylphosphine oxide, preparation and properties of, 20: 22995
with 8-quinolinol, separation of, from solutions, 17: 18213

NIOBIUM COMPOUNDS
crystallography of, with perovskite-like structure, 19: 25014
molecular structure of $NbBr_4(CH_3CN)_2$, 20: 3863(R) (IS-1200(Sect. C))
organic, preparation of dichlorohexaethoxo-bis(pyridine)diniobium(IV) and tetraethoxoniobium(IV), 18: 6840
oxidation of, kinetics of, effects of silicon and titanium on, 17: 8746
preparation and ordering in $A(B'_{0.33}Nb_{0.67})O_3$ perovskite-type, 17: 37201
preparation and properties of heteropoly acids of, 16: 23680
preparation and properties of trinitratoniobium(V) oxide, 17: 21693
preparation of glycollates, by reaction of pentaethoxide with diols, 19: 26371
preparation, properties, and thermal decomposition of dialkylamino-, 16: 11592
preparation, properties, and uses of, review of, 18: 3786
technology and uses of, review, 20: 43817(T) (JPRS-36718)
with tropolone, preparation, properties, and structure, 20: 5538

NIOBIUM COUPLES
Al/Nb, diffusion of aluminum in, 19: 11748
Cu/Nb, fabrication of composite wires of, by drawing, 20: 21298
Cu/Nb, fabrication and properties of superconducting composites of, 20: 23648 (N66-11248)
Cu/Nb, superconducting strip of, current losses in, 20: 46519
Cu/Nb/stainless steel, diffusion in bimetallic tubing of, with copper diffusion barrier, inter-, 20: 11215(R) (NASA-CR-54718)
Fe/Nb/stainless steel, diffusion in bimetallic tubing of, with iron diffusion barrier, inter-, 20: 11215(R) (NASA-CR-54718)
Fe/Nb/stainless steel/V, diffusion in bimetallic tubing of, with iron and vanadium diffusion barriers, inter-, 20: 11215(R) (NASA-CR-54718)
Hf/Nb, interdiffusion in, 18: 42031
Ir/Nb, interdiffusion in, 18: 42031
Mo/Nb, fabrication and performance as thermocouple at high temperature, 19: 22927 (TIM-888)
Mo/Nb, fabrication and performance as high-temperature thermocouple, 19: 22927 (TIM-888)
Mo/Nb, interdiffusion in, 18: 42031
Mo/Nb, performance to 2300°F, 19: 44348 (PWAC-473)
Mo/Ni/Nb/stainless steel, diffusion in bimetallic tubing of, with molybdenum and nickel diffusion barriers, inter-, 20: 11215(R) (NASA-CR-54718)
Nb/Nb–Ti, diffusion at 1300 to 2000°C, inter-, 20: 11227
Nb/Os, interdiffusion in, 18: 42031
Nb/Re, interdiffusion in, 18: 42031
Nb/Re–W, thermoelectric potential at 200 to 1800°C, 19: 37031(R) (GEMP-47A, pp 101-6)
Nb/Sn, fabrication and properties of superconducting composites of, 20: 23648 (N66-11248)
Nb/stainless steel, diffusion in bimetallic tubing of, inter-, 20: 11215(R) (NASA-CR-54718)
Nb/stainless steel, properties of duplex tubing for mercury Rankine boilers, 20: 9495 (NAA-SR-11191)
Nb/Ta, interdiffusion in, 18: 42031
Nb/W, diffusion in polycrystalline, microhardness studies of, 17: 37553
Nb/W, diffusion in single-crystal, 18: 8857
Nb/W, hardness, 18: 8857
Nb/W, interdiffusion in, 18: 42031
Nb/Zr, interdiffusion in, 18: 42031

NIOBIUM ETHOXIDES
spectra of, infrared, 20: 23037

NIOBIUM FLUORIDES
see also Potassium Niobium Fluorides
analysis by potentiometric titration with sodium methylate in methanol, 16: 7530
corrosive effects of pentavalent, on INOR-8, Monel, and nickel, 17: 22111 (BMI-X-229)
corrosive effects on INOR-8, Monel, and nickel, 17: 26944(R) (BMI-1630 (Del.))
crystal structure of NbF_5, 19: 6323
density, self-ionization, and viscosity, 19: 17894
equilibrium with uranium hexafluoride, liquid-vapor, 20: 9045(R) (ORNL-3830, pp 69-96)
heat of formation, 18: 43440(R) (ANL-6800(p.305-25))
heat of formation, 19: 32162
identification in hydrofluoric acid solutions, 17: 10511(R) (ORNL-3320(p.56-82))
nuclear magnetic resonance of niobium-93 in, 19: 13293
preparation and crystal structure, 19: 38640
preparation and properties, 19: 13306
preparation and properties of, 20: 36950
preparation and purification, 16: 17621(T) (AEC-tr-4456(p.14-17))
preparation of hexavalent, by electrolysis, 19: 28315
reactions with bromides, chlorides, and fluorides, 20: 36804
reactions with ethers and organic sulfides, adduct formation in, 19: 17895
reduction by carbon, hydrogen, or metals, methods for, 17: 35950
reduction to niobium using zinc, 20: 9405(P)
separation from uranium hexafluoride by sorption on solid magnesium or sodium fluorides, 20: 27038 (K-1666)
stability of complex, 19: 22228
stability of complex, 16: 5318(T) (CEA-tr-R-1401)
thermodynamic properties, 20: 10816(T) (NASA-TT-F-285)
NbF_5–UF_6, liquid–vapor equilibria in, 20: 20808(R) (ORNL-3916)
NbF_5–UF_6, phase studies on liquid-vapor equilibria in, 20: 45789(R) (ORNL-3945, pp 48-71)
NbF_5–UF_6, vapor pressure of, equipment and procedures for determining, 18: 35644(R) (ORNL-TM-836)

NIOBIUM HYDRIDES
analysis for hydrogen by combustion method, 19: 22150
chemical bonds in, properties of, 20: 12847
crystal structure and magnetic properties, 17: 18074
dissociation pressure of, effects of temperature on, 20: 45691
ductility of solid-solution, 20: 31716(R) (UCRL-16658, pp 121-32)
hydrogen NMR in, 18: 17811
hydrogen vibrations in, (E/T), 19: 5887
neutron inelastic scattering by, spectra of, (E), 19: 23600(R) (RPI-328-20(p.35-9))
neutron inelastic scattering by, determination of localized modes of hydrogen excess in, (E), 20: 20107 (EUR-2734.e)
neutron inelastic scattering by localized oscillation states in, cold,

(E/T), 20: 28670
niobium-93 NMR in, 18: 17811
nuclear magnetic resonance measurements of, 19: 43346
preparation, 20: 26902
spectra of niobium in, L, 19: 6355
structure of beta-, 20: 2365
superconductivity, magnetization, and microstructure at 4.2°K, 19: 9698
thermal capacities at 21 to 386°K, 18: 12051
thermodynamic properties, 20: 10816(T) (NASA-TT-F-285)
NbH–TiH, crystal structure and hydrogen sorption in, 17: 11237

NIOBIUM HYDROXIDES
complex formation with pyrocatechol, 16: 32996
solubility and acidity properties, 18: 1695

NIOBIUM IODIDES
complexes of, with pyridine, structure of, 17: 23297 (IS-544)
crystal structure of alpha, 16: 28938
properties, 19: 13305
properties, 19: 9046(R) (IS-900(Sect.C))
reactions with niobium oxides, phase studies of equilibrium products in, 19: 363
reactions with pyridine, 17: 10500 (IS-385)
reduction to niobium using zinc, 20: 9405(P)
spectra of, electronic, 19: 34160
vaporization at 600 to 700°C, 20: 3863(R) (IS-1200(Sect. C))

NIOBIUM IONS
diffusion in niobium oxides, 18: 5273
electron paramagnetic resonance of tetravalent, 17: 157
electron paramagnetic resonance of tetravalent, in zircon crystals, 18: 9021(T)
fluorescence of, in lanthanum and yttrium niobates and tantalates, 19: 36419
reduction of pentavalent to trivalent, 19: 17841
reduction of pentavalent to tetravalent, electrolytic, 19: 28806
separation by thin-layer ionophoresis, 18: 10185
spectra of, in hydrofluoric acid solutions, infrared and Raman, 17: 32070
states in tartaric acid, 16: 14758

NIOBIUM ISOTOPES
binding energies and energy levels, (T), 19: 6661
distribution and natural carriers of, in sea water, 20: 31422
energy levels, interactions, nuclear moments, and transitions in, 17: 24381 (AD-403411)
exchange in citrate complexes, 17: 14363
gamma reactions on, cross sections for, 19: 12496
isomeric transitions, M_4-type, 16: 22985 (NP-11747)
neutron cross sections, data tape for reactor analysis, 16: 8322 (XDC-59-11-72)
neutron resonance integrals for, 17: 22566 (TID-18590)
nuclear masses and binding energies, 16: 1066
nucleon interactions in, effective, (T), 20: 6337
preparation and properties of radioactive, 19: 4227
production, 17: 18149
production in helium ion and proton reactions with niobium at 240 to 880 Mev, cross sections for, 18: 42745

NIOBIUM ISOTOPES Nb-88
decay properties, 19: 37835(R) (TID-22024)
gamma spectra, (E), 20: 24358(R) (UCRL-16580, pp 1-93)
preparation by irradiation of molybdenum, spectra of, 18: 36593

NIOBIUM ISOTOPES Nb-89
decay properties, 19: 37835(R) (TID-22024)
gamma spectra, (E), 20: 24358(R) (UCRL-16580, pp 1-93)
half life and gamma and positron spectra of, 18: 36593
half life of isomeric, (E), 20: 34610
production in zirconium (p,xn) reactions at 400 Mev, effects of target thickness on, 19: 37835(R) (TID-22024)

NIOBIUM ISOTOPES Nb-90
decay, (E), 19: 43391
decay of isomeric, (E), 19: 5261
decay of isomers of, 17: 7294
decay of 24-sec, effects of chemical state on, (E/T), 20: 24358(R) (UCRL-16580, pp 1-93)
decay of, conversion electron spectra from, (E), 20: 15751
decay scheme of isomeric, 19: 29258 (NP-15050)
electron pair production cross section near threshold, (E), 19: 21252(R) (UCRL-11828(p.35-8))
energy level transitions of very low energy isomeric, (E), 20: 36265
energy levels, (E/T), 19: 21258(R) (UCRL-11828(p.67-71))
energy levels from molybdenum-90 decay, multipolarity, parity, and spin of, (E), 20: 30388
energy levels in, effect of chemical state on lifetime of 24-second isomer, 20: 3088
energy levels of, parity and spin of, (E), 20: 1159 (UCRL-16306)
energy levels of, multipolarity of, (E), 20: 15751
gamma spectra, (E), 19: 16840(R) (IDO-17050)
half life and gamma and positron spectra of, 18: 36593
half life of the isomeric state of, 17: 7294
isomeric transitions in, multipolarities of, (E), 20: 1159 (UCRL-16306)
metabolism of, in rats and rat sarcomas, 20: 1595
nucleon interaction potentials in, shell model calculation of, 17: 40031
production in zirconium (p,xn) reactions at 400 Mev, effects of target thickness on, 19: 37835(R) (TID-22024)

NIOBIUM ISOTOPES Nb-91
core deformability and electric quadrupole moments, 16: 7026
energy level structure in shell model, (T), 20: 12157
energy levels, excitation energies and spins for, 16: 26287 (IS-408)
energy levels from molybdenum-91 decay, (E), 20: 24364
energy levels from the zirconium-91 (p,n) reactions at 13 Mev, isobaric analogue, (E), 20: 46577 (AD-630032)
energy levels in, from proton reactions (p,n) with zirconium-91 at 12.35 Mev, 20: 30480
energy levels of, shell model, 18: 30795
energy levels of, from proton scattering by zirconium-90, (E), 20: 24441
energy levels of, effects of collective vibrational motion on anomalous coupling, 20: 28420
energy levels, configuration mixing, and proton-neutron interaction in, (T), 19: 23678
energy-level transition probabilities of, E2, (T), 20: 3115

NIOBIUM ISOTOPES Nb-92
beta decay of, transitions to vibrational levels in, 18: 36625
decay scheme, 16: 29828 (LADC-5293)
energy level ground-state configuration, 18: 13092
energy levels from niobium-93 (p,d) reactions, p-n residual interaction effects on low-lying, 18: 28574(R) (ORNL-3630(p.18-30))
energy levels of, low-lying, 18: 13096
energy levels of, shell model explanation of low-lying, 18: 28578 (ORNL-3638)
energy levels of, spins and parities of low-lying, 19: 21451
energy levels of, shell model analysis of, (T), 19: 37824(R) (ORNL-3800 (p.50-7))
energy levels of, parity and spin of, (E), 20: 6310
energy levels, configuration mixing, and proton-neutron interaction in, (T), 19: 23678
existence of, in niobium-93 (d,p2n) reaction, 18: 36591
half life of ground state of, 17: 19262
isomers of, 17: 19261
nuclear structure of, neutron-proton residual interaction in, 18: 28578 (ORNL-3638)
nucleon interactions in, 18: 22893
nucleon interaction in, 18: 30788
preparation of high specific activity, 17: 10714
production by gamma reactions (γ,n) at 20 Mev, 17: 30161
production in molybdenum-92 (n,p) reactions, cross sections for, 17: 7101 (NP-12330(p.97-103))
production in reactor by neutron reactions (n,p), 17: 24508
production in 20-Mev linear electron accelerator, purity and yield in, 19: 32836

NIOBIUM ISOTOPES Nb-93
alpha reactions (α,n), model of isomeric ratios in, 19: 22282(R) (NYO-1930-40)
alpha reactions (α,3n), model of isomeric ratios in, 19: 22282(R) (NYO-1930-40)
alpha reactions (α,2n), model of isomeric ratios in, 19: 22282(R) (NYO-1930-40)
alpha reactions (α,n), (α,2n), and (α,3n) to 42 Mev, isomeric ratios from, (E), 19: 41695
alpha reactions (α,n), (α,2n), and (α,2n), statistical model for isomeric ratios in, 19: 41696
alpha reactions (α,xn) with, excitation functions, isomeric ratios, and product recoil ranges for, 17: 16047(R) (TID-18261(p.1-14))
alpha reactions (α,xn), formation of isomeric pairs of technetium isotopes from, 17: 22659
alpha reactions (α,3n) with, technetium-94 production in, 17: 24460
alpha scattering by, 17: 40436(R) (NYO-10063(p.105-15))
beta decay, mass discrepancies from, 16: 26287 (IS-408)
bremsstrahlung reactions (γ,n), (γ,2n), and (γ,p) at 24 Mev, direct photo-effect and evaporation, 17: 38209
bremsstrahlung reactions (γ,n) at 15 to 30 Mev, yields from, 18: 42633 (IFA-M-30)
bremsstrahlung reactions (γ,p) at 32 ± 1 Mev, energy distribution of protons from, 18: 42660
carbon-12 reactions (C-12,N-13) with, angular distributions from, (E), 20: 42153 (JINR-E-2824)
carbon-12 reactions (C-12, N-13) with, angular distributions and cross sections for, (E), 20: 46587 (JINR-P-2794)
deuteron elastic scattering at 15 Mev, optical model for, 19: 14604
deuteron reactions (d,t) at 11 Mev, cross sections for, 18: 13092
deuteron reactions (d,p2n) with, niobium-92 isomer in, 18: 36591

deuteron reactions (d,p) at 10.2 to 12.2 Mev, (E/T), 19: 23670
deuteron reactions (d,n) at 11.8 Mev, total cross sections for, (E), 19: 35438
deuteron reactions (d,t) at 15 Mev, energy levels from, (E), 20: 6310
deuteron reactions at 11.8 Mev, energy spectra from, 20: 40065(R) (BMwF-FB-K-66-01)
deuteron reactions (d,t), analytical uses of, 19: 14494 (ANL-6878 (p.249-75))
electron spin resonance of, in pentachloromethoxoniobate ion, 19: 17884
energy level ground-state configuration, 18: 13096
energy level strength functions for, 16: 26518
energy levels, (E), 20: 21969(R) (ANL-7055, pp 230-3)
energy levels of, cross-section ratios for excitation of, 17: 24488
energy levels of, spins of, 18: 6221
energy levels of, neutron cross sections for production of 0.741-Mev, (E), 20: 6280(R) (ANL-6925, pp 249-51)
energy levels of, effects of collective vibrational motion on anomalous coupling, (T), 20: 28420
Fermi gas coefficient and nuclear temperature, 18: 998 (AD-299005)
gamma emission at 0.741, 0.809, and 0.958 Mev, (E), 20: 6280(R) (ANL-6925, pp 249-51)
gamma reactions (γ,p) on, distributions from, 17: 19371
half life of, determination by direct decay, (E), 19: 37847
Knight shifts of, in molybdenum–niobium–technetium alloys, 18: 8837
magnetic moment, (T), 20: 3118
magnetic resonance in molybdenum–niobium alloys, 17: 16709
neutron capture at 30 to 4000 ev, cross sections, resonance parameters, and strength functions for, (E), 19: 33287
neutron capture by, gamma spectra of p- and s-wave resonances in, 17: 34951
neutron capture by, gamma radiation from thermal, (E), 19: 37805(R) (ORNL-3778(p.44-53))
neutron capture resonances in, parameters of, 18: 24625 (WASH-1046)
neutron capture resonances in, 18: 42622(T) (ANL-6879(p.2-20))
neutron elastic scattering at 1.509 Mev, polarization in, 17: 31410 (TID-19051)
neutron elastic scattering at 4 Mev, polarized, 18: 40511 (NP-14205)
neutron inelastic scattering cross sections, 16: 1023 (KAPL-2163)
neutron inelastic scattering at 6 Mev, compound-nucleus and direct reactions in, 17: 38207
neutron inelastic scattering at 6 Mev, energy spectra for, 18: 998 (AD-299005)
neutron inelastic scattering at 0.3 to 1.5 Mev, cross sections for excitation of 0.74-, 0.81-, 0.96-, and 1.08-Mev levels in, 18: 6221
neutron inelastic scattering at 0.9 to 1.25 Mev, gamma spectra from, (E), 19: 31215(R) (ANL-7010(p.1-19))
neutron inelastic scattering by, gamma emission in, 20: 19805(R) (ANL-7110, pp 1-28)
neutron inelastic scattering, cross sections for excitation by, 19: 33237(R) (ANL-7020(p.226-30))
neutron radiative capture in, optical model for cross sections of, 17: 33048
neutron reactions at 14.6 Mev, mechanisms and shell effects, 16: 12487
neutron reactions (n,α) at 7.0 to 19.8 Mev, cross sections for, 16: 19782
neutron reactions (n,α) at 14.7 Mev, cross sections, 16: 21352 (NP-11667)
neutron reactions (n,2p) at 14.8 Mev, cross section limit, product half life, and Q value for, 17: 2242 (TID-16949)
neutron reactions (n,α) at 14.8 Mev, cross sections for, 17: 2242 (TID-16949)
neutron reactions (n,2n), (n,pγ), and (n,pn) at 14.8 Mev, cross sections for, 17: 2242 (TID-16949)
neutron reactions (n,p) at 14.8 Mev, separation energies for, 17: 2242 (TID-16949)
neutron reactions [(n,αn) + (n,nα)] at 14.8 Mev, cross sections, product half life, and Q value for, 17: 2242 (TID-16949)
neutron reactions (n,γ) at 14.8 Mev, cross sections, product half life, and Q value for, 17: 2242 (TID-16949)
neutron reactions (n,αγ) and (n,αn) at 14.8 Mev, cross sections for, 17: 2242 (TID-16949)
neutron reactions [(n,αn) + (n,nα)], separation energies for, 17: 2242 (TID-16949)
neutron reactions (n,helium-3) at 14.8 Mev, cross section limit, product half life, and Q value for, 17: 2242 (TID-16949)
neutron reactions (n,α), (n,γ), (n,n'α), and (n,2n) at 14.5 Mev, absolute activation cross sections for, 17: 19262
neutron reactions at 2–10 kev, inelastic scattering and radiative capture cross sections for, 17: 29631
neutron reactions (n,nα) at 14.7 Mev, cross section for, 17: 36707
neutron reactions (n,2p) at 14.7 Mev, cross-section limits for, 17: 36707
neutron reactions (n,He³) at 14.7 Mev, cross-section limits for, 17: 36707
neutron reactions (n,γ) at 14.7 Mev, cross sections for, 17: 36707
neutron reactions (n,nα) at 14.8 Mev, cross section for, 18: 1077
neutron reactions (n,2p) at 14.8 Mev, cross-section limits for, 18: 1077
neutron reactions (n,He³) at 14.8 Mev, cross-section limits for, 18: 1077
neutron reactions (n,γ) at 14.8 Mev, cross section of, 18: 1077
neutron reactions (n,γ) with, total radiation widths for s- and p-wave, 18: 11177 (ANL-6797(p.294-300))
neutron reactions (n,α) at 14 Mev, 18: 17057
neutron reactions (n,α) at 14 Mev, angular and energy distributions for, 18: 28640
neutron reactions (n,2n) at 14 Mev, shell effects in, (T), 19: 12536
neutron reactions (n,α), alpha spectrum from, 19: 14533(R) (NYO-1082-1)
neutron reactions (n,γ) with, spectra from, (E), 19: 21330
neutron reactions (n,2n), cross section for, (E), 19: 35378(R) (EANDC(E)-57(U))
neutron reactions to 400 ev, resonance parameters and radiation widths from, (E), 19: 41727
neutron reactions at 1.7 and 2.1 Mev, differential gamma production cross sections for, (E/T), 20: 30360 (WASH-1068)
neutron reactions (n,2n) with, discrepancy between measured and predicted cross sections for, 20: 44616 (CONF-660303, pp 682-9)
neutron resonance capture in, gamma spectra from, 17: 41527(R) (ANL-6720(p.2-15))
neutron resonance capture in, total radiation widths for p- and s-wave, 18: 2936
neutron resonances at 94 to 379 ev, radiation widths of, (E), 20: 3133
neutron scattering at 0.4 to 1.2 Mev, cross sections for, 18: 9331
neutron scattering at 1 to 4 Mev, cross sections for energy level excitation in, 18: 21217
neutron scattering at 3 to 650 kev, cross sections, phase shifts, and strength functions for, (E), 19: 10319
neutron scattering by, excited states from inelastic, (E), 20: 21969(R) (ANL-7055, pp 230-3)
neutron scattering by, gamma rays from inelastic fast, 20: 27316
neutron scattering at 4.0 Mev, polarization angular distributions from, (E), 20: 30360 (WASH-1068)
neutron scattering at 14 Mev, differential elastic cross sections for, (E), 20: 44615 (CONF-660303, pp 675-81)
neutron transmission in, shape elastic cross section for, 17: 38004(T) (AEC-tr-5734(p.27-8))
nuclear magnetic moments, 16: 1054
nuclear magnetic resonance in niobium hydrides, 18: 17811
nuclear magnetic resonance in fluoride solutions, measurement of, 19: 13293
nuclear magnetic relaxation in molybdenum–niobium alloys, 19: 41989
nuclear magnetic resonance in niobium powder, 20: 33607
nuclear spin resonance, 17: 41967
photon reactions at 300-Mev peak, isomer production in, (E/T), 20: 1246
proton elastic scattering at 10.4 to 22.4 Mev, angular distributions and cross sections, 16: 9462
proton reactions (p,d) at 22 Mev, niobium-92 level structure from, 18: 13096
proton reactions (p,d) with, niobium-92 low-lying energy levels from, 18: 28574(R) (ORNL-3630(p.18-30))
proton reactions (p,n) at 7 to 13 Mev, 18: 34859
proton reactions (p,n) at 18.5 Mev, angular distributions of quasielastic, 18: 40587
proton reactions (p,n) with, thresholds for, (E), 19: 6704
proton reactions (p,n) at 2.3 to 11.0 Mev, excitation of isobaric analog states in, (E), 20: 15804
proton reactions (p,n) at 3.0 to 5.8 Mev, strength functions for, (E), 20: 39470(R) (ORNL-3924)
proton reactions (p,n) at 8 to 14 Mev, neutron spectra from, (E), 20: 44739
proton reactions (p,d) with, analytical uses of, 19: 14494 (ANL-6878(p.249-75))
proton reactions at 0.15 and 25 Bev, lithium mass spectra from, (E), 20: 8105
proton reactions (p,γ) in stars, 16: 12308
proton reactions (p,n) at 14.8 Mev, neutron spectra from, 16: 26326 (UCRL-6733)
proton reactions (p,d) at 22 Mev with, deuteron spectrum for, 17: 24053(R) (ORNL-3432)
proton reactions (p,α) at 22 Mev, angular distributions and cross sections for, 17: 26566
proton reactions (p,3p3n) at 30 to 150 Mev, excitation functions for, 17: 29590
proton reactions (p,d) at 22 Mev, excited energy levels in, 17: 38234
proton reactions (p,α) with, pick-up contributions in, 17: 38230
proton reactions (p,d) at 22.3 Mev, distorted-wave analysis of, 17: 38233
proton scattering at 9.4–22.2 Mev, local optical potentials for, 17: 38185
relaxation in niobium metal, (E), 19: 27577
wave function for ground state, 18: 28574(R) (ORNL-3630(p.18-30))
wave functions for, 18: 28578 (ORNL-3638)

NIOBIUM ISOTOPES Nb-94

beta decay of, gamma energies and spectrum shape in, 20: 32518

beta emission from ground and 42-keV states of, 16: 24837
decay of metastable, 17: 2308
decay of 6.6 min. isomers, 16: 2774(R) (IDO-16710)
decay of 6.6-min isomer, 17: 4330(R) (IDO-16781)
decay scheme, 17: 41873 (WASH-1044)
decay to zirconium-94, energy for, 17: 21014
determination in niobium, gamma-spectrometric, (E), 19: 22684 (AE-174)
deuteron reactions (d,p) at 13.6 Mev, proton spectra from, 16: 26356
energy levels, 17: 7257
energy levels, (E), 19: 23670
energy levels of, parity and spin of, (E), 19: 21330
energy levels of, shell model analysis of, (T), 19: 37824(R) (ORNL-3800 (p.50-7))
gamma activity of, discrimination in presence of niobium-95, 20: 11134
gamma dose constants for, 20: 46617
gamma spectra from ground and 42-kev states, 16: 24837
half life, 17: 5320 (AE-81)
half life of metastable state of, 17: 19262
neutron activation cross sections, thermal, 16: 21839(R) (IDO-16760)

NIOBIUM ISOTOPES Nb-95

activity of dust-borne, in Osaka, Japan, Nov. 1962–Dec. 1963, 20: 7275
age and content in fallout, determination of, 17: 39271(T) (AEC-tr-6022)
analysis of mixtures with zirconium-95, beta and gamma scintillation spectrometric, 18: 39117
analytical uses, 18: 33483
beta activity measurements in France, 20: 41189 (CEA-R-3020)
beta decay, 19: 21460
beta decay, gamma circular polarization in, 16: 17085
beta decay, isospin conservation in, 16: 17084
beta decay of, unusually short comparative half life in, 17: 38124
beta decay of, β-γ circular polarization correlation in permitted transitions in, (E), 19: 47605
beta decay of, β-γ circular polarization correlations in, (E), 20: 30543
beta decay of, circular polarization of gamma radiation following, 18: 21309
beta decay of, gamma spectra from, (E), 20: 13859
body burden in Alaska, 18: 20231 (HW-SA-3048)
content and motion in soil, 19: 36661
content in air from Chinese detonations in 1964, 20: 8980(R) (BNWL-36, pp 3.1-122)
content in air over Indian and Pacific Oceans in 1961–62, 19: 20158 (NP-14712)
content in air samples collected at Richland, Wash., 1962, 1963, and 1964, 19: 2541
content in air, bones, food, soil, and water in Italy, 1962, 18: 18040 (BIO/03/63)
content in airborne particles in Cincinnati, May 1962 to Dec. 1963, 19: 4367
content in Alaskan water supplies, 1963, 19: 18164
content in animals, birds, fish, and plants in region of Cape Thompson, Alaska, 1959 to 1962, 20: 7319 (PNE-480)
content in atmosphere over Atlantic Ocean, 1958, 16: 32719
content in atmosphere in 1962, 18: 1975
content in atmosphere and drinking water, Moncloa Station, Spain, 1964, 19: 46597
content in atmosphere, 1962 to 1963, 20: 2049
content in atmosphere, 1962 through mid-1964, 20: 8980(R) (BNWL-36, pp 3.1-122)
content in biosphere of, from fallout, 1959 through 1962, 19: 9367 (IAEA-R-1)
content in brown algae in Black Sea, 18: 4979
content in children and stillborn infants, 17: 27013 (TID-18878)
content in deep bottom ocean feeders, sinking rates for, 18: 8526
content in diet and excreta in Japan, 19: 38894
content in drinking waters in England, 16: 20126
content in dust particles in precipitation, Vienna, Austria, Oct. 1962 to Sept. 1963, 19: 13643
content in environment in Japan, 1961–64, 20: 43615
content in fallout in French territory, 18: 33770 (SCPRI(5)-90)
content in fallout in Dallas, Texas, from Dec. 1962 to July 1963, 19: 28540(R) (TID-21892)
content in fallout from Chinese nuclear test, 19: 32429
content in fallout over Moscow, 1962, 19: 34369
content in fallout particles, 20: 2053
content in fallout, 1963, 20: 5652
content in fallout in USSR, 1962, 20: 29406 (NP-14719)
content in fallout from Chinese nuclear tests, 20: 29423
content in fallout from Chinese nuclear test of May 14, 1965, 20: 33530
content in fallout and plankton of Mediterranean Sea, 1963, 20: 41146
content in fallout from Chinese nuclear test, May 1965, 20: 41130(R) (COO-1407-10)
content in fallout at Vilnius, Soviet Union, 1962, 20: 16700
content in fractionated fallout particles from land surface burst, 20: 31460
content in ground-level air near Moscow, 1960-1962, 19: 13628 (NP-14718)
content in holothuriae, western Mediterranean, 1962, 19: 46611
content in lake sediments and molluska, 19: 1996
content in large fallout particles in Japan, 20: 31412
content in man of, from inhaled irradiated uranium, 19: 10749
content in marine organisms near Columbia River mouth, interspecies differences in, 17: 24866
content in marine environment, 19: 43663
content in marine organisms in northeast Pacific Ocean, 20: 18903 (RLO-1750-3)
content in natural waters, fallout correlations with, 20: 27161
content in nekton and macroplankton in Pacific Ocean off Oregon coast, 18: 1341(R) (TID-19608)
content in organisms and water in Gulf of Mexico, 20: 18200 (NYO-3450-1, pp 109-29)
content in Pacific Ocean surface water near mouth of Columbia River, 20: 18902 (RLO-1725-41)
content in Pacific Ocean sediments near mouth of Columbia River, 20: 18902 (RLO-1725-41)
content in plants and soil, methods for decreasing, 19: 18209
content in plants before and after Salmon Event, 20: 16743 (VUF-1021)
content in rabbit tissues after intravenous injection, 19: 27939
content in rainwater at Ispra during 1963 and 1964, 19: 34373
content in rainwater at Milan following Chinese nuclear explosions, 19: 42543
content in Savannah River water, July through Dec. 1965, 20: 27195(R) (DPST-66-30-1)
content in sedge from Chariot site environment, 19: 25798 (PNE-447)
content in soil in King, Ontario, Oct. 1958 to July 1961, 16: 13375
content in Swedish food, 1962, 18: 23790 (NP-13828)
content in tissues of fin whale captured off Oregon coast, 19: 6936
content in Tyrrhenian Sea plankton, 19: 30411
content in U. S. soil samples, 1962 and 1963, 19: 629 (TID-7696(p.101-10))
content in vegetation in Italy, 1961, 17: 27591 (EUR-223.i)
content in vegetation in Northern Alaska from fallout, 17: 27053 (HW-SA-3050)
content of, in lung specimens, effects of age on, 17: 40492(R) (TID-18790)
content of, in brown algae of Solway Firth, 20: 3662 (PG-Report-650)
content of, in marine organisms, 19: 10732
content of, in tuna from Western Pacific, 1962, 18: 27703 (UWFL-90)
content on air filters at Hanford, methods of gamma spectrometry for monitoring, 19: 620(R) (HW-81746(p.3.51-5))
contents in air in Hanford Works Area, 19: 13626 (HW-SA-3742)
contents in animals and plants from Chariot site environment, 19: 25796 (PNE-445)
contents in animals, plants, rain water, and soils from Chariot site 19: 25797 (PNE-446)
contents in animals and plants from Chariot site environment, 19: 25799(R) (PNE-448)
decay of, branching ratios in, 17: 12802(R) (PR-P-55)
decay of, correction factors for, 17: 24384 (AERE-R-4237)
decay of, calibration of ionization chamber for particles from, 19: 6194
decay patterns in rat tissue, 18: 11604
deposition from helium gas flow at high velocities, 18: 12321
deposition in lungs, calculation of radiation dose from, 19: 22017
deposition on aluminum during corrosion, 17: 8741 (DP-788)
deposition on copper, glass, perspex, platinum, and tin, 16: 7872
deposition on stainless steel in fuel element processing, 18: 23705 (ORNL-TM-837)
deposition on tropospheric aerosols, 20: 31459
detection and measurement of, by 4π-liquid scintillation counting, 19: 11595
determination by coincidence counting, 17: 4845
determination in air by scintillation spectroscopy of gamma spectra, 17: 7778
determination in atmosphere, 19: 4375
determination in aerosols, methods and equipment for, 19: 34258 (NP-15102)
determination in bovine feces, forage, and grain, gamma spectrometric, 19: 32101
determination in cesium-137 sulfate, 16: 23631 (TID-7629(p.209-16))
determination in Chinese cabbage and spinach, 17: 7779
determination in Columbia River, 20: 8980(R) (BNWL-36, pp 3.1-122)
determination in dust samples, spectrometric, 16: 27461
determination in diet and excreta of Japanese, 1962 and 1963, 18: 20232 (JAERI-1057)
determination in dilute waste solutions by computer resolution of gamma spectra, 19: 9063 (ORNL-3744)

determination in decontamination solutions, 19: 32059(R) (IDO-14655)
determination in fallout particles, gamma spectrometric, 19: 17821
determination in food samples by gamma spectroscopy, 19: 15385
determination in forest moss, gamma spectrometric, 19: 42249
determination in fallout, gamma spectrometric, Korea, 1964, 20: 9149
determination in human lungs, whole-body counting, 17: 5704 (TID-12790)
determination in heavy-water moderator by sequential analysis, 18: 27287 (DP-886)
determination in IRL Reactor pool by gamma spectrometry, 17: 40702 (TID-7655(p.107-18))
determination in irradiated MITR fuel elements by gamma spectroscopy, 20: 10764 (MITRE-64)
determination in liquids, gamma spectrometric, 18: 33485
determination in lung tissues, spectrometric, 19: 44292(R) (NP-15173)
determination in man, computer program for processing data from, 16: 27465(R) (NP-11928)
determination in mixtures with zirconium-95, radiometric, 19: 19748 (DP-933)
determination in mixtures with zirconium-95 during chemical separation, gamma spectrometric, 19: 30073 (CEA-R-2729)
determination in man of, in isotope mixtures, γ spectrometric, 20: 6923
determination in newborns, infants, and children, whole-body, 17: 35432
determination in niobium, gamma-spectrometric, (E), 19: 22684 (AE-174)
determination in niobium-95–zirconium-95 samples, gamma-spectrometric, 19: 22684 (AE-174)
determination in Pacific Ocean, 18: 39109
determination in ratio with zirconium-95 in rain water, method for, 17: 38952
determination in rain water, 18: 39506
determination in rain water, 19: 38557
determination in shore sand and sea silt, gamma-spectrometric, 16: 20323 (PG-Report-312)
determination in sediments near mouth of Columbia River, 17: 15530
determination in seaweed and sea water, spectrometric, 17: 32005
determination in sea water, gamma spectrometric, 20: 41145
determination in urine and feces, gamma spectrometric, 18: 33264
determination in water supplies, 19: 324
determination in zirconium-95 mixtures by resolution of complex decay curves, 17: 29009
determination of bomb-produced, in fallout particles, 19: 641
determination of, in soil samples, gamma spectrometric, 17: 18308
determination of inhaled, in man by whole-body gamma spectrometry, 17: 24853
determination of, gamma spectrometric, 19: 32545 (CEA-R-2461)
determination relative to zirconium-95, radiochemical, 19: 9054 (AERE-R-4814)
determination using lithium-drifted germanium detector, 19: 32594
diffusion from chromium-iron alloy at 1000°C, 17: 23946(R) (BMI-X-10039)
diffusion in chromium–iron and chromium–iron–nickel alloys at 600 to 1200°C, 18: 22477(R) (BMI-X-10081)
diffusion in irradiated fuel element cladding alloys and materials at 600 to 1200°C, 20: 21232 (BMI-1763)
diffusion in niobium at 2000 to 2400°C, coefficient for, 18: 4172(R) (ORNL-3470(p.67-74))
diffusion in niobium, tantalum, and beta zirconium, temperature dependence, 18: 27967 (ORNL-3617)
diffusion in niobium, tantalum, and beta-zirconium, 18: 44153 (ORNL-P-425)
diffusion in niobium at 874 to 2400°C, 19: 41064
diffusion in niobium and tantalum, 20: 4385(R) (ORNL-3870, pp 15-19)
diffusion in polycrystalline uranium dioxide at 1100 to 2100°C, 20: 13289
diffusion in pyrolytic graphite, 20: 17107
diffusion in tantalum, submicron sectioning technique for analyzing, 18: 8829
diffusion in tantalum crystals, 18: 44047(R) (ORNL-3670(p.27-30))
diffusion in tantalum at 1050 to 1600°C, 19: 16090
diffusion in tantalum at 920 to 2500°C, 19: 34712
diffusion in uranium, 17: 3471(R) (BMI-X-10017)
diffusion in urania, 18: 4172(R) (ORNL-3470(p.67-74))
diffusion in zirconium crystals at 900 to 1750°C, 17: 29360
diffusion in zirconium at 900 to 1750°C, coefficient for, 18: 4172(R) (ORNL-3470(p.67-74))
diffusion in zirconium at 800, 1000, and 1150°C, 18: 32136(R) (BMI-X-10093)
dispersion from fallout in seawater, 20: 37037
distribution and half life in rats, 16: 27465(R) (NP-11928)
distribution in Columbia River effluent, 19: 46680
distribution in fetal and maternal rabbit tissues, 19: 43883(R) (UCLA-12-565, pp 65-85)
distribution in ground-level aerosols, 19: 13687
distribution in rats and dogs from inhalation, 17: 40510
distribution in rabbit tissues of, fetal and maternal, 19: 22019(R) (UCLA-12-541(p.51-91))
distribution in samples of atmospheric precipitation, effects of sample preparation on, 18: 37372(T) (AEC-tr-6446)
distribution in sea water in Swordfish Program, 20: 18576(R) (TID-22660)
distribution in water and silt of British estuaries, 20: 45224
effects of injected, in rats, pathological, 19: 40384
effects on determination of rhodium-106 and ruthenium-106 using coincidence methods, 20: 43158
effects on plutonium determination in fission product solutions, 20: 10763 (KR-100)
effects on rats, tumorogenic, 18: 13462(T) (JPRS-23559(Del.)(p.28-35))
effects on rats, tumorogenic, 19: 3912(T)
energy levels of, parity and spin of, 19: 47605
energy levels of, effects of collective vibrational motion on anomalous coupling, (T), 20: 28420
excretion by goats, 18: 31118
fractionation in fallout from Chinese and Russian tests, 20: 43528
gamma activity in air, effects of northerly and southerly winds on, 18: 2393
gamma activity of, discrimination in presence of niobium-94, 20: 11134
gamma dose constants for, 20: 46617
gamma dose-rate from, 17: 21925 (AWRE-E-6/63)
gamma dose rate from shielded and unshielded, 18: 18621 (ORNL-3576)
gamma spectra, 16: 12265
gamma spectra, (E), 19: 16840(R) (IDO-17050)
gamma spectra, (E), 20: 36170 (JINR-P-2739)
gamma spectra from terrestrial, time variation, 18: 35746
gamma spectra of, least-squares analysis of, 18: 33926
gamma spectra of, in stratospheric fallout, 19: 22544
half life, 16: 2541
half life, 20: 8076 (NP-15663)
half life of, determination by direct decay, (E), 19: 37847
half life standardization with vibrating reed electrometer, 16: 1053
isomeric yield ratios in uranium-238 fission, 17: 17627(R) (NYO-2304)
isomers of, formation of, in fission, 16: 30930(R) (NYO-2669)
measurement in fallout, 20: 25288
metabolism by dairy cows, 19: 33744
metabolism in fish, 20: 32914
metabolism in rats, after inhalation, 19: 40314
metabolism in rats of, in transient equilibrium with zirconium-95, 20: 6753
metabolism of, in rats and rat sarcomas, 20: 1595
neutron activation cross sections of, upper limit for thermal, 18: 2841(R) (ORNL-3488(p.1-17))
occurrence in marine organisms and particulate material, 17: 30255
preparation and separation from zirconium-95 by ion exchange, 20: 43433
preparation for counting by electrospraying, 16: 5387
production in molybdenum-95 (n,p) reactions, cross sections for, 17: 7101 (NP-12330(p.97-103))
production in proton fission of uranium at 10–85 Mev, cross sections for isomer, 17: 24420
production in zirconium-95 beta decay, activity calculations for various fluxes in zirconium-94 (n,γ) reaction, 17: 26510
production of isomeric, in deuteron reactions (d,n) at 15 Mev, 20: 16508(R) (NYO-2771-13)
radioactivity and yield from uranium fission, gravimetric method of determining, 18: 27288 (KFK-199)
radioactivity standardization in mixtures with zirconium-95, 18: 24042 (AERE-R-4555)
ranges of fission products of, in aluminum, (E), 20: 17721
removal from leafy vegetables, effectiveness of detergents and water for, 18: 5555
retention by reactor coolant sodium, 18: 11383 (NAA-SR-9163)
separation by calcium phosphate–humic acid flocculation, 18: 24982
separation by ion exchange (E), 19: 868
separation by solvent extraction using tributyl phosphate, 17: 37294(T) (AEC-tr-6014)
separation by solvent extraction using butyl phosphate solutions, 18: 6890
separation from drinking water using natural sorbents, 19: 24424
separation from fission product mixtures by ion exchange, design of semiautomatic device for, 18: 1805
separation from fission products by amalgam exchange, radiochemical, 18: 16148
separation from fission products by solvent extraction using TBP, (E), 19: 22417
separation from hydroxides by precipitation, effects of freezing on, 16: 11736
separation from hydrochloric acid by solvent extraction using tribenzylamine, 17: 12370
separation from irradiated uranium oxides using molten sodium chloride, 20: 43454

separation from low-level waste solutions, ion exchange method for, 20: 47083(R) (ORNL-3945, pp 79-106)
separation from nitric acid solutions by solvent extraction with TBP, 16: 23787 (ORNL-3285)
separation from nitrate–nitric acid solutions and zirconium-95 using Vycor glass, 16: 3044
separation from other short-lived uranium fission products, chromatographic, 18: 39393
separation from radioisotopes in aqueous solutions by foam chromatography using colloidal manganese dioxide, 20: 20628
separation from uranium carbide during oxidation reactions, 16: 33071(T,R) (EURAEC-337)
separation from uranium fission products using ring oven method, 19: 11021
separation from waste solutions by flocculation, 16: 21862
separation from waste water by ion exchange on humic acid, 19: 33678
separation from waste solutions by recycle scavenging–precipitation ion exchange process, 20: 10440 (ORNL-3863)
separation from yttrium-90 in food by solvent extraction using di-(2-ethylhexyl) phosphoric acid, 19: 15386
separation from zirconium-95 by ion exchange on tin phosphate, 18: 13922
separation from zirconium-95 by ion exchange on pyrocatechol-*O*,*O*-diacetic acid, 18: 33508
separation from zirconium-95 by solvent extraction using benzene solution of fatty acids, 18: 39116
separation from zirconium by solvent extraction using *N*-benzoyl-*N*-phenylhydroxylamine, 18: 43412
separation from zirconium-95, chromatographic, 19: 44118 (UCRL-16015)
separation from zirconium by solvent extraction using diisobutylcarbinol, 20: 33419
separation of, from nitric acid, efficiency of AMSCO-TBP in, 17: 10739(R) (ORNL-TM-27)
separation of, from americium-241, radiochemical, 17: 19954
separation of zirconium-95 from, by solvent extraction using acetylacetone, 18: 6889
separation using chromatographic paper treated with tri-*n*-octyl phosphate, 17: 35943
shielding power sources of, 19: 21595 (TID-7698(Pt.I)(p.33-248))
sorption by ammonium phosphotungstate, effects of ammonium and sodium salts on, 17: 34062
sorption by degraded kerosene, effects of nitroparaffins on, 20: 33423
sorption by iron trioxide and monodisperse lucite particles, 19: 4124
sorption by PA-2 aluminum alloys and stainless steel, effects of pH on, 20: 25073
sorption by river silts, 18: 35238 (STI/DOC/10/28(p.9-20))
sorption from aqueous solutions by manganese dioxide, 16: 16389
sorption on sediments in river-estuary systems, 20: 39121
sorption reactions of, on minerals, 20: 41178 (AD-635547)
sorption through burns and wounds in rats, 18: 29232
transport in Columbia River, 20: 25290
transport in river-estuary systems, 20: 39121
uptake and distribution in rat tissues, 18: 11604
uptake and excretion by rats, 19: 17472
uptake by beach organisms, 18: 21762
uptake by brain tumors, 18: 1471
uptake by eggs and tissues of chickens following intramuscular and oral administration, 18: 38775(R) (ORO-624)
uptake by food plants under field conditions, 17: 40541
uptake by man following accidental exposure, 20: 9199
uptake, distribution, and excretion by animals, 17: 28637
uptake from fallout by human lungs, 19: 3856
yields in proton fission of uranium-238 at 7.1, 9.4, and 12.0 Mev, 20: 37995
yields in thermal neutron fission of bismuth, lead, thorium, and uranium, 17: 41897
yields of high and low isomeric, in fission of bismuth, lead, thorium, and uranium, 17: 41897

NIOBIUM ISOTOPES Nb-96
beta decay of, gamma spectra from, (E), 19: 45341
beta decay scheme of, 17: 9545
decay of, gamma spectra from, 17: 41961
decay scheme, spin states, and angular correlations for, 17: 9617
decay schemes, molybdenum-96 energy levels, 16: 14030
production in molybdenum-96 (n,p) reactions, cross sections for, 17: 7101 (NP-12330(p.97-103))
production in proton fission of uranium at 10–85 Mev, cross sections for, 17: 24420
yield in alpha fission of thorium-232 at 20 to 40 Mev, (E), 19: 41779
yield in neutron fission of uranium-235 at 14.9 Mev, (E), 19: 41779
yields in thermal neutron fission of bismuth, lead, thorium, and uranium, 17: 41897
yields of, from proton fission of uranium-238 at 12 Mev, 20: 37995

NIOBIUM ISOTOPES Nb-97
activity in fast neutron activation products of zirconium, calculated, 19: 32058(R) (GA-5978)
determination in heavy-water moderator by sequential analysis, 18: 27287 (DP-886)
energy levels, 17: 9606
gamma dose constants for, 20: 46617
gamma spectra, 17: 34966
production in proton fission of uranium at 10–85 Mev, cross sections for, 17: 24420
radioactivity, 19: 17368
use in neutron activation analysis for zirconium, 19: 2255

NIOBIUM ISOTOPES Nb-98
beta decay of, molybdenum-98 levels from, (E), 20: 36201
beta decay scheme for ground-state and isomeric-state, (E), 20: 9960(R) (AEET-228)
decay, (E), 20: 12152
decay, 18: 11195(R) (EANDC(E)-49(L))
half life, (E), 20: 36201

NIOBIUM ISOTOPES Nb-99
decay scheme, 17: 10506(R) (ORNL-3320(p.1-15))
fission yield of isomeric, 17: 22608

NIOBIUM ISOTOPES Nb-100
half life, (E), 20: 36201

NIOBIUM MANGANATES
ion magnetic exchange interactions in, 18: 16048

NIOBIUM MINERALS
see also Pyrochlores
composition and processing, 18: 3977
geochemistry of, in Lueshe carbonatite deposit in Congo Republic, 19: 18137 (EUR-2110.e)
industrial hygiene in mining, 17: 2760(T) (JPRS-19866)
mineralogy and occurrence of niobian eschynite in North China, 17: 3184
mineralogy and paragenesis of carbonatic rare earth deposits, Ravalli County, Montana, 16: 5559
occurrence and properties of niobium–uranium metamict mineral in Powhatan County, Virginia, 19: 44279
prospecting for, in carbonate deposits, by gamma spectroscopy, 19: 30423

NIOBIUM NITRIDES
analysis for nitrogen by reaction with chlorine and measurement of nitrogen released, 19: 17800
analysis, methods for, 19: 24403 (NP-14952)
bonding in, 17: 8082
crystal structure and properties in iron alloys, 19: 22230
crystal structure of, (E), 19: 41051
determination in niobium and niobium alloys by anodic staining, 19: 34107 (ORNL-3821)
determination in niobium by anodic staining, 19: 46929 (MMI-4998, pp 57-64)
electric properties of, effects of non-metallic atoms on, 17: 8854
electric properties of, rigid band model for interpreting, 18: 24137 (NP-13944)
electron structure and physical properties of crystals of, 17: 27875
emissivity, 16: 21077
evaporation rate and vapor pressure at 1100 to 2000°C, 16: 2208(T) (AEC-tr-4865)
extrusion of, development of techniques for, 20: 796
Fermi level, 19: 47009 (NP-15514(Vol.2))
figure of merit and atomic characteristics, 19: 2284
formation in niobium and niobium–zirconium alloy, 19: 13991 (ML-TDR-64-134)
Hall effect, 17: 6520(R) (NP-12373)
hardness and structure, 16: 7916
mechanical and thermodynamic properties of, effects of zirconium on, 20: 37274
preparation and properties, 16: 8749
preparation and properties of, 18: 16498
preparation and properties of, 19: 18472(T) (JPRS-28739)
preparation by decomposition of ammonium fluoroniobate in ammonia, 19: 15541
preparation from niobium powder and nitrogen at 1200 to 1500°C and up to 160 atm, 18: 27454
review, 18: 39899 (LA-2942)
sintering of, electron density in phase lattices and optimal conditions for, 17: 27767
solubility in gamma iron, 16: 10582
solubility products in liquid iron at 1550 to 1750°C, 19: 41065
spectra of niobium in, L, 19: 6355
superconducting critical field measurements, (E), 19: 12434
superconducting properties of evaporated and sputtered films of, 18: 34157
superconducting properties, 19: 20572
superconductivity of platelets and whiskers of, electric and magnetic

transport properties in, (E), 20: 8015
superconductivity of binary alloyed interstitial compounds of, 20: 34444
superconductivity, susceptibility, and thermal capacity of, (E), 20: 34443
thermal conductivity, effects of electronic and crystalline structure, 16: 24208
thermodynamic properties, 20: 10816(T) (NASA-TT-F-285)
thermoemission properties of, 17: 39799
HfN–NbC–NbN, superconducting properties, 20: 17589 (CONF-650922, pp 541-9)
MoC–NbN, superconducting properties, 20: 17589 (CONF-650922, pp 541-9)
NbC–NbN, critical supercurrents in, (E), 19: 39688
NbC–NbN, reflection spectra of, 17: 6520(R) (NP-12373)
NbC–NbN, superconducting critical currents of, (E), 19: 27371
NbC–NbN, superconductivity of platelets and whiskers of, electric and magnetic transport properties in, (E), 20: 8015
NbC–NbN, superconducting properties, 20: 17589 (CONF-650922, pp 541-9)
NbC–NbN, superconductivity of ternary-alloyed interstitial compounds of, 20: 34444
NbC–NbN–VN, superconducting properties, 20: 17589 (CONF-650922, pp 541-9)
NbC–NbN–ZrC, Hall coefficient for solid solutions of, 19: 47009 (NP-15514(Vol.2))
NbC–NbN–ZrN, superconducting properties, 20: 17589 (CONF-650922, pp 541-9)
NbN–TaC, superconducting properties, 20: 17589 (CONF-650922, pp 541-9)
NbN–TiC, superconducting properties, 20: 17589 (CONF-650922, pp 541-9)
NbN–TiN, superconducting properties, 20: 17589 (CONF-650922, pp 541-9)
NbN–VC, superconducting properties, 20: 17589 (CONF-650922, pp 541-9)
NbN–VN, superconducting properties, 20: 17589 (CONF-650922, pp 541-9)
NbN–ZrN, superconductivity of wires of, (E), 20: 2891

NIOBIUM ORES

analysis for niobium by neutron activation, 19: 24420
analysis, spectrographic, 16: 30348
availability of, review of, 17: 29253 (NRC-7129)
consumption, occurrence, trade, and uses, 16: 2034
processing, 16: 30402
processing by reductive chlorination, 20: 4072(P)
resources, mining, and processing, 18: 3977
resources review, 16: 16716 (CNLM-2166)
separation of niobium from low-grade, by chlorination, 19: 28437 (BM-RI-6635)

NIOBIUM OXALATE COMPLEXES

composition and stability, 18: 1665
crystal structure, 17: 3000
preparation and properties, 19: 36376
spectra, infrared, 16: 32982
stability, 16: 17681
thermal decomposition, 17: 3000

NIOBIUM OXIDES

analysis for common impurities by d-c arc excitation, photometric, 19: 26268
analysis for common impurities by fusion and d-c arc excitation, photometric, 19: 26269
analysis for sulfur, luminescent method for, 18: 33513
analysis for tantalum and titanium, spectrographic, 17: 28796 (AEET/ANAL/7)
analysis for tantalum, activation, 19: 4096
analysis for tantalum by neutron activation methods, 19: 32069
analysis for tantalum and titanium, effects of instrumental error on x-ray spectrographic, 20: 8857
analysis for titanium, spectrographic, 18: 17765
analysis for zirconium, 16: 30343
annealing at 125 and 200°C *in vacuo*, effects on electric conductivity and internal friction, 16: 12039
annealing effects on single crystals of, 18: 44163
bonding to alumina, method for, 20: 31669
chlorination at 700 to 1100°C, equilibrium constant for, 16: 1653(T) (AEC-tr-4868)
chlorination by carbon tetrachloride entrained by carbon dioxide at 700°C, 16: 33071(T,R) (EURAEC-337)
chlorination in ore concentrates, 16: 30402
chlorination of, corrosion and reaction rates in processing by, 18: 39386
chlorination of, in presence of graphite powder, kinetics of, 20: 45685
content in zircon from Kyoto Prefecture, Japan, 19: 36296
corrosion by biphenyl, 20: 25491(T) (AECL-2330, pp 179-95)
crystal structure, 16: 4496 (NP-11056(p.16-31))
crystal structure of, vacancy interaction energies in, 17: 35781
crystal structure of NbO_2, 17: 39058
crystal structure of $Nb_{12}O_{29}$ (o-rh), 17: 40784
crystal structure of Nb_2O_5, 19: 6309
crystal structure transformations in, 19: 18501
crystal structure of, electron diffraction study of, 19: 42885(T)
crystal structure of Nb_2O_5, 20: 31746
crystal structure transformations in monocrystals of, 20: 35919
crystal structure of monoclinic $Nb_{12}O_{29}$, 20: 36790
crystal structures of, Nb_2O_5, 20: 29728
crystallization of anodic films of, electron microscope studies on, 19: 975
defect structure of pentavalent alpha, 16: 11651
density of anodically formed, 18: 42042
determination by x-ray fluorescence, 17: 31999
determination in niobium and niobium alloys by anodic staining, 19: 34107 (ORNL-3821)
determination in niobium by anodic staining, 19: 46929 (NKK-4998, pp 57-64)
determination of chlorinated, in fused electrolytic baths, 17: 40689 (AEET/ANAL/15)
diffusion of ions in, 18: 5273
diffusion of oxygen in, 16: 22156
effects on density of sintered uranium dioxide, 18: 35060(R) (ANL-6904)
effects on density of sintered uranium dioxide, 18: 44118
effects on diffusion in uranium dioxide, mechanism of, 20: 37256
effects on electric conductivity of uranium dioxide, 18: 39894 (EURAEC-1110)
effects on electric conductivity of hafnia, 19: 18394 (ML-TDR-64-294)
effects on homomolecular isotopic exchange of carbon monoxide, catalytic, 19: 26328
effects on irradiation performance of urania, 20: 39447 (AECL-2581)
effects on irradiation behavior of sintered uranium dioxide, 17: 41490 (CRFD-1012)
effects on lead titanate–zirconate ceramics at 4 to 77°K, 16: 13605
effects on production of boron nitride by reaction of boron oxide with nitrogen or ammonia, catalytic, 19: 36430(P)
effects on sintering of urania, 19: 43985(R) (ANL-7000, pp 85-110)
effects on thermal conductivity of uranium dioxides, 19: 18448 (AECL-2169)
effects on thermal conductivity of sintered uranium dioxide at 1000 to 2000°C, 19: 46995 (EUR-2424.f)
effects on thermal conductivity of uranium dioxide, 17: 27814(T) (EURAEC-103)
effects on xenon diffusion in urania, 20: 31666
electric conductivity of reduced alpha, at 350 to 1150°K, 16: 22627
electric conductivity at 600 to 1200°C, 17: 3606
electric conductivity of α-Nb_2O_5 and Nb_2O_5, 17: 22212
electric conductivity of nonstoichiometric alpha, at 77 to 1270°K, 17: 8981
electric conductivity of, effect of oxygen vacancies on, 18: 10097
electric conductivity of, avalanche-induced anomalies in, 19: 7921
electric conductivity and thermoelectric properties of liquid, 19: 9684
electrochemistry of passivating films of, formed on metal by polarization, 18: 34063
electron mobility at 900 to 1400°C, 18: 37154
evaporation from niobium surfaces, rates of, 19: 30675(R) (SRIA-132)
formation by oxygen ion bombardment, 19: 27063 (INR-555/XIV)
formation of, free energy of, 18: 14401 (BNL-7553)
free energy of formation at 1050 to 1200°K, 18: 19973
free energy of formation, (E), 19: 17202
growth mechanism and mechanical properties of Nb_2O_5 whiskers, 16: 7918
heat of formation, 16: 25334
heat of formation and enthalpy, 18: 31529
heat of formation of pentavalent, standard, 18: 43517
metallographic and x-ray diffraction studies of, 17: 23944(R) (ARL-62-397)
optical properties of films of, 18: 4252(R) (ORNL-3470(p.55-62))
phase studies, 16: 13568 (ARL-239 (Pt.II))
phase transformation, x-ray studies, 17: 16667
phase transformations in, x-ray studies of, 18: 2283
phase transformations, 20: 11227
phase transitions and x-ray diffraction in, 17: 27788(R) (LRR-41)
phases, metallographic study, 16: 16745
polarography in lithium and lithium sodium metaphosphates at 750 and 730°C, 18: 1516
precipitation from supersaturated niobium-oxygen solid solutions, 18: 27471
preparation and crystal structure of ternary, 17: 32100
preparation and properties of suboxides, 20: 36825
preparation and structure of, 17: 20024
preparation of anodic films of, method for, 18: 32120

preparation of films of, on platinum, 19: 34665
preparation of pentavalent, 16: 1721
preparation of pure, from aqueous solutions containing iron and other impurities, 16: 17775(P)
preparation, properties, and structure, 16: 29390(T) (AEC-tr-5298)
processing of, by chlorination, 20: 7188 (EUR-2088.f)
properties for use as uranium dioxide sintering additives, 17: 546(T,R) (EURAEC-5)
radiation effects on catalytic activity of, in decomposition of hydrogen peroxide, 20: 43364
rare gas release, 16: 4167
reaction with barium carbonates, 18: 22076
reactions at high pressures, solid-phase, 17: 10503 (NP-12359)
reactions with amesicium oxide, properties of ternary oxides formed in, 19: 28286 (KFK-280)
reactions with cerium, thorium, and uranium oxides, x-ray analysis of products of, 17: 8037
reactions with copper oxides, structure of ABO_3 type compound formed in, 19: 46244(R) (TID-22207, Paper D)
reactions with graphite, formation of niobium carbide coatings by, 19: 42835(P)
reactions with graphite, formation of niobium carbide coatings by, 19: 42836(P)
reactions with melted borate, sulfate and chromate salts, 16: 122
reactions with molybdenum oxides, 20: 26864
reactions with niobium carbide in vacuum, 17: 21600
reactions with niobium carbide in arc furnace, 17: 21601
reactions with niobium carbides, kinetics of, 17: 25256
reactions with niobium pentachlorides, 17: 25265
reactions with niobium halides, phase studies of equilibrium products in, 19: 363
reactions with niobium carbides by vacuum reduction process for preparation of niobium metal, 19: 9145
reactions with niobium carbides to prepare crude niobium metal, 19: 9146
reactions with niobium, 20: 16483
reactions with niobium carbides, properties of intermediate products in, 18: 10069
reactions with protactinium oxides, solid-state, 20: 26880
reactions with tiron to form yellow-colored complex, 19: 17908
reactions with tungsten carbide at 1300 to 1400°C, preparation of alloys by, 18: 39833(T)
reactions with uranium oxides, 17: 14244
reactions with uranium(IV-VI) oxides, 19: 22241
reduction by calcium carbide and calcium cyanamide at 1000°C, 17: 28845
reduction by carbon, 16: 1647 (IS-339)
reduction by carbon, equilibria in, 16: 2209(T) (AEC-tr-4867)
reduction by carbon monoxide at 800 to 1050°C, 17: 10661
reduction by carbon, hydrogen, or metals, methods for, 17: 35950
reduction by carbon black, conditions for preparation of niobium by, 18: 35947(T)
reduction by carbon at 1400 to 1600°C, effects of potash and soda on, 20: 16483
reduction by carbon monoxide, 20: 16483
reduction by hydrogen at 760 to 1060°C, kinetics of, 16: 30440
reduction by hydrogen at 1000°C, 20: 16483
reduction of, by calcium and magnesium, 17: 12678
reduction of pentavalent, formation of niobium carbide by, 17: 21692
reduction of pentoxide by carbon at 1600 to 2000°C, 16: 12037
reduction of pentoxide by carbon at 1800°C, 17: 16530(T) (JPRS-18277)
reduction of, thermodynamics of, 17: 14269
reduction of, calciothermic, 19: 15540
reduction of, preparation of alloys in carbothermal, 18: 41948
screening of metal–metal bonds in, effects on overlapping, 18: 17781(T) (AEC-tr-6388)
separation from niobite–tantalite ore by solvent extraction using TBP, 20: 43437
separation from tantalum oxide in Indian columbite and tantalite by solvent extraction, 18: 10188
separation from urania in organic slurries, centrifugal, 20: 36933
sintering of compacts of, isothermal shrinkage in, 16: 31364
solubility of, in nitric acid–hydrofluoric acid solutions at 25°C, 20: 43226
sorptive properties for chloride and potassium ions, effects of pH on, 20: 14651
spectra in low frequency region, infrared, 18: 23549
spectra of nonstoichiometric, reflectance, 18: 12108
stability, 17: 1441
stability of, galvanic cell studies of, 19: 43997(R) (UCRL-11889)
stresses in films of, measurements of, 17: 16685
structure of films of, on niobium oxidized at 400 to 1100°C, 18: 10478(T) (JPRS-22697(p.64-78))
structure of Nb_4O, electron diffraction study on, 20: 876
superconducting properties, 19: 25031
superconductivity of, (E), 19: 16813
surface tension and thermal expansion of pentavalent, 17: 8091
testing for use in shaft seals for potassium space power systems, 20: 2242
thermal energy storage in, in solar-thermionic power supplies, 17: 9113
thermal expansion coefficients of Nb_2O_5 at 20 to 1000°C, 17: 23883
thermal stresses and spalling of films of, on niobium, 17: 23883
thermodynamic properties, 17: 12678
thermodynamic properties of, tables of, 17: 40777(R) (RAD-SR-63-183)
thermodynamic properties, 18: 35939(R) (NP-14192)
thermodynamic properties, 20: 10816(T) (NASA-TT-F-285)
thermodynamic stability at 1030 to 1300°K, 19: 38586 (UCRL-11957)
thermodynamic stability measurements on, using galvanic cells, 20: 31717(R) (UCRL-16658, pp 143-9)
thermodynamics of nonstoichiometric α-Nb_2O_5, 17: 30563
thermoelectric power of nonstoichiometric alpha, 17: 20560 (NP-12698)
thermoelectric properties of tungsten-doped, 16: 29517
thermoluminescence of alpha pentavalent, 16: 9229
vacancy interaction energies in monoxide, 17: 2993
vacancy structure, 16: 22573(R) (AD-266459)
valency changes in films of, on electrodes, 17: 25203
vapor pressure determinations, 16: 30386
Al_2O_3–Nb_2O_5, electric conductivity, 17: 1504
Al_2O_3–NbO, phase formation and properties of $AlNbO_4$, 16: 18057
Al_2O_3–Nb_2O_5, phase studies on, 17: 41454
Al_2O_3–Nb_2O_5, phase studies, 19: 26846
Al_2O_3–Nb_2O_5, phase studies, 19: 41049
Al_2O_3–Nb_2O_5, phase studies, 20: 12833
Al_2O_3–Nb_2O_5, properties and structure of compounds formed in, 18: 34199
Am_2O_3–BaO–Nb_2O_5, preparation, lattice constants, and properties, 19: 32750
AmO_2–Nb_2O_5, crystal structure, preparation, and properties, 19: 32748
Am_2O_3–Nb_2O_5, crystal structure, preparation, and properties, 19: 32749
Am_2O_3–Nb_2O_5, preparation, lattice constants, and properties, 19: 32750
Am_2O_3–Nb_2O_5–TiO_2, preparation, lattice constants, and properties, 19: 32750
As_2O_5–Nb_2O_5, crystal structure of tetragonal phases in, 18: 19942
BaO–Nb_2O_5, formation and properties, 18: 22076
BaO–Nb_2O_5–Pu_2O_3, preparation, lattice constants, and properties, 19: 32750
CaO–Nb_2O_5, crystal structure and phase studies, 16: 24191
CaO–Nb_2O_5, density and surface ductility of fused, at 1200 to 1650°C, 20: 15076
CaO–Nb_2O_5, electric conductivity, 17: 1504
CeO_2–Nb_2O_5, crystal structure, preparation, and properties, 19: 32748
CeO_2–Nb_2O_5, properties and structure of compounds formed in, 18: 34199
Cm_2O_3–Nb_2O_5, preparation, lattice constants, and properties, 19: 32750
CoO–Nb_2O_5, phase diagram, 19: 44711
CoO–Nb_2O_5–Te_2O_5, phase studies, 20: 31734
Cr_2O_3–Nb_2O_5, density and surface ductility of fused, at 1200 to 1650°C, 20: 15076
Cr_2O_3–Nb_2O_5, phase studies, 19: 41049
Cr_2O_3–Nb_2O_5, phase studies, 20: 12833
Cs_2O–Nb_2O_5, crystal structure of phases in, 19: 37059
Dy_2O_3–Nb_2O_5, properties and structure of compounds formed in, 18: 34199
Fe_2O_3–Nb_2O_5, density and surface ductility of fused, at 1200 to 1650°C, 20: 15076
Fe_2O_3–Nb_2O_5, electric conductivity, 17: 1504
Fe_2O_3–Nb_2O_5, phase studies, 19: 30785
FeO–Nb_2O_5, phase studies, 19: 30785
Ga_2O_3–Nb_2O_5, dielectric properties of phases in, 18: 10555
Ga_2O_3–Nb_2O_5, properties and structure of compounds formed in, 18: 34199
Gd_2O_3–Nb_2O_5, properties and structure of compounds formed in, 18: 34199
GeO_2–Nb_2O_5, crystal structure of tetragonal phases in, 18: 19942
In_2O_3–Nb_2O_5, properties and structure of compounds formed in, 18: 34199
La_2O_3–Nb_2O_5, crystal structure, preparation, and properties, 19: 32749
La_2O_3–Nb_2O_5, properties and structure of compounds formed in, 18: 34199
Li_2O–Nb_2O_5, crystal structure of phases in, 19: 37059
Li_2O–Nb_2O_5, electric conductivity, 17: 1504
MoO_3–Nb_2O_5, crystal structure of complex compounds in, 19: 25037
MoO_3–Nb_2O_5, double oxide formation and composition in, after sintering, 18: 12057
MoO_3–Nb_2O_5, phase studies, 19: 41049
NbC–Nb_2O_5, reduction of, electric arc method for, 19: 39133
NbC–Nb_2O_5, reduction of, electric arc method for, 19: 39133
$NbCl_4$–Nb_2O_5, phase studies and properties, 17: 25265
Nb_2O_5–K_2O, crystal structure of phases in, 19: 37059
Nb_2O_5–K_2O, density and surface ductility of fused, at 1200 to 1650°C, 20: 15076
Nb_2O_5–K_2O, electric conductivity, 17: 1504
Nb_2O_5–Na_2O, crystal structure of phases in, 19: 37059
Nb_2O_5–NbO_2F, phase studies at 500 to 800°C, 19: 15468

Nb_2O_5–PaO_2, crystal structure, preparation, and properties, 19: 32748
Nb_2O_5–P_2O_5, crystal structure of tetragonal phases in, 18: 19942
Nb_2O_5–Pr_2O_3, crystal structure, preparation, and properties, 19: 32749
Nb_2O_5–PuO_2, crystal structure, preparation, and properties, 19: 32748
Nb_2O_5–Pu_2O_3, preparation, lattice constants, and properties, 19: 32750
Nb_2O_5–Sc_2O_3, properties and structure of compounds formed in, 18: 34199
Nb_2O_5–SiO_2, phase diagram, 16: 18054
Nb_2O_5–SiO_2–Na_2O, dielectric properties of glasses in, 17: 12686
Nb_2O_5–Sm_2O_3, properties and structure of compounds formed in, 18: 34199
Nb_2O_5–SO_3–H_2O, preparation and solubility constants, 17: 28915
NbO–TaO, analysis for niobium and tantalum, 17: 15857(R) (ORNL-3397(p.57-70))
Nb_2O_5–Ta_2O_5, chlorination in ore concentrates, 17: 16024
Nb_2O_5–Ta_2O_5, crystal structure, 17: 4505
Nb_2O_5–Ta_2O_5, electrolytic reduction of, 17: 16547
Nb_2O_5–Ta_2O_5, phase diagram, 16: 15197 (TID-15382)
Nb_2O_5–Ta_2O_5, phase diagram of, 17: 27788(R) (LRR-41)
Nb_2O_5–Ta_2O_5, phase equilibria in, 18: 8367
Nb_2O_5–Ta_2O_5, phase studies, 19: 41049
NbO_2–TaO_2, preparation and phase studies, 20: 26854
NbO_2–TaO_2–WO_2, phase studies and crystal structure, 19: 9674
Nb_2O_5–ThO_2, crystal structure, preparation, and properties, 19: 32748
Nb_2O_5–TiO_2, crystal structure and equilibria of phases in system, 19: 20569
Nb_2O_5–TiO_2, phase diagrams, 20: 39411
Nb_2O_5–TiO_2, phase studies, 19: 26846
Nb_2O_5–TiO_2, phase studies, 19: 41049
NbO_2–TiO_2, properties of, electric and magnetic, 19: 16175
Nb_2O_5–Tl_2O_3, properties and structure of compounds formed in, 18: 34199
Nb_2O_5–UO_2, crystal structure, preparation, and properties, 19: 32748
Nb_2O_5–U_3O_8, crystal structure at 830 to 1050°K, x-ray diffraction analysis of, (E), 20: 36387
Nb_2O_5–UO_2, density of sintered, 19: 17177(R) (ANL-6965(p.42-83))
Nb_2O_5–U_3O_8, phase transformations in, effects of sintering on, 19: 34697
Nb_2O_5–V_2O_5, crystal structure of tetragonal phases in, 18: 19942
NbO_2–VO_2, crystal structure of double oxide $NbVO_4$, 20: 16982
Nb_2O_5–V_2O_5, double oxide formation and composition in, after sintering, 18: 12057
Nb_2O_5–V_2O_5, electric conductivity, 17: 1504
Nb_2O_5–V_2O_5, phase studies, 19: 26846
Nb_2O_5–V_2O_5, phase studies, 19: 41049
NbO_2–VO_2, properties of tetragonal rutile phase in, electric and magnetic, 19: 16176
Nb_2O_5–WC, reduction to niobium–tungsten alloy by niobium carbide, 20: 29677
Nb_2O_5–WO_3, block principle in phase studies on, 19: 37056
Nb_2O_5–WO_3, crystal structure of complex compounds in, 19: 25037
Nb_2O_5–WO_2, double oxide formation and composition in, after sintering, 18: 12057
Nb_2O_5–WO_2, phase diagrams, 18: 32183
Nb_2O_5–WO_3, phase diagram of, 20: 45012
Nb_2O_5–WO_3, phase studies at 1300 to 1400°C, 19: 37053
Nb_2O_5–WO_3, phase studies, 19: 41049
Nb_2O_5–WO_3, phase studies, 20: 5846
Nb_2O_5–WO_3, phase studies on, 20: 21385
Nb_2O_5–WO_2, preparation and structure, 18: 41462
Nb_2O_5–WO_3, reduction to niobium–tungsten alloy by niobium carbide, 20: 29677
Nb_2O_5–WO_2, space groups and tetragonal unit cell for, 17: 27788(R) (LRR-41)
Nb_2O_5–WO_3, structure of $W_3Nb_{14}O_{44}$ and $W_8Nb_{18}O_{69}$ in, 19: 37055
Nb_2O_5–WO_3, structure of $WNb_{12}O_{33}$ and $W_5Nb_{16}O_{55}$ in, 19: 37054
Nb_2O_5–Y_2O_3, properties and structure of compounds formed in, 18: 34199
Nb_2O_5–ZnO, formation of spinel in, 17: 12597
Nb_2O_5–ZnO, phase studies, 16: 4563
Nb_2O_5–ZnO, phase studies, 19: 26846
Nb_2O_5–ZrO_2, crystal structure of compounds $ZrO_2 \cdot 5Nb_2O_5$ and $ZrO_2 \cdot 7Nb_2O_5$ in, 20: 13281
Nb_2O_5–ZrO_2, phase studies, 19: 26846
Nb_2O_5–ZrO_2, phase studies, 20: 15079
Nb_2O_5–$3WO_3$, crystal structure, 18: 19941
Nd_2O_3–Nb_2O_5, crystal structure, preparation, and properties, 19: 32749
Nd_2O_3–Nb_2O_5, properties and structure of compounds formed in, 18: 34199
NiO–Nb_2O_5, phase diagram, 19: 44711
NiO–Nb_2O_5, phase studies, 19: 26846
NpO_2–Nb_2O_5, crystal structure, preparation, and properties, 19: 32748
PbO–Nb_2O_5, phase studies, 20: 29794
$PbTiO_3$–$PbZrO_3$–Nb_2O_5 system, shock-wave effects on ferroelectric properties of, 17: 552
$PbTiO_3$–$PbZrO_3$–Nb_2O_5, tensile strength of, 20: 828 (SC-DC-65-1588)
$Pb(Zr_{0.65}Ti_{0.35})O_3$–$Nb_2O_5$, radiation effects on crystal structure and electric properties, 19: 47096

NIOBIUM OXYCARBIDES
properties, 18: 10069

NIOBIUM OXYCHLORIDES
chlorination kinetics, 19: 9281(R) (IS-900(Sect.E))
chlorination kinetics, 20: 4077(R) (IS-1200(Sect. E))
chlorination kinetics of, 20: 41064(R) (IS-1500(Sect.E))
electric conductivity in organic solvents, 18: 22081
heat of formation and enthalpy, 18: 31529
properties, 17: 25265
properties in hydrochloric acid solutions, 16: 17634(T) (AEC-tr-4459 (p.77-82))
reactions of, with potassium chloride in vapor phase, 17: 18079
reactions of, with cesium, potassium, and rubidium chloride, 18: 1693
reactions with methanol, methoxide complex formation equilibrium in, 19: 11075
reactions with potassium chloride melts, 17: 1503
reactions with potassium and sodium chlorides, enthalpies of formation of double compounds in, 17: 4550
reactions with potassium and sodium chlorides, 18: 22070
reactions with sodium chloride melts, 17: 1503
reactions with thorium chlorides in melts, tensiometric and thermal analyses, 16: 4169
thermal dissociation and vapor pressure, 16: 16398
CsCl–$NbOCl_3$, thermal analysis of compound formation in, 18: 13782
$NbOCl_3$–RbCl, thermal analysis of compound formation in, 18: 13783

NIOBIUM OXYFLUORIDES
crystal structure, 19: 15469
preparation and properties, 19: 13306
solubility of, in nitric acid–hydrofluoric acid solutions at 25°C, 20: 43226
Nb_2O_5–NbO_2F, phase studies at 500 to 800°C, 19: 15468

NIOBIUM PHOSPHATES
preparation of normal, 16: 30384
preparations and structure of pentavalent, 17: 21711

NIOBIUM PHOSPHIDES
crystal structure, 17: 18738(R) (AFOSR-2645)
crystal structure, 18: 1622
crystal structure, 19: 7945
preparation and high-temperature properties, 16: 12110(R) (TID-14770)
properties, 19: 2802 (NYO-2541-1)
vaporization, 18: 8800(R) (TID-19990(Paper 3))
vaporization behavior, 18: 3430 (TID-19737)

Niobium Potassium Fluorides
see Potassium Niobium Fluorides

NIOBIUM RARE-EARTH TITANATES
preparation and structure, 17: 8836

NIOBIUM SELENIDES
crystal structure of Nb_xSe_y, 19: 6310
crystal structure of, layer polytypism in, 19: 9675
preparation and properties of single crystals of, 16: 31611
preparation by chemical transport in temperature gradient, 19: 26333
structural properties of, 18: 34137
superconducting critical currents in single-crystal, effects of stoichiometry on peak, (E), 20: 17609
superconductivity, 17: 39790
superconductivity in, transition temperatures for, (E), 19: 21195
superconductivity, (E), 20: 13683
Cu–$NbSe_2$, crystal structure of $Cu_{0.4}NbSe_2$, 17: 23310

NIOBIUM SILICIDES
bibliography on phase relations of, 17: 30913 (NP-12972)
bibliography on phase relations of, 18: 10518 (AD-410526)
growth on niobium surfaces, kinetics of diffusion reactions in, 20: 37190
heats of formation, 16: 20394
magnetic susceptibility, 18: 20541
oxidation at reduced pressures, effects of additives on, 20: 41424
oxidation rate of, at 1100°C, 20: 23614
performance as coating on niobium alloys, 20: 5910
phase studies and stability at 1250° to 1500°C, 16: 19410
preparation and properties of superconducting, 17: 18892 (ASD-TDR-62-1111)
solubility in Nb_3Sn at 1300 to 1600°C, 18: 4271
spectra of niobium in, L, 19: 6355
structure and thermoelectric properties, 17: 23987
thermionic emissions at 1300 to 1700°K, 17: 25812
thermodynamic properties, 20: 10816(T) (NASA-TT-F-285)
uses in oxidation-protection coatings for refractory metals, 20: 7517 (PWAC-499)
$MoSi_2$–$NbSi_2$–WSi_2, phase studies, 20: 27542
Nb_5Si_3–W_5Si_3, oxidation and thermal stability of, at high temperatures,

20: 37262
$NbSi_2$–WSi_2, oxidation and thermal stability of, at high temperatures, 20: 37262

NIOBIUM STEEL
carbide formation in, 17: 11209
composition, corrosion resistance, and mechanical properties of, review on, 17: 32508
corrosion by hydrofluoric acid, 16: 20535(R) (IDO-14583)
oxidation by carbon dioxide, tracer studies of carbon deposition in, 18: 41961
reactions with carbon dioxide to 750°C, 19: 22997 (TRG-Report-842)
reactions with uranium dioxide to 800°C, 19: 22997 (TRG-Report-842)
B–C–Cr–Mn–Mo–Ni–Nb–V, precipitation of niobium carbide in, 18: 37726
C–Cr–Mo–Ni–Nb, mechanical properties, effects of low-temperature tempering on, 19: 9647 (AD-604876)
C–Cr–Ni–Nb, precipitation of niobium carbide in, 18: 37726
Cr–Mo–Ni–Nb–V, development as HY-180/210 steel, 20: 5851
Cr–Nb, precipitation in, effects of niobium on, 19: 985
Cr–Ni–Nb, effects of aging at 600 to 800°C on microstructure of, 20: 21355 (TRG-Report-1168)
Cr–Ni–Nb, oxidation resistance of, effects of yttrium on, in carbon dioxide at high temperature, 20: 35914
Cr–Ni–Nb, radiation effects on tensile properties of, at 650 to 800°C, 18: 42128
Cr–Ni–Nb, radiation effects on tensile properties of, at room temperature to 850°C, 18: 42129
Cr–Ni–Nb, radiation effects on, neutron, 19: 7996
Cr–Ni–Nb, radiation effects on stress-rupture of, 20: 13328 (ORNL-TM-1359)
Cr–Ni–Nb, radiation effects on precipitation behavior and tensile properties of, neutron, 20: 33950
Cr–Ni–Nb, radioinduced embrittlement at high temperatures, 18: 5830
Mn–Mo–Ni–Nb, radiation effects on mechanical properties of low-alloy, neutron, 20: 19258 (UJV-1470/65)
Ni–Nb–Ti, properties of Mar-aging, 16: 24153 (DMIC-Memo-156)

NIOBIUM SULFIDES
preparation and properties, 20: 14554
preparation by chemical transport in temperature gradient, 19: 26333
superconductivity, (E), 20: 13683
thermal expansion, 20: 23005
thermodynamic properties, 20: 10816(T) (NASA-TT-F-285)
vaporization of, thermodynamics of, 20: 40796(R) (IS-1500(Sect.C))
Cu–NbS_3, crystal structure of $Cu_{0.33}NbS_3$, 17: 23310
NbS_3–Ag, crystal structure of $Ag_{0.7}NbS_3$, 17: 23310

NIOBIUM SYSTEMS
fabrication of refractory composites of, method for, 19: 28794
Al–B–C–Cr–Mo–Ni–Ta–W–Zr, corrosion and properties of TAZ-8A, 20: 46166 (NASA-TN-D-3597)
Al–B–Nb–Ti–Zr, fabrication and mechanical properties at 70 to 1650°F, 18: 12538(R) (ARF-B201-27)
Al–C–Co–Nb, phase studies, 20: 15103
Al–C–Cr–Nb, phase studies, 20: 15103
Al–C–Cu–Nb, phase studies, 20: 15103
Al–C–Fe–Nb, phase studies, 20: 15103
Al–C–Hf–Nb–Ti, fabrication and mechanical properties at 70 to 1650°F, 18: 12538(R) (ARF-B201-27)
Al–C–Mn–Nb, phase studies, 20: 15103
Al–C–Nb, crystal structure and phase studies, 18: 12706
Al–C–Nb, crystal structure and phase studies of superconducting, 18: 32149(R) (UCRL-11317(p.131-49))
Al–C–Nb, crystal structure and superconductivity of Nb_3Al_2C, 18: 32702
Al–C–Nb, lattice parameters of filled β-manganese structure phases in, 19: 37109
Al–C–Nb, phase studies, 20: 15103
Al–C–Nb, superconducting transitions in, 18: 34283 (UCRL-11390)
Al–C–Nb–Ti, fabrication and tensile properties at 70 and 1600°F, 18: 12538(R) (ARF-B201-27)
Al–C–Nb–V, phase studies, 20: 15103
Al–C–Nb–Zn, phase studies, 20: 15103
Al–C–Ni–Nb, phase studies, 20: 15103
Al–Nb–N, lattice parameters of filled β-manganese structure phases in, 19: 37109
Al–Nb–N, superconductivity of Nb_3Al_2N, 20: 6228
Al–Nb–Si, crystal structure and phase studies, 18: 12704
Al–Nb–Si–Sn, development for use as vanadium alloy coating, 18: 39819(R) (IITRI-B6019-5)
Al–Nb–Si–Ti, oxidation by air at 760 to 1360°C, 17: 27780(R) (DRI-2104)
Al_2O_3–Nb, seals of, development of high-temperature metal-to-ceramic, 19: 44598(R) (GEMP-49A)
Al_2O_3–Nb–V, melting points, 18: 44497(R) (MND-2812-2)
As–Nb, crystal structure of NbAs, 18: 37691
As–Nb, crystal structure of compound in, 19: 23028
As–Nb, phase relations and structures in, 18: 37714
B–C–Nb, preparation and phase studies, 17: 29370
B–Co–Nb, phase studies, 20: 15100
B–Cu–Nb, crystal structure, 20: 14532
Be–Nb–Si, properties for high-temperature applications, 17: 543 (WADD-TR-60-889(Pt.II))
B–Fe–Nb, crystal structure, 20: 14532
B–Mo–Nb–Ti, mechanical and thermal properties of niobium-base systems, 20: 43940
B–Mo–Nb–Ti–Zr, mechanical and thermal properties of niobium-base, 20: 43940
B–Nb, electric and mechanical properties, 18: 24158
B–Nb, mechanical properties, 19: 11734
B–Nb, mechanical properties of, effects of composition on, 20: 11288(T) (AD-622477)
B–Nb, phase studies, 16: 22616
B–Nb, use as brazing alloy, 19: 30690(R) (ML-TDR-64-270)
B–Nb–W, phase studies of, 20: 37261
B–Nb–Zr, neutron radiation effects on, 17: 465
C–Co–Nb, phase studies, 20: 15077
C–Co–Nb, structure of filled Ti_2Ni type compounds in, 19: 37107
C–Cr–Co–Nb–W–Y, oxidation resistance of, at high temperatures, 19: 37155(P)
C–Cr–Fe–Mo–Ni–Nb–Ta–W–V, production of corrosion and oxidation resistant, 18: 12618(P)
C–Cr–Nb, phase studies, 20: 15108
C–Fe–Nb, phase studies, 20: 17086
C–Ga–Nb, crystal structure and phase studies on, 18: 10561
C–Ga–Nb, preparation and structure of T_5M_3X type compound in, 19: 30788
C–Ge–Nb, crystal structure and phase studies on, 18: 10561
C–Ge–Nb, preparation and structure of T_5M_3X type compound in, 19: 30788
C–Hf–Nb, phase diagrams, 20: 13272
C–Hf–Nb, x-ray diffraction of nonmetallic phases chemically extracted from, 19: 7973
C–Hf–Nb–O–W–Y, design improved fabricability and strength at high temperatures, 20: 25610(P)
C–Hf–Nb–V, hardening by annealing, 17: 41428(R) (IITRI-B6007-4)
C–Hf–Nb–V, preparation and properties of dispersion strengthened, 17: 16514(R) (ARF-B6007-1)
C–Hf–Nb–W, fabrication and mechanical properties of, 19: 46940(R) (NP-15444)
C–Hf–Nb–W, phase studies, research program on, 19: 7895(R) (DRI-2198)
C–Hf–Nb–W, properties at very high temperatures, 20: 21412
C–In–Nb, crystal structure of H phase Nb_2InC in, 19: 6339
C–In–Nb, superconductivity of Nb_2InC, 20: 6228
C–Mo–Nb, phase studies of, at 1500 and 1900°C, 16: 13590(T) (AEC-tr-5000)
C–Mo–Nb, phase studies and thermodynamics of, for use at high temperatures, 20: 29774
C–Mo–Nb, phase transformations in, thermodynamics of, 17: 22205
C–Mo–Nb, phase transformations in, thermodynamics of, 18: 44161(T) (AERE-Trans-1009)
C–Mo–Nb–Ta–Ti–W–Zr, creep properties at 1800 to 2200°F of Cb132M, 20: 2333(R) (NASA-CR-54457)
C–Mo–Nb–Ta–W–Zr, erosion by sodium at 400, 1000, and 1500°F of Cb-132M, 20: 769(R) (NASA-CR-54459)
C–Mo–Nb–Ta–W–Zr, extrusion parameters for Cb-132M, 20: 21263(R) (NASA-CR-54911)
C–Mo–Nb–Ta–W–Zr, preparation and specifications for corrosion loop testing, 20: 4380 (NASA-CR-54761)
C–Mo–Nb–Ta–Zr, thermal-mechanical processing of a precipitation-hardenable, dispersion-hardened, 20: 21250
C–Mo–Nb–Ti–Zr, bend and tensile ductility properties of, 20: 21410
C–Mo–Nb–Ti–Zr, corrosion of PWC-533 by boiling potassium, 19: 34640 (CNLM-6246)
C–Mo–Nb–Ti–W, corrosion of tungsten-base Grade 7178, by potassium at 1600°F, 20: 27432(R) (NASA-CR-54892)
C–Mo–Nb–Ti–Zr, extrusion, heat treatment, and rolling of, 19: 32720(R) (AD-609815)
C–Mo–Nb–Ti–Zr, mechanical and metallurgical properties, 19: 32720(R) (AD-609815)
C–Mo–Nb–Ti–Zr, preparation and properties of castings of, 19: 32720(R) (AD-609815)
C–Mo–Nb–Ti–Zr, yield strength of PWC-533, effects of boiling potassium exposure on, 19: 34640 (CNLM-6246)
C–Mo–Nb–W–Zr, corrosion by potassium at 2000 to 2200°F, 18: 24091
C–Mo–Nb–W–Zr, evaluation of protective coatings for, 20: 29651
C–Mo–Nb–W–Zr, thermal properties, 18: 7201 (ASD-TDR-63-597)
C–Mo–Nb–W–Zr, thermal properties to melting point, 20: 878

C–Mo–Nb–Zr, heat treatment of, 20: 14972(P)
C–Nb, metallography, 17: 6525 (TID-7625(p.8-19))
C–Nb, phase diagrams and component interactions, 16: 13601
C–Nb, phase studies, 16: 2210(T) (AEC-tr-4871)
C–Nb, phase studies, 16: 7914
C–Nb, phase studies, 16: 22616
C–Nb, phase studies on, thermal analysis of, (E), 20: 1863
C–Nb, preparation, properties, and uses of, review on, 16: 27640(T) (FTD-TT-62-430)
C–Nb, superconductivity, 17: 41604
C–Nb–N, superconducting properties of, composition dependence of, 20: 34420 (UCRL-16817)
C–Nb–O, phase studies and thermodynamic analysis, 19: 16148
C–Nb–O–W–Y–Zr, design for improved fabricability and strength at high temperatures, 20: 25610(P)
C–Nb–Sn, crystal structure of H phase Nb_3SnC in, 19: 6339
C–Nb–Sn, superconductivity of Nb_2SnC, 20: 6228
C–Nb–Ta–V–Zr, preparation and properties of dispersion strengthened, 17: 16514(R) (ARF-B6007-1)
C–Nb–Ta–Zr, heat treatment of, 20: 14972(P)
C–Nb–Th, corrosion by water at 120 to 260°C, 19: 22889 (ANL-7006)
C–Nb–Ti, analysis for carbon, electron microprobe, 19: 40412 (TIM-924)
C–Nb–Ti, phase diagrams, 20: 13272
C–Nb–Ti–V–Zr, evaluation of properties of, 19: 15995 (IITRI-B231-11)
C–Nb–Ti–V–Zr, mechanical properties, 17: 14809(R) (ARF-B231-8)
C–Nb–Ti–V–Zr, mechanical properties, 17: 41427(R) (IITRI-B231-9)
C–Nb–Ti–V–Zr, mechanical properties and oxidation rate, 19: 32754
C–Nb–Ti–Zr, heat treatment of, 20: 14972(P)
C–Nb–U, phase diagram, 18: 41933 (TID-11295(3rd Ed.))
C–Nb–U, phase diagram, 18: 44116
C–Nb–U, phase diagram, 20: 9552
C–Nb–U, phase studies, 18: 39892 (BMI-1685)
C–Nb–U, phase transformations in, thermodynamics of, 17: 22205
C–Nb–U, phase transformations in, thermodynamics of, 18: 44161(T) (AERE-Trans-1009)
C–Nb–U, vapor pressures to 10,000°R, 20: 8884 (NASA-CR-353)
C–Nb–U, vaporization characteristics at 9,000 and 10,000°R of liquid, calculations, 20: 45626 (NASA-CR-591)
C–Nb–V–Zr, fabrication, 17: 41427(R) (IITRI-B231-9)
C–Nb–V–Zr, hardening by annealing, 17: 41428(R) (IITRI-B-6007-4)
C–Nb–V–Zr, heat treatment of, 20: 14972(P)
C–Nb–V–Zr, mechanical properties, 17: 14809(R) (ARF-B231-8)
C–Nb–V–Zr, preparation and properties of dispersion strengthened, 17: 16514(R) (ARF-B6007-1)
C–Nb–W, fabrication and mechanical properties of, 19: 46940(R) (NP-15444)
C–Nb–W, mechanical properties and preparation, 17: 22150(R) (AD-281728)
C–Nb–W, mechanical properties, 20: 33875 (N-66-16551)
C–Nb–W, phase studies and thermodynamics of, for use at high temperatures, 20: 29774
C–Nb–W–Y–Zr, corrosion by potassium at 2000 to 2200°F, 18: 24091
C–Nb–W–Y–Zr, corrosion by potassium at 2000°F of AS-55, 20: 768(R) (NASA-CR-54226)
C–Nb–W–Y–Zr, microstructure of AS-55 sheet, 19: 13955(R) (WANL-PR-(P)-005)
C–Nb–W–Y–Zr, properties of AS-55 for containment of alkali metals, 17: 41339 (GE-62FPD365)
C–Nb–W–Y–Zr, tensile properties of D-43Y, effects of welds on, 20: 29712(R) (WANL-PR-(P)-009)
C–Nb–W–Y–Zr, weldability study of AS-55, 19: 24957(R) (WANL-PR(P)-006)
C–Nb–W–Y–Zr, weldability of D-43Y, 20: 13264(R) (WANL-PR(P)-008)
C–Nb–W–Zr, aging and recrystallization of D-43, 20: 4301(R) (ORNL-3870, pp 102-35)
C–Nb–W–Zr, aging characteristics of D-43, 19: 13996 (ORNL-P-1051)
C–Nb–W–Zr, bonding of D-43, method for diffusion, 20: 5867
C–Nb–W–Zr, brazing, equipment and methods for, 18: 27938
C–Nb–W–Zr, coatings on D-43, properties of oxidation-resistant, 19: 26801(R) (AD-607530)
C–Nb–W–Zr, contamination of D-43 by residual gases in high vacuum, 18: 39826 (ORNL-3674)
C–Nb–W–Zr, corrosion by potassium at 2000°F of D-43, 20: 768(R) (NASA-CR-54226)
C–Nb–W–Zr, corrosion of D-43, by potassium, 20: 4301(R) (ORNL-3870, pp 102-35)
C–Nb–W–Zr, corrosion of D-43, by lithium, effects of oxygen on, 20: 4301(R) (ORNL-3870, pp 102-35)
C–Nb–W–Zr, corrosion of D-43, by refluxing potassium at 2000°F, stress, 20: 9424(R) (NASA-CR-54844)
C–Nb–W–Zr, corrosion of D-43, by potassium at 2450°F, stress-, 20: 13191(R) (NASA-CR-54476)
C–Nb–W–Zr, corrosion of D-43, by sodium at high temperatures, 20: 25474(R) (BNL-954, pp 122-67)
C–Nb–W–Zr, creep behavior in ultrahigh vacuum at 2000 and 2200°F, 20: 13256 (NASA-TN-D-3222)
C–Nb–W–Zr, creep properties of D-43, 19: 20474(R) (NASA-CR-54281)
C–Nb–W–Zr, ductility of welds in D-43, effects of aging on bend, 20: 4301(R) (ORNL-3870, pp 102-35)
C–Nb–W–Zr, electric conductivity to 1500°C of D-43, 20: 5851
C–Nb–W–Zr, electric conductivity of D-43, at 80 to 400°K, 20: 23749
C–Nb–W–Zr, emissivity to 1500°C of D-43, total hemispherical, 20: 5851
C–Nb–W–Zr, evaluation of protective coatings for, 20: 29651
C–Nb–W–Zr, evaporation losses in high vacuum of D-43, 20: 4301(R) (ORNL-3870, pp 102-35)
C–Nb–W–Zr, extrusion of tubing from, optimization studies, 17: 11140(R) (AMC-TR-7-775(VII))
C–Nb–W–Zr, extrusion of tubes of, 17: 23895(R) (AD-403514)
C–Nb–W–Zr, fabricability, strength, and weldability of, 20: 29763
C–Nb–W–Zr, fabrication into H sections, 18: 7163(R) (NP-13410)
C–Nb–W–Zr, fabrication and properties of sheet, 18: 10497 (RTD-TDR-63-4236)
C–Nb–W–Zr, fabrication by double electrode process, 18: 12562(R) (X63-12299)
C–Nb–W–Zr, fabrication and properties of D-43 strip and foil, 19: 24946 (ASD-TDR-63-829(Pt.II))
C–Nb–W–Zr, fabrication and properties at –325 to 3000°F, 19: 39224(P)
C–Nb–W–Zr, fabrication and mechanical properties of, 19: 46940(R) (NP-15444)
C–Nb–W–Zr, heat treatment of, 20: 14972(P)
C–Nb–W–Zr, mechanical properties of D-43, effects of protective coatings and welding on, 20: 5866
C–Nb–W–Zr, microstructure of D-43, effects of aging on, 20: 17023 (ORNL-TM-1161, pp 208-24)
C–Nb–W–Zr, oxidation and mechanical properties of coated X-110, 17: 39525(R) (AD-416459)
C–Nb–W–Zr, oxidation protection of D-43 by chromium–silicon–titanium coatings at 2000 to 2700°C, 18: 30127 (ASD-TDR-62-934(Pt.II))
C–Nb–W–Zr, preparation and specifications for corrosion loop testing, 20: 4380 (NASA-CR-54761)
C–Nb–W–Zr, properties as space reactor fuel cladding, 18: 9713 (CONF-375-3)
C–Nb–W–Zr, properties of welds in D-43, 19: 40989
C–Nb–W–Zr, properties as hollow turbine vanes, 20: 16963
C–Nb–W–Zr, properties at very high temperatures, 20: 21412
C–Nb–W–Zr, properties of D-43 as bore seal material, 20: 46145 (NASA-CR-54093)
C–Nb–W–Zr, radiation effects on bend properties of D-43, neutron, 18: 32226 (ORNL-TM-880)
C–Nb–W–Zr, rolling of foils of D-43, 19: 7871(R) (AD-422001)
C–Nb–W–Zr, specifications of D-43, for use in corrosion test loop fabrication, 20: 21293 (R-66SD3007)
C–Nb–W–Zr, stress corrosion of D-43 by refluxing potassium, research program on, 19: 20474(R) (NASA-CR-54281)
C–Nb–W–Zr, stress corrosion of D-43 by boiling potassium, research program on, 19: 40970(R) (NASA-CR-54390)
C–Nb–W–Zr, stress-rupture properties of D-43, 19: 40961
C–Nb–W–Zr, tensile properties of welded plates of D-43, 20: 4301(R) (ORNL-3870, pp 102-35)
C–Nb–W–Zr, tensile properties of D-43, 20: 15068
C–Nb–W–Zr, tensile properties of D-43, effects of welds on, 20: 29712(R) (WANL-PR-(P)-009)
C–Nb–W–Zr, tensile properties of D-43, effects of brittle coatings on, 20: 37276
C–Nb–W–Zr, tensile strength of X-110, at 1100 to 1500°C, 17: 30950(R) (NMI-2117)
C–Nb–W–Zr, thermal conductivity of D-43, at 30 to 120°C, 20: 4301(R) (ORNL-3870, pp 102-35)
C–Nb–W–Zr, thermal expansion of D-43, at 80 to 400°K, 20: 23749
C–Nb–W–Zr, thermal properties, 18: 7201 (ASD-TDR-62-597)
C–Nb–W–Zr, weld bend tests of D-43, 19: 13955(R) (WANL-PR-(P)-005)
C–Nb–W–Zr, weld stability in D-43, 20: 5866
C–Nb–W–Zr, weldability study of D-43, 19: 24957(R) (WANL-PR(P)-006)
C–Nb–W–Zr, weldability studies of D-43, 19: 46966(R) (WANL-PR(P)-007)
C–Nb–W–Zr, welding parameters for D-43, electron-beam, 20: 5867
C–Nb–W–Zr, welds in D-43, thermal stability of, 20: 27467
C–Nb–Zn, structure of filled Ti_2Ni type compounds in, 19: 37107
C–Nb–Zr, corrosion of PWC-11 by boiling potassium, 19: 34640 (CNLM-6246)
C–Nb–Zr, corrosion by lithium in niobium–1-zirconium alloy forced-convection loop, 20: 5853 (TIM-898)
C–Nb–Zr, corrosion by potassium at 1070°C, 20: 7518 (PWAC-501)
C–Nb–Zr, development of, with high-temperature strength, 19: 44605

(PWAC-464)
C–Nb–Zr, phase diagrams, 20: 13272
C–Nb–Zr, phase diagrams, 20: 39434
C–Nb–Zr, phase studies on, 18: 34211
C–Nb–Zr, phase studies at 1092 and 1538°C, 20: 4392 (PWAC-461)
C–Nb–Zr, thermal properties to melting point, 20: 878
C–Nb–Zr, x-ray diffraction of nonmetallic phases chemically extracted from, 19: 7973
C–Nb–Zr, yield strength of PWC-11, effects of boiling potassium exposure on, 19: 34640 (CNLM-6246)
C–Ni–Nb, structure of filled Ti_2Ni type compounds in, 19: 37107
C–Ni–Nb–Ti–Zr, creep properties in ultra-high vacuum of AS-30, long-time, 19: 37039(R) (NASA-CR-54393)
Co–Nb–N, structure of filled Ti_2Ni type compounds in, 19: 37107
Co–Nb–O, structure of filled Ti_2Ni type compounds in, 19: 37107
Co–Nb–Si, crystal structure of ternary compounds in, 19: 23096
Co–Nb–Si, crystal structure of compounds in, 19: 41069
Fe–Nb–O, phase studies, 19: 30785
Fe–Nb–O, phase studies at 1180°C, 20: 23691
Fe–Nb–P, phase studies of, 17: 15971
Fe–Nb–Si, effects of carbon content on properties and reduction of, 17: 32492
Ga–Nb–N, preparation and structure of T_5M_3X type compound in, 19: 30788
Ga–Nb–O, crystallographic parameters, 17: 18822
Gd_2O_3–Nb, preparation, 16: 3474(R) (USBM-U-863)
Gd–Nb–O–Ti, crystal structure of $GdTiNbO_6$ in, 20: 26863
Gd_2O_3–Nb, properties of, effects of compacting, sintering, and forging operations on, 16: 17967(R) (USBM-U-887)
Ge–Nb–N, preparation and structure of T_5M_3X type compound in, 19: 30788
Ge–Nb–Si, structure and thermoelectric properties, 17: 23987
graphite–Nb, properties for aerospace applications, 19: 37144
graphite–Nb, properties of, effects of graphite source material on, 20: 33876(R) (N-66-17087)
HfC–Nb, solidus at 2310°C, 19: 44612(R) (USBM-RC-1199)
Hf–Nb–N, precipitation hardening in, effects of heat treatments on, 20: 29759
Hf–Nb–N, properties of, effects of heat treatment on, 17: 34419(R) (WADC-TR-57-344(Pt.VII))
Hf–Nb–N–W, properties of, effects of heat treatment on, 17: 34419(R) (WADC-TR-57-344(Pt.VII))
H–Nb, diffusion of hydrogen in, 20: 2365
H–Nb, magnetic susceptibility at 600 to 900°C, 18: 16502
H–Nb, phase diagram, 19: 23080
H–Nb, phase diagram and tensile properties of, 20: 31667
H–Nb, phase studies and thermal properties, 18: 13776
H–Nb, phase studies of, by x-ray diffraction, 20: 45688
H–Nb, preparation of, for transmission electron microscopy, hydrogen concentration in electrothinning procedures for, 20: 31691
H–Nb, structural phase studies on, 18: 26024
H–Nb, tensile properties of, effects of temperature and strain rate on, 20: 31669
H–Nb, thermodynamic properties of, at 250 to 650°C below 1 atm, 16: 518 (AFOSR-1107)
H–Nb, thermodynamics of excess partial entropy of hydrogen in, 17: 39609
H–Nb–Zr, phase studies, 20: 11225
La–Nb–O–Ti, crystal structure of $LaTiNbO_6$ in, 20: 26863
Li–Nb–O, equilibrium distribution of oxygen in, at 500 to 800°C, 18: 4253(R) (ORNL-3470(p.63-6))
Li–Nb–O, phase studies, 18: 3721 (TIM-696)
Mo–Nb–N–Zr, heat treatment of, 20: 14972(P)
Mo–Nb–O–Zr, heat treatment of, 20: 14972(P)
Mo–Nb–Si, phase diagram and properties of, 20: 23683
Mo–Nb–Si, phase studies and properties of, 19: 39194
Nb–N, degasification of solid solutions of, kinetics of, 20: 13202
Nb–N, dislocation damping interactions in, interstitial, 16: 33491
Nb–N, equilibrium in, 18: 34177
Nb–N, phase equilibria in, 16: 33492
Nb–N, phase studies, 16: 15194 (TID-15145)
Nb–N, phase studies, 18: 39976
Nb–N, phase studies and properties, 19: 986
Nb–N, phase studies at 1600 to 2200°C, 19: 46296
Nb–N, phase studies, 20: 5851
Nb–N, precipitation from supersaturated, kinetics of, 20: 13303
Nb–N, preparation, properties, and uses of, review on, 16: 27640(T) (FTD-TT-62-430)
Nb–N, properties of equilibrium solid solutions in, mechanical and thermodynamic, 19: 13991 (ML-TDR-64-134)
Nb–N, properties of solid solutions of, effects of nitrogen content on, 20: 13302
Nb–N, superconductivity, 17: 41604
Nb–N–O, internal friction studies of interstitial clusters in, 20: 31774
Nb–N–Ta–Zr, heat treatment of, 20: 14972(P)
Nb–N–Ti–Zr, heat treatment of, 20: 14972(P)
Nb–N–V–Zr, heat treatment of, 20: 14972(P)
Nb–N–W–Zr, heat treatment of, 20: 14972(P)
Nb–N–Zn, phase studies, 19: 42872
Nb–N–Zn, structure of filled Ti_2Ni type compounds in, 19: 37107
Nb–N–Zr, equilibrium solid solutions at 1200 to 1800°C in, 20: 2337 (ORNL-P-1677)
Nb–N–Zr, properties of equilibrium solid solutions in, mechanical and thermodynamic, 19: 13991 (ML-TDR-64-134)
Nb–O, internal friction in solid solutions of, 20: 23656 (TRG-Report-1151)
Nb–O, mechanical properties of, 17: 11219
Nb–O, metallography, 17: 6525 (TID-7625(p.8-19))
Nb–O, oxygen clustering in solid solutions of, 20: 4449
Nb–O, partial pressures of oxides formed in solid solutions of, 20: 36836
Nb–O, phase studies, 16: 13610
Nb–O, phase studies, 16: 17631(T) (AEC-tr-4459(p.6-17))
Nb–O, phase studies and properties, 16: 22581 (AROD-2530:1)
Nb–O, phase studies at 500 to 1900°C, 18: 5805
Nb–O, phase studies at 1600 to 2200°C, effect on crystal structure, 19: 46296
Nb–O, precipitation of niobium oxide from supersaturated solid solutions of, 18: 27471
Nb–O, solid-solution clustering of oxygen in, measurements of, 20: 37213
Nb–O, solid-solution clustering of oxygen in, mechanisms of, 20: 37214
Nb–O, superconducting critical fields in, 18: 34704
Nb–O, surface barrier in superconducting, 18: 22842
Nb–O–K, equilibrium distribution of oxygen in, at 500 to 800°C, 18: 4253(R) (ORNL-3470(p.63-6))
Nb–O–Na, equilibrium distribution of oxygen in, at 500 to 800°C, 18: 4253(R) (ORNL-3470(p.63-6))
Nb–O–Ta–Zr, heat treatment of, 20: 14972(P)
Nb–O–Ti, crystal structure of $TiNb_{24}O_{62}$, 20: 11227
Nb–O–Ti, crystal structure and superconductivity at 4.2°K, effects of fabrication and heat treatments on, 20: 37267
Nb–O–Ti–Y, crystal structure of $YTiNbO_6$ in, 20: 26863
Nb–O–Ti–Zr, heat treatment of, 20: 14972(P)
Nb–O–Ti–Zr, phase diagram at 1500°C, 16: 13635
Nb–O–V–Zr, heat treatment of, 20: 14972(P)
Nb–O–W, crystal structure of $Nb_{16}W_{18}O_{94}$ in, 20: 43188
Nb–O–W–Zr, heat treatment of, 20: 14972(P)
Nb–O–Zircaloy-2, phase studies and hardness measurements, 17: 30972 (KAPL-2286)
Nb–O–Zn, phase studies, 19: 42872
Nb–O–Zr, phase studies, 18: 2163(R) (IS-700(Sect.M))
Nb–O–Zr, phase studies on, 18: 34211
Nb–O–Zr, phase studies, 19: 9604(R) (IS-900(Sect.M))
Nb–O–Zr, phase studies, 20: 4297(R) (IS-1200(Sect.M))
Nb–O–Zr, phase studies, 20: 16980
Nb–PuO_2, fabrication of, 17: 19575 (HW-75007(Paper 22))
Nb–$PuSi_x$, fabrication, 17: 35251(R) (BMI-1632(Del.))
Nb–$PuSi_x$, fabrication problems, 17: 40423(R) (BMI-1639(Del.))
Nb–Pu–Si, phase diagram, 17: 14740 (TID-11295(2nd Ed.))
Nb–Pu–Si, properties as reactor fuel, 17: 8763
Nb–Rh–Si, phase study of Cr_3O-type structures in, 19: 44702 (TID-22200)
Nb–Se, phase studies, 19: 7932
Nb–Si, analysis for silicon, spectrophotometric, 19: 46171 (KAPL-M-6492)
Nb–Si, electric and mechanical properties, 18: 24158
Nb–Si, mechanical properties, 19: 11734
Nb–Si, mechanical properties of, effects of composition on, 20: 11288(T) (AD-622477)
Nb–Si, oxidation kinetics, 19: 28757(T) (FTD-TT-64-1154)
Nb–Si, preparation, properties, and uses of, review on, 16: 27640(T) (FTD-TT-62-430)
Nb–Si, preparation and structure of Nb_3Si, 17: 18782
Nb–Si, preparation of superconducting, empiricism for, 18: 14518
Nb–Si–Sn, superconducting properties of Nb_3SnSi, 17: 27861
Nb–Si–V, phase studies, 18: 42088
Nb–Si–W, phase studies on, 18: 14505
Nb–Si–W, phase studies and microstructure, 18: 42091
Nb–Si–W, preparation and properties of, 18: 14505
Nb–Si–W, properties and structure of, 17: 16710
Nb–Te, phase studies, 19: 7932
Nb–Te–Zr, corrosion of, in 680°F water, 17: 16582 (ARF-B198-36)
Nb–Te–Zr, corrosion by water at 680°F, 17: 30905(R) (ARF-B198-42)
Nb–Te–Zr, corrosion and mechanical properties, 17: 34347(R) (IITRI-B198-43)
Nb–Te–Zr, oxidation by steam at 750 and 900°F and water at 680°F,

hydrogen absorption from, 18: 2162(R) (IITRI-B198-46)
Nb–Te–Zr, tensile properties at 68 and 680°F, 17: 30905(R) (ARF-B198-42)
Nb–Te–Zr, tensile properties at 70 and 680°F, 18: 2162(R) (IITRI-B198-46)
Nb–ThO_2, mechanical properties and oxidation rates, 19: 32754
Nb–ThO_2, properties, 19: 26848
Nb–TiC, analysis of, for titanium, titrimetric, 16: 1722
Nb–TiC, corrosion of refractory metal bonded, by potassium at 1600°F, 20: 27432(R) (NASA-CR-54892)
Nb–TiC, wetting by nickel, 18: 7241
Nb–UC, properties as thermionic cell emitters, 17: 27962
Nb–UC, thermionic emission from, 17: 949 (AD-273067)
Nb–UO_2, cladding, fabrication, and testing, 16: 5679 (APEX-276)
Nb–UO_2, cladding with niobium, 18: 3298(R) (ORNL-2221(Pts.1-5)(Del.))
Nb–UO_2, deposition of, by electrophoresis, 16: 30369 (TID-11153)
Nb–UO_2, development of clad, for aircraft reactors, 19: 27768(R) (SCNC-308)
Nb–UO_2, diffusion of aluminum in clad, 16: 7877 (DC-58-2-215)
Nb–UO_2, fabrication and properties, 16: 29335
Nb–UO_2, radiation effects on stability of, 16: 4450(R) (BMI-1546(Del.))
Nb–UO_2, radiation effects on niobium-clad, 17: 11254 (BMI-1608)
Nb–UP, compatibility, 20: 15032(R) (ANL-7152, pp 50-72)
Nb–VC, wetting by nickel, 18: 7241
Ni–Nb–N, structure of filled Ti_2Ni type compounds in, 19: 37107
Ni–Nb–O, structure of filled Ti_2Ni type compounds in, 19: 37107
Sb–Nb–Te, phase studies, 20: 29717

NIOBIUM TELLURIDES
crystal structure of, 18: 34136
crystal structure of Nb_3Te_4, 19: 6310
preparation and chemical and physical properties of, 17: 20009
preparation and properties of single crystals of, 16: 31611
preparation by chemical transport in temperature gradient, 19: 26333

NIOBIUM URANIUM OXIDES
preparation of single crystals of $U_2{}_3Nb_2O_7$, 20: 38892

NITRAMIDES
combustion and thermal decomposition processes in, mechanism of, 18: 25027(T) (LA-tr-64-2)
complexes of HMX, use for HMX determination in admixtures with RDX, 19: 14929 (UCRL-12168)

Nitramine
see Tetryl

Nitramines
see Nitramides

NITRATE COMPLEXES
see also Lead Nitrate Complexes
see also Ruthenium Nitrate Complexes
see also Thorium Nitrate Complexes
see also Uranyl Nitrate Complexes
determination of bidentate and unidentate, from infrared spectra, 20: 3949
preparation and properties of uranium, 16: 27065
rare earth terpyridyl, preparation and infrared spectra of, 20: 16479
structure of metallic, 19: 9046(R) (IS-900(Sect.C))
with beryllium, ion exchange studies of, 19: 46230 (AAEC/E-136)
with hafnium and zirconium, equilibrium and stability constants of, 18: 27414
with plutonium, preparation and stability of, 20: 7206
with plutonium(IV), stability of, 20: 26857
with protactinium V, stability constants of, 18: 13783
with rare earths, formation and stability, 16: 31627
with rare earths in aqueous and organic solutions, 19: 38578 (IA-1014)
with scandium, stability of, extraction and ion exchange studies of, 19: 22223
with silver, properties, 18: 1489(R) (IS-700(Sect.C))
with trivalent lanthanide and actinide ions, stability, 19: 42475
with uranium, spectra of, 18: 16029

NITRATE IONS
charge-transfer band measurements for, in lithium perchlorate at 251°C, 18: 3713(R) (ORNL-3470(p.11-15))
content in waste solutions, method for reducing, 19: 3803(P)
decomposition by pyrosulfate ions in fused potassium nitrate–sodium nitrate, 18: 8323 (IS-742)
determination by coulometric titration, 18: 21957 (HW-SA-2118)
determination in beryllium solutions by cation exchange, 18: 23423
determination in plutonium and uranyl nitrates, volumetric, 17: 15875 (HW-76363)
determination in solution, clathrate method for, 17: 33771 (TID-17223)
determination in water, colorimetric, 17: 5977 (TID-15070)
dissociation in fused nitrates, 18: 200 (IS-618)
effect on primary hydrogen yields in gamma radiolysis of aqueous organic solutions, 20: 43351
effects on contraction regulation by mechanical threshold in frog muscles, 19: 45736
effects on copper determination, 20: 36726
effects on isotopic exchange between iodide and iodate ions, 20: 43248
effects on luminescence from dissolution of irradiated alkali metal halides, 19: 30239
effects on polarographic determination of uranium, 19: 19797
effects on polarographic determination of thorium, 19: 32077
effects on radiolysis of aqueous cysteine solutions, 18: 35608
effects on reduction of iodine-131 retention in mice, specificity of, 19: 25888
effects on separation of americium from magnesium chloride solutions by solvent extraction using triisooctylamine, 20: 18562(R) (EUR-2640.e)
effects on spectrophotometric determination of thorium, 19: 24408
effects on thorium in solutions, 18: 41468
effects on yields in radiolysis of benzyldimethylamine and benzyltrimethylammonium hydroxide, 19: 22299
electrochemical behavior in aliphatic trialkylamines, 17: 14301(T) (AEC-tr-5641)
electron spin resonance in irradiated barium nitrate crystals, 19: 38730
electron spin resonance in x-irradiated sodium nitrate crystals, hyperfine structure from, (E), 20: 15965
energy transitions of, effects of environment on oscillator strength of lowest, 18: 3713(R) (ORNL-3470(p.11-15))
exchange on iron hydroxide, 19: 13525 (KFK-216)
exchange reactions with nitrite ions and nitrogen oxide, 18: 2127(R) (ORNL-3488(p.21-41))
hydration numbers, 17: 30544
isotopic exchange equilibrium calculations, 19: 40460(R) (NYO-3462-1)
lifetimes in ammonium nitrate solutions, determination from infrared and Raman spectra, 20: 324
reactions with atomic hydrogen and polarons radioinduced in ice, 18: 13858
reactions with atomic hydrogen, rate constants for, 19: 22339
reactions with electrons in gamma-radiolyzed water, 19: 439
reactions with rare earths in solutions, 19: 39265(R) (IA-1021)
reduction by iron in alkaline solutions, mechanisms of, 19: 46899(R) (ORNL-3832, pp 33-49)
reduction in presence of zirconium, polarographic, 19: 28238
solvent extraction from nitric–sulfuric acid solutions by trilaurylamine–dodecane, 19: 2203 (EUR-1912.i)
spectra in irradiated urea nitrate, 17: 8186
spectra in molten lithium chlorate, uv, 18: 12068
spectra of, deuterium oxide solvent effects on uv absorption, 18: 43500
spectra of, deuterium isotope effects on infrared, 20: 324
yields in radiolysis of aqueous methanol–sodium nitrate solutions, 18: 43641
yields in radiolysis of lithium nitrate, 20: 20733 (TID-22796)

NITRATES
(See also nitrates of the specific elements.)
see also Alkali Metal Nitrates
see also Ammonium Nitrates
see also Ammonium Uranyl Nitrates
see also Hydrazine Nitrates
see also Neptunyl Nitrates
see also Nitration
see also Plutonyl Nitrates
see also Rare Earth Nitrates
see also Rubidium Uranyl Nitrates
see also Ruthenium Nitrosyl Nitrates
see also Uranyl Nitrates
see also Zirconyl Nitrates
analysis for plutonium by argentic oxidation, ferrous reduction, and dichromate titration, 20: 16405
analysis for rare earths using Arsenazo III, spectrophotometric, 20: 35439
analysis of liquid, for water, 17: 10518(R) (TID-17823)
analysis of solutions of, for plutonium, by x-ray absorption edge method, 20: 20573
anodic depolarization of fused, in bromide, chloride, and cyanide, 17: 10518(R) (TID-17823)
chloride removal and recovery from aqueous solutions of, 17: 8272(P)
combustion of, in pyrotechnic mixture with zirconium, 19: 42518
content in Amazon River, effects on biology, chemistry, and hydrography of Atlantic Ocean, 20: 28878 (NYO-1918-138)
content in Atlantic Ocean, measurements on, 20: 28877 (NYO-1918-124)
content in Atlantic Ocean, measurements on, 20: 28878 (NYO-1918-138)
content in Sargasso Sea, annual and seasonal variations in, 18: 21711 (NYO-3140-1B)
corrosive effects of aqueous solutions of, on yttrium, 20: 23618
determination by controlled potential coulometry, 16: 30326 (HW-SA-2635)
determination by coulometric titration, 20: 14455(R) (ORNL-3889, pp 25-32)
determination in aqueous solutions and solids, titrimetric, 20: 43071 (IDO-14679, pp 75-191)

determination in cesium-137 sulfate, 16: 23631 (TID-7629(p.209-16))
determination in colloidal thoria by uv absorption, 20: 38926
determination in fired thoria, infrared spectroscopic, 20: 14468 (TID-22505)
determination in heavy water moderator, automated, 19: 40406 (CONF-650919-2)
determination in ores using screened methyl red, 16: 18815 (PG-Report-225)
determination in plutonium peroxide and tetrafluoride by infrared spectroscopy, 20: 8850
determination in reactor coolant water, survey of methods for, 18: 1505 (ORNL-TM-724)
determination in thoria gels, ultraviolet absorption, 18: 5215 (TID-19813)
determination in Tramex solutions, methods development for, 19: 28214(R) (ORNL-3739)
determination in uranium(VI) oxides, 16: 8680 (PG-Report-226)
determination in 4-*sec*-butyl-2(α-methylbenzyl)phenol, spectrophotometric, 20: 14455(R) (ORNL-3889, pp 25-32)
determination of, method for, 17: 28801 (IDO-14316(Suppl.4))
dissociation of nitrate ion in fused, 18: 200 (IS-618)
effects on cesium uptake by rice, 17: 30031
effects on dielectric properties of potassium halides, 19: 10680 (NYO-2471-6)
effects on distribution of strontium-90 in water-bearing strata by ground waters, 19: 46602
effects on extraction of uranium with TBP-hexane systems, 16: 5405 (MCW-1456)
effects on radiolysis of ethanol and methanol, 20: 7150
effects on spectrophotometric determination of zinc using 1-(2-thiazolylazo)-2-naphthol, 19: 19814
effects on strontium-89 transport in bean and pea plants, 20: 26625
effects on thermodynamics of uranium solvent extraction by di-2-ethylhexyl phosphoric acid, 18: 12268
electrochemistry of liquid, 18: 12042(R) (TID-20114)
formation effects on radioactivity in aircraft, 16: 27508
formation in radiolysis of glycine in quartz, 18: 20045
heat of formation and ionization potentials, 17: 3010
isotope exchange in systems with nitrogen oxides, 16: 2100 (TID-13427)
metabolism by plants, tracer studies of effects of copper on, 18: 25059(T) (OTS-63-11008(p.6-14))
metabolism in wheat seedlings, 20: 38548(R) (ORO-2410-1)
nitrate removal and recovery from aqueous solutions of, 17: 8272(P)
phase diagrams of, book, 19: 14061
photolysis in acids, mechanisms of, 20: 20360(R) (PRNC-73)
properties for ion exchange in solutions of, 20: 38820
properties of aqueous, from dissolution of clad fuel elements, 17: 16142 (IDO-14602)
radiation effects, formation of intermediate species, 16: 241
radiation effects, measurement of amount and composition of radiation products, 16: 20466 (AERE-R-3409)
radiolysis effects on hydroxylamine at pH 2 to 7, 16: 1811(T) (AEC-tr-4564)
radiolysis of alkaline solutions of, with formate ions, 19: 26447
radiolysis of aqueous, 17: 10509(R) (ORNL-3320(p.30-46))
radiolysis of aqueous solutions, 18: 10162
radiolysis of aqueous solutions of, mechanism of gamma, 19: 19981
radiolysis of aqueous solutions of, at 77°K, yields of hydrogen from gamma, 20: 18748
radiolysis of frozen solutions of, nitrite yields in, 20: 26923(R) (COO-1528-5)
radiolysis of, effects of nitrogen-15 content on neutron, 20: 45754
radiolysis of, products of gamma, 20: 20360(R) (PRNC-73)
reactions with hafnium and zirconium, 16: 30411
salting-out effects in aqueous uranyl nitrate–ether systems, 16: 16462
separation by ion exchange, effects of acids on, 19: 26917(R) (IA-984)
separation from alumina by catalytic action, 18: 17930(R) (IDO-14625)
separation from aqueous solutions, 17: 8272(P)
separation of metal, from nitric acid by solvent extraction using amines, 20: 9049(R) (ORNL-3830, pp 193-221)
separation of rare earths and uranium from fused, by ion exchange, 17: 27500
solvent properties for stainless steel, 16: 23783 (IDO-14584)
spectra, lattice frequencies and rotational barriers in infrared, 16: 20416
spectra of metallic, infrared, 17: 14150 (TID-15842)
thermal decomposition of, application of activated complex theory to, 18: 36900 (UCRL-10791)
thermal stability of anion resins in form of, in vented system, 20: 40877 (RL-SEP-823)
volatility of, in radioactive alumina calcine during high-temperature storage, 20: 14207 (IDO-14670)
yields from gamma radiolysis of ammonium perchlorate, 19: 36483
yields from radiolysis of sodium acid phosphite solutions in sodium nitrate, effects of pH on, 20: 14601
yields from radiolysis of potassium nitrate, effects of lead, strontium, sulfate, and thallium ions on, 20: 43329
Cl^-–NO_3^-–UO_2SO_4, ion exchange equilibria in, 20: 36931
ethanol–nitrates, radiolysis of, yields of primary hydrogen during gamma, 20: 43351
formates–nitrates, radiolysis of, yields of primary hydrogen during gamma, 20: 43351
2-propanol–nitrates, radiolysis of, yields of primary hydrogen during gamma, 20: 43351

NITRATION
hydrogen exchange in, of tritium-labeled toluene, 20: 1950
kinetics of aromatic, 18: 9784 (UCRL-11069)

NITRIC ACID
activity coefficients of 0 to 100 per cent aqueous, ionic and molecular, 18: 27420
analysis for arsenic, neutron activation, 18: 188
analysis for arsenic, copper, and zinc, activation, 18: 25286
analysis for carbon, by combustion-gas chromatography, 19: 17781(R) (ORNL-3750)
analysis for manganese microtraces, activation, 18: 5228
analysis for nitrosylruthenium nitrato and nitro complexes by paper chromatography, 17: 25111 (AERE-R-4292)
analysis for trace impurities, activation, 18: 31390
analysis of aqueous, spectrophotometric, 18: 1614(R) (ORNL-3488 (p.65-90))
analysis of solutions of, for plutonium oxidation states, spectrophotometric, 19: 30084 (RL-SA-33)
analytical use for ion exchange of iron and thorium by amberlite IR-120, 20: 1783
behavior in mixer-settler runs in Eurochemic extraction flowsheet No. 3, 18: 1795 (NP-13272)
complex formation with uranium, effects on separation processes, 17: 14391
complexes with creatinine, radiation effects on spectra of, 18: 12194
content in Purex and Redox solutions, effects on extraction, 17: 238
content in waste solutions, method for reducing, 19: 3803(P)
corrosive effects on copper, effects of group VIII chlorides, 16: 484(R) (AD-256309)
corrosive effects of stainless steel-containing, on Inconel, stainless steels, and titanium, 16: 1854(R) (IDO-14553)
corrosive effects on carbon steel, iodine inhibition, 16: 5676
corrosive effects on austenitic stainless steel, additive effects of Mn, Ce, and Cr on, 16: 13534
corrosive effects with radiation on metals, 16: 17976(R) (EURAEC-94)
corrosive effects on alloys and metals in chemical plants, 16: 20983
corrosive effects on stainless steel (304-L) and titanium (A-55), 16: 30735 (HW-73378)
corrosive effects on Ni-o-nel, stainless steel, steel, tantalum, and titanium at 375°C, 16: 33071(T,R) (EURAEC-337)
corrosive effects on titanium and zirconium, 16: 33441
corrosive effects of, on materials for use in Darex, Sulfex, and Zirflex processes, 16: 32883(R) (ORNL-3314(p.1-39))
corrosive effects on stainless steel, 16: 488(T) (AEC-tr-4683)
corrosive effects of stainless steel-containing boiling, on type 304, 304L, and 309SCb stainless steel, effect of reductants on, 17: 4295(R) (DP-740)
corrosive effects on Coronel, Inconel, nickel, and Ni–O–Nel, 17: 6192(T,R) (EURAEC-382)
corrosive effects of chromium ion containing, on chromium–nickel steel, 17: 14774(T) (AEC-tr-5646)
corrosive effects on construction materials for fuel processing plants, 17: 17451
corrosive effects on chromium–iron and chromium–nickel stainless steel, potentiokinetic studies on, 17: 25729(T) (EURAEC-678)
corrosive effects on stainless steel, 17: 40389
corrosive effects of boiling, on stainless steel, 17: 39494
corrosive effects of aqueous solutions of, on uranium-bearing steels, 18: 2180 (NP-13261(p.207-34))
corrosive effects on aluminum and titanium, 18: 1614(R) (ORNL-3488(p.65-90))
corrosive effects of chloride-ion-containing, on stainless steel, 18: 4202
corrosive effects of chromium-containing, on stainless steel, 18: 8454
corrosive effects of solutions of, on stainless steels, 18: 12581 (HW-78186)
corrosive effects on Hastelloy C, Zircaloy-2, and Zircaloy-4, 18: 14410 (ORNL-3558(p.104-12))
corrosive effects on stainless steel, 18: 16152
corrosive effects on Hastelloy-C, Zircaloy-2, and Zircaloy-4, 18: 22173(R) (ORNL-3591(p.201-4))
corrosive effects on niobium and vanadium, effects of acidity and current density on anodic, 18: 25929
corrosive effects on boron steel, 18: 27983
corrosive effects on type 304 stainless steel, 18: 37620 (ANL-6703

(p.536-65))
corrosive effects on carbon steel, protective effects of zirconium content against, 19: 22903
corrosive effects on platinum–zirconium alloys, 19: 28214(R) (ORNL-3739)
corrosive effects on molybdenum, vanadium, and titanium–vanadium alloys, stress-, 20: 2254 (BM-RI-6680)
corrosive effects on stainless steel, effects of molybdenum and uranium on, 20: 4325 (TB-58)
corrosive effects on stainless steel, 20: 5856
corrosive effects on titanium in pot calciners, 20: 8477(R) (BNWL-139)
corrosive effects on molybdenum, tungsten, and vanadium at 35, 60, and 100°C, 20: 11230 (BM-RI-6715)
corrosive effects on vanadium-base alloys at low temperatures, 20: 11230 (BM-RI-6715)
corrosive effects on molybdenum, tungsten, or vanadium coupled with titanium, galvanic, 20: 11230 (BM-RI-6715)
corrosive effects on types 416 and 430F stainless steels, effects of uranium on, 20: 14983 (NP-15875)
corrosive effects of, on iron-base alloys, mechanisms of stress-, 20: 16968 (COO-1319-33)
corrosive effects of aqueous dichromate solutions of, on chromium–nickel steel, 20: 41418(R) (GEAP-5150)
decomposition effects on cerium chloride complex, kinetics of, 18: 17803
decomposition in Purex waste solutions using sugar, 18: 19445 (HW-76973(Rev.))
destruction in waste solutions, additive effects of sugar on, 17: 36991 (HW-75565)
determination as free acid in uranyl nitrate solutions by anion exchange, 17: 35649
determination in aqueous and organic plutonium purification process solutions, titrimeter design for, 20: 24979 (PG-Report-692)
determination in electrolytic dissolver solutions, conductometric, 17: 18176 (IDO-14603)
determination in kerosene–TBP solutions by potentiometric titration, 18: 15966
determination in organic solvents by solvent extraction using aliphatic sulfoxides, 18: 13939
determination in plutonium and uranyl nitrates, volumetric, 17: 15875 (HW-76363)
determination in solutions of trilaurylamine, 17: 40720 (TID-7655(p.451-64))
determination in solutions of quaternary ammonium nitrates, potentiometric, 20: 5518
determination in uranyl nitrate solutions, potentiometric, 17: 33815
determination in uranium solutions by potentiometric titration, 18: 15966
determination in uranyl nitrate solutions by reactions with potassium carbonate, method for continuous, 19: 2216 (NP-14343(p.IId1-5))
determination of free, in trilaurylamine solutions containing plutonium or thorium nitrates, potentiometric, 19: 26227 (CEA-R-2766)
diffusion into polymers, 18: 25022(T) (ANL-Trans-15)
diffusion of hafnium in, in ion exchange form, 20: 261
diffusion of plutonium and uranium in, activation energies and coefficients of, 18: 10192
dissolution of aluminum in, effects of alloying elements on, 17: 23431 (IDO-14606)
distillation of aqueous solutions of, hydrogen isotope separation in, 16: 22519
distribution between tributyl phosphate and water, temperature effect on, 16: 271(T) (AEC-tr-4852)
distribution between aqueous solutions and tributyl phosphate–Amsco 125-82, 17: 1452
distribution between TBP–Shellsol T and aqueous, 18: 27618(R) (ORNL-TM-833)
distribution coefficients of sodium through neptunium between anion exchange resin and, 16: 3073
distribution in extraction equipment in stages of Purex Process, 20: 7209
distribution in TBP–Amsco 125-82 systems, 16: 1649(R) (ORNL-TM-1)
distribution with uranyl nitrates in extraction with methylcyclohexanones from acid-deficient solutions, equilibrium, 17: 40936
effects on analytical procedures involving uranyl ions, 20: 20630
effects on cation exchange separation of cesium and rubidium, 20: 22909
effects on corrosion of rhenium at 25 and 100°C, 20: 21275
effects on diffusion coefficients of uranyl nitrate solutions, 20: 7104
effects on electrophoresis of bismuth-210, lead-210, and polonium-210, 17: 6153
effects on etching of pyrolytic graphite, 19: 47078 (AD-613643)
effects on ferrous sulfamate at 23 to 55°C, 18: 22004 (DP-871)
effects on ion exchange properties of titanium and zirconium salts, 18: 33535
effects on isomeric transitions in chemical separation of tellurium isomers, 18: 39095
effects on kerosene in Purex Process, 20: 12934
effects on peptization of solid thorium oxide, mechanism of, 20: 16419(T) (UCRL-Trans-1301(L))
effects on polarographic determination of hexavalent uranium in TBP medium, 20: 20631
effects on radiation effects on lithium fluoride monocrystals, 20: 43307
effects on radioprotective effects of sulfhydryl compounds in bacteriophages, 17: 23186
effects on sedimentation rate of uranium(IV–VI) oxide suspensions, 16: 23699
effects on self-diffusion of water at 23°C, 19: 32159
effects on sodium molybdates, 17: 10611(T) (UCRL-Trans-894(L))
effects on solvent extraction of hafnium and zirconium from potassium fluoride solutions using trioctylamine, 17: 14403
effects on solvent properties of hexone for iron, niobium, tantalum, tin, and titanium, 18: 39395
effects on solvent properties of butyl phosphates for hafnium, tantalum, and tungsten, 19: 24446
effects on sorption of americium and rare earths from lithium nitrate solutions by ion exchange resin, 18: 35551
effects on spectrographic sensitivity of impurity determinations in plutonium, 17: 35630(R) (NBL-195)
effects on stainless steel in presence of carbon black and sulfur, 19: 18418(P)
effects on stainless steel, corrosive, 19: 36983
effects on stress corrosion cracking of 18-8 stainless steel in dilute chloride solutions, 18: 20471 (CONF-492-2)
effects on sulfuric acid leaching of uranium from ore, 16: 33059
effects on thorium nitrate complex with triisobutyl phosphate, 20: 26891
electrolytic properties of, with reactor-irradiated platinum electrodes, 18: 27952(R) (EURAEC-926)
elution of calcium from cation resin, 16: 2978
exchange with nitric oxide, enrichment by, 18: 531
hydrolysis of cerium ions in, stability of complex formation in, 19: 30204
isotopic exchange equilibrium calculations, 19: 40460(R) (NYO-3462-1)
isotopic exchange with nitric oxide, effects of additives on nitrogen-15 concentration by, 20: 31639(R) (NYO-755-1, pp 77-129)
isotopic substitution in, partition function ratios at 20 to 2000°K for nitrogen-15 and oxygen-18, 20: 40873(R) (NYO-3462-2)
mass transfer from aqueous solutions to kerosene–tributyl phosphate and triisooctylamine–xylene, 18: 31663(T) (UCRL-Trans-1078)
molar volumes of tributyl phosphate–Amsco 125-82–water solutions, 17: 1453
molecular sizes in TBP, 18: 41588
molecular state of aqueous, NMR studies of, 20: 31221(R) (UCRL-16658, pp 73-87)
neptunium ion behavior with Dowex-1 anion exchange resin in system of, 17: 2992
nitrogen-15 exchange between nitric oxide and, effects of additives on, 18: 2132(R) (TID-19592(Sect.IV))
nitrogen-15 exchange with nitric oxide, mechanisms of, 20: 9362(R) (NYO-755-2, Paper 1)
nitrogen-15 exchange with nitric oxide, effects of acids and salts on, 20: 9363(R) (NYO-755-2, Paper 3)
nitrogen-15 NMR in, chemical shifts in, 18: 23530
oxidation of cerium(IV) in, chronopotentiometry, 16: 2970
oxidation of niobium in, kinetics of, 17: 25246
oxidizing activity in sulfuric acid solutions during reactions with uranium dioxide, 19: 19912
partition between aqueous and tributyl phosphate–hexane phase, 16: 24646
performance of dilute, as HFIR coolant-moderator, 19: 48061 (ORNL-3848)
positron and positronium decay in aqueous solutions of, 19: 4899 (NRS-21)
production by radiolysis of air, 18: 39542
production using radioinduced oxidation of atmospheric nitrogen by fission fragments, (E), 19: 40604
properties as eluant for inorganic ion chromatography on zirconium phosphate paper, 16: 23650
properties for separation of aluminum from D2EHPA, 18: 16377(R) (ORNL-TM-515)
properties for use in elution of uranium from cation exchange resins, 19: 22410
properties for use in ultrasonic cleaning of cobalt-60 from Duralumin and steel-3, 20: 16767
proton paramagnetic resonance in aqueous solutions, 16: 20464
purification of extraction process, 19: 24633(P)
radiation effects on vapor phase reactions with propane, temperature dependence of gamma, 17: 32175
radiation effects on decomposition and formation of, in atmosphere, 20: 25996
radiolysis in High Flux Isotope Reactor, 18: 22013(R) (ORNL-3591 (p.70-6))

radiolysis of, effects of methanol and nitrite radicals on yields from pulse, 20: 43321
reactions of silver nitrate in, 19: 9046(R) (IS-900(Sect.C))
reactions with alkylbenzenes, 20: 9049(R) (ORNL-3830, pp 193-221)
reactions with anion exchange resin and dichromate in contactor, analysis of uncontrolled, 19: 44110 (BNWL-114)
reactions with dextrose and sucrose in waste processing, 18: 45174(R) (MLM-1204)
reactions with graphite, formation of mellitic acid in, 18: 31470
reactions with hydrogen peroxide, effects of plutonium(IV) ions on, 16: 159 (UCRL-6536)
reactions with hydrocarbon diluents for phosphates, scouting experiments on, 19: 46304(R) (ORNL-3832, pp 66-75)
reactions with neptunium-237, 17: 193 (LAMS-2756)
reactions with niobium and zirconium in organophosphorus solvents, 19: 13532(R) (ORNL-TM-1020)
reactions with orthophosphorous acid at 250°C, 16: 2808(R) (ORNL-TM-15)
reactions with ruthenium, 19: 36400
reactions with thorium ions in pores of silica gel, 18: 5279
reactions with trioctylamine, isotope effects in, 18: 23576
reactions with uranium dioxide, composition of gases formed by, 17: 8028
reactions with uranium carbide, 17: 10246(R) (ORNL-TM-403)
reactions with uranium carbides at 25 to 120°C, 19: 22198
reactions with uranium carbides, products of hydrolytic, 20: 9044(R) (ORNL-3830, pp 30-68)
recovery from zirconium oxide preparation process, 19: 36434(P)
reduction of dilute, electrochemical, 18: 37289 (A/CONF.28/P/818)
reduction to ammonia, isotopic effect in electrochemical, 18: 37125
separation by countercurrent extraction, 16: 11805
separation by solvent extraction using butyl phosphate–kerosene, effects of solvent irradiation on, 16: 27127(T) (AEC-tr-5071)
separation by solvent extraction using organophosphoric compounds, 16: 1860(T) (AEC-tr-4671)
separation by solvent extraction, mathematical model of, 17: 18179 (ORNL-TM-358)
separation by solvent extraction using alkyl amines, 17: 20099 (MITNE-30)
separation by solvent extraction with tributyl phosphate, temperature effects on, 17: 20118
separation by solvent extraction using organophosphoric compounds, thermodynamics of, 18: 17957
separation from acid solutions and fission product waste streams by solvent extraction using Alamine-336, 18: 5418 (SRO-56)
separation from aqueous solutions by solvent extraction using di-n-butyl phosphoric acid, 16: 11800
separation from aqueous solutions by solvent extraction with tributyl phosphate, review, 17: 1454
separation from aqueous solutions by dibutyl phosphate extraction, equilibria in, 17: 37304
separation from aqueous solutions by solvent extraction using TBP, mechanisms in, 17: 39193(R) (ORNL-3452(p.215-18))
separation from aqueous solutions by solvent extraction using tributyl phosphate, infrared studies of mechanism of, 18: 13915 (IS-728)
separation from aqueous solutions by solvent extraction with tributyl phosphine oxide, 18: 17927 (EUR-437.f)
separation from aqueous solutions by solvent extraction using long-chain amines, 18: 20107
separation from aqueous solutions by solvent extraction using tri-n-octylamine, 19: 7635
separation from aqueous solution by solvent extraction using long-chain amines and ammonium nitrates, (E), 19: 15677
separation from aqueous solutions by solvent extraction using bis(dihexylphosphinyl)-methane, 19: 24619
separation from aqueous solutions by solvent extraction using bis(2-ethylhexyl) phosphate, TBP, and trioctylamine, 20: 7013 (NP-15649)
separation from cerium by solvent extraction using tridodecylamine, 19: 30133
separation from chlorides by electrolytic means, 16: 11774 (R) (NLCO-685)
separation from metal nitrates by solvent extraction using amines, 20: 9049(R) (ORNL-3830, pp 193-221)
separation from neptunium(IV), plutonium(IV), and thorium(IV) using TBP, TBPO, and TTA mixtures, 16: 10108
separation from neptunium(V) and plutonium(VI) using TBP and TTA mixtures, 16: 10107
separation from nitrate systems using alkyl amines, 17: 3874
separation from nitrate solutions by solvent extraction using amines, 18: 1799(R) (ORNL-3496)
separation from nitrate solutions by solvent extraction using N,N-dialkylamides, 18: 1799(R) (ORNL-3496)
separation from nitrate solutions by solvent extraction using tertiary amines, 19: 30336
separation from protactinium by solvent extraction using TBP, 18: 39184
separation from Purex 1WW solution using primary amines, 16: 11788(R) (ORNL-TM-107)
separation from ruthenium by solvent extraction using 1-naphthol, effects of ferric ions on, 18: 39115
separation from sodium nitrate aqueous solutions by solvent extraction using trilaurylamine, 16: 23791 (TID-16139)
separation from solutions by solvent extraction using trioctyl phosphine oxide in carbon tetrachloride and nitrobenzene, 18: 12259 (UCRL-10971)
separation from thorium nitrate by anion exchange, prediction of loss curves in, 17: 10763
separation from uranium nitrates by TBP, 17: 12379
separation from uranyl chloride and nitrate by solvent extraction using dioctyl sulfoxide, 18: 23716
separation from water by extraction in pulse columns, 20: 41064(R) (IS-1500(Sect.E))
separation of actinide nitrates from, by solvent extraction using dibutyl carbitol and TBP, 19: 22415
separation of americium, curium, and promethium from aqueous, synergistic effects in, 20: 33189(T,R) (ORNL-tr-1240)
separation of benzoic acid from, performance of stacked-clone contactor for, 20: 38998(R) (ORNL-3958)
separation of elements from, by anion exchange, tracer study, 16: 15078
separation of metals from, by sorption on ion exchange papers, 19: 24435
separation of metal ions from, by solvent extraction using tri-n-octylphosphine sulfide, 20: 244
separation of plutonium and uranium from, by solvent extraction using alamine 336 and alamine oxide, 18: 35474
separation of plutonium from aqueous, by solvent extraction, 20: 33188(T,R) (ORNL-tr-1238)
separation of protactinium from, by solvent extraction using tributyl phosphate, 20: 4057
separation of protactinium from, by solvent extraction using tributyl phosphate, 20: 4058
separation of ruthenium from, properties of TBP for, 18: 16377(R) (ORNL-TM-515)
separation of scandium from, by solvent extraction using alkyl phosphates, 19: 40689
separation of strontium from, by adsorption, 16: 1854(R) (IDO-14553)
separation of thorium from, by solvent extraction using benzyl- and cyclohexylalkylamines, 18: 17947
separation of thorium from, by solvent extraction using DBP in chloroform, hexane, and hexol, 18: 22176
separation of thorium from, by solvent extraction using diisopentyl methylphosphonate in benzene, tributyl phosphate, and xylene solutions, 20: 36942
separation of uranium from, by solvent extraction using tridodecylamine, 17: 16155
separation of uranium from aqueous, by solvent extraction, 20: 33189(T,R) (ORNL-tr-1240)
separation of zirconium from, by sorption on silica gel, 19: 30329
separation of zirconium from, by solvent extraction using di- and monoisopentyl esters of methylphosphonic acid, 20: 41051
separation of, from thorium nitrates using TBP, 18: 13944
solubility in bis(2-chloroethyl) ether at 25°C in various electrolytes, 16: 8737
solubility in tributyl phosphate at 25°C, 18: 23712
solvent extraction by tributyl phosphate, temperature dependence, 16: 3070(T) (AEC-tr-4674)
solvent extraction by tributyl phosphate, mechanism, 16: 23797
solvent extraction by tridodecylamine in benzene, 17: 4453
solvent extraction by tributyl phosphate–hexane, mechanism, 17: 25104
solvent extraction by bidentate organophosphorus compounds, 19: 277 (IS-827)
solvent extraction from aqueous solution into TBP–Varsol, pulse column studies of, 19: 20043 (IEA-77)
solvent extraction from solutions by amine–ether systems, 19: 30316 (AERE-R-4440(Pt.2))
solvent partition in tributyl phosphate systems, 16: 25489
solvent partition of pertechnetate anion in diethyl ether, 16: 29041
solvent partition in TBP–uranyl nitrate systems, 17: 10511(R) (ORNL-3320(p.56-82))
solvent partition in aqueous and organic phase in extraction with methylcyclohexanone from acid solution, 17: 40937
solvent partition of uranyl nitrate between aqueous solutions of, and diisoamyl ester of methyl phosphonic acid–TBP, 18: 6902
solvent partition between TBP and water, 18: 17948
solvent partition in aqueous benzene and chloroform solutions containing trioctylamine, 18: 27421
solvent partition between aqueous and organic phases of aliphatic amines in kerosene and xylene, 20: 223 (CEA-R-2760)

solvent properties for molybdic oxide and its hydrates, 16: 168
solvent properties for uranium, 16: 1861(T) (AEC-tr-4874)
solvent properties for thorium, titanium, and zirconium, 16: 1862(T) (AEC-tr-4875)
solvent properties for plutonium dioxide, increase of dissolution rate, 16: 2956(P)
solvent properties for thorium oxide–uranium oxide systems (clad), 16: 7286 (BMI-1560)
solvent properties for nickel base alloys, 16: 11539
solvent properties for molybdenum–uranium reactor fuels, 16: 13135
solvent properties for inorganic ions with tri-n-octyl phosphine oxide, 16: 13136
solvent properties for reactor fuels, 16: 18652(R) (DP-706)
solvent properties for power reactor fuels, 16: 17759 (DP-647)
solvent properties for thorium, 16: 17606
solvent properties for stainless steel, 16: 23787 (IDO-14584)
solvent properties for uranium, 16: 23536
solvent properties for plutonium(IV) and (VI), 16: 25480 (PAN-270/V)
solvent properties for thorium dicarbide at room temperature and 80°C, 16: 25365
solvent properties for molybdenum, 16: 25311 (IG-Memo-466)
solvent properties for uranium dioxide pellets, 16: 30366 (ORNL-3297)
solvent properties for aluminum–uranium alloys, pilot plant study of, 16: 31674 (IDO-14304)
solvent properties for rare earths, 16: 31627
solvent properties for tetravalent plutonium, 17: 239
solvent properties for plutonyl nitrates, 17: 6191(T) (CEA-tr-R-1514)
solvent properties for uranium dioxide pellets, effects of nitrates on dissolution rate, 17: 10246(R) (ORNL-TM-403)
solvent properties for rare earths, 17: 10764
solvent properties for uranium(VI) oxide hydrate at 25 to 350°C, 17: 23346
solvent properties of, for sintered uranium dioxide pellets, 17: 27338
solvent properties for plutonium carbide–uranium carbide fuels, 17: 29027 (LAMS-2884)
solvent properties for scandium nitrates, 17: 32115
solvent properties for aluminum, iron, thorium, and uranium, 17: 32194(R) (TID-19068)
solvent properties for elements, 17: 32194(R) (TID-19068)
solvent properties for thorium oxalate, 17: 35827
solvent properties for urania pellets, 17: 35618(R) (ORNL-TM-545)
solvent properties for plutonia pellets, additive effects of aluminum nitrates and hydrofluoric acid on, 17: 35618(R) (ORNL-TM-545)
solvent properties for thoria–urania compacts, 17: 40389
solvent properties for plutonium and uranium dioxides, 18: 1824
solvent properties for aluminum alloys, 18: 5415(R) (IDO-14599)
solvent properties for ammonium and sodium molybdates, 18: 10191
solvent properties for molybdenum–uranium oxide systems, 18: 13972
solvent properties for antimony, mercury, ruthenium, selenium, and uranium, 18: 27615(R) (MITNE-43)
solvent properties for uranyl nitrates, 18: 29670
solvent properties for lanthanum oxalates, 18: 31523
solvent properties for reactor fuel materials, 18: 31658(R) (IDO-14635)
solvent properties for plutonium dioxide, 18: 36008
solvent properties in paper chromatographic separation of inorganic cations, 18: 39388
solvent properties for uranium carbides at 90°C, off-gases from, 19: 5994 (ORNL-3719)
solvent properties for plutonium, 19: 5783
solvent properties for zirconium, zirconium carbide, and zirconium oxide, 19: 5905
solvent properties for aluminum nitrate, 19: 20042(R) (IDO-14646)
solvent properties for pellets of plutonium dioxide, uranium dioxide, and their mixtures, effects of additives on, 19: 20050 (ORNL-3695)
solvent properties for uranium under anodic polarization conditions, 19: 13533 (RPI-2714-4)
solvent properties for reactor fuel components, 19: 22429
solvent properties for thorium monocarbide at room temperature and 80°C, 19: 28247
solvent properties for uranium spent fuel elements, 19: 41086(P)
solvent properties for thorium and rare earths, 19: 44125
solvent properties for irradiated stainless steel clad plutonium dioxide–uranium dioxide fuels, 19: 46427 (ORNL-3754)
solvent properties for sodium lanthanum sulfate, 19: 46428(R) (ORNL-3847)
solvent properties for uranium, 20: 276(P)
solvent properties for actinium oxalate, 20: 1846
solvent properties for plutonium, uranium, and uranium alloys, 20: 4948(R) (NP-15406)
solvent properties for aluminum-base fuels, 20: 7214(P)
solvent properties for molybdenum–urania systems, (E), 20: 10384(T,R) (EURFNR-3F)
solvent properties for irradiated thoria–urania fuels, 20: 10964
solvent properties of, for plutonium, 20: 36928
solvent properties as eluent in Szilard-Chalmers reactions of trioxalatochromium ions on anion-exchange resin, 20: 45777
solvent properties for tributyl phosphate, 18: 17719
sorption by anion resins, 16: 8821
sorption by colloidal thoria, mechanisms of, 20: 8885(R) (ORNL-3830, pp 275-84)
sorption by thorium dioxide particles, effects of carbon dioxide on, 20: 35480 (ORNL-TM-1536)
sorption by zirconium oxide from dilute aqueous solutions, 18: 6819
sorption effects on thorium in aqueous solutions, 16: 13125 (HW-70536)
sorption of plutonium(IV) from, by Dowex 1x4 anion-exchange resin, kinetics, 19: 36537 (LA-DC-7066)
sorption of zirconium from, by silica gel, 18: 35469
sorptive properties for rare earth and transuranium elements with 1-butanol, 16: 14738
sorptive properties for plutonium in ion exchange resin, 19: 46173 (LA-3357)
spectra in TBP solutions, effects of water on uv absorption, 19: 24439
spectra of deuterium, hydrogen, and nitrogen-14 and -15 in gaseous and solid, vibrational, 19: 7394
spectra of neptunium, plutonium, and uranium hexa- and tetravalent nitrates in, absorption, 16: 2947
spectra of structure of water in, near-infrared, 17: 40803
thorium separation from, by solvent extraction using TBP, 20: 43450
toxic effects on organs and tissues in rat with and without x irradiation, 16: 4004(R) (NP-11020(p.105-16))
use as etchant for uranium, effects on carbon and nitrogen content, 20: 230 (NLCO-965, pp 4.1-5)
use in dissolution of aluminum and aluminum–uranium alloy plates, 20: 438 (RT/CHI(65)23)
use in etching and polishing pyrolytic graphite, 18: 44112
use in leaching fission products from alumina calcine, 20: 40478 (IN-1011)
use in uranium dioxide leaching, 16: 1858(R) (ORNL-TM-32)
use in uranium dissolution, 18: 29800 (HW-46093)
use in uranium dissolution, 19: 44128(P)
use of vapors of, in reprocessing of carbon-containing fuel elements, 19: 44109 (BLG-331)
vapor phase composition, effect of nitrates, 17: 33400
vapor pressure over uranyl nitrate solutions, 19: 32158
volatilization of boron from, effects of mannitol on, 16: 2972
acetic acid–HNO_3, ion exchange equilibrium, 18: 13949
$Al(NO_3)_3$–HF–HNO_3, corrosive effects on type 304L stainless steel and zirconium, 17: 32192(R) (DP-839)
$Al(NO_3)_3$–HF–HNO_3, corrosive effects of boiling, on 304L steel and HAPO-20 alloy, 18: 39841 (HW-80658)
$Al(NO_3)_3$–HF–HNO_3, effects on dissolution of aluminum-canned irradiated thorium dioxide, 20: 43412 (DP-1044)
$Al(NO_3)_3$–HNO_3, analysis for low concentrations of uranium, photometric, 16: 1987
$Al(NO_3)_3$–HNO_3, composition determination, spectrophotometric, 16: 6393
$Al(NO_3)_3$–HNO_3, corrosive effects on hydrofluorinators, 17: 26931(R) (ORNL-TM-453)
$Al(NO_3)_3$–HNO_3–H_2O, distribution coefficients for plutonium between anion exchange resin and, calculation, 19: 20046 (LA-3188)
$Al(NO_3)_3$–HNO_3–$UO_2(NO_3)_2$–H_2O, phase diagrams, 17: 10616
$Al(NO_3)_3$–HNO_3–$UO_2(NO_3)_2$, physical properties, 16: 7611 (DP-653)
$Al(NO_3)_3$–HNO_3, properties for leaching uranium oxides from processed fuels, 20: 9044(R) (ORNL-3830, pp 30-68)
$Al(NO_3)_3$–HNO_3, separation of thorium from, by solvent extraction using TBP, 20: 4060
$Al(NO_3)_3$–HNO_3–$NaNO_3$, separation of americium-243 and curium-244 from, using TBP, 20: 5495 (DP-972)
$Al(NO_3)_3$–HNO_3, sorption of plutonium(IV) from, by Dowex 1x4 anion-exchange resin, kinetics, 19: 36537 (LA-DC-7066)
benzene–HNO_3–H_2O, radiolysis of, 17: 20061
butyl dibutylphosphinate–CCl_4–HNO_3–$UO_2(NO_3)_2$–H_2O, phase separation in, 18: 10187
butyl ether–HNO_3, solvent properties for ruthenium, uranium, and zirconium, 18: 13956
butyl phosphate–HNO_3–$UO_2(NO_3)_2$, analysis of, for uranium, 16: 3033(R) (TID-13917)
butyl phosphate–kerosene–HNO_3–TBP–$UO_2(NO_3)_2$, complex formation and solvent partition in, 18: 10197
butyl phosphate–HNO_3–$UO_2(NO_3)_2$, decomposition kinetics, 16: 16464
butyl phosphate–kerosene–nitric acid, distribution of uranyl phosphate in, 16: 20535(R) (IDO-14583)
butyl phosphate–HNO_3, intermolecular interaction in aqueous, 16: 17697
butyl phosphate–HNO_3, phase studies, 16: 9938
butyl phosphate–HNO_3–$UO_2(NO_3)_2$, phase studies, 16: 33072
butyl phosphate–HNO_3–$UO_2(NO_3)_2$, radiation effects on uranium partition coefficient in, 16: 3033(R) (TID-13917)

butyl phosphate–kerosene–nitric acid, radiolysis of, separation of dibutyl hydrogen and monobutyl dihydrogen phosphates from yields in, 16: 25420(R) (SRIA-62)
butyl phosphate–HNO_3, radiolysis, 16: 3033(R) (TID-13917)
butyl phosphate–HNO_3, solvent behavior of neutron poisons in, 16: 3080
butyl phosphate–HNO_3, solvent properties, 16: 17766
butyl phosphate–HNO_3, solvent properties of, for plutonium(IV) and (VI), 16: 25480 (PAN-270/V)
butyl phosphate–HNO_3, solvent properties of, for hafnium and zirconium, 16: 33074
butyl phosphate–HNO_3, solvent properties for erbium in carbon tetrachloride, 18: 13935
$Ce(NO_3)_3$–$Ce(NO_3)_4$–HNO_3–TBP–H_2O, oxidizing potentials of cerium in, 19: 407
$Ce(NO_3)_4$–HNO_3–TBP–H_2O, method for presenting data on phase diagrams and separations in, 19: 2286
Cr–HBF_4–HF–HNO_3–Zr, solvent properties for uranium–zirconium alloy, 17: 10246(R) (ORNL-TM-403)
Cr–HBF_4–HNO_3–Zr, corrosive effects of, on pre- and de-filmed titanium, 17: 35618(R) (ORNL-TM-545)
dichromate–nitric acid, corrosive effects on austenitic stainless steel, effects of steel composition on, 20: 767(R) (GEAP-4915)
diisoamyl methylphosphonate–nitric acid, solvent properties of, for rare earths in aqueous solutions, 20: 45819
dodecane–HNO_3–TBP–$UO_2(NO_3)_2$–H_2O, equilibrium relations for, for nitric acid-uranyl nitrate extraction, 20: 18844
dodecylamine–HNO_3–trioctylphosphine oxide, distributions coefficients for americium, curium, plutonium, and promethium ions in, 20: 18561 (EUR-2635.d)
ethanol–HNO_3, solvent properties of, for thorium, 16: 17606
$Fe(NO_3)_3$–HNO_3, solvent properties of, for molybdenum–uranium reactor fuels, 16: 13135
F–HNO_3, solvent properties for thorium dioxide–uranium dioxide fuel particles, effects of metals and sulfate on, 20: 18819 (AAEC/E-143)
$Gd(NO_3)_3$–HNO_3–H_2O–$Y(NO_3)_3$, phase studies, 18: 25434
HCl–HF–HNO_3, solvent properties for stainless steel–urania cermets, 19: 36217(R) (IDO-14656)
HCl–HNO_3, corrosive effects of, on molybdenum–tungsten alloys, 16: 17987
HCl–HNO_3, corrosive effects on Hastelloy C, Zircaloy-2, and Zircaloy-4, 18: 14410 (ORNL-3558(p.104-12))
HCl–HNO_3, corrosive effects on Zircaloy-2, 19: 28214(R) (ORNL-3739)
HCl–HNO_3, corrosive effects on platinum–zirconium alloys, 19: 28214(R) (ORNL-3739)
HCl–HNO_3, gas evolution from boiling, 16: 30368 (TID-11021)
HCl–HNO_3, solvent properties of, for iron and nickel, 16: 4221 (IDO-14565)
HCl–HNO_3, solvent properties of, for thorium oxide–uranium oxide systems (clad), 16: 7286 (BMI-1560)
HCl–HNO_3, solvent properties of, for thorium, 16: 17606
HCl–HNO_3, solvent properties for fallout particles, 17: 33532
HCl–HNO_3, solvent properties for cesium-137 in fallout samples, 20: 29081 (NP-14705)
HCl–HNO_3, use for etching charged-particle tracks in silicate crystals, 17: 4999
HCl–HNO_3, use in dissolution of uranium dioxide containing radioiodine, 19: 26453 (KFK-258)
HF–$Hg(NO_3)_2$–HNO_3, solvent properties for irradiated aluminum–plutonium alloys, 18: 22167 (DP-874)
HF–HNO_3, corrosive effects of, on stainless steel (309SCb), 16: 16464
HF–HNO_3, corrosive effects of, on stainless steel (304-L), effects of aluminum nitrate on, 16: 24120 (HW-73211)
HF–HNO_3, corrosive effects on stainless steel, 17: 10246(R) (ORNL-TM-403)
HF–HNO_3, corrosive effects on stainless steel containing boron-10, 17: 32517 (RFP-307)
HF–HNO_3, corrosive effects on stainless steels, 18: 12581 (HW-78186)
HF–HNO_3, corrosive effects on stainless steel vessel during dissolution of zirconium alloy fuel, 18: 35639 (DP-872)
HF–HNO_3, corrosive effects of boiling, on 304L steel and HAPO-20 alloy, 18: 39841 (HW-80658)
HF–HNO_3, corrosive effects on yttrium, 19: 44628
HF–HNO_3, corrosive effects on type-304L stainless steel, effects of aluminum, iron, and thorium ions on, 20: 14982(R) (NLCO-970, pp 6.1-4)
HF–HNO_3, corrosive effects on Corronel 230, 20: 37168(R) (BMI-1771)
HF–HNO_3, effects on corrosion resistant alloys, 20: 37169(R) (BMI-1774)
HF–HNO_3, reactions with zirconium, rate constants for, 19: 34178
HF–HNO_3, solvent properties for plutonium in incinerator ashes, 17: 15521 (HW-72285)
HF–HNO_3, solvent properties for urania pellets, 17: 35618(R) (ORNL-TM-545)
HF–HNO_3, solvent properties for plutonium dioxide, 18: 8447(T) (EURAEC-708)
HF–HNO_3, solvent properties for thorium dioxide–uranium dioxide powders, 18: 25608 (ORNL-TM-867)
HF–HNO_3, solvent properties for thorium and uranium from burned graphite-base fuels, 19: 22406 (ORNL-TM-1096)
HF–HNO_3, solvent properties for reactor fuel components, 19: 22429
HF–HNO_3, solvent properties for ignited plutonium dioxide, 20: 2344 (TRG-Report-1072)
HF–HNO_3, solvent properties for uranyl fluoride at 25°C, 20: 7076
HF–HNO_3, solvent properties for cesium-137 in fallout samples, 20: 29081 (NP-14705)
HF–HNO_3–$Th(NO_3)_4$, corrosive effects of boiling, on 304L steel and HAPO-20 alloy, 18: 39841 (HW-80658)
$Hg(NO_2)_2$–HNO_3, performance for aluminum–plutonium alloy dissolution, 20: 28828 (BNWL-204)
$Hg(NO_3)_2$–HNO_3, solvent properties for SAP, 18: 17938 (RT/CHI(63)-34)
$Hg(NO_3)_2$–HNO_3, solvent properties for aluminum–uranium alloys, 18: 25269(R) (NLCO-905)
$Hg(NO_3)_2$–HNO_3, solvent properties for ATR fuel plates, 19: 24610(R) (IDO-14638)
HNO_3–H_2O, distillation for hydrogen isotope separation, 17: 2681
HNO_3–H_2O, isotope separation factors in distillation of, 17: 2682
HNO_3–H_2SO_4, catalytic effects on nitration of bis(trifluoromethyl)benzene, 18: 31362(R) (UCRL-11213(p.154-61))
HNO_3–H_2SO_4, reactions with bis(trifluoromethyl)benzene, 18: 9784 (UCRL-11069)
HNO_3–H_2SO_4, solvent properties for stainless steel, 19: 11301(P)
HNO_3–H_2SO_4–tridodecylamine, solvent properties for neptunium and plutonium, (E), 19: 15665 (CEA-R-2607)
HNO_3–H_2SO_4–UO_3, oxidation-reduction potentials in, 19: 19912
HNO_3–$K_2Cr_2O_7$, corrosive effects on commercial and pure 18/10 stainless steel at high temperatures, 18: 18320(T,R) (EURAEC-976)
HNO_3–$K_2Cr_2O_7$, corrosive effects of boiling, on high-purity and industrial 18-10 stainless steels, 19: 11690(R) (EURAEC-1213)
HNO_3–$K_2Cr_2O_7$, corrosive effects on austenitic stainless steels, 19: 36977 (APED-4670)
HNO_3–$K_2Cr_2O_7$, corrosive effects on stainless steel, effects of silicon on, 19: 40947(R) (EURAEC-1403)
HNO_3–$K_2Cr_2O_7$, corrosive effects on type 304 stainless steel, effects of reactor irradiation on, 20: 13325(R) (GEAP-4968)
HNO_3–$K_2Cr_2O_7$, radiation effects on corrosive effects of, on type 304 stainless steel, γ, 20: 25616(R) (GEAP-5085)
HNO_3–$Nd(NO_3)_3$–H_2O, phase studies at 25°C, 19: 26305
HNO_3–NH_2SO_3H, solvent properties for plutonium, 17: 15957 (TID-16387)
HNO_3–NO, exchange reactions in equilibrium and isotopic fractionation in, 16: 12007
HNO_3–NO, exchange reactions in, 17: 2686
HNO_3–NO, nitrogen-15 exchange in, 16: 12839
HNO_3–NO, nitrogen-15 fractionation in, effects of temperature on, 20: 40873(R) (NYO-3462-2)
HNO_3–O, reactions with graphite, 19: 28444(R) (ORNL-TM-1094)
HNO_3–oxalic acid, corrosive effects of, on molybdenum–tungsten alloys, 16: 17987
HNO_3–$Pr(NO_3)_3$–H_2O, phase studies at 25°C, 19: 26305
HNO_3–$Pr(NO_3)_3$–$RbNO_3$–H_2O, solubility isotherm at 25°C, 17: 35842
HNO_3–Pu, criticality parameters of water-reflected spheres of, (T), 20: 16031
HNO_3–sulfamic acid, solvent properties of, for plutonium, 16: 25310 (DP-737)
HNO_3–TBP, protactinium species in, 18: 10043 (TID-7675(p.1-15))
HNO_3–TBP, solvent properties for ruthenium nitrosyl nitrates, 17: 8263
HNO_3–TBP, solvent properties for metal nitrates, 17: 37307
HNO_3–TBP, solvent properties for plutonium and uranium, 18: 13966
HNO_3–TBP, solvent properties for ruthenium, uranium, and zirconium, 18: 13956
HNO_3–TBP, solvent properties for californium, europium, fermium, and mendelevium, 18: 23725
HNO_3–TBP, solvent properties for ruthenium, 18: 37292 (A/CONF.28/P/823)
HNO_3–TBP–H_2O, calculation of cascade stagewise conditions for rare earth separation, 18: 20098 (IS-780)
HNO_3–TBP–H_2O, molecular interactions in, 17: 4446 (IS-500(Sect.E))
HNO_3–TBP–H_2O, nitric acid concentration in mixer-settler extractor as function of time, 20: 1953 (IS-T-34)
HNO_3–TBP, phase studies, specific gravity, and viscosity of, 17: 7944
HNO_3–TBP–H_2O, phase studies, specific gravity, and viscosity of, 17: 7944
HNO_3–TBP–$UO_2(NO_3)_2$, hydrodynamic properties and mass transfer, 17: 14409
HNO_3–TBP–$UO_2(NO_3)_2$–H_2O, method for presenting data on phase diagrams and separations in, 19: 2286
HNO_3–tetrahydrofuran, analytical use for combined exchange-solvent

extraction separation of uranium, 20: 14469(R) (TID-22650)
HNO_3–tetrahydrofuran, effects on ion exchange of uranium, 20: 38999 (TID-23229)
HNO_3–tetrabutyl hypophosphate–tetrabutyl pyrophosphate, solvent properties for rare earth and transuranium elements, 19: 540
HNO_3–tetrahydrofuran, solvent properties for uranium, 20: 20811
HNO_3–tetrabutyl ethylene diphosphonate, solvent properties for metals, 17: 40941
HNO_3–tetrabutyl methylene diphosphonate, solvent properties for metals, 17: 40941
HNO_3–$Th(NO_3)_4$–TBP–H_2O, method for presenting data on phase diagrams and separations in, 19: 2286
HNO_3–$Th(NO_3)_4$–TBP–$UO_2(NO_3)_2$–H_2O, phase equilibrium in, 19: 26476
HNO_3–$Th(NO_3)_4$–TBP–H_2O, phase studies, 18: 5268
HNO_3–$Th(NO_3)_4$, protactinium stability in, 18: 10044 (TID-7675(p.35-45))
HNO_3–$Th(NO_3)_4$, separation of uranium-233 from, for Kilorod Program, 17: 35618(R) (ORNL-TM-545)
HNO_3–$Th(NO_3)_4$, separation of protactinium from, 18: 10183 (TID-7675(p.46-56))
HNO_3–$Th(NO_3)_4$, solvent properties of boiling aqueous, for uranium, 17: 35618(R) (ORNL-TM-545)
HNO_3–tributyl phosphate, dielectric constants, 19: 7424
HNO_3–tridodecylamine–$UO_2(NO_3)_2$, thermal decomposition of complexes formed in, 19: 13337
HNO_3–trioctylamine, solvent partition of uranium in, 18: 31488
HNO_3–U, criticality parameters of water-reflected spheres of, (T), 20: 16031
HNO_3–$UO_2(NO_3)_2$, analysis of, conductivity cell design for, 18: 35806 (DP-869)
HNO_3–$UO_2(NO_3)_2$, chemical potentials and solution-vapor equilibrium in, at 25, 35, and 50°C, 19: 19907
HNO_3–$UO_2(NO_3)_2$, corrosive effects on stainless steels at 95°C for 3 years, 18: 39842 (LA-3101)
HNO_3–$UO_2(NO_3)_2$, criticality studies, 19: 19363
HNO_3–$UO_2(NO_3)_2$–H_2O, nitric acid–water partial pressures over, 20: 9052(R) (ORNL-3830, pp 248-51)
HNO_3–$UO_2(NO_3)_2$–H_2O, phase diagrams, 16: 11580 (TID-15080)
HNO_3–$UO_2(NO_3)_2$–H_2O, phase diagram, 20: 38994(R) (AE-232)
HNO_3–$UO_2(NO_3)_2$–H_2O, phase equilibrium in, 17: 10615
HNO_3–$UO_2(NO_3)_2$, phase studies of aqueous solutions of, at 25, 35, and 50°C, isothermal, 19: 393
HNO_3–$UO_2(NO_3)_2$–H_2O, refractive index measurements on, 20: 40804 (KR-108)
HNO_3–$UO_2(NO_3)_2$–H_2O, separation of uranyl nitrate from, using TBP, 19: 4253(R) (ORNL-3627(p.231-2))
HNO_3–$UO_2(NO_3)_2$, solvent properties of, for molybdic oxide and its hydrates, 16: 168
HNO_3–$UO_2(NO_3)_2$–H_2O, vapor pressures of nitric acid and water over, 19: 32158
HNO_3–uranyl acetate, ion exchange equilibrium, 18: 13949
HNO_3–xylene, solvent properties for various elements, 20: 27037 (JAERI-1106)
HNO_3–Zr, corrosive effects of, on titanium, inhibition by chromium(VI)–hydrofluoric acid solutions of, 16: 16464
HNO_3–2-propanol–H_2O, ion exchange of rare earths from, 18: 25395
HNO_3–2-propanol–H_2O, lead complexing in, 18: 25384
HNO_3–2-propanol, sorption of thorium and uranium by ion exchange from, 18: 25383
HNO_3–4-methyl-2-pentanone, electric conductivity of aqueous, 16: 20534(R) (IDO-14574)
H_2O_2–HNO_3, solvent properties for neptunium peroxides, 17: 12227 (TID-16192)
H_2O_2–HNO_3, solvent properties for neptunium peroxide, 18: 344 (DP-594)
hydrazine–HF–HNO_3, solvent properties for plutonium, 20: 33313(P)
kerosene–HNO_3–TBP, degradation and cleanup, 18: 20100 (ORNL-3524)
$La(NO_3)_3$–HNO_3–TBP–H_2O, method for presenting data on phase diagrams and separations in, 19: 2286
$La(NO_3)_3$–HNO_3–H_2O–$Y(NO_3)_3$, phase studies, 18: 25434
$LiNO_3$–HNO_3, separation of americium and promethium from aqueous, by solvent extraction, 20: 33417(T,R) (ORNL-tr-1239)
$LiNO_3$–HNO_3, separation of americium, curium, and promethium from, by solvent extraction, 20: 33418(T,R) (ORNL-tr-1241)
$LiNO_3$–HNO_3, solvent properties for paper chromatographic separation of americium and curium, 19: 34280
$LiNO_3$–methanol–HNO_3, use as solvent in ion-exchange separation of rare earths, 20: 4067
methanol–HNO_3, solvent properties of, for rare earths, scandium, and yttrium, 16: 25280 (TID-15598)
methanol–HNO_3, spectrophotometric analysis for metals, 20: 14469(R) (TID-22650)
methanol–HNO_3, use as eluant in separation of americium and curium by anion exchange, 20: 439(T) (ORNL-tr-893)
mineral oil–HNO_3, flow properties of, in stacked-clone contactor, 20: 45798(R) (ORNL-3945, pp 230-2)
$Nd(NO_3)_3$–HNO_3–H_2O, phase studies at 25°C, 18: 17794
$Nd(NO_3)_3$–HNO_3–$Pr(NO_3)_3$–TBP–H_2O, separation factors for neodymium and praseodymium in, 20: 40904
$Nd(NO_3)_3$–HNO_3–$RbNO_3$–H_2O, solubility isotherm at 25°C, 17: 35842
$Nd(NO_3)_3$–HNO_3–$Pr(NO_3)_3$–TBP–H_2O, solvent distribution of neodymium and praseodymium in, 20: 7004 (IS-T-42)
NH_4F–formic acid–HNO_3, anodic protection effects against corrosion of chromium, iron, molybdenum, and nickel base alloys, 18: 35959
NH_4NO_3–$Gd(NO_3)_3$–HNO_3–H_2O, phase studies, 19: 28334
NH_4NO_3–HNO_3, solvent partition of uranyl nitrate between aqueous solutions of, and diisoamyl ester of methyl phosphonic acid–TBP, 18: 6902
NH_4SCN–HNO_3–TBP, use in chromatographic separation of rare earths, thorium, and uranium, 20: 41045
nitric acid–U–H_2O, criticality data for, 20: 1410 (AHSB(S)HANDBOOK-1(1st.Rev.))
nitric acid–Pu–H_2O, criticality data for, 20: 1410 (AHSB(S)HANDBOOK-1(1st.Rev.))
1-butanol–HNO_3, analytical use in anion exchange separation of cesium and rubidium, 20: 22908
1-butanol–HNO_3, effects on cation exchange separation of cesium and rubidium, 20: 22909
2-ethyl-1-hexanol–HNO_3, flow properties of, in stacked-clone contactor, 20: 45798(R) (ORNL-3945, pp 230-2)
4-methyl-2-pentanone–HNO_3, solvent properties for various elements, 20: 27037 (JAERI-1106)

NITRIDES

(See also nitrides of the specific elements.)
see also Carbonitrides
see also Oxynitrides
see also Rare Earth Nitrides
analysis for carbon, graphite, nitrogen, and oxygen, method for, 19: 46941 (NP-15514(Vol.3))
bibliography on analytical chemistry of certain group IV and V, 19: 46941 (NP-15514(Vol.3))
bibliography on, in field of aerospace, 17: 39459 (AD-296351)
bibliography on properties of refractory, 18: 16481 (UCRL-7559)
book: *Hard Materials*, in German, 18: 7261
book: *High-Temperature Materials*. No. 1, *Materials Index*, 18: 24075
chemical reactions with metals at high temperatures, review on, 20: 39331(T) (UCRL-Trans-10044)
coalescence with alpha–iron, –molybdenum, and –tungsten, 18: 14510
conference on, 18: 37115 (ANL-6856)
conference on compounds of interest in nuclear reactor technology, University of Colorado, Boulder, August 3 to 5, 1964, 19: 7441
crystal structure and properties of metal, of first secondary groups of the periodic system, 16: 20379(T) (UCRL-Trans-817)
data tabulations on, 18: 32079
determination in metals and salts by high-temperature fluorination, 16: 23638 (TID-7629(p.295-307))
development, requirements, and uses for aerospace components, 16: 10425 (ASD-TR-61-322(p.679-709))
developments in high-temperature, 16: 27641(T) (FTD-TT-62-503)
effects on properties of tungsten and tungsten alloys, 17: 1866
entropy of refractory, at 298°K, 18: 27354(R) (ASD-TDR-62-204(Pt.III))
evaporation rate and vapor pressure of, 17: 21691
fabrication of refractory metal, 18: 7263
metallography of types for use above 2500°C, 16: 30803 (TID-11432)
preparation and properties of refractory, review, 17: 14863(T) (JPRS-17446)
preparation of very pure, process for, 19: 4608(P)
preparation, properties, and uses of refractory-metal, 16: 25768(T) (NASA-TT-F-102)
preparation, properties, and uses of, review on, 16: 27640(T) (FTD-TT-62-430)
production and properties of, German book on, 18: 7261
production, properties, and uses of refractory, 19: 47020(T) (AEC-tr-6616)
properties, 17: 1975
properties and structure correlations of, review of, 17: 30987(T) (AEC-tr-5873)
properties and uses of rare-earth, 17: 23999
properties for aerospace applications, handbook, 19: 14063
properties for containment of molten uranium alloys, 20: 20802(R) (ANL-7055, pp 21-98)
properties for high-temperature uses, effects of preparation and fabrication methods on, 20: 7511
properties of, as refractories, 17: 3479 (LAMS-2674(Pt.II))
properties of high-melting, 16: 25835
separation from plutonium by consumable electrode method, 19: 46915 (BNWL-IR-2)
sintering reactions with metals, formation of complex compounds by,

20: 25539
spectra of, effects of chemical combination on soft x-ray K emission bands of nitrogen in, (E), 19: 44944
stability to liquid lithium at 800 to 1500°K, 16: 15200 (TIN-651)
superconducting transition temperatures of metallic, (T), 19: 23565
thermal decomposition of, application of activated complex theory to, 18: 36900 (UCRL-10791)
thermodynamic properties, 18: 12037 (NP-13622)
thermophysical properties, 16: 2204 (WADC-TR-58-476(Vol.IV)(Rev.))
wettability of refractory, by molten metals, 20: 39429

NITRILES
(See also specific nitriles, e.g., Succinonitriles.)
see also Benzonitrile
see also Methacrylonitrile
see also Succinonitriles
carbon-13 nuclear magnetic resonance spectra, chemical shifts in, 20: 26842
catalytic effects on graft polymerization of styrene to cotton fabrics, 18: 31511
determination by titration of amide-converted, 19: 36220(R) (MIT-2098-142)
ionization by electron impact, 16: 17708(R) (TID-14812)
polymerization of chloro-, and oxychloro-, 16: 158(R) (NP-10926)
protective effects against radiation injuries in mice, reaction mechanisms, 17: 10482(R) (NP-12251(p.47-66))
protective effects of, against radiation sickness, review, 17: 14112
protective effects against radiation injuries in mice, 19: 8954(R) (NP-14448(p.65-97))
radiation effects, 17: 12323 (BMI-1610)
radiation effects on, cosmic, 17: 32693
radiation effects on polymers of, neutron, 18: 22122(T) (JPRS-24289 (Del.)(p.41-3))
radiation effects on mechanical properties of elastomeric materials, gamma, 19: 30824 (HW-SA-3629)
radiation effects on elastomers of, gamma, 20: 7170
radiolysis of, electron vs. gamma, 18: 22157
reactions with heavy water and deuterium hydrides, 16: 11594
use of, in development of liquid chemical dosimeter, 17: 30887

NITRITE IONS
bromine ion (Br_3^-) trapping in irradiated potassium bromide crystals containings, 16: 13672
density in lower ionosphere, 18: 21075
determination at low concentration using potassium permanganate, amperometric titration, 16: 25272(R) (TID-16332)
determination in water, colorimetric, 17: 5977 (TID-15070)
effects on dielectric properties of potassium halide crystals, 19: 14914 (NYO-2471-7a)
effects on radiolysis of *p*-nitrosodimethylaniline, 19: 32216
effects on radiolysis of acetylene, 19: 44082
effects on silver yields from gamma radiolysis of silver perchlorate solutions, 20: 26962
electron spin resonance spectra of, in irradiated aqueous sodium hydroxide glasses at 77 to 150°K, 20: 45730
exchange reactions with, nitrate ions and nitrogen oxide, 18: 2127(R) (ORNL-3488(p.21-41))
exchange with chloride in *trans*-dichloro-bis-(triethylphosphine) - platinium(II) complex, 18: 12059
interactions with phonons in potassium chloride crystals at 1 to 100°K, 16: 25996
isotopic exchange equilibrium calculations, 19: 40460(R) (NYO-3462-1)
oxidation by peroxydisulfate ions, 18: 39166(R) (TID-21041)
production in NO^+ in atmosphere, crossed molecular-ion beam interactions for absolute cross section for, (E), 20: 19670
radioinduced production in nitrate solutions, mechanisms of, 19: 46332(R) (ORNL-3832, pp 50-65)
radiolysis of aqueous solutions of, in presence of nitrous oxide, gamma, 19: 26445
radiolysis of aqueous solutions of, pulse, 19: 38728
reactions with atomic hydrogen and polarons radioinduced in ice, 18: 13858
reactions with atomic hydrogen, rate constants for, 19: 22339
reactions with plutonium(VI), 18: 10038 (HW-79354)
reduction by iron in alkaline solutions, mechanisms of, 19: 46899(R) (ORNL-3832, pp 33-49)
scavenging effects on electron and hydrogen yields in irradiated aqueous solutions, 17: 4602
spectra of, deuterium oxide solvent effects on uv absorption, 18: 43500
substitution in chloroamineplatinum(IV) complexes, 16: 165
yields from gamma radiolysis of nitromethane at 77°K, EPR studies of, 19: 40579
yields from gamma radiolysis of aqueous solutions of 2-propanol, 20: 29254
yields from gamma radiolysis of nitrate solutions, at 77°K, 20: 38950
yields in gamma radiolysis of frozen nitrate solutions, 20: 26923(R) (COO-1528-5)
yields in radiolysis of aqueous methanol–sodium nitrate solutions, 18: 43641

NITRITES
see also Isopropyl Nitrites
see also Lithium Nitrites
see also Methyl Nitrites
see also Nitrite Ions
see also Potassium Nitrites
see also Silver Nitrites
see also Sodium Nitrites
content in Atlantic Ocean, measurements on, 20: 28877 (NYO-1918-124)
content in Atlantic Ocean, measurements on, 20: 28878 (NYO-1918-138)
content in Sargasso Sea, annual and seasonal variations in, 18: 21711 (NYO-3140-1B)
decomposition of ethylene glycol dinitrite, thermodynamics, 16: 2933(T) (UCRL-Trans-525(L))
detection in plutonium liquors, device for, 17: 27222(P)
determination by amperometric titration, 17: 35622(R) (TID-19359)
determination in heavy water moderator, automated, 19: 40406 (CONF-650919-2)
determination in nitrate-containing potassium iodide solutions, titrimetric, 20: 14455(R) (ORNL-3889, pp 25-32)
determination of, method for, 17: 28801 (IDO-14316(Suppl.4))
effects on dielectric properties of potassium halides, 19: 10680 (NYO-2471-6)
effects on formation of nitrate radicals in pulse radiolysis of nitrate solutions, 20: 43321
effects on mutation induction in Schizosaccharomyces, protective effects of chloramphenicol against, 20: 36653
formation of, by gamma radiolysis of nitrous oxide, 17: 16441
phase diagrams of, book, 19: 14061
radiation effects on oxidation of hemoglobin in erythrocytes by, 17: 1302
radiation effects on alkaline solutions, 19: 26399
radiolysis of aqueous solutions of, gamma, 18: 22155
radiolysis of aqueous solutions of, at 77°K, yields of hydrogen from gamma, 20: 18748
radiolysis of potassium bromide dispersions of, 17: 10509(R) (ORNL-3320(p.30-46))
reactions with sulfamic acid in titration of uranium(VI), 16: 8678 (ORNL-TM-113)
separation from mixed potassium and sodium nitrates by nitrogen dioxide bubbling, 20: 10272(R) (NAA-SR-9339)
separation of oxygen-18-labeled, from phosphates by ion-exchange chromatography, 19: 42604
yields from gamma radiolysis of ammonium perchlorate, 19: 36483

NITRO COMPOUNDS
determination of organic, micro-, 16: 11528 (UCRL-6639(p.20-8))
effects of nitrofuran on *Escherichia coli*, 19: 33752
effects on activity of leukocyte alkaline phosphatase, toxicity, 20: 5269
effects on iodine-131 exchange between 4-iodoantipyrine and molecular iodine, 19: 24543
effects on iodine-131 exchange between iodine and 1-phenyl-2,3-dimethyl-iodopyrazolone, 20: 18690
effects on radioinduced polymerization reactions of methyl methacrylate, 16: 8789
effects on radioinduced polymerization reactions of vinyl acetate, 16: 8791
effects on radioinduced polymerization of methyl methacrylate, 18: 297
electrochemical reduction of aliphatic, effects of dielectric constant of organic solvents on, 20: 18636(R) (TID-22725)
formation of complex, by nitrous acid reactions with nitrosylruthenium nitrato complexes, 19: 26280 (AERE-R-4769)
nitrogen-14 NMR in, chemical shifts in, 18: 43497
radioactivity of carbon-14-labeled, use of liquid scintillation counter for measuring, 19: 9088
reduction of, effects of uv radiation on catalytic activity of platinum in, 20: 29304
separation by gas chromatography using inorganic salts as column packings, 18: 17931 (IDO-16912)

Nitrobenzene
see Benzene, Nitro-

p-Nitrobenzene-azo-chromotropic Acid, Sodium Salt
see Chromotrope 2B

NITROCELLULOSE
see also Collodion
charged particle track analysis in, methods for, (E), 20: 4251 (USNRDL-TR-917)
determination in mock explosive, method for, 20: 14470 (UCRL-7873)
determination, micro-, 16: 11528 (UCRL-6639(p.20-8))
efficiency for recording individual tracks of low-energy alpha particles, 18: 18188

fission fragment tracks in films of, 18: 2428
fission fragment tracks in, characteristics of, 18: 10411
performance of, for alpha detection, 19: 44384 (CERN-65-4(Vol.II), pp 11-8)
radiation effects on smokeless powder, gamma, 16: 29448

NITROFLUOR PROCESS
development, 19: 36216(R) (BNL-900(p.29-72))
development and flowsheet for, 18: 13974

NITROFORM
formation yields in radioinduced hydrolysis of tetranitromethane, 18: 276(T) (PA-TM-1029)
free radical formation from, electron spin resonance and tracer studies of, 19: 7524
preparation of deuterated using deuterium chloride, 16: 8732

NITROGEN
see also Nitrogen Fixation
absorption of hydrogen Lyman radiation by, 18: 30668
abundance in cosmic radiation, 17: 13010
abundance in cosmic radiation, 17: 13019
abundance in cosmic radiation, 17: 19025(T)
abundance in primary cosmic radiation, 17: 22403 (AD-282243)
abundance in Venus atmosphere, 16: 21228
abundance in 3 Centauri A, 16: 4659
acceleration of plasma by continuous Lorentz forces, 16: 15387
acceleration of plasma of, in crossed-field d-c devices, (E/T), 19: 10431
acoustic-wave production in low-pressure, r-f breakdown for, 18: 28846
additive effects on nuclear resonance in potassium compounds, 16: 31538
additive effects on electron transport in ionized argon, 17: 5515
additive effects on titanium, 17: 16580(P)
additive effects on graphite sputtering by mercury ions, 17: 20659
additive effects on cesium uptake by rice, 17: 30031
additive effects on ductility and electric conductivity of hardened steel, 17: 39545(T,R) (EURAEC-599)
additive effects on properties of hafnium–tantalum–tungsten alloys, 17: 34420(R) (WANL-PR-M-004)
additive effects on melting point of lithium, 18: 595 (ASD-TDR-63-413)
additive effects on oxidation of uranium by water vapor, 18: 10483
additive effects on corrosion resistance of zirconium in steam, 18: 10476(T) (JPRS-22697(p.8-26))
additive effects on lifetime of metastable helium atoms, 18: 26238
additive effects on corrosion of Zircaloy-2 by water and steam, 18: 27884 (KAPL-2000-21(p.VI.1-4))
additive effects on fast-neutron effects in iron and steel, 18: 28041(R) (EURAEC-1046)
alpha energy loss and ionization in, 16: 6931
alpha ion pair production in, 19: 13473
alpha reactions (α,n) with, neutron yields from, 17: 33017
alpha reactions, beryllium-7 production in, 17: 21098
alpha reactions of, spectra from, 19: 26382(R) (RPI-321-1)
alpha reactions with, neutron yields from, 17: 9527
alpha reactions with, energy-level excitation by, 20: 25734
alpha stopping in, energy transfer and scintillations from, 20: 11130
alpha-particle interactions with, properties of recoil ions from, 20: 41622 (SC-DC-66-1564)
alpha-particle molecular stopping cross section at 300 keV to 5 MeV, 20: 46300
analysis for oxygen, 16: 12288
analysis of, effects of hydrogen in mass spectrometric, 17: 2727
analysis of, in plasma jets, 17: 19460(R) (SC-4776(RR))
argon atom scattering by, total cross section for, 17: 34632
argon ion charge exchange in, cross section for, (E), 19: 16419
argon reactions at thermal energies, charge transfer in, 18: 32469
atom concentrations in nonequilibrium supersonic jet from d-c glow discharge, 16: 1270 (AFOSR-1360)
atomic density measurements in afterglow plasma of, 20: 44852 (AD-629924)
atomic self-consistent-field functions for neutral, 16: 33634
atomic wave functions for, with five parameters, 17: 32796
balance in mouse radiation chimeras, 19: 26109(R) (ORINS-49(p.40-62))
balance in mouse radiation chimeras, 20: 38636
bibliography on fluid mechanics and heat transfer, 16: 22305 (UCRL-6807)
boiling burnout and heat transfer in liquid, test of, 20: 47034
boiling data for, nucleate and film, 20: 36993
boiling in, liquid-solid interface effects on nucleation characteristics in, 17: 32828
boiling of upwardly flowing, in heated tube at high vapor qualities, film, 19: 20113 (NP-14895)
boiling of, equation for statistical analysis of heat flux in, nucleate pool, 16: 30564
boiling of, superheat in nucleate, 18: 26461
boiling, relation between bubble diameter and frequency in, 16: 20601
bond length measurement by electron diffraction, 17: 27358
bond lengths and vibrational amplitudes for molecules of, from electron diffraction, 17: 37792
bremsstrahlung dissociation at 250 to 1150 Mev, 16: 7101
bremsstrahlung emission by shock-heated, 17: 34532 (BSD-TDR-63-107)
bremsstrahlung reactions at 30.5 Mev, proton production in, 17: 31540
bubble kinetics in water, 19: 38244 (N64-24160)
carbon ion reactions at 2 to 10 Mev/amu, equilibrium charge-state populations in, (E), 19: 43007
cesium ion elastic scattering at 2.3 to 11.6 ev, (E/T), 20: 17300
charge exchange with aluminum ions at 0.25 to 1.9×10^8 cm/sec, cross sections, 19: 14144 (WL-TDR-64-89)
charge transfer in collisions with ions at 30 to 10,000 ev, cross sections for, 17: 29426
charged-particle density in plasma of, effects of surrounding gas pressure on, (E), 19: 39989(T)
charged-particle reactions with, dE/dx and range-energy graphs for, 20: 46601 (UCRL-2426(Vol.2)(1966 Rev.))
charged-particle reactions with, range-momentum and dP/dx graphs for, 20: 46342 (UCRL-2426(Vol.4)(1966 Ed.))
chemical binding in diatomic molecules of, energies of atomic and molecular orbitals in, 18: 41431
chemical states in lithium and sodium, 19: 39157 (CNLM-6337)
collimation of molecular beams of, (E), 19: 18694
collision integrals and potential energy functions with nitrogen oxides and oxygen, 16: 16853
collisions of molecules of, with alkali metal atoms, ionization produced in, (E), 20: 2639
collisions with excited cyclopropane, energy transfer in, 19: 19938
collisions with helium ions, dissociative charge transfer in, 17: 37753
collisions with metastable argon and helium, 18: 9042
compressibility of liquid, at boiling point, 18: 19929 (CONF-417-20)
compression of, second virial coefficients and volumetric behavior at 0 to −140°C, 17: 28077
condensation and deposition on liquid-helium-cooled surface, trapped atom effects on thermal conductivity, 16: 5261
contact angle hysteresis in gas-aqueous solution-solid system, 17: 35617(R) (NYO-10329)
contact angle with paraffin under water, hysteresis of, 16: 17881(R) (MITS-47)
content in arc-melted rhenium–tungsten ingots, 20: 41429(R) (USBM-RC-1249)
content in Atlantic Ocean, measurements on, 20: 28878 (NYO-1918-138)
content in atmosphere above 100 km, 18: 7617
content in atmosphere, absorption cross section determination of, 18: 30668
content in calf intestine, effects of diet on, 20: 32908(R) (ORO-648, pp 71-90)
content in iodide zirconium, 19: 36558
content in irradiated mice treated with bone marrow injections, 19: 138
content in natural gases, 19: 44239
content in niobium-based alloys, effects of yttrium additions on, 19: 40953 (PWAC-441)
content in Phaseolus, effects of rare earths on, 20: 18237
content in primary cosmic radiation, 19: 20894
content in primary cosmic particles, (E), 19: 25208
content in primary cosmic radiation, at geomagnetic latitude 42° North, 20: 31951
content in rabbit blood during radiation sickness, effects of glycocoll and peptone on, 17: 31975
content in range plants, Miles City, Montana, 1955 to 1960, 19: 45747 (ORNL-TM-1279)
content in snow at South Pole as nitrate and nitrite, 19: 18138
content in stars from CNO bi-cycle, 19: 25128
content in sun, saturation effects on determination of, (T), 19: 18660
content in upper atmosphere, 18: 7616
content in upper atmosphere, from rocket soundings, 18: 37794(T) (NASA-TT-F-141(p.1-21))
content in zirconium, 17: 33819
corrosive effects on high-temperature fatigue characteristics of Hastelloy-X tubing, 16: 10506 (BMI-X-191)
corrosive effects on niobium and vanadium at operating conditions of Dounreay Fast Reactor, 16: 26475 (TID-7622(p.35-56))
corrosive effects on turbine alloys, 16: 32114 (IDO-28591)
corrosive effects on niobium as a function of temperature, 17: 3435
corrosive effects on Hastelloy-X at high temperatures, 17: 3898
corrosive effects of, on iron- and nickel-base alloys, effects of alloying metals on, 17: 20412 (HW-76952)
corrosive effects on niobium at room temperature to 1500°C, 17: 29289
corrosive effects of moist, on magnesium at 350 to 600°C, 18: 2179 (CEA-2280)
corrosive effects on grease-lubricated compressors, 18: 30954(R) (ORNL-3619(p.359-65))
corrosive effects on steels at high temperatures, 18: 35956(R) (MSAR-

64-93)
corrosive effects on steels, development of loop and techniques for studying, 18: 35955(R) (MSAR-60-34)
corrosive effects of moist, on uranium, mechanism of, 18: 44088
corrosive effects on Hastelloy X and Haynes 25 Alloy at 1200°C, 19: 13883(R) (HW-81984(p.9.1-6))
corrosive effects on molybdenum-uranium alloy at high temperatures, radiation effects on, 19: 18540 (SC-RR-65-28)
corrosive effects on superalloys at high temperatures, 19: 46946 (BNWL-100)
corrosive effects on iron- and nickel-base alloys, 20: 9408 (BNWL-154)
corrosive effects on uranium–10 molybdenum alloys, effects of reactor radiation on, 20: 11224
cosmic particle reactions with atmospheric, secondary particles from, (T), 19: 12118
creep effects on nickel, 17: 14838 (NRL-5880)
critical and inversion temperatures, 17: 30460
cryostats, oxygen concentration in, 17: 8036
crystal structure of, isotopic effects on unit-cell volumes, 17: 32106
current sheet microstructure in theta-pinch plasma of, (E/T), 19: 45445
current-sheet structure in plasma jets of, 20: 34718
density and temperature of molecular, in thermosphere, (E), 19: 33136
density in lower ionosphere, 18: 21075
density in lunar atmosphere, equilibrium, 16: 18285
density of, measurement by gamma scattering, (E), 20: 6694(R) (MIT-952-2)
deposition in bones of 30 to 630-day-old white rats, 16: 9913
desorption from iridium, rhodium, and tungsten, flash, 20: 20652 (IS-T-67)
desorption from stainless steel, flash-filament technique for, 16: 31723
detection and measurement using ionization detectors, 16: 28875(T) (AEC-tr-5287)
detection in metals, scanning micro-, 19: 30075 (EUR-1819.e(p.1-14))
detection of molecular beams of, field-ionization detector for, 20: 21089
detection of trapped, in irradiated potassium azides at 77°K, 16: 9273
determination, activation, 16: 2967(R) (TID-14310)
determination as impurity in fused uranium dioxide, 18: 602 (DP-819)
determination as impurity in ultrapure gases, mass spectrometric, 20: 29083(R) (UCRL-14767)
determination as trace impurity in uranium, 18: 29591
determination by activation with charged particles, 16: 20321 (NP-11608)
determination by activation using 14-Mev neutrons, 18: 9966 (CEA-2358)
determination by activation analysis, mobile neutron generator for, 18: 36565
determination by activation using helium-3 ions, 20: 20565 (ORNL-P-1216)
determination by charged-particle reactions at 2 Mev, 20: 43097
determination by fast neutron activation, 17: 4479
determination by helium-3 activation, 18: 31361(R) (UCRL-11213 (p.87-138))
determination by helium-3 activation, 19: 22114
determination by isotopic dilution, 20: 16362
determination by micro-platinum bath vacuum fusion method, 17: 5967 (PG-Report-381)
determination by neutron activation methods, 20: 20596
determination in aluminum, beryllium, iron, and zirconium, activation, 16: 12986
determination in atmosphere in relation to argon using radiation attenuation gages, 17: 27564(R) (NYO-10219)
determination in argon in gas chromatography, electron drift velocity detector for, 18: 33476
determination in alkali metals, review of methods for, 19: 22102 (TIM-900)
determination in argon and helium. 20: 10420 (TIM-824)
determination in argon, properties of gas chromatographic radioionization detectors for, 20: 24989
determination in alkali metals, activation and chemical methods for, 20: 26751 (RAC-1478)
determination in beryllium carbide, methods for, 16: 6366 (NEPA-940)
determination in boron–silicon systems, 16: 23599 (ARL-180)
determination in beryllium, development of mass spectrometric methods for, 19: 7265 (AD-603756)
determination in beryllium, boron, calcium, and sodium, gamma activation, 19: 7339
determination in beryllium by activation, 19: 24415
determination in blood of dogs, 19: 43674 (UCD-472-112, pp 36-43)
determination in boron by activation methods, 20: 3879(R) (MLM-1266)
determination in beryllium by modified combustion-conductometric method, 20: 20556 (AD-626987)
determination in carbon monoxide by high resolution mass spectrometry, 16: 28868 (IS-504)
determination in cesium by photon activation methods, 20: 20645
determination in complex gas mixtures, method using isotopic dilution for spectral, 20: 22954
determination in diamonds by photoactivation, 20: 36746
determination in fused uranium dioxide, Kjeldahl digestion technique for, 17: 17966 (HW-SA-2663)
determination in fertilizers by activation, 18: 21953 (AERE-R-4576)
determination in geothermal bores, fumaroles, and pools in New Zealand, mass spectrometric, 16: 16581
determination in gases of Project Rover test facilities by gas chromatography, 17: 25115 (LADC-5790)
determination in grain products, activation, 20: 7007 (KN-65-186)
determination in helium coolant in Dragon Reactor, evaluation of methods for, 19: 22155
determination in helium at reduced sample pressures by gas chromatography, 20: 1751
determination in helium, method for, 20: 31167(R) (ANL-7175, pp 217-25)
determination in iron, nickel, niobium, uranium, vanadium, and zirconium by hot-vacuum extraction, 17: 14147 (PG-Report-412)
determination in lithium by fluorination using potassium bromotetrafluoride, 16: 28881
determination in lubricants, computer routine for activation, 18: 19918
determination in lubricating oils by neutron activation methods, 18: 39074
determination in lithium, method for, 19: 14765(R) (ANL-6977)
determination in lithium, methods for, 20: 8447 (PWAC-491)
determination in loop-cover argon by diffusion gasometry, 20: 12767 (GEAP-4833)
determination in liquid sodium from recirculating test loops, 20: 41420(R) (MSAR-66-149)
determination in metal alloys, design of modified Kjeldahl apparatus for, 16: 8682 (TID-11411)
determination in molybdenum, niobium, tantalum, and tungsten, review of methods for, 16: 12995
determination in mixtures with fluorine, hydrogen fluoride, and uranium hexafluoride, 17: 1385 (PG-Report-351)
determination in molybdenum, niobium, and tungsten by vacuum extraction, 17: 6022
determination in metals by manometric techniques using inert-gas fusion, 17: 30466 (CONF-14-13)
determination in metals, activation, 17: 39003
determination in metals, vacuum fusion, 18: 33491
determination in metals by vacuum extraction and fusion, review on, 19: 22109
determination in metals, isotope-dilution method for, 19: 40444
determination in metals by helium-3 activation, 19: 46174 (LA-DC-7319)
determination in metal surfaces using deuteron activation analysis, 20: 33238
determination in metals, activation, 20: 38840
determination in metals by carrier-gas fusion extraction, 20: 40796(R) (IS-1500(Sect.C))
determination in nuclear fuels and wastes, gas-chromatographic, 16: 22033
determination in niobium and its alloys, 16: 25294
determination in niobium, tantalum, and tungsten, 18: 10022
determination in niobium and tantalum, 18: 10023
determination in niobium and tantalum, using inert gas fusion-chromatographic method, 19: 15404
determination in organic materials simultaneously with carbon and hydrogen, modifications in gas volumetric, 17: 38950
determination in out-of-pile simulated boiling-water reactor and superheated-steam loops, 17: 40705 (TID-7655(p.147-175))
determination in organic compounds by neutron activation, 20: 33165(T) (AEC-tr-6639, pp 32-5)
determination in purified helium, use of chromatography and radioactive ionization detector for, 18: 31397
determination in petroleum products by radiation absorption, 19: 13214
determination in pure helium, chromatograph for, 19: 28220 (BNWL-12)
determination in petroleum products, x-ray absorption method using iron-55, 19: 28230
determination in plutonium mononitride, methods for, 19: 46164 (AERE-R-5002)
determination in plutonium and uranium carbides and plutonium carbide–uranium carbide cermets with iron or molybdenum, 20: 8873
determination in plasmas, time-resolved profile measurements of, (E), 20: 15872 (IPP-1/41)
determination in plutonium metal, alloys, and compounds, 20: 14440 (LA-3452)
determination in presence of boron by proton activation, 20: 18582
determination in petroleum, activation, 20: 29139
determination in refractory metals, review of methods for, 18: 33515
determination in refractory metals, review of methods for, 18: 33516
determination in rare earths using vacuum fusion, 19: 9046(R) (IS-900 (Sect.C))
determination in refractory metals using carbon-arc chromatographic

methods, 19: 9046(R) (IS-900(Sect.C))
determination in refractory metals by d-c carbon-arc, gas chromatographic technique, 19: 9069
determination in refractory metal nitrides by chlorine release of nitrogen, 19: 17800
determination in refractory borides, carbides, and nitrides, method for, 19: 24403 (NP-14952)
determination in rocks and ores, method for gamma activation, 19: 28277
determination in refractory borides, carbides, and nitrides, method for, 19: 46941 (NP-15514(Vol.3))
determination in refractory metals by gas chromatography, 20: 3863(R) (IS-1200(Sect. C))
determination in surfaces of zinc and zirconium alloys, 17: 7971
determination in sodium, volumetric, 17: 27232 (LA-2892)
determination in steel, 18: 1489(R) (IS-700(Sect.C))
determination in superheated steam, design of gas chromatograph for, 18: 23407 (DP-880)
determination in steel, development of methods for, 19: 9046(R) (IS-900(Sect.C))
determination in steels by isotope dilution method, comparison with vacuum fusion method, 19: 26246
determination in small gas samples, chromatographic, 19: 36227 (AWRE-0-22/65)
determination in stainless steel, method for, 19: 38537 (ACF-7)
determination in steels by platinum-bath vacuum fusion, 20: 3863(R) (IS-1200(Sect. C))
determination in silicates, activation, 20: 26782
determination in solids, mass spectrographic, 20: 38831
determination in steel by x-ray spectrochemical methods, 20: 43161
determination in SAP, methods for, 20: 45574 (EUR-3064.f)
determination in titanium and zirconium nitrides, comparison of hot extraction and Kjeldahl methods for, 20: 40820(T) (IS-Trans-37)
determination in uranium monocarbide, procedures for, 16: 14626 (PWAC-367)
determination in uranium powders, spectrophotometric, 17: 2904 (PG-Report-374)
determination in uranium nitrides using Dumas method, 18: 43366 (AERE-R-4644)
determination in uranium nitrides using Kjeldahl method, 19: 285 (AERE-R-4713)
determination in uranium and its compounds and alloys, methods for, 19: 19823
determination in uranium carbide, 19: 22919(R) (EURAEC-1148)
determination in uranium carbide, method for, 19: 27735(R) (NAA-SR-10850)
determination in uranium dioxide–plutonium dioxide systems, 19: 40438
determination in uranium, effects of nitric acid etching on, 20: 230 (NLCO-965, pp 4.1-5)
determination in uranium nitrides, comparison of Dumas and Kjeldahl methods for, 20: 7025
determination in uranium hexafluoride, spectrographic, 20: 16409
determination in uranium monocarbide, 20: 26770
determination in uranium nitride, comparison of Dumas and Kjeldahl methods for, 20: 43109
determination in vented gases from underground nuclear explosion, apparatus for, 19: 19776 (UCRL-12169)
determination in yttrium, methods for, 20: 4299(R) (ORNL-2711)
determination in zirconium alloys, chemical, 18: 12542(R) (GEAP-4484)
determination of, as impurity in stainless steel, 17: 22114(T,R) (EURAEC-557)
determination of dissolved, in water, 18: 27290 (TID-19180)
determination of, in titanium, vacuum-spectrographic, 16: 29323(T) (AEC-tr-5285)
determination of, in products of biphenyl pyrolysis, chromatographic, 17: 19941 (ORNL-TM-523)
determination of isotopic ratio of, in marsh gas and rocks, 18: 12017
determination of traces in argon, spectrographic, 16: 16570(P)
determination of trace amounts in graphite by proton activation methods, 19: 15371
determination of total, in enriched uranium powder, 19: 36232 (PG-Report-585)
determination of trace amounts of, by reactor neutron activation methods, 20: 26760
determination of urea, in blood serum, micro method, 19: 32060(R) (LF-22)
determination of, quantitative activation, 18: 13713(P)
determination of, factors affecting continuous on line, 20: 1734 (EG-Report-36)
determination of, by alpha scattering methods, 20: 22964
determination of, by neutron activation methods, 20: 29078(R) (AD-633252)
determination of, in helium, chromatograph for continuous, 20: 31210
determination of, in uranium carbide by vacuum fusion, 20: 35417
determination of, on beryllium surfaces by deuteron activation methods, 20: 40812 (ORO-2980-14)
determination of, in gases by deuteron irradiation and neutron time-of-flight spectroscopy, 20: 43115
determination on beryllium surface by deuteron activation methods, 19: 40453
determination using radiometric methods, 18: 29575
determination, activation, 20: 8856
determination, electron microprobe, 19: 40412 (TIM-924)
determination, use of beta ionization detector in chromatographic, 19: 40415(T) (CEA-tr-R-1839)
deuterium and deuteron reactions at 20 Mev, electron detachment in, 18: 24310
deuterium exchange with hydrogen, heat recovery, 16: 2106(P)
deuteron elastic scattering at 13.6 Mev, angular distributions from, 18: 6254
deuteron elastic scattering at 13.6 Mev, angular distributions from, 18: 40632
deuteron elastic scattering at 27 Mev, angular distribution of, (E/T), 19: 33282
deuteron reactions with, electron-capture cross sections for, (E/T), 20: 15886(R) (UCRL-14285)
diagnostics of afterglow plasma of, 18: 34999
diagnostics of discharge plasma of, mass spectrometric sampling probe for, 20: 15915
diagnostics of plasma of, by optical spectra analysis, 18: 21497
diffusion and position energies of interstitial impurities of, in metals, (T), 20: 28679
diffusion and solubility in beryllium, 16: 25757(R) (NMI-9815)
diffusion and solubility of, in beryllium, 17: 22157 (ASD-TDR-62-1018)
diffusion and spin relaxation of cesium in, (E), 19: 41278
diffusion coefficients in carbon tetrachloride, 18: 19963
diffusion coefficients in carbon dioxide, hydrogen, and iodine, temperature dependence of, 19: 34151(T) (ORNL-tr-506)
diffusion from commercial graphite at 1000°C, 17: 4986
diffusion from fused uranium dioxide fuel elements, 17: 28526(R) (DP-845)
diffusion from stored solid plutonium residues, vacuum-drying effects on, 20: 4364 (AERE-M-1644)
diffusion from uranium dioxide pellets at 1000 to 1600°C, 17: 3866
diffusion from urania pellets, kinetics and mechanisms of, 20: 21360 (WCAP-2098)
diffusion from uranium dioxide fuel pellets at 1000 to 1600°C, mechanism of, 18: 7236
diffusion in alumina at high temperatures, 18: 44491(R) (AD-601111)
diffusion in bcc crystals, activation energy for interstitial, (T), 19: 40086
diffusion in beta-zirconium, thermodynamics of, 20: 27509
diffusion in carbon-coated and uncoated uranium carbide–graphite systems, 19: 18475
diffusion in chromium–rhenium alloys, activation energy for, 19: 30642(R) (BMI-1707(Del.))
diffusion in chromium–rhenium alloys, activation energy for short-range, 19: 32676(R) (BMI-1717(Del.))
diffusion in gases, coefficients, 16: 33613
diffusion in graphite, counter, 18: 26061
diffusion in graphite in presence of oxygen, effects of back pressure and pore structure on, 19: 14030
diffusion in hafnium, 16: 2165 (AFOSR-1226)
diffusion in hafnium, coefficient for, 19: 40960
diffusion in latex and neoprene, 18: 25315 (AWRE-0-56/57)
diffusion in molybdenum, activation energy and coefficient of, 19: 9682
diffusion in niobium, alloying effects of zirconium on, 16: 33500
diffusion in oxygen in graphite, 16: 1732 (AERE-R-3814)
diffusion in solid ytterbium, internal friction in interstitial, 18: 26050
diffusion in stainless steel, effects of temperature on, 20: 41419(R) (GMAD-3643-5)
diffusion in tissue-simulating plastics, 18: 13716(R) (ANL-6769(p.21-9))
diffusion in uranium dioxide at 1000 to 1600°C, 18: 42049
diffusion in uranium dioxide, model for, 19: 39219
diffusion in uranium mononitride, activation energy and rate of self-, 20: 4394 (PWAC-477)
diffusion in yttrium at 1235 to 1460°C in electric field, 20: 5599
diffusion in yttrium at 1235 to 1460°C, coefficient for, 20: 21254
diffusion in zirconium, relation to internal friction, 17: 6724
diffusion into urania, coefficient for, 19: 40958
diffusion of charged particles in microwave plasma of, (E), 19: 27642
diffusion of gaseous, in temperature gradients, (E), 19: 39291
diffusion of krypton-85 in, 17: 4524
dissociation and recombination properties of atomic, 17: 5132
dissociation, Lewis number for, 16: 18930
distribution in atmosphere to 430 km, 18: 2409(T) (FTD-TT-63-968)
effect of absorbed, on proton induced electron emission from titanium,

17: 20739
effect on electron energy loss in argon–cesium plasma, (E), 19: 21560
effect on electron attachment to nitrogen dioxide, 19: 32885(R) (AD-610869)
effect on friction between ceramic surfaces at high temperatures, 19: 28826
effect on production of powdered rhenium from rhenium tetrammine chloride, 20: 29672
effect on specific electrical resistivity of tantalum crystals, 19: 39203
effect on stress rupture of type 304 stainless steel at 1250°F, 19: 32733 (NAA-SR-11047)
effects as buffer on spin relaxation of optically pumped cesium, 18: 30403 (NP-14066)
effects as interstitial impurity on corrosion of Zircaloy-2, 20: 25499
effects at high pressure on phosphorus-32 uptake by bean roots, 19: 26022
effects in optical absorption by air at high temperatures, 19: 20832
effects in potassium-sodium reactor coolant, 18: 21661
effects of flowing, on volatilization of fission products from irradiated uranium(IV-VI) oxides, 20: 29211
effects of heat transfer properties of terphenyl coolants, 17: 16228 (NAA-SR-Memo-8064)
effects of impurities of, on mechanical properties and structure of tungsten single crystals, 20: 29793
effects of interstitial, on properties of niobium-vanadium alloys, 16: 12084(R) (ARF-2231-2)
effects of, on dislocations in deformed zirconium, electron microscopic study of, 17: 20482
effects of, on radiation effects on embryo intestine and testis, 16: 20186
effects of sorption of, on low-energy electron diffraction pattern of tungsten single crystals, 20: 23655 (RFP-643)
effects of, on corrosion of zirconium-base alloy by steam, 20: 29660(R) (GEAP-4960)
effects of, on flame emission intensity of barium and strontium, 20: 35487
effects on alkyltin yields in radiolysis of mixtures of 1-bromobutane or 1-bromopentane with tin, 20: 10870 (BMI-1753)
effects on alpha-beta transition in hafnium, 19: 6331
effects on alpha-beta phase transformation in hafnium, 20: 5850
effects on analysis of alkali metals in glove box atmosphere, 20: 7015 (ORNL-TM-1357)
effects on aqueous corrosion resistance of Zircaloy-2, 19: 11682
effects on argon ion-platinum reactions at 22 kev, 17: 25989
effects on atomic hydrogen yields from low-pressure hydrogen discharge, 20: 18663
effects on blood, physiological, 19: 24259 (BNL-898)
effects on boron determination by deuteron or proton activation, 20: 18582
effects on brittleness of tantalum, 20: 15130
effects on brittle-ductile transitions in chromium, 20: 41412(R) (IS-1500(Sect. M))
effects on chlorination of uranium (IV) oxide, 20: 43443
effects on combustion of zirconium droplets in oxygen, explosive,(E), 19: 32050
effects on corrosion of Zircaloy-3 by steam and water, 16: 486 (BM-RI-5865)
effects on corrosion of Zircaloy-2 by steam and water at 750 and 680°F, 16: 10463
effects on corrosion of Zircaloy-2 at high temperatures, 17: 27751 (WAPD-T-1567)
effects on corrosion of Zircaloy-2, 18: 24081 (CONF-509-1)
effects on corrosion by liquid alkali metals, 18: 27890 (NASA-SP-41 (p.49-59))
effects on corrosion of refractory metals by lithium, 18: 27914
effects on corrosion resistance of tantalum to liquid iron–plutonium alloy, 18: 32085 (LADC-6026)
effects on corrosion of consolidated Zircaloy-2 powder by steam and water, 19: 927 (KAPL-3060)
effects on corrosion of niobium by lithium at high temperatures, 20: 4299(R) (ORNL-2711)
effects on corrosion of Zircaloy-2 powders by steam or water, 20: 5851
effects on corrosion of zirconium-base alloys by steam, 20: 14980(R) (GEAP-5065)
effects on corrosion of chromium–iron–zirconium alloy by steam at 300, 400, and 500°C, 20: 31677(R) (GEAP-4840)
effects on creep properties of stainless steel type 304 at high temperatures, 16: 30797 (ORNL-2972)
effects on creep-rupture and tensile properties of niobium, 20: 37218
effects on crystal structure of uranium monocarbide, 20: 39385 (CEA-R-2852)
effects on dark-current drift in phototubes, 19: 22724
effects on deformed zirconium, structural, 16: 33420
effects on density shifts of sodium-23 hyperfine frequency, 19: 30951
effects on ductility of vanadium, 20: 4297(R) (IS-1200(Sect.M))
effects on ductility of low-alloy steel, 20: 27481(R) (EURAEC-1419 and App.)
effects on ductility of chromium–rhenium alloys, 20: 35834(R) (BMI-1767)
effects on dynamic decomposition of rare earth oxalates, 18: 23507
effects on efficiency of electron multiplier, 19: 32413(R) (WERL-2823-17)
effects on efficiency of spark chambers, 17: 23651
effects on electric conductivity of tantalum pentoxide, 19: 23072
effects on electric conductivity of niobium, 19: 30811
effects on electron spin resonance of irradiated silicon oxides, 19: 28384
effects on electron spin resonance signal of activated charcoal, 19: 36332 (IFA-IS-31(1965))
effects on electron energy losses in argon–cesium nonequilibrium plasma, (E), 19: 47737(T)
effects on electronic structure of transition metals and alloys, 20: 31747
effects on enzyme release from x-irradiated lysosomes in rat liver, 20: 38577
effects on equilibria in carbon–uranium system, 19: 14056
effects on fast neutron-irradiated iron and steel, research program on, 19: 44741 (EURAEC-1383)
effects on fast-neutron effects in iron and steel, 18: 37763(R) (EURAEC-1103)
effects on fast-neutron effects on iron and steel, research program on, 19: 44742(R) (EURAEC-1430)
effects on fast-neutron effects on tensile properties of iron and iron–titanium alloys, 20: 13324(R) (EURAEC-1529)
effects on fatigue of molybdenum, 19: 44730
effects on gamma-induced inactivation of transforming DNA, 20: 42818
effects on gas exchange in irradiated pears, 20: 13140(R) (UCD-34P80-3, pp 27-47)
effects on Geiger-Mueller counter pulse attenuation, 19: 30096
effects on genetic response of Drosophila spermatozoa to x radiation, 18: 19647
effects on graphitization of carbon, 19: 28299
effects on Habrobracon eggs in first meiotic metaphase, post-irradiation, 16: 23452
effects on hafnium–niobium–vanadium and niobium–titanium–vanadium alloys, 16: 16712(R) (ARF-2231-3)
effects on heat transfer in Santowax R, 16: 23820 (NAA-SR-Memo-6891)
effects on heavy water decomposition in HBWR moderator, 19: 33604(R) (HPR-57)
effects on heavy water decomposition, 20: 40409(R) (NP-16230)
effects on helium bivalent ion yields in cyclotron sources, impurity, 17: 31222
effects on high-purity vanadium, 16: 19337 (BM-RI-5975)
effects on internal friction peaks in reactor-grade hafnium, 18: 44192
effects on internal friction of niobium, 19: 14053
effects on internal friction in chromium-rhenium alloys, 19: 18420(R) (BMI-1694(Del.))
effects on internal friction in chromium-rhenium alloys, 19: 18421(R) (BMI-1697(Del.))
effects on internal friction in niobium and niobium–titanium alloy, 19: 23035
effects on internal friction of chromium–35 rhenium alloy, 20: 5851
effects on internal friction of recrystallized chromium–0.12 yttrium wires, 20: 7490(R) (BMI-1745, Sect.A)
effects on internal friction of niobium, 20: 11227
effects on internal friction of cold-worked niobium and tantalum, 20: 33893
effects on internal friction of electron-beam refined tantalum, 20: 39420
effects of interstitial, on superconducting critical temperature of niobium, (E), 20: 40025
effects on iodine-128 reaction with methane, 16: 10061
effects on ionization and power loss in theta-pinch plasma, 18: 17167
effects on liquid metal corrosion, mechanisms of, 18: 14401 (BNL-7553)
effects on M-emission bands of molybdenum, niobium, and zirconium, 18: 39197
effects on magnitude of end effects in radiation counters, 19: 30573
effects on Magnox alloy corrosion by carbon dioxide, 20: 7524
effects on maize seeds in water at 3 to 45°C, biological, 20: 14216 (BNL-9859)
effects on mechanical properties of niobium–titanium–vanadium alloys, 16: 2167(R) (ARF-2210-5)
effects on mechanical properties of reactor materials, 16: 22644
effects on mechanical properties of niobium, 17: 32612
effects on mechanical properties of vanadium, 18: 2163(R) (IS-700 (Sect.M))
effects on mechanical properties of chromium, 18: 27956 (IS-745)
effects on mechanical properties of consolidated Zircaloy-2 powder, 19: 6295 (KAPL-3032)

effects on mechanical properties of vanadium, 19: 9658 (IS-994)
effects on mechanical properties of high-melting metals, 19: 11686
effects on mechanical properties of Zircaloy-2, 19: 30784
effects on mechanical properties of chromium, 19: 46912(R) (BMI-1727 (Del.))
effects on mechanical properties of aluminum–copper–iron–tin–titanium–vanadium alloys, 19: 46985 (AD-613651)
effects on mechanical properties of niobium, additive, 20: 5181(R) (ORNL-3029)
effects on mechanical properties of niobium, 17: 20479
effects on metallothermal reduction of titanium and zirconium oxides by magnesium, 20: 7100
effects on microstructure of niobium and tantalum, 17: 36269
effects on microstructure of type 304 stainless steel wire, dilatometric, 20: 41449(R) (EURAEC-1676)
effects on niobium–tantalum weld embrittlement, 16: 3474(R) (USBM-U-863)
effects on niobium–vanadium alloy ductile-to-brittle transitions, 20: 43893 (KAPL-3119)
effects on operation of potassium–sodium heat transfer system in Dounreay reactor, 18: 17310
effects on oxidation of tantalum at 600 to 925°C, 20: 4333
effects on phosphorus uptake by banana leaf disks, effects of light on, 18: 15798
effects on phosphorus-32 uptake by *Eragrostis curvula*, 19: 10780
effects on precipitation of calcium, cerium, and yttrium fluorides, 18: 13766
effects on properties of Zircaloy-2, 18: 44031 (BM-RI-6536)
effects on properties of chromium-yttrium alloys, 20: 37168(R) (BMI-1771)
effects on properties of niobium, 16: 7897 (WADC-TR-57-344(Pt.V))
effects on radiation effects on mechanical properties of iron, 19: 7976(R) (EURAEC-1238)
effects on radiation effects on biological systems, 19: 13026
effects on radiation effects on iron and steel, research program on, 19: 18534(R) (EURAEC-1318)
effects on radiation damage in chicken embryos, 19: 36104
effects on radioinduced chromosome aberrations in Drosophila, 16: 14515
effects on radioinduced mutation frequencies in Drosophila, 17: 35567
effects on radioinduced carbon-14 exchange between carbon dioxide and monoxide, 17: 39161
effects on radioinduced decomposition of plutonium hexafluoride, 18: 43706(R) (ANL-6800(p.197-296))
effects on radioinduced embrittlement of Armco iron, 19: 28871 (EURAEC-1347)
effects on radioinduced decomposition of plutonium hexafluoride, 19: 46325 (ANL-7013)
effects on radioinduced embrittlement of steel, 20: 2474
effects on radioinduced embrittlement of iron, 20: 23801
effects on radioinduced decomposition of 5-bromouracil, 20: 38968
effects on radioisotope fixation in soils, 19: 3832
effects on radiolysis of amino acids, 19: 506
effects on radiolysis of ethylene, 20: 5582
effects on radiosensitivity of Drosophila sperm, 19: 25981
effects on radiosensitivity of roots of *Vicia faba*, 20: 26669
effects on radiosensitivity of Kalanchoe, 20: 31076
effects on reactions of deuterium and hydrogen with oxygen, 17: 39075
effects on reaction of uranium with water, 20: 45683
effects on rolled niobium, structural, 17: 14798
effects on sintering properties of beryllia, 20: 7549 (AAEC/E-138)
effects on solubility of molybdenum and niobium in lithium and potassium, 20: 7579 (TIM-850)
effects on spectra of hydrochloric acid in argon lattice, 20: 12857
effects on stability of europium sulfate, 19: 28332
effects on strain aging and transition temperature in vanadium, 20: 5851
effects on stress corrosion of stainless steel, 19: 24937(R) (EURAEC-1346)
effects on stress-corrosion of austenitic stainless steels, 20: 16969(R) (EURAEC-1579)
effects on structure of niobium by contamination at high temperatures, 20: 4401(T) (ANL-Trans-218)
effects on structure of alpha iron and vanadium, 19: 1951 (BNL-7906)
effects on superconducting current density and resistive transitions in niobium, 18: 22837
effects on tantalum–tungsten alloys, 18: 34059(R) (WANL-PR(Q)-003)
effects on tensile properties of type 304 stainless steel, 20: 27428(R) (EURAEC-1630)
effects on twinning in niobium, 17: 39611
effects on ultrasound aging of wine, 18: 12514
effects on vitality of irradiated Ehrlich ascites tumors, 18: 13555
effects on welding of niobium, 17: 23876(R) (USBM-U-1031)
effects on welding by tungsten inert gas process, 17: 34382
effects on yield strength of niobium, 16: 13612
effects on yields of atomic hydrogen from electric discharge in low-pressure hydrogen, 19: 38590 (UCRL-16050)
effects on Zircaloy-2 corrosion and hydrogen pickup in steam and water, 18: 16440 (WAPD-283)
effects on zirconium corrosion by steam and water, 18: 37632 (A/CONF.28/P/341)
electric arc behavior in, (E), 19: 43454
electric arc performance in, magnetically spun d-c, 17: 24076
electric arc stability in, (E), 19: 6404
electric arcs in gravitationless state in, 20: 6163
electric breakdown in plane-point and plane-wire gaps, 18: 20148
electric breakdown in high-pressure-arc plasma generator, 17: 15343 (AD-277562)
electric breakdown, 18: 32327
electric conductivity at 2000 to 7000°K, effects of seeding with low ionizing potential substances, 16: 21663 (ARL-62-310)
electric conductivity induced by ionization pulse in, 16: 30901(R) (GACD-3178)
electric conductivity of seeded plasma of, 18: 1111 (ARL-63-151 (p.275-93))
electric conductivity of cesium-seeded plasma of, 18: 11318
electric conductivity of alkali-metal-seeded plasma of, (E), 19: 10380 (AEDC-TDR-64-119)
electric conductivity of liquid, (E), 19: 31169 (LA-DC-7026)
electric conductivity of cesium-seeded plasma of, near thermal equilibrium, 17: 33216
electric conductivity of LaB_6 powder suspended in, (T), 20: 41713
electric discharge, radiation intensity at 1250 and 1340 Å, 16: 10752
electric discharge in, electron distribution functions in positive column, 16: 19577
electric discharge in, afterglow temperature and electron collision frequency in, 16: 19463 (AFCRL-984)
electric discharge in, transient intensity pattern in afterglow, 16: 29930
electric discharge in, radiation from, 16: 33654
electric discharge impulse breakdown between coaxial copper electrodes in, at low pressure, 18: 14617
electric discharge in, pinch dynamics of sinusoidally time-dependent currents in, 18: 17160
electric discharges in, effects of electron temperature on dissociation in, 18: 17098
electric discharge in, electron density and collision frequency in afterglow, 18: 17141
electric discharge in, processes in high-voltage, 18: 18468
electric discharge in, triggering mechanism for undervolted, 18: 20149
electric discharge in, theory of self-quenching, 18: 21475
electric discharge in, electron avalanches in, 18: 21490
electric discharge in, electron avalanches in, 18: 21491
electric discharge in, fomative time lags in, 18: 21493
electric discharge in, vortex stabilization of, 18: 21495
electric discharge in crossed fields, rotational properties of, 18: 21501
electric discharge in, ohmic heating in transient, 18: 21522
electric discharge in, photon absorption in, 18: 21474
electric discharge in beams of condensed, 18: 38224
electric discharge behavior in, (E), 19: 5382
electric discharge in, diagnostics of self-quenching cylindrical, (E/T), 19: 11822 (AFCRL-63-343)
electric discharge in, pressure effects on, 19: 16290
electric discharge in, spectroscopic studies of, 19: 23844
electric discharge in, behavior of, in area of sub-normal low pressure, 17: 16802
electric discharge in, ionization processes in, 17: 16812
electric discharge in, dissociative recombination coefficient for, 17: 22711 (AD-283041)
electric discharge in, flash duration in, 17: 36529
electric discharge in, ohmic heating in, 17: 36764
electric discharge in, characteristics of, 17: 38406
electric discharge in, ohmic heating and stability in, 17: 42038 (ARL-63-105)
electric discharge in plasma of, spectral line intensities of trivalent ions in, 17: 42093
electric discharges in gases of, laser-induced, (E), 20: 9844
electric discharge in, electron velocity distribution in low-pressure, (E), 20: 38213
electric discharges in beams of condensed, plasma properties from, 20: 38247
electric discharges in, high-pressure electrodeless, (E), 20: 42509
electric discharge in, intensity of spectral bands from, 20: 44884
electric field effects on cylindrical plasma of, secondary resonances from dipolar, 18: 4660
electric glow discharge in, electromagnetic waves from, 17: 16889
electric polarizability calculation for, by variation-perturbation method, 17: 40799
electric properties of, in semiconducting materials, 16: 33608

electric r-f breakdown of, in nonresonant magnetic fields, 17: 37671
electromagnetic-wave emission from high-temperature nonequilibrium plasma of, energy spectra of, (T), 19: 33424 (R65SD13)
electron absorption and scattering cross sections of, 18: 44450
electron avalanche current in, in electric field, 18: 32940
electron avalanche in, 18: 37856
electron avalanche growth in, visible discharge in, 17: 32786
electron back-diffusion to emitting surface in, 17: 3617
electron beam interactions with, ozone formation and hazards from, 17: 19416 (HW-SA-2664)
electron collisions in, momentum transfer cross sections at low energies, 16: 15630 (NP-11479)
electron collisions with ground and excited states of, 18: 15410
electron collision cross sections at 9.10 and 12.85 ev, 18: 14841
electron collision cross sections and momentum transfer in, 18: 40173
electron collision cross sections for, (E), 19: 37486
electron collisions with, on tungsten surface, 17: 12761(R) (NYO-9813)
electron correlation energy in helium-like atoms of, 18: 5926
electron density in decaying plasma of, 19: 8544
electron detachment from, cross sections for oxygen-ion, 18: 32369
electron diffusion and mobility in, 16: 24281 (NP-11846)
electron diffusion in, at low energies, 16: 24325
electron diffusion coefficient and drift speed in, 18: 16724
electron drift velocity in, at 77 to 443°K, 16: 27742 (NP-11983)
electron drift velocity in gases of, determination of, (E), 19: 18592
electron drift velocity in, (E), 19: 30870
electron drift velocity and mean energy in, determination of, 19: 47124(T) (SLAC-Trans-19)
electron drift velocities in, 17: 7018
electron drift velocity in, at 77.6 and 293°K, 17: 24090
electron drift velocities in, magnetic field effect on, (T), 20: 41628
electron elastic scattering at 295°K, cross sections, 16: 33844
electron elastic scattering by, cross sections for, 18: 32381
electron elastic scattering at 1.5 to 4 ev, resonances in, 18: 32395
electron elastic scattering at low energies, free-electron wave functions for, (T), 20: 11495
electron energies and mobility in gases of, (E), 19: 26953
electron energy distributions in, and rotational excitation, 16: 19569
electron energy distribution in, swarm measurements of, 18: 29768
electron energy losses in, 20: 5542
electron excitation at high pressures, spectra of radiation energy distribution in, 19: 4208
electron excitation and relaxation in molecular, rotational, 17: 25929
electron excitation of molecular, cross section for vibrational, (T), 20: 44125
electron free-free transitions in, method for calculating, 20: 41626
electron inelastic reactions in molecular, collision and momentum transfer cross sections for, 18: 7432
electron inelastic scattering cross sections, 18: 22669 (AROD-3331:5)
electron interactions in plasma afterglow of, probabilities of momentum-transfer (E/T), 19: 3398 (NASA-CR-104)
electron interactions in plasma of, probability of momentum-transfer in, (E/T), 19: 41944
electron-ion attachment and recombination in, 17: 8920(R) (GACD-2461)
electron-ion recombination in, 16: 33946
electron ionization cross sections of, 17: 5142
electron ionization cross sections of molecular, (E), 20: 41652
electron ionization cross sections, 16: 15569
electron loss in electron irradiated, pressure dependence of free, 17: 20646
electron mobility at 0.1 to 100 v cm^{-1} mm-$mercury^{-1}$, 16: 12370
electron multiple scattering by, momentum dependence of, 18: 905
electron multiple scattering at 1000–6000 G-cm, 17: 25939
electron orbitals of molecular, calculation of, 19: 47265
electron pair production in screened nuclear field in, (T), 19: 43280
electron paramagnetic resonance of, in irradiated sodium azide, 17: 35885
electron paramagnetic resonance of free radicals of, in alkali azides, 20: 13970 (AD-611432, pp 135-47)
electron production in, by 30 to 300 ev particles, 18: 10797
electron properties and recombination in ionized, 18: 10767 (RTD-TDR-63-3076)
electron properties to 25,000°K, atomic and ionic, 17: 34559 (RM-3748-PR)
electron reaction with, cross sections for momentum transfer and drift velocities in, 20: 5985 (ORNL-TM-1262)
electron reactions at 1.5 to 4 ev, vibrational excitation in, 16: 8001
electron reactions with atmospheric, excitation and ionization in, 18: 2744
electron reactions with atomic and molecular, ionization cross sections for, 18: 2546
electron reactions at 0.12 to 20 kev, pressure effects on excitation in, 18: 32426
electron reactions at 2 to 3 kev, ionization cross sections for, 18: 32429
electron reactions in discharge afterglow, 18: 32431
electron reactions at 1.7 to 3.5 ev, vibrational excitation in, 18: 34440
electron reactions at 400 to 1500 ev, excitation cross sections for, 18: 44438
electron reactions with, cross sections for rotational excitation in, (T), 19: 8101
electron reactions at low energies, bremsstrahlung from, (T), 19: 16409
electron reactions with, excitation functions for metastable state formation in, 19: 19992
electron reactions with, excitation of long-lived states in, (E), 19: 23320
electron reactions with, emission spectra in, (E), 19: 27064 (LA-3147-MS)
electron reactions with, cross sections for dissociative ionization in, 19: 27078
electron reactions with, cross sections for excitation in, 19: 37466
electron reactions at low energies, energy dependence of ion pair production in, 19: 39375
electron reactions with, classical calculation of cross sections for inelastic, (T), 19: 44947
electron reactions at 20 to 500 ev, excitation and ionization cross sections for, (E), 19: 47245
electron reactions with, vibrational states excited in, 17: 38990
electron reactions with atmospheric, cross sections for, 20: 2859
electron reactions with molecular, ionization cross sections for, (E/T), 20: 5989
electron reactions with molecular, charge transfer in, (E), 20: 9656(R) (GA-6699)
electron reactions with molecular, excitation functions for, (E), 20: 9657 (IPPJ-42)
electron reactions with, excitation total cross sections for, (T), 20: 9661
electron reactions below 0.5 ev, cross sections for, (E), 20: 23897
electron reactions with, primary and afterglow emission from, 20: 29929
electron reactions with rarefied, emission spectra from, (E), 20: 31921
electron recombination rate in heated, temperature dependence of, 17: 31127
electron recombination with oxygen ions in presence of, rate for three-body, 17: 32816
electron scattering by, vibrational excitation in, 18: 16699
electron scattering at 1 to 25 ev, total cross sections for, 18: 32387
electron scattering by, mechanism of excitation and de-excitation of molecular vibration in, 18: 34304
electron scattering by, 18: 40167
electron scattering at low energies, relation to bremsstrahlung of, 19: 8247
electron scattering by atomic, slow, (T), 19: 28988 (58SD222)
electron scattering at low energies by atomic, 17: 13156
electron scattering by atomic and molecular, 17: 34532 (BSD-TDR-63-107)
electron scattering by, spectra from, 17: 36144 (AFCRL-62-1070)
electron scattering by Coulomb field of, phase shift approximation for, 17: 31417
electron scattering by, ionization from, (T), 20: 5982 (AERE-R-5061)
electron scattering at 1 to 25 ev by molecular, total cross sections for, 20: 9678
electron scattering at low energy, resonant, (E), 20: 25743
electron scattering at low energies by molecular, bremsstrahlung effects on resonance, (T), 20: 34096
electron scattering in thin foils of, angular distributions of 100-kev, 20: 35999 (SGAE-PH-40/1966)
electron spin resonance studies of gamma-irradiated, at 4°K, 16: 5239
electron stopping in atmospheric, due to rotational excitation, (T), 19: 41600
electron surface potentials on tungsten crystal faces, 18: 28137
electron temperature in plasma afterglow of, gated microwave radiometer for, 17: 33217
electron temperature of, in afterglow plasma, (E), 20: 44942
electron transitions in ^3S and $^1P^o$ states of, expansion method for E1, 18: 2550
electron transitions in, isotope effects on, 19: 30170
electron transitions of isotopic diatomic molecules of, Franck-Condon factors for, 20: 18658
electron-ion recombination in plasma of, mechanisms of, 18: 40215 (NRC-62-90)
electron-ion recombination in, (E), 19: 19313
electron-ion recombination in plasma of, design and performance of rotating slit-disk device for observing, 20: 34749
electronic collision cross sections and oscillator strengths for, at 10 to 83 ev, 19: 25154
electrons and positive ion drift velocities in, (E), 19: 12096
energy and mass transfer between argon plasma jet and, 20: 15584
energy content of high-temperature, 16: 19256

energy exchange between electron gas and, (T), 20: 39677
energy level transition probabilities of, data compilation on, 20: 31942
energy level transition probabilities and lifetimes in, 20: 37438
energy levels in plasma of, emission and vibration distributions of, (E), 19: 27673
energy levels in, quasibound negative-ion ground-state, (E), 20: 19387
energy levels of, (T), 19: 25168
energy levels of molecular, in aurorae, 18: 28099
energy levels of, Hartree-Fock diagrams for ground-state, (E/T), 19: 8080
energy levels of, hyperfine structure of 2p, (T), 20: 31904 (UCRL-16581)
energy radiated in spectral lines by equilibrium plasma of, (T) 19: 5326(T)
energy storage and transfer in afterglow plasma of, 18: 36720 (RADC-TDR-63-275)
energy transfer to, in iodine fluorescence, 19: 2382
energy transfer with excited argon atoms, cross sections for, 18: 39213
equation of state to 30000°K, 16: 17186
equation-of-state of solid, 17: 2941 (IS-359)
evaporation from titanium, vanadium, and zirconium, 18: 14398
exchange between nitrates and nitrites, 17: 10508(R) (ORNL-3320 (p.22-9))
excitation and reactions of metastable levels, 17: 8914 (AFCRL-62-475)
excitation by electron impact, rotational, (T), 19: 4852
excitation by electron impact, Lyman-Birge-Hopfield bands in spectra from, (E), 19: 9911
excretion, effects of whole-body irradiation on urinary, 16: 14499
explosion tests in gloved box, 20: 41203 (UCRL-16259)
fission fragment energy loss in, 20: 387
fission fragment energy-losses in, (E), 20: 44685
fission fragment reactions with, excitation by, 20: 25734
fission-fragment energy degradation in, (E), 20: 17821
fission-fragment energy loss in, californium-252, (E), 20: 27748
fixation by aurora, contribution to balance in Earth, 19: 18138
fixation by electrochemonuclear process, feasibility, 19: 2201 (BNL-8221)
fixation by fission fragment energy, G value data on, 17: 17945 (BNL-6852)
fixation by *Trichodesmium* plankton, 16: 4029 (TID-12946(App.I, Vol.I))
fixation in lake waters, tracer study, 17: 33600
fixation of, radiochemical process for, 16: 29023
fixation of, development of chemonuclear processes for, 19: 36453 (BNL-8836)
fixation of, development and economics of chemonuclear processes for, 20: 43300
fixation of, magnetohydrodynamic process for, (T), 19: 9982
fixation, radioinduced process for, 16: 17946 (BNL-5728)
fixation, radioinduced process for, 17: 39163(P)
fixation using plasma torch, 20: 45631(R) (ORNL-3945, pp 259-69)
flow and heat transfer, ion motion effects on, 18: 12312 (ASD-TDR-63-842)
flow and heat transfer in transverse electric fields, ionization effects on, 18: 27681
flow characteristics of liquid, discharging into a vacuum, 17: 41661
flow in arc discharge, theory of constricted, 18: 27680
flow in cylindrical wall stabilized arcs, Hagen-Poisville, (T), 19: 26955
flow in heated tube, heat and momentum transfer at high wall-to-bulk temperature ratios in turbulent, 19: 24676 (SU-247-7)
flow in magnetic fields, transverse momentum transport in viscous, (E), 20: 28073
flow in round tubes, effects of large temperature gradients on friction and heat transfer in turbulent, 18: 41624
flow in straight circular tubes during chill-down, two-phase, 20: 10996 (WANL-TNR-154)
flow of liquid-vapor mixtures of, solutions for choking, 17: 28097
flow through electric arcs, radiation from, (E/T), 19: 11823 (ARL-64-49(Pt.II))
flow through tungsten wire meshes, heat transfer and pressure drop correlations, 19: 36610 (NASA-TN-D-2924)
fluorescence from vacuum-uv excited, 18: 28176
fluorescent excitation by α particles, 16: 7962(T) (CEA-tr-A-965)
flux in primary cosmic radiation, (E), 20: 41672
gamma absorption coefficient, 16: 6655
gamma absorption coefficients, 16: 12454
gamma attenuation coefficients at 0.01 to 100 Mev, 20: 36350
gamma ionization rates in ionosphere, 16: 12314
gamma reactions at 170 Mev, absolute yields from, 16: 18529
gamma reactions at 0.01 to 10 Mev, cross sections for, 20: 4996 (AWRE-O-79/65)
gamma reactions with, disintegration and mesons (π) from, 19: 1632
gamma spectra from 14-Mev neutron activation of, determination by, 19: 26241
glow discharges between plane parallel electrodes in, properties of, (E), 20: 36090
Hartree-Fock potential of neutral atoms of, analytical expressions for, 18: 16656
heat of desorption, 17: 33159(R) (ORNL-3472(p.107-18))
heat of vaporization of, calculation from rigid-sphere equation of state, 18: 224
heat transfer and wall friction in small tube at high temperatures, 17: 38447 (TID-7653(Pt.I)(p.74-81))
heat transfer and mass transfer across interface of suddenly pressurized liquid-vapor system, 19: 22499
heat transfer by boiling, in narrow annuli, 19: 9343
heat transfer by, review on boiling, 19: 34324 (NASA-CR-243)
heat transfer coefficients for, 20: 12341
heat transfer for, nucleate boiling, 18: 26462
heat transfer from water to liquid, in heat exchanger, 18: 40979 (LA-DC-6410)
heat transfer in boiling, electroconvection effects on, 16: 25533
heat transfer in boiling, 20: 16610
heat transfer in forced and free convection, effects of electric field on, 16: 27191 (CEA-2122)
heat transfer in, on a heated porous plate, film-boiling, 17: 39255
heat transfer in tubes to liquid, acoustic pressure oscillations in convective, 19: 28501 (LA-DC-6945)
heat transfer to boiling, in straight circular tubes, 20: 10996 (WANL-TNR-154)
helium and hydrogen ion attenuation at 0.1 to 500 Mev, tables for, 20: 41619 (CEA-R-3042)
helium atom reactions at 0.04 to 1 kev, ionization cross sections for, 18: 32450
helium ion energy-range relations in, 18: 14726 (UCRL-10647)
helium ion interactions at 0.133 to 1 Mev, free electron and ion production in, 17: 32731 (TID-19137)
helium ion ionization of, cross sections for, 17: 16886
helium ion ionization of, cross sections for, 17: 32771
helium ion reactions at 0.15-1 Mev, charge transfer and ionization cross sections for, 17: 25865(R) (TID-18705)
helium ion reactions at 0.133 to 1.0 Mev, ionization cross sections for, 18: 42317
helium ion reactions at 0.133 to 1.0 Mev, ionization cross sections for, 18: 42318
helium ion reactions at 0.18 to 1.0, charge transfer and ionization in, 19: 18684(R) (TID-21565)
helium ion reactions at 20 to 120 kev, electron capture in, (E), 19: 39407
helium ion reactions with, helium excited states population in, 20: 7745
helium reactions at 30 to 1000 ev, ionization cross sections for, 18: 36162
helium reactions with, electron kinetic energy from ionization in, (E), 20: 29927
helium-3 scattering at 29 Mev, optical potentials for distorted wave analyses of, 17: 38184
helium-atom and -ion scattering by, electrons and ions from, 20: 11447(R) (TID-22476)
helium–ion reactions at 3 to 600 ev, charge transfer in, 20: 4759
helium-3 elastic scattering at 24 to 29 Mev, 18: 19007
helium-3 reactions (He-3,n) at 19 to 25 Mev, angular distributions and cross sections for, (E), 20: 22132
hydrogen abstraction from bonds with, in ethylenimine, isotope effects on, 20: 23024
hydrogen atom reactions with molecular gases of, emission spectra from, 17: 41641(T)
hydrogen ion interactions with, 17: 37646 (KN-62-133(R))
hydrogen ion reactions at 10 to 180 kev, dissociation in, 18: 24324
hydrogen ion reactions at 25 to 250 kev, charge exchange, dissociation, and ionization in, 18: 32457
hydrogen ion reactions with, Lyman alpha emission from, (E), 19: 8112
hydrogen ion reactions at 10 to 50 kev, equilibrium fractions in, (E), 19: 14243
hydrogen ion reactions at 14.6 Mev, electron detachment from negative, (E), 19: 28999
hydrogen ion reactions with, cross sections for, (E/T), 20: 15886(R) (UCRL-14285)
hydrogen ion reactions with, lifetime of n = 3 hydrogen states from, (E), 20: 29930
hydrogen ion reactions at 20 to 120 kev, ionization cross sections for, 20: 31909
hydrogen ion reactions at 2 to 50 kev, charge exchange and dissociation cross sections for, 20: 41646
hydrogen replacement by, in nitrogen-14 (n,p) reactions in organic compounds, 16: 11741
hydrogen-ion ionization of, cross sections for, 17: 32771
hydrogen-ion reactions at 20.9 Mev, dissociation cross sections for

molecular, (E), 20: 27742
hyperfine structure in atomic, pressure shifts of, 17: 11387
hyperon (Λ^0) reactions, cross sections for hyperfragment formation in, 17: 13601
incorporation in grain and stalk of ripening wheat, tracer study of, 17: 2717
incorporation in tantalum during heat treatment, 19: 18401(R) (WANL-PR(Q)-005)
incorporation in 4-amino-2-hydroxybutyric acid and methyl ester of anthranilic acid, 20: 41024
interactions of gas with plasma at 5 to 200 μ of mercury, 16: 23215
interactions of molecular, with molecular nitrogen ions at 1 to 10 kev, cross sections for emissions from, 18: 12839
interactions with metastable helium atoms, de-excitation cross sections, 16: 30972
interactions with metastable helium atoms, calculation of de-excitation cross sections, 16: 30973
interactions with hydrogen atoms, cross sections for molecular, 20: 44146
internal energies, 16: 22709 (AD-271032)
ion beam reactions with gaseous, charge exchange in, (E), 19: 29008
ion beam reactions with, charge exchange in negative, 20: 7729
ion cyclotron resonance and collision cross sections in weakly ionized, 17: 31604
ion density and velocity in plasma of, from pulsed coaxial gun, (E), 19: 6818
ion drift velocities in, 18: 32473
ion drift velocities in, 18: 32479
ion drift velocity in, 18: 16060
ion energy loss in, below 10 Mev/amu, 17: 671
ion exchange in concentrated hydrochloric and perchloric acids, distribution coefficients for, 18: 17759
ion mobilities in liquid, positive, 18: 34343
ion-neutral reactions in afterglows, 16: 24276 (GA-2824)
ion pair formation by x radiation, mean energy, 16: 246
ion pair production by protons and helium ions, measurement of work/ion pair, 16: 19493
ion pumping mechanism for, in Bayard-Alpert gage, 18: 22241
ion reactions at 0.4 to 2 kev, charge exchange and excitation in, 18: 32449
ion reactions at 0.4 to 2 kev, radiation emission from, 18: 36145
ion reactions at 1 to 30 kev, charge exchange cross sections for alkali metal, (E), 20: 34112
ion reactions at 40 to 1000 ev, beam excitation effects in, 18: 32468
ion reactions with, spectra from, 18: 2523 (AFCRL-816)
ion reactions with, review of charge transfer, 18: 32472
ion reactions with molecular, charge exchange in atmospheric, (E), 20: 9656(R) (GA-6699)
ion reactions with, charge-exchange cross sections for fast negative, 20: 34110
ion reactions with, at 10 to 100 kev, energy losses in, (T), 20: 35998(R) (ORO-2911-7)
ion scattering by, use for production of neutral beams, 19: 2983
ion stopping by, at 50 kev, 18: 32288
ion velocity distribution in, in electric fields, (E), 20: 17298
ion wave propagation in weakly ionized plasma of, damping and phase velocity of, (E), 20: 38294
ion waves in weakly ionized plasma of, longitudinal, (E), 19: 35553
ionic mobility of cesium and rubidium in, at high pressures, (E/T), 22: 16415 (CEA-R-2861)
ionization by alpha particles, slow component in, 17: 16849
ionization by alpha particles, impurity and temperature effects on energy of, 18: 18467
ionization by argon and neon ions, cross sections for dissociative, 18: 40128
ionization by electrons, cross sections and efficiency curve, 16: 1764
ionization by electrons at 1 mm pressure, mass spectrometric study of, 17: 33901
ionization by electron impact, 18: 16720
ionization by electron impact at energies up to 500 ev, cross sections for dissociative, 19: 14127 (FSU-2690-14(Paper 1))
ionization by electron impact, cross sections near threshold, 19: 14128 (FSU-2690-14(Paper 2))
ionization by electron impact, appearance potential for doubly charged molecule ions in, 19: 20807(R) (UCRL-11828(p.201-4))
ionization by electrons at 0.6 to 20 kev, (E/T), 19: 20850
ionization by fast helium atoms and monovalent ions at 15–180 kev, cross sections for, 17: 41649
ionization by gamma radiation and neutrons, 18: 10346(R) (X64-11113)
ionization by heavy ions at 25 to 50 kev, total, (E), 20: 2623
ionization by helium ions and protons at 200 to 900 kev, energy loss per ion pair in, 17: 25881
ionization by helium ions, cross sections for, 17: 36451 (TID-19296)
ionization by helium ions, cross section for, 18: 12829(R) (TID-20169)
ionization by hydrogen atoms and protons at 10 to 180 kev, cross sections, 16: 18277
ionization by protons, cross sections for, 16: 15631 (ORO-539)
ionization equation for optically thin plasma of, (T), 20: 32636
ionization in uniform increasing magnetic yield, (E), 20: 11768 (JUL-327-PP)
ionization of, by electrons at 0.6 to 20 kev, cross sections for, (E/T), 20: 31906
ionization rates in d-c electric fields, (E), 20: 12169 (JUL-322-PP)
ionization by metastable helium atoms, cross sections, 16: 24296
ionization by metastable helium ions, relative cross sections for, 19: 6479
ionization by protons at 0.15 to 1.1 Mev, cross sections, 16: 19559
ionization by x rays at high energies, spectra of, 18: 41506(R) (ML-TDR-64-169)
ionization cross section for, electron-impact, 19: 38630
ionization currents induced by gamma rays, between electrodes, 19: 13726 (NARF-63-16T)
ionization efficiency curves, effects of instrumental factors on, 16: 15296
ionization in atomic and molecular collisions, (E), 19: 14264
ionization in electron-bombardment ion sources, 19: 38838
ionization in microwave discharge in, electron production by collision, (E), 19: 18716
ionization in pulse discharge, 16: 877
ionization of atmospheric, by geomagnetically trapped electrons, 18: 22813
ionization of atomic, by 25- to 750-ev electrons, 16: 33636
ionization of cesium by homogeneous recombination, 16: 1771
ionization of, effect of oxygen and water vapor on, 17: 11047
ionization of molecular by molecular at 30 to 1000 ev, cross sections, 16: 6855
ionization of molecular, during collisions with molecular oxygen, 17: 6864
ionization of, isotope effects on Franck-Condon factors in, 19: 38632
ionization potential in reactions with carbon monoxide ions, 18: 26229
ionization stage of separated beams of, spectral determination of, (E), 19: 37473
isotope content in natural, 18: 13691
isotope effect in crystals, contribution of delayed rotation of the molecule to, 17: 2699
isotope shifts in ultraviolet systems, 17: 35732
isotopic analysis by mass spectrometry, 19: 17843
isotopic analysis of, by emission spectroscopy with photoelectric recording, 20: 16375
isotopic analysis of, by emission spectroscopy, 20: 16376
isotopic exchange in gaseous, effects of gases and silica wool on gamma- and x-ray-induced, 18: 9752 (IA-900)
isotopic exchange between nitrogen and nitrogen oxides, 18: 9752 (IA-900)
leakage in pressure vessels, mechanism and rate, 20: 30810
level control design, 17: 1175(R) (HW-70050(p.31-77))
level control for liquid, 16: 29102 (HW-SA-1993)
level control in Dewar flask, method for, 16: 25413(R) (NP-11882)
level indicator for liquid, 18: 14666 (BNL-6940)
lifetime of radiolytic atomic, 19: 26917(R) (IA-984)
light absorption by fully ionized plasma of, (T), 19: 10390 (IPP-6/27)
light absorption coefficients, monochromatic, 16: 4155 (GA-2528(Vol.III))
light intensity from electron-excited, in auroral storms, 20: 21826
liquefaction of, book, 18: 15122
liquefier description, 16: 2341
lithium halide infrared spectra in matrix of, 18: 27405
lithium ion collisions with molecular, rotational energy levels in nitrogen ions from, (E), 19: 27099
lithium-6 reactions at 0.6 to 3.75 Mev, molecular stopping power for, (E), 19: 23297
loss and production in electric discharges, effects of impurities on, 19: 32048(R) (NP-15073)
loss and uptake by rice, tracer studies of, 19: 31696
magnetic shielding constants, 16: 29523
maser collision processes in, optical, 18: 32484
mass attenuation coefficients at 6 to 12 kev, 16: 28980 (TID-16424)
mass difference with ethylene, (E), 19: 28336
mass difference with methylene, (E), 19: 28336
mass difference with carbon monoxide, (E), 19: 28336
mass spectra of ionized, Aston bands from charge-exchange and dissociation, 16: 19555
mass transfer from potassium–sodium/stainless steel loop to niobium–zirconium alloy at 1250°F, 19: 34640 (CNLM-6246)
mass transfer from type-316 stainless steel to niobium–zirconium alloy by liquid potassium, 20: 2239
mass transfer from stainless steel to niobium and niobium–zirconium

alloy, in potassium–sodium alloy, 20: 5181(R) (ORNL-3029)
meson (K^-) capture by, hyperfragment production in, (E), 19: 10020 (UCRL-11328(Rev.1))
meson (π^-) capture by, two-nucleon emission from, (E), 20: 19842 (UR-875-126, Paper 1)
meson (π^-) reactions at 7.5 Bev, 18: 24390 (JINR-P-1624)
meson (π^-) reactions at 7 Bev, 18: 24391 (JINR-P-1629)
meson (K^-) capture, star properties from, 16: 12357
meson (K^-) capture in emulsion, Auger electron spectra from, 17: 26568
meson (μ^-) capture and decay in, electron spectra, 16: 4725
meson (μ^+) decay asymmetry in, 16: 10958 (NEVIS-99)
meson (π^-) capture by, single charged particle emission in, 17: 11679
meson (π^-) reactions at 7 Bev, meson (η) radiative decay in, 17: 17119 (JINR-P-1164)
meson (π^+) reactions with, quasi-deuteron formation in, 17: 40433(R) (NYO-10063(p.71-89))
meson(μ^-) capture by, lifetimes and rates of, 18: 40572
metabolism by algae, 16: 4029 (TID-12946(App.I,Vol.I))
metabolism by marine algae, fixation rates for, 19: 2020
metabolism during radiation injuries, 16: 16294
metabolism in pigs, effects of vitamin A content of foods on, 19: 17641
metabolism in yeasts, radiation effects, 17: 5881
microwave energy absorption in magnetoplasma of, (E), 19: 37905 (AD-426186)
microwave gyro-interactions in magneto-plasma of, electron cyclotron resonance absorption of energy from, 17: 33215
microwave propagation in plasma of, cyclotron resonance echoes from, (E), 19: 33474
molecular beam production, design and performance of 5- to 1000-ev source for, 16: 7714
molecular properties of (E), 19: 2979
molecular spectra, 16: 15365
molecular structure of, orbital density in, 20: 5524 (ANL-7076)
molecular vibration de-excitation in collisions with atoms or molecules, 16: 12255
momentum transfer on metals at 25 to 550°C, 16: 13692 (HE-150-182)
motion of plasma of, in arc jets, (E), 19: 16295
neon-20 reactions at 200 Mev, in emulsions, (E), 20: 40083
neutron absorption cross section in pitchblende, thermal, 20: 37994
neutron activation of, transport system for in-pile, 19: 19416 (IS-1012)
neutron activation products of, analysis of gamma spectra of fast, 19: 32058(R) (GA-5978)
neutron capture gamma spectrum of, thermal, 17: 41873 (WASH-1044)
neutron cross sections at 0.025 ev to 18 Mev, 16: 24796 (UNC-5002)
neutron cross sections for, 17: 39976 (NARF-62-17T)
neutron cross sections from 0.037 ev to 18 Mev, tables of, 20: 44661 (UNC-5139)
neutron differential scattering cross sections at 14 Mev, 16: 1072
neutron elastic scattering at 1.595 to 3.207 Mev, differential cross sections for, (E), 20: 24354 (ORNL-P-2026)
neutron inelastic removal cross sections, 16: 24408
neutron reactions at 0.1 to 100 Mev, total cross sections for, 16: 11021
neutron reactions (n,α) at 14 Mev, angular distribution of alpha particles from, 17: 19306
neutron reactions (n,γ) with, gamma spectra from fast, 18: 44807
neutron reactions (n,2n) at 14.8 Mev, cross sections for, (E), 19: 12592
neutron reactions (n,n'γ) at 0 to 14 Mev, energy absorption in, 19: 39769 (SC-DC-65-1544)
neutron scattering by, formulas for, 16: 33791 (KR-26)
neutron scattering cross sections at 14 Mev, 17: 33006 (UCRL-7192)
neutron scattering by, angular distribution for, 17: 38028(T) (AEC-tr-5734(p.164-6))
neutron scattering at 14 Mev, 18: 11226
neutron scattering amplitudes for, coherent, (T), 19: 27555
neutron scattering by liquid, quasi-phonon dispersion for cold, (E), 20: 44598
neutron separation energy, (E), 20: 24329(R) (ANL-7108, pp 1-4)
neutron total cross sections at 0.01 to 10 kev, 16: 25586
neutron total cross section of liquid, 18: 38610 (A/CONF.28/P/615)
neutron total cross sections of gaseous and liquid, effects of close-range order on, 18: 40634
neutron total cross section from 90 to 150 Mev, (E), 19: 23808
neutron total cross sections of gaseous and liquid, coherent effects in thermal, 19: 35354
nitrogen ion bombardment of, optical excitation in, 17: 32707 (CONF-46-43)
nitrogen ion motion in, in electric fields, (E), 19: 37218
nitrogen ion reactions, 16: 29881(R) (ORNL-1383)
nitrogen-ion reactions on, distributions from, 17: 12829
nitrogen ion reactions at 2.65 kev, charge transfer cross sections for, (E), 19: 14231 (AFCRL-63-709)
nitrogen ion reactions at 0.14 to 0.7 Mev, energy loss in, (E), 20: 2602
nitrogen-15 EPR and NMR in, (E), 19: 22654 (CEA-R-2506)
nuclear magnetic shielding of the nitrogen atom in molecular, 18: 13111
nuclear magnetic shielding in, theory of, 18: 33563
nuclear quadrupole resonance of nitrogen-14 in solid, at 1.5 to 34.5°K, 16: 16354
nuclear quadrupole resonance, 17: 10592 (IS-520)
nuclear reactions of ionized with nuclei, 16: 29881(R) (ORNL-1383)
nucleation pressure of liquid, as function of temperature, 18: 44680
optical resonance absorption by atomic, in afterglows, 18: 32441
oxidation of magnesium by, 17: 6577
oxygen ion reactions at 15 to 50 kev in, equilibrium fractions for, (E), 19: 18687
oxygen ion reactions at 0.14 to 0.7 Mev, energy loss in, (E), 20: 2602
oxygen reactions with exospheric, interchange coefficients for, 18: 22812
performance for uptake of fission gas in passage through boiling-water reactors, 19: 31516(P)
performance in fission chambers, 20: 5734 (LFEN-NI-19)
performance in heat exchangers for hydrogen liquefaction, 19: 23547
performance in magnetohydrodynamic accelerators, 17: 15011
performance in plasma arc tunnel, (E), 19: 14670 (SC-RR-64-1701)
performance in spark counters for fast neutrons, 19: 15892
phosphorescence of, 18: 37857
photoelectric effect at 852 ev to 40 kev in, cross sections for, (E), 20: 21523
photoionization and absorption cross sections, 18: 16718
photon absorption coefficients and mean opacities, 16: 4153 (GA-2528 (Vol.I))
photon absorption in, 17: 37646 (KN-62-133(R))
photon diffusion in gases of, (T), 19: 42931(T) (ORNL-tr-681)
photon reactions (y,p) at 4.1 to 6.2 Bev, (E), 20: 30432
photon reactions at 6 BeV, antiproton production in, (E), 20: 46348(T) (SLAC-Trans-44)
photon reactions with Coulomb field of, pair production total cross sections for high-energy, (T), 20: 17754
physical properties of liquid, to 50,000 lb/in.^{2}, 18: 15044 (LADC-5956)
physical properties of plasma of, at 8000 to 13,000°K, (E), 19: 14655 (ARL-64-180)
pinch discharge in, instabilities in, 17: 4185
pinch discharge in, axial streams in Z, 18: 21531
pinch discharges in plasma of, structure of large-radius, 17: 35030
pinch-effect collapse in, streamer formation at 1 to 100 μ mercury, 16: 28284
pinch effect in, pressure-dependent characteristics of Z, 17: 21169
plasma afterglow in, 18: 1125 (NASA-TN-D-2226)
plasma column stability in, 17: 20632
plasma jet, performance in arc-heated, 16: 19632
plasma jets in, voltage fluctuations in d-c, (E), 19: 25569
plasma jets of, characteristics of pinch, 17: 33196
plasma jets of, electric current and field distribution in, 17: 33203
plasma jets of, performance of coaxial, 17: 33207
plasma, microwave diagnosis of a partly ionized flow in the presence of a magnetic field, 17: 40211
plasma of, acceleration, 17: 33192
plasma of, electric and microwave properties of seeded, 17: 40155 (ARL-63-159)
plasma of, in positive column at 1 torr, Hall effect and electron drift velocities of, 18: 4678
plasma of, wave patterns in supersonic flow around plate model, 17: 42121
plasma of, containment in DCX-2, 20: 1270(R) (ORNL-3836, pp 15-32)
plasma of, development of emitter electrodes for, (E), 19: 20905 (SC-RR-65-54)
plasma of, measurement of magnetic fields in, by Zeeman effect, 18: 19190
plasma of, microwave diagnostics of high-speed flows of, 18: 19210
plasma of, partition functions and thermodynamic properties of, 18: 28756 (AEDC-TDR-64-22)
plasma of, partition function and thermodynamic properties of, (T), 19: 43430
plasma of, spectra of continuum radiation from arc-heated, 18: 17135
plasma of, temperature measurements by spectroscopic method in, 18: 21406
plasma production in, by follow-cathode electric discharges, 16: 29922
plasma, production of optically thick, 17: 21155
plasma properties of, for use in electro-thermal engines, 17: 9674 (ASD-TDR-62-451)
plasma Z-pinch implosion in, photographic evidence of delayed, 17: 42063
plasmas, effects of magnetic fields on, 16: 9506(R) (ORNL-3239(p.16-46))
plasmas of, electron collision frequency and density in, 17: 19442(R) (AD-283512)
polarization, theoretical basis for calculation, 16: 21121 (AFCRL-1062-I)
positron and positronium decay in, fine structure, 18: 4400 (NP-13341)

positron annihilation in condensed gases of molecular, 17: 26335
positron annihilation in liquid, angular distribution of photons from, (E), 20: 32345
positron annihilation in, (E), 20: 37810
positron mean life in molecular, 18: 707
positron multiple scattering by, momentum dependence of, 18: 905
positron multiple scattering at 1000–6000 G-cm, 17: 25939
positron range distribution in, 18: 4580 (NP-13370)
positronium annihilation and formation in, electric field effects, 16: 13683 (AROD-2211.3)
positronium decay and formation in, 18: 4398 (NP-13329)
positronium decay and formation in, 18: 4399 (NP-13330)
positronium formation in, effects of d-c electric fields, 16: 9324
potential energy curves, 18: 34281 (RM-4034-PR)
precipitation kinetics in chromium–uranium alloys, 20: 35927
preparation of condensed beams of, 17: 1800
pressure in niobium and niobium–zirconium alloy at 1500 to 2100°C, equilibrium, 19: 13991 (ML-TDR-64-134)
pressure of, over beryllium nitride at 1640 to 1950°K, 20: 12830 (UCRL-7802)
production and acceleration of plasma of, in betatrons, (E), 19: 12008
production and trapping in x-irradiated sodium azide at low temperatures, 16: 5250
production in propane radiolysis in presence of nitrous oxide, mechanisms for, 18: 31616
production in radiolysis of nitrous oxide, catalytic effects of beta particles on, 18: 37191 (BNL-874(p.39-40))
production in swimming pool reactors, 16: 26495(T) (TID-7622(p.310-15))
production of beams of molecular, method for, (E), 19: 6446
production of compounds of bound, by radiative processes in aqueous solutions, 20: 25160
production of molecular beams of, by nozzle sources, 18: 40159
production of molecular beams of, by nozzle sources, 18: 40160
production of molecular ions in atmosphere, crossed molecular-ion beam interactions for absolute cross section for, (E), 20: 19670
production of plasmas of, spectroscopic studies of, 20: 17902
production of rotating dielectric plasma of, 18: 36746
production of rotating plasma of, in crossed fields, (E), 20: 30582
production plant using expansion turbines with gas bearings, 19: 42618
properties and reactions in stainless steel, effects of uranium on, 19: 30804
properties as nuclear poison, 16: 7795
properties as plasma burner gas, 17: 22103(T) (AERE-Trans-931)
properties as reactor coolant, 16: 12832
properties as reactor coolant, 16: 23830 (BNL-5377)
properties as working medium in closed-cycle turbine, 20: 42654
properties for use as reactor coolant, 16: 34071 (NYO-9786)
properties for use as reactor coolant, 18: 31002
properties in aluminum–copper–magnesium degassing, 17: 12601
properties of arc-heated plasmas of, electron, 17: 33439
properties of arc plasma of, electrical, thermal, and radiative, (E/T), 19: 5361
properties of, in two-phase flow with mercury, 17: 18257 (ANL-6625)
properties of, thermodynamic and transport, 18: 1112 (ARL-63-151 (p.294-321))
properties of, behind shock waves, 18: 24235
protective effects against radiation injury to bean seedlings, 16: 32866
protective effects against radiation injury to rabbit spermatozoids, 17: 35498
protective effects against radioinduced mutations in Drosophila, 18: 11887
protective effects against x radiation in *E. coli*, 18: 31293
protective effects against radiation in *Vicia faba*, 18: 31294
protective effects of compressed, against radiation damage in bean seedlings, 19: 26139
proton attenuation, 17: 18909 (TID-18436)
proton elastic scattering at 7.6 to 11.8 Mev, polarization in, 20: 6439
proton elastic scattering at 12.6 to 13.6 Mev, angular distribution of polarization from, (E), 20: 30457
proton energy losses in, 18: 16713
proton ionization cross sections, 16: 15569
proton ionization of, cross sections in, 17: 16886
proton reactions, 17: 28686(R) (UCRL-10683(p.1-14))
proton reactions (p,α) at 660 Mev, (E), 19: 27484
proton reactions (p,n) at 15.1 and 18.5 Mev, cross sections for, (E), 20: 46933(R) (ORNL-3973(Vol.2), pp 85-95)
proton reactions at 9 Bev, angular and multiplicity distributions of secondaries from, 16: 28161
proton reactions at 5-130 kev, radiation spectra from, 18: 5924
proton reactions at 97 Mev, delayed emission in, 18: 6189
proton reactions at 220 Mev, cross sections for beryllium-10 production of, 18: 17049
proton reactions at 5 to 130 kev with, spectroscopic study of, 20: 7741
proton reactions at 2 to 35 kev, Balmer-alpha radiation in, (E), 20: 17269
proton reactions at 13 Mev, cross sections for, (E), 20: 19941
proton reactions at 1 to 100 Mev, electron capture by, (T), 20: 27739
proton reactions at 5 to 115 kev, cross sections for electron capture by, (E), 20: 27746
proton reactions at 50 to 200 kev, secondary electron emission in, (E), 20: 29951
proton reactions at 140 Mev, bremsstrahlung production in, (E), 20: 46674
proton reactions following single pass through Van Allen radiation belts, 16: 9761(R) (UCRL-9897(p.131-3))
proton reactions (p,α) at 660 Mev, alpha energy from, 17: 9540
proton reactions with atomic, electron capture in, 17: 22484
proton reactions with, emission and excitation from, 18: 14716 (AFCRL-63-225)
proton reactions with, electron production cross sections for, 18: 14724(R) (TID-20298)
proton reactions with, lithium-6 and -7 fragments from, 18: 16977
proton reactions with molecular, formation of highly excited atomic hydrogen by, (E), 19: 8108
proton reactions with atomic, electron capture in, (T), 19: 34886
proton reactions with, electron-capture cross sections for, (E/T), 20: 15886(R) (UCRL-14285)
proton reactions with, performance of triggered cloud chamber for analyzing, (E), 20: 21063
proton reactions with molecular, emission spectra from, 17: 41641(T)
proton scattering near 100 kev, ionization cross sections, 16: 21218
proton scattering by, isotope effect in, 17: 19247
pumping liquid, in vacuum-system traps, 18: 4370 (TID-18459)
pumping of liquid, centrifugal pump for, 19: 18250
pumping system for liquid, design of automatic, 16: 17779 (TID-15483)
purification, 16: 1856 (K-1477)
purification, 16: 8707 (AERE-R-3710)
purification, 19: 17843
quadrupole moments, 19: 39378
radiation absorption and photoionization cross sections below 1100 Å (E), 19: 3156
radiation absorption coefficient of, photoionization contribution to, (T), 19: 20830
radiation and burn injury effects on content of, in rats, 18: 33381
radiation and/or thermal trauma effects on content of, in rat intestinal mucosa, 20: 12630 (BNL-8383)
radiation attenuation by, critical energies and units for, 17: 38420
radiation doses to tissues from, in solar particle beams in space, 20: 37023 (N-65-33865)
radiation effects on chemical reactions with coal, 16: 570 (NP-10822)
radiation effects on availability in soils, 16: 16176 (NP-11578)
radiation effects on content of, in cell extracts, 16: 32826
radiation effects on liquid, 17: 11264(R) (NP-12388)
radiation effects on liquid, 17: 14317(T) (AERE-Trans-905)
radiation effects on oxidation kinetics of, slow electron, 17: 28947(T) (NP-tr-1035)
radiation effects on oxidation kinetics of, fast electron, 17: 28948(T) (NP-tr-1036)
radiation effects on explosive properties of liquid, 17: 29899
radiation effects on content of, in soils, 17: 39143
radiation effects on fixation in *Azotobacter vinelandii*, 18: 8127
radiation effects on rabbit and rat blood content of, biochemical indexes of chronic low-dose gamma, 18: 13515
radiation effects on fixation in rumen lining, 18: 21893
radiation effects on, dissolved in platinum electrodes, 18: 27952(R) (EURAEC-926)
radiation effects on reactions with reactor graphite, 19: 1008(T) (JPRS-26808(p.157-68))
radiation effects on content of in proteins in muscle tissues in rats, 19: 7157
radiation effects on content of, in rat urine, 19: 2104
radiation effects on fixation of, in *Rizobium japonicum* in symbiosis with soybeans, 19: 12963
radiation effects on content in rat testis, 19: 13072
radiation effects on rat urinary excretion of, protective effects of casein diets against, 19: 19628
radiation effects on production of atomic, 19: 26382(R) (RPI-321-1)
radiation effects on mouse metabolism of, protective effects of bone marrow against x, 19: 31905(R) (ORNL-3768(p.99-108))
radiation effects on metabolism of, in frog liver, 19: 31882
radiation effects on content of, in blood of dogs, 19: 33869
radiation effects on metabolism of, in frogs, 19: 33933
radiation effects on metabolism of total α-amino-, in man, 19: 43852
radiation effects on diffusion in polyethylene, 20: 407
radiation effects on metabolism of, in dogs, β and γ, 20: 5381
radiation effects on content of, in cultured chick embryo heart and intestine, x, 20: 8649

radiation effects on electric conductivity of, 20: 4949(R) (UCRL-14360, pp 85-94)
radiation effects on excretion of, by isolated frog liver, γ, 20: 10551
radiation effects on frog serum content, gamma, 20: 18243 (NIJS-R-454)
radiation effects on distribution of, in mice treated with bone marrow, x, 20: 20407 (ORNL-P-1118)
radiation effects on, effects on algal nitrogen fixation of uv, 20: 20408
radiation effects on content of, in milk after mammary gland exposure in cattle and goats, gamma and x, 20: 22594
radiation effects on metabolism in rat brain, x, 20: 26696
radiation effects on frog liver metabolism of, effects of blood serum, spleen extract, and splenectomy on gamma, 20: 35307
radiation effects on content in soils, effects of soil type on gamma, 20: 40637(R) (ORO-2754-7)
radiation effects on metabolism of, in frog liver, gamma, 20: 42787
radiation effects on oxidation of, electron and ion recombinations in, 20: 43354
radiation effects on content in serum of rabbits, x, 20: 42870
radiation effects on metabolism of, following therapy, x, 20: 45447
radiation effects on free amino acid, in rat liver mitochondria, x, 20: 45339
radiation emission at high temperatures, 16: 4603 (AFSWC-TR-61-72 (Vol.I))
radiation fixation, 16: 10078
radiation fixation of, developments in, 20: 16506 (BNL-10020)
radiation from a-c arc plasma of, 18: 1116 (ARL-63-151(p.388-445))
radiation from arc plasma of, 18: 1114 (ARL-63-151(p.336-79))
radiation from arcs of, analysis of, 19: 44804 (ARL-65-105)
radiation from high-temperature gas of, pressure and temperature dependence of, (E), 20: 32240
radiation from, shock-initiated, 18: 28168
radiation kinetics from nitrous oxide decomposition, 16: 17843
radiation stability effects on oxide fuels, 16: 6698 (WAPD-251)
radiation stopping power of, shell corrections to, (T), 19: 4401 (ORNL-P-659)
radiative rates in plasma of, 18: 42794 (R64SD-41)
radioinduced addition of, to tetrachloroethylene, effects of pressure and temperature on gamma, 20: 33348
radioinduced conductivity in gaseous, 17: 22218(R) (GA-4164)
radioinduced dissociation of, perturbation theory of neutron, 18: 988
radioinduced explosions in liquid, 20: 33333 (N-66-13092)
radioinduced fixation, 17: 25343
radioinduced fixation of, problems in, 18: 41546
radioinduced fixation in air-helium, pressure effects on, 19: 26382(R) (RPI-321-1)
radioinduced fixation of, processes for, 19: 36451(R) (BNL-900(p.73-104))
radioinduced fixation of, equipment for, 19: 47985(P)
radioinduced fixation in nitrogen–oxygen compounds, 20: 25180(R) (BNL-954, pp 84-113)
radioinduced fluorescence of, by light from hydrogen lamp, 18: 283
radioinduced ionization of, electron dosimetry by, 18: 29764
radioinduced isotope exchange in, 19: 36482
radioinduced luminescence in, 17: 37652 (NYO-10691(Pt.1))
radioinduced luminescence of, collisional deactivation of, 19: 13480
radioinduced luminescence of, alpha and fission-fragment, 20: 1933
radioinduced nitrogen-14 and -15 isotopic exchange in gaseous, mechanism of, 18: 23680
radioinduced nitrogen-14–nitrogen-15 isotopic exchange in, 19: 26917(R) (IA-984)
radioinduced oxidation of atmospheric, by fission fragments, (E), 19: 40604
radioinduced oxidation of, yields of molecular and atomic ions in, 20: 45758
radioinduced production of helium and hydrogen in, neutron, 19: 26901
radioinduced production of atomic, effects of nitric oxide on, 20: 3982(R) (AGN-8156)
radioinduced reactions with carbon dioxide and oxygen by fission products, 17: 6161
radioinduced reactions with acetylene, ethylene, and methane, yields in, 17: 29012
radioinduced reactions with steel, 17: 29896
radioinduced reactions with hydrogen, ammonia yields from, 17: 34011
radioinduced reactions with graphite in presence of other gases, 18: 13835 (HW-78948)
radioinduced reactions with oxygen, 18: 31565 (NYO-2546)
radioinduced reactions with hydrocarbons, G-values and mechanisms of, 20: 3982(R) (AGN-8156)
radioinduced spectra from, 19: 26382(R) (RPI-321-1)
radiolysis of purified, spectra of atomic oxygen 5577 Å emission produced by polonium-210 alpha particles in, 18: 22109 (CONF-322-8)
radiolysis of, isotopic exchange in, 20: 31282
radioprotective effects on *Vicia faba* seedlings, 20: 43007
radiosensitivity effects, in *Habrobracon* eggs, 16: 12895
radiosensitivity effects on barley roots, 16: 1528
radiosensitivity effects on germ cells of sex-linked lethal recessives of *Drosophila melanogaster*, 16: 28763 (RT/BIO(62)45)
radiosensitivity effects on mature sperm in *Drosophila virilis*, 16: 9869
radiosensitivity effects on induced Drosophila non-disjunction females and X0 males, 16: 17467
radiosensitivity effects of, on *in vitro* guinea pig cells, 17: 35475
radiosensitivy effects on *E. coli*, 18: 19681
radiosensitivity effects in *Vicia faba*, effects of cold and cyanide on x, 18: 35387(T) (JPRS-25703(p.11-18))
radiosensitivity effects on animal and plant cells, 18: 38977
radiosensitivity effects on cinnamic acid and γ-phenyl ethyl acetate, 19: 11226
radiosensitivity effects on plant growth, 19: 15167
radiosensitivity effects on *E. coli* B, alpha and x, 19: 28047
radiosensitivity effects on Drosophila sperm, x, 19: 29960
radiosensitivity effects on mutation rates in Drosophila, 19: 31670(R) (NIRS-3(p.19-56))
radiosensitivity effects in Drosophila, x, 20: 5338
radiosensitivity effects on chromosomes in bean roots, 20: 10712
radiosensitivity effects on olfactory bulb neurons in rats, 20: 16215 (AD-628443)
radiosensitivity effects on collagen, uv, 20: 23092
radiosensitivity effects on organoleptic properties of fish, gamma, 20: 29583(R) (TID-22515)
radiosensitivity effects on *Thiobacillus thiooxidans*, x, 20: 31139
radiosensitivity effects on male Drosophila, x, 20: 33072
radiosensitivity effects on bacteriophage, x, 20: 38712
radiosensitivity effects on bean sprouts, 19: 7094
radon-219 and radon-220 decay in, properties of recoils from, 20: 29325
reaction with uranium at 400 to 920°C, 17: 18027
reactions between gases and plasma of, ionization in, 18: 36747
reactions of active, with ethylene, 20: 16510(T) (NP-tr-1364)
reactions of atomic, charge transfer and ionization in, 17: 36520
reactions of atomic, with polystyrene, 19: 27735(R) (NAA-SR-10850)
reactions of atomic, with organics, 20: 3982(R) (AGN-8156)
reactions of atomic, with sulfur compounds, 20: 31218(R) (UCRL-16658, pp 1-9)
reactions of atoms of, with sulfur compounds, 19: 10706 (UCRL-11763)
reactions of atoms of, with sulfur compounds, 19: 43997(R) (UCRL-11889)
reactions of atoms in gaseous, exchange, 20: 23075 (NYO-2807-12)
reactions of dry and wet, with lithium, 17: 4522
reactions of, vacuum system in charge exchange chamber for, 19: 16411
reactions of, with ions, atom and charge transfer in, 20: 31224
reactions with acetylene at very low temperatures, 16: 1798
reactions with acetylene, ethylene, and methane, kinetics and mechanisms of, 19: 26382(R) (RPI-321-1)
reactions with air species above 1000°K, 20: 29146 (SC-R-66-885)
reactions with aluminum for preparation of pure aluminum nitride, 18: 12031 (AEET/CD/18)
reactions with argon, neon, and oxygen ions, method for studying interchanges in, 18: 20021
reactions with beryllium at 1000 to 1500°C, kinetics and products of, 18: 25328(R) (SC-DC-64-864)
reactions with beryllium, kinetics, 19: 11051(R) (SC-DC-1432)
reactions with beryllium in simulated launch pad abort environments at 800 to 1500°C, 20: 2341 (SC-DC-65-1637)
reactions with beryllium at 1000 to 1500°C, 20: 5844
reactions with beryllium in group VIII transition metal alloys, 20: 37275
reactions with calcium, iron, magnesium, and silicon, ionization in, 18: 755
reactions with calcium, magnesium, molybdenum, tantalum, and zirconium, combustion, 20: 29641(R) (SC-DC-1691)
reactions with carbon–oxygen–uranium system, 18: 606(R) (NCSC-2663-8)
reactions with carbon-labeled organic molecules, 18: 13840(R) (TID-20203)
reactions with carbon-11, mechanisms of, 19: 7417
reactions with carbon-14-labeled propene, 19: 13425(R) (NYO-2383-12)
reactions with carbon and niobium or tantalum at 1150 to 2370°C, 20: 12845
reactions with carbon at 4.2°K, 20: 18667
reactions with cerium, 17: 6100
reactions with cerium–magnesium alloys at 475 to 600°C, effects of water vapor on, 19: 20485
reactions with chromium, iron and niobium alloys in diffusion zones, electron probe microanalysis, 16: 5281
reactions with deuterium ions, energy dependence of cross sections for, 17: 33912
reactions with deuterium and hydrogen, 18: 12076
reactions with deuterium and hydrogen sulfides, 18: 22052

reactions with excited ions, 16: 6472
reactions with finely divided uranium, 19: 34203(P)
reactions with free radicals in irradiated polytetrafluoroethylene, 16: 3042
reactions with graphite at 2300°K, 16: 25394
reactions with graphite, thermodynamics of, 17: 12226 (TID-15762)
reactions with graphite at 1694 to 2365°K, microwave-activated, 19: 46956 (NP-15514(Vol.1))
reactions with hafnium and zirconium borides and carbides at 3000°K, kinetics and thermodynamics, 16: 25747 (ASD-TDR-62-204(Pt.I))
reactions with Hastelloy X, effects of oil and oxygen on, 17: 14200 (AGN-TM-401)
reactions with helium ions at 300 to 1500 kev, electron loss in, 16: 26021
reactions with helium, ionization cross sections, 16: 26238
reactions with helium and oxygen ions in ionosphere, 18: 21092
reactions with helium and oxygen ions, cross sections and charge exchange rates for, 18: 20810
reactions with helium ions, ionospheric loss processes from, 19: 10179
reactions with helium atoms, charge transfer and ionization in, (E), 20: 17301
reactions with hot tungsten surface at 1710 to 2500°K, energy exchange in, 17: 10609 (UCRL-10504)
reactions with hydrogen in plasma, spectral studies, 16: 30950
reactions with hydrogen ions, atomic and molecular, 18: 28820
reactions with hydrides of cerium, yttrium, and zirconium, (E), 19: 31532 (BMI-X-151)
reactions with INOR-8, effects of oxygen on, 19: 34629(R) (ORNL-3812(p.63-86))
reactions with ionic, calculations of charge exchange and charge exchange and diffusion cross sections for, 18: 34418
reactions with ion source in mass spectrography, 19: 7518
reactions with ions, charge-exchange, 20: 4556
reactions with isoprene, products from, 19: 32048(R) (NP-15073)
reactions with labeled propylene, methods of studying, 17: 14315(R) (TID-18027)
reactions with lanthanum to form lanthanum nitride, 18: 31514
reactions with lithium and barium nitrides, 19: 7361(T) (AERE-Trans-1011)
reactions with magnesium borides at high temperatures, 16: 17694
reactions with molten uranium–zirconium particles, disintegration properties of, 20: 14169 (AFWL-TDR-64-75)
reactions with molybdenum–zirconium alloys, nitride formation in, 20: 29632
reactions with niobium and tantalum during annealing and melting, 19: 40490
reactions with niobium–zirconium alloy in potassium–sodium environment at 1250°F, 19: 44626 (TIM-896)
reactions with niobium, embrittling effects of, 19: 46296
reactions with niobium at high temperatures, 20: 4299(R) (ORNL-2711)
reactions with niobium and tantalum carbides at 1150 to 2370°C, 20: 12845
reactions with nitrogen oxide and nitrogen-15, 16: 25362
reactions with nitrogen ions and other cations, cross sections for, 18: 41391
reactions with nitrogen ions in cathode region of glow discharge, 19: 38637
reactions with nuclei at 1.47 Mev, alpha and proton angular distributions and energy spectra for, 17: 38293
reactions with oxygen at 400 to 5000°K, calculated efficiencies of, 19: 4107 (ORNL-TM-968)
reactions with oxygen in ionosphere, 19: 35227 (AD-609844)
reactions with plutonium and uranium carbides during grinding and sintering, 20: 27441 (CEA-R-2997)
reactions with plutonium dioxide and uranium dioxide, effects of carbon on, 20: 37207
reactions with radioisotope-containment materials in launch pad abort environments, 20: 19192 (SC-DC-65-1918)
reactions with radioisotope-containment materials in launch pad abort environment, 20: 39312 (SC-CR-66-2044)
reactions with rare gases at high pressure, spectra of, 17: 4527
reactions with rare gases in discharges and afterglows, 18: 32494
reactions with refractory alloys at 900°C, 19: 24064(R) (ANL-6997)
reactions with revolving surfaces, 18: 40154
reactions with sodium, spin relaxation cross sections for, 18: 30418
reactions with sodium at 190 to 385°C, 19: 17176(R) (ANL-6965(p.1-41))
reactions with tantalum in sputtering, properties of films formed by, 20: 29745
reactions with thorium carbide, iodide, and nitride at 300 to 900°C, impurity transfer and self-gettering in, 19: 6328
reactions with tungsten, kinetics, 16: 22059 (UCRL-10135)
reactions with uranium carbide, kinetics, 16: 32994
reactions with uranium carbide and uranium-carbon-oxygen systems, 17: 32486(R) (NCSC-2663-13)
reactions with uranium carbide, kinetics of nitride formation in, 18: 204 (NAA-SR-8388)
reactions with uranyl bromide monohydrate during thermal decomposition, 18: 41390
reactions with uranium carbide, 19: 11293
reactions with uranium carbide, 19: 36337 (NAA-SR-11235)
reactions with uranium carbide powders, 20: 9395
reactions with uranium hydrides, 20: 13227
reactions with uranium carbide at 550 to 1050°C, 20: 14994
reactions with uranium dioxide and carbon to produce uranium mononitride, 20: 23593
reactions with uranium carbide, effects of hydrogen on, 20: 40870 (NAA-SR-Memo-7310)
reactions with uranium at 470 to 1000°C, composition of uranium nitrides produced by, 20: 43191
reactions with zirconium in air by flash-heating, 18: 41393
reactions with zirconium, effects of pressure and temperature on, 19: 11722(R) (EURAEC-1099)
reactions with zirconium at 1400 to 1700°C, 19: 19877
reactions with zirconium droplets, flash heating effects on combustion and explosive, 20: 12826 (SC-RR-65-569)
reactions with zirconium at 750 to 1000°C, kinetics of, 20: 27439
reactivity with niobium–zirconium alloys at 578 to 1202°C, 18: 4255(R) (ORNL-3470(p.98-125))
recombination coefficient of neutral atomic, 17: 16888
recombination coefficients into low-lying states of, radiative, 18: 14754
reduction of alkali halides by high-frequency electric discharge in, role of electrons in, 19: 39181
refractive index at 1 atmosphere and 0°C, 16: 8897 (AERE-R-3867)
refractive index and dispersion for Cherenkov counters (E), 19: 2268 (ANL-6916)
relaxation of potassium-seeded plasma of, to steady state, 20: 32657
relaxation strength in niobium, anisotropy of Snoek, (E), 20: 13980
release from amino acids using ninhydrin, nitrogen-15 determination by, 20: 40824
removal from argon by reactions with titanium, 17: 36860(R) (ANL-6648)
removal from vanadium by cerium, 19: 22875(T) (JPRS-28849(p.166-78))
resonance in laser-induced plasma of, optical frequency, (E/T), 20: 13942
scattering by surfaces, decrease of frictional resistance in, 18: 40155
scattering by surfaces, normal momentum transfer in, 18: 40156
scattering of cesium ions by, angular distribution of elastic, 19: 46161(R) (ORNL-3832, pp 116-50)
scattering of potassium chloride molecules by, 18: 20627(R) (NP-13815)
scavenging in molybdenum and tungsten preparation, 16: 25696(R) (DRI-2010)
scintillations in, alpha-induced, 18: 13831(R) (ANL-6769(p.55-8))
sensitivity and operating point of liquid, in bubble chambers, 17: 25648
separation from argon, krypton, and xenon by gas chromatography, 16: 4228 (USNRDL-TR-535)
separation from argon on hot titanium sponge, 18: 17921(R) (ANL-6725(p.31-88))
separation from argon by gettering on hot titanium sponge, 18: 33678(R) (ANL-6875)
separation from argon on hot titanium sponge, 18: 43359(R) (ANL-6800 (p.43-196))
separation from argon by titanium gettering, 19: 14765(R) (ANL-6977)
separation from argon, pilot plant design for, 19: 15662(R) (ANL-6900 (p.45-142))
separation from argon by hot titanium sponge, 19: 32279(R) (ANL-7020(p.3-99))
separation from argon using titanium sponges, 20: 5594(R) (ANL-6925, pp 21-106)
separation from argon by titanium gettering, 20: 20802(R) (ANL-7055, pp 21-98)
separation from compounds for isotopic analysis by high-frequency discharge, 19: 17843
separation from hafnium by electron-beam melting, 19: 4582 (BM-RI-6560)
separation from helium, 18: 1608 (JAERI-4025)
separation from interstitial positions in hafnium, thorium, titanium, and zirconium, 19: 36564(P)
separation from lutetium by electrotransport, 20: 4297(R) (IS-1200 (Sect.M))
separation from niobium by electrolysis, 18: 35926 (BM-RI-6506)
separation from niobium by degassing reactions at 1600 to 2300°C, 18: 39977
separation from nitrogen by gettering on hot titanium sponge, 19: 40177(R) (ANL-7046(p.1-35))
separation from niobium and tantalum, degasification processes for, 20: 29633
separation from other atmospheric gases, chromatographic, 18: 29799 (CEA-2361)

separation from oxygen and rare gases by sorption on zeolite, gas chromatographic, 18: 41328
separation from oxygen by gas chromatography, 20: 40805(R) (MLM-1325, pp 63-70)
separation from rare gases, use of tritium-metal sponge as gettering agent for, 20: 29329 (ANL-7128)
separation from thorium by electrotransport, 20: 41412(R) (IS-1500 (Sect. M))
separation from thorium by electrotransport, 20: 43820
separation from titanium by zone melting, 18: 8456
separation of interstitial impurities of, from bcc metals, technique for, 20: 23641(R) (AROD-4074:2)
separation of, from argon by titanium gettering, 20: 31314(R) (ANL-7175, pp 1-41)
shock wave velocities in, models for, 18: 32945
shock waves in, radiation behind, 17: 32705 (BSD-TDR-63-102)
shock waves in, uv radiation from, 17: 13643
Slater-Condon parameters of, determined from spectral data, 17: 31118
solubility in beryllium, 17: 20474
solubility in boron–iron systems, 16: 21073
solubility in chromium–rhenium alloy, internal friction study of, 19: 6243 (BMI-1703)
solubility in chromium and chromium–rhenium alloys, effects of quenching on, 19: 13871(R) (BMI-1691(Del.))
solubility in chromium-base chromium–yttrium alloys, 20: 37169(R) (BMI-1774)
solubility in iron alloys with niobium, tantalum, titanium, vanadium, and and zirconium, 19: 41065
solubility in metals, review on, 19: 22109
solubility in niobium, 18: 34177
solubility in niobium, 19: 30675(R) (SRIA-132)
solubility in niobium at 450 to 1000°C, 20: 13303
solubility in niobium, 20: 31250
solubility in Santowax-OM1, 20: 20708 (AEET-213)
solubility in stainless steel at 1000°F, effects of ammonia–hydrogen ratio on, 19: 40968(R) (EURAEC-1424)
solubility in tantalum at 350 to 2300°C, 18: 33595
solubility in tungsten, 20: 39098(R) (WERL-2823-21)
solubility in uranium nitride, thermodynamics of, 19: 7449
solubility in uranium mononitride, 20: 4303(R) (ORNL-3870, pp 164-70)
solubility in uranium monocarbide, 20: 9548
solubility in yttrium, 20: 13180(R) (IS-RD-4)
solvent properties of liquid, for hydrogen, 20: 31251
sorption by barium sulfate (labeled and unlabeled), 17: 14277
sorption by cathode tube at low pressures, effects of magnetic field on electrical, 18: 27694(T) (ORNL-tr-150)
sorption by evaporated molybdenum films, 19: 40463(R) (SRIA-426-5)
sorption by evaporated zirconium films, 18: 29668
sorption by gamma-irradiated quartz, 20: 43302
sorption by irradiated and unirradiated synthetic zeolites, 18: 43702
sorption by liquid iron, effects of surface-active elements on, 20: 29623(R) (TID-22970, pp 121-256)
sorption by materials, pore volume determination by, 16: 23641 (TID-7629(p.345-56))
sorption by molybdenum film, 17: 35706(R) (TID-19307)
sorption by molybdenum film and niobium filament in ultrahigh vacuum and constant pressure, 18: 22002 (CONF-209-26)
sorption by molybdenum, 18: 44200
sorption by molybdenum films at −195 and −185°C, 19: 11052(R) (SRIA-135)
sorption by molybdenum films at low temperatures, mechanism of chemi-, 19: 26822 (TID-20853)
sorption by molybdenum films, 19: 29812(R) (SRIA-425-4)
sorption by molybdenum films in ultrahigh vacuum, kinetics of, 20: 21351(R) (SRIA-425-8)
sorption by niobium in vacuum, research program, 17: 10602(R) (TID-16820)
sorption by niobium at high temperatures and low pressures, 18: 12041 (TID-19489)
sorption by niobium in ultrahigh vacuum, 18: 35958(R) (SRIA-126)
sorption by niobium, 18: 41933 (TID-11295(3rd Ed.))
sorption by niobium–zirconium alloy, 18: 44049(R) (ORNL-3670(p.77-111))
sorption by niobium in ultrahigh vacuum to 1800°C, 19: 906(R) (TID-21114)
sorption by niobium, 19: 30675(R) (SRIA-132)
sorption by niobium at 25 to 1800°C and 6×10^{-9} to 6×10^{-5} torr, 19: 47031
sorption by niobium at very low pressures, 20: 775(R) (SRIA-425-6, pp 10-33)
sorption by niobium–1 zirconium alloy, kinetics of, 20: 4301(R) (ORNL-3870, pp 102-35)
sorption by niobium, 20: 5851
sorption by niobium, 20: 8887(R) (SRIA-425-7)
sorption by niobium surfaces, kinetics of, 20: 21351(R) (SRIA-425-8)
sorption by niobium at 10^{-5} to 10^{-8} torr and 1400 to 1900°K, 20: 29178
sorption by silica gel, gamma radiation effects on, 18: 37196(T) (AEC-tr-6398(p.222-5))
sorption by solids, use in measurement of pore size distribution, 17: 1422 (TID-17044)
sorption by synthetic zeolite for gas chromatography, effects of lithium, potassium, and sodium on, 18: 41328
sorption by titanium films in getter pumping of vacuum systems, 16: 3098 (ORNL-3217)
sorption by tungsten, 18: 27373
sorption by uranium trioxide, 19: 2352
sorption by vapor-deposited titanium films at −195 and 10°C, 16: 9511(R) (ORNL-3239(p.85-95))
sorption by vapor-deposited titanium films, probability factors for, 18: 4329(R) (ORNL-3470(p.237-9))
sorption by vapor-deposited titanium films, 18: 14591 (ORNL-3481)
sorption by zeolite at 21°C, 16: 31719 (UCRL-6396)
sorption by zeolites at low pressures and temperatures, 20: 43499
sorption effects on ductile-to-brittle transition in alloyed and unalloyed refractory metals, 16: 25751 (DMIC-Memo-155)
sorption of electron-impact-activated, 19: 7507
sorption of hydrogen on films of solid, 16: 10679 (UCRL-6626)
sorption of thermally activated, by tungsten filament, 20: 12549(R) (TID-21555)
sorption on activated carbon, isotherms for cryo-, 18: 8513
sorption on heterogeneous surface below 10^{-10} torr, 20: 45876
sorption on homogeneous surface above 10^{-10} torr, 20: 45876
sorption on molybdenum films, 18: 2405(R) (TID-19665)
sorption on molybdenum films, sticking probability determination in, 19: 32131
sorption on tungsten, effects of surface structure on, 19: 22201
sorption on Vycor porous glass at 77.7°K, 16: 16385
spectra as impurity in silicon, absorption, 19: 33513 (AD-611194)
spectra at zero scattering angle, electron-impact, 19: 7399
spectra at 1080 to 1520 Å, absorption, 19: 22863(R) (AD-606809)
spectra at 30 ev, energy losses in electron-impact, 20: 43288(R) (CALT-532-1)
spectra, electron collision study of excitation functions, 16: 22145
spectra excitation by products from electric discharge in helium, 18: 16719
spectra from plasma of, Stark widths of, 20: 44931
spectra in airglow, 20: 32289
spectra in artificial aurora, 18: 21073
spectra in auroral, use for determinations of temperatures, 17: 12458
spectra in d-c arc between iron electrodes at low currents, 19: 28296
spectra in electric arcs, 18: 11347
spectra in mixtures with oxygen, negative ions in afterglow, 18: 21093
spectra in polar auroras, atomic emission, 19: 16739
spectra in polar-cap absorption events, emission, 17: 14504
spectra in primary cosmic radiation, intensity and rigidity, 17: 12956
spectra in pulsed glow discharge, second positive electron band system of, 19: 14268
spectra in silicon carbide crystals, photoluminescence, 16: 33009
spectra in silicon lattices, absorption, 18: 2254
spectra in type-B red aurora, emission, 19: 23513
spectra lines from ion excited, rotational structure of, 20: 37471
spectra of arc-heated plasma of, radiation data from, (E), 20: 22167(R) (AD-622391)
spectra of atmospheric, x-ray excitation of first negative and second positive band, (E), 20: 6181 (AD-619288)
spectra of, excited by electron impact, 18: 801
spectra of foil-excited beams of, 20: 31903 (N-66-16702)
spectra of graphite vapor, mercury, and sulfur isolated in, at high temperatures, 20: 1818 (UCRL-11976)
spectra of high-speed excited atomic, at 2700 to 6600 A, (E), 20: 39593
spectra of highly ionized, in high-temperature plasma, 16: 33925 (ARL-62-399)
spectra of, hyperfine splitting in ESR, 17: 8070
spectra of, in magnetically confined vacuum arc, 17: 34071
spectra of ionized, operation of theta-pinch discharge as light source for, 20: 25631
spectra of molecular, in auroras, (E), 19: 33133
spectra of molecular, at 720 to 830 A, 18: 28240
spectra of multiply ionized, 18: 14739
spectra of nitrogen-14 in solid, effects of nitrogen-15 on nuclear quadrupole resonance, 17: 12837
spectra of nitrogen-14 in vacuum uv region in isotope shifts in, 18: 42302
spectra of, radio-frequency excited, 17: 34641
spectra of shock-heated, excitation mechanisms in, 18: 32493
spectra of sulfur molecules in solid, u-v absorption, (E), 19: 45480 (UCRL-10771)

spectra of, accelerator methods for obtaining optical atomic, 18: 28254
spectra of, behind shock waves, (E), 19: 20676
spectra of, effects of chemical combination on soft x-ray K emission bands of, (E), 19: 44944
spectra of, hyperfine splitting in ESR, 18: 31474
spectra of, isotope shifts and vibrational structure of weaker systems in, 18: 33568
spectra of, wavelengths of Lyman lines in, 20: 25731
spectra of, x-ray excitation of first negative and second positive bands of, 20: 21834
spectral absorption coefficients of, 18: 42806
spectral line emission from plasma of, Stark broadening of, 19: 41941
spectral line intensity in auroral arcs at middle latitudes, (E), 19: 18996
spectral line shifts and Stark width measurements in plasma of, 19: 39952 (AFCRL-65-348)
spectral-line profile in theta-pinch hydrogen plasma, (E), 20: 20061
spectrum, fluorescent x-ray, 16: 13358
spectrum of molecular, in polar auroras, 19: 16740
spectrum of, molecular excitation potentials in, 19: 25155
sputtering of gold in upper atmosphere, 18: 43142
stability of inhomogeneous plasma of, (E), 20: 10191(T)
sticking factors for, on titanium film, 17: 17337(R) (ORNL-3392 (p.86-8))
stopping power for recoil ions from alpha reactions (α,n), 16: 26243
storage in cryogenic vessels in space vehicles, 17: 9123
storage of liquid, high-pressure cryogenic vessels for, 18: 44699
temperature distribution in plasma jets in, 18: 1117 (ARL-63-151 (p.446-59))
temperature measurements in static flowing, electron-beam method, 16: 6536
temperature behind reflected shock waves, 18: 24236
thermal capacity of liquid, at boiling point, 18: 19929 (CONF-417-20)
thermal conductivity and viscosity, 16: 18933
thermal conductivity to 380°C, application of frequency response analysis to, 16: 18935
thermal conductivity and viscosity of liquid, at critical point, 17: 25849 (LADC-5791)
thermal conductivity, 18: 22476(R) (BATT-4673-Q13)
thermal conductivity of partially ionized gases of, 18: 28166
thermal conductivity at 20 to −195°C and 1 to 500 atm, 19: 13284(T) (LA-tr-65-1)
thermal conductivity of compressed, at 0 to 300°C and 1 to 500 kg/cm², 19: 16264(T) (LA-tr-65-4)
thermal conductivity at 1000 to 20,000°K, (T), 20: 13644
thermal conductivity of liquid, 20: 19614 (N-65-17283)
thermal conductivity at 750°C, 20: 20651(R) (CU-2660-26)
thermal conductivity of high-temperature gas of, pressure and temperature dependence of, (E), 20: 32240
thermal diffusion in columns, comparison with carbon monoxide, 17: 2690
thermal diffusion in refractory metals, 20: 29769
thermal properties at 2600°F, 17: 18769(R) (TID-18334)
thermodynamic and transport properties at 500 to 15000°K, calculations for, 16: 15381
thermodynamic critical point exponents of, quantum theory of corresponding states for, (E/T), 19: 32806
thermodynamic functions of Morse oscillator of, anharmonic and quantal effects in, 18: 37128
thermodynamic properties, graphs and tables, 16: 23664 (ASD-TR-61-625)
thermodynamic properties at high temperatures, review, 16: 25300 (ARL-62-358)
thermodynamic properties, 17: 30552
thermodynamic properties at 64 to 300°K and 0.1 to 200 atm, 18: 21095(R) (NBS-8239)
thermodynamic properties of plasma of, 18: 24742 (ANL-6802(p.15-18))
thermodynamic properties of, (T), 20: 1265 (NBS-3346)
thermodynamic properties of equilibrium solid solutions of, in niobium–zirconium at 1200 to 1800°C, 20: 13263 (ORNL-TM-1355)
thermodynamics of, at high pressures and temperatures, 20: 45624 (JUL-383-RB)
thermoluminescence of solid, after electron bombardment at 4.2°K, 16: 19496
tracer studies on soil organic, 20: 42795
transfer from stainless steels to niobium–zirconium alloys in potassium, 20: 2270
transfer system for liquid, automatic, 17: 12391 (BNL-764)
transport coefficients at high temperatures, 16: 25880 (ARL-62-328)
transport coefficients for partially ionized, 18: 28166
transport properties, 16: 14143(R) (RAD-SR-62-11)
transport properties at 1000 to 24000°K, calculations for, 16: 15382
transport properties, 16: 3553
transport properties in pure gaseous and liquid, 16: 18933
transport properties of, influence of magnetic field, 17: 9016
transport properties of gaseous, magnetic field effects on, 20: 7118
treatment for chemical combination, 16: 20580(P)
triton energy losses in, 16: 2491 (TID-14145)
triton ranges and stopping cross sections in, 17: 17212
triton scattering and slowing-down by, at 2.7 Mev, 16: 27782
ultraviolet emission from molecular, in auroras, (T), 19: 18981
ultraviolet refractive indices of gaseous, Cherenkov radiation method for vacuum, 17: 28028
ultraviolet refractive indices of gaseous, Rayleigh scattering method for vacuum, 17: 28029
uptake and incorporation by *Vicia faba*, tracer study of, 17: 2718
uptake by niobium–zirconium alloys in liquid metals, 20: 41419(R) (GMAD-3643-5)
uptake by plants from ammonia and nitrates, tracer studies of effects of copper on, 18: 25059(T) (OTS-63-11008(p.6-14))
uptake by rat blood and organs from organic and inorganic salts, tracer study, 17: 2716
uptake by refractory metals from vacuum, 18: 14355 (CONF-373-7)
uptake by rice, tracer study of, 20: 12592(R) (NP-15671)
urea, content in blood of deer and sheep, 20: 40541(R) (UCD-34P104-3)
use as carrier gas in radon sorption studies on wood charcoal, 18: 23462(T) (SC-T-64-616)
use as carrier in plasmochemistry, 20: 38314
use as tracer, survey, 16: 1359
use in calibration of vacuum gages, 16: 7625 (CF-61-5-109(Suppl.3))
use in gas bearings, 20: 43469 (TID-23350)
use in inductive plasma furnaces, 17: 35041
use in space simulators, supply systems for, 17: 28078
use of liquid, as coolant for 300-kgauss pulsed-field magnet coils, 16: 15421
vapor pressure of liquid, isotopic effects on, 16: 18905
vapor pressure of liquid, up to critical point, 18: 3722 (UCRL-7167)
vapor pressure of, from chemical reactions in sol-gel fuels, 20: 14512 (ORNL-TM-1418)
vapor pressure up to critical point, 18: 41374 (UCRL-7167(Rev.I))
viscosity of molecular, saturated-liquid, 20: 39940
viscosity of, excess transport property determination from, 19: 17865
viscosity to 1000°C, measurement of, 18: 27387(T)
wave functions for, first-order solutions of Hartree-Fock, 18: 2548
wave functions for molecular, localized self-consistent field orbitals in, (T), 19: 18681 (IS-1107)
weight loss measurements of liquid, in Dewars at 3 to 20 psi, 17: 36347(R) (NARF-62-18P)
x-ray attenuation by diatomic, coefficients for soft, 17: 22433 (NP-12661)
x-ray scattering by, theory, 17: 27953
x-ray scattering by, diffraction of, 18: 4615
x-ray spectrum from mesic (μ), 17: 22264(R) (ANL-6679)
yielded in gamma radiolysis of nitrous oxide, 17: 16441
yields from aqueous systems irradiated with recoils from reactions of thermal neutrons with boron-10, 19: 36514
yields from gamma radiolysis of carbon tetrachloride in ammonia solutions, 19: 36477
yields from gamma radiolysis of alkaline solutions of nitrous oxide in aliphatic alcohols, 20: 26937
yields from radioinduced oxidation of potassium iodide solutions saturated with nitrous oxide, 20: 7140
yields from radiolysis of ammonia at 25 and −196°C, 19: 22383
yields from radiolysis of aqueous solutions of nitrous oxide, 19: 28407
yields from radiolysis of ammonia, 20: 4021
yields in gamma radiolysis of aqueous potassium iodide-nitrous oxide solutions, 20: 392
yields in gamma radiolysis of aqueous nitrous oxide-sodium tellurite solutions, 20: 393
yields in gamma radiolysis of hydrazine, Hydyne, and RP-1 rocket fuels, 20: 25118 (AD-632461)
yields in gamma radiolysis of nitroalkanes, 20: 33362
yields in nitrogen-13 recoil reactions, 16: 11759
yields in nitrous oxide gamma dosimeters, effects of cell diameter on, 19: 2633
yields in photo- and radiation chemistry of mineral acid glasses, effects of iron ions and nitrous oxide on, 19: 46394
yields in radiolysis of aqueous solutions of propanol containing nitrous oxide, 18: 20058
yields in radiolysis of nitrous oxide aqueous solutions, effects of added solutes on, 18: 31601
yields in radiolysis of methylhydrazine, 19: 30237 (USNRDL-TR-843)
yields in radiolysis of ammonia–deuterium, 19: 46324(R) (AGN-8132)
yields in radiolysis of gaseous nitrous oxide, 20: 12884(R) (RRL-2310-171)
yields in x radiolysis of dimethylhydrazine and hydrazine, 18: 35589 (NASA-TN-D-2452)
yields of atomic, in electron radiolysis of nitrogen–propene systems,

20: 23071(R) (AGN-8169)
yields of, in gamma radiolysis of dinitrogen tetroxide, 17: 23381 (PA-TR-3072)

NITROGEN COMPOUNDS
see also Chemical Warfare Agents
analysis for nitrogen-15 by mass spectroscopy, 19: 36282
bibliography on inorganic binary, 18: 6794(R) (TID-19898(App.II))
bonds in, electron repulsions in abnormally weak, 18: 1619 (UCRL-10920)
chemical binding in diatomic hydride molecules, energy partitioning between atomic and molecular orbitals in, 18: 41430
combustion of, Hopcalite-catalyzed, 18: 40988(R) (NRL-6053)
content in Bear Creek waters, determination, 17: 26932(R) (ORNL-TM-516)
graphitization of heterocyclic, mechanism and properties for, 18: 35934 (ML-TDR-64-125(Vol.I))
hydrogen exchange in heterocyclic, 18: 10134
isotopic analysis of nitrogen from, procedures for, 20: 16376
nitrogen-14 NMR in, chemical shifts in, 18: 43497
production of N_2O^+ in mass spectrometer ion source, 20: 38902
radiation effects on content in blood and urine of dogs, partial-body x, 20: 42939
radioinduced polymerization of unsaturated bases, 17: 25840(P)
reaction with diborane and its derivatives, 16: 17682
review of nitrogen-15-labeled, 17: 8202
spectra of, infrared, 18: 1489(R) (IS-700(Sect. C))
spectra of, infrared, 20: 3863(R) (IS-1200(Sect. C))
synthesis, 19: 8952(R) (AD-601838)
valence frequency location of double-bond isotopic, 16: 28930(T) (AEC-tr-5283)

NITROGEN FIXATION
development of chemonuclear processes, 18: 33122 (A/CONF.28/P/292)
effects of calcium, cobalt, molybdenum, and strontium on, in Nostoc, 18: 33237
effects of irradiated nitrogen gas on, by Azotobacter, review of, 18: 19721
effects of uv-irradiated nitrogen on algal, 20: 20408
radioinduced, effects of temperature on, 19: 26382(R) (RPI-321-1)
tracer study in rice, 20: 12592(R) (NP-15671)

NITROGEN FLUORIDES
molecular structure of difluorodiazine, electron-diffraction analysis of, 19: 24531
preparation and structure of N_2F_2, 19: 22252
production of N_2F_2 and N_2F_4, 16: 16402(P)
reactions with ethylene, 16: 6253 (ARGMA-TN-2H1N-30)
stability of, radiation and thermal effects on, 17: 10516 (ORNL-TM-475)
structure and properties, 19: 32048(R) (NP-15073)
synthesis in nitrogen plasma jets, (E), 19: 24532
use in photosensitive gas phase etching process for semiconductors, 17: 29277(P)

NITROGEN IONS
acceleration, 16: 29880(R) (ORNL-1345)
acceleration in electromagnetic and static magnetic field gradients, continuous, 18: 28802
acceleration of negative, 17: 25857(R) (PR-P-56(p.4-18))
angular distributions of, from deuteron with fluorine-19 and oxygen-18, (E), 19: 25549
beam production and focusing of multicharge, 18: 8967
charge exchange and dissociation interactions of doubly charged molecular, with nitrogen molecules, 17: 39783
charge exchange and dissociation collisions of doubly charged molecular, 17: 39783
charge transfer in, cross sections for, 16: 4602 (AD-258147)
charge transfer with nitrogen, nitric oxide, and oxygen at 30 to 10,000 ev, cross sections for, 17: 29426
charge transfer with atomic oxygen at 50 to 10,000 ev, cross sections for, 17: 29427
content and reactions in ionosphere, (T), 19: 45173
content in outer ionosphere, 20: 39950
deionization in atmosphere, studies of kinetics of, 18: 37114 (AFCRL-64-496)
density of molecular monovalent, in high auroral rays, (E), 19: 25422(T)
detection of trapped molecular, in irradiated potassium azides at 77°K, 16: 9273
detection using photographic emulsions, 18: 37521
determination in plasma condensations, mass-spectrographic, (E), 19: 5288(T) (AEC-tr-6518(p.146-53))
dissociation of molecular, in scattering by copper crystals, (E), 19: 37234
dosimetry using nuclear emulsions, photomicrography of ion tracks in, 20: 9263
drift velocities in nitrogen, 18: 32479
effects on electric properties of germanium surface layers, (E), 19: 16239(T)
electron absorption and scattering cross sections of, 18: 44450
electron affinities of, relativistic and nonrelativistic, 17: 27996
electron density matrix in trivalent, generalized product functions for, 17: 22378
electron loss by, at 2.6 to 12 × 10^8 cm/sec, 16: 32231
electron reactions in discharge afterglow, 18: 32431
electron reactions with, classical calculation of cross sections for inelastic, (T), 19: 44947
electron reactions with, excitation cross sections for, (T), 20: 31929
electron recombination with ionospheric, parameters for, 18: 28480
electron spin resonance spectra of, in nitrate-doped alkali halide crystals, 18: 31530
electron transition probabilities of, $2s$-$2p^0$, (E), 19: 25173
electron transitions in, collision cross sections for dipolar, 20: 2598
electron transitions in, oscillator strengths for probability of, (T), 20: 15275
electron triplet splitting of 2p, 18: 28238(T) (ANL-Trans-25)
energy distribution of fragment, 18: 25763
energy level transition probabilities and lifetimes in, 20: 37438
energy levels and wave functions for, (T), 19: 16370 (UCRL-7943-T)
energy levels in molecular, rotational, (E), 19: 27099
energy levels of, (T), 20: 11450 (UCRL-7842-T)
energy levels of pentavalent and trivalent, electron distance correlation for ground-state, 17: 25864 (SCTM-58-63(91))
energy loss in gases and solids, 16: 12295
excitation of molecular, by electron and ion impact, (E), 19: 41279
formation and stability of positive molecular, 16: 19556
formation of doubly charged atomic, from singly charged ions by electron impact, cross section for, 17: 39784
Hartree-Fock wave functions and oscillator strengths for configurations of, 18: 7412
hyperfine splitting of ground state, 17: 20747
interactions with hydrogen ions at 20 to 250 kev, cross sections for inelastic, (E), 20: 41666
ionization after passage through solids, auto-, (E), 20: 17262(T)
ionization in beams, determination from spectral emission lines, (E), 19: 20857
ionization of argon by 8 to 100 kev, 18: 26217
ionization of atomic, by 25- to 750-ev electrons, 16: 33636
ionization of nitrogen by 25- to 50-kev, total, (E), 20: 2623
light scattering by molecular monovalent, in upper atmosphere, (E), 19: 22746
lithium ion reactions at 1 to 3 kev, rotational energy distribution measurements, 16: 2366
mobilities of atomic and molecular, 18: 16058
mobilities of, in electric field of 1 to 4 volts/cm, 18: 16057
mobility, 18: 16060
motion in nitrogen in electric fields, (E), 19: 37218
nuclear quadrupole coupling in, 19: 11086
oscillator strengths, 18: 28168
oxidation by peroxydisulfate ions in aqueous solution, kinetics of, 20: 1571(R) (TID-22186)
photodissociation cross sections for molecular, 18: 31640
photoionization of optical electrons in, transition cross sections for, 18: 40136
photoionization of negative, cross section for, 19: 11213(T)
polarizability and shielding factor for, dipole, (T), 20: 37440
potential energy curves for molecular, 18: 34281 (RM-4034-PR)
production and acceleration of multicharged, 16: 11911
production and acceleration of beams of, 20: 13804
production by cosmic protons at 57 and 100 kev in ionosphere, 16: 27872
production by geomagnetically trapped electrons, 18: 22813
production by hot cathode oscillator discharge for heavy-ion cyclotrons, 19: 37360
production in ionsophere, (E/T), 19: 18971(T) (FTD-TT-64-1316 (p.75-101))
production of atomic, mechanisms of ionospheric, 18: 11096
production of excited, in electron reactions with air, (E), 19: 14272
production of molecular, in presence of helium, 17: 20695
production of pentavalent, by electron bombardment, (T), 20: 5982 (AERE-R-5061)
production of pulsed multicharged, 16: 11912
properties at 500 to 15000°K, calculations for thermodynamic and transport, 16: 15381
proton reactions at 1 Mev, rotational energy distribution measurements, 16: 2366
radioinduced formation of N_T in sodium azides, ESR studies of x, 20: 40966
radioinduced N_2^- as defect in sodium azide, ESR spectral studies on, 20: 15942 (NYO-2150-11)
range-energy relations in matter, (E), 19: 9893 (NAS-NRC-PUB-1133 (p.173-86))
ranges in gold, 17: 21065

ranges in nickel and silver at 0.4 and 2.5 Mev, (E), 19: 41269
ranges in solids at 50 to 500 kev, 16: 18247
reaction with deuterium hydrides, cross sections and velocity spectra for, 19: 37468
reactions of atomic and molecular, with oxygen molecules, charge transfer and dissociation in, 19: 32885(R) (AD-610869)
reactions of beams of, with niobium, 19: 27063 (INR-555/XIV)
reactions of excited, charge exchange and dissociation in, (E), 19: 8071
reactions of molecular, with molecular nitrogen at 1 to 10 kev, cross sections for emissions from, 18: 12839
reactions of monatomic singly charged, with nitrogen at 10 to 65 kev, rotational and vibrational excitation of singly charged molecular nitrogen ions in, (E), 20: 2618
reactions of nitric oxide with atomic and molecular, charge transfer, 20: 44127
reactions of positive monatomic and diatomic, with molybdenum surfaces, secondary-electron yields from, 20: 2628
reactions of, with light nuclei at various energies, 16: 32175(R) (ORNL-1531)
reactions of, with cobalt-59 at 3 to 10 Mev, 16: 33692 (TID-16687)
reactions of, with molecules, atom and charge transfer in, 20: 31224
reactions on nitrogen molecules, distributions from, 17: 12829
reactions on 25-Å platinum films at 24 Mev, mechanisms of, 16: 22754
reactions with aluminum, copper, and tantalum, two- and three-neutron reactions in, 17: 2323
reactions with argon at thermal energies, charge transfer in, 18: 32469
reactions with argon, hydrogen, and nitrogen, charge transfer in, 18: 41391
reactions with argon, charge exchange in, (E), 19: 16419
reactions with argon, nitrogen, and helium at 0.14 to 0.7 Mev, energy loss in, 20: 2602
reactions with argon and nitrogen, charge-exchange, 20: 4556
reactions with argon, krypton, neon, and xenon, cross sections for, (E), 20: 25747
reactions with argon and nitrogen gases at 10 to 100 kev, energy losses in, (T), 20: 35998(R) (ORO-2911-7)
reactions with atmospheric gases, charge exchange in, 20: 9656(R) (GA-6699)
reactions with atoms and ions at 0.4 to 2 kev, radiation emission from, 18: 36145
reactions with beryllium and molybdenum, secondary ion emission, 16: 16880
reactions with carbon films, optical atomic spectra from, 18: 28254
reactions with carbon-12, 18: 30716 (CEA-2298)
reactions with carbon tetrachloride and tetrafluoride in mass spectrometer, 19: 13484
reactions with carbon monoxide, charge-transfer excitation in slow, (E), 20: 2631
reactions with deuterium, energy dependence of cross sections for, 17: 33912
reactions with deuterium beams, angular distributions and cross sections in, 19: 27079
reactions with deuterium in crossed beam, cross sections for, 19: 32885(R) (AD-610869)
reactions with deuterium and hydrogen molecules, spectra of N_2D^+ and N_2H^+ in, (E), 19: 41252
reactions with ethylene molecules at 200 and 400 kev, mass spectra of fragments from, 18: 34433
reactions with even-even nuclei at 36 to 53 Mev, Coulomb excitation of energy levels in, 16: 33826
reactions with even-even nuclei at 44 and 52 Mev, 18: 7718
reactions with gases and solids below 1 Mev, range and stopping power determinations, 16: 10954 (EFINS-61-68)
reactions with gases, charge exchange in, (E), 19: 29008
reactions with gases, charge-exchange cross sections for, 20: 34110
reactions with germanium at 46, 67, and 82 kev, inversion layer production in, 19: 20625
reactions with gold and lutetium, K x-ray spectra from, (E), 20: 24359(R) (UCRL-16580, pp 95-106)
reactions with hydrogen, charge transfer and ionization in, 17: 36520
reactions with hydrogen molecules at 5 to 100 ev, cross sections for inelastic, 20: 9685
reactions with lanthanum-139 and praseodymium-141 at 52 Mev, level excitation in, (E), 19: 27469
reactions with molecular nitrogen ions at 10 to 65 kev, rotational and vibrational excitation in, (E), 19: 41279
reactions with nitrogen, optical excitation in, 17: 32707 (CONF-46-43)
reactions with nitrogen at 40 to 1000 ev, beam excitation effects in, 18: 32468
reactions with nitrogen at 0.4 to 2 kev, charge exchange and excitation in, 18: 32449
reactions with nitrogen, calculations of charge exchange and charge exchange and diffusion cross sections for, 18: 34418
reactions with nitrogen at 2.65 kev, charge transfer cross sections for, (E), 19: 14231 (AFCRL-63-709)
reactions with nitrogen molecules in cathode region of glow discharge, 19: 38637
reactions with nuclei at 30 to 42 Mev, Coulomb excitation of energy levels in, 16: 33823
reactions with nuclei, cross sections for isotope production in, 18: 18868 (CERN-64-17)
reactions with oxygen in ionosphere, thermal, 18: 21092
reactions with palladium-104 at 42 Mev, Coulomb excitation of energy levels in, 16: 33824
reactions with selenium-77, titanium-47, and vanadium-51 at 16.5 and 18.3 Mev, angular distribution of gamma radiation from excited levels from, 16: 33827
reactions with tungsten at 10–140 kev, secondary electron emission from, 17: 29473
reactions with tungsten at 50–200 ev, Auger electron ejection from, 17: 41621
reactions with tungsten surfaces, electron ejection by, 18: 20777
recombination coefficients, 19: 32885(R) (AD-610869)
recombination of diatomic positive, with electrons, 18: 34259 (AD-434907)
recombination with electrons, effects of water vapor, 16: 12218 (NASA-TN-D-1191)
rotational and vibrational excitation of singly charged molecular, by monatomic ions at 10 to 65 kev, (E), 20: 2618
rotational temperatures in auroral atmosphere from 80 to 160 km, (E), 20: 1096
scattering by gases, neutral beams from (E), 19: 2983
scattering by hydrogen molecules at 3 to 100 ev, cross sections for inelastic, (E), 20: 11467
scattering by nuclei at 11 Mev, Coulomb excitation in, 18: 38128
scattering by odd-A nuclei at 16.2 and 17.7 Mev, Coulomb excitation in, (E), 20: 15759
scattering on gold, nickel, and silver, energy loss in, (E/T), 20: 9668
Slater-Condon parameters of, determined from spectral data, 17: 31118
source for multicharged, performance of, 17: 2352
spectra in deuterium plasma, 16: 14183
spectra in plasma, 17: 24594
spectra of trivalent, in plasma discharge, 17: 42093
spectral line intensities of lithium-like, 18: 17185
spectrum of molecular, in polar auroras, 19: 16740
sputtering of copper, mechanisms and yields, 16: 13741
sputtering of copper by, effects of pressure and temperature on, 16: 31730
sputtering of copper by, at oblique angles and 0.5 to 7 kev, (E/T), 19: 26919 (N64-18080)
sputtering on metals at 0.5 to 4 kev, momentum accommodation in, 18: 20782
sputtering on tungsten, 19: 34884
sputtering ratio for polycrystalline copper, 16: 9114
sputtering reactions with copper, iron, molybdenum, nickel and tungsten at 0 to 8 kev, 16: 587 (NASA-TR-R-105)
temperature of stellarator, Doppler effect, 16: 7211
temperatures in ionospheric plasma, 18: 28480
transport properties at 1000 to 24000°K, calculations for, 16: 15382
valency of accelerated, effects of density on average, 18: 769
Van der Waals cohesion on tungsten, 19: 16112
velocity distribution in nitrogen in electric fields, (E), 20: 17298
wave functions for, 18: 4407
wave functions for tetravalent, ground-state, 20: 25730

NITROGEN ISOTOPES
abundance ratios of, emission spectrometric methods for determining, 20: 35189
analysis by electron paramagnetic resonance, 16: 5285
biological effects of, nuclear-mass, 18: 33258
concentration of nitrogen-14/-15 molecules by thermal diffusion, 20: 16931
concentration of, methods for, 18: 35919
content in uranium fuel elements, 17: 24618 (EUR-238.e)
detection of environmental, use of photographic film detectors for, 18: 39704
determination in ammonium salts, micromethod for, 17: 2722
determination in water of Melusine Reactor cooling system, design of power channel for, 17: 22906 (CEA-2211)
distribution between gaseous nitrogen oxides and liquid organic solutions, 20: 16486
effects on decomposition of diazonium salts, 19: 865(R) (ORNL-3679 (p.23-38))
effects on thermal decomposition of 2,2'-azobis(2-methylpropionitrile), 19: 46899(R) (ORNL-3832, pp 33-49)
equilibration reactions on tungsten, 19: 46289
equilibria in systems of carbon dioxide with primary and secondary amines, 17: 10521
exchange between ammonium nitrate and urea, measurement of, 17: 2705

exchange between nitric oxide and nitric acid, 18: 16403
exchange equilibrium between nitric oxide and nitrate salts, fractionation factors for, 16: 12007
exchange in nitric oxide–nitrate systems, 16: 2100 (TID-13427)
exchange in nitric oxide, catalysis of, 17: 23335
exchange in nitrogen compounds, mechanism for, 16: 3310(T) (AEC-tr-4497(p.17-29))
exchange in nitrogen oxides, effects of pressure and temperature on, 17: 30505 (CONF-14-22)
exchange in nitrogen and nitrogen oxides, 18: 9752 (IA-900)
exchange of, between gaseous and liquid nitrogen oxides, 17: 20044
exchange reactions in various compounds and systems, 18: 2127(R) (ORNL-3488(p.21-41))
fractionation in gaseous absorption, 17: 4511
helium-3 elastic scattering by, optical model for, 17: 5364
incorporation in nitroquinoline 1-oxide and quinoline 1-oxide, 19: 32192
mass analyses, design of assembly for, 16: 6611
nucleon configuration mixing, (E), 20: 42204
nucleon scattering at high energies by, cross sections for, 17: 15280
potential constants and thermodynamic properties of oxides of, at 200 to 2000°K, 16: 30381
preparation, determination, and properties of radioactive, 16: 1349
production in fast neutron reactions with oxygen, 19: 7607
production of, availability and cost of, 19: 22844 (ORNL-TM-1047(p.23-9))
properties for tracer use in biology, 19: 43707
properties of hyperfragments of, review, 18: 16963
proton decay, 18: 18876 (KFK-185)
radioinduced exchange of, in nitrogen gas, 19: 36482
ratio of, in marsh gas and rocks, 18: 12017
ratios of, from radiolysis of nitrogen-15-labeled nitrous oxide, 19: 26404
reactions with praseodymium-141, 17: 41871 (UCRL-10541)
separation by distillation of nitric oxide at low temperatures, 17: 23808
separation by distillation and exchange, 19: 13850
separation by exchange of nitric oxide with non-aqueous solutions of nitric oxide complexes, 16: 463
separation by exchange, separation factors for, 16: 12839
separation by ion exchange chromatography, 16: 10374
separation by ion exchange, 17: 23810
separation by ion exchange, 17: 23811
separation by ion exchange methods, coefficients for, 19: 11643
separation by ion exchange of amines on cation exchanger, 19: 22840 (IS-1059)
separation during production of concentrated nitric acid by direct methods, 16: 24079
separation factor in nitrogen oxide–methane systems, 16: 29300
separation factors for, on ion exchangers, 19: 20433
separation in nitrogen monoxide–nitrosyl bromide systems, 16: 22520
separation of, by transdiffusion, optimum conditions for, 17: 14709
separation of, in vortex tube, 17: 18657
separation of, research in Japan on, 20: 25469(T) (K-Trans-17)
separation of, thermodynamic effects in, (E/T), 19: 9568 (NP-14359)
sorption by iridium, rhodium, and tungsten, isotopic mixing during, 20: 20652 (IS-T-67)
vapor pressure ratios in nitrous oxide, structural effect in, 16: 1761

NITROGEN ISOTOPES N-12

beta decay, 18: 21306
beta decay matrix elements for, 18: 42724
beta decay of, branching ratio and half life for, 17: 17236
beta decay of, branching ratio to 7.6-Mev level of carbon-12, 17: 17237
beta decay of, carbon-12 recoil momentum spectrum from, (T), 20: 34646
beta decay of, conserved-vector-current theory for, 18: 34752(R) (CU(PNPL)-234)
beta decay of, end-point energy and ft value for, 18: 15262
beta decay of, f values for, 19: 37795 (NP-15109)
beta decay of, G parity non-invariance from, (T), 19: 31275
beta decay of, matrix elements for, 20: 19940
beta decay of, nuclear matrix elements for, (T), 19: 5204
beta decay of, phase-space integrals for, (T), 20: 17732
beta decay of, with alpha decay of carbon-12, (E), 20: 46665
beta spectra, 17: 15251(R) (CU(PNPL)-220)
beta spectra of, comparison to boron-12, 16: 28145
beta spectra of, comparison with boron-12 to test conserved-vector-current theory, 18: 1090
beta spectra of, test for conserved vector current theory with, 17: 17237
beta spectra of, test for conserved vector current theory in, 17: 19363
beta spectrum, 17: 36669 (WASH-1042)
beta spectrum analysis using spherical tensor calculations, 18: 9434
decay of, comparison of beta spectra with boron-12, 17: 7141 (TID-15182)
decay spectra, effects of pseudoscalar interaction and weak magnetism on shape of, 16: 19764
energy levels, 17: 881
energy levels, (E), 20: 13808
energy levels and equilibrium form, 18: 30832
energy levels from boron-10 (He^3,n) reactions, 18: 15261
energy levels of, shell model LS coupling, 18: 26624
half life, 17: 26574
harmonic oscillator constant in, 16: 13994
mass difference with carbon-12, 18: 15262
mass from threshold energy for carbon-12 (p,n) reactions, (E), 20: 44811
nuclear deformation parameters and energy levels for, 18: 21307
positron decay of, alpha-particle spectra from, 17: 22631
production by secondary nuclear reactions, 19: 30267
production in neutrino reactions on carbon-12, 16: 18517

NITROGEN ISOTOPES N-13

angular distributions and ranges from magnesium-24 (N^{14},N^{13}) reaction, 16: 21416
beta decay half life (E), 19: 3295
beta decay of, model for relative period of, 17: 29632
beta emission in stars, 16: 23016
chemistry of recoils, from carbon-12 (d,n) reactions, 16: 11759
decay of, K-capture to positron ratios for, (E), 20: 15712 (CONF-233 (Vol.2), pp 359-64)
decay, computed, 19: 32058(R) (GA-5978)
determination for neutron flux measurements, 16: 4864
determination in hydrocarbons by fast neutron irradiation, 16: 7494
determination of short-lived, gas flow activation and automatic radiogas chromatography for, 20: 25017
electric dipole resonance (E), 19: 1609
emission in nitrogen-14 reactions (N^{14},N^{13}) with boron-10 at 28 Mev, angular distributions and ranges for, 17: 26597
energy level from carbon-12 (p,p'γ) reactions, parity and spin of, (E), 20: 32438
energy level transitions in, (E), 20: 6405
energy levels, 16: 12434(R) (NIRL/R/15)
energy levels, 17: 881
energy levels, 17: 2276
energy levels, 17: 38169
energy levels, (E), 20: 38053
energy levels, (E), 20: 42204
energy levels and equilibrium form, 18: 30832
energy levels from proton reactions with oxygen-16 at 146 Mev, 16: 17088
energy levels from boron-11 (He-3, n) reactions at 1.3 to 5.8 Mev, 20: 4925
energy levels from helium-3 reactions (He-3,d) with boron-10 at 5.8 Mev, resonance, (E), 20: 10078
energy levels from boron-10 (He-3,$p\gamma$) reactions at 4.5 to 9.0 Mev, giant resonance, (E), 20: 28418
energy levels from boron-10 (He-3,p) reactions at 1.2 to 12 Mev, excited, (E), 20: 32527
energy levels in intermediate bond model, wave functions for, 18: 28618
energy levels near 7-Mev excitation, 17: 36692
energy levels near 7-Mev excitation, 17: 36693
energy levels of, anomalous parity in, 18: 2946
energy levels of, Coulomb energy differences between carbon-13 and, 17: 36691
energy levels of, excitation functions for ground and 3.5-Mev, 17: 33044
energy levels of single-particle states, unified model, 16: 1083
energy levels of, search for above-threshold $\frac{5}{2}$, 17: 40014
energy levels of, wave functions for, 18: 36621
energy levels of, parity and spin of ground-state, 20: 6326
energy levels of, use of Hamada-Johnston potential for, (T), 20: 22102
energy levels of, lowest $T = \frac{3}{2}$, (E/T), 20: 24358(R) (UCRL-16580, pp 1-93)
energy levels of, lifetime of, (E), 20: 44731
energy levels, properties below 3.6 Mev, 16: 4783
energy parameters of two-body interactions in various nuclear configurations, 18: 14823
energy spectra of 1 p shell, determination using Hamada-Johnston potential, (E/T), 20: 30354(R) (ORNL-3940, pp 62-9)
gamma spectra of, to first-excited and ground states, 17: 7153
half life, 20: 16331 (GA-6568)
harmonic oscillator constant in, 16: 13994
hazards from, at linear electron accelerators, 20: 9172 (CONF-650616-28)
helium-3 reactions (He-3,$p\gamma$) at 15.1 Mev, excitation and resonances in, 18: 21336
incorporation in organic compounds by recoil techniques, 19: 32241
mass shifts with carbon-13, from splitting of SU(3) isospin multiplets, 18: 12935
monitoring airborne, from electron linacs, 20: 5774
neutron separation energy for, (E), 19: 39862

nuclear deformation parameters and energy levels for, 18: 21307
nuclear magnetic dipole moment of, 17: 15257 (PUC-1963-96)
nuclear magnetic moment and spin, 18: 40579
nuclear spin measurements by atomic beam methods, 16: 29809
nucleon emission from, reduced widths in shell-model intermediate coupling, (T), 20: 15830
positron decay scheme, 17: 4157
preparation and properties of, for use as tracer in pulmonary function studies, 18: 35414 (TID-7678(p.213-36))
production and recoils in deuteron reactions with benzene, 16: 10051(R) (TID-15003)
production and use for lung function studies, 20: 26735
production by deuteron reactions (d,n) in benzene and carbon tetrafluoride, chemical effects of, 19: 13484
production by oxygen-16 (p,α) reactions in water-moderated reactor, 18: 30763
production by photodisintegration and electrodisintegration of oxygen-16, excitation curves, 16: 21377
production by reactions (B-10,Be-9) and (B-11,Be-10) on carbon-12 at 105 and 115.5 Mev, proton transfer in, (E), 19: 43393
production by secondary nuclear reactions, 19: 30267
production in (α,n) reaction in NRX reactor, 16: 3691
production in atmosphere at 100-Mev electron linear accelerator, radiation hazards from, 20: 27210(R) (UCRL-14680)
production in carbon-12 (d,n) measurement of neutron flux by, 17: 9505 (NP-12441)
production in carbon-12(d,n) reactions in alcohols, 16: 13108
production in carbon-12(d,n) reaction, polarization of neutrons from, 17: 17264
production in deuteron reactions with carbon, detection, 18: 18222
production in helium-3 reactions with carbon-12, 17: 854
production in linear electron accelerator, concentration guides and monitoring for, 19: 20204 (RPI-328-25)
production in man during high-energy radiotherapy, 19: 40392 (NYO-3364-6)
production in operation of linear accelerator, 18: 14683 (TID-7677 (p.208-21))
production in oxygen-16 reactions with rhodium-103 at 160 Mev, angular distributions for, 17: 38279
production in proton reactions at 0.25 to 5 Bev, fragment, 19: 43365
production in proton spallation of aluminum at 28 Bev, cross sections, 16: 29842(BNL-6034)
production in tunnel of Frascati electron linear accelerator, (T), 19: 44866 (LNF-65/21)
production in Van Allen proton reactions, 16: 9761(R) (UCRL-9897 (p.131-3))
production of, in neutron reactions with normal and heavy water, (E), 20: 45728
reactions with sodium azide, activities of yields in recoil, 18: 33663
spectra of recoil, from deuteron reactions with carbon-12, (E), 20: 17820
spectrum of, from nitrogen-14 reactions with lead-207, 17: 36649 (CONF-62-12)
tracer use for measurement of blood circulation in lungs, 19: 46070
use in medical diagnostics, 19: 46136
use in medicine of cyclotron-produced, 20: 18515

NITROGEN ISOTOPES N-14

abundance in massive stars, effects of helium and hydrogen burning on, (T), 19: 41242
alpha elastic and inelastic scattering at 40.5 Mev, angular distributions for, (E), 20: 30450
alpha elastic scattering at 1.0 to 2.4 Mev cross sections, 16: 3743
alpha elastic scattering at 15 to 22.7 Mev, angular distribution from, 17: 13539
alpha elastic scattering at 65 Mev, 18: 21260
alpha reactions (α,d) at 4 Mev, angular distributions for, 18: 15299
alpha reactions (α,γ) with, in CH stars, 18: 30383
alpha reactions (α,d) at 45 to 50 Mev, highly populated levels in, 18: 34779 (UCRL-11341)
alpha reactions (α,Li-6) at 42 Mev (E/T), 19: 3337
alpha reactions (α,d) with, (T), 19: 17008
alpha reactions (α,d) at 40 Mev, deuteron transfer recoil effects in, (T), 19: 33339
alpha reactions (α,d) at 42 to 53 Mev, deuteron energy spectra from, (E), 20: 12061
alpha reactions (α,d) at 42 to 53 Mev, energy spectra from, (E), 20: 24358(R) (UCRL-16580, pp 1-93)
alpha reactions (α,d) at 48 Mev, angular distributions, 16: 8203
alpha reactions (α,d) on, residual energy levels from, 17: 9548
alpha reactions (α,d) and (α,Li^6) at 42 Mev, 17: 21097
alpha reactions (α,p) at 22 Mev, angular distributions from, 17: 28288
alpha reactions (α,d) at 47 Mev, energy levels excited in, 17: 38289
alpha scattering at 19 Mev, distributions from, 17: 876
alpha scattering at 40.5 Mev, inelastic, (E), 20: 24360(R) (UCRL-16580, pp 107-48)
alpha scattering by, differential cross sections for, 17: 31404 (INSJ-57)
baryon capture in emulsions, computer program for kinematics of, 19: 29231 (CERN-65-6)
binding energy of, using Hartree-Fock self-consistent-field model, 19: 17026
boron-10 reactions at 30 to 90 Mev, cross sections for 3α production in, 18: 6277
boron-10 reactions with, alpha-particle clusters in, (E), 20: 12004(T)
boron-10 reactions (B-10,3α) at 100 Mev in photoemulsions, mechanism of, (E), 20: 13891
boron-10 reactions at 100 Mev with emulsion nuclei of, 6α production in direct, (E), 20: 28468
boron-11 reactions (B-11,B-10) and (B-11,Be-10) at 115 Mev, fractional parentage of boron-11 ground state from, (E), 20: 36214
bremsstrahlung reactions (γ,α) at 21.5 Mev, cross sections for, 18: 30778
bremsstrahlung reactions at 170 Mev with, distributions from, 18: 38084(T) (AEC-tr-6398(p.164-88))
charge dependence of nuclear forces and energy differences in the A = 14 isobaric spin triplet, 18: 4612
charged-particle reactions with, amplitude singularities in knockon and stripping, (T), 20: 21997 (INSJ-96)
content in natural nitrogen, 18: 13691
content in star surface during helium burning, nitrogen-14/carbon-12 ratio, (T), 19: 9843
coupling constants with protons in ammonium ion, 16: 7976
decay of, electromagnetic transitions in, 18: 19101
detection, scintillation efficiency of sodium iodide crystals for, 16: 3847(R) (ORNL-3193(p.74-8))
deuteron elastic scattering and reactions (d,p) at 27 Mev, 16: 24831
deuteron elastic scattering by, absolute cross sections for, 17: 24402 (TID-18633)
deuteron elastic scattering at 0.7 to 2.1 Mev, (E/T), 19: 3361
deuteron elastic scattering at 28.5 Mev, (E/T), 20: 42389
deuteron reactions (d,p) at 15.2 and 13.8 Mev, angular distributions, 16: 2537
deuteron reactions (d,α) at 14.7 Mev, angular distribution from, 16: 6000
deuteron reactions (d,γ) at 20 Mev, 16: 5944
deuteron reactions (d,α) and (d,p), measurement of Q_0 values for, 16: 11038
deuteron reactions (d,n), cross sections at 1 to 1.7 Mev, 16: 12444(R) (TID-15124)
deuteron reactions (d,p) at 27 Mev, angular distribution of protons and elastically scattered deuterons, 16: 21355 (NP-11697)
deuteron reactions (d,p) at 2 Mev, stripping analysis, 16: 24841
deuteron reactions (d,p) at 0.75 to 1.10 Mev, angular distributions from, 16: 31076
deuteron reactions (d,α) at 1 to 3 Mev, 17: 4079
deuteron reactions (d,p), angular distribution and excitation curves for, 17: 7159
deuteron reactions (d,n), neutron polarization in, 17: 11633(R) (TID-17534)
deuteron reactions(d,n), neutron polarization from, 17: 17125 (TID-18137)
deuteron reactions (d,n) at 1.32 Mev, polarization of neutrons from, 17: 17127 (TID-18256)
deuteron reactions (d,p) on, knock-out mechanism in, 17: 17168
deuteron reactions (d,n) at 0 to 700 kev, neutron yield curve for, 17: 24496
deuteron reactions (d,n) at 5 Mev, hyperfine structure, nuclear magnetic dipole moment, and spin from, 17: 28311
deuteron reactions (d,γ) at 21.4–25.0 Mev, giant resonances in, 17: 38278
deuteron reactions (d,p) at 13.6 Mev, proton asymmetries in polarized, 18: 6275
deuteron reactions (d,n), Distorted Wave Born Approximation theory of angular distributions from, 18: 6198
deuteron reactions (d,α) at 24 Mev, 18: 9320 (UCRL-10993)
deuteron reactions (d,α) at 1.8 Mev, carbon-12 energy level decay in, 18: 9359
deuteron reactions (d,p) model for, 18: 17053
deuteron reactions (d,α) with, differential cross sections for, 18: 21157(R) (AFOSR-5284)
deuteron reactions (d,n) at energies up to 3.8 Mev, angular distributions and yields of neutrons from, 18: 26673
deuteron reactions (d,α), theoretical and experimental angular distributions, 18: 26675
deuteron reactions (d,p), energy levels from, 18: 32329
deuteron reactions (d,α) at 1 to 2.5 Mev, angular distributions and excitation functions for, 18: 38122
deuteron reactions (d,γ) at 1.50 Mev, giant resonances in (E/T), 19: 1684
deuteron reactions (d,α) at 0.9 to 1.2 Mev (E), 19: 1605
deuteron reactions (d,n), angular distributions from (E), 19: 3277
deuteron reactions (d,α) at 2 to 12 Mev, angular distributions, cross

sections, and excitation functions for, (E), 19: 5133 (NP-14500)
deuteron reactions (d,α) at 24 Mev, alpha spectra from, 19: 10363
deuteron reactions (d,p) at 0.75 to 1.10 Mev, analysis of angular distribution of protons from, 19: 12495(T) (AEC-tr-6227/3(p.167-72))
deuteron reactions (d,α) with, isobaric spin selection rule in, (E), 19: 16919
deuteron reactions (d,α) at 15 Mev with, cross sections for, (E), 19: 23643
deuteron reactions (d,α) at 4 and 7.2 Mev, angular and energy distributions from, (E), 19: 25531
deuteron reactions (d,n) at 1.65 to 2.90 Mev, polarization from, (E), 19: 27511
deuteron reactions (d,n) at 1 to 3 Mev, angular distributions from, (T), 19: 27522
deuteron reactions (d,p) at 0.717 to 1.740 Mev, angular distributions for, (E), 19: 29274
deuteron reactions (d,n) at 3.7 Mev, neutron polarization in, (E), 19: 33366
deuteron reactions (d,p) at 1.3 to 5.5 Mev, nitrogen-15 excited levels from, (E), 19: 47604
deuteron reactions (d,α) at 24 Mev, energy spectra from, (E), 20: 1211
deuteron reactions (d,γ) at 0.5 to 5.5 Mev, excitation curves and angular distributions from, (E), 20: 4884
deuteron reactions at 1.9 to 6.7 Mev, bound states from, (E), 20: 4905
deuteron reactions (d,α) at 11.8 and 12.0 Mev, (E), 20: 6369
deuteron reactions (d,pγ) with, gamma spectra from, (E), 20: 5928(R) (PR-P-66)
deuteron reactions with, oxygen-15 gamma transitions from, (E), 20: 6318
deuteron reactions (d,p) at 200 to 350 kev, proton angular distributions in, (E), 20: 12096
deuteron reactions (d,α) at 24 Mev, energy spectra from, (E/T), 20: 24358(R) (UCRL-16580, pp 1-93)
deuteron reactions (d,p) at 1.3 to 5.0 Mev, differential cross sections for, (E), 20: 28362
deuteron reactions (d,p) at 4 Mev, nitrogen-15 levels from, (E), 20: 32501
deuteron reactions (d,n) at 1.173, 1.797, and 2.098 Mev, angular distributions and excitation functions for, (E), 20: 38144
deuteron reactions (d,p) at low energy, distorted-wave analysis of, (T), 20: 40122
deuteron reactions (d,nγ) with oxygen-15 energy levels from, (E), 20: 42346
deuteron reactions (d,p) with, nitrogen-15 energy levels from, (E), 20: 42369
deuteron reactions (d,α) with, alpha energy spectra from, (E), 20: 42389
deuteron reactions (d,t) and (d,He-3) with, cross sections for, (E), 20: 44794
deuteron scattering cross sections at 2.1 Mev, 17: 11633(R) (TID-17534)
deuteron scattering at 0.7–2.1 Mev, angular distributions and cross sections for, 17: 33086
effects on fractional decomposition of diazonium salts, 19: 38690
effects on Franck-Condon factors for electron transitions in nitrogen molecules, 20: 18658
effects on vibrational frequencies in polyglycine, 18: 31490
electromagnetic transitions in, from carbon-13 (d,n) reactions at 1.9–3.1 Mev, 17: 40107
electromagnetic transitions in, multipolarity of, 18: 6238
electron elastic scattering at 160 to 420 Mev, shell model for, 19: 17029
electron elastic scattering to 230 Mev, magnetic form factors from, (E), 20: 22120
electron energy levels of, 2^3P, (T), 19: 12083
electron inelastic scattering by, excitation of M1 transitions by, 18: 13095
electron inelastic scattering at 121 and 180 Mev, 18: 34825
electron inelastic scattering at 50 Mev, energy levels from, (E), 20: 28346
electron magnetic elastic scattering at 41.5 Mev, 17: 7222
electron scattering by, study of nuclear magnetic transitions by inelastic, 17: 19078
electron scattering at high energies, deformation parameter variation in, 18: 7741
electron spin resonance, 19: 37469
electronic charge distribution at high energy, 17: 11388
energy level at 10.43 Mev, gamma decay scheme of, 18: 21261
energy level at 7.03 Mev, properties of, (E), 20: 38083
energy level at 9.17 Mev, gamma spectra of, 19: 1630
energy level excitation by electron inelastic scattering at 180°, (E/T), 20: 24322 (AD-624Z70)
energy level excitation in meson ($\pi^{\pm}$) reactions ($\pi^{\pm}$,2n) with oxygen-16, (E), 20: 38070
energy level lifetimes from helium-3 reactions (He-3,pγ) with carbon-12 at 4.7 Mev, (E), 20: 36211
energy level lifetimes from tritium (C-12,nγ) reactions at 12 and 17.75 Mev, 20: 38008(R) (AECL-2595)
energy-level population at 2.31 Mev in, by deuteron reactions (d,α) with oxygen-16, 18: 2906
energy level population in (α,d) reactions, 18: 34779 (UCRL-11341)
energy level transitions in, quadrupole-dipole mixture in, (E), 19: 12568
energy level transitions in, mixing ratios in 5.10-Mev, (E), 19: 19168
energy level transitions from carbon-14 beta decay, wave functions for rate of, 20: 26150
energy levels, 16: 7051
energy levels, 17: 881
energy levels, 18: 17060
energy levels, 18: 21336
energy levels, 18: 34825
energy levels, (E), 20: 9991(T)
energy levels, (E), 20: 12061
energy levels, (E), 20: 40112
energy levels, (E), 20: 42400
energy levels and dipole gamma spectra, 16: 21452
energy levels and equilibrium form, 18: 30832
energy levels at 2.31, 3.95, and 5.10 Mev, mean lives of, (E), 20: 3045
energy levels at 5.83 Mev and 5.10 Mev, relative parity of, 16: 29815
energy levels at 5.83 and 6.44 Mev, lifetime of, 18: 19102
energy levels at 5.10 and 5.83 Mev, lifetimes and gamma decay strengths of, (E), 20: 38075
energy levels at 6.44, 7.03, and 9.17 Mev, 17: 11714
energy levels, configuration mixing in ground-state and first excited state, 16: 28090
energy levels from oxygen-14 beta decay, 17: 841
energy levels from proton reactions with carbon-13, 17: 2329
energy levels from deuteron reactions (d,d) and (d,p) with carbon-12 at 0.9–5.0 Mev, excited, 17: 26527
energy levels from proton reactions (p,γ) with carbon-13 at 0.60 to 1.8 Mev, (E), 19: 41740
energy levels from carbon-13 proton reactions, (E), 20: 13898
energy levels from proton elastic scattering by carbon-13 at 1.0 to 2.6 Mev, 20: 22123
energy levels from oxygen-16 (d,α) reactions (E), 20: 22160
energy levels from carbon-12 (d,pγ) reactions, (E), 20: 22087
energy levels from carbon-12 (d,n) and (d,p) reactions, (E), 20: 24393
energy levels from lithium-6 and -7 reactions with boron-10 and -11 at 3.05 Mev, (E), 20: 26167
energy levels from helium-3 reactions (He-3,α) with nitrogen-14 at 39.8 Mev, (E), 20: 30438
energy levels from carbon-13 (d,n) and (He-3,d) reactions, 20: 30481
energy levels from lithium-6 and -7 reactions with boron-10 and -11, 20: 30519
energy levels from carbon-12 (d,d) reactions, parity and spin of, (E), 20: 36194
energy levels from carbon-13 (d,n) and (He-3,d) reactions, (E), 20: 44601(R) (ANL-7218)
energy levels from proton inelastic scattering at 7 to 11 Mev, (E), 20: 44840
energy levels in intermediate bond model, wave functions for, 18: 28618
energy levels in, decay scheme for 10.43-Mev, 18: 36686
energy levels in, isospin selection rules for transitions of 5.10-Mev, (T), 19: 39856
energy levels of, 19: 47603
energy levels of, anomalous parity in, 18: 2946
energy levels of, configuration mixing in ground-state, 17: 24450
energy levels of, excitation of $(d_{5/2})^2$, 17: 9548
energy levels of, from the reaction nitrogen-15(helium-3,α)nitrogen-14, 17: 4083
energy levels of, M1-transitions in, 17: 4119
energy levels of, parity of 5.83-Mev, 17: 26590
energy levels of, search for excited state at 2.31 Mev in, 17: 15251(R) (CU(PNPL)-220)
energy levels of, shell-model calculation of low, 17: 22620
energy levels of, shell-model calculations of odd-parity, 17: 41970
energy levels of, spin-orbit splitting from two-nucleon potential in, 18: 6190
energy levels of, $(d_{3/2})^2$, 18: 16933 (ANL-6848(p.182-7))
energy levels of, properties of ground and low-lying, 18: 19097
energy levels of, tensor force effects on, 18: 34838
energy levels of, wave functions for, 18: 36621
energy levels of, cross sections for proton-capture excitation of, 18: 36687
energy levels of, analysis of carbon-12 (α,d) reactions for, (E), 19: 8460
energy levels of, deuteron, neutron, and proton emission by, (E/T), 19: 17012
energy levels of, parity and spin for, (E), 19: 19196
energy levels of, spin of, (E), 19: 35433
energy levels of, from deuteron reactions (d,α) with oxygen-16 at 15 Mev, (E), 19: 35452
energy levels of, effective interactions for 1p, (T), 19: 43307

energy levels of, use of Hamada-Johnston potential for, (T), 20: 22102
energy levels of, finite Fermi-system theory for, 20: 24472
energy levels of, shell-model potential parameters for low-lying, (T), 20: 38145
energy parameters of two-body interactions in various nuclear configurations, 18: 14823
energy-range relations at 0.4 to 6 Mev, 16: 8003
energy separation and nuclear-force charge dependence in, isobaric-triplet, 18: 26618
energy spectra of 1 p shell, determination using Hamada-Johnston potential, (E/T), 20: 30354(R) (ORNL-3940, pp 62-9)
energy-level spins and transitions, (E), 20: 42252
energy-level transitions in, branching ratios for, (E), 20: 42231
energy-level transitions in, mixing ratios for, (T), 20: 44784
exchange equilibrium calculations in oxy-nitrogen molecules, 19: 40460(R) (NYO-3462-1)
exchange reactions between nitrogen oxides, equilibrium constants and frequencies of, 19: 4136
exchange with nitrogen-15 in radiolysis of gaseous nitrogen, 20: 31282
excited states in, from deuteron reactions in carbon-12, 17: 11623 (NP-12496)
fluorine isotope reactions (F^{19},F^{18}) up to 43 Mev, 16: 21428
gamma absorption, energy of giant resonance in, 16: 13976
gamma decay of 10.22-Mev level in, 17: 31450
gamma reactions (γ,p) at 15.5 to 30.5 Mev, 18: 26633
gamma reactions (γ,α) at 16 to 21 Mev, cross sections for, 18: 30730(R) (NP-14096(p.7-15))
gamma reactions at 170 Mev, absolute yields from, 16: 18529
gamma reactions (γ,n), (γ,p), and (γ,np), cross sections, 16: 24834
gamma reactions (γ,pα) around 120 Mev, cross sections, 16: 29827
gamma reactions (γ,n) at 30.5 Mev, neutron spectra from, 17: 11756
gamma reactions (γ,np) with, nucleon-nucleon correlations from, 17: 29598
gamma reactions (γ,2n), (γ,2p), (γ,2p4n), (γ,4pn), (γ,4p2n), cross sections for, 17: 34991
gamma reactions (γ,d) with, threshold shift for fast deuteron emission in, 17: 41985
helium nucleus reactions (He^3,α) at 1.50 to 1.65 Mev, 16: 3743
helium nucleus reactions (helium-3,α), 17: 11721
helium-3 reactions on, distributions from, 17: 5363
helium-3 reactions (He^3,p) at 2.5 to 5.5 Mev, angular distribution and excitation curves for, 17: 24475
helium-3 reactions (He^3,pγ) with, gamma and proton spectra for, 17: 38588 (CU(PNPL)-227(p.35-48))
helium-3 reactions (He^3,n) with, differential cross section for, 17: 41873 (WASH-1044)
helium-3 elastic scattering at 16.6 to 36.6 Mev, differential cross sections for, (E), 19: 33382
helium-3 reactions (He-3,α) at 5.2 Mev, alpha angular distribution from 18: 18979
helium-3 reactions (He-3,n) at 25 Mev, spectra of, 18: 24650
helium-3 reactions (He-3,n) at 3.5 and 6.2 Mev, spectra from, (E), 19: 16987
helium-3 reactions (He-3,α) with, (E), 19: 39941
helium-3 reactions (He-3,p) at 6 to 15 Mev, oxygen-16 levels from, 18: 15281
helium-3 reactions (He-3,α) at 25.7 and 27.0 Mev, angular distributions from, (E), 20: 6326
helium-3 reactions (He-3,α) with, nucleon cluster substitution in, (T), 20: 10033
helium-3 reactions (He-3,α) with, association replacement amplitudes for, (T), 20: 15838
helium-3 reactions (He-3,α) at 12 Mev, Q value for, 20: 16331 (GA-6568)
helium-3 reactions (He-3,p) with, double nucleon transfer in, (T), 20: 28294
hyperfine coupling constants in chloronitrobenzene, effects of metal ions on, 18: 16068
hyperfine interactions in ESR-spectra of heterocyclic anions, 17: 8076
hyperfine structure in, 16: 26318
hyperfine structure of, in electron paramagnetic resonance, 17: 4533
hyperfine structure in paramagnetic resonance spectra of chromium pentacyanonitrosyl, 18: 31435(R) (UCRL-11317(p.52-78))
hyperon (Λ) binding in, 16: 33760
hyperons (Σ^-) reactions with, C^{14} production in, 17: 9243
ion reactions with, neutron-transfer mechanisms in, (E), 19: 37823(R) (ORNL-3800(p.1-49))
ionization for cyclotrons, pulsed sources for, 19: 23224
lifetime in hydrogen burning stars, 17: 3914
magnetic resonance spectra coupled with proton magnetic resonance spectra in formamide, picolines, and pyridine, 19: 17877
mass, 19: 28336
meson (K^-) capture at 440 Mev/c, Y_0^* production in, 18: 11244
meson (π^-) absorption by, at rest in emulsion, 18: 16978
meson (π^-) absorption by, products of, (E), 19: 19220
meson (π^-) reactions with, charge exchange in, (E), 20: 37740 (JINR-P-2780)
meson ($\pi^\pm$) reactions (π^+,2p) at 106 Mev, two-hole states in, (E), 19: 25513
meson ($\pi^\pm$) reactions (π^-,2n) and (π^+,2p) with, carbon-12 energy level excitation in, (E), 20: 38070
meson (π^+) reactions at 80 Mev, cross section for, (E), 19: 21279
meson (π^+) reactions (π^+,2p) at 80 Mev, angular distributions and cross sections for, (E), 19: 33385
meson capture in emulsions, computer program for kinematics of, 19: 29231 (CERN-65-6)
neutron capture by, gamma spectra from, 20: 4999(R) (ORNL-2599)
neutron capture cross sections at 10, 15, and 60 kev, 17: 9158
neutron capture cross section of, thermal, 18: 6159 (LADC-5990)
neutron-capture gamma spectra, 16: 18434
neutron elastic scattering at 14 Mev, optical model analysis of, 18: 1048
neutron elastic scattering by, optical model calculations for, 18: 30729 (NP-14056)
neutron elastic scattering at 4.5 to 14.5 Mev, cross sections for, (T), 19: 35396 (NP-15095)
neutron nonelastic reactions at 13 to 21 Mev, cross sections for, (E), 20: 11985
neutron reactions (n,d), transitions in, 16: 3668 (NYO-7864)
neutron reactions (n,p), cross sections and resonance integrals, 16: 4757
neutron reactions (n,p), replacement events in organic compounds from, 16: 11741
neutron reactions (n,p) in crystalline solids, distribution of carbon-14 from, 16: 23734
neutron reactions (n,d) at 14 Mev, cross sections for, 17: 2242 (TID-16949)
neutron reactions with, gamma production in thermal, 17: 4210 (DASA-1318)
neutron reactions (n,d) at 14.1 Mev, angular distributions of, 17: 11716
neutron reactions (n,2n) at 14.1 Mev, cross sections for, 17: 15299
neutron reactions (n,p) with, cross section for thermal, 17: 22561 (NP-12658)
neutron reactions (n,α) with, angular distribution for, 18: 2840 (NYO-9766)
neutron reactions (n,2n) with, cross section for, 18: 11195(R) (EANDC(E)-49(L))
neutron reactions (n,p) with, recoil chemistry of carbon-14 in hydrazine dihydrochloride and sulfate, 18: 12151 (TID-20192)
neutron reactions (n,α) at 14 Mev, nuclear shell effects in cross sections for, 18: 18977
neutron reactions (n,p) with, in atmosphere, 18: 20817
neutron reactions (n,2n) at 12.5 to 19.6 Mev, cross sections for, 18: 24602 (NP-13930(p.43-9))
neutron reactions (n,α) with, cross sections for fast, 18: 24643
neutron reactions (n,xγ) at 14.8 Mev, cross sections and spectrum for, 18: 30736(R) (TID-20658)
neutron reactions (n,p) with, energy dependence of, 18: 40631
neutron reactions (n,p) with, 18: 40493
neutron reactions (n,α) at 14 Mev (E/T), 19: 1557 (NP-14297)
neutron reactions (n,p) in hydrazine salts, recoil chemistry of carbon-14 produced by, 19: 431 (TID-21121)
neutron reactions (n,2n) with, cross sections for, (E), 19: 5230
neutron reactions (n,2n) at 12.6 to 19.6 Mev, excitation functions for, (E), 19: 6669
neutron reactions (n,p) in ammonium chloride, effects of post-irradiation treatment on product spectrum of, 19: 11172 (TID-21590)
neutron reactions (n,t), energy levels of carbon-12 from, 19: 14533(R) (NYO-1082-1)
neutron reactions (n,p), use in carbon-14 labeling of, 19: 26457
neutron reactions with, angular and energy distributions in fast, (E), 19: 33279
neutron reactions (n,p) in air, ionization yields of, (E), 19: 35420
neutron reactions (n,2n) at 14.6 Mev, total cross sections for, (E), 19: 39797
neutron reactions (n,2n) at 14.1 Mev, cross sections for, (E), 19: 45325
neutron reactions (n,$\alpha\gamma$), (n,dγ), and (n,pγ) at 14.8 Mev, gamma angular distributions from, (E/T), 19: 47593(R) (TID-22012, pp 156-75)
neutron reactions (n,α) and (n,t) with, angular distributions from, (E/T), 20: 8078(R) (NYO-1082-2)
neutron reactions (n,p) with, excitation functions for, (E), 20: 13741
neutron reactions (n,d) at 14 Mev, (E), 20: 38150
neutron reactions with, beryllium-7 production in, (E), 20: 41276 (UCRL-16769)
neutron reactions (n,p) with, Szilard-Chalmers effect in, 20: 45720
neutron reactions (n,p) at 14.7 Mev, cross section for, (E), 20: 46614
neutron reactions (n,2n) at 13.56 to 14.7 Mev, excitation functions for, (E),

20: 46614
neutron reactions (n,2n) at 14.6 Mev, cross section for, (E), 20: 46614
neutron scattering at 4.5 to 11.6 Mev, optical model analysis of elastic, (T), 19: 5132 (NP-14480)
neutron scattering at 1.595 to 3.25 Mev, differential cross sections for elastic, 20: 34681
neutron scattering at 1.78 to 3.21 Mev, differential cross sections for, (E), 20: 39470(R) (ORNL-3924)
neutron total cross sections at 4.5 to 14.5 Mev, (T), 19: 35396 (NP-15095)
neutron total cross sections at 80 to 150 Mev, (E), 20: 34583
nitrogen-14 reactions on, neutron transfer in, 17: 15266
nitrogen-14 reactions (N^{14},N^{15}) at 18 Mev, neutron transfer mechanisms in, 17: 38228
nitrogen-14 reactions with, analysis of, 18: 24618 (NYO-1807-8)
nitrogen-14 reactions (N-14,N-13) at 6.62 Mev, neutron reduced widths from, (E), 19: 21387
nitrogen-14 reactions (N-14,N-13) at 4.7 to 9.4 Mev, neutron tunneling mechanism in, (E), 19: 21388
nitrogen-14 reactions (N-14,F-18) with, analysis of, (E), 19: 37823(R) (ORNL-3800(p.1-49))
nitrogen-14 reactions (N-14,N-13) with, cross sections, (E), 19: 37823(R) (ORNL-3800(p.1-49))
nitrogen-14 reactions (N-14,N-13) below Coulomb barrier, (E), 19: 43390
nitrogen-14 reactions (N-14,N-13) at 9.0 to 18.0 Mev, neutron transfer cross sections for, 18: 7770
nitrogen-14 reactions (N-14,N-13) at 9 to 16 Mev, ground-state neutron transfer in, 18: 9410
nitrogen-14 reactions (N-14, N-13) with particle transfer model for, 20: 4851
nitrogen-14 reactions (N-14, N-13) with, total cross sections for, (E), 20: 12057
nitrogen-14 reactions (N-14,N-13) with, angular distributions and cross sections for, (T), 20: 13830
nuclear charge distribution, mean-square radius, 16: 18529
nuclear deformation parameters and energy levels for, 18: 21307
nuclear excitation by 180° electron scattering, 17: 5388
nuclear magnetic moment, 18: 13111
nuclear magnetic resonance shifts in terbium and thulium nitrides, 16: 31620
nuclear magnetic resonance in organic compounds, chemical shifts in, 18: 43497
nuclear magnetic resonance in rare-earth nitrates and transition-metal nitrates, 20: 12325
nuclear quadrupolar relaxation of, in quaternary ammonium compounds, 19: 34177
nuclear quadrupole resonance in nitrogen (solid) at 1.5 to 34.5°K, 16: 16354
nuclear quadrupole relaxation in organic compounds, 18: 33615
nuclear quadrupole resonance in hexamethylenetetramine, molecular rotations from (E), 19: 2337
nuclear quadrupole coupling constant for, in polyatomic molecules, 19: 11086
nuclear quadrupole resonance, 19: 31448(R) (RPI-3030-3)
nuclear quadrupole coupling constants in deuterated and normal crystalline ammonia, (E), 19: 45483
nuclear spin resonance, 17: 41967
nucleon pairing forces in, non-canonical transformation for calculation, 16: 21509
nucleon scattering by, differential cross section and polarization for, (T), 20: 3091
nucleon spatial correlations in, 19: 19152
oxygen-16 reactions at 6.3 to 12 Mev, compound nucleus formation, 16: 7041
production and separation of, method for, 20: 11191 (JEN-150-DQ/I-51)
production and trapping in x-irradiated sodium azide at low temperatures, 16: 5250
production by carbon-12 reactions at 6.5 to 11 Mev, angular distributions and excitation functions in, 17: 38087 (NYO-10034)
production by secondary nuclear reactions, 19: 30267
production in (α,n) reactions on boron-11, energy levels from, 17: 2252
production in carbon-13 (p,γ) reactions, 7.6 Mev resonance in, 17: 15269
production in deuteron reactions on oxygen-16, distributions, 18: 7078
production in lithium-6 and -7 reactions with boron-10 and -11, 20: 30519
production in oxygen-16 reactions at 10 Mev, differential cross sections, 16: 10999
production in oxygen-16 (B-10,3α) reactions, angular distributions from, (E), 20: 17815)
production in tissue by proton activation, 17: 31851 (BNL-6989)
proton activation of, in mice, 18: 15828
proton capture cross sections, 18: 32330
proton elastic scattering at 1–2 Mev, differential cross sections for, 17: 29589
proton elastic scattering at 31 Mev, differential cross sections for, 18: 32796
proton elastic scattering at 4.9 Mev to 10.1 Mev, polarization from elastic, (E), 20: 15783
proton elastic scattering at 1.0 to 2.9 Mev, angular distributsions for, (E/T), 20: 28283 (PD-261)
proton inelastic scattering at 185 Mev, cross sections for spin-flip, 16: 18520
proton inelastic scattering by, dipole-resonance effects on, 17: 11734
proton inelastic scattering at 10.2 Mev, angular distributions and total cross sections for, 18: 6242
proton inelastic scattering at 9.15 to 10.45 Mev, energy level excitation in, 18: 26605
proton inelastic scattering at 19 Mev, (E), 20: 1183
proton quasi-elastic scattering by, 18: 1012 (JINR-P-1357)
proton radiative capture in odd-parity states of, 18: 28674
proton reactions (p,n), excitation function of total cross section for, 18: 17061
proton reactions (p,γ) at 210 to 1070 kev, cascades in, 18: 18976
proton reactions (p,d) at 18.5 Mev, 18: 18979
proton reactions (p,n) with, yields in, 18: 21336
proton reactions (p,pd) with, shell-model calculations for, 18: 28619
proton reactions (p,pd) with, fragmentation theory for, 18: 40536
proton reactions (p,pn) and (p,2p2n) at 15 to 155 Mev, excitation functions for, 18: 44770
proton reactions (p,n) at 155 Mev (E/T), 19: 3313
proton reactions (p,α) in mixtures of nitrogen with alkanes and hydrogen, recoil reactions of carbon-11 produced in, 19: 2370 (BNL-8537)
proton reactions (p,α) with, for determination of trace amounts of nitrogen in graphite, 19: 15371
proton reactions (p,n) with, threshold of, (E), 19: 23683
proton reactions (p,2p) at 19 Mev, (E), 20: 1183
proton reactions (p,γ) at 0.97 to 1.96 Mev, performance of anticoincidence shielded gamma spectrometer for detecting, (E), 20: 4233 (AD-618676)
proton reactions (p,2p) at 460 Mev, (E/T), 20: 11948 (AD-624318)
proton reactions (p,2p) at 140 Mev, energy spectra and angular correlation distributions from, (E), 20: 17741
proton reactions (p,dp) with, 3α decay of excited nucleus from, 20: 22033
proton reactions (p,γ) at 0.85 to 1.96 Mev, oxygen-15 energy levels from, (E), 20: 42258
proton reactions (p,d) at 156 Mev, nitrogen-13 energy levels from, (E), 20: 42204
proton reactions at 100 Mev angular correlation and energy of multicharged lithium-6 and lithium-7 particles produced by, 17: 21092
proton reactions at 155 Mev, isotope dilution measurements of lithium-6 production in, 17: 38973
proton reactions at 155 Mev, cross sections for, 18: 4613
proton reactions at 2.2 Bev, beryllium-12 production in, (E), 19: 19184
proton reactions at 2.2 Bev with, cross sections for beryllium-7 production in, 19: 47625
proton reactions (p,2p) and (p,n) at 150 Mev, gamma radiation from, 16: 4859
proton reactions(p,α) in ammonia gas, 16: 29001
proton reactions (p,2p), hole excitation spectra from, 16: 29871
proton reactions (p,np), cross sections for, 17: 7188
proton reactions (p,α), use of, in studying recoil chemistry of carbon, 17: 19250
proton reactions (p,n) at 10 Mev, isospin potential in, 17: 38201
proton reactions (p,γ) at 800 kev, non-resonant emission in, 18: 9356
proton scattering at 1 to 2 Mev, cross sections, 16: 5868
proton scattering at 10.5 Mev, 18: 16951(R) (TID-20311)
radioinduced exchange with nitrogen-15, use in dosimeters, 20: 2520(R) (IA-920)
radioinduced isotopic exchange with nitrogen-15 in gaseous nitrogen, mechanism of, 18: 23680
reactions (N-14,α) with nuclei at 27 Mev, angular momentum effects in, 18: 24726
reactions (N-14,α) with aluminum-27, oxygen-16, and sodium-23, quantum mechanical spin-cutoff parameters for, 18: 28573(R) (ORNL-3630(p.1-17))
reactions (N-14,α) with lithium-6 and -7 at 27.6 Mev, differential cross sections for, 18: 36660
reactions (N-14,α) with aluminum-27 and oxygen-16, cross sections, (T), 19: 10255 (ORNL-TM-971)
reactions (N-14, B-10) with beryllium-9 at 30 Mev, proton transfer recoil effects in, (T), 19: 33339
reactions (N-14, B-10) with beryllium-9 at 30 Mev, alpha transfer recoil effects in, (T), 19: 33339
reactions (N-14, C-13) with beryllium-9 at 20 to 30 Mev, angular distributions from, 20: 40065(R) (BMwF-FB-K-66-01)
reactions (N-14, F-18) with oxygen-16 at 20 to 33 Mev, angular distributions from, (E), 20: 32429
reactions (N-14, N-13) with zinc-68, isomeric ratios in, 19: 22282(R) (NYO-1930-40)

reactions (N-14, N-13) with boron-10 and nitrogen-14, total cross sections for, (E), 20: 12057
reactions (N-14,F-18) with nuclei, analysis of, (E), 19: 37823(R) (ORNL-3800(p.1-49))
reactions (N-14,F-18) with aluminum-27 at 65.0 to 107.3 Mev, (E), 20: 42156 (JINR-P-2813)
reactions (N-14,γ) with phosphorus-31 at 27 Mev, 16: 29853
reactions (N-14,N-15) with scandium-45 at 27.5 Mev, excitation functions for, 18: 28573(R) (ORNL-3630(p.1-17))
reactions (N-14,N-13) with phosphorus-31 at 27.5 Mev, excitation functions for, 18: 28573(R) (ORNL-3630(p.1-17))
reactions (N-14,N-13) with rhodium at 10 Mev, differential cross sections for, 18: 34951
reactions (N-14, N-13) with gold-197 at 69 to 133 Mev, diffraction model for, 18: 42709
reactions (N-14, N-13) with rhodium-103 at 140 Mev, diffraction model for, 18: 42709
reactions (N-14,N-13) with nuclei, cross sections, (E), 19: 37823(R) (ORNL-3800(p.1-49))
reactions (N-14,N-13) with nuclei, neutron-reduced widths in, (E), 19: 37823(R) (ORNL-3800(p.1-49))
reactions (N-14,N-15) and (N-14,O-15) with nuclei, 17: 19339
reactions (N-14,N-13) with nitrogen-14 at 9 to 16 Mev, ground-state neutron transfer in, 18: 9410
reactions (N-14,N-13) with boron-10 and calcium-40 at 8 to 16 Mev, cross sections for, (E/T), 20: 30353(R) (ORNL-3940, pp 1-61)
reactions (N-14,N-15) and (N-14,O-15) with carbon-12 at 148 Mev, isospin purity in, (E), 20: 36214
reactions (N-14,O-15) with aluminum-27, oxygen-16, and sodium-23 at 27.5 Mev, excitation functions for, 18: 28573(R) (ORNL-3630(p.1-17))
reactions (N-14,p2n) with sodium-23, excitation functions for, 18: 28573(R) (ORNL-3630(p.1-17))
reactions (n-14,2p) with carbon-12 at 20 to 65 Mev, excitation functions and isomeric yield for, (E), 19: 29242 (JINR-E-2012)
reactions (N-14,3n) with indium-115 at 52 Mev, barium-126 energy levels from, (E), 19: 45285 (UCRL-16040)
reactions (N-14,5n) with holmium-165 and terbium-159, final-state rotational energy levels from, 18: 44738 (UCRL-11402)
reactions (N-14,5n) with indium-115 at 84 Mev, barium-124 energy levels from, (E), 19: 45285 (UCRL-16040)
reactions (N-14,5n) with cesium-133, angular momentum effects on excitation functions for, (E), 20: 17784
reactions (N-14,N-13) with magnesium-25, indirect interaction theory for, 17: 20991 (TID-18504)
reactions (N^{14},α) on lithium-6 at 27.5 Mev, angular distributions for, 17: 38279
reactions (N^{14},C^{13}) and (N^{14},N^{13}) with boron-10 at 28 Mev, carbon-11 and nitrogen-13 angular distributions and ranges from, 17: 26597
reactions (N^{14},C^{13}), (N^{14},N^{13}), and (N^{14},O^{15}) on nuclei, cross sections for nucleon transfer in, 17: 38279
reactions (N^{14},N^{15}) with lead-207 at 132 Mev, neutron transfer in, 17: 36649 (CONF-62-12)
reactions (N^{14},N^{15}) with nitrogen-14 at 12 Mev, 17: 36650 (CONF-62-13)
reactions (N^{14},5n) with cesium-133 at 79.8 and 105.4 Mev, samarium-142 recoil range from, 17: 33094
reactions on bismuth-209 and gold-197 at 7.1 to 10.5 Mev/nucleon, 16: 3744
reactions on cobalt-59 and manganese-55, mechanisms for, 16: 33891
reactions with aluminum-27 at 8.0 to 147.0 Mev, excitation functions, 16: 9460
reactions with aluminum, copper, gold, nickel, and tantalum, neutron transfer in, 16: 26221 (JINR-P-973)
reactions with aluminum, carbon, copper, and tantalum nuclei, nitrogen-17 production in, 16: 17153
reactions with aluminum, copper, and tantalum, nitrogen-17 production in, 16: 27381
reactions with antimony-121 at 80.9 to 144.2 Mev, ion recoil ranges in aluminum from, (E), 20: 28425
reactions with beryllium-9 at 20 to 30 Mev, heavy-product angular distributions from, (E), 19: 33286
reactions with beryllium-9 at 25 Mev, beryllium, boron, carbon, and lithium spectra from, 20: 40065(R) (BMwF-FB-K-66-01)
reactions with bismuth-209 and gold-197, fission, 17: 17225
reactions with boron-10 and boron-11 at 27.5 Mev, proton transfer, 16: 9459
reactions with boron-10, boron-11, magnesium-24, and nitrogen-14 at 28 Mev, nucleon transfer in, 16: 21575
reactions with bromine and silver in emulsions, recoil range-energy ratio for, (E), 19: 43360
reactions with carbon-12 and nitrogen-14, rates for thermonuclear, 16: 23016
reactions with carbon-12, mechanisms and spins in, 17: 12802(R) (PR-P-55)
reactions with carbon-12 at 133.8 Mev, cross sections for, 16: 15669
reactions with cesium-133 at 140 Mev, cesium isotope production in, 20: 19927
reactions with chlorine-35, phosphorus-31 and sulfur-32, scandium-44 isomeric yield ratios for, 17: 24053(R) (ORNL-3432)
reactions with chlorine-35, cross sections for isotope production in, 17: 24053(R) (ORNL-3432)
reactions with chlorine-35, phosphorus-31, and sulfur-32 at 30 to 42 Mev, scandium-44 isomer pair production in, (E), 19: 21392
reactions with complex nuclei, recoil-range evidence for compound-nucleus formation in, 17: 4088
reactions with fluorine-19 and oxygen-16 at 21.4 to 27.4, angular distributions from, 16: 21625
reactions with gold-197, product distribution in, 17: 24391 (JINR-P-1238)
reactions with gold-197 and silver-107 at 70 to 130 Mev, cross sections for, 19: 1554 (JINR-P-1745)
reactions with heavy nuclei, angular momentum effects on neutron emission in, 17: 26470 (UCRL-10767)
reactions with holmium-165, fission, (E/T), 19: 21259(R) (UCRL-11828(p.77-80))
reactions with lead-207 and lead-208, energy level selection in neutron transfer in, 16: 21536
reactions with light nuclei at 9.6 Mev, gamma spectra of transfer, 18: 24721
reactions with lithium-6 and lithium-7, 16: 31128(R) (ORNL-3257)
reactions with lithium-6 and -7 at 7.7 to 27.5 Mev, cross sections for fluorine-18, oxygen-15, and -19 production in, 18: 28573(R) (ORNL-3630(p.1-17))
reactions with magnesium-24, angular distribution and ranges of nitrogen-13 from, 16: 21416
reactions with nickel-58, angular momentum effects in, 17: 36657 (JINR-P-1347)
reactions with nitrogen-14, cross sections for nitrogen-13 production in, 17: 9580
reactions with nitrogen-14, cross section for nucleon-transfer, 17: 20992 (TID-18508)
reactions with nitrogen-14, neutron reduced widths from, 18: 16929 (ANL-6848(p.160-7))
reactions with nitrogen-14 in nitrate-doped alkali halide crystals, 18: 31530
reactions with nitrogen-15 on tungsten, equilibration, 19: 46289
reactions with nuclei, terbium-149 isomeric excitation functions from, 17: 26573
reactions with nuclei, cross sections for nucleon transfer in, 17: 38292
reactions with nuclei at 27.5 Mev, single-nucleon transfer excitation functions for, 18: 24716
reactions with nuclei at 27 Mev, angular-momentum effects in compound-nucleus, (E), 19: 12590
reactions with nuclei, scandium-44 isomeric state from, (E), 19: 37823(R) (ORNL-3800(p.1-49))
reactions with nuclei, excitation functions for nucleon-transfer, (E/T), 19: 47586 (ORNL-TM-1218)
reactions with nuclei at 20 to 42 Mev, excitation functions for alpha- and nucleon-transfer, (E), 19: 47667
reactions with phosphorus-31 and sulfur-32, production of scandium in, 17: 38108
reactions with photoplates, blackening effects in, (E), 19: 6781
reactions with platinum-198 at 60 to 110 Mev, products from, 16: 24854 (UCRL-9950)
reactions with praseodymium-141, equilibrium charge distribution in, 17: 24750(R) (UCRL-10624)
reactions with rare earths, effective charge distribution from, 18: 24624 (UCRL-10806)
reactions with tantalum at 140 Mev, production of platinum isotopes in, 19: 23656
reactions with tellurium-128, cross sections for tellurium-127 and -129 production in, 18: 13839(R) (TID-20201)
reactions with tellurium-128 and zinc-68 at 40 to 150 Mev, isomeric pair production ratios in, 19: 41674 (NYO-1930-44)
reactions with tin-120 at 138.2 Mev, ion recoil ranges in aluminum from, (E), 20: 28425
reactions with uranium-238, production of actinium-225 and -226 from, 16: 25411 (JINR-P-978)
reactions with uranium-238 to 10.4 Mev/nucleon, 17: 833
scattering by aluminum at 0.3 Mev/nucleon, angular distributions from multiple, (E), 20: 25749
scattering by beryllium-9 and carbon-12, optical model description of elastic, 17: 31542
scattering by bismuth-209, 17: 22558 (JINR-P-1244)
scattering by carbon-12 and nitrogen-14, cross sections for differential elastic, 16: 10729
scattering by carbon-12 and nitrogen-14, experimental and theoretical cross sections for elastic, 17: 20989 (TID-18505)

scattering by carbon, electronic stopping cross sections in, 17: 37670
scattering by carbon-12 and nitrogen-14, cross sections for elastic, 18: 24674
scattering by erbium-167 at 50 Mev, Coulomb excitation of 532-kev level in, 16: 33829
scattering by even-even nuclei at 37 Mev, double coulomb excitation in, 18: 28601
scattering by even tin isotopes at 52.5 Mev, coulomb excitation of E3 transitions in, 18: 28602
scattering by gold-197, optical model calculation of differential cross section for elastic, 17: 22550 (BNL-6931)
scattering by lead-208, elastic, 17: 34990
scattering by lead-206, -207, and -208, elastic, 16: 29843
scattering by nuclei, strong absorption model for elastic, 18: 26563
scattering by nuclei, diffraction mechanism for elastic, 18: 34848
scattering by nuclei, Coulomb excitation in inelastic, (E), 20: 19959
scattering by samarium-152 and selenium-78, 2^+ level excitation in, (T), 20: 15768
scattering by samarium-152 and tungsten-186, Coulomb excitation from inelastic, (E), 20: 30488
scattering by zirconium-90 and zirconium-96 at 44 Mev, Coulomb energy-level excitation in, (E), 19: 39942
separation by exchange reactions, 16: 29295(R) (NYO-8771)
separation from nitrogen-15 in hydrochloric acid–nitric oxide complex, 16: 32021
separation from nitrogen-15 by thermal diffusion, 17: 30895(R) (NYO-8772)
separation from nitrogen-15, 18: 37584 (A/CONF.28/P/491)
separation from nitrogen-15 by thermal diffusion, optimal conditions for, 18: 39779 (IFA-30-IS)
separation from nitrogen-15 by ion exchange in amine systems, 19: 9046(R) (IS-900(Sect.C))
separation from nitrogen-15 by ion exchange, effects of ion exchange material and solvent on, 19: 20433
separation from nitrogen-15 by thermal diffusion, 19: 24908
separation from nitrogen-15 in reactions of chromium ions with cobalt ammine complexes, 19: 36369
sorption on tungsten in presence of nitrogen-15, isotope mixing in, 19: 32150
spectra in alkali metal–ammonia solutions, Knight shifts and relaxation times in, 19: 7386
spectra in gaseous and solid nitric acid, vibrational, 19: 7394
spectra in solid nitrogen, effects of nitrogen-15 on nuclear quadrupole resonance, 17: 12837
spectra in vacuum uv region in nitrogen, isotope shifts in, 18: 42302
spectra of molecular, at 720 to 830 A, 18: 28240
spectra of, vibration quantum number assignment of $D^3\Pi_g$–$A^3\Pi_u$ bands in, 18: 3749
spectroscopy, 16: 32458(R) (LAL-1035)
spin-lattice relaxation in hexamethylenetetramine, 19: 22220
structure, from lithium-6 reactions with carbon-12, 16: 24851
thermal diffusion factors for systems of mixed diatomic molecules of, with nitrogen-15, 20: 25034 (IFA-IS-35)
tritium reactions (t,α) and (t,d_0), differential cross sections for, 16: 4611(R) (NP-11098)
triton reactions (t,α), (t,d), (t,p), and (t,t) at 1 to 2 Mev, differential cross sections for, 18: 21282
triton reactions (t,p) at 1195 Mev, nitrogen-16 energy levels from, (E), 20: 44730
triton reactions (t,α) and (t,n) on, cross sections for, 16: 33897
use as polarized proton detector, 20: 27305
viscosity coefficient from 78 to 300°K, (E), 19: 5847
x-ray spectra of μ- and π-mesic atoms of, (E), 20: 34103
N-14–N-15, thermal diffusion factors for, as function of temperature, 20: 25034 (IFA-IS-35)

NITROGEN ISOTOPES N-15

alpha elastic and inelastic scattering at 40.5 Mev, angular distributions for, (E), 20: 30450
alpha elastic scattering at 40.2 Mev, cross sections for, 18: 32749 (UCRL-11378)
alpha reactions (α,d) at 45 to 50 Mev, highly populated levels in, 18: 34779 (UCRL-11341)
alpha reactions (α,d) at 42 to 53 Mev, deuteron energy spectra from, (E), 20: 12061
alpha reactions (α,d) at 42 to 53 Mev, energy spectra from, (E), 20: 24358(R) (UCRL-16580, pp 1-93)
alpha reactions (α,Li-7) at 42 Mev, angular distributions from, (E/T), 20: 28284 (RLO-1388-5)
alpha reactions (α,d), 16: 20305(R) (UCRL-10023)
alpha reactions (α,d) at 47 Mev, energy levels excited in, 17: 38289
alpha reactions (α,d) on, residual energy levels from, 17: 9548
alpha scattering at 40.5 Mev, inelastic, (E), 20: 24360(R) (UCRL-16580, pp 107-48)
alpha scattering by octupole levels in, at 40.6 Mev, (E/T), 19: 21268(R) (UCRL-11828(p.129-31))
boron-11 reactions (B-11,B-10) and (B-11,Be-10) at 115 Mev, fractional parentage of boron-11 ground state from, (E), 20: 36214
bremsstrahlung reactions (γ,p) at 19 to 30.5 Mev, cross sections and photoproton energy spectra for, 18: 32856
charged-particle reactions with, amplitude singularities in knockon and stripping, (T), 20: 21997 (INSJ-96)
concentration by exchange between nitrogen oxides using carbon tetrachloride–freon 112 solvents, 20: 31638(R) (NYO-755-1, pp 12-76)
concentration by exchange between nitric acid and nitric oxide, effects of additives on, 20: 31639(R) (NYO-755-1, pp 77-129)
concentration of, noncorrosive packing for exchange-column, 18: 12522 (PAN-458/XVI)
content in natural nitrogen, 18: 13691
content in soils, 19: 6089
content of, in alkaloids, amides, and amino acids, significance of excess, 17: 23043
core deformability and electric quadrupole moments, 16: 7026
determination by spectroscopy, elimination of interfering background, 16: 12987
determination in amino acids in legume root nodules, use of ninhydrin in colorimetric, 20: 40824
determination in gases by spectrography, step-filters for, 20: 12807
determination in gases, by proton irradiation and neutron time-of-flight spectroscopy, 20: 43115
determination in inorganic and organic compounds, mass-spectrometric, 20: 29131
determination in nitrogen compounds by mass spectrometry, 19: 36282
determination in 0.38 to 20.0 percent range, spectrographic method for, 20: 36772
determination of, method for, 18: 37070 (A/CONF.28/P/825)
deuteron reactions (d,n) at 1.25 Mev, angular distributions and differential cross sections, 16: 12418 (AD-262135)
deuteron reactions (d,α) and (d,p), measurement of Q_0 values for, 16: 11039
deuteron reactions (d,n) at 2.5–3.0 Mev, angular distributions and energy level excitation in, 17: 38231
deuteron reactions (d,p) with, study of excited levels in nitrogen-16 from, 17: 41908
deuteron reactions (d,p) with, energy-level studies from, 17: 40434(R) (NYO-10063(p.90-8))
deuteron reactions (d,p) at 3 Mev, studies of nitrogen-16 produced by, 19: 9771(R) (PR-P-63)
deuteron reactions (d,α) at 1 to 2.5 Mev, (E), 19: 14578
deuteron reactions (d,p) at 7.5 Mev, angular distributions from, (E), 19: 36220(R) (MIT-2098-142)
deuteron reactions (d,n) at 1.6 to 3.0 Mev, neutron polarization from, (E), 20: 30427
deuteron reactions (d,α) at 0.8 to 1.8 Mev, oxygen-17 energy levels from, (E), 20: 42295
deuteron reactions (d,p) at 11.98 Mev, nitrogen-16 energy levels from, (E), 20: 44730
doublet splitting in 1p shell due to tensor interaction, 16: 9466
doublet splitting in, due to spin-orbit interaction, 19: 10360
effects on cobalt-59 magnetic shielding in potassium cyanocobaltates, (E/T), 19: 10269
effects on ESR signals in photosynthetic organisms, 19: 31686
effects on fractional decomposition of diazonium salts, 19: 38690
effects on Franck-Condon factors for electron transitions in nitrogen molecules, 20: 18658
effects on infrared spectra of lysine hydrochlorides, tetramethylenediamine, and pentamethylenediamine, 19: 30223
effects on radiation stability of azides and nitrates, 20: 45754
effects on rice cultivation, 20: 23534 (AECD/Ag/2)
effects on vibrational frequencies in polyglycine, 18: 31490
electron energy levels of, 2^3P, (T), 19: 12083
electron spin resonance, 19: 37469
electron spin resonance of, in gamma-irradiated potassium sulfamate, 20: 40955
emission in oxygen reactions (O-16,N-15) with aluminum-27 at 30 Mev, angular distributions for, 18: 24718
energy level at 6.32 Mev, spin of, 18: 18990
energy level at 7.57 Mev, 16: 29834
energy level at 9.83 Mev, gamma spectra of, 19: 1630
energy level de-excitation in, formed in nitrogen-15 (d,p) reactions, 17: 7159
energy level excitation by 40-Mev alpha particles, collective excitations in, 18: 32749 (UCRL-11378)
energy level lifetimes from helium-3 reactions (He-3,pγ) with carbon-13 at 4.5 to 5.5 Mev, (E), 20: 36211
energy level structure of, (E/T), 19: 6637 (NOLTR-64-46)
energy level transitions in, probability for two-quantum (E), 19: 3323

energy level transitions in, mixing ratios for, (E), 20: 6378
energy level transitions in, destructive interference of hole and collective E2, (T), 20: 10067
energy levels, 17: 881
energy levels, 18: 32329
energy levels, 18: 40631
energy levels, (E), 20: 34576
energy levels, (E), 20: 42369
energy levels, 18: 24625 (WASH-1046)
energy levels and equilibrium form, 18: 30832
energy levels excited by (α,p) reactions on carbon-12, 16: 21417
energy levels from deuteron beam reactions with light nuclei, 16: 11040
energy levels from proton reactions with fluorine-19 at 143 Mev, 16: 17088
energy levels from carbon-14 (d,n) reactions, 18: 18965
energy levels from gamma reactions (γ,p) with oxygen-16 at 21.3 to 43.7 Mev, (E), 20: 3107
energy levels from helium-3 reactions (He-3,pγ) with carbon-13 at 4.95 and 5.25 Mev, (E), 20: 13819
energy levels from boron-11 (α,n) reactions, parity and spin of, (E), 20: 15790
energy levels from lithium-6 and -7 reactions with boron-10 and -11 at 3.05 Mev, (E), 20: 26167
energy levels from helium-3 reactions (He-3, pγ) with carbon-13 at 3.0 Mev, (E), 20: 32495
energy levels from deuteron reactions (d,p) with nitrogen-14 at 4 Mev, (E) 20: 32501
energy levels from helium-3 reactions (He-3,p) with carbon-13 at 4.0 Mev, (E), 20: '32501
energy levels from oxygen-16 (γ,pγ') reaction, (E), 20: 42343
energy levels in, collective retardation in 6.33-Mev, $^1/_2^-$, (E/T), 19: 43329
energy levels in, particle-hole matrix-elements for, (T), 20: 10051
energy levels, L-S potential in spin-orbit splitting, 16: 31070 (TID-12043)
energy levels of, (E), 20: 19273(R) (BNL-929, pp 3-43)
energy levels of, (E/T), 20: 30353(R) (ORNL-3940, pp 1-61)
energy levels of, Coulomb energy differences between oxygen-15 and, 17: 36691
energy levels of, from alpha reactions (α,p) with boron-11 at 2.5–5.0 Mev, 17: 31472
energy levels of, spin-orbit splitting from two-nucleon potential in, 18: 6190
energy levels of, parity and spin for, (E), 19: 19196
energy levels of, gamma transitions from doublet, (E), 19: 19204
energy levels of, analysis of spurious states owing to center-of-mass motion, (T), 19: 39812
energy levels of, from carbon-12 (t,α) reactions, (E), 19: 41706
energy levels of, parity and spin of excited, (E), 19: 47604
energy levels of, from oxygen-16 giant dipole resonance de-excitation, (E), 20: 3074
energy levels of, lifetime, parity, and spin of, (E), 20: 5928(R) (PR-P-66)
energy levels of, gamma rays from first two excited, (E), 20: 6318
energy levels of, Hartree-Fock calculations for, (T), 20: 40138
energy parameters of two-body interactions in various nuclear configurations, 18: 14823
energy-level transitions in, 6.33-Mev, (T), 20: 44783
energy-level transitions in, mixing ratios for, (T), 20: 44784
enrichment by chemical exchange in nitric acid–nitric oxide systems, 17: 2686
enrichment of, in marine algae, 19: 2020
exchange between nitric acid and nitric oxide in bubble cap column, effects of additives on, 18: 2132(R) (TID-19592(Sect.IV))
exchange between nitric acid and nitric oxide, mechanisms of, 20: 9362(R) (NYO-755-2, Paper 1)
exchange between nitric acid and nitric oxide, effects of acids and salts on, 20: 9363(R) (NYO-755-2, Paper 3)
exchange equilibrium calculations in oxy-nitrogen molecules, 19: 40460(R) (NYO-3462-1)
exchange in nitrous oxide, 16: 1761
exchange of, between nitric acid and nitric oxide in aqueous solution, oxygen-18 concentration in, 17: 18656
exchange of, in reactions of active nitrogen with nitric oxide, 16: 25362
exchange reactions between nitrogen oxides, equilibrium constants and frequencies of, 19: 4136
exchange with nitrogen-14 in radiolysis of gaseous nitrogen, 20: 31282
fractionation in nitric acid–nitric oxide system, effects of temperature on, 20: 40873(R) (NYO-3462-2)
gamma reactions (γ,p) at 24.5 and 31 Mev, proton spectra from, 17: 28294
gamma spectra and energy levels, 16: 18434
gamma transitions in, spectra from, 19: 26922(R) (PR-P-64)
gamma transitions in, angular distributions and intensities of (E), 20: 4905
harmonic oscillator constant in, 16: 13994
helium nucleus reactions (He^3) with, 16: 30924(R) (CU(PNPL)-214)
helium nucleus reactions (helium-3α), 17: 4083
helium-3 reactions (He^3,d) and (He^3,p) with, 17: 15251(R) (CU(PNPL)-220)
helium-3 reactions (He-3,d) and (He-3,p) with, distributions from, (E), 19: 37815(R) (ORNL-3778(p.104-10))
helium-3 reactions (He-3,α) at 39.8 Mev, nitrogen-14 levels from, (E), 20: 30438
hyperfine structure in, 16: 26318
incorporation in DL-β-methylaspartic acid, 19: 22266(T)
incorporation in nitrous oxide, methods for, 19: 30235(R) (RPI-321-2)
incorporation in substituted quinolines, methods for, 19: 28429
incorporation in thiazole to study ring geometry, 18: 43595
incorporation in 2-picolyl ketones, 20: 45782
incorporation into inorganic compounds, review, 17: 8202
incorporation of, into rat proteins from labeled glycine, 20: 38600(R) (TID-23034)
isotope effects of, in organic reaction mechanisms, use of successive labeling technique for studies on, 18: 39341
isotope effects on characteristic frequencies of amino acids, 17: 23379
isotope effects on elimination reactions of quaternary ammonium salts with ethoxide ions, 17: 28925
isotope effects on decomposition of *p*-nitrophenethyltrimethylammonium iodide in solutions, 18: 6839 (TID-19838)
labeling positions in ricinine, mass spectral studies on, 20: 43382
lifetime in hydrogen burning stars, 17: 3914
magnetic resonance in nitrogen, analysis of EPR and NMR, (E), 19: 22654 (CEA-R-2506)
neutron binding energy, 18: 11166 (ANL-6797(p.179-82))
neutron elastic scattering at 1.9 to 3.5 Mev, cross sections for, 16: 21394
neutron elastic scattering up to 10 Mev with formation of compound particle-hole states, resonances in, 18: 18890
neutron elastic scattering at 440 to 1960 kev, angular distributions for, 18: 28643
neutron reactions (n,γ) with, resonance, 18: 11182 (ANL-6797(p.342-57))
neutron reactions (n,d), effects of compound nucleus processes on, 19: 14533(R) (NYO-1082-1)
neutron reactions (n,d) at 14.1 and 14.8 Mev, angular distributions from, (E/T), 20: 8078(R) (NYO-1082-2)
neutron reactions (n,p) at 14.8 Mev, cross sections for, (E), 20: 36212
neutron reactions (n,d) at 14 Mev, (E), 20: 38150
neutron scattering at 1 to 12 Mev, cross sections for, (T), 20: 6426
neutron separation energy, (E), 20: 24329(R) (ANL-7108, pp 1-4)
neutron total cross sections of, fast, 18: 24625 (WASH-1046)
neutron total cross sections at 0.45 to 2.20 Mev, 18: 36674
neutron total cross sections at 3.2 to 6.6 Mev, (E), 20: 9981 (WASH-1064)
nuclear deformation parameters and energy levels for, 18: 21307
nuclear magnetic dipole moment, (T), 19: 21322
nuclear magnetic moment, 18: 13111
nuclear magnetic moment, (T), 19: 6667
nuclear magnetic moment corrections for, perturbation theory for, 20: 13838
nuclear magnetic resonance in compounds, chemical shifts in, 18: 23530
nuclear magnetic resonance in liquids, chemical shifts of, 18: 27399
nuclear magnetic resonance of, in nitrogen molecules (E), 19: 2979
nuclear state alignment of, 17: 11703
nucleon clustering in, reduced widths for, 18: 28680
nucleon clustering in, theory of, 18: 32851
production and separation of, method for, 20: 11191 (JEN-150-DQ/I-51)
production by nitrogen-14 reactions (N-14,N-13) below Coulomb barrier, (E), 19: 43390
production by NITROX method during sulfuric acid production, 20: 35569 (INR-674/XVI/J)
production by secondary nuclear reactions, 19: 30267
production, design of plant using Hitrox process for, 16: 3367 (AERE-Z/R-2629)
production in lithium-6 and -7 reactions with boron-10 and -11, 20: 30519
production in oxygen-16 reactions at 10 Mev, differential cross sections, 16: 10999
production of, methods for, 19: 46413
proton capture by, gamma yield from, 18: 14590(R) (NIRL/R/60)
proton reactions (p,γ) with, resonance, 18: 11182 (ANL-6797(p.342-57))
proton reactions (p,γ) at 4 to 14 Mev, structure of giant dipole resonance in, 18: 19051
proton reactions (p,α) at 15.16 Mev, analysis of, 18: 28630
proton reactions (p,$\alpha\gamma$) with, threshold energy for, 18: 28633
proton reactions (p,n) at 6.9 to 12.3 Mev, neutron polarization in,

18: 38072 (UCRL-7676)
proton reactions (p,n) at 18.5 Mev, angular distributions of quasielastic, 18: 40587
proton reactions (p,α) with, analysis of (E/T), 19: 1690
proton reactions (p,γ) with, giant dipole resonances in, (E/T), 19: 6665
proton reactions (p,n) at 6.9 to 12.3 Mev, neutron polarization from, (E/T), 19: 10338
proton reactions (p,α) with, cross section fluctuations in, (E), 19: 14499 (ANL-6878(p.457-77))
proton reactions (p,α$_0$) and (p,γ$_0$) with, theory for, 19: 39805
proton reactions (p,n) with, neutron polarization in, 19: 47710
proton reactions (p,α) at 3 to 12 Mev, direct-reaction analysis of angular distributions from, (E/T), 20: 3061
proton reactions (p,α) with, angular distributions for, (E), 20: 4849(R) (UCRL-14360, pp 1-50)
proton reactions (p,t) at 43.7 Mev, (E), 20: 12036
proton reactions (p,He-3) at 43.7 Mev, (E), 20: 12036
proton reactions (p,α) at 6.70 to 15.16 Mev, cross sections for, (E), 20: 19818 (INSJ-95)
proton reactions (p,t) with, angular distributions and energy spectra from, 20: 24358(R) (UCRL-16580, pp 1-93)
proton reactions (p, He-3) with, angular distributions and energy spectra from, 20: 24358(R) (UCRL-16580, pp 1-93)
proton reactions (p,α) at 340 to 470 kev, angular-distribution energy dependence from polarized, (E), 20: 24476
proton reactions (p,γ) with, oxygen-16 energy levels from, (E), 20: 42342
proton reactions at 2.2 Bev, beryllium-12 production in, (E), 19: 19184
proton reactions at 2.2 Bev with, cross sections for beryllium-7 production in, 19: 47625
proton reactions (p,n) and (p,γ), cross sections, 16: 12211(R) (CU(PNPL)-208)
proton reactions (p,γ), excitation and giant dipole resonance in, 16: 21510
proton reactions (p,αγ), gamma yield curve for, 17: 21065
proton reactions (p,α) at 7–15 Mev, angular distributions from carbon-12 ground and first excited state in, 17: 38295
proton reactions (p,n) with, Lane optical model analysis of, 17: 39984 (UCRL-7229)
proton reactions (p,γ) on, branching ratios from, 17: 41919
proton reactions (p,α) at 3.5 to 12.5 Mev, angular distributions and excitation curves, 18: 1087
proton reactions with, research on, 17: 29392(R) (NP-12951)
proton reactions with, oxygen-16 excitation in, 18: 38103
proton reactions with, 3⁻ continuum states of oxygen-16 from, (T), 20: 38102
radioinduced exchange with nitrogen-14, use in dosimeters, 20: 2520(R) (IA-920)
radioinduced isotopic exchange with nitrogen-14 in gaseous nitrogen, mechanism of, 18: 23680
reactions (N-15,xn) with thulium-169, beta decay of osmium-180 from, (E), 20: 42284
reactions (N-15,4n) with americium-243 at 75 to 90 Mev, nobellum-254 production in, (E), 20: 11969 (JINR-P-2471)
reactions with aluminum, copper, gold, nickel, and tantalum, neutron transfer in, 16: 26221 (JINR-P-973)
reactions with aluminum, copper, and tantalum, nitrogen-17 production in, 16: 27381
reactions with complex nuclei, recoil-range evidence for compound-nucleus formation in, 17: 4088
reactions with heavy nuclei at 102 Mev, neutron pickup in, (E), 20: 22001 (JINR-P-2555)
reactions with nitrogen-14 on tungsten, equilibration, 19: 46289
reactions with nuclei, production of nitrogen-17 in, 16: 7130
reactions with nuclei, terbium-149 isomeric excitation functions from, 17: 26573
reactions with nuclei, cross sections for nucleon transfer in, 17: 38292
reactions with zirconium isotopes, two-neutron transfer in, 17: 38080 (JINR-P-1273)
reactions with zirconium-94, -92, and -90 at 70 to 120 Mev, cross sections for two-neutron transfer in, 18: 6260
role in soil organic matter research, 20: 42795
separation by exchange reactions, 16: 29295(R) (NYO-8771)
separation by exchange between nitric oxide and nitrogen tetroxide complexes, 18: 2121(R) (TID-19592(Sect.III))
separation by ligand exchange, method for, 19: 24447
separation by nitric oxide-nitric acid exchange, 18: 37578 (A/CONF.28/P/388)
separation by nitric oxide distillation, 19: 11648
separation by thermal diffusion, 16: 3374
separation from nitrogen isotopes in exchange-distillation systems, 16: 2101(R) (TID-13776)
separation from nitrogen-14 in hydrochloric acid–nitric oxide complex, 16: 32021
separation from nitrogen-14 by thermal diffusion, 17: 30895(R) (NYO-8772)
separation from nitrogen-14, 18: 37584 (A/CONF.28/P/491)
separation from nitrogen-14 by thermal diffusion, optimal conditions for, 18: 39779 (IFA-30-IS)
separation from nitrogen-14 by ion exchange in amine systems, 19: 9046(R) (IS-900(Sect.C))
separation from nitrogen-14 by ion exchange, effects of ion exchange material and solvent on, 19: 20433
separation from nitrogen-14 by thermal diffusion, 19: 24908
separation from nitrogen-14 in reactions of chromium ions with cobalt ammine complexes, 19: 36369
separation from other nitrogen isotopes, optimal conditions for, 17: 29235
separation from other nitrogen isotopes by thermal diffusion, 17: 29237
separation from other nitrogen isotopes by chemical exchange, mass transfer in, 17: 32470
separation from other nitrogen isotopes, review of methods for, 19: 11642
separation from other isotopes by exchange, 20: 9361(R) (NYO-755-2)
separation from other isotopes by exchange between nitrogen oxides, carrier effects on, 20: 9362(R) (NYO-755-2, Paper 1)
separation from other isotopes by exchange between nitrogen oxides, effects of carbon tetrachloride carrier on, 20: 9365(R) (NYO-755-2, Paper 6)
separation from other nitrogen isotopes by chemical exchange between nitric solutions and nitrous vapors, 20: 16443
separation of, chemical exchange reactions for, 17: 23819
separation of, in acid exchange columns, 17: 389(R) (TID-16834)
sorption on tungsten in presence of nitrogen-14, isotope mixing in, 19: 32150
spectra in ATP, effects of magnesium and zinc on, 20: 29083(R) (UCRL-14767)
spectra in gaseous and solid nitric acid, vibrational, 19: 7394
spectra in thiotrithiazyl cations, NMR, 20: 31218(R) (UCRL-16658, pp 1-9)
spectra of molecular, at 720 to 830 A, 18: 28240
spectra of, vibration quantum number assignment of $D^2\Pi_g$–$A^2\Pi_u$ bands in, 18: 3749
spectra of, isotope shifts and vibrational structure of weaker systems in, 18: 33568
spectra of, method for measurement of content ratio by mass, 19: 22224
spectral effects in nuclear quadrupole resonance of nitrogen-14 in solid nitrogen, 17: 12837
spectrum of shifts in ultraviolet systems of, 17: 35732
spin-spin coupling with hydrogen in quinoline 1-oxide or nitroquinoline 1-oxide, 19: 32192
substitution in nitrogen compounds, partition function ratios at 20 to 2000°K for, 20: 40873(R) (NYO-3462-2)
synthesis in early history of solar system, 16: 24658
thermal diffusion factors for systems of mixed diatomic molecules of, with nitrogen-14, 20: 25034 (IFA-IS-35)
tracer use in electron microscopy using nuclear reactions, 19: 45741
tracer uses in biology, 18: 36915
translocation in soybean seedlings, 17: 24871
triton reactions (t,p) at 2 Mev, 18: 15270
uptake of ammonium sulfate-incorporated, by rice, 20: 12592(R) (NP-15671)
uptake of ammonium sulfate-incorporated, by rice, 20: 12593(R) (NP-15672)
use as internal standard in determination of argon-40 in minerals, 19: 43960
use as tracer in studies of nitrogen cycle in lakes, 17: 33600
use in measurements of self-diffusion in liquid ammonia, 19: 38579 (JUL-238-PC)
use in nutritional research, 20: 10560
use in study of fertilizer utilization by maize, 20: 9(R) (STI/DOC/10/42, pp 61-9)
use of urea-incorporated, combined with carbon-14-labeled carbonate for measuring rate of urea synthesis, 20: 10559
viscosity coefficient from 78 to 300°K, (E), 19: 5847
N-14–N-15, thermal diffusion factors for, as function of temperature, 20: 25034 (IFA-IS-35)

NITROGEN ISOTOPES N-16

activity in water coolant of EWA research reactor, power measurement by, 20: 32870
activity monitoring of, for determining power of Polish EWA research reactor, 20: 47073
activity of, design of coincidence counters for, 20: 2139
activity of, from neutron reactions (n,p) with oxygen-16, (T), 19: 14847 (WAPD-BT-31(p.37-42))
beta decay of, G invariance in, 17: 33095
beta decay of, gamma spectroscopy of product from, 19: 23646
beta spectrum analysis using spherical tensor calculations, 18: 9434
chemical behavior in Halden Boiling Reactor, 18: 38479 (A/CONF.28/P/

595)
chemistry of neutron-reaction-produced, 19: 11224
content in reactor coolants, power-level determination from, 20: 14019
decay in cooling water of Danish Research Reactor DR-2, design of tank for, 18: 6527 (RISO-32)
detection and measurement of, Cherenkov detector performance in, 19: 30081(R) (NBL-216)
determination in light-water reactor, power measurements from, 18: 45081 (CEA-R-2533)
distribution between steam and water in boiling reactors, 20: 6638
effects on reactor primary cooling system shielding design, 19: 45601(R) (WCAP-3750)
energy in isobaric multiplets (T), 19: 3368
energy levels, 16: 21394
energy levels, 17: 881
energy levels, 17: 41908
energy levels, 18: 21352
energy levels, (E), 20: 42369
energy levels from deuteron beam reactions with light nuclei, 16: 11040
energy levels from lithium-6 and -7 reactions with boron-10 and -11 at 3.05 Mev, (E), 20: 26167
energy levels from lithium-6 and -7 reactions with boron-10 and -11, 20: 30519
energy levels from helium-3 reactions (He-3,p) with carbon-14 at 4.0 and 4.5 Mev, 20: 32501
energy levels of, produced by neutron scattering on nitrogen-15, resonance energies and widths of negative-parity, 18: 18890
energy levels of, produced by neutron scattering on nitrogen-15, resonance energies and widths of negative-parity, 18: 18890
energy levels of, parity and spin for, 18: 28643
energy levels of, parity and spins for, 18: 36674
energy levels of, detection of T = 2, (E), 19: 5196
energy-level structure, (E), 20: 44730
gamma decay of excited, 17: 41908
gamma dose constants for, 20: 46617
gamma emission by, 18: 8313
gamma spectra, 17: 9549
gamma spectra, 17: 34966
gamma spectra to 8 Mev, 18: 15951(R) (GA-4855)
gamma spectrum, high energy, 16: 7493
half life, 16: 26213 (AE-78)
half life, 17: 5352
half life, 18: 18989
half life, (E), 19: 29315
half life, (E), 19: 39813
half life, (E), 20: 12019
internal conversion coefficient for 120-kev first-excited to ground state transition in, K, 17: 41908
internal conversion coefficient for 120-kev transition, K, 18: 21352
lifetime measurement, 17: 21011
meson (μ) capture by, partial rates for, (T), 20: 46768
meson (μ) capture, shell-model analysis, 16: 23088
monitoring in reactor coolant for core neutron flux indicator, 20: 10430
neutron reactions (n,α) at 14 Mev, nuclear shell effects in cross sections for, 18: 18977
nuclear properties, 19: 9771(R) (PR-P-63)
nucleon interaction potentials in, shell model calculation of, 17: 40031
preparation by fast neutron reactions of oxygen, 18: 29694 (IA-913)
production and reactions of, 20: 2520(R) (IA-920)
production by secondary nuclear reactions, 19: 30267
production in lithium-6 and -7 reactions with boron-10 and -11, 20: 30519
production in nitrogen-15 neutron-pickup reactions with heavy nuclei, cross sections for, (E), 20: 22001 (JINR-P-2555)
production in oxygen-16 reactions at 10 Mev, differential cross sections, 16: 10999
production of ground state, from meson (μ^-) capture by oxygen-16, probabilities of, 20: 36154 (AD-635312)
recoil reactions with oxygen, 19: 7607
specific activity, evaluation by diffusion calculations, 16: 24590
specific activity, determination of required neutron activating flux in reactor coolants, 16: 28423 (WAPD-T-1456)

NITROGEN ISOTOPES N-17

beta decay of, to oxygen-17 bound states, 18: 15270
beta decay to bound oxygen-17 levels, 18: 1003 (CONF-250-2)
decay of, reactor power monitoring using, 18: 19440
decay scheme, 17: 35253(R) (IA-775)
decay scheme, 18: 2841(R) (ORNL-3488(p.1-17))
energy level structure, (E), 19: 43396
energy levels, 17: 881
energy levels and gamma spectra, (E), 19: 8449
energy levels from lithium-7 reactions with boron-11 at 3.05 Mev, (E), 20: 26167
energy levels from lithium-6 and -7 reactions with boron-10 and -11, 20: 30519
energy levels of, negative-parity, 18: 32277(R) (PR-P-61)
energy levels of, negative-parity, 19: 1053(R) (PR-P-62)
energy levels of, low-lying negative parity, (T), 20: 32398
mass of, isobaric formula for, 19: 1623
neutron decay in reactor coolant water, power monitor using, (E), 19: 29655
neutron emission from, spectrographic determination of delayed, 18: 2841(R) (ORNL-3488(p.1-17))
neutron emission of, determination of oxygen-18 by measurement of delayed, 17: 14166
neutron source properties, delayed, 17: 41124
production by neon-20 and nitrogen-14 reactions with aluminum, carbon, copper, and tantalum, 16: 17153
production by proton reactions with target masses $20 \leq A \leq 240$, cross sections for, 20: 18556(R) (BNL-929, pp 66-82)
production by secondary nuclear reactions, 19: 30267
production for use as neutron source, 20: 4802 (IDO-17115)
production in boron-11 (Li-7,p) reactions, three-parameter analysis of, (E), 19: 8449
production in heavy ion reactions with nuclei, 16: 7130
production in heavy-ion reactions with nuclei, 16: 27381
production in nitrogen-14 and -15 reactions with aluminum, copper, and tantalum, 16: 26221 (JINR-P-973)
production in proton reactions at 1.0 and 2.8 Bev, cross sections for, (E), 19: 41780
production in reactor water by (n,p) and (n,d) reactions with oxygen-17 and oxygen-18, cross sections for, 17: 20983 (IA-755)
production in 3-Bev proton reactions with various targets, 19: 23355(R) (BNL-867(p.1-117))
use as delayed neutron source for determination of oil-water interface, 20: 43553

NITROGEN ISOTOPES N-18

existence, search for, 17: 35253(R) (IA-775)
production and properties, (E), 19: 5225

NITROGEN MUSTARDS

see also Chlorambucil
see also Diethylamine, 2,2'-Dichloro-N-Methyl-
biological effects in *Escherichia coli*, chemical protection against, 16: 16297
derivatives, distribution and excretion in cancer therapy, 16: 7371
effectiveness in tumor treatment, 17: 17835
effectiveness with autologous bone marrow transfusion in therapy of malignancies in man, 19: 12896
effects combined with radiotherapy on carcinomas in rabbit legs, 19: 13165
effects of nitromin on virus production in chicken sarcomas, 20: 35303
effects of novoembichine combined with x radiation on amino acid accumulation in *Mycobacterium cyaneum* 416, 20: 31005
effects of, on somatic segregation from heterozygous diploids of *Penicillium chrysogenum*, 17: 17886
effects of radiation and, on cells, 17: 25024
effects of tritium-labeled, on inoperable tumors, 20: 36705
effects of, on growth and cell division of *Escherichia coli*, 18: 27064(R) (ORNL-3601(p.92-7))
effects of, on nucleic acid synthesis in rabbit thymus, 18: 17473 (NYO-2565-1)
effects of, protective effects of bone marrow infusions and aminoethyl-isothiuronium against, lethal, 17: 7934
effects on antigenicity of bone marrow transplants in mice, 20: 42995
effects on bacteriophages, inactivating, 20: 14267
effects on barley, mutagenic, 19: 87
effects on bone marrow function in dogs, 20: 3652
effects on bone marrow in dogs, pathological, 20: 45481
effects on brain development in rat embryos, 18: 15834
effects on chromosome aberration induction in carcinoma and sarcoma cells, effects of nicotinamide on, 20: 40550
effects on content and molecular structure of glycogen in rat liver, 18: 29353
effects on DNA mitosis and synthesis on onion root tips, 18: 29399
effects on DNA molecule, site and mechanism of action, 20: 42821
effects on DNA synthesis, 18: 1398
effects on Drosophila, genetic, 17: 27099
effects on Drosophila, mutagenic, 16: 28680
effects on embryonic intestine of chicken cultivated *in vitro*, 20: 20372
effects on erythrocyte content in rat blood, 19: 19489
effects on giant cell formation in RCP cell strain, 20: 5323
effects on glycogen content of rat liver, 19: 8879
effects on growth, nucleic acid and protein synthesis, and survival of mammal cells, 17: 35505
effects on growth of mouse tumors, 18: 1323 (TID-19670)
effects on growth of mammalian cells in culture, synergistic effects of x radiation on, 18: 43277

effects on growth of lymphoma cells in culture, tracer study, 20: 18462
effects on Habrobracon, genetic, 16: 31406
effects on hematopoietic system of rats, pathological, 20: 5296(R) (NP-15585)
effects on hypoxanthine production by microorganisms, 18: 10177(P)
effects on induction of dental lesions in rats, mechanism of, 19: 38325
effects on induction of leukopenia in rabbits, 20: 5315
effects on intestinal vascular permeability, 16: 1503
effects on intestinal glucose absorption, 16: 5178
effects on intestines in rats, use of polyvinylpyrrolidone leakage for measurement of, 19: 10891
effects on leukemia cells, cytotoxic, 20: 3736
effects on leukocyte metabolism, 16: 20062
effects on life spans of mice, 17: 33754
effects on lungs, protective effects of AET against carcinogenic, 19: 31678(R) (ORNL-3768(p.137-45))
effects on lymphoid and myeloid leukemia incidence in mice, 20: 6788 (ORNL-P-1703)
effects on mammalian cells in tissue culture, 17: 23124
effects on mice and monkeys, effects of thioglycollic acid derivatives on toxic, 20: 18474
effects on mice, effects of mycelia-derived nucleotides on, 20: 18452
effects on mice, genetic, 16: 5207
effects on mice, protective effects of AET against, 18: 11881
effects on microorganisms, lethal, 19: 76(R) (UCRL-11387(Suppl.) (p.19-51))
effects on mitosis in RCP cell strain, 20: 5323
effects on mitotic index and succinic dehydrogenase activity in hepatomas, 16: 14560
effects on morphology and physiology of rat spleen, 18: 15822
effects on phytohemagglutinin-treated leukocytes, 18: 1407
effects on plants, genetic, 19: 3927
effects on radiotherapy of tumors in rats, 18: 43348
effects on rat liver glycogen levels, 18: 13470
effects on rats, biological, 20: 22732
effects on repair of DNA replication in uv-irradiated *E. coli*, 19: 24368
effects on reproductive capacity of HeLa and L cells, 18: 43306
effects on Saccharomyces radiosensitivity, mutagenic, 20: 5360
effects on survival of animal cells in culture, 20: 1617(R) (NP-15149)
effects on tissue regeneration of amphibians, 20: 20440(R) (EUR-2643.f)
effects on trace element content in spleen in rats, 17: 40547(R) (NYO-10569)
effects on treatment of transplanted lung tumors in rats, 19: 28150
effects on *Vicia faba* seeds, 16: 1595
effects on whole-body radiation damage to blood vessels in rat mesentery, 19: 17501
effects on yeasts, effects of plating time on recovery from, 18: 8183
labeling with carbon-14 and tritium, 19: 31771
metabolism of labeled, 19: 31771
preparation of boron-containing, 20: 38745(R) (NYO-3267-3)
protective effects of cystamine and cysteamine against, in tissue culture cells, 16: 12887
protective effects of dietary, against radiation injuries in rats, 17: 19872
protective effects of, against radiation injuries in mice, 18: 31278
protective effects with radioprotective compounds against leukemia in mice, 19: 8962
radiation effects on genetics of *Neurospora crassa* exposed to, visible, 17: 10455
radiation effects in bacteria and yeast exposed to, uv and x, 18: 1416
radiosensitivity effects on mouse tumor cells, gamma, 18: 35389
sensitivity of *Vicia faba* bean roots to, 17: 21503
therapeutic effects of homogenates of, on tumors, 19: 10963
tooth lesions induced by, in rats, 19: 45845
toxic effects of merophan in rat bone marrow, protective effects of cysteine against, 19: 22000
toxic effects of, protective effects of aminoethylisothiuronium against, 16: 17418
toxic effects on *E. coli*, recovery from lethal, 19: 19485
toxicity of, in cats, rabbits, and rats, 20: 43
urease inactivation, effects of amino acids, buffer salts, and proteins on, 16: 1531
use for therapy of lymphomas, 20: 43014(R) (RLO-581-10, pp 33-6)
use to determine biologic activity of radioprotective compounds, 17: 35409

NITROGEN OXIDES

analysis of mixtures of, spectrophotometric method for, 20: 16486
bond length measurement by electron diffraction, 17: 27358
bond lengths and vibrational amplitudes for molecules of, from electron diffraction, 17: 37792
catalytic decomposition, 16: 14693(R) (TID-15365)
catalytic effects on radiolysis of carbon dioxide, 19: 2400
catalytic reduction, 16: 14693(R) (TID-15365)
charge transfer in collisions with ions at 30 to 10,000 ev, cross sections for, 17: 29426
charge transfer of ions of, with atomic oxygen at 50 to 10,000 ev, cross sections for, 17: 29427
combustion of, Hopcalite-catalyzed, 18: 40988(R) (NRL-6053)
complexes of nitrous anhydride with hydrofluoric acid, electron diffraction of structure of, 19: 22264 (IS-T-8)
complexes with anhydrous uranyl nitrate, spectra and thermal decomposition of, 18: 39220
complexes with iron, kinetics of formation of, 20: 12884(R) (RRL-2310-171)
concentration in ionospheric D region, electron density for determining, 20: 44436
content and production in upper atmosphere, 19: 14120
content and reactions in ionosphere, (T), 19: 45173
content in upper atmosphere, 18: 7616
content in upper atmosphere, from rocket soundings, 18: 37794(T) (NASA-TT-F-141(p.1-21))
decomposition of, effects of aluminum oxide catalyst on, 17: 18011 (TID-18423)
decomposition of nitrous oxide using oxide catalysts, 17: 41333(R) (ANL-6677)
decomposition of nitrous oxide using oxide catalysts, 18: 25893(R) (ANL-6868(p.355-72))
decomposition of nitrous, catalytic properties of chromium and magnesium oxides for, 19: 44680(R) (ANL-7000, pp 227-32)
decomposition of, catalytic effects of cobalt oxide on, 20: 20365
deionization of ions of, in atmosphere, studies of kinetics of, 18: 37114 (AFCRL-64-496)
determination by gas chromatography, 18: 13629(R) (ORNL-3537 (p.17-23))
determination in atmosphere using radioactive clathrate techniques, 20: 29142
determination in clouds and precipitation on Zugspitzplatt August 15 to September 21, 1955, 16: 25625
determination in nuclear fuels and wastes, gas-chromatographic, 16: 22033
determination in off-gases from waste calcination facility, 19: 32059(R) (IDO-14655)
determination in superheated steam, design of gas chromatograph for, 18: 23407 (DP-880)
determination of, in the atmosphere, radiometric, 16: 32917 (ASD-TR-61-654)
determination of, factors affecting continuous on line, 20: 1734 (EG-Report-36)
determination of, radioluminescent method for, 20: 22952
determination of, in presence of hydrogen, methane, and nitrogen by gas chromatography, 20: 40805(R) (MLM-1325, pp 63-70)
determination using labeled sodium chlorite-clathrates, effects of moisture on, 18: 17866(R) (NYO-2766)
disproportionation of divalent, 17: 30895(R) (NYO-8772)
distillation for separation of nitrogen and oxygen isotopes, 19: 11648
effects as electron scavenger in pulse radiolysis of cyclohexane solutions of aromatics, 20: 7144
effects as impurity on performance of carbon dioxide-filled proportional detectors, 18: 7068
effects in optical absorption by air at high temperatures, 19: 20832
effects in radiation biology, electron spin resonance studies, 20: 40597
effects of nitric-oxide on neutron reactions (n,γ) on sulfur-34 in gaseous sulfur compounds, 17: 23386 (UCRL-10360(Rev.))
effects of nitric oxide on ionic reactions in radiolysis of methane, 18: 6858
effects of nitric and nitrous, on radiolysis of polyethylene and polypropylene, 18: 16093
effects of nitrous oxide on radiation effects on polyethylene and polyisobutene, 17: 30208
effects of nitrous, on radioinduced crosslinking in polymeric materials, 17: 40898(P)
effects of nitrous oxide on radioinduced cross linking of polyethylene, 18: 35612
effects of N_2O as electron scavenger in propane radiolysis, 20: 25125(R) (RRL-2310-174)
effects of, on speed of radioinduced crosslinking of polyethylene, 17: 18123
effects of radical scavenging by, on radioinduced reactions, 20: 23113
effects of tetravalent, on isotopic composition of carbon dioxide in atmosphere, 17: 25436
effects of, on gamma radiolysis of liquid methanol, 19: 36466
effects on annealing of recoil damage in neutron-irradiated cobalt complexes, 20: 38965
effects on anoxic radiosensitivity of *Shigella sonnei*, 16: 21959
effects on argon ion-platinum reactions at 22 kev, 17: 25989
effects on chemical equilibrium and rate of solvation of charge groups in aromatic compounds, 18: 33613

effects on corrosion of stainless steel by nitric acid, 16: 266(R) (DP-626)
effects on electron spin resonance spectra of irradiated acrylamide and methacrylamide, 16: 8781
effects on electron spin resonance of irradiated silicon oxides, 19: 28384
effects on fission fragment radiolysis of nitrogen–methane systems, 20: 23071(R) (AGN-8169)
effects on gamma radiolysis of 2-propanol, 20: 18766
effects on gamma radiolysis of polypropylene, 20: 18770
effects on gamma radiolysis of cyclohexane, 20: 33359
effects on gas-phase radiolysis of cyclobutane and deuterated cyclobutane, 20: 12894
effects on hydrogen yields in electron radiolysis of methanol vapor, 19: 11210
effects on hydrogen yields in propane radiolysis, 19: 46396
effects on hydrogen yields from radiolysis of hydrogen sulfide, 20: 4017
effects on hydrogen yields from gamma radiolysis of cyclohexane, 20: 29270
effects on hydroxyl radical yields from gamma radiolysis of aqueous benzene solutions, 20: 25158
effects on iodine-128 reaction with methane, 16: 10061
effects on oxygen effect in irradiated barley seed, 20: 5298(R) (RLO-353-4)
effects on paramagnetic defects in gamma-irradiated high-surface-area silica, ESR studies of, 20: 27608
effects on photosensitized decomposition of deuterated and normal cyclobutane, 20: 38941(R) (RRL-2310-182)
effects on products formed in radiolysis of ethylene, 19: 22331
effects on propane radiolysis, 18: 31616
effects on pulse radiolysis of ferrocyanide solutions, 19: 20009
effects on quenching of energy spectra in determination of carbon-14, sulfur-35, and tritium, 20: 36771
effects on radiation chemistry of polymethylmethacrylate, 18: 1777
effects on radiation effects on biological systems, 19: 13026
effects on radiation chemistry of polypropylene, 19: 34216(R) (COO-1088-12)
effects on radical yields from radiolysis of water, 19: 26446
effects on radioinduced degradation of polyisobutylene, 17: 35879
effects on radioinduced isomerization of 2-butene, 18: 23666
effects on radioinduced isomerization of 2-butene, 19: 17967
effects on radioinduced carbon dioxide-graphite reactions, (E), 19: 19953 (AERE-R-4201)
effects on radioinduced isotopic exchange in nitrogen, 19: 36482
effects on radioinduced crosslinking of polyethylene, polypropylene, and ethylene-propylene copolymers, 20: 402
effects on radioinduced crosslinking of polyethylene, 20: 4010
effects on radioinduced oxidation of aqueous solutions of potassium iodide, 20: 7140
effects on radioinduced surface activity of γ-octahydro-1,3,5,7-tetranitro-1,3,5,7-tetrazocine, 20: 16504 (AD-627846)
effects on radioinduced polymerization of solid methane, 20: 29314
effects on radioinduced decomposition of 5-bromouracil, 20: 38968
effects on radioinduced crosslinking of polyethylene, 18: 13861
effects on radiolysis of liquid cyclohexane, 16: 27071
effects on radiolysis of liquid cumene, 16: 27072
effects on radiolysis of methanol, 17: 12322 (ARL-90)
effects on radiolysis of organic compounds in aqueous solutions, 17: 39151
effects on radiolysis of aqueous solutions, 18: 1765
effects on radiolysis of ammonia, 18: 29788
effects on radiolysis of carbon dioxide, 18: 31565 (NYO-2546)
effects on radiolysis of ethane at high densities, 19: 17994
effects on radiolysis of gaseous mixtures of cyclohexane and deuterated cyclohexane, 19: 42538
effects on radiolysis yields in ethylene, 19: 46324(R) (AGN-8132)
effects on radiolysis of cyclohexane vapor at 100°C, mechanism of, 20: 377
effects on radiolysis of aminobenzoic acid and pyridoxal-5-phosphate, 20: 7164
effects on radiolysis of cyclopentane, 20: 14599
effects on reactions of hydroxyl radicals with iodide ions in pulse radiolysis, 19: 26444
effects on reactions of photolyzed carbon dioxide with graphite, 20: 23097
effects on sulfur-35 exchange between sulfur dioxide and sulfuric acid, 19: 26330
effects on yields in radiolysis of aqueous 2-propanol, 18: 20058
effects on yields with organic solutes in radiolysis of deuterated sodium formate aqueous solutions, 18: 31602
effects on yields from radiolysis of water vapor, 19: 22376
effects on yields from gamma radiolysis of deuterated hydrogen sulfide in hexane, 19: 28368
effects on yields from gamma radiolysis of 2-methyltetrahydrofuran, 19: 28406
effects on yields in photo- and radiation chemistry of mineral acid glasses, 19: 46394
effects on yields in radiolysis of benzyldimethylamine and benzyltrimethylammonium hydroxide, 19: 22299
electron attachment and recombination in ionized, 18: 10767 (RTD-TDR-63-3076)
electron attachment in gases containing, 19: 32885(R) (AD-610869)
electron beam collisions with, emission spectra from, 18: 16700
electron drift velocity in, slow, 16: 19470 (NP-11617)
electron drift velocity in nitrous oxide at 77 to 443°K, 16: 27742 (NP-11983)
electron elastic scattering at 295°K by nitrous, cross sections, 16: 33844
electron energy levels of, determination of, using infrared lasers, (E), 20: 30734(R) (TID-22970, pp 1-63)
electron-ion attachment and recombination in, 17: 8920(R) (GACD-2461)
electron paramagnetic resonance spectra of trapped radicals of, in sodium nitrate, 19: 15590
electron reactions with, vibrational states excited in, 17: 38990
electron reactions with, cross sections for dissociative ionization in, 19: 27078
electron reactions with, classical calculation of cross sections for inelastic, (T), 19: 44947
electron reactions with, vibrational excitation in fast, (E/T), 20: 2638
electron reactions with, rate constants for hydrated, 18: 23691
electron recombination with positive ions of, in shock-heated air, 18: 42184
electron scattering by, spectra from, 17: 36144 (AFCRL-62-1070)
electron spin resonance of $N_2O_2^-$ radical, in irradiated sodium nitroprussiade, 20: 7156
electron transfer reactions with negative ions, 16: 6471
electron transitions in, isotope effects on, 19: 30170
energy transfer to, in iodine fluorescence, 19: 2382
exchange between nitric acid and nitric oxide, enrichment of oxygen-18 by, 18: 531
exchange of gaseous with non-aqueous solutions of complexes, nitrogen and oxygen isotope separations in, 16: 463
exchange reactions between nitric oxide and calcium nitrate, equilibrium and isotopic fractionation in, 16: 12007
exchange reactions with nitrate and nitrite ions, 18: 2127(R) (ORNL-3488(p.21-41))
fine structure and magnetic coupling, 18: 27397
fluorescence from vacuum-uv excited, 18: 28176
force constants of isotopic, 16: 22133(T)
formation by radioinduced nitrogen fixation, problems in, 18: 41546
formation during fast neutron reactions with oxygen, 18: 29694 (IA-913)
formation in neutron-irradiated liquid air, 16: 24587
handling of, 20: 1727 (NASA-SP-5032)
heat of vaporization of, calculation from rigid-sphere equation of state, 18: 224
helium atom reactions with, electron kinetic energy from ionization in, (E), 20: 29927
hydrogen ion reactions at 10 to 50 kev, equilibrium fractions in, (E), 19: 14243
hydrogen reactions at 3 to 30 kev, electron loss and formation of slow anions in, (E), 20: 11509
ion reactions with, charge exchange in atmospheric, (E), 20: 9656(R) (GA-6699)
ionization by electron impact, appearance potential for doubly charged molecule ions in, 19: 20807(R) (UCRL-11828(p.201-4))
ionization by electrons, (E), 19: 34770 (AD-612806)
ionization by krypton ions, cross sections for dissociative, 18: 40128
ionization cross section for, electron-impact, 19: 38630
ionization cross sections for negative-ion formation, electron-impact, 19: 38631
ionization efficiencies, electron impact-induced, 16: 16409(R) (TID-15424)
ionization in ionosphere, (E/T), 19: 18971(T) (FTD-TT-64-1316 (p.75-101))
ionization of nitric oxide by electron impact at energies up to 500 ev, cross sections for dissociative, 19: 14127 (FSU-2690-14(Paper 1))
ionization of, isotope effects on Franck-Condon factors in, 19: 38632
isotope effects among gas- and liquid-phase, 20: 9361(R) (NYO-755-2)
isotope effects in dual temperature systems, 17: 389(R) (TID-16834)
isotope exchange between nitric oxide and nitric acid in aqueous solution, oxygen-18 concentration in, 17: 18656
isotope exchange in systems with nitrates, 16: 2100 (TID-13427)
isotope exchange in nitrous oxide, 16: 1761
isotope exchange in systems with nitrosyl bromide, 16: 22520
isotope exchange in, 17: 23819
isotope exchange in, catalysis of, 17: 23335

isotope exchange in, nitrogen and oxygen, 16: 29295(R) (NYO-8771)
isotope exchange reactions of, equilibrium constants and frequencies of, 19: 4136
isotope separation in hydrochloric acid complex of, 16: 32021
isotopic exchange of nitrogen between nitrogen and, 18: 9752 (IA-900)
isotopic exchange equilibrium calculations, 19: 40460(R) (NYO-3462-1)
isotopic exchange reactions of, nitrogen-15 concentration by, 20: 31638(R) (NYO-755-1, pp 12-76)
isotopic exchange with nitric acid, effects of additives on nitrogen-15 concentration by, 20: 31639(R) (NYO-755-1, pp 77-129)
isotopic substitution in, partition function ratios at 20 to 2000°K for nitrogen-15 and oxygen-18, 20: 40873(R) (NYO-3462-2)
meson (μ^+) decay asymmetry in nitrous oxide, 16: 10958 (NEVIS-99)
molecular vibration de-excitation in collisions with atoms or molecules, 16: 12255
molecule scattering by, cross sections for inelastic, 19: 14265
neutralization of gaseous ions of, 17: 35263(R) (UCRL-10706(p.1-110))
nitrogen isotope distribution between gaseous and liquid phases of, 20: 16486
nitrogen isotope exchange in, 16: 29295(R) (NYO-8771)
nitrogen isotope exchange between gaseous and liquid, 17: 20044
nitrogen isotope exchange in, effects of pressure and temperature on, 17: 30505 (CONF-14-22)
nitrogen-15 exchange between nitric oxide and nitrogen tetroxide complexes, 18: 2131(R) (TID-19592(Sect.III))
nitrogen-15 exchange between nitric acid and, effects of additives on, 18: 2132(R) (TID-19592(Sect.IV))
nitrogen-15 exchange with nitric acid, effects of acids and salts on, 20: 9363(R) (NYO-755-2, Paper 3)
nitrogen-15 exchange in, effects of carbon tetrachloride carrier on, 20: 9365(R) (NYO-755-2, Paper 6)
nitrogen-15 exchange with nitric acid, mechanisms of, 20: 9362(R) (NYO-755-2)
oxidation of graphite by, kinetic anisotropy in, 18: 25932
oxygen ion reactions at 15 to 50 kev in, equilibrium fractions for, (E), 19: 18687
oxygen-18 exchange, equilibrium constants and partition function ratios for, 16: 18876
oxygen-18 exchange reactions with, rate and spectra of, 18: 22048
photoionization efficiency curves of, fine structure and measurement of ionization potentials from, 17: 37752
photoionization of nitric oxide, calculation of ion-electron dissociative recombination rate constant from, 16: 11719
photoionization of dioxide, 16: 18954
photolysis of di-, kinetics of flash, 19: 42461 (SC-R-65-956)
photolysis of dioxide at 3130 and 4050 Å, 17: 1536
photolysis of, mechanisms of ultraviolet, 20: 31221(R) (UCRL-16658, pp 73-87)
photon absorption in, 17: 37646 (KN-62-133(R))
positron annihilation in, 18: 34752(R) (CU(PNPL)-234)
positron annihilation rates in nitric, second-order phenomena in, (E), 19: 35172
positronium quenching in, ortho-, 16: 5912
potential constants and thermodynamic properties of isotopic, at 200 to 2000°K, 16: 30381
potential energy curves for nitric oxide molecules and ions, 18: 34281 (RM-4034-PR)
potential energy functions with nitrogen and oxygen, 16: 16853
potential energy of NO molecules, 16: 13700 (NP-11429)
preparation by chemonuclear processes, 18: 3843
preparation by photolysis of cerium nitrate in nitric acid solutions, electron exchange kinetics in, 18: 31467
preparation from air using reactor as energy source, 19: 36469
preparation of nitrogen-15-labeled, 19: 30235(R) (RPI-321-2)
production and quenching of nitric oxide in continuous flow furnace, 19: 42815
production by chemonuclear synthesis, 20: 40988
production in gamma radiolysis of frozen sodium nitrate solutions, 18: 43638
production in plasma, 17: 9708
production in plasma jets, 20: 17959
production in reactor irradiated nitrogen–oxygen systems, 17: 25337
production in reactors, conditions for, 19: 441
production in tunnel of Frascati electron linear accelerator, (T), 19: 44866 (LNF-65/21)
production of ionic and molecular, by chemical reactions in ionosphere, 19: 35227 (AD-609844)
production of the tetroxide from a nitrogen-oxygen mixture, radiochemical process for, 16: 29023
production of, in gamma radiolysis of sodium nitrites, (E), 19: 24563
production using radioinduced oxidation of atmospheric nitrogen by fission fragments, (E), 19: 40604
properties as electron scavenger in radiolysis of hydrocarbons, 20: 16515
properties as gamma dosimeter, 20: 14870
properties as scavenger of water radiolysis products, 19: 38720
properties of nitric oxide as radiation dosimeter, 19: 13433
protective effects of nitrous oxide against whole-body radiation in mice, 16: 28842
protective effects against radiation in *Vicia faba*, 18: 31294
quadrupole moments, 19: 39378
quenching effects of nitric oxide on radiofluorescence of tryptophan and tyrosine, 19: 19970(T)
quenching effects on positronium in organic liquids, kinetics of, 20: 18662
radiation chemistry, 18: 31565 (NYO-2546)
radiation effects on reactions, 16: 208(R) (NYO-9967)
radiation effects on aqueous solutions, 16: 1811(T) (AEC-tr-4564)
radiation effects on properties as dosimeter, 17: 35253(R) (IA-775)
radiation effects on, in dosimeters, 18: 11512(R) (NARF-63-9p)
radiation effects on ESR spectra of di- and tri-, in lead nitrate, 18: 16087
radiation effects on paramagnetic resonance spectra of NO_3, in potassium nitrates, 19: 4210
radiation effects on production of, 19: 26382(R) (RPI-321-1)
radiation effects on gaseous nitrous oxide, yields in, 20: 12884(R) (RRL-2310-171)
radiation effects on formation of, in upper atmosphere, 20: 25996
radiation effects on, effects of electric fields, pressure, and temperature on electron, 20: 26959
radioinduced chain reactions of nitrous oxide with hydrogen in aqueous solutions, 18: 27524
radioinduced decomposition, reaction mechanisms in, 17: 39163(P)
radioinduced formation in air and nitrogen–oxygen as measure of radiation dose, 17: 39111
radioinduced formation in radiolysis of dry air, conditions for maximum, 18: 13896
radioinduced formation of, in air, 18: 25718
radioinduced formation of, 19: 23355(R) (BNL-867(p.1-117))
radioinduced formation of, around high-power gamma facility, ventilation calculations for, 20: 5670
radioinduced in atmospheres of industrial radiation facilities, 19: 38884
radioinduced ionization of, electron dosimetry by, 18: 29764
radioinduced luminescence in, 17: 37652 (NYO-10691(Pt.1))
radioinduced production of, G-values for, 20: 20177(R) (BNL-929, pp 83-105)
radioinduced reactions with cyclohexane, 17: 35895
radioinduced reactions with Teflon, electron spin resonance studies of, 18: 23648(T,R) (AEC-tr-6316(p.534-7))
radioinduced reactions with acrylamide and methacrylamide monomers and polymers, 18: 23650(T,R) (AEC-tr-6316(p.567-72))
radioinduced reactions of nitric oxide with cyclohexane, products of gamma, 18: 29731(T,R) (AEC-tr-6231(p.269-73))
radioinduced reactions with hydroxyl radical in aqueous solutions, absolute values of rate constants for, 18: 37223
radioinduced synthesis, 19: 15565(R) (BNL-841(p.43-51))
radiolysis effects of nitrous oxide on hydroxyl radical yields in aqueous benzene, 18: 20047
radiolysis nitrogen-15-labeled, mechanism of gamma, 19: 26404
radiolysis of aqueous solutions of, mechanisms for gamma, 18: 3854
radiolysis of aqueous solutions of nitrous oxide, 18: 31563 (AD-429919)
radiolysis of aqueous solutions of nitrous oxide, effects of added solutes on, 18: 31601
radiolysis of aqueous solutions of, in presence of nitrite ions, gamma, 19: 26445
radiolysis of aqueous solutions of, yields from, 19: 28407
radiolysis of dinitrogen tetroxide, effects of oxygen on products in, 17: 23381 (PA-TR-3072)
radiolysis of liquid nitrous, G values for, 16: 20514
radiolysis of liquid nitrogen tetroxide, effects of nitric oxide and oxygen on yields in, 20: 380
radiolysis of nitrous oxide, nitrite and nitrogen yields in, 17: 16441
radiolysis of nitrous oxide, effects of cell diameter on nitrogen yield in gamma, 19: 20329 (USNRDL-TR-806)
radiolysis of, spectra of negative ions in, 17: 20057(R) (TID-18500)
radiolysis of 2-propanol in, gamma, 20: 43318
radiolysis of, catalytic effects of beta particles on, 18: 37191 (BNL-874(p.39-40))
radiolysis of, effects of transition metal cations on, 19: 39265(R) (IA-1021)
radiolysis of, heat generation by alpha, 19: 15826 (MLM-1163(p.I-1-12))
radiolysis of, in 2-propanol, effects of potassium hydroxide on yields from gamma, 20: 26937
radiolysis of, in-pile gamma dosimeter using, 18: 31576
radioprotective effects of, in biological systems, 20: 5296(R) (NP-15585)

radioprotective effects on *Vicia faba* seedlings, 20: 43007
radiosensitivity effects, in *Shigella flexneri*, 16: 12894
radiosensitivity effects on Drosophila sperm, 17: 7885
radiosensitivity effects in bacteria, 18: 3590
radiosensitivity effects on mice, 18: 11878
radiosensitivity effects in bacteriophage, x, 18: 15901
radiosensitivity effects on animal and plant cells, 18: 38977
radiosensitivity effects of free-radical, on *Escherichia coli*, 19: 7194
radiosensitivity effects on *E. coli*, 19: 26059
radiosensitivity effects on seeds and spores, 19: 29886(R) (ANL-6971 (p.29-46))
radiosensitivity effects of, on seeds, 20: 3759
radiosensitivity effects on *Bacillus megaterium* spores, 20: 18434
radiosensitivity effects on rat erythrocyte membranes, x, 20: 24943
reaction with radioisotope containment materials in launch pad abort environments, 20: 39312 (SC-CR-66-2044)
reactions of nitric oxides with gaseous sulfur compounds, sulfur-35 activity in, 16: 28982 (UCRL-10360)
reactions of nitric oxide with free radicals radioinduced in Teflon, electron spin resonance spectra of, 18: 5388
reactions of nitrous oxide with photolytic and radiolytic products, 18: 9752 (IA-900)
reactions of nitrous oxide with tungsten at high temperatures and low pressures, kinetics, 19: 34149 (UCRL-16019)
reactions of tetravalent, with anhydrous barium, calcium, and strontium nitrates, 17: 15995
reactions with active nitrogen, tracer studies, 16: 25362
reactions with atomic and molecular ions of oxygen and nitrogen, charge transfer, 20: 44127
reactions with beryllium, kinetics, 19: 11051(R) (SC-DC-64-1432)
reactions with beryllium in simulated launch pad abort environments at 800 to 1500°C, 20: 2341 (SC-DC-65-1637)
reactions with carbon-11, mechanisms of, 19: 7417
reactions with electrons in gamma-radiolyzed water, 19: 439
reactions with ethyl and methyl radicals, preparation of nitrosoethane and methane by, 16: 11725
reactions with free radicals in irradiated polytetrafluoroethylene, 16: 3042
reactions with free radicals from irradiated polytetrafluoroethylene, 18: 8435
reactions with glovebox materials, 19: 28215 (RFP-531)
reactions with graphite, lamellar compounds formed in, 19: 7473
reactions with hexafluorides of molybdenum, tungsten, and uranium, 17: 1417 (GAT-T-970)
reactions with high-strength forged beryllium, 19: 23107
reactions with hydrofluoric acid, gaseous products, 16: 30357 (BNL-6231)
reactions with hydrated electrons, 20: 7164
reactions with irradiated cyclohexane, formation of nitroso-monomer in, 16: 13104
reactions with lanthanum, terbium, and vanadium sesquioxides and praseodymium chromite, 16: 10018
reactions with molybdenum, tungsten, and uranium hexafluorides, 16: 4156 (GAT-T-552(Rev.1))
reactions with molybdenum, tungsten, and uranium hexafluorides, 16: 25339 (GAT-T-969)
reactions with molybdenum hexafluoride, tungsten hexafluoride, and uranium hexafluoride, 17: 7993 (GAT-T-971)
reactions with muonium, cross sections for, 20: 29177
reactions with muonium, review of, 20: 41661
reactions with neptunium(IV) chloride and neptunium trioxide hydrates, 20: 33295
reactions with powdered polymethyl methacrylate, ESR spectra of, 19: 22355
reactions with radioisotope-containment materials in launch pad abort environments, 20: 19192 (SC-DC-65-1918)
reactions with rare gas ions, cross sections for, 19: 13324
reactions with scandium chlorides, 20: 29214
reactions with silica gel, radioinduced, 16: 13664
reactions with tungsten, kinetics, 16: 22059 (UCRL-10135)
reactions with tungsten, 20: 31718(R) (UCRL-16658, pp 149-54)
reactions with xenon fluorides at 300 to 350°K and 0.1 to 30 mm, kinetics of, 18: 29642
reactivity of tetra-, with stabilizers for nitrate ester explosives, 19: 3807 (LADC-6130)
recombination of positive ions of, with electrons, 18: 34259 (AD-434907)
recovery from Purex plant dissolvers, tests of condenser-absorber designs for, 19: 26458 (BNWL-53)
recovery in uranium dissolution, 18: 29800 (HW-46093)
reduction of, by hydrogen and methane, effects of zinc-promoted copper chromate catalyst on, 17: 18011 (TID-18423)
scavenging deuterated methyl radicals by nitric, at low temperature, 17: 27337
shock waves in, uv radiation from, 17: 13643
sorption by neutron-irradiated magnesium and nickel oxides, 17: 18152
sorption of hydrogen on solidified films, 16: 10679 (UCRL-6626)
spectra, electron collision study of excitation functions, 16: 22145
spectra, Franck-Condon factor arrays for band, 16: 22129
spectra from 13-kev electron excited, emission, 20: 37466(T)
spectra of mixed, effects of partial pressures on absorbance, 20: 9363(R) (NYO-755-2, Paper 3)
spectra of nitrogen-14, -15, and oxygen-16 labeled, infrared, 18: 22055
spectra of nitrous, containing nitrogen-14 and -15, 19: 5915
spectra of x-ray-produced, in potassium azides, 16: 33047
spectra of x-ray excited, trapped in solid rare gases, 20: 18016
spectra of, infrared, 19: 32048(R) (NP-15073)
spectra of, *L*-uncoupling effects on EPR, 20: 29194
spectra of, metastable peaks in mass, 20: 22859(R) (UCRL-16580, pp 149-205)
spectra of, polarization in visible absorption, 19: 2412
spectral effects of nitrous, on hydrated electron in sodium carbonate, 17: 1436
spectrum in polar auroras, 19: 16740
spectrum of nitrogen-15-labeled nitrous oxide, mass, 19: 17861 (TID-21648)
synthesis from nitrogen, development of chemonuclear, 19: 36453 (BNL-8836)
thermal conductivity and viscosity for nitric oxide, 16: 18933
thermal dissociation of molecules of, in shock wave, (T), 19: 29010
thermodynamic and transport properties at 500 to 15000°K, calculations for, 16: 15381
toxic effects of dioxide, mechanisms and indexes of response in, 16: 12863
toxicity of, 20: 1727 (NASA-SP-5032)
transport properties at 1000 to 24000°K, calculations for, 16: 15382
uptake by human brain during anesthesia, 18: 19522
use for gamma dosimetry, 18: 4115
use for processing uranium and vanadium ores, 19: 44129(P)
use of nitrous oxide in gamma dosimetry, 16: 17843
use of nitrous oxide for radiation dosimetry, 19: 11170(R) (TID-21443)
use of nitrous, for gamma dosimetry, 19: 2633
use of nitrous, for low gamma dosimetry, 19: 46332(R) (ORNL-3832, pp 50-65)
uses for chemical dosimetry of gamma radiation, 17: 20364
uses for electron dosimetry, 20: 26959
uses for purification of mixed potassium and sodium nitrates from nitrites and water, 20: 10272(R) (NAA-SR-9339)
vapor pressure of, isotope effects on, 17: 17944 (BNL-6279)
vapor pressure of liquid, up to critical point, 18: 3722 (UCRL-7167)
vapor pressure up to critical point, 18: 41374 (UCRL-7167(Rev.I))
vapor pressures in isotopic systems of, 17: 23334
vibrational mean-square amplitudes in dioxides, 16: 6423
yield in radiolysis of liquid air by fast neutrons, 17: 25303
yields in gamma radiolysis of tetranitromethane at 77°K, EPR spectra of, 20: 23104
yields in gamma radiolysis of nitroalkanes, 20: 33362
yields in nitrogen-13 recoil reactions, 16: 11759
yields in radiolysis of liquid nitrogen tetroxide, effects of nitric oxide and oxygen on yields in, 20: 380
yields in radiolysis of propene, competitive electron capture between tetrafluoroethylene and, 20: 38941(R) (RRL-2310-182)
yields in reactions of nitrogen with oxygen at 400 to 5000°K, 19: 4107 (ORNL-TM-968)
yields of, in gamma radiolysis of dinitrogen tetroxide, 17: 23381 (PA-TR-3072)
air–He–NO_2, radiolysis, 17: 40855(R) (TID-19512)
Ar–methane–NO, positron annihilation rates in gases of, (E), 19: 35172
Ar–N_2O, alpha ionization of, 17: 24052 (ORNL-3422)
Ar–NO_2, electron-ion attachment and recombination in, 17: 8920(R) (GACD-2461)
Ar–NO, mutual charge neutralization of ions in, pressure dependence at 10 to 600 torr, 18: 7407 (UCRL-10904)
Ar–NO, positron annihilation rates in gases of, (E), 19: 35172
benzene–N_2O–H_2O, production of biphenyl–terphenyl mixtures in radiolysis of, 20: 10930(P)
CO_2–N_2O, oxygen-18 exchange in photolysis of, 18: 12192
D–NO, mutual charge neutralization of ions in, pressure dependence at 10 to 600 torr, 18: 7407 (UCRL-10904)
ethane–d_6–NO, effects of density and electric field on radiolysis of, 19: 7555
ethane–ethane–d_6–NO, effects of density and electric fields on radiolysis of, 19: 7555
ethanol–NO–H_2O, radiolysis of, nitrous oxide yields from, 20: 23168
ethylene–methane–NO, radiolysis of, 19: 46324(R) (AGN-8132)
He–NO_2, electron-ion attachment and recombination in, 17: 8920(R) (GACD-2461)
He–NO, mutual charge neutralization of ions in, pressure dependence at

10 to 600 torr, 18: 7407 (UCRL-10904)
HF–NO, chemical properties, 16: 20042(R) (BNL-696)
HF–NO_2, corrosive effects on monel and nickel, 18: 3671(R) (BNL-799 (p.26-54))
HF–NO_2, corrosive effects on Monel and nickel, 18: 11958(R) (BNL-823 (p.20-47))
HF–N_2O_4, corrosive effects on monel and nickel, 19: 15331(R) (BNL-841(p.18-42))
HF–NO_2, corrosive effects on Monel and nickel, 19: 36216(R) (BNL-900(p.29-72))
HF–N_2O_3, corrosive effects on Monel and nickel, 20: 20177(R) (BNL-929, pp 83-105)
H–NO, electrical properties of ionized flames in, 16: 15386
H–NO, electromagnetic properties of, in high-temperature ionized flames, 16: 14135 (AFOSR-990)
H–NO, flame ionization in, 16: 13679 (AFOSR-825)
H–NO, mutual charge neutralization of ions in, pressure dependence at 10 to 600 torr, 18: 7407 (UCRL-10904)
H–NO, nuclear spin lattice relaxation in, 19: 39378
H–N_2O, nuclear spin lattice relaxation in, 19: 39378
H–NO, proton spin-lattice relaxation in, 16: 18887
H–N_2O, radiolysis of aqueous solutions of, chain reaction in, 19: 28407
HNO_3–NO, exchange reactions in equilibrium and isotopic fractionation in, 16: 12007
HNO_3–NO, exchange reactions in, 17: 2686
HNO_3–NO, nitrogen-15 exchange in, 16: 12839
HNO_3–NO, nitrogen-15 fractionation in, effects of temperature on, 20: 40873(R) (NYO-3462-2)
KI–N_2O, yields in gamma radiolysis of aqueous solutions of, 20: 392
Kr–NO, mutual charge neutralization of ions in, pressure dependence at 10 to 600 torr, 18: 7407 (UCRL-10904)
methanol–NO–H_2O, radiolysis of, nitrous oxide yields from, 20: 23168
methanol–nitrogen oxides, synthesis of glycol from, radiochemical, 18: 33629
NiO–N_2O_5–UO_3–H_2O, formation of NiO·3UO_3 at 300°C in, 18: 12084
N–NO, mutual charge neutralization of ions in, pressure dependence at 10 to 600 torr, 18: 7407 (UCRL-10904)
N–NO, radiolysis of, 19: 46324(R) (AGN-8132)
N_2O–H_2O, radioinduced hydroxyl radicals in, 20: 10924
NO–NO_2, charge neutralization of ions in, rate constant for, 18: 7407 (UCRL-10904)
NO_2–N_2O, ratio changes in in-pile loops, 19: 26382(R) (RPI-321-1)
NO–rare gas, charge neutralization of ions in mixtures of, 19: 9796
NO–SF_6, recombination rates for gaseous, 18: 33555
NO–SO_3–UO_3–H_2O, uranyl sulfate liquid–liquid immiscibility in, above 300°C, 16: 10022
NO–^4Xe, mutual charge neutralization of ions in, pressure dependence at 10 to 600 torr, 18: 7407 (UCRL-10904)
NO–2-propanol–H_2O, radiolysis of, nitrous oxide yields from, 20: 23168
2,2-dimethylpropene–NO_2, photolysis and pyrolysis, free radical reactions in, 18: 25329 (TID-20645)

NITROGEN SYSTEMS

crystal structure of transition metal alloys, 16: 2259
heat transfer in graphite suspensions, 17: 14447(R) (BAW-1181)
phase studies of transition metal alloy, 16: 16768
thermal diffusion factors for nitrogen-14- and -15-labeled diatomic molecules of, 20: 25034 (IFA-IS-35)
acetylene–N–O, electron density in sulfur hexafluoride seeded flame plasma of, (E), 19: 40016
Al–C–Cu–H–N–Sn–Ti–V–Zr, mechanical properties of, 19: 46985 (AD-613651)
Al–N, flow of suspensions of, in process-heat reactor systems, 19: 17333(R) (TID-21596)
Al–Nb–N, lattice parameters of filled β-manganese structure phases in, 19: 37109
Al–Nb–N, superconductivity of Nb_3Al_2N, 20: 6228
Ar–N, alpha stopping in, energy transfer and scintillations from, 20: 11130
Ar–N, corrosive effects on structural alloys at 900°C, 19: 32279(R) (ANL-7020(p.3-99))
Ar–N, corrosive effects on structural alloys and metals at 900°C, 20: 20802(R) (ANL-7055, pp 21-98)
Ar–N, electric discharge in, constriction, volt-ampere characteristics, and volume recombination of the positive column of, 16: 21179
Ar–N, ionization by electron impact, 18: 16720
Ar–N, luminescence from columnar electron-ion recombination following alpha particle or fission fragment ionization in, 16: 13824
Ar–N, mixing at high temperatures, (E), 19: 40231 (LA-3229, pp 149-76)
Ar–N, nitridation of uranium–zirconium droplets in, 18: 24933 (AFSWC-TDR-63-51)
Ar–N, nitriding effects on refractory alloys at 950°C, 19: 14765(R) (ANL-6977)
Ar–N, phase behavior of, equation of state for, 19: 42957
Ar–N, positron and positronium decay in, fine structure, 18: 4400 (NP-13341)
Ar–N, positronium annihilation and formation in, electric field effects on, 16: 13683 (AROD-2211.3)
Ar–N, positronium decay and formation in, 18: 4398 (NP-13329)
Ar–N, positronium decay and formation in, 18: 4399 (NP-13330)
Ar–N, radioinduced luminescence of, 3-Mev-electron, 19: 26395
Ar–N, scintillation from alpha-excited, pulse-height spectra of, 19: 20313(R) (ANL-6938(p.9-20))
Ar–N–O, corrosive effects on niobium, titanium, Zircaloy-2, and zirconium at 20°C, 18: 37639(R) (EURAEC-1130)
Ar–N–O, forbidden auroral radiation from Tesla discharges in, 18: 28174
B–C–N, reactions with fluorocarbons at high pressures and temperatures, 19: 32048(R) (NP-15073)
benzene–N, radiolysis yields in, 19: 46324(R) (AGN-8132)
C–Hf–Mo–N–Re–Ta–W–Zr, creep properties at 2400°F, 19: 18401(R) (WANL-PR(Q)-005)
C–Hf–Mo–N–Re–Ta–W–Zr, development of dispersion-strengthened tantalum-base, 20: 21240(R) (WANL-PR-(Q)-006)
C–Hf–Mo–N–Re–Ta–W–Zr, effects of heat treatment on hardness of, 19: 18401(R) (WANL-PR(Q)-005)
C–Hf–Mo–N–Ta–W–Zr, effects of heat treatment on hardness of, 19: 18401(R) (WANL-PR(Q)-005)
C–Hf–N–Re–Ta–W, hardness at room temperature, 19: 18401(R) (WANL-PR(Q)-005)
chlorotrifluoromethane–N, distribution ratio in vortex flow, 20: 20293 (JPL-TR-32-808)
Cl–N, positron resonance annihilation in, (E), 19: 33026
Cl–N, properties in aluminum alloy degassing, 17: 12601
C–N, spectra of diatomic, in plasma jets, (E), 19: 41287
C–Nb–N, superconducting properties of, composition dependence of, 20: 34420 (UCRL-16817)
C–N–O–Pu–U, corrosion by water at 550°F, 20: 4327(R) (UNC-5138)
C–N–O–Pu–U, phase studies, 20: 9550
C–N–O–Pu–U, preparation of single-phase compositions of, 20: 4327(R) (UNC-5138)
C–N–O–U, crystal structure and phase studies, 18: 2165(R) (NCSC-2663-14)
C–N–O–U, crystal structure of solid solutions in, 20: 39385 (CEA-R-2852)
C–N–O–U, fabrication and properties, 18: 2165(R) (NCSC-2663-14)
C–N–O–U, fabrication, phase studies, and properties of, 20: 9496(R) (NCSC-2663-19)
C–N–O–U, phase studies, 18: 12651(R) (NCSC-2663-15)
C–N–O–U, preparation and high-temperature properties of stoichiometric, 20: 41429(R) (USBM-RC-1249)
C–N–O–U, properties of, as inclusion in uranium metal, 17: 18765(R) (NYO-10354)
C–N–O–U, research program plans on phase relations and uses in fuels, 18: 14384(R) (USBM-U-1091)
C–N–Ti, Hall coefficients, 19: 47009 (NP-15514(Vol.2))
C–N–U, crystal structure and phase studies, 18: 2165(R) (NCSC-2663-14)
C–N–U, phase diagram and stability of, 18: 33576
C–N–U, phase studies, 17: 14830(R) (NCSC-2663-9)
C–N–U, phase studies, 19: 11758
C–N–U, phase studies, 20: 29749
C–N–U, thermodynamic properties, 17: 18849
C–N–U, thermodynamics of formation of $UC_{1-x}N_x$ in, 17: 32132
coal–N, compressibility of suspensions of, 17: 42354(R) (TID-19443)
CO_2–glass–N, heat transfer in glass-bead suspensions, 20: 14671(R) (TID-22394)
CO–H–N, radioinduced reactions in, 20: 3982(R) (AGN-8156)
CO–H–N, radiolysis yields in, 19: 46324(R) (AGN-8132)
Co–Mg–N, crystal structure, 16: 2259
CO_2–N, dielectric loss coefficient, 18: 5847(R) (NP-13401)
CO–N, diffusion in, 17: 39076
CO_2–N, mass transfer in turbulent systems of, 18: 22222 (IS-738)
CO_2–N, radiation and thermal effects on, analysis for product yields in, 20: 23071(R) (AGN-8169)
CO–N, radiolysis, 18: 35586 (AERE-R-4198)
CO_2–N, temperature dependence of dielectric loss properties of, 18: 20627(R) (NP-13815)
Co–Nb–N, structure of filled Ti_2Ni type compounds in, 19: 37107
CO_2–N–O, physical properties, calculated, 19: 11045 (ANL-6951)
Co–N–Zn, crystal structure, 16: 2259
Co–N–Zn, phase studies, 16: 16768
Cr–N, scavenging effects of metals on, 18: 12692
Cs–N, excitation transfer in, 17: 9019
DH–N, electron reactions with, cross sections for secondary ion formation in, 19: 19995
D–N, diffusion in, 17: 39076
D–N, electron-induced ion-molecule reactions in, formation of N_2D^+

ions in, 17: 40853 (TID-18176)
ethane–N, radiolysis yields in, 19: 46324(R) (AGN-8132)
ethylene–N, alpha-particle interactions with, properties of recoil ions from, 20: 41622 (SC-DC-66-1564)
ethylene–N, radiolysis yields in, 19: 46324(R) (AGN-8132)
ethylene–methane–N, radiolysis of, 19: 46324(R) (AGN-8132)
ethylene–N, radiolysis of, 19: 46324(R) (AGN-8132)
Fe–Mo–N, preparation of kryptonates of Moly-Perma-Foil by diffusion, 20: 18570(R) (NYO-2757-5)
Fe–N, dispersion hardening in, effect of pre-aging on, 16: 10598
Fe–N, radiation effects on internal friction, 17: 34557(R) (ORNL-3480(p.117-42))
Fe–N, radiation effects on engineering properties of, 18: 32216 (A/CONF.28/P/242)
Fe–N, radiation effects on nitride precipitation in, 19: 37173 (ORNL-P-1448)
Fe–N, radiation-enhanced nitrogen losses from solid-solution, neutron, 19: 1004(R) (ORNL-3676(p.125-56))
Fe–N, stress relaxation, 17: 5040(R) (ORNL-3364(p.125-50))
F–N, corrosive effects on nickel at 450 and 500°C, 18: 15426(R) (ANL-6810)
F–N, corrosive effects on nickel having weldments, 18: 24813(R) (ANL-6880(p.49-67))
F–N, use in removal of actinide halides from alumina, 20: 41062(P)
Ga–Nb–N, preparation and structure of T_5M_3X type compound in, 19: 30788
Ga–N–Ta, preparation and structure of T_5M_3X type compound in, 19: 30788
Ga–N–V, lattice parameters of filled β-manganese structure phases in, 19: 37109
Ge–Nb–N, preparation and structure of T_5M_3X type compound in, 19: 30788
Ge–N–Ta, preparation and structure of T_5M_3X type compound in, 19: 30788
graphite–N, circulation in heat-transfer loop, 17: 42360(R) (TID-19553)
graphite–N, compressibility of suspensions, 17: 42355(R) (TID-19475)
graphite–N, compressibility of suspensions of, 17: 42354(R) (TID-19443)
graphite–N, density of, densitometers for measuring, 16: 22329(R) (TID-16021)
graphite–N, density of, design of device for measuring, 16: 33155(R) (TID-16753)
graphite-N, density of, design of measuring device for, 17: 16386(R) (TID-18162)
graphite–N, density of flowing streams of, instrument for measuring, 18: 5466(R) (TID-19815)
graphite–N, deposition in heat exchangers, effects of bentonite on, 18: 15584(R) (TID-20319)
graphite–N, deposition in heat exchangers, 18: 33123(R) (TID-20830)
graphite–N, effects on candidate HTLTR materials at 1000 and 1200°C, 19: 40966 (BNWL-92)
graphite–N, particle degradation in circulation of, 18: 1277(R) (TID-19574)
graphite–N, radiation effects on, reactor, 19: 13421(R) (HW-81984 (p.6.1-14))
HCl–N, corrosive effects on nickel at 450°C, 18: 15426(R) (ANL-6810)
HCl–N, corrosive effects on nickel having weldments, 18: 24813(R) (ANL-6880(p.49-67))
He–N, analysis of ionized, 17: 4457 (GA-3358)
He–N, compressibility at high pressures at 25°C, 19: 19840 (LA-3250)
He–N, heat transfer and mass transfer across interface of suddenly pressurized liquid-vapor phases, 19: 22499
He–N, performance for irradiation capsule temperature control, 20: 6680 (ORNL-TM-1319)
He–N, phase equilibria in gas–solid, at low temperatures, 16: 32248
He–N, radioinduced collisions in, by 10-kev electron beam, 19: 11194
He–N, second virial coefficients and volumetric behavior at 0 to −140°C, 17: 28077
He–N, spectra of singly ionized nitrogen in plasma of, Stark profiles of, (E), 20: 3215
He–N, thermal conductivity of effects of temperature on, 19: 42804(R) (GEAP-3771-16)
Hf–In–N, superconductivity of Hf_2InN, 20: 6228
Hf–Nb–N, precipitation hardening in, effects of heat treatments on, 20: 29759
Hf–Nb–N, properties of, effects of heat treatment on, 17: 34419(R) (WADC-TR-57-344(Pt.VII))
Hf–Nb–N–W, properties of, effects of heat treatment on, 17: 34419(R) (WADC-TR-57-344(Pt.VII))
HF–N–O, solvent properties for chromium and stainless steel, 19: 31462(R) (ANL-7028)
Hf–N–Re–Ta–W–Zr, hardness at room temperature, 19: 18401(R) (WANL-PR(Q)-005)
Hf–N–Zn, structure of filled Ti_2Ni type compounds in, 19: 37107
Hg–N, flow characteristics for two-phase, 17: 27535 (BNL-801)
Hg–N, flow of circulating and non-circulating, slip ratios in, 19: 36622
Hg–N, heat transfer in two-phase flow of, 17: 18265 (NAA-SR-8171)
H–N, analysis of ionized, 17: 4457 (GA-3358)
H–N, distribution ratio in vortex flow, 20: 20293 (JPL-TR-32-808)
H–N, effects on melting points of plutonia–urania, 20: 29621(R) (NYMEC-3524-17)
H–N, ion-neutral reactions in afterglows in, 16: 24276 (GA-2824)
H–N, magnetic shielding constants for NH molecule in, 16: 29523
H–N, mass spectra of ion-molecule reactions in, (E), 19: 42481
H–N, molecular energies, forces, and internuclear distances of, 18: 22059
H–N, nuclear spin lattice relaxation in, 19: 39378
H–N, phase equilibria in gas–solid, at low temperatures, 16: 32248
H–N, proton spin-lattice relaxation in, 16: 18887
H–N, reduction of uranium trioxides, kinetics of, 17: 23356
H–N–Ti , phase studies, 19: 27735(R) (NAA-SR-10850)
In–N–Ti, superconductivity of Ti_2InN, 20: 6228
Kr–N, electric discharge in, constriction, volt-ampere characteristics, and volume recombination of the positive column of, 16: 21179
Kr–N, electron reactions at 50 kev, luminescence from, (E), 19: 41246
Kr–N, radioinduced luminescence of, 3-Mev-electron, 19: 26395
Kr–N, thermal diffusion in, 16: 3561
LaB_6–N, electric conductivity of suspensions of, in MHD cells, 20: 21575
methane–N, electron avalanche in discharges in, 18: 21491
methane–N, electron drift velocity and mean energy in, determination of, 19: 47124(T) (SLAC-Trans-19)
methane–N, fission fragment effects on, effects of nitric oxide and temperature on, 20: 23071(R) (AGN-8169)
methane–N, phosphorescence of, 18: 37857
methane–N, radiolysis of, 19: 46324(R) (AGN-8132)
methane–N, radiolysis in fissiochemical loop, 19: 46324(R) (AGN-8132)
methane–N, radiolysis of, products from fission-fragment, 20: 3982(R) (AGN-8156)
methane–N, radiolysis of, products from electron, 20: 3982(R) (AGN-8156)
methane–N, spectra of ion molecule reactions in deuterated, 20: 23071(R) (AGN-8169)
Mo–N, superconductivity, 17: 41604
Mo–Nb–N–Zr, heat treatment of, 20: 14972(P)
Mo–N–Re–Ta–W–Zr, effects of heat treatment on hardness of, 19: 18401(R) (WANL-PR(Q)-005)
Nb–N, degasification of solid solutions of, kinetics of, 20: 13202
Nb–N, dislocation damping interactions in, interstitial, 16: 33491
Nb–N, equilibrium in, 18: 34177
Nb–N, phase equilibria in, 16: 33492
Nb–N, phase studies, 16: 15194 (TID-15145)
Nb–N, phase studies, 18: 39976
Nb–N, phase studies and properties, 19: 986
Nb–N, phase studies at 1600 to 2200°C, 19: 46296
Nb–N, phase studies, 20: 5851
Nb–N, precipitation from supersaturated, kinetics of, 20: 13303
Nb–N, preparation, properties, and uses of, review on, 16: 27640(T) (FTD-TT-62-430)
Nb–N, properties of equilibrium solid solutions in, mechanical and thermodynamic, 19: 13991 (ML-TDR-64-134)
Nb–N, properties of solid solutions of, effects of nitrogen content on, 20: 13302
Nb–N, superconductivity, 17: 41604
Nb–N–O, internal friction studies of interstitial clusters in, 20: 31774
Nb–N–Ta–Zr, heat treatment of, 20: 14972(P)
Nb–N–Ti–Zr, heat treatment of, 20: 14972(P)
Nb–N–V–Zr, heat treatment of, 20: 14972(P)
Nb–N–W–Zr, heat treatment of, 20: 14972(P)
Nb–N–Zn, phase studies, 19: 42872
Nb–N–Zn, structure of filled Ti_2Ni type compounds in, 19: 37107
Nb–N–Zr, equilibrium solid solutions at 1200 to 1800°C in, 20: 2337 (ORNL-P-1677)
Nb–N–Zr, properties of equilibrium solid solutions in, mechanical and thermodynamic, 19: 13991 (ML-TDR-64-134)
NH_3–H–N, radiolysis of ammonia in, proton, 18: 17917
NH_3–N, diffusion in, 17: 39076
NH_3–N, spectra of nitrogen-14 Knight shifts and relaxation times in, 19: 7386
N–H_2O, hydrodynamic characteristics in circular tubes, 19: 1875(R) (EURAEC-1011)
N–H_2O, oxidative effects on uranium, mechanism of, 20: 16986
N–H_2O, radiation effects on oxidation of reactor graphite, 19: 1008(T) (JPRS-26808(p.157-68))
N–H_2O, radiation effects on production of ammonia in, effects of acidity on γ and uv, 20: 31289
N–H_2O, yields from d-c discharges in, 18: 20013

Ni–Nb–N, structure of filled Ti_2Ni type compounds in, 19: 37107
N–NO, mutual charge neutralization of ions in, pressure dependence of 10 to 600 torr, 18: 7407 (UCRL-10904)
N–NO, radiolysis of, 19: 46324(R) (AGN-8132)
N–O, alpha reactions of, spectra from, 19: 26382(R) (RPI-321-1)
N–O, analysis for fluorine and hydrofluoric acid, chromatographic, 20: 45789(R) (ORNL-3945, pp 48-71)
N–O, chemical reactions during high temperature rapid quenching of, 19: 44041
N–O, combustion of plutonium alloys and sodium in, properties of aerosols from, 20: 35668 (LA-3491)
N–O, corrosive effects of, on turbine alloys, 16: 32114 (IDO-28591)
N–O, corrosive effects on nickel at 500°C, 18: 15426(R) (ANL-6810)
N–O, corrosive effects on nickel having weldments, 18: 24813(R) (ANL-6880(p.49-67))
N–O, corrosive effects on INOR-8 at 1300 and 1400°F, 20: 4308(R) (ORNL-3870, pp 243-60)
N–O, diffraction of x-ray scattering by, 18: 4615
N–O, electric breakdown in plane-point and plane-wire gaps, 18: 20148
N–O, electric discharge in, ionizing radiation from, 16: 12288
N–O, electron-ion attachment and recombination in, 17: 8920(R) (GACD-2461)
N–O, heat transfer and mass transfer across interface of suddenly pressurized liquid-vapor phases, 19: 22499
N–O, ion-neutral reactions in afterglows in, 16: 24276 (GA-2824)
N–O, oxidizing effects on irradiated graphite, 18: 38247 (A/CONF.28/P/185)
N–O, plasma of, development of emitter electrodes for, (E), 19: 20905 (SC-RR-65-54)
N–O, preparation and use in thermodynamic studies of uranium oxides, 19: 28298
N–O, radiation effects on reactions in, 16: 208(R) (NYO-9967)
N–O, radiation effects on production of carbon-14 and nitric oxides in, 17: 25337
N–O, radiation effects on optical spectra of, electron, 18: 24300(R) (NP-13953)
N–O, radiation effects on, gamma, 19: 36451(R) (BNL-900(p.73-104))
N–O, radioinduced formation of nitric oxide in, as measure of radiation dose, 17: 39111
N–O, radioinduced nitrogen fixation in, 19: 2395
N–O, radioinduced luminescence of, collisional deactivation of, 19: 13480
N–O, radiolysis of, 17: 10509(R) (ORNL-3320(p.30-46))
N–O, radiolysis at 77°K, ozone yields from, 18: 1725(R) (ORNL-3488 (p.42-54))
N–O, radiolysis of, ozone formation in, 18: 20095
N–O, radiolysis of, fission fragment, 19: 15565(R) (BNL-841(p.43-51))
N–O, radiolysis of liquid, formation of ozone in, 19: 23163(R) (ORNL-3650(p.111-86))
N–O, radiolysis of, decontamination of products from fission-fragment, 20: 40951(RPI-321-6)
N–O, reactions with tantalum in simulated atmospheric re-entry, 19: 4626 (SC-RR-64-575)
N–O, reactions with nuclear graphite at 575, 595, and 655°C, 19: 30680
N–O, reactions with graphite, effects of water vapor on kinetics of, 20: 23608
N–O, sorption by niobium, 20: 5851
N–O–H_2O, oxidative effects on uranium, mechanism of, 20: 16986
N–O–U, crystal structure and phase studies, 18: 2165(R) (NCSC-2663-14)
N–propene, radiolysis yields in, 19: 46324(R) (AGN-8132)
N–propene, radiolysis of, nitrogen atom yields in electron, 20: 23071(R) (AGN-8169)
N–Pu, phase studies, 17: 28565(R) (LAMS-2915)
N–Pu, structure, 17: 3536
N–Pu–U, preparation of powders of, from arc-cast plutonium–uranium alloy, 20: 7491(R) (BMI-1745, Sect.B)
N–Pu–U, properties of hot-pressed powders of, 20: 7491(R) (BMI-1745, Sect.B)
N–Pu–U, properties of hot-pressed powders of, 20: 14957(R) (BMI-1754)
N–rare gases, alpha reactions of, spectra from, 19: 26382(R) (RPI-321-1)
N–Re–Ta–W–Zr, creep properties at 2400°F, 19: 18401(R) (WANL-PR(Q)-005)
N–Ru–Zr, structure of filled Ti_2Ni type compounds in, 19: 37107
N–stainless steel, flow of suspensions of, in process-heat reactor systems, 19: 17333(R) (TID-21596)
N–T, thermal diffusion factors and mutual diffusion coefficients for, composition dependence of, 18: 8933
N–Ta, preparation, properties, and uses of, review on, 16: 27640(T) (FTD-TT-62-430)
N–Ta–W–Zr, effects of heat treatment on hardness of, 19: 18401(R) (WANL-PR(Q)-005)
N–Tc, composition and structure of phases in, 18: 18381
N–Th, preparation, properties, and uses of, review on, 16: 27640(T) (FTD-TT-62-430)
N–Ti, elastic modulus variations and internal friction in iodide-refined, 16: 13629
N–Ti, preparation, properties, and uses of, review on, 16: 27640(T) (FTD-TT-62-430)
N–Ti–Zn, structure of filled Ti_2Ni type compounds in, 19: 37107
N–Ti–Zr, tensile properties at room temperature, 18: 18380
N–trichlorotrifluoroethane, flow of circulating and non-circulating, slip ratios in, 19: 36622
N–U, metallographic tests on arc melted, 20: 29775
N–U, phase diagrams, 18: 34035(R) (BMI-X-10053)
N–U, phase diagrams, 20: 13286
N–U, phase relations and thermodynamics in, 19: 885 (BMI-1692)
N–U, phase studies, 18: 542(R) (BMI-X-10061)
N–U, phase studies, 18: 2234(R) (UNC-5060)
N–U, phase studies on, 18: 7237
N–U, phase studies, 18: 22478 (CONF-45-3)
N–U, phase studies, 18: 32035(R) (BMI-X-10073)
N–U, phase studies, 18: 32037(R) (BMI-X-10092)
N–U, preparation, properties, and uses of, review on, 16: 27640(T) (FTD-TT-62-430)
N–V, preparation, properties, and uses of, review on, 16: 27640(T) (FTD-TT-62-430)
N–V–Zn, lattice parameters of filled β-manganese structure phases in, 19: 37109
N–Xe, electric discharge in, constriction, volt-ampere characteristics, and volume recombination of the positive column of, 16: 21179
N–Xe, electron reactions at 50 kev, luminescence from, (E), 19: 41246
N–Y, oxidation in air at 500 to 1400°C, 19: 2750
N–Y, phase studies, 20: 41412(R) (IS-1500(Sect. M))
N–Zn–Zr, structure of filled Ti_2Ni type compounds in, 19: 37107
N–Zr, preparation, properties, and uses of, review on, 16: 27640(T) (FTD-TT-62-430)
N–Zr, superconductivity, 17: 41604
Nitrogen Trifluorides
see Nitrogen Fluorides

NITROGEN TRITIDES
spectra of, ν_1 and ν_3 bands of, 18: 1640
spectra of, vibrational bands in infrared, 17: 32048 (TID-19213)

NITRONES
reactions of, photochemical, 18: 17854(R) (UCRL-11046(p.159-98))

NITROSO COMPOUNDS
(For inorganic nitroso compounds see Nitrosyl Compounds and specific compounds, e.g., Ruthenium Nitrosyls.)
see also Nitrosyl Compounds
see also Ruthenium Nitrosyls
preparation of deuterated and nitrogen-15-labeled *cis*- and *trans*-dimers of ethane and methane, 16: 11725
spectra of aqueous solutions of nitrosodisulfonate, ESR, 20: 43184 (UCRL-17064)

NITROSYL BROMIDES
isotopic exchange equilibrium calculations, 19: 40460(R) (NYO-3462-1)
isotopic substitution in, partition function ratios at 20 to 2000°K for nitrogen-15 and oxygen-18, 20: 40873(R) (NYO-3462-2)

NITROSYL CHLORIDES
chlorine-36 exchange from, to metal chlorides, 17: 15996
corrosive effects on monel and nickel, 18: 3671(R) (BNL-799(p.26-54))
determination in nuclear fuels and wastes, gas-chromatographic, 16: 22033
isotopic exchange equilibrium calculations, 19: 40460(R) (NYO-3462-1)
isotopic substitution in, partition function ratios at 20 to 2000°K for nitrogen-15 and oxygen-18, 20: 40873(R) (NYO-3462-2)
oxygen-18 exchange, equilibrium constants and partition function ratios for, 16: 18876
radioinduced reactions with cyclohexane, mechanisms, 16: 7586
radioinduced reactions with cyclohexane and 2,3-dimethylbutane, effects of solvents on, 18: 1731 (TID-19671)
radiolysis in cyclohexane and 2,3-dimethylbutane, yields in, 16: 27035(R) (NYO-10200)
reactions with hydrofluoric acid, NOF · 3.1 HF production in, 17: 31795(R) (BNL-782(p.18-43))
reactions with hydrofluoric acid, 18: 3671(R) (BNL-799(p.26-54))
reactions with molybdenum hexafluoride, tungsten hexafluoride, and uranium hexafluoride, 17: 7993 (GAT-T-971)
reactions with molybdenum, tungsten, and uranium hexafluorides, 18: 5272
transport properties, 16: 3553
use in solar regenerative fuel cell system, 16: 16480 (WADD-TR-60-821(Pt.II))
HF–NOCl, corrosive effects on Zircaloy-2, 18: 3671(R) (BNL-799 (p.26-54))

NITROSYL COMPOUNDS
see also Ruthenium Nitrosyls
isotope exchange in systems with nitrogen monoxide, 16: 22520
nuclear double resonance in potassium nitrosyl sulfonates, 16: 31538
spectra of pentacyanonitrosylchromium(II) ion, electron spin resonance, 19: 40465 (UCRL-16175)
structure of $K_3Mn(CN)_5NO$, 16: 23570
volatility, 17: 31795(R) (BNL-782(p.18-43))
with iron, covalency and nuclear isomer shift in, 18: 39228
NITROSYL FLUORIDES
see also Uranium Nitrosyl Fluorides
electric conductivity of hydrofluoric acid solutions of, 17: 2461(R) (BNL-731(p.18-46))
isotopic exchange equilibrium calculations, 19: 40460(R) (NYO-3462-1)
isotopic substitution in, partition function ratios at 20 to 2000°K for nitrogen-15 and oxygen-18, 20: 40873(R) (NYO-3462-2)
radiolysis of, synthesis of fluid propellants by fission-fragment, 18: 17865(R) (NP-13764)
reactions with glass and mercury, 17: 3574(R) (NP-12212)
reactions with hydrofluoric acid, metals, and uranium carbide and oxide, products of, 16: 30357 (BNL-6231)
reactions with molybdenum hexafluoride, tungsten hexafluoride, and uranium hexafluoride, 17: 7993 (GAT-T-971)
reactions with molybdenum, tungsten, and uranium hexafluorides, 18: 5272
reactions with uranium salts, 18: 6882 (BNL-7572)
solvent properties of NOF·3.1HF aziotrope for uranium(IV) oxides, 17: 31795(R) (BNL-782(p.18-43))
HF–NOF, corrosive effects on aluminum alloy 1100 and Zircaloy-2, 18: 3671(R) (BNL-799(p.26-54))
HF–NOF, preparation and properties, 18: 3671(R) (BNL-799(p.26-54))
HF–NOF, use in fuel element reprocessing, 18: 37299(P)
Nitrosyl Ruthenium Nitrates
see Ruthenium Nitrosyl Nitrates
Nitrosyl Uranium Fluorides
see Uranium Nitrosyl Fluorides
NITROUS ACID
effects on algae, patterns of expression of mutagenic, 20: 16294
effects on Aspergillus, genetic, 20: 26680
effects on Aspergillus, mutagenic, 17: 31893
effects on *Bacillus subtilis*, 20: 26688
effects on bacteriophage, biological, 19: 33840
effects on cytolytic and transforming abilities of Polyoma virus, 20: 38702
effects on DNA in pneumococci and streptococci, mutagenic, 20: 6835
effects on *E. coli*, effects of uv on, 18: 27115
effects on mutagenesis in isolated DNA from *B. subtilis*, 19: 19542
effects on mutations in *E. coli*, mechanism of, 19: 33912
effects on mutation induction in *Schizosaccharomyces pombe*, 19: 42266
effects on neurospora, mechanism of mutagenic, 17: 35453(R) (TID-19287)
effects on pyrimidine mutation induction in *Salmonella typhimurium*, genetic analysis of, 19: 45878
effects on reproduction and transformation of polyoma virus, 19: 36052
effects on Saccharomyces radiosensitivity, mutagenic, 20: 5360
effects on TBP-Amsco, extraction of niobium and zirconium, 19: 13532(R) (ORNL-TM-1020)
formation and nature, 18: 9752 (IA-900)
formation by radiolysis of aqueous benzene, 20: 36881
isomerization in solid nitrogen matrix, infrared-induced, 18: 302
isotopic exchange equilibrium calculations, 19: 40460(R) (NYO-3462-1)
isotopic substitution in, partition function ratios at 20 to 2000°K for nitrogen-15 and oxygen-18, 20: 40873(R) (NYO-3462-2)
mutation induction in *Neurospora crassa* by, spectra of allelic complementation and leakiness in, 19: 8862
reactions with nitrosylruthenium nitrato complexes, formation of nitro complexes by, 19: 26280 (AERE-R-4769)
reactions with uranium dioxide in sulfuric acid solutions, 19: 28335
NITROXIDE
di-*t*-butyl-, radiosensitivity effects on *E. coli* B/r, 19: 43875
di-*tert*-butyl-, toxic effects in HeLa cells in culture, 20: 26622
di-*tert*-butyl, EPR and NMR spectra in, (E), 19: 22654 (CEA-R-2506)
t-butyl-2,6-dimethoxyphenyl-, radiosensitivity effects on *E. coli* B/r, 19: 43875
tetramethylpentamethylene-, radiosensitivity effects on *E. coli* B/r, 19: 43875
NITROXY FLUORIDES
isotopic substitution in, partition function ratios at 20 to 2000°K for nitrogen-15 and oxygen-18, 20: 40873(R) (NYO-3462-2)
NITROXYL
production in photolysis of ammonia in solid carbon dioxide, spectra of, 17: 8167
spectra of deuterium-labeled and normal, absorption, 16: 13031
NITRYL CHLORIDES
isotopic exchange equilibrium calculations, 19: 40460(R) (NYO-3462-1)
isotopic substitution in, partition function ratios at 20 to 2000°K for nitrogen-15 and oxygen-18, 20: 40873(R) (NYO-3462-2)
NITRYL FLUORIDES (NO_2F)
isotopic exchange equilibrium calculations, 19: 40460(R) (NYO-3462-1)
isotopic substitution in, partition function ratios at 20 to 2000°K for nitrogen-15 and oxygen-18, 20: 40873(R) (NYO-3462-2)
radiolysis of, synthesis of fluid propellants by fission-fragment, 18: 17865(R) (NP-13764)
reactions with molybdenum hexafluoride, tungsten hexafluoride, and uranium hexafluoride, 17: 7993 (GAT-T-971)
reactions with molybdenum, tungsten, and uranium hexafluorides, 18: 5272
thermodynamic properties, 16: 26644(R) (NP-11755)
NOBELIUM
see also Actinides
discovery of, review of, 19: 18686
fission of, data on spontaneous, 17: 19396
production, 20: 16543
production in heavy-ion nuclear reactions, review of, 20: 15740
production of, review of methods for, 20: 20796
properties and separation of, review on, 19: 4161
synthesis of, 17: 16085
NOBELIUM ISOTOPES
fission barriers and half lives of, spontaneous, (T), 20: 28357
production in neon-22 reactions (Ne-22,xn) with uranium-238, cross sections for, (E), 20: 13889
NOBELIUM ISOTOPES No-254
alpha decay of, energy and half life of, (E), 20: 11968 (JINR-P-2470)
alpha decay of, half life for, (E), 20: 11969 (JINR-P-2471)
decay, (E), 20: 28299
production in americium-243 (N-15,4n) and uranium-238 (Ne-22,6n) reactions, (E), 20: 11969 (JINR-P-2471)
production in neon-22 reactions (Ne-22,xn) with uranium-238, cross sections for, (E), 20: 13889
properties, (E), 20: 28298
NOBELIUM ISOTOPES No-255
production in neon-22 reactions (Ne-22,xn) with uranium-238, cross sections for, (E), 20: 13889
NOBELIUM ISOTOPES No-256
fission half life of, spontaneous, 18: 21183 (JINR-P-1580)
half life, (E), 20: 46775
half life, (E), 20: 13778 (JINR-P-2525)
production and half life, 18: 2839 (JINR-P-1383)
production in neon-22 reactions (Ne-22,xn) with uranium-238, cross sections for, (E), 20: 13889
production in oxygen-18 reactions with plutonium-242, (E), 20: 13778 (JINR-P-2525)
synthesis and half life, 17: 34897
Noble Gases
see Rare Gases
NOISE
see also Circuit Noise
see also Sound
absorption of cosmic, in polar-cap regions, 16: 18204
absorption of cosmic, sunrise and sunset effects on aurora and geomagnetic storm-associated, 17: 23541
absorption of cosmic radio, in ionosphere, 17: 28016
absorption of cosmic radio, auroral chorus activity and K-index correlation to ionospheric, 17: 28122
absorption of cosmic, mechanism of smooth auroral, 19: 14429
analysis of electric, for determination of kinetics in pool-type reactors, 17: 12775(R) (ORNL-3360(p.68-72))
analysis of electronic, method for, 19: 32680(R) (IDO-17052)
analysis of reactor, 18: 13193
analysis of reactor, kinetics model for, 19: 31460(R) (ANL-7010 (p.179-233))
analysis of, in bubbling electrolytic cell, 19: 725 (IDO-16975)
contamination of signal by optimum quantization of, 17: 35260(R) (TID-19135)
control of industrial, 19: 40806 (RL-SA-37)
discrimination against, in nuclear magnetic resonance spectra by continuous averaging, 17: 32363
effects on auditory nerve responses, 16: 4610(R) (TID-14435)
effects on capillary permeability, 18: 43267
effects on cardiac activity in dogs, 20: 1629
effects on gravitational radiation detection, 18: 11013
effects on measurement of coulomb scattering in nuclear emulsions, 19: 2965
elimination of pulses of, from scintillation counters, 16: 22358
emission from hot plasma, electron temperature from, 17: 42094
emission in low-pressure electrodeless discharges in air, radiation effects

on spectra of, 17: 34577
emission of r-f, by plasma, 18: 7807
filters for electronic, optimization of, 19: 39270(R) (TID-21894)
from probes immersed in gas discharges, h-f, 18: 7820
generation at 1 to 10 kc of white, in exosphere, 16: 21231
generation of cyclotron, in exosphere, 17: 24228
generation of radiofrequency, by ion engines, 17: 31780
geomagnetic storm effects on cosmic radio, Ahmedabad, India, 16: 8047 (NP-11232(p.172-8))
in instrumentation systems, 17: 10915 (TID-17749)
in nuclear systems, research at University of Florida on, 18: 11487
in total-activity measurements, optimum discriminator bias for minimum, 16: 29157
intensity and spectrum of acoustic, from chain reacting systems in power reactors, (T), 20: 36219
intensity of cosmic, in Ethiopia and Ghana, 17: 34677
intensity of cosmic, off Chile coast July 9, 1962, 17: 34679
measurement in plasma by two-frequency correlation method, 20: 4991
measurement of, computer analysis of performance of linear and square-law detectors for, 17: 10916 (TID-17788)
measurement of decimetric, 18: 43915
measurement of linear and square-law detectors for, 19: 31460(R) (ANL-7010(p.179-233))
measurement of, errors in, 18: 25760
measurement of, errors in, 19: 31460(R) (ANL-7010(p.179-233))
occurrence of high-frequency auroral, relation to geomagnetic disturbances, 20: 21835
of gas discharges, 17: 11829 (ASD-TR-61-179(Vol.I))
power radiation by nonequilibrium cylindrical plasma, 16: 19586
production and propagation in xenon low-pressure plasma, 19: 3412
production in coaxial cables by gammas and neutrons, 18: 37518 (USAELRDL-TR-2334)
production in power reactors, sources of, 18: 35155 (TID-7679(p.357-68))
production of acoustic, in nucleate boiling, 17: 32251 (TRG-Report-549)
production of r-f, in ionosphere during ionization by corpuscular streams, (T), 20: 28108(T)
propagation along plasma column, (E/T), 19: 5353
propagation from magnetic field penetration in superconductors, 17: 39746
propagation in electrical cables by nuclear pulse irradiation, 17: 34519
propagation in electron beams in crossed fields, (T), 19: 6401
propagation in maser amplifiers, sources for, 18: 922
propagation in photomultiplier tubes, reduction of, 18: 5586
propagation of microwave, from sheath rotation instability in plasma discharge, 17: 38380
properties in lithium-drifted silicon radiation detectors, 18: 14278
quantum, in linear amplifiers, 17: 3286
radio anomalies of, from high-altitude explosions, 17: 23520
reduction in electromagnetic test systems, methods development for, 19: 31462(R) (ANL-7028)
reduction in nuclear magnetic resonance spectra, methods for, 19: 43997(R) (UCRL-11889)
reduction in silicon semiconductor detectors by internal carrier multiplication, 20: 33666
reduction of four-die swager, engineering drawings for enclosure for, 19: 6287
removal of space-charge fast-wave, using resonators, 18: 23848
research programs on electron device, 20: 14227(R) (TID-22419)
response of nonlinear time-variant control systems to, 18: 4063
source of, design of predictable, 19: 1956(R) (IDO-16994)
spectrum of, from nonequilibrium plasma in longitudinal fields, 17: 21185
spectrum of random television, 17: 21401(R) (TID-18585)
spectrum of reactor, analysis method development, 17: 17623(R) (IDO-16827)
standards on limiting, in industrial areas, 16: 29252(T) (JPRS-14621)
suppression in photomultiplier tubes, design and performance of system for, 17: 29203 (UCRL-68886)
suppression of photomultiplier, method for, 17: 27657 (UCRL-6886 (Rev.1))
transfer function measurements in nonlinear systems, 18: 12430
transmission in hot cells, development of system for, 17: 25388 (ORNL-TM-565)
use in fast-reactor measurements, 18: 35158 (TID-7679(p.469-500))
use in reactor shutdown reactivity measurements, 18: 35072 (TID-7679 (p.135-54))
use of acoustic emission for detection of metal overstress in reactor pressure systems, 20: 11001 (BNWL-SA-438)
use of reactor, for measurement of spatially dependent transfer function, 18: 11377

Nomenclature
see Glossaries

NOMOGRAPHS
description of, for finding simple probabilities, (T), 19: 13862 (SC-R-64-1348)
development for airborne radioactivity sampling, 18: 5548(R) (UCRL-7450)
development for correction coefficient in activation analysis, 19: 24412
for absolute beta activity determination, 16: 6604
for calculating angular correlation in nuclear reactions, 18: 32754
for calculating tellurium-132 activity for iodine-132 production, 16: 27090 (BLG-78)
for charged particle ranges in silicon, 16: 29541
for conversion between neutron spectrometric units, 16: 29717
for determining activity of radioisotopes, 16: 32628
for determining shock wave attenuation in tunnels, 16: 17349(T) (AEC-tr-5025)
for estimation of microcuries and millimicrograms from counts per minute, 19: 38749
for linear accelerator design, 19: 11884
for neutron time-of-flight spectrometry, 16: 22363
for nuclear reaction kinematics, 18: 28576 (ORNL-3636)
for nuclear reaction kinematics, 19: 16855(R) (ORNL-3714(Vol.I) (p.1-30))
performance of, for measuring radiation dosage to patient in fluoroscopy, 17: 35564

Non-Destructive Testing
see Materials Testing

NONADECANOIC ACID
sorption by annealed and oxidized copper and nickel single crystals, 20: 1570 (TID-22150)

NONANAL
effects on flavor of irradiated beef, 20: 39299
effects on off-flavor in radiosterilized beef, 20: 7467 (NP-15658)

NONANE
bond dissociation energies and ionization potentials of, calculation of, 18: 43489
carbon-13 chemical shifts in, from proton decoupled magnetic resonance spectra, 18: 8405
determination in kerosene by vapor-phase chromatography, 17: 6195
effects on radioluminescence of luminescent compounds, 19: 15624(T)
electron reactions in ethylene mixture, cross sections for momentum transfer and drift velocities in, 20: 5985 (ORNL-TM-1262)
mass spectroscopy of, first-order constant for metastable ion decay in, 18: 12013
polarization of irradiated, high voltage relaxation, 17: 27469
radiation effects on reactions with carbon dioxide, 19: 38727(T)
radioinduced reactions of, with carbon dioxide, yields in, 17: 27458
radiolysis at 77°K, luminescence spectra of electron, 18: 13888(T)
radiolysis of, electron, 18: 37215(T) (AEC-tr-6398(p.505-11))

NONANOIC ACID
radiolysis of, formation of carbonyls by gamma and ultraviolet, 17: 21748
radiolysis of, ESR spectra of, 18: 35599

1-NONANOL
hexadecafluoro-, radiolysis of, ESR spectra from gamma, 20: 372
solvent properties for rare earth nitrates, 19: 7644

NONELECTROLYTES
see also Electrolytes
solution of, review properties of, 17: 2953 (UCRL-6357)
spectroscopy of solutions of, 17: 2953 (UCRL-6357)

Nonyl Alcohol
see 1-Nonanol

n-Nonyl Aldehyde
see Nonanal

NONYLAMINE
preparation of carbon-14-labeled, 17: 21750

Noradrenaline
see Arterenol

19-NORANDROSTENOLONE
effects on acute radiation disease in rats, 19: 19624
phenyl propionate, protective effects of, against x radiation in rats, 18: 19779

NORBORANAMINE
reactions of, deamination, 17: 10510(R) (ORNL-3320(p.47-55))

NORBORNANE, BROMO-
exo-, solvolysis of, deuterium isotope effects on, 20: 352

7-NORBORNANECARBOXYLIC ACID, 1,7-DIMETHYL-2-OXO-
labeling with deuterium, octant rule for, 20: 33324

NORBORNANOL
deuterium scrambling in stereochemical equilibration of, 20: 45704
labeling with deuterium, 20: 45704

2-NORBORNENE
5-methylene, labeling with carbon-14 by Wittig reaction, 19: 28351

NORLEUCINE
ionization potential, 20: 3863(R) (IS-1200(Sect. C))
preparation of sulfur-35-labeled, by reactions with sulfur-35 recoil atoms,

19: 40619
radiolysis in presence of nitrogen or oxygen, mechanisms of, 19: 506
radiolysis of aqueous solutions of, mechanism of, 18: 6855
reactions with sulfur-35, formation of labeled methionine in, 20: 20786
synthesis and transformation in uv photolysis of organic compounds in mixtures with ammonium compounds, 18: 23204(T) (JPRS-24164(p.19-42))

NORMORPHINE
excretion of tritium-labeled, by dogs and monkeys, 17: 15601
preparation of tritium-labeled, 17: 15601
transformation of, from tritium-labeled morphine, 17: 15602

Normorphine, *N*-Allyl-
see Nalorphine

19-Nortestosterone Phenylpropionate
see Estr-4-en-3-one, 17 β-hydroxy-, phenylpropionate

NORTH AMERICA
effects of 20,000-MT nuclear attack on, ecological, 20: 2081 (BNL-917, pp 39-60)
effects of 20,000-MT nuclear attack on, physical, 20: 2078 (BNL-917, pp 1-10)
evolution during post-Turonian time, 20: 43500(R) (COO-689-60)
fallout monitoring for tritium content, 1961–1962, 17: 41059
fallout monitoring, 1963 and 1964, 18: 35784
fallout monitoring along 80th Meridian (West), 1957 through 1962, 18: 35785
fallout monitoring along 80th Meridian (West), 1963, 18: 35786
fallout monitoring, 1963 and 1964, 18: 35791
fallout monitoring, 1964, 18: 37383
fallout monitoring, 1964, 18: 37384
fallout monitoring, 1963 and 1964, 18: 41644(R) (HASL-149)
fallout monitoring, 1964, 19: 637
fallout monitoring, 1964, 19: 7712
fallout monitoring, 1963, 19: 18144(R) (HASL-156)
fallout monitoring, 1964, 19: 18157
fallout monitoring, 1964, 19: 22552
fallout monitoring, 1964, 19: 22554
fallout monitoring, 1964, 19: 22557
fallout monitoring, 1964, 19: 22562
fallout monitoring, 1965, 20: 18914
fallout monitoring, 1965, 20: 18915
fallout monitoring, 1965, 20: 18918
fallout monitoring, 1965, 20: 29428
fallout monitoring, 1965, 20: 29431
fallout monitoring, 1965, 20: 29434
geochronology, 20: 29397 (NAS-NRC-1276)
lithium-6/-7 ratios in natural sources from, 19: 32418
radiation monitoring of atmosphere in, 19: 42677

NORTH CAROLINA
(See also headings of the form North Carolina (Mitchell Co.))
analysis of river water in, for trace elements, 20: 45880(R) (YALE-2912-12)
deuterium content in rainfall in, Nov. 1 and 2, 1963, 19: 47112
fallout monitoring in Great Smoky Mountains in, 18: 419 (TID-19618 (App.E))
hydrographic, sediment, and faunal survey of Bogue Sound area, 17: 31817(R) (TID-19122)
mineral cycling in ecosystems of western, 18: 11 (TID-19618(p.38-112))

NORTH CAROLINA (MITCHELL CO.)
ages of uranium minerals in Spruce Pine District, 16: 29197

NORTH CAROLINA RESEARCH REACTOR
neutron spectra from, measurement using Fermi chopper, 20: 2994

NORTH DAKOTA
strontium-90 content in milk of Mandan-Minot region of, 20: 5678
studies of uranium-bearing lignites from, mineralogical, petrographical, and paleobotanical, 19: 26568 (NYO-10361)
uranium occurrence in southwestern part of Williston Basin, 19: 30434

NORTH SEA
radioactive contamination of Inner Oslofjord, dispersion factors in, 19: 24810
strontium-90 content of surface waters of, 1961, 18: 22248(T) (JPRS-24281)

NORTHERN IRELAND
iodine-131 content in cattle thyroid, Nov. 1961, 16: 11423

NORTHERN RHODESIA
age determinations of minerals and rocks in, review on, 18: 43793
sulfur-34 content in sulfide deposits in, 19: 36657
uranium minerals in, age of, 17: 32265

Northern States Power Co. Reactor
see Sioux Falls Power Reactor

NORTHWEST TERRITORIES
ages of uranium minerals in Eldorado Mine, 16: 29197
solar eclipse observations July 20, 1963, 19: 18973

NORVALINE
preparation of sulfur-35-labeled, by reactions with sulfur-35 recoil atoms, 19: 40619
protective effects against uv radiation in *Hansenula wingei*, 18: 43303
radiochemical degradation of, 18: 1744
radiolysis in presence of nitrogen or oxygen, mechanisms of, 19: 506
reactions with sulfur-35, formation of labeled methionine in, 20: 20786
synthesis and transformation in uv photolysis of organic compounds in mixtures with ammonium compounds, 18: 23204(T) (JPRS-24164 (p.19-42))
thermodynamic properties of, in water and heavy water, 19: 46318
vapor pressure, 18: 15678 (IS-790)

NORWAY
activation of soils and rocks in, 19: 308
age estimation of minerals in eclogites of, by potassium argon and rubidium–strontium methods, 20: 20891
carbon-14 contamination in, 19: 32483
cesium-137 content in man, source of, 17: 7771
cesium-137 body burdens to school boys in, 19: 6980
cesium-137 content in milk, correlation with precipitation, 19: 26534 (NYO-3364-4)
cesium-137 content in air in, effects of precipitation on, 19: 28549
cesium-137 content in man, meat, and milk in, 1962 through 1965, 20: 29432
cesium-137 content in milk from, March 1962 to 1966, 20: 41132 (NYO-3364-20)
cesium-137 content in beer from, 20: 45957 (NYO-3364-23)
cesium-137 uptake by man in, hazards from, 20: 22795
dose in houses in, 19: 20218
ecology of aquatic environment in, 19: 8740(R) (IAEA-R-37-5)
fallout content in milk during 1961, measurement of, 17: 15614 (A/AC.82/G/L.810)
fallout from radioactive cloud over, Nov. 1962, 18: 27712
fallout monitoring, 1956 to 1961, 17: 29116 (A/AC.82/G/L.769)
fallout monitoring, 1957 to 1959, 17: 37054 (FFIK-IR-K-253)
fallout monitoring, 1960 through 1964, 20: 31465
fallout monitoring, 1960 to 1961, 16: 394 (AERE-R-3766)
fallout monitoring, 1961 to 1964, 20: 2054
fallout monitoring, 1962 to 1965, 19: 36653 (NYO-3364-5)
fallout monitoring, 1963 and 1964, 19: 36652 (NYO-3364-3)
fallout monitoring, 1963 through 1965, 20: 14739 (TID-22655)
fallout monitoring, 1964, 19: 26533 (NYO-3364-1)
food irradiation research in, 19: 11624
fuel element reprocessing pilot plant research, Kjeller, 20: 16569
geochronology of basement complex in, determination by uranium-lead isotopic ages, 19: 22567(R) (NYO-1669-10)
geology of base rock, 16: 16577 (TID-14861(Vols.I&II))
monitoring for cesium-137 body burden and content in milk in, 18: 1361
monitoring of atmospheric cesium-137 in, during Oct. 1937, 17: 32275
nuclear power development and uses in, 19: 48114
operations at Kjeller, Oct.-Dec. 1964, 19: 29808(R) (KR-94)
personnel monitoring at atomic energy plants in, 1962, 18: 6968 (AE-126)
Precambrian rock age estimation by zircon method in, 18: 14067(R) (NYO-7243)
radioactive contamination of Inner Oslofjord, dispersion factors in, 19: 24810
radioisotope uses in, economics of industrial, 20: 27377
reactor program, 16: 2706
reactors in, competence of Norwegian industry in construction of, 17: 22810
reactors in, contribution of industry to construction of, 17: 22811
research activities at Institutt for Atomenergi, Kjeller Research Establishment, Lillestrom, Norway, 16: 2298(R) (KR-10)
research programs of Institutt for Atomenergi, 1961, 16: 26645 (NP-11911)

Norwegian–Dutch Heavy Water Reactor
see JEEP Reactor

NORWEGIAN SEA
radioactivity of organisms at bottom of, variations in, 20: 29424
strontium-90 content in surface water of, 1962 and 1963, 19: 24722

NOSE
iodine-131 content in, after thyroid cancer radiotherapy, 20: 18512
radiation effects on neurons in dog, polonium-210 and strontium-90, 18: 13463(T) (JPRS-23559(Del.)(p.36-42))
radiation effects of inhaled strontium-90 on virus production in dog, 20: 8636(R) (LF-28, pp 230-5)
radiation effects from inhaled strontium-90 on production of bacterial flora in dog, 20: 8637(R) (LF-28, pp 236-49)
radiation effects on olfactory neuron response, x, 20: 20431 (AD-630323)
radiation sickness and blood loss effects on phosphorus-32 uptake by rabbit, 19: 38431
radioinduced malpighian epitheliomas in, 18: 29448
radiosensitivity effects of gases in, on olfactory bulb neurons in rats,

20: 16215 (AD-628443)
radiosensitivity of, 19: 13074
radiotherapy of benign and malignant tumors of, prospects for, 19: 31968
radiotherapy of carcinoma of, 19: 28148
radiotherapy of chronic diseases of, by radon inhalation, 19: 38528
radiotherapy of, technique for, 18: 3636
radiotherapy of tumors on, effectiveness, 18: 17712
radiotherapy of tumors in region of, use of fast electrons for, 20: 45554
radiotherapy of, late effects on central nervous system from, 19: 45983
treatment of tumors of, by radiation and methotrexate, 20: 40782

Notohp (Massless particle of spin 1)
see Bosons

NOVA SCOTIA
age of granitic rock in, 18: 4001(R) (NYO-10517(p.143-5))

Novocaine
see Procaine

NOZZLES
see also Rocket Motor Nozzles
analysis of nozzle-to-shell attachments, 18: 15535(R) (ORNL-3523(p.361-413))
attachment to gas-cooled-reactor pressure vessels, 18: 30995(R) (ORNL-3619(p.278-335))
attachment to spherical shells, stress analysis of, 20: 35600(R) (ORNL-3951, pp 164-8)
calibration and fabrication of small-diameter, 16: 10127 (DC-60-6-37)
cavitation in mercury flows through Venturi, 18: 27673
cladding bores of, welding techniques for, 20: 16617
condensation of metal vapors in, 17: 8345
cooling at very high heat fluxes, study of forced-convection nucleate boiling of water for, 16: 31795 (NASA-TN-D-1214)
crack propagation in pressure vessel, effects of bending fatigue cycling on, 19: 13999(R) (SWRI-1228-43)
design and operation of pneumatic atomizing, 18: 41304(R) (ORNL-TM-775)
design and performance for fused salt atomizing, 16: 11503(R) (ORNL-TM-34)
design and performance of air, for lifting water from storage tanks, 18: 31658(R) (IDO-14635)
design for electrothermal thrustor using wire-coil heat exchanger, 19: 44220 (N64-31011)
design for expansion of very low quality steam, 16: 14882 (UCRL-6152)
design for molecular beam production, 18: 10359
design for pressure vessels, 17: 37326(P)
design for pressurizers and steam generators, stress analysis for, (T), 20: 30928
design of two-orifice, for steam generating plants, 17: 31747(P)
development for gas-cooled reactor temperature measuring system, 20: 36491(R) (ORNL-3951, pp 197-216)
development for Poodle propulsion system, 20: 41396(R) (STL-517-0042)
development of refractory, for high-temperature thermometry in gases, 19: 20277 (ORNL-P-1068)
effect on internal and external pressures in spherical pressure vessels, theory evaluation for, 20: 43467 (TID-23343)
effects on reactor accident containment, limiting, 20: 5034 (NOLTR-63-140)
effects on stresses in spherical pressure vessel, 20: 43491 (ORNL-P-2472)
flexibility in spherical heads, 20: 43468 (TID-23344)
flow and kinetics of DeLaval, 17: 3562 (AD-273540)
flow of dissociated and ionized hydrogen in, equilibrium in, 19: 20124
flow of two-phase fluid through, 18: 16178(R) (TID-20336)
flow through, two-phase, 18: 15663(R) (ANL-6808)
fluid flow in electric-arc, thermal boundary layer growth in, 18: 14052
fluid flow measurements in horizontal, converging-diverging analysis of two-phase, two-component, 17: 35984 (ANL-6754)
fluid flow through, composed of four plane walls, 18: 27666
fluid flows through, analysis of two-phase, 18: 26824(R) (ANL-6885)
gas jet compression shocks near, 16: 22735(T) (AEC-tr-5196)
gas stream separation in, 16: 32022 (KFK-78)
insertion in inlet and outlet ducts of pressure tubes, to limit speed of escaping coolant, 18: 32992(P)
inspection of pressure-vessel, ultrasonic devices for, 20: 42636(R) (SWRI-1228-4-22)
ionization nonequilibrium in expanding quasi one-dimensional airflows through hypersonic, 16: 10686
isotope separation in gases in supersonic jet, calculations of, 19: 20434
joining to spherical surfaces, stress analysis for, (T), 19: 22457 (ORNL-3755)
limit pressure of radial, in spherical shell, 19: 9288 (WAPD-T-1636)
magnetohydrodynamic flow through, sonic line of, (T), 19: 8018
magnetohydrodynamic flow patterns in, (T), 19: 14135 (NP-14785)
materials in male connectors for fuel reprocessing, evaluation of ACI# CD_4M Cu stainless steel as, 19: 44607 (RL-SEP-508)
molecular beam production by, shock wave effects on, 18: 40158
performance for molecular beam production, 18: 40159
performance for molecular beam production, 18: 40160
performance of constricted-arc discharges in supersonic, 17: 40203
performance of nitrided steel, in steam at 1050°F, 19: 38183(R) (ORNL-3807, pp 238-48))
performance of, influence of geometry on, 20: 39021 (K-1665)
plasma ejection from axial, pinched, 20: 4138
plasma expansion in Laval, isentropic, (T), 20: 1295
plasma flow in converging-diverging, with crossed fields, 17: 2372
plasma flow in magnetic annular-arc, 17: 959 (NP-12160)
plasma flow in MPD cell, nonequilibrium, (T), 19: 27131 (IRD-64-36(Pt.3))
plasma flow in, one-dimensional fully ionized, (T), 19: 40048
pumping characteristics of magnetohydrodynamic, 18: 35060(R) (ANL-6904)
seal for, performance tests of self-tightening Dome, 18: 10216 (HW-79205)
shock location during two-phase flow in overexpanded, 16: 7663 (UCRL-6676)
stress concentration factor in spherical pressure vessels, 20: 1364
stress distribution in hemispherical pressure vessel with single radially attached, 20: 459 (ORNL-3817)
stress in pressure vessel, 17: 6246 (NYO-10147)
stress patterns of radial attachements of, to hemispherical shells, 19: 44144 (TID-22134)
stresses around, in reactor pressure vessels, 19: 31482
stresses at connections on pressure vessel, effect of external bending moments and pressures, 16: 7632(R) (NYO-9666)
stresses at connections of, on pressure vessels, effects of bending couples, internal pressure, and thrust on, 17: 23461(R) (NYO-10151)
stresses at connections on pressure vessels, research program on, 17: 35960(R) (NYO-10150)
stresses at connections in pressure vessels, effects of combined loads on, 17: 37315(R) (NYO-10149)
stresses at connections on pressure vessels, effects of bending couples, internal pressure, and thrust on, 18: 4909(R) (NYO-10598)
stresses in pressure-vessel-attached, 19: 38082(R) (ORNL-3807, pp 177-88)
stresses in, thickness dependence of, 20: 10280
stresses on spherical-shell-attached, analysis of, 19: 25761(R) (ORNL-3731(p.229-35))
testing aluminum nitrate-feed, for fluidized-bed calciner, 16: 16022 (IDO-14568)
testing converging-diverging, 20: 29974(R) (ANL-7190, pp 167-75)
testing of stainless-steel, 17: 14613(R) (ORNL-3378(p.47-62))
tests of pneumatic atomizing, in fluidized-bed calciner, 18: 45150 (IDO-14631)
theory of, for gaseous isotope separation, 16: 12004(T) (KFH-tr-60)
theory of, for gaseous isotope separation, 16: 25687(T) (AEC-tr-5069)
thermal relaxation of flow in, 16: 1931
thermal stress analysis of reactor pressure vessel, 19: 17296
thermal stress analysis of PM-2A and SM-1A vessel coolant, equations for, 19: 29618 (AP-Note-436)
thrust of partly ionized gas flowing through, 16: 33589
use in isokinetic sampling of particles in air streams, 20: 39103(R) (BNWL-235-3, pp 51-69)
uses for temperature measurement in flowing gases, 18: 27755(R) (ORNL-3578(p.78-95))
uses of ejector, for cleaning metallic filters, 20: 14645
welding of stainless steel to carbon steel pipes, fatigue strength of, 20: 39404 (SWRI-1228-4-20)

NPD REACTOR
(Canada)
carbon steel conditioning for, 17: 26791 (TID-7641(p.326-50))
component fabrication, 17: 3860
component fabrication, 18: 3167 (AECL-1682(p.71-102))
component testing, 17: 1104 (AECL-1599(p.7-20))
components and fuel developments, survey, 16: 9609 (AECL-1318 (Paper 4))
construction, 17: 1106 (AECL-1599(p.32-9))
control, 17: 3859
control and instrumentation of, bibliography on, 20: 47044
control area description, 16: 34096
control system, 18: 3164 (AECL-1682(p.11-25))
control system for, 20: 3533
coolant line rupture in boiler room of NPD-2, anticipated pressures from, 19: 3610 (AECL-1930)
coolant pump seal deflection in, evaluation of primary, 18: 33096 (AECL-1988)
coolant-moderator radiolysis in, 18: 38243 (A/CONF.28/P/20)
cooling system chemistry, 18: 1228 (AECL-1841)
cooling system fabrication, pressure testing, and early operation,

18: 3280
cooling system of, operating experience with, 19: 21698
core design for, (E), 19: 17241
description, 16: 9606 (AECL-1318(Paper 1))
description, 17: 15443 (AECL-1675)
description, 18: 3163 (AECL-1682(p.1-9))
description and operating experience, 19: 3662
description, commissioning, and early operation, 17: 33359
description of, 17: 3856
description of, 19: 45694(R) (AECL-2251)
design and characteristics, 16: 21832
design and economic prospects for, 17: 10099
design and operating experience, 17: 4322
design and operation, 18: 3162 (AECL-1682)
design and operation data, 19: 33704
design and performance, 20: 1485
design changes for increasing power output, 17: 1108 (AECL-1599(p.43-53))
design data and drawings, 16: 14345
design description and startup, 17: 2596
design implications, analysis, 16: 9607 (AEC-1318(Paper 2))
design, public relations release, 16: 21792 (AECL-1458)
development and operation, 17: 13784
development and operation of, review, 18: 35171
development and performance of, 19: 38217
development of, manufacture of components for, 17: 1105 (AECL-1599 (p.21-31))
development of, bibliography on, 19: 19379 (AECL-2205)
development of, survey, 19: 29697
electric system of, design review, 20: 1507
electrical system design, 16: 34094
environs monitoring, 20: 14738 (NP-15853, pp 21-33)
environs monitoring of, March 1966, 20: 33556 (NP-16124)
environs monitoring, January 1966, 20: 29053 (NP-15951)
environs monitoring, April 1965, 20: 41136
fuel assemblies for, engineering and performance of, 18: 38383 (A/CONF.28/P/18)
fuel bundle design for, hydraulic and thermal characteristics of, 17: 42370
fuel bundle dimensional stability measurements using linear differential transformers, 17: 331 (FD-86)
fuel development for, status, 20: 42618 (66-CNA-312)
fuel element compatibility with fuel-handling equipment, 18: 2272
fuel element development for, 17: 3857
fuel element experimental lattice parameters in heavy water, 17: 3738
fuel element fabrication, end cap welding in, 17: 14799
fuel element fabrication, 18: 3166 (AECL-1682(p.53-69))
fuel element irradiation testing for, 18: 22523 (CRFD-1179)
fuel element irradiation tests for, 19: 2878
fuel element manufacturing development for, 17: 34390
fuel element performance in one year of operation, 17: 36958
fuel element testing for, design of compression rig for, 17: 35170 (CRE-1155)
fuel elements from, inspection of, 20: 3496
fuel handling control system for, 17: 31745
fuel pellet fabrication, 16: 5678 (AECL-1382)
fuel scheduling and reactivity, 18: 38569 (A/CONF.28/P/9)
heat transfer system for, fabrication and testing of high-pressure heavy-water, 19: 5485 (R63CAP-71)
loading of, on-power fueling system for, 18: 3165 (AECL-1682(p.27-51))
loading of, system for on-power, 17: 3858
loading process compatibility, 18: 9704
materials performance in, 17: 36960
nuclear characteristics, 18: 3268
nuclear characteristics, 18: 4823
operating experience from June 1962 to March 1963, 17: 33337
operating experience, Oct. 1962 to Sept. 1963, 17: 42327 (AECL-1807 (p.7-15))
operating experience, 19: 17297
operation, 16: 31294
operation and startup of, 17: 1127 (NP-12157)
operation and startup of, 17: 17402 (AECL-1684)
operation aspects, survey, 16: 9608 (AECL-1318(Paper 3))
operation from startup to fuel equilibrium, computer simulation, 16: 24932 (CRRP-1087)
operation of, performance and reliability of, 18: 3277
operation of, nuclear performance of fuel in, 18: 11443 (TID-7672(p.95-122)
operation of, review of experience in, 20: 16097
performance, 18: 38568 (A/CONF.28/P/8)
performance and reliability of, 18: 4822
performance evaluation, 20: 30891
personnel training program for, 17: 33343
pressure tube burst testing for, 17: 42341 (CRRCE-1152)
process systems in, review of, 20: 8421
radiation effects on Zircaloy-2 fuel cladding and pressure tubes for, neutron, 18: 37732 (A/CONF.28/P/21)
radiation protection program for, 17: 318
reactivity excursion of, analysis of, 19: 19377 (AECL-2155)
reactivity of mockup lattice of, with enriched fuel, 19: 19378 (AECL-2157)
safety features (E), 19: 1862 (AECL-2073)
shielding design and properties for, (E), 19: 14860
staff training program, outline, 16: 9610 (AECL-1318(Paper 5))
startup, 17: 1107 (AECL-1599(p.40-2))
startup, 17: 3861
systems in, chemical engineering role in, 19: 44155
vapor relief system dynamic response characteristics, 16: 9697 (MSAR-62-05)
welding of components for, 17: 12631 (NP-12539)

NPD-2 REACTOR

calandria fabrication for, methods of welding aluminum in, 17: 14796
environs monitoring, April 1965, 20: 41136
safety hazards analysis for, 18: 4782 (AECL-1813)

NPR (New Production Reactor)
see Hanford Production Reactors (N)

NRL ISOCHRONOUS CYCLOTRON

beam control and handling system for, 19: 37271
beam focusing system for, 19: 37380
bending magnets for, calculations for, 19: 39317 (NRL-6248)
data collection and handling systems for, 19: 37336
description, 19: 37332
description of sector-focusing, 19: 37332
development, 20: 17169(R) (AD-628928)

NRL RESEARCH REACTOR

control rod behavior during 1-Mw operation, 16: 4615(R) (NP-11098 (p.30-4))
control system, transistorized current amplifier design for, 16: 15785 (NRL-5763)
neutron flux spectrum for pneumatic tube system in, 20: 16335(R) (NBS-TN-276)
neutron spectra in modified, slow, 17: 12030
use of, 17: 10170

NRU REACTOR

(Canada)
contamination control for accident at, 19: 24798
control of, computer, 19: 42148 (AECL-2216)
control of, two-computer system for direct, 20: 12511
control program for, time-optimal on-off digital computer, 20: 8475
control rod performance, 18: 40765 (IOI-265)
control rods, development of stainless steel magnet for, 16: 14221 (CRE-1062)
control using dual-computer system, system in failures, 20: 35167
coolant flow monitoring in, solid-state circuitry for, 18: 36847 (AECL-1974)
coolant leak repair using epoxy resin, 17: 42338 (AECL-1844)
coolant loop for, design of steam–water, 20: 26530 (AECL-2415)
coolant-moderator radiolysis in, 18: 38243 (A/CONF.28/P/20)
cooling system leak in, casting an epoxy resin to repair, 18: 3358
cooling system of, deposition of aluminum and uranium in, 18: 1291 (AECL-1840)
cooling system of, behavior of aluminum and uranium in, 18: 3381
design and safety analysis, 16: 21793 (AECL-1495)
design data and drawings, 16: 14349
development and operation of, review, 18: 35171
development of, survey, (E), 19: 43548
experimental facilities and research program, 17: 13836
fuel change-over to enriched uranium, 18: 23109
fuel element critical heat flux measurements in U-1 loop, 20: 8372
fuel element fabrication, Mark XIV fuel bars, 16: 13545 (FD-77)
fuel of, conversion from natural to fully enriched uranium, 18: 19427 (IOI-259)
fuel rod fabrication and irradiation testing, 17: 22931 (TID-7642 (p.398-424))
fuel rod uranium-235 distribution, automatic scanner for checking, 16: 8977
fuel rods, design and development of 19-element, 16: 14230 (FD-74)
fuel rods, production records, 16: 12774 (FD-78)
gamma-ray resonant scatter facility, 19: 9771(R) (PR-P-63)
in-pile loops in, design of, 17: 10136
instrumentation, 16: 1997
maintenance problems, 18: 3072
maintenance scheduling, PERT program for, 16: 25081 (CRIO-1091)
neutron flux detectors for, self-powered, 19: 42148 (AECL-2216)
operation, 16: 31294
operation of, safety aspects of, 17: 1082

operation procedures for, 20: 30935
orifice sections, evaluation of corrosion in, 16: 8302 (CRE-1048)
poisoning by xenon, reduction of shutdown time from, 18: 21687
power distributions and reactivity in converted, calculation of, (E/T), 19: 14881 (CRRP-1209)
pressure tube creep in, equipment for measuring, 20: 36451 (AECL-2568)
pressure-tube in-pile inspection, 18: 4704
pressure vessel of, health physics aspects for changing, 20: 26531 (AECL-2420)
radioisotope production in, 20: 39282 (DP-1066(Vol.1), pp III.3-32)
safety in operation procedures for, 16: 26614 (AECL-1486)
safety of, control of tritium hazards in, 18: 1979
safety system performance, 17: 13733
shutdown functions for, 19: 29790
shutdown of, extension of time-to-poison in, 17: 7536 (CRIO-1115)
shutdown of, mode optimization for planned startup, 20: 40423
tritium hazards at, safety program for, 17: 14541
uses, 18: 38567 (A/CONF.28/P/2)

NRX REACTOR
(Canada)
calandria tube leaks in, repairs on, 18: 19423 (AECL-1881)
contamination control for accident at, 19: 24798
coolant radioactivity, 17: 10126 (CRDC-1126)
coolant-moderator radiolysis in, 18: 38243 (A/CONF.28/P/20)
corrosion product deposition on fuel, 16: 3409 (RLI-5(Rev.))
description, 16: 9694 (CRIO-1043)
description of, 19: 45694(R) (AECL-2251)
design and safety analysis, 16: 21793 (AECL-1495)
design data and drawings, 16: 14346
development and operation, review, 17: 17402 (AECL-1684)
development and operation of, review, 18: 35171
development of, survey, (E), 19: 43548
environs monitoring, April 1965, 20: 41136
experimental facilities for fog- and steam-cooling study, 17: 289
experimental facilities and research program, 17: 13836
fission product release from 1952 accident, estimation, 18: 15604 (CRDC-1177)
fuel burnup in, computer program for calculating, 20: 3583 (CRT-1187 B)
fuel burnup, long-term reactivity changes, 16: 9251 (AERE-R-3787)
fuel element burnup in, methods for determining, 18: 10001
fuel element design and performance, review, 16: 16669
fuel element fabrication of metal, 16: 12070 (FD-76)
fuel element preparation by aluminum reduction of uranium dioxide, 16: 10430 (CRRM-1065)
fuel element preparation for, plutonium-containing, 17: 16570
fuel irradiation in, effects on fissile isotope content, 19: 9729 (CRT-1187(Pt.A))
fuel irradiation testing in, 20: 2429 (ORNL-3837)
fuel pin preparation and performance, thorium oxide–uranium oxide, 16: 11503(R) (ORNL-TM-34)
fuel replacement using uranium dioxide rods, 18: 1293 (AECL-1843)
fuel rod analysis for burnup, 19: 10506 (CRR-861)
fuel rod fabrication, solid-pellet uranium dioxide, 16: 12069 (FD-72)
fuel rod fabrication and testing, 16: 15156 (FD-73)
fuel rod fabrication, review, 17: 16556
fuel rods, development for booster elements, 16: 13544 (FD-75)
fuel rupture in, location using gamma spectrometers, 20: 5109 (AECL-2360)
gamma dose rate in, following shutdown, 20: 35145 (AECL-2563)
hazards of cobalt spill at, July 1958, 17: 17594 (IOI-158)
heat transfer in loop of, 19: 31602 (AECL-2247)
in-pile creep testing machine for, 16: 8972 (CRRL-1054)
in-pile loop operation for organic-coolant studies in, 17: 32662 (CRFD-1132)
in-pile loops in, design of, 17: 10136
instrumentation, 16: 1997
insulation test in X-7 loop on coolant tubes, 16: 18617 (EXP-NRX-70103)
maintenance problems, 18: 3072
neutron dosimetry and flux measurements in, methods for, 19: 19415 (CRC-1210)
neutron dosimetry in, 20: 11145
neutron flux axial distribution and various moderator levels, thermal, 16: 17232 (CRC-1058)
neutron reactions and spectra, 17: 31758
neutron spectra in, threshold-detector measurement of fast, 18: 35836 (CRC-1101)
operating problems, 18: 1292 (AECL-1842)
operation, 16: 31294
operation of, safety aspects of, 17: 1082
operation of, safety in, 17: 20256
operation procedures for, 20: 30935
pressure tube creep in, equipment for measuring, 20: 36451 (AECL-2568)
radiation dosimetry in biological cavity of, neutron and gamma, 18: 38727
radioisotope production in, 20: 39282 (DP-1066(Vol.1), pp III.3-32)
safety in operation procedures for, 16: 26614 (AECL-1486)
safety system performance, 17: 13733
shutdown of, performance of electromechanical rods for, 20: 8460 (IOI-296)
stack dilution tests, 16: 20858 (AECL-1518)
use for electric power and water desalination, economics of, 20: 20290 (NP-15920)
uses, 18: 38567 (A/CONF.28/P/2)

NRX Reactors (Nuclear Rocket Propulsion Experiment)
see Rocket Reactors

NTA
see Acetic Acid, Nitrilotri-

NTG (Nuclear Test Gadge)
see Exponential Piles

NUCLEAR AIRCRAFT
see also Aircraft Reactors
see also Nuclear Aircraft Power Plants
characteristics of surface effect ships, 20: 38526
characteristics of lighter than air vehicles, 20: 38526
design analysis of subsonic logistic, with helium-cooled reactor, 18: 13317 (NASA-TM-X-28)
design of lighter-than-air, (T), 20: 30927
development, 20: 4999(R) (ORNL-2599)
development, 20: 5181(R) (ORNL-3029)
development of folded-flow reactors for, 17: 2583 (NP-12087)
dose rates in crew compartment of, (T), 20: 5181(R) (ORNL-3029)
gamma dose rates in crew compartment of, 20: 4999(R) (ORNL-2599)
materials of, radioinduced heating in, 16: 32117 (NARF-62-12T)
neutron dose rates in crew compartment, computer program for calculating fast, 20: 4299(R) (ORNL-2711)
neutron fluxes and dose rates in shield compartment of, 20: 4999(R) (ORNL-2599)
piping system for, flexibility and stress analysis of potassium–sodium, 19: 22509 (PWAC-123)
propulsion, critical evaluation, 16: 15932
research programs on, review of, 20: 8450
review of economic and development possibilities in, 17: 24697
shielding arrangement for, 19: 5537(P)
shielding arrangement for, 19: 43595(P)
survey, 19: 42632

NUCLEAR AIRCRAFT POWER PLANTS
see also Aircraft Reactors
see also Nuclear Aircraft
construction and defects of, 17: 24704
control, automatic, 16: 327 (AD-255794)
control system for turbojet and turboprop, 16: 23314 (DC-55-7-71)
control system for, analysis of, 18: 24935 (APEX-260)
criticality studies on P127 offset twin-engine design mockup, 18: 24845 (APEX-638)
design and cycle analysis of liquid circulating fuel and ternary heat-transfer system, 16: 7281 (APEX-135)
design and development, 17: 7606(R) (ORNL-1515)
design of shielding for AC-series, 16: 8371 (XDC-54-7-20)
design using two reactors cooled and moderated by decomposable hydride, 20: 28807(P)
development, 20: 4999(R) (ORNL-2599)
development, 20: 5181(R) (ORNL-3029)
fuel element stress analysis, concentric-ring, 18: 33059 (DC-60-1-60)
fuel element stress analysis, 18: 32038 (DC-60-2-285)
heat exchanger design for, 18: 33754(P)
maintenance of, method for, 20: 22486
operation of, problems in, 19: 10629
porous plug shielding experiments, 18: 15593 (NARF-58-28R)
shielding experiments, 18: 15594 (NARF-58-29R)
shielding experiments, 18: 15595 (NARF-58-40R)

NUCLEAR BATTERIES
see also Photoelectric Cells
see also Radioactive Voltage Generators
see also Systems for Nuclear Auxiliary Power (SNAP)
analysis of cerium-144 cell, 18: 529 (NASA-TN-D-2070)
bibliography, 16: 6259 (TID-3561(Rev.1))
bibliography, 17: 11322 (NP-12429)
bibliography, 19: 9961 (AED-C-15-03)
bibliography, Direct Energy Conversion Literature Abstracts, 16: 9288 (NP-11302)
bibliography, Direct Energy Conversion Literature Abstracts, 16: 15269 (NP-11455)
bibliography on, 18: 5974 (AED-C-15-02)
bibliography on U. S. developed, 17: 14930 (CEA-Bib-33)
book: *Radioisotopic Power Generation*, 19: 2692

burnup at high altitudes, contamination of troposphere by, 20: 39306 (DP-1066(Vol.1), pp V.17-25)
characteristics for space vehicles, 16: 20033
characteristics of thermionic, in ion propulsion systems, 17: 10215
conference, 20: 21583
containers for, impact testing of, 19: 44298(R) (SC-RR-65-9)
course work and experiments on, 17: 26239
description of, for uses in space vehicles, 16: 28633
description of, for space power uses, 17: 33391
description of triode, with fissionable-material-coated cathodes, 17: 5068
design, 17: 5162(P)
design, 17: 12751(R) (ARF-1214-1)
design, 20: 25776(P)
design, 18: 37872 (A/CONF.28/P/318)
design and characteristics, review, 16: 25667
design and operation of, 17: 9150(P)
design and operation of, review, 17: 20282
design and performance review, 16: 19224
design and performance of NAP-100, 17: 4353 (AFSWC-TDR-61-99)
design and performance, 18: 825
design and promethium-147 semiconductor, 18: 27827
design and use of isotope-fueled, review, 18: 32507 (A/CONF.28/P/217)
design for direct conversion of fission heat to electric energy, 16: 25972
design of alpha-emitting heat source, 18: 24049(P)
design of beta emitter-photovoltaic, for space uses, 17: 18215(R) (ASD-TDR-63-244)
design of Beta-2, for meteorological station, 19: 34606
design of casing for, 16: 20583(P)
design of electrochemical, 18: 32512 (JüL-144-PC)
design of fission, 16: 28589(P)
design of gas-filled thermionic, 17: 17586(P)
design of high-voltage, 18: 42352
design of portable, 16: 30543(P)
design of semiconductor, 17: 27531(P)
design of, using electron-voltaic effect, 18: 9068 (SC-DC-3530)
design of 60-watt thermoelectric, 18: 32514 (NP-14068)
design using solar cells with promethium-147 beta sources, 20: 2206
design using strontium-90, 19: 46897(P)
design using waste solutions, 20: 9360(P)
destruction during re-entry from space, RFD-1 test results, (E), 19: 8661 (SC-RR-64-516)
development, 18: 8700 (NYO-10689)
development, 18: 14793
development, 18: 44007
development, 20: 27390
development, 20: 44169
development, 19: 2716(R) (BMI-1681(Del.))
development and uses, 16: 3359(T) (FTD-TT-61-72)
development for manned space stations, 19: 10009
development for space uses, 17: 10213
development for space vehicles, 18: 5973 (AD-423714)
development for space vehicles, 18: 5980
development for space propulsion systems, 18: 24358 (ANL-6802 (p.89-99))
development for space power systems, status of, 18: 34001
development for use with thermoelectric cells, for space, (E), 19: 16444(R) (AFAPL-TR-64-135)
development of cesium double-diode, 18: 12858(R) (MND-2945-4)
development of fission-electric cells, 17: 16189
development of fission-electric cells, 18: 24372(R) (TID-20575)
development of isotope-heated thermionic cells, 20: 15294 (CONF-640921, pp 9-45)
development of mixed fission product-fueled thermoelectric, 18: 32510 (GIC-2605-2)
development of promethium-147, 19: 13871(R) (BMI-1691(Del.))
development of promethium-147, 19: 30642(R) (BMI-1707(Del.))
development of thermoelectric, for space uses, 18: 24351(R) (AD-427285)
development of 5-watt thermoelectric, 17: 37660(R) (TID-19333)
development status of radioisotope-fueled, for use on lunar surface, 20: 19132 (N-65-24571)
development, (E), 19: 4882(P)
developments for space applications, 17: 6551
electrical energy production by, methods and uses of, 18: 827
electricity production from reactor fission products, 18: 26254
energy conversion in, review, 19: 41319
fabrication and performance of promethium-147, 19: 15972 (BMI-1709)
fabrication and properties of strontium-90-fueled, 17: 29854(R) (MND-2584-4)
fabrication of cesium-137 borosilicate-glass, (E), 19: 22839 (ORNL-3669)
feasibility of promethium-147–silicon, 20: 11546 (SC-RR-65-671)
fuel burnup during re-entry of, from space, (E/T), 19: 17350 (RTD-TDR-63-3002)
heat exchangers for, performance of direct-contact, 17: 8103
magnetron effect from cathodes in plasma diodes in, geometric dependence of, 18: 26256
modification and performance of SNAP-7A, (E), 19: 28713 (MND-3043-1)
operation of thermionic converter in-pile, heat transfer study for, 18: 30478 (BAW-1267)
performance for electric-power and life-support systems on spacecraft, (E/T), 20: 5820 (NASA-CR-316)
performance for space vehicle uses, 17: 41607
performance for thermionic, thermoelectric, and thermophotovoltaic energy conversion, (E/T), 19: 20904 (BLG-317)
performance in gamma-radioisotope thrustors, (E), 19: 28715
performance in integrated space thrustors, 18: 27829
performance in satellites, 17: 2637
performance in space vehicles, 17: 10212
performance in space propulsion systems, review, 17: 10214
performance in space propulsion systems, review, 17: 17611
performance of krypton-85, 20: 37159
performance of radioactive regenerative fuel cell, electrochemical aspects of, 18: 14790
performance of, using alpha, beta, and gamma emitters, 18: 27828
power output of, computer program for calculating, 20: 9358 (ORNL-3826)
promethium-147 thermal power in, 19: 18368
properties, 17: 26101
properties and shielding, 18: 18621 (ORNL-3576)
properties and uses of, for direct conversion of energy into electricity, 18: 34500
properties in lunar vehicle power system, 20: 45870
properties of fuel compounds and encapsulation materials for radio-isotope heat sources, 18: 9066 (MND-P-2975)
properties of plutonium compounds as, 19: 24058
properties of promethium as fuel in, summary, 19: 39069 (BNWL-C-45)
properties of, review of, 18: 2564 (DL-55)
properties of, comparison with solar cells, 20: 39306 (DP-1066(Vol.1), pp V.17-25)
radiation hazards from space, 19: 11422 (RSG-A-1)
radioisotope selection for use as heat sources in, 18: 12519 (HW-78658)
radioisotope selection for, 18: 32514 (NP-14068)
radioisotopes for, comparison and needs for, 17: 15517
review, 17: 37749
review, 18: 32514 (NP-14068)
safety analysis for 10-watt strontium-90-fueled generator, 16: 11997 (MND-P-2614)
safety analysis of strontium-90-fueled, 16: 11996 (MND-P-2613)
shielding for space uses for payload protection, 18: 11362
strontium-90 leach rates from strontium titanate-fueled, in sea water, (E), 19: 28716
strontium-90 preparation for, 18: 14334
use in fail safe timing circuits, 19: 44364(P)
use in mobile power units, evaluation and survey, 16: 13682 (ANL-6483)
use in space propulsion systems, 17: 6543
use of radioisotopes in, economics of, 19: 20415

NUCLEAR CHEMISTRY

(See also specific elements, isotopes, and compounds.)
see also Radiation Chemistry
see also Radiochemistry
see also Tracer Techniques
analyses in, uses of x-ray-absorption methods in, 17: 33790 (EUR-270.e)
bibliography on, French publications, 1956 to 1961, 19: 19738(T)
book: *Annual Review of Nuclear Science*, 17: 17637
book: *Basic Concepts of Nuclear Chemistry*, 17: 37290
book: *Chemistry in Nuclear Technology*, 17: 28792
book: *Nuclear and Radiochemistry, Fundamentals, Practical Methods, and Technical Application*, 16: 7602
book: *Nuclear Chemistry*, 17: 32815
book: *Nuclear Chemistry. Study of Radioactive Nuclei and Nuclear Reactions*, 20: 24487
book: *Nuclear Chemistry*, 20: 43056(T) (JPRS-36943)
book: *Nuclear Techniques in Analytical Chemistry*, 19: 19822
book: *Physical Nuclear Chemistry*, in German, 18: 33676
conference on applications of computers to nuclear and radiochemistry, 17: 18660 (NAS-NS-3107)
conference on nuclear reactor chemistry, Gatlinburg, Tenn., October 10 to 12, 1961, 16: 26472 (TID-7622)
conference on nuclear and radiation chemistry, 20: 43356
conference on, Bombay, India, March 16 to 19, 1964, 20: 25166
development trends, 16: 20484
developments and prospects, 16: 10088
developments at Carnegie Institute of Technology, 16: 1808(R) (TID-12849)

effects of nuclear transformations, conference, 16: 6465 (STI/PUB/34 (Vol.I))
effects of nuclear transformations in inorganic solids, chemical, 20: 7131
handbook of laboratory experiments, 16: 2092 (ANL-6421)
mass spectrometer and radioisotope separator uses in, 20: 25181
processes in, for nuclear energy development, 17: 28960
radioisotope decay measurements in, multidimensional pulse analyser use in, 20: 2142
research at Lajos Kossuth Univ., Hungary, 18: 35438
research at Saha Institute, review of, 20: 9605
research in, 17: 28247(R) (TID-18788)
research in Soviet Union, literature survey, 19: 27767 (ORNL-TM-1133)
research programs at Hahn-Meitner Institute for Nuclear Research, 1961, 16: 25083 (HMI-B-22)
research programs progress at MIT, 16: 26646(R) (NYO-2668)
research programs on, at Hahn-Meitner Institute for Nuclear Research, 17: 37002(R) (HMI-B-26)
research programs and facilities for, at MIT, 17: 40429(R) (NYO-10063(p.23-51))
research programs in, at MIT, 18: 19837(R) (MIT-905-1)
research programs on, Hahn-Meitner Institute for Kernforschung, 1963, 18: 33182(R) (HMI-B-34)
research programs at Carnegie Institute in, 18: 43601(R) (TID-21007)
research programs on, at ORNL, 19: 23163(R) (ORNL-3650(p.111-86))
research programs on, 20: 31165(R) (HMI-B-46)
research progress 1961, 16: 11689(R) (TID-15020)
research progress at Carnegie Institute of Technology, 16: 26876(R) (TID-16290)
research progress on, at MIT, 17: 20563 (NYO-10062)
research progress in, at MIT, May 1, 1963, 17: 40426(R) (NYO-10063)
research progress on, summary of 1963 AEC, 18: 11550
review of recoil, 16: 15079

Nuclear Data
see Data Tabulations

Nuclear Dipole Moments
see Moments

NUCLEAR ELECTRIC MOMENTS
see also Nuclear Magnetic Moments
analysis from beta decay, survey, 18: 26679
analysis of quadrupole, using computers, (T), 19: 21246 (TID-21697)
calculation of quadrupole, for first excited state of spherical nuclei, (T), 20: 44812
calculations of quadrupole, for near-spherical nuclei, (T), 19: 47573 (IAE-717)
determination of partial multipole, by direct reaction sum rules, (T), 19: 5221
effects on forbidden transitions in hydrogenlike transitions, 17: 5124(T)
hexadecapole, in ions, second-order quadrupole effect in, 16: 29559 (BNL-6038)
interactions of, effect on nuclear magnetic resonance, 17: 24388 (IS-519)
interactions with external electrostatic field, 17: 15255 (IS-475)
internal conversion of monopole, Born approximation of, 17: 22648
investigation by pulse techniques, 16: 22953
measurement, 17: 17306
measurement of dipole, by interaction with external electrostatic field, 18: 2914
measurement of quadrupole, for excited states, method for, (T), 20: 42303
measurement of sexadecapole, 19: 1622
measurement of, Mossbauer and angular correlation methods for, 18: 30854
orientation of, review of dynamic and static methods for, 17: 5056
perturbations in angular correlations, 17: 19120
polarization induced by quadrupole, in mu-mesic atoms, 17: 36687
quadrupole, calculations, 16: 19512(T)
quadrupole coupling constants in alkali halide crystals, 16: 24654
quadrupole, effects on nuclear relaxation in potassium iodide crystals, 16: 22779
quadrupole, of even-even nuclei, calculations of, 17: 31546
resonances in, design of detector for, 18: 14179
tables, 18: 30864
theory, 18: 30843

NUCLEAR EMULSIONS
see also Photographic Emulsions
see also Photographic Film
see also Photographic Film Detectors
aging by controlled temperatures, effects of, 19: 44402 (CERN-65-4 (Vol.II), pp IV5-15)
aging effects in ultra-fine, 18: 23918
alpha interactions in, mean-free-path for, 18: 40187
alpha reactions at 900 Mev, 18: 24619 (NYO-10269)
alpha reactions at 10^{13} ev/nucleon, angular distributions from, 18: 38129
alpha track length and radon-220 diffusion in, effects of exposure in organic liquids on, 19: 15880
alpha track profiles in, 17: 32888
alpha-particle track registration and discrimination in, 19: 44425 (CERN-65-4(Vol.II), pp VIII17-26)
alpha, deuteron, neutron, and proton reactions with, star production in, (E), 20: 8069 (JINR-P-2383)
analysis for silver by x-ray fluorescence, use of gamma-excited x-ray sources for, 19: 15376
analysis of double-star short-range hyperfragments in, method for, 18: 24445
analysis of multiple scattering and track curvature in, device for, 18: 24003
analysis of, from polar-orbiting satellites, 19: 9775(R) (UCRL-11466)
analysis of, from polar-orbiting satellites, 19: 25265(R) (UCRL-11776)
angular distribution measurements in, instrument effects, 16: 10206
antiproton annihilation in, meson (π) emission in, 17: 31305
antiproton annihilation and production in, (E), 19: 18771
antiproton elastic scattering at 3 Bev/c by nuclei in, amplitudes for, (E/T), 20: 32467
antiproton interactions with nucleons at 725 Mev/c in, particle distributions from, (E), 20: 19465
antiproton reactions at 3 Bev/c, double-hyperfragment production in, 18: 44759
antiproton reactions at 3.0 Bev/c, amplitude for small-angle, (T), 20: 8106
antiproton scattering cross sections at 0 to 250 Mev, 16: 16922 (AD-261903)
area scanning of, method for efficiency determination of, 18: 8657
argon-ion scattering in, particle-track production and momentum transfer in, (E), 20: 3063
autoradiographic image production in liquid, effects of development time and temperature on, 18: 36937
background eradication by fading after development, 17: 23780
background eradication in developed, 17: 36421 (NP-13020(p.278-81))
background-insensitive, for fission studies, 16: 25558 (JINR-P-979)
beta multiplet production in x-irradiated, 16: 13916
book: *Nuclear Photography*, 17: 17635
book: *Nuclear Research Emulsions*. Vol. I. *Techniques and Theory*, 18: 31972
boron-11 range-energy relations in, 18: 24643
bremsstrahlung reactions in, electron pair opening angle in, (E), 20: 32006
californium-252 fission fragment stopping in Ilford K-5, 16: 17078
carbon-13 range-energy relations in, 18: 24643
cascade showers in, determination of energy of electromagnetic, 18: 36635
cascade showers in, energy of cosmic-ray initiated, 20: 21556
characteristics and preparation, 16: 3194(T) (JPRS-8937(p.120-6))
charged particle interactions in, design of gap meter for measuring, 16: 343 (PAN-240/VI)
charged particle ionization density in carbon-, hydrogen-, and oxygen-enriched, 19: 44435 (CERN-65-4(Vol.II), pp IX62-5)
charged-particle multiple scattering in, 17: 32931
charged particle momentum determination in, method for low-momentum, 20: 25795
charged-particle range spread in, equation for heavy, 17: 41301
charged particle reactions with electrons in, 18: 23908
charged particle scattering in, multiple, 16: 24702
charged-particle scattering in, analysis of multiple Coulomb, 17: 19326
charged-particle tracks in, 16: 27331
charged particle tracks in, ionization measurements on fast, 17: 30861
charged-particle differentiation in, by means of ionization parameters and tracks, 19: 9511
charged-particle image formation in, exciton mechanism in, (T), 20: 13082
charged-particle reactions with silver bromide in, latent image formation in, 19: 44387 (CERN-65-4(Vol.II), pp III1-10)
clearing using ammonium salts, 16: 13321
coagulation of fine-grain, by synthetic polymers, 19: 44400 (CERN-65-4(Vol.II), pp III31-56)
compositions of commercial, 19: 837
contraction factor of, method for measuring, 19: 44444 (CERN-65-4 (Vol.II), pp X67-73)
coordinate grids for, 17: 41296
cosmic meson (π^-) and proton reactions at $\geq$14 Bev, momentum spectra of secondary show particles from, 17: 41713 (TID-19500)
cosmic nuclei reactions with, shower production from heavy, 20: 25752
cosmic nuclei reactions in, charge spectra from heavy, 20: 27767
cosmic nucleon interactions with nucleons in, isobar production in, 18: 42402
cosmic nucleon interactions in, spectra from, (E), 20: 13345(R) (NP-15772)
cosmic nucleon interactions at 25 and 10^3 Bev in, isobar production from, (T), 20: 37675
cosmic nucleon reactions at $\geq 10^{16}$ ev, high-energy gamma flux from, 17: 26273

cosmic particle fragmentation and secondary jets at 1 to 15 Tev in, 18: 16728 (BNL-7534(p.2-28))
cosmic particle interactions in, secondary particle production in, 18: 34492
cosmic particle interactions with nucleons in, multiplicity frequency distributions in secondary, 18: 42401
cosmic particle interactions in, at 300 km, (E), 19: 20893
cosmic particle reactions in, meson production in nucleon interactions in heavy, 17: 26269 (PAN-398/VI)
cosmic particle reactions with, helium-3 and triton energy spectra for, 17: 29608
cosmic particle reactions at 25 Bev, azimuthal distribution of shower particles produced in, 17: 41720
cosmic particle reactions in, analysis of, 18: 42713
cosmic particle reactions in, double maximum angular distributions and asymmetry in, 18: 42714
cosmic particle reactions at high energies, meson (π^0) production in, (E/T), 19: 27439 (PAN-551/VI)
cosmic particle reactions in, secondary particle angular distributions in, (T), 19: 34906
cosmic particle reactions at 5 to 10 Tev, meson (π^0) production in, (E), 19: 34910
cosmic proton elastic scattering by nuclei at 3 Tev in, cross section upper limit for elastic, (E), 20: 37666
cosmic proton reactions at 24 Bev, azimuthal symmetry of meson shower particles from, 17: 20821
cosmic radiation interactions in, gamma spectra and high energy jets in, 16: 2392 (INSJ-42)
cosmic radiation reactions, studies in satellites with polar orbits, 16: 2293 (AFCRL-285)
cosmic radiation reactions in, 18: 42712
cosmic radiation sampling at different altitudes by, simultaneous, 17: 34712
cosmic ray interactions at high altitudes, volumetric rate of star production in, 16: 19659 (TID-15699)
cosmic-ray reactions in, rate of star production in, 18: 2558
cosmic-particle reactions with heavy nuclei in, slow particle production in high-energy, 20: 30371
Coulomb scattering in, effects of distortion and noise on measurement of, 19: 2965
data processing equipment for, 19: 22786
deposition of thin layers of, on electron microscope preparations, 17: 27644
description of types of, 17: 18520 (CERN-63-3(p.129-50))
detection and analysis of neutron reactions (n,p) in nickel by, 17: 31545
detection of 10 to 100 kev ions in, 17: 3337
developers for fine-grain, evaluation of, 19: 44404 (CERN-65-4(Vol.II) pp IV23-31)
developing of, changes in alpha and electron tracks during, 18: 23924
development, 19: 44379 (CERN-65-4(Vol.I), pp 29-41)
development and performance as radiation dosimeters, 16: 13311(T) (NP-tr-868)
development as detector for high-energy accelerator experiments, 20: 37077 (UCR-34P107-34)
development by electrodialysis, 18: 23927
development for alpha decay studies, 19: 14620
development for detecting charged particles, 20: 21060
development for particle detection, 19: 13746
development methods, 16: 10252
development near minimum-ionization plateau, 16: 6561
development of exposed, aboard satellites, 18: 23957
development of high-density PR-2, 16: 7695
development of high-space-resolution, 17: 11333 (TID-17640)
development of highly sensitive, by bromination of silver hydrosol in gelatin, 18: 33962
development of Ilford C2 and K2, 16: 21145
development of tracks with minimum of ionization, kinetics, 16: 1940 (NP-10988)
development of unsupported layers of, wet-method, 18: 23926
development of very sensitive, using bromination of silver hydrosols, 18: 37513 (NP-14166)
development of, effects of additives on distortion in ultrasonic-oscillation, 19: 40884
development techniques for maximum track visibility in, 18: 23937
development techniques for, after exposure in space probes, 18: 23956
discriminating capacity of, use of superproportional mercury amplifier for increase in, 19: 464
discrimination between gamma and particle tracks in, 18: 23912
discrimination between gamma background and protons in, 18: 23929
discrimination between alpha particles and protons in, using super-proportional intensification, 18: 23931
discrimination between alpha particles and protons in, 18: 23932
discrimination between alpha particles and protons in, 18: 23933
discrimination between low-energy deuterons and protons in, 18: 23943
discrimination of charged particles in, 17: 3325
distortion and spurious scattering in, 18: 41782
distortion during development of, reduction of, 18: 23556
distortion in, effects on measurements at high momenta, 16: 24718
distortion in, effects of drying methods on, 16: 29540
distortion in NIKFI-R, humidity-temperature effects on, 19: 11541
distortion in, determination of, 19: 6189
distortion prevention in, by resin treatments, 17: 41251
efficiency for dosimetry of mixed radiation, 18: 8566
efficiency in multiplate proton cameras, 18: 25866
efficiency of ionization measurements in, 19: 11552
electromagnetic cascades in, energy determination of, 18: 39696
electron conversion spectra techniques for, 16: 10249
electron energy losses from ionization in, 18: 20391
electron ionization losses in, 19: 44432 (CERN-65-4(Vol.II)(pp.IX41-3))
electron ionization losses in, 19: 44428 (CERN-65-4(Vol.II)(pp.IX9-13))
electron multiple scattering in, center-of-gravity and sum methods for calculating, 17: 29510
electron radiation length in, at 800 Mev, 18: 26295
electron reactions at 800 Mev, radiation length from, (E), 19: 16960
electron scattering at 1 Bev by, shower distributions from, 17: 9225
electron-photon cascades in, Monte Carlo calculations of, 19: 1600
elementary particle scattering, effects of higher order differences in measurements on reduction of spurious, 16: 26090 (NYO-10233)
elementary particle interactions in, asymmetry in low multiplicity jets from, 17: 9200 (PAN-342/VI)
elementary particle scattering in, optimum multiple, (T), 19: 16858 (UCRL-11535)
elementary-particle interactions in, at high energies, 20: 38168
energy resolution and statistics for neutron, 16: 23934
energy response to neutrons and properties of Eastman Type A (NTA), 16: 30599 (UCRL-9513)
exposure configurations for neutron, plates, 17: 36347(R) (NARF-62-18P)
exposure to cosmic radiation by rockets, 17: 5194
fading in neutron, gamma-induced, 18: 16359
fog and track density in Agfa-K 5 effect of amidol concentrations in developer on, 16: 22351
for momentum measurements of high-energy particles, use of 200-kilogauss pulsed magnetic field in, 16: 19502
gamma reactions (γ,α) with nuclei in, angular distributions in, (E), 19: 33264
grain-counting in, charged particle discrimination by, 17: 5110
grain densities of highly ionized particle tracks in, photomicrographic techniques for measuring, 17: 10919 (USNRDL-TR-591)
grain density and ionization loss in, 17: 18526 (CERN-63-3(p.225-44))
grain density on track of ionizing particles, formula for calculation, 16: 10687
grain diameter and sensitivity relation, 16: 339 (NP-10962)
grain diameter, effect of excess silver ions during preparation on, 16: 18213
grain dimensions and structure in alpha- and beta-irradiated, 18: 31971
grain measurements in, digitized micrometer eyepiece for, 18: 43961
granulation curves and sensitivities of, 18: 23909
handling, 17: 18521 (CERN-63-3(p.155-65))
heavy ion discrimination in, 18: 23954
hyperfragment production in, by mesons(π^-) on nuclei, 17: 15135
hyperon (Σ^-) reactions at rest, hypernuclei from, 19: 25499
hyperon (Σ^-) capture at rest in, hyperfragment production from, (E), 20: 34628
hyperon (Σ^-) capture at rest in, hyperfragment production from, (E), 20: 34629
hyperon (Ξ^-) capture in, hyperfragment production by, 20: 24326 (AD-626056)
hyperon (Σ) interactions in, sign of nuclear potential, 16: 21483
hyperon (Σ^-) reactions in, production of mesons (π^-) by, 16: 3664 (AFOSR-856)
hyperon (Σ^-) absorption, hyperon (Λ^0) trapping from, 16: 18487
hypersensitization by triethanolamine, 18: 41436
image-development and sensitization centers in, effects of acid treatment, 16: 30612
image dispersion in, exposed to alpha particles, electrons, and light, 19: 22762
image eradication in, for low-intensity radiation detection, 18: 23921
image etching in, in stop-bath, 18: 23928
image fading in K.5, effects of storage conditions on latent, 17: 2076
image fading in, at −20 and +20°C, relation to grain density of, 17: 22280 (USNRDL-TR-610)
image formation in, latensification of, 19: 44391 (CERN-65-4(Vol.II), pp II29-42)
images on, photometric analysis of, 18: 23914
impregnation of, with radioisotopes, mechanism of, 17: 14696

impregnation with uranium salts, 18: 23553
impurities on surface of, method for removing, 18: 2061
instrument for moving plates of, 18: 23847
interactions in, determination of virtual number, 16: 12334 (JINR-P-839)
interactions in, measurement of spurious, 16: 8122
interactions (p-p) in, identification of, 18: 5991 (JINR-P-1430)
interpretation of events in, 16: 13693 (JINR-P-864)
ion attenuation by, heavy, 17: 18909 (TID-18436)
ion attenuation in, grain densities for heavy, 17: 39417 (USNRDL-TR-657)
ion beam reactions with, effects of energy and mass on grain darkening in, 18: 23916
ion range-momentum relations in, heavy, (T), 19: 34520
ion reactions at 10.4 Mev/nucleon, range-momentum relation for heavy recoil ions in, (E), 19: 39883
ion track width measurements in, charge determination from thin-down, 20: 43706
ion track widths in, measurement of, 19: 44434 (CERN-65-4(Vol.II), pp IX48-61)
ion tracks in, photomicrography of heavy, 20: 9263
ion tracks in, registration mechanisms of heavy, 20: 5755
ionization by charged particles, velocity dependence of, 20: 23876 (CERN-65-24(Vol.2), pp 89-106)
ionization-mass measurements using, 16: 8066 (NP-11232(p.353-9))
ionization parameters of, effect of drying speed on, 17: 20676
irradiation in CERN synchrotron, technical problems connected with, 17: 18518 (CERN-63-3(p.103-10))
irradiation in CERN synchrotron, general problems connected with, 17: 18517 (CERN-63-3(p.95-102))
loading with bismuth, 16: 19504
loading with bismuth, techniques for, 16: 22727 (NP-11766)
loading with lithium, 17: 29879(R) (IA-822)
measurements in, design of microscope stages for, 16: 299 (PAN-238/VI)
measurements in, effects of high magnetic field on, 17: 18529 (CERN-63-3(p.297-314))
mesic atoms decay modes in, relative probabilities, 16: 21534
meson (K^o) absorption cross sections in Ilford G5, 18: 30713(R) (AFOSR-4999)
meson (K^-) and (π^-) reactions at 1.5 and 17.2 Bev/c, hyperfragment production in, (E), 19: 5143
meson (K^-) and (π^-) and proton reactions at 1.5 to 25 Bev, lithium-8 energy spectra from, (E), 20: 15792
meson (K^-) capture at 440 Mev/c, Y_0^* production in, 18: 11244
meson (K^-) capture in, models for hyperfragment production in, 18: 36652
meson (K^-) capture by nuclei in, hyperfragments from, 19: 5184
meson (K^-) capture at rest, (T), 19: 5222
meson (K^-) capture in, short-range hyperfragment production in, (E/T), 19: 54342
meson (K^-) capture at rest, Y_0^* (1405) production in, (E), 20: 6051
meson (K^-) capture in, hypernuclei from, (E), 20: 34628
meson (K^-) capture in, hypernuclei from, (E), 20: 34629
meson (K^-) capture in, hyperfragments, hyperons, and meson (π) production in, 20: 44657 (UCRL-16602)
meson (K^-) interactions at 0 to 180 Mev in, 18: 14854
meson (K^-) interactions at 1.5 Bev/c in lithium-loaded, hyperfragment production in, 18: 20938
meson (K^-) interactions in, correlations of meson (π) production and decay chains in, (E), 20: 13487
meson (K^-) reactions in, hyperfragment production in, 18: 11215 (NP-13541)
meson (K^-) reactions in, nonmesic hyperfragment production in, 18: 24654
meson (K^-) reactions in, hyperon (Σ) production in, 18: 24415
meson (K^-) reactions at 1.5 Bev/c, lithium-8 fragments from, 18: 26636
meson (K^-) reactions at 3.5 Bev/c, hyperfragment production in, 18: 30787
meson (K^-) reactions at 1.3 and 1.5 Bev/c, lithium-8 production in, 18: 36653
meson (K^-) reactions in, ($\Sigma-\pi$) resonances in, 18: 36266
meson (K^-) reactions at 1.5 Bev/c, hyperon (Ξ^-) production in, 18: 38134
meson (K^-) reactions at 1.5 Bev/c, hyperon (Ξ^-) production in, 18: 38135
meson (K^-) reactions at 800 to 3500 Mev/c, short-range hyperfragments in, 18: 44819
meson (K^-) reactions with nuclei in, at 3 Bev/c, 18: 44550
meson (K^-) reactions at 1.3 and 1.5 Bev in, production of lithium-8 fragments in (E), 19: 1664
meson (K^-) reactions in, hyperfragments produced in (E/T), 19: 1665
meson (K^-) reactions with, hyperfragments from (E), 19: 1666
meson (K^-) reactions with, hyperfragment production in (E), 19: 1667
meson (K^-) reactions at 0.8 to 3.5 Bev/c, short-range hyperfragment production in, (E), 19: 16967
meson (K^-) reactions at rest, hyperon (Σ) and meson (π) production in, (T), 19: 19151
meson (K^-) reactions with, hyperfragment production in, (E), 19: 21365
meson (K^-) reactions at 0.8 to 3.0 Bev/c, lithium-8 emission in, (E), 19: 21389
meson (K^-) reactions at 1.3 and 1.5 Bev/c, hyperfragment and lithium-8 production in, (E), 19: 27444
meson (K^-) reactions at 800 Mev/c, heavy spallation hyperfragments in, (E), 19: 33292
meson (K^-) reactions with, hyperfragment production in, (E), 19: 35491
meson (K^-) reactions at 2.3 Bev/c, hyperfragment production in, (E), 19: 37830 (TID-21937)
meson (K^-) reactions in, review on, 20: 11991
meson (K^-) reactions at 3.0 and 5.0 Bev/c, hyperfragment production from, (E), 20: 17752
meson (K^-) reactions in, hyperfragments from, (E), 20: 22161
meson (K^-) reactions at 800 Mev/c in, hyperfragment production from, (E), 20: 26102
meson (K^-) reactions at 1.5 Bev/c with heavy nuclei in, $_{\Lambda}He^7$ and $_{\Lambda}Li^7$ production in, 20: 30368
meson (K^-) reactions at 1.5 Bev, Λ-hyperfragment production in, (E), 20: 30448
meson (K^-) reactions, at 1.5 Bev/c in, hyperfragment production and mesic decay from, (E), 20: 32491
meson (K^-) reactions at 5.0 Bev/c with nuclei in, lithium-8 emission in, (E), 20: 32469
meson (K^-) scattering at 21 Mev, differential and total cross sections for, (E), 19: 35443
meson (K^-), meson (π^-), and proton reactions in, hyperfragment production in, 19: 1668
meson (K^+) elastic scattering at 320 Mev, optical model analysis of elastic, (T), 19: 27569
meson (μ^-) capture in, charged-particle production in, 19: 33386
meson (μ^-) interactions in, at 5 Bev/c, (E/T), 19: 23476
meson (μ^-) scattering at 8 Bev/c, single, (E/T), 19: 16871
meson (μ^+) depolarization quenching in, as function of longitudinal magnetic field, (E/T), 19: 45079
meson (μ^+) depolarization in targets of, (E), 19: 45080
meson (μ) and proton multiple scattering in, 18: 34627
meson (μ) inelastic scattering at 5 Bev/c, (E), 20: 13526
meson (μ) scattering at 2.5 and 5.0 Bev/c in, distributions from inelastic, (E), 20: 7815
meson (π^-) absorption by light nuclei in, 18: 16978
meson (π^-) absorption by nuclei in Ilford G-5, 18: 24582 (AD-439331)
meson (π^-) and (π^+) scattering at 4 Bev/c, interference effects between Coulomb and nuclear, (E), 19: 25508
meson (π^-) and proton spurious scattering in, track distortion from, (E), 19: 37787 (IFA-CR-52)
meson (π^-) elastic single scattering in, detection of, 18: 23947
meson (π^-) reactions at 7.5 Bev, fragment production in, 18: 11280
meson (π^-) reactions at 16.2 Bev/c, meson (π) multiple production in, 18: 28750
meson (π^-) reactions at 4.5 Bev, beryllium-8 production in, 18: 30758
meson (π^-) reactions in, coherent multiple meson (π) production in, 18: 32806
meson (π^-) reactions with, heavy fragment emission in, 18: 34811
meson (π^-) reactions at 4.5 Bev, lithium-8 emission from, 18: 44758
meson (π^-) reactions in, at 4.5 Bev, recoil studies of heavy fragments from (E), 19: 1614
meson (π^-) reactions in, mass spectrum of charged particles from, (E), 19: 8213
meson (π^-) reactions at 3.5 Bev/c, hyperfragment production in, (E), 19: 16966
meson (π^-) reactions at 17 Bev/c, secondary particles in, (E), 19: 19148
meson (π^-) reactions in, at rest, (E), 19: 27501
meson (π^-) reactions at 68 Mev, proton energy spectra from, (E), 19: 35454
meson (π^-) reactions at 17 Bev, production of A_1 in, 19: 43126
meson (π^+) reactions in, meson (π^0) intensity from, 19: 44439 (CERN-65-4(Vol.II), pp X37-43)
meson (π^+) reactions at 7.2 Bev/c, meson (K) production in, 20: 1224
meson (π^-) reactions at 4.4 Bev, cascade showers from, (E), 20: 9775
meson (π^-) reactions at 16.3 Bev, angular distributions from, (E/T), 20: 11602
meson (π^-) reactions with heavy nuclei at 17.2 Bev/c in, cross sections for, (E), 20: 13893
meson (π^-) reactions at 3.85 Bev/c, meson (π) production in, 20: 26085 (JINR-P-2624)
meson (π^-) reactions (π^-,3π) at 17.2 Bev/c, mechanism for coherent, (E/T), 20: 26127
meson (π^-) reactions at 3.8 Bev, slow meson (π) production in, (E), 20: 30501
meson (π^-) reactions at 300 Bev, $_{\Lambda}B^{12}$ production in, (E), 20: 32412
meson (π^-) reactions at 50 to 176 Mev, total cross sections for double charge-exchange, (E), 20: 38012 (JINR-P-2806)
meson (π^-) reactions at 17 Bev/c, electron pair production from, (E),

20: 41814
meson (π^-) scattering in, distortion and noise effects on, 18: 16348
meson (π^-) spurious scattering at 17 Bev/c, 19: 44416 (CERN-65-4 (Vol.II), pp VI53-62)
meson ($\pi^\pm$) range in, at 78 and 90 Mev/c, 20: 41826
meson (π^0) ionization losses in, 19: 44428 (CERN-65-4(Vol.II), pp IX9-13)
meson (π) and proton ionization losses in, (E/T), 19: 12622
meson (π) and proton reactions at 5 to 30 Bev/c, particle distributions in, (E), 19: 23693
meson (π) ranges in (E), 19: 3029 (UCRL-11518)
meson (π) reactions at 4.5 Bev, excited fragments from, 18: 38082(T) (AEC-tr-6398(p.153-6))
meson (π) reactions at 40 to 87 Mev, double charge exchange in, (E), 19: 10243 (JINR-P-1837)
meson (π) reactions at 7.5 Bev, alpha, deuteron, and triton distributions from, (E), 19: 19222
meson (π) reactions with nuclei in, intranuclear cascades from, (E/T), 20: 6287 (JINR-P-2373)
meson (π) reactions at 7.5 Bev, production of high-energy fragments in, (E), 20: 17715
meson (π) reactions at 17.5 Bev, helium particle emission in, (E), 20: 17716
meson (π) reactions at 17 Bev/c, deuteron and triton production in, (E), 20: 25813
meson (K^-) capture in, effects of nuclear mass, 16: 26084 (NP-11623)
meson (K^-) capture by, hyperon (Σ^+) production in, 16: 27952
meson (K^-) interactions in, characteristics and cross section, 16: 8063 (NP-11232(p.327-36))
meson (K^-) interactions with nucleons at 830 Mev/c in, hyperfragment ($A \gtrsim 40$) production, 16: 27988
meson (K^-) interactions in, analysis of in-flight, 16: 8064 (NP-11232 (p.337-45))
meson (K^-) interactions in, pair production (Σ-π) in, 17: 39907
meson (K^-) reactions in, 17: 18530 (CERN-63-3(p.315-23))
meson (K^-) reactions at 500 Mev/c, hyperfragment production in, 17: 24483
meson (K^-) reactions at 800 Mev/c, hyperfragment ($A \gtrsim 60$) production in, 17: 26555
meson (K^-) reactions at 50–300 Mev/c, hyperfragment production in, 17: 26557
meson (K^-) reactions with carbon-12 in, Y_0^*(1405) production in, 17: 29542
meson (K^-) reactions in, hyperfragment production from, 17: 34942
meson (K^-) reactions at 800 Mev/c, hypernuclei production in, 17: 41917
meson (K^-) reactions at 800 Mev/c, production of short-range hyper-fragments in, 18: 2755
meson (K^-) reactions at 800 Mev/c, hyperfragment production in, 18: 9365
meson (K^+) reactions at 2.3 Bev/c with, double-hyperfragment event in, 18: 2656
meson (μ^-) and (π^-) scattering at 8.2 and 16.2 Bev/c, respectively, angular distributions, 16: 8123
meson (μ^+) depolarization in, effects of electric field, 16: 31046
meson (π^0) lifetime in, 17: 18531 (CERN-63-3(p.325-37))
meson (π^-) absorption and scattering at 5.7 Bev, 16: 16964 (NP-11592 (Vol.I)(p.291-4))
meson (π^-) capture in, neutron energy spectra from, 17: 26543
meson ($\pi^\mp$) interaction lengths and elastic scattering at 300 Mev, 16: 21406
meson (π^-) interactions at 4.2 Bev in, meson (π^0) production from, 18: 9110
meson (π^-) reactions in, Auger electrons from, 17: 13525
meson (π^-) reactions with bromine and silver in, angular distribution of relativistic particles from 16-Bev, 17: 26462 (PAN-367/VI)
meson (π^-) reactions at 4.6 Bev/c, lithium-9 decay in, 17: 28274
meson (π^-) reactions at 17.2 Bev/c, hyperfragments from, 17: 29617
meson ($\pi^\mp$) reactions at 4.5 Bev, 17: 36663 (TID-19329)
meson reactions in, asymmetric jet formation by, 18: 40614
mesons (K^-) reactions at 800 Mev/c with, computer analysis of, 20: 2520(R) (IA-920)
mesons (μ^-) elastic scattering in, 17: 31383
mesons (π), absorption and scattering at 5.7 Bev/c, small angle, 17: 16980
microscopy of, automation of, 17: 18525 (CERN-63-3(p.221-4))
microscopy of, survey of equipment for, 17: 18523 (CERN-63-3 (p.199-209))
neon-20 reactions with bromine and silver in, models for, 18: 17010
neon-20 reactions with nuclei in, at 200 Mev, (E), 20: 40083
neutrino interactions in, location and analysis of, (E), 20: 6052
neutrino interactions in, method for determining, 20: 21609 (CERN-65-32, pp 175-80)
neutron reactions (n,α) with bromine and silver at 18.3 Mev in, angular distributions and energy spectra from, (E), 20: 26209
neutron star identification in, method for, (E), 19: 46767 (TID-22256)
nitrogen-14 reactions with bromine and silver in, recoil range-energy ratio for, (E), 19: 43360
nucleon interactions with protons in, at 10^{10} ev, distributions of secondary particles from, 18: 6037
nucleon interactions in, mean-free-path for, 18: 40187
nucleon interactions with nucleons in, particle-track distributions from, (E), 20: 17357
nucleon interactions at high energy in, energy spectra of, (T), 20: 24024
nucleon reactions in, asymmetric jet formation by, 18: 40614
nucleon-proton interactions at 30 Bev/c in, models for jets from, (E/T), 20: 6039 (INSJ-90)
orientation of cosmic-ray, design of device for, 19: 25192
particle absorption by nuclei in, hyperfragments from, 18: 16979
particle Coulomb scattering measurements in, effects of spurious scattering and track distortions on, 19: 44414 (CERN-65-4(Vol.II), pp VI31-6)
particle discrimination and loading techniques for, 19: 24865
particle entrance coordinates for, system for determining, 17: 23679
particle interactions in, 18: 16732(T) (FTD-TT-64-90(p.163-76))
particle ionization and momentum in, automatic measurement of, 18: 41844
particle ionization losses in, 19: 44430 (CERN-65-4(Vol.II), pp IX23-31)
particle jets in, Landau hydrodynamic process in, (T), 19: 43073(T)
particle mean-free paths at high energies in, 16: 13880
particle moment in, method for measurement of high-energy, 17: 34246
particle momentum measurements in, 16: 5903
particle momentum determinations in, at high energies, 18: 23945
particle momentum determination in, method for, 19: 44427 (CERN-65-4 (Vol.II), pp VIII34-7)
particle momentum determination in, method for slow, 19: 44424 (CERN-65-4(Vol.II), pp VIII9-16)
particle multiple scattering constant in, effect of cell length on, 20: 16833
particle scattering measurements in, Coulomb and spurious effects on, 19: 44413 (CERN-65-4(Vol.II), pp VI23-30)
particle scattering measurements in, device for multiple, 19: 44418 (CERN-65-4(Vol.II), pp VIII5-19)
particle scattering constant determination in, method for, 19: 44429 (CERN-65-4(Vol.II), pp IX14-22)
particle scattering constant of cell length dependence of, 19: 44431 (CERN-65-4(Vol.II), pp IX22-40)
particle scattering in, non-planarity effects in spurious, (E), 20: 2145
particle spurious scattering and track distortion in, 18: 10393
particle stopping power of Russian, uniformity in, 20: 33716
particle track analysis in, microscope for, 18: 23940
particle track analysis in, semi-automatic methods for, 18: 23941
particle track analysis in, automatic device for, 19: 44421 (CERN-65-4 (Vol.II), pp VII35-7)
particle track analysis in, design of automatic following microscope for, 20: 27287
particle track angular distributions, 16: 32339
particle track artificial construction in, by Monte Carlo method, 19: 44433 (CERN-65-4(Vol.II), pp IX44-7)
particle track curvatures in, device for measuring, 19: 44418 (CERN-65-4(Vol.II), pp VIII5-19)
particle track density in, statistics for analyzing, 16: 19509
particle track developer for, properties of amidol-pyrogallol, 20: 41340
particle track distortion in NIKFI-R, effects of fixation methods on, 16: 22354
particle track distortions in, uniform, 19: 34547
particle track distortion in, successive differences for analyzing, 19: 44411 (CERN-65-4(Vol.II), pp VII-8)
particle track distortion in, 20: 7384
particle track discrimination in, amplification method for, 20: 25391
particle track discrimenation by electron microscopy, 20: 43731
particle track grain densities, 16: 20677
particle track horizontal projection lengthening in, effects of drying, using alcohol on, 17: 12567
particle track intensification in, methods for, 20: 19026 (INSJ-94)
particle track length measurement in, design of micrometer for micro-scope with optical, 19: 39000
particle track lengths in, effects of pH of impregnating solution on alpha, 19: 40597
particle track location in, using spark chambers, 19: 44445 (CERN-65-4 (Vol.II), pp X74-83)
particle track measurements in, errors due to microscopic field curvature, 17: 23767
particle track measurements in, semiautomatic apparatus for, 19: 44417 (CERN-65-4(Vol.II), pp VIII1-14)
particle track measurements in, apparatus development for, 19: 44422 (CERN-65-4(Vol.II), pp VII39-42)

particle track measurements in, semi-automatic microscope for, 20: 23477
particle track photographic techniques for, 18: 35834 (BNL-7282)
particle track profile measurement for, method for, 20: 33621 (IS-T-87)
particle track resolution in, electron microscopy for, 19: 44423 (CERN-65-4(Vol.II), pp VIII8)
particle track structure in, distribution of bundle length in, 20: 31522
particle track width measurements in, method for, 19: 13762
particle track width measurements in, charge determination from, 19: 42723
particle tracks in, statistical analysis, 16: 3639
particle tracks in, analysis of, 17: 22041
particle tracks in, semi-automatic apparatus for analysis of, 17: 30806
particle tracks in irradiated, developed, and re-irradiated, 18: 2047
particle tracks in, determination of particle charges from, 18: 2063
particle tracks in, effects of multiple scattering on, 18: 2065
particle tracks in, photomicrography of, 18: 5677
particle tracks in, effects of development parameters on spurious, 18: 23935
particle tracks in, analysis of spurious, 18: 23936
particle tracks in, discrimination of, 18: 41768 (INSJ-77)
particle tracks in, 18: 41781
particle tracks in, device for measuring, 18: 43964
particle tracks in, measurement of $Z \geq 3$, 18: 43965
particle tracks in NIKFI-R, detection of spurious scattering in, 19: 4510
particle tracks in, device for automatic following of, 19: 39017
particle tracks in, semiautomatic device for analyzing, 19: 44419 (CERN-65-4(Vol.II), pp VII20-7)
particle tracks in, computer for angle and range measurements of, 19: 44420 (CERN-65-4(Vol.II), pp VII28-34)
particle tracks in, use of electron microscopes for observing, 19: 44426 (CERN-65-4(Vol.II), pp VIII27-33)
particle tracks in, semi-automatic device for measuring, 20: 7432
particle trajectories in, 17: 18524 (CERN-63-3(p.211-19))
performance and properties for dosimetry, 19: 40889
performance as detectors on sounding rockets, 18: 23955
performance for accelerator monitoring, 20: 13367 (UCRL-16445(Rev.))
performance for alpha and proton detection and discrimination, 18: 20362
performance for analyzing fast-neutron fission of thorium-232, 18: 23959
performance for cosmic particle studies in space, 19: 44436 (CERN-65-4(Vol.II), pp X13-18)
performance for determination of amplitude of elastic p-p scattering, 19: 31089
performance for determination of high-energy secondary particles, 19: 33051
performance for detecting geomagnetically trapped protons, 19: 44437 (CERN-65-4(Vol.II), pp X19-32)
performance for discriminating between high-energy particles, 18: 23911
performance for fast-neutron spectrometry, 17: 34293
performance for fast-neutron spectroscopy, 18: 23960
performance for fallout monitoring, 19: 34479
performance for fast neutron spectra measurements, 20: 29848 (CONF-651109, pp 199-212)
performance for gamma, hyperon (Λ), meson (K), and proton detection, 19: 44443 (CERN-65-4(Vol.II), pp X61-6)
performance for low-energy recoil scattering experiments, 19: 44438 (CERN-65-4(Vol.II), pp X33-6)
performance for measuring alpha distributions from proton collisions with nuclei, 18: 23948
performance for measuring beta distributions from fission fragments, 19: 44441 (CERN-65-4(Vol.II), pp X47-53)
performance for neutron spectroscopy from 20 to 30 Mev, (E/T), 19: 46769 (UCRL-16325)
performance for nuclear-reaction studies at accelerators, 18: 24261
performance for nuclear fission studies, 18: 23958
performance for particle detection, 20: 29534
performance for study of proton reactions with hydrogen jets, 19: 44443 (CERN-65-4(Vol.II), pp X61-6)
performance for stray neutron spectra, 20: 29522 (CONF-651109, pp 286-305)
performance in electron beam dose density measurements, 16: 14929(T) (NP-tr-872)
performance in system with spark chambers for determining point of incidence of particles, 20: 31569
performance in 48-kOe magnetic fields, 18: 23946
performance of Agfa, Gevaert, and Ilford L4 for alpha and beta particles, 19: 44389 (CERN-65-4(Vol.II), pp III7-18)
performance of boron-impregnated type K-2, for neutron detection, 20: 16891
performance of Eastman Type A, for neutron dosimetry, 17: 34146 (CONF-67-18)
performance of ionographic, for fast reactor neutron spectra analysis, 20: 35790
performance of thick-pellicle, 18: 2064
performance of tungsten-loaded, 18: 23920
performance under proton dynamic polarization conditions, 19: 44442 (CERN-65-4(Vol.II), pp X57-60)
performance, with incorporated filamentary and powdered targets, 16: 16967 (NP-11592(Vol.I)(p.307-25))
photographic properties and grain formation, 18: 23490
photographic properties of, effects of moisture on stability of, 18: 23922
photon reactions at 1.16, 1.29, and 1.35 Bev, 16: 8761 (TID-14850)
photon reactions in, triplet/pair ratio for electron production in, 20: 27279
photon reactions with electron and nuclear fields in Ilford G-5, opening angle for triplet and pair production from, (E), 20: 27278
photon showers in, angular and radial distribution of particles in, 17: 13112
positron ionization losses in, 19: 44432 (CERN-65-4(Vol.II), pp IX41-3)
preparation and performance of silver bromide–polyvinyl alcohol, 16: 30614
preparation and properties, 17: 18615
preparation and properties of gold-sensitized, 18: 18242
preparation and processing of ionographic, 18: 23496
preparation and properties of fine-grained, 18: 23498
preparation and properties of, 20: 2158
preparation by ammonia maturing, grain growth in, 18: 23493
preparation by continuous reaction of silver nitrate, potassium bromide, and gelatin in 1-ml mixer, 18: 23494
preparation by Ostwald maturing, 18: 23492
preparation for underground cosmic radiation studies, 19: 44397 (CERN-65-4(Vol.II), pp III5-11)
preparation for use in electron microscopy, 18: 23845
preparation of beryllium-loaded, 16: 7119
preparation of bismuth-, diamond-, and lithium-loaded, 19: 44399 (CERN-65-4(Vol.II), pp III17-20)
preparation of carbon-loaded, for meson (K) stopping, 19: 44398 (CERN-65-4(Vol.II), pp III12-16)
preparation of fine-grain silver bromide, 16: 13838(P)
preparation of Mylar-supported thin sheets of, 18: 23925
preparation of proton-sensitive, 16: 3193(T) (JPRS-8937(p.109-19))
preparation of thorium- and uranium-containing, 20: 14877
preparation of uranyl acetate-loaded, 17: 11039
preparation of, with very fine granulation, 17: 32407
preparation of 94% silver bromide concentration, 19: 44396 (CERN-65-4(Vol.II), pp III1-4)
preparation of, having sensitivity varying with dose, 18: 23923
preparation, processing, and reading in measurements of neutron spectra, 16: 22327 (NARF-61-36T)
preparation, relation between silver bromide crystal size and gelatin concentration, 16: 10195 (UCRL-6048-T)
preparation with self-contained developing agent, 19: 44408 (CERN-65-4(Vol.II), pp V9-16)
processing, 17: 18522 (CERN-63-3(p.169-97))
processing and examination in, physicochemical and instrument effects on, 20: 25428
processing, design of apparatus for, 16: 25504 (PAN-293/I-A)
processing of, automatic equipment for isothermal, 19: 44409 (CERN-65-4(Vol.II), pp V17-21)
processing of, automatic, 20: 7352
processing of, developers for, 19: 44407 (CERN-65-4(Vol.II), pp V1-9)
processing of, electrodialyzer for, 19: 44410 (CERN-65-4(Vol.II), pp V22-32)
processing of, exposure and sensitivity effects on, 20: 39202 (IFA-PN-17)
processing of, gelatin layer swelling in, 20: 46086
processing of, ultrasonic, 18: 30045
processing thick and thin plates, 16: 1973
production and performance of silver halide precipitates as, 18: 20414
properties and uses of, review, 18: 23905
properties as alpha monitor, 18: 37528
properties as personnel dosimeter, 17: 22699
properties as radiation detector, 17: 30868
properties evaluation for use in personnel monitoring for detecting fast neutrons, 17: 8606
properties for optimal measurement of low-range particle mass, 18: 41843
properties for particle identification, 17: 37442
properties in accelerator experimentation, 16: 25907 (LNF-62/37 (p.180-3))
properties in alpha source monitoring, 18: 27731
properties of fine-grain, effects of silver content on, 18: 43521
properties of fine-grain polyvinylacetals, 19: 44400 (CERN-65-4 (Vol.II), pp III21-56)
properties of fine-grain PR-2, 19: 44404 (CERN-65-4(Vol.II), IV23-31)
properties of gold and silver halide, latent image formation and threshold

oxidation in, 19: 44393 (CERN-65-4(Vol.II), pp II50-63)
properties of ion-sensitive, for mass spectrography, 18: 39148
properties of ion-sensitive, for mass spectrography, 19: 43979
properties of lithium acetate-loaded, 18: 23919
properties of NIKFI and ORWO, 19: 44403 (CERN-65-4(Vol.II), pp IV16-22)
properties of ORWO-K5 type, 19: 7438
properties of, effects of preparation method on, 18: 23489
properties of, effects of sodium salts of sulfosuccinic acid esters as surface-active agents on, 18: 23495
properties of, review of, 19: 44380 (CERN-65-4(Vol.I), pp 45-63)
proton energy-range relationship in Agfa-K2, 16: 23859(T) (CEA-tr-A-1119)
proton fission of silver and bromine nuclei at 1 to 3 Bev, 16: 18515
proton inelastic interactions in, optical model parameters for, 17: 36637 (AERI-P/R-3)
proton interactions with nucleons in, at 25 Bev, 17: 13532
proton interactions in, at 27 Bev, 17: 26304
proton interactions with nucleons in, effective target mass distribution for 28-Bev, 17: 32965
proton interactions in, selective criteria for, (E), 19: 10093
proton interactions at 9 Mev in, hyperon ($\Sigma^{\pm}$) production and decay, (E), 19: 41350
proton interactions at 30.5 Bev in, anisotropy in multiple meson emission in, 19: 45054
proton interactions at 25 Bev in, multiple fragment emission in, 20: 41827
proton interactions at 24 Bev/c, method of analysis of mechanism for inelastic, 20: 44192(T)
proton multiple scattering at 27 Bev, 18: 17062
proton multiple scattering in, at 5 to 24 Bev/c, (E), 19: 23806
proton range in Agfa K2, at 6.50 Mev, 17: 34753
proton range-energy relation in K2, from 4 to 9 Mev, (E), 19: 34518
proton ranges in Agfa K2, 16: 6556
proton ranges in Ilford K-1, at 0.3 to 1.2 Mev, 18: 20372
proton ranges in, energy dependence of, 18: 16344
proton reactions at 9 Bev in, angle and energy measurements of, 17: 6971
proton reactions at 25 Bev/c, hyperfragment production in, 17: 29593
proton reactions at 25 Bev/c, unstable fragment emission in, 17: 29607
proton reactions at 27 Bev in, meson (π) production in, 18: 15311
proton reactions at 16 to 2800 Bev, meson (π) production in, 18: 16775
proton reactions at 9 and 24 Bev, lithium-8 production in, 18: 32795
proton reactions at 2 to 9 Bev, fragment angular correlations for, 18: 34940
proton reactions at 9 and 24 Bev, lithium-8 production in, 18: 36653
proton reactions at 25 Bev, heavy ions emitted in, 18: 44811
proton reactions at 660 Mev with bromine and silver in, angular correlation of fragments from, 18: 44753
proton reactions at 600 Mev, distributions from spallation (E/T), 19: 3257
proton reactions at 25 Bev, hyperfragment production in, (E), 19: 5143
proton reactions at 19.8 Bev/c, shower particles from, (E), 19: 12264
proton reactions at 19.7 Bev/c, gamma spectra fine structure from, (E), 19: 12614
proton reactions at 24 Bev/c, emission of fast deuterons in, (E), 19: 27419 (INR-601/VI/PH)
proton reactions at 6.2 and 22.5 Bev, angular and momentum distributions from, (E), 19: 29282
proton reactions at 12.8 Bev in, cascade particle production in, 19: 31249
proton reactions at 28 Bev, angular distribution of shower tracks in, (E), 19: 31265
proton reactions at 19.8 Bev, analysis of, (E), 19: 31308
proton reactions at 6.2 to 25 Bev, statistical calculations for, 19: 43274 (JINR-P-2279)
proton reactions at 9 Bev with heavy nuclei in, with large energy transfer, (E), 20: 3047
proton reactions at 27 Bev, (E), 20: 10095
proton reactions at 28 Bev, lithium-8 production from, (E/T), 20: 17753
proton reactions at 9 Bev with, cascade effects on alpha yields in, (E), 20: 17713
proton reactions at 23 and 24 Bev/c, deuteron and triton production in, (E), 20: 25813
proton reactions at 13.8 Bev/c with bromine and silver in, intranuclear cascades from, (E), 20: 28397
proton reactions at 12.8 Bev with heavy nuclei in, angular distributions of secondaries from, (E), 20: 30364
proton reactions at 9 Bev with, slow meson (π^+) production from, (E), 20: 30370
proton reactions at 10 to 20 Bev with, emission of fast helium nuclei, (E), 20: 30496
proton reactions at 1 to 30 Bev in, calculations for, 20: 39828
proton reactions in, at 25 Bev, 17: 13529
proton reactions in, at 9 Bev, cross section for lithium-8 formation from, 17: 21024
proton reactions in, plate distortion from, 17: 22012
proton reactions on bound nuclear neutrons in, 5.1-Bev cross sections, 16: 27931
proton reactions on heavy nuclei in, at 24 Bev, 17: 17161
proton reactions (p,n) at 9 Bev, 17: 3973
proton reactions with bromine and silver in, boron-8 and lithium-8 emission frequency in 9 and 24 Bev, 17: 26464 (PAN-397/VI)
proton reactions with, deuteron, helium-3 and triton production in, 17: 33091
proton reactions with bromine and silver in, emission of short-range fragments in 2- and 9-Bev, 18: 11279
proton reactions with heavy nuclei of, 25-Bev, 18: 40546
proton reactions with heavy nuclei in, at 25 Bev/c in a strong magnetic field, 18: 44814
proton reactions with bromine and silver at 25 Bev/c in, lithium-8 recoil from, (E), 20: 17748
proton reactions with heavy and light nuclei at high energies in, method for discriminating, (T), 20: 26106
proton reactions with nuclei at 9 Bev in, hammertracks from, (E), 20: 26202
proton recoil in, neutron spectra measurement by, 18: 13028 (AWRE-NR-5/63)
proton recoil spectra induced by fast neutrons in, 16: 5528
proton recoil track length in, 16: 6989
proton recoil tracks in, sampling bias in scanning, 19: 44464 (UCRL-11703)
proton scattering track analysis at 27 Mev, 16: 6934
proton scattering at 6.2 Bev in, 17: 32907 (NYO-10271)
proton scattering in, spurious, 17: 41916
proton scattering at 19.8 and 24 Bev/c in, spurious, 18: 10922
proton scattering in NIKFI-R, coefficients for 9-Bev, 18: 16339
proton scattering at 12 and 24 Bev/c, amplitudes for, (E), 19: 8436
proton scattering in, small-angle elastic, (E/T), 20: 15314 (RT/FI(65)35)
proton scattering-amplitude measurements in, at 12 and 24 Bev/c, (E), 19: 10253 (NP-14626)
proton spurious scattering in, ultrasonic processing for reducing, 18: 30044
proton spurious scattering at 24 Bev, 18: 33963
proton spurious scattering at 24 Bev, (E/T), 19: 8438
proton spurious scattering and track distorion in, 19: 44412 (CERN-65-4(Vol.II), pp VI11-21)
proton spurious scattering in, 19: 44415 (CERN-65-4(Vol.II), pp VI37-52)
proton star identification in, method for, (E), 19: 46767 (TID-22256)
proton stopping in, scattering in, 18: 16552(R) (UCRL-11132)
proton-induced showers at 24 Bev in, angular distributions from, (E), 20: 6325
radiation dosimetry using, effects of humidity and temperature on, 17: 36054
radiation dosimetry of personnel using, 18: 16357
radiation effects on exposed, developed, and dried gelatin of, 17: 10703
radiation effects at −75 to 50°C, 19: 5966
radiation effects on dispersion of latent images in, alpha particle, electrons, and light, 19: 44388 (CERN-65-4(Vol.II), pp III1-16)
radiation effects at −75 to 50°C, y, 20: 23124
radiation effects on, x, 20: 27616
reactions in, scanning methods for, 18: 18221
reactions with emulsion nuclei, nuclear structure of $6 \leq Z \leq 9$, 17: 34708
research with, at CERN accelerators, 17: 34995 (CERN-63-22)
response of, in film badges with multi-element filters, 18: 22336 (LA-3001)
scanning and evaluation, design of automatic apparatus for, 16: 4264
scanning equipment for, automatic, 16: 27318
scanning in measurement of neutron spectra in reactors, digitized microscope for, 19: 34440
scanning methods and statistics of measurements in, 17: 18528 (CERN-63-3(p.275-96))
scanning of, automatic, 17: 6476
scanning of, automatic device for, 17: 23703
scanning of bubble-chamber, device for ionization measurements in, 18: 24002
scanning of nuclear spectra registered in, reliability of fractional, 20: 41315
scanning of, automatic apparatus for, 18: 10426
scanning of, automatic system for, 18: 29945
scanning of, statistical methods in, 18: 23944
scanning of, statistics of, 18: 33892
scanning procedure for absolute neutron yields, (E), 19: 46817
scattering at long cell lengths, meson (π) and proton, 18: 28343
scattering data from, design of instrument for calculation and registration, 16: 342 (PAN-239/VI)
scattering in, analysis of distortion in multiple, 20: 46090

scattering in, design and construction of device for automatic measurement of multiple, 16: 15537
scattering in, formulas for elimination of spurious, 20: 7423
scattering in, lateral displacement limit effects on determination of mean multiple Coulomb, (E), 20: 43690
scattering measurements in, 17: 18527 (CERN-63-3(p.245-74))
scattering measurements in, problems of small-angle elastic, 17: 18532 (CERN-63-3(p.339-59))
scattering measurements in, effects of distortion and noise on multiple Coulomb, 19: 9936
scattering measurements in, digitally controlled device for multiple, 16: 19108
Schwarzschild exponent for ions of medium mass, 16: 29588
sensitivities in, heating effects on, 16: 20685
sensitivities to charged particles and light photons, 18: 23910
sensitivity and sensitization of, role of metals in, (T), 20: 11121
sensitivity at liquid hydrogen and nitrogen temperatures, 19: 44401 (CERN-65-1(Vol.II), pp IV1-4)
sensitivity centers in, sizes and structures of, 18: 23913
sensitivity centers and latent image distributions in, 19: 44392 (CERN-65-4(Vol.II), pp II44-9)
sensitivity during irradiation, effects of hydrogen ions, 16: 30464
sensitivity, effect of temperatures between 20 and 110°C, 16: 6558
sensitivity, effects of foreign ions adsorbed on silver bromide microcrystals, 16: 10205
sensitivity for beta particles, 19: 46832
sensitivity measurements, using 10-Mev electron beams, 16: 8916(T) (CEA-tr-R-1417)
sensitivity of, as function of temperature, 17: 28168
sensitivity of hydrogen-filled, 17: 23790
sensitivity of Ilford L-4, for beta particles, 19: 32089
sensitivity of Ilford K5, at low temperatures, 19: 44405 (CERN-65-4 (Vol.II), pp IV33-40)
sensitivity of silver bromide crystals in, 18: 20336 (NP-13851)
sensitivity of silver halide, 18: 35633
sensitivity of silver bromide, effects of gold on high-intensity reciprocity law in, 19: 30174
sensitivity of triethylamine-sensitized, for uranium-233 alpha radiation, 20: 41341
sensitivity of, effects of ripening processes on, 18: 23497
sensitivity of, effects of ripening on, 18: 41874
sensitivity of, effects of concentration and pH of developer on, 19: 18031
sensitivity of, effects of polyethylene glycols on, 19: 20014
sensitivity of, for x-ray films, 18: 15938
sensitivity of, for *in vivo* stomach autoradiography, 19: 13182
sensitivity of, latent image parameters for, 20: 37121
sensitivity of, materials study for hyper-, 19: 44406 (CERN-65-4 (Vol.II), pp IV41-5)
sensitivity of, method for increasing, 19: 44390 (CERN-65-4(Vol.II), pp II19-28)
sensitivity of, performance of gold and triethanolamine for improvement of, 19: 44395 (CERN-65-4(Vol.II), pp II75-87)
sensitivity of, processes for increasing, 19: 44394 (CERN-65-4(Vol.II), pp II65-74)
sensitization by gold sodium thiocyanate complexes, 16: 31847
sensitization by iron sulfates and triethanolamine, 18: 23550
sensitization mechanisms in layers of, 18: 23551
sensitization of silver bromide, 16: 29129
sensitization of, using dyestuffs, 18: 23499
shock electrons produced in, by 26-Bev protons, 17: 9214
shrinkage coefficient determination, 16: 1966
silver bromide electron energy sensitivity in, threshold for, 20: 37122
slicing of, to study cosmic-ray nuclei, (E), 20: 46319
stars in, apparatus for measuring double-center, 18: 39667
statistical corrections for utilization of powders in, 16: 1999
swelling during preparation of, methods of measuring and reducing, 18: 23555
techniques for, 17: 18510 (CERN-63-3)
techniques for, in high-energy nuclear physics, 17: 18511 (CERN-63-3(p.1-15))
techniques for, for high-energy particle accelerators, 18: 20966
techniques in uses of, description of, (E), 19: 15859 (JINR-E-1866)
testing for use in cyclotrons, 20: 13345(R) (NP-15772)
track analysis in, using pulsed magnetic fields, 16: 27785
track analysis in, electronic instruments for, 18: 23939
track analysis in, automatic devices for, 18: 23942
track analysis in, working accuracies for, 18: 23949
track analysis in, geometry factors for recoil-proton, (T), 19: 22699 (UCRL-11296)
track analysis in, surface-angle method for dipping, 20: 23490
track distortion in, effects of guard rings on, 18: 23938
track measurements in, performance of KSM-1 microscope for, 17: 18565
track photometric profiles in, heavy-particle, 16: 10250
track profile measurement in, design of micro- densitometer for, 17: 1771
track profiles in, 16: 7707
tracks in, blob distributions in relativistic, 18: 23953
tracks in, discrimination between alpha and bremsstrahlung, 18: 23930
tracks in, distortions and spurious scatterings in, 18: 23950
tracks in, distortions and spurious scatterings in, 18: 23951
tracks in, in relativistic ionization-loss region, 18: 23952
tracks of multiply scattered particles in, spurious effects in, 18: 23934
use as fast neutron dosimeter, 17: 6323 (UCRL-9967)
use for cosmic shower analysis, 20: 21555
use for determination of radium and uranium in solutions, 17: 6003
use for determination of radon in gases, 18: 176
use for determining neutron spectra from beryllium–lead-210 source, 18: 36564
use for dosimetry of fast neutrons, methodological errors in, 17: 27692
use for electron detection in beta spectroscopy, 19: 32564
use for identification of cosmic nuclei with $Z > 5$, 18: 44483
use for measurement of alpha activity in solutions, 20: 11044
use for measuring anisotropic fast neutron spectra, 19: 20374
use for monitoring accelerator radiation, 20: 41276 (UCRL-16769)
use for neutron dosimetry in accelerator environment, 20: 41543 (RPP-R-2)
use for neutron spectral measurements, 17: 8648
use for neutron spectra measurements, 19: 18269 (UCRL-11599(Rev.))
use for nucleon interaction cross sections, 18: 39673
use for spectral analysis of fast and intermediate neutrons, 19: 11532
use for thorium determinations, 17: 31988(T) (CEA-tr-A-1197)
use in ALRR neutron spectra analysis, 20: 42681(R) (IS-1500(Sect. R))
use in autoradiography, 20: 11002
use in beta spectroscopy of individual electrons, 17: 25644
use in bubble chambers, 20: 23507
use in calibration of fission neutron spectrometric system, 18: 16358
use in cameras for scattering measurements on gas and solid targets, 20: 27317
use in cosmic shower measurements, (E), 19: 13756
use in cosmic-ray energy spectra measurements, 20: 4569
use in detection and measurement of elementary particles, 19: 44381 (CERN-65-4(Vol.I), pp 79-87)
use in determination of natural alpha-active aerosols, 20: 9154
use in elastic scattering experiments at high energy, 18: 20897 (CERN-64-6(p.31-48))
use in electron-track counting for beta spectroscopy, 16: 27264 (UCRL-9809)
use in elementary particle studies at CERN, 19: 44382 (CERN-65-4 (Vol.I), pp 105-10)
use in estimating stray neutron spectra near particle accelerators, 17: 14660
use in high-energy interaction studies, 18: 20901 (CERN-64-6(p.125-42))
use in mass spectrographic analysis of plasma, (E), 19: 5288(T) (AEC-tr-6518(p.146-53))
use in measurement of neutron spectra, 19: 44448 (HASL-162)
use in measurement of hyperon (Λ^0) magnetic moment, 20: 29534
use in momentum measurement of high-energy particles, 17: 14681
use in momentum measurements on cosmic charged particles, 20: 27347
use in neutron angular distribution measurements, 19: 836
use in neutron dosimetry near bare pulsed reactor, 18: 31917 (UCRL-10907)
use in neutron dosimetry, 20: 43671 (ORNL-P-2467)
use in neutron personnel dosimetry, sources of error in, 17: 16434
use in neutron spectral measurements in reactor cores, 16: 18441
use in neutron spectrometers, 20: 4249 (UCRL-16311)
use in radioautograms made with tritium, 18: 1338
use in radioisotope identification, 18: 8288(T) (AEC-tr-6049(p.75-99))
use in space research, (E), 20: 41803(R) (UCRL-16863)
use in spectroscopy of (γ,α) reactions, (E), 19: 16879
use in studies of particle interactions, errors in, (T), 19: 37617
use of large stacks of, in cosmic-radiation studies, 18: 40203
use of melted, in radioautography, 16: 1345
use with spark chambers for cosmic radiation detection, 18: 39674
use with spark chambers for cosmic radiation studies, 18: 39695
uses for determination of meson (π) contamination of meson (μ) beams, 18: 42410
uses for spectrometry of fast and intermediate neutrons, 18: 30747
uses in determination of proton beam qualities and intensities in CERN linear accelerator, 18: 42213
uses in neutron dose measurements for personnel, sources of error in, 18: 23961
x-ray reactions at 5 to 90 Mev, pair and triplet production in, 16: 11029

NUCLEAR ENGINEERING

see also Reactor Engineering
bibliography of bibliographies on, 17: 19741
book: *Advances in Nuclear Science and Technology*, Vol. 2, 18: 22992

book: *Advances in Nuclear Science and Technology*, Vol. 1, 17: 2516
book: *Annual Review of Nuclear Science. 11.*, 17: 5053
book: *Annual Review of Nuclear Science*, 17: 17637
book: *Atomic Engineering*, Vol. V, in French, 20: 8813
book: *Chemistry in Nuclear Technology*, 17: 28792
book: *Concrete for Shielding Nuclear Installations*, 20: 46171
book: *Dictionary of Nuclear Science and Techniques* (E/T), 19: 1985
book: *Nuclear Engineering Fundamentals*, 18: 10210
book: *Nuclear Glossary. English-French, French-English* (E/T), 19: 1984
book: *Nuclear Power Engineering*, 17: 5630
book: *Principles of Radiation Protection Engineering*, 19: 46683(T)
book: *Progress in Nuclear Energy. Technology, Engineering, and Safety. IV.*, 16: 12829
book: *Progress in Nuclear Energy. Technology, Engineering and Safety. III.*, 16: 12690
book: *Radioisotopic Methods for Investigation of Processes Inside Boilers*, in Russian, 19: 20418
book: *World Nuclear Directory*, 19: 8718
chemistry of, 19: 9050
compilation of U. S. nuclear standards for 1964, 20: 12559
conference, 20: 25228
conference on applications in construction industry, 17: 41180(T) (AEC-tr-5632)
conference on applications in wood, paper, and pulp industries, 19: 2684
conference on education, 17: 10247 (TID-7638)
conference on nuclear technology, France-Japan, Tokyo, Nov. 12 to 14, 1962, 19: 40302
conference on, France-Japan, Nov. 12 to 14, 1962, 17: 33267
conferences on, index to 1957 through 1963, 18: 25005 (TID-4043 (Rev.1))
course work and experiments in direct radiation-to-electrical energy conversion, 17: 26239
curriculum at University of Michigan on interaction of radiation and matter, 16: 13888
data analysis in, uses of computers for, 18: 37472 (A/CONF.28/P/633)
data for use in, 17: 4270
design methods for nuclear industry facilities, 17: 29977
design of sea water desalination plants using reactors, 20: 35103
design techniques utilizing computers, 16: 21833
development in France, 19: 12888
development in Germany, government promotion of, 20: 10492
development in Soviet Union, 19: 21762 (RM-2163(RAND))
development of facilities for, research in U. S. on, 20: 33558 (ORNL-NSIC-10)
development status in Japan, 20: 7217
development, summary of EURATOM program for July to Sept. 1962, 17: 17441
developments, US-EURATOM joint research program, 16: 14382
developmental operations in, summary of, 18: 2403(R) (PR-P-58)
developments and problems of gas turbine engines for use in, 16: 8378
developments and problems of gas turbine engines for, 16: 28573(T) (FTD-TT-62-620)
developments at Ames Lab. July 1, 1960 to June 30, 1961, 16: 11352(R) (IS-348)
developments at Brookhaven, 17: 31793(R) (BNL-782)
developments in Belgium, 3-year summary, 18: 6555(R) (NP-13390)
education of Navy Civil Engineer Corps officers in, 16: 28665
education program on, in Mexico, 17: 24815
educational programs for radiation science and engineering in colleges, 18: 6556 (NYO-10690)
educational programs for, 18: 19481 (TID-7671)
educational use of subcritical assemblies, panel discussion, 16: 6919 (TID-7619(p.239-59))
elastomer and plastic uses in, 20: 23094
electron-beam melting and welding in, 18: 20491
engineering materials list, 16: 3100 (TID-4100(1st Rev., Suppl.14))
engineering materials list, 16: 14846 (TID-4100(1st Rev., Suppl.15))
engineering materials list, 17: 3087 (TID-4100(1st Rev., Suppl.16))
engineering materials list, 17: 34070 (TID-4100(1st Rev.)(Suppl. 17))
engineering materials list, 18: 368 (TID-4100(1st Rev., Suppl.18))
engineering materials list, 18: 376 (TID-4100(1st Rev., Suppl.19))
engineering materials list, cumulative drawing number index for, 18: 8463 (TID-4101)
engineering materials list, 18: 13985 (TID-4100(Suppl.20))
engineering materials list, cumulative indexes for, 18: 13986 (TID-4102)
engineering materials list, 18: 26987 (TID-4100(Suppl. 21))
engineering materials list, 18: 35661 (TID-4100(Suppl.23))
engineering materials list, 18: 39407 (TID-4100(Suppl.22))
engineering materials list, 19: 559 (TID-4100(Suppl.24))
engineering materials list supplement, 19: 9807 (TID-4100(Suppl.25))
engineering materials list, cumulative drawing number index for, 19: 9286 (TID-4101(Rev.1))
engineering materials list, 19: 30352 (TID-4100(Suppl.27))
engineering materials list, 19: 32334 (TID-4100(Suppl.28))
engineering materials list, 20: 464 (TID-4100(Suppl. 29))
engineering materials list, cumulative indexes for, 20: 5608 (TID-4102 (1st Rev.))
engineering materials list, 20: 18854 (TID-4100(Suppl. 32))
engineering materials list, 20: 27070 (TID-4100(Suppl.33))
engineering properties of materials used in irradiation experiments, 18: 10536 (NAA-SR-Memo-8499)
equipment design for safety in chemical, effects of criticality control on, 20: 26431
facility for research in, description of isolated, 17: 41100
instrumentation for, description of standardized modularized, (E), 19: 22661 (KFK-275)
manual, 16: 885
materials development for, survey of, 17: 4973
materials for, 17: 36212
materials for use in, powder metallurgy, 19: 22938
materials for use in, survey of, 20: 41413
materials for, use of plastic, 20: 43471
materials handbook, 16: 16036
metals for process equipment in, review on, 17: 39556
neutron group constants for courses in, computer program for calculating, 20: 34957
nuclear facility construction techniques for containment, shielding, and cleanliness, 17: 31744
nuclear research facility siting, in Netherlands, 17: 41099
optimization studies in, based on Maximum Principle, 19: 14799
political aspects of facility site selection, 17: 41097
power spectral density in, indirect measurements of, 18: 4742 (LADC-5845)
program of SORIN nuclear research center, 17: 13838
programs in American universities, 17: 13840
programs in Great Britain, 18: 9667
radiation protection in, review, 17: 41078
radioactivity monitoring near installations, 17: 41083
remote-control problems in nuclear plants, 16: 27278 (RT/ING(62)5)
research facilities of Italian CNEN, 16: 30174
research facilities for, Casaccia, Italy, 20: 36540
research in, review, (E), 19: 31464 (IDO-17042)
research organizations and programs, 17: 13841
research program at Brookhaven in 1961, 16: 4606(R) (BNL-682)
research program at University of Florida, 17: 13839
research program at Rensselaer Polytechnic Inst., 18: 9802
research programs on, summary of, 17: 2459(R) (BNL-731)
research programs on, 17: 12057(R) (BNL-742(p.1-85))
research programs on, Euratom-U. S., 18: 1184
research programs at BNL on, July 1962 to July 1963, 18: 7987(R) (BNL-806(p.3-90))
research programs on, at Karlsruhe Nuclear Research Centre, 19: 17442
research programs at BNL, 1964, 19: 36949(R) (BNL-900(p.121-97))
research programs on, 19: 40396(R) (HMI-B-39)
research programs on, 19: 48059(R) (IDO-17081)
research progress in joint EURATOM-US programs, 16: 34014
research progress in, Boris Kidric Institute of Nuclear Sciences, Belgrade, Yugoslavia, 18: 26989(T) (AEC-tr-6227/1)
role of government in nuclear education, 16: 28664
role of the university in nuclear training and education, 16: 28663
safety criteria in processing-plant and reactor siting, 17: 41084
siting criteria for facilities, future trends in, 17: 41105
siting facilities at NRTS, 17: 41101
siting of facilities, effects on agricultural interests, 17: 41089
siting of facilities, role of public health officials in, 17: 41098
status of, January 1962, 17: 4376 (TID-14912)
summary of NORA Project from June to November 1962, 17: 17555(R) (TID-18108)
survey, 19: 24000
thermodynamic properties of nuclear materials, tables of, 19: 19983
training in, in Western Europe, 17: 5661
training in, in Mexico, 17: 24816
training programs for, analysis of, 17: 1172
training programs for technologists in Japan, 18: 33208
use in nuclear medicine, 16: 28696
use of concrete mixed with brown iron ores in, 17: 19596
use of non-conventional lubricants and bearing materials in, conference on, 18: 22998
use of reactor safeguards reports in courses on, 20: 34874
use of special isotopes in teaching, 17: 26234
Nuclear Engineering Test Reactor (USAF)
see Air Force Engineering Test Reactor
Nuclear Explosions
see Atomic Explosions

Nuclear Forces
see Nuclear Theory
Nuclear Fuels Testing Reactor
see Lynchburg Test Reactor
Nuclear Fusion Reactions
see Thermonuclear Reactions
NUCLEAR HEATING PLANTS
see also Nuclear Power Plants
coolant purification in boiling-water, survey of ion-exchange methods for, 20: 3539 (ACNP-65558(Rev.1))
design and uses of, 19: 25745
design for use in oil wells, 20: 6651(P)
design for water desalinization, 17: 28499
designs and status, review on, 18: 7852 (HW-66666(Rev.2))
development status, 1963, 18: 35066 (STI/DOC/10/28(p.73-7))
developments in, 1965, 19: 44307
economics, 18: 7954
economics of small dual-purpose, 20: 18124
economics of, effects of industrial price reform on, 19: 25746
heat transfer equipment in, design of, 17: 9942(P)
heat transfer system in, design of, 17: 9919(P)
turbines for dual-purpose, flexibility of back-pressure, 20: 3540 (ACNP-65573)
use for conversion of coal to pipeline gas, economics of, 18: 29101
use for water desalination, economic implications of, 18: 21665
use in process industries, 16: 31231
uses in water desalination, 18: 19402
uses of high- and low-temperature, survey, 16: 4424 (TID-8537)
NUCLEAR INDUCTION
use for measuring weak magnetic fields, 18: 4068(P)
use in determining nuclear magnetic moments, comparison with hyperfine structure method, 20: 44695
NUCLEAR ISOMERS
see also Isomeric Transition
decay by spontaneous fission, (E), 20: 46653
effects of nuclear polarizability on shifts on, 16: 28098
equilibrium deformations of $Z \geq 50$ and $N \leq 82$, 18: 36629
existence with quantized vortices in superfluid model, (T), 20: 40106(T)
formation ratios of, in (n,γ) reactions with germanium-76 and selenium-82, effects of energy on, 20: 44816
gamma energies and half lives of 5- to 1000-μsec, (E), 20: 15856
half lives and production of, (E), 19: 31260
half lives of hafnium-178, hafnium-179, tungsten-183, and ytterbium-177, (E), 20: 15688 (AD-620384)
half lives of msec and μsec, 18: 38112
half lives of rare-earth, (E), 19: 31219 (IS-1071)
half lives of 5 to 1000-μsec, 19: 10329
half lives of, measurement in 1- to 10,000-μsec range, 18: 21249
lifetimes of radioelement-daughter, measurement of, 18: 34770 (NP-14115)
lifetimes of ultra-shortlived, measurement using semiconductor detectors, 18: 24025
Mossbauer study of isomer shifts, 18: 14640
neutron reactions (n,n′), cross sections and uses of, 18: 29790(T) (AEC-tr-5187)
photoproduction of, use in gamma dosimetry, 20: 37079
production in alpha reactions with gadolinium, indium, molybdenum, samarium, tantalum, and zirconium at 24 Mev, (E), 20: 46717
ratios in reactions, Fermi-gas and superconductor models for, 18: 44780
separation of, effects of medium on chemical, 18: 39095
spins of three-particle states in spherical, with odd A, 20: 38136
structure of spontaneously fissioning, (T), 20: 13777 (JINR-E-2515)
structure of spontaneously fissioning, (T), 20: 46788
transition probabilities in core of, 18: 28597
use of, in production of polarized particle beams, 17: 11640(R) (TID-17720(p.79-89))
uses, 16: 2519
yield ratios of, 17: 9498 (ANL-6598)
NUCLEAR MAGNETIC MOMENTS
see also Nuclear Electric Moments
alignment of, in nuclear gyroscopes, (T), 19: 20279 (RTD-TDR-63-4001)
analysis from beta decay, survey, 18: 26679
analysis of dipole, determined with NMR, (T), 19: 47606
analysis using computers, (T), 19: 21246 (TID-21697)
calculation of, 20: 17733
calculation of quadrupole, (T), 19: 39791
calculation of, correction of Nilsson wave function for, 19: 29264
correlation of nuclear structure and, (T), 19: 23653
detection and measurement of, using gamma correlations, 17: 2255
detection and measurement of, using gamma correlations, 17: 2256
determination for radioisotopes from radiation angular distributions, (T), 19: 27454
determination from hyperfine structure and nuclear induction measurements, accuracy of, 20: 44695
determination of multiple, molecular beam technique for, 19: 6714
determination of partial multipole, by direct reaction sum rules, (T), 19: 5221
determination of, wave-function operators for, 17: 40124
determination using optical double resonance, 20: 1237
deviations from Schmidt lines in odd-A nuclei, 16: 1054
directional correlation attenuation coefficients for combined magnetic dipole and electric quadrupole interactions, for I = 1 and I = 2 states, 17: 15259 (TID-17089(Pt.I))
directional correlation attenuation coefficients for combined magnetic dipole and electric quadrupole interactions, for I = 3/2 and I = 5/2 states, 17: 15260 (TID-17089(Pt.II))
effects on cross sections of pair photoproduction on nuclei, (T), 20: 19968
equations for octupole, in spherical nuclei, 20: 8149
equipment for measuring quadrupole relaxation, 16: 31861
equipment for studying proton relaxation in liquids in weak fields, 16: 31862
hyperfine interaction due to, of electrons with large g factors, 16: 1795
interaction with extra-nuclear fields, perturbed angular correlations from, 17: 22573
interactions of, in alkali halide molecules, 19: 23655
interactions with electronic magnetic moments, dynamic polarization effects in, 16: 28046
interactions with electron magnetic moments, hyperfine, 16: 32408
interactions with nuclear magnetic fields in solids, effects on Mössbauer spectra, (T), 19: 33525
investigation by pulse techniques, 16: 22953
magnetic field dependence of, (E), 19: 37870
measurement, 17: 17306
measurement by gamma resonance scattering, 18: 36575 (NP-14084)
measurement for $f_{7/2}$ shell nuclei, 18: 1073
measurement in excited states by resonance fluorescence methods, 16: 21448
measurement in short-lived excited states, 16: 10907
measurement of dipole, using perturbed γ–γ angular correlations, (T), 20: 40125
measurement of dynamic nuclear polarization, 17: 7164
measurement of sexadecapole, 19: 1622
measurement of, equipment for, 18: 11268
measurement of, method for, 18: 30857
measurement of, Mossbauer and angular correlation methods for, 18: 30854
measurement of, review, (E), 20: 6282 (CERN-64-13(Vol.4), pp 97-136)
measurements from hyperfine structure, effects of core polarization on, 17: 40256
meson exchange effects on, in three-body systems, 19: 25543
of excited nuclear energy levels, 17: 24435
of mirror nuclei, 16: 3730
orientation of, review of dynamic and static methods for, 17: 5056
orientation of, description of 9.5-kOe magnet for, (E), 20: 5715 (AEET-227)
pair-interaction effects, 16: 21433
polarization of, thermodynamic approach to, 18: 32808
quadrupole, calculations, 16: 19512(T)
quadrupole coupling constants in alkali halide crystals, 16: 24654
regularities of, in odd-A nuclei, 17: 22630
relation to scattering cross sections, 18: 18941
relaxation in 3-body systems, 18: 17076
review, 18: 30842
scattering by, electron bremsstrahlung in, 18: 42773
screening of, constants for anti-, 17: 30545(T)
shell model explanation of, 18: 6289
spin gyromagnetic ratio for nucleons, effective, (E), 20: 40073 (LA-DC-8065)
tables, 18: 30864
theory, 18: 30843
theory, 18: 36695
theory of, of excited nuclear energy levels, 17: 24436
theory of, nucleon interaction effects in, 18: 28734
use in coupling constant analysis of solids, 18: 8351
NUCLEAR MAGNETIC RESONANCE
see also Nuclear Induction
see also Nuclear Quadrupole Resonance
acoustic power effects on lines of, saturation in, (T), 19: 35447
acoustic saturation of, 18: 42719
analysis of high resolution spectra of, by nuclear Overhauser effect and transitory selective irradiation methods, 18: 34309
analysis of liquids and solids by, 17: 10946
analysis of spectra for chemical shifts, 17: 15007
analysis of spectra, theory of magnetic multiple resonance spectra from,

18: 42307
analysis of spectra, decomposition of peaks in, 19: 43997(R) (UCRL-11889)
analysis of, Overhauser effects in, 19: 25490
band width and chemical shift in, solvent effects on, 18: 39182
bibliography and review on spectrometry, 16: 14705
book: *An Introduction to Spin-Spin Splitting in High-resolution Nuclear Magnetic Resonance Spectra*, 17: 3648
book: *Developments in Applied Spectroscopy*, Vol. 3, 19: 11041
book: *Formula Index to NMR Literature Data, Vol. 1, References Prior to 1961*, 19: 24526
book: *Formula Index to NMR Literature Data. Vol. 2: 1961–1962 References*, 20: 36842
book: *High Resolution Nuclear Magnetic Resonance Spectroscopy, Vol. I*, 20: 41255
book: *Interpretation of NMR Spectra*, 19: 21462
book: *Magnetic Resonance at High Pressure*, 18: 22584
book: *Nuclear Magnetic Relaxation*, 19: 19228
book: *Nuclear Magnetic Resonance and Relaxation in Solids*, 20: 3316
book: *Nuclear Magnetic Resonance Methods*, 20: 29498
book: *Nuclear Magnetic Resonances in Chemistry*, 20: 33308
book: *Nuclear Orientation*, a collection of reprints, 18: 24706
book: *Nuclear Resonance in Magnetic Materials*, 18: 44843
book: *Quantum Radiofrequency Physics*, 20: 925(T)
book: *Theory of Nuclear Magnetic Resonance*, 20: 46797(T)
bridge for pulsed, design of radiofrequency, 17: 14635
calculation of, slide-rule for frequency, 20: 8066 (INR-618/XV/I)
calculations for ferri- and ferromagnetic materials, 18: 30303 (CEA-R-2336)
calculations of, using double resonance methods with stochastic perturbation, 18: 2418
chemical exchange effects on, 18: 29616
chemical shifts in, theory of, 18: 41470
classification and analysis of, 20: 44680
conference on high-resolution, 18: 30752
conference on magnetic and electric resonance and relaxation, Eindhoven, July, 1962, 18: 18492
coupling constants in, nuclear, 19: 5152
coupling constants in, perturbation theory for extreme, (T), 19: 44945
data analysis for, in liquid metals, 20: 7744
detection at low temperatures, equipment for, 19: 39011
detection of broad resonances, low-frequency super-regenerative oscillators for, 18: 18160
detection of, design of instrument for, 18: 14179
detection of, equipment sensitive to continuous transverse fields for, 18: 44771
detection of, spectrometer for, 20: 7382
detection using modified spectrometer for improving signal-to-noise ratio, 20: 43640
detection using spectrometer sensitive to weak transverse static fields, 20: 4255
detection with twin-T bridge system, sensitivity of, 18: 477 (NP-13198)
determination in polar fluids, 18: 6828
determination in silicon by ultrasonics, 17: 16779 (ISS-62/17)
double resonance studies of sodium–ammonia solutions, 18: 26154
double resonance technique, experiments and theory, 18: 38197
effect of anisotropic shift and nuclear quadrupole interactions on, 17: 24388 (IS-519)
effects of chemical exchange processes on spectra, 17: 626
effects of intramolecular exchange processes on spectra, 17: 625
electric field effects on, 18: 17065(T)
electron transfer effects on spectra of, 18: 16027
electron-spin-echo envelope modulation, (E/T), 19: 6710
energy levels and line intensities of NQR, in single crystals, (T), 20: 3284
equipment design with resonance control, 16: 20705(P)
equipment for detecting, 16: 23962(P)
equipment for determining magnetic properties of drilling mud, 16: 27407(P)
equipment for measurement of electron double, at 12500 gauss, 18: 29956
equipment for observation, theory, 16: 3191(T) (CEA-tr-A-996)
equipment for pulsed measurements in solids, 17: 21985
equipment for well logging, 16: 23961(P)
equipment, magnet design for detectors, 16: 14987(P)
equipment, principles, and uses of, 16: 32436
frequency dependence on equipment parameters of, 18: 37479(T) (AEC-tr-6398(p.314-21))
frequency shifts in, due to radiation field, 18: 6247
generators for, theory of flow-type, 18: 31526
in antiferromagnetic Bloch wall, effects of bound spin wave excitation on, 17: 2936 (AD-276118)
in crystals due to hindered rotations, 17: 31212
in ferromagnetic alloys and metals, (T), 19: 5886
in ferromagnetic alloys, properties of, 20: 36359(R) (TID-22992)
in ferromagnetic transition metals, nuclear magnetic relaxation associated with, 18: 32273 (NP-14118)
in metal single crystals, 17: 1926 (D1-82-0194)
in metals, review, 16: 9469
internuclear coupling constants in, effects of temperature and solvents on, 19: 19888
Knight shift in, crystal symmetry effects on anisotropic, 18: 35562
Knight shifts of alkali metals, theory, 17: 635
Knight shifts of boron-11, in metal hexaborides, 17: 32083
Kronig-Kramers relations in, 18: 24659
lectures, 18: 43151 (ISS-63/50)
line broadening of, effect of paramagnetic impurities on temperature dependence of, (T), 19: 15526
line narrowing in, by rotating r-f field, 20: 8164
line shape analysis by lattice harmonics, 17: 5134
line shapes for metallic powders, Knight shifts in, 19: 7429
linewidth in magnetic materials, correlation effect on, 17: 31206
magnetic field boundaries of nuclear polarization from nuclear relaxation dispersion, 19: 23786
magnetic field inhomogeneities, correction for high-resolution spectroscopy, 17: 6418
measurement, design, and performance of high-frequency spectrometers for, 16: 30622
measurement in aqueous alkaline earth metal solutions, design of apparatus for, 19: 8114
measurement in enriched tin-119 hollow cylindrical monocrystals, (E), 19: 40990
measurement in fluids, wall effects in, 19: 32811
measurement in intermetallic compounds and solid solutions, 18: 26522(R) (ANL-6868(p.326-30))
measurement in liquids, design and characteristics of spectrometer for, 18: 18142
measurement in liquids, high-resolution probe for, 19: 42699
measurement in paramagnetic materials, ENDOR spectrometer for, 20: 32525
measurement in rapidly rotating solids, 20: 4931
measurement in rotating solids, design of resonance spectrometer for, 20: 28683
measurement in solids, high-resolution, 18: 30753
measurement in solids, system for, 19: 26643
measurement in solids, stable autodyne pickup circuit for, 20: 29492
measurement in very weak magnetic fields, 17: 32390
measurement of, correlating chart movement and sweep in, 18: 4077(P)
measurement of, design of instrument for, 18: 4074(P)
measurement of electron double, in fields up to 12500 gauss, 18: 30824
measurement of, equipment for, 17: 8566(P)
measurement of, magnetic field inhomogeneity compensation in spectrometer for, 17: 32367
measurement of, using low-field spectrometers, 17: 7126 (NP-12330 (p.259-76))
measurement of, cryostat for, 18: 29663
measurement of, design of 3 spectrometers for, 19: 14162
measurement of, for studying molecular motions in solids, 20: 18672
measurement of, magnetic field stabilization in, 18: 39577
measurement of, magnetometer design for (E/T), 19: 718 (CEA-R-2383)
measurement of, noise suppression in, 18: 19995
measurement of, performance of INDOR technique for, 20: 42529
measurement of, techniques in, 20: 1166
measurement, sample holder for, 16: 20703(P)
measurement to 0.3°K, equipment for, 19: 35342
measurement using flow-type detecting elements, conditions for maximum signal from, 17: 39735
measurement using flow-type detecting element, shift in signal for, 17: 39736
measurement using flow-type detecting element, acceleration of polarization of liquids for, 17: 39737
measurements at high temperature, furnace and probe assemblies for, 18: 25758
measurements for nuclei with large spin, nuclear quadrupole interaction effects on, 18: 2401(R) (IS-700(Sect.P))
measurements in intermetallic phase, methods for, 18: 44229
measurements in weak field, spectrometer for, 19: 6153
measurements of pulsed, circuits for, 19: 42695
measurements of, equipment for spin echo, 19: 13794
measurements of, flux stabilizer for spectrometer for, 19: 13717
measurements of, superconducting Helmholtz coils for, 19: 745
measurements using wideline spectrometer, advantages of sideband technique in, 17: 3274 (UCRL-9791)
model of effects, electrical, 16: 28062 (CEA-2025)
modes in magnetic materials, theory of, 17: 11379
modulation of, mutation of spins in, 19: 11094
neighbor anisotropy effect in nuclear magnetic shielding, 17: 36436

(NP-13020(p.448-50))
neutron-scattering effects on para-, (E/T), 19: 8398 (JINR-P-1840)
noise reduction in spectra, 19: 43997(R) (UCRL-11889)
nuclear polarization effects on, (T), 19: 42001
observation in solids, equipment for, 17: 41569(T) (JPRS-21326 (p.69-80))
observations in unstable magnetic fields, 16: 6588
of acoustic spin-phonon coupling of electron and nuclear spins in solids, 16: 18275
of metals, 17: 32569 (CONF-54-1)
of nucleotides, 18: 43444(R) (LA-3132-MS(p.233-5))
of polar liquids in electric fields, 18: 15711(R) (TID-20256)
optical pumping cycle in, experimental verification of quantum theory of, 17: 17132
pressure effects, in cobalt complexes and manganese fluoride, 17: 2738
probes for, development of high-temperature, 18: 41870
properties in solids, multiple-phase transients in, (T), 19: 10347
pulse methods and spin-stabilized spectrometer arrangement for double, 20: 28312
pulsed measurements in, use of analog-to-digital converter for accurate, 17: 37875
quadrupolar signals of, intensity and shape of, 17: 14272
quantum transitions in, role of multiple, 18: 13081
quantum transition enhancement in, method for double, 18: 24644
radiofrequency field effects in double, 20: 28314
relaxation effects in double, (T), 19: 8462
relaxation in crystals near Curie temperature, 17: 5402
relaxation in solids, effects of magnetic field on spin-lattice, (E/T), 20: 34866
relaxation in two-spin systems, (T), 19: 6717
relaxation in, linearized equations for, 19: 41751
relaxation of, effects of paramagnetic-ion relaxation on, 16: 33013
relaxation of, arbitrary spin equations for multipole, (T), 20: 8308
relaxation of, effect of molecular rotational motion on, 19: 25507
relaxation rates in transition metals from dipolar and orbital interactions of d- and p-bands, 17: 34585
relaxation time measurements, Carr-Purcell method, 16: 6024
relaxation time of, spin-echo measurement devices for, 19: 35497
relaxation time of oriented atoms in, effect of surface inhibitors on, (T), 20: 32417
relaxation times in liquids, thermal, (E), 19: 15511
relaxation times in gases, h-f modulation and saturated scattering for measuring, 20: 19869
research programs on, 16: 30172(R) (TID-16489)
research programs on, 17: 6801(R) (TID-17303)
review and bibliography on, 17: 41967
review of chemical applications of double resonance method, 17: 17957
review on, 18: 11225
sample orientation for spectrum measurements, 16: 20701(P)
shielding by neighboring atoms, 18: 21232
shielding constants for, in 2-, 3-, and 4-electron atoms and ions, 18: 21233
signal enhancement in, by dynamic nuclear polarization, 18: 15194 (EUR-483.e)
signal fine structure, nutation in, 16: 25965(T) (JPRS-13656(p.260-78))
signal shape in solids, (T), 19: 8422
signals at $2\omega_2-\omega_1$ in double, (T), 19: 45307
spectra from liquids and solids, narrow-line, 20: 28619
spectra from, use of double-quantum transitions in assignment of, 17: 35750
spectra from, method for least squares analysis of, 19: 5869
spectra in rapidly rotating solids, 16: 26974
spectra in superconductors, shape of, 18: 18848
spectral line width in flow-probe measurement of magnetic fields, 19: 26934
spectra of, analysis of high-resolution, 17: 28293
spectra of complex organic compounds, interpretation of, 18: 4618
spectra of double, for nuclei with spin ½, (T), 20: 40103
spectra of fluorine in halogenated ethanes, 19: 5934 (UCRL-11649)
spectra of four-membered ring compounds, analysis, 19: 46247 (UCRL-16349)
spectra of organic compounds, data recordings of, 20: 14459(R) (ORNL-3889, pp 44-6)
spectra of, use of Overhauser effect in analysis of high resolution, 17: 32129
spectra of, computer programs for analysis of, 20: 3645 (UCRL-16344)
spectra of, device for recording accurate, 18: 27784(P)
spectra recording of, magnetic-field pulse modulation method for, 20: 43657
spectra, principles and uses of, 18: 12002
spectral analysis of, by method of subspectral transformations, 19: 28307
spectral analysis of, performance of double-resonance spectrometer for, 20: 2109
spectral line shapes of, 18: 22885
spectrometer design for, 16: 6608
spectrometer design for high resolution, 16: 17875(P)
spectrometer design with control probe for keeping magnetic field constant, 16: 17876(P)
spectrometer design for comparing two samples, 16: 20704(P)
spectrometer design with frequency sweep for all nuclei, 17: 18578
spectrometer design for spin decoupling experiments, 17: 18579
spectrometer design for solids, 17: 25570
spectrometer design for, 18: 14183
spectrometer for, design of quartz autogenerator for, 17: 41214
spectrometer for moving elongated materials, 16: 17865(P)
spectrometer for measuring, modifications to, for proton relaxation measurements, 17: 40427(R) (NYO-10063(p.1-6))
spectrometer for quadrupole, design of cryostat and transducer for, 17: 41216
spectrometer for, resolving power and sensitivity of, 19: 46157(R) (MLM-1254)
spectrometer for, broad-line, 20: 33607
spectrometer, use of modulation in high-resolution, 17: 6421
spectroscopy for nuclei exchanging between different rotational isomers, 17: 35263(R) (UCRL-10706(p.1-110))
spectroscopy, improvement of signal-to-noise ratio by continuous averaging in, 17: 32363
spectroscopy in superconducting magnetic fields, 18: 43920
spectroscopy of double, method for, 18: 27409
spectroscopy, review on long-range H^1–H^1 spin-spin coupling in, 18: 24234
spin coupling in, review on, 19: 5153
spin coupling mechanism in, 17: 35263(R) (UCRL-10706(p.1-110))
spin-echo measurements in, 16: 14966
spin-echo measurement in weak magnetic field, 16: 14967
spin Hamiltonian coupling constants for, 19: 14251
spin temperature measurements from double, 17: 26602
splittings in, use of double-irradiation method for assignment of, 19: 13446
survey of, in chemical substances, 17: 25962
theory, 17: 33929
theory, 20: 28618
theory and uses of, developments in, 19: 367
theory for two-quantum resonance spectrum of nuclear spin I = 1 in anisotropic medium, 19: 7432
theory, in paramagnetic media, 16: 7138
theory in paramagnetic media, 16: 16887
theory of, by spin-rotational interactions in liquids, 17: 31194
theory of double, 18: 44295
theory of high-resolution, in presence of weak radio-frequency field, 17: 6076
theory of nuclear magnetic shielding in molecules, 17: 36437 (NP-13020(p.451-3))
theory of, correlations and oscillations in relaxation of model spin system for, 18: 40576
theory of, in precessing frame for solids, 18: 32267 (COO-1198-175)
use for crystal structure analysis, 20: 26341 (CEA-Bib-67)
use for determination of optical purity of α-deuterated primary alcohols, 20: 43254
use for inertial navigation, 19: 735
use for inhomogeneous field measurements, 19: 44353(T) (SLAC-Trans-22)
use for isotope analysis of deuterated organic compounds, 17: 8109
use for magnetic field measurements, 17: 8562(P)
use for magnetic field measurements, 19: 26938
use for magnetic field measurement, nuclear spin alignment by nutation in, (E/T), 19: 26935
use for magnetic field measurements in CERN storage ring, equipment for, 20: 31817 (CERN-66-15)
use for measurement of homogeneous and inhomogeneous magnetic fields, (E), 20: 2112
use for measuring inhomogeneous magnetic fields, effect of nuclear nutation on, (E/T), 19: 26933
use for type-II superconductor investigations, 20: 44517(T)
use in biochemistry, review, 18: 43192
use in burnup analysis of reactor fuels, 18: 24856(R) (GEAP-4430)
use in calibration of superconducting magnets, 19: 29156 (NYO-2150-4)
use in crystallography, comparison of electronic resonance scattering with, 19: 34707
use in determination of gyromagnetic ratios, (E/T), 19: 35502
use in determining relative signs of nuclear spin coupling constants, 17: 18934
use in determining nuclear spin temperatures, 18: 9283
use in determining flow rate of liquids in pipes, 18: 39723(T)

(AEC-tr-6390(p.15-18))
use in determining volume of stream of liquid in pipe with variable cross section, 18: 39724(T) (AEC-tr-6390(p.19-21))
use in fast-neutron flux measurement, 20: 11169(P)
use in magnetic field measurements with continuous-flow transducers, 20: 7351
use in maser for frequencies below 50 Mc, 17: 16908(P)
use in measurement and stabilization of inhomogeneous magnetic fields, 18: 37477(T) (AEC-tr-6398(p.306-10))
use in metallographic studies, 19: 4599
use in nuclear dipole moment studies, (T), 19: 47606
use in nuclear gyroscope, 18: 5604(P)
use in nuclear gyroscope, 18: 5605(P)
use in observation of atomic motion in solids, 19: 25176
use in protein studies, deuterated organisms for, 20: 16165
use in studies of radiation damage in solids, 16: 13645(R) (TID-15230)
use in studies of radiation damage in solids, 17: 18863(R) (TID-18438)
use in studies of ligand exchange rates in metal complexes, 19: 352 (UCRL-11584)
use in studies of radiation damage in solids, 19: 20620(R) (NYO-2024-8)
use in well logging, 20: 45931(P)
use of, in studies of hydrogen bonding, 16: 30378(T) (HW-tr-42)
use of polarized-neutron capture and β-decay anisotropy for NMR of short-lived nuclides, 18: 11188 (ANL-6797(p.397-403))
use of single nutation-pickup in measurement of magnetic field of strong d-c with direct dependence, 18: 37478(T) (AEC-tr-6398(p.311-13))
use of spin-echo, for studies of restricted diffusion, 17: 33943
use of, for molecular weight determinations, 20: 26747 (LA-DC-7143)
use of, in chemical exchange studies, 20: 31218(R) (UCRL-16658, pp 1-9)
use to control chemical and distillation processes, 16: 26951(P)
use to determine manganese ion in pyruvate carboxylase, 20: 42773
use to stabilize weak inhomogeneous magnetic fields, 19: 26930
uses in inorganic chemistry studies, 16: 26887
uses in organic chemistry, 17: 18101
uses in organic chemistry, 18: 6844
uses in studying reaction rates and mechanisms, 19: 22219
uses of electron double, 18: 29615
uses of, in flowing liquids, 19: 44813(T) (NP-tr-1307)
vibrational corrections to second, 17: 36493

NUCLEAR MATERIALS MANAGEMENT

absorptiometric determination of boron in uranyl nitrate liquor, 18: 13641 (PG-Report-521)
accidents in fuel fabrication and radioisotope processing plants, theoretical possibilities and consequences of, 18: 25711 (ORNL-3441)
accounting systems for, at AECL, 19: 47906 (AECL-2282)
analysis and constitution of plutonium-uranium alloy, 18: 29568(T) (EURAEC-1014)
analysis and sampling methods for, economics of, 20: 20647
analysis of fuel plates for uranium-235 by gamma-ray scintillation spectrometry, 19: 13263
analysis of fuels for plutonium and uranium concentrations and isotopic abundances, 19: 7267 (APED-4527)
analysis of fuels for plutonium-239 by neutron transmission measurements, 20: 233 (SGAE-PH-28/1965)
analysis of irradiated fuel elements for plutonium and uranium-235, development of nondestructive method for, 19: 7272(R) (IAEA-R87-1)
analysis of irradiated fuel elements for plutonium and uranium-235, development of nondestructive method for, 19: 7273(R) (IAEA-R87-2)
analysis of irradiated fuel elements for fission products by gamma spectrometry, 20: 236(T) (AEC-tr-6621)
analysis of mixed fissionable isotopes, radiometric, 20: 12814(P)
analysis of uranium for uranium-235, gamma spectrometric, 19: 7278 (RT/CHI(64)-18)
analysis of uranium fuels and ores, 19: 31696
analytic problems in uranium refining, 18: 25619
analytical methods used at CANEL, manual of, 19: 42426 (TIM-936)
Aqueous Reprocessing Chemistry for Irradiated Fuels, Symposium on, Brussels, 1963, 18: 13954
assay of fuel pins and residues, calorimetric methods for, 19: 13197 (ANL-6771)
auto-catalytic criticality excursion in an array of fissile units, 18: 14775 (AHSB(S)R-68)
automated accounting system used at Hanford, 18: 29812 (HW-SA-3546)
autoradiography of plutonium oxide–uranium oxide compacts, 20: 31212
bibliography on radiation effects on solid uranium-based nuclear fuel materials, 18: 16529 (VDIT-16(4.1))
bibliography on, annotated, 19: 39101 (TID-3315)
blending of materials for isotopic adjustment of uranium-235 assay, experiences in, 19: 17768 (TID-21330)
blending of uranium tetrafluoride production lots, model for, 19: 2204 (NLCO-935)
book: *Reactor Handbook. Vol. IV: Engineering*, 18: 38257
breeding potentials for TARGET with thorium/uranium-233, 19: 3623 (GAMD-4592)
breeding ratio of plutonium in EBR-I, 18: 33097 (ANL-6789)
burnup analysis by gamma scanning, 20: 5093
burnup analysis of reactor fuels, 18: 15487(R) (GEAP-4361)
burnup analysis of nuclear fuels, 19: 1853(R) (GEAP-4621)
burnup analysis of reactor fuels, development of methods for, 19: 10510(R) (GEAP-4716)
burnup calculations for fuel used in plutonium recycle program, 19: 8617(R) (GEAP-4729)
burnup calculations for reactor fuels, 20: 16061(R) (BAW-296)
burnup determination in fuels, development of methods for, 19: 9060(R) (IDO-14649)
burnup determination in fuels, using stable fission products, 19: 28222 (IDO-14642)
burnup determination in reactor fuels, mass spectrometric, 19: 28225 (SGAE-PH-11/1964)
burnup determination by praseodymium-144 gamma activity, 19: 35735
burnup measurement in fuels, development of techniques for, 19: 45542(R) (BAW-272)
burnup measurements on fuels for, nondestructive methods of, 20: 11004
calculation of working capital invested in fuel cycles and its interest charges, 18: 13280 (CEA-2325)
charges for uranium-235-enriched and depleted uranium as hexafluoride, list of base, 18: 45190 (TID-21015)
comparison of four titrimetric methods for assaying plutonium, 19: 4058 (LA-DC-6722)
comparison of published methods for analysis of irradiated and unirradiated fuel samples, 18: 15960 (SGAE-PH/CH-1/1964)
computer use for auditing data centralization in, 20: 20965
conference on, 20: 20944 (STI-PUB-110)
conference on, 18: 43125 (TID-7700)
conference on transport of radioactive materials, 19: 663 (AHSB(A)-R-8)
conference on, Buffalo, New York, June 17 to 19, 1963, 20: 20366
conference on, Pittsburgh, Penn., May 4-6, 1964, 19: 13694
control and inventory in, criteria for, 20: 20966
control in fabrication of enriched uranium fuels, 19: 34656 (ORNL-P-1431)
control of uranium fuel element fabrication, systems for, 19: 39130 (RFP-507)
control program for reprocessing enriched uranium scrap, 19: 38758 (Y-KA-7)
conversion of plutonium nitrate to plutonium tetrafluoride, 18: 13718 (HW-SA-2880)
critical dimensions of systems containing plutonium-239, uranium-233, and -235, 18: 30958 (TID-7028)
critical mass of plutonium-238, 19: 25246(R) (HW-84369(p.53-4))
critical sizes of cubic arrays of interacting fissionable units, comparison of theory and experiment for, 18: 32506 (DP-868)
criticality calculations for regular arrays, 19: 44977 (IDO-17095)
criticality control in chemical processing department at Hanford, administration of, 19: 46433 (RL-SA-43)
criticality control and safety of fissionable materials, 20: 2095
criticality control in fuel processing operations, use of reactor physics calculation methods in, 20: 10969
criticality control and safety in, relation of, 20: 20974
criticality evaluation of packages for transport of fissile materials, 19: 40828 (SC-RR-65-98, pp 679-90)
criticality of annular cylinders containing plutonium solutions, 18: 34494 (CEA-R-2495)
criticality of container arrays of plutonium nitrate, 19: 18733 (BNWL-19)
criticality of cubic arrays, 18: 44490
criticality of low-assay uranium compounds in array of shipping containers, 19: 40819 (SC-RR-65-98, pp 330-56)
criticality of plutonium nitrates in spherical geometry, 19: 25245(R) (HW-84369(p.45-51))
criticality problems in fissionable materials handling, 19: 18737
criticality safety procedures, 19: 40807 (RL-SEP-389(Rev.))
criticality studies of aqueous uranyl nitrate solutions, 18: 18613
criticality studies for fuel element handling and storage, 20: 3379 (ORNL-TM-1207)
cycle development for gas-cooled reactors, 19: 38082(R) (ORNL-3807, pp 177-88)
data processing by random-access electronic equipment, 18: 43131 (TID-7700(p.98-109))
design study for 2500-Mw(th) breeder, 18: 29032 (ACNP-64503)
design study of 1000-Mw(e) liquid-metal fast breeder reactor, 18: 29035 (CEND-200(Vol.I))
design study of 1000-Mw(e) liquid-metal fast breeder reactor, 18: 29036 (CEND-200(Vol.II))
design study of 1000-Mw(e) liquid-metal fast breeder reactor, 18: 29038 (GEAP-4418(Vol.I))
design study of 1000-Mw(e) liquid-metal fast breeder reactor, 18: 29039

(GEAP-4418(Vol.II))
design study of 1000-Mw(e) liquid-metal fast breeder reactor, 18: 29061 (WCAP-3251-1)
determination of free carbon in uranium carbide, 18: 11971 (PG-Report-526)
determination of plutonium-239, uranium-233, and uranium-235 by fission counting, 20: 228 (LA-DC-7439)
determination of plutonium and uranium in nuclear fuel cycles, evaluation of methods for, 20: 14447 (NBL-231)
determination of thorium-230 in thorium, 18: 39110
determination of uranium-235 enrichment of flat fuel plates, 19: 6852
determination of uranium-235 enrichment in low-enriched uranium dioxide, 19: 7317
determination of zirconium in ignited uranium/zirconium residues, 18: 13640 (PG-Report-515)
development of pyrometallurgical fuel-processing methods, 18: 17921(R) (ANL-6725(p.31-88))
disposal, inventory, and shipment at HNPF, 19: 33609(R) (TID-21861)
economic aspects, 20: 10967
economic comparison of fuel fabrication processes used in the High Power Density Program, 18: 12597 (GEAP-4294)
economic criteria for, 20: 12562
economics of plutonium, thorium, and uranium fueled reactors, 18: 24858(R) (HW-80560F)
economics of uranium enrichment by gaseous diffusion, 18: 24054(T) (ORNL-tr-134)
economy of nuclear fuels, 18: 26904
engineering-scale study of fluid-bed fluoride volatility process, 18: 17924(R) (ANL-6725(p.131-90))
engineering-scale study of fluid-bed fluoride volatility process, 18: 43706(R) (ANL-6800(p.197-296))
fabrication cost estimate for uranium dioxide and uranium dioxide–plutonium dioxide fuel, 18: 13246 (GEAP-3824)
fabrication costs of plutonium-enriched fuel elements, 18: 32103 (HW-SA-3543)
fabrication of fuels for organic cooled reactors, 19: 33601(R) (DP-965)
fissile interactions, eigenvalue matrix treatment of, 18: 16737 (HW-80213)
fuel alloy separation processes, 19: 15662(R) (ANL-6900(p.45-142))
fuel analysis for plutonium and uranium-233 during burnup, (E), 19: 25704 (HW-76195)
fuel assay, feasibility of nondestructive methods for, 19: 38547 (TID-21475)
fuel burnup determination by perturbation technique, 19: 5552
fuel burnup determination in reactors, methods for accurate, (E), 19: 21667(R) (GEAP-4776)
fuel cycle costs, 19: 38081(R) (HW-84609(p.3.1-16))
fuel cycle economics of fast reactors, 18: 33057 (A/CONF.28/P/248)
fuel cycle economics, 18: 45052
fuel cycles and private ownership, 19: 1857
fuel cycles in organic-moderated reactors, 18: 24859 (TID-20593)
fuel depletion analysis using LEOPARD program, (T), 19: 12762 (WCAP-3269-26)
fuel economics for nuclear power complexes, 18: 45030 (ORNL-P-365)
fuel element assay method, 20: 7014 (NP-15688)
fuel inventory calculations for Elk River, methods for, 19: 29610 (ACNP-64519(Rev.))
fuel management and inventory in EBR-II, 19: 42075 (ANL-6735)
fuel policy for pool-type reactor, 18: 33152(T) (CEA-R-2458)
fuel processing facilities for EBR-II, 18: 43359(R) (ANL-6800(p.43-196))
fuel recovery by volatility processes, 19: 15663(R) (ANL-6900(p.143-202))
fuel uniformity in sandwich plates, 19: 22511
fuel-processing facilities for EBR-II, 18: 17922(R) (ANL-6725(p.88-99))
fueling nuclear power complexes, 19: 3659
gamma counting of unirradiated fuel elements, 20: 3464
gamma scintillation spectrometry for inspection of fuels, 19: 22512
impact and static tests on 15-ton cask for shipping irradiated fuels, 18: 10301 (DP-843)
in analysis methods, ORNL Master Analytical Manual, 18: 23410 (TID-7015(Suppl.6))
in chemical processing of radioisotopes, 18: 25607 (ORNL-3633)
in fluoride volatility processing, 19: 4247(R) (ORNL-3627(p.29-72))
in in-plant systems, use of pulsed neutron sources for, 19: 6125 (HW-80913)
in power reactor fuel processing, 19: 4246(R) (ORNL-3627(p.1-28))
in radioactive waste management avoiding environmental disposal, 18: 26979
in transportation of radioactive materials, 18: 25713 (VDDIT-89)
indexes to ORNL Master Analytical Manual, 18: 25271 (TID-7015 (Indexes)(Rev.1))
inventory and statistical procedures for, 20: 35181 (SRIA-115P49-1)
inventory in reactor accidents, 20: 12333
inventory management, survey of mathematical approaches to, 18: 43127 (TID-7700(p.8-29))
inventory management at ORNL, 18: 43128 (TID-7700(p.30-40))
isotopic analysis of uranium, 19: 330
isotopic analysis of low-burnup plutonium fuels, (E), 19: 10514 (HW-83431)
isotopic analysis by mass spectroscopy, errors in, 20: 10795
isotopic analysis methods for, of plutonium and uranium, 20: 20978
isotopic analysis, automation of mass spectrometers for, 19: 46181 (WAPD-T-1769)
isotopic content of operating fuel elements, methods for calculating, 20: 20979
laboratory studies of fluoride volatility processes, 18: 17923(R) (ANL-6725(p.113-31))
material balances for nuclear power, comparison, 19: 29635 (EUR-2412.e)
materials balances in Kilorod program, 20: 27040(R) (ORNL-3831)
materials management processing methods for fast reactor fuels, 19: 40177(R) (ANL-7046(p.1-35))
measurement of content of fissile material using thermal neutrons, 18: 41362(P)
measurement of oxygen-to-metal ratio in uranium and plutonium dioxide solid solutions, 18: 11962 (GEAP-4271)
measurement quality, statistical control of, 19: 34102 (BNWL-SA-3)
method for identification and inspection of irradiated fuel elements, 20: 20970
method for power-breeder reactor using thorium–uranium fuel cycle, 19: 43531(P)
method of calculating nuclear fuel cycle costs, 18: 45005
method of controlling and determining concentration in uranium manufacture, 18: 12272(P)
method of fuel management optimization, 19: 33639
methods for analysis, measurement, and sampling in separation plants at Windscale, 20: 20972
methods for direct inventory during fuel cycle, 20: 26450
methods for fission product, relation of waste solution storage to economics of, 20: 22517
methods for inventory in conversion plant, 20: 20971
methods for plutonium at Rocky Flats, Colo., 20: 18948 (RFP-720)
methods for 1965 AEC Report to Congress on, 20: 24825
methods for, economics of, 20: 38416
methods for, in processing ores and concentrates, 20: 10968
methods for, review of, 19: 18210
methods of ENEA, 19: 10677(R) (NP-14552)
methods of, at Windscale New Separation Plant, 20: 20830
methods of, based on materials balance, 20: 10970
methods of, for EBR-II fuel, 20: 12452
methods of, for economic processing of radioactive residues, 20: 20833
methods of, for enriched uranium chemical processing facility, 20: 20832
methods of, for power reactors, 20: 12451
methods of, for research establishment, Lucas Heights, Australia, 20: 12560
methods of, in Eurochemic's Mol fuel reprocessing facility, 20: 20831
methods of, in fabrication of enriched fuel elements, 20: 21313
methods of, in fluoride volatility process, 19: 13537
methods of, in fuel element fabrication plant, 20: 11262
methods of, in production, distribution, recycle, and reprocessing, UKAEA, 20: 22528
methods of, in USA, 19: 15809
methods of, using internal audit, 20: 22529
methods used in Italian power stations and research institutions, 20: 20964
methods used in uranothorianite processing unit of Bouchet Plant, France, 20: 20969
neptunium purification facilities at the Hanford Purex plant, 18: 10180 (HW-SA-3282)
neptunium recovery facility at the Hanford Purex plant, 18: 13912 (HW-SA-2928)
neptunium recovery and purification at Hanford, 18: 13913 (HW-SA-3283)
neutron radiography of irradiated fuel, 18: 20591
nondestructive assay of nuclear fuels, 18: 15494(R) (SWRI-1321-1)
nondestructive determination of burnup in nuclear fuels, 19: 9056 (CEA-R-2542)
nondestructive testing of fuel elements, 19: 32551(R) (NP-14962)
nonnuclear uses for depleted uranium, 18: 15730
nuclear safety research, 19: 13671(R) (WASH-1052)
operations in isotopes separation, summary, 18: 27811(R) (ORNL-TM-198)
operations in waste processing, 18: 19448(R) (ORNL-TM-757)
organization of auditing in fuel element fabrication plant, 20: 20967
Plutonium Abstracts, Vol. 4, No. 1, 18: 17353 (HW-68600-35)
plutonium and uranium recovery from irradiated fuels, 19: 35604(R) (ANL-7045(p.1-23))

plutonium and uranium recovery by volatility processes, 19: 35605(R) (ANL-7045(p.24-48))
plutonium assay in irradiated fuels by isotopic dilution, 19: 4057 (EURAEC-1159)
plutonium assay, comparison of titrimetric methods for accurate, 18: 27285 (AWRE-O-10/64)
plutonium determination using isotopic dilution, 18: 41311 (CEA-R-2563)
plutonium determination in spent fuels, metal, alloys, and compounds, review of methods for, 19: 38542 (LA-DC-6938)
plutonium determination in, methods for, 20: 20976
plutonium handling and shipping, measurement problems in, 19: 38535 (RFP-508)
plutonium nitrate solution analysis, study of shipper-receiver differences in, 19: 282 (RFP-436)
plutonium nitrate shipping packages, 19: 4402 (RFP-437)
plutonium nitrate shipping containers, design for reduced weight and cost, 19: 40825 (SC-RR-65-98, pp 609-19)
plutonium oxidation-reduction titrations, 18: 11963 (HW-53368(Suppl.1))
plutonium pricing, 19: 5595
plutonium recovery from irradiated uranium fuels, 18: 12279(P)
plutonium recycle program at Hanford, 18: 15608 (HW-SA-3321)
plutonium-239 determination in irradiated fuels, 20: 10796
preparation of plutonium trifluoride, 18: 12119(P)
preparation of uranium monocarbide, 18: 12118(P)
procedures at Chinon power plant, 19: 45607
procedures for Berkeley and Bradwell fuels, 20: 3530
process vessel calibration for, 19: 38756 (RFP-488)
processing methods for irradiated fuels, 19: 40112(R) (ANL-7046 (p.36-66))
processing scraps of highly-enriched aluminum–uranium alloys, 19: 13538
production of transneptunium isotopes in high neutron fluxes, (T), 19: 13845 (ANL-6932)
program at AECL, 18: 35801
program for, by USAEC, 20: 22527
program for, in United States, technical support activities of, 20: 12561
programming methods for fuel management optimization, 18: 29010
protactinium and uranium recovery from molten fluoride systems by oxide precipitation, 18: 13931
quantitative autoradiography for plutonium fuel analysis, 18: 27334
reactor fuel burnup monitors, (E), 19: 30524 (NP-14972)
reactor fuel composition and reactivity changes during burnup, (T), 19: 19350 (AD-605022)
reactor fuel cost reduction, 18: 24866
reactor fuel cycle costs, 18: 35151 (ORNL-TM-564)
reactor fuel inventory and control, 20: 3536
recovery of neptunium-237 from a Purex-type plant, 18: 13910 (HW-56675(Del.))
regulations for transport of nuclear fuel materials and reactor fuel elements in Great Britain, 19: 669 (AHSB(A)-R-8(p.37-45))
regulations for transport of fissionable material, 19: 672 (AHSB(A)-R-8 (p.59-62))
role in assurance of nuclear safety, 18: 33799 (CONF-620-2)
safety control in chemical processing facilities of Savannah River Plant, 20: 431 (CONF-651103-7)
safety criteria for handling materials, 18: 31830
sampling methods in French nuclear industry, 20: 20973
sampling of enriched uranium hexafluoride for analysis, 19: 36230 (K-P-3248)
sampling program for, in uranium refining and machining, 20: 16140
scope of, for typical power reactor in U. S., 20: 20968
separation of thorium and uranium from perchloric acid solutions, 18: 9970 (IS-777)
separation of uranium hexafluoride from a gas mixture, 18: 12278(P)
shipment of radioactive materials, packaging and regulatory problems in, 19: 13666 (LA-DC-6866)
shipping containers for fissionable materials, 19: 15697 (ORNL-P-869)
shipping container for fissile materials, design and tests of Class I, 19: 18193 (HW-SA-3995)
shipping container for fissile materials, impact tests of, 19: 26491 (LAMS-2983(Suppl.))
shipping irradiated fuel assemblies from Yankee reactor, experience in, 19: 19392 (WCAP-6062)
shipping of plutonium oxides, study of shipper-receiver differences in, 19: 42425 (RFP-502)
shipping packages for plutonium di-oxide, 19: 30443 (RFP-501)
specifications for high-density nuclear-grade uranium dioxide, 18: 12545 (HW-74204(Rev.1))
specifications for swage-compacted mixed oxide fuel elements for PRTR, 18: 16452 (HW-79290)
spectrographic determination of boron in cast uranium metal, 18: 11970 (PG-Report-464)
spectrographic determination of tantalum in plutonium, 18: 13620 (HW-79738)
spent fuel shipping cask for PM-1 and PM-3A, 18: 16225 (MND-M-1856)
standards for plutonium, AEC, 20: 33549 (CONF-660308, pp 131-42)
statistical quality control in manufacturing reactor fuel elements, 18: 11418
status of U. S. program to establish primary standard for plutonium, 19: 4059 (LA-DC-6723)
subcontracts for fuel element fabrication, responsibility clauses in, 18: 43126 (TID-7700(p.1-7))
system for chemical processing industry, 18: 39367 (HW-SA-3672)
thorium fuel cycle process development, 19: 38755(R) (ORNL-3611)
tritium disposal in fuel processing wastes, 18: 24978 (ORNL-TM-851)
uranium conservation by breeder reactors, 19: 3703
uranium determination in waste solutions from fuel reprocessing, 19: 7290
uranium determination for, review of methods for, 20: 18619
uranium determination in, methods for, 20: 20977
uranium distribution in fuel plates, 19: 17377
uranium distribution in solid homogeneous critical assembly fuel, method for measurement of, 20: 227 (KAPL-M-6448)
uranium feedsite data processing, computer program for, 18: 18287 (HW-80806)
uranium isotopic analysis, 18: 29565 (NLCO-904)
uranium isotopic ratio measurement errors caused by ion interactions with impurity molecules, 18: 11965 (K-1400)
uranium material balance in ion exchange, 19: 36889(R) (MLM-1250)
uranium ore reserves and fuel cycle costs, comparison for conventional and breeder reactors, 19: 3660
uranium processing and control at Watertown Arsenal, 18: 10455 (WAL-MS-55)
uranium processing at NLCO, 18: 25269(R) (NLCO-905)
uranium processing at NLCO, 18: 43378(R) (NLCO-920)
uranium resource conservation by breeder reactors, 19: 3702
uranium-233–thorium-232 cycle in fast reactors, 18: 13303(T) (AEC-tr-6336)
uranium-235 determination in absolute air filters, nondestructive method for, 18:25270 (NYO-10726)
uranium-235 determination in SNAP fuel rods, nondestructive, 19: 30080 (NAA-SR-9600(Vol.III))
uranium-235 determination in combustible waste and air filters by gamma counting, gage for, 20: 31174 (WAPD-T-1905)
uranium-235 enrichment in uranium fuels, instrument for measuring, 19: 769 (HW-83427)
uranium-235 enrichment measurement in aluminum–silicon fuel elements, nondestructive tester for, 19: 8618 (HW-78153)
use of uranium dioxide in power reactors, survey of problems of, 18: 14368 (HW-SA-3110)
vibration and vibration-swaging fabrication of plutonium-enriched fuels, 18: 12603(T) (AEC-tr-6312)
waste management practices, review, 18: 45149 (HW-SA-3575)

NUCLEAR MODELS

accuracy of superfluid, for strongly deformed element properties using, 17: 17113 (JINR-E-1154)
adiabatic approximation for inelastic scattering, 16: 14023
agreement from nucleon indistinguishability in, 17: 17120
alpha decay rates and, 19: 19101
alpha decay rates of deformed even-even nuclei in, (T), 19: 39793
alpha-particle, for scattering of electrons, 18: 6271
alpha reduced widths in superfluid, with projected wave functions, (T), 20: 1150 (IFA-FT-55)
alpha scattering on complex nuclei in smooth cutoff, analysis of, 18: 24712
alpha-cluster, geometry of, 18: 18943
analysis of alpha, 17: 7189
analysis of alpha, for beryllium-9, 18: 9428
analysis of octet, for baryon charge and R-inversion, 17: 35253(R) (IA-775)
analysis of optical and statistical, 18: 10702
analysis using terminology of high-energy elementary-particle physics, (T), 19: 14500 (ANL-6878(p.481-504))
angular momentum distribution in Thomas-Fermi, 18: 26578
angular velocity corrections to cranking, 19: 23741
anisotropic harmonic-oscillator, collective effects in, 16: 23087
applicability of deformed and spherical, criteria for, 19: 17047
asymmetric-rotator model for odd-A, 16: 19799
basic concepts of, summary of, 16: 29787 (UCRL-10046)
behavior in strongly deformed regions, 17: 34972
beta decay theory for $7 \leq A \leq 39$, 17: 29632
beta decay transitions, 18: 26679
beta transitions in Nilsson model, matrix element of, 20: 13831
bibliography on, 18: 42765
bibliography on, 18: 42766
bibliography on, 20: 22011 (TID-22771)
binding energies from, 19: 17028

binding energies, radii, and surface diffuseness of atomic nuclei, 18: 32758
book: *Contemporary Models of Atomic Nuclei*, 16: 3748
book: *Contemporary Models of the Atomic Nucleus*, 19: 21463
book: *Coulomb Excitation*, 20: 15848
book: *Les Modeles en Spectroscopie Nucleaire*, 20: 3139
book: *Nuclear and Radiochemistry*. Second Ed., 18: 33455
book: *Nuclear Structure and Electromagnetic Interactions*, 20: 3147
book: *Nuclear Theory. Pairing Force Correlations and Collective Motion*, 19: 19227
book: *Physics of the Nucleus*, 17: 17280
book: *Strong-Interaction Physics*. (T), 19: 1657
bound states in short-range central potentials, (T), 20: 4708(R) (UCRL-14360, pp 50-73)
boundary-condition, application to Brueckner theory, 17: 39987
Brueckner-Bethe-Goldstone reaction-matrix theory in, 20: 34648
californium-252 spontaneous fission prompt neutron statistics from, 18: 24651
characteristics and capabilities of, review, 18: 44838
charge density for $Z \leq 20$, 17: 29633
classical self-consistent, 17: 26595
cluster and shell, comparison for lithium-6, 16: 21429
cluster arrangement in alpha particle, rules for, 17: 38158
cluster model for beta decay of carbon-10, 18: 1068
collective dipole excitations in, 17: 15292
collective potential-energy surface for quasi-spin, calculation of, 17: 17254
collective states of even-even nuclei ($228 \leq A \leq 254$) in superfluid, energy of octupole, 17: 40086
comparison of cluster, shell, and unified, for 1p-shell nuclei, 16: 26247
comparison of DAVYDOV, with conventional, 16: 29769 (JAERI-1020 (p.142-52))
comparison of Davydov and rotation-vibration, 18: 21323
compound nucleus, parameters for calculation of neutron cross sections using, 20: 15863
conversion coefficients in core-excitation, penetration effects on M1, 20: 36247
deformations in pairing-plus-quadrupole, j-shell, 18: 24614 (NP-13941)
deformed-core, results for beta decay from, 18: 18955
description for collective vibrations of nuclei, 20: 17711
description, for properties of light nuclei ($4 < A \leq 40$), 16: 31116
description of close-packed-spheron, 20: 4918
description of inexpensive, for educational purposes, 19: 29331
description of odd-A 1p shell nuclei using strong-coupling rotational, (T), 20: 46679
description of self-consistent, 16: 3742
description of, combining collective giant-dipole-resonance model and unified model, (T), 19: 6629 (AD-600710)
description of, combining cluster model and shell model, 20: 30377
description of, for calculation of equilibrium nuclear shape, (T), 20: 40136
description, with washed-out nuclear boundaries, 16: 31115
development, 20: 21961 (AD-624028)
development and results of asymmetric-rotor, 16: 21460
development for deformed nuclei, (T), 20: 19986
development for stripping reactors, 17: 38223
development for vibrational states, 20: 15851
development of, for predicting asymmetry in mass distribution of fission fragments, 17: 19387
development of generalized cluster, 16: 17073 (SUI-61-6)
development of modified statistical, for finite nuclei, 18: 36602
development of single-particle, for deformed odd-mass nuclei, 18: 38118
development of single-particle, 20: 28441
development of superfluid, 16: 33835
distributions from reactions in statistical, 17: 11675
effectiveness of superfluidity, in explaining properties of nuclear matter, 17: 31416
eigenstates of pairing-force Hamiltonian for many-boson system with N-body interaction in, 18: 21034
energy gap in cubical, (T), 19: 12561
energy level densities and nucleon correlations in, high-energy behavior of, 17: 24446
energy level density in superfluid, odd-even effects in, (T), 19: 23667
energy level density in independent-particle, angular-momentum dependence of, (T), 20: 12012
energy level density in statistical, 20: 34668
energy level determination using deuteron reactions (d,d') and (d,p), review on, 19: 16892
energy levels from Nilsson, (T), 19: 12524
energy levels in alpha-particle, low-lying, 17: 2288
energy levels in cranking, higher order corrections to rotational, (T), 19: 47680
energy levels in core-excitation, quasi-particle, 20: 17814
energy levels in hydrodynamic, particle-hole wave equations for, 18: 42699
energy levels in isobaric multiplets, (T), 20: 46705
energy levels in odd-A nuclei from, predictions for copper-63 and -65, 17: 24495
energy levels in single-particle, 20: 6431
energy levels in, excitation and study of collective, 18: 17020
energy levels in, five-dimensional quasispin for pairing hamiltonian in J-T scheme of, 19: 41687
energy levels of beryllium-9 in cluster, 16: 26272
energy levels of deformed nuclei with rotation-vibration interaction, (E), 20: 46766
energy levels of even-even nuclei in alpha-particle, 19: 1619
energy levels of heavy nuclei, statistical theory for, 19: 17027
energy levels of lithium-6 in 3-body, 16: 31093
energy levels of light nuclei from cluster, 17: 9621
energy levels of medium-weight nuclei, 0^+, (T), 20: 44647 (NIJS-R-484)
energy levels of odd nuclei in asymmetric rotator model with intermediate coupling, 17: 26531
energy levels with high angular momenta in single-particle, (T), 19: 27546
energy spectrum of center of gravity, in second order, 17: 7508
energy width variations near threshold, interpretation by, 16: 21543
energy-level spectra for deformed, Hartree-Fock approximation for rotational, 19: 45364
energy-level transitions in BCS theory, matrix elements for, 20: 46654
evaluation of statistical and optical, for neutron scattering by bismuth-209, 18: 13123
evaporation, analysis of alpha energy spectra from proton reactions, 16: 7112
excitation in deformed, β-vibration effects on multiple Coulomb, (T), 19: 10341
Fermi-liquid theory and Green-function method for spherical, 20: 6425
fission in unified, angular momentum effects in (E/T), 19: 1679
fission theory using adiabatic, 18: 9445
for beta decay and energy levels of nuclei with $150 < A < 190$, 16: 32416
for binary-fission mechanisms, 18: 21186 (KR-64(Sect.II))
for collective single-particle excitations in even-even nuclei, 20: 24461
for deformed nuclei, 18: 36692
for electron beam interactions with plasmas, 16: 4610(R) (TID-14435)
for energy level E2 transitions of even-even nuclei, 20: 30372
for first 0+ energy levels, in near-magic and magic nuclei, 16: 5980
for gamma branching ratios of even-even spherical nuclei, 16: 33868
for gamma branching ratios of even-even spherical nuclei, 16: 33870
for giant-resonance structure in photonuclear reactions, 16: 32434
for giant resonance properties of deformed nuclei, 16: 33858
for heavy nuclei, review on, 19: 1656
for high-energy nuclear reactions, 18: 42717
for level density near threshold, (T), 19: 8472
for lithium-6, testing of, (T), 19: 21368
for quasiparticle interactions in even-even nuclei, 19: 23632 (UCRL-11225)
for vibrational even nuclei, 18: 6215
for vibrational spectra, time-dependent Hartree-Fock theory in, 20: 36205
formalism for Nilsson, with single-particle and collective mixing, 20: 36246
formalism for phenomenological, 19: 3281
formalism of peripheral, for meson (π) photoproduction, 20: 24013 (DESY-66/2)
formulation for deformed nuclei using quadrupole force and pairing force, (T), 20: 46669
formulation of Independent-Pair, variational principal connection with, 18: 21330
formulation of statistical compound-nucleus, (T), 20: 42269
formulation of statistical, (T), 20: 44698
fragmentation mechanisms in, 18: 38081(T) (AEC-tr-6398(p.139-52))
gamma E-2 transitions in even-even and odd-even nuclei, 17: 41965
gamma E1 transitions in single-particle, for $A \geq 16$, 17: 2263
gamma E1 transition probabilities in deformed odd-A nuclei in, 17: 13507
generalization of Wilkins', 18: 40530
generalized rotation-vibration model for deformed even nuclei, 17: 5331
Goldberger, Gell-Mann model, 18: 28456
group theoretic approach to 2s-1d shell nuclei, (T), 20: 34645
Hartree-Fock self-consistent-field method for, 19: 17026
hole self-energy corrections in Brueckner theory, 20: 42244
independent particle, of odd-A nuclei, 16: 22985 (NP-11747)
independent-particle, for predicting E_3 type isomeric transitions for odd A nuclei, 16: 31066 (NP-11746)
intrinsic symmetries of rotational states, 17: 7206
isobaric correspondence between nuclear states, 16: 4856
isomer shifts of Mössbauer spectra in, 17: 13254
isomerism probabilities in statistical, 17: 28343
K-matrix, for multichannel resonances, 18: 9162

magnetic and orbital moments from quasicrystalline, (T), 19: 23654
many-body perturbation methods and summation of bubble graphs for, 16: 21512
mass differences in T = ½ nuclear isobaric quartets, 19: 1623
mass formula and deformations in modified liquid-drop, 20: 24401
mass formula for diffuse nuclear surfaces, semi-empirical, 18: 32767
mass formula from ground-state energy in superfluid, 19: 43290
mass of deformed nuclei in, parameters for collective hamiltonian for, 20: 24471
meson (μ) capture in shell and statistical, 17: 19293
meson (π) composite, meson (π) mass treatment by, 16: 2459
meson (π^+) capture by light nuclei, nucleon pair correlations from spectra of, 17: 41987
Mittay-Lefleur, theory of integral transformations for, 19: 3255
motion equations for single-nucleon relativistic, solution of, 17: 29581
Nambu for elementary particles, nucleon mass treatment by, 16: 2459
neon-21 low-lying positive-parity states from core-particle coupling, 17: 41950
neutron cross section calculations with combinatorial, gap, and gas, in kev region, 17: 34859
neutron scattering cross section calculations from, value of, 20: 26092 (ORNL-P-2072)
neutron strength functions and widths in, 17: 19222 (TID-16603)
neutron strength functions from rigid ellipsoidal and vibrational, s-wave, 17: 29599
nonspherical rectangular-well, nuclear equilibrium shapes in, 16: 18530
nuclear deformation on gross structure, Nilsson model determination, 16: 4842
nuclear deformation in spheron, prolate, (T), 20: 8137
nuclear isomers with quantized vortices in superfluid, (T), 20: 40106(T)
nuclear matrix calculation formalism for, 19: 16852(R) (NP-14647)
nuclear moments of inertia in superfluid, (T), 20: 40102
nuclear motion in unified, collective, 20: 36189
nuclear structure of sodium-24 in unified, 18: 19031
nuclear structure in close-packed-spheron, (T), 20: 1218
nuclear structure of odd-A nuclei in superfluid, 20: 11961 (INR-602/VII/PH)
nucleon binding energies, energy levels, and potentials for self-consistent, 18: 21358
nucleon correlations in superfluid, four-body, (T), 19: 33253
nucleon coupling to axial symmetric core in deformed odd-even, hamiltonian for, 19: 33896
nucleon energy levels in superfluid, partially projected functions for, 18: 7706
nucleon interactions with nucleon clusters in nuclei, high energy, 17: 7209
nucleon interactions in nuclear matter, velocity-dependent potential for, (T), 20: 46722
nucleon momentum distribution from quasi-deuteron, 17: 11695
nucleon-nucleon potential for nuclear matter calculations, velocity-dependent, 17: 40088
nucleon pairing energy in alpha-particle, with degenerate shells, 20: 8087 (ZFK-TPH-16)
nucleon pairing models with and without particle number conservation, 19: 12497
nucleon-nucleon and Yukawa potentials in, eigenvalues of Lippmann-Schwinger kernel for, (T), 20: 13836
nucleon-phonon interactions in nuclei, (T), 20: 44638 (JINR-E-2772)
of beryllium-9 nucleus, 18: 21349
of photonuclear reactions, 17: 36405 (NP-13020(p.129-44))
parameters of generalized diffraction, at 660 Mev, 17: 11307 (JINR-P-1009)
parity in asymmetric top, of deformed even-even nuclei, (T), 20: 44781
particle number conservation in pairing, 18: 28689
performance of cluster and shell, in light nuclei, 17: 13591
performance of compound-nucleus, for analyzing reactions, (E), 19: 17014
perturbation theory for deformation in light nuclei in Nilsson, 20: 15809
phosphorus-29 energy levels with strong- and weak-coupling models, 18: 26594
polar Fermi-liquid approximation for Migdal, 19: 27292
potential form in, self-consistent, 20: 19965
potential in boundary-condition, hard-core, (T), 20: 17772
potentials in single-particle, nonlocal, 20: 6430
potentials in, effects of short-range repulsive forces on, 19: 39814
potentials with local and nonlocal interactions, isospin dependence of, (T), 20: 44691
potentials with local and nonlocal interactions, isospin-dependent, (T), 20: 44844
properties, 17: 38012(T) (AEC-tr-5734(p.69-70))
properties, 20: 3149
properties comparison and evaluation, 19: 14544
properties of compound-nucleus, clarification of, 18: 4527 (CONF-285-4)
properties of heavy nuclei in unified, 18: 4585 (UCRL-8783(Rev.))
properties of statistical, lectures on, 18: 21190 (KR-64(Sect.VII))
properties of superfluid, 18: 9438
properties of systems of like nucleons in, 17: 2281
proton decay systematics in semi-empirical, for Z > 50, 19: 1621
proton scattering in, by deformed nuclei, 17: 2271
quadrupole effects in Elliott oscillator, 18: 6253
quantum theory of many-particle, 20: 9604
quasi-particle interactions in spherical nuclei, 18: 9321 (UCRL-11080)
radii as functions of N and Z in, 17: 36678
radii as functions of N and Z in, 17: 36679
reaction cross section calculations in, method for, (T), 19: 39935
reaction matrix in Brueckner, method for calculation of, 20: 38160
reactions in statistical, compound, 17: 38206
reactions in unified, 19: 17010
relation between drop and statistical models for equilibrium distribution of nucleon density, 18: 6265
relation between shell and other, lecture on, 17: 17302
relation between the shell model and the rotation-vibration model, 17: 7220
relation between the shell model and the rotation-vibration model, 17: 7221
relation to shell model, lecture on, 17: 17305
reproduction of rotational bands by alpha-particle, 17: 5374
research on, 20: 33970(R) (ORO-2915-61)
research programs on, uses of sector-focused cyclotrons in, 17: 38321 (CERN-63-19(p.85-92))
residual forces in single particle, 16: 29645 (NP-11901)
review, 16: 15698
review, 18: 26667
review, 19: 43369
review, 20: 38118
review for few-nucleon systems, 19: 17069
review of, 19: 10374
review of Elliott model, 16: 24825
review of recent major developments in low-energy, 18: 19062
review of rotational, 20: 38164
rotating development, 16: 12452
rotation in cranking, unified derivation for, 20: 15828
rotation-vibration, for odd-A nuclei, 20: 6441
self-consistent classical, 17: 879
self-energy of Bogoliubov quasi-particle in superfluid, 18: 34687
semiatomic, for properties of odd-A nuclei, 17: 22629
shape of deformed nuclei, Bohr-Mottelson vs. asymmetric-rotor models for 18: 18934
spectra in, effects of collective excitations on single-particle, 16: 26269
spectra of nuclei with A ≤ 60 in, multipole vibrational, 18: 16981
spherical complex-potential, for slow-neutron scattering, 16: 28039
statistical analysis of thermal neutron fission of uranium-235, 17: 41927
statistical, for compound nuclear reactions, review of, 17: 17640
statistical, for particle production, 16: 2433
statistical interpretation of high-energy reaction excitation functions, (T), 19: 31222 (LA-3266)
statistical properties of eigenvalues and eigenvectors of, 17: 24385 (AWRE-NR-3/63)
statistical properties of compound nuclear states in, (T), 19: 17013
statistical, with account of correlations, 17: 7284
statistical, development of, 18: 24633
statistical, for energy-level fluctuations and distributions of widths, 18: 11178 (ANL-6797(p.302-21))
statistical, for multiple-production interactions, (T), 19: 45041 (TPJU-12/65)
statistical, for scission of uranium-236, 18: 42720
statistical, use in nuclear reaction theory, 18: 18938
strong coupling model, verification of predictions from half-life measurements, 18: 9435
superconducting, use for describing residual interactions in shell model, 17: 33064
superconductivity, determination of states in strongly deformed nuclei by, 17: 40009
superfluid, alpha reduced widths in, 18: 7686 (NP-13422)
superfluid, derivation of self-consistent field in, 16: 31080
superfluid, for pairing energy in Weizsäcker mass formula, 17: 40077
superfluid, moment of inertia for even-even nuclei in, 17: 24390 (JINR-P-1216)
superfluid, use in study of strongly deformed nuclei, 16: 4827
superfluid, comparison with energy level structures of indium-117, praseodymium-143, and tin-117, (E), 20: 40159
superfluid, for reduced widths in helium-3- triton-producing reactions, (T), 19: 6713
superfluid, for single quasiparticle states, 19: 17052
superfluid, odd-even effect in nuclear level density in (T), 19: 1601
superfluidity, 18: 11233
survey, 16: 1058

survey of, 17: 19221 (PUC-1963-95)
symmetry relations of collective, 19: 9767(R) (IS-900(Sect.P))
testing asymmetric rotator and vibrational, 19: 14645
theory, 20: 19987
theory for analysis of break-up processes in elementary particle collisions, 16: 2485 (NP-10958)
theory for excited-core, 20: 30484
theory of adiabatic and statistical, for fission, 18: 38199
theory of collective, for nonspherical nuclei, 20: 8091
theory of nuclear surfaces, using Fermi-gas model, 16: 23058
theory of rotation vibration, 19: 29285
theory of self-consistent cranking, for higher rotational states, 20: 6416
theory of statistical, for fast neutron reactions and scattering, 17: 34857
theory of statistical, high-energy limit in, 19: 31289
theory of superfluid, for spontaneous fission, 20: 4876
theory of, review of, 19: 19102
transformation in superconductive, accuracy of u-v, 17: 28242 (JINR-P-1259)
transport coefficients of square well potential, 17: 36665 (UCRL-7376)
unified description of collective-shell vibrations, 16: 26277
unitary symmetry, mass of Z^- particle in, 18: 26315
uranium-239 partial radiation widths in statistical, fluctuations in, 17: 40085
use for constructing wave functions and testing electromagnetic properties of nuclei, 20: 3148
use in study of odd-A nuclei in the 2s-1d shell, 20: 34642
use in studying low-lying states, 18: 11160 (ANL-6797(p.58-78))
use of peripheral, in study of structure of light nuclei, 18: 11213 (LNF-63/47(p.249-50))
use of single particle Nilsson model for odd-A nuclei in 1d-2s shell, 16: 29752 (EFINS-62-26)
use of strong-coupling rotational, for lithium-7, 17: 19321
uses for estimating single-particle effects in nuclear reactions, 19: 14543
uses of cluster, in compound-nucleus theory of reactions, (T), 19: 17012
uses with single-nucleon-transfer reactions, for nuclear-structure analyses, (T), 19: 14494 (ANL-6878(p.249-75))
validity of, 17: 21211
validity of compound-nucleus statistical, in helium-3 reactions with iron-56, 20: 10090
validity of Thomas-Fermi, 20: 2819
velocity-dependent potentials in, 18: 21223
vibration spectra of even-even spherical nuclei in, 17: 17137
vibrational states in spherical, two-phonon, 18: 28664
wave function for nuclear ensemble, particle number fluctuations in BCS, 19: 18949
wave function for beryllium-8 cluster, distortion of, (T), 20: 10014
wave functions for deformed, superconductivity, 19: 23635

NUCLEAR MODELS (COLLECTIVE)

asymmetric core, for 2s-1d shell of odd-A, 17: 26596
Bohr-Mottelson theory comparison with ytterbium-166 → thulium-166 → erbium-166 decay chain, 16: 4828
Bohr-Mottelson hydrodynamical, for rotational states in deformed even-even nuclei, 19: 17046
book: *Contemporary Models of the Atomic Nucleus*, 19: 21463
book: *Nuclear Theory. Pairing Force Correlations and Collective Motion*, 19: 19227
book: *Unified Theory of Nuclear Models*. (T), 19: 1655
calculations using variational method, (T), 20: 38108
characteristics of asymmetric-core, for odd-A nuclei, 16: 21459
Coulomb excitation with heavy ions, multiple, 17: 33087
derivation of residual-interaction terms in deuteron stripping reactions (d,p), 17: 41921
description of dynamic, for odd-A nuclei, (T), 19: 6629 (AD-600710)
development and properties, 19: 43282
development for deformed odd-mass nuclei, 18: 38118
development for negative parity states in even-even nuclei, 20: 10096
development for negative parity states in deformed even nuclei, 19: 27535
differential cross sections in, 17: 11699
energy level excitation by alpha and helium-3 scattering (T), 19: 3250
energy level parameters in, relation to shell model, 20: 36174 (PUC-937-163)
energy level structure of odd-A nuclei in, nitrogen-15 experiment for, 18: 32749 (UCRL-11378)
energy level structure for $150 < A < 190$ and $228 \leq A \leq 254$ nuclei in, 2+, 18: 34760 (JINR-E-1696)
energy level symmetries for mass-40 nuclei in, 18: 34897
energy level transition probabilities in, electromagnetic, 18: 34761 (JINR-E-1703)
energy levels and transition probabilities as function of rotation frequency of deformed nuclei in, 18: 28615
energy levels in nonspherical nuclei, vibrational, 16: 1085
energy levels in phenomenological deformed, rotation and vibration, 19: 12603
energy levels of deformed odd-even nuclei in, 18: 28611
energy levels of light nuclei in, properties of low-lying, (T), 19: 14519 (CONF-640301(p.165-81))
energy levels of odd-mass nuclei with spin-½ considered as asymmetric rotors, 18: 30714 (BLG-223)
energy levels of single-particle states in light nuclei, 16: 1083
excitation of collective states by heavy-particle inelastic scattering, (T), 19: 21234 (JINR-P-1908)
excitations in, description using model fermion system, (T), 19: 6635 (JINR-P-1830)
excitations of collective rotational and vibrational states in, (T), 19: 14518 (CONF-640301(p.143-64))
for energy levels and gamma spectra of even-even nuclei, 16: 33850
for energy levels of spherical nuclei, 16: 33872
for vibrational energy levels of even-even nuclei, 16: 33873
formulation of breathing-mode, (T), 20: 38170
formulation with breathing-mode state, (T), 20: 42245
fragmentation of nuclei by high-energy particle scattering in, "shock-wave" mechanism for, 18: 28621
gamma absorption by heavy nuclei in, 18: 13090
gamma transitions in even nuclei in, 17: 17172
gamma transitions after neutron capture in, 18: 11167 (ANL-6797 (p.194-210))
hamiltonian of, microscopic method for collective excitation, (T), 19: 10291
iron-57 structure in "core-excited state model", 18: 32750 (USNRDL-TR-742)
isobaric states in, description of transitions between, 19: 1631
many-body problem in, 18: 44731 (LA-DC-6098)
mass scheme for elementary particles, resonances, and hyperfragments using, 18: 14963
modes of motion for translationally invariant interactions, 16: 8293
motions in giant photonuclear resonance, 16: 4840
nuclear potential energy in, 20: 28289 (UCRL-16768)
nuclear spectra from, collective effects in, 17: 4110
nuclei physical quantity calculations from, computer programs for even-even, 20: 6278 (AD-623877)
nucleon potentials for, (T), 19: 14514 (CONF-640301(p.22-38))
octupole vibrations of deformed even-mass, 18: 18991
parameters for even-even deformed nuclei in, 17: 11732
photon emission, analysis of (M1 + E2), 16: 1068
properties of heavy spherical nuclei in, 18: 9329
properties of, lectures on, 18: 21189 (KR-64(Sect.VI))
properties of, lectures on, 18: 21191 (KR-64(Sect.VIII))
relation to shell models, 17: 24512
review, 18: 36690
scattering, cross sections for inelastic diffraction, 17: 7205
single-particle aspects of, residual forces in, 18: 42645 (NP-14338)
structure of states of even deformed nuclei in, (T), 19: 8397 (JINR-P-1811)
symmetry in rotational, sum rule and energy relations from, (T), 19: 10279
testing excited-core odd-A, by copper-63(p,p') and nickel-62(p,p') reactions, 17: 19335
theory of, dynamic, 18: 19095
use for describing residual interactions in shell model, 17: 33064
use for level parity and spin assignments, 20: 15726 (ORNL-P-1957)
use in calculating neutron scattering on sodium-23 at 0 to 4 Mev, 18: 24597 (NP-13930(p.15))
use in predicting excited states in sodium-23, 18: 21327
uses of, for interpreting dipole excitation of nuclei, 17: 22585
vibrational motions of spherical odd nuclei in (T), 19: 3317
vibrational spectra of even-even nuclei in, 18: 42758
vibrational states of spherical nuclei in, 17: 17285
wave function calculations in, variational methods for, 17: 2297
wave functions in, calculation from model Hamiltonian, 16: 28356

NUCLEAR MODELS (DROP)

asymmetry of fission, (T), 20: 46632
charged particles emission in, 18: 26629
configurations of rotating, with high angular momentum, 18: 24733
corrections for shell effects, (T), 20: 46610(T) (ANL-Trans-353)
decay of high angular momentum, gamma distributions from electromagnetic, 19: 27545
deformation energies and fission behavior in, 16: 24803
deformation energy and fission behavior in, 17: 28262
deformation energy of charged liquid drop, 17: 41532(R) (ANL-6720 (p.59-66))
development and properties of, 20: 34657
electron scattering by quantized, theory, 16: 18507
energy level transition densities in, surface oscillations in, (T), 19: 6716
equilibrium configuration, approximate method for calculating, 16: 19898

equilibrium configuration and fission barrier for, at high angular momentum, 17: 17241
equilibrium shapes in, 16: 33863
equilibrium shapes of rotating charged drop, 17: 28258 (UCRL-10775)
equilibrium shapes from, 18: 11286
equilibrium shapes from, stability of, 18: 11287
fission calculations by, 17: 33009(T) (UCRL-Trans-978)
fission in, (T), 19: 37873
fission in, angular momentum effects in (E/T), 19: 1679
fission in, nuclear moment of inertia at, (T), 19: 37894
fission in, theory for, 18: 34778 (UCRL-11338)
fission in, theory of, 19: 35430
fission of axisymmetric nuclei in, (T), 19: 6698
fission product distributions in, shell effects on, (T), 20: 6308(T) (ANL-Trans-243)
fission properties in, (T), 19: 37836 (UCRL-11338(Rev.1))
fission-barrier energies and shapes in, (T), 19: 41767
for shape of fissioning nuclei at saddle point, (T), 19: 19096(T) (ANL-Trans-157)
mass formulas from, (T), 19: 29346
nuclear equilibrium shapes for, symmetrical, 18: 9362
nuclear moment of inertia at fission saddle point in, (T), 20: 17849
nuclear reaction theory from, 20: 4879
nucleon binding energies in single-particle, 17: 19231(T) (AEC-tr-5702)
nucleon shell effects on energy of nuclei in, 20: 26215
of axially symmetric nuclei fission, 19: 26917(R) (IA-984)
performance for describing fission reactions, 18: 21194 (KR-64 (Sect.XV))
review, 19: 3248
statistical model approximation by quasi-static, 17: 36670(T) (AEC-tr-5955)
surface diffuseness in, 16: 33874
symmetrical shapes of equilibrium in, 16: 32448
theory for asymmetric fission, 20: 28319
theory for fission, 18: 38199
thermodynamics of, superfluid phase transitions in, 17: 38214
uniformly charged liquid, saddle-point shapes for, 17: 22264(R) (ANL-6679)
use in calculating density distribution in nucleus, 18: 32857
validity for alpha fission, 18: 2848 (UCRL-11006)
variational problems in, invariant trial functions for solving, 17: 20985 (JINR-P-1187)
variational problems in superfluid, projection operators for, 17: 32738
with compressibility, 17: 22569(T) (AEC-tr-5783)
zero-point oscillations in, 18: 15216

NUCLEAR MODELS (OPTICAL)

alpha elastic scattering by carbon-12 at 48 Mev, 18: 32747(R) (UCRL-11213(p.64-86))
alpha inelastic scattering in extended, excitation of collective modes in, 17: 38257
alpha scattering on complex nuclei, analysis of, 18: 24712
analysis for elastic scattering of 10-Mev protons, 17: 24750(R) (UCRL-10624)
analysis of (He-3,t) reactions, 18: 26596
analysis of deuteron elastic scattering by nuclei at 1 to 20 Mev, 16: 12514
analysis of deuteron elastic scattering angular distributions at 11–27 Mev, 17: 40104
analysis of direct photonuclear effect cross sections and polarization, 16: 12575
analysis of neutron scattering by deformed nuclei, at high energies, 16: 8228
application to light nuclei, 18: 30729 (NP-14056)
average resonance parameters in, 17: 7244
bibliography on, annotated, 18: 30728 (NP-14055)
book: *Contemporary Models of the Atomic Nucleus*, 19: 21463
book: *Optical Model of The Atomic Nucleus*, 19: 35508(T)
book: *The Optical Model in Nuclear and Particle Physics*, 17: 33108
book: *The Optical Model of Elastic Scattering*, 18: 15303
book: *Unified Theory of Nuclear Models*. (T), 19: 1655
calculation of deuteron stripping cross sections and angular distributions, 18: 9437
calculation of proton-induced reaction cross sections, 16: 2492(R) (TID-14186)
calculations for neutron elastic scattering by calcium at 0.7 to 18 Mev, 16: 33846
collective potential in, effects on S- and P-wave strength functions, 16: 26334
complex effective mass in calculation of the potential of, 16: 26229 (PAN-304/VII)
cross sections for compound-nucleus formation, resonance contributions to calculations, 16: 21624
cross sections for virtual mesons (π), 18: 30821
cross sections for compound-nucleus reactions in, 19: 17011
cross sections in, energy-independent strength function for, 18: 15268
density distribution in light nuclei, (T), 19: 31256
description of proton reactions (p,n), 16: 11034
deuteron and nucleon potentials in, real parts of, (T), 19: 23712
deuteron and nucleon potential calculations in, (T), 20: 11570(T) (ANL-Trans-258)
deuteron elastic scattering analysis of 11.0 and 11.8 Mev, 17: 38192
deuteron elastic scattering in, potential for, 17: 38203
deuteron elastic scattering in, energy dependence of angular distributions from, 18: 1052
deuteron elastic scattering at 27.5 Mev, 18: 19003
deuteron potential in adiabatic approximation, (T), 20: 46655
deuteron reactions (d,p) with silicon-28 at 15 Mev, parameter variation effects on angular distributions and polarizations in, 17: 38251
deuteron reactions at 11.8 and 19.6 Mev, parameters for, 18: 1051
deuteron scattering on nickel at 21.6 Mev, polarization predictions for, 17: 38247
deuteron scattering on nickel at 21.6 Mev, parameters for, 17: 38190
deuteron stripping reaction parameters in, 16: 26300
development and properties, 17: 17279
development for meson (π) elastic scattering, (T), 20: 42319
effects of form factor distortion in, 17: 40025
effects on barrier penetration of nuclei, (E), 20: 10047
energy level scattering studies, velocity-dependent nuclear potentials for, 16: 2497 (UCRL-6552)
evaluation for neutron reaction studies, 18: 24594 (NP-13930(p.1-5))
exact solution of equations of, for analysis of (p,n) reactions, 20: 42243
fitting to proton elastic scattering angular distributions, 16: 7955(R) (PR-P-51)
for deuteron elastic scattering at 22 Mev by calcium, absence of tensor term in, 18: 9378
for nuclei with polynomial potential, 16: 7140
for proton inelastic scattering by complex nuclei, distorted-wave approximation for, 17: 26629
formulation and history, review, 20: 40162
fringe absorption relation to neutron strength function, 16: 26212
heavy ion scattering analysis with, 17: 22550 (BNL-6931)
helium-3 elastic scattering by metals at 20 Mev, differential cross sections, 18: 26681
isobaric states in, description of transitions between, 19: 1631
multiple scattering corrections to the optical potential, 16: 28104
neutron absorption in, shell model effects in, 18: 38155
neutron absorption cross sections for nuclei with $20 \leq A \leq 240$ from 0.1 to 25 Mev, (T), 20: 46583 (IKF-17)
neutron elastic scattering at 0.275 to 0.85 Mev, analysis for $A \sim 100$, 18: 6241
neutron elastic scattering in, analysis of, 18: 15221
neutron elastic scattering by lead and molybdenum at 3.3 and 3.7 Mev, analysis of, 18: 15222
neutron elastic scattering in, 18: 34828
neutron inelastic scattering and radiative capture in, cross sections for, 17: 33048
neutron P-wave strength functions in, 17: 724
neutron reaction cross sections for medium and heavy nuclei in, 18: 42673
neutron reactions (n,α) and (n,p) with nuclei ($23 \leq A \leq 77$) at 5–25 Mev, statistical analysis of cross sections for, 17: 38212
neutron reactions below 1 Mev in spherical nuclei, 17: 40042
neutron scattering on carbon-12 at 30 Mev, wave-function localization in, 17: 38183
neutron scattering on carbon-12 and oxygen-16 in, bound states in, 18: 6211
neutron scattering and absorption cross section calculations by, 18: 26663
neutron scattering by uranium-238 in rotational, fast, 18: 38133
neutron states in deformed optical potential, 20: 38126
neutron strength calculations for s- and p-wave functions, 16: 6949
neutron strength functions in, 16: 1015
neutron strength functions in, collective vibration effects on p and s-wave, 17: 38197
neutron surface absorption by, low-energy, 17: 7212
neutron transmission in, 17: 32968 (BNL-765)
neutron transport cross sections in, 17: 17472
neutron-reaction (n,α) and (n,p) cross sections from, 18: 28666
nuclear cross sections in, computer program for, 19: 31221 (KAPL-3085)
nuclear potential in, 16: 29874
nuclear surface by analysis, 18: 40610
nucleon elastic scattering in, 18: 30836
nucleon interactions in, one pion exchange approximation to potential for, 17: 38191
optical potential of heavy nuclei, 17: 2324
parameters for neutron scattering by zirconium, 16: 8169 (TID-14569)

parameters for nucleon–nuclei interactions, (T), 19: 27503
parameters for proton reactions, 16: 12434(R) (NIRL/R/15)
parameters of, s-wave transmission coefficient effects of, 18: 34866
particle scattering with excitation of collective energy levels, (T), 20: 8151
phase relations between partial waves in, 17: 849
potential and reduction factor for nonlocal wave function in, Perey effect for equivalent local, (T), 20: 13811
potential calculation for nucleon-nucleus reactions, 16: 10832
potential, calculation of imaginary part for nucleon-nucleus reactions, 17: 22663
potential expressions for meson (π) scattering by nuclei, second-order, 16: 7074
potential expression for (p,p) scattering by heavy and light nuclei, 17: 9539
potential for alpha reactions with cobalt-59, (E/T), 20: 19815 (INP-440/PL)
potential for excited states in, using Fermi gas model, 20: 3116
potential for nucleon scattering, 18: 13064
potential for nucleon scattering, (T), 19: 16931
potential for particle scattering, universal, (T), 19: 27572
potential for rearrangement reactions, 16: 17132
potential for spin-spin interaction in nucleon-nuclei reactions, low-energy, (T), 20: 6395
potential for, energy and isotopic spin dependence of, 18: 11257
potential for, energy-dependent nonlocal, (T), 20: 46641
potential, including surface absorption effects, 16: 23089
potential of, isotopic spin dependence of, 17: 29618
potential of, pairing correlation and, 17: 13517
potential of, reciprocity relations for, 18: 12971 (NASA-TN-D-1985)
potential parameters for deuterons, 18: 6229
potential parameters for deuterons, 20: 12095
potential, shape of imaginary part, 16: 21540
potentials and two-body forces in, charge-exchange effects on, 17: 2278
potentials for alpha elastic scattering by nuclei, 18: 32836
potentials for composite particles, approximate relations for strengths and shapes of, 20: 42280
potentials for high-energy two-nucleon interactions, 16: 19691
potentials for nucleon elastic scattering at high energies, nonlocal and target-momentum effects on, 18: 7772
potentials for nucleus-nucleus elastic scattering, 18: 32836
potentials for nucleon scattering, surface and nonlocal corrections to, 18: 42782
potentials for nucleon and complex scattering in (T), 19: 3239 (MIT-2098-67)
potentials for two-body scattering at relativistic energies, 20: 34594
potentials in, ambiguities for strongly absorbed particle scattering from, 17: 34944
potentials in, dependence on isobaric spin, 16: 26285
potentials in, distorted wave analyses from complex, 17: 38184
potentials in elastic scattering, S-matrix formalism for, 20: 12021
potentials in, for proton elastic scattering, 16: 31119
potentials in, for nuclear reactions and scattering, 16: 33798
potentials in, for (p,n) reactions, 17: 2279
potentials in, for nucleon scattering by nuclei, 17: 2280
potentials in, foundation of effective complex, 17: 38181
potentials in, Green's function techniques for, 17: 38200
potentials in, nucleon scattering for equivalent local and nonlocal, 17: 38185
potentials in, radial distributions of imaginary, 17: 19319
potentials in, analysis of, 20: 34607
potentials in, effects of non-locality in off-diagonal, (T), 19: 29299
potentials in, energy dependence and nonlocality of, (T), 20: 15829
potentials in, for nuclear spectroscopy, 20: 12047
potentials in, radial distribution of imaginary part of, (T), 20: 12129
potentials in, spin-orbit part of, (T), 20: 22116
potentials of, local energy approximation for nonlocal, 18: 28683
potentials of, relation to nuclear–matter dissipation constants, 18: 15316
potentials without Coulomb correction, symmetry term in, (T), 20: 46675
properties of isobaric analog states in, from (p,n) reactions, (E/T), 19: 14493 (ANL-6878(p.215-29))
proton elastic scattering, at 8 to 17 Mev, 16: 4803
proton elastic scattering at 10 Mev, cross section analysis for, 17: 38193
proton elastic scattering by copper at 12.29 Mev in, 18: 19054
proton elastic scattering by nuclei at 30.3 Mev, differential cross sections for, 18: 36631
proton elastic scattering by nuclei at 30 Mev, polarization in, 18: 36633
proton inelastic scattering in, excitation of collective states in, 18: 2898
proton penetrabilities and cross sections in, 18: 15175 (CEA-2379)
proton reactions (p,n) with mirror nuclei in, polarization in, 18: 38072 (UCRL-7676)
proton reactions (p,α) and (p,He^3) at 3–12 Mev, cross sections and excitation curves for, 17: 38294
proton reactions (p,n) in, isospin potential from, 17: 38201
proton scattering analyses in generalized, 17: 19342
proton scattering in, parameters and wave functions for, 17: 38198
proton scattering on copper at 7–17 Mev, surface absorption in, 17: 38199
proton scattering by nuclei at 30 Mev, total cross sections for, 18: 36632
proton scattering parameters in, experimental uncertainty of, (T), 20: 17768
reaction cross sections in, (T), 19: 6632 (JINR-P-1795)
relativistic characteristics of, 20: 15730(R) (RHEL/R-112, pp 67-98)
resonance structures in generalized, from neutron scattering by spin-zero nuclei, 20: 24469
review of, 20: 24418
role of deformation parameter in, from elastic differential proton scattering cross sections of heavy nuclei, 18: 2915
S- and P-wave strength in surface absorption, 18: 18988
scattering between mirror states in, charge-exchange quasi-elastic, 17: 38188
scattering in, elastic, 18: 36698
scattering of spinless charged particles by even-even nuclei, calculations, 18: 26678
scattering theory for, matrix elements and parity rules for inelastic, 18: 26651
second-order potential for nucleon-nucleus scattering, 16: 28093
single-particle radiation transitions in, 19: 21442
spin-orbit coupling in, determination from P-wave strength functions, 17: 26637
survey of recent data, 16: 3747
theory of, formal, 17: 17067
theory of low-energy nuclear reactions, 17: 11740
theory of neutron reactions and scattering, 17: 34852
threshold effect in elastic scattering according to, 17: 4092
triton elastic scattering by light nuclei in, 18: 19022
use for analysis of elastic scattering and direct nuclear reactions, 20: 19989
use for calculating transmission coefficients and absorption cross sections for neutrons and protons, 18: 24595 (NP-13930(p.6-13))
use for description of low-energy excitations in nuclear matter, 18: 40582
use for level parity and spin assignments, 20: 15726 (ORNL-P-1957)
use for proton differential elastic scattering cross sections, 20: 21963 (AD-626656)
use for proton inelastic scattering calculations, 20: 11974 (ORNL-P-960)
use in analysis of scattering of 14-Mev neutrons by light nuclei, 18: 1048
use in analysis of spin-zero elastic scattering, computer program for, 18: 18878 (NASA-TN-D-2120)
use in analysis of deuteron elastic scattering, (E/T), 20: 3053
use in analysis of polarized proton scattering data, 20: 34672
use in analysis of neutron scattering by nuclei, 20: 34673
use in analysis of neutron scattering cross section data, 20: 41796(R) (MIT-2098-251, pp 74-103)
use in calculating neutron scattering on sodium-23 to 0 to 4 Mev, 18: 24597 (NP-13930(p.15))
use in calculation of neutron cross sections, 17: 2269
use in calculation of neutron elastic scattering cross sections, 18: 32726 (AERE-R-4649)
use in calculation of neutron cross sections, 18: 40507 (KAPL-3020)
use in interpretation of meson (π)-nucleus interactions in the π-mesic atom, 18: 15203 (NP-13679)
use in localization of direct interactions of nucleons within nuclei, 18: 2923
use in neutron cross section calculations, 18: 38055 (TID-20943)
use in neutron scattering analysis, 17: 13536
use in neutron scattering by polarized deformed nuclei, 18: 19017
use in neutron scattering analysis of nitrogen-14, 19: 5132 (NP-14480)
use in nuclear structure analysis, (T), 20: 21978 (BNL-948, pp 454-524)
use in nucleon scattering at medium energy, 18: 38080(T) (AEC-tr-6398 (p.120-5))
use in proton scattering studies at 30 Mev (E/T), 19: 3315
uses for computer analysis of reactions, (T), 19: 31232 (ORNL-TM-1117)
uses for nuclear analyses, 20: 15730(R) (RHEL/R-112, pp 67-98)
wave equations for inelastic particle scattering in, hamiltonian and lagrangian formalism for, 20: 34548
wave functions for strongly absorbing nuclei, 16: 2510

NUCLEAR MODELS (SHELL)

alpha cluster reduced widths in light nuclei, 18: 24588 (JINR-P-1595)
alpha clusters in, single-pole Majorana forces and nucleon coupling in, 18: 28617
alpha decay in, hindrance of, (T), 19: 16978
alpha decay of deformed nuclei, (T), 19: 47597 (UCRL-16187)
alpha decay rate near lead-208, 17: 29601
analysis from quasi-free scattering, review of, (T), 20: 10082
analysis of oxygen energy level spectra by, 17: 28302

approximation for, quasi-particle random-phase, 18: 18883(R) (TID-20378(Sect.2))
beta decays of odd nuclei in, neutron-proton pairing effects on (E/T), 19: 3311
beta-decay asymmetry parameters and signs of beta moments in, 20: 10097
binding energies in, configuration mixing effects on, 20: 28416
binding energies of 1p shell in harmonic oscillator, U_3 symmetry and clustering for, 20: 26146
binding energies of s-d shell nuclei, quadrupole correlations in, (T), 20: 44818
binding-energy differences in mirror nuclei, (T), 20: 46776
book: *Contemporary Models of the Atomic Nucleus*, 19: 21463
book: *Group Theoretical Methods in Shell Models of the Nucleus*, 19: 21444
book: *Nuclear Shell Theory*, 17: 15309
book: *Unified Theory of Nuclear Models*. (T), 19: 1655
calcium-42 energy-level spectrum in, effects of deformed states in, (T), 20: 13839
calculation of nuclear matrix elements for beta decay, 16: 8179
calculations, 19: 9771(R) (PR-P-63)
calculations in, boundary-condition constraints for, 19: 27557
calculations in, computer program for, 19: 45254 (CST-1213)
calculations in, graphic method in, 19: 27509
calculations of alpha decay rates of spheroidal even nuclei, 16: 32417
calculations of alpha decay rates near lead-208 by simplified, 17: 24403 (UCRL-10414)
calculations of lead-208 excited states in, 16: 32428
calculations of nuclear energy levels by, 17: 4109
calculations of two-body forces, 18: 17054
calculations with, fractional parental coefficients for, 17: 31543
cluster-coupling, for oxygen-16, 17: 21073
coefficients of translation-invariant, genealogical, 18: 9346
collective effects in, nucleon-potential models for, (T), 19: 14514 (CONF-640301(p.22-38))
collective excitations of spherical nuclei, 16: 8190
collective motion in even-even deformed nuclei in, 17: 11732
collective motions in, effects of spin-dependent forces on, 16: 23093
collective motions in, 17: 24512
collective particle effects in, 16: 2484 (NP-10931)
collective states with unlike pair excitations, 18: 30826
comparisons with alpha-model, 17: 7189
compound nuclear states in, from unified nuclear reaction theory, 18: 34773 (NP-14190)
configuration centroid energies and widths for ds shell, (T), 20: 46712
configuration mixing effects in carbon-14, (T), 20: 12155
configuration mixing in, (T), 20: 24332(R) (ANL-7108, pp 67-73)
configuration-mixing effects on stripping reactions, (T), 19: 6706
core deformability and electric quadrupole moments, 16: 7026
correlation corrections for amplitudes in, 19: 14601
deformation of light 1p nuclei in, 18: 42725
deformations in, uses in calcium spectroscopy, 20: 9974 (PUC-937-171)
derivation of residual-interaction terms in deuteron stripping reactions (d,p), 17: 41921
description of light nuclei using Brueckner model, nucleon-nucleon interactions in, (T), 20: 46652 (ORNL-P-2468)
description of, with collective and superconducting corrections, 17: 33064
deuteron and triton reduced widths in, 18: 38139
deuteron potential in adiabatic approximation, (T), 20: 46655
deuteron stripping in, 17: 40036
deuteron wave function in, 20: 19273(R) (BNL-929, pp 3-43)
development and properties of, 20: 34657
doublet splittings in, nucleon-nucleon potentials from, 17: 40031
effectiveness of, in explaining properties of nuclear matter, 17: 31416
electron conversion probabilities in, 18: 11271
electron inelastic scattering calculations for, isospin selection rules for, (T), 19: 31270
energy calculations in, 18: 36691
energy level calculations, 17: 11739
energy level calculations of single-particle states in, 17: 40118
energy level calculations for $28 \leq A \leq 40$, 18: 32782
energy level calculations for $28 \leq A \leq 40$, 18: 32783
energy level calculations for $28 < A \leq 40$, 18: 36697
energy level calculations for $90 \lesssim A \lesssim 100$, 19: 23163(R) (ORNL-3650 (p.111-86))
energy level calculations from, $28 < A \leq 40$, 20: 6295 (NP-15647)
energy level calculations for odd tin isotopes, 20: 21962 (AD-624214)
energy level parameters in, relation to collective model, 20: 36174 (PUC-937-163)
energy level properties in, for A = 28 to 40, (T), 19: 14512 (CONF-640301(p.1-12))
energy level properties of oxygen-16, ground state, (T), 20: 13785 (ORNL-TM-1374)
energy level shifts in, (T), 19: 16980
energy level spacings in, parameters for, 17: 38163
energy level spin-orbit splitting from two-nucleon potentials in, 18: 6190
energy level structure of nuclei with $29 \leq A \leq 40$, (T), 20: 1231
energy level structure of niobium-91, (T), 20: 12157
energy level transitions in spherical nuclei, branching ratios for (T), 19: 1694
energy level transition calculations for even nuclei, E0, 20: 13746 (AD-626681)
energy levels and transition rates in, 18: 42627(R) (ANL-6879(p.88-113))
energy levels and potential in, single-particle, 20: 26198
energy levels from, computer program for bound, 19: 19082 (CRT-1213)
energy levels in bounded isotropic harmonic oscillator potential in, 18: 42656
energy levels in continuum region, (T), 20: 46650
energy levels in, studies using (p,d) pickup reactions, 16: 26258
energy levels in silicon-28, particle-hole, 18: 19086
energy levels in 1p shell with abnormal parity, wave functions for (T) 19: 3334
energy levels in, particle-hole wave equations for, 18: 42699
energy levels in, one-nucleon (T), 19: 3279
energy levels in, single-particle, (T), 19: 29353
energy levels in, jj-coupling model for spurious, (T), 19: 39812
energy levels in, four-body operator for classification of, (T), 19: 47678
energy levels in, analog states for, 20: 9978(R) (TID-22462)
energy levels in, neutron single-particle, (T), 20: 19849
energy levels in, fractional parentage coefficients for f^3 and f^4 configurations of, 20: 30365
energy levels in, elimination of spurious, 20: 30514
energy levels in, spin-spin coupling and shell closure for, 20: 36187
energy levels in, isobaric analog, 20: 36198
energy levels of lithium-6 in intermediate-coupling, 16: 26276
energy levels of light nuclei in, properties of low-lying, (T), 19: 14519 (CONF-640301(p.165-81))
energy levels of nuclei having several 2s–1d nucleons in, 19: 27437 (NRL-6256)
energy levels of polonium-212 in, (E), 20: 24358(R) (UCRL-16580, pp 1-93)
energy levels of two-dimensional nuclei in, 20: 19854
energy levels in, review of collective vibrations in, (T), 20: 10079
energy levels, threshold and rearrangement-energy effects, 16: 12485
energy of nucleus as function of deformation and nucleon number, 20: 9965 (IAE-878)
energy splittings of spin-orbit doublets in, 16: 33884
energy-level transitions in nuclei with A = 14 to 18, mixing ratios for, (T), 20: 44784
estimation of magnetic moments in odd A nuclei, 16: 1054
even parity energy levels in oxygen-16 in jj-coupling, 19: 39806
excitations of collective rotational and vibrational states in, (T), 19: 14518 (CONF-640301(p.143-64))
extension to describe inelastic nucleon scattering, 19: 14642
fission product distributions in, (T), 20: 6308(T) (ANL-Trans-243)
fission theory as Markov process in, corrections for, 20: 30428
fluorine-18 even-parity levels in, 18: 24685
fluorine-19 energy levels in, negative-parity, 18: 26592
for energy levels of iron-57, 16: 33854
for nuclei with $28 \leq Z \leq 82$ by, with simple residual forces, 17: 24381 (AD-603411)
for systems of identical nucleons, (T), 20: 24386
forces in, Schroedinger equation solution for realistic, (T), 20: 10052
formulation of and connection with other nuclear models, lecture on, 17: 17302
formulation of and connections with other models, 17: 17305
foundations of, 17: 19333
foundations of, 18: 42770
fractional parentage coefficients, in multi-shell configuration, 16: 1079
gamma emission in, analysis of *l*-forbidden M1, 17: 21045
gamma E1 absorption, effects of mass number, 16: 19784
gamma reactions (*γ*,d) with light nuclei, threshold shift for fast deuteron emission in, 17: 41985
gamma transition probabilities in, effects of residual interactions, 16: 21432
generalized quasi-spin in neutron-proton systems, 20: 3046
Green's functions in classical, 18: 24615 (NP-13959)
Hartree-Fock calculations with parity mixing, (T), 20: 40138
hole-particle interactions in, 17: 7192
interaction matrix elements in, 17: 17217
interactions of nuclei in, single-particle representation of deformed orbitals in s-d shell, 18: 2913
intermediate coupling application to 1p shell, 16: 11014
isobaric analog states of heavy nuclei in, energy calculations with

neutron pairing effects, 18: 28635
lithium-6 wave function in, configuration mixing in, (T), 19: 16930
many-body problem in configuration-mixing and intermediate-coupling, 18: 44731 (LA-DC-6098)
many-nucleon states in, seniority-reduced-isospin scheme for, (T), 19: 29310
many-nucleon systems in, 18: 34826
mass formula in, semi-empirical, (T), 19: 8428
mass formulas from, (T), 19: 29346
mass-12 energy levels from, 18: 26624
matrix elements for nucleon configurations, particle number dependence of, 19: 16921
matrix elements for central and tensor interactions in, tables of reduced, 20: 26134
matrix elements for $(1d_{5/2}, 2s_{1/2})$ configuration in oxygen isotopes, (T), 20: 44749
matrix elements in SU3 classification scheme, calculation of, 17: 19346
meson (π) elastic scattering cross sections in, 18: 44801
meson (μ) nuclear capture analysis by, 16: 23088
meson (π^-) capture in studies on, 17: 11687
motion of many-body systems in, separation of center-of-mass, 18: 28690
negative parity states in (2s,1d) shell, 17: 33092
neon-20 energy levels from, 18: 36666
neutron cross section calculations with statistical, in kev region, 17: 34859
neutron-proton interaction between states of the same l in, 16: 28152
neutron resonance scattering structures in continuum, configuration mixing in, 18: 26531 (LADC-6007)
neutron scattering analysis by harmonic oscillator potentials, 16: 3662
neutron scattering resonances in, with formation of particle-hole states, 18: 18890
neutron-proton interaction in, 18: 38115
neutron-proton interactions in j-j coupling, effective, (T), 19: 35431
neutron-proton residual interaction in, experiment and theoretical interpretation for, 18: 28578 (ORNL-3638)
nitrogen-14 lower levels in, 17: 22620
nuclear bound states in nonlocal, 20: 42301
nuclear forces in isobaric triplet A = 6, charge independence of, (T), 19: 5181
nuclear quadrupole moments correction estimations, 16: 8240
nuclear spectra in, Brueckner-Bethe-Goldstone theory for, 20: 34648
nuclear spectra in, intermediate coupling calculations for, 20: 36188
nuclear surface oscillations of, semi-classical description of, 17: 40019
nucleon binding energies in, pairing corrections to, (T), 19: 29347
nucleon clustering in, 18: 4606
nucleon clustering in, reduced widths for, 18: 34891
nucleon clustering in, reduced widths for, 18: 28680
nucleon coupling parameters in, sensitivity of, 20: 4835 (JINR-P-2287)
nucleon energy spectra in, for spherical nuclei, 16: 28114
nucleon grouping in shell-model states, fractional parentage coefficients for three-particle, 18: 24621 (PAN-449/VII)
nucleon grouping in oxygen-16, 19: 8494
nucleon interactions in chlorine-38 and potassium-40, 17: 24507
nucleon interactions in oxygen isotopes, effective, 17: 33100
nucleon interactions in, 18: 34869
nucleon interactions in, representation of residual, 18: 44545
nucleon interactions and configuration mixing in, 19: 25541
nucleon interactions in $2s_{1/2}1d_{3/2}$ shell, surface delta interaction approximation of, 20: 30423
nucleon interactions in single j-shell with charge-independent pairing force, calculations using BCS method, (T), 20: 44734
nucleon orbital fractional parentage coefficients in 2s-1d shell, SU(3), 19: 45266 (JINR-E-2285)
nucleon pairing approximation for $f_{7/2}^-$ and $p_{3/2}^+$ shells, (T), 20: 44684
nucleon pairing correlations in, conservation of nucleon number in formalism for, (T), 20: 10027
nucleon pairing energies, 16: 3700
nucleon pairing energies for residual interactions in, 17: 24504
nucleon pairing energy in alpha-particle models with degenerate shells, 20: 8087 (ZFK-TPH-16)
nucleon pairing forces in, 16: 23078
nucleon pairing interactions in translationally invariant, group-theoretical treatment for, 20: 44699
nucleon pickup reactions in, calculations for, 18: 36605
nucleon recoupling and fractional parentage in 2s-1d shell, SU_3, 19: 3310
nucleon shells in nuclei with Z > 82 and N > 126, closed, (T), 20: 44640 (JINR-P-2793)
nucleon shells of nuclei with N ≥ 126 and Z ≥ 82, (T), 20: 44774
nucleon systems in, wave functions for self-bound, (T), 19: 8475
nucleon systems, Talmi coefficients for motion isolation, 16: 3627
of complex nuclei, 19: 32048(R) (NP-15073)
oxygen-16 energy levels in unitary, (T), 19: 6682
oxygen-16 energy levels in, 20: 24358(R) (UCRL-16580, pp 1-93)
oxygen-16 odd-parity levels from, 18: 24649
oxygen-18 energy levels from, potentials for, 18: 26639
oxygen-18 even-parity levels in, 18: 24685
pairing correlations in gamma transitions using, 18: 15251
pairing energies in superfluid, 18: 9371
parentage coefficients in, 3-nucleon $\langle p^n|p^{n-1},p^1\rangle$ fractional, 18: 30742
Pauli exclusion principle in, development and application of, 19: 21275
performance for describing fission reactions, 18: 21194 (KR-64 (Sect.XV))
performance in light and heavy nuclei, 17: 13591
photonuclear reactions in, spin-orbit effects on, 17: 7167
photoproton production cross sections in, 19: 14528 (LAL-1120)
physical concepts and uses, review, 16: 18177 (NP-11463(Pt.1) (p.139-47))
potassium-40 energy levels from, 18: 24634
potential boundary diffusion in, 16: 18176 (NP-11463(Pt.1)(p.133-7))
potential for Hartree-Fock, calculations of effective, 18: 11219 (TID-20105)
potential for one-nucleon definite j-value state in, (T), 20: 15791
potential for structure calculations, 19: 16969
potential parameters for calculations using, 20: 38145
potentials for calculation of nuclear properties, (T), 20: 42247
potentials for gamma spectra in, for two nucleon pairs outside closed shells, 16: 23094
potentials in, effective range of residual, 17: 40116
potentials of, local energy approximation for nonlocal, 18: 28683
potentials without Coulomb correction, symmetry term in, (T), 20: 46675
properties, 20: 3149
properties and uses of, (T), 19: 37205(R) (ORNL-3778)
properties of heavy spherical nuclei in, 18: 9329
properties of 28 < N < 50, 20: 6435
properties of, lectures on, 18: 21188 (KR-64(Sect.V))
proton momentum distributions in, 16: 26273
quadrupole vibration effects on l-forbidden M1 transitions, 17: 34881 (NP-13050)
random-phase approximation for singular hard-core potentials in, 19: 14602
reaction matrix for, calculation of effective, 20: 30354(R) (ORNL-3940, pp 62-9)
research progress on, 17: 41532(R) (ANL-6720(p.59-66))
research progress on, 18: 15172(R) (AROD-1784 : 31)
resonance in Bloch shell, thermal motion effects on, 18: 6185(T) (SC-T-526)
resonance reactions in, 18: 11182 (ANL-6797(p.342-57))
review, 18: 6289
review, 18: 40629
rotation and vibration effects in calculations by, 16: 21622
S-state interactions of, pairing-type properties for, 18: 9382
scattering analysis in, inelastic, 20: 12008
scattering in, computer programs for Slater integrals for inelastic, 19: 1565 (ORNL-TM-964)
seniority scheme for degenerate levels, (T), 19: 6649
single-nucleon damping of collective vibrations in, 17: 24179
single-particle energy changes from pair-distribution variation, 16: 3682
single-particle aspects of, residual forces in, 18: 42645 (NP-14338)
solutions for pairing plus quadrupole-quadrupole interactions, 16: 21507
spatial symmetry in, jj-coupled wave-function classification from, (T), 20: 19932
spectra of giant dipole resonances in light nuclei, 18: 22918
spectroscopy in the $1f_{7/2}$ shell, 18: 21275
spin-orbit interactions in, 18: 21192 (KR-64(Sect.IX))
spurious-state exclusion using normal coordinates, 16: 11134
surface properties of nuclei with near-full shells, 16: 1080
tensor-force effects in, 17: 34887 (UCRL-10865)
theory for compound nuclear reactions, 20: 8128
theory for resonance states in nuclear reactions, 19: 19195
theory of, many-body foundations of, 20: 13790
three-particle j = 7/2 shell in, fractional parentage coefficients for, 18: 36580 (UCRL-7506)
use for crystal lattice dynamics analysis, 20: 26347 (NP-16010, pp 42-101)
use in analysis of scattering of low-energy nucleons by nuclei, (T), 19: 33250 (TID-21869)
use in calculating properties of bismuth-208, lead-208, and thallium-208, 18: 42775
use in calculation of moments of inertia, 18: 2912
use in calculation of nuclear properties, 18: 28575(R) (ORNL-3630 (p.31-7))
use in description of tin isotopes, (T), 20: 30521
use in description of nuclear analog states, (T), 20: 38025
use in nuclear structure theory, 17: 41896
use in nuclear structure theory, 18: 20972

use in nuclear structure theory, 19: 31253
use in R-matrix calculations, 16: 32522 (UCRL-10432)
use in study of core polarization in transfer reactions, 20: 15852
use in study of properties of 1d2s-nuclei, 18: 36574 (KFKI-1491-F)
use in studying low-lying states, 18: 11160 (ANL-6797(p.58-78))
use in studying many-particle systems with translational invariance, 19: 47399
use of J-J coupling in analysis of odd-odd ground state spins in, 16: 29763 (JAERI-1020(p.89-96))
use with reaction matrix in calculations of binding energies and excitation energies of nickel isotopes, (T), 20: 38066
uses for analysis of isobaric-spin effects, 19: 14491 (ANL-6878(p.181-206))
uses for energy level calculations, (T), 19: 37824(R) (ORNL-3800(p.50-7))
uses for nuclear analyses, 20: 15730(R) (RHEL/R-112, pp 67-98)
uses of single-particle, 20: 26199
vibrational states of spherical nuclei in, 17: 17285
wave-function calculation of alpha-decay constants, 16: 10998
wave function calculations, 17: 32930
wave function for l-forbidden beta emission in relativistic, 16: 17122
wave function intermediate couplings in deuteron reactions (d,p) with beryllium-9, 16: 11006
wave functions for 2s-1d shell in, 18: 15293
wave functions for, short-range correlations in (T), 19: 3247
wave functions for calcium isotopes, single-particle, 20: 42270
wave functions in, development of, 17: 40125
wave functions in, effects of center-of-mass motion on, 18: 2403(R) (PR-P-58)
wave functions in, U(3)-group classification of oscillator, 20: 22079
wave-function classification using SU(3) group, (T), 20: 40163
Wigner supermultiplets, theory, 16: 31075(T) (CEA-tr-A-1154)

Nuclear Moments
see Moments

NUCLEAR PARTICLES
see also Elementary Particles
see also Nucleons
see also Radiation
acceleration by electromagnetic waves, conditions for, 17: 41815
book: *Counting Statistics of Nuclear Particles*, 17: 39447(T)
coupling of elastically and inelastically scattered waves for E2 excitations, 16: 4857
cross sections for, method for calculating, 17: 14713 (IA-777)
data recording system for, 25-input pulse-height, 16: 27251 (CTSL-35)
detection and measurement, characteristics of surface-barrier diodes for, 16: 5526
detection and measurement, design of particle identification system, 16: 20799
detection and measurement of heavy, spectrometer for, 17: 41283
detection and measurement using silicon detectors, energy resolution for, 18: 20395
detection of beams of, using electroluminescent image intensifier, 18: 35868
detection of $Z \geq 3$, in emulsions, 18: 43965
detection of, counting statistics for, 18: 33964
discriminator for, 17: 8663(P)
disintegration and S function poles of compound, 17: 24758
effects of accelerated, on Staphylococcus growth in chicken muscle, 17: 39364
emission of polarized heavy, circular polarization of gamma rays following, 17: 19271
flux of, across surface of uniformly emitting cylinder, 17: 39973 (EUR-205.f)
ground-state properties of self-bound many-particle system of Hartree-Fock and Puff-Martin approximations for, 17: 9499 (ANL-6623)
identification, detector system for, 16: 5530
identification of, equipment for, 20: 23427(R) (UCRL-16580, pp 219-50)
interactions at high energies, models for, 17: 32952
interactions, theory of strong, 16: 17066 (IA-698)
interactions with strange particles, review of strong, 17: 5054
optical potentials for composite (T), 19: 1603
passage through potential barrier in tunnel effect, 17: 9535
polarization of Dirac, beams in reciprocal effect with external field, 17: 41816
production in cosmic showers, 18: 18609
production in cosmic showers, determination of, 18: 28299
production in proton reactions at 10 to 33 Bev with internal targets in AGS, 17: 37989
production of many, theory, 16: 21270(T) (UCRL-Trans-825)
production of polarized beams of, 17: 11640(R) (TID-17720(p.79-89))
scattering by collective nuclei, coupled-channel calculations for, (T), 19: 47685
scattering by nuclei, phase relations for, 17: 31463
scattering cross sections, analytical properties of elastic, 16: 15647
use of heavy, with high energy for radiotherapy, 19: 17728

NUCLEAR PHYSICS
abstracts on low-energy, 16: 29746 (AERE-R-4131)
analysis of intermediate coupling, 17: 7140 (TID-14921)
analysis of monoenergetic Boltzmann equation, Lagrangian variational, 17: 28412
analysis of monoenergetic Boltzmann equation, self-adjoint transformation in Lagrangian variational, 17: 28413
analysis of new isobaric spin group, 16: 16990 (NP-11592(Vol.I)(p.503-6))
approximate γ_5 invariance in strong interaction theory, 16: 12457
Belgian production and research programs, review, 16: 17352(T) (AEC-tr-5030)
beta decay processes in, theory of, 17: 4111
bibliography on, 19: 31213 (AD-608695)
bibliography on, 20: 19803 (AED-C-12-13(Pt.1))
bibliography on high-energy, 20: 17153 (AED-C-23-05)
bibliography on high-energy, 20: 17154 (AED-C-23-06)
bibliography on high-energy, 20: 17155 (AED-C-23-07)
bibliography on high-energy, 20: 19804 (AED-C-12-13(Pt.2))
bibliography on high-energy, 20: 23807 (AED-C-23-08(Pt.2))
bibliography on high-energy, 20: 23806 (AED-C-23-08(Pt.1))
bibliography on measuring instruments and methods for, 18: 475 (AED-C-06-08)
bibliography on measuring instruments and measuring methods used in, 18: 7025 (AED-C-06-09)
bibliography on, at Warsaw Center, 1945–63, 19: 28915(R) (INR/517/I/PL)
book: *A Collection of Problems in Atomic and Nuclear Physics*, 20: 11376(T)
book: *A Manual of Experiments in Reactor Physics*, 17: 29735
book: *A Textbook of Nuclear Physics*, 19: 25544
book: *An Introduction to Transport Theory*, 17: 15227
book: *Angular Momentum*, 17: 22394
book: *Annual Review of Nuclear Science. 11.*, 17: 5053
book: *Annual Review of Nuclear Science*, 17: 17637
book: *Annual Review of Nuclear Science*. Vol. 13, 18: 10635
book: *Applied Nuclear Geophysics*, 17: 20225
book: *Applied Nuclear Physics*, 18: 32300
book: *Atomic and Nuclear Physics*, 17: 24174
book: *Atomic and Nuclear Physics. An Introduction*, 18: 32299
book: *Atoms, Molecules, and Nuclei*, 17: 41658
book: *Atoms, Radiation and Nuclei*, 19: 2916
book: *Concepts of Nuclear Physics*, 19: 39951
book: *Concise Dictionary of Atomics*, 19: 2915
book: *Constants in Nuclear Physics*, 18: 17255
book: *Electronic Equipment in Nuclear Physics*, 17: 6426
book: *Electronic Equipment in Nuclear Physics*, in Russian, 19: 11490
book: *Elements de Physique Nucleaire*, 16: 28170
book: *Group Theory*, 16: 16639
book: *Hilbert Space with Nuclear Functions*, in German, 18: 21341
book: *Introduction to Nuclear Physics*, 17: 19407
book: *Introductory Nuclear Reactor Theory*, 17: 33266
book: *Investigation of High Energy and Elementary Particle Physics*, 17: 41644
book: *Landolt-Bornstein Numerical Data and Functional Relationships in Science and Technology. New Series. Vol. I, Energy Levels of Nuclei: A = 5 to A = 257*, 16: 26366
book: *Lectures on Nuclear Interactions. I.*, 18: 40646
book: *Lectures on Nuclear Interactions. II.*, 18: 40650
book: *Multichannel Analyzers for Nuclear Physics*, 18: 30065
book: *Neitronnaya Fizika* (Neutron Physics), in Russian, 16: 29722
book: *Nuclear Chemistry and Its Applications*, 18: 6874(T)
book: *Nuclear Orientation*, a collection of reprints, 18: 24706
book: *Nuclear Physics. Part B.*, 17: 19406
book: *Nuclear Physics*, 17: 28344
book: *Nuclear Physics*, 18: 11293
book: *Nuclear Physics and the Fundamental Particles*, 18: 13117
book: *Nuclear Physics. An Introduction*, 18: 32874
book: *Nuclear Physics*, 18: 40645
book: *Nuclear Physics and Meson Physics*, 19: 3110
book: *Nuclear Physics Laboratory Manual with an Introduction to Measurement Fundamentals*, 19: 12624
book: *Nuclear Physics Detection Instruments and Their Application*, (In Chinese), 20: 19086
book: *Nuclear Physics. Mechanism of Nuclear Reactions*, 20: 32538
book: *Nuclear Properties of the Heavy Elements*, 19: 1656
book: *Nuclear Radiation Physics*, 17: 26642
book: *Physical Nuclear Chemistry*, in German, 18: 33676
book: *Physics of the Nucleus*, 17: 17280
book: *Problems of Elementary Particle and Nuclear Physics*, 17: 19183
book: *Progress in Nuclear Physics*, Vol. 9, 18: 14660
book: *Radioactive Transmutation of Nuclei and Atomic Shells*, in

Russian, 18: 17096
book: *Selected Topics in Nuclear Spectroscopy*, 18: 36688
book: *Symmetry Groups in Nuclear and Particle Physics*, 20: 19591
book: *Tables of Coulomb Wave Functions (Whittaker Functions)*, 19: 21117(T)
book: *Textbook on Nuclear Physics. Vol. I. Experimental Methods*, in German, 18: 10661
book: *Textbook on Nuclear Physics. Vol. II. Physics of Atomic Nuclei*, in German, 18: 10662
book: *The Atomic Nucleus*, 18: 13125(T)
book: *The Lightest Atomic Nuclei*, in Russian, 18: 17097
book: *The Optical Model in Nuclear and Particle Physics*, 17: 33108
book: *The Theory of Fundamental Processes*, 16: 26453
book: *The Universe of Time and Space*, 18: 18556
book: *Theory of the Fission Chain Reaction*, 18: 995
calculation of retardation density and thermal flux in scattering medium with fast neutron source, 17: 32984
calculations for multiple Coulomb excitation cross sections, 16: 12442 (TID-15078)
calculations in, computer programs for, 19: 45251 (BNL-9108)
cascade showers in, secondary particle energy spectra in, (T), 19: 32920
charge conjugation invariance in, test of, 17: 39919
Clebsch-Gordan coefficients for $j_3 = 5/2$, 3, and 7/2, 18: 38162
collective effects in nuclear spectra, 17: 4110
commutation relations in non-Abelian gauge fields, 16: 11135
computer programs for calculations in, use of auxiliary storage with, 20: 34497
computer uses in, 19: 18383(R) (TID-21595)
computer uses in experimental, 18: 18483
conference, 18: 16561
conference, 20: 12112
conference, 20: 17871
conference, 20: 19980
conference on, 17: 3650
conference on, 19: 1673
conference on, 19: 17025
conference on, 20: 42337
conference on analytical chemistry in nuclear reactor technology, Gatlinburg, Tenn., October 10 to 12,1961, 16: 23613 (TID-7629)
conference on, Bombay, Feb. 27–Mar. 2, 1963, 17: 36388 (NP-13020)
conference on, by Joint Institute for Nuclear Investigations, Dubna, May 1962, summary, 17: 9211
conference on elementary particle interactions, (I–V), Kiev, July 1959, 16: 10908
conference on elementary particle interactions, (VI–IX), Kiev, July 1959, 16: 10922
conference on low and medium energies, Strasbourg, May 23–25, 1961, 16: 13748
conference on low and medium energies, Strasbourg, May 23–25, 1961, 16: 5807
conference on neutron physics, Karlsruhe, Germany, Oct. 8 to 10, 1963, 18: 24567 (NP-13930)
conference on polarization processes below 50 Mev, 17: 2224 (NIRL/R/16)
conference on theoretical physics, 20: 24088
conference on uses of reactor neutrons in, 18: 10621 (ANL-6797)
conference on utilization of research reactors, IAEA, Bangkok, Dec. 17 to 21, 1962, 18: 15635
conference on, Frascati, Italy, May 6–9, 1963, 18: 10625 (LNF-63/47)
conference, Rutherford Jubilee, Manchester, 1961, 16: 21462
connection with cosmology, cosmic numbers for, 17: 19008
conservation laws of, 17: 39788
continuum in, space-time, 17: 36457 (UCRL-10891)
cross-section probability distributions, 17: 9584
data analysis for multiparameter experiments in, zone-selection technique for, 20: 33700
data analysis for, least squares techniques for, 20: 41518
data analysis systems using PDP-5 computers, 20: 19840 (UCRL-16723)
data analysis using on-line PDP-7 computer, 20: 38176
data handling from, design of buffer stores for, (E), 19: 11655 (EUR-2160.e)
data handling system for, engineering drawings of, 19: 2586
data measurements in, progress of Euratom, 17: 20555(R) (EANDC(E)-38(L))
data processing, automatic experiment conditions for, 16: 27366
data processing in, 18: 23849
data processing in, use of digital computers for, 20: 17708
data processing in, 20: 17709
data processing system using digital computer, 20: 2996
data recording system for, automatic, 16: 14935
data recording system for, 25-input pulse-height, 16: 27251 (CTSL-35)
data representation, 18: 24987 (AEEW-M-426)
data simulation in, use of on-line computer for, 18: 21158 (BNL-7836)
data storage systems for nuclear codes, secondary, 20: 43804 (LA-3546)
decay of quantum system, theory of spontaneous, 16: 25964(T) (JPRS-13656(p.233-59))
design of tool-holding winch with tool-changing capability, 16: 27180(P)
determination of the analytical region, 16: 15761 (JINR-P-225)
development in Free Europe, 16: 14
development in Soviet Union, 19: 21762 (RM-2163(RAND))
development, Nov. 1961, 16: 4959(R) (ANL-6473)
development of, review of progress at Warsaw Center in, 16: 25950 (PAN-279/1-A)
development of, summary for AECL, 16: 32176(R) (PR-P-53)
development of theoretical, Brown University summary, 16: 23850(R) (TID-16074)
development trends, 16: 20484
developments, 17: 31091(R) (UCRL-10862)
developments at ANL, November and December, 1961, 16: 9277(R) (ANL-6455)
developments at Naval Research Laboratory, 17: 38618(R) (NP-13150)
developments in, annual report of CEA, 20: 14223(R) (NP-15723)
developments using ETR and MTR, 16: 9696(R) (IDO-16733)
education in, development of laboratories for, 17: 24817
education of Navy Civil Engineer Corps officers in, 16: 28665
education program on, in Mexico, 17: 24815
electromagnetic cross sections for electron and nuclear research, 18: 26684
electromagnetic properties of light nuclei, theory of, 17: 4112
elementary particle interactions and properties, review, 16: 23254
energy analyses in natural dimension system for, 18: 4336
energy from fission, review, 16: 16655
energy-level distributions in, statistical theory for, 16: 32415
equipment for, 16: 23174
equipment for low-energy, 19: 47629
experimental and theoretical studies on particle reactions, 16: 25910(R) (NP-11749)
experimental techniques in, 17: 4114
experiments, design of electronic equipment for, 16: 27280 (RT/EL(62)12)
experiments in, book on, 20: 7743
experiments in, data acquisition systems for, 19: 26752
experiments in, for student use, 20: 19850
experiments in, statistical behavior of content addressable memories for, 19: 32671
experiments, testing of electronic systems for, 16: 23918 (UCRL-9982)
fine structure constants, 18: 34921
fine structure constant, 18: 38181
French production and research programs, review, 16: 17351(T) (AEC-tr-5029)
gamma energies of radionuclides, table, 17: 20797
gauge invariance and correlated boson fields, 17: 6969
Green function methods in, 19: 1650
high-energy, review on, 19: 30953
impulse approximation in, 17: 4217
induced radiation processes in classical and quantum theories, 17: 31666
inert atmosphere production and uses in, 16: 25517
instrumentation, 16: 2495(R) (TID-14256)
instrumentation for, control and testing of multichannel, 19: 839
instrumentation for, description of standardized, (E), 19: 20262 (KFK-259)
instrumentation for, bibliography, 19: 44366 (AED-C-06-12)
instrumentation for experiments in, control system for, 20: 20995
instruments and measuring techniques in, bibliography on, 20: 25377 (AED-C-06-13)
interaction of matter and radiation, curriculum at University of Michigan, 16: 13888
interrelations of nuclear structure with elementary particle physics, 17: 5395
isotope separator and mass spectrometer uses in, 19: 9781
isotopic gauge invariance of vector field of zero eigenmass, 16: 19890
Italian program, 16: 9738
lectures on, 17: 40122
lectures on basic concepts of, 19: 35394 (N64-29785)
lectures on high energy physics given at Sixth Summer Meeting of Nuclear Physicists, Hercegnovi, Yugoslavia, July to August 1961, Vol. I., 16: 29647 (NP-11950(Vol.I))
lectures on high energy physics given at Sixth Summer Meeting of Nuclear Physicists, Hercegnovi, Yugoslavia, July to August 1961, Vol. II., 16: 29653 (NP-11950(Vol.II))
lectures on photo-, 16: 10959 (NP-11355)
lectures on theoretical aspects at Brandeis University 1960 summer institute, 16: 1173
lifetime determinations in, statistical analysis on methods of, 17: 13600
location of neutron single-particle levels from stripping reactions,

17: 40118
manual of laboratory experiments on reactors, 16: 7237 (ANL-6410)
mass spectroscopy uses in, 19: 2245
matrix element growth in the axiomatic method, 16: 10956 (JINR-D-694)
matter in, mass spectroscopy of smallest quantities of, 19: 14214
measurement methods in, 16: 14938
measurement of lifetimes of excited nuclear states using delayed gammas, 17: 6958 (UCRL-7091)
measurements in, application of Poisson statistics to, 19: 25491
measurements in, uses of computers integrated in equipment for, 19: 23166
measures in dual space of nuclear space, rotationally invariant, 18: 40555
measuring techniques in, bibliography, 19: 44366 (AED-C-06-12)
method for studying the fission process at a specific excitation energy, 17: 24415
methods for spectroscopic averaging, 20: 46710
methods for spectroscopic averaging, combinatorial, (T), 20: 46711
minimization of hamiltonian expectation value, method for, 18: 38110
Mössbauer effect applications in, 20: 6293 (NP-15603)
Mössabauer effect uses in, review of advances in, 20: 22327
multiparameter analyzers in low-energy, 17: 38586 (CU(PNPL)-227 (p.22-5))
multiparametric analyses in, use of integral computer for, 18: 24063
neutron spectroscopy in, 16: 14041
neutron-scattering methods for studies of, low-energy, 20: 34506
normal coordinates in, 16: 11134
nuclear data information center, bulletin of IAEA, 20: 44665(T) (INDSWG-101)
nuclear dynamic polarization in, double resonance and statistical-thermodynamic description of, 17: 24393 (LNF-63/15)
nuclear matter calculations and phenomenological potentials, 17: 4085
nuclear moments of inertia in, determination of, 17: 38206
nuclear potential, long-range, 17: 24477
numerical solution to coupled BCS equations, 17: 22559 (LADC-5551)
particle passage through potential barrier in tunnel effect, 17: 9535
photonuclear resonances in deformed nuclei, 17: 4115
principles of, in medical uses of radiation, 17: 7710
properties of nuclear matter, 17: 40002
Puff-Martin model generalization for many-fermion systems, compressibility and symmetry energy, 16: 7104
pulse analyzers for, conference on multiparameter, 17: 38583 (CU(PNPL)-227)
Racah and Z coefficients, table, 17: 24392 (LAMS-1739)
representation of rotation matrices, graphical method for, 20: 40120
research, (E/T), 20: 5928(R) (PR-P-66)
research, 20: 9597 (ANL-7029)
research, (T), 20: 4475(R) (ANL-7081, pp 95-119)
research, 20: 6034 (CERN-64-13(Vol.4))
research, 20: 19811 (EUR-2465.i)
research, (E), 20: 6296(R) (ORNL-3858(Vol.1), pp 1-12)
research, (E/T), 19: 47587(R) (TID-22012)
research, 19: 39788(R) (UCRL-12204, pp 1-27)
research, (E/T), 20: 13347(R) (UCRL-16511)
research activities at Harvard University, 19: 35371(R) (AD-612914)
research and development on, 17: 6532 (WADC-TR-53-373(Suppl.9))
research at CERN, 19: 42927(R) (NP-15281)
research at CERN center, 19: 35617
research at CERN, 1965, 20: 37308(R) (NP-16226)
research at Frascati, 20: 2521 (LNF-65/28)
research at JEEP reactor facility, 20: 20332
research at Kurchatov Atomic Energy Institute, 16: 3754
research at LRL, (T), 20: 41803(R) (UCRL-16863)
research at Orsay, 20: 13364(R) (LAL-1148)
research at Saha Institute, review of, 20: 9605
research at Seibersdorf, 20: 16127
research at Warsaw 1945 to 63, review of experimental, 19: 3242 (PAN-517/I)
research capabilities at General Dynamics/Fort Worth, 16: 18163 (NARF-61-8T)
research facilities for, Casaccia, Italy, 20: 36540
research in, 17: 17123(R) (TID-18127)
research in Czechoslovakia, 16: 2341
research in England, 20: 4504(R) (NP-15420)
research in Germany, government promotion of, 20: 10492
research in high-energy, 17: 11331(R) (TID-17023)
research in high-energy, review, (E/T), 19: 41337 (NYO-2262-95)
research in, hyperfragment, 17: 32901 (EFINS-63-32)
research in hypernuclear, future, 17: 32901 (EFINS-63-32)
research in low-energy, review of, 20: 43764
research in reactor physics in Japan, 18: 42885
research in, review of, 17: 3390(R) (WADC-TR-53-373(Suppl.8))
research in, thermal neutron uses in, 17: 36658 (LADC-5951)
research in, using reactors, 17: 35185
research in, status of, 19: 45372
research on, using isotopic composition of extraterrestrial and terrestrial material, 20: 37369
research in, 460-Mev synchrocyclotron, 20: 4577 (AD-618067)
research on, (E/T), 20: 17651(R) (AD-612192)
research on, 19: 16819(R) (ORNL-3714(Vol.I))
research on, 19: 41678(R) (PR-P-65)
research on high energy report of Joint Committee on Atomic Energy on, 20: 1241
research on high-energy, summary for university of Tokyo, 20: 13345(R) (NP-15772)
research on, in Germany, 17: 5698
research on low-energy, summary, 18: 30520(R) (TID-20720)
research on theoretical, July 1963 to July 1964 at BNL, 19: 23355(R) (BNL-867(p.1-117))
research on, at Interuniversity Institute of Nuclear Sciences, 20: 6695(R) (NP-15607)
research on, bibliography for, (E/T), 19: 44812(R) (UCRL-16099)
research on, in CEA, 20: 10471(R) (NP-15720)
research on, in Great Britain, 20: 10472 (NP-15721)
research on, in Rumania, 19: 45705 (NP-15193)
research on, review, (E/T), 19: 35876
research on, review, 19: 37822(R) (ORNL-3800)
research program, 16: 2495(R) (TID-14256)
research program, 16: 9360(R) (TID-14827)
research program, 18: 24959 (NP-13910)
research program at Kjeller Research Institute, Norway, 17: 35187
research program at Warsaw center from 1945, 19: 12599
research program at Joint Institute of Nuclear Studies, review of, 20: 34160
research program in Poland, 19: 11846
research program in low-energy, at Krakow center, 19: 12598
research program, National Bureau of Standards, 16: 4608 (NBS-TN-92)
research program on, summary for European Nuclear Energy Agency, 17: 1045(R) (NP-12101)
research program of Nuclear Chemistry Division of Lawrence Radiation Laboratory, 19: 19735(R) (UCRL-11828)
research program using Van de Graaff accelerators, 20: 21463 (BNL-948, pp 685-91)
research programs, summary for July to Sept 1961, 16: 12212(R) (CU(PNPL)-213)
research programs, summary for 1961, 16: 14376(R) (HW-70000)
research programs, 16: 18124(R) (UCRL-10113)
research programs in underdeveloped countries, use of reactors in, 16: 18421
research programs at NRL, 16: 21130(R) (NP-11643)
research programs in low-energy, summary for Pennsylvania State University, 16: 24794(R) (TID-15211)
research programs, 16: 25886 (LNF-62/37)
research programs progress at MIT, 16: 26646(R) (NYO-2668)
research programs at Institute for Nuclear Study, University of Tokyo, April 1960 to March 1962, 16: 28645(R) (NP-11960)
research programs at National Laboratories of Frascati, Italy, 16: 29877(R) (LNF-62/30)
research programs at Nevis Cyclotron Laboratory, review, 16: 29642(R) (NEVIS-100)
research programs in Warsaw, Poland, 16: 30975
research programs at Israel Research Laboratories, 16: 30162(R) (IA-726)
research programs on high-energy, summary of, 16: 32454 (60-RL-2345E)
research programs on, summary for Ames Laboratory, 17: 4448 (IS-500 (Sect.P))
research programs on nuclear properties of various elements, 17: 14933 (EANDC(OR)-19(L))
research programs on, at Laboratory of Nuclear Studies, Osaka University, Japan, 17: 14946(R) (OU-LNS-62-01)
research programs on, in Soviet Union, organization and literature of, 17: 28589 (EUR-236.e)
research programs of U. S. Army on, 1962 summary, 17: 33413(R) (NP-12967)
research programs at Rutherford High Energy Laboratory, 1961–62, 17: 34998(R) (NP-13002)
research programs on, uses of sector-focused cyclotrons in, 17: 38321 (CERN-63-19(p.85-92))
research programs on, at Hahn-Meitner Institute for Nuclear Research, 17: 37002(R) (HMI-B-26)
research programs at ENEA in, 17: 37006(R) (NP-13095)
research programs on, at Seibersdorf Reactor Center, 17: 38498
research programs at CERN in, 17: 41555(R) (NP-13209)
research programs in theoretical, at MIT, 17: 40437(R) (NYO-10063 (p.116-25))
research programs on, at New Zealand's Institute of Nuclear Sciences, 18: 1317(R) (NP-13210)
research programs in low-energy, at 66 sites throughout the world,

18: 2400 (INSJ-62)
research programs at BNL on, July 1962 to July 1963, 18: 7987(R) (BNL-806(p.3-90))
research programs on, in Israel, 18: 9752 (IA-900)
research programs on, at Atomic Energy Establishment, Trombay, India, 18: 15638
research programs on, at reactor centers in developing countries, 18: 15651
research programs at Rutherford High Energy Laboratory, 1962–63, 18: 18506(R) (NP-13787)
research programs on, Hahn-Meitner Institute for Kernforschung, 1963, 18: 33182(R) (HMI-B-34)
research programs on, in British universities, 18: 38250 (A/CONF.28/P/564)
research programs at CERN in, 18: 42157(R) (NP-14228)
research programs on, 19: 9775(R) (UCRL-11466)
research programs at ENEA in, 19: 10677(R) (NP-14552)
research programs on, at Karlsruhe Nuclear Research Centre, 19: 17442
research programs on, 19: 23209(R) (RPI-328-20)
research programs data acquisition in, 19: 23809
research programs using Van De Graaff accelerator in Pakistan, 19: 25089 (AECD/EP/1)
research programs on, 19: 25265(R) (UCRL-11776)
research programs at Frascati National Laboratory, 19: 28917(R) (LNF-64/69)
research programs on, at Japanese universities, 1964, 19: 37211
research programs on, 19: 40396(R) (HMI-B-39)
research programs on high-energy, equipment and methods for, 19: 47326
research programs on, at Risö, Denmark, 20: 3646
research programs on, using Kyoto University cyclotron, 20: 22524
research programs in India, 20: 26588(R) (NP-15950)
research programs on, 20: 28864(R) (NP-15976)
research programs on, 20: 31165(R) (HMI-B-46)
research programs in India on, 1965–1966, 20: 36539(R) (NP-16171)
research progress at Washington University, St. Louis, 16: 1018(R) (AFOSR-1396)
research progress, 16: 5108(R) (TID-14418)
research progress at ORNL, February 1, 1961 to January 31, 1962, 16: 22986(R) (ORNL-3268)
research progress at Purdue Research Foundation, 16: 25953(R) (TID-16079)
research progress at Chalk River, 16: 33583(R) (PR-P-54)
research progress on, at MIT, 17: 20563 (NYO-10062)
research progress at ORNL, 17: 26427(R) (ORNL-3425)
research progress at Chalk River, 17: 32722(R) (PR-P-57)
research progress in, at MIT, May 1, 1963, 17: 40426(R) (NYO-10063)
research progress in, at ANL, Oct. 1963, 18: 3038(R) (ANL-6801)
research progress on, EURATOM, 18: 11195(R) (EANDC(E)-49(L))
research progress on, summary of 1963 AEC, 18: 11550
research progress on, 18: 16552(R) (UCRL-11132)
research progress at Iowa State Univ. in, 18: 18882(R) (TID-20378)
research progress on, 18: 23139(R) (NP-13876)
research progress, (E/T), 19: 43110
research progress, 20: 24328(R) (ANL-7108)
research progress at ORNL, 20: 46240 (ORNL-3973(Vol.1))
research, status and prospects in Australia, 16: 4604 (ANU/P-235)
research using pulsed neutrons in, review on developments in, 19: 1528
research using thermal neutrons, advanced course on, 18: 21185 (KR-64)
research with Saclay tandem accelerator, scattering chamber for, 19: 34439
resonance poles and mass differences within unitary multiplets, 18: 9162
review, 17: 26477
review of basic, 17: 29120 (MRL-TDR-62-61)
review of recent major developments in low-energy, 18: 19062
review of research at University of Edinburgh on, 20: 5239
review of, Rutherford memorial lecture, 19: 16287
role of government in nuclear education, 16: 28664
role of the university in nuclear training and education, 16: 28663
rotation of gamma-vibration interaction in rare earths, 16: 33793 (PAN-325/VII)
S-matrix theory, lectures on, 16: 9560 (UCRL-9875(Vol.I))
scattering amplitude determination in, theory of two-body, 17: 9254
search for Dirac magnetic poles, 16: 13698 (NP-11363)
self-bound finite systems in, 18: 38166
shell model spectra in nuclei, 17: 4109
singularities in partial wave amplitudes for interactions of two-ingoing and two-outgoing particles, 16: 16970 (NP-11592(Vol.I)(p.337-42))
solution of kinetic equations in, application of the stationary phase method in, 17: 11308 (JINR-P-1113)
spectra of low- and high-density fermion systems, excitation, 16: 22884
spectral representation of Feynman amplitude for fourth-order diagrams, double, 16: 15762 (JINR-P-449)
spectroscopy in, lectures on nuclear, 17: 4107
standards in, fifth meeting of European-American Nuclear Data Committee on, 17: 39970 (EANDC-28(L))
statistical theory of multiple particle production, formulation of, 17: 41749
summary, 18: 17375
superconductive pairing correlations, effect on alpha decay rates, 16: 27901 (JINR-E-945)
symmetry terms in optical potential, 17: 17204
symposium, 17: 7087 (NP-12330)
tables of eigenvalues and eigenvectors of Hamiltonian, 17: 605 (TID-15749)
teaching of, experiments for use in, 19: 47621
terminology, 20: 3096
terminology of, relations with terminology of high-energy elementary-particle physics, (T), 19: 14500 (ANL-6878(p.481-504))
theoretical aspects of high-energy, 18: 14805 (JINR-E-1436)
theory, discussion of dualisms in quantum physics, 16: 15763
theory of fission, developments in, 16: 32392 (LADC-5267)
theory of, Hartree-Fock approximation in, 17: 40123
theory of many-particle systems, 17: 9499 (ANL-6623)
theory of nuclear matter, 17: 4113
theory of Regge poles, 16: 18594 (CERN-62-13)
theory of selection rule $\Delta Q = \Delta S$, testing, 16: 16953 (NP-11592(Vol.I)(p.209-15))
theory of, elementary particle analogies in, 20: 19994
time measurements in, electronic systems for, 19: 36782
time-reversal quantum mechanics in, 18: 22792
training in, in Western Europe, 17: 5661
transactions of the American Nuclear Society 1962 Meeting, Boston, 16: 24338
transformation matrix for isotropic harmonic oscillator eigenvectors, 18: 34807
transition matrix for nucleon-nucleon scattering in, 16: 31072 (TID-16473)
transition probability and relaxation time for particles, relation of (T), 19: 3244
units for, 20: 4539 (UCRL-11444)
units for, system of, 19: 37207
universal Fermi interaction predictions for complex nuclei, 17: 9582
use of multiparameter analyzers in, 17: 32348
use of on-line computers in low-energy experiments in, 20: 22031
use of oriented nuclei in, 16: 19501
use of polarized neutrons in, 18: 12929
volume effects in, 17: 7103 (NP-12330(p.109-18))
wave functions of systems with many degrees of freedom, 16: 29985
Whittaker functions and logarithmic derivatives, 17: 24459

NUCLEAR POWER

see also Nuclear Aircraft
see also Nuclear Aircraft Power Plants
see also Nuclear Power Plants
air pollution by fuel cycle in, review of possible, 19: 10546 (HW-SA-3683)
book: *Atomic Power in the National Economy*, in Russian, 19: 10595
book: *Chemical Processing in the Atomic Energy Industry*, 18: 39398
book: *Civilian Nuclear Power, Economic Issues and Policy Formation*, 17: 19656
book: *Fact Book on U. S. Nuclear Power Projects*, 19: 35801
book: *From the Atomic Nucleus to the Nuclear Power Station*, in German, 18: 26943
book: *Nuclear Energy Technology. Introduction to the Physics and Technology of Nuclear Energy Production*, 16: 8385
book: *Nuclear Energy and Nuclear Power Plants*, in German, 17: 22897
book: *Nuclear Energy in Space*, 19: 1930
book: *Nuclear Power, Today and Tomorrow*, 16: 6233
book: *Nuclear Power Systems. An Introductory Text*, 18: 23077
book: *Nuclear Power Technology*, 18: 38546
book: *Proceedings of the Atomic Industrial Forum 1964 Annual Conference*, Vol. I, 19: 17327
book: *Summary of Nuclear Energy*, 18: 17375
book: *The Economics of Nuclear Power*, 19: 38214
competitive, long term prospects for, 16: 9616 (AECL-1318(Paper 11))
conference, 16: 9605 (AECL-1318)
conference, 19: 5505
conference, 20: 5154
conference at Montreal, May 1963, 17: 42325 (AECL-1789)
conference, Chicago, March 1961, 16: 2761
conference on, 17: 19657
conference on, 20: 5161
conference on, AECL, Chalk River, Ontario, September 24, 1962, 17: 1103 (AECL-1599)
conference on Canadian, 17: 42326 (AECL-1807)
conference on development and applications, 20: 47096

conference on, in Chicago, Nov. 1961, 16: 18727
Congressional hearings on, 17: 19661
considerations for Ontario hydro system, 16: 9612 (AECL-1318 (Paper 7))
contribution to total Italian power needs, 16: 11370
conversion into electrochemical energy, 18: 32512 (JüL-144-PC)
cost analysis of kilowatt hour, 17: 10250
cost calculations, 16: 16034
cost calculations, graphs for rapid, 16: 30117
cost evaluation in national power programs, computer program for, 19: 25731 (TRG-Report-894)
cost per kilowatt-hour of, 19: 17289
current trends in, 17: 22969 (TID-7656)
design using two reactors cooled and moderated by decomposable hydride, 20: 28807(P)
development, 19: 38205
development, 20: 5167
development, 20: 12431
development, 20: 21097
development and economics, 16: 31353
development and economics in France, 20: 45166
development and expansion in Canada, 18: 41002
development and integration into eletric power complex in Pacific Northwest, 16: 26653
development and prospects of, in United Kingdom, 17: 19640
development and prospects for central-station, in U. S., 20: 45175
development and research programs for, need for, 19: 14815 (CONF-631201(p.36-40))
development and research program in United Kingdom, 20: 5150
development and trends in Canada, 17: 15443 (AECL-1675)
development and uses, 19: 38219
development and uses of, in Italy, 19: 45724
development and uses in Soviet Union, 20: 20182(T) (AEC-tr-6700)
development by European Nuclear Energy Agency members, review on, 20: 26587(R) (NP-15919)
development, economics, and legal aspects of, 17: 2599
development for communications satellites, survey, 17: 4363
development for desalination, 20: 24776
development for propulsion, 19: 1987
development for space systems, 17: 31768
development for space applications, 20: 47058
development for undersea uses, 17: 15385(R) (ANL-6683)
development for undersea uses, review of, 20: 40362
development in Argentina, 18: 38503 (A/CONF.28/P/715)
development in Brazil, prospects for, 20: 40487 (NP-16229)
development in Britain, 17: 5664
development in Britain, 20: 26479
development in Canada, 17: 13784
development in Canada, 18: 13277 (AECL-1882)
development in Canada, 18: 40918
development in Canada, 1965 to 1985, 18: 41005
development in Canada, long- and short-term aspects of, 18: 41007
development in Canada, future, 20: 1454 (AECL-2293)
development in Canada, industrial effects on, 20: 45245
development in Colorado, 20: 35089
development in Czechoslovakia, 17: 40368
development in Eastern Germany since 1955, 17: 10083
development in Europe, conference on, 17: 2740
development in Europe, 17: 35252 (HW-SA-2841)
development in Europe, role of state in, 18: 21644(T) (AEC-tr-6385)
development in Europe, 19: 38201
development in Europe, industrial, 19: 45723
development in European countries, 20: 35044
development in Federal Republic of Germany, 18: 43042
development in France, 18: 38385 (A/CONF.28/P/31)
development in France, Great Britain, and United States, review of, 19: 17439
development in France, 19: 31565
development in free world, 18: 426 (EUR-414.e)
development in Germany, 19: 40204
development in Great Britain, 18: 45063
development in Great Britain, 20: 22450
development in Great Britain, 20: 28777
development in Great Britain, 20: 28778
development in India, 18: 38704 (A/CONF.28/P/741)
development in India, 19: 25737
development in India, 20: 26588(R) (NP-15950)
development in Italy, 20: 26475
development in Italy, 16: 30118 (RT/EC(62)7)
development in Japan, 18: 38701 (A/CONF.28/P/577)
development in Japan, 19: 33627
development in Philippine Islands, economic and technical aspects of, 18: 23073
development in Russia, 18: 38442 (A/CONF.28/P/316)
development in Russia, 18: 43046
development in Soviet Union, 19: 1919
development in Soviet Union, 20: 28779
development in Soviet Union, economic aspects of, 20: 38512
development in Spain, 17: 10
development in Switzerland, survey of, 17: 24650
development in Switzerland, 20: 22421
development in the U.S., relations with uranium reserves, 17: 19611(R) (DP-825)
development in U. S., fact book on, 18: 15527 (NP-13723)
development in U. S., governmental and industrial support for, 19: 10599
development in U.S.S.R., 18: 38431 (A/CONF.28/P/294)
development in United States, survey of, 18: 4809
development in United Kingdom, 18: 38474 (A/CONF.28/P/559)
development in United Kingdom, 18: 38475 (A/CONF.28/P/561)
development in United States, 1964, 19: 27891
development in USSR, 16: 2839
development in Victoria, Australia, evaluation of, 18: 26929
development in Yugoslavia, 19: 38211
development in Yugoslavia, 20: 1491
development of, 19: 36695
development of, chemical processes in, 17: 28960
development of controlled thermonuclear reactions for, 16: 2763
development of, for use in space programs, 17: 22954 (TID-18558)
development of, in Sweden, review on, 17: 22866
development of low-cost, 17: 35271
development of, survey of selected countries, 17: 7663 (NP-12329)
development of, conference on, 18: 45058
development of, conference on, 20: 5166
development of, effects of reactor siting policies on, 19: 33600 (CONF-650201(p.288-92))
development of, energy conversion cycles in, 19: 42121
development of, future, 18: 11459
development of, government participation in, 19: 1917
development of, international, 18: 38432 (A/CONF.28/P/295)
development of, international, 19: 1920
development of, international progress in, 19: 10713
development of, national plans for, 18: 45042
development of, national plans for, 19: 1912
development of, neutron cross section data requirements for, 20: 32839
development of, review of, 18: 35178
development of, review on, 18: 36819
development of, survey on, 19: 38200
development of, United States program for, 20: 3492
development of, world forecast for, 19: 35813
development planning of, 17: 28595
development potential, review of, 17: 13776 (DL-50)
development programs for, report to Congress on, 1962, 17: 40439
development programs in Japan, commercial, 18: 40904
development program in U. K., 20: 45179
development program and status in U. K., 20: 45179
development, review, 16: 31356
development, role of International Atomic Energy Agency in, 16: 31359
development, roles of Atomic Energy of Canada Ltd. and Canadian Nuclear Association in, 16: 31358
development status for manned orbital space stations, 18: 39419
development status, 18: 40905
development status in Italy, 19: 40200
development status, 20: 20283
development trends in West Germany, survey of, 17: 24693
development, economics, and feasibility, 18: 40889
developments in, 17: 13787
developments in, as potential market for uranium, 17: 26957
developments in Switzerland, 18: 35082
developments in, 1965, 19: 44307
developments, 1962, 17: 5662
economic analysis of binary cycle using steam and Freon-12, 17: 33351
economic and industrial aspects of, conference on, 19: 24221
economic and other environmental considerations in reactor evaluation, 16: 12766
economic and social aspects in relation to trade unions, conference, 16: 11354 (NP-11417)
economic and social aspects, 16: 11286
economic aspects and production problems, 17: 24701
economic aspects and role of engineer in, 19: 17441
economic aspects in systems consisting mostly of conventional plants, 16: 5051
economic aspects in electric utility systems, 17: 33348
economic aspects of production, 16: 1294(T) (AEC-tr-4141(p.1-32))
economic aspects of nuclear ship propulsion, 16: 3949
economic aspects of development of, 16: 18730
economic aspects of, effects of nuclear insurance rates on, 16: 21733

economic aspects of, in Pakistan, 16: 31361
economic aspects of, in Tennessee, 17: 4377
economic aspects of combined production of electricity and heat, 18: 38393 (A/CONF.28/P/46)
economic aspects of continuance of Civilian Nuclear Power Program, 17: 28532 (SRIA-65)
economic aspects of fuel processing for, 19: 11291
economic aspects of, data tables on world-wide, 17: 26856 (GC(V)/INF/38)
economic effects of pooling and growth in electric utility industry on, 16: 31304
economic evaluation, 18: 19383
economic evaluation of future development of, 18: 33112
economic of, long-term, 18: 4936
economic prospects, 17: 2521
economic prospects for, in France, 20: 14151
economic, social, and technical aspects of, in Italy, 17: 7671
economic survey and total energy needs of Italy, 16: 11369
economics, 17: 35269
economics, 18: 36820
economics, 19: 3659
economics and potential of uranium use for, 17: 11968
economics and prospects of, in EURATOM countries, 17: 10251
economics and prospects for, 20: 10398
economics and prospects of, 20: 38487 (AECL-2584)
economics for under-developed countries, 18: 38704 (A/CONF.28/P/741)
economics in Europe, 16: 23360
economics in Iowa power system, analysis, 18: 26944
economics of, 18: 3239
economics of Canadian, 1970 to 1985, 18: 41008
economics of French, 19: 17292
economics of, influence of steam-cycle performance on, 17: 33356
economics of, review of long-term, 18: 9659
economics of, role of fuel reprocessing in, 17: 8232 (BNL-5479)
economics of, utility system conditions affecting, 18: 9668
economics of, bibliography on, 19: 19404
economics of, evaluation of, 20: 35096
economics of, fuel cycle effects on, 20: 45099
economics of, in France, 20: 32889
economics of, in Japan, 18: 40901
economics of, in Sweden, 18: 38703 (A/CONF.28/P/604)
economics of, uranium depletion effects and requirements in, 19: 31563
economics of, with uranium from ocean and rocks, 18: 26917 (DM-72)
economy, effects of waste management costs on future, 18: 33161 (A/CONF.28/P/868)
French program, part played by C.E.A., 17: 12074
fuel cell development for, 16: 2762
fuel costs in Europe, survey of, 17: 38541 (DPR/INF-272)
fuel costs in future, comparison with coal costs, 17: 22877
fuel cycle cost analysis for Senn reactor, 18: 4801 (NYO-9992)
fuel cycle costs, effects of stainless steel and Zircaloy cladding on, 19: 17264 (AD-422953)
fuel economics, bibliography on, 19: 6850 (AED-C-24-01)
fuel utilization in, problem of efficient, 18: 3283
future prospects for Portugal, 18: 24922
generating capacities for, listing by country, 20: 14222(R) (NP-15612)
generation and use of explosion-produced, 16: 12820 (UCRL-Trans-790(L))
generation of, economics of, 18: 33113
generation problems of space vehicles, 16: 5091
growth in Canada and U. S., 16: 24978 (DL-49)
growth of civilian, estimated, 19: 40194 (WASH-1055)
industrial activities, 1963, 19: 855
industrial development of, Federal Republic of Germany, 18: 43144
insurance against risks in, 18: 37453
introduction into less-developed countries, 16: 5063
maritime uses of, 19: 1931
material balances in, 19: 29635 (EUR-2412.e)
needs and prospects in Israel, 18: 21739
performance of Berkeley, Bradwell, and Hunterston, 19: 48019
potential of, for space operations, 17: 10185 (AD-275297(p. 15-17))
production and uses of, forecast of future, 19: 45725
production in gas-cooled reactors, optimization of, 18: 1273
production in German Republic, USA, and western Europe, fuel economics and sources for, 20: 24671
production of, review of problems in, 16: 34085
production of, classification and evaluation of, 20: 1494
production of, protection against release of radioactivity to biosphere in, 19: 4410
production of, review of developments in, 18: 26931
production of, uranium economics for, 19: 9393
production prospects in Italy, 16: 32592
production, prospects and contending reactor types for, 17: 1110 (AECL-1599(p.69-82))
production, review, 16: 28655(R) (JPRS-14284)
program in United States, report to the President, 17: 5631
program of, initiation of, 18: 38414 (A/CONF.28/P/131)
prospects and programs in Great Britain, 18: 21740
prospects for use of, in Pakistan, 16: 29076 (STI/DOC/10/7)
prospects for use of, in Israel, 18: 11437 (IA-795)
prospects in Australia, 18: 38523 (A/CONF.28/P/866)
prospects in European Atomic Energy Community, 18: 43027 (EUR-1887.f)
prospects in Latin America, 19: 24127
prospects in Tasmania, 18: 19498
public acceptance of, problem of, 19: 33597 (CONF-650201(p.247-53))
public control, significance and limits, 16: 11371
public education aspects of, 19: 14862
public understanding, 19: 33528 (CONF-650201(p.257-9))
research in Czechoslovakia, 16: 2746
research in Rumania, 17: 31811
research on military uses of, in France, 20: 45239(R) (NP-16267)
research program for Whiteshell Nuclear Research Establishment, 17: 9
research programs in U. S., 20: 5151
research programs in United Kingdom, 20: 5152
research progress in Australia, 1960 and 1961, 16: 20044 (NP-11606)
review of policies toward and economic and technological status of, 19: 24219
review on British nuclear industry, 19: 40300
role in India, 18: 38509 (A/CONF.28/P/746)
role in Spanish power grid, 18: 38521 (A/CONF.28/P/863)
role in U.S. Merchant Marine, 18: 35203 (NP-14139)
safety, 19: 713
safety aspects of, review, 16: 19206
safety in space, outline of standards and evaluation of, 19: 20206 (TID-7698(Pt.I)(p.31-2))
status, 20: 20282
survey of future prospects of, 18: 9670
systems for, makeup of future, 19: 31563
thermodynamics of reactor coolants for power generation, 17: 5615
transformation into chemical energy, economics and technology of, 18: 33629
transmission of, development of thermal radiation focusing guide for, 17: 3573(R) (NP-12206)
use for desalination of sea water, economics of, 19: 21707 (ORNL-TM-432)
use for extraction of water from rocks, comparison of solar power with, 19: 34360 (AD-608225)
use for industrial development, 20: 20363
use for methanol synthesis in mobile energy depot system, 19: 13195 (BNL-8808)
use for sea water desalination, evaluation, 19: 21708 (ORNL-TM-465)
use for synthesis of methanol fuel in mobile energy depot system, 19: 276 (BNL-8489)
use in Canada, effect of fossil fuel transportation costs on, 20: 45177
use in desalination, economic aspects of, 20: 6649
use in electrochemonuclear production of ammonia, 19: 2201 (BNL-8221)
use in electrochemonuclear production of chemicals, 19: 12770 (BNL-8754)
use in expanding utility systems, economics of, 20: 45178
use in industrial chemical production, 19: 3704
use in small portable and automotive power supplies, survey of energy conversion devices for economical, 16: 13682 (ANL-6483)
use in space, hazards from, 20: 18949 (SC-DC-1369)
uses, 19: 3485
uses in aerospace technology, 16: 15950
uses in industrial processes, 20: 30786(R) (ANL-7190)
uses in space exploration, 16: 15943
uses in space exploration, radiation safety problems in, 16: 15949
uses of, college course on, 20: 3329
uses of, economics of industrial, 20: 45631(R) (ORNL-3945, pp 259-69)
uses of, survey of prospects for, 19: 24216
utilization in northern Chile, 16: 7271

Nuclear Power Demonstration Reactor
see NPD Reactor

NUCLEAR POWER PLANTS
see also Nuclear Heating Plants
see also Power Reactors
accident, radioactivity release from total loss of coolant, 16: 22487
accidents in, arrangement for preventing pressure buildup in steam-releasing, 17: 28550(P)
accidents in, use of turbogenerator shut-down energy in, 20: 1492
automation of, review of status of, 19: 27787
automation of, use of computers in, 18: 13305
availability summary, 20: 35059
bibliography on, for ships, 18: 38559 (AED-C-22-02)

boiler and piping corrosion in steam–water, 20: 10399
boiler control principles for, 18: 3960
boiler design, 16: 8854(P)
boiler design and operation in, 16: 20622(P)
boiler design and performance for, 17: 34084
boiler design for gas-cooled-reactor, 18: 26941
boiler design for, 19: 35667(P)
boiler for, limits of fault detection in, 20: 23260
boiler system design for, 17: 29819(P)
boiler transient analysis, mathematical model for, 19: 28505 (WAPD-T-1648)
boiler, design of stable, 19: 12742
boilers for, design of water-tube, 17: 8308(P)
boilers for, design of sodium-heated, 20: 12389 (BAW-1280-28(Vol.1))
boilers for, development of sodium-heated, 20: 12392 (BAW-1280-28(Vol.4))
book: *Analysis of Thermodynamic Cycle of Atomic Power Plants*, 19: 27805
book: *Atomic Power Plants*, 18: 11462
book: *Costs and Prospects of Nuclear Power*, 19: 3706
book: *Dosimetric and Special Technological Rules for Nuclear Power*, 16: 20903
book: *International Marketing of Nuclear Power Plants*, 20: 18117
book: *Nuclear Power Systems. An Introductory Text*, 18: 23077
book: *Nuclear Power Plants. Design, Operating Experience and Economics*, 18: 33114
book: *Radioisotopic Power Generation*, 19: 2692
book: *Technological and Thermotechnical Control of Nuclear Power Stations*, 20: 18118
book: *The First 10 Years of the First Atomic Power Plant in USSR*, 19: 5507
book: *The Story of the Construction of Berkeley Nuclear Power Station*, 17: 36946
book: *Thermal Power Engineering for Nuclear Installations*, 16: 26605(T) (FTD-TT-61-241)
book: *Thermodynamic Cycles of Atomic Electric Power Plants*, 17: 29814
book: *Thermodynamic Cycles of Nuclear Power Stations*, 20: 24765(T)
book: *Water Circuit in Thermal Power Stations*, 19: 35633
burnup of spacecraft-housed, during re-entry, (E/T), 19: 17350 (RTD-TDR-63-3002)
cathode development for nuclear-thermionic, 18: 35929(R) (GA-4769 (Pt.I))
characteristics and circuit design of Belgian, 17: 36941
characteristics of Russian, at Beloyarsk and Voronezh Oblast, 16: 3952
characteristics of mercury binary-cycle, 16: 31303
check-out procedures before start-up of Latina, 17: 28537
competitive position in energy market, review, 17: 15479
computer installation for, description of Saturn, 16: 4448
condenser design for surplus steam, 18: 21663(P)
condenser for boiling-water, performance of air-cooled, 17: 33303 (CEND-139)
conference, 20: 5154
conference, 20: 20281
construction and cost of German 237-Mw KRB, 19: 24092(R) (TID-21501)
construction and operation of, in Sweden, 17: 22867
construction and operation of, review of licensing procedures for, 19: 29817
construction cost analysis, 20: 40402 (EUR-2993.d)
construction costs, 20: 18102
construction in Pakistan, feasibility of, with participation of German reactor industry, 17: 29809
construction in under-developed nations, advantages, 16: 26648
construction of Dungeness, 17: 24708
construction of, effects of earthquakes on, 18: 9701
construction of Japanese Power Demonstration Reactor (JPDR), 18: 19384
construction of large demonstration, review of arguments for and against, 17: 15477
construction of marine, nondestructive testing in, 18: 35206
construction of MZFR, 20: 5138
construction of Saint-Laurent-des-Eaux, 19: 42119
construction of 15-Mw installation at Kahl, Germany, 16: 14332
construction of 252-Mw Lingen, 20: 5139
construction of, use of optical instruments in, 20: 18114
construction of, use of network planning technique in, 20: 30907
construction problems and operation of Berkeley, 17: 22889
construction problems of Bradwell, 17: 22890
construction problem of Kahl, 17: 26878
construction program for, economics of, 17: 10082
construction techniques for, survey of, 17: 31744
containment and safeguards design criteria, 18: 33091 (A/CONF.28/P/276)
containment costs for, 20: 30815
containment of underground, 16: 1258
containment of underground, 16: 28569(T) (AEC-tr-5218)
containment system for, pressure-suppression, 20: 30833(P)
containment vessel for, fabrication and testing of spherical, 19: 13686
containment vibration analysis for, 19: 38210
control and operation, 17: 19647
control and transient performance tests on RWE Plant, Kahl, Germany, 17: 10100
control by computers, 16: 31310
control equipment for, design of automatic safety, 19: 20103
control of boiling water reactor, 16: 6152(P)
control of lunar, telemetry system for, 20: 24746
control of pressurized-water, 18: 40884
control of single-cycle, having a steam-generating reactor, 18: 23081(P)
control of, survey of objectives and methods in, 17: 10077
control of, survey of semiconductor devices for, 17: 41227
control of, computer, 19: 29611 (AECL-1539)
control of, use of static programming of digital data handling in, 20: 18121
control system and instrumentation for Czechoslovakian A 1, 20: 3534
control system design for British, 16: 9682
control system design, environmental effects, 16: 11244
control system for, automatic, 18: 7862 (RT/EL(63)-10)
control system for Army, feasibility of universal, 18: 11381 (IDO-10039)
control system for, load-response, 19: 35819(P)
control system for, having two load medium circuits, 20: 3357(P)
control system for, load-response, 20: 30832(P)
control system for, load–response, 20: 35099(P)
control system for, 20: 40432(P)
control system of first Soviet, 18: 36826
control, system using digital computers, 16: 20016
control system using digital computers, 16: 20017
control systems for Canadian, 20: 3533
control using on-line computers, 20: 35074
control using on-line computers, 20: 35075
coolant circuit design for load variation at constant heat output in reactor, 16: 6235(P)
coolant combustion and explosion prevention in, organic, 20: 24764
coolant control in boiling, 17: 42282(P)
coolant cycle analysis for, using supercritical steam-cooled reactors, 20: 12415 (TID-22545, pp 54-65)
coolant flow control method for, 19: 29701(P)
coolant flow control system for, 20: 28809(P)
coolant flow control system for, 20: 36502(P)
coolant flow control system for, 20: 36505(P)
coolant flow system for, 19: 35821(P)
coolant leakage from steam generators in gas-cooled, radiometric determination of, 20: 28785
coolant purification, protection of installations for gas, 19: 31579(P)
coolant purification in boiling-water, survey of ion-exchange methods for, 20: 3539 (ACNP-65558(Rev.1))
coolant regeneration in water-cooled and moderated, optimum temperature for, 16: 28582
coolant systems in, failures in, 18: 11466
coolant temperature determination for boiling reactors with superheating, feed-water, 20: 28780
cooling system design for sodium cooled, 16: 32598(P)
cooling system design for, 16: 32599(P)
cooling system design for space, 17: 20174(R) (TID-17707)
cooling systems of, pressure control device for primary circuit of, 20: 1520(P)
corrosion problems, review, 17: 11133 (TID-16561)
corrosion problems, review, 17: 20419
cost analysis for, 18: 31014
cost analysis for European, capital and power, 19: 5496
cost analysis of electricity and plutonium from, computer program for, 17: 10061 (TRG-Report-198)
cost analysis of electricity and plutonium from, computer program for, 17: 23852 (TRG-Report-198(Suppl.1))
cost and efficiency of 500- and 1000-Mw(e), effects of steam pressure and temperature on, 19: 14765(R) (ANL-6977)
cost calculation, equation for, 16: 5035
cost calculation for, methodology, 16: 18674
cost calculation methodology, 16: 21828
cost calculations, 16: 15929
cost comparison of biphenyl and steam, 16: 34090
cost data on, capital and operational, 18: 1238 (GC(VI)/INF/53)
cost, effect of variation of components on kilowatt-hour, 16: 12764
cost estimation of, guide for, 17: 31735 (TID-7025(Suppl.1))
cost evaluation of 1000-Mwe molten salt converter power plants, 18: 30997 (SL-1954)
cost evaluation, use of guide in, 17: 12010

cost factors for British designs, 16: 26606
cost factors, guide for estimating, 16: 24990 (TID-7025(Vol.1))
cost factors of buildings, improvements, and land, guide for estimating, 16: 24991 (TID-7025(Vol.2))
cost factors of equipment, guide for estimating, 16: 24992 (TID-7025 (Vol.3))
cost factors of fuel in, guide for estimating, 16: 24993 (TID-7025(Vol.4))
cost factors of power production in, guide for estimating, 16: 24994 (TID-7025(Vol.5))
cost structure of kilowatt price, fixed and variable, 16: 7303
cost studies on large steam-electric, 20: 30875(R) (ANL-7190, pp 143-55)
costs analysis, 16: 12760
costs analysis and methods of estimating generating costs, 16: 7305 (STI/DOC/10/5)
costs, comparison with conventional power plants, 16: 5050
costs for, analysis of, 18: 38382 (A/CONF.28/P/11)
costs of, economic factors affecting, 17: 22863
costs of one- and two-reactor 150- to 1000-Mwe, (T), 19: 31550 (NYO-3289-1)
costs of RISE, effect of power conversion efficiency on, 20: 43799 (NP-16281)
criticality accidents in, alarm system for detecting, 19: 44321
current generation costs in, effect of interest rates, taxes, and amortization time on, 18: 4807
defense against nuclear attack, comparison with coal-fired systems, 17: 7656 (BNL-6080)
description, 16: 34103(P)
description and cost analysis of 1800-Mw(e) heavy-water, 17: 33332
description of boiling water, 17: 10104
description of direct-conversion, using triode concept, 17: 5068
description of German AEG projects, 17: 24695
description of Kahl installation, 17: 22878
description of multi-kwe nuclear-thermoelectric, for space, (E/T), 19: 29771
description of radioisotope-powered pulsed engine, 18: 27830
description of Russian Arbus 750-kw(e) organic-moderated, 18: 38436 (A/CONF.28/P/307)
description of Soviet-100 Mw(e) with boiling water graphite reactor and high pressure steam superheater, 16: 9684
description of 450-Mw(e) spectral-shift-control, 17: 13790
description of 525-Mw(e) sodium-graphite, 17: 7623
description of, for direct nuclear-to-laser power conversion, 18: 28312
design, 16: 6197(P)
design, 16: 21834(P)
design, 17: 2606(P)
design, 17: 28558(P)
design, (E), 19: 8649(P)
design, 19: 31575(P)
design, 20: 36501(P)
design and characteristics of Berkeley and Bradwell, review, 17: 42366
design and construction of experimental, at Kahl, Germany, 16: 9681
design and construction, 17: 7617
design and construction of, at Ardennes, France, 17: 42380
design and construction of, economic aspects, 18: 6498
design and cost calculations for heavy water, computer program, 16: 27545 (DP-707)
design and cost estimates to 4-unit heavy-water, 17: 33360
design and development of maritime, 16: 34068(R) (GEMP-144)
design and development, 17: 5622
design and development, 17: 5624
design and development, 17: 5625
design and development of Latina, 18: 24923
design and development of Gundremmingen, in 1963, 18: 26918(R) (EUR-1802.d)
design and development, (E), 19: 5514(P)
design and development of 237-Mw KRB, 19: 10573(R) (TID-21407)
design and development of French, 19: 12788(T) (RISLEY-Trans-287)
design and development of SENA, 19: 24091(R) (TID-21500)
design and dynamic analysis of, aseismatic, 19: 17315
design and economics of heavy-water-moderated, trends in, 17: 36948
design and economic aspects of Inland Antarctic station, 17: 40334 (ACNP-63809(Vol.I))
design and economic aspects of Lingen, at Darme, Germany, 19: 27785
design and evaluation of 1000-Mw(e), with circulating fuel gaseous core reactor, 20: 5128 (TID-22225)
design and operation for supplying variable grid loads, 16: 11310(P)
design and operation, 18: 17314(P)
design and performance of compact thermionic, for space applications, 16: 26598 (NAA-SR-7144)
design and safety, in passenger ship, 16: 3298
design at Fairport, Ontario, 18: 45040
design concept of 300-Mw(e) graphite-moderated boiling-water superheat, 17: 2518
design concepts for thermionic, 17: 22857 (MND-2903(Vol.I))
design data estimation, statistical methods for, 16: 14330
design data for 300- and 1000-Mw(e) sodium graphite, 17: 2594
design description of Douglas Point station, 16: 20008
design description of Swedish 235-Mw(e) rock-vessel, 17: 4311
design development of Agesta and Marviken, in Sweden, 17: 22869
design evaluation of 200-Mw(e) Gamma, 16: 1239 (DANATOM-04-61)
design feasibility of unattended 300-kw(e), 17: 24677 (GEAP-3474)
design feasibility and economics of 1000-Mw(e) pressurized-water, 19: 35797
design for continued operation after reactor shutdown, 18: 7951(P)
design for direct conversion, 17: 28560(P)
design for gas-cooled reactors, 16: 14335(P)
design for improved cycle efficiency, 16: 3954(P)
design for improved efficiency with inorganic fluid coolant, 18: 13310(P)
design for improved efficiency, 18: 26951(P)
design for improved thermal efficiency, 19: 25741(P)
design for improved thermal efficiency, 19: 25743(P)
design for increased steam generation capacity, 17: 21351(P)
design for Japanese nuclear-powered ship, 20: 24783
design for Lenin icebreaker, 16: 11239(T) (JPRS-12183(p.11-34))
design for lunar base mission, 19: 10631
design for Mambucaba, Brazil, 16: 7280
design for manned lunar bases, 18: 36811(R) (WANL-PR(S)001-A)
design for moderator heat transmission to steam cycle, 16: 32600(P)
design for moderator heat transmission to steam cycle, 16: 32601(P)
design for once-through steam generation, 20: 30931(P)
design for operation at low temperatures and pressures, 16: 20020(P)
design for preventing pressure rise in containment vessel in event of accident, 16: 17867(P)
design for producing superheated vapor, 16: 34099(P)
design for simplified fluid circulation, 19: 27808(P)
design for simplified coolant circulation, 20: 26509(P)
design for superheated steam, 16: 21835(P)
design for superheated steam, 17: 2607(P)
design for superheated steam, 17: 13801(P)
design for thermoelectric, for underwater applications, 18: 24903 (NP-13900(Sect.10))
design for thorium fuel, 18: 15511 (ACNP-62548)
design for use with MHD generators, 20: 47024
design for water desalination, 19: 45635
design for 70,000 ton tanker, 16: 32590
design incorporating gas turbines, 18: 40878
design of, at Mol, Belgium, 18: 1261
design of beryllium-moderated gas-cooled, 17: 10118(P)
design of boiling mercury, for use in airless environment, 17: 22902(P)
design of boiling-reactor, 17: 28555(P)
design of boiling-water, built by General Electric, 17: 36951
design of Brayton-cycle, for space, 17: 35233
design of Brayton-cycle, for space vehicles, 19: 48048 (GE-65SD4251)
design of compact, 17: 26857 (GEAP-3962)
design of device for compensating sudden load changes in, 17: 26884(P)
design of dual-purpose, 20: 47042(P)
design of Dungeness B, 19: 47995 (NP-15473)
design of Dungeness B, 20: 20280
design of earthquake-resistant, in Japan, 16: 23328
design of earthquake-resistant, Calder Hall type, 17: 42378
design of earthquake resistant, 20: 28792
design of first Czech, (E), 19: 14852(T) (ORNL-tr-402)
design of floating, factors in, 19: 24134
design of, for a lunar mobile surface vehicle, 17: 4348 (61SPC3)
design of Garigliano, 18: 36821
design of gas-cooled reactor with heat exchanger, 16: 15995(P)
design of gas cooled, 19: 35730(P)
design of German 300-Mw pressurized-water, 19: 45609
design of, having two primary circuits, 16: 31317(P)
design of heat transfer system, 16: 28594(P)
design of large Swedish, 18: 38485 (A/CONF.28/P/605)
design of Latina, 18: 11458
design of layout for, 20: 24759
design of magnetohydrodynamic, 17: 12002
design of marine, using steam jet propulsion, 19: 40255(P)
design of mobile boiling-water, 18: 6504(P)
design of multipass superheated-steam-cooled, 17: 29815(P)
design of nuclear-thermionic, 17: 17586(P)
design of, operating experience for, 18: 9697
design of, optimalization of parameters in, 17: 7619
design of phosphorus sulfide cooled, 18: 3238
design of phosphorus sesquisulfide-cooled portable thermoelectric, 18: 12880
design of phosphorus sulfide-cooled thermoelectric, conceptual, 18: 24902 (NP-13900(Sect.9))
design of portable, 18: 38439 (A/CONF.28/P/310)

design of potassium–steam binary vapor cycle molten-salt, 20: 47025
design of pressurized-water, for superheating, 16: 3922(P)
design of pressurized-water marine, 17: 38560
design of radioisotope, for aircraft, land vehicles, and ships, 20: 46128(P)
design of, review of safeguards for, 17: 1075
design of Russian, at Voronezh, 16: 32624 (KR-24)
design of steam-generating, 17: 2602(P)
design of steam generator for use in, 20: 1517(P)
design of steam-operated, 16: 31320(P)
design of Swiss NOK, 20: 1490
design of thermionic, 18: 24927
design of thermionic-reactor, for space vehicles, 19: 3728 (PWA-2319)
design of thermoelectric, for underwater applications, 19: 45627
design of TRIKT-50 thermionic, for space, 20: 12482
design of two-region fission-electric reactor, (E), 19: 24086 (JPL-TR-32-685)
design of underground, in rock, 17: 24710(P)
design of unified modular, 18: 19406 (CEND-169)
design of, using a pressure-tube reactor, 17: 40372
design of vapor-cooled, 17: 29817(P)
design of water-cooled portable thermoelectric, 18: 12881
design of water-cooled double-cycle, efficient selections of parameters for, 19: 10594
design of, with superheating, 17: 28549
design of Wylfa, 18: 11457
design of 1-Mw thermionic space, 17: 35222 (PWA-2240)
design of 100-kwe thermoelectric, 18: 3237
design of 100-Mw(e) natural-circulation boiling-water, 16: 14317 (TID-15057)
design of 1000-Mwe, reference, 19: 24089(R) (SRO-114)
design of 15-Mw(e), for Austria, 19: 45581 (NP-15291)
design of 150-Mw, with vaporizing reactor, 17: 10084
design of 150-Mwe Hungarian, 16: 20009
design of 237-Mwe German, at Gundremmingen, 18: 9664
design of 3.25-Mw nuclear-thermionic, for space, (E), 19: 10623 (PWA-2351(Vol.I))
design of 300-kwe capsule reactor, 16: 1241 (GEAP-3485)
design of 300 Mw multiple boiling-superheat, 17: 15464 (SL-1812)
design of 500 Mev(e), using organic-cooled, heavy-water-moderated reactor, 18: 11430 (CEND-175(Vol.II))
design of 500 Mw(e), 19: 25734 (WAPD-LPR-154)
design of 500-Mw(e) Candu-type, 18: 38379 (A/CONF.28/P/6)
design of, dynamic problems in structural, 20: 8432
design of, engineering techniques in, (E), 19: 17284(T) (ORNL-tr-405)
design of, guide for planning in, 19: 24114
design of, optimization program for, 20: 6605 (GAMD-6673)
design of, optimum parameters for, 18: 36828
design of, using electrochemical heat conversion, 19: 17251(P)
design of, using HWOCR concept, 20: 42621 (CONF-660516-16)
design optimization of organic-cooled, 17: 11979(R) (DP-805)
design optimization, 17: 26099
design optimization using gradients, 18: 38481 (A/CONF.28/P/599)
design optimization of dual-purpose desalination, 19: 29647 (ORNL-P-1151)
design optimization of gas-turbine, 20: 12422
design parameters for gas-cooled, optimum, 20: 10404
design requirements for manned lunar power station, 18: 26956 (MTP-ASTR-A-63-8)
design study of dual-purpose heavy-water, for sea water distillation, 18: 21632 (DP-866)
design study of fission-electric cell-reactor, 20: 3577
design study of fluid engine conversion system for, 18: 6492 (NYO-10398)
design techniques utilizing computers, 16: 21833
design using advanced gas-cooled reactor, 20: 28781
design, using chemical fuel cells, 17: 2605(P)
design using gas-cooled semihomogeneous reactor, 18: 23071
design using gas-cooled heavy-water-moderated pressure-tube reactor, 19: 42112
design using heavy water moderated reactors, 19: 40211
design using molten-salt reactor with potassium–steam binary vapor cycle, 20: 24737 (ORNL-P-2052)
design using ORGEL reactors, optimization of, 18: 1235 (EUR-466.d)
design using pressurized coolant expansion in turbine, 18: 9706(P)
design using pressurized water reactor and steam generator, 20: 30911(P)
design using steam-cooled heavy-water-moderated reactor, 20: 28789
design using steam turbine driven circulator for reactor coolant, 20: 28811(P)
design using two differently pressured boilers, 20: 5171(P)
design using two primary cooling circuits, 19: 33648(P)
design using vapor-cooled heterogeneous reactor, 20: 16106(P)
design using water-moderated reactor, 20: 24774(P)
design using 500 Mw(e) breeder reactors, 19: 25733 (WAPD-LPR-141)
design with auxiliary superheater, 16: 34102(P)
design with constant coolant temperature at reactor inlet, 16: 26611(P)
design with cooling of pump motor, 18: 35191(P)
design with dual cooling circuits, 20: 22458
design with pressure-tube reactor, 17: 26886(P)
design with steam-cooled reactor, 17: 21355(P)
design with superheating reactor, 16: 1226(P)
design with two cooling cycles, 17: 29818(P)
design with two primary circuits for generating superheated steam, 17: 26885(P)
design without expansion joints, 16: 6237(P)
design, reliability for space applications, 18: 29117
destruction during re-entry from space, RFD-1 test results, (E), 19: 8661 (SC-RR-64-516)
development, 17: 21264
development, 19: 33612
development, 19: 38205
development, 20: 35046
development and cost of long-range program, 18: 38490 (A/CONF.28/P/636)
development and economic aspects of small, 16: 5054
development and economic aspects of ENEA, 17: 37006(R) (NP-13095)
development and economics of, review of, 17: 36944
development and economics of military, (E), 19: 10575 (WL-TDR-64-25)
development and economics of, 20: 5168
development and economic aspects of, in European Atomic Energy Community, 20: 10282
development and economics of, for communications satellites, 20: 29608
development and economics of, in France, 20: 32889
development and future use in Europe, analysis of, 20: 40443
development and introduction in electric networks in Europe, 20: 10388
development and operation of ENEA, July 1963 to July 1964, 19: 10677(R) (NP-14552)
development and prospects of, review of, 20: 1481
development and selection of type of, for Yugoslavia, 17: 11976
development and shielding for space vehicles, 16: 20236
development and testing of thermionic, summary, 18: 7956(R) (GA-3992(Pt.I))
development and testing of Latina station, 18: 26921(R) (EUR-1810.i)
development and testing of nuclear-thermoelectric, 18: 26251(R) (AD-437280)
development and testing of nuclear-thermionic, 18: 36228(R) (GEST-2033)
development and use of, public health aspects of, 18: 43853
development and utilization in Spain, 20: 1576
development data on western European, 20: 40441
development for desalination, 19: 38212
development for electric space propulsion, 18: 31027
development for space vehicles, 16: 17327
development for space propulsion, survey, 16: 31339
development for space vehicles, 18: 13322
development for space flight, economics and technical problems in, 18: 13323
development for space vehicles, (E/T), 19: 38836 (NASA-SP-79)
development for space, 20: 12484
development for use as maritime steam generator, 16: 28530 (GEMP-107)
development for water desalination and electricity production, 19: 33631
development for water desalination and power, 19: 42124
development in Austria, 19: 48010
development in Belgium, 19: 48113
development in Canada, review of, 18: 35171
development in Canada by private industry, 18: 41004
development in Common Market countries, 20: 10395
development in Czechoslovakia, 16: 8384
development in Denmark, 19: 48004
development in EURATOM, industrial aspects of, 18: 43025(R) (EUR-1850.e(p.135-9))
development in EURATOM, status of, 18: 43026(R) (EUR-1850.e (p.141-51))
development in Europe, 1963, 19: 17289
development in Europe, review of conditions for, 19: 45610
development in European Atomic Energy Community, target program for, 19: 48003
development in Federal Republic of Germany, 18: 9798
development in France, 19: 45580 (NP-15283)
development in France, 19: 48006
development in Great Britain, 17: 36937
development in Great Britain, 19: 48007
development in Great Britain, review of, 20: 12427
development in India, 20: 32817

development in Israel for sea water desalination, economic and technical advantages for, 20: 45188
development in Italy, prospects for, 19: 45622
development in Italy, 19: 48008
development in Japan, 19: 39064
development in Netherlands, 19: 47923
development in Soviet Union, 19: 21762 (RM-2163(RAND))
development in Spain, 19: 48011
development in Spain, problems in, 20: 5158
development in Sweden, 19: 8647
development in Sweden, 20: 26477
development in Switzerland, 19: 48009
development in U. S., economic analysis of, 20: 45175
development in U.S.A., outline, 19: 45615
development in United Kingdom, 16: 20012
development in United Kingdom, uses of DIDO reactors in, 17: 5636
development in United States, 20: 30885
development in USSR and abroad, survey, 17: 13789
development in USSR, survey, 18: 19396
development in Western Europe, review, 19: 31656
development in Yugoslavia, 19: 38211
development of Beloyarsk, in Ural Mountains, 17: 21324
development of Canadian, 19: 21781
development of Canadian, 19: 45694(R) (AECL-2251)
development of cermet emitters for nuclear-thermionic, 18: 29015
development of closed-cycle gas-turbine, 20: 28783
development of d-c–to–d-c converters for nuclear-thermionic, 18: 34497(R) (NP-12888(Vol.5))
development of direct-cycle steam-superheating, 20: 5113 (CONF-650602-59)
development of Dungeness-B 1200-Mw(e), 19: 48020
development of, economic aspects of, 17: 1045(R) (NP-12101)
development of Euratom, 17: 42343(R) (EUR-420.e)
development of fast breeder reactors for, 19: 5492
development of fission-electric, 18: 28310
development of Garigliano station, quarterly summary, 17: 28530(R) (NP-12909)
development of Garigliano station, quarterly summary, 17: 29791(R) (GEAP-4218)
development of Garigliano station for increased power output, quarterly summary No. 3, 17: 33311 (GEAP-4306)
development of Garigliano station, quarterly summary No. 4, 18: 1242(R) (GEAP-4389)
development of Garigliano station, quarterly summary No. 5, 18: 11434(R) (GEAP-4486)
development of, in Finland, 17: 22870
development of, in Sweden, contribution of private industry to, 17: 22868
development of Japanese, 19: 48043
development of, joint US-EURATOM progress on, October 1 to December 31, 1962, 17: 24663
development of Karachi, status, 20: 45101(R) (66-CNA-305)
development of large turbo-, for space vehicles, 18: 4840
development of low-temperature nuclear-thermionic, 18: 30474(R) (AD-428884)
development of magnetohydrodynamic, 17: 37001(R) (ANL-6780)
development of nuclear-MHD gas-cycle, 18: 12853(R) (AD-409905)
development of nuclear-thermionic, for lunar bases, 18: 28311
development of nuclear-thermionic, 18: 37869 (A/CONF.28/P/132)
development of nuclear-magnetoplasmadynamic, 18: 37870 (A/CONF.28/P/133)
development of nuclear-thermionic, 18: 38392 (A/CONF.28/P/44)
development of nuclear-thermionic, 18: 44499(R) (MND-2812-4)
development of nuclear-thermionic, 18: 44497(R) (MND-2812-2)
development of nuclear-regenerative fuel cells, (E), 19: 14286(R) (AD-422728)
development of nuclear-thermionic double-diode, (E), 19: 14295(R) (MND-3149-2)
development of nuclear-thermionic noble-gas plasma diodes, (E/T), 19: 16440(R) (AD-609177)
development of nuclear-thermionic noble-gas plasma diodes, (E/T), 19: 16366(R) (AD-609177(Sect.A))
development of nuclear-thermionic, (E), 19: 30978 (LA-DC-7073)
development of nuclear-thermionic, (E), 19: 35008
development of nuclear-thermionic, 20: 15294 (CONF-640921, pp 9-45)
development of Rankine-turboelectric and in-core thermionic, for unmanned spacecraft, 19: 3713 (64SD892)
development of Rooppur, 18: 38480 (A/CONF.28/P/597)
development of thermionic, 18: 6490 (MND-2903(Vol.II))
development of thermoelectric, for space uses, 18: 24351(R) (AD-427285)
development of thermoelectric, for space, (E), 19: 16444(R) (AFAPL-TR-64-135)
development of thermionic, summary, 18: 24369(R) (NP-13892)
development of 300 Mw(e), in Finland, 19: 48005
development of, economic and technical aspects of, 18: 38505 (A/CONF.28/P/731)
development of, effects of magnetohydrodynamic generators on, 19: 48013
development of, Euratom studies of industry grouping for, 19: 48118
development of, in Federal Republic of Germany, 18: 43043
development of, international cooperation in, 18: 33069 (A/CONF.28/P/193)
development of, in European Atomic Energy Community, 20: 18180
development of, in India, 20: 36539(R) (NP-16171)
development of, neutron cross section data requirements for, 20: 32839
development of, review of uranium requirements for, 20: 12558
development of, review of industrial aspects of, 20: 24827
development of, supercritical steams cycles in, 19: 42121
development of, 1965 Report to Congress on, 20: 24825
development perspectives of Russian, 20: 5149
development program for superheating, 17: 7624
development prospects for, 20: 8423
development status review, 16: 28587
development studies on, in Denmark, 17: 22871
development, survey, 16: 9685
development, technical and economic, 16: 32585
development, 1962, 17: 5662
digital computers in, 16: 1993
dynamic analysis of gas turbine, digital, 18: 3177 (GAMD-489)
dynamic stability analyses of, 18: 38448 (A/CONF.28/P/371)
dynamics analysis of Beloyarsk, 17: 42364
economic analysis of heavy water-moderated, 17: 33331
economic and technical risks in operation of, 18: 21645
economic and technical data on, 18: 40883
economic and technical aspects of, survey of, 19: 10579
economic and technical aspects of Dungeness-B, 19: 48023
economic and technical appraisal of Dungeness B, 20: 20279
economic aspects, 16: 30110 (RT/EC(62)1)
economic aspects, 17: 33334
economic aspects, 19: 10582
economic aspects, 19: 10595
economic aspects, 20: 26592
economic aspects and cost evaluation, 16: 5049
economic aspects and predictions of future use of, 20: 35095
economic aspects in electric utility systems, 17: 33348
economic aspects in electric utility systems, 18: 17305
economic aspects in Europe, 1970 to 1979, Euratom estimates of, 19: 38319
economic aspects of use of, in chemical industry, 17: 24700
economic aspects of site selection for, 17: 26866 (NYO-10280)
economic aspects of European, 18: 15571
economic aspects of large, 18: 26993
economic aspects of, 19: 10594
economic aspects of dual-purpose desalination plants, 19: 38185 (ORNL-P-1278)
economic aspects of, in Japan, 19: 38204
economic aspects of, effects of fuel reserves and costs of tubing on, 19: 47979
economic aspects of, in Soviet Union, 19: 48014
economic aspects of, in coordinated networks, 20: 1488
economic aspects of, in Britain, 20: 10396
economic aspects of, 20: 36945
economic assessment of combinations of, method for, 17: 15483
economic assessment of large dual-purpose, for sea water distillation, 18: 19403
economic assessment of large dual-purpose, for desalination, 18: 36834
economic comparison with coal-fired plants, 16: 31282
economic comparison to conventional power plants, 19: 33630
economic comparison of boiling-water and gas-cooled reactors for, 20: 12432
economic effects of, in electric power grids, 18: 6487 (EUR-468.i)
economic efficiency of gas circulators for, with gas-cooled heavy-water reactors, 20: 28784
economic feasibility of merchant-vessel, 18: 43058 (EUR-586.d(App.))
economic feasibility of Canadian, (E), 19: 12768 (AECL-2069)
economic feasibility of, factors affecting, 20: 47020
economic integration into electric systems, 19: 21695
economic justifications for small, in isolated regions, 16: 5066
economic potential in Germany, 16: 20007
economic prospects in Spain, review, 17: 35159
economic trends of, 20: 28738 (AECL-2534)
economics, 18: 33113
economics, 20: 14121 (EUR-2453.f)
economics, 20: 10276(R) (NP-15580)
economics, 20: 14133 (NP-15587)
economics and design of Karachi, 18: 35183

economics and efficiency of gas-cooled reactor turbine, effects of cycle parameters on, 16: 34001 (Y-1396)
economics and evaluation of nuclear defense capabilities of, 17: 33361
economics and future uses of, summary, 18: 33068 (A/CONF.28/P/192)
economics and growth in free world, 20: 32808 (TID-22973)
economics and load factor of thermal, 18: 38470 (A/CONF.28/P/546)
economics and prospects for, 20: 10398
economics and prospects for, model analysis of, 20: 45128
economics and status, 18: 36818
economics and status of dual-purpose, 20: 45189
economics and thermal efficiency of superheated, 18: 36825
economics and thermal efficiency of, 19: 27805
economics and use of large-scaled, 18: 4802 (TID-7683(p.36))
economics for electricity and water production, 18: 19394
economics for Portuguese power system, 18: 38702 (A/CONF.28/P/598)
economics for 1000-Mw(e) pressurized water, reference, 19: 42102 (WCAP-2385(Vol.I))
economics in Germany, 20: 14130 (KFK-366)
economics in United Kingdom and USA, 19: 38213
economics of, 19: 17288
economics of, 20: 35013 (CONF-660308, pp 196-201)
economics of advanced, 20: 28782
economics of desalination-power, 20: 45187
economics of dual-purpose desalination, 20: 20292
economics of Dungeness B, 19: 47996 (NP-15474)
economics of electric utility expansion using, 16: 30121
economics of equipment and fuel cost for, 19: 35631
water and electricity, effect of maximum brine temperature on, 17: 19632 (ORNL-TM-536)
economics of heavy-water-reactor, 18: 11432(R) (DP-875)
economics of integration of, into existing electrical networks,
economics of heavy-water-cooled and -moderated, for the production of 19: 24115
economics of low-capacity, 20: 18107
economics of mixed ownership of dual-purpose power-desalination plants, 18: 13290 (ORNL-TM-787)
economics of small electric-desalination, (T), 19: 29685
economics of small dual-purpose, for electricity and sea water desalination, 20: 35105
economics of steam as coolant in, 18: 31002
economics of, analysis of future, 20: 12440
economics of, bibliography on, 20: 24738 (PEL-97)
economics of, calculation of size for optimum, 18: 26934
economics of, calculation method for, 20: 32814
economics of, compared to fossil-fueled plants, 19: 31569
economics of, computer program for calculating, 20: 32743 (ORNL-3944)
economics of, comparison with fossil-fuel and hydro plants, 20: 38511
economics of, comparison with coal- and oil-fired power plants, 20: 38520
economics of, effects of safety problems on, 19: 33596 (CONF-650201 (p.110-24))
economics of, for domestic power production, 18: 31004
economics of, for Canada, 18: 38378 (A/CONF.28/P/1)
economics of, for expanding utility systems, 20: 45178
economics of, for undersea mining operations, 20: 45927
economics of, in Czechoslovakia, (E), 19: 14853(T) (ORNL-tr-403)
economics of, method for analysis of, 18: 21656
economics of, survey, 18: 31010
effects on regional industrial development, 20: 10496
efficiency comparisons with conventional plants, 19: 38195 (ZfK-RN-30)
efficiency of, with supplemental oil combustion, 19: 12791
efficiency using gas turbines, 20: 38513
efficiency using liquid-metal MHD power cycles, 20: 29980
effluent monitoring at, gaseous, 18: 8593
electric characteristics of nuclear-thermionic noble-gas plasma diodes, (T), 19: 16249(R) (AD-609177(Sec.B))
electric design considerations for closed cycle water, 17: 21327
electric systems of foreign, 20: 1507
electrical characteristics, using thermionic- and turbo-generators, 16: 28626
electrical system of Hunterston, 16: 34091
electrical system design for NPD reactor, 16: 34094
electrical system for dual-cycle boiling-water reactor, 17: 15488
electricity and heat production by small, 16: 5065
electrodes for nuclear-thermionic, 18: 16742(R) (GA-4804)
energy conversion in, MHD, 17: 28548
energy conversion in, methods for direct, 20: 10406
energy transfer in, 19: 22498(T)
energy transformation in, efficiency of, 20: 32813
engineering aspects, 16: 31706
engineering aspects of dual-purpose, 20: 35104
engineering features of, civil, 17: 1140
engineering problems in, review of conventional, 17: 42381
engineering to meet daily and yearly load needs, 16: 12761
environmental monitoring program for, at Indian Point, N. Y., 17: 18400
environs monitoring, 16: 7779
environs monitoring of Enrico Fermi, 17: 23561
environs monitoring in England, 18: 6775
environs monitoring program at, in England, 18: 8588
environs monitoring at Berkeley, district survey program for, 18: 8601
equipment for Yugoslavia, possibility of domestic manufacture of, 17: 11976
equipment for, laboratory for industrial-scale testing, 19: 38197
evaluation for electric propulsion, problems in, 18: 13320
evaluation for space flight, 16: 29265
evaluation of 300-Mw(e) heavy water, research program on, 18: 9651(R) (SL-1974-1)
evaluation of, factors in, 20: 35094
experimental loop for Kahl, constructional and assembly problems in installation of, 18: 28938
experimental studies in Kurchatov, Russia, 18: 38441 (A/CONF.28/P/314)
fabrication and installation of steam system, heat exchangers, and piping for Japanese Power Development Reactor, 18: 19386
fabrication of cesium-137 borosilicate-glass, (E), 19: 22839 (ORNL-3669)
fabrication of Kahl, materials used in, 17: 22881
fabrication of Kahl, civil engineering experiences in, 17: 22882
feasibility for water desalination, 19: 31571
feasibility of barge-mounted, 18: 36801 (AD-437833)
feasibility of breeder-reactor, long-range analysis, 18: 4936
feasibility of MHD-reactor, 20: 14132 (LA-3368)
feasibility of offshore, for desalination, 20: 10413 (ORNL-TM-1329)
feasibility of steam, for lunar base operation, 19: 3611 (ASTRA-G-39.2)
feasibility of 1000-Mw(e) boiling-water, 19: 3625 (GEAP-4476(Vol.I))
feasibility of 1000-Mw(e) boiling-water, 19: 3626 (GEAP-4476(Vol.II))
feasibility of 1000-Mw(e) boiling-water, 19: 3627 (GEAP-4476(Vol.III))
feasibility of 1000-Mw(e) pressurized water, 19: 42102 (WCAP-2385 (Vol.I))
feasibility of 1000-Mw(e) pressurized water, 19: 42103 (WCAP-2385(Vol. II))
feasibility of, in heavily populated areas, 19: 40207
feed water pre-heating temperature for, methods for computation of, 17: 18238
filter testing of ventilation system in, 19: 22602 (RISO-94)
fission product release following loss-of-coolant accident in, calculation of, 19: 31567
fluid flow stability analyses in radiator manifolds for space, 18: 3300 (PWA-2227(Vol.2))
frequency regulation by, in Swedish power system, 18: 38486 (A/CONF.28/P/606)
fuel costs, calculation, 17: 4315
fuel cycle costs in, method for calculating, 18: 45005
fuel cycle costs of, 18: 38370 (A/CONF.28/P/570)
fuel cycle economics, 16: 5055
fuel cycling capital costs, calculation in France, 18: 13280 (CEA-2325)
fuel economics, 18: 42969
fuel element development for nuclear-thermionic, 18: 12851(R) (AD-409015)
fuel element examination at Latina, hot laboratory for, 18: 30996 (RT/ING(64)-4)
fuel elements for lunar, mechanical analysis of, 18: 24943
fuel for Berkeley and Bradwell, 17: 22891
fuel for, economic factors in obtaining, 17: 5610
fuel management in SENN, effects on plant cost, 18: 9649 (NYO-9990)
fuels and materials for advanced, development of, 16: 30854
fuels for nuclear-thermionic, development of coated-urania, 18: 28018
fuels for, projected availabilities of, 18: 33173 (A/CONF.28/P/256)
future of, in developing countries, 18: 6500
gas circulation in, gas injection into bearings from cleaning circuit for, 18: 33119(P)
gas circulator motors and generators in Calder Hall, operating experience, 16: 34092
gas turbine design for, 19: 3757
gas turbine performance in, 20: 25235
hazards evaluation of, public health considerations in, 19: 11466
hazards summary for Southern California Edison Coast nuclear station, 17: 14532 (NP-12513)
hazards summary of Inland Antarctic station, 17: 40335 (ACNP-63809(Vol.II))
health physics and safety programs for, in Great Britain, 18: 10314
health physics experience at Chapelcross, 16: 31995
health physics experience at Chapelcross, 17: 30760
health zone around, method for determining, 17: 36942
heat exchange in vaporizer, thermodynamic analysis, 16: 8878(T) (AEC-tr-4943)

heat exchanger and steam generator design and operation for 30-Mw sodium cooled, 17: 265 (APAE-112(Vol.IV))
heat-exchanger design for small, 17: 30650(P)
heat exchanger design for, 19: 29700(P)
heat exchanger development for, 18: 23076
heat exchanger for, design of, 17: 10016(P)
heat rejection by space, research on, 17: 27535 (BNL-801)
heat transfer control, 17: 4686(P)
heat transfer in, methods for, 17: 37338
heat transfer in nuclear-heated tube bundles in, (T), 19: 18113 (LA-3167)
heat transfer, research programs of British at CERL, 16: 4310
heat transfer systems for space-vehicle auxiliary, 18: 29844(R) (SAN-409-1)
heat utilization system for, 19: 14863(P)
hydrodynamic losses in radiator manifolds of Rankine-cycle space, analysis of, 18: 3299 (PWA-2227(Vol.1))
in European Nuclear Energy Agency countries, listing of, 20: 26587(R) (NP-15919)
industrial development of, conference on, 19: 28711
industry in Canada, general survey, 20: 45102 (66-CNA-320)
instrumentation and control of, feasibility of unified digital system for, 20: 38508 (NYO-2764-2)
instrumentation at Berkeley, 16: 34086
instrumentation for, as factor in power cost, 16: 30630
instrumentation for, design of non-nuclear and nuclear, 18: 31003
insulation problems for, materials and techniques for, 20: 3487
integration into utility system, problems of, 20: 45182
introduction of, into power supply with conventional power plants, 17: 22862
ion generation rates in nuclear-thermionic argon–cesium, (E), 19: 16442(R) (AD-609177(Sect.E))
kinetics of nuclear-thermionic, for space vehicles, transient, 20: 35143
kinetics of, analog calculations of, 18: 44987
kinetics using coupled-core superheating boiling-water reactors, 20: 36463 (CONF-650413, pp 544-65)
leak detection and measurement in, 18: 35207
leak tightness of buildings, criteria, 17: 19658
licensing of, public safety aspects of, 20: 22434
licensing procedures in France, decree for, 19: 10464
list of, built or planned in European Atomic Energy Community, 17: 24743 (EUR-183.e)
lists of, worldwide, 20: 14222(R) (NP-15612)
locks in, control of isolation, 19: 11425
lubricants for, evaluation of properties of, 17: 24709
lubrication requirements for, 16: 1210
magnetohydrodynamic generators in, 18: 828
magnetohydrodynamic generators for, status of, 19: 25257
magnetohydrodynamic generator for, 20: 17328
maintenance and operation, 18: 38262
marine, safety of, 18: 10320
materials for, development of steel plate, 19: 38196(T) (NSJ-tr-37)
materials for, review, 20: 30815
materials management in Italian, 20: 20964
materials problems for, survey of, 18: 10464
materials, properties of steel, 16: 13619
materials, uses of reinforced plastic, 16: 10447
medium-temperature reactor development for medium-capacity, 16: 5059
monitoring of environs, 17: 12493 (CRER-1120)
monitoring procedure for personnel at, in Kahl, Germany, 18: 1965
mounting submarine, external vs internal, 20: 6664
neutron flux measuring equipment for Hinkley Point, 16: 34088
operating experience of Kahl station from 1961 to 1963, 17: 33338
operating experience of *Lenin* icebreaker from 1959 to 1963, 18: 38552 (A/CONF.28/P/313)
operating using benzene as coolant-moderator and working medium, 19: 31576(P)
operation and performance of, at Berkeley and Bradwell, England, 19: 5495
operation conditions for small and medium, in Argentina, 16: 5067
operation experience of first Soviet, 16: 3948(T) (FTD-TT-61-151)
operation in water-filled containment, rupture tests of, 18: 30942 (BAW-3198-2)
operation of AEC, 16: 3950
operation of C.E.G.B., personnel recruitment and training for, 17: 40399
operation of, comparison with conventional stations, 17: 19646
operation of electrical equipment in Belgian BR-3, 18: 29100
operation of first Russian, 17: 36957
operation of gas-cooled, effect of departure from optimum, on economics, 17: 13772 (AAEC/TM-171)
operation of Kahl Station, Germany, 16: 31298
operation of Kahl Station, Germany, 16: 31283
operation of, organization of group, for, 17: 10092
operation of PWR, conditions for minimum specific power cost in, (T), 20: 22448
operation of, radiation protection measures for, 17: 18443
operation of Saxton, 18: 29097
operation of simulated Rankine-cycle, for space applications, 17: 28574(R) (PWA-2197)
operation of sodium-cooled, 18: 29098
operation of, selection of personnel for, 19: 42098 (RT/PROT(65)24)
operation probability calculations, 16: 18645 (AFSWC-TDR-61-100 (Vols. I & II))
operation probability, 17: 22886
operation using benzene as coolant-moderator and working medium, 19: 31580(P)
operation with conventional plants, economics of integrated, 20: 35092
operation with conventional plants, economics of integrated, 20: 47049
operational effectiveness for use at Nike X launch facilities, 18: 33095 (AD-430158)
operations, survey of experience in UK, USA, and USSR, 16: 5038
optimization of preheating temperature of feed water for, 17: 33329
parameters of dynamic behavior of, 17: 7529 (AEEW-R-179)
parameters using ORGEL reactors, optimum, 18: 1234 (EUR-464.f)
performance analysis of turbo-generator power cycle using reacting gas, 16: 11330 (ERR-SD-135)
performance as power source for ion thrustors for spacecraft, (T), 19: 26521 (APL-TDR-64-52(Vol.II))
performance comparison of gas-cycle, for space vehicles, 17: 31778
performance compared to conventional power plants, 18: 19388
performance efficiency enhancement for arctic installations, 16: 18668(R) (RADC-TR-59-77)
performance evaluation of, computer program for, 20: 10373 (GAMD-6674)
performance factors of, preventative maintenance and, 20: 42655
performance for propulsion of icebreakers, 17: 13788
performance for space propulsion, 16: 28630
performance for space propulsion, 17: 13850
performance in electricity-generating networks, 18: 33172 (A/CONF.28/P/216)
performance in integrated space thrustors, 18: 27829
performance in space vehicles, 17: 10212
performance in space propulsion systems, review, 17: 10214
performance in spacecraft ion engines, testing facility for, 18: 39418
performance of boiling-water, 18: 9673
performance of first Soviet, 18: 36824
performance of Kahl, 18: 23070
performance of nuclear-electric space propulsion systems, 16: 9709 (JPL-TR-32-158)
performance of nuclear reactors and heat exchangers in space, research on, 17: 18273(R) (TID-18028)
performance of nuclear-thermionic, 18: 33052 (A/CONF.28/P/219)
performance of spacecraft, integration studies for, 18: 4831 (ASD-TDR-63-428(Pt.I))
performance of spacecraft, integration studies for, 18: 4832 (ASD-TDR-63-428(Pt.II))
performance of, using thermionic cells, (T), 19: 24140
performance with hydrogen for spacecraft propulsion, (E/T), 19: 17346 (NASA-CR-59366)
personnel in, statistical evaluation of hemograms of, 18: 8580
personnel requirements and training, 16: 5046
personnel training program for NPD, 17: 33343
personnel training for Selni, 18: 9692
planning for accidents, 19: 46703
plutonium use in, accounting for, 18: 1263
potassium-steam binary vapor cycle for molten-salt, design study, 18: 40869 (ORNL-3584)
power conversion systems for lunar, 19: 29768
power conversion systems for lunar, 20: 1516
power cost function studies, 16: 20005
power failure, automatic start-up of standby engine in event of, 16: 12771(P)
power failure or shut-down in pressurized water, emergency dynamic behavior in, 20: 1495
power generating system for, 19: 35820(P)
power regulation, 16: 6236(P)
power system for, design of emergency, 20: 24742
pressure suppression containment apparatus for, 17: 26883(P)
pressure vessel design practices for, summary, 16: 15918 (SL-1532A)
pressure vessels for, analysis of prestressed-concrete, (T), 19: 29683
pressure vessels for British, construction and testing of prestressed concrete, 20: 1358
problems of monotube boilers, 18: 38500 (A/CONF.28/P/696)
process systems in, application of chemical engineering to, 20: 8421

progress report on EURATOM-SIMEA, 17: 38542(R) (EUR-330.i)
properties and economics of boiling-water reactors for use as, 17: 42374
protection from water vapor, adsorption system for, 18: 7934
pumps for, description and uses, 16: 12692
radiation detection and control in, apparatus for, 17: 2513
radiation dose rates in environs of, long-range estimates of, 17: 1095
radiation dose rate measurements in Kahl, 17: 22879
radiation dose rate measurements in Kahl, 17: 22880
radiation dosimetry and safety problems in, 20: 11042
radiation hazards control in, 16: 19190
radiation hazards in, insurance aspects of, 19: 9429
radiation hygiene in and around, 17: 34162
radiation monitoring at first Soviet, 18: 36827
radiation monitoring in, instrumentation for, 20: 14864
radiation protection practices in German, 16: 5618
radiation protection in, relation of design and operation to, 19: 24808
radiation protection procedures at, 20: 8417
radiation protection at, methods for, 20: 23388
radiation protection standards at, in U. S., 20: 46000
radiator design for space, 18: 23779
radiator design for heat rejection from, on spacecraft, (T), 19: 40731 (AD-609969)
radioactive contamination in, methods for prevention of, 19: 24805
radioactive contamination of personnel in, medical control in, 19: 24806
radioactive contamination in Japan from, environmental, 20: 33584
radioactivity in exhaust air from, maximum permissible, 19: 28583
radioactivity release to atmosphere from, 19: 12794
radioactivity release from, calculation of limits of permissible, 19: 34411
radiological safety analysis computer program, 20: 37167 (IDO-17151)
raw material preparation for, role of engineer in, 19: 17441
reactivity of, computer model development for analysis of, 20: 7501(R) (TID-22426)
reactor containers for, safety requirements for, 18: 21647
reactor simulators for, use of MNB-1 and MN-7 analog computers as, 19: 22860
reactors for Dungeness B, economic and technical assessment of advanced gas-cooled and boiling-water, 20: 8430
regenerative preheating temperature of water in, with double circulation, 17: 40351
repair of space, feasibility of, 19: 3743
research on thermionic, 17: 27535 (BNL-801)
review, 17: 13791
review, 18: 35180
review of British, 17: 24690
safety, 16: 25010
safety analysis, 20: 22536
safety analysis of space, ground-based, 18: 1955 (SC-DC-3248)
safety and technical problems of mobile and stationary, review, 16: 14333
safety criteria and site selection for, problems of applying fixed formulas for, 18: 6960
safety criteria for, 18: 37470
safety economics in, 18: 15572
safety evaluation, 16: 22488
safety hazards from, review of, 19: 11440
safety in, review of, 18: 41695
safety measures for, economics of, 17: 8477
safety of aerospace, conference on, 18: 8551 (SC-DC-3553)
safety of, analysis of loss-of-coolant accident in, 17: 5618
safety of, review of evaluation methods, 17: 1099
safety of, developments in, 18: 43848
safety of, engineering aspects of, 20: 22437
safety of, insurance view of, 19: 32453 (CONF-650201(p.23-31))
safety of, protective systems for, 20: 10401
safety of, research in U. S. on, 20: 33558 (ORNL-NSIC-10)
safety of, roles of engineered safeguards and siting in, 18: 33116
safety procedures for, 16: 27473(T) (JPRS-14449)
safety requirements for site selection, 16: 30108
safety system description for Berkeley, 16: 32550
safety systems for, design and evaluation of, 20: 22358
safety techniques for, in merchant vessels, 17: 3255
shutdown of, heat removal during, 19: 38225(P)
simulation of, design of transistorized analog-digital converter for, 17: 29725 (RT/EL(63)4)
simulation of Sizewell, use of analog computers for, 17: 22894
simulation of, concepts and methods of, 20: 18106
simulation, uses of analog computers for, 16: 9584(T) (CEA-tr-R-1420)
simulator design and performance for complex optimalization of, automatic, 17: 4319
simulator designs for, 17: 1058
site evaluation for, environmental radioactive contamination as factor in, 17: 14527 (HW-SA-2809)
site evaluation for Mexican, 17: 19662
site evaluation of Sizewell, Suffolk, 16: 28585
site requirements for, 17: 9894
site selection, 19: 32463 (CONF-650201(p.192-200))
site selection criteria, 17: 19660
site selection criteria, 18: 23072
site selection for, survey of factors in, 19: 22565
site selection for, survey of factors in, 19: 22566
site selection for, 20: 16709
site selection, quantitative method for, 17: 19659
site tests at Sizewell, 16: 28581
siting considerations, 19: 33599 (CONF-650201(p.277-87))
siting criteria for, 17: 41104
siting in Sweden, 18: 37393 (A/CONF.28/P/611)
siting of, safety considerations in, 17: 41086
siting of, cost penalty of remote, 19: 33595 (CONF-650201(p.102-9))
siting of, problems in, 19: 32450 (CONF-650201(p.1-7))
siting of, public-acceptance and technical aspects of, 18: 39512
siting of, radiation control criteria in, 18: 40881
siting on western coast, experiences in, 19: 32440 (CONF-650201(p.81-97))
size of future, 17: 28541
stability analysis of supercritical-pressure, 18: 19378 (WCAP-2258)
stability analysis of, using linear techniques, (T), 19: 10574 (WCAP-2565)
stability calculations for, using water-cooled reactors, (T), 19: 31548 (NP-14894)
stack disposal control system for, design and performance of meteorologically operated, 18: 11501
staffing and operation costs, 16: 5045
staffing of, requirements for, 18: 3287
startup accident at, problems of, 18: 3204
startup and operation of first unit of Beloyarsk, Russia, 18: 38437 (A/CONF.28/P/308)
startup and transient operation of Rankine-cycle space, analysis of simulated, 18: 3301 (PWA-2227(Vol.3))
startup and transient operation of Rankine-cycle, for space, 19: 3729 (PWA-2342)
startup conditions of Beloyarsk, 20: 3486
startup of, computer program for, 17: 23856 (WCAP-3722(Vol.I))
startup of, computer program for, 17: 23857 (WCAP-3722(Vol.II))
startup of Latina, 18: 9686
startup of pressurized water, using natural circulation, digital computer analysis of, 16: 30122
startup of, delays in, 19: 24118
steam cycle analysis in, dual-pressure, 17: 29038 (DEG-Report-201)
steam cycle conditions for, economic aspects of, 19: 24122
steam cycle optimization for large sodium-graphite, 18: 40840 (NAA-SR-9488)
steam cycle optimization for 1000-Mw(e) sodium-cooled, 19: 5489 (TID-21292)
steam cycle with reheater for SELNI station, 16: 18675
steam generating system for, design of, 19: 33650(P)
steam generation in, temperature-enthalpy diagram for analysis of, 20: 45174
steam generator control system for, 20: 24773(P)
steam generator design for, 17: 31717(P)
steam generator design for, 17: 31746(P)
steam generator design for, 17: 31747(P)
steam generator for, heat transfer and pressure losses in, 19: 38206
steam generator operation in, 17: 29806(T) (AEC-tr-5887)
steam generator parameters for PWR, 19: 33642
steam generator tubes for, nondestructive testing of, 20: 14160
steam handling in, 17: 4755(P)
steam pressurizer surge tank behavior, 16: 24503
steam yield in, effects of humidity and regeneration cycle on saturated, 18: 7938
structural elements for, review on, 17: 17583
superheat-reheat programs and concepts, review of, 17: 33353
superheater for, 19: 35822(P)
superheater for, design of nuclear, 19: 38224(P)
superheaters for, advantages of conventional, 16: 32587
superheaters for, development of fossil-fueled, 18: 38492 (A/CONF.28/P/672)
superheaters for, design using auxiliary liquid, 19: 45630(P)
supervision, signal recording and display arrangement design for, 16: 16561(P)
survey of space, 18: 9721
temperature distribution in, nondimensional curves for determination of transient, 20: 24760
temperature optimization in, economics and technical aspects of, 20: 8403
temperature-scanning equipment for Hinkley Point, 16: 34087
thermal analysis, (T), 19: 8609
thermal analysis of, combined with thermal power plants, 18: 7935

thermal aspects of, analysis of, 17: 37339
thermal cycle of gas-cooled reactor, 16: 15941
thermal efficiency of combined thermoelectric, 17: 26873
thermal problems with heavy water gas-cooled reactor, review, 16: 6228(T) (CEA-tr-X-422)
thermal shocks in main gas ducts, 16: 1255(T) (CEA-tr-X-413)
thermionic converters for space, review of, 18: 2580
thermodynamic analysis for increased efficiency, 17: 2517
thermodynamic cycle parameters of, analysis and calculation, 16: 34084
thermodynamic cycle of reactor-magnetohydrodynamic generator, 17: 16188
thermodynamic cycles of, with magnetohydrodynamic generator, 17: 40350(T) (JPRS-21241)
thermodynamics of French, 18: 35169
thermodynamics of two-coolant-cycle, 19: 5493
training programs, 16: 30123
transportation of, analysis of aircraft capabilities for, (T), 19: 24065 (AFWL-TDR-64-81)
turbine design and performance for, closed-cycle gas, 20: 3343
turbine design and performance, 20: 38521
turbine design for, 18: 33753
turbine development for, gas, 19: 35780(R) (TID-21842)
turbine exhaust wetness reduction in, methods for, 18: 25660
turbine processes for, comparative study, 16: 22291
turbines for dual-purpose, flexibility of back-pressure, 20: 3540 (ACNP-65573)
turbines for, closed-cycle gas, 19: 47987 (AD-612409)
turbines for, use of closed-cycle gas, 20: 42654
turbopump operations analysis in hydrogen-fueled rockets, 20: 7247 (D-910093-19)
use as power source for undersea missions, 20: 45830
use for heat production in Czechoslovakia, 19: 12787(T) (ORNL-tr-404)
use for production of electricity in western Europe, 20: 40442
use in desalination of sea water, 20: 28813
use in digital computers in French, 19: 40203
use in electrical systems of Europe, 20: 10390
use in France, future, 18: 38391 (A/CONF.28/P/43)
use in manned Mars flights, 20: 45871
use in manned space flight, 20: 12492
use in sea water desalination, economic aspects of, 19: 45606
use in surface-effect ships, 18: 35215
use in underground installations, 17: 26865 (NP-12873)
use of boiling potassium in space, 19: 5396 (ORNL-3605(Vol.1) (p.1-2))
use of dual purpose, with reverse osmosis, 19: 42120
use of dual-purpose, for production of power and desalted water in southern Tunisia, 19: 14861
use of dual-purpose desalination, for Northeast U. S. water supplies, 20: 45186 (NP-16148)
use of gas turbines in, 17: 25397
use of gas turbine in boiling-water-reactor, 18: 26942
use of mercury–steam binary power cycle in, 18: 26949
use offshore for desalination of sea water, 20: 12453 (TID-22330 (Vol.2))
uses for small, 16: 5060
uses in electrochemonuclear processes, 20: 36506 (BNL-959)
uses of diphenyl instead of steam in, 17: 19654
uses of General Electric 630A, 18: 40802
valve design for, 16: 33109(P)
vibrations in, computer studies, 17: 3353(ANL-6319(Rev.))
waste discharge from, wind effects on diffusion of radioactive gases in, 19: 18555
waste discharge monitoring for control of radioactivity releases from, 18: 8596
waste disposal, 17: 13873
waste disposal from, in Great Britian, site evaluation for, 20: 47090
waste disposal practices of UKAEA, 16: 11351
waste handling at, 19: 31622
waste treatment at Latina station, 16: 8442
welding in, 16: 2154
welding in, requirements for quality control in, 19: 22922 (HW-SA-3510)
welding problems in Japan, 19: 12798
welding processes, 16: 507

Nuclear Quadrupole Moments
see Moments

NUCLEAR QUADRUPOLE RESONANCE
detection and measurement of, design of alternating-magnetic-field generators for, 17: 4794
detection and measurement of, pulse method for, 19: 21430
detection of, equipment for, 18: 19994
development and uses of, review of, 17: 4443 (AFOSR-2542)
development and uses in analytical chemistry, 20: 20578
line shape distortion due to apparatus factors, 16: 27751(T) (JPRS-14515(p.201-19))
measurement and experimental uses of, review of, 19: 12505
measurement of, design of automatic spectrometer for, 17: 23617
measurement of, data recorder pen recentering circuit for, 18: 18158
measurement using polarized neutrons, 16: 29856
nuclear induction theory and absorption methods in, (E/T), 20: 41648
perturbations in solid-state coupling constants, 16: 7537
principles and applications of Mössbauer effect, 17: 14967
quench frequency effects on, of chlorine-35 and iodine-127, 18: 31448
relaxation of, (T), 20: 8309
relaxation time for, 18: 17814
second moment of, for spin ⅝ nuclei, 17: 38140(T)
spectra in asymmetric field gradients, (T), 20: 4867
spectra, measurements at low temperatures, 17: 23730
spectrometers for, development of, 19: 9530
spin-lattice relaxation in single crystals for I = ⅝, 20: 24447
temperature and volume dependence of, 17: 37833
temperature dependence of, in chlorine compounds, 17: 26249
temperature dependence in chlorine-35, use as thermometer, 18: 29632
theory and experimental observation, review, 16: 21169
theory for nuclei in solids, 20: 38019
trace relations for tensors relating electric fields and elastic strains to, 17: 657
use for studies of chemical bonds in solids, 16: 27643
use of, in determining crystal defects, 17: 613(T) (JPRS-15740 (p.203-19))
uses in chemistry, 20: 20699
Zeeman effect of spectrum, in crystalline powder, 16: 1760

Nuclear Radiation
see Radiation

Nuclear Reaction Chambers
see Radiation Target Chambers

NUCLEAR REACTIONS
(Specific reactions may be found under headings for participating nuclei and particles and where content justifies it under nuclei and particles produced. See also headings for specific types of reactions such as Spallation)
see also Fission
see also Spallation
see also Thermonuclear Reactions
alpha emission in spallation, effect of alpha substructure on, (T), 20: 32455
alpha transfer, Freiman-Yang tests for, 18: 22902
alpha-cluster emission in quasifree scattering, (T), 20: 8112
amplitude for deuteron stripping in dispersion and distorted-wave Born approximations, 18: 38164
amplitude of deuteron stripping, in Coulomb approximation, 20: 22028
amplitudes above the Bev region, "multicenter" peripheral model for, 16: 26116
amplitudes and angular correlations for (p,2p) and (e,e'p) on light and medium nuclei, 16: 19810
amplitudes and triple angular correlations for, 18: 40625
amplitudes for (d,n) stripping, (T), 20: 17704
amplitudes for final-state interactions in, Aitchison equation for, 20: 12016
amplitudes for production processes in, (T), 19: 20925 (ICTP-64/3)
amplitudes for stripping, importance of interaction range in knockout, 17: 31495
amplitudes for three-body scattering, 16: 27786
amplitudes in, polarization and zeros of, 20: 25938
amplitudes, kinematic branch points of n-line scattering graphs, 16: 21208
amplitudes of direct, diagram summation method for, (T), 19: 33362
amplitudes of direct, Feynman graph method for, 20: 6383
amplitudes of direct particle-redistribution, 20: 19974
amplitudes of, for configuration mixing in continuum, (T), 19: 25516
amplitudes of, Green's causality functions for, (T), 19: 31101
analysis by distorted-wave calculations, 19: 14486 (ANL-6878(p.23-60))
analysis, generalized cluster model for, 16: 17073 (SUI-61-6)
analysis in emulsion in pulsed magnetic fields, 16: 27785
analysis in light nuclei, (E/T), 19: 8401 (TID-21338)
analysis of (d,p) and (p,d), effects of D-wave deuteron states on, 20: 15730(R) (RHEL/R-112, pp 67-98)
analysis of (n,α), 18: 34810
analysis of (p,n), exact solution of optical-model equations for, 20: 42243
analysis of (p,2p) and other knockout, for nuclear structure, (E), 19: 39904
analysis of breakup, using approximate model, 16: 26270
analysis of, by unnatural-parity state production, 17: 9589
analysis of complex, design of semiconductor detector for, 18: 30016
analysis of compound, statistical-model, 17: 38206
analysis of compound, shell-model, (T), 20: 8128
analysis of d-p stripping, using prior-form DWBA method, (T),

19: 37802(R) (ORNL-3778(p.28))
analysis of, design of magnetic stereo-spectrograph for, 17: 24776
analysis of direct, using distorted-wave Born approximation, 18: 32880
analysis of direct, theories for, 18: 36699
analysis of direct, methods of analyticity and unitarity for, 19: 45340
analysis of, double-focusing spectrometer for, 18: 2007
analysis of elastic scattering and direct, optical model, 20: 19989
analysis of few-nucleon reactions with A ≤ 4, 16: 6029
analysis of (helium-3,p) and (α,n), 17: 5396
analysis of high-energy coherent, 17: 19382
analysis of high-energy, using detectors with on-line computers, (E), 19: 46806
analysis of, MONSTER program for, 17: 28246 (NDA-Memo-2123-1)
analysis of multichannel, 16: 18604
analysis of, multidimensional chain for, 17: 29206
analysis of neutron-induced, using computers, 19: 14506 (BNL-8710)
analysis of neutron-generating, on light nuclei, 18: 11232
analysis of nucleon transfer, 18: 24618 (NYO-1807-8)
analysis of (p,d) pickup, for studies of filled shell model states, 16: 26258
analysis of pickup and stripping, 18: 21204 (LADC-6302)
analysis of quasi-elastic, distorted-wave, 17: 13537
analysis of stripping, using distorted-wave Born approximation, (T), 19: 39910
analysis of two-nucleon stripping, method for, 18: 16934 (ANL-6848(p.188-98))
analysis of, cluster model, 20: 28438
analysis of, coincidence counter for, 18: 35886
analysis of, computer programs for, 18: 34752(R) (CU(PNPL)-234)
analysis of, design of broad-range magnetic spectrograph system for, 20: 41306
analysis of, design of circuit for data cutoff at preset value for, 20: 41244
analysis of, performance of computers for, 18: 18275
analysis of, using multidimensional analyzer, 18: 16321
analysis of, using multidimensional analyzer, 18: 16322
analysis of, using PDP 1 computer with time sharing, (E), 19: 46807
analysis of, with deuteron-triton build-up structure, 18: 11227
analysis of, with polarized particle beams and targets, 20: 28435
analysis using bubble chambers, (E), 19: 26660 (JINR-E-1855)
analysis using compiler language computer programs, (E), 19: 4579
analysis using nsec-pulsed accelerators, 17: 17282
analysis using terminology of high-energy elementary-particle physics, (T), 19: 14500 (ANL-6878(p.481-504))
analytic properties of direct interactions, 16: 28102
analytic theory of subCoulomb stripping, 20: 10011
angular correlations, theory, 16: 1069
angular correlations in statistical, 16: 8193
angular correlations in particle emission, effects of statistical perturbations, 16: 26250
angular correlation analysis of, coefficients for triple, 17: 17104 (CRP-615(Rev.))
angular correlation experiments, determination of distribution in, 18: 4542 (KFK-135)
angular correlations in, 18: 6291
angular correlation in, nomogram for calculating kinematic elements of, 18: 32754
angular correlation analysis in compound nucleus, (T), 19: 29275
angular correlations in, detector correction factors for, (T), 19: 40900
angular correlations in direct and resonance, intermediate coupling parameters for, 20: 4835 (JINR-P-2287)
angular correlations and polarization in pickup, (T), 20: 28378
angular correlations for, techniques for, 20: 38179
angular distributions in, lectures on theories for, 16: 10964 (UCRL-5701)
angular distribution data for, computer program for analysis of, 16: 26227 (ORNL-3251)
angular distributions from, design of polygonal magnetic analyzer and spectrograph for determining, 16: 33207
angular distribution of products from transfer, 17: 24391 (JINR-P-1238)
angular distributions from, double spectrographic technique for measuring, 17: 24775
angular distributions and Q-values for, 17: 28239 (ANL-6718)
angular distributions and momenta from three-particle final state interaction, 18: 15283
angular distributions and spectra of (d,t), with light nuclei, 18: 18881 (NP-13784)
angular distributions from, method for measuring, 18: 30767
angular distributions for direct, 18: 36613
angular distribution measurements on, target chamber for, 18: 41804
angular distributions from one-nucleon-transfer, 19: 1553 (JINR-P-1743)
angular distributions from, multidetector data handling in, 19: 11570
angular distributions in multinucleon transfer, (T), 19: 12539
angular distribution of compound nucleus decay products in direct, (T), 19: 14542(T) (ANL-Trans-156)
angular distribution for (α,p), total angular momentum transfer effects in, (E/T), 19: 19210
angular distribution of decay products from compound nucleus in direct, 19: 33375
angular distribution of fragments from, at 76 Mev to 25 Bev, (T), 20: 3111
angular distributions and cross sections for two-particle, computer program for, 20: 4844 (ORNL-TM-1234)
angular distributions from neutron pickup, J dependence of, (E/T), 20: 9975 (PUC-937-174)
angular distributions in (p,d), form-factor calculations for, (T), 20: 10056
angular distributions in surface, adiabatic approximation for, 20: 22062
angular distributions of products from one- and two-nucleon transfer, (T), 20: 26101
angular distributions and polarization from, summation and integration of spherical harmonics for, 20: 32437
angular distributions from, computer program for, 20: 36180 (USC-136-100)
angular distributions from, quantum theory of, 20: 46612
angular moments in, 21-j coefficients for, (T), 19: 19156
angular momentum effects in, 17: 36657 (JINR-P-1347)
angular momentum effects in compound, 17: 38094 (UCRL-10850)
angular momentum effects in, 18: 6183 (UCRL-11049)
angular momentum weight factors, 18: 21212 (PAN-445/VI)
angular-momentum-projection conservation in, 18: 22908
atomic ionization from charged-particle, K-shell, (T), 20: 7726
average compound nucleus reactions in the continuum, 18: 2903
average resonance parameters and the optical model, 17: 7244
back-angle peaking and exchange effects in (d,p) and (d,n), 16: 28088
barrier penetration in, diffuse nuclear edge optical model effects on, (T), 20: 10047
bibliography, 16: 9433 (NP-11294)
bibliography on, 20: 19803 (AED-C-12-13(Pt.1))
bibliography on, 20: 22011 (TID-22771)
bibliography on beryllium, 20: 3007 (CEA-Bib-32)
bibliography on capture, 19: 5262
bibliography on chemical effects of transformations, 17: 27421 (NP-12894)
bibliography on cross sections for neutron-induced threshold, 18: 34753(R) (EANDC(E)-50(L))
bibliography on low-energy, 18: 42765
bibliography on low-energy, 18: 42766
bibliography on photodisintegration and photoproduction, 17: 39982 (NP-13139)
bibliography on photo-, 18: 19125
bibliography on research on, at Hungarian Academy of Sciences, 17: 31810
book: *Collision Theory*, 18: 28419
book: *Distribution of Radioactivity in Some Organic Compounds, Labeled by the Reaction $^{14}N(n,p)^{14}C$*, 18: 41556
book: *Effects of High Energy Particles on Nuclear Reactions*, 17: 15311
book: *From the Atomic Nucleus to the Nuclear Power Station*, in German, 18: 26943
book: *High Energy Nuclear Reactions*, 20: 12111
book: *Introduction to the Atomic Nucleus*, 19: 23802
book: *Kinematics of Nuclear Reactions*, 18: 34956
book: *Nuclear and Radiochemistry*. Second Ed., 18: 33455
book: *Nuclear Chemistry. Study of Radioactive Nuclei and Nuclear Reactions*, 20: 24487
book: *Nuclear Chemistry*, 20: 43056(T) (JPRS-36943)
book: *Nuclear Physics. Mechanism of Nuclear Reactions*, 20: 32538
book: *Nuclear Reactions. Volume II*, 17: 17281
book: *Nuclear Reactions at Low and Medium Energies*, 17: 29637
book: *Nuclear Reactions, Volume I*, 18: 6287
book: *Nuclear Structure and Electromagnetic Interactions*, 20: 3147
book: *Strong-Interaction Physics*. (T), 19: 1657
book: *Textbook on Nuclear Physics. Vol. II. Physics of Atomic Nuclei*, in German, 18: 10662
book: *The Optical Model in Nuclear and Particle Physics*, 17: 33108
book: *Theory of Direct Nuclear Reactions*, 18: 4628
Born approximation for stripping, second term in, 18: 28593
calculation of low-energy intranuclear cascades, 17: 31526
calculation of (n,α) reactions with even-even nuclei using a direct interaction process, 17: 39994
calculation of two-nucleon stripping, 16: 28079
calculations for, comparison of DWBA and SCA, 18: 28636
calculations for, boundary-condition constraints for shell-model, 19: 27557
calculations of cross sections of, formulas for, 16: 33962
calculations of direct, finite-range distorted-wave Born-approximations for, 16: 21579
calculations of intranuclear-cascades in, (T), 19: 21239 (LA-3206)
calculations on direct, 20: 19947
cascade showers in, secondary particle energy spectra in, (T),

19: 32920
characteristics of weak, 16: 18101 (NP-11463(Pt.2)(p.195-211))
charge exchange, use of t-matrix for free bound system in, 17: 20987 (LA-2805)
charge transfer and ion-atom interchange collisions in high-energy, 17: 40131
charge transfer in, exact numerical solution for asymmetric, 18: 32811
charged particle emission, measurements using solid-angle filters, 16: 8932
charged-particle absorption with formation of compound nuclei, (T), 20: 38020
charged-particle identification in low-yield, instrument for, 20: 33696
charged-particle spectra from, computer program for decomposition of, 20: 44656 (TID-23315)
chemical effects, 16: 11740
chemical effects, review, 16: 6466
cluster effects in, 16: 21572
coincidence measurements in, use of Chase two-dimensional analyzer for, 17: 36112 (BNL-6518)
collision integral for anisotropic neutron chain-type, 20: 36213
comparison of alpha and proton, 17: 26533
competition between gamma and proton emission from compound nucleus in, 17: 26478
complex singularities of the amplitudes for direct, 17: 9615
compound nuclei in, heavy-ion studies of (E/T), 19: 1563 (ORNL-P-514)
compound nucleus formation and decay, 16: 8222
compound statistical features in, review, 17: 17640
compound systems in heavy ion, angular moments and cross sections for, 18: 1011 (JINR-P-1351)
conference on complex nuclei, 18: 24707
core excitation in stripping, (T), 20: 13816
core polarization in, shell-model and sum-rule calculations of, 20: 15852
corrections for center-of-mass motion for heavy nuclei, 16: 14035
correlation effects in ground-state, (T), 19: 41814
correlation effects and polarization in, orientation effects on, (T), 20: 24372
cosmic particle, in meteorites, 17: 5060
cosmic-particle, mesons (π^0) from, 17: 11454
cosmic protons, gamma production cross sections at 30 to 300 Mev, 16: 29620
Coulomb displacement energies from isobaric analog resonances in proton-induced, (E), 20: 42262
Coulomb distortions in L = 0 stripping, 18: 18986
Coulomb excitation, effects of elastic scattering resonances, 16: 19798
Coulomb excitation processes and applications, review of, 18: 11222
Coulomb interactions and penetration factors in, 18: 18978
Coulomb interactions in, energy spectrum for, (T), 19: 29302
Coulomb wave functions for, 17: 24314
coupling potential in direct, 17: 24492
cross-section calculations, relation of optical model and resonance theory, 16: 21624
cross-section fluctuations in, angular cross-correlation function for, 18: 4631
cross section fluctuation in, relation of intensity fluctuations in radio astronomy to, 18: 16637
cross section fluctuation in, direct reaction contribution to, 18: 16938 (ANL-6848(p.228-9))
cross section fluctuations in, theory of, 18: 19067
cross section fluctuations in, finite energy range and modulation effects in, 18: 30796
cross section fluctuations in, finite-sample-size effects in, (T), 19: 41762
cross section fluctuation analysis for, effects of finite range of data on, 19: 43333
cross section fluctuations in, theory of Ericson statistical, 20: 34667
cross section for alpha-stripping, 17: 24468
cross section measurements by radioactivity counting, system for, 19: 34441
cross section of direct, in vicinity of singularities, 17: 26544
cross section ratios for (n,γ), isomeric, 17: 832
cross section requirement for astrophysics, 20: 41600
cross sections and polarization in (d,n), 18: 18950
cross sections and spectroscopic amplitudes for direct inelastic scattering and charge exchange, 20: 22067
cross sections at high energies, 16: 22943
cross sections at high energies, effects of Regge poles on, 17: 9274
cross sections, contribution of multiquantum exchange terms to ratio of total (e,N) to total (γ,N), 16: 12523
cross sections, contribution of multiquantum exchange terms to ratio of total (e,π) to total (γ,π), 16: 21469
cross sections for photo-, formula for calculating, 16: 28060
cross sections for low momentum transfer type, in complex nuclei at high energies, 16: 28092
cross sections for (n,p) at 2 to 5 Mev, theoretical calculation of, 16: 32396 (NP-11745)
cross sections for three-particle production in, 17: 2295
cross sections for, effects of final-state scattering on, 17: 5356
cross sections for direct, perturbation theory for, 17: 5360
cross sections for (n,2n), 17: 15299
cross sections for (n,α), statistical model calculations of, 17: 17206
cross sections for deuteron, activation, 17: 17216
cross sections for pair producing bremsstrahlung, 17: 17105 (DESY-A-2.96)
cross sections for zero-spin, probability distribution in heavy nuclei, 17: 24499
cross sections for (n,α), (n,d), (n,He^3), (n,nα), (n,2n), (n,np), (n,p), and (n,t) at 14–15 Mev, 17: 26422 (EUR-122.e)
cross sections for, fluctuations in high-energy, 17: 29614
cross sections for charged particle, 17: 34886 (UCRL-10783)
cross sections for, dispersion relations in, 17: 34906
cross sections for photo-, for light nuclei, 17: 40117
cross sections for, statistical theory of fluctuations in, 17: 39986
cross sections for rare, induced by 14.8-Mev neutrons, 18: 1077
cross sections for, intermediate structure in energy dependence of, 18: 2938
cross sections for neutron, 18: 9307 (CEA-2380)
cross sections for (α,n), up to 11 Mev for nuclei of A = 27 to 120, 18: 9412
cross sections for, mean square fluctuations in, 18: 11255
cross sections for (n,α), statistical-model, 18: 17058
cross sections for, fluctuations in, 18: 17078
cross sections for neutron, 18: 16947 (NP-13661)
cross sections for, 18: 17255
cross sections for high-energy, 18: 18868 (CERN-64-17)
cross sections for, approximation method based on R-matrix theory, 18: 21304
cross sections for, statistical theory of, 18: 32837
cross sections for, fluctuations in, 18: 34893
cross sections for (N,2N), literature survey on, 18: 40514
cross sections for, methods of calculation of, 18: 42649 (TID-7050(p.24-89))
cross sections for, optical-model calculations of, (T), 19: 6632 (JINR-P-1795)
cross sections for gamma-induced, 19: 12496
cross sections for direct radiative capture, (T), 19: 12541
cross sections for compound-nucleus, calculations of average, (T), 19: 17011
cross sections for, nomograms for Breit-Wigner formula for, (T), 19: 16868
cross sections for, computer calculations of, (E), 19: 19080 (ANL-6978)
cross sections for, summary of research by U. S. laboratories on, 19: 19095 (WASH-1053)
cross sections for, effect of polarization on fluctuation in, (T), 19: 29289
cross sections for, review of those pertinent to reactor design, (E/T), 19: 29321
cross sections for sulfur-33, 19: 31788(R) (ORNL-3768(p.33-57))
cross sections for, energy dependence of fluctuations in, (T), 19: 35458
cross sections for, probability distributions of total, (T), 19: 35459
cross sections for, resonant backward peaks in, (T), 19: 35474
cross sections for compound nucleus formation, (T), 19: 37889
cross sections for, calculation in optical model, (T), 19: 39935
cross sections for, AEC program on, 19: 45288 (WASH-1056)
cross sections for, tabulation of, 20: 9981 (WASH-1064)
cross sections for helium-3, table on, (E), 20: 14661(R) (ORNL-3889, pp 48-70)
cross sections for compound nucleus, computer program for calculating, 20: 17672 (AERE-R-5053)
cross sections for photo-, methods for measuring, 20: 19991
cross sections for, statistical description of fluctuations in, (T), 20: 21987 (BNL-948, pp 826-75)
cross sections for, probability distribution of maxima and minima of, (T), 20: 40113
cross sections for, probability distributions for extremes of, (T), 20: 42395
cross sections for stripping, graphical method for calculation of differential, 20: 42397
cross sections for, statistical theory of fluctuations in, 20: 42194
cross sections for direct spin dependence of differential, (T), 20: 44773
cross sections for, systematics near shell closure, (T), 20: 46658
cross sections for, spurious intermediate resonances in randomly generated, (T), 20: 46713
cross sections in vicinity of reaction singularities, 16: 28047
cross sections, independence of isotopic spin values at high energies, 16: 2549
cross sections near thresholds, in attractive Coulomb fields, 17: 33083
cross sections near threshold of, resonances in, (T), 19: 27512
cross sections of (n,γ), calculation, 16: 19766

cross sections of photo-, yield function solution for, 17: 41865 (IS-607)
cross sections of threshold, 18: 42659
cross sections of photo-, effects of velocity-dependent forces on, 18: 42740
cross sections of photo-, yield-curve measurement for, (E/T), 19: 10356
cross sections of two-nucleon knock-on and stripping, structure-factor effects on, (T), 19: 41819
cross sections of direct cluster-replacement, contribution of excited states of virtual nucleus to, (T), 20: 19967
cross-section fluctuations in statistical model, (T), 20: 46581 (CEA-R-2876)
cross-section measurements in, experimental-resolution effect on widths of fluctuation correlation function for, (T), 19: 41734
cryogenic disruption, for space propulsion, (T), 19: 36637 (NP-15148)
Dalitz diagrams for, with three particles in final state, 17: 13555
data comparators for analyzing, design of digital, 20: 29485 (EUR-2799.e)
data handling from, design of buffer stores for, (E), 19: 11655 (EUR-2160.e)
data on, at Aldermaston Library, 17: 36638 (AWRE-O-70/63)
data recording for multiparameter, magnetic tape, 19: 20255 (EUR-2119.e)
data table for neutron-induced, 17: 21033
density and potential functions for studying particle-nucleus interactions, 18: 7722
description of neutrino-emitting, in stars, 18: 44344
detection and measurement in bubble chambers, 17: 12570
detection and measurement of high-energy, using emulsions, 18: 23905
detection and measurement of, performance of counters for, (T), 19: 5160
detection in nuclear emulsion, scanning methods for, 18: 18221
detection of (γ,α), in nuclear emulsion, 18: 23930
detection of distorted and spurious, in nuclear emulsion, 18: 41782
deuteron (d,n) and (d,p), knock-out mechanism in, 17: 17168
deuteron emission from, reduced widths for, 20: 26189
deuteron stripping, effects of spin-orbit distortion, 16: 26284
deuteron stripping, with light and medium nuclei, polarization of protons from, 17: 7286
deuteron stripping, polarization effects on, 17: 19312
deuteron stripping and shell model, 17: 40036
deuteron stripping, effects of active nucleons in, 18: 38091
deuteron stripping, finite range effects in, 19: 1618
deuteron stripping, L-space localization in, 20: 6394
deuteron stripping, target-excitation effects in, (T), 20: 32497
differential cross sections for heavy ion stripping, 16: 8192
diffraction in 10- to 30-Mev, spin-orbit coupling in, (T), 20: 4827 (CEA-Bib-60)
diffraction mechanism for direct, 18: 9381
diffraction scattering, effects of washed-out nuclear boundaries on, 16: 31115
Dirac-Coulomb integrals for zero energy-loss, evaluation of, 19: 32048(R) (NP-15073)
direct, by single particle modes, 16: 21266 (NP-11680)
direct, calculations and experimental evidence for, 16: 21547
direct, dispersion method applied to, 17: 17304
direct interaction processes in, 17: 7094 (NP-12330(p.46-52))
direct interactions in low-energy, 17: 7091(NP-12330(p.22-34))
direct interactions in heavy-ion, 18: 34856
direct, lecture on application of, 17: 17302
direct process, review, 16: 21546
direct processes in (p,α), (E), 19: 14499 (ANL-6878(p.457-77))
direct, theories and possible developments in, 17: 17303
direct, theory for cross sections of, 17: 33085
directional correlation measurements, variances in, 17: 33031
dispersion relations for direct, 16: 8188
dispersion relations and kinematics for general production processes, 16: 31017 (UCRL-9553)
dispersion relations for direct, (T), 19: 47684
distorted-wave approximation for stripping, 17: 24053(R) (ORNL-3432)
distorted-wave calculations of (d,p) angular distributions in stripping, 18: 9437
distorted wave theory of heavy particle stripping, 16: 28072
distorted-wave Born approximations, 18: 18947
distorted-wave Born approximation and stripping matrix element with finite range, 18: 26626
distorted-wave theory of stripping, finite-range effects in, 18: 24667
distorted-wave theory of deuteron stripping, 18: 32799
distortion of incident and emergent waves in direct, 16: 21550
distribution functions for simultaneous three-body emission, 16: 23052
distributions for stripping, Born approximation for, (E/T), 19: 8399 (NP-14543)
distributions from (γ,n) and (γ,p) spin-orbit effects on, 17: 7167
distributions from, measurement of angular, 18: 21250
distributions from intranuclear-cascade, (T), 19: 19088 (ORNL-TM-1033)
distributions from, computer analysis using Hauser-Feshbach theory, (T), 19: 31232 (ORNL-TM-1117)
distributions in Tev jets, models for, (E/T), 19: 12493 (PAN-537/VI)
distributions of mesons (π) from high-energy, 19: 5127 (INSJ-79)
double-stripping (t,p) at 7 to 13 Mev, 18: 19019
double-stripping (t,p) at 7 to 13 Mev, 18: 19020
double-stripping (t,p) at 7 to 13 Mev, 18: 19021
doublet parity and its conservation in electromagnetic and weak interactions, 16: 22887
effect in universe evolution, 17: 34661 (JINR-P-1326)
effect of deuteron internal structure on Coulomb stripping, 18: 42641 (KFKI-1491/G)
effects in astrophysics, 19: 42974 (NEIC-RR-10)
effects of polarization on Ericson fluctuations in, (T), 20: 42396
effects of resonances on direct, 18: 44816
effects of, review of chemical, 20: 9019
electrodisintegration and photoeffect, relation between cross sections for, 18: 2920
electromagnetic cross sections for electron and nuclear research, 18: 26684
emissions from, statistical model for, 16: 12505
emissions from, computer analysis of distributions of, 18: 2511
energies of, calculation of, 20: 15853
energy balance in fission, 16: 6006
energy determinations for, status of, 19: 29350
energy distribution in daughter nuclei, 16: 6469
energy estimations for high-energy, 18: 42717
energy level excitation of deformed nuclei by multiple Coulomb processes, 17: 26483
energy level excitation in spherical nuclei in stripping, collective, (T), 20: 6353
energy level reduced neutron width determination by, 17: 33066
energy level widths of compound nuclei, determination in continuum region, (T), 20: 42164 (LA-DC-8083)
energy levels from quasi-elastic, alpha model evaluation of, 17: 7189
energy levels in, shell model analysis of resonance, (T), 19: 19195
energy of, determination of, 17: 15098
energy production by, equation for, 19: 5150
energy production from, review on, 19: 12649
energy Q values for, for target mass numbers $A \leq 70$, 19: 31280
energy relations in secondary, 17: 2242 (TID-16949)
energy transitions in, isomeric, 19: 9230
energy-level excitation in compound-nucleus, data analysis for widths in, (T), 19: 45343
energy-level widths of compound nuclei in continuum energy region, (T), 20: 46690
equations for finite-range Coulomb stripping and heavy-ion transfer, 20: 12091
equipment for inducing, design of, 17: 42152(P)
escape of recoil nuclei, probability, 16: 7123
evaluation of four-particle reactions in three dimensions, 18: 2899
evaporation of neutrons from, on excited nuclei, 17: 17162
evaporation processes in (p,n), at 42 to 150 Mev, 16: 23096
evaporation processes in (α,n), at 11 to 20 Mev, 16: 23100
evaporation, distributions from 400-Mev neutron-induced, 18: 30751
excitation functions for compound-nucleus, 16: 33900
excitation functions and energy spectra of (n,α), statistical analysis of, 18: 17057
excitation functions for high-energy, interpretation of, (T), 19: 31222 (LA-3266)
excitation functions for, statistical-model analysis of fluctuations in, 20: 22054
excitation functions for, errors in fluctuation analysis, (T), 20: 44745
excitation of double analog states in (p,n), (E/T), 20: 10031
excitation of giant dipole resonance in (p,γ), (T), 19: 14520 (CONF-640301(p.182-218))
experimental studies of resonance, review of, 18: 6293
few-nucleon problems in, 17: 41990
Feynman amplitudes for nonrelativistic processes, 17: 7524
field model of, 19: 27467
field theoretic methods in direct interaction theory, 17: 36411 (NP-13020(p.174-85))
fields of, description of, by Lobachevskii's kinematics and geometry, 17: 19512
fine structure of photo, NMR method for, 19: 21282
form factors for stripping, (T), 19: 41746
formalism for rearrangement, Born series for symmetric interaction in, 20: 13798
formalism of direct knock-out, at intermediate energies, 17: 31395 (CONF-46-23)
formation of deuterons from proton bombardment of nuclei at 25 to 30 Bev, 17: 7258
forward and backward selection rule in a class of inelastic collisions, 17: 35072

forward peaking of fast photoneutron angular distributions, 18: 19038
fragment emission in, model for, 19: 5141
fragment emission in high-energy, mechanism of light, (T), 20: 13880
fragmentation in, cascade model of, (T), 19: 19221
fragmentation mechanism in high-energy, 18: 28621
g-shifts in electron paramagnetic resonance in F-centers by, 18: 29784
gamma-absorption giant resonances in, on deformed nuclei, 16: 33858
gamma and neutron emission from compound nucleus in, (T), 20: 12048
gamma angular correlations from, book on, 20: 8167
gamma angular correlations in, use in energy level structure analysis, (E/T), 20: 12150
gamma angular correlations from, performance of detectors for measuring, 20: 38184
gamma angular distribution analysis, calculation of coefficients for, 17: 33033
gamma circular polarization in stripping, (E/T), 20: 17726
gamma emission in, method for evaluating angular distributions of, 18: 13073
gamma emission mechanism in heavy-ion, (T), 20: 26216
gamma polarization from deuteron stripping, (T), 20: 22006 (KFKI-600)
gamma reactions (γ,tn), experimental apparatus and techniques for studying, 18: 32757
gamma resonance effects in (p,γ), 16: 21452
gamma resonance effects in (n,γ), 16: 21454
gamma spectra from high-energy, 16: 21389
gamma spectra from neutron-capture, 20: 36191
gamma spectra from, use in mean-life measurements, (T), 20: 42379
gamma transitions involving continuum states, 16: 21451
gamma-ray angular distribution analysis using counter array, 19: 9771(R) (PR-P-63)
geometric effects in stripping, 18: 18910
giant resonances in photo-, 17: 24432
graph sequences in theory of, summation of complex and ladder, 20: 10022
heat flow and neutron flux measurements in, sensing device design for, 16: 14975(P)
heating in, partial, 17: 38211
heavy-ion, models for gamma distributions and yields, 16: 21457
heavy-ion reaction mechanisms, 18: 6290
helicity inversion in, 16: 29637 (JINR-D-1016)
high-energy cross sections for elements uranium to zinc, 16: 19747 (CERN-62-9)
hyperon and meson(π) production in high-energy, 17: 15297
impact parameters in high-energy, 17: 13531
induced by deuterons at 20 Mev, 17: 31548
inelastic effects in, theory for, 17: 41873 (WASH-1044)
interaction in the initial and final states in direct, 17: 9608
interactions of unstable particles with nucleons in high-energy, 18: 7520
intermediate states in, K-shell ionization probability for lifetime of, 18: 2897
invariance violation in nonresonant statistical, time-reversal, (T), 20: 46693
invariance violation in compound-nucleus, time-reversal, (T), 20: 46694
invariant variables for n particles and phase-space volume element, 18: 21305
isobaric analog resonances in, shell-model theory of, 20: 36198
isobaric analog states from (p,n), (E/T), 19: 14493 (ANL-6878 (p. 215-29))
isobaric properties of (p,n), on heavy nuclei, 17: 2282
isomer ratios in, in Fermi gas and superconductor models, 18: 44780
isomer yield ratios for, 17: 9498 (ANL-6598)
isospin effects in light nuclei, review on, 20: 44834
isospin selection rules for (α,d) and (α,α′), effects of Coulomb interaction on, 20: 32484
isospin–multiplet production by, nuclear analog states in, 18: 28706
isotope yields from, measurement using mass spectrometry, (E), 20: 8105
Jacobi coordinates in formal resonance theory, 17: 38099
jet distributions from 10^{13}-ev cosmic-particle, 17: 6919
kinematic study of, Fano-Racah formalism for, 20: 30396
kinematics nomogram for low-energy, 18: 28576 (ORNL-3636)
kinematics of high-energy relativistic, 18: 6158 (JINR-P-1320)
kinematics of multiparticle, relativistic and nonrelativistic, 19: 31225 (NIJS-R-429)
kinematics of, computer programs for UMC-1 for, 20: 6285 (INP-414/PL)
kinematics of, having three-particle final states, 20: 6333
knock-on, formulas for angular distribution, angular correlation, and polarization, 17: 19249
lithium-6 and -7 induced, angular distributions, cross sections, and energy spectra for, 17: 38281
local heating model of direct, 18: 13839(R) (TID-20201)
magnitude of two-nucleon stripping, calculation by pairing interaction model, 16: 21604
mass defect, calculation of reaction energy from, 16: 33848
mathematical analysis of break-up processes, 16: 2485 (NP-10958)
matrix calculation using separation method, 16: 5933
matrix calculations in Brueckner theory, method for, 20: 38160
matrix for, Brueckner approximation for closed-shell nuclei, (T), 19: 37801(R) (ORNL-3778(p.24-5))
measurement of, background reduction using cyclotron D voltage regulator, 16: 33254
measurement of compound-nucleus behavior in, (E), 19: 17014
measurements on high-energy, using cosmic radiation, 18: 36190
mechanism and isospin selection rules in light nuclei, involving virtual photons, (T), 20: 44744
mechanism at 5 to 20 Mev, 16: 1061
mechanism of direct and resonance, 16: 24799(T) (AEC-tr-5160)
mechanism of direct transfer, 20: 8092
mechanism of direct, at high energies, 20: 11377
mechanism of proton-transfer, (E), 20: 42153 (JINR-E-2824)
mechanism of the (d,t) reaction, 18: 1041
mechanism of three-body, 20: 8138
mechanism of two-nucleon-transfer, (T), 20: 42290
mechanisms for charged-particle production at high energies by nucleus-induced, (T), 19: 10246 (JINR-P-1881)
mechanisms for (d,α), at 15 Mev, 16: 32422
mechanisms for multiple neutron production in, 17: 41901
mechanisms for stellar helium-burning, 17: 9159
mechanisms for, effects of density and temperature on, 18: 40600
mechanisms for, review of, 20: 34658
mechanisms in heavy-ion-induced, 17: 28258 (UCRL-10775)
mechanisms in helium-3–light nucleus, 17: 4116
mechanisms in (p,pn), 16: 28042
mechanisms in quasi-particle, 18: 9321 (UCRL-11080)
mechanisms in stripping, direct, (T), 19: 5137
mechanisms, lecture, 17: 9538
mechanisms of (N,2N), review of, 19: 19103
mechanisms of, at 40 Mev and lower, survey of, 17: 2239 (NIRL/R/16 (p.53-5))
mechanisms of, calculation by one-dimensional theory of showers, 17: 7183
mechanisms of compound-nucleus and direct, mutual relations of, 17: 38205
mechanisms of complex-nuclei, (E/T), 19: 5128 (JINR-D-1798)
mechanisms of compound nucleus, (T), 20: 19988
mechanisms of, conference on, 17: 38171
mechanisms of direct, effects of Exclusion Principle on, (T), 19: 27581
mechanisms of, in stars, 17: 24197
mechanisms of (n,t), 16: 7048
mechanisms of nucleon–nuclei, at 1 to 50 Mev, 18: 19107
mechanisms of nucleon-nuclei interactions at 100 to 1000 Bev, 18: 34764 (JINR-P-1678)
mechanisms of solar-flare, 18: 44400
mechanisms of three-particle, (T), 19: 39894
mechanisms of, angular correlations of excitation functions in, 18: 26634
mechanisms of, elementary terms defined for, 20: 36184
meson multiple production in, model for, 17: 5399
meson (π^0) production modes in, from photon-nucleon direct interaction, 18: 9420
meson production in high-energy jets, 17: 19159
model for compressed nuclei in, statistical, (T), 20: 42269
model for (d,p) stripping, 18: 6162 (NP-13348)
model for deuteron stripping, angular distribution calculations in, (T), 20: 13851
model for deuteron stripping, (T), 20: 46630
model for direct, 18: 42653
model for direct knock-out, 20: 8162
model for direct, diffraction, 20: 8160
model for high-energy multiple-production, 17: 13375
model for isobaric-spin effects in, shell, 19: 14491 (ANL-6878(p.181-206))
model for jets from high-energy, 2-center, 16: 33869
model for multiple meson production in high-energy, 17: 9441
model for, partial equilibrium, 17: 29392(R) (NP-12951)
model for stripping, 17: 38223
model for stripping, 18: 17053
model for stripping, validity of DWBA in three-body, 19: 41777
model for ultra-high-energy, in extensive air showers, 18: 2560
model for, heavy-ion-induced transfer, diffraction, (T), 20: 44757
models for (n,α), in direct interactions, 18: 34769 (NP-14085)
models for, clarification of compound-nucleus, 18: 4527 (CONF-285-4)
models for, computer parameter search code for, 16: 3873(R) (ORNL-3193(p.250-3))
models for direct, description of field-theoretical, (T), 19: 8395 (ISS-64-31)
models for direct, diffraction, 20: 25942

models for heavy-ion, 20: 8092
models for helium-3- and triton-producing, (T), 19: 6713
models for high-energy, comparisons between, 17: 32952
models for multiple meson production in, 16: 33736
models for two-nucleon stripping, 18: 15256
models for, diffraction, (T), 20: 21980 (BNL-948, pp 561-609)
models of, use for educational purposes, 19: 29331
momentum transfer measurements in, 17: 19322
momentum transfer singularities in graphs for low-energy, 18: 7742
Monte Carlo calculation of intranuclear cascades at 50 to 350 Mev, 17: 12782(R) (ORNL-3360(p.137-81))
Monte Carlo calculation of neutron production in proton-induced, at 0.3 to 1 Bev, 18: 34961
multinuclear transfer in, distribution of products from, 18: 34763 (JINR-P-1675)
multinucleon transfer between complex nuclei, 17: 11737
mutual excitation, semi-classical treatment of, 17: 33022
nature and importance of, review on, 18: 26572
neutron coupling in transfer, 17: 7155
neutron distributions from, theory of, 17: 34984
neutron emission in compound-nucleus, 17: 9593
neutron emission in compound-nucleus, (T), 19: 21245 (ORNL-TM-196)
neutron emission in, separation energies for double, (T), 20: 28452
neutron evaporation from compound nuclei, angular momentum effects in, 18: 28628
neutron experiments with a tandem accelerator, 18: 6156 (CONF-354-1)
neutron-neutron phase-shift determination, by analysis of neutron pair production, 16: 19689
neutron, pairing-energy effects on 14.5-Mev (n,p), 16: 23103
neutron production in, for activation analysis, 20: 16332 (GA-6691)
neutron reactions (n,α) at 14 Mev, effects of nuclear shell on cross sections, 18: 4632
neutron reactions (n,γ) with nuclei, relation between cross section and scattering length for, 18: 34762 (JINR-P-1671)
neutron reactions (n,α), (n,d),(n,p), and (n,t) at 14 Mev, measurement of cross sections for, 18: 44768
neutron resonances in heavy nuclei, 18: 6295
neutron transfer cross sections in, for arbitrary Q, 16: 29870
neutron transfer in, 17: 36650 (CONF-62-13)
neutron-transfer, theory using Saxon-Woods potentials, 17: 15266
neutron tunneling transfer in, 20: 6387
neutron-capture gamma radiation from, measurement techniques for, 19: 45375
neutron-proton potential in Coulomb stripping, finite-range, 18: 16911 (ANL-6848(p.43-50))
neutron-transfer in heavy-ion, studies of (E/T), 19: 1563 (ORNL-P-514)
nuclear alignment in heavy-ion, use in nuclear spectroscopy, 20: 34603
nuclear energy-level densities in, effects of pairing correlations on, 18: 19018
nuclear excited states from direct (p,n), 16: 33860
nuclear polarization effects in direct, 16: 4763
nuclear recoil momentum in evaporation, calculation of, 19: 31251
nuclear structure determinations from, review of, 18: 13116
nuclear surface-layer effects on low-energy, 16: 19809
nucleon cluster exchange in, cross sections for, 17: 38280
nucleon correlation effects on direct (T), 19: 1644
nucleon distributions from 660-Mev-proton-induced, 18: 42634 (JINR-P-1713)
nucleon exchange in, tunneling theory for, 18: 36671
nucleon excitation classification of resonant, 17: 39974 (INSJ-59)
nucleon group structure and, 18: 11235
nucleon indistinguishability in, 16: 21623
nucleon knock-out distribution from, excitation energy, nuclear volume, and recoil momentum for, (T), 20: 13892
nucleon–nucleon correlation effects on photo-, 16: 31117
nucleon–nucleon correlation effects on photo-, 16: 31118
nucleon pair transfer between light nuclide and nucleus, correlations in, (E/T), 19: 21266(R) (UCRL-11828(p.108-9))
nucleon pickup and stripping strengths for fixed target, single-, (T), 19: 23731
nucleon polarization in direct, 19: 5149
nucleon polarization from, symmetry defects in measurement of, 20: 28321
nucleon potentials in photo-dipole approximation in nonlocal, (T), 20: 15842
nucleon reduced widths and charge independence in, 16: 23090
nucleon transfer in, mechanisms of, 18: 11223
nucleon transfer in, 19: 41795
nucleon transfer in, mechanism of, (T), 20: 4850
nucleon transfer in, modified energy matrix method for one-dimensional model for, 20: 4852
nucleon transfer in, single, (T), 20: 21971 (BNL-948, pp 1-65)
nucleon transfer in, multi-, (T), 20: 21972 (BNL-948, pp 86-174)
nucleon transfer in, isobaric spin in, (T), 20: 30343 (COO-1371-30)
nucleon transfer in, many-body, (E/T), 20: 32547
nucleon transfer probability in, theory, 16: 21555
nucleon transfer strengths in, multipole sum rules for single, (T), 20: 1190
observation through particle tracks in solids, 16: 33404
occurrence in dense media, rate of, (T), 19: 25143
occurrences in star evolutions, 16: 18114 (NP-11463(Pt.3)(p.419-29))
on star surfaces, effects on electromagnetic activity, 20: 37399
optical giant resonances in, physical reasons for, 16: 7077
optical-model evaluation of neutron-produced, 18: 24594 (NP-13930 (p.1-5))
oriented nuclei and polarized beams in, 17: 38138
origin of heavy-particle stripping, 17: 5397
overlap integral for deuteron-induced, 19: 1651
pair correlations in two-gamma processes, 17: 7190
pair production conversion coefficients in, review on, 17: 21103
pair production, cross section calculations for, 18: 26380
parity nonconservation in strong, 16: 3750
parity nonconservation studies for, 18: 40504 (EUR-1643.e(p.196-203))
parity-spin relations in, 17: 24469
partial equilibrium model for, 16: 12516
partial waves in multi-particle production, 16: 1078
particle correlations in, conference on, 19: 39893
particle emission in, 17: 36645 (CERN-63-28(p.105-42))
particle energy distribution from, Galilean transformation of continuous, (T), 20: 11952 (COO-238-46)
particle energy distributions in, laboratory to center-of-mass transformation for continuous, (T), 20: 12011
particle identification in, statistical approach for, 16: 33724
particle production amplitudes in, representations for, 17: 9222
particle production in, unitary description of multiple, (T), 19: 37612(T)
particle production in, fluctuations in differential polarizations of, (T), 20: 30397
particle track distributions from, code for analysis of, 20: 7794 (JINR-P-2399)
peripheral model for (p,d), far above 1 Bev, 16: 24843
phase-shift analysis of single-channel, 17: 26484
phase-space integral in statistical model for multiple-production, classical, 20: 8113
photo-, dipole sum rules for N = Z, 17: 34989
photo-, effects of collective dipole excitations on, 17: 15292
photo-, excitation by protons, 17: 11734
photo-, giant dipole resonances in, 17: 7305
photo-, giant resonance in, 16: 3703
photo-, giant resonance effects in, 17: 17284
photo-, giant resonance in, 17: 19366
photo-, on unfilled-shell nuclei, 17: 17160
photo-, phonon-excitation effects in giant resonance region, 16: 29873
photo-, relation of collective and shell descriptions, 16: 12576
photo-, sum rules for high-energy, 17: 34927
photo-, tensor effects on sum rule for, 17: 11733
photo-, analysis of, 20: 3151
photo-, delayed neutron yields in, (T), 19: 5145
photo-, handbook of, 18: 30706 (AD-428207)
photoeffect and optical model, direct, 16: 12575
photoeffect, survey, 16: 1059
photofission, quasi-deuteron model for, 16: 32430
photon channels in, (T), 19: 25492
photon emission in nucleon-nucleus elastic scattering, 16: 31095
photonuclear, giant-resonance structure in, 16: 32434
photoproduction, nuclear size effects in, 17: 40111
polarization correlations in direct, (T), 20: 4849(R) (UCRL-14360, pp 1-50)
polarization effects, indirect, 16: 4801
polarization effects in, 16: 21548
polarization effects in direct, on polarized nuclei, 17: 4099
polarization effects in, 17: 11662
polarization effects in direct, with polarized targets, 17: 38243
polarization effects in direct, 18: 40609
polarization effects in (γ,N), (T), 20: 38175
polarization in, 18: 6291
polarization in, channel coupling theory, 16: 12453
polarization in direct, correlations between incoming and outgoing, 16: 21590
polarization in direct, theory of, 18: 34853
polarization in, helicity formalism for, 16: 29651 (NP-11950(Vol.I) (p.208-60))
polarization in, experimental developments on, 19: 45337
polarization of nuclei in direct, with spin-orbit interaction, 17: 22647
polarization of targets for charged-particle, methods for, 17: 38244
polarization phenomena in, 17: 36413 (NP-13020(p.201-13))
polarized nuclei in direct, 16: 21574
poles and residues of statistical collision matrix (T), 19: 3357

potential barrier model for, parabolic, (T), 20: 32423
potential scattering, with complex angular momentum and energy, 16: 24310
potentials for (p,n), optical model, 17: 29618
potentials with hard cores in, 17: 9541
probabilities of double conversion and internal Compton effect, 17: 5405
processes in, effects of compound nucleus formation on, 18: 4614
product angular distributions from, computer program for, 19: 15981(R) (ORNL-3714(Vol.I)(p.70-7))
product energy measurement, description of detector system for, 16: 5530
product identification and energy measurement from heavy-ion induced, 20: 27288
product mass discrimination in, method for, 18: 42624(R) (ANL-6879 (p.35-63))
product mass distributions in, random flight theory for, 18: 32822
production in stars by hydromagnetic shocks, 18: 5898
production of short-lived radioisotopes by, energy function chart for, 20: 36739
production of, electric discharge vessel for, (E), 19: 5263(P)
production of, electron discharge device for, 20: 39509(P)
products from, analysis of, in cyclotron chambers, 17: 17135
products from, magnetic analyzer for, 17: 29392(R) (NP-12951)
products of, continuous chamber for observing, 17: 32393(P)
products of, nomogram for correlation between escape angles of, 17: 13493
products of, method for identification of, 18: 32281(R) (UCRL-11213 (p.139-53))
projection operators for rearrangement in, (T), 20: 6312
properties above 10^{14} ev, 16: 18310
properties at 3×10^{14} ev, of cosmic particles on nuclei, 16: 26296
properties of direct, computer program for calculating, 18: 13053 (NASA-TN-D-2170)
properties of photo-, review of, 20: 8090
properties of stellar, book on, 20: 11436
properties of stellar, 20: 37392
properties of, involving incident and outgoing particles having A = 1 to 3, (E/T), 19: 21238 (LA-3205)
proton, at 3 to 25 Bev, cross sections, 16: 26274
proton capture, calculation of resonance widths in, 17: 5346
proton, distributions of charge-2 fragments from, 18: 4601
proton emission from, delayed, 18: 11230
proton inelastic scattering, direct-reaction model, 16: 19791
proton (p,n), direct mechanisms for, 17: 17226
proton potential anomaly in, 17: 31483
proton reactions (p,2p) at 155 Mev, realistic distorted-wave calculations of angular correlations in, 17: 38195
proton, lithium isotopes from fragmentation and spallation, 18: 16977
proton, short-lived elementary particles from high-energy, 18: 30754
Q-value determination for, from resonance energies, 19: 29364
Q-value measurements at MIT, 19: 29360
Q-value measurements at National University of Mexico, 19: 29361
Q-value measurements for (d,p) and (d,t), 19: 29362
Q-value measurements at MIT, review of, 20: 31808
Q-values for three-body final-state, for Z = 3 to 20 (T), 19: 1564 (ORNL-TM-938)
radial variation of the absorbing part of the nuclear optical potential, 17: 5398
radiative transitions from, 20: 3150
radiative, of mesons (π) with complex nuclei, 18: 30721 (JINR-P-1663)
radioisotope production by secondary, 19: 30267
range theory for heavy-ion, 18: 2527
rates at high densities, calculation of, 20: 40157
rates in white-dwarf stars, (T), 20: 34075
rates of, cross sections for calculating, 17: 32994 (CONF-39-37)
rates of nonresonant, at stellar temperatures, (T), 20: 15221
rearrangement collisions in Born approximation, 16: 10986
rearrangement collisions, calculation methods, 17: 2335
rearrangement in compound and direct, model for, 16: 17132
recoil nuclei from, analysis by semiconductor detectors, 18: 18222
recoil products of, diffusion measurements for determination of, 20: 43073 (JINR-P-2804)
recoil range evidence for compound-nucleus formation in complex, 17: 4088
recoil studies of compound-nucleus and partial-momentum-transfer, 18: 34782 (UCRL-11563)
reconstruction of, computer techniques for, 20: 19839 (UCRL-16478)
reduced widths in direct, determination of, 16: 4821
relations between differential cross sections for photon and electron disintegration, 18: 36638
research, new method involving strangeness excess, 16: 10990
research on, at Johns Hopkins Univ., 17: 11635(R) (TID-17720)
research on, monthly summary, 17: 19510(R) (TID-18344)
research on nucleon pickup, 17: 41530(R) (ANL-6720(p.43-7))
research on, on-line computer uses in, 17: 38606 (CU(PNPL)-227 (p.162-5))
research on 1 to 3 Mev, survey on, 17: 41855 (AFCRL-62-162)
research program at CERN, 1961, 16: 30929 (NP-12003)
research programs on meson-induced, 16: 20305(R) (UCRL-10023)
research programs at Orsay linear accelerator, 16: 21646(R) (LAL-1010)
research programs at Orsay linear accelerator, 16: 21647(R) (LAL-1021)
research programs on, uses of sector-focused cyclotrons in, 17: 38321 (CERN-63-19(p.85-92))
research programs at Bartol Research Foundation on (E/T), 19: 1568(R) (TID-21113)
research programs on, 19: 31459(R) (ANL-7010)
research programs on neutron, review of, 19: 31207
research programs on, 20: 41511(R) (RLO-1388-501)
research progress, 16: 24699(R) (TID-15820)
research progress at Purdue Research Foundation, 16: 25953(R) (TID-16079)
research progress on, 18: 21712(R) (NYO-10065)
research review, 20: 38109
resonance and threshold energies for, 19: 29359
resonance behavior of isospin-forbidden, 20: 38045
resonance energies in, determination of, 19: 29358
resonance theory of, 17: 41532(R) (ANL-6720(p.59-66))
resonance width fluctuations in, Porter-Thomas distribution for, 20: 1188
resonance-mode effects on channel coupling in, (T), 20: 6426
resonances in, (T), 19: 19153
resonances in compound-state, 17: 5268
resonances in neutron-induced, with aligned nuclei, 18: 4540 (JINR-P-1369)
resonances in photo-, width of giant, 18: 21206 (NP-13813)
resonances in, fine structure in, (T), 20: 12087
resonances in, isobaric analog, (E/T), 19: 39875
resonances in, theory of giant dipole, 19: 37900
resonant particle transfer in elastic, 16: 26299
review, 17: 817
review, 17: 26477
review of electron- and photon-induced, with light nuclei, 20: 42340
review of recent major developments in low-energy, 18: 19062
scattering effects in direct, inelastic, 18: 38165
selection rules for, nucleon associations in SU(3) scheme for, 20: 3117
shell effects in 14-Mev (n,p), 18: 44789
shell model intermediate coupling theory for, 18: 6289
shell-model theory for, boundary-condition constraint method for, 19: 43354
single-particles effects in low-energy, (T), 19: 14543
solar flare, effects on light elements on, 18: 18544
spectra from, computer program for processing pulse-height, 17: 30855 (ORNL-3405)
spectrometry of (n,α), using solid state detectors, 17: 30850 (EUR-222.f)
spectroscopic information from direct, 20: 8086 (ZFK-TPH-15)
spectroscopy of 2-nucleon-transfer, 18: 9320 (UCRL-10993)
spin effects in, triangle inequalities for, 17: 5544
spin-orbit interaction and polarization phenomena in direct, 16: 15699
spin-orbit splitting and tensor force, 16: 24829
spin path mutual exchange in stripping, 18: 34873
spin-orbit interactions in stripping, 18: 21366
spins from single-nucleon-transfer, on spin-zero nuclei, (E), 19: 14495 (ANL-6878(p.279-301))
spirality inversion in, 17: 9610
splitting of E1 giant resonance into two peaks, 17: 7253
statistical analysis of 2-center meson jets from, 17: 15111
statistical analysis, 17: 17471
statistical emission in, 16: 26516
statistical model of, theoretical work on, 17: 2243(R) (TID-17083)
statistical properties of compound-nucleus, (T), 19: 17013
statistical theory of, 18: 6294
statistics of, fluctuations in Monte Carlo, 18: 13056 (ORNL-TM-771)
stellar, element-building in, 17: 24199
stripping amplitudes and cross sections, 16: 18179 (NP-11463(Pt.1) (p.159-69))
stripping amplitudes for heavy-particle, distorted wave calculations of, 17: 24461
stripping, applications of polology to, 17: 7255
stripping, location of neutron single-particle levels from, 17: 40118
stripping processes with strong absorption, 17: 21055
stripping processes, review of, 18: 11223
stripping, computer program for distorted wave analysis of, 20: 12095
stripping, configuration-mixing effects on, (T), 19: 6706
stripping, effects of two-particle excitation in, (T), 20: 46771
stripping, finite-range effects in double, 20: 24404
stripping, polarization of emergent protons from, 18: 16994
stripping, surface reactions in, 18: 30740(T) (UCRL-Trans-1079)

strong and weak interactions, review of recent experimental and theoretical results on, 17: 37942
structure amplitudes from two-nucleon transfer, (T), 19: 8459
structure effects survey, 16: 1058
structure effects in lithium-ion, with light nuclei, (T), 20: 38014
structure in direct theory, at 10^3 to 10^4 Mev, 17: 7186
studies of high-energy, 19: 37835(R) (TID-22024)
studies of, using electromagnetic separation in continential Europe, 18: 16950 (SGAE-PH-2/1964)
survey of, for use as neutron sources, 17: 15249 (BNL-6765)
survey of scattering and reaction experiments with medium-energy alpha particles and nucleons, 18: 6296
systematics of effective cross sections of neutron-produced, in the medium-energy region, 18: 24601 (NP-13930(p.41-2))
target orientation optimization for, computer program for, 20: 4842 (NASA-TN-D-3116)
theories for, quantum, 20: 11511
theory, 16: 9311
theory, 16: 29656 (NP-11950(Vol.II)(p.425-84))
theory, 18: 18938
theory, 18: 26667
theory, 19: 29283
theory, effects of physical properties on channel radii, 16: 19786
theory for (α,p), improvement of knock-out, 18: 18961
theory for (He-3,d) and (t,d), distorted-wave, (T), 19: 37824(R) (ORNL-3800(p.50-7))
theory for (He-3,p), distorted-wave Born approximation in, 20: 12127
theory for arbitrary spin, 20: 32382 (UCRL-14592-T(Rev.1))
theory for cluster stripping, distorted wave, 19: 39829
theory for deuteron stripping, 20: 3070
theory for direct, 20: 22018
theory for direct photo-, resonance effects in, (T), 20: 26206
theory for direct transfer, 20: 28376
theory for direct, dispersion, 20: 19990
theory for direct, at medium energies, 20: 28372
theory for high-energy, (T), 19: 5200
theory for intermediate structure in, channel coupling, 19: 19171
theory for knockout and stripping, 18: 18880 (NP-13773)
theory for multi-nucleon stripping, cross sections for, 20: 28376
theory for multichannel, derivation of effective-range in, 16: 32433
theory for neutron reactions below 5 Mev, 16: 23145
theory for one-meson-exchange, distorted-wave, 20: 17474
theory for (p,n), 17: 2279
theory for pickup (p,d), 17: 11492 (TID-16044)
theory for pickup and stripping, quasi-particle, 20: 17814
theory for stripping, with emission of slow particles, 19: 41664 (JINR-P-2193)
theory for two nucleon pickup and stripping, 20: 30483
theory for two-step (p,2p), 18: 15208 (TID-20226)
theory for, channels projection operator and Pauli principle in, 20: 15744
theory for, description of unified, 19: 17010
theory for, extension of scattering theory to, 20: 46609 (ZFK-TPH-20)
theory for, inelastic effects in, (T), 20: 17692 (ORNL-TM-1414)
theory for, R- and S-matrix, 20: 19893
theory for, shell-model calculations in continuum, (T), 20: 4882
theory from liquid drop model, 20: 4879
theory of (α,d), 19: 8474
theory of (α,d) and (d,α), 19: 17008
theory of (p,pd), at high energies, 18: 18967
theory of, application of time-dependent formalism to, 17: 34902
theory of charged-particle stripping, Coulomb distortions in, 18: 26646
theory of compound, random phase approximation for, 17: 40127
theory of compound nucleus, high angular momentum states in, 18: 24733
theory of Coulomb stripping, 17: 31521
theory of Coulomb excitation, review of, 18: 18887 (ZFK-PHA-11)
theory of cross section fluctuation in statistical, 17: 26430(R) (ORNL-3425(p.10))
theory of (d,p) stripping, on even-even spherical nuclei, 16: 31121
theory of deuteron stripping, 20: 46752
theory of direct and resonance, short-range interaction, 20: 32387
theory of direct, exchange terms in, 18: 2877
theory of direct, Feynman nonrelativistic diagram in, 16: 28033 (NP-11833)
theory of direct interaction, 17: 11669
theory of direct stripping, 20: 38023
theory of direct, zero-range distorted-wave formalism, 16: 9435 (ORNL-3240)
theory of direct, relation of distorted-wave and dispersion, 18: 30737 (UCRL-7478-T)
theory of direct, spin-orbit effects in distorted-wave, 18: 34835
theory of direct, diffraction mechanism in, 18: 34848
theory of direct, Treiman-Yang criterion in, 19: 3286
theory of direct, unified, 19: 10268
theory of direct, Coulomb effects in, 20: 24473
theory of direct, using three-body collision theory, 20: 44654 (PUC-937-227)
theory of doorway states in, 20: 34666
theory of double-stripping (t,p), zero-range distorted-wave, 18: 19023
theory of elastic and inelastic, 16: 33798
theory of finite-range distorted-wave calculations for, 18: 6235
theory of inelastic scattering of identical nuclei, 20: 30493
theory of intermediate structure in, 20: 21988 (BNL-947, pp 876-904)
theory of intermediate structures in, 20: 34667
theory of isobaric analogue resonances, 20: 46637
theory of isometric ratios in compound, 18: 13839(R) (TID-20201)
theory of isospin forbidden, cross section fluctuations in, 19: 8445
theory of low-energy, 17: 11740
theory of low-energy, 18: 34754 (HMI-B-35)
theory of low-energy, 19: 36220(R) (MIT-2098-142)
theory of many-channel, 16: 26345
theory of multi-particle, general relativistic, 17: 26288 (PAN-401/VII)
theory of multichannel, surface effects in, 19: 19193
theory of neutron-induced, 19: 31215(R) (ANL-7010(p.1-19))
theory of nuclear evaporation, 17: 15277
theory of nucleon cluster stripping, 17: 9614
theory of, one-level approximations in, 17: 22578
theory of photo-, 17: 36405 (NP-13020(p.129-44))
theory of photo-, unified, 18: 13054 (NP-13560)
theory of photo-, in strongly deformed nuclei, 20: 8173
theory of photodisintegration, direct-interaction, 18: 21266
theory of pickup and stripping, below Coulomb barrier, 20: 6352
theory of polarization in direct, 18: 36624
theory of polarization in direct, semiclassical, 20: 3049
theory of, R-matrix, 17: 38113
theory of rearrangement processes in, neutron tunneling in, 18: 34894
theory of rearrangement, coupled equations for, 20: 12045
theory of resonance, 18: 6292
theory of resonance, dispersion relations for, 18: 36616
theory of resonance, Coulomb barriers and cross sections in (T), 19: 1689
theory of resonance, 19: 1575
theory of resonance, 20: 32428
theory of shell-model resonance, 18: 11182 (ANL-6797(p.342-57))
theory of, statistical, 17: 32727(R) (PR-P-57(p.69-85))
theory of, statistical, 17: 41892
theory of stellar, 20: 7706
theory of stripping, 18: 36617
theory of stripping, 18: 42627(R) (ANL-6879(p.88-113))
theory of stripping, Coulomb wave, 19: 5162
theory of stripping, 19: 37841
theory of stripping, 20: 1228
theory of, strongly coupled channel, 17: 40081
theory of, studies at MIT on, 17: 40437(R) (NYO-10063(p.116-25))
theory of transfer, local energy approximation for finite range effects in, 18: 28683
theory of, two-level approximation for eigenvalue, 17: 24418
theory of two-nucleon stripping, DWBA for, 20: 13814
theory of two-step (p,2p), 20: 12006
theory of, unified, 16: 28043
theory of, unified, 18: 9440
theory of, without boundary conditions, 17: 22264(R) (ANL-6679)
theory of, antisymmetrization of unified, 18: 32790
theory of, antisymmetrization of unified, 18: 34773 (NP-14190)
theory of, bibliography on, 18: 21353
theory of, channel coupling in, 20: 44653 (PUC-937-219)
theory of, completeness of set of eigenstates of non-Hermitian operators in, 20: 44707
theory of, corrections in distorted-wave, 20: 21979 (BNL-948, pp 525-60)
theory of, development of, 19: 14544
theory of, diffuse nuclear edges in barrier penetration, 19: 9771(R) (PR-P-63)
theory of, eigenchannel, 20: 30449
theory of, elementary particle, 18: 15305
theory of, formulation of, 19: 3280
theory of, in stellar interiors, 20: 4534
theory of, independence hypothesis in statistical, 18: 26529 (BNL-8020)
theory of, open and closed channels and unitarity in, 18: 36619
theory of, partial equilibrium model in, (T), 19: 5183
theory of, projection operators in unified, 20: 13850
theory of, quantum Green function in, 19: 33377
theory of, quantum, 19: 43375
theory of, research programs on, 20: 41796(R) (MIT-2098-251, pp 74-103)
theory of, review on direct-interaction and compound-nucleus, 18: 40612
theory of, review of, 19: 17036
theory of, review of recent developments in, 20: 42339

theory of, single-level approximation of R-matrix, 19: 25478
theory of, status of, 18: 40647
theory of, studies at MIT on, (T), 19: 5569(R) (MIT-2098-64)
theory of, time dependent, 18: 17088
theory of, time-dependent equations in, 20: 22024
theory of, unified, 20: 4837 (JINR-P-2310)
theory of, using cluster and compound-nucleus models, 19: 17012
theory of, using few-level approximations, 19: 39805
theory of, with multibody exit channels, 20: 21981 (BNL-948, pp 610-84)
threshold effects in average cross sections according to R-matrix theory, 17: 7236
threshold effects in, research on, 20: 19802(R) (AD-630042)
threshold rate normalization to sulfur, 17: 36347(R) (NARF-62-18P)
thresholds for, tabulation, (E), 19: 14539 (TID-21627)
time and energy aspects in, 18: 32774
time delay in compound-nucleus and direct, method for measuring, 17: 38216
time delay in compound-nucleus and direct, bremsstrahlung techniques for measuring, 17: 38217
time delay of compound-nucleus component in, cross section correlation function for, 18: 4629
transition matrix for scattering of free particles by systems of identical bound particles, 16: 21312
triple angular correlation and time reversal invariance, 16: 4851
unified theory of photo-, 18: 21364
unified theory of, application to elastic neutron scattering by nitrogen-15, 18: 18890
use for production of gamma masers, 17: 36614
use in determination of energy level structure of heavy nuclei, 20: 1229
use in distinguishing between chemically bound and free hydrogen, 20: 20653 (JINR-P-2558)
use in microanalysis, 18: 13625 (LAL-1053)
use in neutron measurement, 18: 16356
use in nuclear structure studies, review of, 20: 46618
use of (n,γ), for nuclear physics studies, 18: 24607 (NP-13930(p.104-8))
use of accelerators in studying, 18: 15386
use of polarized neutrons in, 18: 12929
use of recoil methods for short lifetime measurements, 16: 21441
use of two-nucleon-transfer, in nuclear structure analyses, (E/T), 20: 1232
used in neutron dosimetry, 18: 16355
uses of (d,p) and (d,t), for nuclear analyses, 18: 32881
uses of deuteron-transfer, for nuclear spectroscopy, (E/T), 19: 14497 (ANL-6878(p.353-422))
uses of direct, for nuclear spectroscopy, (E/T), 19: 14485 (ANL-6878)
uses of many-nucleon-transfer, for nuclear-structure analyses, (T), 19: 14496 (ANL-6878(p.335-50))
uses of secondary, in radiochemistry, 20: 18807
uses of single-nucleon-transfer, for nuclear-structure analyses, (T), 19: 14494 (ANL-6878(p.249-75))
uses of two-nucleon-transfer, for nuclear spectroscopy, (T), 19: 14498 (ANL-6878(p.425-48))
vertex function kinematic structure of, Lorentz transformations in, 16: 24860
vertex parts of the amplitudes for direct, 17: 2327
wave amplitudes for zero angular momentum stripping, Coulomb, 18: 6240
wave functions for (d,p) stripping, three-body, 20: 28386
wave functions in direct, overlap integrals and single-particle, (T), 19: 41728
wave functions in two-nucleon stripping, (T), 20: 12086
width fluctuation factor for, correlated multichannel distribution for, (T), 20: 13824
widths of, analysis of, 17: 9585
yield curves for, atomic effects on, 17: 32998 (CONF-52-3)
yields, calculation by statistical method, 16: 15645
yields from, electromagnetic separation of, 18: 36595
yields in, Fortran program for IBM 704 computation of relative isomer, 17: 19215 (ANL-6662)
yields of, methods for improving, (T), 19: 43377

Nuclear Reactors

see Reactors

Nuclear Rockets

see Rockets

NUCLEAR SHOWERS

analysis of cascade, by solving inverse problem, (T), 19: 41710
calculations of intranuclear, (T), 19: 21239 (LA-3206)
data on, computer codes for analyzing, 17: 24395 (ORNL-3433)
description of, for incident energies up to 1 Tev, (E/T), 19: 6633 (JINR-P-1796)
distributions in intranuclear, from 17-Bev mesons, (π), (E/T), 20: 6287 (JINR-P-2373)
distributions in nucleon-pion, in iron from 1- and 3-Bev protons, (T), 20: 5927 (ORNL-P-1733)
distributions in 1- to 3-Bev proton-produced, (E), 20: 3015 (NASA-SP-71, pp 357-62)
fragment distributions in proton-induced, charge-2, 18: 4601
parameters of proton-induced, in baryte concretes, 17: 12791(R) (ORNL-3360(p.241-8))
production and properties of high-energy, (T), 19: 41709
spectra in cosmic, at 12 to 450 Bev (E), 19: 1201

Nuclear Spallation

see Spallation

NUCLEAR SPECTRA

analyses for T = 0 and T = 2 states for four-particle configurations of S-state interactions, 18: 9382
analyses of evaporation of compound nuclei, role of level density parameters in, 18: 28627
analysis of, group theory for, 18: 2958
analysis of, 2-nucleon-transfer, 18: 9320 (UCRL-10993)
analysis of, approximation methods and pairing forces in, 18: 21216
analysis of, asymptotic reduced-width amplitude distributions for, 19: 35415
analysis of, method for least squares, 19: 5869
analysis of, Racah algebra for, 19: 45315
analysis using direct reactions, conference, (E/T), 19: 14485 (ANL-6678)
band structure of, 18: 44728 (INSJ-71)
book: *Les Modeles en Spectroscopie Nucleaire*, 20: 3139
book: *Statistical Theories of Spectra*, 19: 35507
calculation using deformations in shell model, (T), 20: 9974 (PUC-937-171)
coincidence measurements of complicated, evaluation of, 17: 38097
conference on, 18: 16905 (ANL-6848)
correction to rotational, (T), 20: 12088
determination using emulsions, reliability of fractional scanning for, 20: 41315
drift-correcting computer subroutine for, 19: 11660
effects of collective excitations on single-particle, 16: 26269
effects of nonspherical states in, 20: 8091
emission by oriented nuclei at low temperatures, 16: 32245
energy level calculations for, random-phase approximation validity for, 17: 36662 (TID-17785)
energy level spacing distributions for, of complex nuclei, 18: 28745
fine and hyperfine structure of, 18: 28609
inequality method for unfolding continuous-energy, 17: 26199
interpretation using excitation modes, (T), 20: 19993
levels in, spacing distribution and correlations between, 18: 2955
measurement and recording of, magnetic-tape system for, 20: 25360
measurement of, data acquisition systems for, 20: 6307 (UCRL-16439)
measurement of, development of equipment for, 20: 1252
measurement using nuclear emulsions, 19: 44448 (HASL-162)
monitor for two-parameter, design of integrating storage display, 20: 46011 (EUR-3117.e)
of M1 transitions, 17: 4119
properties of, conference on statistical, 18: 2953
recording device for, 18: 27784(P)
relation to nucleon-nucleon forces, 17: 24177
research progress, review, 16: 21621
research progress at Purdue Research Foundation, 16: 25953(R) (TID-16079)
research progress on, 18: 15172(R) (AROD-1784:31)
rotational, at high momenta, 20: 3103
rotational, nonadiabatic effects of, 20: 32492
rotational, of nuclei with small asymmetry (T), 19: 1604
stability in, 20: 40108
stabilization of recording systems for, 18: 32281(R) (UCRL-11213 (p.139-53))
theory of unitary matrix ensembles, 20: 38033
theory of, eigenfunction expansions for, 20: 36161 (IC-66/62)
theory of, optical-model potential and hole-particle model for, 20: 12047
variations of the decoupling parameters for ½ rotational bands for very deformed nuclei, 16: 29813
wave equation with rotational invariance and broken SU(E) symmetry for, Schroedinger, 20: 34403

NUCLEAR SPIN

book: *Nuclear Orientation*, a collection of reprints, 18: 24706
book: *Nuclear Spin-Parity Assignments*, 20: 46801
chains, quantum mechanical models for antiferromagnetic, 16: 5785
coupling constant for, alternant molecular orbital expressions for, 20: 14543
coupling constants for, molecular orbital theory of, 18: 44773
coupling in NMR, 19: 5153
coupling mechanism in nuclei, 17: 35263(R) (UCRL-10706(p.1-110))
coupling of, between geminal hydrogen atoms, 19: 11097
coupling to electrons in solids, nuclear magnetic resonance of spin-phonon, 16: 18275

cross section independence of isotopic, at high energies, 16: 2549
diffusion in crystals and magnetic relaxation, 16: 23156
diffusion in irradiated polymers, 19: 22308
distribution function of energy levels in system of normal paramagnetics, 16: 7121
dynamics of ferromagnetic, 16: 26013
effect on differential cross sections for direct reactions, (T), 20: 44773
effects in extracting alkali spin-exchange cross sections from Zeeman optical-pumping signals, (T), 19: 39879
effects on fission fragment angular distribution, 16: 3706
effects on neutron elastic scattering by nuclei with Z = 4 to 92, (E), 20: 46794
effects on nuclear quadrupole relaxation time, 18: 17814
effects on Regge pole position, 17: 11485 (NP-12478)
electron nonequilibrium in systems of, 16: 22953
energy level density dependence on, 18: 6257
energy levels and intensities of, in single crystals, 17: 24072(T) (JPRS-19316(p.162-76))
excitation in nuclei, giant resonance in, 16: 32452
fission resonance width effects, 16: 24348
in molecular crystals, 16: 2354
inertial moment in strongly deformed nuclei, effect of Pauli exclusion principle on, (T), 19: 16955
inertial moment in excited superfluid nuclei, (T), 19: 19126
inertial moments of asymmetric nuclei, (T), 19: 39831
interactions in paramagnetic crystals, 16: 22811
interactions with electron spin in paramagnetic media, 16: 7138
interactions with ultrasounds, 17: 6792(R) (ISS 62/14)
interactions with orbital momenta in deformed nuclei, 18: 18942
interactions with electron spin, energy of, (T), 19: 20695
isobaric, purity in heavy nuclei, 17: 13568
magnetic properties of, in solids, 17: 525 (AFCRL-922)
measurements of acoustical and optical waves of, in magnetites, 16: 31582 (AECL-1575)
mixing between systems of, dynamic polarization in, 17: 40099
moments of, determination of inertial, 17: 38206
mutation of moment vector of groups of, by modulation of nuclear magnetic double resonance, 19: 11094
nuclear relaxation as a probe of electron spin correlation, 17: 6856
of three-particle isomeric states in spherical nuclei with odd A, 20: 38136
orientation of, by cooling, 17: 21018
orientation of, review of dynamic and static methods for, 17: 5056
oscillations in antiferromagnetics, 19: 47903
polarization in lithium and sodium, Overhauser, 17: 41944
polarization in semiconductor lattice near paramagnetic impurities, r-f suppression of, 18: 34334
polarization of, schemes for dynamic, 17: 21019
polarization of, dynamic, 18: 32808
polarization spin diffusion effects on, 16: 18276
polarization time in solid dielectrics, electron-resonance excitation in, 18: 26652
prediction of ground-state, empirical rules for, 18: 7755
radioinduced in nucleic acids and bases, gamma and x, 17: 39125
relation to statistics in electromagnetic fields, 16: 12346
relation to statistics in relativistic quantum field theory, 16: 12375
relaxation in dilute gases, (T), 20: 11784
relaxation in gases, 19: 39378
relaxation in liquid and solid methane, isotope effects in, (E), 19: 32191
relaxation in molecular crystals, 18: 29660
relaxation mechanisms for, non-perturbative interactions in, 17: 34946
relaxation of a rotating pair of, 17: 26609
relaxation of, Fokker-Planck equation for, 17: 842
relaxation of, in two-spin systems, 17: 843
relaxation of, semiclassical density-matrix theory of, 18: 38092
relaxation of, stochastic equations for, 20: 30249
relaxation time in viscous media, calculation of paramagnetic, 16: 32450
relaxation time in metals, temperature dependence of, 18: 2450
resonance of, use in radiation effects studies, 17: 22222 (MMPP-NPC-1-3)
resonance of, measurement and experimental uses of, 19: 12505
resonance spectral study, 16: 17552 (AD-263735)
shift behavior of, in pionic decay of hyperons, 17: 31382
static theory of spin resonance saturation, 17: 3631
statistics relation, 16: 3621
tables, 18: 30864
temperature measurements below 1°K using, method for, 19: 25451
temperature of, double resonance method for determining, 17: 26602
testing of isotopic, by strong interactions, 16: 29663 (UCRL-10290)
theory of antiferro- and ferro-magnetism in cubic clusters of, 17: 5027 (AD-273950)
theory of cross-relaxation systems, quantum statistical, 16: 18536
theory of Raman analog of electronic and, induction and echo, 20: 41640(T)
theory of spin pumping and relaxation in systems with a low concentration of electron spin resonance centers, 16: 29568
theory of, Thomas classical, 17: 15296
theory of, spin operators in, 19: 9767(R) (IS-900(Sect.P))
translation of, in Lobachevsky space, 17: 9290
wave properties in magnetites, 16: 25979

NUCLEAR STRUCTURE

see also Nuclear Models

alpha cluster and nuclear surface, 16: 18521
alpha clusters in, evidence for, 17: 26593
alpha clusters in, quadrupole moment as measure of existence of, 18: 7715
alpha clusters in, geometrical positions of, 18: 18943
alpha clusters in, single-pole Majorana forces and nucleon coupling in, 18: 28617
alpha clusters in, helium-3 beam probe study of, 18: 44739 (UCRL-11598)
alpha, detection by (p,α) reactions on bismuth-209, 18: 7728
alpha-alpha potentials for forces in, (T), 20: 22061
amplitudes for two-nucleon transfer reaction, structure, (T), 19: 8459
analyses using electron linear accelerators, survey on, 20: 1233
analysis by alpha inelastic scattering, (E), 19: 47608
analysis by inelastic electron scattering with orientation effects, 17: 24182
analysis by neutrons, conference on, 20: 34656
analysis by optical model studies of elastic scattering, 16: 21529
analysis equations for, (T), 20: 19273(R) (BNL-929, pp 3-43)
analysis for light nuclei, by (p,2p) reactions at 155 Mev, 16: 31094
analysis for light nuclei, (γ,p) and (p,2p) reactions for, 17: 24503
analysis for light and medium nuclei, conference, (E/T), 19: 14511 (CONF-640301)
analysis for tritons, using separable potentials, (T), 20: 12130
analysis from beta decay measurements, 20: 30536
analysis from electron magnetic scattering by nuclei, 20: 24451
analysis from inelastic electron-scattering experiments, 17: 24181
analysis from quasi-free scattering, review of, (T), 20: 10082
analysis of, computer methods in, 17: 24513
analysis of deuteron reactions for, (T), 19: 17033
analysis of intermediate coupling, 17: 7140 (TID-14921)
analysis of reactions of deuteron-triton built-up nuclei, 18: 11227
analysis of, cluster model, 20: 28438
analysis of, conference on, 19: 41671 (LADC-6186)
analysis of, graphic method in shell model, 19: 27509
analysis of, instrumentation for, 20: 39240
analysis of, relation with elementary-particle physics, 19: 32956
analysis of, using nuclear models, 20: 34657
analysis, review, 16: 29751 (BNL-5013)
analysis using (p,2p) and other knock-out reactions, (E), 19: 39904
analysis using beta decay data, (E/T), 20: 12113
analysis using Brookhaven Cosmotron, 20: 28267 (BNL-10135)
analysis using conversion electron-gamma directional correlations, (T), 20: 36225
analysis using deuteron-transfer reactions, (E/T), 19: 14497 (ANL-6878(p.353-422))
analysis using distorted-wave Born approximation, 18: 32880
analysis using DWBA and optical model, (T), 20: 21978 (BNL-948, pp 454-524)
analysis using fast-neutron reactions, survey on, 20: 9973 (NP-15816)
analysis using fast neutron reactions and scattering, 20: 12132
analysis using heavy-ion reactions and scattering, 20: 21992 (BNL-948, pp 1045-1134)
analysis using inelastic neutron scattering, 20: 34659
analysis using inverse gap equation and phenomenological approach, 20: 28411
analysis using many-nucleon-transfer reactions, (T), 19: 14496 (ANL-6878(p.335-50))
analysis using meson (π) reactions with nuclei, 19: 45339
analysis using neutron capture gamma rays, 20: 34660
analysis using proton capture, 20: 21986 (BNL-948, pp 763-825)
analysis using single-nucleon-transfer reactions, (T), 19: 14494 (ANL-6878(p.249-75))
analysis using terminology of high-energy elementary-particle physics, (T), 19: 14500 (ANL-6878(p.481-504))
analysis using two-nucleon-transfer reactions, (T), 19: 14498 (ANL-6878(p.425-48))
analysis using two-nucleon-transfer reactions, (E/T), 20: 1232
angular correlation methods in, multipole mixing of gamma transitions in, 18: 36569 (INSJ-66)
angular momentum dependence of the effective two-body nuclear interaction, 17: 36403 (NP-13020(p.121-4))
axial asymmetry in, 18: 21225
bibliography on, 18: 42765
bibliography on, 18: 42766

bibliography on, 20: 19803 (AED-C-12-13(Pt.1))
binding energy at equilibrium density, off-energy-shell effects in Brueckner theory for, 19: 47666
Bohr-Mottelson and asymmetric-rotor models for shape of deformed, 18: 18934
book: *Coulomb Excitation*, 20: 15848
book: *Les Modeles en Spectroscopie Nucleaire*, 20: 3139
book: *Nuclear Chemistry. Study of Radioactive Nuclei and Nuclear Reactions*, 20: 24487
book: *Nuclear Structure and Electromagnetic Interactions*, 20: 3147
book: *Nuclidic Masses and Binding Energy of Nuclei*, 19: 31313
book: *Structure of Matter*, 19: 41829(T)
calculation of neutron bound states using a nonlocal single-particle model, 17: 41943
calculations for finite nuclei using Hartree-Fock approximation, (T), 20: 34564
calculations for, boundary-condition constraints for shell-model, 19: 27557
calculations using shell model, boundary-condition constraint method for, 20: 21989 (BNL-948, pp 905-27)
calculations using shell model, potentials for, (T), 20: 42247
calculations using projection techniques, (T), 20: 46664
closed-shell effects on cluster singularities of the nucleon-nucleus vertex part, 18: 11241
collective excitation of zero spin and, 16: 2552
collective E0 transitions and nuclear shape, 17: 41905
conference, 20: 15749
conference on, 20: 19952
configuration mixing in sd-shell nuclei, (T), 20: 12128
construction of low-energy nuclear potentials, 17: 5380
core excitations in nondeformed odd-A nuclei, 17: 36399 (NP-13020 (p.85-91))
Coriolis interactions in odd-odd nuclei, 18: 36581 (UCRL-11379)
correlation energy in, wave function for short-range three-body, 19: 47665
correlation of nuclear moments and, (T), 19: 23653
Coulomb energies of lower excited levels in light mirror nuclei, 17: 36691
deformation calculations for, near N = 18, 18: 34781 (UCRL-11376)
deformation in $90 \leq N \leq 120$ nuclei, close-packed-spheron theory for prolate, (T), 20: 8137
deformation of heavy nuclei, (T), 20: 24385
deformations in medium and heavy nuclei, (T), 20: 19986
deformations in rare earth and light nuclei, self-consistent calculation for, 20: 15843
determination by electron scattering on nuclear protons, 16: 21471
determination by electron-gamma correlation measurements, 17: 9524
determination by electron scattering, 17: 36642 (CERN-63-28(p.37-46))
determination by neutron reactions (n,γ) with nuclei, 18: 32876
determination by proton reactions and scattering, 17: 36644 (CERN-63-28(p.73-104))
determination by reactions of oriented nuclei and polarized beams, 17: 38138
determination for s-d shell nuclei, 18: 1091
determination from interactions of fast nucleons with nuclei, 16: 21464
determination from nuclear reactions in Bev range, 17: 38306
determination from proton reactions (p,d) with nuclei ($12 \leq A \leq 48$) at 40 Mev, 17: 40110
determination from shell model, 17: 40125
determination from reactions, review of, 18: 13116
determination from nucleon–nuclei interactions at 1 to 50 Mev, 18: 19107
determination from internal conversion, (T), 20: 36223
determination in electron inelastic scattering on nuclei at high energies, 17: 38261
determination in odd transition-region nuclei from E2 and M1 transitions, (T), 20: 9995(T)
determination in proton reactions (p,n), (p,p), (p,pn), and (p,2p) with nuclei at 100–200 Mev, 17: 38304
determination of, 17: 36647 (CERN-63-28(p.175-84))
determination of, conference on, 17: 36640 (CERN-63-28)
determination of, from proton reaction Q values, 16: 29774 (JAERI-1020 (p.194-200))
determination of, group theory for, 18: 2958
determination of states in strongly deformed nuclei on the basis of the superconductivity model, 17: 40009
determination of, use of strange particles in, 17: 36641 (CERN-63-28 (p.1-36))
determination of, using mesons(μ), 17: 36646 (CERN-63-28(p.143-71))
determination of, fast neutron spectroscopy for, 18: 13112
determination using meson(π) interactions, 17: 36643 (CERN-63-28 (p.47-72))
determination using polarized nucleon elastic scattering, 20: 3014 (LA-DC-7386)
determination using Λ hyperfragments, 20: 24463
determination using mass spectrometry, (T), 20: 28452
determination using meson (μ^-) capture studies, 20: 42317
determination using electron inelastic scattering, review of, 20: 44679
deuteron properties in nuclear matter, 16: 21403
development and periodicity in, 17: 15279
discovery of exclusion of electrons from, 18: 4446
effects in lithium-ion reactions with light nuclei, (T), 20: 38014
effects of dynamic, on internal conversion, review of, 20: 6332
effects of finite, dimensions of nucleus on polarization of particles during pair production and bremsstrahlung radiation, 18: 7716
effects of pairing correlations on nuclear level densities, 18: 19018
effects of shell structure on level densities in continuum, 20: 22070
effects on charge distribution in spherical nuclei, (T), 20: 38043
effects on coefficient of internal conversion of gamma rays, 17: 22584
effects on diffraction dissociation of complex nuclei, 18: 38137
effects on internal pair formation, 18: 26581
effects on K-internal conversion, evidence for, 19: 14641
effects on multichannel reactions, (T), 19: 19193
effects on neutrino reactions with nuclei, (T), 20: 12100
effects on radiative corrections to beta decay, 18: 28741
effects on spectra of mesic atoms, 18: 21331
eigenstates of pairing-force hamiltonian for deformed nuclei, (T), 19: 21347
electric multipole conversion in, Born approximation for, 17: 22648
electromagnetic form factors for helium-3 and tritium, 18: 40596
electron inelastic scattering for correlation, (T), 19: 14601
energy gap in, hard-core effects on, 16: 2543
energy level calculations for praseodymium isotopes, nucleon interactions in, 20: 12124
energy level density model, analysis by (p,γ) reactions, 16: 19797
energy level densities in, measurement by inelastic neutron scattering, 17: 11708
energy level densities in, band structures from variations in, 18: 44728 (INSJ-71)
energy level distributions, 17: 19285
energy level identification in light nuclei by photodisintegration cross sections, 20: 38138
energy level schemes of nonspherical nuclei in accordance with the independent particle model, 17: 34969
energy level spacings in, neutron s-resonance determinations of, 17: 38163
energy level spacing distributions in, computer program for eigenvalue, 18: 32014 (BNL-863)
energy level spectra for complex nuclei, 18: 28745
energy level structure for $150 < A < 190$ and $228 \leq A \leq 254$, collective, 18: 34760 (JINR-E-1696)
energy level systematics for even-even nuclei, 18: 42757
energy levels from Coulomb excitation, gamma emission from, 18: 34965
energy levels in even-even nuclei, seniority-zero spin-zero, 18: 44746
energy levels in nonspherical odd-mass nuclei, 17: 40005
energy levels in, delayed-coincidence measurements of lifetimes of first-excited, 18: 34772 (NP-14184)
energy levels in, one-quasiparticle, 18: 42640 (KFKI-1467/r)
energy levels in, many-particle Green function theory for composition of giant-dipole, 19: 45334
energy levels of light nuclei, shell effects in Coulomb displacement energies of, (T), 20: 11963 (INSJ-91)
energy levels of nonaxial odd-mass nuclei, 18: 21180 (JINR-P-1574)
energy levels of nuclei, one- and two-phonon, (T), 20: 12123
energy levels of two-dimensional nuclei, 20: 19854
energy levels of 2s1d nuclei, (E), 19: 5130 (KFKI-15/1963)
energy levels with high spin, gamma cascade from, (T), 20: 13847
equilibrium form of light nuclei, 18: 30832
equilibrium parameters of light nuclei, 18: 21307
excitation of rotational levels by nucleon scattering, 18: 16959
fine structure in masses of heavy odd-A nuclei, 17: 13510
fission studies on, review of, 19: 27539
five-body problem in, independent pair model of, 16: 26452
formation and excitation energies of nuclei, (T), 19: 23652
generalized rotation-vibration model for deformed even nuclei, 17: 5331
group theory in, invariant operators in, 17: 13666
group-theory and model-interaction methods for, in 2s-1d shell, 19: 41729
Hartree-Fock theory, tensor-force and spin-orbit coupling in, 17: 40030
investigation by meson (K^-) capture, 17: 7232
investigation of, using heavy ion projectiles, 16: 29780 (JAERI-1020 (p.229-35))
isobaric multiplets in light nuclei, 20: 42355
isomer shift and structure of metastable nuclear states, 20: 3138
isotope shift of charge radius, anomalous, (T), 20: 38101
isotope shift theory and, 17: 36711
level parameters from (γ,p) reactions, 17: 40080
level spacings in, formula for, 18: 2957

localization of direct interactions for, (T), 19: 14603
localized solutions of the Bethe-Goldstone equation for two nucleons in nuclear matter, 17: 26746
location of quasistationary single-particle states in nuclei with A = 5 to 240, 17: 40012
magnetic and orbital moments from quasicrystalline, (T), 19: 23654
many-body problem in, 16: 21530
many-body problem, boundary condition model for, 16: 21541
many-body problem in configuration-mixing and intermediate-coupling shell models, 18: 44731 (LA-DC-6098)
masses and neutron separation energies of even-even nuclei, 17: 38102
matrix elements for n-p interactions and the odd-group model for heavy nuclei, 16: 28146
matrix elements of nuclear two-particle interaction operators in, 18: 44727 (BNL-871)
measurement of nuclear matter distribution by meson (π^0) photoproduction, 17: 33106
measurements, interpretation of gross, 16: 21583
measurements near $1f_{7/2}$ shell using (p,d) and (p,t) reactions, 20: 46596 (PUC-937-211)
meson theory for forces in, review of, 19: 23765
model for odd-parity states in even nuclei, 16: 28077
model for rotational states in deformed nuclei, 18: 44832
model for, close-packed-spheron, (T), 20: 1218
model interaction matrices for 2s-1d shell for A = 18 and 20, 19: 41730
models of low-lying states, 18: 11160 (ANL-6797(p.58-78))
models of, residual forces in single-particle, 18: 42645 (NP-14338)
monopole force effects on, (T), 19: 16917
multipole moments of rounded charge distribution, 18: 19025
neutron-proton interaction between states of the same l in, 16: 28152
neutron resonance parameters and radiation widths for medium-weight nuclei (E/T), 19: 3238 (JINR-P-1771)
neutron shell configuration study for $23 \leq Z \leq 28$ nuclei from (p,d) reactions, 18: 21291
nuclear forces in, phenomenological treatment of, 20: 17727
nuclear forces in, phenomenological treatment of, 20: 17728
nuclear matter studies using quantum statistics, 16: 3731
nuclear radii derived from alpha-decay theory taking into account pair correlations of the superconducting type, 17: 40010
nucleon cluster reduced widths for, 18: 34891
nucleon clustering and the shell model, 18: 4606
nucleon clusters in, dissociation of, 17: 38280
nucleon form factors in the configuration space, 16: 2658
nucleon grouping in shell-model states, fractional parentage coefficients for three-particle, 18: 24621 (PAN-449/VII)
nucleon magic numbers in, (T), 20: 4872
nucleon pairing correlations for heavy nuclei, 19: 23671
nucleon pairing correlations in L = 0 state, 20: 12131
nucleon pairing hamiltonian in, symmetry properties of, 18: 34890
nucleon pairing-correlation model for, 20: 26115
nucleon quadrupole and pairing forces in, (T), 20: 17801
nucleon recoupling and fractional parentage in 2s-1d shell, SU_3, 19: 3310
nucleon subshell closures at 56 neutrons in, 18: 40506 (IS-878)
nucleon-nucleon potential scattering parameters in, 19: 1552 (JINR-P-1728)
octupole deformation in rare earths and actinides, 16: 3745
octupole deformation in even-even medium-mass nuclei, 17: 36703
of beta-instability region nuclei, 20: 19884
of heavy spherical nuclei, (T), 20: 21975 (BNL-948, pp 269-336)
of light nuclei, use of peripheral model in study of, 18: 11213 (LNF-63/47(p.249-50))
of light spherical nuclei, 20: 21974 (BNL-948, pp 222-68)
of nuclear quasimolecules, 18: 38170
of nuclei with A = 46 to 70, study using (p,t) reactions, 19: 3363
of strongly deformed light nuclei, (E/T), 20: 21976 (BNL-948, pp 337-79)
of strongly deformed heavy nuclei, (E/T), 20: 21977 (BNL-948, pp 380-453)
of upper surface of nuclei, 17: 24434
optical anisotropy and surface shape of nuclei, 17: 7302
optical model in the interior of nuclei, 18: 2923
optical potential and effective interaction for inelastic alpha scattering, (T), 19: 12550
pairing correlations in deformed nuclei, 18: 24692
pairing correlations in nuclear surface layer, 18: 24630
parentage coefficients in, 3-nucleon $\langle p^n | p^{n-3}, p^3 \rangle$ fractional, 18: 30742
parity states in (2s,1d) shells, negative, 17: 33092
particle correlations in, internal conversion coefficients for, 20: 36240
particle polarization effect of, 17: 40003
perturbation theory and nuclear matter, 18: 2878
potential barrier penetration in two-proton decay, Coulomb, (T), 19: 19174
potential well in, bound states for particle motion in, 20: 8141
potentials at short ranges, from deuteron elastic scattering, 18: 17041
potentials for Hartree-Fock calculations of, singular, (T), 20: 17791
potentials of finite nuclei, Hartree-Fock calculations of, 19: 37800(R) (ORNL-3778(p.22-3))
principles of, 16: 28170
probe for, nucleon scattering at high energies as, 17: 26428(R) (ORNL-3425(p.1-2))
problems in, 19: 47629
properties, limitations and needs in instrumentation and techniques for studying, 16: 21605
properties of nuclear matter, 16: 15374
quadrupole surface resonances in spherical nuclei, 20: 38039
quantitative nuclear evaporation theory and the nuclear potential, 17: 36708
Racah 12-j coefficients, tables of, 17: 13481 (BLG-142)
radius and surface thickness measurements using heavy-ion elastic scattering, (E/T), 19: 33251 (UCRL-11781)
random-matrix theory in, eigenvalue distributions from ensembles in (T), 19: 1054 (PUC-1964-153)
reference spectrum method for nuclear matter, 17: 7214
relation between beta-gamma angular correlations and, 19: 12506
relation between drop and statistical models for equilibrium distribution of nucleon density, 18: 6265
relation between the shell model and the rotation-vibration model, 17: 7220
relation between the shell model and the rotation-vibration model, 17: 7221
relation of elementary particle physics to, 17: 5395
relation to beta decay matrix elements, 17: 36396 (NP-13020(p.62-8))
relation to beta spectrum shapes of non-unique first forbidden transitions, 19: 12064
relation to fission processes, 18: 7786
research on, prospects through 1967, 17: 15310
research program on, AEC, 18: 16413 (TID-4005(Pts.3&4, Rev.2))
research program on, 18: 30710(R) (AFOSR-4920)
research programs on, 17: 12057(R) (BNL-742(p.1-85))
research programs on, using Van de Graaff accelerators, 19: 33704
research programs on, 20: 19273(R) (BNL-929, pp 3-43)
research programs on, 20: 41511(R) (RLO-1388-501)
research progress on, EURATOM, 18: 11195(R) (EANDC(E)-49(L))
research progress on, 18: 15172(R) (AROD-1784 : 31)
research progress on, 18: 21712(R) (NYO-10065)
research progress and techniques for nuclei with $16 \leq A \leq 56$, 20: 46755
research techniques, review of, 20: 46618
review, 16: 15698
review, 19: 23649
review of basic unresolved problems in, 18: 11212 (LNF-63/47(p.247-9))
review of theoretical aspects for light nuclei, 20: 42338
rotational motion in deformed potential, 19: 23774
second-order effects of nuclear magnetic fields on, 17: 11617 (BNL-6205)
self-consistent-field calculation of, 17: 13504
semi-classical description of nuclear surface oscillations, 17: 40019
shell theory of, energy levels in bounded isotropic harmonic oscillator potential in, 18: 42656
shell-model description of nuclear analog states, (T), 20: 38025
single-particle effects in, 18: 40512 (NP-14239)
single-particle states in, hamiltonians for (T), 19: 3234 (JINR-P-1744)
single-particle wave functions in Woods-Saxon potential well in, computer program for, 19: 1565 (ORNL-TM-964)
sizes of 1p-shell nuclei, 20: 34580
spectroscopy in the $1f_{7/2}$ shell, 18: 21275
spin rules for lower multiplet states of spherical odd-odd nuclei, (T), 20: 42289
studies of, using ion beams, 18: 32777
superconductivity theory for, statistical behavior of, 17: 31218
surface calculation using special single-particle wave functions, 17: 2306
surface layer effects on low-energy reactions and scattering, 16: 19809
survey, 17: 26482
symmetrical shapes of nuclear equilibrium, 17: 2247(T) (AEC-tr-5493)
symmetry for, quasi-spin representations of the orthogonal group R(5), 20: 44676
symmetry in, calculations on prolate-axial, 18: 18956
systematics of, from oxygen-16 to calcium-40, 18: 7785
systematics of, calculation of, 20: 15853
theoretical studies, 19: 35510
theory, 17: 36402 (NP-13020(p.108-20))
theory, 18: 24684
theory for heavy spherical nuclei, 20: 21975 (BNL-948, pp 269-336)
theory for intermediate structure in nuclear reactions, channel coupling, 19: 19171
theory for odd-A nuclei with $62 \leq Z \leq 76$, 20: 11961 (INR-602/VII/PH)

theory for, BCS, 18: 36664
theory of Fermi fluid consisting of two types of particles to the nucleus, 17: 7303
theory of, from high-energy particle reactions, 17: 7186
theory of intermediate, 18: 16941 (ANL-6848(p.241-8))
theory of, relations of nucleon scattering with target nucleus energy level in, 16: 29772 (JAERI-1020(p.175-83))
theory of, statistical, 17: 38011(T) (AEC-tr-5734(p.62-8))
theory of, using shell model, 17: 41896
theory of, bibliography on, 18: 21353
theory of, close-packed-spheron, (T), 20: 4918
theory of, core excitations in quasi-particle, 20: 17814
theory of, development of, 19: 19218
theory of, extended boson approximation in, 19: 1645
theory of, group theory for, 20: 1236
theory of, in relation to atomic mass measurements, review, 20: 31808
theory of, inelastic electron scattering in, 19: 21448
theory of, meson (μ) capture in, 18: 36703
theory of, quasi-particle approximation in, 20: 6433
theory of, research progress on, 18: 42627(R) (ANL-6879(p.88-113))
theory of, review of, 19: 19102
theory of, self-consistent calculations in, (T), 20: 12122
theory of, shell model in, 19: 31253
theory of, status of, 18: 40647
theory of, status of, 20: 30511
three-nucleon clusters in nuclear matter, 17: 7215
three-quasiparticle states in deformed nuclei, 18: 1009 (JINR-P-1338)
three-particle $j = \frac{7}{2}$ shell in, fractional parentage coefficients for, 18: 36580 (UCRL-7506)
transitions in, electron scattering analysis of magnetic, 17: 19078
two nuclear models in a strongly deformed region, 17: 34972
two-nucleon potentials in nuclear matter, 19: 1571 (TID-21247)
two-particle radial matrix elements for j-j coupling hamiltonian in, calculation of coefficients for, 18: 36566 (BNL-7191)
use of absorption and resonant diffusion of monochromatic gamma radiation in study of, 18: 11208 (LNF-63/47(p.188-94))
use of Coulomb excitation in studies of, 16: 29779 (JAERI-1020(p.215-28))
use of nuclear shell theory in, 18: 20972
use of (p,d) reactions with medium-mass nuclei in study of, 18: 1088
use of proton reactions in study of, 16: 29776 (JAERI-1020(p.203-5))
validity of the supermultiplet model of nuclear states, 17: 41931
variational approach to collective motion, 20: 38108
vibration-rotation interaction in deformed nuclei, 18: 42647 (PAN-508/VII)
vibrational motions of spherical odd nuclei in, collective description of (T), 19: 3317
volume effects on, 17: 7103 (NP-12330(p.109-18))
widths of bound single-particle states, 17: 29623

NUCLEAR SUBMARINES
aerosol control in atmosphere of, using electrostatic precipitators, 16: 29221 (TID-7627(p.102-15))
air particulate activity measurements on, 18: 10299 (AD-401763)
atmosphere control methods, 16: 4372 (ONR-9(Vol.3)(p.1018-33))
atmosphere control in, 17: 21930 (NRL-5800)
atmosphere control in, 18: 40988(R) (NRL-6053)
atmosphere purification and control on, 16: 33988(R) (NRL-5630)
atmosphere purification and control in, research on, 19: 29751(R) (NRL-6251)
atmospheric integrity on, maintenance of, 18: 4046
book: *Atomic Submarines*, 18: 19418
design, economics, and performance of commercial, 19: 12834
fission product release from Thresher, monitoring of, 18: 41678 (NOLTR-64-21)
health hazards in operation of Polaris, evaluation of, 17: 12509
monitoring atmosphere of, for aromatic hydrocarbons, 20: 27214
propulsion of, radioisotope and reactor, 19: 45662
safety of, 18: 10320
waste disposal from, marine contamination from, 20: 23396

Nuclear Superheaters
see Superheaters (Nuclear)

Nuclear Technology
see Nuclear Engineering

Nuclear Test Gauge (NTG)
see Exponential Piles

NUCLEAR TEST REACTOR
(General Electric.)
design description and service available, 16: 14336 (APED-3855)
safety performance of, evaluation of, 19: 38207

NUCLEAR THEORY
see also Nuclear Models
absolute log *ft* values for first-forbidden transitions of odd-mass nuclei in $150 < A < 190$ region, 19: 1606
alpha decay of even-even nuclei, 18: 15271
alpha-nucleon interaction phase shifts in, 17: 5216
amplitudes of 2-particle processes, rate of decrease of, 17: 9412
analysis of the virtual deuteron by the Lee model, 17: 8935(R) (NP-12415(p.22-9))
analytic properties of direct interactions, 16: 28102
angular correlation of gamma rays following allowed beta transitions, 17: 36397 (NP-13020(p.69-74))
angular correlation of gamma radiation in inelastic diffraction scattering, 18: 18996
angular cross-correlation function of nuclear cross-section fluctuations, 18: 4631
angular momenta coupling in two-particle states in deformed even-even nuclei, 16: 21423
angular momentum dependence of the effective two-body nuclear interaction, 17: 36403 (NP-13020(p.121-4))
anharmonic effects on collective oscillations in spherical even, 18: 44833
anharmonic oscillations of spherical nuclei, 18: 18921
anticommutator for field corresponding to spin 3/2 on Einstein space, 16: 4950
antisymmetric wave functions of nucleon systems, 18: 2873
application of ordinary perturbation theory to nuclear matter, 18: 2878
application of self-consistent field methods to rotational motion in sd shell nuclei, 18: 19093
application of theory of a Fermi fluid consisting of two types of particles to the nucleus, 17: 7303
approximations in many-body systems, self-consistent, 19: 16269
approximations of nuclear transfer theory, 17: 20992 (TID-18508)
asymmetric charge transfer in, exact numerical solution for, 18: 32811
asymptotic behavior of vortex part for mesons, 16: 13864 (JINR-P-888)
asymptotic behavior of the Vertex part in pseudoscalar meson theory, 17: 7505
attenuation factors from electron collisions, method for the calculation, 17: 14970
average resonance parameters and the optical model, 17: 7244
baryon charge and R-inversion in the octet model, 16: 18470 (IA-725)
baryonic–muonic current interactions in, $\Delta S = 0$, 20: 30141
BCS treatment of nuclear matter, 17: 22559 (LADC-5551)
beta decay, 19: 14573
beta decay in mirror nuclei, 18: 44748
beta-decay transition probabilities and magnetic moments in the $f_{7/2}$ shell, 18: 1073
beta spectra and partially-conserved axial-vector current, 19: 21340
beta transitions in, computer program for calculating nuclear matrix elements from, 18: 15193 (CONF-417-13)
beta transitions in even-even nuclei, allowed, 18: 30823
beta transitions in Nilsson model, matrix elements for, 20: 13831
Bethe-Salpeter equation and conservation laws for finite nuclei, 20: 13789
bibliography, 17: 22779
bibliography, 17: 22780
bibliography on, 18: 21353
bibliography on low-energy, 18: 42765
bibliography on low-energy, 18: 42766
binding energies and phase shifts in, separable potentials from, 20: 10074
binding energies for, for D, P, and S wave forces, 20: 42281
binding energy of hyperon(Λ) in nuclear matter, 18: 40589
binding energy of nuclear matter, 18: 42686
Bohr-Mottelson and asymmetric-rotor models for shape of deformed, 18: 18934
book: *Annual Review of Nuclear Science*, 19: 18582
book: *Contemporary Models of Atomic Nuclei*, 16: 3748
book: *Dynamic Nuclear Orientation*, 18: 11294
book: *Elementary Quantum Field Theory*, 16: 27853
book: *Group Theory; The Application to Quantum Mechanics*, 18: 11024
book: *Introduction to the Atomic Nucleus*, 19: 23802
book: *Lectures in Theoretical Physics, V*, 18: 2462
book: *Lectures on Field Theory and the Many-Body Problem*, 16: 2644
book: *Lectures on Nuclear Theory*, 17: 28415
book: *Lectures on Nuclear Many-body Problem*, 19: 14635
book: *Nuclear Forces*, 20: 8159
book: *Nuclear Interactions*, 18: 26667
book: *Nuclear Orientation*, a collection of reprints, 18: 24706
book: *Nuclear Reactions, Volume I*, 18: 6287
book: *Nuclear Shell Theory*, 17: 15309
book: *Nuclear Theory. Pairing Force Correlations and Collective Motion*, 19: 19227
book: *Nuclei and Particles*, 19: 25538
book: *On the Interaction Between Atomic Nuclei and Electrons*, 17: 28345
book: *Perturbation Theory and the Nuclear Many Body Problem*,

16: 26023
book: *Physics of the Nucleus*, 17: 17280
book: *Quantum Mechanics. III. Radiation and High Energy Physics*, 16: 15369
book: *The Atomic Nucleus*, 19: 33397
book: *The Theory of Finite Fermi Systems and Properties of Atomic Nuclei*, 20: 13632
book: *Unified Theory of Nuclear Models*. (T), 19: 1655
boson contributions to nuclear forces in, 17: 13589
bound states in short-range central potentials, (T), 19: 41439
boundary condition model of nuclear forces, 16: 21478
boundary-value problems in, solutions to ordinary second-order nonlinear differential equations for, 18: 34269 (JINR-P-1682)
Brueckner many-body theory of nucleus, 16: 18175 (NP-11463(Pt.1) (p.119-32))
Brueckner's many-body, review, 16: 18174 (NP-11463(Pt.1)(p.75-117))
calculation method for electromagnetic transition probabilities, 18: 13085
calculation of binding energy for hard core potential, variational procedure for, 18: 4622
calculation of moments of inertia using the shell model, 18: 2912
calculation of (n,α) reactions with even-even nuclei using a direct interaction process, 17: 39994
calculation of neutron bound states using a nonlocal single-particle model, 17: 41943
calculation of nonaxial rotational wave functions and energy levels of odd-A nuclei, 18: 2950
calculation of nuclear moments of inertia by Nilsson model, 16: 7023
calculation of the optical potential with the nucleon-nucleon phase shifts in the Thomas-Fermi approximation, 16: 28040
cause of disappearance of the renormalized charge in the Lee model, 16: 1166
charge dependence of nuclear forces and energy differences in the A = 14 isobaric spin triplet, 18: 4612
charge dependence of nuclear forces, 18: 9416
charge dependence of nuclear forces and ΔT = ±1 Fermi transitions, 18: 19024
charge independence of nuclear forces and its relation to the study of light nuclei, 17: 995 (ZFK-TPH-4)
charge independence of nuclear forces, 18: 40649
charge independence of nuclear forces in isobaric triplet A = 6, (T), 19: 5181
charge symmetrical pairing correlations in light nuclei, 18: 32819
charge-independent nucleon pairing correlations in, 18: 18972
classes of quadrupole magnetic gamma transitions, 16: 21376
classification of many-particle states, 17: 20581 (UCRL-10022 (p.151-62))
classification of excited states of even-even nuclei, 18: 21303
closed-shell effects on cluster singularities of the nucleon-nucleus vertex part, 18: 11241
coefficients of spin and isospin mixtures of effective nucleon-nucleon force, 20: 42348
collective effects and elastic scattering from odd-mass nuclei, 17: 33051
collective excitations in superfluid nuclear matter, 16: 4818
collective excitations of non-spherical nuclei, 16: 4823
collective excitations for neutron-proton energy gap, 18: 19059
collective excitation of unlike pair states in heavier nuclei, 18: 30826
collective model wave functions, 16: 28356
collective motion in, 18: 2881
collective M1 transitions in, nonexistence of, 18: 17073
collective properties of nuclei, lecture on aspects of, 17: 17308
collective vibrations, shell-model calculations of single-nucleon damping of, 17: 24179
comparison of formulas for nuclear temperature, 17: 29879(R) (IA-822)
comparison of the Davydov theory with the model of axial-symmetric top with rotation-vibration interaction for deformed e-e nuclei, 18: 21323
complex effective mass in calculation of the optical model potential, 16: 26229 (PAN-304/VII)
complex singularities of the amplitudes for direct nuclear reactions, 17: 9615
complexity of the spin-orbit interaction potential between nucleons and nuclei, 17: 9612
compound nuclear states in, antisymmetrized shell-model description of, 18: 34773 (NP-14190)
compound nuclear states in, 19: 21283
conference on high-energy physics, 17: 9303
connection of Independent-Pair model with variational principals, 18: 21330
conservation of particle number in the nuclear pairing model, 18: 28689
conserved vector current hypothesis in, test of, 17: 13422
construction of low-energy nuclear potentials, 17: 5380
core excitations in nondeformed odd-A nuclei, 17: 36399 (NP-13020 (p.85-91))
corrections for distorted-wave Born approximations, 20: 19273(R) (BNL-929, pp 3-43)
correlation of fission-fragment energy fine structure with semiempirical mass surface, 18: 9419
Coulomb energies of lower excited levels in light mirror nuclei, 17: 36691
Coulomb excitation in deformed nuclei, 18: 24641
Coulomb self-energy of axial figures, 17: 31509
coupling between dipole and quadrupole oscillations of nuclei, 18: 30790
coupling between shell model excitations and cluster excitations in light nuclei, 18: 24588 (JINR-P-1595)
coupling constants, upper limits for, 16: 28348
coupling constants for Yukawa forces in, 17: 19108
cross-section fluctuations in, 18: 19067
data on M4 transitions, 18: 26208
decay and formation of compound nuclei, independence of, 19: 19100
decay by emission of two protons, 18: 42678
decay theory of closely coupled unstable states, 20: 15816
deformations of nuclei, models for calculating equilibrium, 20: 12125
deformed-core model results for nuclear beta moments, 18: 18955
degrees of freedom in, 18: 11229
delta-function potential in a box, 17: 11910
density and potential functions for studying particle-nucleus interactions, 18: 7722
density-energy relations in nuclear matter, 17: 997
derivation of Bethe-Salpeter equation in symmetric meson theory, (T), 19: 6516 (JINR-P-1715)
description of high-energy interactions in, 17: 32952
description of superconducting-superfluid Fermi-fluid, 17: 28069
determination of nuclear matrix elements for forbidden transitions from ratio of electron capture to positron emission, 18: 24629
determination of Regge-poles, 16: 27902 (JINR-E-961)
determination of states in strongly deformed nuclei on the basis of the superconductivity model, 17: 40009
determination of the isobaric states in models with a fixed nucleon, 17: 21026
deuteron and nucleon form factors in, 19: 1255
deuteron electromagnetic structure in, 20: 6304 (TID-22401)
deuteron scattering in nuclear matter, 18: 36604
development of, 16: 30930(R) (NYO-2669)
direct interaction processes, importance of indirect interactions in, 17: 20991 (TID-18507)
dispersion calculations in, using two-meson approximation, 16: 29991
dispersion theory and the nuclear many-body problem in (T), 19: 1613
dispersive bonding theory, 16: 17031
distorted-wave effects in proton inelastic scattering, 17: 26629
dynamic, of the collective model, 18: 19095
dynamical, of internal parameters for nuclear collective motion, 17: 21051
effect of meson (*π-π*) interactions on nuclear forces, 16: 29695
effect of rotation on pair correlation in nuclei, 16: 1074
effect of short-range repulsion in nuclear matter, 18: 42687
effect of surface layer and deformation of nucleus on reduced E0 conversion probability, (T), 19: 8483
effect of three-body force on binding of three nucleons, 17: 34933
effective hamiltonian for nuclear matter, 20: 38160
effective nuclear interaction for the 1p shell, 19: 19095 (WASH-1053)
effectiveness of shell and superfluidity models in explaining nuclear properties, 17: 31416
effects of anharmonic terms in oscillations of spherical nuclei, 18: 22916
effects of Coulomb field on energy of electrons emitted in beta decay, 17: 26630
effects of exchange on M/L capture ratios, 17: 31523
effects of finite dimensions of nucleus on polarization of particles during pair production and bremsstrahlung radiation, 18: 7716
effects of finite nuclear dimensions on unique first-forbidden transitions, 18: 24638
effects of nuclear polarizability on isotope and isomer shifts, 16: 28098
effects of pairing correlations on nuclear level densities, 18: 19018
effects of pairing correlations and Coriolis force on E2 ΔK = 1 transitions, 20: 38041
effects of resonances on direct processes, 18: 44816
effects of superconducting pairing relations in, 17: 17307
eigenfunctions for spherical and deformed Saxon-Woods potentials, 20: 38078
eigenfunctions of the pairing hamiltonian, 18: 19094
eigenstates of asymmetric odd-A nuclei, 18: 4623
eigenstates of pairing-force Hamiltonian for many-boson system with N-body interaction in, 18: 21034
eigenstates of pairing-force hamiltonian for deformed nuclei, (T), 19: 21347

eigenvalues of the nuclear pairing Hamiltonian, 17: 38421
electric monopole (E0) transitions in, probability determination of, 17: 41905
electric quadrupole transitions in deformed even-even nuclei, 20: 38127
electrical monopole transitions in nonspherical nuclei, 18: 44804
electrodisintegration and photoeffect, relation between cross sections for, 18: 2920
electromagnetic form factors for helium-3 and tritium, 18: 40596
electromagnetic lifetimes and properties of nuclear states, 16: 21431 (NAS-NRC-Pub-974)
electromagnetic multipole moments of deformed odd-A nuclei, 18: 4626
electromagnetic structure of helium-3 and tritium, 17: 34959
empirical relation for alpha decay energies of medium-heavy elements, 17: 36404 (NP-13020(p.125-8))
empirical relation for alpha decay energies of medium-heavy elements, 18: 1035
energy gap at Fermi surface of nuclear matter, 19: 21273
energy gap in finite nuclei, slab model calculation of, 18: 11262
energy gap in finite nuclear systems, 20: 22112
energy gap in finite nuclei, 20: 38113
energy gap in nuclear matter, 18: 9429
energy-level and potential calculations, 16: 9561
energy level coupling schemes in odd-mass nuclei, (T), 20: 13825
energy level excitation of deformed nuclei by multiple Coulomb processes, 17: 26483
energy level E2 transitions of even-even nuclei, 20: 30372
energy level spacing, dependence on A and Z, 16: 12555
energy-level spacings in odd-mass deformed nuclei, 17: 2277
energy level systematics for even-even nuclei, 18: 42757
energy level transitions in deformed odd-mass nuclei, E1 $\Delta K = 0$, 20: 38040
energy level wave functions of 1p-shell nuclei in the intermediate bond model, 18: 28618
energy levels and spins of odd-mass nuclei, 16: 31092
energy levels and transition probabilities as function of rotation frequency in collective model, 18: 28615
energy levels in alpha transitions, 17: 4070
energy levels in a square well with hard core, 17: 33001 (CONF-128-1)
energy levels in, determination from neutron-capture gamma spectra, 17: 5058
energy levels in even-even nuclei, seniority-zero spin-zero, 18: 44746
energy levels in nonspherical odd-mass nuclei, 17: 40005
energy levels in, statistical distributions of, 17: 2451
energy levels in, applications of nuclear models to, 18: 11160 (ANL-6797(p.58-78))
energy levels in, time-dependent Hartree-Fock theory for vibrational, 20: 36205
energy levels of even-even strongly deformed nuclei in region $228 \leq A \leq 254$, 18: 21178 (JINR-P-1568)
energy levels of heavy odd-odd nuclei, pair correlation and nucleon interaction in, 18: 28616
energy levels of N-particle quantum systems in, 16: 26441
energy levels of nonaxial odd-mass nuclei, 18: 21180 (JINR-P-1574)
energy levels of oxygen-18, calculation from free-nucleon potentials, 16: 21365
energy levels of odd-mass nuclei, vibrational, 19: 23696
energy levels of three interacting nucleons in, 18: 44542
energy levels of vibrating particle in f7/2 shell, 18: 17075
energy of nuclear matter in ground state, 18: 16960
equilibrium deformations of isomers in region $50 \cong Z$ and $N \cong 82$, 18: 36629
equilibrium figures and fission of a rotating nucleus, 17: 7298
equilibrium form of light nuclei, 18: 30832
equilibrium parameters of light nuclei, 18: 21307
exchange magnetic moment in three-body nuclei, 18: 17074
exchange terms in direct nuclear reaction theory, 18: 2877
excitation of rotational levels in alpha decay, 17: 2249(T) (UCRL-Trans-258)
excitation operators and intrinsic hamiltonians in, 19: 21289
E2-M1 mixing ratio in $2^+ \rightarrow 2^+$ transition, 17: 36398 (NP-13020(p.80-4))
fermion hard-core interactions in nuclear matter, 17: 19327
few-nucleon problems in, 17: 41990
field theoretic methods in direct interaction theory, 17: 36411 (NP-13020(p.174-85))
fission fragment angular distributions by exact power series, 16: 29847
fission of nuclei, asymmetric, 19: 3245
fission symmetry, 16: 12572
fission-threshold and fragment-excitation energies, 16: 26361
fluctuations in nuclear cross sections, 18: 34893
for odd A nuclei, dynamic collective, 19: 6720
forces and spin-orbit coupling in, effect of scalar mesons on, (T), 19: 19154
forces and zero-range saturation mixture in, particle-hole matrix elements for Wigner, 20: 19873
forces due to π-π interaction, 16: 2439
forces in finite nuclei, saturation of, 20: 42208
forces in nuclear reaction, velocity-dependent, 16: 21619
forces in nucleus, review of model development for, 16: 21463
forces in p-shell configurations in, three-body, 20: 22092
forces in shell model for, Schroedinger equation solution for realistic, (T), 20: 10052
forces in, bootstrap hypothesis for, 20: 25887 (PAEC(A)PH-663-a)
forces in, charge dependence of, 20: 34527 (RLO-1388B-6)
forces in, determination of, (T), 20: 19981
forces in, equations for, 20: 25791 (PAEC(A)PH-663)
forces in, formulation of meson theory of, 20: 36218
forces in, isotopic structure of parity nonconserving, (T), 20: 9992(T)
forces in, many-body, 20: 8118
forces in, meson resonance effects on, 20: 15817
forces in, momentum-dependent, 20: 13792
forces in, nuclear reaction method for time invariance of, 20: 30505
forces in, origin of repulsive core in, (T), 20: 13879
forces in, oscillator brackets for Hartree-Fock calculations for two-body, 20: 17744
forces in, parity nonconservation effects induced by, (T), 20: 9724(T)
forces in, repulsive core of, 20: 24450
forces in, time-reversal invariance test for, (E), 20: 19906
form factors for medium and heavy nuclei, 18: 34928
formalism for nuclear reactions, antisymmetrization in unified, 18: 32790
four-particle wave function in the SU(3) scheme, 18: 21215 (UJV-1002-63)
fourth-order diagrams in many-body systems, 18: 15252
fractional parentage coefficients for wave functions in, 19: 6650
gamma stability of axially asymmetric nuclear deformation, 16: 2548
gamma transitions in, effect of pairing correlation on, 18: 15251
gauge invariance of mass doublet fields, 16: 14210
generalized Hartree-Fock method in, accuracy of, 18: 6268
generalized quasi-spin in neutron–proton systems, 20: 3046
geometric positions of alpha clusters in the nucleus, 18: 18943
gravitational wave emission by elementary particles, 16: 18607
Green functions and transition probabilities in odd nuclei, 20: 3104
Green's function method in, 18: 36577 (NP-14202)
Green's function method in, lecture on, 19: 37903
Green's functions in classical, 18: 24615 (NP-13959)
ground-state energy of odd-fermion systems in, 18: 24631
ground-state energy of nuclear matter, long-range force corrections to, 18: 42685
Hartree-Fock approximation in, stability of, 19: 21440
Hartree-Fock calculations for spherical nuclei, 18: 22871 (CONF-502-1)
Hartree-Fock field and method of projection in, 20: 13826
higher-order spacing distributions for a class of unitary ensembles, 18: 24679
hole-particle interactions in light nuclei, 18: 4608
hyperon (Λ) binding energy in nuclear matter, 18: 19111
imaginary part of the optical potential, 17: 22663
improved superconductivity approximation for the pairing interaction in nuclei, 18: 19098
impulses of nucleon pairs in, solution of Bethe-Goldstone equation for, 17: 28330
impurities in isobaric analog states, 18: 40558
independence hypothesis in statistical theory of nuclear reactions, 18: 26529 (BNL-8020)
interaction in the initial and final states in direct nuclear reactions, 17: 9608
interactions between systems with arbitrary angular momenta, 18: 14981
interactions in even spherical nuclei, quasi-particle, 19: 14584
interactions in nuclear matter, velocity-dependent, 17: 17164
interactions of nonevaporated nucleons in deformed nuclei, 18: 18905
interactions of particles with potential fields, superbarrier reflection, 16: 864
internal pair emission from aligned nuclei, 18: 15249
internal pairs from aligned nuclei, 17: 31508
interpretation of spin-½ nuclei as asymmetric rotors, 18: 30714 (BLG-223)
intrinsic excitation of even-even nuclei, 17: 13577
isobaric analog states and the shell model, 18: 28635
isobaric multiplets in light nuclei, 20: 42355
isobaric properties of heavy nuclei, 17: 2282
isobaric spin without charge space for, 20: 22019
isomer shift and structure of metastable nuclear states, 20: 3138
isomeric transition probabilities in odd-odd spherical nuclei, 18: 15214
isotopic spin validity as quantum number in, for large Z, 16: 26304
lectures, 18: 24593 (NP-13925)
localized solutions of the Bethe-Goldstone equation for two nucleons in nuclear matter, 17: 26746
location of quasistationary single-particle states in nuclei with A = 5 to

240, 17: 40012
Low equations in, solution of nonregularized, 18: 11199 (JINR-P-1445)
magnetic moments of nuclei, effects of pair interactions, 16: 21433
Majorana forces and nucleon coupling in light nuclei, 18: 28617
many-body problem in, with nonuniform density, 17: 7260
many-body problem in, boundary-condition model for, 17: 39987
many-body systems in, variational principle for, 17: 42166
many-body theory of the nucleus, 18: 6288
many-body forces in heavy nuclei, internucleon potentials from, 18: 15291
many-body forces in, Monte Carlo investigation of Schroedinger equation for, 18: 22800
many-body problem and dispersion theory, 18: 18937
many-body problem in, preparation method for, 19: 23645
many-body problem in, effective interaction in, 20: 13791
many-particle systems with translational invariance, approximation for, 19: 3336
mass and pairing energy calculations for heavy nuclei, 16: 33882
mass constancy for low moments, 16: 21700
mass differences of neutrons and protons in, 17: 13381
mass formula in 1p shell, isobaric, 19: 3371
matrix elements and wave functions for transition-region nuclei, generator coordinate method for, 20: 22081
matrix elements for n-p interactions and the odd-group model for heavy nuclei, 16: 28146
matrix elements for nuclear interaction operators, 17: 38112
matrix elements for one- and two-body operators, (T), 19: 6649
matrix elements for allowed unfavored transitions in, (T), 19: 47622
matrix representation of energy levels, exponential ensemble for random, (T), 19: 14557
measurement of induced pseudoscalar coupling constants in, 18: 42718
measures in dual space of nuclear space, rotationally invariant, 18: 40555
measuring process in quantum, 17: 15151
mechanisms for decay by proton emission, 19: 10245 (JINR-P-1863)
meson (μ) capture rates in 2s-1d nuclei, 18: 21277
meson (π)–nucleon interaction in, 19: 6528
meson (π)–nucleon interactions, one-particle-exchange models for, (T), 19: 41375
meson, effects of almost-conserved currents on pseudoscalar, 17: 15136
meson field equations in, modified Yukawa potential and Riemannian space-time for scalar, 19: 31264
meson, ghost-scattering effects in, 16: 32319
meson (K) and (π) clouds around antibaryons and baryons, symmetry properties of, 17: 11547
meson theories in, properties of static, 17: 19089
meson theory for nuclear forces, review, 16: 15373
mesons and hard core in nuclear forces, 16: 17044
method for studying the optical anisotropy and shape of the surface of nuclei, 17: 7302
methods in meson, quasi-optical, 18: 10967
microscopic description of collective levels of nonspherical, 17: 2326
model for high-energy collisions, single-virtual-particle exchange, 16: 13896
model for nucleon-nucleon interaction, 19: 4987
model for odd-parity states in even nuclei, 16: 28077
model for potential barrier penetration, 19: 19099
model for rotational states in deformed nuclei, 18: 44832
modes of motion, in nuclear many-body systems, 16: 8293
moments of inertia of a heated nucleus and angular anisotropy of the fission fragments, 17: 7301
moments of inertia and simplified wave functions for nuclei, 18: 34927
moments of nucleons, sum rules for, 20: 40130
momentum distribution and pair correlation function, 17: 24409
Monte Carlo calculations of ground state of three- and four-body nuclei, 17: 868
motion of nuclei, methods for describing rotational, 19: 14627
multiple Coulomb excitation of rotational states of nonaxial even-even nuclei, 18: 21177 (JINR-P-1563)
multiple scattering theory, 17: 36412 (NP-13020(p.186-200))
multipole deformability of nuclei of rounded charge distribution, 18: 19025
M1-E2 mixing ratios in 2^+-2 transition in even-even nuclei as a test of the purity of vibrational states, 17: 41913
necessity of axial asymmetry in some nuclei, 18: 21225
neutron beta-decay parameters in, 18: 21128 (KR-64(Sect.XXVI))
neutron evaporation from compound nuclei, angular momentum effects in, 18: 28628
neutron half life in, 18: 21129 (KR-64(Sect.XXVII))
neutron states in deformed optical potential, 20: 38126
neutron-transfer reactions in, using Saxon-Woods potentials, 17: 15266
neutron–neutron interaction parameters in, crossed-beam measurements of, 19: 1259
neutron-proton correlation effects in spherical even nuclei, 20: 42195
neutron-proton residual interaction in, experiment and theoretical interpretation for, 18: 28578 (ORNL-3638)
new symmetries for strong interactions, 16: 17127
non-relativistic rotator and zero strangeness, 16: 22888
nonsingular formulations of the Brueckner approximation for an infinite Fermi system, 16: 29855
nuclear coulomb potentials in, from neutron scattering, (T), 19: 6699
nuclear force and energy gap in finite nuclei, 18: 36649
nuclear force properties in Brueckner theory, 16: 29807
nuclear forces and bremsstrahlung emission, 17: 31409 (NP-12965)
nuclear forces and OBEC model, 18: 38168
nuclear forces, effects of charge, 16: 24301
nuclear forces in, 18: 40648
nuclear forces in, charge asymmetry of, 18: 36648
nuclear forces in, multipion resonance contributions to intermediate-range, 18: 42651 (UCRL-7553-T)
nuclear forces in, ωNN and ϕNN coupling constants in, 19: 19161
nuclear forces in, hard core of, 19: 29093
nuclear forces in, phenomenological treatment of, 20: 17727
nuclear forces, relation to meson (ω) and (ρ^0) mass spectra, 16: 27953
nuclear level density, energy dependence of, 18: 32826
nuclear magnetic relaxation of three-spin systems, 18: 17076
nuclear masses and interaction amplitudes in, relation between, 20: 3102
nuclear matter at low density, 16: 17063 (CEA-2086)
nuclear matter binding energy and two-nucleon potential, 18: 40537
nuclear matter binding energy sensitivity to two-nucleon potential, 19: 10365
nuclear matter calculations and phenomenological potentials, 17: 4085
nuclear matter studies using quantum statistics, 16: 3731
nuclear molecule consisting of two C_6^{12} nuclei, 16: 21220
nuclear pairing energies in superfluid model of nuclei, 18: 9371
nuclear particle spin effects on forces in, review of, 20: 37332
nuclear potential in non-local theory, contribution of bipion and tripion to, 17: 15276
nuclear potential energy and single-particle density matrix, 18: 44813
nuclear potential in, nomograms for, 19: 16868
nuclear potentials in, quadratic momentum dependence of, 20: 12103
nuclear radii derived from alpha-decay theory taking into account pair correlations of the superconducting type, 17: 40010
nuclear reactions of intermediate-energy neutrinos, 16: 21425
nuclear tensor operators for, matrix elements of integrable, 19: 29298
nuclear vibrations in, time-dependent Hartree-Fock theory for, 20: 22068
nucleon binding energy in three-body systems, (T), 19: 8455
nucleon bound states in, Bethe-Salpeter equation for two-body, 20: 13876
nucleon clustering and the shell model, 18: 4606
nucleon clusters in light nuclei, 18: 21247
nucleon-correlation calculations in, 17: 19083
nucleon effective two-body potential in nuclei, 16: 3738
nucleon electromagnetic form factors in, 16: 33758
nucleon electromagnetic structure in, 17: 34819
nucleon electromagnetic structure studies, (E/T), 19: 12168 (NP-14540)
nucleon form factors in, representation by scattering theory, 16: 33743
nucleon form factors in, effects of high-energy limits on, 16: 33747
nucleon form factors in strong coupling meson, 17: 9296
nucleon form factors in strong-coupling, 17: 19134
nucleon form-factor measurements in, 17: 34822
nucleon form factors in, effects of mesons (ρ) on, 17: 41790
nucleon ground-state energy in fixed-source meson theory, 16: 13899
nucleon grouping in shell-model states, fractional parentage coefficients for three-particle, 18: 24621 (PAN-449/VII)
nucleon interactions in, axial-vector form factors for, 17: 15115
nucleon interactions in, effects of spin-orbit forces on, 17: 19074
nucleon interactions in, models for inelastic, 17: 19079
nucleon interactions in, numerical methods for many-body, 18: 2403(R) (PR-P-58)
nucleon interactions in, S-matrix for, 18: 4444
nucleon interactions in, on the basis of electron scattering by nuclei, 18: 6272
nucleon interactions in a harmonic oscillator potential, two-body, 18: 15250
nucleon interactions in odd-odd deformed nuclei, effects on $0^+(T = 1)$ levels, 18: 19092
nucleon interaction forces in (T), 19: 1696
nucleon interaction in nuclei, soft-core, 19: 3335
nucleon interaction-potential parameters in, (T), 19: 8405 (UCRL-7155(Rev.I))
nucleon interaction potentials in, description of singlet-even, (T), 19: 10258(R) (TID-21335(p.151-60))
nucleon interaction forces in, parity non-conserving, 19: 35376 (CONF-641210-17)
nucleon isobar excitation in, 17: 31647 (NP-12975(p.93-114))

nucleon magnetic properties in, models for, 17: 11558
nucleon mass differences in, 17: 15140
nucleon-nucleon effective interactions in finite nuclei, 17: 5366
nucleon-nucleon forces, coupling and phase parameters, 16: 4799
nucleon-nucleon interactions in, effects of velocity-dependent potentials on, 17: 2289
nucleon-nucleon interaction potentials in, review, 17: 5055
nucleon-nucleon interactions in, dispersion relations for, 17: 13448
nucleon-nucleon spin-orbit interactions in, 17: 2179
nucleon–nucleon triplet–even potentials and scalar form factor, 16: 20305(R) (UCRL-10023)
nucleon pair correlations and level widths, 16: 4819
nucleon pair potentials in, singlet-even, 19: 6544
nucleon pairing correlations in, effect on beta decay, 17: 24178
nucleon pairing in finite nuclei, variational derivation of equation for, 20: 15742
nucleon pairing interactions in nuclei, number-conserving approximations for, 20: 32494
nucleon potentials without hard cores in, 16: 26251
nucleon potentials in, one-pion-exchange approximation for, 17: 2280
nucleon potentials in, for high energies, 19: 14325 (UCRL-1011)
nucleon quadrupole and pairing forces in, (T), 20: 17801
nucleon relations to (3,3) resonance, 17: 5262
nucleon states in shell model, many-body, (T), 19: 29310
nucleon structure in, three-meson (π) contributions to, 17: 9272
nucleon structure in, 3-meson (π) effects on isoscalar, 17: 11559
nucleon structure in, effects of meson (π) resonances on, 17: 20885
nucleon tunneling, applicability of, 18: 24617 (NYO-1807-7)
nucleon 2-pion-exchange potentials in, 17: 19124
nucleon-nucleon interactions inside light nuclei, 18: 21345
nucleon-nucleon phase shifts and potentials in (T), 19: 1647
nucleus-nucleus rearrangement scattering, 18: 15259
octupole deformation in even-even medium-mass nuclei, 17: 36703
octupole vibrations of deformed even-mass nuclei, 18: 18991
octupole vibrations in spherical nuclei, 18: 30757
odd-even effect in nuclear level density in superfluid model of nucleus (T), 19: 1601
of cluster stripping reaction, 17: 9614
of Coulomb stripping, 17: 31521
of deuteron elastic scattering by complex nuclei at high energies, 20: 3044
of direct photodisintegration, 18: 21266
of even-even nonspherical nuclei, precision of Bogolyubov method, 16: 26218 (JINR-P-923)
of fission using liquid drop and adiabatic models, 18: 9445
of giant resonances in spherical nuclei, 20: 24486
of nonspherical nuclei in accordance with the independent-particle model, 17: 34969
of resonance reactions, 18: 6292
of self-bound finite systems, 18: 38166
of single-particle excitations and vibrations, 17: 24177
optical model for virtual mesons (π), 18: 30821
optical model in the interior of nuclei, 18: 2923
optical potential of heavy nuclei, 17: 2324
optical potential in, shape of symmetry term in, 18: 9373
optical potential in, shape of imaginary, 18: 9374
optical potentials and macroscopic dissipation constants, 18: 15316
optical potentials for composite particles (T), 19: 1603
optical-model description of low-energy excitations in nuclear matter, 18: 40582
pairing and quadrupole interactions in configurations j^n, 18: 6222
pairing correlations in deformed nuclei, 18: 24692
pairing correlations in nuclear surface layer, 18: 24630
pairing correlations in excited nuclei with specified angular momentum, 18: 34930
pairing energies in spherical and deformed light nuclei, B.C.S. plus Hartree-Fock model for, 17: 40064
parentage coefficients in, 3-nucleon $\langle p^m|p^{m-s},p^s\rangle$ fractional, 18: 30742
parity mixing in single-nucleon orbitals, properties of wave functions from, 20: 22080
parity nonconservation in, 18: 7764
partial wave amplitudes as functions of angular momentum, 17: 9408
partial wave analysis in, method for, 17: 9418
partial waves with complex angular momenta and their moving singularities, 17: 9411
particle penetration of potential barriers, (T), 19: 41533
particle scattering by complex nuclear potential, 16: 19790
peripheral collision theory based on the S matrix, 17: 20584 (UCRL-10022(p.191-3))
perturbation of resonance energy levels in, 18: 16997
phase-shift analysis of single-channel reactions, 17: 26484
phenomenalistic, status of, 18: 32766
photodisintegration of the three-body system, 18: 4611
photonuclear reaction sum rules in, tensor effects on, 17: 11733
poles in meson (π)-nucleon amplitudes in, 17: 19133
possibility of symmetric and asymmetric fission, 17: 2325
potential barrier penetration in, 19: 27459
potential of triplet even state in, non-static, 19: 23778
potentials for binding and saturation of nuclear matter, 20: 30434
potentials in, analyticity of complex Yukawa, 17: 2422
potentials in axiomatic quantum field theory, 18: 17050
potentials in nucleon scattering and many-body problem, nonstatic, 18: 19002
potentials in, effects of short-range repulsive forces on, 19: 39814
potentials in, nonstatic, 19: 23775
potentials in, T matrix for screened Coulomb, 20: 19827 (N-65-21644)
potentials in, variational method for approximating, 19: 1646
potentials of finite nuclei, Hartree-Fock calculations of, 19: 37800(R) (ORNL-3778(p.22-3))
potentials with hard cores in, 17: 9541
prediction of most probable nuclear charge of primary fission products, 17: 26616
probabilities of electromagnetic transitions from collective to ground states of even-even strongly deformed nuclei, 18: 34761 (JINR-E-1703)
probabilities of forbidden gamma transitions, calculation, 16: 7023
probability of double gamma emission, 18: 11238
properties of light nuclei ($4 < A \leq 40$), 16: 31116
properties of nuclear matter, 16: 15374
properties of nuclear matter, 17: 40002
properties of nuclear matter, ground-state, 20: 42249
properties of odd-mass nuclei having a $j = \frac{1}{2}$ particle coupled to a vibrating core, 18: 6220
proton capture resonances in nuclei, single state interpretation of, (T), 19: 5228
proton electromagnetic form factors in, analytic continuation of, (T), 19: 41388
proton form factors and resonances in, 18: 15317
proton-proton phase shifts in, 18: 30521(R) (TID-20720(Paper 3))
proton–proton phase shifts in, 18: 30522(R) (TID-20720(Paper 4))
proton–proton phase shifts in, 18: 30523(R) (TID-20720(Paper 5))
pseudoscalar interaction in beta decay, 17: 4118
quadrupole energy levels of deformed even-even nuclei, 18: 18870 (JINR-E-1534)
quadrupole surface resonances in spherical nuclei, 20: 38039
quantitative nuclear evaporation theory and the nuclear potential, 17: 36708
quantum-mechanical three-body problem in, coordinates for, (T), 19: 12347
quantum, of nuclear collective rotation, 20: 3048
quasar model for gas clouds in dense star clusters, 19: 47199
quasi-deuteron model and the internal momentum distribution of nucleons in carbon-12, 17: 11695
quasi-spin and the n-dependence of shell-model matrix elements, 19: 19095 (WASH-1053)
quasioptical quantum field theory for scattering amplitude, Regge asymptotic behavior in, 17: 13349 (JINR-P-1149)
radial equations of an arbitrary-spin particle interacting with a central potential, 18: 14980
radial variation of the absorbing part of the nuclear optical potential, 17: 5398
radiative corrections to muon and nucleon decay, analysis by dispersion and perturbation theory, 17: 22520
range of nuclear force, 19: 6684
reaction cross sections near thresholds, Coulomb-field effects on, 17: 33083
reaction mechanisms in, effects of density and temperature on, 18: 40600
reactions in, using few-level approximations, 19: 39805
reciprocity between nucleons and (3,3) resonances, Chew theory of, 17: 4007
reduced widths and strength functions in, 19: 17009
reference spectrum method for nuclear matter, 17: 7214
reference spectrum method of calculating single-particle energies of nuclear matter, 17: 38144
reformulation of theory of pairing correlations in, 17: 9817 (NP-12352)
Regge pole positions in, calculation of, 17: 9409
Regge poles as consequences of analyticity and unitarity, 17: 9410
Regge poles in, applications of, 17: 9414
Regge poles in quantum electrodynamics, 17: 13341 (JINR-E-1122)
Regge trajectories for Yukawa potentials, 16: 33699 (UCRL-10216)
regularity in enhancement phenomenon of allowed beta transitions to even-even nuclei, 19: 1642
relation between beta decay and nuclear structure, 17: 36396 (NP-13020(p.62-8))
relation between drop and statistical models for equilibrium distribution of nucleon density, 18: 6265

relation between optical model and the resonance theory, 18: 15268
relation between the shell model and the rotation-vibration model, 17: 7220
relation between the shell model and the rotation-vibration model, 17: 7221
relation of bispinor and spinor theory in Riemann space, 17: 11931
relativistic strong coupling, 16: 17013
representation of the potential of two nucleons, 17: 24757
representations of semisimple Lie groups, (T), 19: 8263
representations of semisimple Lie groups, (T), 19: 8264
research, 17: 20594(R) (UCRL-10572)
research facilities of Italian CNEN, 16: 30174
research on, monthly summary, 17: 19510(R) (TID-18344)
research program on, AEC, 18: 16413 (TID-4005(Pts.3&4, Rev.2))
research programs on, at Univ. of Pennsylvania, 18: 42377(R) (TID-21014)
research programs on, 20: 41796(R) (MIT-2098-251, pp 74-103)
research progress on, 18: 8920(R) (TID-19940(p.119-39))
research progress on, EURATOM, 18: 11195(R) (EANDC(E)-49(L))
research progress on, 18: 10628(R) (TID-20068)
research progress on, 18: 21712(R) (NYO-10065)
resolution of Boltzmann equation, 17: 15382
resonance excitation in fluorescence, (T), 19: 12551
resonance reactions in, 18: 11182 (ANL-6797(p.342-57))
review of statistical, 18: 6294
review of the statistical model, 18: 6294
rotation operators in, polynomial expressions for finite, 18: 44787
rotation-vibration interaction in deformed even-even nuclei, 20: 38156
rotational energies for the asymmetric rotor model for odd-mass nuclei, 16: 29822 (UCRL-9876)
rotational motion of nuclei, 18: 6297
rotational motion in, 18: 44834
rotational spectra of nuclei with small asymmetry (T), 19: 1604
rule $(2I + 1)$ and the statistical compound nucleus, 16: 23075
S- and P-wave strength functions and surface absorption optical model, 18: 18988
Sargent rule and Fermi theory of beta decay, 18: 42657
scattering amplitude singularities in potential theory, (T), 19: 41550
scattering matrix, multichannel resonance states and resonance poles, 18: 9162
selected topics in, lectures on, 17: 17302
self-consistent field problem, 16: 18176 (NP-11463(Pt.1)(p.133-7))
semi-classical description of nuclear surface oscillations, 17: 40019
separability of center-of-mass motion in the nuclear shell model, 18: 28690
shape of dipole resonance in deformed nuclei, 17: 9611
significance of Coulomb excitation in, review of, 18: 18887 (ZFK-PHA-11)
simulation of the hard core by a velocity dependence, 17: 11921
single-meson interactions, 16: 5859 (JINR-P-699)
single-particle excitations in, model hamiltonians for, 20: 3099
single-particle states in, hamiltonians for (T), 19: 3234 (JINR-P-1744)
single-particle l-forbidden transitions in, 20: 3100
solution of many-body K matrix in, for Yukawa potential, (T), 19: 4935
solutions of Yang-Mills field, static and spherically symmetric, 16: 26449
spin dependence of resonance level density, 18: 6257
spin-orbit forces in proton interactions, 16: 19716
spin pumping and relaxation in systems with a low concentration of electron spin resonance centers, 16: 29568
spin-orbit interactions in deformed nuclei, 18: 18942
spin-orbit splitting of giant resonance, 18: 38187
spirality inversion in nuclear reactions, 17: 9610
splitting of E1 giant resonance into two peaks, 17: 7253
spurious state in beta vibrations of deformed nuclei, 17: 5381
spurious states in calculations of collective excitations, 16: 28116
statistical model of meson theory, 16: 28327
statistical nuclear model with correlations accounted for, 17: 7284
statistical theory of nuclear states and transitions, 18: 11178 (ANL-6797(p.302-21))
statistical theory of nuclear collision cross sections, 18: 32837
statistical theory of compound nucleus formation and decay, 19: 19095 (WASH-1053)
stripping and knockout amplitudes from Gaussian interactions of finite range, 18: 18880 (NP-13773)
strong absorption model for elastic nuclear scattering, 18: 1032
strong absorption model for elastic nuclear scattering, 18: 6186
strong and weak interactions of bound Λ particles, 17: 32900 (EFINS-63-29)
strong interaction theory without elementary particles, 17: 9413
structure of finite nuclei, 19: 16969
structure of 1^-, $T = 1$ states of light nuclei, analysis using E1 sum rules, 20: 8065 (INP-426/PL)
sum rules for high-energy photonuclear absorption, 17: 34927
super-high energy multiple production of particles, multiperipheral model evaluation of cross sections for, 17: 15084 (PAN-368/VII)
superconductivity in metals having spherical nuclei, 17: 13133
superfluid properties of nuclei in, 17: 11735
superfluidity and excited states of spherical odd-A nuclei, 18: 7723
superfluidity of nuclear matter, 18: 28620
superfluidity of nuclear atoms in the lead-208 region (T), 19: 3270
superfluidity-type pair interactions in, 18: 11233
surface properties of large nuclei in, reference-spectrum analysis of, (T), 19: 6690
surface properties of nuclear matter, calculation by reference spectrum method, 19: 10359
survey of high-energy interactions, 18: 14805 (JINR-E-1436)
survey of recent results on internal conversion, 17: 36390 (NP-13020 (p.27-33))
symmetrical shapes of nuclear equilibrium, 17: 2247(T) (AEC-tr-5493)
symmetries at high energies, 17: 20582 (UCRL-10022(p.163-7))
symmetry energy and isotopic spin dependence of single-particle potential in, 18: 21287
symmetry properties of Nogami's modified pairing hamiltonian, 18: 34890
systematics of l-forbidden M1 transitions, 18: 44815
t-matrix formalism in, 19: 39871
tables of Clebsch-Gordan coefficients, 16: 21348 (IFA/FT/40)
tables of identical-particle fractional parentage coefficients, 20: 26137
Talmi transformation and related formulas in, 20: 21226
temperature of nuclear matter, critical, 19: 43284
theory of nuclear matter, 16: 2628
theory of nuclear matter, 17: 21213
theory of orientation, 17: 21211
three-body effect in nuclear matter to all orders of perturbation, 17: 31504
three-nucleon clusters in nuclear matter, 17: 7215
threshold effects in average cross sections according to R-matrix theory, 17: 7236
time and energy aspects in nuclear reactions, 18: 32774
time invariance of nuclear forces, 17: 38022(T) (AEC-tr-5734(p.104-6))
time reversal invariance in strong interactions, 16: 2656
transformation permutation group matrix and construction of coordinate wave function of a multishell configuration, 16: 1168
transition frequencies and probabilities in, phenomenological approach to, 18: 6267
transport coefficients, microscopic determination, 16: 24921
treatment of nuclear phenomena, nuclear models for, 17: 15307
triton ground-state wave functions, 17: 24180
triton, matrix elements of quadratic LS operator in, 16: 24833
two-body potentials, $J = 2 - 0$ energy level splittings, 16: 2507
two-level approximation for eigenvalue, 17: 24418
two nuclear models in a strongly deformed region, 17: 34972
two-quantum transitions in nuclei, 17: 40057
two-body tensor force and Pauli exclusion principle in nuclear matter, 18: 21344
uncoupled nuclear matter approximation, 18: 32834
unified theory of nuclear reactions, 16: 28043
unified, of photonuclear reactions, 18: 21364
unitary ensemble in, reduced width amplitude distribution for, 17: 38114
unitary symmetry consequences, 16: 17030
use of group theory in, 20: 1236
vacuum polarization induced by the nuclear quadrupole moment in mu-mesic atoms, 17: 36687
validity of the supermultiplet model of nuclear states, 17: 41931
variant theory of higher symmetry for baryon strong interactions, 16: 2458
variation principles for nuclear rotations, 16: 12451
variational approach to collective motion, 20: 38108
variational method for random phase approximation, 18: 44839
variational shell-model methods for deformed orbitals, 18: 2913
variations of the decoupling parameters for $^1/_2$ rotational bands for very deformed nuclei, 16: 29813
vector gauge field unification, 18: 21060
velocity-dependent nuclear forces and their effects in nuclear matter, 16: 21535
velocity dependent nuclear forces and the repulsive core as the possible consequence of classical relativistic effects, 16: 28081
velocity-dependent p-p potential model, 17: 26383
velocity-dependent nucleon-nucleon potentials and saturation of nuclear matter, 18: 21223
vertex parts of the amplitudes for direct nuclear processes, 17: 2327
very high-energy phenomena, summary of CERN conference on, 17: 20566 (UCRL-10022(p.3-7))
very high-energy phenomena, possible contributions from experiments with 300-Bev proton accelerator, 17: 20572 (UCRL-10022(p.83-8))
vibration-rotation interaction in deformed nuclei, 18: 42647 (PAN-508/

VII)
vibrations of nonspherical nuclei, 18: 18920
vibrations of nuclei, collective, 19: 14628
wave equations for, 19: 9767(R) (IS-900(Sect.P))
wave functions for superposed bound-state Yukawa potentials, 16: 23146
wave functions for (p,n) reactions in, 17: 2279
wave functions for defining finite nuclear dimensions, relativistic, 19: 12503
wave functions in, derivation of single-particle, 16: 33883
wave functions in the $1f_{7/2}$ shell, 18: 30733 (NYO-9891)
wave functions in ,particle-number conserving method for BCS, 20: 12050
wave functions of one-particle systems without definite parity in, Hartree-Fock theory of, 17: 40030
weak interactions, 17: 22432 (NP-12610)
weak non-leptonic interactions in quark model, 18: 32583
width of giant resonances in heavy nuclei, 18: 21206 (NP-13813)
Wigner coefficients in rotation group R_4, 19: 6656
zero-point oscillations in the drop model, 18: 15216

Nuclear Vapotron
see Reactor Fuel Elements

Nuclear Weapons
see Weapons

Nucleation
see Phase Studies

NUCLEI
absorption potential for, radial distribution of, 18: 34854
abundance and source spectra of $Z \geq 3$, in galactic cosmic radiation, 20: 41673
abundance of cosmic, heavier than lithium, 17: 22403 (AD-282243)
abundance of, in primary cosmic radiation, 17: 34711
abundance of medium-weight, in solar cosmic radiation, 17: 18357 (TID-7652(p.33-43))
abundance of $Z > 2$, in primary cosmic radiation, (E), 19: 23331
abundance tables, 17: 24397 (SCR-245A)
abundances in cosmic radiation above atmosphere, 16: 21250
abundances in solar system, mass law dependence on nucleosynthesis, 20: 44070 (LA-DC-7885)
abundances in stellar convective cores, (T), 20: 9635
abundances of A ~90 in solar system, (T), 19: 6433
abundances of $Z \geq 4$, in primary cosmic radiation, (E), 20: 17321
acceleration in Brookhaven AGS, experiments with, 17: 11784 (BNL-6673)
alignment and polarization of I = 1, 18: 26598
alignment of even, by alpha inelastic scattering, 16: 32420
alpha bombardment of heavy, neutron spectra from, 17: 20994 (UCRL-7233)
alpha branching in heavy, weak, 18: 7698 (UCRL-11028)
alpha cluster arrangement in, rules for determining, 17: 38158
alpha cluster isolation in p-shell, (T), 19: 14586
alpha clustering in, (T), 20: 32542
alpha clustering potentials for, (T), 20: 22061
alpha clusters in light, quadrupole moment as measure of existence of, 18: 7715
alpha clusters in light, coupling of Majorana forces for, 18: 28617
alpha decay energies of, variation with neutron number, 20: 17729
alpha decay ground-state transitions in A > 190, energy of, 18: 36614
alpha decay in crystals, research using shadow effect, 20: 40135
alpha decay of, alpha-gamma angular correlations in, 17: 32446
alpha decay of deformed, (E), 19: 16913
alpha decay of deformed, (T), 19: 47597 (UCRL-16187)
alpha decay of deformed, reduced widths in, (T), 20: 1150 (IFA-FT-55)
alpha decay of deformed even-even, Coulomb interaction effects on, (T), 20: 8174
alpha decay of even-even, alpha surface distribution in, 17: 21013
alpha decay of even-even, barrier penetrability effects of nonlocal potentials in, 17: 26565
alpha decay of even-even, theory of correlations in, 17: 31490
alpha decay of even-even, hindrance and availability of nuclear surface states in, 18: 15271
alpha decay of even- and odd-mass, (T), 19: 39789
alpha decay of heavy, self-consistent potential and radius for, 16: 18506
alpha decay of heavy odd-A, effects of fine-mass-structure on, 17: 13510
alpha decay of heavy, barrier penetrabilities in, 18: 7685 (NP-13421)
alpha decay of N = 127, (T), 20: 42287
alpha decay of odd-mass, calculation, 18: 32745(R) (UCRL-11213(p.1-48))
alpha decay of spherical, calculation, 18: 32745(R) (UCRL-11213(p.1-48))
alpha decay of, alpha energies in, 19: 29356
alpha decay of, barrier penetrabilities in, (T), 19: 21411
alpha decay of, K-shell atomic ionization from, (T), 20: 7726
alpha decay of, reduced width for, (T), 19: 14569
alpha decay of, tunnel effect in, (T), 20: 38117
alpha decay rates of spheroidal, calculation of hindrance factors, 16: 21533
alpha decay rates of spheroidal even, shell-model analysis of, 16: 32417
alpha decay rates of deformed even-even, shell model calculations of, (T), 19: 39793
alpha decay systematics for medium-heavy beta-stable, 17: 7199
alpha elastic and inelastic scattering at 22.2 Mev by intermediate, angular distributions from, (E), 19: 45312
alpha elastic quadrupole scattering by polarized, at 16 and 24 Mev, (T), 20: 42235
alpha elastic scattering by, optical potentials for, 18: 32836
alpha elastic scattering by light, exchange contribution to, 18: 34801
alpha elastic scattering by, phase shift and complex potential description of, (T), 19: 33327
alpha elastic scattering by, distorted-wave model in, (E/T), 20: 1238
alpha elastic scattering at 24.7 Mev, optical-model analysis of, (E/T), 20: 30413
alpha emission by, quantum theory for, 17: 31412(T) (AEC-tr-5915)
alpha emission from heavy, effects of nuclear deformations on, 16: 1081
alpha emission from heavy, internal probability densities for, 16: 18521
alpha emission from 1p shell of fractional parentage, coefficients for, (T), 20: 15741
alpha emission intensities in heavy, Landau equation for, 16: 23072
alpha inelastic scattering by, gamma distributions from, 16: 32421
alpha inelastic scattering by, analysis of, 17: 31642 (NP-12975 (p.14-25))
alpha inelastic scattering by spherical even, three-phonon vibrational levels from, 17: 40028
alpha inelastic scattering by, 18: 40608
alpha inelastic scattering by even, polarizations from, 18: 42668
alpha inelastic scattering by deformed, Drozdov-Blair model for, 19: 17036
alpha inelastic scattering by even-even, reverse rotation of gamma angular pattern in, (T), 19: 33320
alpha inelastic scattering at 44 Mev, data on collective states from, (E), 19: 47608
alpha inelastic scattering by deformed, rotational excitation and gamma angular pattern from, (T), 20: 13848
alpha inelastic scattering at 25 Mev, angular distributions from, (T), 20: 19816 (INP-441/PL)
alpha inelastic scattering by, rotation of gamma angular distribution pattern in, (T), 20: 26235
alpha inelastic scattering by, computer program for analysis of, 20: 32544
alpha inelastic scattering by even-even $46 \leq A \leq 64$, vibrational energy levels from, (E/T), 20: 44795
alpha inelastic scattering by, in the region iron-54 to zinc-68, 16: 29471(R) (ANL-6574)
for, 17: 31494
alpha inelastic scattering, validity of distorted-wave Born approximation
alpha mean lifetimes in, 17: 9540
alpha particle elastic scattering by light, cross sections, 18: 17019
alpha particle formation in, during alpha decay, 18: 42658
alpha particle scattering by, excitation of two-phonon states by inelastic, 16: 29839
alpha particle scattering by vibrational, 16: 32410
alpha-particle scattering by, inelastic, 17: 5382
alpha-particle scattering by, inelastic, 17: 5383
alpha reactions (α,n) with medium-weight, 18: 7696(R) (ORNL-TM-761)
alpha reactions (α,d), (α,He-3), (α,n), (α,p), and (α,t) with, polarization in direct, 18: 36624
alpha reactions (α,2α) with light, cluster model for, 18: 36639
alpha reactions (α,α'), (α,d), (α,He-3), (α,Li-6), and (α,t) with, diffraction model for direct, 18: 36657
alpha reactions (α,d) with light, mechanism of, (T), 19: 8474
alpha reactions (α,d) with, selection rules for, (T), 19: 8443
alpha reactions (α,d) with, cross sections for, (T), 19: 17032
alpha reactions (α,n) with, performance as neutron source, (E), 20: 4802 (IDO-17115)
alpha reactions (α,α') and (α,d) with, effects of Coulomb interaction on, (T), 20: 32484
alpha reactions (d,p) at 30.5 Mev, proton spectra from, (E), 20: 30472
alpha reactions (α,d), angular distributions, 16: 8202
alpha reactions (α,t), forward-peaking transitions in, 16: 21558
alpha reactions (α,2α) at 0.915 Bev, clusters in, 17: 26593
alpha reactions (α,n) up to 11 Mev with A = 27 to 120, cross sections for, 18: 9412
alpha reactions at 10^{13} ev/nucleon, angular distributions, 16: 21404
alpha reactions at 14–20 Mev, excitation of collective octupole states in $106 \leq A \leq 154$, 17: 24440
alpha reactions at 10^{13} ev/nucleon, angular distributions from, 18: 38129
alpha reactions with galactic, x-ray emission from, 18: 28226
alpha reactions with, three-body bound states from, (T), 19: 10247 (JINR-P-1882)
alpha reactions with, bibliography, (E/T), 19: 25473 (LYCEN/6416/1)

alpha reactions with light, polonium, 19: 33278
alpha reactions with, amplitude singularities in knockon and stripping, (T), 20: 21997 (INSJ-96)
alpha scattering at 30 Mev, optical potential for, (T), 19: 5179
alpha scattering by light, exchange effects in, 17: 31464
alpha scattering by, multiparametric modular circuitry for detection of, 18: 33936
alpha scattering by, study of phase rule in angular distributions, (E/T), 19: 21269(R) (UCRL-11828(p.132-3))
alpha scattering by, angular distributions and excitation from, 20: 4824(R) (ANL-7081, pp 70-7)
alpha scattering by light ($6 \leq A \leq 40$), data compilation on, (E), 20: 12099
alpha scattering by odd-mass, amplitudes for, (T), 20: 28332
alpha scattering by spherical even-even, quadrupole and octupole energy-level transitions from, (E/T), 20: 44799
alpha scattering by, collective excitations in, (T), 19: 3250
alpha scattering, distorted wave theory for inelastic, 16: 23043
alpha stripping from, cross section for, 17: 24468
alpha transition rates in, absolute, (T), 19: 23788
alpha transitions in, reduced widths for, 18: 7686 (NP-13422)
alpha transitions in spherical, (T), 20: 6376
alpha-cluster knock-out reactions on heavy and medium, quasifree scattering in, (T), 20: 8112
alpha-decay barrier penetrabilities with Igo potential for even-mass, 20: 32399
alpha-particle interactions in, three-body, (T), 20: 34567
alpha, deuteron, neutron, and proton reactions with emulsion, star production in, (E), 20: 8069 (JINR-P-2383)
analog states in heavy, compound nuclear resonance observation of, 18: 28752
analog states of, widths of isobaric, 18: 40558
analysis of deformed, use of effective interactions in, 18: 2918
analysis of $1f_{7/2}$ mixing in, 16: 33697 (TID-16749)
angular momenta coupling in two-particle states in deformed even-even, 16: 21423
angular momentum distributions in, (T), 19: 27448
angular momentum of, nonadiabatic correction to rotational, 16: 32444
angular-momentum distributions in, following intranuclear cascades, (T), 19: 19088 (ORNL-TM-1033)
anisotropic magnetic shift and nuclear quadrupole interactions in, effects on nuclear magnetic resonance, 17: 24388 (IS-519)
antineutrino inelastic reactions with, cross section asymptotic behavior for production of mesons (π^+) and (π^-) in, 17: 41826
antineutrino reactions with, structure effects in, 18: 36656
antineutrino reactions at high energy, meson (μ^+) and positron distributions from, (T), 19: 14555
antineutrino reactions at high energies, boson nonproduction in, 16: 26130
antinucleon annihilation in light, recoil momentum distribution in, (T), 20: 8109
antiparticle and particle scattering at high energies, differential cross sections for, 18: 21333
antiproton annihilation on, meson (π) distributions from, 17: 3971
antiproton reactions during slowing-down, 16: 18532
antiproton reactions with complex, mean-free-path for, 18: 18900
antiproton reactions at 3 Bev/c, double-hyperfragment production in, 18: 44759
antiproton reactions at 3.0 Bev/c, amplitude for small-angle, (T), 20: 8106
antiproton refraction effects on absorption cross section, 16: 2426
approximations for single closed shell, quasi-particle random phase, 18: 18883(R) (TID-20378(Sect.2))
axial asymmetry of heavy, 18: 32277(R) (PR-P-61)
barrier penetration in, diffuse nuclear edge optical model effects on, (T), 20: 10047
beta and gamma transition probabilities of, survey, 20: 8081 (ORNL-P-1736)
beta decay, (T), 20: 30535
beta decay ($\frac{1}{2}+ \rightleftharpoons \frac{1}{2}-$) in $150 < A < 190$, 18: 40565
beta decay and magnetic dipole transitions in $1f_{7/2}$, seniority selection rules for, 17: 41959
beta decay energy of $16 \leq A \leq 249$, isobaric analysis of total, 17: 26517
beta decay in odd-odd, 18: 9343
beta decay in stars, photon-induced, (T), 20: 31878
beta decay in stellar interiors, photon-induced, (T), 20: 4530
beta decay matrix elements for, assuming partial conservation of axial vector current, 18: 42724
beta decay near closed shells, pair-correlation effects on, 17: 17182
beta decay of, book, 17: 9618
beta decay of complex, Goldberger-Treiman relation for, 19: 41774
beta decay of, effects of finite nuclear size on, 17: 834
beta decay of, electromagnetic multipole theory for, 17: 19378
beta decay of, electromagnetic emission of atomic electrons in, 18: 6270
beta decay of, experimental analysis of, 17: 4114
beta decay of heavy, core polarization effects on, 18: 9386
beta decay of heavy, role of neutron-proton correlations in, 19: 12507
beta decay of, induced effects in, 17: 33095
beta decay of mirror, theory, 18: 44748
beta decay of neutron-deficient, (T), 20: 28391
beta decay of neutron-deficient, with positron emission, (T), 20: 46623
beta decay of odd-odd, first-forbidden (T), 19: 3333
beta decay of odd-mass, l-forbidden transitions in, (T), 19: 16928
beta decay of odd, neutron-proton pairing effects on (E/T), 19: 3311
beta decay of oriented, problems in, (T), 20: 4933
beta decay of oriented, nuclear reorientation before gamma emission in, (T), 20: 44688
beta decay of polarized, produced by capture of polarized neutrons, 18: 21201 (KR-64(Sect.XXVIII))
beta decay of, properties of second-forbidden Coulomb, 17: 15294
beta decay of spherical, collective level excitation in, (T), 20: 6353
beta decay of, theory of anomalous spectra in allowed, 17: 5370
beta decay of, theory of vector interactions in, 17: 5400
beta decay of, theory using exact electron wave functions, 17: 17177
beta decay of $3 \leq Z \leq 36$, excitation and ionization of daughter atoms by, 20: 28451
beta decay of, allowed and forbidden transitions in, (T), 20: 3090
beta decay of, analysis using Geiger counters, (E), 19: 40903
beta decay of, β-γ angular correlations in, (E/T), 20: 7404
beta decay of, β–γ circular polarization correlations of allowed and first-forbidden, 20: 46799
beta decay of, conference on, 20: 30534
beta decay of, coupling constants in, (T), 20: 10069
beta decay of, delayed proton spectra from, 20: 28269 (BNL-10196)
beta decay of, diffuse surface boundary effects on, (T), 19: 12504
beta decay of, double, 20: 32562
beta decay of, effects of strong interactions between nucleons on forbidden, 20: 15836
beta decay of, effect of Coulomb field on, (T), 20: 15716 (CONF-233 (Vol.3), pp 529-37)
beta decay of, electron screening corrections to Fermi function for allowed, (T), 20: 46731
beta decay of, interacting quasiparticle method for, (T), 20: 3101
beta decay of, internal bremsstrahlung spectra in, (T), 20: 13761 (CONF-233(Vol.4), pp 656-68)
beta decay of, isobaric spin conservation in, (T), 20: 19837 (UCRL-14750-T)
beta decay of, Langer effect in, (T), 19: 14624
beta decay of, lectures on theory of, 18: 21187 (KR-64(Sect.IV))
beta decay of, matrix elements for first-forbidden, (E/T), 20: 30522
beta decay of, matrix elements for first-forbidden, 20: 32393
beta decay of, momentum distribution of recoil nuclei in, (T), 20: 46780
beta decay of, nuclear structure from, 20: 30536
beta decay of, renormalizable vector boson theory for allowed, 19: 5136
beta decay of, screening effects on, 19: 1597
beta decay of, sum rules for, (T), 20: 34602
beta decay of, theory for, 18: 36693
beta decay of, vector current conservation in, 18: 36701
beta decay probabilities for transition-region, 20: 10059
beta decay, pseudoscalar interaction in, 16: 17080
beta decay schemes and energy levels of, for $150 < A < 190$, 16: 32416
beta decay systematics in heavy, 17: 17148
beta decay theory for, 18: 34752(R) (CU(PNPL)-234)
beta decay transitions in strongly-deformed, 16: 7142
beta-decay transition probabilities and magnetic moments for $f_{7/2}$ shell, 18: 1073
beta emission calculations, 16: 10974
beta emission from, momenta dependence of helicity of, (E/T), 20: 19806 pp 313-25)
beta emission from oriented, 18: 4582 (NP-13378)
beta-gamma emission through virtual states, 17: 41873 (WASH-1044)
beta spectra of, effects of backscattering on measurement of, 18: 7076
beta transition probability for odd-Z, effect of structural changes on, 20: 34545
beta transitions ($0^+ \leftrightarrow 0^-$) in, 18: 34808
beta transitions in even-even, mechanisms for 0^+ excited and ground-state, 17: 31533
beta transitions in, correction functions for super-allowed, 18: 11218 (TID-20049)
beta transitions in, computer program for calculating nuclear matrix elements from, 18: 15193 (CONF-417-13)
beta transitions in even-even, 18: 30823
beta transitions in even-even, regularity in enhancement phenomenon of (T), 19: 1642
beta transitions in odd-A, log ft values for first-forbidden, (T), 19: 23769
beta transitions in, allowed and first-forbidden, (E/T), 20: 12113

beta transitions in, Nilsson model for matrix elements of, 20: 13831
beta transitions in $11 \leq A \leq 63$ odd, theory of finite Fermi systems for, 20: 13887
beta transitions in, higher-order effects in allowed, (E), 20: 17678 (COO-1420-113)
beta transitions in, single-particle matrix elements for first-forbidden, (T), 20: 40124
beta transitions in, second-forbidden contributions to isospin-forbidden, (T), 20: 46701
beta transitions in, exchange electric moments for, (T), 19: 45363
beta transitions of, coulomb matrices and spin conservation in allowed, 18: 28665
binding energies, (T), 20: 44703
binding energies and spectra of $f_{7/2}$-shell, 18: 4605
binding energies and masses in rare-earth region, 18: 7724
binding energies in 1p shell, U_3 symmetry and clustering in harmonic oscillator shell model for, 20: 26146
binding energies of, relations for, 18: 34812
binding energies of three- and four-nucleon, (T), 19: 12534
binding energies of, density matrix method for calculating, (T), 19: 14588
binding energies of, systematics of, (T), 19: 17028
binding energies of light, (T), 19: 19223
binding energies of, Bethe-Weizsacker relation for, 19: 43363
binding energies of, neutron-proton interaction effects on, (T), 19: 43383
binding energies of closed-shell, Bethe-Goldstone equation for, (T), 20: 11997
binding energies of, methods of calculating, (E/T), 20: 17158(R) (ORNL-3900, pp 82-149)
binding energies of heavy, nonlocal potential calculation of, 20: 30508
binding energies of, calculation using K-matrix theory, 20: 40119
binding energies of s-d shell, quadrupole correlation in, (T), 20: 44818
binding energies, radii, and surface diffuseness of, 18: 32758
binding energy and mass of, with A = 143 to 177, (E), 19: 29367
binding energy and quadrupole-quadrupole interaction in, (T), 20: 8126
binding energy at equilibrium density, off-energy-shell effects in Brueckner theory for, 19: 47666
binding energy for, soft-core potential in, (T), 20: 24449
binding energy of nuclear matter, 18: 42686
binding energy of three-nucleon, (T), 19: 23779
binding energy of nuclear molecule held together by neutron, (T), 19: 37852
binding energy of 1p-shell, deformation effects in ground-state, (T), 20: 1170
binding energy of, (T), 20: 32559
binding energy parameters for, from realistic two-nucleon potentials, (T), 20: 13840
binding-energy differences in mirror, calculations using shell model, (T), 20: 46776
book: *Beta Decay*, 20: 46800
book: *Dynamic Nuclear Orientation*, 18: 11294
book: *From the Atomic Nucleus to the Nuclear Power Station*, in German, 18: 26943
book: *Introduction to the Atomic Nucleus*, 19: 23802
book: *Isobar Nuclei with A = 140*, 16: 31125
book: *Nuclear Chemistry. Study of Radioactive Nuclei and Nuclear Reactions*, 20: 24487
book: *Nuclear Forces*, 20: 8159
book: *Nuclear Orientation*, a collection of reprints, 18: 24706
book: *Nuclear Spin-Parity Assignments*, 20: 46801
book: *Nuclidic Masses and Binding Energy of Nuclei*, 19: 31313
book: *Oriented Nuclei. Polarized Targets and Beams*, 19: 25083
book: *Physics of Nuclear Fission*, in Russian, 17: 19386
book: *Radioactive Transmutation of Nuclei and Atomic Shells*, in Russian, 18: 17096
book: *Textbook on Nuclear Physics. Vol. II. Physics of Atomic Nuclei*, in German, 18: 10662
book: *The Atomic Nucleus*, 18: 13125(T)
book: *The Nuclear Properties of the Heavy Elements. II. Detailed Radioactivity Properties*, 19: 1659
book: *The Nuclear Properties of the Heavy Elements. III. Fission Phenomena*, 19: 1660
book: *The Theory of Finite Fermi Systems and Properties of Atomic Nuclei*, 20: 13632
book: *Unified Theory of Nuclear Models*. (T), 19: 1655
boron-11 reactions with $232 \leq A \leq 256$, high angular momentum effects on lifetime of products from, 17: 38282
boson inelastic diffraction scattering by, complex angular momentum method for spin-zero, (T), 20: 17817
bound-state ($\bar{K}$-nucleus) existence, 18: 9151
bremsstrahlung emission by, contribution to radiative processes, (T), 20: 30516
bremsstrahlung excitation of, resonance fluorescence from, 18: 34852
bremsstrahlung polarization in fields of, 16: 32449
bremsstrahlung reactions with, cross sections for pair production in, 17: 17105 (DESY-A-2.96)
bremsstrahlung reactions with $77 < A < 199$, isomer production in, 17: 34910
bremsstrahlung reactions in Bev range, nuclear size effect on, 17: 40111
bremsstrahlung reactions (γ,N) with, effect of velocity-dependent forces on cross sections for, 18: 42740
bremsstrahlung reactions with Coulomb field of, pair production in, (T), 20: 6072
bremsstrahlung reactions at 2 Bev, quantum electrodynamic violation in wide angle pair production from, (E), 20: 42327
bremsstrahlung scattering, resonant, 16: 24703
burning of light, in non-hydrogenic stars, 17: 13269
carbon-12 reactions with, total cross sections for, 17: 28256 (UCRL-10766)
charge and energy spectra of $2 \leq Z \leq 8$, in primary cosmic radiation at solar minimum, 1965, 20: 23909
charge and magnetization distribution in, from hyperfine structure, 17: 40128
charge and mass distributions in, compressibility and polarizability effects on, (T), 19: 33374
charge distribution in, 16: 2499(T) (AEC-tr-4141(p.91-100))
charge distributions of, integrals for multipole moments of rounded, 18: 7695 (ORNL-3525)
charge distribution in cosmic radiation (E), 19: 2998
charge distribution of, in primary cosmic radiation, (E), 19: 34929
charge distribution of deformed, from x-ray spectra from μ-mesic atoms of, (T), 20: 17756
charge distribution in spherical, structure effects on, (T), 20: 38043
charge distribution in, isotopic shift of, (T), 20: 38101
charge distribution of deformed, determination from meson (μ-) hfs spectra, (T), 20: 42308
charge radius of spherical, structure effects in, (T), 20: 32561
charge spectra of, in primary cosmic radiation, (E), 19: 47277
charge symmetrical pairing correlations in light, 18: 32819
charged particle and neutron beam reactions with, technique for angular distribution measurements from, 20: 9786
charged particle and electromagnetic radiation reactions with, form factors for, 20: 28440
charged particle Coulomb scattering by, 17: 22503
charged particle elastic scattering by, strong absorption model for, 18: 26563
charged particle emission, deformed model for, 18: 26629
charged particle elastic scattering amplitudes at high energies, (T), 19: 8407(T) (NP-14468)
charged particle elastic scattering by, computer program for differential cross sections for, 20: 30348 (INP-446/PL)
charged particle inelastic scattering by, analytic uses of, 19: 14489 (ANL-6878(p.143-73))
charged particle reactions on, momentum transfer from, 17: 19322
charged particle reactions at 3×10^{11} ev, angular distribution from, 17: 21085
charged particle reactions with, neutron threshold energies from, 17: 34862
charged-particle reactions with, concept of nuclear density and potential in, 18: 7722
charged particle reactions with, Coulomb excitation in, (T), 20: 8082 (ORNL-P-1793)
charged particle reactions with, mechanisms for, 20: 34658
charged particle reactions with, in crystals, effects of crystal structure on, 18: 42316
charged particle scattering, multiple Coulomb, 16: 7070
charged-particle scattering by, analysis of multiple Coulomb, 17: 19326
charged particle scattering by even-even, optical model calculations of spinless, 18: 26678
charged particle scattering by, relativistic outgoing wave functions for, (T), 19: 5188
charged-particle and neutron reactions with heavy and medium, rates of, (T), 20: 11989
charged-particle absorption with formation of compound nuclei, (T), 20: 38020
charged-particle emission by heavy, evaporation theory for, 19: 39936
charged-particle elastic scattering by light, at low energies, (E/T), 19: 43371
charged-particle elastic scattering by, conversion factors for calculating angular distributions from, 20: 28322
charged-particle elastic scattering by spherically symmetric potential of, critical potential for, (T), 20: 36193
charged-particle elastic scattering by, critical potential perturbation for, (T), 20: 42173
charged-particle inelastic scattering by, analytic expressions for, (T), 20: 15743
charged-particle reactions with, Coulomb excitation in, 18: 13105

charged-particle reactions with, vacuum chamber for investigating, 18: 30822
charged-particle reactions with, analysis of (E/T), 19: 1686
charged-particle reactions in Coulomb field of, electron pair production in, (T), 19: 23799
charged-particle reactions in Coulomb field of, (T), 20: 3153
charged-particle reactions with, cross sections and level studies from, 20: 4822(R) (ANL-7081, pp 22-35)
charged-particle reactions with, angular momentum transfer, cross sections, and level studies from, 20: 4823(R) (ANL-7081, pp 36-69)
charged-particle reactions and scattering, Fraunhofer and Fresnel diffraction in, (T), 20: 6359
charged-particle reactions with, K-shell atomic ionization from, (T), 20: 7726
charged-particle reactions with Coulomb field of, bremsstrahlung production in, (T), 20: 7736
charged-particle reactions at high energies, fragmentation in, 20: 11377
charged-particle reactions with, finite range Coulomb stripping and heavy-ion transfer in, (T), 20: 12091
charged-particle reactions at high energy with heavy, light fragment emission in, (T), 20: 13880
charged-particle reactions with, energy levels and gamma spectra from, 20: 36190
charged-particle stripping reactions with, Coulomb distortions in neutron capture in, 18: 26646
charged-particle scattering by, amplitudes and cross sections for small-angle, (T), 19: 21233 (JINR-E-1992)
charged-particle scattering by Coulomb fields of, amplitudes for, (T), 19: 21425
charged-particle scattering by, Coulombic modified effective-range theory for, 19: 27554
charged-particle stripping reactions with, slow particle emission in, (T), 19: 41664 (JINR-P-2193)
charged-particle scattering by, radial relativistic Coulomb integrals for, (T), 20: 6375
charged-particle scattering by, collective-state excitation in, (T), 20: 15763
charged-particle scattering by, ionization losses in, (T), 20: 21515 (JINR-P-2615)
charged-particle scattering by, spin-½, (T), 20: 36156 (COO-1573-1)
charged-particle, direct radiative capture, (T), 19: 12541
cluster wave functions for, interpretation of generalized, 16: 21398
collection of recoil, electrostatic (E), 19: 3339
collective effects and elastic scattering from odd-mass, 17: 33051
collective excitations of zero spin, effects of structure on, 16: 2552
collective excitations for $N \neq Z$, 18: 19059
collective excitations of, review on, (T), 19: 16888
collective g-factor for strong deformed, formula for, 18: 34939
collective levels and deformations of, having 82 to 90 neutrons, 16: 12466
collective motion and neutron resonance spacing in highly excited, 16: 21513
collective motion in, coefficients of SU_3 group for, 17: 11928
collective motion in, dynamic theory of internal parameters for, 17: 21051
collective motion in even-even deformed, 17: 11732
collective motion and deformation energies of heavy, 20: 22065
collective motions, effects of spin-dependent forces on, 16: 23093
collective motions of, variational calculations of, 17: 2297
collective oscillations and pairing correlations in, 19: 10374
collective particle effects in, relation to shell model, 16: 2484 (NP-10931)
collective phenomena in, theory of, 17: 4110
collective properties in anisotropic harmonic-oscillator model, 16: 23087
collective properties of, effects of pairing and quadrupole interactions on, 17: 2281
collective properties of, lecture on aspects of, 17: 17308
collective properties of, from pairing and quadrupole interactions in nucleon configuration $j^n = (\frac{9}{2})^4$, 18: 6222
collective states of deformed, energies of octupole, 18: 1007 (JINR-E-1356)
collective vibrations of even-even spheroidal, theory of, 16: 29787 (UCRL-10046)
collective vibrations of even-even, with $A \approx 30$, 17: 7104 (NP-12330 (p.119-21))
collective vibrations in $A \approx 30$, 17: 11661
collective vibrations of, single-nucleon damping of, 17: 24179
composition of $Z \geq 3$, in primary cosmic radiation, 20: 41672
compound, isobaric analog states as resonances of, 18: 22927
compression of, neutrino spectra from neutron production in, (T), 20: 8097
concentration behavior of, in neutron fluxes, relations of, with time, 16: 32028 (ORNL-TM-361)
conference on nuclear spectroscopy, 19: 27463
conference on spectroscopy and structure of, 20: 15749
conference on spectra and structure of, 20: 19952
configuration centroid energies and widths for ds shell, (T), 20: 46712
configuration mixing effects in shell-model, (T), 20: 12155
configuration mixing in shell model, (T), 20: 24332(R) (ANL-7108, pp 67-73)
content in cosmic radiation, 19: 30972
content in solar radiation (E), 19: 2953
contents in reactors, computer determination of, 17: 33244 (ORNL-TM-361(Add.))
contents in stars, 17: 24197
conversion-electron directional correlations in, interference particle parameter for, 18: 6237
conversion electrons from, angular correlations of, (T), 19: 27488
conversion electrons from, review of data on, 20: 17795
core deformability and electric quadrupole moments, 16: 7026
core excitations in nondeformed odd-A, 17: 36399 (NP-13020(p.85-91))
core isomerism in, (T), 19: 17051
correlation energy of, wave function for short-range three-body, 19: 47665
cosmic meson (μ) reactions at high energies, multiple meson (π) production in, (E), 19: 35445
cosmic meson (μ) reactions with energy losses from relativistic, (T), 20: 37707
cosmic meson (μ) reactions at 58 mwe underground, fast neutron differential energy spectrum from, (E), 20: 37710
cosmic meson (π^-) reactions at ≥ 14 Bev, momentum spectra of secondary particles from, 17: 41713 (TID-19500)
cosmic meson (μ) interactions, with energy transfers >300 Bev, 16: 5902
cosmic meson (μ) reactions above 2 Bev/c, photonuclear cross sections for, 17: 24253
cosmic meson reactions at 3200 m, spectra of events from, 16: 27874
cosmic nucleon reactions, cloud chamber studies at 3860 m, 16: 27873
cosmic nucleon reactions with heavy, slow-particle production in, 17: 9511 (PAN-348/VI)
cosmic nucleon reactions at $\gtrsim 10^{13}$ ev, high-energy gamma flux from, 17: 26273
cosmic nucleon reactions with, isobar production in, 18: 44820
cosmic nucleon reactions with atmospheric, showers from, (T), 19: 41300
cosmic nucleon reactions at high energies, models for, 20: 23982
cosmic nucleon reactions with air, models for EAS, 20: 46318
cosmic nucleon reactions at 100 to 1000 BeV, cascade mechanism in, 20: 46356
cosmic particle interactions, azimuthal distributions of jets from, 16: 5898
cosmic particle reactions, heavy, 16: 5850
cosmic particle reactions with heavy, azimuthal angular distribution, 16: 13962 (PAN-253/VI)
cosmic-particle reactions at 3×10^{14} ev in emulsion, 16: 26296
cosmic particle reactions on, jet distributions from 10^{13}-ev, 17: 6919
cosmic-particle reactions on, mesons (π^0) from, 17: 11454
cosmic particle reactions with atmospheric, cascades from, 17: 13110
cosmic particle reactions with emulsion, meson production in nucleon interactions in heavy, 17: 26269 (PAN-398/VI)
cosmic particle reactions with, helium-3 and triton energy spectra for, 17: 29608
cosmic particle reactions with scintillator, at 41 Bev, angular distributions from, 18: 2562
cosmic particle reactions with, analysis of, 18: 42713
cosmic particle reactions with, double maximum angular distributions and asymmetry in, 18: 42714
cosmic particle reactions at high energies, meson (π^0) production in, (E/T), 19: 27439 (PAN-551/VI)
cosmic particle reactions at 70 to 700 Bev, inelasticity of, (E), 19: 27461
cosmic particle reactions with, diffraction dissociation in, (E/T), 19: 32914
cosmic particle reactions with, secondary particle energy and intensity from, (T), 19: 34908
cosmic particle reactions at 5 to 10 Tev, meson (π^0) production in, (E), 19: 34910
cosmic particle reactions above 10 Bev, model for inelastic, (T), 20: 21999 (JINR-P-2552)
cosmic proton interactions with intergalactic, proton production in, (T), 19: 14275 (NASA-CR-149)
cosmic proton reactions with, departure from isotropy in meson production in, 17: 24254
cosmic proton reactions with, neutron transport from, 18: 28538
cosmic proton reactions with interstellar, proton spectra from, (T), 19: 12106 (NASA-CR-150)
cosmic proton reactions with complex, angular distribution of secondary particles from, 20: 25760
cosmic radiation reactions with emulsion, 18: 42712
cosmic ray reactions in atmosphere at 10^{13} to 10^{14} ev, energy spectra of showers from, 16: 27876

cosmic ray reactions in air at 10^{15} ev, shower production in, 16: 27881
cosmic ray reactions, angular distribution of meson jets from, 16: 27890
cosmic-ray reactions with emulsion, rate of star production in, 18: 2558
cosmic shower nuclear-active component reactions with light, young-air, (E), 20: 37755
cosmic-nucleon reactions with, at 10^{11}–10^{13} ev, 18: 40618
cosmic-ray reactions with atmospheric, spectra from, (E/T), 19: 41291
Coulomb energies of light, 17: 7090 (NP-12330(p.17-21))
Coulomb energy in light (T), 19: 3371
Coulomb excitation of, use of, in investigation of low-lying energy states, 16: 29779 (JAERI-1020(p.215-28))
Coulomb excitation of, review, 18: 11222
Coulomb excitation of 4^+ levels in nonspherical even-even, double, 18: 28601
Coulomb excitation of even, second-order, 18: 32827
Coulomb excitation of even-even, 18: 36675
Coulomb field of, screening by bound electrons, (T), 19: 37853
Coulomb interactions in, energy spectrum for, (T), 19: 29302
coupling constants between, review on, 19: 5152
coupling of giant resonances and surface oscillations in light, (T), 20: 42271
coupling scheme in light, variation with radius, 18: 4604
coupling schemes and effective interactions in, 17: 11739
coupling schemes for, surface delta interaction in, (T), 19: 41686
coupling to electrons, signs of constants for hyperfine, (E/T), 19: 12086
critical temperature for high-energy behavior of even-even, 17: 24506
cross sections of, optical-model calculations of, (T), 19: 6632 (JINR-P-1795)
cross-section resonance effects on fissionable, 18: 38009 (A/CONF. 28/P/357)
data summary, chart of nuclides, second edition, 1961, 16: 21430
data tables, 16: 17154
decay and formation of intermediate, intrinsic parity-spin relations for, 17: 24469
decay and formation of compound nucleus system in nuclear reactions, independence of, 18: 26529 (BNL-8020)
decay and formation of compound, independence of, (T), 19: 19100
decay and particle emission, effects of statistical perturbations on angular correlations, 16: 26250
decay and production of mirror, 17: 34999 (NP-13064)
decay and structure of, review on, 19: 23649
decay, angular correlation and Mössbauer effect studies, 16: 25953(R) (TID-16079)
decay by alpha emission, theory of, 16: 33796(UCRL-10434)
decay by electron capture, use of calibrated gamma spectrometer for measuring, 20: 15747
decay by emission of two protons, theory for, 18: 42678
decay channels of, analysis of reaction widths in, 17: 9585
decay constants for, errors in determination of, 18: 6170 (NP-13439)
decay, effects of paired correlations of superconducting type on alpha, 16: 31079
decay energy systematics of heavy, 16: 32402 (UCRL-9524)
decay in reactors, computer analysis of, (T), 19: 12490 (ORNL-3689)
decay of, analysis of multicomponent time-dependent spectra from, 17: 20981 (HW-75806)
decay of analyticity and unitarity for analysis of two-body, 19: 45340
decay of compound, (T), 20: 38020
decay of compound, after direct nuclear reaction, (T), 19: 14542(T) (ANL-Trans-156)
decay of deformed, 17: 19221 (PUC-1963-95)
decay of deformed, alpha and beta, (T), 19: 12603
decay of deformed, electromagnetic, (E/T), 20: 20365
decay of, effect of recoil asymmetry on motion during, 17: 812
decay of, effects of nuclear structure on internal conversion of gamma rays in, 17: 22584
decay of, emission of delayed protons in, 17: 19246
decay of excited states in, study of gamma-gamma angular correlation in, 17: 2243(R) (TID-17083)
decay of heavy, lifetimes for alpha, beta, and spontaneous-fission, (T), 20: 22043
decay of high-angular-momentum, gamma spectra from single-particle electromagnetic, (T), 19: 47655
decay of light, orbital Young diagram restrictions on cluster, 18: 30789
decay of loosely bound, Coulomb effects on vertex parts in, (T), 19: 45146
decay of neutron-deficient, emission of delayed protons in positron, 17: 7169
decay of odd-mass, half lives for, 18: 18936
decay of radioactive, spectral shape in exponential, (T), 19: 39304
decay of, statistical properties, 17: 29990
decay of, superfluidity effects in alpha, 17: 22581
decay of $T = -3/2$, log ft values for, (T), 19: 21379
decay of $Z > 50$, two-proton, (T), 20: 12028
decay of $49 \leq Z \leq 73$, conversion electron angular-correlation parameters for, (T), 20: 26205
decay of 6-quasiparticle isomeric states of odd-odd, with $A \sim 240$, 18: 28613
decay of, angular correlation measurements in, (T), 19: 40900
decay of, angular correlations in, 20: 1166
decay of, calculation of member yields from chain, (E), 19: 10241 (AERE-M-1464)
decay of, calculation of gamma-gamma angular correlations for, (T), 20: 30341 (AECL-2529)
decay of, cluster model calculations of, (T), 20: 28438
decay of, correlation functions for, (T), 20: 24372
decay of, directional correlations of gamma and positron emitted in pair-conversion, (T), 19: 43378
decay of, effect of high spin on electromagnetic, (T), 20: 32374(R) (IITRI-578P25-15)
decay of, formation of internal pairs in M1 transitions (T), 19: 3258
decay of, gamma-gamma angular correlations for, (T), 20: 22010(R) (NYO-72-28)
decay of, helicity representation for angular correlations with recoil effect in, 19: 47610
decay of, internal bremsstrahlung spectra from electron-capture, (T), 20: 13760 (CONF-233(Vol.4), pp 637-55)
decay of, mechanisms of proton emission in, (T), 19: 10245 (JINR-P-1863)
decay of, optimization of counters for measuring, (E/T), 19: 44503
decay of, perturbed angular correlation of triple gamma cascades from, (T), 20: 22015
decay of, spin relaxation in gamma angular correlations of, 18: 24653
decay of, spontaneous, (E), 19: 43110
decay of, statistical distributions for, 20: 19851
decay of, systematics of, 20: 40108
decay of, theory for beta and gamma, 18: 36689
decay of, three-body, 18: 24625 (WASH-1046)
decay of, unperturbed directional correlations in, 20: 46582 (COO-1420-126(Vol.1))
decay processes of, hydrodynamic models of, 18: 13079
decay products of compound, angular distribution in direct reactions for, 19: 33375
decay properties of, use of isotope separator with synchrocyclotron for study of, 20: 19885
decay rates of, effects of laser beam on, (E/T), 20: 12102
decay scheme of, methods for determining, 20: 36185
decay schemes for deformed, book, (E), 19: 10256 (RISO-92)
decay theory of closely coupled unstable states in, 20: 15816
decoupling parameters for $^1/_4$ rotational bands for very deformed, variations of, 16: 29813
deformation alteration by rotation, 17: 17134
deformation and mass of, tables of, 20: 36177 (UCRL-11980)
deformation at high angular momentum of compound, calculation by liquid drop model, 16: 21508
deformation effects in 1p-shell nuclei, 20: 1170
deformation in even-even $60 \leq A \leq 150$, octupole, 17: 36703
deformation in even-A ($84 \leq N \geq 98$), mass effect associated with, 18: 24681
deformation in heavy, space symmetry of wave functions for equilibrium, (T), 20: 11970 (JINR-P-2473)
deformation in light, perturbation theory for, 20: 15809
deformation in 50- to 82-proton region, observations, 16: 7118
deformation of, effects of quadrupole interaction on prolate, 18: 6253
deformation of heavy, Y_{40}, 18: 32745(R) (UCRL-11213(p.1-48))
deformation of heavy, calculation of axially asymmetric equilibrium, 19: 9771(R) (PR-P-63)
deformation of heavy, Y_{40} contribution to, (T), 19: 17000
deformation of heavy, (T), 20: 24385
deformation of j-shell of, in pairing-plus-quadrupole model, 18: 24614 (NP-13941)
deformation of light 1p, shell-model calculations of, 18: 42725
deformation of $N \leq 82$ and $Z \geq 50$, equilibrium, 18: 36629
deformation of, oblate, 18: 9305 (AD-290788)
deformation of, close-packed-spheron theory for, (T), 20: 4918
deformation of, in pairing model, 19: 12497
deformation of, measurement of sexadecapole, 19: 1622
deformation of, review of theory of, 20: 40136
deformation of, tensor force effect in, (T), 19: 6663
deformation parameters for even-even, 20: 17730
deformation shapes of rare earth and light, self-consistent calculation for, 20: 15843
deformation, calculations, 18: 32745(R) (UCRL-11213(p.1-48))
deformations and masses of, modified liquid-drop model for, 20: 24401
deformations and quadrupole moments of $84 \leq Z \leq 100$, ground-state equilibrium, 17: 31418
deformations in medium and heavy, (T), 20: 19986

deformations of, systematics of, 17: 15308
deformations of, models for calculating equilibrium, (T), 20: 12125
deformed odd-odd, separation of members of the doublet of, 17: 15274
delayed-neutron precursors, effects of angular momentum and energies on occurrence, 16: 11697(R) (TID-15020(p.49-56))
density and potential of, analytical functions for, 18: 7722
density distributions and energies of, Fermi-Thomas-type K-matrix calculations of, 17: 24457
density distribution in, drop model calculations of, 18: 32857
density distribution in light, (T), 19: 31256
description of analog states using shell model, (T), 20: 38025
description of deformed, using single-particle model with energy-dependent potential, (T), 20: 44830
description of ground state, using random phase approximation, (T), 20: 44766
description of odd-A 1p shell, using strong-coupling rotational model, (T), 20: 46679
description of rotating, 16: 26305
description of, diagram for, 19: 23163(R) (ORNL-3650(p.111-86))
description using statistical approximation with momentum-dependent forces, (T), 20: 40115
description using Hartree-Fock approximation with density-dependent two-nucleon interaction, (T), 20: 44785
description using liquid-drop model, shell corrections to, (T), 20: 46610(T) (ANL-Trans-353)
detection and identification of cosmic, with $Z > 5$, 18: 44483
detection and measurement of $Z > 2$, silicon surface-barrier detector for, 20: 11124(T)
detection of recoil, electronic equipment for, 18: 41834
determination of isobaric, using alpha scattering, 19: 29240 (INP-402/PL)
determination of the isobaric states in models with a fixed nucleon, 17: 21026
deuteron (d,p) reactions with, impulse approximation for calculating, 19: 47631
deuteron diffraction reactions with, deuteron internal-structure effects on, (T), 20: 25854
deuteron double elastic scattering by, polarization parameters from, (T), 20: 17805
deuteron elastic and inelastic scattering at 15 Mev, (E/T), 20: 15850
deuteron elastic scattering by low-mass, cross sections and polarizations in, 16: 17130
deuteron elastic scattering by, effect of the nuclear electric field on elastic, 17: 5384
deuteron elastic scattering by, angular distributions and polarization in, 17: 26461 (PAN-241)
deuteron elastic scattering from $13 \leq Z \leq 82$, angular distributions from 15-Mev, 17: 26575
deuteron elastic scattering on $12 \leq Z \leq 90$ at 11.8 Mev, atomic weight dependence of cross sections for, 17: 34940
deuteron elastic scattering at 11–27 Mev, optical-model analysis of angular distributions from, 17: 40104
deuteron elastic scattering at 11.8 Mev by $Z = 45$ to 52, closed-shell anomaly in cross sections for, 18: 4603
deuteron elastic scattering by, polarization in, 18: 6230
deuteron elastic scattering at 10 Mev, 18: 26561
deuteron elastic scattering by complex, angular distribution of polarization in, 18: 40639
deuteron elastic scattering by complex, theory of, 18: 42780
deuteron elastic scattering by, distorted-wave model in, (E/T), 20: 1238
deuteron elastic scattering by complex, at high energies, (T), 20: 3044
deuteron elastic scattering by, spin-orbit interaction in optical model for, 20: 8140
deuteron elastic scattering by, method for calculating cross sections for, (T), 20: 10068
deuteron elastic scattering in Coulomb fields of, (T), 20: 25796
deuteron elastic scattering by, deuteron internal-structure effects on differential cross section for, (T), 20: 25854
deuteron elastic scattering by $Z = 22$ to 29, at 13.6 Mev, optical-model analysis of, (T), 20: 42294
deuteron elastic scattering by, optical model for, (T), 20: 44846
deuteron optical potential in, (T), 20: 4879
deuteron reactions (d,n) and (d,p), nuclear superfluidity effects, 16: 1084
deuteron reactions (d,p), excitation of rotational levels in, 16: 2551
deuteron reactions (d,p), determination of reduced width in, 16: 4821
deuteron reactions (d,p) and (d,n), angular correlations of possible conversion electrons in, 16: 14006
deuteron reactions (d,p) proton spin-orbit distortion effects in, 16: 21600
deuteron reactions (d,n) and (d,p), structure effects in, 16: 21584
deuteron reactions (d,p), graphs for determining reduced widths in, 16: 21356 (NYO-2666)
deuteron reactions (d,p), model for, 16: 28140
deuteron reactions (d,t) with $1f_{\frac{7}{2}}$, seniority mixing in, 17: 839
deuteron reactions (d,p) with, cross sections for, 17: 846
deuteron reactions at 22.4 Mev, total cross sections for, 17: 13554
deuteron reactions with arbitrarily oriented, polarization in direct, 17: 17244
deuteron reactions in deformed, geometric effect in stripping, 17: 22555 (JINR-P-1214)
deuteron reactions (d,p) with $A \leq 48$, proton angular distributions from distorted-wave Born approximation for, 17: 26588
deuteron, reactions with cross sections for, 17: 29575 (PAN-242)
deuteron reactions (d,d) and (d,p) and proton scattering on, angular distributions and polarizations for, 17: 33036
deuteron reactions (d,p) with, Coulomb interaction effects in, 17: 33067
deuteron reactions (d,ny) with, coincidence methods for, 17: 34864
deuteron reactions (d,p) at 13.6 Mev, angular distributions, differential cross sections, and interaction radius for, 17: 38187
deuteron reactions (d,pn) with heavy, cross section for, 17: 38095(T) (AEC-tr-5981)
deuteron reactions (d,N) with, exchange effects in, 18: 2860
deuteron reactions (d,py) with, polology for angular correlations in, 18: 19087
deuteron reactions (d,t) with light, angular distributions and spectra from, 18: 18881 (NP-13784)
deuteron reactions (d,n) with, spin-orbit interactions in, 18: 21366
deuteron reactions (d,np), polarization effects in, 18: 30834
deuteron reactions (d,p) with, distorted-wave theory of, 18: 32799
deuteron reactions (d,p) and (d,t) with, analytic uses of, 18: 32881
deuteron reactions (d,xy), spin path mutual exchange in, 18: 34873
deuteron reactions (d,p) with, theory of, 18: 36617
deuteron reactions (d,He-3), (d,n), (d,p), and (d,t) with, polarization in direct, 18: 36624
deuteron reactions (d,p) with, diffraction model for direct, 18: 36657
deuteron reactions (d,n) with medium-weight, 18: 42624(R) (ANL-6879 (p.35-63))
deuteron reactions (d,n) and (d,p) with, finite-range interaction effects in, 18: 42641 (KFKI-1491/G)
deuteron reactions (d,p) with, total angular momentum of residual states from angular distributions in, 18: 42744
deuteron reactions with, finite-range effects in stripping, 19: 1618
deuteron reactions with, overlap integral for, 19: 1651
deuteron reactions (d,α), (d,d^+), (d,He-3), (d,p), and (d,t) with, (T), 19: 17033
deuteron reactions (d,p) on absorptive, (T), 19: 17036
deuteron reactions with, excitation cross sections for, (T), 19: 16884
deuteron reactions (d,α) and (d,p) with, direct, (T), 19: 23685
deuteron reactions (d,py) with, spin-orbit coupling in, (T), 19: 23707
deuteron reactions (d,n) with, thresholds for, (T), 19: 23727
deuteron reactions (d,np) with light, angular and energy distributions from, (T), 19: 27481
deuteron reactions (d,p) with, DWBA approximation for, 19: 33271
deuteron reactions (d,p) with, prior-form DWBA analysis of, (T), 19: 37802(R) (ORNL-3778(p.28))
deuteron reactions (d,p) in Coulomb field of, spectroscopic factors for, (T), 19: 41739
deuteron reactions (d,p) with medium-weight nuclei at 28 Mev, isobaric analog states from, (E/T), 19: 41772
deuteron reactions (d,α), differential cross sections for, (T), 19: 41817
deuteron reactions (d,p) with, equation for matrix element of, 19: 47630
deuteron reactions (d,α) with, distorted-wave model in, (E/T), 20: 1238
deuteron reactions at low energies, formalism for stripping, (T), 20: 3070
deuteron reactions (d,p) with $88 \leq N \leq 90$, effect of deformation change on cross sections for, 20: 3125
deuteron reactions (d,He-3) with, level studies from, 20: 4824(R) (ANL-7081, pp 70-7)
deuteron reactions (d,p) at 10 to 30 Mev, spin-orbit coupling in, (T), 20: 4827 (CEA-Bib-60)
deuteron reactions (d,p) with, effect of deformation change on capture probabilities in, (T), 20: 8176
deuteron reactions (d,d'), (d,p), and (d,t) with actinide, spectrographic analysis of, (E), 20: 9961(R) (ANL-7029, pp 1-3)
deuteron reactions (d,n), analytic theory of subCoulomb, 20: 10011
deuteron reactions at 15-Mev, isomer production in, (E), 20: 15856
deuteron reactions (d,p) with, effects of D-wave deuteron states on, (T), 20: 15730(R) (RHEL/R-112, pp 67-98)
deuteron reactions (d,n) with, amplitudes for, (T), 20: 17704
deuteron reactions (d,n) with, neutron production for activation analysis in, 20: 16332 (GA-6691)
deuteron reactions (d,p), amplitudes for, (T), 20: 19974
deuteron reactions (d,p) with, sensitivity to truncated potential, (T), 20: 19925
deuteron reactions with, amplitude singularities in knockon and stripping, (T), 20: 21997 (INSJ-96)
deuteron reactions (d,Ny) with, gamma polarization from, (T), 20: 22006

(KFKI-600)
deuteron reactions (d,p) with, amplitudes in Coulomb approximation for, 20: 22028
deuteron reactions with, effect of asymmetry of deuteron charge center on, (T), 20: 24371
deuteron reactions with, effects of $^3D_1$ state on reduced widths for, (T), 20: 24452
deuteron reactions with Coulomb field of, disintegration in, 20: 26218
deuteron reactions (d,p) with, single-particle reduced widths from, (T), 20: 26164
deuteron reactions (d,p) with, three-body wave function for, 20: 28386
deuteron reactions (d,p) with, angular distributions and polarization from, (E/T), 20: 28387
deuteron reactions (d,n) with, amplitudes for, (T), 20: 30426
deuteron reactions (d,He-3) and (d,t) with, isobaric spin in, (T), 20: 30343 (COO-1371-30)
deuteron reactions with, many-body nucleon transfer in, (E/T), 20: 32547
deuteron reactions (d,p) with even-even spherical, vibrational energy levels from, (E/T), 20: 44797
deuteron reactions and scattering on, isospin effects on, 20: 44834
deuteron reactions (d,n) and (d,p), (T), 20: 46752
deuteron reactions (d,p) with, model for, (T), 20: 46630
deuteron reactions with, optical model potentials for, (T), 19: 23712
deuteron reactions with, amplitudes for, (T), 19: 5211
deuteron scattering by non-spherical, Drozdov-Blair diffraction model for, 16: 19750 (PAN-261/VII)
deuteron scattering on nonspherical, deformation of arbitrary multipolarity from, 16: 26228 (PAN-300/VII)
deuteron scattering by light, 17: 10240(R) (NP-12208)
deuteron scattering by complex, 17: 17122 (PUC-1962-78)
deuteron scattering by non-spherical, diffraction model for, 17: 19234
deuteron scattering on potential fields of, 17: 38186
deuteron scattering by, theory of, 18: 36604
deuteron scattering by, elastic and inelastic, (T), 19: 31298
deuteron scattering by, rotational-state excitation in, (T), 19: 33359
deuteron scattering by non-spherical, analysis of diffractive, (T), 20: 1153 (INR-605/VII/PL)
deuteron scattering by nonspherical, (T), 20: 3026
deuteron splitting in field of deformed, 17: 17247
deuteron splitting in fields of deformed, 18: 9350
deuteron stripping reactions, on aligned and unaligned, 16: 4800
deuteron stripping on non-axial, 16: 26350
deuteron stripping reactions (d,p) on even-even spherical, theory, 16: 31121
deuteron stripping in Coulomb field of heavy, classical description of, 17: 11630 (TID-15924)
deuteron stripping reactions on, polarization effects in, 17: 19312
deuteron stripping reactions on, S-matrix reduction for amplitudes of, 17: 22642
deuteron stripping reactions (d,p), residual-interaction terms in, 17: 41921
deuteron stripping reactions with, inelastic effects in, 18: 24652
deuteron stripping reactions with, polarization in, 18: 34853
deuteron stripping reactions with, cross section for, (E), 19: 5569(R) (MIT-2098-64)
deuteron stripping reactions with, effects of inelastic scattering on, (E), 19: 16855(R) (ORNL-3714(Vol.I)(p.1-30))
deuteron stripping reactions on, distorted-wave Born approximation for three-body, (T), 19: 39910
deuteron stripping reactions with, L-space localization in, 20: 6394
deuteron stripping reactions with, angular distribution calculations for, (T), 20: 13851
deuteron stripping reactions with odd-n, spectroscopic factors from, (T), 20: 13865
deuteron stripping reactions with, neutron single-particle states from, (T), 20: 19849
deuteron stripping reactions with, correlation effects and polarization in, (T), 20: 24372
deuteron widths in 1p-shell, estimates by harmonic oscillator wave functions, 16: 21354 (NP-11682)
diamagnetic shielding by conduction electrons in metals, 16: 21215
diamagnetic shielding of, in metals, 17: 681
dimensions of, polarization effects of finite, 17: 40003
dipole excitation, 16: 23157
dipole excitations of, collective interpretation of, 17: 22585
dipole polarization parameters, 16: 2553
dipole resonance formation in spheroidal, surface vibration effects in, (T), 19: 5209
dipole resonance in 1d-2s shell, 18: 40556
dipole resonances in light, proton-capture study of, 18: 19050
dipole resonances in light, proton-capture study of, 18: 19051
Dirac particle scattering by Coulomb fields of, 19: 1283
disintegration of, relations between electron and photon, 18: 36638
disintegration rate determination from beta-gamma coincidences, absolute, (E/T), 19: 5233
distortion of even-even $82 \leq A \leq 126$, from isotope shift data, 17: 40078
distribution in cosmic radiation, charge and energy, (E), 19: 6482
distribution of hyper, in emulsions exposed to mesons (K^-), 19: 9767(R) (IS-900(Sect.P))
distributions of cosmic, with $Z = 2$ to 10, 18: 2063
distributions of recoil, device for measuring angular and energy, 20: 32526
dynamic properties of light, Feshbach theory for, 20: 8104
effect of compound, on Coulomb excitation, 17: 21001
effect of configuration mixing on M4 transitions of (T), 19: 1643
effect of rotation on pair correlation in, 16: 1074
effect of short-range repulsion in nuclear matter, 18: 42687
effective interaction in 1P shell, Hamada-Johnston potential for, 20: 26153
effects of heavy solar-flare, on low-shielding space systems, 20: 16300
electric-dipole transitions (forbidden) in heavy, anomalous internal conversion, 16: 7076
electric dipole transitions in, theory of internal pair formation for, 18: 26581
electric monopole transitions in nonspherical, (T), 19: 41812
electric quadrupole transitions in odd-mass spherical ($28 \leq Z \leq 82$), 18: 7757
electric quadrupole moments and gamma transitions in rotational band of deformed, Hill-Wheeler integrals for, 18: 28584
electric quadrupole moments of rotational bands in deformed, 18: 28738
electric quadrupole moments and transitions in even and odd-mass, 19: 43325
electric quadrupole moment and spectral isotopic shift calculations of near-spherical, (T), 19: 47573 (IAE-717)
electric transitions and quadrupole moment of, relation of scattering cross sections to, 18: 18941
electrical monopole transitions in nonspherical, 18: 44804
electrodisintegration and photoeffect, relation between cross sections for, 18: 2920
electromagnetic form factors of three-nucleon, (T), 20: 3119
electromagnetic multipole moments of deformed odd-A, 18: 4626
electromagnetic properties of light, theory of, 17: 4112
electromagnetic properties, 17: 17306
electromagnetic properties of nuclear models and wave functions for, 20: 3148
electromagnetic transitions in, sum rules for, 16: 12481
electromagnetic transitions in deformed odd-odd, 17: 11654
electromagnetic transition probabilities for, projection method for calculation of, 18: 13085
electromagnetic-wave scattering by inhomogeneous spherical, 16: 33640
electron and positron scattering by spinless, deviations from electrodynamics in, 20: 34257
electron and x-ray excitation of, use of low-energy, 20: 13782 (ORNL-P-1927)
electron back-scattering by, Bothe diffusion theory of, 18: 30838
electron backscattering from, formulas for equivalent atomic number of complex targets for saturation in, 18: 26660
electron capture, bremsstrahlung-gamma ray correlations, 16: 19796
electron capture by aligned, effects of K-shell hole on alignment, 16: 33861
electron capture by, internal moderating radiation in, 18: 6203
electron capture by, exchange and overlap effects in orbital, (T), 19: 23818
electron capture by, processes from, 20: 15693 (CONF-233(Vol.1))
electron capture by, review of orbital, (E/T), 20: 15695 (CONF-233 (Vol.1), pp 30-56)
electron capture decay of, bremsstrahlung emission in, 18: 18930
electron capture decay of, positron emission in, 18: 18931
electron capture decay of $Z = 40$ to 90, (T), 19: 12517
electron capture in, K-electron emission during K, (T), 19: 41825
electron capture probabilities of, orbital-M, (T), 19: 10328
electron capture ratios, M/L, 20: 40153
electron conversion in, probabilities of E0, 18: 11271
electron elastic and inelastic scattering by 1p- and 2s1d-shell, alpha-particle model for, (T), 20: 8150
electron elastic scattering by, polarization in, 16: 23049
electron elastic scattering by, theory of relativistic Coulomb, 17: 7520
electron elastic scattering by, Green's function and optical potential analysis of, 17: 7187
electron elastic scattering by, radiative tail in, 18: 13110
electron elastic scattering by, radiative tail in, 18: 15320
electron elastic scattering by, relativistic approximation for high-energy, 18: 15285
electron elastic scattering by, magnetic moment effects in, (T), 19: 12532

electron elastic scattering by p-shell, modified oscillator distribution for, (T), 19: 17029
electron elastic scattering by magnetic moments of light, shell model for high-energy, 19: 41694
electron elastic scattering by, monopole excitation in, (T), 19: 43301
electron elastic scattering by, cross sections for, 20: 1156 (JINR-P-2370)
electron elastic scattering at high and low energies, phase shifts for, (T), 20: 2635
electron elastic scattering by, electric and magnetic moment effects in, (T), 20: 4840 (LAL-1140)
electron elastic scattering at high energies, amplitudes for, (T), 20: 24365
electron elastic scattering by, with a Fermi charge distribution, (T), 20: 38139
electron elastic scattering at high energies, phase shifts for, (T), 20: 44675
electron elastic-scattering form factors for d-shell, (T), 20: 42376
electron energy level in field of, wave equations for (T), 19: 1435
electron energy levels of, group theory classification of g^N, 20: 37437
electron inelastic scattering, sum rules for, 16: 11030
electron inelastic scattering, single-particle excitations, 16: 24825
electron inelastic scattering by, partial-wave analysis of, 17: 840
electron inelastic scattering by heavy, pair correlation function in, 17: 24410
electron inelastic scattering from $40 \leq A \leq 200$, cross sections for relativistic, 17: 24454
electron inelastic scattering at high energies, isospin selection rules for, 17: 28326
electron inelastic scattering by, single-particle excitations from, 17: 34949
electron inelastic scattering at high energies, nuclear structure data from, 17: 38261
electron inelastic scattering by, radiative corrections to, 18: 1031
electron inelastic scattering by, with an alpha-particle core and a weakly bound neutron, 18: 6271
electron inelastic scattering at high energies, radiative corrections to, 18: 9422
electron inelastic scattering by, orientation and polarization effects on excitation in, 18: 19039
electron inelastic scattering by, nucleon pair-correlation functions from, 18: 21356
electron inelastic scattering by oriented, differential cross section for polarized, 18: 21181 (JINR-P-1575)
electron inelastic scattering by, partial-wave analysis of, 18: 24669
electron inelastic scattering by, photon distributions from, 19: 1635
electron inelastic scattering by, correlation structure from, (T), 19: 14601
electron inelastic scattering by, analysis of cross section for, 19: 21452
electron inelastic scattering, differential cross sections for, (T), 19: 25502
electron inelastic scattering by, two-nucleon correlations in, (T), 19: 33288
electron inelastic scattering by, radiative corrections to, (T), 19: 41752
electron inelastic scattering by, amplitude for, (T), 20: 3124
electron inelastic scattering by, two-nucleon correlation functions and cross sections for, (T), 20: 6424
electron inelastic scattering by closed shell, (E/T), 20: 8169
electron inelastic scattering by, amplitudes for, (T), 20: 13775 (JINR-P-2490)
electron inelastic scattering by heavy excitation of giant multipole resonances in, (T), 20: 13832
electron inelastic scattering by light, relations between E1 sum rules and form factors for, (T), 20: 15746
electron inelastic scattering by, electron and nucleon angular distributions for giant resonance decay from, (T), 20: 17757
electron inelastic scattering by, two-nucleon correlation functions from cross sections for, (T), 20: 21996 (FTI-142/T-016)
electron inelastic scattering by, two-particle correlation functions from, (T), 20: 24398
electron inelastic scattering by heavy, giant multipole resonances in, (T), 20: 26224
electron inelastic scattering at high energies, 20: 28437
electron inelastic scattering by, parity and spin of energy levels from, 20: 34683
electron inelastic scattering at 1 to 10 Mev, partial wave analysis of, (T), 20: 40150
electron inelastic scattering at high energies, radiative corrections to, 20: 42095
electron inelastic scattering by light, sum rule for, (T), 20: 44636 (INP-479/PL)
electron inelastic scattering by nuclei, review of nuclear structure determination from, 20: 44679
electron inelastic scattering with excitation of collective levels, (T), 20: 46791
electron interactions in Coulomb field, relativistic spherical-wave solutions, 16: 18605
electron interactions in Coulomb field of, equations for, (T), 19: 14244
electron interactions in Coulomb field of, (T), 20: 24462
electron magnetic scattering by, (T), 20: 4831 (HEPL-272)
electron multiple scattering at relativistic energies, (T), 20: 30509
electron noncoherent scattering, 16: 7139
electron pair conversion in, screening effects on coefficient for, 18: 6285
electron pair photoproduction in Coulomb field of, radiative corrections for, 18: 40337
electron polarization in fields of, 16: 32449
electron radial functions and tangents of phase shifts for $1 \leq Z \leq 10$, 20: 22009 (NBS-MON-81)
electron radiative transitions in Coulomb field of, 18: 12830
electron reactions near 1 Bev, meson (μ) pair production in, 16: 18381
electron reactions with alkali halide crystal, double-resonance spectrum for hyperfine F-center, 16: 24317
electron reactions with, in magnetic crystals, 17: 24150
electron reactions with, 17: 28345
electron reactions with, cross sections for meson (π) production in, 17: 32913 (TID-7668(Sect.V))
electron reactions (e,e' p) with, Monte Carlo analysis of experimental conditions, 18: 32732 (ISS-64/8)
electron reactions with, angular correlations in disintegration in, (T), 19: 10306
electron reactions with, first Born approximation including anapole for, (T), 20: 4612
electron reactions with Coulomb field of, cross sections for meson (μ^-) production in, (T), 20: 6089
electron reactions (e,e' p) with, Monte Carlo analysis of, 20: 6286 (ISS-65/10)
electron reactions (e,pe) above 300 Mev, cross sections and structure from, (T), 20: 10082
electron reactions with heavy deformed, dipole-giant resonances from high-energy, (T), 20: 12015
electron reactions with, internal pair production in, (E/T), 20: 15696 (CONF-233(Vol.1), pp 60-86)
electron reactions (e,e'p) with, kinematics of, 20: 26083 (ISS-65/49)
electron reactions (e,e'α), (e,e'n), and (e,e'p) with, 20: 36167 (ISS-66/20)
electron reactions at 300 kev, asymmetry function for external bremsstrahlung from transversely polarized, (E), 20: 41662
electron reactions at 300 kev, bremsstrahlung angular distributions from, (E), 20: 46692
electron scattering, inelastic form factors, 16: 4713
electron scattering, effects of bremsstrahlung and nuclear excitation, 16: 5872
electron scattering at high energies by heavy, phase-shift formulas for, 16: 8172
electron scattering form factors, 16: 12524
electron scattering, symmetrical behavior in transition from particle to antiparticle, 16: 12525
electron scattering at 300 to 1000 Mev, proton emission and angular and energy correlations, 16: 17094
electron scattering by Coulomb field, radiative corrections, 16: 18503
electron scattering, momentum transfer and Pauli correlations in, 16: 21474
electron scattering at high energies, charge density distributions from, 16: 23129
electron scattering, form factors for elastic and inelastic, 16: 24862
electron scattering, effects of charge on bremsstrahlung emission in, 16: 26348
electron scattering, studies of effective charge in, 16: 29748 (AFOSR-TN-3065)
electron scattering, cross sections for excitation of individual-particle states in, 16: 29749 (AFOSR-TN-3066)
electron scattering by Coulomb fields of, wave functions for, 16: 32538
electron scattering by, cross sections for E0 transitions in, 17: 7269
electron scattering at 1 Bev by, shower distributions from, 17: 9225
electron scattering by, partial-wave analysis of, 17: 11710
electron scattering from, review of inelastic, 17: 17638
electron scattering by, elastic and inelastic, 17: 18950
electron scattering at high energies, angular dependence of cross section corrections for relativistic, 17: 22597
electron scattering on $1 \leq Z \leq 83$, charge density distributions from, 17: 34968
electron scattering at high energy, nuclear structure determination by, 17: 36642 (CERN-63-28(p.37-46))
electron scattering by, effects of intranuclear particle interactions on cross sections for, 18: 6272
electron scattering by nonspherical, 18: 9344
electron scattering at 180° by, review of experimental data on, 18: 11211 (LNF-63/47(p.205-13))

electron scattering by Coulomb field of, wave function for Dirac, 18: 15306
electron scattering by, meson (π) contribution to inelastic, 18: 19034
electron scattering at high energies, energy losses in, 18: 21302
electron scattering by Coulomb fields of, double bremsstrahlung in, 18: 24704
electron scattering by, relaxation paths for elastic, 18: 26371
electron scattering by, magnetic moment effects on bremsstrahlung in, 18: 40590
electron scattering by Coulomb field of, inverse bremsstrahlung in, 18: 40592
electron scattering by, modified WKB approximation for phase shifts in (T), 19: 1581
electron scattering by Coulomb field of, relativistic (T), 19: 1582
electron scattering by, cross sections for inelastic (T), 19: 3291
electron scattering by, bremsstrahlung spectra from, (E), 19: 6545
electron scattering by, cross sections for bremsstrahlung emission in, (T), 19: 8183
electron scattering by complex, (T), 19: 8434
electron scattering by, distorted-wave analysis of, (T), 19: 10258(R) (TID-21335(p.151-60))
electron scattering at high energies, distorted-wave approximation for, (T), 19: 12593
electron scattering at 200 Mev by nonspherical, cross sections for, (T), 19: 12519
electron scattering by, magnetic and size effects on bremsstrahlung from, (T), 19: 16990
electron scattering by, cross sections for case of no excitation, (T), 19: 16401
electron scattering by, theory of, 19: 21448
electron scattering by, electron screening effect in, (E), 19: 30961
electron scattering at 180° and relativistic energies, (E), 19: 35392 (LAL-1132)
electron scattering by, meson (π) production in, (T), 19: 39621
electron scattering by, cross sections for, (T), 19: 41510
electron scattering by, polarization effects in, (T), 20: 996 (NP-15204)
electron scattering by, (T), 20: 3152
electron scattering by, differential cross section for trident electron pair production from, (T), 20: 4604
electron scattering by nuclei at high energy, multipole expansion of, (T), 20: 10017
electron scattering by, analysis near 180°, (E), 20: 13089
electron scattering by aligned deformed, amplitudes for high-energy, (T), 20: 22124
electron scattering by, magnetic form factors and nuclear properties from, 20: 24451
electron scattering by, amplitudes for relativistic Coulomb, (T), 20: 26222
electron scattering by, nuclear property determination using, 20: 32405
electron scattering by deformed, at high energies, (T), 20: 34647
electron scattering by, cross sections for inelastic, 20: 44208
electron scattering by, solution of Dirac equation using Green functions, (T), 20: 44847
electron scattering by Coulomb field of, phase shifts in, (T), 19: 10307
electron scattering by, 18: 11210 (LNF-63/47(p.199-204))
electron scattering by stellar, neutrino pair production in, 17: 41708
electron scattering cross sections, 16: 24863
electron scattering by, 16: 13890
electron shell electrostatic potential at, in diatomic molecules, (T), 19: 20836(T)
electron transitions in Coulomb field of, cross sections for radiative, 17: 24413
electron-pair photoproduction in, radiative, (T), 20: 8156
electron-positron pair emission from aligned, 18: 15249
electronic radial functions at nuclear surface and tangents of phase shifts, tables, 16: 4753 (ORNL-3207)
elementary particle scattering by, quantum field theory of, 17: 13485 (JINR-E-1145)
elementary particle reactions with, intermediate structure in energy dependence of cross sections for, 18: 2938
elementary particle reactions with, fragment emission in, 18: 15185 (CERN-64-1(p.123-9))
elementary particle reactions with, to form artificial elements, 18: 22886
elementary particle reactions with, book on, 18: 34956
elementary particle scattering by, relativistic Coulomb Green functions for, (T), 19: 12621
elementary particle scattering by emulsion, optimum multiple, (T), 19: 16858 (UCRL-11535)
elementary particle inelastic scattering at high energy, amplitudes for, (T), 19: 27429 (JINR-P-2037)
elementary particle inelastic scattering by, odd-even angular momentum anomaly in, (T), 19: 31228 (NYO-1807-10)
elementary particle scattering by, polarization-asymmetry in spin-flip inelastic, (T), 20: 3076
elementary particle reactions with, unified theory for, 20: 4837 (JINR-P-2310)
elementary particle reactions in nuclear Coulomb fields of, (T), 20: 15562
elementary particle elastic scattering by, phase-shift analysis for 0- and ½-spin, (T), 20: 17693 (ORNL-TM-1464)
elementary particle coherent reactions at high energies, (T), 20: 26237
elementary particle scattering at 0 to 320 Mev, effect of $^3S_1-^3D_1$ coupling on $^3D_1$ phase shift in, 20: 27969 (UCRL-14885-T)
elementary particle scattering by, coupled equations for rearrangement, 20: 32388
elementary particle reactions with, computer program for angular distributions from, 20: 36180 (USC-136-100)
elementary-particle reactions at low-momentum transfer, coherence properties for, 20: 22145
emission by sun and propagation in interplanetary space, 20: 23849
emission in nuclear reactions, separation energies for double, (T), 20: 28452
emission of light, in nuclear reactions, (E/T), 19: 5141
energies and masses of, for A = 84 to 125, 17: 19298
energies of A = 84 to 125, 17: 19298
energy and flux of solar ejected, with $3 \leq A \leq 18$, 17: 24220
energy distribution following heavy particle emission, 16: 6469
energy distributions of recoil, in nucleon evaporation, (T), 19: 33378
energy gap and effective hamiltonian in finite, 17: 21074
energy gap and pairing energies in spherical, (T), 20: 10024
energy gap at Fermi surface of, 19: 21273
energy gap for soft core potentials of, (T), 19: 39857
energy gap in BCS theory, surface effects on, (T), 20: 46682
energy gap in cubical model for, (T), 19: 12561
energy gap in finite, slab model calculation of, 18: 11262
energy gap in finite, 18: 36649
energy gap in finite systems of, 20: 22112
energy gap in nuclear matter, 18: 9429
energy gaps of finite, (T), 19: 41826
energy level and lifetime measurements by pulsed-beam methods, 16: 21435
energy level and lifetime measurements using r-f deflection methods, 16: 21438
energy level and mass systematics of $1f_{7/2}$-shell, 18: 2872
energy level calculations for, centrifugal nuclear stretching in classical, 18: 38149
energy level calculations for, using soft-core potential, 19: 3335
energy level charge distributions in, from isomer shift in Mössbauer effect, 19: 35456
energy level collective excitations in spherical, structure of, 18: 28737
energy level configurations in, doublets from, 17: 7105 (NP-12330 (p.122-5))
energy-level corrections and transition probabilities in deformed even-even, 17: 22601
energy level Coulomb excitation in deformed, theory of, 18: 24641
energy level deformation vibrations in even-even, effects on E2 branching ratios in, (T), 19: 21384
energy level deformation and transition probabilities, (T), 20: 24384
energy level densities in, effects of spin on, 16: 33853
energy level densities in, measurement by inelastic neutron scattering, 17: 11708
energy level densities of, for interacting Fermi system, 17: 26545
energy level density, 17: 29604
energy level densities in excited, 17: 31393 (CONF-46-6)
energy level density in, high-angular momentum cut-off in, 17: 32999 (CONF-62-7)
energy level densities in excited, expression using Eckart-Bethe potential shape for, 17: 36708
energy level densities of, from superfluidity properties, 17: 38215
energy level density statistical fluctuations in compound, nuclear cross section variations from, 17: 40046
energy level densities of, dependence on spin magnitude, 18: 6257
energy level densities of A = 40 to 70, 18: 26597
energy level density in, energy dependence of, 18: 32826
energy level density in, in single-particle model, 18: 38105
energy level density of, angular momentum dependence of, 18: 40613
energy level density in, odd-even effect in (T), 19: 1601
energy level density in, odd-even effect of pairing correlation in, (T), 19: 21364
energy level density in, odd-even effects in, (T), 19: 23667
energy level densities in Z < 30, (T), 19: 29368
energy level densities of, (T), 19: 29377
energy level densities and thermodynamic functions of deformed even, (T), 19: 33361
energy level densities in light, (T), 19: 33268

energy level density in, statistical analysis of, 19: 41655 (BNL-934)
energy level density of, pairing effects on, (T), 19: 47616
energy level density of, independent particle model for angular-momentum dependence of, (T), 20: 12012
energy level density in, calculation of, 20: 32432
energy level density in, shell structure effects on, 20: 34591
energy level density in, statistical model for, 20: 34668
energy level density in, methods for determining, 20: 38157
energy level determination using deuteron reactions (d,d') and (d,p), review on, 19: 16892
energy level displacement in K = 0 band of odd-odd deformed, effects of scattering on, 17: 7146 (UCRL-9764)
energy level distances in two-body problem, 16: 8238
energy-level distributions in, statistical theory for, 16: 32415
energy level distribution and repulsion effect for eigenvalues of random matrices, (T), 19: 35475
energy level electromagnetic transitions in spherical, effective multipole fields in, (T), 19: 33373
energy level energies in Bopp approximation, (T), 19: 21412
energy level excitation and measurement using resonant scattering of gamma radiation of variable energy, 17: 7229
energy level excitation of deformed, by multiple Coulomb processes, 17: 26483
energy level excitation in, spectroscopic studies of, 20: 1252
energy level excitation in spherical, collective, 20: 6353
energy level excitation of deformed even-even, cross sections for giant resonances in, (T), 20: 8171
energy level excitation modes in, coupling of, (T), 20: 19993
energy level excitation by direct interactions, 20: 21990 (BNL-948, pp 928-1004)
energy level excitation by Coulomb scattering of heavy ions, 20: 21991 (BNL-948, pp 1005-44)
energy level identification in light, by photodisintegration cross sections, 20: 38138
energy level in odd-A deformed, in rare earth region, collective, 20: 15833
energy level interaction effects on shape of giant dipole line in spherical, dipole-quadrupole, (T), 19: 45314
energy-level lifetime measurements using gamma resonance fluorescence, 16: 21442
energy-level lifetimes, from Coulomb-excitation analysis, 16: 21444
energy level lifetime measurements by Doppler attenuation, 18: 11249
energy level lifetimes of, resonance gamma scattering techniques for measuring second, (E), 19: 6643
energy level lifetimes, counter for measuring nanosecond, 19: 15907
energy level lifetimes of, recoil measurements of nanosecond, 20: 42180
energy level mixing in external fields, interference phenomena in, 19: 45270 (JINR-P-2248)
energy level parameters in odd-A 2s-1d shell, (E/T), 20: 34642
energy level properties of, low-background neutron source for determining, (E), 20: 28236 (NP-16039)
energy level spacing, dependence on A and Z, 16: 12555
energy level spacings near A = 50, 16: 13967
energy-level spacings in odd-mass deformed, 17: 2277
energy level spacings in, neutron s-resonance determinations of, 17: 38163
energy level spacing distribution of, formula for, 18: 2957
energy level spacings and spin assignments in, neutron spectroscopic studies of, 19: 31207
energy-level spectra, higher-random-phase approximation for spherical, 16: 26330
energy level spectra for even-even, in the region $16 \leq A \leq 40$, 17: 21072
energy level spectra for complex, 18: 28745
energy level spectra of odd-odd deformed, (T), 19: 29230 (CEA-R-2730)
energy level spectra of, self-consistent perturbation of Hartree-Fock-Bogoliubov equations for rotational, 19: 41685
energy-level spin-orbit splitting in deformed odd-mass, 16: 31083
energy level spins, determination from neutron resonance capture gamma spectra, 16: 14058
energy level splitting in electric and magnetic field interactions with electromagnetic movements, 16: 8210
energy level splitting in odd-odd deformed, 16: 29781 (JINR-P-999)
energy level splitting from electric quadrupole and magnetic dipole interactions in, 17: 31425
energy level structure from electron scattering at 300 to 1000 Mev, 16: 17094
energy level structure for $150 < A < 190$ and $228 \leq A \leq 254$, collective, 18: 34760 (JINR-E-1696)
energy level structure of heavy, determination using nuclear reactions, 20: 1229
energy level structure of, with $29 \leq A \leq 40$ in shell model, (T), 20: 1231
energy level structure of, analysis using gamma angular correlations in nuclear reactions, (E/T), 20: 12150
energy level structure of closed-shell, (T), 20: 12157
energy level structure of deformed even-even, rotational, (T), 20: 12088
energy level structure of even-even, collective, (T), 20: 19950
energy level systematics of even-even, 18: 42757
energy level transitions in light, form factors for strong M1, 18: 24675
energy level transitions in light, form factors for M1, 18: 24676
energy level transitions in, probabilities for M1, 18: 28598
energy level transitions of odd, effects of pairing correlations on E1, 18: 30741(T) (UCRL-Trans-1081)
energy level transitions in deformed and spherical, E1 (E), 19: 1676
energy level transitions in spherical, shell model analysis of branching ratios for (T), 19: 1694
energy level transitions in, angular momentum operator for, (T), 19: 5159
energy level transitions in, effects of Coriolis forces and pair correlations on E1, (T), 19: 5210
energy level transitions in deformed, pairing correlation effects on E1, (T), 19: 14525 (JINR-P-1907)
energy level transitions in, giant resonance, (T), 19: 17018
energy level transitions in odd, probability of E2 and M1, (T), 19: 19127
energy level transitions in heavy, finite size effects on x rays from, (T), 19: 23798
energy level transitions in odd-mass nonaxial, electromagnetic, (T), 19: 27425 (JINR-P-2003)
energy level transition probabilities for even- and odd-A deformed and spherical, E1, 19: 31214 (AD-613472)
energy level transition probabilities for, electromagnetic, (T), 19: 37888
energy level transitions in even-even, E_2–M_1 mixing ratios of, (E), 19: 43361
energy level transition probabilities and relaxation time for, (T), 19: 3244
energy level transitions in, pulse correlation of two cascade quanta for mixed, (T), 20: 4871(T)
energy level transition probabilities in medium and heavy, review of data on E1, 20: 10081
energy level transition probabilities in deformed odd A actinide and rare earth, (E/T), 20: 11951 (AE-205)
energy level transitions in even-even, L subshell ratios of E2, 20: 12035
energy level transition probabilities in even-even, E2, (E), 20: 12083
energy level transitions in even-even, conversion coefficients of E2, (E), 20: 12112
energy level transitions in even, E0, (T), 20: 13746 (AD-626681)
energy level transitions and octupole vibrations in odd-mass rare-earth region, E1, (T), 20: 13820
energy level transitions in deformed, effect of pairing correlations on E-1, (T), 20: 15764
energy level transitions in deformed odd, delayed E1, (T), 20: 15765
energy level transition probabilities in deformed odd, pairing correlations in E1, (T), 20: 15766
energy level transitions in, P violation in, (E/T), 20: 17444(T)
energy level transitions in, effects of atomic hyperfine interactions on, (T), 20: 17686 (JINR-P-2512)
energy level transitions in, energy-weighted sum rule for M1, (T), 20: 17690 (NP-15899)
energy level transitions in, multi-photon, (T), 20: 17401
energy level transition probabilities for even-even, E2, 20: 17730
energy level transitions in odd, probabilities for E2 and M1, (T), 20: 19976
energy level transitions in deformed odd, probabilities for E2 and E3, (T), 20: 19824 (JINR-P-2540)
energy level transitions in, determination of multipolarities from internal pair correlation measurements, 20: 21985 (BNL-948, pp 757-62)
energy level transitions in even, M1, (T), 20: 22085
energy level transitions in, isobaric spin selection rules for, 20: 24333 (BNL-10075)
energy level transitions in spherical, coupling of surface quadrupole vibrations to giant dipole resonance, 20: 24486
energy level transitions in, precision tests of T invariance in, (T), 20: 24439
energy level transition probabilities in deformed odd-mass, (E/T), 20: 24390
energy level transitions in, giant dipole, (T), 20: 26233
energy level transitions in, multipole radiation from, (T), 20: 26234
energy level transitions in deformed, anomalous E1, (T), 20: 26204
energy level transitions in lead region of odd-A, quasiparticle description of multipole, 20: 26116
energy level transitions in odd-mass deformed, effect of Coriolis force on E1, 20: 26145
energy level transitions in aligned, tabulation of angular correlation coefficients for, 20: 28261 (AD-631954)
energy level transitions of, competition between M1 and E2 of, (T), 20: 32374(R) (IITRI-578P25-15)
energy level transitions of even, collective M1, (T), 20: 32420(T)
energy level transition probabilities in single closed shell, (T),

20: 32426
energy level transitions of 1p-shell, single-particle E2, 20: 34581
energy level transitions of, penetration effects in internal conversion for, (T), 20: 36256
energy level transitions in $49 \leq Z \leq 69$, L subshell conversion matrix elements for, (T), 20: 36267
energy level transitions in, particle parameters for L-shell conversion electrons from, 20: 36268
energy level transitions in, particle parameters for L-shell conversion electrons from, 20: 36269
energy level transitions in deformed region, anomalous E2, (T), 20: 36246
energy level transitions in, conversion coefficients for high multipole, 20: 36249
energy level transitions of, particle parameters from pure, 20: 36254
energy level transitions of rare earth; L subshell measurements of retarded dipole, 20: 36261
energy level transitions in even-even, anomalies in internal conversion coefficients of E2, 20: 36232
energy level transitions in Coulomb excitation, angular correlations for E2 and E3, (T), 20: 38032
energy level transitions in deformed odd-mass, E1 $\Delta K = 0$, (T), 20: 38040
energy level transitions in deformed odd-mass, E2 $\Delta K = 1$, (T), 20: 38041
energy level transitions in deformed even-even, E2, (T), 20: 38127
energy level transitions in even-even, EO, (T), 20: 40116
energy level transitions in, statistical method for study of triple cascades, 20: 40160
energy level transitions of, multipolarity in electromagnetic, (E), 20: 42384
energy level transitions in deformed, analysis of giant E1 resonance by rpa in, 16: 26253
energy level wave functions for 1p-shell, in intermediate bond model, 18: 28618
energy level widths in, effects of cluster structure on virtual-resonance, 20: 38013
energy levels and vibrations in even-even, 16: 21494
energy levels and transitions for A = 5 to 257, tables, 16: 26366
energy levels and spins of odd-mass, with small non-axiality, 16: 31092
energy levels and ground state properties of $f_{3/2}$, 17: 24480
energy levels and E2 transitions in spherical, 17: 26487
energy levels and nonaxial rotational wave functions of odd-A, calculational methods for, 18: 2950
energy levels and transitions in, statistical properties of, 18: 11178 (ANL-6797(p.302-21))
energy levels and two-body interactions in, 18: 14823
energy levels and transition probabilities as function of rotation frequency in collective model, 18: 28615
energy levels and equilibrium form of light, 18: 30832
energy levels and vibrational spectra of even-even, 18: 42758
energy levels and transitions in, gamma vibrational, (T), 19: 14597
energy levels and wave functions for spin ½, with $C_{3v} \times C_i$ symmetry, 20: 7092
energy levels and pairing correlations in, band structure of, 20: 19855
energy levels at high excitation energy, data analysis for widths of compound-nucleus, (T), 19: 45343
energy levels densities in, with A near 140, 18: 7683 (NP-13419)
energy levels, effects of angular momentum on stability and energy of excited, 16: 23036
energy levels, energy shifts between, 16: 3682
energy levels for N = 82 to 88, l-forbidden proton M1-transitions of, 17: 13543
energy levels for $184 \leqq A \leqq 192$, 19: 17781(R) (ORNL-3750)
energy levels for $28 < A \leq 40$, shell model calculations for, 20: 6295 (NP-15647)
energy levels from neutron-capture gamma spectroscopy, 20: 36191
energy levels, gross-structure properties of (1d,2s)-shell, 16: 23123
energy levels in alpha-cluster, 0^+, (T), 19: 25548
energy levels in A = 15, positive parity T = ½, 19: 47694
energy levels in A = 16, isospin quintuplet, 20: 30440
energy levels in complex, statistical distributions on, 17: 2451
energy levels in continuum region, calculations using shell model, (T), 20: 46650
energy levels in deformed, three-quasiparticle, 18: 1009 (JINR-P-1338)
energy levels in deformed even-even, rotational bands of two-quasiparticle, 18: 34907
energy levels in deformed, vibration-rotation corrections to, 18: 42647 (PAN-508/VII)
energy levels in deformed even-even, Bohr-Mottelson model for rotational, 19: 17046
energy levels in deformed, rotation vibration, (T), 19: 29285
energy levels in deformed, rotational, (T), 19: 31300
energy levels in even-even, 17: 7655(R) (ANL-6600)
energy levels in even-even, splitting of two-quasiparticle, 17: 9502 (JINR-P-1068)
energy levels in even-even, seniority-zero spin-zero, 18: 44746
energy levels in even-even $142 \leq A \leq 152$, energy systematics from 3^- and 4^+, 20: 12081
energy levels in even, E2 transitions between high-spin rotational, (T), 20: 13801
energy levels in even-even, collective single-particle excitations of, 20: 24461
energy levels in isobaric multiplets, (T), 20: 46705
energy levels in light, calculation by cluster model, 16: 21496
energy levels in medium-weight even, excitation of second 2^+, 16: 23142
energy levels in nonspherical, vibrational, 16: 1085
energy levels in nonspherical, negative parity, 16: 12578
energy levels in Nilsson potential, (T), 20: 30392
energy levels in odd-neutron, between N = 89 to 113, 17: 24053(R) (ORNL-3432)
energy levels in odd-mass, coupling schemes for, (T), 20: 13825
energy levels in spherical, intensity ratios and interval rules for vibrational, (T), 20: 8130
energy levels in, with A = 5 to 240, location of quasistationary single-particle, 17: 40012
energy levels in weakly deformed, coherent effect in, (T), 19: 33354
energy levels in 1p shell with abnormal parity, wave functions for (T), 19: 3334
energy levels in 1p-shell, Coulomb energy differences in, (T), 20: 28410
energy levels in, properties of high-spin rotational, 18: 15288
energy levels in, with specified angular momentum and pairing correlations, 18: 34930
energy levels in, particle-hole wave equations for, 18: 42699
energy levels in, five-dimensional quasispin for pairing hamiltonian in J-T scheme of, 19: 41687
energy levels in, gamma resonance absorption analysis of, 19: 43336
energy levels in, four-body operator for classification of, (T), 19: 47678
energy levels in, eigenstates of pairing hamiltonian for single-particle, 20: 12051
energy levels in, microscopic models for vibrational, (T), 20: 15851
energy levels in, excitation of alpha-cluster, (T), 20: 17802
energy levels in, pairing vibrations of, (T), 20: 22075
energy levels in, quadrupole-quadrupole interaction of $(1^1/_2)^n$, 20: 26155
energy levels, measurement of lifetimes of 10^{-10} to 10^{-15} sec, 16: 21441
energy levels, method of solving Schroedinger equation having smoothly varying potential for, 16: 29745
energy levels near threshold, shell model calculations, 16: 12485
energy levels of, (T), 20: 30350 (JINR-P-2682)
energy levels of A = 12, in shell model with LS coupling, 18: 26624
energy levels of A = 40 to 50, systematics of 3- and 5-, (E), 20: 38100
energy levels of A = 37, T = ½ multiplet, (E), 20: 44659 (UCRL-16990)
energy levels of A = 24, T = 2, (E), 20: 44758
energy levels of A = 16, T = 2, (T), 20: 46688
energy levels of A = 15 and 17, T = ½, (T), 20: 46688
energy levels of A = 40, particle-hole, (T), 20: 46777
energy levels of, binding energy of ground-state, 17: 26524
energy levels of closed-shell, 17: 7088 (NP-12330(p.1-14))
energy levels of, correlations in decay of, 17: 9524
energy levels of, capture gamma detection of resonance, 18: 9310 (IA-863)
energy levels of complex, statistical higher-order spacing distributions for hamiltonian unitary ensembles of, 18: 24679
energy levels of closed-shell, collective, (T), 19: 21415
energy levels of deformed, conversion process of, 17: 9568
energy levels of deformed even, perturbation corrections to, 17: 11665
energy levels of, double internal conversion transitions of, 17: 13548
energy levels of, drop model of ground-state, 17: 22569(T) (AEC-tr-5783)
energy levels of, density and phase transitions of excited, 17: 24505
energy levels of, determination of reduced neutron widths of, 17: 33066
energy levels of deformed, collective motion in rotational, 18: 15307
energy levels of deformed even-even, energies of quadrupole, 18: 18870 (JINR-E-1534)
energy levels of deformed even-even, two-quasiparticle, 18: 21178 (JINR-P-1568)
energy levels of deformed, multiple Coulomb excitation of, 18: 24728
energy levels of deformed, with $164 \leq A < 190$, 18: 28568 (JINR-E-1621)
energy levels of deformed odd-even, properties of vibrational, 18: 28611
energy levels of deformed, rotation and vibration, (T), 19: 12603
energy levels of deformed odd-mass, (T), 19: 14575
energy levels of deformed even-even, 2^+, (T), 19: 16878
energy levels of deformed even-even, octupole, (T), 19: 16889
energy levels of deformed even-even, with A = 164 to 190, (T), 19: 16890
energy levels of deformed, cranking model and perturbation calculation for rotational, (T), 19: 21349
energy levels of deformed odd-odd, doublet $K^\pm$, (T), 19: 21370
energy levels of deformed, corrections to cranking model for, 19: 23741
energy levels of deformed odd-A, coupling between rotation and single-particle, (T), 19: 27491

energy levels of deformed even-even, collective nonrotational, (T), 19: 29244 (JINR-P-1973)
energy levels of deformed odd-mass, collective nonrotational, (T), 19: 29248 (JINR-P-2045)
energy levels of deformed, interactions of rotational and vibrational, (T), 19: 37876(T)
energy levels of deformed even-even, review on non-rotational collective, 20: 1165
energy levels of deformed even-even, symmetry rules for, (E/T), 20: 4476(R) (IS-1200(Sect.P))
energy levels of deformed, cranking model for higher rotational, (T), 20: 6416
energy levels of deformed ($176 \leq A \leq 190$), collective, (T), 20: 21998 (JINR-E-2579)
energy levels of deformed even-even, rotation-vibration interaction in, (T), 20: 38156
energy levels of deformed, M1 transitions of rotational, (E), 20: 40072 (LA-DC-8061)
energy levels of deformed odd-A, with $229 \leq A \leq 255$, collective, (T), 20: 42154 (JINR-E-2857)
energy levels of deformed even-even octupole vibrational, (T), 20: 44825
energy levels of deformed even-even, rotational, (T), 20: 44843
energy levels of deformed, (T), 20: 46686
energy levels of deformed, with rotation-vibration interaction, (T), 20: 46766
energy levels of even, model for odd-parity states in, 16: 28077
energy levels of even-even, model for collective vibrational, 16: 33873
energy levels of even, for neutron numbers 82, 84, 86, and 88, 17: 9547
energy levels of excited, projection theorem for, 17: 21036
energy levels of even-even, reduced probability for E2 transitions in rotational, 17: 24419
energy levels of even deformed, beta vibration effects on collective, 17: 31405 (INSJ-58)
energy levels of, excitation of octupole, by proton scattering, 17: 34926
energy levels of even-even, 5^-, 17: 39996
energy levels of, external field effects on electromagnetic transition angular correlations in, 17: 41650
energy levels of, electric monopole transitions between, 18: 6252
energy levels of even deformed, 18: 9345
energy levels of even-even, multiple Coulomb excitation of rotational, 18: 21177 (JINR-P-1563)
energy levels of even-even, 18: 21303
energy levels of even-even, interpretation of 5^-, 18: 26579
energy levels of even-even, vibrational, 18: 34933
energy levels of even-even deformed, electromagnetic transitions of collective, 18: 34761 (JINR-E-1703)
energy levels of even-even, measurement of lifetimes of first-excited, 18: 34772 (NP-14184)
energy levels of even-A, for $A = 184$ to 192, 18: 42674
energy levels of even-even, in alpha-particle model, 19: 1619
energy levels of even-even spherical, properties of excited (E), 19: 1674
energy levels of even-even spheroidal, vibrational, (T), 19: 17049
energy levels of even-even, beta transitions to 5^-, (E), 19: 19122
energy levels of even-even, negative parity, (T), 20: 10096
energy levels of even-even spherical, second-vibrational, (T), 20: 13793
energy levels of even-even, pair-correlation model for, 20: 19966
energy levels of even-even, E1 transitions from octupole, (T), 20: 19979
energy levels of even-even deformed, high-spin rotational, (E/T), 20: 19953
energy levels of even-even, alpha-cluster wave function for ground state, 20: 22093
energy levels of even, g_s factors for, (T), 20: 22085
energy levels of even-even, E2 transitions from 3^+, (E/T), 20: 30372
energy levels of even-even for $228 \leq A \leq 254$, octupole, (T), 20: 34524 (JINR-P-2712)
energy levels of equivalent $j = 9/2$ nuclear configurations, classification using group theory, 20: 40082
energy levels of even-even, with $228 \leq A \leq 254$, octupole, (T), 20: 44751
energy levels of even-even, (T), 20: 44788
energy levels of even-even spherical, vibrational, (T), 20: 44797
energy levels of $f_{7/2}$, with four nucleons outside closed shell, configuration-mixing calculation of, 18: 19030
energy levels of f7/2-shell regions, (E/T), 19: 36220(R) (MIT-2098-142)
energy levels of, hole-particle interactions in collective, 17: 7192
energy levels of heavy even, properties of first-excited 2^+, 17: 15289
energy levels of heavy, with unlike pair excitations, 18: 30826
energy levels of heavy, statistical theory of, 19: 17027
energy levels of heavy, quadrupole giant resonance, (T), 19: 33363
energy levels of heavy, isospin for, (T), 19: 43382
energy levels of heavy, rotational, (T), 19: 45285 (UCRL-16040)
energy levels of hard-core, with neutron excess, (T), 20: 28290
energy levels of heavy, (γ,n) reactions for studying, 20: 44631 (CONF-660303, pp 1064-72)
energy levels of interference phenomena in quantum transitions of, 18: 6251
energy levels of light, 17: 881
energy levels of light, with constant neutron excess, relations with nuclidic masses, 17: 19216 (IS-494)
energy levels of light, 17: 22264(R) (ANL-6679)
energy levels of light, models for collective rotational and vibrational, (T), 19: 14518 (CONF-640301(p.143-64))
energy levels of light, collective and shell models for low-lying, (T), 19: 14519 (CONF-640301(p.165-81))
energy levels of light, mixed symmetry state contribution in, (T), 19: 29305
energy levels of light, collective model for vibrational, 19: 43364
energy levels of light, collective, (T), 20: 1227
energy levels of light, form factors for 1^-, $T = 1$, 20: 8065 (INP-426/PL)
energy levels of light, shell effects in Coulomb displacement energies of, (T), 20: 11963 (INSJ-91)
energy levels of light, hamiltonian reduction for lowest, 20: 24381
energy levels of light, tensor and vector Coulomb energies of, 20: 32499
energy levels of light even-even, systematics of 0^+, (T), 20: 32522
energy levels of light, Brueckner-Bethe-Goldstone theory for, 20: 34648
energy levels of, mathematical techniques in calculation of, 17: 4108
energy levels of, model for resonance, 17: 33001 (CONF-128-1)
energy levels of, method for spin determination for, 17: 38013(T) (AEC-tr-5734(p.71))
energy levels of mixtures of two types of, (E/T), 19: 5198
energy levels of medium-weight, 0^+, (T), 20: 44647 (NIJS-R-484)
energy levels of non-spherical, analysis of vibrational, 16: 23098
energy levels of neutron-deficient odd-man, 17: 847
energy levels of nonspherical, independent-particle model for, 17: 34969
energy levels of nonspherical, vibrational, 17: 40044
energy levels of nonspherical odd, electromagnetic transition probabilities and rotational and single-particle excitations in, 17: 40119
energy levels of nonspherical odd-mass, summary of models for, 17: 40005
energy levels of nonspherical, 18: 43151 (ISS-63/50)
energy levels of nonspherical, low-lying, (T), 20: 8091
energy levels of neutron deficient, for $39 \leq Z \leq 49$, 20: 15727 (PPAD-572F)
energy levels of $N = 82$, surface delta interaction for, 20: 26169
energy levels of nonspherical, microscopic description of collective, 17: 2326
energy levels of odd-A, study by Coulomb excitation, 16: 26230 (TID-16058)
energy levels of odd-mass, conversion properties of M1 transitions of, 17: 13559
energy levels of odd-odd, 17: 34887 (UCRL-10865)
energy levels of odd-A, f7/2-particle vibrations and, 18: 17075
energy levels of odd-odd, 18: 21180 (JINR-P-1574)
energy levels of odd, with small nonaxiality, 18: 21231
energy levels of odd, BCS determination of ground-state, 18: 24631
energy levels of odd-mass, three-particle isomeric, 18: 28614
energy levels of odd-odd heavy, analysis of nondiagonal matrix elements for, 18: 28616
energy levels of odd-mass, interpretation of spin-½, as asymmetric rotors, 18: 30714 (BLG-223)
energy levels of odd-mass, multiple Coulomb excitation probabilities for rotational, 18: 42710
energy levels of odd-mass, vibrational, (T), 19: 23696
energy levels of odd-A spherical, (T), 19: 37875(T)
energy levels of odd-odd deformed, neutron-proton residual interaction for, (T), 20: 8115
energy levels of odd-odd light deformed, unified model wave functions for low-lying rotational, (T), 20: 15814
energy levels of odd, transverse spin polarization effects on, (T), 20: 17682 (INP-428/PL)
energy levels of odd deformed for $153 \leq A \leq 187$, structure of, (T), 20: 19821 (JINR-E-2561)
energy levels of odd-odd deformed, phonon-quasiparticle interactions in, (T), 20: 28419
energy levels of odd-odd deformed, phonon-quasiparticle interactions in, 20: 28605 (JINR-P-2622)
energy levels of odd-mass deformed, transverse spin polarization effects on, (T), 20: 32447
energy levels of odd, energy ratios and spins of, (T), 20: 38022
energy levels of odd-A rare-earth, vibrational, (T), 20: 40118
energy levels of odd-A spherical, calculations using phonon-quasi-particle coupling theory, 20: 46670
energy levels of odd-even $1f_{7/2}$-shell, negative-parity, (T), 20: 46739
energy levels of octupole band, rotational, (E), 20: 46773
energy levels of, probabilities for isomeric, 17: 28343
energy levels of, relations of, with band structure and mass number,

16: 29761 (JAERI-1020(p.66-74))
energy levels of, resonant scattering of gamma rays by, 17: 13560
energy levels of, random-phase approximation accuracy for, 17: 36662 (TID-17785)
energy levels of rotational, analysis of low-lying, (T), 20: 19273(R) (BNL-929, pp 3-43)
energy levels of spin ½ odd, asymmetric-rotor theory for, 16: 5988
energy levels of spherical, model for, 16: 33872
energy levels of, shell model calculations of, 17: 4109
energy levels of, statistical theory for, 17: 38011(T) (AEC-tr-5734 (p.62-8))
energy levels of, slow-neutron-excited, 17: 38012(T) (AEC-tr-5734 (p.69-70))
energy levels of, single-particle states in (1f,2p), 17: 38172
energy levels of strongly deformed, accuracy of superconductivity model in calculating properties of, 17: 40009
energy levels of, statistical model for partial radiation widths of, 17: 41536(R) (ANL-6767)
energy levels of, statistical fluctuations in, 18: 6209
energy levels of spin-2, -3 and -4, quadrupole, 18: 15212(T) (JPRS-23436(p.151-64))
energy levels of spherical odd-odd, theoretical, 18: 32745(R) (UCRL-11213(p.1-48))
energy levels of spherical, 18: 32748 (UCRL-11373)
energy levels of sd-shell, in shell model, 18: 38111
energy levels of spherical even, anharmonic effects on collective oscillations in, (T), 19: 17005
energy levels of spherical, structure of 3^-, (T), 19: 35504
energy levels of spherical, variational calculation of collective, (T), 19: 41702
energy levels of s-d shell, parity and spin determinations for, 20: 1230
energy levels of spherical, two-phonon quadrupole-octupole energy levels of, 20: 28358
energy levels of spherical odd-odd, spin rules for multiplet, (T), 20: 42289
energy levels of spherical odd-mass, wave functions for collective properties of low-lying, 20: 44742
energy levels of spherical, quadrupole moments of, (T), 20: 44812
energy levels of, theory of, 17: 4113
energy levels of three-nucleon, matrix elements of three velocity-dependent operators for arbitrary, 20: 17746
energy levels of two-dimensional, in shell model, 20: 19854
energy levels of transition-region, generator coordinate method for matrix elements and wave functions for, 20: 22081
energy levels of vibrational, static quadrupole moment of 2^+, (T), 20: 46720
energy levels of weakly deformed, in first-order perturbation theory, 19: 45257 (IAE-811)
energy levels of $Z \geq 20$, shell description of, 18: 21275
energy levels of 1p-shell, use of Hamada-Johnston potential for, (T), 20: 22102
energy levels of $16 \leq Z \leq 20$, shell-model calculations of odd-parity, 20: 30407
energy levels of $2 \leq A \leq 27$, spin prediction rules for ground-state, 18: 7755
energy levels of $28 < A \leq 40$, 18: 36697
energy levels of 2s1d-shell, (E), 19: 5130 (KFKI-15/1963)
energy levels of $5 \leq A \leq 10$, 20: 12023
energy levels of $6 \leq A \leq 9$, intermediate coupling shell-model calculations for, 20: 32436
energy levels of, use of nuclear models in studying low-lying, 18: 11160 (ANL-6797(p.58-78))
energy levels of, effect of electromagnetic fields on, 18: 11198 (JINR-P-1222)
energy levels of, intermediate-coupling wave functions for, 18: 11246
energy levels of, perturbation of resonance, 18: 16997
energy levels of, excitation and study of collective, 18: 17020
energy levels of, quasi-particle approximation for spurious, 18: 17082
energy levels of, pairing hamiltonian for, 18: 19094
energy levels of, rotational motion in, 18: 19093
energy levels of, approximations for, 18: 21216
energy levels of, lifetimes of, 18: 30865
energy levels of, methods for calculating densities of, 18: 24596 (NP-13930(p.14))
energy levels of, moments and spins for, 18: 30864
energy levels of, shell-model calculations of isobaric analog, 18: 28635
energy levels of, statistics of intervals and widths of, 18: 24598 (NP-13930(p.17-25))
energy levels of, symmetrization in Coulomb excitation of, 18: 24731
energy levels of, lifetimes of, 18: 32776
energy levels of, potential shape dependence of lower, 18: 34906
energy levels of, approximations for low, 18: 34959
energy levels of, particle fluctuations in pairing wave functions for, 18: 34839
energy levels of, energy gap in rotational, 18: 38145
energy levels of, measurement of lifetimes of nanosecond, 18: 38070 (NP-14171)
energy levels of, inelastic excitation of collective, 18: 40651
energy levels of, neutron single-particle effects on, 18: 40512 (NP-14239)
energy levels of, perturbative calculation of one-quasiparticle, 18: 42640 (KFKI-1467/r)
energy levels of, from bounded isotropic harmonic oscillator potential, 18: 42656
energy levels of, asymptotic densities in statistical ensembles for, 18: 42728
energy levels of, with small asymmetry (T), 19: 1604
energy levels of, analysis by angular correlations, (E/T), 19: 5191
energy levels of, description of collective, (T), 19: 6635 (JINR-P-1830)
energy levels of, shell model using Talmi transformation for, 19: 10130
energy levels of, giant dipole resonance damping in, (T), 19: 10366
energy levels of, beam-pulsing method for lifetimes of metastable, 19: 12512
energy levels of, Fermi system description of, 19: 17015
energy levels of, computer program for shell model calculations of bound, 19: 19082 (CRT-1213)
energy levels of, electromagnetic moments of excited, 19: 19105
energy levels of, isospin structure of low lying collective octupole vibrations in, (T), 19: 21351
energy levels of, lifetime measurements on short-lived, 19: 21369
energy levels of, pairing hamiltonian for seniority-zero excited, (T), 19: 21385
energy levels of, analysis using triple correlations in (p,γγ) reactions, (E), 19: 23628 (NRL-6186)
energy levels of, collective excitation of, (T), 19: 23771
energy levels of, deformed, rotational, 19: 23774
energy levels of, axially symmetric regions in s-d shell, (T), 19: 27547
energy levels of, collective model for negative parity, 19: 27535
energy levels of, isobaric analog, 19: 29250 (KFK-296)
energy levels of, single-particle, (T), 19: 29353
energy levels of, classification by quasi-spin in LS coupling, (T), 19: 29280
energy levels of, collective modes for ground-state, (T), 19: 33324
energy levels of, matrix elements for configuration mixing in, (T), 19: 34881
energy levels of, odd-mass deformed, collective nonrotational, (T), 19: 35464
energy levels of, asymptotic reduced-width amplitude distributions for, 19: 35415
energy levels of, computer program for analysis of resonance, 19: 37902
energy levels of, effects of temperature on, (T), 19: 40112(R) (ANL-7046(p.36-66))
energy levels of, analysis of spurious states owing to center-of-mass motion, (T), 19: 39812
energy levels of, excitation energies of isobaric-analog, (T), 19: 43314
energy levels of, many-particle Green function theory for composition of giant-dipole, 19: 45334
energy levels of, effective interactions for 1p, (T), 19: 43307
energy levels of, capture gamma detection of, (E), 20: 2520(R) (IA-920)
energy levels of, random phase approximation for ground-state, (T), 20: 3085
energy levels of, measurement of lifetimes of excited, (T), 20: 4917
energy levels of, self-consistent theory of bounded rotational, 20: 6344
energy levels of, parity and spin assignment by Coulomb excitation, (T), 20: 8082 (ORNL-P-1793)
energy levels of, isobaric splitting of dipole, (T), 20: 8125
energy levels of, giant resonance location in, (T), 20: 8170
energy levels of, electromagnetic properties of excited, (E), 20: 9978(R) (TID-22462)
energy levels of, review of collective vibrations in, (T), 20: 10079
energy levels of, method for measuring widths of 2^+, 20: 12147
energy levels of, Tamm-Dancoff method for collective, (T), 20: 11966 (JINR-P-2432)
energy levels of, nucleon pairing correlations in $L = 0$, (T), 20: 12131
energy levels of, one- and two-phonon, (T), 20: 12123
energy levels of, parity and spin assignment by DWBA method, 20: 15726 (ORNL-P-1957)
energy levels of, unified derivation of cranking model and Peierls-Yoccoz method for rotational, (T), 20: 15828
energy levels of, statistics of random-matrix eigenvalues for, (T), 20: 15784
energy levels of, lifetimes of, (E), 20: 17676 (CEA-R-2810)
energy levels of, model for collective vibrations of, 20: 17711
energy levels of, structure from isomeric transitions in, (T), 20: 19970
energy levels of, parity mixing in, (E), 20: 19836 (SGAE-PH-36/1965)
energy levels of, g-factor and lifetime determination of excited, (E),

20: 19846
energy levels of, measurement of widths of, 20: 19948
energy levels of, spin assignment using gamma-particle correlations, 20: 21983 (BNL-948, pp 741-50)
energy levels of, spin assignment using gamma-gamma correlations, 20: 21984 (BNL-948, pp 751-6)
energy levels of, quasiparticle random-phase approximation for, 20: 22147
energy levels of, equilibrium deformations in excited, (T), 20: 22005 (JINR-P-2596)
energy levels of, gamma correlation methods determining magnetic dipole moment of, 20: 22025
energy levels of, parity mixing in single-nucleon, 20: 22080
energy levels of, g-factor measurements for excited, (E/T), 20: 24358(R) (UCRL-16580, pp 1-93)
energy levels of, spherical, giant resonances in, (T), 20: 26225
energy levels of, tables of reduced matrix elements for shell-theory analysis of, 20: 26134
energy levels of, pairing correlations in rotational, (T), 20: 28364
energy levels of, quadrupole motion in, (T), 20: 28289 (UCRL-16768)
energy levels of, theory for, (T), 20: 28289 (UCRL-16768)
energy levels of, determination from delayed proton emission following beta decay, 20: 28269 (BNL-10196)
energy levels of, BCS wave functions for, 20: 28411
energy levels of, configuration mixing effects on, (T), 20: 28416
energy levels of, effects of collective vibrational motion on anomalous coupling $\frac{1}{2}^+$ and $\frac{3}{2}^+$, 20: 28420
energy levels of, giant resonance, (T), 20: 28439
energy levels of, single-particle description of giant E1 resonance, (T), 20: 28385
energy levels of, random-phase approximation for particle-hole, (T), 20: 30398
energy levels of, rotational, (T), 20: 32492
energy levels of, projection operator for studying isospin of, 20: 32533
energy levels of, spin assignment from triple correlations from, (T), 20: 32372 (COO-1120-43)
energy levels of, macroscopic and microscopic descriptions of dipole, 20: 32448
energy levels of, Heisenberg uncertainty principle for determining, (T), 20: 31910
energy levels of, use of neutron resonance parameters for determining, 20: 34662
energy levels of, Wood-Saxon potentials for, 20: 36182 (ZFK-TPH-19)
energy levels of, g factor measurement by resonant scattering, (T), 20: 38079
energy levels of, $f_{7/2}$, (E), 20: 42166(R) (MIT-2098-251, pp 37-49)
energy levels of, density of, (T), 20: 42222
energy levels of, lifetime measurements using gamma Doppler shift, (T), 20: 44724
energy levels of, isobaric analogue, (T), 20: 44777
energy levels of, description of rotational, (T), 20: 44810
energy levels of, Coulomb damping of isobaric analogue resonances, (T), 20: 46662
energy levels of, spin determination for isobaric analogue resonances using proton elastic scattering, (T), 20: 46663
energy levels of, effects of ground-state correlations on particle-hole, (T), 20: 46715
energy levels of, isobaric analogue, (T), 20: 46637
energy levels populated by Coulomb excitation in, angular distribution of gamma rays from, 18: 34965
energy levels, statistical theory of complex, 16: 12473
energy levels, statistical theory of complex, 16: 12474
energy levels, statistical theory of complex, 16: 12475
energy levels with high angular momenta in single-particle model for, (T), 19: 27546
energy levels with hard core interaction with neutron excess, ground-state, (T), 20: 3079
energy levels, calculation using Green's functions, 19: 9771(R) (PR-P-63)
energy levels, gamma absorption and stimulated emission from, 18: 42359 (AD-600270)
energy levels, Nilsson model for, (T), 19: 12524
energy of ground state in, supermultiplet model for, 17: 41931
energy of large, correction by Brueckner's theory, 17: 21020
energy of nuclear matter in ground state, 18: 16960
energy of stable and radioactive, spatial representation, 16: 12521
energy of, nucleon shell effects on, 20: 26215
energy of, shell effects on, (T), 20: 9965 (IAE-878)
energy shifts of giant resonances in, effects of E1 overtones on, 16: 33906
energy spectra and flux of low-energy heavy, of cosmic radiation, (E), 20: 44458
energy spectra for high excitation of even-even, 16: 10957 (JINR-P-826)
energy spectra from solar flares, 20: 5969
energy spectra of $Z \geq 6$, in primary cosmic radiation, (E), 20: 7770
energy spectrum of $Z \geq 6$, in cosmic radiation, (E), 19: 4867
energy splittings of spin-orbit doublets in, 16: 33884
energy states of deformed, large-spin rotational, (E/T), 20: 3008 (COO-1420-104)
energy width variations near threshold, cluster model interpretation, 16: 21543
energy-level densities in, effects of pairing correlations on, 18: 19018
energy-level densities in, effects of shell structure on, 20: 22070
energy-level lifetimes, B (E2) values and deformation parameters for $60 \leq Z \leq 68$ even-even rotational, 20: 12082
energy-level lifetimes from delayed-coincidence measurements, computer program for calculation of, 20: 46584 (INP-472/PL)
energy-level lifetimes of, measurement of nanosecond, (E), 20: 46607 (ZFK-PHA-19)
energy-level spacing distributions in, 18: 26587
energy-level spectra of, statistical theory of, 18: 26588
energy-level spectra of deformed, Hartree-Fock approximation for rotational, (T), 19: 45364
energy-level spectra of odd-odd spherical, low-lying, (T), 19: 47658
energy-level structure with $N = 29$ and $22 \leq Z \leq 26$, calculations using shell model with configuration mixing, (T), 20: 42201
energy-level transitions in, measurement techniques for, (E), 20: 42381
energy-level transitions in $A = 15$, mixing ratios of, mirror, (T), 20: 44783
energy-level transitions in even-even spherical, octupole and quadrupole, 20: 44799
energy-level transitions in BCS theory, matrix elements for, 20: 46654
energy-level transitions in deformed, L conversion intensity ratios in E2, (E), 20: 46673
energy-level transitions in deformed, gamma angular distributions from, (T), 20: 46721
energy-level transitions in, nuclear parameters from angular correlations in E0, (T), 20: 46770
energy-level transitions in deformed odd-A, E2 and E3, (T), 20: 46779
energy-level transitions with conversion of two shell electrons, two-quantum, (T), 20: 46781
energy-level transitions in odd-A deformed $59 \leq Z \leq 80$, effects of pairing correlations on E1, (T), 20: 46608 (ZFK-PHA-21)
energy-level widths of compound nuclei in continuum energy region, (T), 20: 46690
entropy of spin ½ system of, in magnetic fields, 19: 41713
equilibrium figures and fission of rotating, 17: 7298
equilibrium shapes in nonspherical rectangular-well models, 16: 18530
equilibrium shapes of, in quasistatic fission model, 16: 26358
equilibrium shapes of, in liquid-drop model, 16: 33863
even-even, behavior of, in the vibrational region, 16: 29766 (JAERI-1020(p.123-8))
even-even, collective vibration of spherical, 16: 29764 (JAERI-1020 (p.97-113))
even-even, models for excited states in the region of neutron number 82 for, 16: 29759 (JAERI-1020(p.50-4))
even-even, relative phase of E2 and M1 transitions between 1st and 2nd 2^+ states of, 16: 29765 (JAERI-1020(p.114-22))
even-even spherical, analysis of vibrational states of, 16: 29758 (JAERI-1020(p.38-49))
even-even spheroidal, summary of recent data on, 16: 29760 (JAERI-1020(p.55-65))
even-parity-alpha decay of nonaxial, 17: 31546
excitated states of odd-odd, with small nonaxiality, 17: 9596
excitation and formation energies of, (T), 19: 23651
excitation by Coulomb scattering, (T), 20: 46589 (NP-16185)
excitation by electromagnetic and nuclear fields of slow particles, (T), 19: 14610
excitation by heavy ions, third order reorientation effect in Coulomb, 17: 20990 (TID-18506)
excitation by low-energy electrons, test of Robl theory of, 19: 21455
excitation by slow charged particles, cross section for, 17: 17267
excitation frequencies in, dispersion equation for collective, 17: 40044
excitation in deformed, β-vibration effects on multiple Coulomb, (T), 19: 10341
excitation in even, double Coulomb, 17: 24448
excitation level packing near the thresholds of light, 17: 17099
excitation of, dispersion formulas for, 17: 34906
excitation of even-even, intrinsic, 17: 13577
excitation of even-even, with single closed shells, (E), 20: 46695
excitation of strongly deformed, effect of surface gamma vibrations on dipole, (T), 19: 33360
excitation of 2^+ levels in even-even, interference effects in Coulomb, (T), 20: 15768
excitation of, review of Coulomb, 18: 18887 (ZFK-PHA-11)
excitation probabilities of rotational band in even-even, Coulomb, (T), 19: 23664

excitations and vibrations in closed-shell, 17: 24177
excitations, collective-model wave functions for, 16: 28356
excitations in scattering fast particles, collective, 17: 7184
excitations in, spurious states in collective, 16: 28116
excitations of p-shell, dipole, 18: 36637
excitations of, properties of collective dipole, 17: 15292
excitations of spherical, Fermi-liquid theory and Green-function method for collective, 20: 6425
excitations of, Fermi-liquid model for collective, 18: 26612
excited and ground states of strongly deformed, analysis of, 16: 28028 (JINR-E-918)
excited state lifetimes, Doppler shift method for measurement of, 19: 9771(R) (PR-P-63)
excited states of, measurements using pulsed beam accelerator and coincidence methods, 17: 6450
excited states of, review, 17: 17638
excited states of, mass effects on, 17: 31406 (IS-695)
excited states of, uv-transformation method for, 18: 6268
excited states of even-even, solution for first 0+, 19: 1053(R) (PR-P-62)
existence of isomeric, with quantized vortices in superfluid model, (T), 20: 40106(T)
E1 transitions in, for $A \geq 16$, 17: 2263
E2-M1 mixing ratio in $2^+ \rightarrow 2^+$ transition, 17: 36398 (NP-13020(p.80-4))
Fermi gas coefficients and nuclear temperatures of $56 \leq A \leq 238$, 17: 38207
fermion elastic scattering by, models for, 17: 17186
fermion scattering by, matrix elements for polarized, 18: 42705
field interactions, iteration method for neutral scalar, 16: 24847
fields acting on, in solids, 17: 13480 (AFOSR-2929)
fission at high energies, fragmentation in, 18: 26608
fission barriers and particle binding energies of, liquid-drop model for, 20: 24402
fission barriers and half lives of trans-radium elements ($224 \leq A \leq 276$), spontaneous, (T), 20: 28357
fission barriers in rotating, 16: 23155
fission fragment asymmetry, 16: 12572
fission half lives of, superfluid model for spontaneous, (T), 20: 4876
fission of, angular anisotropy of, 17: 19392
fission of axisymmetric, drop model for, (T), 19: 6698
fission of even-even complex, channel effect in, (E), 19: 8411
fission of even-even, channel analysis of neutron-induced, (E), 19: 19095 (WASH-1053)
fission of even-even compound, coupling effects in, (T), 19: 37839(T) (ANL-Trans-195)
fission of, gamma and neutron emission in, 17: 19393
fission of heavy compound, ternary, 17: 28257 (UCRL-10772)
fission of heavy, cross section for Coulomb, 17: 41875
fission of heavy even-even, systematics of spontaneous, 18: 40604
fission of heavy, models and theories for binary, 18: 21186 (KR-64 (Sect.II))
fission of heavy, prompt neutron emission in, (T), 19: 19129
fission of heavy, review of chemical studies of low-energy, 19: 20033
fission of heavy, review of chemical studies on low-energy, 20: 12920
fission of heavy, analysis using mica sandwiches, 20: 13099
fission of, neutron spectrometric studies of, 17: 19399
fission of odd-even and even-odd, probabilities of spontaneous, (E), 20: 34533
fission of oriented, (E/T), 19: 37205(R) (ORNL-3778)
fission of, review of spontaneous, 17: 19396
fission of, statistical theory of, 17: 19388
fission of $Z \geq 98$, spontaneous, 17: 5326 (UCRL-10474)
fission of, analysis using nuclear emulsions, 18: 23958
fission of, close-packed-spheron theory for, (T), 20: 4918
fission of, corrections to calculation of fission-fragment yields in, (T), 20: 44819
fission of, effects of transition states on, (T), 19: 14526 (LA-DC-6670)
fission of, energy release in low-energy, (E/T), 19: 21224 (AECL-2160)
fission of, liquid-drop model with shell effects for energy and mass spectra from, (T), 20: 6308(T) (ANL-Trans-243)
fission of, moment of inertia at, (T), 19: 37894
fission of, neutron distributions from, 18: 21197 (KR-64(Sect.XVIII))
fission of, neutron emission from, (T), 20: 6313
fission of, pair correlation effect on parameters for, (T), 20: 4876
fission of, pairing effects on angular distributions of fragments from, (T), 20: 26203
fission of, primary charge distribution in low-energy, (T), 20: 22013(T) (ANL-Trans-296)
fission of, quasimolecular-state mechanism for, (T), 19: 37796 (NP-15230)
fission of, review of processes in, 19: 33270
fission of, saddle-point shape in, (T), 20: 10072
fission of, spontaneous, 19: 45271 (JINR-P-2265)
fission of, theory of asymmetric, 19: 3245
fission of, theory using Markov process, 20: 12116
fission of, theory using single-particle model, 20: 42272
fission product symmetry for heavy and light, 16: 5925 (JINR-P-786)
fission, theory for low-excitation energy, 17: 17283
fission thresholds of heavy, phenomenological model for, 19: 37840(T) (ANL-Trans-196)
fission, two-mode analysis of, 17: 19385
fluorine-19 reactions with, cross sections for single neutron transfer in, 17: 38279
flux and energy spectra of heavy, in primary cosmic radiation, (E), 19: 34928
flux and energy spectrum of heavy, in primary cosmic radiation, (E), 19: 34930
flux intensity ratios of multiply charged, in primary cosmic radiation, (E), 19: 47277
Fock method for rotational, (T), 19: 23684
force mechanisms of, inter-nucleon, 19: 32048(R) (NP-15073)
forces in, electron-neutrino pair exchange and, 17: 24484
forces in, statistical theory, 16: 12210(R) (ANL-6488)
forces in, velocity dependent, 16: 21703
forces in, charge dependence of, 18: 36694
forces in, charge independence of, 18: 40649
forces in, charge dependence of, 18: 44781
forces in, effect of meson resonances on, 20: 15817
forces in, meson (I^0) contribution to, (T), 19: 14626
forces in, oscillator brackets for Hartree-Fock calculations for two-body, 20: 17744
forces in, particle-hole matrix elements for Wigner and zero-range, 20: 19873
form factors for heavy and medium, 18: 34928
formation and excitation energies of, (T), 19: 23652
formation of compound, determination of time for, 16: 9428 (JINR-P-822)
formation of light, mechanism for, 17: 17149
formation time for compound, 16: 23153
g-factor measurements for excited, analysis of differential method of, 16: 29783 (NP-11956)
g factor measurements on, internal perturbation effects on, 18: 30850
gamma absorption and emission in crystals, phonon effects on, 17: 11658
gamma absorption and emission by, recoilless, 17: 13223
gamma absorption and emission processes in, projection operator formalism for, 17: 33013
gamma absorption and scattering by, in crystals, theory of resonance, 18: 4355
gamma absorption and scattering by, research at RC-1 reactor, 20: 20334
gamma absorption by, cross section giant resonances in, 18: 22875 (UCRL-7740)
gamma absorption by nucleon pairs in heavy, total cross section for, 18: 34925
gamma absorption by, in diatomic lattices, 19: 23768
gamma absorption by, total cross section for, (T), 19: 39873
gamma absorption cross sections for light, 18: 40513 (NP-14241)
gamma absorption in, and resonance fluorescence, 17: 5404
gamma activation, 16: 23045
gamma and neutron emission in decay of compound, effect of spin on, (T), 20: 12048
gamma angular correlation data on aligned, method for analysis of, 18: 26637
gamma angular correlations for, multipole mixing in, 18: 36569 (INSJ-66)
gamma angular correlations from, corrections to, 19: 9482 (NASA-TN-D-2549)
gamma angular correlations from, testing symmetries by, (T), 20: 44806
gamma angular distributions from oriented, 17: 5069
gamma capture cross sections for light, measurement by transmission, (T), 19: 37878(T)
gamma cascades from high-spin levels in, angular distribution and spectra of, (T), 20: 13847
gamma cascades in, analysis using directional and polarization correlations, 20: 46743
gamma decay of even-even spherical, branching ratios for, 16: 33868
gamma decay of even-even spherical, branching ratios for, 16: 33870
gamma decay of, effects of pairing correlations on, 18: 15251
gamma decay, spectra of double, 16: 23092
gamma elastic scattering by Z = 72 at 92 to 0.511 Mev, (E), 20: 44829
gamma elastic scattering and (p,γ) reactions, giant resonance behavior in, 16: 21455
gamma emission by compound, 16: 23153
gamma emission by spherical, analysis of collective E3 and E4, 16: 26271
gamma emission by compound, at high angular momenta, 16: 26364
gamma emission by, effect of pair correlations in two-gamma, 17: 7190
gamma emission by, recoilless, 17: 13222
gamma emission by, frequency shifts in Mössbauer spectra, 17: 13226
gamma emission by, frequency modulation in Mossbauer spectra,

17: 13227
gamma emission by aligned, correlation coefficients for double, 17: 17286
gamma emission by, analysis of *l*-forbidden M1, 17: 21045
gamma emission by, circular polarization analysis by resonance absorption, 17: 34936
gamma emission by high angular momentum, angular distribution of, 17: 36655 (IITRI-A6034-1)
gamma emission by polarized, correlation of cascade, (T), 19: 45280 (NP-15457)
gamma emission by, measurement of gamma–gamma correlations in, 19: 835
gamma emission by, mass-change effect on Mössbauer spectrum after, (T), 19: 21422
gamma emission by, effects of neutron number on radiative width, (E), 19: 23626 (JINR-P-1995)
gamma emission by, angular correlations in, (T), 19: 41698
gamma emission by, measurement using lithium–drifted germanium detectors, (E), 20: 17158(R) (ORNL-3900, pp 82-149)
gamma emission from excited states of odd-A rotational, 16: 33901
gamma emission from fission-produced, 17: 877
gamma emission from, theory of stimulated, 18: 16952 (TID-20313)
gamma emission from, where level energy surfaces intersect, 19: 33254
gamma emission from, time-dependent perturbations in angular correlations of, (T), 19: 35466
gamma emission from oriented, 18: 4582 (NP-13378)
gamma emission in 0^+–0^+ transitions in, double, 18: 34752(R) (CU(PNPL)-234)
gamma emission in crystals, spontaneous, (T), 19: 17024
gamma emission, angular correlations in, 18: 16953(R) (TID-20352)
gamma emission, magnitude of dipolar and quadrupolar, 16: 21363(T) (UCRL-Trans-822(L))
gamma E1 absorption by closed-shell, mass-number effects, 16: 19784
gamma E1 spectra of odd-A, in rare earth region, 16: 21458
gamma inelastic scattering by, isomeric cross section dependence on absorber material and shape for, (E), 20: 34558
gamma inelastic scattering by Coulomb fields, 16: 12577
gamma inelastic scattering by, mechanism of, 17: 9613
gamma inelastic scattering by even-mass, angular correlation in, 18: 18996
gamma interactions with coulomb fields of, meson (π) pairs from, 18: 42416
gamma internal conversion coefficients at threshold in, Coulomb field effects on K-shell, 17: 33047
gamma lifetimes of, determination by delayed-coincidence method, 17: 5354
gamma magnetic transitions in deformed, orbit-flip effects on, 17: 5350
gamma Mossbauer scattering by impurity, in solids, 17: 28340
gamma Mössbauer spectra in infinite crystals, 17: 33084
gamma Mössbauer transmission, 16: 11015
gamma oscillations in deformed, potential energy of, 17: 11748
gamma perturbed angular correlations from, circular polarization measurements in, 20: 36175 (RT-FI-(66)8)
gamma radiation by, possibility of maser action in, 17: 34986
gamma radiation from, measurement of internal conversion coefficients of, (E), 19: 30522 (IS-1159)
gamma-ray spectra following neutron capture in, 17: 31549
gamma reactions (γ,n) with $(50 < A < 200)$, 18: 34935
gamma reactions (γ,n) with heavy, damping of giant resonances in, (T), 19: 25532
gamma reactions (γ,n) with, 19: 31207
gamma reactions (γ,α) with emulsion, angular distributions in, (E), 19: 33264
gamma reactions (γ,n) with light, cross sections for, 19: 37831(R) (TID-21940)
gamma reactions (γ,α) with light, (T), 19: 39934
gamma reactions (γ,n) with, polarization effects in, (T), 20: 38175
gamma reactions (γ,n) and (γ,p) with medium and heavy, mechanism of, (E), 20: 44778
gamma reactions at high energies, forbidden e-μ pair production, 16: 24724
gamma reactions at 90 Mev, electron multiplets from, 17: 875
gamma reactions at 6 Mev, electron pair production in, 18: 18994
gamma reactions at $(0.5 \text{ to } 2.0) \times 10^9$ °K at 10^{-2} to 10^2 g cm^{-3}, rates of, 16: 26341
gamma reactions, boson production cross sections for, 16: 26362
gamma reactions (γ,π), cross sections for, 17: 6975
gamma reactions (γ,n) and (γ,p) on, spin-orbit effects in, 17: 7167
gamma reactions (γ,π°) on Coulomb fields of, 17: 17184
gamma reactions (γ,α), (γ,n), and (γ,p) with, energy-range relation for recoiling atoms from, 17: 31053
gamma reactions, meson (π^0) photoproduction in, 16: 25893 (LNF-62/37 (p.57-71))
gamma reactions on odd, polarization of nucleons from, 16: 33864
gamma reactions on deformed, structure of giant resonance in, 16: 33858
gamma reactions on, electron pair production in, 17: 7304
gamma reactions on, giant dipole resonances in, 17: 7305
gamma reactions on, tensor effects on nucleon production in, 17: 11733
gamma reactions on unfilled-shell, giant resonances in, 17: 17160
gamma reactions on, mesons (π) from, 17: 17163
gamma reactions on, giant resonance effects in, 17: 17284
gamma reactions on N = Z, dipole sum rules for, 17: 34989
gamma reactions, theory of deuteron production in, 16: 17071 (NP-11564)
gamma reactions with, giant-resonance structure in, 16: 32434
gamma reactions with, yields of, 17: 4081
gamma reactions with, meson (π^-) and (π^+) production cross sections for, 17: 24443
gamma reactions with light, cross sections for, 17: 40117
gamma reactions with, yield function solution for cross sections of, 17: 41865 (IS-607)
gamma reactions with, equipment and method for measuring yields from, 18: 1076
gamma reactions with, Thomas-Reiche-Kuhn sum rule for, (T), 19: 5217
gamma reactions with, electron pair production in, (E), 19: 23625(R) (HUX-2752-1)
gamma reactions with, neutron production in, (E), 20: 4802 (IDO-17115)
gamma reactions with, electron emission from, (E), 20: 35993 (AECL-2567)
gamma reactions with, cross section libraries for, 18: 37597 (A/CONF.28/P/168)
gamma resonance absorption, apparatus for measurement of Mössbauer effect, 16: 5514
gamma resonance absorption, effects of nucleon pair forces on, 16: 13976
gamma resonance absorption in, energy levels from, 17: 38160
gamma resonance absorption and emission by, (T), 19: 12479 (AFCRL-64-840)
gamma resonance absorption by, uses of superconducting magnets in studies of, (E), 19: 14507 (BNL-8745)
gamma resonance absorption at high pressures, methods for analyzing, (E), 19: 21231 (COO-1198-255)
gamma resonance emission by, 17: 38066 (JINR-P-1231(p.7-16))
gamma resonance reactions with, methods for studying, 17: 33034
gamma resonance scattering by (E/T), 19: 1675
gamma resonance scattering by heavy and medium, 19: 26917(R) (IA-984)
gamma resonant scattering by, use of (n,γ) reactions as sources for, 18: 30765
gamma resonant scattering by, cross sections for neutron-capture, (E), 20: 30467
gamma scattering at low energies, dispersion relations for, 16: 29872
gamma scattering at 2 to 6 Bev, electron pairs from, (T), 19: 14522 (DESY-64/12)
gamma scattering by, Mössbauer-*vs*-Rayleigh interference in, 17: 9232
gamma scattering by, interference between Mössbauer and Rayleigh, 17: 13251
gamma scattering by, cross sections for electron-positron production in, 17: 15103
gamma scattering by, isomeric states from, 17: 29953
gamma scattering by, Z dependence of Rayleigh, 18: 34417
gamma scattering by, Mössbauer and Rayleigh, (T), 19: 27576
gamma scattering by, spectroscopy of, 19: 35476
gamma scattering by, resonance, (E), 20: 13771 (IA-1050)
gamma scattering by, Mössbauer, 20: 26194
gamma scattering by, electron-pair production in, (E/T), 20: 29996
gamma scattering cross sections for $30 \leq Z \leq 90$, Mössbauer resonance, (E/T), 19: 36220(R) (MIT-2098-142)
gamma scattering from oriented nonspherical, anisotropy, 16: 12566
gamma spectra in crystals, temperature effects on Mössbauer, 17: 13231
gamma spectra in deformed odd-A, probabilities for E1, 17: 13507
gamma spectra in powdered crystals, Mössbauer line broadening for measuring, 19: 39876
gamma spectra in two-photon monopole transitions of, 18: 9326
gamma spectra of, determination of small shifts in Mössbauer, 17: 13248
gamma spectra of, Fermi-fluid theory for, 17: 28069
gamma spectra of neutron-deficient, 20: 44634(R) (IDO-17188)
gamma spectra of, with two nucleon pairs outside closed shells, 16: 23094
gamma spectra of $181 \leq A \leq 194$, (E), 20: 33718
gamma spectra of, intensities of low-energy lines in, 18: 16320
gamma spectra of, effects of mesons (μ^-) in electronic orbits on, 18: 44797
gamma spectra of, relative intensities in, (T), 19: 8392 (IS-993)
gamma transition in, hindrance factor for, for isotopes with neutron or proton number 50 and 82, 16: 29767 (JAERI-1020(p.129-37))
gamma transition multipolarities in, determination using internal conversion coefficients, 19: 27487

gamma transitions, effects of momenta in, 16: 2524
gamma transitions (⅞⁺ to ½⁻), 16: 8239
gamma transitions in deformed even, coupling of K = 2 band to ground state rotational band, 16: 21521
gamma transitions in even, E2/M1 mixing ratios in, 17: 17172
gamma transitions in, from band with K = 3⁺ to principal rotational band, 17: 26503
gamma transitions of, two-quantum, 17: 40057
gamma transitions in even-even and odd-even, quadrupole E-2, 17: 41965
gamma transitions in vibrational even, probability ratio of E2, 18: 6215
gamma transitions in Z = N type even-even, 18: 18929
gamma transitions in, internal conversion in, coefficients for strongly forbidden, 18: 28733
gamma transitions in, measurement of multipolarity of, (E), 19: 10367
gamma transitions in, independent particle model for M4, 19: 17051
gamma transitions in, survey on, 19: 31311
gamma transitions of, determination of internal conversion coefficients of, (E), 19: 44501
gamma transitions in, exchange electric moments for, (T), 19: 45363
gamma-gamma cascades in, installation for studying, 19: 14563
generalized Nilsson diagram, 16: 8235
generalized quasi-spin in neutron–proton systems, 20: 3046
ground state deformation equilibrium in rare earth, 16: 6009
ground-state energy of nuclear matter, long-range force corrections to, 18: 42685
gyromagnetic ratios for even-odd, 16: 1087
gyromagnetic ratios of excited-state, device for measurement of, 18: 11268
gyromagnetic ratios of excited, measurement of, 18: 36575 (NP-14084)
gyromagnetic ratios and magnetic dipole transitions of deformed even-even, (T), 19: 21410
gyromagnetic ratios of deformed odd-A, 20: 44791
half life of short-lived, measurement of, 17: 30085
half lives, evaluation of time correlation method of measurement, 16: 26215 (AROD-2543.5)
half lives of short-lived isomeric states of, 18: 21249
half lives of, determination by direct decay, (E), 19: 37847
Hartree-Fock approximation for, generalized, (T), 20: 24387
heavy ion reactions, production of nitrogen-17 in, 16: 7130
heavy ion reactions, fragmentation in, 16: 21634
heavy ion reactions with, cross sections for compound-nucleus formation in, 17: 41877
heavy ion scattering by, 17: 41876
heavy-ion reactions with heavy, production of transcurium elements by, 20: 15740
helium nucleus reactions (He^3), mechanism and relative magnitudes of double stripping and pickup, 16: 31068 (PUC-1962-77)
helium-3 reactions (He^3,α) with, enhancement of large orbital angular momentum in, 17: 38172
helium-3 reactions (He^3,n) and (He^3,p) with, double stripping mechanisms in, 17: 38225
helium-3 scattering at 29 Mev, optical model analysis, 16: 21538
helium-3 and -4 scattering by even-mass, amplitudes for, (T), 20: 28331
helium-3 and triton emission by, superfluid model for reduced widths for, 20: 38116
helium-3 elastic scattering by, optical model for, 19: 23163(R) (ORNL-3650(p.111-86))
helium-3 inelastic scattering by, DWBA analysis of, (T), 19: 39885
helium-3 reactions (He-3,p) with spheroidal, cross sections for, 18: 36609
helium-3 reactions (He-3,d), (He-3,α), and (He-3,p) with, polarization in direct, 18: 36624
helium-3 reactions (He-3,d) and (He-3,α) with, diffraction model for direct, 18: 36657
helium-3 reactions with, selection rules for two-nucleon stripping, (T), 19: 8443
helium-3 reactions with light, excitation functions for, (E), 19: 37880(T)
helium-3 reactions (He-3,α) with light, angular distributions in direct, (T), 20: 3121
helium-3 reactions with, angular distributions from, 20: 4824(R) (ANL-7081, pp 70-7)
helium-3 reactions (He-3,p) with, distorted-wave Born approximation for, (T), 20: 12127
helium-3 reactions (He-3,n) with light, angular distributions for direct, (T), 20: 15798
helium-3 reactions at 10 Mev, properties of, (T), 20: 24336 (CEA-Bib-68)
helium-3 reactions (He-3,d) with calculations using distorted-wave theory, 20: 42250
helium-3 reactions (He-3,n) with angular distributions for, (T), 20: 42290
helium-3 scattering by, collective excitations in, (T), 19: 3250
helium-3 scattering from deformed, as test for coupling potential complexity in direct interactions, 17: 24492
hole-particle interactions in light, 18: 4608
hyperfine interactions of magnetic moment of displaced, with S electron, 16: 7122
hyperfine structure in ENDOR spectra of, invariants method for, (T), 19: 43479
hyperfragment and hyperon (Λ) reactions with heavy, (T), 20: 30503
hyperfragment scattering on heavy, Coulomb spallation in, (T), 19: 41815
hypernuclei decay in Coulomb field of, (T), 19: 12618
hyperon (Λ^0) reactions with A = 40 to 100, 18: 44594
hyperon (Λ) and proton binding energies in, (E), 20: 22161
hyperon (Λ) binding energy in, 18: 19111
hyperon (Λ) binding energy in, 20: 28477
hyperon (Λ) binding energies in, (T), 20: 44702
hyperon (Λ) binding energies in, (T), 20: 44703
hyperon (Λ) binding energy in, (T), 20: 46689
hyperon (Λ) binding energy, (T), 20: 46697
hyperon (Λ) binding energy in, 18: 40589
hyperon (Λ) capture by heavy, (T), 19: 12618
hyperon (Λ) trapping in, 18: 26623
hyperon (Λ) well-depths for, 18: 15188 (CERN-64-1(p.173-90))
hyperon (Λ)-nucleon interactions in, (T), 19: 16962
hyperon (Λ)–nucleon interactions in, 20: 8098
hyperon (Σ^-) reactions at rest, hypernuclei from, 19: 25499
hyperon (Σ^-) capture by, hyperfragment production in, 16: 8067 (NP-11232(p.360-6))
hyperon (Λ) reactions, Coulomb excitation in, 17: 5286
hyperon (Λ^0) binding energies in, for A = 50 to 80, 17: 19332
hyperon reactions with, 17: 19324
hyperon (Ξ^-) capture by light, double fragment production in, 17: 31361
identification, detector system for, 16: 5530
inertia moment of even-even, superfluid model calculation of, 17: 24390 (JINR-P-1216)
inertia moments of, review of calculations of, 17: 17068
inertia moments of excited even-even and odd, (T), 20: 9988
inertial moment calculations for, accuracy of cranking model, 18: 1016 (JINR-P-1386)
inertial moments of asymmetric, (T), 19: 39831
intensity and spectra of cosmic, in IYQS, (E), 20: 23963
intensity increases of heavy cosmic, accompanied by solar x-ray bursts, 20: 29965
intensity modulation of heavy primary cosmic, (E), 19: 25210
intensity of low-energy heavy, (E), 19: 23342
intensity variations of cosmic, over one solar cycle, 18: 42342
interaction in s-d shell of, 18: 14592(R) (PR-P-60)
interactions, effects of charge polarization on pure Coulomb, 16: 9470
interactions in nuclear matter, velocity-dependent, 17: 17164
interactions, nonconservation of parity and fission in strong, 16: 3750
interactions of, deformed-orbitals in the s-d shell variational model of single-particle, 18: 2913
interactions of heavy, with cosmic fragments at energies greater than 1000 Bev, 18: 26378
interactions of high energy nucleons with, 17: 7209
interactions of two spin-½, fusion, (T), 19: 18768
interactions with electron magnetic moments, hyperfine, 16: 32408
interactions with electrons in cesium, magnetic, (E), 20: 23639 (AD-625687)
interior characteristics of, model for, 17: 849
internal conversion coefficients for cascade decay to second levels, 16: 22366
internal conversion of gamma spectra of, theory, 17: 19383
internal conversion (K) coefficients in deformed even, 18: 18995
internal conversion in, structural effects in, (E), 19: 16913
internal conversion coefficients for $5 \leq Z \leq 95$, (T), 19: 27548
internal conversion matrix elements, (T), 19: 27466
internal conversion in, nuclear structure effects on L-shell, (T), 19: 27486
internal conversion coefficients for Z = 80 and 81, M, (T), 19: 33393
internal conversion coefficients of, measurements of, 19: 37826 (ORNL-P-1248)
internal conversion in, coefficients for L-shell, 19: 43341
internal conversion coefficients of E2 transitions in, (T), 19: 45369
internal conversion in, review of dynamic structure effects in, 20: 6332
internal conversion in, correlation of electron polarization in, (T), 20: 13802(T)
internal conversion coefficients for $2^+ \rightarrow 0^+$ transitions in deformed, E2, (E), 20: 15745
internal conversion coefficients for high-energy transitions in, 20: 24389
internal conversion coefficients for, calculations using relativistic Hartree-Fock model, (T), 20: 46699
internal pair production in oriented, calculation of, 19: 25545
interparticle interactions in even-even, 17: 17214
intrinsic symmetries of rotational states, 17: 7206
ion beam reactions with, method of recording resonance capture spectra

from, 16: 3665 (BRL-TN-1394)
ion elastic scattering by, quasi-classical analysis of heavy, 17: 17115 (JINR-P-1153)
ion elastic scattering by, nuclear radius and surface-thickness analysis from, (E/T), 19: 33251 (UCRL-11781)
ion elastic scattering by complex, mechanism of heavy, 20: 8092
ion elastic scattering by, spin-½, (T), 20: 9984
ion fission of $176 \leq A \leq 209$, energy and mass distributions from, (E), 20: 13861
ion inelastic scattering by, excitation of collective states in, (T), 19: 21353
ion inelastic scattering by complex, cross sections for heavy, (T), 19: 27427 (JINR-P-2030)
ion inelastic scattering by complex, collective-level excitation in, (T), 19: 35383 (JINR-P-2142)
ion inelastic scattering by, matrix elements for, (T), 20: 4839 (JINR-P-2333)
ion inelastic scattering by complex, dynamic deformation in heavy, (T), 20: 13794
ion inelastic scattering by, gamma-ion angular correlations in, (T), 20: 15767
ion reactions and scattering on, review on, 20: 21992 (BNL-948, pp 1045-1134)
ion reactions with heavy and medium, heavy, 16: 17134
ion reactions with, multiple Coulomb excitation from heavy, 17: 33087
ion reactions with, compound systems in heavy, 18: 1011 (JINR-P-1351)
ion reactions with, neutron transfer and compound-nucleus formation in heavy (E/T), 19: 1563 (ORNL-P-514)
ion reactions with, nucleon transfer in, (E), 19: 27573
ion reactions with, many-nucleon transfer in, 19: 41795
ion reactions with, neutron angular distributions from heavy, (T), 20: 8089(T) (BNL-tr-30)
ion reactions with, mechanisms of heavy, 20: 11377
ion reactions with, method for calculating isomeric cross sections for, 20: 32374(R) (IITRI-578P25-15)
ion scattering by, optical model analysis of heavy, 17: 22550 (BNL-6931)
ion scattering by even-even, reorientation effect in Coulomb excitation in, (T), 20: 4901
ion scattering by, energy level excitation by, 18: 18873 (JINR-P-1532)
ion scattering by, reorientation effect in, 18: 24625 (WASH-1046)
ion scattering by, microscopic description of, (T), 20: 22118
ion scattering by, multiple Coulomb excitation in, (T), 20: 26129
ion scattering by, gamma angular distribution from rotational levels excited in, (T), 20: 28457
ion scattering by, calculations using optical model, (T), 20: 46667
ion stopping power of medium and heavy, at 10 to 100 Mev, (E), 19: 25475(R) (ORNL-TM-1044)
isobaric excited states in medium-A, non-mirror, even, 16: 26333 (UCRL-6830)
isobaric mass formula and Coulomb energies in 1p shell of, 20: 38174
isobaric spin without charge space for, 20: 22019
isobaric states in heavy, 17: 2282
isomeric states of, spontaneously fissioning, (E), 20: 13777 (JINR-E-2515)
isomeric transition of odd-A, M_4-type, 16: 22985 (NP-11747)
isomeric transitions of E_3 type for odd A, 16: 31066 (NP-11746)
isomeric transitions in odd-odd spherical, calculation of probabilities of, 18: 15214
isospin multiplets in nuclear analog states, 18: 28706
isotopic effects on spectra, 17: 27396
isotopic spectral shifts and compressibility of deformed, 16: 18531
isotopic spin of heavy, validity as quantum number, 16: 26304
kinematical properties of deformed, for $152 \leq A \leq 185$, 17: 21002
knock-on and stripping reactions, structure-factor effects on cross sections of two-nucleon, (T), 19: 41819
lepton pair production in, two-virtual-photon exchange in, (T), 19: 12178
lepton reactions with Coulomb field of, lepton pair production in, 16: 1086
lepton reactions with Coulomb fields of, charged vector boson production in, 16: 23154
lepton reactions with fields of, boson and meson (μ) production in, 17: 22644
lepton reactions with Coulomb field of, vector-meson emission in, (T), 19: 35395 (NP-14993)
level densities, spin cut-off parameters in, 16: 4748 (AWRE-NR/P-2/61)
lifetime measurement, delayed coincidence for submillimicrosecond, 17: 14669
lifetime measurements of, beta spectrometer for short, 17: 30863
lifetime measurements to 10^{-11} sec, beta spectrometer for, 17: 30864
lifetime of intermediate states in, (T), 20: 42288
lifetime of intermediate states in nuclear reactions, (T), 20: 42288
lifetimes of excited states in, back-scattering techniques for measuring, 17: 26613
lifetimes of, methods for estimating short, 17: 41763
lifetimes of undiscovered, prediction of, 20: 22043
light emission in nuclear reactions, (E/T), 19: 5141
light scattering by coulomb field of, angular distribution of, 18: 42503
lithium reactions (Li-6,α), (Li-6,d), (Li-7,α), and (Li-7,t) with, mechanisms for, (T), 19: 45264 (JINR-E-2243)
lithium-6 and -7 reactions with, angular distributions, cross sections, and energy spectra for, 17: 38281
lithium-ion reactions with light, structure effects in, (T), 20: 38014
lithium-6 reactions (Li-6,α) with, deuteron threshold states in, (T), 19: 33244 (JINR-P-2079)
magnetic and orbital moments of quasicrystalline, (T), 19: 23654
magnetic and quadrupole resonances in, computer analysis of, (T), 19: 21246 (TID-21697)
magnetic dipole moments of conjugate, (T), 19: 21322
magnetic dipole moments of, measurement using perturbed γ–γ angular correlations, (T), 20: 40125
magnetic dipole-dipole relaxation for spin ½, effects of internal molecular motion on, 19: 16381
magnetic field effects on, in paramagnetic materials, 18: 30863
magnetic field fluctuations in magnetic materials, (T), 19: 43384
magnetic fields of, effects on atomic energy levels, 17: 824
magnetic fields of, method for measuring hyperfine, 19: 16998
magnetic fields of, para-, (T), 20: 1235
magnetic fields of ferromagnetic-lattice solute, hyperfine, 20: 22859(R) (UCRL-16580, pp 149-205)
magnetic moment and orbital angular momentum for structure of, (T), 19: 23653
magnetic moment corrections to second order for mirror, perturbation theory for, 20: 13838
magnetic moment distribution in odd-A, regularities in, 17: 22630
magnetic moment measurement of short-lived excited states, 16: 10907
magnetic moment measurement of, review, 20: 6282 (CERN-64-13(Vol.4), pp 97-136)
magnetic moments, 18: 36695
magnetic moments, effects of pair interactions, 16: 21433
magnetic moments of mirror, 16: 3730
magnetic moments of excited states of, from gamma correlations, 17: 2255
magnetic moments of excited states of, from gamma correlations, 17: 2256
magnetic moments of excited, review, 17: 15278
magnetic moments of, nucleon interaction effects on, 18: 28734
magnetic moments of odd-A deformed, spin-polarization effect on, (T), 19: 29238 (INP-361)
magnetic moments of spherical, (T), 19: 41804(T)
magnetic moments of spherical, corrections to equation for, 20: 3118
magnetic moments of spherical, octupole, (T), 20: 8149
magnetic moments of light, 20: 15439
magnetic moments of, first and second order corrections to, 20: 24391
magnetic octupole moments in, 20: 6277 (AD-619952)
magnetic parameters for deformed, with $A = 153$ to 187, 17: 17199
magnetic properties of, review, 17: 13174
magnetic properties of strongly deformed, (T), 19: 29239 (INP-362)
magnetic relaxation and resonances in superconductors, 18: 15092
magnetic relaxation times in gases, h-f modulation and saturated scattering for measuring, 20: 19869
magnetic relaxation in crystals, 20: 28678
magnetic resonance spectra in polar fluids, 18: 6828
magnetic resonance of, book, 18: 40080
magnetic resonance of, theory of double, 18: 44295
magnetic resonance in, effects of neutron scattering on para-, (E/T), 19: 8398 (JINR-P-1840)
magnetic shielding of, by neighboring atom, 18: 21232
magnetic shielding constants for, of 2-, 3-, and 4-electron atoms, 18: 21233
magnetic shielding of impurity, in metals, 18: 30855
magnetization in atomic, ultrasonic saturation effects on, 17: 24490
magnetization of spin system in step magnetic field, 18: 6169 (NP-13426)
many-body theory of, 18: 6288
many-particle evaporation spectra from highly excited, integral equations for numerical computation of, 17: 36708
many-body forces in heavy, 18: 15291
mass and pairing energy calculations for heavy, 16: 33882
mass calculations, by covariant Weizsacker-Williams formalism, 16: 12552
mass corrections to 1964 tables of alpha–beta decay chain into bismuth-213, 20: 22154
mass defects in heavy, calculation of, 20: 26099(T) (ORNL-tr-1102)
mass difference of mirror, (T), 19: 12619
mass differences between, in $T = 3/2$ isobaric quartets, 19: 1623

mass differences in even near-to-magic, (T), 19: 33358
mass differences of, even- and odd-mass effects in, (T), 19: 43302
mass equation for (T), 19: 3354
mass equations for, experimental data comparison with, 18: 22864 (ANL-6814)
mass equations for, semi-empirical, (T), 20: 44814
mass formula for, (T), 19: 29348
mass formula for compressible, (T), 19: 8473
mass formula for isobaric analog states of A = 24, charge-independent, 18: 38140
mass formula for, including shape effects, (T), 19: 29349
mass formula from ground-state energy in superfluid, 19: 43290
mass formulas and deformation energies for, 20: 24409
mass formulas and regularities, 20: 42323
mass formulas for, semi-empirical, (T), 19: 29346
mass formulas for, statistical problems in calculating, 19: 29351
mass formulas for, role of symmetry energy in, (T), 19: 33269
mass law, (T), 20: 12090
mass laws for, (T), 19: 29345
mass of A = 13 T = $\frac{3}{2}$, testing of isobaric mass multiplet equation on, (E/T), 20: 12036
mass of deformed, parameters for collective hamiltonian for, 20: 24471
mass of deformed, electromagnetic, (T), 20: 32548
mass of, ratio of effective to real, 18: 9360
mass of Z = 13 to 110, from Wing-Fong's mass-excess equation, 18: 40502 (ANL-6886)
mass of, electromagnetic, (E/T), 20: 24325 (AD-625706)
mass ratios for A > 200, 16: 6008
mass ratios for A = 70 to 200, 16: 6007
mass relations between, beta-transition frequencies for, 20: 3102
mass surfaces of, spacing in superfluid nuclear model, 18: 9371
mass systematics, 20: 21990 (BNL-948, pp 928-1004)
mass table for, extended, 17: 36639 (BNL-7160)
mass tables, 16: 17087
mass tables for, shell model semi-empirical, (T), 19: 8428
mass tables, relative, 16: 17086
masses and neutron separation energies of even-even, 17: 38102
masses and nucleon pairing correlations for spherical, 20: 30491
masses and Q values for A = 1 to 255, tabulation of, 18: 32727 (BNL-846)
masses of A = 84 to 125, 17: 19298
masses of, for mass numbers 3 to 240, 18: 8348
masses of, based on carbon-12, 19: 9928
masses of, determination of, 19: 29355
matrix elements for three-nucleon, (T), 19: 43322
matrix elements for, effect of particle number fluctuations on, 20: 22103
mean-life measurements from gamma-ray transitions, (T), 20: 42379
measurement of heavy cosmic, in emulsions, 19: 32048(R) (NP-15073)
meson ($\bar{K}^0$) absorption by Ilford G5 emulsion, cross sections for, 18: 30713(R) (AFOSR-4999)
meson (K^-) absorption by emulsion, (E), 19: 23467
meson (K^-) capture by nucleons in complex, 18: 36615
meson (K^-) capture by, models for hyperfragment production in, 18: 36652
meson (K^-) capture at rest by, hyperfragments from, 19: 5184
meson (K^-) capture at rest, (T), 19: 5222
meson (K^-) capture by, hyperfragment production in, (E), 19: 10020 (UCRL-11328(Rev.1))
meson (K^-) capture by emulsion, production of Y_0^* (1405) in, (E), 20: 6051
meson (K^-) capture at rest by light, (E), 20: 42386
meson (K^-) capture in, hyperfragments, hyperons, and meson (π) production in, 20: 44657 (UCRL-16602)
meson (K^-) capture, production of hyperfragments in, 16: 8067 (NP-11232 (p.360-6))
meson (K^-) reactions with emulsion, hyperfragment production in, 18: 11215 (NP-13541)
meson (K^-) reactions with complex, 18: 16552(R) (UCRL-11132)
meson (K^-) reactions with, hyperon (Σ) production in, 18: 24415
meson (K^-) reactions at 1.5 Bev/c, lithium-8 fragments from, 18: 26636
meson (K^-) reactions at 3.5 Bev/c, hyperfragment production in, 18: 30787
meson (K^-) reactions with emulsion, hyperfragments from, 18: 32807
meson (K^-) reactions with, ($\Sigma-\pi$) resonances in, 18: 36266
meson (K^-) reactions at 1.5 Bev/c, hyperon (Ξ^-) production in, 18: 38134
meson (K^-) reactions at 1.5 Bev/c, hyperon (Ξ^-) production in, 18: 38135
meson (K^-) reactions at 800 to 3500 Mev/c, short-range hyperfragments in, 18: 44819
meson (K^-) reactions with, ($\Sigma\pi$) resonance at 1405 Mev in (E), 19: 1344
meson (K^-) reactions at 0.8 to 3.5 Bev/c, short-range hyperfragment production in, (E), 19: 16967
meson (K^-) reactions at rest, hyperon (Σ) and meson (π) production in, (T), 19: 19151
meson (K^-) reactions with emulsion, hyperfragment production in, (E), 19: 21365
meson (K^-) reactions at 0.8 to 3.0 Bev/c, lithium-8 emission in, (E), 19: 21389
meson (K^-) reactions at 1.3 and 1.5 Bev/c, hyperfragment and lithium-8 production in, (E), 19: 27444
meson (K^-) reactions at 800 Mev/c, heavy spallation hyperfragments in, (E), 19: 33292
meson (K^-) reactions with, hyperfragment production in, (E), 19: 35491
meson (K^-) reactions at 2.3 Bev/c, hyperfragment production in, (E), 19: 37830 (TID-21937)
meson (K^-) reactions with emulsion, heavy hyperfragments from, (E), 19: 37859
meson (K^-) reactions with, at rest, 19: 47708
meson (K^-) reactions with emulsion, hyperfragment production in, (E/T), 19: 47648
meson (K^-) reactions with emulsion, at 5 Bev/c, hyperfragment and lithium-8 production in, (E), 20: 3062
meson (K^-) reactions with emulsion, Y_0^* production in capture, (E), 20: 3064
meson (K^-) reactions with emulsion, heavy hypernuclei from, (E), 20: 6294 (NP-15617)
meson (K^-) reactions with emulsion, review on, 20: 11991
meson (K^-) reactions with light, hyperon (Λ) and (Σ) production from, 20: 22033
meson (K^-) reactions in emulsions at 800 Mev/c, hyperfragment production from, (E), 20: 26102
meson (K^-) reactions with heavy, at 1.5 Bev/c, hyperfragments from, 20: 30368
meson (K^-) reactions on, 17: 19324
meson (K^-) reactions with emulsion, hyperfragment production in, (E), 19: 5143
meson (K^-) scattering at 21 Mev, differential and total cross sections for, (E), 19: 35443
meson (K^+) elastic scattering at 320 Mev, optical model analysis of elastic, (T), 19: 27569
meson (μ^-) capture, coupling constants in, 18: 26523 (BNL-837(p.292-7))
meson (μ^-) capture on, radiative, (T), 19: 16964
meson (μ^-) capture by complex, relativistic effects in, (T), 19: 19194
meson (μ^-) capture by light, probability of, (T), 19: 27434 (JINR-P-2063)
meson (μ^-) capture by proton pairs in, (E/T), 19: 41753
meson (μ^-) capture reactions with, elementary-particle model for, 20: 1207
meson (μ^-) capture by spherical, (T), 20: 8155
meson (μ^-) capture by complex, (T), 20: 24339 (COO-720-060)
meson (μ^-) capture rates in complex, (E), 20: 28348
meson (μ^-) capture rates in heavy, closure approximation for, 20: 30454
meson (μ^-) capture by spherical, (T), 20: 30494
meson (μ^-) capture by, $\Delta S = 0$ neutron current coupling in, 20: 30141
meson (μ^-) capture by protons in 2s-1d, 20: 38166
meson (μ^-) capture by, neutron angular distributions from, (E), 20: 40096
meson (μ^-) capture by deformed, nuclear charge distribution determination from hfs spectra from, (E), 20: 42308
meson (μ^-) capture by deformed and spherical, x-ray spectra from, (E), 20: 42309
meson (μ^-) capture by, review of, 20: 42317
meson (μ^-) capture by complex, rates for, (E), 20: 42318
meson (μ^-) capture by nuclei, mass dependence of average neutron emission from, (E/T), 20: 42174
meson (μ^-) radiative capture by, polarization in, 18: 21310
meson (μ^-) scattering at 8 Bev/c, single, (E/T), 19: 16871
meson (μ) and neutrino reaction in Coulomb field of, polarization effects in intermediate boson production in, 18: 7533
meson (μ) capture by, Goldberger-Treiman relation for, 18: 15304
meson (μ) capture by 2s-1d, Nilsson model calculations of rate of, 18: 21277
meson (μ) capture by heavy, theory of, 18: 24658
meson (μ) capture by, 18: 36703
meson (μ) capture by deformed, 18: 38167
meson (μ) capture by, in nuclear emulsion, 18: 42410
meson (μ) capture by (T), 19: 1419 (NP-14404(p.188-201))
meson (μ) capture by, nuclear matrix elements for, (T), 19: 5232
meson (μ) capture by, G-parity violation in, (T), 19: 6648
meson (μ) capture by, gamma-neutrino correlation in first-forbidden, (T), 19: 21378
meson (μ) capture in, coupling constants for, (T), 19: 31227 (NP-15026)
meson (μ) capture by, decay of collective states excited in, (T), 19: 41769
meson (μ) capture by complex, correlation functions in, (T), 19: 47656
meson (μ) capture by complex, (T), 20: 8062(R) (COO-720-058)
meson (μ) capture by, (T), 20: 12100
meson (μ) capture by, G-parity violation in, (T), 20: 13877
meson (μ) capture by, review on, 20: 19459
meson (μ) capture by, coupling constants in, (T), 20: 24382

meson (μ) capture by complex, effects of giant resonances in, 20: 40151
meson (μ) capture by complex, (T), 20: 46768
meson (μ) pair production at high energies, (T), 20: 27951
meson (μ) reactions with Coulomb field of, electron pair production in, (T), 19: 41486(T)
meson (μ) reactions above 300 Tev, evidence for, (E), 19: 45368
meson (μ) reactions with, first Born approximations including anapole for, (T), 20: 4612
meson (μ) reactions at 5 to 50 Bev, 20: 6007 (CONF-640919, pp 143-8)
meson (μ) reactions with, cosmic, (T), 20: 11975 (PAM-6502)
meson (μ) scattering by nuclei at high energies, cross sections for electron pair production from, (T), 20: 27841
meson (μ) total capture rates in light, (T), 19: 6681
meson (π^-) absorption by emulsion, 18: 24582 (AD-439331)
meson (π^-) absorption by shell-model effects on evaporation processes for neutron emission in, 18: 32733 (ISS-64/10)
meson (π^-) absorption by light, products of, (E), 19: 19220
meson (π^-) and (π^+) scattering at 4 Bev/c, interference effects between Coulomb and nuclear, (E), 19: 25508
meson (π^-) absorption in heavy, s-orbit, (T), 19: 33260
meson (π^-) charge exchange on complex, 18: 13045 (JINR-P-1470)
meson (π^-) capture by, nucleon pair emission in, (T), 19: 47679
meson (π^-) capture by, yields and energy spectra from, (E/T), 20: 6292 (NP-15601)
meson (π^-) capture in light, energy spectra and yields from, (T), 20: 26219
meson (π^-) capture by, radiative, (T), 20: 28414
meson (π^-) capture by, angular correlations of particles from, (T), 20: 30504
meson (π^-) capture by complex, radiative, (T), 20: 38064
meson (π^-) capture by, radiative, (T), 20: 42385
meson (π^-) reactions at 16.2 Bev/c, meson (π) multiple production in, 18: 28750
meson (π^-) reactions at 4.5 Bev, beryllium-8 production in, 18: 30758
meson (π^-) radiative capture by complex, spectra from, 18: 30721 (JINR-P-1663)
meson (π^-) reactions with emulsion, multiple-π production in, 18: 32806
meson (π^-) reactions with, heavy fragment emission in, 18: 34811
meson (π^-) reactions at 4.5 Bev, lithium-8 emission from, 18: 44758
meson (π^-) reactions at 3.5 Bev/c, hyperfragment production in, (E), 19: 16966
meson (π^-) reactions at 17 Bev/c, secondary particles in, (E), 19: 19148
meson (π^-) reactions at 68 Mev, proton energy spectra from, (E), 19: 35454
meson (π^-) reactions with emulsion, coherent meson (π) production in, (E/T), 19: 37882(T)
meson (π^-) reactions at 17 Bev, production of A_1 in, 19: 43126
meson (π^+) reactions at 7.2 Bev/c, meson (K) production in, 20: 1224
meson (π^-) reactions (π^-,π^0) on complex, excitation functions for, (T), 20: 4910
meson (π^-) reactions with emulsion, effective particle mass from diffraction dissociation, (T), 20: 7878
meson (π^-) reactions at 16.3 Bev, angular distributions from, (E/T), 20: 11602
meson (π^-) reactions (π^-,2N) with, momentum distribution from, (T), 20: 13874
meson (π^-) reactions at 3.85 Bev/c, meson (π) production in, 20: 26085 (JINR-P-2624)
meson (π^-) reactions (π^-,3π) at 17.2 Bev/c in emulsions, mechanism for coherent, (E/T), 20: 26127
meson (π^+) reactions at 7.2 Bev/c with heavy, meson (K^-) and (K^+) production cross sections for, (E), 20: 28460
meson (π^-) reactions at 16 Bev/c with complex, multipion resonance production from, (E), 20: 37822
meson (π^-) reactions at 50 to 176 Mev, total cross sections for double charge-exchange, (E), 20: 38012 (JINR-P-2806)
meson (π^-) reactions (π^-,2n) and (π^-,np) with light, neutron-neutron and neutron pair angular distributions from, (E), 20: 42313
meson (π^-) reactions in nuclear emulsions at 1.7 Bev/c, proton spectra from, 20: 46932(R) (ORNL-3973(Vol.2), pp 71-84)
meson (π^+) reactions in light, phenomenological analysis of, 20: 41665
meson (π^-) reactions at 16.2 Bev/c, coherent meson (π) trident production in, (E), 19: 47355
meson (π^-) reactions with emulsion, hyperfragment production in, (E), 19: 5143
meson ($\pi^\pm$) scattering at low energies, double-charge-exchange, (T), 19: 41773
meson ($\pi^\pm$) reactions ($\pi^\pm$,2N) with light, (T), 20: 46789
meson (π^+) reactions (π^+,π^-), model for, 19: 47660
meson (π^+) reactions, double-charge-exchange cross sections for, (T), 20: 15813
meson (π) absorption by, in mesic atoms, calculation of rates of, 18: 15232
meson (π) absorption cross sections up to 800 Mev, (T), 20: 32078
meson (π) and nucleon reactions with complex, 18: 7690(R) (ORNL-3499(Vol.II)(p.54-6))
meson (π) and nucleon reactions at 2 to 10 Bev, cascade showers from, 20: 8079 (ORNL-3855)
meson (π) and proton reactions at 5 to 30 Bev/c, particle distributions in, (E), 19: 23693
meson (π) capture by, two-nucleon emission from, (T), 20: 19843 (UR-875-126, Paper 2)
meson (π) elastic scattering by, double charge exchange in, 18: 15192 (CONF-399-2)
meson (π) elastic scattering by, double charge exchange in, 18: 16939 (ANL-6848(p.236-9))
meson (π) elastic scattering at 65 to 150 Mev, mechanisms for, 18: 44801
meson (π) elastic scattering on, electromagnetic form factor from, (T), 20: 13878
meson (π) elastic scattering by, optical models for, (T), 20: 42319
meson (π) interactions with nucleons in emulsion, intranuclear cascades from, (E/T), 20: 6287 (JINR-P-2373)
meson (π) optical properties in, low-energy, (T), 20: 22021
meson (π) quasi-elastic scattering by, nucleon correlation effects on, (T), 20: 15827
meson (π) reactions in, meson (3π) formation in, 18: 26300
meson (π) reactions at 4.5 Bev, excited fragments from, 18: 38082(T) (AEC-tr-6398(p.153-6))
meson (π) reactions with, meson (ρ) coherent production in, 18: 44821
meson (π) reactions with, nucleon emission in (T), 19: 1683
meson (π) reactions with emulsion, charge exchange in, (E), 19: 10243 (JINR-P-1837)
meson (π) reactions with, three-meson–(π) distribution from, 19: 1280
meson (π) reactions with, charge-exchange, (T), 19: 31302
meson (π) reactions below 200 Mev with, nuclear structure from, 19: 45339
meson (π) reactions with light, double charge exchange in, 20: 22033
meson (π) reactions at low energies, (T), 20: 42312
meson (π) reactions at high energies with Coulomb field of, meson (ω) production from, (T), 20: 46385
meson (π) reactions at 2 to 10 BeV, 19: 17159(R) (ORNL-3714 (Vol.II)(p.97-118))
meson (π) scattering at 30 to 150 Mev/c, Coulomb effects in, 18: 28730
meson (π)-nucleon interactions in, (T), 19: 29306
meson (π)–nucleon interactions in, elastic, (E/T), 20: 19444 (LYCEN-6527)
meson (ξ) scattering by, (T), 19: 23362 (JINR-P-1993)
meson capture of, conference on, 20: 42304
meson exchange currents in light, tests of, 20: 24435
meson (K) differential scattering cross sections for, 16: 29683
meson(K)–nucleon scattering in, dispersion relations for low-energy, 17: 21075
meson (K) reactions at 800 Mev, hyperfragments from, 18: 9315 (NP-13483)
meson (K^-) absorption at rest, in emulsion, 16: 5900
meson (K^-) absorption, hyperon effects, 16: 16980 (NP-11592(Vol.I) (p.389-94))
meson (K^-) capture at rest, hyperon production, 16: 9374
meson (K^-) capture, hyperon (Λ^0) emission in, 16: 10854
meson (K^-) capture by, effects of atomic weight, 16: 26084 (NP-11623)
meson (K^-) capture by complex, nuclear matter distribution and orbit distortion in, 17: 24442
meson (K^-) capture by complex, validity of multi-nucleon process in, 17: 24494
meson (K^-) capture by, for nuclear structure measurement, 17: 7232
meson (K^-) capture by light, hyperon (Σ)-meson (π) pair production in, 17: 13411
meson (K^-) interactions with nucleons in, Y_0^* production in, 18: 9368
meson (K^-) reactions at 1.15 Bev/c, energy distributions from, 16: 12355
meson (K^-) reactions in emulsions at 500 Mev/c, hyperfragment and hyperon production in, 16: 22886
meson (K^-) reactions, $_\Lambda Be^9$ production in, 16: 26312
meson (K^-) reactions at 300 Mev/c, hyperon (Λ^0) production in, 16: 27947
meson (K^-) reactions at 1.3 and 1.5 Mev, hyperfragment production in, 17: 17191
meson (K^-) reactions at 500 Mev/c, hyperfragment production in, 17: 24483
meson (K^-) reactions at 800 Mev/c, hyperfragment ($A \gtrsim 60$) production in, 17: 26555
meson (K^-) reactions at 50–300 Mev/c, hyperfragment production in, 17: 26557
meson (K^-) reactions at 1.455 Bev/c, hyperons (Ξ^0) and (Ξ^-) production in, 17: 26334
meson (K^-) reactions at 800 Mev/c, hyperon (Λ) beta decay branching ratio from, 17: 28192
meson (K^-) reactions at 800 Mev/c, hypernuclei production in, 17: 41917

meson (K^-) reactions at 800 Mev/c, production of short-range hyperfragments, 18: 2755
meson (K^-) reactions at 800 Mev/c, hyperfragment production in, 18: 9365
meson (K^-) scattering at low energies, 16: 4691 (TID-13768)
meson (K^-) scattering differential cross sections and optical potentials, 16: 12337 (NP-11175)
meson (K^-) scattering by, cross sections for, 16: 33812
meson (K^+) elastic scattering in emulsions at 260 Mev, cross sections for, 16: 27994
meson (K^+) reactions with, in emulsions at 240 to 300 Mev, 16: 8068 (NP-11232(p.367-72))
meson (K^+) reactions at 2.3 Bev/c with, double-hyperfragment event in, 18: 2656
meson (μ) capture by, 16: 21609
meson (μ) capture by, theory of, 17: 9582
meson (μ) capture by complex, hyperfine effects in, 17: 17229
meson (μ) capture by complex, models for, 17: 19293
meson(μ) capture by, nuclear structure research by, 17: 36646 (CERN-63-28(p.143-71))
meson (μ) capture in heavy, neutron emission in, 16: 18486
meson (μ) photoproduction in Coulomb field of, 16: 25931 (NP-11977 (p.90-2))
meson (μ) reactions on, mesons (π) from, 17: 28341
meson (μ^-) capture rates, 16: 24826
meson (μ^-) capture by, photon angular distributions from, 16: 26236
meson (μ^-) capture by, radiative, 17: 9394
meson (μ^-) capture by $40 \leq Z \leq 70$, lifetime and rates for, 17: 40083
meson (μ^-) capture by, interaction constants for, 17: 41936
meson (μ^-) capture by complex, gamma spectra from, 18: 6194
meson (μ^-) capture by, coupling constants in, 18: 9312 (JINR-E-1457)
meson (μ^-) reactions with heavy, particle emission in, 16: 7100
meson (ω^0) and (ρ^0) and photon interactions with Coulomb field of, meson (ω^0) and (ρ^0) production in, 18: 9169
meson (π) and nucleon nonelastic reactions with complex, data survey for, 17: 34883 (ORNL-3455)
meson (π) capture by complex, isobar mechanism for, 17: 26577
meson (π) peripheral reactions on, production of meson (π) pairs by, 16: 32321
meson (π) reactions at 4.15 Bev, mechanism for nuclear evaporation in, 16: 4881
meson (π) reactions with, nucleon pair production in, 16: 26089 (NP-11832)
meson (π) reactions in heavy, 16: 26340
meson (π) reactions with, nuclear research using, 17: 36643 (CERN-63-28(p.47-72))
meson (π) reactions at 7 Bev, tunnel mechanism for, 17: 40038
meson (π) scattering, optical model potential to the second order, 16: 7074
meson (π^0) photoproduction on complex, 17: 9517 (UCRL-10417)
meson (π^0) photoproduction from complex, 18: 9420
meson (π^-) absorption by complex, 17: 17108 (ISS-62/21)
meson (π^-) absorption by, nucleon emission from, 17: 19080
meson (π^-) and proton reactions on, up to 10 Bev, 16: 33752
meson (π^-) capture by complex, neutron spectrum from, 16: 25902 (LNF-62/37(p.138-42))
meson (π^-) capture in complex, 17: 6793(R) (ISS 62/14)
meson (π^-) capture by, two-hole excitation studies using, 17: 11687
meson (π^-) capture by light, formation of protons, deuterons, and tritons from, 17: 17273
meson (π^-) capture in complex, 17: 22418 (ISS-62/7)
meson (π^-) capture by emulsion, neutron energy spectra from, 17: 26543
meson (π^-) capture at rest by complex, 17: 34734 (NYO-10278)
meson (π^-) capture by, nuclear structure from two-nucleon emission in, 17: 38175
meson (π^-) inelastic reactions with, cross section asymptotic behavior for production of intermediate vector mesons in, 17: 41826
meson (π^-) inelastic scattering cross sections at high energies, 18: 1092
meson (π^-) interactions with, at 4.5 Bev, 17: 5214
meson (π^-) reactions at 4.5 Bev, angular distribution of secondary particles in, 16: 2413(T) (JPRS-10727)
meson (π^-) reactions at 2 Bev/c on, distributions from, 17: 2173
meson (π^-) reactions on, Auger electrons from, 17: 13525
meson(π^-) reactions on emulsion, hyperfragments from, 17: 15135
meson(π^-) reactions at 4.5 Bev, emission of lithium-8, beryllium, and boron fragments from, 17: 19354
meson (π^-) reactions on, at 16.2 Bev/c, 17: 19086
meson (π^-) reactions with, mass spectra for, 17: 26425 (NP-12886)
meson (π^-) reactions at 4.6 Bev/c, lithium-9 decay in, 17: 28274
meson (π^-) reactions at 17.2 Bev/c, hyperfragments from, 17: 29617
meson (π^-) reactions at 4.5 Bev in emulsion, 17: 36663 (TID-19329)
meson (π^-) scattering at 960 Mev/c, 16: 19770
meson (π^-) scattering in, 16: 24682 (JINR-P-868)
meson (π^-) scattering at 4.5 Bev by emulsion, cross sections, 16: 27968
meson reactions at 1.3 and 1.5 Bev/c, hyperfragments from, 18: 40548
meson reactions with, tests of unitary symmetry from, 20: 38009 (BNL-10420)
meson theory for forces in, review of, 19: 23765
mesons (μ) reactions, spin-dependence of capture, 16: 21610
mesons (μ) scattering, 16: 8060 (NP-11232(p.302-7))
mesons (π) absorption, 16: 23134
model for deformation and fission, drop, 16: 24803
model for deformed even, rotation-vibration, 17: 5331
model for deformed, using quadrupole force and pairing force, (T), 20: 46669
model for light, 18: 34833
model for light, Hartree-Fock self-consistent-field, 19: 17026
model for odd-A, asymmetric-core collective, 16: 21459
model for odd-A, eigenstates of asymmetric, 18: 4623
model for odd-A, semiatomic, 17: 22629
model for odd-mass 1d-2s shell, single particle Nilsson, 17: 11660
model for, superfluid, (T), 19: 39687
model interaction matrices for 2s-1d shell for A = 18 and 20, 19: 41730
model of deformed even-even, parity in asymmetric top, (T), 20: 44781
model of deformed, description of quasi-molecular states in independent-particle, 20: 34532
models for, 20: 3149
models for deformed, 18: 36692
models for even-even, development of asymmetric-rotor, 16: 21460
models for, review, 17: 13591
models for, lectures on collective, 18: 21191 (KR-64(Sect.VIII))
models for, spin-orbit terms in, 18: 21192 (KR-64(Sect.IX))
modulation of heavy cosmic, 18: 20813 (AD-434176)
moment of inertia of large systems of, with pairing forces, 16: 28166
moment of inertia of, Fermi theory for, 20: 15835
moments of inertia, calculation by approximate second quantization, 16: 21387
moments of inertia of heated, 17: 7301
moments of inertia and odd-even shift for K = 0 rotation bands of odd, 17: 19275
moments of inertia of, calculation using the shell model, 18: 2912
moments of inertia and quadrupole moments of even-even and odd, for Z = 60 to 94, 18: 6297
moments of inertia and wave functions for, with pairing interaction, 18: 34927
moments of inertia of strongly deformed, (T), 20: 32416
moments of inertia of deformed, (T), 20: 40102
momentum distribution in, relation to correlation structure, 16: 21531
momentum distribution and pair correlation function, 17: 24409
monopole force effects in light, (T), 19: 16917
Mössbauer effect in, tables, (T), 20: 9977 (TID-22403)
Mössbauer line shapes, in solid solutions, 16: 1077
Mossbauer scattering by, determination of recoilless fractions in, (T), 19: 10354
Mössbauer spectra with fluctuating hyperfine magnetic fields, (T), 20: 40152
motion in, many-body techniques for collective, 17: 40126
motion in triatomic molecules, quantum mechanical study of, 19: 16696
motion of, model for rotational, 17: 31536
motion of, methods for describing rotational, (T), 19: 14627
multiparticle excitations in intermediate compound states of, 18: 17079
M1-E2 mixing ratios in 2^+-2 transitions in even-even, test for purity of vibrational states in, 17: 41913
neon nucleus reactions at 200 Mev, effects of temporary nuclear structure, 16: 5965
neon nucleus reactions at 200 Mev, α particles and protons from, 16: 5966
neon-20 reactions with emulsion, at 200 Mev, (E), 20: 40083
neutrino absorption in Coulomb field of, cross section for high-energy, 17: 20999
neutrino absorption by, collective vibrations from, (T), 19: 12567
neutrino emission in transitions of stellar, 18: 18551(T)
neutrino inelastic reactions with, cross section asymptotic behavior for meson (π) production in, 17: 41826
neutrino interactions with neutrons in, analysis of elastic, 18: 13040 (CERN-63-37(p.203-13))
neutrino interactions in electromagnetic field of, direct production of lepton pairs from, (T), 20: 25858
neutrino pair emission by excited, 18: 34932
neutrino quasi-elastic scattering by, (T), 20: 44740
neutrino quasielastic scattering by, transverse muon polarization from, 20: 32468
neutrino reactions at 1 Bev, particle production cross sections, 16: 27965
neutrino reactions, 17: 17018
neutrino reactions on, multiple meson production from, 17: 19176

neutrino reactions with, intermediate boson production in, 17: 29546
neutrino reactions with, polarization of bosons produced in, 17: 31317
neutrino reactions with Coulomb intermediate boson production in, 18: 2653
neutrino reactions with, lepton pair production in, 18: 11256
neutrino reactions with Coulomb field of, vector boson production in, 18: 12896 (CERN-63-37(p.179-201))
neutrino reactions in universe, theory of, 18: 24348
neutrino reactions, W production in meson (μ)-, 18: 26269 (BNL-837 (p.257-65))
neutrino reactions with, structure effects in, 18: 36656
neutrino reactions at 60 Bev, meson (π) pair production in, 18: 40642
neutrino reactions with Coulomb field of, lepton pair production in, 18: 44552
neutrino reactions with, polarization of mesons (μ^-) from, (E/T), 19: 5201
neutrino reactions at high energies, intermediate boson production in, (E/T), 19: 33049
neutrino reactions with, induced transformations in, 19: 34984
neutrino reactions with, cross sections for, 19: 39943
neutrino reactions with nucleons in, meson (π) production in, (T), 19: 41754
neutrino reactions with, nuclear structure effects in, (T), 20: 12100
neutrino reactions (ν,μ) with, test for time reversal violation in, (T), 20: 13835
neutrino reactions at high energies, boson non-production in, 16: 26130
neutrino scattering near 1 Bev, lepton pair production cross sections, 16: 29705
neutrino scattering by, bremsstrahlung from, (T), 19: 8482
neutrino scattering by Coulomb field of, lepton pair production in, (T), 19: 45027 (NP-15199)
neutron absorption coefficients of excited, optical potential for estimating, 16: 32445
neutron absorption by, Doppler broadened cross sections for resonance, 17: 24383 (AEEW-R-226)
neutron absorption by, Monte Carlo analysis of thermal, (T), 19: 10223 (WAPD-T-1734)
neutron absorption cross sections for, Doppler-broadened, (T), 20: 21951
neutron absorption cross sections for $20 \leq A \leq 240$, from 0.1 to 25 Mev, calculations using optical model, (T), 20: 46583 (IKF-17)
neutron absorption cross sections and transmission coefficients, optical model calculations of, 18: 24595 (NP-13930(p.6-13))
neutron binding energies in, with A = 81 to 209, 18: 30813
neutron binding energies for A = 91 to 209, 18: 34966
neutron binding energies in A = 91 to 209, (E), 19: 29362
neutron binding energies in $86 \leq N \leq 92$, 20: 3098
neutron binding in, with A = 92 to 132, 19: 29366
neutron capture at binding energies by, levels from, 18: 42650 (TID-21144)
neutron capture by, measurement of, 16: 27367
neutron capture by, gamma polarization following thermal, 16: 29806
neutron capture by, gamma production in, 17: 5058
neutron capture by heavy, gamma spectra from, 17: 13590
neutron capture by, statistical analysis of levels in, 17: 28282
neutron capture by, effects on nuclide abundances, 17: 32869
neutron capture by $15 \leq A \leq 100$, cross sections for M1 transition in slow, 17: 38196
neutron capture by, electron distributions from, 18: 20332 (KR-64 (Sect.XII))
neutron capture by, gamma spectra from thermal, 18: 21193 (KR-64 (Sect.XIV))
neutron capture by, gamma spectra from, 18: 26666
neutron capture by, resonance self-shielding corrections for, 18: 30766
neutron capture by, structure studies by gamma emission following, 18: 32876
neutron capture by, probability of large cross sections for (T), 19: 3373
neutron capture by, gamma spectroscopy from, 19: 4505
neutron capture by, energy levels in s and p, (E/T), 19: 12553
neutron capture by, effects of resonance interference in, (T), 19: 21335
neutron capture by, gamma spectra from, 19: 23163(R) (ORNL-3650(p.111-86))
neutron capture by, precise absolute intensity determination of gamma rays from, (T), 19: 27505
neutron capture by, gamma emission from, 19: 31267
neutron capture by, radiation spectroscopy in, 19: 31310
neutron capture by, in stars, (T), 19: 41235
neutron capture by, gamma spectra from, 20: 1252
neutron capture by, resonance scattering of gammas from, (E), 20: 13771 (IA-1050)
neutron capture by, method for analysis of γ-γ cascades from, (E), 20: 13062 (IEA-96)
neutron capture by, gamma production data for, 20: 15725 (NP-14855)
neutron capture by, resonance widths in, (E), 20: 17676 (CEA-R-2810)
neutron capture by, computer program for resonance parameters from, 20: 24340 (GA-5816)
neutron capture by, cross sections for nucleosynthesis in, 20: 24350 (LA-DC-7774)
neutron capture by, average level widths of compound nucleus from, (E), 20: 32424
neutron capture by, analysis of gamma spectra from thermal, 20: 34660
neutron capture by mechanisms in fast, 20: 34669
neutron capture by $23 \leq A \leq 209$, at 14.7 Mev, (E), 20: 46614
neutron capture cross sections of light, measurement of fast, 17: 24473
neutron capture cross sections for, regularities in, 18: 44735 (NRL-6124)
neutron capture cross sections of, measurement, 19: 4517
neutron capture cross sections at 25 kev, nucleon number parity effect on, (T), 19: 33284
neutron capture cross sections at 5 to 100 kev, review of, 19: 37825 (ORNL-P-1226)
neutron capture cross sections, 20: 26095 (SGAE-PH-34/1965)
neutron capture gamma spectra from, 16: 14054
neutron capture in medium-weight, transition partial-width fluctuations from, 16: 14056
neutron capture in resonance region, data analysis method for, (T), 19: 35434
neutron capture to 50 kev, energy dependence of radiative (E/T), 19: 3391
neutron cross section measurements on fissionable, status of, 17: 15252 (EANDC(US)-28(L))
neutron cross sections for, 17: 41860 (HW-75716(Vol.1))
neutron cross sections of, tabulation of, 18: 4538 (EANDC(UK)-26U)
neutron cross sections for fissile, expressions for, 18: 18865 (ANL-6792(p.695-709))
neutron cross sections, Hanford library revisions for, 18: 29144 (HW-75715)
neutron cross sections for Z = 1 to 20, 18: 44726 (BNL-325(2nd Ed.) (Suppl.2)(Vol.I))
neutron cross sections for, computer program for, 19: 3375
neutron cross sections of, tables, (E), 19: 8406 (UNC-5090)
neutron cross sections at stellar temperatures, 19: 12604
neutron cross sections for, methods for measuring fast, 19: 14529 (MMPP-FRPC-64-2)
neutron cross sections of, availability for reactor calculations, (E), 19: 21225 (AECL-2168)
neutron cross sections for $Z \geq 94$, measurement of, 19: 29326
neutron cross sections of, computer analysis, (E/T), 19: 31200 (WAPD-TM-501)
neutron cross sections for, (E), 19: 31244 (ZfK-RN-23)
neutron cross sections for, echoes, giant resonances, and size resonances in, (T), 19: 33315
neutron cross sections for fissionable, evaluation of, 20: 1160 (WAPD-T-1847)
neutron cross sections of, tabulations, (E), 20: 3018 (NYO-72-27)
neutron cross sections of, energy dependence of, (T), 20: 6404
neutron cross sections and resonance integrals for heavy, 20: 44602 (BNL-982)
neutron cross sections of $6 \leq A \leq 27$, at 0 to 16 Mev, calculations using local optical potential with average parameters, (T), 20: 46555 (LA-3538(Vol.1))
neutron cross sections of $28 \leq A \leq 240$, at 0 to 16 Mev, calculations using local optical potential with average parameters, (T), 20: 46556 (LA-3538(Vol.2))
neutron definite j-value state for, shell model for single, (T), 20: 15791
neutron diffraction by, review of, 17: 5059
neutron elastic and inelastic scattering at 0.5 to 3 Mev, 18: 30835
neutron elastic scattering by hard-sphere, total cross sections, 16: 18419
neutron elastic scattering by, 17: 17094 (TID-18277)
neutron elastic scattering by nonspherical, 17: 17246
neutron elastic scattering at 1.509 Mev, polarization in, 17: 31410 (TID-19051)
neutron elastic scattering on, techniques for angular distribution measurements from fast, 17: 34851
neutron elastic scattering by, intermediate state lifetime from K-shell ionization probability in, 18: 2897
neutron elastic scattering by medium, polarization in, 18: 2846(R) (TID-19709)
neutron elastic scattering by complex, optical model analysis of, 18: 15221
neutron elastic scattering at 1 Mev, optical model analysis of, 18: 34828
neutron elastic scattering by spherical, polarization in, 18: 42702
neutron elastic scattering at 14 Mev, measurement of cross sections for, 18: 44768
neutron elastic scattering at 0.1 to 14 Mev, angular distribution coefficients for, 19: 14540 (TID-21629)
neutron elastic scattering, unified theory for, 19: 17036
neutron elastic scattering by, asymptotic approximation for, (T),

19: 27540
neutron elastic scattering on, model for, (E/T), 19: 47581 (LA-DC-6730)
neutron elastic scattering at 0.8 Mev, cross sections for, (T), 20: 15770
neutron elastic scattering at 0.3 to 0.8 Mev, angular distributions from, (E), 20: 22023
neutron elastic scattering at 3.4 Mev, charge and mass dependence of polarization for, (T), 20: 26207
neutron elastic scattering by Z = 13 to 92, cross sections for, 20: 44669(T) (INDSWG-101, pp 109-57)
neutron elastic scattering by Z = 4 to 92, angular distributions from, (E), 20: 46794
neutron elastic scattering by Z = 13 to 83, at 3.2 Mev, (E/T), 20: 46644
neutron elastic scattering and polarization to 50 MeV, bibliography on, 19: 35390 (LA-3281)
neutron emission by compound, 17: 9593
neutron emission by compound, computer analysis of, (T), 19: 21245 (ORNL-TM-196)
neutron evaporation from excited distributions, 17: 17162
neutron evaporation spectra from, angular momentum effects in, 18: 28628
neutron Fermi energy in A ≳ 200, 18: 19118
neutron fission cross sections for, twenty-six-group (E/T), 19: 3374
neutron fission lifetime of compound, 16: 32394 (LADC-5367)
neutron fission of, charge and mass distributions from thermal, 18: 21195 (KR-64(Sect.XVI))
neutron fission of, delayed neutrons from fast, (T), 19: 27436 (NP-14833)
neutron fission of, channel theory of, 20: 34661
neutron inelastic scattering on non-spherical, 17: 17248
neutron inelastic scattering at 14 Mev by closed-shell, level density and nuclear temperature from fast, 17: 31492
neutron inelastic scattering on, excitation functions for fast, 17: 34856
neutron inelastic scattering on, gamma detection techniques for fast, 17: 34858
neutron inelastic scattering at 6 Mev, energy spectra for, 18: 998 (AD-299005)
neutron inelastic scattering at 6 Mev, 18: 999 (AD-299028)
neutron inelastic scattering cross sections at high energies, 18: 1092
neutron inelastic scattering by many-body systems of, self-diffusion in incoherent, 18: 6149
neutron inelastic scattering by, with two extra nucleons, 18: 18906
neutron inelastic scattering by heavy and medium, 18: 38146
neutron inelastic scattering by heavy and medium, 18: 44777
neutron inelastic scattering by, analysis of thermal, (T), 19: 5160
neutron inelastic scattering at low energies, methods for measurement of, 19: 33235 (AERE-R-4263)
neutron inelastic scattering probabilities for multigroup reactor analysis, fast, (T), 19: 37768 (WCAP-3269-34)
neutron inelastic scattering by, computer program for matrices of, (T), 19: 47544 (KAPL-M-6467)
neutron inelastic scattering at high energies, direct-interaction, (T) 20: 3256
neutron inelastic scattering by, equation of state from, (T), 20: 6379
neutron inelastic scattering by A = 12 to 209, at 14 Mev, (E), 20: 8153
neutron inelastic scattering at 8 Mev by A = 208, excitation of 3⁻ collective state, (E/T), 20: 13870
neutron inelastic scattering at 0.8 to 4.1 Mev, nuclear shell effects on, (E), 20: 22023
neutron inelastic scattering by, intensity measurements for thermal, (T), 20: 24314
neutron inelastic scattering by, gamma differential cross sections for, (T), 20: 28343
neutron inelastic scattering by, method for low-background, (E), 20: 28236 (NP-16039)
neutron inelastic scattering by, analysis of, 20: 34659
neutron inelastic scattering by Z = 3 to 92, cross sections for, 20: 44668(R) (INDSWG-101, pp 73-108)
neutron inelastic scattering by light, computer program for calculations using evaporation model, 20: 46560 (ORNL-TM-1552)
neutron infinitely dilute resonance integrals, (T), 19: 33234 (AAEC/TM-270)
neutron levels in, correlation of positions of, 19: 47583 (NP-15467)
neutron multiple capture by, fluctuations in, 18: 30759
neutron penetrabilities and reaction cross sections for, 18: 9307 (CEA-2380)
neutron-proton interaction energy in odd-odd, 16: 32446
neutron radiative capture cross sections for, 17: 17222
neutron radiative capture, spectra from thermal, 18: 4627
neutron radiative capture by, gamma elastic scattering from thermal, 18: 32792
neutron radiative capture by, multiple scattering corrections for, (T), 20: 11967 (JINR-P-2455)
neutron reaction (n,2a) with medium and heavy, cross sections for, (T), 20: 1187
neutron reaction and scattering constants for Z = 97 to 200, 17: 41861 (HW-75716(Vol.2))
neutron reaction and scattering data for Z = 196 through 240, 17: 41862 (HW-75716(Vol.3))
neutron reactions (n,α) and (n,p), cross sections and Q-values, 16: 1017 (AE-58)
neutron reactions (n,p) at 14 Mev, cross sections for, 16: 12477
neutron reactions (n,γ), gamma resonance effects, 16: 21454
neutron reactions (n,α), (n,2n), and (n,p) around Z = 40, cross sections, 16: 21586
neutron reactions at 30 kev, gamma spectra from, 16: 22991(R) (ORNL-3268(p.43-7))
neutron reactions below 5 Mev, resonance theory, 16: 23145
neutron reactions at 2 to 5 Mev, cross section fluctuations near A = 30, 16: 24845
neutron reactions (n,γ), isotopic effect of secondary reactions of recoil atoms in, 16: 24861
neutron reactions (n,γ) in, spectroscopy of, 16: 29777 (JAERI-1020 (p.206-11))
neutron reactions, generalized nuclear model for, 16: 33843
neutron reactions with thirty even-even, at 0.8 to 3.3 Mev, calculations of inelastic cross sections for, 16: 2493 (TID-14206)
neutron reactions (n,γ) at 0.025 ev, recoil energies from, 17: 5001
neutron reactions (n,α) and (n,p) at 14.5 Mev, cross-section calculations by statistical theory for, 17: 11754
neutron reactions (n,α) with, statistical model calculation of cross sections for, 17: 17206
neutron reactions on, strength functions and widths for, 17: 19222 (TID-16603)
neutron reactions with, angular distributions for fast, 17: 28240 (BNL-400(Vols.I and II))
neutron reactions, correlation of cross section and product activity, 17: 31441
neutron reactions at intermediate energies, theory of, 17: 32990
neutron reactions with, resonance processes in fast, 17: 34853
neutron reactions with, polarization effects in fast, 17: 34854
neutron reactions with, statistical-model theory for fast, 17: 34857
neutron reactions (n,α) at 14 Mev, cross section trends in, 17: 36409 (NP-13020(p.166-8))
neutron reactions (n,α) and (n,p) with 12 < A < 150, cross section behavior in 14 to 15-Mev, 17: 38162
neutron reactions (n,α) and (n,p) with 23 ≤ A ≤ 77 at 5–25 Mev, statistical model analysis of cross sections for, 17: 38212
neutron reactions below 1 Mev with spherical, optical model for, 17: 40042
neutron reactions (n,α) with even-even, theoretical calculations using direct interaction processes, 17: 39994
neutron reactions and scattering on, cross section computer program for, 18: 1018 (KAPL-M-NCF-4)
neutron reactions on, Doppler-broadened cross sections for, 18: 4586 (WAPD-T-1626)
neutron reactions with aligned, resonances in, 18: 4540 (JINR-P-1369)
neutron reactions with, effects of crystalline fields on resonant, 18: 6164 (NP-13354)
neutron reactions (n,γ) with 110 ≤ A ≤ 140 and 180 ≤ A ≤ 200, gamma-ray M1 transitions from, 18: 11169 (ANL-6797(p.220-9))
neutron reactions at 14 Mev, 18: 13636(R) (ORNL-3537(p.71-105))
neutron reactions with, radiation widths for resonance, 18: 17033
neutron reactions with spin-½, scattering widths for resonance, 18: 17034
neutron reactions (n,α) at 14 Mev, statistical analysis of excitation functions and energy spectra, 18: 17057
neutron reactions (n,α) at 14 Mev, statistical model cross section for, 18: 17058
neutron reactions (n,γ) with, gamma spectra from, 18: 20333 (KR-64 (Sect.XX))
neutron reactions with polarized, resonance effects in, 18: 21127 (KR-64(Sect.XXV))
neutron reactions (n,γ) with, gamma-gamma angular correlations from, 18: 21199 (KR-64(Sect.XXI))
neutron reactions (n,γ) with, polarization of photons from, 18: 21200 (KR-64(Sect.XXII))
neutron reactions with, optical studies of, 18: 24594 (NP-13930(p.1-5))
neutron reactions at 14 Mev, systematics of cross sections for, 18: 24601 (NP-13930(p.41-2))
neutron reactions at 14.7 Mev, activation cross section measurements in, 18: 24613 (NP-13930(p.139))
neutron reactions (n,γ) with, studies of compound nucleus decay and nuclear structure in, 18: 24607 (NP-13930(p.104-8))
neutron reactions (n,α) and (n,p), cross sections for, 18: 28666
neutron reactions with, promulgation of cross sections for, 18: 28541
neutron reactions (n,α) at 14 Mev, total cross sections for, 18: 34887
neutron reactions with, bibliography on cross sections for, 18: 34753(R)

(EANDC(E)-50(L))
neutron reactions (n,γ) with, relation between cross section and scattering length for, 18: 34762 (JINR-P-1671)
neutron reactions (n,d) and (n,t) with, polarization in direct, 18: 36624
neutron reactions (n,α) at 14 Mev, statistical model anomalies for, 18: 38156
neutron reactions with, in reactor for radioisotope production, 18: 39781(T) (AEC-tr-6390(p.488-92))
neutron reactions with medium and heavy, optical potentials for, 18: 42673
neutron reactions (n,p) at 50 to 150 Mev, 18: 42695
neutron reactions (n,α) at 14.5 Mev with $6 \leq Z \leq 30$, 18: 44779
neutron reactions (n,p) at 14 Mev, shell effects in, 18: 44789
neutron reactions with light, total effective cross sections for (E), 19: 1654
neutron reactions with, Doppler-broadened cross sections for (T), 19: 1537
neutron reactions with, 19: 1987
neutron reactions with polarized, precession in, (T), 19: 5254
neutron reactions with, computer analysis of cross section data for, 19: 8390 (AEEW-M-347)
neutron reactions (n,γ) with, level studies from, 20: 4821(R) (ANL-7081, pp 2-21)
neutron reactions (n,γ) with, spectra from, (E), 19: 8670
neutron reactions (n,γ) with, experimental study of, 18: 38071 (NP-14214)
neutron reactions with, multigroup flux-weighted cross sections for, (T), 19: 10220 (GEMP-329)
neutron reactions at 14 Mev for $Z < 31$, distributions from, (E), 19: 10254 (ORNL-3672)
neutron reactions with computer analysis of yields from, (T), 19: 12489 (ORNL-3673)
neutron reactions with, (T), 19: 11590
neutron reactions (n,2n) at 14 Mev, shell effects in, (T), 19: 12536
neutron reactions (n,d) with, variational treatment of, (T), 19: 12528
neutron reactions (n,2n) with, statistical model analysis of cross sections for, (T), 19: 14503 (BNL-897)
neutron reactions with, computer analysis of cross sections and resonances of, (E), 19: 14506 (BNL-8710)
neutron reactions with, cross sections for fast, (T), 19: 16851 (NAA-SR-Memo-10544)
neutron reactions (n,α) and (n,p) at 14 Mev, shell effects in, (T), 19: 17040
neutron reactions (n,d) and (n,p) with, scintillation telescopes for, 19: 15891
neutron reactions with, scintillation spectrometer for charged-particle emission in, 19: 15894
neutron reactions with, cross sections for, (T), 19: 21228 (ANL-6970)
neutron reactions with, chain element activity in intermittent, (T), 19: 21226 (AEET/HP/Th-19)
neutron reactions with, computer analysis of cross sections for, (T), 19: 25472 (KAPL-M-6424)
neutron reactions (n,p) with, cross sections for, (T), 19: 29323
neutron reactions (n,γ) with, spin cut-off coefficient for, (T), 19: 29341
neutron reactions with, beam paramagnetic resonance in, (T), 19: 29343
neutron reactions to 20 Mev, graphs of excitation functions for, 19: 31226 (NP-15018)
neutron reactions (n,γ) in Mev, range, level density from compound-range, level density from compound-nucleus, (T), 19: 35448
neutron reactions (n,p) with closed-shell, effective two-body interactions in, (T), 19: 35470
neutron reactions with, cross sections for, 19: 35506
neutron reactions (n,γ) in, thermal reactors gamma spectra from, (E), 19: 35849 (RT/FI(64)-16)
neutron reactions with, cross sections for gamma production in, (T), 19: 43269 (GEMP-360)
neutron reactions with, activation rate reduction to differential spectrum in thermal, (T), 19: 43327
neutron reactions to 80 kev, resonance parameters in, (E), 19: 45296
neutron reactions with, effective cross section factors for, (T), 19: 47577 (IDO-17107)
neutron reactions with, cross section and polarization studies from, 20: 4822(R) (ANL-7081, pp 22-35)
neutron reactions (n,γ) with, gamma spectra from, (T), 20: 6427
neutron reactions with, code for multigroup transfer matrices in, (T), 20: 8043 (TID-22447)
neutron reactions (n,γ) at 0.1 to 15 Mev, cross section tabulations for, 20: 8084 (UCRL-14007(Rev.1))
neutron reactions with, survey on, 20: 9973 (NP-15816)
neutron reactions with, structure analysis using fast, 20: 12132
neutron reactions (n,p) with light, at 14.8 Mev, (E), 20: 12133
neutron reactions (n,2n) with, cross sections for, (E/T), 20: 12040
neutron reactions with, width fluctuation factor for, (T), 20: 13824
neutron reactions with, computer programs for charged particle cross sections from, 20: 17671 (AEEW-M-611)
neutron reactions (n,n′) and (n,p) with excited, cross sections for direct, (T), 20: 17714
neutron reactions (n,γ) with, research at RC-1 reactor, 20: 20334
neutron reactions (n,α), (n,2n), (n,np), (n,p) and (n,t) below 20 Mev, excitations for fast, (E/T), 20: 19883
neutron reactions at 14 Mev, design and performance of counter telescope for, 20: 21054
neutron reactions (n,αn′) with heavy, direct, (T), 20: 22018
neutron reactions up to 100 Mev, cross-section energy-dependence model for, 20: 24360(R) (UCRL-16580, pp 107-48)
neutron reactions with, giant resonances in, (T), 20: 24383
neutron reactions with, semiconductor performance for charged particle detection from, 20: 25376 (AECD/EP-9)
neutron reactions with nonfissile, cross section analysis for, 20: 28282 (ORNL-P-2091)
neutron reactions with, review of cross section research on, (E/T), 20: 30349 (JAERI-1102)
neutron reactions with, survey of fast, 20: 32535
neutron reactions (n,γ) with, method for calculating cross sections for, 20: 32374(R) (IITRI-578P25-15)
neutron reactions at 14 Mev, cross sections, Q-values, and sensitivities for, 20: 32380 (SC-RR-66-229)
neutron reactions (n,2n) with, cross section for, (T), 20: 34623
neutron reactions with, mechanisms for, 20: 34658
neutron reactions with, strength functions for, 20: 34663
neutron reactions with, resonances and strength functions from, 20: 34665
neutron reactions with, resonance parameters from, (T), 20: 36160 (GA-7060)
neutron reactions with, collision integral for anisotropic chain-type, 20: 36213
neutron reactions (n,α), (n,2n), (n,p), and (n,t) with nuclei, cross sections for, (E), 20: 40069(R) (EANDC(E)-66(U))
neutron reactions (n,α) and (n,p) with, cross sections for, (E), 20: 40069(R) (EANDC(E)-66(U))
neutron reactions with charged-particle emission, review on thermal, 20: 44666(T) (INDSWG-101, pp 1-22)
neutron reactions with $Z = 13$ to 28, with charged-particle emission, 20: 44671(T) (INDSWG-101, pp 164-223)
neutron reactions with $Z = 11$ to 16, fluctuations in total cross sections for, (E), 20: 44743
neutron reactions in reactors, computer analysis of, (T), 19: 12490 (ORNL-3689)
neutron reactions with, cross section libraries for, 18: 37597 (A/CONF.28/P/168)
neutron removal cross sections for, 18: 34888
neutron resonance widths in, 17: 13487 (JINR-P-1130)
neutron resonance parameters of, statistical analysis of, 18: 2954
neutron resonance capture in 2s-1d, 18: 7696(R) (ORNL-TM-761)
neutron resonance spins in, method for determination of, 18: 21164 (CONF-481-36)
neutron resonance capture by, effects on neutron velocity distributions, 18: 28544
neutron resonance integrals for, computer program for, 18: 30083 (AEEW-R-323)
neutron resonance integrals for, level separation corrections to, (T), 19: 27538
neutron resonance absorption by, 19: 31207
neutron resonance parameters for, least squares analysis of, 19: 37758 (BNL-9243)
neutron resonance cross sections, approximate Doppler broadening of isolated, (T), 19: 43275 (LA-3315)
neutron resonance absorption in homogeneous media with heavy moderators, (T), 20: 11941
neutron resonance integrals for, second order approximations for effective, 20: 17650 (AAEC/E-144)
neutron resonance absorption by measurement of, cross sections for, 20: 19812 (GA-6919)
neutron resonance absorption in unresolved region, computer program for, 20: 21940 (GAMD-6908)
neutron resonance properties in fast and intermediate reactors, self-screening, (T), 20: 34531
neutron resonance absorption by, Doppler broadening in, 20: 34551
neutron resonance parameters for $Z = 18$ to 95, 20: 44667(T) (INDSWG-101, pp 23-72a)
neutron resonance integrals for, computer program for, 20: 6291 (NAA-SR-Memo-11538)
neutron resonance elastic scattering, 16: 23109
neutron resonances in heavy, cross sections for, 18: 6295
neutron resonances in, 18: 11195(R) (EANDC(E)-49(L))
neutron resonances of, determination of parameters for, 20: 34662
neutron S-wave strength functions of spherical, (T), 19: 21327
neutron scattering at 0.4 to 24 Mev, optical model for, 16: 3872(R)

(ORNL-3193(p.237-50))
neutron scattering, effects of atomic weight on polarization, 16: 4793
neutron scattering at high energies, by deformed, 16: 8228
neutron scattering at 1 to 5 Mev, inelastic, 16: 9413 (CEA-2083)
neutron scattering at thermal energies, calculation using complex potential, 16: 13935
neutron scattering at 2.09 Mev, optical model analysis of polarization by, 16: 21539
neutron scattering, wave distortion in inelastic, 16: 21591
neutron scattering, non-local potential model for, 16: 21390
neutron scattering at high energies by light, resonance, 16: 26521
neutron scattering, S- and P-wave strength functions for A = 34 to 242, 16: 26334
neutron scattering cross sections for spherical, with complex potentials, 16: 28039
neutron scattering at 3.5 Mev, polarization in, 16: 32438
neutron scattering by even-even, search for selectively excited spin-zero states by, 17: 7075 (AROD-2577:2)
neutron scattering by, compound and direct contributions to polarization in, 17: 11752
neutron scattering at 14 Mev by, cross sections for, 17: 15286
neutron scattering by harmonically bound protons in, 17: 19228 (TID-18424)
neutron scattering by statistical, time-dependent motions of, 17: 21216
neutron scattering below 10 ev, spins of resonant states from, 17: 26604
neutron scattering by, effects of polarization on, 17: 34894
neutron scattering by, polarized, 17: 36414 (NP-13020(p.214-26))
neutron scattering by A near 100, optical model analysis of, 18: 7676 (CONF-340-3)
neutron scattering by A near 20, 18: 7677 (CONF-340-6)
neutron scattering by Coulomb field of, 18: 15213
neutron scattering by polarized deformed, optical-model cross sections for, 18: 19017
neutron scattering by polarized, in ferromagnetic materials, 18: 24580
neutron scattering at small angles, cross section increase in, 18: 26519
neutron scattering by, effect of non-axially symmetric deformation on thermal, 18: 34787
neutron scattering at small angles near s-wave resonance, polarization in, 18: 40586
neutron scattering by, polarization from, (T), 19: 6699
neutron scattering by deformed, inelastic, 19: 10361
neutron scattering by, transfer matrices for, (T), 19: 19087 (NAA-SR-Memo-9055)
neutron scattering by bound, asymptotic formulas for, (T), 19: 19107
neutron scattering by, boundary diffusion effects on cross sections for slow, (T), 19: 21424
neutron scattering at 14 Mev by Z = 12 to 83, cross sections for inelastic, (E), 19: 25475(R) (ORNL-TM-1044)
neutron scattering by polarized, in electric or magnetic fields, (T), 19: 27426 (JINR-P-2026)
neutron scattering by, cross sections, (E/T), 19: 29322
neutron scattering by, non-spherical optical model for, (T), 19: 33238 (CONF-650524-1)
neutron scattering on polarized, review of polarized, 19: 35373 (BNL-903)
neutron scattering by, electrodynamic effects in Coulomb, (T), 19: 41334 (JINR-P-2229)
neutron scattering by nonspherical, optical model analysis of, (T), 19: 43276 (NAA-SR-Memo-11456)
neutron scattering by, Coulomb field and magnetic moment interactions in, 19: 47115(R) (ANL-6983)
neutron scattering by polarized, in external magnetic field, (T), 20: 3120
neutron scattering by Coulomb field of, polarization determination from, (T), 20: 4832 (IAE-901)
neutron scattering by, p-wave phase shifts in small-angle, (T), 20: 4909
neutron scattering by, computer program for angular data from, 20: 9972 (NAA-SR-11231)
neutron scattering by, in matter, (T), 20: 13734
neutron scattering by, gamma production data for, 20: 15725 (NP-14855)
neutron scattering at low energies, intermediate structure in, (T), 20: 21988 (BNL-948, pp 876-904)
neutron scattering by even-even, at 2.5 Mev, (T), 20: 24338 (CONF-660411-1)
neutron scattering by, polarization from, (E), 20: 24362(T) (ANL-Trans-294)
neutron scattering by spin-zero, generalized optical model for resonances in, (T), 20: 24469
neutron scattering by, resonance effects on spectra from, (T), 20: 24313
neutron scattering by, technique for measuring resonance, 20: 30358(R) (RPI-328-56, pp 1-48)
neutron scattering by, optical model analysis of, 20: 34673
neutron scattering by, slowing down parameters and Legendre polynomial coefficients for, 20: 37988 (WAPD-TM-572)
neutron scattering by, computer program for solving T matrices for, 20: 44663 (WAPD-TM-571)
neutron scattering by, spin-orbit effects in, (T), 20: 44780
neutron separation energies in even-A ($84 \leq N \geq 98$), 18: 24681
neutron single-particle states in, energies of, 17: 17231
neutron states in deformed optical potential, 20: 38126
neutron strength functions of ellipsoidal, s-wave, 17: 29599
neutron strength functions for, optical model for, 18: 7678 (CONF-346-5)
neutron strength function in nonsymmetric deformed, S-wave, 18: 16956 (ZFK-TPH-7)
neutron strength function of, with A = 220 to 246, 18: 42622(R) (ANL-6879(p.2-20))
neutron strength functions of, method for estimating, 20: 38038
neutron surface absorption by, low-energy, 17: 7212
neutron total cross sections of, measurement of, (E), 19: 18098 (KAPL-3074)
neutron total cross sections at 2 to 15 Mev, substructure in giant resonances in, (E), 19: 33239 (HW-SA-3588)
neutron transmission through polarized, polarized, 18: 36696
neutron-proton interaction in, 18: 34915
neutron-proton interactions in, isobaric states in, (T), 19: 21304
neutron-proton interactions in, short-range, (T), 20: 38056
neutron-proton pairing in, generalized Bogolyubov transformation for, (T), 19: 19160
neutron-proton pairing correlations in spherical even, 20: 38177
neutron-proton pairing correlation effects in even-even spherical, with $40 < A < 70$, (T), 20: 42195
neutron-proton ratio in, formula for, 18: 22883
nitrogen-14 reactions with, cross sections for single neutron transfer in, 17: 38279
nonaxiality of deformed even-even (T), 19: 3278
nuclear binding and particle separation energies for $22 \leq Z \leq 120$, 20: 6290 (LA-3280)
nuclear binding energies in, reference spectrum determination of, 17: 19350
nuclear charge division, fission energy tables for calculation, 16: 19755 (UCRL-9883(Rev.))
nuclear data for A = 21 to 212, 20: 46634
nuclear data sheets for A = 186, revised, 20: 44713
nuclear data sheets for A = 187, revised, 20: 44714
nuclear data sheets for A = 188, revised, 20: 44715
nuclear data sheets for A = 189, revised, 20: 44716
nuclear forces, effects of charge, 16: 24301
nuclear forces in, Brueckner theory for, 16: 29807
nuclear interactions in, equilibrium shape from, 18: 36683
nuclear magnetic double-resonance spectra of spin ½, (T), 20: 40103
nuclear magnetic resonance, effects of dipole-dipole coupling on double, 16: 32397 (NP-12012)
nuclear magnetic relaxation and resonance in liquids, 17: 822
nuclear magnetic relaxation of spin-½, dipole interactions in spherical molecules, 17: 26584
nuclear magnetic resonance of weakly coupled, role of multiple quantum transitions in, 18: 13081
nuclear magnetic relaxation of three spin-½, 18: 17076
nuclear matter binding energy and two-nucleon potential, 18: 40537
nuclear pairing correlations in, variational approach to, 20: 26108
nuclear particle scattering by collective, coupled-channel calculations for, (T), 19: 47685
nuclear potential in light, charge-dependent, 17: 21100
nuclear properties of light ($4 < A \leq 40$), 16: 31116
nuclear quadrupole resonance for spin ½, second moment of, 17: 38140(T)
nuclear scattering by, narrow resonances in, 17: 36661 (PUC-1962-90)
nuclear structure of odd-A, with $62 \leq Z \leq 76$, (T), 20: 11961 (INR-602/VII/PH)
nuclear tensor operators for, matrix elements of integrable, 19: 29298
nucleon absorption cross sections and transmission coefficients for, in optical model, 18: 42762
nucleon absorptive potential in heavy, spatial distribution of, 18: 7674 (CONF-327-7)
nucleon angular momentum distribution in, 18: 26578
nucleon binding and pairing energies in, effects of shell closure on, 19: 10358
nucleon binding energy and distribution in, 17: 11736
nucleon binding energies in single-particle model of, 17: 19231(T) (AEC-tr-5702)
nucleon binding energy in $6 \leq Z \leq 100$, formula for, 17: 28273
nucleon binding energies in, formula for, 18: 22883
nucleon binding energies in, pairing corrections to, (T), 19: 29347
nucleon binding energies in A = 69 to 100, 19: 29365
nucleon binding energies in, four-particle Bethe-Faddeev equation for, (T), 20: 10057
nucleon binding energies in, systematics of, 20: 17729
nucleon binding energies in, measurement of, 20: 28445

nucleon binding energy in, (T), 20: 34577
nucleon binding energy in, calculation using K-matrix theory, 20: 44727
nucleon binding in, three-nucleon state in, 16: 31122
nucleon binding in, potentials for saturation, 20: 30434
nucleon bond energies in $174 \leq m \leq 239$, 16: 10967(T) (FTD-TT-61-175 (p.15-24))
nucleon capture by, analysis of gamma spectra from, 18: 21202 (KR-64(Sect.XXXII))
nucleon cluster structure and Coulomb energy difference of mirror, (T), 20: 10063
nucleon clustering in, connection to shell-model wave function, 18: 4606
nucleon clustering in light, effects on nuclear reactions, 18: 21247
nucleon clustering in light, review on, 19: 16886
nucleon clustering in light, review on, 20: 17707
nucleon clusters in, 18: 40610
nucleon collisions with, model for high-energy, 17: 19542
nucleon conservation, 16: 26328
nucleon-correlation calculations in, 17: 19083
nucleon correlations in, linear quasi-particle theory for, 19: 5208
nucleon correlations in, method for studying, 20: 8160
nucleon coupling in, spin-independent, (T), 19: 10273
nucleon coupling to axial symmetric core in model for deformed odd-even, 19: 33896
nucleon densities of, (T), 19: 27450
nucleon density distribution in, effects of exponential, Gaussian, and Yukawaian interactions on, 18: 24633
nucleon distributions in, analysis by meson (π^0) photoproduction on, 17: 33073
nucleon distributions and wave functions in light, (T), 19: 8393 (ISS-64/24)
nucleon elastic and inelastic scattering by shell, 18: 30836
nucleon elastic scattering at high energies, gamma production, 16: 3712
nucleon elastic scattering, low-energy photons from, 16: 31095
nucleon elastic scattering by, mechanism for resonances in, 17: 26608
nucleon elastic scattering on, interference of compound and direct, 17: 40130
nucleon elastic scattering by, 17: 41820
nucleon elastic scattering at high energies, nonlocal and target-momentum effects on optical potential for, 18: 7772
nucleon elastic scattering by, monopole excitation in, (T), 19: 43301
nucleon elastic scattering below 50 Mev, data survey for polarized, 20: 3014 (LA-DC-7386)
nucleon energy spectra in spherical, shell model analysis, 16: 28114
nucleon exchange reactions between complex, 17: 11737
nucleon forces in, origin of repulsive core in, (T), 20: 13879
nucleon inelastic scattering by, amplitudes in, 17: 11731
nucleon inelastic scattering by, test of impulse approximation for, 17: 28300
nucleon inelastic scattering by, detection of direct interaction contribution in, 17: 31488
nucleon inelastic scattering by, exchange effects in, 18: 2860
nucleon inelastic scattering by deformed, in collective model, 18: 34865
nucleon inelastic scattering at 50 to 150 Mev, 18: 42695
nucleon inelastic scattering by, angular distributions from, 20: 10083
nucleon inelastic scattering by, microscopic description of, (T), 20: 22118
nucleon inelastic scattering via compound nucleus mechanism, review of gamma angular distributions from, 20: 38178
nucleon inelastic scattering from, validity of distorted-wave Born approximation for, 17: 31494
nucleon interaction matrix elements and the odd-group model for heavy, 16: 28146
nucleon interactions with heavy, 16: 7143
nucleon interaction matrix elements and the odd-group model for heavy, 16: 28146
nucleon interactions in photographic emulsions at high energies, angular distribution of jets from, 17: 9522
nucleon interactions in A = 6, energy level spectra from free, 17: 24412
nucleon interactions with surface nucleons in, mechanisms for, 17: 38178
nucleon interactions in, boundary-condition model for forces in two-body, 18: 7760
nucleon interactions in deformed, 18: 18905
nucleon interactions inside light, calculation of energy levels using, 18: 21345
nucleon interactions in, shell-model analysis of, 18: 38115
nucleon interactions in, representation of residual, 18: 44545
nucleon interaction forces in (T), 19: 1696
nucleon interaction-potential parameters in, (T), 19: 8405 (UCRL-7155(Rev.I))
nucleon interactions in, BCS and RPA calculations for, (T), 19: 16984
nucleon interactions in, shell-model study of, 19: 25541
nucleon interaction energy of odd-odd, multiplet splitting and, (T), 19: 27489
nucleon interactions in, SU(3) model for s-state, (T), 19: 45247(R) (ANL-6877,pp 29-31)
nucleon interaction potentials in, shell model calculations for, (T), 20: 3058
nucleon interactions in finite, energy levels from effective, (T), 20: 8133
nucleon interactions in, perturbation theory for, 20: 9971 (MIT-2098-201)
nucleon interactions in, correlated basis functions for, (T), 20: 11492
nucleon interactions in, hard-core potential in boundary-condition model for, (T), 20: 17772
nucleon interactions in p-shell configurations in, three-body, 20: 22092
nucleon interactions in, separation distance for effective, (T), 20: 22122
nucleon interactions in, hamiltonian for, 20: 24381
nucleon interactions in mixed degenerate orbits of, generalized seniority scheme for identical, 20: 26168
nucleon interactions in, nonlinear field equation for, 20: 30361
nucleon interactions in $2s_{1/2}1d_{3/2}$ shell, surface delta interaction approximation of, 20: 30423
nucleon interactions in, integral operators and S-matrix for scalar dispersion in, 20: 32537
nucleon interactions in, two-body matrix element for Gaussian, 20: 32461
nucleon interaction with complex, at high energies, (T), 20: 37790
nucleon interactions in single j-shell with charge-independent pairing force, calculations using BCS method, (T), 20: 44734
nucleon interactions in, long range multipole forces in, 20: 46340 (PUC-937-224)
nucleon isospin pairing correlations in light, (E), 19: 43349
nucleon level density in, p-shell, 17: 17070
nucleon magic numbers in, structural basis for, (T), 20: 4872
nucleon magnetic moment in, sum rule for, 19: 29246 (JINR-P-2019)
nucleon magnetic properties in, method for studying, 19: 19113
nucleon momentum distribution in, effects of optical potential on, 17: 830
nucleon momentum distribution in, (T), 19: 45279 (NP-15415)
nucleon motion in deformed light, 16: 12463
nucleon motion in strongly deformed, 16: 23151
nucleon nonlocal interactions in, dipole photoabsorption cross section increase from, 17: 40120
nucleon packing fraction of, ambiguities in, 20: 28318
nucleon pair correlations and final-state interactions in, 20: 38015
nucleon pair transfer between light nuclide and, correlations in, (E/T), 19: 21266(R) (UCRL-11828(p.108-9))
nucleon pairing approximation for $f_{7/2}^-$ and $p_{3/2}^+$ shells, (T), 20: 44684
nucleon pairing correlations in, effect on beta decay, 17: 24178
nucleon pairing correlations in, charge-independent, 18: 18972
nucleon pairing correlations in, (T), 19: 21381
nucleon pairing correlations and structure for heavy, 19: 23671
nucleon pairing correlations in, effect of nuclear rotation on, (T), 19: 39858
nucleon pairing correlation at high moments, 20: 3103
nucleon pairing correlations in, conservation of nucleon number in formalism for, 20: 10027
nucleon pairing correlations in light, four-body, (T), 20: 12013
nucleon pairing correlations in odd-mass, effects of rotational motion on, 20: 22148
nucleon pairing correlations in, coupling effects of nuclear rotation on, 20: 36199
nucleon pairing effect in, 18: 15172(R) (AROD-1784:31)
nucleon pairing energies in, 17: 13516
nucleon pairing force ratio to field-producing force in, 16: 17106
nucleon pairing forces in, theory, 17: 36713
nucleon pairing forces in strongly deformed, effects on intrinsic excitation in, (T), 19: 8484
nucleon pairing force of deformed, superconductivity wave functions for, (T), 19: 23635
nucleon pairing forces in, (T), 20: 3066
nucleon pairing hamiltonian for, symmetry properties of, 18: 34890
nucleon pairing in, and optical model potential, 17: 13517
nucleon pairing interactions in, approximation for, 18: 19098
nucleon pairing interactions in, method for calculating, 18: 44783
nucleon pairing in, theory for, 18: 44785
nucleon pairing interaction in, (T), 19: 6657
nucleon pairing interactions in, charge-independent, (T), 19: 17007
nucleon pairing interactions in, superconductivity theory of, 19: 23735
nucleon pairing in, effect on two-particle penetration through centrifugal barrier, 19: 33376
nucleon pairing in, R(5) and R(8) groups in quasi-spin formalism for, 19: 41839
nucleon pairing interactions in, superconductivity theory of, 19: 41843
nucleon pairing interactions in, Bogolyubov compensation method and variational principle for, (T), 20: 6343
nucleon pairing interactions in, stability of solutions of Hartree-Bogolyubov equations for, 20: 10026
nucleon pairing interactions in, (T), 20: 12049

nucleon pairing infinite, variational derivation of equation for, (T), 20: 15742
nucleon pairing interactions in, approximation for, (T), 20: 17765
nucleon pairing interactions in, eigenstates for J = 0, T = 1, charge-independent, 20: 22121
nucleon pairing interactions in, number-conserving approximations for theory of, 20: 32494
nucleon pairing interaction in, superconductivity approximation for, 20: 32397
nucleon pairing in, quasi-particle triples as exact solution of Lee model for, 20: 46396
nucleon pairing-correlation model of, one-body matrix elements and wave functions in, 20: 26115
nucleon pairing-force Hamiltonian for, exact eigenstates of, 19: 35414
nucleon pairs in, solution of Bethe-Goldstone equation for impulses of, 17: 28330
nucleon potential in, parity nonconservation by, 18: 40559
nucleon potentials in, charge-exchange effects on, 17: 2278
nucleon potentials in, soft core, (T), 19: 16934
nucleon pulse distribution, 16: 7025
nucleon quadrupole and pairing forces in d-s shell of, (T), 20: 17801
nucleon reaction for A ≤ 4, analysis, 16: 6029
nucleon reaction potential calculations, 16: 10832
nucleon reactions to 16 Mev, cross sections and energy spectra for, 16: 12505
nucleon reactions, optical potential calculations, 16: 13964 (PAN-258/VII)
nucleon reactions, optical potential calculations, 16: 13965 (PAN-281/VII)
nucleon reactions at intermediate energies, model for, 16: 17131
nucleon reactions at high energy, determination of nuclear structure from, 16: 21464
nucleon reactions, coefficient of inelasticity for, 16: 31114
nucleon reactions above 100 Bev on heavy, mesons from, 16: 32314
nucleon reactions with nonaxial, reduced widths of rotational states in, 16: 33841
nucleon reactions with even, tables of cross-section functions for double Coulomb excitation in, 17: 792 (AWRE-NR/P-2/62)
nucleon reactions with light, optical potential calculation for, 17: 7188
nucleon reactions with, momentum transfer to mesons (π) in, 17: 13336
nucleon reactions with complex, mechanisms of, 17: 18376 (TID-7652 (p.409-32))
nucleon reactions with spherical spin-zero at 40–180 Mev, comparison of exact solution and semi-classical approximation for, 17: 31421
nucleon reactions on, models for inelastic, 17: 33064
nucleon reactions with, mechanisms of compound-nucleus and direct, 17: 38205
nucleon reactions with, theory of compound-nucleus and direct, 18: 9440
nucleon reactions at 1 to 50 Mev, nuclear structure studies from, 18: 19107
nucleon reactions with complex, cross sections and energy conservation for, 18: 34952
nucleon reactions at 100 to 1000 Bev, mechanisms of, 18: 34764 (JINR-P-1678)
nucleon reactions above 10^{12} ev, heavy particle production in, 18: 40524
nucleon reactions at high energies, helium-3 and triton emission in, (E/T), 19: 8435
nucleon reactions with, nucleon-alpha cascades from, (T), 19: 21372
nucleon reactions at high energies, charge exchange in, (E), 19: 27433 (JINR-P-2060)
nucleon reactions at 10^{11} to 10^{13} ev, (T), 19: 27460
nucleon reactions with, optical model parameters for, (T), 19: 27503
nucleon reactions at very high energies, 19: 27182
nucleon reactions with, gamma spectra calculations for inelastic, 19: 41954 (NP-15338)
nucleon reactions with, (T), 19: 43374
nucleon reactions at high energies, nucleon production in, 20: 3259
nucleon reactions with, spin-spin interaction in low-energy optical potential for, (T), 20: 6395
nucleon reactions at 0.1 to 25 Mev, data tabulations on polarization in, 20: 11965 (JINR-P-2426)
nucleon reactions at high energies, mechanisms of, 20: 12111
nucleon reactions with, DWBA for two-body stripping, (T), 20: 13814
nucleon reactions with, dependence of EAS characteristics on model for, 20: 23945
nucleon reactions with, SU(3) symmetry for meson (η^0) multiple production in, 20: 24380(T)
nucleon reactions in cosmic showers, upper limit for passive-state, (T), 20: 25755(T)
nucleon reactions at high energies, in cosmic showers, (T), 20: 25806(T)
nucleon reactions with, heavy particle stripping in, (T), 20: 32444
nucleon reactions with, theory of doorway states in, 20: 34666
nucleon reactions with, isobaric analog resonances in, (T), 20: 36198
nucleon reactions above 10 Bev, internuclear cascade model for inelastic, 20: 38122
nucleon reactions above 10^{12} ev, angular distribution of secondaries from, (E), 20: 44286
nucleon reactions with, amplitudes for, (T), 19: 5211
nucleon reactions with, optical model potentials for, (T), 19: 23712
nucleon reactions at 2 to 10 Bev, 19: 17159(R) (ORNL-3714(Vol.II)) (p.97-118))
nucleon reactions, multiple particle production in, 19: 1652
nucleon reactions, composite particle production in, 19: 36220(R) (MIT-2098-142)
nucleon scattering, operator impulse approximation, 16: 8234
nucleon scattering at 300 Mev, quasi-elastic, 16: 9371
nucleon scattering at high energies by heavy, differential cross sections for, 16: 12506
nucleon scattering at high energies, Regge poles, 16: 15696
nucleon scattering at high energies, Pauli exclusion effects in, 16: 17121
nucleon scattering cross sections, channel coupling in, 16: 17101
nucleon scattering, cross section relation to optical potential imaginary component, 16: 17104
nucleon scattering, radial dependence of optical potential for, 16: 21477
nucleon scattering, optical potential radial dependence in, 16: 21364
nucleon scattering at 3 to 25 Bev, model for, 16: 21391
nucleon scattering by, optical potential for, 16: 28040
nucleon scattering by, second-order optical potential for, 16: 28093
nucleon scattering by, corrections to the optical potential for, 16: 28104
nucleon scattering amplitudes for, 17: 7080 (JINR-P-1024)
nucleon scattering by light, cross sections for, 17: 15280
nucleon scattering by, one-pion-exchange effects on, 17: 2280
nucleon scattering by, Regge pole application to, 17: 9414
nucleon scattering by, surface corrections to the high-energy optical potential for, 17: 13434
nucleon scattering by, theory for, 17: 31282 (PUC-1963-110)
nucleon scattering by, theory of, 17: 36412 (NP-13020(p.186-200))
nucleon scattering on, Green potential for, 17: 11527
nucleon scattering at high energies, identity effects in multiple, 18: 7747
nucleon scattering by, impulse approximation optical model for, 18: 16953(R) (TID-20352)
nucleon scattering by, nuclear rotational levels from, 18: 16959
nucleon scattering by, two-body formulation of problems in, 18: 21337
nucleon scattering by, optical potential for, 18: 42782
nucleon scattering by computer program for angular distributions from, 18: 44737 (ORNL-TM-930)
nucleon scattering by, Slater integrals and form factors for inelastic single-particle, 19: 1565 (ORNL-TM-964)
nucleon scattering by excited, coupled-channel resonances in (T), 19: 1566 (PUC-1964-154)
nucleon scattering at low energies, evaluation of models for, 19: 14544
nucleon scattering by, localization of direct interactions in, (T), 19: 14603
nucleon scattering by, optical model potential for, (T), 19: 16931
nucleon scattering by, parameters for, (T), 19: 20937(T) (TID-21672)
nucleon scattering at low energies, survey on, (T), 19: 31247
nucleon scattering by, particle-hole analysis of, (T), 19: 33250 (TID-21869)
nucleon scattering by, rotational-state excitation in, (T), 19: 33359
nucleon scattering at low energies on, quantum Green function for, (T), 19: 33377
nucleon scattering by, optical-model analysis of, (E/T), 19: 35510
nucleon scattering by, (T), 19: 43374
nucleon scattering by, shell-model calculations for, (T), 20: 4882
nucleon scattering by, errors in optical model analysis of, 20: 6296(R) (ORNL-3858(Vol.1), pp 1-12)
nucleon scattering by, resonance-mode effects on channel coupling in, (T), 20: 6426
nucleon scattering by, shell model for, 20: 6434
nucleon scattering by, high-energy approximation for nonlocal potentials in, 20: 19573
nucleon scattering at low energies, compound nucleus properties from resonance, (T), 20: 24468
nucleon scattering by complex, off-shell amplitudes for, (T), 20: 28374
nucleon scattering by, computer program for gamma angular distributions from, 20: 36220
nucleon scattering by solution of Schroedinger equation using Green-function method, (T), 20: 44836
nucleon shells in Z > 82 and N > 126, closed, (T), 20: 44640 (JINR-P-2793)
nucleon shells of N ≥ 126 and Z ≥ 82, calculations using diffuse potential well, (T), 20: 44774
nucleon single-particle potential for, nonlocal, 20: 6430
nucleon spin interaction with rotation in odd nonaxial, 18: 2949
nucleon spin-orbit interaction potential with, complexity of, 17: 9612

nucleon spiral correlation for light, 17: 38161
nucleon surface delta interaction in single closed shell spherical, correlation with pairing plus quadrupole model, 20: 28412
nucleon transfer reactions between, (T), 20: 4850
nucleon triplet-even potentials in, phase shifts for singular, 17: 40032
nucleon tunneling in, theory for, 18: 24617 (NYO-1807-7)
nucleon two-body forces in, 18: 42756
nucleon wave functions for, structural effects of principal quantum number on, (T), 19: 45365
nucleon 4-body interactions in, single-shell, 18: 34863
nucleon-nucleon interaction on Fermi surface of, (T), 19: 16861
nucleon-nucleon interaction in, charge dependence of, (T), 19: 21373
nucleon-nucleon interactions in, resonance density in, (T), 19: 27174
nucleon-nucleon interactions in, core excitation effects on residual, (T), 19: 31301
nucleon-nucleon interaction in, tensor, (T), 19: 39872
nucleon-nucleon interactions in, (T), 19: 43374
nucleon-nucleon interactions in, core polarization effects in two-body, (T), 20: 1186
nucleon-nucleon interaction in, research using nucleon inelastic scattering, (T), 20: 38120
nucleon-nucleon interactions in light, (T), 20: 44652 (ORNL-P-2468)
nucleon-nucleon interactions in, (T), 20: 44760
nucleon-nucleon potentials in, space-parity nonconserving, (E/T), 19: 33371
nucleon-nucleon potentials in, repulsive core, 20: 24450
nucleon-nucleon potentials for Hartree-Fock calculations, (T), 20: 42208
nucleon-nucleon potentials and saturation of nuclear matter, velocity-dependent, 18: 21223
nucleon-pair binding energies in, 19: 29354
nucleon-pair correlation function of, (T), 19: 31314
nucleon-phonon interactions in spherical, (T), 19: 37874(T)
nucleon-phonon interactions in, (T), 20: 44678
nucleon-proton interactions at 30 Bev/c in, models for jets from, (E/T), 20: 6039 (INSJ-90)
nucleons in, SU_3 wave functions for sd-shell, 18: 38172
nucleus inelastic scattering by, collective levels from, (T), 20: 3013 (JINR-P-2331)
nutation effects on NMR measurement of magnetic fields, (E/T), 19: 26933
octupole states in even-even, dependence of excitation energy on atomic number for, 16: 21523
octupole vibrations of deformed even-mass, 18: 18991
octupole vibrations in even-even, liquid-drop-model studies, 18: 30757
odd mass, energy levels and transition probabilities in the mass region 41 to 147 in, 16: 29755 (JAERI-1020(p.1-17))
odd mass, energy levels in the mass regions 150 to 190 and >225 in, 16: 29756 (JAERI-1020(p.18-25))
odd-odd, ground state analysis using the J-J coupling model in, 16: 29763 (JAERI-1020(p.89-96))
odd-odd, structure studies in the mass range 40 or greater of, 16: 29757 (JAERI-1020(p.26-37))
optical anisotropy and shape of the surface of, method for studying, 17: 7302
optical potential of heavy, 17: 2324
optical potential of, calculation of imaginary part of, 17: 7143 (TID-17357(Pt.II))
optical potential for excited states of, Fermi gas model for, 20: 3116
optical potentials and macroscopic dissipation constants, 18: 15316
orientation and polarization, 16: 18121(R) (RADC-TN-61-199)
orientation at low temperatures, 16: 32245
orientation by adiabatic demagnetization, system for, 19: 6158
orientation by high magnetic fields, 16: 15448
orientation by optical pumping, hfs effects on, (T), 19: 8420
orientation in beta–gamma decay, 18: 4528 (CONF-303-9)
orientation in external fields, review of, 19: 35373 (BNL-903)
orientation in heavy-ion reactions, use in nuclear spectroscopy, 20: 34603
orientation, low-temperature methods for, 16: 3746
orientation of, design of helium-3 cryostat for, 17: 28092
orientation of, lectures on, 17: 4057 (NP-12247(Pt.A))
orientation of, lectures on, 17: 4058 (NP-12247(Pt.B))
orientation of, review of dynamic and static methods for, 17: 5056
orientation of spin-1, 20: 32390
orientation of, study by r-f spectroscopy, 17: 36389 (NP-13020(p.1-26))
orientation of, angular momentum operators in, 18: 19080
orientation of, deformation cooling for, 18: 24703
orientation of, method for, 18: 36685
oriented, use in nuclear physics research, 16: 19501
origin of bypassed, 17: 13594(T)
origin of, in solar system, (T), 20: 29909
oscillations in, review of experimental evidence for collective, 16: 21492
oscillations in spherical even, anharmonic effects on collective, 18: 44833
oscillations in spherical even-even, collective, (T), 19: 33352
oscillations in, Pauli principle effects on collective, (T), 19: 29304
oscillations in, two-component collective, (T), 20: 24458
oscillations of, collective motion in surface, 18: 2881
oscillations of deformed, dispersion equation for collective frequencies of octupole, (T), 20: 24470
oscillations of even-even, coupling of dipole and quadrupole, 18: 30790
oscillations of heavy, theory of compressible, 19: 3282
oscillations of spherical, anharmonic, 18: 18921
oscillations of spherical, effects of anharmonic terms on, 18: 22916
oscillations, theory of collective, 16: 21493
oscillator-strengths sum for, effects of hard core on, 17: 11753
Overhauser effect in spin-1, 19: 16863
oxygen-16 reactions with, total cross sections for, 17: 28256 (UCRL-10766)
pair correlation, quadrupole-quadrupole interactions, and superfluidity in odd-A, 18: 7723
pair correlations and energy levels in near-magic, 16: 8186
pair emission from aligned, 17: 31508
pairing correlations in, 16: 21491
pairing correlations between like nucleons in strongly deformed, 18: 24692
pairing correlations in surface layer of, 18: 24630
pairing correlations in light, charge symmetric, (T), 19: 5203
pairing force approximation, 16: 4855
pairing-force calculations for deformed, refined, 17: 24750(R) (UCRL-10624)
pairing forces and energy levels in near-magic, 16: 8187
pairing forces, approximations to, 16: 8189
pairing interaction in, (T), 19: 28962(R) (NIRL/R/81)
pairing model, conserved particle number in, 18: 32745(R) (UCRL-11213 (p.1-48))
pairing-force strength, comparison of exact and BCS calculations of, 18: 32745(R) (UCRL-11213(p.1-48))
parities of, use of deuteron scattering data in calculating, 20: 15850
parity states in (2s,1d) shell of, shell model study of negative, 17: 33092
particle absorption by, hyperfragments from, 18: 16979
particle behavior in, dynamical correlation, 16: 9407
particle capture by, collective model for direct radiative, 20: 34670
particle cascade reactions with, at high energies, 18: 1010 (JINR-P-1341)
particle diffraction scattering by, with washed-out nuclear boundaries, 16: 31115
particle diffraction at 660 Mev by, model for, 17: 19377
particle diffraction scattering by, nuclear surface diffuseness effect on, (T), 19: 10289
particle diffraction scattering by, cross section for, (T), 19: 37899
particle diffraction scattering with excitation of collective states, (T), 20: 38143
particle elastic scattering by, variational calculations for, 17: 7507
particle elastic scattering by, strong absorption model for charged and neutral, 18: 1032
particle elastic scattering by, optical model for, 18: 15303
particle elastic scattering by, approximation calculations for, 18: 44296
particle elastic scattering by, polarization in, (T), 19: 19181
particle elastic scattering by, optical model for heavy, (T), 19: 19212
particle elastic scattering angular distributions, conversion function for calculating, 19: 35372 (ANU-P/349)
particle elastic scattering by, formal theory for, 19: 39821
particle elastic scattering by, interaction-region model for, 20: 36207
particle elastic scattering by, blast-nucleus model for compound, (T), 19: 23706
particle elastic scattering by, strong-absorption model for polarization in spin-½, 18: 24636
particle emission from rotating, 16: 23040
particle inelastic scattering by, with monopole and quadrupole excitations, 16: 14023
particle inelastic scattering by, excitation of two-phonon states in, 18: 11267
particle inelastic scattering by, collective-state excitation in, (T), 19: 21234 (JINR-P-1908)
particle inelastic scattering by, shell model for, 20: 12008
particle inelastic scattering by, (T), 20: 21973 (BNL-948, pp 175-221)
particle inelastic scattering by, strong absorption model for, 20: 22086
particle inelastic scattering by, polarization and asymmetry in inelastic, (T), 20: 30492
particle inelastic scattering by, matrix elements for heavy-, 20: 32383
particle inelastic diffraction scattering with excitation of collective states, (T), 20: 38142
particle inelastic diffraction scattering with excitation of monopole oscillations, (T), 20: 46778
particle inelastic scattering by complex, strong absorption model for

charged and neutral, 18: 6186
particle interactions with delta-function potential, 17: 11910
particle interactions in, effects on scattering cross section, 18: 6272
particle interactions in spherical even-even, quasi-, 18: 32745(R) (UCRL-11213(p.1-48))
particle interactions in even-even quasiparticle theory for, 19: 23632 (UCRL-11225)
particle model of, analysis of independent, 16: 29762 (JAERI-1020 (p.75-88))
particle model of scattering from collective states of, 17: 11699
particle polarization by, size effects in, 16: 19815
particle reabsorption, fast secondary, 16: 17123
particle reactions at high energy, inelastic, 17: 15311
particle reactions at high energies on, mesons from, 17: 19159
particle reactions at high energies on, coherent, 17: 19382
particle reactions with, angular distributions from, 18: 21250
particle reactions with, theory for high-energy, (T), 19: 5200
particle reactions at high energies with, meson (π) distributions from, 19: 5127 (INSJ-79)
particle reactions near 1 Tev, calculations and measurements of, (E/T), 19: 6633 (JINR-P-1796)
particle reactions with, helium-3 and triton production in, (T), 19: 6713
particle reactions with, kinematics of, (T), 19: 8394 (ISS-64/27)
particle reactions at Tev energies, jets from, 19: 12493 (PAN-537/VI)
particle reactions with, tabulation of thresholds for, (E), 19: 14539 (TID-21627)
particle reactions with spin-zero, spins of states from, (E), 19: 14495 (ANL-6878(p.279-301))
particle reactions with, average cross sections for compound-nucleus, (T), 19: 17011
particle reactions with, models using cluster and compound-nucleus models for, (T), 19: 17012
particle reactions with, computer calculations of cross sections for, (E), 19: 19080 (ANL-6978)
particle reactions at variable beam intensities, radiation from, (T), 19: 21235 (JINR-P-1950)
particle reactions with, optical-model computer analysis of, 19: 31221 (KAPL-3085)
particle reactions at high energies, multiple meson production from, (T), 19: 41708
particle reactions at high energies, analysis of jets from, (T), 19: 41709
particle reactions with, statistical model for multiple production in, (T), 19: 45041 (TPJU-12/65)
particle reactions with, gamma angular distributions following electromagnetic excitation by, (T), 20: 24414
particle scattering by, classical cross sections for, 17: 618
particle scattering by, cross sections for elastic, 17: 7205
particle scattering by, amplitudes for, 17: 19178
particle scattering by, effects of particle-hole excitations in, 17: 21060
particle scattering from, partial wave analysis for relativistic charged spinless, 17: 22451
particle scattering by extended, distribution for large momentum transfer, 17: 22551 (CERN-63-9)
particle scattering by heavy, phase relations for, 17: 31463
particle scattering by, effects of multiple, 18: 2065
particle scattering by, S-wave phase shifts for, 18: 6020
particle scattering by potential fields of, 18: 44606
particle scattering by emulsion, detection of spurious, 19: 4510
particle scattering by, computer analysis of geometrical factors in, (T), 19: 9897 (UCRL-7734)
particle scattering by, optical model for, (T), 19: 27572
particle scattering with excitation of collective energy levels, (T), 20: 8151
particle scattering on regular systems of, resonance levels in, (T), 20: 9967 (IAE-940)
particle scattering by nucleons of, (T), 20: 12100
particle scattering by complex, analysis of diffraction, (T), 20: 17816
particle scattering by, transfer theorem for multichannel, 20: 32409
particle scattering by, optical model for inelastic, 20: 34548
particle scattering by, calculations using diffraction model, (T), 20: 46590 (NP-16309)
particle scattering at large angles by light, with strong absorption, (T), 20: 46646
particle scattering by, inelastic models of, 16: 29771 (JAERI-1020 (p.155-74))
particle spurious scattering by, in emulsion, 18: 41782
periodic system of, 17: 17287
phase shift definition from elastic scattering experiments, 16: 28048
phonon-quasiparticle interactions in odd spherical, (T), 19: 29309
photo nuclear resonance in strongly deformed, calculations for, 17: 19366
photo-excitation of, development of gamma sources for, 20: 34682
photoabsorption by, dipole theory of, 18: 42632 (IAE-613)
photodisintegration of, compound and direct effects in, 17: 24411
photodisintegration of, bibliography on, 18: 19125
photodisintegration of mass-3, theoretical calculations on, 20: 19946
photodisintegration of three-particle, structure effects on, 20: 26135(T)
photodissociation in nuclear emulsions at 1.16, 1.29, and 1.35 Bev, 16: 8761 (TID-14850)
photofission of heavy, at 200 to 730 Mev, (E), 20: 13345(R) (NP-15772)
photofission of heavy, delayed neutron yields in, (E), 20: 28300
photofission of, quasi-deuteron model for, 16: 32430
photoinduced gamma emission from, method for observing two-photon photoeffect in laser, (T), 20: 34539
photon absorption by, dynamic collective theory for, 18: 11216 (NP-13561)
photon absorption by, giant resonance in dipole, (T), 19: 16918
photon absorption by neutron-proton pairs in, (T), 19: 21274
photon absorption by, giant quadrupole resonance in, (T), 20: 15823
photon absorption by, Fermi liquid theory for, 20: 32539
photon coalescence in the Coulomb field of, 17: 21093
photon elastic scattering by Coulomb fields of, 17: 19384
photon elastic scattering and coupling in coulomb field of, (T), 19: 12545
photon emission, analysis of (M1 + E2), 16: 1068
photon interactions with Coulomb field of, cross section for two photon production in, (T), 20: 32031
photon reaction resonances in heavy, width of giant, 18: 21206 (NP-13813)
photon reactions (γ,π^0) with complex, theory of, 18: 17063
photon reactions (γ,N) with, unified theory for, 18: 21364
photon reactions ($\gamma,n\pi$) to 200 Mev, cross sections for, (T), 19: 10295
photon reactions (γ,K^+) with complex, spectral distribution from, (T), 19: 35393 (LNF-65/6)
photon reactions (γ,n) and (γ,p) with heavy, isospin selection rules in, (T), 20: 1226
photon reactions (γ,N) with deformed, models for polarization from, 20: 8111
photon reactions at 10 to 5000 Mev, electron pair production in, (E), 20: 29990 (JINR-P-2667)
photon reactions in light, effects of nucleon group structure on, 18: 11235
photon reactions in field of, electron pair production by, 18: 36576 (NP-14167)
photon reactions in coulomb field of, electron pair production in, 18: 42386
photon reactions in, effect of dynamical correlations on, 19: 41844
photon reactions to 7 Mev, electric dipole ground-state transition width strength functions for, 16: 8167 (NP-11174)
photon reactions, vector meson pair production in, 18: 5989 (JINR-P-1403)
photon reactions with heavy, 16: 25949 (NP-11977(p.144-6))
photon reactions with, proton distributions from, 17: 32440
photon reactions with stellar, neutretto emission from, 18: 2517
photon reactions with, unified theory for, 18: 13054 (NP-13560)
photon reactions with, effect of quadrupole collective motions on dipole resonance in, 18: 34908
photon reactions with, cross section for, (T), 19: 14334
photon reactions with light, meson (π) production in, (T), 19: 33387
photon reactions with Coulomb field of, photon-pair production in, (E/T), 19: 41784
photon reactions with, meson (π^0) production in, (E), 19: 46788
photon reactions with, analysis of, 20: 3151
photon reactions with, resonance-mode effects on channel coupling in, (T), 20: 6426
photon reactions with, review on, 20: 8090
photon reactions with heavy, Levinger-Bethe sum rules for dynamical correlations in, (T), 20: 13873
photon reactions with, dipole approximation in nonlocal potential for, (T), 20: 15842
photon reactions with, giant resonance in, (E/T), 20: 17706
photon reactions with field of, nuclear magnetic effects on pair production in, (T), 20: 19968
photon reactions with, total absorption cross sections for, (T), 20: 19991
photon reactions with, resonance effects in direct, (T), 20: 26206
photon reactions with, neutron production in, 20: 34671
photon scattering in crystals, 16: 8182
photon scattering by, time-dependent, 18: 9427
photon scattering by Coulomb fields of, electron pair production in, 18: 19124
photon scattering by Coulomb fields of, electron pair production in, 18: 18744
photon scattering by Coulomb field of, gauge invariant calculation of, 19: 21119
photon scattering by oriented, (T), 20: 38055
photon splitting in fields of, 16: 32451
photon splitting in electric field of, cross section for, (T), 20: 15339

photoneutron emission by Z = 24 to 33, 18: 38152
photonuclear reactions, effects of nucleon–nucleon interactions on, 16: 31117
photonuclear reactions, effects of nucleon–nucleon interactions on, 16: 31118
photonuclear reactions in deformed, 17: 4115
photonuclear resonance energy for deformed and spherical, 16: 4840
photonuclear resonance calculations for, 16: 28060
photoproduction of mesons (π) on, amplitude for low-energy, 17: 17274
photoproduction of mesons (π) on, impulse approximation theory for, 19: 1558 (NP-14404(p.140-59))
photoreactions on, cross sections for, (E/T), 19: 10356
photoreactions on, giant resonances of, (E/T), 20: 20365
photoreactions with deformed, (T), 19: 12603
physical properties, 16: 4358
physical properties of oriented, general form of second order tensor for, (T), 20: 33879 (NLCO-946, pp 63-7)
polarizability of, effects on isotope and isomer shifts, 16: 28098
polarizability of, 17: 7025
polarization, application to production of polarized targets, 16: 12456
polarization at low temperatures, dynamic, 18: 34717
polarization, based on gamma scattering amplitude, 16: 24782 (JINR-P-967)
polarization by direct currents in semiconductors, (T), 20: 8311
polarization by electron-nucleus dipolar coupling, (T), 20: 15819
polarization by rotation, 17: 21057
polarization effects on nuclear magnetic resonance and Mössbauer spectra, 19: 42001
polarization enhancement in helium-3, 17: 31544
polarization, factors influencing dynamic, 16: 28046
polarization for use as targets, 18: 44831
polarization from dispersion of nuclear magnetic relaxation, high field boundaries, 19: 23786
polarization, in crystals rotating in magnetic fields, 16: 4774
polarization in crystals, dynamic, 20: 28678
polarization in direct reactions, effects of, 17: 38243
polarization in liquids by relaxation interactions, 18: 15194 (EUR-483.e)
polarization in organic solvents, Overhauser effect in, 19: 20869
polarization in paramagnetic solutions, ENDOR spectrometer for measuring, 20: 32525
polarization in solid deuterium, method for, 20: 12104
polarization in solids by solid-state effect, (E/T), 20: 38402
polarization in solutions of diphenylpicrylhydrazyl, dynamic, (E), 20: 45678
polarization methods for, magnetic, 17: 17121 (LNF-62/102)
polarization of, by optical pumping techniques, 17: 34640
polarization of, for charged particle reactions, 17: 38244
polarization of, generalized expression for dynamic, 17: 36438 (NP-13020(p.454-9))
polarization of, in direct reactions, 17: 22647
polarization of, in flow-type nuclear resonance detecting element, acceleration of, 17: 39737
polarization of magnetic, 17: 7267(T)
polarization of, measurement of dynamic, 17: 7126 (NP-12330(p.259-76))
polarization of, measurement of dynamic, 17: 7164
polarization of, review of dynamic methods for, 17: 13592
polarization of, review of methods for, 17: 42002
polarization of spin-1, (T), 20: 26107
polarization of, using magnetic resonance, 17: 7123 (NP-12330(p.224-41))
polarization of, by capture of polarized neutrons, 18: 11188 (ANL-6797(p.397-403))
polarization of, method for measuring, 18: 39578
polarization of, minimum entropy production in dynamic (T), 19: 1576
polarization of, performance of autodyne installation for measuring dynamic, 20: 41249
polarization of, quantum-statistical theory of dynamic, 20: 17819
polarization of, review of dynamic methods for, 19: 19104
polarized, preparation of targets containing, 16: 4771
positron capture by stellar, neutrino pair production in, 17: 41708
positron decay of, energy relations and forbidden character of, 18: 21227
positron inelastic scattering, 16: 19817
positron scattering by, cross sections for E0 transitions in, 17: 7269
positron scattering by, cross sections for, (T), 19: 41510
positron scattering, 16: 13890
positron scattering cross sections, 16: 24863
positron scattering by, 18: 11210 (LNF-63/47(p.199-204))
positron single-quantum annihilation in fields of, 17: 19082
potential and reduction factor for nonlocal wave function for, Perey effect for equivalent local, (T), 20: 13811
potential at, electron-produced electrostatic, 18: 20744(T)
potential, calculation of three-body, 16: 11009
potential calculations for finite, using Hartree-Fock methods, 19: 37800(R) (ORNL-3778(p.22-3))
potential energy surface-crossing transitions, 16: 6835
potential fields of, multipole expansions of Coulomb, 17: 14958
potential in optical model, including surface-absorption effects, 16: 23089
potential of, anomalous solutions to Dirac and Schroedinger equations for Coulomb, 17: 26579
potential of, non-locality of optical, 17: 21039
potential of, calculation of parameters for repulsive, 16: 33842
potential well of, bound states for particle motion in, 20: 8141
potentials at low energies, radial distribution of imaginary part of optical, (T), 20: 12129
potentials for nonlocal interactions, approximations to, (T), 19: 16945
potentials, in optical model, 16: 29874
potentials in, random-phase approximation for singular hard-core, 19: 14602
potentials in, reduced diagonal matrix elements for, 20: 8102
potentials of, quantum properties of hard-core, 17: 9541
potentials of, radial distributions of imaginary optical, 17: 19319
potentials of, effects of short-range repulsive forces on, (T), 19: 39814
potentials of, equilibrium distributions of, (T), 19: 16842 (IFA-MC-7)
potentials of, Hartree-Fock approximation for average, (T), 19: 14545
potentials of, nomograms for, (T), 19: 16868
precession of spinning, in nonuniform magnetic field, 18: 9239
principles of, review on, 19: 2916
production and decay of heavy, research using thermonuclear explosions, (E), 20: 38093
production in neutron stars, neutron and proton chemical potentials for, 20: 44074
production in stars having no helium, 17: 19009
production of compound transuranic, in heavy ion reactions with heavy nuclei, (T), 19: 45286 (UJV-1293/65)
production of delayed-proton emitting, possibility of, 18: 24736
production of heavy, in thermonuclear explosions, (T), 19: 41765
production of proton-emitting, 18: 24737
production of very heavy, 17: 5326 (UCRL-10474)
production of 4- and 6-neutron, in calcium-48 reactions, 18: 24616 (NP-13964)
production of, in N = 184 and Z = 126 region, (T), 20: 30367
production of, reaction cross sections for, 18: 18868 (CERN-64-17)
properties and shell effects of, determination from neighboring nuclide properties, 20: 42278
properties, Brueckner theory calculations, 16: 18175 (NP-11463(Pt.1) (p.119-32))
properties, derivations of self-consistent field in superfluid nuclear model for explaining, 16: 31080
properties, determination using Monte Carlo method, 16: 21382
properties determined by mass spectroscopy, review of, 17: 17649
properties of beta-unstable, methods for investigating, 20: 40109
properties of deformed, 20: 20365
properties of, effects of superconducting pairing correlations on, 17: 17307
properties of, effectiveness of shell and superfluidity models for explaining, 17: 31416
properties of, effects of superconducting pairing correlations on, 18: 9438
properties of even-even, 19: 1562(R) (ORNL-3679(p.1-18))
properties of even-even, microscopic and phenomenological analysis of, 20: 21961 (AD-624028)
properties of excited states, electric and magnetic, 16: 21446
properties of finite, theory of, 17: 7249
properties of finite, Hartree-Fock calculations of, (T), 20: 24323 (AD-624314)
properties of finite, Hartree-Fock method for, 20: 42328
properties of ground-state, volume, 17: 22623
properties of ground-state, surface, 17: 22624
properties of heavy, in shell and unified models, 18: 4585 (UCRL-8783(Rev.))
properties of heavy spherical, models for, 18: 9329
properties of heavy, 19: 1656
properties of highly deformed even-even, 16: 11036
properties of light, calculation of, 18: 34807
properties of, methods for calculating, 17: 32727(R) (PR-P-57(p.69-85))
properties of nuclear matter, 17: 40002
properties of odd-A, single particle Nilsson model for describing, 16: 29752 (EFINS-62-26)
properties of odd-A, between N = 89 and 113, 17: 24053(R) (ORNL-3432)
properties of odd and odd-odd, 17: 26506
properties of odd-mass, Bayman-Silverberg model for j = ½ particle/hole coupling by quadrupole-quadrupole forces to quadrupole vibrating cores, 18: 6220
properties of odd-A, dynamic-collective model for, (T), 19: 6629 (AD-600710)
properties of, prospects for research on, 17: 15310

properties of, self-consistent models for, 17: 879
properties of spherical, computer program for Hartree-Fock, 18: 22871 (CONF-502-1)
properties of spherical, (T), 19: 10364
properties of states of even deformed, (T), 19: 8397 (JINR-P-1811)
properties of strongly deformed, superfluidity model, 16: 4827
properties of strongly-deformed, accuracy of superfluid model for, 17: 17113 (JINR-E-1154)
properties of very strange, 18: 21184 (JINR-P-1583)
properties of, volume effects on, 17: 7103 (NP-12330(p.109-18))
properties of $139 \leq A \leq 177$, $54 \leq Z \leq 108$, (T), 20: 22042
properties of 2s-1d shell, group theoretic model for, 20: 34645
properties of, analysis using deuteron-transfer reactions, (E/T), 19: 14497 (ANL-6878(p.353-422))
properties of, analysis using two-nucleon-transfer reactions, (T), 19: 14498 (ANL-6878(p.425-48))
properties of, calculation using boundary-condition model, (T), 20: 30523
properties of, isobaric spin effects on, (T), 19: 14491 (ANL-6878(p.181-206))
properties of, periodic system of, 18: 38063 (A/CONF.28/P/583)
properties of, performance of models for describing, 18: 44838
properties of, review of reduced widths and strength functions, (T), 19: 17009
properties of, review of, 20: 11512(T)
properties of, shell-model calculations for A = 28 to 40, (T), 19: 14512 (CONF-640301(p.1-12))
properties of, solution for Brownian motion of random-matrix eigenvalues 20: 15785
properties of, tabulations of, (E), 19: 37205(R) (ORNL-3778)
properties of, with momentum-dependent forces, (T), 20: 13792
properties of, with velocity-dependent two-body potential, 20: 19874
properties, studies by collective model and intermediate coupling, 16: 23042
properties, study by Mössbauer effect, 16: 21447
properties survey, 16: 1058
proton absorption cross sections and transmission coefficients, optical model calculations of, 18: 24595 (NP-13930(p.6-13))
proton and deuteron reactions with, polarization in, (E), 19: 10113
proton bombardment of heavy, neutron spectra from, 17: 20994 (UCRL-7233)
proton decay, (E), 19: 21271(T) (KFK-tr-161)
proton decay of light neutron-deficient, 18: 18876 (KFK-185)
proton decay of neutron-deficient, with $Z > 50$, 19: 1621
proton decay of $Z > 50$, 18: 34767 (JINR-P-1706)
proton decay of, following bombardment by heavy ions or fast protons, 19: 47628
proton decay of, observation of, 18: 28567 (JINR-D-1570)
proton delayed emission from odd-Z, with $51 \leq Z \leq 81$, (T), 20: 26124
proton elastic and inelastic scattering at 11-Mev by medium-weight, (E), 19: 16855(R) (ORNL-3714(Vol.I)(p.1-30))
proton elastic and inelastic scattering to 3 Mev by light, review of, 19: 29226 (AECD/EP/2)
proton elastic and inelastic scattering by, analogue-state resonances in, (T), 20: 44796
proton elastic scattering at 8.7 Bev, in emulsion, 16: 955
proton elastic scattering, optical model for, 16: 4803
proton elastic scattering by complex, polarization in, 18: 24625 (WASH-1046)
proton elastic scattering at 10.5 and 14.5 Mev from, optical model potential for, (E/T), 19: 41682
proton elastic scattering at 10.5 and 14.5 Mev, neutron-nucleus potential from polarized, (E/T), 19: 47581 (LA-DC-6730)
proton elastic scattering at 10 to 20 Mev by medium, spin-orbit potential for polarization from, (T), 20: 22116
proton elastic scattering at high energies, review of, 20: 21593 (CERN-65-24(Vol.1), pp 65-80)
proton elastic scattering at 7 to 22 Mev, nonlocal optical potentials for, 20: 26149
proton elastic scattering by, apparatus for analysis of, (E), 20: 28280 (LYCEN-6610)
proton elastic scattering by, optical model potential for, 20: 28307
proton elastic scattering by, analog state resonance in, (T), 20: 28281 (ORNL-P-2074)
proton elastic scattering at 18.5 and 20.5 Mev, optical-model analysis of polarization from, (E/T), 20: 32523
proton elastic scattering by nuclei, neutron-nucleus potential from polarized, 20: 34672
proton elastic scattering at 30 Mev, optical-model analysis of, (T), 20: 42255
proton elastic scattering by, interference effects in Coulomb and nuclear polarized, (T), 20: 44741
proton elastic scattering by spin-zero, isobaric analogue resonances in, (T), 20: 46663
proton elastic scattering and polarization to 50 Mev, bibliography on, 19: 35390 (LA-3281)
proton emission by decaying, 17: 7082 (JINR-P-1072)
proton emission by light neutron-deficient (E/T), 19: 1615
proton emission from light, with $N < Z$, (T), 19: 23669
proton emission from even, neutron-deficient, transmutation from spontaneous two-body, (T), 20: 28454
proton emission in two-proton nuclei, 16: 4846
proton evaporation from excited, (T), 20: 4897
proton fission at high energy, 16: 1082
proton fission at high energies, methods for detecting, (E), 19: 7782 (CERN-64-49)
proton inelastic scattering, excitation of 1-p states by, 16: 4852
proton inelastic scattering by light, effects of nuclear protons on, 16: 18533
proton inelastic scattering, direct-reaction model, 16: 19791
proton inelastic scattering by complex, distorted wave effects in, 16: 29821
proton inelastic scattering by, distorted-wave approximation for, 17: 26629
proton inelastic scattering by complex, angular distributions for mesons (π) from, 17: 28304
proton inelastic scattering at 28 Bev, optical model parameters for, 17: 36637 (AERI-P/R-3)
proton inelastic scattering by even-even, level structure from, 19: 17043
proton inelastic scattering by, breakdown of phase rule for, (T), 19: 23728
proton inelastic scattering by, optical potentials for, (T), 19: 29299
proton inelastic scattering at 155 Mev by light even, cross sections for, (T), 20: 15897
proton inelastic scattering by even-even, angular correlation for 4^+-state excitation in, (T), 20: 24457
proton interactions with nucleons in, at 8.7 Bev, 16: 954
proton interactions in light, at 460 Mev, (E/T), 20: 11948 (AD-624318)
proton multiple scattering at 27 Bev, 18: 17062
proton polarization by complex, 45-Mev, (E), 20: 6274 (AD-619061)
proton quasi-elastic scattering by light, fragmentation in, 18: 1012 (JINR-P-1357)
proton quasi-elastic scattering at 160 Mev, (E/T), 20: 46725
proton reactions (p,γ,γ) with, complexity of angular correlations in, 18: 30770
proton reactions (p,n) with heavy, calculation of neutron production in, 18: 32277(R) (PR-P-61)
proton reactions (p,d), (p,He-3), and (p,t) with, polarization in direct, 18: 36624
proton reactions (p,pα) with light, cluster model for, 18: 36639
proton reactions (p,n) with, equipment for measuring angular distributions of, 18: 39669
proton reactions (p,n) with, optical-model analysis of, 19: 1631
proton reactions (p,t) with A = 46 to 70 (E/T), 19: 3363
proton reactions (p,n) with, neutron polarization in, 19: 5149
proton reactions (p,d) with, variational treatment of, (T), 19: 12528
proton reactions (p,n) with, isobaric analog states from, (E/T), 19: 14493 (ANL-6878(p.215-29))
proton reactions (p,γ) with, compound and direct processes in, (T), 19: 16914
proton reactions (p,γ) with, collective vibrations in, (T), 19: 16936
proton reactions (p,n) with $37 \leq A \leq 112$, threshold limits for, (E), 19: 19095 (WASH-1053)
proton reactions (p,$\gamma\gamma$) with, triple correlations in, (E), 19: 23628 (NRL-6186)
proton reactions (p,γ) with, (T), 19: 23727
proton reactions (p,pd) with, cluster model formalism for, (T), 19: 27575
proton reactions (p,n) with, optical model potentials for, (T), 19: 29299
proton reactions (p,2p) and (p,pα) at 100 Mev, momentum distributions in, 19: 33272
proton reactions (p,2p) with, nuclear structure from, (E), 19: 39904
proton reactions (p,2n) with vibrational, conversion electron spectra from, (E), 20: 1173
proton reactions (p,n) with $70 \leq A \leq 165$, Coulomb displacement energies from, (E), 20: 4849(R) (UCRL-14360, pp 1-50)
proton reactions (p,2n), (p,pα), and (p,2p), cross sections for, (T), 20: 4897
proton reactions (p,γ) with $56 \leq Z \leq 77$ at 10.5 Mev, isomeric transitions in, 20: 5928(R) (PR-P-66)
proton reactions (p,d) with, projection operators for, (T), 20: 6312
proton reactions (p,d) with, J dependence of, (E/T), 20: 9975 (PUC-937-174)
proton reactions (p,n) with, excitation of double analog states in, (E/T), 20: 10031
proton reactions (p,2p) above 100 Mev, cross sections and structure from, (T), 20: 10082
proton reactions (p,2p) with, two-step, (T), 20: 12006

proton reactions (p,2n) with odd-Z, conversion electrons from, (E/T), 20: 13345(R) (NP-15772)
proton reactions (p,pd) with, momentum distribution from, (T), 20: 13874
proton reactions (p,d) with, effects of D-wave deuteron states on, (T), 20: 15730(R) (RHEL/R-112, pp 67-98)
proton reactions (p,2p) with, diproton model for, 20: 15730(R) (RHEL/R-112, pp 67-98)
proton reactions (p,n) with, charge exchange properties of, (E/T), 20: 19838 (UCRL-14760-T)
proton reactions (p,t) with, two-nucleon transfer theory for, 20: 19926
proton reactions (p,n) at 5.5 and 9.5 Mev with $90 \lesssim A \leq 209$, cross sections and strength functions for, 20: 26181
proton reactions (p,pα) and (p,pd), finite-range effects in, (T), 20: 28442
proton reactions (p,xn) and (p,p(x-1)n) at 40 to 100 Mev, inelastic scattering model for, 20: 30446
proton reactions (p,n) with $90 \lesssim A \lesssim 209$, cross sections for, 20: 34513(R) (ANL-7179)
proton reactions (p,α) at 28 Mev with medium-weight, (E), 20: 34639
proton reactions (p,2n) with translational and vibrational, anomalous K/L ratio of conversion electrons from, (E), 20: 36230
proton reactions (p,n) with exact solution of optical-model equations for, (T), 20: 42243
proton reactions (p,2p) with, calculations using distorted-wave t-matrix approximation, (T), 20: 42215
proton reactions (p,d) with, form factors for DWBA calculations of, 20: 42221
proton reactions above 20 Bev, meson (π) production in, 16: 990
proton reactions at 9 Bev, azimuthal distributions of jets from, 16: 5898
proton reactions at 150 Mev, direct-interaction analysis, 16: 5959
proton reactions, angular and frequency distributions from, 16: 2544
proton reactions at 23.5 Bev on light, asymmetric meson showers from, 16: 8095 (IFA-EM-45)
proton reactions at 0.4 to 27 Bev, angular distributions from, 16: 12508
proton reactions at 10 Bev, antinucleon spectra from, 16: 15623 (JINR-P-302)
proton reactions at 25 Bev, hyperfragment production in, 16: 23029
proton reactions at 25 Bev, emission of beryllium-8 in, 16: 23026
proton reactions at 1 Bev/c on emulsion, in pulsed magnetic fields, 16: 27785
proton reactions at 9 Bev, emission of doubly-charged high-energy particles following, 16: 27936
proton reactions at 22 Mev, charged-particle spectra from, 16: 27369
proton reactions at 9 Bev, calculation of particle production in, 16: 33837
proton reactions at 9 Bev, lithium-8 double emission in, 16: 21415
proton reactions at 9 Bev with, angle and energy measurements of, 17: 6971
proton reactions at 9 Bev, meson (π) production in, 17: 9558
proton reactions at 26.7 Bev, meson production in, 17: 11611 (AD-277387)
proton reactions at 27 Bev, determination of primary energy in, 17: 15098
proton reactions at 9 Bev, correlation of nucleons struck and emitted in, 17: 19269
proton reactions at 3 Tev on, mean free path for, 17: 19023
proton reactions at 9 Bev, momentum of mesons (K) and (π) from hyperfragment production in, 17: 20936
proton reactions at high energy, fragment emission in, 17: 36645 (CERN-63-28(p.105-42))
proton reactions at 76 to 350 Mev, angular dependence of multicharged particle production in, 17: 38153
proton reactions at 9 Bev, helium isotope production in, 17: 41966
proton reactions at 25 Bev/c, hyperfragment production in, 17: 29593
proton reactions at 25 Bev/c, unstable fragment emission in, 17: 29607
proton reactions at 22 Bev, charge-2 fragments from, 18: 4601
proton reactions at 27 Bev on emulsions, meson (π) production in, 18: 15311
proton reactions at 16 to 2800 Bev, meson (π) production in, 18: 16775
proton reactions at 75 to 350 Mev, formation of multiply charged particles in, 18: 22925
proton reactions at 23.4 Bev, quarks in, 18: 22736 (UCB-64-2)
proton reactions at 9 and 24 Bev, lithium-8 production in, 18: 32795
proton reactions at 660 Mev, cascade nucleons from, 18: 42634 (JINR-P-1713)
proton reactions at 19.8 Bev/c, shower particles from, (E), 19: 12264
proton reactions at 19.7 Bev/c, gamma spectra fine structure from, (E), 19: 12614
proton reactions at 25 to 200 Mev, gamma spectra from, (T), 19: 25547
proton reactions at 24 Bev/c, emission of fast deuterons in, (E), 19: 27419 (INR-601/VI/PH)
proton reactions at 6.2 and 22.5 Bev, angular and momentum distributions from, (E), 19: 29282
proton reactions at 12.8 Bev in, cascade particle production in, 19: 31249
proton reactions at 19.8 Bev, analysis of, (E), 19: 31308
proton reactions at 25 to 30 Bev, helium-3 and triton emission in, (T), 19: 35446
proton reactions at 1.0 and 2.8 Bev, cross sections for lithium-9, carbon-16, and nitrogen-17 production in, (E), 19: 41780
proton reactions at 6.2 to 25 Bev, statistical calculations for, 19: 43274 (JINR-P-2279)
proton reactions at 10 and 20 Bev/c, in steel, (T), 19: 45317
proton reactions at high energies, ion production in, 20: 11377
proton reactions at 7 to 14 Mev, neutron cross sections from, (T), 20: 26097 (UCRL-14568)
proton reactions at 1 to 30 Bev with emulsion, calculations for, 20: 39828
proton reactions at 140 Mev, bremsstrahlung production in, (E), 20: 46674
proton reactions at (0.5 to 2.0) × 10^9 °K at 10^{-4} to 10^2 g cm^{-3}, rates of, 16: 26341
proton reactions at ≥ 14 BeV, momentum spectra of secondary particles from, 17: 41713 (TID-19500)
proton reactions, cascade production, 16: 8760(R) (TID-14830)
proton reactions far above 1 Bev, peripheral model, 16: 24843
proton reactions in thin targets (Z = 4 to 50) at 32 Mev, neutron yields from, 16: 21479
proton reactions near 10 Mev, cross sections for, 17: 13542
proton reactions on neutrons in, 5.1-Bev cross sections, 16: 27931
proton reactions on cosmic, radioisotopes from, 17: 9177
proton reactions on, at 24 Bev in emulsion, 17: 17161
proton reactions (p,n), (p,2n), and (p,xp) at 100 to 400 Mev, 16: 1808(R) (TID-12849)
proton reactions (p,pγ) at high energies, 16: 5962
proton reactions (p,n), isobaric-state widths in, 16: 19805
proton reactions (p,γ), gamma resonance effects, 16: 21452
proton reactions (p,2p) at 150 Mev, binding energy and shell structure determinations from, 16: 21487
proton reactions (p,n) with mirror, angular distributions and excitation curves from, 16: 21582
proton reactions (p,γ) of, spectroscopic uses of, 16: 29775 (JAERI-1020 (p.201-2))
proton reactions (p,γ), in analysis of use of, as giant resonance in (γ,p) reactions, 16: 29776 (JAERI-1020(p.203-5))
proton reactions (p,n), nuclear excited states from direct, 16: 33860
proton reactions (p,n) on, theory for, 17: 2279
proton reactions (p,α) at 18 Mev, review, 17: 4061 (PUC-1962-88)
proton reactions (p,p'γ), angular correlation symmetries in, 17: 11684
proton reactions (p,n) on even-even, for A = 40 to 82, 17: 17226
proton reactions (p,n), beta transitions in model for, 17: 17189
proton reactions (p,d) in isobaric, analog states in, 17: 19361
proton reactions (p,n), (p,p), (p,pn), and (p,2p) at 100–200 Mev, nuclear structure data from, 17: 38304
proton reactions (p,d) with, distorted-wave Born approximation for stripping to virtual levels in, 17: 38236
proton reactions (p,n) with $27 \leq A \leq 93$, isobaric analog excitation in, 17: 38172
proton reactions (p,t) with, Regge pole theory for di-neutron exchange in, 17: 38226
proton reactions (p,d) with $12 \leq A \leq 48$ at 40 Mev, nuclear structure from, 17: 40110
proton reactions (p,d) with N = 28, 18: 9319(R) (TID-19940(p.22-76))
proton reactions (p,2p) with p-shell, angular correlations in, 18: 9421
proton reactions with, mesons (π) and strange particle production in, 16: 26089 (NP-11832)
proton reactions with emulsion, at 25 Bev, 17: 13529
proton reactions with, secondary particles from, 17: 18377 (TID-7652 (p.523-94))
proton reactions with, nuclear research by, 17: 36644 (CERN-63-28 (p.73-104))
proton reactions with, cross sections and penetrabilities for, 18: 15175 (CEA-2379)
proton reactions with heavy, fragment production in, 18: 15187 (CERN-64-1(p.131-45))
proton reactions with nucleons in, distributions from 6-Bev, 18: 19110
proton reactions with galactic, x-ray emission from, 18: 28226
proton reactions with, short-lived elementary particles from, 18: 30754
proton reactions with, through analog states, 18: 38154
proton reactions with heavy emulsion, 25-Bev, 18: 40546
proton reactions with light and medium, distributions from, (E), 19: 10257(R) (TID-21335(p.33-107))
proton reactions with, experimental plans for, 19: 26922(R) (PR-P-64)
proton reactions with emulsion, at 27 Bev, (E), 20: 10095
proton reactions with, in meteorites, 20: 11377
proton reactions with, pickup effects in, (E/T), 20: 17158(R) (ORNL-3900, pp 82-149)
proton reactions with, amplitude singularities in knockon and stripping, (T), 20: 21997 (INSJ-96)

proton reactions with emulsion, at 9 Bev, hammertracks from, (E), 20: 26202
proton reactions with, nucleon-alpha cascades from, (T), 20: 32455
proton reactions with Z = 6 to 92 at 660 Mev, cascade nucleon emission in, (E), 20: 42299
proton reactions with $22 \leq Z \leq 50$, at 14.5 Mev, total cross sections for, (E), 20: 42162 (LA-DC-8075)
proton reactions with $10 \leq Z \leq 20$, resonance strengths for, (E), 20: 42182
proton reactions with emulsion, hyperfragment production in, (E),
proton reactions with, polarization in, (E), 19: 10113
19: 5143
proton scattering at 50 Mev, theoretical studies of slit, 16: 21639
proton scattering by, polarization and triple reactions in elastic, 17: 2233 (NIRL/R/16(p.31-3))
proton scattering by deformed, cross sections for fast, 17: 2271
proton scattering at 740-Mev, polarization in, 17: 20594(R) (UCRL-10572)
proton scattering by, neutron, prong, proton angular distributions and spectra for, 17: 22564 (ORNL-3383)
proton scattering from spheroidal boundary diffused potential of, cross sections for elastic, 17: 22582
proton scattering from $7 \leq A \leq 209$, asymmetry and polarization in elastic and inelastic, 17: 24514
proton scattering by light, approximation for absorption in, 17: 29585
proton scattering by, diffuse potential effects on widths for resonant, 17: 38089 (TID-17643)
proton scattering by, noncoplanar quasi-free, 18: 2862
proton scattering by, Coulomb excitation in inelastic, 18: 10702
proton scattering by, intermediate resonances in, 18: 16926 (ANL-6848(p.143-6))
proton scattering at small angles by, multiple effects in, 18: 21242
proton scattering at high energies, energy losses in, 18: 21302
proton scattering in Bev range, Coulomb effects in, 18: 28730
proton scattering by light lp-shell, deuteron emission in quasielastic, 18: 28619
proton scattering at 12 and 24 Bev/c, amplitudes for, (E), 19: 8436
proton scattering at 12 and 24 Bev/c, amplitudes for, (E), 19: 10253 (NP-14626)
proton scattering at 50 to 150 Mev, measurements of polarization from, (E/T), 19: 33236 (AERE-R-4896)
proton scattering at 667 Mev, double, (E), 19: 41666 (JINR-P-2233)
proton scattering at ~20 Bev, analysis of small-angle, 20: 5720 (CERN-65-33)
proton scattering by, optical model parameters for, (T), 20: 17768
proton scattering by, finite geometry corrections for differential cross sections for, 20: 27311
proton scattering by nuclei at high energies, coherent elastic and incoherent inelastic, (T), 20: 28428
proton scattering by, nonlocal potential for optical-model analysis of, 20: 30408
proton scattering by A = 44 to 74, isobaric analogue states from, (E), 20: 44761
proton scattering at 180 Mev, optical-model potential for, (T), 20: 46639
proton scattering by Coulomb field of, phase shifts in, (T), 19: 10307
proton spallation of emulsion, angular correlation of fragments in, 18: 21229
proton total cross sections of Z = 4 to 92 at 99 Mev, (E), 20: 44687
proton-neutron interactions in heavy, 18: 22926
pseudopotentials of hard-sphere, (T), 19: 39651
quadrupolar deformation of heavy, 18: 16949 (NP-13735)
quadrupole charges and E2 transition probabilities of, (T), 20: 3115
quadrupole excitations of even-even spherical, by proton-neutron interactions, 16: 17150
quadrupole moment of odd-A spherical, effects of quasi-particle interactions on, 18: 32745(R) (UCRL-11213(p.1-48))
quadrupole moments correction estimations, 16: 8240
quadrupole moments of, spectroscopic determination of, (E/T), 19: 8421
quadrupole moments of $150 < A < 188$, correction of Nilsson wave function for calculating, 19: 29264
quadrupole moments of nearly spherical, (T), 19: 37877(T)
quadrupole moments of odd spherical, (T), 19: 37887
quadrupole moments, (T), 19: 39791
quadrupole oscillations of spherical, anharmonic effects of, 16: 26359
quadrupole oscillations of spherical, anharmonic corrections to, 17: 13518
quadrupole oscillations of spherical, secondary quantization concept for, (T), 19: 6642
quadrupole vibration in spherical, high phonon states of, 17: 11685
quantum states in crystal, field theory for angular-momentum, 18: 6057 (AD-400614)
quasi-particle interactions in even spherical, (T), 19: 14584
radiation absorption by, density and transparency distributions in high-energy, 18: 6409
radiation effects on disassembly of mitotic organelles in, microbeam, 19: 10896
radiation emission recoil in solids, 16: 12517
radiation emission by, electric quadrupole and magnetic dipole interaction effects on angular correlations of, 17: 31428
radiation from, intensity variations produced by variable-intensity particle bombardment, (T), 19: 21235 (JINR-P-1950)
radiation widths, statistical theory, 16: 10969(T) (NSF-62-35(1))
radiative dipole transitions in heated, energy dependence of width of, (T), 20: 3114
radiative transitions of, probability of electric multipole relativistic, (T), 20: 3026
radii of closed-shell, Bethe-Goldstone equation for, (T), 20: 11997
radii of, formula for, 17: 36678
radii of, formula for, 17: 36679
radii of, odd-even staggering in isotopic shift of, (T), 20: 28423
radii of, systematics of, (T), 19: 27449
radioactive, magnetic moment measurements of, by optical pumping techniques, 17: 34640
radioactivities of, nomograph for determining neutron-induced, 17: 34029
radioactivity of electron-capturing, absolute measurement of, 20: 15690 (CEA-R-2813)
radioactivity of, absolute determination of, (T), 20: 13805
radioinduced in activation of, in fish embryos, effects on cytochrome oxidase activity of, 17: 12140(T)
reaction amplitudes and triple angular correlations for, 18: 40625
reaction cross sections for, mean square fluctuations in, 18: 11255
reaction matrix calculations for closed-shell, in Brueckner approximation, (T), 19: 37801(R) (ORNL-3778(p.24-5))
reaction matrix calculations using separation method, 16: 11132
reaction matrix in doubly magic, Bethe-Goldstone Equation for t, 19: 29243 (JINR-E-2047)
reaction matrix theory for, 17: 7211
reaction mechanism in light, involving virtual photons, (T), 20: 44744
reactions at high energies, gamma spectra from, 16: 21389
reactions between complex, conference on, 18: 24707
reactions between complex, double transfer processes in direct, 20: 28377
reactions in nuclear emulsions, radii for, 18: 34964
reactions, nucleon reduced widths in, 16: 23090
reactions of complex, product charge distributions for, 17: 28253 (UCRL-10741)
reactions of complex, internal ionization after, 17: 36668 (UCRL-10888)
reactions of complex, delayed proton emission in, 18: 24736
reactions of cosmic-ray, in graphite, (E), 19: 34925
reactions of, effects of second-order isotope shift on, 17: 16803
reactions of heavy, corrections for center-of-mass motion, 16: 14035
reactions of heavy, at 5000 Bev, 17: 32893
reactions of heavy even-even, with neutrons, 20: 22520(R) (NAA-SR-11805)
reactions of identical, neutron tunneling transfer in, 20: 6387
reactions of identical, theory of inelastic, 20: 30493
reactions of light with heavy, cross sections for elastic, 17: 34990
reactions of light, 18: 32776
reactions of light, 18: 40648
reactions of particles with, computer analysis of, (T), 19: 31232 (ORNL-TM-1117)
reactions of polarized identical, exchange effects in elastic, (T), 20: 9994(T)
reactions of spherical, quasi-particle, 18: 9321 (UCRL-11080)
reactions of, with heavy ions, models and theory of, 16: 29780 (JAERI-1020(p.229-35))
reactions of, analysis using distorted-wave Born approximation, 18: 32880
reactions of, analysis using terminology of high-energy elementary-particle physics, (T), 19: 14500 (ANL-6878(p.481-504))
reactions of, chemical and physical effects of, 19: 9230
reactions of, compound-nucleus behavior in, (E), 19: 17014
reactions of, nucleon transfer in, (T), 19: 20937(R) (TID-21672)
reactions of, status report on pick-up and stripping, 16: 29773 (JAERI-1020(p.184-93))
reactions on, effects of Coulomb field on cross sections, 17: 33083
reactions on, kinematics of relativistic, 18: 6158 (JINR-P-1320)
reactions on, multiple neutron production in, 17: 41901
reactions on, perturbation theory for cross sections of direct, 17: 5360
reactions on polarized, analysis of direct, 17: 4099
reactions on, theory of elastic and inelastic, 16: 33798
reactions on, theory for cross sections of direct, 17: 33085
reactions on, three-particle production cross sections in, 17: 2295
reactions with complex nuclei, cluster-transfer, (T), 19: 41764
reactions with crystal-structure paramagnetic centers, polarization from, 16: 18276
reactions with deuteron beams (d,α) and (d,p), determination of excitation

energies and primary intermediates for, 16: 11040
reactions with electrons, dipole-coupling, 18: 11294
reactions with emulsion, hyperfragment production in 3 Bev/c, 18: 44550
reactions with emulsion nuclei, jets from, 19: 3348
reactions with emulsion nuclei at high energy (E), 19: 3349
reactions with heavy ions, 17: 28258 (UCRL-10775)
reactions with high-energy particles, fragmentation mechanisms in, 18: 38081(T) (AEC-tr-6398(p.139-52))
reactions with, indirect interaction effects on direct, 17: 20991 (TID-18507)
reactions with ions, properties of isomeric states of thallium produced in, 17: 28255 (UCRL-10764)
reactions with nuclei at high energies, inelasticity in, 16: 16920
reactions with nuclei at $>5 \times 10^{10}$ ev/nucleon, showers from, 16: 27877
reactions with nuclei, tables of cross-section functions for double Coulomb excitation in, 17: 792 (AWRE-NR/P-2/62)
reactions with nuclei $10 \leq A \leq 19$, terbium-149 isomeric excitation functions from, 17: 26573
reactions with nuclei, model for alpha distribution in, 17: 38082 (JINR-P-1291)
reactions with nuclei, neutron tunneling in Coulomb field in, 18: 34894
reactions with nuclei, angular distributions in multinucleon-transfer, (T), 19: 12539
reactions with nuclei, neutrino momentum distribution in, (T), 19: 19131
reactions with nuclei at high energy, neutrino production in, (T), 19: 19132
reactions with nuclei, diffraction effects on angular distributions for nucleon-transfer, 20: 28276 (JINR-P-2664)
reactions with nuclei, parabolic potential barrier model for, 20: 32423
reactions with nuclei at high energies, cross section for, 17: 3931 (AFCRL-1089)
reactions with nuclei, nucleon transfer rearrangement processes in, 18: 15259
reactions with nuclei, mechanisms of, (E/T), 19: 5128 (JINR-D-1798)
reactions with nuclei, binding-neutron potential for, (T), 19: 37852
reactions with nuclei, neutron transfer in, 17: 15266
reactions with nuclei, mechanisms of high-energy charged-particle production in, (T), 19: 10246 (JINR-P-1881)
reactions with oriented, review on, 17: 38138
reactions with paramagnetic ions, magnetic relaxation in, 16: 15680
reactions with protons at 24 Bev in strong pulsed magnetic field, quasi-nucleon interactions in, 20: 44280
reactions with targets, neutrino momentum distribution in, (T), 19: 25488
reactions with targets, neutrino momentum and space distributions in, (T), 19: 25489
reactions with tritons, effects of spin on, 20: 25120(R) (BNL-954, pp 114-21)
reactions with 14-Mev neutrons for activation analysis, 20: 38838
reactions with, configuration-mixing effects on stripping, (T), 19: 6706
relaxation near paramagnetic centers in irradiated polymers, 19: 22308
relaxation of spin systems, spin-spin coupling dependence of magnetic, 18: 28244
relaxation phenomena in crystals, lattice phonon-quadrupole interactions in, (T), 20: 30749
relaxation times, free nuclear induction device for measurement of longitudinal, 19: 4439
research on, at ANL, 17: 41532(R) (ANL-6720(p.59-66))
research using Mössbauer effect, 20: 34630
resonances in solids, design of detector for, 18: 14179
resonating fluorescence, dispersion effects connected to absorption of, 17: 14969
rotation bands in odd-mass, decoupling effect and odd-even shift in, 17: 33046
rotation of axially-symmetric deformed, 16: 12451
rotation of, current and magnetic field from, (T), 20: 44833
rotation states of deformed axial symmetry in even, 17: 19282
rotation theory, 16: 12646
rotation-vibration interaction in deformed, 16: 29863
rotational and vibrational states of even–even, non-spherical, 16: 4822
rotational energies for the asymmetric rotor model for odd-mass, 16: 29822 (UCRL-9876)
rotational energy levels associated with two-particle states in deformed even-even, 18: 28612
rotational levels of even-even, intrinsic excitation of, 17: 6956 (TID-13705)
rotational motion of, models for, 18: 44834
rotational potentials, Hartree-Fock equations in, 16: 17102
rotational spectra, non-adiabatic parameter, 16: 21386
rotational spectra, 16: 23118
rotational states and tensor of inertia of heavy, nuclear-model determination, 16: 21503
rotational states of non-axial odd, 17: 36710
rotational states in, theory of, 18: 6297
rotational states of odd nonaxial, 18: 9351
rotational states in deformed, model for, 18: 44832
scattering by nuclei, long-range interaction potential in elastic, 18: 24674
scattering by nuclei, optical potentials for elastic, 18: 32836
scattering by, analysis of inelastic, 18: 36699
scattering by, optical model analysis of elastic, 18: 36698
scattering by, theory of resonance, 18: 44571
scattering by, time correlation functions for, (T), 19: 43376
scattering cross sections for heavy, probability distributions of, 17: 24499
scattering from spherical deformable, neutral-particle, 17: 24400 (TID-16301)
scattering model for, inelastic, 20: 24360(R) (UCRL-16580, pp 107-48)
scattering of complex, quasi-classical analysis of elastic, 17: 22558 (JINR-P-1244)
scattering of complex, collective level excitation in inelastic, (T), 20: 13890
scattering of complex, angular distributions from inelastic, 20: 30502
scattering of spin-0 and spin-½, phase shifts for, 17: 11570
separable nonlocal interactions in, 16: 28070
separation of long-lived isomeric, 17: 1794
separation of reaction-yield, electromagnetic, 18: 36595
shape of deformed, Bohr-Mottelson and asymmetric-rotor models for, 18: 18934
shape of dipole resonance in deformed, 17: 9611
shape of fissioning, in liquid-drop model, (T), 19: 19096(T) (ANL-Trans-157)
shape of, equilibrium, 18: 36683
shell structure and Roche nuclear density, 17: 33010
shell structure of, from resonance peaks in (p,n) reactions, 17: 11681
single-particle energies of, reference spectrum method of calculating, 17: 38144
single-particle excitations in, model hamiltonians for, 20: 3099
size correction for relativistic Thomas-Fermi atomic model, mass limit effects of, 17: 34961
sizes of 1p-shell, 20: 34580
spallation in high-energy particle scattering, "shock-wave" mechanisms for, 18: 28621
spectra for Z = 7 to 94, K-LL Auger-electron, 17: 9544
spectra, hyperfine structure splitting and isotope shift, 16: 32406(T) (NP-tr-916)
spectra of cosmic, at 3260 m altitude, 17: 32892
spectra of cosmic helium, energy and mass, 18: 40179
spectra of, deformation effects on isotopic shift of lines in, 18: 6283
spectra of deformed even, one-parameter description of collective, 16: 17108
spectra of deformed even-even, comparison of Davydov theory with rotation-vibration model for, 18: 21323
spectra of giant dipole resonances in light, 18: 22918
spectra of heavy primary cosmic, 17: 6931
spectra of light, from hole-excitation levels, 16: 29871
spectra of odd-odd, effect of tensor forces on, (T), 19: 27464
spectra of spherical even-even, models for vibrational, 17: 17137
spectra of, theory of, for closed shells, 16: 32390 (CEA-2177)
spectra of two-particle excitations in, 16: 21522
spectra of $2s_{1/2} - 1d_{1/2}$, shell model for, (T), 19: 47600
spectra of $6 \leq Z \leq 20$, in cosmic radiation, (E), 19: 41310
spectra of, semiclassical description of vibrational, 18: 16981
spectra of, signals at $2\omega_2 - \omega_1$ in double NMR, (T), 19: 45307
spectra of, Zeeman effect in NQR, (E), 19: 17067
spherical, with simple residual forces, 17: 24381 (AD-403411)
spin alignment by nonresonant nutation, NMR measurement of magnetic fields using, (E/T), 19: 26935
spin and quadrupole interaction in, via optical phonon virtual field, (T), 20: 17818
spin coupling of, review on, 19: 5153
spin diffusion in electron-nuclear double resonance, (T), 20: 12311
spin interactions with electrons, energy of, (T), 19: 20695
spin interactions between, excitation energy in, (T), 20: 46303
spin of strongly deformed, effect of Pauli exclusion principle on moment of inertia of, (T), 19: 16955
spin-orbit splitting and tensor force, 16: 24829
spin-orbit splitting, pion theoretic L-S potential in, 16: 31070 (TID-12043)
spin-orbit splitting in spherical, 17: 21047
spin polarization of, effect of magnetic induction on, (E), 20: 26221
spin purity in heavy, isobaric, 17: 13568
spin scattering of, bibliography on, 19: 20828
spin systems in r-f magnetic fields, (T), 19: 23660
spin wave excitation in, giant resonance in, 16: 32452
spin-lattice relaxation of, 18: 11294
spin-lattice relaxation times of, for spins ⅞ and ⅝, 19: 12510

spin-orbit interactions in deformed, 18: 18942
spin-spin relaxation in crystal fields, 18: 14621
spinor particle scattering in Coulomb fields of, 16: 991
spins of odd-odd, j-j coupling odd-group model for, 19: 43362
stability of, 20: 40108
stability of Z = 126, A = 310, shell model calculations for, 20: 32482
stability of, neutron excess effects on equilibrium, (T), 20: 44674
stability of, relation of magic numbers to, 19: 21275
statistical properties of compound states of, (T), 19: 17013
strange particle reactions with, 18: 15290
strength parameter correlation with beta bands in even, electric monopole, (T), 20: 38180
stretching deformed, centrifugal, (E/T), 20: 20365
strong interactions of, book (T), 19: 1657
structure and symplectic symmetry of, in region $40 \leq A \leq 56$, 19: 21437
structure calculations for finite, using Hartree-Fock approximation, (T), 20: 34564
structure, effects of deuteron-type, 16: 21403
structure of A = 37 and 38, intermediate coupling shell model for, 20: 38111
structure of atomic, development of theory of, 19: 19218
structure of beta-unstable, 20: 19884
structure of deformed, in region of N = 18, 18: 34781 (UCRL-11376)
structure of deformed even-even, computer programs for collective model calculations of, 20: 6278 (AD-623877)
structure of finite, reaction matrix theory for, 19: 16969
structure of heavy spherical, (T), 20: 21975 (BNL-948, pp 269-336)
structure of, in the mass range above 40, 16: 29754 (JAERI-1020)
structure of light, representations of, 17: 15307
structure of light and medium, conference, (E/T), 19: 14511 (CONF-640301)
structure of light, (T), 19: 39932
structure of light spherical, 20: 21974 (BNL-948, pp 222-68)
structure of mass 18, shell model calculations, 16: 21631
structure of odd deformed, theory of low-energy-level, (E/T), 19: 14638
structure of odd transition-region, from E2 and M1 transition properties, (T), 20: 9995(T)
structure of s-d shell, 18: 1091
structure of sd-shell, configuration mixing and independent particle motion in, (T), 20: 12128
structure of spontaneously fissioning isomeric, (T), 20: 46788
structure of strongly deformed light, (E/T), 20: 21976 (BNL-948, pp 337-79)
structure of strongly deformed heavy, (E/T), 20: 21977 (BNL-948, pp 380-453)
structure of $16 \leq A \leq 56$, 20: 46755
structure of 82-neutron, 17: 857
structure of, analysis using proton capture, 20: 21986 (BNL-948, pp 763-825)
structure of, determination from isobaric analog states, (E/T), 20: 17158(T) (ORNL-3900, pp 82-149)
structure studies by proton reactions, 16: 31128(R) (ORNL-3257)
superconductivity of metals composed of spherical, 17: 13133
superconductivity theory for, effects on particle number nonconservation in, 18: 28689
superfluid pairing correlations in excited states of deformed, 16: 5926 (JINR-P-801)
superfluid phase transitions in, 17: 38214
superfluid properties of, 17: 11735
superfluidity in, 18: 34864
superfluidity, theory using independent pair approximation, 16: 9568
superfluidity-type pair interactions in, 18: 11233
surface diffuseness of, liquid-drop model for, 16: 33874
surface layer effects on low-energy reactions and scattering, 16: 19809
surface of, semi-empirical mass formula for diffuse, 18: 32767
surface penetrability of, from S-wave strength functions, 17: 40105
surface properties, determination by low-energy particles, 16: 16811(R) (PR-P-52)
surface properties, model based on Fermi-gas model, 16: 23058
surface properties of large, reference-spectrum analysis of, (T), 19: 6690
surface resonances in spherical, quadrupole, (T), 20: 38039
surface structure, methods for determining, 16: 21528
surface structure of heavy alpha-emitting, (T), 20: 42275
surface tension of, Fermi-gas model for, 20: 32470
surface vibration excitation, two-phonon, 16: 11013
symmetry energy and isotopic spin dependence of single-particle potential in neutron-excess, 18: 21287
synthesis in neutron reactions in stars, 20: 34674
synthesis in supernova envelope, alpha and proton reaction rates for $20 \leq A \leq 40$, 17: 34693
synthesis of heavy, possible source of neutrons for, 17: 13594(T)
synthesis of Z > 20, neutron and proton capture processes for, 17: 41706(T)
systematics of elementary particles and, 19: 23375
systematics of, from oxygen-16 to calcium-40, 18: 7785
systematics of light, review on, 19: 35503
temperature of, comparison of formulas for, 17: 29879(R) (IA-822)
theory, Brueckner's many-body, 16: 18174 (NP-11463(Pt.1)(p.75-117))
theory for deformed, rotation-vibration, 18: 15206 (TID-20224)
theory of, application of projection theorem to, of low-mass-number, 16: 31067 (NYO-9536)
theory of compound, statistical, 17: 48192
theory of compound, review on, 19: 21283
theory of compound, statistical, 19: 37202(R) (BNL-900(p.1-28))
theory of even-even nonspherical, 16: 32447
theory of heavy, statistical, 16: 28160
theory of odd A, dynamic collective, 19: 6720
theory of, on basis of Fermi liquid of two types of fermions, 17: 12826
theory of rotations, 16: 11042
theory of rotations, 16: 11043
theory of rotations, 16: 11044
theory of seniority mixing in $1f_{7/2}$, 16: 29471(R) (ANL-6574)
theory of, studies at MIT on, 17: 40437(R) (NYO-10063(p.116-25))
theory of, interacting quasi-particles in, 18: 36577 (NP-14202)
theory of, studies at MIT on, (T), 19: 5569(R) (MIT-2098-64)
tracks of heavy, in nuclear emulsions, 16: 10250
transformation into neutron gases at high densities, 16: 18535
transformations of, theory of integral, for Mittag-Lefleur model, 19: 3255
transition frequencies and probabilities in, phenomenological approach to, 18: 6267
transition probabilities for, effects of dipole polarization on, 17: 7191
transition probabilities from first 2^+ states of even-even, 17: 11674
transition probabilities in light, measurement of E2, 18: 32778
transition probabilities of, determination by Coulomb excitation, (E/T), 19: 8400 (NP-14574)
transition probabilities in odd, Green functions and, 20: 3104
transition spectra in, Alaga's rules for electromagnetic, 18: 26628
transitions (E1) in Z = 30, 63, and 82, positron formation in, 16: 17098
transitions in, deformation retardation of L-forbidden M1, 17: 40000
transitions in deformed even, branching ratio of E2, 17: 7208
transitions in deformed odd and odd-odd, 17: 17146
transitions in deformed, probabilities of E1 and M2, 17: 38084 (JINR-P-1303)
transitions in deformed, particle parameters of E2, (E), 19: 21399
transitions in even-even, K-conversion coefficients of E2, 17: 38091(R) (TID-19350)
transitions in even-even, M_1--E_2 mixing ratio of $2^+ \rightarrow 2$, 18: 26580
transitions in even-even, E2, (E/T), 19: 14554
transitions in even-even, E2/E1 mixing ratios of $2^+ \rightarrow 2^+$, 19: 21419
transitions in light, strong M1, 17: 22619
transitions in light, E2 and E3, 18: 8919(R) (PR-P-59(p.65-78))
transitions in light, $\Delta T = 0$, 18: 34858
transitions in mixing ratios for $2^{+*} \rightarrow 2^+$, 17: 24465
transitions in odd rare-earth, shell effects on E1, (T), 19: 12498
transitions in, probabilities of radiationless, 16: 15697
transitions in, probabilities of double conversion and internal Compton effect, 17: 5405
transitions in, l-forbidden M1, 17: 38091(R) (TID-19350)
transitions in, geometrical corrections for angular correlation measurements on, (T), 19: 36845
transitions in, matrix elements for, (T), 19: 47622
transitions in, single-particle l-forbidden, 20: 3100
transitions of, quadrupole vibration effects on l-forbidden M1, 17: 34881 (NP-13050)
transitions probabilities for excited odd, with small nonaxiality, 18: 2948
transmutation by arc discharge or irradiation, 16: 5394(P)
transmutation of, spontaneous two-proton, 17: 13524
transmutation theory of, computer program for analysis of, 19: 25696(R) (HW-84369(p.11-19))
triton reaction (t,p) with, selection rules for, (T), 19: 8443
triton reactions (t,d), (t,n), and (t,p) with, polarization in direct, 18: 36624
triton reactions (t,p) with, direct, (T), 19: 23685
triton reactions (t,d) in Coulomb field of, spectroscopic factors for, (T), 19: 41739
triton reactions (t,p), differential cross sections for, (T), 19: 41817
triton reactions (t,p) with light, angular distributions in direct, (T), 20: 3121
triton reactions (t,p) with, properties of, (T), 20: 11972 (NP-15716)
triton reactions (t,p) with light, angular distributions for direct, (T), 20: 15798
triton reactions (t,p) with, two-nucleon transfer theory for, 20: 19926
triton reactions (t,p) with, finite-range effects in, (T), 20: 24404
triton reactions (t,d) and (t,p) with, absolute cross sections for, (T), 20: 28327
triton reactions (t,d) with, calculations using distorted-wave theory, 20: 42250

triton reactions (t,p) with, angular distributions from, 20: 42290
triton reactions, mechanism and relative magnitudes of double stripping and pickup, 16: 31068 (PUC-1962-77)
triton reactions (t,n) and (t,p) with, double stripping mechanisms in, 17: 38225
triton reactions with, amplitude singularities in knockon and stripping, (T), 20: 21997 (INSJ-96)
triton scattering from deformed, as test for coupling potential complexity in direct interactions, 17: 24492
two-body potentials, J = 2 – 0 energy level splittings, 16: 2507
two-nucleon potential, analytical solutions, 16: 8211
two-nucleon potential for singlet-even states, 16: 8212
two-body tensor force and Pauli exclusion principle in nuclear matter, 18: 21344
two-phonon triplets in vibrational, quadrupole (T), 19: 3331
uncoupled nuclear matter approximation, 18: 32834
use of aligned, as gyroscopes, 16: 20654
uses in research on strange particles, 17: 36641 (CERN-63-28(p.1-36))
vibration levels in nonspherical, 18: 18920
vibration of spherical, introduction of inharmonic terms in calculating, 16: 23027
vibration of spherical, ground-state effects of zero-point, 17: 24438
vibrational states of spherical, models for, 17: 17285
vibrations in, collective, (T), 19: 14628
vibrations of, description of collective, using shell model wave functions, 16: 26277
vibrations of spheroidal even-even, octupole, 16: 24302
wave function, dispersion calculations of "peripheral," 16: 28338
wave functions, (E), 19: 10257(R) (TID-21335(p.33-107))
wave functions for, with $1f_{7/2}$-level neutrons and protons, 16: 7090
wave functions for, derivation of single-particle, 16: 33883
wave functions for 2s-1d shells of, 18: 15293
wave functions for, perturbation calculations of degenerate, 18: 16800
wave functions for low-energy particles in, Coulomb, 18: 24682
wave functions for two-particle $1f_{7/2}$ shell, 18: 30733 (NYO-9891)
wave functions for light, one-particle, 18: 30833
wave functions for, BCS, 18: 36664
wave functions for, particle-number conserving-method for BCS, 20: 12050
wave functions for medium and heavy, (T), 20: 19985
wave functions for light, generalized Bogoliubov transformation for, 20: 24436
wave functions for three-nucleon, 20: 26160
wave functions for three-nucleon states of, (T), 20: 42209
wave functions for three-body, orthonormal expansion of, (T), 20: 44692
wave functions in s-d shell of, 4-particle, 18: 21215 (UJV-1002-63)
wave functions in light, charge-dependent nuclear, (T), 19: 47679
wave functions of, effects of center-of-mass motion on shell-model, 18: 2403(R) (PR-P-58)
x-ray reactions at 5 to 90 Mev, pair and triplet production in, 16: 11029
x-ray resonance elastic scattering, 16: 23109
yields of isobaric (A = 72), in proton reactions with molybdenum-96, ruthenium-96, and zirconium-96 at 1.8 Bev, 18: 7761
Zeeman interactions in diamagnetic crystals in external magnetic fields, 18: 11294

NUCLEI (CELLS)

see also Chromosomes
see also Cytology
see also Genetics
see also Mitochondria
see also Mitosis
see also Nucleic Acids
see also Nucleotides

association of alkali metal and alkaline earth cations with, in dog kidney cells, 20: 35224
chromosome analysis in photographs of, using flying-spot devices, (E), 19: 38910 (CERN-65-11(p.43-56))
concentration of disulfides and sulfhydryl compounds by liver and thymus, 19: 26150
desoxyribonuclease activity of rat liver, 18: 9785 (USNRDL-TR-688)
desoxyribonucleic acid content of, effects on radiosensitivity, 19: 5663
DNA content in liver cells of xenogenic radiation chimeras, 19: 31856
effects of actinomycin on specific activity of RNA in, 20: 8613
effects of DNA content of, on radiosensitivity of ciliates, 18: 35321(R) (TID-20937)
effects of growth on gamma-irradiated culture media on human leukocyte, 20: 45331
effects of nitrogen mustard on RCP strain, 20: 5323
effects of nuclear surface area on radiosensitivity of plants, 16: 31523
effects of ozone on mouse and rabbit myocardial, 18: 33334
effects of ploidy in guinea pigs, 20: 18260
effects of radiation sickness on neurosecretory, in rat adrenal, hypothalamus, and thyroid glands, 20: 35313
effects of size of plant, on radiosensitivity of pollen, γ, 20: 18384
effects of testosterone on, in rat kidney cells, 19: 6944(R) (ANL-6906 (p.106-9))
effects of thioacetamide on, of rat liver, 19: 6943(R) (ANL-6906(p.102-5))
effects on radiosensitivity in Spathidia, 19: 42261 (TID-22124)
enzyme activity of mitochondria, 16: 2872 (TID-14283)
enzymes in rat-liver radiosensitivity of, 17: 7853
function and replication, tracer study, 17: 23011
gamma crystallins in Salamander lens, 20: 40499(R) (ORNL-3922, pp 69-79)
hematin synthesis by, in erythrocytes, 19: 5587 (TID-19797)
incorporation of tritium labeled amino acids into, in mice, 17: 31887
injuries to mouse bone marrow and spleen, from x rays in combination with acceleration or vibrations, 20: 42986
isolation from mammalian cells in tissue culture, 20: 18204(R) (LA-3432, pp 130-77)
isolation of, for trace-metal studies, 18: 41051
isolation of, in *Vicia faba* cells, 18: 45178 (ORNL-P-483)
macromolecular synthesis in mammalian, 20: 40534(R) (NYO-3621-1)
modification of rat thyroid, during β-induced neoplasia, 20: 42857(R) (TID-23228)
molecular transport through membranes of, 18: 17399(R) (ANL-6790 (p.138-44))
nucleic acid synthesis in isolated, tracer study, 20: 18204(R) (LA-3432, pp 130-77)
nucleoplasm stratification in Pelomyxa, by centrifugation, 18: 23197(R) (ANL-6823(p.169-73))
phosphorus-32 uptake by RNA in amoeba, 18: 11582
preparation of amoeba, for toxicity test systems, 20: 42997(R) (ANL-7136, pp 191-204)
properties of proteins in, 20: 42702(R) (ANL-7136, pp 243-55)
properties of wheat seed, microspectrophotometric study of, 20: 40631(R) (ORNL-3922, pp 161-6)
protective effects of post-irradiation oxygen starvation against injuries to, in rat thymocytes exposed to x rays, 20: 42989
protein biosynthesis in, 20: 40567
protein characteristics, 16: 11445(R) (ANL-6464(p.88-9))
radiation damage to thymocyte, 20: 40549
radiation dose received from incorporation of tritium-labeled thymidine, 16: 20222
radiation dose to mouse testes, following tritiated thymidine injection, 18: 25069
radiation dose to bone marrow, from injected tritiated thymidine, autoradiographic determination, 20: 40743 (BNL-9374)
radiation dosimetry of labeled DNA in, beta, 19: 38873 (BNL-9331)
radiation effects on mitosis of nucleolus in grasshopper embryo, ultraviolet, 16: 1622
radiation effects mechanism, 16: 2887 (A/AC.82/G/L.636)
radiation effects on Habrobracon eggs, uv and x, 16: 1621
radiation effects on metabolism of ribonucleic acid and proteins, 16: 14518
radiation effects, continuous ultraviolet, 16: 6339
radiation effects, 16: 20142
radiation effects, 16: 26762
radiation effects on phosphate-transfer reactions, 16: 30227
radiation effects on metabolism, 16: 30273
radiation effects on phosphate metabolism, 16: 30276
radiation effects on synthesis of desoxyribonucleic acid, tracer study, 17: 75
radiation effects on nucleotide content in tumor cells, 17: 1190
radiation effects, 17: 1284
radiation effects on neurons in supraoptic, in rats, 17: 7868
radiation effects on loss of protein nitrogen and DNA decomposition in isolated liver, in rats, 17: 24958
radiation effects on protein content, 17: 27157
radiation effects on nucleoli in Chang liver cells, 17: 27063 (TID-18846)
radiation effects on structure of, in tumor cells, 17: 35555
radiation effects on incorporation of tritiated thymidine into, 17: 37087
radiation effects on ultraviolet fluorescence of, x, 17: 37093
radiation effects on KB tumor, x, 17: 38817
radiation effects on size of monkey heart, x, 17: 38833
radiation effects on, 17: 40636
radiation effects on sulfhydryl groups in rat thymus, protective effects of oxidized glutathione against, 18: 129
radiation effects on thiol groups in rat thymus, 18: 3517
radiation effects on ATPase activity in mouse tumor, x, 18: 3534
radiation effects on rat neuron area of, gamma, 18: 5115
radiation effects on human blood, beta, 18: 5193
radiation effects on synthesis of histone and DNA in, 18: 8151
radiation effects on enzyme activity in liver, 18: 9870
radiation effects on ultrastructure of rat liver, x, 18: 11772
radiation effects, 18: 11809
radiation effects, 18: 11810
radiation effects, 18: 11812

radiation effects on sorghum, gamma and x, 18: 13534
radiation effects on relation to cytoplasm, review, 18: 15867
radiation effects on mitosis in, x, 18: 17599
radiation effects on, in Walker carcinomas, 18: 19699
radiation effects on amino acid incorporation by proteins of rat thymus, x, 18: 23259
radiation effects on dimensions of, in leaf tissue of sugar beets, 18: 25136
radiation effects on nucleic acid synthesis in, tracer study of, 18: 31132(T) (JPRS-25233)
radiation effects on nuclei of mouse liver cells, x, 18: 33350
radiation effects on somatic, moderate-dose, 18: 38796
radiation effects on rat spinal, proton, 18: 38917
radiation effects on structure of, in rat thymus, 18: 41185
radiation effects on Allium, quantitative study of x, 18: 41197
radiation effects on protein metabolism in, of rat liver, 19: 5661
radiation effects on chromatin structure and histone components of rat thymocyte, 19: 7077
radiation effects on histone localization and structure in rat thymocytes, 19: 7078
radiation effects on formation of giant, in mouse tumors, 19: 8939
radiation effects on, in brain cells, 19: 10786(R) (TID-21440)
radiation effects on rat thymus, x, 19: 12993
radiation effects on carbon-14-labeled-leucine uptake by, in regenerating rat liver, 19: 15138
radiation effects on plant, gamma, 19: 15166
radiation effects on histone synthesis in mouse tumors by inhibition of DNA replication, 19: 15052
radiation effects on RNA metabolism in Ehrlich ascites and thymocyte, x, 19: 15063
radiation effects on human embryo culture, low dose, 19: 17611
radiation effects on, 19: 17566
radiation effects on physico-chemistry and structure of, in bone marrow cultures, 19: 17620
radiation effects on sorptive properties of rat thymus, protective effects of AET against, 19: 17690
radiation effects on secretory activity of, in brain hypothalamic area of rabbits, 19: 19509(T) (JPRS-29250(p.9-13))
radiation effects on mitosis suppression in *Tradescantia paludosa*, 19: 19579
radiation effects on Amoeba, uv, 19: 31796(R) (ORNL-3768(p.187-94))
radiation effects on ribonucleic acid metabolism, tracer study, 19: 35967
radiation effects on, beta, 19: 38873 (BNL-9331)
radiation effects on bone marrow, synergistic effects of vibration, 19: 38358 (AD-612660)
radiation effects on rabbit, biochemical, 19: 40375
radiation effects on interphase, in developing Misgurnus fetuses, 19: 42319
radiation effects on, in frog skin, 19: 42257(R) (COO-1080-1)
radiation effects on morphology of erythrocyte, in salamanders, 19: 43730
radiation effects on droplet nuclei in staphylococcus , uv, 19: 43736
radiation effects on Triton erythroblast, x, 19: 45925
radiation effects on morphology of, in *Cannabis sativa* seedlings, 19: 45940
radiation effects on, biological, 19: 45992
radiation effects on thymidine metabolism in, 19: 45808(R) (NYO-901-36)
radiation effects on morphology of lymphocyte, 20: 1612 (EUR-2505. e)
radiation effects on phosphorylation in tumor, x, 20: 1626
radiation effects on, in tissue culture, uv, 20: 6793(T) (JPRS-33170, pp 211-16)
radiation effects on tumor, early x, 20: 6882
radiation effects on rat bone marrow and thymus, effects of calcium and phosphate contents on, 20: 6906 (EUR-2485.e)
radiation effects on, of normal and neoplastic oral cells, x, 20: 8750
radiation effects on specific activity of RNA in, x, 20: 8613
radiation effects on DNA-ase activity in animal, 20: 10591
radiation effects on mouse spleen, x, 20: 12681
radiation effects on ultrastructure of, 20: 14335
radiation effects on structure of rat thymocytes, x, 20: 18455
radiation effects on rat leukocyte, protective effects of B vitamins on beta, 20: 18499
radiation effects on potassium and sodium content of animal, x, 20: 20422
radiation effects on rat leukocyte, protective effects of B vitamins on beta, 20: 18499
radiation effects on nerve cell, radio wave, 20: 22592
radiation effects on chicken heart myoblast, x, 20: 24936
radiation effects on, in cultured leukocytes, 20: 28920
radiation effects on paramecia, x, 20: 29007
radiation effects on guinea pig, x, 20: 28976
radiation effects on DNA synthesis in HeLa cells by exposure of, α, 20: 32937
radiation effects on HeLa, morphology of γ, 20: 32985
radiation effects on, in duodenal crypt epithelium of mice, x, 20: 33007
radiation effects on virus-transformed hamster cells to produce multiple, x, 20: 35255
radiation effects on nucleoli in tissue culture cells, uv, 20: 36592
radiation effects from incorporated tritium on, biological, 20: 38624
radiation effects on thymidine metabolism in mouse thyroid, 20: 40616(R) (NYO-901-54, pp 48-50)
radiation effects in rats on male germ cell, following exposure at birth, x, 20: 40683
radiation effects on HeLa, effects of trenimon on γ, 20: 40704
radiation effects on size of, in human salivary glands, following cobalt-60 therapy, 20: 40644
radiation effects on volume of *Paramecium caudatum* macro-, uv, 20: 42800(T) (ORNL-tr-1289)
radiation effects on human thyroid β and x, 20: 42857(R) (TID-23228)
radiation effects on thymocyte, effects of phosphate metabolism and respiration on x, 20: 42928
radiation injuries, 16: 12937(T) (JPRS-12712)
radiation lesions in, significance in relation to cytoplasmic lesions, 17: 38872
radiation, growth, and aging effects on size of, in ascites tumor cells, 18: 13554
radioinduced changes in human, during various cell phases, x, 17: 30358
radioinduced decomposition of globulin, histone, and nucleic acids in, 16: 23468
radioinduced depletion of, in bone marrow, spleen, and thymus of young mice, γ, 20: 14365
radioinduced inhibition of pycnosis in rat thymocyte, x, 19: 28000
radioinduced luminescence of chemicals, 17: 27065 (UCRL-10724)
radioinduced pyknotic degeneration of retinal, x, 20: 42958
radiosensitivity in plants, 16: 31510 (BNL-5381)
radiosensitivity of enzymes, 16: 16219
radiosensitivity of adenosine triphosphate synthesis of thymic, in rats, 17: 38796
radiosensitivity of glycolytic enzymes in, in thymus cells of mice and rats, 17: 40573
radiosensitivity of, in normal and neoplastic cells, 18: 5043
radiosensitivity of, effects of cell volume ratio to volume, 18: 38775(R) (ORO-624)
radiosensitivity of conidia of *Neurospora crassa*, relation of karyokinetic stage to, 19: 7066
radiosensitivity of, in gemmae of *Marchantia polymorpha* L., effects of volume on, 19: 7119
radiosensitivity of mammalian, x, 20: 22668
ribonucleic acid loss from, carbon-14 tracer study, 18: 21799
ribonucleoprotein isolation and purification, 16: 11390 (TID-15142)
role of, in radiation effects on cathepsin activity in *Misgurnus fossilis* embryos, 19: 17518(T)
ruthenium metabolism in, of rat liver cells, tracer study of, 18: 41049
sodium-22 uptake by Chironomus salivary gland, 20: 24850
soluble proteins in rat liver, factors affecting, 18: 23192(R) (ANL-6823(p.124-7))
structure of bacterial, effects of uranyl ions on, 20: 20392
synthesis of protein and desoxyribonucleic acid, effects of radiation, 16: 26798
uptake of tritium by, radiation dose to cell from, 19: 25826
uridine triphosphate uptake by fish liver, carbon-14-labeled, 19: 31681(R) (ORNL-3768(p.164-76))
volume in Paramecium clones, variations in, 19: 31788(R) (ORNL-3768 (p.33-57))
volume in tree species, variations of, 19: 14946
volume of plant, effects on radiosensitivity, 18: 17472 (BNL-7866)
volume of, effects on radiosensitivity of plant cells, 20: 1610 (BNL-9611)

NUCLEIC ACIDS
see also Guanylic Acid
see also Ribonucleic Acid
analysis for adenine, cytosine, and guanine, polarographic and voltammetric methods for, 16: 6370 (TID-14465)
analysis for carbon-14 and tritium by liquid scintillation counting, use of hyamine–toluene–water system for, 19: 24466
analysis for trace elements, activation, 18: 19892
analysis of tobacco mosaic virus, for trace elements, neutron-activation, 18: 21764 (SGAE-BL-4/1964)
analysis of, automated chromatographic, 18: 15954(R) (LAMS-3034 (p.313-18))
analysis of, chromatographic, 20: 18205(R) (LA-3432, pp 178-262)
base composition of fractions of, in root cells of Vicia, 20: 40631(R) (ORNL-3922, pp 161-6)
base sequence determinations for, use of exoenzymes for, 18: 17406(R) (UCRL-11046(p.27-42))
β-thioethylamino derivatives of constituents of, use of, as radiation-

protection agents, 17: 14046
biosynthesis of carbon-14-labeled, in *Chlorella*, 17: 30016
book: *Progress in Nucleic Acid Research*, 19: 31694
chromosome aberrations induced in mice by, comparison of radiation with, 18: 33309
conference on radiation effects, 17: 30381
content in irradiated testes, 16: 65
content in irradiated rats, effects of methandrostenolone on, 20: 8735
content in liver, effects of central nervous system irradiation on, 16: 2895
content in organs of healthy and irradiated rats, effect of sodium gallate on, 17: 24900(T) (JPRS-19355)
content in *Pseudomonas aeruginosa*, 19: 19503(R) (NP-14933)
content in regenerating and irradiated extremities of salamanders, 17: 7834
content in scorpion and insects, relation to radiosensitivity, 17: 33656
content in viruses, effects on radioinduced inactivation, 20: 14387
desalting of, by metal hydroxide precipitation, 18: 27010(R) (ORNL-3601(p.174-86))
determination and separation in sea urchin embryos, methods for, 20: 8508(R) (EUR-2589.e)
determination in single cells, photometric, 18: 4968(R) (UCRL-11033 (p.118-25))
deuterium effects on thermal transition, 17: 21432
distribution of, in mutants of Neurospora, 20: 6777(R) (ORNL-3853, pp 54-61)
effects in animal radiation sickness, 20: 24829(R) (NEIC-RR-17)
effects of Acridine Orange and incorporated phosphorus-32 on viral, 20: 33058
effects of phosphorus-32- and -33-labeled, on *E. coli* mortality, 20: 24912
effects of virus on properties of, in irradiated tissue cultures, 18: 27199
effects on recovery of irradiated bone marrow cells, 20: 40634 (ORNL-P-2312)
effects on rejoining of radioinduced chromosome breaks in Trillium, 19: 8869
exchange in plant food reserves, gamma-ray effects, 16: 21941
formation in bacteria, reaction mechanisms, 16: 7449
fractionation, 16: 28743(R) (NYO-10152)
induction of leukemia by injection with, from mouse leukemic tissue, 20: 45511(R) (UCLA-12-595, pp 33-66)
interactions with cystamine and cystamine derivatives of, 19: 35909
metabolism by bacteriophages, 20: 5250(R) (UR-668, pp 110-16)
metabolism by growing oocytes, radioautographic study of, 19: 1988 (EUR-1836.e)
metabolism in anucleated and nucleated sea urchin eggs, 20: 8508(R) (EUR-2589.e)
metabolism in brain, autoradiographic tracer study in chicks, pigeons, rats, and cats, 18: 43187 (TID-19605)
metabolism in irradiated rats, effects of injected native liver DNA on, 17: 15797
metabolism in man, tracer studies, 16: 28743(R) (NYO-10152)
metabolism in nerve tissues, 16: 9811(R) (TID-14972)
metabolism in Neurospora, 16: 30
metabolism in rat liver, effects of plutonium on, 17: 30279
metabolism in rat liver, effects of antimetabolites on, 19: 33815
metabolism of, 20: 18185(R) (BNL-929, pp 126-47)
metabolism of, control mechanisms for, 18: 36866 (BNL-7213)
metabolism of, in liver of tumor-bearing rats, 19: 3838
metabolism of, in nuclei of liver cells, effects of thioacetamide on, 19: 6943(R) (ANL-6906(p.102-5))
metabolism of, tracer studies using tritium, 19: 19515
molecular structure of, (E/T), 20: 30734(R) (TID-22970, pp 1-63)
phosphorus-32 uptake in sunflowers by, effects of boron, 16: 26700
phosphorus-32 uptake by, 17: 28645
phosphorus-32 uptake by, in embryonic stages of barley, 17: 28649
photochemical reactions of, in microorganisms, 19: 42212 (NYO-3424-1)
photochemistry, 18: 17386(R) (UCRL-11046(p.210-15))
photochemistry of, 18: 41509(R) (TID-21044)
photochemistry of, review of biological implications of ultraviolet, 18: 31130 (ORNL-P-85)
photochemistry of, review, 19: 18032
photosensitization of, effects of furocoumarins on, 20: 18469
physical properties of, 19: 42212 (NYO-3424-1)
physiological chemistry of, 19: 46158(R) (NYO-910-23, pp 112-82)
polymerization of, enzyme reactions for, 20: 18205(R) (LA-3432, pp 178-262)
precursors of, protective effects against radiation injuries in mice, 19: 43866
preparation of carbon-14-labeled, by use of yeast, 18: 38746
protective effects against radiation injuries in mice, 16: 25253
protective effects against radiation damage to regenerative capacity of extremities of salamanders, 16: 26794
protective effects against radioinduced leukopenia in rabbits, 18: 23373
protective effects with pentoxyl against radiation effects on blood formation in guinea pigs, rabbits, and rats, 18: 27225
protective effects of *Escherichia coli*, against radiation injuries of guinea pigs and rats, 19: 33981
radiation and radioinduced toxin effects on composition of, in rabbit tissues, 19: 8923
radiation chemistry, reaction mechanisms, 16: 30264
radiation chemistry, 17: 24987
radiation chemistry, 18: 11627 (CONF-81-5)
radiation chemistry of, 19: 46417
radiation effects on structure in thymus nucleoprotein, 16: 1543
radiation effects on chromophore group, 16: 1474(T) (JPRS-10170 (p.69-89))
radiation effects, 16: 9902
radiation effects on synthesis, 16: 12937(T) (JPRS-12712)
radiation effects on metabolism, 16: 14518
radiation effects on metabolism in mice, gamma and x, 16: 25212
radiation effects on metabolism in spleen, testis, and thymus in mice, protective effects of AET and MEA against, 16: 25255
radiation effects on constituents of, 16: 26687(R) (UCRL-10156)
radiation effects on metabolism of, 16: 26846
radiation effects on metabolism in *Azotobacter agile*, 16: 30226(T) (JPRS-15220)
radiation effects in bacteria, 17: 212
radiation effects on levels in uterus and vagina of prepubertal mice submitted to induced hyperplasia, 17: 1262
radiation effects, 17: 1284
radiation effects on content in regenerating liver, 17: 1289
radiation effects, 17: 1306
radiation effects on, in rat liver, 17: 2866
radiation effects on, 17: 4561(R) (UCRL-10350)
radiation effects on synthesis of, in rats, 17: 12161
radiation effects on phosphorus-32 uptake by, in *E. coli*, 17: 12141
radiation effects on aqueous solutions of, 17: 15771
radiation effects on translocation in germinating barley, 17: 15775
radiation effects on binding of chromium-51 by liver, 17: 27084
radiation effects on magnetic properties of, 17: 27432
radiation effects on content of, in onions, 17: 33667
radiation effects on trace element content in, in yeast, 17: 35540
radiation effects on skeletal muscle metabolism of, x, 17: 37068(T) (JPRS-20997)
radiation effects on ultraviolet, 17: 40557
radiation effects on metabolism of, in rats and guinea pigs, 18: 49(T) (JPRS-21472(Del.))
radiation effects on sunflower, gamma, 18: 6678
radiation effects on content in organs of guinea pigs, 18: 8220
radiation effects on, review, 18: 9842
radiation effects on, in fish embryos, 18: 11722
radiation effects on, tracer studies of, 18: 11804
radiation effects on potato, gamma, 18: 14307
radiation effects on, in yeasts, 18: 17867 (SGAE-BL-1/1964)
radiation effects on levels of rabbit, 18: 21884
radiation effects on synthesis of, in strain L cells, gamma, 18: 25209
radiation effects on nuclease decomposition of, in presence of trace elements, 18: 25085 (SGAE-BL-5/1964)
radiation effects on metabolism of, in barley seed embryos, 18: 25175
radiation effects on, 18: 27086
radiation effects on content of, in spleen of rats and mice, 18: 27192
radiation effects on synthesis of, 18: 29307
radiation effects on Triturus egg, beta, 18: 31161
radiation effects on synthesis of, in rat spleen, 18: 33382
radiation effects on content of, in gonads of rats, 18: 38939
radiation effects on, in guinea pig epidermis, 18: 43223(R) (NYO-1727-1)
radiation effects on synthesis of, in mammals, 18: 43276
radiation effects on synthesis of, in epidermis of guinea pigs, 19: 123
radiation effects on phosphorus-32 uptake by rat, x, 19: 3970
radiation effects on, 19: 9220
radiation effects on neurological, 19: 10786(R) (TID-21440)
radiation effects on chemistry and structure of, review on, 19: 13024
radiation effects on content in rat liver, 19: 13054
radiation effects on, EPR spectra of, 19: 13086
radiation effects on aqueous solutions of, 19: 22385
radiation effects on content of, in rat pituitary, 19: 24352
radiation effects on, electron spin resonance method for studying, 19: 28106
radiation effects on metabolism of, 19: 29917
radiation effects on content in *Escherichia coli*, 19: 29923
radiation effects on, photochemical, x, 19: 31876
radiation effects on thermoluminescence and magnetic properties of, 19: 36022
radiation effects on, in cucumber leaves, 19: 42325
radiation effects on fish gonad, α, 19: 43769
radiation effects on synthesis in ϕX174-infected *E. coli*, tracer study

of x, 19: 45851
radiation effects on bacteriophage, EPR spectra, 19: 38365
radiation effects on metabolism of, in rat lens, tracer study, 20: 89
radiation effects on plant metabolism of, 20: 1648
radiation effects on content of, in developing chick embryos, x, 20: 5306
radiation effects on synthesis of, tracer study in cultured cells, uv, 20: 6816
radiation effects on phosphate levels in Phycomyces, x, 20: 14264
radiation effects on, in growing plant cells, 20: 14383
radiation effects on metabolism of, 20: 16160 (UCRL-14739(Pt.2))
radiation effects on primer function of, 20: 16160 (UCRL-14739(Pt.2))
radiation effects on properties of virus, uv, 20: 16206
radiation effects on properties of virus, uv, 20: 16207
radiation effects on metabolism of, x, 20: 22794 (EUR-2769.f)
radiation effects on synthesis in rat thymus, x, 20: 28953
radiation effects on content of, in *E. coli*, x, 20: 31023
radiation effects on, uv, 20: 31039
radiation effects on, uv, 20: 32936
radiation target size of single-stranded, 17: 35457(R) (TID-19345)
radioactive carbon-14-labeled, retention from embryonic stage throughout life span, 16: 26825
radioactivity of tritium-labeled, liquid-scintillation counting of, 19: 9072
radioinduced castration effects on, x, 18: 19731
radioinduced changes in, in *Escherichia coli*, 18: 27153
radioinduced decomposition of constituents of, reactions in, 16: 28981 (UCRL-10053)
radioinduced free radicals, paramagnetic resonance spectra, 16: 31483(T)
radioinduced free radicals in dry, 17: 110
radioinduced free radicals in, 17: 15767
radioinduced free radicals in, 17: 25012
radioinduced free radicals in, 19: 5957
radioinduced inactivation of, target theory for, 19: 26058
radioinduced nuclear spin in, gamma and x, 17: 39125
radioinduced phosphatase activity on poly-, uv, 19: 31853
radioinduced radicals, 17: 19845
radioinduced radicals in dry, ESR of gamma and x, 20: 1623
radiolysis, 16: 20515
radiolysis of aqueous solutions of, review on, 19: 30276
radiosensitivity effects of content of, on bacteria, 18: 33310
radiosensitivity effects of irradiated, 19: 45729(R) (NYO-910-23, pp 1-111)
radiosensitivity of infectious, of tobacco mosaic viruses, 18: 25159
reactions with aminoacridines, 18: 43151 (ISS-63/50)
reactions with hydrated electrons and hydroxyl radicals, rates of, 20: 10917
reactions with hydrogen atoms, 20: 45322(R) (UCLA-12-595, pp 6-28)
reactions with radionuclides, injuries from, 20: 16160 (UCRL-14739 (Pt.2))
separation by paper chromatography, 16: 5117(R) (UCRL-9900)
separation from bacteriophages, method for, 19: 31683(R) (UCRL-11833 (p.26-8))
separation from *Escherichia coli*, 19: 4250(R) (ORNL-3627(p.177-208))
separation from *Escherichia coli* KL-9 by extraction using sodium arsenate, 19: 29923
separation of, chromatographic, 18: 15780(R) (LAMS-3034(p.350-72))
separation of, tracer studies of, 18: 43586
spectra of derivatives of computer analysis of infrared and ultraviolet, 18: 43375(R) (LA-3132-MS(p.249-51))
structure from radiosensitivity effects, 16: 7406 (BNL-675(p.1-17))
structure of, 19: 29849(R) (ANL-6971(p.1-28))
structure of, use of electron microscopy in studies of, 19: 19455 (CONF-640204(p.44-62))
synthesis and storage of tritiated, 20: 2 (EUR-2419.1)
synthesis by isolated rat diaphragm, effects of corticosteroids, tracer study, 16: 28802
synthesis during hepatic regeneration, tracer study, 17: 24895(R) (TID-18721)
synthesis in cultured bone marrow cells from patients with leukemia, myeloma, or polycythemia, tracer study, 20: 30971 (ORINS-45)
synthesis in isolated nuclei from mammalian cells, tracer study, 20: 18204(R) (LA-3432, pp 130-77)
synthesis in maize seedlings, 18: 27011(R) (ORNL-3601(p.188-206))
synthesis in rat liver, effects of plutonium on, 17: 30278
synthesis in regenerating thymus and liver, tracer study of, 17: 33736
synthesis in *Vibrio cholerae*, effects of ultraviolet radiation and chloramphenicol on, 18: 9862
synthesis of, effects of irradiated *S. typhimurium* on, 17: 15777
synthesis of, enzyme reactions in, 17: 33511(R) (TID-19143)
synthesis of nucleotide phosphate and adenosine triphosphate by seedlings, effects of light, 16: 26816
synthesis of, control mechanisms for, 20: 36555(R) (NYO-2643-22)
synthesis of, in barley seed, 18: 17361(R) (TID-20353)
synthesis of, in *Tetrahymena pyriformis*, 18: 27005(R) (ORNL-3601(p.60-8))
synthesis of, tracer studies, 18: 13444(R) (CU-1304-1)
synthesis rate of, effects on radiosensitivity of *Escherichia coli*, 18: 6695
synthesis, reaction mechanisms, 17: 32
viral and transforming-principle, 16: 32643(R) (UCRL-10211(p.9-15))
Nucleometer
see Rate Meters
NUCLEON SHOWERS
alpha emission in, by direct interaction, (T), 19: 21372
calculation of meson-, for accelerator shield design, 17: 9646 (ORNL-3289)
calculations for meson (π^-) reactions with emulsion nuclei at 17 Bev, (T), 20: 38060
calculations of intranuclear, (T), 19: 21239 (LA-3206)
development, cascade theory, 16: 18106 (NP-11463(Pt.2)(p.255-60))
distributions in, 19: 10452 (CERN-64-47)
distributions in meson–nucleon cascades, (T), 19: 18751 (ORNL-3734)
distributions in, produced by 10- to 1000-Bev protons, (T), 19: 10452 (CERN-64-47)
energy spectra in meson (π)-nucleon, from 2- to 10-Bev primaries, 20: 8079 (ORNL-3855)
equations for, perturbation method for solving, 17: 31281 (ORNL-3467)
particle energies and distributions, computer analysis, 16: 3885(R) (ORNL-3193(p.323-4))
production by proton reactions with nuclei from Z = 6 to 92 at 660 Mev, (E), 20: 42299
production by 82- to 156-Mev protons on nuclei, 18: 16974
production in proton reactions with iron at 1 and 3 Bev, (T), 20: 3258
production of meson–nucleon, by 10- and 20-Bev/c protons in steel, (T), 19: 45317
NUCLEONS
see also Antinucleons
see also Baryons, Resonance
see also Cosmic Nucleons
see also Neutrons
see also Protons
absorption by carbon at 300 to 970 Mev, cross sections for, (T), 19: 19121
absorption of, spatial distribution of potential for, 18: 7674 (CONF-327-7)
angular distributions of excited, from cosmic showers, 16: 27878
angular distributions in alpha-nuclear showers, 16: 27880
angular momentum distribution in nuclei, 18: 26578
angular momentum of, in nuclei, (T), 19: 27448
annihilation by antinucleons, 16: 10812 (CERN-61-30)
annihilation by antinucleons, production of mesons (π) in, 16: 9408
annihilation, heavy meson production in, 17: 20857
annihilation of, perturbation theory of, 17: 20858
annihilation on antiprotons, hyperon pair production by, 16: 27959
annihilation on antibaryons, distributions from, 17: 11547
beta decay in systems of one, two, and three, (T), 19: 10045
beta decay of bare, modes in, 17: 745
binding and pairing energies in nuclei, effects of shell closure on, 19: 10358
binding and pairing energies in nuclei with A = 143 to 177, (E), 19: 29367
binding and scattering of three-body system of, 18: 18935
binding energies in tritons, 16: 15589
binding energies in single-particle model of nuclei, 17: 19231(T) (AEC-tr-5702)
binding energies in nuclei, formula for, 18: 22883
binding energies in oxygen-16, 18: 24635
binding energies in hypernuclei, 18: 34857
binding energies in few-body systems with velocity-dependent potentials, (T), 19: 6675
binding energies in nuclei with A = 69 to 100, 19: 29365
binding energies in nuclei, measurement of, 20: 28445
binding energies in nuclei, 17: 11736
binding energies of pairs of, in nuclei, 19: 29354
binding energies of, Hartree-Fock calculations of, 19: 43340
binding energies, energy levels, and potentials of, from self-consistent, model, 18: 21358
binding energy and coupling constant for two-body systems of, Bethe-Salpeter equation for, 20: 13876
binding energy and mass relationships for, 20: 25791 (PAEC(A)PH-663)
binding energy and wave functions for three-body systems of, (T), 20: 36210
binding energy in nuclear matter, 18: 40537
binding energy in three-body systems, (T), 19: 8455
binding energy in nuclei, pairing corrections to, (T), 19: 29347
binding energy in nuclei, four-particle Bethe-Faddeev equation for, (T), 20: 10057
binding energy in nuclei, (T), 20: 34577

binding energy in nuclei, calculation using K-matrix theory, 20: 44727
binding energy of, reference spectrum determination of, 17: 19350
binding energy of, formula for nuclei $6 \leq Z \leq 100$, 17: 28273
binding energy of, variational procedure for calculation of, 18: 4622
binding energy of ground-state three-body system of, upper and lower bounds of, 18: 21048
binding energy of ground-state three-body system of, (T), 19: 14588
binding energy of three bound-state, (T), 19: 33052
binding energy of three-body system of, (T), 19: 39926
binding energy of system of four, (T), 19: 43348
binding in nuclei, three-body, 16: 31122
binding of three, effect of three-body force on, 17: 34933
bond energies in nuclei of, $174 \leq m \leq 239$, 16: 10967(T) (FTD-TT-61-175(p.15-24))
book: *Fundamental Particles*, 19: 21072
book: *The Nucleon-Nucleon Interaction. Experimental and Phenomenological Aspects*, 17: 39941
book: *The Two-Nucleon Interaction*, 18: 909
bound-state ($\bar{K}NN$) existence, 18: 9151
bound state of three, binding energy and wave function of, 16: 33716
bound state problem, calculation of the three-body forces in, 16: 19720
bound states in 3-body systems having separable potentials, 16: 22890
capture and emission in shell model intermediate coupling theory of nuclear reactions, 18: 6289
capture by nuclei at 10 to 40 Mev, cross sections and mechanism for direct, (T), 20: 17737
capture in (d,He-3) reactions on nuclei near A = 40, 18: 16931 (ANL-6848(p.177))
cascades from, analysis of meson, 18: 7474(R) (ORNL-3499(Vol.II)(p.23-4))
cascades from, calculations of meson, 18: 7360(R) (ORNL-3499(Vol.II)(p.24-5))
charge density of, pseudoscalar, 17: 36570 (CONF-122-9)
charge distribution in meson (π)-nucleon systems, (T), 20: 37791
charge form factors of, in static model (T), 19: 1371
charge, hypercharge, and mass spectra, model for nondegenerate, 16: 27980
charge independence and symmetry, and reduced widths, 16: 23090
charge structure, 17: 41533(R) (ANL-6720(p.67-75))
classification and notation for, 17: 9371
classification of, review, 19: 27273
cluster emission in nuclear reactions, (T), 19: 19221
cluster substitution in nuclear reactions, (T), 20: 10033
clustering in beryllium-8, carbon-12, and oxygen-16, (T), 19: 19141
clustering in light nuclei, review on, 19: 16886
clustering in light nuclei, review on, 20: 17707
clustering in nuclei, effects on nuclear reactions, 18: 21247
clustering in nuclei, reduced widths for, 18: 28680
clustering in nuclei, theory of, 18: 32851
clustering in peripheral nuclear region, (E), 19: 16887
clustering of, connection to shell-model wave function, 18: 4606
collisions with nuclei, model for high-energy, 17: 19542
configuration in nuclei, spherical-shell, (T), 19: 27449
configuration in nuclei, magic numbers for, (T), 20: 4872
core potential parameters of, effects of variations of, 18: 18670
correlation functions for electron-nucleus scattering, two-nucleon, 16: 11030
correlation functions for, in photon reactions (γ,np) with light nuclei, 17: 29598
correlations in nuclei, (T), 20: 24398
coupling constant of, with mesons, 18: 24411
coupling in nuclei, spin-orbit, 16: 8238
coupling to anharmonic surface vibrations of nickel-62, in copper-63, (T), 20: 26125
coupling to massive photons in elastic scattering, 20: 32046
coupling to mesons (ω), 17: 13410
coupling to mesons (π), (E), 20: 25781(R) (COO-1195-56)
coupling to spherical core, energy spectrum, 17: 7508
coupling to spin-j core, doublets from, 17: 40031
currents between one- and two-body states, 18: 22879
decay modes of, life time limits for, 17: 13465
decay of, CVC in leptonic, 19: 16674
decay of, G_2 and SU_2 symmetry for, 18: 900
decay of, effects of mesons (ω) and (ρ^0) mixtures on spin and parity in, 17: 34800
decay of, radiative corrections to, analysis by dispersion and perturbation techniques for, 17: 22520
decay of, unitary symmetry in leptonic, 19: 16673
decay rates of, conserved currents in, 17: 5219
density equilibrium distribution of, in quasiclassical statistical model, 18: 6265
description in Regge-pole and conventional field theory, 17: 4006
description of, formulation of quaternion, 17: 32716(R) (NP-12996(p.23-8))
dispersion relation subtraction constants from meson (π) interactions, 16: 18359
distribution from knock-out reactions, excitation energy, nuclear volume, and recoil momentum for, (T), 20: 13892
distributions and wave functions in deuterons and light nuclei, (T), 19: 8393 (ISS-64/24)
distributions in nuclei, analysis by meson (π^0) photoproduction on, 17: 33073
doses in tissue from 100- to 400-Mev, 18: 6714(R) (ORNL-3499(Vol.II)(p.56-60))
dosimetry of, in transverse shielding of 45-Bev electron accelerator, 17: 15322 (ORNL-3365)
doublets of, prediction by quaternion formulation of wave functions, 17: 24191
dynamics in helium-3 and tritium ground states, form factors for, 18: 2937
effects of three-, on binding energy of nuclear matter, 17: 31547
effects on diffraction scattering, 18: 32580
electric charge radius of, 18: 20976
electric dipole moment of, 18: 32594
electric dipole moment of, (T), 19: 12202
electric dipole moment of, (T), 19: 29124
electric dipole moment, (T), 19: 32997
electric dipole moments of, in intermediate vector boson theory, 20: 17372
electromagnetic form factors for, 16: 25896 (LNF-62/37(p.81-8))
electromagnetic form factors at high energies, 16: 26133
electromagnetic form factors, 16: 27971
electromagnetic form factors for, 16: 32331
electromagnetic form factors of, effects of high-energy limits on, 16: 33747
electromagnetic form factors of, representation by scattering theory, 16: 33743
electromagnetic form factors of, 17: 5274
electromagnetic form factors at high momentum transfer for, 18: 14897
electromagnetic form factors of, Regge representation for, 18: 21009
electromagnetic form factors of, (T), 19: 12320
electromagnetic form factors, (T), 19: 12321
electromagnetic form factors of, extrapolation of, (E/T), 19: 39458 (CONF-796(Paper 24))
electromagnetic form factors of, $\bar{U}(12)$ theory for $(56,\bar{56})^-$ contribution to, 20: 9735
electromagnetic properties of, use of Lee model in computation of, 17: 26386
electromagnetic properties of, SU(4) symmetry for, 19: 41397
electromagnetic structure, meson (π) interaction relation to, 16: 999
electromagnetic structure, meson (ρ) effects on, 16: 8144
electromagnetic structure, π-π interaction resonance effects on, 16: 12380
electromagnetic structure of, 3-meson (π) effects on isoscalar, 17: 11559
electromagnetic structure of, effects of vector mesons on, (T), 19: 10258(R) (TID-21335(p.151-60))
electromagnetic structure of, review, (E/T), 19: 12168 (NP-14540)
electromagnetic structure of, effects of meson (K) interactions with meson (π) on, 17: 13464
electromagnetic structure of, from electron scattering studies, 17: 34819
electromagnetic structure of, 17: 34822
electromagnetic structure of, effects of mesons (ρ) on, 17: 41790
electromagnetic structure of, review of, (T), 20: 11579
emission from nuclei following proton bombardment at 660 Mev, distributions from, 18: 42634 (JINR-P-1713)
emission from nuclei, adiabatic separation energies for, (T), 19: 16844 (ISS-64/36)
emission from nuclei, reduced widths in shell model intermediate coupling, (T), 20: 15830
emission in deuteron photodisintegration at 11.23 to 127.38 Mev, phase parameters from, 18: 42394
emission in meson (π^-) capture by nuclei, nuclear structure from two-particle, 17: 38175
emission in meson (π^-) capture by nuclei, correlations from, 18: 34851
emission in meson (π) reactions with nuclei (T), 19: 1683
emission in meson (π^-) capture by nuclei $3 \leq Z \leq 13$, angular distributions from double, (E), 20: 19842 (UR-875-126, Paper 1)
emission in meson (π) capture by light nuclei, (T), 20: 19843 (UR-875-126, Paper 2)
emission in neon-20 reactions with tantalum at 160 Mev, 18: 24717
emission in nuclear electrodisintegration, angular correlations in, (T), 19: 10306
emission in nucleon-stimulated decay of hyperfragments, 18: 40334
emission in proton reactions with slabs of aluminum, carbon, lead, and nickel, 20: 28596
emission of, from nuclei in meson (π^-) capture, 17: 11687
emission of pairs of, in meson (π^-) capture by nuclei, (T), 19: 47679
energies in heavy even-even nuclei, effects on spontaneous fission,

18: 40604
energies of, in light nuclei, 17: 38161
energies of many-body systems of, in Bopp approximation, 19: 21412
energy gap in systems of interacting, (T), 19: 41826
energy in fixed-source meson theory, ground-state, 16: 13899
energy levels and isobars of, rotation, (T), 19: 23383
energy levels in closed-shell nuclei, 17: 7088 (NP-12330(p.1-14))
energy levels in nuclear models (superfluid), partially projected functions for, 18: 7706
energy levels of equivalent j = ½ configurations, classification using group theory, 20: 40082
energy levels of three-body system of, matrix elements of three velocity-dependent operators for arbitrary, 20: 17746
energy loss in hydrogen due to strong interactions, 17: 9287
energy of hard core system of, with neutron excess, (T), 20: 25783 (INR-662/VII/PH)
energy states in bounded isotropic harmonic oscillator potential, 18: 42656
equilibrium states of systems with gravitational forces, (T), 19: 12059
evaporation from nuclei, energy distribution of recoil nuclei in, (T), 19: 33378
exchange at high energies, methods for studying, 18: 2581 (AD-299108)
exchange currents in, test for, 18: 37907
exchange in direct nuclear reactions, (T), 20: 28376
exchange in direct nuclear reactions, double, (T), 20: 28377
exchange in heavy ion reactions with nuclei, delayed neutron activity method for, 17: 38292
exchange in meson (π)-nucleon interactions, 18: 32600
exchange in nitrogen-14 reactions with nuclei at 27.5 Mev, excitation functions for, 18: 24716
exchange in nuclear reactions, tunneling theory for, 18: 36671
exchange in nuclear reactions, interference effects in, (E/T), 19: 5256
exchange in nuclear reactions, (T), 19: 41805(T)
exchange in nuclear reactions, mechanism of, 20: 4850
exchange in nuclear reactions, one-dimensional tunneling model for, 20: 4851
exchange in nuclear reactions, modified energy matrix method for, 20: 4852
exchange in nuclear reactions, (T), 20: 21972 (BNL-948, pp 86-174)
exchange in pickup and stripping reactions, two-body, (T), 20: 30483
exchange of clusters of, in nuclear reactions, 17: 38280
exchange of resonance state, in meson (π)–nucleon interactions, 18: 6028
exchange of single, in nuclear reactions, (T), 20: 21971 (BNL-948, pp 1-65)
exchange of virtual, in meson (π^-) interactions with protons at 4.13 and 4.95 Bev/c, 17: 41802
exchange reactions between complex nuclei, 17: 11737
excitation in photonuclear giant resonance, 18: 22875 (UCRL-7740)
excitation of, in very high-energy collisions, 17: 9436
excitations and resonances in nuclear reactions, 16: 12516
excited state decay modes, 18: 40292
excited states of, evidence for, 17: 22437 (SLAC-13)
existence of heavy unstable, possibility of, 19: 47398
experiments on, survey of, 18: 6296
field equations for multiplets of, transformation invariance in free, 17: 24292
form factor for, axial-vector, 17: 31289 (TID-19105)
form factor for, electromagnetic, 19: 47318
form factor for, sum rule calculation of isovector, 20: 30037
form factor of, isovector part of, (T), 20: 24056
form factors, 17: 32909 (TID-7668(Sect.I))
form factors, 18: 37960
form factors, 18: 37987
form factors, 18: 40314
form factors, (T), 19: 35034
form factors, (T), 20: 27912
form factors, 18: 37879 (NP-14173)
form factors, analysis of scalar, 16: 6980
form factors, development of models for, 16: 8096 (JINR-D-774)
form factors, effect of inelastic processes in meson (π)–meson (π) scattering on, 17: 28198
form factors for, 16: 23129
form factors for electromagnetic and weak transitions, relation to vector meson form factors, 16: 2450
form factors for, effects of π-π interaction in electromagnetic, 16: 22957
form factors for, high-energy behavior of, 17: 9346
form factors for, in helicity representation, 16: 29694
form factors for, interpretation and notation of, 17: 9346
form factors for, review of theory of, 17: 9465
form factors for, meson (ϕ) contribution to, (T), 20: 11598
form factors for, electromagnetic and weak, (T), 20: 13447 (IC/65/95)
form factors for, current algebra for coupling constants for, 20: 15308 (IC/66/18)
form factors for, relations in SU(6) for electromagnetic, 20: 24153
form factors for, sum rules for electromagnetic, 20: 25782 (DESY-66/8)
form factors for, proportionality of electric and magnetic, (T), 20: 27863
form factors for, choice of F or G electromagnetic, 20: 36050
form factors for, electric and magnetic, (T), 20: 44269
form factors for, from singularities in redundant variables of sum rules, 20: 44362
form factors in strong-coupling meson theory, 17: 19134
form factors in the configuration space, 16: 2658
form factors of, in strong coupling meson theory, 17: 9296
form factors of, isospin density effects on isovector, 17: 26308
form factors of, meson (ρ) effects on electromagnetic, 17: 22494
form factors of, ($K\bar{K}$) and ($\pi\rho$) contributions to isoscalar, (T), 19: 47371
form factors of, (56,$\overline{56}$) contribution to, (T), 20: 4642 (IC/65/78)
form factors of, asymptotic decrease of, (T), 20: 24027
form factors of, contributions of (K-K) interaction intermediate states to, 18: 2671
form factors of, corrections for inelastic deuteron-electron interaction effects on, (T), 20: 11646
form factors of, determination for time-like momentum transfer, (T), 19: 39590
form factors of, determination using electron scattering, 20: 15439
form factors of, determination using electron scattering, 20: 15440
form factors of, determination by cosmic particle momentum transfer analysis, 20: 39781
form factors of, effect of scalar dipion resonance on axial, 18: 14910
form factors of, electromagnetic, 18: 37927
form factors of, equality of, 18: 37977
form factors of, electromagnetic, (T), 19: 25386
form factors of, electromagnetic, (T), 20: 13479(T)
form factors of, electromagnetic, (E), 20: 15306(R) (CEAL-1026)
form factors of, electromagnetic and weak, (T), 20: 21651
form factors of, electromagnetic, 20: 24008 (CERN-65-24(Vol.2), pp 67-87)
form factors of, electromagnetic, (T), 20: 24005 (CERN-65-24(Vol.2), pp 1-17)
form factors of, electromagnetic, (T), 20: 32033
form factors of, effect of meson (π)-meson (π) interactions on electromagnetic, (T), 20: 37801
form factors of, electromagnetic, 20: 41952
form factors of, electric and magnetic, 17: 39940
form factors of, fundamental length in, 18: 36279
form factors of, from electroproduction of mesons (π), (T), 20: 36039 (N-66-18134)
form factors of, Green function approximation scheme for, (T), 19: 12187
form factors of, isovector, 18: 16781
form factors of, in strong-coupling meson theory, 18: 37930
form factors of, isovector, 18: 42385
form factors of, isovector, (T), 20: 9709 (COO-427-42)
form factors of, isospin exchange relations for, (T), 20: 15449
form factors of, isotopic vector electric and magnetic, (T), 20: 25850
form factors of, quark model for electric and magnetic, 20: 36035 (JINR-P-2757)
form factors of, review of Stanford research on, 20: 6277 (AD-619952)
form factors of, relations for, (T), 20: 15492
form factors of, review on, 20: 19529
form factors of, spectral function for electromagnetic, (T), 19: 8146
form factors of, theory of, 18: 37959
form factors of, vector meson model for, (T), 20: 11627
form factors, Regge theory for, 19: 8233
gamma absorption by pairs of, in helium-4, 17: 24464
gamma absorption by pairs of nuclear, 18: 34925
gravitational wave emission, 16: 18607
gravitational wave emission by, 16: 26176
grouping in shell-model states, fractional parentage coefficients for three-particle, 18: 24621 (PAN-449/VII)
indistinguishability in nuclei, nuclear-model agreement from, 16: 17120
interacting systems of, singularity of t-matrix of, 17: 7006
interaction amplitudes of, coupling constants for elastic, 17: 9189 (JINR-P-1087)
interaction amplitudes for three-particle systems, 17: 37971
interaction forces, 16: 13976
interaction of four, in same shell, 18: 34863
interaction parameters, in shell model, 16: 33854
interaction phase shifts for, 16: 15580
interaction potential determination method, 16: 2444
interaction potential, three-body, 16: 11009
interaction potentials, 16: 15540
interaction potentials from dispersion relations, 16: 18382
interaction potentials in nuclei, phase shifts for singular, 17: 40032
interaction potentials of, existence of parity-nonconserving, (E),

19: 14331(T) (CEA-tr-R-1814)
interaction potentials in nuclei, shell model calculations for, (T), 20: 3068
interaction resonances of, classification of, 17: 750
interaction resonance state ($\bar{K}$-N) coupling to (Σ-π), 17: 28136 (BNL-6363)
interaction resonant states of, classification and transition system for, 17: 37931 (JINR-P-1282)
interaction resonances of, review on, 18: 34636
interaction resonances with mesons (π), form factors of N*, (T), 20: 24014 (DESY-66/4)
interaction with meson fields, magnetic moment addition in, 16: 22877
interaction with nucleons, polarization in elastic, 16: 10821
interaction with nucleons at high energy, one meson (π) exchange model for, 17: 20866
interactions, 18: 10850 (JINR-P-1469)
interactions above 10 Bev, magnetic monopole production cross sections, 16: 9375
interactions above 100 Bev, kinetics, 16: 22902
interactions above 400 Mev, phase shifts for, 17: 19153
interactions above 1 Bev, phase-shift analysis of, (T), 20: 9777
interactions and α-β potential, two-body, 16: 31122
interactions and properties of, model for, 17: 7016
interactions and spectra in spherical nuclei, shell model analysis, 16: 28114
interactions at cosmic-radiation energies and at less than 30 Bev, meson (π) production in, 16: 8108
interactions at high energies, cross-section constancy, 16: 5889
interactions at high energies, multiple-meson-production model for, 16: 22903
interactions at high energies, cross sections for inelastic, 16: 32343
interactions at high energies, 2-center model for jets from, 16: 33869
interactions at high energies, azimuthal angular distribution of secondary particles from, 17: 7019
interactions at high energy, experimental and theoretical data on elastic, 17: 11507
interactions at high energies angular distributions of meson (π) secondaries in jets from, 18: 7525
interactions at high energies, method of analysis of, 18: 40205
interactions at high energies, total cross sections for, (T), 19: 8147
interactions at high energies, Regge trajectories for, (T), 19: 21063
interactions at high energy, Regge-pole hypothesis in asymptotic amplitudes for, 19: 39478 (NP-15210)
interactions at high energies, isobar production in, (T), 19: 39508
interactions at high energies, SU(3) for multiple meson production in, (T), 20: 17345 (JINR-P-2531)
interactions at low energies, effective range parameters for potential, (T), 19: 14313 (JINR-E-1894)
interactions at low energies, two-body, (T), 19: 16476 (NP-14680)
interactions at small distances, analytical solutions for potential, 16: 8211
interactions at ultrarelativistic energies, comparison of methods for primary energy determinations in, 17: 15098
interactions at 0 to 400 Mev, effects of pion resonance exchange in, 18: 14954
interactions at 10^{12} ev, angular distributions, 16: 21404
interactions at 10^3 to 10^6 Bev, angular distribution of secondary particles in, (T), 19: 25280
interactions at 12 to 450 Bev, inelastic effects in (E), 19: 1201
interactions at 23 to 630 Mev of polarized, spin correlation tensors for, (T), 20: 7796 (JINR-P-2407)
interactions at 3×10^{12} ev, Monte Carlo analysis of, 18: 12948
interactions at 300 Bev, cross sections, (T), 19: 41358
interactions at 400 to 900 Mev, meson production in, 16: 12333 (JINR-P-226)
interactions at 6 Bev to 10 Tev, multiple charged particle production in, 18: 9119
interactions at 95 to 310 Mev, triplet-even potentials for, 16: 26126
interactions below 315 Mev, potential model for, 16: 22896
interactions, Brueckner theory for nuclear forces in, 16: 29807
interactions, corrections to shell model, 16: 4819
interactions, coupling constants and dispersion relations, 16: 2648
interactions, coupling and phase parameters, 16: 4799
interactions, dispersion theory of, 16: 17038
interactions, dispersion relation electrostatic corrections for, 16: 24751
interactions, effects of mesons (ζ) on, 16: 32320
interactions, field theory, 16: 2462
interactions in carbon, ratio of charged to neutral, 16: 17114
interactions in deformed nuclei, 18: 18905
interactions in deformed nuclei, vibrational-rotational, 18: 34950
interactions in few-nucleon systems, final-state, 18: 28563 (BNL-7982)
interactions in finite nuclei, effects on energy levels, 17: 5366
interactions in four-body systems at low energies, 18: 34619
interactions in G_2 symmetry scheme, reciprocal bootstrap properties of, (T), 19: 4925
interactions in heavy cosmic particle reactions in emulsions, meson production from, 17: 26269 (PAN-398/VI)
interactions in helium-3 and tritium, binding energy from three-particle, (T), 19: 43379
interactions in interior of nuclei, optical model for, 18: 2923
interactions in many-body systems of, bound states in, (T), 19: 25383
interactions in many-body systems of, (T), 20: 19274 (N-65-16830)
interactions in mixed degenerate orbits, generalized seniority scheme for, 20: 26168
interactions in molybdenum, niobium, technetium, yttrium, and zirconium isotopes, effective, (T), 20: 6337
interactions in nuclei, effective two-body potentials, 16: 3738
interactions in nuclei, pairing force ratio to field-producing force, 16: 17106
interactions in nuclei, effects on gamma transition probabilities, 16: 21432
interactions in nuclei, dipole-dipole, 16: 23157
interactions in nuclei, effects on photonuclear reactions, 16: 31117
interactions in nuclei, boundary-condition model for forces in two-body, 18: 7760
interactions in nuclei, two-body forces in, 18: 17054
interactions in nuclei, approximation for pairing, 18: 19098
interactions in nuclei, density distributions from exponential, Gaussian, and Yukawaian, 18: 24633
interactions in nuclei, potentials for, 18: 26638
interactions in nuclei, effects on magnetic moments, 18: 28734
interactions in nuclei, equilibrium shape from, 18: 36683
interactions in nuclear matter, effective, 18: 42695
interactions in nuclei, forces from (T), 19: 1696
interactions in nuclear matter, two-particle potentials for, 19: 1571 (TID-21247)
interactions in nuclei, soft-core (T), 19: 3335
interactions in nuclei, potential parameters for, (T), 19: 8405 (UCRL-7155(Rev.I))
interactions in nuclei, spin-independent coupling in, (T), 19: 10273
interactions in nuclei, (T), 19: 12625
interactions in nuclei, self-consistent treatment of, (T), 19: 12497
interactions in nuclear matter, effective, (T), 19: 12564
interactions in nuclei, isobaric spin effects on, (T), 19: 14491 (ANL-6878(p.181-206))
interactions in nuclei, BCS and RPA calculations for, (T), 19: 16984
interactions in nuclei, charge-independent pairing, (T), 19: 17007
interactions in nuclei, (T), 19: 16931
interactions in nuclei, soft core potentials in, (T), 19: 16934
interactions in nuclei, (T), 19: 23645
interactions in nuclei, superconductivity theory of pairing, 19: 23735
interactions in nuclei, review of meson theory for, 19: 23765
interactions in nuclear matter, three-body, (T), 19: 25527
interactions in nuclei, shell-model study of, 19: 25541
interactions in nuclei, (T), 19: 29093
interactions in nuclei, parity non-conserving, 19: 35376 (CONF-641210-17)
interactions in nuclei, t-matrix formalism for, (T), 19: 39871
interactions in nuclei, tensor, (T), 19: 39872
interactions in nuclei, superconductivity theory of pairing, 19: 41843
interactions in nuclei, SU(3) model for s-state, (T), 19: 45247(R) (ANL-6877,pp 29-31)
interactions in nuclei, effects on photonuclear reactions, 16: 31118
interactions in nuclei, self-consistent model for, 17: 879
interactions in nuclei, effective, 17: 11739
interactions in nuclear matter, velocity-dependent, 17: 17164
interactions in nuclei, calculations of correlations, 17: 19083
interactions in nuclei, dipole photoabsorption cross section increase from nonlocal, 17: 40120
interactions in nuclei, pairing energy for charge-independent, 20: 8087 (ZFK-TPH-16)
interactions in nuclei, correlated basis functions for, (T), 20: 11492
interactions in nuclei, effects on beta decay of strong, (T), 20: 13886
interactions in nuclei, effects on meson (π)-induced nuclear reactions, (T), 20: 15827
interactions in nuclei, effects on forbidden beta transitions of strong, 20: 15836
interactions in nuclei, statistics of random-matrix eigenvalues for, (T), 20: 15784
interactions in nuclei, phenomenological treatment of, 20: 17728
interactions in nuclei, velocity-dependent potential for, 20: 19874
interactions in nuclei, separation distance for effective, (T), 20: 22122
interactions in nuclei, hamiltonian for, 20: 24381
interactions in nuclei, hard-core, (T), 20: 28290
interactions in nuclei, surface delta, (T), 20: 28412
interactions in nuclei, nonlinear field equation for, 20: 30361
interactions in nuclei, integral operators and S-matrix for scalar dis-

persion in, 20: 32537
interactions in nuclei, two-body matrix element for Gaussian, 20: 32461
interactions in nuclei, group theoretic model for, 20: 34645
interactions in nuclei, pair correlations and final-state, 20: 38015
interactions in nuclei, symmetry of self-consistent field, (T), 20: 40136
interactions in nuclei, pairing approximation for $f_{7/2}^{-}$ and $p_{3/2}^{+}$ shells, (E), 20: 44684
interactions in nuclei, (T), 20: 44844
interactions in nuclei, velocity-dependent potential for, (T), 20: 46722
interactions in nuclei, (T), 20: 46400
interactions in odd-odd deformed nuclei, effects on 0 (T = 1) levels in, 18: 19092
interactions in oxygen isotopes, model for effective, 17: 33100
interactions in oxygen-18, velocity-dependent potentials for, 18: 26639
interactions in oxygen-16, properties of odd-parity states from effective, 20: 30412
interactions in praseodymium isotopes, (T), 20: 12124
interactions in saturated nuclear matter, velocity-dependent, 17: 40088
interactions in single nuclear j-shell with charge-independent pairing force, calculations using BCS method, (T), 20: 44734
interactions in superfluid state of nuclear matter, hamiltonian for strong, 18: 7748
interactions in superfluid nuclear model, four-body correlations in, (T), 19: 33253
interactions in symmetric pseudoscalar fields, 17: 17047
interactions in three-body systems of, theory for, 18: 36320
interactions in three-nucleon sound systems, 19: 1559 (NP-14404(p.160-4))
interactions in three-body systems of, with separable potentials, (T), 19: 20986
interactions in three-body system of, binding energy for, (T), 19: 23779
interactions in 1p shell nuclei, Hamada-Johnson potential for effective, 20: 26153
interactions in $2s_{1/2}1d_{3/2}$ shell nuclei, surface delta interaction of, 20: 30423
interactions, meson (π) form factor effects in peripheral, 16: 3648
interactions, meson (π) exchange potentials from, 16: 18387
interactions, meson (π) production in, 16: 22950
interactions, model for inelastic, 16: 2463
interactions of, amplitudes in, 17: 7080 (JINR-P-1024)
interactions of, amplitude residue in vacuum pole trajectory, 17: 20900
interactions of, boundary-condition model for, 17: 39987
interactions of bound, with mesons (π), elastic, (E/T), 20: 19444 (LYCEN-6527)
interactions of, bremsstrahlung mechanism for multiple meson (π) production in, 17: 29518
interactions of, complex Yukawa potentials for, 17: 2422
interactions of, coupled partial-wave-dispersion relation and meson (ρ) and (ω) contributions to, 17: 20918
interactions of, dispersion relations for, 17: 13448
interactions of, effects of nucleon magnetic moments on, 16: 33767
interactions of, effects of velocity-dependent potentials on, 17: 2289
interactions of, effects of spin-orbit forces in, 17: 19074
interactions of external, with nonaxial nuclear rotation, 18: 2949
interactions of fields of, with scalar meson fields, 18: 40262
interactions of four identical, quantum electrodynamics of pairing and quadrupole, 18: 6222
interactions of four, bound states in, 19: 12176
interactions of, Hamiltonian for derivation of self-consistent field in superfluid nuclear model for, 16: 31080
interactions of, in deuterium electrodisintegration, 17: 26341
interactions of, meson (π) multiple production in, 17: 2187
interactions of, meson (π)-nucleon interpretation of, 17: 29522
interactions of, models for inelastic, 17: 19079
interactions of, nonlocal even parity, 17: 28187
interactions of, nuclear matter behavior from residual, 17: 9574
interactions of, nuclear matter ground-state binding energy from velocity-dependent, 17: 26524
interactions of, numerical analyses of, 18: 2403(R) (PR-P-58)
interactions of, numerical methods for many-body, 18: 8919(R) (PR-P-59 (p.65-78))
interactions of, one pion exchange approximation to optical model potential for, 17: 38191
interactions of, parity in ($K\Sigma N$), 17: 9384
interactions of, particle emission in, 18: 5944 (PAN-454/VI)
interactions of pairs of, spin-orbit effects in, 18: 21192 (KR-64(Sect. IX))
interactions of pairs of, composite meson (π) model for, 19: 23384
interactions of, phase shifts for, 17: 26307
interactions of, pseudoscalar potential for, 18: 7493
interactions of, review of models and potentials for, 17: 5055
interactions of relativistic, multiple meson production in, (T), 19: 41708
interactions of, S-matrix for, 18: 4444
interactions of, single mesons (π) from, 17: 19110
interactions of, spin-orbit effects on, 17: 2179
interactions of, sum rules for nucleon form factors in, 17: 37943
interactions of systems of like, collective effects in, 17: 2281
interactions of three, bound-state, 18: 18907
interactions of three, classification of energy levels in, 18: 44542
interactions of three- and four-body systems of, (T), 19: 27201
interactions of three, matrix elements for bound state in, (T), 19: 43322
interactions of three-body systems of, in p-shell configurations, 20: 22092
interactions of two, approaches to study of, 17: 15150
interactions of two, absorption and polarization in, 17: 19152
interactions of two, symmetry properties of, (T), 19: 6553
interactions of, with nucleons, calculation of angular and radial parts, 16: 33679 (BLG-72)
interactions of, with mesons (K), formulation by many channel N over D method, 17: 13467
interactions of, with hyperons (Λ) in Fermi distribution, low energy optical potentials for, 17: 13468
interactions of, with neutrons in Fermi distribution, low energy optical parameters for, 17: 13468
interactions of, with full recoil, 17: 20870
interactions of, with photons, 17: 22431 (NP-12591(Pt.II))
interactions of, 2-pion-exchange potentials for, 17: 19124
interactions of, Azimov conditions for elastic, 18: 10941
interactions of, amplitudes for three-body, (T), 19: 16486
interactions of, amplitude of three-body, (T), 19: 31079
interactions of, boundary condition model for strong, 18: 37890
interactions of, characteristics of spin-orbit, 18: 16960
interactions of, charge exchange mechanism for elastic, 18: 32585
interactions of, CP violation in strong, (T), 19: 32997
interactions of, canonical decomposition of generalized Bogoliubov transformation, (T), 19: 35136
interactions of, dispersion theoretic calculation of two-pion exchange in, 20: 9778
interactions of, dispersion sum rules for electromagnetic and strong, (T), 20: 41793 (JINR-E-2822)
interactions of, electrodynamics of weak, 18: 28740
interactions of, effects of final states on kinematics of, (E/T), 19: 14310 (BNL-8526)
interactions of, effects of short-range repulsions on nuclear potentials, (T), 19: 39814
interactions of, Faddeev equations for three-body, (T), 20: 15343
interactions of, Hamada-Johnston potential for bound-state, (T), 19: 39570
interactions of, irreducible spin-tensor operators for amplitudes of, (T), 19: 6560
interactions of, inelasticity and p-wave dispersion relations for, (T), 19: 8172
interactions of, lower energy bound for form factor decay for large momentum transfer in, (T), 20: 44257
interactions of, models for intranuclear and extranuclear, (T), 19: 14514 (CONF-640301(p.22-38))
interactions of, meson (π) theory of relativistic, 19: 27257
interactions of, mesic gauge invariance and symmetries for, 20: 7910
interactions of, meson (π)-interaction effects on potential for three-body, (T), 20: 11650
interactions of, methods for analysing, (T), 20: 19981
interactions of, multiple meson (π) production in, (T), 20: 36059
interactions of, nonrelativistic and relativistic amplitudes for, 18: 36327
interactions of, nonrelativistic potentials from S-matrix theory for, 19: 27216
interactions of, nonsingular energy-dependent potential for, 20: 30060
interactions of, nonlocal potential for, 20: 30061
interactions of, potentials for meson resonances in, 18: 34539
interactions of, phase shifts and potentials in (T), 19: 1647
interactions of, properties of (T), 19: 1241
interactions of, polarization effects on isobar production in, (T), 19: 18780
interactions of, pole approximation for one-meson exchanges in, (T), 19: 25263 (IS-987)
interactions of, production amplitudes for, (T), 19: 27223
interactions of, quantum-mechanical three-body, (T), 19: 12347
interactions of, research progress on, 18: 16953(R) (TID-20352)
interactions of, Regge poles in, 18: 20988
interactions of, shell-model, 18: 34869
interactions of, selection rule for strange particle production in, (T), 19: 4971
interactions of, singlet-even potentials for, (T), 19: 6544
interactions of, singlet-even potentials for, (T), 19: 10258(R) (TID-21335(p.151-60))
interactions of, spin-dependent amplitudes for, (E/T), 19: 45032 (NP-15452)

interactions of, saturation of local commutation relations of vector and axial currents for, 20: 25911
interactions of, short-range theory for, 20: 32387
interactions of, S-matrix elements in theory for, 20: 32168
interactions of, theory for, 18: 26667
interactions of, two-body, 19: 23772
interactions of, three-body, (E), 19: 35493
interactions of, two-pion-exchange potential for three-body, 20: 41838
interactions of, vanishing amplitudes in, 18: 40397
interactions of, velocity dependence of potentials for, 19: 1255
interactions of, with polarized beam and target, (T), 20: 11671
interactions of, weak axial-vector currents for, 20: 41981
interactions, partial-wave dispersion relations, 16: 12381
interactions, potential for singlet-even states, 16: 8212
interactions, potential containing central, tensor, and spin-orbit terms, 16: 18378
interactions, potential composed of direct and exchange Yukawa potentials, 16: 21402
interactions, potentials without hard cores for, 16: 26251
interactions, relations to nuclear reaction potentials, 16: 10832
interactions, single meson theory, 16: 5859 (JINR-P-699)
interactions, singlet phase shifts in, 16: 10867
interactions, single hyperon production in weak, 16: 12400
interactions to 100 Bev, effective target masses in, 16: 21271
interactions, two-meson (π) exchange potentials in, 16: 18386
interactions, velocity-dependent forces in, 16: 21703
interactions with mesons (K), phase shifts for peripheral, 16: 961
interactions with gamma radiations, low-energy limit of scattering amplitude and crossing symmetry, 16: 966
interactions with mesons (π), calculation of amplitude taking into account π–π interaction, 16: 973
interactions with mesons (π), total cross sections, 16: 981
interactions with mesons (π), phase shift calculations from one-dimensional representation, 16: 1000
interactions with nucleons, energy spectra of secondaries, 16: 2419
interactions with mesons (K^+) at 0.8 to 2.9 Bev/c, cross sections, 16: 2305(R) (UCRL-9704)
interactions with mesons (π), coupling constant, 16: 3634
interactions with antinucleons, potential range, 16: 3632
interactions with nucleons at 10 to 310 Mev, shape-independent theory, 16: 3630
interactions with mesons, inelastic scattering, 16: 4692 (TID-13955)
interactions with mesons ($\bar{K}$), pion-hyperon production and scattering, 16: 4692 (TID-13955)
interactions with nucleons, partial-wave amplitude properties for high angular momentum, 16: 4705
interactions with mesons (π) and nucleons, effective-target-mass model, 16: 4711
interactions with mesons (π^-) at 7 to 8 Bev, cross sections, 16: 4689 (JINR-P-765)
interactions with mesons ($K_{\pi 3}$), 16: 4728
interactions with mesons (K^-), analysis, 16: 4734
interactions with mesons (π^-) at 7 to 8 Bev cross sections, 16: 4736
interactions with mesons (π) at 0.2 to 1.4 Bev, resonances, 16: 5879
interactions with mesons (π), relation to pion photoproduction on nucleons, 16: 5915
interactions with heavy nuclei, theory, 16: 7143
interactions with mesons (π), dispersion relations for, 16: 6958
interactions with mesons (π^-) at 7 to 8 Bev, cross sections, 16: 6927(T) (NP-tr-836)
interactions with photons, dispersion relations for, 16: 6958
interactions with nucleons, double-maximum angular distributions in high-energy, 16: 7013 (IFA-EM-42)
interactions with mesons (π) at high energies, π-π interaction dominance in, 16: 5880
interactions with mesons (π), dispersion relations, 16: 4707
interactions with mesons (π^-) at 6.8 Bev, inelastic, 16: 5862 (JINR-P-789)
interactions with protons at 9 Bev, secondary particle angular and energy characteristics, 16: 4726
interactions with mesons (π) and nucleons at high energies, characteristics, 16: 8052 (NP-11232(p.219-35))
interactions with mesons (ρ), coupling constant, 16: 8138
interactions with nucleons, application to scattering by nuclei, 16: 8234
interactions with mesons (π), development of models for, 16: 8096 (JINR-D-774)
interactions with mesons (K), meson (μ) mass calculations in, 16: 8107
interactions with antinucleons, meson (π) production in, 16: 8108
interactions with mesons (π), meson (π) production in, 16: 8108
interactions with mesons (π) at 5 Bev, structure model, 16: 8138
interactions with nucleons, dispersion relations and resonances in many-pion systems, 16: 8147
interactions with mesons (π), hyperon and meson isobar production, 16: 8148
interactions with nucleons, one-boson-exchange potentials, 16: 8149
interactions with nucleons, amplitude momentum-space integral equations, 16: 8150
interactions with mesons (π) at Bev energies, isotopic spin relations in hyperon production, 16: 9432 (NP-11280)
interactions with nucleons, bibliography on scattering, 16: 9354 (AERE-BIB-135)
interactions with mesons (π) at high energies, 16: 9370
interactions with nucleons at above 10^{13} ev, angular distributions and energies, 16: 9380
interactions with mesons (π), general unitarity application, 16: 9383
interactions with mesons (K^-), 16: 9406
interactions with mesons (π), scattering and single-pion production, 16: 10910
interactions with mesons (π), and nucleons, strong coupling effects, 16: 10914
interactions with hyperons (Λ) in hyperfragments, 16: 10921
interactions with mesons, formalism for two-nucleon systems, 16: 10823
interactions with nucleons, branching ratios, 16: 10835
interactions with mesons (π) below 1 Bev, multiple meson (π) production in, 16: 10841
interactions with photons below 1 Bev, multiple meson (π) production in, 16: 10841
interactions with bosons, dispersion relations, 16: 10864
interactions with electrons, form factors, 16: 10886
interactions with mesons and nucleons, dynamical model, 16: 12351
interactions with nucleons, complex phase-shift analysis, 16: 12352
interactions with mesons (π), partial-wave amplitudes in, 16: 12362
interactions with meson (ρ^0), isovector form factors for, 16: 12367
interactions with hyperons (Λ), parameters, 16: 12368
interactions with protons, meson (π^+) production in, 16: 12369
interactions with nucleons, isotopic spin relations, 16: 12382
interactions with mesons (π), isotopic spin relations, 16: 12382
interactions with protons at 9 Bev, 16: 12392
interactions with mesons (π) at high energies, inelastic, 16: 12398
interactions with mesons (π) and photons near threshold, 16: 12399
interactions with nucleons, deuteron production, 16: 12431 (JINR-P-850)
interactions with bosons, theory, 16: 12435 (NP-11376)
interactions with mesons, differences in total cross sections at high energies, 16: 12210(R) (ANL-6488)
interactions with mesons (π), model for hyperon (Λ) production, 16: 12556
interactions with neutrinos, pion production cross sections, 16: 12558
interactions with neutrinos, weak processes during, 16: 12563
interactions with mesons (μ), coupling constants, 16: 12565
interactions with electrons, polarization effects in, 16: 13878
interactions with mesons (π), chirality conservation, 16: 13891
interactions with mesons (π) and nucleons, high-energy inelastic peripheral, 16: 13896
interactions with mesons (K) and (π), isobar mechanism, 16: 13900
interactions with mesons (K^+), amplitudes for, 16: 33708
interactions with mesons (π), effects of acnodes of Landau curves, 16: 13902
interactions with mesons (ρ), coupling strength, 16: 13903
interactions with mesons (π^-), coupling strength, 16: 13903
interactions with mesons (π), meson (π) production at low energies, 16: 13904
interactions with mesons (π), amplitudes in higher-resonance region, 16: 15539
interactions with mesons (π), resonance properties, 16: 15551
interactions with hyperons (Σ) and mesons (K^-), hyperon (Λ^0) decay asymmetries from, 16: 15556
interactions with mesons, cross sections for, 16: 15575
interactions with mesons (K^-) and (K^+), meson (π)-exchange relations to potential in, 16: 15581
interactions with leptons at low energies, form factors for, 16: 15597
interactions with mesons (π) and nucleons, meson theory for, 16: 15373
interactions with electrons, inelastic form factors, 16: 4713
interactions with electrons, form factors from, 16: 10917
interactions with mesons (π) and nucleons to 10 Bev, multiple particle production in, 16: 2413(T) (JPRS-10727)
interactions with primary and secondary particles, 16: 17123
interactions with scalar mesons, solution of low equation, 16: 17224
interactions with mesons (π), phase-space integral for 25 Bev collision, 16: 17020
interactions with mesons (π) and photons, coincidence measurements from, 16: 17036
interactions with mesons (K^-), cross-section maxima in, 16: 17043
interactions with antinucleons and nucleons, core phenomena in, 16: 17044
interactions with mesons (π), phenomenological description, 16: 17052

interactions with nucleons, intermediate region potential, 16: 16972 (NP-11592(Vol.I)(p.347-9))
interactions with mesons (π), phase shifts at 0 to 350 Mev, 16: 16988 (NP-11592(Vol.I)(p.461))
interactions with mesons (π) at 20 Bev, photon emission in, 16: 17014
interactions with mesons (π) at 400 to 1500 Mev, mechanisms, 16: 16989 (NP-11592(Vol.I)(p.467-83))
interactions with hyperons (Λ), binding energies, 16: 17015
interactions with mesons (π) and nucleons at high energies, cross sections for elastic, 16: 18400
interactions with V particles, eigenvalue functions for, 16: 18355
interactions with mesons (π) at 300 to 600 Mev, pion production cross sections, 16: 18374
interactions with deuterons, corrections to the impulse approximation, 16: 18375
interactions with mesons (π), contributions to nucleon–nucleon potentials, 16: 18382
interactions with gamma rays, Compton-scattering dispersion relations, 16: 18516
interactions with antinucleons, pseudoscalar meson theory, 16: 18171 (NP-11463(Pt.1)(p.49-52))
interactions with photons, amplitude integral equations for, 16: 18326
interactions with mesons (π) at low energies, π–π resonance effects on, 16: 18335
interactions with mesons (π) at 3 Bev, particle production in, 16: 18353
interactions with antinucleons, hyperon (Λ) pair production in, 16: 18354
interactions with deuteron, spin states in, 16: 19674 (JINR-P-858)
interactions with mesons (K^+) at 0.8 to 2.9 Bev/c, cross sections, 16: 19679 (UCRL-10130)
interactions with mesons (π), isobar approximation of production processes in inelastic, 16: 19682
interactions with baryons, model, 16: 19688
interactions with mesons (π) at 7.3 Bev, angular distributions, 16: 19692
interactions with mesons, multiplet models, 16: 19711
interactions with mesons and nucleons, spin structure of high-energy scattering amplitudes, 16: 19713
interactions with hyperons (Λ), 16: 21465
interactions with hyperons (Λ), forces in, 16: 21470
interactions with nucleons, charge independence of nuclear forces and pseudoscalar coupling in, 16: 21473
interactions with nucleons below inelastic threshold, 16: 21480
interactions with mesons and nucleons, three-meson (π) resonance in, 16: 21620
interactions with mesons (π) to 100 Bev, effective target masses in, 16: 21271
interactions with mesons (K^+) at 50 to 210 Mev, amplitudes for, 16: 21296
interactions with mesons (K^-), partial-wave dispersion relations in, 16: 21299
interactions with mesons at 10^{10} to 10^{13} ev, angular distributions, 16: 21308
interactions with mesons (π) and nucleons, dispersion relations for, 16: 23251
interactions with mesons (K), effects of hyperon parities and meson resonances on scattering, 16: 22852 (NP-11761)
interactions with mesons (π), coupling constant for, 16: 22892
interactions with mesons (K), and nucleons, one-meson-exchange domination by lowest partial waves in, 16: 22893
interactions with alpha particles, correlation effects in, 16: 22905
interactions with mesons (π), partial-wave dispersion relations for, 16: 22916
interactions with mesons (π), π–Λ resonance production from, 16: 22917
interactions with protons at 10^{10} ev, and multiplicity from angular distribution, 16: 22922
interactions with particles at high energies, cross sections, 16: 22943
interactions with mesons (π^-), bound quasielastic, 16: 22944
interactions with neutrinos, 16: 22949
interactions with mesons (π^-), angular distribution, 16: 24682 (JINR-P-868)
interactions with nucleons, phase shifts for scattering, 16: 24708
interactions with mesons (π^-) at 7 Bev, inelastic low-multiplicity, 16: 24715
interactions with mesons (π^-) at 7 Bev, inelastic, 16: 24716
interactions with mesons (π^-) at 7.5 Bev, inelastic, 16: 24717
interactions with mesons (π^-) at 6.8 Bev/c, inelastic, 16: 24718
interactions with mesons (π) and nucleons at high energies, elastic cross sections, 16: 24721
interactions with antinucleons, selection rules for integral-isospin meson production in, 16: 24735
interactions with mesons (K) and nucleons, cross sections, 16: 25877(R) (ANL-6534)
interactions with nucleons at 1 Bev, elastic, 16: 26071 (JINR-P-817)
interactions with antinucleons at 1 Bev, elastic, 16: 26071 (JINR-P-817)
interactions with mesons (π), regularization of equations for, 16: 26072 (JINR-P-891)
interactions with mesons (π), 16: 26076 (JINR-P-938)
interactions with mesons (π), dispersion relations for, 16: 26077 (JINR-P-949)
interactions with mesons (π^-) at 7 Bev, properties of mesons (π^0) formed in inelastic, 16: 26081 (JINR-P-974)
interactions with mesons (π), form factors for, 16: 26089 (NP-11832)
interactions with hyperons and mesons (K), form factors for, 16: 26089 (NP-11832)
interactions with hyperons and nucleons, global symmetry and scattering, 16: 26091 (NYO-10234)
interactions with photons, meson (π) photoproduction amplitude integral equations, 16: 26094
interactions with mesons (π), coupling constant for, 16: 26105
interactions with antinucleons and hyperons (Λ), dispersion relations, 16: 26110
interactions with antineutrinos and neutrinos at high energies, boson nonproduction in, 16: 26130
interactions with mesons ($\bar{K}$), S-wave scattering amplitudes, 16: 26137
interactions with mesons (π), vertex function in, 16: 26144
interactions with nucleons at 3.3 to 7.8 Bev/c, total cross sections for, 16: 26145
interactions with mesons (π), complex angular momentum plane singularities in, 16: 26153
interactions with mesons (K^-), resonances from, 16: 26161
interactions with hyperons (Λ), heavy-meson single exchange force in, 16: 26165
interactions with mesons (π), amplitude relation to π-π amplitudes, 16: 26169
interactions with bosons, meson multiple production in, 16: 26170
interactions with mesons (π), meson (π) production in, 16: 26174
interactions with mesons (ω), coupling constant for, 16: 26175
interactions with nucleons in nuclear matter, complex effective mass in optical potential model scattering, 16: 26229 (PAN-304/VII)
interactions with mesons and nucleons at high energies, spin amplitude in, 16: 26191
interactions with mesons (π) and nucleons in heavy nuclei, 16: 26340
interactions with hyperons (Λ), spin dependence of, 16: 26344
interactions with neutrino, meson (π) production in, 16: 26074 (JINR-P-905)
interactions with nucleons at $>5 \times 10^{10}$ ev/nucleon, showers from, 16: 27877
interactions with mesons (π), Regge poles and scattering amplitudes in, 16: 27915 (UCRL-10254)
interactions with nucleons at ultra relativistic energies, transverse moment at 27 Bev, 16: 27922
interactions with nucleons, meson (π) production in, 16: 27940
interactions with mesons (π) with charge exchange, unsubtracted dispersion relation for, 16: 27946
interactions with photons, partial-wave dispersion relations for, 16: 27948
interactions with mesons (K^-) at low energies, Y* effects on S-wave parameters in, 16: 27949
interactions with mesons (π) and nucleons at high energies, spectra from ultrarelativistic, 16: 27951
interactions with mesons, symmetry schemes for, 16: 27958
interactions with mesons, symmetry schemes for, 16: 27960
interactions with neutrinos at 0 to 5 Bev, cross sections for inelastic, 16: 27973
interactions with mesons (μ^-), electron emission from, 16: 27365
interactions with mesons (π), coupling constants for, 16: 28327
interactions with nuclei, dispersion-theoretical coupling constants, 16: 28338
interactions with mesons (π), partial wave dispersion relations for amplitudes in, 16: 27910 (NP-11839)
interactions with nucleons at 210 Mev, 16: 27911 (NYO-10036)
interactions with photons at 1.05 Bev, parity conservation in, 16: 27981
interactions with nucleons at high energies, cross-section relation to energy resolution in, 16: 27986
interactions with mesons (K^-) in emulsions at 830 Mev/c, hyperfragment ($A \gtrsim 40$) production in, 16: 27988
interactions with neutrinos at high energies, search for anomalous, 16: 27990
interactions with mesons (π) below 1 Bev, production amplitudes and unitarity in, 16: 27996
interactions with neutrinos, meson (π) production in, 16: 28001
interactions with neutrinos, meson (π) production in, 16: 28002
interactions with antinucleons, Pauli exclusion principle relation to, 16: 28007
interactions with nucleons, velocity dependent nuclear forces and the repulsive core as the possible consequence of classical relativistic effects, 16: 28081

interactions with antinucleons, dispersion relations for, 16: 28006
interactions with hyperons, lectures, 16: 29635 (EFINS-62-9)
interactions with nucleons at 40, 95, 147, 210, and 310 Mev, phase analysis of, 16: 29639 (JINR-P-1011)
interactions with mesons (π), relation to meson (π) scattering, 16: 29649 (NP-11950(Vol.I)(p.113-72))
interactions with mesons (π), static model for, 16: 29650 (NP-11950 (Vol.I)(p.173-207))
interactions with mesons (π) at 500 to 1500 Mev, 16: 29652 (NP-11950 (Vol.I)(p.261-74))
interactions with mesons (π) and nucleons, analyticity properties of scattering amplitudes in, 16: 29654 (NP-11950(Vol.II)(p.275-354))
interactions with mesons (π) and photons, Mandelstam representation for, 16: 29655 (NP-11950(Vol.II)(p.355-424))
interactions with mesons (π), dispersion relations in, 16: 29675
interactions with photons, dispersion relations in, 16: 29677
interactions with electrons, form factors for, 16: 29694
interactions with mesons (π), form factors for, 16: 29694
interactions with hyperons, potential term, 16: 29696
interactions with mesons (K), hyperon-meson (π) resonances in, 16: 29697
interactions with electrons at 6 Bev, 16: 31010 (KFK-83)
interactions with antinucleons and nucleons, contributions of Regge poles to, 16: 31023 (UCRL-10331)
interactions with gamma radiation, resonance model for meson (K) production from, 16: 31043 (NYO-10133)
interactions with mesons, resonances in, 16: 31044
interactions with mesons (π) at 2 to 20 Bev/c, elastic cross sections, 16: 31047
interactions with nucleons, coefficient of inelasticity for, 16: 31114
interactions with photons, meson (K) production in, 16: 32276 (NP-12035)
interactions with antinucleons, Born approximation calculations for, 16: 32277 (NYO-9288)
interactions with mesons (π) and nucleons, isobaric model for, 16: 32305
interactions with mesons (π), effects of 2π vector mesons on, 16: 32316
interactions with mesons (π), effects of π-π resonances on, 16: 32330
interactions with mesons (π) and photons, resonance effects on, 16: 32334
interactions with mesons (π) at medium energies, amplitudes for, 16: 32313
interactions with deuterons, off-the-energy-shell effects in, 16: 33691 (TID-16625)
interactions with mesons (π), S-wave, 16: 33706
interactions with mesons (π), strange-particle production in, 16: 33737
interactions with hyperons (Λ) and (Σ), parameters for, 16: 33745
interactions with mesons ($\bar{K}$), effects on π-Λ and π-Σ amplitudes, 16: 33772
interactions with mesons (K^-) at 1.1 Bev/c, 16: 2305(R) (UCRL-9704)
interactions with mesons (K), relation to antihyperon excited state, 16: 5894
interactions with mesons (μ), parity nonconservation in, 16: 5864(T) (UCRL-Trans-759)
interactions with hyperons, effects of hyperon (Λ)-meson (π) resonance in inelastic, 16: 6965
interactions with mesons (π^-) at 6.8 Bev, inelastic, 16: 6996
interactions with mesons (μ), electron production rates in, 16: 10891
interactions with mesons (π), asymptotic behavior of scattering amplitude, 16: 13862 (JINR-D-900)
interactions with nucleons, meson (π) resonances in scattering potential, 16: 14014
interactions with protons in nuclei at 8.7 Bev, meson (π) and proton distributions from, 16: 954
interactions with antinucleons, effects on π-π interactions, 17: 780
interactions with antihyperons, selection rules for annihilation, 17: 5289
interactions with alpha particles, separable-potential model for, 17: 5216
interactions with antinucleons, angular distributions of, 17: 5221
interactions with antinucleons, bound states in, 17: 9293
interactions with antinucleons and nucleons, spin structure of amplitudes of, 17: 9416
interactions with antinucleons and mesons (π), review, 17: 9461
interactions with antinucleons and nucleons, cross sections for antinucleon production in, 17: 13345 (JINR-P-1132)
interactions with antibaryons, baryons, and mesons, symmetries in, 17: 13454
interactions with antinucleons, hyperon isobars from, 17: 16995
interactions with antinucleons, resonance model of, 17: 28197
interactions with antinucleons, meson (π) as bound state from, 17: 29525
interactions with antinucleons and nucleons, asymptotic behavior of, 17: 34779
interactions with antineutrinos and neutrinos, meson production in, 17: 37970
interactions with antinucleons and nucleons, effects of heavy mesons on, 17: 37985
interactions with baryons and mesons, spinor formalism for, 17: 9221
interactions with baryons and mesons, symmetries in strong, 17: 9277
interactions with baryons and mesons, Regge asymptotic amplitudes for, 17: 17046
interactions with baryons, Regge hypothesis for multiple meson production in, 17: 34806
interactions with bosons and nucleons, polarization measurements for Regge cuts in, 17: 39897
interactions with deuterons, polarization effects in, 17: 2230 (NIRL/R/16(p.17-22))
interactions with deuterons at high energy, elastic, 17: 15086 (TID-16474)
interactions with deuterons at 30–50 Mev, amplitude and cross-section singularities in breakup, 17: 26340
interactions with deuterons, phase-shift ambiguities in, 17: 32946
interactions with deuterons, amplitudes in, 17: 37971
interactions with electrons and neutrinos, meson (π) production in, 17: 743
interactions with electrons, review of theory of, 17: 9465
interactions with electrons, mesons (π) from, 17: 19105
interactions with electrons, data fitting analysis, 17: 24184
interactions with electrons, cross section for, 17: 24410
interactions with electrons, Reggeian cross sections for, 17: 31329
interactions with electrons, electric and magnetic form factors from hard-core and meson (ω), (ϕ), and (ρ) effects in, 17: 41800
interactions with gamma radiation, dispersion relations for production of mesons (K) in, 17: 39857
interactions with hyperons (Λ) and (Σ), effective-range theory for, 17: 726
interactions with hyperons (Λ), meson (π) contribution to, 17: 5247
interactions with hyperons, mass-difference and strangeness effects in, 17: 5220
interactions with hyperons, potentials for, 17: 9383
angular distribution of jets from, 17: 9522
interactions with hyperons (Λ^o), exchange, 17: 13601
interactions with hyperons (Λ^o) in ${}_{\Lambda}H^3$ and ${}_{\Lambda}H^4$, 17: 17014
interactions with hyperons, potential models and scattering cross sections for, 17: 22522
interactions with hyperons (Λ), two-meson (π)-exchange contribution to, 17: 26348
interactions with hyperons (Λ) and (Σ), coupling and potentials in, 17: 29538
interactions with hyperons (Λ), (Σ), and (Ξ) and mesons (K) and (π), coupling constants for strong, 17: 31373
interactions with hyperons (Λ), structure of weak, 17: 32903 (EFINS-63-39)
interactions with hyperons (Λ) and mesons (K) and (π), vertex functions for, 17: 34809
interactions with hyperons, isobars in binding, 17: 37952
interactions with hyperons (Λ) in ${}_{\Lambda}H^3$, effects of hard-core and three-body forces on well-depth parameter of, 17: 39861
interactions with hyperons (λ), 17: 41758
interactions with light nuclei at high energy, 17: 7209
interactions with leptons, lecture on theory of weak, 17: 17302
interactions with leptons, theory of weak, 17: 17309
interactions with mesons (π), 17: 768
interactions with mesons (π), prediction of meson (π)–meson (π) phase shifts from, 17: 769
interactions with mesons (π), $I = \frac{1}{2}$, $J = \frac{1}{2}$ state in, 17: 771
interactions with mesons (π), meson (π) production in, 17: 781
interactions with mesons (π), dispersion relations for elastic, 17: 2163 (JINR-P-1043)
interactions with mesons (π^-) at 2 Bev/c, distributions from, 17: 2173
interactions with mesons ($\bar{K}$), strange particle production from, 17: 2177
interactions with mesons, fixed-fermion field theory for, 17: 5210
interactions with mesons, higher symmetries of, 17: 5224
interactions with mesons (K) and antimesons (K), effect of ρ and ω exchanges on, 17: 5246
interactions with mesons (π), resonances in, 17: 5268
interactions with mesons (π) and nucleons, production of mesons (α) in, 17: 5276
interactions with mesons (π), spin rotation effects in, 17: 6985
interactions with mesons (π), dispersion relations in, 17: 7010
interactions with mesons (π), effect of π-π interactions on s and p waves of, 17: 7024
interactions with mesons (π), interaction constant for, 17: 7027
interactions with mesons through large angles, Regge fermion poles in, 17: 7034
interactions with mesons (π), gauge groups and symmetries of the isospace associated with nonrelativistic rotator, 17: 6970
interactions with mesons (π), dispersion-theoretical approach to diffraction, 17: 9202 (PAN-359/VII)
interactions with mesons ($\bar{K}$), amplitudes for, 17: 9276

interactions with mesons (π^-), meson (K^0) production in, 17: 9282
interactions with mesons (π), production of slow mesons (π) in, 17: 9289
interactions with mesons (π), phase shift calculations for, 17: 9335
interactions with mesons (π), γ_5 invariance in, 17: 9338
interactions with mesons (π), meson (π-π) interactions in, 17: 9339
interactions with mesons (π^-), strange particle correlations in, 17: 9360
interactions with mesons (K), s-wave scattering parameters for, 17: 9383
interactions with mesons (π), analysis of, 17: 9409
interactions with mesons (π), Regge pole application to, 17: 9414
interactions with mesons (π^-), peripheral effects in, 17: 9433
interactions with mesons (π^-) at 7 Bev, inelastic, 17: 9435
interactions with mesons and nucleons, dispersion relations for, 17: 9455
interactions with mesons (π) and nucleons, review of theories of, 17: 9463
interactions with mesons (π), review of data on, 17: 9474
interactions with mesons at large angles, amplitudes of, 17: 9415
interactions with mesons, effects of Regge poles on, 17: 11466 (CERN-62-33)
interactions with mesons(π), differential cross sections for meson(π) production in, 17: 11476 (JINR-P-1111)
interactions with mesons(K) at high energy, total cross sections and Regge poles for, 17: 11493 (TID-16216)
interactions with mesons (K), and meson (Yβ) scattering amplitude in, 17: 11514
interactions with mesons (π), two-pion exchange terms in, for states T = 0 and T = 1, 17: 11544
interactions with mesons (π), Regge poles in, 17: 11546
interactions with mesons (π), Riemann-Cauchy relations in theory of, 17: 11571
interactions with mesons (π), effect of meson (π-π) resonance in, 17: 11578
interactions with mesons, code for numerical analysis of, 17: 12786(R) (ORNL-3360(p.215-20))
interactions with mesons, analytic cascade equations for, 17: 12787(R) (ORNL-3360(p.221-4))
interactions with mesons (π) and nucleons at high energies, target mass in, 17: 13121
interactions with mesons (π) and nucleons, review of theories of, 17: 13126
interactions with mesons (π), resonances in, 17: 13455
interactions with mesons ($\bar{K}$), resonances in, 17: 13367
interactions with mesons (π), dispersion relations for, 17: 13377
interactions with mesons (π), effect of (π-π) resonances on low-energy, 17: 13385
interactions with mesons (π), gauge invariance in isobaric model for, 17: 13396
interactions with mesons(π), relativistic effects in low-energy, 17: 15120
interactions with mesons ($\bar{K}$), effects on K^--p interactions, 17: 15133
interactions with mesons(π), resonances in, 17: 15139
interactions with mesons (π) and nucleons, models for peripheral, 17: 15079 (NP-12566)
interactions with mesons (K), effects of resonances in, 17: 15117
interactions with mesons (π^-), mechanism for gamma production in inelastic, 17: 17192
interactions with mesons (π) and nucleons, production of hyperons and mesons (K) in, 17: 16953 (JINR-P-1163)
interactions with mesons (π) and nucleons, analyticity and unitarity conditions in, 17: 16955 (NYO-10238)
interactions with mesons, physical diagrams for vertex portions of, 17: 16966
interactions with mesons (π), Regge-pole analysis of, 17: 17038
interactions with mesons (K) and (π), angular distribution of particles produced near threshold in, 17: 17098
interactions with mesons, Regge trajectories in, 17: 16770(R) (ANL-6666)
interactions with mesons (π), chirality and structure of, 17: 16989
interactions with mesons (π), amplitudes for, 17: 19133
interactions with mesons (π), theory of J = 3/2, I = 1/2 resonance, 17: 19138
interactions with mesons (π), empirical systematics for, 17: 19151
interactions with mesons (π), resonance effects on, 17: 19154
interactions with mesons (π), distributions from, 17: 19169
interactions with mesons (π), model for higher resonances in, 17: 19539
interactions with mesons (K^-), 17: 19324
interactions with mesons (π^-), at 16.2 Bev/c, 17: 19086
interactions with mesons (π), model for large-angle elastic, 17: 19091
interactions with mesons (π), dispersion theory of diffraction, 17: 19077
interactions with mesons (π), meson (π-π) interaction effects on partial waves of, 17: 20839 (JINR-E-1189)
interactions with mesons (π), coupling constants for, 17: 20847 (JINR-P-1207)
interactions with mesons (π), asymptotic properties and zero of forward scattering amplitude in, 17: 20852
interactions with mesons (K^-), (K^0), (π^-), and (π^+), effect of ($\bar{K}$-K) resonance in, 17: 20871
interactions with mesons (π), effect of S-wave (π-π) interactions on, 17: 20872
interactions with mesons (π), coupling constants for, 17: 20883
interactions with mesons (π^-), production of excited mesons (K) in, 17: 20891
interactions with mesons (K) at low energies, contributions of mesons (ρ) and (ω) to scattering amplitudes of, 17: 20893
interactions with mesons (π), partial wave dispersion relations for, 17: 20948
interactions with mesons(K^-) and(K^+) in nuclei, dispersion relations for low-energy, 17: 21075
interactions with mesons (π), effects of π-π interactions on, 17: 20879
interactions with mesons (π^-) at 7 Bev, gamma production in, 17: 20934
interactions with mesons (π), momentum transfer in, 17: 22435 (NP-12730)
interactions with mesons (π) at 7 Bev, particle generation in, 17: 22444
interactions with mesons (π), forward scattering amplitudes in, 17: 22496
interactions with mesons (π), domains of analyticity for, 17: 22504
interactions with mesons (K), domains of analyticity for, 17: 22504
interactions with mesons (π) and nucleons at 2 to 28 Bev, 17: 22505
interactions with mesons (π), model for final-state, 17: 22517
interactions with mesons (K) and mesons (π), application of Boundary Condition Model to, 17: 24188
interactions with meson (π), cross sections and systematic behavior in, 17: 24263 (BNL-6934)
interactions with mesons(K), vector meson exchange effects on amplitudes of S-wave, 17: 24350
interactions with mesons(π) in octet boson–octet fermion model, amplitudes for, 17: 24354
interactions with mesons (π), charge independence in, 17: 24514
interactions with mesons (π), spinor Regge pole exchange in, 17: 26320
interactions with mesons (π), inner Coulomb corrections to phase shifts in, 17: 26324
interactions with mesons ($\bar{K}$) and (π) at high energies, double-charge exchange cross sections for, 17: 26326
interactions with mesons (π) at high energies, fermion Regge pole analysis of cross section and polarization in, 17: 26331
interactions with mesons ($K\pi_3$) in fermion decay models, 17: 26346
interactions with mesons (π), overlapping resonances in final states of, 17: 26353
interactions with mesons (π), model for single π production in, 17: 26359
interactions with mesons, algebraic equations for describing, 17: 28142 (JINR-E-1262)
interactions with mesons (K), resonance, 17: 28172
interactions with mesons (π^-) at 7 Bev, peripheral, 17: 28208
interactions with mesons (π) and nucleons, amplitudes for, 17: 28212
interactions with mesons (K) at high energy, 17: 29504 (UCRL-10834)
interactions with mesons (π), parity and spin of 2190-Mev resonance, 17: 29505 (UCRL-10894)
interactions with mesons (π), resonance properties of, 17: 29506
interactions with mesons (π^-), parameters of inelastic, 17: 29515
interactions with mesons (π), coupling constant for, 17: 29521
interactions with mesons (π), energy jets in, 17: 29522
interactions with mesons (π) in isobar decay, Q values for, 17: 29531
interactions with mesons (π) at 2 Bev, meson (f^0) effects in, 17: 29532
interactions with mesons ($\bar{K}$), bound state effects in meson (K^-) reactions with deuterium and hydrogen, 17: 29535
interactions with mesons (π), spin-orbit forces in, 17: 29550
interactions with mesons (π), Regge trajectories in, 17: 29551
interactions with mesons (π) in the boundary-condition model, inelastic effects on S waves in, 17: 31334
interactions with mesons (π), chirality conservation and soft-meson (π), production in, 17: 31353
interactions with mesons (π), method for analyzing, 17: 31366
interactions with mesons ($\bar{K}$), two-channel formalism for S-wave, 17: 31372
interactions with mesons (π), generalization of Minami ambiguity for, 17: 31375
interactions with mesons (π), analyticity regions of Feynman integrals in, 17: 31379
interactions with mesons (K), analyticity regions of Feynman integrals in, 17: 31379
interactions with mesons (π) and nucleons at 10^{13} ev, effective target mass for, 17: 31380
interactions with mesons (π), partial wave amplitudes for, 17: 32899 (CONF-46-80)
interactions with mesons (π) at $\leq$ 3 Bev, strange particle production cross sections in, 17: 32920
interactions with mesons (π^-) at 6.8 and 8.0 Bev/c, hyperon (Ξ^-) production in, 17: 32945
interactions with mesons (π) at low energy, S-wave dispersion relation in,

17: 32949
interactions with mesons (π), unitarity in, 17: 34726 (ISS-63/34)
interactions with mesons (π) at low energies, meson (π) production effect in, 17: 34746
interactions with mesons (π), resonance-state production effects on polarization in, 17: 34747
interactions with mesons (π) following proton-proton quasielastic scattering at high energies, 17: 34782
interactions with mesons (π), coupling constants for, 17: 34798
interactions with mesons (K), Sawada transformation for multichannel, 17: 34807
interactions with mesons (π^-) at 6.8 Bev, inelastic, 17: 34813
interactions with mesons(π) at intermediate energies, resonance production in, 17: 36571 (EFINS-62-61)
interactions with mesons(π), resonances in, 17: 36582 (TID-19336)
interactions with mesons($\bar{K}$) at low energies, Y_0^* production in, 17: 36605
interactions with mesons, theory of, 17: 36619
interactions with mesons, multiple production of mesons in, 17: 36620
interactions with mesons (π), meson (π-π) interaction contribution to, 17: 37975
interactions with mesons (π), resonance in, 17: 37980
interactions with mesons (π), dispersion relations for $\pi + N \rightarrow \pi + \pi + N$, 17: 37988
interactions with mesons (π^-) at 2.66 Bev, inelastic, 17: 38151
interactions with mesons (K^-) in the Mandelstam representation, study of K* Regge trajectory from, 17: 39839
interactions with mesons (π), modified phase shift analysis of, 17: 39845 (NP-13114)
interactions with mesons ($\pi^\pm$), meson and baryon exchange diagrams for, 17: 39880
interactions with mesons (K^-), mechanisms for, 17: 39894
interactions with meson fields, ground-state energy of two-body system, 17: 39926
interactions with mesons (π), formulation of Chew-Low theory for, 17: 41748
interactions with mesons (π^-) at 6, 11, and 18 Bev/c, correlations in strange-particle pairs produced by, 17: 41765
interactions with mesons (π), meson (π) interaction effects on invariant amplitude in, 17: 41803
interactions with mesons, statistical theory, 17: 41819
interactions with meson (π), 17: 41819
interactions with mesons (π) in emulsion at 7.5 Bev, inelastic, 17: 41823
interactions with mesons (π), fermion Regge poles and polarization phenomena in, 17: 41828
interactions with mesons, 17: 41533(R) (ANL-6720(p.67-75))
interactions with nucleons at low energies, pion-nucleon resonance of, 17: 730
interactions with neutrinos, cross sections, 17: 2145 (JINR-E-1032)
interactions with nucleons, effects of Regge poles on polarization in, 17: 2168 (TID-17205)
interactions with nuclei at high energies, meson production in, 17: 3931 (AFCRL-1089)
interactions with nucleons in nuclei, construction of low-energy potentials for, 17: 5380
interactions with nucleons at very high energies, production of jets based on the fireball model, 17: 5231
interactions with nucleons, diffraction effects in, 17: 5243
interactions with nucleons in momentum space, phase shifts in, 17: 5271
interactions with nucleons at high energies, semi-phenomenological model for meson (π) production in, 17: 6984
interactions with neutrinos, meson (π) production amplitudes for, 17: 7023
interactions with nucleons at 40, 95, 147, and 310 kev, phase-shift analysis of, 17: 7027
interactions with nucleons, inelastic, 17: 7040
interactions with nucleons at 9 Bev, angle and energy measurements of, 17: 6971
interactions with nucleons in nuclear matter, intermediate coupling in, 17: 7140 (TID-14921)
interactions with nucleons at 660 Mev, amplitudes in, 17: 9612
interactions with nucleons, production of slow mesons (π) in, 17: 9289
interactions with nucleons in the two-meson approximation including π-π interaction effect, 17: 9291
interactions with nucleons, amplitudes of, 17: 9310
interactions with nucleons at 40 to 310 Mev, phase shift analysis of, 17: 9311
interactions with nucleons, charge independence of, 17: 9334
interactions with nucleons, theory of, 17: 9331
interactions with nucleons, calculations of potentials for, 17: 9332
interactions with nucleons, Regge pole applications to, 17: 9414
interactions with nucleons at high energy, field-theoretical models of, 17: 9422
interactions with neutrinos, cross section for, 17: 9439
interactions with nucleons below 1 Bev, review, 17: 9462
interactions with nucleons, review of data on, 17: 9474
interactions with nucleons, vector mesons in, 17: 11491 (TID-15930)
interactions with nucleons at high energy, cross sections for, 17: 11493 (TID-16216)
interactions with nucleons, single meson (π) production in peripheral, 17: 11515
interactions with nucleons, Green potential for, 17: 11527
interactions with nucleons, theory of, 17: 11568
interactions with neutrinos and antineutrinos, cross sections for, 17: 11563
interactions with nucleons at 0.5 to 2 Bev, meson (π) production in, 17: 12784(R) (ORNL-3360(p.199-203))
interactions with nucleons at high energies, two-center model for, 17: 13116
interactions with nucleons, model for multiple meson production in, 17: 13117
interactions with nucleons at high energies, statistical analysis of angular distributions in, 17: 13118
interactions with nucleons at high energies, theory of multiple meson production in, 17: 13119
interactions with nucleons at high energies, theory of, 17: 13124
interactions with nucleons at 300 Bev, characteristics of, 17: 13125
interactions with neutrons, resonance widths in, 17: 13487 (JINR-P-1130)
interactions with nucleons at low energy, amplitude and phase shifts in, 17: 13351 (NP-12514)
interactions with nucleons at 25 Bev, elastic-inelastic ratio for, 17: 13389
interactions with nucleons at 0 to 400 Mev, relativistic dispersion relations in phase shifts of elastic, 17: 13443
interactions with nucleons and nuclei, investigation of, 17: 17123(R) (TID-18127)
interactions with nucleons, meson (π) resonance model of, 17: 16948 (JINR-D-1128)
interactions with nucleons at 100 Bev, energy distribution of mesons (π) from, 17: 16971
interactions with nucleons, coupling constant and spectral functions of scattering amplitude for, 17: 17054
interactions with nucleons at low energies, nucleon core and, 17: 19056
interactions with nucleons, Regge trajectories in, 17: 20564(R) (TID-18442)
interactions with nucleons at 147 Mev, phase shift analysis of, 17: 20846 (JINR-P-1206)
interactions with nucleons, Regge poles in high-energy, 17: 20914
interactions with nucleons, scattering amplitudes from Regge poles in, 17: 20941
interactions with nucleons, dispersion relations for partial wave amplitudes for, 17: 22423 (JINR-P-1205)
interactions with nucleons at 660 Mev, phase-shift analysis of, 17: 22426 (JINR-P-1221)
interactions with nucleons, cross sectional energy dependence and momentum transfer in, 17: 22435 (NP-12730)
interactions with nucleons and photons, integral representation of amplitude of, 17: 22445
interactions with neutrinos, cross sections for, 17: 28151 (NEVIS-111)
interactions with nucleons, solution of Bethe-Goldstone equation for hard-core potential in, 17: 28330
interactions with neutrinos, polarization of bosons produced in, 17: 31317
interactions with nucleons at high energies, range of, 17: 31339
interactions with nucleons at very high energies, range of, 17: 31347
interactions with nucleons, analyticity regions of Feynman integrals in, 17: 31379
interactions with nucleons, peripheral model for, 17: 36381 (ISS-63/29(p.13-21))
interactions with nucleons, multiperipheral model for asymptotic behavior of amplitudes of elastic, 17: 39874
interactions with neutrinos, Regge pole domination of, 17: 39887
interactions with mesons, perturbation theory for, 17: 41743 (NP-13127)
interactions with nucleons in the presence of a hard core, transition for, 17: 41752
interactions with neutrinos, unitary symmetry of weak current structure in, 17: 41781
interactions with nucleons, importance of many-body forces in, 17: 41990
interactions with photons, and mesons by, radiation damping in, 17: 11916
interactions with protons at 25 Bev, 17: 13532
interactions with photons, isobaric model for, 17: 13388
interactions with photons, strange particles from, 17: 19107
interactions with particles, amplitudes for, 17: 19178

interactions with protons at 28 Bev, Dirac pole production in, 17: 26420 (CERN-63-13)
interactions with photons, unitary symmetry model for pseudoscalar meson production in, 17: 28149 (LNF-63/21)
interactions with photons, electron pair production in, 17: 32711 (LNF-62/113)
interactions with photons, amplitude for, 17: 32962
interactions with protons at 28 Bev, effective target mass distribution for, 17: 32965
interactions with photons, model for resonance state production in, 17: 32966
interactions with photons at high energy, Compton effect in, 17: 36623
interactions with protons at 26.7 Bev/c, effective target-mass distribution in inelastic, 17: 39865
interactions with protons at 28 Bev, meson (π) production in, 17: 41735 (AERI-P/R-7)
interactions with photons at high energies, 17: 41738 (CTSL-40)
interactions with pseudoscalar particles, minimal coupling in, 17: 41766
interactions with protons in emulsions, analysis of, 17: 41822
interactions with photons at high energies, meson (π) production in, 17: 41842
interactions with hyperons (Λ), 17: 41758
interactions with antiprotons, symmetry relations for, 18: 834 (AFOSR-2326)
interactions with mesons (π), forward amplitude zeroes for, 18: 841 (JINR-P-1336)
interactions with nucleons at 630 Mev, phase-shift analysis of, 18: 847 (JINR-P-1375)
interactions with nucleons, phase shift energy dependence in, 18: 848 (JINR-P-1376)
interactions with photons, amplitude for virtual Compton, 18: 851 (JINR-P-1389)
interactions with nucleons, polarization in, 18: 853 (JINR-P-1404)
interactions with mesons (K^+), partial amplitudes for, 18: 856 (PAN-387/VII)
interactions with mesons (K^-), 18: 862(R) (TID-19590)
interactions with mesons (π^-), (π-π) resonances in inelastic, 18: 865 (UCRL-10731)
interactions with photons, dispersion relations for, 18: 872
interactions with mesons (π) at high energies, Regge trajectories from backscattering, 18: 881
interactions with mesons (π) in the c.m. energy plane, partial-wave dispersion relations for, 18: 886
interactions with gamma radiation, meson (π) production in, 18: 888
interactions with mesons (π), isotopic symmetry in, bootstrap requirement for, 18: 890
interactions with mesons (π), optical model for resonance, 18: 897
interactions with gamma radiation, meson (π) production in, 18: 903
interactions with antinucleons, resonance model for, 18: 911
interactions with mesons (π), self-consistent calculation of coupling constant in, 18: 912
interactions with deuterons, bibliography on, 18: 833 (AERE-Bib-142)
interactions with mesons(π) at 7.5 Bev/c, separation of peripheral and central collisions in, 18: 2596
interactions with pseudoscalar mesons, static three-body nuclear forces in, 18: 2599
interactions with mesons (π) relativistically invariant partial-wave analysis of, 18: 2613
interactions with mesons (K^0), asymptotic properties of scattering amplitudes in, 18: 2624
interactions with mesons (ρ), electric coupling constant for, 18: 2663
interactions with nucleons at 4 Bev, total cross section for inelastic, 18: 2680
interactions with mesons (π^-) at 16.2 Bev/c, separation of central and peripheral, 18: 2616
interactions with mesons, energy multiplication in, 18: 2611
interactions with antinucleons, angular correlations in annihilation, 18: 4439
interactions with mesons (π), book on, 18: 4464(T)
interactions with photons, book on (γ,π), 18: 4464(T)
interactions with electrons, neutron-proton mass difference from, 18: 5996
interactions with photons and vector mesons, Regge poles in, 18: 6026
interactions with mesons (π), model for meson (ρ) and N* exchange in, 18: 6028
interactions with mesons (π) at low energies, coupling constant and P-wave phase shifts in, 18: 6029
interactions with protons in nuclear emulsions, distributions of secondary particles from, 18: 6037
interactions with mesons (π) at high energies, description by fermion Regge poles, 18: 6040
interactions with mesons (π), use in analysis of meson (π) photoproduction, 18: 6044
interactions with antinucleons and nucleons, annihilation effects on cross sections for, 18: 6050
interactions with gamma rays, Regge poles in amplitudes of (γ,π), 18: 6051
interactions with nucleons in nuclei, 18: 6272
interactions with hyperons (Λ), binding energy from, 18: 6245
interactions with photons, Compton effect at ($\frac{3}{2},\frac{3}{2}$) resonance in, 18: 6003
interactions with mesons (π) at 15–600 Mev, interpolative formulas for phase shifts in, 18: 7557
interactions with mesons (π), dispersion relation treatment of, 18: 7472 (NP-13451)
interactions with meson (π), bremsstrahlung emission in, 18: 7475 (TID-19854)
interactions with photons, angular momentum analysis of ($\gamma,\pi^-\pi^+$), 18: 7495
interactions with mesons (π), mass correlations to orbital angular momentum in resonance states from, 18: 7496
interactions with mesons (π) at 3 Bev, information theory for multiple particle production in, 18: 7498
interactions with photons, strip approximation for (γ,π), 18: 7499
interactions with unstable particles in nuclei, 18: 7520
interactions with mesons (π), zero momentum-transfer dispersion relations for elastic, 18: 7522
interactions with nucleons by one-pion exchange, explanation by meson (π) reggeization, 18: 7523
interactions with nucleons, potential for, 18: 7527
interactions with hyperons (Λ) at low and intermediate energies, binding energies from, 18: 7529
interactions with hyperons (Λ) in hypertriton, binding energies from, 18: 7535
interactions with hyperons (Λ), effects of baryon resonances on forces on, 18: 7541
interactions with mesons (π), ($\frac{3}{2},\frac{3}{2}$) resonance effect and two-pion-exchange process in, 18: 7549
interactions with mesons (π) in hyperon (Λ) decay, diagonalization for mixture, 18: 7550
interactions with neutrinos at high energies, one-neutrino hypothesis for, 18: 7555
interactions with mesons (π) at low energies, parameters and phase shifts for, 18: 7556
interactions with mesons (π), quantum numbers of resonance states in, 18: 7540
interactions with antimesons (K) in I = 1 $P_{3/2}$ channel, cross sections for, 18: 7560
interactions with protons at 14 Bev, 18: 9084 (NP-13484)
interactions with mesons (K^-) in nuclei, Y_1^* production in, 18: 9368
interactions with mesons (π), energy-momentum transfers in inelastic, 18: 9113
interactions with mesons (π), one-meson (π)-exchange model for, 18: 9114
interactions with mesons (π) at 6 Bev to 1 Tev, multiple charged particle production in, 18: 9119
interactions with mesons (K^-) at 350 to 450 Mev/c, Y_1^* resonances in, 18: 9143
interactions with antinucleons at 20 to 120 Mev, angular distributions and cross sections for, 18: 9154
interactions with mesons (π), N* Regge pole and (3,3) phase shifts in, 18: 9168
interactions with mesons (π), variational technique for partial-wave dispersion relations for, 18: 9176
interactions with pseudoscalar mesons, pseudoscalar and vector exchanges in vector meson production from, 18: 9177
interactions with mesons (π), partial-wave s-singularity of production amplitude in fourth-order diagram of, 18: 9188
interactions with nucleons at 52 Mev, spin correlation measurements in, 18: 9189
interactions with mesons (π), interpretation of N_{33} resonance in, 18: 9193
interactions with neutrinos, cross sections for production of heavy vector mesons, 18: 9202
interactions with nucleons, energy-momentum transfers in inelastic, 18: 9113
interactions with deuterons, optical theory for, 18: 10852 (JINR-P-1484)
interactions with gamma radiation at 1 Bev, meson (η^0) and meson (π^0) production in, 18: 10857 (LNF-63/47(p.58-61))
interactions with photons, amplitudes in virtual Compton, 18: 10886
interactions with mesons (π), zeros in forward amplitude of, 18: 10888
interactions with nucleons, hyperon production in, 18: 10916
interactions with electrons, strange particle production in, 18: 10928
interactions with mesons (K^-), Y* (1765 Mev) production in, 18: 10931
interactions with nucleons, charge dependence of phase shifts in, 18: 10944

interactions with nucleons, scattering amplitude and meson resonances in, 18: 10953
interactions with antinucleons, diffraction patterns for inelastic, 18: 10958
interactions with nucleons, amplitudes for, 18: 10965
interactions with mesons, theory of, 18: 10967
interactions with nucleons, potential for, 18: 11219 (TID-20105)
interactions with nucleons, theory of, 18: 11266
interactions with electrons, 18: 10681(R) (CEAL-1009)
interactions with neutrinos, spark chamber performance for, 18: 12448 (CERN-63-37(p.43-75))
interactions with mesons (K) and (π), amplitudes for, 18: 12911 (PAN-451/VII)
interactions with mesons (K^-), resonance (K^*) decay and production in, 18: 12936
interactions with mesons (π), singularities in final-state interactions in, 18: 12941
interactions with nucleons at high energies, strip approximation of, 18: 12960
interactions with gamma radiation, resonance model for meson (K) production in, 18: 12962
interactions with nucleons, theory for, 18: 15172(R) (AROD-1784:31)
interactions with nucleons in common harmonic oscillator potential modified by two-body potential, 18: 15250
interactions with mesons (π), study of internucleon potentials from, 18: 15291
interactions with hyperons, meson theory for, 18: 14800 (CERN-64-1(p.191-9))
interactions with mesons (π), meson (ρ)-nucleon coupling in, 18: 14801 (CONF-22-32)
interactions with mesons (ρ), resonance, 18: 14801 (CONF-22-32)
interactions with nucleons, pole approximation for, 18: 14812 (JINR-P-1511)
interactions with mesons (π), crossing relations for helicity amplitudes for, 18: 14825
interactions with nucleons at 1 Tev, effective target-mass distribution for, 18: 14857
interactions with mesons (π), secondary diffraction peak in elastic, 18: 14896
interactions with antineutrinos and neutrinos, unitary universal model for, 18: 14904
interactions with mesons (π) at 0 to 700 Mev, inelastic effects in, 18: 14939
interactions with gamma radiation, meson (K) production in, 18: 14886
interactions with mesons (π); Regge pole hypothesis in, 18: 14932
interactions with photons, meson (π) production in, 18: 16798
interactions with protons at 16 to 2800 Bev, meson (π) production in, 18: 16775
interactions with mesons (π^-) at 6.1 to 18.1 Bev/c, strange particle production in, 18: 16776
interactions with mesons (π) at low energies, ($\frac{3}{2}$, $\frac{3}{2}$) resonances in 18: 16777
interactions with mesons (θ), Lee model for, 18: 16778
interactions with mesons (π) at high energies, Regge pole formalism for, 18: 16779
interactions with mesons (π) at low energies, meson (ρ) effects on, 18: 16781
interactions with mesons (π), 556-Mev p_{11} resonance, 18: 16791
interactions with nucleons, nonstatic potentials in, 18: 19002
interactions with nucleons, one- and two-pion and boson contributions to, 18: 18656
interactions with nucleons, Born amplitude corrections for, 18: 18716
interactions with electrons at high energies, meson (π) production in, 18: 18740
interactions with protons at 6 Bev, distributions from intranuclear, 18: 19110
interactions with photons, meson (ω) and (ρ) production in, 18: 18635 (DESY-64/1)
interactions with mesons (π) and nucleons at high energies, inelastic, 18: 18639 (JINR-P-1524)
interactions with nucleons, computer programs for calculating, 18: 18647(R) (TID-20378(Sect.1))
interactions with hyperons (Λ) in reaction ($K^- + d \rightarrow \pi + \Lambda + N$), 18: 18679
interactions with gamma radiation, meson (π) production in Regge-pole theory, 18: 18680
interactions with nucleons at fixed momentum transfer, scattering-amplitude bounds for, 18: 18682
interactions with leptons, effects of nuclear structure in peratization method for, 18: 18683
interactions with mesons (π), isotopic splitting of spin state in, 18: 18690
interactions with gamma radiation, anomalies in (γ,π), 18: 18733
interactions with gamma radiation at high energies, strange particle production in, 18: 18735
interactions with mesons (π), detection of final state in, 18: 20401
interactions with mesons (π), resonances in, 18: 21005
interactions with mesons (π), S-wave scattering lengths using N/D method for, 18: 20937
interactions with mesons (π), Regge trajectories for, 18: 20940
interactions with mesons (π), coupling constant on Regge trajectory for, 18: 20948
interactions with mesons (π) at 170 to 600 Mev, model for single meson (π) production in, 18: 20964
interactions with nucleons at 30 to 10^6 Bev, particle production in, 18: 20969
interactions with mesons (π), Regge poles in, 18: 20988
interactions with nucleons, meson (ω) coupling in, 18: 21001
interactions with hypersons (Λ), π-K resonance in, 18: 21003
interactions with mesons (π), resonances in, 18: 21004
interactions with electrons, quantum electrodynamics of, 18: 21014
interactions with mesons ($\overline{K}$), motion of poles in resonance, 18: 21016
interactions with mesons (K), S-wave, 18: 21020
interactions with nucleons inside light nuclei, use in calculation of energy levels, 18: 21345
interactions with nucleons, velocity-dependent potentials in, 18: 21223
interactions with nucleons, variational principal connection with Independent-Pair Model for, 18: 21330
interactions with nucleons, amplitudes for, 18: 20913 (TID-20483)
interactions with hyperons, amplitudes for, 18: 20913 (TID-20483)
interactions with deuterons in three-body potential problem, integral equation for amplitude for, 18: 20930
interactions with mesons (π^-) at 17 Bev/c, 18: 20891 (AD-433625)
interactions with mesons (π) at low energies, analysis of, 18: 22727 (NP-13860)
interactions with nucleons, 18: 22728(R) (NP-13870)
interactions with mesons (K^-), correlated nucleon pairs in, 18: 22769
interactions with mesons ($\overline{K}$), hyperon decay in, 18: 22770
interactions with mesons (π) at low energies, amplitudes for, 18: 22778
interactions with mesons (π), second resonance in elastic, 18: 22779
interactions with antihyperons (Λ) and antinucleons, 18: 22782
interactions with mesons (π), single-meson exchange in, 18: 24477
interactions with nucleons, single-meson exchange in, 18: 24477
interactions with antinucleons, optical model for, 18: 24481
interactions with leptons, scattering amplitudes for, 18: 24419
interactions with mesons (π), coupling constants for, 18: 24423
interactions with antinucleons and nucleons, analysis of total cross sections including channel-crossing for, 18: 24452
interactions with antinucleons, meson (π) form factors from, 18: 24471
interactions with mesons, phase-shift linearization of differential cross sections for, 18: 24472
interactions with mesons (π), mechanisms of low-energy, 18: 24474
interactions with mesons (π^-) at 7 Bev, 18: 24391 (JINR-P-1629)
interactions with meson (π^-), parity conservation in hyperon (Λ^0) production in, 18: 24394 (NEVIS-122)
interactions with nucleons near 140 Mev, phase-shift analysis of, 18: 24403 (UCRL-7563-T)
interactions with antinucleons and mesons (K) and (π) at high energies, parameters for, 18: 24384 (JINR-P-1577)
interactions with nucleons at high energies, parameters for, 18: 24384 (JINR-P-1577)
interactions with mesons (π), constants and coupling in shell-model, 18: 24414
interactions with nucleons, meson (π) production in resonant, 18: 24479
interactions with mesons (π^+), meson (f^0) spin from, 18: 24466
interactions with gamma radiation, polarization dependence of single meson (π) production in, 18: 26276 (DESY-64/6)
interactions with hyperons (Λ), detection of resonances in, 18: 26277(R) (ORNL-3582(p.127-8))
interactions with mesons (π), production processes in, 18: 26281
interactions with mesons (π), models for elastic, 18: 26281
interactions with mesons (π) at low energies, equations for, 18: 26299
interactions with mesons (μ), meson (π) production in, 18: 26305
interactions with mesons (π), mesons (ρ) in, 18: 26348
interactions with mesons (π), resonance effects in, 18: 26352
interactions with bosons, isobar production in, 18: 26358
interactions with nucleons in nuclear matter, Moszkowski and Scott approximation of Brueckner's many-body theory of, 18: 26369
interactions with photons, meson (π) production in, 18: 26372
interactions with photons, production of mesons (ω) and mesons (ρ) in, 18: 26373
interactions with photons at high energy, Regge poles in pion production in, 18: 26385
interactions with neutrinos (μ), upper limits for, 18: 26321
interactions with hyperons (Λ) in hyperfragments, strength parameter for, 18: 28652

interactions with hyperons (Λ) in hypertriton, strength of, 18: 28749
interactions with mesons (π), parity conservation and unitary symmetry in, 18: 28342
interactions with mesons (π), bootstrap equations for static model of resonance, 18: 28352
interactions with mesons (π), diagrams for resonance, 18: 28357
interactions with mesons (π), coupling constants for, 18: 28359
interactions with neutral vector mesons, vector-spinor bootstrap in theory of, 18: 28361
interactions with mesons (π), meson (ρ) effects on phase shifts in, 18: 28368
interactions with hyperons (Λ), charge symmetry in, 18: 28369
interactions with nucleons, coupling constants and partial wave scattering amplitudes for, 18: 28415
interactions with nucleons, resonances in, 18: 28416
interactions with hyperons (Λ), two-pion-exchange contribution to, 18: 28418
interactions with mesons (π), field theory model for, 18: 28456
interactions with nucleons at 5 Tev, meson emission asymmetry, inelasticity, and multiplicity in, 18: 30515(R) (NP-14096(p.1-4))
interactions with antinucleons, effects on p-p phase shifts, 18: 30522(R) (TID-20720(Paper 4))
interactions with mesons(π) below 1 Bev, final-state interaction model for single-meson(π) state interaction model for single-meson(π) production in, 18: 30527 (TID-20773)
interactions with hyperons (Λ) and mesons (π), CP invariant theory for, 18: 30557
interactions with hyperons (Σ), hyperon (Λ^0) production in, 18: 30577
interactions with nucleons with one-boson exchange, 18: 30582
interactions with electromagnetic fields in photodisintegration processes, multipoles in, 18: 30731 (NYO-1807-13)
interactions with mesons (π), phase shifts for, 18: 30593
interactions with nucleons, two-particle, 18: 30594
interactions with mesons (π), vector meson exchange model for, 18: 30596
interactions with nucleons at 10 Mev, resonance effects in, 18: 30604
interactions with mesons (π), Chew-Low's method for $\pi + N \rightarrow N + 2\pi$, 18: 30612
interactions with deuterons, corrections to diffraction-scattering, 18: 30579
interactions with electrons and photons at high energies, strange-particle production in, 18: 32528 (IFA-HE-53)
interactions with θ particles in Lee model, nonanalytic cut off functions for, 18: 32546
interactions with hyperons, 18: 32549
interactions with mesons (π), B resonance in, 18: 32550
interactions with nucleons, $^1S_0$ virtual bound state of, 18: 32556
interactions with mesons (π), determination of coupling constant for, 18: 32562
interactions with mesons (π), reciprocal bootstrap mechanism in resonance, 18: 32568
interactions with mesons (π) at low energy, phase shifts for, 18: 32575
interactions with nucleons, inelastic effects in, 18: 32592
interactions with mesons (π), one-nucleon exchange in, 18: 32600
interactions with mesons (π^0), model for resonances in, 18: 32608
interactions with mesons, resonance models for, 18: 32620
interactions with mesons (π^-) at 6.8 Bev, inelastic, 18: 32621
interactions with deuterons and mesons (π), bound states in, 18: 32623
interactions with mesons, asymptotic scattering amplitudes for, 18: 32626
interactions with electrons, mesons, nucleons, and photons, dispersion relations for, 18: 32629
interactions with mesons (π), meson (φ) production in, 18: 32664
interactions with mesons (π), relativistic corrections to s- and p-wave, 18: 34507 (JINR-E-1686)
interactions with mesons (π), secondary-particle production in, 18: 34509 (NP-14086)
interactions with mesons (π), complex singularities in amplitude for, 18: 34524
interactions with deuterons, amplitudes for break-up, 18: 34535
interactions with nucleons, singlet-state phase shifts for, 18: 34546
interactions with mesons (π), maximum coupling constant for, 18: 34548
interactions with pseudoscalar mesons, fermion Regge trajectories for, 18: 34558
interactions with neutrinos, conserved vector current testing by, 18: 34561
interactions with mesons ($\bar{K}^0$), assuming Y$_1^*$ Regge particle, 18: 34571
interactions with mesons (π) below 500 Mev, analysis of, 18: 34604
interactions with mesons (π), meson (f^0) contribution to, 18: 34611
interactions with deuterons, optical theorem for, 18: 34618
interactions with tritons, amplitudes for, 18: 34619
interactions with mesons (π) at low energies, phase shifts in, 18: 34621
interactions with nucleons, baryon production analysis of, 18: 34632
interactions with mesons (π), production of mesons (ω^0) and (ρ) in, 18: 34622
interactions with mesons (K^-) in complex nuclei, 18: 36615
interactions with mesons (π), threshold effects for meson (ρ) production in, 18: 36263
interactions with mesons (π), model for nonlocal, 18: 36264
interactions with hyperons (Λ), potentials from single-particle exchanges in, 18: 39274
interactions with mesons (K), resonances in, 18: 36285
interactions with mesons, s-wave, 18: 36289
interactions with mesons (π), amplitude for, 18: 36290
interactions with antinucleons at 30 to 280 Mev, model for, 18: 36294
interactions with protons at 2.95 Bev, resonance production in, 18: 36303
interactions with mesons, $\frac{3}{2}$ -baryon production in, 18: 36306
interactions with photons at high energies, meson (π) production in, 18: 36317
interactions with mesons (π), theory for three-body, 18: 36320
interactions with neutrinos, meson (μ) pair production in, 18: 36344
interactions with protons at 24 Bev, secondary particle angular distributions in, 18: 36352
interactions with neutrinos, J = ½ isobar production in, 18: 37909
interactions with nucleons with nonlocal separable potentials, exclusion principle in, 18: 37874 (64-RL-3604-M)
interactions with mesons (K), ($\bar{K}$), and (π), model for strong, 18: 37890
interactions with nucleons near 50 Mev, phase-shift analysis of, 18: 37902
interactions with mesons (π), strong coupling meson theory for resonances in, 18: 37930
interactions with nucleons, 18: 37937
interactions with mesons ($\bar{K}$), masses of resonances in, 18: 37948
interactions with mesons (π) at low energies, p-wave resonances in, 18: 37952
interactions with mesons (π), meson (π-π) contribution to, 18: 37964
interactions with nucleons, theory for, 18: 37966
interactions with nucleons, Regge trajectories in, 18: 37974
interactions with mesons (π), 18: 37977
interactions with nucleons, asymptotic cross sections for, 18: 37983
interactions with nucleons, 18: 37987
interactions with mesons (π), decay of N*, 18: 40258
interactions with mesons, double-peripheral model for elastic, 18: 40275
interactions with neutrinos, electron production in, 18: 40280
interactions with mesons (π^-) at 7.5 Bev, 18: 40287
interactions with mesons (π^-) at 6.8 Bev/c, 18: 40288
interactions with mesons (π^-) at 6.8 and 7.5 Bev/c, mesons (π^0) from, 18: 40289
interactions with mesons ($\bar{K}$) and (π), selection rules and W, symmetry for, 18: 40319
interactions with mesons (π) and protons at 2–25 Bev, review, 18: 40361
interactions with nucleons, review of recent data and theory on, 18: 40362
interactions with nucleons, theory of, 18: 40363
interactions with nucleons at high energies, theory of, 18: 40372
interactions with mesons (π) at high energies, theory of, 18: 40372
interactions with protons, angular distribution and inelasticity for, 18: 40373
interactions with mesons (π), momentum distributions for, 18: 40373
interactions with protons, asymmetry and Lorenz factors of, 18: 40373
interactions with deuterons, helium-3, nucleons, and tritons, 18: 40648
interactions with nucleons, charge independence, 18: 40649
interactions with electrons at high-energies, cross sections for inelastic, 18: 40278
interactions with mesons (π), resonance N* production in, 18: 40240 (UCRL-11423)
interactions with nucleons above 10^{12} ev, heavy-particle production in, 18: 40524
interactions with protons, fractionally charged particles from, 18: 42446
interactions with mesons (π), criteria for bound state in, 18: 42457
interactions with hyperons (Λ), two-pion-exchange contribution to, 18: 42459
interactions with photons, meson (π) production in, 18: 42460
interactions with hyperons at low momentum, 18: 42365 (JINR-E-1790)
interactions with mesons (π) above 1 Bev/c, 18: 42366 (JINR-E-1802)
interactions with mesons ($\pi^\pm$) at 0 to 700 Mev, phase-shift analysis of, 18: 42378 (UCRL-7846)
interactions with electrons, meson (π) production in, 18: 42385
interactions with mesons (π^-) at 4.4 Bev, transverse momentum of mesons (π^-) and (π^+) emitted in, 18: 42395
interactions with cosmic nucleons, transverse momentum of secondary particles in, 18: 42398
interactions with secondary cosmic particles, multiplicity frequency distributions in, 18: 42401
interactions with cosmic nucleons in emulsions, isobar production in, 18: 42402
interactions with mesons (π), phase shifts in, 18: 42408
interactions with mesons (π), models for resonances in, 18: 42412

interactions with nucleons, resonances at 1238 to 1690 Mev in, 18: 42419
interactions with mesons (π), asymptotic parameters for, 18: 42426
interactions with mesons (π) at 1 to 6 Bev, resonances in, 18: 42430
interactions with mesons (π), separation of variables in, 18: 42437
interactions with mesons (π), effects of meson (ρ) production on amplitudes for, 18: 42439
interactions with mesons, theory of, 18: 42627(R) (ANL-6879(p.88-113))
interactions with nucleons near 140 Mev, multipion resonances in, 18: 42651 (UCRL-7553-T)
interactions with nucleons in nuclear surface, model for, 18: 42653
interactions with mesons(μ^-) in nuclei, 18: 42718
interactions with mesons(K^-), hyperon (Λ) production in, 18: 44522 (UCRL-11432)
interactions with nucleons, charge dependence in, 18: 44782
interactions with photons, meson (π) production by, 18: 44572
interactions with photons, meson (π) production in, 18: 44538
interactions with nucleons, isobar production in, 18: 44543
interactions with hyperons (Λ), long-range effects in, 18: 44544
interactions with mesons (π), resonance poles in Lee model for, 18: 44557
interactions with mesons (K) and (π), secondary diffraction peaks in, 18: 44562
interactions with hyperons (Λ^0), in nuclei having A = 40 to 100, 18: 44594
interactions with mesons (π) above 20 Bev, forward amplitudes for, 18: 44599
interactions with nucleons at high energies, four-momentum transfers in (T), 19: 1193 (PAN-498/VI)
interactions with mesons (π), thresholds for N^*_{33} resonance in (T), 19: 1236 (UCRL-11622)
interactions with neutral vector mesons, asymptotic behavior of Feynman integrals for (T), 19: 1243
interactions with mesons (K), parameters for s-wave, 19: 1274
interactions with mesons (K), vector-meson effects in (T), 19: 1293
interactions with deuterons, three-body effects in, 19: 1260
interactions with protons at 3.5 Bev (E), 19: 1339
interactions with mesons (π), phase shift analysis of (E/T), 19: 1369
interactions with mesons (π^-) at 6.1 Bev (E), 19: 1397
interactions with mesons (π), scattering model for (T), 19: 1379
interactions with mesons (π^-) at 6.1 and 18.1 Bev, 3-π production in (E), 19: 1398
interactions with protons at 22 Bev, meson (π) and meson (K) distribution from (E/T), 19: 1400
interactions with electrons in quantum field theory, 19: 1424 (NP-14404 (p.271-99))
interactions with nucleons in nuclei, potentials for, 19: 1552 (JINR-P-1728)
interactions with nucleons, 19: 3345
interactions with nucleons in emulsions at high energy, 19: 3348
interactions with mesons (π) and nucleons at 0.8 to 10 Bev, statistical model calculations for, 19: 3028 (ORNL-3713)
interactions with mesons (π) and nucleons, models for peripheral (T), 19: 3035
interactions with mesons (π) at 5 Bev/c, meson-exchange study of particle production in (T), 19: 3048
interactions with photons, meson (π) production in (E/T), 19: 3049
interactions with nucleons above 10^{13} ev, angular distribution of secondary particles in (T), 19: 3055
interactions with mesons (π), N^* isobar and meson (ρ) effects on (T), 19: 3076
interactions with nucleons (E), 19: 3079
interactions with nucleons, inelastic unitarity effects in (T), 19: 3083
interactions with neutrinos (E/T), 19: 2941
interactions with nucleons, scattering lengths for (T), 19: 3099
interactions with nucleons, optical potentials for (T), 19: 3239 (MIT-2098-67)
interactions with nucleons and mesons (π), statistical model calculations of distributions from, 19: 4900 (ORNL-3716)
interactions with mesons (π), at 600 to 900 Mev, (E), 19: 5572(R) (PPAD-525-D)
interactions with nucleons below 1 Bev, (E/T), 19: 4892 (JINR-P-1785)
interactions with mesons (π) below 1 Bev, (E/T), 19: 4892 (JINR-P-1785)
interactions with mesons (π), (T), 19: 4893 (JINR-P-1788)
interactions with mesons (π) above 1 Bev, (T), 19: 4895 (JINR-P-1792)
interactions with mesons (π^-) at 10 Bev, inelastic, (E), 19: 4905
interactions with mesons (π), self-consistency in, (T), 19: 4913
interactions with hyperons (Λ), S-wave, 19: 4937
interactions with neutrinos in liquids, (E), 19: 4947
interactions with mesons (π) near 1500 Mev, model for resonance, 19: 4952
interactions with mesons (π) at high energies, (T), 19: 4956
interactions with mesons (π), coupling constants for, 19: 4957
interactions with mesons (π) to 700 Mev, P_{33} state in, (T), 19: 4961
interactions with photons at high energies, cross sections for, (T), 19: 4968
interactions with antinucleons and mesons (π), selection rule for strange particle production in, (T), 19: 4971
interactions with neutrinos, N^* production in, (T), 19: 4981
interactions with nucleons, one-boson-exchange model for, 19: 4986
interactions with mesons (π), phase-shift analysis and dispersion relations for, (T), 19: 4997
interactions with mesons (π), local field theory of, (T), 19: 5016 (JINR-P-1793)
interactions with antinucleons, particle spectrum from annihilation, (T), 19: 6526
interactions with mesons (π) in nuclei, (T), 19: 6528
interactions with protons, meson (π^+) and (π^0) production in, (T), 19: 6536
interactions with mesons (K) and (π), A-invariance in, (T), 19: 6543
interactions with mesons (π), self-consistent calculations of, 19: 6549
interactions with mesons (π), vertex functions for, (T), 19: 6550
interactions with mesons (K), (π), and nucleons, models for, (T), 19: 6551
interactions with mesons (π) at low energy, un-Reggeized strip approximation for, (T), 19: 8160
interactions with antineutrinos and neutrinos, unitary symmetry for SU(3) relations in, (T), 19: 8165
interactions with mesons (π), meson (η) production in, (T), 19: 8182
interactions with antinucleons, meson (W) production in annihilation, (T), 19: 8193
interactions with mesons (π), ρ-exchange model for N^* production in, (T), 19: 8206
interactions with mesons (π), N^*_{11} (1400) production in, (T), 19: 8209
interactions with nucleons above 10^{13} ev, angular distribution of shower particles from, (E), 19: 8214
interactions with hyperons (Λ) at low and intermediate energies, binding energies from, (T), 19: 8220
interactions with mesons (π), dispersion method for, (T), 19: 8225
interactions with electrons, dispersion relations for, (T), 19: 8225
interactions with mesons, vertex functions for, (T), 19: 8281
interactions with mesons (π) in Lagrangian field theories, spectral functions for, (T), 19: 8289
interactions with neutrino, intermediate bosons in, (E), 19: 8149
interactions with mesons (π), model, (T), 19: 8150
interactions with hyperons (Λ) at low energy, potentials in, (T), 19: 8152
interactions with hyperons (Λ), potential of, (T), 19: 8154
interactions with mesons (π^-) in xenon at 9 Bev/c, (E), 19: 8446
interactions with mesons (π), distributions from inelastic, (E/T), 19: 10014 (IFA-HE/54)
interactions with mesons (π), Lorentz-covariant Low equation for, (T), 19: 10031
interactions with mesons (π), Regge pole method for, (T), 19: 10035
interactions with mesons (K), dispersion relation for amplitudes in, 19: 10039
interactions with nucleons at 300 Bev, meson (π) production in, (E), 19: 10048
interactions with hyperons (Λ), two-meson (π)-exchange contribution to, (T), 19: 10050
interactions with mesons (K), Y^*_1 Regge pole in, (T), 19: 10053
interactions with mesons (K^+) at 900 Mev/c, one meson (π) production in, 19: 10064
interactions with neutrinos, PC violation in meson (π) production in, (T), 19: 10073
interactions with mesons (π) at high energies, amplitudes and total cross sections for, (T), 19: 10076
interactions with hyperons (Λ), cross sections and potential for, (T), 19: 10080
interactions with antinucleons, meson (π) resonances in, (T), 19: 10104
interactions with mesons (π^-) at 17 Bev, (E), 19: 10108
interactions with bosons, gradient-coupling models for, 19: 5033
interactions with mesons (π) and photons, form factors from, (T), 19: 12187
interactions with deuterons at 155 Mev, analysis of elastic, (T), 19: 12193
interactions with hyperons (Λ), analysis of scattering cross sections for, (T), 19: 12195
interactions with mesons (π), 1400-Mev resonance in, (T), 19: 12198
interactions with mesons (π), absorption in final-state, (T), 19: 12205
interactions with mesons (π), axial vector current in, (T), 19: 12229
interactions with mesons (π) and nucleons at high energies, inelastic peripheral, (T), 19: 12250
interactions with photons, analysis of, (T), 19: 12252
interactions with neutrinos, lepton emission in, (T), 19: 12253
interactions with mesons (π) and photons, polarization effects on single isobar production in, (T), 19: 12262
interactions with protons in emulsions at 19.8 Bev/c, shower particles

from, (E), 19: 12264
interactions with mesons (π) at high energy, Regge poles for backscattering in, (T), 19: 12305
interactions with deuterons, diagram summing method for short-range, (T), 19: 12318
interactions with photons, meson (π) production in, (T), 19: 12380
interactions with hyperons (Λ) in hyperfragments, analysis of, (T), 19: 12530
interactions with mesons (π) at 12 and 18 Bev/c, dibosons from, (E), 19: 14405 (TID-21409)
interactions with mesons (π), hard photon emission mechanism for, (T), 19: 14317 (JINR-P-1896)
interactions with mesons (π^-) at 6 to 18 Bev/c, strange particle production in, (E), 19: 14322 (NP-14637)
interactions with mesons (π) at low energy, resonances in, (T), 19: 14337
interactions with antinucleons at 0.1 to 1.3 Bev, (T), 19: 14340
interactions with mesons (π^-) at 7.5 Bev, isospin analysis of, (T), 19: 14342
interactions with mesons (π), meson (K) pair production in, (T), 19: 14354
interactions with mesons (π^-) at 10 Bev, (E), 19: 14366
interactions with electrons at high energy, (T), 19: 14386
interactions with nucleons, soft-core potential in, (T), 19: 14387
interactions with nucleons at high energy, momentum transfer in, (T), 19: 14388
interactions with nucleons, validity of Bethe-Salpeter equation for, (T), 19: 14385
interactions with mesons (π), phase shift analysis of, (T), 19: 16482 (UCRL-11849)
interactions with mesons, cascade equations for, 19: 17159(R) (ORNL-3714(Vol.II)(p.97-118))
interactions with mesons (π) and nucleons, statistical model calculations of, 19: 17159(R) (ORNL-3714(Vol.II)(p.97-118))
interactions with mesons (π), small momentum transfer in inelastic, (T), 19: 16487
interactions with hyperons (Λ) in hyperfragments, model for, (T), 19: 16541
interactions with hyperons (Λ) at low energies, N/D calculations for elastic, (T), 19: 16548
interactions with intermediate vector bosons, (T), 19: 16563
interactions with mesons (π^-) at 12 and 18 Bev/c, meson (ρ^0) production in, (E/T), 19: 16613
interactions with mesons (K), total cross sections for, (T), 19: 16615
interactions with mesons (K) and (π), s-wave virtual states in amplitudes for, (T), 19: 16621
interactions with mesons (π) and nucleons, p-wave dispersion relation for, (T), 19: 16623
interactions with nucleons, boson mass width effects on, (T), 19: 16638
interactions with mesons (π) and photons at high energies, inelastic, (T), 19: 16646
interactions with nucleons at low energy, (T), 19: 16651
interactions with gamma photons and mesons (π), $N^*_{3/2}$ production in, (T), 19: 16686
interactions with hyperons (Λ) in nuclei, (T), 19: 16962
interactions with nucleons, review of few-body systems in, 19: 17069
interactions with nucleons on nuclear Fermi surface, (T), 19: 16861
interactions with antihyperons, cross section calculations for, (T), 19: 18755 (UR-875-28)
interactions with mesons (ω) and (ϕ), coupling constants for, (T), 19: 19161
interactions with mesons (π), algebra for describing, (T), 19: 18775
interactions with deuterons, final-state, (T), 19: 18788
interactions with mesons (π) at high energies, cross sections and Regge poles for, (T), 19: 18790
interactions with photons, meson (ρ) effects on meson (π) production in, (T), 19: 18813
interactions with neutrinos, meson (K) and (π) peripheral production in, (T), 19: 18815
interactions with mesons (η) and (π), coupling constants for, (T), 19: 18817
interactions with antinucleons, boson production in central, (T), 19: 18822
interactions with mesons (π), physical sum rules on real part of amplitude for, (T), 19: 18852
interactions with mesons (π) at 0 to 800 Mev, energy-dependent phase shift analysis of, (T), 19: 18870
interactions with mesons (π) at high energies, total cross sections for, (T), 19: 18877
interactions with nucleons, velocity-dependent potentials for, (T), 19: 18895
interactions with mesons (π), (3,3) partial-wave amplitude in, (T), 19: 18907
interactions with mesons (π) and nucleons, dispersion relations for, (E), 19: 18915
interactions with mesons (π) and nucleons, parameters for, (T), 19: 20937(R) (TID-21672)
interactions with nucleons, computer calculation of matrix elements of, (T), 19: 20938(R) (UCRL-11828(p.9-10))
interactions with mesons (π) and nucleons, coupling constants for, (T), 19: 20917 (IC/65/3)
interactions with elementary particles, production amplitudes in, (T), 19: 20925 (ICTP-64/3)
interactions with neutrinos, neutral weak currents in, (T), 19: 20988
interactions with mesons (π), production of massive neutral gauge particle in, (T), 19: 20989
interactions with mesons (π), position and width of N* (1688) in, (T), 19: 20992
interactions with mesons (π), N^*_{33} resonance in, (T), 19: 21000
interactions with antinucleons, mesons (π), and nucleons, phase of forward amplitudes for, (T), 19: 21010
interactions with antinucleons, mesons (π), and nucleons, selection rules for final states in, (T), 19: 21023
interactions with mesons (μ^-) at 5 Bev/c, meson (π) production in, (E), 19: 21037
interactions with antinucleons at rest, SU(12) symmetry model predictions for annihilation, (T), 19: 21039
interactions with nucleons, Treiman-Yang criterion for, (T), 19: 21046
interactions with mesons (π), complex angular momentum in, (T), 19: 21048
interactions with mesons (π), Jacob-Wick method for scattering amplitude in, (T), 19: 21052
interactions with nucleons, Jacob-Wick method for scattering amplitude in, (T), 19: 21052
interactions with antinucleons, Jacob-Wick method for scattering amplitude in, (T), 19: 21052
interactions with mesons (π^-) at 6.8 Bev/c, angular and momentum distributions in, (E), 19: 21062
interactions with mesons (K) and (π) at high energies, Regge trajectories for, (T), 19: 21063
interactions with mesons (π), kinematic analysis of, 19: 21076
interactions with mesons (π), Regge trajectories in, 19: 21077
interactions with nucleons, charge dependence of, (T), 19: 21373
interactions with mesons (π), solution of integral equation for, 19: 20445
interactions with antinucleons and mesons (π), absorptive corrections to one-meson-exchange model for, (T), 19: 23441
interactions with hyperons (Λ), strangeness changing in, (T), 19: 23459
interactions with mesons (π), OBEC model for phase shift analysis of low-energy, 19: 23460
interactions with mesons (K) at high energies, strange particle production in, (T), 19: 23466
interactions with mesons (π) at low energy, vertices in (πN) and ($\bar{N}$D), (T), 19: 23468
interactions with neutrinos, single meson (K) and (π) production in, (T), 19: 23477
interactions with mesons (π), quantum numbers of isobars in, (T), 19: 23368
interactions with protons at low energy, meson (π) production in, (T), 19: 23369
interactions with mesons (π), amplitudes of production processes in, (T), 19: 23388
interactions with mesons (π) at resonance energies, phase shifts in, (T), 19: 23396
interactions with mesons (π^+) at 3.25 Bev/c, exchange mechanism for meson (ω) production in, (E), 19: 23397
interactions with deuterons at 40 and 150 Mev, D-state and pickup effects in, (T), 19: 23406
interactions with mesons (π) at 650 Mev, short-range, (T), 19: 23411
interactions with nucleons, nonstatic potential in, 19: 23775
interactions with mesons (π), effects of meson (π) final-state interactions on amplitudes for, (T), 19: 25276
interactions with mesons (π^-) at 7 Bev/c, proton spectra from inelastic, (T), 19: 25281
interactions with mesons (π) and photons, spin structure of five-point amplitudes in, (T), 19: 25282
interactions with antineutrinos, Cabibbo theory for, 19: 25291
interactions with neutrinos, N* production in, (T), 19: 25292
interactions with mesons (π), meson (π) production in, (T), 19: 25301
interactions with mesons (π) and nucleons, effective target mass in, (T), 19: 25308
interactions with mesons (π), spin propagators in, (T), 19: 25309
interactions with neutrinos, meson production in, (T), 19: 25315
interactions with antinucleons, bound states and Regge trajectories in vector meson exchange model for, 19: 25321
interactions with mesons (π) at 0 to 350 Mev, phase-shift analysis of, (T), 19: 25352

interactions with nucleons in nuclei at 10^{11} to 10^{13} ev, (T), 19: 27460
interactions with mesons (π), Chew-Low equations and phases in, (T), 19: 27144 (JINR-P-1964)
interactions with mesons (π) at high energy, pole diagrams for, (T), 19: 27147 (JINR-P-1979)
interactions with nucleons in nuclei, resonance density in, (T), 19: 27174
interactions with mesons (π) and nucleons at very high energies, 19: 27182
interactions with tritons, nonrelativistic, (T), 19: 27201
interactions with mesons (π), analytic continuation of amplitudes for, (T), 19: 27212
interactions with hyperons (Λ) at low energies, N/D method for, (T), 19: 27220
interactions with mesons (π), coupling constants for, (T), 19: 27222
interactions with mesons (π) and nucleons, residues of Regge poles in, (T), 19: 27228
interactions with mesons (π), internal symmetries in bootstrap dispersion relations for, (T), 19: 27233
interactions with mesons (π), inelastic unitarity contributions to scattering lengths in, (T), 19: 27238
interactions with mesons (π), coupling in, (T), 19: 27256
interactions with hyperons (Λ), one-meson contribution to cross section of, (E), 19: 26917(R) (IA-984)
interactions with mesons (π), meson (K) and (ρ) coupling constants from, (T), 19: 27281
interactions with nucleons, attractive–repulsive potentials for, 19: 28912(R) (ANL-6819)
interactions with mesons (π) in nuclei, (T), 19: 29306
interactions with nucleons, potentials in, (T), 19: 29307
interactions with hyperons (Λ), theory of two-pion exchanges in, 19: 28962(R) (NIRL/R/81)
interactions with antinucleons, $\bar{U}(12)$ symmetry in four-meson annihilation, (T), 19: 29053 (IC/65/47)
interactions with nucleons, potentials for heavy-meson exchange in, (T), 19: 29063 (JINR-P-2048)
interactions with mesons (η) and (π), coupling constants for, (T), 19: 29072 (NP-15014)
interactions with electrons at high energies, meson (K) production in, (T), 19: 29080
interactions with mesons (π), meson (ρ) production in, (T), 19: 29091
interactions with nucleons, boson wave excitation in, (T), 19: 29092
interactions with nucleons, two-pion exchange in, (T), 19: 29095
interactions with nucleons in U(12) symmetry, 19: 31007 (IC/65/50)
interactions with mesons, coupling constants for, (T), 19: 31039
interactions with mesons (π), K-matrix model of peripheral, (T), 19: 31043
interactions with nucleons, boson-exchange effects in, (T), 19: 31067
interactions with mesons (π), meson (π) final-state interactions in, (T), 19: 31008 (LA-3171)
interactions with mesons (π), coupling constants for, (T), 19: 31014 (UCRL-7942)
interactions with mesons (π), Regge dynamics in (T), 19: 31016 (UCRL-16115)
interactions with mesons (π), peripheral model for meson (ρ) production in, 19: 31002 (CONF-550-97)
interactions with pseudoscalar mesons, (T), 19: 31129
interactions with nucleons in nuclei, core excitation effects on residual, (T), 19: 31301
interactions with mesons (π), coupling constants for, (T), 19: 31041
interactions with mesons (K) and (π), microscopic non-causality in, (T), 19: 32949 (LADC-6480)
interactions with electrons, strange particle production in, (T), 19: 32958
interactions with mesons (π), multichannel approach to high-energy peripheral, (T), 19: 33016
interactions with electrons, meson (π) production in, (T), 19: 33032
interactions with mesons (π) and nucleons, hyperon production in, (T), 19: 33064
interactions with nucleons at 0 to 350 Mev, phase-parameters for, 19: 32048(R) (NP-15073)
interactions with holes in silicon, hyperfine, (T), 19: 34729
interactions with mesons (π) and protons at 7 to 20 Bev, inelastic, 19: 34909
interactions with mesons (π) and nucleons, Monte-Carlo method for inelastic, 19: 35028 (JINR-P-2140)
interactions with antineutrinos unitary symmetry for baryon resonance formation in, 19: 35059(T)
interactions with neutrinos, form factors and polarization effects in, (T), 19: 35081
interactions with mesons (π), $J = \frac{1}{2}$, $T = \frac{1}{2}$ phase shifts in, (T), 19: 35091
interactions with nucleons, parity violation in, (E), 19: 35114
interactions with mesons (π), p-wave amplitude effects on bootstrap calculations of, (T), 19: 35124
interactions with neutrinos, cross sections and form factors for, (T), 19: 35128
interactions with mesons (π), three-body forces in, (T), 19: 35145
interactions with mesons (K) and (π) at 2 to 3 Bev/c, peripheral production and resonance decay in, (T), 19: 35152
interactions with mesons (K) at low energies, s-wave, (T), 19: 35157
interactions with antinucleons at high energies, annihilation, (T), 19: 35173
interactions with Y* at high energies, annihilation, (T), 19: 35173
interactions with mesons (π^-) at 6.8 Bev/c, meson (π^0) production in, (E), 19: 35175
interactions with mesons (π), resonances in, (E/T), 19: 35181
interactions with mesons ($\bar{K}$) at low energies, Y* resonance in, (T), 19: 35035
interactions with mesons (π), internal invariance and symmetry groups for, 19: 35039
interactions with mesons (π), algebraic equations for, 19: 35050
interactions with nucleons, radial wave equations for trinucleon bound-state, 19: 37523 (COO-1371-1)
interactions with photons, dispersion relations for meson (π) production in, (T), 19: 37541 (UCRL-7953-T)
interactions with mesons (π) at 300 to 700 Mev, phase-shift analyses of, 19: 37546 (UCRL-12383)
interactions with phonons in spherical nuclei, (T), 19: 37874(T)
interactions with collective excitations in odd-A nuclei, (T), 19: 37875(T)
interactions with mesons (π) at 20 to 340 Mev, phase-shift analysis of elastic, (T), 19: 37584
interactions with neutrons at 2.6 to 8.3 Bev, total cross sections for, (E), 19: 37610(T)
interactions with mesons (π) at 7.5 Bev, meson (π) production in, (T), 19: 37611(T)
interactions with deuterons at low and medium energies, inelastic, (T), 19: 37614
interactions with nucleons at low energies, (T), 19: 37615
interactions with nucleons at very high energies, charge exchange in, (T), 19: 37624
interactions with nucleons, charge independence in low-energy, 19: 37639
interactions with mesons, asymptotic amplitudes of, (T), 19: 37657
interactions with nucleons, unitarity of amplitudes for elastic, 19: 37550
interactions with nucleons at 1 to 3 Bev, analysis of, 19: 37559
interactions with mesons (K) and (π), resonances in three-particle production, (T), 19: 37649
interactions with antineutrinos, CERN experiments on, 19: 39612
interactions with mesons (π^+) amplitudes for elastic, (T), 19: 39621
interactions with nucleons at 400 Mev, phase shift analysis for, (T), 19: 39469 (JINR-P-2170)
interactions with photons, meson (π) production in, (T), 19: 39498
interactions with nucleons, general operator potential for, 19: 39504
interactions with neutrinos, resonance production in, (T), 19: 39517
interactions with vector mesons, complex angular momentum in, (T), 19: 39518
interactions with nucleons, SU(6) predictions for, 19: 39532
interactions with mesons (π), peripheral production and decay of mesons (ρ) in, (E/T), 19: 39576
interactions with mesons (K), peripheral production and decay of K* in, (E/T), 19: 39576
interactions with mesons (K) at low energies, model for, (T), 19: 39592
interactions with mesons (π) at high energies, analyses of final-state, (E/T), 19: 39574
interactions with vector bosons, complex angular momentum in, (T), 19: 39518
interactions with mesons (π), reciprocal bootstrap in, (T), 19: 41422
interactions with mesons (π^+) and (π^-) at 300 to 700 Mev, amplitudes for, (E), 19: 41442
interactions with antinucleons at rest, $\bar{U}(12)$ predictions for four-meson production in annihilation, (T), 19: 41463
interactions with mesons (π) at low energies, (T), 19: 41498
interactions with mesons (K), resonance effects in, (T), 19: 41506
interactions with mesons (π) below 1 Bev, single meson (π) production in, (T), 19: 41509
interactions with hyperons, book on, 19: 41513
interactions with cosmic neutrinos, meson (μ) production in, (E), 19: 41306
interactions with photons, production of mesons (ω) and (ρ) in, 19: 41321 (AECD/TP/4)
interactions with mesons (π) at high energies, optical model for backward, (T), 19: 41332 (JINR-P-2220)
interactions with protons, polarization tensor for double, (T), 19: 41333 (JINR-P-2227)
interactions with mesons (π), one-particle-exchange models for, (T), 19: 41375
interactions with mesons (π), meson (ρ^0) and meson (ω_8) effects in, (T),

19: 41380
interactions with mesons (π), form factors from, (T), 19: 41385
interactions with mesons (π), absorptive corrections and form factors in peripheral model for ($N\rho$), 19: 41400
interactions with neutrinos, meson (π) production in, (T), 19: 41754
interactions with mesons (K) and (π) at high energies, Regge-pole models for, (T), 19: 41426
interactions with nucleons in nuclei, (T), 19: 43374
interactions with mesons (π), N/D method for J = ⅝, T = ½ phase shifts in, (T), 19: 43081
interactions with mesons at high energy, real part of forward scattering amplitude for, (T), 19: 43117
interactions with pseudoscalar mesons, unitary symmetry for amplitudes and cross sections of, (T), 19: 43184
interactions with antiprotons, antineutron production in, (E), 19: 43077
interactions with mesons (π), SU(3) symmetry for $N\pi\pi$ state in, 19: 43082
interactions with mesons (π) and nucleons at high energy, nucleon structure in, (T), 19: 43103
interactions with mesons (π), meson (η) production in, (E/T), 19: 43114
interactions with antinucleons, non-Reggeization of vector meson in, (T), 19: 43131
interactions with mesons (π), mechanism for T = ½ and ⅝ recurrences in, 19: 43137
interactions with mesons (K) or (π), theory of $N^{\dagger}_{1/2}$ and $Y^{\dagger}_{1}$ production in, 19: 43144
interactions with neutrinos ($\nu\mu$), cross section for pion production in, (T), 19: 43158
interactions with scalar photons, perturbation expansion for Compton, 19: 43160
interactions with gamma radiation, γnp coupling constants from, (E/T), 19: 43162
interactions with mesons (π^-) at 2.8 Bev/c, $K^0\bar{K}^0$ resonance production in, (E), 19: 43048 (NP-15377)
interactions with nucleons at high energies, resonance production in, (T), 19: 45037 (TID-21316)
interactions with nucleons at high energies, polarization and Regge poles in, (T), 19: 45044 (UCRL-16186)
interactions with antinucleons at high energies, polarization and Regge poles in, (T), 19: 45044 (UCRL-16186)
interactions with nucleons, relativistic particle-wave dispersion relations for elastic, 19: 45084
interactions with mesons (K) and (π) at high energy, absorption model for charge-exchange, (T), 19: 45087
interactions with mesons (π) at high energy, multiple production in elastic, (T), 19: 45091
interactions with mesons (π) below 1 Bev, phase shift analysis of, (T), 19: 45100
interactions with protons, amplitudes and deuteron polarization from, (T), 19: 45017 (JINR-P-2267)
interactions with mesons, form factors from off-shell effects in, (T), 19: 45067
interactions with mesons (π), one-trajectory exchange for amplitudes of, (T), 19: 45074
interactions with mesons (K) and mesons (π) at high energies, polarization and Regge poles in, (T), 19: 45044 (UCRL-16186)
interactions with mesons (π), resonance in static, (T), 19: 47298 (AD-613934)
interactions with charged particles, peripheral electromagnetic, (T), 19: 47318
interactions with hyperons (Σ) at low energy, T = ½ bound state in, (T), 19: 47348
interactions with mesons (π), model for P_{11}-state strong, 19: 47350
interactions with photons at high energy, total cross section for (πN), (T), 19: 47353
interactions with mesons (K^0), scattering length for $S_{1/2}$ T = 0, (T), 19: 47365
interactions with mesons (π), restriction on forward amplitudes of, (T), 19: 47375
interactions with mesons (π), fixed-variable dispersion relations for, (T), 19: 47388
interactions with gamma rays at high energies, meson production and momentum-transfer distributions in, (T), 19: 47389
interactions with mesons (π) calculation using Regge trajectory, 19: 47395
interactions with mesons (π), meson (η) production in, (T), 19: 47401
interactions with mesons (π), analysis of data for, 19: 47404
interactions with deuterons, (T), 19: 39585
interactions with neutrinos, SU(6) for N^* and Y^*_1 production in, 20: 1020
interactions with nucleons, two-meson (π) exchange contribution to phase shifts in, (T), 20: 1029
interactions with nucleons in nuclei, core polarization effects in two-body, (T), 20: 1186
interactions with gamma rays, meson (π) production amplitude from, (T), 20: 2695
interactions with mesons (π) at 0 to 20 Bev, data review for, 20: 2725
interactions with nucleons, one-boson-exchange model for, (T), 20: 2726
interactions with gamma radiation at 165 to 230 Mev, amplitude and cross sections for meson (π^+) production, (E/T), 20: 2737
interactions with nucleons at 300 to 700 Mev, polarization parameters of, (E), 20: 4590 (UCRL-11926)
interactions with nucleons below 350 Mev, models for, (T), 20: 4849(R) (UCRL-14360, pp 1-50)
interactions with antinucleons, potential model for, (T), 20: 4849(R) (UCRL-14360, pp 1-50)
interactions with nucleons, phase-shift analysis of, (T), 20: 4849(R) (UCRL-14360, pp 1-50)
interactions with mesons ($\pi^{\pm}$), phase-shift analysis of, (T), 20: 4849(R) (UCRL-14360, pp 1-50)
interactions with mesons (π), amplitude of vector meson production in, (T), 20: 4584 (JINR-P-2380)
interactions with mesons (π), three-channel N/D equations in pole approximation for, 20: 4593
interactions with mesons (π), Dashen-Lee sum rules for intermediate state in, (T), 20: 4598
interactions with nucleons, SU(12) predictions for, (T), 20: 4605
interactions with photons, spin-1 meson production from, (T), 20: 4610
interactions with antiprotons at rest, SU(6) symmetry in two-meson annihilation, (T), 20: 4615
interactions with protons, polarized hydrogen target for, 20: 4637
interactions with mesons at high energy, sum rule for cross sections of, (T), 20: 4678
interactions with protons at 30 Bev/c, models for jets from, (E/T), 20: 6039 (INSJ-90)
interactions with nucleons, time-reversal noninvariant potential for, 20: 6047
interactions with nucleons in I = 0 S = 1 state, N/D method for s-wave, 20: 6049
interactions with nucleons, bremsstrahlung theory of multiple meson production in, 20: 6053
interactions with mesons (π), virtuality effects on, (T), 20: 6054
interactions with photons, SU(6) and SU(6)W for meson production in, 20: 6055
interactions with neutrinos, baryon resonance production in, (T), 20: 6065
interactions with mesons (K) and (π), single and double resonance production in, (T), 20: 6069
interactions with photons, spin correlations in vector meson production in, (T), 20: 6076
interactions with mesons and nucleons at high energy, total cross section differences for, (T), 20: 6082
interactions with mesons (π), calculation of higher resonance energies in, 20: 6096
interactions with alpha particles in spherical nuclei, (T), 20: 6376
interactions with mesons (π), solutions of Chew-Low equations for, 20: 6106 (JINR-P-2369)
interactions with hyperon (Λ), (T), 20: 6283 (CERN-64-13(Vol.4), pp 137-86)
interactions with mesons (π) in emulsion nuclei, intranuclear cascades from, (E/T), 20: 6287 (JINR-P-2373)
interactions with protons at 24 Bev, angular distributions from shower, (E), 20: 6325
interactions with hyperons (Λ) in nuclei, 20: 8098
interactions with antinucleons in light nuclei, nuclear recoil momentum distribution in annihilation, (T), 20: 8109
interactions with protons at 23.2 to 630 Mev, polarization tensor for, (T), 20: 7789 (JINR-P-2349)
interactions with nucleons at 600 Mev, meson (π^+) production in polarized, (E/T), 20: 7791 (JINR-P-2382)
interactions with photons, quark model for absorption in, (T), 20: 7797 (JINR-P-2439)
interactions with mesons (π), analytic continuation of Froissart-Gribov amplitude for, 20: 7817
interactions with nucleons in OBE model, π-π (720) S-wave resonance in, 20: 7818
interactions with virtual mesons (π), (T), 20: 7822
interactions with photons, $SU(6)_w$ symmetry model for, 20: 7825
interactions with antinucleons, model for annihilation, 20: 7826
interactions with mesons (π), dispersion relations for, (T), 20: 7830
interactions with mesons (π^-) at 6.1 Bev/c, angular and mass distributions from, (E), 20: 7836
interactions with mesons (π), generated unitarity relations for amplitudes of multichannel, (T), 20: 7837
interactions with mesons (π) at 746 to 1148 Mev, phase shift analysis of, (T), 20: 7843
interactions with mesons (π) at low energy, mass of N_{33} from, (T),

20: 7851
interactions with nucleons at high energies, amplitudes for, (T), 20: 7876
interactions with photons, U(6W) for collinear production of 0^- and 1^- mesons in, 20: 7904
interactions with photons, SU(3) ⊗ SU(3) ⊗ U(1) symmetry for production amplitudes in coplanar, 20: 7905
interactions with nucleons at 0.17 to 310 Mev, phase shifts in, (T), 20: 7788 (JINR-E-2440)
interactions with nucleons in nuclei, perturbation theory for, 20: 9971 (MIT-2098-201)
interactions with protons at 27 Bev, (E), 20: 10095
interactions with mesons (π^-) at 4.4 Bev, secondary particles from, (E), 20: 9775
interactions with deuterons at 90, 156, and 310 Mev, cross sections and polarization from elastic, (E/T), 20: 9780
interactions with neutrinos, cross-section calculations for, 20: 9784
interactions with mesons (π), sum rule for coupling constant for, (T), 20: 9791 (IC/65/91)
interactions with mesons (π), regularization of Chew-Low equations for amplitude of, (T), 20: 9717
interactions with mesons (π), π-π distributions and meson (f^0) from, (E), 20: 9730
interactions with mesons (K^-) and (R^0) to 300 Mev/c, effective-range analysis of, (T), 20: 9733
interactions with mesons (π) at high energies, model for elastic and exchange, (T), 20: 9739
interactions with cosmic mesons (μ) in lead at high energies, electromagnetic, (E), 20: 11528
interactions with mesons (π) at 290 to 905 Mev, cross sections for N* production in, (T), 20: 11562 (JINR-P-2454)
interactions with photons, meson (π) production in, (T), 20: 11572
interactions with mesons (π^-) at low energies, cross sections for scalar, (T), 20: 11574
interactions with mesons (π), self-consistency condition for πNN-vertex function in, 20: 11576
interactions with antineutrinos and neutrinos, nonpolarized lepton state from, (T), 20: 11577
interactions with hyperons, mass splitting effects in, (T), 20: 11586(T)
interactions with hyperon (Λ), analysis of light hyperfragments for cross sections for, (T), 20: 11594
interactions with photons, vector meson production in, (T), 20: 11595
interactions with mesons (π), triangle graphs for three-particle production in, (T), 20: 11596
interactions with nucleons, heavy-meson exchange in, (T), 20: 11597
interactions with mesons (π), meson (ϕ)-nucleon coupling in, (T), 20: 11598
interactions with mesons (ϕ), coupling constants for, (T), 20: 11598
interactions with mesons (π^-) in emulsions at 16.3 Bev, angular distributions from, (E/T), 20: 11602
interactions with antinucleons and mesons (π), ABC anomaly for amplitudes of, (T), 20: 11604
interactions with photons, SU(6) symmetry for particle production in, (T), 20: 11635
interactions with electrons, cross sections for, (T), 20: 11636
interactions with mesons (π), N/D calculation with inelastic unitarity for, (T), 20: 11643
interactions with mesons (π), Regge poles for, (T), 20: 11647
interactions with mesons(π), self-consistent method for vertex functions for, (T), 20: 11730
interactions with photons, SU(6) symmetry for meson production in, (T), 20: 11581(T)
interactions with mesons ($\bar{K}$), $Y_0^*(1815)$ production from, (T), 20: 11632
interactions with nucleons, data tabulations on polarization in low-energy, 20: 11965 (JINR-P-2426)
interactions with cosmic mesons (μ), (T), 20: 11975 (PAM-6502)
interactions with hyperons (Λ) in hypertritons, cross sections for, (T), 20: 12084
interactions with nucleons, spin structure of, (T), 20: 13455 (UCRL-14240-T)
interactions with mesons, scattering matrix for, (T), 20: 13448 (JINR-E-2521)
interactions with mesons (π) up to 500 Mev, quasipotential method for, (T), 20: 13467
interactions with vector mesons, (T), 20: 13479(T)
interactions with nucleons, phase-space volumes for, (T), 20: 13481
interactions with mesons (π), phase-space volumes for, (T), 20: 13481
interactions with hyperons (Λ), charge-asymmetry effects in, (T), 20: 13485
interactions with mesons (π^-) and (π^+), phase-shift analysis and spin-flip dispersion relations for, (T), 20: 13492
interactions with hyperons (Λ^0), hypernucleus nonmesic decay for, (T), 20: 13501
interactions with mesons at high energies, elementary-particle structure from backward-scattering, 20: 13510
interactions with nucleons at 400 Mev, phase-shift analysis of, (E/T) 20: 13516
interactions with nucleons, cross sections for, (T), 20: 13528
interactions with leptons, permutation symmetry in isospace for weak, 20: 13596
interactions with mesons (π) and nucleons in Bev range, partial-wave analysis of, (T), 20: 13513
interactions with nucleons, momentum-dependent potential for, (T), 20: 13792
interactions with nucleons, eigenvalues of Lippmann-Schwinger kernel for, (T), 20: 13836
interactions with nucleons in nuclei, binding-energy parameters from potentials for realistic two-body, (T), 20: 13840
interactions with nucleons, origin of repulsive core from, (T), 20: 13879
interactions with nucleons, effect of meson-resonance exchange on, 20: 15817
interactions with mesons (K^-) at high energies, resonances in, (E), 20: 15414
interactions with mesons, peripheral model for, (T), 20: 15419
interactions with mesons (K), testing broken M(12) symmetry by vector exchange in, (T), 20: 15421
interactions with photons at low energies, meson (π) production in, (T), 20: 15441
interactions with mesons, renormalization theory for, 20: 15453
interactions with mesons, N/D method for, 20: 15466
interactions with mesons (π), rescattering correction for three-body final-state, (T), 20: 15476
interactions with photons, dispersion sum rules for meson (π) production in, (T), 20: 15503
interactions with mesons (π) at low energies, dispersion theory of, 20: 15522
interactions with mesons, classical limit of cross sections for, (T), 20: 15563
interactions with mesons (π), pseudoscalar and scalar, (T), 20: 15325
interactions with mesons (π), mass and coupling constant for, 20: 15352
interactions with mesons (π), meson (ρ) exchange in, (T), 20: 15364
interactions with mesons (π), review of, 20: 15371
interactions with mesons (π), dispersion relations for low-energy, (T), 20: 15385
interactions with deuteron, amplitude for inelastic, (T), 20: 15386
interactions with neutrinos, lepton production in, (T), 20: 15387
interactions with weak intermediate bosons, (T), 20: 15396
interactions with mesons ($\pi^\pm$) at 1.7 Bev/c, meson (ω) and (ρ^0) production and decay in, (E), 20: 15403
interactions with mesons (π) at 1.68 Bev/c, $Y_0^*(1405)$ and $Y_1^*(1358)$ production in, (E), 20: 15404
interactions with mesons (π), amplitudes for, (T), 20: 15312 (MIT-2096-86)
interactions with hyperons (Λ) in hypernuclei, nuclear contraction effects from, (T), 20: 15826
interactions with mesons (π) and (K), Ü(12) symmetry for, 20: 15390
interactions with meson field, high-energy successive, (T), 20: 17418
interactions with mesons (π) and nucleons, inelastic effects on cross sections for elastic, (T), 20: 17419
interactions with mesons (π) and nucleons, dynamical equations for, 20: 17420
interactions with nucleons, velocity-dependent potential from amplitude of low-energy, (T), 20: 17449
interactions with hyperons in broken SU(3), sum rules for S-state amplitudes for, 20: 17468
interactions with mesons (π), coupling constants for, (T), 20: 17336 (AECD/TP-5)
interactions with nucleons, T-invariance tests in, (T), 20: 17337 (AERE-R-5138)
interactions with neutrons, scattering lengths for, (T), 20: 17350 (N-65-19395)
interactions with mesons (π), inelastic effects on P_{11} phase shift in, (T), 20: 17355
interactions with nucleons in nuclear emulsions, particle-track distributions from, (E), 20: 17357
interactions with mesons (π) at high energies, optical model for backward, (T), 20: 17373
interactions with photons, current algebra for meson (π) production from, (T), 20: 17375
interactions with mesons (π), effect of dipion resonances on amplitude for, (T), 20: 17388
interactions with antiprotons, meson production in annihilation, (T), 20: 17396
interactions with mesons (π), coupled-channel Schroedinger equation model for, 20: 17397
interactions with electrons and mesons (μ), inelastic, (T), 20: 17399
interactions with photons, cross sections for vector meson production

in, (T), 20: 17414
interactions with mesons (π), minimal singularity in axiomatic approach to charge-symmetry, (T), 20: 17416
interactions with charged leptons, tests of C and T invariances in, 20: 17392
interactions with nucleons in nuclei, hard-core potential in boundary-condition model for, (T), 20: 17772
interactions with nucleons in nuclei with N = 29 and 30, properties from effective, (T), 20: 17735
interactions with photons, polarization coefficients for meson (K) and (π) production from, (T), 20: 17407
interactions with photons, meson (π) production in, (T), 20: 19447 (UCRL-14614-T)
interactions with nucleons, review of, 20: 19454 (YALE-1807-33)
interactions with nucleons at 23.1 Mev, phase shift analysis for, (E), 20: 19442 (JINR-E-2609)
interactions with antiprotons in emulsions at 725 Mev/c, particle distributions from, (E), 20: 19465
interactions with mesons (π^-) at 17.2 Bev, mass distributions from, (T), 20: 19472
interactions with nucleons, p-wave analysis of N* and meson (π) production in, 20: 19476
interactions with nucleons, peripheral model for N* production in, 20: 19477
interactions with neutrinos, asymmetries in meson (π) production in, 20: 19478
interactions with mesons (π) at 300 to 700 Mev, absorption parameters and phase shifts for, (T), 20: 19481
interactions with hyperons (Λ), unitary symmetry for structure of weak, 20: 19489
interactions with mesons (π), dynamics with invariant collinear vertices, analyticity, and unitarity for low-energy strong, (T), 20: 19491
interactions with deuterons, asymmetry and multiple scattering in, (T), 20: 19492
interactions with photons, multipoles in meson (π^0) production from, (E/T), 20: 19493
interactions with mesons (ρ^0), total cross section for, 20: 19506
interactions with photons, T-invariance violations in, (T), 20: 19513
interactions with scalar and vector mesons, coupling constants for, (T), 20: 19521
interactions with mesons (π) at low energies, analysis using dispersion relations, (T), 20: 19522
interactions with neutrinos at high energies, semileptonic, (T), 20: 19527
interactions with mesons (π), SU(3) symmetry in bootstrap model for, 20: 19564
interactions with photons, isotopic relations for meson (K) and (π) production amplitudes from, (T), 20: 19518
interactions with antineutrinos, spark chamber experiments on, 20: 21607 (CERN-65-32, pp 161-8)
interactions with nucleons, T-matrix for, (T), 20: 21617 (JINR-P-2546)
interactions with phonons, Schroedinger equation solution for, (T), 20: 21619 (JINR-P-2567)
interactions with nucleons, one-boson exchange model parameters from, (T), 20: 21621 (JINR-P-2584)
interactions with nucleons, bounds for correction to Born term for, 20: 21635
interactions with neutrinos, asymmetries in meson (π) production from, (T), 20: 21638
interactions with mesons (π), absorption model for 2^+-meson production in, 20: 21644
interactions with polarized bremsstrahlung at 475 to 750 Mev, meson (π^+) production from, (E), 20: 21660
interactions with mesons (π), threshold factor in p-wave dispersion relations for, 20: 21667
interactions with mesons (π), p-wave amplitudes for off-shell, 20: 21672
interactions with mesons (K) in 27-fold representation, dynamics of, 20: 21674
interactions with mesons (π^-) at 6.8 Bev, inelastic, (E/T), 20: 21693
interactions with mesons (π), mass splittings from, 20: 21758
interactions with mesons (π), Lie algebra for isobar-coupling, 20: 21759
interactions with photons, analysis of, (T), 20: 21587 (AD-623564)
interactions with neutrinos at high energies, intermediate boson production in, (E), 20: 21595 (CERN-65-32, pp 1-10)
interactions with neutrinos, (T), 20: 21598 (CERN-65-32, pp 79-82)
interactions with nucleons, boundary condition methods for nuclear matter, 20: 22022
interactions with hyperons (Λ), research on, 20: 22033
interactions with electrons at high momentum transfer, (T), 20: 24005 (CERN-65-24(Vol.2), pp 1-17)
interactions with photons at low energies, meson (π) production in, (T), 20: 24007 (CERN-65-24(Vol.2), pp 55-66)
interactions with nucleons in emulsions at high energy, energy spectra of, (T), 20: 24024
interactions with mesons (π), Fourier-Bessel representation for helicity amplitudes of, (T), 20: 24031
interactions with electrons, sum rules from local commutation relations of currents for, 20: 24036
interactions with hyperons (Λ) and (Σ), N/D calculation of polarization and cross sections for, 20: 24038
interactions with photons, time-reversal invariance in meson (π^+) production from, (T), 20: 24039
interactions with mesons (π), electromagnetic correlations to low-energy, (T), 20: 24040
interactions with mesons (π) at high energies, minimum in differential cross sections of, (T), 20: 24048
interactions with photons, quark model for N* production in, (T), 20: 24051
interactions with mesons (π), pole model of resonance production in, (T), 20: 24079
interactions with mesons (π), phase-shift analysis of, (E/T), 20: 24087
interactions with nucleons at 5000 Bev, isobar production in, (T), 20: 24122
interactions with photons, polarization from, (E), 20: 24362(T) (ANL-Trans-294)
interactions with photons, charge-dependent corrections for meson (π) production in, (T), 20: 24034
interactions with nucleons in nuclei, repulsive-core potential for, 20: 24450
interactions with leptons, (E/T), 20: 24260
interactions with mesons (π), dispersion analysis of elastic, (E/T), 20: 25785 (JINR-P-2582)
interactions with nucleons, relativistic reconstruction of scattering matrix for, 20: 25786 (JINR-P-2630)
interactions with mesons (π), high-energy behavior of charge-exchange forward amplitude for, 20: 25825
interactions with mesons (K), nucleon-hyperon (Λ)--meson (K) coupling constants from dispersion relations for, 20: 25827
interactions with nucleons at intermediate energies, electrostatic effects in, 20: 25832
interactions with mesons (π), multiple meson (π) production in, (T), 20: 25839
interactions with mesons (π), parity conservation in, (T), 20: 25841
interactions with nucleons, amplitude for mesons (π) and deuteron production in, 20: 25863
interactions with nucleons at high energies, polarization effects in, 20: 25866
interactions with mesons (π) in SU(4) spin-isospin symmetry, 20: 25876
interactions with mesons (π), semiclassical peripheral model for, 20: 25877
interactions with nucleons, dispersion analysis of elastic, (E/T), 20: 25785 (JINR-P-2582)
interactions with electrons, meson (π) production in, (T), 20: 27940
interactions with electrons, isobar model for meson (π) production in, (T), 20: 27941
interactions with electrons, N* resonance production in, (T), 20: 27947
interactions with mesons (π), sum rules of chiral algebra for $N^*N\pi$ coupling constants in, 20: 27999
interactions with mesons (π), at 1 to 10 Bev, phase-space factors for, 20: 27808
interactions with deuterons at low and medium energies, impulse approximation amplitudes for inelastic, (T), 20: 27810
interactions with hyperons (Λ), charge symmetry breaking and particle mixing in, 20: 27818
interactions with mesons (π), resonant amplitudes from elastic and inelastic, (T), 20: 27821
interactions with nucleons, four-pole boson exchange model for, 20: 27830
interactions with mesons (π), P_{33} amplitude for, (T), 20: 27831
interactions with electrons and photons at 1300 Mev, meson (π) production amplitudes for, (T), 20: 27847
interactions with mesons (K), exact N/D method for phase shifts for, 20: 27855
interactions with photons via spin-J resonance with, isobar model for spin-0 meson production from, (T), 20: 27857
interactions with mesons (π) below 1 Bev, model for single meson (π) production from, 20: 27861
interactions with nucleons, hard core isospin independence in, (T), 20: 27863
interactions with antinucleons, mesons, and nucleons, total cross sections for, (T), 20: 27872
interactions with mesons (K) and (π) and nucleons, differential cross sections and structures of, (T), 20: 27874
interactions with mesons (π) at low energies, dispersion relations for s-wave, (T), 20: 27881
interactions with electrons, matrix elements for, (T), 20: 27890
interactions with nucleons, dispersion relations in nonlinear spinor

theory for, 20: 27892
interactions with mesons (π^-) in oxygen-16, absorption probability for, (T), 20: 28351
interactions with mesons (π), p-wave dispersion relations for, (T), 20: 30073
interactions with mesons (μ), inelastic, (T), 20: 30076
interactions with mesons (π^-) at 3.7 Bev/c, A_1 and A_2 resonance production in, (E), 20: 30078
interactions with protons at 9 Bev, peripheral model for, (E/T), 20: 30080
interactions with mesons (π), N/D calculations of p-wave amplitudes for, (T), 20: 30158
interactions with nucleons at 0 to 300 Mev, pole contributions to, (T), 20: 29985 (CONF-640509(Pt.1), Paper 1)
interactions with mesons (π), amplitudes for, (T), 20: 29986 (CONF-640509(Pt.1), Paper 2)
interactions with mesons (μ), cross sections for, (E/T), 20: 29994
interactions with protons, quark production in, (T), 20: 29999(T)
interactions with antinucleons, quark model for annihilation, 20: 30005
interactions with mesons (π), amplitudes for, 20: 30006
interactions with mesons (K), dispersion relations and symmetry groups for, 20: 30018
interactions with mesons (π^-) at 12 and 18 Bev, meson (ρ^0) and dipion production in, (E), 20: 30025
interactions with mesons (π), zero-effective-range analysis for meson (η^0) production in, 20: 30033
interactions with mesons (π), production and properties of mesons A_1 and A_2 from, (E/T), 20: 30023
interactions with photons, SU(6) symmetry predictions for N* production in, 20: 30043
interactions with nucleons, dispersion theory calculations for, 20: 32008
interactions with mesons (π) and nucleons, inelastic unitarity in eigenstates of total angular momentum for, 20: 32014
interactions with photons, T violation in $N^*_{\frac{1}{2}}$ production in, (T), 20: 32020
interactions with mesons (π), boundary-condition model for P_{33} resonance in, 20: 32023
interactions with mesons ($\bar{K}$) at low energies, N/D method for s-wave, 20: 32024
interactions with photons, mesons (ω) and (ρ) production in, (T), 20: 31984 (IC-66/54)
interactions with mesons (π) at high energies, forward dispersion relations for, 20: 32026
interactions with nucleons, charge-dependent effects in $^1S_0$ scattering lengths for, 20: 32030
interactions with mesons (π), asymptotic behavior of amplitudes for elastic, (T), 20: 32032
interactions with photons, asymptotic behavior of amplitudes for elastic, (T), 20: 32032
interactions with leptons, C-violating effects in electromagnetic inelastic, 20: 32042
interactions with photons, high-energy theory for Compton, 20: 32054
interactions with electrons, (ω-ϕ) mixing angle from elastic, (E/T), 20: 32058
interactions with nucleons, meson (π) correlation effects in two meson (π)-exchange contribution for, (T), 20: 32073
interactions with neutrinos, baryon resonance production in, 20: 32080
interactions with mesons (π), amplitudes for $N^*_{\frac{1}{2}}$ and $N^*_{\frac{3}{2}}$ production in, (T), 20: 32091
interactions with mesons (π), Mandelstam representation and elastic unitarity for amplitudes of, 20: 32095
interactions with antineutrinos, amplitudes and selection rules for inelastic, (T), 20: 32090
interactions with neutrinos at high energies, inelastic, 20: 34146 (CU-1932-256)
interactions with mesons (π) at high energies, ρ Regge residues in charge exchange, 20: 34154(R) (UCR-34P107-33)
interactions with mesons (π) at high energies, I = 0 D-wave $\pi\pi$ resonance in, 20: 34154(R) (UCR-34P107-33)
interactions with nucleons, charge dependence and symmetry properties of, 20: 34527 (RLO-1388B-6)
interactions with electrons and positrons, deviations from electrodynamics in, 20: 34257
interactions with mesons(η), (T), 20: 34221
interactions with photons, meson(η) production in, (T), 20: 34221
interactions with nucleons at 0.8 to 1.4 Bev, moduli of elastic amplitudes and partial-wave absorption in, 20: 34151 (ISS-66/15)
interactions with neutrinos, W meson production in, 20: 34157 (UJV-1576)
interactions with neutrons, analysis of, 20: 34179
interactions with mesons(K), effective-range parameters for, 20: 34199
interactions with nucleons in U(3) × U(3) symmetry, mass-splitting effects on, (T), 20: 34223
interactions with mesons(π), effects of ABC exchange on, (T), 20: 34225
interactions with electrons and photons, meson(π) production in, (T), 20: 34250
interactions with mesons(π) and nucleons, cross sections for quark production in, (T), 20: 34193
interactions with nucleons, multiple meson(π) production in, (T), 20: 34183
interactions with nucleons at 0.8 to 1.4 Bev, meson(π) production in, 20: 34151 (ISS-66/15)
interactions with photons, production of mesons and π-N resonances in, (T), 20: 36025 (DESY-66/9)
interactions with nucleons at 400 Mev, phase shift analysis of, (T), 20: 36033 (JINR-E-2743)
interactions with nucleons in nuclei, research using nucleon inelastic scattering, (T), 20: 38120
interactions with mesons (π), Regge-pole model for charge-exchange, 20: 37761
interactions with nucleons, SU(12)$_L$ predictions for amplitudes of, (E/T), 20: 37772
interactions with nucleons, zero-energy solution with tensor forces for, 20: 37782
interactions with complex nuclei at high energies, model for, 20: 37790
interactions with mesons (π), C, P, and T invariances in bootstrap mechanism for, 20: 37794
interactions with mesons (π), electromagnetic form factors from, (T), 20: 37801
interactions with mesons (π) at 500 to 600 Mev, amplitudes for, 20: 37803
interactions with photons at high energies, meson (ω) production in, (T), 20: 37807
interactions with mesons (π), Regge dynamics in, (T), 20: 37809
interactions with nucleons, isobaric spin dependence of, 20: 37811
interactions with mesons (π), Regge recurrence parity assignments in, (T), 20: 39749 (COO-881-77)
interactions with mesons (π^-) at 7 Bev, momentum spectra of secondary particles from, (E/T), 20: 39751 (JINR-E-2738)
interactions with nucleons at 14.5 Mev, phase-shift analysis of, 20: 39756 (JINR-P-2742)
interactions with mesons (K), K* production threshold from, (T), 20: 39778
interactions with nucleons in double-peripheral model, cross section for W-meson production in, (T), 20: 39797
interactions with mesons (π), crossing in backward cone and threshold regions in, 20: 39798
interactions with nucleons, analyticity of partial-wave amplitudes for, 20: 39799
interactions with mesons (π), graphical method for charge independence in strong, 20: 39800
interactions with mesons (π), analysis for Λ-K^0 production, (E/T), 20: 39803
interactions with nucleons, Regge-pole model for cross-channel amplitudes of, (E/T), 20: 39806
interactions with photons, reciprocity relation as test of C and T invariance in, 20: 39810
interactions with mesons (π), sum rule for axial-vector coupling-constant renormalization in, 20: 39814
interactions with mesons (π) at 290 to 905 Mev, cross sections for $N^*_{\frac{3}{2}}$ production in, (E/T), 20: 39827
interactions with mesons (π), model for, 20: 39839
interactions with mesons (K), (T), 20: 39840
interactions with antinucleons, deuteron exchange effect in, (T), 20: 39841
interactions with nucleons, cross sections and polarization parameters for, (E/T), 20: 39844
interactions with nucleons, effects of NN* channel on elastic, (T), 20: 39848
interactions with polarized protons at 23.1 to 630 Mev, polarization tensor, 20: 39909
interactions with mesons (π), effect of $\pi\pi$-scattering annihilation channels on, 20: 39776(T)
interactions with nucleons in nuclei, (T), 20: 40115
interactions with nucleons in M(12) symmetry, SU(3) symmetry breaking effects in, 20: 41973
interactions with mesons (π) at 300 Mev, phase shift analysis of, (E), 20: 41794 (JINR-E-2860)
interactions with photons, SU(6) symmetry for meson production in, (T), 20: 41812
interactions with mesons (π) in nuclei at low energies, (T), 20: 42312
interactions with mesons (π), modified one-nucleon exchange model for, 20: 41815

interactions with mesons (π), Schroedinger theory for static, 20: 41418
interactions with photons, two-meson (π) exchange in, (T), 20: 41821
interactions with mesons (π^-) at 12 and 18 Bev/c, recoil states from inelastic meson (ρ^0) production in, (E), 20: 41828
interactions with protons at 20 Bev/c, multiple meson production, (E/T), 20: 41829
interactions with mesons (K) and (π), scattering lengths for, (T), 20: 41846
interactions with mesons (π), consistency condition on strong, 20: 41861
interactions with mesons (π) at low energies, modified effective-range approximation for, 20: 41864
interactions with mesons (π), meson (η) production and interaction from, (T), 20: 41866
interactions with mesons (η) from meson (π)-nucleon interactions, (T), 20: 41866
interactions with photons, vector dominance approximation for meson production in, 20: 41869
interactions with nucleons, two-pion-exchange effects in, (T), 20: 41873
interactions with mesons (π), consistency of nucleon-nucleon interactions with, (T), 20: 41873
interactions with mesons (π), quark model for $N\frac{3}{2}_3 N\pi$ vertex in, 20: 41876
interactions with mesons (π), meson (π)-nucleon and meson (ρ) coupling constants from scattering lengths in, (T), 20: 41885
interactions with antinucleons, intermediate boson production in annihilation, (T), 20: 41892
interactions with hyperons (Λ), repulsive core in S state in, (T), 20: 41894
interactions with massless vector photons, large t limit for sixth-order diagrams for Compton, 20: 41897
interactions with mesons (K), cross sections for, (T), 20: 41898
interactions with nucleons, one-boson exchange potentials for, (T), 20: 41899
interactions with mesons (π) and photons, theory of three particle production in, 20: 41900
interactions with photons, isospin amplitudes for S-state meson (π^0) production in, 20: 41906
interactions with mesons (π^-), cross section lower limit for, (E), 20: 41910
interactions with mesons (π), phase shift analyses for, 20: 41913
interactions with nucleons in light nuclei, (T), 20: 44652 (ORNL-P-2468)
interactions with phonons in nuclei, (T), 20: 44638 (JINR-P-2772)
interactions with phonons in nuclei, (T), 20: 44678
interactions with nucleons, effects of strong correlations on weak, (T), 20: 44760
interactions with electrons, particle production from inelastic, (T), 20: 44180
interactions with mesons (π), P-wave resonances in Chew-Low model for, 20: 44186
interactions with nucleons, phase-shift analysis of, (E/T), 20: 44191(T)
interactions with mesons (π) at high energies, polarization in charge-exchange, (T), 20: 44201
interactions with neutrino at 1 Bev, particle production cross sections, 16: 27965
interactions with nucleons to 10 Bev, 16: 33752
interactions with nucleons, S-matrix theory for nonrelativistic, 20: 44209
interactions with photons near threshold, meson production in, (T), 20: 44211
interactions with nucleons, ρ' trajectory contribution to charge-exchange, 20: 44222
interactions with photons, quark model for baryon resonance and meson production from, 20: 44239
interactions with nucleons at low energies, two-meson (π) exchange potential in, (T), 20: 44271
interactions with deuterons, differential cross sections for inelastic, (T), 20: 44275
interactions with neutrinos (ν_μ), polarized N* production from, (T), 20: 44276
interactions with protons in emulsions at 24 Bev in strong, pulsed magnetic field, 20: 44280
interactions with mesons (π), general solution of Chew-Low equations for partial waves in, 20: 44281
interactions with mesons (π) at high energies, backward and forward peaks for elastic, (T), 20: 44267
interactions with neutrinos, differential cross sections for lepton polarization and N* production in, (T), 20: 46334 (IS-T-96)
interactions with antineutrinos, differential cross sections for lepton polarization and N* production in, (T), 20: 46334 (IS-T-96)
interactions with nucleons in nuclei, long range multipole forces in, 20: 46340 (PUC-937-224)
interactions with antinucleons and nucleons, on-shell and off-shell methods for T-matrix for, 20: 46392 (UCSD-10P10-9)
interactions with hyperons (Λ) in hypernuclei, (T), 20: 46689
interactions with mesons (π^-) crossing symmetry and spin states for, (T), 20: 46378
interactions with neutrinos, collinear meson production in SU(6) from, (T), 20: 46383
interactions with mesons (π), reconstruction of reaction amplitude for vector production from, 20: 46384
interactions with mesons, scattering matrix for, 20: 46386
interactions with mesons (π), vertex function and Mandelstam representation for, 20: 46354
interactions with mesons (π), P_{11} phase shifts for, 20: 46355
interactions with, deuteron pole in amplitude for, (T), 19: 37570
interactions, variant theory of higher symmetry for strong, 16: 2458
isobar relative energies and widths, low-lying, 16: 9405
isospin pairing correlations in light nuclei, (T), 19: 43349
isospin space for fields of, 20: 13611
isospin-$\frac{1}{2}$ and -$\frac{1}{2}$ states of, detection of, 16: 33761
isospins and seniorities for three, in $j = \frac{7}{2}$ shell, 18: 36580 (UCRL-7506)
lepton capture, μ–e^- symmetry in, 16: 28126
level density in p-shell, calculation of, 17: 17070
lifetime of bound, lower limits for, (E), 20: 4853
lifetime of solar, 19: 37452
magnetic moment corrections by central and tensor forces, mathematical analysis, 16: 18318 (AFOSR-1568)
magnetic moment in global symmetry model, anomalous, 16: 29693
magnetic moment of bound, sum rule for, 19: 29246 (JINR-P-2019)
magnetic moment of, sum rule for isovector, (T), 20: 9811
magnetic moment of, dispersion-theoretical calculation of, 20: 17390
magnetic moment of, anomalous, (T), 20: 19525
magnetic moment operator in SU(6) for, covariant, 20: 32053
magnetic moment ratio of, (T), 20: 6074
magnetic moments, (T), 20: 25817
magnetic moments from strange-particle interactions at high energies, 16: 24739
magnetic moments in SU(4) supermultiplet model, 19: 25344
magnetic moments of, meson (η), (ω), and (ρ) effects on, 16: 26164
magnetic moments of, self-consistent calculation of isovector part of, 20: 2704
magnetic moments of, sum rule for, (T), 20: 27866
magnetic moments of, sum rules for photoproduction amplitude correlations with, 20: 39879
magnetic properties of, models for, 17: 11558
magnetic properties in nuclei, method for studying, 19: 19113
many-body problem in quantum mechanics, Coriolis coupling in, (E), 19: 39948
mass approximation of hyperon (Ξ) mass in antihyperon (Λ) decay, 16: 4718
mass difference (N–N*), Bethe-Salpeter equation in static bootstrap model for, (T), 19: 43149
mass difference estimate, form factors for, 16: 10860
mass difference of, model for electromagnetic, 20: 32057
mass differences and isobar states, 16: 4712
mass formulas in SU(6) symmetry scheme, 18: 42450
mass, Nambu model treatment, 16: 2459
mass of N*, 17: 19071
mass of, self-consistent calculation of, 18: 912
mass of, calculation in unified nonlinear theory, (T), 19: 5001
mass ratio to mesons (π), calculation from dispersion relations, 18: 2623
mass spectra in quantum field theory, 17: 15131
mass splitting of, electromagnetic, (T), 20: 34210
mass systematics of, equations for, 16: 32336
matrix elements in shell model calculations on, particle number dependence of, (T), 19: 16921
mesic form factor of, 17: 7505
meson (K^-) capture, 16: 10906
meson (μ) capture by, pseudoscalar coupling magnitude in, 18: 34551
meson (μ) capture by, scalar coupling constant in, (T), 19: 8084
meson (μ) capture by, form factors in, (T), 19: 12316
meson (π^-) absorption by pairs of, in heavy nuclei, (T), 19: 33260
meson (π^-) capture by, in propane, 18: 24475
meson (π) emission by, in nuclear reactions, (T), 19: 16489
meson (π) distributions in, 18: 9146
meson (π) forward scattering, dispersion relations, 16: 16991 (NP-11592(Vol.I)(p.485-6))
meson (π) photoproduction on, amplitudes, 16: 5905
meson (π) photoproduction on, transition amplitudes, 16: 5915
meson (π) photoproduction on, partial wave dispersion relations for, 17: 20948
meson spectrum in fast, peripheral, 16: 17016
model for baryon-isobar excited states, 17: 11557
model for systems of identical, shell, (T), 20: 24386
model for, bootstrap with N*(1238) in self-consistent, 20: 19457
model for, reformulation for meson-atomic, 20: 17356

model of, deuteron magnetic moment from, (T), 19: 45049
moments of, sum rules for, 20: 40130
momentum components of nuclear, high, 17: 22602
momentum distribution in carbon-12, 17: 11695
momentum in nuclei, effects of optical potential on, 17: 830
motion in deformed light nuclei, 16: 12463
motion in nonaxial oscillator potential, 18: 21307
motion in nonaxial oscillator potential, nuclear equilibrium form in, 18: 30832
motion in nuclear matter, (T), 19: 14545
motion in nuclear potential well, bound states for, 20: 8141
motion in strongly deformed nuclei, 16: 23151
motion of many-body systems of, symmetric group theory for, 18: 12919
motions in nuclear matter, solution of Bethe-Goldstone equation for, 17: 26746
multiple pair formation and supernovae explosions, 16: 22827
neutrino absorption by (E/T), 19: 2941
number conservation in quantum field theory, 17: 5270
orbital fractional parentage coefficients in 2s-1d shell, SU(3), 19: 45266 (JINR-E-2285)
pair annihilation into mesons, scattering amplitude relations for, 17: 19526
pair correlations in light nuclei, nuclear model for small-range, 17: 41987
pair production in meson (π) reactions with nuclei, 16: 26089 (NP-11832)
pair production in annihilation of polarized electrons and positrons, (T), 19: 43067
pair production in photon-photon interactions, (T), 20: 37758
pair transfer between nucleus and light nuclide, correlations in, (E/T), 19: 21266(R) (UCRL-11828(p.108-9))
pair-correlation functions from electron inelastic scattering by nuclei, 18: 21356
pair-correlation functions in nuclei, (T), 19: 31314
pairing and quadrupole-quadrupole interactions in nuclei, shell model for, 16: 21507
pairing correlations in nuclei, charge-independent, 18: 18972
pairing correlations in deformed nuclei, 18: 24692
pairing correlations in excited nuclei, 18: 34930
pairing correlations in heavy nuclei, (T), 19: 23671
pairing correlations in nuclei, effects of nuclear rotation on, (T), 19: 39858
pairing correlations in nuclei, method for studying, 20: 8160
pairing correlations in nuclei, formalism for, (T), 20: 10027
pairing correlations in light nuclei, four-body, (T), 20: 12013
pairing correlations in L = 0 states, (T), 20: 12131
pairing correlations in odd-mass, effects of rotational motion on, 20: 22148
pairing correlations in nuclei, generalized Bogoliubov transformation for, 20: 24426
pairing correlations in spherical even nuclei, 20: 38177
pairing effects on fission of even-even compound nuclei near threshold, (T), 20: 17847
pairing energies for residual interactions in shell models, 17: 24504
pairing energies in shell models, 16: 3700
pairing energies in superfluid model of nuclei, 18: 9371
pairing forces in the shell model, 16: 23078
pairing forces in strongly deformed nuclei, effects on intrinsic excitation in, (T), 19: 8484
pairing forces in nuclei, (T), 20: 3066
pairing forces in light nuclei, residual, 17: 17275
pairing forces near closed shells, non-canonical transformation for calculation, 16: 21509
pairing in even lead isotopes, 17: 29616
pairing in finite nuclei, variational derivation of equation for, (T), 20: 15742
pairing in nuclei, optical model potential and, 17: 13517
pairing in nuclei, Lipkin's treatment of forces in, 17: 36713
pairing in nuclei, symmetry properties of hamiltonian for, 18: 34890
pairing in nuclei, method for calculating, 18: 44783
pairing in nuclei, theory for, 18: 44785
pairing in nuclei, effect on two-particle penetration through centrifugal barrier, 19: 33376
pairing in nuclei, R(5) and R(8) groups in quasi-spin formalism for, 19: 41839
pairing in nuclei, quasi-particle triples as exact solution of Lee model for, 20: 46396
pairing in spherical nuclei, (T), 20: 30491
pairing interaction in nuclei, (T), 19: 6657
pairing interactions in nuclei, effects on level densities, (T), 19: 47616
pairing interactions in nuclei, Bogolyubov compensation method and variational principle for, (T), 20: 6343
pairing interactions in nuclei, stability of solutions of Hartree-Bogolyubov equations for charge-independent pairing, 20: 10026
pairing interactions in nuclei, (T), 20: 12049
pairing interactions in nuclei, approximation for, (T), 20: 17765
pairing interactions in nuclei, eigenstates for J = 0, T = 1, charge-independent, 20: 22121
pairing interactions in nuclei, number-conserving approximations for, 20: 32494
pairing interaction in nuclei, superconductivity approximation for, 20: 32397
pairing interactions in translationally invariant shell model, group-theoretical treatment of, 20: 44699
pairing relations for, effects of superconducting, 17: 17307
pairing-force Hamiltonian for, exact eigenstates of, 19: 35414
parities (relative), 16: 10844
parity and spin of, 17: 32941
parity nonconservation by potential between, spatial, 18: 40559
parity of ($K\Lambda N$) and ($K\Sigma N$), 17: 9467
particle scattering by, in nuclei, (T), 20: 12100
photon reactions with, meson (π) production amplitudes for, (T), 20: 41996
photoproduction of Z^- resonance, unitary symmetry in, 18: 2627
photoproduction on nuclei, unified theory for, 18: 21364
photoproduction on nuclei, effect of velocity-dependent forces on cross sections for, 18: 42740
photoproduction on strongly deformed nuclei, (T), 20: 8173
photoproduction on deformed nuclei, polarization from, (T), 20: 8111
photoproduction on nuclei, polarization effects in, (T), 20: 38175
photoproduction sum rules, (T), 20: 25817
plasma of antinucleons and, production in supernova, 18: 4661(T)
polarizabilities of, experimental and theoretical data on electric and magnetic, 16: 33721
polarizability of, 17: 7025
polarizability of, electromagnetic, 18: 37971
polarizability of, from Compton effect, (T), 19: 10060
polarization, 17: 36413 (NP-13020(p.201-13))
polarization, based on gamma scattering amplitude, 16: 24782 (JINR-P-967)
polarization, electric and magnetic, 16: 5860 (JINR-P-771)
polarization from knock-out reactions, 17: 31395 (CONF-46-23)
polarization from deuteron spallation in nuclear electromagnetic fields, (T), 20: 26201
polarization from nuclear reactions, symmetry defects in measurement of, 20: 28321
polarization in back scattering from photoproduction of mesons (π) on hydrogen, 16: 32275 (NP-12034)
polarization in direct nuclear reactions, 19: 5149
polarization in gamma reactions (γ,N$\pi^{\pm}$) with nuclei, 18: 19009
polarization of, 18: 11294
polarization, problems, 16: 2415
potential between two fixed, 16: 10976
potential between two, Low equation for, 17: 26511
potential calculations for, optical model, 20: 11570(T) (ANL-Trans-258)
potential in nuclei, reaction matrix theory for, 17: 7211
potential in nuclei, nonlocal single-particle, 20: 6430
potential of, due to mesons (K) in nonlocal interaction theory, 17: 20862
potential of two, conditions for representation of, 17: 24757
potential of two, sensitivity of nuclear matter binding energy to, (T), 19: 10365
potentials for singlet-even states, velocity-dependent, 19: 41841
potentials for, description of high-energy, (T), 19: 14325 (UCRL-1011)
potentials in nuclei, charge-exchange effects on, 17: 2278
potentials, theoretical analysis, 16: 7235
production by elementary particle processes in special relativity, 19: 44895
production by gamma reactions on odd nuclei, polarization in, 16: 33864
production by proton reactions with aluminum, beryllium, and iron at 30 Bev, 17: 7259
production by 24-Bev proton beam incident on heavy concrete, 17: 11489 (ORNL-3367)
production in meson (π) reactions with beryllium-9, cross sections for, 18: 24587 (JINR-P-1584)
production in meson (K^+)-proton interactions at 1.3 and 5 Bev, (T), 19: 4907
production in meson (π^+)-proton interactions at 2 Bev/c, (E), 20: 11672
production in nuclear reactions, model for multiple, 16: 33736
production in nucleon reactions with nuclei at high energies, cross sections for, 20: 3259
production in photon interactions, 16: 27948
production in proton-meson (π) interactions at 910 Mev, resonance, 16: 12378
production in steady-state universe, selection rules for, 17: 41783
production of ($\bar{K}2\pi N$), 18: 30589
production of antinucleons and, by photons, dispersion relations in, 16: 29677
production of $\bar{N}^*_{3/2}$ in antiproton–proton interactions at 3.25 and 3.69 Bev/c,

18: 14947
production of clusters in gamma reactions (γ,pt) with carbon-12, 16: 3704
production of isobaric, effects on (π-π) scattering in (π⁻-p) interactions, 17: 24353
production of N* in meson (K_2^0)-proton interactions at 2 Bev/c, 18: 14948
production of N*⁺⁺ in meson (π⁻)-proton interactions at 4 Bev/c, cross sections for, 18: 16774
production of N* in meson (π⁻)-proton interactions at 7 to 8 Bev, 18: 18734
production of N* in neutrino interactions, SU(6) symmetry for, (T), 19: 18832
production of N*, in cosmic nucleon reactions with nuclei, 18: 44820
production of N*, in proton-proton interactions at 7.1 Bev/c, (E), 19: 16526
production of nucleon–meson cascade by 200-Bev proton reactions with iron, (T), 19: 41955 (ORNL-TM-1121)
production of nucleon-pion, showers in iron by 1- and 3-Bev protons, (T), 20: 5927 (ORNL-P-1733)
production of N_{33}^* (1238) in meson (K^+)-proton interactions at 1.96 Bev/c, 17: 41745 (UCRL-10954)
production of N_{33}^*, in meson (K^+)–proton interactions at 1.14 Bev/c, 18: 6033
production of pairs by photons, open cosmological model for multiple, 16: 26097
production of resonance states in meson (K^+)-proton interactions at 1.96 Bev/c, meson (π) exchange in, 17: 39895
properties, 17: 28160 (UCRL-10842)
properties in nuclear matter, 16: 15374
properties of G_n multiplets for, decay and electromagnetic, 18: 7537
properties of isobaric, 16: 16998 (NP-11592(Vol.II)(p.57-85))
properties of systems of nonidentical, quasi-spin formalism for quantum, 18: 40411
properties of, covariant analysis of quark commutators and electromagnetic couplings for, 20: 46358
properties of, model for, 19: 16645
properties of, symmetrization postulate for, 18: 40317
properties of, theory of, 18: 11137 (ANL-6797(p.2-14))
reactions (N,d) and (N,N') with nuclei, amplitudes for, (T), 19: 5211
reactions (N,2N) with nuclei above 100 Mev, review of mechanisms of, 19: 19103
reactions in accelerator shielding, meson showers from, 17: 19418 (ORNL-3412)
reactions on carbon near 1 Tev, inelastic, 17: 19373
reactions on heavy emulsion nuclei above 100 Bev, mesons for, 16: 32314
reactions on nuclei, models for inelastic, 17: 33064
reactions with accelerator shielding, meson cascades from, (T), 20: 24576 (ORNL-TM-951)
reactions with aluminum at 30 to 400 Mev, Monte Carlo cascade calculations for, (T), 20: 8274 (LNF-65/30)
reactions with carbon-12 at 185 Mev, distortion effects in 15.1-Mev level excitation in inelastic, 17: 26428(R) (ORNL-3425(p.1-2))
reactions with carbon-13, fluorine-19, and tin-118, optical-model wave functions for, (T), 20: 13817
reactions with carbon and lead, cascade showers from, (T), 20: 44152
reactions with complex nuclei, computer program for calculation of, 17: 12782(R) (ORNL-3360(p.137-81))
reactions with complex nuclei, angular distributions and spectra from, 17: 18376 (TID-7652(p.409-32))
reactions with complex nuclei, data survey for nonelastic, 17: 34883 (ORNL-3455)
reactions with complex nuclei, gamma production cross sections for, 17: 41873 (WASH-1044)
reactions with complex nuclei at 25 to 400 Mev, cascade and evaporation, 18: 7689(R) (ORNL-3499(Vol.II)(p.31-53))
reactions with complex nuclei, literature survey on, 18: 7690(R) (ORNL-3499(Vol.II)(p.54-6))
reactions with complex nuclei at 1 to 50 Mev, nuclear structure studies from, 18: 19107
reactions with complex nuclei, cross sections and energy conservation for, 18: 34952
reactions with deuterium, helium, and hydrogen, antinucleon production in, 16: 23050
reactions with even nuclei, tables of cross-section functions for double Coulomb excitation in, 17: 792 (AWRE-NR/P-2/62)
reactions with heavy nuclei in photographic emulsions at high energies, angular distribution of jets from, 17: 9522
reactions with helium-4, spin coupling analysis for, (T), 20: 11978 (UCRL-7961-T)
reactions with hypernuclei of A ≥ 3, two meson (π)-exchange contribution to three-body, 18: 2648
reactions with iron nuclei, secondary particles from, 18: 40617
reactions with light nuclei, optical potential calculation for, 17: 7188
reactions with nuclei for A ≤ 4, analysis, 16: 6029
reactions with nuclei at 100 Bev, data analysis, 16: 10994
reactions with nuclei, potential calculation, 16: 10832
reactions with nuclei to 16 Mev, cross sections and energy spectra for, 16: 12505
reactions with nuclei, optical potential calculations, 16: 13964 (PAN-258/VII)
reactions with nuclei, optical potential calculations, 16: 13965 (PAN-281/VII)
reactions with nuclei at intermediate energies, model for, 16: 17131
reactions with nuclei, determination of nuclear structure from, 16: 21464
reactions with nuclei, distinguishability in, 16: 21623
reactions with nuclei in photographic emulsions at 10^{12} ev, 16: 24662 (PAN-291/VI)
reactions with nuclear collective excitation, 17: 7193
reactions with nuclei, momentum transfer to mesons (π) in, 17: 13336
reactions with nuclei, intranuclear cascades from, 17: 22564 (ORNL-3383)
reactions with nuclei, mechanisms of compound-nucleus and direct, 17: 38205
reactions with nuclei, transverse momentum distributions in, 17: 41820
reactions with nuclei at high energies, "shock-wave" fragmentation mechanism during, 18: 28621
reactions with nuclei at 100 to 1000 Bev, mechanisms of, 18: 34764 (JINR-P-1678)
reactions with nuclei above 10^{13} ev, heavy-particle production in, 18: 40524
reactions with nuclei, multiple particle production in, 19: 1652
reactions with nuclei at high energy, helium-3 and triton emission in, (E/T), 19: 8435
reactions with nuclei at 2 to 10 Bev, calculation of, 19: 17159(R) (ORNL-3714(Vol.II)(p.97-118))
reactions with nuclei, neutrino momentum distribution in, (T), 19: 19131
reactions with nuclei at high energy, neutrino production in, (T), 19: 19132
reactions with nuclei, optical model potentials for, (T), 19: 23712
reactions with nuclei at high energies, charge exchange in, (E), 19: 27433 (JINR-P-2060)
reactions with nuclei at 10^{11} to 10^{12} ev, (T), 19: 27460
reactions with nuclei, optical model parameters for, (T), 19: 27503
reactions with nuclei at very high energies, 19: 27182
reactions with nuclei at high energies, analysis of jets from, (T), 19: 41709
reactions with nuclei, gamma spectra calculations for inelastic, 19: 41954 (NP-15338)
reactions with nuclei, (T), 19: 43374
reactions with nuclei, spin-spin interaction in low-energy optical potential for, (T), 20: 6395
reactions with nuclei at 2 to 10 Bev, meson (π)-nucleon cascades from, 20: 8079 (ORNL-3855)
reactions with nuclei at 0.1 to 25 Mev, data tabulations on polarization in, 20: 11965 (JINR-P-2426)
reactions with nuclei at high energies, mechanisms of, 20: 12111
reactions with nuclei, DWBA for two-body stripping, (T), 20: 13814
reactions with nuclei, core polarization effects in, (T), 20: 15852
reactions with nuclei, SU(3) symmetry for meson (η^0) multiple production in, 20: 24380(T)
reactions with nuclei in cosmic showers, upper limit for passive-state, (T), 20: 25755(T)
reactions with nuclei at high energies, in cosmic showers, (T), 20: 25806(T)
reactions with nuclei, heavy particle stripping in, (T), 20: 32444
reactions with nuclei, isobaric analog resonances in, (T), 20: 36198
reactions with nuclei above 10 Bev, internuclear cascade model for inelastic, 20: 38122
reactions with nuclei, approximate relations for strengths and shapes of optical potentials for, 20: 42280
reactions with nuclei, coefficient of inelasticity for, 16: 31114
reactions with nuclei, composite particle production in, 19: 36220(R) (MIT-2098-142)
reactions with nuclei to 10 BeV, 16: 33752
reactions with spherical spin-zero nuclei at 40–180 Mev, comparison of exact solution and semi-classical approximation for, 17: 31421
reactions with targets, neutrino momentum distribution in, (T), 19: 25488
reactions with targets, neutrino momentum and space distributions in, (T), 19: 25489
reciprocity between, and (3,3) resonances, 17: 4007
research on, review of, 18: 28336
resonance (N* and Y*) production model, 18: 24456
resonance (N-π) production in proton-proton inelastic scattering at 3.6 to 11.8 Bev/c, 18: 12933
resonance (πN) at 1350 Mev, possible existence of J = ¾, 18: 24453

resonance (π^+p) at 1922 Mev, production in proton-proton peripheral collisions, 18: 20927
resonance (π-N) at 1400 Mev, evidence for existence of, 18: 12934
resonance ($\frac{3}{2}$,$\frac{3}{2}$) anti-isobar production in antiproton-neutron interactions at 1.96 Bev/c, 18: 44510 (BNL-8268)
resonance in baryon system with strangeness −3, production of, 18: 4452
resonance models and symmetries of, octet and Sakata, 18: 20994
resonance (N*) production in meson (K^+)–proton interactions at 1.96 Bev/c, 18: 5995 (UCRL-11068)
resonance N_{33} in meson (π)-nucleon scattering, theoretical interpretation of, 18: 9193
resonance pole at 1238 Mev, splitting of SU(3) multiplets in channel decay of, 18: 12935
resonance production of N^*_{33}, by proton interactions with electrons and mesons (K^+), 17: 41785
resonance states of, classification of, 17: 39938
resonance states of, G_3 and SU_3 symmetry for, 18: 900
resonance states of, properties of N***, 18: 2677
resonance states of, classification of N* in hypercharge space, 18: 6011
resonance states of, decay and electromagnetic properties of G_3 multiplets for N*, 18: 7537
resonance states of, mass formula for, 18: 9147
resonance states of, theories for production of, 18: 9197
resonance states of, bilocal field theory of, 18: 14834
resonance states of, SU(3) symmetry for $N^*_{3/2}$, 18: 36328
resonance states of, sum rules for decay of N*, 18: 36333
resonance states of, mass difference (N**-N***) in SU3, 18: 40253 11543(Rev.))
resonance states of, mass equations for, 18: 40279
resonance states of, production in cosmic nucleon interactions in emulsions, 18: 42402
resonances ($N^*_{3/2}$), baryon-boson levels in, 18: 22771
resonances and threshold mass numerologies in, 16: 17028
resonances as unitary multiplets, 16: 17029
resonances in baryon system with strangeness of S = 1, 17: 9282
resonances of, review of properties of, 18: 18676
resonant state formation and decay, angular correlations in, 17: 41791
scattering amplitudes, integral representation for, 16: 12376
scattering amplitudes for, integral representation of, 17: 2166 (JINR-P-1060)
scattering amplitude of nucleon interactions, analysis of coupling constant and spectral functions in, 17: 11472 (JINR-P-1046)
scattering, angular distributions in, 17: 36347(R) (NARF-62-18P)
scattering by aluminum-27 and silicon-28, core excitation model for inelastic, (E/T), 19: 37854
scattering by beryllium and carbon at 140 Mev, parametrization analysis for elastic, (T), 20: 17740
scattering by carbon-12 at 120 to 150 Mev, coupling scheme variation with radius in light nuclei, 18: 4604
scattering by carbon-12 at 20 Mev, optical potential for, (T), 20: 12047
scattering by carbon-12 at 185 Mev, inelastic, (T), 20: 38120
scattering by complex nuclei below 50 Mev, data survey for elastic polarized, 20: 3014 (LA-DC-7386)
scattering by complex nuclei, off-shell amplitudes for, (T), 20: 28374
scattering by deformed nuclei, inelastic, 18: 34865
scattering by even-even nuclei via compound nucleus mechanism, review of gamma angular distributions from inelastic, 20: 38178
scattering by heavy nuclei at high energies, differential cross sections for, 16: 12506
scattering by helium-4 at 0–40 Mev, nuclear forces from elastic, 18: 7779
scattering by light nuclei, amplitudes, 16: 5870
scattering by light nuclei at high energies, cross sections for, 17: 15280
scattering by light nuclei at 180 Mev, (T), 19: 31256
scattering by lithium-6 at high energy, exact distorted wave calculations for inelastic, 17: 24479
scattering by magnesium isotopes, models for inelastic, 18: 2403(R) (PR-P-58)
scattering by nitrogen-14, differential cross section and polarization for, (T), 20: 3091
scattering by nuclei at high energies, gamma production in elastic, 16: 3712
scattering by nuclei, polarization effects in indirect, 16: 4801
scattering by nuclei, operator impulse approximation, 16: 8234
scattering by nuclei at ~300 Mev, angular distributions for quasi-elastic, 16: 9371
scattering by nuclei at 147 to 220 Mev, differential cross sections and polarizations in elastic, 16: 13996
scattering by nuclei at high energies, Regge poles, 16: 15696
scattering by nuclei at high energies, Pauli exclusion effects in, 16: 17121
scattering by nuclei, cross section relation to channel coupling, 16: 17101
scattering by nuclei, cross section relation to optical potential imaginary component, 16: 17104
scattering by nucleons, effects of meson (π) exchange, 16: 18319 (AFOSR-2117)
scattering by nucleons at high energies and small angles, theory, 16: 21125(R) (ANL-6517)
scattering by nuclei, radial dependence of optical potential for, 16: 21477
scattering by nuclei, optical potential radial dependence in, 16: 21364
scattering by nuclei at 3 to 25 Bev, model for, 16: 21391
scattering by nucleons, theory of non-local effects, 16: 24794(R) (TID-15211)
scattering by nuclei, optical potential for, 16: 28040
scattering by nuclei, second-order optical potential for, 16: 28093
scattering by nuclei, corrections to the optical potential for, 16: 28104
scattering by nuclear density fluctuations, in optical model, 16: 29874
scattering by nuclei, low-energy photons from elastic, 16: 31095
scattering by nuclei, one-pion-exchange effects on, 17: 2280
scattering by nuclei, radial variation of the absorbing part of the nuclear optical potential in, 17: 5398
scattering by nuclei, amplitudes in, 17: 7080 (JINR-P-1024)
scattering by nuclei, Regge pole application to, 17: 9414
scattering by nuclei, amplitudes in inelastic, 17: 11731
scattering by nuclei, surface corrections to the high-energy optical potential for, 17: 13434
scattering by nuclei, mechanism for resonances in elastic, 17: 26608
scattering by nuclei at high energies, test of impulse approximation for inelastic, 17: 28300
scattering by nuclei at low energies, detection of direct interaction contribution in inelastic, 17: 31488
scattering by nuclei, validity of distorted-wave Born approximation for inelastic, 17: 31494
scattering by nuclei, theory for, 17: 31282 (PUC-1963-110)
scattering by nuclei, theory of, 17: 36412 (NP-13020(p.186-200))
scattering by nuclei, narrow resonances in, 17: 36661 (PUC-1962-90)
scattering by nuclei, exchange effects in elastic, 18: 2860
scattering by nuclei at medium energies, survey of experiments on, 18: 6296
scattering by nuclei at high energies, identity effects in multiple, 18: 7747
scattering by nuclei at high energies, nonlocal and target-momentum effects on optical potential for elastic, 18: 7772
scattering by nuclei, theory of compound-nucleus and direct, 18: 9440
scattering by nuclei, polarization in high-energy inelastic, 18: 15289
scattering by nuclei, optical model for elastic, 18: 15303
scattering by nuclei, nuclear rotational levels from, 18: 16959
scattering by nuclei, two-body formulation of problems in, 18: 21337
scattering by nuclear matter, collective excitations in, 18: 26612
scattering by nuclei with shell properties, elastic and inelastic, 18: 30836
scattering by nuclei at 50 to 150 Mev, inelastic, 18: 42695
scattering by nuclei, optical potential for, 18: 42782
scattering by nuclei, Slater integrals and form factors for inelastic single-particle, 19: 1565 (ORNL-TM-964)
scattering by nuclei in two states, coupled-channel resonances in (T), 19: 1566 (PUC-1964-154)
scattering by nucleons, meson exchange in, 19: 9767(R) (IS-900(Sect.P))
scattering by nuclei at low energies, evaluation of models for, 19: 14544
scattering by nuclei, localization of direct interactions in, (T), 19: 14603
scattering by nuclei, optical model potential for, (T), 19: 16931
scattering by nuclei, optical model for elastic, (T), 19: 19212
scattering by nuclei, collective effects of SU_3 classification in inelastic, (T), 19: 19216
scattering by nuclei, parameters for, (T), 19: 20937(R) (TID-21672)
scattering by nuclei at 14 to 24 Mev, optical model analysis of, (T), 19: 23700
scattering by nuclei at low energies, survey on, (T), 19: 31247
scattering by nuclei, particle-hole analysis of, (T), 19: 33250 (TID-21869)
scattering by nuclei, rotational-state excitation in, (T), 19: 33359
scattering by nuclei at low energies, Green function for, (T), 19: 33377
scattering by nuclei, optical-model analysis of, (E/T), 19: 35510
scattering by nuclei, (T), 19: 43374
scattering by nuclei, monopole excitation in elastic, (T), 19: 43301
scattering by nuclear Coulomb field, lepton pair production in, (T), 19: 45027 (NP-15199)
scattering by nuclei, shell-model calculations for, (T), 20: 4882
scattering by nuclei, resonance-mode effects on channel coupling in, (T), 20: 6426
scattering by nuclei, shell model for, 20: 6434
scattering by nucleons, theory of, 20: 20365
scattering by nuclei, high-energy approximation for nonlocal potentials in, 20: 19573

scattering by nuclei, microscopic description of, (T), 20: 22118
scattering by nuclei, diffraction, (T), 20: 26238
scattering by nuclei $3 \leq A \leq 5$, polarization from elastic, 20: 34516 (COO-7-0365)
scattering by nuclei, computer program for gamma angular distributions from, 20: 36220
scattering by nuclei, calculations using diffraction model, (T), 20: 46590 (NP-16309)
scattering cross sections for, asymptotic relations for, 17: 28218
scattering, Feyaman diagram majorization for, 16: 22951 17: 28155 (ORNL-3429)
scattering from nonlocal optical potentials, computer program for,
scattering of, by nucleons, development of transition matrix for analysis of, 16: 31072 (TID-16473)
scattering of, by nuclei, analogy of electron scattering by atoms, 16: 33682 (BNL-6332)
scattering of, inelastic, 17: 41820
scattering of, optical potentials obtained from analyses of elastic, 17: 17204
scattering of polarized, FORTRAN program for analysis of left-right asymmetry in, 16: 938 (ANL-6420)
scattering of, polarization of inelastic, 17: 9288
scattering of, relations of inelastic, with target nucleus energy level, 16: 29772 (JAERI-1020(p.175-83))
scattering of, strip approximation to Mandelstam representation of, 17: 11498 (UCRL-10028)
scattering of, bremsstrahlung from, 18: 18962
scattering of, nuclear shell model description of inelastic, 19: 14642
scattering of, quadratic momentum dependence of nuclear potential in, 20: 12103
scattering of, solution of Schroedinger equations using Green-function method, (T), 20: 44836
scattering of, theory of first-passage distributions for cascade, 20: 20101
scattering on nuclei, interference of compound and direct elastic, 17: 40130
scattering on nuclei, optical potential depth for, 18: 13064
screening in deuterium nuclei, 16: 13880
size effects on Coulomb energy of helium-3 and tritons, finite, 17: 829
spectra from proton reactions with elements at 160 and 450 Mev, (T), 20: 3260
spectra of low- and high-density systems of, excitation, 16: 22884
spectral functions for, determination of isotopic, (T), 20: 27850
spin effects on multiple particle production, 16: 22934
spin gyromagnetic ratio for, effective, (E), 20: 40073 (LA-DC-8065)
spin interaction effect in deuteron stripping, 17: 5375
spin-orbit interaction potential between nuclei and, complexity of, 17: 9612
spin-orbit potential, effects on light isotope electromagnetic processes, 16: 2511
spin-orbit potentials for, triplet-even, 18: 34931
stability measurements, 16: 26328
strength functions in nuclear matter, (T), 20: 4879
structure, 16: 4722
structure, 16: 18379
structure, effects of meson (π) resonances on, 17: 20885
structure, electromagnetic aspects, 16: 16997 (NP-11592(Vol.II)(p.33-55))
structure, isoscalar-component form factors for, 16: 18384
structure, meson (π) model, 16: 15532 (JINR-P-427)
structure of, calculation of electromagnetic, 17: 26389
structure of, effects of multi-meson (π) resonances on isoscalar, 17: 41776
structure of groups of, photonuclear reaction effects of, 18: 11235
structure of, review of experiments on, 18: 5998
structure of, three-meson (π) contributions to electromagnetic, 17: 9272
structure of, three-pion contribution to isoscalar electromagnetic, 18: 9195
structure of three-body systems of, electron scattering studies of, 20: 1234
structure of, conference on, 18: 37958
structure of, electromagnetic, (E), 19: 37667
structure of, from inelastic electron-deuteron scattering experiments, 18: 20945
structure of, meson (μ) probing of, 18: 37969
structure of, resonance models for electromagnetic, 18: 40321
structure of, review, 18: 40363
structure, role of mesons (π) in, 16: 15540
structure, solution of non-linear differential equation for, 16: 13505
structure, theory, 16: 16941 (NP-11592(Vol.I)(p.121-37))
structure, theory of electric, 16: 16996 (NP-11592(Vol.II)(p.21-31))
structure, 3-π resonance contribution to isoscalar, 16: 9392
superconducting systems of, Hartree-Fock method for, 17: 21207
symmetry for, electromagnetic form factors from, (T), 20: 17455
symmetry for, Wigner's supermultiplet theory in framework of SU_6, 19: 25333
systems of interacting, Green function formalism for, (T), 19: 16965
systems of, in shell-model potential with residual pairing forces, 18: 34826
theoretical nature of, relationship of (3,3) resonance to, 17: 5262
theory, 17: 22432 (NP-12610)
theory, eightfold-way assignments in, 17: 17043
theory of many-body systems of, hole self-energy corrections in Brueckner, (T), 20: 42244
theory of N**, as member of unitary symmetry octet, 18: 40312
theory of, quantum, 18: 831 (AD-420626)
theory of self-bound finite system of, 18: 38166
theory of three-body system of, (T), 19: 39923
theory of three-body systems of, p-wave, 20: 46730
three-body correlations and charge form factors, 17: 11583
transfer in deuteron reactions with nuclei, many-body, (E/T), 20: 32547
transfer in heavy ion collisions, parameters for, (T), 19: 20937(R) (TID-21672)
transfer in heavy ion reactions with nuclei, 19: 41795
transfer in ion reactions with nuclei, (E), 19: 27573
transfer in nuclear reactions, transform relation for strengths of, (T), 19: 23731
transfer in nuclei-nuclei reactions, theory of, 17: 20992 (TID-18508)
transfer in oxygen-16 reactions (O^{16},F^{16}), (O^{16},F^{17}), and (O^{16},O^{18}) with aluminum-27 at 36 Mev, 16: 8232
transfer in reactions, analysis of, 18: 24618 (NYO-1807-8)
transfer reactions, virtual coulomb excitation in, 16: 9436 (TID-14211)
transfer reactions of, use in (p,t) reaction correlations, (T), 20: 24360(R) (UCRL-16580, pp 107-48)
transfer strengths in nuclear reactions, multipole sum rules for single, (T), 20: 1190
transfer theory for, 17: 17123(R) (TID-18127)
transitions in nuclei, nuclear core dipole excitation effects on, 17: 7191
transport at 400 to 50 Mev, computer program for, 18: 36578 (ORNL-3610)
transport by shielding, calculations of, 17: 22694
transport through shielding, IBM-7090 Monte Carlo codes for, 17: 18379 (TID-7652(p.608-18))
triplet formation with hyperons, 16: 10902
tunneling theory for, 18: 24617 (NYO-1807-7)
two-nucleon center-of-mass systems, Schrödinger equation for, 16: 6959
vector charge and magnetic moment form factors of, 17: 763
wave function for three-body systems of, properties of bound-state, 20: 26160
wave functions for systems of, antisymmetric, 18: 2873
wave functions for system of three, 18: 30592
wave functions for sd-shell, SU_3, 18: 38172
wave functions for three-body systems of, 19: 18928
wave functions for orbital, structural effects of principal quantum number on, (T), 19: 45365
wave functions for three-body systems of, (T), 20: 42209
wave functions of n-identical system of, isospin and spin from relative coordinate symmetry in, 17: 24309
wave functions of systems of, antisymmetric, 17: 29517
wave functions of SU_3 symmetry in 2s-1d shell, 19: 3310
wave-functions in nuclei, (T), 19: 27579
Wigner supermultiplets, theory, 16: 31075(T) (CEA-tr-A-1154)

NUCLEOPROTEINS

deoxy-, radiation effects on *E. coli*, 19: 19576
deoxyribopoly-, radiation effects on, in animal tissues, x, 19: 29933
desoxy, radiation effects on solutions of, β, 20: 38581
desoxyribo-, radiation effects on structure of, 19: 42307
desoxyribo-, radiation effects on, at molecular and supermolecular levels, 20: 28908
incorporation of tritiated arginine, lysine, and tryptophan in *Vicia faba* roots, 17: 24852
interactions with cystamine and cystamine derivatives of, 19: 35909
iron-59 uptake by yeast ribosomes and ribonucleic acid, 17: 1229
isolation and purification from carcinosarcoma, 16: 21874
properties in rat liver microsomes, chemical and physical, 16: 11389 (TID-15141)
properties, electric and magnetic, 16: 11586(T) (JPRS-12342)
radiation chemistry, ultraviolet fluorescence microscopic studies, 16: 30269
radiation damage, repair using cysteamine, 16: 8587
radiation effects on molecular weight and shape of thymus, gamma, 16: 1543
radiation effects on structure, 16: 1471(T) (JPRS-10170(p.1-23))
radiation effects, 16: 9902
radiation effects in lymphatic and parenchymatous tissues, 16: 23468
radiation effects in central nervous system, 16: 30303
radiation effects on aqueous solutions of, 17: 15771
radiation effects on, 17: 15789
radiation effects on, protective effects of cysteamine against, 17: 23233

radiation effects on, 17: 25023
radiation effects on content of, in organs and tissues in chickens, 17: 31955
radiation effects on ribosomes in *E. coli*, 17: 35483
radiation effects on rat thymocyte, light, uv, x, 18: 17505
radiation effects on properties of, 18: 17570
radiation effects on rabbit agglutinins, restoration effects of immune donor, 18: 19765
radiation effects on RNA synthesis by deoxy-, 18: 35356
radiation effects on rate of removal for rat thymus nuclei, 18: 41185
radiation effects on chemistry and structure of, review on, 19: 13024
radiation effects on calf thymus deoxyribo-, 19: 13083
radiation effects on, EPR spectra of, 19: 13086
radiation effects on physico-chemistry and structure of, in bone marrow cultures, 19: 17620
radiation effects on mouse ribo-, x, 19: 26154
radiation effects on synthesis in rat adrenal cortex, 19: 33914
radiation effects on synthesis of, by gonocytes in rat testes, 19: 38370
radiation effects on Tetrahymena, x, 20: 5267
radiation effects on, x, 20: 6762
radiation effects on density of, x, 20: 8595
radiation effects on structure and content of, in rabbit corneas, β and x, 20: 32961
radiation effects on, in regenerating rat liver DNA, mechanism of x, 20: 36593
radiation effects on, electron spin resonance studies, 20: 40598
radiation effects on, in spleen in mice, 17: 15706
radiation effects on DNA in, protective effects of albumin against, 20: 14277
radiation sensitivity, from liver, spleen, and thymus, 16: 4071
radioinduced degradation of thymus deoxyribonucleohistone, mechanism of, 18: 1762
radioinduced free radicals, 16: 30265
radioinduced free radicals in nucleohistone, x, 20: 14592
radiolysis of aqueous solutions of, review on, 19: 30276
radiosensitivity of mouse thymus deoxyribo-, effects of sodium dodecyl sulfate on, 19: 146
radiosensitivity of artificial, composed of polyadenylic acid–polyuridylic acid/bovine gamma–globulin, 19: 17551
staining of, chromatin affinity for lead hydroxide and uranyl acetate in, 17: 21436
synthesis in normal and tumorous cells, 20: 18264
synthesis in normal and tumorous cells, 20: 18265
synthesis in normal and tumorous cells, 20: 18266
synthesis in normal and tumorous cells, 20: 18267

NUCLEOSIDASES

radiation effects on activity of, in uterine cervical cancer tissues, 20: 35358

NUCLEOSIDES

see also Adenosine
see also Adenosine, Deoxy-
see also Cytidine
see also Cytidine,2'-Deoxy-
see also Guanosine
see also Inosine
see also Uridine
see also Uridines, 2'-Deoxy-
amino-, effects of injected, on catalase activity of blood and liver of rats, 19: 6938(R) (ANL-6906(p.70-2))
analysis for tritium by beta counting, 16: 1302(R) (LAMS-2627(p.45-50))
analysis of, ion exchange chromatographic micro-, 20: 6699(R) (ORNL-3853, pp 151-4)
content in urine of irradiated rats, 20: 42807
content of, in Neurospora conidia, effects of germination and growth on, 20: 6777(R) (ORNL-3853, pp 54-61)
degradation of tritium-labeled, 16: 1304(R) (LAMS-2627(p.57-65))
deoxyribo-, synthesis of carbon-14-labeled, 16: 30313 (LADC-5345)
determination in fish of, 20: 9315 (CONF-651024, pp 10-13)
determination of iodine-125- or iodine-131-labeled, by thin-layer chromatography and counting, 19: 22131
effects on thymine utilization by *E. coli*, 20: 42716(R) (UCRL-16246, pp 164-7)
electron spin resonance spectrometry of irradiated, 20: 40593
labeling 9-(α,β-D-2'-deoxyribofuranosyl)-2-amino-6-mercaptopurine with tritium by isotopic exchange with benzene or toluene, 19: 28349
metabolism in microorganisms, 16: 8529
optical rotation of dinucleoside phosphates, 19: 48104 (UCRL-16278)
optical rotation of dinucleoside phosphates, 19: 48104 (UCRL-16278)
phospho-, contents in organs of irradiated rats, 18: 19702
preparation of carbon-14-labeled, by use of yeast, 18: 38746
pyrimidine, radiolysis of aqueous solutions of, γ, 20: 10899
radiation effects on inhibition of phosphorylase, in rat erythrocytes, 18: 8174
radiation effects on metabolism of, 18: 41103
radiation effects on bacteriophage, EPR spectra, 19: 38365
radiation effects on composition of, in messenger RNA in *Pseudomonas effusa*, 19: 43744
radiation effects on deoxyriboside excretion in urine by dogs, pigs, and sheep, gamma, 20: 36604
radiation effects on rat, x, 18: 82
radioinduced free radicals in, radioprotective effect of, 18: 1463
radioinduced free radicals in, 19: 5955
radiolysis of aqueous solutions and *in vacuo*, ESR spectra of yields in, 19: 11215
radiolysis of aqueous solutions of, review on, 19: 30276
radiolysis of solutions of, NMR spectra of electron beam and gamma, 19: 11216
radiolysis of tritium-labeled, effects of low temperature and scavengers on self-, 20: 16533
radiosensitivity effects of solid phase, electron spin resonance study of, 19: 31825
radiosensitivity effects of bromouracildesoxyriboside and iodouracil-desoxyriboside on *Herpes simplex* virus in HeLa cell cultures, 20: 5363
radiosensitivity of, electron spin resonance studies of, 19: 3921
reactions with hydrated electrons and hydroxyl radicals, rates of, 20: 10917
reactions with hydrogen atoms, 20: 45322(R) (UCLA-12-595, pp 6-28)
ribo-, 5-monophosphate, labeling with carbon-14 in algae, 20: 8966
role of 5-bromouridine desoxyriboside in radiation death of mammalian cells, 17: 35538
sensitivity effects of cytosine arabinoside on murine leukemic cells, 19: 15050
separation by paper chromatography, 16: 5117(R) (UCRL-9900)
spectra of, computer analysis of infrared and ultraviolet, 18: 43375(R) (LA-3132-MS(p.249-51))
synthesis of purine, method for, 19: 46158(R) (NYO-910-23, pp 112-82)
5'-monophosphate, labeling with phosphorus-32, 20: 31307

NUCLEOTIDES

see also Nucleic Acids
acid-soluble, effects of hybridization on embryonic frog, 19: 31704(R) (ORNL-3768(p.157-63))
acid-soluble, isolation from Tetrahymena, 19: 31679(R) (ORNL-3768 (p.146-8))
analysis for carbon-14 and tritium by liquid scintillation counting, use of hyamine–toluene–water system for, 19: 24466
analysis of, chromatographic, 20: 18205(R) (LA-3432, pp 178-262)
anticoagulant properties of, effects of base composition on, 19: 14938
anticomplementary properties of synthetic polyinosinic acid, 19: 14940
biological properties of, 18: 33222
concentration in rat organs, effect of cysteine on radioinduced modifications, 16: 8624
content in fish tissue, methods for measurement of, 20: 29583(R) (TID-22515)
content in yeast cells, effects of growth conditions on, 20: 6696(R) (ORNL-3853, pp 66-77)
content of, in Neurospora conidia, effects of germination and growth on, 20: 6777(R) (ORNL-3853, pp 54-61)
dephosphorylation by thorium and zirconium ions, 19: 19876
determination in tissue extracts, design of automated system for, 18: 11515 (ORNL-3502)
determination of, in enzymatic digests of DNA by neutron activation, 20: 38816
developmental effects on sea urchin adenosine, 18: 33270(R) (NIRS-2(p.23-6))
effect of chemical structure on conformation of pyridine in solutions, 18: 27012(R) (ORNL-3601(p.207-9))
effects of deuterium oxide on hypochromicity of synthetic polymers of, 20: 35204
effects of mycelia-derived, on toxic effects of nitrogen mustard in mice, 20: 18452
effects of radiophosphorus on composition of, in plants, 20: 40548
effects of thorium and zirconium ions on, 19: 60
effects on deuterium–hydrogen exchange in chicken heart lactic dehydrogenase, 19: 17462
enzyme reactions in, 18: 27010(R) (ORNL-3601(p.174-86))
epimerization of uridine diphosphate galactose, tritium isotope effect in, 19: 28350
flavin, photoreduction of, 18: 17387(R) (UCRL-11046(p.227-37))
fluorescence of intracellular pyridine, effects of radioprotective compounds on, 20: 31122
gamma dose effects on phosphate uptake by, in lymphoid tissue, 20: 38585
genetic code for, during synthesis of messenger ribonucleic acid, 19: 40296 (TID-21856)
hydrolysis by apyrase of, tracer study, 19: 35935

hydrolysis of, catalytic effects of thorium and zirconium ions on, 19: 43708
incorporation of uridine, into microsome ribonucleic acid, tracer study, 16: 8528
inhibition of valyl-tRNA synthetase by oligo-, 20: 40503(R) (ORNL-3922, pp 137-45)
isolation of labeled free, from yeast by radiophotosynthesis, 17: 7758
labeling by exposure to tritium gas, 17: 18472
labeling of phosphorus of, by neutron activation, 17: 12335
labeling phosphorus in, by neutron activation, 16: 20494
metabolism in brine shrimp during embryogenesis, 20: 6720(R) (ORNL-3853, pp 143-50)
metabolism in microorganisms, 16: 8529
metabolism in rat liver, 17: 7800(R) (TID-17580)
metabolism of, in amphibian eggs, tracer study of, 20: 6720(R) (ORNL-3853, pp 143-50)
nicotinamide adenine, effects on radiosensitivity of enzymes, 20: 20514
nicotinamide adenine dinucleotide phosphate, effects of glucose-6-phosphate and radioprotectors on rat liver metabolism of, 18: 11581
nicotinamide-adenine-di-, radiation effects on formation of N^1-oxide by decomposition of, 19: 44062
nicotinamide-adenine-N^1-oxide-di-, preparation by radioinduced decomposition of nicotinamide adenine dinucleotide, 19: 44062
nomenclature of oligo-, 18: 15745(R) (LAMS-3034(p.326-8))
nuclear magnetic resonance spectra of, 18: 43444(R) (LA-3132-MS (p.233-5))
oligo-, ion exchange chromatography of, 19: 31703(R) (ORNL-3768 (p.154-6))
oligo-, preparation of triphosphates of, 18: 43541(R) (LA-3132-MS (p.242-4))
origin in cell-free viral synthesis, 18: 21725(R) (TID-20437)
oxidation and radioisotope labeling of Ehrlich ascite, effects of metabolic inhibitors on, 19: 14974
oxidation of, fluorometric study of, 20: 6723(R) (ORNL-3853, pp 175-6)
oxidative phosphorylation, fluorescence polarization during, 20: 45322(R) (UCLA-12-595, pp 6-28)
phosphate metabolism in erythrocyte, tracer study, 19: 33748
phospho-, contents in organs of irradiated rats, 18: 19702
phosphorus-32 uptake by, in *Penicillium chrysogenum*, 19: 25852
poly-, exciton bonds of helical, nature of, 17: 40846
poly-, preparation of high-molecular-weight, 18: 1325(R) (UCRL-10934)
poly-, symmetry and spectral properties of helical, 17: 40846
poly-, energy band structure in Hueckel approximation, 18: 22041
polymerization of 5'-thymidylic acid, 18: 43542(R) (LA-3132-MS(p.252-7))
polymerization of 5'-thymidylic acid, 18: 43543(R) (LA-3132-MS(p.258-62))
polymerization of, tracer studies of reaction mechanisms for, 18: 36872 (BNL-7292)
polymerization of, enzyme reactions for, 20: 18205(R) (LA-3432, pp 178-262)
pool size in experiments with tritiated thymidine, problem on, 16: 20104
preparation of carbon-14-labeled, by use of yeast, 18: 38746
properties of, 19: 2006(R) (ORNL-3700(p.148-9))
properties of synthetic, biological, 19: 31662(R) (ACRH-23(p.87-98))
properties of synthetic, biological, 19: 31663(R) (ACRH-23(p.99-109))
properties of synthetic, biological, 19: 31664(R) (ACRH-23(p.110-17))
protective effects of injected, against radiation injuries in mice, 19: 33967
proton equilibrium distribution and tunneling rate in hydrogen bonds of, 19: 2157
pyridine, complex formation with peroxidases, 19: 27853 (ORNL-P-1212)
pyridine, radiation effects on intracellular oxidation-reduction states of, in mouse and rat organs, 20: 22708
pyrimidine, radiolysis of aqueous solutions of, γ, 20: 10899
radiation chemistry of, 20: 18295(R) (UCLA-12-576, pp 27-56)
radiation effects on metabolism, 16: 9859(T)
radiation effects on content in liver of rats, 17: 34
radiation effects on content in tumor cells, 17: 1190
radiation effects, 17: 5877
radiation effects on metabolism in liver, whole-body exposure, 17: 5879
radiation effects on metabolism in liver, tracer study, 17: 5879
radiation effects on loss of, from lymphocytes in rat thymus, 17: 23110
radiation effects on thymocyte, 17: 27085
radiation effects on metabolism of, in lymph system, tracer study of, 17: 31932
radiation effects on, in spinal ganglia of rats, 17: 35499
radiation effects on, 17: 40553
radiation effects on urine content of, in rats, 18: 6665
radiation effects on metabolism of, 18: 41103
radiation effects on synthesis of, 18: 43276
radiation effects on bacteria as affected by DNA content of, review, 19: 179
radiation effects on content of, in rat liver, 19: 17523
radiation effects on rat liver content of, orotic acid effects on, 19: 17674
radiation effects on metabolism of, in rat liver, 19: 27976
radiation effects on pyridine, in rat liver, 19: 29919
radiation effects in bacteria, uv, 19: 35949(R) (TID-22039)
radiation effects on, in processed fish, 19: 36878
radiation effects on bacteriophage, EPR spectra, 19: 38365
radiation effects on, 19: 43682(R) (UCLA-12-565, pp 33-57)
radiation effects on, in intestine and liver cells, 20: 16230(R) (TID-22644)
radiation effects on magnetic resonance of, x, 20: 18274
radiation effects on $NADH_2$ oxidation in suspensions of cattle heart mitochondria, 20: 20496
radiation effects on aqueous solutions of, review on, 20: 20728 (PB-181506, pp 49-58)
radiation effects on formation of cyclo-, in adenosine monophosphate, γ and x, 20: 32950
radiation effects on nicotinamide adenine, in rat thymocytes, x, 20: 36590
radiation effects on levels of reduced pyridine, in rat liver homogenates, γ, 20: 40583
radiation effects on bone marrow concentration, ionizing, 20: 42822
radiation effects on rat blood, whole-body x, 20: 42955
radiation effects on, in aqueous solution, gamma, 20: 45322(R) (UCLA-12-595, pp 6-28)
radiation sorption from chromatographic eluants, continuous flow analyzer for recording ultraviolet, 18: 19870
radioinduced free radicals in, 19: 5956
radioinduced free radicals in aqueous solutions of flavin mono-, gamma, 19: 36455 (BNWL-SA-199)
radioinduced free radicals in poly-, ESR study of, 20: 23162
radioinduced free radicals in aqueous solution of flavin mono-, gamma, 20: 33331 (BNWL-SA-712)
radioinduced incorporation of labeled, in cold polynucleotides, gamma, 19: 36090
radioinduced polymerization of, gamma, 19: 36517
radioinduced polymerization of, gamma, 19: 36090
radioinduced pyrimidine dimers in poly-, dI:dC, spectra of uv, 19: 28061
radiolysis of aqueous solutions of, review on, 19: 30276
radiosensitivity effects of solid phase, electron spin resonance study of, 19: 31825
radiosensitivity of, in Ehrlich tumors, 17: 35478
radiosensitivity of, electron spin resonance studies of, 19: 3921
reactions with hydrated electrons and hydroxyl radicals, rates of, 20: 10917
reactions with hydrogen atoms, 20: 45322(R) (UCLA-12-595, pp 6-28)
reactions with uranyl ions, 20: 5237(R) (UR-668, pp 55-109)
ribosemono-, radiosensitivity effects on survival time in mice, gamma, 19: 13098
ribosemono-, radiosensitivity effects on marrow cells in mouse spleens, gamma, 19: 13098
role of pyridine coenzyme in radiation protection, 20: 18274
separation by capillary column chromatography, 19: 45730(R) (ORNL-3752)
separation by capillary column, chromatography, 19: 2005(R) (ORNL-3700(p.134-47))
separation by paper chromatography, 16: 5117(R) (UCRL-9900)
separation of carbon-14-labeled, electrophoretic method for, 18: 1333
separation of oligo- and poly-, by ion exchange chromatographic method, 19: 2006(R) (ORNL-3700(p.148-9))
separation of oligo-, by gel filtration, 20: 6699(R) (ORNL-3853, pp 151-4)
spectra of, computer analysis of infrared and ultraviolet, 18: 43375(R) (LA-3132-MS(p.249-51))
structure of, computer program for calculating three-dimensional, 20: 39470(R) (ORNL-3924)
synthesis of carbon-14-labeled pyrimidine, in rat liver, 19: 4176(T) (AEC-tr-6227/2(p.131-7))
synthesis of oligo-, with cytosine and thymine bases, 18: 15779(R) (LAMS-3034(p.329-49))
synthesis, tracer study, 17: 26982
tritium uptake by, in tumor cells, 20: 22545 (CONF-640413, pp 128-31)
ultraviolet radiation effects on dimer formation, 17: 27079
yields in enzymatic hydrolysis of uv irradiated DNA, 19: 7055

NUCLEOTIDES, DESOXY-

biological properties of, 19: 31703(R) (ORNL-3768(p.154-6))
biosynthetic poly-, preparation and uses of, 19: 31703(R) (ORNL-3768(p.154-6))
effects on radiosensitivity of cells, 16: 17456
electron spin resonance spectrometry of irradiated, 20: 40593
enzymatic synthesis, tracer studies, 16: 1375
oligo-, transferase system, characterization and purification of, 19: 31704(R) (ORNL-3768(p.157-63))
photoreactivability of uv-irradiated, 19: 36503

preparation of triphosphates, 18: 43541(R) (LA-3132-MS(p.242-4))
preparation of, using desoxynucleotidyl transferase from calf thymus, 18: 27032(R) (ORNL-3601(p.173))
radioinduced release in tissues, time course of, 19: 29933

NUCLEOTIDES, DIHYDRODIPHOSPHOPYRIDINE
biological effects on respiration of homogenized liver of irradiated rats, 16: 30290
radiation effects, gamma, 16: 18952

NUCLEOTIDES, PYRIDINE DIPHOSPHATE
diphosphopyridine, radiation effects on metabolism in liver and Ehrlich ascites tumor cells in mice, 17: 68
effects of free radicals and radiations on, molecular mechanisms in, 20: 35251
effects of, on activity of hydrogen dehydrogenase, exchange reactions and kinetics of, 17: 19793
effects of ultraviolet radiation on peroxide content, 16: 31481
effects on leukopoiesis, 20: 26620
effects on phosphate and rubidium uptake by isolated cells of bean seedlings and tobacco leaves, 20: 14217 (COO-888-43)
labeling with carbon-14 or tritium, 19: 11143
metabolic repair of radioinduced chromosome aberrations in Tradescantia by, 16: 30252
protective effects against radiation injury in chick embryos, 17: 5914
protective effects against radiation damage to embryonal cells, 19: 7184
protective effects of injected, against radiation injuries in rats, 19: 46020
radiation effects on activity in kidney, abdominal exposure, 16: 55
radiation effects on oxidized, mechanism, 16: 18952
radiation effects on content of, in tumor cells, 17: 33639
radiation effects on sulfhydryl content of, in rat liver, 17: 33640(T)
radiation effects on reactions of enzyme-coupled, x, 17: 33625
radiation effects on rat, x, 17: 38762
radiation effects on, x, 18: 6852
radiation effects on content of, in ascites tumors, 18: 27079
radiation effects on synthesis of, in ascites tumor cells, x, 18: 27087
radiation effects on content of, in organs and tumors of rats, 18: 27148
radiation effects on distribution in sarcoma cells of, x, 18: 29378
radiation effects on content of, in chick embryo heart, 19: 3922
radiation effects on content of, in ascites tumor cells, 19: 15051
radiation effects on binding titratable sulfhydryl group loss in glutamate and lactate dehydrogenase solutions, 19: 25848
radiation effects on content of, in ascites tumor cells, 19: 28041
radiation effects on content in sarcoma cells, x, 20: 14370
radiation effects on content of, in Ehrlich ascites carcinoma cells, x, 20: 18270
radiation effects on, ESR and thermoluminescence studies of, 20: 29249
radiation effects on metabolism of, in Ehrlich ascites and Yoshida sarcoma tumor cells, x, 20: 35259
radiation effects on metabolism of, in rat bone marrow and peripheral blood, x, 20: 42788
radiation effects on metabolism in liver and Ehrlich ascites tumor cells in mice, 17: 68
radiolysis, 18: 3821
radiosensitivity effects on cell membrane permeability, gamma, 18: 13508
radiosensitivity effects in rats, 20: 18504
radiosensitivity effects in man and rats, 20: 18535
reactions in malic dehydrogenase, effects of deuterium on alpha and beta stereoisomers of, 16: 31395(R) (ANL-6535(p.96-9))
reduction mechanisms in rat liver slices, 20: 42759
relation to sodium ion efflux from rat liver slices, 20: 42758

NUCLEOTIDES, PYRIDINE TRIPHOSPHATE
chemical and radiation effects on, in tumor cells, 17: 27035
effect of, on sulfur-35 incorporation by amino acids, 17: 37048
labeling with carbon-14 or tritium, 19: 11143
metabolic repair of radioinduced chromosome aberrations in Tradescantia by, 16: 30252
radiation effects on, in chloroplasts, 17: 10458
radiation effects on concentration of oxidized and reduced, in rat organs, 20: 18343
radiation effects on metabolism of, in rat bone marrow and peripheral blood, x, 20: 42788
reduction and formation of ATP by spinach chloroplasts, 18: 23198(R) (ANL-6823(p.191-8))
reduction in irradiated chloroplasts, quantum efficiencies of spectra of, 16: 31402(R) (ANL-6535(p.142-3))
relation to sodium ion efflux from rat liver slices, 20: 42758

NUTRIENTS
assimilation by plant roots from soil, effects of soil management practices on, 18: 19515 (NP-13796)
bibliography on nutrition and radiation injury, 16: 17436 (AD-266312)
biochemical circulation of, in Sargasso Sea, 18: 17382(R) (NYO-3140-1A)
biochemical circulation of, in Sargasso Sea, role of phytoplankton in, 18: 19471(R) (NYO-3140-1)
book: *Value of Nutrition in Prophylaxis of Radiation Sickness*, 17: 28777
content in Mediterranean Sea, 20: 43508(R) (NP-16179)
content in seawater, tracer techniques for measuring, 20: 20368 (CONF-640309-1)
cycling in ecosystems, tracer study, 17: 33552
cycling through ecosystems, computer calculation, 17: 33553
distribution in man, tracer studies using whole-body counting, 18: 27050
distribution in Pacific Ocean near mouth of Columbia River, 20: 18902 (RLO-1725-41)
distribution in soils, tracer studies of, 20: 3710(R) (EUR-2493.e)
effects of maternal, on embryonic and fetal development in sheep, 18: 38775(R) (ORO-624)
effects of maternal, on pigs, 18: 38775(R) (ORO-624)
effects of starvation on life span of mice, 20: 42840(R) (ANL-7136, pp 164-90)
effects on growth of pea seedlings in vermiculite, 18: 36868 (BNL-7246)
effects on iodine-131 metabolism by cattle, 20: 598 (NP-15568)
effects on metabolism in chickens, 19: 8763
effects on radiation effects on metabolic processes in rats, 17: 31838
effects on radiosensitivity of animals, 19: 21971
effects on radiosensitivity of chromosomes in plant cells, 19: 33874
foliar absorption of, 18: 13377 (TID-20184)
foliar absorption of, mechanisms for, 20: 14219 (COO-888-47)
in survival foods, 18: 16237
intestinal absorption of, effects of hookworm infection in man, 18: 21724(R) (TID-20404)
leaching and recycling in plants and forests, 20: 29451(R) (NYO-2598-29)
leaching from plants, tracer study effects of injury on, 19: 3875
leaching from plants of, during mist propagation, tracer study, 20: 21 (NYO-2598-25)
maintenance of, in radiation injury of head, in mice, 17: 28667(R) (ACRH-19(p.49-53))
metabolism in animals, tracer studies of, 20: 3685
movement of plant, through soil systems, tracer study, 20: 6726 (STI/DOC/10/48)
permeation through plant foliage, effects of urea on, 20: 14218 (COO-888-44)
plant, transfer in forest litter, tracer studies, 17: 33589
plant uptake of, from irradiated soils, 18: 29363
plant, foliar absorption of, 18: 15671 (CONF-411-1)
radiation effects on soil, 18: 29363
radiation effects on, in meat, 18: 35311(R) (NP-14188)
radiation effects on intestinal absorption of, in man, 20: 3851
radiation effects on, in clams, 20: 9330 (CONF-651024, pp 85-7)
radiosensitivity effects on plants, 16: 18787
radiosensitivity effects in plants of, y, 20: 6868
radiosensitivity effects on conifer-hardwood forests, fast-neutron, 20: 12672
root uptake of, tracer study in sunflowers, 19: 33777
tracer studies on requirements of man for selected, using whole-body counting, 18: 36940
transport in soils, tracer techniques for measuring, 20: 33540
uptake by plants from soil, tracer study, 20: 20389 (STI-PUB-108)
uptake by plants from soil, tracer study, 20: 6726 (STI/DOC/10/48)

Nuts
see Bolts and Nuts

NYASALAND
radiation effects on Chilwa islanders in, background, 19: 31823
radioactive geological areas on Chilwa Island, effects on population, 16: 16173

Nylon
see Amide Polymers

DEPOSITORIES OF USAEC REPORTS

In Countries Other than the U.S.

ARGENTINA
Buenos Aires, Comisión Nacional de Energía Atómica
AUSTRALIA
Canberra, Australian National Library
Sutherland, New South Wales, Australian Atomic Energy Commission
AUSTRIA
Vienna, Zentral Bibliothek der Physikalischen Institute der Universität
BELGIUM
Mol-Donk, Centre d'Etude de l'Energie Nucleaire
BOLIVIA
La Paz, Comisión Nacional de Energiá Nuclear
BRAZIL
Rio de Janeiro, Instituto Brasileiro de Bibliografia e Documentacao
São Paulo, Instituto de Energia Atomica, Cidade Universitaria São Paulo
BURMA
Rangoon, Union of Burma Applied Research Institute, Atomic Energy Center Library
CANADA
Hamilton, McMaster University
Ottawa, National Research Council Library
Vancouver, University of British Columbia
CHILE
Santiago, Departamento de Fisica, Universidad de Chile
CHINA
Hsinchu, Taiwan, Free China, National Tsing Hua University
COLOMBIA
Bogota, Instituto De Asuntos Nucleares
COSTA RICA
San Pedro, University of Costa Rica Library
DENMARK
Risö, Danish Atomic Energy Commission
ECUADOR
Quito, Escuela Politécnica Nacional
EL SALVADOR
San Salvador, Universidad de El Salvador, Biblioteca de Energia Nuclear
FINLAND
Helsinki, Teknillisen Korkeakoulun Kirjasto
FRANCE
Gif-sur-Yvette, Centre d'Etudes Nucléaires de Saclay
Paris, Académie des Sciences
GERMANY
Berlin, Hahn-Meitner-Institut für Kernforschung Berlin
Frankfurt/Main, Gmelin-Institut
Munich, Technische Hochschule, Bibliothek
GHANA
Accra, University College of Ghana
GREECE
Athens, Nuclear Research Center "Democritus"
GUATEMALA
Guatemala, Comisión Nacional de Energía Nuclear
INDIA
Bombay, Department of Atomic Energy
INDONESIA
Djogjakarta, Java, Science Faculty Gadjah Mada University
IRAN
Tehran, Tehran University Nuclear Centre
IRAQ
Baghdad, Iraqi Atomic Energy Commission
IRELAND
Dublin, University College
ISRAEL
Rehovoth, Israel Atomic Energy Commission
ITALY
Rome, Centro di Studi Nucleari della Casaccia
Rome, Comitato Nazionale per l'Energia Nucleare
JAPAN
Tokyo, National Diet Library
KOREA
Seoul, Office of Atomic Energy
LEBANON
Beirut, Lebanese National Council for Scientific Research
LUXEMBOURG
Luxembourg, Ministry of Transport and Electricity
MALAYSIA
Kuala Lumpur, University of Malaysia
MEXICO
Mexico, D.F., Comisión Nacional de Energía Nuclear
NETHERLANDS
The Hague, Reactor Centrum Nederland
NEW ZEALAND
Lower Hutt, Institute of Nuclear Sciences
NIGERIA
Ibadan, University of Ibadan
NORWAY
Lillestrom, Institutt för Atomenergi
PAKISTAN
Islamabad, Pakistan Institute of Nuclear Science and Technology
PERU
Lima, Junta de Control de Energia Atomica
PHILIPPINE REPUBLIC
Manila, Philippine Atomic Energy Commission
POLAND
Warsaw, Biura Pelnomocnika Rzadu do Spraw Wykorzystania Energii Jadrowej
PORTUGAL
Sacavem, Junta de Energía Nuclear
REPUBLIC OF SOUTH AFRICA
Pretoria, Atomic Energy Board Library
REPUBLIC OF THE CONGO
Leopoldville, Université Lovanium
SPAIN
Madrid, Junta de Energía Nuclear, Biblioteca Documentación y Publicaciones, Ciudad Universitaria
SWEDEN
Nyköping, Aktiebolaget Atomenergi
SWITZERLAND
Zürich, Eidgenössische Technische Hochschule, Bibliothek
THAILAND
Bangkok, Office of the Thai Atomic Energy Commission, Department of Science
TURKEY
Ankara, Turkish Atomic Energy Commission, Atomic Energy Library
UNITED ARAB REPUBLIC
Cairo, Atomic Energy Commission
UNITED KINGDOM
Birmingham, Central Library
Boston Spa, National Lending Library for Science and Technology
Kingston upon Hull, Central Library
Liverpool, Central Library
London, Central Library, Acton
London, National Reference Library
London, Science Museum Library, South Kensington
Manchester, Central Library
Newcastle upon Tyne, Central Library
Nottingham, Central Library
Sheffield, Central Library
URUGUAY
Montevideo, Comision Nacional de Energia Atomica
VENEZUELA
Caracas, Instituto Venezolano de Investigaciones Científicas
VIET-NAM
Saigon, Atomic Energy Office
YUGOSLAVIA
Belgrade, Federal Commission for Nuclear Energy

In International Agencies

AUSTRIA
Vienna, International Atomic Energy Agency
BELGIUM
Brussels, La Bibliotheque EURATOM
FRANCE
Paris, European Nuclear Energy Agency, O.E.C.D.
ITALY
Ispra, EURATOM Research Center
SWITZERLAND
Geneva, United Nations Library

UNITED STATES
GOVERNMENT PRINTING OFFICE
DIVISION OF PUBLIC DOCUMENTS
WASHINGTON, D.C. 20402

OFFICIAL BUSINESS

POSTAGE AND FEES PAID
U.S. GOVERNMENT PRINTING OFFICE

TECHNICAL PROGRESS REVIEWS

The Division of Technical Information, U. S. Atomic Energy Commission, also publishes the Technical Progress Reviews, a series of four quarterly journals on nuclear technology. These journals, compiled by specialists and recognized authorities, summarize, evaluate, and reference the progress of development in four important fields.

Isotopes and Radiation Technology P. S. Baker, A. F. Rupp, and associates, Oak Ridge National Laboratory. Reviews AEC-sponsored projects and related significant worldwide developments in radioisotopes and radiation technology.

Nuclear Safety Wm. B. Cottrell, W. H. Jordan, J. P. Blakely, and associates, Nuclear Safety Information Center, Oak Ridge National Laboratory. Covers topics relevant to the analysis and control of hazards associated with nuclear reactors and with operations involving fissionable materials and the products of nuclear fission.

Power Reactor Technology Argonne National Laboratory. Reviews research, development, design practices, and operating experiences associated with power reactors, including aerospace applications.

Reactor Materials E. M. Simons and associates, Battelle Memorial Institute. Covers the properties, behavior, and fabrication processes of materials used in nuclear reactors and associated equipment.

Availability

SUBSCRIPTION RATE: The Technical Progress Reviews may be purchased from the Superintendent of Documents, U. S. Government Printing Office, Washington, D. C. 20402. *Nuclear Safety* at $3.00 per year for each subscription or $1.00 per issue; each of the other journals at $2.50 per year or $0.70 per issue.

POSTAGE: Postpaid within the United States, Canada, Mexico, and all Central and South American countries except Argentina, Brazil, Guyana, French Guiana, Surinam, and British Honduras. For these Central and South American countries and all other countries, add $0.75 for each annual subscription or $0.20 for a single issue.

REMITTANCE: Payment should be by check, money order, or document coupons and MUST accompany order. Remittances from foreign countries should be made by international money order or draft on an American bank payable to the Superintendent of Documents or by UNESCO book coupons.